Athens, Greece
Divani Caravel Hotel
25–26 September 2013

34th AIVC Conference
3nd TightVent Conference
2nd Cool Roofs' Conference
1st venticool Conference

Energy conservation technologies for mitigation and adaptation in the built environment: the role of ventilation strategies and smart materials

PROCEEDINGS

In cooperation with:

INIVE

NATIONAL & KAPODISTRIAN UNIVERSITY OF ATHENS
Faculty of Physics
Department of Environmental Physics & Meteorology

Technical University of Crete

Acknowledgments

The conference organisers gratefully acknowledge the support from:

AIVC with its member countries : Belgium, Czech Republic, Denmark, Finland, France, Germany, Greece, Italy, Japan, the Netherlands, New Zealand, Norway, Poland, Portugal, Republic of Korea, Sweden and USA.

Since 1980, the annual AIVC conferences have been the meeting point for presenting and discussing major developments and results regarding infiltration and ventilation in buildings. AIVC contributes to the programme development, selection of speakers and dissemination of the results. pdf files of the papers of older conferences can be found in AIRBASE. See www.aivc.org.

TightVent Europe

The TightVent Europe 'Building and Ductwork Airtightness Platform' was launched in January 2011. It aims at facilitating exchanges and progress on building and ductwork airtightness issues, including the production and dissemination of policy oriented reference documents and the organization of conferences, workshops, webinars, etc. The platform has been initiated by INIVE EEIG (International Network for Information on Ventilation and Energy Performance) and receives active support from the following organisations: Aeroseal, Buildings Performance Institute Europe,BlowerDoor GmbH, European Climate Foundation, Eurima, Lindab, Retrotec, Soudal, Tremco illbruck, and Wienerberger. listed below. More information can be found on www.tightvent.eu.

venticool

The international ventilative cooling platform, venticool (venticool.eu) was launched in October 2012 to accelerate the uptake of ventilative cooling by raising awareness, sharing experience and steering research and development efforts in the field of ventilative cooling. The platform supports better guidance for the appropriate implementation of ventilative cooling strategies as well as adequate credit for such strategies in building regulations. The platform philosophy is pull resources together and to avoid duplicating efforts to maximize the impact of existing and new initiatives. venticool will join forces with organizations with significant experience and/or well identified in the field of ventilation and thermal comfort like AIVC (www.aivc.org) and REHVA (www.rehva.eu). Venticool has been initiated by INIVE EEIG (International Network for Information on Ventilation and Energy Performance) with the financial and/or technical support of the following partners: Agoria-NAVENTA, ES-SO, Eurima, Velux and Window Master.

ECRC

The ECRC (www.coolroofs-eu.eu) is a not-for-profit association whose initiatives are driven and paid for by members. It is a voluntary organization that brings value by promoting the benefits of cool roofing products to regulators, policy makers, consumers and other stakeholders.

Established in 2011, and with more than 25 members around Europe, ECRC believes that Cool Roofs can make an important contribution to mitigating climate change through reducing the urban heat island effect and increasing the sustainability of buildings. For this reason, the ECRC promotes the certification of Cool Roof products and their use across Europe.

INIVE EEIG (International Network for Information on Ventilation and Energy performance)

INIVE was founded in 2001.

INIVE is a registered European Economic Interest Grouping (EEIG), whereby from a legal viewpoint its full members act together as a single organisation and bring together the best available knowledge from its member organisations. The present full members are all leading organisations in the building sector, with expertise in building technology, human sciences and dissemination/publishing of information. They also actively conduct research in this field - the development of new knowledge will always be important for INIVE members.

INIVE has multiple aims, including the collection and efficient storage of relevant information, providing guidance and identifying major trends, developing intelligent systems to provide the world of construction with useful knowledge in the area of energy efficiency, indoor climate and ventilation. Building energy-performance regulations are another major area of interest for the INIVE members, especially the implementation of the European Energy Performance of Buildings Directive.

With respect to the dissemination of information, INIVE EEIG aims for the widest possible distribution of information.

The following organisations are members of INIVE EEIG (www.inive.org):

BBRI - Belgian Building Research Institute - Belgium
CETIAT - Centre Technique des Industries Aérauliques et Thermiques - France
CSTB - Centre Scientifique et Technique du Bâtiment - France
IBP - Fraunhofer Institute for Building Physics - Germany
SINTEF - SINTEF Building and Infrastructure - Norway
NKUA - National & Kapodistrian University of Athens - Greece
TNO - TNO Built Environment and Geosciences, business unit Building and Construction - Netherlands

The following organisations are associated members.

CIMNE - International Center for Numerical Methods in Engineering, Barcelona, Spain
eERG - End-use Efficiency Research Group, Politecnico di Milano, Italy
ENTPE - Ecole Nationale des Travaux Publics de l'Etat, Vaulx en Velin, France
TMT US - Grupo Termotecnia, Universidad de Sevilla, Spain

TUC

The Technical University of Crete (TUC) was founded in Chania in 1977 and admitted its first students in 1984. Since its foundation, the Technical University of Crete is at the forefront in the development of modern engineering skills and specializations, as well as in the research for advanced technologies and their connection with the industrial and productive units of the country. The Environmental Engineering Department of TUC targets to provide advanced, high-quality education and research means concerning environmental engineering issues, as well as to prepare qualified engineering scientists capable of contributing in the measurement, monitoring, assessment, and treatment of problems caused by human intervention in the environment.

Technical University of Crete

GROUP BUILDING ENVIRONMENTAL RESEARCH – UNIVERSITY OF ATHENS

The Group of Building Environmental Research, (GRBES), operates under the frame of the Section of Applied Physics, Department of Physics of the University of Athens. It carries out specific research and development programs on the field of environmental quality of the built environment. In parallel, offers education and training to under and post graduate students, and prepares educational material and books on the field of energy and environment.

It works on topics related to: Development of Intelligent Materials, Energy Performance of Buildings, Solar Energy Systems and Techniques, Energy Efficient Technologies, Indoor Environmental Quality, IT Technologies applied to Buildings, Urban Environmental Quality, Energy and Environmental Rating.

The Group is organised around five laboratories: Intelligent Materials, Outdoor Components Testing, Daylighting and Solar Radiation, Intelligent Buildings, Ventilation and Indoor Air Quality, Urban Environment. All laboratories are located in the open field experimental facility of the University of Athens. The Group is equipped with all the necessary infrastructure to perform experimental studies on the field of environmental quality of the build environment.

The Group is working on specific International projects aiming to apply and demonstrate energy efficient technologies. Simulation techniques are used to optimise the efficiency of the energy systems while the finalized projects are monitored in details to experimentally assess their energy and environmental performance.

By using its modern and complete experimental facilities the Group has undertaken many audits aiming to identify energy and environmental problems in the built environment. Specific and optimised solutions are then prepared and proposed for implementation.

Design advice on energy and environmental performance of new projects aiming to present a high environmental quality is offered by the Group. Many prestigious International and National projects have been undertaken and completed in collaboration with well-known professionals.

NATIONAL & KAPODISTRIAN UNIVERSITY OF ATHENS
Faculty of Physics
Department of Environmental Physics & Meteorology
University Campus, Building PHYS-V, 157 84, Zografos, Athens, GREECE
Tel.: +30 210 7276830, Fax.: +30 210 7295281

TABLE OF CONTENTS

MODEL PROJECTED HEAT EXTREMES AND AIR POLLUTION IN THE MEDITERRANEAN AND MIDDLE EAST IN THE TWENTY-FIRST CENTURY

Jos LELIEVELD

ABSTRACT

The Mediterranean and Middle East region is exposed to strong climatic gradients between its temperate north and arid south. We present model results, which suggest that across the Balkan Peninsula and Turkey climate change is particularly rapid, and especially summer temperatures are expected to increase strongly. Very hot summers that occurred only rarely in the recent past are projected to become common by the middle and the end of the century. As a result, the number of heat wave days may increase drastically. Furthermore, conditions in the region are conducive for photochemical air pollution. Our model projections suggest strongly increasing ozone formation, a confounding health risk factor particularly in urban areas. This adds to the high concentrations of aerosol particles from natural (desert dust) and anthropogenic sources. The heat extremes may have strong impacts, especially in the Middle East where environmental stresses are plentiful.

OPTIMIZATION OF NIGHTTIME VENTILATION PARAMETERS TO REDUCE BUILDING ENERGY CONSUMPTION BY INTEGRATING DOE2 AND MATLAB

Hashem Akbari* and Hatef Aria

Concordia University

1455 De Maisonneuve Blvd. W.
Montreal, QC H3G 1M8
Canada

**Corresponding author: hakbari@encs.concordia.ca*

ABSTRACT

The nighttime ventilation strategy uses the outdoor cold air during the night to cool the building mass. The cooled building mass then is used as a heat sink during the next hot day. Mechanical nighttime ventilation requires a fan for the outside air ventilation. The energy use by the fan reduces the potential cooling energy savings. Higher nighttime ventilation flow rate and its duration decrease required cooling energy during next hot day in the building, also they increase fan energy consumption. In an optimal nighttime ventilation operation, these parameters need to be optimized based on each day outdoor temperature variation.

We have developed an algorithm to optimize fan flow rate by integrating DOE2 (building energy simulation software) with MATLAB's genetic algorithm (GA). In our developed algorithm MATLAB can send desired values of optimization variable for different hours to DOE2 to simulate building energy use, also MATLAB can receive building energy consumption and other data from DOE2 for the optimization. This online connection between DOE2 and MATLAB create powerful building optimization tool. This optimization tool can be used for finding optimal solution of nighttime ventilation fan flow rates and maximizing energy savings. Also, by using this tool nighttime optimization can be easily applied to different buildings and systems. Nighttime ventilation can be investigated in DOE2 by considering effective parameters such as: 1) nighttime ventilation duration, 2) nighttime ventilation fan flow rate, 3) outdoor temperature set-point, and 4) temperature difference between outdoor and indoor. Optimization results show outdoor temperature between 10 to 18 °C and temperature difference more than 8 °C are appropriate for nighttime ventilation.

Keywords

Nighttime ventilation, building energy, optimization, integration

1 INTRODUCTION

Nighttime ventilation is a strategy used for reducing cooling energy consumption in buildings. Many studies have investigated the effect of nighttime ventilation in different climates [1-4]. The nighttime ventilation strategy uses the nighttime outdoor cold air to cool the thermal mass of the building. During the next day, the cooled thermal mass is used as a heat sink. For mechanical nighttime ventilation a fan is needed to bring in outdoor air during the night that allows control of outside air ventilation. The energy use by the fan, in turn, reduces the potential cooling energy savings.

Parameters that specify nighttime ventilation effectiveness are classified into three main categories [5-7]: building parameters (thermal mass), technical parameters (outdoor air flow rate, nighttime ventilation duration), and climatic parameters (outside temperature, humidity, and solar radiation).

Higher nighttime ventilation flow rates and duration can decrease building cooling energy consumption, also they increase fan energy consumption. In an optimal control operation, these parameters need to be optimized. For nighttime ventilation to be effective, building thermal mass is a necessary requirement, therefore, in buildings with low thermal mass nighttime ventilation is not efficient.

Various studies have evaluated the effect of different parameters such as climate, air flow rate, and thermal mass, on effectiveness of nighttime ventilation and occupant comfort [8-11]. However, fewer studies considered duration of nighttime ventilation [15, 16]. Most studies have used simplified method of building model or optimization. Developing an accurate method of optimization that can be applied in all types of buildings still needs more investigation.

To study the potential of nighttime ventilation, Wang et al. [18] evaluated the important factors influencing nighttime ventilation performance such as ventilation rate and duration, building mass and climatic conditions. They used EnergyPlus to simulate the indoor thermal environment and energy consumption in typical office buildings with mechanical nighttime ventilation in three cities in northern China. They results show that with night ventilation rate of 10 ach, the mean radiant temperature of the indoor surface decreased by up to 3.9 ℃ and longer duration of operation, the more efficient the night ventilation strategy becomes A variety of optimization methods have been applied in building control problems such as, linear and non-linear optimization (LP & NLP) [12,13], genetic algorithm optimization technique [14, 15, 16], and dynamic programming (DP) [17]. The most common method used in building optimization is genetic algorithm (GA) that is a search technique used in computing to find solutions to optimization problems.

Congradac and Kulic [19] discussed IAQ and energy savings potential of the HVAC system through the application of the GA. Their results showed up to 20% energy savings for chiller. They applied results from optimization problem with Matlab to EnergyPlus model of the building and introduce this model as a reliable model for optimization.

The objective of this paper is to assess the performance of mechanical nighttime ventilation cooling and optimize nighttime fan flow rate in typical conditioned office buildings. An hourly building energy simulation model, DOE2.1E [20, 21], was used to calculate building energy consumtion. In addition, the MATLAB software was integrated with DOE2 for optimization of outdoor fan flow rate during the night. Genetic algorithm was used in MATLAB as the optimization method. The effects of various parameters such as outdoor temperature, indoor-outdoor temperature difference and nighttime ventilation duration were studied to evaluate the effectiveness of nighttime ventilation.

2 METHODOLOGY

Nighttime ventilation is optimized by integrating MATLAB as an optimization software and DOE2 as building energy calculation software. Genetic algorithm (GA) was chosen for optimization method since it is a stochastic method and does not require an exact equation of objective function. In this integration GA method generate a set of flow rates for different hours during the night and sends them to DOE2. DOE2 calculates building energy consumption for the entire day base on the specified nighttime fan flow rates and returns the

results to GA. This process is continued until GA reaches to its maximum iteration and GA introduces final set of nighttime fan flow rates that optimized building energy consumption.

The results of this optimization were used to investigate the effect influencing parameters such as ioutdoor temperature, indoor-outdoor temperature difference, and nighttime ventilation duration.

2.1 **Building model**

The selected prototype building is a one-story office building with 5 zones and a plenum. The total floor area is 464.5 m^2 (5000 ft^2) with a height of 2.4 m (8 ft). There is no shade from other nearby facilities. The building is built with medium weight construction. Interior loads are surface mounted fluorescent lighting at 16 W/m^2, equipment at 10.8 W/m^2, and peak occupancy of 9.3 m^2 (100 ft^2) per person. Infiltration is 0.25 air changes per hour (ACH). Design temperatures for cooling and heating are set at 25.5°C (78 °F), and 21°C (70 °F), respectively. A single variable air volume system serves the entire building. The system has a variable speed fan motor, and VAV boxes with a minimum stop of 30%. The cooling and heating system operate from 8am to 6pm weekdays and is off during nights and weekends. HVAC plant works with gas fired hot water generator and reciprocating air cooled chiller. Detail of building construction and systems are shown in Table 1.

Table 1: Detail of building description

Parameters	**Description**
Floor area [m^2] (ft^2)	464.5 (5000)
Wall construction	Wood shingles, plywood, R-11 fiber insulation, gypsum board
Roof construction	Roof gravel, built-up roofing, R-3 to R-30 mineral board insulation, wood sheathing ceiling
Window glass	0.6 cm plate double pane
Door glass	1.3 cm plate single pane
Interior loads	Lighting=16 W/m^2, equipment = 10.8 W/m^2, people = 9.3 m^2 (100 ft^2) per person
Interior partitions [W/m^2K] (BTU/hr ft^2 F)	U-value = 8.5 (1.5)
Infiltration	0.25 ACH
Chiller	Reciprocating air cooled chiller (COP=3.65)
Boiler	Gas fired hot water boiler (Eff = 85%)

2.2 **External temperature conditions:**

Outdoor temperature has a strong effect on the effectiveness of ventilation. During the air conditioning period, from June 1 to August 31, the maximum, minimum and average outside air temperatures are shown in Table 2 for Montreal. In this paper optimization is applied on weekdays of July.

Table 2: The maximum, minimum and average outside air temperatures for investigated cities

	Jun			**Jul**			**Aug**		
City	**Max T [°C] (°F)**	**Min T [°C] (°F)**	**Ave T [°C] (°F)**	**Max T [°C] (°F)**	**Min T [°C] (°F)**	**Ave T [°C] (°F)**	**Max T [°C] (°F)**	**Min T [°C] (°F)**	**Ave T [°C] (°F)**
Montreal	30 (86)	7.2 (45)	18.5 (65.4)	31.6 (89)	8.3 (47)	20.7 (69.2)	28.9 (84)	7.7 (46)	19.5 (67.2)

2.3 **Optimization method (Genetic algorithm)**

Genetic Algorithms (GA) are stochastic search algorithms that borrow some concepts from nature. At the start of the algorithm, an initial population is generated, either randomly or according to some rules. The reproduction operator selects population members (set of

optimization variables) from the previous population to be parents for new members. This parenthood selection can range from a totally random process to one that is based by the member's fitness value (value of objective function for each member).

Each new generation are formed by the action of genetic operators on the older population. Finally, the members of the population pool are compared via their fitness value to choose optimal solution. A GA is left to progress through generations, until certain criteria (such as a fixed number of generations, or a time limit) are met [22].

2.4 **Integrating DOE2 and MATLAB**

Building energy use and cost analysis tool (DOE2.1E) was used for building simulation. DOE2 is a widely used, validated and accepted freeware building energy analysis program. It can calculate the energy use and cost for all types of buildings; it has a complete library and weather data; and most importantly it has available source code with possibility to add functions. For MATLAB and DOE2 integrating, first, GA generates chromosomes that are matrices of nighttime fan flow rates. These matrices include fan flow rates from one hour before working hours (7am) to five hour before working hours (3am). Each of these chromosomes has five elements that fill with a number between zero and one. These numbers show the fraction of that hour fan flow rate to maximum possible fan flow rate. After that MATLAB calls AWK (a text-processing programme) and create an input file of DOE2 base on each of these chromosomes. Finally DOE2 is run and building energy consumption is return to MATLAB for that chromosome as a fitness value. Figure 1 shows optimization process.

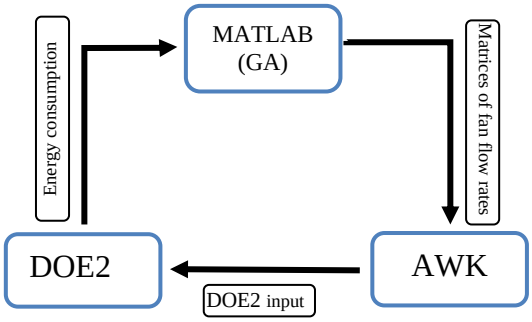

Figure 1: Optimization process

Result and Discussion

Nighttime fan flow rates optimization was applied for five hours before working hours during the summer (Jun, July and August) at Montreal. The results for days with energy savings during summer are listed in Table 3. These results show total energy savings up to 8% and cooling energy saving up to 23%. These savings happened in a day with high diurnal temperature range and average temperature near 17 ˚C.

The results for total-building and cooling-energy consumption with and without nighttime ventilation during some days of summer are shown in Figures 2 and 3.

Table 3: Daily weather conditions and optimization results during summer in Montreal

Day No.	Date	Diurnal ave temp.	Diurnal temp. range	Night ave temp.	Ave fan flow rate fraction	Energy savings (kWh)	Cooling savings (kWh)	% Energy savings	% Cooling savings
1	8-Jun	20.2	13.9	14.0	0.4	2.1	6.7	2.0	9.7
2	10-Jun	23.4	14.4	17.4	0.3	0.8	4.5	0.5	4.2
3	13-Jun	13.6	8.9	10.0	0.3	1.2	1.1	1.9	6.2
4	14-Jun	17.1	16.1	10.2	0.6	7.8	13.6	8.1	23.0
5	15-Jun	19.9	15.0	13.3	0.7	5.5	13.8	4.3	16.6
6	16-Jun	20.0	8.3	16.6	0.4	1.9	7.3	1.6	10.1
7	17-Jun	22.1	11.7	17.1	0.4	0.1	5.3	0.1	5.8
8	22-Jun	19.4	11.1	14.8	0.4	1.4	5.8	1.4	9.0
9	23-Jun	20.1	12.8	14.1	0.5	4.5	10.6	3.9	14.2
10	24-Jun	22.5	15.6	15.7	0.5	2.4	10.0	1.7	10.5
11	28-Jun	16.6	15.0	10.0	0.1	1.1	2.4	1.7	6.3
12	29-Jun	16.7	9.4	13.6	0.5	3.7	8.7	4.9	22.1
13	6-Jul	17.4	8.9	14.0	0.3	1.2	4.3	1.1	6.7
14	7-Jul	19.3	11.1	14.7	0.5	2.8	8.3	2.2	10.8
15	8-Jul	20.1	10.6	15.7	0.4	1.9	6.4	1.4	7.2
16	14-Jul	20.6	11.1	16.7	0.5	1.3	7.6	1.1	10.2
17	22-Jul	15.7	9.4	13.0	0.2	0.4	2.3	0.5	6.2
18	27-Jul	17.2	13.9	10.8	0.4	1.6	6.2	2.1	14.2
19	28-Jul	20.0	12.2	14.7	0.5	1.7	7.9	1.5	10.8
20	29-Jul	21.3	8.9	17.3	0.4	1.7	6.2	1.3	7.4
21	5-Aug	19.9	12.2	14.3	0.4	2.5	7.3	2.2	10.4
22	11-Aug	20.4	12.8	14.3	0.5	4.4	11.3	3.2	12.8
23	12-Aug	20.0	11.1	16.2	0.5	2.5	9.1	1.9	10.9
24	18-Aug	18.8	10.6	15.1	0.2	0.6	3.1	0.7	5.4
25	19-Aug	22.2	12.2	16.4	0.4	0.6	5.9	0.4	6.5
26	22-Aug	19.9	12.2	14.7	0.9	7.3	15.5	4.4	15.4
27	23-Aug	18.8	8.3	16.7	0.4	0.6	6.4	0.5	8.9
28	25-Aug	15.2	11.7	9.8	0.1	0.8	1.6	1.7	5.9
29	26-Aug	15.9	12.8	11.9	0.4	1.3	6.5	2.1	19.7
30	30-Aug	18.5	11.1	13.8	0.4	1.1	6.2	1.4	12.8

Figure 4 shows total energy savings percentage verses outdoor average and diurnal temperature range. Base on the results at constant outdoor average temperature, energy savings increase when there is a higher temperature range. Also the results show that higher energy savings happened at outdoor average temperature between 15 ˚C and 22 ˚C and energy savings decrease when outdoor average temperature is out of this range.

Figures 5 and 6 show results for fan flow rates during the night between hour 7 (7am) and hour 3 (3 am) verses outdoor temperature at that specific hour and temperature difference between indoor and outdoor. The results show that minimum suitable temperature difference between outdoor and indoor to apply nighttime ventilation is 8 ˚C. Using the outdoor air with temperature difference less than 8 ˚C cannot reduce building energy consumption. Also, outdoor temperature between 10 ˚C and 18˚C are appropriate for nighttime ventilation and energy savings of nighttime ventilation reduce significantly when outdoor temperature is out of this range.

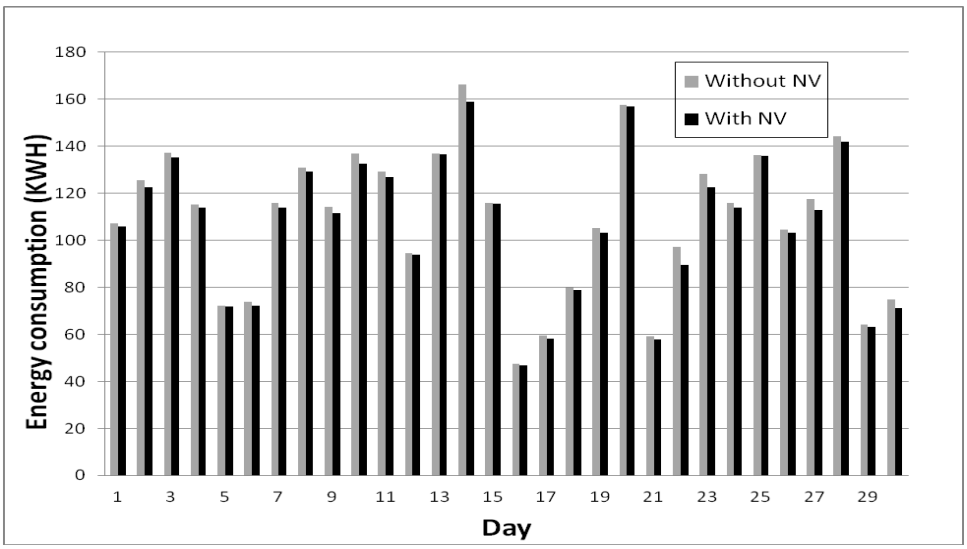

Figure 2: Building total energy consumption with and without nighttime ventilation during summer in Montreal

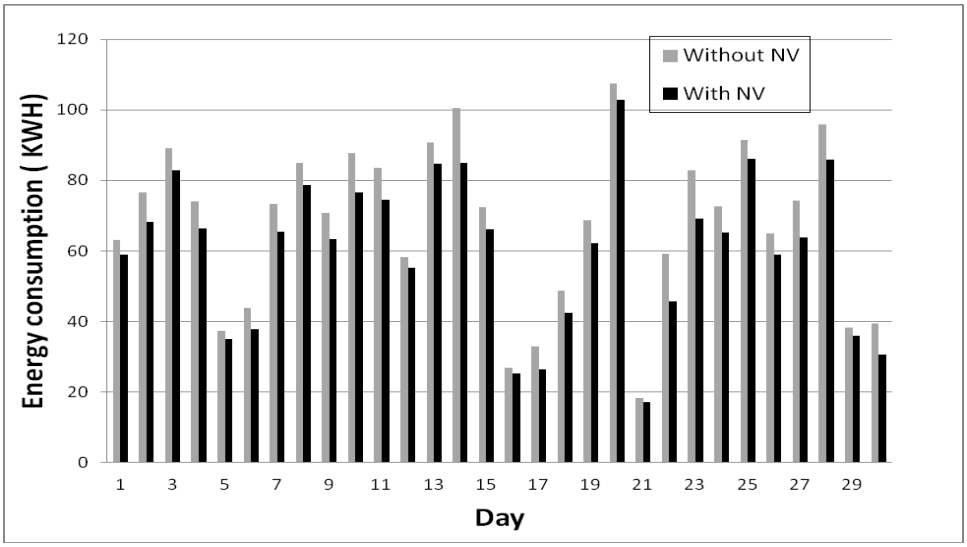

Figure 3: Building cooling energy consumption with and without nighttime ventilation during the summer in Montreal

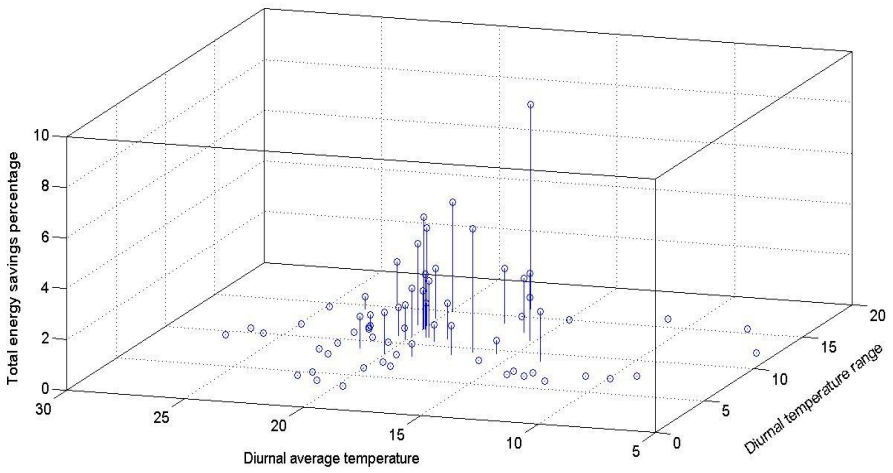

Figure 4: total energy saving percentage verses diurnal outdoor average temperature and diurnal temperature range.

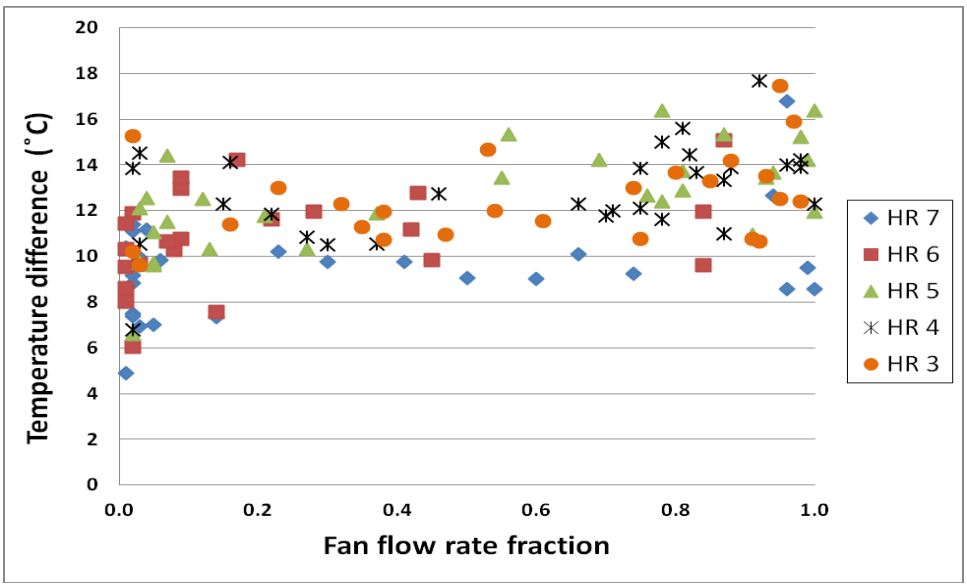

Figure 5: Nighttime fan flow rate fraction versus temperature difference between outdoor and indoor temperature for 5 hours before working hour during summer in Montreal

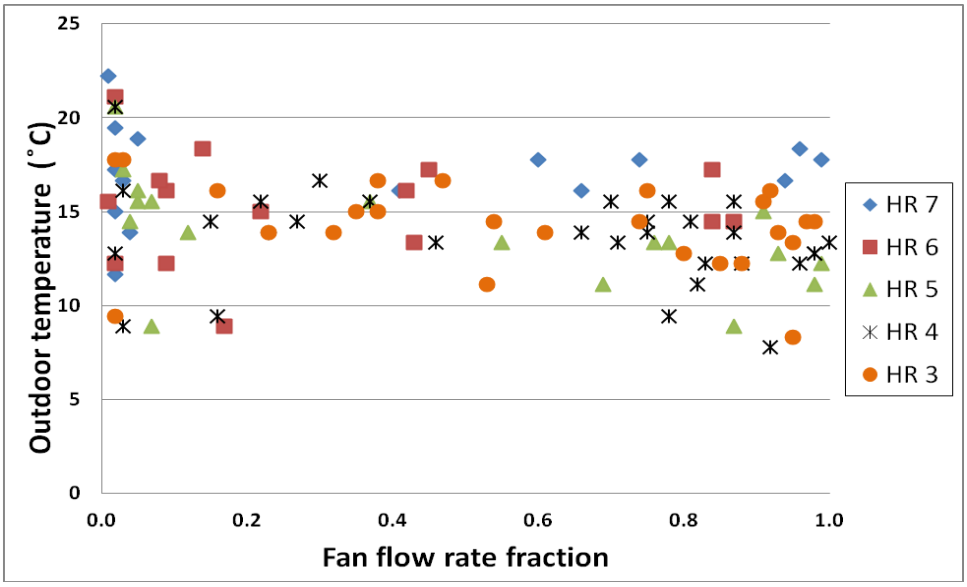

Figure 6: Nighttime fan flow rate fraction versus temperature difference between outdoor and indoor temperature for 5 hours before working hour during summer in Montreal

To better understand of nighttime ventilation optimization, the hourly results for fan flow rates for some days with higher energy savings potential are shown in Figures (7-10). The results show that optimization is converging towards an indoor temperature of about 23 ˚C at the beginning of the day. To reach this goal, optimization uses higher fan flow rates during hours with lower outdoor air temperatures and higher temperature differences between outdoor and indoor.

3 CONCLUSIONS

We have integrated DOE2 and MATLAB to optimize building energy use and nighttime fan flow rates. The results of this optimization were used to investigate the effect of outdoor temperature, indoor-outdoor temperature difference and nighttime ventilation duration.

Nighttime fan flow rates optimization was applied for five hours before working hours during the summer (June, July and August) in an office building in Montreal. The results show that nighttime ventilation decrease total energy consumption up to 8% and cooling energy

consumption up to 23%. These savings occurred in days with high diurnal temperature range and average temperature near 17 ˚C. Higher energy savings are calculated for days with an outdoor average temperature between 15 ˚C and 22 ˚C.

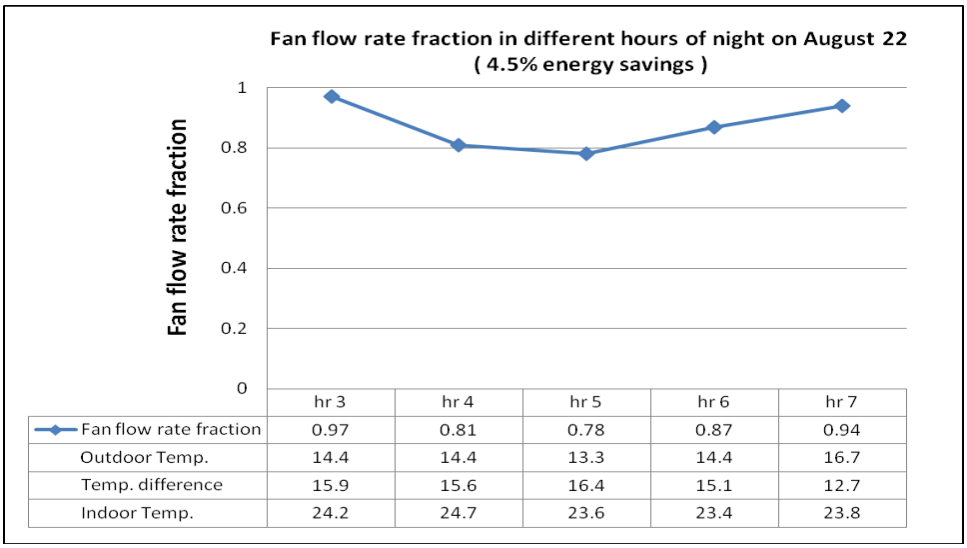

	hr 3	hr 4	hr 5	hr 6	hr 7
Fan flow rate fraction	0.97	0.81	0.78	0.87	0.94
Outdoor Temp.	14.4	14.4	13.3	14.4	16.7
Temp. difference	15.9	15.6	16.4	15.1	12.7
Indoor Temp.	24.2	24.7	23.6	23.4	23.8

Figure 7: Hourly fan flow rate fraction and temperatures from 3am to 7am for August 22 in Montreal

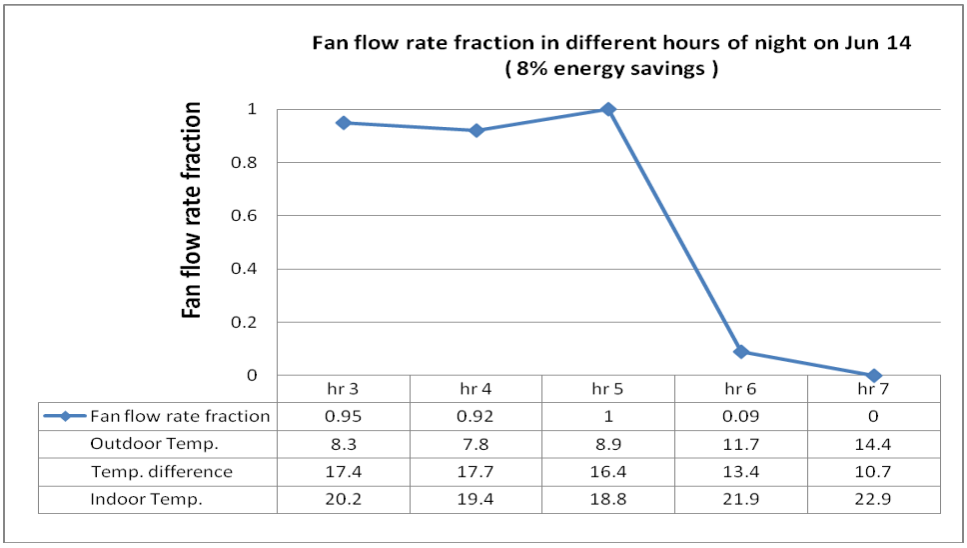

	hr 3	hr 4	hr 5	hr 6	hr 7
Fan flow rate fraction	0.95	0.92	1	0.09	0
Outdoor Temp.	8.3	7.8	8.9	11.7	14.4
Temp. difference	17.4	17.7	16.4	13.4	10.7
Indoor Temp.	20.2	19.4	18.8	21.9	22.9

Figure 8: Hourly fan flow rate fraction and temperatures from 3am to 7am for Jun 14 in Montreal

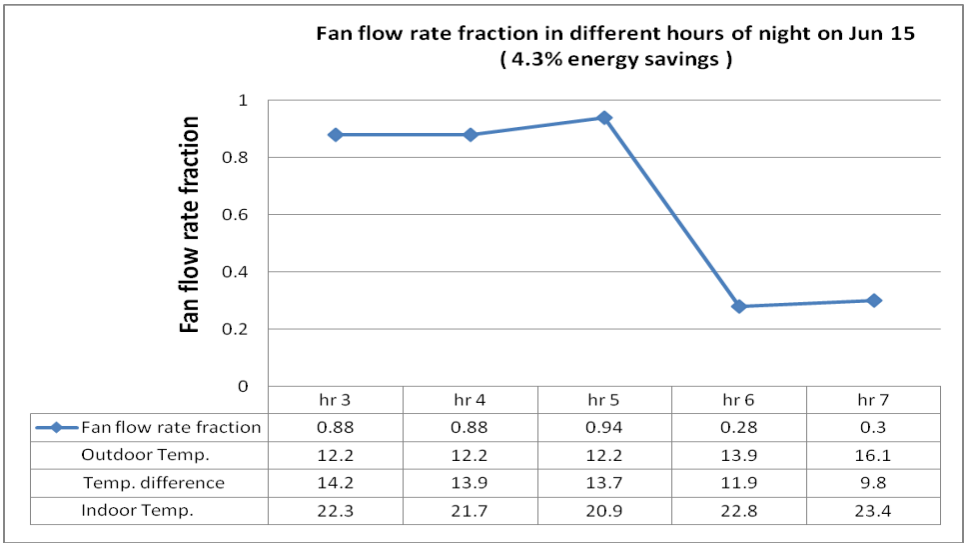

	hr 3	hr 4	hr 5	hr 6	hr 7
Fan flow rate fraction	0.88	0.88	0.94	0.28	0.3
Outdoor Temp.	12.2	12.2	12.2	13.9	16.1
Temp. difference	14.2	13.9	13.7	11.9	9.8
Indoor Temp.	22.3	21.7	20.9	22.8	23.4

Figure 9: Hourly fan flow rate fraction and temperatures from 3am to 7am for Jun 15 in Montreal

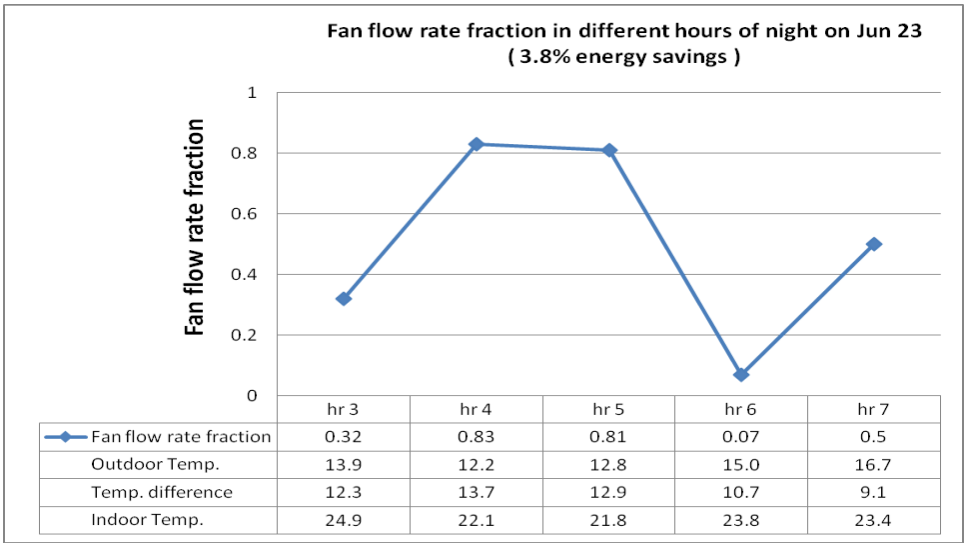

Figure 10: Hourly fan flow rate fraction and temperatures from 3am to 7am for Jun 23 in Montreal

4 ACKNOWLEDGEMENTS

This work was in part supported by an internal grant from the Faculty of Engineering and Computer Science at Concordia University, Montreal, Canada and by a Discovery Grant from Natural Sciences and Engineering Research Council of Canada (NSERC).

5 REFERENCES

[1] M. Kolokotroni, A. Aronis, Cooling-energy reduction in air conditioned offices by using night ventilation, Applied Energy 63 (4) (1999) 241–253.
[2] E. Gratia, I. Bruyere, A. De Herde, How to use natural ventilation to cool narrow office buildings, Building and Environment 39 (10) (2004) 1157–1170.
[3] E. Shaviv, A. Yezioro, I.G. Capeluto, Thermal mass and night ventilation as passive cooling design strategy, Renewable Energy 24 (3–4) (2001) 445–452.
[4] B. Givoni, Performance and applicability of passive and low-energy cooling systems, Energy and Buildings, 17 (1991) 177-199.
[5] G. Agas, T. Matsaggos, On the use of the atmospheric heat sinks for heat dissipation, Energy and Buildings 17 (1991) 321-329.
[6] A.N. Ayoob, J.L. Izard, Study of comfort in atrium design, Renewable Energy 5 Part II (1994) 1002-1005.
[7] B. Givoni, Effectiveness of mass and night ventilation in lowering the indoor daytime temperatures, Energy and Buildings 28 (1) (1998) 25–32.
[8] J. Pfafferott, S. Herkel, M. Jaschke, Design of passive cooling by night ventilation: evaluation of a parametric model and building simulation with measurements, Energy and Buildings 35 (11) (2003) 1129– 1143.
[9] N. Artmann, H. Manz, P. Heiselberg, Parameter study on performance of building cooling by night-time ventilation, Renewable Energy 33 (12) (2008) 2589–2598.
[10] L. Yang, Y. Li, Cooling load reduction by using thermal mass and night ventilation, Energy and Buildings 40 (2008) 2052–2058.
[11] V. Geros, M. Santamouris, A. Tsangrasoulis, G. Guarracino, Experimental evaluation of night ventilation phenomena, Energy and Buildings 29 (2) (1999) 141–154.
[12] M. Gwerder, J. Tödtli, Predictive control for integrated room automation, 8th REHVA World Congress for Building Technologies – CLIMA 2005, Lausanne, 2005
[13] F.G. Uctug, E. Yukseltan, A linear programming approach to household energy conservation: Efficient allocation of budget, Energy and Buildings 49, 200–208, 2012

[14] L. Magnier, F. Haghighat, Multiobjective optimization of building design using TRNSYS simulations, genetic algorithms, and artificial neural network, Building and Environment 45, 739–746, 2010
[15] L. G. Caldas, L. K. Norford, Genetic Algorithms for Optimization of Building Envelopes and the Design and Control of HVAC Systems, Journal of Solar Energy Engineering, Vol. 125 / 343, 2003
[16] W. Wang, R. Zmeureanu, H. Rivard, Applying multi-objective genetic algorithms in green building design optimization, Building and Environment 40, 1512–1525, 2005
[17] T. Nagai, Dynamic Optimization Technique for Control of HVAC System Utilizaint Building Thermal Storage. Energy Conversion and Management, 999–1014, 1999.
[18] Z. Wang, L. Yi, F. Gao, Night ventilation control strategies in office buildings, Solar Energy 83 (2009) 1902–1913.
[19] V. Congradac, F. Kulic, HVAC system optimization with CO2 concentration control using genetic algorithms, Energy and Buildings 41, 571–577, 2009.
[20] DOE-2 Supplement (Version 2.1E), Berkeley, CA, USA: Lawrence Berkeley Laboratory, 1994.
[21] DOE-2, Lawrence Berkeley National Laboratory DOE-2 website 2007, Online at http://simulationresearch.lbl.gov/dirsoft/d2whatis.html.
[22] T. Bäck, Evolutionary Algorithms in Theory and Practice: Evolution Strategies Evolutionary Programming, Genetic Algorithms. Oxford University Press, N.Y.,1996.

HIGH PERFORMANCE INSULATION MATERIALS

Karim GHAZI WAKILI,Samuel BRUNNER, Thomas STAHL

ABSTRACT

Energy use for heating and cooling of the existing building stock in Europe makes about 35 to 40% of the final energy consumption and produces 36% of greenhouse gas emission. Knowing that the rate of new buildings per year is slightly more than 1%, it is no wonder that retrofitting the building stock has become a crucial topic on the road to reach the EU energy and CO_2 emission targets for 2020 and beyond. The use of high performance insulation materials with a thermal resistance of 3-4 higher than conventional insulations is one of the major paths to be taken to reach these goals. The presentation will start with the state-of-the-art of high performance insulation materials for building applications namely vacuum insulation panels, aerogel based products and nano-structured foams. Then, experiences with some demonstration objects and their monitoring by will be summarized and finally future technical and scientific challenges such as potential degradation processes and structural fragility as well as possibilities and risks of a widespread application will be discussed.

The overview will also include the major objectives of a new IEA Annex presumably starting in 2014 and dealing with the long-term performance of super-insulations in building components and systems and the major outcome of the 11th International Vacuum Insulation Symposium (IVIS2013) held in September 2013 at Empa Switzerland.

SHIFTING PEAK COOLING LOAD USING THERMAL STORAGE TECHNOLOGY

Branislav Todorovic,
professor of University Belgrade, president of Serbian HVAC Society, editor-in-chief of Elsevier's journal Energy&Buildings, former president of REHVA, ASHRAE fellow.

ABSTRACT.

There are growing trends of energy use in buildings and these trends are now moved to the hot part of a year, which becomes more critical when space air conditioning is concerned. HVAC industry and sciences are investigating how summer energy needs could be minimized to lower cooling load amount and to achieve nearly zero cooling load buildings, when outside heat sources are concerned. Going in this direction one possibility which is very much occupying researchers, is practical use of thermal energy storage in building, which could be stored as the sensible, latent or thermo chemical heat storage process. Latent storage is most promising one, storing energy in phase change material. The storage could be as a passive or active storing system. In the paper are presented some of the examples of the latent heat storage applications based on the new published articles in the scientific publications.

.

PHASE CHANGE MATERIALS FOR THERMAL STORAGING

Reduction of cooling loads is not only by thermal insulation but also by implementation of phase change materials (PCM) for thermal storage. For such purposes PCM began to be used since more then 3 decades, since the year 1980 . These materials could be organic (fatty acids , paraffin, non paraffin), inorganic (salt hydrate, metallic), or eutectic materials which are minimum melting compositions of two or more organic or inorganic materials in all combinations (organic-organic, organic-inorganic, inorganic-inorganic). Materials to be used as PCM must have large latent heat per 1kg, high thermal conductivity and range of the melting-freezing temperature 15-30C or even higher, which correspond to the outside summer daily temperature range. Beside these conditions, PCM shall have small volume's change during phase change process, high nucleation rate to avoid supper cooling of the liquid phase, high rate of crystal growth, and complete reversible freeze-melting cycle.

The application of PCM options for cooling effects is integration in buildings envelopes to increase thermal mass or to be installed in HVAC systems with natural-free ventilation, systems with encapsulated PCM what is a group of passive systems since no additional energy is needed. If mechanical ventilation is involved, then a system is no more passive, but active.

The classical refrigeration can be eliminated or replaced in some periods of day time by the systems with phase change materials which can be integrated into building elements as in walls and ceilings, increasing building's thermal mass. But PCM can also be a part of AC equipment presentive active systems as needing additional energy use.

For free cooling it is important that temperature between day and night is about 15K and if it is existing a good air circulation. Free cooling system is storiging "outdoor cold" during night period of lowest temperature. Use of air conditioning system, or ventilation one, in the buildings or rooms in which are cooling load varying during a day, electrical needs significantly varies having its peak load during a day. In such a case load can be shifted to a night time with low electricity tariff.

Air conditioning systems usually combine cooled ceiling , microencapsulated PCM slurry storage and evaporative cooling technologies . Such systems can effectively achieve the target- shifting the part of cooling load from the daytime to night time as an energy saving and economy- air-conditioning system.

PCM IN PASSIVE AND ACTIVE COLING SYSTEMS

The paper (2) is studying composite materials containing phase change materials as mixing PCM macro encapsulation or microcapsules with shape stabilized traditional construction materials as gypsum or concrete.

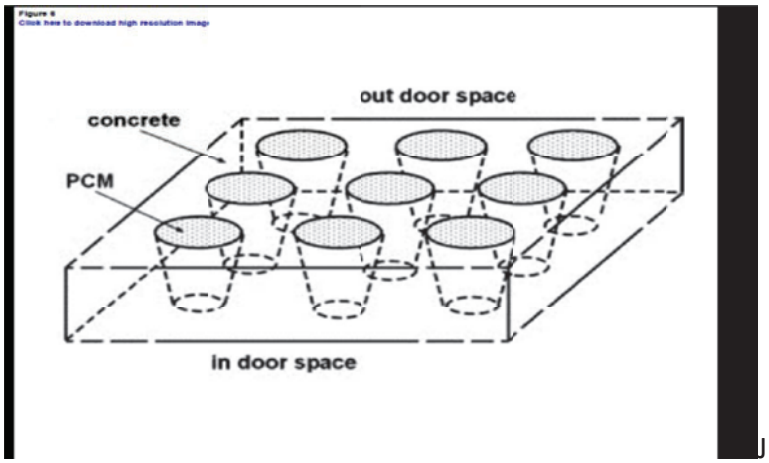

Figure 1. Holes in ceiling or roof filled by PCM

When micro encapsulation is used to integrate a PCM in building structure the capsule shell prevent any physical or chemical interaction between the PCM and the structure. Simplest passive cooling system with encapsulated PCM is presented on the figure 1.

The holes in the conrete ceiling or roof are filled with PCM. With a maximum PCM mass fraction of about 25-30% or in material as high density as polyethylene, a mass fraction of PCM can be up to 70% or more.

H.M.Chou, C.R.Chen and V.L.Nguyen (3) were investigating solar influence through metal sheet roofs as a passive type of energy storing system. High level of absorption could be reduced with light roof colors till 30% but with implementation of metal-sheet roof using PCM , much more. It was found that when PCM which has melting temperature 46,3C and latent heat capacity of 90kJ/kg was used to cover 48% of the roofing surface with ambient temperature 25C., the energy saving rate was to 52,7% in relation of 43% with normal insulated roof. Phase change material is inserted in between insulation layers and metal sheet roofing and is improving also thermal insulation effect This system is designed for hot areas with and also there where are high sunny regions. (Figure 2)

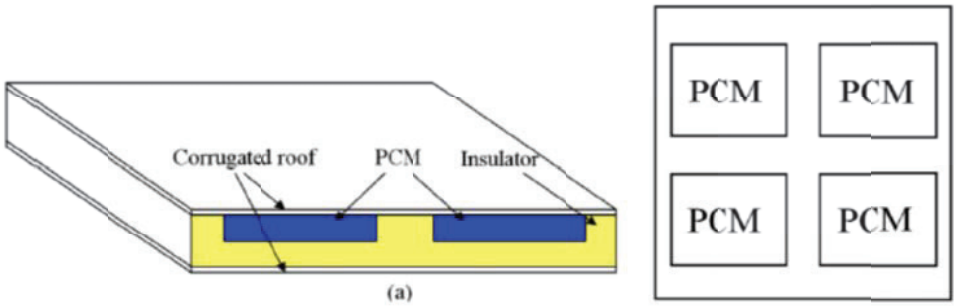

Fig. 2. Novel design structure of the corrugated roofing a) 3D view; b) Top view

Simulation results of variation of energy saving ratio with varied PCM amount

PCM weight (kg)	δ (%)	PCM dimension thickness× width× length (mm^3)	$\xi_{\#2}$(%)	$\xi_{\#3}$(%)
1*	48*	7×180×240*	43.1*	52.7*
1.5	48	10.5×180×240	43.1	51.3
1.5	72	7×270×240	43.1	53.6
2	48	14×180×240	43.1	48.9
2	64	10.5×240×240	43.1	51.0
2	100	6.7×300×300	43.1	53.9

Table 1. Energy saving ratio only with insulation and combining with PCM

Average diameter of micro capsules is 5 microns, shell width d=0,1 -0,2 microns, PCM is mixture of heptadecane, octadecane and nonadecane; material of the shell is of Poly

-methil- metacrilate with melting temperature which varies according to composition of the mixture: 21-26C.

In Hong Kong at City University , for very long time is going research program for implementation of PCM . They proposed air conditioning system with cold ceiling and with microencapsulated PCM slurry storage tank . It was selected hexadecane C16H34 with melting temperature 18C and latent heat of 224kJ/kg . (Fig.3.). The experiment and simulation showed that in Hong Kong climate, such a system can decrease daily electricity demand for 1/3.

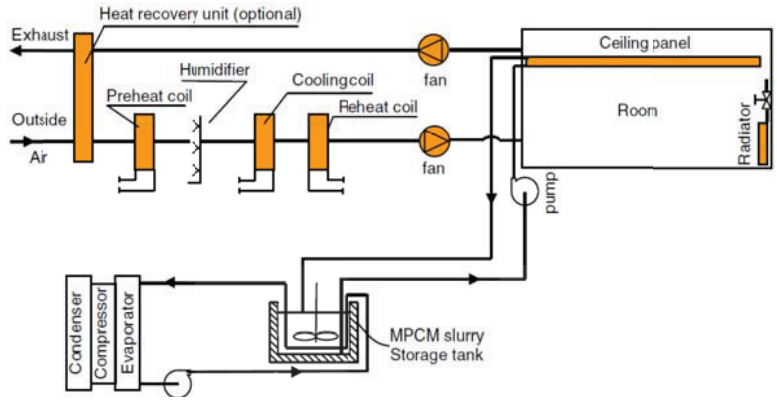

Fig. 3. Cooled ceiling with PCM slurry

Another system for cutting paek electrical energy needs for cooling is described and investuigated by Japans T. Condo and T. Ibamoto (4). Rock wool PCM ceiling board was enhansed by adding mislocpsulate PCM having melting temperarure at about 25C .Their system is working in three different modes: during the night cold air from air handing unit cirkuletes into the ceiling and chills PCM ceiling board and cold is srored for next day peak time when air from the room flows through space above ceiling cham ber to the AHU.Air is precooled and and maxinum thermal load was about 85% of that using the rock wool ceiing board only.

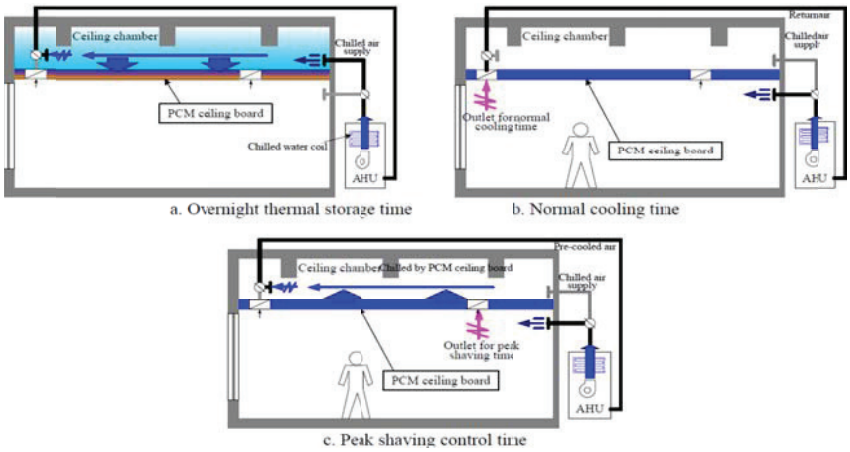

Fig.4. Cutting peak energy for cooling

It is interesting investigation done at Hong Kong polytechnic, which could be named as one of scientific centre having good postgraduate program for MPCM slurry use for air conditioning. The last investigation was to use nocturnal sky radiation for next day cooling of the ceiling panel (Fig 5.)

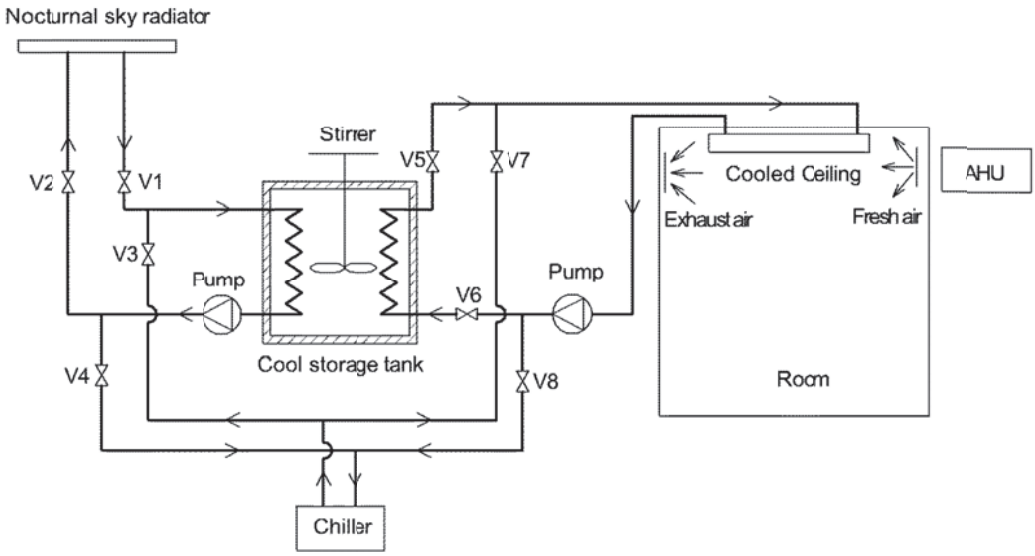

Fig. 5.Storaging nocturnal sky radiation for next day cutting peak cooling load

PCM REDUCING COOLING LOAD THROUGH WINDOWS

Regarding building's cooling load the weakest" part of the envelopes are windows and glassed parts of fasades. The authors from Brunel University in UK (B.L. Gowreesunker, S.B. Stankovic, S.A.Tassou and P.A.Kyriacou) have investigated thermal and optical performances of PCM in glassed units and compared with standard double glazed window.

They have found that during rapid phase change of PCM or changes in temperature the transimitance spectra from PCM is unstable. When there are stable conditions, visible transmission was 90% during the period of liquid phase but 40% in a solid phase. The scattering effects are dominant in the solid phase, in the liquid phase radiation absorption dominates. During mushy phase the optical properties that are not scattering in luiquid phase depends of the liquid fraction. The use of PCM within double glazed window improves the thermal mass during phase change regarding standard double double glazing. PCM visual aspects changes as the material changes phase and it is translutant in the solid phase and transparent in the liquid phase (Fig. 6.) .

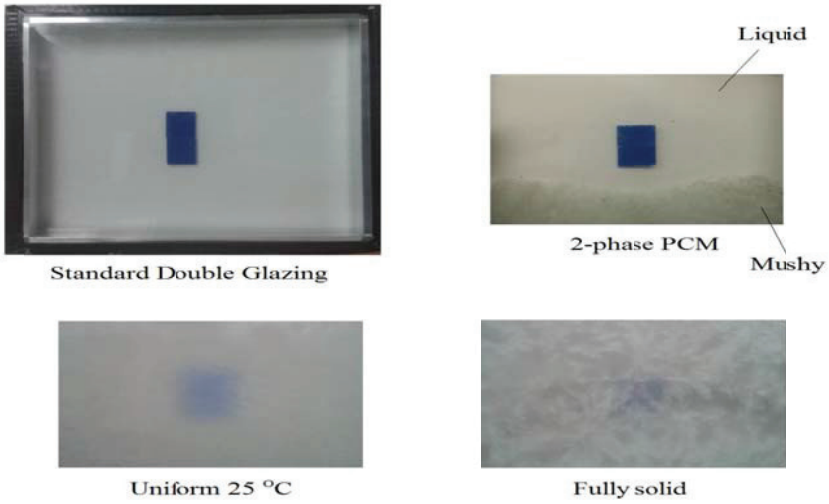

Fig.6. Visual characteristics of dfifferent PHC phases

CONCLUSION

Cooling load of building should be more reduced in the future and also shifted out of the time when there is the peak of cooling needs. At the time of a day when there is economically more convenient. Concerning this task, use of phase change materials are offering very promising possibility, but there is a need of additional efforts for investigation of PCM having appropriate thermal characteristics. That means to produce PCM concerning daily temperature range in various locations, stabile volume, constant thermal parameters . As the windows are the greatest energy losers in winter but also in summer regarding high heat gains from outside temperature and specially from solar radiation, there is a need to find such PCM materials combination to get PCM which will have also favourable optical characteristics.

References

1. E.Osterman, V.V.Tyagi, , V.Butala, at all, Review of PCM based cooling technologies for buildings, Energy&Buildings, Vol 49 (2012)
2. Yomasso Toppi.Livio Mazzarella. Gypsum based composite materials with micro-encapsulated PCM. Energy&Buildings 57 (2013) .
3. H.M.Chou, C.R.Chen and V.L.Nguyen A new design of metalsheet cool roof using PCM, Energy&Buildings, Vol.57 (2013).
4. T.Condo, T. Ibamoto, Reaserch on thermal storage using rock woolphse change material ceiling bioard, ASHRAE Transactions 2006.
6. Zhang S**,** Nocturnal Sky Radiative Cooling and MPCM Slurry Thermal Storage, PHD dissertation, Hong Kong Polytehnik.2012
7. B.L.Gowreesunker, S.B.Stankovic,S.A.Tassou.P.A Kiriacou. Experimental and numerical investigation of the optical and thermal aspects of a PCM glazed unit. Energy&Buildings, 2013 ,

PREFERRED AIR VELOCITY AND LOCAL COOLING EFFECT OF DESK FANS IN WARM ENVIRONMENTS

Angela Simone*[1] and Bjarne W. Olesen[1]

1 International Center for Indoor Environment and Energy,
Department of Civil Engineering at
Technical University of Denmark
Nils Koppels Allé, building 402 2nd floor
2800Kgs.Lyngby, Denmark
**Corresponding author: asi@byg.dtu.dk*

ABSTRACT

Common experiences, standards, and laboratory studies show that increased air velocity helps to offset warm sensation due to high environmental temperatures. In warm climate regions the opening of windows and the use of desk or ceiling fans are the most common systems to generate increased airflows to compensate for higher environmental temperatures at the expense of no or relatively low energy consumption.
When using desk fans, local air movement is generated around the occupant and a certain cooling effect is perceived. The impact of the local air movement generated by different air flow patterns, and the possibility to keep comfortable conditions for the occupants in warm environments were evaluated in studies with human subjects.
In an office-like climatic chamber, the effect of higher air velocity was investigated at room temperatures between 26°C to 34°C and at constant absolute humidity of 12.2 g/kg. By a thermal manikin the effect of direct air movement generated by a personal desk fan at 26 °C, 28 °C, or 30 °C room temperatures and the achievable thermal comfort was also analyzed.
Results show that it is possible to offset warm sensation within a range of indoor conditions using increased air velocity. Besides, higher air velocities and personal control increase the acceptability of the indoor environment at higher air temperatures with a limited energy consumption compared to full air conditioning during summer seasons in warmer countries. Comparing the study with Danish subjects with previous findings with Chinese subjects showed that subjects used to warmer climate could accept higher air velocities and felt less uncomfortable.

KEYWORDS

Thermal comfort, air velocity, personal control, desk fan

1 INTRODUCTION

Thermal comfort Standards ISO 7730-2005, ISO 15251/2007 and ASHRAE 55-2010, for indoor environments include air movement limits that protect the occupants of being exposed to draught problems and discomfort. The limits of air movement are dependent on air turbulence (Tu) and frequencies, while the direction is not considered.
Fanger and Pedersen (1977) and Zhou et al. (2002) demonstrated that the impact on human sensation of draught is higher at frequencies between 0.2-0.6 Hz, while it is not significant at

frequencies below 0.1 Hz, as well reported in Tanabe and Kimura (1994) study, and at frequencies higher of 1 Hz.

When considering the direction, Fanger et al. (1974) demonstrated by the human subjects experiment for seated occupants that there is no influence of the direction of air flow on creating thermal comfort even though the heat loss measured by the thermal manikin was higher when the air motion was from front. Later, Zhou (1999) in a similar experiment found that the draught rating (DR) reported at 26 ˚C was lower from the front airflow movement and the reason could be due to a weaker natural convection in front of a seated person which has a ticker boundary layer in front than at the back (Homma and Yakiyama, 1988). Therefore subjects may naturally prefer the airflow from the front that often occurs in the daily life when walking, cycling, etc.

Many previous laboratory and field studies (Rohles et al. 1974, Tanabe and Kimura 1989, Scheatzle et al. 1989, Fountain 1991, Fountain et al. 1994, Mayer 1992, Arens et al. 1998, Zhang et al. 2007, Zhou et al. 2006, Cândido et al. 2010, Cattarin et al. 2012) have demonstrated that higher air movement can compensate for warmer temperatures in make people more comfortable.

The ISO Standard 7730-2005 and ASHRAE Standard 55-2010 adopted a model that provide a conservative upper limit for air velocity that protects occupants who are sensitive to air movement, occupants who feel cooler than neutral, or occupants who are occupied mostly with sedentary work.

In Standard ISO 7730-2005 it is also recognized that: “People used to working and living in warm climates can more easily accept and maintain a higher work performance in hot environments than those living in colder climates.” For that reason, as numerous studies show, in warm environments people seem to be less sensitive to draught than the predicted by DR model and as consequences higher air velocity could be used for obtaining neutral environment at higher temperatures.

In Naturally Ventilated buildings (NV) during summer time there was no sensation of draught and 80.6% of people wanted more air movement (Yang and Zhang, 2009) increasing to 90% and 96% in Baizhan et al. (2010) and Zhang et al. (2007) studies. Besides, those last two studies observed that the demand for less air movement under cool sensation is much smaller (30%) than the overwhelming demand for more air movement at warm sensation (80%).

The increase of air velocity can be achieved by windows opening, ceiling or free standing fans (including desk fan) at the expense of no or relatively low energy consumption (Koranteg and Mahdavi 2011, Aynsley 2007, Yamtraipat et al. 2006, Schiavon and Melikov 2009, Sun et al. 2013).

It is known that those solutions are often used in NV buildings in warm countries, like in the Mediterranean, Asian, or South America, where the people are used to natural ventilation systems and they can easily adapt and accept environments with air temperatures up to 28 ˚C (Cândido et al. 2012, Kubo et al. 1997, Zhang et al. 2010, Feriadi end Wong 2004).

Today higher level of air velocities are allowed in ASHRAE Standard 55 (2010) but only under personal control of the occupants. Feriadi and Wong (2004) reported that the occupant control focusing on preferred air velocity can provide a higher percentage of people satisfied while Boerstra et al. (2013) found a significant positive correlation with overall comfort in summer and perceived air quality when control on ventilation is allowed.

Perception of control, behavioural actions and human expectation studies (Feriadi and Wong 2004, Weiwei et al. 2012), mainly referring to warm environments acceptability, reported the increase of fan usage for cooling with the increase of temperature.

The adaptation at warmer room temperature with the use of the desk fans as support for cooling, with the perspective of lower energy consumption, was investigated in this study. In particular, the evaluation of comfortable and acceptable environment for the occupants was studied when increased local air velocity and/or preferred air velocity was provided.

In this paper, some results of human subject study are presented. The preferred air velocities at different room temperatures and their capability to offset warm sensation and to provide comfortable and acceptable environment for Scandinavians are presented.

2 METHOD

The experiment was carried out in a climatic chamber that reproduces a typical office room with dimensions 5.9*5.8*3.2 m^3, located at the International Centre for Indoor Environment and Energy, Technical University of Denmark (ICIEE-DTU). The same chamber with similar setup of Cattarin (2012) study was used, providing occupants with a view on the outdoors garden. The office had eight workplaces, each workplace having a desk, office chair, desk lamp, desk fan, and laptop. A partition between the right and left side was located in the middle of the room in order to avoid any influence at the back of each occupant due to the air movement generated by the desk fan of another person (see Figure 1).

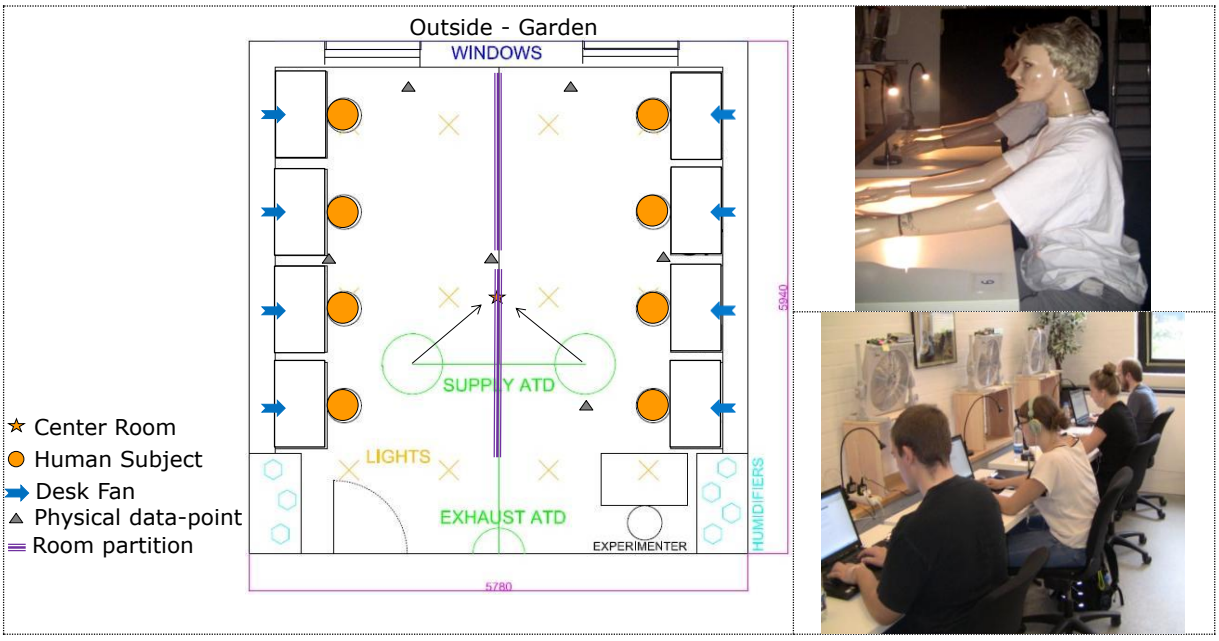

Figure 1: Sketch and setup of the experimental chamber (left) and view of workplace with thermal manikins (right-up) and participants (right-down)

Air and globe temperature sensors, developed at the ICIEE-DTU according Simone et al. (2007) with an accuracy of ±0.3 °C, omnidirectional anemometers with accuracy of ±0.05 m/s and HOBO humidity sensors with accuracy of ±5% were used during the experiments to record the physical parameters in different locations of the room (see Figure 1) and at different heights above the floor (mainly at 0.1, 0.6, 1.1 m and 1.7 m).
Skin temperatures of the occupants were recorded by iButtons sensors (as suggested by van Marken Lichtenbelt et al. 2006, and Smith et al. 2010). Particular the forehead was measured in order to estimate the local cooling effect generated by the fan. Four points schema suggested by the Standard ISO 9886 (2003) was used for estimating the average body skin temperature.
During the experimental session, working tasks were given to the participants so that an activity level of 1.2 met could be maintaned. The type of clothes worn by the occupants resulted in a clothing insulation of 0.5-0.6 clo-value. A ventilation system was used to provide fresh air and keep a room background air velocity of 0.15-0.18 m/s just below the suggested limit in ISO 7730 (2005). Air humidity and operative temperature were controlled by the

main conditioning system in order to provide the required values for the different experimental environments that were investigated.
The absolute humidity was kept constant at 12.2 g/kg and room temperature of 26 ˚C, 28 ˚C, 30 ˚C, 32 ˚C and 34 ˚C were investigated.
At the room temperature conditions of 26 ˚C, 28 ˚C and 30 ˚C, two thermal manikins were used to evaluate the cooling effect provided by the higher constant air velocity. They have been placed at the desks in the same experimental room (see Figure 1) exposed to the investigated conditions. Body parts equivalent temperatures and heat losses were recorded. Based on those data the acceptability of the thermal environment was estimated together with the PMV index and by the human occupants´ responses.
A total of 27 Danes participated in the experiments. Their average anthropometric data is reported in Table 1. The participants spent 15 minutes in the pre-test room at low activity level. The exposure to the warm environmental conditions lasted 2 hours for each room temperature settings.

Table 1. Anthropometric data of participants attending the study

Sex	No. of subjects	Age (years)	Height (cm)	Weight (kg)	Du Bois area (m^2)	Body Mass Index (BMI)
females	11	22 ± 5	167 ± 13	59 ± 11	1.66 ± 0.15	21.4 ± 4.7
males	16	24 ± 9	178 ± 9	72 ± 24	1.89 ± 0.22	22.9 ± 8.4
females + males	27	23 ± 10	173 ± 19	66 ± 30	1.78 ± 0.33	22.1 ± 9.2

As shown in Figure 2, the occupants had a period in which they could adapt to the heat followed by the local exposure of 15 minutes at the constant air flow, provided by the desk fans in direction to the face. The air speed settings of the fans, at constant air flow, were random.

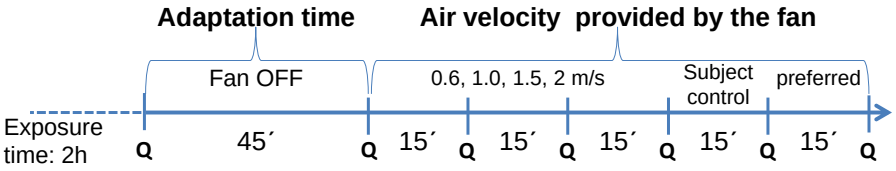

Figure 2: Time Schedule of the Experiments

The used desk fan, see Figure 1, is a prototype of fan developed at Tsinghua University in China, which can generate different type of air flow, at very high air velocity and different turbulent intensity, as explained in Zhou et al. (2006). In this experiment, aimed for evaluating the cooling impact on the occupant, the turbulence intensity of 22% of the constant air flow, at sample frequency of 10 Hz, was measured at the face location of the participants. In addition the participants, after one hour and thirty minutes in the experimental chamber, could regulate the air velocity by using a dimmer switch that provides a continuous variation of the air speed. Along the experiment, at each change (see Figure 2), the subjects were asked to fill in the provided questionnaires (Q) giving us information regarding: thermal environment (thermal comfort, thermal acceptability, air movement preference, etc.), air quality (perception of air quality, air humidity, etc.), experienced sick building symptoms (dry eyes, irritated throat and nose irritation, etc.), and etc.

3 RESULTS AND DISCUSSIONS

The dry heat losses of the thermal manikin at steady-state conditions were measured when the airflow generated by the fan was at 0 m/s, 0.6 m/s, 1 m/s, and 1.5 m/s of constant air velocities in direction of the occupant face (80 cm perpendicular distance at 1.2 m above the

floor) and at three investigated room temperatures of 26 ˚C, 28 ˚C, and 30 ˚C (see Figure 3a and 3b). Average values of the equivalent temperatures and dry heat loss of the whole body and the head are reported in Table 2, where the heat loss at the head region was calculated as an average of the heat loss from the neck, face and crown. Thus, the influence of the airflow direction is diminished. The heat transfer coefficient (dry heat loss) for the head was approximately 4.5 W/m^{2}K, while for the face 5.6 W/m^{2}K which is similar to values measured by Homma and Yakiyama (1988) and Zhou (1999). The heat loss increased as the air velocity increased from 0.6 m/s to 1.5 m/s. As expected the increase of air velocity had higher impact at the face with no any perception at the lower body parts, as shown in Figure 3(3a and 3b) when the room temperature was 26 ˚C. Besides, the cooling effect was higher at 26 ˚C than at 28 ˚C and 30 ˚C, which is shown by the body part heat loss in Figure 4. Whole body temperature only decreased 1 K by 1.5 m/s while head temperature decreased 3.6 K.

Table 2: Whole body and head region T_{eq}s and heat losses at different room temperature and constant air velocity

		Equivalent temperature (°C)			**Heat loss (W/m^2)**		
	t_a (°C)	26	28	30	26	28	30
whole body	no fan	24.9	27.8	29.7	47.3	35.1	27.5
	0.6 m/s	24.7	27.5	29.2	48.2	36.6	29.6
	1 m/s	24.3	26.9	29	49.7	39.1	30.3
	1.5 m/s	-	26.5	28.8	-	40.4	31.3
head	no fan	23.9	26.6	28.7	45.5	35.6	28.1
	0.6 m/s	21.4	24.5	26.7	54.6	43.2	35.4
	1 m/s	19.6	22.7	25.9	61.2	49.7	38.1
	1.5 m/s	-	21.6	25.1	-	53.8	41.1

a)

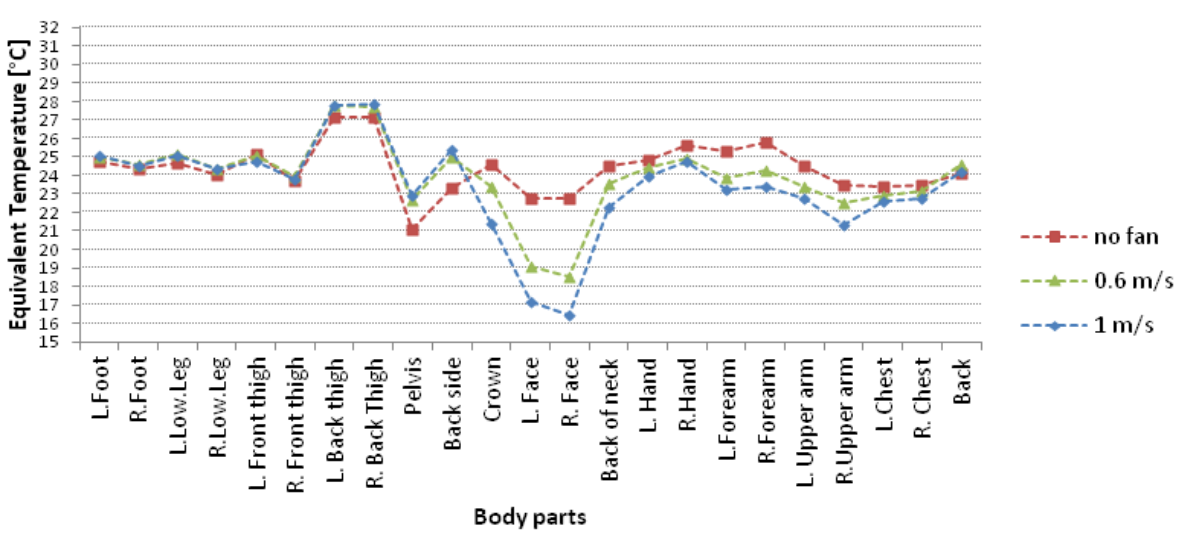

b)

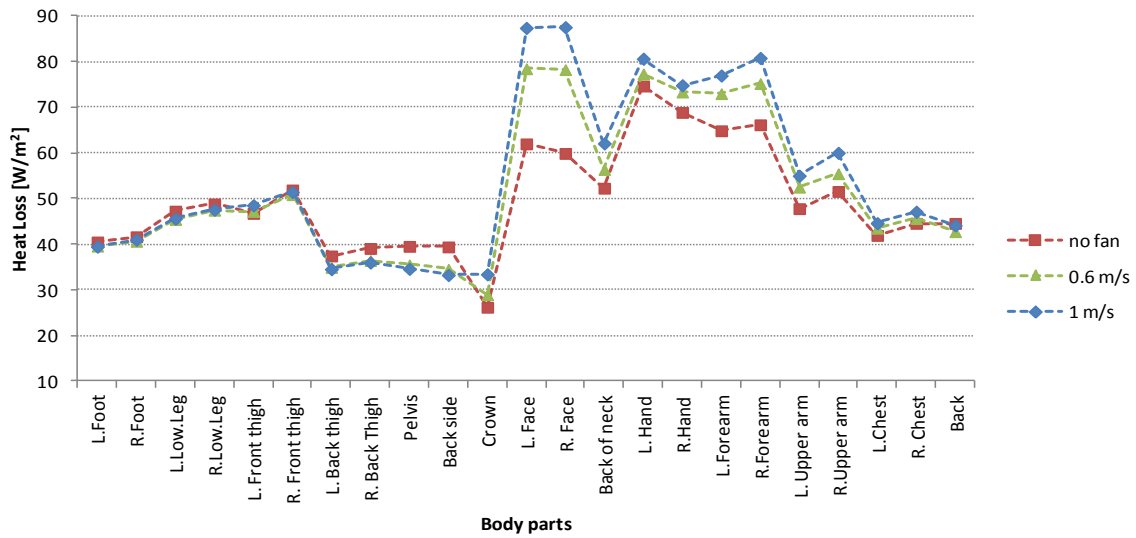

Figure 3: Equivalent Temperature (T_{eq}) and body parts Heat Losses at 26°C exposure and different air velocities

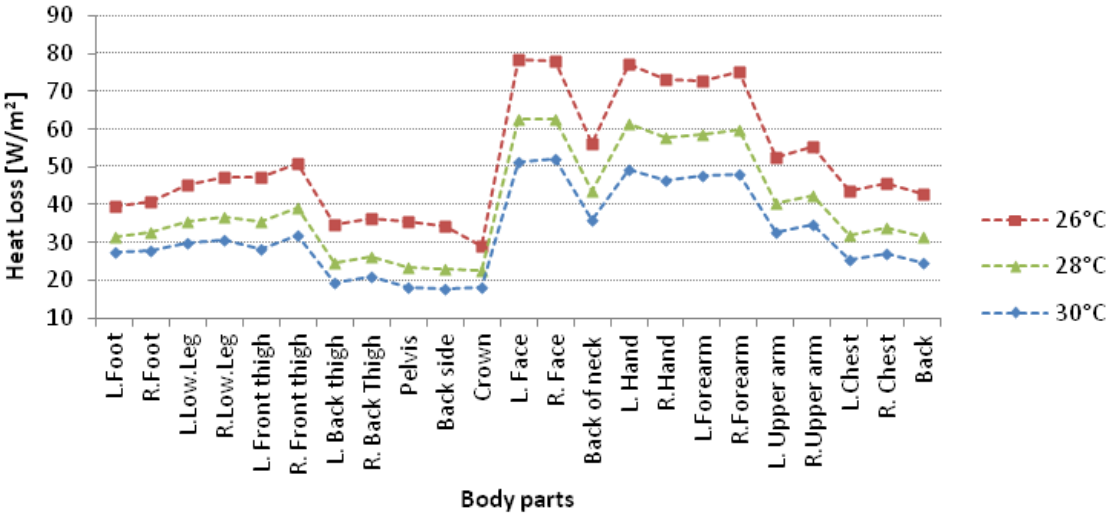

Figure 4: Body parts heat losses at 26 °C, 28°C, and 30 °C room temperature and 0.6 m/s of constant air velocity

The measurements performed with the thermal manikin show that the cooling effect decreases with the increase of the environmental temperature, and it increased with the increase of the constant air velocity resulting in higher head heat losses.

Following the experiments with thermal manikins, the human subjects´ experiments were performed to evaluate which are the right combination of air temperature and constant air velocity that can provide thermal comfort and no draught problems.

Previous studies, as shown in Figure 5, reported preferred air velocity to offset warm environments higher than 0.18 m/s suggested by ISO Standards 7730 (2005) for building category B. In Figure 5 are reported the preferred air velocities obtained, at almost the same experimental set up, for the Scandinavian human subjects´ experiment of Cattarin et al. (2012) and the present study.

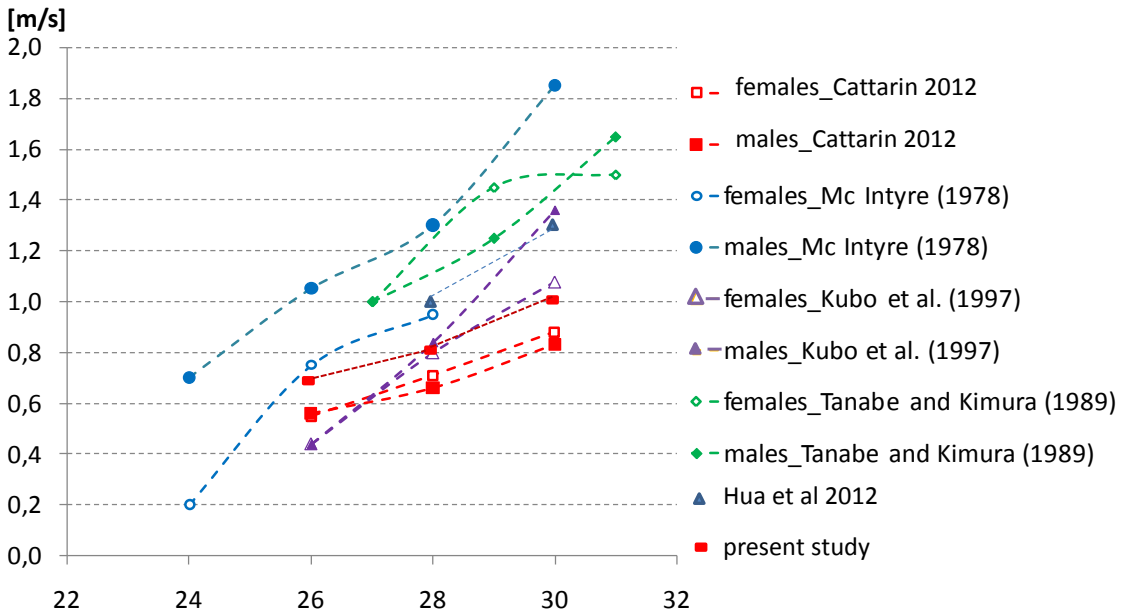

Figure 5: Preferred Air Velocities from Human Subjects Experiments

The two human subjects´ experiments, having 32 and 27 Scandinavian participants (in Cattarin et al. 2012 and in the present study) present slightly different results. This could be due to the different type of fan used, where later a larger diameter and the possibility to provide higher air velocity (>1.2 m/s). As reported in Table 3, the results of the 2nd experiments had on average circa 0.1 m/s higher preferred air velocity and higher percentage of dissatisfaction (PD). However, only at environmental temperatures of 26 ˚C and 28 ˚C the higher air velocity helped to offset the warm sensation by achieving neutral thermal conditions (TSV< ±0.5) and low dissatisfaction (PD) as reported in Table 3 and shown in Figure 5. The local air velocity decreased the subjective thermal sensation (TSV) of one step in the evaluation scale of thermal comfort, while the estimated thermal comfort through the measured equivalent temperature (PMV_{TEQ}) resulted closer to neutral. However, at temperatures higher than 28 ˚C, the preferred local air movement was not enough to fulfil the occupants cooling needs as the environment was assessed warm and additional physiological complains, like eye dryness and nose irritation, were expressed through the questionnaires.

Table 3: Scandinavian Human Subjects Results

	1st experiment (Cattarin et al., 2012)			**2nd experiment**		
t_a (˚C)	**v_a (m/s)**	**TSV (-)**	**PD (%)**	**v_a (m/s)**	**TSV (-)**	**PD (%)**
26	0.56	0.0	4	0.70	-0.1	19
28	0.69	0.5	10	0.82	0.3	12
30	0.85	1.3	55	1.03	0.9	35
32	-	-	-	1.5	1.2	49
34	-	-	-	1.7	1.6	63

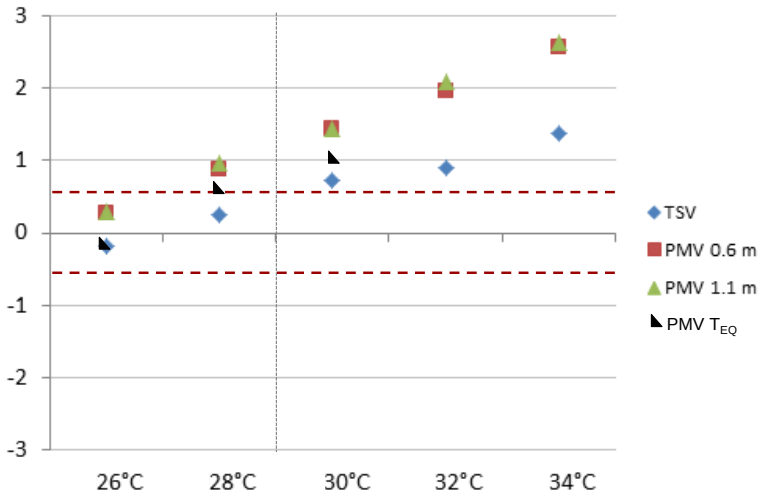

Figure 6: Evaluation (TSV) and Estimation (PMV) of Studied Thermal Comfort Environments

Comparing the present results of preferred local air velocities with the one obtained in a subjects experiment conducted with Chinese population (Zhou et al. 2006) it appear clear the different preference with higher air velocity and capability to adapt and achieve comfortable conditions, even at 30 ˚C, from the Chinese population.
Even if the Scandinavians appeared keen to higher air velocities to offset warm environments, they showed lower capability of adaptation maybe due to their daily exposure to colder environments.

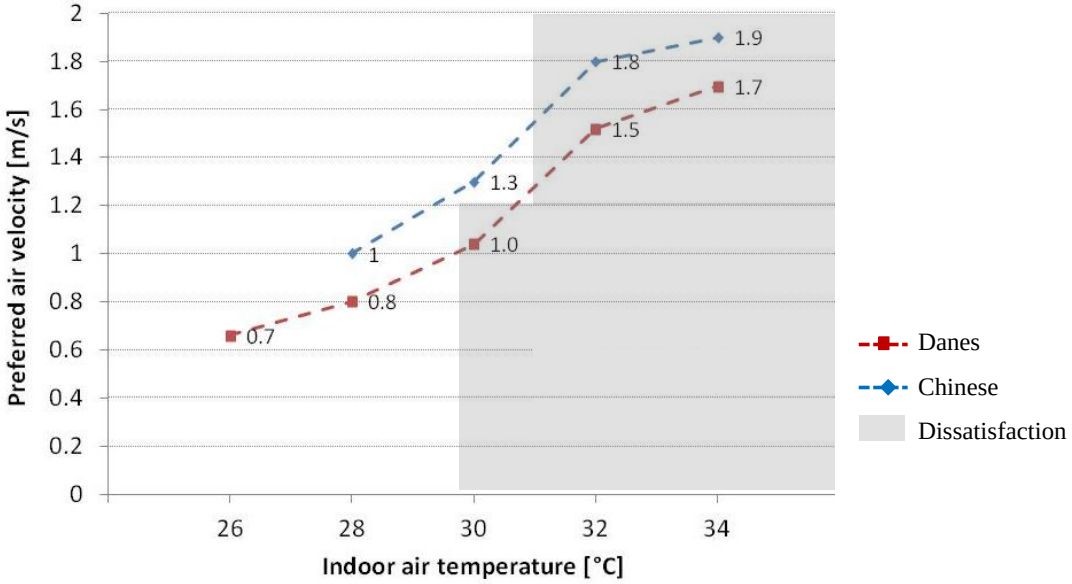

Figure 7: Subjective preference of local air velocity and comparison between Danish and Chinese participants

4 CONCLUSIONS

In this study the occupants, at sedentary positions, were exposed to an increased room temperature and local front air movement provided by a desk fan.
Higher local air velocity compensates higher room temperature at 28 ˚C and ˚30 C, resulting in neutral thermal environment.
Significant individual difference in the preferred air velocities was found which indicates that people differ and that personal control is important.

Comparing the present study with Danes and the one with Chinese subjects under similar experimental conditions, it shows acceptability and preferences in terms of neutral thermal environment.

5 ACKNOWLEDGEMENTS

This work is collectively sponsored by the Danish Agency for Science, Technology and Innovation and the Ministry of Science and Technology of P.R.China in the Sino-Danish collaborated research project: "Activating the Building Construction for Building Environment Control" (Danish International DSF project no. 09-71598, Chinese international collaboration project no. 2010DFA62410).

6 REFERENCES

Arens, E., Tengfang, X., Miura, K., Zhang, H., Fountain, M., Bauman, F., (1998). A study of occupant cooling by personally controlled air movement. Energy and Buildings, 27(1), 45-59.

ASHRAE Standard 55 (2010). Thermal environmental conditions for human occupancy.

Aynsley, R. (2007). Circulating fans for summer and winter comfort and indoor energy efficiency. Environment Design Guide.

Baizhan, L., Tan, M., Liu, H., Ma, X., Zhang, W. (2010). Occupant's perception and preference of thermal environment in free-running buildings in China. Indoor Built Environ, 19 (4), 405-412.

Boerstra, A., Beuker, T., Loomans, M., Hensen, J. (2013). Impact of available and perceived control on comfort and health in European offices. Architectural Science Review, Vol. 56 (1), 30–41.

Brager, G., Paliaga, G., de Dear, R. (2004). Operable Windows, Personal Control, and Occupant Comfort. ASHRAE Transaction, Vol.110 (2), 17-35.

Cattarin, G., Simone, A., Olesen, B.W. (2012). Human preference and acceptance of increased air velocity to offset warm sensation at increased room temperatures. In Proceedings of: AIVC 2012.

Cândido, C., de Dear, R.J., Lamberts, R., Bittencourt, L. (2010). Air movement acceptability limits and thermal comfort in Brazil's hot humid climate zone. Buildings and Environments 45, 222-229.

Cândido, C., de Dear, R., Ohba, M. (2012). Effects of artificially induced heat acclimatization on subjects' thermal and air movement preferences. Building and Environment 2012, 49, 251-258.

De Dear, R. (2004). Thermal comfort in practice. Indoor Air 2004, 14 (suppl 7), 32-39.

Fanger, P.O. and Pedersen, C.J.K. (1977). Discomfort due to air velocities in spaces. Proc. Of Meeting of Commission B1,B2,E1 of Int. Instit. Refrig: 1977, 4, 289-296.

Fanger, P.O., Ostergaard, J., Olesen, S., Lund Madsen, T.H. (1974). The effect on man´s comfort of a uniform air flow from different directions. ASHRAE Transaction, 2, 142-157

Feriadi, H. and Wong, N.H. (2004). Thermal comfort for naturally ventilated houses in Indonesia. Energy and Buildings, Vol. 36, 614-626.

Fountain, M.E. (1991). Laboratory studies of the effect of air movement on thermal comfort:a comparison and discussionof methods. ASHRAE Transaction, 97, 863-873.

Fountain, M.E., Arens, E., de Dear, R., Bauman, F., Miura, K. (1994). Locally controlled air movement preferred in warm isothermal environments. ASHRAE Trans., Vol 14 (1), 937-949.

Homma, H., and Yakiyama, M. (1988). Examination of free convection around occupant´s body caused by its metabolic heat. ASHRAE Transaction, 94, 104-124.

Hua, J., Ouyang, Q., Wang, Y., Li, H., Zhu, Y. (2012). A dynamic air supply device used to produce simulated natural wind in an indoor environment. Building and Environment 47, 349-356.

ISO 9886 (2003) Ergonomics- Evaluation of thermal strain by physiological measurements

ISO 7730 (2005). Moderate thermal environments. Determination of the PMV and PPD indices and specification of the conditions for thermal comfort.

ISO 15251 (2007). Indoor environmental input parameters for design and assessment of energy performance of buildings- addressing indoor air quality, thermal environment, lighting and acoustics.

Koranteg, C. and Mahdavi, A. (2011). An investigation into the thermal performance of office buildings in Ghana. Energy & Build. 43, 555-563.

Kubo, H., Isoda, N., Enomoto-Koshimizu, H. (1997). Cooling effect of preferred air velocity in muggy conditions. Building and Environment 1997, 32 (3), 211-218.

Mayer, E. (1992). New measurements of the convective heat transfer coefficients: influences on turbulence, mean air velocity and geometry of human body. In Proceedings of Roomvent´92, 3,263-276.

McIntyre, D.A. (1978). Preferred air speeds for comfort in warm conditions. ASHRAE transactions 1978, 84 (2), 264-277.

Olesen, B.W. (2007). The philosophy behind EN 15251: indoor environmental criteria for design and calculation of energy performance of buildings. Energy and Buildings 39 (7), 740-749.

Rohles, F.H., Woods, J.E., Nevins, R.G. (1974). The effects of air movement and temperature on the thermal sensations of sedentary man. ASHRAE Transaction, 80 (1)

Scheatzle, D.G., Wu, H., Yellott, J. (1989). Extending the summer comfort envelope with ceiling fans in hot, arid climates. ASHRAE Trans. 95, 269-279.

Schiavon, S and Melikov, AK (2009). Introduction of a Cooling-fan efficiency index. ASHRAE HVAC&R Research, 15 (6), 1121-1138.

Simone, A., Olesen, B.W., Babiak, J., Bullo, M., Langkilde, G. (2007). Operative temperature control of radiant surface heating and cooling systems. In: Proc. Clima 2007, Helsinki.

Smith, A.D.H., Crabtree, D.R., Bilzon, J.L.J., Walsh, N.P. (2010). The validity of wireless iButtons and thermistors for human skin temperature measurement. Physiol. Meas. 31, 95-114.

Sun, C., Giles, H., Xu, G., Lan, L., Lian, Z., (2013). Investigation on thermal comfort and energy conservation of local ventilation. HVAC&R Research, accepted manuscript.

Tanabe, S. and Kimura, K. (1989). Importance of air movement for thermal comfort under hot and humid conditions. ASHRAE Conference, Kuala Lumpur

Tanabe, S. and Kimura, K. (1994). Effect of air temperature, humidity, and air movement on thermal comfort under hot humid conditions. ASHRAE Transaction, 100, 953-969

van Marken Lichtenbelt, W.D., Daanen, H.A.M., Wouters, L., Fronczek, R., Raymann, R.J.E.M., Severens, N.M.V. and Van Somenen, E.J.W. (2006). Evaluation on wireless determination of skin temperature using iButtons. Physiol. and Behaviour 88, 489-497.

Zhang, H., Arens, E., Fard, S.A., Huizenga, C., Paliaga, G., Brager, G., Zagreus, L. (2007). Air movement preferences observed in office buildings. Int. J. Biometeorology, Vol. 51, 349–360.

Zhang, Y., Wang, J., Chen, H., Zhang, J., Meng, Q. (2010). Thermal comfort in naturally-ventilated buildings in hot-humid area of China. Building and environment 2010, 45, 2562-2570

Zhou, G., Melikov, A.K., Fanger, P.O. (2002). Impact of equivalent frequency on the sensation of draught. Roomvent´02, paper 242.

Zhou, G. (1999). Human perception of air movement- Impact of frequency and airflow direction on sensation of draught. Ph.D. Thesis at ICIEE-DTU, Denmark.

Zhou, X., Ouyang, Q., Lin, G., Zhu, Y. (2006). Impact of dynamic airflow on human thermal response. Indoor Air, Vol. 16, 348–355.

Weiwei, L., Zheng, Y., Deng, Q., Yang, L. (2012). Human thermal adaptive behavior in naturally ventilated offices for different outdoor air temperatures: a case study in Changsha China. Building and Environment 2012, 50, 76-89.

Yamtraipat, N., Khedari, J., Hirunlabh, J., Kunchornrat, J. (2006). Assessment of Thailand indoor set-point impact on energy consumption and environment. Energy policy 34, 765-770.

Yang, W. and Zhang, G. (2009). Air movement preferences observed in naturally ventilated buildings in humid subtropical climate zone in China. Int J. Biometeorol, 53, 563-573.

INDOOR AIR AND THERMAL ENVIRONMENT OF ENVIRONMENT-FRIENDLY HOUSE BY PASSIVE DESIGN IN JAPAN

Tomoyuki Endo [*1], Masayuki Otsuka [1], Yusuke Minami [2], and Tetsuya Umeno [2]

1 Kanto Gakuin University
1-50-1 Mutsuurahigashi, Kanazawa-ku
Yokohama city, Kanagawa,Japan
**Corresponding author: endo@kanto-gakuin.ac.jp*

2 Sekisui House Ltd.
4-15-1 Akasaka, Minato-ku
Tokyo, Japan

ABSTRACT

In recent years, with actualization of a global warming issue, the need for simultaneous pursuit of progress of comfort in living space at residential house and energy saving is now becoming greater and greater. In this study, we investigated the indoor thermal environment and air distribution by natural ventilation at earth sweet home in summer, middle and winter seasons in Japan. This house is designed so that the effect of natural ventilation may become high. We report the results with focus on the effects of indoor thermal and air environment by opening window in middle season. By using a skylight, it is showed that the cross-ventilated air volume is increased and the effect of SET* fall is high at the second floor room in this house. Also, this house is planed that the bathroom and the changing room protrude on the north side. Since this bulge has achieved the window catcher's effect, it has succeeded in passing indoor the wind is blown from the east side which is a predominant wind direction in this region. As a result, in indoor habitation space, it turned out that the air distribution environment of suitable wind velocity is formed in the wide range. Moreover, it is shown by here that the effect of the SET* fall by a cross-ventilated air is high similarly. In addition, we report that effects of heating insulation of whole in house, double sliding screen and thermal storage floor in summer and winter season too. As a result, through every year, to outside-air-temperature change, change of room temperature is small and has proved insulative effect, and also indoor thermal environment is improved by using double sliding screen in both seasons. And, the improvement effect of the thermal environment is acquired by gaining solar radiation heat from thermal storage floor in this measured house. From here onwards, it is thought that the energy saving effect of winter is fully expectable by gaining solar radiation heat from thermal storage floor.

KEYWORDS

Passive design, Natural ventilation, Cross-ventilation, Taiko-shoji, Thermal storage floor

1 INTRODUCTION

In recent years, Japan has an increasing demand for the compatibility between residential comfort and energy saving. That leads an increase of the number of the study cases about environment-friendly house, and double skins and solar chimneys recently receive much attention. In addition, the technological innovation in building equipments such as solar power generation and fuel cells is outstanding, and an idea of the energy storage with electric vehicles has appeared. However, the primary mind of architectural environmental engineering is that architectural planning methods (passive methods) predominantly make indoors comfortable and architectural equipments works complementally. So, it can be said that the effect of passive methods greatly influence on the effects of architectural equipments and the amount of consumption energy. This study therefore conducted a survey of an environment-friendly house which has some devices on the floor planning and kinds of passive technologies are installed on the house itself.

2 THE OUTLINE OF THE HOUSE

Fig.1 shows the floor plan and Table 1 shows the outline of the house. This house has no wall dividing rooms. A garage and SOHO are placed in the eastside of the house, but this study sets only the area west to the stairs for the target in this survey. In Japan, the solar elevation in summer is high and it is low in winter, so the balcony on the first floor functions as the eave for the living room on the ground floor. The eave enables to block sun rays in summer and to take sunlight inside of the room in winter. The floor of Room 1 adjacent to the veranda-like porch is a concrete thermal storage floor. Woods in the southern garden and the wall greening block the sun rays in summer. Twofold shoji screens (Taiko-shoji) which involve airspace between them are installed inside of each window. The floor plan of the house also considers the gain of the cross-ventilation airflow. The wall surface of the washroom in the north functions as a wind catcher to send airflow effectively into the living room.

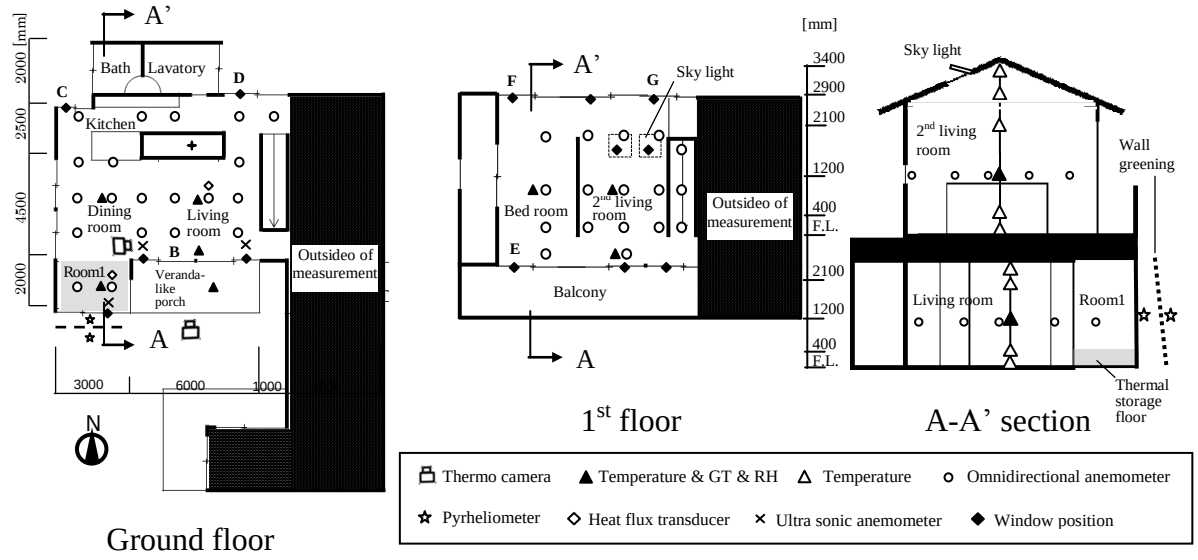

Figure 1. Plan, section and measurement point

Table 1. Outline of objective house

Location	**Architecture**	**Measurement area**
Kanagawa pref. JP	Two-story wooden house	Ground floor: 80.25 [m^2], 1st floor: 45.50 [m^2]
Thermal storage floor spec		
Contexture: Tile (15mm) + Mortar (30mm) + Concrete (450mm)		
Taiko-shoji spec		
Contexture: Shoji paper (3mm) + Airspace (30mm) + Shoji paper (3mm), Shoji material: Wahron paper		
Sky light spec		
Low-e pair glass + inner window shade, Size: 970 [mm] * 970 [mm]		

3 OUTLINE AND RESULTS OF THE SURVEY

The survey was conducted in the 3 periods: summer (Aug.), mid-time (Sep. – Oct.), and winter (Dec. – Feb.). The main measurement items are shown in Table 2. Indoor temperature was measured with thermocouples and thermo recorders. Air velocity was measured with 3D ultrasonic anemometer and thermal omnidirectional anemometer. pyrheliometer were set in the front and back of the wall greening. A heat flux transducer was placed on the surface of the floor of Room 1 to measure heat flows. The followings are the detail conditions in each measurement periods.

Table 2. Measurement item and points

Item	Instrument	Measurement points	Interval
Indoor temp.	Thermocouple	GF: Ceiling, FL+0, 400, 1200, 2100 [mm] 1F: Ceiling, FL+0, 400, 1200, 2100, 2900, 3400 [mm]	1 [min]
Globe temp.	Globe thermometer	All rooms: FL+1200 [mm]	1 [min]
Heat flux	Heat flux transducer	Living room floor, Room1 floor	1 [min]
Solar radiation	Pyrheliometer	FL+1200 [mm	1 [min]
Indoor RH	Thermo recorder	All rooms	30 [min]
Indoor air velocity	Omnidirectional anemometer	FL+1200 [mm	1 [min]
Air velocity through window	Ultrasonic anemometer	Center of each window	1 [sec]
Outdoor climate		Wather observation station (Yokohama)	10 [min]

3.1 Outline of summertime measurement

The measurement in summer was conducted from August 8th till 22nd in 2011. From Aug. 8th till 17th was the period for the fundamental performance measurement of the house, and the distribution of indoor temperatures were examined without opening windows and Taiko-shoji. From Aug. 18th till 22nd, the measurement was conducted under the condition which assumes real-life situations, and indoor environment was controlled by using of windows, Taiko-shoji, and air conditioning. In this summertime measurement, adiabatic effectiveness of the building and Taiko-shoji, and insolation shielding effectiveness of the wall greening were considered.

3.2 Results and discussion of the summertime measurement

(1) The building's adiabatic effectiveness

Fig. 2 shows the temperature changes in vertical direction in the center of the living room on ground floor. The maximum difference in vertical direction was about 2 degrees C, and it can be judged as small. The change of indoor temperature in whole day was about 3 degree C on the ground floor, and it can be said as small. The first floor showed similar findings to the ground floor. From the results of temperature measurements in several measurement points, generally uniform thermal environment was formed, and this building's adiabatic effectiveness is considered to be high.

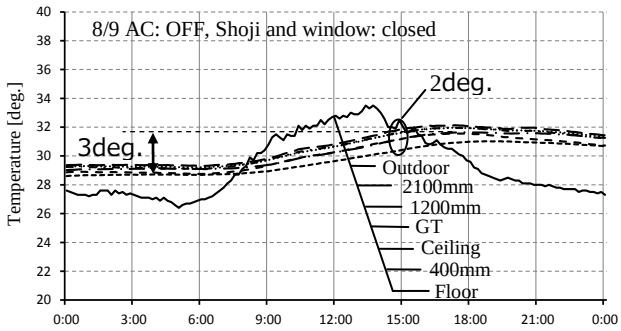

Figure 2. Temperature change at living room

(2) Adiabatic effectiveness of Taiko-shoji

Fig. 3 shows the deference (= Δ t) between the external temperature and the indoor temperature in the center of the living room on the ground floor (1200 mm height). The data

of Aug. 11th when Taiko-shoji were open from 9 a.m. to 6 p.m. was compared with that of Aug. 9th when Taiko-shoji were closed all day. The deference between the external and indoor temperature (=⊿t) on Aug. 11th rose and close to 0 line because of opening Taiko-shoji. Closing Taiko-shoji enables inside of room insusceptible to external temperature, so it is a good way to enhance adiabatic effectiveness.

(3) Insolation shielding effectiveness of the wall greening

Room 1 has no eaves to take a lot of sunlight into inside of it, and insolation in summer seems to influence on its indoor condition. Therefore, wall greening were installed in front of the window to consider their insolation shielding effectiveness. Fig. 4 shows the results of the amount of isolation in front and back of the green. Inside of the wall greening, the amount of isolation decreased more than 300W/m2 (about 50% shielding effectiveness) in daytime. From this result, thermal load shielding effectiveness of the wall greening is big and have potential for energy saving effect.

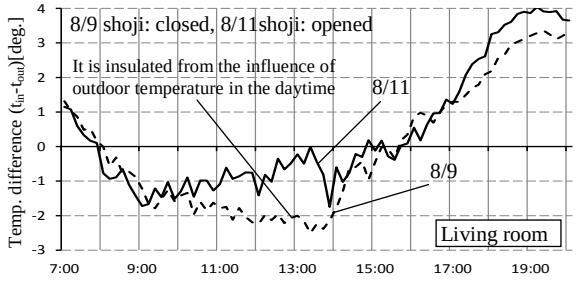

Figure 3. Heat insulating effect of Taiko-shoji

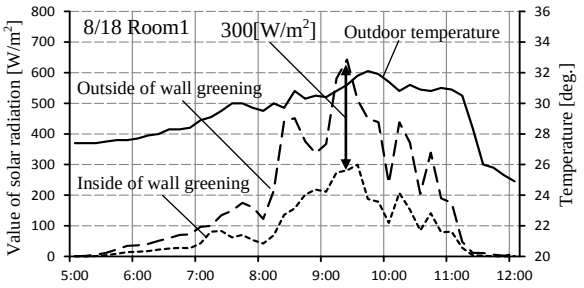

Figure 4. Insolation shielding effectiveness of the wall greening

(4) Consideration with integrated values of temperature differences

Table 3 shows the integrated values (degree C・hour) of the differences between indoor temperature with or without Taiko-shoji from 9 a.m. to 6 p.m. (in the center of each room , 1200mm height) and preset temperature of air conditioning (28 degree C). However, the data in the condition that the indoor temperature falls below the preset temperature were cut off. It is found from the table that about 17 (degree C・hour) decreased on the ground and first floor by closing Taiko-shoji. From this result, it can be said that Taiko-shoji has inhibiting effect of indoor temperature increase.

Table 3. Integrated values of temperature differences (Indoor temp. – 28 deg.) [degree * hour]

Condition		Ground floor		1st floor	
AC	Shoji	Dining room	Living room	Bed room	Living room
OFF	Opened	44	45	69	66
	Closed	28	27	52	49
ON	Opened	0.3	0.4	-	-
	Closed	0.2	0.2	-	-

3.3 Outline of mid-term measurement

Mid-term measurement was conducted from Sep. 27th till Oct. 5th. In this season, external temperature decreases, and indoor environment can be improved with cross-ventilation. Windows were opened from 9:30 a.m. to 6:00 p.m. in this measurement. The windows which were chosen for opening are presented as A through G in Fig 1. Opening space of each

window were shown in Table 4. Temperature, globe temperature (GT), and relative humidity were measured in the center of each room. To examine the indoor air velocity distribution, thermal omnidirectional anemometer were placed at almost regular intervals as in Fig. 1 (25 points on ground floor, 18 points on 1st floor, 1200mm height). In addition, amount of passing air at the windows were measured by setting 3D ultrasonic anemometer at the center and in front of the window. SET was calculated with the values of temperature, GT, and relative humidity which were measured in the middle (1200mm) height in the room, and the average value of air velocity at 1200 mm height. The amount of clothing was set at 0.6 clo, and the amount of metabolism was set at 1 met. With combination use of the skylight which is characteristics of this house, the 8 patterns of window openings as in Table 5 were compared one another.

Table 4. Window opening area

	Window position						
	A	**B**	**C**	**D**	**E**	**F**	**G**
Area [m^2]	2.46	1.48	0.97	1.96	0.58	0.33	0.96

Table 5. Window opening pattern

Window	**mode0**	**mode1**	**mode2**	**mode3**	**mode4**	**mode5**	**mode6**	**mode7**
GF all	Closed	Opened	Opened	Opened	Opened	Closed	Closed	Opened
1F all	Closed	Opened	Opened	Closed	Closed	Opened	Opened	Opened(south side only)
Skylight	Closed	Closed	Opened	Closed	Opened	Closed	Opened	Closed

3.4 Results and discussion of mid-term measurement

(1) Comparison of amount of passing airflow at window

Table 6 shows the comparison of the air velocity in each opening pattern, and Table 7 shows the amount of airflow with and without the skylight. The data only in the case that the external wind direction and air velocity were almost equal were extracted for this comparison. The amount of passing air was at maximum in mode 2, and it was at minimum in mode 5. The windows of the wall surfaces on 1F are small, so it is found that opening these windows does not bring a big cross-ventilation effect. The amount of passing air increased by 35% in mode 2 in which the skylight is opened with all other windows compared with mode 1 with all the windows except of the skylight opened.

Table 6. Air volume through windows [unit: m^3/h]

Window Position	**mode1**	**mode2**	**mode3**	**mode4**	**mode5**	**mode6**	**mode7**
South side	4793	6243	6580	5531	1968	2013	3905
North side	7399	10146	9039	7979	2355	4127	4282

Table 7. Air volume ratio depend on the presence or absence of skylight

Window Position	**Mode2 / mode1**	**Mode4 / mode3**	**mode6 / mode5**
South side	1.30	0.84	1.02
North side	1.37	0.88	1.75

Besides, the results of measurements with tracer-gas shows that air change rate increased by 1.5 times in the living room on the first floor by opening the skylight (Table 8). The results of this measurement show that opening both the skylight and windows on surface wall are expected to have a decreasing effect of indoor temperature and energy saving effects with air conditioning, in the case that external temperature is lower than indoor temperature.

Table 8. Air change rate of 1st floor living room

Ventilation Number [-/h]	mode1	Mode2
Living room (1st Floor)	25.31	38.58

(2) Distribution of indoor air velocity

The distribution of indoor airflow velocity of each floor in mode 1 and 2 were shown in Fig. 5 and 6 respectively. In mode2, the air velocity at the northern window and the southern window is 1.5 and 1.8 times respectively as faster as that in mode 1 because of the influence of opening the skylight. In addition, the main wind direction during the measurements was north to east, and the eastern surface wall of the washing room works as a wind catcher in the northern part of the ground floor. So, the air velocity become very fast at the opening D on the ground floor. The average air velocity of each room is in Table 9. The result was different from that of passing air amount that the average air velocity was relatively big in mode 3 for the ground floor and in mode 5 for the 1st floor. In the residential area on the 1st floor, the average air velocity didn't change in mode 5 and 6 regardless of the additional opening of the skylight in mode 6. The factor of this result can be that airflow passed along with the surface walls and didn't pass through the residential area.

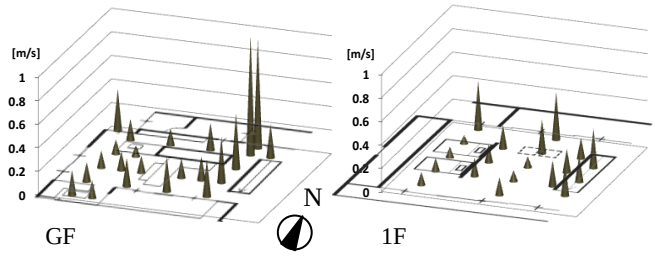

Figure 5. Indoor air velocity distribution (mode1)

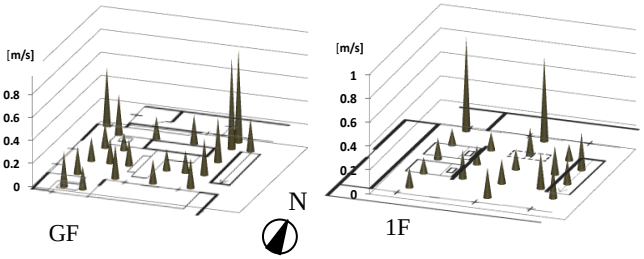

Figure 6. Indoor air velocity distribution (mode2)

Table 9. Averaged air velocity in each room [unit: m/s]

Room		mode1	mode2	mode3	mode4	mode5	mode6	mode7
GF	Dining room	0.15	0.21	0.26	0.18	-	-	0.15
	Living room	0.21	0.21	0.26	0.39	-	-	0.21
	Room1	0.17	0.23	0.51	0.31	-	-	0.19
1F	Living room	0.19	0.22	0.05	0.11	0.30	0.16	0.06
	Bed room	0.12	0.15	0.04	0.06	0.21	0.14	0.05

(3) Consideration with integrated values of temperature differences

Table 10 shows the integrated values (degree C・hour) of the differences between indoor temperature in each mode (in the center of each room , 1200mm height) and the external temperature from 9 a.m. to 6 p.m. Mode 0 with no window opened resulted in 27 degree C in average on the ground floor and 36 degree C in average on the 1st floor. By opening windows,

the temperature decreased both in the ground and 1st floor. In addition, the results of mode 5 and 6 show that opening skylight with the other windows decrease the temperature on the 1st floor more greatly than only the windows on surface walls. As mentioned above, energy saving effect is expected by opening both the skylights and windows on surface walls in the condition that external temperature is lower than indoor temperature.

Table 10. Integrated values of temperature differences (Indoor temp. – Outdoor temp.) [degree * hour]

Room		Mode0	Mode1	Mode2	Mode3	Mode4	Mode5	Mode6	Mode7
GF	Dining room	24	5	10	8	10	-	-	7
	Living room	28	7	11	9	10	-	-	8
	Room1	28	11	14	8	10	-	-	45
1F	Living room	34	13	14	-	-	20	15	24
	Bed room	38	17	17	-	-	23	18	21

(4) Comparison of SET* decreasing effect

In this part, SET* decreasing effect was considered with the formula in Fig. 7. Table 11 is the results of SET* decreasing effect in each mode. In the living room on the ground floor, with and without opening the skylight didn't show any apparent difference. In living room on the 1st floor, opening the skylight leaded indoor air velocity and produced bigger SET* decreasing effect than temperature difference decreasing effect mentioned before. Especially, SET* decreasing effect enhanced immediately after opening windows, so the thermal comfort enhancing effect of opening windows is considered to be great.

$$\text{Decrease ratio of the SET*} = \frac{\text{SET* in situation window closed} - \text{SET* in situation window opened}}{\text{Time taken to SET* decrease}}$$

Figure 7. Equation of decrease ratio of SET* [unit: degree / min]

Table 11. Decrease ratio of SET* results [degree / min]

	Mode0	Mode1	Mode2	Mode3	Mode4	Mode7
Living room (GF)	-0.01	-0.13	-0.13	-0.19	-0.17	-0.08
Living room (1F)	-0.01	-0.07	-0.20	-0.01	-0.10	-0.08

3.5 Outline of wintertime measurement

The wintertime measurement was conducted in the two times: from Dec. 26th, 2011 to Jan. 5th, 2012, and from Feb. 14th to 21st in 2012. Throughout the measurement period, the windows were not opened, and indoor environment was controlled by Taiko-shoji, floor heating, and air conditioning. This measurement reports the adiabatic effectiveness of the building and Taiko-shoji, and the effect of thermal storage floor.

3.6 Results and discussion of wintertime measurement

(1) The building's adiabatic effectiveness

Fig. 8 is the temperature distribution in vertical direction in the center of living room on the 1st floor. This is on the day with windows closed and without heaters, but Taiko-shoji in the living room on the ground floor was opened from 9 a.m. to 6 p.m. The temperature difference in vertical direction was about 2 or 3 degree C, that of whole day was about 6 degree C at maximum, and that at the same measurement point was about 4 degree C at maximum. These

changes are smaller than the external temperature changes, so the indoor temperature is not relatively influenced by the external temperature.

(2) Adiabatic effectiveness of Taiko-shoji

Fig. 9 is the temperature changes in the center of the living room on the ground floor on Dec. 31st, when Taiko-shoji was closed whole day. By closing Taiko-shoji, the difference of indoor temperature distribution became smaller. The differences in one day and at the same measurement point also became smaller as about 4 and 2 degree C at maximum respectively. Fig. 10 shows the difference between the indoor and external temperature in the living room (1200mm height) on the 1st floor in 2 cases: Case 1 in which Taiko-shoji was closed from 6 p.m. to 9 a.m. in the next morning, and Case 2 in which Taiko-shoji was opened in the same period of time. In Case 2, the indoor temperature drastically fell in about 4 degree C from midnight, and dropped in about 8 degree C at maximum after that. In Case 1, however, a rapid decrease of indoor temperature was not found, and the temperature showed gradual decline for 9 a.m. in the next morning.

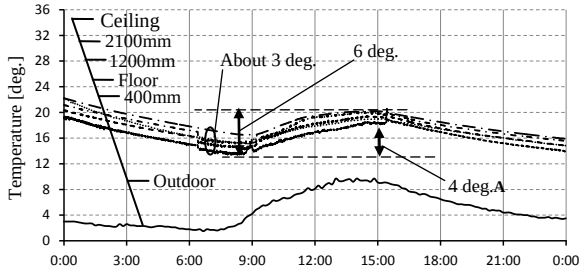

Figure 8. Temperature change at living room (12/27)

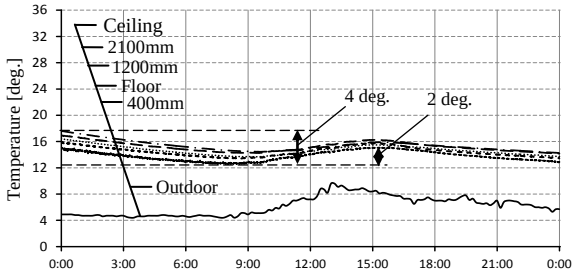

Figure 9. Temperature change at living room (12/31)

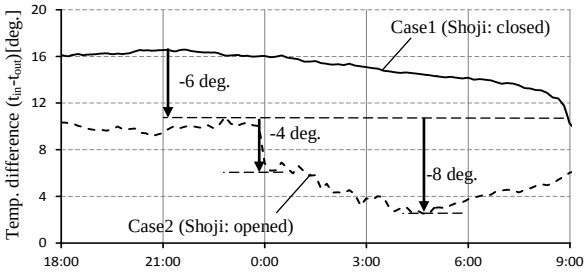

Figure 10. Heat insulating effect of Taiko-shoji

(3) Indoor environmental enhancing effect of insolation intake

The picture and thermal image of the southern window in the living room on the ground floor, which were took in out of doors, were shown in Fig. 11. In wintertime, sunlight penetrates into the surface of the window, and the temperature of surface window near the floor was about 25 degree C higher than that of the center of the window. Fig. 12 shows the picture and thermal image of the same area, which were took from the inside of the room. The floor was heated by sunlight and the temperature increased about 12 degree C. These results show the thermal environmental enhancing effect with insolation around the windows in wintertime.

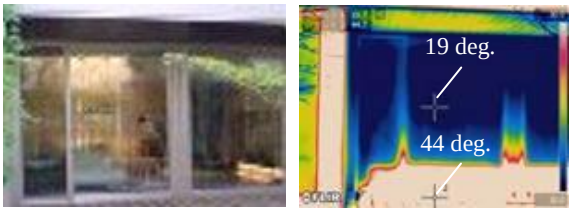

Figure 11. Picture and thermal image at veranda-like porch

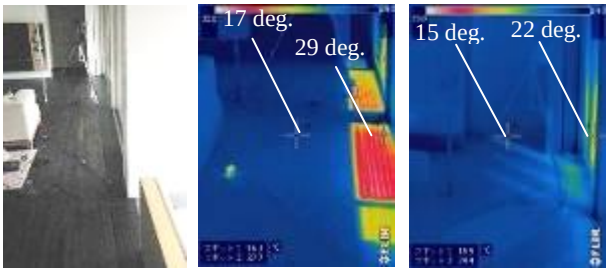

Figure 12. Picture and thermal image at south side perimeter in living room

Picture Thermal image at 12 a.m. Thermal image at 4 p.m.

(4) The effect of thermal storage floor

1) Consideration on surface floor temperature

Fig. 13 shows the surface temperature of the thermal storage floor of Room 1 and wooded floor of the living room on the ground floor. At 4 p.m. on 16th, the surface temperatures were 13 degree C in the living room and 15 degree C in Room 1. After floor heating worked, the temperature of the living room floor rapidly increased, but the thermal storage floor gradually increased. In night after floor heating stopped, the way of surface floor temperature decreasing differed because of the thermal storage effect. Besides, the surface floor temperature at noon on 19th were 15 degree C in the living room, but it increased to 30 degree C in thermal storage floor even when floor heating didn't work then. These results show that thermal storage floor can intake sunlight and function like floor heating.

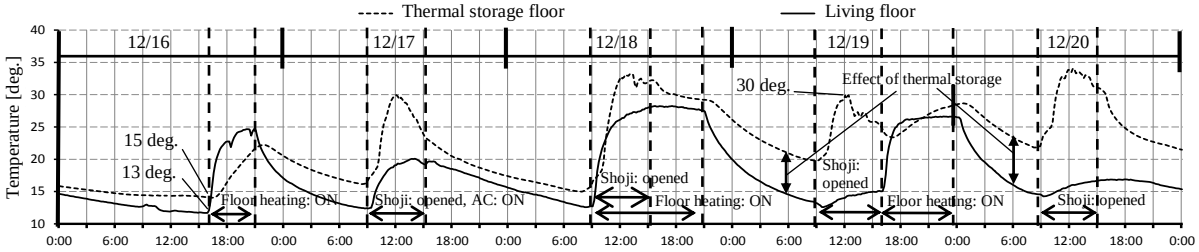

Figure 13. Floor temperature change

2) Consideration on the difference between surface floor and indoor temperature

Fig. 14 shows the difference between the surface floor and indoor temperature in Room 1 and the living room on the ground floor. The temperature of the thermal storage floor was always higher than that of indoor. In converse, it has already found that the temperature of thermal storage floor was always lower than that of indoor in summertime.

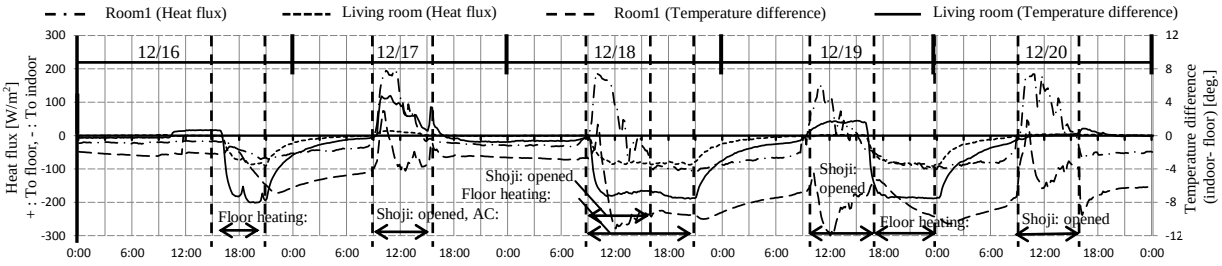

Figure 14. Heat flux and Temperature difference (indoor – floor surface) change

3) Consideration on heat flux

Fig. 14 shows the results of heat flux transducers set on the surface floor of the thermal storage floor and floor of living room floor. From this figure, heat flew in the surface of thermal storage floor and was stored in daytime, and the floor emitted heat into the room in night.

(5) Consideration with integrated values of temperature differences

Table 12 and 13 show the integrated values of the differences between indoor temperature of each room on the ground floor (in the center of each room, 1200mm height) and the preset temperature of heaters (22 degree C). Table 12 shows the comparison of opening and closing

Taiko-shoji from 9 a.m. to 4 p.m. With closing Taiko-shoji and without heaters, the values was 67 (degree C *hour) in each room. With opening Taiko-shoji, the values decreased to 45 (degree C *hour) in the living and dining room, and to 32 (degree C *hour), less than half of closing case, in Room 1. Table 13 compares the results of during 4 p.m. to 9 p.m. based on the 2 condition in earlier time than 4 p.m. (Taiko-shoji was closed after 4 p.m. in both cases.). When Taiko-shoji was opened by 4 p.m., heat stored in daytime was maintained. The integrated value of this case was about 50 % of that of the case without opening Taiko-shoji in daytime. From these results, appropriate opening and closing Taiko-shoji was found to increase the enhancing effectiveness of indoor thermal environment, so heating load can be reduced and energy saving effect can be expected.

Table 12. Integrated values of temperature differences between 9 a.m.-4 p.m. [degree * hour]

Situation between 9 a.m. – 4 p.m.	Dining room	Living room	Room1
Shoji : closed, AC : OFF	66	66	69
Shoji : opened, AC : OFF	45	46	32

Table 13. Integrated values of temperature differences between 4 p.m.-9 p.m. [degree * hour]

Situation before 4 p.m.	Dining room	Living room	Room1
Shoji : closed, AC : OFF	33	33	39
Shoji : opened, AC : OFF	18	19	19

4 CONCLUSION

The results of measurements in whole year revealed that the building's adiabatic performance is high. Taiko-shoji is an effective way to enhance adiabatic effect, and appropriate use of it leads a big energy saving effect in wintertime. In mid-term, the combined use of the skylight increased amount of airflow and significantly boost the effectiveness for comfort. The east surface wall of the northern washing room in the house played a big role of wind catcher, and induced great amount of airflow into the rooms. With the devises in floor plan like this house, increase of amount of passing air become possible, and cooling load can be reduced by emitting excess heat inside of the rooms with cross-ventilation when the external temperature is lower than that of indoor. In addition, the sense of airflow is expected to improve comfort. Comfort enhancement brings raise of the residents' awareness in window opening. Therefore, daily opening windows from the mid-term of April and May can delay the beginning period of cooling use in summertime.

5 REFERENCES

Institute for Building Environment and Energy Conservation (2005). Design Guideline to Low Energy Housing with Validated Effectiveness.

Yasunobu W.(2012). Effect of cross-ventilation in environmentally symbiotic house with double-deck engawa、AIJ J. Techol. Des. Vol. 18, No.39, 607-612

Nao N.(2012). Study on effect of passive design and energy saving in detached house Part1 - Part3., Summaries of Tech\nical Papers of Annual Meeting D-2, Architectural Institute of Japan, 483-488

EVALUATING THE PERFORMANCE OF SELECTED THERMO-PHYSIOLOGICAL INDICES ON QUANTIFYING BIOCLIMATIC CONDITIONS FOR PEDESTRIANS IN A STREET CANYON

Katerina Pantavou[*1], Mattheos Santamouris[1]

1 Faculty of Physics, Department of Environmental Physics and Meteorology , University of Athens
Building Physics 5
University Campus – Zografou, Athens, Greece
**Corresponding author: kpantav@phys.uoa.gr*

ABSTRACT

A large number of indices have been developed to assess human bioclimatic conditions. The indices that could be considered valid in all climate and seasons are those that are based on calculations involving the heat balance equation. The aim of the present study is to evaluate the performance of selected existing indices based on body's energy balance, in an outdoor built environment. A field questionnaire survey was carried out simultaneously with microclimatic measurements in a street canyon located in the centre of Athens, Greece. The experiments that lasted 2 days, were performed in July while the interviews were conducted in randomly selected people passing by or visiting the measurements sites. The values produced by COMFA, PET and UTCI were compared to the actual thermal sensation that was indicated on a 7-point thermal sensation scale by the respondents. The results showed a significant relationship between predicted and actual thermal sensation. However indices' estimates deviated from the actual thermal sensation. The maximum percentage of correct predictions was about 37% while UTCI predicted thermal sensation better than COMFA or PET.

KEYWORDS

Thermal sensation, outdoors, predictive models, questionnaire survey

1 INTRODUCTION

Urbanization and designers' interest on internal thermal comfort, with respect to low energy consumption, led to a great number of studies on indoor thermal sensation. The models developed to estimate thermal sensation indoors were used also, without any modification, to outdoor environments. However, studies on outdoor thermal sensation demonstrated that thermal sensation differed from that predicted by the indoor models, due to unrealistic approaches such as lack of solar radiation and still air conditions (Höppe, 2002).
More recently the environmental quality of outdoor urban spaces has drawn a lot of attention for reducing heat island effect (Santamouris, 2013; 2012; Santamouris et al, 2011) and managing the potential of sun and wind due to the mutual obstructions between buildings as well as improving microclimate outdoors that influence both the bioclimatological conditions indoors and the function of the space; thus several models have been developed in the context of outdoor thermal sensation. Among the proposed ones, the state of the art in the assessment of thermal environment are the thermo-physiological indices that are based on heat balance

equations. Often the predictions among the models differ (Blazejczyk et al, 2012; Jones, 2002) or the predictions of an index differ depending on the climate while there is a discrepancy between the predicted and the actual (Monteiro and Alucci, 2006; Lin and Matzarakis, 2008; Cheng et al, 2012; Pantavou et al, 2013). Lin and Matzarakis (2008) and Cohen et al (2013) calibrated Physiological Equivalent Temperature (PET) index, in order to improve its predictability while they identified differences in PET boundaries in Western/Middle Europe, Tel Aviv and Taiwan assessment scale.

Nevertheless bioclimatic models remain important tools for assessing human thermal sensation and are widely used (Pantavou et al, 2011; Theoharatos et al, 2010; Lin and Matzarakis, 2008; Gaitani et al, 2007) so it is essential to be aware of their applicability as well as to identify the model that predicts the most accurate thermal sensation in the climatic zone of interest. The aim of the present study is to evaluate the adequacy of three different models on quantifying thermal sensation in Mediterranean climates. All three theoretical models examined, Comfort Formula (COMFA), Physiological Equivalent Temperature (PET) and Universal Thermal Climate Index (UTCI), are based on human energy balance and are designed for the prediction of thermal sensation outdoors.

COMFA (Brown and Gillespie 1986, 1995) is based on estimating the energy budget of a person. PET (Höppe, 1999) is based on a two node model, the Munich Energy-balance Model for Individuals (MEMI). It is defined as the air temperature at which, in a typical indoor setting (with a water vapour pressure of 12 hPa and light air (0.1 m s^{-1}), the heat budget of the body (80 W activity, in addition to the basic metabolism: thermal resistance of clothing of 0.9 clo) is balanced with the same core and skin temperature that occurs when under the outdoor conditions to be assessed. Universal Thermal Climate Index (UTCI) (COST Action 730) is based on a multi-node model of human thermoregulation and it is independent of person's characteristics (e.g. age, gender). It is expressed as an equivalent ambient temperature (°C) of a reference environment providing the same physiological response of a reference person, as in the actual environment

2 MATERIALS AND METHODS

Field questionnaire surveys were performed simultaneously with microclimatic measurements for two days in July, one day during morning-midday and one during afternoon–evening, at the pedestrianized part of Ermou Street which is the busiest shopping street in central Athens, Greece. A mobile meteorological station equipped with a Rotronic S3CO3 thermo-hygrometer, a Second Wind C3 anemometer, two Kipp & Zonen CM3 pyranometers, an ECO pyrgeometer and a grey globe thermometer (PVC sphere, 40 mm diameter with an emissivity of 0.3) were monitoring air temperature (T_{air}), relative humidity (RH), average wind speed (WS), down-welling ($SR_{\downarrow}$) and reflected ($SR_{\uparrow}$) solar radiation down-welling and ground total radiation ($TR_{\downarrow}$, $TR_{\uparrow}$) on a horizontal plane as well as globe temperature (T_{globe}) at the height of 1.1m above the ground. The data were stored on a CR10X Campbell Scientific data logger at 1 min intervals.

The interviews were based on a structured questionnaire and were conducted in people passing by or visiting the site. The questionnaire included questions related to personal characteristics of the interviewees such as clothing, main activity during the last half hour, gender, age, height and weight as well as the main question of thermal sensation vote (TSV) in which the respondents were asked to assess their thermal sensation based on ASHRAE 7-point scale (3, cold; 2, cool; 1, slightly cool; 0, neutral; 1, slightly warm; 2, warm; 3, hot).

2.1 Additional data and data processing

Hourly data of atmospheric pressure as well as per minute data of total and diffuse solar radiation were obtained by the Institute of Environment and Sustainable Development, National Observatory of Athens (Thissio Station).
The provided data of solar radiation were used to evaluate diffuse solar radiation at the measurement site. Moreover, down-welling and up-welling long-wave radiation on a horizontal plane ($IR_{\downarrow}, IR_{\uparrow}$) were estimated using the data of $SR_{\downarrow}$, $SR_{\uparrow}$, $TR_{\downarrow}$ and $TR_{\uparrow}$. Mean radiant temperature (T_{mrt}) was calculated using the data of T_{air}, T_{globe} and WS (Thorsson et al, 2007) while the wind speed at 10 m height was estimated using the formula (Stull, 2000):

$$WS_{10m} = WS\frac{\ln(10/z_0)}{\ln(z/z_0)} \quad (1)$$

where z is wind speed at the measured height in m, z_0 is the aerodynamic roughness length in m and was set at 0,01 m (Jendrintzky et al, 2000).
The respondents' clothing insulation (I_{cl}, in clo) and metabolic rate (M, in $W \cdot m^{-2}$) were estimated by the clothing description and the type of activity in accordance to ISO 9920 and ISO 8996 respectively.
A Matlab (MATLAB R2010a, The MathWorks Inc.) code was developed for the calculation of the indices COMFA, PET and UTCI consistent with weather measured data. The analysis was performed on the 3 min average of the meteorological values since that was the estimated time for completing a questionnaire.

Table 1: Assessement scale of COMFA and temperature thresholds used in PET and UTCI

Thermal Sensation	**COMFA ($W \cdot m^{-2}$)**	**PET (^oC)**	**PET_{Med} (^oC)**	**UTCI (^oC)**	**TSV**
Very cold		<4	<8		-3
Cold	≤−201	4-8	8 to 12	-27 to -13	
Cool	−200 to −121	8-13	12 to 15	-13 to 0	-2
Slightly cool	−51 to −120	13-18	15 to 19	0 to 9	-1
Neutral	−50 to +50	18-23	19 to 26	9 to 26	0
Slightly warm	51 to +120	23-29	26 to 28		1
Warm	+121 to +200	29-35	28 to 34	26 to 32	2
Hot	≥+201	35-41	34 to 40	32 to 38	
Very hot		>41	>40	38 to 46	3
Extreme hot				>46	

2.2 Data analysis

The aim of the study is to evaluate the performance of COMFA, PET and UTCI consistent with weather measured data in an outdoor Mediterranean built environment. Therefore, the analysis focused on the comparison of the predictions of the three selected models with TSV. Three criteria were established: 1) the correlation between models' predictions and TSV 2) the correlation between models' class prediction and TSV and 3) the percentage of correct predictions. The first two criteria verify the model's sensibility, showing how well the model's value or class predictions vary in function to variations of TSV while they were assessed by the measure of correlation, Spearman rho, and the symmetrical measure of association, Gamma, respectively. The third criterion concerns the percentage of correct predictions, showing model's good performance, and it was validated by cross-tabulation analysis.
In order to apply the second and third criteria, the indices' assessment scales adjusted to the 7-point scale of TSV (from -3 to 3) based on the verbal description of thermal sensation. For

example, the extreme categories such as extreme hot / cold merged to the categories -3 and +3 respectively. In the case of UTCI that contain the sense of thermal stress, the assessment scale was modified according to Epstein and Moran (2006) who described thermal sensation compared to thermal physiological effects. Two assessment scales of PET were considered; the classification for Western/Middle European (PET) (Matzarakis and Mayer, 1996) as well as for the Mediterranean climate (PET_{Med}) (Cohen et al, 2013). Table 1 shows the assessment scales of the indices as well as the respective level of TSV.

3 RESULTS

Totally 313 interviews were performed in typical summer weather conditions. Air temperature ranged between 22.6 ^{o}C and 35.3 ^{o}C, relative humidity measured from 33% to 74% while the wind was kept low, apart from few gusts recorded by the anemometer. About 58% of the interviewees were males whereas 88.2% were from 18 to 64 years old indicating a very low percentage of children and elderly people in the sample. TSVs varied from -1 to +3. Some of 1.6% of the TSVs were 'slightly cool' while the largest percentage of votes (41%) were observed in class 'warm' (+2).

Table 2: Indices range during the field surveys

A Index	Minimum	Maximum	Mean	Std Dev	B Index	Minimum	Maximum
COMFA ($W \cdot m^{-2}$)	-54	288	29	66	COMFA	-1	+3
PET (^{o}C)	24.7	40.1	33.4	2.5	PET	+1	+3
UTCI (^{o}C)	26.4	36.9	33.0	1.8	PET_{Med}	0	+3
					UTCI	+2	+3

Table 2 presents indices' range during the surveys. COMFA values ranged correctly according to TSVs, between classes -1 and +3 (Table 2B), whereas PET and UTCI range differed from that of TSV. The PET_{Med} showed better predictions (between classes 0 and +3) compared to PET, while UTCI values varied between classes +2 and +3 indicating that TSV is overestimated.

To evaluate the performance of the three models, the correlation coefficients between the models' predictions and TSV as well as the percentage of correct predictions were estimated (Table 3). Higher correlation coefficient (0.36) was observed in the case of UTCI. The results remained the same when ranked indices values were considered. UTCI predicted with greater success the TSV (Gamma=0.45) compared to COMFA, PET and PET_{Med}, while PET_{Med} was the index with the highest percentage of correct predictions. Nevertheless the cross-tabulation of the results (Fig. 1) demonstrates reduced predictability of the models in the categories -1, 0 and 1, and apart from UTCI it is observed a tendency of thermal sensation to be classified in class +2.

Table 3: Spearman's correlation coefficients and cross-tabulation statistics of models' predictions and thermal sensation vote.

				Normalized values			
Index	**Correlation coefficient**	**Gamma Statistic**	**Correct predictions (%)**	**Correlation coefficient**	**Gamma Statistic**	**Correct predictions (%)**	**Total**
COMFA	0.28	0.31	15.4	0.78	0.69	0.41	1.88
PET	0.14	0.18	36.6	0.39	0.40	0.98	1.77
PET_{Med}		0.25	37.2	0.39	0.56	1.00	1.94
UTCI	0.36	0.45	33.6	1.00	1.00	0.90	2.90

In order to have an objective measure of comparison between models, the correlation coefficients and the percentage of correct predictions were normalized. As a reference value was set the maximum value per criterion. The sum of the three normalized values reveals an index on which the models can be compared and classified with respect to their applicability to Mediterranean climate (Table 3). According to our limited sample and the criteria posed in this study, UTCI showed better reproduction of TSV compared to COMFA and PET. This result is in agreement with Monteiro and Alucci (2006) who considered that is preferable to use a model with better correlation between the model and the TSV instead of using the one with the greater percentage of correct predictions because when the first model is calibrated has a good potential to correctly predict thermal sensation.

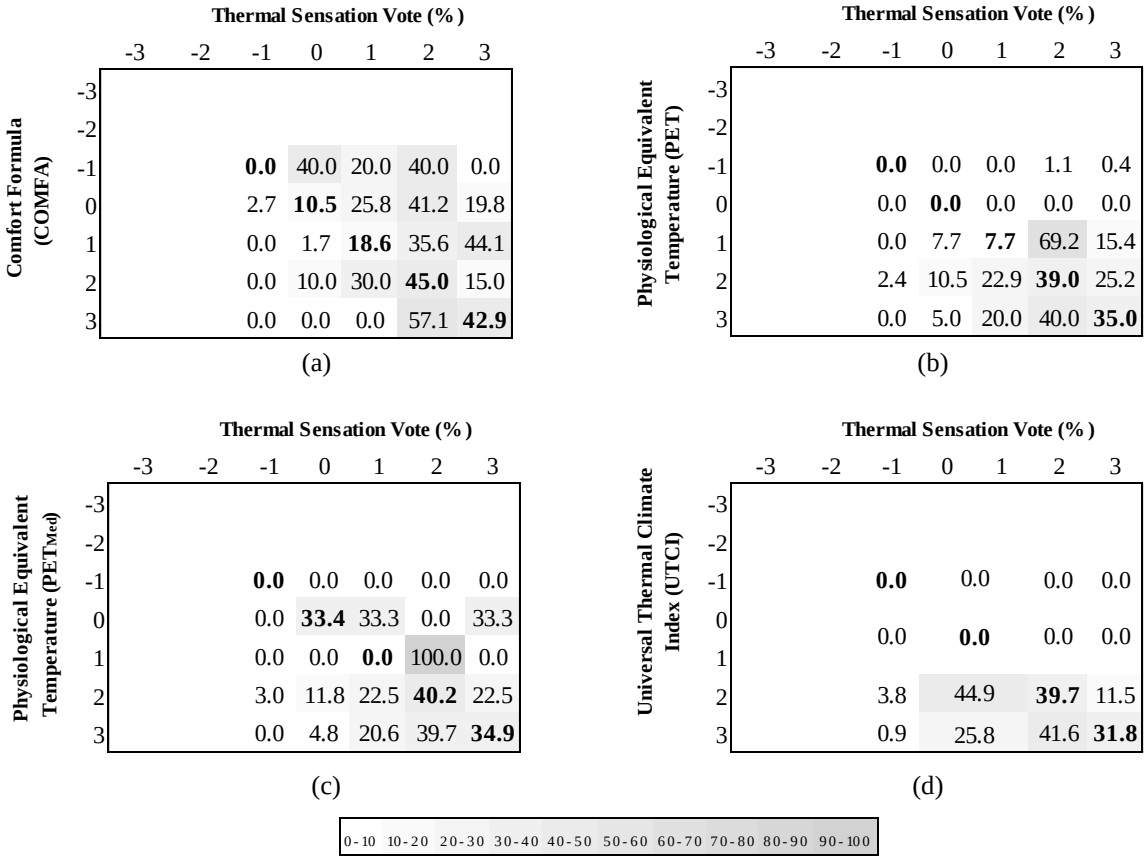

Figure 1: Distribution of predicted in relation to thermal sensation votes (each row adds to 100%)

The same method was applied considering mean TSV per 10 $W \cdot m^{-2}$ in the case of COMFA and $1^{o}C$ in the case of PET and UTCI. Spearman's correlation coefficients were estimated between rounded indices values and mean TSV at the corresponding intervals, while cross-tabulations were developed based on indices' classes and rounded mean TSV. The results are

Table 4: Spearman's correlation coefficients and cross-tabulation statistics of models' predictions and mean thermal sensation vote.

				Normalized values			
Index	**Correlation coefficient**	**Gamma Statistic**	**Correct predictions (%)**	**Correlation coefficient**	**Gamma Statistic**	**Correct predictions (%)**	**Total**
COMFA	0.45	0.28	17.2	0.47	0.28	0.31	1.05
PET	0.68	1	56.3	0.71	1.00	1.00	2.71
PET_{Med}		1	50.0	0.71	1.00	0.89	2.60
UTCI	0.96	1	27.3	1.00	1.00	0.48	2.48

are demonstrated in Table 4. PET predicted successful about 56% of mean TSV and according to the criteria posed reproduced mean TSV best of all models. The percentage of correct predictions of UTCI in the case of mean TSV (27.3%) was lower than that in the case of TSV (33.6%).

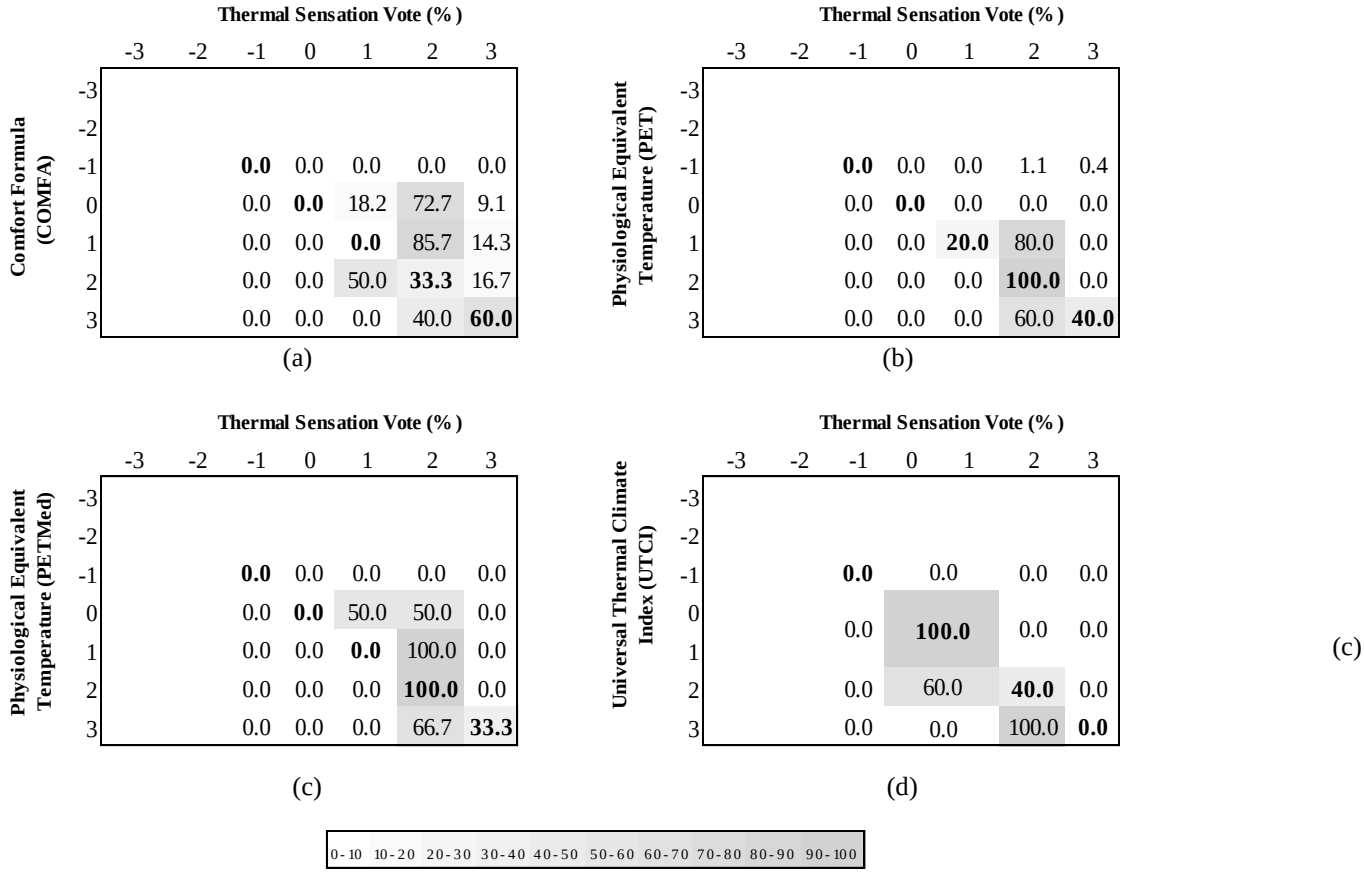

Figure 2: Distribution of predicted in relation to mean thermal sensation votes (each row adds to 100%)

The cross-tabulation of the predicted and mean TSV showed that the range of PET (1 to 3) was in accordance with mean TSV and its predictions were improved in classes +2 and +3. COMFA tended to underestimate mean TSV, failing to successfully reproduce class +1 while UTCI tended to overestimate mean TSV reproducing fairly well the class 'neutral'.

4 CONCLUSIONS

The present study demonstrates the early results of a survey on urban thermal sensation focusing on the comparison of three outdoor thermal sensation predictive models, COMFA, PET and UTCI. According to the method followed, the criteria posed and our limited sample, UTCI showed better applicability in the case of Mediterranean climate compared to COMFA and PET while PET reproduced best of all models the mean thermal sensation vote. Nevertheless, all the models demonstrated relative low percentage of correct predictions, indicating that the calibration of the models with empirical data is possible to provide better results.

Further research should be undertaken with a larger sample size and including data from all seasons.

5 REFERENCES

Blazejczyk, K. Epstein, Y. Jendritzky, G. Staiger, H. Tinz, B. (2012). Comparison of UTCI to selected thermal indices. *International Journal of Biometeorology 56*(3), 515-535.

Brown, RD. Gillespie, TJ. (1986). Estimating Outdoor Thermal Comfort Using a Cylindrical Radiation Thermometer and an Energy Budget Model. *International Journal of Biometeorology 30(1)*, 43-52.

Brown, RD. Gillespie, TJ. (1995). *Microclimate landscape design*. New York:Wiley.

Cheng, V. Ng, E. Chan, C. Givoni, B. (2012) Outdoor thermal comfort study in a sub-tropical climate: a longitudinal study based in Hong Kong. *International Journal of Biometeorology 56*, 43–56.

Cohen, P. Potchter, O. Matzarakis, A. (2013). Human thermal perception of Coastal Mediterranean outdoor urban environments. *Applied Geography 37*, 1-10.

COST Action 730 on UTCI http://www.utci.org/index.php. Accessed March 2013.

Gaitani, N. Michalakakou, G. Santamouris, M. (2007). On the use of bioclimatic architecture principles in order to improve thermal comfort conditions in outdoor spaces. *Building and Environment 42(1)*, 317–24.

Höppe, P. (1999). The physiological equivalent temperature – a universal index for the biometeorological assessment of the thermal environment. *International Journal of Biometeorology 43*, 71–75.

Höppe, P. (2002) Different aspects of assessing indoor and outdoor thermal comfort. *Energy and Buildings 34*, 661-665.

ISO 9920. (1993). *Ergonomics-estimation of the thermal characteristics of a clothing ensemble*. Geneva: International Standards Organisation.

ISO 8996. (2004). *Ergonomics-determination of metabolic heat production*. Geneva: International Standards Organisation.

Jendritzky, G. Staiger, H. Bucher, K. Graetz, A. Laschewski, G. (2000). *The Perceived Temperature: The Method of the Deutscher Wetterdienst for the Assessment of Cold Stress and Heat Load for the Human Body*. Internet Workshop on Windchill, hosted by Environment Canada.

Jones, BW. (2002). Capabilities and limitations of thermal models for use in thermal comfort standards. *Energy and Buildings*, *34*, 653-659.

Lin, TP. Matzarakis, A. (2008). Tourism climate and thermal comfort in Sun Moon Lake, Taiwan. *International Journal of Biometeorology 52*, 281-290.

Matzarakis, A. Mayer, H. (1996). Another kind of environmental stress: thermal stress. *WHO News 18*, 7–10.

Monteiro, L. Alucci, MP. (2006). Outdoor thermal comfort: comparison of results of empirical field research and predictive models simulation. Windsor International Conference: Comfort and energy use in buildings.

Pantavou, K. Theoharatos, G. Mavrakis, A. Santamouris, M. (2011). Evaluating thermal comfort conditions and health responses during an extremely hot summer in Athens. *Building and Environment 46(2)*, 339-344.

Pantavou, K. Theoharatos, G. Santamouris, M. Asimakopoulos, D. (2013) Outdoor thermal sensation in a Mediterranean climate and a comparison with UTCI. *Building and Environment 66*, 82-95.

Santamouris, M. (2012). Cooling the cities-a review of reflective and green roof mitigation technologies to fight heat island and improve comfort in urban environments. *Solar Energy* [inpress].

Santamouris, M. (2013) Using cool pavements as a mitigation strategy to fight urban heat island-A review of the actual developments. *Renewable and Sustainable Energy Reviews 26*, 224-240.

Santamouris, M. Synnefa, A. Karlessi, T. (2011) Using advanced cool materials in the urban built environment to mitigate heat islands and improve thermal comfort conditions. *Solar Energy 85*, 3085–102.

Theoharatos, G. Pantavou, K. Mavrakis, A. Spanou, A. Katavoutas, G. Efstathiou, P. Mpekas, P. Asimakopoulos, D. (2010). Heat waves observed in 2007 in Athens, Greece: synoptic conditions, bioclimatological assessment, air quality levels and health effects. *Environmental Research 110(2)*,152-161.

Stull, R.B. (2000). *Meteorology for scientists and engineers*. Pacific Grove: Brooks/Cole Thomson Learning.

Thorsson, S. Lindberg, F. Eliasson, I. Holmer, B. (2007). Different methods for estimating the mean radiant temperature in an outdoor urban setting. *International Journal of Climatology 27*, 1983–1993.

NATURAL VENTILATION IN HOSPITAL WARDS OF SEMI-ARID CLIMATES: A CASE FOR ACCEPTABLE INDOOR AIR QUALITY AND PATIENTS' HEALTH

Mohammed Alhaji Mohammed[*1], Steve JM Dudek[1], and Neveen Hamza[1],

[1] *School of Architecture, Planning and Landscape, Newcastle University, NE1 7RU, Newcastle Upon Tyne, UK*
**Corresponding author's e-mail address: a.m.mohammed@ncl.ac.uk*

ABSTRACT

Owing to the growing concern about indoor air quality (IAQ) globally in hospitals, especially after the recent outbreak of diseases like severe acute respiratory syndrome (SARS), Swine Flu (H1N1) and other airborne infections such as Tuberculosis, the quest for energy efficient ventilation system is growing. To provide acceptable indoor air quality that is capable of removing indoor air contaminants in hospital wards, sustainable ventilation strategy is required. Therefore, this paper tends to exploit the possibilities of using natural ventilation strategies in providing acceptable indoor air quality in hospital wards of semi-arid climates. The study established that, Mosquito insects, Harmattan dust, and high temperatures are the three major factors militating against the achievement of natural ventilation in semi-arid climates of Nigeria. Mosquito insects remain the only source of Malaria parasites that kills thousands of people in the tropics, while the inhalation of Harmattan dust causes cardiovascular and respiratory diseases.

To achieve the objectives of this study, a comprehensive literature review, full-scale measurement and field survey have been conducted. The results obtained from the field measurement shows that none of the hospitals measured achieved the required ventilation rates of 6 ACH as enshrined by AHSREA. Moreover, the survey results for the five hospitals studied shows that more than 80% and 90% of the respondents have admitted the presence of Harmattan dust and mosquitoes respectively in the hospital multi-bed wards. Therefore, the design of sustainable natural ventilation that can remove indoor contaminants while excluding outdoor pollutants in the hospital wards of semi-arid climates without compromising occupants comfort is essential.

KEYWORDS

Natural Ventilation, indoor air quality, Mosquito, Harmattan dust, semi-arid

1 INTRODUCTION

Nowadays, the quest for energy efficient natural ventilation system design is growing due to the increasing concern about carbon emission, indoor air quality and health, especially in hospital multi-bed wards. Moreover, this concern has instigated the professionals in building system design to intensify efforts in proposing different ventilation strategies to achieve healthy and acceptable indoor air quality.

The adoption of natural ventilation system was informed by the prevalent energy shortage in the study area. Despite the abundant resources to generate energy in Nigeria, due to the poor planning, maintenance and management of the energy sector, it has been difficult to fulfil the electricity generation and supply demands of its population. The electricity demand extremely exceeds the supply, and even the supply remains unreliable (Sambo, 2008). The total grid installed capacity produced by Nigerian power stations was 8,876 MW with only 3,653 MW available as at December 2009, hence, the available power supply is less than 41% of the total installed capacity (Emovon, et al. 2011). Moreover, the 2009 International Energy Agency (IEA) records shows that the electrification rate for the whole country was about 45% to 50%, thus, depriving approximately 76 million people access to electricity.

According to a World Bank report, the yearly (2007–2008) average power outages experienced in Nigeria was 46 days, and an outage last for about 6 hours on average. In addition to problems such as insufficient maintenance, inadequate feedstock and insufficient transmission network, high population growth combined with underinvestment in the electricity sector have also resulted in increased power demand without any substantial growth in production (IEA, 2012).

Nigeria's location on the southern fringe of the Sahara makes it more vulnerable to numerous climatic problems including Harmattan dust, mosquitoes and high temperatures. The mosquito insect and Harmattan dust usually seize the advantage of the openings provided for natural ventilation to find their way into the building indoor spaces. Moreover, the consequences of these Harmattan dust and mosquitoes are more destructive in hospital environment compared to any other type of facility. This is because, hospital wards accommodates immunosuppressed and immunocompromised group of people due certain ailments. These group of people are easy to be infected by diseases especially Malaria, which solely caused by mosquitoes. Furthermore, Harmattan dust will help in deteriorating patients' sickness especially those with respiratory diseases.

2 CHARACTERISTICS OF SEMI-ARID CLIMATES

The environmental parameters for building design for tropical countries such as Nigeria are quite contrary with temperate regions due to the difference in climate and weather conditions. Climate references are required for the design of buildings in semi-arid climates to achieve acceptable indoor air quality and thermal comfort. Therefore, to accomplish indoor air quality and thermal comfort requirements with the presence of mosquitoes and Harmattan dust in hospital wards, the climatic parameters have to be considered right from the design stage. Three major parameters should be considered when designing for natural ventilation in semi-arid climates including Harmattan dust, Mosquitoes and high ambient temperatures.

Harmattan is a fugitive dust transported by dry North-East trade wind that usually blows across Nigeria between November and March annually and diminishing southwards. The consequences of this dust are higher in the Nigerian semi-arid climatic zone being situated in the Northern boarders of the country. The relationship between dust particles concentration and its effect on human health is established in literature, particularly linking cardiovascular and respiratory diseases to Dust outbreaks (Kwon et al. 2002, Chen et al. 2004, Meng and Lu, 2007). The dust particles size varies with location, depending on the proximity of the collection center from the dust origin in the Sahara desert. The mean sizes of dust samples collected in Nigeria for two Harmattan seasons are 2.7μm and 4.4 μm, respectively (Chineke and Chiemeka 2009). However, the elemental composition of Harmattan dust in Nigeria was measured using neutron activation analysis to determine the concentrations of 29 elements, with iron (Fe), aluminum (Al), and potassium (k) being among the highest at 61 mg g-1, 431 mg g-1, and 15 mg g-1, respectively (Adepetu et al. 1988).

Mosquitoes are cold-blooded insects that have the same body temperature as the surrounding environment. There are only three species out of more than 3,000 species of mosquitoes that are largely responsible for the spread of human infections including; Anopheles, Culex and Aedes. The Anopheles mosquitoes are found in the study area (Maiduguri, Nigeria), and are the only species known for transmitting the malaria parasite (National Geographic, 2013). The average lifespan of a Mosquito is from 2 weeks to 6 months and its average size is 0.3 to 2 cm, with average weight of 2.5 mg) (National Geographic, 2013).

The consideration of high outdoor air temperatures that exceed human comfort thresholds creates a challenge in designing natural ventilation strategies for acceptable thermal comfort in semi-arid climates. In the dry season the temperature in Maiduguri (Study area) peaks with

wide diurnal and annual ranges of dry bulb temperatures, with the hottest months of April, May and June. Dry bulb temperatures can exceed 43^{o}C but falls to a mean of 24^{o}C or 29^{o}C with the start of the rainfall (Maxlock Group Nigeria, 1976).
Since, the thermal comfort and human preferences are related to acclimatisation to local conditions the neutrality temperature of the study area (Maiduguri) has been estimated using the outdoor average ambience temperature using the formula Tn = 17.8 + 0.31Toav (Szokolay, 2008). The thermal neutrality temperature of Maiduguri is found to be 26.7^{o}C, and considering a temperature band of ±2.5 as recommended in Szokolay, S. V. (2008), the thermal comfort zone will fall between 24.2^{o}C and 29.2^{o}C. Figure 1 illustrates the annual ambient temperature in the study area in relation to the neutrality temperature range. The ambient average temperatures that are within the comfort zone includes February, August and November, while the remaining nine months are out of the comfort temperature zone.

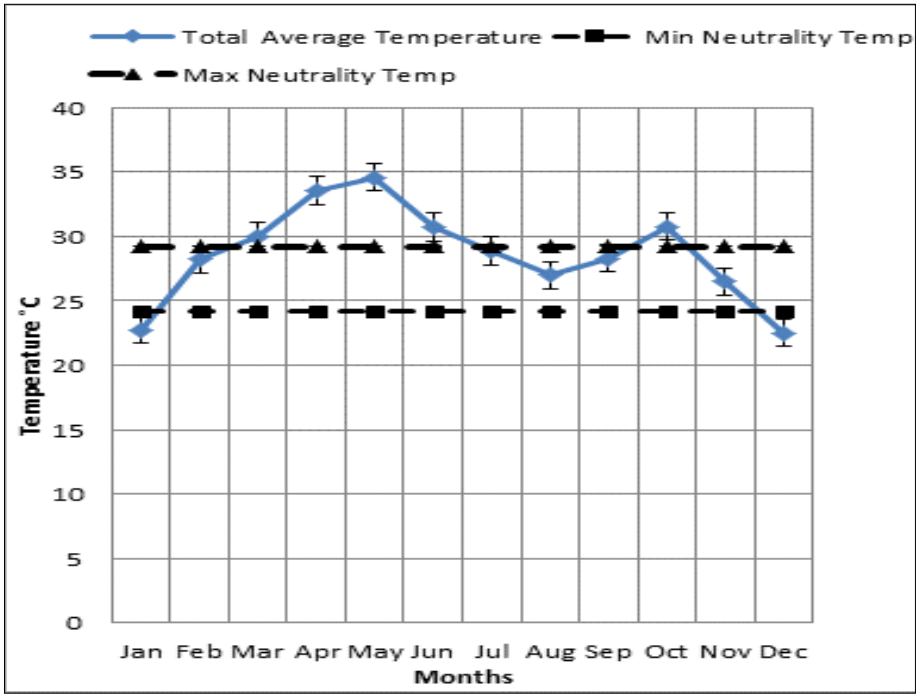

Figure 1: Total Average Ambience Temperature of the Study Area in Relation to Neutrality Temperature Zone

3 INDOOR AIR QUALITY AND NATURAL VENTILATIONS IN HOSPITAL MULTI-BED WARDS

The quality of indoor air dictates the health status of an environment and its occupants. As clean indoor air quality is critical for healthy indoor environment. Poor indoor environmental qualities are responsible for many health problems including allergies, eye irritations, and respiratory problems (Yau, et al, 2011). Various indoor air contaminants exist in hospital multi-bed wards. These contaminants are very difficult to predict as they generate from both indoor and outdoor sources, and contain different types of substances (Hobday, R. 2011). Indoor air contaminants especially those with outdoor sources are largely dependent on climatic condition of the environment, whereas contaminants with indoor sources are largely originates from furniture, building materials, chemicals and human body.
The achievement of acceptable indoor air quality and thermal comfort passively, while excluding unwanted parameters such as mosquitoes and Harmattan dust in the semi-arid climates is a difficult task that requires a holistic approach. The exclusion of these unwanted

parameters are easy to realize when using mechanical means for ventilation, as the need for opening large ventilators to the outside is not required. Regrettably, there is insufficient energy in the study area to cater for such demands. Therefore, there is a salient need to explore the possibility of using natural ventilation for achieving acceptable indoor air quality and thermal comfort.

Natural ventilation is usually driven by natural forces such as wind, thermal buoyancy force owing to variations in indoor and outdoor air density, which force in fresh air from outside through custom-made building envelope openings (Atkinson, 2009). It relies on the pressure differences caused by either wind or the buoyancy effect created by temperature or humidity difference to move fresh air through buildings. The use of natural ventilation in buildings becomes an increasingly attractive means of cutting energy cost and achieving acceptable quality of indoor environment, due to the improvement on the cost and environmental consequences of energy utilization (Walker, 2010). However, the performance and condition of ventilation in hospitals have great impact on the perceived indoor air quality (Hellagren, U. et al, 2011).

4 HEALTH CONSEQUENCES OF OUTDOOR POLLUTANTS IN HOPSITAL MULTI-BED WARDS IN SEMI-ARID CLIMATES

The two major outdoor pollutants in the hospitals of semi-arid climates are Harmattan dust and Mosquitoes.

4.1 Health consequences of Harmattan Dust

The respiration of airborne dust particles in form particulate matter of less than 2.5 micrometres in size is known as a health hazard, particularly at ambient concentrations as reported for many West African countries (Ogunseitan, 2007). These airborne dust particles usually affect human health, as a result of their impact on local and regional air qualities (Anuforom, 2007). The relationship between dust particles concentration and its effect on human health has already been established in the literature, particularly linking cardiovascular and respiratory diseases to Dust outbreaks (Kwon et al. 2002, Chen et al. 2004, Meng and Lu, 2007). Likewise, study by Yoo, et al. (2008), established that children with mild asthma reported more respiratory symptoms during dust days, often requiring the use of bronchodilator compared to clean days. Furthermore, Harmattan winds and more humid conditions usually experienced during dry season in North Eastern Nigeria are believed to be responsible for an increase in positive ions and other gases in the air triggering migraine head pain. When an interview was conducted among margarine sufferers in this region, 46% and 38% of the respondents mostly experienced migraine attack during warmest months and Harmattan season respectively (Timothy, et al. 2011)

Environmental Protection Agency (EPA) in Unites State of America issued final guidelines on 29th March, 2007 for regions to clean up their air that, the presence of Fine particles or "PM2.5" in the air can ignite heart and lung diseases and have been connected to premature death and a range of severe health complications including heart attacks, chronic bronchitis and asthma attacks (Ogunseitan, 2007).

4.2 Health consequences of Mosquitoes

Malaria is the most parasitic infectious disease in the world, is transmitted by mosquitoes which breed in fresh or rarely salty water. It symptoms include fever, headache, chills, muscle aches, tiredness, nausea and vomiting, diarrhoea, and jaundice. It could also lead to

convulsions, coma, severe anaemia and kidney failure. The severity and range of symptoms is determined by the specific type of malaria. In the absence of prompt and effective treatment, malaria can evolve into a severe cerebral form leading to death. Moreover, malaria is among the five leading causes of death in children under the age of 5 in Africa (WHO, 2001). Figure 2 shows the control of Malaria in Africa.

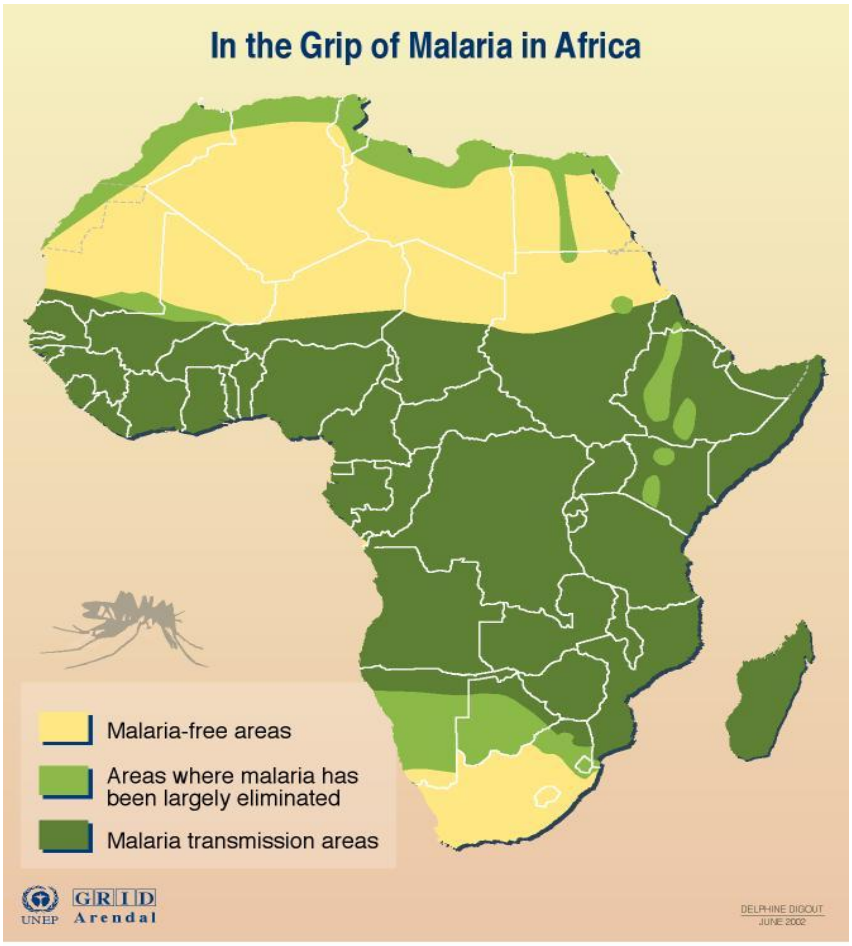

Sources: A. Platt McGinn, *Malaria, Mosquitoes, and DDT*, World Watch, Vol.15. No.3, May-June 2002.

Figure 2: The Control of Malaria in Africa

5 CASE STUDY

5.1 Physical Measurement

Four hospital wards were selected in the study area Maiduguri and the Air Change Rates (ACR) in these hospital wards was measured using tracer gas (Concentration decay) techniques with CO_2 as the tracer gas. The concentration decay method is usually done by releasing a small amount of gas initially, after which there is no injection of gas throughout the measurement period (Etheridge and Sandberg 1996). Once the injected tracer gas is mixed with the space air, the concentration is measured at a regular time interval (Laussman and Helm 2011). Concentration decay is the most commonly used method in practice, which provides a direct measurement of the nominal time constant or the air change rate and gives unbiased estimate of the mean airflow rate. Typical procedure that has been used for conducting concentration decay tracer gas measurement is illustrated in Figure 3.
The results obtained from these measurements were used to estimate the air change rates in the selected hospitals multi-bed wards using the mathematical expression in equation 1. The

result shows that the air change rates (ACR) in all the measured hospital wards are below the standard ACR of 6 ACH set aside by AHSRAE (Ninomura and Bartley, 2001). The ACR measurement result is illustrated in Figure 4.

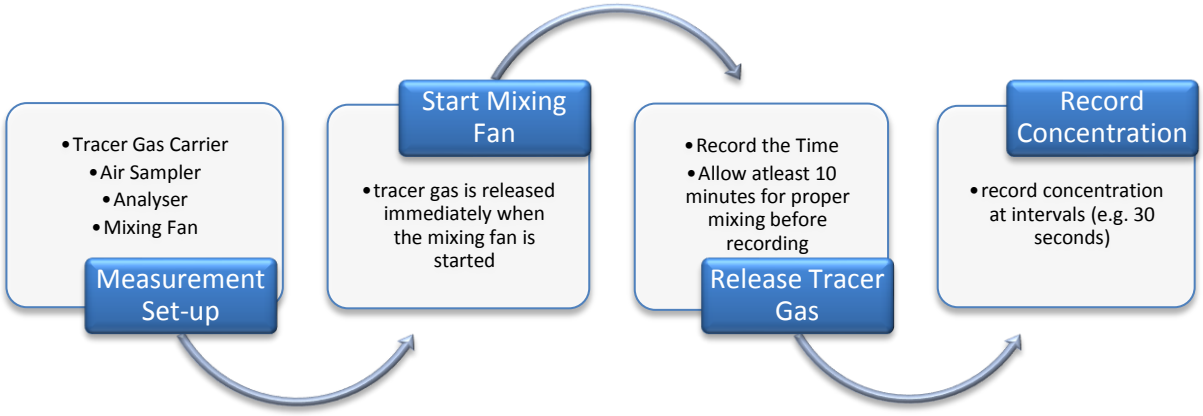

Figure 3: Procedures for conducting concentration decay tracer gas measurement

$$N = \frac{\ln C(0) - \ln C(\tau 1)}{\tau 1} \quad (1)$$

Where
N = Air Change Rate
C = Tracer Gas Concentration in Rooms
τ = Time (h)

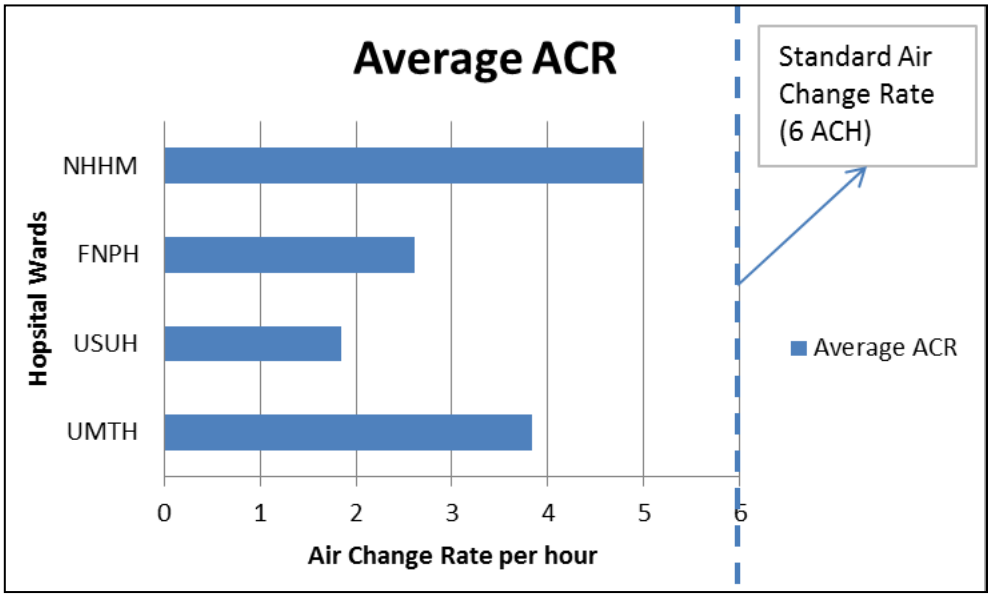

Figure 4: Air change rates in four hospitals in the study area compared to the standard

5.2 Psychosocial Perception

Questionnaire survey has been conducted among the immediate occupants of the hospital multi-bed wards including medical doctors, nurses and other healthcare workers. The respondents were asked about their perception on Harmattan dust and mosquitoes in the

hospital wards. Both Harmattan dust and mosquitoes usually penetrates through windows, doors and air-conditions openings.

The availability of dust particles within hospital wards has great consequences on the patients' health condition. According to the result of the survey conducted to ascertain the level of dust within the hospital wards, by asking the respondents "Do you normally experience dust problem in the wards?" about 97% have agreed they experience dust problems in the wards and the remaining 3% don't experience any dust problem as illustrated in Figure 5.

Moreover, when the respondent to the survey to ascertain the level of mosquito problem in the hospital wards were asked "Do you usually experience Mosquito problem in the wards?" 99% of the respondents said they are facing mosquito problems in the multi bed wards, while the remaining 1% said they are not as shown in Figure 6.

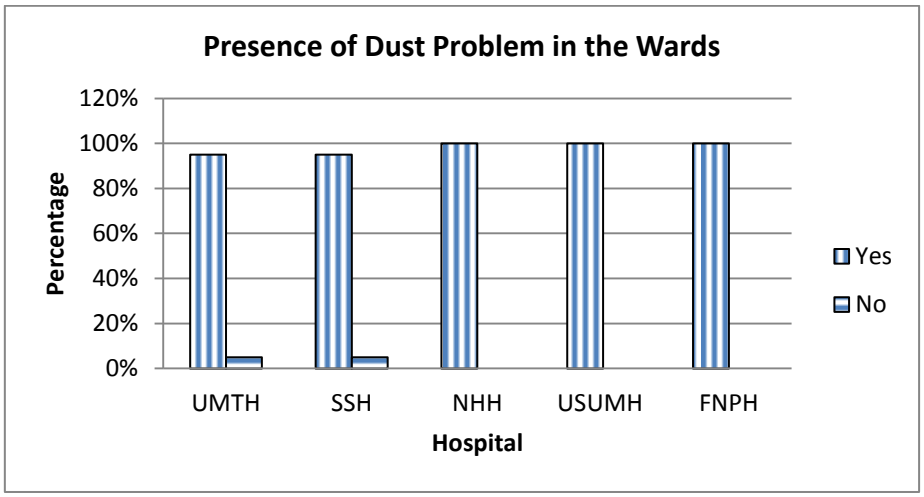

Figure 5: Dust problems in the hospital wards

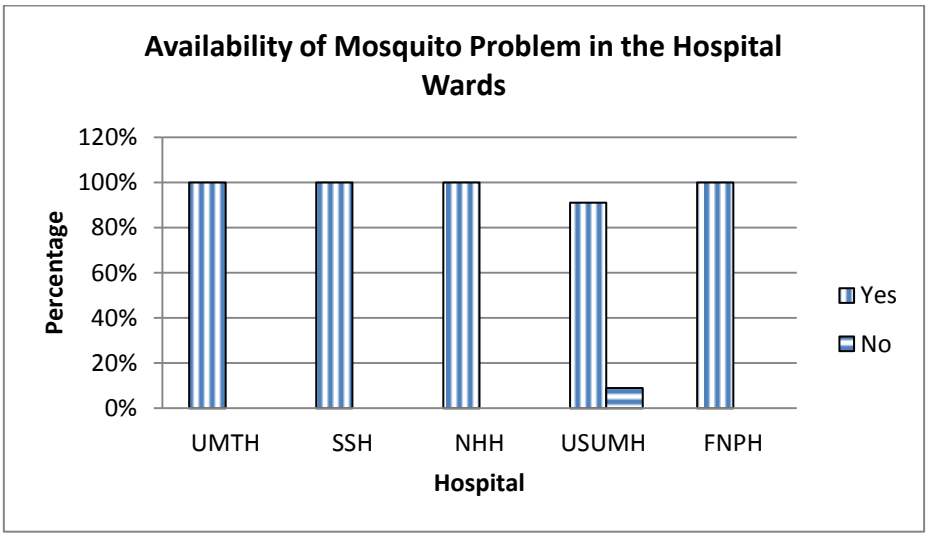

Figure 6: Mosquito problems in the hospital wards

6 DISCUSSION AND CONCLUSION

This paper examined the status of acceptable indoor air quality in the hospital multi-bed wards of semi-arid climates. It tends to exploit the possibilities of using natural ventilation strategies in providing acceptable indoor air quality in hospital wards of semi-arid climates. The study established that, Mosquito insects, Harmattan dust, and high temperatures are the

three major factors militating against the achievement of natural ventilation in semi-arid climates of Nigeria. The mosquito insect and Harmattan dust usually seize the advantage of the openings provided for natural ventilation to find their way into the building indoor spaces. Mosquito insects remain the only source of Malaria parasites that kills thousands of people in the tropics, while the inhalation of Harmattan dust causes cardiovascular and respiratory diseases.

To achieve the objectives of this study, a comprehensive literature review, full-scale measurement, and field survey have been conducted. The consequences of Harmattan dust and mosquitoes are more destructive in hospital environment compared to any other type of facility. This is because, hospital wards accommodates immunosuppressed and immunocompromised group of people due certain ailments. These group of people are easy to be infected by diseases especially Malaria. Moreover, Harmattan dust will help in deteriorating patients' sickness especially those with respiratory diseases.

The results obtained from the field measurement shows that none of the hospitals measured achieved the required ventilation rates of 6 ACH as enshrined by AHSREA. Moreover, the survey results for the five hospitals studied shows that more than 80% and 90% of the respondents have admitted the presence of Harmattan dust and mosquitoes respectively in the hospital multi-bed wards.

Therefore, the design of sustainable natural ventilation that can remove indoor contaminants while excluding outdoor pollutants in the hospital wards of semi-arid climates without compromising occupants comfort is essential.

7 REFERENCES

Adepetu J. A., Asubiojo O. I. Iskander F. Y., and Bauer T. L. (1988). Elemental Composition of Nigerian Harmattan Dust. *Journal of Radioanalytical and Nuclear Chemistry,* Articles, Vol. 121, No. I, 141-147

Anuforom A. C. (2007) "Spatial distribution and temporal variability of Harmattan dust haze in sub-Sahel West Africa" *Atmospheric Environment,* Vol. 41, Page 9079–9090.

Atkinson, J (2009). *Natural Ventilation for Infection Control in Health-care Settings.* World Health Organization publication/guidelines, WHO press, http://www.who.int/water_sanitation_health/publications/natural_ventilation/en/index.html

Awadzi T. W. and Breuning-Madsen H. (2007). Harmattan Dust Deposited in Ghana within 2000–2005. *West Africa Journal of Applied Ecology,* Vol. 11 (2007), pp. 173–188

Chen Y. S., Sheen P. C., Chen E. R., Liu Y. K., Wu T. N., and Yang C. Y. (2004). Effects of Asian dust storm events on daily mortality in Taipei, Taiwan. *Environmental Research,* Vol. 95, Page 151–155.

Chineke T. C. and Chiemeka I. U. (2009). Harmattan Particulate Concentration and Health Impacts in Sub-Saharan Africa. *African Physical Review,* Vol. 3: 0018

EIA (2012). *Nigeria: Independent Statistics and Analysis of Energy Sector.* A report of the Energy Information Administration (EIA), United State Department of Energy, Washington ULR: http://www.eia.gov/countries/cab.cfm?fips=NI accessed on 10th January, 2013

Emovon, I., Adeyeri, M.K. and Kareem, B. (2011). Power generation in Nigeria; Problems and solution. *presented at the 2011 International Conference of Nigerian Association for Energy Economics*, Abuja, Nigeria

EPA (2010). *An Introduction to Indoor Air Quality (IAQ).* United States Environmental protection Agency (EPA), Indoor Environments Division Administrative Office, http://www.epa.gov/iaq/ia-intro.html Accessed on 19th January, 2010

Etheridge, D. W., and Sandberg, M. (1996) *Building Ventilation: Theory and Measurement.* John Wiley and Sons Ltd. West Sussex, Engand

Hellagren U., Hyvarinen M., Holopainen R., and Reijula K. (2011). Perceived Indoor Air Quality, Air-Rated Symptoms and Ventilation in Finnish Hospitals. *International Journal of Occupational Medicine and Environmental Health*, Vol. 24, No 1, Page 48-56.

Hobday, R. (2011). Indoor environmental quality in refurbishment. *Historic Scotland Technical Paper 12*, www.historic- scotland.gov.uk/technical papers, research report

Kwon H. J., Cho S. H., Chun Y., Lagarde F., and Pershagen G. (2002). Effects of the Asian dust events on daily mortality in Seoul, Korea. Environmental Research, Vol. 90, Page 1–5.

Laussmann, D., and Helm, D., (2011). *Chemistry, Emission Control, Radioactive Pollution and Indoor Air Quality: Air Change Measurements Using Tracer Gases.* Edited by Mazzeo N. A. InTech publishers, Janeza, Croatia

Maxlock Group Nigeria (1976). *surveys and planning reports for Borno state government*. Warministers press Ltd, U.K.

Meng Z. Q., and Lu B. (2007). Dust events as a risk factor for daily hospitalization for respiratory and cardiovascular diseases in Minqin, China. *Atmospheric Environment,* Vol. 41, Page 7048-7058.

National Geographic (2013). *Animals: Mosquito Culicidae.* National Geographic Society, USA. http://animals.nationalgeographic.com/animals/bugs/mosquito/ Accessed on 8th January, 2013.

Ninomura, P.P.E., and Bartley, J. (2001). New Ventilation Guidelines for Health-Care Facilities. *ASHRAE Journal*, w.w.w.ashraejournal.org

Ogunseitan O. A. (2007). Harmattan Haze and Environmental Health. *African Journal of Environmental Science and Technology* Vol. 1 (4)

Sambo A. S. (2008). Matching Electricity Supply with Demand in Nigeria. *Publication of the International Association for Energy Economics*, Fourth Quarter 2008.

Szokolay, S. V. (2008). *Introduction to Architectural Science: The Basis of Sustainable Development.* Architectural Press, Elsevier. Oxford, UK

Timothy S. Y., Kwanashie H. O., Nyandaiti Y. W., Watila M., Mava Y., Sadiq G. U., Maspalma D. I., Bwala A. Y., Abdussalam B. (2011). Impact of Weather Conditions on Migraine Headache in North-Eastern Nigeria. *International Journal of Pharmacy and Pharmaceutical Sciences,* Vol 3, Suppl 3, Page 133-136

Walker, A. (2010). *Natural Ventilations.* Whole Building Design Guide, National Institute of Building Sciences, Washington, http://www.wbdg.org/resources/naturalventilation.php, accessed on 14th November, 2011

WHO (2001). *Water Sanitation and Health (WSH): Water-related diseas.* Prepared for World Water Day 2001. Reviewed by staff and experts from the cluster on Communicable Diseases (CDS), and the Water, Sanitation and Health Unit (WSH), World Health Organization (WHO), Geneva, http://www.who.int/water_sanitation_health/diseases/malaria/en/# accessed on 2nd February, 2012

Yau, H. Y., Chandrasegaranm, D., and Badarudin, A. (2011). The Ventilation of Multiple-Bed Hospitals in the Tropics: A Review. *Building and Environment,* Vol. 46, Page 1125-1132

Yoo Y., Choung J. T., Yu J. H., Kim D. K, and Koh Y. Y. (2008). Acute effects of Asian dust events on respiratory symptoms and peak expiratory flow in children with mild asthma. *Journal of Korean Medical Science,* Vol. 23, Page 66–71.

INDIVIDUAL APPRECIATION OF AIR CONDITIONED SURROUNINGS

Samuel Hassid
Technion- Israel of Technology
Faculty of Civil and Environmental Eng.
Haifa, Israel
**Corresponding author: cvrhasd@tx.technion.ac.il*

ABSTRACT

This work is based on the RESHYVENT project in which the effectiveness of hybrid (i.e. combined natural and mechanical ventilation) was measured and investigated in the urban canyon of Athens, Greece – the most important conclusion being that natural ventilation is dominant. It is suggested that the individual reaction to Air Conditioned Buildings should be better investigated, since many people ask for the comfort associated with natural ventilation.

KEYWORDS

Air Conditioning, Ventilation Natural and Mechanical

1 INTRODUCTION

Till 20 years ago air condition in Mediterranean Countries – and among them Israel - was the exception and was used almost exclusively in offices and even there only for higher level staff. For most people, the main "passive" cooling method was ventilation – be it during the day, so that even though the temperature may rise, the subjective evaluation of the environment was that it became cooler, or as a result of night cooling. The last method was particularly used in Israel and in dry regions, when the best policy was to close the windows during the day and open them during the night. During this period requests from the Israeli ministry of energy for investigating the energy performance of buildings were turned down because it was thought that the investment was not justified.

Despite with the start of some passive cooling research in which Mediterranean Countries played a leading role (PASCOOL), in the 1990ies Israel, together with all the Mediterranean countries, were characterized by an explosion in Air Conditioning. On one hand, air conditioning entered the residential sector (where it is today the rule rather than the exception, since it means that the air conditioners can be used for heating during the winter, where the COP means that the electrical energy consumption is reduced) and on the other hand, the development (in Israel) of many shopping centers to which the commercial establishments have moved means a multiplication of AC energy consumption and also of top demand during the summer months – which in many cases bring all the reserve energy production capability of Israel to zero in the hottest days of the summer, but also during the Hamsins of the spring and autumn.

2 THE AIR CONDITIONING EXPLOSION OF THE 1990S AND 2000S

Despite the start of some passive cooling research in which Mediterranean Countries played a leading role (PASCOOL), in the 1990ies Israel, together with all the Mediterranean countries, were characterized by an explosion in Air Conditioning. On one hand, air conditioning

entered the residential sector (where it is today the rule rather than the exception, since it means that the air conditioners can be used for heating during the winter, where the COP means that the electrical energy consumption is reduced) and on the other hand, the development (in Israel) of many shopping centers to which the commercial establishments have moved result in a rapid i of AC energy consumption and also of top demand during the summer months – which in many cases bring all the reserve energy production capability of Israel to zero in the hottest days of the summer, but also during the Hamsins days of the spring.

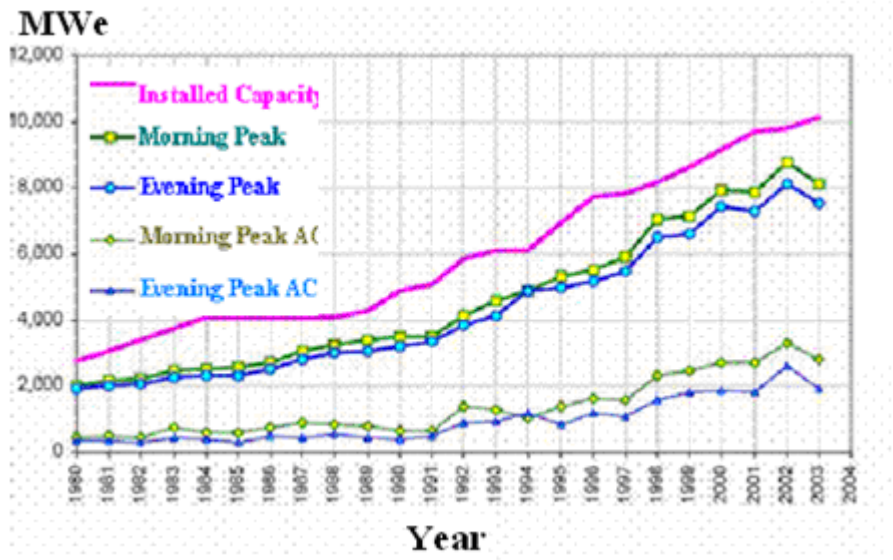

Fig. 1. Peak demand and grid capacity in Israel.

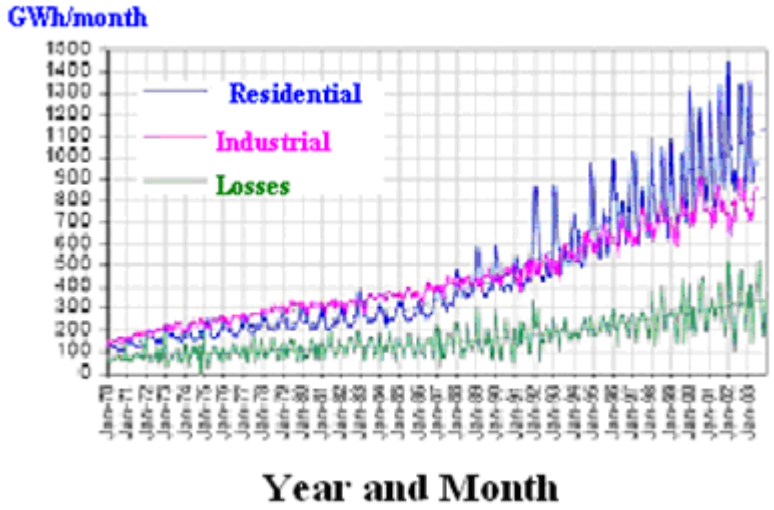

Fig. 2. Monthly electricity consumption in Israel according for different tarifs

The electric grid has difficulties keeping in line just ahead of peak demand, Israel being particularly vulnerable because of the insular nature of its grid. Last summer power stoppages were prevented because that particular summer was very mild – but power stoppages are on the horizon. Building more power plants is opposed by many environmentalist associations.

The increase in peak energy demand and the monthly energy consumption are shown in Figures and 2 on the basis of Ref. 4.

3. INDIVIDUAL REACTION TO AIR CONDITIONING

The psychological acceptance of air conditioning by the public has been mixed. Mediterranean life is based to a large extent on open windows – especially for hot thermal discomfort, but to some extent during winter too. People tend to a large extent to ask for open windows, even if air-conditioning is operated. This often leads to strong arguments between occupants, some of whom want the windows closed and some demand the windows open. The real reason for this attitude is not clear. One could argue that the problem is the internal air quality (IAQ) or the sick building syndrome, but this is not necessarily true – increasing the make-up outside air is not a substitute for open windows. The circulation that can be achieved using internal fans is not either.

In Israel there have been several examples of civil servants in prestigious government buildings designed to serve as an example of energy conservation in both Jerusalem and Haifa leading a “revolt” of sorts by people demanding openable windows – some of them even saying that they will achieve their goal "whatever it takes", the implication being even by force – an attitude totally unsuited for what is perceived as one of the most conservative parts of the population (See Ref. 3). The result was several strikes and work stoppages in both Jerusalem and Haifa. “We became blue out of suffocation” is an exaggerated, but common expression. Senior staff admit that they try to fix meetings outside the building in pursuit of an opportunity to leave the building. Experts express apparently opposing opinions, some putting the blame on the air conditioning system and other expressing a different opinion. It was finally decided to have in some of those buildings at least 20 % openable windows, at an enormous cost – but this was not implemented.

All around the Mediterranean coolness is associated with open windows. The author has often expressed his frustration when he is teaching a course in Climatology of Buildings in his Faculty Building– including a lecture on ventilation – which was supposed to be a Intelligent Building and students keep on opening the windows of an air-conditioned room. On another occasion, during his work in a research institution specializing in energy efficient buildings the very students of energy efficiency including ventilation techniques also kept on opening the windows – the claim being that otherwise the air is "scruffy", perhaps an inexact term, which does however express non-satisfaction with the indoor air quality. The author has also witnessed in a bus a violent clash between two passengers on opening a window when the bus was air-conditioned.

4. THE RESHYVENT PROJECT

The RESHYVENT (Residential Hybrid Ventilation) project is a multi-participant EU-funded project (between the years 2003 and 2005) which focused on Hybrid (combined natural and mechanical) Ventilation for the domestic sector in the residential sector in Urban Environments. The author was involved in the part of the RESHYVENT project that was carried out in Athens, Greece during the summer of 2003 in which the effect of several ventilation strategies were investigated during the Greek summer in the urban canyons in Athens under different climatic conditions. The project involved many measurements of ventilation rate (using the multiple tracer gas method to measure ventilation through the decay of two tracer gasses in the different rooms of the apartments).

In all those experiments it was found that Natural Ventilation is far more often than not a far more effective method of ventilation than mechanical or partly mechanical ventilation. Although this could not be measured – it was found that in rooms naturally ventilated the personal thermal comfort was far better than in the case of mechanical ventilation, even if the doors were open making communication between the rooms free. Even in the case of rather small wind velocities the ventilation rates were rather bigger for natural ventilation in comparison to hybrid and mechanical ventilation.

Although the target of the experimental program was not the calculation of the thermal comfort, but rather the ventilation rate, it was obvious that natural ventilation is not only far more effective but also results in higher velocities, felt through the entire room, rather than in the vicinity of the vents. The exception was in the case of one-sided ventilation during the time of very small outside velocities. The above results were only little affected by the urban canyon phenomena which did not prevent in most cases an effective ventilation.

5. DISCUSSION AND CONCLUSIONS

It can be concluded from the previous sections that the thermal comfort as perceived by many individuals is very much dependent on whether the environment is under natural or artificial ventilation. It is proposed to repeat a program similar to RESHYVENT but focusing on the criteria for thermal comfort during the summer. It would be advisable to include in this study both air conditioned and non-air-conditioned environments and ask for human appreciation of the environment – even if air-conditioning is combined with open windows – in order to address the problems of thermal comfort under summer conditions without preconceived ideas.

6. REFERENCES

1. Niachou K. (2007). *A study of natural and hybrid ventilation in the urban environment – Experimental and Theoretical Study in Urban Canyons*. PhD Thesis, Athens University, Physics Department – Environment and Meteorology Sector.

2. Niachou K., Hassid S. , Santamouris M. and Livada I. (2008). Experimental Performance Investigation of Natural, Mechanical and Hybrid Ventilation in the Urban Environment. *Building and Environment, 43*, 1373-1382.

3. http://hagada.org.il/hagada/html/modules.php?name=News&file=article&sid=4918 (On the reaction of civil servants on the air quality in some air-conditioned buildings in Israel)

4. http://www.neaman.org.il/publications/publication_item.asp?fid=590&parent_fid=490&iid=2587 (on the Development of Air Conditioning in Israel)

5. http://www.aivc.org/medias/pdf/LitList%2033_Reshyvent.pdf (on RESHYVENT)

A STUDY ON THE THERMAL ENVIRONMENT IN GREEK PRIMARY SCHOOLS BASED ON QUESTIONNAIRES AND CONCURENT MEASUREMENTS

Paraskevi Vivian Dorizas*, Margarita-Niki Assimakopoulos, Constantinos Helmis, and Mattheos Santamouris

Faculty of Physics, Departments of Environmental Physics and Meteorology, University of Athens, University Campus,
Athens, 157 84, Greece
**Corresponding author: p.dorizas@phys.uoa.gr*

ABSTRACT

The present study investigates the indoor thermal comfort perceived by students through a questionnaire survey conducted during spring 2013 in naturally ventilated primary schools in Athens. Thermal environment parameters such as air temperature, relative humidity, air velocity and mean radiant temperature were simultaneously measured. Then, Fanger's indices of Predicted Mean Vote (PMV) and Percentage of People Dissatisfied (PPD) were calculated by using clothing and metabolic rates. The main purpose of this work is the evaluation of the ability of the answers from students to be sufficient to assess the thermal environment of classrooms. The possible associations between subjective thermal sensation votes and objective measurements are examined by comparing students' answers based on the seven point thermal sensation scale and the results taken by the calculated indices of PMV and PPD.

KEYWORDS

Thermal comfort, Questionnaires, PMV, PPD, Schools

1 INTRODUCTION

Several recent studies have shown that inadequate thermal conditions in classrooms can affect students' performance and attendance (Mendell and Heath, 2005). There is also a number of studies carried on in offices where the adult thermal perception has been evaluated (de Dear and Brager 1998). Since there in an argue on children's ability to understand and express their feelings in a sensible way (Walker, 2001), thermal comfort field studies conducted in school classrooms are usually focused in the ages between thirteen and seventeen (Wong and Khoo, 2003). The study conducted by Humpreys (1977) is one of the few that did a survey on children of younger ages and found that they were capable of perceiving the thermal environment. However, there are limited studies on how children perceive, evaluate and accept the prevailing thermal conditions in school classrooms (Teli et al., 2013).

In the present paper the thermal comfort of the indoor environment of Greek Primary schools is investigated. The aims of this study are: (1) to investigate the thermal comfort votes (thermal sensation, acceptability and preference) of primary school students, (2) to assess the combination of votes of the thermal sensation versus the acceptability and preference and to examine whether significant gender differences appear in thermal comfort preferences, (3) to investigate if any kind (qualitative or quantitative) of correlation exist between the subjective answers from the questionnaires and the objective measurements, and if the correlation do exist to conclude on whether the answers from children of the certain age are representative for the evaluation of the thermal conditions of the classrooms.

2 SURVEY AND MONITORING METHODOLOGY

This field study was conducted in nine primary schools of the Attika basin in Greece during April and May 2013 (Figure 1 & Table 1). The survey was performed on a mid-season, (outside heating season) in order to assess the thermal comfort conditions into a free- running mode of the school buildings (Teli et al., 2013). The study includes students' questionnaire survey and simultaneous measurements of environmental variables affecting thermal comfort. All students participating in the survey were at the same age of eleven years old.

Figure 1: Map of Attika (left) and locations of schools (right)

Table 1: Schools characteristics and measurement periods

School name	School code name	Measurement period (Number of measurement days)	Year of construction	Classroom's floor area (m^2)	Classroom's volume (m^3)	Classroom's number of Students	Classrooms' orientation
Acharnae 14	1	1-5/4/13 (5 days)	2001	53	165	17	North
Thrakomakedones 1	14	8-12/4/13 (5 days)	1978	64	198	25	Northwest
Axharnae 4	4	14-18/4/13&24/4/13 (5 days)	1986	50	155	24	Southwest

Pallini 3	3	19&22/4/13 (2 days)	-	46	137	25	West
Acharnae 18	18	23/4/13 (1 day)	1991	47	138	18	South
Acharnae 12	12	13-17/5/13 (5 days)	1980	49	157	25	South
Thrakomakedones 2	2	20-24/5/13 (5 days)	2003	50	162	25	East
Acharnae 8	8	27-29/5/13 (3 days)	1999	52	159	19	West
Acharnae 11	11	31/5/13 (1day)	1994	55	172	15	South

2.1 Subjective Approach- Questionnaire Survey

The thermal perception of the students was assessed through subjective questionnaires. The questionnaire consisted of two sections: personal data and thermal comfort sensation. The personal data included questions regarding their age and gender. The part of thermal comfort sensation included three questions. In the first question, the participants were asked to evaluate their thermal sensation according to the American Society of Heating, Refrigerating and Air-Conditioning Engineers (ASHRAE) rating 7-point scale (cold, cool, slightly cool, neutral, slightly warm, warm, hot) (ASHRAE 55, 2005). The ASHRAE rating scale was chosen instead of the Bedford scale (much too cool, too cool, comfortably cool, comfortable, comfortably warm, too warm, much too warm) as it was considered easier for the students to understand (Teli et al. 2013). The second and third questions were associated to the thermal preference (3-point McIntyre Thermal Preference Scale: warmer, no change, cooler) and acceptability (acceptable, unacceptable) of the thermal conditions (de Dear and Brager 1998).

The questionnaires were handed out to students once every day at approximately the same time (10:15), 15 min after the pupils came into the classrooms right after a 20 min break. 667 questionnaires were collected in total from a sample of 193 students from whom only two did not want to participate to the survey. It should be mentioned that there were cases that the same students filled the same questionnaires more than one time, depending on the days of the survey's duration (Table 1, columns 2 &3). During the days when the students had gymnastics right before, the questionnaires were handed out one hour later in order to avoid the influence of the thermal sensation by the vigorous exercise instead of the classroom's thermal environment.

2.2 Objective Approach- Measurements

The measurements of the physical parameters affecting the thermal environment were carried out using the INNOVA 1221, thermal comfort data logger which is connected to a PC with the dedicated application software INNOVA 7701 software for the real time measurements (LumaSense Technologies). INNOVA 1221 is complied with ISO 7730/ CEN 27730 and ASHRAE 55. This instrument uses several transducers such as: air temperature, humidity, air velocity, wet bulb globe temperature (WBGT), operative temperature which are simultaneously collecting data. These data are used to calculate key parameters necessary to assess the thermal comfort environment such as predicted mean vote (PMV) and predicted percentage dissatisfied (PPD) indexes, given the Metabolic rate (MET) and Clothing insulation value (CLO). For this case these values assumed to be equal to: MET=1.2 and CLO=0.8 that corresponds to sedentary activity and light daily wear clothing respectively according to ISO EN 7730. All the parameters were measured at height 1.1m above the floor

according to the standard ISO 7726:1998 for seated people and the sampling interval was 5 min.

3 RESULTS AND DISCUSSION

3.1 Subjective Analysis by means of questionnaires

3.1.1 Thermal perception of students

The frequency distributions of the thermal sensation votes in each of the nine schools of measurement are shown in Figure 2. As it can be seen the greater amount of answers lies between neutral and the positive answers of warmth and resembles a half-normal distribution. In overall, the students characterized the thermal environment mostly as warm. In school 18 all students evaluated the thermal environment as neutral. More than 50% of the students in school 2 and less than half of the students in schools 3, 8 and 11 felt slightly warm during the survey. Approximately 20% of the students in school 1 and 10% of the ones in school 14 felt slightly cool. About 5% of the students in school 14 felt cold while the same percentage of students in schools 4, 3, 12 and 2 felt hot. A significant percentage exceeding 20% of students, in school 8 felt hot.

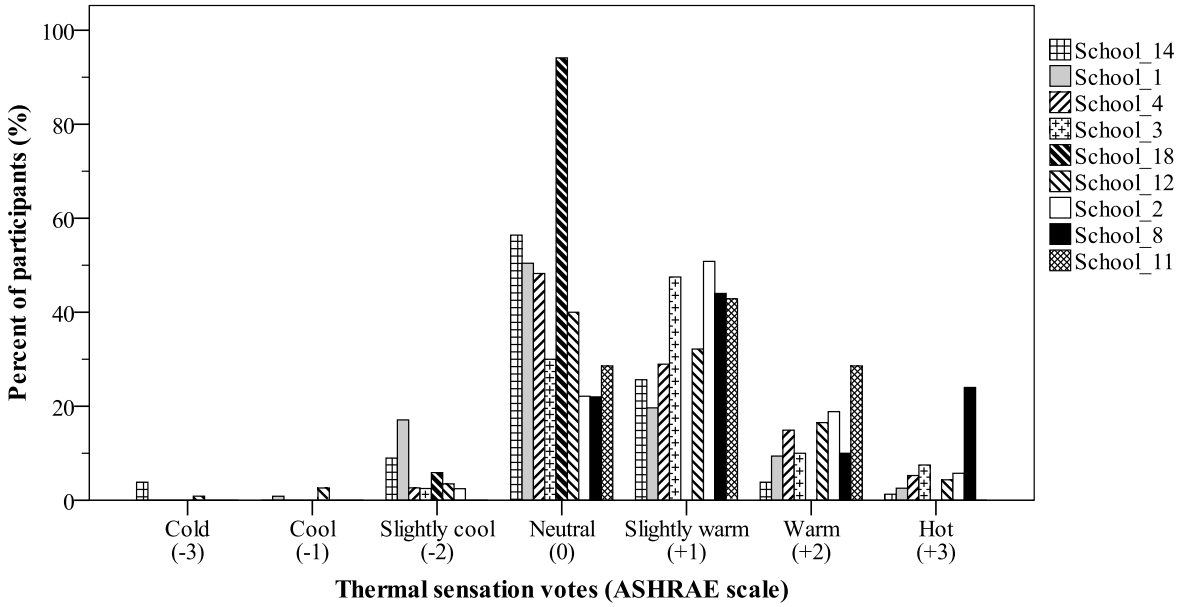

Figure 2: Distribution of the thermal sensation votes of students in all the schools

3.1.2 Thermal preference of students

Figure 3 presents the distribution of the thermal preference votes on the three-point thermal preference scale in each of the nine schools of measurements. More than 70% of the votes in schools 3, 2 and 8 preferred a cooler environment. Approximately half of the responds in schools 14, 1, 4, 18 and 11 didn't prefer any change in the thermal environment. The distribution in school 1 approaches a normal distribution. Less than 10% of the votes in schools 14, 4, 18, 12 and 8 preferred warmer thermal environment.

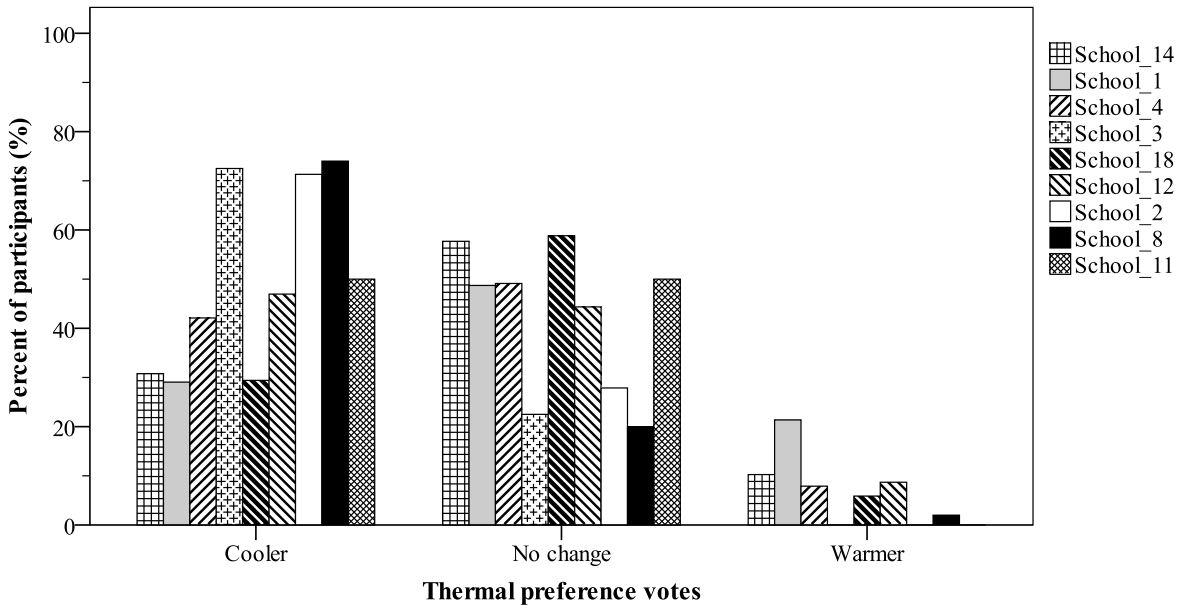

Figure 3: Distribution of the thermal preference votes of students in all schools

3.1.3 Thermal acceptability of students

Acceptable seemed to be the thermal environment for the majority of the students (Figure 4). In school 18, all students evaluated the thermal environment as acceptable. However, approximately 30% of the votes and only in schools 2 and 8 considered the thermal environment as unacceptable. In schools 14, 1, 4, 3, 12 and 11 the unacceptable votes were less than 20%.

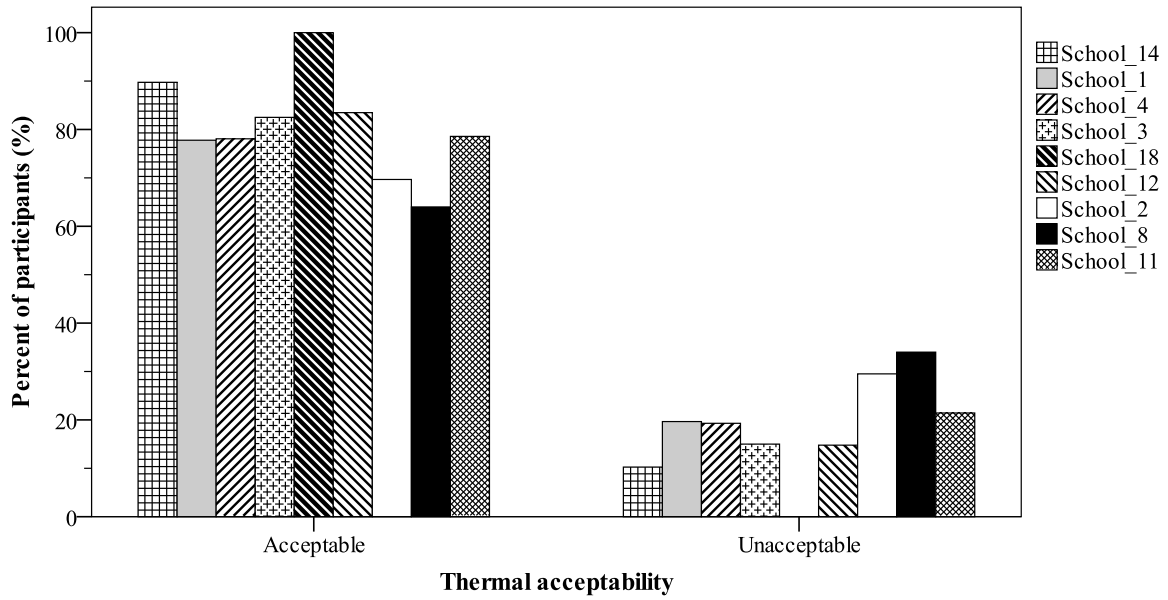

Figure 4: Distribution of the thermal acceptability votes of students in all schools

In the following three paragraphs the individual data sets from each of the schools have been considered as a united single sample so as to examine the combination of the thermal comfort evaluation questions.

3.1.4 Thermal sensation vs acceptability for the entire data set

In figure 5 the thermal sensation votes are presented versus the thermal acceptability for all the schools. Approximatelly 43% of the participants in the survey characterized the thermal environment as neutral from which a mimor 3% strangely considered it as unacceptable. The unacceptable votes lie mostly on the positive axis of the thermal sensation scale. It is worth mentioning that a small percentage of 3% feeling hot, and 8% feeling warm, seemed to accept the thermal environment.

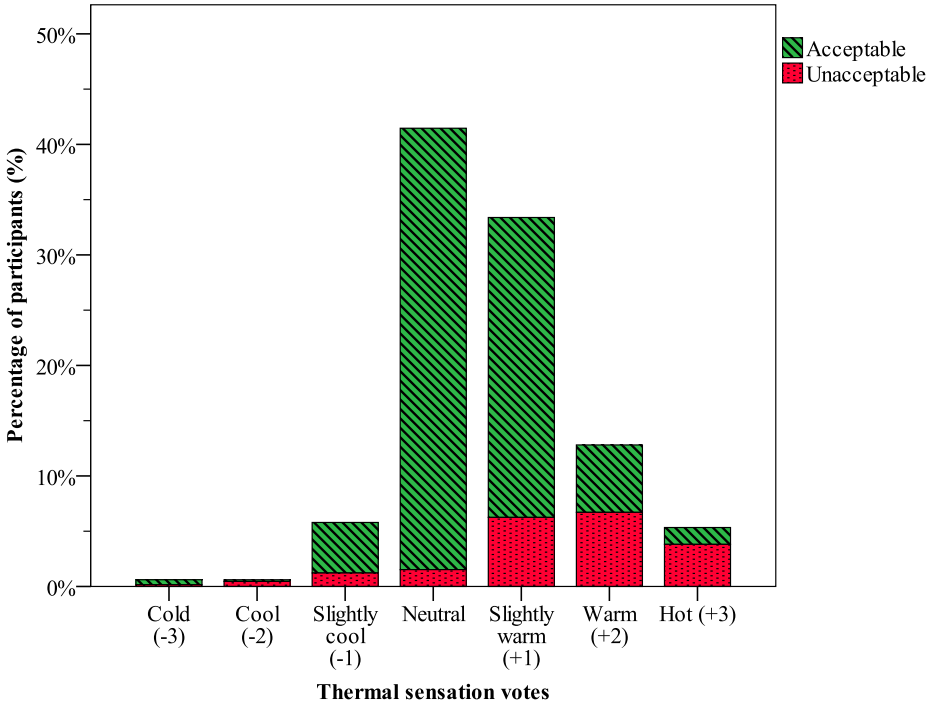

Figure 5: Thermal sensation votes versus thermal acceptability of all the schools

3.1.5 Thermal sensation vs gender for the entire data set

The thermal sensation is presented versus the gender in figure 6. Overall, the thermal sensation of girls and boys do not differ a lot. The greater differences however, between the two genders seemed to be for the votes of ‘slightly warm’ and ‘hot’. Also greater proportion of girls than boys felt slightly cool. The greater amount of both girls and boys felt neutral however the percentage of boys was slightly higher.

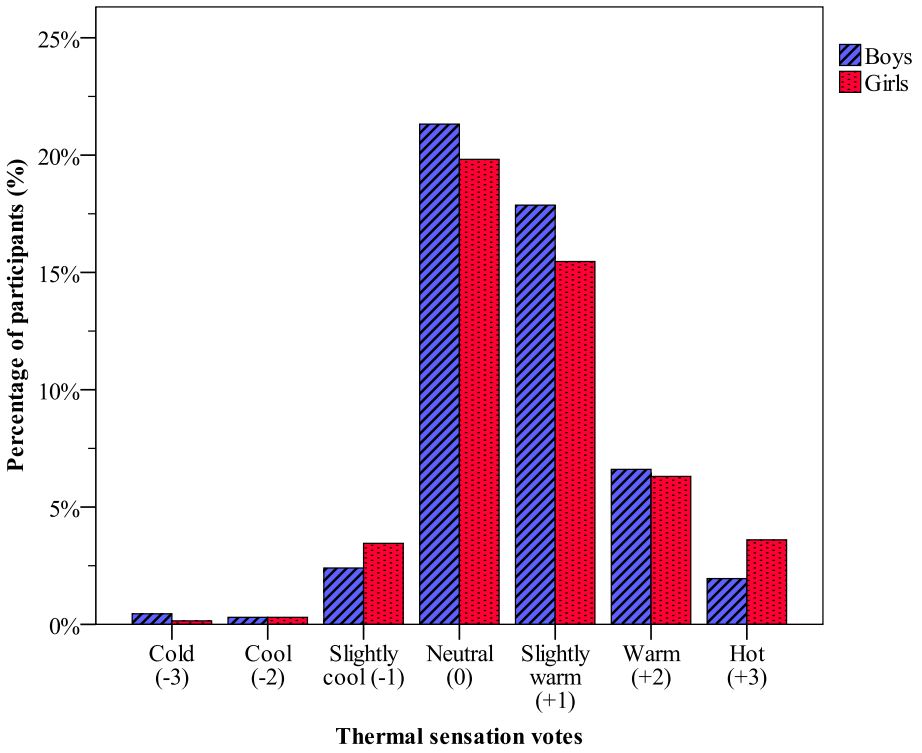

Figure 6: Thermal sensation votes versus gender of all the schools

3.1.6 Thermal preference vs acceptability for the entire data set

In Figure 7 the thermal preference is shown versus the acceptability. Approximately half of the responders preferred a cooler environment during the survey from which more than 15% evaluated the thermal environment as unacceptable. About 43% didn't want any change in the thermal conditions, from which 3% characterized them unacceptable. Less than 10% of the total students would prefer a warmer environment from which more than half accepted the thermal conditions.

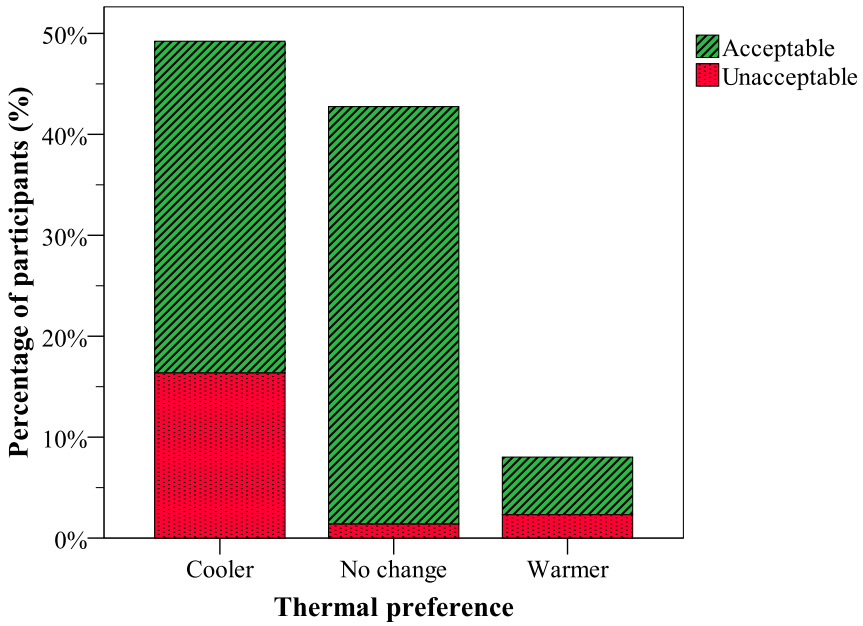

Figure 7: Thermal preference votes versus thermal acceptability of all the schools

3.2 Comparison of subjective answers from questionnaires to objective measurements-PPD

In the following section the correlation between the results from the objective measurements and the subjective answers from the questionnaires is presented. In order to make a reliable comparison between the two variables, the following methodology was followed. The calculated PPD value by the INNOVA 7701, was estimated only for the same 15 min period the students were filling in the questionnaires. Fanger's approach was followed in order to calculate the PPD from the subjective questionnaires, in which those who have voted ±2 or ±3 on the thermal sensation scale were considered as dis-satisfied (Fanger 1970). A single value of the subjective PPD was estimated from each day of measurement, which is compared to the corresponding 15 min averaged value obtained from the instrument, and is presented in Figure 8 in a temporal fluctuation diagram. There aren't any significant similarities between the subjective answers from the questionnaires and the objective measurements. There is a clear divergence in the trends in the two variables, meaning that the objective measurements are not representative of the actual percentage of dissatisfied considering Fanger's approach.

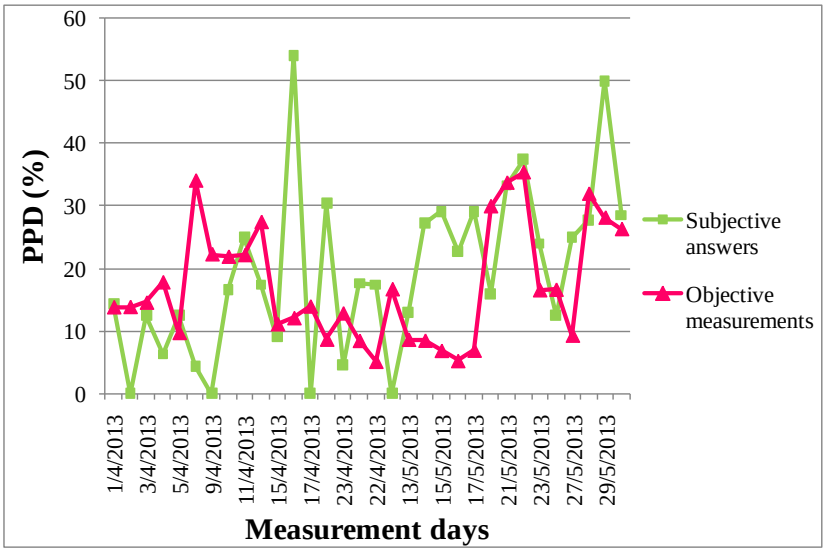

Figure 8: Temporal variation of the PPD indexes obtained from the measurements (Objective) and the questionnaires (Subjective)

3.3 Correlation between the subjective answers from questionnaires-TSV and the objective measurements-PMV

The measured Predicted Mean Vote (PMV) is presented versus the averaged Thermal Sensation vote (TSV) from the questionnaires in a scatter plot diagram in Figure 9. The TSV on the vertical axis arise from the daily mean value of the 7-point thermal sensation votes and it is presented versus the averaged 15 min of calculated PMV by the measuring instrument. As shown in Figure 9, a moderate correlation stands for these two variables ($r^2 \approx 0.5$), which encourages a further investigation of the correlations between the PMV, PPD and TSV indexes.

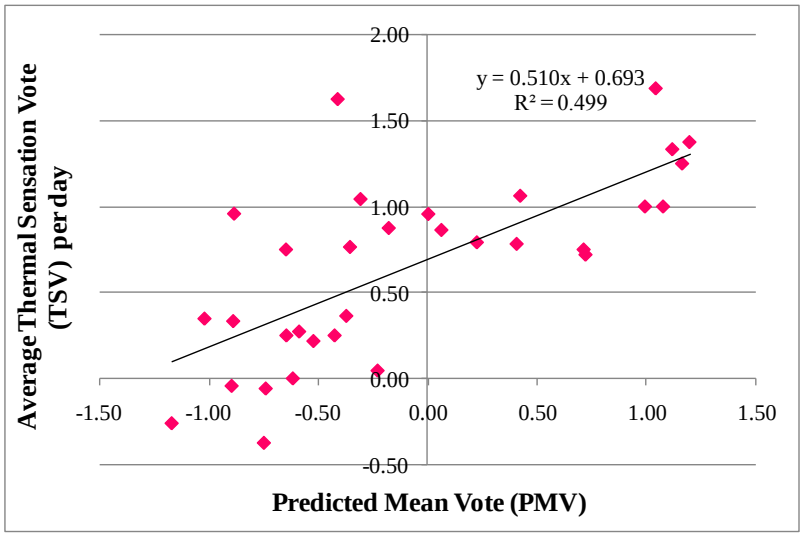

Figure 9: Scatter plot

Table 2 gives the Pearson's and Spearman's correlation coefficients between the objective and subjective TSV, PMV and PPD indexes. Significant Pearson correlation coefficients stand for the following cases; subjective TSV and objective PMV (r^2= 0.707), subjective TSV and subjective PPD (r^2= 0.826) and objective PMV and subjective PPD (r^2= 0.539). As for Spearman's rho correlation coefficients, they are significant for the same cases as Pearson's coefficients. In particular, significant correlations found for: subjective TSV and objective PMV (r^2= 0.726), subjective TSV and subjective PPD (r^2= 0.822) and objective PMV and subjective PPD (r^2= 0.611). It should be mentioned that all these cases were studied at the level of significance 0.01.

Table 2: Pearson and Spearman's correlation coefficients (N=32, same as the measurement days)

	Pearson correlation coefficient				**Spearman's rho correlation coefficient**			
	Subjective TSV	Objective PMV	Subjective PPD	Objective PPD	Subjective TSV	Objective PMV	Subjective PPD	Objective PPD
Subjective TSV	1	0.707**	0.826**	0.146	1	0.726**	0.822**	0.055
Objective PMV		1	0.539**	0.302		1	0.611**	0.015
Subjective PPD			1	0.130			1	-0.025
Objective PPD				1				1

**Correlation is significant at the level of significance: 0.01

4 CONCLUSIONS

The main conclusions arisen from this study are summarized further bellow: 1. the thermal sensation votes in the majority of the schools lied on the positive axis of the 7-point scale, indicating a rather warm environment, 2. About half of the students in most of the schools didn't prefer any change in the thermal conditions; however there were cases where the preference of a cooler environment exceeded 70% of the participants. 3. The thermal environment for most of the students seemed acceptable for the majority of the schools. 4. Most of the thermal unacceptable votes lied on the positive axis of 'warm' on the 7-point

thermal sensation scale. 5. The thermal sensation of boys and girls was not significantly different. 6. Approximately half of the responders in all schools preferred a cooler environment from which more than half of them evaluated it as acceptable and about 40% of the responders didn't prefer any change in the thermal environment. 7. The temporal variation of the subjective and objective PPD indexes was compared and their trend lines seemed to differ by far. 8. The objective PMV was then compared to the subjective TSV of students and a moderate correlation was found between them. 9. Significant correlation coefficients were found between: the subjective TSV and objective PMV, the subjective TSV and PPD and for the objective PMV and subjective PPD. These correlations indicate that students at this age are capable to fully understand and evaluate the thermal environment of their classrooms.

5 ACKNOWLEDGEMENTS

This research has been co-financed by the European Union (European Social Fund – ESF) and Greek national funds through the Operational Program "Education and Lifelong Learning" of the National Strategic Reference Framework (NSRF) - Research Funding Program: Heracleitus II. Investing in knowledge society through the European Social Fund. We are greatly indebted to the school directors, pupils and parents without whose consent this study would have not been possible.

6 REFERENCES

ASHRAE (2005). *ASHRAE Handbook: Fundamentals*. Atlanta, GA, American Society of Heating, Refrigerating and Air-Conditioning Engineers, Inc.

ASHRAE 55 (2010). *Thermal environmental conditions for human occupancy.* ANSI/ASRAE Standard 55. Atlanta: American Society of Heating, Refrigerating, and Air-Conditioning Engineers, Inc.

de Dear, R. J. and Brager, G. S. (1998). *Developing an adaptive model of thermal comfort and preference.* San Francisco, CA, USA, ASHRAE.

Fanger, P.O. (1970). *Thermal Comfort.* Danish Technical Press, Copenhagen, Denmark.

Humphreys, M.A. (1977). A study of the thermal comfort of primary schools children in summer. *Building and Environment*, 12, 231-239.

ISO 7726 (1998). *Ergonomics of the thermal environment-instrurments for measuring physical quantities*. Gevene: International Organization of Standardization.

ISO 7730 (2005). *Ergonomicas of the thermal environment-Analytical determination and interpretation of thermal comfort using calculation of the PMV and PPD indices and local thermal comfort criteria.* Brussels: International Organization of Standardization

Mendell M.J. and Heath G.A (2005). Do Indoor Pollutants and Thermal Conditions in Schools Influence Student Performance? A critical Review of the Literature. *Indoor Air* 15: 27-32

Teli, D., James, P. A. B. and Jentsch, M. F. (2013). Thermal comfort in naturally ventilated primary school classrooms. *Building Research and Information* 41(3): 301-316.

Wong, N.H. and Khoo, S.S. (2003). Thermal comfort in classrooms in the tropics. *Energy and Buildings*, 35, 337-351

COMBINING THERMAL INERTIA, INSULATION AND VENTILATION STRATEGIES FOR IMPROVING INDOOR SUMMER THERMAL COMFORT

Gianpiero Evola[1], Luigi Marletta[*1], Fabio Sicurella[2] and Vladimir Tanasiev[3]

1 Department of Industrial Engineering
University of Catania
Viale A. Doria 6,
95125 Catania, Italy

**Corresponding author: gevola@unict.it*

2 Tech-Inn
Via Caronda 300
95129 Catania, Italy

3 Department of Production and Energy Use
Polytechnic University of Bucharest
313 Splaiul Independentei
060042, Bucharest , Romania

ABSTRACT

A good level of thermal insulation and an adequate thermal capacity of the building envelope are essential to achieve good energy performance. Many studies have been conducted about this topic, mostly focused on the reduction of energy losses, peak load control and energy savings. Nevertheless, very few studies were realized addressing both insulation and inertia of the building envelope in a thermal comfort perspective, and taking into account the combined effect of different ventilation strategies.
What is the right combination of insulation thickness, heat capacity and night ventilation, in order to achieve better thermal comfort? How to exploit effectively the passive energy potential of the envelope? Of course the answer is not unique since too many parameters influence the building dynamic response under real weather condition. Nevertheless, in this paper a number of simulated results will be reported showing, for a real building with concrete walls, the combined effect of wall thickness, insulation level and outdoor ventilation rates on thermal comfort. These simulations were run under continental climate conditions (UK), and the results show the synergic effect of some strategies to achieve thermal comfort as well as their individual impact on it.

KEYWORDS

Thermal inertia, thermal comfort, ventilation strategies, dynamic simulation, insulation

1 INTRODUCTION

Although the definition of the insulation thickness that is necessary to comply with European or national standards is relatively easy, the management and the exploitation of the thermal inertia of a building is a much harder task, since this is influenced by many factors, linked not only to the thermal properties of the walls, but also to other boundary conditions (weather, heat gains, duration of the heating/cooling cycle).
The heat capacity of the building envelope has inspired many studies since dynamic numerical simulation became accessible and time-cost acceptable. Most of these works are based on an energy saving perspective for HVAC: as an example, see (Aste et al., 2009), (Orosa et al., 2012), (Ozel, 2011) and the works written by Tsilingiris. All these studies report

the thermal behaviour of different heavy walls in simple case studies, under particular boundary conditions and for energy or economic purposes.
However, there are very few works that take into account the actual potential of the thermal capacity of the building envelope, as well as its combination with the level of insulation, in a thermal comfort perspective. In fact, as long as the building is treated as being coupled with an HVAC system, its transient behaviour will be under-exploited and its potential for passive cooling masked or distorted.
In the present work some results concerning the design of new heavy-weight energy-performing houses through numerical simulation will be presented. A parametric analysis has been performed in order to understand the effect of the thermal capacity of concrete walls on indoor thermal comfort in the warm season, when coupled with different insulation thickness or ventilation strategies. To this aim, the building has been simulated in a free-running mode, which exalts the transient behaviour of the envelope as well as its potential for passive cooling.

2 METHODOLOGY

The main goal of this paper is to show the role of the thermal capacity of the building envelope, the insulation layer and the ventilation strategies for improving summer thermal comfort in buildings. To this aim, a parametric approach was followed in order to explore not only the individual contribution of each technical solution, but also possible synergic effects.
The results of the simulations were interpreted through the calculation of some indicators, recently introduced in (Sicurella et Evola, 2012), namely the *Intensity of Thermal Discomfort* (ITD) and the *Frequency of Thermal Discomfort* (FTD). The ITD represents the time integral of the difference between the current operative temperature and a threshold value that defines the upper limit for comfort; on the other hand, the FTD is the percentage of time during which thermal comfort is not accomplished, as the previously mentioned threshold value is exceeded.
In this study, the definition of the threshold value is based on the adaptive approach, as described in (EN Standard 15251, 2007); in particular, the threshold operative temperature corresponds to the upper limit of Category I, that is the most restrictive one. The threshold value is not constant in time, but it should be determined daily as a function of the running mean outdoor air temperature. In order to use these indicators, the building is simulated in a free-running mode so as to obtain the time profile of the indoor operative temperature, i.e. the main parameter associated with thermal comfort according to the adaptive approach (Nicol et al., 2002). As the building is supposed to be used for residential purposes, the calculation of the indicators is based on the 24-h profile of the operative temperature.
Thanks to this approach, the comparison between the different design solutions will be based on physical and measurable parameters, thus allowing an easy but comprehensive identification of the best strategies needed to achieve summer thermal comfort.

3 CASE STUDY

The methodology described in the previous paragraph was applied during the design stage of real two-storey houses for residential use (see Fig. 1), whose construction is in progress near London (UK). Each house is about 65 m^2 in surface and has two floors: the ground floor hosts the living room, a kitchen, a hall and a WC, whereas in the first floor there are a landing, two bedrooms and one bathroom. The main façades are due north and south.
One of the objectives of the project was to understand the real potential of massive constructions to achieve both energy savings and thermal comfort. The results concerning the energy demand are presented in (Sicurella and Tanasiev, 2012): a correct design of the

envelope allowed reducing the specific energy demand for heating by only 2%, whereas the cooling demand could be reduced by approximately 10%, in coherence with other previous works.
Anyway, the present paper wants to focus on thermal comfort, and therefore to investigate on the individual contribution of each technical solution (thermal inertia, insulation, ventilation) as well as their synergic effects. As a reference configuration, in order to achieve excellent winter performance, the massive exterior wall (200 mm concrete) was covered with 300 mm of extruded polystyrene. For the ground floor, that is made by 250 mm of concrete, a 300-mm layer of extruded polystyrene was added, while the roof was composed of tiles, extruded polystyrene (300 mm) and plywood. Table 1 reports the main physical characteristics of the opaque envelope. As concerns the windows, they have a triple glazing with a wooden frame. Their U-value is 1.32 $W \cdot m^{-2} \cdot K^{-1}$, and the g-value is 0.48.
The house is a residential building, whose internal gains (occupancy, lighting, electric equipment) have an average value of 3.06 $W \cdot m^{-2}$, that is typical for new high-performance buildings. The weather data used for the simulations are those of London Gatwick; the simulations were run by using Energy Plus 6.1, through the interface Open-Studio for Google SketchUp and a time step of fifteen minutes was set.

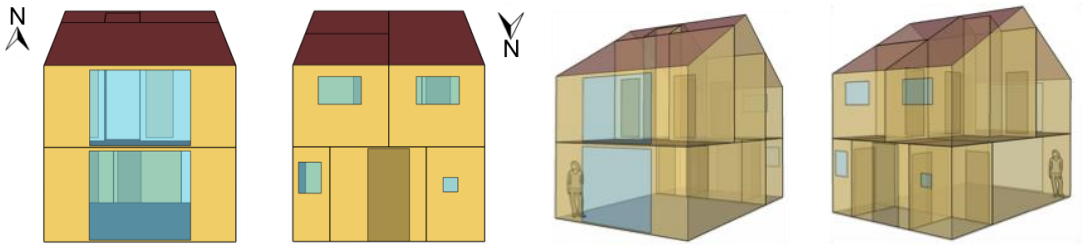

Figure 1: Waterford house, exterior (north view) and interior view (south view)

Table 1: Main features of the simulated building envelope (reference configuration).
The materials are listed from the outer to the inner layer.

	Components	Thickness [cm]	ρ [kg·m^{-3}]	c_p [J·kg^{-1}·K^{-1}]	λ [W·m^{-1}·K^{-1}]	U [W·m^{-2}·K^{-1}]
Exterior walls	Lime sand render	3	1600	1000	0.8	0.11
	Extruded polystyrene	30	35	1400	0.034	
	Concrete	20	2300	880	1.8	
Ground floor	Sand and gravel	5	1950	1045	2	0.11
	Polyethylene	0.01	920	2200	0.33	
	Extruded polystyrene	30	35	1400	0.034	
	Polyethylene	0.01	920	2200	0.33	
	Concrete	25	2300	880	1.8	
	Ceramic	2	2300	1000	1.3	
Roof	Tiles	2.5	1602	1464	1	0.11
	Extruded polystyrene	30	35	1400	0.034	
	Polyethylene	0.01	920	2200	0.33	
	Plywood	1.8	700	1420	0.15	
Internal walls	Concrete	10	2300	880	1.8	3.27

3.1 Parametric analysis

A parametric analysis was performed in order to understand how the insulation of the envelope, the thickness of the concrete slab and the ventilation rate might influence the summer thermal comfort.

To this purpose, seven different solutions for the opaque envelope were considered, by varying the thickness L_c of the concrete slab (for walls and ground floor) from 100 mm to 300 mm, and the thickness L_{in} of the insulation layer from 150 mm to 300 mm. For the sake of comparison, only one case without insulation was considered, but actually this solution is not practically feasible as it would lead to great disadvantages in winter.
For each envelope solution, Table 2 reports the U-value and the values of two dynamic transfer properties, i.e. the *decrement factor* (f) and *the time shift* (φ): they respectively measure the attenuation and the time delay of the thermal wave transferred into the building, if compared to the thermal wave acting on the outer surface of the building. The calculation is conducted according to (ISO 13786, 2007).
As concerns the ventilation of the building, several scenarios were considered, characterized by different values and different time profiles for the air change rate *n*. In any case, ventilation is supposed to be provided through mechanical means.
All the combinations defined in this parametric analysis are reported in Table 3.

Table 2: Main transfer properties for the envelope solutions considered in the parametric analysis.

Concrete slab	**Insulation**	**U** **[W·m^{-2}·K^{-1}]**	***f*** **[-]**	**φ** **[h]**
L_c = 200 mm	L_{in} = 0 mm	3.14	0.46	6.1
L_c = 100 mm	L_{in} = 150 mm	0.21	0.40	7.1
L_c = 100 mm	L_{in} = 300 mm	0.11	0.28	11.0
L_c = 200 mm	L_{in} = 150 mm	0.21	0.19	9.4
L_c = 200 mm	L_{in} = 300 mm	0.11	0.13	13.2
L_c = 300 mm	L_{in} = 150 mm	0.21	0.10	11.7
L_c = 300 mm	L_{in} = 300 mm	0.11	0.07	15.5

Table 3: Combinations used in the parametric analysis.

Case nr	**Concrete slab thickness**	**Insulation thickness**	**Ventilation rate**	**Time schedule for ventilation**	**Comments**
1	200 mm	0 mm	n = 0 h^{-1}	00:00 – 24:00	*Role of the insulation*
2	200 mm	150 mm	n = 0 h^{-1}	00:00 – 24:00	
3	200 mm	300 mm	n = 0 h^{-1}	00:00 – 24:00	
4	100 mm	150 mm	n = 2 h^{-1}	00:00 – 24:00	*Role of the slab thickness (L_{in} = 150 mm)*
5	200 mm	150 mm	n = 2 h^{-1}	00:00 – 24:00	
6	300 mm	150 mm	n = 2 h^{-1}	00:00 – 24:00	
7	100 mm	300 mm	n = 2 h^{-1}	00:00 – 24:00	*Role of the slab thickness (L_{in} = 300 mm)*
8	200 mm	300 mm	n = 2 h^{-1}	00:00 – 24:00	
9	300 mm	300 mm	n = 2 h^{-1}	00:00 – 24:00	
10	200 mm	300 mm	n = 0.5 h^{-1} n = 2.0 h^{-1}	06:00 – 22:00 otherwise	*Mechanical ventilation only at night (two schedules)*
11	200 mm	300 mm	n = 0.5 h^{-1} n = 2.0 h^{-1}	08:00 – 20:00 otherwise	

4 RESULTS AND DISCUSSION

4.1 The role of the insulation and the thermal mass

The results of the simulations for all the cases listed in Table 3, in terms of Intensity of Thermal Discomfort (ITD) and Frequency of Thermal Discomfort (FTD), are shown in Fig. 2. As discussed in the following, many elements can be drawn from the analysis of this graph.
First of all, the comparison between cases nr. 1 to nr. 3 suggests that, when no ventilation is allowed (n = 0 h^{-1}), an increase in the insulation thickness implies a considerable worsening of the thermal comfort perceived by the occupants. In fact, the overall ITD in summer grows from 10100 °C·day^{-1} to 13500 °C·day^{-1}, when increasing the insulation thickness from 0 mm (case nr. 1) to 300 mm (case nr. 3). This means that the intensity of the thermal discomfort in the sample building, i.e. the average overheating beyond a comfort threshold, increases up to 30% due to the positioning of a thick insulation layer.
The room overheating occurring in case nr. 3 can also be observed in Fig. 3a, where for each day in July the hourly operative temperatures in a representative room during the occupancy period are reported. As one can observe, the operative temperature ranges from 28°C to 32°C, and never falls within the acceptable range for comfort, included between the solid lines. As a consequence, the Frequency of Thermal Discomfort in this case is FTD = 100% (see Fig. 2).
Here, one can understand that the very low thermal transmittance determined by the envelope insulation (U < 0.21 W·m^{-2}·K^{-1}) prevents the heat generated by internal and solar gains from being effectively transferred to the outdoors, especially at night, when the outer temperature is likely to be lower than the indoor temperature. This problem is emphasized by the absence of ventilation. However, even if case nr. 1 presents better results, it is not practically feasible, as the absence of insulation implies a very high thermal transmittance (U = 3.4 W·m^{-2}·K^{-1}), that would strongly affect the energy performance in winter.
In addition, when looking at cases nr. 4 to nr. 6 in Fig. 2, it is possible to remark that an increase in the thickness of the concrete slab from 100 mm to 300 mm, while keeping the same insulation layer (150 mm) and a constant ventilation rate (n = 2 h^{-1}), determines a reduction in the ITD of about 7% (from 11500 °C·day^{-1} to 10700 °C·day^{-1}). The same trend emerges through cases nr. 7 to nr. 9, i.e. when the insulation thickness is 300 mm: in this case, the potential reduction in the ITD due to a thicker concrete slab amounts to about 11% (from 15600 °C·day^{-1} in case nr. 7 to 13900 °C·day^{-1} in case nr. 9).
These results testify the importance of thermal mass for improving the response of the building to both internal heat gains and outdoor thermal waves in summer. This is also highlighted in Table 2, where the cases with a higher slab thickness are also those that present lower values of the decrement factor f and higher values of the time shift φ.

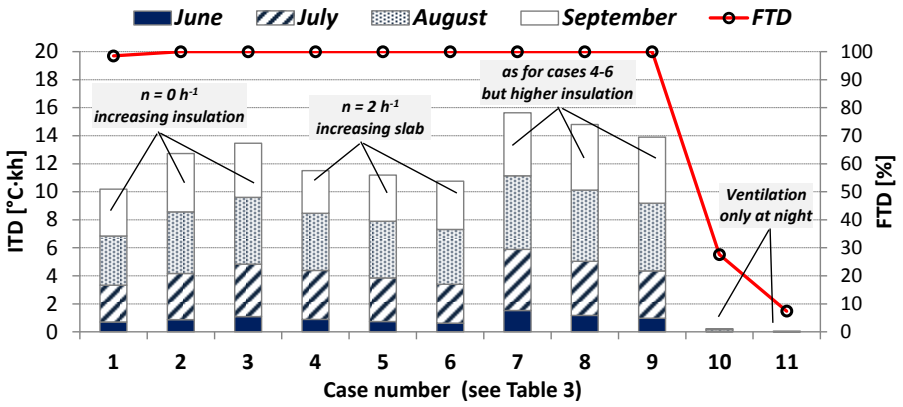

Figure 2: Values of the ITD and the FTD for all the cases considered in the parametric analysis.

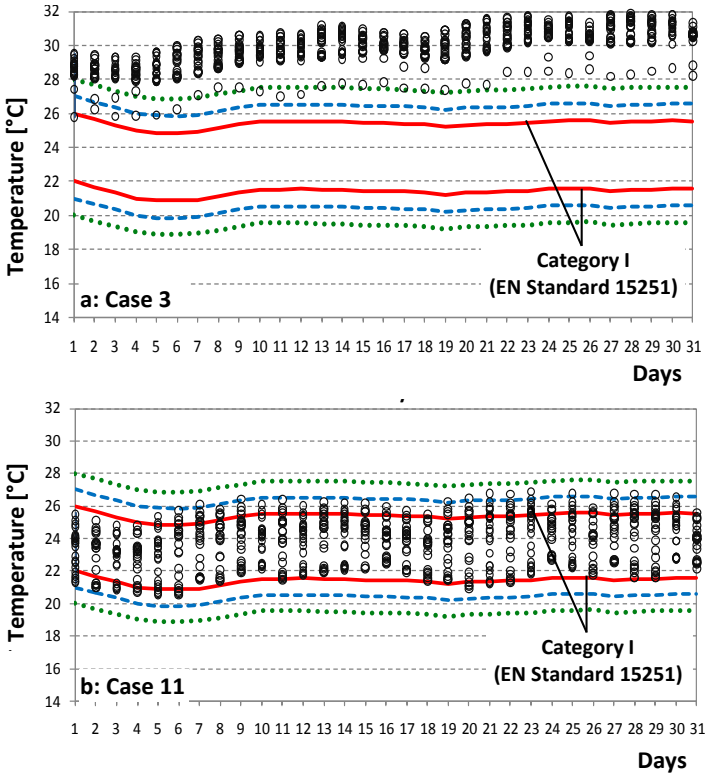

Figure 3: Distribution of the operative temperature in July (a: case 3; b: case 11)

Furthermore, if one compares in Fig. 2 the cases having the same concrete slab but different insulation thickness, it is evident that a higher insulation determines a lower thermal comfort. As an example, ITD = 11200 °C·day-1 in case nr. 5 (200 mm of concrete and 150 mm of insulation) and ITD = 14800 °C·day-1 in case nr. 8 (200 mm of concrete and 300 mm of insulation): thus, the installation of a very thick insulation introduces an increase of 24% in the ITD. This confirms what already remarked form case nr. 1 to case nr. 3, that is to say the negative effect of an excessive envelope insulation on the dissipation of heat gains in summer.

4.2 The role of ventilation: definition of appropriate strategies

Now, what is not fully explained by the results shown in Fig. 2 is the role of ventilation. Actually, if one compares case nr. 2 (n = 0 h^{-1}) to case nr. 5 (n = 2 h^{-1}), that present different ventilation rates but the same thickness of concrete slab (200 mm) and insulation (150 mm), it seems that the higher ventilation rate adopted in case nr. 5 determines better comfort conditions. Indeed, the ITD drops from 12700 °C·day-1 in case nr. 2 to 11200 °C·day-1 in case nr. 5 (-12%). However, a different message emerges if comparing case nr. 3 (n = 0 h^{-1}) to case nr. 8 (n = 2 h^{-1}), where the thickness of insulation is 300 mm. In this case, it seems that higher ventilation rates should imply worse comfort conditions.
The reason for this behaviour is most likely due to the fact that an intense ventilation during the daytime, i.e. when the outdoor temperature is usually higher than indoor temperature, may have negative effects on the room comfort. This is more likely to occur if the insulation layer is thick, since in this case the operative temperature tends to be high, as already discussed in the previous section.
This remark introduces the need to choose an appropriate ventilation strategy for massive buildings. This issue has been tackled through cases nr. 10 and nr. 11: here, starting from the

configuration of case nr. 8 (200 mm of concrete, 300 mm of insulation), the ventilation of the building was limited to a specific time interval at night. In particular, case nr. 10 implies an air change rate n = 2 h^{-1} from 22:00 to 06:00, whereas during the daytime mechanical ventilation is switched off, and a low air change rate (n = 0.5 h^{-1}) is considered to describe infiltration through leaks. On the other hand, in case nr. 11 mechanical ventilation is kept for a longer period at night (12 hours, from 20:00 to 08:00).
As shown in Fig. 2, in both cases the seasonal value of the ITD is now close to 0, whereas the Frequency of Thermal Discomfort is very low (FTD = 27.6% for case nr. 10 and FTD = 7.4% for case nr. 11). This proves that these ventilation strategies are very effective for improving summer thermal comfort in the sample building. Further proof of this statement comes from Fig. 3b: here, one can observe that throughout the whole month of July the operative temperature for case nr. 11 lies very frequently within the comfort range defined by Category I of the international standard EN 15251.
In conclusion, the results presented in this section illustrate the need of practising an intense ventilation of the building only at night, when the outdoor temperature is low, hence the potential for discharging the heat released by the thermal mass is high. On the contrary, ventilation during the daytime should be limited to a minimum rate for hygienic purposes, since it is likely to produce a room overheating.

4.3 Other remarks on the role of the thermal mass

The results presented in Section 4.1 show the importance of thermal mass for improving the thermal response of the building in summer, especially in terms of comfort for the occupants.
However, it is also interesting to remark that the role of thermal mass is far less significant in winter. Indeed, other simulations were run in order to calculate the energy demand for space heating while varying the thickness of the concrete slab from 100 mm to 300 mm (with 50 mm step). The results show that the specific energy demand for heating decreases very weakly from 35.4 to 34.8 $kWh \cdot m^{-2} \cdot y^{-1}$ (less than 2%) and reveal that, for a well-insulated envelope, the effect of the thermal mass of the walls is almost negligible

Table 4: Thickness of the concrete slab vs. energy demand for space heating (L_{in} = 300 mm)

Slab thickness	**100 mm**	**150 mm**	**200 mm**	**250 mm**	**300 mm**
Energy needs for heating [$kWh\ m^{-2}\ y^{-1}$]	35.4	35.3	35.1	35.0	34.8

5 CONCLUSIONS

The exploitation of the building thermal mass and of appropriate ventilation strategies have often been treated in an energy saving or economical perspective, while few studies have been made in order to understand their individual and synergic effect on thermal comfort.
In the present work the effect of ventilation strategies, insulation thickness and thermal capacity of the envelope on thermal comfort was investigated by means of dynamic simulations for a real sample building in continental climate.
The results underline the major role played by night ventilation, that is essential to discharge the heat released by the opaque envelope, thus keeping a comfortable indoor temperature. On the contrary, ventilation should be avoided during the daytime, as it might be responsible for room overheating.
Moreover, an excessive thickness of the insulation layer, despite being very effective for reducing energy needs in winter, is a cause of overheating and thermal discomfort in summer.

Hence, a good compromise should be determined for the thickness of the envelope insulation, with the support of dynamic simulations.
As concerns the thermal capacity of the building envelope, in this case study it seems to have a slight effect on thermal comfort if not assisted by an appropriate ventilation strategy; in addition, a heavier structure seems more effective for improving thermal comfort when coupled with a smaller insulation layer. In any case, the role of the thermal capacity is secondary to that of ventilation.
Further investigations are in progress in order determine the combined effect of solar shadings, ventilation and thermal inertia on thermal comfort for historical buildings located in the Mediterranean area. The results will be reported in future papers.

6 REFERENCES

Aste, N., Angelotti, A., Buzzetti, M., (2009). The influence of the external walls thermal inertia on the energy performance of well insulated building, *Energy and Building* 41, 1181-1187.

EN Standard 15251 (2007), Indoor environmental input parameters for design and assessment of energy performance of buildings addressing indoor air quality, thermal environment, lighting and acoustics.

ISO Standard 13786, (2007). Thermal performance of building components. Dynamic thermal characteristics. Calculation methods.

Nicol, J.F., Humphreys, M.A., (2002). Adaptive thermal comfort and sustainable thermal standards for buildings, *Energy and Buildings* 34, 563-572.

Orosa, J.A., Oliveira, A.C., (2012). A field study on building inertia and its effects on indoor thermal environment, *Renewable Energy* 37, 89-96.

Ozel, M. (2011). Effect of wall orientation on the optimum insulation thickness by using a dynamic method, *Applied Energy* 88, 2429-2435.

Ozel, M. (2011). Thermal performance and optimum insulation thickness of building walls with different structure materials, *Applied Thermal Engineering* 31, 3854-3863.

Sicurella, F., Evola, G., Wurtz, E., (2012). A statistical approach for the evaluation of thermal and visual comfort in free-running buildings, *Energy and Buildings* 47, 402-410.

Sicurella, F., Tanasiev, V., Wurtz, E., (2012). Achieving energy savings and thermal comfort by coupling insulation, thermal inertia and ventilation strategies: a case study, Proceedings of the AUGC-IBPSA Conference 2012.

Tsilingiris, P.T. (2003). Thermal flywheel effects on the time varying conduction heat transfer through structural walls, *Energy and Buildings* 35, 1037-1047.

Tsilingiris, P.T. (2004). On the thermal time constant of structural walls, *Applied Thermal Engineering* 24, 743-757.

Tsilingiris, P.T. (2006). The influence of heat capacity and its spatial distribution on the transient wall thermal behaviour under the effect of harmonically time-varying driving forces, *Building and Environment* 41, 590-601.

Tsilingiris, P.T. (2006). Wall heat loss from intermittently conditioned spaces. The dynamic influence of structural and operational parameters, *Energy and Buildings* 38, 1022-1031.

US Department of Energy, (2011). Energy Plus version 6.1, http://apps1.eere.energy.gov/buildings/energyplus

ASSESSMENT OF INTEGRATED PV SHADING SYSTEMS FOR ENERGY SAVINGS AND INTERIOR COMFORT CONDITIONS IN MEDITERRANEAN COUNTRIES

Maria Mandalaki[1*], Theocharis Tsoutsos[2], Nikos Papamanolis[3]

1 Technical University of Crete
Environmental Engineering School
Polytechnioupoli, Kounoupidiana 73100
Chania, Crete, Greece
**Corresponding author: mandalaki@arch.tuc.gr*

2 Technical University of Crete
Environmental Engineering School
Polytechnioupoli, Kounoupidiana 73100
Chania, Crete, Greece

3 Technical University of Crete
Architectural Engineering School
Polytechnioupoli, Kounoupidiana 73100
Chania, Crete, Greece

ABSTRACT

Fixed shading systems are saving energy by reducing the cooling loads of the space they shade, but can be a source of energy losses due to the increased need of daylight that they create. Aim of this paper is the comparative assessment of different typologies of buildings' shading systems with integrated photovoltaics. The assessment is focused on their energy efficiency and degree of internal visual comfort conditions that they can ensure. The purpose of the comparison is to optimize the combination of shading systems and their integrated solar cells. Especially for office units, due to the specific demands for visual comfort and the increased needs for quality lighting, balancing the above mentioned facts is more crucial.

Shading systems are grouped and studied according to their energy savings (production and reduction of cooling loads) and to the quality of the visual interior environment. For the study computer simulations are used for the energy loads (needs/production) and both computer simulation and experimental physical models are used for the daylighting assessment. Moreover, through this research, the effect of specific geometrical characteristic of the photovoltaic modules installed is analyzed in relation to the energy produced and to the resulting visual conditions.

KEYWORDS: energy balance, shading systems, BIPV, visual comfort

1. INTRODUCTION

The main objective of this paper is to evaluate fixed shading systems with integrated photovoltaics (PV) facing south in Mediterranean countries according to their ability to save energy and to provide visual comfort. For this purpose we focus the experimental work mainly on three areas: balancing energy consumption with the resulting thermal comfort, daylight quality and energy production for office units.

This research concerns the determination of best performing systems in terms of low energy needs for heating, cooling and electric light needs of the shaded space. We examine both the energy needs for heating the space and the energy needs for cooling the space for yearly-fixed thermostat settings range between 21.6 and 24.1 C, for office hours of 9:00 to 17:00 for five days per week (Sanea & Zedan, 2008). We examine electric light needs when daylight levels fall under 500 lux on the desk level (Boyce & Raynham, 2009)

We mostly compared the two groups of shading systems, the louvers systems and the systems that allow view to outside. Analytically we categorize them to:

a. Shading systems that allow transparency: Canopy horizontal, Canopy horizontal double, Brise Soleil full façade, Brise Soleil Semi façade, Surrounding Shade, Canopy Louvers, Canopy Inclined Single and

b. Shading systems that obstruct view to outside: Canopy Inclined double, Brise Soleil Semi Façade with Louvers, Louvers Vertical, Louvers Horizontal, Louvers Horizontal inwards inclined, Louvers Horizontal Outwards Inclined.

2. EVALUATING VISUAL COMFORT CONDITIONS

2.1. Comparison of physical model and simulation tools

The comparison between measurements on physical models and simulations can be a complicated task, especially in cases when the physical model has been tested in real sky conditions. For this reason, research has been carried out and we have arrived at some basic conclusions with reference to the measurements from the validated simulation tool used and the measurements from the constructed model. In general the physical model overestimates the values in comparison with the simulation tool (Mardaljevic, 2001). In some cases the overestimation is in the range of 10%.

When the divergence between the two models is in the range of 300% and over this is due to the rapid changeability of the daylight and to the small divergence of positioning the sensor in relation to the simulated model. In cases where the sun is higher in the sky (summer solstice) the divergence is higher. Moreover, in the complicated geometries of Venetian blind systems the divergences become even higher. It is important to mention that in contrast with the reported data by Mardaljevic (2001) the differences between measurements in a physical

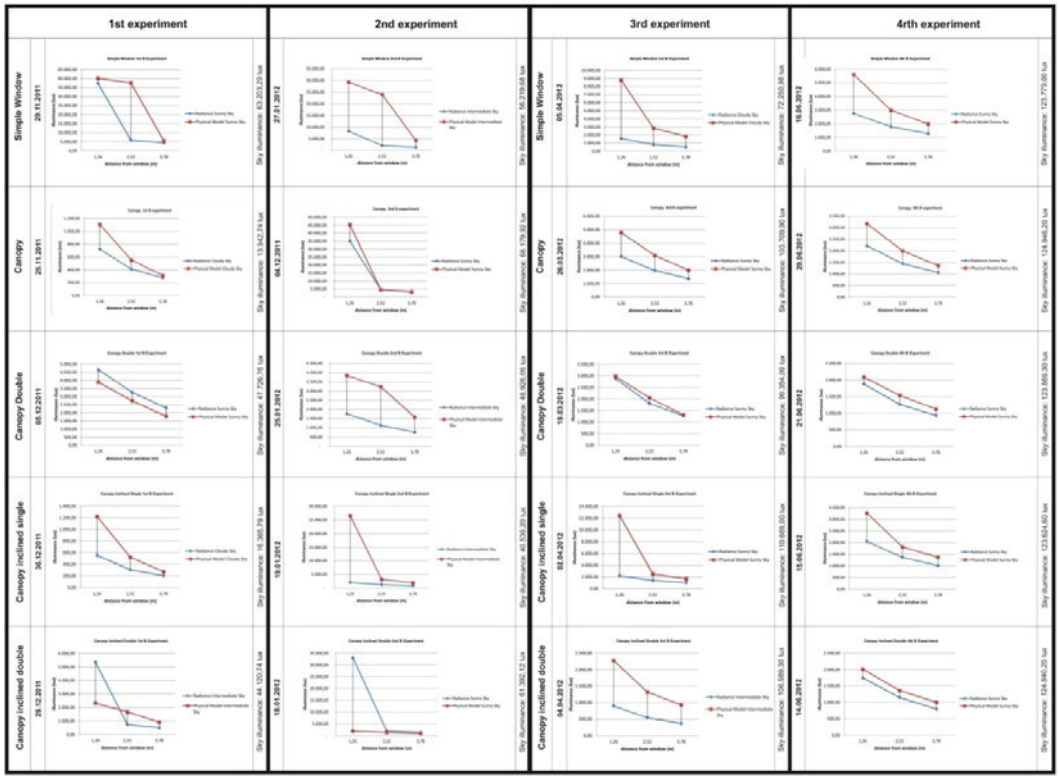

model and measurements in simulations are higher in positions near the window and not at the back of the room (Fig. 1).

Figure 1: Comparison of results of simulations and measurements with physical models of 44.92% WWR for Chania Latitude

2.2. Evaluation of Daylight Autonomy Levels

Regarding Daylight Autonomy (DA) for daylight levels above 500lux, systems allowing outside view perform better than louvers systems. From the first group of shading systems (transparent systems) **Canopy louvers** and **Brise soleil** systems perform better while the **Surrounding shade** has the lowest value of DA. In the second group of shading systems **Louvers vertical** and **Louvers horizontal** perform better when compared with **Louvers Horizontal Outwards Inclined** (Fig.2).

The higher the DA the lower the energy needs for electric lighting.

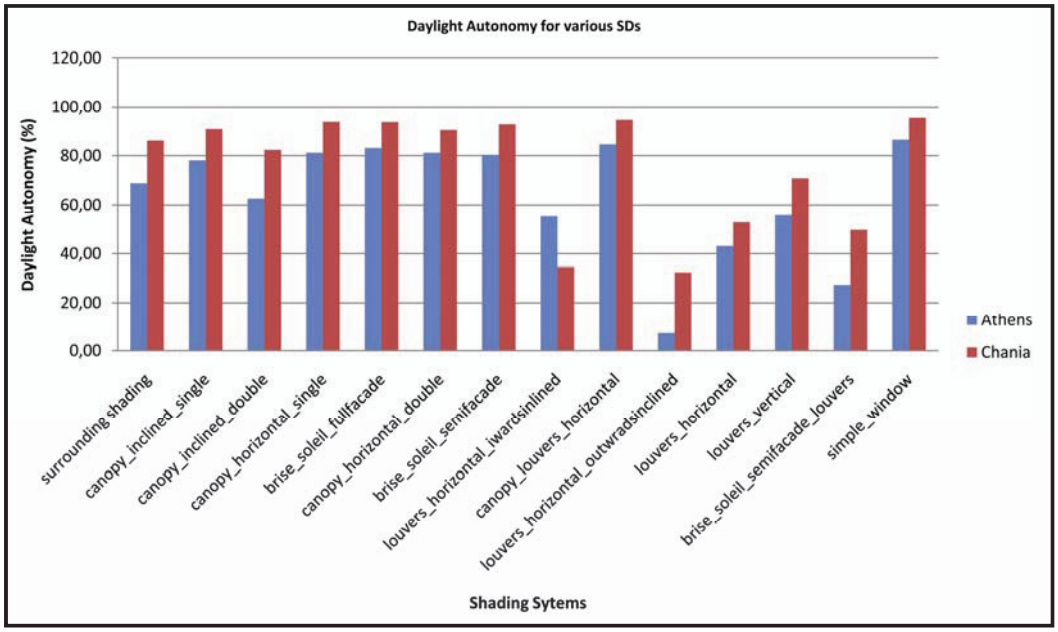

Figure 2: Comparison of Daylight Autonomy for Athens and Chania

2.3. Comparison of Daylight quality in terms of Useful Daylight Illuminance (UDI)

Useful Daylight illuminance (UDI) is defined by Mardaljevic (2001). We assess three basic statistical values: UDI 100 -2000 (the mean value of the UDI), the UDI 100, (the percentage of the time of the year when the space has daylight under 100 lux; this level is considered very low) and the UDI 2000, (the percentage of the time of the year that the space has daylight above 2000lux; these levels of daylight are considered to result in uncomfortable comfort conditions).

Amongst transparent façade systems Surrounding Shade seems to perform well because it has high UDI 100 - 2,000 values, low UDI 100 value and low UDI 2,000 value in comparison to other transparent shading systems. Additionally Canopy Double systems Inclined or not perform well in relation to the three examined UDI values, but lower than Surrounding Shade. Façade shading systems and especially louvers systems perform better in terms of high percentage of UDI 100-2,000. Amongst these systems, Louvers Horizontal has the highest UDI 100 -2,000 and simultaneously the lowest UDI 100 (Fig. 3).

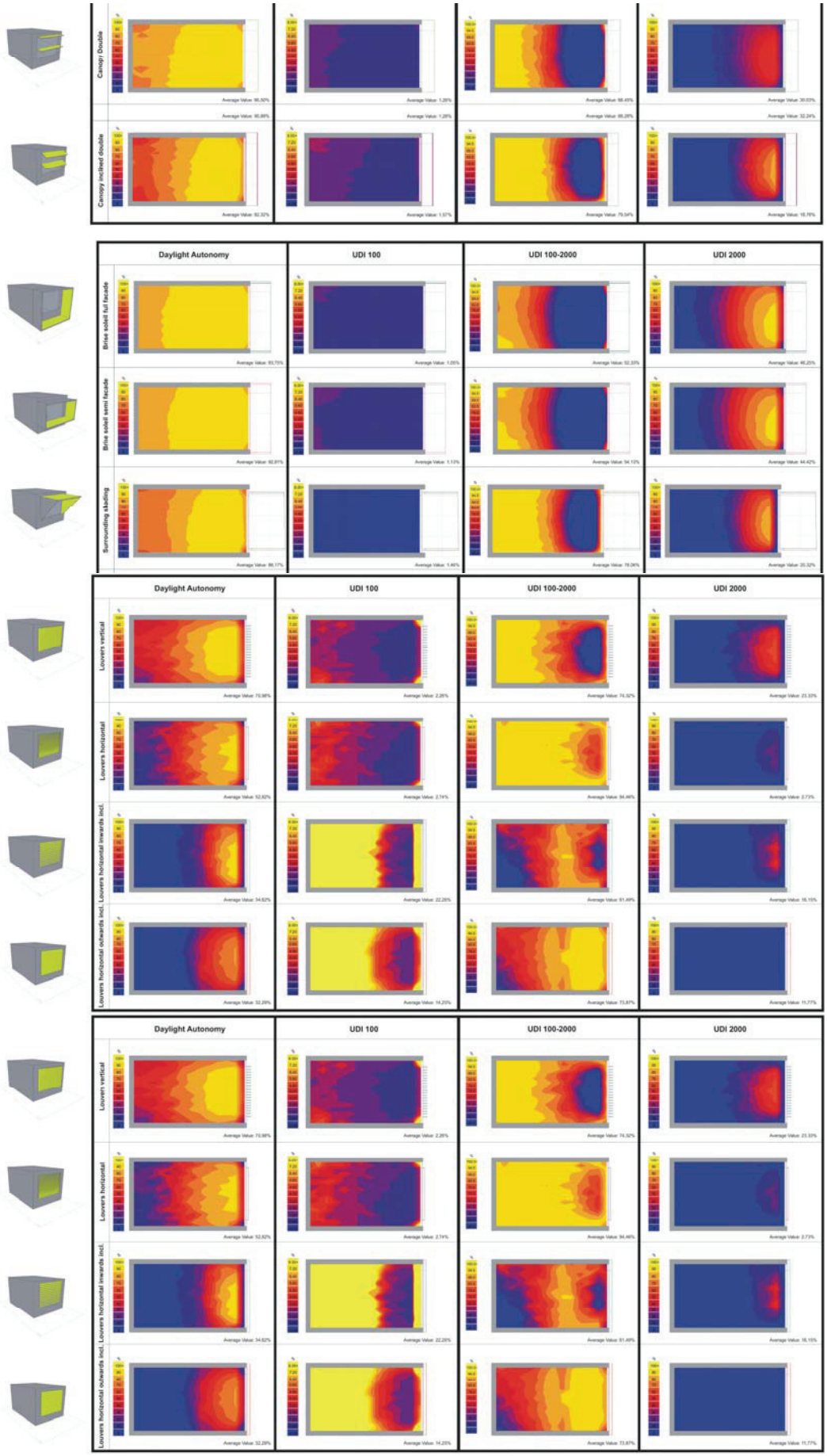

Figure 3: Comparison of UDI values in relation to DA values for all SDs examined for the case of Chania

2.4. Comparison of Daylight quality in terms of Glare

Daylight Glare Index (DGI) is defined by Baker & Steemers (1993). Values below 16 are considered to result in an imperceptible visual environment. Originally we selected the "worst viewing position" for the simulations. In theory, the worst viewing position is the one that has the highest vertical viewing angle of the window that constitutes the main light source of the space in question, and the one with the widest viewing angle onto the surface of the window (Meresi, 2010). Only some systems can result in values below 16 and these are presented here in sequence starting from the best performing: Canopy louvers, Louvers vertical, Brise Soleil Full Façade and Canopy horizontal (Fig. 4).

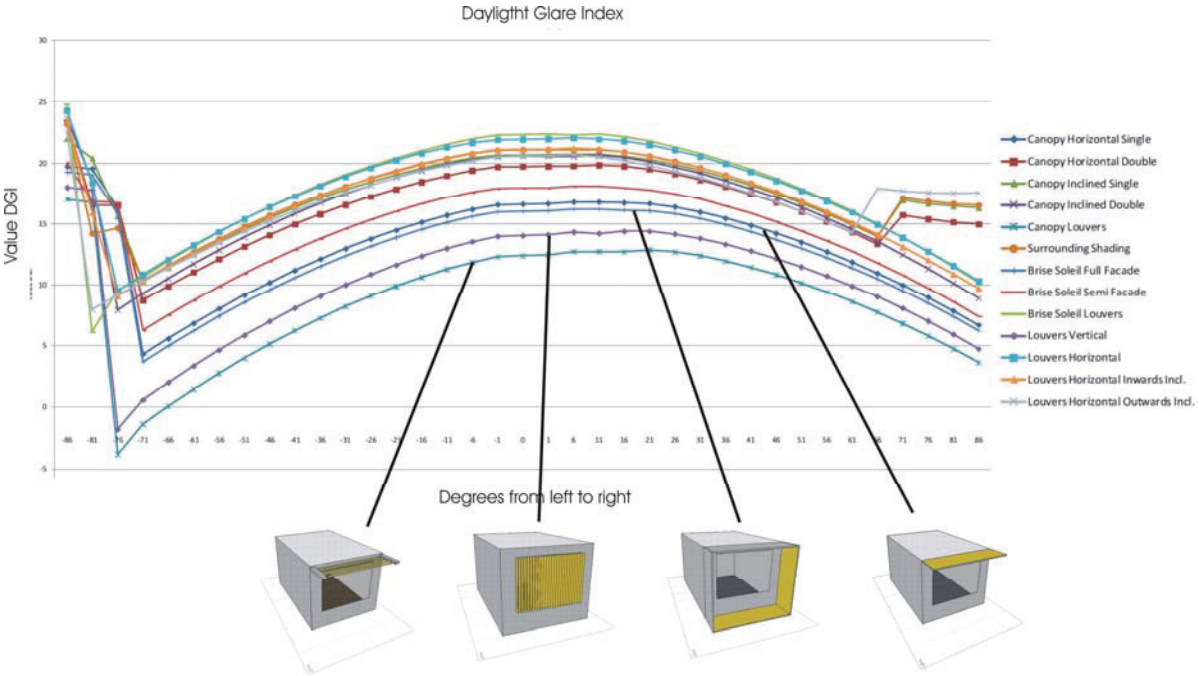

Figure 4: DGI values for the 21 December at 12:00 o'clock for all examined systems in relation to the angle of view for the camera away from window

3. BALANCING ENERGY SAVINGS AND VISUAL COMFORT

The system of Surrounding Shade is performing extremely well in terms of low energy needs, has proved to perform well in terms of daylight quality for positions away from the window and has good performance of UDI values. On the other hand, the System of Brise Soleil full facade that is performing well in terms of energy needs for thermal comfort (but lower than the surrounding shade) performs very well in all daylight quality values examined. Similar results can be extracted for Brise Soleil semi facade system. If we examine the systems in terms of daylight performance the system of Canopy Louvers has very good performance according to energy savings for lighting and according to visual comfort in positions away from window and acceptable visual conditions near the window. At the same time this system performs low in terms of energy savings for heating and cooling the space. Additionally it is important to mention that the systems of Canopy double horizontal or inclined seems to have an acceptable performance for all examined values but cannot be a valuable solution due to the resulting moderate environment in terms of comfort and of energy savings.

4. DISCUSSION AND CONCLUSIONS

In order to evaluate the performance of the examined shading systems a table is being created that incorporates all the examined values related with visual comfort and energy savings (Fig.5). It is obvious that the system of **Surrounding shade** is performing extremely

well in terms of low energy needs, has proved to perform well in terms of daylight quality for positions away from the window and has good performance of UDI values. On the other hand, the System of **Brise – Soleil full facade** that is performing well in terms of energy needs for thermal comfort (but lower than the surrounding shade) performs very well in all daylight quality values examined.

We have attempted to combine the different and occasionally contradicting properties of the various shading systems examined in relation to their ability to save energy and to provide high quality of daylight. We have concluded that the systems of Surrounding shade and of Brise Soleil Full and Semi facade can best achieve these two goals. The only disadvantage is that they cannot ensure comfortable daylight conditions away of the window of the examined room.

It is remarkable that the systems of Louvers which have proved to perform very well in office units tare unsuitable for integration of PV, due to the fact that their energy production becomes very low when PVs are integrated.

We recommend that when considering PV integration for shading systems in office buildings Surrounding shade and Brise - Soleil Systems should be considered as a valuable solution.

	UDI	DGI Away from window	DA	Energy Needs For H + C
	LOW - 1	BEST - 2	BEST - 2	LOW
	MIDDLE	LOW - 4	BEST - 5	LOW - 3
	MIDDLE	MIDDLE	BEST - 3	MIDDLE
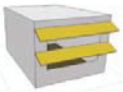	BEST	MIDDLE	MIDDLE	MIDDLE
	LOW - 2	BEST	BEST	LOW - 1
	MIDDLE	BEST - 3	BEST - 1	BEST - 1
	MIDDLE	MIDDLE	BEST - 1	BEST - 2
	BEST	LOW	LOW - 1	BEST - 3
	BEST	LOW - 3	BEST - 3	BEST
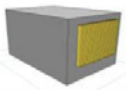	MIDDLE	BEST - 1	LOW- 2	MIDDLE
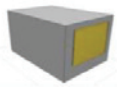	BEST	LOW - 1	LOW- 2	MIDDLE
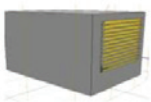	LOW	LOW - 2	LOW	LOW - 2
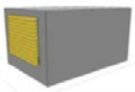	LOW	LOW -3	LOW	MIDDLE

Figure 7: Comparative assessment of shading systems

5. REFERENCES

Al-Sanea, S.A. and Zedan, M.F. (2008). Optimized monthly-fixed thermostat-setting scheme for maximum energy - savings and thermal comfort in air- conditioned spaces. *Applied Energy , 85*, 2008, 326 - 246.

Baker N., Fanchiotti A. & Steemers K. (1993). *Daylighting in Architecture. A European Reference Book.* Brussels. James x James.

Boyce P. and Raynham P. (2009). *SLL Lighting Handbook,* London. The Society of Light and Lighting.

Mardaljevic, J. (2001). The BRE-IDMP dataset: a new benchmark for the validation of illuminance prediction techniques. Lighting Research and Technology 33, 117 - 136.

Meresi, K. (2010). Energy Savings in schools through daylighting. Thessaloniki, Polytechnic School of Thessaloniki.

THE THERMAL COMFORT AND IAQ OF RECENT DUTCH ENERGY EFFICIENT OFFICE BUILDINGS WITH THERMAL ACTIVATE BUILDING SYSTEMS

Wim Zeiler, Koen Smelt and Gert Boxem

TU Eindhoven
Den Dolech 2
Eindhoven, Netherlands
w.zeiler@bwk.tue.nl

ABSTRACT

The need for more energy efficient Heating Ventilation and Air Conditioning systems led to a search for new systems for heating, cooling and ventilation of buildings. Strong reduction of energy consumption within the built environment is necessary because of the growing effects of depletion of fossil fuel and global warming. This lead to a almost standard concept of energy efficient office buildings in the Netherlands. That concept exists of heat pumps and LTES aquifers combined with thermally activated building systems (TABS). Though there are many studies about TABS behaviour they are mainly based on simulations and only a very few actual field studies have been performed on the ventilation performance, draft and the perceived comfort of the ventilation in combination with TABS. Therefore measurements were done and questionnaires held to determine the perceived comfort and IAQ in three recently completed office buildings with the energy efficient TABS concept. The results showed that in one office the percentage of predicted satisfied persons would be more than 40% and the others respectively around 20% and around10%. The results of the held questionnaires also showed that the three buildings score on average 4 on a scale from 1 to 7 for the aspects of perceived indoor comfort, so the occupants were slightly more dissatisfied with the performance of the TABS.

KEYWORDS

Thermal comfort, Indoor Air Quality, Termal Activated Buildings Systems

1 INTRODUCTION

During the last years global warming, the deterioration of the environment and the limited amount of fossil energy have focussed the attention to the development of more energy efficient systems for heating and cooling (De Carli et al 2003). Main principle of modern building design is, besides a healthy and comfortable indoor climate, a low energy consumption and durability. Thermally Activated Building Systems (TABS) have emerged as energy efficient ways for cooling and heating of buildings (Gwerder et al 2008, Olessen 2012). Different names are given to the system; thermally activated building systems or parts or components (Weber 2005), concrete core conditioning (Koschenz, 1999), thermo active core systems (TACS). In Dutch, the name betonkernactivering or bouwdeelactivering is used primarily. TABS uses the capacity of the massive floor or wall to cool or heat the building. Plastic pipes are positioned between the reinforcement and concrete is poured over. Depending on temperature difference between supply and room, the concrete is absorbing the heat in the room or heating the room. The temperature span is near comfort temperature, approximately between 18 and 25 ^{o}C. Precaution has to be taken in cooling mode, since

condensation on the surface has to be prevented. For ventilation Hybrid ventilation is a energy efficient solution (Delsante and Vik 2000). Hybrid ventilation has access to two ventilation modes (natural ventilation and mechanical ventilation) in one system and as such exploits benefits of both modes (Heiselberg 2002). Advanced hybrid ventilation technology fulfils the high requirements on indoor environmental performance and the increasing need for energy savings by optimizing the balancing between indoor air quality, thermal comfort, energy use and environmental impact (Heiselberg 2002). Natural ventilation is difficult to control in winter therefore often hybrid ventilation is chosen as a solution for ventilation with mechanical supply in winter. For the generation of heat or cold heat pumps are preferred because they can use low temperature energy sources from the environment. To create a good energy efficiency performance for a heat pump it is necessary to have a small difference in temperature level of the energy source and the needed heat or cold. This is best done by using low temperature heating and high temperature cooling systems. For such systems large surface areas are required to exchange enough energy to the room of a building. TABS are a good solution because their large surface area's to exchange heat or cold allows to transform the generated small temperature differences being generated by the heat or cold generation. Therefore, Hybrid ventilation and TABS in combination with a heat pump is often used in present buildings. This system uses the building mass to heat and cool the building. Water filled pipes are embedded in the core of the concrete slab. Water near comfort temperature is used. Slow accumulation of concrete results in small adaptation possibilities in order to meet the needs of users. Much research has been done in simulations of TABS still for us the questions remains if simulations are enough especially with systems like TABS. One of the possible drawbacks with this system is that the use of small temperature differences results in low thermal driving forces to compensate for locally appearing unexpected cold air flow through cavities cause by building defects such as "cold bridges", insufficient insulation on specific details or unexpected behaviour of occupants. Such aspects do not occur in simulations but only in real life situations. As such a field test gives much clearer picture of the practical resulting comfort of such systems compared to simulation tests which are often used to look into the expected behaviour of such innovative systems.

2 MEASUREMENTS IN 3 OFFICES

Human thermal comfort is affected by a number of parameters, namely according to Franger's comfort equation, and the respective standard EN ISO 7730 (ISO 2005). Underlying the resulting predicted mean vote (PMV) or the predicted percentage dissatisfied (PPD) was calculated based on the six parameters: air temperature, radiant temperature, relative air velocity, humidity, clothing and activity. In three offices measurements were done according to NEN-EN-ISO 7726 (ISO 1998) to determine the personal thermal comfort of occupants in relation to the six above mentioned parameters. Measurements were done in one office space in each of the three selected recently completed office buildings in the Netherlands. Table 1 provides an overview of the used measurement equipment.

Table 1: Used measurement equipment

Type of measurement	Equipment	Brand	TU/e ID	Range
Temperature	Sensor	EE80	2335	0° - 40°C
Radiant temperature	Black sphere PT100	-	612	-100° - 300°C
Relative humidity	Sensor	EE80	2335	0 - 100%
Air velocity	Omni speedometer	Sensor HT428	708	0.05 - 5 m/s
CO_2 -concentration	Sensor	EE80	2335	0 - 5000 ppm
Log data	Data logger 2F8	Grant 2020 series	1816	n.v.t.

Process data	Laptop	Dell Latitude C840	1629	n.v.t.

Besides the PPD extra attention was given to the occurrence of draft. Roughly, it is advised to keep the average air speed lower than 0.15 m/s. However, there is also a relation between the air speed and turbulence intensity. Fanger determined the relation between draught and persons dissatisfied:

$$DR = (34 - T_a).(\bar{v} - 0.05)^{0.62}.(37.\bar{v}.Tu + 3.14) \quad (1)$$

$$Tu = \frac{\sigma}{v} * 100 \quad (2)$$

Where:

DR=	Draught rate	(%)
v=	average air speed	(m/s)
Tu=	relative turbulence intensity	(-)
σ=	standard deviation of fluctuations in air speed	(-)

In offices as a standard 15% DR is recommended.

Building A

Users	170
Completed	2011
Floor space	14.000 m²
Ventilation	Hybride
Heating/cooling	TABS

This is an environmental research building, see Fig. 1, inspired by the Cradle to Cradle (C2C) principles the design and construction of the building was taken one step further than most sustainable buildings built to date in the Netherlands. The designers Claus and Kaan Architects were instructed to keep as close to this philosophy as possible and had to meet a number of stringent material specifications. For example the hull is made of durable concrete without any artificial additives and no sealant, solvents or such like were used in the process. Using materials such as wood, glass, steel, flax, ground limestone and granular debris creates a streamlined building with an open and natural appearance. Efforts towards energy efficiency cover two areas: reducing consumption and sustainable production, both of which lead to a reduction in CO2 emissions. Hybrid ventilation system was installed with natural supply and mechanical exhaust. Heating is delivered through concrete core activation.

Figure 1. Building A with the setup of the measurement equipment

Building B

Users	150
Completed	2009
Floor space	6.500 m²
Ventilation	Mechanical
Heating/cooling	Thermal Activated building Systems

This is a municipality building of a middle seized town in the Netherlands, see Fig. 2. It has an electrical heat pump with an Aquifer Thermal Storage system and Thermal Activated Building System integrated in the floor for heating and cooling.

Figure 2. Building B with the setup of the measurement equipment

Building C

Users	600
Completed	2000
Floor space	3.700 m²
Ventilation	Mechanisch
Heating/cooling	Thermal Activated Building Systems

This building is an office of one of the biggest building services contracting companies in the Netherlands, see Fig. 3. It also as an electrical heat pump with Aquifer Thermal Energy Storage and Thermal Activated building Systems for heating and cooling.

Figure 3. Building c with the setup of the measurement equipment

Users opinion is of great importance. First of all, perception of indoor climate is important for determining whether users are comfortable. Secondly it is important how the interaction with the system is experienced. The users were asked to rate different aspects of the comfort. Distinction was made between summer and winter. The questionnaire used is based on the

validated list which has been developed in the Health Optimisation Protocol for Energy-efficient Buildings research (Hoope 2001)

3 RESULTS

3.1 Measurements

Building A

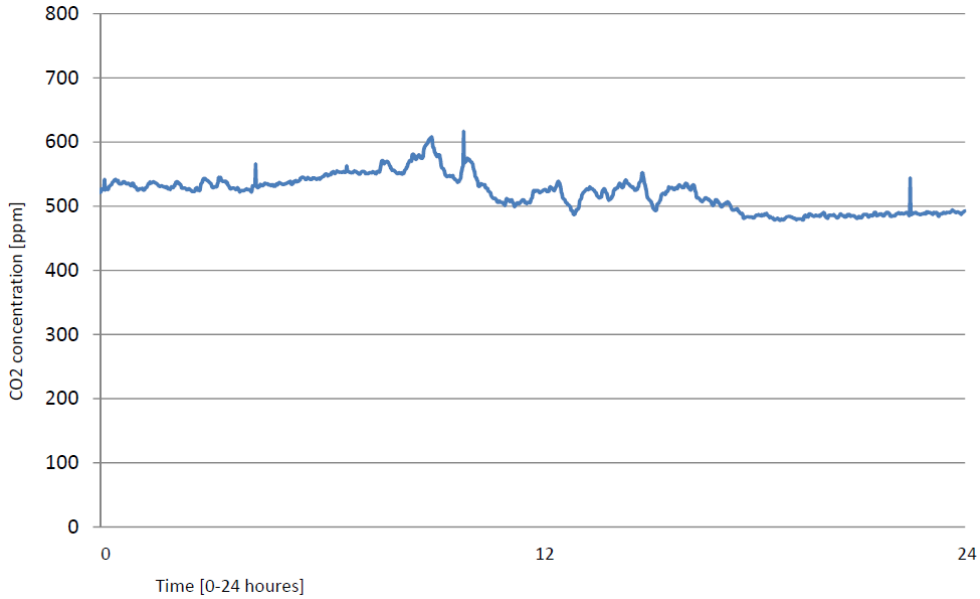

Figure 4. CO_2 concentration during one working day in office A

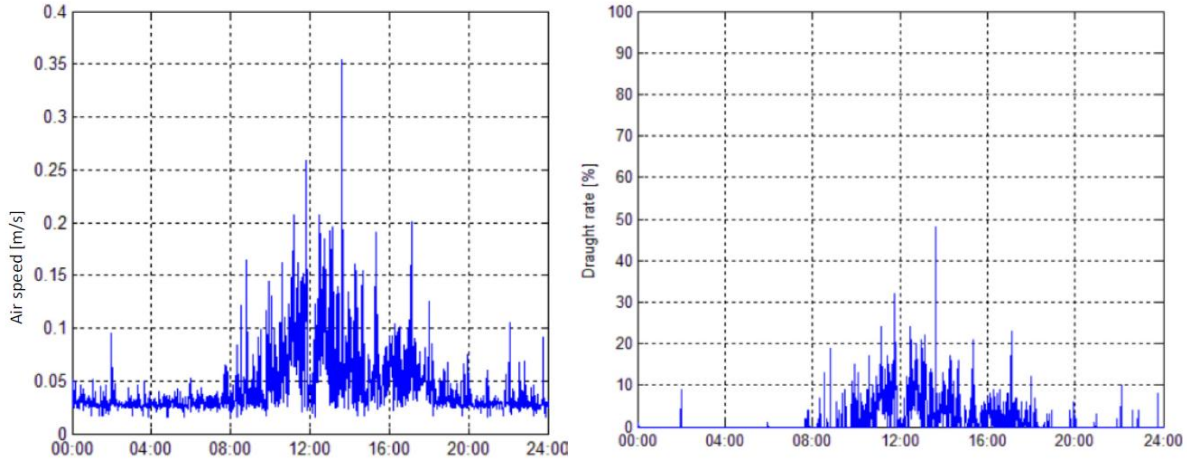

Figure 5. Air speed and draught rate in office A

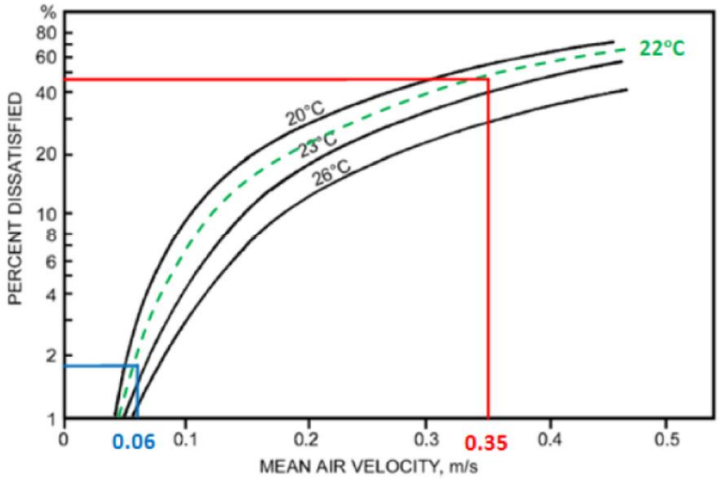

Figure 6. Percentage dissatisfied based on air temperature and minimum and maximum mean air velocity in office A

Building B

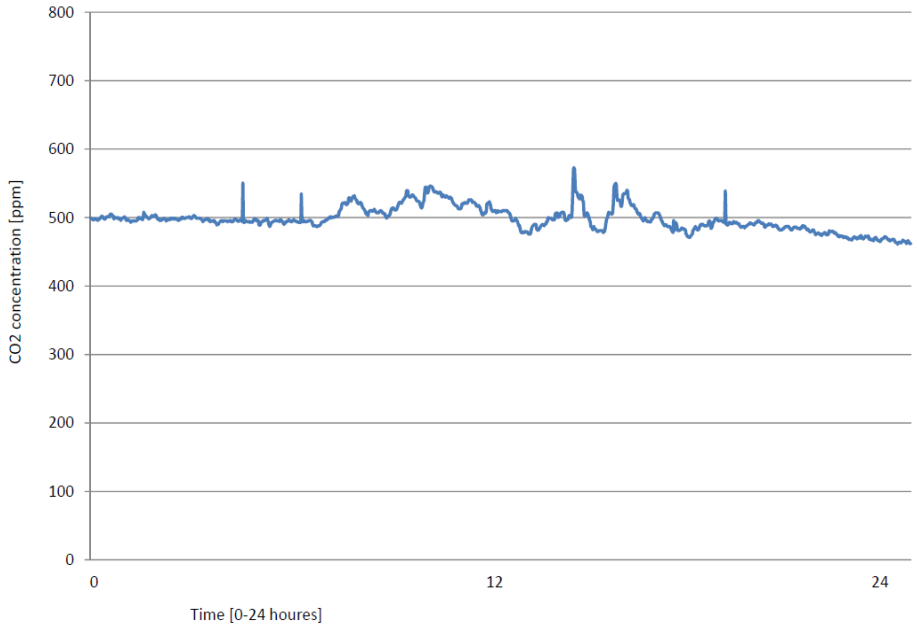

Figure 7. CO_2 concentration during one working day in building B

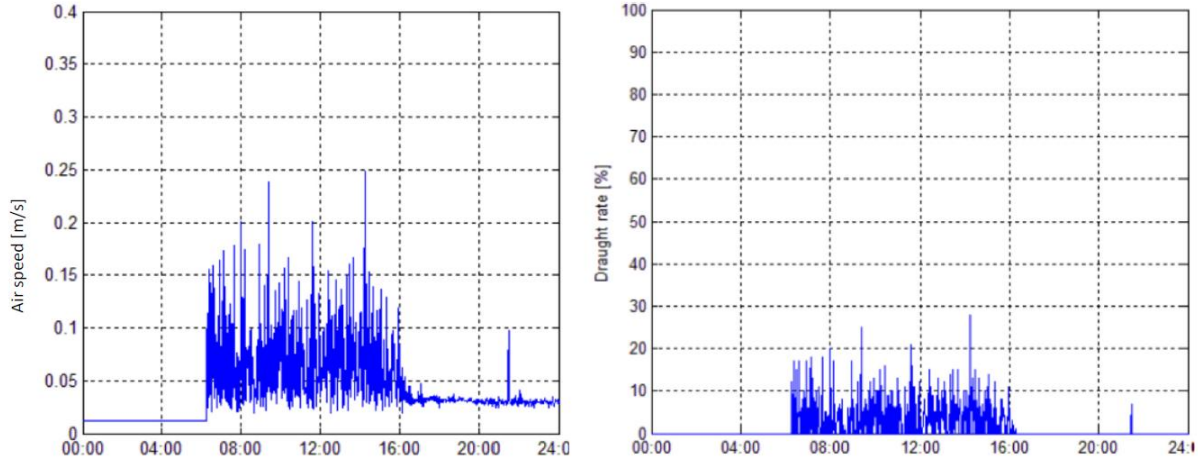

Figure 8. Air speed and draught rate in office B

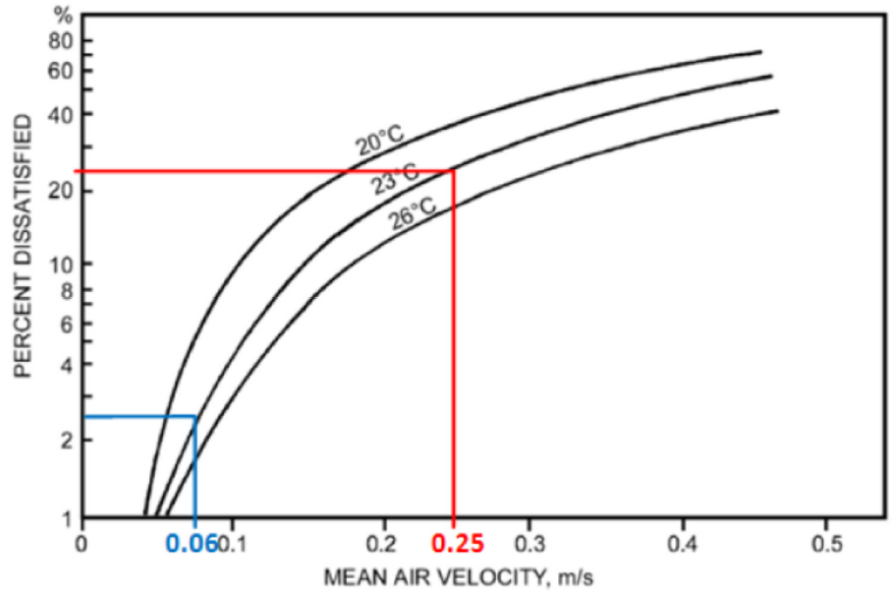

Figure 9. Percentage dissatisfied based on air temperature and minimum and maximum mean air velocity in office B

Building C

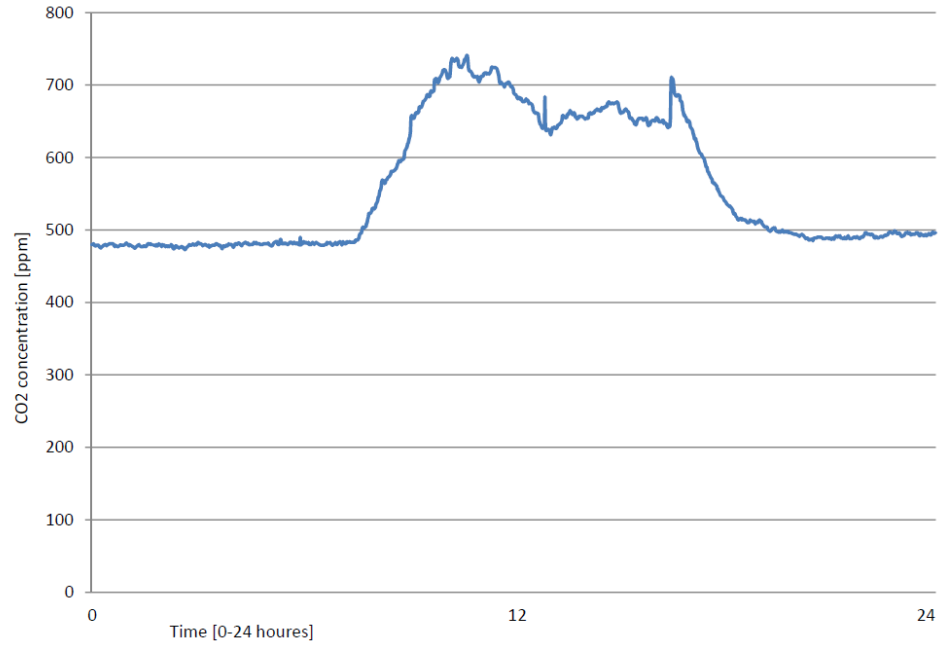

Figure 10. CO_2 concentration during one working day in building C

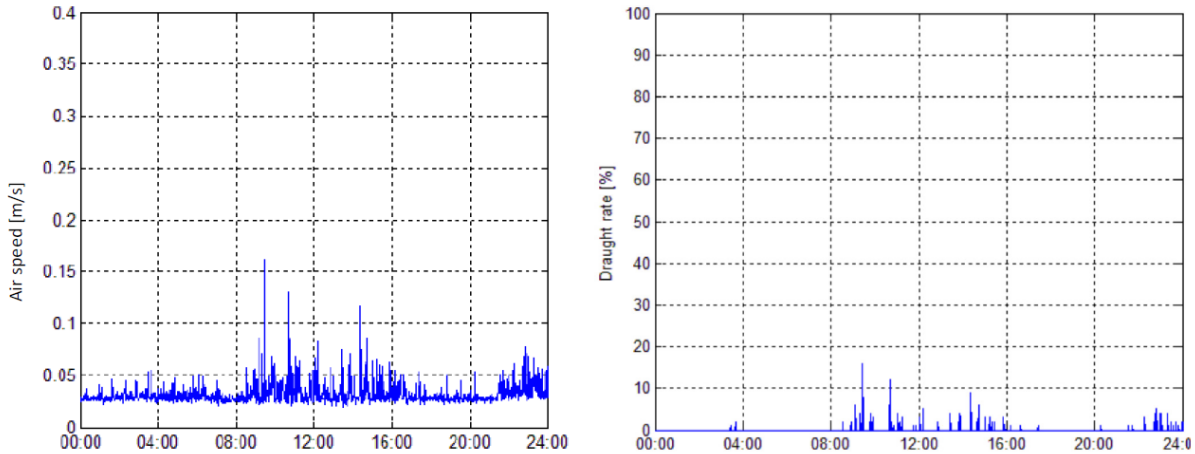

Figure 11. Air speed and draught rate in office C

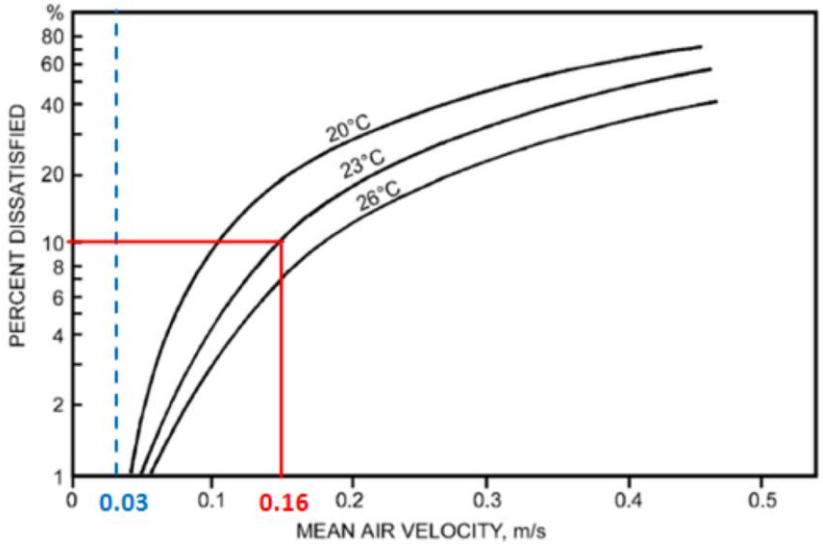

Figure 12. Percentage dissatisfied based on air temperature and minimum and maximum mean air velocity in office C

3.2 Questionnaires

The response for the buildings was nearly the same: 15(A), B(14) and C (14) and represent around 70% of the people in the direct area of the measurements.

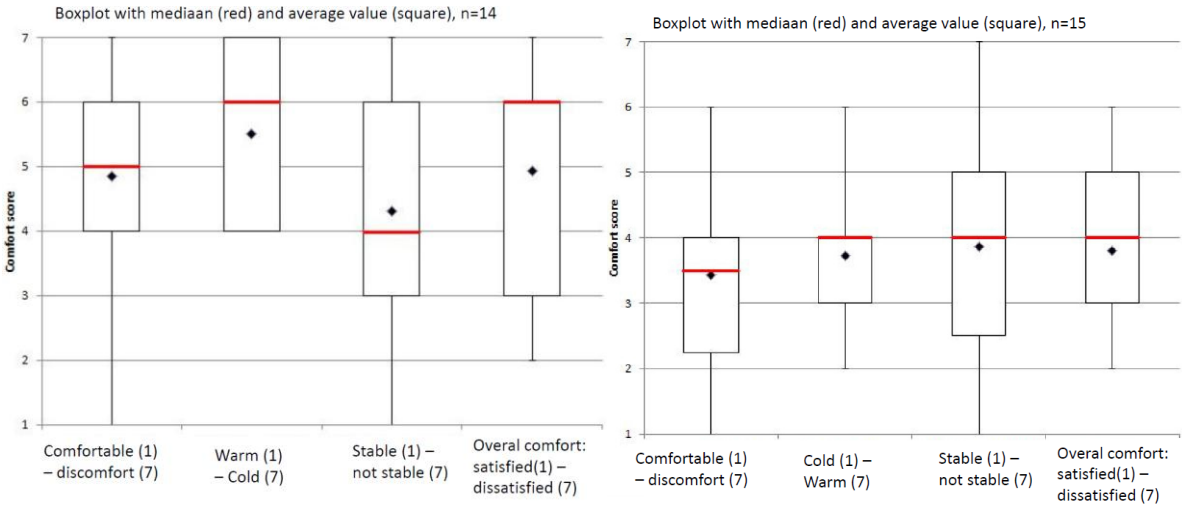

Figure 13. Office building A results winter and summer questionnaires

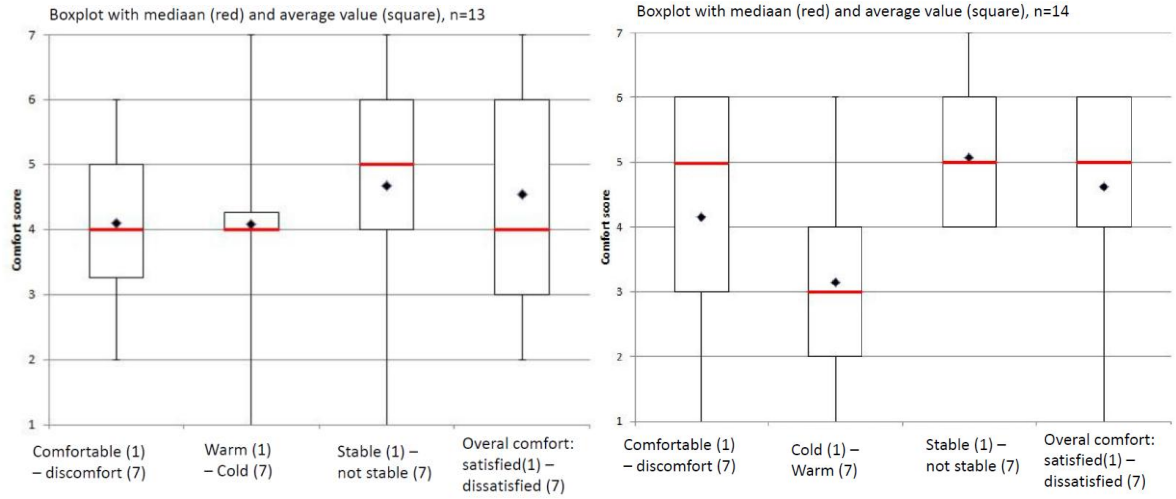

Figure 14. Office building B results winter and summer questionnaires

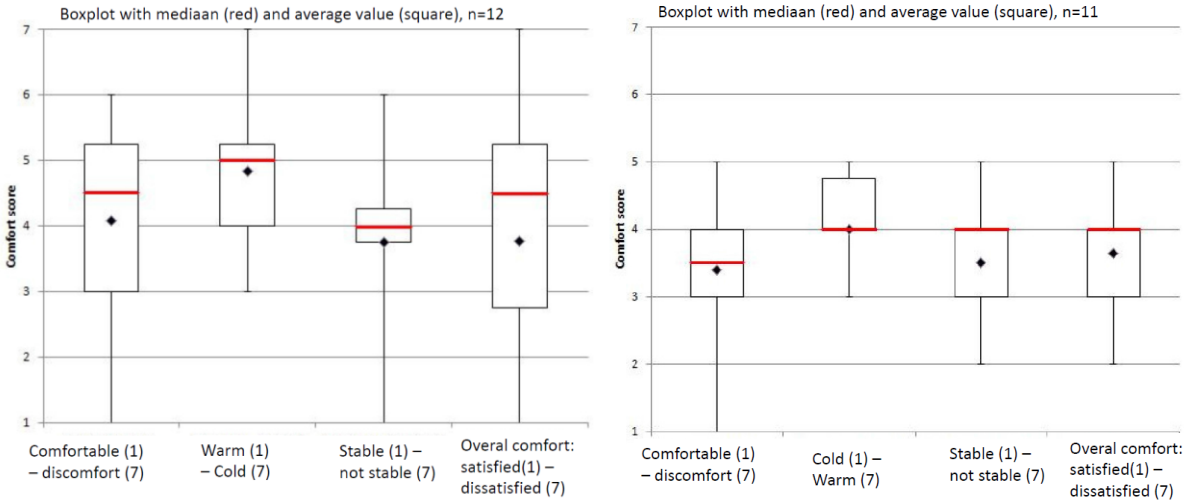

Figure 15. Office building C results winter and summer questionnaires

4 CONCLUSIONS

Air Quality

A relatively good indicator for the level of ventilation and indoor air quality is the CO2-concentration. The results presented in Fig. 4, 7and show that there are very low CO2 concentration levels within the measured office buildings. Definitely the mechanical ventilation does its work rather well.

Air speed

The figures 5, 8 and 11 give the measured air speed in an office. Guidelines give a maximum air speed of 0.15 m/s (Fanger 1970). The figures show that only in one case, office C, the air speed is always within these boundaries.

Draft

From Fig. 5, 8 and 11 it can be concluded that building C has an exceptional low draft rate, were as in building A and B the draft rate is around on aravege 10%.

PPD

PPD (predicted percentage dissatisfied (ISO 2005)), is calculated using metabolic rate of 65 W/m2 and clothing value of 1. From Fig. 6, 9 and 12 it is concluded that especially in building A there is unacceptable high draft rate where also building B shows a high draft rate.

Questionnaires

The results of the questionnaire for respectively temperature, stability of temperature, air speed, humidity, freshness and smell of the air showed on average not a very high rated satisfaction (on average around 4 on a scale from 1 (good) to 7 (bad).

Figure 13 to 15 show that the temperature is not quite acceptable during the winter (average scores resp 5.5, 4 and 4.8 on a scale from 1 to 7). The air speed stability, with an average score of 4 is also considered moderate comfortable.

Measurements and questionnaires provided an insight in the effects of TABS on the thermal climate itself and the individual perception. The following conclusions can be drawn from the measurements: TABS can assure an acceptable indoor temperature. Precaution has to be taken with the Hybrid Ventilation integration in the building façade. Since for TABS supply temperatures close to comfort temperature are used, there is little room for mistakes. Cold air

from thermal bridges and natural supply ventilation cannot be counterbalanced by TABS. In the examined building, users keep ventilation grilles shut in order to prevent cold supply air from causing discomfort. However, this results in a climate where no planned ventilation takes place. The result of the measurements showed that extra care should be taken to the quality of detail finishing of the outer walls and facades. Often their quality is not as good as expected with major draw backs to the comfort of occupants.
Simulations are often used to study the influence of different aspects related to the use of TABS (Koschenz 1999). These simulations use per example the TRNSYS building simulation program (TRNSYS 2005), in which the Resisantance-Capacitance (RC) modelling approach (Weber and Johannesson 2005) for TABS has been gradually developed (Olesen et al 2006, Lehman et al 2007, Gwerder et al 2008, Ma et al 2013). However this field study, as well as an earlier field study (van Schijndel 2006) showed that in practice TABS encounter many in simulation unforeseen aspects which are sometimes critical for its functioning. Also in the study by Rijksen et al (2010) they found deviations between measurements and simulations due to to malfunctioning of some TABS. This because, especially with TABS the margin for the driving heating or cooling capacities are limited. Therefore the installed capacities should be not too much optimized based on simulation results but a safety factor should be applied to install some more capacity to be able to deal with practical imperfections.
The measurements and questionnaires provided an insight in the effects of TABS on the thermal indoor climate and individual perceived perception. The following conclusions can be drawn from the measurements: TABS itself can assure an acceptable indoor environment what temperature and indoor quality.

5 REFERENCES

De Carli, M., Hauser, G., Schmidt, D., Zecchin, P., Zecchin, R. (2003), An innovative building bsased on active thermal slab sysgtems. In: Proceedings to the 58th ATI National Conference on Building Physics, 9-12 September 2003, San Martino di Castrozza, Italy

Delsante, A., Vik, T.A.(editors), (2000) Hybrid Ventilation, State-of-the-art review, IEA-ECBCS Annex 35 HybVent report, http://hybvent.civil.auc.dk/puplications/sotar.pdf

EN ISO 7730, 2005, Ergonomics of the thermal environment – analytical determination and interpretation of thermal comfort using calculations of the PMV and PPD indices and local thermal comfort criteria, CEN (European Committee for Standardization)

Fanger, P.O.(1970), Thermal comfort, PhD Thesis, McGraw-Hill Book Co.

Gwerder, M., Lehmann, B., Tödtl, J., Renggli, F. (2008), Control of thermally-activated building systems (TABS), Applied Energy 85: 565-581

Heiselberg, P. (editor), (2002), Principles of Hybrid Ventilation, Aalborg University, Aalborg, Denmark, august 2002, http://hybvent.civil.auc.dk/

HOPE, 2001, Health Optimisation Protocol for Energy-efficient Buildings: Pre-normative and socio-economic research to create healthy and energy-efficient buildings, EU: NNE5-2001-00032

ISO, 1998, Standard 7726, Ergonomics of the thermal environment – Instruments for measuring physical quantities, second edition 1998.

Koschenz, M.(1999), Interaction of an air system with concrete core conditioning, Energy and Buildings 30(1999)139-145

Lehman, B., Dorer, V., Koschenz, M. (2007), Application range of thermally activated building systems tabs, Energy and Buildings 39: 593-598

Ma, P., Wang, L., Guo, N. (2013), Modeling of TABS-based thermally manageable buildings in Simulink, Applid Energy 104: 791-800

Olesen, B.W., Carli, M. de, Scarpa, M., Koschenz, M., (2006). Dynamic evaluation of the cooling capacity of thermo-active building systems, ASHRAE transactions 112(1): 350-357

Olessen, B.W.(2012), Using Building Mass to Heat and Cool, ASHRAE Journal February 2012: 44- 52

Rijksen D.O., Wisse C.J., Schijndel A.W.M.van, (2010), Reducing peak requirements for cooling by using thermally activated building systems, Energy and Buildings 42: 298-304

Schijndel, H.M. van, (2006), Individual Comfort with Termally Activated Building Systems, MSc-thesis, june 2006, Technische Universiteit Eindhoven

TRNSYS 16, Transient System Simulation Program, SEL, University of Wisconsin USA, TRANSSOLAR, Stuttgart, 2005.

Weber, T., G. Johannesson, G.(2005), An optimized RC-network for thermally activated building components, Building and Environment 40: 1–14.

HEAT RECOVERY VENTILATION WITH CLOSED-LOOP GROUND HEAT EXCHANGE

Bart Cremers

Zehnder Group Nederland
Lingenstraat 2
8028 PM Zwolle, The Netherlands
bart.cremers@zehndergroup.com

ABSTRACT

In this article, it will be shown how heat recovery ventilation with closed-loop ground heat exchange performs in practice, in a residential building in Nijeveen, The Netherlands. A state diagram is presented to explain when heat recovery and/or ground heat exchange is used during the year.
The correlation between ground temperatures and air temperatures shows how the ground preheats the incoming outdoor air from -13°C to 0°C in winter, and precools the incoming outdoor air from 30°C to 23°C in summer. After preheating or precooling, the outdoor air enters the ventilation unit where heat is recovered (only in winter) and the air is distributed to the rooms.
The benefit of heat recovery in winter is expressed in terms of avoided heating relative to ventilation without heat recovery and results in 3899 kWh. The benefit in summer is expressed as free cooling, with reference to the indoor temperature, and results in 950 kWh.

KEYWORDS

residential heat recovery ventilation, ground heat exchange, monitoring, seasonal performance factor, bypass

1 INTRODUCTION

Ventilation of modern residential buildings is often combined with additional technologies to bring fresh air into the building in the most comfortable and energy efficient way. As such, balanced ventilation with heat recovery can be combined with ground heat exchange. Because the ground temperature reacts slower than the air temperature, often the ground can be used to preheat the incoming outdoor air in winter, and precool the incoming outdoor air in summer. In this article, the results will be shown how balanced ventilation with closed-loop ground heat exchange performs in practice, in a residential building in Nijeveen, The Netherlands.

2 TWO TYPES OF GROUND HEAT EXCHANGE

Two variations of ground heat exchange systems exist. First, an open system where outdoor air is led through pipes in the ground, before entering the building and going through the heat recovery unit. For a description of the open system, see the references (Cremers, 2012).

Second, a closed system (see fig. 1) where outdoor air is led through an air-liquid heat exchanger before entering the heat recovery unit. The liquid is a glycol-water mixture that is flowing through a tube. Most part of the tube is horizontally installed in the ground (ground collector) where the liquid picks up the heat (or cold) from the ground (Vollebregt, 2011 and Stege, 2012).

Figure 1: Representation of the ventilation system. Green: outdoor air; Red: supply air; Yellow: extract air; Brown: exhaust air; Grey: the ground collector with glycol-water mixture.

Closed-loop ground heat exchange is preferred, because it is easier to install, and less prone to damage because of natural settling of the ground or digging into the ground after installation. The closed-loop system also avoids potential microbial growth problems. Last, closed-loop ground heat exchange needs less area as it can be installed in a meandering pattern.

3 EXPLANATION OF THE TECHNOLOGY

Balanced ventilation with heat recovery and ground heat exchange is explained using fig. 2. The horizontal axis shows the outdoor temperature. The black line is the desired indoor temperature. For heat recovery ventilation, the green line represents the supply temperature of the fresh air that enters bedrooms and living room via supply air grilles.

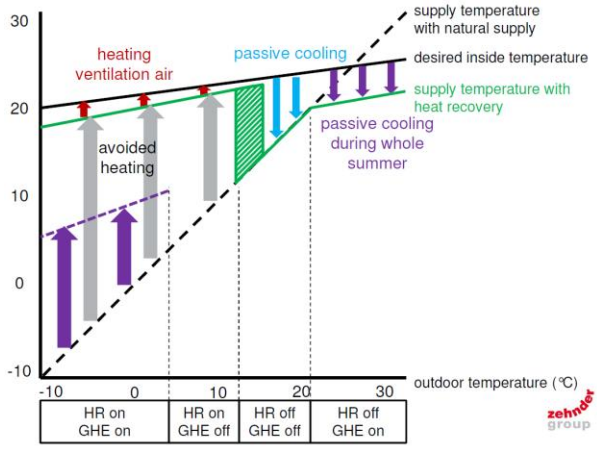

Figure 2: Schematic principle of balanced ventilation with heat recovery (HR) and ground heat exchange (GHE).

In winter, the necessary heating to bring the incoming fresh air to the desired temperature (red arrows) is low. The avoided heating when compared without heat recovery is shown by the grey arrows. This saves costs for heating the internal climate. Ground heat is used when possible to keep the heat recovery unit free of condensation and ice so that the mass balance is maintained.

Under certain conditions, the bypass is opened automatically to prevent too high supply air temperatures. Now, the fresh air enters the rooms without energy exchange. The green line follows the dashed black line. This is called free cooling as the supply air temperature is below the indoor air temperature (blue arrows).

In summer, the ground temperature is lower than the outdoor air, and even lower than the indoor temperature. Thanks to the ground heat exchange, free cooling is therefore available throughout the summer and this raises the comfort level in every room of the house (purple arrows).

Ground heat exchange is not used for outdoor temperatures between 7°C and 23°C, but these values can be changed according to the location.

4 THE MONITORED HOUSE

In Nijeveen (The Netherlands), the ventilation of a residential building has been monitored for a full year. For the monitoring period, the heat recovery ventilation had a fixed amount of fresh air of 220 m3/h. The closed loop ground heat exchange consists of the unit ComfoFond-L (positioned next to a heat recovery unit) and the ground collector. In this project the ground collector is a 100 m long polyethylene tube with an outer/inner diameter of 25/17 mm. The collector is installed at a depth of 1.20 m in the ground and filled with a glycol-water mixture.

The collector tube is going from the unit in the attic straight down to the basement floor. At the front door of the house it is entering the ground and runs around the house to the backyard. In the backyard it makes a few turns and goes back along the same side of the house and up to the attic again. It is advisable to respect a minimal tube spacing of 60 cm, but in this project the distance is 30 cm in some segments.

Ground heat exchange is automatically switched on/off by a pump in the ComfoFond-L unit. In this project, the pump is running for outdoor temperatures below 7 °C and above 16 °C. The fresh air is distributed throughout the house by round metal ducts branching off to the various rooms. Stale air is returning from kitchen, toilets and bathroom to the heat recovery unit again before being exhausted to the outside.

Flow rates, temperatures and settings of the ventilation system have been collected with an interval of 1 minute, and afterwards 1 hour averages are calculated to give statistical results for July 2011 until August 2012. In spring 2012, some data is missing because of hardware problems with the monitoring equipment.

5 VENTILATION WITH GROUND HEAT EXCHANGE IN PRACTICE

In fig. 3, the ground temperature at 1.20 m depth and the outdoor air temperature are shown. The dampening effect of the ground is visible. At this depth, the ground temperature varies between 5 and 16 °C for outdoor air temperatures between -15 and 35 °C.

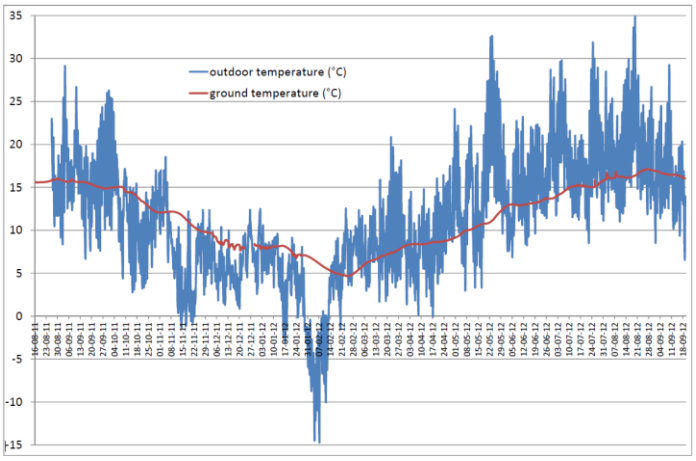

Figure 3: Ground temperature (1.20 m depth) and outdoor air temperature.

There are four possible states for this ventilation system (see also fig. 2), depending on whether heat recovery (HR) is used and/or ground heat exchange (GHE) is used. Fig. 4 shows that in the cold season heat recovery is used, with ground heat exchange whenever the outdoor air was below 7 °C (mostly at night, and during cold days). In the warm season heat recovery is not used (ventilation with bypass open), and for outdoor air temperature higher than 16 °C the ground cools the fresh air even further (afternoons and warm nights). In this project with the mild Dutch sea climate, ground heat exchange is used during 55% of the monitored time.

The preheating and precooling effect of the ground heat exchange is shown in fig. 5a. For outdoor temperatures lower than 7 °C, the fresh air is preheated by the ground. For outdoor temperatures higher than 16 °C, the fresh air is precooled by the ground.

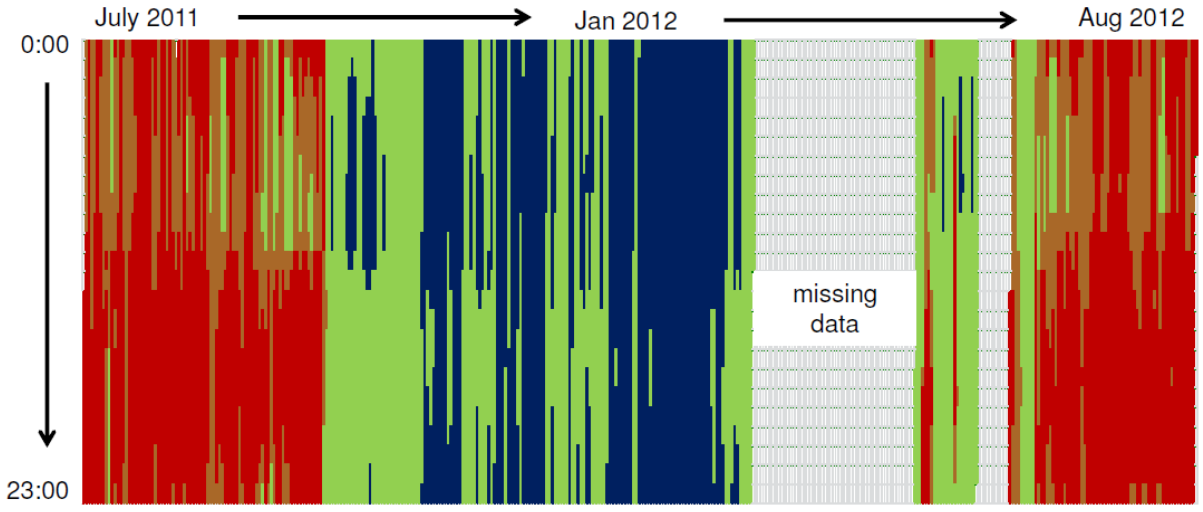

Figure 4: State diagram. Blue: HR on, GHE on; Green: HR on, GHE off; Orange: HR off, GHE off; Red: HR off, GHE on.

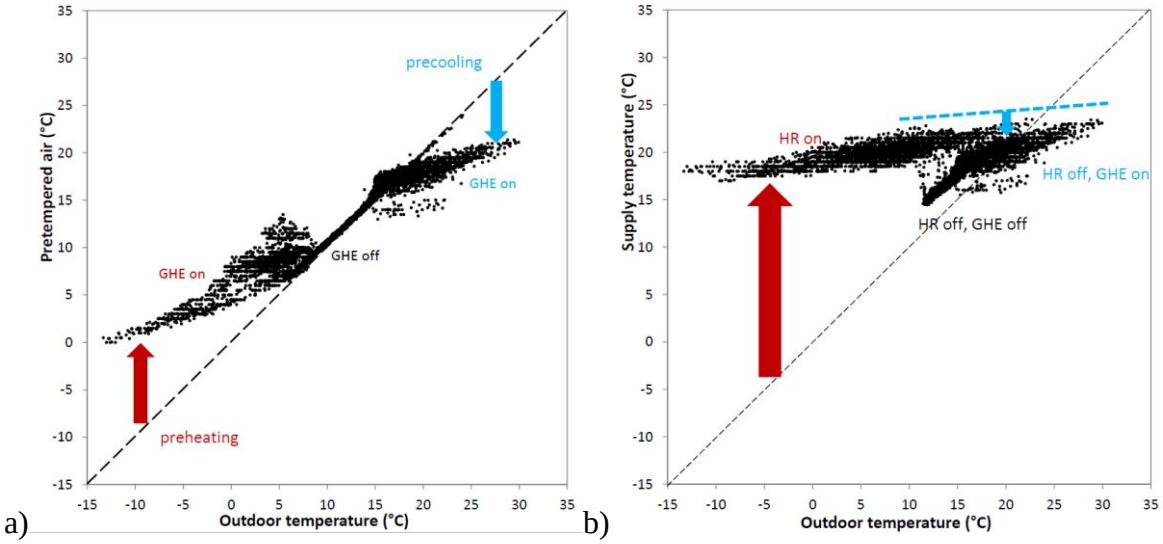

Figure 5: a) Air temperature after ground heat exchange and b) supply temperature as a function of outdoor air temperature.

Optimal performance would be that the air temperature is preheated in winter to 5°C (minimal ground temperature) and precooled in summer to 16°C (maximal ground temperature). In this project the air temperature is minimally 0°C and maximally 21°C. Detailed analysis has shown that the performance of the ground heat exchange could be improved with better positioning of the ground collector. The collector should be laid out more evenly in the ground, respecting a minimum distance between two tubes of 60 cm.

After the heat recovery unit, the fresh air is increased in temperature when the heat recovery is on (see fig. 5b). Even with outdoor temperatures as cold as -13 °C, the fresh air is brought to the living rooms at a comfortable 17 °C. This reflects the huge energy saving capacity, as the heat demand for ventilation is decreased enormously. In fact, the average heat recovery efficiency is measured as 92% over the entire heat recovery season.

If the heat recovery is off, the ground heat exchange helps to keep the fresh air temperature low, so that the supply temperature is always lower than the indoor temperature. This means free cooling for the whole warm season, and not only during cool summer nights. The free cooling helps to keep the cooling load of the house low in summer, in the same way as proper shading equipment.

6 ENERGY SAVING

The performance of the ventilation system in terms of energy is given in table 1. The seasonal performance index SPF is calculated as the energy gain divided by the energy consumption, both inside and outside the heat recovery season.

The energy saving of the heat recovery is calculated in terms of avoided heating. The reference situation is that fresh air comes in at the same temperature as the outdoor air. The avoided heating thanks to heat recovery is calculated using the difference between supply air and outdoor air and the actual air flow rate. This saving is achieved using electrical energy by the fans of the heat recovery unit and the pump of the ComfoFond-L ground heat exchanger in the heat recovery season.

With heat recovery off, the free cooling for the house is calculated using the difference between indoor temperature and supply temperature and the actual flow rate. This free cooling is again achieved using electrical energy by the fans of the heat recovery unit and the pump of the ComfoFond-L ground heat exchanger outside the heat recovery season.

For this monitored installation, the values of the SPF inside en outside heat recovery season of 7 and 2 respectively are quite low compared to the reported 17 and 8 (Cremers, 2012). This is because the fans and the pump take more energy. The first due to from resistance in the air distribution system and the second due to a higher pump speed setting than necessary.

Table 1: Annual energy benefit of heat recovery ventilation and seasonal performance factors

	Energy gain	**Electrical consumption**	**Seasonal Performance Factor SPF**
Avoided heating load	3899 kWh	593 kWh	7
Free cooling load	950 kWh	408 kWh	2

7 CONCLUSIONS

The combination of a balanced ventilation unit with heat recovery and ground heat exchange can provide ventilation which is both energy efficient and comfortable.

In the cold season, the ground heat exchange in combination with heat recovery ensures that fresh air is brought into the rooms in a stable and comfortable way, whilst keeping the heating demand for ventilation low. In the warm season, the ground heat exchange ensures free cooling for the whole summer (not only cool summer nights), keeping the cooling load of the house low. Along with proper shading measures in the house, the ventilation system with ground heat exchange also prevents overheating of the house.

8 REFERENCES

Cremers, B.E. (2012). Long term monitoring of residential heat recovery ventilation with ground heat exchange, REHVA Journal, August 2012, 41–46.

Stege, C. ter (2012). Geen bevriezing of oververhitting bij ventileren met aardwarmte (in Dutch), *Gawalo*, November 2012, 14–17.

Vollebregt, R. (2011). Koelen zonder energiegebruik door zomernachtventilatie (in Dutch), *Verwarming & Ventilatie*, May 2011, 268–271.

IMPACT OF CLIMATE CHANGE ON A NATURALLY NIGHT VENTILATED RESIDENTIAL BUILDING, GREECE.

Theofanis Psomas[1], Peter Holzer[2], Mattheos Santamouris[3]

1 Danube University, Department for Building and Environment
Dr. Karl Dorrek Str. 30
Krems, Austria, th.psomas@gmail.com

2 Institute of Building Research and Innovation
Luftbadgasse 3/8
Vienna, Austria

3 National and Kapodistrian University, Physics Department, Group Building Environmental Research
Panepistimioupolis, Zografou
Athens, Greece

ABSTRACT

The climate of Greece is typical Mediterranean with wet, cool winters and hot, dry summers. The temperature range is on average between 5°C to 35°C without many extreme temperatures and weather events. The cool sea breeze on the islands makes summer conditions milder. According to researchers and assessment reports of the United Nations climate change is inevitable in the 21st century. Regional climate models related to Greece show low uncertainties. As far as Greece is concerned, this climate change will be related to an increase in the ambient surface temperature and to a decrease in the annual precipitation. Wind patterns show that they will not change significantly. No significant changes are expected also for global radiation.
In this paper a typical single family two storey detached residential building for five occupants, in the hottest area of Greece – Rhodos island, is thermally optimized with various processes – strategies and the effect of the night natural flush ventilation. The cooling and heating demands of the building are less than 15 kWh/m²/yr (nearly zero). For the dynamic thermal simulation and performance of the examined building, the TAS software has been used. The thermal simulations for this paper run with the most updated weather data from Meteonorm software. In addition thermal demands of the same building are checked with the use of future data from the same source, for different emission scenarios, until 2050, per decade. In general, the A1B medium – emission scenario, which is the most pessimistic for the area, assumes rapid economic growth, increase of the population and social interactions until the middle of the century and more efficient technologies with a balance across all sources. The heating and cooling demands of the future compared with the present situation. Finally new night ventilation patterns are checked for optimization purposes for the A1B emission scenario at the end of the examined period.

KEYWORDS

single family building, building performance simulation, night ventilation, climate change, Mediterranean – Greece.

1 INTRODUCTION

The built environment offers the largest potential of cost – effective energy and greenhouse gas emission savings [1]. In Greece the continually increasing building sector, before the economic recession of 2010, was responsible on average for 30% to 35% of the greenhouse gas emissions and for 35% to 40% of the total energy consumption, mainly through electricity [2]. The Greek households consume more energy (mainly electricity) than the households

from countries with similar Mediterranean climate and weather, like Portugal, Spain, Cyprus and Malta [3]. The greatest percentage of the buildings constructed before 90's without insulation and they are single family or multifamily buildings. Passive systems for heating or cooling and bioclimatic design are not part of the construction process. The main reason for these results is the absence, until 2010 and TOTEE/KENAK, of modern non conservative legislation [4].

There is no doubt that the energy performance of a building is straight related with the climate of a region [5]. The great advantage of Greece compared to the other countries is the mild Mediterranean climate that helps to relatively balance energy needs compared to northern countries [6]. In general, the year may be mainly divided into two seasons, the cold and rainy winter period, from November to the middle of April and the warm, drought period from the middle of May to October. In addition, the winter weather is often interrupted by sunny days. Rains in Greece even during the winter period, do not last for many days. During the hot and drought period the weather is constant, the sky is cloudless and it never rains, except for a few intervals of intense, short – lasted storms. Finally the high temperatures are tempered by the cool sea breeze of the northern winds blowing in the sea. Spring usually does not last long.

This advantage of Greece will not be very important as it approaches the new world, the world of the "climate change". According to researchers and assessment reports of the United Nations (IPCC) climate change is unequivocal [7]. During the last 150 years, 129 out of a total 274 days with temperature over 37 °C were in the period 1998 – 2007 in Greece [8]. Also, in the same period there were 19 extreme heatwaves events out of a total of 52 in the last 150 years. The increased number of events was accompanied with an increase in the intensity and the duration. The regional climate models related to Mediterranean Sea and Greece show low uncertainties [9]. As far as Greece is concerned, this climate change will be related to an increase in the ambient surface temperature and to a decrease in the annual precipitation [10]. Wind patterns show that they will not change significantly. No significant changes are expected also for global radiation. These changes would have serious impacts on local communities, on the environment – ecosystems, on the agriculture and tourism. There is no doubt that this climate change will have also a serious impact on building performance and occupant comfort. This situation will affect mainly low income households, especially during the period of the economic recession. Results of assessment reports related to possible emission greenhouse gas future scenarios.

This paper deals with the subject how the climate change will affect the thermal demand of an efficient single family detached building, like the nearly zero energy building (cooling and heating demand under 15 kWh/m^2) in the hottest area of Greece, Rhodos island (zone A). The thermal performance of the building is optimized with the use of the extra movable shadings strategy during the mornings and the natural night ventilation strategy during all year. It is goal is to display the importance of design not just for today but for the whole life cycle of a building, through representative dynamic future weather data. Finally different ventilation strategies – patterns are simulated for the worst scenario in 2050.

For this paper three emission scenarios is used (A1B, A2, B1). In general, the A1B emission scenario assumes rapid economic growth, increase of the population and social interactions until the middle of the century and more efficient technologies with a balance across all sources. The A2 emission scenario family assumes a preservation of the local structure and economic development, an increase in population rates and a smaller increase in technological changes. The B1 scenario assumes similar population pattern as the A1 family scenario and social and environmental sustainability. Economic structures focus on services and information and technologies are more efficient [11]. The warming at the end of the 21st century for Greece is in range of about 3 °C to 6 °C for the A2, 3 °C to 5.5 °C for the A1B and 2.5 °C to 4.5 °C for the B1 scenarios [10]. Also with A2 and A1B scenarios is estimated a

decrease in precipitation up to 30% in southern Greece. These values are more pessimistic than the average Mediterranean values of the global climate models.

2 METHODOLOGY – BUILDING DESIGN SETTINGS

The paper is split in three parts. At the first part is presented all the initial high efficient structural and physical characteristics of the building. At this building is applied the strategies of the extra movable shadings and the one of the night ventilation during all year. All these characteristics arise by the Greek regulations and by the Greek Center of Renewable Energy Sources (CRES), which is the research center responsible for sustainable and ecological development in Greece. The building is simulated with weather data exported from the Meteonorm software version 7.0.16. As far as the initial design process the output of the software is stochastically interpolated "typical" year for temperature until 2009 and for radiation until 2005. These data are the most updated weather data for simulations in Greece. At the second part the same building with all the characteristics is simulated with various data sets from the future (every decade from Meteonorm) for different emission scenarios (A2, A1B, B1). Finally for the worst case, in 2050, different ventilation patterns are simulated. For the dynamic thermal simulation and performance of the examined single family building in one of the hottest areas of Greece, the Rhodos island, the Thermal analysis software or Tas (EDSL Ltd.) version 9.2.1.3 and the response function method has been used.

2.1 Design of the energy efficient building

For the designing of the single family residential building of this paper is used:
1) Minimum exposed surfaces and compact design
2) Sufficient and continuous thermal airtight insulation for the walls and the roof ($U=0.2W/m^2K$) and the ground floor ($U=0.8W/m^2K$) of the building, exceeding the minimum limits of Greek regulations for the thermal transmittance of the building elements. The building envelope is designed with infiltrations of 0.7 ach.
3) The long axis of the building is set to be at the west – east axis. There are no openings on the west and east sides. Losses from the west and east directions are net higher than the others during winter and the danger of overheating and glaring because of the solar sunshine during summer is high. The main façade for purposes of solar gains and daylight comfort, faces the south direction. Direct passive heating systems, like Trombe wall and sun spaces, are not used because the low heating requirements of the building.
4) For the decreasing of solar gains in summer, extended fixed shading (double length compared with the opening) and pergolas are applied for the southward orientated apertures. Fixed shading is designed to cover the openings at the highest points of the sun from 16th of April until 31st October.
5) Double glazing air filled with low emissivity in high quality openable vertical windows with a wooden frame is used ($U_g=1.5W/m^2K$, $g=0.6$).
6) The prevailing cold North winds creating efficient cross – ventilation to the building mainly for the summer and the spring. The night flush ventilation (0:00 – 5:00) is an important cooling strategy for the whole year. The high ceiling (2.6 m) and the open stair wells achieve temperature stratification and a vertical air movement through the building.
7) Rooms with limited use and lower temperature requirements during the day (closets, corridors, warehouses, bathrooms etc.) are located in the northern part of the building. The living room is located on the southern part of the ground floor.
The building covers all the needs of a typical Greek family with five occupants. The total floor area of the building is 143.38 m² and the total volume 440.89 m³. The compactness (surface/volume) of the building is 0.65.

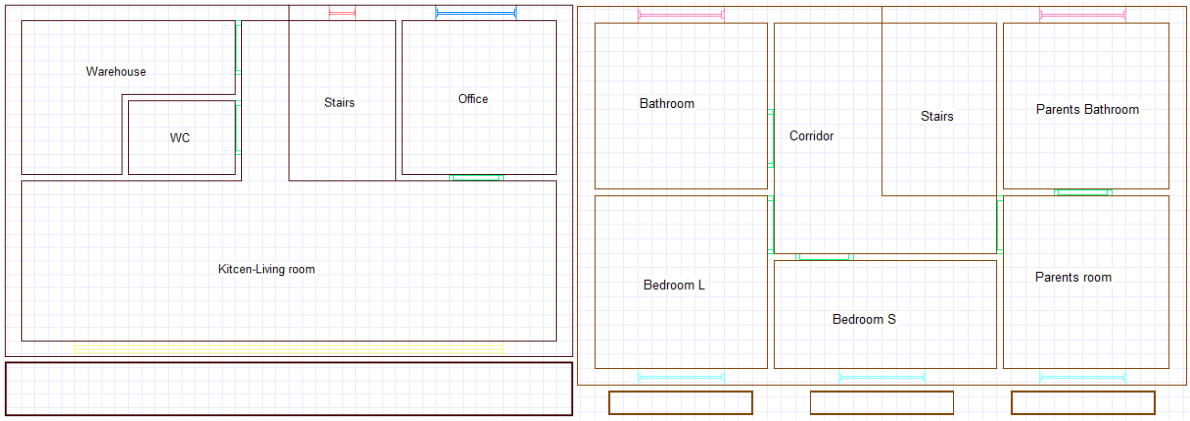

Figure 1: Plans (ground floor and upper floor) of the building (North direction is upwards).

The internal conditions are due to the Greek and European regulations [12]. The temperature band is set to be between 20 °C and 26 °C for all of year and day round. Lower and upper limit regarding the relative humidity is applied, which is the 40% and the 90% also for the whole year and day round. The movable shadings are applied at the southern openings during the morning (working hours) for the spring and the summer. For the optimization process, the night flush ventilation is applied for five hours at night. Every day of the year at night all apertures automatically start to open when the internal temperature of the zone is over 20.5 °C (fully opened at 21 °C) and the temperature outside is below the interior temperature. In Fig.2 the psychrometric chart of the updated weather data for Rhodos island, from Meteonorm, is presented. The prevailing strong cold northern or western winds mild the summer extreme conditions.

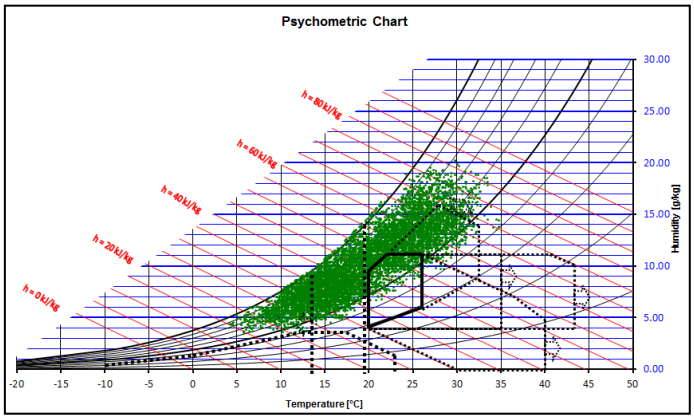

Figure 2: Psychrometric chart of the "typical" year of the most representative weather data of Rhodos island – Greece [13].

2.2 Future climate change and scenarios

This building, with all the characteristics, is simulated with various dynamic data sets from the future for different emission scenarios. The average, maximum and minimum values for temperature and relative humidity of the present and future weather data, for three different emission scenarios, for Rhodos island in Table 1 are presented. The A1B scenario, which is the medium critical scenario for IPCC, presents the highest increase until 2050 as far as the average and the maximum temperature. The relative humidity as far as the upper and lower bands remains almost constant. The "typical" year of the measured solar radiation in Fig.3 is

presented. The future changes of global radiation in the Mediterranean region are less than 4% increase until 2100 [14].

Table 1: Present and future weather data from Meteonorm software for different emission scenarios of Rhodos island – Greece.

a/a	Average Temperature (°C)	Minimum Temperature (°C)	Maximum Temperature (°C)	Minimum R. Humidity (%)	Maximum R. Humidity (%)
Present Data	19.5	3.6	34.8	39	100
A2/2020	19.8	4.7	35.5	35	100
A2/2030	20.2	5.0	36.2	34	100
A2/2040	20.4	4.6	36.3	34	100
A2/2050	20.8	5.5	37.0	34	100
A1B/2020	19.8	4.1	35.5	34	100
A1B/2030	20.2	4.6	36.3	34	100
A1B/2040	20.5	5.0	36.3	34	100
A1B/2050	20.9	5.3	37.2	34	100
B1/2020	19.8	4.2	35.5	33	100
B1/2030	20.1	4.5	36.2	34	100
B1/2040	20.2	4.6	36.2	35	100
B1/2050	20.5	4.9	36.5	34	100

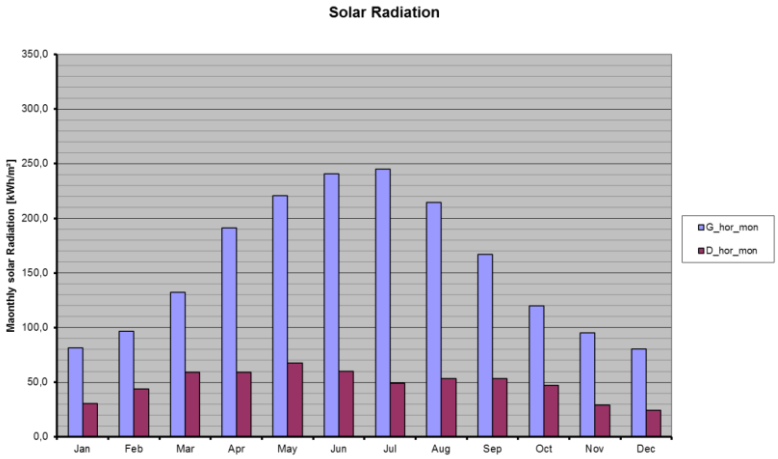

Figure 3: "Typical" year of the solar radiation (global and diffused), until 2005, of Rhodos island – Greece [13].

2.3 Different night ventilation patterns

Finally for the most pessimistic scenario, in 2050, different night ventilation patterns are simulated. The night flush ventilation at the initial building is from 0:00 am to 5:00 am. The thermal demand for different sets of night hours is checked. Also the effect on the thermal demand of the open internal doors for cross ventilation is simulated. Finally different ventilation patters as far as the apertures of the upper or ground floor and the north or the south façade are calculated.

3 RESULTS

The Fig. 4 below presents the results for the cooling demand of the energy efficient single family two storey detached building of Rhodos island in kWhs, for every month for the three steps of optimization. The annual cooling demand for every step is 29.7 kWh/m²/yr, 18.4 kWh/m²/yr and 11.8 kWh/m²/yr respectively. The specific heating demand is annually less than 0.3 kWh/m²/yr and only in January and February (not presented). For March, April, May and December the thermal demand (cooling – heating) is zero. The second and third steps

show an annual decrease in thermal demand of 38% and 34% respectively (59% in total). Also the cooling period is shortened from April – December to June – November. The shading process is critical from May to October and the natural ventilation process in June and from September to November.

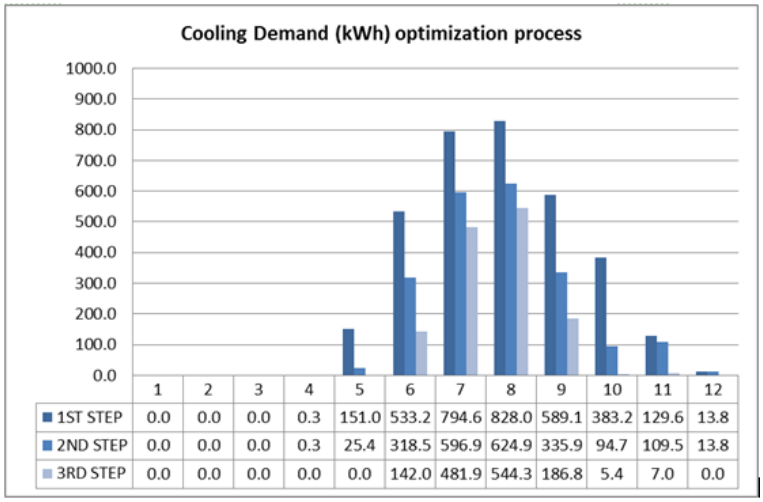

	1	2	3	4	5	6	7	8	9	10	11	12
1ST STEP	0.0	0.0	0.0	0.3	151.0	533.2	794.6	828.0	589.1	383.2	129.6	13.8
2ND STEP	0.0	0.0	0.0	0.3	25.4	318.5	596.9	624.9	335.9	94.7	109.5	13.8
3RD STEP	0.0	0.0	0.0	0.0	0.0	142.0	481.9	544.3	186.8	5.4	7.0	0.0

Figure 4: Monthly cooling demand (kWhs) for the three steps of optimization process of the energy building, of Rhodos island – Greece.

In the following Fig. 5 – 8 the cooling demand for every future scenario and every decade of simulation until 2050 for the optimized energy efficient NZE building of Rhodos island are presented. The cooling demand increases in every year and in every scenario until 2050. In 2020 the highest increase of the cooling demand is presented in scenario B1 (41.4% - optimistic scenario). Until 2050 the highest increases are presented in scenario A1B (109.2%) and in scenario A2 (96.5%), always compared with the results of the designed initial building. In summary the scenario with the greatest changes in cooling and heating demand is the A1B (104.6%).

For the A2 future scenario, even as early as 2020 the cooling demand extends from May to November. The maximum sensible cooling peak load is increased too from 2.5 kW to 3 kW in 2050. The highest cooling demand for the A2 and A1B future scenario occurs in August except for 2050 when it takes place in July. The cooling demand is higher in September than in June for every scenario and decade.

The annual cooling demand in the A1B future scenario is always higher than the demand in A2 future scenarios for every year until 2050. The peak cooling load remains constant on average until 2050 at 2.3 – 2.5 kW. From 2030 and afterwards the cooling period is extended from November to December.

Concerning the B1 future scenario apart from 2020 the cooling demand is always lower than the other scenarios for every year and almost every month. The cooling period does not include December and always August is the month with the highest demand. The sensible cooling peak load remains constant on average until 2040 at 2.2 kW and increased in 2050 at 2.9 kW. In Table 2 all the specific heating and cooling results of the simulations as a summarization are presented.

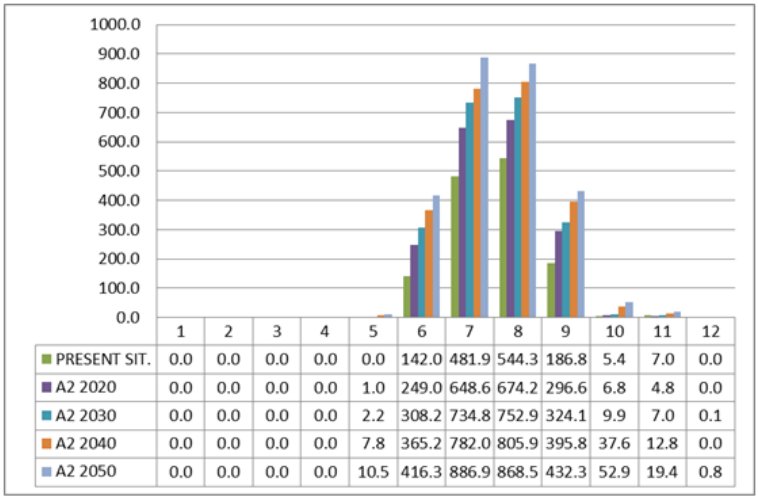

	1	2	3	4	5	6	7	8	9	10	11	12
PRESENT SIT.	0.0	0.0	0.0	0.0	0.0	142.0	481.9	544.3	186.8	5.4	7.0	0.0
A2 2020	0.0	0.0	0.0	0.0	1.0	249.0	648.6	674.2	296.6	6.8	4.8	0.0
A2 2030	0.0	0.0	0.0	0.0	2.2	308.2	734.8	752.9	324.1	9.9	7.0	0.1
A2 2040	0.0	0.0	0.0	0.0	7.8	365.2	782.0	805.9	395.8	37.6	12.8	0.0
A2 2050	0.0	0.0	0.0	0.0	10.5	416.3	886.9	868.5	432.3	52.9	19.4	0.8

Figure 5: Monthly cooling demand (kWh) for the energy efficient building, for A2 scenario until 2050, of Rhodos island – Greece.

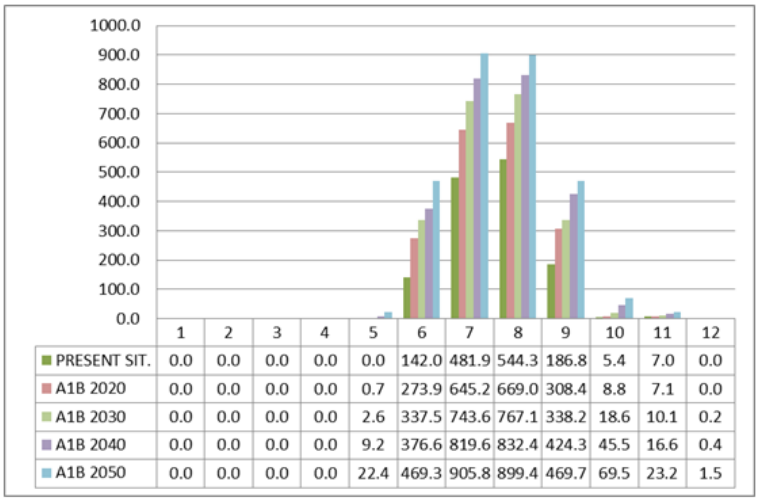

	1	2	3	4	5	6	7	8	9	10	11	12
PRESENT SIT.	0.0	0.0	0.0	0.0	0.0	142.0	481.9	544.3	186.8	5.4	7.0	0.0
A1B 2020	0.0	0.0	0.0	0.0	0.7	273.9	645.2	669.0	308.4	8.8	7.1	0.0
A1B 2030	0.0	0.0	0.0	0.0	2.6	337.5	743.6	767.1	338.2	18.6	10.1	0.2
A1B 2040	0.0	0.0	0.0	0.0	9.2	376.6	819.6	832.4	424.3	45.5	16.6	0.4
A1B 2050	0.0	0.0	0.0	0.0	22.4	469.3	905.8	899.4	469.7	69.5	23.2	1.5

Figure 6: Monthly cooling demand (kWh) for the energy efficient building, for A1B scenario until 2050, of Rhodos island – Greece.

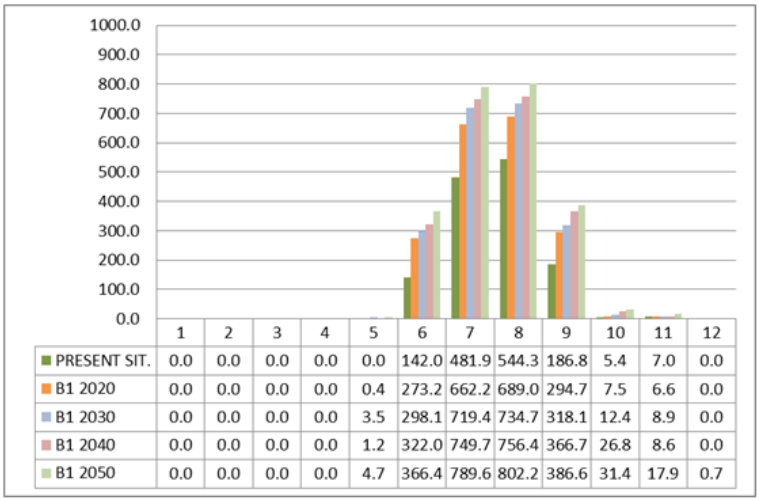

	1	2	3	4	5	6	7	8	9	10	11	12
PRESENT SIT.	0.0	0.0	0.0	0.0	0.0	142.0	481.9	544.3	186.8	5.4	7.0	0.0
B1 2020	0.0	0.0	0.0	0.0	0.4	273.2	662.2	689.0	294.7	7.5	6.6	0.0
B1 2030	0.0	0.0	0.0	0.0	3.5	298.1	719.4	734.7	318.1	12.4	8.9	0.0
B1 2040	0.0	0.0	0.0	0.0	1.2	322.0	749.7	756.4	366.7	26.8	8.6	0.0
B1 2050	0.0	0.0	0.0	0.0	4.7	366.4	789.6	802.2	386.6	31.4	17.9	0.7

Figure 7: Monthly cooling demand (kWh) for the energy efficient building, for B1 scenario until 2050, of Rhodos island – Greece.

Table 2: Specific heating and cooling demand (kWh/m²/yr) for the optimization process and every future scenario until 2050 for the building, of Rhodos island – Greece.

a/a	Heating	Cooling				
Step 1	0.1	29.7				
Step 2	0.1	18.4				
Step 3	0.3	11.8				
a/a	**A2-Heating**	**A2-Cooling**	**A1B-Heating**	**A1B-Cooling**	**B1-Heating**	**B1-Cooling**
2020	0.3	16.3	0.3	16.6	0.3	16.8
2030	0.2	18.5	0.2	19.2	0.2	18.2
2040	0.1	20.9	0.1	21.9	0.2	19.3
2050	0.1	23.3	0.1	24.8	0.1	20.8

Table 3: Specific heating and cooling demand (kWh/m²/yr) for different opening hours for all the apertures of the building, of Rhodos island – Greece.

a/a	Specific Heating Demand (kWh/m^2)	Specific Cooling Demand (kWh/m^2)
00:00-01:00	0.0	29.5
00:00-02:00	0.0	27.9
00:00-03:00	0.0	26.6
00:00-04:00	0.0	25.6
00:00-05:00	0.1	24.8
01:00-02:00	0.0	29.3
01:00-03:00	0.0	27.7
01:00-04:00	0.0	26.4
01:00-05:00	0.0	25.4
02:00-03:00	0.0	29.2
02:00-04:00	0.0	27.6
02:00-05:00	0.0	26.3
03:00-04:00	0.0	29.2
03:00-05:00	0.0	27.5
04:00-05:00	0.0	29.2

In Tables 3 – 4 all the specific heating and cooling demands for different opening patterns of all apertures as far as the time and the season of operation for night ventilation are presented. Also different patterns of night ventilation as far as the apertures of different facades are simulated (Table 5). As it was expected the maximum hours of application of night ventilation during all year decrease the cooling demand of the building. The open internal doors help the cross ventilation and decrease significantly the cooling demand of the building, more than the cooling demand of every zone – room separately (Table 5). The apertures of the upper floor (7.5 m^2), as expected, are more important for ventilation cooling than those of the ground floor (15 m^2). Finally the apertures of the south façade (17.7 m^2) are more important for cooling purposes than those of the north façade (4.75 m^2). The explanation of this larger increase in efficiency is the four times larger size of the apertures compared to the northern one.

Table 4: Specific heating and cooling demand (kWh/m²/yr) for different seasons of application of the night ventilation for the building, of Rhodos island – Greece.

a/a	Specific Heating Demand (kWh/m^2)	Specific Cooling Demand (kWh/m^2)
Annual	0.1	24.8
Spring-Summer-Autumn	0.0	26.7
Spring and Autumn	0.0	29.0
Summer	0.0	29.0

Table 5: Specific heating and cooling demand (kWh/m²/yr) for different strategies – orientations of application of the night ventilation for the building, of Rhodos island – Greece.

a/a	Specific Heating Demand (kWh/m^2)	Specific Cooling Demand (kWh/m^2)
Internal Doors	0.1	23.9
Upper Floor openings	0.0	25.2
Ground Floor openings	0.0	25.6
North Façade openings	0.0	25.7
South Façade openings	0.0	24.4

4 CONCLUSIONS

The Greek – Mediterranean climate offers excellent weather conditions for thermally efficient, carbon neutral, fuel's independent and low budget family houses. The absence of extreme uncomfortable temperatures and the refreshing summer cool breeze help the bioclimatic design of really efficient energy buildings. In a dynamic situation, like climate change, the use of meteorological data from previous years, as for Greece from 2003 (TOTEE/KENAK), is not precise and scientifically acceptable. The climate change will significantly affect the thermal demands (mainly cooling) and non significantly the cooling loads, of a highly efficient NZE building in one of the hottest regions of Greece and Mediterranean Sea (Rhodos island) with an increase of more than 90% in 2050 on average. The cooling period is also extended. The increase of the cooling demand even from the first decade is really impressive (on average close to 40%). This is probably because the "typical" weather year used for the initial design utilizes data from a longer period than the last year (2009). For this reason the weather characteristics are milder than these of the present years and those of the next decades. Also in the summer warm period September is included (hotter than June). Mainly, because of the low standards of performance – construction of the old buildings in the area, the thermal demands will increase seriously due to weather changes, especially affecting low income households.

In contrast with the assumption of the IPCC for the Mediterranean Sea, the worst results in thermal demands for the area of the South Aegean with scenario A1B (medium) and then with scenario A2 (pessimistic) are presented. Only in the first decade (2020) scenario B1 (optimistic) is the leading worst scenario. The great increase in the first sets of simulation for 2020, as far as thermal demand, confirms the dramatically changed conditions of the weather and the climate. The decrease in precipitation and the changes of the drought periods have to be included in our design beyond the thermal simulations. This change of the parameter do not observed at the future meteorological data of Meteonorm.

The structural characteristics of this building like orientation, compactness, insulation, airtightness and shadings may be used as reference for the hottest areas of Greece. The used strategies of movable shadings and night natural cross ventilation are critical for the optimization of the thermal results close to the higher levels of international energy standards.

This paper is a contribution to deal with the effects of climate change in the thermal demands of a building, in Greece. For further research the investigation of the thermal demands of the future conditions until the end of the century is suggested, with outputs from meteorological regional climate models (not software – black boxes) and more greenhouse gas emission scenarios. The same research will be interesting for the coldest regions of Greece, too.

5 REFERENCES

1. Robert, A., Kummert, M. (2012). Designing net-zero energy buildings for the future climate, not for the past. *Building and Environment, 55*, 150-158.
2. Asimakopoulos, D., Santamouris, M., Farrou, I., Laskari, M., Saliari, M., Zannis, G., Tiggas, T. (2011). *Danger and results of climate change to the building environment.* Athens: Bank of Greece.
3. Balaras, C., Gaglia, A., Georgopoulou, E., Mirasgedis, S., Sarafidis, Y., Lalas, D. (2007). European residential buildings and empirical assessment of the Hellenic building stock, energy consumption, emissions and potential energy savings. *Building and Environment, 42*, 1298-1314.
4. Dascalaki, G., Balaras, C., Gaglia, A., Droutsa, K., Kontoyiannidis, S. (2012). Energy performance of buildings – EPBD in Greece. *Energy Policy, 45*, 469-477.
5. de Wilde, P., Coley, D. (2012). The implications of a changing climate for buildings. *Build Environ, 55*, 1-7.
6. Peel, M.C., Finlayson, B.L., McMahon, T.A. (2007). *Updated world map of the Köppen – Geiger climate classification.* Melbourne.
7. Solomon, S., Qin, D., Manning, M., Chen, Z., Marquis, M., Averyt, K., Tignor, M., Miller, H.L. (2007). *Summary for Policymakers. The Physical Science Basis. Contribution of Working Group I to the Fourth Assessment Report of the IPCC.* New York: Cambridge University Press.
8. Founta, D., Aber, J. (2011). *Journal in Press.*
9. Christensen, J.H., Hewitson, B., Busuioc, A., Chen, A., Gao, X., Held, I., Jones, R., Kolli, R.K., Kwon, W.T., Laprise, R., Magana Rueda, V., Mearns, L., Menéndez, C.G., Raisanen, J., Rinke, A., Sarr, A., Whetton, P. (2007). *Regional Climate Projections. In: Climate Change 2007: The Physical Science Basis. Contribution of Working Group I to the Fourth Assessment Report of the IPCC.* New York: Cambridge University Press.
10. Tolika, C.K., Zanis, P., Anagnostopoulou, C. (2012). Regional climate change scenarios for Greece, future temperature and precipitation projections from Ensembles of RCM's. *Global Nest, 14* (4), 407-421.
11. Nakicenovic, N., Davidson, O., Davis, G., Grübler, A., Kram, T., Rovere, E. L., Metz, B., Morita, T., Pepper, W., Pitcher, H., Sankovski, A., Shukla, P., Swart, R., Watson, R., Dadi, Z. (2000). *Summary for Policymakers. Emissions Scenarios. A Special Report of Working Group III of the IPCC.* New York.
12. TOTEE – KENAK 20701 – 1, 2, 3. (2010). *Technical energy regulations of Chamber of Greece.* Athens.
13. Holzer, P. (2011). *Climate data tool.* Educational material of M.Sc. of Future Building Solutions, Danube University. Krems.
14. Remund, J., Muller, S., Kunz, S., Schilter, C. (2012). *Meteonorm manual version 7. Handbook part I and II.* Bern.

ENERGY SAVING EFFECT OF THE ERV (ENERGY RECOVERY VENTILATOR) WITH OUTDOOR AIR COOLING

Joonghoon Lee[1], Doosam Song[*2], Joowook Kim[3], Junghun Lee[4]

1 Samsung C&T
1312-20 Seocho 2-dong
Seoul, Korea

2 Sungkyunkwan University
300 Cheon-cheon-dong
Sunwon, Korea
**Corresponding author: dssong@skku.edu*

3 Graduate School, University of Colorado
40 UCB, Boulder
Colorado 80309-0040, USA

4 Graduate School, Sungkyunkwan University
300 Cheon-cheon-dong
Sunwon, Korea

Note: the contact addresses may be re-arranged

ABSTRACT

Maintaining an IAQ with fresh in school building is very important because the good IAQ can keep the student in health and improve the academic performance. Since school buildings are very dense and require a lot of fresh air, the need for ventilation has become obvious. While opening a window does provide fresh air, which is undesirable for the indoor climate and for energy efficiency under severe outdoor condition. ERV (Energy Recovery Ventilation) technology offers an optimal solution: fresh air, better climate control and energy efficiency. However, when the outdoor air condition is favourable to control the indoor environment such as spring and autumn in Korea, heat exchange in ERV would rather increase the cooling load than diminish. Economizer cycle control which using the outdoor air in controlling the indoor thermal environment has many benefit in terms of energy saving and IAQ control.
In this study, the ERV with outdoor air cooling mode is suggested. And then the system control characteristics and energy saving effect were analyzed using the simulation method.

KEYWORDS

ERV, Outdoor air cooling, Energy saving, TRNSYS

1 INTRODUCTION

Good Indoor Air Quality (IAQ) of school buildings is an important factor to maintain healthy indoor environments and to improve the student's academic performance. Because the population density of the school is high and the students spent a long time in class. Poor indoor air quality can cause many adverse health effects such as respiratory symptoms, asthma (Mi et al., 2006). The ventilation requirement in school buildings is specified in the "School Health & Hygiene Law" in Korea. School buildings should be ventilated at the air flow rate of more than 21.6 [CMH/person] by opening the windows or operating mechanical ventilation systems (Lee YG, 2008).
However, introducing the outdoor air for ventilation results in increased heating and cooling demands in sever outdoor condition. Energy Recovery Ventilators (ERV) is a good solution in

conflicted interests between ventilation and energy saving. ERV have been equipped in most of the newly constructed school building in Korea from 2007. ERV, however, occasionally rather results in the increase of the cooling load because unnecessary heat recovery makes the cool and comfort outdoor air into hot and discomfort air.
In this study, the ERV with outdoor air cooling or economizer cycle is suggested. And the energy saving effect of the proposed system was analyzed by simulation method. In this paper, the system configuration, the system control characteristics and energy saving effect of the proposed system were described.

2 OUTLINE OF THE ERV WITH OUTDOOR AIR COOLING

2.1 System configuration

This system consists of the ceiling mounted air-conditioner (VRF, Variable Refrigerant Flow) and ERV (Energy Recovery Ventilator) with economizer cycle. It is similar to the previous VRF air conditioner with ERV (here after, VRF AC+ERV) in system structure, but the control logic for ERV is different in both systems. The ERV with economizer cycle is controlled based on the outdoor air condition. Economizer cycle control (Ke and Mumma, 1997) is a method to control the indoor environment using the outdoor air by introducing outdoor air without heat recovery when the outdoor air temperature or enthalpy is lower than that of the indoor set-point. The economizer cycle control can be categorized as 'temperature based control' and 'enthalpy based control' depending on its control method generally used for HVAC system.
The proposed system (VRF AC+ERV with economizer cycle) is operated like the previous "VRF AC+ERV" when the outdoor conditions are not favourable as shown in Fig. 1-(b). In this condition, the outdoor air is wholly induced with heat recovery, and VRF AC is operated for cooling or heating. However, when the outdoor conditions are favourable, the outdoor air is induced directly without heat recovery, and used for cooling as well as improvement of IAQ (see Fig. 1-(a)).

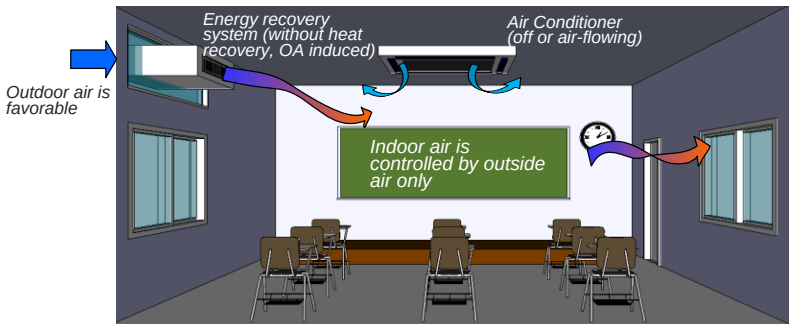

(a) Economizer cycle control mode : The indoor air is controlled by outside air only

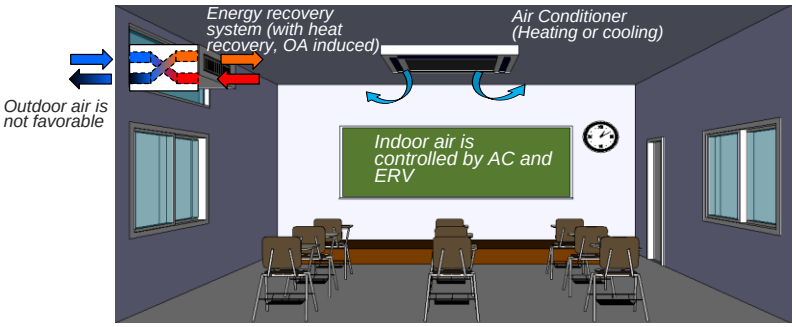

(b) AC + ERV mode : The outdoor air is introduced with heat recovery

Figure 1: System outline

2.2 System control logic

Fig. 2 shows the logic of "VRF AC+ERV with economizer cycle". When the outdoor air condition is comfortable, outdoor air is induced without heat recovery at the maximum ventilation rate through ERV as shown on phase 1. In this condition, indoor thermal environment is controlled by the outdoor air. On the while, outdoor air is induced through heat recovery at the minimum ventilation rate when the outdoor condition is not favorable. In phase 2, AC is operated for cooling when indoor air temperature is higher than *Tiset*, and it stops when indoor air temperature is lower than *Tiset*.

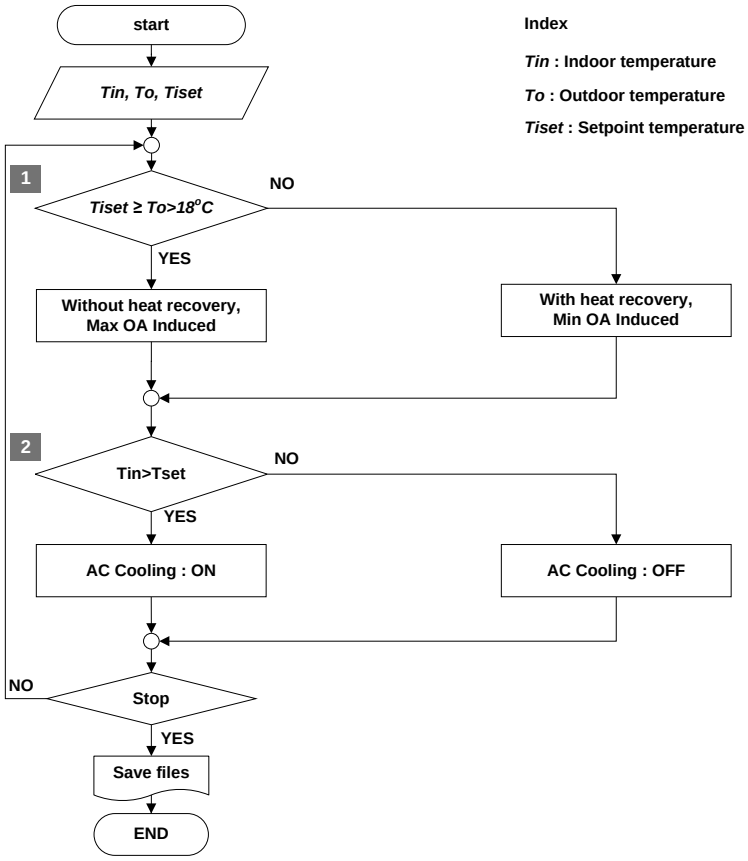

Figure 2: System control logic

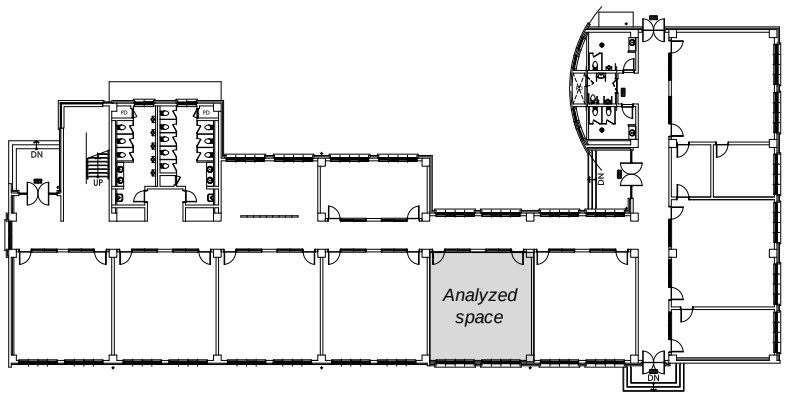

Figure 3: Analyzed space

3 ANALYSIS OF THE INDOOR CONTROL AND ENERGY CONSUMPTION BEHAVIROS

3.1 Simulation conditions

The analyzed school building was a J high school located at Gimpo, Korea, and the classroom is on the second floor in the middle of the school building with the size of 67.24 m^2. Table 1 shows the simulation conditions. The capacity and electricity consumption data of AC and ERV systems installed in the analyzed classroom are described in Table 2 and 3.

Table 1: Simulation Conditions

<table>
<tr><td>Weather data</td><td colspan="2">Seoul, Korea (TMY2)</td></tr>
<tr><td>Heating set point</td><td colspan="2">22 °C (dead band 1 °C)</td></tr>
<tr><td>Cooling set point</td><td colspan="2">26 °C (dead band 1 °C)</td></tr>
<tr><td>Heat gain</td><td>Persons</td><td>▪ Occupants : 35 Person
▪ Activity level : Seated, very light writing
▪ Internal Heat Gain : Sensible heat 65(W), Latent heat 55(W)
▪ Occupancy Schedule
 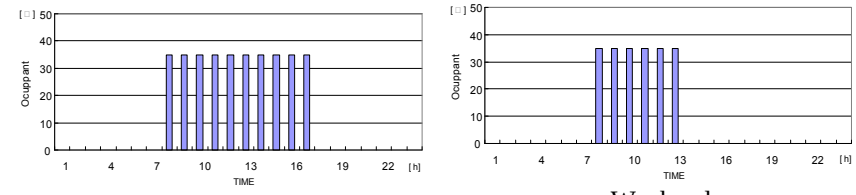

Weekday Weekend</td></tr>
<tr><td></td><td>Lighting power</td><td>▪ Density : 15 (W/m^2)
▪ Schedule
 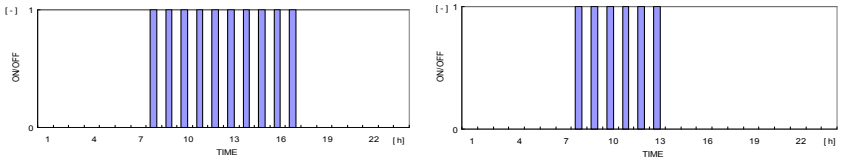

Weekday Weekend</td></tr>
<tr><td>Air-flow rate of ERV</td><td colspan="2">800 (CMH)</td></tr>
<tr><td>System operation schedule</td><td colspan="2">Weekday 08:00 ~ 17:00 (on), other hour (off)
Saturday 08:00 ~ 13:00 (on), other hour (off)
Sunday and holiday (off)</td></tr>
</table>

Table 2: VRF AC System information

		Max	Min
Performance	Capacity (HP)	5	
	Cooling (Kcal/h)	12,470	
	Heating (Kcal/h)	14,020	
Air flow rate (CMM)		29	19.33
Electrical demand	Outdoor unit (W)	7,192	7,109
	Indoor unit (W)	85	10

Table 3: ERV System

Air Flow rate (CMH)			800
Electrical demand (W)			290
Heat recovery performance (%)	Sensible heat	Cooling	71
		Heating	82
	Latent heat	Cooling	44
		heating	65

Table 4: Simulation Cases

Cases	Operation mode
Case 1	AC + mechanical ventilator
Case 2	AC + ERV (Normal control)
Case 3	AC + ERV (Economizer cycle control)

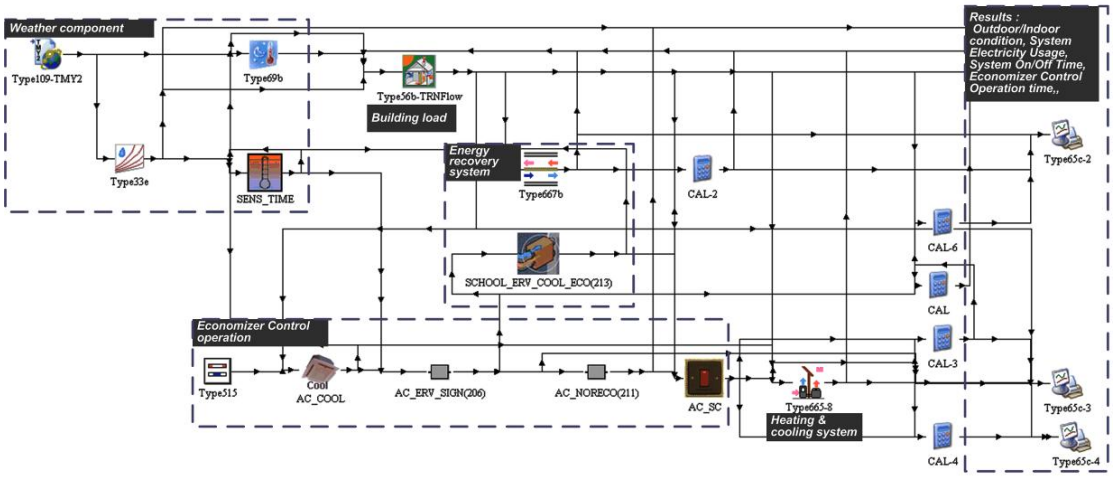

Figure 4*:* Layout of economizer control with AC and ERV in TRNSYS

Fig. 4 depicts the layout of the simulation modeling by TRNSYS. A module provided by the TRNSYS program was used for weather conditions, indoor temperature condition setting, building modeling, AC and ERV system modeling, and energy consumption output module for the simulation (TRNSYS, 2007).

However, the system control modules such as economizer cycle control and AC and ERV system control module were newly developed for the simulation of this study.

Table 4 shows the simulation cases analyzed in this study. In Case 1, the classroom is equipped with AC and mechanical ventilator. In Case 2, the classroom is equipped with AC and ERV, and the ERV is controlled with normal control (heat recovery only). In Case 3, the proposed system in this study, the classroom is equipped with AC and ERV, and the ERV is controlled with heat recovery mode and outdoor air cooling (economizer cycle) mode.

3.2 Results

The system control and energy consumption behaviours of the analyzed cases were analyzed.

3.2.1 System control behaviours

Fig. 5 shows the system control characteristics in the cooling period, and Fig. 6 shows that in the intermediate period.

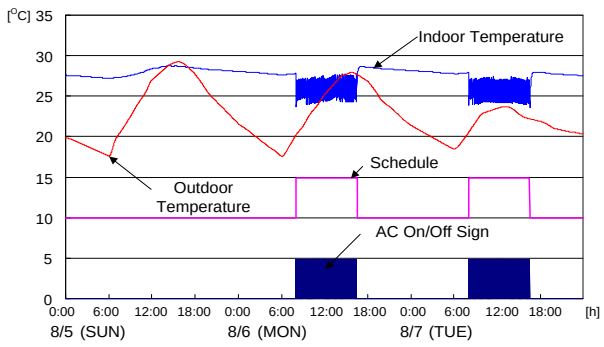

(a) Case 1 (AC+Mechanical Ventilator)

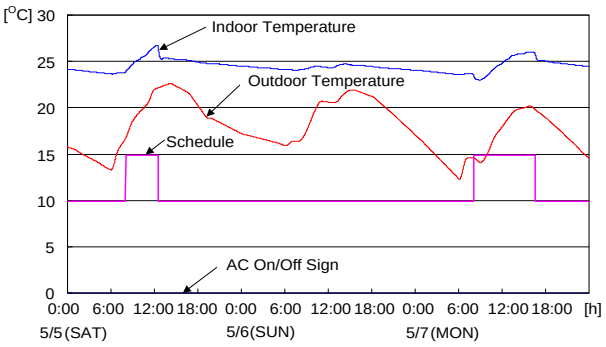

(a) Case 1 (AC+Mechanical Ventilator)

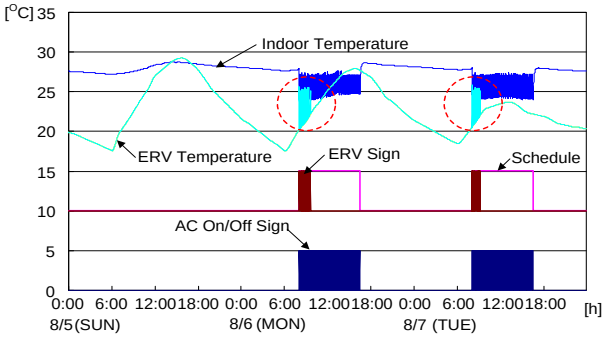

(b) Case 2 (AC+ERV)

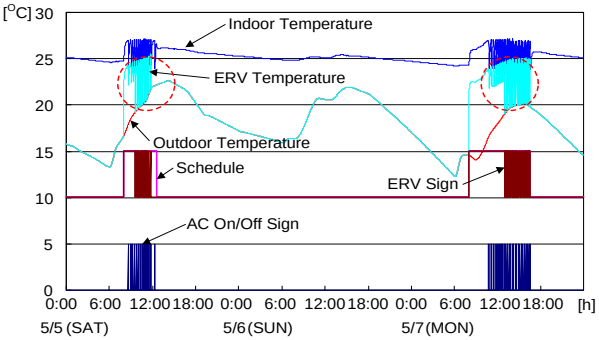

(b) Case 2 (AC+ERV)

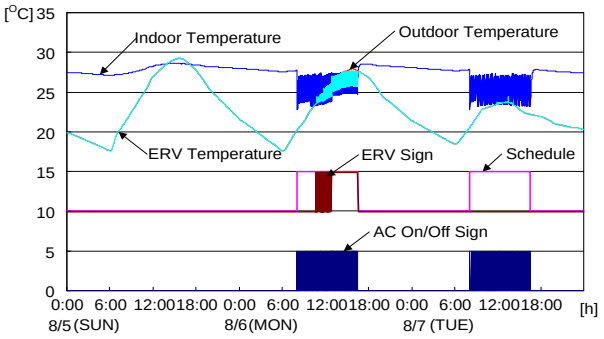

(c) Case 3 (AC+ERV with economizer control)

Figure 5: Cooling season control

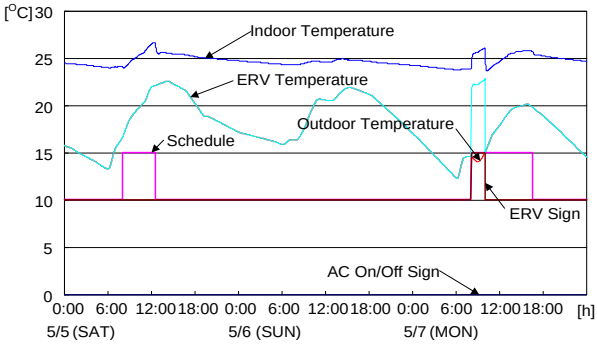

(c) Case 3 (AC+ERV with economizer control)

Figure 6: Intermediate season control

In cooling period (Fig. 5), the average indoor temperature was controlled by 26°C in daytime in weekday. As shown in Fig. 5-(b), the temperature of the supply air from ERV was rather higher than that of the outdoor air temperature. This is because of the unnecessary heat exchange in ERV. This resulted in the increase in the operation hour of AC in Case 2.

In intermediate period (Fig. 6), also the temperature of the supply air from ERV was rather higher than that of the outdoor air temperature in Case 2 (Fig. 6-(b)).
In Case 3, the temperature of the supply air from ERV was same with the outdoor when the outdoor air was lower than indoor set-point temperature in cooling and intermediate season.

3.2.2 Energy consumption

Energy consumption was calculated from the operation hours of AC and ERV, and the monthly and annul electricity consumption of each case were estimated and analyzed.

Fig. 7 shows the monthly electricity consumptions of AC and ERV. In the heating period (November ~ March) of Case 1, the electricity consumption was the highest because the heating load was boosted by the induction of the outdoor air at low temperature. In Case 2 and 3, on the other hand, the great reduction in the electricity consumption of AC is observed because of ventilation through heat recovery.

In the intermediate and cooling period (April~October), the monthly electricity consumption of Case 3 which the outdoor air cooling (economizer control) was applied showed reduction compared to Case 1 and 2. While the energy consumption in Case 2 was higher than that in Case 1, which is the result of the increased indoor cooling load caused by the unnecessary heat exchange in ERV.

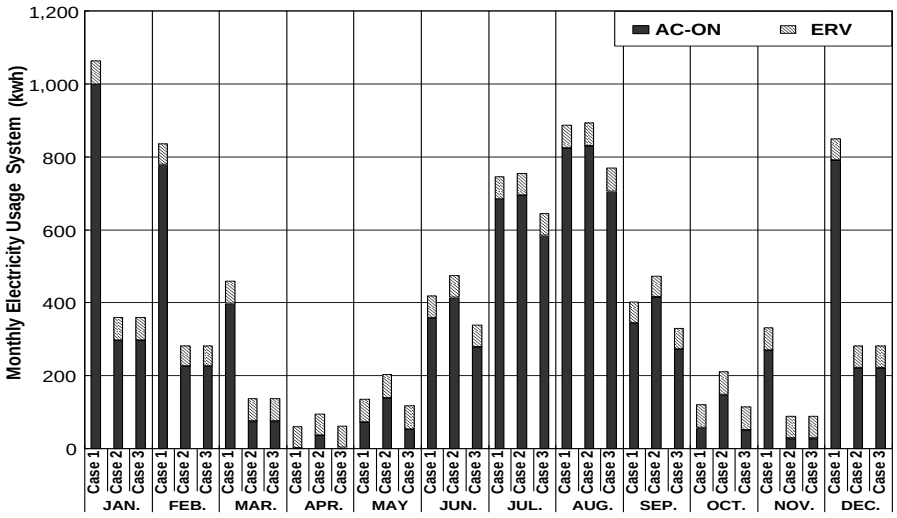

Figure 7: Monthly electric requirements for heating, cooling and ventilation

Fig. 8 represents the annual electricity consumptions of AC and ERV, showing the reduction in annual total electricity consumptions of the system by about 32.6% and 44.1% respectively in Case 2 and 3 compared to that in Case 1. With the outdoor air cooling mode in Case 3, the energy demand of AC was decreased by about 20.7% compared to that of the Case 2.

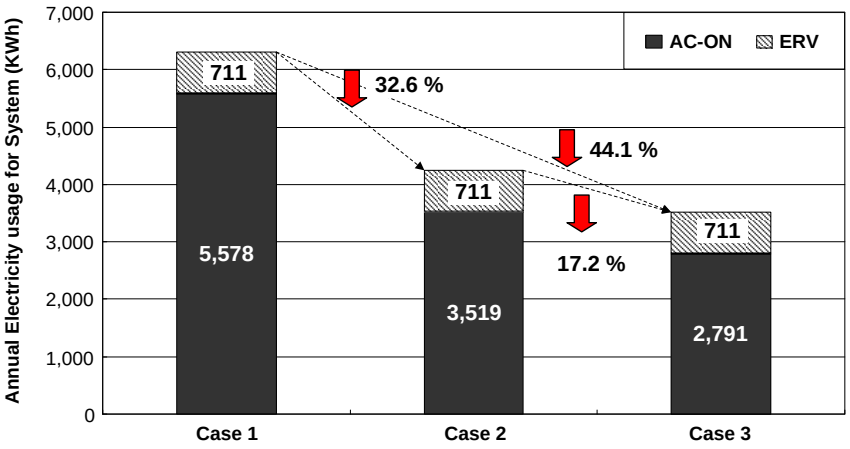

Figure 8: Annual electric requirements for heating, cooling and ventilation

4 CONCLUSIONS

In this study, the ERV with outdoor air cooling or economizer cycle is suggested. And the energy saving effect of the proposed system was analyzed by simulation method. The system control characteristics and energy saving effect of the proposed system were analyzed through the TRSNSYS simulation. The analysis results are as follows;

1) When operated by ERV with economizer cycle (Case 3), about 50% reduction in annual AC operation hour resulted compared to Case 1 (AC+ Mechanical ventilation, without heat recovery), and about 44.1% reduction in electricity consumption resulted. Compared to Case 2 (AC+ERV Normal control), about 20.7% reduction in annual AC operation hour and about 17.2% reduction in electricity consumption resulted.

2) AC+ERV with economizer cycle suggested by this study was verified as a method to minimize the energy consumption as well as to keep the indoor environment comfort and clean compared to the previous operation method of systems in the school buildings.

5 ACKNOWLEDGEMENTS

This work was supported by the National Research Foundation of Korea(NRF) grant funded by the Korea government(MSIP) (NO.2005-0049406).

6 REFERENCES

Mi YH, Norback D, Tao J, Mi YL, Ferm M: Current asthma and respiratory symptoms among pupils in Shanghai, China: influence of building ventilation, nitrogen dioxide, ozone, and formaldehyde in classrooms: Indoor Air 2006;16:454–464.

Lee YG, Kim S., Trends in the Korean building ventilation market and drivers for change. AIVC Information Paper no. 26, May 2008: 1-10. Available from : http://www.aivc.org/medias/pdf/Free_VIPs/VIP26_Korea.pdf

Ke YP, Mumma SA. Using carbon dioxide measurements to determine occupancy for ventilation control. ASHRAE Transactions 1997;103(1):365–74.

TRNSYS, TRNSYS16 Reference Manual, Solar Energy Laboratory, University of Wisconsin-Madison, 2007.

DOUBLE-SKIN SYSTEM OF ROOM-SIDE AIR GAP APPLIED TO DETACHED HOUSE (PART 1): SIMULATION ANALYSIS FOR REDUCTION OF COOLING LOAD IN THE FORCED VENTILATED WALL OF DETACHED HOUSE

Kan Lin[1], Shinsuke Kato[*2], Togo Yoshidomi[3], and Kyosuke Hiyama[4]

1 Graduate School of The University of Tokyo
7-3-1, Hongo, Bunkyo-ku,
Tokyo, Japan

2 IIS, The University of Tokyo
4-6-1 Komaba, Meguro-Ku,
Tokyo, Japan
**Corresponding author: kato@iis.u-tokyo.ac.jp*

3 Graduate School of The University of Tokyo
7-3-1, Hongo, Bunkyo-ku,
Tokyo, Japan

4 Yamaguchi University
1677-1, Yoshida, Yamaguchi-shi,
Yamaguchi, Japan

ABSTRACT

Detached residential wooden houses are a common type of housing in Japan. Decay of wooden components within the walls caused by condensation or defective flushing, is sometimes an issue. To solve this problem, a double-skin system with a room-side air gap was developed. In this system, during summer, the airflow that is driven by ventilation fans moves through the room-side air gap in the wall, and removes heat load either from the inner surface of the insulation material, or from the surface adjacent to the rooms inside. The purpose of this study is to evaluate the flow rate in the ventilated wall, controlled by ventilation fans. The airflow in the ventilated wall removes heat from the surface of the wall and influences occupants' thermal comfort. Therefore, it is important to develop an expression for flow rate in the wall. An airflow-energy simulation program was used to predict flow rates in the ventilated wall, and the performance of air-flows in several exterior walls of the house was investigated under various conditions. The results verify that the flow rate in the ventilated walls increased with the ventilation fan speed. By using forced ventilation, the cooling load was reduced by 10% to 20%.

KEYWORDS

Double-skin system, Detached house, Simulation, Forced ventilation, Cooling load

1 INTRODUCTION

Wooden detached houses, which have wood-based structural insulation materials for walls and flooring, are widely used in Japan. However, many problems exist with this type of home construction. For example, during the summer period, incoming solar radiation is not equally distributed, leading to uneven indoor temperature distribution. In the winter period, indoor humidity is closely related to the durability of the building envelope. Moisture leaking from the interior rooms increases the risk of condensation on the walls, because the surface temperature of the wall is low. Condensation on the walls may cause the wood used in the houses' construction to decay. In addition to condensation from interior rooms, water vapour condenses on wooden window frames, and rainwater can leak through the roof and walls. The

increased moisture is absorbed by the wooden structure of the house, and reduces the endurance and strength of the wood, and also accelerates its decay.

To remove the moisture between the external and internal walls, a double-skin system is commonly installed to detached houses. A double-skin system consists of a multi-layered façade, with a buffer space used for ventilation. Air flow in the ventilated wall is controlled by ventilation fans set atop the roof. This system can integrate the mechanical ventilation with natural ventilation so that air can move freely in the buffer space.

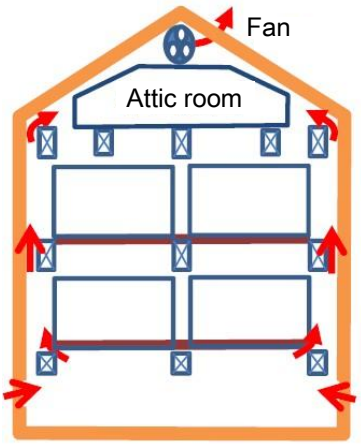

Figure 1: Double-skin system of room-side air gap with ventilated wall applied to detached house

In summer, air vents in the basement are opened and the ventilation fans on top of the roof are turned on to facilitate airflow through the ventilated wall, and out the roof. Airflow in the ventilated wall removes heat from solar radiation and from the internal wall. The airflow discharges heat in the wall and attic space, while obtaining cold heat from the ground under the floor. This ensures that the rooms are kept in moderate temperature and comfort.

Although houses using this system have been built for about 30 years in Japan, only a few studies have been conducted on them. Using a simulation of a model house from previous research, Ozaki et al. analyzed the airflow speed in the wall, as well as the airflow in the space under the floor during the summer period. However, there is hardly any information available regarding the actual airflow and thermal effects of this system. For this reason, it is difficult to select appropriate strategies to maintain airflow rate in the ventilated wall.

The objective of this study is to understand the basic properties of the double-skin system, temperature drop, and reduction in cooling load during the summer period by performing a ventilation network simulation. To perform calculations during the summer period, we used a network simulation by creating two building models with spaces in the air gap and rooms of the house that were regarded as independent nodes. The impact of each element to the airflow rate was estimated, and the cooling load reduction effect of the system was examined in the simulation.

The results show the relationship between different patterns of the airflow rate and reduction in the cooling load. The reduction in the cooling load increased with the flow rate of the ventilation fans. In addition, natural indoor temperature drop effects became more significant with the increase in the flow rate of the ventilation fans.

2 MATERIALS AND METHODS

2.1 Simulation Software

To calculate the airflow in the buffer space, we used the variable energy calculation software TRNSYS17, and its add-on program TRNFlow. TRNFlow is designed based on COMIS3.1, a ventilation network calculation software, and can perform the iterative calculations by resolving the movement of the air and heat at the same time in TRNSYS.

2.2 Building Model

In this research, the house model (4th region) proposed by IBEC, Institute for Building Environment and Energy Conservation, as a standard detached house in Japan was used in the simulation. This house model is a two-story house with 120.07 m^2 total floor area, and it is intended for a four-person family. There are several spaces divided by rooms, as shown in figure 2. Occupants' schedules as well as the lighting, equipment, ventilation, and air

conditioning are based on the investigation. The dimensions and the basic configuration of the building were set based on this model. In addition, the dimensions of the air gap in the ventilated wall were set based on the real house.

The air gap in the ventilated wall is shown in figure 3. The area of the air gap in which air moves upwards is represented as the blue portion. Grooves are arranged on the surface of the insulation material in equal intervals. These create openings between the insulation and the other components, so that air flows freely. The air gap is divided into several zones by resistance parts, such as vents or these openings. In such zones, the flow path is narrower than the open air gap. For the calculations by TRNFlow, we modeled the air gap as an "airnode," and defined any resistance parts as an "airlink." For each airlink, the relationship of the mass flow rate and the pressure difference is calculated based on equation (1). In equation (1), a common formula for ventilation, the value of $C_{s,}$ for each airlink, was decided by fixing α to 0.6 as a typical value. Also determined was the opening area A of the airlink, from the actual specification of this house. The value of n was determined to be 0.5, from the above substitution for the opening area, which is reflected in equation (2).

$$\dot{m} = C_s \cdot (\Delta p)^n \tag{1}$$

$$\dot{m} = aA\sqrt{2r \cdot \Delta p} \tag{2}$$

$\dot{m}$: Δp mass flow rate [kg / h], α: pressure difference [Pa], C_s: flow coefficient [-],
A: opening area [m^2], ρ: air density [kg/m^3]

In this simulation, a simple building model that does not take into account the air infiltration, was used; neither air leaking into the rooms, nor outside air from the gas passage is considered. A simple network that connects the air gap to the outside air was created, as shown in figure 4.

With this model, it is possible to estimate the potential of the maximum amount of airflow generated by mechanical ventilation, regardless of the influence of air infiltration. On the other hand, because heat from solar radiation and internal heat cannot be discharged by infiltration, simulation results may show that the room temperature is higher than the actual environment.

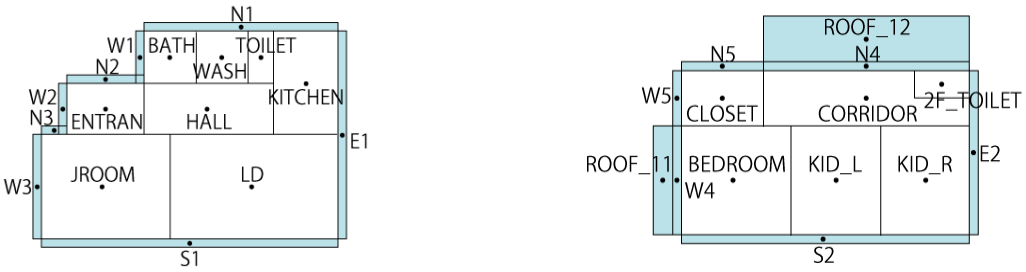

Figure 2: Zones and airnodes of the building model in TRNSYS

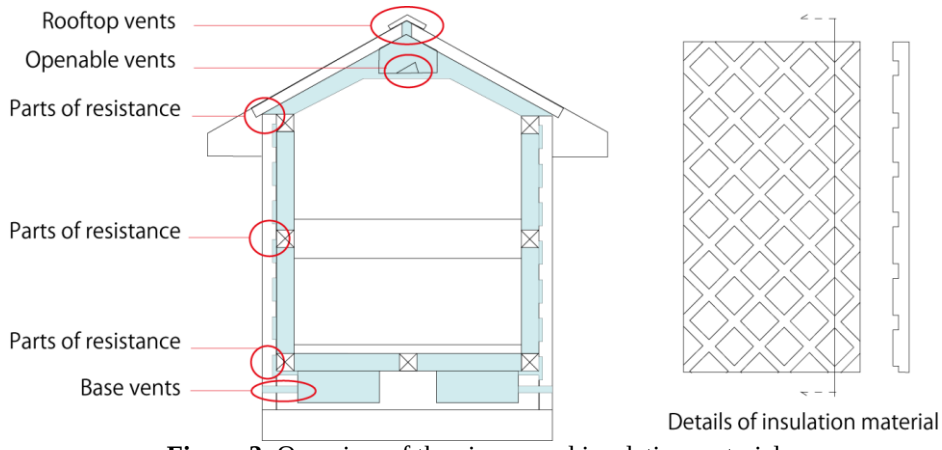

Figure 3: Overview of the air gap and insulation material

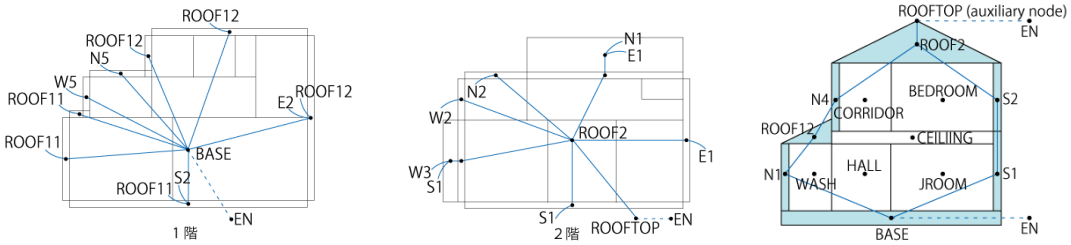

Figure 4 : Overview of airlinks in TRNFlow

Table 1: Building Properties

Wall of external side	Extruded polystyrene foam = 50 mm + Air layer = 15 mm + Tile = 10 mm
Wall of internal side	Gypsum board = 13 mm
Air gap thickness	120 mm
Roof	Extruded polystyrene foam = 50 mm + Air layer = 30 mm + Plywood = 10 mm + Slate = 5 mm
Base	EPS 50 mm + RC 150 mm + EPS 50 mm
Internal wall, Ceiling, Floor	U = 3.125 W/m^{2}K, 4.082 W/m^{2}K, 4.082 W/m^{2}K
Window, double-glazing	U = 1.8 W/m^{2}K, Shading coefficient = 0.5
Infiltration	None

Table 2: Ventilated Wall Setting

Opening area A [m^2]	Part of resistance in the air gap	0.00396 m^2/m (opening area per unit length wall)
	Ventilation unit at the rooftop to outside	0.0919
	Attic space to the ventilation unit at the rooftop	0.0755
	Outside to under-floor space	0.0720
Constants		α = 0.6, ρ = 1.2, n = 0.5

Table 3: Calculation Conditions

Internal heat gain	Exists (based on the schedule by IBEC)
Ventilation	None
Air-conditioning	None, Exists (based on the schedule by IBEC)
Surface temperature in the under-floor space	20°C
Weather data	Expanded AMeDAS standard data (2000) , Tokyo
External wind	None
Calculation period	7/21–8/20, 6/1–9/30 (plus 3 days for run-up period)

Table 4: Simulation Cases

	Flow rate of the attic fan (m^3/h)	**Multiplier (-)**
Case 0	0 (off)	-
Case 1	150	1/2

Case 2	300	1
Case 3	600	2

2.3 Calculation Conditions

The calculation conditions used in this study are listed in Table 1 through Table 4. Table 1 lists the properties of the walls, air gap, windows, etc. The conditions of the ventilated wall are listed in Table 2, and the calculation conditions are listed in Table 3. For evaluating the airflow rate, four cases under different flow rates are supposed. To estimate effects under different airflow rates, the flow rate of the basic case (Case 0) is set to 0 m^3/h, and the main flow rate is set to 300 m^3/h (Case 2). Other cases are multiplied by 0.5 or 2, respectively. The simulation cases are listed in Table 4.

To estimate the properties of airflow in the ventilated wall at natural room temperature, the simulation was first performed without air-conditioning. Then, calculations were carried out with air conditioning, and the effect of cooling load reduction due to heat loss carried by airflow in the wall was estimated. The air-conditioning temperature was set to 28°C, and a total of five rooms—living room, kitchen, bedroom, and two children's rooms—were regarded as air-conditioned.

As shown in Table 3, the schedule of internal heat generation, ventilation, and air-conditioning was set according to the criteria of the IBEC standard. The ground surface temperature of the subfloor space was set to 20°C, in reference to the results of past measurements. For weather data, including external wind, AMeDAS' expansion 2000 standard data in Tokyo was used. The calculation period was 7/21–8/20 (plus 3 days for run-up period) in the study of airflow rate, and was 6/1–9/30 (plus 3 days for run-up period) in the study of the cooling load reduction effect.

3 RESULTS

The average flow rate for each wall is shown in Figure 5. The bars with black frames represent the second floor, and the bars without black frames represent the ground floor. The figure shows positive airflow in all walls, and flow direction along a wall (upward direction) is considered positive. For the case in which the flow rate is 300 m^3/h, the average velocity is 54.0 cm/s on the first floor and 66.9 cm/s on the second floor. When the flow rate changes from 300 m^3/h to 150 m^3/h and then to 600 m^3/h, the average flow rate in this period changes by a factor of 0.5 and 2, respectively.

Figure 6 shows the results of a natural indoor temperature and the temperature decrease for Case 2, in which the airflow rate is 300 m^3/h. The temperature in the living room drops by 1.5–3.5°C. The temperature in the roof changes drastically, and the biggest drop is as much as 4.8°C. Also, the average indoor temperature decline is about 2.6°C over the same period.

Figure 7 shows the flow rate of each wall during the representative days, by direction. Based on the graph, the flow rate for each wall is affected by the outdoor temperature. The flow rates in the walls N1, N3, W1, and W3 are low when compared to the other walls, which range from 45 to 50 cm/s.

Figure 8 shows the temperature decreasing in six airnodes. The effect of the temperature decrease in each room is especially remarkable. However, the temperature of the base airnode rises when the flow rate of the ventilated walls is increased. When outdoor air goes through the base airnode, outdoor air is cooled and the base airnode obtains heat from the outdoor air. The largest temperature decrease, 5.4°C, appears on the airnode of roof2, which is at the top of the house. Over a period of time, a decrease of 2.0°C in the indoor temperature can be achieved when the flow rate is 150 m^3/h; 2.6°C, when it is 300 m^3/h; and 4.7°C, when it is 600 m^3/h.

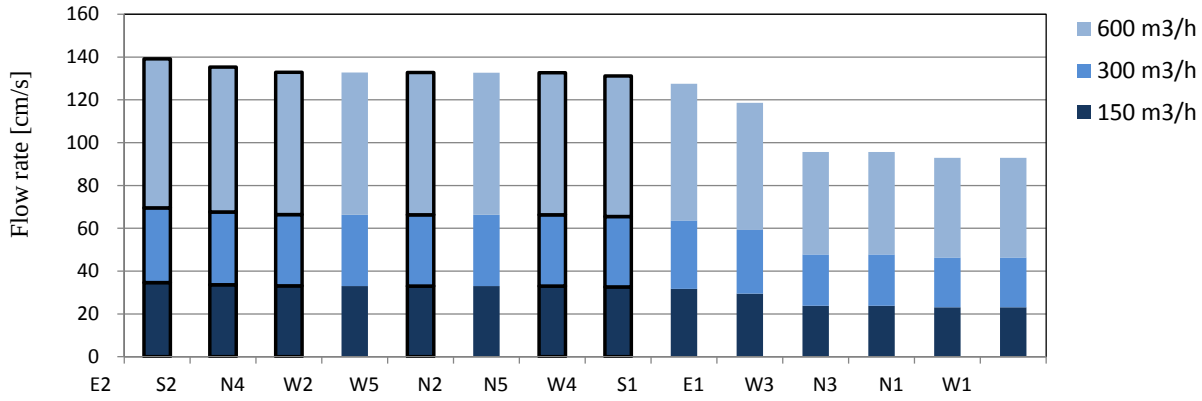

Figure 5: Average flow rate of each wall

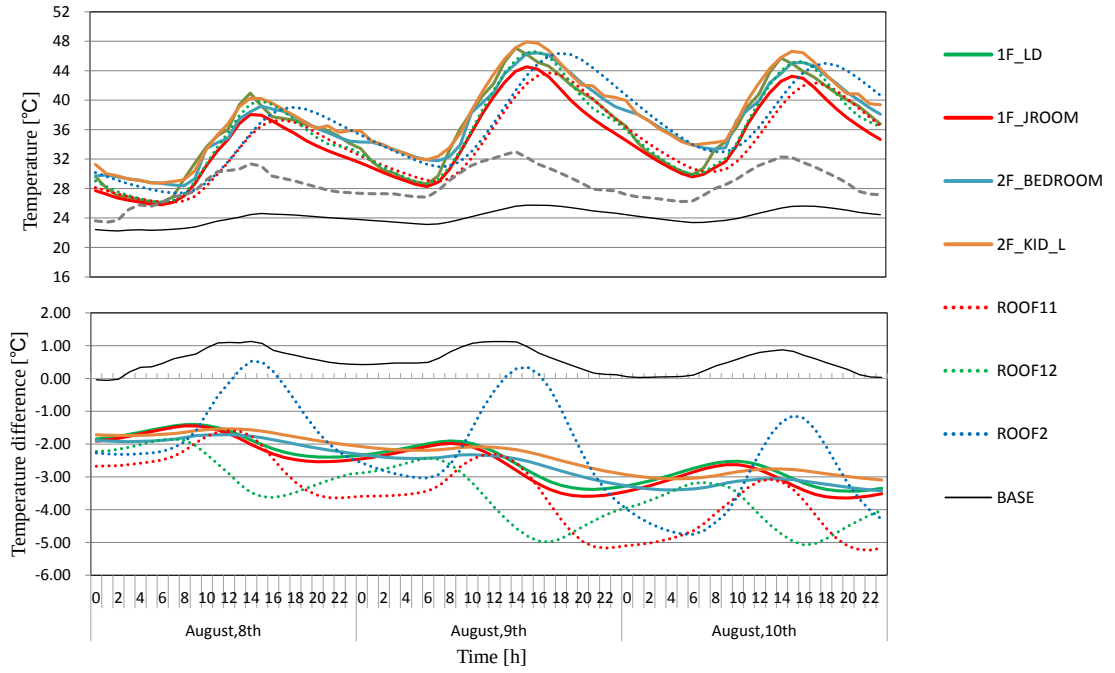

Figure 6: Temperature decrease during representative days (Case 2, 300 m^3/h)

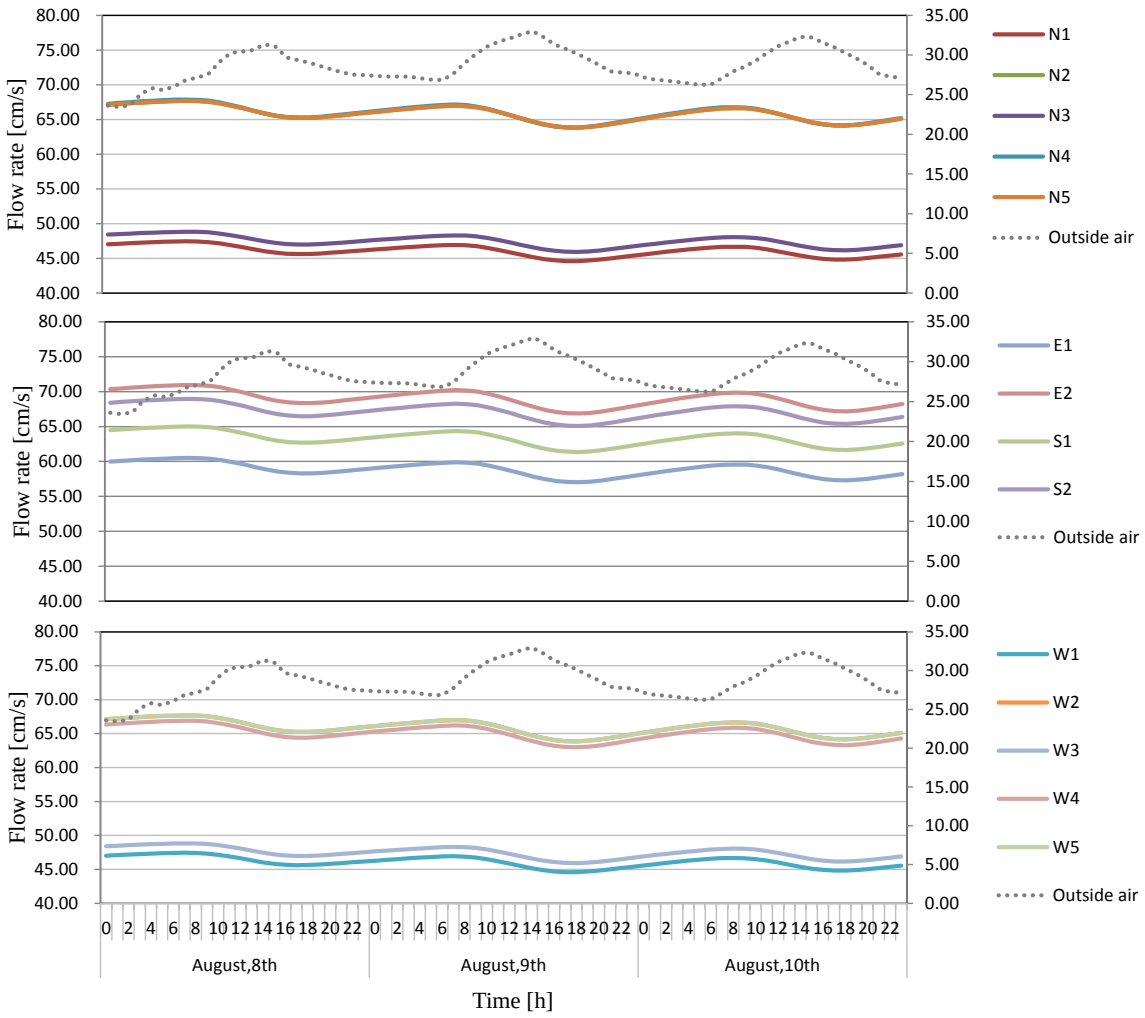

Figure 7: Flow rate for each wall during representative days (Case 2, 300 m^3/h)

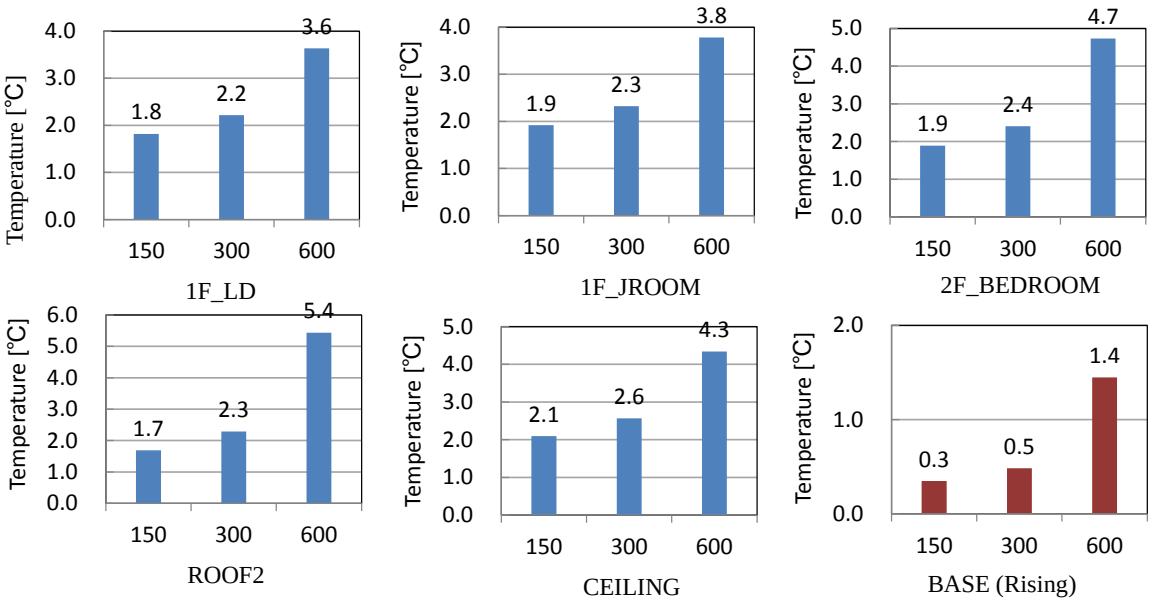

Figure 8: Temperature Decreasing in Each Airnode

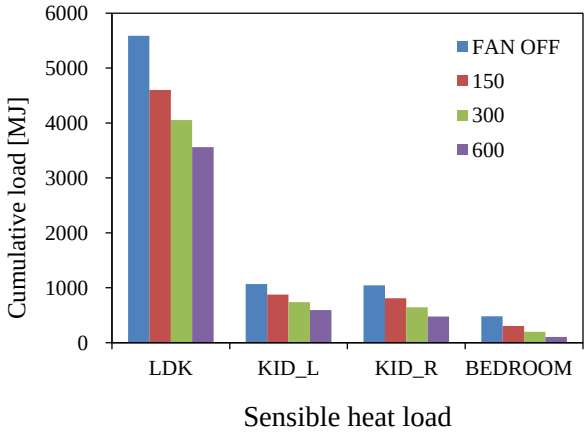

Figure 9: Total cooling load in each room

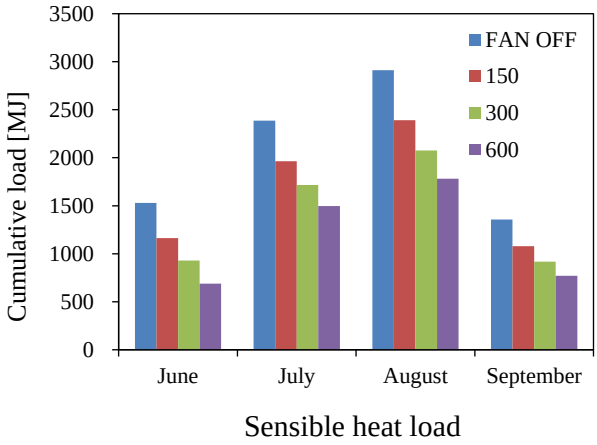

Figure 10: Total cooling load in each month

Figure 9 shows the total cooling load in the ventilated walls for each room and flow rate, for the case with air-conditioning set at 28°C. Results for the four rooms are shown in the graph. The dining room (LDK) receives the largest cooling load reduction because it consumes the most energy among the four rooms. The average cooling load reduction for the dining room from June to September was reduced by 27%.

Figure 10 shows the total cooling load from June to September for each month. The cooling load was reduced for the cases with flow rates equal to 150 m^3/h, 300 m^3/h and 600 m^3/h, and the average cooling load during the period from June to September was reduced by 19%, 31%, and 42%, respectively. The reduction was largest in June and September in which the temperature was lowest. The cooling load was reduced by 28% for a flow rate of 300 m^3/h, even in August, which is the hottest month.

4 CONCLUSIONS

In this study, we evaluated the airflow rate in the air gap of a double-skin cooling system, the cooling load reduction, and the temperature decrease by performing a ventilation network simulation. When changing the airflow of the fan, cooling is improved as the ventilation quantity increases. If the flow rate changes by a factor of 0.5 and 2, the average flow along the

wall changes by a factor of 0.5 and 2, respectively. In general, the cooling effect is greater when the flow rate is higher. Over a period of time, a decrease in 2.0°C in the indoor temperature can be achieved when the flow rate is 150 m^3/h; 2.6°C, when it is 300 m^3/h; and 4.7°C, when it is 600 m^3/h, respectively. The cooling load was reduced for the cases with flow rates of 150 m^3/h, 300 m^3/h, and 600 m^3/h, and the average cooling load during the period from June to September was reduced by 19%, 31%, and 42%, respectively. Reduction was largest in June and September, when the temperatures were the lowest. The cooling load was reduced by 28% for a ventilated flow rate of 300 m^3/h, even in August, which is the hottest month.

It was found that the total period cooling load is reduced while the ventilated wall is working and the air-conditioning is on. It seems that this effect is mainly because the air-conditioning settling time was reduced by the room temperature drops. As a result, it is expected that the cooling load reduction effect is dependent on the flow rate of the ventilated wall and the cooling load supplied from subfloor ground surface Therefore, a further simulation of geothermal heat is necessary for future study. Furthermore, because heat from solar radiation and internal heat cannot be discharged by infiltration, the simulation result shows the the room temperature is higher than that of the actual environment. To evaluate the influence of infiltration, a simulation that considers infiltration between the interior-exterior wall interface and between the wall-room interface is needed in further research.

5 REFERENCES

Ozaki, A. (1992). Heat and water transfer through an ventilated structure using urethane panels [in Japanese]. *Summaries of technical papers of Annual Meeting Architectural Institute of Japan, D,* 945-946.

Institute for Building Environment and Energy Conservation. (2009). *Description of the energy consumption calculation method in the standards of judgment of the housing business building owners* [in Japanese].

Kurabuchi, T. (2009). Wind tunnel experiments on surface wind pressure and cross-ventilation flow rate in densely populated residential area: study on proper design method of locating windows aiming at utilization of cross-ventilation in densely populated residential area (part 1) [in Japanese]. *Journal of environmental engineering 74(642), 951-956*.

NATIONAL SRVEY ON VENTILATION SYSTEM AND OCCUPANTS' HEALTH IN JAPAN

Kenichi Hasegawa*[1] and Hiroshi Yoshino[2]

1 Akita Prefectural University,
Faculty of Systems Science and Technology
84-4, Ebinokuchi, Tsuchiya-aza,
Yurihonjyo, Akita, Japan

2 Tohoku University,
Department of Architecture and Building Science
6-6-11-1203, Aramaki-aza, Aoba, Aoba-ku,
Sendai, Miyagi, Japan

**Corresponding author:*

Note : the contact addresses may be re-arranged

ABSTRACT

The indoor environment and occupants' health of approximately 5,000 residential buildings were investigated by a questionnaire covering entire Japan. The purpose of this survey is to clarify the association between indoor air pollution and adverse health effect, and to study effective ways of keeping indoor air clear with ventilation systems in house. Questionnaires were distributed to 7,812 occupants living in a house with a mechanical ventilation system across 47 Prefectures in Japan on February 2012 using internet survey web site. The questionnaires were completed and returned within 5 days by occupants. The contents of the 50-question survey addressed the indoor environment, installed equipment, the type of ventilation system, occupant behaviour, shelter performance of the building, occupant characteristics, health related QOL (SF8 Health Survey Japanese version provided by Institute for Health Outcomes & Process Evaluation Research) and health problems such as respiratory symptoms, allergic diseases and chemical sensitivities. As a result, the total number of respondents was 5,265 and the response ratio was 67.4%. Also the actual conditions of both the perception of thermal environment, dryness, wetness and air quality and house characteristics such as thermal performance on envelopes, heating system and ventilation system have been clarified, and several problems related to using ventilation systems have been grasped.

This paper described the outline of investigation and the results obtained from the questionnaire survey. In particular, the features of the home environment and occupants health conditions with health related QOL were shown and the association between indoor dampness such as mould growth and ventilation system were discussed through a multivariable regression analysis. This survey revealed the ratio of the type of an installed ventilation system and the pattern of using it in Japan and the possibility of the association between adverse health effect and indoor environmental factors such as inadequate ventilation.

KEYWORDS

Ventilation system, Occupants' behaviour and health, Indoor Air Quality, Questionnaire survey in Japan, Health related QOL

INTRODUCTION

It is important to maintain adequate air change rate in indoor for keeping the occupants healthy in dwellings. In Japan so called "sick house problem" has happened in 2000's, and the indoor concentration of chemical substance such as formaldehyde had been higher than the guideline in many newly built dwellings. After this affair, revision of the Building Standard Law was approved on July, 2002, and the installation of mechanical ventilation has been needed in any dwellings [1].

In order to clarify the actual conditions such as installation and occupants' operation of the ventilation system and to study effective ways of keeping indoor air clear with a ventilation system in a dwelling, a questionnaire about the ventilation system and indoor environment covering entire Japan were conducted to the approximately 5,000 dwellings. Questionnaires

were distributed to 7,812 occupants living in a house with a mechanical ventilation system across 47 Prefectures in Japan on February 2012 using internet survey web site. The questionnaires were completed and returned within 5 days by occupants. The contents of the 50-question survey addressed the indoor environment, installed equipment, the type of ventilation system, occupant behaviour, shelter performance of the building, occupant characteristics, health related QOL [2] and health problems such as respiratory symptoms, allergic diseases and chemical sensitivities.
This paper described the outline of a questionnaire survey and the results obtained from the survey. In particular, the features of the home environment and occupants health conditions with health related QOL were shown and the association between health problems and influencing factors were discussed through a multi-regression analysis. This survey revealed the ratio of the type of an installed ventilation system and the pattern of using it in Japan and the possibility of the association between adverse health effect and indoor environmental factors such as inadequate ventilation.

METHOD

Outline of survey

Questionnaires were distributed to 7,812 occupants using internet survey web site on February 2012. The investigated houses were detached house and apartment house which were completed after 2003 and were installed a mechanical ventilation system. The questionnaires were completed and returned within 5 days by occupants. In this paper, investigated areas were divided into six kinds of regions according to heating degree days as shown in Figure 1. Table 1 shows the investigated areas (Region I, II, III, IV, V+VI), the number of questionnaires sent and respondents. The total number of respondents was 5,265 and the response ratio was 67.4%.
The contents of the 50-question survey addressed the indoor environment, installed equipment, the type of ventilation system, occupant behaviour, shelter performance of the building, occupants' characteristics, health related QOL [2] and self-reported health problems such as respiratory symptoms, backache, stiff shoulder, mental symptoms and so on. The SF8 in Japanese version which was provided by Institute for Health Outcomes & Process Evaluation Research was used as a simple tool with which to evaluate the health related QOL using eight kinds of questions. The health rerated QOL was assessed from the viewpoints of physical function, body pain, general health perception, vitality, mental health and so on, and were calculated by a combination of scale answers to specific questions.

Statistical analysis

We analyzed the data using the Statistical Package for the Social Sciences (SPSS). Associations between indoor dampness such as mould growth and condensation on the surface of windows and the factors related to ventilation system were estimated using logistic regression models. Odds ratios were estimated including the 95% confidence interval (CI). Indoor environment factors selected from the results of the single regression analysis were estimated in multiple logistic regression models with a P value <0.2 as representing significance.

Table 1. Investigated area, number of questionnaires distributed and response.

Region	Distributed Questionnaires	No. of Respondents	Response[%]
Region I	787	526	67.4
Region II	641	417	
Region III	1,279	990	
Region IV	4,816	3,235	
Region V, VI	289	97	
Total	7,812	5,265	

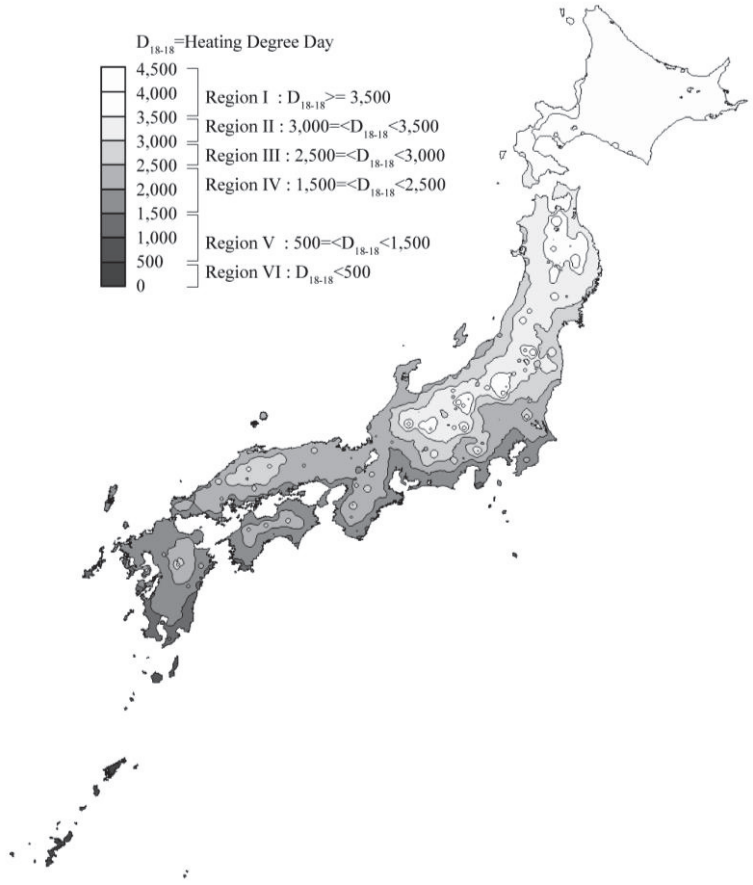

Figure 1. Heating degree days (D_{18-18}) and areas of investigated houses.

RESULTS AND DISCUSSION

Table 2 shows characteristics and indoor environment of investigated houses in each regions determined from the questionnaire.

Building characteristics

Most of the respondents were from 30s to 40s, and about 50% of respondents were male and female. Thermal performance of dwellings in accordance with the equivalent of 1992's standard dwellings was around 50% of all. The dwellings to fulfil newly standard was around 20% in each area.

Vented kerosene burners and central heating system were used as the source of winter heat in Region I and II, which are cold climatic regions in winter. On the other hand, in Region III to VI, unvented kerosene heaters were still being used in around 20% of dwellings. About 50% of dwellings in Region IV to VI used air conditioning during winter. A ventilation system of a mechanical exhaust and supply with and without a heat recovery was installed in about 30% of all dwellings. Type of a mechanical exhaust was used more than a mechanical exhaust and supply.

Around 40% of dwellings operated a mechanical ventilation system all the time during winter, while around 50% operated it intermittently. There were dwellings which didn't operate a mechanical ventilation system. Table 3 shows reasons for not operating a mechanical ventilation system. In Region I to IV about 40% of dwellings felt cold when operating a ventilation system. 30 to 40% of dwellings didn't operate a ventilation system for economizing on electric power. A few occupants thought that outdoor air pollutants such as

pollen and airborne dust entered into indoor rooms with operating a mechanical ventilation system. Around 40% of dwellings were cleaning a ventilation system regularly.

Table 2. Characteristics and indoor environment of investigated housing

Items \ Region	Region I [n(%)] (N=526)	Region II [n(%)] (N=417)	Region III [n(%)] (N=990)	Region IV [n(%)] (N=3,235)	Region V, VI [n(%)] (N=97)
Age groupe					
20-29	23 (4.4)	24 (5.8)	46 (4.6)	150 (4.6)	4 (4.1)
30-39	224 (42.6)	169 (40.5)	431 (43.5)	1,383 (42.8)	36 (37.1)
40-49	185 (35.2)	155 (37.2)	336 (33.9)	1,093 (33.8)	34 (35.1)
50-59	66 (12.5)	49 (11.8)	111 (11.2)	401 (12.4)	16 (16.5)
60-	28 (5.3)	20 (4.8)	66 (6.7)	208 (6.4)	7 (7.2)
Gender					
Male	262 (49.8)	182 (43.6)	480 (48.5)	1,586 (49.0)	52 (53.6)
Female	264 (50.2)	235 (56.4)	510 (51.5)	1,649 (51.0)	45 (46.4)
Housing type					
Detached	265 (50.4)	305 (73.1)	540 (54.5)	1,707 (52.8)	61 (62.9)
Apartment	261 (49.6)	112 (26.9)	450 (45.5)	1,528 (47.2)	36 (37.1)
Thermal insulation level					
Equivalent of 1980's standard	148 (28.1)	105 (25.2)	301 (30.4)	946 (29.2)	26 (26.8)
Equivalent of 1992's standard	265 (50.4)	200 (48.0)	457 (46.2)	1,536 (47.5)	49 (50.5)
Equivalent of 1999's standard	80 (15.2)	84 (20.1)	165 (16.7)	532 (16.4)	18 (18.6)
No data	33 (6.3)	28 (6.7)	67 (6.8)	221 (6.8)	4 (4.1)
Main heating equipment in a living room					
Vented kerosene or gas heater	116 (22.1)	124 (29.7)	58 (5.9)	40 (1.2)	1 (1.0)
Unvented kerosene or gas heater	56 (10.6)	79 (18.9)	334 (33.7)	917 (28.3)	21 (21.6)
Electric heater	87 (16.5)	86 (20.6)	143 (14.4)	219 (6.8)	5 (5.2)
Central heating system	225 (42.8)	74 (17.7)	66 (6.7)	33 (1.0)	0 (0.0)
Floor heating	30 (5.7)	20 (4.8)	81 (8.2)	412 (12.7)	4 (4.1)
Air conditioning	4 (0.8)	32 (7.7)	292 (29.5)	1,506 (46.6)	51 (52.6)
Others	8 (1.5)	2 (0.5)	16 (1.6)	108 (3.3)	15 (15.5)
Ventilation system in rooms					
Mechanical exhaust and supply	75 (14.3)	82 (19.7)	192 (19.4)	669 (20.7)	24 (24.7)
Mechanical ventilation with heat recovery	56 (10.6)	62 (14.9)	111 (11.2)	286 (8.8)	6 (6.2)
Mechanical exhaust using fans on walls	264 (50.2)	216 (51.8)	415 (41.9)	1,286 (39.8)	45 (46.4)
Mechanical exhaust using ductwork system	131 (24.9)	57 (13.7)	272 (27.5)	994 (30.7)	22 (22.7)
Pattern of operating the ventilation system during winter					
Using all the time	222 (42.2)	180 (43.2)	356 (36.0)	980 (30.3)	36 (37.1)
Intermittently	239 (45.4)	198 (47.5)	514 (51.9)	1,780 (55.0)	50 (51.5)
Not using	38 (7.2)	31 (7.4)	91 (9.2)	339 (4.2)	8 (8.2)
Others	27 (5.1)	8 (1.9)	29 (2.9)	136 (4.2)	3 (3.1)
Cleaning of ventilation system regularly					
Yes	191 (36.7)	168 (40.5)	385 (39.4)	1,369 (43.0)	54 (57.4)
No	330 (63.3)	247 (59.5)	529 (60.6)	1,818 (57.0)	40 (42.6)
Vapor condensation on the glass surface in a living room during winter					
Observed, clouded	36 (6.8)	37 (8.9)	77 (7.8)	342 (10.6)	10 (10.3)
Observed, drop of water attaching	131 (24.9)	113 (27.1)	287 (29.0)	936 (28.9)	24 (24.7)
Observed, drop of water flowing	54 (10.3)	53 (12.7)	149 (15.1)	434 (13.4)	8 (8.2)
Not observed	305 (58.0)	214 (51.3)	477 (48.2)	1,523 (47.1)	55 (56.7)
Visible mould during winter					
Observed, in a living room and/or bed room	63 (12.0)	82 (19.7)	141 (14.2)	364 (11.3)	14 (14.4)
Observed, in a bathroom	112 (21.3)	151 (36.2)	328 (33.1)	1,018 (31.5)	37 (38.1)
Observed, in a kitchen	20 (3.8)	24 (5.8)	52 (5.3)	141 (4.4)	7 (7.2)
Observerd, other rooms	43 (8.2)	50 (12.0)	100 (10.1)	278 (8.6)	14 (14.4)
Not observed	360 (68.4)	218 (52.3)	584 (59.0)	1,985 (61.4)	51 (52.6)
Percept of odor in indoor					
Mold	18 (3.4)	28 (6.7)	44 (4.4)	161 (5.0)	8 (8.2)
Garbage	28 (5.3)	33 (7.9)	46 (4.6)	166 (5.1)	2 (2.1)
Tobacco smoke	26 (4.9)	25 (6.0)	38 (3.8)	142 (4.4)	2 (2.1)
Chemical material from furniture etc.	5 (1.0)	11 (2.6)	23 (2.3)	72 (2.2)	3 (3.1)
Pet	43 (8.2)	28 (6.7)	55 (5.6)	205 (6.3)	4 (4.1)
Not perceived	225 (42.8)	161 (38.6)	440 (44.4)	1,455 (45.0)	43 (44.3)

Table 3. Reasons for not operating a mechanical ventilation system

Items \ Region	Region I [n(%)] (N=276)	Region II [n(%)] (N=228)	Region III [n(%)] (N=601)	Region IV [n(%)] (N=2,113)	Region V, VI [n(%)] (N=58)
Reason for not operating the ventilation system					
Heat loss with operating it	76 (27.5)	64 (28.1)	153 (25.5)	512 (24.2)	9 (15.5)
Feeling cold with operating it	129 (46.7)	99 (36.9)	222 (36.9)	800 (37.9)	17 (29.3)
Entering pollen or dust from outdoor air	13 (4.7)	16 (7.0)	63 (10.5)	217 (10.3)	2 (3.4)
Economizing on electric power	77 (27.9)	75 (32.9)	209 (34.8)	839 (39.7)	25 (43.1)
Feeling noise when operating it	35 (12.7)	39 (17.1)	91 (15.1)	374 (17.7)	10 (17.2)
Not necessary to use it	87 (31.5)	79 (34.6)	215 (35.8)	781 (37.0)	27 (46.6)

Indoor air quality and health conditions

Vapour condensation on the glass surface in a living room was “Not observed” around 50% of all dwellings, 8.2 to 15.1% of them observed vapour condensation with drop of water flowing. Mould was visible on the surface of building envelopes in living room and bed room in 11.3 to 19.7% of all dwellings. About 40% of dwellings observed mould growth on the surface in rooms. Occupants perceived odour in indoor such as mould, garage, tobacco smoke, chemical material, pet and so on.

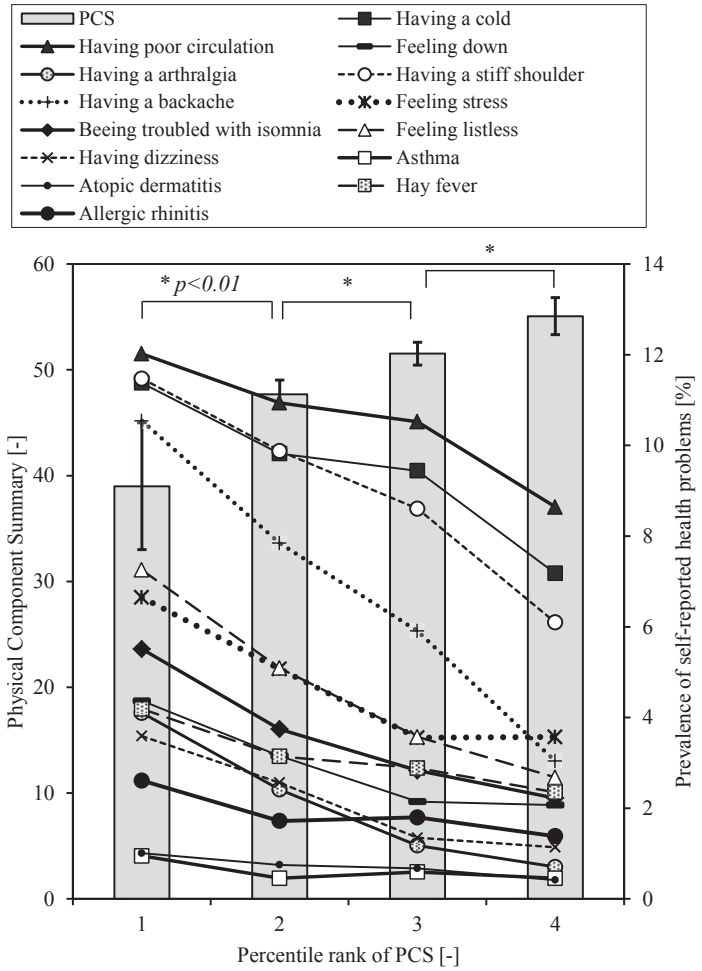

Figure 2. The prevalence of self-reported health problems and its association with health related QOL

Figure 2 shows prevalence of disease and its association with health related QOL. The health rerated QOL was assessed by Physical component summary (PCS) from the eight kinds of scales such as physical function, body pain and so on. PCS of each occupant was calculated using self-reported score to eight kinds of scales. The PCS score had an average score of 50.0 and the level of health related QOL was rising according as the PCS score was increasing

more than 50.0. In this paper all data were distributed among 25% percentile rank of the PCS score. Rank 1 included lower score than 25 % percentile rank. Rank 2 was between 25% and 50% percentile rank and Rank 3 was between 50 and 75%. Rank 4 included occupants accessed as higher score than 75% percentile rank. Each 'Percentile rank of PCS' in Figure 2 shows averaged score in the range each rank. The averaged PCS score was significantly increasing when 'Percentile rank of PCS' was high.

It was recognized that prevalence of self-reported health problems was associated with 'Percentile rank of PCS'. The lower the prevalence of health problems was, the higher 'Percentile rank of PCS' became. Therefore health related QOL could represent the inclusive health condition on the basis of occupants' self-reported answers.

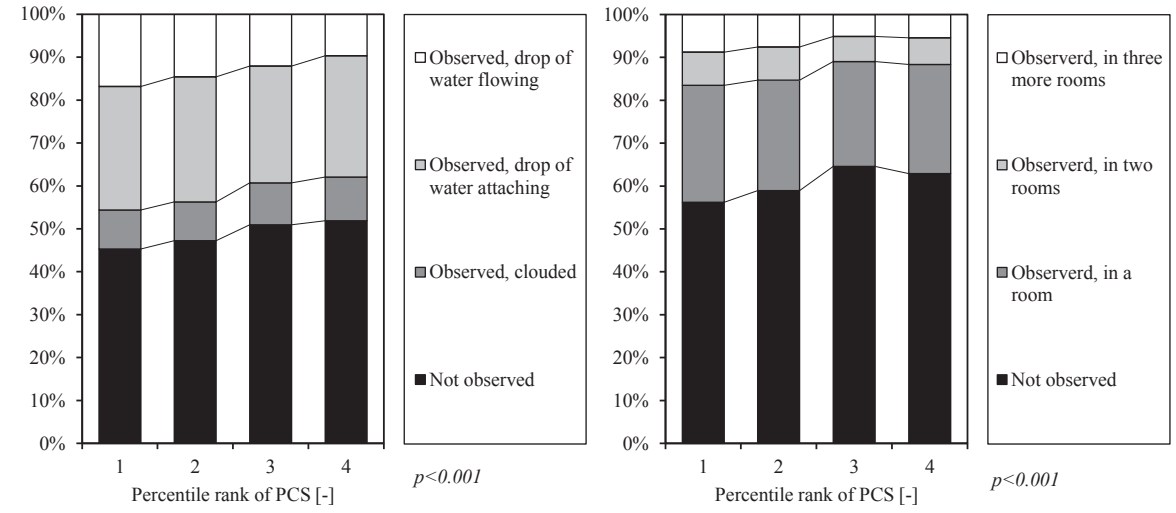

(a) Vapour condensation on the glass surface in a living room during winter.

(b) Visible mould during winter.

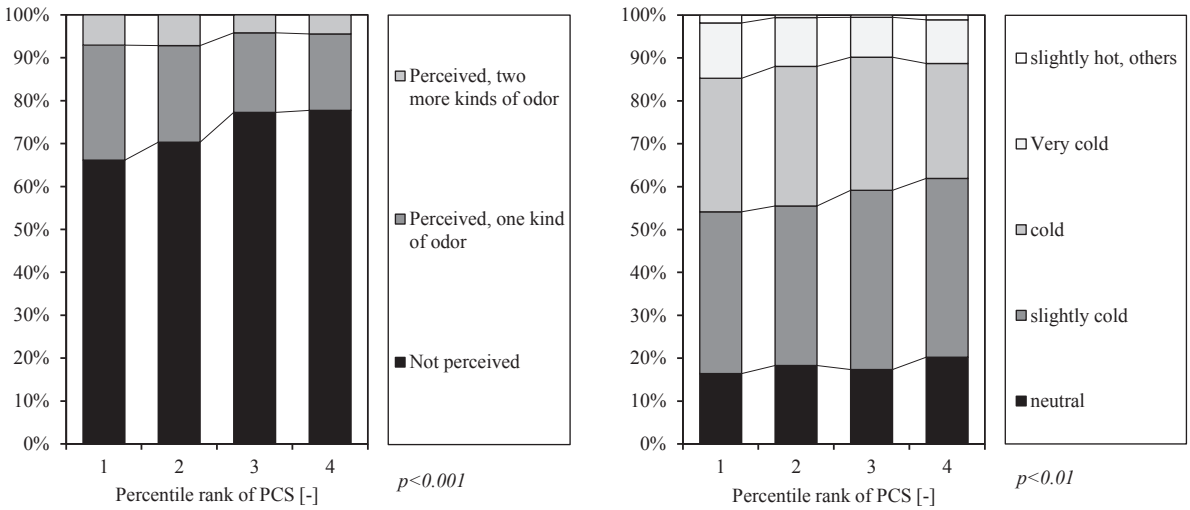

(c) Perception of odour in indoor.

(d) Feel thermally comfortable in the morning

Figure 3. Association between percentage rank of PCS and indoor environment

Occupants' health and indoor environment

Proportion of respondents regarding indoor environmental quality due to health related QOL are shown in Figure 3. Vapour condensation on the glass surface and visible mould growth in rooms significantly decreased when 'Percentile rank of PCS' was rising. Also perception of odour in indoor and feeling thermally uncomfortable in the morning gradually reduced according as 'Percentile rank of PCS' was rising. These results indicated indoor dampness

related to the indoor environmental quality was significantly associated with occupants' health conditions.

Ventilation system and Indoor environmental factors related health

Associations between ventilation system and indoor dampness related to occupants' health are shown in Table 4. Adjusted ORs were calculated using a multivariable regression models adjusted for area (Region I-VI) of housing location. We selected several variable factors related to ventilation system such as the type of ventilation system, pattern of operating a ventilation system, cleaning of a ventilation system and feeling thermally comfortable.

The adjusted ORs for mechanical ventilation with heat recovery (OR=0.7, 95% CI=0.51-0.96) was statistically significant for not visible mould in rooms. This result indicates that this type of ventilation system was operating more effectively due to prevent dampness in rooms than the other types. The adjusted ORs for operating intermittently a ventilation system (OR =2.10, 95% CI=1.84-2.38) and not using it (OR=2.21, 95% CI=1.76-2.78) were statistically significant for visible vapour condensation on the surface openings. With less frequency in use of a ventilation system, the adjusted ORs for vapour condensation, visible mould and mouldy odour were larger. The risks of vapour condensation and visible mould in rooms increased with pattern of operating a ventilation system ($p<0.001$). The adjusted ORs for not cleaning of a ventilation system (OR=1.21, 95% CI=1.08-1.38) was statistically significant for occurring vapour condensation. Feeling thermally comfortable in the morning increased the risks of vapour condensation, visible mould and mouldy odour in rooms with the adjusted ORs of 0.16-0.65 ($p<0.001$). Indoor thermal environment in the morning was affected by thermally insulation levels of building envelopes. It indicated that dwellings of occupants' feeling cold in rooms in the morning didn't have enough thermally performance of building envelopes. Therefore vapour condensation and visible mould in rooms could occur easily.

CONCLUSION

In order to clarify the actual conditions of installed ventilation system and to study effective ways of keeping indoor air clear with a ventilation system in a house, a questionnaire survey were conducted to the approximately 5,000 dwellings in Japan. Vapour condensation on the glass surface and visible mould growth in rooms significantly decreased when health related QOL was rising. These results indicated indoor dampness was significantly associated with occupants' health conditions. Through a multivariable regression analysis, it was revealed that the mechanical ventilation with heat recovery was operating more effectively due to prevent dampness in rooms than the other types. In addition, the risks of occurring vapour condensation and visible mould growth increased with pattern of operating a ventilation system.

ACKNOWLEDGEMENTS

The authors would like to thank the residents who were involved in this study for their helpful cooperation. This project was conducted as one of the activities of the Research Project for Creation of Housing that Promotes Health and Well-being (Chair: Prof. Shuzo Murakami). This study was supported by the Grants-in-Aid for Scientific Research of the Ministry of Education, Culture, Sports, Science & Technology in Japan.

REFERENCES

[1] Sawachi, T. and Tajima, M. 2008. Trends in the Japanese building ventilation market and derivers for change, *Ventilation Information Paper*, No.25, AIVC, 1-16.

[2] Fukuhara S, Suzukamo Y. 2004. Manual of the SF-8 Japanese version, Institute for Health Outcomes & Process Evaluation Research, Kyoto.

Table 4. Association between vapour condensation, visible mould, perception of mouldy odour, and factors related indoor ventilation.

Variable factor	Vapor condensation		Mould in rooms		Perception of mouldy odor	
	visible/not visible (N=5,062)	Adjusted OR (95% CI)	visible/not visible (N=5,062)	Adjusted OR (95% CI)	perceptible/not perceptible (N=5,062)	Adjusted OR (95% CI)
Type of ventilation system						
Mechanical exhaust	2,253 / 1,344	1.00 (Ref.)	468 / 3,129	1.00 (Ref.)	27 / 476	1.00 (Ref.)
Mechanical ventilation with heat recovery	290 / 213	0.82 (0.67-1.00)	80 / 453	0.70 (0.51-0.96)*	41 / 921	1.07 (0.70-1.63)
Mechanical exhaust and supply	640 / 322	0.99 (0.85-1.16)	128 / 834	0.86 (0.69-1.07)	179 / 3,418	0.72 (0.51-1.03)
Pattern of operating a ventilation system						
Using all the time	880 / 894	1.00 (Ref.)	153 / 1,621	1.00 (Ref.)	55 / 1,719	1.00 (Ref.)
Intermittently	1,937 / 844	2.10 (1.84-2.38)***	406 / 2,375	1.74 (1.43-2.14)***	162 / 2,619	1.82 (1.32-2.50)***
Not using	366 / 141	2.21 (1.76-2.78)***	87 / 420	2.01 (1.49-2.71)***	30 / 477	1.85 (1.15-2.97)*
Cleaning of a ventilation system regularly						
Yes	1,752 / 1,212	1.00 (Ref.)	326 / 2,638	1.00 (Ref.)	136 / 2,828	1.00 (Ref.)
No	1,431 / 667	1.21 (1.08-1.38)**	320 / 1,778	1.23 (1.03-1.46)*	111 / 1,987	0.96 (0.74-1.26)
Feel thermally comfortable in the morning						
Very cold	437 / 115	1.00 (Ref.)	137 / 415	1.00 (Ref.)	60 / 492	1.00 (Ref.)
cold	1,096 / 441	0.65 (0.52-0.83)***	221 / 1,316	0.52 (0.41-0.67)***	90 / 1,447	0.50 (0.35-0.71)***
slightly cold	1,227 / 781	0.44 (0.35-0.56)***	211 / 1,797	0.38 (0.29-0.48)***	78 / 1,930	0.33 (0.23-0.47)***
neutral	407 / 507	0.25 (0.19-0.32)***	67 / 847	0.24 (0.17-0.33)***	17 / 897	0.16 (0.09-0.27)***
slightly hot, others	16 / 35	0.16 (0.08-0.30)***	10 / 41	0.73 (0.35-1.53)	2 /49	0.34 (0.08-1.45)

Note: ***p<0.001, ** p<0.01, * p<0.05, + p<0.1 ; Adjusted for Area(Region I - VI). Ref.=referent.

ENERGY EFFICIENCY & IAQ ASPECTS OF THE SCHOOL BUILDINGS IN GREECE

Niki Gaitani*, Mat Santamouris

National & Kapodistrian University of Athens, Greece
**Corresponding author: ngaitani@phys.uoa.gr*

ABSTRACT

The present article deals with the energy classification and the environmental evaluation of the school buildings in Greece. The energy performance of the school buildings, in relation to the normalized annual consumption for heating regarding floor area and climatic conditions, was rated using clustering technique (K-means algorithm) and an energy classification tool developed. The audited school buildings were classified into five energy categories. To investigate the potential for energy savings a methodology for the definition of the characteristics of the typical building for each energy class of the school sector has been developed using multivariate statistical techniques. It is based on a selection of seven variables that influence the energy performance of the building and has been mainly carried out using principal components analysis techniques (PCA). For the evaluation of indoor temperatures, the heating loads and the potential for energy conservation interventions, the typical buildings in each class have been simulated for a typical meteorological year, using TRNSYS. The measurements of indoor air quality concerned in concentrations of monoxide (CO) and carbon dioxide (CO_2), as well as in the organic volatile compounds (TVOCs) in 83 classrooms. Thermal comfort conditions have been calculated using the indoor measurements of the meteorological parameters. The research has shown that school buildings suffer from important IAQ problems while their energy consumption and global environmental quality can be improved considerably. The conclusions obtained promote a general energy and environmental evaluation of the school buildings in Greece.

KEYWORDS

Schools, Energy efficiency, IAQ, Cluster analysis, PCA

1 INTRODUCTION

Energy efficiency and IAQ are key points of environmental policy and energy strategy in Europe. As EPBD came into force, European regulation on buildings has been implemented in different ways in European Union Member States and various techniques have been proposed to develop rating schemes (Roulet 2002, Santamouris 2005, Santamouris 2007, Corgnati S. P.,2008, Gaitani N., 2010).

In Greece, since May 2008 the Law 3661 on "Measures to reduce energy consumption in buildings and other provisions" in line with Directive 2001/91/EC has been adopted. The Regulation for Buildings Energy Performance (KENAK) based primarily in European Standard ISO/EN 13790, has been incorporated within national legislation and expected to comprise an integral part of all future developments in the building sector in Greece.

Greece currently has 15,446 schools of which 4,500 are over 45 years old. The total energy consumption of school buildings is around 270.000 MWh. In parallel, the insular and mountainous character of the country and the resulted student population moving to bigger urban centers constantly generates new school infrastructure demand. The result is the

constant need to build new schools and to implement actions to improve the quality of existing school facilities.
The Greek school buildings are divided into two categories: those that were built before 1960 and are usually stone with a wooden roof and the ones that were built after 1960 and represent typologies of Greek School Buildings Organisation SA (SBO). These typologies generally have similar construction features in all climatic zones of the country; are built with concrete and bricks and have metal frames. The different typologies show many similarities mainly in construction but also in the proportions of classes, corridors and other spaces. Basic differences usually occur in the number and arrangement of classrooms.
The design may be linear or Γ shaped, or less commonly Π shaped. Commonly, the schools encountered in compact arrangement, with rooms arranged around a central inner space.
The linear buildings and those that are arranged in Γ shaped, showing the rooms face in the yard, or outdoor with an enclosed hallway toward the rear or, more rarely, open hallway from the main side. The typologies appear with 1, 2, or 3 floors according to the school building program.
The research is based on data collection using energy audits of secondary education public school buildings. The distribution of questionnaires to all the prefectures of Greece conducted in collaboration with the SBO and the Greek Ministry of Education. The method of free sample (Haphazard sampling) was used. The data set represents 33% of the entire population of secondary education school buildings and is distributed in all the prefectures of Greece, while 23% of the sample originates from Attica. The collected data were quantitatively and qualitatively.
The present article deals with the energy classification and the environmental evaluation of the school buildings in Greece. The energy performance of the school buildings, in relation to the normalized annual consumption for heating regarding floor area and climatic conditions, was rated using a clustering technique (K-means algorithm) and an energy classification tool developed. The audited school buildings were classified into five energy classes. In order to identify best practices, set energy performance goals and predict internal conditions, thermal simulations were applied with TRNSYS software for a year in every typical building of each energy class.
The main contribution of the present study is the assessment of energy conservation potentials in schools taking into account the environmental quality issues.

2 ENERGY PERFORMANCE

The research was based principally on data collection using energy audits in a sample of 1190 secondary education public school buildings. The auditing techniques were used to create a database on the energy use for heating in the school field and contained data such as the annual consumption for heating and lighting, the area of the building, the number of students and professors, the installed power of the boiler, the manufacturing year of the building and the schedule of operation.
The majority of the school buildings in Greece (98%) are not heated with other carriers than oil. Furthermore, the classrooms in Greek schools are not equipped with electrical heating or cooling systems. For general lighting the interior school spaces rely mainly on daylight during daily operation. The percentage of electricity refers to the energy consumption by office and other electrical energy-consuming equipment. Most schools of the sample were 25 years of age and the heating system on average calculated 18 years.
The oil values for space heating of the school buildings measured in litters converted in kWh multiplied by the factor 11.2 kWh/L) according to the Greek legislation. The schools on an

average have 18 internal spaces (classes, workshops and offices), 246 students and 32 students.

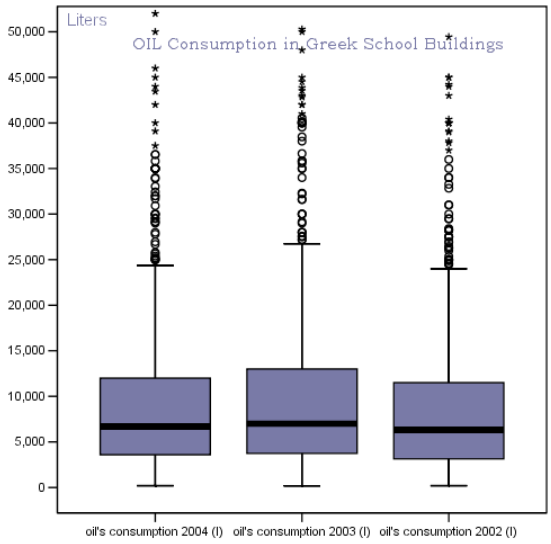

Figure 1: Box plot of energy consumption for space heating with oil [three school years]

As shown in Fig 1 the median values of energy consumption for space heating with oil ranged between 6300-7000 L.

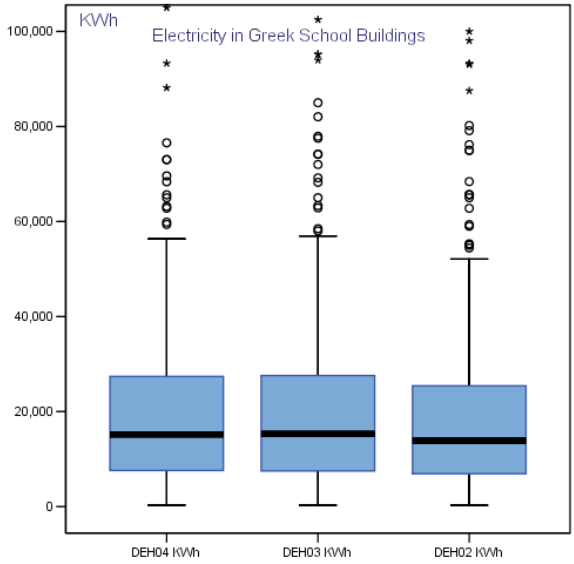

Figure 2: Box plot of energy consumption for electricity [three school years]

The median values of energy consumption for electricity ranged between 13.925-15.252 kWh (see Fig 2). The average power of the boiler was calculated 350 kW and the average heated area of the schools was 1772m^2. Also, the average power of the lamps was found to be 387kW.

2.1 Energy consumption for heating

The majority of schools in Greece (98%) were not heated with other carriers than oil. The classrooms were not equipped with electrical heating (nor cooling) systems. The focus was on oil conservation used for space heating. The energy performance of the school buildings, in relation to the normalized annual consumption for heating regarding floor area and climatic conditions, was rated using a clustering technique (K-means algorithm, Afifi AA., Clark,

1996.) and an energy classification tool developed (Gaitani N., 2010). The annual consumption for space heating has been divided by the total heated floor area, (to get energy per unit area, kWh/m^2) in order to enable a comparison with buildings of different size. In order to normalize the impact of climate on energy consumption the degree-days method was applied on energy use for heating with a base temperature of 18.5°C (Papakostas 2005, Yael 2009).

Table 1: Normalized annual consumption for heating with oil in kWh/m^{2}y

		$OILN_{04}$ kWh/m^{2}y	$OILN_{03}$ kWh/m^{2}y	$OILN_{02}$ kWh/m^{2}y
N	**Valid**	944	918	901
	Missing	247	273	290
Mean		63.8	65.8	61.0
Median		47.9	49.5	45.7
Std. Deviation		61.9	61.5	59.9
Percentiles	**25**	29.9	31.2	27.7
	50	47.9	49.5	45.7
	75	77.3	79.6	73.7

The mean normalized energy consumption for heating with oil was calculated for three years (Table 1): 61.0 kWh/m^{2}y, 65.8 kWh/m^{2}y and 63.8 kWh/m^{2}y respectively.

As the data set is skewed the median is preferred to other measures of central tendency. Moreover, it is the most appropriate measure of central tendency when the data has outliers (Hoaglin D C., 1986). Here, the median of the normalized energy consumption for heating was calculated for the three years respectively: 45.7kWh/m^{2}y, 49.5kWh/m^{2}y, and 47.9kWh/m^{2}y.

The energy performance of the school buildings, in relation to the normalized annual consumption for heating regarding floor area and climatic conditions, was rated using K-means algorithm and the audited school buildings were classified into five energy classes A–E. The average annual energy consumption for heating in school buildings for the three examined years, in class A was varied in a range of 18-22 kWh/m^{2}y and the median 19-23kWh/m^{2}y. For energy class B, the corresponding values were 37-42 kWh/m^{2}y and 40-42kWh/m^{2}y, respectively. In class C was calculated 57-62kWh/m^{2}y (mean) and 58-62kWh/m^{2}y (median), in class D, 85-89kWh/m^{2}y and 84-87 kWh/m^{2}y and finally in class E 119-124kWh/m^{2}y and 117-123kWh/m^{2}y, respectively.

The consumption for heating with oil was high, given the limited operation hours of schools and the mild climate of the country. Furthermore, this consumption usually does not cover the actual needs for heating, as most schools do not meet the thermal comfort conditions during operation.

All non-insulated elements (i.e. non-insulated columns, beams, ledges) contributed to increased thermal losses during winter and increased thermal gains during the warm period and intensify the feeling of thermal discomfort. The large air infiltration from cracks and openings uncontrolled ventilation produced excessive fuel consumption and cold conditions in the halls. Also, the random orientation of buildings, according to the available land did not provide the necessary insolation schools, nor to avoid overheating in combination with insufficient shading.

The orientation should be a crucial issue in the creation of a building with low energy efficiency. School buildings with favourable orientation in classrooms (north and south orientation) had a smaller load for heating.

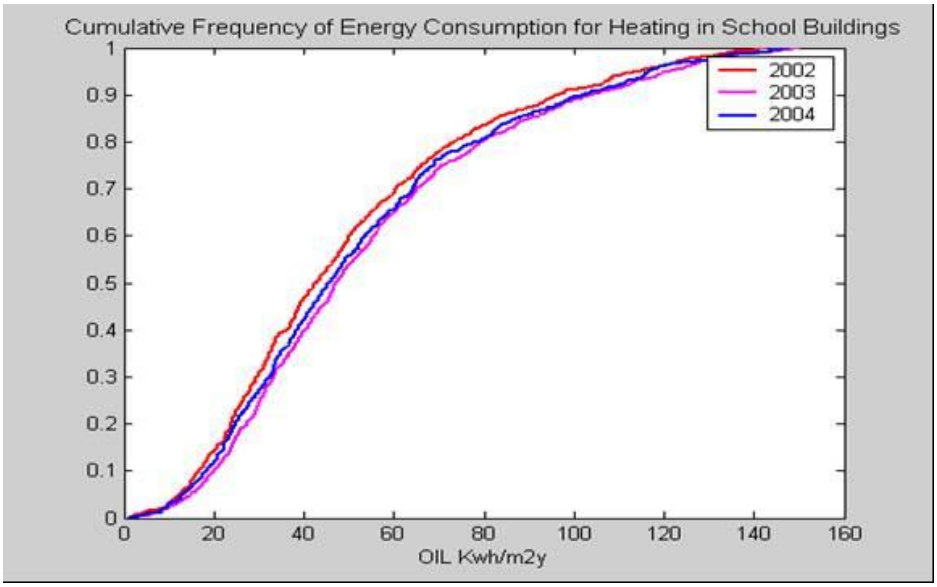

Figure 3: Cumulative frequency distribution of the normalized energy consumption for heating with oil in kWh/m^2y (after the removal of outliers-Tukey method)

Fig 3 illustrates the cumulative frequency curve of the normalized energy consumption for heating with oil in kWh/m^2y. 50% of schools consume for space heating with oil, less than 50 kWh per square meter annually.

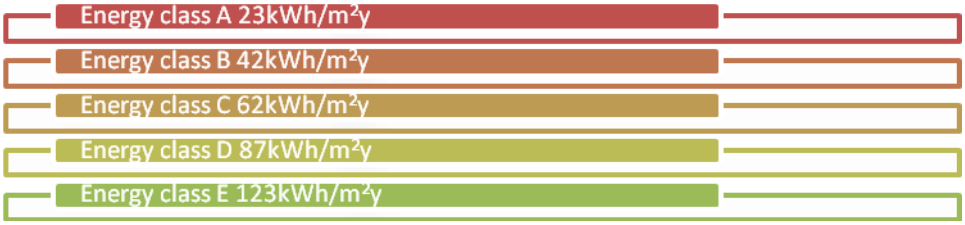

Figure 4: Benchmarks of the normalized energy consumption for heating with oil in kWh/m^2y in each energy class

In order to acquire in-depth data on energy consumption levels the benchmarks for each class were calculated as shown in Fig 4. To evaluate the potential energy conservation, the typical characteristics of school buildings belonging to an energy class have to be identified. A methodology based on the use of the principal components analysis (PCA, Jolliffe IT., 1993) has been developed. The method allows to define in an accurate way the typical building of each energy class and thus to perform analysis on the potential energy savings for the specific group of school buildings.

For the definition of the typical building in each one of the five energy classes, seven variables have been selected:

- Heated surface (m^2)
- Age of the building (years)
- Insulation of the building (0 for non-insulated, 1 for insulated)
- Number of classrooms
- Number of students
- School's operating hours per day
- Age of the heating system (years)

The characterization of the typical school among a seven variables sample, has being performed as the closest to the medians in the principal components' coordinate system. The Euclidian distance performed in the seven dimensional PCs coordinate system and the five reference schools are presented in Fig 5.


Figure 5: The examined reference school buildings (A-E class)

2.2 Best practices for energy efficiency

In order to set energy performance goals and predict internal conditions, thermal simulations were applied with TRNSYS 15.1 software for a year in every typical building of each energy class. The models have been calibrated to the real consumption as obtained from the bills. The simulated heating load varied in the range of 22.3-50.7 kWh/m^2y while the corresponding cooling load, in case of AC fluctuated between 6.9-18.9 kWh/m^2y. Several scenarios were examined.

Following the adoption of energy choices in class A, the annual heating load was varied in a range of 18kWh/m^2y-27kWh/m^2y. The potential of the reduction of the energy load for heating calculated between 7 and 40%.

For the reference building in class B the annual heating load was varied in a range of 26kWh/m^2y-34kWh/m^2y. Energy savings could be achieved by a combination of interventions, were accounted for 26%.

With implementation of the proposed interventions energy saving class C, the annual heating load for the representative building was varied in a range of 20kWh/m^2y-47kWh/m^2y. The reduction of thermal losses of the cracks proved the most effective method of reducing the thermal load. Specifically, the reduction of thermal exchanges the cracks calculated that can reduce the heat load of 34%. The final examined scenario with all the proposed interventions calculated in savings of 59%.

From the simulations for the reference building in class D emerged annual heating loads by 26kWh/m^2y to 65kWh/m^2y. The largest reduction of annual consumption for heating, with a 63% calculated for the simultaneous implementation of all actions.

Finally, the annual heating load in the representative building of E class was varied in a range of 23kWh/m^2y-110kWh/m^2y. The main reduction of annual consumption for heating, with a change of 80%, calculated for all the scenario of the combined solutions.

A considered efficient intervention was the replacement of the windows with new, better quality with lower U (u-value) and solar heat gains (g-value). More specifically, for the simulation low-e double window glazing was chosen. The efficient thermal insulation through the use of up-to-date double glazing was important, as the blinds covering an average area of 30% on the sides of school buildings contributed at a rate of 10% in energy consumption for heating.

The insulation accounted only for 35% of the buildings in class A, B; C, D, and class E buildings were non-insulated. The remaining surface either created thermal bridges or was covered by window frames. The thermal insulation of the external wall could contribute to energy saving per year to 32%. Furthermore, external insulation may ensure less fluctuation of indoor temperatures and therefore better thermal comfort conditions in classrooms.

Modern boilers and heating systems are designed to have minimal thermal losses and yield 0.8-0.9 means that the losses are on the order of 10-20%. The heat recovery process could contribute to a reduction in consumption for heating ranging from 5 to 15%.
The most effective method of reducing the thermal load was associated with the reduction of heat loss from the cracks. Consequently, the airtightness of frames or replacement of gastight doors and frames should be a technical priority in old school buildings as they were accounted for 23-44% reduction in the heating load.

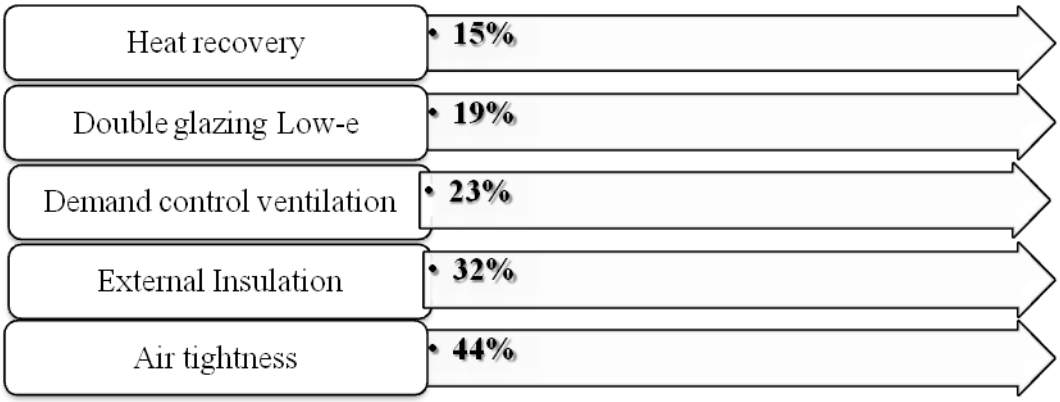

Figure 6: Benchmarks of the normalized energy consumption for heating with oil in kWh/m^2y in each energy class

As it can be seen (Fig 6) the energy saving for heating load may be reduced up to 50% with simple energy measures. The evaluation of various energy saving techniques, revealed an opportunity for an overall reduction in consumption for heating of 15-80%. The rational operation and maintenance of school buildings should be integrated also into a global Action Plan.

3 INDOOR AIR QUALITY ASPECTS

Together with the energy demand one should consider the general requirements of indoor climate conditions, in order to avoid possible adverse consequences (Santamouris, 2008). The school buildings in general are characterized by a high density of people per unit area, which is associated with increased concentrations of certain pollutants and therefore with reduced attentiveness of students and less ability to learn. Moreover, students are a vulnerable group necessitating a special attention. Characterized by:

- Greater respiratory rate compared with adults
- Lower weight
- Higher levels of physical activity
- The human lung continues to develop until adolescence

Measurements of air quality were conducted within ten school buildings in the Greater Athens area. Hourly measurements of ambient indoor and outdoor temperature and relative humidity have been performed, while indoor air velocity and infiltration have been also monitored. Furthermore, CO_2, CO, TVOCs were measured in 83 examined classrooms.

3.1 Ventilation

The monitoring strategy to evaluate air flow rates in classrooms was the concentration decay method (tracer gas). Measurements of infiltration rate were performed using SF_6 tracer gas when classrooms were empty and the windows closed. Then measurements were repeated during the breaks when most of the windows were opened (opening of windows is very

common practice in mild climates) and classrooms were empty. Thus the max & min ventilation rates were estimated. Infiltration in all schools varied between 0.1 to 0.9ACH with a mean value close to 0.4ACH. Combined air flow rates (natural ventilation & infiltration) varied between 1.3-12.1ACH with a mean value of 2.2ACH (see Table 2).

Table 2: Infiltration & ventilation rates

School number	Infiltration (ACH)	Infiltration & natural ventilation (ACH)
1	0.1	3.5
2	0.2	2.8
3	0.4	9.0
4	1.2	4.6
5	1.9	6.9
6	0.1	7.4
7	0.2	1.7
8	0.3	3.8
9	0.9	7.3
10	0.3	2.4
11	0.5	12.1
12	0.9	10.2
13	1.3	6.0
14	0.4	11.7
15	0.4	1.3
16	0.4	1.4
17	0.3	2.0
18	0.2	4.8

3.2 Indoor Air

As it concerns indoor air quality, measurements have been performed according to experimental protocol in 83 classrooms of the examined schools (Table 3).

Table 3: Minimum, average and maximum measured values of CO, CO_2 and TVOC's concentration per school building, number of classrooms and percentage exceeding the threshold limit values

	Min	Average	Max	Number of classrooms & percentage that exceed the acceptable limit	Min	Average	Max	Number of classrooms & percentage that exceed the acceptable limit	Min	Average	Max	Number of classrooms & percentage that exceed the acceptable limit	Number of classrooms & percentage that exceed at least one limit, in total
1	0,28	0,67	1,05	0/8 (0%)	413	675	1298	4/8 (50%)	0,14	0,40	0,78	8/8 (100%)	8/8 (100%)
2	0,74	1,42	2,67	0/9 (0%)	867	1258	1628	9/9 (100%)	0,00	0,60	1,32	8/9 (89%)	9/9 (100%)
3	0,30	1,09	3,10	0/8 (0%)	424	813	1664	5/8 (63%)	0,23	1,34	3,62	8/8 (100%)	8/8 (100%)
4	0,52	0,92	1,45	0/12 (0%)	105	661	1133	6/12 (50%)	0,01	0,76	1,53	11/12 (92%)	11/12 (92%)
5	0,25	0,36	0,44	0/3 (0%)	367	602	1040	1/3 (33%)	0,24	0,93	2,15	3/3(100%)	3/3 (100%)
6	0,14	0,57	1,15	0/11 (0%)	396	598	846	5/11 (45%)	0,05	0,60	1,68	11/11 (100%)	11/11 (100%)
7	0,28	0,88	1,70	0/7 (0%)	446	833	1373	4/7 (57%)	0,02	0,74	2,55	4/7 (57%)	5/7 (71%)
8	0,19	0,32	0,61	0/10 (0%)	363	576	786	7/10 (70%)	0,02	0,08	0,21	9/10 (90%)	9/10 (90%)
9	1,27	1,70	2,25	0/8 (0%)	408	600	1246	3/8 (38%)	0,58	1,28	2,29	8/8 (100%)	8/8 (100%)
10	3,80	4,08	4,47	0/7 (0%)	772	1070	1873	7/7 (100%)	1,42	2,45	5,34	7/7 (100%)	7/7 (100%)
Sum				0/83 (0%)				51/83 (61%)				77/83 (93%)	79/83 (95%)

Regarding the CO_2 concentrations, while the measured values were not considered to impose healthy risks, were measured in high levels related to inadequate ventilation. All CO concentration values were measured below the international limits (concentration limit for CO according to ASHRAE is 9ppm for an eight hour exposure). In 7 out of 10 schools, TVOCs were measured in the classrooms above the recommended limit values.

3.3 Thermal Comfort Conditions

The mean values of the air temperature in the classes, varied in the range of 19.4°C-26.0°C. The majority of the examined school buildings (60%) showed minimum value above 21.0°C and in accordance with the European standard prEN 15251:2006, guarantee an adequate level of thermal comfort. The wet bulb globe temperature is a heat stress indicator that considers the effects of temperature, humidity & radiant energy.

Table 4: WBGT index calculated values

A/α	Minimum WBGT (°C)	Average WBGT (°C)	Maximum WBGT (°C)
1	19	21	22
2	14	15	16
3	21	22	22
4	18	20	21
5	19	21	23
6	19	21	23
7	16	18	19
8	19	21	23
9	22	22	23
10	14	16	18

The average value of the calculated WBGT index was ranged from 15˚C to 22˚C. For the examined schools the WBGT values were lower than the considerate limits (as shown in the Table 4) and therefore persons are not subjected to heat stress.

Table 5: CP index calculated values

A/α	Minimum CP (mcal $cm^{-2}sec^{-1}$)	Average CP (mcal $cm^{-2}sec^{-1}$)	Maximum CP (mcal $cm^{-2}sec^{-1}$)
1	4.30	5.21	5.90
2	6.70	7.07	7.30
3	4.70	5.06	6.10
4	5.30	5.91	7.30
5	4.50	5.20	6.20
6	3.80	4.55	5.70
7	5.80	6.27	7.10
8	4.00	4.78	5.90
9	4.00	4.70	6.40
10	6.60	7.36	8.20

The cooling power calculated values was varied in the range 4.6-7.4mcal*cm^{-2}*sec^{-1} of irritating warm environment to tolerable cold environment, with the majority of the mean values in the range of adequate warm environment (see Table 5).
The same period the outdoor air temperature was varied in the range of 17.5°C-27.5°C. A comparison of the measurements has shown that the mean indoor air temperature did not differ significantly from the corresponding values in the external environment. This is an indication of insufficient heating due to a grade and continuous opening of windows which generates thermal energy losses.

4 CONCLUDING REMARKS

The main objectives of this research included the assessment of energy conservation potentials in schools in view of the environmental quality issues. The research has shown that school buildings feature indoor air quality problems while their energy consumption and

global environmental quality could be improved significantly. The energy consumption of school buildings may be reduced up to 50 % with simple energy measures (great potential for energy conservation).The conclusions obtained endorse a general energy evaluation for space heating for the Greek school buildings. The clustering in five classes could be used for energy saving techniques applied from the decision makers.

5 ACKNOWLEDGEMENTS

The authors are grateful to the Greek School Buildings Organisation SA (SBO) and the Ministry of Education for the collaboration in the distribution of the energy audits.

6 REFERENCES

Roulet C. A., Flourentzou F., Labben H H., Santamouris M., Koronaki I., Daskalaki E., et al. (2002). ORME: A multi-criteria rating methodology for buildings. *Building and Environment*, 37, 579-586.

Santamouris M.(2005). *Energy Rating of Residential Buildings*, Earhscan, London.

Santamouris M, Mihalakakou G, Patargias P, Gaitani N, Sfakianaki K, Papaglastra M, et al. (2007) Using Intelligent Clustering Techniques to Classify the Energy Performance of School Buildings. *Energy and Buildings*, 39 (1), 45-51.

Corgnati S. P., Corrado V., Filippi M., (2008). A method for heating consumption assessment in existing buildings: A field survey concerning 120 Italian schools. *Energy and Buildings*, 40, 801–809.

Gaitani N, Santamouris M, Mihalakakou G, Patargias P, 2010. Using principal component and cluster analysis in the heating evaluation of the school building sector *Applied Energy*, 87(6), 2079-2086.

Santamouris,M., A. Synnefa, M. Asssimakopoulos, I. Livada, K. Pavlou, M. Papaglastra, N. Gaitani, D. Kolokotsa, V. Assimakopoulos, (2008). Experimental investigation of the air flow and indoor carbon dioxide concentration in classrooms with intermittent natural ventilation, *Energy and Buildings*, 40 (10), 2008, 1833-1843.

Papakostas K., Kyriakis N., 2005. Heating and cooling degree hours for Athens and Thessaloniki, Greece. *Renewable Energy*, 30 (12), 1873-1880.

Yael V. P., Capeluto, I.G.(2009). Climatic considerations in school building design in the hot–humid climate for reducing energy consumption. *Applied Energy*, 86, 340-348.

Hoaglin D C., Iglewicz B., Tukey J W., (1986). Performance of Some Resistant Rules for Outlier Labelling, 81, 991-999.

Afifi AA., Clark, 1996. *Computer Aided Multivariate Analysis*, London: Chapman & Hall.

TRNSYS 15.1, A transient system simulation program developed from Solar Energy Laboratory, University of Wisconcin–Madison and Transsolar of Stuttgart, 20.

Jolliffe IT., 1993. Principal Component analysis: A beginner's guide – II. Pitfalls, myths and extensions Weather 48, 246-253.

HEALTH ISSUES IN RELATION TO BUILDING DAMPNESS IN EUROPEAN SOCIAL HOUSING

Stavroula Karatasou*[1], Marina Laskari[1], and Mat Santamouris[1]

1 Group Building Environmental Studies
Department of Applied Physics, National and
Kapodistrian University of Athens
Athens, Greece
**Corresponding author: skarat@phys.uoa.gr*

ABSTRACT

Scientific evidence exists of an association between dampness and mould in buildings and of an increased risk of health effects for occupants, usually associated with the respiratory system. It is difficult to establish the exact prevalence of residential dampness, but according to WHO, it is likely to be in the order of 10-50%.
The aim of this study is to examine the frequency of indoor dampness in social housing in different European countries, and whether dampness in these residential buildings is related to health issues such as asthma or allergies. Both, dampness (condensation on windows and /or walls and mould growth) and symptoms were surveyed by standardized questionnaires filled-out by the household occupants. In total, 215 residences are included in the study. Results indicate that dampness is around 16% and that mould is significantly related to asthma or other respiratory symptoms and allergies (odds ratio (OR) around 2.6)).

KEYWORDS

Dampness, mould growth, asthma, odds ratio

1 INTRODUCTION

Respiratory symptoms and asthma are among common diseases in Europe and worldwide. The prevalence of asthma has increased during last decades, and there are indications that this may be partially due to allergic and non-allergic reaction to indoor environment.
Several cross-sectional studies during the last years have observed an increased risk of respiratory symptoms and other diseases which are related to exposure to mould in damp or mouldy buildings: condensation on cold surfaces, permanent dampness in the building construction or episodes of water leakage and high indoor air humidity facilitate microbial growth (Peat et al. 2008; Norback et al. 1999).
Scientific evidence exists of relation between these symptoms and to exposure to mould in damp or mouldy buildings (Bornehag 2001; Bornehag 2004; WHO 2009; IOM 2004; Muddari 2007). Bornehag (2001) lists 51 studies, in most of which a relationship exists between self-reported dampness and asthma, coughing and wheezing, with odds ratios (OR) ranging from 1.4 to 2.2.
According to the review of the Institute of Medicine (IOM) of the National Academy of Sciences (IOM, 2004), dampness problems are common and excessive indoor dampness consists a public health problem: building dampness may cause the building to become contaminated with microorganisms such as mould or bacteria, which might in-turn cause adverse health effects. Building dampness could also cause increased emissions of some chemical pollutants from materials and surfaces (IOM, 2004). Research has not yet

determined the exact causal agent(s) (IOM, 2004). The increased risk associated with building dampness suggests a potentially large public health problem. Most available data indicate that at least 20% of homes have dampness problems or visible mould.
In their analysis, Muradi and Fisk (2004) found sufficient evidence of a relationship between dampness or mould exposure and upper respiratory symptoms, as well as significant health and economic risks in the USA.
The present study is a part of the EC funded ICE-WISH project which commenced in 2011 with the primary objective of improving energy efficiency in social housing using ICTs, while ensuring that the conservation measures will have no adverse influence on Indoor Environmental Quality (IEQ). Of equal importance to the project, is the quantification of the improvements in IEQ, as well as the identification of possible non-energy benefits for the participants, such as the prevention of adverse health effects that can result from dampness and mould.
The study consists of quantitative surveys matched with a set of measured parameters (indoor air temperature, indoor air humidity and indoor CO_2 concentrations), and is designed to follow a longitudinal design approach, i.e. occupant surveys and relevant data collection will be performed before, a few months after, and at least one year after the ICE-WISH service implementation.
This paper presents results from the baseline survey, conducted in late 2011 to 2012 within seven European countries: Belgium, Denmark, France, Germany, Italy, Poland, and Spain.
The aim of the work presented in this paper is to examine the frequency of indoor dampness in social housing in different European countries, and whether dampness in these residential buildings is related to health issues such as asthma, stroke or other circulatory problems, rheumatisms, skin symptoms or allergies.

2 DATA AND METHOD

To ensure European replication, the sampling frame consists of a population of low income occupants living in social housing across 7 different European countries. A total of 215 households have completed the tenant questionnaire.
This questionnaire covered a broad range of topics, including demographics and socioeconomics, smoking habits and time spent in the home. The analysis presented here focuses on the health issues and dampness and mould conditions present in individual dwellings which were also specifically addressed in the questionnaire. The analysis is based on participants' responses.
Symptoms related questions:
The participants were asked whether they or anyone in the household suffer from any of the following symptoms: (a) 'asthma or other respiratory problems', (b) 'stroke or other circulatory problem', (c) 'rheumatism or other joint problem', (d) 'Eczema or other skin condition', (e) 'allergies', (f) 'colour blindness' and (g) 'requires use of a wheel chair'.
Symptoms included in the following analysis are: Asthma (asthma or other respiratory problems); Stroke (stroke or other circulatory problems); Skin (Eczema or other skin condition), and; Allergies. Participants were asked if they suffer from any of the above health issues. For each symptom, there were only two answers: "yes" or "no".
Building's dampness condition related questions:
The questionnaire included also queries about the dampness conditions in dwellings. In particular, participants were asked if they have noticed: condensation on the windows/walls/ceilings; damp patches on the walls/ceiling; mould on the walls/ceiling, and mould on the furniture, carpets or clothes.
The question on dampness conditions was repeated for the following room types: kitchen, bathroom, bedroom, living-room and any other space. Thus, in total, respondents had to

answer 20 items concerning dampness conditions in their household (4 dampness conditions for 5 different space types). For each question, there were again only two answers: "yes" or "no".
For the 215 tenant questionnaires, binary logistic regression analysis was applied and odds ratio with 95% confidence intervals (OR: 95% CI) were calculated.

3 RESULTS

Table 1 shows symptoms and dampness conditions observed from the results of the survey. Namely, asthma or other respiratory symptoms were found for 15.9% of the studied households, stroke or other circulatory symptoms were found in 7.7% of the households while, rheumatism symptoms, skin symptoms and allergies were found in 13.3%, 7.2% and 30.3%, of those studied, respectively. The most prevalent symptoms are allergies and asthma. There are no statistically significant differences in any of the symptoms between different countries, except for rheumatism (Fisher's exact test =28.464; $p<0.001$). Nonetheless, variations are observed among the studied countries in asthma symptoms with distribution ranging from 0% in Italy to 41.7% in France.
Of the total of 215 households that participated in the study, 22.3% reported condensation on windows, walls and/or ceilings, and 16.7% reported mould growth (9.8% had damp patches, 7.9% had mould on walls/ceilings and 1.4% had mould on furniture (Table 1)). There are no statistically significant differences in any of the symptoms between different countries.

Table 1: Descriptive overview of the European Countries included in the study

	Belgium	**Denmark**	**France**	**Germany**	**Italy**	**Poland (EG)**	**Spain**	**Poland (CG)**	**Total estimate**
Symptoms									
Asthma	20.0%	12.0%	41.7%	8.3%	.0%	6.7%	22.2%	26.7%	15.9%
Stroke	4.0%	24.0%	25.0%	8.3%	.0%	3.3%	3.7%	3.3%	7.7%
Rheumatism	16.0%	20.0%	58.3%	16.7%	.0%	3.3%	18.5%	.0%	13.3%
Skin	4.0%	24.0%	8.3%	12.5%	.0%	3.3%	7.4%	.0%	7.2%
Allergies	28.0%	20.0%	41.7%	41.7%	31.8%	30.0%	25.9%	30.0%	30.3%
Dampness Conditions									
Condensation	27.6%	33.3%	19.0%	48.3%	18.2%	.0%	29.6%	3.3%	22.3%
Damp patches	17.2%	17.9%	19.0%	16.7%	29.2%	13.3%	20.7%	3.3%	9.8%
Mould structure	6.9%	7.4%	.0%	13.8%	18.2%	.0%	14.8%	3.3%	7.9%
Mould Furniture	.0%	.0%	.0%	3.4%	.0%	.0%	7.4%	.0%	1.4%

Dampness conditions are more prevalent in bedrooms and bathrooms (Table 2), and they involve mainly condensation problems in walls, windows and/or ceilings. Mould growth in structure components is more prevalent in bathrooms, while mould growth on furniture and carpets is more prevalent in bedrooms (Table 3).

Table 2: Dampness frequency per room type

Room Type	**Dampness per room type (n=215) (%)**
Kitchen	15.8
Bathroom	**18.2**
Living Room	13.9
Bedroom	**19.4**

Other Place	8.5

Table 3: Dampness conditions per room type

	Condensation	Damp patches	Mould /Structure	Mould/Furniture
Kitchen	14.0	3.7	3.0	0.6
Bathroom	15.2	**5.5**	**4.9**	0.6
Living Room	12.2	4.9	3.0	0.6
Bedroom	**15.9**	5.5	3.0	**1.8**
Other space	7.3	3.0	2.4	**1.8**

In a further analysis, mould in structures and mould in furniture were grouped together to form the constructed variable "mould growth". The values for "mould growth" were defined as 1, if the answer was positive to the existence of mould on structure or mould on furniture, and 0, if the answer was negative.

Results of the binary logistic regression are presented in Table 4. As observed from Table 4, there is a statistically significant association between damp patches and asthma (OR, 3.437 (95% CI, 1.072-11.022)) and between damp patches and skin symptoms (OR, 4.752 (95% CI, 1.285-7.573)). None of rheumatism, stroke or other circulatory symptoms are associated with any of the dampness conditions. Allergies on the other hand, are significantly related to condensation.

Table 4 Each symptom related to the building dampness conditions (OR (95% CI))

	OR (95% CI)		
Symptom	**Condensation**	**Damp patches**	**Mould growth**
Asthma	1.657 (.638-4.303)	**3.437 (1.072-11.022)****	2.588 (.750-8.937)
Stroke	0.736 (.193-2.804)	1.661(.336-8.210)	.761(.092-6.268)
Rheumatisms	1.723 (.718-4.133)	.689 (.148-3.209)	.744 (.159-3.487)
Skin	3.036 (.999 9.221)	**4.752 (1.285-7.573)***	1.792 (.360-8.911)
Allergies	**2.108 (1.005-4.422)***	1.250 (.413-3.784)	1.376 (.449-4.219)

Next, to address dose response relationships between symptoms and exposure to dampness, the OR for category I and category II were calculated. Categories are defined as follows: Category 1, if the answer included any one of the four dampness conditions; Category 2, if the answer included all dampness conditions. The results of the calculations are summarized in Table 5. It can be observed that, as the level of dampness increases, the OR for asthma and allergies symptoms increases also.

Table 5 Each Symptom related to the building dampness conditions. Category I any of the dampness conditions, Category II both dampness conditions (OR (95% CI))

Symptom	**OR (95% CI)**	
	Category I	**Category II**
Asthma	**2.671 (1.055-6.762)***	1.330 (0.339-5.221)
Skin	2.688 (0.856-8.440)	1.472(0.28-7.747)

Allergies	1.886 (0.913-3.897)	**2.689 (1.094-6.610)****

4 CONCLUSIONS

In total 215 households were examined in the present study, within seven different European countries.

Building dampness was reported by 16% of the population in this study, while condensation in structural parts of dwellings was reported by 22% of the same population. These percentages are based on self-reported questionnaires with no objective measurement of conditions or symptoms.

The most prevalent symptoms among participants are allergies and asthma.

Main results of this study indicate an increased risk of asthma and allergies (ORs of around 2.7). The increased prevalence of asthma and other respiratory symptoms is predominately present for participants reporting damp patches, while allergies are more prevalent for participants reporting all conditions of dampness.

No association was found between dampness conditions and stroke or other circulatory symptoms and rheumatism. This could indicate that building dampness does not cause these symptoms.

We conclude that building dampness is not a common problem in the countries participating in this study, but in cases where dampness is present there is also an increased prevalence of asthma and allergies. With regards to the considerable scientific evidence that dampness and mould do affect peoples' health, it is clear that the consideration of corrective, preventive and/or remedial actions is necessary for the reduction of this health risk.

5 ACKNOWLEDGEMENTS

The authors gratefully acknowledge partners from the ICE-WISH Project: Kristien Van Hemelryck and Bernard Wallyn from VMSW (Belgium); Rie Øhlenschlæger, Lulu Grønlund and Palle Jørgensen from RING (Denmark); Benoit Jehl from OPAC38 (France); Juergen Nitschke and Wolfgang Pfeuffer from Joseph-Stiftung (Germany); Alain Lusardi and Gianfranco Tofanelli from CasaQualita (Italy); Martyna Sikora and Marta Kęsik from the City of Warsaw (Poland); Txari Vallejo, Oihana Hernaez and Atin Eugenia from Bilbao-Viviendas (Spain), and; Lorna Hamilton and Ranjit Bassi from BRE. The project was made possible through funding from the European Commission.

6 REFERENCES

Bornehag, C.G., Sundell, J., Bonini, S.,Custovic, A., Malmberg, P., Skerfving, S.,Sigsgaard, T. and Verhoef, J. (2001). Dampness in buildings and health. Nordicinterdisciplinary review of the scientificevidence on associations between exposure to dampness and health effects.NORDDAMP. *Indoor Air*, 11, 72–86.

Bornehag, C.G., Blomquist, G., Gyntelberg,F., Jarvholm, B., Malmberg, P., Nordvall,L., Nielsen, A., Pershagen, G. And Sundell, J. (2004) Dampness in buildings as a risk factor for health effects, EUROPO.A multidisciplinary review of the literature (1998–2000) on dampness and mite exposure in buildings and health effects, *Indoor Air*, 14, 243–257.

Institute of Medicine (IOM), (2004). Board on Health Promotion and Disease Prevention, Committee on Damp Indoor Spaces and Health. Damp indoor spaces and health, Washington, DC: The National Academies Press, available at: http://www.nap.edu.

Mudarri, D., Fisk, W.J. (2007). Public health and economic impact of dampness and mold. Indoor Air, 17, 226–235.

Norback, D., Bjornsson E., Janson C., Palmgren U., Boman G. (1999). Current asthma and biochemical signs of inflammation in relation to building dampness in dwellings. *Int J Tuberc Lung Dis*, 3, 368–376.

Peat, J.K, Dickerson J., Li J. (1998). Effects of damp and mould in the home on respiratory health: a review of the literature. *Allergy*, 53, 120–128.

WHO 2009 WHO. WHO guidelines for indoor air quality: dampness and mould. World Health Organization.

SANITARY ASPECTS OF DOMESTIC VENTILATION SYSTEMS: AN *IN SITU* STUDY

Joris Van Herreweghe*, Samuel Caillou, Marilyn Roger and Karla Dinne

Belgian Building Research Institute (BBRI),
Avenue Pierre Holoffe 21, 1342 Limelette, Belgium
*Corresponding author: joris.van.herreweghe@bbri.be

ABSTRACT

With the continuous improvement of the energy performance of buildings, ventilation plays a crucial role in the control of pollutants from indoor sources and related comfort and health effects. However, the ventilation system itself could possibly also be a source of indoor air pollutants such as microbial contaminants. Profound scientific and technical knowledge on the impact of the design, installation and maintenance on the real performances of ventilation systems is currently lacking. Therefore within a collaborative research project at the Belgian Building Research Institute (BBRI) the acoustic performance, energy consumption, air quality and ease of maintenance of five exhaust ventilation systems and twenty-eight balanced ventilation systems were evaluated *in situ*. Within this paper the results of the microbial analysis of the air quality part are presented. Different air sampling techniques were used to evaluate the supply and the indoor air in relation to the outdoor air. The impact of the accumulation and development of micro-organisms within the ventilation systems, especially in the ducts, the filters and if present on controllable supply grids, was also evaluated. The results indicate that the outdoor air quality has a major influence on the quality of the supplied and indoor air, especially for the mould load. However, human activity and the indoor environment tend to have a high impact on the indoor bacterial load. Exhaust ventilation systems were found to hardly alter the quality of the supplied air, leaving the indoor air microbial quality largely dependent on the outdoor air quality. In contrast balanced ventilation systems are capable of reducing the mould load, and to a lesser extend the bacterial load, of the supplied air. Filtration of the supplied air in the first place serves to protect the ventilation system from becoming dirtied. Nevertheless, the observed reduction in mould load of the supplied air within balanced ventilation systems can be regarded as an asset. However, the effectiveness of this filtration/protection was found to be largely dependent on the quality of the filters, filter housing (by-pass leakiness) and their state. These findings underscore the importance of a rational design, a proper installation and the importance of good maintenance.

KEYWORDS: Mechanical ventilation, air quality, moulds, bacteria

ABBREVIATIONS: EvS: Exhaust ventilation System, BvS: Balanced ventilations System, CFU: colony forming units;

1 INTRODUCTION

People spend on average more than 90% of their time indoors. In general, indoor air is more polluted than outdoor air (Tilborghs *et al.* 2009). Moreover, some indoor air pollutants, from chemical, biochemical as well as microbial origin, are recognized as important risk factors for our health. This especially holds true for the so called YEPI's (young, elderly, pregnant and immunodeficient), which in addition spend even more time indoors. Therefore, the absolute importance of indoor air quality is widely recognized by local (Tilborghs *et al.* 2009), European (European Commission 2003) as well as international organizations (World Health Organization 2009).

Ventilation is of utmost importance and even becoming more important for several reasons. First and foremost for the supply of fresh air and oxygen and the removal of humidity, since the latter might in turn cause mould and off odour issues. Further, ventilation also prevents the accumulation of harmful substances emitted by materials, although priority should be given to the use of low emitting materials. Last but not least, the continuously improving energy efficiency of buildings and its related increased air tightness resulted in an enhanced dependency on mechanical ventilation systems.

Basically two main mechanical ventilation systems can be distinguished. An exhaust ventilation system (further abbreviated as: EvS) comprises a natural supply through adjustable supply grids in windows or walls, an air flow through the house and mechanical extraction in the humid places of the house. A balanced ventilation system (BvS) consists of a mechanical supply and extraction with heath recycling and air filtration. In a variant of this system the supply air is sucked in through a traditional Canadian well (= earth heat exchanger). Alternatively, the supplied air might also be cooled or heated (depending on the season) by a glycol driven earth heat exchanger (hydraulic Canadian well).

Obviously these systems themselves might also have an influence on the sanitary aspects of the supplied and indoor air. Therefore the aim of this research project was to investigate this influence through system- and air sampling in 33 residential buildings equipped with a mechanical ventilation system (5X EvS and 28X BvS), but without visible dampness/moisture or mould problems.

2 MATERIALS AND METHODS

Different air sampling techniques were used to evaluate the supply and the indoor air in relation to the outdoor air. All samples were collected at the maximal ventilation capacity of the system. The supply air was sampled at the tip of supply duct in the living room, after removal of the supply valve. Indoor air was sampled in the living room on the coffee table. For viable fungal and bacterial air contaminants, an Air Sampler (RCS Plus, Biotest Hycon®) equipped with Hycon® agar Strips (Total count (TC) and Yeast and Mould (YM)) was used. A sticky surface sampler, Air-O-Cell®, was used to determine the total fungal particulate load of the air samples. The impact of the accumulation and development of micro-organisms within the ventilation systems, especially in the ducts, the filters and if present on controllable supply grids, was evaluated by ATP-tests, surface sampling as Swab and Rodac, in addition to culturing methods. Moulds were identified based on microscopic examination of tape samples taken directly from the surface or culture plates/agar strips. Concerning the statistical analysis, outliers were defined as values < Q1 (quartile) - 1.5xIQR (Inter Quartile Range) or > Q3 + 1,5xIQR. Mould removal efficiency was calculated as follows: $= (1 - \frac{\text{Supply}}{\text{outdoor}})$ x100

3 RESULTS AND DISCUSSION

The interpretation of microbial air sample data is far from standardized and a frame of reference is still lacking. Instead a number of arbitrary numeric standards for "acceptable" levels of indoor micro-organisms have been proposed, but none of them is currently generally accepted. Current interpretation is based on the comparison of the types and levels of micro-organisms detected indoors versus those in matched outdoor samples. Ideally, there should be no difference in the types observed indoors and outdoors, and additionally the indoor levels should be lower (Codina *et al.* 2008). This forms the general rule of thumb that was used to interpret the obtained measurements in this study.

3.1 Seasonal influences

Although the outdoor environment is regarded as a good source of clean and fresh air, the outdoor air is already loaded with biological (moulds, bacteria, pollen,…) and chemical contaminants. This however doesn't pose direct problems for healthy people, but means that when outdoor air is used by a ventilation system, it always forms a potential source of eventual problems. The amount of micro-organisms in the outdoor air does not remain constant, but is influenced by the geographical location, climate and meteorological conditions (Codina *et al.* 2008). Since our collections were spread throughout the year, they should anyhow reflect the seasonal influences.

As expected the fungal load in the viable air samples was clearly influenced by the seasons (data not shown). Based on the comparison of the median of the seasonal subpopulations, higher outdoor levels were observed in autumn and the highest levels in summer. Winter accounted for the lowest levels. Independent on the system type (EvS or BvS), the indoor fungal levels were observed to be linked to the outdoor levels, although the supply and indoor air were generally less loaded than the outdoor air. This observation is less clear for winter time, which might be due to the overall lower microbial load of the outdoor air in this season.
In contrast, no clear seasonal influence could be observed for the bacterial load of the collected viable air samples. Furthermore, the indoor air was always observed to be more loaded than the supply and outdoor air. These results suggest that the indoor environment (dust, human activity,…) itself might largely contribute to the bacterial load of the indoor air. This assumption is supported by other studies and our own findings (see 3.3.1).

For both system types, 57% of all samples were collected during autumn and summer. For EvS 43% was additionally collected in spring, while for BvS 22% of all samples were collected in winter and 21% in spring. In spite of this dissimilarity, no significant differences were observed for the outdoor fungal levels between the datasets for both systems. This means that both datasets can be compared, although keeping the difference in sample size in mind.

3.2 Exhaust ventilation systems

3.2.1 Viable bacteria

As can be seen in Figure 1 below, the bacterial load in the indoor air (288;366 CFU/m³: Median (M); Average (Av)) is slightly higher than the load in the supply air (263;245) and both are more charged than the outdoor air (100;170). However, these differences are not significant based on a one way ANOVA statistical analysis ($\alpha = 0.05$). Little bacteria were found on the adjustable supply grids (Swab analysis, data not shown). This means that the higher bacterial load in the supply air in comparison to the outdoor air cannot be attributed to accumulation of bacteria on the supply grids. However, when sampling supply air at an

adjustable supply grid, there is always a risk to aspirate indoor air due to the limited dimensions and accessibility of these grids. This might be a possible reason for the higher bacterial load in the supply samples in comparison to the outdoor samples.

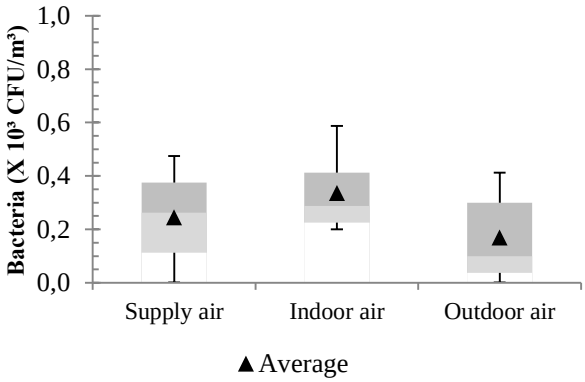

Figure 1: Box-whisker plot of the viable bacterial load expressed in CFU/m³ determined by RCS air sampling for EvS.

3.2.2 Viable moulds

Unlike our observations for the bacterial load, the indoor air is the least charged with mould particles (306;329), followed by the supply air (513;548) and the outdoor air (819;848) (see Figure 2: A). As can be seen from Figure 2B a direct relationship between the supply- and outdoor air was observed for the EvS. This actually forms a logical finding, since in Ev systems the outdoor air is just passed through an adjustable supply grid, which theoretically doesn't alter the microbial composition of the outdoor air. It also means that the sanitary performance of an Ev system is more seasonal dependent. This was clearly illustrated in our dataset by three different measurements for the same Ev system in three different seasons. While the measurements for spring and autumn are quite normal, the measurements for the summer time form an outlier in this dataset for all three collected air samples (Supply, Indoor and Outdoor) (No.1 2nd (summer) in Figure 2A). Furthermore, the value for the ATP-measurement on the outside of the adjustable supply grid exceeded the overall observed values. Finally, Air-O-Cell analysis confirmed the massive presence of *Cladosporium* spp. spores in all three samples.

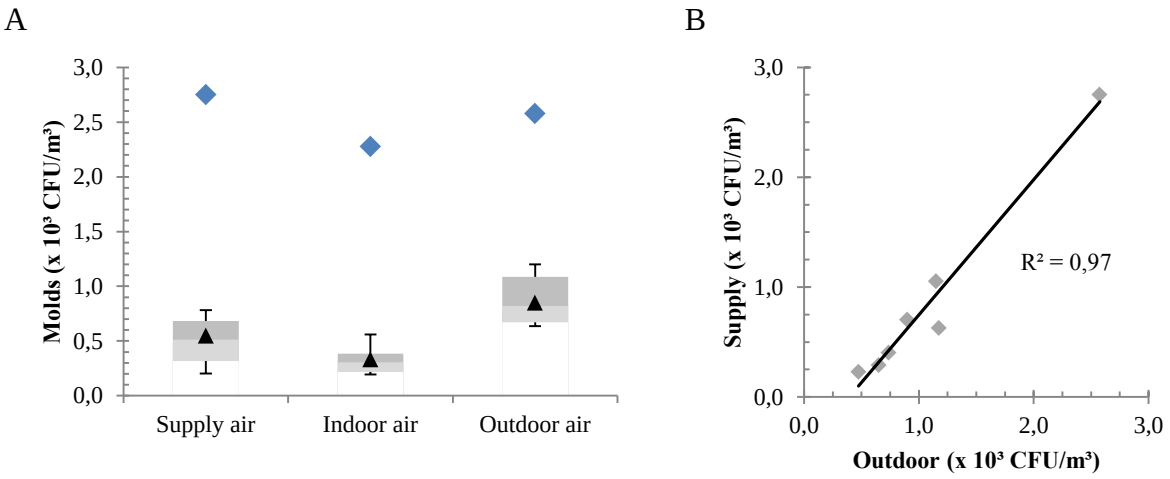

Figure 2: A) Box-whisker plot of the viable mould load expressed in CFU/m³ determined by RCS air sampling for EvS. Legend: ▲ average ◆ outlier No.1 2nd (summer). The outlier was excluded from the dataset for the descriptive statistical analysis. B) Viable mould load in the supply air in function of the outdoor air, both expressed in CFU/m³.

3.3 Balanced ventilation systems

3.3.1 Viable bacteria

For balanced ventilation systems the indoor air was found to contain more bacteria (325;467) than, in descending order, the outdoor (125;205) and the supply air (25;63) (see Figure 3A). The bacterial load in the supply air was observed to be significantly reduced (one way ANOVA, Tukey Post-hoc test, $\alpha = 0.05$) in comparison to the outdoor air. This reduction is most likely due to the presence of the air filters in the ventilation systems. These filters are coarse- or fine dust filters, which in the first place serve to protect the interior of the ventilation system, but additionally can be used to alter the microbial composition of the supplied air. The diameter of bacteria ranges from 0,5 µm to 2 µm. Technically spoken this means that the typical filter types present in Bv. systems (see Table 1 in appendix) do not restrain bacteria on a large scale, based on impact retention. However, the bulk effect of a dusty filter or electrostic interaction between the filter and the bacterium can result in bacterial removal. One outlier in our dataset (No.20) is directly in line with this hypothesis due to the fact that the filters were changed not long ago before the measurements (no bulk effect) in combination with a high outdoor bacterial load. Another outlier (No.16) comprises the measurement on a system equipped with very old (> 2.5 years) G3 sock filters, which is a filter type vulnerable to leakiness. Furthermore, a study of Möritz *et al.* (2001) demonstrated that F7 type air filters were able to retain airborne bacteria and moulds with an efficiency of 70-80% when the outdoor air was relatively dry (<80% RH) and warm (>12°C).
On the other hand, although the supplied air is reduced in its bacterial load, the indoor air contains a significantly (P-value < 0.0001) higher amount of bacteria in comparison to the supply (see Figure 3B) and the outdoor air. This actually means that the relatively clean supply air gets again loaded with bacteria coming from the indoor environment (indoor dust,…) and human activity. Two studies (Hospodsky *et al.* 2012, Qian *et al.* 2012) have already shown that direct human shedding (skin, hair and nostrils) and resuspended floor dust are the most important sources of indoor bacteria whenever a room is occupied. Since the major source of bacteria can be found indoors, there is no direct need for filter types with higher bacterial retention efficiency.

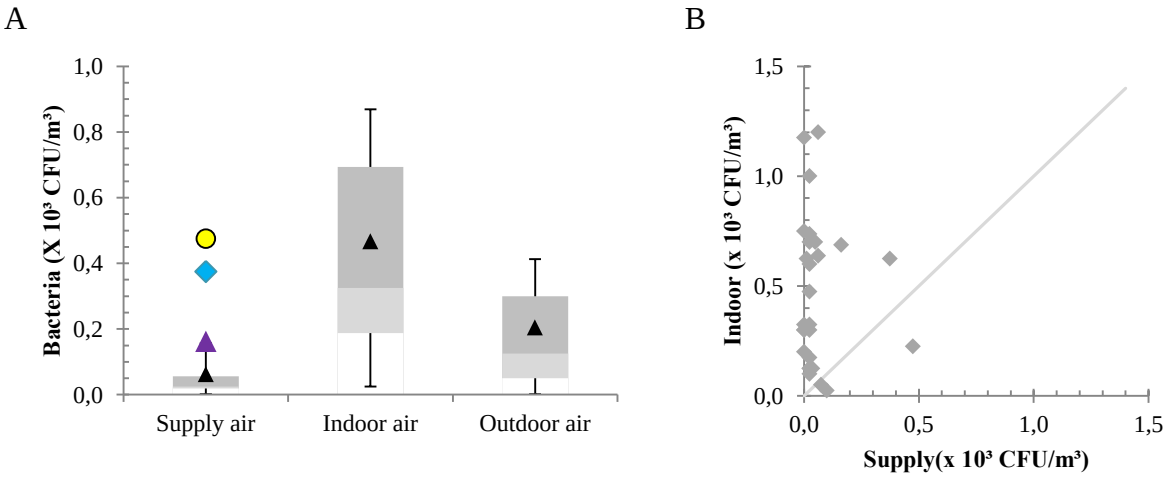

Figure 3: A) Box-whisker plot of the viable bacterial load determined by RCS air sampling for BvS. Legend: ▲ average, Outliers are shown as a separate data point: ◆ No.16 (autumn), ○ No.20 (autumn), ▲ No.35 (winter) B) Viable bacterial load in the supply air in function of the outdoor air

3.3.2 Viable moulds

As indicated in Figure 4A the supply air (163;365) in balanced ventilation systems is less loaded with mould particles than the indoor air (250;505) and the outdoor air (663;1016) respectively. The fact that the supplied air contains fewer moulds than the outdoor air is the result of the filters present in the system (see Figure 4B). These are, depending on their type, theoretically capable of retaining mould spores (2-10µm (Baily 2005)) based on impact retention. Apparently the relative clean supply air gets again slightly loaded with moulds. The potential sources for this phenomenon are materials present indoors like plants, kitchen waste, dust as well as an additional air change rate independent of the ventilation system (open doors and windows, air leakages in the building envelope,…). All exceptional values (outliers Figure 4A) can be attributed to samples collected in autumn and summer, the two seasons with the highest outdoor mould levels (see 3.1). For No.2 an exceptional high mould load was observed in the outdoor air sample, which was collected in summer time. Although the filters present in the system (G4 type) reduced the outdoor mould load with nearly 70%, still high mould levels were found in the supply and indoor air samples. On the other hand for exception No.19, which is also characterised by a high mould load in the outdoor air, the filters (G4) still remove the vast majority of the mould load (96.7%) resulting in no exceptional values for supply and indoor samples (See section 3.3.3 for a description of the other exceptions). Figure 4 B represents the number of moulds (x 10^3 CFU/m^3) in the indoor air in function of the number in the outdoor air. The vast majority of the samples can be found beneath the grey line (indicating an indoor/outdoor value of 1), meaning that the indoor air contains fewer moulds than the related outdoor sample (see section 3.3.3. for a description of the exceptions).

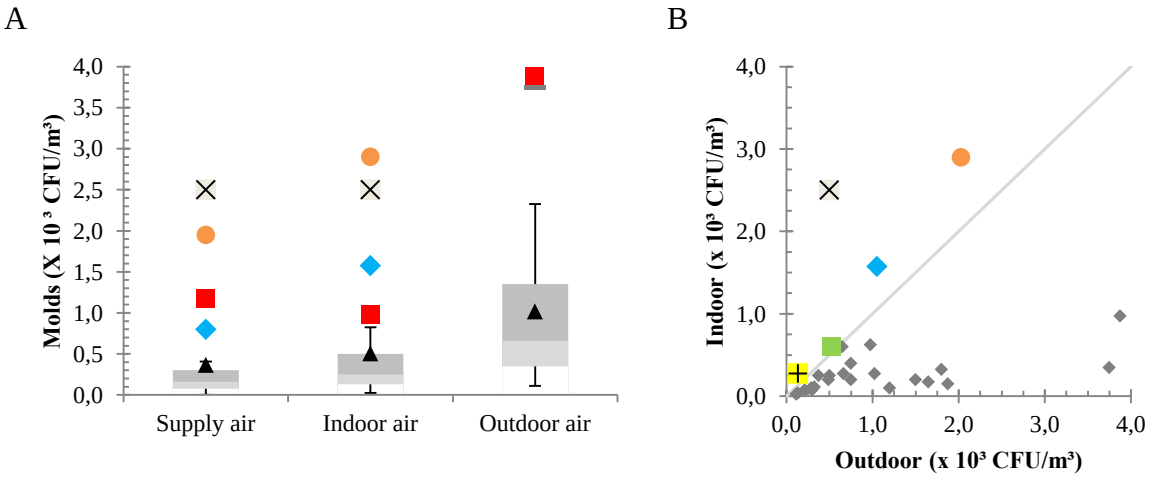

Figure 4: A) Box-whisker plot of the viable mould load expressed in CFU/m^3 determined by RCS air sampling. Outliers are shown as a separate data point: ▲ average, ■ No.2 2nd (summer), ● No.15 (summer), ◆ No.16 (autumn), ▬ No.19 (autumn), ✕ No.37 (under construction) B) Viable bacterial load in the supply air in function of the outdoor air. Legend: ● No.15, ◆ No.16, ■ No.21, ✚ No.34 and ✕ No.37

3.3.3 Filter analysis and performance

Filters present in ventilation systems in the first place serve to protect the interior of the ventilation system, but additionally can be used to improve the quality of the supplied air. Within this project no direct performance measurements were conducted on the filters. However, comparison of the supplied air in relation to the outdoor air gives an impression of the filter performance, although any influence of the duct system is also included (see Figure 5 A). As can be seen from Figure 5A, the mould load of the supplied air is generally reduced

in comparison to the outdoor air. Only two out of 28 samples have a supply/outdoor value >1 (No.34: house with serious construction errors, No.37 house under construction) and one has a S/O value ≈1 which could be due to leaking filters (by-pass leakage). The mould removal efficiency increases with a decreasing mesh size, although the differences between the finest filters (or combination of a coarse and fine dust filter) is rather small (see Figure 5 B). As can be seen from Figure 5 C, the mould removal efficiency of the filters tends to decrease in function of their age. In any case, old filters form a potential contamination risk (see No.16 in Figure 5 C), but also new filters may not function properly. For example point No.15 in Figure 5 C represents a filter of 52 days old with a mould removal efficiency of 3.7% which is most likely related to the fact that it is a sock filter, which is a filter type vulnerable to leakiness. Further point No.21 in Figure 5 C, represents a system with wrongly installed filters and a vertical supply air intake, resulting in clear visual pollution of the system. Finally point No.34 represents a house with serious constructions errors and a potential mould source in the ventilation ducts.

For balanced ventilation systems equipped with a Canadian well, large amounts of bacteria were observed on the pulsion filters (4 out of 6 cases; Rodac and Swap analysis; data not shown). So far, no clear influence on the bacterial load of the supply air was observed, however all samples for these systems were collected in winter time. The appearance of condensation in the Canadian well in summertime might form a potential risk for high levels of bacteria in the supply air of these types of systems, but this remains to be investigated.

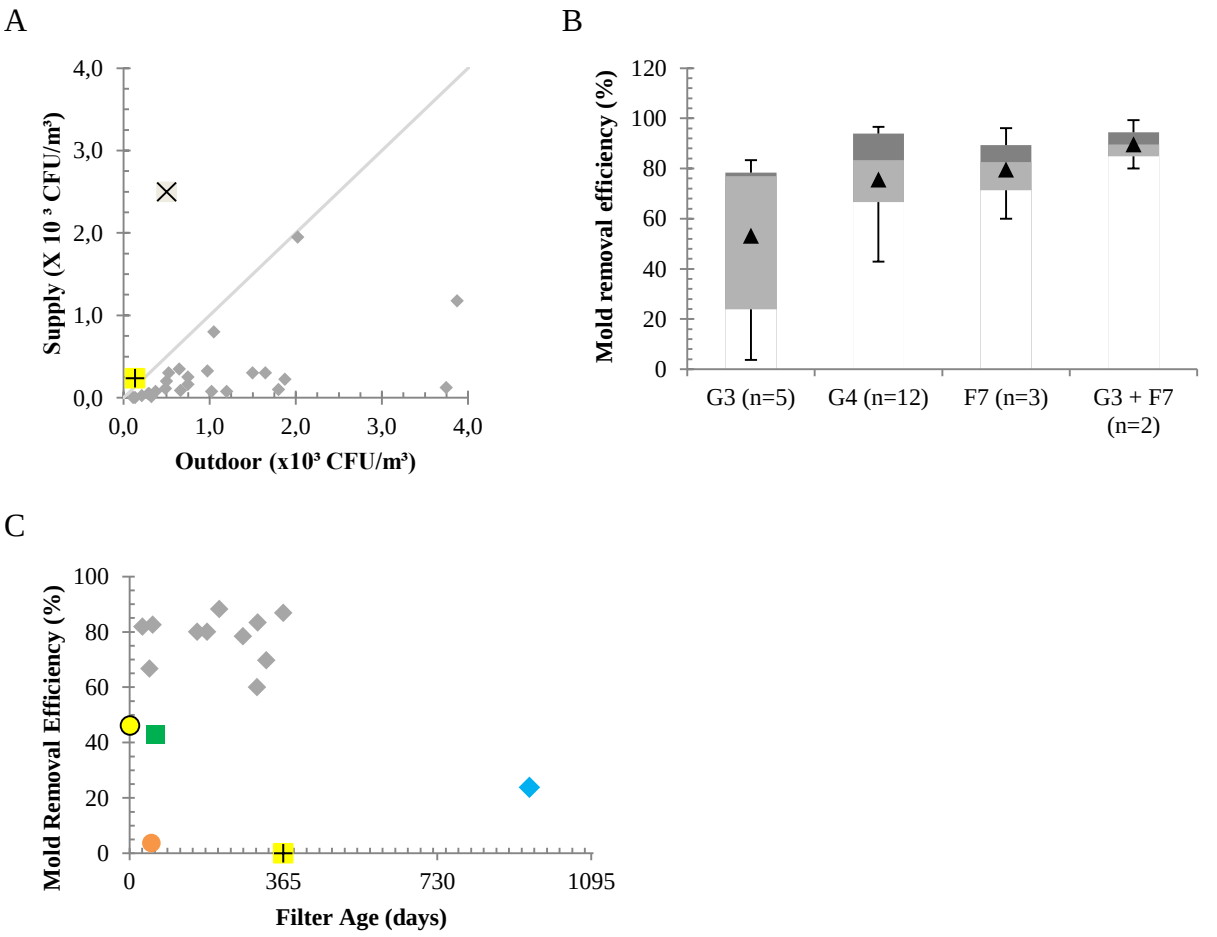

Figure 5 A) Viable mould load in the supply air in function of the outdoor air. Legend: + No.34 and × No.37 B) Mould removal efficiency (%) versus filter type present in the system (exceptions No34, 37 and 15 were excluded from the graph), ▲ average. C) Mould removal efficiency in function of the filter age. Legend: ● No.15; ◆ No.16; ○ No. 20; ■ No. 21; + No.34.

3.4 Most commonly identified mould genera

As mentioned earlier, the interpretation of the microbial viable air sample data was based on the assumption that the indoor microbial levels should be lower than the outdoor levels and there should ideally be no difference in the mould types present in both samples. In the majority of the samples no distinct differences were observed in the identified mould genera. *Aspergillus* (Supply: 33%, Indoor: 31% and Outdoor: 34%), *Cladosporium* (65%,72%,89%) and *Penicillium* (70%,86%, 69%) were the most abundantly identified mould genera. The frequency of occurrence in the different samples is shown between brackets. The fact that these genera were the most abundant is however not surprising, since the spores of these moulds are relatively small and easily airborne. As a result these spores are also easily collected by air sampling. Moreover, samples were collected in houses without visible mould and dampness problems, rendering the chance of collecting the spores of associated mould genera, which are usually larger and less airborne, less likely.

4 CONCLUSIONS AND RECOMMENDATIONS

For both systems the bacterial load in the indoor air samples was higher than in the outdoor and supply samples. These results suggest that human activity has a higher impact on the indoor bacterial load than the supply from outdoors through the ventilation system. For both systems the mould load in the outdoor air was higher than the load in the indoor and supply air. However, for the exhaust systems the supply air is more loaded than the indoor air and the mould content of the supply- and indoor air was found to be directly related to that of the outdoor air. No direct relation between the number of bacteria and moulds present on the adjustable supply grids and extraction ducts and the microbial load of the supplied and indoor air was observed for EvS. This however does not exclude the necessity of maintenance. In contrast, for the balanced systems the indoor air contained a slightly higher mould load in comparison to the supply air. The supply air was drastically reduced in mould load in comparison to the outdoor air, which is due to the supply filter present in balanced ventilation systems. Furthermore, seasonal variations have an influence on the hygienic quality of the supplied air by the ventilation system. This influence is clearer in exhaust systems in comparison to balanced systems. Although the effect of the outdoor air on the quality of the supplied air for balanced systems largely depends on quality of filters and their airtightness.

Based on the results of our *in situ* measurements as well as on on-site observations the following recommendations can be formulated to prevent ventilation systems from becoming microbially contaminated and finally in the worst case a potential indoor microbial source. These recommendations are categorized in three subgroups related to: the design, installation and maintenance of the system.

Design:

As concluded earlier (see point 3.3.1), the major source of bacteria can be found indoors. Therefore, there is no direct need for filter types with higher bacterial removal efficiency. Further a coarse dust filter (type G4) has already a satisfying mould removal efficiency and is sufficient to protect the system (see Table 1 and Figure 5 C). On the other hand, leaking filters have a baleful influence on the microbial quality of the supply air. Therefore priority should be given to the airtightness of the filters and the combination of the filter and its housing in the system, rather than the improvement of their efficiency. This includes: avoiding the use of sock filter types which are vulnerable to leakiness, preventing the possibility of incorrect installation, prevention of air passing around the filters (by-pass), provide a good accessibility

to the filters in order to facilitate maintenance. Whenever more efficient filters are desired, an F7 fine dust filter can be combined with an inline coarse dust filter (G3 or G4) in front of the exchange unit

Installation:

A vertical supply air intake should be avoided in order to prevent the accumulation of dirt on the pulsion site of the system (ducts, heat exchanger and filter). Also the filters are at risk to become wet, which might result in microbial growth. Further, a certain distance between the fresh air intake and the exhaust of the consumed air and other exhausts (chimney, aeration of wastewater,…) should be respected. It is absolutely not recommended to launch the system in a building under construction (see outlier No.37 in Figures 4 and 5). Finally, the ducts should be protected against possible contamination shortly after production and remain covered during storage, transport, installation and until occupation of the house.

Maintenance:

For a balanced ventilation system, the state of the filters has a direct impact on the microbial quality of the supply air. Therefore it is recommended to clean the filters every 2 to 3 months using a vacuum cleaner, ideally equipped with a HEPA14 filter. Once a year, the filter pair should be replaced, preferably before winter time. Additionally the grill of the supply air intake and the supply and extraction mouths should be cleaned. For the ducts, a regular inspection and/or cleaning (rigid ducts) or replacement (flexible ducts) is recommended.

Exhaust ventilation systems require less maintenance, but a 3 monthly based inspection and yearly cleaning of the controllable supply grids and extraction ducts is recommend.

5 APPENDIX

Table 1: Air filters typically used in balanced ventilation systems and their characteristics according to Filtration Engineering Ltd (Cheshire, UK) using test standard BS EN 779

Intended removal	Filter class	Nearly 100% retention for particles	Average performance according to EN779
Coarse dust	G3	>5µm	80-90% Arrestance
	G4	>5 µm	≥ 90% Arrestance
Fine dust	F7	>2 µm	80-90% Efficiency

6 ACKNOWLEDGEMENTS

The authors wish to thank the Agency for Innovation by Science and Technology in Flanders (IWT) for the financial support.

7 REFERENCES

Baily, H. S. (2005). *Fungal Contamination: A Manual For Investigation, Remediation And Control.*

Codina, R., R. W. Fox, R. F. Lockey, P. DeMarco and A. Bagg (2008). Typical levels of airborne fungal spores in houses without obvious moisture problems during a rainy season in Florida, USA. *Journal of Investigational Allergology and Clinical Immunology* **18**(3): 156-162.

European Commission (2003). V*entilation, Good Indoor Air Quality and Rational Use of Energy*. (Report No 23). Retrieved june 2013 from: http://ihcp.jrc.ec.europa.eu/our_activities/public-health/indoor_air_quality/eca/eca_report_23

Hospodsky, D., J. Qian, W. W. Nazaroff, N. Yamamoto, K. Bibby, H. Rismani-Yazdi and J. Peccia (2012). Human occupancy as a source of indoor airborne bacteria. *PLoS One* **7**(4).

Möritz, M., H. Peters, B. Nipko and H. Rüden (2001). Capability of air filters to retain airborne bacteria and moulds in heating, ventilating and air-conditioning (HVAC) systems. *International Journal of Hygiene and Environmental Health* **203**(5–6): 401-409.

Qian, J., D. Hospodsky, N. Yamamoto, W. W. Nazaroff and J. Peccia (2012). Size-resolved emission rates of airborne bacteria and fungi in an occupied classroom. *Indoor Air* **22**(4): 339-351.

Tilborghs, G., D. Wildemeersch and K. De Schrijver (2009). *Wonen en Gezondheid*. Vlaams Agenschap Zorg en Gezondheid. Retreived june 2013 from: http://www.belgium.be/nl/publicaties/publ_wonen_en_gezondheid.jsp

World Health Organization (2009). WHO guidelines for indoor air quality : dampness and mould [edited by Elisabeth Heseltine and Jerome Rosen]. Copenhagen.

AIRTIGHTNESS AND VENTILATION OF SOCIAL HOUSING IN IRELAND – A REVIEW OF FIELD MEASUREMENTS AND OCCUPANT PERSPECTIVES PRE- AND POST- RETROFIT

Derek Sinnott[1], Mark Dyer

TrinityHaus
Trinity College Dublin,
Dublin 2, Ireland
[1]dsinnott@wit.ie

ABSTRACT

Airtightness and controlled ventilation are important factors affecting energy use and indoor air quality. Airtightness tests were carried out on nine naturally ventilated social houses in Ireland. Subsequently, four of the houses were retested following energy efficient upgrading. The upgrading largely consisted of improving fabric insulation and where required the mandatory installation of passive wall vents. Interviews were conducted with the occupants to gain their perspectives of airtightness and ventilation in their homes. The occupants of the upgraded houses were interviewed pre- and post- the process.

The paper compares the results obtained to that assumed in the Dwelling Energy Assessment Procedure (DEAP), which is Ireland's National Methodology for calculating the energy performance of dwellings. The location of the most onerous visible air leakage paths, identified using a smoke pencil are presented.

As an unintentional side-effect, fabric upgrading considerably improved the airtightness of the dwellings. However, due to lack of cognisance of airtightness principles, simple airtightness techniques which would further improve results were not integrated into the upgrading process. The survey revealed that although occupants understand that ventilation is important, their understanding of required ventilation levels and control is limited. Airtightness levels in one house were high, but the house was under-ventilated resulting in condensation and potential for mould growth on external walls. Whilst a number of houses had considerable levels of uncontrolled infiltration leading to occupant comfort levels being compromised. Overall occupants were happy with the upgrading but had a number of concerns about the newly installed passive vents.

The paper takes a novel approach combining quantitative and qualitative data gaining an insight into occupant attitude and behaviour. The paper highlights the importance airtightness and controlled ventilation in naturally ventilated houses. The paper discusses the potential to reduced air leakage to a level where mechanical ventilation with recovery (MVHR) becomes viable and can be integrated as part of the upgrading process.

KEYWORDS

Ventilation, Dwelling Airtightness, Testing, Occupant Perspective

1 INTRODUCTION

Social housing, accounts for approximately 8.6% (130000 units) of all housing in Ireland (ICSH, 2006). Nationally, Local Authorities are in the process of upgrading their older exiting housing stock, aspiring to increase living and comfort standards for occupants in unison with reducing energy use in the dwelling. This paper forms part of a study focused on the assessment energy use patterns in Irish social housing and the real effect of fabric upgrading.

It is a well-recognised in temperate climates, like Ireland, that a large proportion of heat loss from dwellings is as a result of air infiltration. However, there has been little attention given to improving airtightness as part of standard retrofitting strategies.

Building technologies and technical standards continually advancing, but to date there is little research relating to user interface with these buildings and a particular lack of knowledge relating to airtightness and ventilation.
This paper evaluates the technical findings from airtightness testing, comparing measured modelled airtightness levels and compliance with Building Regulations. The outcome of energy efficient retrofitting is then assessed and combined with surveys of occupant perspective of airtightness, existing practices and perceived effect of upgrading the houses.

2 BACKGROUND

While climate corrected energy use for each dwelling in Ireland decreased by 28% from 1990 to 2011, mainly as a result of improved energy performance of new housing stock, overall the housing stock has been identified as being one of the least energy efficient in the EU-27 (Lapillonne *et al.*, 2012, Howley *et al.*, 2012). In 2011 the "average" dwelling consumed 19,875 kWh of energy, based on climate corrected data, approximately 60% of which was used for space heating (Howley *et al.*, 2012, Janssen, 2004). Considering estimated heat loss due to 'easily avoidable air leakage' accounts for between 5 and 10%, up to 2000kWh of heat energy per dwelling is wasted annually in Ireland (DEHLG, 2008a).
Approximately 50% of the current Irish housing stock was built pre- 1979, when the minimum energy performance building regulations were introduced and mandatory airtightness testing was first introduced for new dwellings in 2008. Consequently, as a result of the recent downturn in Irish construction, almost all dwellings in Ireland have being constructed prior to any minimum mandatory airtightness levels. Technical Guidance Document (TGD) Part L states 'To avoid excessive heat losses, reasonable care should be taken to limit the air permeability of the envelope of each dwelling' and set a reasonable air permeability upper limit of $10m^3/hr/m^2$(DEHLG, 2008b). In 2011, this limit was revised down, to a not very onerous, 7 $m^3/hr/m^2$ (DEHLG, 2011). Unsurprisingly, there is still no minimum airtightness standard when upgrading existing dwellings. However, cognisance must be paid to the point made by the Energy Saving Trust (EST, 2005) that air permeability in dwellings is made up from a myriad of entry points in the fabric and making airtightness improvements difficult when retrofitting.
Ireland's temperate oceanic climate and average annual temperature of about 9^0 Celsius (C), summer mean maximums and minimums of about 19^0 C and 2.5^0 C respectively, means that dwellings are predominately naturally ventilated (MET Eireann, 2012). Due to Ireland's geographical location and exposure to the Atlantic Ocean to the west there is significant wind speed climate variation. However, Technical Guidance Document Part F – Ventilation (DEHLG, 2009), dictates a uniform standard irrespective of location. Though a small country, this uniformity is not optimal from a technical design standpoint. Consequently, there is no guarantee of sufficient ventilation all year around, with excessive heat loss on cold and windy days and risk of overheating on calm warm days. The relationship between airtightness and space heating demand is complicated by occupant behaviour and their routine of opening and closing windows and vents.

3 DWELLING ENERGY ASSESSMENT PROCEDURE

To comply with the European Directive 2002/91/EC, Ireland has adopted the Dwelling Energy Assessment Procedure (DEAP) as the official methodology for calculating the energy performance of buildings. The DEAP calculation framework, based on IS EN 13790, draws heavily on the calculation procedures and tabulated data of the UK Standard Assessment Procedure (SAP), itself based on the BRE Domestic Energy Model (BREDEM), and is adapted for Irish conditions (BRE, 2009). The methodology applies equations and algorithms

to estimate natural airtightness levels of the dwelling based on dwelling profile, including number of stories, structure type, presence of suspended wooden ground floors, and the level of draught stripping of the windows and doors. This natural airtightness is used energy performance calculation. If airtightness test results are available, DEAP uses the (Kronvall, 1978) derived "rule of thumb" method where the natural infiltration rate is 1/20 of the air permeability under test conditions. This study uses the DEAP methodology estimated results for each dwelling, multiplied by 20, to give an estimate of air permeability under test conditions, q50.

4 DWELLING TYPOLOGY AND OCCUPANT PROFILE

The nine single family local authority owned semi-detached and terraced houses were built circa 1980. Combined terrace and semi-detached houses account for the largest proportion, 44.8%, of dwellings in Ireland (CSO, 2007). The occupancy profile outlined in Table 1 is typical for social housing units in Ireland with a number of parents and children, older couples and people living on their own. The average floor area of the three-bedroom two-storey (Figure 1a) and two bedroom single storey houses (Figure 1b) is $80m^2$ and $50m^2$ respectively, with the exception of house D which has a single storey extension to the rear, giving an increased floor area of $87m^2$. All dwellings have load bearing external cavity walls and are naturally ventilated. Ground floors are slab-on-grade with suspended timber first floors. Ground floor internal walls are of solid block construction, with stud partitions at first floor level. The attic space is of typical cold roof construction with insulation between ceiling joists. Previous refurbishment schemes upgraded all windows to double glazing and back boiler heating systems were replaced with natural gas central heating. Where passive wall vents were not installed during original construction, windows with integrated trickle vents were fitted. There is no mechanical ventilation in the kitchen or bathrooms.

In 2012, four of the nine two-storey houses in this study were upgraded by the local authority as part of the Social Housing Improvement Programme (SHIP). This central government funding can only be drawn down by a local authority if they carry out eligible energy efficiency works. Eligible upgrading pertinent to airtightness undertaken in the case study houses included:

- placing full-fill cavity wall insulation;
- laying 300mm of attic insulation to meet the current Part L building regulations;
- replacing existing open fires with a Stanley Cara 'Insert Stove';

Table 1: Dwelling and occupant profile

Dwelling	Classif-ication	Orient-ation	Number of Occupants	Occupant age				
				5 – 17	18 – 25	26 – 45	46 – 55	56 – 65
A	2[1],T[2]	E-W	1				F	
B	2,S	E-W	2					F[3]M[4]
C	2,S	E-W	3	M	M	F		
D	2,T	E-W	3		M		F M	
E	2,T	N-S	3	M F		F		
F	2,S	N-S	3	M F		F		
G	2,T	N-S	1				F	
H	1,S	N-S	1					F
J	1,S	N-S	2					M F

[1] 1 or 2 storey high [2] T = Terrace, S = Semi-detached [3] Female [4] Male

(a) three-bedroom two-storey

(b) two bedroom single storey

Figure 1: Typical case study dwellings

- draught stripping around attic hatch and fitting two holding down latches. Replacing existing window and door draught stripping where compromised or missing;
- in compliance with Part F of the building regulations (DEHLG, 2009), where necessary, background passive ventilation was installed with constant open vents fitted to the kitchen and living room and 'Hit & Miss' vents fitted to all other rooms. In each of the houses a new mechanical wall vent were installed to the main bathroom with an automatic overrun (after switch off), located on external wall wired into bathroom light switch;
- where vents were in place, the opening was cleaned and new vent covers provided internally and externally;
- House B and D had all windows and doors replaced.

With the exception of draught stripping there is a clear absent of any intentional airtightness improvement works.

5 AIR PERMEABILITY TESTING

The location of individual air-leakage paths are often difficult to identify by visual inspection, in dwellings. Thus, assessing the building envelope as a whole, using the standardised blower door test, is the only reliable means of assessing building air-tightness. Due to the variety of methods used to deal with intentional openings during testing, direct comparison of blower door test results between countries is often difficult (Carrié and Rosenthal, 2008, Caillou and Van Orshoven, 2010). In 2012, standardised blower door tests were carried out on the nine case study houses to establish airtightness characteristics pre- upgrading and repeated on the four upgraded houses approximately one month after completion. Testing was carried out in accordance with ATTMA (The Air Tightness Testing and Measurement Association) Technical Standard for dwellings (ATTMA, 2010). The Technical Standard is generally compliant with IS EN 13829:2001 Thermal performance of buildings – Determination of air permeability of buildings – Fan pressurization method. Prior to testing, dwellings were surveyed and the internal envelope area (AE) and volume (V) accurately calculated. Testing to determine the air permeability was largely compliant with Method B, of EN 13829; external doors and windows, intentional vents, attic hatches, letterbox and extract fans were closed but not sealed; open fireplaces were sealed.

The Retrotec Q46 Automated Blower-Door used for the tests has Maximum Flow at 50 Pascal test pressure of 9,514m^3/h and Minimum Flow at 10 Pascal of 65m^3/h and incorporates regulated variable frequency speed controllers to prove a stable speed control, making it suitable for testing dwellings. The fan was secured to the front door using the Retrotec soft panel frame. Pressure and flow rate were controlled using a laptop, connected to a DM-2A Automatic Micro-manometer, which controlled the fan. In addition to the DM-2 the test this

software continuously logged a number of parameters including fan flow, test pressure and the area measurements.
Both pressurisation and depressurisation test cycles were undertaken to a pressure differential across the envelope of 55 Pascals. A software generated best fit straight line was used to automatically calculate the air permeability at 50 Pascals. The average of both results was recorded as the air permeability for the building. Averaged results are an important component of the test as leakage paths have complicated shape and different aerodynamic characteristics depending upon air flow direction. The 'value effect' can also occur where by a component can be pushed up during pressurisation and pulled down generating a seal during depressurisation. Stephen (Stephen, 1998) has shown that pressurisation and depressurisation results can differ by up to 20%. During testing, wind speed and ambient temperature conditions were measured using a hand held thermo-anemometer to ensure compliance with IS EN 13829:2001. Simultaneously with the airtightness testing in-depth visual and smoke pencil testing was carried out to identify the key air leakage locations. Though it is easy to visually identify a number of common leakage paths it is assumed that up to about 70% of the air leakage is through cracks and other invisibale locations (Stephen, 2000).

6 TEST AND INSPECTION RESULTS

Pre-upgrading air leakage paths identified by the smoke pencil test and simple observations were similar to those identified in previous research (Sinnott and Dyer, 2012, EST, 2005, Sherman and Chan, 2003, Jaggs and Scivyer, 2006). The most significant and easily accessible leakage paths from the perspective of upgrading, identified in Figure 2, are:

(a) the waste and services pipes enclosed within a timber box-out which penetrates directly into the unheated attic space;
(b) unsealed penetrations in timber first floor. There is typically an unsealed path along the floor joists and into the empty cavity space;
(c) penetrations into the stud partition walls allowing air to transfer to the attic into the floor void;
(d) poorly maintained and sealed attic hatches;
(e) poorly maintained window and door seals.

Considering poor and under-ventilation, many of the existing passive wall vents had been partially or fully obstructed. Figure 2(f) shows a vent which had been painted over a number of times. Also a number of vents were completely blocked by miscellaneous items and debris.

The results of the testing pre- and post- upgrading are presented in Figure 3. The DEAP calculated airtightness of the houses ranged from 8.4 $m^3/hr/m^2$, for both single storey houses, H & J, to 11.2 $m^3/hr/m^2$ for house F. The variation in predicted airtightness is based predominantly on number of storeys and percentage draught stripping.
The results demonstrate the large range in measured air permeability from 3.9 – 17.1$m^3/hr/m^2$. The 10.9 $m^3/hr/m^2$ mean results is consistent with the findings of a similar study by Sinnott and Dyer (Sinnott and Dyer, 2012). Overall 44% of the results exceeded DEAP predicted airtightness levels. For house C which had the highest measured air permeability of 19.7$m^3/hr/m^2$, DEAP underestimated the result by 47%. Superficially this house is identical to the other two storey houses. However, during testing the dwelling occupant explained that to limit cold draughts she places towels around the kitchen units. A visual inspection identified a large hole under the counter where pipework enters the internal service duct, shown in Figure 4(a), allowing uncontrolled airflow from the attic into the room. Figure 4(b) shows a missing floor board under the bath and a number of pipes from the hotpress and penetrations through

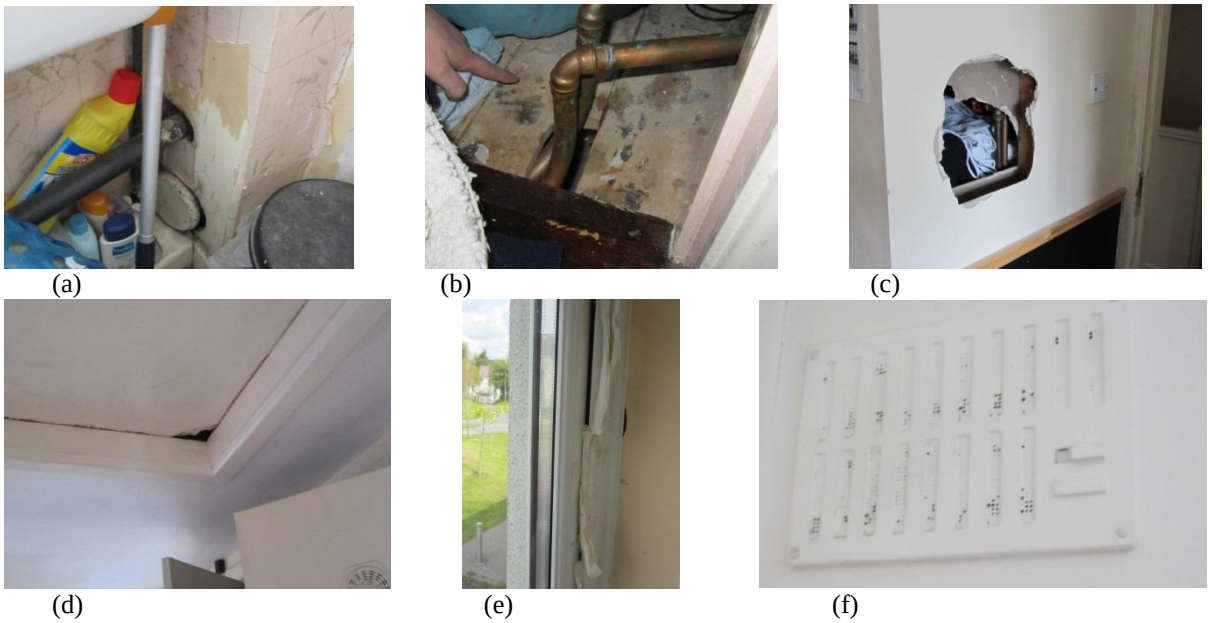

Figure 2: Typical leakage paths identified during inspection

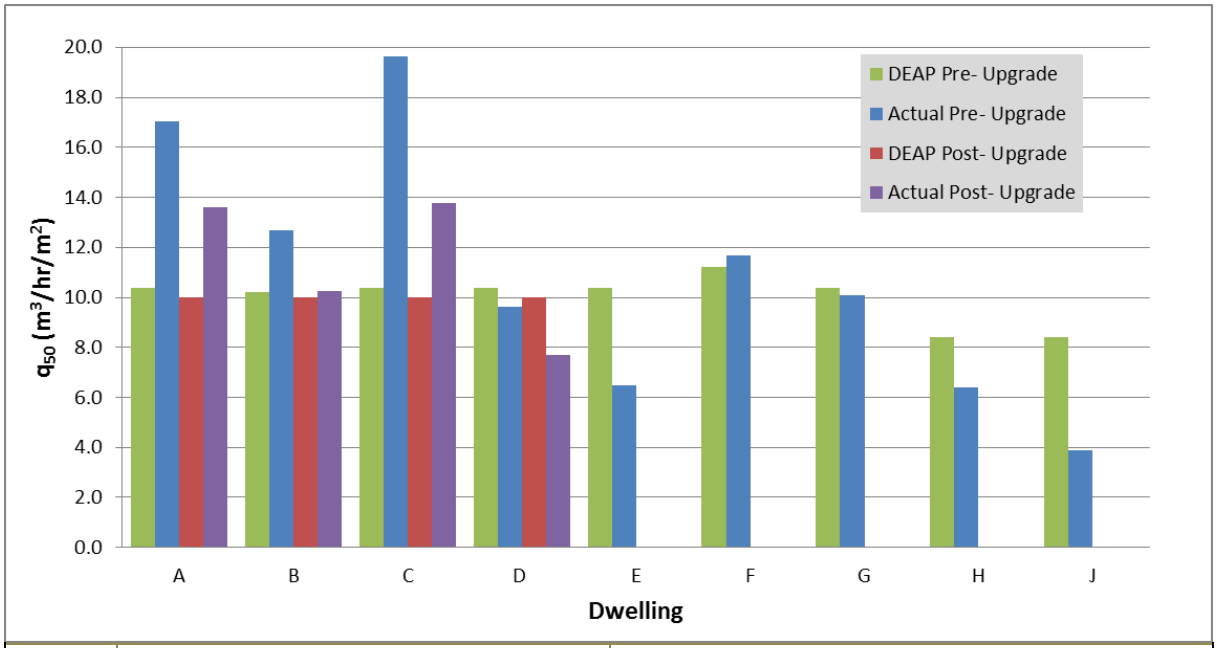

Dwelling	Pre - Retrofit			Post - Retrofit			
	% Draught Stripped	DEAP Calculated, Q_{50} $[m^3/h.m^2]$	Measured, Q_{50} $[m^3/h.m^2]$	% Draught Stripped	DEAP Calculated, Q_{50} $[m^3/h.m^2]$	Measured, Q_{50} $[m^3/h.m^2]$	Improvement [%]
A	90	10.4	17.1	100	10.0	13.6	20.2
B	93	10.2	12.7	100	10.0	10.2	19.3
C	90	10.4	19.7	100	10.0	13.8	29.9
D	88	10.4	9.6	100	10.0	7.7	20.2
E	90	10.4	6.5	100			
F	70	11.2	11.7	100			
G	90	10.4	10.1	100			
H	88	8.4	6.4	100			
J	90	8.4	3.9	100			

Figure 3: Measured and DEAP esitmated dwelling airtightness

the walls such as the extractor from the tumble dryeras shown in Figure 4(c) provide leakage paths. Figure 2(c) shows a large hole in the bedroom timber stud wall allows air to leak into the wall space.

(a) (b) (c)

Figure 4: House C major leakage paths

Sub-dividing the dwellings by number of storeys reveals that the two single storey houses not only performed better than predicted by DEAP, but achieved the highest levels of airtightness. House J seems to have an optional result at 3.9 $m^3/hr/m^2$; less than 50% of that predicted by DEAP. However, during the testing the occupants stated as a means of minimising heat loss they had blocked up as many vents, gaps, and holes as that they could. Without any form of mechanical ventilation house is under-ventilated, made evident by a number of issues including, noticeable stale air upon entry, high humidity levels resulting in condensation and staining on the north facing external walls, as shown in Figure 5. Without regular drying, with a towel, the occupants report that mould growth can be prevalent.

Figure 5: Staining on external wall due to condensation

House H, identical footprint to house J, at 6.4$m^3/hr/m^2$, again performed better than DEAP predicted but there was no evidence of condensation or mould growth, demonstrating that the house is adequately ventilated, whilst being relatively airtight.

Airtightness improvement works were not specified, with the exception of draught stripping to the windows and attic hatch. However, the upgrading had a positive effect on airtightness by between 19.3 and 29.9%, with an average airtightness improvement of 22.4%. Though the four houses are not statistically significant the pattern is clearly positive. Notably, post upgrading, 3 houses still exceed the DEAP calculated values. DEAP calculated overall improvement of less than 4%, from 10.4 to 10 $m^3/hr/m^2$, by providing 100% draught stripping. It is clear in this study that the methodology underestimates the positive effect of upgrading. The real improvement in airtightness is as a result of a number of works carried out including, upgrading a number of windows and doors, the full-fill cavity wall insulation which acts in some way to seal the myriad of crack and block easy leakage from around floor joists into the cavity space, the fixing of the attic hatches and replacement of the open fires with stoves.

7 SURVEY RESULTS

Interviews were conducted with all adult occupants in each of the nine households to establish their perceived living and comfort standards and to gain their perspectives of airtightness and ventilation in their homes. The semi-structured interviews were undertaken in the occupant's home and rather than a question and answer sessions were conversational in form. Interviews were repeated with the four houses post- upgrading to establish if there was a benefit to the indoor environment. The interviews were digitally recorded and relevant sections analysed in detail and the key findings are presented in this paper.

The nature of social housing means occupants in general spend more time in the homes than private homeowners, either due to lack of employment as a result of the recession or lack of disposable income. On average each house is occupied by at least one occupant 22 hours per day. Overall, the householders believe they have a 'fairly good' to 'very good' standard of living. However, a number of the occupants suffer from chronic health problems such as diabetes. As a result, they say they feel the cold more. Overwhelmingly the householder's express that their priority is to run the house with minimal expense. Consequently, they are keen to maintain heat within their homes, even if it means compromising airflow by blocking up vents or leaving window trickle vents closed. In general occupants who are local authority tenants have done little or no remedial work to prevent heat loss through infiltration citing: they are not capable of carrying out the works; they do not have the money to hire a professional and ultimately the onus is on the council.

7.1 Pre-upgrading

A number of the households complained of draughts throughout the house and over the winter period they need place draught excluders at the front and rear doors. House D stated that given a particular wind direction they can feel draughts around the 'poorly fitted windows, doors and attic hatch'. The occupants of house C, which has the worst overall test result of 19.7m^3/hr/m^2 place towels around the kitchen units under the sink during winter. As shown in Figure 4a the service duct seems to be the worst offender. Somewhat surprisingly the adult female says that always sleeps with the window slightly open, regardless of season. This may be a sign of under ventilation in the bedroom, which has no passive vents.

The issue of the service duct was raised in a number of the two storey houses. In house B, the occupants have rearranged their home so that the service duct is in the corner of their living room and the draughts cause some discomfort when sitting on the sofa. The occupants also say that the passive vent above the food preparation area in the kitchen 'make it's very cold when working ….it's awful'.

The real outlier is house J. The female occupant suffers from chronic osteoarthritis and finds mobility difficult. As a result she feels the cold very much and keeps the ambient temperature in the house very high. The occupants have blocked up as many air leakage paths as they could. Consequently, a wave of stale and humid air hits the visitor upon entering the house. The male occupant believes that the dwelling environment contributes to his wife's illness but they have no option as they have to keep the temperature up.

7.2 Post-upgrading

In general terms all the occupants are happy with the upgrading saying that they feel that their houses are warmer. However, a number of issues were raised during the second interview. The female occupant of house A says her bedroom is 'freezing' because if the installation of the new wall vents in each room. Before the upgrading there were trickle vents in the windows but they were always closed 'to keep the heat in'. The householder also says 'with

the vents you can't enjoy the television because of the noise' from breeze moving through the vents. Overall she describes the upgrading as positive but 'the only thing I can't stand are the air vents ….. the noise drives me bananas'.
The occupants of house B, which always had wall vents, were disappointed that there was no improvement made to the service duct and there is still substantial air ingress resulting in discomfort. They are happy with the new windows and doors. The vent in the kitchen was moved to a different location which has 'improved the working environment'. The new mechanical vent in the bathroom worked initially, but the external grill was later replaced and some expanding foam was inadvertently deposited around the blades, preventing it from working and partially blocking the vent pipe.
The female adult in house C really does not like the newly installed vents and because it causes draughts in the house and she can also hear noise coming from the street 'which is very annoying'. Following the second scheduled interview she now plans to block up at least some of the vents. However, she still 'has the habit' of opening her bedroom window at night.
Again, the occupants of house D occupants find their house warmer 'but the new vents were causing problems'. There is a newly installed vent in the sitting room and the adult male says 'it was freezing sitting under the one in the sitting room..... now it is sealed with tape. The extractor fan in the bathroom is also turned off and sealed with tape because 'it was too noisy when having a bath'. The occupants open the window to purge the room with fresh air when required.

8 CONCLUSIONS

This paper combines quantitative air permeability results with qualitative interview data, gaining a whole house integrated understanding of building airtightness and its effect on indoor environment. The uniform nature of the houses makes the sample unrepresentative of the national housing stock. However, the vast majority of houses in Ireland are of cavity wall, cold roof construction and it could be expected that similar trends would be revealed through widespread testing.
Typical expected leakage paths were prevalent; however, anomalies were found in each house. Johnston (Johnston *et al.*, 2011) suggests that achieving $6m^3/hr/m^2$, with good design, using existing techniques at little increased cost is genuinely achievable for new build. Due to the number of inaccessible leakage paths this would be challenging for existing dwellings. Nevertheless, there is considerable scope to improve airtightness when upgrading by simply paying attention to detail, sealing around all pipes and penetrations, improving window seals, sealing conduits and being generally aware of airtightness improvements.
Broadly occupants have a negative attitude towards design vents, viewing them as letting heat out and noise in. It is clear that the adoption of a user centred design approach when developing a ventilation strategy for new and existing dwellings is the only way to remove the potential for occupant discomfort.
All houses pre- and post- retrofitting, excluding House J, excessed $5m^3/hr/m^2$, which is generally considered to be the threshold when MVHR becomes viable. Traditional upgrading practices are disruptive to the householder offering an opportune time to improve airtightness levels to a standard where MVHR could be implemented. The local authority should consider installing an MVHR in House J, as it already surpasses this threshold and would improve air quality and occupant comfort.
It is clear that DEAP needs to include a greater number of variables where calculating airtightness to yield realistic results. The first step to enhance this model is through extensive testing of a range of buildings and development of a national database. The failure of the majority of the houses to meet the minimum airtightness standards set down for new

construction should be seen as a potential opportunity to achieve real energy reduction when upgrading houses.

9 REFERENCES

ATTMA, 2010. Measuring air permeability of building envelopes (Dwellings): Technical Standard 1. Northampton, UK: The Air Tightness Testing and Measurement Association (ATTMA), BINDT.

BRE, 2009. The Government's Standard Assessment Procedure for Energy Rating of Dwellings. British Research Establishment.

CSO, 2007. Census 2006: Volumne 6 - Housing. Central Statistics Office: Stationery Office, Dublin, Ireland.

DEHLG, 2008a. Limiting Thermal Bridging and Air Infiltration - Acceptable Construction Details. Department of Environment, Heritage and Local Government. Dublin.

DEHLG, 2008b. Technical Guidance Part L - Building Regulations 2007 - Conservation of Fuel and Energy - Dwellings. Department of Environment Heritage and Local Government, Dublin.

DEHLG, 2009. Technical Guidance Document F, Building Regulations - Ventilation. Department of Environment, Heritage and Local Government. Dublin.

DEHLG, 2011. Technical Guidance Part L - Building Regulations 2011 - Conservation of Fuel and Energy - Dwellings. Department of Environment Heritage and Local Government, Dublin.

EST, 2005. Improving airtightness in dwellings. Energy Saving Trust: UK.

Howley, M., Dennehy, E., Gallachóir, B. Ó. & Holland, M. 2012. Energy in Ireland 1990 – 2011. Energy Policy Statistical Support Unit (EPSSU) of Sustainable Energy Authority of Ireland

ICSH, 2006. ICSH Background Paper Housing Issues. Irish Council for Social Housing.

Jaggs, M. & Scivyer, C. 2006. Achieving airtightness: General principles. GBG 67 Part 1. British Research Establishment.

Janssen, R. 2004. Towards Energy Efficient Buildings in Europe - Final report. European Alliance of Companies for Energy Efficiency in Buildings (EuroACE), Brussels.

Johnston, D., Miles-Shenton, D., Bell, M. & Wingfield, J. 2011. Airtightness of buildings — towards higher performance: Final Report — Domestic Sector Airtightness. Department for Communities and Local Government, London, UK.

Kronvall, J. 1978. Testing of houses for air leakage using a pressure method. *ASHRAE Transactions,* 84**,** 72-79.

Lapillonne, B., Sebi, C. & Pollier, K. 2012. Energy Efficiency Trends for Households in theEU. Enerdata - An Analysis Based on the ODYSSEE Database.

Met Eireann. 2012. *Climate of Ireland* [Online]. Met Eireann Available: http://www.met.ie/climate/climate-of-ireland.asp.

Sherman, M. H. & Chan, W. R. 2003. Building airtightness: research and practice. *Lawrence Berkeley National Laboratory, LBNL-53356.*

Sinnott, D. & Dyer, M. 2012. Air-tightness field data for dwellings in Ireland. *Building and Environment,* 51**,** 269-275.

Stephen, R. 1998. Airtightness in UK dwellings: BRE's test results and their significance. London: Construction Research Communications Ltd.

Stephen, R. 2000. *Airtightness in UK Dwellings*. BRE Information Paper IP 1/00, January 2000. Garston, Watford, Building Research Establishment.

AIRTIGHTNESS QUALITY MANAGEMENT SCHEME IN FRANCE: ASSESSMENT AFTER 5 YEARS OPERATION

Sandrine Charrier[*1], Jocelyne Ponthieux[2], Alexis Huet[2]

1 Centre d'Etudes Techniques de l'Equipement de Lyon
46 rue Saint Théobald. F – 38081 L'ISLE D'ABEAU Cedex, France

2 Centre d'Etudes Techniques de l'Equipement de Lyon
Boulevard Bernard Giberstein 71400 AUTUN Cedex, France

**Corresponding author:*
sandrine2.charrier@developpement-durable.gouv.fr

ABSTRACT

From 2006 till 2012, the 2005 energy performance (EP) regulation (RT 2005) did not entail any obligation to justify the envelope airtightness level. As a consequence, asking for the certification of airtightness quality management approaches was a voluntary request from constructors. Thus, they might be allowed to take into account a better-than-default value into the thermal calculation. Since 2012, French 2012 EP regulation (RT 2012) requires building airtightness level to be justified, with two ways of justification. Either the constructor performs systematic measurements on each building, or the constructor proves that a certified quality management approach is implemented. Thus, since 2012, the number of requests for airtightness quality management certification has significantly increased.

In order to evaluate the airtightness quality management approaches, the French State has created a specific national committee. It aims at authorizing constructors to justify their buildings airtightness level through a quality management approach. The CETE de Lyon is in charge of this committee.

This paper will present and analyze the evolution of the committee processes and statistics, concurrently with the French EP regulation. The first part will focus on an assessment of the committee validation process. It will also present the evolution of the number of requests and certifications, since 2006. Results show that compared to each previous year (2006-2011), the number of RT 2012 requests in 2012, has been multiplied by 4. Moreover, the number of RT 2012 certifications is, by June 2013, higher than the whole RT 2005 certifications delivered over 6 years. The second part will present the control process implemented by the committee on certified constructors. First, it will present the self-declared airtightness values that are presented by constructors in their yearly renewal files. Then, it will focus on results of the control campaign set up by the committee. Results show that the majority of measured dwellings meet the required airtightness level. Nevertheless, results of that control campaign show that approved constructors do not entirely implement their quality management approach.

The paper concludes with the committee process improvements. These improvements must meet the increasing number of requests, without losing quality reputation of these approaches. The State will continue to inspect certified constructors in two ways. Yearly files analysis will focus more on the actual implementation of airtightness quality approach. The control campaign will be maintained because of its impact on constructors. A question is now set on the need to externalize this quality management approach committee because of the number of requests. The process could be the same as the airtightness measurement qualification made in France, a few years ago.

KEYWORDS

1 INTRODUCTION

French energy performance (EP) regulation is frequently revised in order to reduce buildings energy consumption. Now, the airtightness value of building envelope must be taken into consideration in the thermic calculation to obtain low-energy-consumption buildings.

French EP regulation allows two ways to justify the airtightness value of the building envelope for residential buildings. Either the constructor performs systematic measurements on each building, or the constructor proves that a certified quality management (QM) approach is implemented. QM approach presents the advantage of enabling constructors to carry out measures on a restricted sample of their production. Since 2006, the French State has implemented a committee (named the Annex VII committee) in charge of examining these approaches and proposing the certification. The certification allows constructors to justify the airtightness value of their buildings through a QM approach. The CETE de Lyon is in charge of this committee.

In the 2005 version of the French EP regulation (RT 2005), a certified QM approach enabled approved constructors to use a better-than-default-value in their regular thermic calculation. Thus, constructors could use a 0.8 $m^3/h/m^2$ ($Q_{4PaSurf}$) envelope airtightness value, instead of the 1.3 $m^3/h/m^2$ default value (for single dwellings). In that process, RT 2005 QM approaches were a voluntary constructors' approach. Since January 1st 2013, the 2012 version of the French EP regulation (RT 2012) has required the airtightness level of residential buildings to be justified to a lower-than-required value. Consequently, constructors must justify the airtightness value of their buildings. This new regulation has led more constructors to implement QM approaches.

This papers aims at presenting quantitative and organizational evolutions noted by the committee after more than 5 years of activity. The paper will also present control result evolutions on certified constructors.

This paper is organized as follows. Section 2 presents the committee process and its organizational and quantitative evolutions. Section 3 deals with results for different controls implemented by the committee so that the certified QM approaches are reliable. Section 4 closes the paper by looking at future evolutions of the committee organization.

2 COMMITTEE PROCESS AND ITS EVOLUTION

This section presents firstly the evolution of the QM approach philosophy between RT 2005 and RT 2012. Then, the evolutions of the request and certification numbers are presented. At the same time, the committee organization had to evolve to meet the demand. This evolution is presented in the final section.

2.1 A successful approach in RT 2005

Since 2006, RT 2005 has enabled constructors to justify the airtightness value of a building envelope with a certified QM approach. The regulation text (JO, 2006) describes what is expected in the QM approach. The following points describe what is mainly expected in a RT 2005 QM approach in order to be approved:

- Construction type of buildings concerned
- Organizational elements
- Description of "who does what"
- Craftsmen's contractual involvement and training
- Documents that allow the tracing of each step of the QM approach
- Site supervision documents
- Documents that trace actions in case of non-compliance
- Bar chart of airtightness measured values on a sample of buildings concerned.

The Annex VII committee is composed of national airtightness experts. When a QM approach is submitted, experts base their analysis on an evaluation grid detailed for each point required. The RT 2005 grid includes 11 evaluation criteria. The evaluation grid mentions the criterion type, the expert detailed observations, the consulted files and the final expert opinion (compliance, non-compliance, some additional justifications to be given or advice).

From 2006 to 2012, 28 requests have been submitted to the committee, and 24 RT 2005 QM approach certifications were delivered. As a consequence, this first implementation of QM approach in EP regulation has been successful and constructors gave an enthusiastic and positive welcome to these approaches. Indeed, in RT 2005, as it remained a constructors' voluntary approach, submitting an airtightness QM approach was the proof of an actual motivation to implement a good quality in construction. At the same time, approved constructors were rewarded with being allowed to use a better-than-default-value in their thermic calculation. This enabled them to justify lower-energy-consumption buildings than traditional ones. This success enabled the French State to keep that possibility in the 2012 EP version (RT 2012).

Considering QM approach, RT 2012 regulation is more precise and more demanding. Indeed, thanks to RT 2005 experience, the French State reinforced expectations on key steps in order to guarantee the QM approach reliability. All RT 2005 required point remain in the 2012 version, but they must be more detailed, from the point of view of the organisation, of the traceability, and of the actual implementation. For instance, dealing with craftsmen's training, RT 2012 QM approach must a) provide the training support, b) detail how the constructor plans their craftsmen's training, so as to guarantee everyone's training, c) describe and provide the document that enables the constructor to be sure that anybody concerned by the QM approach is trained d) provide this document filled out. The same method applies to the traceability of non-compliant points and of the actions taken in that case. Furthermore, an independent ISO 9001 audit must be carried out in the approach, sites supervisions and measures documents must be provided for some constructions. JO (JO, 2010) describes all the points that must be taken into consideration in RT 2012 QM approach. The RT 2012 evaluation grid is composed of 27 evaluation criteria. Thus, having a certified RT 2005 airtightness QM approach is useful to implement a RT 2012 one, but is not enough to acquire the RT 2012 certification. Finally, the positive experience of RT 2005 certified approaches contributed to a positive welcome of RT 2012 processes, and to a similar mobilisation for their implementation.

2.2 An important increase in the number of requests with the RT 2012

As introduced in the previous section, the number of RT 2012 QM certification has been motivated by the RT 2005 positive experience. Figure 1 presents the evolution in the number of requests from 2006 to 2013.

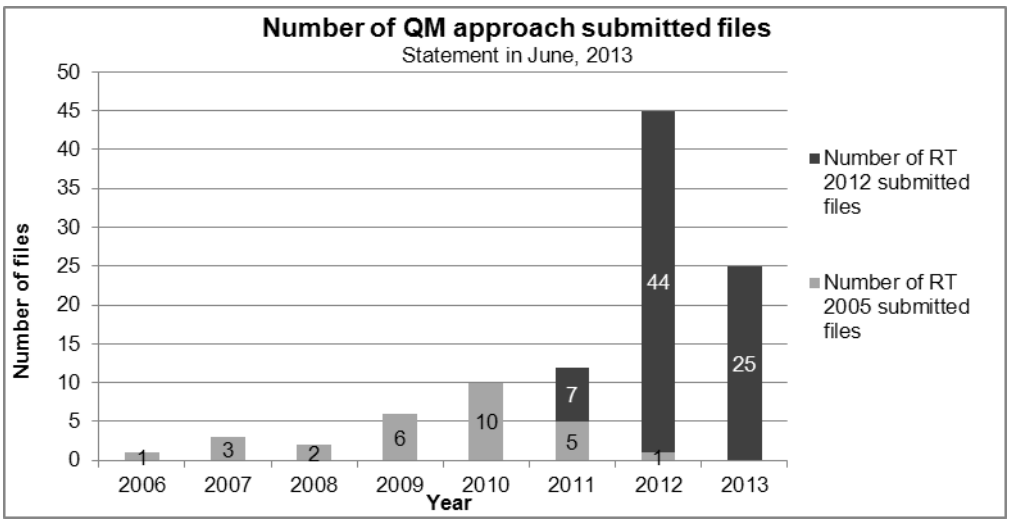

Figure 1: Number of QM approach submitted files. Statement in June 2013.

RT 2012 QM approaches can be submitted since 2012. During the period of application of RT 2005, 28 requests were submitted over 6 years, from 2006 to 2012. In 2010 and 2011, around 10 requests were received per year. The evolution between RT 2005 and RT 2012 QM approaches is indicated by a multiplication by 4 of the number of requests between 2011 and 2012 and by 5 between 2011 and 2013. Thus, as in RT 2005, around ten files were received per year. The Annex VII committee now receives around 50 files per year for the RT 2012.

This growth can be explained 1) by the RT 2012 that requires building airtightness to be justified, 2) by the RT 2005 QM positive experience.
Moreover, it must be noted that the RT 2005 QM approaches were a voluntary constructor approach that enabled them to have lower-energy-buildings than traditional ones. On the contrary, with the RT 2012, the QM approaches being one of the possibilities to be in accordance with regulation, QM approaches seem to be submitted more in order to comply with regulation than to have a real quality in construction.

2.3 A consecutive evolution of the committee organisation

The Annex VII committee had to evolve to meet the growing demand of QM approach certifications. The number of evaluation meetings of the Annex VII committee doubled between 2011 and 2012, going from 5 per year until 2011, to 10 per year since 2012. Moreover, the number of analysed files per meeting has increased since 2011. It multiplied by 4 between 2011 and 2013. As a consequence, the number of yearly analysed files was 18 in 2011, 68 in 2012, and is already about 70 at mid-2013. It must be noted that, at present, before obtaining the certification, a request need to be evaluated at least three times by the committee.

The Annex VII committee has needed to evolve to meet the increasing demand. The main evolutions in the committee organization are the followings:

- The number of experts doubled between 2011 and 2012, evolving from 6 to 12. The increase was regular and required, for each new expert, some time before performing a complete QM approach evaluation.
- Each file is analyzed by two experts, before the committee meeting. For their evaluation, the experts complete the assessment grid presented in.2.1.

- Before the meeting, the two experts compare their evaluation. In the case of discordant criteria, they agree on a common position that they will present to the committee.
- At present, 4 main private engineering departments are contracted with constructors to implement their QM approach. Each office proposes a similar approach to each constructor. Thus, the committee analyses very similar files, for which only the constructors' appropriation and adaptation to their practices differ. As a consequence, while the committee is examining a file, every other expert gives their observations. This enables the committee to identify repetitive observations on similar files and to send homogeneous evaluations, after each meeting.
- Moreover, after each committee, a grid is filled in with those repetitive observations. This grid is sent to each expert before their evaluation. This enables each expert, and then the committee, to be homogeneous with previous analysis.
- Finally, a personal grid of repetitive observations is sent to each private engineering department every 6 months, so that their services take into consideration repetitive observations permanently.

It may be noted that the evolution mentioned above made the meetings more efficient and enabled the committee 1) to analyze more files per meeting 2) and to guarantee homogenous analysis. But it can also be noted that some evolutions are required, mainly from private engineering departments. Among the 4 main private engineering departments, after having received the evaluation grids, 2 usually make the constructor QM approaches evolve. On the opposite, 2 do not make all of the constructor QM approaches evolve.

Regarding delays, with RT 2012 that expects a more precise approach, constructors need at least 3 committee evaluations before obtaining their certification. We can expect that, with the organization described above, private engineering departments will finally produce quasi perfect QM approaches. This should soon enable constructors to need only two committee evaluations, that is to say the average delay that was observed at the end of RT 2005 evaluations. At the present time, the average delay observed between the first file submission and the certification is 10 months. This delay did not evolve with the years. Indeed, while the number of required committee evaluations before obtaining the certification grew up, the number of committee meetings and their efficiency evolved at the same time. Nevertheless, since mid-2012, we observe a growing delay between the file submitting date and the first committee evaluation date. Indeed, the average delay observed before mid-2012 was 30 days. It has regularly grown up since that period, and the delay is now around 80 days.

To conclude, Figure 2 presents the evolution of the number of delivered certifications, between 2008 and 2013. The number of RT 2012 QM approach certifications is about 27 at mid-2013. This means that the number of RT 2012 certifications delivered over 1.5 years is the same as the number of RT 2005 certifications delivered over 6 years. With that tendency, about 45 certifications can be expected at the end of 2013. From that point of view, the committee organization evolution is a success.

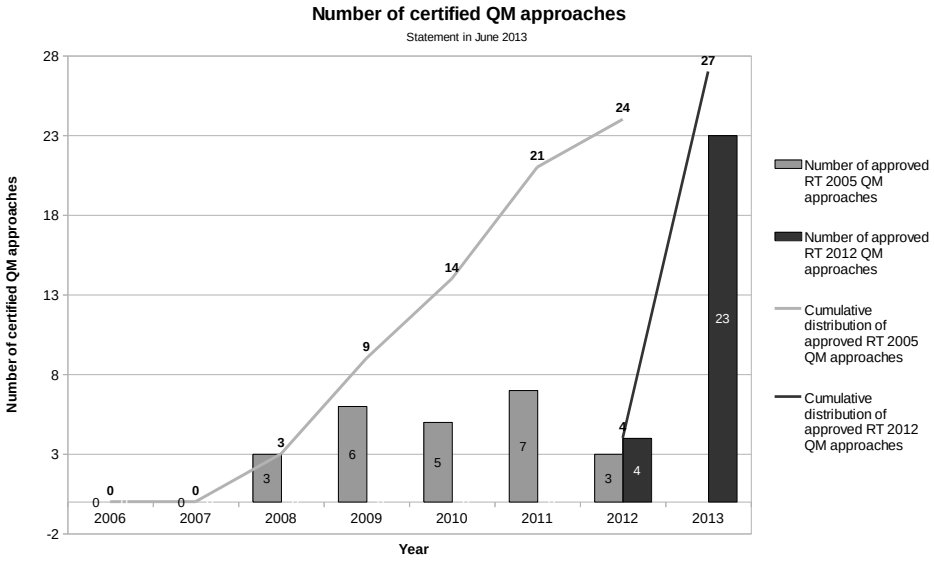

Figure 2: Number of delivered certifications. Statement in June 2013.

Regarding the number of buildings yearly produced in accordance with a QM approach, this number was approximately 6000 with RT 2005 approaches. With the present tendencies, we can expect that RT 2012 certified applicants will represent around 40000 buildings, that is to say around 20% of the national residential building production.

We can see that the RT 2012 QM approaches are a famous process. However, we must bear in mind that the control of their actual implementation is essential, in order to guarantee their reliability.

3 CONTROL PROCESS ON CERTIFIED QM APPROACHES

Once the QM approach is certified, it is important to check regularly whether the certified approach is implemented and fulfilled. Thus, the French regulation had foreseen the submission of a yearly renewal file to the Annexe VII committee, in order to control regularly the actual implementation. In addition of the process, the Annexe VII committee set up a control campaign in 2011, in order to reinforce the verification of the implementation of certified QM approaches. The next section will present the yearly renewal file process and results. Then, the control campaign process and results will be presented.

3.1 Yearly files analysis

Each year, every certified constructor must give a renewal file to the Annex VII committee, so that the actual implementation of their approach is proven. This file must contain 1) the actual QM approach, 2) the fulfilled application files, 3) test results on the previous year sample. The Annex VII committee evaluates the content of the files and the measure results, thanks to an evaluation grid.

This section deals with the test results that are sent by constructors. More precisely, it presents measured values carried out until the end of 2011. Results on 2012 cannot be presented. Indeed, in 2013, the yearly files analysis has been limited because of the RT 2012 certification requirements. These first results, that concern 12 certified constructors, enabled the Annex VII committee to evaluate whether constructors improved their measure results year after year.

Figure 3 shows the evolution in the measured values, for the 12 approved constructors together.

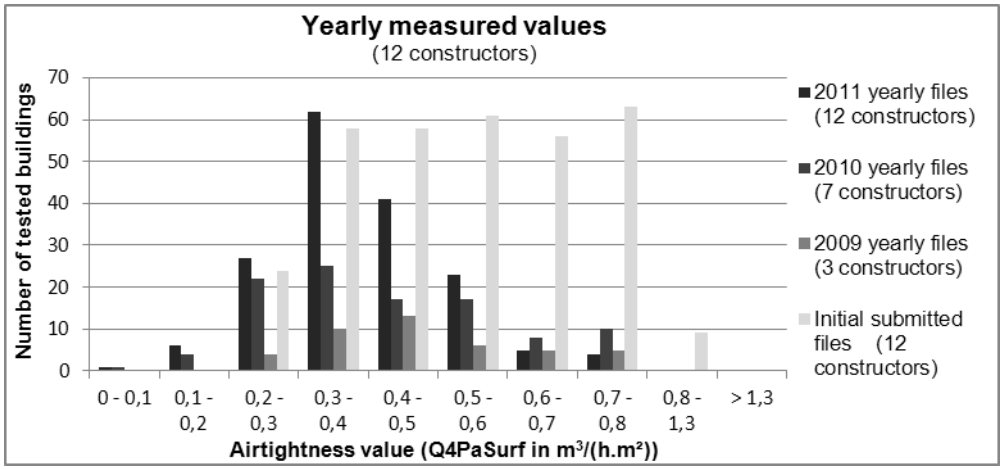

Figure 3: Yearly measured values, all constructors together. From 2008 to 2011.

Figure 3 shows that, year by year, the certified constructors improve their measure results. Indeed, if we compare the evolution of the results, from 2008 to 2011, it can be noted that the peak of the bar graphs tends to lower airtightness values. This indicates that the QM approach implementation enables constructors to improve their measure results and more generally the quality in their construction. Moreover, year by year, a lower number of measured values close to the 0.8 $m^3/(h.m^2)$ limit value is observed. This global result is positive. However, for the yearly renewal file analysis, each constructor's bar graph must be analysed.

Among the 12 certified constructors, 2 presented some warning results because of the number of measured values close to the 0.8 $m^3/(h.m^2)$ limit value. As the results comply with the regulation, the committee could only address a word of warning to those 2 constructors. Figure 4 shows a type of warning bar graph.

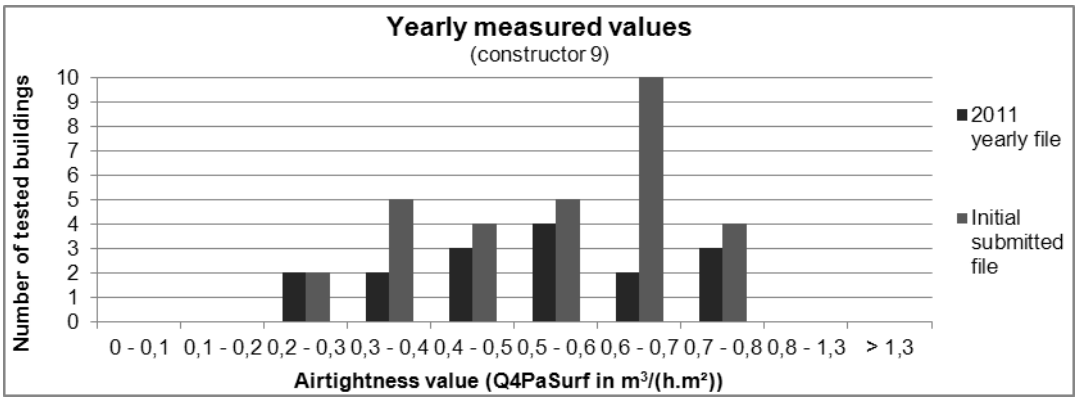

Figure 4: Yearly measured values for constructor 9, in 2010 and 2011.

On the other hand, among the 12 constructors, 10 presented yearly bar graphs that illustrated an actual improvement in the measure results. Figure 5 gives an example of a constructor good measured result. Indeed, the graph shows a regular movement of the peak of measures toward lower values. Moreover, it can be noted that each year, there are fewer measured values close to the limit one.

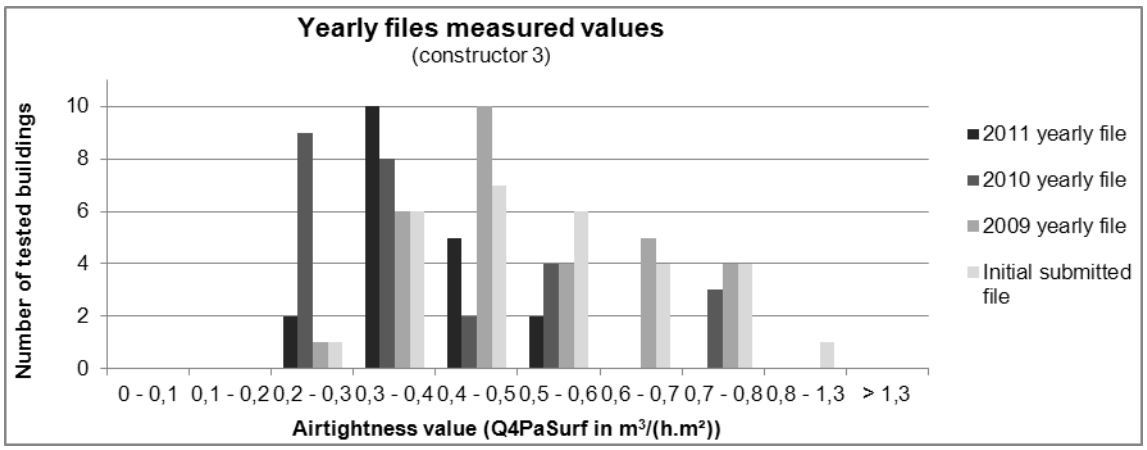

Figure 5: Yearly measured values for constructor 3. From 2008 to 2011.

The yearly renewal file analysis enables the Annex VII committee to check whether the certified QM approach is implemented and fulfilled. However, with the RT 2012 approach submission files, the RT 2005 approved constructors did not really collaborate for their 2012 yearly renewal file. Indeed, in 2012, some constructors did not answer to the committee's requests on their yearly files. Moreover, in 2013, considering the RT 2012 important demand, the committee decided, not to require renewal files from constructors who were setting out RT 2012 QM approach.

As a consequence, since 2012, the committee has not been able to analyse all the yearly renewal files. Nevertheless, considering the number of QM certifications, it appears essential to keep the yearly renewal files analysis. Indeed, it enables the committee 1) to have a look on the evolution of measured values, 2) to check whether the QM approach is really implemented by constructor. Moreover, as each certified constructor will submit every year a renewal file, the management of the QM approach certification must evolve so as to meet this future demand.

3.2 Control campaign results: good results for a majority of the controlled constructors, two failing constructors

In addition of the yearly file analysis, the Annex VII committee wished to set up in-situ controls, carried out by state employees. The first control campaign occurred in 2011 and 2012 and is described by Charrier (Charrier, 2013). The control campaign was divided in two types of control:

- a quantitative control that consisted in measuring a part of the approved constructors' production,
- a qualitative control that consisted in requiring all the documents produced in the frame of the certified QM approach, for randomly selected buildings.

Results of that control campaign are presented in Charrier (Charrier, 2013) and summed up in a double label, presented in Figure 6.

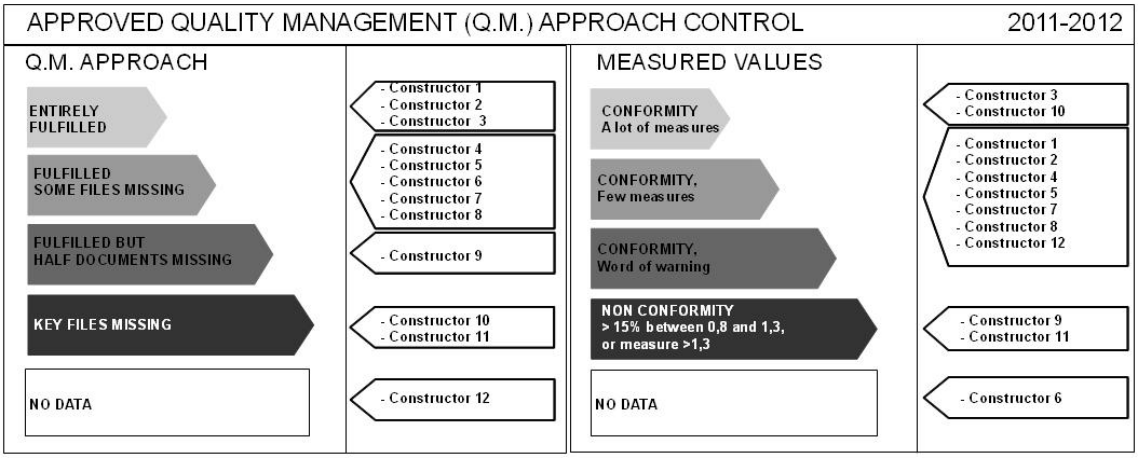

Figure 6: Double label summing up the first control campaign results

The double label illustrates the results of both controls: qualitative and quantitative one. Some results of the control campaign are:

- Two constructors have difficulty in implementing their certified QM approach (constructors 9 and 11).
- For 75% of the controlled constructors, the certified QM approach is not entirely implemented. For some of them (25%), lots of important files are missing. This means that the quality management approach does not seem to be applied and fulfilled. This reveals that constructors seem to consider that a good quality in construction is not helpful in obtaining values that comply with regulation. The quality in construction mentioned by Debrabander (Debrabander, 2011) is essential in QM approach and seems to be forgotten by constructors.

The control campaign was welcomed positively by approved constructors. However, the actual implementation of the certified approach has not been proved for 75% of controlled constructors. As a consequence, some evolutions are planned for the next control campaign that will occur in 2013 and 2014. For instance, an actual in situ audit, based on ISO 9001 processes and realised in constructors' headquarters, could be one of the possibilities to reinforce the in situ control.

3.3 Comparison between yearly files and control campaign results

During the control campaign, it could be noted that two constructors had difficulty in fulfilling their certified QM approach. So as to see whether this non-compliance could have been foreseen with the yearly files, a comparison between both results was made. This also enabled us to compare both types of control.

The analysis shows that the two types of control are complementary. Indeed, for constructor 11, the peak of measured values moved toward the quality direction. As a consequence we could not have noted any lack of conformity with the certified approach. On the contrary, for constructor 9, we might have felt a type of laxity in the actual implementation of the approach. However, as all yearly file results complied with regulation, the Annex VII committee could not expect more and could only have a word of warning. Figure 7 shows that constructor 9 presented in their 2011 yearly file some warning results. Indeed, 3 measures (20%) were above the limit value.

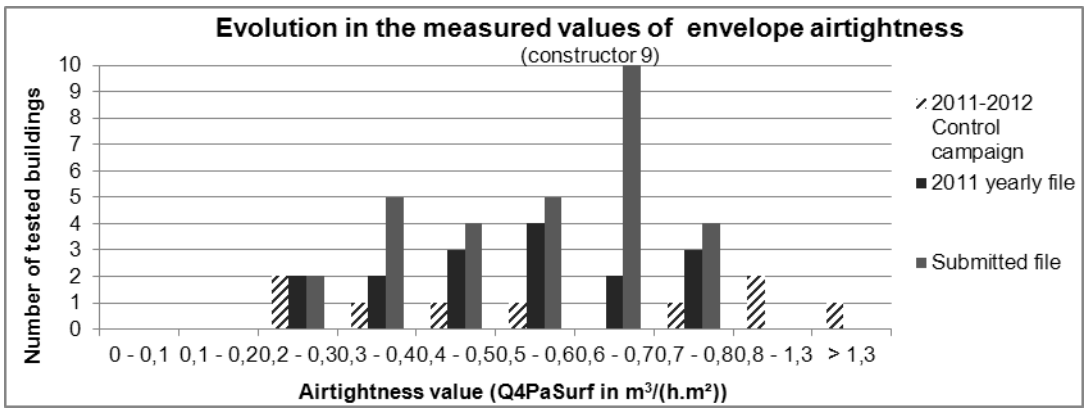

Figure 7: Measured results of both controls for constructor 9

The conclusion of that comparison is that both controls are essential so that the certified QM approaches are reliable:

- The yearly renewal file enables the committee to carry out a file analysis of the QM approach actual implementation,
- The control campaign enables the committee to set up in situ controls and measures on a sample of constructors' production, to see how the QM approach is applied in the "actual life".

Finally, the next control campaign should not concern all of the approved constructors. As a consequence, it seems even more important to continue on carrying out yearly files control.

4 CONCLUSIONS

The number of QM approach submitted files has been multiplied by 5 since 2011. This illustrates the success of RT 2005 QM approaches, and the constructors wish to comply with regulation. To meet that growing demand, the Annex VII committee has evolved to be more efficient in its file evaluations and in the delays between the date of subscription and the date of certification. This led to 27 RT 2012 certifications, obtained over 1.5 years, compared to the 24 RT005 certifications, obtained over 5 years.

In order to guarantee the certified QM approach reliability, the French State implemented two types of control: 1) yearly renewal file analysis, 2) and a control campaign. These two types of control are complementary and must be continued and reinforced.

As Leprince (Leprince, 2011) described the necessity of the evolution of the airtightness measurers' qualification in 2010, it seems that the Annex VII committee should evolve in the same direction. Indeed, the State set out the quality management approach certification. Then, considering the number of requests, the RT 2005 and RT 2012 QM approaches have been successful. In order to 1) guarantee the QM approach reliability, 2) be able to meet the growing demand, 3) implement a reliable yearly renewal file analysis, the Annex VII committee should be dedicated to a private entity that would be able to meet the important demand. The private body is not yet defined, but the necessity of such a transfer is obvious. Moreover, in that possibility, control campaigns could be let to state employees so as to guarantee neutral control. In the future control campaigns there could be more in situ controls, with for instance an in situ audit based on ISO 9001 processes and realized at the constructors' headquarters.

To conclude, quality management approach are now available for the airtightness of ventilation ducts. We can expect that the committee in charge of certifying QM approaches, and constructors, will benefit from the 5 years of envelope airtightness experience. This is another important step in the QM approach and EP regulation that the State must accompany.

5 ACKNOWLEDGEMENTS

The contribution of the CETE de Lyon to the implementation of this quality framework is funded by the ministry of ecology, sustainable development and energy (MEDDE). The responsibility for the content of this publication lies with the authors. It does not necessarily reflect the opinion of the Ministry.
1) All national experts that participate to constructor file analysis and to the committee's meetings 2) and all the CETE civil servants that contributed to the quality management control campaign 2011-2012, are gratefully acknowledged for their mobilisation and contributions.

6 REFERENCES

Leprince, V., Carrié, R., Olivier, M. (2011). The quality framework for air-tightness measurers in France : assessment after 3 years operation, 32nd AIVC Conference and 1st TightVent Conference, 12-13 October 2011, Brussels, Belgium.

Charrier, S., Huet, A., Biaunier, J.(2013). *Control of airtightness quality management scheme in France: results, lessons and future developments*. 34th AIVC Conference and 3rd TightVent Conference, 25-26 September 2013, Athens, Greece

Debrabander, C., Neutens,K. (2011). *The power of quality*, 32nd AIVC Conference and 1st TightVent Conference, 12-13 October 2011, Brussels, Belgium.

Arrêté du 26 octobre 2010 relatif aux caractéristiques thermiques et aux exigences de performance énergétique des bâtiments nouveaux et des parties nouvelles de bâtiments, JO 27 octobre 2010

Arrêté du 24 mai 2006 relatif aux caractéristiques thermiques des bâtiments nouveaux et des parties nouvelles de bâtiments, JO 25 mai 2006

PRELIMINARY ANALYSIS OF A FRENCH BUILDINGS AIRTIGHTNESS DATABASE

Adeline Bailly*[1], Yizhe Jiang[1], Gaëlle Guyot[1], and Florian Desfougères[1]

1 Centre d'Etudes Techniques de l'Equipement de Lyon
46 rue Saint Théobald. F – 38081 L'Isle d'Abeau Cedex, France

**Corresponding author:*
adeline2.bailly@developpement-durable.gouv.fr

ABSTRACT

Pushed at first by the labels backed onto the 2005 French energy performance (EP) regulation, and later on by the 2012 energy performance regulation, which imposes envelope airtightness requirements for any new dwellings, and pulled by a growing interest for low-energy labels, an important market transformation is observed in France on envelope airtightness measurement.
A framework has been set to supervise the authorized measurers' activities. Within this framework, the measurers must fill a standard register for each measurement they perform. Every year, since 2006, this file has to be sent to CETE de Lyon to set a database. It represented around 31.000 envelope airtightness data in August 2013 and around 100.000 new data are expected each year with the new EP regulation.
In 2013, a database and specific tools have been developed in order to make the most of this numerous data. Five airtightness indicators (Q_{4Pa_Surf}, n_{50}, NL, w_4, ELA_n) can be analysed through 20 parameters concerning: region and climate zone, building use, certification/label, building age, construction mode and main material, insulation type, ventilation system, heating system, measurement devices, method of the measurement, local measured (envelope or part of building), floor area and volume.
This paper describes the database, and presents some preliminary analysis about residential and non-residential buildings envelope airtightness based on the impact of several parameters: label and connected applicable airtightness requirement, building volume, ventilation system and main material.

KEYWORDS

Airtightness, database, measurement

INTRODUCTION

In France, air-leakage measurements of buildings envelopes have been increasing in recent years, pushed by some low-energy labels such as BBC-Effinergie, Passiv'Haus and Minergie. Furthermore, since January 1st 2013, the new French energy performance regulation (RT2012) is in effect. Therefore, airtightness measurements are now expected to represent about 100 000 data each year. Indeed, according to the RT2012, each residential building envelope has to respect some performance targets, and to justify its airtightness. The EP regulation imposes different requirements for the French indicator Q_{4Pa_Surf} (the air permeability at 4 Pa divided by the loss surfaces area excluding basement floor):

- 0.6 $m^3.h^{-1}.m^{-2}$ for single family houses (corresponds to an n_{50} = 2.4 h^{-1} for a ratio V/A*=1.3)

- 1 $m^3.h^{-1}.m^{-2}$ for multi-family dwellings (corresponds to an n_{50} = 2.3 h^{-1} for a ratio V/A* =2.3).

**The ratio V/A=Volume/ loss surfaces area excluding basement floor. The previous values correspond to the average of database ratio for these kinds of building*

Moreover, a new label has been introduced: Effinergie Plus, with more restrictive requirements:

- 0.6 $m^3.h^{-1}.m^{-2}$ for single family houses;
- 0.8 $m^3.h^{-1}.m^{-2}$ (sampling measurement) or 1 $m^3.h^{-1}.m^{-2}$ (entire building envelope measurement) for multi-family dwellings;
- compulsory measurement for non-residential building with a volume of less than 3 000 m^3, without requirement.

In this context, any air leakage measurement has to be done by a certified operator. According to the authorization process [1], each operator has to complete a professional register that includes results of all air leakage measurements he has done. This register is one of the main sources of data to study airtightness in French constructions.

This paper first explains the framework of the airtightness database developed by the CETE de Lyon from certified operators registers. Secondly, it describes the main properties of measured buildings, including distributions by use, year of construction and main material, for residential and non-residential buildings. Then, this article presents a state of the art of French buildings airtightness developed from this database, according to indicators such as buildings use, label candidacy and ventilation system.

1 DATABASE: DATA AND OPERATING SYSTEM

For each measurement, French certified operators have to include all information concerning label and connected applicable airtightness requirement, building volume and cold wall area, ventilation system, structure and insulation type, and measurement season into a standardized Excel spreadsheet. The database includes all information of operators register and more. It extracts geographical data (region, climate zone) and, when data are complete, calculates the value of five airtightness indicators:

$$Q_{4Pa\_Surf} = \frac{C_L * 4^n}{A_{Tbat}} \quad (1) \qquad n_{50} = \frac{C_L * 50^n}{Volume} \quad (2) \qquad w4_{Pa} = \frac{Q_{4Pa\_Surf} * A_{Tbat}}{Area} \quad (3)$$

$$ELA_{4Pa} = \sqrt{\frac{\rho}{2 * 4Pa}} * Q_{4Pa\_Surf} \quad (4) \qquad NL = 1000 * \left(\frac{ELA_{4Pa}}{Area}\right) * (numbers of . floors)^{0,3} \quad (5)$$

with A_{Tbat} = loss surfaces area excluding basement floor *(m^2)*, *Area* = Floor area *(m^2)*, C_L=air leakage coefficient *($m^3.h^{-1}.Pa^{-n}$)*, n = air flow exponent and ρ = air density *($kg.m^{-3}$)*.

According to each case, (1) and (2) could be included in recorded data or calculated: if the building is measured to obtain the Passiv'Haus label, the airtightness indicator is n_{50}; else, it is Q_{4Pa_Surf}. Indicators (3), (4) and (5) are calculated by the database tool.

2 FIRST RESULTS

2.1 Location and properties of measured buildings

On August, 2013, the database includes about 31 000 measurements. For some of them (about 4 200), the building region has not been identified. Figure 1 presents the distribution of the others measurements by region. Even if regions have different area and density, this map reveals that measurements are not equally distributed on the French territory. Indeed, some examples can be given:

- two regions are responsible for respectively 6% and 8% of the national residential constructions, and count about respectively 10% and 13% of measurements;
- one region is responsible for 8% of the national residential constructions and counts only 3% of measurements.

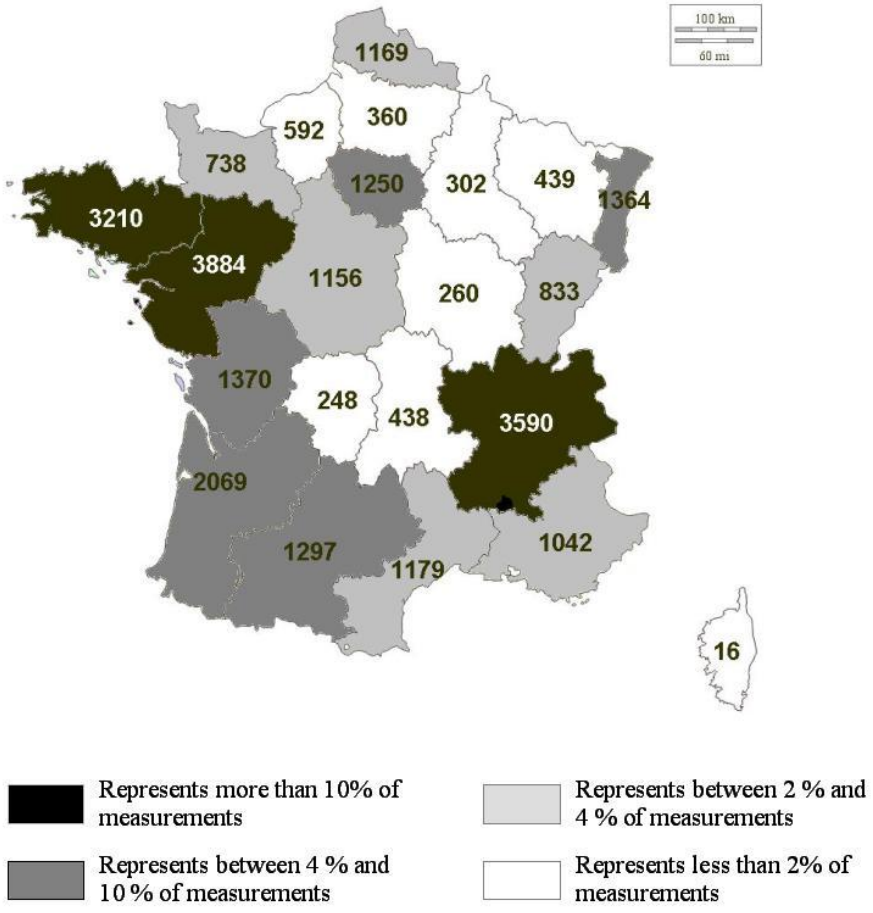

Figure 1: Distribution of measured buildings in France

The database includes non-residential buildings (about 1250 records) and residential buildings (about 29 000 records); mainly new constructions, with very different volumes, uses and structures. The following figures give the distribution of those buildings.

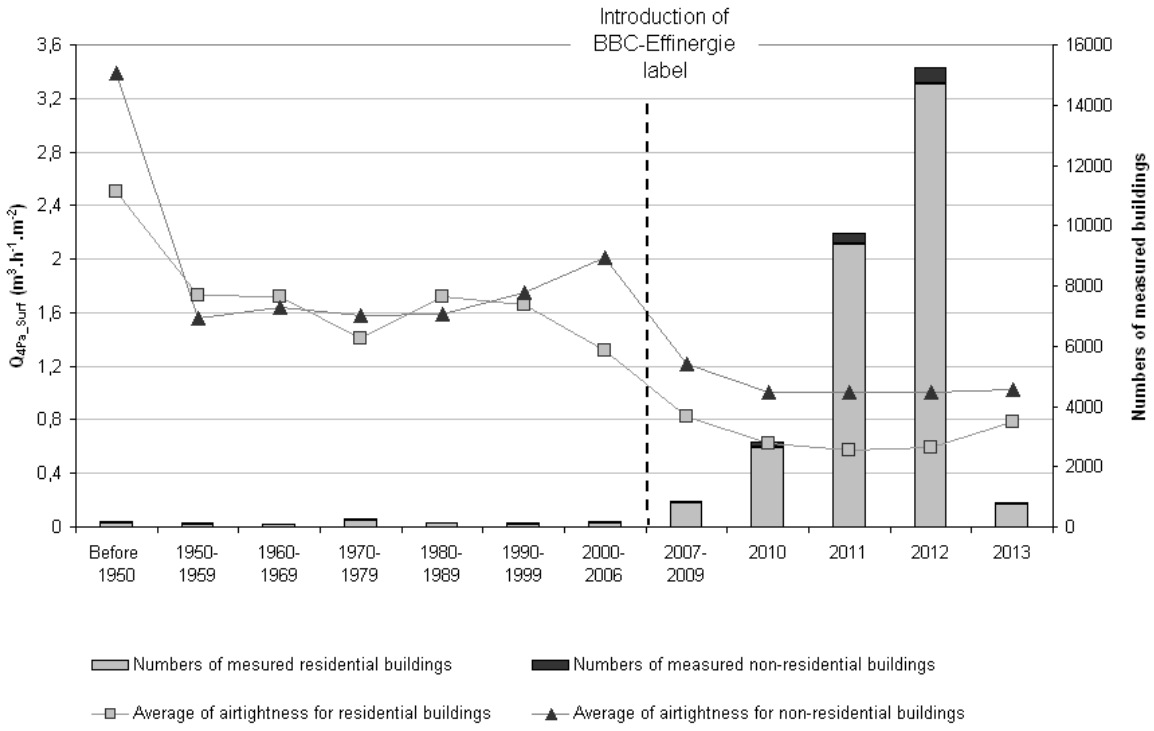

For example, measured buildings include 852 buildings built between 2007 and 2009: 809 residential buildings for which the average airtightness is 0.82 $m^3.h^{-1}.m^{-2}$, and 43 non-residential buildings for which the average airtightness is 1.21 $m^3.h^{-1}.m^{-2}$.

Figure 2: Airtightness performance depending on the construction year of measured buildings

Most of the measurements have been done on recent buildings: figure 2 shows that more than 97 % of them have been built since 2000 (94 % since 2010). These figures should be analysed regarding the two last EP regulation years: 2000, and 2005 (applied for constructions built from 2007). Even if they did not include airtightness requirement, good air leakage measurement results may be rewarded in the EP-calculation. Furthermore, during these years, labels have encouraged to reinforce the envelope airtightness (BBC-Effinergie label: 2007).

Figure 2 shows that buildings are more and more airtight until 2011. The average airtightness is a bit higher in 2012 and still increases in 2013 for residential buildings. It is explained by the part of single-family houses and multi-family dwellings in this sample.

Table 1: Selection of residential buildings samples for the last few years

Construction year of residential buildings	**2010**	**2011**	**2012**	**2013**
Part of single-family houses	84%	77%	60%	44%
Part of multi-family dwellings	16%	23%	40%	56%

The measured buildings built in 2012 include 40% of multi-family dwellings, 56% in 2013. This kind of building has not the same requirement than single-family houses, which explains why the average of residential building airtightness is higher in 2012 and 2013.

Figure 3 represents the distribution of buildings measured volumes for residential and non-residential constructions.

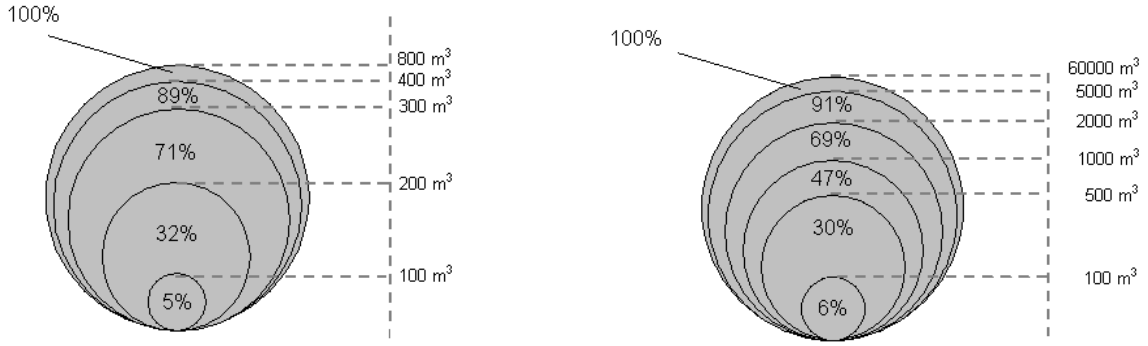

(a) (b)

Figure 3: Distribution of measured volumes for residential (a) and non-residential buildings (b)

A blower-door can generally provide between 7 000 and 8 000 $m^3.h^{-1}$. With this kind of equipment, measuring a non-residential building of more than 2 000 m^3 (n_{50} must be lower than about 3.5 h^{-1}) could be very difficult: it could require rare and more expensive material, or several blower-doors. This limit can explain why most of measured non-residential buildings (about 70%) are below 2 000 m^3. On the other hand, residential buildings should be more airtight so it should be possible to measure large volumes with a "Blower Door". Nevertheless, the regulation authorizes sampling measurements for multi-family dwellings. This method is often easier and so, few entire buildings are measured.

The following paragraph describes the distributions of measured buildings by uses and kind of principal material. Residential buildings include two groups: single-family houses and multi-family dwellings. These categories are distinguished into the French EP regulation, which imposes distinct target values for them. Figure 4 shows the distribution of the main materials used in France to build these two kinds of constructions. For both, the market share of concrete and brick are important. However, 17% of the single family houses measured have used wood as their main material, whereas wood constructions represent only about 10% of the new single-family houses in France, in 2011 [2].

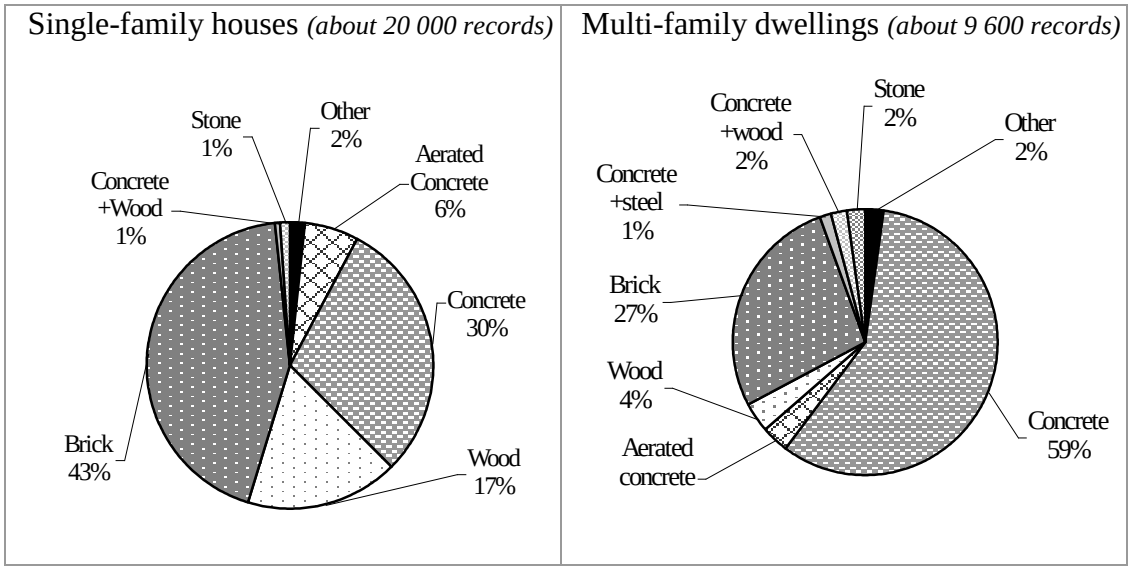

Figure 4: Distribution of main materials for measured residential buildings

Therefore, there is a bias in the database. Indeed, 79% of the measured houses were applicant for a BBC-Effinergie label, whereas the market share for this label was about 13% in 2012 for new single-family houses. For multi-family dwellings, wood constructions represent only 4% of the measured buildings, which is consistent with the French market, even if 88% of the database applied for a BBC-Effinergie label (against 70% for the national market).

The next figure describes the distribution of non-residential buildings into the database. In 2011, some data were analysed [3], describing the distribution of 188 measured non-residential buildings. In 2013, the database includes about 1250 measurement results. The distributions are similar, with a majority of office buildings and schools. Concrete is still the main used material, and wood is the second one. In France, the market share for wood in constructions is less than 5%. Like for houses, the greater use of wood in this sample is explained by the important part of buildings applying for a label in this database (74%).

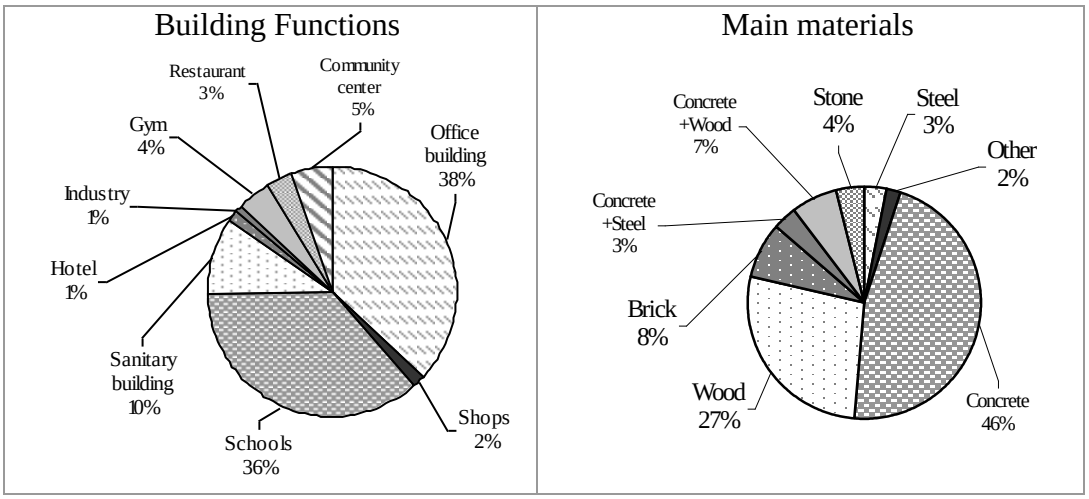

Figure 5: Distribution of measured non-residential buildings

2.2 The airtightness performance of the French buildings

The first figure of this part shows airtightness performance of all database measurements depending on the main material of buildings. According to last graphs, concrete and brick are the main material of most buildings: respectively 39% and 34% of the sample. Their airtightness performance is quite good: the airtightness of 63% of concrete buildings and 76% of brickwork buildings is lower than 0.6 $m^3.h^{-1}.m^{-2}$, like 74% of wooden buildings. For this three construction systems, between 76% and 86% of buildings have been applying for a label. This is an important bias in this result: for example, buildings built with stone present the worse airtightness performance, but only 52% on them (in the database sample) have been applying for the BBC-Effinergie label. The BBC-Effinergie label importance for residential buildings is the next point of this paper.

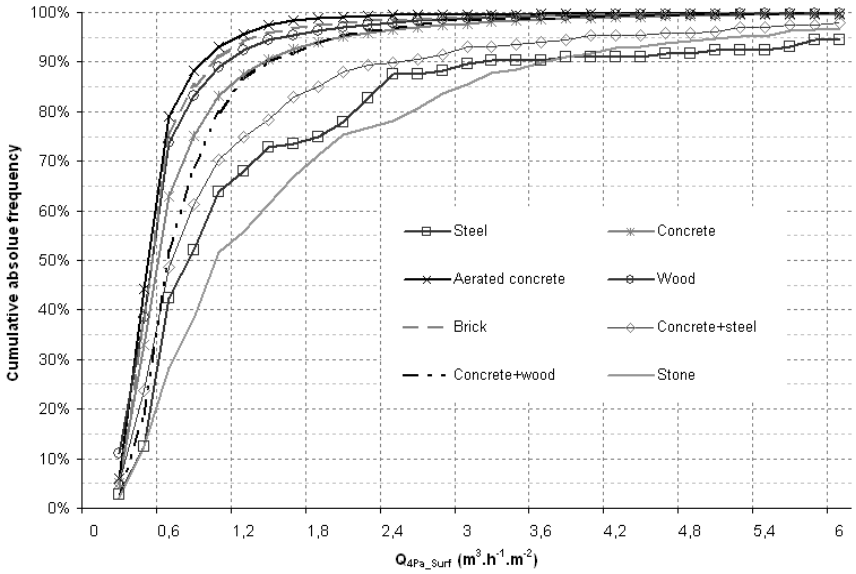

Figure 6: Airtightness performance of French buildings depending on main material

Residential Building

The average airtightness for single-family houses is 0.57 $m^3.h^{-1}.m^{-2}$, and 0.81 $m^3.h^{-1}.m^{-2}$ for multi-family dwellings. The figures 6 and 7 distinguish three different cases: buildings applying for a BBC-Effinergie label, constructions applying for other label (such as Passiv'Haus and Minergie,), and buildings without a label candidacy.

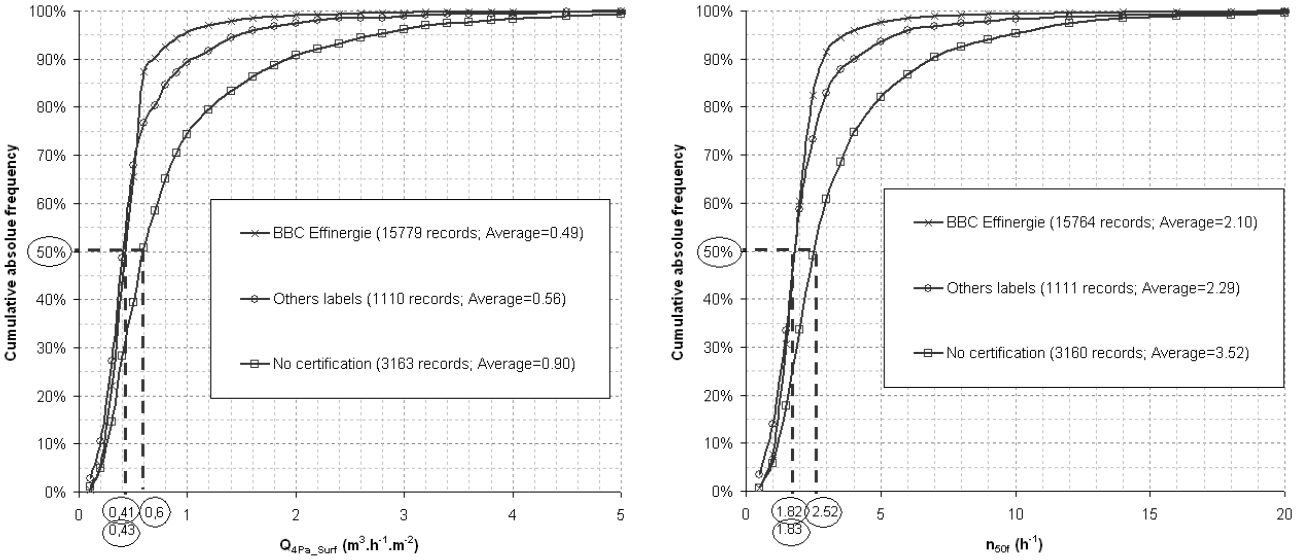

Figure 7: Airtightness performance of single-family houses

Those figures show that the average airtightness for houses applying for a label is under the limit value of the RT2012 (0.6 $m^3.h^{-1}.m^{-2}$), like for others labels. However, the average of

"usual" houses is 0.9 $m^3.h^{-1}.m^{-2}$. This average is expected to decline for the next few years to respect the EP regulation. They also show that airtightness of 95% of houses applying for BBC Effinergie is lower than 1 $m^3.h^{-1}.m^{-2}$ against 89% of houses applying for an other label, and only 74% for houses without any label candidacy.

The interaction between airtightness envelope building performance and mechanical ventilation systems directly impact on energy consumptions due to air exchange and indoor air quality. The next figure shows the airtightness performance for the three main ventilation systems: balanced ventilation, simple-exhaust ventilation and natural ventilation.

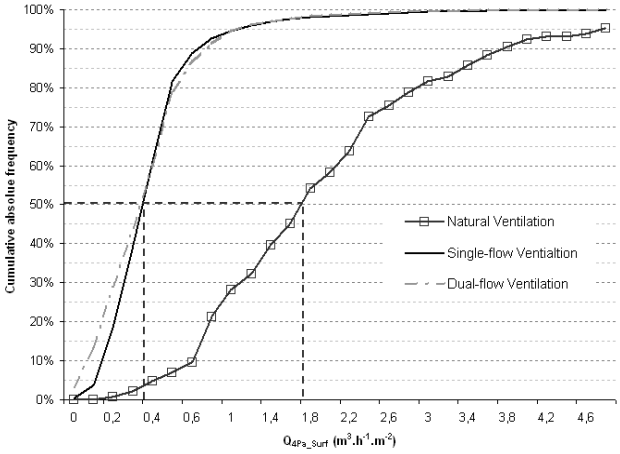

Figure 8: Airtightness envelope of single-family houses depending on ventilation system

As Guyot et al (2010) [4] have explained, the balanced ventilation generalization in European Nordic countries is mainly responsible for a long-standing airtightness interest. Figure 8 shows that for 50% of houses with either single-flow ventilation or dual-flow ventilation, the airtightness is lower than 0.44 $m^3.h^{-1}.m^{-2}$, and for about 80%, it is lower than 0.6 $m^3.h^{-1}.m^{-2}$. These systems are widely used in recent constructions, whereas natural ventilation is very difficult to install in order to respect label and new regulation requirements [5]. Therefore, results of this system mostly correspond to older houses, which may explain that 50% of measured houses airtightness is higher than 1.88 $m^3.h^{-1}.m^{-2}$.

Non-residential Buildings

A similar study has been conducted for non-residential buildings. The main figures are included in Table 2. The BBC-Effinergie buildings represent 32% of the non-residential constructions in this sample, and 12% was applying for an other label. Even if there is no airtightness requirement for most of those labels, it is assumed that a low-energy consumption building may have better airtightness performance than buildings without this kind of certification, which explains the following figures.

Table 2: Main figures for non-residential buildings airtightness

	BBC-Effinergie	**No certification**
Q_{4Pa_Surf} $(m^3.h^{-1}.m^2)$		
Average	1.05	2.0
Standard deviation	1.78	2.63
Median	0.74	1.15
n_{50} (h^{-1})		
Average	2.68	3.73

Standard deviation	3.03	4.05
Median	1.86	2.32

The non-residential sample includes many different building uses; next figure describes the airtightness performance depending on the building function. The five building functions represented in this figure were chosen using the size of the sample (more than 50 records).

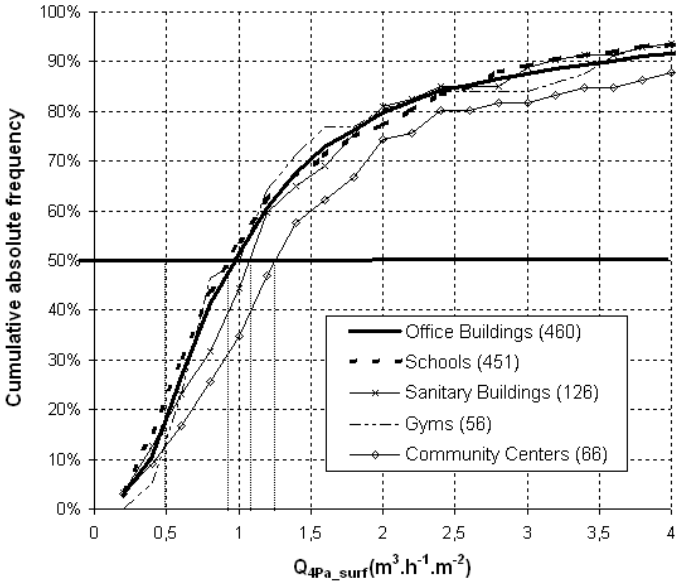

Figure 9: Distribution of measured airtightness for the main groups of non-residential buildings

The median airtightness is quite close for the five groups of non-residential buildings: the airtightness of 50% of the office buildings is lower than 1 $m^3.h^{-1}.m^{-2}$, and lower than 1.3 $m^3.h^{-1}.m^{-2}$ for community centers. Nevertheless, the curves are different: office buildings curve is more concave than community centers curve, which shows better knowledge and implementation of airtightness treatment for office buildings.

The two next graphics illustrate the airtightness performance for office buildings and multi-family dwellings, two comparative kinds of construction.

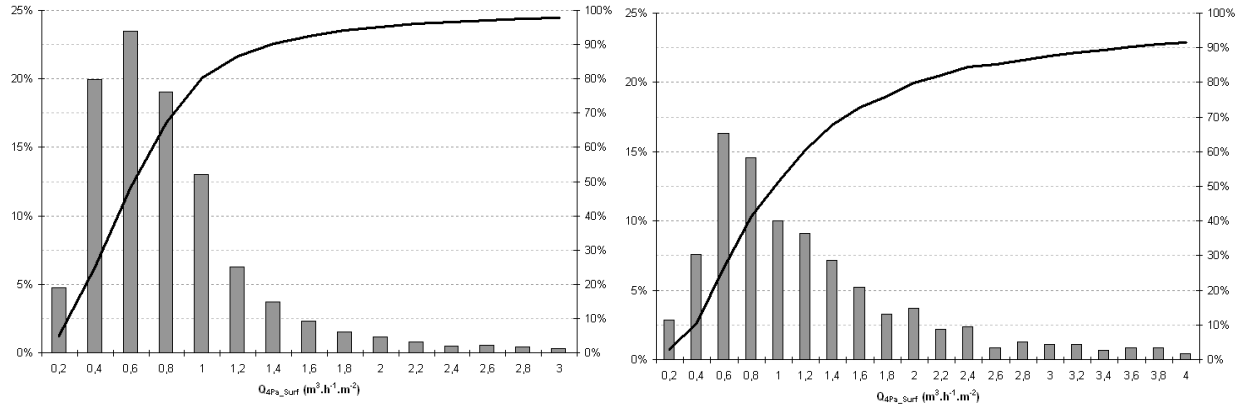

(a) (b)

Figure 10: Multi-family dwellings and office buildings (b) airtightness performance

The multi-family dwellings yield courses is smoother, with about 9 600 records (against 460 records for office buildings). As it was expected, multi-family dwellings are more airtight (average=1.01 $m^3.h^{-1}.m^{-2}$) than office buildings (average=1,73 $m^3.h^{-1}.m^{-2}$). But these figures

also show that good airtightness performance is more often respected by multi-family dwellings: most of their airtightness results (80%) are under 1 $m^3.h^{-1}.m^{-2}$, whereas about 30% of office buildings measured results are more than 1.6 $m^3.h^{-1}.m^{-2}$. Nevertheless, there is not airtightness requirement for offices building, which explain the difference performance.

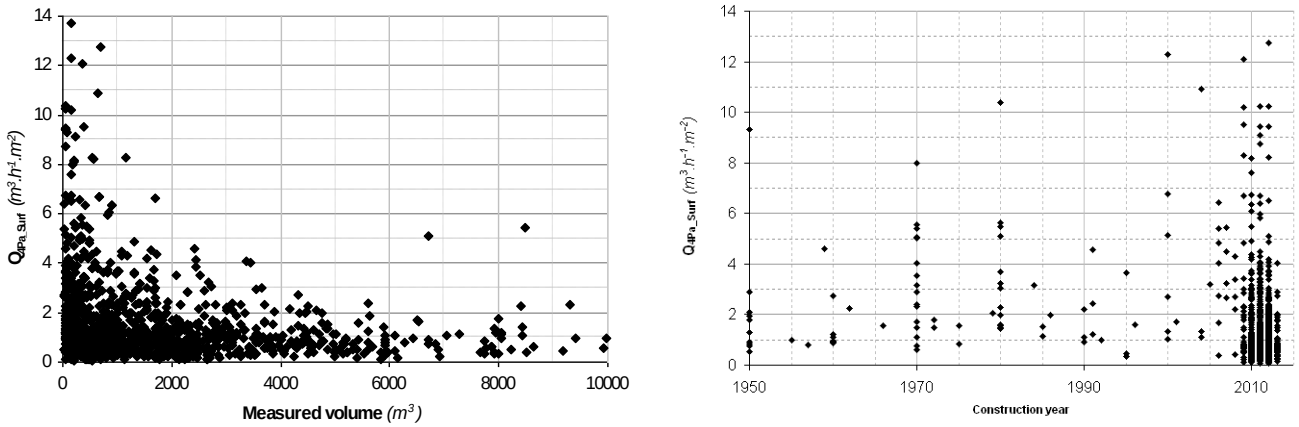

(a) (b)

Figure 11: non-residential buildings airtightness depending on the measured volume and construction year

Figure 11 describes the airtightness performance of non-residential buildings depending on their volume and construction year. It shows that airtightness could be treated as well for large buildings than for smaller. Even if the airtightness level is still high (25% of the non-residential buildings airtightness exceed 1,8 $m^3.h^{-1}.m^{-2}$), large volumes do not seem to be the worst.

2.3 Additional results

The database could provide further analysis, including airtightness coefficients. Last figure represents the distribution of the air flow exponent (n) or pressure exponent for the 31 000 measurements of the database.

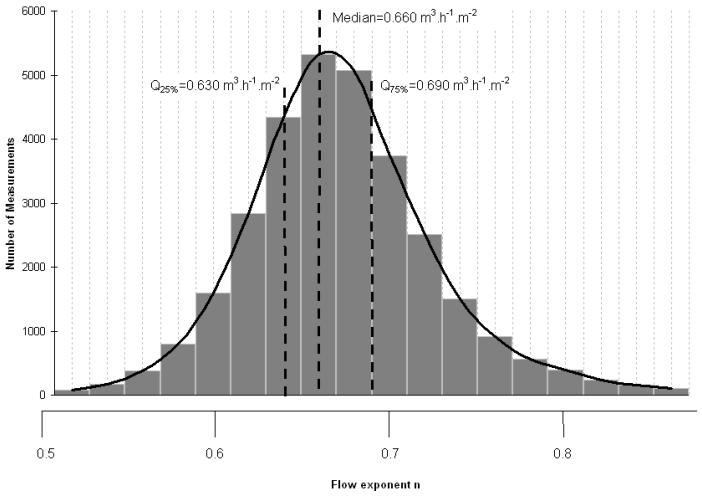

The average exponent is 0.663 $m^3.h^{-1}.m^{-2}$ with a standard deviation of 0.060 $m^3.h^{-1}.m^{-2}$. Those figures match the commonly used default value (n=0.67) and previous studies results [6].

3 CONCLUSIONS

This objective of this study was to realize a state of the art of French airtightness buildings through analysis of more than 31 000 results of air leakage measurement. The database has been developed in recent months. Moreover, thanks to the new French EP-regulation, about 100 000 measurements are expected to be performed each year. Statistical studies should be conducted, more diverse and reliable.

This data tool is a main source to monitor the buildings airtightness performance, including the impact of the new EP-regulation. It will also allow us to analyse air leakages distribution and occurrence, in order to understand how to reinforce buildings envelope airtightness. Then, it will be an important trusted way to estimate the feasibility to add new requirements on airtightness for next labels and EP-regulation.

Figure 12: Distribution of air flow exponents from about 31 000 airtightness measurements

4 ACKNOWLEDGEMENTS

The contribution of the CETE de Lyon is funded by the ministry for ecology, sustainable development and energy (MEDDE).
The sole responsibility for the content of this publication lies with the author. It does not necessarily reflect the opinion of the Ministry.
On January 1st, 2014, the CETE de Lyon will merge to become the CEREMA.

5 REFERENCES

[1] F.R Carrié, S. Charrier and V. Leprince. *Implementation of measurement and quality frameworks in the French regulation for achieving airtight envelopes*, 31th AIVC Conference, 26-28 October 2010, Seoul Korea.

[2] Observatoire économique de France Bois Forêt. *Enquête nationale de recensement des constructions bois*. 2nd Rencontres Bois Construction du Limousin – 26 November 2012.

[3]V. Leprince, A. Bailly, F.R. Carrié and M. Olivier. *State of the art of a non-residential buildings air-tightness and impact on the energy consumption*. 32nd AIVC Conference and 1st TightVent Conference, 12-13 October 2011, Brussels.

[4] G. Guyot, F.R. Carrié, M. Fleury, B. Rosenthal, W. Walther, J. Shemeikka, N. Heijmans, P. Van den Bossche, D. Van Orshoven, C. Mees, A. Tormod, P. G. Schild. *An Overview of the market transformation on envelope and ductwork airtightness in 5 European countries*. Report of the ASIEPI Project, http://www.asiepi.eu/wp-5-airtightness/available-reports0.html, 32p. 2010.

[5] R. Jobert and G. Guyot. *Detailed analysis of regulatory compliance controls of 1287 dwellings ventilation systems*. AIVC International Workshop: Ventilative Cooling, 19-20 March 2013, Brussels.

[6] I.S. Walker, M.H. Sherman, K. Joh. and W.R. Chan. *Applying Large Datasets to Developing a Better Understanding of Air Leakage Measurement in Homes*. International Journal of Ventilation, March 2013.

[7] M.I. Montoya, E. Pastor, F.R. Carrié, G. Guyot and E. Planas. (2009). *Air leakage in Catalan dwellings: Developing an airtightness model and leakage airflow predictions*. Building and Environment, June 2010.

[8] Laverge J. ans A. Janssens. *Optimization of design flow rates and component sizing for residential ventilation*. Building and Environment, 65, p.81-89. 2013.

A STOCHASTIC APPROACH TO PREDICT THE RELATIONSHIP BETWEEN DWELLING PERMEABILITY AND INFILTRATION IN ENGLISH APARTMENTS

Benjamin Jones[*1], Zaid Chalabi[2], Payel Das[3], Michael Davies[3], Ian Hamilton[4], Robert Lowe[4], Anna Mavrogianni[3], Darren Robinson[1], Clive Shrubsole[3], Jonathon Taylor[3]

1 Department of Architecture and Built Environment
Lenton Firs House, University of Nottingham
NG7 2RD, United Kingdom
**Corresponding author:*
benjamin.jones@nottingham.ac.uk

2 London School of Hygiene
and Tropical Medicine
15-17 Tavistock Place
London, WC1H 9SH, United Kingdom

3 Bartlett School of Graduate Studies
University College London
Central House, 14 Upper Woburn Place
London, WC1H 0NN, United Kingdom

4 Energy Institute
University College London
Central House, 14 Upper Woburn Place
London, WC1H 0NN, United Kingdom

ABSTRACT

Reducing adventitious infiltration in order to save energy is important and is highlighted by the building standards of many countries. This operational infiltration is often inferred via the measurement of the air leakage rate at a pressure differential of 50 Pascals. Some building codes, such as the UK's Standard Assessment Procedure, assume a simple relationship between the air leakage rate and mean infiltration rate during the heating season, the so-called *leakage-infiltration ratio*, which is scaled to account for the physical and environmental properties of a dwelling. The scaling does not take account of the permeability of party walls in conjoined dwellings and so cannot be used to differentiate between the infiltration of unconditioned ambient air that requires heating, and conditioned air from an adjacent dwelling that does not. This article evaluates the leakage infiltration ratio in apartments, which share a large proportion of their envelope area with other dwellings. A stochastic approach is used that applies a theoretical model of adventitious infiltration to predict the distribution of the mean infiltration rate and total heat loss during heating hours for a sample of apartments of the English housing stock (a subset of the UK stock) for two extreme assumptions of party wall permeability. Knowledge of party wall permeability is not provided by a standard measurement of air leakage but is shown to be vital for making informed decisions on the implementation of energy efficiency measures. Accordingly, this paper provides probability distribution functions of operational infiltration in English apartments that can be used to help the policy makers of any country whose housing stock contains a large proportion of conjoined dwellings.

KEYWORDS

Ventilation, House, Stock, Model, Monte-Carlo

1 INTRODUCTION

The infiltration of cold air through adventitious openings located in the envelope of a dwelling, known as air leakage paths (ALPs), is thought to be a significant contributor to its heating load. However, determining a mean infiltration rate during the heating season is time

consuming, invasive, expensive, and technically difficult. Therefore, it is often inferred from a measurement of the air leakage rate (ALR), V_{50} (m^3/s) or M_{50} (kg^3/s), the rate of airflow through the fabric of a building at a steady high pressure difference, normally 50 Pascals (Pa), when the effects of wind and buoyancy are effectively eliminated (Etheridge; 2012). The ALR is often scaled by dwelling volume to give an *air change rate* at 50 Pa, N_{50} (h^{-1}), or by dwelling envelope area, A_{env} (m^2), to give an *air permeability*, P_{50} ($m^3/h/m^2$). In order to be useful, the ALR must be converted to an operational infiltration rate, and although there are several methods of doing this, the most common for dwellings is the *rule-of-thumb* known as the *leakage-infiltration ratio*, *L*, given by Sherman (1998) as:

$$V_{50} \;\; V_I = M_{50} \;\; M_I = N_{50} \;\; N_I \;\; \approx L \qquad (1)$$

Here, the subscripts *50* and *I* indicate parameters measured at a steady pressure differential of 50Pa and under operational conditions, respectively. The parameter *L* is a variable but is often taken to be equal to 20 when Equation (1) is known as the *rule-of-20*. However, *L* must not be considered to be a constant but should be scaled according to factors such as dwelling height air leakage path (ALP) size, shielding, and climate (Sherman, 1987). The UK government's method for assessing and comparing the energy and environmental performance of dwellings is known as the Standard Assessment Procedure (SAP). SAP uses the *rule-of-20* as a starting point to obtain an initial dwelling infiltration rate from the measured ALR. Further infiltration is added if chimney, flues, and fans are present. The figure is revised further according to local shielding, and mechanical ventilation. Other building codes make similar assumptions; for example, MoEoF (2012).

There are obvious problems with Equation (1). Firstly, the ALR is a physical property of a dwelling that indicates the resistance of its fabric to airflow (Jones *et al.*, 2013a) at high pressure whereas operational infiltration occurs at pressure differences that are both dynamic and an order of magnitude lower. Furthermore, the *rule-of-20* was derived from measurements made in dwellings in the USA (Sherman, 1998) whose climatic conditions and dwelling properties are different from typical European houses. For example, detached dwellings comprise the majority (~86%) of the U.S. stock (Sherman & Matson, 1997) whereas semi-detached houses and apartments comprise >50% of the English housing stock (DCLG, 2011). A dwelling of either of these latter types shares some of its walls, known as party walls, with adjacent dwellings. However, when building codes scale the ALR they do not take account the permeability of party walls in conjoined dwellings and so cannot differentiate between the infiltration of unconditioned ambient air that requires heating, and conditioned air from an adjacent dwelling that does not. When measuring the ALR, Jones *et al.* (2013a) propose that one can make two extreme assumptions about the permeability of party walls at 50Pa: A(1) party walls are permeable and so airflow to and from adjacent dwellings does occur; or A(2) party walls are impermeable and so airflow to and from adjacent dwellings does not occur. They then use two archetypal English dwellings to investigate the potential consequences of these assumptions using a theoretical model. They predict for assumption A(1) that the leakage-infiltration is significantly higher than that used by building codes whereas for assumption A(2) the leakage-infiltration ratio is predicted to be close to that used in practice. The consequences of these findings are two-fold. Firstly, if A(1) is true, then operational heat losses are less than those predicted by building codes (such as SAP), and government funded schemes (such as the UK's Green Deal) that aim to tighten the European housing stock could have longer payback periods than expected. Secondly, if A(2) is true, government funded schemes that aim to tighten the European housing stock are appropriate. This predicted dichotomy of outcomes introduces great uncertainty into the effectiveness of any policy that aims to reduce energy consumption through fabric tightening.

An investigation of the variation of infiltration rates found in a stock of dwellings could be used to determine its exfiltration heat loss. Estimated probability distribution functions of

infiltration and heat loss are useful tools with which policy makers can determine the likely effectiveness of fabric tightening schemes. Accordingly, this paper asks the questions: how can one predict distributions of infiltration rates for a housing stock and what effects do the extreme assumptions about the permeability of party walls have on them?

2 METHODS

There are no known large scale measurements or predictions of heating season infiltration rates in English dwellings and so a modelling approach is proposed. Distributions of infiltration rates in U.S. dwellings have been predicted by Persily *et al.* (2010), and their study offers useful guidance. An infiltration model requires three things: a model of dwelling infiltration and exfiltration, knowledge of the properties of a large representative sample of of a dwelling stock that can be applied to the model, and a suitable statistical approach that enables the stock variability to be captured. In this section the three requirements are discussed using the English housing stock as a case study, although the approach is readily transferable to housing stocks in other countries. A single dwelling type is used to answer the research question "what effects do the extreme assumptions on the permeability of party walls have on a distribution of infiltration rates?" Here, apartments (defined as low-rise with $\leq$3 stories) are used because they can share up to 5 of their external surfaces with another dwelling and so any difference between predictions for the two permeability assumptions A(1) and A(2) is expected to be clearly observed. If a difference is observed, the method proposed here can be applied to all other dwelling types encompassing the whole stock.

2.1 Modelling infiltration and exfiltration heat loss

For any model there is always a trade-off between model complexity and data requirements (and potential input error) with computational speed. Variations in the predictions of a model are a function of variability and uncertainties in the inputs to the model (parametric uncertainty) and uncertainty in the model itself (structural uncertainty). Striking the right balance in this trade-off must be addressed when considering the model's tasks; for example, when modelling a stock of dwellings the sample size is expected to be large and so a computationally fast model is desirable. Furthermore, the variation in geometry types across a stock dictates that the model should also be versatile. A final requirement is that the workings and limitations of the model must be documented and its predictions compared against empirical data or, less desirably, corroborated against the predictions of other models.

This paper applies DOMVENT3D, a model of infiltration and exfiltration through any number of façades that assumes two things about façades: all are uniformly porous; the pressure distribution over one is linear. DOMVENT3D integrates the airflow rate in the vertical plane to predict the total airflow rate through any number of façades (Jones *et al.*, 2013). DOMVENT3D makes further assumptions about the dwelling. Following Etheridge (2012), it assumes that all rooms of a dwelling are interconnected and that its internal doors are open so that a dwelling can be treated as a single-zone, thus reducing model complexity. Each horizontal and vertical surface of the external envelope requires only a single flow equation linked by a continuity equation, thus reducing computational time. DOMVENT3D's final assumption follows Jones *et al.* (2013a) who state that adjacent dwellings are assumed to experience identical environmental conditions and thus have the same internal pressure. Therefore, airflow through permeable party walls and floors does not occur under operational conditions and so is only considered through external surfaces. DOMVENT3D is implemented using bespoke MATLAB code (MathWorks, 2013). Its assumptions, merits, limitations, and the corroboration of its predictions are discussed widely by Jones *et al.* (2013a,b).

DOMVENT3D requires inputs that may be unique to each dwelling or are general to a sub-stock of dwellings bounded by geographic region. Unique inputs comprise the flow exponent, internal air density, the dimensions of all permeable external vertical (façades) and horizontal (ceilings and floors) surfaces, scaled wind speed, and façade wind pressure coefficients. General inputs are the ambient air temperature, regional wind speed, and wind orientation. Sources of data are discussed in Section 2.2.
Once the infiltration and exfiltration rates are predicted by DOMVENT 3D, the exfiltration heat loss (W) at an instant in time is calculated by

$$H\ t\ = M_I c \Delta T\ _{T_{ext} \leq\ T_{int} - 3} \quad (1)$$

where M_I is as defined above, c is the specific heat capacity of air ($\mathrm{J kg^{-1} K^{-1}}$) and ΔT is the difference between the internal and ambient air temperatures. The internal air temperature, T_{int} (ºC), of an average unheated English house is, on average, 3ºC higher than the ambient air temperature, T_{ext} (ºC), and so the heating system is assumed to function only when the ambient air temperature is ≤3ºC below the internal air temperature (Hamilton *et al.*, 2011). Heat loss is only calculated when the heating system is "on". Equation (1) is integrated over the entire heating season to estimate the total heat loss, H_I (kWh) via exfiltration.

2.2 Model inputs

The English housing stock is comprised of 22.3 million dwellings, of which a statistically representative sample of 16,150 dwellings is documented by the 2009 English housing survey (DCLG, 2011). Each sample is weighted so that the sum of the weights equals 22.3m, and provides geographic, geometric, and environmental information. However, the inputs to DOMVENT3D are not always explicitly available despite the data rich EHS. Therefore, metadata must be derived either from the EHS and other sources, or assumed. Data inputs to DOMVENT3D may be divided into four distinct types: geographic (location), geometric (dwelling dimensions, block dimensions, orientation), physical parameters (air permeability, flow exponent, and façade pressure coefficients), and environmental (local wind speed and direction, internal and ambient temperatures, terrain type, and local shielding). We now discuss each data type in turn beginning with geographic data.

2.2.1 Geographic metadata

The EHS indicates the region in which each sample is located and allows suitable weather data to be chosen. The CIBSE Test Reference Year (TRY) weather data set (CISBE, 2002) provides synthesised typical weather years for 10 English regions and is suitable for analysing the environmental performance of buildings. Accordingly, each EHS region is mapped to an appropriate CIBSE TRY region and where more than one CIBSE region is located in an EHS region the CIBSE region is chosen randomly (with equal probability) from the set of possible regions.

2.2.2 Geometric metadata

The EHS assumes that two connecting cuboids can reasonably represent the geometry of ~98% of English dwellings. The proportion of each surface shared with another dwelling is recorded and we note that this does not always add to 100%; for example, a terrace might be staggered in the horizontal plane. The cuboid model is constructed following the Cambridge Housing Model (CHM) (Hughes *et al.*, 2012) that applies SAP to estimate energy use and CO_2 emissions in the English stock. Although the EHS gives the number of stories in an apartment block and the location of the apartment within the block, it is desirable to assume that the vertical location of the apartment is a random variable uniformly sampled between the

boundaries of the block dimensions and commensurate with the number of apartment floors (some have several floors). Dwelling orientation is not given by the EHS and so it is assumed to be a uniformly distributed random variable between 0 and 360 degrees. Other geometric parameters must also be assumed. For example, the number of dwellings in a block of apartments is not always given by the EHS but this parameter informs the calculation of physical parameters, such as wind pressure coefficients (see Section 2.2.3). In the absence of any direct measurement of block aspect ratio, it is arbitrarily assumed to be a uniformly distributed random variable between 3 and 20. Using variable inputs introduces a distribution of outputs so a sensitivity analysis is undertaken in Section 5 to evaluate their impact on the predictions of DOMVENT3D.

2.2.3 Physical metadata

To the best of the authors' knowledge, there are no large-scale measurements of operational infiltration rates in the English housing stock. However, there are a limited number of databases of P_{50} values for U.K. dwellings (Pan, 2010); for example, Pan (2010) gives air permeability values for 287 *new* English houses constructed after 2006, and Stephen (1998) gives air permeability values for 384 U.K. dwellings (also reported in Orme *et al.*, 1998) constructed before 2000. Although U.K. housing developments constructed after 2006 are required to record the air permeability of a proportion of them (HM Government, 2010) new dwellings represent a small percentage of the total stock, ~4% (DCLG, 2011). Therefore, there is only a cursory knowledge of the operational infiltration rates one expects to find in the majority of English dwellings. In their model of infiltration in U.S. dwellings, Persily *et al.* (2010) assign a permeability value to a dwelling according to its age and type, representing an appropriate approach. However, the limited quantity of empirical data for English dwellings makes this approach impossible. Instead, inverse cumulative distribution functions are formed from the published histograms (for all dwelling types) of Pan (2010) and Stephen (1998) using Piecewise Cubic Hermite Interpolating Polynomials and are applied if a dwelling is constructed pre-2000 and post-2000, respectively. It is acknowledged that Pan's data is for post 2006 houses, but this is the best compromise that the EHS dwelling age distribution allows.

The flow exponent variable characterises the airflow regime through an ALP and is a function of its geometry and surface roughness. Its value affects both the pressure difference across an ALP and the airflow rate through it. Most infiltration models assume a constant value of 0.66 (Orme *et al.*, 1998), but Sherman (1998) shows that a mean value of μ=0.65 with a standard deviation of σ=0.08 best represents more than 1900 measurements made in U.S. dwellings. Sherman's distribution is very similar to the smaller international AIVC data set (Orme *et al.*, 1998) and so is applied with confidence as a Gaussian random variable.

Wind pressure coefficients are defined for the horizontal and vertical surfaces. For the latter, the algorithm of Swami and Chandra (1987) gives a normalized average wind pressure coefficient for long-walled low-rise dwellings and is a function of the angle of incidence of the wind (for wind direction see Section 2.2.1), local sheltering (Section 2.2.4), and the block aspect ratio (Section 2.2.2). The coefficient is then scaled to account for local shielding (Section 2.2.4). Horizontal surfaces are assumed to be completely shielded from the effects of the wind following Sherman and Grimsrud (1980).

2.2.4 Environmental metadata

Local wind speed, wind direction, and ambient air temperature are taken from an appropriate CIBSE TRY file (see Section 2.2.2) but the wind speed must be scaled according to the terrain and dwelling height using a standard power law formula (BSI, 1991). Dwelling height is obtained from the cuboid model and the terrain is indicated by the EHS. The four BSI

terrain types and the local wind pressure shielding coefficients (Section 2.2.3) of Deru and Burns (2002) are mapped to the six EHS terrain types with format EHS (BSI){Deru and Burns}: city (city){very heavy}, urban (urban){heavy}, suburban town (urban){heavy}, rural residential (urban){moderate}, village centre (urban){moderate}, rural (country with scattered wind breaks){light}.
DOMVENT3D is not a thermal model and so the internal air temperature must be prescribed. Here, a constant value of 18.5°C is chosen following Palmer *et al.* (2011) who estimate this figure for the U.K. domestic average internal air temperature in 2005. There is no evidence of a fluctuation of this value and so it is assumed to be a constant.

2.3 Stochastic methods

A Monte Carlo (MC) approach is used to predict distributions of winter infiltration and heat loss in English apartments and their sensitivity to model inputs. There are four stochastic inputs to DOMVENT3D: the EHS sample (using dwelling weight), dwelling orientation, air permeability, and a flow exponent. Twenty sets of the four inputs are chosen at a time using a Latin Hypercube. Each set is applied to DOMVENT3D to predict N_I (h^{-1}). The total sample size increases incrementally according to the set size, which is arbitrarily chosen to minimize calculation time. After each set of predictions are made, the mean (μ) and standard deviation (σ) of N_I for the whole sample are calculated and used to decide if a stopping criterion has been met. The number of samples is deemed adequate if the change in σ from one set of 20 samples to the next is less than 0.1%. The model is run twice because a distribution is required for each of the two permeability assumptions, A(1) and A(2).

3 RESULTS

Table 1: Statistical summary of mean infiltration rate (h^{-1}) and total winter heat loss (MWh) samples. Assumption A(1): permeable party walls. Assumption A(2): impermeable party walls.

Statistical measure	Mean Infiltration Rate, N_I (h^{-1}) Permeability Assumption		Total Heat Loss, H_I (MWh) Permeability Assumption	
	A(1)	A(2)	A(1)	A(2)
Minimum	0.00	0.02	0.00	0.03
2% centile	0.01	0.03	0.02	0.08
25%	0.05	0.14	0.12	0.39
50%	0.12	0.29	0.30	0.75
75%	0.22	0.48	0.59	1.29
98%	0.54	1.08	1.70	3.11
Maximum	0.74	1.60	6.47	8.28
Mean, μ	0.15	0.34	0.45	0.96
Standard deviation, σ	0.13	0.25	0.56	0.82
Mode	0.03	0.11	0.06	0.47

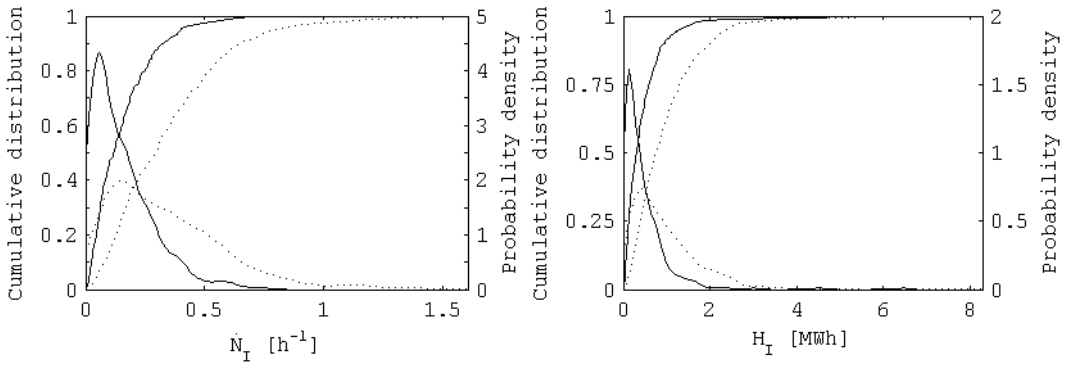

Figure 1a (left) and 1b (right): Predicted cumulative distributions and probability density functions of mean infiltration rate (left) and total winter heat loss (right). □ □ □ □ □ , Assumption A(1); ·····, A(2).

Figure 1a shows the predicted cumulative distributions (CDF) and probability density functions (PDF) of the mean infiltration rate, N_I (h^{-1}) in English apartments during the heating season for both permeability assumptions. Figure 1b shows the same for total winter heat loss, H_I (MWh). Table 1 gives descriptive statistics for each sample and extreme permeability assumption. The number of samples required were 360 and 860 for permeability assumptions A(1) and A(2), respectively.

Table 1 and Figures 1a and 1b show that all distributions are positively skewed and so median values are used herein. A clear difference between the predictions made for each of the two permeability assumptions is observed. One-sided Kolmogorov-Smirnov tests of the null hypothesis that the A(1) and A(2) samples come from populations with the same distributions compared against the alternative that the A(1) CDFs are larger than the A(2) CDFs are rejected (at significance p <0.05) for both N_I ($p = 6 \times 10^{-33}$) and H_I ($p = 3 \times 10^{-31}$).

N_I and H_I are predicted to be lower for permeability assumption A(1) than for A(2), and that assumption A(2) increases the variance of the sample. The difference in predicted mean winter infiltration for A(1) and A(2) is explained by considering both assumptions applied to an apartment of fixed permeability with at least one party wall. Whatever the permeability assumption of the party walls, the total leakage area (equal to the sum of the cross sectional areas of all ALPs) of the apartment is identical because the permeability is fixed. If assumption A(1) is made and the party walls are permeable then the total leakage area is uniformly distributed over all surfaces of the apartment's envelope. If assumption A(2) is made and the party walls are impermeable then the total leakage area is only uniformly distributed over the exposed surfaces, A_I (m^2) of the apartment's envelope, thus increasing the operational infiltration rate. Jones *et al.* (2013a) show that the ratio of the predicted infiltration rate for the two permeability assumptions is equal to a ratio of permeable envelope area at a pressure differential of 50 Pascals A_{50} (m^2), where

$$A_{50,A(1)} \; A_{50,A(2)} = N_{I,A(2)} \; N_{I,A(1)} \tag{2}$$

Here, the subscripts indicate the pressure differential and the permeability assumption. Equation (2) shows that for apartments, the ratio is likely to be ≫1 because apartments tend to have more than one party wall and so $A_{50,A(1)} \gg A_{50,A(2)}$. For detached houses, one expects the ratio to approach unity because they have no party walls and so $A_{50,A(1)} \approx A_{50,A(2)}$. Note that Equation (2) is valid for a single dwelling and not for an entire distribution. Therefore it is reassuring that Table 2 shows that Equation (2) is approximately true for the sample medians of the two permeability assumptions. Table 2 also shows that the median air permeability, apartment volume, envelope area, and exposed envelope area for both samples are also similar because they are unaffected by the permeability assumptions.

The difference in variance between the samples (indicated by σ) is attributable to the variation of A_{50} governed by the permeability assumptions. For the A(1) sample, $A_{50} = A_{env}$ for the vast majority of cases (ground floor apartments with impermeable solid floors are an exception), whereas for the A(2) sample, $A_{50} \neq A_{env}$ for the vast majority of cases (when at least one party wall is assumed), they vary instead between $0 \ll A_{50} \ll A_{env}$.

Table 2: Meadian values of key descriptive parameters of sampled apartments. Assumption A(1): permeable party walls. Assumption A(2): impermeable party walls.

Sample median	A(1)	A(2)
Air permeability, P_{50} ($m^3/h/m^2$)	9.4	9.1
Apartment volume (m^3)	132.3	134.6
Envelope area, A_{env} (m^2)	184.2	185.6
A_I (m^2)	63.8	60.7
A_{50} (m^2)	161.9	60.7
$A_{50,A(1)} \; A_{50,A(2)}$		2.7
$N_{I,A(2)} \; N_{I,A(1)}$		2.5

A_{50}, permeable envelope area at a pressure differential of 50 Pascals.
A_I, exposed envelope area able to transfer mass under operational conditions

Table 3: Predicted leakage infiltration ratio L and performance statistics.
Assumption A(1): permeable party walls. Assumption A(2): impermeable party walls.

	A(1)	A(2)
L	66.90	32.07
R^2	0.01	0.41
RMSE	7.33	5.43
MAE	26.01	25.14

Figure 1 suggests that 97% and 78% of apartments for permeability assumptions A(1) and A(2), respectively, have a mean infiltration rate below 0.5ac/h. This is significant because 0.5ac/h is a threshold ventilation rate (all be it with great uncertainty), recommended by many European countries, above which some negative health effects reduce (Jones *et al.*, 2013a). This suggests that English apartments should be fitted with purpose provided ventilation to minimize health risks to occupants and is an important consideration for policy makers.
Table 1 shows that the median total heat losses are 300kWh and 748kWh for permeability assumptions A(1) and A(2), respectively. For assumption A(1) and A(2) this is equivalent to running approximately three and eight 11W light bulbs non-stop for an entire year, respectively, or equivalent to the continuous occupancy by a single adult (assuming 100W per adult) for approximately 34% and 85% of a year, respectively.

4 ASSESSING THE LEAKAGE INFILTRATION RATIO

Equation (1) is evaluated by the linear regression of N_I and N_{50} to estimate L and by the calculation of key performance statistics: R^2, Root Mean Squared Error (RMSE), and Maximum Absolute Error (MAE). Values of L are given in Table 3 by permeability assumption along with the performance statistics. These statistics imply that $L \neq 20$ and that Equation (1) is a poor model of the relationship between N_I and N_{50} in English apartments, whatever the permeability assumption. This outcome suggests that building codes that apply Equation (1) with $L = 20$ (in the first instance) could be over predicting exfiltration heat loss in apartments. However, it is acknowledged that sub-groups of these samples may exhibit a correlation but further work is required to determine if it is appropriate for building codes to scale L (as described in Section 1) or if another type of relationship is needed.
An alternative model of the relationship between N_I and N_{50} may be required. In the long term, an exhaustive field survey is required to give a reliable empirical basis for the prediction of N_I from dwelling characteristics. In the short term, further work could apply meta-modelling techniques, such as multiple linear regression, that minimize the prediction errors in a least-squares sense and that use the predictions given here as training and validation data.

5 SENSITIVITY ANALYSIS

Table 4: Sensitivity of outputs to inputs, confidence, and rank of key model inputs.

Outputs	**Mean infiltration rate, N_I**			**Total heat loss, H_I**		
Inputs	τ	p	**rank**	τ	p	**rank**
Air permeability, P_{50} ($m^3/h/m^2$)	0.54	0.00	1	0.53	0.00	1
Airflow exponent	-0.35	0.00	2	-0.35	0.00	2
A_{50} (m^2)	-0.22	0.00	3	-0.19	0.00	3
Mean wind speed at dwelling height (m/s)	0.08	0.00	4	0.09	0.00	4
Orientation (º)	-0.04	0.02	5	-0.05	0.01	5
Apartment volume (m^3)	-0.03	0.16	6	0.04	0.03	7
Block aspect ratio	0.02	0.33	7	0.02	0.24	8
Mean temperature difference, ΔT (ºC)	-0.01	0.66	8	-0.01	0.52	9
A_I (m^2)	0.00	0.90	9	0.05	0.02	6

A_{50}, permeable envelope area at a pressure differential of 50 Pascals.
A_I, exposed envelope area able to transfer mass under operational conditions.

It could be argued that the salient assertions made in Sections 3 and 4 are dependent upon the assumptions made in Section 2. Accordingly, a sensitivity analysis is used to determine the

relative importance of inputs. All of the inputs are perturbed simultaneously by the Monte Carlo sampling method (see Section 2.3) and so any interactions between them (including those that are synergistic) are accounted for (Lomas and Eppel; 1992). To test the dependence of the inputs on the outputs N_I and H_I, the Kendall τ correlation coefficient (a number between ± 1) is used. Here, $\tau = 1$ indicates perfect positive correlation between the input and the output, whereas $\tau = -1$ indicates perfect negative correlation. Inputs are ranked by τ where the lowest rank is the most significant; see Table 4. The inputs assessed in Table 4 are continuous numerical variables that are uncorrelated with each other; for example, P_{50} ($m^3/h/m^2$) is considered instead of envelope area, A_{env}. Moreover, the inputs are chosen to represent implicitly the geographic, geometric, environmental, physical, and terrain parameters discussed in Section 2, thus avoiding the need to test categorical variables, such as the region.

Table 4 evaluates both samples in concert using MATLAB's "`corr`" function (with "`kendall`" as an input) to test for a non-zero correlation between the input and the output, assuming that the null-hypothesis is true. Table 4 shows that N_I is sensitive to 5 of the 9 inputs (at $p < 0.05$) and H_I is sensitive to 6 of the 9 inputs. Both outputs are most sensitive to P_{50} whose limitations are identified in Section 2.2.3. The accuracy of the predictions given here could be improved with more robust distributions of P_{50} by dwelling type and age. It is reassuring that the model is insensitive to block geometry, given that its imposed limits are arbitrary (see Section 2.2.2), and to the mean temperature difference, ΔT, given the uncertainty in the variance of the internal air temperature (Section 2.2.4).

6 CONCLUSIONS

This paper provides a stochastic method for predicting distributions of mean infiltration rates in winter and total winter heat loss in a stock of dwellings. The method is used to investigate mean winter time infiltration rates in apartments, which share at least one wall with another dwelling, based on two extreme assumptions of party wall permeability. The first assumes that the party walls are permeable whereas the second assumes that they are not. A clear statistical difference between the distributions for each of the two permeability assumptions is predicted. The distributions show that the mean infiltration rate and total heat loss are significantly less for the first assumption than for the second, and that at least 78% of apartments require additional purpose provided ventilation to limit negative health consequences.

Concern is raised about the use of the *leakage-infiltration* ratio predict an apartment's mean winter infiltration rate from a measurement of its air leakage rate. This is independent of the assumption of party wall permeability, because the *leakage-infiltration* ratio cannot account for the variation in geographic, geometric, environmental, physical, and terrain parameters unless it is scaled. Further work is required to reassess the use of the relationship by building codes.

The modelling approach detailed here can be applied to any stock of dwellings. The application of the approach to apartments highlights significant health and energy ramifications. The predicted distributions of the mean infiltration rate and total heat loss in winter for the two extremes of party wall permeability are a useful tool with which policy makers of any country whose housing stock contains apartments can make informed decisions about fabric tightness and exfiltration heat loss.

ACKNOWLEDGEMENTS

The authors are grateful to the European Commission for its funding of the PURGE project by its 7th Framework Programme under grant agreement number 265325.

REFERENCES

BSI (1991). BS5925:1991. Code of Practice for Ventilation Principles and Designing for Natural Ventilation. British Standards Institution, London.

DCLG (2011). English Housing Survey: Headline report 2009-10. London, Department for Communities and Local Government.

Deru, M.P. and Burns, P.J. (2003). Infiltration and natural ventilation model for whole building energy simulation of residential buildings. *ASHRAE Transactions* 109(2), 801-811.

Etheridge, D.W. (2012). *Natural Ventilation of Buildings: Theory, Measurement and Design*, John Wiley and Sons.

Hamilton, I., *et al.* (2011). The impact of housing energy efficiency improvements on reduced exposure to cold — the 'temperature take back factor'. *Building Services Engineering Research and Technology* 32(1), 85-98.

HM Government (2010). The Building Regulations 2000 (2010 edition): Approved Document L1A: Conservation of fuel and power in new dwellings. Crown Copyright 2010.

Hughes, M., *et al.* . (2012). Converting English Housing Survey Data for Use in Energy Models, Cambridge Architectural Research Ltd. and University College London.

Jones, B.M., *et al.* (2013a). The Effect of Party Wall Permeability on Estimations of Infiltration from Air Leakage. *International Journal of Ventilation* 12(1): 17-29.

Jones, B.M., Lowe, R.J., Davies, M., Chalabi, Z., Das, P. and Ridley, I. (2013b). Modelling uniformly porous façades to predict dwelling infiltration rates. *Building Services Engineering Research and Technology*. Accepted for publication.

Lomas, K.J., and Eppel, H. (1992). Sensitivity analysis techniques for building thermal simulation programs. *Energy and Buildings* 19(1): 21-44.

MathWorks (2013). MATLAB Version 8.1.0.604 (R2013a). Natick, Massachusetts: The MathWorks Inc.

Palmer, J. and Cooper, I. (2011). Domestic Energy Fact File 2011, Department of Energy and Climate Change.

Ministry of the Environment of Finland (2012). National Building Code of Finland, Part D5: Calculation of power and energy needs for heating of buildings, Department of the Built Environment, Ministry of the Environment, Finland.

Orme, M., Liddament, M.W. and Wilson, A. (1998). TN 44: Numerical Data for Air Infiltration and Natural Ventilation Calculations, Air Infiltration and Ventilation Centre.

Pan, W. (2010). Relationships between air-tightness and its influencing factors of post-2006 new-build dwellings in the UK. *Building and Environment* 45(11), 2387-2399.

Persily, A., Musser, A. and Emmerich, S.J. (2010). Modeled infiltration rate distributions for U.S. housing. *Indoor Air* 20(6), 473-485.

Sherman, M.H. and Grimsrud, D.T. (1980). Infiltration–pressurization correlation: simplified physical modelling. Lawrence Berkeley Laboratory Report LBL-10163.

Sherman, M.H. (1987). Estimation of infiltration from leakage and climate indicators. *Energy and Buildings* 10(1), 81-86.

Sherman, M.H., and Matson, N. (1997) Residential ventilation and energy characteristics. *ASHRAE Transactions* 103(1), 717-730.

Sherman, M.H. and Dickerhoff, D.J. (1998). Airtightness of U.S. dwellings. *ASHRAE Transactions* 104(4), 1359-1367.

Stephen, R. (1998). Airtightness in UK dwellings: BRE's test results and their significance, Building Research Establishment.

Swami, M. and Chandra, S. (1987). Procedures for Calculating Natural Ventilation Airflow Rates in Buildings, ASHRAE.

THE CLIMATE EFFECTS OF INCREASING THE ALBEDO OF ROOFS IN A COLD REGION

Hashem Akbari and Ali Gholizadeh Touchaei

Heat Island Group
Building, Civil and Environmental Engineering Department
Concordia University

1455 De Maisonneuve Blvd. W.,

Montreal, Quebec, Canada

ABSTRACT

Urban heat island (UHI) phenomenon has been observed in many populated cities located in cold regions (e.g., Montreal in Canada) during summer. One of the well-known strategies to mitigate the temperature rise of urban areas is increasing their albedo. Roofs cover about 25% of urban areas and increasing their reflectivity would have significant effect on the total energy budget of a city. Changing the surface energy budget can directly affect the air temperature near ground and the vertical wind speed. We have studied the effect of increasing the albedo of roofs on the air and skin temperature distributions of the Greater Montreal area. We performed simulations for one-day summer episode (12 July 2005) using Weather Research and Forecasting (WRF) mesoscale model. The WRF solver (version 3.4.1) is coupled with three different Urban Canopy Models (UCMs): slab, single-layer, and multi-layer. The slab UCM is a one-dimensional model where the surface properties of urban areas (e.g. albedo, thermal storage, etc.) are kept constant. The single-layer UCM considers the albedo of different urban surfaces (i.e. roof, road, and wall), the wind effect in the canopy, and radiation trapping between buildings. Multi-layer UCM has the ability of simulating the effect of turbulence and momentum sink, to estimate the vertical heat exchange more accurately.

We used all three UCMs by increasing the roof albedo from 0.2 to 0.8 and compared the results. All models simulated a well-defined UHI over areas with high concentration of roofs. They predicted a maximum air temperature decrease of about 1 ºC by implementing cool roofs. The difference between the skin (surface) temperature of urban area and its surrounding was about 9 K. The maximum air temperature difference between the urban and suburban areas was about 4 K.

KEYWORDS

Urban Heat Island, Urban Canopy Model, Albedo, Mitigation Strategies.

1 INTRODUCTION

Urban areas are usually warmer than their surroundings; this phenomenon is called urban heat island (UHI) (Keefer, 2012). Figure 1 illustrates the typical surface temperature variation along a city, maximum temperature occurs in its urban area. UHI can increase the average air temperature of an urban area 1-3K more than its surrounding (EPA, 2012). UHI have considerable nocturnal effect (Figure 2) and the temperature difference can be as high as 12K (Oke, 1987; Roth et al., 1989). UHI affects a large vertical region above cities, for instance, Bornstein (1968) reported the temperature difference between New York City and its surrounding have been extended over 500 m in mornings.

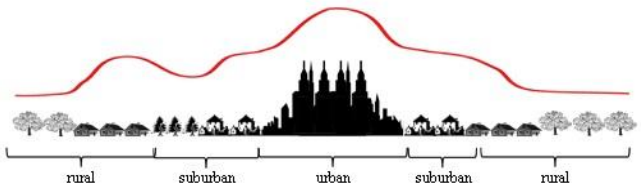

Figure 1: Typical variation of surface temperature along a city and occurrence of the UHI

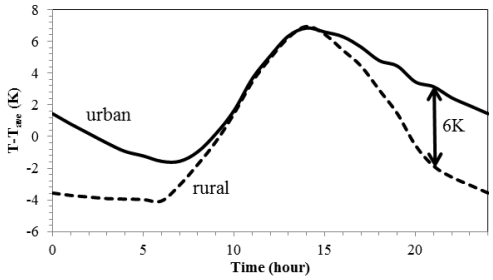

Figure 2: Typical temporal variation of urban and rural surface temperature from its daily average

Two main strategies to mitigate UHI are: 1) cool surfaces and 2) vegetating surfaces (including roofs). The focus of this paper is on studying the effect of cool surfaces on urban climate.

Cool materials have both high solar reflectance and high thermal emittance (Levinson et al., 2005). Using cool materials for roofs and pavements decreases the heat absorption of urban surfaces. The reflectivity of urban surfaces is known as "Albedo" and increasing the albedo can reduce the temperature of the urban areas and consequently the UHI intensity.

Here, the effect of increasing roofs reflectivity in Montreal is simulated by using three standard urban canopy models (UCM) of Weather Research and Forecasting model (WRF). Multi-layer UCM (ML-UCM) is more accurate than other types of UCM because it can consider the effect of turbulence. However, other two types of UCM (slab and single layer) are much faster in computation time. Applicability of slab model and single layer UCM (SL-UCM) for urban climate modeling is compared to ML-UCM. All UCMs coupled with WRF to simulate a single day in summer and characterize UHI at 2-m height. The skin temperature distribution is also quantified.

2 SIMULATION

WRF version 3.4.1 was used for the simulation of the urban climate. For Greater Montreal, the simulation domain was 100×100 km centered at ~45.5º N and ~73.6º W [Figure 3 shows the areas of interest cropped from the original domain]. Size of the grids was in the order of a neighborhood (333×333 m). Figure 3 shows the satellite image of the selected city (on left) and its land-use categories (on right). Land-use was standard 24-catagoryUSGS implemented within WRF. Urban areas of the city are illustrated in Figure 3 in black. Simulation period started from 11-July-2005 1200 UTC [11-July-2005 0800 LST] to 13-July-2005 1200 UTC [13-July-2005 0800 LST]. First 16 hours is considered as spin-up time and outputs of next 24 hours of simulations analyzed [July 12th LST]. Initial and boundary conditions of the simulations extracted from 3-hourly, high resolution 32 km, North America Regional Reanalysis (NARR) data (Mesinger et al., 2006).

Planetary boundary layer (PBL) accounts for the exchange of vertical heat and momentum from the ground on the whole air column of the grid cell. Surface-layer model provides

interaction between lower level (from land-surface model) and PBL. A Land-Surface Model (LSM) provides information of heat and moisture fluxes on land points and sea ice using atmospheric feedback of other schemes in a simulation (it can be considered as a boundary condition for PBL). LSM updates surface variables (e.g. the ground temperature, soil temperature profile, soil moisture profile, snow cover, and canopy properties) in each iteration step as independent variables. PBL is simulated by Mellor-Yamada-Janjic scheme (Janjic, 1990; 1994) using ETA similarity theory (surface layer scheme) (Janjic, 2002). Only available option in WRF for land-surface scheme is Noah-LSM (Chen & Dudhia, 2001). Microphysics models calculate the process of transforming water from one form (rain, snow, graupel, vapor, etc.) to another form. In general, water vapor creates cloud water and cloud ice to shape snow, rain and other types of precipitation. Lin scheme (Lin, et al., 1983) was used as the microphysics option comprises six classes of hydrometeors. Cumulus model estimate the effect of cloud convection in a grid. Grell 3D option based on the Grell-Devenyi ensemble scheme (Grell & Devenyi, 2002) was used for cumulus parameterization. Radiation models determine different radiation processes in the atmosphere (incoming shortwave from the sky, longwave radiation from clouds, absorption by aerosols in the atmosphere, etc.). A new rapid radiative transfer model (named "RRTMG") was selected to simulate the longwave radiation (Clough, et al., 2005). Goddard scheme was employed to estimate the shortwave radiation by considering the effect of ozone and cloud (Chou & Suarez, 1994).

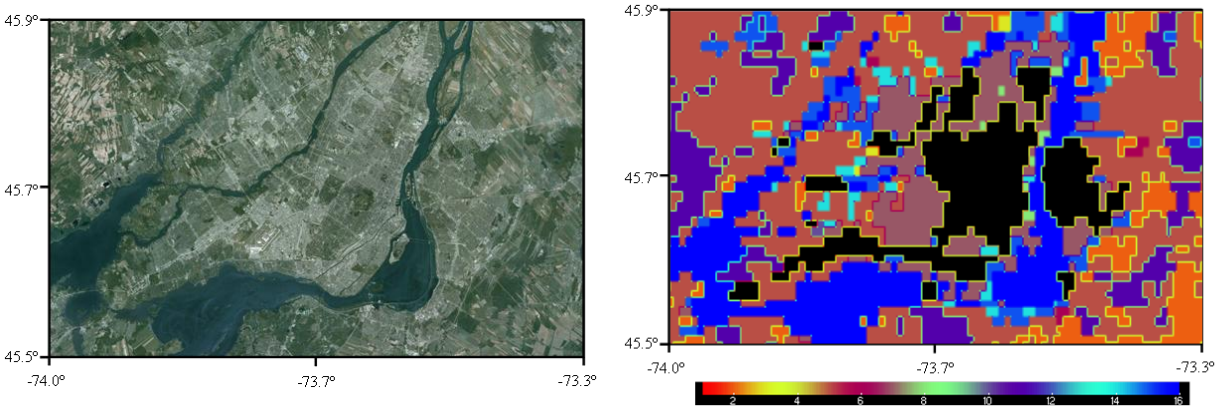

(a) (b)

Figure 3: (a) Simulation domain (http://maps.google.ca) and (b) Land Use Land Cover (LULC) of Greater Montreal extracted from USGS dataset (Black regions are urban areas)

Simulations were performed without applying any damping option (a method to increase the stability of mesoscale model by reducing the vertical velocity) according to the short period of running. Positive definite advection options for turbulent kinetic energy (TKE), moisture, and scalars were activated. Monthly background albedo is the standard input of the software and it is based on measurements of the advanced very high resolution radiometer (AVHRR). In slab model, albedo of the urban areas is considered to be 0.15 (this value is corrected from 0.18 by Liu et al. (2006) to account for radiation trapping in the canopy). In single and multi-layer UCMs, albedo of urban areas is estimated based on albedo of urban surfaces (i.e. roof, wall, and road). By default, all urban surfaces are considered to be 20% reflective. However, the effective albedo of the urban area changes during a day by the position of sun.

3 RESULTS AND DISCUSSIONS

Results are divided into three parts: 1) evaluation of UCMs, 2) observation of UHI in Montreal, and 3) effect of increasing surface albedo on urban temperature.

3.1 Evaluation of UCMs

Simulation of a case with ML-UCM increases the computation time 30-40% respect to the time needed for slab model and SL-UCM. Figure 4 shows the average air and skin temperatures difference between ML-UCM with other two models. Based on these simulations, the temperature difference is up to 1 K is observed. Although SL-UCM and slab model in WRF tested for mesoscale modeling, for fine-resolution and the scale of urban they are not appropriate. Hence, we used ML-UCM in the rest of the study. Our simulations for other cities than Montreal produced similar results.

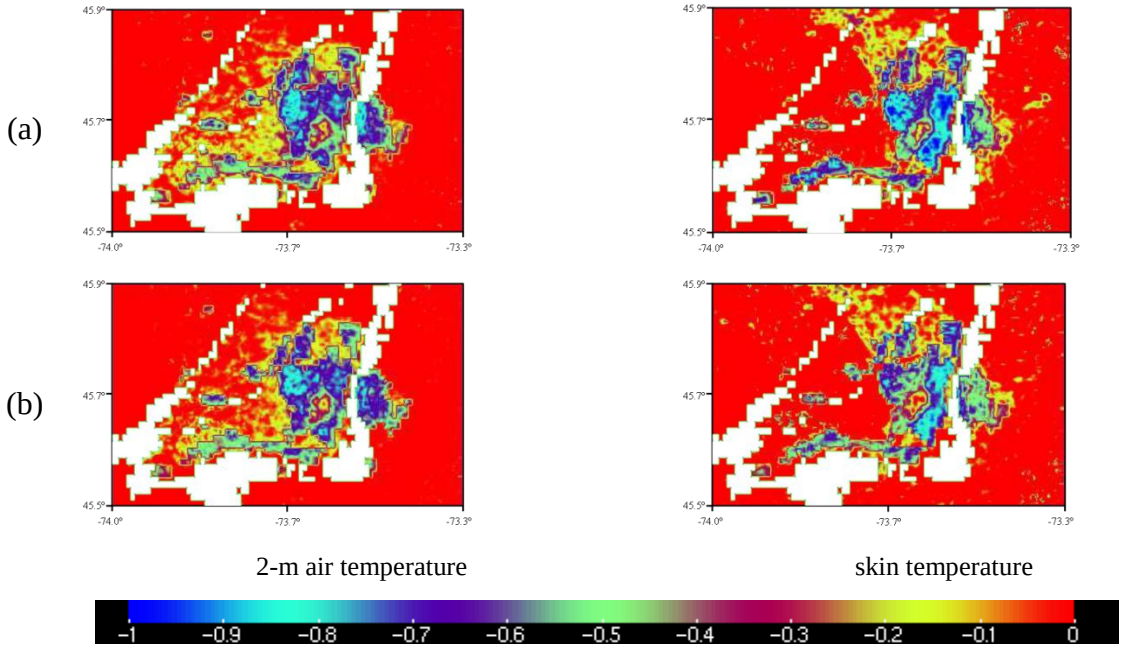

Figure 4: 2-m air temperature and skin temperature difference between (a) Multi-layer UCM and Single-layer UCM, and (b) Multi-layer UCM and slab model of Greater Montreal in 12-July-2005

3.2 Observation of UHI in Montreal

To find the difference between the air and skin temperatures of urban and rural areas, some random points in each region were selected. We considered the mean of these points as the temperature of that region. Skin and 2-m air temperatures of Montreal are shown in Figure 5. For the Greater Montreal, maximum difference between the skin temperature of urban areas and rural areas is about 9 K and it is occurred at 1 PM. Thermal storage of the urban surfaces delay the maximum difference of 2-m air temperature to the evenings. As shown in Figure 5, Montreal experienced a 2-m air temperature difference of about 4 K at 8 PM.

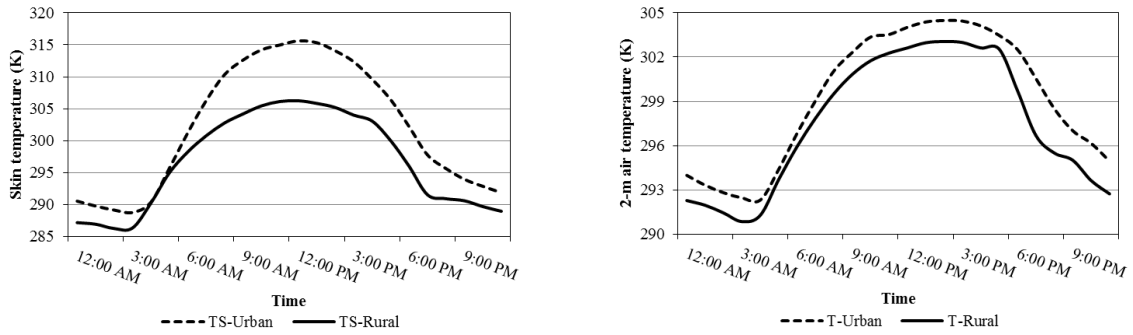

(a) (b)

Figure 5: Temporal variation of (a) skin temperature and (b) 2-m air temperature (K) in urban and rural areas of Greater Montreal in 12-July-2005 using ML-UCM for CTRL case.

3.3 Effect of increasing the albedo on urban temperature

We simulated the effect of increasing the roof albedo (from 0.2 to 0.8) on the air and skin temperatures. Figure 6 illustrates the results of mean 2-m air and skin temperatures of Greater Montreal. Simulations were performed for all three UCMs to compare their performance in characterizing the modification of the surface. In the slab model, albedo of urban areas increased by 0.2 (0.35×0.6≈0.2); roofs considered to cover 35% of the urban area. Increasing albedo of roofs decreased the air temperature of the city about 0.3 K. This value is the change in average temperature, peak temperature reduction is more than that (~2 K)

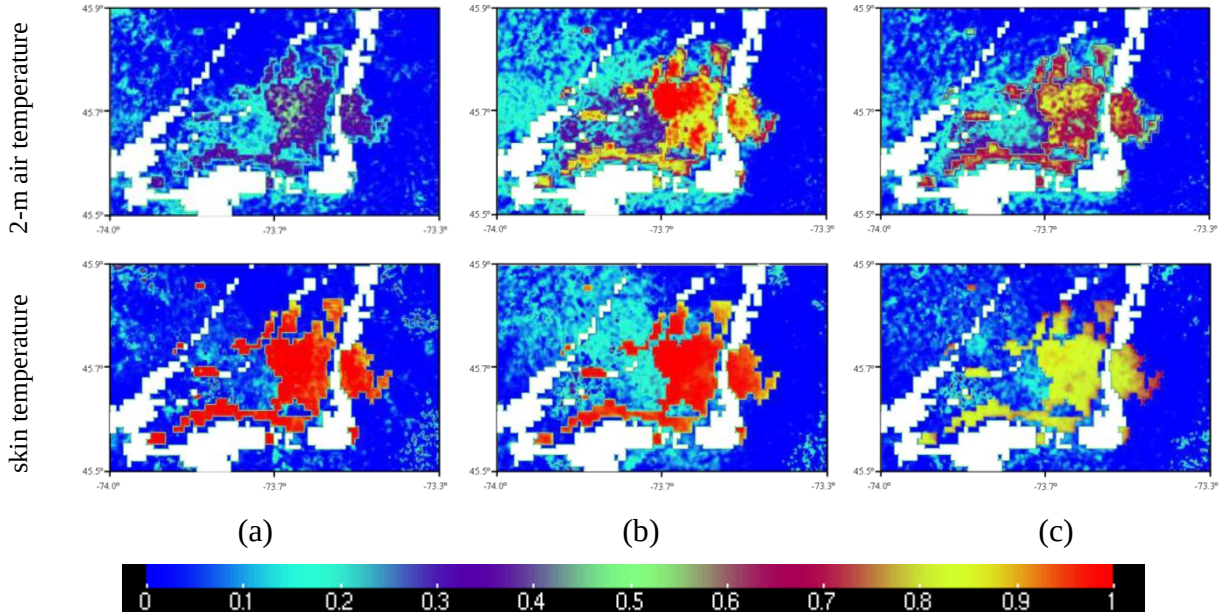

Figure 6: 2-m air temperature and skin temperature difference between CTRL and ALBEDO of Greater Montreal in 12-July-2005. (a) Multi-layer UCM, (b) Single-layer UCM, and (c) slab model.

4 CONCLUSIONS

Applicability of using different urban canopy models for urban climate simulation is investigated. Slab model and SL-UCM overestimated skin and 2-m air temperature by about 1 K compared to ML-UCM. Although Slab model and SL-UCM proved to be effective in large-scale climate simulation, they are not appropriate for urban climate simulations. Consequently, ML-UCM is used to simulate UHI in the city of Montreal. UHI is well observed in urban areas of Montreal. The maximum difference between urban and rural areas air temperature occurred in the evening. Intensity of UHI was about 4 K and 9 K considering 2-m air temperature and skin temperature, respectively. Increasing the albedo of roofs from 0.2 to 0.8 decreased the average air temperature of urban areas of Montreal by 0.3 K. Maximum decrease of air temperature was about 2 K in the evening (8 pm). Simulations indicated the effectiveness of implementing cool roofs in lowering the summertime temperatures in Montreal.

5 ACKNOWLEDGEMENTS

Funding for this research was provided by the National Science and Engineering Research Council of Canada under discovery program.

6 REFERENCES

Bornstein, R. D. (1968). Observation of Urban Heat Island Effect in New York City. *Journal of Applied Meteorology, 7,* 575-583.

Chen, F., & Dudhia, J. (2001). Coupling an Advanced Land Surface–Hydrology Model with the Penn State–NCAR MM5 Modeling System. Part I: Model Implementation and Sensitivity. *Monthly Weather Review, 129*, 569-585.

Chou, M. D., & Suarez, M. J. (1994). *An efficient thermal infrared radiation parameterization for use in general circulation models.* NASA Tech. Memo. 104606, 3, 85pp.

Clough, S., Shephard, M., Mlawer, E., Delamere, J., Iacono, M., Cady-Pereira, K., et al. (2005). Atmospheric Radiative Transfer Modeling: a Summary of the AER Codes. *Journal of Quantitative Spectroscopy & Radiative Transfer, 91* , 233–244.

EPA. (2012, 08 31). *Heat Island Effect*. Retrieved 09 04, 2012, from United States Environmental Protection Agency: http://www.epa.gov/hiri/

Grell, G. A., & Devenyi, D. (2002). A generalized approach to parameterizing convection combining ensemble and data assimilation techniques. *Geophys. Res. Lett., 29*(14), Article 1693.

Janjic, Z. (1990). The Step-mountain Coordinate: Physics Package. *Mon Weather Rev, 118*, 1429–1443.

Janjic, Z. (1994). The Step-Mountain Eta Coordinate Model: Further Developements of the Convection, Viscous Sublayer, and Turbulence Closure Schemes. *Monthly Weather Review, 122*, 927-945.

Janjic, Z. (2002). *Nonsingular Implementation of the Mellor-Yamada Level 2.5 Scheme in the NCEP Meso model.* Camp Springs, MD,: National Centers for Environmental Prediction.

Keefer, T. (2012). *AMS glossary*. Retrieved 09 04, 2012, from urban heat island: http://amsglossary.allenpress.com/glossary/search?id=urban-heat-island1

Levinson, R., Akbari, H., & Berdahl, P. (2005). Solar spectral optical properties of pigments, part II: Survey of common colorants. *Solar Energy Materials & Solar Cells, 89*(4), 351-389.

Levinson, R., Akbari, H., & Berdahl, P. (2010). Measuring solar reflectance—Part I: Defining a metric that accurately predicts solar heat gain. *Solar Energy, 84*, 1717-1744.

Lin, Y.-L., Farley, R. D., & Orville, H. D. (1983). Bulk Parameterization of the Snow Field in a Cloud Model. *Journal of Climate and Applied Meteorology, 22*, 1065-1092.

Liu, Y., Chen, F., Warner, T., & Basara, J. (2006). Verification of a Mesoscale Data-Assimilation and Forecasting System for the Oklahoma City Area During the Joint Urban 2003 Field Project. *Journal of Applied Meteorology and Climatology, 45*, 912-929.

Mesinger et al., F. (2006). North American Regional Reanalysis. *Bulletin of Amererican Meteorological Society, 87*(3), 343–360.

Oke, T. R. (1987). *Boundary Layer Climates.* New York: Routledge.

Roth, M., Oke, T., & Emery, W. (1989). Satellite-Derived Urban Heat Islands from Three Coastal Cities and the Utilization of such Data in Urban Climatology. *International Journal of Remote Sensing, 10*, 1699-1720.

Statistcs Canada. (2011, 05 05). *From urban areas to population centres*. Retrieved 09 04, 2012, from Statistics Canada: http://www.statcan.gc.ca/subjects-sujets/standard-norme/sgc-cgt/urban-urbain-eng.htm

U.S. Census Bureau. (2011, 02 18). *Geographic Terms and Concepts - Urban and Rural*. Retrieved 09 04, 2012, from U.S. Department of Commerce: http://www.census.gov/geo/www/2010census/gtc/gtc_urbanrural.html

United Nations. (2011). *2009–2010 Demographic Yearbook.* New York, NY: United Nations.

INTERLABORATORY COMPARISON OF COOL ROOFING MATERIAL MEASUREMENT METHODS

Afroditi Synnefa*[1], Alexandros Pantazaras[1], Mat Santamouris[1], Emmanuel Bozonnet[2], Max Doya[2], Michele Zinzi[3], Alberto Muscio[4], Antonio Libbra[4], Chiara Ferrari[4], Valentina Coccia[5], Federico Rossi[5], Denia Kolokotsa[6]

1 National and Kapodistrian University of Athens
Physics Dept., Section Applied Physics
Building of Physics - 5, University Campus
157 84 Athens, Greece
**Corresponding author: asynnefa@phys.uoa.gr*

2 La Rochelle University
LaSIE - Pôle Sciences et Technologie
Avenue Michel Crépeau 17042
LA ROCHELLE Cedex 1, France

3 ENEA - UTEE ERT
s.p. 104 - st. 113
Via Anguillarese, 301
00123 Rome, Italy

4 EELab - Dipartimento di Ingegneria "Enzo Ferrari"
Università di Modena e Reggio Emilia
Via Vignolese, 905/B
41125 Modena, Italy

5 CIRIAF - Interuniversitary Research Center on Pollution from Physical Agents "Mauro Felli"
Via G. Duranti,
6706125 Perugia, Italy

6 Technical University of Crete
Technical University Campus, Kounoupidiana,
73100 Chania, Greece

ABSTRACT

The present study aims at investigating different methodologies and standards for measuring and calculating solar reflectance and infrared emittance, the two main properties characterizing cool roofing materials. In order to achieve this goal, an interlaboratory comparison testing has been set up among several laboratories that are members of the European Cool Roofs Council. The measurement methods practiced by the labs include measurement of the reflectivity by using spectrophotometers equipped with integrating spheres and reflectometers and measurement of the emissivity using different emissometer devices and FTIR spectrometers equipped with integrating spheres. Seventeen different samples representing the range of commercially available roofing materials and covering the full range of reflectance and emittance values have been selected and tested. The results of this study provide information on the suitability of the various methods to be used for cool roof products assessment. This work could potentially lead to the adoption of a European Cool Roof Standard.

KEYWORDS

Solar reflectance, infrared emittance, measurement standards, cool roofs, interlaboratory testing

1 INTRODUCTION

Cool roofs can give an important contribution to mitigate climate change, reduce the urban heat island effect and increase the sustainability of buildings. Cool roofs technology has long been applied in the U.S. where there are measurement standards related to cool roofs, it is a part of the energy code in many states, and organizations like the U.S. EPA Energy Star, the U.S. Cool Roof Rating Council, programs (e.g. LEED) and incentives are promoting it. Cool roofs technology is also applied and promoted in other countries around the world like Japan,

Australia, Brazil, India etc. In Europe, the foundation of the European Cool Roofs Council (ECRC) has given an important boost in the cool roofs technology and market. The ECRC is a non-profit association aiming at developing scientific knowledge and research in relation to "cool roof" technology and promoting the the use of cool roof products and materials in Europe, including developing a product rating programme for such products and materials. The foundation of the ECRC was supported by the IEE Project "Cool Roofs" (IEE/07/475/SI2.499428).

One of the core objectives of the ECRC is the development of a Product Rating Programme, in which roofing product manufacturers will be able to label various roof products with radiative property values rated under a strict programme administered by the ECRC. Code bodies, architects, building owners and specifiers can have credible radiative properties data provided by the ECRC Product Rated Programme. The radiative properties that will be reported by this product rating program are the solar reflectance and the infrared emittance. There exist several measurement methods for the determination of the solar reflectance and the infrared emittance. They can be measured using portable instruments i.e. reflectometers and emissometers in accordance with procedures defined in the ASTM C1549 (2004), ASTM E1918 (2006), ASTM C1371 (2010) and EN 15976 (2011) standards. They can also be determined using spectrophotometric techniques described in several standards like ASHRAE 74 (1988), ASTM E903 (1996), ASTM E1585 (1993), CIE 130 (1998), EN 410 (1998), EN 12898 (2001), EN 14500 (2008) and ISO 9050 (1990).

In order to provide the ECRC with information regarding its product rating programme under development, an interlaboratory comparison (ILC) of the measurement methods of reflectance and emittance (emissivity) has been organised and conducted. The main objective of this ILC is to compare different measurement methodologies for measuring and calculating solar reflectance (SR) and infrared emittance (e), mainly ASTM and European (EN) standards, and provide information on their suitability to be used for cool roof products assessment. This paper describes the main aspects of this ILC and discusses the first results.

2 EXPERIMENTAL DETAILS

The following sections report the details of the samples that have been tested for this ILC and also the process and measurement methods that have been followed.

2.1 Sample description

A set of 17 samples that represents the range of commercially available roofing materials was selected to be measured by the labs like coatings, membranes, tiles, shingles and metal products. These samples were selected to cover the full range of reflectance and emittance values. Consequently, the selected samples include white and black, coloured and cool coloured, variegated, profiled and rough and smooth surfaced products. The details of samples used for the ILC are given in Table 1.

All product samples have been prepared following specific guidelines. More specifically, field applied coatings were applied on an aluminium panel at the minimum dry mil thickness or coverage recommended by the manufacturer for use in the field. Factory applied coatings were also applied on an aluminium panel. The rest of the products were not applied on a substrate and tiles were provided as full uncut tiles. The size for all the samples was 10cmx15cm, except for tiles that were provided as full uncut tiles. An additional set of samples at the size of 22cmx22cm was prepared to be used with a large integrating sphere by one of the labs. In total 275 samples have been prepared and were measured for the purpose of this ILC.

Table 1: The samples measured for the ILC

Product type	Sample description	Sample code	Characteristics
Coating	Waterborne elastomeric acrylic coating	S1	White, smooth
	Elastomeric waterproof coating	S2	NIR reflecting black, smooth
	Elastomeric waterproof coating	S3	Black, smooth
	Elastomeric waterproof coating	S4	NIR reflecting brown, smooth
	Aluminium-thermoplastic hydrocarbon based roof coating	S5	Aluminium, smooth
Asphalt membrane (modified bitumen)	Granulated bituminous membrane	S6	White, rough
	Granulated bituminous membrane	S7	Black, rough
	Granulated bituminous membrane	S8	Green, rough
Shingle	Multicoloured asphalt shingle	S9	Red, rough
Single ply membrane	FPO membrane	S10	White, smooth
Concrete tile	High profile multi-colour coated tile	S11	Multicoloured, profiled, Rough
	Curved profile tile, monocolour	S12	Profiled, smooth
	Flat monocolour tile	S13	smooth
Metal roof	Prepainted metal	S14	Silver, smooth
	Prepainted metal	S15	Dark brown, slight textured finish
	Prepainted metal	S16	Off white, Smooth
	Bare pretreated metal	S17	Silver, Smooth

2.2 ILC participating labs and instrumentation

In total 12 Labs have participated at the ILC. The instrumentation used by the labs includes spectrophotometers equipped with integrating spheres of 150mm diameter, reflectometers and two portable emissometers (the Devices and Services Emissometer and the INGLAS TIR100-2 referred to as EN 15976 emissometer). Measurements were also performed using a spectrophotometer with an integrating sphere of 75cm diameter by one lab. Table 2 includes a short description of the labs and the instrumentation availability.

Table 2: The samples measured for the ILC

	Spectrophotometer	Reflectometer	ASTM C1371 Emissometer	EN 15976 Emissometer
Lab 1		x	x	
Lab 2		x	x	x
Lab 3	x		x	
Lab 4	x		x	
Lab 5		x	x	
Lab 6	x		x	
Lab 8	x		x	
Lab 9	x	x	x	

Lab 10	x		x	
Lab 11	x		x	
Lab 12				x

In order to minimize efforts and sample distribution costs, two measurement rounds (6 labs performing the measurements in each round) have been carried out using the same sets of samples.

3 MEASUREMENT METHODOLOGY

The two radiative properties that were measured by the labs were the solar reflectance and the infrared emittance. The different measurement methodologies followed by the labs are described in the following sections.

3.1 Solar reflectance

The solar reflectance was measured and/or calculated in two different ways:
a) Spectrophotometer with an integrating sphere
Measurements were conducted according to ASTM E903 (1996) or EN 14500 (2008). The solar reflectance was then calculated using all the following reference solar spectra:

- ✓ ASTM E891-87 (1992) or ASTM G159-98 (1998)
- ✓ ASTM Standard G173-03 (2008)
- ✓ CIE 85-1989 (The reference solar spectrum given in EN 410 (2011) – Glass in building. Determination of luminous and solar characteristics of glazing)

b) Reflectometer
Measurements were conducted according to ASTM C1549-04 (2004)
The solar reflectance of variegated products was determined according to the methodology described in the CRRC-1 Method #1: Standard Practice for Measuring Solar Reflectance of a Flat, Opaque, and Heterogeneous Surface Using a Portable Solar Reflectometer (CRRC-1 Standard, 2008).
The solar reflectance of tiles was determined using either the CRRC-1 Method #1 or the Template method as described in the CRRC-1 Standard (2008).

3.2 Infrared emittance

The infrared emittance was measured in two different ways:

a) D&S Emissometer
Measurements were conducted using equipment and procedures in accordance with ASTM C1371 (2010).

b) EN 15976 emissometer
Measurements were conducted using equipment and procedures in accordance with EN 15976 (2011)

4 ILC RESULTS

4.1 Homogeneity test

In order to check for any inhomogeneities between the samples to be tested by the labs, an initial characterisation of their radiative properties was performed by 4 labs using one of the

methods for determining SR and e. More specifically, all the samples per product type were measured by a single lab.
The homogeneity of the samples was determined and checked using the statistical criteria according to ISO13528 (2005). The samples that were found to present inhomogenities were replaced by new ones. The final homogeneity check showed that the set of samples to be measured was suitable for the ILC.

4.2 Solar reflectance evaluation

The first step of the statistical analysis consisted of detecting and removing outlier data (ISO Guide 43, 1997). The Grubb's test (significance level equal to 0.05) was used to determine whether the larger or smaller observation in a set of data is an outlier. Five outliers were detected and removed from the datasets corresponding to the spectrophotometric measurements and three outliers were detected and removed from the datasets corresponding to the reflectometer measurements.

a) Spectrophotometer measurements:

Measurements with spectrophotometers equipped with integrating spheres were performed according to ASTME903 (1996) and the solar reflectance was calculated using the solar spectra mentioned in section 3.1.
The average values (AVG), standard deviation (STDEV) and coefficient of variance (C.V.) for solar reflectance values have been determined for each sample and are reported in Table 3. N represents the number of labs that have measured the specific sample.

Table 3: The results of the statistical evaluation of the solar reflectance measured according to ASTME903(1996)

Samples	N	Total Solar Reflectance (TSR) (ASTME903)									ΔSR	
		E891			G173			EN410			E891 – G173	E891 – EN410
		AVG	STDEV	CV	AVG	STDEV	CV	AVG	STDEV	CV		
S1	6	86	1.11	0.01	85	0.67	0.01	83	0.99	0.01	1	3
S2	7	21	2.07	0.10	20	0.98	0.05	18	0.54	0.03	1	3
S3	7	4	0.38	0.09	4	0.36	0.08	4	0.41	0.10	0	0
S4	7	42	1.72	0.04	40	0.97	0.02	38	0.54	0.01	2	4
S5	7	76	2.16	0.03	76	1.97	0.03	76	1.94	0.03	0	0
S6	7	31	1.29	0.04	31	1.04	0.03	31	1.24	0.04	0	0
S7	7	6	0.49	0.08	6	0.42	0.07	6	0.43	0.07	0	0
S8	7	11	1.11	0.10	10	0.80	0.08	10	0.54	0.05	1	1
S9	7	16	1.00	0.06	15	0.92	0.06	15	0.78	0.05	1	1
S10	6	86	1.33	0.02	86	0.83	0.01	85	0.56	0.01	0	1
S12*	4	30	2.83	0.09	28	0.97	0.03	27	0.63	0.02	2	3
S13*	3	38	2.00	0.05	36	1.26	0.03	35	0.59	0.02	2	3
S14	6	51	1.63	0.03	51	0.73	0.01	50	0.72	0.01	0	1
S15	7	13	0.49	0.04	13	0.41	0.03	13	0.42	0.03	0	0
S16	6	53	1.03	0.02	53	0.58	0.01	52	0.64	0.01	0	1
S17	7	57	3.10	0.05	57	3.22	0.06	57	3.07	0.05	0	0

A first observation from this work is that profiled and variegated tile samples cannot be measured with a spectrophotometer. The samples S12 and S13 represent a monocolour profiled and a monocolour flat tile. Four of the participating labs have cut smaller pieces of the full uncut tiles in order to be able to place them in the spectrophotometer port. These results are only indicative (marked with an asterisk in Table 3) and further investigation is

necessary to explore the possibility of a spectrophotometer to accurately measure variegated and profiled products if smaller and flat samples are provided.
The differences in the average TSR values calculated with the three different solar spectra were also calculated for each sample and are included in Table 3. It was found that the highest differences were observed between the ASTM E891 and the EN 410 solar spectra. Also, the highest difference was observed for the sample S4 which is a near infrared reflective brown coating. This can be explained if we examine the spectral characteristics of the different spectra summarised in Table 4.

Table 4: Summary of the three solar spectral irradiances specified by the two ASTM and the CIE standards.

Standard	Description	NIR (%)
ASTM E891-87 (1992)	Hazy sky AM1.5 beam-normal irradiance	58.1
ASTM G173-03 (2003)	Clear sky AM1.5 beam-normal irradiance	54.3
CIE 85(1989)	Global radiation, AM1	49.5

The NIR solar irradiance (700-2500nm) as calculated for the ASTM E891 is by 8.6%NIRSR higher than that of the CIE standard, which explains the higher differences observed between the two standards and the fact that a higher difference was observed for the NIR reflective sample. It is obvious that the choice of the solar spectrum for the calculation of solar reflectance affects the calculated SR value especially for spectrally selective materials. It should be pointed out however that the observed differences are lower or equal to the total uncertainty quoted in the ASTME903, which is equal to ±3-4%TSR and includes potential differences from the use of different solar spectra.
Finally, an average standard deviation for each calculation method (E891, G173 and EN410) was evaluated as 1.5%TSR, 1%TSR and 0.9%TSR respectively. This result demonstrates that there is a very good inter-laboratory agreement when using the same method and calculation procedure since these errors fall well within the expanded uncertainties quoted in the ASTM E903 standard (total uncertainty according to ASTME903 equals with ±3-4%TSR).

b) Reflectometer measurements:

The solar reflectance of the samples was also measured by using a reflectometer according to the ASTM C1549 by four labs. The average values (AVG), standard deviation (STDEV) and coefficient of variance (CV) for solar reflectance values have been determined for each sample and are reported in Table 5. The average standard deviation of all the measurements is 0.87%TSR indicating a good inter-laboratory agreement when using this measurement method.
The results of the reflectometer measurements were compared with the results obtained with the spectrophotometer. The difference in the solar reflectance values obtained with the two standards (ASTM C1549 and ASTM E903) is also reported in Table 5. The highest absolute differences between the two methods were observed for the NIR reflective black sample (S2) and the bare aluminium sample (S17) and were equal to 3 and 5%TSR respectively. It should be pointed out though that the observed differences are comparable to the measurement methods' uncertainty which is estimated to be about 4%TSR.
In addition, the relation between the determination of TSR by reflectometer (ASTM C1549) and spectrophotometer (ASTM E903, using the solar spectrum of a) ASTM E891 and b) ASTM G173) are shown in Figure 1. The data show that although there are differences as great as 5% in the absolute values achieved using the two different methods on the same samples, the overall trends are very similar. The regression analysis gave an R^2 value of 0.996

when the ASTM E891 solar spectrum was used and an R^2 value of 0.995 for the ASTM G173 solar spectrum. The results indicate a strong and positive correlation between the two test methods.

Table 5: of the statistical evaluation of the solar reflectance measured according to ASTM C1549 (2004)

Samples	N	Total Solar Reflectance (ASTMC1549)			E903 - C1549
		AVG	STDEV	CV	
S1	4	85	1.94	0.02	1
S2	4	24	1.50	0.06	-3
S3	4	4	0.00	0.00	0
S4	3	43	0.98	0.02	-1
S5	4	77	1.04	0.01	-1
S6	4	31	1.31	0.04	0
S7	4	6	0.05	0.01	0
S8	4	11	0.48	0.04	0
S9	4	16	0.44	0.03	0
S10	4	85	0.53	0.01	NA
S11	4	19	1.24	0.06	1
S12	3	30	0.00	0.00	0
S13	3	40	0.00	0.00	-2
S14	4	49	0.35	0.01	2
S15	4	13	0.49	0.04	0
S16	4	53	0.49	0.01	0
S17	4	62	4.03	0.06	-5

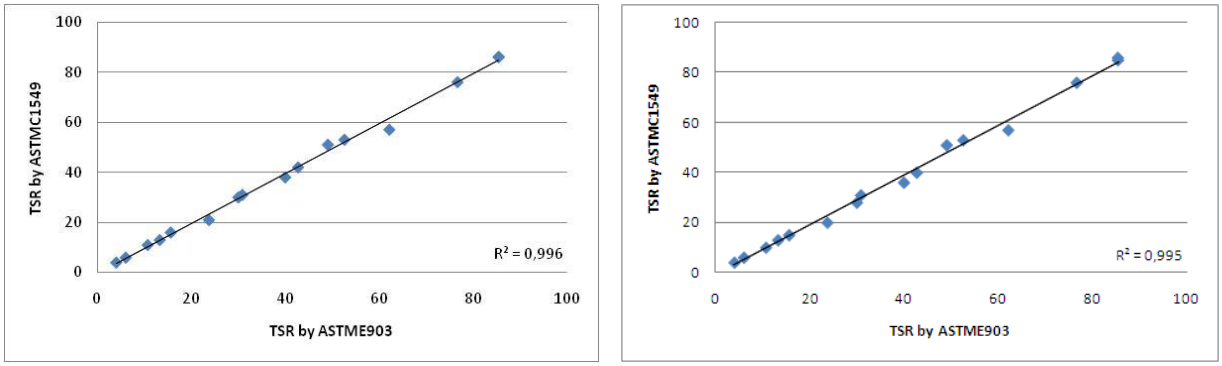

a) b)

Figure 1: Relation between the estimate of TSR by reflectomer (ASTMC1549) and spectrophotometer (ASTM E903, using the solar spectrum of a) ASTM E891 and b) ASTM G173)

Finally, comparing the TSR results for the samples obtained by the lab that has used the spectrophotometer with the large diameter integrating sphere with the average TSR values obtained by the labs using the small diameter integrating spheres, it was observed that the absolute differences between these values range between 0-1.1%TSR. The comparison of the TSR results for the samples obtained by the spectrophotometer with the large diameter integrating sphere with the average values obtained with the ASTMC1549 range between 0-4%TSR. These results and the R^2 values calculated (Figure 2) indicate a strong correlation between these test methods.

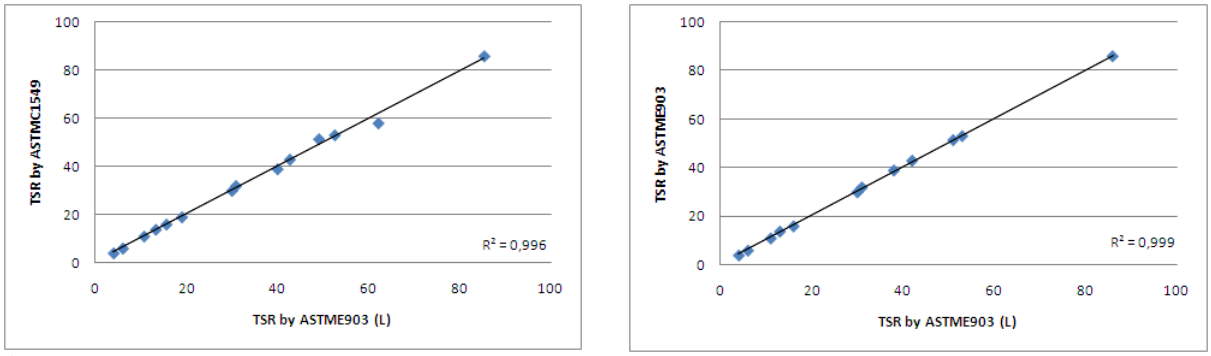

a) b)

Figure 2: Relation between the estimate of TSR a spectrophotometer with a large diameter integrating sphere (ASTM E903(L), using the solar spectrum of ASTM E891 and a) by reflectometer (ASTM C1549) and b) by a spectrophotometer with a small diameter integrating sphere (ASTM E903, using the solar spectrum of ASTM E891)

4.3 Infrared emittance evaluation

The first step of the statistical analysis consisted of detecting and removing outlier data (ISO Guide 43, 1997). The Grubb's test (significance level equal to 0.05) was used again to determine whether the larger or smaller observations in a set of data are an outlier. Three outliers were detected and removed from the datasets corresponding to the measurements with the D&S emissometer and two outliers were detected and removed from the datasets corresponding to the EN15976 measurements.

Table 6 contains the measurement results for the 17 samples as well as the average (AVG), standard deviation (STDEV) and the coefficient of variation (CV) that have been calculated from the different labs, for each method. N indicates the number of labs that have the performed the specific measurement on the specific sample.

The standard deviations range from 0.01 to 0.04 emittance units for the measurements of the emissivity with an average standard deviation of ±0.02. When considered in the context of the determined expanded uncertainty for this procedure (calculated at ±0.04 emittance units), the data indicate that there is good consistency in the measured thermal emissivity between the participating laboratories.

Also, as it can be observed few labs were able to measure the emissivity of the profiled tile samples. These measurements present several difficulties. First these are low conductivity samples and because they are large they cannot be applied on the D&S emissometer heat sink. Second, for the profiled tiles, the detector of the emissometer is not completely in contact with sample as there is not a wide enough flat area on the sample to perform the measurement correctly. For the first problem there exist a method called the "slide method" that is proposed by the manufacturer and it was followed by the labs. For the second problem, there is a special adapter that can be used that provides a smaller port size reducing errors due to the non-flat surface geometry by permitting good contact of the detector and sample. The remaining error due to the cylindrical shape can then be approximately corrected. Not all the labs were equipped with this adapter. The EN15976 emissometer is not fit for measuring low conductivity and profiled samples and only one lab tried to perform the measurement with instrument. This explains the high differences in the emissivity values measured by the two standards for the Samples S11 and S12

Finally, the relation between the determination of e by the ASTM C1371 and the EN 15976 is shown in Figure 2. The data shows that although there are differences as high as 0.08 in the absolute emissivity values achieved using the two different methods on the same samples, the overall trends are quite similar. The regression analysis gave an R^2 value of 0.991. The results

indicate a strong correlation between the two test methods. This means that both standards can be used to measure the emissivity of flat roof products.

Table 6: Results of the statistical evaluation of the infrared emittance measured according to the ASTM C1371 and the EN 15976

Samples	Infrared emittance (e)								Δe
	ASTMC1371				EN15976				ASTMC1371 – EN15976
	N	AVG	STDEV	CV	N	AVG	STDEV	CV	
S1	9	0.88	0.03	0.03	3	0.91	0.01	0.01	-0.03
S2	10	0.87	0.03	0.03	3	0.90	0.01	0.01	-0.03
S3	9	0.90	0.01	0.01	3	0.93	0.02	0.02	-0.03
S4	9	0.88	0.01	0.02	3	0.89	0.01	0.01	-0.01
S5	10	0.24	0.04	0.16	3	0.19	0.02	0.11	0.05
S6	9	0.89	0.02	0.03	3	0.93	0.03	0.03	-0.04
S7	9	0.87	0.02	0.03	3	0.92	0.01	0.01	-0.05
S8	9	0.91	0.02	0.03	3	0.95	0.01	0.01	-0.04
S9	9	0.91	0.02	0.02	2	0.95	0.00	0.00	-0.04
S10	9	0.88	0.02	0.02	2	0.93	0.00	0.00	-0.05
S11	4	0.90	0.03	0.03	1	0.97	NA	NA	-0.07
S12	5	0.92	0.03	0.03	1	1.00	NA	NA	-0.08
S13	6	0.83	0.02	0.03	2	0.83	0.01	0.02	0
S14	9	0.71	0.04	0.06	3	0.67	0.02	0.02	0.04
S15	9	0.86	0.01	0.01	3	0.90	0.02	0.02	-0.04
S16	9	0.85	0.02	0.03	3	0.89	0.01	0.01	-0.04
S17	8	0.06	0.01	0.24	3	0.05	0.02	0.33	0.01

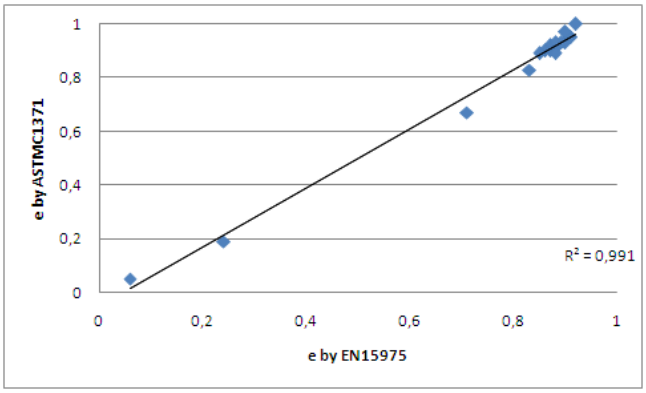

Figure 3: Relation between the determination of emissivity by the ASTM C1371 and the EN 15976.

5 CONCLUSIONS

This paper presents the results of an interlaboratory comparison aiming at investigating the suitability of different measurement methods and standards in determining the radiative properties, *i.e.* the solar reflectance and infrared emittance, of roofing materials. Regarding the measurement of reflectance using a spectrophotometer equipped with an integrating sphere and the differences in the average TSR values determined by using three different solar irradiance spectra (ASTM E891, ASTM G173 and EN 410), it was found that the observed differences are in the range of 0-4%TSR and they are more important for spectrally selective materials. These differences contribute to the total uncertainty of the measurement method indicating that the use of single solar spectrum would provide comparable and "fair" results in the framework of a product rating programme. It was also found that profiled and variegated

tile samples provided as full uncut tiles cannot be measured with a spectrophotometer. Further investigation is needed to assess the suitability of spectrophotometers in measuring the TSR of variegated and profiled samples if smaller dimension samples are provided. The regression analysis performed gave a strong correlation between the TSR determined by a spectrophotometer (ASTM E903) and a reflectometer (ASTM C1549). A strong correlation was also found between the determination of TSR with a spectrophotometer with a large diameter integrating sphere and by both reflectometers (ASTM C1549) and spectrophotometers with ~~a~~ small diameter integrating sphere. The ASTM C1371 and EN 15976 standards give comparable results for infrared emittance of flat roof products

6 ACKNOWLEDGEMENTS

This interlaboratory comparison testing has been conducted by the European Cool Roofs Council's Technical Committee with the valuable contributions of the ECRC members.

7 REFERENCES

ASHRAE 74 (1988), Method of measuring solar optical properties of materials, ISSN 1041-2336, ASHRAE, 1988.

ASTM C1371-04a(2010)e1 – Standard Test Method for Determination of Emittance of Materials Near Room Temperature Using Portable Emissometers, ASTM International, West Conshohocken, PA.

ASTM C1549-04(2004) – Standard Test Method for Determination of Solar Reflectance Near Ambient Temperature Using a Portable Solar Reflectometer, ASTM International.

ASTM E 903-96 (1996) – Standard Test Method for Solar Absorptance, Reflectance, and Transmittance of Materials Using Integrating Spheres, ASTM International.

ASTM E1585 (1993) – Standard Test Method for Measurement and Calculating Emittance of Architectural Flat Glass Products Using Spectrometric Measurements (withdrawn 2002) , ASTM International.

ASTM E1918-06 (2006) – Standard Test Method for Measuring Solar Reflectance of Horizontal and Low-Sloped Surfaces in the Field, ASTM International.

ASTM E891-87(1992) – Tables for Terrestrial Direct Normal Solar Spectral Irradiance Tables for Air Mass 1.5, ASTM International. [Note: Currently a withdrawn standard]

ASTM G159-98(1998) – Standard Tables for References Solar Spectral Irradiance at Air Mass 1.5: Direct Normal and Hemispherical for a 37° Tilted Surface, ASTM International.

ASTM G173-03(2008) – Standard Tables for Reference Solar Spectral Irradiances: Direct Normal and Hemispherical on 37° Tilted Surface, ASTM International.

CIE 130(1998), Practical methods for the measurement of reflectance and transmittance, ISBN 978 3 900734 88 6.

CRRC-1 Standard (2008), 2008 Cool Roof Rating Council, Inc. Available on line at: http://coolroofs.org/documents/CRRC-1-2012_Standard.pdf

EN 410 (1998) – Glass in Building – Determination of luminous and solar characteristics of glazing.

EN673 (2002):2002 – Glass in building – Determination of thermal transmittance (U value) – Calculation method.

ISO 10292(1994) – Glass in building – Calculation of steady-state U values (thermal transmittance) of multiple glazing.

EN 12898 (2001) – Determination of the emissivity, European Committee for Standardisation, CEN/TC 129.

EN 14500 (2008) – Blinds and shutters – Thermal and visual comfort – Test and calculation methods.

EN 15976(2011) – Flexible sheets for waterproofing. Determination of emissivity

ISO 9050 (1990) – 'Glass in Building: Determination of Light Transmittance, Solar Direct Transmittance, Energy Transmittance and Ultra-violet Transmittance, and Related Glazing Factors' Genève, Switzerland, 1990.

ISO 13528 (2005) – Statistical methods for use in proficiency testing by interlaboratory comparisons, Genève, Switzerland.

ISO/IEC Guide 43(1997) – Proficiency testing by interlaboratory comparisons, Genève, Switzerland.

Websites:

Cool Roof Rating Council: http://coolroofs.org/
European Cool Roofs Council: http://coolroofcouncil.eu/
IEE Project “Cool Roofs”: http://www.coolroofs-eu.eu/
Devices and Services Co.: http://www.devicesandservices.com/prod03.htm
INGLAS: http://www.tir100.de/
LEED: http://www.usgbc.org/leed
U.S. EPA Energy Star:
http://www.energystar.gov/index.cfm?fuseaction=find_a_product.showProductGroup&pgw_code=RO

DEVELOPMENT AND ANALYSIS OF INORGANIC COATING FOR ENERGY SAVING FOR BUILDINGS

Konstantinos Gobakis[1], Dionysia Kolokotsa[1], Noni Maravelaki-Kalaitzaki[2], Stratos Lionakis[2], Vasilios Perdikatsis[3], Matheos Santamouris[4]

1 School of Environmental Engineering, Technical University of Crete Kounoudipiana Crete, Greece

2 School of Architecture, Technical University of Crete Kounoudipiana Crete, Greece

3 School of Mineral Resources Engineering, Technical University of Crete Kounoudipiana Crete, Greece

4 Physics Department Section of Applied Physics, Physics Department National and Kapodistrian University of Athens Build. Physics 5 15784 Athens, Greece

ABSTRACT

Buildings account for 40% of Europe's energy use and a third of its greenhouse gas emissions. Building materials currently used in the construction of building have low solar reflectance, leading to an increase of surface temperature of the building. The aim of the present study is to develop various inorganic and colour change coatings for increasing the solar reflectance of buildings. A series of inorganic coatings are examined and tested. Their thermal properties are estimated by infrared thermography, surface temperature measurements, emissometer and chemical properties by X-ray diffraction and Fourier transform infrared spectroscopy.

KEYWORDS

Cool materials, inorganic, thermochromic

Heat island is the more documented climatic change phenomenon (Cartalis C. 2001). Important research has been carried out to document its strength and its influence on the urban climate (Santamouris 2007; Akbari et al. 1999). Heat island intensity in hot climates may rise up to 10^{o}C (Livada et al. 2002; Mihalakakou et al. 2002) , resulting in increased discomfort, higher pollution levels while it has a serious impact on the cooling energy consumption of buildings (Hassid et al. 2000). Increased urban temperatures, exacerbate the peak electricity demand for cooling and decrease the efficiency of air conditioners, while it reduces considerably the cooling potential of natural and night ventilation techniques (Geros V. 2005) and increases the urban ecological footprint.

Another significant effort towards energy conservation for buildings and urban structures is the research for cool materials (e.g. reflecting tiles, membranes, colors) and coatings as a passive cooling technique (Synnefa et al. 2007; Oke et al. 1991; Zinzi 2010). Those materials target to minimize the surface temperature in roofs, masonries and pavements through the increase of solar reflectance and infrared emittance(Asaeda et al. 1996). Coatings with specific optical properties, such as increased reflectance and/or emittance resulting in lower surface temperatures are developed and tested. Even though the tested coatings range from cool materials, thermochromic, phase change materials, etc. (Bretz & Akbari 1997; Karlessi et al. 2009). Nevertheless, corrosion can effectively diminish their performance. This issue intensifies the need for resistant materials. Based on the above, the study of lime renders', mortars' and natural paints' thermo-physical properties are of a major importance. Although various studies can be found (Veiga et al. 2009; Hernández-Olivares & Mayor-Lobo 2011) that quantify their density, thermal conductivity, etc., there is a significant lack of information concerning their optical properties and their contribution to energy conservation. While the

optical properties of common colorants and materials for the built environment (Doulos et al. 2004; Papadopoulos et al. 2008) are studied in the past, the natural materials and coatings' optical characteristics and their potential role as a passive solar technique is still under study.

To this end, the aim of the present work is to examine the performance of mineral-based coatings as a passive solar technique that contributes to buildings' energy efficiency. This is achieved by investigating the optical properties and thermal behavior of these coatings in an attempt to lower the surface temperature of the built environment thus increasing energy efficiency. Mortars and plasters consisting of lime and/or natural hydraulic lime with pozzolanic additions as binders, inorganic additive such as calcite powder and aggregates of carbonate nature are designed and tested. The surface temperature of the developed samples is measured using infrared thermography and surface thermocouples. A series of measurements is also performed for the evaluation of the solar reflectance and infrared emittance of the samples. The energy efficiency of the developed samples is finally investigated using simulation techniques.

1 MATERIALS AND METHODS

1.1 Design concepts and technical specifications of coatings

The studied plasters are commonly used either in the building construction sector or in the restoration of historic buildings. The aim of the present section is to describe the development procedure and technical specifications of the various mineral based samples tested.

The approach of making the samples is similar to that is used in the real world with some modifications in order to shorten the developing time. The development of the samples is separated into two different stages. The first stage of process was the preparation of the substrate. Sample carriers were constructed with dimensions 9cm x 9cm x 3cm from sheet metal with thickness of 0.5mm. The substrate was created inside the carriers with a thickness of 2.7 – 2.8 cm using 28% Portland cement, 56% limestone and 16% water (Figure). On the top, a large amount of cotton was placed. The cotton was regular moistened with water to ensure proper curing of cement for a five days period. The second stage of the proses was the development of various coactions on top of the substrate which will be analytical presented later.

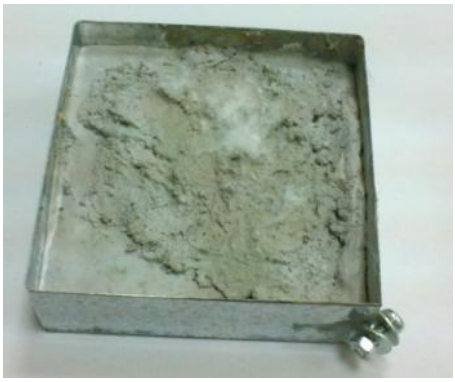

Figure 1 Sample carrier with substrate

1.2 Mineral-based coating binders lime renders and paintings

1.2.1 Mineral based binders

The binders used are made of natural hydraulic lime (NHL), produced by calcining agillaceous or siliceous lime stones at temperatures of 900 - 1200 °C. These temperatures are higher than those typically used for the production of quick lime (CaO), typically around 1000 °C, but much lower than those used to produce cement (typically around 1400 °C). Natural hydraulic lime conforming to EN459 as a moderately hydraulic lime, is typically used for repointing/rendering and building works on most masonry types. These limes have become increasingly popular over the last decade due to their superiority in strength and weathering resistance compared to fat limes. Pozzolan or pozzolanic materials can react with calcium hydroxide to form hydraulic compounds acting as binders, which enhance the strength gain of hydrated, hydraulic and NHL mortars. In particular, pozzolan additions to a lime arc indicated by the letter Z following the lime designation e.g. NHL-3.5Z (BS EN 459-1:2001).

The calcined temperature of the raw materials of NHL is much lower than the required for the cement. Therefore, NHL can be considered as more environmentally-friendly hydraulic binder, because of the lower energy required to be produced comparing to the Ordinary Portlant Cement (OPC) and other cements.

1.2.2 Marble powders

Two different white marble powders were used on this experiment. The first one is a dolomite marble powder (DMP) (Ganguly 2010) originated from Kavala, Greece. The grading is following the standard EN13139 with maximum particle size of 250μm. X-Ray Diffraction (XRD) was performed for the verification of its composition ().

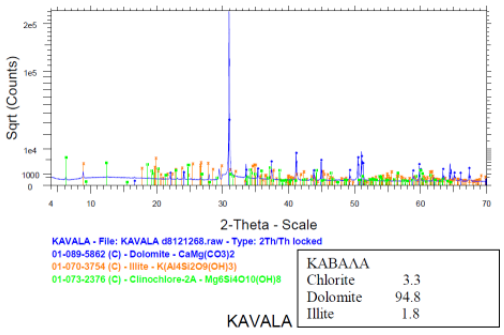

Figure 2 XRD dolomite marble powder

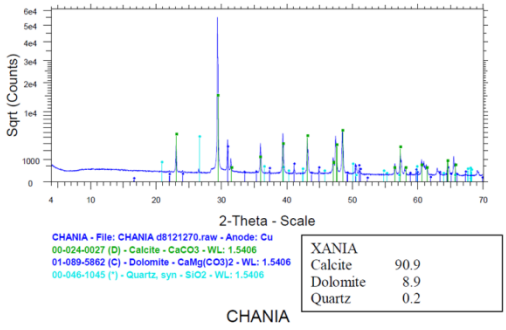

Figure 3 XRD limestone marble powder

The second is a limestone marble powered (LMP) originated from Chania, Greece. The grading is following the standard EN13139 with maximum particle size of 250μm. X-Ray Diffraction (XRD) was also done for the second marble powder (

Figure).

Among the specific characteristics of these renders it can be mentioned the high water permeability and resistance to UV radiation, weathering parameters and fungi's growth.. All these properties establish the above mentioned lime renders as appropriate finishing layers for masonry applications

1.2.3 Glass beads

The glass beads (GB) are predominantly used in road markings and have the ability to reflect incident radiation. They are made of SiO_2 (71-73%), Na_2O (13-15%), MgO (3-5%),CaO (8-10%), Al_2O_3 (0.5-2%) other (<2%) with a refractive index of 1.5 to 1.55, diameter of 180 – 850μm and roundness >80% following the EN 1424 standard. This sample was not tested by XRD. Because glass is amorphous and due to the fact that was accompanied by certificate by the manufacturer.

Figure 4 Glass beads

1.2.4 Inorganic thermochromic pigment

Thermochromic is called the chemical whose colour depends depending on the ambient temperature. Following literature survey inorganic compounds were chosen for the specific research. The chemical competition of this compound is $(Et_2NH_2)_2CuCl_4$. The compound is showing a vivid green colour at a low temperature and a bright yellow colour in relatively high ambient temperatures (Figure 5). The pigment's composition was verified using XRD. Using the crystal structure of the pigment, a simulated pattern were produced and compared with the experimental data.

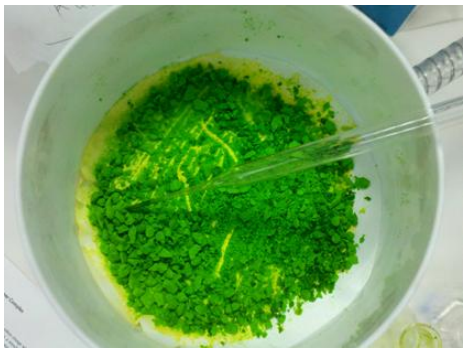

Figure 5 Thermochromic pigment in ambient temperature

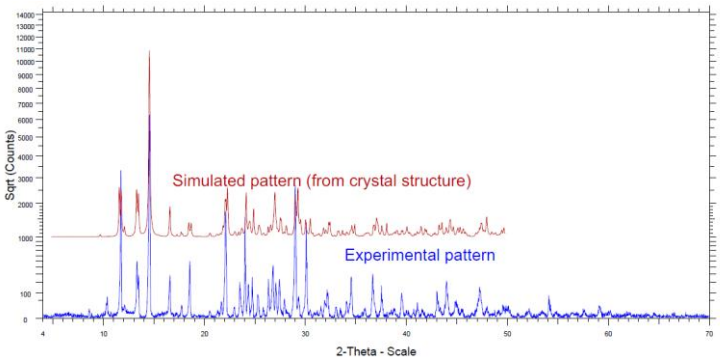

Figure 6 XRD of thermochromic pigment

1.3 Creation of samples

The sample names and composition are tabulated in Table 1. All the samples were cured for one month in stable humidity and temperature conditions (RH = 50 ± 5% and T = 22 ± 2^{o}C). A smooth and even surface was achieved for all samples with sanding proses (Figure 7). The thermochromic pigment was applied by a water solution (**Error! Reference source not found.**7).

Figure 7 Examined samples at the experimental site

Table 1: Composition, codenames of the studied samples.

Sample Code	Finishing	Ratio per volume	Type	Group
WCM-DMP	WCM/L/DMP	1/1/2	Render	1
WCM-LMP	WCM/L/LMP	1/1/2		
NHL-DMP	NHL/L/DMP	1/1/2		
NHL -LMP	NHL/L/LMP	1/1/2		
NHL -LMP-GB	NHL/L/LMP/GB	1/1/1.8/0.2		2
NHL -DMP-GB	NHL/L/DMP/GB	1/1/1.8/0.2		
P-TC	P	1	Paint	3

NHL, natural hydraulic lime NHL with pozzolanic additives; P, plaster; WCM, white Portland cement; L, hydrated lime; W, water.

Figure 8 Preparing thermochromic sample

2 EXPERIMENTAL PROCEDURE

2.1 Methodology and instrumentation

The analysis of the coatings' optical and thermal characteristics is divided into four phases:

1. K-type surface temperature thermocouples arc then used to measure the various samples surface temperature.
2. The solar reflectance and infrared emittance arc measured using a Cary 5000 spectrophotometer with integrating sphere and
3. Devices and Services emissometer.

The surface mounted thermocouples arc characterized by:

- Resolution: -200 to +200 (0.1 °C).
- Operating temperature and humidity: 0-50 °C and 0- 80%.
- Accuracy: -200 °C to 200 °C (±2% reading +1 °C)

The surface mounted K type thermocouples include an embedded thin insulation layer by silicon rubber to avoid the solar radiation influence. A small amount of thermal paste was placed between the K type thermocouple and the sample surface. The solar reflectance and infrared emittance arc measured using a Cary 5000 spectrophotometer with integrating sphere and a Devices and Services emissometer respectively.

3 RESULTS AND DISCUSSION

3.1 Results of surface temperatures measured using K type thermocouples

A series of surface measurements are performed using the K-type thermocouples. Due to limited number of data loggers the surface temperature measurements took place during different days of summer 2013. In order to be able to compare the results, the difference between the surface temperature of the samples and the air temperature is calculated and utilized. Also for competition reasons a Portland cement substrate were present on all measurements and is plotted on all figures. The results of the 1st Group are depicted in Figure 9. The samples of the 1st Group with the lowest surface temperature are NHL-DMP followed by WCM-DMP with a difference of 2.5°C from the heist surface temperature differences witch was recorded for WCM-LMP. Also the lowest average temperature differences were observed by NHL-DMP followed by WCM-DMP with a difference of almost 1°C witch was recorded for WCM-LMP.

The surface temperature differences for the 2nd Group are depicted on Figure 10. Regarding this group glass, beads were inserted as part of the composition. The NHL – DMP-GB had better performance than NLG-LMP-GB. Also NHL-DMP-GB had the lowest temperature of all the samples that were tested.

The surface temperature differences for the 3rd Group are depicted on Figure 11 Surface temperature measurement of the 3st Group The P-TC demonstrated lower temperature compared to the plaster. Also due to the very calm summer in the experiment location there was not possible the turning temperature to be reached.

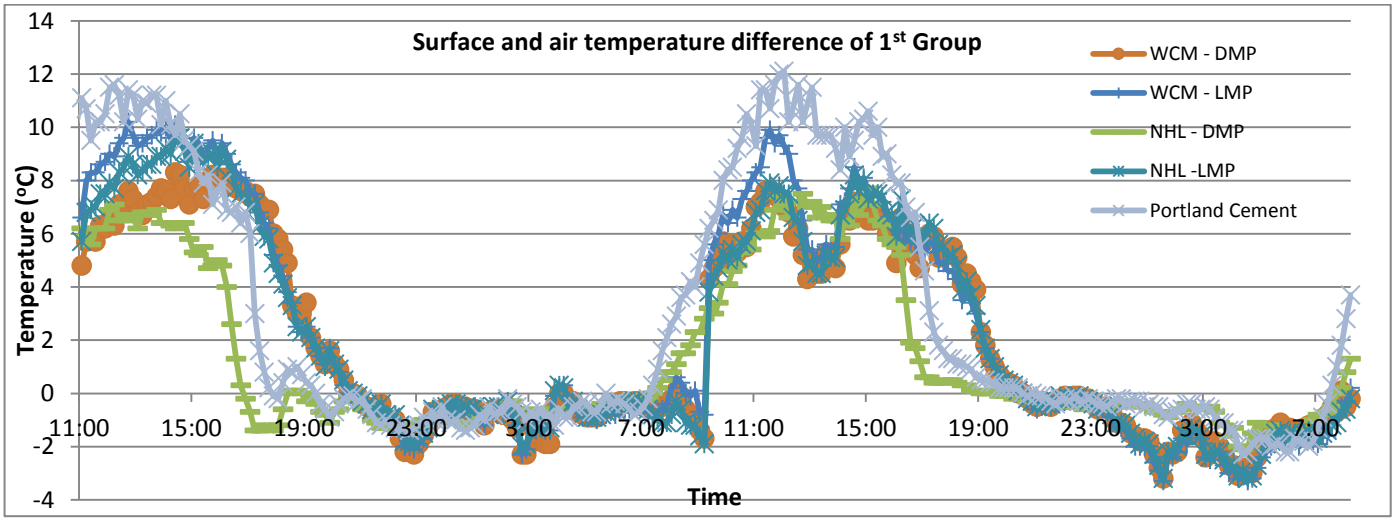

Figure 9 Surface temperature measurement of the 1st Group

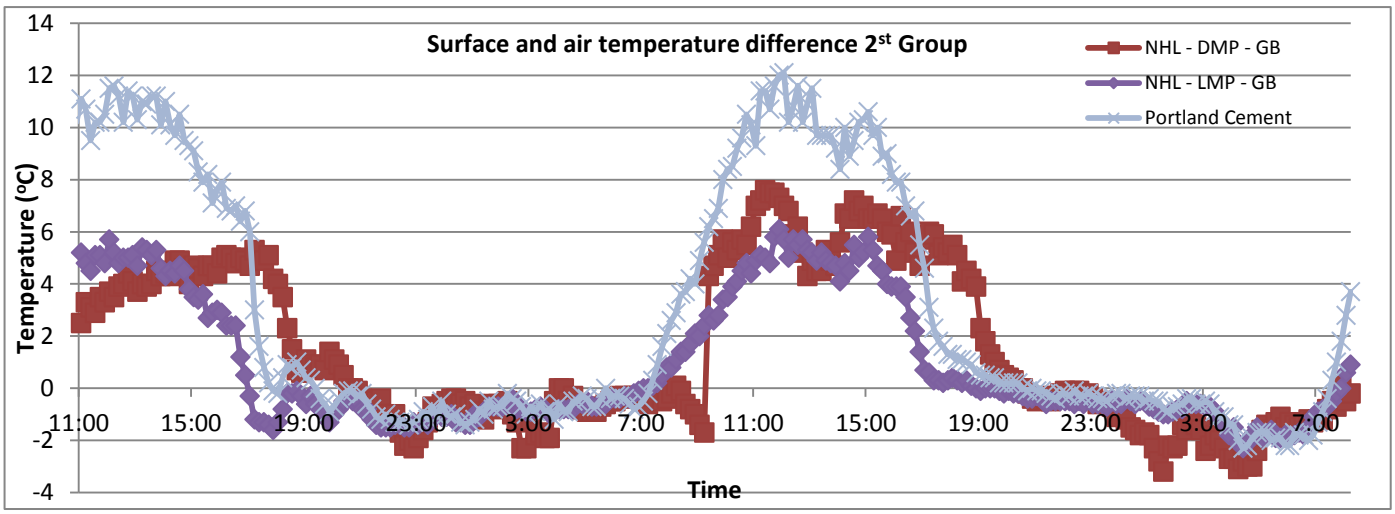

Figure 10 Surface temperature measurement of the 2st Group

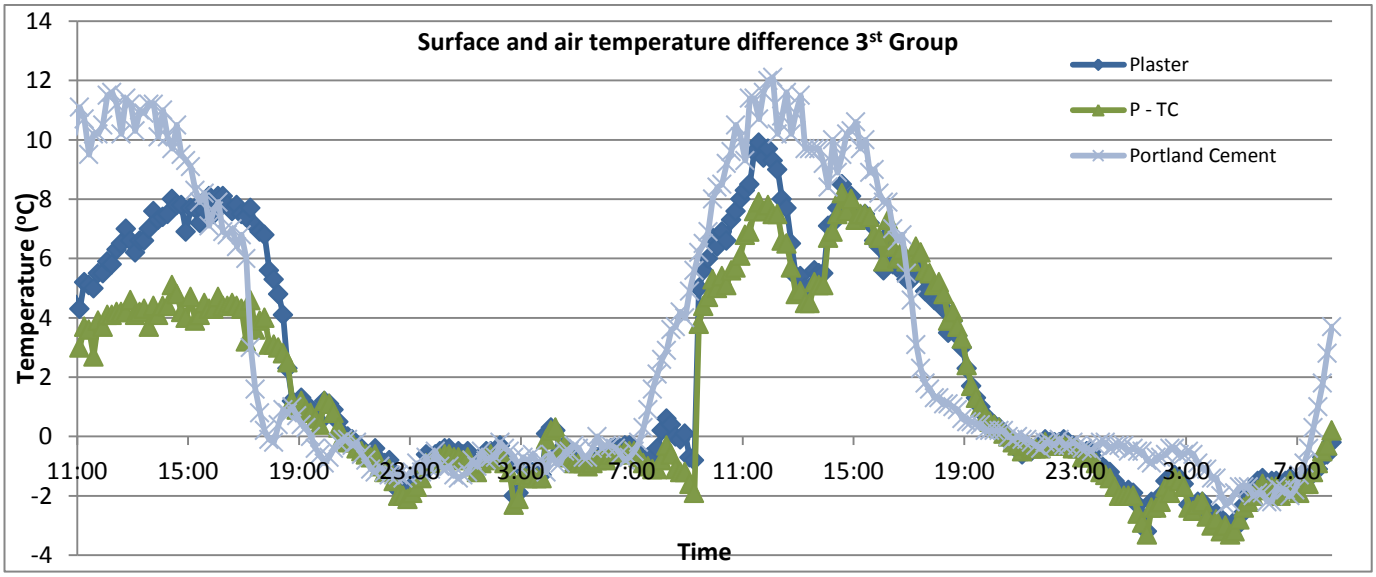

Figure 11 Surface temperature measurement of the 3st Group

3.2 Experimental results of the solar reflectance and infrared emittance

In this specific section the optical properties i.e. the solar reflectance and infrared emittance of the samples are measured. The sola reflectance results for the first, second and third group are depicted in Figure 12 and Figure 13. The total, infrared (IR), ultraviolet (UV), visible (VIS) solar reflectance, as well as infrared emittance are also tabulated in Table 2. The results for all samples show increased SR_{IR} which is in accordance with the surface temperature measurements.

The samples with increased solar reflectance and infrared emittance are with white cement. The additional of glass beads give a small increase on solar reflectance. The addtition of the thermochromic compound did not change the solar reflectivity of the plaster.

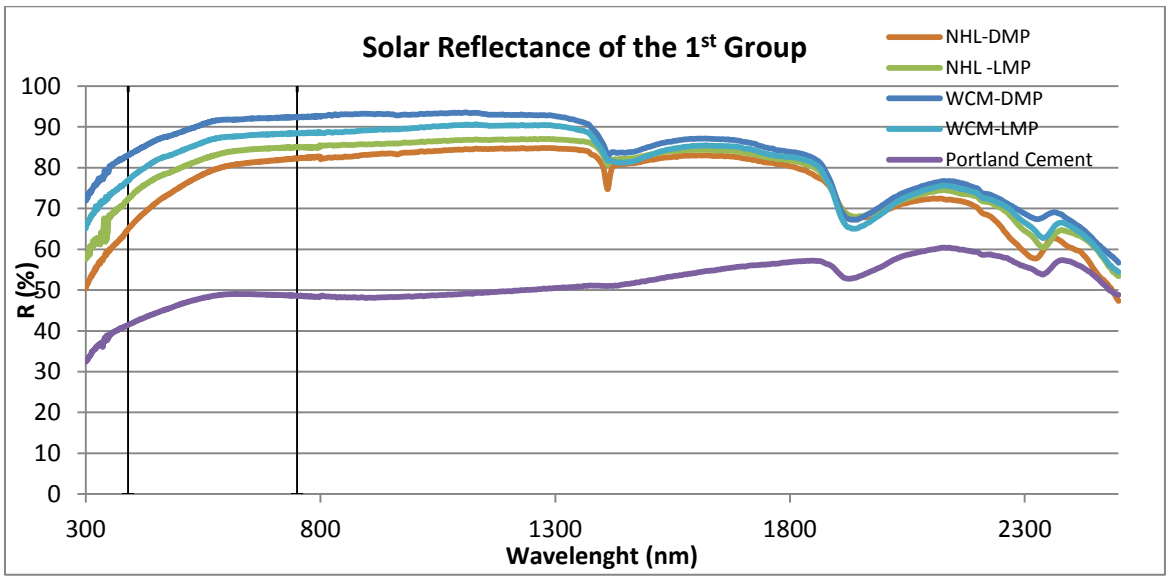

Figure 12 Solar Reflectance of the 1st Group

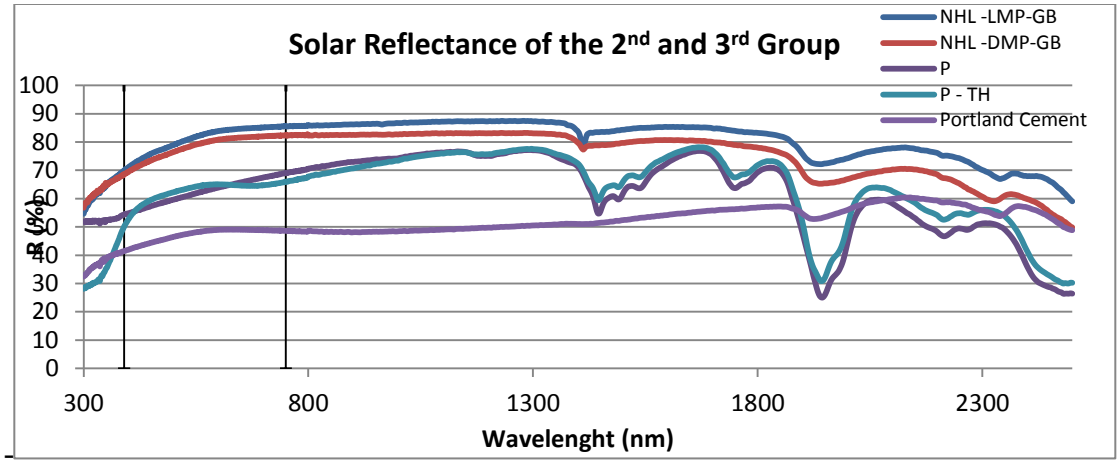

Figure 13 Solar Reflectance of the 2nd and 3rd Group

Table 2 Solar reflectance and infrared emittance of the various samples.

Sample Name	SR (%)	SR_{IR} (%)	SR_{VIS} (%)	SR_{UV} (%)	E (%)
WCM-DMP	89	90	90	78	0.83
WCM-LMP	86	86	85	71	0.81
NHL-LMP	82	84	81	64	0.88
NHL–DMP	79	81	77	57	0.88
NHL-LMP-GB	83	85	81	62	0.88
NHL-DMP-GB	80	81	78	63	0.85
P	66	70	62	52	0.85
P+TH	66	69	63	34	0.87
Portland Cement	49	50	47	37	0.78

4 CONCLUSIONS

The present study examined the thermal and optical properties, of a series of mineral based coatings. By examining the overall experimental results, the samples with dolomic marble powder where with natural hydraulic lime with pozzolanic additions. The addition of glass beads improved the overall performance of the sample. Therefore, the use of such coatings can be included in hot climates' construction due to their thermal performance, UV behavior and chemical composition.

The first experiments with the inorganic thermochromic pigment were very promising. Next the stability of long term exposure to solar radiation must be examined.

5 ACKNOWLEDGEMENTS

The research leading to these results has received funding from the Technical University of Crete, Research Committee under grant agreement n° 80710 (Development of cool materials for energy savings in buildings).

6 REFERENCES

Akbari, H., Konopacki, S. & Pomerantz, M., 1999. Cooling energy savings potential of reflective roofs for residential and commercial buildings in the United States. *Energy*, 24(5), pp.391–407.

Asaeda, T., Ca, V.T. & Wake, A., 1996. Heat storage of pavement and its effect on the lower atmosphere. *Atmospheric Environment*, 30(3), pp.413–427.

Bretz, S.E. & Akbari, H., 1997. Long-term performance of high-albedo roof coatings. *Energy and Buildings*, 25(2), pp.159–167.

Cartalis C., S.A.P.M.T.A.S.M., 2001. Modifications in energy demand in urban areas as a result of climate changes: An assessment for the southeast Mediterranean region. *Energy Conversion and Management*, 42(14), pp.1647–1656.

Doulos, L., Santamouris, M. & Livada, I., 2004. Passive cooling of outdoor urban spaces. The role of materials. *Solar Energy*, 77(2), pp.231–249.

Ganguly, A., 2010. *Fundamentals of Inorganic Chemistry*, Pearson Education India. Available at: http://books.google.gr/books?id=lTcNk8MsHrkC.

Geros V., S.M.K.S.T.A.P.N., 2005. On the cooling potential of night ventilation techniques in the urban environment. *Energy and Buildings*, 37(3), pp.243–257.

Hassid, S. et al., 2000. Effect of the Athens heat island on air conditioning load. *Energy and Buildings*, 32(2), pp.131–141.

Hernández-Olivares, F. & Mayor-Lobo, P., 2011. Experimental assessment of commercial one-coat renders for buildings faades. *Construction and Building Materials*, 25(1), pp.156–162.

Karlessi, T. et al., 2009. Development and testing of thermochromic coatings for buildings and urban structures. *Solar Energy*, 83(4), pp.538–551.

Livada, I. et al., 2002. Determination of places in the great Athens area where the heat island effect is observed. *Theoretical and Applied Climatology*, 71(3-4), pp.219–230.

Mihalakakou, G. et al., 2002. Application of neural networks to the simulation of the heat island over Athens, Greece, using synoptic types as a predictor. *Journal of Applied Meteorology*, 41(5), pp.519–527.

Oke, T.R. et al., 1991. Simulation of surface urban heat islands under "ideal" conditions at night part 2: Diagnosis of causation. *Boundary-Layer Meteorology*, 56(4), pp.339–358.

Papadopoulos, A.M., Oxizidis, S. & Papathanasiou, L., 2008. Developing a new library of materials and structural elements for the simulative evaluation of buildings' energy performance. *Building and Environment*, 43(5), pp.710–719.

Santamouris, M., 2007. Heat island research in Europe: the state of the art. *Advances in Building Energy Research*, 1(1), pp.123–150.

Synnefa, A., Santamouris, M. & Akbari, H., 2007. Estimating the effect of using cool coatings on energy loads and thermal comfort in residential buildings in various climatic conditions. *Energy and Buildings*, 39(11), pp.1167–1174.

Veiga, M.R., Velosa, A. & Magalhães, A., 2009. Experimental applications of mortars with pozzolanic additions: Characterization and performance evaluation. *Construction and Building Materials*, 23(1), pp.318–327.

Zinzi, M., 2010. Cool materials and cool roofs: Potentialities in Mediterranean buildings. *Advances in Building Energy Research*, 4(1), pp.201–266.

STUDY ON THE APPROPRIATE SELECTION OF URBAN HEAT ISLAND MEASURE TECHNOLOGIES TO URBAN BLOCK PROPERTIES

Hideki Takebayashi[*1], Yutaro Kimura[2] and Sae Kyogoku[2]

1 Kobe University
Rokkodai 1-1, Nada
Kobe 657-8501, Japan
**Corresponding author: thideki@kobe-u.ac.jp*

2 Kobe University
Rokkodai 1-1, Nada
Kobe 657-8501, Japan

ABSTRACT

Toward the appropriate selection of urban heat island measures technology in the street canyon, the introduction effects of the technologies in the typical street canyon are analysed by the model calculation. It is appropriate to use street trees for the improvement of the thermal environment on the sidewalk and high reflectance paint or water-retentive pavement for the reduction of surface temperature on the roadway. Reduction of solar radiation gain to the sidewalk pavement surface is dependent on the location and area of the shadows by street tree. Shadows by street tree are likely to occur on the northern sidewalk of the east-west road than the eastern (or western) sidewalk of the north-south road. While the shadow by the street tree is occurred on the sidewalk, the area of the shadow is proportional to the square of the width of tree crown (the radius) and inversely proportional to the distance of each tree. It is necessary to be considered a priority according to the road orientation and time zone primarily used by pedestrian.

KEYWORDS

Urban Heat Island, Radiant Environment, Street Canyon, Properties of Urban Block

1 INTRODUCTION

Various urban heat island measure technologies have been proposed and the performance of each technology has been evaluated. Toward the appropriate selection of urban heat island measures technology, relationship between where the technology has been introduced and the effect by the introduction of technology must be studied. In order to understand where these technologies should be introduced, the relationships between the properties of urban canopy components and the radiant environment in an urban street canyon are examined in previous paper by the authors (Takebayashi and Moriyama, 2012). As a consequence, the top priorities for the implementation of urban heat island measures are the roofs, the north sides of east-west roads, and the center of north-south roads. From the view point of introduction of appropriate technique for each place, it is analysed the relationship between benefits by heat island measure technique and places it was introduced. Objective techniques are street tree, green wall, high reflectance paint and water-retentive pavement, which are pointed out benefits are relatively large in previous study (Takebayashi and Moriyama, 2012). Objective places are road and wall surface. The roof surface has the highest priority for urban heat island measure due to the highest solar radiation gain. However, surface temperature distribution is relatively small because the shading effects by the penthouse or surrounding

buildings are not so remarkable. So, the benefits by the heat island measure technique are as similar as the results of previous study which has been carried out on the horizontal surface (Takebayashi and Moriyama, 2007). The evaluation index is surface temperature distribution on the road and wall. Surface heat budget and radiation transfer are calculated in the typical street canyon model. The parameters of the street canyon are orientation and width of the street.

2 RADIATION TRANSFER AND SURFACE HEAT BUDGET MODEL IN THE URBAN CANOPY

2.1 Outline of the calculation model

The urban canopy components—roofs, walls, and roads—are divided into grids, and for each surface, direct, diffuse, and reflected solar radiation and infrared radiation are calculated. Sky view factors from each surface and view factors between the surfaces are calculated by the Monte Carlo method. Mutual radiation between the surfaces is calculated using Gebhart's absorption factors. It is assumed that all surfaces are uniform diffuse reflectors and only one reflected radiation flux is included within the calculation. The objective condition is a sunny summer day, when the normal direct solar radiation is calculated by Bouguer's equation, the horizontal diffuse solar radiation is calculated by Nagata's equation, and the infrared radiation from the sky is calculated by Brunt's equation. The surface heat budget for each surface is calculated and the one-dimensional heat conduction equation is estimated for each wall, roof, and road.

Surface heat budget on each surface:

$$R_n = V + lE + A \tag{1}$$

where R_n is net radiation [Wm^{-2}], V is sensible heat flux [Wm^{-2}], lE is latent heat flux [Wm^{-2}], and A is conduction heat flux [Wm^{-2}].

One-dimensional heat conduction equation:

$$C_p\gamma \frac{\partial T}{\partial t} = \lambda \frac{\partial^2 T}{\partial x^2} \tag{2}$$

where $C_p\gamma$ is heat capacity [$Jm^{-3}K^{-1}$)]; λ is thermal conductivity [$Wm^{-1}K^{-1}$]; T is the temperature of the wall, roof, or road [K]; t is time [s]; and x is the distance to the wall, roof, or road [m].

A typical sunny summer day, August 4, 2011, was set for the weather conditions. It was selected from hot days Japan meteorological agency issued a warning. The criteria is more than 35°C in daily maximum air temperature. Observation data that were recorded at the Kobe meteorological observatory (34°41.8′ N, 135°12.7′ E) were used. Local distribution of wind velocity in the urban canyon was not considered and the convective heat transfer coefficient was assumed to be a constant with a value of 12.5 $Wm^{-2}K^{-1}$. It can be discussed mainly the impact of radiation heat exchange in the street canyon. Initial surface and inner temperatures of each component were set at 27°C, and the calculations were repeated twice on the same day to consider the effects of heat storage.

The walls and roofs were assumed to be 0.3 mm thick concrete and the roads were assumed to have 0.2 mm thick asphalt and 0.35 mm thick soil. Parameters regarding heat conduction are set based on previous study results by the authors (Takebayashi and Moriyama, 2012); solar reflectance, emissivity, thermal conductivity, heat capacity of concrete are 0.2, 0.95, 1.64 $Wm^{-1}K^{-1}$, 1.93 $MJm^{-3}K^{-1}$, and solar reflectance, emissivity, thermal conductivity, heat capacity of asphalt are 0.1, 1.0, 0.74 $Wm^{-1}K^{-1}$, 2.1 $MJm^{-3}K^{-1}$, and thermal conductivity, heat capacity of soil are 0.62 $Wm^{-1}K^{-1}$, 1.58 $MJm^{-3}K^{-1}$.

2.2 Outline of the urban canopy model and heat island measure techniques

From the results of the previous study, the characteristics of road surface temperature in the street canyon can be explained by the typical two-dimensional street canyon model represented by the building height and road width. It is necessary to distinguish east-west road and north-south road, and thermal characteristics of both roads are overlaid on the intersection. In this paper, north-south road and east-west road whose width is 20 m (narrow), 30 m (middle), 50 m (wide) are selected to the objective road, with constant building height 30 m, by referring to the typical urban block of Kobe city. They are treated as a two-dimensional street canyon model. However, because the street trees are assumed to be planted continuously along the road in the two-dimensional street canyon model, the examination of changing the arrangement interval of the street tree is carried out in the next chapter. Outline of street canyon model with street tree and green wall is shown in figure 1. Both side buildings with 30 m height are located by 1 m set back from the road, and the sidewalk with 3 m width is in the front of them. Street tree with 2 m width is located between the roadway and sidewalk. The widths of the roadway are 10 m, 20 m, 40 m and it is equally divided to three for analysis. Mesh interval for calculation is 0.5 m constant in both horizontal and vertical directions.

Objective heat island measure techniques are street tree, green wall, high reflectance paint and water-retentive pavement. The height of street tree, the height under the tree crown, solar radiation shielding factor of leaves, evaporative efficiency of leaves are 10 m, 2.5 m, 0.8, 0.3, respectively. The height of green wall is 5 m which is 0.5 m away from the wall. Solar radiation shielding factor of leaves, evaporative efficiency of leaves are 0.8, 0.3, respectively. The reflectance of high reflectance paint is 0.4 which is painted on asphalt road surface. The evaporative efficiency of water-retentive pavement is 0.3 which is changed from asphalt road surface. It is continuous water supply type pavement with the irrigation equipment.

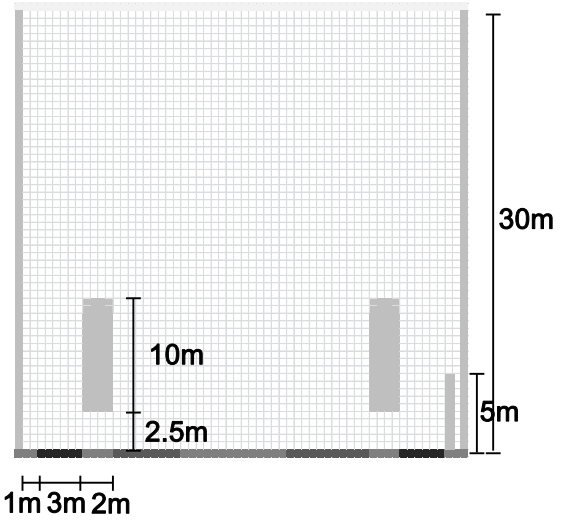

Figure 1: Outline of street canyon model with street tree and green wall

2.3 Calculation results

The daily mean surface temperature is averaged along each side sidewalk, each side roadway and center of roadway, from the calculation results of introducing the countermeasure technology. And, the daily mean wall surface temperature is used for the green wall examination. Benefit of each technology is occurred at different time depending on the introducing location. Some technologies influence on night temperature by the thermal storage of road and wall materials. In this study, it is assumed that the daily mean surface temperature represents not only the thermal environment during the day, but also heat storage effect during the night. For example, the benefit by high reflectance paint is about 7 K during the day and about 0.5 K during the night on the center of the north-south road, then it is about 1 K on daily average.

Daily average surface temperature reduction by street tree is shown in figure 2. The benefit on the northern sidewalk of the east-west road is greater than the others. The benefit on the eastern and western sidewalk of the north-south road is greater than the others. It means that the improvement of thermal environment on the pedestrian space is remarkable.

Daily average surface temperature reduction by green wall is shown in figure 3. The benefit of the east-west road on the north side wall is larger than the south side wall. And the difference due to the road width is not sure. The difference of the benefit of the north-south road between the west and east side wall is small. And, the benefit on large road width is larger than the others. The benefit on the wall which is received large solar radiation is greater than the others.

Daily average surface temperature reduction by high reflectance paint and water-retentive pavement are shown in figures 4 and 5. The benefits by both high reflectance paint and water-retentive pavement are larger on the center of north-south road and from the center to northern side of east-west road where the solar radiation gain is large. The difference of benefits by between water-retentive pavement and high reflectance paint is depending on the evaporation efficiency of water-retentive pavement, solar reflectance of high reflectance paint and weather condition.

Daily average surface temperature reduction by street tree, high reflectance paint and water-retentive pavement are shown in figure 6. As described above, the benefit by both high reflectance paint and water-retentive pavement appears mainly on the roadway. On the other hand, the benefit by street tree is concentrated mainly on the sidewalk. Since the benefit by street tree is caused by solar radiation shielding by the tree crown, the shadows by canopy occur mainly on the sidewalk. Therefore, it can be said that the introduction of water-retentive pavement and high reflectance paint on the roadway is more appropriate for the road surface temperature reduction and the introduction of roadside tree is more appropriate for the thermal environment improvement on the sidewalk. Technology by solar radiation shielding on the wall such as green wall is suitable to the wall surface temperature reduction.

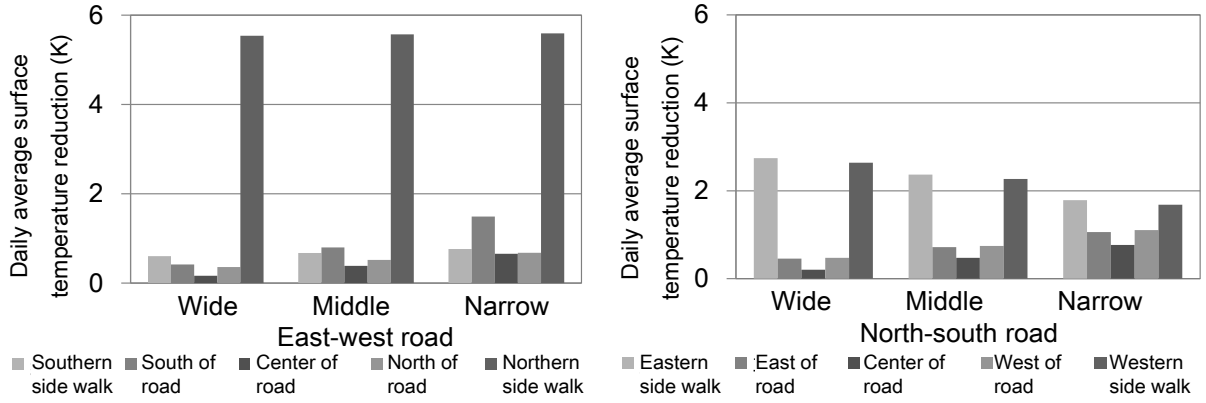

Figure 2: Daily average surface temperature reduction by street tree

(Left: east-west road, Right: north-south road)

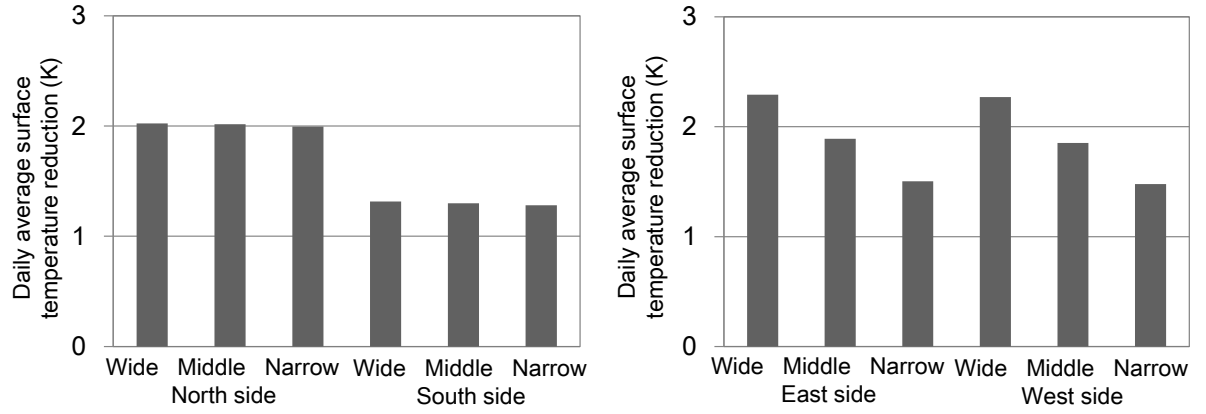

Figure 3: Daily average surface temperature reduction by green wall

(Left: east-west road, Right: north-south road)

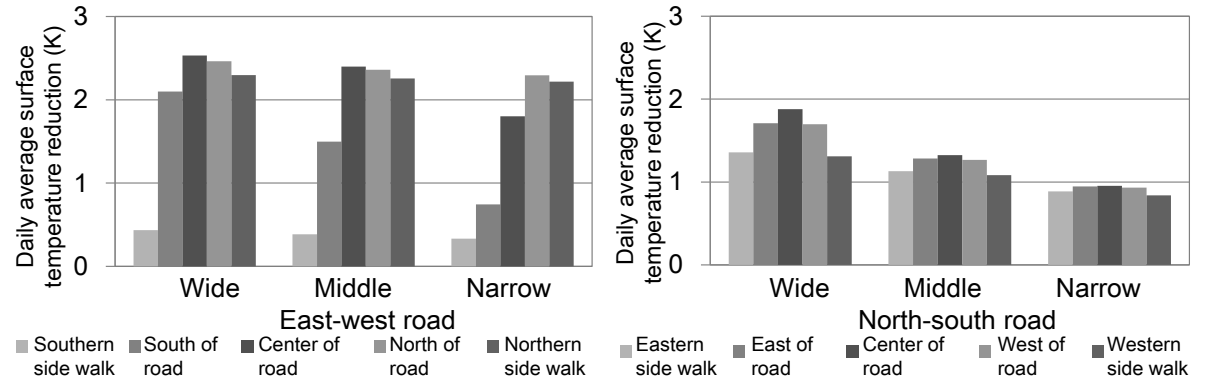

Figure 4: Daily average surface temperature reduction by high reflectance paint

(Left: east-west road, Right: north-south road)

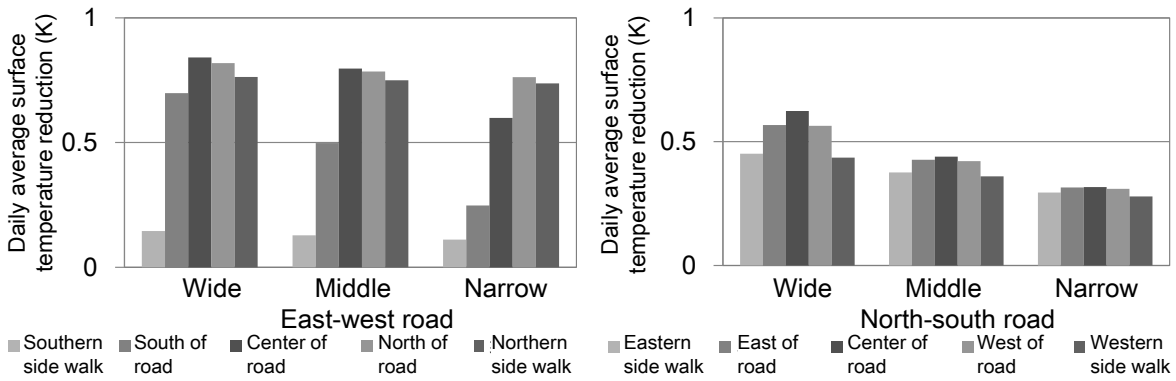

Figure 5: Daily average surface temperature reduction by water-retentive pavement

(Left: east-west road, Right: north-south road)

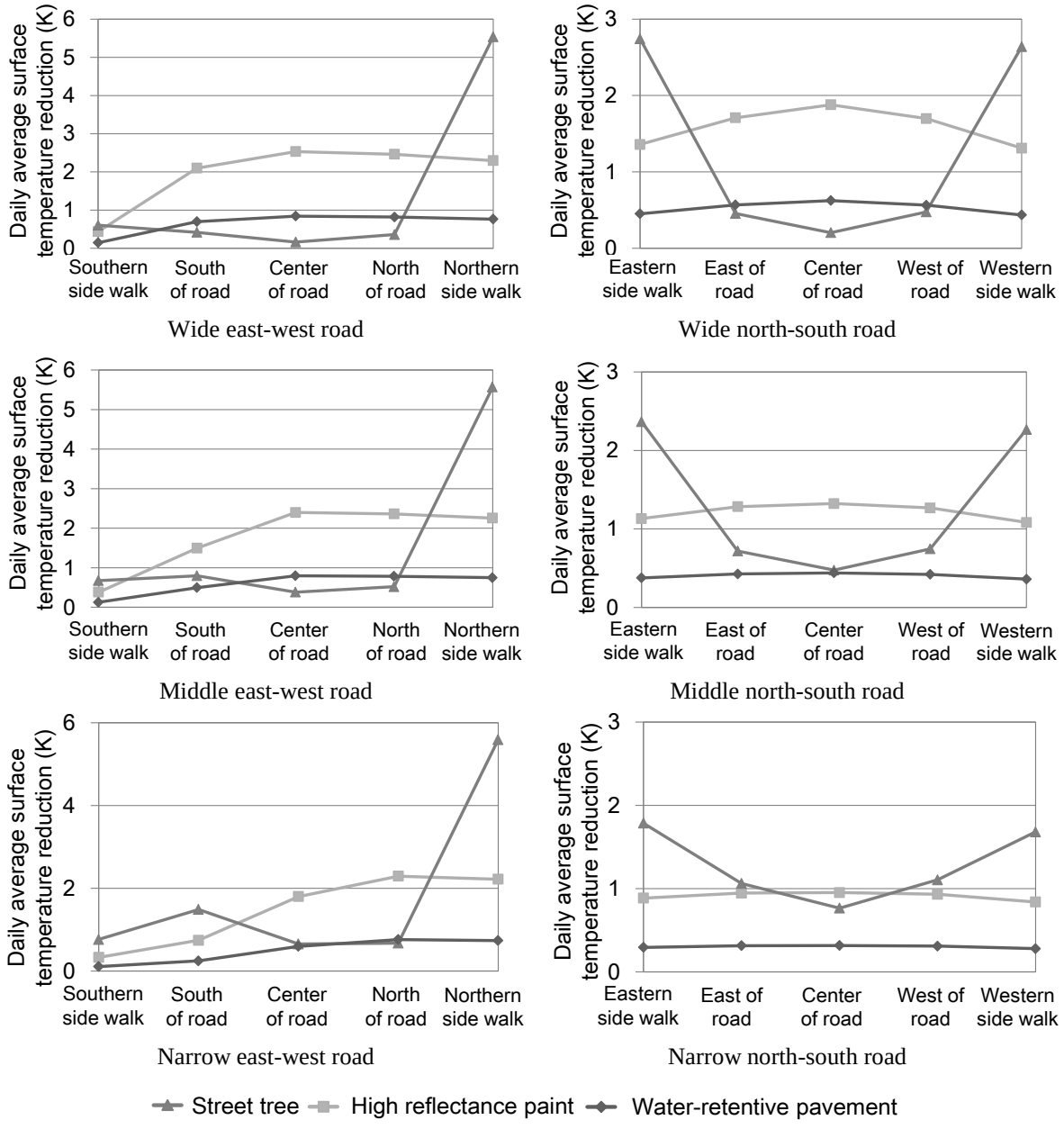

Figure 6: Daily average surface temperature reduction by street tree, high reflectance paint and water-retentive pavement

3 CALCULATION IN THE CASE OF CHANGING STREET TREE LAYOUT

The relationship between street tree layout and the thermal environmental improvement is analysed for the appropriate introduction policy of roadside trees. The calculation results of MRT at 12:00, 15:00, 17:00 on typical sunny day in summer are used for the examination.

3.1 Calculation method of the solar radiation shielding by roadside tree

The shape and solar transmittance of the tree crown are calculated from the survey results of street trees in Kobe city. Street tree model and objective urban block are shown in figure 7. It is assumed that street crown is floating in the air, the solar transmittance uniform in the entire crown with no change by the time. The building height is 18 m. The ArcGIS tool is used for the solar radiation shielding calculation on the road surface. At first, the visible area of the upper hemisphere is calculated considering the influence of surrounding buildings or street trees at the object road surface, then the direct solar radiation is calculated by the overlay of the solar orbit chart and the visible area, and the diffuse solar radiation is calculated by the overlay of the whole sky divided chart and the visible area. The reflected solar radiation is not taken into account.
Parameter of street tree layout is shown in table 1 and location of street trees is shown in figure 8. The diameter of the cylinder of the street tree model is the tree crown width (A) and the distance between each cylinder is tree interval (B). As a result of pre-calculation of the solar radiation gain as parameters as the tree crown width, the height of the tree and the solar radiation transmittance, the tree crown width is most sensitive to the solar radiation gain on the road surface, and the height of the tree is next. In this paper, we focus on the street trees layout mainly, but also on the tree crown width. And, we focus on the direct effect by solar radiation and ignore the mutual radiation exchange.

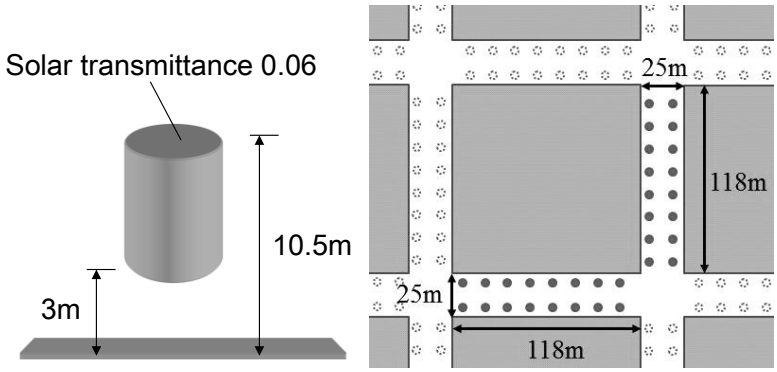

Figure 7: Street tree model and objective urban block (building height is 18 m)

Table 1: Parameter of street tree layout

Tree crown width (A)	Tree interval (B)
4 m	6, 8, 10, 12 m
6 m	8, 10, 12 m

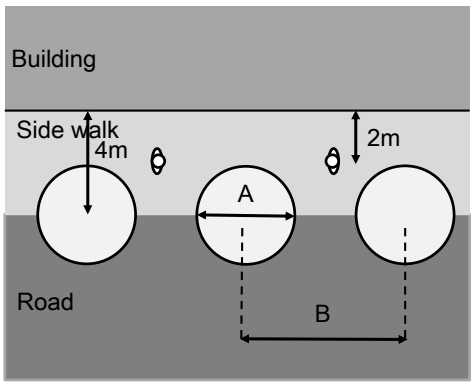

Figure 8: Location of street trees (A: crown width, B: tree interval)

3.2 Calculation results of solar radiation gain

Solar radiation gain averaged along the street at 12:00 in several tree interval cases is shown in figure 9. Solar radiation gain from 11:30 to 12:30 is averaged along the sidewalk. In the case of large tree crown width and small tree interval, solar radiation gain is small due to large proportion of the shaded area. The reduction of solar radiation gain on the northern sidewalk of the east-west road is greater than that on the eastern sidewalk of the north-south road, because half of the shadow by the roadside tree occurs on the driveway at the eastern sidewalk of the north-south road.

Solar radiation gain averaged along the street at 15:00 in several tree interval cases is shown in figure 10. Since solar radiation is less than 12:00, the reducing of solar radiation gain due to the change of street tree layout is also small, but the trend of the reduction of solar radiation gain is as same as 12:00. The reduction of solar radiation gain on the northern sidewalk of the east-west road is greater than the eastern sidewalk of the north-south road as well as 12:00, because many part of shadow occurs on the northern sidewalk of the east-west road than on the eastern sidewalk of the north-south road.

The reduction of the solar radiation gain on the sidewalk depends on the area and the position of the shadow by street trees. The shadow tends to occur on the northern sidewalk of the east-west road than the eastern sidewalk of the north-south road, because the shadow on the eastern side of the north-south road is on the wall and roadway as compared to the northern side of the east-west road.

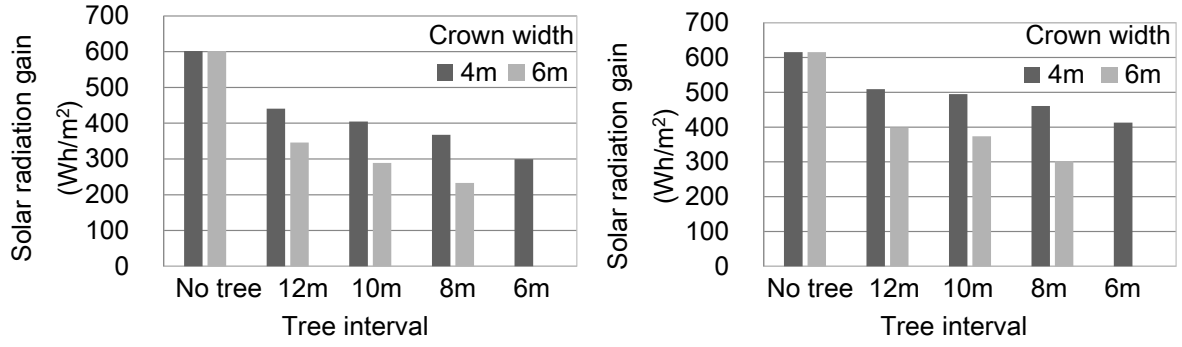

Figure 9: Solar radiation gain averaged along the street at 12:00 in several tree interval cases

(Left: northern sidewalk of east-west road, Right: eastern sidewalk of north-south road)

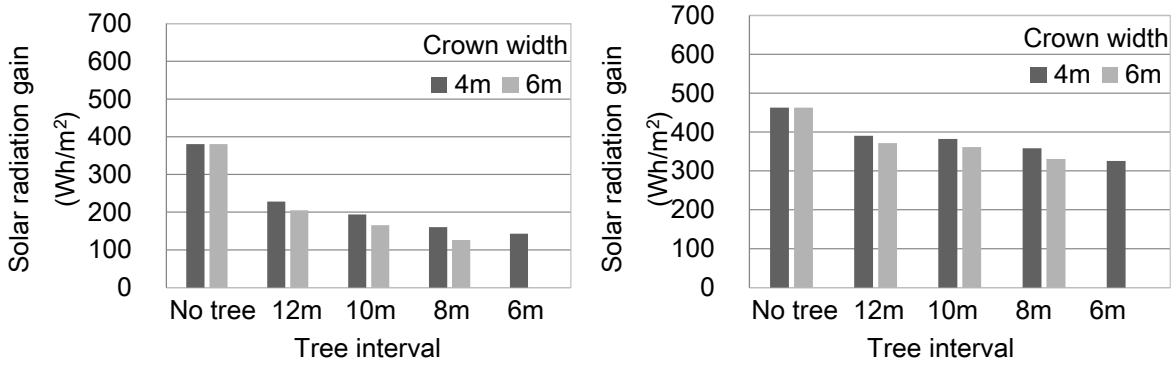

Figure 10: Solar radiation gain averaged along the street at 15:00 in several tree interval cases

(Left: northern sidewalk of east-west road, Right: eastern sidewalk of north-south road)

3.3 Calculation results of MRT

MRT averaged along the street at 15:00 in several tree interval cases is shown in figure 11. The tree crown width is 4m. The calculation results by considering only the influence of the long wave radiation and those with the short wave radiation are separately shown. It is assumed that human body is cube, the weighting factor for upper and lower surface is 0.024 and that for side surface is 0.238 concerning for solar radiation gain area, the solar absorptance of the human body is 0.5, the human body walks on the center of the sidewalk, and MRT is averaged along the sidewalk.

The influence by the reduction of short wave radiation gain is significant for MRT. The influence by the difference of the street tree layout is mainly due to the difference of the short wave radiation on the human body. The reduction of MRT is greater on the northern sidewalk of the east-west road than on the eastern sidewalk of the north-south road. Because shadow of the roadside trees occurs on the perpendicular direction to the eastern sidewalk of the north-south road and on the parallel direction to the northern sidewalk of the east-west road, the area where the human body enters under the influence of shadow is large on the northern sidewalk of the east-west road.

The reduction of MRT on the sidewalk depends on the area where the human body enters under the influence of shadow. The shadow tends to occur on the perpendicular direction to the eastern sidewalk of the north-south road and on the parallel direction to the northern sidewalk of the east-west road. So, the shadow area on the northern sidewalk of the east-west road is larger than on the eastern (western) sidewalk of the north-south road.

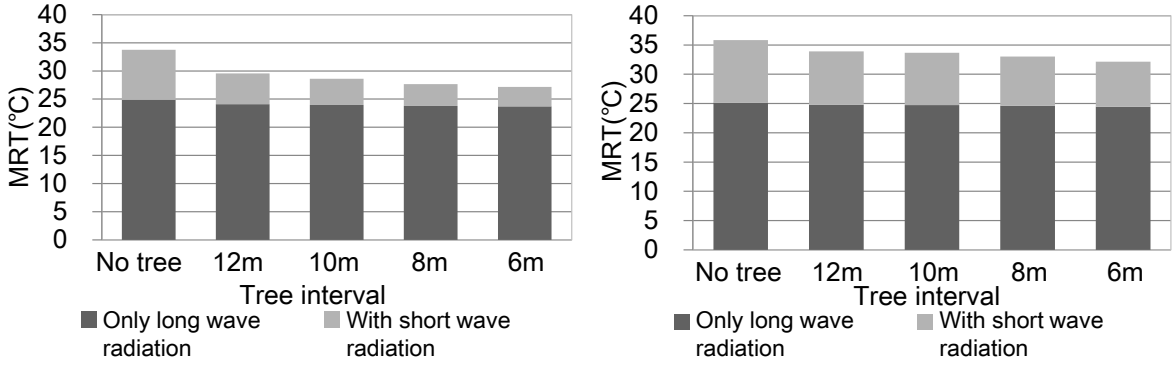

Figure 11: MRT averaged along the street at 15:00 in several tree interval cases (crown width is 4 m)

(Left: northern sidewalk of east-west road, Right: eastern sidewalk of north-south road)

4 CONCLUSIONS

From the view point of introduction of appropriate technique for each place, it is analysed the relationship between benefits by heat island measure technique and places it was introduced. Findings are as follows.

- The benefit by street tree is expected mainly for the sidewalk.
- The benefit by green wall is expected mainly for the wall surface.
- The benefit by high reflectance paint and water-retentive pavement is expected mainly for the roadway. The difference between high reflectance paint and water-retentive pavement depends on solar reflectance, evaporative efficiency and weather condition.
- The shadow by street tree is more significant to the thermal environment on the sidewalk. In the case of large tree crown or small tree interval, shadow is large and thermal environment is improved. Shadow tends to occur on the northern sidewalk than the eastern (western) sidewalk.

In conclusion, from the viewpoint of thermal environmental improvement, street tree is suitable for the sidewalk and high reflectance paint and water-retentive pavement is suitable for the roadway.

5 REFERENCES

Takebayashi, H., Moriyama, M. (2012). Relationship between the properties of an urban street canyon and its radiant environment: Introduction of appropriate urban heat island mitigation technologies. *Solar Energy, 86,* 2255-2261.

Takebayashi, H., Moriyama, M. (2012). Study on a Simple Evaluation Method of Urban Heat Island Mitigation Technology Using Upper Air Data. *Journal of Heat Island Institute International, 7(2),* 102-110.

Takebayashi, H., Moriyama, M. (2007). Surface heat budget on green roof and high reflection roof for mitigation of urban heat island. *Building and Environment, 42, 2971-2979.*

Takebayashi, H., Moriyama, M. (2012). Study on Surface Heat Budget of Various Pavements for Urban Heat Island Mitigation. *Advances in Materials Science and Engineering, 2012.*

PASSIVE COOLING DISSIPATION TECHNIQUES FOR BUILDINGS AND OTHER STRUCTURES: THE STATE OF THE ART

M. Santamouris[1], D. Kolokotsa[2]

1 University of Athens, Physics Department, Group Building Environmental Studies, Athens, Greece

2 Technical University of Crete, School of Environmental Engineering , GR 73100, Crete, Greece

Note: the contact addresses may be re-arranged

Abstract

Passive cooling in the built environment is now reaching is phase of maturity. Passive cooling is achieved by the use of techniques for solar and heat control, heat amortization and heat dissipation. Modulation of heat gain deals with the thermal storage capacity of the building structure, while heat dissipation techniques deal with the potential for disposal of excess heat of the building to an environmental sink of lower temperature, like the ground, water, and ambient air or sky. The aim of the present paper is to underline and review the recent state of the art technologies for passive cooling dissipation techniques in the built environment and their contribution in the improvement of the indoor environmental quality as well as in the reduction of cooling needs. The paper starts with a short introduction in passive cooling and continues with the analysis of advanced heat dissipation techniques such as ground cooling, evaporative cooling, and night ventilation in the built environment. The various technologies are compared versus their contribution to energy efficiency and users' comfort. Future trends and prospects are discussed.

Keywords: passive cooling, heat dissipation, ground cooling, evaporative cooling, ventilative cooling

1 INTRODUCTION

Buildings present a very high energy consumption compared to the other economic sectors. Although percentages vary from country to country, buildings are responsible for about 30-45% of the global energy demand. As a result of the application of very intensive energy savings' measures and technologies, the thermal performance of buildings during the winter period has been tremendously improved mainly in the developed world. On the contrary, because of the increasing standards of life, the affordability of air conditioning, the universalization of modern architecture and also the temperature increase in the urban environment and the global climatic change, the energy needs for cooling have increased in a rather dramatic way (Antinucci et al. 1992).

The serious penetration of air conditioning has an important impact on the absolute energy consumption of buildings. Studies have shown that refrigeration and air conditioning are responsible for about 15 % of the total electricity consumption in the world(Confederation of International Contractors' Associations 2002), while in Europe air conditioning increases in average the total energy consumption of commercial buildings to about 40 kWh/m2/y (Dascalaki and Santamouris 2002; Sfakianaki et al. 2011).

Passive cooling is a multilayered and multidisciplinary process. A framework that is widely accepted for passive cooling is under the frame of three steps: Prevention of heat gains, modulation of heat gains and heat dissipation. Important research has been carried out on the field of passive cooling of buildings. Existing experience has shown that passive cooling provides excellent thermal comfort and indoor air quality, together with very low energy consumption. New materials, systems and techniques have been developed, applied and are now commercially available (Santamouris et al. 2007). In parallel, passive cooling techniques and systems are extensively used in outdoor spaces to improve local microclimate and fight urban heat island (Gaitani, Mihalakakou, and Santamouris 2007; Santamouris et al. 2012; Santamouris, Synnefa, and Karlessi 2011).

Heat dissipation techniques deal with the disposal of the excess heat of a building to a sink characterized by lower temperature, like the ambient air, the water, the ground and the sky.

Effective dissipation of the excess heat depends on two main pre-conditions: a) The availability of a proper environmental heat sink with sufficient temperature difference for the transfer of heat and b) the efficient thermal coupling between the building and the sink.
The present paper aims to present the state of the art on heat dissipation passive cooling techniques. The main scientific and technical developments on ground, ventilative and evaporative cooling are presented and discussed. Examples of application are presented while the main future priorities are discussed.

2 THE USE OF THE GROUND AS A HEAT SINK

It is well known that the temperature of the ground at a depth of about 2.5 to 3 m remains fairly constant and low around the year(Mihalakakou, Santamouris, and Asimakopoulos 1992; Mihalakakou 1997). The idea to dissipate the excess heat from a building to a natural sink like the ground is known from the ancient time (Santamouris and Assimakopoulos 1997). The most common technique to couple buildings and other structures with the ground is the use of underground air tunnels, known as earth to air heat exchangers (EATHE). Earth to air heat exchangers consist of pipes which are buried in the soil while an air circulation system forces the air through the pipes and eventually mixes it with the indoor air of the building or the agricultural greenhouse.
The performance of the EATHE system varies as a function of its characteristics such as the length and the diameter of the pipe, the air flow rate, the depth where the system is buried, the thermal characteristics of the soil, the pipes' material, etc. (Jacovides, Santamouris, and Mihalakakou 1996; Mihalakakou, Santamouris, and Asimakopoulos 1994b, 1994c)
Hundreds of studies have been performed in order to develop models able to predict the efficiency of the earth to air heat exchangers, to analyse the experimental performance of pilot applications and to report the global performance of real scale case studies. At the initial stage of the research many problems associated to the use of ground pipes were reported. Most of them dealt with the accumulation of water inside the tubes, problems of indoor air quality, lack of efficient and dynamic control during the operation, etc. However, recent applications have overcome efficiently the initial barriers and given the quality and the quantity of the available actual knowledge and information, it may be concluded that EATHE is a very mature and quite efficient technology. Evaluation of many real case studies described in (Anon 1997), has shown that for moderate climates the seasonal energy performance of the EATHE systems is close to 8-10 kWh/m2 of ground coupling area, while the peak cooling capacity at air temperature close to 32 °C is estimated at 45 W/m2 of ground coupling area.Many applications of earth to air heat exchangers are available around the world and several scientific works have been published reporting design data and monitoring results. Existing works refer either to the use of EATHE systems in buildings or agricultural greenhouses. It is evident that the degree of information provided for each case is different and is almost impossible to homogenize the results or extract comparative conclusions. However, it is important to collect all available information, classify it and report the major results and conclusions from each project. In the following sections, data and results from 30 building projects and twenty agricultural greenhouse applications of EATHE are given.
Almost twenty different publications have been identified reporting application of EATHE systems in agricultural greenhouses. Review of 14 agricultural greenhouses equipped with earth to air heat exchangers is given in (Santamouris, Mihalakakou, Balaras, et al. 1995). The characteristics of the reported greenhouses are given in Table 3. The used earth to air heat exchangers were buried at depths varying between 50 and 200 cm. The heat exchangers are constructed using plastic, aluminium or concrete pipes. The projects have been monitored and information on the winter performance of the used systems is given in (Santamouris, Mihalakakou, Balaras, et al. 1995).
A system of earth to air heat exchangers consisting of 20 pipes buried at 2m depth and 15 long has been installed in an agricultural greenhouse of 150 m2 in Greece, (Mavroyanopoulos

and Kyritsis 1986). The greenhouse was monitored only during the winter period where the EATHE system had an important contribution. In another experiment described in (Hollmuller 2001), 24 PVC pipes of 11 m length running at 80 cm below the ground have been installed in an experimental greenhouse in Switzerland. Data on the cooling potential of the system are not given.

Tenths of models have been developed to predict the thermal performance of earth to air heat exchangers. Proposed models are either deterministic where the thermal problem is described through appropriate equations as well as data driven where intelligent techniques like neural networks are used to predict the exit temperature from the exchanger, based on training of the models with appropriate experimental data. Deterministic models may be analytical or numerical. Analytical models propose algebraic equations to predict mainly the exit temperature from the exchangers, while analytical models are usually transient and propose a set of differential equations that describe heat and mass transfer phenomena. Numerical models may be of one, two or three dimensions. According to (Tittelein, Achard, and Wurtz 2009), numerical models may be classified as type A or type B. In type A models it is considered that part of the ground is influenced by the exchanger, while in type B models the whole geometrical area is considered. In the following sections the main models proposed are described and reviewed.

Heat transfer phenomena related to EATHE involves mainly a full analysis of the conduction phenomena in the ground and convection phenomena inside the pipe. A complete description of the proposed models to consider heat conduction in the ground is given in (Zoras 2009).

A comparative analysis of nine simulation models to predict the thermal performance of earth to air heat exchangers is given in (van de Brake 2008). It is found that the models described in (Hollmuller 2001) and (Mihalakakou, Santamouris, and Asimakopoulos 1994a) are validated and found to be accurate within 1% of existing published data.

A new methodology to calculate the contribution of earth to air heat exchangers to buildings is proposed in (Santamouris, Mihalakakou, Argiriou, et al. 1995).

The method is based on the principle of balance point temperature and is validated using TRNSYS simulations. The method may be used as an hourly based simplified simulation accurate model to design the coupling of buildings with EATHE and size their specific quantitative characteristics. The method is further extended to couple buildings with both EATHE and night ventilation techniques. The basic characteristics of the method are similar as in (Santamouris, Mihalakakou, Argiriou, et al. 1995). The new extended method is validated against detailed simulations performed with TRNSYS.

Research described in (Misra et al. 2012) has evaluated the performance of EATHE when coupled with the condenser of a conventional air conditioning system. The experiment has been carried out in India and comprised a 60 m long horizontal cylindrical PVC pipe buried at 3.7 m depth. The air at the exit of the exchanger was either directly circulated in a room together with the air from a conventional air conditioner or it was used for cooling the condenser tubes of an 1.5 TR window air conditioner. The experiment It was found that when the air is used to cool the condenser the achieved energy conservation was close to 18 %, while when both system supplied in parallel the room, the corresponding energy saving was around 6 %.

3 EVAPORATIVE COOLING

Evaporative cooling is extensively used as a passive cooling technique in the built environment. The air movement over a wetted surface causes some of the water to evaporate. This evaporation results in a reduced temperature and an increased vapour content in the air. The increase of the surface area increases the evaporation, resulting in a significant cooling effect. There are two basic types of evaporative air cooling techniques:

- The direct evaporative coolers that are commonly used for residential buildings. In this type of evaporative cooling the reduction of temperature is followed by an increase of moisture content.
- The indirect systems where the evaporative cooling is delivered across a heat exchanger, which keeps the cool moist air separated from the room. This system does not cause an increase of the air humidity.

The limit of the evaporative cooling potential is given by the wet bulb temperature of the air to be cooled. Some researchers (Givoni 1992), (Evyatar 2007) though indicate that this theoretical limit is rarely reached and that the maximum output of the most evaporative coolers is at least 2°C warmer than the wet bulb. Therefore the climatic criterion for the applicability of evaporative cooling is the ambient wet bulb temperature.

Direct evaporative cooling is the simplest and oldest form of air conditioning. It is performed using a fan to draw hot outside air into the building by passing it from an evaporative pad (see Figure 2). Direct evaporative cooling is quite simple and cheap commonly used for residential applications to cool the air by increasing its moisture content of the air (Bom et al. 1999). Typical commercial evaporative coolers have an effectiveness of 50-70%.

Since the major drawback for DEC is the wet bulb temperature limitation, research efforts the last decades are mainly focusing on the improvement of the DEC's effectiveness by various configurations targeting to expand their application in more humid climates.

For the improvement of DEC's effectiveness the following alternatives are proposed in chronological order:

- Water falls over films proposed by Giabaklou et al (Giabaklou and Ballinger 1996) while exposing maximum surface area to the passing air flow.
- The use of micronisers is proposed for the Passive Down-draught Evaporative Cooling (PDEC) configuration studied by (Bowman et al. 2000) and (Robinson et al. 2004).
- An evapo-reflective roof to reduce passive cooling in buildings for hot arid climates has been proposed in (Ben Cheikh and Bouchair 2004).
- A direct evaporative cooler that operates either with natural wind flow or with wind catchers is described in (Qiu and Riffat 2006).
- Water evaporative walls are proposed in (Naticchia et al. 2010) and (He and Hoyano 2010) on 2010 and 2011.
- A wet porous cooling plate as a building wall is proposed in (Chen and Liu 2010; Chen 2011) where cooling is performed via evaporation of the porous material.

Therefore direct evaporative cooling can be considered a very effective solution for hot and arid climatic conditions. When humidity is increased other evaporative cooling configurations can be a viable solution.

For hot humid climates the indoor temperature conditions should be kept lower than outdoors. In these regions where usually the outdoor temperature fluctuations are small and the humidity is considerably high throughout the whole day, direct evaporative cooling is not effective. The indirect evaporative coolers (IEC) can be an alternative option.

IEC usually incorporates an air to air heat exchanger to remove heat from the air without adding moisture. In IEC the hot outside air is passed through a series of horizontal tubes that are wetted on the outside. A secondary air stream blows over the outside of the coils and exhausts the warm, moist air to the outdoors. The outside air is cooled without adding moisture as it passes through the tubes. Indirect evaporative cooling typically has an effectiveness of almost 75%. There are various configurations that can increase effectiveness even higher than 100%, i.e. cooling the supply air to a level below the wet-bulb temperature.

An evolution of the simple DEC is the so called two stage evaporative cooling (Bourne 2004) as depicted in Figure 4. The two stage evaporative coolers pre-cool the air before it goes through the evaporative pad. The overall system has 70% effectiveness for its indirect part and 90% effectiveness for the direct part (Anon 2007) while the relative humidity of the cool

air is between 50-70%. Two-stage evaporative coolers can reduce energy consumption by 60% to 75%.
Significant research efforts for the improvement of DEC's effectiveness are performed by various researchers the last decade.
Based on the above, indirect evaporative cooling techniques can be low energy solutions for medium and large buildings where passive cooling techniques cannot reach the required comfort conditions (Belding and Delmas 1997; Costelloe and Finn 2007; Elzaidabi 2009; Joudi and Mehdi 2000; Kim et al. 2011; Navon and Arkin 1994). Such systems require energy for the fan power for the air flow. On the one hand this fan power can be up to 20% less due to lower air velocities required and on the other hand the main reduction of the energy demand is attributed to the replacement of the conventional air conditioning system. Based on future projections performed in (Smith and Harpham 2010) and (Hanby and Smith 2012) climate change will deteriorate the energy demand for cooling in areas which are less vulnerable nowadays and the dependence on mechanical cooling will be increased. This research showed that the evaporative cooling and especially the IEC are suitable solutions for more extreme conditions due to increase in wet bulb temperature depression. The projections are tested under the UK climatic conditions and it is proved by simulations that the 'drier' UK climate provides an opportunity to offset the impact of increased cooling demands through wider application of indirect evaporative coolers.
Based on the state of the art review, evaporative cooling is a viable and attractive passive cooling technique for various climatic conditions while a considerable effort is put in the improvement of systems' effectiveness and applicability (Navon and Arkin 1994). Moreover there is a significant environmental and economic benefit in using EC over conventional air conditioning due to the it's increased energy efficiency.

4 VENTILATION AS A PASSIVE COOLING TECHNIQUE

Night ventilation or nocturnal convective cooling exploits the cold night air to cool down the building's absorbed heat gains during daytime and reduce the daytime temperature rise. Night ventilation can either be driven by natural forces – i.e. stack or wind pressure difference, or may be sometimes supported by a small fan power to provide sufficient airflow at times when the natural forces are weak. As a consequence, temperature peaks are reduced or even postponed. The efficiency of the technique is mainly based on the relative difference between the outdoor and indoor temperatures during the night period. However, for a given place, the cooling potential of night ventilation techniques depends on the air flow rate, the thermal capacity of the building and the appropriate coupling of the thermal mass and the air flow.
Various studies prove night ventilation effectiveness. In (Givoni 1991, 1992) Givoni argues that the night ventilation technique is efficient particularly for arid regions where day time ventilation is insufficient to ensure thermal comfort. Kolokotroni and Aronis in (Kolokotroni and Aronis 1999) introduce some variables for the building such as building mass, glazing ratio, solar and internal gains, orientation and demonstrate that the optimization of the building design for night ventilation according to these parameters can cause an abatement of about 20-25% of the air conditioning energy consumption. The effectiveness of night ventilation techniques is determined by the prevailing climatic conditions, the microclimate, the building characteristics and the location. The outdoor temperature, the relative humidity and the wind speed are the environmental parameters that influence the successful application of night ventilation techniques (Geros et al. 2005; Santamouris et al. 1996).
Santamouris et al (Santamouris, Sfakianaki, and Pavlou 2010) pointed out that the application of night ventilation techniques to residential buildings may lead to a decrease of cooling loads almost 40 kWh/m^2/y with an average contribution of 12 kWh/m^2/y. In urban areas though, the Urban Heat Island (UHI) phenomenon deteriorates quality of life and has a direct impact on the energy demand, the environmental conditions and, consequently, on ventilation effectiveness. The increased urban temperatures (Livada et al. 2002; Livada, Santamouris, and

Assimakopoulos 2007) exacerbate the cooling load of buildings, increase the peak electricity demand for cooling, decrease the efficiency of air conditioners,(Cartalis et al. 2001; Santamouris et al. 2001) and create an emerge necessity for passive cooling.
To better understand the relative phenomena and also quantify the impact of night ventilation techniques, important experimental and theoretical research has been carried out (Santamouris et al. 2010). Various studies are performed reporting the contribution of night ventilation to passive cooling either in real buildings or in test experimental conditions. Moreover a series of simulation studies can be found targeting to the quantification of night ventilation in the reduction of cooling demand together with improvement of indoor comfort.
Based on the above, night ventilation can be categorized based on the type of study, i.e. simulation based or experimental based as well as based on the building types studied.
Ventilative cooling is studied for various building types including offices, residential, industrial, etc. The aim of the present section is to review the applicability of night ventilation for various dwellings.A significant number of studies are focusing on the energy efficiency and applicability of night ventilation cooling in office buildings under various climatic conditions (Blondeau, Spérandio, and Allard 1997) showed a reduction of diurnal variation from 1.5 to 2°C, resulting in a significant comfort improvement for the occupants. The same results can be found by Birtles et al (Birtles, Kolokotroni, and Perera 1996) in London region.
An office building in Germany is monitored versus its ventilation in (Pfafferott, Herkel, and Wambsganß 2004). Adequate thermal insulation and moderate window dimensions guarantee a low heating and cooling energy demand. Two buildings (the Institute of Criminology building and the English Faculty building) with night-time natural ventilation strategies in Cambridge, UK, were selected for a pilot field study. The buildings were designed by architects Allies + Morrison (London, UK) with engineers Buro Happold (London, UK)(Yun and Steemers 2010).
Therefore night ventilative cooling is a very effective method to reduce the air conditioning demand for office buildings and improve thermal comfort during daytime regardless the climatic conditions. In order to increase the night ventilation cooling performance and ensure that the required window opening will be performed on a regular basis, the night ventilation strategy should be integrated to the office buildings energy management system and control if applicable.
Regarding residential buildings the following studies are found: The ventilation effectiveness is studied in (Golneshan and Yaghoubi 1990) regarding the residential buildings of Iran. The effectiveness of night ventilation technique for residential buildings in hot-humid climate of Malaysia is analysed in (Kubota, Chyee, and Ahmad 2009).Two hundred fourteen air conditioned residential buildings using night ventilation techniques have been analysed in (Santamouris et al. 2010). Based on the above residential buildings' energy efficiency can be considerably enhanced by night ventilation strategies and minimise the use of air conditioning. Moreover the specific passive cooling technique can contribute to an improvement of indoor thermal comfort for low income households where the air conditioning is not an option due to economic restrictions.

5 CONCLUSIONS

The energy consumption of the buildings is quite high and may increase considerably in the future because of the improving standards of life and increasing penetration of air conditioning.
Urban climate change and heat island effect is another important source enhancing the use of air conditioning and increasing peak electricity demand. .
Important research has been carried out that has resulted in the development of alternative to air conditioning systems, techniques and materials. The proposed technologies, known as passive cooling can provide comfort in non-air conditioned buildings and decrease considerably the cooling load of thermostatically controlled buildings. In parallel, passive

cooling techniques and systems may be used to improve the outdoor urban environment and fight heat island.

The proposed technologies have been tested in demonstration and real scale applications with excellent results. The efficiency of the proposed passive cooling systems is found to be high while their environmental quality is excellent. Expected energy savings may reach 70 % compared to a conventional air conditioned building while substantial improvements have been measured in outdoor spaces.. Based on the research developments many of the proposed systems and in particular the heat dissipation systems have been commercialised and are available to the public.It is evident that further research is necessary in order to optimise the existing systems and develop new ones.

6 REFERENCES

Anon. 1997. "Selection guidance for low energy cooling technologies. International Energy Agency, Energy Conservation in Buildings and Community Systems Programme, Annex 28 Low Energy Cooling, Subtask 2 Report 1."

Anon. 2007. "ASHRAE Handbook - Heating, Ventilating, and Air-Conditioning Applications."

Antinucci, M. et al. 1992. "PASSIVE AND HYBRID COOLING OF BUILDINGS – STATE OF THE ART." *International Journal of Solar Energy* 11(3-4):251–71.

Belding, William A., and Marc P. F. Delmas. 1997. "Novel desiccant cooling system using indirect evaporative cooler." Pp. 841–47 in *ASHRAE Transactions*, vol. 103.

Birtles, A. B., M. Kolokotroni, and M. D. A. E. S. Perera. 1996. "Night cooling and ventilation design for office-type buildings." *Renewable Energy* 8(1-4):259–63.

Blondeau, P., M. Spérandio, and F. Allard. 1997. "Night ventilation for building cooling in summer." *Solar Energy* 61(5):327–35.

Bom, Gert Jan, Robert Foster, Ebel Dijkstra, and Marja Tummers. 1999. *Evaporative Air-Conditioning: Applications for Environmentally Friendly Cooling Published*. World Bank Technical Papers 421.

Bourne, R. C. 2004. "Developement of an improved two-stage enaporative cooling system."

Bowman, N. T., H. Eppel, K. J. Lomas, D. Robinson, and M. J. Cook. 2000. "Passive downdraught evaporative cooling: I. Concept and precedents." *Indoor and Built Environment* 9(5):284–90.

Van de Brake, J. 2008. "Old technology for new buildings, a study on earth-to-air heat exchangers." University of Technology Eindhoven.

Cartalis, C., A. Synodinou, M. Proedrou, A. Tsangrassoulis, and M. Santamouris. 2001. "Modifications in energy demand in urban areas as a result of climate changes: an assessment for the southeast Mediterranean region." *Energy Conversion and Management* 42(14):1647–56.

Ben Cheikh, Hamida, and Ammar Bouchair. 2004. "Passive cooling by evapo-reflective roof for hot dry climates." *Renewable Energy* 29(11):1877–86.

Chen, W. 2011. "Thermal analysis on the cooling performance of a wet porous evaporative plate for building." *Energy Conversion and Management* 52(5):2217–26.

Chen, W., and W. Liu. 2010. "Thermal analysis on the cooling performance of a porous evaporative plate for building." *Heat Transfer - Asian Research* 39(2):127–40.

Confederation of International Contractors' Associations, ed. 2002. *Industry as a partner for sustainable development-Refrigeration*. UNEP.

Costelloe, B., and D. Finn. 2007. "Thermal effectiveness characteristics of low approach indirect evaporative cooling systems in buildings." *Energy and Buildings* 39(12):1235–43.

Dascalaki, E., and M. Santamouris. 2002. "On the potential of retrofitting scenarios for offices." *Building and Environment* 37(6):557–67.

Elzaidabi, Abdalla Ali Mohamed. 2009. “Low energy, wind catcher assisted indirect-evaporative cooling system for building applications.”

Evyatar, Erell. 2007. “Evaporative cooling.” in *Advances in Passive Cooling*, edited by Mattheos Santamouris. London: James and James.

Gaitani, N., G. Mihalakakou, and M. Santamouris. 2007. “On the use of bioclimatic architecture principles in order to improve thermal comfort conditions in outdoor spaces.” *Building and Environment* 42(1):317–24.

Geros, V., M. Santamouris, S. Karatasou, A. Tsangrassoulis, and N. Papanikolaou. 2005. “On the cooling potential of night ventilation techniques in the urban environment.” *Energy and Buildings* 37(3):243–57.

Giabaklou, Zahra, and John A. Ballinger. 1996. “A Passive Evaporative Natural Ventilation.” *Science* 31(6):503–7.

Givoni, B. 1991. “Performance and applicability of passive and low-energy cooling systems.” *Energy and Buildings* 17(3):177–99.

Givoni, B. 1992. “Comfort, climate analysis and building design guidelines.” *Energy and Buildings* 18(1):11–23.

Golneshan, A. A., and M. A. Yaghoubi. 1990. “Simulation of ventilation strategies of a residential building in hot arid regions of Iran.” *Energy and Buildings* 14(3):201–5.

Hanby, V. I., and S. T. Smith. 2012. “Simulation of the future performance of low-energy evaporative cooling systems using UKCP09 climate projections.” *Building and Environment* 55:110–16.

He, Jiang, and Akira Hoyano. 2010. “Experimental study of cooling effects of a passive evaporative cooling wall constructed of porous ceramics with high water soaking-up ability.” *Building and Environment* 45(2):461–72.

Hollmuller, P. 2001. “Cooling and preheating with buried pipe systems: monitoring, simulation and economic aspects.” *Energy and Buildings* 33(5):509–18.

Jacovides, P., M. Santamouris, and G. Mihalakakou. 1996. “ON THE GROUND TEMPERATURE APPLICATIONS PROFILE FOR PASSIVE COOLING IN BUILDINGS.” *Solar Energy* 57(3):167–75.

Joudi, K. A., and S. M. Mehdi. 2000. “Application of indirect evaporative cooling to variable domestic cooling load.” *Energy Conversion and Management* 41(17):1931–51.

Kim, M. H., J. H. Kim, O. H. Kwon, A. S. Choi, and J. W. Jeong. 2011. “Energy conservation potential of an indirect and direct evaporative cooling assisted 100% outdoor air system.” *Building Services Engineering Research and Technology* 32(4):345–60.

Kolokotroni, M., and A. Aronis. 1999. “Cooling-energy reduction in air-conditioned offices by using night ventilation.” *Applied Energy* 63(4):241–53.

Kubota, T., D. T. H. Chyee, and S. Ahmad. 2009. “The effects of night ventilation technique on indoor thermal environment for residential buildings in hot-humid climate of Malaysia.” *Energy and Buildings* 41(8):829–39.

Livada, I., M. Santamouris, and M. Assimakopoulos. 2007. “On the variability of summer air temperature during the last 28 years in Athens.” *Journal of Geophysical Research D Atmospheres* 112(12).

Livada, I., M. Santamouris, K. Niachou, N. Papanikolaou, and G. Mihalakakou. 2002. “Determination of places in the great Athens area where the heat island effect is observed.” *Theoretical and Applied Climatology* 71(3-4):219–30.

Mavroyanopoulos, G. N., and S. Kyritsis. 1986. “The performance of a greenhouse heated by an earth-air heat exchanger.” *Agricultural and Forest Meteorology* 36(3):263–68.

Mihalakakou, G. 1997. “On the application of the energy balance equation to predict ground temperature profiles.” *Solar Energy* 60(3-4):181–90.

Mihalakakou, G., M. Santamouris, and D. Asimakopoulos. 1992. “Modelling the earth temperature using multiyear measurements.” *Energy and Buildings* 19(1):1–9.

Mihalakakou, G., M. Santamouris, and D. Asimakopoulos. 1994a. “Modelling the thermal performance of earth-to-air heat exchangers.” *Solar Energy* 53(3):301–5.

Mihalakakou, G., M. Santamouris, and D. Asimakopoulos. 1994b. “On the cooling potential of earth to air heat exchangers.” *Energy Conversion and Management* 35(5):395–402.

Mihalakakou, G., M. Santamouris, and D. Asimakopoulos. 1994c. “Use of the ground for heat dissipation.” *Energy* 19(1):17–25.

Misra, R., V. Bansal, G. D. Agarwal, J. Mathur, and T. Aseri. 2012. “Thermal performance investigation of hybrid earth air tunnel heat exchanger.” *Energy and Buildings* 49:531–35.

Naticchia, B., M. D’Orazio, A. Carbonari, and I. Persico. 2010. “Energy performance evaluation of a novel evaporative cooling technique.” *Energy and Buildings* 42(10):1926–38.

Navon, R., and H. Arkin. 1994. “Feasibility of direct-indirect evaporative cooling for residences, based on studies with a desert cooler.” *Building and Environment* 29(3):393–99.

Pfafferott, J., S. Herkel, and M. Wambsganß. 2004. “Design, monitoring and evaluation of a low energy office building with passive cooling by night ventilation.” *Energy and Buildings* 36(5):455–65.

Qiu, G. Q., and S. B. Riffat. 2006. “Novel design and modelling of an evaporative cooling system for buildings.” *International Journal of Energy Research* 30(12):985–99.

Robinson, D., K. J. Lomas, M. J. Cook, and H. Eppel. 2004. “Passive down-draught evaporative cooling: Thermal modelling of an office building.” *Indoor and Built Environment* 13(3):205–21.

Santamouris, M., G. Mihalakakou, C. A. Balaras, et al. 1995. “Use of buried pipes for energy conservation in cooling of agricultural greenhouses.” *Solar Energy* 55(2):111–24.

Santamouris, M. et al. 2001. “On the impact of urban climate on the energy consumption of buildings.” *Solar Energy* 70(3):201–16.

Santamouris, M. et al. 2012. “Using cool paving materials to improve microclimate of urban areas-Design realization and results of the Flisvos project.” *Building and Environment* 53:128–36.

Santamouris, M., and DN Assimakopoulos, eds. 1997. *Passive Cooling of Buildings*. London, UK: James & James (Science Publishers) Ltd.

Santamouris, M., G. Mihalakakou, A. Argiriou, and D. Asimakopoulos. 1996. “On the efficiency of night ventilation techniques for thermostatically controlled buildings.” *Solar Energy* 56(6):479–83.

Santamouris, M., G. Mihalakakou, A. Argiriou, and D. N. Asimakopoulos. 1995. “On the performance of buildings coupled with earth to air heat exchangers.” *Solar Energy* 54(6):375–80.

Santamouris, M., K. Pavlou, A. Synnefa, K. Niachou, and D. Kolokotsa. 2007. “Recent progress on passive cooling techniques. Advanced technological developments to improve survivability levels in low-income households.” *Energy and Buildings* 39(7):859–66.

Santamouris, M., A. Sfakianaki, and K. Pavlou. 2010. “On the efficiency of night ventilation techniques applied to residential buildings.” *Energy and Buildings* 42(8):1309–13.

Santamouris, M., A. Synnefa, and T. Karlessi. 2011. “Using advanced cool materials in the urban built environment to mitigate heat islands and improve thermal comfort conditions.” *Solar Energy* 85(12):3085–3102.

Sfakianaki, A. et al. 2011. “Energy consumption variation due to different thermal comfort categorization introduced by European standard EN 15251 for new building design and major rehabilitations.” *International Journal of Ventilation* 10(2):195–204.

Smith, S. Th, and C. Harpham. 2010. “A probabilistic analysis of the future potential of evaporative cooling systems in a temperate climate.” *Energy and Buildings* 43(2-3):507–16.

Tittelein, Pierre, Gilbert Achard, and Etienne Wurtz. 2009. “Modelling earth-to-air heat exchanger behaviour with the convolutive response factors method.” *Applied Energy* 86(9):1683–91.

Yun, G. Y., and K. Steemers. 2010. “Night-time naturally ventilated offices: Statistical simulations of window-use patterns from field monitoring.” *Solar Energy* 84(7):1216–31.

Zoras, S. 2009. “A review of building earth-contact heat transfer.” *Advances in Building Energy Research* 3(1):289–314.

EXPERIMENTAL ANALYSIS OF DIFFERENT OPERATIONAL CONFIGURATIONS FOR SINGLE SIDED NATURAL VENTILATION AS PART OF A LOW ENERGY RETROFIT

Paul D O'Sullivan[*1, 2], Maria Kolokotroni [2]

1. *Department of Process, Energy & Transport, School of Mechanical Engineering, Cork Institute of Technology, Cork, Rossa Avenue, Bishopstown, Cork, Ireland*
2. *Howell Building, Mechanical Engineering, School of Engineering and Design, Brunel University, Uxbridge UB8 3PH, United Kingdom*

**Corresponding author: paul.osullivan@cit.ie*

ABSTRACT

Non-invasive, scalable, building retrofit solutions are amongst the most likely large scale adoption techniques to assist in climate change adaptation in the existing built environment, particularly in university type buildings where rehousing live activities will prove costly. Natural ventilation is an attractive retrofit strategy due to the low impact nature of the installation. A number of internal environmental criteria that are important to ventilative cooling strategies can be substantially modified as a result of an external retrofit solution. These include ventilation rate, internal thermal stratification, diurnal thermal stability, surface and air temperature variations etc. More generally, additional factors that can influence single sided natural ventilation performance related to the building microclimate are wind speed and direction, outdoor temperature profile, turbulent characteristics of the wind and pressure differences across the building envelope. This paper presents results from full scale performance testing of the natural ventilation system of a deep retrofit solution applied to an existing 1970s precast concrete building in south of Ireland. The solution presented is modular, scalable, externally applied and incorporates opaque and transparent elements as well as integrated automated and manual ventilation openings. The paper outlines different operational configurations for the single sided natural ventilation system and the respective effect these configurations have on internal environment based on full scale testing under dynamic outdoors conditions. Results are based on data collected for two single sided, direct gain cellular offices, one in the existing building that has not been retrofitted which acts as the control space, and the other one retrofitted to a very high standard. Four different types of ventilation configuration are summarised. The findings show that thermal stratification has been found to be substantially modified post retrofit although the relative magnitude is still significant in the retrofit due to reduced indoor temperatures while the amplitude of diurnal indoor air temperature has been effectively eliminated. The ventilation rate is also considerably lower in the retrofit spaces under some configurations. Each configuration is classified based on findings.

KEYWORDS

Ventilation rate, single sided ventilation, retro-fit, stack effect, stratification factor, thermal time constant

1 INTRODUCTION

Ventilative cooling coupled with exposed thermal mass is widely accepted as an important strategy for reducing summer overheating in non-domestic buildings. Extended monitoring has shown that naturally ventilated buildings typically use less than 50% of the corresponding energy consumption of air conditioned buildings and assessment of ventilative cooling techniques in Europe have shown they may contribute highly to reducing the cooling needs of buildings (Kolokotroni et al 1996a, 1996b; 2002) and be an effective tool for tackling climate change adaptation in existing buildings. Recently, focus for market activation in the construction sector has shifted towards dealing with the overhaul of the existing building stock. Article 9 of the EPBD (European Union 2010) brings in refurbished buildings under

the near zero-energy umbrella by requiring member states to develop policies in order to stimulate the transformation of refurbished buildings into near zero-energy buildings (NZEB). The Irish National Energy Efficiency Action Plan 2013-2020 (DCENR 2013) report has identified refurbishment of existing public sector buildings as a key focus. The report states that there are over 10,000 existing public sector buildings in Ireland and a key strategy for delivering retrofit projects may be through Energy Performance Contracting. Cork Institute of Technology (CIT) have recently completed a pilot project for a low energy retrofit of their existing 29,000m^2 teaching building constructed in 1974. The retrofit pilot covered 1.5% of the total building floor area. The project scope consisted of design and installation of a structurally independent external envelope solution. O'Sullivan et al (O'Sullivan et al. 2013) have summarised details of the design and specification of the retrofit solution. In this paper work is summarised from experimental measurements of ventilation rates under different ventilation opening configurations in a single sided isolated office space within the retrofit. The objective is to investigate whether modification in both the building thermophysical properties and ventilation opening design has influenced ventilation rates and the internal environment and under what conditions is performance enhanced. A control space in the existing building has been identified and utilised for comparative purposes.

Figure 1: The recently completed retrofit pilot project at B-Block CIT (a) retrofit space (b) control space

Section 3 of the paper summarises details regarding the existing building, completed retrofit strategy, natural ventilation system and operational configurations. Section 4 provides information about the ventilation rate (ACH^{-1}) tests including experiment setup, results and analysis. Sections 5 summarises findings from comparative studies of the internal environment in the control space and retrofit space. Results are categorised according to the four configurations detailed in section 4.2.

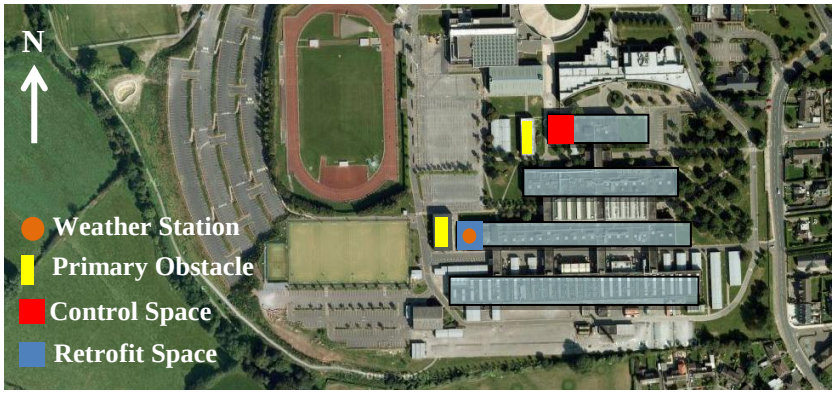

W.Dir	Cp
0.00	-0.255
45.00	-0.140
90.00	-0.128
135.00	-0.139
180.00	-0.264
225.00	0.132
270.00	0.053
315.00	0.103

Figure 2: Site Location of Control and Retrofit Space & associated surface wind pressure coefficients, C_p

2 LOCAL CLIMATE (2013 & LONG TERM)

Ambient air temperature, solar radiation and wind speed 95th Percentile values for May – September 2013 are presented in Table 1. Cork Airport TMY3 data also shown for comparison and was generated using Meteonorm 7 software []. Weather data used for the analysis in this paper was obtained from a weather station located on the roof of the retrofit

space, set 6.0m in from the edge of the building and at an elevation of 8.0m above the finished roof level.

Table 1: Local Climate at CIT

Month	Cork Airport TMY3 95th Percentile			Summer 2013 95th Percentile**		
	G_h (Wh/m^2)	T_a (°C)	WS (m/s)	G_h (Wh/m^2)	T_a (°C)	WS (m/s)
May	742	17.2	10.0	730	16.0	6.3
June	815	19.5	9.3	826	20.6	5.0
July	707	20.7	9.0	795	25.0	4.3
August†	662	20.0	9.3	567	19.1	4.7
September*	574	19.4	9.0	-	-	-

† Data up to 15th August only for short term; *Data not yet available for short term; **Data taken from zero2020 weather station

3 DESCRIPTION OF CONTROL SPACE & LOW ENERGY RETROFIT

3.1 Envelope Components

The external envelope retrofit solution involved the installation of a new external façade, independently supported at the base and tied into the structure at certain locations. The solution can be sub-divided into three broad modular categories; Roof module, opaque wall module and the fenestration module comprising both the glazing and ventilation openings. O'Sullivan et al (O'Sullivan et al. 2013) have already outlined in some detail the component specifications elsewhere. Figure 3 below provides information on the final wall build up and external retrofit solution applied. It should be noted that the entire existing structure has remained in place as part of the solution. The main thermophysical properties for the existing building and the retrofit components are summarised in table 1.

Table 2: Thermophysical properties of opaque external retrofit solution & fenestration module

	Description	Dim. (mm)	Location	ω/φ (W/mK) / h	f (W/mK)	U_{wall} (W/m^{2}K)	$U_{fenestr.}$ (W/m^{2}K)
1	Existing Internal Block	100	Control Space	5.49 / 1.017	0.608	3.633	6.0
2	BASF Wall-tite Spray Foam	86					
3	Existing aggregate panel	125					
4	Air gap	30					
5	Kingspan benchmark ceramic granite panel	12	Retrofit Space	5.92 / 0.963	0.004	0.090	0.84
6	Kingspan support rail	37					
7	Kingspan KS 1100 insulated panel	125					
8	AMS support mullion	125					

Figure 3: (a) Opaque Retrofit module, (b) fenestration module (including ventilation inlets)

3.2 Ventilation System

For most enclosed spaces in the existing building the ventilation system is based on single sided top hung pivoting window sections. There is generally one opening window per structural grid. These are the original 1974 windows. In the retrofit space fenestration system, the ventilation module uses a flush faced external louvre with individual air inlet sections.

Inside this louvre ventilation is supplied using dedicated insulated doors controlled either manually or automated based on conditions in the enclosed spaces (see Table 3). The overall thermal transmittance performance of this unit including doors and linear transmittance is 0.84 W/m^{2}k, according to IS EN 10077-2:2003 (NSAI 2012). The new fenestration module resulted in an overall opaque/transparent area ratio reduction of 20%. Unwanted ventilation through adventitious openings has also been greatly reduced. The retrofit envelope air permeability was tested in accordance with BS EN 13829:2001. The envelope achieved an air permeability of 1.76 (m^3/hr)/m^2 at 50Pa building pressure. The existing structure was measured as 14.77 (m^3/hr)/m^2. Details of the different ventilation opening configurations including are highlighted in Table 3 below.

Table 3: Summary of ventilation opening data & operating configurations

Location & Information	Configuration & operating mode	Vent Opening Type	A_{eff} A_{eff}/A_w	Schematic Envelope Flow Model
Existing building First Floor D-Block Single office Room D259 ***(Control Space)***	CS/1.0/M		0.32 m^2 3.7%	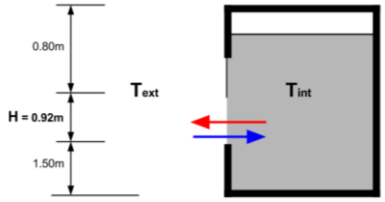
Retrofit building First Floor B-Block Single Office West Facing Room FF-03 ***(Retrofit Space)***	RE/2.0/M		0.21 m^2 2.4%	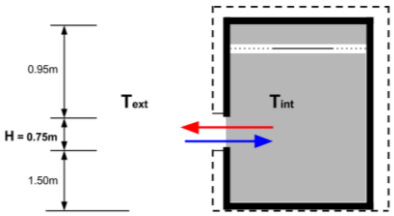
	RE/3.0/A		0.21 m^2 2.4%	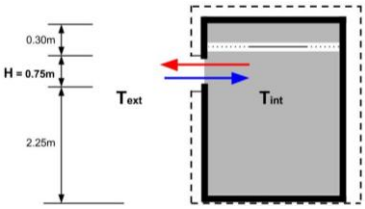
	RE/4.0/M/A		0.42 m^2 4.9%	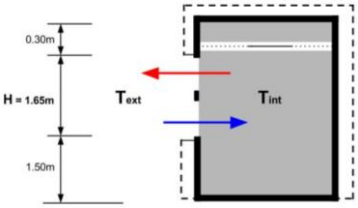

CS=Control Space; RE = Retrofit Space; M = Manual; A=Automated with manual override

4 VENTILATION RATE (ACH^{-1}) MEASUREMENT

4.1 Tracer Gas Concentration (TGC) Decay technique

The ventilation rate for the control space and retrofit space was measured using a single zone TGC decay technique. TGC decay techniques are among the most efficient to assess airflow patterns within buildings. They consist of 'marking' the air with a tracer gas (Roulet, 2007). Carbon Dioxide (CO_2) was chosen as the tracer gas for this work due to the ease of use, availability of analysis equipment, its density being similar to air and cost. CO_2 qualities as a tracer are summarised in Table 7.2 of Roulet (Roulet 2007). One main concern when using CO_2 as a tracer gas can be the presence of a large background concentration and, if constant, account must be taken for this in analysis of data by substituting the difference between

indoor and outdoor concentration for indoor concentration in the analysis (Persily 1997). For each of the tests presented in this work outdoor CO_2 concentrations during the test and indoor zone CO_2 concentrations prior to the test start were monitored and test start time concentration levels adjusted accordingly. Overall average outdoor CO_2 concentration during testing (as a percentage of the indoor concentration for each configuration) are summarised in Table 4. Occupant generated CO_2 if present in the zone during the test must also be accounted for in the analysis. Occupant CO_2 generation rates were calculated using ASHRAE Fundamentals (ASHRAE 2009). Based on specific information relating to the occupant the volumetric generation rate of CO_2 was calculated according to

$$Q_{O_2} = {}^{MA_D}/_{21(0.23RQ + 0.77)} \quad (1)$$

Where Q_{O_2} is the volumetric consumption rate, RQ is the respiratory quotient and gives the ratio of CO_2 generation to O_2 consumption, (taken as 0.83); M is the metabolic rate in W/m^2 and A_D is the DuBois surface area (calculated as $02.02m^{0.425}l^{0.725}$). Where an occupant was present in the zone, the occupant generation rate was assumed to be constant during the test period and I_{occ} was to be incorporated into the concentration mass balance equation where I is the injection rate of a particular source (kg/s). For the TGC decay technique a suitable quantity of tracer gas is injected to achieve a measureable initial concentration, $C_{initial}(t_0)$. After the initial pulse injection period, the injection is stopped and $I_{pulse} = 0$,. Once the pulse injection has stopped the tracer gas is then mixed within the zone until the average uniformity concentration difference for the test reaches an acceptable level. The tracer gas is then monitored using a gas analyser from the test start time until the test end time, in this instance once the concentration has returned at or close to the pre-test concentration levels. Based on Sherman (Sherman 1990) by solving the continuity equation for tracer gas it can be found that tracer gas concentration decays with time according to:

$$C = C(t_0)\, e^{(-Nt)} \quad (2)$$

And Including occupant generated CO_2 during the test the average N can be calculated from:

$$N = \frac{1}{T}\, ln\left(\frac{C_{final}}{C_{initial}}\right) - \left(\frac{\overline{I_{occ}}}{C}\right)$$

4.1 Experiment setup and Test conditions

35 TGC Decay tests were completed in total. Table 4 outlines the breakdown of tests completed for each operational configuration. Tests were completed in accordance with the procedure set out in ASTM E741-11 (2011). Two tracer gas sampling locations were used within the zone being tested. A single injection point was used. This was a standard CO_2 cylinder and heated flow regulator. CO_2 concentration analysers were AlphaSense IRC-A1 Non Dispersive Infra-Red (NDIR) Sensors. As CO_2 is denser than air ($\sigma = 1.53$) the gas was actively mixed as it entered the space. A maximum 10% acceptable uniformity of concentration criteria between both sampling locations in accordance with ASTM E741-11 was used to determine when there had been sufficient mixing. Figure 4 describes the equipment layout for both the control space tests and retrofit space tests.

Table 4: Schedule of experimental tests and conditions

Config.	No of tests	Range of test durations	Average Conc. uniformity	Start PPM Range (Adj.)	End PPM Range (Adj.)	Average B.G. PPM (%)
CS/1.0/M	13	24 – 90 min	5.11 %	2776-5743	386-1286	10.3
RE/2.0/M	6	26 – 77 min	3.10 %	3129-4687	495-1583	12.3
RE/3.0/A	3	31 – 50 min	3.47 %	3105-3787	865-1424	13.4
RE/4.0/A/M	13	30 – 161 min	4.73 %	2546-4198	334-1179	13.0

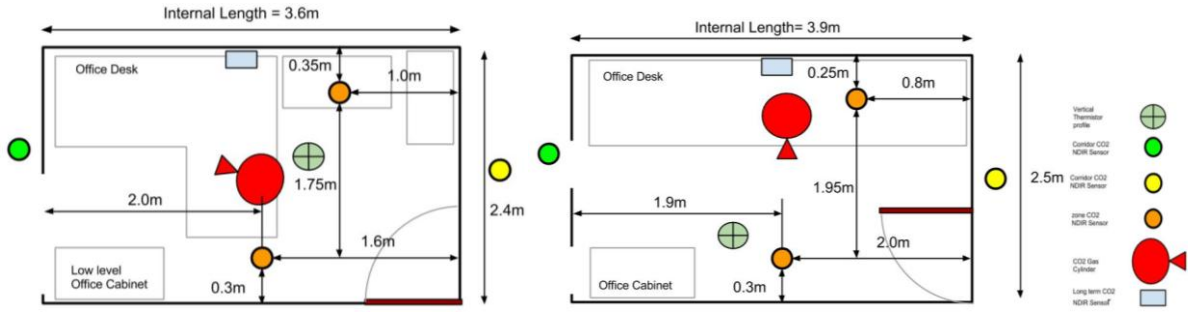

Figure 4: TCG Decay test equipment locations (a) control space (b) retrofit space

The time period of each test varied based on the configuration. Figure 5 shows results from two of the tests showing three stages; injection, mixing and stabilisation of concentration and concentration decay rate.

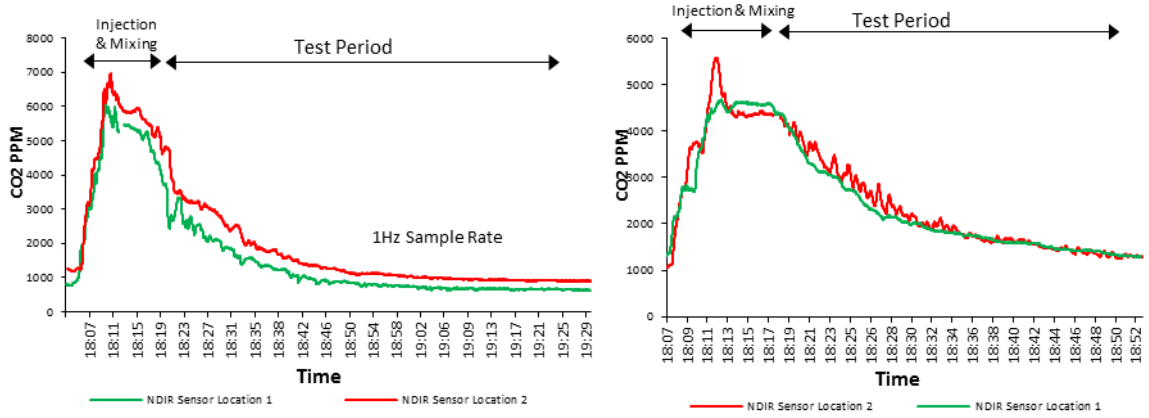

Figure 5: PPM Profile for TGC Decay Test (a) 12 RE/4.0/A/M & (b) Test 26 CS/1.0/M

4.2 Results & Analysis

Table 1 contains summary data regarding the 35 tests. Having measured the ventilation using the TGC decay technique the purpose of the investigation was to understand whether the dominant forces were different for the different configurations under similar conditions. The highest range of ACH^{-1} can be seen to occur in the control space. It produced the highest ACH^{-1} and on average had higher ACH^{-1} under similar conditions.

Table 5: ACH^{-1} Controlled Test Results Overview

Test Config.	Max ACH^{-1}	Min ACH^{-1}	Std. Dev.	Ave ACH^{-1}	Occ. < 3.0 ACH	Occ. < 1.5 ACH	WS Range (m/s)	No. of Windward/ Leeward tests	ΔT_{ie} Range
CS/1.0/M	4.70	1.16	1.19	2.81	7	4	1.41-5.20	9/4	4.2-8.9
RE/2.0/M	3.59	1.28	0.89	2.14	1	2	1.36-5.24	4/2	0.5-5.5
RE/3.0/A	2.75	1.13	0.89	1.73	0	2	3.33-4.24	1/2	1.1-5.3
RE/4.0/A&M	3.70	0.54	0.94	2.52	5	3	1.52-4.47	7/6	0.4-7.1

Envelope temperature differences were generally higher for the CS tests. Under each of the three configurations in the RE space there is a large variation in ventilation rate with average ACH^{-1} generally less than 2.0 ACH^{-1} for Config RE/2.0/M & RE/3.0/M. For the full height configuration RE/4.0/M/A, 40% of tests were above 3.0 ACH^{-1}. Overall these are still low ventilation rates and will impact on the thermal time constant, heat transfer to and from the structure and indoor air freshness. The retrofit space had lower ACH^{-1} than the control space potentially due to reduced wind effect from the flush faced louvres and reduced temperature differences. The two main forces that can give rise to ventilation rates are stack effect, generated by temperature difference across the building envelope and pressure at the building

surface due to wind effect (magnitude and direction). Single sided ventilation rates due to these combined forces can be described using a number of semi-empirical models. Warren (1978) proposed 2 separate correlations for stack and wind effect, taking the larger of the two to quantify ventilation rate. Dascalaki (1996) proposed an alternative correlation to take account of wind effects. More recently Larsen and Heiselberg (Larsen & Heiselberg 2008) proposed a more complex correlation that takes account of the thermal effects, wind speed & direction. Larsen & Heiselberg found that the dominating force differs between wind speed and ΔT_{ie} depending on the ratio between these forces and the wind direction. Based on this further analysis of the results above is needed. In attempting to quantify these combined forces, Warren (1978) proposed the use of 3 dimensionless values in order to study the strength of stack effect in contributing to the ventilation rate in single sided ventilation. The Archimedes number, $Ar = (Gr/Re^2)$ is a measure of the relative strength of buoyancy and inertia forces described as:

$$Ar^{0.5} = \frac{\Delta T g H}{T v_{wind}^2} \tag{3}$$

By plotting the Archimedes number as a function of Flow number, F, it is possible to see whether stack effect or wind effect is dominant for each measured ventilation rate.

$$F = \frac{q_{ACH}}{A_{eff} v_{wind}} \tag{4}$$

The use of a flow number due to thermal stack effect alone, F_{th}, is introduced to the plot. K is a function of opening discharge coefficient and depending on whether an orifice law or quadratic law is used K will vary. We have taken K= 0.2 (based on a $C_d = 0.61$) for the opening

$$F_{th} = K.Ar^{0.5} \tag{5}$$

The Warren chart in figure 6 suggests that for a large number of the tests the ventilation was either equal to or less than the stack ventilation rate.

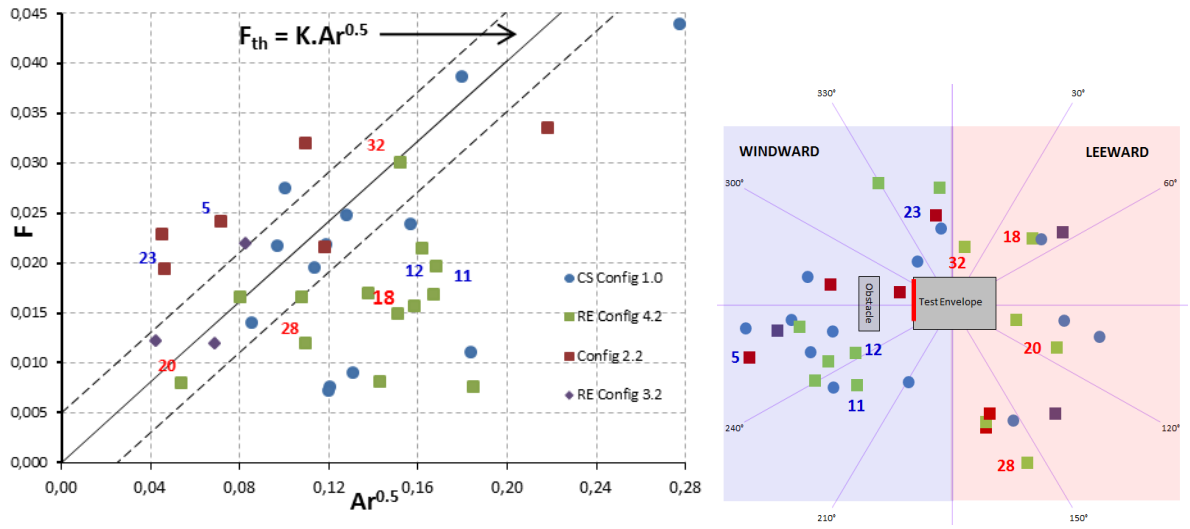

Figure 6: Warren Plot & Wind Direction/Wind Speed for each test categorised according to configuration

Figure 6 also contains a plot showing wind direction and magnitude for each of the tests, colour coded according to configuration. Some test values have been numbered according to the test reference. Blue represent windward and red leeward tests. It is clear from the results shown that both windward and leeward directions are opposing stack effect for RE/4.0/A/M and all test results are at or below stack ventilation rates. Where there is leeward winds these were with ΔT_{ie} values of 0.4°C - 4.4°C. Caciolo et al (Caciolo et al. 2011) reported that from experimental tests of single side ventilation at low wind speeds stack effect was more dominant creating turbulence at the opening. Test 11 & 12 had windward conditions but wind

speeds were relatively low. A Recirculation zone is likely present for leeward tests with no mixing layer thus reducing wind effect on ACH^{-1}. For RE/2.0 the low height dimension suggests stack effect wasn't sufficiently established across opening and wind effect was more dominant.

5 INTERNAL ENVIRONMENT

5.1 Zonal Thermal Stratification

According to Etheridge (2011) while stratification has practical importance in that it affects envelope flows it is not as important as the mean temperature of air and surrounding surfaces, i.e. if these temperatures are outside an acceptable range then stratification is of secondary importance. However it can be viewed as a source of uncertainty when modelling zone ventilation and temperatures and using a single node technique and some understanding of the likely effects should be established. Li (2002) proposes three possible "good" profiles for vertical air temperature profiles; linear, a two layer profile & a mixed profile. A simple linear temperature profile can be described using the following Kappa model (BSim2000) which uses a k function for varying gradients of stratification, $k = T_f - T_o / T_R - T_o$.:

$$T = T_0 + (T_R - T_0)\left(\frac{z}{H}(1-k)+k\right) \quad (6)$$

Li (2002) also stated that the effect of thermal stratification on airflow can be very significant and ignoring it can lead to significant under estimation of the neutral levels in a building. In un-insulated or poorly insulated buildings stratification may also affect heat transfer between inside air and walls, modifying ventilation flow rates. In order to investigate what level of thermal stratification was present in the existing building and how the retrofit strategy has modified this vertical temperature profile was measured during each of the ACH^{-1} tests and for an extended period covering 9th June 2013-23rd July 2013. This data was useful for studying stack driven ventilation rate and analysing the conditions that result in higher stratified air than normal in each zone. It can assist in quantifying the uncertainty in air temperature prediction when using multi zone airflow networks models for existing and low energy retrofit buildings. Comparison of stratification profiles for retrofit configurations are presented in figure 7. Figure 8 shows the effect of high external temperatures & night cooling for the retrofit space. The data was obtained during a particularly warm period with external temperatures reaching 10 year highs. Etheridge (2011) mentions the use of the dimensionless stratification factor (*StrFr*) to also characterise its relative strength in a single zone compared to envelope temperature difference:

$$\frac{\Delta T_s}{\Delta T_{ie}} = \frac{T_H - T_0}{T_{H/2} - T_E} \quad (7)$$

Both these values have been calculated and tabulated for ACH^{-1} tests that were highlighted as being stack dominant in the Warren plot in section 4 above. Longer term *StrFr* are also shown in table 7 below.

5.2 Instrument setup

Hanwell Radio-logger RL4000 wireless data loggers and precision thermistors with an accuracy of +/- 0.1°C between -25°C to 50°C were used for vertical temperature distributions. Measurements were recorded every 10 minutes in the retrofit space and every 5 minutes in the control space. Measurements were taken at 8 vertical positions from floor to false ceiling level spaced evenly throughout the 3.2m height. Surface and air temperatures are continuously logged using Gemini Tiny-tag data loggers.

5.1 Results & Analysis

Figure 7 highlights vertical temperature profiles for the RE configurations. Note these have differing opening heights. They are plotted for similar *StrFr* in (a) and the largest test value in

(b) (same relative strength). RE/4.0/A/M demonstrates the largest temperature gradient in each case though RE/3.0/A is very similar in (b).

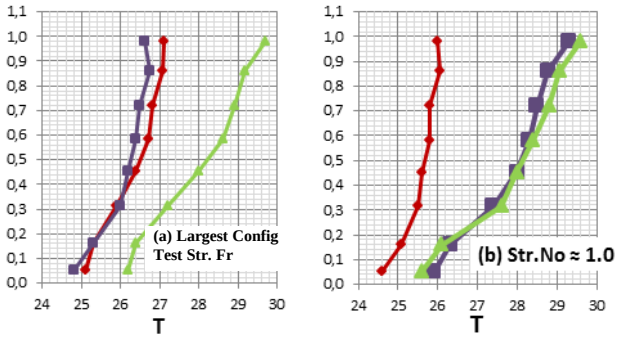

Figure 7: Vertical Stratification RE config during ACH Tests 16, 23, 20 (colour as per Config)

Table 6 below summarises the vertical temperature gradients, kappa values and *StrFr* for each test that was seen to have stack dominated ventilation flow based on Warren plot results earlier. All CS tests that demonstrated strong stack effects have small stratification numbers while the opposite is the case for the RE space. This indicates that in the CS ΔT_{ie} was always stronger than ΔT_s and suggests stratification is potentially of secondary importance (other than affecting heat transfer at the zone surfaces) to envelope flows. In the RE space, although T_{int} was generally lower and ΔT_{ie} & ΔT_s both individually lower than the CS, results suggest stratification may still play a significant role in the thermal dynamics of the internal zone.

Table 6: Stratification Profiles for Stack Dominated Tests based on Warren plot

Location/Config	Test	*StrFr*	$\|F-F_{th}\|$	Km^{-1}	Kappa Range
CS/1.0	3	0.227	0.002	0.49	0.95
CS/1.0	4	0.551	0.002	0.94	0.76
CS/1.0	27	0.565	0.001	1.00	0.72
CS/1.0	2	0.621	0.003	1.81	0.64
RE/2.0	29	0.700	0.002	1.30	0.57
CS/1.0	14	1.051	0.003	3.20	0.38
RE/3.0	25	1.111	0.002	1.20	0.31
RE/3.0	16	1.125	0.004	0.60	0.13
RE/4.0	32	1.438	0.001	0.80	0.01
RE/4.0	24	1.809	0.000	1.20	0.01

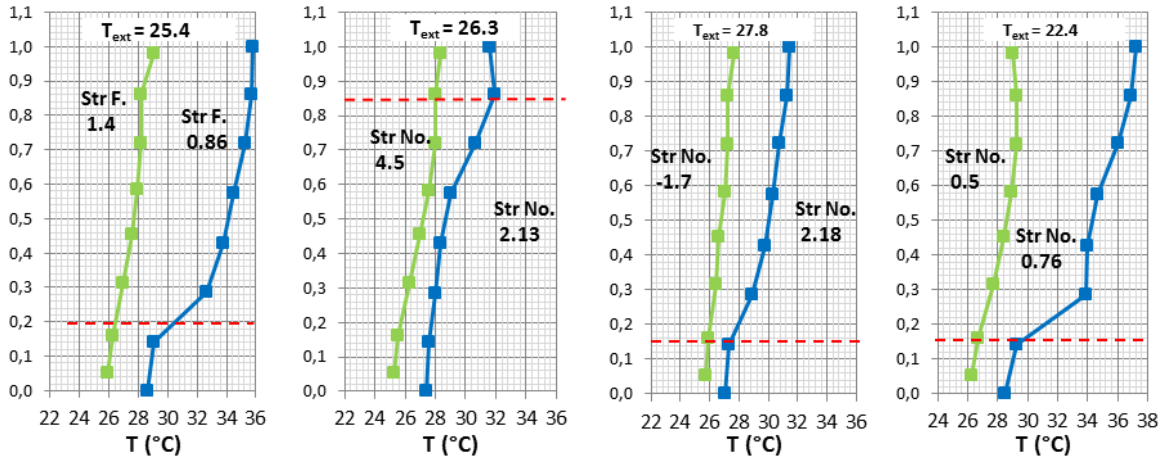

Figure 8: RE vs. CS stratification for (a) 10-Jul 16:45 (b) 12-Jul 15:30 (c) 13-Jul 16:50 (d) 18-Jul 20:00

Considering some specific dates, 10th July had night cooling (NC) activated in RE and blinds fully closed but no NC in CS; 12th July had NC activated in RE and CS with blinds in RE fully closed and CS internal blinds 50% closed; 13th July is a Saturday with window open 24hrs in CS but only RE/3.0/A Config active all weekend in RE space. 18th July had NC in

both spaces. On 10th July even though there's a high ΔT_s it still isn't more dominant than ΔT_{ie} and less significant, while the RE space has a lower temp diff but a StrFr > 1. Night cooling resulted in mean zone temp 2.5K above T_{ext} but outside acceptable ranges. On 12th July *StrFr* is very strong in RE mainly due to ΔT_{ie} but again suggests the vertical temperature profile is important to understanding ventilation coupling with thermal mass at different heights (WS = 2.7 ms^{-1} WD = parallel to envelope 196°). T_{ext} on 13th July is one of the highest recorded during the summer 2013 period and *StrFr* for RE space is -1.7, ($T_{int} < T_{ext}$).

Table 7: 20th June – 19th July 2013 Percentile Values *Str.Fr ($\Delta T_s/\Delta T_{ie}$)* Data

Space.	Occupied hours (09:00-18:00)				Unoccupied Hours (18:00-09:00)			
	50th	75th	95th	% occ hrs >1	50th	75th	95th	% occ hrs>1
Control	0.411	0.691	1.19	9.0%	0.192	0.333	0.622	0.0%
Retrofit	0.202	0.609	2.59	14.5%	0.157	0.290	0.611	2.2%

Table 7 shows how stratification is substantially reduced during overnight periods. The 95th percentile value for unoccupied hours of 0.611 is largely based on conditions up to around 21:00 each evening where there is still significant stratification. Both spaces monitored are west facing and this suggests an association with incident solar irradiation and the occurrence of peak conditions later in the evenings. Most of the peak conditions take place at this time even though peak day time air temperatures occur as early as 11:45. The retrofit occupied hours 95th percentile value of 2.59 does highlight that there is stratification still present in the space and it has a significant relative strength compared to ΔT_{ie}. Temperatures at the surface of the exposed roof slab are often 2-3°C higher than would be reported based on a mid-level zone thermostat which can be significant in ventilate cooling of a low energy space.

5.2 Thermal time constant & T_{int} time lag

While the envelope structure has undergone a major external material upgrade with a significant reduction in decrement factor (0.608 to 0.004) the internal thermal mass in contact with the zone air has largely remained unchanged other than part exposure of the roof slab in the retrofit though perforated ceiling tiles. It should be noted there is also a difference in quantity of thermal mass between CS and RE with CS only having one internal block-work wall while RE has two. The zone thermal time constant described below, is plotted for each ACH^{-1} test result as a function of flow number, *F*, shown in figure 9.

$$\tau = \left[\left(\rho C_p Vol \right)_{air} / \left(\rho C_p Vol \right)_{mass} \right] \quad (8)$$

Higher τ values are seen in the RE, even a similar F values. Table 8 presents a comparison of daily maximum & minimum internal temperatures for RE & CS with the corresponding hour of occurrence for 8th – 14th July 2013. If NC was present on the previous night this is indicated by the symbol (*Config RE/4.0/M/A & ** Config RE/3.0/A) adjacent to Max T_{int}.

Table 8: Measured $T_{H/2(peak)}$ Time Lag during week 8th-14th July 2013

Day	External		RE				CS			
	Max T_{ext} (°C)	Occ. (hr)	Max T_{int} (°C)	Occ. (hr)	Min T_{int} (°C)	Occ. (hr)	Max T_{int} (°C)	Occ. (hr)	Min T_{int} (°C)	Occ. (hr)
8th	25.4	16:35	29.0	18:50	24.4	06:00	36.8	19:35	25.0	05:40
9th	27.1	14:40	28.6	18:40	25.5	23:40	36.1	19:00	26.8	07:05
10th	26.4	13:00	29.1*	19:50	22.8	07:10	36.5	19:25	28.0	06:10
11th	23.9	11:45	30.0*	18:40	22.8	06:50	-*	-	25.0	07:40
12th	26.4	15:15	28.0*	19:00	22.0	06:30	35.6*	17:35	-	-
13th	27.8	14:20	28.4**	18:40	25.1	06:20	36.1*	17:45	24.3	07:45
14th	25.8	16:55	27.9**	20:00	25.8	07:20	33.9*	17:20	25.7	23:40

Table 9: $T_{H/2}$ Peak Daily Air Temperatures and Diurnal Variation (20th June – 19th July 2013)

Space.	hrs>25°C (%Σhrs)*	hrs>28°C (%Σhrs)*	95th Perc. $\Delta T_{ext(24hr)}$	50th Perc. $\Delta T_{ext(24hr)}$
Control	34	17		
Retrofit	33	3.5		

**Based on 981 working hours May-September*

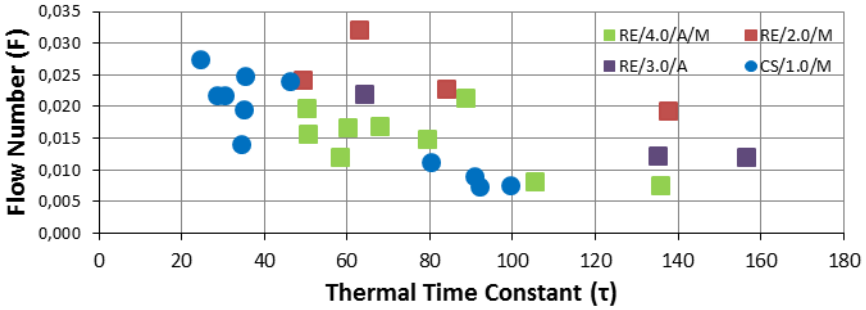

Figure 9: τ vs. F based on each controlled ACH^{-1} test

6 CONCLUSIONS

While the current results and analyses are not yet definitive it is clear from current findings that the retrofit works have modified the internal environment and ventilation rate for isolated spaces with single sided ventilation. The largest ACH^{-1} rates measured in the retrofit space were still lower than the existing building under similar conditions. Error analysis and uncertainty of results also still needs to be quantified. The analysis suggests ventilation rates were either dominated by stack effect or lower than the rate due to stack effect indicating some counteracting force during these tests. More tests are needed to better understand how different forces affect ventilation performance in the RE, particularly for configurations RE/2.0/M & RE/3.0/A. In the CS when there were windward conditions with wind speeds > $4ms^{-1}$ these tests still displayed flow numbers very close to F_{th} (ΔT_{ie} > 6.5K in both tests). In the RE space leeward tests were generally stack dominant or lower. However, there were results that had flow numbers very close to F_{th} with both high and low wind speeds and windward and leeward conditions. This suggests that the influence of wind conditions on ventilation rates is complicated by local obstacles at the site nearby the CS and RE spaces. More analysis and additional testing is required to establish to what extent wind conditions are affecting ventilation rate. What is clear is for configuration RE/4.0/A/M, which is the proposed summer cooling arrangement; nearly all measurements of ventilation rate were lower than stack effect alone. Regarding Internal thermal environment, this has been modified with the mean zone temperature substantially reduced. Diurnal temperature amplitude has also been reduced. This is as expected. ΔT_s had a lower magnitude in the RE but had higher *StrFr* values suggesting it had a higher relative strength compared to the existing building. Night cooling didn't appear to have a measurable influence on the RE space which may be due to low ventilation rates at night, something that may need to be studied further. In the CS when night cooling was used $T_{int(max)}$ magnitude didn't change but the hour of occurrence shifted back to earlier in the day. This is probably due to ventilating the space in the evening time when high solar gains are present as opposed to the night cooling, although $T_{int(min)}$ were moderately reduced.

7 ACKNOWLEDGEMENTS

The original pilot project works was supported through a grant from the Department of Education and Skills, Ireland. The authors wish to acknowledge the co-work of the pilot project design and research team in the design and development phases of the pilot project, Mr Fergus Delaney for providing the dynamic thermal response factors in Table 2 and Mr Turlough Clancy for the Image in Figure 3(a).

8 REFERENCES

ASHRAE, 2009. *2009 ASHRAE HANDBOOK - Fundamentals*,

ASTM E741-11 (2011), 'Standard Test Method for Determining Air Change in a Single Zone by Means of a Tracer Gas Dilution'.

Caciolo, M., Stabat, P. & Marchio, D., 2011. Full scale experimental study of single-sided ventilation : Analysis of stack and wind effects. *Energy & Buildings*, 43(7), pp.1765–1773.

Dascalaki (1996)

DCENR, 2013. *Irelands Second National Energy Efficiency Action Plan*,

Etheridge, D. (2011). Natural Ventilation of Buildings: Theory, Measurement and Design ISBN: 978-0-470-66035-5, Chapter 6 - Internal air motion, zonal models and stratification. 180-183

European Union, 2010. Directive 2010/31/EU. , pp.13–35.

Kolokotroni, M.,Webb, B.C. and Hayes, S.D. (1996b)'Summer cooling for office-type buildings by night ventilation' in Proceedings of the 17th AIVC Conference on Optimum Ventilation and Air Flow Control in Buildings, Gothenburg, Sweden, 17-20 September, vol 2, pp591-599

Kolokotroni M., Watkins R., Santamouris, M., Niachou, K., Allard, F., Belarbit, R., Ghiaus, C., Alvarev, S. and Salmeron, J.M. (2002)'Lissen: Passive ventilation cooling in urban buildings: An estimation of potential environmental impact benefits', in Proceedings of the EIPC 2002 Conference, Lyon, France

Larsen, T.S. & Heiselberg, P., 2008. Single-sided natural ventilation driven by wind pressure and temperature difference. *Energy and Buildings*, 40(6), pp.1031–1040.

Li, Y. (2002) ' Integrating thermal stratification into natural and hybrid ventilation analysis' Technical Report TR15, IEA-ECB&CS Annex 35, pg1-38

NSAI, 2012. ISO 10077-2:2012 Thermal performance of windows, doors and shutters - Calculation of thermal transmittance - Part 2 : Numerical method for frames,

O'Sullivan, P. et al., 2013. Design and Performance of an External Building Envelope Retrofit Solution For a Grid Optimised Concrete Structure: A Case Study. In *IMC30 Conference Proceedings 2013*.

Persily, A. (1997) 'Evaluating Building IAQ and Ventilation with Indoor Carbon Dioxide', ASHRAE TRANSACTIONS 1997, V.103, Pt 2

Roulet, C.A., (2007). Ventilation and Airflow in Buildings: Methods for Diagnosis and Evaluation, BEST (Buildings Energy and Solar Technology). Chapter 7 - Common methods and techniques, pg 133

Sherman, M., 1990. Tracer Gas Techniques for Measuring Ventilation in a Single Zone. *Building and Environment*, 25(4), pp.365–374.

Warren, P.R., 'Ventilation through openings on one wall only'. Proceedings of the International Centre for Heat and Mass Transfer Conference - 'Energy Conservation in Heating, Cooling and Ventilating Buildings, Dubrovnik, August 29 - September 2, 1977. Volume 1, pp 189-206. Publ. Hemisphere Publishing Corporation, Washington.

List of figures and tables

VENTILATIVE COOLING OF RESIDENTIAL BUILDINGS: STRATEGIES, MEASUREMENT RESULTS AND LESSONS-LEARNED FROM THREE ACTIVE HOUSES IN AUSTRIA, GERMANY AND DENMARK

Peter Foldbjerg*, Thorbjørn Asmussen

VELUX A/S, Daylight Energy and Indoor Climate, Ådalsvej 99,
2970 Hørsholm, Denmark
**Corresponding author: peter.foldbjerg@velux.com*

ABSTRACT

The thermal comfort of the residential buildings Home for Life in Denmark, LichtAktiv Haus in Germnay and Sunlighthouse in Austria is investigated with a particular focus on the strategies used to achieve good thermal comfort, and the role of solar shading and natural ventilation. The houses are three of six buildings in the Model Home 2020 project. They have generous daylight conditions, and are designed to be energy efficient and CO_2 neutral with a good indoor environment. The living rooms in all three houses have high daylight levels and have been selected for the detailed analyses for this reason. The thermal environment is evaluated according to the Active House specification (based on the adaptive method of EN 15251), and it is found that the house reach category 1 for the summer situation. Some undercooling occurs in Sunlighthouse and Home for Life during winter, which is caused by occupant preferences or incomplete commissioning. It is found that ventilative cooling through window openings play a particularly important role in maintaining thermal comfort in all three houses and that both window openings and external solar shading is used frequently.

KEYWORDS

Thermal comfort; ventilative cooling; residential buildings; natural ventilation; solar shading

1 INTRODUCTION

Five single-family houses in five European countries were built between 2009 and 2011 as a result of the Model Home 2020 project. Home for Life, Denmark, was completed in spring 2009, followed by Sunlighthouse (SLH) in Austria and LichtAktiv Haus (LAH) in Germany in 2011. Home for Life and Sunlighthouse are new buildings while LichtAktiv Haus is a refurbishment and extension of an existing house. The three houses have been occupied by test families in one-year periods, and measurements have been made during the period (Foldbjerg 2012, 2013). This paper focuses on the consolidated learnings from the three houses.

The houses follow the Active House principles (Eriksen, 2011) which mean that a balanced priority of energy use, indoor environment and connection to the external environment must be made. The design has particularly focused on excellent indoor environment and a very low

use of energy. There is a particular focus on good daylight conditions and fresh air from natural ventilation.

Measurements of IEQ include light, thermal conditions, indoor air quality, occupant presence and all occupant interactions with the building installations, including all operations of windows and solar shading. The present deals with thermal comfort, particularly the natural ventilation system and the solar shading. Use of natural ventilation for summer comfort is based on ventilative cooling principles (venticool, 2013).

The presented results focus on thermal conditions, effectiveness and experience with the applied strategies. Some demonstration houses in Scandinavia have experienced problems with overheating, often due to insufficient solar shading and use of natural ventilation (Isaksson, 2006 and Larsen, 2012).

All three houses use natural ventilation in the warm part of the year. Home for Life and Sunlighthouse use mechanical HRV during cold periods, while LichtAktiv Haus is using natural ventilation all year. There is external automatic solar shading on all windows towards South, and overhangs are used where appropriate.

Figure 1. Home for Life (left). Sunlighthouse (middle). LichtAktiv Haus (right)

Each room is an individual zone in the control system, and each room is controlled individually. There are sensors for humidity, temperature, CO_2 and presence in each room. The building occupants can override the automatic controls, including ventilation and solar shading at any time. Override buttons are installed in each room, and no restrictions have been given to the occupants. As house owners they have reported a motivation to minimise energy use on an overall level, and to maximise IEQ on a day-to-day basis.

The recorded temperature data is evaluated according to the Active House specification (Eriksen, 2011), which is based on the adaptive approach of EN 15251 (CEN, 2007). The results presented here are based on the measurements and analyses for the period in which test families have occupied the houses. For Sunlighthouse and LichtAktiv Haus data collection for this paper stopped in October 2012.

2 RESULTS

Figure 2 shows thermal comfort categories for the three houses. Home for Life experiences low temperatures (undercooling) in most rooms, but no overheating except for the bedroom. All rooms except the bedroom achieve category 1 when overheating is disregarded. LichtAktiv Haus experiences undercooling in the top-floor library, possibly in periods when the room is not used. The kitchen-living room and bedroom does not experience much undercooling. The children's rooms (Room 1 and Room 2) experience undercooling for more

than 5% of the investigated period. No main rooms experience overheating for more than 5% of the time, and therefore achieve category 1 with regards to overheating.

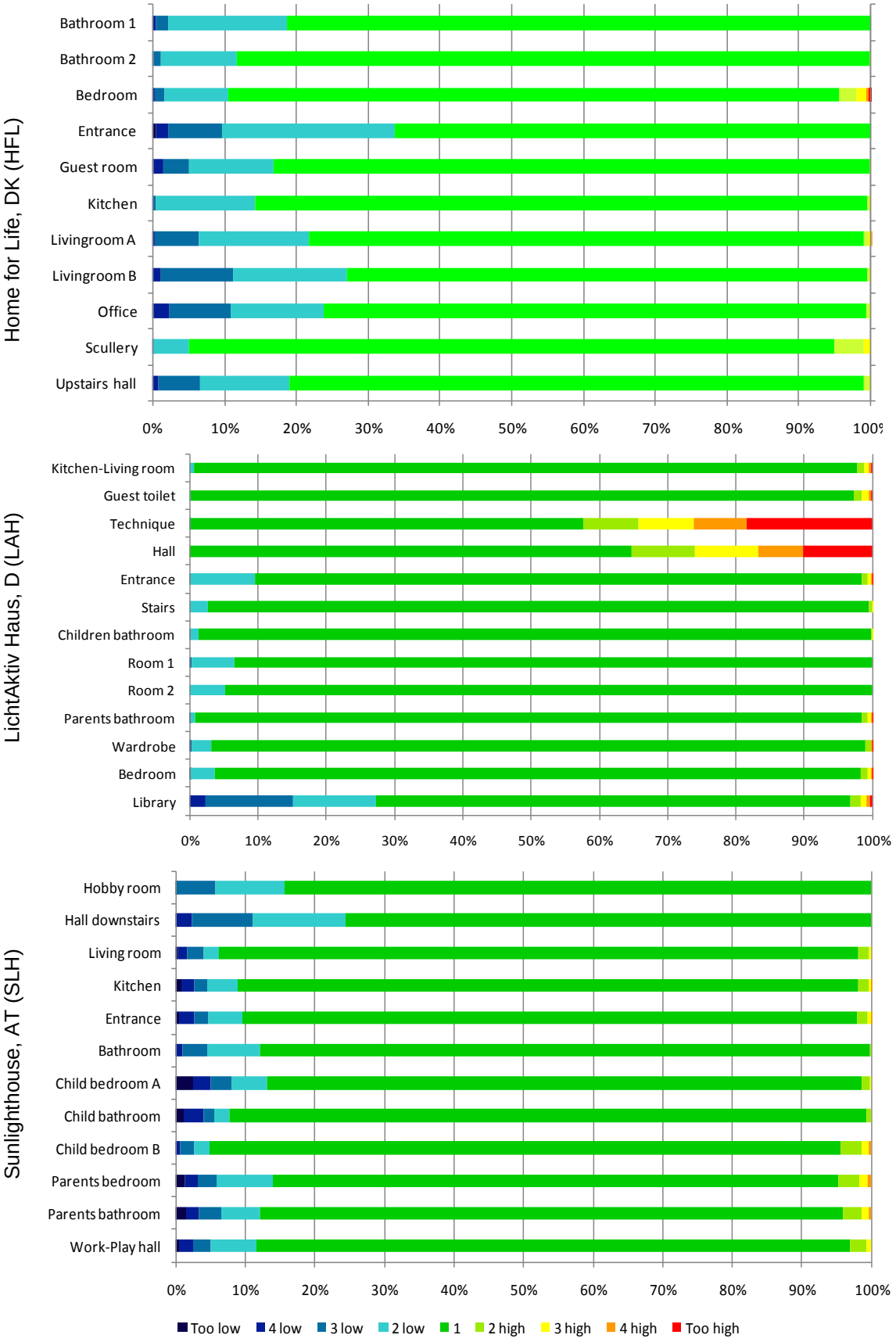

Figure 2. Home for Life, LichtAktiv Haus and Sunlighthouse. Thermal comfort for each of the rooms evaluated according to Active House specification (based on adaptive method of EN 15251). Criteria are differentiated between high and low temperatures.

Sunlighthouse experiences substantial undercooling in all main rooms for 5-15% of the investigated period. Overheating is limited, and all main rooms achieve category 1 with regards to overheating.

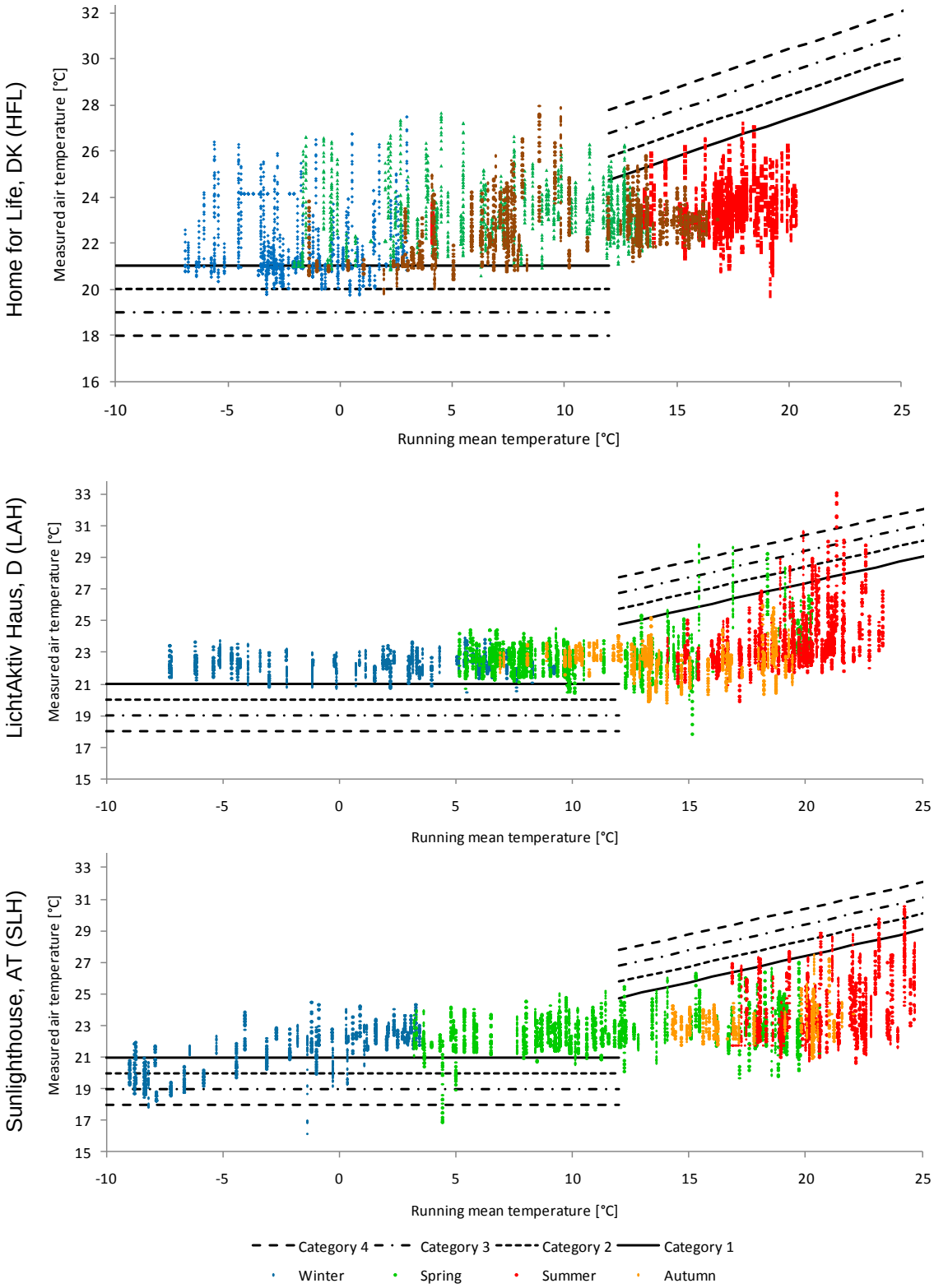

Figure 3. Livingroom in HFL, LAH and SLH. Indoor temperatures in the living room plotted against running mean temperature for each hour of the year including the Active House category limits. The dots are coloured to represent a season.

The focus of the present paper is on the performance related to ventilative cooling and potential overheating. The further analyses will focus on the performance of the combined living and dining room, which have large glazed areas in each of the three houses, and therefore these rooms are investigated further. Figure 3 shows the indoor temperature at each hour of the year plotted against the running mean outdoor temperature as defined in EN 15251.

For Home for Life the temperatures during cold periods drop below the category 1 limit (21°C) for a substantial part of the time, but with only a few hours below the category 2 limit (20°C). During transition periods, only few hours below category 1 are seen. For LichtAktiv Haus it is seen that temperatures below the category 1 limit (21°C) occur both in winter and in the transition periods. The occupants have reported discomfort due to undercooling during airings at outdoor temperatures below 0 °C. For Sunlighthouse more pronounced undercooling is observed, particularly during the coldest part of the year.

In Home for Life, high temperatures are seen more in the transition periods than during the warmer summer period. This is expected to be caused by the control system, which maximises solar gains in "spring" mode, while it prioritizes thermal comfort in "summer" mode by minimizing solar gains. For Sunlighthouse, no episodes with temperatures above 26°C are seen during winter or in the transition periods. For LichtAktiv Haus, no overheating was seen in winter, but three episodes of spring overheating (light green dots are seen). This happens when the outdoor temperature is below 26°C, and the most likely cause is the same control system phenomena as was seen for Home for Life. Some summertime overheating is observed for LichtAktiv Haus, with some episodes where category 3 is exceeded. Only few episodes with summertime overheating are observed for Sunlighthouse.

Relatively low temperatures are observed for all three houses during summer, with episodes with temperature drops below 21 °C. This is suspected to be caused by night cooling, where the temperature decreases during the night to reduce overheating the following day, which in some situations lead to temperatures in the morning between 20 °C and 21 °C.

The variation over time-of-day and time-of-year is further investigated in Figure 4, which is using temporal maps to plot each hour of the year according to day-of-year and time-of-day. For Home for Life it is seen that the episodes during winter with temperatures below category 1 can last for several days during the winter, but that in many of the episodes, the temperature reaches category 1 between 12:00 and 20:00, possibly due to solar gains. During summer, only few episodes with temperatures beyond category 1 are observed. For LichAktiv Haus, no wintertime undercooling of importance is seen. The episodes with summertime overheating are short with a span of 2-3 days. The overheating occurs during the afternoon between 12:00 and 22:00 with temperatures reaching even category 4. For Sunlighthouse, substantial undercooling occurs mainly during one week at the end of January, during which the house was not yet occupied by the family, and in a period when the heat pump system was not functioning properly. In June, a few episodes with overheating where temperatures reach category 3 are observed between 16:00 and 23:00. These episodes last for 2-3 days.

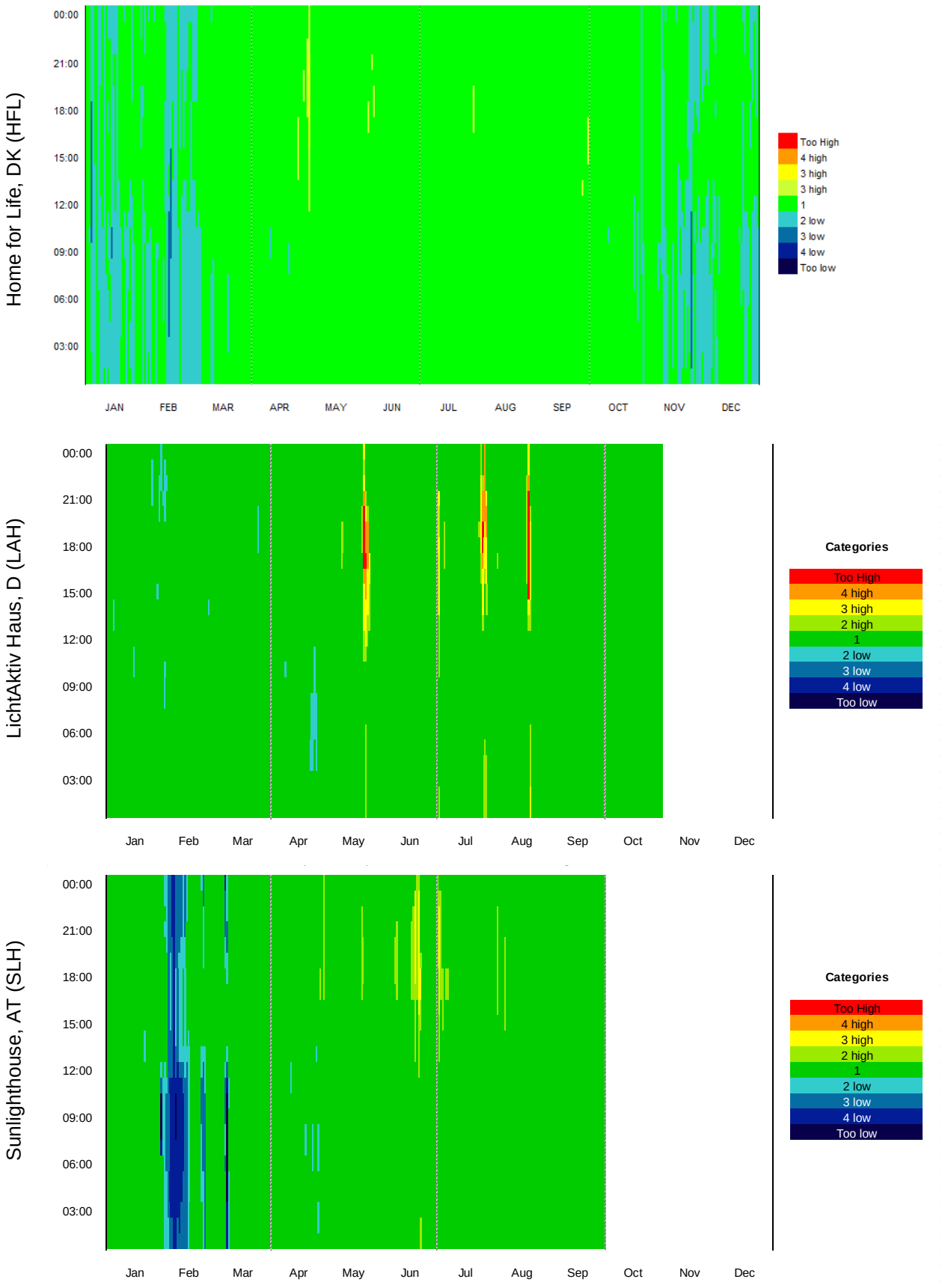

Figure 4.Living room in HFL, LAH and SLH. The comfort category of each hour of the year is plotted as a temporal map

To investigate the role of window openings in maintaining comfort, Figure 5 is used. A simplified comfort definition is imposed for the sake of the analysis, so that category 1 or 2 is considered “Comfort” while categories 3 and 4 are considered “Discomfort”. The figure shows if any windows where active during each hour.

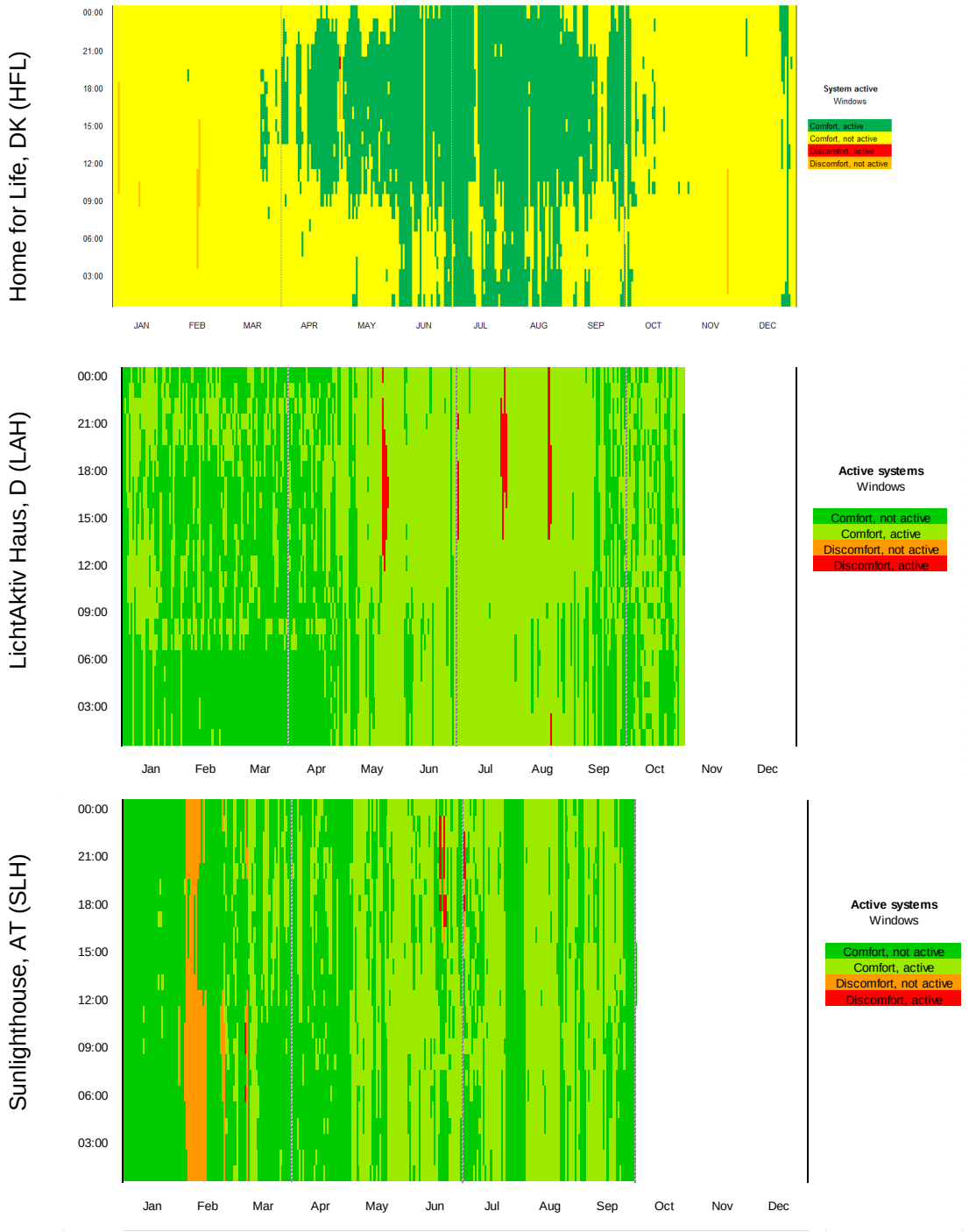

Figure 5. Living room in HFL, LAH and SLH. Temporal map showing comfort or discomfort and if windows were open or closed (active or not active).

Figure 5 shows that in LichtAktiv Haus windows are used for airings on most days in the winter at 6:00 to 8:00 and in the evening between 20:00 and 22:00, which can be expected, as the house is based on natural ventilation all year. Home for Life and Sunlighthouse use

mechanical ventilation during winter, and in these houses windows were not open during the winter episodes with temperatures below category 1, indicating that these episodes were not caused by window airings. In interviews, the occupants of Home for Life have reported that they decided to have a room temperature of 20-21 ^{o}C to reduce heating consumption. The episodes with winter temperatures below category 1 can thus be attributed to user preferences.

A few episodes with red colour are seen during summer for all three houses in the late afternoon, indicating that overheating occurred and that windows were opened, but that this was not sufficient to maintain category 1 or 2.

Figure 5 further shows that during the summer, windows are almost permanently open and that category 1 or 2 is maintained during these hours. This tendency applies to daytime as well as night-time, and indicates that windows are used for automatic night cooling and that the occupants are not closing the windows by overriding the control system.

Also in the transition periods (March to May and September to October) windows are used to a large extent. In Home for Life and LichtAktiv Haus the windows are mainly used during daytime, while they are used in 24-hour cycles in Sunlighthouse.

3 CONCLUSIONS

The houses are evaluated according to the Active House specification, which uses the same methodology and criteria as EN 15251 with regards to thermal comfort. For all three houses, there is more undercooling than overheating, but not to a large extent, and most main rooms end in category 2 or 3. The undercooling has simple explanations. In HFL it is an active choice of the occupants to have a temperature between 20°C and 21°C. In SLH the undercooling occurs during a week here the house was not yet commissioned and occupied, and where the heat pump was not yet in proper operation. LAH experiences practically no undercooling which means that natural ventilation is applied without adverse effect on thermal comfort, as the occupants could have decided to close windows. The conclusions in the following refer to the combined dining and living room, which is exposed to the most solar gains.

In all three houses, the minimum indoor temperature does not increase with outdoor temperature during summer. This is most likely caused by night cooling, which cools down the building to reduce the maximum temperature on the following day. The occupants could have deactivated the night cooling if they were uncomfortable with it, which indicates that in these buildings the occupants accept lower summer temperatures than suggested by the adaptive approach.

In LAH (Germany) and HFL (Denmark), some episodes with temperatures above 26°C are seen on days during the transition periods. This is explained by the different priorities of the control system, which priorities energy in “Spring/autumn” mode, and thermal comfort in “summer” mode.

All three houses have generous daylight conditions, which could have caused overheating. However, little overheating is seen, which is attributed to the active use of ventilative cooling by solar shading and natural ventilation. The role of windows is investigated, and in all three houses, window openings occurred at the same time as acceptable thermal comfort during the

summer period. This indicates that window openings have contributed to achieving and maintaining good thermal conditions.

4 REFERENCES

CEN (2007). CEN Standard EN 15251:2007. *Indoor environmental input parameters for design and assessment of energy performance of buildings addressing indoor air quality, thermal environment, lighting and acoustics*. European Committee for Standardisation.

Eriksen, K.E. et al (2011). *Active House – Specification*. Active House Alliance. 2011.

Foldbjerg, P., Worm, A. and Feifer, L. (2012). Strategies for Controlling Thermal Comfort in a Danish Low Energy Building: System Configuration and Results from 2 Years of Measurements. In *Proceedings of AIVC 2012*, Copenhagen.

Foldbjerg, P., Rasmussen, C. And Asmussen, T. (2013). Thermal Comfort in two European Active Houses: Analysis of the Effects of Solar Shading and Ventilative Cooling. Proceedings af Clima 2013, Prague.

Isaksson, C. and Karlsson, F. (2006) Indoor Climate in low-energy houses – an interdisciplinary investigation. *Building and Environment*, Volume 41, Issue 12, December 2006

Larsen, T.S. and Jensen, R.L (2012). *The Comfort Houses - Measurements and analysis of the indoor environment and energy consumption in 8 passive houses 2008-2011*. Aalborg University.

Venticool, the European platform for ventilative cooling. Published by Venticool. Last accessed August 2013. http://venticool.eu/faqs/.

EVALUATION OF VENTILATIVE COOLING IN A SINGLE FAMILY HOUSE

Bruno Peuportier[1], Karsten Duer[2], Christoffer Plesner[2] and Nicolas Dupin[3]

1 ARMINES, CES
60 boulevard Saint-Michel
75272 Paris Cedex 06, France

2 VELUX
Aadalsvej 99
2970 Horshom, Denmark
**Corresponding author: karsten.duer@velux.com*

3 VELUX
1, rue Paul Cézanne B.P. 20
91421 Morangis Cedex, France

ABSTRACT

A characterization and modeling process has been conducted in order to better account for ventilative cooling in the evaluation of energy performance of buildings. The proposed approach has been tested using a monitored zero energy Active House (Maison Air et lumière) located near Paris.

The air flow characteristics of a pivoted roof window have been evaluated using a test chamber installed in the CES laboratory. A CFD calculation has been used to model the air movements inside the chamber and derive the relevant location for the pressure sensors. The air flow rate has been measured as well as the pressure difference on both sides of the window. A flow coefficient and a flow exponent of a power law equation have been identified for different window opening angles.

Flow rates have been evaluated in "Maison Air et lumière" using an air flow model (CONTAM) with the characteristics evaluated previously. These results were compared with on site tracer gas measurements.

Indoor air temperatures in the house have been evaluated using dynamic thermal simulation complemented with air flow calculation (PLEIADES+COMFIE) in order to evaluate the potential of ventilative cooling.

Around 5K indoor temperature reduction has been obtained by the use of ventilative cooling, both by simulation and measurement: with similar outdoor conditions, the interior air temperature of the house was 5K lower using ventilative cooling than without any opening of windows.

The air exchange rates were between 10 and 22 air change per hour even with limited wind velocities (between 2 and 3 m/s) and low temperature difference between outside and inside (0-3 K). An acceptable correlation was found between calculations and measurements.

The overall consistency between calculation results and measurements shows that this process, including the evaluation of air flow characteristics and the use of combined thermal and air-flow simulation, is feasible. The aim is to progress towards assessing the effects of ventilative cooling. Such a process could be used in a regulatory calculation, provided that this calculation integrates an appropriate model.

KEYWORDS

Ventilative cooling, Thermal simulation, airflow simulation, measurements, characterization of air flow

1 INTRODUCTION

Low energy buildings, being highly insulated, are subject to important overheating risks if no proper cooling strategy is implemented. Thermal simulation as well as experimental studies has shown the large potential of ventilative cooling [Ghiaus, 2005]. One barrier against this approach is the difficulty of evaluating air flows. Appropriate calculation methods and characterization of openings are needed, so that these systems can be dealt with in design, regulation and certification tools.

The present work aims at studying a characterization and modelling process allowing natural ventilation to be accounted for in the evaluation of energy performance and thermal comfort of buildings. The approach is tested using the monitoring system of the zero energy Active House Maison Air et Lumière, located near Paris.

In summary, the following steps have been performed.

- A test bench has been used to characterize the air flow features of a roof window (such features of roof windows are not well described in literature)
- These air flow features have then been used for numerical simulations of the air flows and air temperatures in the building
- On site measurements of air flows and air temperatures have been performed in order to get realistic data about natural ventilation and its contribution to summer comfort
- Comparisons between simulations and on site measurements have been performed in order to validate the models used to evaluate air flow rates through windows. These comparisons are also used for checking the relevancy of numerical simulations in terms of summer comfort

2 LABORATORY MEASUREMENTS

2.1 Description of the method

Before performing on site tests, a test bench has been built in the laboratory in order to identify air flow characteristics of a roof window. A ventilator is used to create a pressure difference in a test cell divided in two compartments. A roof window has been installed between the two compartments. The pressure difference $\Delta P = (P1-P2)$ is measured, as well as the air flow rate Q. The air flow rate and pressure difference have been varied in order to get a curve and to derive characteristics C and n of the roof window corresponding to the following equation [Axley, 2002], [Walton, 2010]:

$$Q = C\,(P2 - P1)^n \tag{1}$$

The flow coefficient C, depend on the size and opening angle of the window. In a first approximation, C can be considered proportional to the section S corresponding to the geometrical opening section, which is commonly assumed using a discharge coefficient C_d (i.e. $C = C_d*S*(2/\rho)^n$, ρ being the air density). ΔP is in the range from 0.05 to 10 Pa. In the real house, it may be lower, depending on wind conditions, but it is hoped that the values of C_d and n will not vary too much. The laboratory test therefore provides two parameters that can be used in the analysis of on-site measurements, and that can be refined using a calibration step.

The correlation between ΔP and Q is derived from the measurements at different window opening areas. From equation (1) follows that

$$\ln Q = n*\ln\Delta P + \ln C \tag{2}$$

2.2 Laboratory test results

An example of a fully opened window is shown in figure 1 in a double logarithmic presentation. n equals the slope of the curve, ie. n = 0.45 and lnC = -1.14 leading to C = 0.32
Similar analysis is performed for all six opening areas and shown in table 1.

100% opening refers to the maximum opening length of the actuator ~200 mm opening.

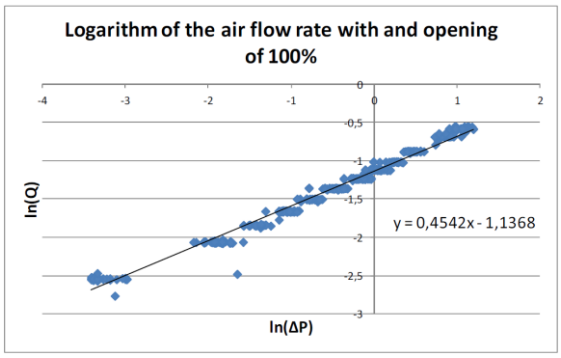

Figure 1. Air flow rate vs pressure difference for 100% opening length of the roof window.

With the assumption that the opening area *S* is around 0.07m² for 50% opening percent, we find a C_d value $C_d = C / S * (\rho/2)^{0,5}$ of around 0.75, which is near the standard values [Etheridge, 1996].

Table 1 Air flow characteristics of the roof window

Window opening percent [%]	n coefficient	C coefficient
50	0.49	0.074
60	0.46	0.12
70	0.45	0.17
80	0.48	0.22
90	0.45	0.27
100	0.45	0.32

3 ON SITE MEASUREMENTS

3.1 Description of the building

The 130 m² floor area extends over two storeys. The house is highly insulated and designed as a net zero energy Active House. Concrete slabs on the ground floor and first floor provide thermal mass. The window-floor ratio is nearly 1:3. All windows are equipped with dynamic solar protection and the operation of all systems in the building (heating, ventilation, shading window-opening, lighting etc) is fully automated.

.

3.2 Measurements

Several tracer gas techniques can be found in the literature [Sherman, 1990]. CO2 concentration decay measurements have been performed in order to evaluate the air flow rate in the house and to compare it with values calculated using the laboratory characterization of the roof windows. Concentration decay is a widely used method to measure the air change rate in a building because it is the easiest to set up, it uses less tracer gas and it gives accurate results [Baptista, 1999].
In a second step, temperature measurements allow thermal simulation results to be compared in order to study the validation of the complete approach to evaluate ventilative cooling.

The house is equipped with a detailed monitoring and logging system providing event-driven data on indoor air temperatures and weather data. In addition the following sensors have been implemented:

- Anemometers and pressure difference (at different times for vertical and roof windows),
- Tracer gas concentration meters.

Tracer gas decay involves injecting a small amount of tracer gas, mixing it with the room air and then measuring the decay in gas concentration with time. The tracer gas was released inside the building and mixed with the inside air by use of a ventilator. The duration of each tracer gas measurement was 10 min including the release and decay. The experiments were carried out in both the living room on the ground floor and the south bedroom on the upper floor. For each room two scenarios have been adopted.

- Scenario n°1: Windows and doors are opened.
- Scenario n°2: Windows opened and doors closed.

3.3 On site air change measurements

For each room, the tracer gas tests have been executed during the morning noted (am) and the afternoon noted (pm). Therefore, four experiments have been conducted in each room.

Figure 2 shows as an example the relative CO_2 concentrations (CO2 concentration above outdoor level), measured in the living room for the two scenarios: internal doors being opened (blue curve) or closed (green curve). The continuous lines and the dashed lines correspond to respectively the measurements during the morning and the afternoon.

The air change rate is calculated from the tracer gas decay curve assuming the air-leakage rate remains constant throughout the measurement period and the incoming air mixes well with the indoor air.

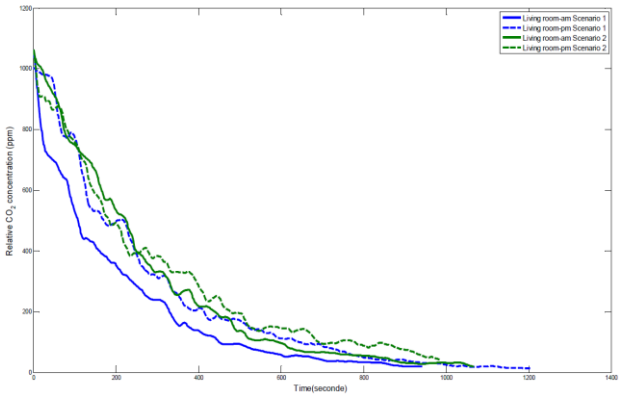

Figure 2. Relative CO_2 concentration in the living room during CO_2 decay test

The calculation of the air change rate is deduced from the general tracer gas mass balance equation [Cheong, 2001]:

$$V*dC_{int}(t) / dt = S(t) – Q(t) * (C_{int}(t) – C_{out}(t)) \quad (3)$$

where:

- $C_{int}(t)$ is the CO_2 concentration of indoor air (ppm)
- $C_{out}(t)$ is the CO_2 concentration of outdoor air (ppm)
- S(t) is the injection of tracer gas into the room (m^3*h^{-1})
- V is the indoor air volume (m^3)
- Q(t) the air flow rate (m^3*h^{-1})

Integration of (3) leads to an exponential function relating the concentration to the time, the air change rate being in the exponent: $(C_{int}(t) – C_{out}(t)) = C*e^{-Q*t/V}$ where C is a constant.

A linear regression is fitted : Log ($C_{int}(t) - C_{out}(t)$) = a t + b. The logarithm of the relative tracer-gas concentration is plotted against elapsed time. The slope of the line (a) is equal to the air change rate (Q/V, in ACH, i.e. Air Change rate per Hour) and b is a constant.
The relative CO_2 concentration profiles in the log-scale are presented for the living room in figure 3. Similar data have been derived for all scenarios and the results are shown in table 2 together with simulated values.

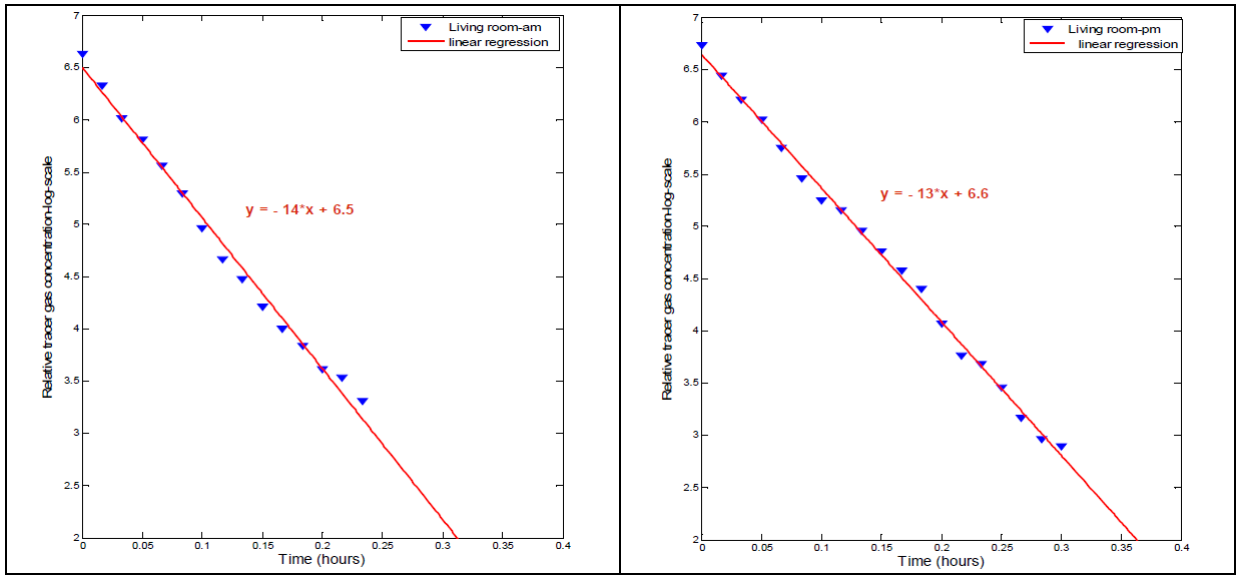

Figure 3 Relative CO_2 concentration profile in the living room. Morning (left) shows 14 ACH and afternoon (right) 13 ACH.

3.4 On site indoor temperature measurements

Inside air temperature measurements have been performed from 23 July to 20 August 2012, according to four scenarios successively:

- No natural ventilation (all windows closed), from 23 to 26 July
- With natural ventilation (all roof windows and top vertical windows are constantly open), without movable shading and with internal doors open (to get the maximal effect of natural ventilation), from 27 July to 3 August,
- With natural ventilation, with movable shading and internal doors closed (to get the minimal effect of natural ventilation), from 4 to 7 August (tracer gas and pressure difference measurements have been performed from 8 to 10 August),
- With natural ventilation, with controlled movable shading and internal doors closed, from 13 to 20 August.

4 AIR FLOW SIMULATIONS

Complementing monitoring results, numerical simulation constitutes another way to better understand the behavior of a building. Studying natural ventilation is improved by using both thermal and air-flow models.
Air flow simulation requires information about pressures on the external sides of the windows. These pressures can be evaluated in terms of the wind velocity and direction using pressure coefficients, C_p. We use the software “Cp generator” [cpgen.bouw.tno.nl/cp/] to find the values of C_p for all the 14 windows in the building.
The input file of the C_p generator software needs information such as the orientation of the house, the roughness of the terrain for different direction of the wind, some obstacles near the studied building, the direction in degrees of the north arrow as well as a short description of

the house, the roof and where the C_p value are to be calculated. The main problem comes from the description of the roof of the house. Only one pitched roof description is available, and it is not possible to have three different roofs in a row like in the investigated house. That's why we chose a unique angle of the roof of 45°.

4.1 Air flow simulations using CONTAM

Knowing the geometry of the house, wind pressure coefficients and the characterization of the windows, it is possible to perform an air flow simulation of the house and to compare the results with the values obtained from the tracer gas experimentation.
The air flow simulation is done using CONTAM7 [Axley, 2002] and [Walton, 2010], a multizone indoor air quality and ventilation analysis software. It allows the simulation of infiltration, windows, and room-to room airflows in building systems driven by mechanical means, wind pressures acting on the exterior of the building, and buoyancy effects induced by the indoor and outdoor air temperature difference.

The simulation model of the house is simplified and takes into account five thermal and air flow zones: The living room and the mezzanine, each of the bedrooms and the bathroom at the first floor.
14 windows are modeled, and the corresponding C_p values have been calculated with "Cp generator". There are also 4 doors between the living room-mezzanine and all the other rooms. Each of these openings is modeled by a power law corresponding to a leakage area. For each item, a leakage area is given by the cross section of the window or the opened area of the door. The power law is then standard as in equation (1) with $C = C_d*S*(2/\rho)^n$.

The C_d coefficient is 0.6 for a vertical window [Walton, 2010] and 0.75 for a roof window (obtained via the laboratory test), and the flow exponent *n* is 0.65 for a vertical window and 0.5 for a roof window. The closed door has a standard value for the C_d coefficient of 0.6, and a flow exponent of 0.65 [Walton, 2010] with a leakage area of 0.03 m². An open door has the same parameters but a flow area of 2 m².

For each tracer gas experiment, the same case is simulated with CONTAM. The following table shows the results of air flow for the tracer gas experiments and using the software CONTAM. The results are given in (ach) with a volume of the living room + mezzanine zone of 340 m3 and the volume of the south bedroom at the first floor of 35 m3.

The power law model used for the window is not valid for the experiment in the bed room with closed doors. The stack effect is less important due to the closed door - a very small air flow is going under the door. The power law being a one way flow model, the air flow in the bedroom calculated using CONTAM is very small (0.6 ach for the morning case, 2 ach for the afternoon case) compared to the measured (13.4 ach for the morning case, 13.2 ach for the afternoon case). The stack effect being small, the opening model is different in these two cases: a two way flow model is used with two openings. One opening is the upper part of the open roof window, the other corresponds to the lower part. No laboratory test was done for this model, so the C_d coefficient used is a standard value given by CONTAM: 0.7, the flow exponent *n* being automatically 0.5. The results for two way flow are shown with * in table 2.

Table 2 Measured and simulated air change per hour (ACH)

		South bedroom temp	North bedroom temp	Bath room temp	Wind speed m/s	Tracer Gas ACH	Simulated CONTAM ACH
Morning	Closed door	23.7	21.3	22.5	3.6	13.4	13.9*
	Open door	23.7	21.3	22.5	2.8	22.5	20.6
Afternoon	Closed door	27.1	26.5	26.2	2.3	13.2	16.6*
	Open door	27.1	26.5	26.2	2.3	19.8	19.5
Morning	Closed door	24.2	22.5	23.3	3.6	13.4	14
	Open door	24.2	22.5	23.3	3.6	14.6	17.4
Afternoon	Closed door	26.5	25.2	25	2.9	10.6	13.2
	Open door	27	26.1	25.6	2.8	13.1	17

4.2 Thermal simulation of the house

A dynamic thermal simulation tool is used to evaluate temperature profiles in the house [Peuportier, 1990], which has been modeled using five thermal zones (identical to the air flow simulation). In this highly insulated building the effects of the ventilation flow rate is clearly visible in the calculated indoor temperatures.

The air change rate has a large influence on the temperature profiles. It can therefore be calibrated by minimizing the discrepancy between measured temperature profiles and simulation results [Mejri, 2011] using the climatic data corresponding to on site measurements (external temperature and solar radiation). This constitutes a third way to evaluate the global air exchange rate, and may be helpful to refine the characteristics evaluated in the laboratory benchmark, by taking into account the actual conditions in the real house. However such calibration step has not been conducted in the present study.

Another added value of numerical simulation is that once the model has been calibrated, temperature profiles with and without ventilative cooling can be compared under the same climatic conditions, in order to evaluate the effects of ventilative cooling.

Three simulations are conducted:

- Interior doors opened with the opening of the windows on July 26th
- Interior doors closed with the opening of the windows on July 26th
- Interior doors opened without any opening of the windows (in order to see the effect of absent natural ventilation)

Figure 4 presents the results of the first simulation for the ground floor bed room. The windows are opened during the 26th of July, at midnight for the simulation and during the morning in the measurements, therefore the results are different: this is a transition day.

During the first three days corresponding to the closed windows period, the temperature profile from the simulation follows the same tendency as the measured temperature inside the house but 0.5°C to 2°C higher or lower depending on the thermal zone. As the opening of the windows in the simulated case happens earlier during the night on the 26th day, the simulated temperature decreases more than the temperature inside the house, this is the transition day.

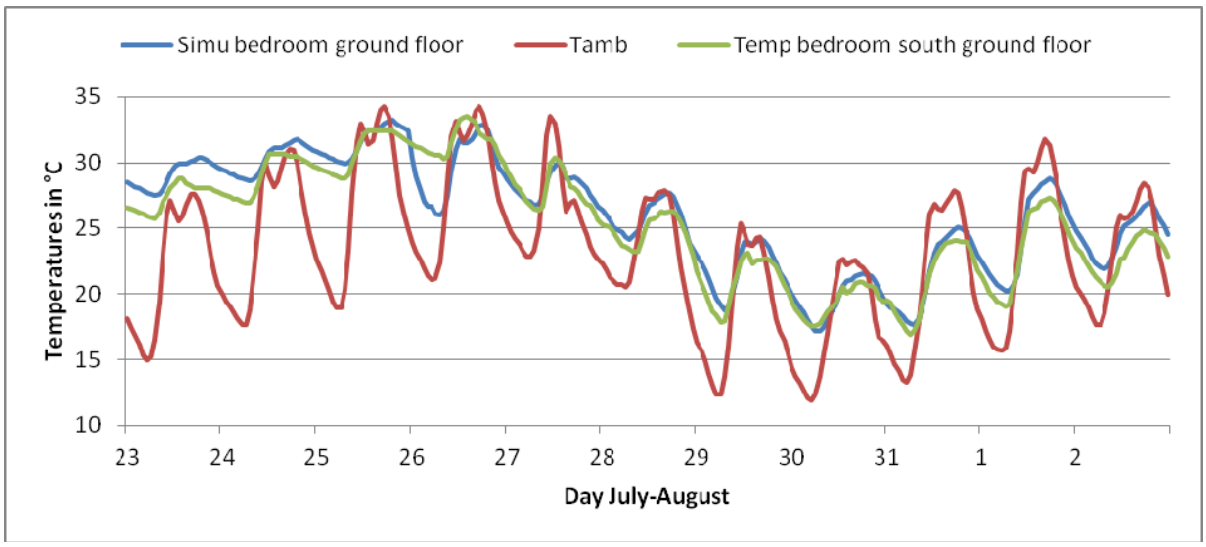

Figure 4 Example of simulated and measured indoor temperature in the ground floor bed room. Simulated indoor temperature in blue, measured in green and external temperature in red. Windows all closed until 26th – all open after, internal doors open.

After that it is possible to see the effect of the natural ventilation with the decrease of the temperature in a similar way for the simulation and the measurements.
The closed doors simulation results are presented in figure 5. The results are in line with the previous: Good correspondence between measured and simulated indoor sir temperatures.

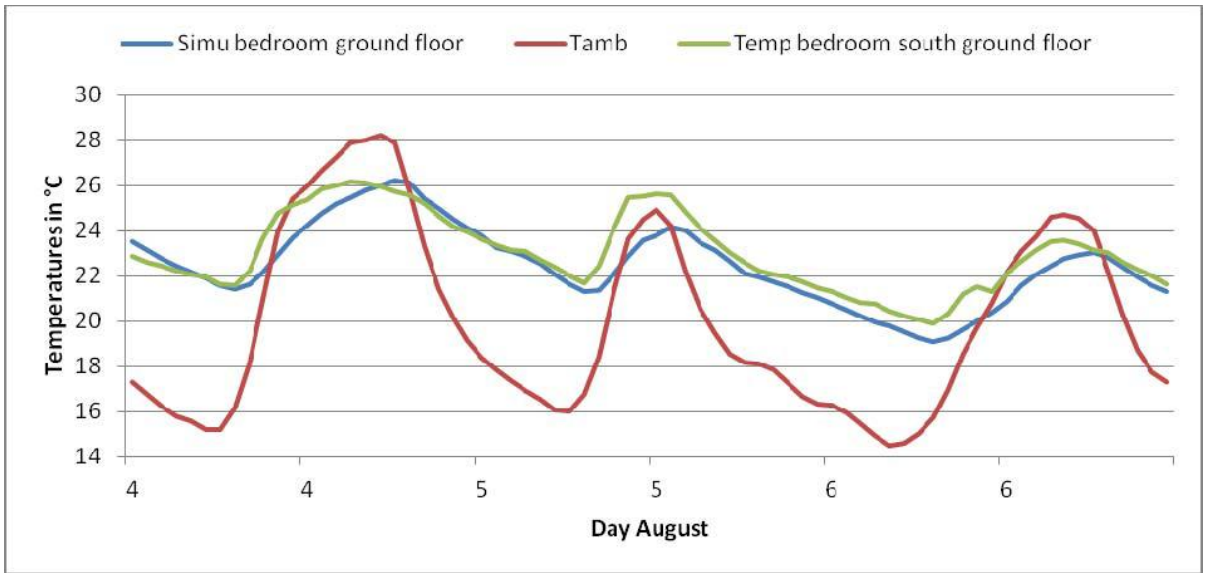

Figure 5 Example of simulated and measured indoor temperature in the ground floor bed room. All windows are open and all internal doors closed.

A third simulation has been conducted with the windows closed during all the period from July the 23rd to August the 2nd. It allows the comparison of the temperature with and without natural ventilative cooling. The results are shown in figure 6 for two thermal zones, the ground floor bedroom and the living room + mezzanine zone. The effect of natural ventilation is very important; there is around 5°C in difference between the indoor temperatures with and without the windows opening. We can see that the temperature when the windows are opened follows the ambient temperature but with smaller variations.

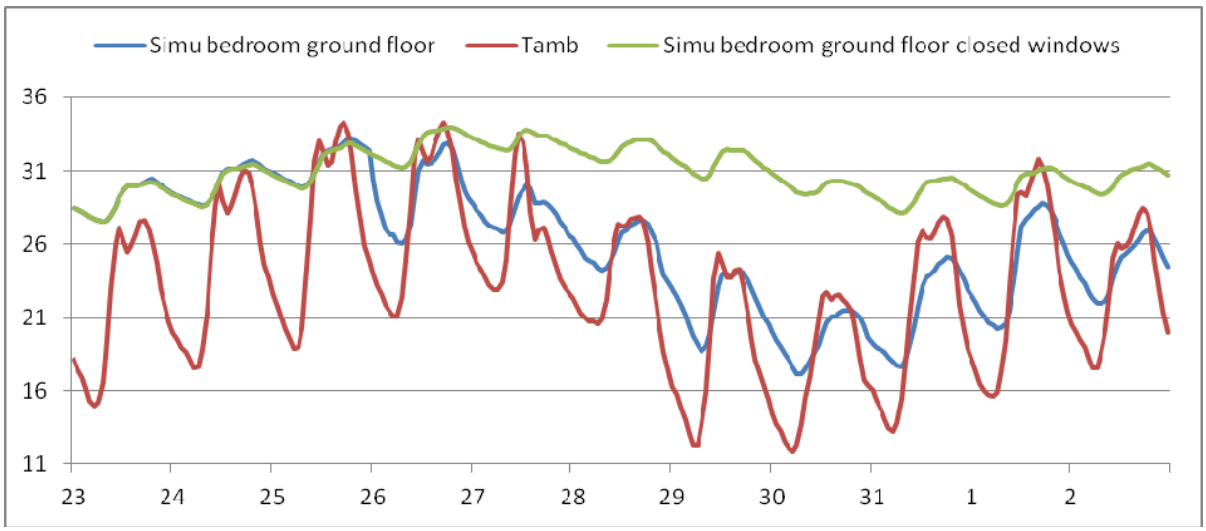

Figure 6 Simulated indoor air temperatures of the ground floor bedroom. Green: All windows closed. Blue: all windows opened from 26th of July. Red: Ambient temperature.

The work done on the thermal simulation of the house with a natural ventilation module could be improved by a calibration of the ventilative part of the thermal model, especially the C_p coefficients which are very difficult to measure or calculate. However, we are able to characterize the effect of the natural ventilation on the « Air et lumière » house, showing a large difference with and without the opening of the windows. This improved thermal comfort will be even better if the windows are opened only during the night, to take advantage of the night free cooling and avoiding venting with warm outdoor air.

5 CONCLUSIONS

The measurements performed in Maison Air et Lumière have shown that during the period without ventilation (end of July 2012), the temperature has reached 35°C. Ventilative cooling allowed a rapid reduction of this overheating, and temperatures stayed within the comfort interval (less than 27°C in the occupied rooms) during the rest of the measurements period. This shows that during summer, ventilative cooling is efficient.

10-22 ACH was measured even with times of low temperature differences and relatively low wind speed (between 2 and 3 m/s). In addition air flow rates were simulated in CONTAM for similar boundary conditions. Simulated and measured air flow rates correspond rather well with an average difference of 10% and local differences up to 30%.

In complement of measurements, dynamic thermal simulations have shown to reproduce the resulting indoor air temperature well with average difference between measured and calculated overheating of around 1K (average difference between indoor and outdoor temperatures). Thermal simulation has been used to evaluate the effects of ventilative cooling by comparing temperature profiles with and without ventilation during the same period, i.e. in the same climatic conditions. According to these results, indoor temperatures were decreased by about 5°C thanks to ventilative cooling. A further decrease will occur if the ventilation is controlled to avoid venting during warm periods.

The comparison between simulations and measurements gives confidence in the reliability of the model regarding both the evaluation of temperatures and flow rates even without detailed model calibration.

The consistency between calculations and measurements show that this process, including the evaluation of air flow characteristics using a laboratory test bench and the use of combined thermal and air flow simulation, is feasible and allows the effects of ventilative cooling to be assessed in a project. Such a process could be used in a regulatory calculation, provided that this calculation integrates an appropriate thermal and air-flow model.

6 ACKNOWLEDGEMENTS

The researchers who have contributed in this work at CES are Bérenger Favre (thermo-aeraulic simulation), Michaël Cohen (laboratory benchmark and on site measurements), Eric Vorger (CFD calculations), Olfa Mejri (interpretation of on site measures), and Maxime Robillart (data acquisition).

7 REFERENCES

Axley, J., Progress Toward a General Analytical Method for Predicting Indoor Air Pollution in Buildings Indoor Air Quality Modeling Phase III Report, NBSIR 88-3814. National Bureau of Standards, 1988.

Axley, J.M. 2001. Residential passive ventilation systems : Evaluation and design. Technical Note n° 54, Air Infiltration and Ventilation Center, Coventry, 158 p, 2001

Axley J. W. Emmerich S. J. and Walton G. N., 2002, Modeling the Performance of a Naturally Ventilated Commercial Building with a Multizone Coupled Thermal/Airflow Simulation Tool, *ASHRAE Transactions 2002, V. 108, Annual Meeting. Proceedings. Honolulu, 1-16 pp*

Baptista F. J.; Bailey B. J.; Randall J. M.; Meneses J. F., 1999, Greenhouse Ventilation Rate: Theory and Measurement with Tracer Gas Techniques, Journal of Agricultural Engineering Research 72 363-374.

Cheong K.W., 2001, Airflow measurements for balancing of air distribution system- tracer-gas technique as an alternative?, Building and Environment 36 955–964

Ghiaus C., Allard F., 2005, Natural Ventilation In The Urban Environment: Assessment And Design, *Earthscan, London, 241 p*

Mejri O., Palomo Del Barrio E., Ghrab-Morcos N., 2011, Energy performance assessment of occupied buildings using model identification techniques, *Energy and Buildings 43 285-299*

Peuportier B. and Blanc Sommereux I., 1990, Simulation tool with its expert interface for the thermal design of multizone buildings, *International Journal of Solar Energy 8 109-120*

Sherman M.H., 1990, Tracer gas techniques for measuring ventilation in a single zone, *Building and Environment 25-4 365-374*

Walton G. N. and Dols W. S., CONTAM User Guide and Program Documentation, report NISTIR 7251, Gaithersburg,2010

SECURING THE QUALITY OF VENTILATION SYSTEMS IN RESIDENTIAL BUILDINGS: EXISTING APPROACHES IN VARIOUS COUNTRIES

Paul Van Den Bossche[1], Arnold Janssens[2], Dirk Saelens[3]

1 Belgian Building Research Institute, www.wtcb.be
Avenue Pierre Holoffe 21, B-1342 Limelette, Belgium
Corresponding author: pvdb@bbri.be

2 Ghent University, Faculty of Engineering and Architecture, Research group building physics, construction and services
Jozef Plateaustraat 22, B-9000 Gent, Belgium

3 KU Leuven, Department of Civil Engineering, Building Physics Section
Kasteelpark Arenberg 40, B-3001 Leuven, Belgium

ABSTRACT

In March 2013 an international workshop was organized in Brussels to discuss existing approaches to secure the quality of residential ventilation systems in various countries. In the past large-scale field studies have shown evidence that installation quality of residential ventilation systems is typically insufficient, so it is important to develop frameworks to improve the situation. In total 13 experts presented the status and perspectives in their country, with a major focus on the voluntary and regulatory schemes developed to secure the quality of ventilation systems in residential construction practice. These schemes intend to influence different steps in the process of the realisation and use of ventilation systems: training, products and systems development, design, installation en commissioning, use, maintenance and inspection.
This article gives a synthesis of the various applied quality approaches, together with practical experience in these countries. A critical review of the pros and cons of existing quality approaches presented at the Brussels workshop is given. Some examples of solutions to tackle the challenges in ventilation system quality will be discussed more in detail. Finally the applicability of the approaches in the Belgian context is discussed.

1 INTRODUCTION

Ventilation of dwellings plays an important role in the recast of European energy performance requirements towards "Nearly Zero Energy Buildings", because of the need for providing a good air quality in highly insulated and airtight buildings in an energy efficient way. In the meanwhile shortcomings of ventilation systems in operation are frequently reported. Sometimes there is a big gap between the theoretical performance and the performance in actual operation. Typical problems are:

- Insufficient air flow rates
- Poor balancing of air flow rates
- Noise complaints
- Poor quality of supply air
- Inadequate operation by the occupants

Many of these problems are related to a poor design or installation, lack of maintenance, and to a lesser extent, poor product quality. The need for high quality remains an important issue, and could be defined as 'to meet the end-user expectations'. The occupant requires a comfortable and healthy living area with regard to temperature, light, noise, safety,… and of course also with regard to the air quality. The ventilation system should be easy in daily use and have an acceptable cost. Considering costs, both investment costs and operation costs need an assessment. Operation cost is defined by maintenance costs and energy cost.

The authorities in the Flemish region (Belgium) initiated some studies (Caillou et al. 2011, 2012, 2013; Stranger et al. 2012) that confirmed the existence of aforementioned problems. The following recommendations were formulated (VEA 2013):

- Raise public awareness of the importance of ventilation system use and maintenance
- Increase attention to a correct dimensioning of the system
- Offer quality guarantee through performance testing
- Increase attention to noise problems

Partly based on these recommendations, the energy authorities in the Flemish Region (VEA - Vlaams Energieagentschap) initiated a project to evaluate the willingness to introduce a quality approach for ventilation systems. This project is commonly conducted by BBRI, Ghent University, Leuven University, INIVE and ICEE. As part of this project, an international workshop 'Securing the quality of ventilation systems in residential buildings: status and perspectives' has been organized on March 18-19 in 2013 (AIVC 2013). The results of the workshop will be made available in the form of edited proceedings, which contain an overview of the quality assurance approaches in each of the participating countries. This paper reports on the obtained results.

Apparently almost every aspect to realize high quality residential ventilation systems is available: ventilation standards, in most countries part of the building code or the EPBD regulation, performance requirements (air flow rates, energy consumption, comfort aspects such as noise levels), product and system standards (and product databases and labels), design and installation guidelines, testing and compliance standards and guidelines, educational and qualification programmes for installers,… However, there is increasing evidence (Caillou et al. 2012, Stranger et al. 2012, De Brauwere et al. 2010, AIVC 2013) that these instruments, although they are necessary preconditions, do not automatically lead to good quality installations. Reasons for this might be:

- Lack of collaboration and continuity at different stages of design and construction
- Lack of knowledge, awareness and care for quality at different stages
- Savings on investments: lack of willingness to pay for quality
- Lack of training of specific installers and commissioners, no training requirements
- Limited enforcement of legislation

Apart from the aforementioned instruments, there is a need for an integrated quality approach to ensure all available tools are used to end up in quality. These quality approaches can interact with one or more steps or parameters that interfere with the final ventilation system performance on site.

Below some important parameters which influence the final ventilation system performance are listed (see fig 1).

- The consecutive actions in the construction process, all of which affect the as-built situation of the ventilation system: design, selection of products and systems, the installation work and the commissioning.
- User behaviour: use of controllers; selection and use of polluting products like furniture, carpets, …; opening of windows,…
- Maintenance (after inspection if applicable)

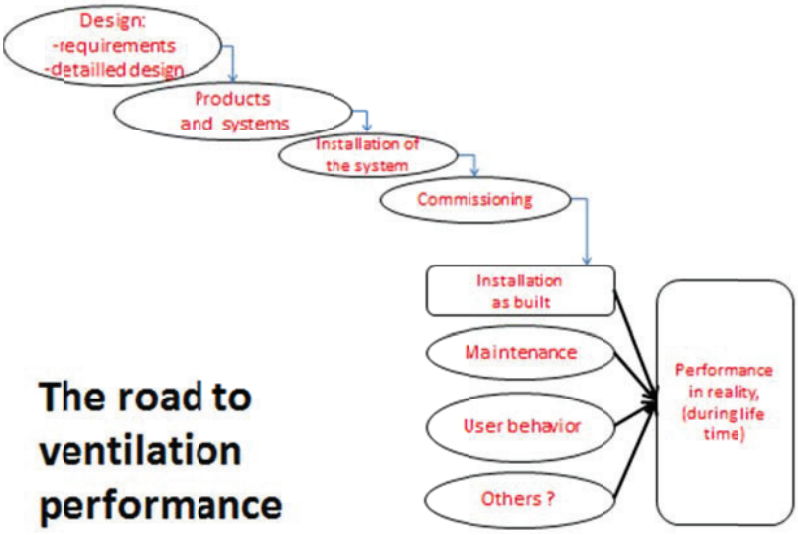

Figure 1: Parameters influencing the final ventilation system performance

2 INTERNATIONAL SITUATION

The intention of the aforementioned international workshop was to get an overview of the international situation regarding the following questions:

- What is the knowledge regarding the quality of ventilation systems in residential buildings in various countries?
- What is the status with existing approaches to improve the quality of these systems?
- What can we learn from targeted efforts to characterize or monitor real ventilation system performance?
- How can quality frameworks help to improve the situation and how can they converge with existing regulations or programmes?

Based on the answers, the pros and cons of existing approaches were discussed and ways to improve the situation with key experts from various countries were explored.
Following countries were represented at the workshop with a paper: Belgium, Canada, Germany, Estonia, Finland, France, the Netherlands, Norway, Poland, Romania, United Kingdom, United States, Sweden.
As an illustration, next paragraphs report some approaches used in 2 countries, selected at random.

2.1 Canada (Fig. 2)

In Canada, ventilation is a part of the obligatory building code. A voluntary 3 day contractor training exists that can lead to certification of ventilation installer. Local authorities are deemed to perform a compliance check with the building codes at key construction stages.
Products can get an HVI (Home Ventilating Institute) product certification on a voluntary basis in which rating of product performance in accordance with standards is required. No independent compliance check or permanent follow-up is provided.
On a voluntary basis, contractors can obtain a HRAI (Heating, Refrigeration and Air Conditioning Institute of Canada) contractor certification for 5 years. This requires passing an exam with at least 75 % and signing a certification agreement where the contractor commits to install in accordance with the aforementioned training. No third party compliance check of installations is provided. Withdrawal of the certification however, is possible after complaints. Inspection of installations in use are sometimes performed, in case of homes put for sale.

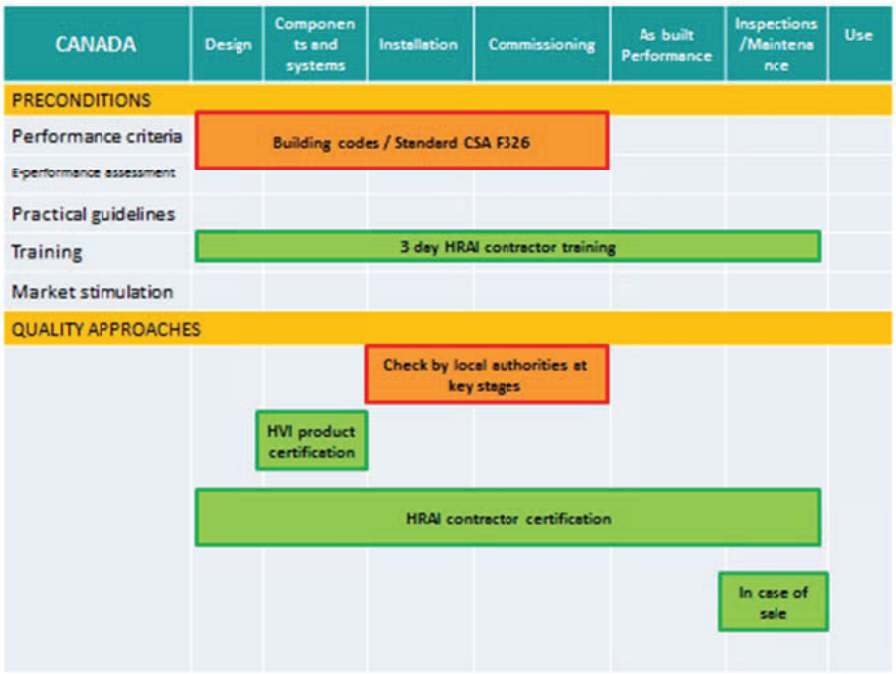

Figure 2: Preconditions and quality approaches in Canada

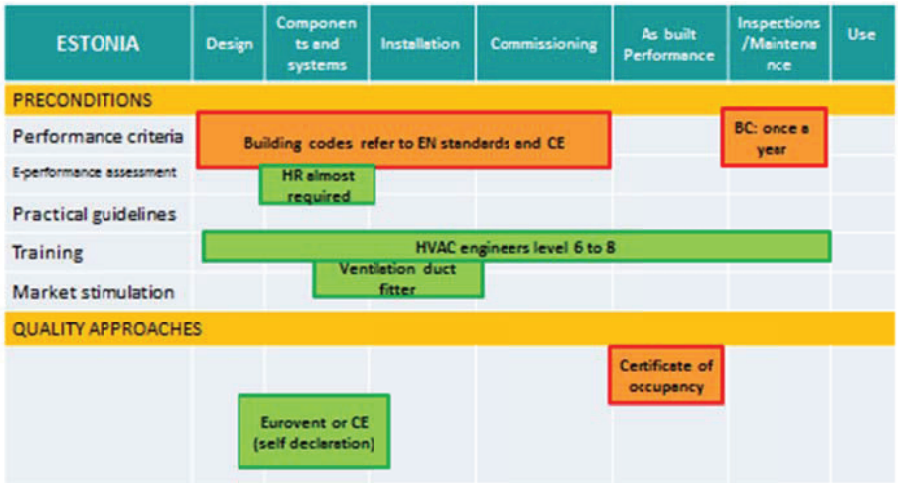

Figure 3: Preconditions and quality approaches in Estonia

2.2 Estonia (Fig. 3)

In Estonia, ventilation is a part of the obligatory building code, which refers to EN standards and to Finnish requirements. There is a requirement that installations are maintained once a year, but this is rarely done in practice. Ventilation characteristics are taken into account in the energy performance assessment, which makes the use of Heat Recovery ventilation (HR) almost obligatory in order to meet energy performance requirements. Engineers are educated, there is a ventilation duct fitter qualification, but 75 % of the installers do not apply for it.

A certificate of occupancy is needed before a newly built house is put into use. For detached houses, commissioning can be done by the house owner himself; the authorities lack competence to check for compliance. Product performances are mostly 'self-declared'.

3 OVERVIEW QUALITY APPROACHES

Various quality approaches can be identified. They can be classified as necessary preconditions, as process improvements or as as-built evaluations. A number of interesting quality approaches were identified during the workshop, for each of them we mention some additional conditions to be fulfilled in order to make them work as intended.

3.1 Preconditions

A first precondition is the availability of clear quality criteria for which there is an agreement among the whole sector. As much as possible, these criteria are performance based on the condition they can be evaluated in practice. If these criteria are part of legislation, they should enable enforcement of this legislation. A link between ventilation aspects and the energy performance assessment can be a strong asset. In different countries the approach might differ a lot: from pure intentions and design conditions having effect on the energy performance to as-built approaches in which on-site measured performance (e.g. air flow rates, fan power) are a part of the calculation.
Example:

- Ventilation is part of the building codes to some extent in most countries.

In most countries a lot of guidelines on how to design, install, commission ventilation installations is available. An important issue however is whether this information is practical and directly applicable by the contractors.

The professional competences of various persons, active in the process chain, need to be increased. There might be a need for training of different profiles, such as: designers, installers, commissioners, inspectors, maintenance technicians,... The training shouldn't concentrate only on knowledge, but should be directed towards skills and attitudes.
The training approach can be limited to training on its own, or can require theoretical and practical exams and can end up in certification. Competence certification certifies that persons have obtained the required skills in the field of ventilation. The certification should also confirm or proof the ability of the person to conduct a certain function and should therefore be a continuous process. Training or competence certification schemes can be voluntary but also compulsory, e.g. when only certified persons are allowed to develop certain professional activities.
Examples:

- HRAI contractor certification ((Heating, Refrigeration and Air Conditioning Institute of Canada)
- OVK inspectors (Sweden, OVK = Compulsory Ventilation Inspection)
- License designers and supervisors (Poland)
- Competent person (UK)

3.2 Process improvements

Before attributing a building permit, the design could be checked, avoiding big mistakes from the start of the construction process. This approach requires that the ventilation system design is already done in a sufficient detailed way at the time of the building permit request, which is normally not the case. The method also requires that the authorities are competent in ventilation matter. Another drawback for this approach is that it gives little guarantee on the as-built result.

Examples:

- Check at building permit (Finland, the Netherlands)
- State Inspectorate (Romania)

With product and system characteristics declaration comparable data of various products are available for the designer. This should facilitate a proper selection, best suited to the application. In some cases this classification is limited to some reliable data on energy performance and flow characteristics – in that case the quality aspect is limited to 'quality of data'. Some approaches include additional quality aspects, such as cleanliness, hygiene, acoustical performance and can end up in labelling or certification in which minimum performance levels should be obtained.

With regard to the reliability of the declared performance data, different level approaches can be encountered. In a number of cases data are a result of an initial type testing (ITT), through self-declaration of the manufacturer or performed by a third party laboratory test, on one available sample or through a set of statistically selected samples. As a result, the reliability of the data might differ a lot. A real certification goes beyond an instant snapshot but evaluates the evolution in time through e.g. Factory Process Control (FPC). For some private labels neither the testing procedures, nor the certification process are publicly available, which makes an evaluation of the value of the label difficult. Because most manufacturers also act on an international level, the availability of uniform schemes across EU would be an important asset.
Examples:

- HVI (Home Ventilating Institute) certification (Canada and US)
- EPBD product database (Belgium)
- NF VMC, CSTBat (France)
- TUV-RLT (Germany)
- M1 cleanliness (Finland)
- Product characteristics SAP (Standard Assessment Procedure, UK)
- Eurovent-certification (Europe)

Innovation with regard to products or systems can play an important role in quality improvement. A product can be easy to install or maintain, systems can be self-calibrating, reducing the need of commissioning and the risk of mistakes.

With a follow-up in the installation phase, the authorities may check the compliance with the legal requirements or the building permit. It is crucial to conduct these visits at key stages in the building construction. The impact on the quality aspect is rather low: quality is more than 'legal compliance'. In general authorities lack the competence to go into detail, and often the visits are poorly sampled.
Examples:

- Compliance check at key stages (Canada)
- As a part of EPBD compliance (Belgium)

Whole company certification is an integrated approach in which the company is assisted to keep every step of the process under control. Elements are person competence assurance, organisation, management, document and complaint treatment. Such an ISO 9001-like approach seems to be limited to companies of a certain scale.
Examples:

- Qualibat, Qualifelec (France)

- Company registration (Norway)
- Specialist certification (Romania)
- Cleaning companies (Germany)

3.3 As-built evaluation

As-built performance evaluation looks at the final result, without bothering about the process needed to realize it. Evaluation can be limited to compliance with mandatory requirements or can be extended to additional quality issues. The evaluation may include visual, qualitative checks as well as measurements (air flow rates, electric power, acoustics, …). Document availability, e.g. user and maintenance manuals, can be added.
Various concepts may be used as different persons may perform the evaluation:

- Each installation is checked by a third party or by the authorities
- Sample checks are conducted at ventilations systems, installed by contractors. This can also be performed in a framework to label installers or for whole company certification.
- Declared by house-owner

Such an approach can be voluntary or mandatory. In some cases it will lead to a 'certificate of occupancy' in which the authorities allow to put the house into use. It requires a systematic and serious organisation with competent evaluators.
Examples

- Permit to use (Estonia)
- Acceptance before putting into use (Poland)
- VPK (voluntary Ventilation Performance Check, the Netherlands)
- OVK (mandatory Ventilation Inspection, Sweden)

This approach is a close to end user expectations approach, which gives, compared to process approaches, much more liberty when selecting solutions. It gives however direct feedback to the contractor, who might have to improve his process of realisation.

Even an excellent installation at the moment of commissioning, doesn't guarantee a good operation during the total service life. In some countries, regular maintenance is mandatory, but some lack a compliance framework. Inspections after a predetermined time can be helpful in order to define necessary repairs, replacements and maintenance. It could be part of an energy audit, required when putting the dwelling for sale or rent, but detailed ventilation performance isn't always included.
Examples

- OVK, but not for small dwellings (Sweden)
- Some housing companies (UK)
- At sale/rent (Belgium, Canada)
- As part of energy audit (Estonia)
- For passive stack by chimneys-sweeps (Poland)

3.4 Drivers for better quality

An important discussion point for the afore mentioned quality approaches is to make sure the approach enters into action, is correctly used and leads to actual quality improvement for the market as a whole (and isn't limited to a small niche market). Quality approaches may be imposed with fines in case of non-compliance or incentives can be created.

How far should legislation go to support quality? Legislation can be directed to requirements for design, products, commissioning, inspection or maintenance. Legislation can require minimum skills for ventilation contractors or specialists. Legislation can require an as-built performance evaluation or regular inspections and maintenance. The effect of pure mandatory requirements depends in practice on the country culture. In some countries the existence of a law suffices to have effect, in other countries systematic enforcement is needed. In some countries (e.g. The Netherlands) the authorities avoid enforcing requirements and leave the improvement of the quality of ventilation systems up to market commitments.
Generally speaking, financial incentives can generate an effect. Unfortunately, nowadays the authorities have to reduce this kind of spending.

Good quality ventilation systems can also be valorised in energy performance calculations. Various ventilation characteristics might improve the final performance. When not introduced, (more unfavourable) default values will be used to perform calculations. Examples are the flow capacity of natural ventilation openings, type and power of fans, temperature effectiveness of heat exchangers, a proven flow balance. Because of the need to further improve the energy performance of buildings in the next decade, favouring high quality ventilation systems in the EPBD calculation is an indirect way to enhance quality. It is important that this assessment refers as much as possible to the as-built situation, to avoid a merely 'paper quality'.
Example:

- As-built data as a base for E-level calculation (EPBD implementation in Belgium)

Finally, it is important to raise awareness by the users that good ventilation is important for everybody and to get support from the public for the various quality approaches. It is indeed the end-user who will have to pay additional costs!

4 APPROACHES FOR BELGIUM

Within the aforementioned VEA-project (search for quality approaches, supported by the whole ventilation sector), a number of quality approaches will be evaluated and discussed. Without looking too much ahead, following approaches might be withheld:

- Reinforce ventilation quality aspects into the EPB-legislation and the energy performance calculation. It doesn't seem to be realistic to increase the application control by the administration itself, but a link with the declaration of conformity might be made.
- Make training available for various professional levels: architects, installers, craftsmen and performance evaluators.
- Organize a system to deliver a declaration of conformity for each installation. This approach declares for each individual installation:
    - The conformity with the legal or additional performance requirements.
    - All relevant data enabling to calculate the ventilation aspects in the energy performance calculation: product performances such as flow rate capacities, auto-control capacities, fan power,… or system measurements such as measured flow rates.

5 CONCLUSIONS

Although market maturity might differ from country to country, various countries report the same kind of problems regarding residential ventilation systems. Almost every country in this review is looking for approaches to improve quality in the field. To solve the problem as a

whole, improvement can be expected from a well selected set of complementary quality approaches. Fully voluntary measures might not work too well, some kind of official enforcement will be required.

6 ACKNOWLEDGEMENTS

The authors wish to thank the Flemish Energy Administration (Vlaams Energieagentschap - VEA) for their financial support to the aforementioned project.

7 REFERENCES

Caillou S., Van den Bossche P., (BBRI) 2011. Ventilation systems: monitoring of performances on site. Presented at the Passive House Symposium 2011, 7 October 2011, Brussels

Caillou S., Van den Bossche P., (BBRI) 2013. On site performance of ventilations systems – Scientific report OPTIVENT, July 2013, Brussels

Caillou S, Dinne K., Wuyts D., Van den Bossche P. .(BBRI), 2012. Performances of ventilation systems: on site measurements related to energy efficiency, comfort and health. Presented at the 33rd AIVC conference "Optimising Ventilative Cooling and Airtightness for [Nearly] Zero-Energy Buildings, IAQ and Comfort", 10-11 October 2012, Copenhagen, Denmark.

De Brauwere S., Van de Velde S., 2010. Meting van luchtdichtheid en binnenluchtkwaliteit in nieuwbouwwoningen (bouwjaar 2006-2009) (Assessment of airtightness and IAQ in dwellings, in Dutch). Masterthesis, Faculty of Engineering and Architecture, Ghent University.

Quest vzw, 2011. Beoordelingsrichtlijn voor installatiebedrijven van ventilatiesystemen met warmterecuperatie (Review requirements for installation companies of ventilation systems with heat recovery, in Dutch and French) Quest, www.q4q.be

Stranger M., Verbeke S., Verbeke L., Geyskens F., Swinnen R., Goelen E. (VITO), Täubel M., Hyvärinen A. (THL, Finland), Laverge J., Janssens A. (UGent), Wuyts D., Ingelaere B. (BBRI). 2012. Clean Air, Low Energy. "Exploratory research on the quality of the indoor environment in energy-efficient buildings: the influence of outdoor environment and ventilation" VEA-LNE.

Tweejaarlijkse evaluatie energieprestatieregelgeving-versie 13 juni 2013 – VEA Brussel

AIVC, 2013, Securing the quality of ventilation systems in residential buildings: status and perspectives' (2013) workshop proceedings, March 18-19, 2013, AIVC/Tightvent Europe, Brussels

OVERVIEW OF THE UK RESIDENTIAL VENTILATION MARKET AND INITIATIVES TO IMPROVE THE QUALITY OF THE INSTALLED SYSTEMS

Alan Gilbert, BA IEng MIET PInst NDT

BSRIA
Old Bracknell Lane West
Bracknell, Berkshire
RG12 7AH UK
alan.gilbert@bsria.co.uk

ABSTRACT

New homes currently being built within the UK all incorporate some type of ventilation system, the majority of which are of the fixed mechanical fan type. These generally come in three generic designs know as single room background ventilators, continuous mechanical systems and continuous mechanical systems with heat recovery. Installation, inspection and commissioning of these systems is covered by Building Regulations, and there are training schemes in-place which allow individuals to become Competent Persons to undertake these tasks.

Regulation 42 of the Building Regulations 2010 requires builders to provide evidence appertaining to the installation, inspection and commissioning process to be lodged with the Building Control Body within 5 days of the tests being carried out. The method of testing and reporting is described in a Domestic Ventilation Compliance Guide, but since 2010 there has been a growing body of evidence cataloguing problems with the quality of work being undertaken. This has led to organisations such as BSRIA developing initiatives to assist all the parties involved in the design, installation, inspection, and commissioning processes to improve their outputs.

KEYWORDS

Ventilation, fans, dwellings, residential housing, UK Building Regulations 2010, Building Control Body, Approved Document Part F, Mechanical Heat Recovery, MVHR, MEV, SAP Appendix Q, DCLG, Domestic Ventilation Compliance Guide, BSRIA, BG46/2013

INTRODUCTION

The UK housing sector can be considered as being well developed with approximately 130,000 dwellings being completed in the 12 month period ending 31st March 2012, and the majority of these contained fixed mechanical ventilation systems. The market is dominated by a number of large-scale national developers building more than 500 homes each annually. The self-build market in the UK currently contributes about 12 per cent of total new housing and this includes those who appoint a builder to do the construction work on a plot of land. In 2012 there was an estimated 27.4 million dwellings in the UK, with 17.4 million privately

owned, 4.7 million privately rented, 2.7 million rented from housing authorities with the remainder rented from local authorities. [1]

Statistics relating to the stock profile are produced on a regular basis by the UK National Statistics Office, and are published by the Department for Communities and Local Government (DCLG). Data can be extracted from these statistics in many forms, for example approximately one-in-five dwellings in the UK were built before 1919, with the majority of all dwellings (80%) houses or bungalows, and 95% of dwellings were of traditional masonry or timber construction; the majority of these were cavity brick/block. Non-traditional construction is often seen as synonymous with social housing but half of these dwellings are actually in the private sector. These statistics do not contain any data relating to ventilation systems installed into the dwelling, so the size of the market is ascertained by independent research such as that conducted by BSRIA who obtain data from manufacturers and suppliers through robust survey techniques.

RESIDENTIAL VENTILATION MARKET

To comply with the current UK Building Regulations all new domestic homes are built with some type of ventilation system incorporated. These ventilation systems are categorised into four groups as defined in Table 1.

Type	Description	Background ventilation	Comments
System 1	Background ventilators and intermittent extract fans including single room heat recovery ventilators	Yes	Size as per tables in Regulations based on floor area and number of bedrooms
System 2	Passive stack ventilation (PSV)	Yes	As above
System 3	Continuous mechanical extract (MEV): centralised and de-centralised	Yes and No	Size as per tables in Regulations or if air permeability >5$m^3/(m.^2)$ none is required
System 4	Continuous mechanical supply and extract with heat recovery (MVHR): centralised and single room	No	

Table 1: Ventilation system type description

It should be noted that other types of ventilation systems such as Demand Control Ventilation (DCV) are allowed to be used within the UK, but the design must be shown to achieve certain criteria such as the removal rate of moisture and other indoor air pollutants to the satisfaction of the Building Control Body.

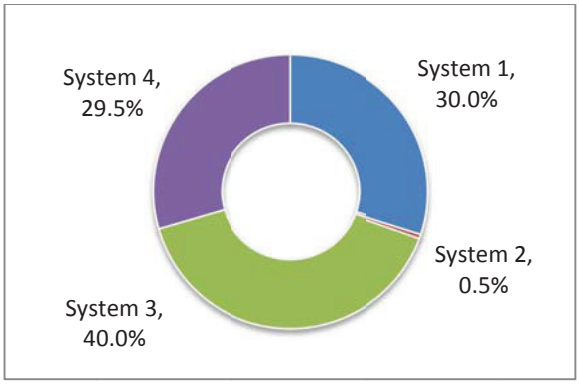

Graph 1: Estimated percentage mix of ventilation system types installed in new build in 2012

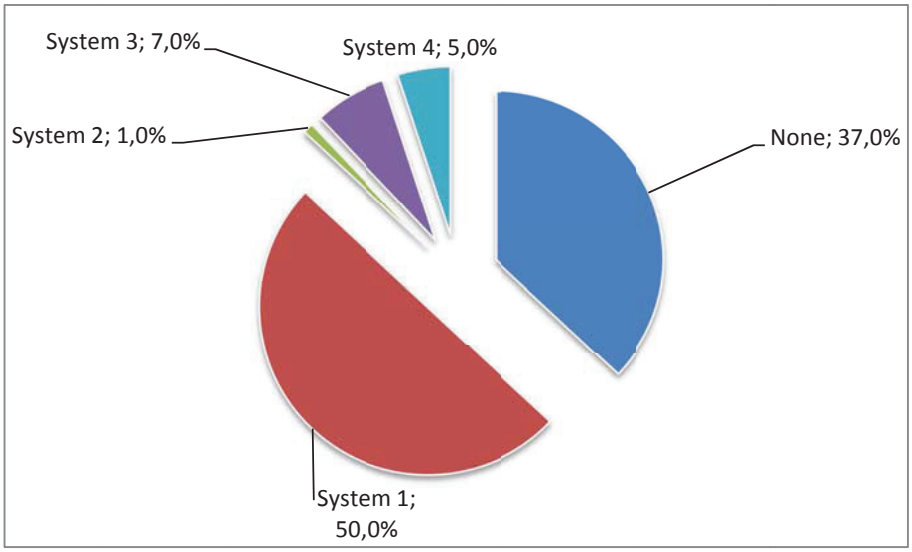

Graph 2: Estimated percentage mix of ventilation system types in total UK housing stock

Within the UK there are separate Building Regulations published in England and Wales, Scotland and Northern Ireland along with their second tier guidance documents. In general terms these are all similar in nature, and for the purposes of this paper the Regulations in each of the regions should all be considered as being equal.

Approved Document F [2] which came into force in October 2010 deals with the functional requirements for ventilation systems. It states "There shall be adequate means of ventilation provided for people in the building" and "Fixed systems for mechanical ventilation and any associated controls must be commissioned by testing and adjusted as necessary". These Regulations cover the broad requirements for the systems, and are not designed to be comprehensive. For this there is a separate Domestic Compliance Ventilation Guide [3] which gives users more details and assistance on how to comply with the Regulations.

PRODUCTS

Background ventilators and intermittent extract fans, have no certification schemes in-place to uniformly define the product characteristics. Responsible manufacturers do however understand the role they can play in the quality of the installation, and provide system designers, installers and commissioners with a plethora of information in regard to how the products perform, along with how they should be used and installed. This often includes within their product manuals a replication of the details contained in the Building Regulations Ventilation Compliance Guide regarding installation, inspection and commissioning requirements.

For Mechanical Ventilation with Heat Recovery (MVHR) and Mechanical Extract Ventilation (MEV) systems uniform product characteristics are available via the Standard Assessment Procedure (SAP) Appendix Q. This data is available via a searchable website of performance data for technologies as well as products. The website also includes test and calculation methodologies that can be used to measure product performance

SAP is the methodology used by the Department of Energy & Climate Change (DECC) to assess and compare the energy and environmental performance of new dwellings. Its purpose

is to provide accurate and reliable assessments of dwelling energy performances that are needed to underpin energy and environmental policy initiatives. SAP quantifies a dwelling's performance in terms of; energy use per unit floor area, a fuel-cost based energy efficiency rating (the SAP rating) and emissions of CO_2.

With the exception of products that are listed in SAP Appendix Q there are no product labelling schemes defining product characteristics such as energy efficiency or fan performance in place within the UK. SAP Appendix Q requires products to display, the unique SAP identifier, the technology category, the brand name and model.

DESIGN

Whilst the design of ventilation systems is critical in obtaining correct operation, there are no national dedicated training schemes operating within the UK for designers. Many manufacturers do nevertheless offer a design service for their own systems based on meeting the requirements contained within the Building Regulations, and there are free practical guidance documents issued by organisations such as the NHBC Foundation (National House-Building Council) to help the industry meet the considerable design challenges [4][5]. Further guidance in the form of a new chapter (3.2), within the separate NHBC Standards is due for imminent publication, and this will detail a number of requirements in relation to the design of MVHR systems. Where these requirements are broken down into three general categories to aid the various parties in the build process; design, materials and site work. Topic areas covered include:-

- MVHR location, the positioning of air valves and the locking of these after commissioning
- Controls
- Use of flexible ducting
- Position of terminals (minimum distance between inlet and outlet)
- Control of condensation and the use of insulated duct materials
- Protection of the system from the cold
- Compatibility of the system with other building elements
- Maximum noise levels
- Cleaning
- Definitions for summer bypass mode

NHBC is a warranty and insurance provider that provided standards for UK house-building for new and newly converted homes.

INSTALLATION AND COMMISSIONING

The UK Building Regulations state that ventilation systems should be "commissioned by testing" and the associated Compliance Guide details what this entails. It also states that a copy of all the completed documentation should form part of the systems Operation and Maintenance manual which should be left in the dwelling.

Both installation and commissioning are undertaken by the completion of a series of questions on a form which are broken down in to three main sections:-

Part 1 – System details and declarations (manufacturer, make model serial numbers)
Part 2a – Installation details (type of ductwork, description of controls i.e. central, PIR etc., installation engineer's details)
Part 2b – Inspection of installation (general overview of system and visual of specifics such as condensate connections, duct insulation, inspector details)
Part 3 – Air flow measurement test and commissioning details (detailed breakdown of the design air flow rates and the measured air flow rates in each room at both low and high fan speeds where applicable, the test instrument used, date of last UKAS (ISO 17025) calibration, test engineers details).

For each installation all the parts of the forms need to be completed, and as a minimum Part 3 should be submitted to the Building Control Body (BCB) as evidence that the installation has been correctly tested and commissioned.

It should be noted that commissioning does not normally include any fan power measurements, even though there is guidance on the maximum allowable figures for fans contained within the 2010 edition of the Domestic Building Services Compliance Guide. This document is similar to the Domestic Ventilation Compliance Guide, and is specifically designed to assist persons installing fixed building services in comply with the Building Regulations.

Value	Description
0.5 W/(l/s)	Intermittent extract systems
0.7 W/(l/s)	Continuous extract systems
0.5 W/(l/s)	Continuous supply systems
1.5 W/(l/s)	Continuous supply and extract with heat recovery systems

Table 2: Domestic Building Services Compliance Guide maximum specific fan power values for new and replacement systems

There are no current requirements contained in the Building Regulations for the assessment of noise levels from ventilation systems. However, the generally accepted criterion for noise is that when systems are set to run at their "normal" rate it should not exceed:-

- 30dB LAeq,T when measured in bedrooms and living rooms
- 35dB LAeq,T when measured in all other rooms (unless the room is solely intended for plant/mechanical services usage)

A single training course designed to meet the requirements of the manufacturers for the installation, inspection, testing, commissioning and provision of information for fixed domestic ventilation systems exists in the UK. This is organised by BPEC Services Ltd, and it is run by the majority of the UK ventilation system suppliers. The 2 day course includes a short examination, and if the candidate is successful they can register with a number of different bodies to become a Competent Person.

Competent Persons are able to record their registration number / details on the forms that are submitted to the Building Control Bodies, and in doing this it allows the in-use figures in SAP Appendix Q to be used. If the person undertaking the test is not registered then a penalty is applied within the SAP calculation giving a different less favourable energy rating for the dwelling.

MAINTENANCE

Despite incorrectly installed ventilation systems having the capability of affecting the health of the occupants, and poor installations having a direct adverse impact on the cost of running the system, there is no large scale maintenance schemes operated within the UK for residential ventilation systems. Many would consider that this is as a result of very little information made available to the residents when they take occupancy of their home, but with the majority of the UK housing stock privately owned getting the message out to a wide audience of the importance of maintenance could be considered as an extremely difficult task. Individuals who have installed retrofit MVHR systems could be considered as being more aware of the need for maintenance, but there is growing evidence from manufacturers of systems that this is not being applied as the reported sales of replacement filters is low compared to systems in the market.

The only exception to this trend is that some local housing authorities are now playing a more active role in maintenance with systems in place that automatically link the replacement of filters in MVHR systems to their yearly inspections of the dwellings they rent. But, these schemes can be considered to be in the minority especially when considering the number of systems installed.

INSPECTIONS

Similar to the maintenance of systems, there are no dedicated schemes in-place within the UK for the regular inspection of residential ventilation systems, and there are no standards for training, labelling or certification schemes for any inspectors. There is an inspection process as part of the initial installation process and details are recorded on the installation and inspection sheet provided within the Domestic Ventilation Compliance Guide.

THE QUALITY OF INSTALLED VENTILATION SYSTEMS

Closing the gap between design and as-built performance of new homes is the subject of a major industry review for UK Government in 2013. [6] Whilst the interim report has not specifically identified ventilation systems as having a specific problem, the taskforce is aware of a growing body of evidence cataloguing problems with the quality of work being undertaken. They are therefore due to explore why this is occurring, and their future work is likely to include areas such as:-

- The availability of appropriate design input
- Use of inappropriate value engineering within the build process (lowest price not quality wins)
- Self-regulation of subcontractors especially during design and installation phases
- Ignorance or disregard of UK Building Regulations
- Supervision of mechanical & electrical subcontractors by qualified practitioners at all stages of the build process
- Enforcement of Building Regulations by the Building Control Bodies. [(1)]

[(1)] The BCB's are currently operating an amnesty regarding ventilation systems and the quality of the documentation they are provided by the builder as they have not been able to fully enforce the Building Regulations. This is primarily due to lack of guidance, but this amnesty is due to expire on 1 January 2014.

Some of the evidence available to the task group includes data undertaken by BSRIA in late 2011 on domestic ventilation system failures. Here a small independent study on 40 random properties constructed by different builders, with various ventilation systems employed to the requirements contained in 2010 version of Building Regulations to assess their performance characteristics. Where, an example of the testing can be seen in image 1. It found that that 95% of everything initially evaluated failed to meet the requirements of the Building Regulations with some installations having a number of failure modes.

Value	Description
33 (82.5%)	Ductwork incorrectly fitted (kinked / bent / poor joints / excessive length)
10 (25%)	Undersized fans to meet the minimum ventilation requirement
6 (15%)	Insufficient fans or terminal outlets for dwelling type
3	No boost function
3	Incorrect installation data
2	Missing ductwork
1	Blocked ductwork

Table 3: Ventilation system failure modes in a study of 40 dwellings

In undertaking this work it became evident that the test instrumentation used in commissioning out in the field was not meeting the requirements contained in the Compliance Guide. More specifically they were not UKAS (ISO 17025) calibrated for air volume. Some meters were calibrated for air velocity, not volume, but most equipment had no calibrations at all. The measurement instruments often failed to meet the 5% accuracy requirement, with some having a 1 l/s scale resolution that equated to a best measurement capability of 16.6% at 6.0l/s, the minimum rate specified for sanitary accommodation (WC cloakrooms etc.). Furthermore it became apparent that the influence of the measuring system employed could significantly affect the performance of the fan system itself, which is a finding similar to other studies conducted. [7] [8]

A further in-house study in early 2013 on 242 dwelling by BSRIA found that a similar percentage level of failures were still evident in new properties. There were however improvements in the figures amongst a number of the smaller builders for whom the Building Control Bodies were enforcing the Building Regulations in place. It should be noted that this in-house study was primarily focused on determining if the fitted system achieved the design air flow rates rather than the nature of any failure mode, but in overall terms the data set showed:-

- System 1 installations - The vast majority of properties had reduced fan performance figures due to poorly fitted ductwork particularly excessive lengths of the flexible type.
- System 3 installations - Unlike system 1 most installations met the requirements for airflow performance but this was due to the capability of the systems having variable speed fans and the engineer able to alter the flow rates during commissioning process.
- System 4 installations – Most systems were out of balance i.e. the supply and extract rates differed by figures >10% which would lead to poor system heat recovery performance.

Image 1: Assessment of ventilation system performance using a powered flow hood assembly

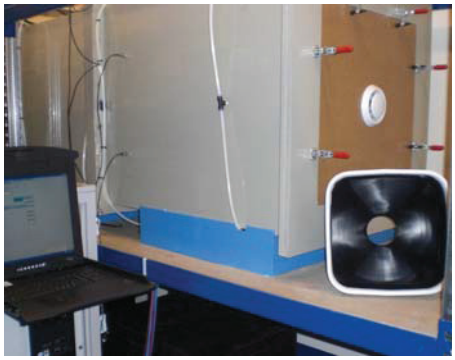
Image 2: BSRIA UKAS (ISO 17025) accredited air volume test facility

Further testing within the BSRIA laboratories on their UKAS (ISO 17025) accredited test facilities, see image 2, into the influence of the measuring system on the ventilation system, revealed that the use of the traditional 100mm vane anemometer and plastic hood assemblies produced significantly variable results. An example of which can be found in graph 1. Further investigation into this phenomena resulted in the publication of a BSRIA guide to measuring airflow rates in domestic ventilation systems [9], and this specifies that there are two methods that should be used for domestic installations – the unconditional method and the conditional method.

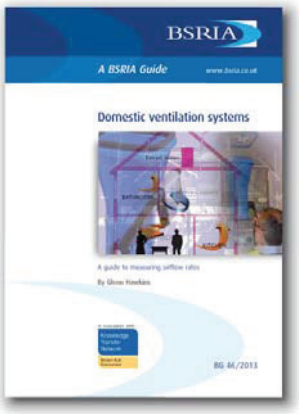

Image 3 BSRIA document BG 46/2013 – A guide to measuring airflow rates

The unconditional method of airflow measurement uses a powered flow hood assembly, and is deemed as the preferred method in all installation scenarios because of its accuracy and simplicity. As the name suggests, it is a method that is free from site specific conditions such as fan type, model, airflow direction and instrumentation characteristics.

Whilst the unconditional method of airflow measurement is the preferred method for all type of domestic system, the conditional method employing systems such as a vane anemometer & hood can still be employed for some types of installation. However, as its name implies there is need to take into account specific site conditions such as the fan performance characteristics, the resistance to airflow created by the measurement device and assorted correction and conversion factors depending on the type of measuring equipment used. These correction factors are currently not available as every system is different, and only where a house builder is able to standardise on a dwelling type and a specific ventilation system type, will correction factors become available.

Following the publication of the BSRIA guide a number of organisations within the UK recognised the importance of using the correct instrumentation for taking measurements from domestic ventilation systems, along with appropriateness of the training being conducted and value of the data being recorded by the test engineers. The Good Homes Alliance, a trade organisation for housing developers for example run a seminar on "Making ventilation systems work", and similarly the installation of systems was a seminar subject area covered at ECOBUILD the largest UK building exhibition held in March each year. Furthermore, BPEC are currently in the process of revising their training course to include additional materials relating to the use of test equipment specifically when testing Type 1 (intermittent extract) fan systems. Likewise NHBC have produced a guidance note on Type 1 systems for builders so they can demonstrate compliance with the Building Regulations to satisfy the Building Control Bodies and discharge their obligations under Section 42. Where, this document is includes a third method of testing not covered detailed in the BSRIA guide that is based on using vane anemometers in plastic hoods and a table of empirical benchmark performance figures for determining system failures.

CONCLUSIONS

Based on the studies BSRIA has undertaken it can be inferred that there are a large number of newly installed ventilation systems within the UK do not comply with the requirements contained in the Building Regulations which is due to a number of factors occurring throughout the design, installation and commissioning processes.

Over recent months BSRIA has seen some improvements in the number of ventilation systems meeting the airflow requirements within Building Regulations which is especially true amongst a number of the smaller builders for whom the Building Control Bodies are enforcing the minimum legal requirements. But, the overall level of poor performance should still be considered as unacceptably high with improvement a necessary requirement as opposed being "nice to achieve".

With ventilation system performance regularly compromised with inappropriate value engineering taking place during the build process without reference to the original design specification, inadequate installation inspection and commissioning along with the use of instrumentation providing data that was wholly incorrect, any softly-softly approach to change is going to be a problematic issue if the construction industry is to ever build better homes and to meet the carbon reduction challenges ahead. Nevertheless, some positive steps

have occurred within the industry during the early half of 2013 in regards to change. The production of a freely available BSRIA flow measurement guide is one such example, but it is only the firm implementation of the existing Regulations by the Building Control officers that are likely to result in any significant improvements in the overall build quality of new dwellings coming onto the market.

REFERENCES

[1] Dwelling Stock Estimates, Department for Communities and Local Government www.gov.uk

[2] The Building Regulations 2010, Approved Document F Means of ventilation, HM Government

[3] Domestic Ventilation Compliance Guide 2010, Department for Communities and Local Government, ISBN 978-1-85946-378-9

[4] Part F 2010 – where to start – An introduction for house builders and designers, NHBC Foundation, ISBN 978-0-9568415-3-7

[5] Designing Homes for the 21st Century – Lessons for Low Energy Design, NHBC Foundation, ISBN 978-1-84806-331-0

[6] Closing the gap between design and as-build performance, new homes – Interim progress report July 2013, Zero Carbon Hub, Free download from www.zerocarbonhub.org

[7] Evaluation of flow hood measurements for residential register flows, Walker, I.S., Wray, C.P., Dickerhoff, D.J., and Sherman, M.H. Energy Performance of Buildings Group Lawrence Berkley national Laboratory

[8] Mechanical ventilation in recently built Dutch homes: technical shortcomings, possibilities for improvement, perceived indoor environment and health effects
Jaap Balvers, Rik Bogers, Rob Jongeneel, Irene van Kamp, Atze Boerstra, Froukje van Dijken

[9] Domestic ventilation systems, A guide to measuring airflow rates, BSRIA document BG46/2013, free download www.bsria.co.uk or ISBN 978-0-86022-720-5

DETAILED ANALYSIS OF REGULATORY COMPLIANCE CONTROLS OF 1287 DWELLINGS VENTILATION SYSTEMS

Romuald Jobert [1], Gaëlle Guyot [*2]

[1]*CETE de Lyon*
48 rue St Théobald BP128
38081 L'Isle d'Abeau Cedex, France

[*1]*Corresponding author:*
gaelle.guyot@developpement-durable.gouv.fr

Note: the contact addresses may be re-arranged

ABSTRACT

Ventilation's historical goal has been to assure sufficient air change rates in buildings from a hygienic point of view. Regarding its potential impact on energy consumption, ventilation is being reconsidered. An important challenge for low energy buildings lies in the need to master airflows through the building envelope.

In this framework, the recent French energy performance (EP) regulation (2012) imposes envelope airtightness requirements for any new dwellings. As the dwelling airing is also governed by a 30-years-old regulation, this EP-regulation does not include any new requirement on ventilation rates.

In this context, actors in the building's sector are reflecting on the risk, with this generation of high performance airtight dwellings, of generating an unhealthy indoor air environment.

The "VIA-Qualité" project focuses on low energy, single-family dwellings. It proposes developing quality management (QM) approaches (ISO 9001) with the goal of increasing both on-site ventilation and indoor air quality. Such QM approaches, when applied to the individual home builder sector, appear to be promising. The benefits would be to: 1- Improve ventilation system performance, especially thanks to rigorous monitoring from conception to installation; 2- Limit indoor internal pollution sources, monitoring materials selection; 3- Increase final users understanding.

In France, the individual home builders sector accounts for more than 90 % of new single-family dwellings. Such QM approaches in envelope airtightness field are already being used by individual home builders, with respect to Annexe VII of the French EP-regulation. Feedback from these experiences shows that such approaches are both succesfull and affordable for either small or large individual home builder.

The first step in this project consists in increasing our knowledge of the actual performance of ventilation systems, once they have been installed and in-use in the buildings.

To this end, we analysed data from government building compliance regulatory controls, related to several laws, including energy performance and dwellings airing. Dysfunction analysis observed in a sample of 1287 dwellings allowed us to establish a more accurate picture of the quality of on-site ventilation systems. From a overall point of view, we observed that 68% of the single-family dwellings analysed do not comply with the regulation. A deeper analysis has allowed us to understand more specifically what are the underlying technical and organizational reasons for such results.

Firstly, this paper introduces the VIA-Qualité project objectives. Then, it rapidly presents the framework of French regulation compliance controls and the content of its underexploited database. The main part of this paper then presents the results of the detailed analysis of dysfunctions compilation observed on the sample, along 6 groups and 28 indicators. Finally, first proposals for ventilation installation improvement are presented.

KEYWORDS

Ventilation, airflow measurement, indoor air quality, regulatory checks, performance

1 INTRODUCTION

In order to insure a good indoor air quality, including a proper humidity level in buildings, adequate air change rate is necessary. On the other side, building energy performance requires to rethink of ventilation and air change rates, because of their impact on thermal losses:
1) New ventilation systems technologies, such as Demand-Controlled Ventilation (DCV) systems, aim at restricting airflows to the minimum level for healthy buildings. 2) Envelope airtightness treatment becomes essential, especially for low energy dwellings (Erhorn, 2008). Indeed, envelope air leakage entails thermal losses, but also modifies theoretical voluntary airflows circuits in building: airtight rooms may be short-circuited in case of other very leaky rooms. In France, the recent thermal regulation (RT2012) generalizes low energy dwellings and imposes envelope airtightness requirement for any new dwellings. For a single-family dwelling, the requirement is Q_{4Pa_Surf}=0.6 $m^3.h^{-1}.m^{-2}$, that is around n_{50}=2.3 h^{-1}.

This energy performance-regulation does not include any new requirement on ventilation rates. Dwellings airing are concerned by another 30 years old regulation (JO, 1982).
In this context, building's sector wonders about the risk for a generation of performing airtight dwellings to contribute to an unhealthy indoor air. Some questions are emerging in this way: are former regulations ventilation airflows in former regulations sufficient to provide a healthy indoor air in these new airtight dwellings ? For these dwellings, what are the consequences of dysfunctional-working ventilation installations ? What do we know exactly about the actual efficiency of those ventilation systems, once they are installed and in-use in the buildings ?

Some answers are given in recent research projects. The QUAD-BBC project (Boulanger, 2012) confirmed that envelope airtightness drives to a better indoor air quality, thanks to a better mastering of the theoretical airflows circuits in buildings. This project has also confirmed the need for increased airflows during cooking period.
Moreover, a growing number of actors, namely around the Healthvent project (Wargocki, 2012), agree about the idea that ventilation is not a panacea. To achieve a good indoor air quality, contributing to healthy buildings, reduce buildings pollutant sources is a priority.

The "VIA-Qualité" project focuses on low energy, single-family dwellings. It proposes developing quality management (QM) approaches (ISO 9001) with the goal of increasing both on-site ventilation and indoor air quality.

As a first step of this project, and in order to evaluate the ventilation system efficiency, we analyzed available data from regulation compliance controls, related to several regulations, including energy performance (RT2005 & 2012) and dwelling airing (1982-1983). Dysfunctions analysis of a 1287 dwellings sample allows us to establish an accurate picture of on-site ventilation systems quality. This original first analysis represents an essential step towards the final goal: find solutions to increase ventilation installation quality.

First, the paper presents quickly the "VIA-Qualité" project. Then, the framework of French regulation compliance controls and the content of this precious database. After that, it gives an overview of the analyzed sample. Finally, results of the detailed analysis of dysfunctions compilation are presented, leading to some proposals for ventilation installation improvement.

2 THE "VIA-QUALITE" PROJECT

The “VIA-Qualité” project (2013-2016) focuses on low energy, single-family dwellings. It proposes developing quality management (QM) approaches (ISO 9001) with the goal of increasing both on-site ventilation and indoor air quality. Such QM approaches, when applied to the individual home builder sector, appear to be promising. The benefits would be to: 1- Improve ventilation system performance, especially thanks to rigorous monitoring from conception to installation; 2- Limit indoor internal pollution sources, monitoring materials selection; 3- Increase final users understanding.

In France, the individual home builders sector accounts for more than 90 % of new single-family dwellings. Such QM approaches in envelope airtightness field are already being used by individual home builders, with respect to Annexe VII of the French EP-regulation. Feedback from these experiences shows that such approaches are both succesfull and affordable for either small or large individual home builder (Carrié R. et al, 2007) (Charrier S. et al, 2013).

The first step in this project consists in increasing our knowledge of the actual performance of ventilation systems, once they have been installed and in-use in the buildings. To this end, we analysed data from government building compliance regulatory controls, related to several laws, including energy performance and dwellings airing.

3 STUDY OF A SAMPLE OF BUILDING REGULATORY COMPLIANCE CHECKS

3.1 Building regulatory compliance checks: a precious source of field data

In France, building’s owner is legally responsible for the compliance with regulations: when asking for a building permit, he has to sign a commitment to comply with building regulations. Then, he must be able to prove that this building complies with these regulations.

Both during building construction and up to 3 years after commissioning, French authorities have the legal power to proceed to a regulatory compulsory check of any building. Controls are performed by sworn-in and specifically qualified government employees. Their qualification process includes technical and regulatory trainings, and a minimal number of controls performed under a senior employee supervision. The final qualification can be addressed only after a 3 years experience.

Several regulations are controlled, including energy performance and airing. The control is based on plans analysis, specifications analysis and calculations, on-site visit, visit at commissioning. Non-compliance with construction regulations is an offence, and controllers’ reports are sent to national authorities and to general attorney. Financial penalties may go up to 45k€ (75k€ if repeated). Prison term or banning from practicing may be decided. In general, no penal, no direct financial sanctions are sentenced, but the building’s owner must undertake remedial actions to comply with regulation, sometimes very costly. An extensive description of the control process is given in (Lecointre et al, 2009).

The French dwellings airing regulation (JO, 1982) requires a general and continuous airing system. It describes the compulsory general layouts of ventilation installation. It also sets exhaust airflows in each humid room, depending on the total number of rooms in the dwelling. Total airflows drive to around 0.5 h^{-1} global air change rate in the dwelling. This

regulation has been modified in 1983 in order to reduce these airflows in case of demand-controlled ventilation system (DCV), for instance based on humidity. In this case, controls include also additional specific technical guidelines.

This regulatory compliance control includes two sections:

- "What can be seen and operated observation": control of the ventilation system installation, as well as of the whole ventilation equipments set;
- "Exhaust and supply airflows measurements»: check of airflow or pressure difference at air vents (global minimal airflow in dwelling, minimal airflow in kitchen, peak airflow in kitchen, peak airflow in other humid rooms).

The French construction technical regulation observatory (ORTEC) compiles these control data on both sections. In its last report, ORTEC published the following national statistics (CSTB, ORTEC, 2009):

- 50% of the controlled buildings do not meet the requirements in terms of ventilation mounting, with entails a system dysfunction;
- 43% of the controlled buildings do not comply with the regulatory airflow rates, especially concerning exhaust airflows that are insufficient for 36% of the buildings and excessive in 7%.

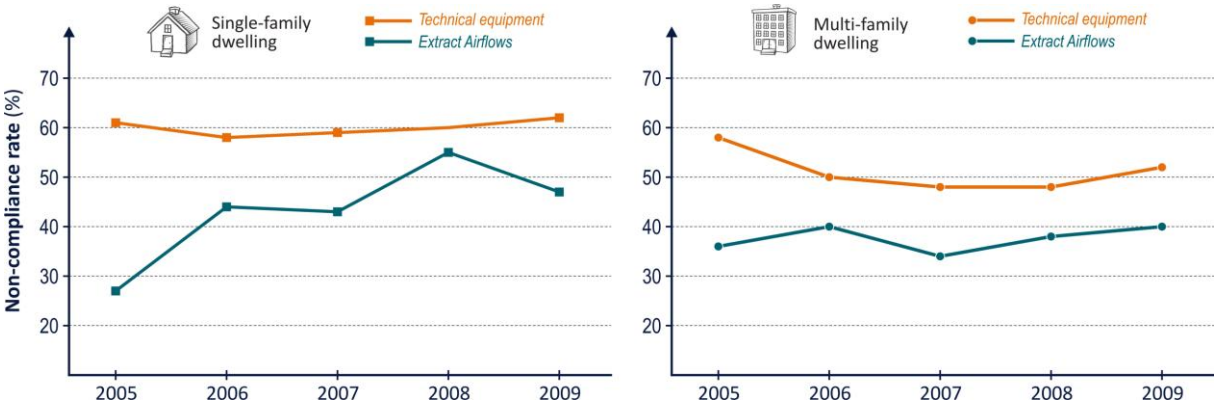

Figure 1: Annual distribution of non-compliance rates, for each type of dwelling, source: ORTEC, CSTB, 2009

However, these national published data are only statistical and mainly analyze "pass-or-fail" tests results. And yet, because comprehensive control reports fully describe all observed non-compliances, even when not related to the regulations, original data are far more detailed and include precise descriptions of the different causes, which affect ventilation performance.
As a result, beyond the regulatory aspect, these detailed reports constitute a potentially important technical database. This paper presents the first results using those data to explain the sources of on-site ventilation dysfunctions.

3.2 Description of the analyzed sample

We exhaustively analysed 373 control reports performed between 2008 and 2011, by the technical civil servants network of the Ministry in charge of the Construction's sector. These 373 compliance checks reports concern 1287 dwellings, situated in different climate zones, and include by 88% of multi-family new dwellings (Figure 2).

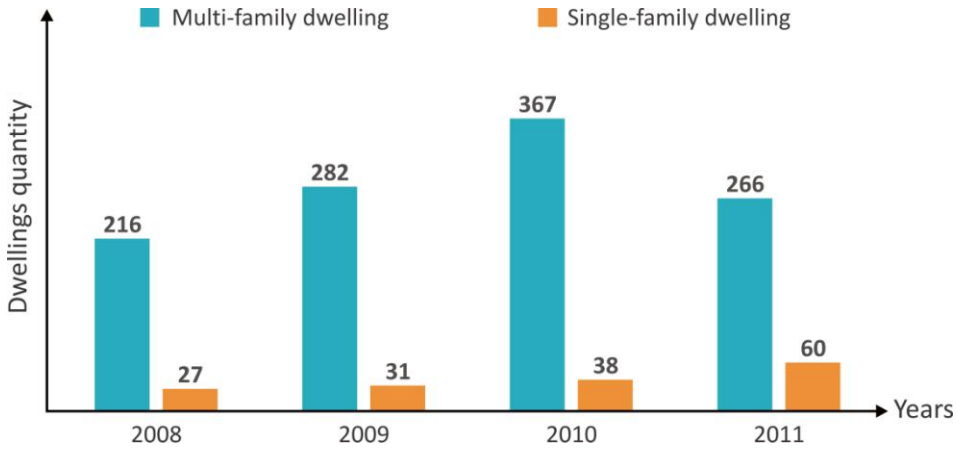

Figure 2: Dwelling type repartition analysed per year

Nearly all dwellings of the sample are equipped with simple exhaust mechanical ventilation. Humidity demand-controlled ventilation accounts for 74% of the sample. Balanced ventilation is found only in 10 single-family dwellings. This distribution (Figure 3) gives a good characterisation of the new dwellings stock in France, since the implementation of the 2005 thermal regulation (RT2005).

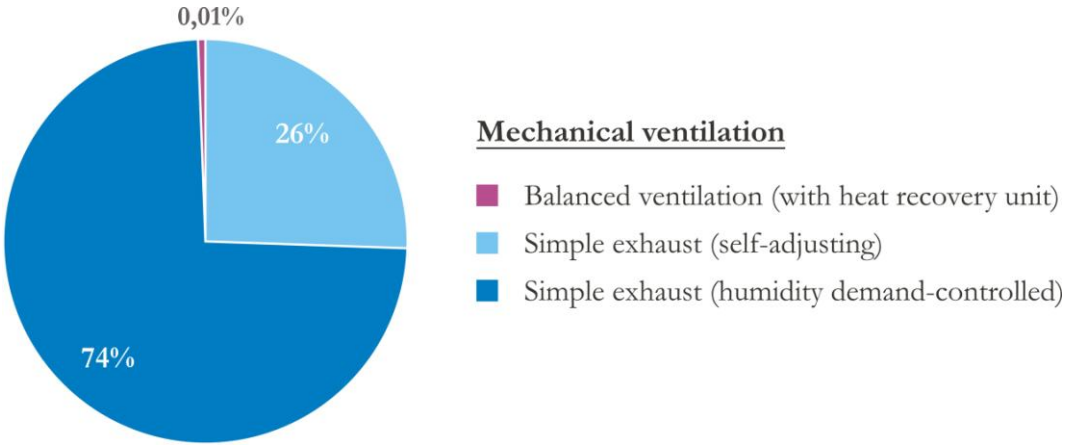

Figure 3: Ventilation system repartition in the analysed sample

The statistic analysis of this sample reveals that 604 dwellings out of 1287, that is 47% of the sample, do not comply with the airing regulation. It also means that 47% of the sample present at least one non-compliance remark. The non-compliance rate is 68% for single-family dwellings, and 44% for multi-family dwellings. These results confirm the national trend (CSTB, ORTEC, 2009).

Among non-complying dwellings, around 1/3 get only one non-compliance point, 1/3 two non-compliance points, and the last third obtain more than 3 non-compliance points.

4 ANALYSIS OF OBSERVED VENTILATION DYSFUNCTIONS

4.1 Global analysis

Based on the analysis of 373 control reports, the first part of the study consisted in drawing up and classifying all the dysfunctions observed during the controls into a 28 dysfunction points

list. These 28 points have then been distributed into 6 representative categories for the main mechanical ventilation system elements: airflow/pressure (DCV) measurement, air inlet, air outlet, system configuration, ventilation fan, ducts (Figure 4), (Table1).

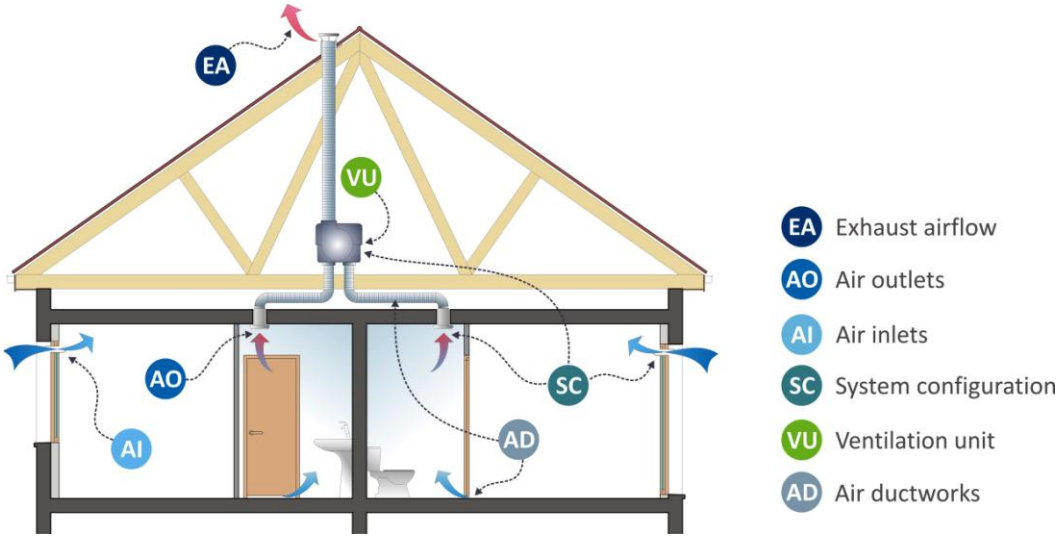

Figure 4: Dysfunctions classifying per category

Statistical analysis shows that the 604 non-complying dwellings account for 1246 non-compliance or dysfunctions points (Figure 5),. These points directly or indirectly contribute to a bad ventilation functioning, and also affect indoor air quality.

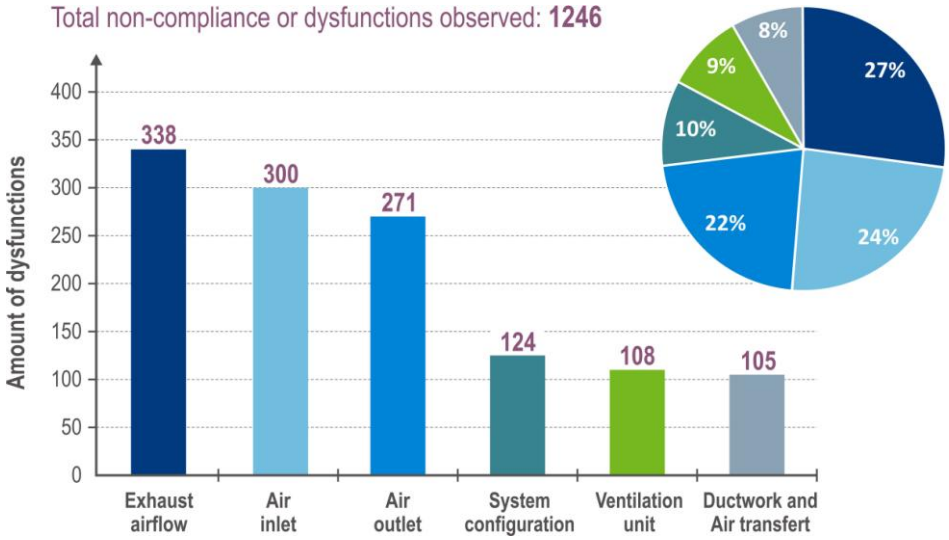

Figure 5: Number of non-compliance or dysfunctions items per category

We can notice that 46% dysfunctions are due to a bad quality of the ventilation mounting terminal devices, that are air inlets (24%) and air outlets (22%). As for air inlets, the most frequently observed dysfunctions are: lack of module, insufficient module quantity, and non-compliance with characteristics of the module (airflows).

And yet, on site, terminal devices comply with specific technical terms and conditions and are delivered with plans supplied by the main contractor. The problem lies with the quality of functional layouts mounting, often neglected.

The second important heading (around 1/3) concerns exhaust airflows. Among them, 85% non-compliance cases are due to insufficient minimal airflows, 15% to total excessive exhaust airflows. The frequent causes of these dysfunctions are: implementation of non-complying air outlet, non-adapted airflows regarding the size of the dwelling, bad quality of ventilation ducts mounting (air leakage and pressure losses).

Dysfunctions type		Amount	(%)
EA	**Air inlets**	**300**	**100**
EA1	Absence of air inlets modules	153	51
EA2	The Implementation of air inlets does not comply with prescribed rules and regulations	54	18
EA3	Presence of inlet air in a humid or service room	36	12
EA4	No mortises in window frames or incorrect size	28	9
EA5	Air inlet excess in the main rooms	17	6
EA6	Obturation of air inlets in one or more rooms	12	4
SA	**Air outlets**	**271**	**100**
SA1	The air outlets does not comply with regulation requirements	102	38
SA2	Control for changing peak flow missing or inaccessible	57	21
SA3	Dysfunction of air outlets equipped with presence detectors	41	15
SA4	Absence of air outlets in one or more rooms	39	14
SA5	Location of air outlets does not comply with regulation and technical requirements	32	12
QE	**Exhaust airflows**	**338**	**100**
QE1	The pressure measures at the air outlets are not correct	196	58
QE2	The exhaust airflows at the air outlets are not correct	142	42
SY	**System configuration**	**124**	**100**
SY1	The system configuration does not comply with the technical note requirements	74	60
SY2	Interversion of air inlet and air outlet	34	27
SY3	The system configuration does not comply with the standardized calculations of thermal regulations	16	13
GX	**Ventilation unit**	**108**	**100**
GX1	The warning signal which indicates ventilation failure is absent	55	51
GX2	The warning signal which indicates ventilation failure is not identified	34	31
GX3	Malfunction or failure of the ventilation unit	14	13
GX4	unsuitable Ventilation unit location and non-compliance with the acoustic requirements	4	4
GX5	Electrical protection group VMC is not independent of other circuit	1	1
CA	**Ductwork and air transfer**	**105**	**100**
CA1	Absence of transfer grids or doors undercut	49	47
CA2	Fouled air discharge in the attic	22	21
CA3	Extracting fouled air ducts are crushed or bent	17	16
CA4	Connecting ducts and duct fittings system are not airtight	17	16
Total of dysfunctions observed		**1246**	**100**

Table 1: Repartition and amount of dysfunctions observed by main mechanical ventilation system elements categories

4.2 Analysis of first reasons behind these dysfunctions

In most cases, observed dysfunctions are due to lack of attention at the mounting step. But they are also due to imperfections during the project managing process and during the decision chain whenever the ventilation installation process is concerned. Indeed, there is a real lack of continuity between program step, design, mounting, and also material and component furniture.

During the execution phase, the lack of ventilation installation quality is due to the actors' dispersion inside multiple technical lots. Thus, in the process of execution phase contracting procedures, ventilation is rarely defined as a specific lot. As a result, the ventilation different components installation is generally divided up among different building trades and no one is/feels responsible for the final result.

We also observed that ventilation installation verification is rarely planned during the construction phase, and that its control at commissioning is not systematic or most incomplete. Therefore, it appears that ventilation commissioning is an absolutely necessary step to ensure a well working installation upon receipt, with an in-use performance corresponding to the planned one. Recent guides (CETIAT, 2012) describe precisely these receipt procedures.
For further information on quality of ventilation systems in residential buildings, see also another French paper (Mouradian, 2013).
The on-going "VIA-Qualité" project will go further on reasons and solutions to improve ventilation systems quality once there are installed.

5 CONCLUSIONS

This analysis confirms that, even if adapted industrial solutions are available, ventilation system dysfunctions are very frequently observed in dwellings, which entails the reliability of these installations. Unfortunately, we found out that, just like in France, other countries (Boersta, 2012; Caillou, 2012) also observe that in-site ventilation system mounting is often far from the hoped quality.
This first analysis, based on French regulatory compliance controls and performed only on airing regulation (among 7 other regulations including energy performance), gives clear information about ventilation dysfunctions localisation and qualification. Up to now, only 1287 dwellings have been analysed. In 2013, an important project will harmonize data collection which goal will be to implement a robust database including all other information obtained from building regulation compliance checks.

very low energy dwellings (OQAI, 2011) even if some ongoing projects aim at increasing knowledge on this subject. But one thing is for sure: even if indoor pollution sources are minimized, the more airtight the dwellings will become, the more essential the need for guaranties on in-site ventilation installation quality will become. In this way, the French Effinergie+ label plans to reinforce ventilation controls, introducing ventilation airflows and duct leakage measurements at commissioning.

The main stake now consists in determining the ultimate causes for ventilation dysfunctions, and manage major projects to develop tools leading to better practices at every stage of the construction. For instance, many dysfunctions could be avoided through the implementation of quality management tools. With such tools, one could pretty easily, but efficiently, control

ventilation system at each stage of the building construction: from design to installation, even including maintenance and final use.

6 ACKNOWLEDGEMENTS

The authors are very grateful to the French ministry for ecology, sustainable development, and energy (MEDDE), for their support during this study. The sole responsibility for the content of this publication lies with the authors. It does not necessarily reflect the opinion of the Ministry.

The "Via-Qualité" project is supported by ADEME, région Rhône-Alpes, and French ministry for ecology, sustainable development, and energy (MEDDE).

7 REFERENCES

Erhorn H., Erhorn-Kluttig H., Carrié F.R. (2008). *Airtightness requirements for high-performance buildings*. Conference paper, AIVC, Kyoto, Japan, 6 p.

Boulanger X. et al. (2012). *Lessons learned on ventilation systems from the IAQ calculations on tight energy performant buildings*. Conference paper, AIVC, Tightvent, Copenhague, Denmark, 7 p.

Wargocki P, Hartmann T. (2012). *Health-Based ventilation Guidelines for Europe*. HealthVent project, AIVC, Tightvent, Copenhague, Denmark.

W. Lecointre, R. Carrié and G. Guyot. (2009). *"France : Impact, compliance and control of legislation"*. Information paper P176, www.buildup.eu.

JO, *Arrêté du 24 mars 1982 consolidée relatif à l'aération des logements : aération générale ou permanente*. JO du 15 novembre 1983.

CSTB, Rapport de synthèse de l'ORTEC, Période 2005-2009. Rubrique "aération des logements", 2009.

Caré I., Chaffois P., Henry P. (2012). *Guide de bonnes pratiques des mesures de débit d'air sur site pour les installateurs de ventilation*. CETIAT, France, 49 p.

Mouradian L., Brière E. (2013). *Quality of ventilation systems in residential buildings - Status and perspectives in France*. In: proceedings of the AIVC workshop "Securing the quality of ventilation systems in residential buildings", Brussels.

Boersta A. (2012). *Residential ventilation system performance : outcomes of a field study in the Netherlands*. Conference paper, AIVC, Tightvent, Copenhague, Denmark, 7 p.

Caillou S. (2012). *Performances of ventilation systems : on site measurements related to energy efficiency*, comfort and health. Conference paper, AIVC, Tightvent, Copenhague, Denmark, 7 p.

Jobert R. (2012). "*La ventilation mécanique des bâtiments résidentiels neufs : État de l'art général - Analyse qualitative et technique des dysfonctionnements*". Mémoire professionnel, France, 125p.

Carrié R. et al. (2007). *Performance de la ventilation et du bâti*. Rapport final phase 1 et 2, Association air.h, France, 109 p.

Charrier S., Huet A., Biaunier J. (2013). *Airtightness quality management scheme in France: assessment after 5 years operation*. 34th AIVC Conference and 3rd TightVent Conference, Athens, Greece, 2013, 11 p.

Charrier S., Ponthieux J. (2013). *Control of airtightness quality management scheme in France: results, lessons and future developments*. 34th AIVC Conferenceand 3rd TightVent Conference, Athens, Greece, 2013, 11p.

OQAI Campagne sur 7 logements BBC

Effinergie association, www.effinergie.fr.

EFFECT OF AGEING PROCESSES ON SOLAR REFLECTIVITY OF CLAY ROOF TILES

Chiara Ferrari*[1,2], Ali Gholizadeh Touchaei[2], Mohamad Sleiman[3], Antonio Libbra[1], Alberto Muscio[1], Cristina Siligardi[1], Hashem Akbari[2]

[1]*Dept. of Engineering "Enzo Ferrari"*
University of Modena and Reggio Emilia
Via Vignolese 905
41125 Modena (ITALY)
**Corresponding author: Chiara.ferrari@unimore.it*

[2]*Heat Island Group, Building, Civil and Environmental Engineering Department*
Concordia University
1455 de Maisonneuve Blv. West
Montreal, Quebec, Canada H3G 1MB

[3]*Heat Island Group,*
Lawrence Berkeley National Laboratory
One Cyclotron Road,
Berkeley, CA 94720, U.S.A

ABSTRACT

Clay roof tiles are widely used as roofing materials because of their good mechanical and aesthetical properties. The exposure to atmospheric agents and, most of all, to pollutants and smog affects negatively the solar reflectance of a tile surface. The aim of this study is to analyze the influence of ageing on the solar reflectance of clay roof tiles. We studied samples provided by manufacturer in Greece and USA. Samples were coated with either organic or inorganic coatings. Natural ageing processes were used for samples with inorganic coating, and artificial ageing simulation was performed on all samples. Samples were naturally aged in a test farm in Arizona, with an exposure time of 3 years. In artificial ageing processes, the surface of the tiles was subjected to the application of two different mixtures simulating exposure to i) Arizona weathering agents such as clay, salts and soot and ii) Arizona, Florida and Ohio weathering agents through an average mixture made by clay, salts, particulate organic matter and soot. The amount of soiling mixture deposited on the surface of the samples was aimed at reproducing a 3 years exposure. Soiled samples were subjected to air blowing and rinsing under running water to simulate the wind and rain effects, respectively. The effects of both natural ageing and artificial soiling on the surface reflectivity of the clay roof tiles were assessed in the UV-Vis-NIR range (range from 300 to 2500 nm). The two different soiling conditions were found to affect significantly the solar reflectance of the samples, in particular the samples soiled with the average mixture present a decrease up to 0.20, while Arizona weathering condition affects the solar reflectance up to 0.05, and neither air blowing nor rinsing seem to permit a significant recovery of the surface properties. All solar reflectance measurements were computed by averaging the spectral reflectivity weighted by the AM1GH solar spectral irradiance.

KEYWORDS

Cool roof, Natural ageing, Accelerated ageing, Clay roof tiles, Cleaning processes

1 INTRODUCTION

Building materials are deeply subjected to atmospheric factors and ageing, therefore not only good aesthetical and surface properties but also mechanical ones are required. The combination of the features of ceramic products, their shock resistance properties, and the design of a coating characterized by excellent solar reflective behavior make roof tiles an ideal product to be applied on modern buildings. Cool roof tiles have the potentials of saving energy, limiting summer overheating, and mitigating the urban heat island effect (Konopacki et al 1997; Akbari, 2006; Levinson & Akbari, 2010).
Building products characterized by high solar reflectance and high thermal emittance are commonly defined cool roofs (Akbari, 2012; Santamouris, 2012). In this study, in particular, our attention will be focused on solar

reflectance analysis. To improve the integration in the city skyline, solar reflective coatings can be integrated with pigments that reproduce the desired colors with just a small compromise: the slight decrease of the reflectance properties of the final product in comparison with a light colored coating. (Akbari, 2005).

Studies about ageing processes affecting roof materials were carried out in the last 15 years. In particular Bretz et al (Bretz, 1997) demonstrated that the loss in solar reflectance due to ageing of solar reflective coatings is not a significant barrier to the use of these materials for the improvement of energy efficiency in buildings. The study was carried out in collaboration with three different suppliers, analyzing three different coatings made by a white polymer coating with an acrylic base, a white acrylic-based coating and a white cementitious coating applied on horizontal and gently sloped (<25%) roofs. Albedo values were measured in the warmest hours of the day, in clear days using a pyranometer, and reflectance measurements were carried out with a double beam spectrophotometer with 150 mm integrating sphere according to ASTM Standard Test Method E903-96 (ASTM, 1996). The main finding of that paper was that the change in albedo depends mainly on the coating, the surface texture, the slope of the roof and the nearby sources of dirt and debris, quantifying the albedo loss in 0.15 during the first year and much more gradual decline after the first year of ageing. Bretz et al. assume also that the albedo can be restored from 90 to 100% of the estimated original value just washing the surfaces.

Levinson et al (Levinson, 2005) studied the effect of cleaning processes on the reflectance and, in general, on solar heat gains of light colored roofing membranes. In that study white or light grey PVC membrane samples taken from roofs across the United States were analyzed. On the sample surface was found black carbon and inorganic carbon. These contaminants reduce the solar reflectance of the membranes. To analyze the influence of several cleaning processes on the solar reflectance values, the sample surfaces were firstly wiped to simulate wind action, then rinsed to simulate rain action, and as a third step the surfaces were washed simulating a homemade cleaning process using a phosphate-free dishwashing detergent. As a final step all the surfaces were treated with a mixture of sodium hypochlorite and sodium hydroxide to simulate professional cleaning processes. After rinsing and washing processes almost all the dirt deposited on the surface was removed except for thin layers of organic carbon and some isolated dark spots of biomass. Bleaching processes cleared these last two ones recovering the loss of solar reflectance.

The same cleaning processes were used by Akbari et al. (Akbari, 2005) studying unweathered and weathered single ply roofing membranes collected from various sites across the US and Canada. In that study, 16 samples were analyzed at LBNL, following all the cleaning processes concerning the weathered samples surface treatment, and 25 samples were studied at NRC, applying just wiping processes on the samples surface. All cleaning processes were effective with recovery of almost 90% of their unweathered reflectivity. In some cases, an anti-algae product was required to restore the reflectivity level.

Among several studies concerning solar properties of building materials, Berdahl et al (Berdahl, 2012) highlighted how solar reflectance changes during sample exposure to weathering agents. Asphalt shingles with granules coated by inorganic metal oxide pigment were studies. The very stable nature of the coatings helps to keep the properties of the granules constant on time, but initial solar reflectance values changed due to the loss of processing oils which coat the granules. These oils are particularly sensible to UV induced Photo Oxidation, which produces dark hydrophilic substances that are removed by rain or dew. Both hot dry and hot humid climates were considered in this study: in hot dry climates the changes in solar reflectance are mainly related to the annual cycle of accumulation of atmospheric particles and their removal by wind and rain; in hot humid climate, instead, algae grow easily on granule surfaces, creating coatings which reduce reflectance by as much as 0.06 after 3 years. In this case anti-algae additive addition to the asphalt shingles is suggested. If algae growth is absent, solar reflectance does not change deeply in the first year (0.02 or less).

Considering the importance of the atmospheric particles deposited on the roof tiles, Cheng et al (Cheng, 2012) studied the nature of dust deposited during natural ageing processes. According to that study, the knowledge taken from Bretz (Bretz, 1997) concerning the black and organic carbon deposited by ageing and weathering processes on the roofing material was integrated with the definition of two different kind of atmospheric particles belonging from rural and urban/industrial sites. Moreover Cheng et al performed elemental analysis on atmospheric particle and they highlighted that Fe is the most abundant contaminant, and Fe, Cr and C are the major contributors to the change of solar reflectance on soiled samples (after 4.1 year exposure)

Accelerate ageing experiments (Sleiman, 2010) have been formulated to simulate the natural weathering conditions. On the sample surface a suspension of water and soiling agents is sprayed with a nozzle. Artificial soiling mixture is made by sooty particles, salty particles and organic particulate matters trying to reproduce, in the most repeatable way possible, particles that can be found in the atmosphere. After the deposition of a known amount of soiling mixture, the samples will be dried under a heating lamp. The soiling mixture recipe is aimed at reproducing in a quite standard way a natural one, but it must be integrated with insoluble dust surrogate to optimize the wet and dry deposition and create a mixture that can be industrially adoptable. This mixture should be flexible and tunable to better represent different climate zones across the globe.

This study is aimed at applying the results of previous studies (Libbra, 2011), which were carried out on polymeric materials and asphalt shingles, to ceramic roof tiles considering both the study of natural and accelerated ageing influence. More specifically, the studies were carried out on clay roof tile, coating fired clay

samples with a white basecoat and a semi-colored topcoat both of them made by organic materials. They also compared organic coatings with inorganic materials such as ceramics, which offer better reflection and durability properties than organic coating for wavelengths above 1100-1700nm. They however highlighted how these materials cannot be applied to existing tiles on site but they could be used to coat new tiles during the manufacturing process.

2 EXPERIMENTAL STUDY

In this study, all the samples were collected both from the United States (California) and European (Greece) suppliers, which provided samples both unweathered and weathered. For weathered samples, suppliers gave us information about the place of ageing and the time of ageing.
No information is provided concerning the weathering roof slope. On all samples solar reflectivity measurements are carried out through both UV-Vis-NiR spectrophotometer with a 150 mm integrating sphere and reflectometer analysis. In second instance, some unweathered samples will be artificially aged thanks to the use of an accelerated soiling device that mimics natural exposure of roofing materials (Sleiman et al, 2010).
The accelerated ageing process is carried out just on the samples from California and Greece in order to confirm the correspondence between artificial and natural ageing. The influence of the same accelerating ageing process on two different coated tiles, taking as reference the inorganic and unglazed coating for the Californian samples and the organic coating for the Greek samples, was also analyzed.
The approach in the studies regarding the influence of different cleaning process carried out by Levinson et al (2005) and Akbari et al (2005), must probably be modified considering that in typical buildings it is not practical to clean with phosphate free soap and bleaching agents a roof made by traditional clay roof tile. For this reason, artificially and naturally aged samples are modified with two different cleaning processes with increasing influence on the surface state, starting from a wiping process to simulate wind action through rinsing to simulate rain action. After each step, solar reflectance of the samples is measured once again with both a UV-Vis-NiR Spectrophotometer with a 150 mm integrating sphere and a reflectometer.
These operations allow us to discover the influence of natural ageing on ceramic roof tiles, evaluate the influence of atmospheric agents on both natural and artificially aged surfaces, and understand how the same accelerated ageing protocols will influence the solar properties of different coated clay roof tiles.

2.1 Roof tiles samples

Two different macro-set of samples were used in order to carry out this study: from California we received four set of samples made by 5 fresh and 5 3-years-aged coupon; from Greece we received four set of samples made by 4 fresh samples (Tab.1).
All the samples, like traditional terracotta red ceramics, present a substrate made by ceramic material obtained by mixing quartz, feldspar $CaCO_3$ and different clays. In order to reduce the cost of the finished product, raw material sources located close to the tile plant are used; this often affects the quality of the clay due to the high levels of iron.
All samples, both fresh and aged, were in good mechanical conditions.

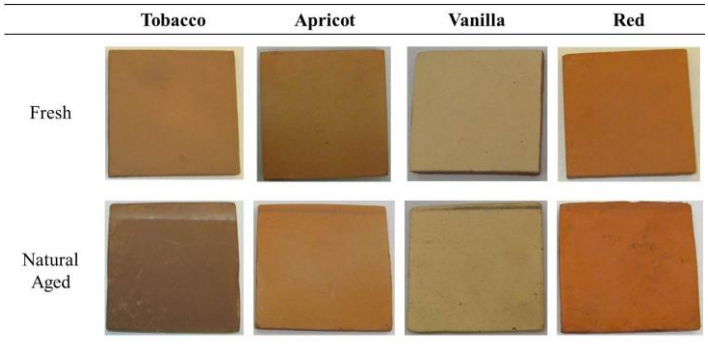

Figure 1: Samples from California

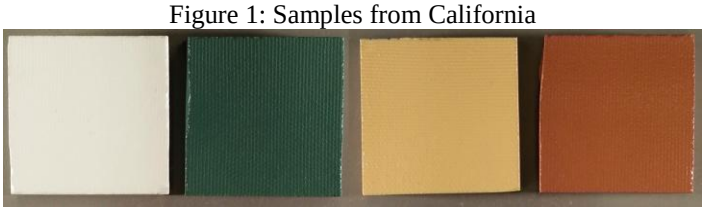
Figure 2: Samples from Greece

Table 1: Samples from Greece and California

Location	Color	Condition	Place of ageing	Time of ageing	Substrate nature	Coating nature
California	Tobacco	Unweathered	N/A	N/A	Clay tile	Inorganic
		Weathered	Arizona	08.2007/09.2010	Clay tile	Inorganic
	Vanilla	Unweathered	N/A	N/A	Clay tile	Inorganic
		Weathered	Arizona	08.2007/09.2010	Clay tile	Inorganic
	Apricot	Unweathered	N/A	N/A	Clay tile	Inorganic
		Weathered	Arizona	08.2007/09.2010	Clay tile	Inorganic
	Red	Unweathered	N/A	N/A	Clay tile	Inorganic
		Weathered	Arizona	08.2007/09.2010	Clay tile	Inorganic
Greece	Beige	Unweathered	N/A	N/A	Clay tile	Organic (Paint)
	Brown	Unweathered	N/A	N/A	Clay tile	Organic (Paint)
	Green	Unweathered	N/A	N/A	Clay tile	Organic (Paint)
	White	Unweathered	N/A	N/A	Clay tile	Organic (Paint)

3 METHODOLOGY

As reported in Levinson (2010) and Levinson (2010a), the near-normal hemispherical solar spectral reflectance (300–2500 nm @ 5-nm intervals) and the total reflectance corresponding to air-mass 1 global horizontal radiation (AM1GH) of a 10mm^2 area at the center of each sample were measured according to ASTM Standard E903 (ASTM, 1996), using a PerkinElmer Lambda 1050 UV/Visible/NIR Spectrometer with 150 mm integrating sphere.
The global solar reflectance of each tile was estimated as the mean of ASTM Standard C1549 air-mass 1.5 solar reflectance (ASTM, 2002) measured with a Devices & Services Solar Spectrum Reflectometer (model SSR-ER v.6) at several 2.5-cm diameter spots (five per samples from California, four per samples from Greece) over the whole sample area.

3.1 Samples preparation

In a first step the solar reflectance was measured for both weathered and unweathered samples as received by the suppliers. The unweathered samples from California and Greece were, then, artificially weathered in the LBNL laboratories applying three different conditions identified as “After weatherometer”, “Arizona” and “Average”. On a first set made by one coupon from each sample a 24 hours weathering cycle was applied with a QUV/SPRAY from Q-LAB (website on references) according to ASTM G154 (ASTM, 2012). The cycle was made by 8 hours of UV light exposure at the conditions of 0.89 W/m^2 and T=60°C, and 4 hours of water condensation at T=50°C, repeated twice.
Other two sets made by one coupon from each sample were artificially soiled applying, after a 24 hours weathering cycle as described above, Arizona soiling condition (Fig. 3) and an Average (Fig. 4) of the soiling conditions presented in the three location selected by the CRRC as a reference for the weathered samples (Ohio, Arizona and Florida) (Tab. 2).

Figure 3: Samples from Greece after accelerated ageing simulating (Arizona weathering conditions)

Figure 4: Samples from Greece after accelerated ageing simulating (average weathering conditions)

Table 2: Soiling mixture wt% composition

	Dust	**Salts**	**POM**	**Soot**
Arizona Mixture	79 wt%	20 wt%	0 wt%	1 wt%
Average Mixture	47 wt%	20 wt%	28 wt%	5 wt%

After the weatherometer exposure, all the samples were dried for one hour under a heating lamp; once the surface was completely dried, the soiling mixture was applied on the samples surface through a device, which allows to deposit, through a spray nozzle, a mixture of soiling agents in aqueous suspension put in a pressurized vessel and, once ageing was applied, all the artificially soiled samples were dried under heating lamp for 1 hour in order to bind the soiling mixture to the surface and then they were treated with another 24 hours weathering cycle, and then dried again.
Both naturally and artificially aged coupons were treated with two different surface processes which tried to simulate the most common natural weathering agents, i.e. wind and rain. The surface of the samples was blown with a hairdryer set on cold air flux to simulate wind and was rinsed under cold running water to simulate rain. Both processes were applied for two minutes on each coupon and after each process the samples were dried under a heating lamp. Solar reflectance was measured with both the spectrophotometer and the reflectometer. These processes yielded eleven different cleaning steps for each sample analyzed considering the two cleaning mechanism shown above and both the unweathered, the samples just weathered, the naturally soiled, the two artificially soiled, and their respective artificially weathered conditions.

4 RESULTS AND DISCUSSION

The samples images (Fig. 3 and Fig. 4) show how the soil layer affects visibly the surface. It is interesting to notice the different deposition patterns of Arizona and Average soiling mixture on the samples surface. Only organic coated surfaces pictures are shown here, since because of the very homogeneous surface structure, the soiling layer is more visible than on the samples with inorganic coatings. Measured spectral reflectance of all the samples in each step are reported in Table 3 for inorganic coatings and in Table 4 for the inorganic ones.
Analyzing inorganic coatings, the lighter colored samples such as vanilla and apricot present higher loss after soiling, moreover the differences between Arizona natural and artificial ageing range from 0.05 to 0.11 except for tobacco samples which present a difference of 0.017 between natural and artificial soiling. Analyzing the cleaning steps the higher gain both in Wiping and Rinsing is reached by apricot sample which in Artificial Arizona soiling recovered 0.007 and in Natural Arizona soiling recovered 0.012 in solar reflectance. In order to better analyze the reflectance gain through the different cleaning steps, in Tab. 5 the ratios between the unsoiled solar reflectance and the different reflectance values measured according to ASTM E903 (ASTM, 96) are reported.

Table 3: Reflectance of samples with inorganic coating

Sample	Status	ASTM C1549	Δ	ASTM E903	Δ
Tobacco	Unweathered	0.361	0.002	0.345	0.001
	After weatherometer	0.346	0.004	0.339	0.003
	Soiled Arizona	0.349	0.002	0.341	0.001
	Wiped Arizona	0.351	0.002	0.341	0.001
	Rinsed Arizona	0.352	0.003	0.340	0.002
	Soiled Natural	0.338	0.003	0.322	0.003
	Wiped Natural	0.337	0.003	0.317	0.003
	Rinsed Natural	0.338	0.003	0.317	0.002
	Soiled Average	0.318	0.001	0.307	0.001
	Wiped Average	0.319	0.001	0.307	0.001
	Rinsed Average	0.319	0.002	0.308	0.001
Vanilla	Unweathered	0.525	0.005	0.537	0.002
	After weatherometer	0.511	0.004	0.521	0.003
	Soiled Arizona	0.522	0.002	0.507	0.003
	Wiped Arizona	0.522	0.002	0.508	0.001
	Rinsed Arizona	0.523	0.002	0.508	0.001
	Soiled Natural	0.528	0.003	0.515	0.002
	Wiped Natural	0.527	0.004	0.514	0.007
	Rinsed Natural	0.526	0.005	0.518	0.002
	Soiled Average	0.478	0.003	0.466	0.002
	Wiped Average	0.479	0.003	0.465	0.005
	Rinsed Average	0.479	0.004	0.465	0.005
Apricot	Unweathered	0.406	0.003	0.413	0.001
	After weatherometer	0.391	0.006	0.374	0.001
	Soiled Arizona	0.395	0.001	0.381	0.002
	Wiped Arizona	0.396	0.002	0.381	0.003
	Rinsed Arizona	0.396	0.002	0.382	0.001
	Soiled Natural	0.401	0.004	0.385	0.007
	Wiped Natural	0.403	0.003	0.388	0.003
	Rinsed Natural	0.402	0.004	0.397	0.010
	Soiled Average	0.372	0.003	0.367	0.003
	Wiped Average	0.372	0.004	0.365	0.005
	Rinsed Average	0.372	0.004	0.362	0.002
Red	Unweathered	0.376	0.001	0.381	0.001
	After weatherometer	0.377	0.003	0.365	0.002
	Soiled Arizona	0.368	0.001	0.352	0.006
	Wiped Arizona	0.369	0.001	0.352	0.005
	Rinsed Arizona	0.370	0.001	0.351	0.004
	Soiled Natural	0.377	0.003	0.361	0.004
	Wiped Natural	0.372	0.002	0.359	0.004
	Rinsed Natural	0.372	0.002	0.377	0.003
	Soiled Average	0.353	0.001	0.340	0.004
	Wiped Average	0.355	0.001	0.341	0.003
	Rinsed Average	0.355	0.002	0.338	0.002

Concerning the samples coated with organic layers, the beige samples present a higher loss in solar reflectance when treated with Arizona mixture, while the brown sample presents the lower one. The brown sample presents also the lower loss in solar reflectance considering the surfaces treated with average mixture, while the white one presents the higher loss. Considering the cleaning steps, the higher gain is reached by the white samples rinsed after average soiling mixture exposure, but the gain is as small as 0.001.

Table 4: Reflectance of samples with organic coating

Sample	Status	ASTM C1549	Δ	ASTM E903	Δ
Beige	Unweathered	0.646	0.001	0.659	0.002
	After weatherometer	0.645	0.003	0.659	0.002
	Soiled Arizona	0.636	0.003	0.650	0.000
	Wiped Arizona	0.635	0.006	0.651	0.000
	Rinsed Arizona	0.633	0.004	0.648	0.002
	Soiled Average	0.543	0.004	0.555	0.002
	Wiped Average	0.543	0.001	0.541	0.002
	Rinsed Average	0.543	0.005	0.558	0.006
Brown	Unweathered	0.379	0.001	0.382	0.000
	After weatherometer	0.380	0.001	0.384	0.000
	Soiled Arizona	0.378	0.002	0.382	0.000
	Wiped Arizona	0.379	0.001	0.382	0.000
	Rinsed Arizona	0.378	0.001	0.382	0.000
	Soiled Average	0.332	0.004	0.337	0.000
	Wiped Average	0.330	0.011	0.326	0.002
	Rinsed Average	0.335	0.003	0.340	0.000
Green	Unweathered	0.302	0.001	0.311	0.000
	After weatherometer	0.300	0.001	0.311	0.000
	Soiled Arizona	0.298	0.002	0.309	0.002
	Wiped Arizona	0.298	0.002	0.309	0.002
	Rinsed Arizona	0.297	0.002	0.309	0.000
	Soiled Average	0.260	0.004	0.270	0.002
	Wiped Average	0.260	0.001	0.262	0.002
	Rinsed Average	0.261	0.004	0.271	0.000
White	Unweathered	0.842	0.001	0.867	0.004
	After weatherometer	0.847	0.001	0.871	0.002
	Soiled Arizona	0.838	0.003	0.864	0.002
	Wiped Arizona	0.840	0.002	0.865	0.000
	Rinsed Arizona	0.837	0.002	0.863	0.002
	Soiled Average	0.673	0.005	0.689	0.002
	Wiped Average	0.672	0.007	0.665	0.002
	Rinsed Average	0.672	0.006	0.698	0.020

Table 5:– Solar reflectance R_0 and solar reflectance ratio R_n/R_0 of all the samples in each experimental step (all solar reflectance values in this table were measured via ASTM E903)

	Solar reflectance R_0	Solar reflectance ratio R_n/R_0									
	Unsoiled	After weatherometer	Soiled Arizona	Wiped Arizona	Rinsed Arizona	Soiled Natural	Wiped Natural	Rinsed Natural	Soiled Average	Wiped Average	Rinsed Average
Tobacco	0.345	0.983	0.983	0.989	0.986	0.934	0.921	0.921	0.891	0.892	0.893
Vanilla	0.537	0.969	0.969	0.945	0.945	0.958	0.956	0.964	0.868	0.865	0.865
Apricot	0.413	0.904	0.904	0.921	0.925	0.932	0.939	0.959	0.887	0.882	0.875
Red	0.381	0.960	0.960	0.924	0.922	0.947	0.944	0.991	0.894	0.897	0.889
Beige	0.659	1.000	0.986	0.988	0.983	N/A	N/A	N/A	0.842	0.821	0.847
Brown	0.382	1.004	1.000	1.000	1.000	N/A	N/A	N/A	0.882	0.853	0.890
Green	0.311	1.000	0.994	0.994	0.994	N/A	N/A	N/A	0.868	0.842	0.871
White	0.867	1.005	0.997	0.998	0.995	N/A	N/A	N/A	0.795	0.767	0.805

Only organic coatings pictures are shown in Figs. 2-4 because, for samples with inorganic coatings, due to the higher roughness of the surface, the soiling mixture deposition did not affect visibly the surface of the coupons. The two soiling mixtures were applied using the same setup and the same protocol, however it is interesting to notice how they create two completely different patterns on the two surfaces. This can be due to the different chemical composition of the mixtures. The peculiar surface morphology of the two coupons, in addition, affected the distribution of the soiling droplets on the surfaces, according to what is evident in Fig. 4.

Considering samples with inorganic coating, the difference between natural and artificial Arizona soiling is up to 0.01 for data measured with ASTM C1549 (ASTM, 2002) and up to 0.02 for data measured with ASTM E903 (ASTM, 96). Moreover, the ratio between the reflectance values measured for unweathered and soiled samples after the various cleaning processes, applied both on natural and accelerated aged samples, remains almost constant.

Looking at the different cleaning process, there is not a big recovery of solar reflectance neither after wiping nor after rinsing. On light color samples (vanilla, apricot, beige, and white) observations can be made easier if compared with other coupons and, analyzing the ratio of solar reflectance values measured on unsoiled and soiled samples, for each group of samples (organic and inorganic), the lighter samples are more influenced by the different soiling treatments.
Finally, inorganic coated samples are characterized by higher heterogeneity if compared with organic coated ones. However, this feature does not affect the feasibility of the study.

5 CONCLUSIONS

The aim of this study was to investigate how accelerated ageing can affect solar reflectance of samples, characterized with both inorganic (4 coupons) and organic (4 coupons) and how natural weathering agents such as rain and wind, simulated in laboratory through wiping and rinsing processes, can eventually restore the solar reflectance.
The different soiling and cleaning processes show a good reproducibility of the process but also that the soiling mixture adheres to the fresh substrate in a way that excellently simulates the real soiling conditions of the naturally aged samples.
Contrary to what is shown in Levinson et al (2005) concerning single ply membrane, cleaning processes do not seem to restore the solar reflectance of the samples, however washing and bleaching processes were not suitable for these samples since they cannot be applied to roofs covered with clay based tiles. A suitable reason of this lack in recovery of solar reflectance can be attributed to the morphology of the samples. For this reason microstructural, mineralogical and chemical analyses will be carried out on all the samples, both unsoiled and soiled, in order to better understand this particular behavior.

6 ACKNOWLEDGEMENTS

This work was in-part funded by the National Science and Engineering Research Council of Canada under discovery program. Dr. Afroditi Synnefa, Mr. Yoshi Suzuki, and MCA tiles, Mr. Prokopis Perdikin, and Abolin Polymer are gratefully acknowledged for their support.

7 REFERENCES

- Akbari,H. (2005). Energy Saving Potentials and Air Quality Benefits of Urban Heat IslandMitigation. *Lawrence Berkeley National Laboratory Report LBNL,* Berkeley, CA.
- Akbari, H., Berhe, A., Levinson, R., Graveline, S., Foley, K., Delgado, A.H., and Paroli, R.M. (2005). Aging and weathering of cool roofing membranes. *Proceedings of the First International Conference on Passive and Low Energy Cooling for the Built Environment*, May 17, 2005, Athens, Greece, Also published as *Lawrence Berkeley National Laboratory Report LBNL-58055*, Berkeley, CA.
- Akbari, H., and Matthews, H.D. (2012). Global cooling updates: Reflective roofs and pavements, *Energy & Buildings*, 55, 2-6.
- ASTM (1996). ASTM E 903-96 – Standard test method for solar absorptance, reflectance, and transmittance of materials using integrating spheres. *Standard of the American Society for Testing and Materials.*
- ASTM (2002). ASTM C 1549-02 – Standard test method for determination of solar reflectance near ambient temperature using a portable solar reflectometer. *Standard of the American Society for Testing and Materials.*
- ASTM (2003). ASTM G 173-03 – Standard tables for reference solar spectral irradiance at air mass 1.5: direct normal and hemispherical on 37° tilted surface. *Standard of the American Society for Testing and Materials.*
- ASTM(2012). ASTM G154-12a – Standard Practice for Operating Fluorescent Ultraviolet (UV) Lamp Apparatus for Exposure of Nonmetallic Materials. *Standard of the American Society for Testing and Materials.*
- Berdahl, P., Akbari, H., Levinson, R., Jacobs, J., Klink, F., and Everman, R. (2012). Three-year weathering tests on asphalt shingles: Solar reflectance. *Solar Energy Materials and Solar Cells*, 99, 277-281.
- Bretz, S., and Akbari, H. (1997). Long-term performance of high-albedo roof coatings. *Energy & Buildings*, 25, 159-167.
- Cheng, M.D., Miller, W., New, J., and Berdahl, P. (2012). Understanding the long-term effects of environmental exposure on roof reflectance in California. *Construction and Building Materials* 26, 516–526 (2012)

- Kolopacki, S.J., Akbari H., Pomerantz M., Gabersek, S., and Gartland, L.M. (1997). Cooling Energy Savings Potential of Light-Colored Roofs for Residential and Commercial Buildings in 11 US Metropolitan Areas. *Lawrence Berkeley National Laboratory Report LBNL-39433,* Berkeley, CA.
- Levinson, R., and Akbari, H. (2010). Potential benefits of cool roofs on commercial buildings: conserving energy, saving money, and reducing emission of greenhouse gases and air pollutants. *Energy Efficiency*, 3(1), 53-109.
- Levinson, R., Akbari, H., and Berdahl, P. (2010a). Measuring solar reflectance – Part I: defining a metric that accurately predicts solar heat gain. *Solar Energy*, 84, 1717-1744.
- Levinson, R., Berdahl, P., Berhe, A., and Akbari, H. (2005). Effects of soiling and cleaning on the reflectance and solar heat gain of a light-colored roofing membrane. *Atmospheric Environment*, 39, 7807-7824. Also published as *Lawrence Berkeley National Laboratory Report LBNL-57555*, Berkeley, CA.
- Levinson, R., Berdahl, P., Akbari, H., Miller, W., Joedicke, I., Reilly, J., Suzuki, Y., and Vondran, M. (2007). Methods of creating solar-reflective nonwhite surfaces and their application to residential roofing materials. *Solar Energy Materials and Solar Cells*, 91, 304–314.
- Levinson, R., Akbari, H., Berdahl, P., Wood, K., Skilton, W., and J. Petersheim, J. (2010). A novel technique for the production of cool colored concrete tile and asphalt shingle roofing products. *Solar Energy Materials & Solar Cells*, 94, 946-954.
- Libbra, A., Tarozzi, L., Muscio, A., and Corticelli, M.A. (2011). Spectral Response Data for Development of Cool Coloured Tile Coverings. *Optics and Laser Technology*, 43(2), 394-400.
- Libbra, A., Muscio, A., Siligardi, C., and Tartarini, P. (2011). Assessment and improvement of the performance of antisolar surfaces and coatings. *Progress in Organic Coatings*, 72, 73-80.
- Q-Lab (2013). QUV ACCELERATED WEATHERING TESTER. Retrievable in 2013 at the web address: http://www.q-lab.com/products/quv-weathering-tester/quv
- Santamouris, M. (2012). Cooling the cities – A review of reflective and green roof mitigation technologies to fight heat island and improve comfort in urban environments. *Solar Energy*, In press (2012).doi:10.1016/j.solener.2012.07.003.
- Sleiman, M., Kirchstetter, T., Berdahl, P., Gilbert, H., Francois, D., Spears, M., Levinson, R., Destaillats, H., and Akbari, H.(2010).Development of an accelerated soiling method that mimics natural exposure of roofing materials.*Proceedings of the 3rd International Passive and Low Energy Cooling for the Built Environment (Palenc 2010),* September 29 to October 1, 2010, Rhodes, Greece, pp. 19-21.

FIELD OBSERVAION OF COOLING ENERGY SAVING BY THE HIGH REFLECTANCE PAINT

Chihiro YAMADA[1], Hideki TAKEBAYASHI[1], Etsuko ISHII[1], and Katsuo MIKI[2]

1 Gradeuate School of Engineering, Kobe University
1-1,Rokkodai-cyo,Nada-ku, Kobe,
657-8501 Japan

2 Miki Coating Design Office
1-64-1-1810,Kishiki-cyo,Omiya-ku, Saitama,
330-0843 Japan
**Corresponding author: wa43827@db4.so-net.ne.jp*

Note: the contact addresses may be re-arranged

ABSTRACT

Cooling energy savings in a building with the roof coated by high reflectance paint are examined. It is difficult to recognize the cooling energy savings by using the data observed every hour. It is assumed that factors affecting to cooling energy load are the internal heat generation, the set temperature, weather conditions, etc. From the analysis on the relationship between in-outdoor air temperature difference and electric power consumption for air conditioner, which are averaged and integrated into every day, the reduction of electric power consumption by high reflectance paint coating is estimated about 72Wh/m^2/day.

KEYWORDS

High reflectance paint, Cooling energy savings, Field observation

1 INTRODUCTION

Nowadays, high reflectance paint is becoming famous in Japan for the mitigation of heat island phenomenon. The evaluation method of high reflectance paint is established in the JIS (Japanese Industrial Standards) [(1)(2)]. Although the mitigation effect for heat island phenomenon by high reflectance paint has been evaluated in many studies[(3)], the cooling energy saving in the building actually used by high reflectance paint is evaluated in few studies, because the cooling energy saving in the typical office or residential building with high thermal insulation performance is generally recognized small[(4)]. However, it cannot be ignored in the building with low thermal insulation performance, such as factory, warehouse and gymnasium. In this study, we analysed the cooling energy saving by high reflectance paint in a building actually used.

The cooling energy saving in the building by heat island mitigation technologies, such as green wall, green roof, high reflectance paint has been studied by several researchers(5)(6). In those studies, they conducted controlled experiments using same two prefabricated houses without internal heat generation, in order to compare the difference of energy consumption with or without the heat island mitigation technologies in same weather condition. However, it is required by building owner or manager that the cooling energy saving by high reflectance paint in the building actually used on site.

Akbari et al analyzed the cooling energy saving in buildings actually used in California such as shop, school and refrigerated warehouse. They concluded that the savings are

70Wh/m^2/day, 42-48Wh/m^2/day, 57-81Wh/m^2/day, respectively, from measurement results in summer[7]. We have carried out similar experiments in Japan.

It is recognized that introduction of high reflectance paint to buildings without high thermal insulation performance such as factory, warehouse, gymnasium is one of the energy saving measures. At that time, it is necessary to analyze the introduction effect for high reflectance paint. In this study, we analyzed the cooling energy saving in a building actually used based on measured results.

2 OUTLINE OF CASE STUDY BUILDING AND MEASUREMENT

General office buildings have relatively large window area ratio and small roof area ratio to the total envelope surface area. And, they have much internal heat generation from their apparatus and so on. So, the ratio of cooling load by heat conduction from roof is small in the total cooling load. In this study, the objective building is a small (floor area is 60m^2) two story research building (1st floor is piloti) in Kobe University (see Figure 1 and Table 1). It is expected that the objective building have large possibility to achieve cooling energy saving by high reflectance paint due to small window area ratio (15%) and large roof area ratio (25-30%) to total envelope surface area.

The experiment was carried out in rooms 1 and 2. The air conditioners in both rooms were continuously running for 24 hours. The roof consists of concrete slab (thickness is 100mm), above the ceiling (depth is 575mm) and ceiling (height from the floor is 2730mm) and it has no heat insulating material. We measured surface temperature of under and upper the slab and ceiling, room temperature (at 1200mm height), and power consumption of the air conditioner. Cross section of measurement point of temperature is shown in Figure 2. In order to avoid the influence of insolation, roof surface temperature was measured by infrared thermometer, and other measurement elements were measured by thermistor thermometer. The certificate cooling capacities of air conditioners in rooms 1 and 2 are 7.1 kW and 14.5 kW. Power consumption was measured by clamp type power meter (HIOKI3168-98) at the power distribution panel. We measured temperature and power data at one minute interval and averaged for temperature and integrated for power consumption over ten minutes.

We conducted measurement from July 12 to September 26, 2011 and from July 12 to September 26, 2012. High reflectance paint was painted on August 2, 2011. Cooling energy saving is evaluated by the comparison of the measurement results of before and after painting. The albedo of objective paint is 86.9% (300 – 2500 nm wavelength, by JISK5602). The albedo measured by the pyranometer with white and black board which solar radiation is known was 16.9% before painting, 86.9% immediately after painting and 76.1% one year after painting[8]. These are averaged value of measurement results at three points on the roof surface (east, middle and west point).

Measurement results of the temperature under the slab, upper and under the ceiling, in the room of room 1, outdoor air temperature and solar radiation are shown in figure 3. The temperature under the slab is from 40 to 27 deg. C and the maximum temperature is occurred around 18:00 due to the thermal storage of the slab. The temperature reduction on the roof surface is around 30 K at maximum after painting. Measurement results of the cooling energy consumption and solar radiation are shown in figure 4. It is difficult to recognize the cooling energy saving, based on the comparison in typical day even if solar radiation is similar to each other.

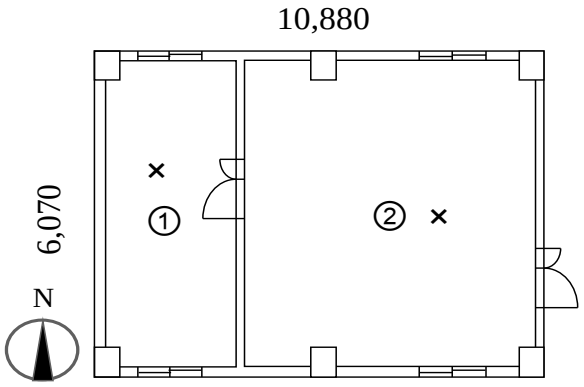

Table 1: Thermal load characteristics of objective rooms

	Roof ratio	Wall ratio	Window ratio	Heat generation	Set temperature
Room 1	25.3%	27.7%	6.4%	W/m^2	26 deg. C before 15:00, Aug. 8, 2011 25 deg. C after 15:00, Aug. 8, 2011 25deg. C through 2012
Room 2	29.7%	27.4%	3.9%	W/m^2	

Figure 1: Facade and plan (2nd floor) of objective building (x: measurement point in Figure 2)

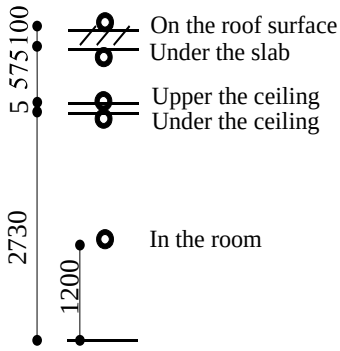

Figure 2: Cross section of measurement point of temperature

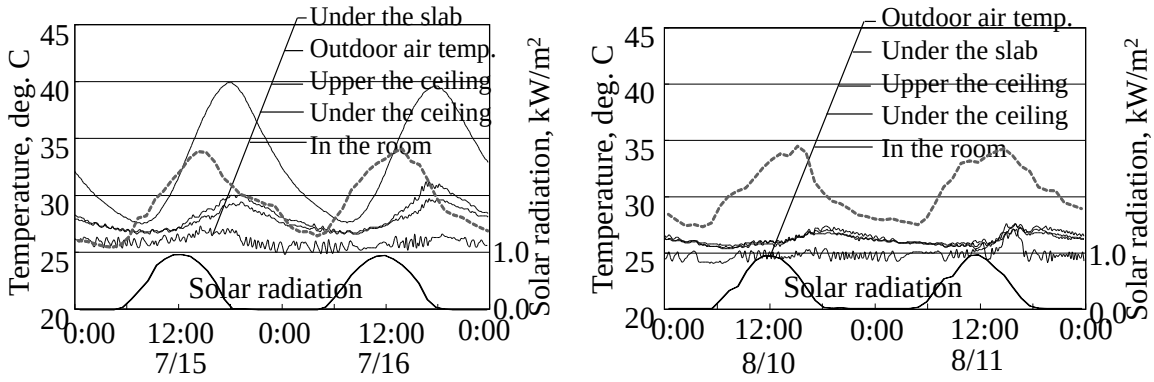

Figure 3: Measurement results of the temperature under the slab, upper and under the ceiling, in the room of room 1, outdoor air temperature and solar radiation (left: before painting, right: after painting)

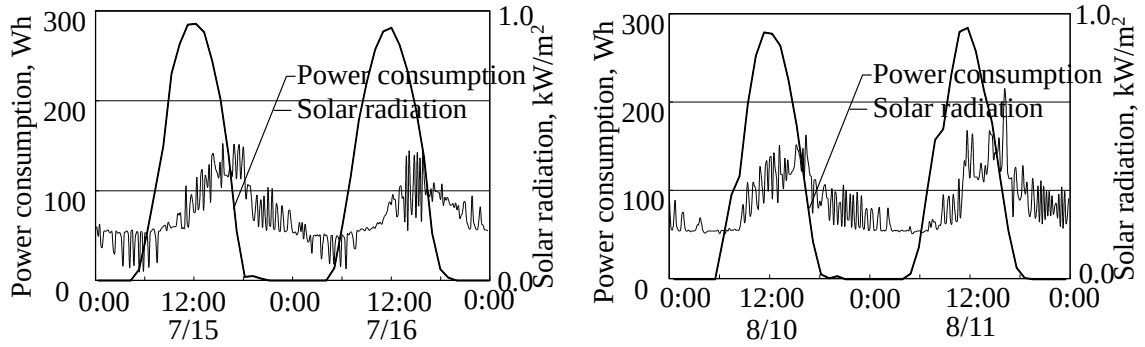

Figure 4: Measurement results of the cooling energy consumption and solar radiation (left: before painting, right: after painting)

3 EVALUATION METHOD OF COOLING ENERGY SAVING BY HIGH REFLECTANCE PAINT

We analyse the cooling energy saving with difference of cooling power consumption between before and after painting. Every hour relationships between outdoor to room air temperature difference and cooling power consumption are shown in figure 5. The data of before painting is black point, and that of after painting is white point. The sol–air temperature changes larger after painting influenced by solar radiation, but power consumption doesn't change so much after painting. Air temperature difference is averaged in one hour and power consumption is integrated in one hour. Since the temperature under the slab reaches maximum around evening, it is difficult to recognize the relationship between temperature difference and power consumption by every hour data.

We analyse the relationship between daily averaged outdoor to room air temperature difference and daily integrated cooling power consumption, by referring to the method of Akbari et al. The evaluation of cooling energy saving by high reflectance paint is mainly influenced by following factors.

- internal heat generation
- set temperature of air conditioner
- weather condition (air temperature, solar radiation)

Because the object of this study is the evaluation of cooling energy saving in the building actually used, we didn't instruct the users how to use the room. Accordingly, the measurement results are affected by above three factors. However, the differences of internal heat generation and set temperature of air conditioner are not so large.

Cooling power consumption influenced by internal heat generation, set temperature of air conditioner and weather condition is shown as follows.

$$E=A\times I+ B\times \Delta T + C \quad (1)$$

where E is the daily integrated cooling power consumption (Wh/day), I is the daily integrated solar radiation (Wh/day), ΔT is the daily averaged temperature difference between outdoor and room (K), A is the coefficient related to absorptivity, B is the coefficient related to thermal condauctiance, and C is the internal heat generation. In the case that these coefficients are large, cooling power consumption becomes large. Strictly speaking, we should use the difference of enthalpy instead of ΔT and consider the coefficient of performance of air conditioner. In this study, we measured E, I, ΔT. It is assumed that B and

C don't change by painting. The influence by set temperature of air conditioner is reflected in ΔT and the influence by weather condition is reflected in ΔT and *I*. In following chapter, we will analyze measurement results using equation (1).

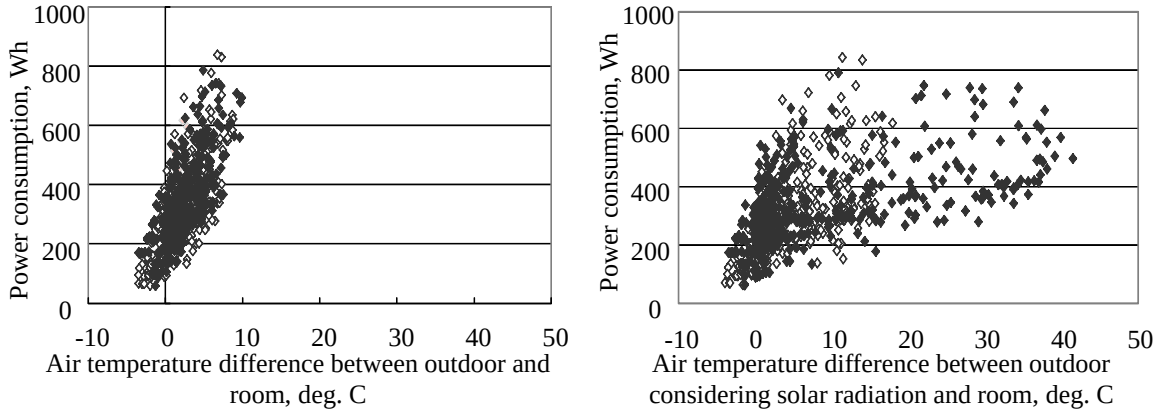

Figure 5: Every hour relationship between outdoor to room air temperature difference and cooling power consumption (black: before painting, white: after painting) (left: air temperature difference without considering solar radiation effect, right: air temperature difference with considering solar radiation effect)

4 EXAMINATION OF COOLING ENERGY SAVING BY HIGH REFLECTANCE PAINT

Every day relationship between outdoor to room air temperature difference and cooling power consumption is shown in left of figure 6. Since both slopes of regression equations of before and after painting are similar, cooling power consumption is influenced by outdoor air temperature. And, it is also influenced by set temperature of air conditioner, which was changed during measurement period. Every day relationship between solar radiation and the intercept of regression equation in left of figure 6 is shown in right of figure 6. Cooling power consumption doesn't change after painting even if the daily integrated solar radiation is large. When the daily integrated solar radiation is relatively large, the cooling energy saving is about 1.6kWh/day (72Wh/m^2/day).

The coefficient *B* before painting is as mostly same as that after painting in left of figure 6, so it is assumed that the influences by ΔT to power consumption are similar before and after painting. The coefficient *A* after painting is nearly 0 in right of figure 6, so it is assumed that the influence by solar radiation to cooling power consumption may be neglected after painting. Since the internal heat generation was not controlled during measurement, the coefficient *C* is not similar before and after painting in right of figure 6. We only have information on the use of the rooms shown in Table 1. Even if using the data measured in the building actually used, the analysis results have captured the approximate characteristics of cooling energy consumption.

Regression equations of cooling power consumption by air temperature difference between outdoor and room before, after and one year after painting in rooms 1 and 2 are shown in Table 2. Cooling power consumption and its saving in table 2 are divided by floor area (room 1 is 22.5m^2, room 2 is 43.5m^2). Because slopes of regression equation (coefficient *B*) of before, after and one year after painting are relatively similar in each room, the influences by ΔT to cooling power consumption are similar in each room. In room 1, coefficients *B* are almost similar both after and one year after painting. Cooling energy saving in room 2 is smaller than that in room 1. The internal heat generation ratio to the total cooling load in room 2 is larger than that in room 1, because floor area in room 2 is approximately twice as large as room 1. Since slopes of regression equation (coefficient *B*) in room 2 are smaller than room 1, it is not so much influenced by external weather condition in room 2.

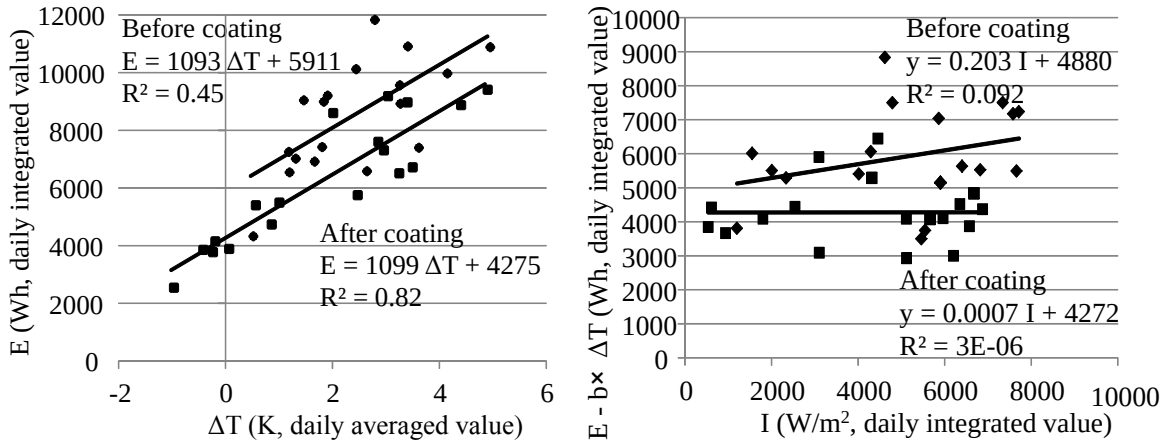

Figure 6: Relation per day between air temperature difference between outdoor and room and cooling power consumption(left), Relation per day between the integrated of the day solar radiation and cooling consumption(right)

Table 2: Regression equations of cooling power consumption by air temperature difference between outdoor and room before, after and one year after painting in rooms 1 and 2

		Regression equation	Energy saving
Room 1	Before painting*	*E=48.6ΔT+262.7* *(R^2=0.45)*	-
	After painting**	*E=50.3ΔT+190.8* *(R^2=0.82)*	72Wh/m^2/day
	One year after painting***	*E=48.0ΔT+171.6* *(R^2=0.82)*	91Wh/m^2/day
Room 2	Before painting*	*E=26.7ΔT+151.3* *(R^2=0.54)*	-
	After painting**	*E=27.6ΔT+116.6* *(R^2=0.60)*	35Wh/m^2/day
	One year after painting***	*E=26.9ΔT+142.8* *(R^2=0.77)*	9Wh/m^2/day

*before painting: from July12 to July 31, 2011
**after painting: from August 3 to September 26, 2011
***one year after painting: from July 12 to September 26, 2012

5 CONCLUSION

In this study, we analyzed the cooling energy saving by high reflectance paint in a building actually used based on measured results. It is assumed that factors influencing on cooling energy are the internal heat generation, set temperature of air conditioner, and weather condition. Considering these factors, we analyzed the relationship between daily integrated solar radiation and cooling power consumption, and the relationship between outdoor to room daily averaged temperature difference and cooling power consumption.

By analysis of the relationship between outdoor to room daily averaged temperature difference and cooling power consumption, cooling power consumption saving by high reflectance paint is estimated around 1.6kWh/day (72Wh/m^2/day). Similar result is confirmed one year after painting. Even if we use results measured in a building actually used, we could evaluate approximate energy savings. However, under the condition in that ΔT is relatively

large, cooling power consumption tends to be more larger. Therefore, we may have to consider change of the coefficient of performance of the air conditioner.

6 ACKNOWLEDGEMENTS

This measurement was supported by Center for Environmental Management in Kobe University.

7 REFERENCES

(1) Japanese Industrial Standards, JIS K 5602, Way to measure of albedo of paint (2008)

(2) Japanese Industrial Standards, JIS K 5675, High reflectanace paint for roof (2011)

(3) Hideki Takebayashi, Yasushi Kondo, Development of evaluation tool for public benefit－Simple evaluation system of cool roof for proper promotion (Part 2)－, AIJ Journal of Technology and Design, 33(2010), pp.589-594.

(4) Yasushi Kondo, Yasuhiro Nagasawa, Maiko Irimajiri, Reduction of solar heat gain of building, urban area and vending machines by high reflective paint, The Society of Heating, Air-Conditioner Sanitary Engineers of Japan, No.78(2000), pp15-24.

(5) Hisanobu Kawashima, Chihiro Kato, Yoshihiro Yarita, Hidetsugu Kurooka, Tsuneaki Ishima, Field experimental results on the rooftop green with the textile mats- The power saving effect of air-conditioner in summer - Journal of Heat Island Institute International Vol.6 (2011), pp.1-7.

(6) Mariko Yamasaki, Akio Mizutani, Tetsuo Ohsawa, Cooling load reduction effect of green roof and green wall in the case of building with thermal thin wall, AIJ Journal of Technology and Design, 29(2009), pp.155-158.

(7) Hashem Akbari, Ronnen Levinson, Leo Rainer, Monitoring the energy-use effects of cool roofs on California commercial buildings, Energy and Buildings, 37(2005), pp.1007-1016.

(8) Yasutaka Murata, Koji Sakai, Hiroshi Kanamori, Hideki Takebayashi, Yoh Matsuo, Masakazu Moriyama, Atsumasa Yoshida, Masatoshi Nishioka, Naomichi Yano, Ryosaku Shimizu, Katsuo Miki, Toshikazu Murase, Hashem Akbari, A study on insolation reflectivity measurement of the cool painting surface : A proposal of measuring method by the 2 point correction and accuracy testing on the horizontal surface, Journal of Environmental Engineering (Transaction of AIJ), (2008), pp1209-1215.

COMPOSITE MATERIALS FOR RENOVATION OF ROOFS IN EXISTING BUILDINGS

Stella Chadiarakou[1*], Agis Papadopoulos[2], Mattheos Santamouris[3]

1 *Dr. Mechanical Engineer, FIBRAN S.A. P.O.Box 40306, GR-56010, Thessaloniki, Greece, stellah@fibran.gr*

2 *Process Equipment Design Laboratory, Department of Mechanical Engineering Aristotle University Thessaloniki, GR- 54124 Thessaloniki, Greece, e-mail: agis@eng.auth.gr*

3 *University of Athens Physics Department – Section of Applied Physics Building Physics 5, University Campus, GR-15784 Athens, Greece, e-mail: msantam@phys.uoa.gr*

**Corresponding author: stellah@fibran.gr*

ABSTRACT

The EPBD directive (91/2002/EU) paved the way for the European Union member states to develop and apply a holistic approach on the building's energy performance. It is documented that buildings' energy consumption represents 40% of the total energy consumption in Europe, a significant figure when compared to the industry and transportation sector. Respectively the CO2 emissions are calculated to be around 30%. A series of published data indicates that the uninsulated or poorly insulated roofs account for up to 25% of energy losses. Taking into consideration the significant downturn of new constructions monitored all over Europe after 2008, energy refurbishment of the existing building stock appears as a nodal point towards the mitigation of the energy consumption.

In particular for retrofitting insulation solutions for the roof we need to apply insulation with regard of the technical parameters of the roof. Thus, a combination of a board of extruded polystyrene with a ceramic tile would provide effective thermal protection. Moreover, a material like this can be characterized as cool material because of its light colour and the high reflectance. Application of this kind of material in existing roofs in Greek buildings indicated a reduction on the energy consumption and an amelioration of the temperature of the apartment below the roof.

In this paper, the results of the application of the composite material are presented along with its technical characteristics.

KEYWORDS

Energy performance, Roof insulation, Composite insulation materials

1. INTRODUCTION

EPBD directive defined the way to reduce energy consumption by improving the buildings envelope. Though it captures only 10% of the potential from buildings, a fully extended EPBD could reduce total emissions from buildings by 460 million tons a year, more than the EU commitment under the Kyoto Protocol [Ecofys II - 2004 and V - 2005]. With new buildings only representing 1% of the building stock and with the normal renovation cycle for buildings being 30 years, there is no time to lose in terms of bringing both new built and renovation standards up to speed.

The building sector is, together with transportation, the major energy consumer. In the OECD countries this consumption was in 2004 close to 28 trillion of Btu's and accounted

nearly the 20% of the total energy consumption (IEA, 2007). In particular, the Greek building stock consists of 4.3 million dwellings (Theodoridiou et al, 2012 a), whereby only 26% were constructed after the implementation of the first Greek Insulation Law (TIR, 1979). Thus, approximately 3 million dwellings are lacking insulation in the building's envelope. Data indicates that uninsulated or poorly insulated roofs account for approximately 25% of conductivity energy losses from the envelope as such (figure1).

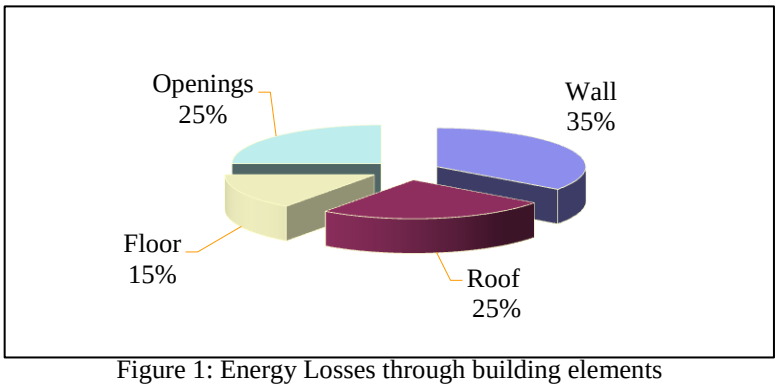

Figure 1: Energy Losses through building elements

In this direction, Greece has put in 2008 into force thelaw on energy performance of buildings, Law 3661/2008 which harmonized the European Directive on Energy Performance of Buildings (EPBD) 91/2002/EC. The Energy Regulation deriving from this legislation, foresees, adequate thermal protection of the building's envelopel, to be achieved mainly with the implementation of the increased thickness of thermal insulation, as well as the use of state of the art materials and construction solutions, as those are are the main tool towards the mitigation of the energy consumption in buildings and the reduction of environmental impacts. In early 2013 the EPBD recast (21/2010/EU) was harmonized by means of Law 4122/2013; the revised Energy Regulation is expected to become valid by the end of 2013.

In the present paper, we are focusing on the retrofitting insulation of roof elements, mainly with the use of composite insulation materials. Based on the results of a research performed in 500 apartments, we have studied 6 simulation scenarios with thicknesses from 100-300mm of insulation material, extruded polystyrene.

2. GREEK RESIDENTIAL BUILDINGS

There are some 4.4 million dwellings in Greece; out of those more than 3.2 millions are in urban areas [Statistical Services, 2002]. The vast majority of urban residential buildings have the shape of multi-storey apartment buildings and was constructed since the 1970's. They feature three to five floors of residential uses, rarely reaching up to seven. On the ground floor lie the main entrance, the building's utilities and either an open sided parking area where the residents park their cars (pilotis) or shops if there is commercial activity in the area [Papamanolis, 2004].

According to the classification discussed by Theodoridou [Theodoridou et al, 2011 b] most Greek residential buildings constructed after 1946 in have balconies in the form of projected overhangs. They are met in several widths usually narrower in older buildings and wider in later constructions, sometimes up to 2.5 m. The Greek urban residential building stock can be classified in three categories regarding the thermal protection of the buildings' envelopes. The first category includes the buildings constructed before 1979, which are not thermally insulated at all since they were constructed before the implementation of the national Thermal Insulation Regulation. The second category includes the buildings constructed during the period 1980 – 1990, which are considered to be partially insulated. As

a rule they feature limited, if at all, insulation on the load bearing structure. Finally, the third category includes buildings constructed from 1991 until today and they can be considered to be, at least in most of the cases, fully insulated (Chadiarakou,2007).

Almost all apartment buildings have accessible flat roofs, used as terraces. They are constructed as conventional flat roofs or as upside-down ones (inverted). Until the early 1980s the conventional flat roof was the rule, as the roof was utilized for auxiliary uses making accessibility and mechanical strength properties a prerequisite. but Since then the inverted roof began to establish itself on the market, as flat roofs are rarely used for any purposes other than installing solar collectors and TV and satellite dishes. In the latter case the thermal insulation is placed above the dampness proofing and not below it. The final layer is usually gravel or pavement plates or even terrazzo. The inverted rood presents for the Greek climatic conditions a series of advantages, in terms of energy performance, water proofing performance, construction cost and maintainability. The results have been recognized early enough, but the traditional conservatism of the building sector combined with the aforementioned usage restriction of the 1960s' and 1970s' did not make the inverted roof popular until the early 2000s [Papadopoulos, 1998]. Not rarely, in colder regions in Northern Greece, apartment buildings may be found with tiled roofs resting on inclined concrete slabs. [Chadiarakou,2007]).

3. STATISTICAL DATA OF GREEK RESIDENTIAL BUILDINGS

The research started in 2005 and finished in 2007. The measurements took place in Thessaloniki, the second biggest city in Greece, situated in the North, with a Mediterranean climate. The city's climate has a heating demand of 2,184 degree days, αρε whilst the design maximum and minimum temperatures are 34,8°C and -4,2 °C respectively [Papakostas et al, 2004]. The research was carried out via a questionnaire, where the owners of the apartments provided information on its technical characteristics, the number of occupants and the energy bills for electrical and thermal consumption.

The analysis focused on the energy consumption of the constructions. The classes that was used was as described above. The annual electrical energy consumption per surface and person show stability through the three classes. Thus, the total energy (Figure 2) is present without any significant reduction and varies apporoximately around 100 kWh per surface and person through all the classes. (Chadiarakou, 2013). New thermal insulation law has applied new lower limits of thermal transmittance (table 1) which is leading to new higher thicknesses of insulation (table 2)

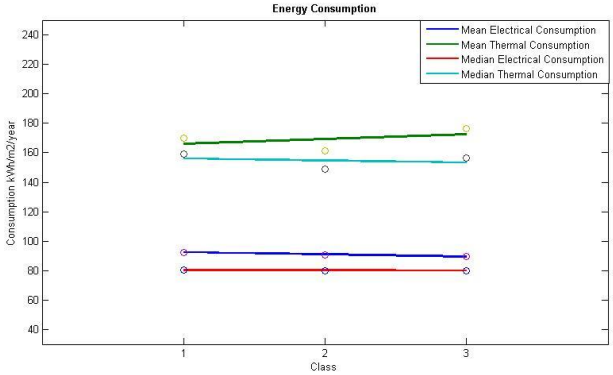

Figure 2: Total energy Consumption in Residences in Greece

Table 1: Comparison of U values in old and New Greek Regulation

Building Element\Climatic Zone	A		B		C		D
Regulation	Old	New	Old	New	Old	New	New
Vertical Element (Wall)	0,7	0,6	0,7	0,5	0,7	0,45	0,4
Horizontal Element (Roof)	0,5	0,5	0,5	0,45	0,5	0,40	0,35
Windows		3,2		3,0		2,8	2,6
Km	1,9		1,9		1,9		

Table 2: Comparison of U values in old and New Greek Regulation (old value with red color)

	A	B	C	D
Climatic Zone				
Minimum Thickness	cm	cm	cm	cm
Roof	6 /4	7 / 5	7 / 5	10 / 7
Wall	5 / 4	6 / 5	7 / 5	8 / 6
Concrete element	5 / 4	6 / 5	7 / 6	8/ 7

4. RETROFITTING INSULATION SOLUTIONS

Retrofitting insulation scenarios faced several difficulties concerning the type of the building, the adjacency with the neighboring buildings and its own architecture. Thus, even though walls seem to be the first choice for the retrofitting insulates solution; in reality it is not possible. Some of the reasons are very narrow balconies which do not allow external insulation with the adequate thickness, the distance with the neibhoring buildings which limits the possibility of external insulation. Therefore, the next best possible scenarios include the insulation of the roof. Flat roof are in most cases open unused spaces. A small percent might have the solar collectors on the roof. The retrofitting scenario that could be used is the one of inverted roof (figure 3). The majority of flat roofs acquire rather new water proofing, so the solution acquire only the insulation and the final layer.

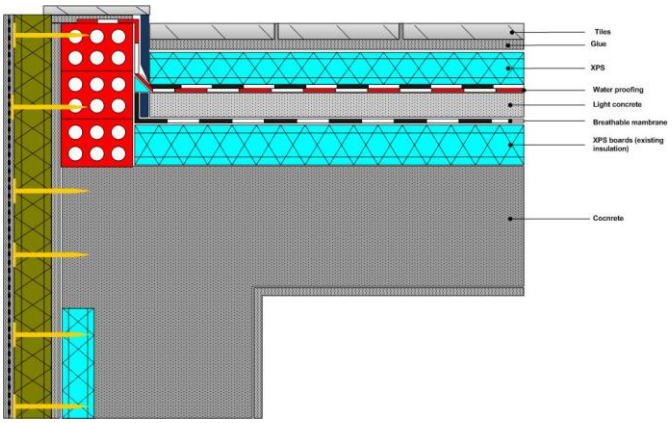

Figure 3: Retrofit insulation on Flat Roof

We need to take into consideration a few limitations for the roof thermal insulation. First of all is the weight of the total construction. The problem is focused on the fact that the majority of the buildings have been constructed before the year 2000, when the requirements according to the seismic control regulation was not as strict as they are today. Thus, the

insulation solution should comply to strict limitations with respect to itse weight. The best solution is in theory the use of a composite insulation material with ceramic tile which are light enough and has a layer of thermal insulation up to 100mm. Detailed photo of the material is shown in figure 4. The composite material includes a layer of extruded polystyrene with thermal conductivity of 0.033 W/mK (up to 60mm) and 0.034 W/mK (for thicknesses 60-100mm) and a ceramic tile usually in light white of ivory color. The white ceramic tile can be characterized as cool material.

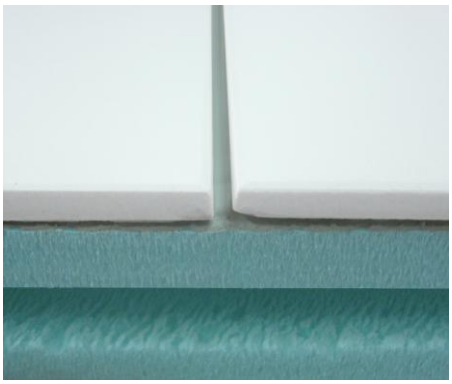

Figure 4: Detailed photo of composite material

Figure 5: Retrofit insulation on Flat Roof

5. SIMULATION SCENARIOS

The simulation scenarios were performed on a typical building for Greece. The simulation scenarios enclose insulation scenarios from 50-300mm thickness in all elements (table 3). The simulation program that we have used was Energy Plus version 3.1.0.027 through design program Design Builder. Energy Plus included a number of innovative simulation features such as variable time steps, user-configurable modular systems that were integrated with a heat and mass balance-based zone simulation and input and output data structures tailored to facilitate third party module and interface development.

Table 3: Insulation thickness of simulation scenarios

Scenarios	Thickness of Insulation			
	Wall	Concrete element	**Roof**	Floor
Basic	50mm	30mm	**60mm**	50mm
Scenario 1	60mm	60mm	**100mm**	50mm
Scenario 2	100mm	100mm	**100mm**	100mm
Scenario 3	150mm	150mm	**150mm**	150mm
Scenario 4	200mm	200mm	**200mm**	200mm
Scenario 5	250mm	250mm	**250mm**	250mm
Scenario 6	300mm	300mm	**300mm**	300mm

Other planned simulation capabilities are multy zone airflow, and electric power and solar thermal and photovoltaic simulation. Loads calculated (by a heat balance engine) at a user-specified time step (15-min) are passed to the building systems simulation module at the same time step. The building systems simulation module, with a variable time step (down to seconds), calculates heating and cooling system and plant and electrical system response (Drury B, 2001).

Integrated simulation also allows evaluating a number of processes:

- Realistic system controls
- Moisture adsorption and desorption in building elements
- Radiant heating and cooling systems
- inter zone air flow

In particular, we have explored through simulation the amelioration of the energy losses from building envelope. Furthermore, we have monitored the thermal comfort through

the different scenarios. It must be stressed that the simulation model is structured based on the new thermal insulation law (KENAK).

Moreover, we need to emphasize on the fact that we have applied scenarios only on different insulation levels, keeping heating and cooling system steady. In the same context, the glazing system remains steady on the basis that it fulfills the requirements of KENAK (U value of 2,8 W/m^{2}K). The typical building consists of 7 floors and 6 apartments. The building is free of all sides.

In order to start the simulation we need to define the parameters, therefore to create a schedule under the guidelines of KENAK. Moreover, schedules for occupancy profile, appliances, lighting and domestic hot water (DHW).

To be more specific, occupancy profile specifies that habitants are in the apartment from 00:00 until 9:00 and then from 14:00 until 24:00. Totally, 18 hours per day. It is important to note that the time period between 9:00 in the morning until 14:00 at noon is the typical one, when all the members of the family are either at school or at work. As for appliances profile, this is set from 18:00 to 21:00, a total time of 4 hours per day. Lighting profile is the same as the occupancy one and DHW is set for 2 hours per day.

As a result the U value (table 4) of the elements is mitigating to the limits of the nearly zero buildings requirements.

Table 4: U value for the simulation scenarios

U value	Basic	Scenario 1	Scenario 2	Scenario 3	Scenario 4	Scenario 5	Scenario 6
Walls Bricks	0,646	0,316	0,237	0,181	0,146	0,123	0,106
Walls Concrete	0,801	0,349	0,255	0,191	0,153	0,127	0,109
Walls Last Floor	0,569	0,297	0,226	0,174	0,142	0,119	0,103
Floors (ext)	0,546	0,307	0,222	0,172	0,14	0,118	0,102
Flat Roof	**0,336**	**0,237**	**0,237**	**0,181**	**0,122**	**0,105**	**0,093**

The maximum reduction of the thermal losses has been calculated to 72%. Especially, for scenario 3 the mitigation is 57%, while actual amount of the kWh saved from scenario 3 to scenario 6 is just 3 kWh/m2 (Figure 6)

Figure 7 presents the distribution of thermal losses for the flat roof is 14,18 kWh/m2. The fluctuation of values in scenario 1 and 2 is justified because we have used the same thickness of insulation. Generally, the reduction has a maximum value of 58%, while for scenario 3 are 28%.

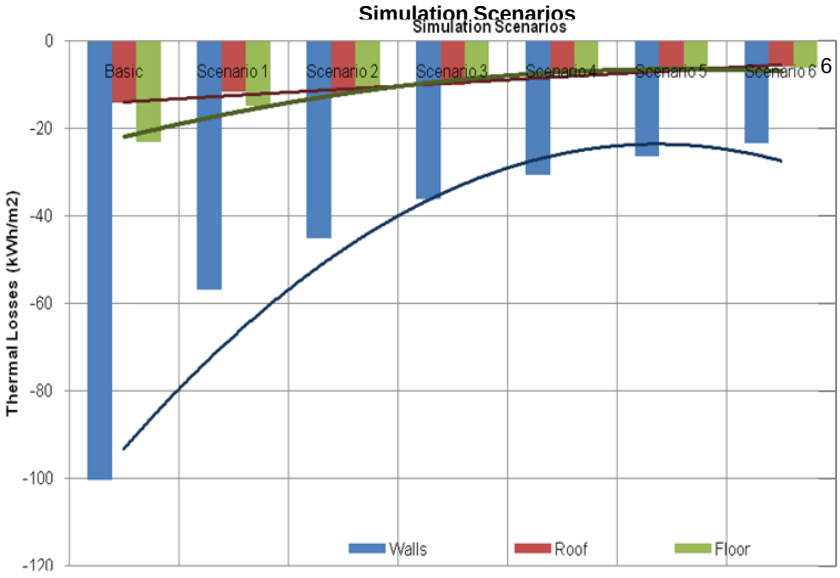

Figure 6: Thermal Losses of the building elements through simulation scenarios

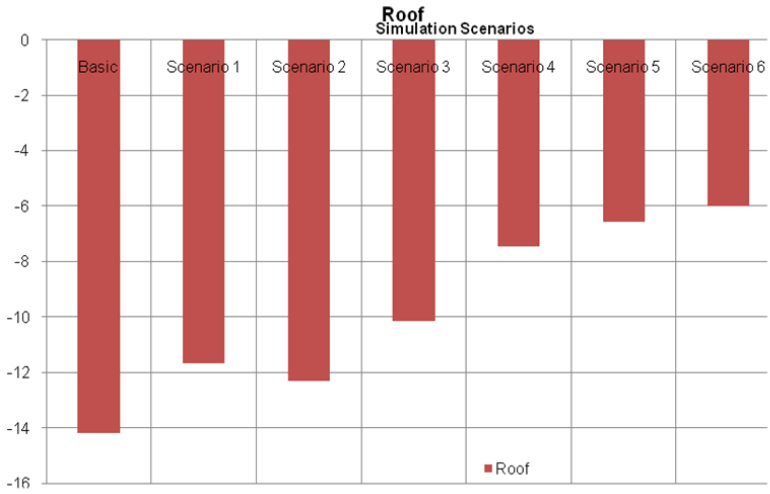

Figure 7: Thermal Losses of the building elements through simulation scenarios

6. CONCLUSIONS

The building stock of Greece requires innovating solutions for retrofitting insulation solutions for the building shell. Roof accounts approximately 25% of the energy losses and are most of the times open spaces which can be very easily insulated. Taking into consideration, the limitation regarding the weight of the applied insulation solution, a composite material of ceramic tile with extruded polystyrene could be the perfect solution. Simulation scenarios with insulation up to 300 mm provide max thermal losses reduction of 14,18 kWh/m2 in total while in comparison to un- insulated roofs the use of 150 mm provides a reduction of 28%.

7. REFERENCES

Eurima, Ecofys 2007 Δεν είναι επαρκής, σελίδα, τόπος κλπ

Thermal Insulation Law (TIR) Ministry of Public Work. Regulation on the Thermal Insulation of Buildings. Official Government Gazette (OGG) 362D/-4-07-1979,pp 3969-4035

Theodoridou I., Papadopoulos A.M. and Hegger M. (2011), Statistical analysis of the Greek residential building stock, Energy and Buildings 43, 9, 2422-2428.

Theodoridou I., Papadopoulos A.M. and Hegger M. (2011), A typological classification of the Greek building stock, Energy and Buildings 43, 10, 2779-2787.
(KENAK) Ministry of Development, Measures to reduce energy consumption buildings and other provisions. Official Hellenic Journal -OHJ 89A/19-05-2008, pp 1371-1377

National Statistical Service of Greece, 2001 census, Detailed Report, Athens, 2002.

Papadopoulos A. (1998), Inverted flat roof: the behavior of extruded polystyrene in time, Technika Chronika, Scientific Review I, 18, 1, 53-63. (in Greek)

Papakostas K.T., Papadopoulos A.M. and Vlahakis I. (2004), Optimization of thermal protection ın residential buildings using the variable base degree days method, International Journal of Sustainable Energy 24, 1, 19-32.

Papamanolis N. The main construction characteristics of contemporary urban residential building in Greece, Building and Environment 2004;40: 391-398.

S. Chadiarakou, A.Papadopoulos, A. Karamanos, M.Santamouris, Energy performance of residential buildings in Greece38th International, Congress on Heating Refrigeration and Air-Conditioning Belgrade, 2007

S. Chadiarakou, M. Santamouris, Field survey on multy- family buildings in order to depict their energy characteristic, RES, CYPRUS, 2013

Drury B. Crawleya, et all, EnergyPlus: creating a new-generation building energy simulation program, Energy and Buildings 33,pp 319-333, 2001

COOLING ROOFS THROUGH LOW TEMPERATURE SOLAR-HEAT TRANSFORMATIONS IN HYDROPHILIC POROUS MATERIALS

D. Karamanis[*,1], E. Vardoulakis[1], E. Kyritsi[1], V. Kapsalis[1], G. Gorgolis[1], S. Krimpalis[1], G. Mihalakakou[1], N. Ökte[2]

1 Department of Environmental & Natural Resources Management, University of Patras Seferi 2, 30100 Greece

2 Department of Chemistry, Boğaziçi University, Bebek 34342, Istanbul, Turkey

**Corresponding author: dkaraman@cc.uoi.gr*

ABSTRACT

The principle of roofs cooling through the water vapour adsorption-desorption cycle in porous materials is presented. In order to study the effect, porous materials of natural origin or synthesized at our lab, were characterized at the micro-scale with SEM, XRD, UV-VIS-NIR spectrometry, thermal and water-vapour adsorption measurements and tested at the urban scale in a wind tunnel of controlled environmental conditions and simulated sun. In the later, the difference of temperature increase under simulated solar irradiation (300 W/m^2) between a highly hydrophilic mesoporous sample and marble dust with comparable reflectance was almost 5 °C in the first irradiation hours and reduced to 2 °C at the end of irradiation.

KEYWORDS

Solar cooling, hydrophilic materials, solar-heat transformation, solar multifunctional nanocomposites

1 INTRODUCTION

Rapid urbanization and economic development in many countries during the last century resulted in microclimate changes of cities, mainly due to man-made constructions. High temperatures appear during the summer and form a serious societal problem (Santamouris, 2013). For example, the mean temperature in Tokyo during the last 100 years has been raised 3 to 4 ^oC, while there has been an increase to the number of the nights in which the temperature in Tokyo is over 25 ^oC, from 10 to 40 during the last decade (Okada et al., 2008). In Athens, temperature differences between urban and suburban stations up to 10 ^oC have been observed (Santamouris et al., 1999). Even in smaller cities in Greece, the temperature differences between the urban and rural areas seem to be high (Kolokotsa et al., 2009; Vardoulakis et al., 2013). This temperature increase due to the urban heat island phenomenon can be quantified by measuring the maximum temperature difference between urban and suburban areas which is specified as heat island intensity.

Consequences of this phenomenon are energy consumption increase due to air-conditioning, thermal discomfort inside the city environment, growth in peak energy demand and money loss (Akbari et al., 1997, Nikolaidis et al., 2009), even heat related deaths in some cases (Johnson and Wilson, 2009). The accumulation of heat inside the urban spar is clearly involved with the urban design and structure density of building in cities. Heat island effect is mainly caused by the reduction of wind speed, due to the high rise building development, which results in low convective heat removal. Moreover, the reduction of permeability of the ground and the usage of materials that absorb and store solar radiation increase the heat

capacity of the cities and diminish the cooling effect of evaporation. Due to the lack of green areas, it was reported that evapotraspiration in Tokyo has been reduced by 38% from 1972 to 1995 (Kondoh et al., 2000). Additionally, an important factor for the heat island appearance is waste heat generated from low energy efficient devices, factories and automobiles, the anthropogenic heat.

Much research was carried out to solve the problem and reduce the energy consumption in buildings. Proposals like the reduction of anthropogenic heat and the proper urban design were recommended. Constraining this problem requires a combination of countermeasures since presented techniques so far have advantages and disadvantages. Increasing the area of green tract land or the surface area of water (eg. artificial lakes and ponds) prevent the heat island phenomenon. However, the high land value of urban space limits the wide applicability of these methods. On the contrary, roofs provide an excellent space to apply mitigation techniques and save buildings' energy consumption (Santamouris, 2012). Roof surfaces are a key element of the heat exchange in city environment, since they take up a great percentage of urban area (up to 20%) and are exposed to solar radiation for many hours every day. For arid areas, almost 50% of the heat load in the building comes from the roof (Nahar et al., 1997), so it is of great importance to understand and reduce the heat movement and storage during a daytime cycle, due to radiation, conduction and convection at roof surface (Meyn et al., 2009). In this direction, the most important mitigation technologies are cool or reflective roofs and green roofs (Santamouris, 2012). Both technologies can lower the surface temperatures of roofs and thus decrease the corresponding sensible heat flux to the atmosphere. However, there are important considerations for both technologies. For example, reflective coatings over roof reduce cooling loads by 18 to 93% (Synnefa et al., 2007) but their reflectivity reduces even 15% during the first year of the application due to weathering (Bretz et al., 1997). Although the cost of green roofs has been highly reduced, the need of water for the irrigation and drainage systems as well as the required intensive maintenance and the dependence on the local climate conditions can limit their worldwide applicability. Therefore, new and more efficient materials and procedures have to be developed (Santamouris, 2012).

Evaporative cooling is a well known and efficient technique in passive cooling (Alvarado et al., 2009) and many methods have been studied by applying a thin film of water over the roof (Sanjay et al., 2008) or by using phase change materials for heating and cooling the building (Pasupathy et al., 2007). During the last years, intensive research about evaporative cooling has been developed and mainly concentrated on the use of natural porous materials for roof-surface treatment (Meng et al., 2005, Okada et al., 2009, Wanphen et al., 2009). According to the evaporative cooling principle, rainwater or humidity adsorbed from porous materials during rainfall or during high humidity nights, can be stored inside small pores and channels in a porous material. Reversely, during a sunny day, humidity stored inside the pores, is released and maintains roof surface temperature at low levels due to latent heat of water evaporation. Lowering the roof surface temperature is important, since heat transfer inside the building reduces as well. Also, there are many indirect benefits like water retention during a heavy rainfall, increase of thermal insulation of the building and removal of many polluting elements. Moreover, roof material degradation due to high roof temperatures is reduced, while relative humidity in winter changes environmental climate to more wet states, resulting in reduction of diseases spread like influenza (Okada et al., 2008).

In order to choose the appropriate material for applications of evaporative cooling, a set of properties must be satisfied:

- Ability to absorb water or vapour at different relative pressure
- High water retention
- Thermal, hydrothermal and ageing stability
- Being locally available and inexpensive
- Environmentally non toxic and easily to handle
- Easy construction into required shape and size for roof application
- Added ability for CO_2 and toxic pollutants sorption
- Easy scale-up production

The principle of building integrated evaporative cooling has been validated with the addition of liquid water in natural porous materials and irradiation from a metal halide lamp (500 W/m^2) (Wanphen et al., 2009), synthetic and aluminum pillared clays (Vardoulakis et al., 2011) or modified lignite fly ash (Karamanis et al., 2012) with metal halide lamp (~100 W/m^2) and pHEMA polymer and sun simulation of class A, AM1.5 (Rotzetter et a., 2012). Recently, we showed that the principle can be applied by moisture sorption on the highly hydrophilic natural sepiolite (Karamanis et al., 2012). With overnight uptake of water vapor on porous sepiolite in 70% relative humidity (to resemble the night outdoor condition), lower surface temperatures were observed under low simulated solar irradiation in comparison to concrete due to heat absorption for water evaporation and desorption with the accompanied mass reduction. Sepiolite, a fibrous magnesian silicate made up of talk-like layers arranged in long ribbons stuck together to form the fibers, adsorbs water vapor on the external surfaces, in microporous channels and inter-fiber micropores and in larger pores that are also present between fibers (Karamanis et al., 2012). In addition, we have seen that by in situ buildup of TiO_2 in sepiolite (Karamanis et al., 2012) or ZnO nanoparticles on the surface of fly ash cenospheres (Ökte et al., 2013), the water vapour adsorption capacity of the porous matrix is retained while the photoresponsive can be used for pollutants photocatalytic degradation. This simultaneous multifunction is possible since different parts of the solar spectrum are being utilized, ie. UV-VIS for photodegradation and VIS-IR for providing the thermal energy for phase changes. *Obviously, the design of appropriate materials for roof covering with combined properties of high reflectance (especially in the visible range), moisture sorption and evaporation through infrared absorbance and self cleaning through ultraviolet absorbance could contribute significantly to the reduction of the heat flux entering the building from the roof.*

In the selection of the hydrophilic porous matrix, it is customary to distinguish between water vapor adsorption in the micropores of porous materials (pore widths of less than 2 nm) and mesopores (2-50 nm). In the former, micropore filling (and cooperative filling) is the dominant mechanism. Recent investigations in low-temperature solar energy storage applications with water sorption on microporous aluminophosphates have shown that the driving force for the water sorption process is the formation of highly ordered water clusters in the micropores (Ristic et al., 2012). Due to the strong water confinement, temperatures of up to 140 ° C are needed for water desorption and these can be reached by solar thermal collectors (e.g., evacuated tube collectors). In the mesoporous materials, the exothermic process of capillary condensation is observed (preceded by a molecular layering on the pore walls) with the appearance of a dense liquid-like state in mesoporous adsorbents for chemical potential lower than its bulk saturating value. In cylindrical mesopores, the adsorbant is confined in two dimensions, the confinement effects are greater and capillary condensation is observed at lower pressures. A similar phenomenon occurs on desorption, with the system persisting in the liquid state at chemical potentials (pressures) below the true equilibrium value. Therefore, the principle of solar cooling with the mesoporous materials can be extended to account for all the phase changes within the adsorption-condensation-evaporation-desorption cycle as: after overnight water vapor adsorption and capillary condensation, liquid water in the mesopores will be desorbed in lower temperatures than the bulk liquids due to solar radiation absorption for providing the sensible and latent heats as well as the heat of desorption. In this way, the temperature of the mesoporous material surface should be highly reduced after these low-temperature solar-heat transformations.

In this work, we studied the interaction of solar irradiation with porous materials of natural origin or synthetic (purchased or prepared) in comparison to PCMs and materials used in the external building surfaces. The interaction was studied with UV-VIS-NIR reflectance-absorbance spectroscopy as a function of the incident wavelength (200-2500 nm) and in a wind tunnel of adjustable environmental parameters as mass and temperature variation under simulated radiation. Prior to the interaction experiments, all materials were characterized with different techniques while their thermal and optical properties were also determined.

2 EXPERIMENTAL

A mesoporous material was prepared and characterized with techniques like X-ray diffraction (XRD) and nitrogen adsorption–desorption isotherms. Since TiO_2 is a well known photoresponsive material with self-cleaning properties and in order to test the variability of the porous matrix in water vapour adsorption, TiO_2 nanoparticles were in situ prepared in the mesoporous sample through the sol-gel method with low Ti concentration (7 wt% as deduced from SEM-EDX measurements). Their surface morphology was determined by scanning electron microscopy with energy-dispersive X-ray spectroscopy (SEM-EDX). The thermogravimetry (TG) and differential thermogravimetry (DTG) measurements was performed on a STA 449C (Netzch-Gerätebau, GmbH, Germany) thermal analyzer. The heating range was from ambient temperature up to 150 °C, with a heating rate of 2 °C min^{-1} under synthetic air flow. Prior to measurements, the samples were put in desiccators of specific relative humidity. The optical characterization of the samples with pre-determined adsorbed water vapor was conducted by a UV/VIS/NIR spectrophotometer (Lambda 950 of PerkinElmer fitted with a 150 mm diameter InGaAs integrating sphere that collects both specular and diffuse radiation) over the solar spectrum (200–2500 nm). The equipment was calibrated with a set of Labsphere certified standards while the ASTM G173-03 reference spectrum was used to normalize the data. Thermal conductivity of the samples was measured by a KD2 Pro meter (Decagon Devices) using the transient line heat source method while infrared emmitance was recorded with a high resolution thermographic camera (VarioCAM). Water adsorption capacity of the produced materials was examined as a function of relative humidity and time. In the moisture sorption isotherms, samples were placed in desiccators with saturated salt solutions for controlling relative humidity while temperature was air-conditionally controlled at 25°C. Prior to measurements, samples were dried to constant mass in an air-circulated oven at 105°C. In order to determine the sorption isotherms, the samples were periodically weighed and the moisture content was calculated as the difference of mass measurements in different time periods and the initial dry state.

The water sorption properties and the associated surface temperature reduction were conducted in an in-house designed and built wind tunnel of controllable conditions of air relative humidity, temperature and wind flow (Vardoulakis et al., 2011). The wind tunnel consists of five parts: the setting entrance, the contraction zone, the diffuser, the test section and the fan housing. Wind flow (m^3 h^{-1}), relative humidity (%) and temperature (°C) of air inside the tunnel, the weight of the sample and the temperatures of the T-type thermocouples at the surface and middle layers of the sample cell are recorded by a CR1000 data logger (Campbell Scientific). The solar radiation can be simulated with a metal halide lamp or two 80 W Philips xenon lamps or a recently acquired 1 sun solar simulator (LOT-ORIEL). The reflected radiation and the power stability of the lamps are monitored by an inverted ISO second-class pyranometer on the top of the test section of the tunnel. The incoming radiation at the test cell position (typical 6x6x3 cm^3 but several volumes are available) is measured with a portable digital solar meter. Every material test is lasted at least for 48 h. In the morning the lamp is turned on for a period of 12 h and the cycle is repeated for one more day. The relative humidity is raised to 70% at night with lamp off. In this work, typical soil (used in green roofs) and marble dust (calcium carbonate) were also tested for comparison purposes.

3 RESULTS & DISCUSSION

The materials' morphology was of mesoporous structure with pore diameter in the corresponding region. In Fig. 1, the absorption spectra of the MESO sample after the adsorption of water vapor at different humidity, are shown. In the same figure, the spectra of

the MESO sample and the TiO_2-MESO composite as stored in room conditions are also included. In the NIR region of the spectrum for the MESO sample saturated at 75% relative humidity (RH), four main maxima located at c. 970 nm, c. 1190 nm, c. 1450 nm and c. 1930 nm are clearly observed, indicating the water vapor condensation within the mesopores. These maxima correspond to the second overtone of the OH stretching band ($3\nu_{1,3}$), the combination of the first overtone of the O–H stretching and the OH-bending band ($2\nu_{1,3}+\nu_2$), first overtone of the OH-stretching band ($2\nu_{1,3}$) and combination of the OH-stretching band and the O-H bending band ($2\nu_{1,3}+\nu_2$), respectively. In the MESO sample saturated at 33% of RH, the intensity of the maxima is much lower due to the reduction of the adsorbed water vapor. By normalizing the absorption data with the solar spectral irradiance ASTM G-173, an increase of the NIR to TOTAL absorption ratio from 31% to 42% was calculated for the two samples at 33% and 93% RH, respectively. The same peaks are also observed for the pure MESO and the TiO_2-MESO composite (Fig 1). Since room RH varies between 40-60%, the peaks intensity of the room stored samples is within the respective of the samples at 33% and 75% of RH. The buildup of the TiO_2 nanoparticles on the MESO surfaces retained the IR spectrum, increased the reflectance in the VIS due to white titania and the absorbance in the UV due to the TiO_2 photocatalytic action under UV light. Therefore, the TiO_2-MESO composite improved its optical properties towards its utilization in multifunctional applications. The absorption spectra of marble dust ($CaCO_3$) that is used as external building surface, is also shown in Fig. 1. The marble dust shows the highest reflectance of all the studied materials, indicating its suitability as a "cool" reflective material. In addition, the intense 1412 nm peak in the $CaCO_3$ spectrum as well as others of lower intensity, are mainly due to water bound in the structure since are observed in both dried and room stored samples.

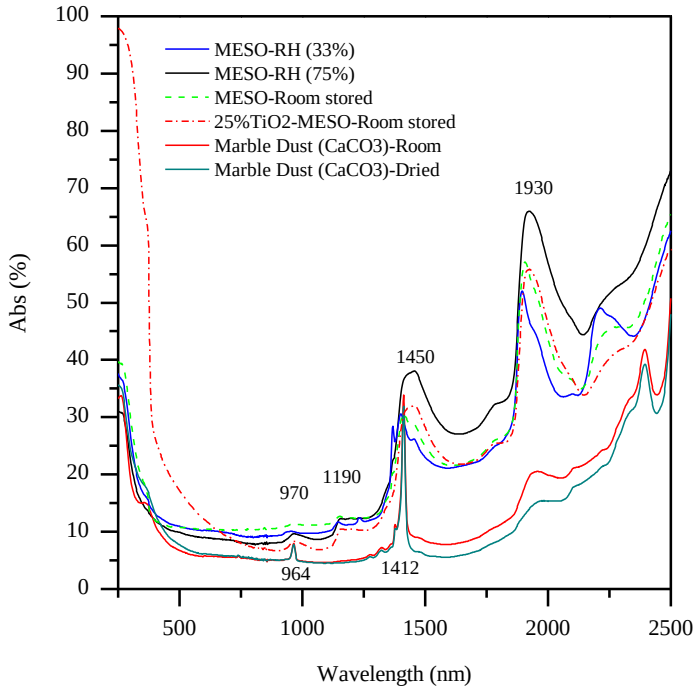

Figure 1. Absorbance spectra of the MESO and 25%TiO_2-MESO materials as room stored, MESO after water vapor adsorption 33% and 75% of RH and marble dust ($CaCO_3$) as received (room stored) and after drying.

According to the thermogravimetric results of Fig. 2, there is one major endothermic peak of temperature around 55 °C where the physisorbed and condensed water is released from the mesoporous material. This "free water" bound due to condensation is being removed by the low temperature heating fluxes through evaporation and desorption from the pores. In contrast, water molecules bound to materials like zeolites through the adsorption bonds of physical adsorption demand higher heats of desorption but also higher temperatures for their removal

from materials' pores. In the proposed application of materials integration in building surfaces, the temperature rise of an absorbing building surface with 0.05 reflectance can be about 34 -50 °C warmer than the ambient air in full sunlight. Therefore, the mesostructured samples are appropriate for such applications and almost all of the sorbed water is expected to be removed under the summer solar radiation. Furthermore, the thermal conductivity of the MESO material at room conditions was measured 0.16 W m^{-1} K^{-1} and was reduced to 0.099 W m^{-1} K^{-1} after drying the sample at 200 °C for 2 h.

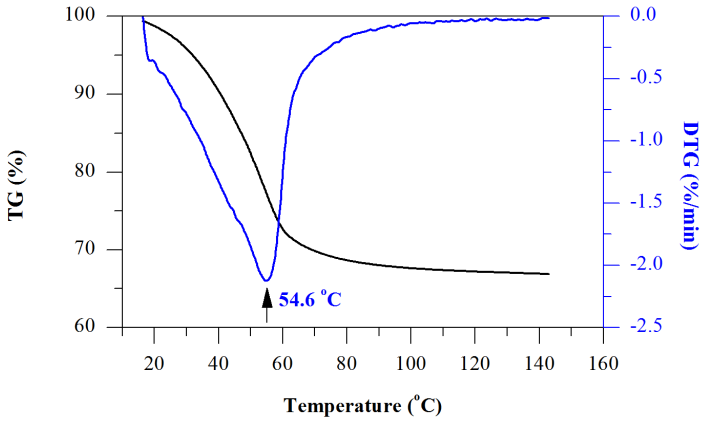

Figure 2. TG and DTG curves of the MESO material after water vapor adsorption at 75% RH.

The hydrophilicity of the MESO samples and the supported TiO_2 nanocatalyst was investigated by the water vapor adsorption isotherms. Fig. 3 shows the water vapor sorption isotherm of the tested materials at 25 °C. For comparison purposes, soil, marble dust ($CaCO_3$) and silica gel isotherm curves are also included. Water vapor sorption in soil and marble dust was very low in the whole scale of relative pressures. The isotherms of silica gel and MESO samples showed different type behaviour. The silica sorption isotherm was of type I in the IUPAC classification indicating a highly hydrophilic material with water vapor sorption ability up to 0.25 g g^{-1}.

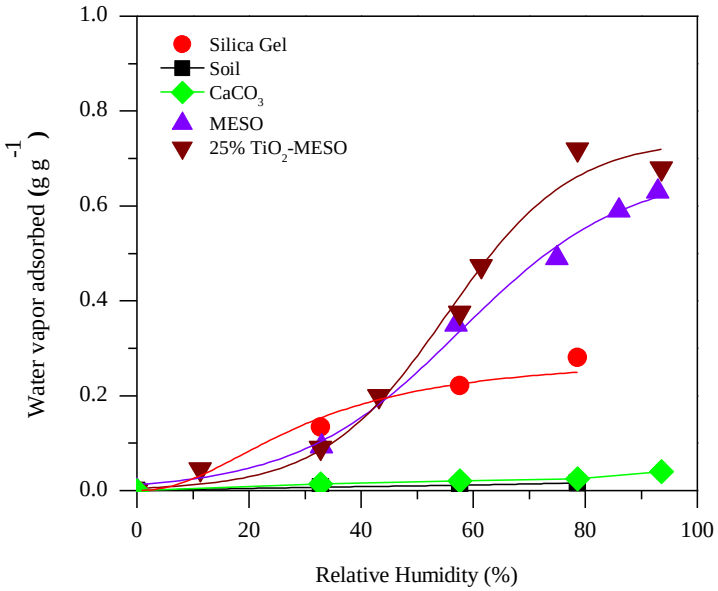

Figure 3: Water vapor adsorption isotherms on the MESO samples, TiO_2-MESO, soil, silica gel and $CaCO_3$ at 25 °C.

In contrast, the water adsorption isotherm on the MESO samples was of type V. This is indicative of a relatively hydrophobic character in the low-pressure region of the adsorption

isotherm but with a capillary condensation step 0.55-0.6 relative pressure leading to a total filling of the pore volume and thus to a type-V isotherm (with maximum uptake more than 0.6 g g^{-1} at 93 % RH). Upon TiO_2 in situ buildup on the MESO sample, the hydrophilicity of the composite was maintained and the catalyst still exhibited a type V isotherm (Fig. 3).

The MESO material was further tested in the wind tunnel under simulated solar irradiation in comparison to soil and marble dust. The radiation was provided by two low power xenon lamps over the top of the wind tunnel. The incoming radiation at the test cell position was measured at several points of the cell with an average of 300 W m^{-2}. Every material test lasted at least for 48 h. In the morning, the lamp was turned on for a period of 12 h and the cycle was repeated for one more day. The relative humidity was raised to 70% at night with lamp off. The weight variation curve of the samples revealed that the soil and marble masses remained almost constant at night with increased RH while the MESO mass increased more than 15 % within the 12 hours period. Upon irradiation its mass decreased almost exponentially due to the evaporation and desorption of night sorbed water.

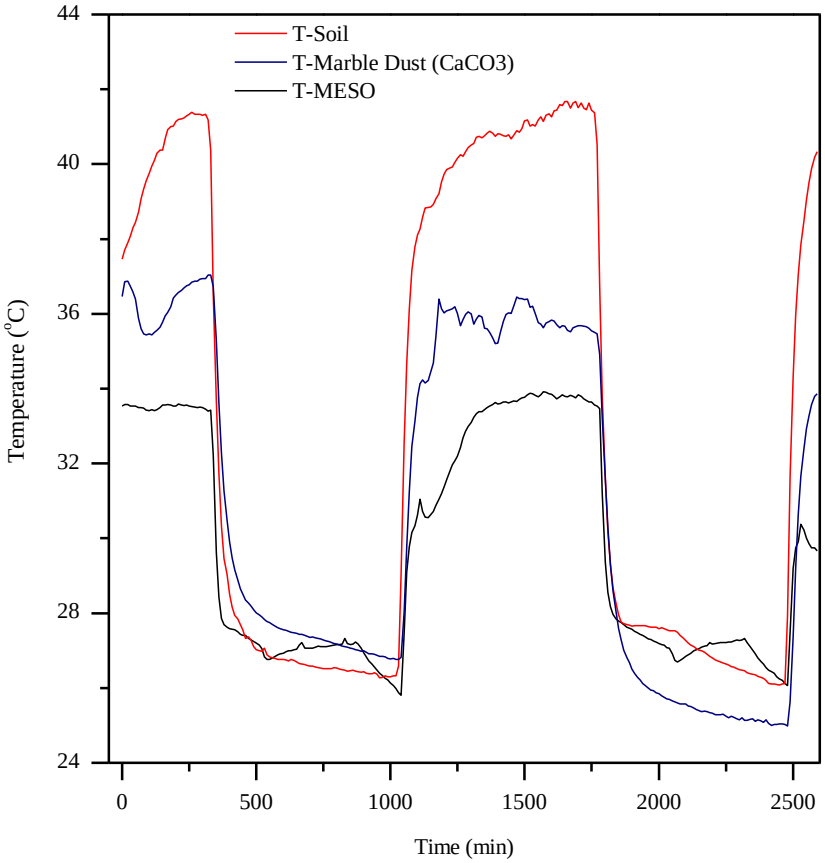

Figure 4: Temperature increase inside the MESO, soil and $CaCO_3$ samples due to low simulated solar irradiation (average 300 W m^{-2}).

Fig. 4 shows the measured temperature increase in the cyclic experiments with simulated solar radiation of two continuous cycles, starting from the first lamp on as the zero time. The difference of temperature increase under simulated solar irradiation between the MESO sample and marble dust with comparable reflectance was almost 5 °C in the first irradiation hours and reduced to 2 °C at the end of irradiation. The MESO difference with the soil sample was even higher. By considering a latent heat of 2300 kJ kg^{-1} for water vaporization at the attained material temperatures, the observed MESO mass reduction of 1 g (13% of the initial mass) corresponds to 2.3 kJ of absorbed energy for water evaporation or half of the absorbed incoming radiation. The evaporation term was absent in $CaCO_3$ that exhibits comparable

reflectance to MESO and very small in soil with the very low reflectance. These results indicate the material's suitability for the proposed application of evaporative cooling.

4 CONCLUSIONS

Key factor in reducing energy consumption in buildings is the materials used in the building sector. In order to sustain our natural resources through the utilization of the abundant solar energy, new cooling principles should be applied and, if possible, be integrated in the building from the manufacturing phase. In this work, the solar-heat transformation for the evaporation of night adsorbed and condensed water vapor in novel highly hydrophilic mesoporous materials of high reflectance has been found to contribute significantly in the temperature reduction of the irradiated surface and consequently, the heat flux transferred through the surface. Although some direct applications of the hydrophilic materials could be investigated like the cooling effect of materials' addition in green roofs, further combined research and development is needed for their technological implementation and building integration.

5 ACKNOWLEDGEMENTS

This work has been supported by the University of Western Greece, Latsis Foundation and GSRT programmes of Hrakleitos II, Greece-Turkey Bilateral Program and ARISTEIA I ("Operational Programme Education and Lifelong Learning co-funded by the European Social Fund (ESF) and National Resources). Thanks are due to the Horizontal Network of Laboratories of the University of Ioannina and Bogazici University for the help in materials' characterization.

6 REFERENCES

Akbari, H., Bretz, S., Kurn, D. and Hanford, J. (1997). Peak power and cooling energy savings of high-albedo roofs. *Energy and Buildings* 25 (2), 117- 126.

Alvarado, J., Terrell, W. and Johnson, M. (1999). Passive cooling systems for cement-based roofs. *Building and Environment,* 44 (9), 1869-1875.

Bretz, S. and Akbari, H. (1997). Long-term performance of high-albedo roof coatings. *Energy and Buildings*, 25 (2), 159-167.

Johnson, D.P. and Wilson, J.S. (2009). The socio-spatial dynamics of extreme urban heat events: The case of heat-related deaths in Philadelphia. *Applied Geography*, 29, 419-434.

Karamanis, D., Vardoulakis, E. (2012) Application of zeolitic materials prepared from fly ash to water vapor adsorption for solar cooling. *Applied Energy*, 97, 334-339.

Karamanis, D., Vardoulakis, E., Kyritsi, E., Ökte, N. (2012). Surface solar cooling through water vapor desorption from photo-responsive sepiolite nanocomposites. *Energy Conversion and Management*, 63, 118-122.

Kolokotsa, D., Psomas, A. and Karapidakis E., (2009). Urban heat island in southern Europe: The case study of Hania, Crete. *Solar Energy*, 83 (10) 1871-1883.

Kondoh, A. and Nishiyama, J. (2000). Changes in hydrological cycle due to urbanization in the suburb of Tokyo Metropolitan area, Japan. *Advances in Space Research*, 26 (7), 1173-1176.

Meng, Q, Hu, W. (2005). Roof cooling effect with humid porous medium. *Energy and Buildings*, 37, 1-9

Meyn, S. and Oke, T. (2009). Heat fluxes through roofs and their relevance to estimates of urban heat storage. *Energy and buildings* 41, 745-752.

Nahar, N.M., Sharma, P. and Purohit, M.M. (1997). Studies on solar passive cooling techniques for arid areas. *Energy Conversion & Management*, 40, 89-95.

Nikolaidis, Y., Pilavachi, P. and Chletsis, A. (2009). Economic evaluation of energy saving measures in a common type of Greek building. *Applied Energy*, 86 (12), 2550-2559.

Okada, K., Matsui, S., Isobe, T., Kameshima, Y. and Nakajima, A. (2008). Water-retention properties of porous ceramics prepared from mixtures of allophone and vermiculite for materials to counteract heat island effects. *Ceramics International*, 34 (2), 345-350.

Okada, K., Ooyama, A., Isobe, T., Kameshima,Y, Nakajima, A. and MacKenzie, K. (2009). Water retention properties of porous geopolymers for use in cooling applications. *Journal of the European Society*, 29, 1917-1923.

Ökte, N., Karamanis, D. A novel photoresponsive ZnO-flyash nanocomposite for environmental and energy applications. (2013) *Applied Catalysis B: Environmental*, 142-143, 538-552.

Pasupathy, A. and Velraj, R. (2007). Effect of double layer phase change material in building roof for round thermal management. *Energy and Building*, 40, 193-203.

Ristic, A., Logar, N., Henninger, S., Kaucic, V. (2012) The performance of small-pore microporous aluminophosphates in low-temperature solar energy storage: the structure–property relationship. *Advanced Functional Materials*, 22, 1952-1957.

Rotzetter, A.C.C., Schumacher, C.M., Bubenhofer, S.B., Grass, R.N., Gerber, L.C., Zeltner, M., Stark, W.J. (2012). Thermoresponsive polymer induced sweating surfaces as an efficient way to passively cool buildings. *Advanced Materials*, 24, 5352–5356.

Sanjay,J., and Chand, P. (2008). Passive cooling techniques of buildings: Past and present- A review, *Engineering Energy*, 4, 37-46

Santamouris, M., Michalakakou, G., Papanikolaou, N. and Assimakopoulos, DN (1999). A neural network approach for modelling the heat island phenomenon in urban areas during the summer period. *Geophysical Research Letters*, 26 (3), 337-340.

Santamouris, M. (2012). Cooling the cities – A review of reflective and green roof mitigation technologies to fight heat island and improve comfort in urban environments. *Solar Energy*, (in press).

Santamouris, M. (2013). Using cool pavements as a mitigation strategy to fight urban heat island—A review of the actual developments. *Renewable Sustainable Energy Reviews*, 26, 224-240.

Synnefa, A., Santamouris, M. and Akbari, H. (2007). Estimating the effect of using cool coatings on energy loads and thermal comfort in residential buildings in various climatic conditions. *Energy and Buildings* 39 (11), 1167-1174.

Vardoulakis, E., Karamanis, D., Fotiadi, A., Mihalakakou, G. (2013). The urban heat island effect in a small Mediterranean city of high summer temperatures and cooling energy demands. *Solar Energy*, 94, 128-144.

Vardoulakis, E., Karamanis, D., Mihalakakou, G., Assimakopoulos, M.N. (2011). Solar cooling with aluminium pillared clays. *Solar Energy Materials and Solar Cells*, 95, 2363–70.

Wanphen S. and Nagano K. (2009) "Experimental study of the performance of porous materials to moderate the roof surface temperature by its evaporative cooling effect", *Building and Environment* **44** pp338-351.

PARAMETRIC ANALYSIS OF ENVIRONMENTALLY RESPONSIVE STRATEGIES FOR BUILDING ENVELOPES SPECIFIC FOR HOT HYPERARID REGIONS

Alex Cicelsky[1], Isaac A. Meir[*2]

1Center for Creative Ecology
Kibbutz Lotan
D.N. Hevel Eilot 88855
Israel

2 The Jacob Blaustein Institutes for Desert Research
Ben-Gurion University of the Negev
Desert Architecture & Urban Planning
Sede Boqer Campus, Israel
**Corresponding author: sakis@bgu.ac.il*

ABSTRACT

The deep hot hyperarid valley between Israel and Jordan presents unique design and construction challenges in terms of energy conservation and thermal comfort. Winters are relatively mild, summers are extremely hot during the day and at night the air temperature remains above 25°C. Such conditions present real challenges in this sparsely populated yet rapidly developing region. Such development depends on the ability to provide acceptable indoor environments at a low energy investment. Potential solutions were investigated through a parametric analysis including physical and operational elements aiming at establishing benchmarks for free running and low energy buildings under extreme conditions. First, building performance was simulated for a limited number of parameters. Additional operational and physical parameters were introduced and results compared. The data were analyzed to determine the best performing options for building assemblies.

Results of permutations investigated confirmed that simulated conventional building systems did not allow for free running operation and that mechanical systems for both heating and cooling were needed. This research concluded that it is imperative to extensively insulate building envelopes in order for them to be free running in the winter. Buildings need extensive shading in the transition seasons to allow for free running operation and avoid overheating. Buildings with complete shade, high efficiency window systems and levels of insulation above and beyond those currently employed when simulated with summer climate conditions had significantly lower energy consumption requirements for mechanical cooling than other building designs. The research showed that energy efficiency in this region is a function of particular combination of extensive insulation, full shade, high performance windows, air tight buildings and seasonal operation of window shutters utilized together.

KEYWORDS

Free-running buildings, hyperarid environment, insulation, thermal mass, ventilation

1 INTRODUCTION

Settlement in hyper-arid regions has usually been scarce and sparse, yet the continuous processes of desertification and climate change on the one hand, alongside human expansion and search for new places to settle on the other hand, are bringing more people closer or inside deserts, and often bring the deserts to the doorsteps of people used to much more temperate climates. Urbanization and population growth processes are also exacerbating housing related issues in such regions. The need to provide sustainable, low energy housing in

deserts is thus becoming all the more pressing, as has been stressed in a number of recent publications (e.g., Beer et al., 2012; Meir et al., 2012).

The case study dealt with in this paper is the Southern Arava Valley, part of the long Afro-Asian Rift, a natural border between Israel and Jordan. To the north lies the Dead Sea (over 400m below Mean Sea Level – MSL), and to the south the port city of Eilat on the Red Sea coast, with a higher middle part rising to appr. 210m above MSL. It is considered one of the climatically harshest parts of Israel. Its climate is unique in Israel and unusual when compared to deserts worldwide. Winters are relatively mild, frost is rare and no occurrences of snow have been recorded within the valley. Winter daily maxima range between 21-23°C, and night minima between 9-11°C. Rarely do temperatures go below 5°C, and the absolute minimum registered ever was 1.2°C. Summers are extremely hot during the day with temperatures often reaching 42°C and above, and at night the air temperature remains above 25°C, with katabatic winds from the cliffs to the west often keeping it higher. The absolute maximum registered was above 47°C. Only one out of four nights reaches a minimum temperature below 24°C. During the summer and transition seasons months relative humidity may go as low as 10% and below (Bitan and Rubin, 1991), though in recent years there have been anecdotal reports of high relative humidity, which renders climatic conditions nearly unbearable without mechanical cooling.

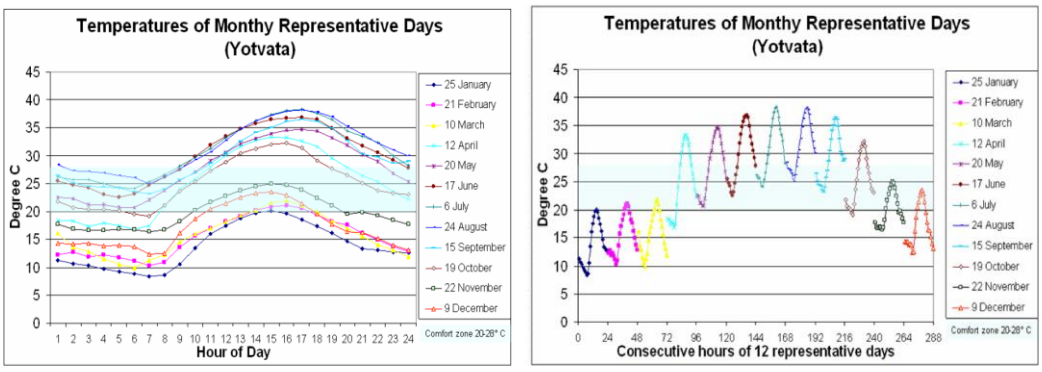

Figure 1: Left: external temperatures of representative days from Typical Meteorological Year (TMY). Right: temperature measurements of representative days for each month selected from the Yotvata TMY. The consecutive hours in the graph are multiples of 24 times the numerical month of the year (– after Faiman et al., 2004).

The region of Eilot Regional Council stretching 102 km northwards from the port city of Eilat on the Red Sea has been traditionally sparsely populated. Within the valley nine modern communities have been established in the past 50 years along with limited industrial, commercial and municipal facilities. The region has announced its commitment in the next decade to become energy independent using solar technologies and other alternative and renewable resources electricity production. The master plan for the region calls for tripling the population of around 3,000 residents in the next decade. Both of these goals depend on building housing units in each of the existing communities. The existing models of housing are recognized as energy inefficient and inappropriate for the region. This is because they are copies of units built in (but not necessarily planned to be adapted to) other regions of the country and either transported to the Arava or built in situ according to plans that only marginally relate to the particular extreme climate. Common building types and technologies include concrete, flat roofed non-insulated houses which were marginally improved post construction by the addition of "thermal" external plaster (a mix of cement with polystyrene beads, applied to exterior concrete walls); aerated autoclaved concrete (AAC) blocks; introduction of the most basic model of double glazed windows (in aluminum frames with no thermal breaks); and roof shading. Recently, lightweight housing units have been introduced.

In all cases, the level of satisfaction has not increased and HVAC use is high. The development of architectural strategies that are particular to this region with an emphasis on energy efficiency should be recognized as a component in the renewable energy plan and the physical development master plan of the regional council and the communities.

Residents of the southern Arava are quite aware that heating and cooling systems and their associated costs are inseparable with living in this region. Winter days, normally sunny and often moderate are pleasant outdoor, but marginally tolerable indoor, while nights are cold and internal walls and windows feel very cold. Temperatures in the spring and fall are moderate during day and night, allowing daily ventilation, with windows open or closed at night. Summer daytime cooling can begin as early as late April and even March during sandstorms with hot wind events blowing up from Africa. By late May air conditioners are running during the day and night until cool nighttime breezes begin again in September. In Israel residential buildings, and public and commercial ones account for 30.0% and 32.4% respectively of the overall annual electricity consumption (IEC 2011). Summer air conditioning accounts for appr. 16% of the overall electricity consumption in Israel (40% of the May-Oct. summer electricity use). A case study surveyed in the Arava (Kibbutz Grofit) showed cooling loads comprised 49% of the annual residential electricity use (46% of the Apr.-Oct. summer electricity use) (Daniels, 2009).

The goal of the research presented here was to determine the components of residential buildings that would allow houses to be heated passively using solar gain and to be cooled using less energy than that currently needed for mechanical cooling. An analysis of the southern Arava's climate presented three seasonal conditions that must be addressed when designing free running as well as low energy use buildings: a clear or partially cloudy skied winter during which sufficient heating can be provided using solar gain; spring and fall with comfortable ambient temperatures and risks of overheating from solar gain; and summer in which ambient temperatures are above comfort levels during the day and most nights.

2 TOOLS AND METHODS

The research methodology selected to determine energy efficient building design guidelines was a parametric analysis of operational as well as physical elements.

2.1 Parameters

A 100 m^2 building with internal height of 3 m, of one zone (no internal differentiation between thermal zones or rooms), was modified in accordance with the variations of physical building element parameters. The climate data for each month were taken from the Typical Meteorological Year (TMY) file of the Yotvata Israel Meteorological Service (IMS) station. Data sets of simulated interior temperatures for each set of parameters were created by the QUICK II simulation software for each month of data. The building element parameters selected for this project appear in Table 1. There were 55,296 possible combinations of these building elements and operational scenarios. Instead of running all the possible permutations and comparing all of the results, a progressive method parametric analysis was employed. The process began with simulating building performance for a limited number of parameters. The data were analyzed to determine the best performing options out of the simulation set. This process was repeated as additional parameters were added to the building assembly.

Operational parameters, for example shuttering windows completely during warm spring days to avoid overheating, are as significant to the free running operation of a building as are

building elements such as wall and roof insulation. Within the time limitations of this work and because of the understanding that numerous combinations of parameters were inappropriate for this climate, it was decided to progressively compare parameters instead of running all the possible permutations and comparing all of the results. The process began with collecting site specific climatic data from the IMS, which are not readily accessible, and selecting naturally occurring representative days for each month of a standardized TMY.

2.2 Simulation tool

The computer program selected for the parametric analysis of the building system was QUICK II, developed by the Centre for Experimental and Numerical Thermoflow, University of Pretoria, South Africa (Mathews et al., 1994a; Mathews et al., 1994b; Mathews, 1997), which was validated for local use in collaboration with the Desert Architecture and Urban Planning Unit of the Jacob Blaustein Institutes for Desert Research, Ben Gurion University (Mathews et al., 1997).

Table 1: Parameters analyzed in this research.

Geometry	Square bldg 10/10m	Rectangular bldg 20/5m		
Orientation	N-S axis	E-W axis		
Construction	Lightweight [LW]: wood frame drywall construction envelope walls and roof (low thermal mass)	Medium weight [MW]: 22 cm thick AAC block envelope walls and roof (medium thermal mass)	Heavyweight [HW]: 20 cm thick cast concrete envelope walls and roof (high thermal mass)	
Wall shading	Unshaded/none	N, S walls shaded during all daylight hours	E, W walls shaded during all daylight hours	N, S, E, W walls shaded during all daylight hours
Roof shading	Flat, un-shaded roof	Shaded, well ventilated roof	Unventilated clay terracotta tile roof	Well ventilated clay terracotta tile roof
Insulation	Un-insulated [0] - No thermal insulation on walls/roof	Insulated [5] - 5cm layer of external thermal insulation (expanded polystyrene) on walls/roof	Insulated [10]- 10cm layer of external thermal insulation (expanded polystyrene) on walls/roof	Insulated [20] - 20cm layer of external thermal insulation (expanded polystyrene) on walls/roof
Window size	6 m^2 on N, S walls	6 m^2on N, 12 m^2on S walls		
Window treatment	Glazed openings not shaded by shutters	Glazed openings shaded by shutters	Seasonal operation of shutters – summer/closed in daytime; winter/opened in daytime.	
Window insulation	Low: single glazing	High: triple glazing		
Ventilation – Air Changes per Hour (ACH)	10 ACH	20 ACH	30 ACH	50 ACH
Finish	Light color: reflective white finish of external walls/roof (absorption coefficient = 0.3)	Medium color: dark brown finish on external walls/roof (absorption coefficient = 0.65)	Dark color: dark brown finish on external walls/roof (absorption coefficient = 0.8)	

The program functions by simulating the effect of seasonal external climate (radiation, temperature, humidity and wind) on the building envelope (physical and thermal properties of components and materials) and calculates the internal temperature of the building for a representative day of each month. The program also derives the energy consumption needed by mechanical heating and cooling systems for reaching/maintaining set temperatures. The process began with simulating building performance for a limited number of parameters. Additional operational and physical parameters were added and the results compared. The data were analyzed to determine the best performing options for building assemblies.

3 RESULTS AND DISCUSSION

The results of the permutations investigated confirmed that simulated conventional building systems did not allow for free running operation and that mechanical heating and cooling systems were needed for significant parts of the year. The conclusion of the research was that it is imperative to extensively insulate building envelopes in order for them to be free running in the winter. Buildings need extensive shading in the transition seasons to allow for free running operation and avoid overheating. Buildings with complete shade, high efficiency window systems and levels of insulation above and beyond those currently employed when simulated with summer climate conditions had significantly lower energy consumption requirements for mechanical cooling than other building designs. The research showed that energy efficiency in this region is a function of particular combination of extensive insulation, full shade, high performance windows, air tight buildings and seasonal operation of window shutters utilized together.

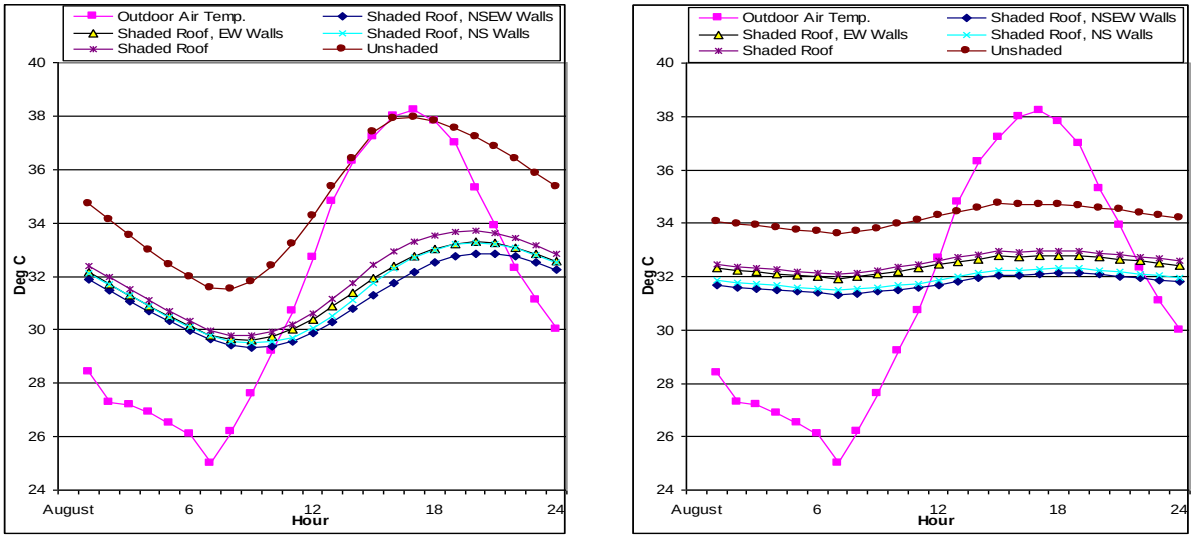

Figure 2: Effect of shading on buildings with increasing insulation on walls and roof in summer (August). Buildings had 6m^2 south facing windows and 200mm concrete walls and ceiling. Left: non-insulated; right: 50 mm polystyrene insulation.

The climatically advantageous geometry was a rectangular rather than a square building unit. The walls of the rectangular building had 25% greater surface area than the square building, which could be considered detrimental in a region where reduction (in summertime) of the surface area to volume ration would be preferential. However, the rectangular building allowed for substantially lowered wall area exposure in the summer when properly oriented. The preferred orientation of the rectangular building was along the east-west axis so as to make expanded solar gain options available in the winter and to reduce exposed east and west walls in the summer.

Wall shade in the winter months was not beneficial for the building. Nevertheless if the building was warmer because of un-shaded walls (not including windows) it suggested heat gain through the walls which is not a positive characteristic of the external envelope. Analysis of roof construction strategies showed that the insulated roofs were a necessity for reducing conduction of energy through the envelope. Shading of the roof, along with its insulation reduced internal heat in most months of the year. Ventilated roof shading options correlated with lower energy use for cooling in the summer.

Window size - for winter solar gain $6m^2$ of south facing windows for a $100m^2$ building proved insufficient for solar gain needed to raise simulated interior temperatures above the lower threshold for thermal comfort (20°C). Increasing the window area to $12m^2$ increased the internal temperatures and was sufficient when highly insulated windows were used. In summer larger windows were associated with increased simulated internal temperatures. In practice reflective and insulated external shutters would reduce this effect.

Higher performing windows (low conductivity/high insulation, in this study taken as U=3 and 1.5 W/m^2K; R= 0.333 and 0.666 m^2K/W for double and triple glazing, respectively) were associated with higher interior temperatures in the winter and lower energy use in the summer when mechanical cooling was employed. Better tools with a higher resolution based on a more complex analysis of glazing systems could be used to determine the cost/benefit ratio for windows. This is of particular interest because of the high cost of good glazing options.

Ventilation was simulated on a hypothetical building system that should be more appropriate for the southern Arava because of its high interior mass and large level of insulation and shading. The effectiveness of night time ventilation for cooling the building increased as air speed increased. The question of utility of night time cooling in the summer is one relating to personal preferences and acclimation to the high ambient temperatures. In general, and in accordance with ASHRAE standards for populations in industrialized countries, thermal comfort would only be reached by maintaining high air flow ventilation during the few hours that temperatures were below, but near the upper threshold of thermal comfort (28°C). For most of the summer day ventilation from outdoors could not be used.

Three commonly used construction techniques were compared in the summer in order to determine their relative efficiency in energy use for cooling. Commonly used roofing systems were also parameters simulated. The lowest energy use was associated with the heavy weight building with high levels of insulation. Lightweight and heavy weight buildings with low levels of insulation had similar energy usages. Lightweight buildings with unventilated roofs needed more energy to cool. The simulated building built from AAC blocks, marketed as an environmentally superior material, demanded more energy for cooling than all of the other options. A medium color of external surfaces (absorption coefficient = 0.65) was used throughout the analysis process. A final check of the response to light or dark colored surfaces on the best performing envelope showed that even in full shade darker colors would absorb and conduct heat to the interior of the building due to reflected and diffuse radiation.

Therefore it is preferable to use light colors on buildings in the southern Arava in particular because the airborne dust is dark and all textured surfaces will become darker in time. The parametric analysis process used ended with the selections of a building that incorporates many architectural elements in use in the southern Arava, but not necessarily incorporated into one building. The results suggest that such incorporation should produce a building which would be energy efficient because of its appropriateness to this specific environment.

Further research could determine what the effect of trade-offs would make, for example lowering the internal mass while adding more insulation. This would be useful when examining the functioning of alternative building materials and technologies, such as the straw bale and earth plaster domes recently built in Kibbutz Lotan (Golding, 2010). Apparently these un-shaded and dark colored buildings which have 5cm of earth mass on the interior and 50cm of straw insulation, when cooled to 25°C in the summer using air conditioners, do not heat up from conduction of heat through the walls and have very small daily temperature fluxes due to infiltration of hot air. This would be a case of reaching energy use goals by using levels of insulation beyond those addressed in this analysis.

Table 2: Simulated cooling loads for buildings with same geometry, shading and windows as a function of different wall components: 5x20m (100m^2) buildings oriented on EW axis; single glazed windows: 6m^2 north facing, 12m^2 south facing; windows, walls and roofs shaded. Set temperature 25ºC, 24 h/day, August.

Wall and roof	200mm concrete	200mm concrete	AAC	19mm gypsum wallboard	19mm gypsum wallboard
Insulation of wall and roof	200mm XPS	50mm XPS	-	50mm fibreglass batt	50mm fibreglass batt
Roof	Well ventilated, no mass	Well ventilated, no mass	Well ventilated, no mass	Clay tile, unventilated	Well ventilated, no mass
Daily (24h) energy consumption, August typical day [kWh]	27.82	53.61	79.96	62.69	51.66

4 CONCLUSIONS: BUILDING DESIGN GUIDELINES FOR FUTURE CONSTRUCTION

The conclusion of this research is that it is imperative to dictate extensive envelope insulation, insulated windows and doors units and frames with low infiltration and low convective heat loss in order to make the buildings free running during all winter months. Extensively shading the insulated envelope and windows in accordance with daily ambient temperatures and solar radiation levels allows for free running operation of buildings during the transition seasons. Significant reductions in energy consumption in the summer months can be realized by completely shading the buildings, utilizing high efficiency window systems, preventing convective heat gain from infiltration and ventilation and enveloping the building with levels of insulation above and beyond those currently employed.

This research proved building design guidelines would have a significant impact on the thermal performance of buildings in the southern Arava and subsequent minimization of energy consumption to employ auxiliary heating and cooling when they incorporate:

- a significant increase of exterior insulation on all types of building construction systems (this research simulated insulation thickness of up to 20cm of expanded polystyrene U=0.035W/m°C);
- employment of full shading of the building envelope in the summer months;
- integration of operable, insulated, externally ventilated and highly reflective external window shading on all windows;
- the advantages of high efficiency double and even triple glazed windows assuming high quality of construction and installation.

Additional energy savings design techniques should be utilized in particular to reduce convective heat gain and loss. These include:

- entrance halls "air locks" with double sets of insulated doors;
- heat exchangers for use with A/C units to supply fresh, heated/cooled air at ACH levels that meet standards.

This project suggests that issues of boundary cases of insulation and mass should be evaluated again when designing buildings for the southern Arava. The following discussion and estimates are based on 2009-10 prices and tariffs. Material cost makes up a relatively small portion of total cost of construction. The cost of standard construction in the southern Arava is around $\$1200/m^2$, therefore a $100m^2$ house would cost around $120,000. The cost of 200mm XPS at $\$50/m^3$ (around $50m^3$ is needed) is $2,500 or 2% of the total cost. At energy prices at the time of the research ($0.15/kWhr) average yearly heating and cooling costs for the $80m^2$ kibbutz houses (see Kibbutz Grofit residential energy use, Daniels, 2009) is approximately $580/year per household. The payback period could be calculated as function of energy saved by having the insulation. If the energy savings would be 30% then the payback period would be 14 years. These preliminary calculations illustrate that implementing energy savings strategies in building design can be cost efficient in the short to medium term, yet energy price rises since then (0.18 $/kWh, June 1, 2013) shorten the insulation payback period even more.

This research showed that commonly accepted architectural norms should be reevaluated when building in the southern Arava, as well as in similar hyper arid regions. Recent building in the southern Arava has disregarded design norms that were shown in this research to have been beneficial to energy efficiency. These include building houses along the east-west axis so as to shade each other (and, if connected, reduce external surfaces), high and well ventilated roofs of light colored materials and painting buildings white. However, use of light hue reflective finish materials dictates shading them extensively to avoid high reflectance and glare, making the use of outdoor spaces thermally and visually uncomfortable even in winter days, and could negatively affect neighboring buildings by exacerbating cooling loads.

These design directives should not be lost in the name of expedient building or "personal choice" instead of following local building strategies. Each of these elements plays a part in the mosaic of components in designing an energy efficient building in this particularly extreme climate. All of the components need to be included if reduction of energy use for heating and cooling is to be achieved.

5 ACKNOWLEDGEMENTS

This research was carried out within the graduate program of the Albert Katz International School for Desert Studies of the Jacob Blaustein Institutes for Desert Research, Ben Gurion University of the Negev. The active support and cooperation of the Arava Institute for Environmental Studies, the Tzel HaTamar Association, and Kibbutz Lotan's Center for Creative Ecology is kindly acknowledged.

6 REFERENCES

Beer, A., S. Tually, M. Krohen, J. Law (2012). *Australia's Country Towns 2050: What Will A Climate Adapted Settlement Pattern Look Like?* Preliminary Report. National Climate Change Adaptation Research Facility. Adelaide: Center for Housing, Urban and regional Planning, University of Adelaide.

Bitan, A. and S. Rubin (1991). *Climatic Atlas of Israel for Physical and Environmental Planning and Design.* Tel Aviv: Ramot.

Daniels, R. (2009). *Kibbutz Grofit electricity use in 50 metered houses, 2008*. Kibbutz Grofit: Accounting Office.

Faiman, D., D. Feuermann, P. Ibbetson, B. Medwed, A. Zemel, A. Ianetz, V. Liubansky, I. Setter , S. Suraqui (2004). The Negev Radiation Survey. *J. Solar Energy Engineering* 126(3): 906-914.

Golding, J.Y. (2010). *Assessing the Thermal Behaviour of Straw Bale and Mud Geodesic Domes in the Southern Arava: A Hot-Arid Zone Case Study*. Master's thesis, submitted to the Albert Katz International School for Desert Studies (AKIS), Ben-Gurion University of the Negev, Sede Boqer Campus.

IEC (2011). *Statistical Report*. Haifa: Israel Electric Corporation.

Mathews, E.(1997). *QUICK II*. Pretoria: Transfer of Energy Mass and Momentum International (Pty) Ltd.

Mathews, E., P. Richards, C. Lombard (1994a). A first-order thermal model for building design. *Energy and Buildings* 21(2): 133-145.

Mathews, E., Shuttleworth, A. and Rousseau P. (1994). Validation and further development of a novel thermal analysis method. *Building and Environment* 29(2): 207-215.

Mathews, E., Y. Etzion, E. van Heerden, S. Weggelaar, E. Erell, D. Pearlmutter, I.A. Meir (1997). A novel thermal simulation model and its application on naturally ventilated desert buildings. *Building and Environment* 32(5): 447-456.

Meir, I.A., A. Peeters, D. Pearlmutter, S. Halassa, Y. Garb, J.M. Davis (2012). Green Building Standards in MENA: An assessment of regional constraints, needs and trends. *J. Advances in Building Energy Research* 5: 1-39.

A LOW-ENERGY INNOVATIVE SYSTEM FOR SPACE COOLING

G. Mihalakakou[1*], and H. S. Bagiorgas[1]

1 University of Patras, Department of Environmental and Natural Resources Management, 2 G. Sepheris Str., 30100 Agrinio, Greece

**Corresponding author: pmichala@cc.uoi.gr*

ABSTRACT

A lightweight aluminium nocturnal radiator, painted with an appropriate paint, was established on the roof of the Department of Environmental & Natural Resources Management in Agrinio, in Western Greece. The dynamic thermal performance of the system during summer months was calculated using an accurate mathematical model, based on the heat transferred from the air circulating inside the radiator to the ambient air. Furthermore, an extensive validation process was carried out. Thus, the experimental air temperature values at the radiator's outlet were compared with the theoretical ones and a very good agreement was achieved. The validation procedure was extended for two different radiator's paints and it was found that there is a significant impact of the paints' emissivities on the system's efficiency.

Moreover, the more effective lightweight nocturnal radiator was used to provide space cooling or pre-cooling for the building of the University. Indoor air temperature values of the thermal zone connected with the radiator were compared with those of a similar zone without any cooling system and the results demonstrated a remarkable effectiveness of the system.

KEYWORDS

Passive cooling**,** radiative cooling, sky temperature, clear sky emissivity, metallic nocturnal radiator.

1. INTRODUCTION

Passive cooling of buildings can achieve remarkable thermal comfort during summer with a great reduction of cooling loads (Givoni, 1994; Cook, 1989). Heat dissipation techniques are based on the transfer of a buildings' excess heat to a lower temperature environmental sink, as the ambient air, water, ground and sky (Santamouris and Assimakopoulos, 1996). In case the sink is the sky, heat dissipation is carried out by long wave radiation from a building to the sky (radiative cooling) (Mihalakakou et al, 1998). The sky temperature is usually lower than the temperature of the most objects on the earth, so, any ordinary surface that "sees" the sky has a net long wave radiant loss (Givoni, 1982; Mostrell and Givoni, 1982). Despite this

radiative loss, the surface doesn't obtain lower temperature throughout the 24-hour daily cycle, as the incoming solar radiation during the daytime is greater than the net long wave radiation loss. This daytime disadvantage of radiative cooling is being eliminated if the radiating surface is not the building envelope directly (as happens in so-called direct, or passive radiative cooling), but a specific radiator with a suitable heat transfer medium circulating through it at the appropriate time – nocturnal radiator (as in so-called hybrid radiative cooling) (Givoni, 1994; Cook, 1989).

In the present study, a lightweight nocturnal radiator is placed on the roof of the 10 m height building of the Environmental and Natural Resources Management Department of University of Patras, in Agrinio (Western Greece). As a first step of the construction of the metallic panel of the radiator, we use a folded long aluminium tube, painted with an appropriate white paint of high emissivity (Figure 1).

Figure 1: Metalic base with the folded aluminium tube.

Then the aforementioned tube is been pressed both to its up and down surfaces, in order to obtain a flat appearance - instead of the cylindrical shape – with a width of 1 cm in the flat sides. One end of the tube is sited at one corner of the rectangular panel formation, carrying a small fan, which – when it operates – drives air masses through the parallel tubes. The fan is connected to the power supply through a time starter, in order to operate only at nocturnal hours (10.00 pm to 06.00 am). The other end of the tube is adapted to an appropriate window opening. The use of silicon glue keeps the tube well fitted to the window opening. The air mass through the radiator loses heat by convection to the metallic surface above, becomes cooler and finally is transferred into the building's interior, in an office of the university building, driven by the fan.

The above mentioned procedure has been repeated once more for the construction of a similar radiator panel, but, this time, the paint used has a higher emissivity. Finally, two similar radiator panels are ready to be used and the only difference between them is in their optical properties.

The main objectives of the present paper is primarily to present, describe and analyse an experimental performance of a metallic nocturnal radiator placed on the roof of University of Ioannina, in Agrinio, Greece, and secondly to compare the experimental data with the ones calculated using a mathematical model able to simulate the thermal performance of the radiator. Moreover, the cooling potential of the nocturnal radiator was investigated during the present research as the radiator was connected to the building of University and it was used to cool a specific thermal zone. Thus, the feasibility and the effectiveness of the cooling system was investigated and analysed.

2. MODELING OF THE NOCTURNAL RADIATOR

The dynamic thermal performance of the nocturnal radiator has been calculated using an accurate mathematical model. Modelling of water and air based radiators for cooling purposes can be considered to be quite similar with that of water-based solar collectors (Santamouris and Assimakopoulos, 1996; Mihalakakou et al, 1998; Ito and Miura, 1989).

The convective heat exchange due to wind, q_{win}, between the radiator and the ambient air is given by the following expression (Santamouris and Assimakopoulos, 1996; Mihalakakou et al, 1998):

$$q_{win} = h_{win}(T_r - T_a) \quad (1)$$

where h_{win} is the convective heat transfer coefficient and T_r and T_a are the radiator and ambient absolute temperatures respectively (K).

The convective heat transfer coefficient h_{win} is a function of the wind velocity v and, in case of nocturnal radiator with no wind screen, is calculated from the following expressions:

$$h_{win} = 5.7 + 3.8v \quad if \ v < 4ms^{-1}$$

$$h_{win} = 7.3v^{0.8} \quad if \ v > 4ms^{-1}$$

The radiative heat flux of the radiator to the sky could be incorporated into the "ambient" heat flux q_{amb} of the radiator, which includes both convective and radiative heat flux and is calculated by the following formulation:

$$q_{amb} = h_e(T_r - T_{th}) \quad (2)$$

where h_e is an effective heat transfer coefficient and T_{th} is the threshold absolute temperature.

The effective heat transfer coefficient h_e can be calculated as follows:

$$h_e = h_{win} + h_{rad} \quad (3)$$

In the previous expression h_{rad} is the radiative heat transfer coefficient, given by the following expression:

$$h_{rad} = 0.00000022\tau\varepsilon T_a^2 \quad (4)$$

where τ is the infrared transmittance of the wind screen (if there isn't any wind screen, then: τ = 1), ε is the infrared emissivity of the radiator plate and T_α is the absolute ambient temperature (K)

Generally, threshold temperature or stagnation temperature, (T_{th} in K or θ_{th} in ºC), is the temperature a surface will drop to without any heat being added to the surface. In case of the nocturnal radiator is the minimum stagnation temperature the radiator can achieve, constrained to be no less than 1ºC below the ambient dew point temperature.

Threshold temperature θ_{th} (ºC) can be calculated using the following formula:

$$\theta_{th} = \theta_a - 0.00000005\sigma(1-\varepsilon_s)\frac{\theta_a^4}{h_e} \quad (5)$$

where θ_α is the ambient temperature (ºC) and ε_s is the sky emissivity.

Sky emissivity ε_s was calculated using the clear sky emissivity ε_{cs}, with a correction factor c which is used in case that the sky isn't clear and there is cloudiness (Clark, 1981):

$$\varepsilon_c = c\varepsilon_{cs} \quad (6)$$

If sky is clear, then c=1. Many different long wave radiation parameterization methods have been used in order to calculate clear sky emissivity ε_{cs} (Brutsaert, 1975;

Berdahl and Martin, 1984). The Swinbank formula (Swinbank, 1963) was used in the present research, as ε_{cs} is dependent only from the ambient temperature:

$$\varepsilon_{cs} = 9.36.10^{-6} T_a^2 \quad (7)$$

The outlet temperature θ_{out} (^{o}C) of the flowing air (when the air exits the tube) can be calculated by the following equation (Ito and Miura, 1989):

$$\theta_{out} = \theta_{th} + (\theta_{in} - \theta_{th}) e^{-\frac{UA}{mc_p}} \quad (8)$$

where θ_{in} is the inlet temperature of the heat transfer fluid (^{o}C), U is the overall heat transfer coefficient between the fluid circulating under the radiator and the ambient air (W m^{-2} K^{-1}), A is the surface of the radiator plate (m^2), m is the mass flow rate (kg s^{-1}) and c_p is the specific heat of the fluid (J kg^{-1} K^{-1}).

For the specific characteristics of the radiator, Eq. (8) is transferred to the following formulation (Santamouris and Asimakopoulos, 1996):

$$\theta_{out} = \theta_{th} + (\theta_{in} - \theta_{th}) e^{-\frac{Uw}{1173zu}} \quad (9)$$

where w is the width of the radiator plate (m), z is the height of the duct (m) and u is the air velocity of the circulating air under the radiator plate (ms^{-1}). The overall heat transfer coefficient U can be calculated by the overall thermal resistance R as:

$$U = \frac{1}{R} \text{ (W}^{-1}\text{ m}^2\text{ K)}$$

The overall thermal resistance R is the combination of individual thermal resistances (Kreith and Bohn, 1986): $R = R_r + R_e + R_a$ [R_r is the resistance of the radiator plate, given by: $R_r = \frac{d}{k}$, where d is the thickness of the radiator plate (m) and k is the radiator's thermal conductivity (k=236 Wm^{-1}K^{-1}), R_e is the effective resistance: $R_e = \frac{1}{h_e}$ and R_a is the resistance between the circulating air and the radiator: $R_a = \frac{1}{h}$, where h is the corresponding heat transfer coefficient between the radiator and the circulating air under the radiator].

Finally, the overall heat transfer coefficient U can be calculated using the following expression:

$$U = \frac{1}{\frac{1}{h_e} + \frac{1}{h} + \frac{d}{k}}$$

The heat transfer coefficient h can be determined from the values of hydraulic diameter D_h and the air velocity u of the circulating air into the tube.

The hydraulic diameter D_h can be calculated as follows (Santamouris and Asimakopoulos, 1996):

$$D_h = 2w[z/(w+z)].$$

3. RESULTS AND DISCUSSION

During the validation process the obtained experimental data were compared with those calculated with the mathematical model presented in Chapter 2 (theoretical ones) and this process was carried out for two similar radiators, painted with paints of different emissivities, in order to investigate the impact of different materials' optical parameters on the system efficiency. This procedure was performed for a quite long

experimental period, in order to achieve safe results. During these time intervals, temperature at the radiator's outlet was monitored continuously with a self-recorded sensor, placed at the exit of the tube. After the validation process, in order to estimate the cooling effect of the radiator with the most efficient paint, the indoor temperature of the office connected with the radiator was monitored, as well as the temperature of a neighbouring office with the same structural and size characteristics, without any cooling system in operation.

Figure 2a shows the temporal variation of hourly theoretical and experimental air temperature values at the outlet of the radiator painted with a paint of emissivity 0.71, for the hours of the radiator's operation (nocturnal hours). The hours in the horizontal axis of the diagram are the nocturnal hours only (from 10.00 pm to 06.00 am), so the first 9 hours on the axis, from 1 to 9 are the nocturnal hours of the first randomly selected day (from the 25th of August at 10.00 pm to the 26th of August at 06.00 am), the next 9 hours from 10 to 18 are the corresponding nocturnal hours of the second selected day etc. As shown, the calculated values perform well with the experimental ones for every time interval of this 10-days demonstration. Figure 2b also shows the temporal variation of hourly theoretical and experimental air temperature values at the outlet of the radiator painted with a paint of emissivity 0.93, for the hours of the radiator's operation (nocturnal hours). The time interval presented in the horizontal axis is a randomly selected 10-days period, where there is a great agreement between theoretical and experimental values and this agreement was achieved for the whole set of measured and theoretical data, as well. The comparisons of the experimental air temperature values at the radiator's outlet with the calculated ones, for both paints, for the whole time of the each radiator's operation (10 days) showed an excellent agreement in both occasions, while the linear regression analysis confirmed this observation (R^2 = 0.9648 and R^2 = 0.9766 for the paints of 0.71 and 0.93 emissivities, respectively).

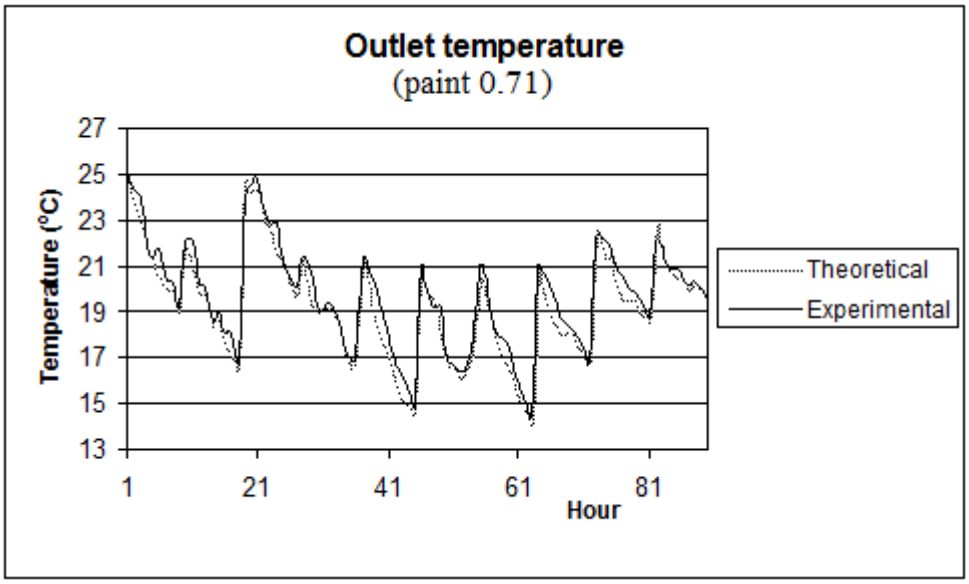

Figure 2a: Temporal variation of the measured (experimental) and calculated (theoretical) air temperature values at the radiator's exit for 10 selected days, when the radiator is painted with a paint of emissivity 0.71.

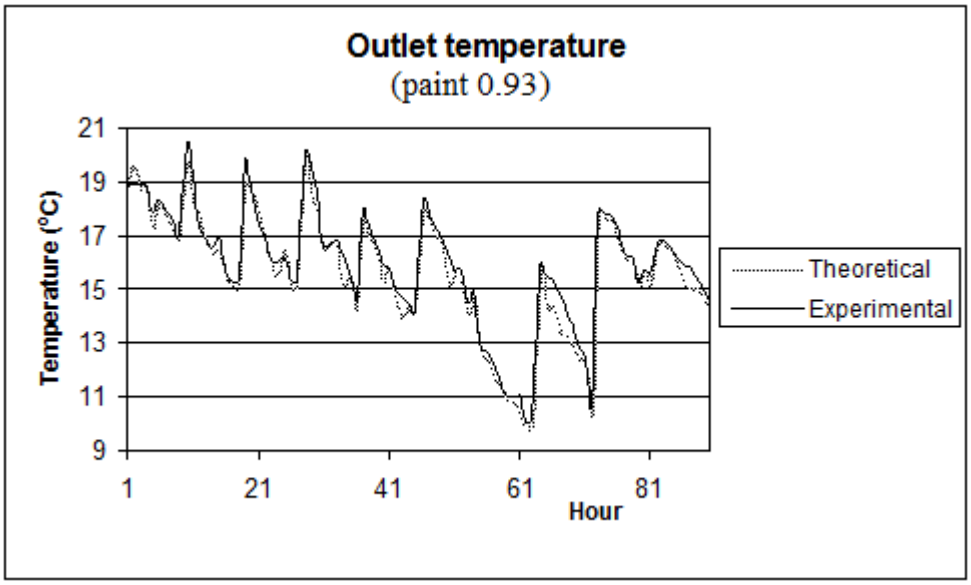

Figure 2b: Temporal variation of the measured (experimental) and calculated (theoretical) air temperature values at the radiator's exit for 10 selected days, when the radiator is painted with a paint of emissivity 0.93.

Tables 1a and 1b presents analytically the correlation coefficient values for the theoretical and experimental temperatures for each day of the experiment particularly, for both radiators. These high values ($0.959278<CC<0.988345$ for the paint with emissivity 0.71 and $0.957786<CC<0.986548$ for the paint with emissivity 0.93) also demonstrate the strong agreement between them in both occasions.

Table 1a. Correlation coefficient of theoretical and experimental data (paint 0.71)

Day	CC
1	0.974169
2	0.977206
3	0.959278
4	0.959417
5	0.979823
6	0.977007
7	0.988345
8	0.959616
9	0.960218
10	0.967170

Table 1b. Correlation coefficient of theoretical and experimental data (paint 0.93)

Day	CC
1	0.958693
2	0.978610
3	0.977582
4	0.966045
5	0.986137
6	0.978473
7	0.967282
8	0.961923
9	0.986548
10	0.957786

From the presented results, two essential conclusions can be extracted:

a. the radiator with the paint of 0.71 emissivity is less "effective" in the achievement of lower temperatures than the radiator with the paint of 0.93 emissivity. As shown in Figures 2a and 2b, the differences between theoretical and experimental values at lower temperatures are greater for the radiator with the less emissive paint. So, for the 0.71 paint these differences are: 0.43, 0.41 and 0.42 ^{o}C at the 18th, 45th and 63rd hour respectively (Figure 2a), when for the paint 0.93 these differences are: 0.28, 0.20 and 0.29 ^{o}C at the 18th, 45th and 63rd hour respectively (Figure 2b).

b. there is a better agreement between theoretical and experimental temperatures for the radiator with the more emissive paint: $R^2 = 0.9648$ for the radiator with the 0.71 paint and $R^2 = 0.9766$ for the radiator with the 0.93 paint.

The above mentioned analysis shows that the emissivity of the radiator have significant influence on the system's efficiency.

Afterwards, the air cooled by the nocturnal radiator was transferred as ventilation into an office of the experimented building in order to provide space cooling. The radiator used is the one with the more effective paint (0.93). The indoor air temperature inside the ventilated office was monitored during the experimental period on a 24-hour basis. Moreover, the indoor air temperature of a neighboring office, with similar orientation, construction and internal gains elements, was measured on a 24-hour basis too, in order to estimate the system cooling capacity. During the experimental period there was not any cooling system operated in that second office.

Figure 3 shows the 24-hour temporal variation of the indoor air temperature values at both rooms, the room connected with the nocturnal radiator and that not equipped with any cooling system for 5 randomly selected days – 120 hours (from the 15th of September at 10.00 pm to the 20th of September at 10.00 pm).

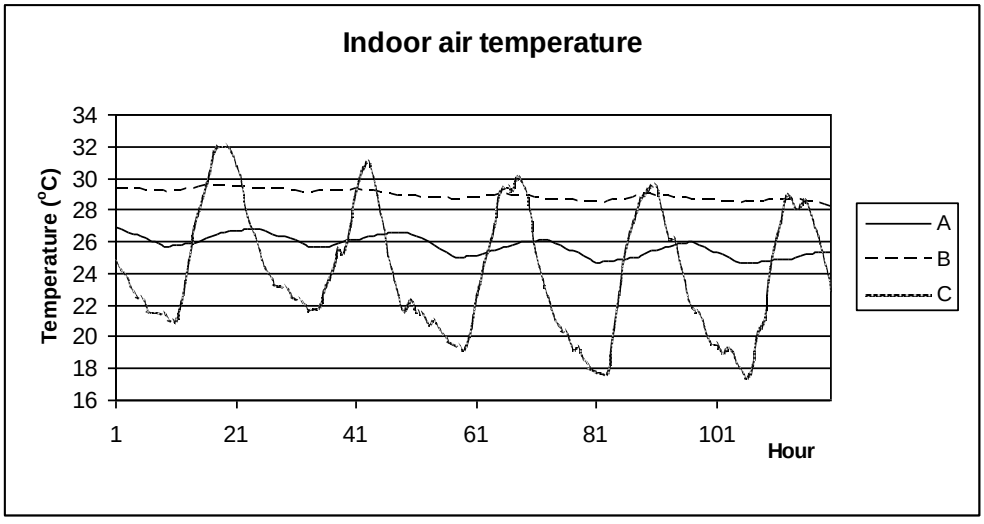

Figure 3: Temporal variation of the indoor air temperature values at both rooms, the room connected with the nocturnal radiator (A), and that not equipped with any cooling system (B) for 5 randomly selected days of the experimental time period (from the 15th of September at 10.00 pm to the 20th of September at 06.00 am), and ambient temperature for the same period (C).

As shown, the temperature difference between the two rooms fluctuated between 4 ºC at the late nocturnal hours, to 2.5 ºC at daily hours. This daily temperature difference is remarkable, despite the fact that the radiator doesn't operate and is due to the thermal inertia of the building. Especially, for every night this difference take its

highest value at the last observation (at 06.00 am), when the fan still operates and the ambient and the radiator outlet temperature take its lowest values. At the presented 5-day period, this peak (at 06.00 am) difference increases as the temperature difference between the indoor temperature of the room without any cooling system and the radiator outlet temperature increases. This conclusion is clearly depicted in Table 2, which shows numerically these temperature differences at the "peak" hours (06.00 am).

Table 2. Indoor and outdoor temperature differences

Hour	T_{room2}-T_{amb} (^oC)	T_{room2}-T_{room1} (^oC)
9	7.69	3.41
33	7.42	3.36
57	9.07	3.53
81	10.60	3.79
105	10.46	3.75

T_{room1} = temperature of the room connected with the radiator (^oC)

T_{room2} = temperature of the room not equipped with any cooling system (^oC)

T_{amb} = ambient temperature (^oC)

Similar results were achieved for the whole experimental period. Thus, the nocturnal radiation system could be effectively used in order to remarkably reduce the energy consumption for space cooling.

4. REFERENCES

Berdahl, P. and Martin, M. (1984). Emissivity of clear skies. *Solar Energy*, 32(5), 663-664.

Brutsaert, W. (1975). On a derivable formula for long-wave radiation from clear skies. *Water Resources Research*, 11(5), 742–744.

Clark, E. (1981) *Passive/hybrid comfort cooling by thermal radiation*. Proceedings of the International Passive and Hybrid Cooling Conference. Miami Beach, FL, pp. 682-714.

Cook, J. (1989). *Passive Cooling*. MIT Press.

Givoni, B. (1982). Cooling by longwave radiation. *Passive Solar Journal*, 1, 131-150.

Givoni, B. (1994). *Passive and Low Energy Cooling of Buildings*. New York: John Wiley and Sons.

Ito, S. and Miura, N. (1989). Studies of radiative cooling systems for storing thermal energy. *ASME Journal of Solar Energy Engineering*, 111(3), 251-257.

Kreith, F. and Bohn, M. (1986) Principles of heat transfer. New York: Happer & Row.

Mihalakakou, G., Ferrante, A. and Lewis, J.O. (1998). The cooling potential of a metallic nocturnal radiator. *Energy and Buildings*,28(3), 251–256.

Mostrell, M. and Givoni, B. (1982). Wind screens in radiant cooling. *Passive Solar Journal*, 1, 229-238.

Santamouris, M. and Asimakopoulos, D.N. (1996). *Passive Cooling of Buildings*. London: James & James.

Swinbank, W.C. (1963). Longwave radiation from clear skies. Quarterly Journal of the Royal Meteorological Society, 89(381), 339-348.

DOUBLE FACADES: COMFORT AND VENTILATION AT AN EXTREME COMPLEX CASE STUDY

Wim Zeiler, Joep Richter and Gert Boxem

TU Eindhoven
Den Dolech 2
Eindhoven, Netherlands
w.zeiler@bwk.tue.nl

ABSTRACT

In a Dutch project the double façade became an integral part of the ventilation concepts aa well as the heating system by trying to optimize the heat gain within the cavity during spring and autumn. The study shows how variable facade parameters influence the energy flows coming through the facade, in order to optimize the indoor environment for the comfort of the individual occupant. How can the facade make optimal use of the free incoming energy flows to maximize the comfort level of the individual building occupant at minimal energy use? The type of façade described as a second skin façade is characterised by a single glass layer on the outside and an isolated façade layer on the inside. The application of the single glass layer as a second skin around the insulated layer results in an air cavity between these two layers of around 0.9 m. The property that distinguishes a second skin façade from other DSF is that it relies on natural ventilation of the cavity, in comparison to other facades which use mechanical systems to induce the airflow. The advantage of merely using natural ventilation in the façade cavity is the lower energy consumption. However, it also results in some unresolved issues which require further attention. The researched was focussed the behaviour of the highly complex shaped second skin facade of a Dutch office building, and its thermal comfort impact on the building user. During 3 weeks different measurements were done to determine the main characteristics of the glass and the cavity of the facade. A key difference between a second skin facade, as well as other climate facades, and more traditional opaque facades is its dynamic behaviour. DSF have several adjustable properties, such as the shading device and ventilation mode, and because various physical processes take place in the air cavity, these facades can show very dynamic behaviour. In case of a second skin facade this dynamic behaviour is especially of interest since its cavity airflow merely relies on temperature differences and wind effects to induce the ventilation in the cavity, resulting in very limited control and highly erratic behaviour. The complex form of the facade in combination with the large atrium and exhaust only ventilation of the offices in the case study led to a problematic thermal indoor environment.

KEYWORDS

Please provide a maximum of five keywords which reflect the content of the paper

1 INTRODUCTION

A building envelope is critical to the energy performance and comfort of its occupants. As more buildings are becoming better insulated, lesser energy in the nearest future would be needed to counter excessive gains/losses through the envelope(Kalmar and Kalmar 2012). However, there is a shift towards the impact of the glazed area of building envelopes on energy consumption and comfort (Tsikaloudaki et al 2012). From the energy and comfort perspective, glazed components of a building's façade can act as both the strongest and weakest element (Clarke et al 1998). Although glazed areas of building envelopes are not the only factors that influence both physical and physiological comfort of building occupants, its

influence on both energy consumption and physical comfort becomes significant when building occupants due to innate need to be in contact with nature (Boyce et al., 2003)are situated close to the glazed surface area for extended periods. The interior surface temperature of glass, the most commonly used glazing material due to its thermal properties is highly susceptible to changes in the outdoor weather and compared to other opaque elements of the building façade, is a lot more vulnerable to energy flows (Tsikaloudaki et al., 2012). Variations in outdoor weather conditions influences the interior surface temperature of glass significantly affecting the radiant heat exchange between an occupant the environment (Arens et al., 2006).

The façade of a building is one of its most distinct features, defining not only a buildings aesthetics, but also separating the indoor environment for the outdoor climate as a large part of the building shell. As a result of this, a façade strongly affects the comfort level and energy use of a building. Improving the performance of the façade is therefore aspired in order to further improve the quality of a buildings indoor environment while also reducing its energy consumption. In modern buildings the facade is often considered as part of the climate system, since its performance greatly affects the indoor climate and thus comfort and energy use. The second skin principle offers excellent possibilities to improve the comfort level and energy use of existing buildings, by applying the second skin to its current facade.

In today's modern architecture, highly glazed envelopes are a common feature of non-residential buildings and for more efficient control of energy gains through glazing components on the facade of adequately insulated building envelopes, various active façade building systems have been proposed (Altan et al., 2009). One of the common systems available in practice today is the naturally controlled double skin façade system which relies on the stack effect. The potential of this system lies in the possibility of obtaining a dynamic behaviour by creating a naturally ventilated air-gap between two glazed layers with the possibility also to locate a shading device within the gap to protect against direct solar radiation(Serra et al., 2010). In recent years a good deal of research has been done on the energy performance of the double skin façade (Pappas and Zhai 2008, Hashemi et al. 2010, Gratia and de Herde 2007, Jiru and Haghighat 2008, Saelens et al. 2008, de Siva and Gomes 2008, Chan et al. 2009, Jini et al. 2011, Lou et al. 2012),

For efficient control of heat flux through the glazing into the building interior in temperate climates, the air flow through the cavity should be high in summer but low in winter. However due to dependence on environmental wind conditions, in practice large mechanical systems have to compensate for excessive gains or occupants would have to tolerate some level of discomfort due to varying radiant temperature resulting from varying glass surface temperatures. In the design of building control strategy in temperate climates regions as that in the Netherlands, designers often only consider the effect of extreme weather changes in winter and summer but little attention is placed on the periods in-between this extremes such as autumn and spring with rapid frequent variations in outdoor weather conditions. In highly glazed building envelopes this frequent changes in the outdoor climate may affect the radiant temperature, which has a major influence on thermal comfort(Dong et al 2010).

Despite all these positive effects associated with the application of the second skin façade to buildings, sometimes realized applications are linked with comfort problems (Lyons 2000. Poirazis 2006, Hwang and Shu 2011, Joe et al 2013) The inducement for this study originates from a building in the Netherlands, displayed in Fig. 1. Occupants of this building complained about the quality of the indoor environment, especially the thermal environment. It was discovered that the behavior of the applied second skin was not in accordance with its design,

and the presumption is made that this could be the cause of a part of the comfort complains. Considering all the positive and negative implications associated with a second skin facade made it a very interesting subject for further study.

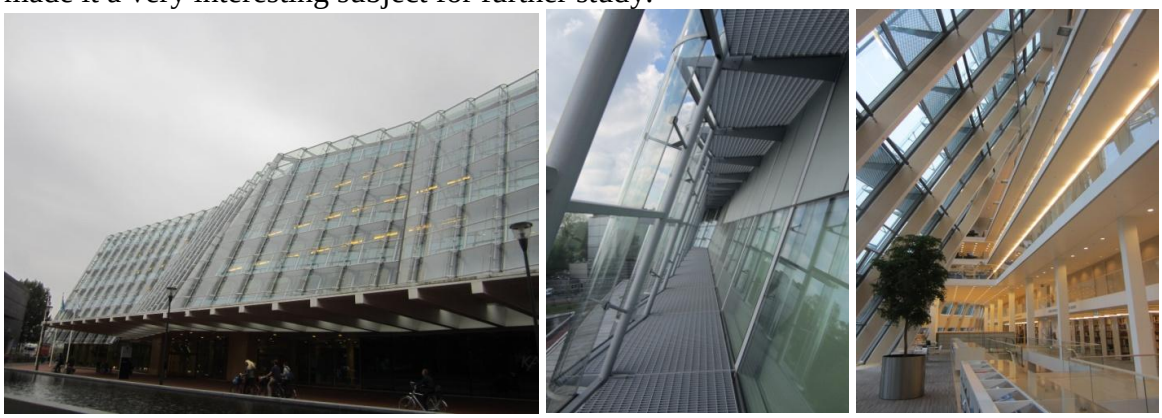

Figure 1: Outside of the façade, the cavatity of the DSF and the atrium behind the DSF

In subsequent sections of this paper, preliminary results from measurement obtained from a modern naturally controlled highly glazed office building in the Netherlands is presented. The impact of frequent variations in the outdoor weather , particularly the effect of direct solar radiation and daylight on occupants working near the glass façade is discussed.

2 MEASUREMENTS

During a period of nearly two weeks, from April 5th till April 17th 2013, the temperatures within the cavity were measured as well as the indoor solar radiation in the horizontal plans as well as parallel to the window. The surface temperatures (T_s) of both sides of both panes are measured in one line and not too close to the window frame. The different sensors that are used for the measurements can be found in table 1. Since the measurements continue for one week, the data is stored with data loggers. Two different data loggers are used. One data logger is used for the parameters that are measured in the office space and one for the parameters that are measured in the cavity and outside the building. This data logger has a wireless connection with transmitters that are connected to the sensors, which makes it possible to station the data logger inside and the sensors and transmitters outside and in the cavity.

Table 1: Sensors used by measurements

Parameter	Sensor	Accuracy
Temperature	NTC thermistor Sensor data DC 95	calibrated sensitivity
Solar radiation	Pyranometer (CM5 and CM11)	1 %
Air velocity	Dantec 54R10	calibrated sensitivity

The air temperatures (T_a) in the cavity are measured at three levels: 2nd floor, 3th floor and 4th floor. The pyranometer and air temperature sensor to measure the outside conditions are placed on appropriate positions on the roof, where there are no obstructions. The air temperatures inside are measured at 0.5 m from the façade at a height of 1.10 m. The air velocities are measured on the same positions as the air temperature at 0.5 m from the façade at a height of 1.10 m. The horizontal radiation asymmetry (T_{ra}) is measured at 0.5 m from the façade at a height of about 1.1 m and the vertical radiation asymmetry is measured at the same distance from the façade at a height of about 1.1 m. The solar radiation inside is measured vertically at a minimum distance of the façade, see Fig. 2 and for the set-up Fig. 3. The

airflow through the outlet grills at the top of the cavity were measured as well as the air flow through the open windows on the 4th floor, see Fig. 4

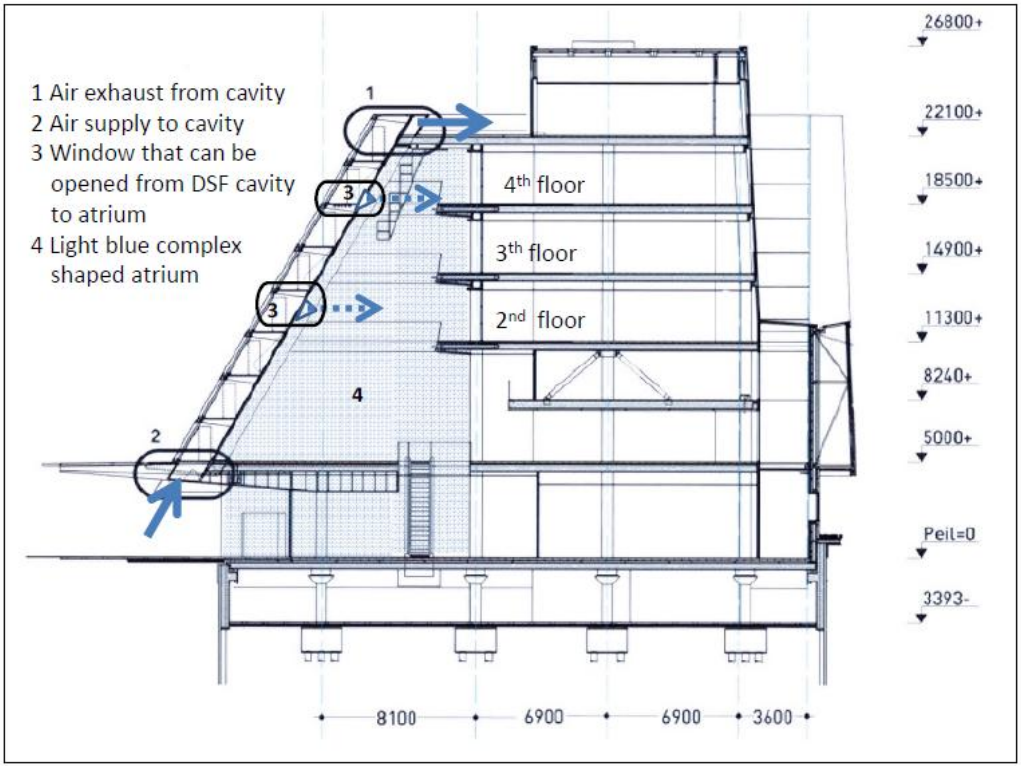

Figure 2: The schematic representation of the ventilation supply from the cavity to the atrium

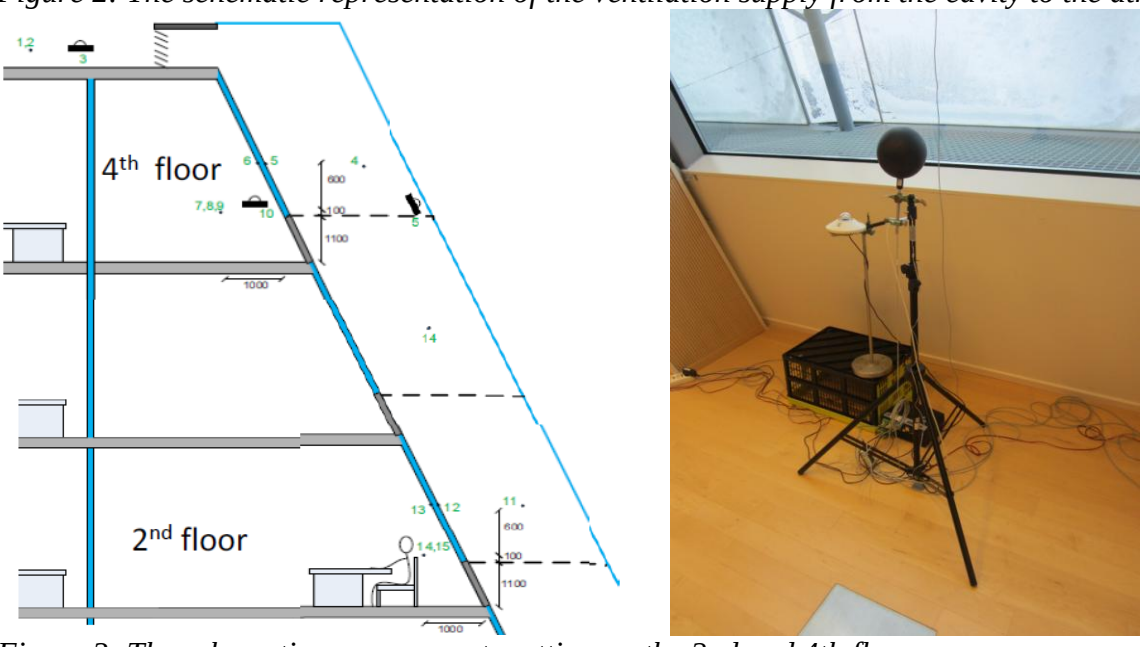

Figure 3: The schematic measurements setting on the 2nd and 4th floor

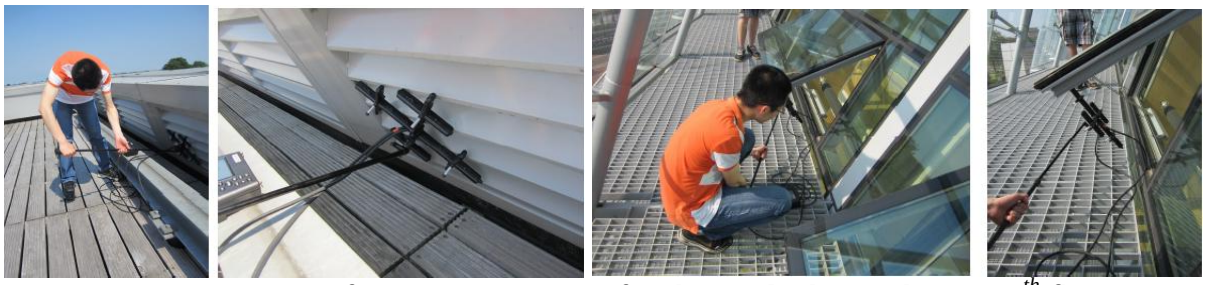

Figure 4. Measurements of air quantities at roof outlets and inlet windows on 4th floor

3 QUESTIONNAIRE

In addition to the field measurements a questionnaire was held in the case building, which was aimed at determining the actual comfort that was perceived by the building users. In this questionnaire several comfort issues were addressed, including thermal comfort. The main purpose of the questionnaire was to establish the perceived comfort by the building users, and to determine whether there were differences between different floors and locations in the building. The building occupants at the second, fourth, and fifth floor were asked to fill out the questionnaire. The second and fourth floor both adjoin the second skin facade, whereas the fifth floor does not. By distinguishing between different floors it is possible to determine if there are differences present in the comfort perception of the building users at the floor near the top of the facade. Finally, a distinction between the building users near the second skin facade and the rest of the building user was made, in order to see if there are differences present. In the questionnaire the users were asked about several comfort aspects during both winter and summer conditions. For the response to the above stated topic a 7-point scale was applied, allowing the subjects to give a rating to each of aspects. Although there was still a difference present between these scales, which require a short explanation because a distinction between ambiguous and unambiguous voting scales is present in the questionnaire. For the unambiguous aspects (thermal comfort) the highest score lies in the extremity of the voting scale, whereas for ambiguous aspects (sensation) this lies in the middle of the voting scale. The distribution of the responses of the questionnaire is provided in table 2.

	1	2	3	4	5	6	7	
Comfortabel	☐	☐	☐	☐	☐	☐	☐	Oncomfortabel
To hot	☐	☐	☐	☐	☐	☐	☐	Too cold

Figure 5. Example of two aspects on the 7-point scale.

Table 2:The distribution of the questionnaire respondents

Total participants	*78*	**<20 year**	*1*
Male	*49*	**20 – 30 year**	*9*
Female	*28*	**31 – 40 year**	*10*
2nd floor	*36*	**41 – 50 year**	*26*
4th floor	*34*	**51 – 60 year**	*28*
5th floor	*10*	**>60 year**	*6*

4. RESULTS

4.1 Measurements air flows

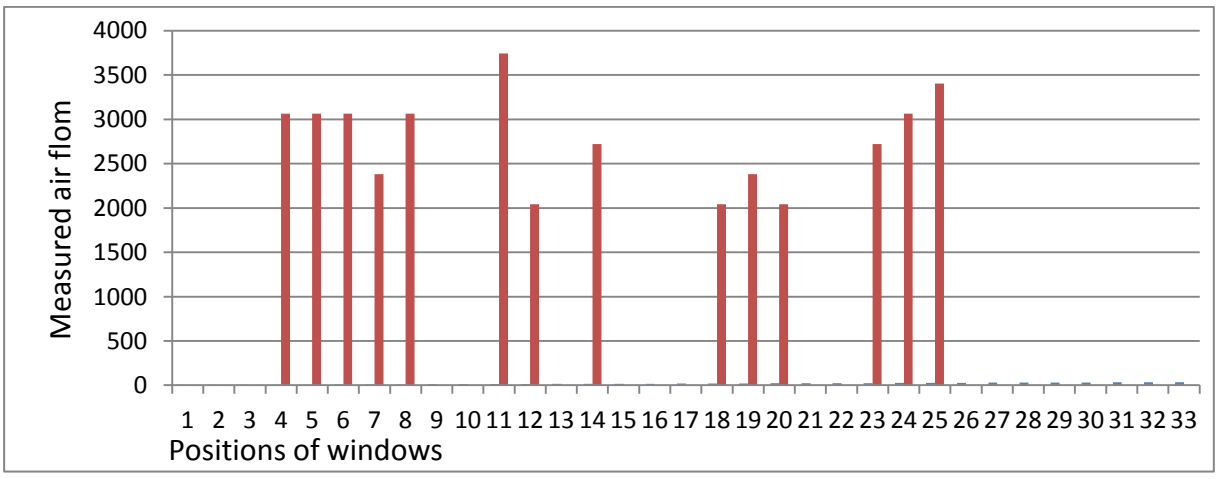

Figure 6. Measured air flow through the windows in the cavity on the 4th floor

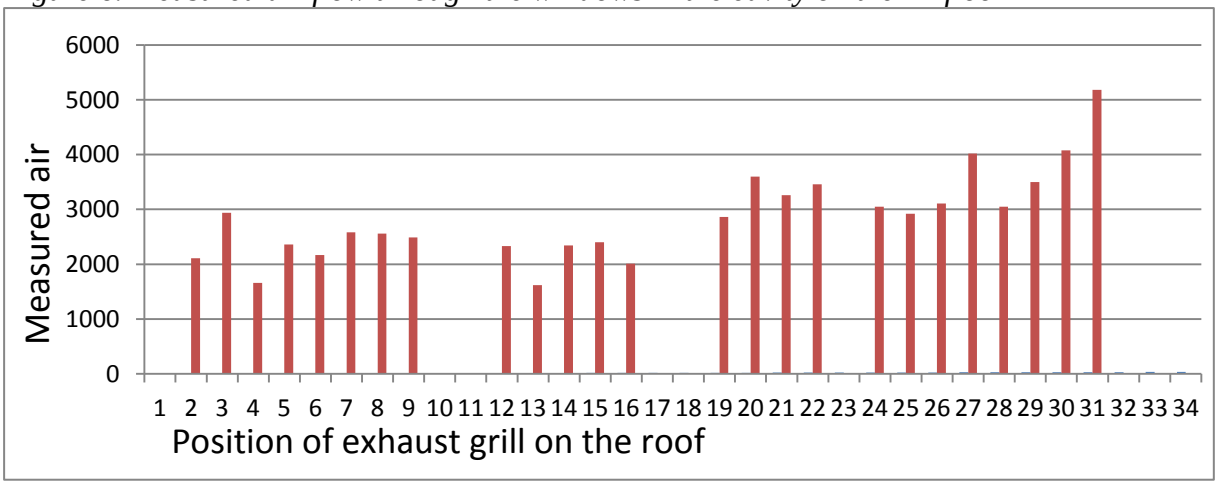

Figure 7. Measured air flow through the exhaust grilles in the cavity on the roof

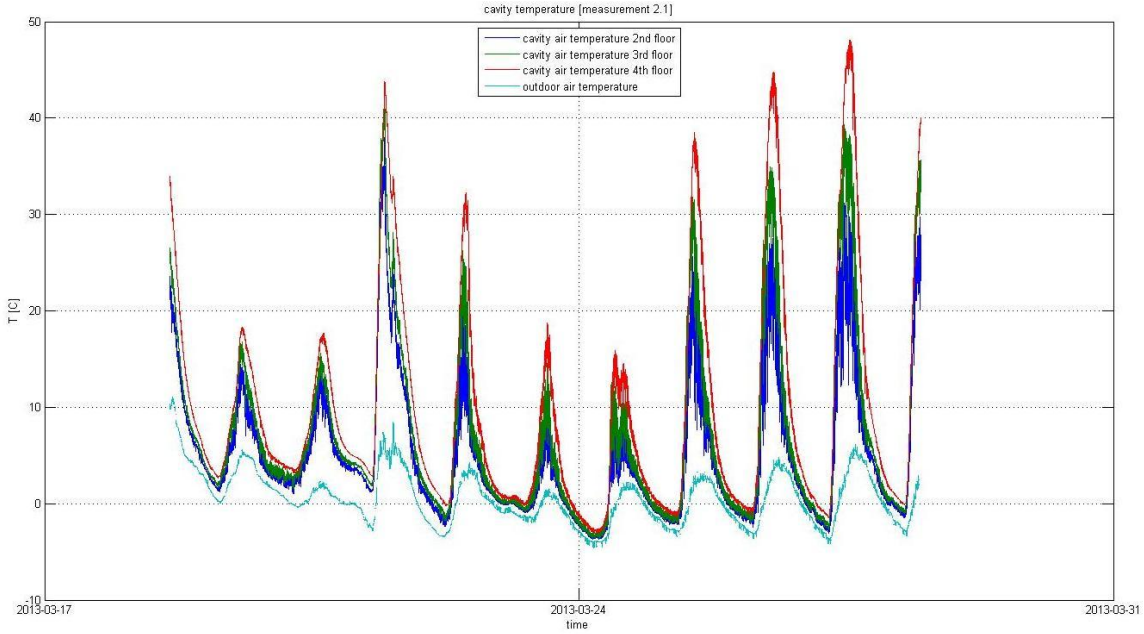

Figure 8. The increase in cavity temperature on the 2nd, 3rd, and 4th floor in comparison to the outdoor temperature of the second measurement period.

Important is the cavity temperature increase due to the solar radiation and the fast changes to the thermal indoor conditions for the occupants. The correlated dissatisfaction between radiant temperature and air temperature is presented in Fig. 9. The lines represent the range of perceived thermal comfort (Lusden and Freymark 1951).

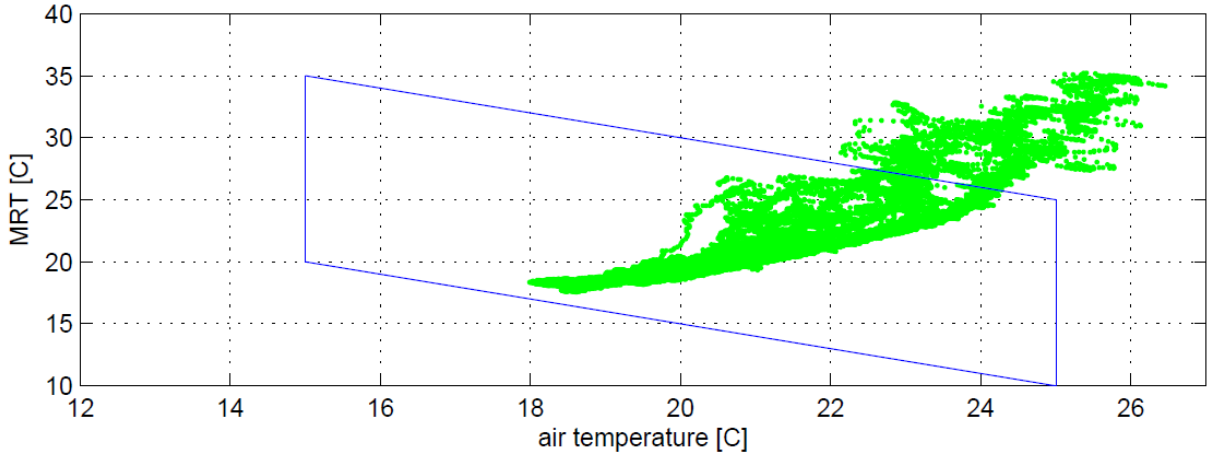

Figure 9: Ration between radiant temperature and air temperature of 4th floor

4.2 Questionnaire results

In figures 10 and 11, the results of the questionnaire are provided, where the figures displays the results for winter time and in summer time.

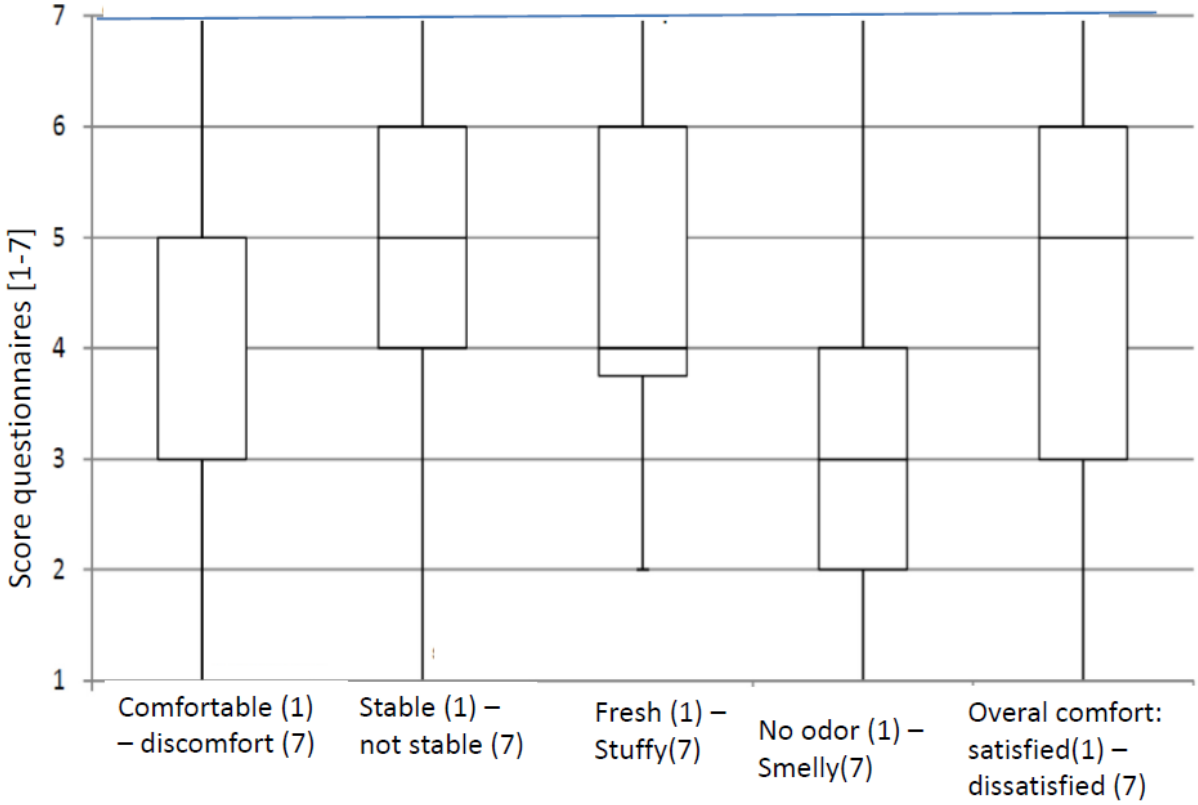

Figure 10: Results questionnaires perceived indoor air quality aspects in winter

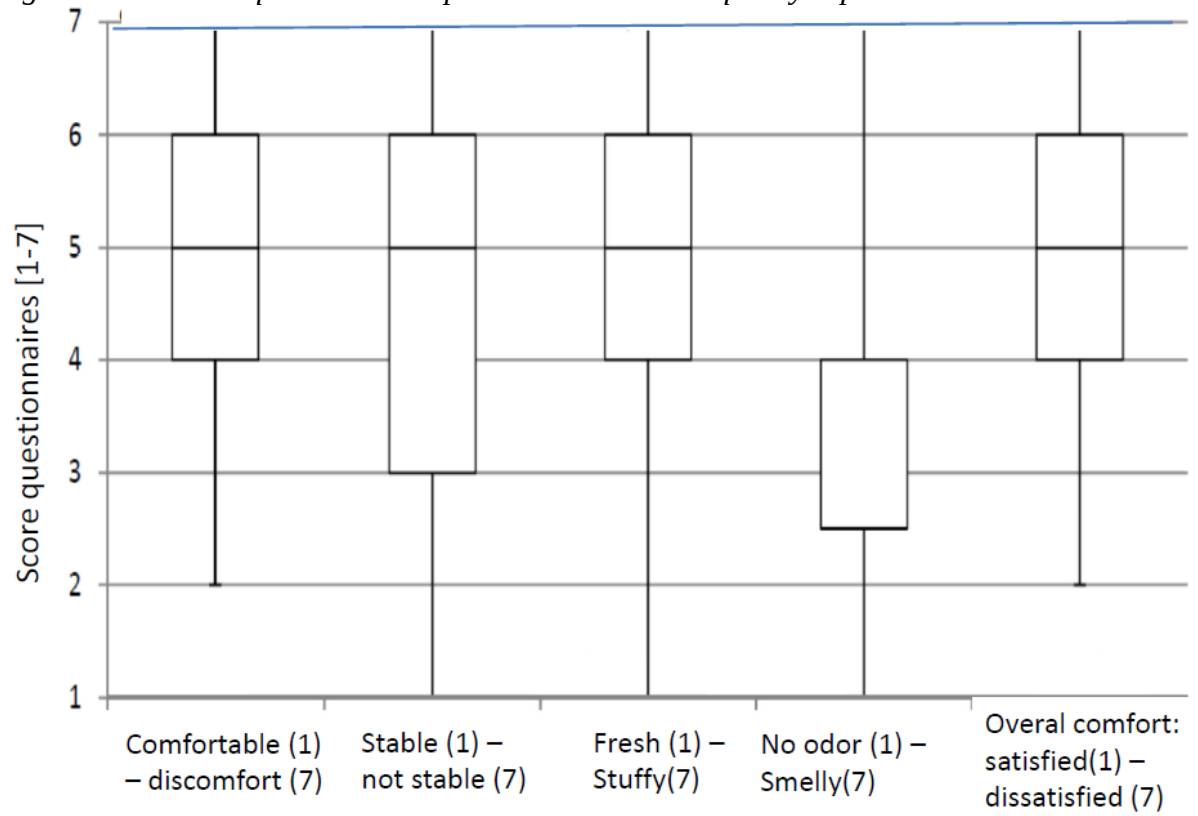

Figure 11: Results questionnaires perceived indoor air quality aspects in summer

4 CONCLUSIONS

The real behaviour of air flows within the cavity of a double façade and within the building itself due to ventilation from the cavity to the building is extremely complex. An important influencing factor is the fluctuations in wind strength and wind direction resulting in a stochastic fluctuation of the wind pressure, see the measured air volume in Fig. 6 and 7. Due to the complex shape of the building there was quite a difference in the air volume through the windows and outlet grills on different positions, see Fig. 12.

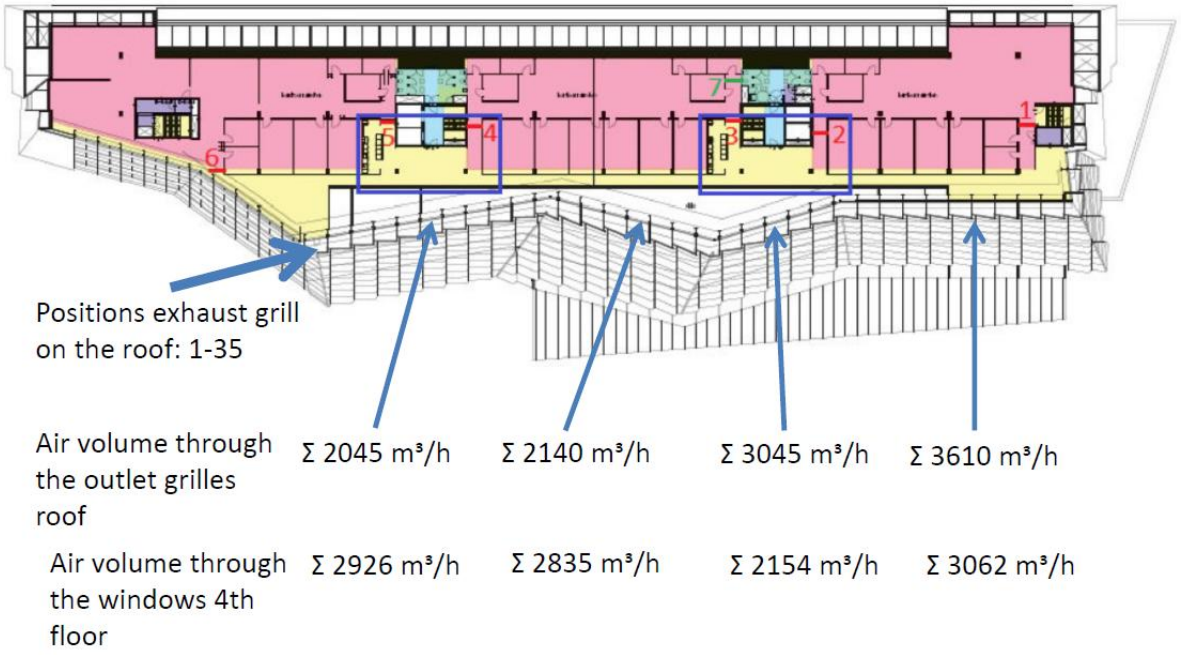

Figure 12: The different air flows through windows and outlet grilles

As a result the air flow inside the cavity of the examined building was restricted due to wind pressure on the outlet grilles on top of the roof. and as a result the temperature increase within the cavity over several floors was enormous. This increase was directly related to the solar radiation, see Fig. 13.

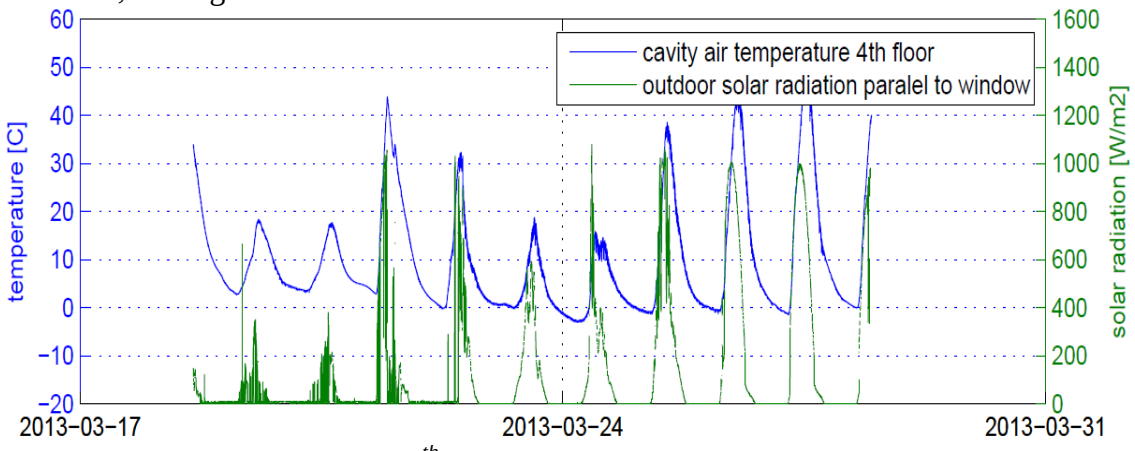

Figure 13: Cavity temperature 4th floor versus outdoor solar radiation

As a result the cooling load for the building was much higher than calculated and also the perceived thermal comfort especially in summer was rather poor. Although there are many simulation studies about the behaviour of double facades, in real live the effects of wind in combination with complex building shapes can lead to real problematic situations in practice to control and balance the ventilation is such buildings.

5 REFERENCES

Altan H., Ward I., J. Mohelnikova J., Vajkay F., 2009, An internal assessment of the thermal comfort and daylighting conditions of a naturally ventilated building with an active glazed facade in a temperate climate'. Energy and Buildings 41(1): 36-50.

Arens E., Huizenga C., Zhang H., Mattelaer P., Yu T., 2006, Window performance for human thermal comfort'. Report to the national fenestration rating council. Berkeley: centre for the built environment, university of California.

Boyce P., Hunter C., Howlett O., 2003, The benefits of Daylight through windows, Available from: http:// www.Irc.rpi.edu/programs/dayligthdivideneds/pdf/daylightBenefitd.pdf.

Chan A.L.S., Chow T.T., Fong K.F., Lin Z., 2009, Investigation on energy performance of double skin façade in Hong Kong, Energy and Buildings 41: 1135-1142

Clarke J., Janak M., Ruyssevelt P., 1998, Assessing the overall performance of advanced glazing systems'. Solar Energy 63(4): 231-241.

Dong K., Moa P., Dong H., Seung Y., Myoung S., Kwang W., 2010, Effect of MRT variation on the energy consumption in a PMV-controlled office, Building and Environment 45:1914-1922.

Gratia E., Herde A. de, 2007, Greenhouse effect in double-skin facade, Energy and Buildings 39:199-211

Hashemi N., Fayaz R., Sarshar m., 2010, Thermal behavior of a ventilated double skin façade in hot arid climate, Energy and Buildings 42: 1823-1832

Hwang R., Shu S., 2011,Building envelope regulations on thermal comfort in glass facades buildings and energy-saving potential for PMV-based comfort control, Building and Environment 46:824-834

Jini T.E., Tao Y.X., Haghighat F., 2011, Airflow and heat transfer in double skin facades, Energy and Buildings 43:2760-2766

Jiru T.E., Haghighat F., 2008, Modeling ventilated double skin façade-A zonal approach, Energy and Buildings 40: 1567-1576

Joe J., Choi W., Kwon H., Huh J., 2013, Load characteristics and operation strategies of building integrated with multi-story double skin facade, Energy and Buildings, 60:185-198

Kalmar F., Kalmar T., 2012, Interrelation between mean radiant temperature and room geometry', Energy and Buildings 55:414-421.

Lou W., Huang M., Zhang M., Lin N., 2012, Experimental and zoanal modeling for wind pressures on double-skin facades of a tall building, Energy and Buildings 54:179-192

Lusden F.P., Freymark H., 1951, Darstellung der Raumbehaglichkeit für den einfachen praktischen Gebrauch. Gesundheits Ingenieur 72(16): 271-273

Lyons P.R., 2000, Window performance for human thermal comfort, ASHRAE Transactions :594-602

Pappas A., Zhai Z., 2008, Numerical investigation on thermal performance and correlations of double skin façade with buoyancy-driven airflow, Energy and Buildings 40:466-475

Poirazis H., 2006, Double skin facades, a literature review, IEA Task 34 ECBCS Annex 43

Saelens D., Roels S., Hens H., 2008, Strategies to improve the energy performances of multiple-skin facades, Building and Environment 43:638-650

Serra V., Zanghirella F., Perino M., 2010, Experimental evaluation of a climate façade: Energy efficiency and thermal comfort performance, Energy and Buildings 42: 50-62.

Siva F.M.de, Gomes M.G., 2008, Gap inner pressures in multi-story double skin facades, Energy and Buildings 40: 1553-1559

Tsikaloudaki k., Laskos k., Theodosiou T., Bikas D., 2012, Assessing cooling energy performance of windows for office buildings in the Mediterranean zone, Energy and Buildings 49:192-199.

DOUBLE-SKIN SYSTEM OF ROOM-SIDE AIR GAP APPLIED TO DETACHED HOUSE (PART 2): SIMULATION ANALYSIS TO REDUCE COOLING LOAD THROUGH NATURAL VENTILATION IN WALL

Togo Yoshidomi[1], Shinsuke Kato[*2], Kan Lin[3], and Kyosuke Hiyama[4]

1 Graduate School of The University of Tokyo
7-3-1, Hongo, Bunkyo-ku,
Tokyo, Japan

2 IIS, The University of Tokyo
4-6-1 Komaba, Meguro-Ku,
Tokyo, Japan
**Corresponding author: kato@iis.u-tokyo.ac.jp*

3 Graduate School of The University of Tokyo
7-3-1, Hongo, Bunkyo-ku,
Tokyo, Japan

4 Yamaguchi University
1677-1, Yoshida, Yamaguchi-shi,
Yamaguchi, Japan

ABSTRACT

In Japan, wooden detached residential houses are common; the wood components within a wall may undergo decay because of condensation in the wall or flushing defects, which can be a concern. The temperature distribution throughout the house, such as a high temperature in the attic space, can cause discomfort to the occupants. A double-skin system of room-side air gaps is considered to be an effective technique to handle these problems. In this system, during the summer, the airflow driven by natural ventilation moves through the room-side air gap in the wall and removes heat load from the inner surface of the insulation material or from the surface adjacent to the rooms inside. Although this system has been applied to many houses, further study on the design specifications for parts of the ventilation route is still required. In this study, airflow network simulation was carried out using TRNFlow to evaluate the performance of this system under different conditions. A standard residential house model was simulated by considering conditions of summer. On the basis of the results, it was verified that the total airflow rate exhausted from the rooftop vent fluctuates with the ambient temperature; the flow rate distribution in different walls was also determined. Sensitivity analysis was performed on each part of the ventilation route with different opening areas; the opening area of the wall was found to have more effect than the rooftop and base vents on the total amount of airflow. When wind is blowing outside, the total flow rate increases. When there is no wind outside and the windows are closed, this system reduces the cooling load of an ordinary detached house by 15.5%.

KEYWORDS

Double-skin system, Detached house, Simulation, Natural ventilation, Cooling load

1 INTRODUCTION

In Japan, wooden detached houses, which have a wooden structure and insulation material, are popular. However, several problems are associated with this type of house. In the summer, a temperature distribution can be caused by heat from solar radiation. In the winter period, if the house is not sufficiently airtight, moist air leaking from the room is cooled by the outside air, and condensation occurs in the wall. This condensation may cause the wooden structure to decay. To remove moisture in the wall, vent layers are now often installed outside the insulation material to exhaust the moisture, and Hokoi (Hokoi, 2011) has done measurements and calculations.

The double-skin system of a room-side air gap, which places the vent layer inside the insulation material, has also been applied to detached houses. The air gap extends to envelope

the entire house, and ventilated air can move freely in the gap. The airflow pattern in the air gap differs in the summer and winter. In the summer, air vents at the top of the roof and sides of the base are opened to introduce and discharge outside air. When the air in the air gap is heated by solar radiation and rooms inside the wall, an upward driving force is generated because of buoyancy. Thus, a flow is induced where outside air is introduced through vents at the base; it moves upward through the wall and flows out through the roof. This airflow discharges heat in the wall and attic space while being cooled by the ground under the floor, so the rooms are kept at a comfortably moderate temperature and. In the winter, all of the vents are closed to increase thermal insulation and air circulation in the air gap.

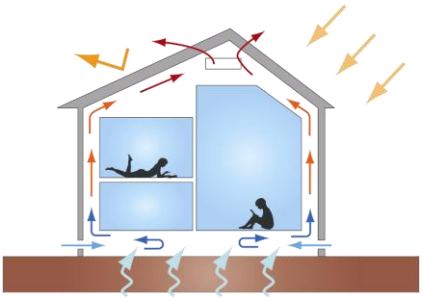

Figure 1: Double-skin system of room-side air gap applied to detached house

Although some houses in Japan have been built using this system for about 30 years, few studies have examined the system in detail. Ozaki et al. measured temperature and humidity in the air gap in wall of an experimental house during the summer rainy season.

However, there have been no studies on how to obtain sufficient airflow and the effects of introducing this system. With respect to the airflow rate, quantifying the effects of the air gap specifications and outside disturbances is necessary. With regard to the air gap specifications, both the opening areas with the smallest cross-sections in the air gap and the leakage area of the entire house are considered. Since the smallest cross-sections in the air gap can play a major role in determining the overall ventilation resistance of the entire air gap, the airflow rate may get affected if different opening areas are used for these parts. If the leakage area is increased, infiltration of the air gap, rooms, and outside air will increase, and the airflow rate of the original route will decrease. With regard to outside disturbances, external wind was considered. The effect of external wind seems to depend on the relationship between the vent position and the wind pressure coefficient distribution of the outer wall surface along with the wind speed and direction. With respect to the effect of introducing the system, quantifying the effect on the thermal environment is necessary. This can be confirmed by verifying that the natural room temperature and air-conditioning load decrease during the summer period when this system is introduced. When air-conditioning is on, some of the cooling air supplied by the air-conditioner will be ejected outside by the airflow, so the air-conditioning load might actually increase. Therefore, examining the effect on the load reduction due to the shortened air-conditioning time is also necessary.

This study aimed to determine the basic properties of the double-skin system of a room-side gap during the summer through the simulation of a ventilation network. We created two building models in which spaces in the air gap and rooms of the house were treated as individual nodes. The impact of each element on the airflow rate was estimated, and the effect of introducing this system was simulated. For the airflow rate, a sensitivity analysis was performed on the opening area of each airflow resistance part by using a building model without infiltration. The results show the relationship between the airflow rate and different opening area patterns. For the external wind, the impact on the airflow rate was examined under several conditions. The effect of infiltration on the airflow rate was estimated by comparing a model of a general detached house with infiltration to the model with no infiltration. For the introduction effect, the natural room temperature for the middle of summer was calculated using the model with infiltration, and the decrease in the natural room temperature was estimated when the system was used. We calculated the air-conditioning load using the same model and compared it to the result for the case when there was no airflow in the wall. Preventing condensation inside the wall by considering the humidifying capacity of the wall is outside the scope of this study.

2 METHODS

2.1 Simulation Software

To calculate the airflow in the air gap, we used the unsteady energy calculation software TRNSYS17 and its add-on program TRNFlow. TRNFlow is based on COMIS3.1, which is a ventilation network calculation software that can iteratively solve the movement of air and heat simultaneously on TRNSYS. We used this software to solve the airflow in the air gap.

2.2 Building Models

We used the standard house model (fourth region) proposed by IBEC, Institute for Building Environment and Energy Conservation, to represent a standard detached house in Japan. This model has two stories and a total floor area of 120.07 m^2. A family of four people is supposed to live in there. Schedules for the occupants, lighting, equipment, ventilation, and air-conditioning were based on the survey results. We set up the dimensions and basic configuration of the building according to this model.

We modeled the air gap, which may significantly affect the calculation of airflow in the wall, as follows. In figure 3, the area of the air gap where air moves around is represented in blue. Grooves are placed at equal intervals on the surface of the insulation used in the walls; these grooves ensure that openings between the insulation and other components do not impede airflow. The air gap can be divided into several zones by the resistance parts such as vents or these openings, where the flow path is narrower than other parts. For the TRNFlow calculations, we modeled the air gap by defining this zone as "air node" and defining the resistance part as "air link." For each air link, the relationship between the mass flow rate and pressure difference was calculated according to equation (1). In equation (2), which is the common formula for ventilation, the value of C_s for each air link was determined by fixing α to 0.6, which is a typical value, and determining the opening area A of the air link from the actual specifications of the house. The value of n was determined to be 0.5 from the correspondence between formula (1) and equation (2).

$$\dot{m} = C_s \cdot (\Delta p)^n \tag{1}$$

$$\dot{m} = aA\sqrt{2r \cdot \Delta p} \tag{2}$$

m□: Δp mass flow rate [kg / h], α: pressure difference [Pa], C_s: flow coefficient [-],
A: opening area [m2], ρ: air density [kg/m^3]

In this study, two building models with different air link networks were created: a "simple model" that does not consider infiltration and a "detailed model" that does. In the simple model, the leakage of air into the rooms or outside air from the air gap is not considered; a simple network that connects the air gap to the outside air was created, as shown in figure 4 and 5. This model can be used to estimate the potential maximum airflow generated by buoyancy ventilation without depending on the amount of infiltration. However, because heat from solar radiation and internal heat cannot be discharged by infiltration, the calculated room temperature may be higher than the actual environment. On the other hand, the detailed model considers infiltration between air nodes; the network is shown in figure 6. The typical C-value of this house was assumed to be 2 cm^2/m^2; values for surfaces were allocated to the walls, openings such as windows and doors, and the ventilation equipment. The allocation percentage was determined by referring to the measured data of a general detached house. This model is suitable for calculating the room temperature and air-conditioning load because its approach considers the actual environment. However, the results calculated with this model depend on the size and distribution of the opening areas.

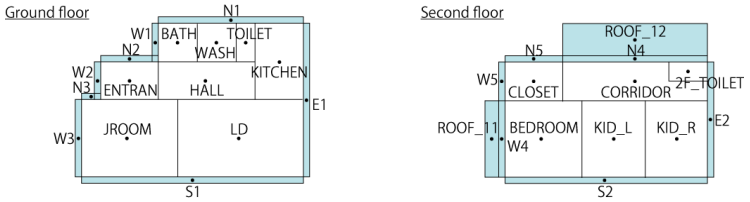

Figure 2: Zones and air nodes of the building model in TRNSYS

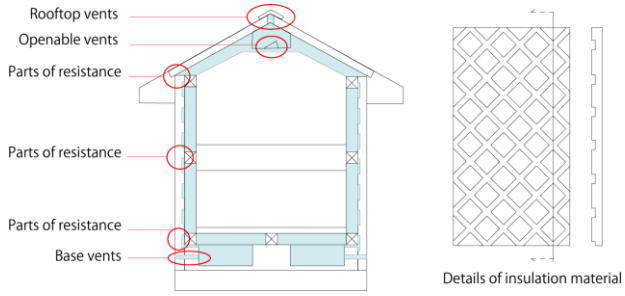

Figure 3: Overview of air gap and insulation material

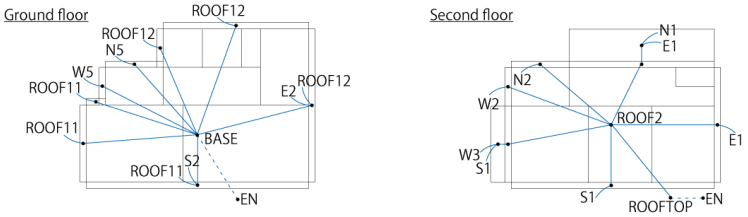

Figure 4: All air links set in TRNFlow (simple model)

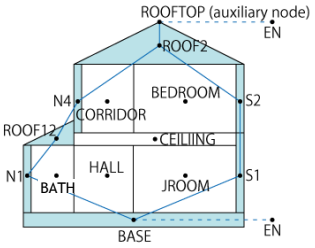

Figure 5: Overview of air links (simple model)

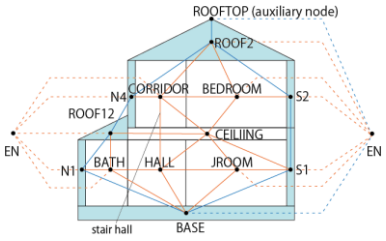

Figure 6: Overview of air links (detailed model)

Table 1: Calculation conditions for building

Wall of external side	Extruded polystyrene foam 50 mm + Air layer 15 mm + Tile 10 mm
Wall of internal side	Gypsum board 13 mm
Air gap thickness	120 mm
Roof	Extruded polystyrene foam 50 mm + Air layer 30 mm + Plywood 10 mm + Slate 5 mm
Base	EPS 50 mm + RC150 mm + EPS 50 mm
Internal wall, Ceiling, Floor	U = 3.125 W/m^{2}K, 4.082 W/m^{2}K, 4.082 W/m^{2}K
Window	Double-glazing U = 1.8 W/m^{2}K, Shading coefficient = 0.5
Infiltration	None

Table 2: Calculation conditions for air gap

Opening area A [m^2]	Openings in the wall	0.00299 m^2/m (opening area per unit length wall)
	Roof vents (Vents at the rooftop)	0.0919
	Roof vents (Mechanical opening/closing unit in the attic space)	0.0755
	Base vents	0.0720
Constants		$\alpha = 0.6$, $\rho = 1.2$, $n = 0.5$

Table 3: Opening areas of infiltration (detailed model)

Opening areas of whole house1	Total floor area	120.07 m^2	
	C-value	2 cm^2/m^2	
	Opening area of whole house	240 cm^2	
Allocation of opening areas	Structure	94 cm^2	39%
	Opening	67 cm^2	28%
	Ventilating facilities	79 cm^2	33%
	(contains local ventilation)	64 cm^2	27 %
	(contains overall ventilation)	15 cm^2	6 %

2.3 Calculation Conditions

The calculation conditions are listed in Tables 4–8. To examine the airflow rate, two sensitivity analyses were carried out on the airflow rate for different opening areas of resistance parts and different external wind conditions. To examine the properties of the airflow rate, the simple model was used in these analyses. Table 4 lists the cases for the opening area. Eleven cases were calculated; the values of the opening areas for three elements—walls, rooftop vents, and base vents—were multiplied by 5 or 0.5. To examine the external wind, wind pressure coefficients C_p around the rooftop and base vents were set according to the specifications listed in Table 5. Each C_p value was determined using the average value, obtained from literature, for the wind pressure coefficient distribution of the building surface at the portion corresponding to each vent. Because the wind pressure coefficient varies according to objects around the building, we also used wind pressure coefficients under the conditions of surrounding buildings being present or absent. Table 6 lists the cases for the external wind. When there are surrounding buildings, wind pressure

Table 4: Cases for sensitivity analysis of opening area in air gap

	Resistance in air gap	Rooftop vents	Base vents
Case 1	-	-	-
Case 2	×5	-	-
Case 3	-	×5	-
Case 4	-	-	×5
Case 5	×0.5	-	-
Case 6	-	×0.5	-
Case 7	-	-	×0.5
Case 8	-	×5	×5
Case 9	-	×0.5	×0.5
Case 10	×5	×5	×5
Case 11	×0.5	×0.5	×0.5

Table 5: Calculation conditions of wind pressure coefficients

	Vents		Wind direction			
	Location	Direction	North	East	South	West
Case 12 (with surrounding building)	Rooftop vents	North	0	0	-0.18	0
		South	-0.18	0	0	0
	Base vents	North	0	0.01	0.05	0
		East	0.05	0.1	0.05	0.03
		South	0.05	0	0	0.01
		West	0.05	0.03	0.05	0.1
Case 13 (without surrounding building)	Rooftop vents	North	-0.2	-0.25	-0.55	-0.25
		South	-0.55	-0.25	-0.2	-0.25
	Base vents	North	-0.7	-0.3	0.22	-0.3
		East	-0.4	0.6	-0.4	-0.15
		South	0.22	-0.3	0.7	-0.3
		West	-0.4	-0.15	-0.4	0.6

Table 6: Cases for sensitivity analysis of external wind

	External wind	Surrounding building
Case 1	None	N/A
Case 12	Exist	Exist
Case 13	Exist	None

Table 7: Cases for introduction effect

	Airflow	Air-conditioning
Case 21	Exist	None
Case 22	Exist	Exist
Case 23	None	None
Case 24	None	Exist

Table 8: Calculation conditions

Internal heat gain	Exist (based on schedule by IBEC)
Ventilation	None, Exist (based on schedule by IBEC)
Air-conditioning	None, Exist (based on schedule by IBEC)
Surface temperature under floor space	20℃
Weather data	Expanded AMeDAS standard data (2000) Tokyo
External wind	None, Exist (based on weather data)
Calculation period	Jul. 21–Aug. 20, Jun. 1–Sep. 30 (plus 3 days for run-up period)

coefficient is generally smaller, and the impact of wind is reduced. In case 12, surrounding buildings were considered; buildings of the same shape were assumed to be arranged according to a density with a gross building coverage ratio of 40%, which is equivalent to the most overcrowded residential area in Tokyo.

To examine the effect of introducing the system, the detailed model was used to obtain a room temperature close to that of the actual environment. Table 7 lists the cases for the introduction effect. First, the airflow rate and natural room temperature were calculated without air-conditioning. Airflow rates calculated on the basis of the simple and detailed models were compared to examine the effect of infiltration. The results for the cases with and without airflow in the wall were then compared, and the effect of lowering the natural room temperature by means of airflow in the wall was examined. The calculation for the case without airflow was performed by removing all air links from the detailed model. Finally, to calculate the air-conditioned state, the effect of reducing the air-conditioning load due to airflow in the wall was estimated. The temperature was set to 28°C, and five rooms (i.e., living room, kitchen, bedroom, and two children's rooms) were air-conditioned. This time opening of windows when ambient temperature is lower than room temperature is not considered.

The other calculation conditions that were used are listed in Table 8. The schedules for internal heat generation, ventilation, and air-conditioning were set according to the criteria of the IBEC standard. Ventilation was used only in the detailed model. The ground surface temperature under the floor space was set to 20°C on the basis of past measurement results. For weather data, including for external wind, the expanded AMeDAS 2000 standard data for Tokyo was used. The calculation periods were July 21–August 20 (plus 3 days for the run-up period) to study the airflow rate and June 1–September 30 (plus 3 d for the run-up period) to study the introduction effect.

3 RESULTS

3.1 Airflow Rate

First, the results of the representative case 1 are shown to demonstrate the basic properties of the airflow rate: airflow rate of S1, the south side wall on the ground floor, and rooftop vents (figure 2), room temperature of LD, a living-dining room on the south side (figure 5), and outside temperature during representative days (August 8– 10; figure 7). The airflow rate in the rising direction within the network is represented as a positive value. The average airflow rate during the period was 114.8 m^3/h. The room temperature changed almost simultaneously with the outside air temperature, and peak hours were the same. On the other hand, the changes in airflow rate of the rooftop vents occurred 2–3 h later than the changes in the temperature. The airflow rate of S1, which can be taken as representative of each wall, changed almost proportionally to the flow rate of the rooftop vents. We discuss the time delay in section 4. Figure 8 shows the average flow rate per unit length of wall over the period for each wall. The light-colored bar represents the ground floor, whereas the dark-colored bar represents the second floor. The airflow rate was positive throughout the wall. The average airflow rate on the ground floor was 3.14 (m^3/h)/m, and the average on the second floor was 3.80 (m^3/h)/m.

Figure 9 shows the sensitivity analysis results for the opening areas. The bar graphs represent the airflow rates of the rooftop vents. The airflow rates of case 1 and the cases where the opening areas changed by 5× and 0.5× are shown together. In cases 2–7, only one element was changed; the results were highly sensitive to changes in the wall, rooftop vents, and base vents, in descending order. The changes in airflow rate were smaller than the ratio of the changes in the opening areas. In cases 8–11, multiple elements were changed. The change in airflow rate was significantly greater when all three elements were changed (case 10); the change in airflow rate was close to the change in opening area ratio (0.54×) in case 11.

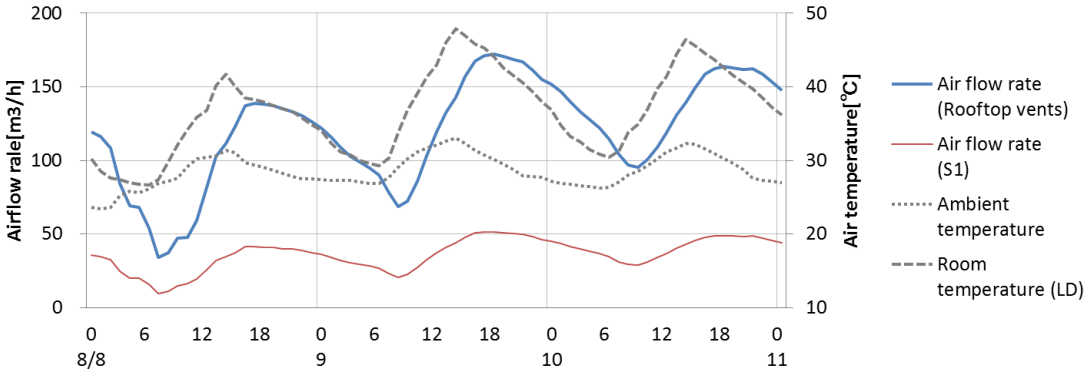

Figure 7: Airflow rate and ambient and room temperatures on representative days

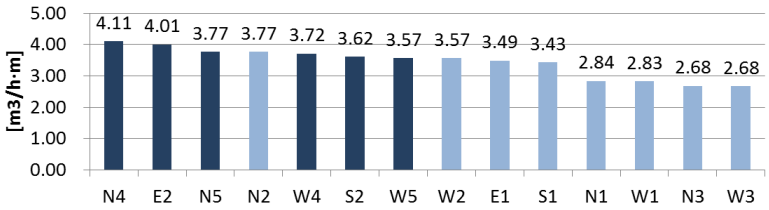

Figure 8: Airflow rate per unit length wall of each wall

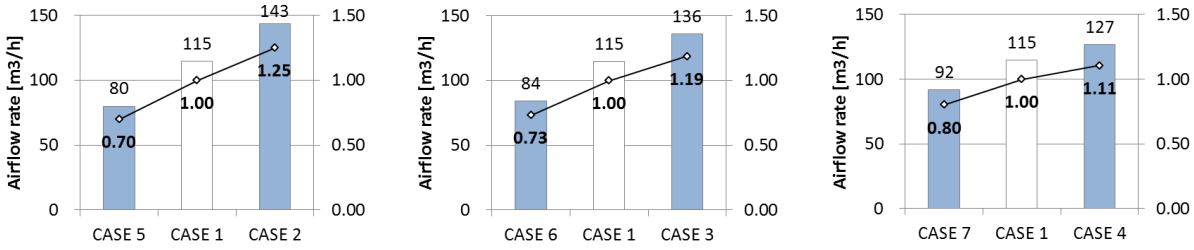

Resistance in air gap changed

Rooftop vents changed

Base vents changed

Rooftop vents and base vents changed

All three elements changed

Figure 9: Average airflow rate over period

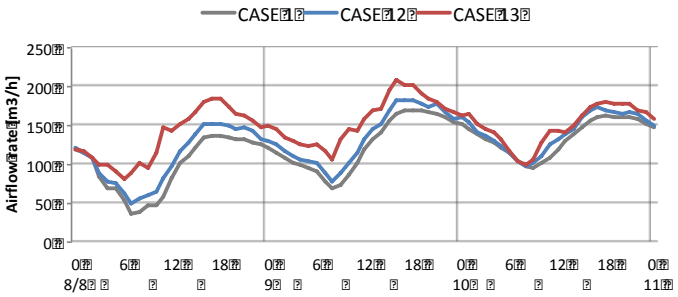

Figure 20: Airflow rate in the representative days

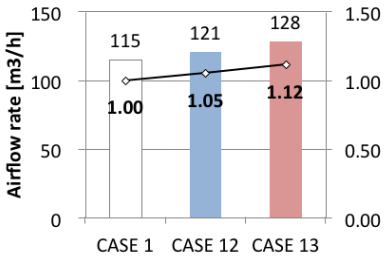

Figure 31: Period average airflow rate

Figures 10 and 11 show the sensitivity analysis results for external wind. The line and bar graphs indicate the airflow rate of the rooftop vents. Figure 10 shows the change in airflow over time during the representative days; the airflow rate fluctuated proportionally in all cases. Figure 11 shows the average airflow over the period in each case. Compared with the case of

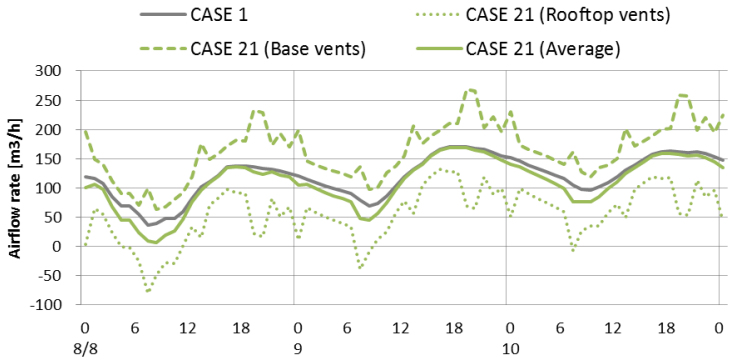

Figure 12: Airflow rate during representative days

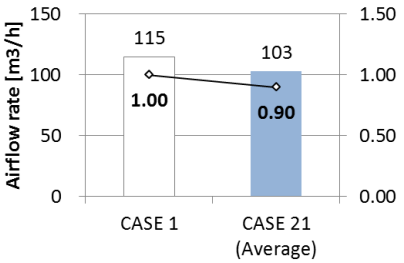

Figure 43: Average airflow rate over period

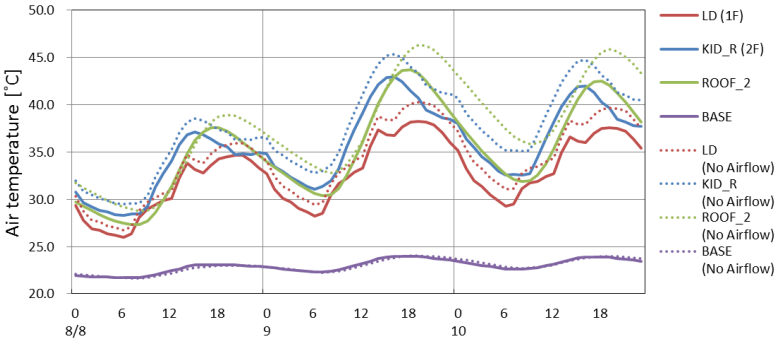

Figure 54: Natural room temperature during representative days

Table 9: Differences in average natural temperature over period by airflow in air gap

Zone	Average temperature difference
Average of 1F	-1.53
Average of 2F	-1.87
Rooftop vents (1F and 2F)	-2.43
Under floor space	1.03

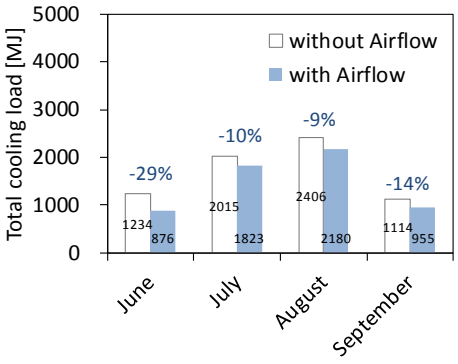

Figure 16: Total cooling load in each month

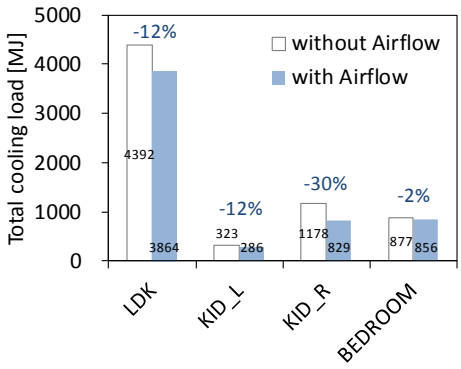

Figure 17: Average cooling load in each room over period

no wind, the average airflow increased by 5% for the case with surrounding buildings and increased a further 5% for the case with no surrounding buildings.

3.2 Introduction Effect

The detailed model that considers infiltration was used to examine the introduction effect. Figure 12 compares the airflow rates of the detailed model (case 21) and simple model (case 1) over time. In case 1, the airflow rates of the base vents and rooftop vents were equal; they are represented by a gray line. In case 21, the airflow rates of the base vents and rooftop vents were different; they are represented by dotted lines. The average airflow rates of the base vents and rooftop vents can be assumed to represent the airflow characteristics throughout the building in case 21; the change in this value over time showed properties similar to those of case 1. Figure 13 shows the average airflow over the period of both cases. For case 21, this average value was used. In case 21, when infiltration was considered, the airflow rate decreased by 10%.

The details for the natural room temperature during the representative days are given in Table 9 and Figure 14. Solid lines represent the natural room temperature for the case when there is airflow (case 21), and the dotted lines represent the natural room temperature for the case without airflow (case 23). The temperature was higher on the second floor than on the first floor. The average natural room temperature on the first floor decreased 1.5 °C with airflow, and that of the second floor decreased 1.9 °C. While the average temperature of the attic spaces for the first and second floors decreased 2.4 °C, the average under the floor space rose 1.0 °C.

Figure 16 shows the total cooling load for each month when the air-conditioning was set at 28°C. The monthly total cooling load of the whole house with airflow (case 22) and without airflow (case 24) is represented in the graph. The cooling load was reduced when there was airflow throughout the month; from June to September, it was reduced by an average of 15.5%. The reduction was large in June and September, which had low temperatures; even in August, which was the hottest month, saw the cooling load reduced by 9%. Figure 17 also shows the total cooling load for each room from June to September. The amount of reduction varied in each room; it was 2%–30%.

4 DISCUSSION

4.1 Airflow rate

Figures 7 and 8 show that the airflow rate in the representative case was uniform in each wall, and the variation in airflow over time in each wall was approximately proportional to the airflow rate of the rooftop vents. Therefore, the variation in airflow of the whole building can be represented by the airflow rate of the rooftop vents; the airflow rates were thus compared by using the airflow rates of the rooftop vents.

The flow rate of the rooftop vents changed 2-3 hours after the outside air temperature. This is considered to be due to effects that heat stored in the wall is discharged by the airflow. In other words, heat from hot outside air and solar radiation stored in the components on the outside of the air gap leads to air temperature rise in the air gap and an increase in the pressure difference between the inside and outside, and contributes to the delay of the airflow. On the other hand, it is considered that because the influence of the heat storage to the room is reduced by the airflow, room temperature changed in the same phase as the outside air temperature. Therefore, possibility of controlling the flow of heat stored in the wall into the rooms by controlling the airflow is suggested. For example, the cold heat is stored in the wall by the airflow at night, also in the morning the airflow is stopped to take the stored cold heat into the rooms, and in the afternoon the airflow is resumed to keep the stored heat by the sunlight from flowing in the room. By performing these operations, improving of the energy saving effect by the airflow can be expected.

In the sensitivity analysis of the vent opening area, the magnitude of the sensitivity of the opening areas of each portion in the air gap became clear. Although the magnitude of the sensitivity varied in cases, especially when the opening areas of all elements were changed in the same manner, the airflow rate changed significantly. The airflow rate increased 1.39 times when two elements were changed in case 8; the airflow rate increased 3.34 times when three elements were changed in case 10. When the opening area was changed to 0.5×, the airflow rate was significantly reduced by only changing one or two elements (cases 5–7, 9, and 11). This result seems to show that the flow rate of the whole air gap depends on the magnitude of the resistance at points where the airflow resistance is high. The airflow increased when there was an external wind, and the airflow became particularly large when there were no surrounding buildings. This is because the wind pressure coefficient, listed in Table 5, was lower at the rooftop vents than that at the base vents, and more work was required to draw the air out of the air gap. Since this pressure difference was higher for the case without surrounding building than for the case with them, the increase in airflow rate became larger.

4.2 Introduction Effect

The magnitude of the effect of infiltration on the airflow rate was estimated by comparing the results of the simple and detailed models (Figure 13). When the C-value was 2 cm^2/m^2 and the opening area was assumed to be allocated as listed in Table 3, the airflow rate was reduced by 10% with infiltration. The natural room temperature was lowered whenever there was airflow. While the temperature under the floor space was increased by the outside airflow, the temperature in the attic space dropped as more hot air was discharged. The introduction effect was expected to be dependent on the cooling supplied from the ground surface under the floor to the air gap. Although the ground surface temperature was set to 20°C on the basis of past measurement results, a detailed simulation of geothermal heat is necessary for future study.

When air-conditioning was used, the total period of the air-conditioning load was reduced. We should note that there was no opening of windows in this calculation. Figure 18 shows the total time that air-conditioning was active for each month. This value was reduced when there was airflow, and this trend was close to the result of cooling load (Figure 16). Therefore, the reduction in the cooling load period is mainly due to the reduction in air-conditioning time.

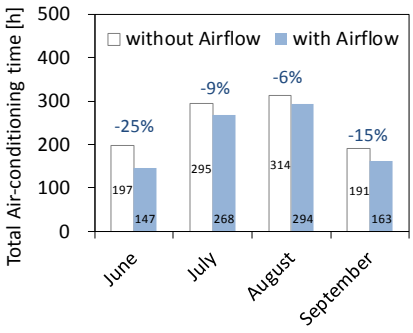

Figure 18: Total air-conditioning time in each month

5 CONCLUSIONS

We simulated a ventilation network to examine the airflow rate in the air gap and the introduction effect. In the simple model, infiltration was not considered, and it was found that the air rose uniformly in any wall surface; it was discharged from roof vents. The airflow rate changed 2–3 h after the outside air temperature. Sensitivity analysis of the opening areas in the air gap for the airflow rate showed high sensitivity to changes in the wall, rooftop vents, and base vents, in descending order. The airflow rate changed significantly when the opening areas of all three elements were changed similarly. Sensitivity analysis of the external wind effect on the airflow rate showed that the airflow rate increased in the case with an external wind compared to the case without an external wind. In particular, the case of no surrounding buildings caused the pressure difference between the inlet and outlet of the vents to increase, and the airflow rate increased significantly.

We examined the effect of introducing the double-skin system of room-side air gap by using a detailed model that considers infiltration. When this system was introduced, the natural room temperature was lowered throughout the summer compared to the case without ventilation. However, since the room temperature still exceeded the comfort zone in the summer, air-conditioning was required. The total cooling load of the period was reduced when there was airflow in the wall with air-conditioning. This effect is mainly due to the reduction in air-conditioning time caused by the drop in room temperature. The introduction effect was assumed to depend on the cooling supplied from the ground surface under the floor to the air gap, so a detailed simulation of geothermal heat is necessary for future study.

6 REFERENCES

Hokoi, S. (2011). Survey of Ventilation Volume in the Vented Air Space of Exterior Walls [in Japanese]. *Summaries of technical papers of Annual Meeting Architectural Institute of Japan, D-2,* 839-840.

Ozaki, A. (1992). Heat and water transfer through an ventilated structure using urethane panels [in Japanese]. *Summaries of technical papers of Annual Meeting Architectural Institute of Japan, D,* 945-946.

Institute for Building Environment and Energy Conservation. (2009). *Description of the energy consumption calculation method in the standards of judgment of the housing business building owners* [in Japanese]. http://ees.ibec.or.jp/documents/img/kaisetsu200903_all_ver2.pdf

Kurabuchi, T. (2009). Wind tunnel experiments on surface wind pressure and cross-ventilation flow rate in densely populated residential area: study on proper design method of locating windows aiming at utilization of cross-ventilation in densely populated residential area (part 1) [in Japanese]. *Journal of environmental engineering 74(642), 951-956*.

BUILDING ENVELOPE DESIGN FOR CLIMATE CHANGE MITIGATION: A CASE-STUDY OF HOTELS IN GREECE

Ifigenia Farrou[*1], Maria Kolokotroni[2], Mat Santamouris[3]

1 Brunel University
Howell Building, Mechanical Engineering
School of Engineering and Design
Uxbridge, Middlesex
UB8 3PH, UK
** Corresponding author: ifarrou@hotmail.com*

2 Brunel University
Howell Building, Mechanical Engineering
School of Engineering and Design
Uxbridge, Middlesex
UB8 3PH, UK

3 National and Kapodistrian University of Athens
Physics Department
Group Building Environmental Research
Panepistimioupolis, 15784 Athens, Greece

ABSTRACT

Future climate change might have a tremendous impact on energy use, ventilative cooling strategies and thermal comfort in buildings, since these parameters are strongly correlated with the external weather conditions.
This paper will present results of a study of the impact future climate change scenarios as developed by the Intergovermental Panel on Climate Change (IPPC) and implemented in weather files for specific future time slices (2020, 2050 and 2080) on the design of the external envelope of a hotel building in Greece. Three climatic regions of Greece are considered.
The impact of climate change on the building is assessed via hourly simulations using a calibrated model developed using the software TRNSYS. The model was calibrated using measured energy use data from an existing hotel building. Future climate weather files were constructed for the three climatic regions using METEONORM data and the 'morphing' method using a weather generator software (Weather Generator v1).. The heating and cooling loads (kWh/m^2/yr) of the building are calculated using monitored climatic data for the years 1970-2010 and future climatic files for the years 2020, 2050 and 2080. Two modes of buildings are studied: a. all year operated, and b. seasonally operated. The effectiveness of the most energy efficient techniques is investigated for the three climatic zones of Greece via a parametric study. The climate change mitigation strategies examined are described by the principles: 'blow away' (intelligently controlled night and day ventilation), 'switch off'; (shading), 'reflect' (cool materials) 'reflect and switch off' (glazing), 'switch off & absorb' (insulation) and 'convection' (ceiling fans). For each principle, a parametric analysis was carried out to define the 'optimum' buildings in each climatic period.
Results indicate an increase of the cooling load by 15% in year 2020, 34% in year 2050 and 63% in year 2080. On the other hand heating load is expected to decrease by 14% in year 2020, 29% in year 2050 and 46% in year 2080.
It was found that different strategies can be applied to all year and seasonally operated buildings for the most energy efficient performance. These include:
a. For all year operated buildings: high levels of insulation, double low e glazing, intelligently controlled night and day ventilation, ceiling fans and shading. The building of year 2050 would need more shading and the building of year 2080 would need additional shading and cool materials.
b.For seasonally operated buildings: Intelligently controlled night and day ventilation, cool materials, ceiling fans, shading and double low e glazing. Only the building of year 2080 would need insulation.

KEYWORDS

Climate change, generation of future files, morphing method, mitigation strategies, degree days

1 INTRODUCTION

Future climate change is defined by an increase in the Greenhouse Gas emissions (GHG) and in turn in the global mean temperatures (IPPC 2011; European Environment Agency 2004). The evaluation of the climate change is uncertain since the climate process is not totally predictable and the socio-economic development is a complex procedure. However, using projections of greenhouse gas emissions in the future, several scenarios have been modeled combining possible future CO_2 concentration and social-economic development in order to predict possible increase of mean temperature. The main aim of these scenarios is to achieve stabilization of the GHG concentration in the future.
The main objective of this paper is to assess the impact of the climate change on the energy demand of a hotel building using real climatic data and future climate change scenarios as developed by the Intergovernmental Panel on Climate Change (IPPC) and implemented in weather files for specific future time slices (2020, 2050 and 2080) on the design of the external envelope of a hotel building in Greece.

2 LITERATURE

The energy use in buildings is correlated to the external temperature. As this relation is non-linear, the method of the degree days is used to calculate the energy consumption of buildings according to the variations of the external temperature. (Ch. Giannakopoulos et al 2009; Committee for the Study of the Climate Change Impact 2011; CIBSE 2006a; Cartalis et al 2001; Tselepidaki et al 1994). Accumulation of a large number of degree days above the base temperature indicates intense need for cooling whereas accumulation of a large number of degree days below the base temperature implies intense need for heating. The differences in the cumulative numbers of CDDs and HDDs between the reference and the future period show the changes in the energy demand of buildings.
It is predicted that due to the climate change and the increase of the air temperature, more cooling will be required in the Mediterranean countries. The increase in cooling requirements will be larger over Southern Spain, the Eastern parts of Greece, Western Turkey and more so over Cyprus/North Africa. Until now, the increase of the cooling requirements in Greece is correlated to the increased use of air-conditioning and the associated problems of supply of electric power during the peak periods (i.e. blackout) and the sick -building syndrome.
On the other hand, the heating requirements will be decreased during all seasons, especially spring and winter. Continental areas of Europe like Northern Spain, central Italy, Greece and Turkey will require less heating. (Ch. Giannakopoulos et al 2009; Committee for the Study of the Climate Change Impact 2011).
Many studies focus on simulations using projected future files in order to predict the impact of the climate change on the building energy use. (Oxizidis et al 2008; Eames et al 2012; Guan 2009; Guan 2012; Mark F. Jentsch et al 2008, Kolokotroni et al 2012, Giannakidis, G et al 2011). In the literature four methods appear for the preparation of future weather data, these include: the extrapolating statistic method, the morphing procedure based on the imposed offset method, the stochastic weather model and global climate models. The comparison and analysis of these four methods conclude that the ‘morphing’ method is the one most reliable for building simulations (Belcher, Hacker, and Powell 2005; Guan 2009).

3 METHODOLOGY

The impact of the climate change is computed by modelling a hotel building. The building is a real building and is located in climatic zone B of Greece. The simulations are carried out using the software TRNSYS. The impact of the climate change is assessed a. for the period 1970 – 2010 using real climatic data for the area of Athens, provided by the Hellenic National Meteorological Service and b. for the years 2020, 2050 and 2080 using generated future files

for Patra (climatic zone B), Thessaloniki (climatic zone C) and Iraklio of Crete (climatic zone A). Future climate weather files are constructed for the three climatic regions A,B and C using METEONORM data and the 'morphing' method using a weather generator software (Weather Generator v1).Then climate change mitigation strategies are defined for an optimum building envelope design for climatic zone B. The effectiveness of these strategies is also assessed for the climatic zones A, C of Greece. It is found that different strategies can be applied to all year and seasonally operated buildings for the most energy efficient performance

3.1 Description of the simulated building

The hotel building taken into consideration is located in Peloponese, in the Loggos area, 7.5 klm away from the city of Aegio, and west of Athens (Greece). Its construction dates back to 1972. The hotel offers 115 rooms, reception area, restaurant and kitchen facilities, lounge with bar, and one meeting room. The hotel operates from April to October and occasionally, during the heating period, i.e. during the Christmas holidays. The hotel is a freestanding building and located next to the sea. The building has a rectangular layout with the main facades facing northwest and southeast.

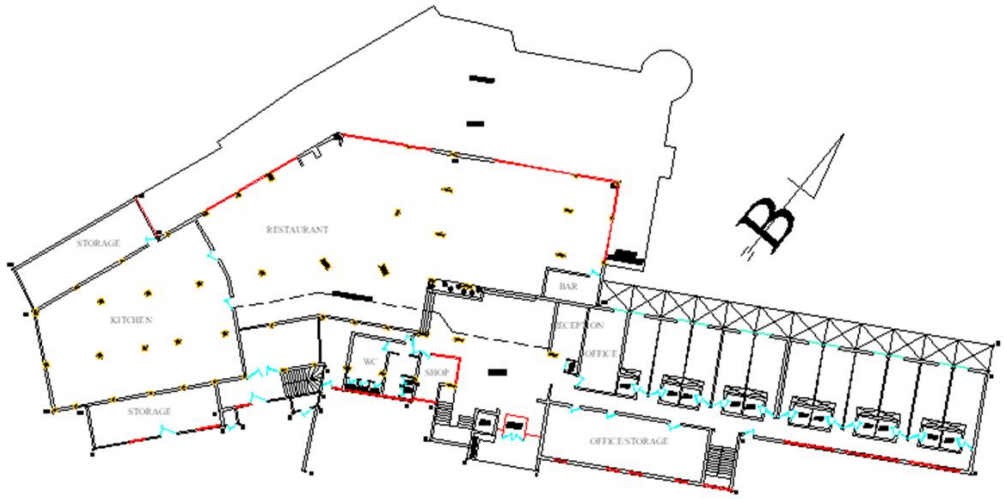

Figure 1 Ground floor

The building elements have no insulation and the u-values do not comply with the national legislation EPBD (Table 1).

Table 1: U-values of the building elements considered in the simulations

Building element - U-value (W/m^2K)	**Typical U values for constructions before 1979 TOTEE 20701-1/2010 ppg 46/47)**	**Required u-value (TOTEE 20701-1/2010) for climatic zone B (ppg 43 table 3.3a)**
External wall: Plaster – brick – plaster, with plaster externally & internally	2.20	0.50
External wall-concrete frame, with plaster externally & internally	3.40	0.50
Roof: Plaster - concrete – plaste	3.05	0.45
Floor (concrete slab) to external air	2.75	0.45
Ground floor : concrete slab	3.10	0.90
Windows (glazing & frame)		
Common areas: single with aluminum frame	Ugl:5.68	3.00

	Ufr: 7.00	
Corridors to the rooms (facing south): double with aluminum frame	Ugl: 2.95 Ufr: 7.00	3.00
Beds: single with wooden frame	Ugl:5.68 Ufr: 2.20	3.00
Infiltration	0.44ach (according to the Technical Guidelines TOTEE 20701-1/2010)	

The building systems of the hotel building are shown in Table 2:

Table 2: Building systems of the hotel building

Building systems of the hotel building	
Heating	Central heating is with gas via radiators and operates in the rooms and the common areas of the hotel. Central heating operates occasionally during the heating period, when the hotel is open, i.e. during the Christmas period. (Design temperature 20°C)
Cooling	A/C split units in each room. There is no cooling in the common areas. (Design temperature 26°C)
Ventilation	All areas of the hotel are naturally ventilated via openable windows. No mechanical ventilation is installed in the main areas of the hotel.
DHW	Flat plate solar collectors are used for DHW
Airflow rates	Common areas: 9 m3/h/m2, Rooms: 1.2 m3/h/m2 (according to the Technical Guidelines TOTEE 20701-1/2010)

The floor slabs provide shading to the southeast and northwest windows (Table 3)

Table 3: Shading factors calculated according to the Technical Guidelines TOTEE 20701-1/2010

Shading factor (according to the Technical Guidelines TOTEE 20701-1/2010)				
Rooms	1st and 2nd floor	3rd and 4nd floor	2.85m height	3.75m height
Windows southeast	0.43	0.14		
Windows northwest			0.28	0.2

3.2 Generation of Future Climate files

The future files for the building simulations are generated using the CCWorldWeather Generator tool, developed by Southampton University (Southampton University 2010; M.F. Jentsch 2010; Mark F. Jentsch, Bahaj, and James 2008). The tool uses the 'morphing method', developed by Belcher et al. (Belcher, Hacker, and Powell 2005). The 'morphing' methodology is published by the Chartered Institution of Building Services Engineers (CIBSE) and is utilised as a baseline for transforming current CIBSE Test Reference Years (TRY) and Design Summer Years (DSY) into climate change weather years (Mark F. Jentsch, Bahaj, and James 2008).

The algorithms used in the morphing method are described by the following equations (Belcher, Hacker, and Powell 2005; Chan 2011):

- $x = xo + \Delta xm$, (shift) (1)
- $x = \alpha_m xo$ (linear stretch) (2)
- $x = xo + \Delta xm + \alpha m \times (xo - (xo)m)$ (a combination of shift and stretch) (3)

where:

x_o: the existing hourly climatic data,

Δxm : the absolute change in monthly-mean climatic variable for month m,

α_m : the fractional change in monthly –mean climatic variable for month m and

$(xo)_m$: the climatic variable xo average over month m.

The tool enables the generation of future climatic files ready for use in building simulation programs. It is Microsoft Excel based and transforms 'present-day' EPW or TMY files into

future files (Mark F. Jentsch, Bahaj, and James 2008). The toolkit uses IPCC TAR model summary data of the HadCM3 A2 experiment ensemble which is available from the IPCC Data Distribution Centre.

3.3 Mitigation strategies

In order to tackle the climate change, a number of energy efficient techniques are studied for each climatic period. The energy efficient strategies that are studied for the hotel building are based on the example given in CIBSE TM36 (Hacker et al 2005) and are summarised below:

Table 4: Climate change mitigation strategies for the hotel building

Principle	Type of Principle	Techniques
switch off	Passive cooling	Shading, double low emission glazing
absorb & switch off	Passive cooling	adding insulation in walls & roof
Reflect	Passive cooling	cool materials & double low e glazing
blow away	Passive cooling	Intelligent night and day time control
Convection	Hybrid cooling	using ceiling fans

Five principles are used to tackle the energy increase and overheating of the hotel: 'switch off', 'absorb', 'reflect', 'blow away' and 'convect'. The principle 'switch off' is realized with the control of solar gains in the interior of the building, with the use of external shading and the use of energy efficient glazing. The 'switch off & absorb' principle is approached with the addition of external insulation in the non-insulated fabric. Energy efficient glazing summarizes both principles 'switch off' and reflect' by removing and 'reflecting' the undesirable solar gains. Apart from the glazing, the 'reflect' option is also illustrated by increasing the reflectance of the external surfaces and relieving indoor spaces from excessive peak temperatures. The 'blow away' principle is illustrated by an 'intelligent' ventilation system and the use of automated control in the daytime and nighttime ventilation according to the external temperature and the indoor temperature of each zone. In addition to the minimum airflow rates in each zone of the hotel as defined by the national legislation, extra fresh air is supplied in the areas of the hotel according to the external temperature and the internal temperature, both at day and night. The convection principle is illustrated with the use of ceiling fans by blowing the 'cool' air downwards to the occupied zone and extending the thermal comfort zone without the use of air conditioning.
For every principle different scenarios are simulated as shown in Table 5, in order to define the most energy efficient ones.

Table 5: Energy efficient techniques for the upgrade of the building envelope of the demonstration hotel as a response to the climate change

Principle	Technique	Description
Absorb & switch off- (insulation)	National legislation	U roof=0.45W/m^{2}K, Uwalls=0.5 W/m2K
	7 cm	U roof=0.45W/m^{2}K, Uwalls=0.34 W/m2K
	10 cm	U roof=0.32W/m^{2}K, Uwalls=0.25 W/m2K
	12 cm	U roof=0.27W/m^{2}K, Uwalls=0.21 W/m2K
Switch off & reflect – (glazing)	Double glazing	U=2.95 W/m^{2}K, g=0.8
	Double low –e	U=1.8 W/m^{2}K, g=0.6
	Double low e	U=1.8 W/m^{2}K, g=0.45
	Double low –e & argon	U=1.43 W/m^{2}K, g=0.6
	Double low e	U=1.06 W/m^{2}K, g=0.55
Switch off – (shading)	Shading to corridors	Shading factor 0.5
	Shading to corridors	Shading factor 0.7
	Shading to corridors	Shading factor 0.8
	Shading to corridors & rooms	Shading factor 0.8 & 0.5
	Shading to corridors & rooms	Shading factor 0.8 & 0.7

Reflect – (cool materials)	External walls	Solar absorptance:0.2
	External walls & roofs	Solar absorptance:0.2
Blow away – (ventilation)	Day time	Indoor temp of each zone > 23°C & external temperature < 25°C, may-sept
	Day time	Indoor temp of each zone > 23°C & external temp< internal temp, may-sept
	Night time	Ventilation at a constant rate from 23:00 – 7:00, for the period may-sept
	Night time	Ventilation when the indoor temp of each zone > 23°C, 23:00 – 7:00, may -sept
	Night time	Ventilation when the outdoor temp >15°C, 23:00 – 7:00, may-sept
Convection – (ceiling fans)	Hybrid cooling	Cooling setpoint at 27.5°C instead of 26°C, increase of 1°C assuming that the fans cover 60% of the thermal zone – TOTEE 20701-1

4 ANALYSIS OF CLIMATIC FILES

The climatic data is analysed with the mean degree hours using the formulas below as given in CIBSE TM1 41:

$$D_d = \frac{\sum_{j=1}^{24}\left(\theta_b - \theta_{o,j}\right)_{\left((\theta_b-\theta_{o,j})>0\right)}}{24} \quad \text{HDD} \quad (4)$$

$$D_d = \frac{\sum_{j=1}^{24}\left(\theta_{o,j} - \theta_b\right)_{\left((\theta_{o,j}-\theta_b)>0\right)}}{24} \quad \text{CDD} \quad (5)$$

Where:
Dd is the daily degree-days for one day, θb is the base temperature and θo,j is the outdoor temperature in hour j. Only the positive values are taken. (CIBSE 2006a)
As default by the Technical Chamber of Greece, the base temperature for heating degree days is 18°C and 26 °C for cooling degree days (Technical Chamber of Greece 20701-3/ 2010).

4.1 Period 1970 – 2010

Table 6: Mean degree hours for the area of Athens for the period 1970-2010

Mean degree hours for the area of Athens											
	CDD	**HDD**		**CDD**	**HDD**		**CDD**	**HDD**		**CDD**	**HDD**
1970	128	1159	**1981**	124	1101	**1991**	153	1261	**2001**	282	996
1971	118	1178	**1982**	122	1273	**1992**	191	1189	**2002**	223	1032
1972	139	1120	**1983**	87	1260	**1993**	276	1013	**2003**	281	1217
1973	160	1127	**1984**	95	1156	**1994**	201	1069	**2004**	184	1099
1974	136	1134	**1985**	145	1093	**1995**	200	1145	**2005**	196	1161
1975	68	1171	**1986**	169	1067	**1996**	165	1171	**2006**	234	1242
1976	162	996	**1987**	203	1234	**1997**	275	1098	**2007**	313	1052
1977	114	1082	**1988**	222	1180	**1998**	262	914	**2008**	308	1026
1978	131	1024	**1989**	133	1139	**1999**	271	1023	**2009**	209	954
1979	131	1138	**1990**	190	993	**2000**	153	1261	**2010**	278	805
1980	128	1159									

An increasing trend characterizes the mean cooling degree days and a decreasing trend characterises the heating degree days. Between the years 1970 – 2010 the increase in the mean cooling degree hours is calculated to 78% whereas the decrease of the heating degree days is 18%.

4.2 Generated future files 2020, 2050 and 2080

❖ Heating and Cooling Degree days

Table 7: Cooling and heating mean degree hours for Patra, Iraklio and Thessaloniki, for present climatic file and years 2020, 2050 and 2080

Heating (base temp 18 °C) and Cooling (base temp 26°C) Degree Days				**Variation % from present**			**Variation in degree days**		
	Patra	**Thes.**	**Iraklio**	**Patra**	**Thes.**	**Iraklio**	**Patra**	**Thes.**	**Iraklio**
Present									
CCD	169	141	122						
HDD	1121	2123	871						
2020									
CCD	200	177	159	**19**	**25**	**31**	**32**	**36**	**38**
HDD	990	1961	753	-12	-8	-13	-130	-162	-118
2050									
CCD	250	**218**	**212**	**48**	**54**	**75**	**82**	**77**	**91**
HDD	851	1812	631	-24	-15	-28	-269	-311	-240
2080									
CCD	330	**289**	**302**	**96**	**104**	**149**	**161**	**147**	**181**
HDD	681	1607	478	-39	-24	-45	-440	-517	-393

❖ Night- time cooling degree days

Table 8: Night-time cooling degree days for Patra, Iraklio and Thessaloniki, for present climatic file and years 2020, 2050 and 2080

Night Cooling (base temp 20°C) Degree Days				**Variation % from present**			**Variation in degree days**		
	Patra	**Thes.**	**Iraklio**	**Patra**	**Thes.**	**Iraklio**	**Patra**	**Thes.**	**Iraklio**
Present									
CCD	101	64	143						
2020									
CCD	126	85	172	25	33	20	25	21	29
2050									
CCD	157	109	211	55	70	48	56	45	68
2080									
CCD	206	149	273	104	133	91	105	85	130

The weather analysis of the three climatic zones shows that in all areas there will be an increase in the cooling degree days and a decrease in the heating degree days, predicting an increase in the cooling energy demand and decrease in the heating energy demand respectively. Iraklio (zone A) has the maximum number of night cooling degree days, the highest values of solar radiation and wind speed at present and in the future and presents the smallest diurnal differences. On the other hand, Thessaloniki (zone C) presents the maximum number of heating degree days along with the lowest values of solar radiation. Patra has the maximum cooling degree days and large diurnal differences. Also in all areas, relative humidity is increasing with the years. Thessaloniki is the most humid city during the winter and spring months apart from the months May –August when Patra is the most humid area.

5 SIMULATION RESULTS

5.1 Impact of the climate change on the hotel building using real monitored data

Using real monitored data for the period 1970 – 2010 for the area of Athens, the simulation results show an increase of the cooling loads of the hotel building by 33% and a decrease in the heating demand by 22% in 2010 compared to 1970.

5.2 Impact of the climate change on the hotel building using generated future files

Using generated future files for the area of Patra, results indicate an increase of the cooling load of the building by 15% in year 2020, 34% in year 2050 and 63% in year 2080. On the other hand heating load is expected to decrease by 14% in year 2020, 29% in year 2050 and 46% in year 2080.

5.3 Mitigation strategies for an optimum building envelope design

The most energy efficient techniques as these are defined by the simulations are applied to the hotel building (in climatic zone B) in order to define the 'optimum' building' for the present day, period 2020, 2050 and 2080. For the purposes of the study, two modes of building operation are considered:

- ❖ All year operation.

The selected principles and energy techniques are those that have the best benefit for the building for both the heating and cooling period. The optimum buildings with all year operation comprise: Insulation (10cm) in external walls and roof, double low e glazing (U=1.8 W/m2K, g=0.45), intelligently controlled night ventilation, intelligently controlled day ventilation, ceiling fans in the rooms, and shading to the corridors. The optimum building for present day and the optimum building for year 2020 comprise the same energy techniques. The optimum building for year 2050 comprises more shading. The optimum building for year 2080 includes even more shading and is also equipped with cool materials on the walls.
The heating and cooling loads of the optimum buildings based on the simulation results are:

Table 9: Heating and cooling loads (kWh/m2/yr) for the optimum building with all year operation

Optimum buildings – ALL YEAR operated		
	Heating Loads (kWh/m^2/yr)	**Cooling Loads (kWh/m^2/yr)**
Present day	21	8
2020	16	11
2050	13	15
2080	9	22

- ❖ Seasonal operation.

In that case the building is operating during the months May to September. The simulations are carried out for the whole year but heating, cooling, ventilation and all internal gains (lighting, people) are operating only for the months May – September whereas for the months January – April and October to December the systems and internal gains are set to 0. The 'optimum' buildings comprise: Intelligently controlled night ventilation, cool materials, ceiling fans, intelligently controlled day ventilation, shading and double low e glazing. The optimum building for the present day and year 2020 comprise the same energy techniques. The optimum building for year 2050 differs in the type of night ventilation control. The optimum building for year 2080 is also equipped with insulation.
The heating and cooling loads of the optimum buildings based on the simulation results are:

Table 10 Heating and cooling loads (kWh/m2/yr) for the optimum building with seasonal operation

Optimum buildings – SEASONALLY operated		
Heating, cooling ventilation Operation May - Sept	**Heating Loads (kWh/m^2/yr)**	**Cooling Loads (kWh/m^2/yr)**
Present day	1	6
2020	1	8

2050	1	13
2080	1	19

5.4 Effectiveness of the proposed measures in different climatic regions

The effectiveness of the proposed measures is investigated for the area of Thessaloniki (climatic zone C) and Iraklio -island Crete (climatic zone A), shown in Table 11 & Table 12:

Table 11 Heating and cooling loads for the 'all year operated' optimum buildings for the 3 climatic zones

OPTIMUM BUILDINGS – ALL YEAR OPERATED						
	HEATING LOADS kWh/m^2/yr			**COOLING LOADS kWh/m^2/yr**		
	Patra	**Thessaloniki**	**Iraklio**	**Patra**	**Thessaloniki**	**Iraklio**
present day	21	58	12	8	4	10
2020	16	53	9	11	6	14
2050	13	48	7	15	9	19
2080	9	41	4	22	14	29

Table 12 Heating and cooling loads for the 'seasonally operated' optimum buildings for the 3 climatic zones

OPTIMUM BUILDINGS – SEASONALLY OPERATED						
	HEATING LOADS kWh/m^2/yr			**COOLING LOADS kWh/m^2/yr**		
	Patra	**Thessaloniki**	**Iraklio**	**Patra**	**Thessaloniki**	**Iraklio**
present day	1	2	1	6	3	6
2020	1	2	1	8	5	9
2050	1	2	0	13	8	15
2080	1	2	0	19	13	24

6 DISCUSSION

The simulations show that optimum buildings in Iraklio present the highest cooling energy demand, whereas optimum buildings in Thessaloniki present the highest heating energy demand.

From the climatic analysis, it seems that Patra (climatic zone B) presents maximum cooling degree days, large diurnal differences and small night time temperatures. As a result, during the year, Patra is cooler than Iraklio, and presents the mildest climatic characteristics, compared to Thessaloniki and Iraklio. As the most energy efficient techniques were selected for the optimum buildings of that climatic zone (B), it seems that in terms of cooling the techniques are performing very well for buildings in Thessaloniki (that is cooler area than Patra) but not so well for buildings in Iraklio that in overall is warmer area than Patra. Therefore, the optimum buildings in Thessaloniki present nearly zero cooling loads, ranging from 4 kWh/m^2/yr in present year to 14 kWh/m^2/yr in year 2080. However in areas as Iraklio with higher night time temperatures and solar radiation than Patra, optimum buildings present quite high energy demand for cooling, ranging for the 'all year' operated building from 10 kWh/m^2/yr (present) to 29 kWh/m^2/yr (year 2080) and for the 'seasonally' operated building from 6 kWh/m^2/yr (present) to 24 kWh/m^2/yr (year 2080). For this area and especially for the long term future (2080) more drastic climate change solutions are required; the development of a design strategy based on the principles 'switch off', 'reflect' and 'blow away' would help for the removal of solar gains and excessive heat gains. This strategy could include even more shading, different type of glazing (reflecting), cool materials of better performance and

probably exploitation of the wind patterns of the area with another strategy/control of daytime and nighttime ventilation.
In terms of heating loads, the optimum buildings in areas colder than Patra with more HDD, i.e.Thessaloniki, are not well equipped with the specific mitigation strategies and require high energy demand that ranges between 58 kWh/m^2/yr in present to 41 kWh/m^2/yr in year 2080. The selected energy techniques are not coping with the climate of this area, more efficient strategies are in need to tackle the climate change. A design strategy based on the 'switch off and absorb' principle would provide higher level of insulations, combined with a more appropriate glazing that would prevent heat losses, the minimization of shading and the avoidance of cool materials. On the hand, the optimum buildings of areas with less HDD than Patra, i.e. Iraklio, would present almost zero heating energy demand in 2080.
The climatic analysis of the forecast future years shows that the decrease in heating degree days is almost double than the increase of the cooling degree days. This results in increase of the cooling demand and decrease of the heating demand in the future. Taking into consideration that cooling mainly relies on electricity; this signifies a modification on the use of the primary energy and a shift towards electrical power. Other alternatives like renewable energy source should be considered for the generation of electrical energy.
The simulations were performed taking into consideration current conventional mitigation measures, thus passive cooling techniques that focus on the upgrade of the building envelope and deal with the control of heat transfer (switch off and absorb principle), solar control (switch off and reflect principle), heat gain (thermal storage capacity, absorb principle), heat dissipation (blow away principle) and the adjustment of the cooling set point (convection principle). With the implementation of the above climate change adaptation methods a significant reduction of the building energy demand is achieved in both the cooling and heating season but still the building presents rather high cooling in the long term future. This may indicate the inefficiency of the conventional mitigation methods to cope with the climate change and the necessity to develop further the technical characteristics of the current technologies to cope with severe climatic characteristics, in the long term future.

7 CONCLUSIONS

The climate change and in particular the increase of the air temperature has a significant impact on the energy demand of the hotel building, an increase of the cooling loads and a decrease of the heating loads. Between the three climatic regions, the optimum buildings require more cooling in climatic zone A and extra mitigation strategies are in need based on the principles 'switch off', 'reflect' and 'blow away' to cope with the increased solar gains. In terms of heating, the optimum buildings in climatic zone C require extra mitigation strategies based on the 'switch off and absorb' principle to cope with the heat losses through the building envelope. Additionally, it was found that different strategies can be applied to all year and seasonally operated buildings for the most energy efficient performance. Therefore, for an all year operated building, extra shading and cool materials are required in time, whereas for a seasonally operated building insulation is required for the long term future, i.e. after year 2080.
The simulation results show that cooling loads of optimum buildings are rather high in 2050 and 2080, meaning that the current technologies are not efficient enough to cope with the climate change in the long term future. Additionally, in terms of heating, optimum buildings are not very efficient in areas with severe climatic conditions. Therefore, for a better result the energy efficient building envelope design should be combined with the use of energy efficient plant.

8 REFERENCES

Cartalis, C, A Synodinou, M Proedrou, A Tsangrassoulis, and M Santamouris. 2001. 'Modifications in energy demand in urban areas as a result of climate changes: an assessment for the southeast Mediterranean region'. Energy Conversion and Management 42 (14): 1647–1656. doi:10.1016/S0196-8904(00)00156-4.

CIBSE 2006. *Degree-days: theory and application TM41:2006*.

Eames, M., T. Kershaw, and D. Coley. 2012. 'A comparison of future weather created from morphed observed weather and created by a weather generator'. Building and Environment 56: 252–264. doi:10.1016/j.buildenv.2012.03.006.

European Environment Agency. 2004. 'Impact of Europe 's changing climate'.

Giannakidis, G., D.A. Asimakopoulos, M Santamouris, I. Farrou, M. Laskari, M. Saliari, G. Zanis, et al 2011. 'Modelling the energy demand projection of the building sector in Greece in the 21st century'. In Press.

Giannakopoulos, Ch., P. Hadjinicolaou, Ch. Zerefos, and G. Demosthenous. 2009. 'Changing Energy Requrements in the Mediterranean Under Changing Climatic Conditions'. Energies 2: 805–815.

Guan, Lisa. 2009. 'Preparation of future weather data to study the impact of climate change on buildings'. Building and Environment 44 (4): 793–800. doi:10.1016/j.buildenv.2008.05.021.

Guan, Lisa.. 2012. 'Energy use, indoor temperature and possible adaptation strategies for air-conditioned office buildings in face of global warming'. Building and Environment 55: 8–19. doi:10.1016/j.buildenv.2011.11.013.

Hacker, J., M. Holmes, S. Belcher, and G. Davies. 2005. 'CIBSE TM36:2005 Climate change and the indoor environment: impacts and adaptation'.

IPPC, Intergovermental Panel on climate change. 2011. 'IPPC Special Report on Renewable Energy Sourves and Climate Change Mitigation, Final Release'.

Jentsch, M.F. 2010. 'Climate Change Weather File Generators. Technical reference manual for the CCWeatherGen and CCWorldWeatherGen tools'.

Jentsch, Mark F., AbuBakr S. Bahaj, and Patrick A.B. James. 2008. 'Climate change future proofing of buildings—Generation and assessment of building simulation weather files'. Energy and Buildings 40 (12): 2148–2168. doi:10.1016/j.enbuild.2008.06.005.

Kolokotroni, M., X. Ren, M. Davies, and A. Mavrogianni. 2012. 'London 's urban heat island: Impact on current and future energy consumption in office buildings'. Energy and Buildings 47: 302–311. doi:10.1016/j.enbuild.2011.12.019.

Oxizidis, S., A.V. Dudek, and A.M. Papadopoulos. 2008. 'A computational method to assess the impact of urban climate on buildings using modeled climatic data'. Energy and Buildings 40 (3): 215–223. doi:10.1016/j.enbuild.2007.02.018.

Southampton University. 2010. ‘Manual, CCWorldWeatherGen Climate change world weather File generator’.

Technical Chamber of Greece 20701-1/. 2010. ‘Technical Directive - Technical Chamber of Greece T.O.T.E.E. 20701-1/2010 Analytical Specifications of Parameters for the calculation of the Energy Performance of Buildings and the issue of Energy Certificate’.

Technical Chamber of Greece 20701-3/. 2010. Technical Directive - Technical Chamber of Greece T.O.T.E.E. 20701-3/2010 Climatic Data of Greek Regions.

Tselepidaki, I., M. Santamouris, D.N. Asimakopoulos, and S. Kontoyiannidis. 1994. ‘On the variability of cooling degree-days in an urban environment: application to Athens, Greece’. Energy and Buildings 21 (2): 93–99. doi:10.1016/0378-7788(94)90002-7.

THE EFFECT OF A NOVEL ROOF POND TO THE INDOOR AIR TEMPERATURE FOR PASSIVE COOLING

Artemisia Spanaki*[1], Dionysia Kolokotsa[2], Theocharis Tsoutsos[2], Ilias Zacharopoulos[1]

1 National Technical University of Athens, School of Architecture, Department of Architectural Technology, 42 Patission Street, 10682 Athens, Grecce

2 Technical University of Crete, Environmental Engineering Department, 73100 Chania, Crete, Greece

**Corresponding author: e-mail address Spanakiart@hotmail.com*

ABSTRACT

The effect of a new passive cooling device to the indoor air is analyzed based both to experimental and simulating results. The tested device is a ventilated pond protected with an aluminum layer, placed on the roof of the examined building. The indoor air temperature of the building has been recorded, before and after the placement of the roof cooling technique. The record indoor air temperature is analyzed, in regard to the ambient conditions. Furthermore, the record indoor air temperature before the application of roof cooling technique has been assessed in order to create the digital model of the building, using the TRNSYS software. The climatic data of the experimental period are applied to the simulating model, in order to estimate the indoor air temperature that the building would have without the tested roof cooling technique. According to the simulation, the daily indoor air temperature fluctuation for the building without any roof treatment varies from 4.8 to 8.2^{o}C, while the corresponding values after the application of the Ventilated pond with Aluminum layer are significantly reduced, varying from 1.6 to 3.1^{o}C.

KEYWORDS

Roof Ponds, indirect evaporative cooling

1 INTRODUCTION

Evaporative cooling is widely considered as an effective passive cooling technique [Givoni, 2011]. Cooling towers [Givoni, 1997, Hamza 1995], cooling radiators [Erell, 1999, Dimoudi, 2006] and roof ponds are only few evaporative cooling techniques.

Roof ponds are an effective passive cooling and heating technique. A number of pond variations have been proposed differing in terms of function and constructional characteristics (e.g. water circulation, movable insulation, spraying system, protective materials etc [Spanaki et al, 2011].

Ventilated pond protected by a reflective layer has been proposed in small scale experiments [Spanaki et al, 2012]. According to the experimental results, the system results lower bottom pond temperatures comparing to other ponds, protected with different materials.
The present study aims to investigate the performance of the ventilated pond protected with reflective layer, in terms of indoor air temperature reduction. The system is placed on the roof of a small building, while the bottom pond and the indoor air temperatures are both recorded.
The records of the indoor air temperature of the building before the application of the investigated system on the roof are used in order to simulate the building. The simulating model is used in order to calculate the temperatures that the building would have without any roof treatment.
The aim of the present study is to assess the effectiveness of the ventilated pond with aluminium layer in terms of indoor air temperature.

2. DESCRIPTION OF THE INVESTIGATED POND

Roof pond is consisted by a wooden frame on roof's perimeter, as shown in Figure 1. The pond is filled with water up to 0.10-0.12m deep while water level is kept constant by a floater as shown in Figure 2. The aluminium layer is placed on wooden beams, as shown on Figures 3 and 4. The aluminium layer placed above water layer, reflecting solar radiation during daytime.

Figure 1: Wooden frame is the pond's perimeter.

Figure 2: Nylon for pond waterproofing and floater.

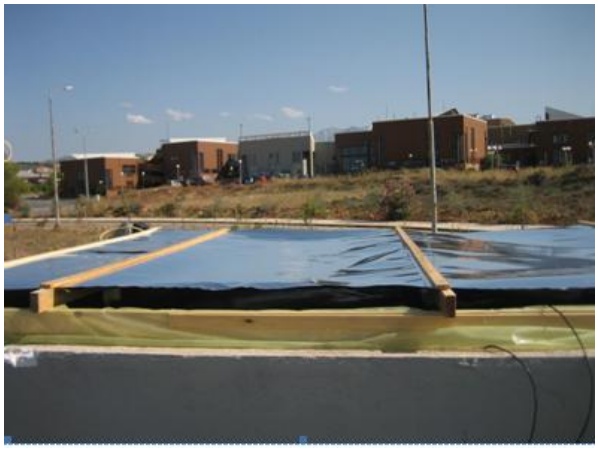

Figure 3: Ventilated Roof pond with aluminium layer.

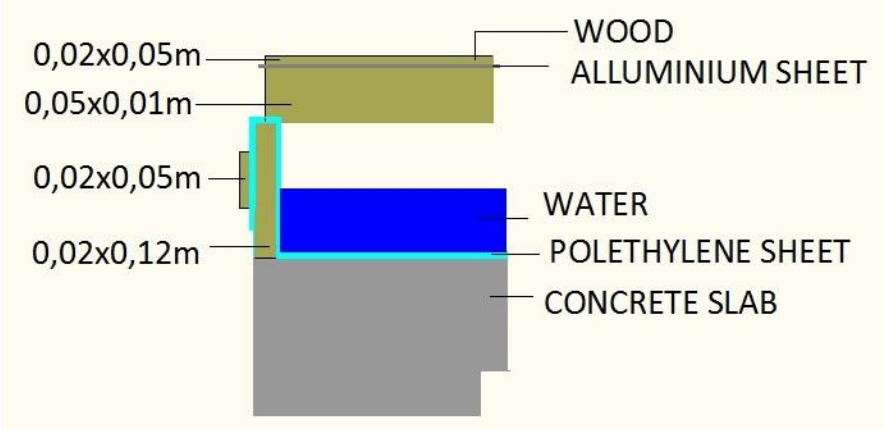

Figure 4: Section of the Ventilated Roof pond with aluminium layer.

3. BUILDING DESCRIPTION

The small building that is record during the experiments is shown on Figure 5. The area of the roof is 6m^2, as shown on Figures 6 a and b. Section of building envelope are shown on Figures 7 a and b. The roof is partly insulated, as shown in the infrared photo on Figure 8.

Figure 5: Photo of the building with the investigated pond on the roof.

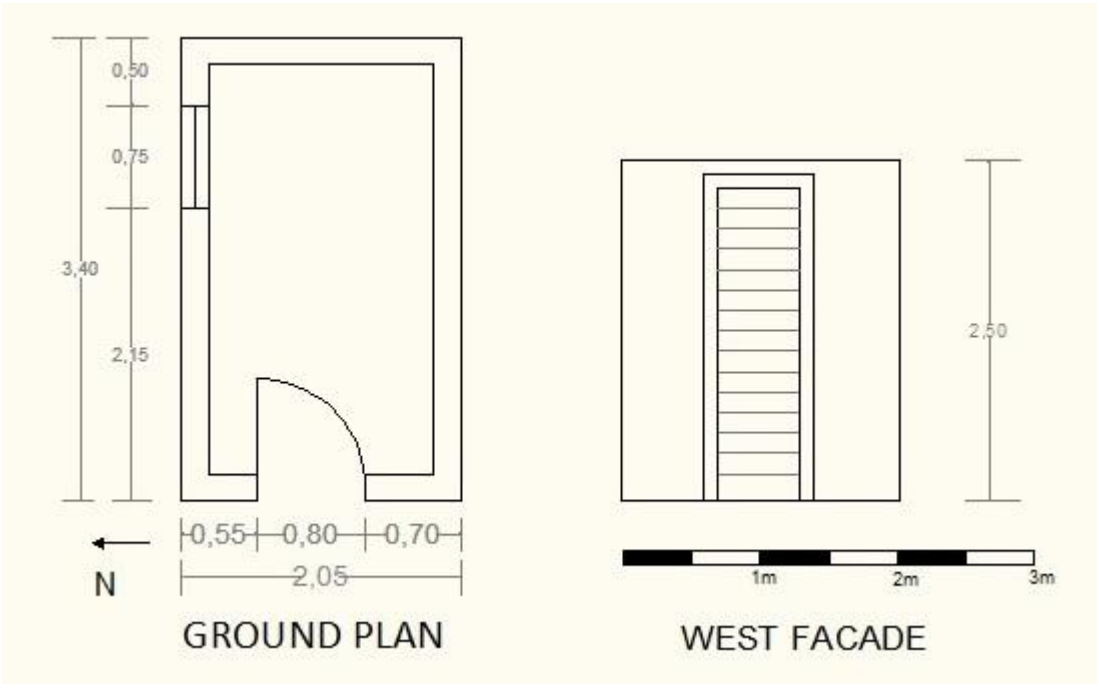

Figures 6 (a) Ground Plan and (b) west facade of the building.

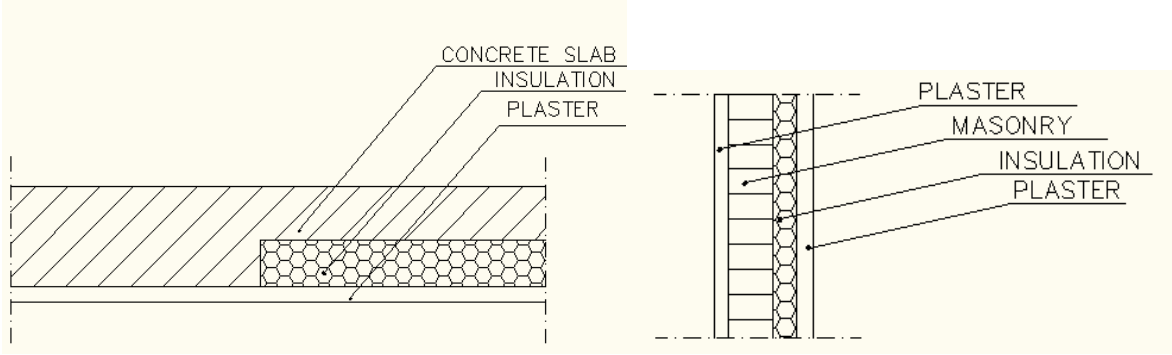

Figures 7 (a) Roof and (b) Wall section of the building.

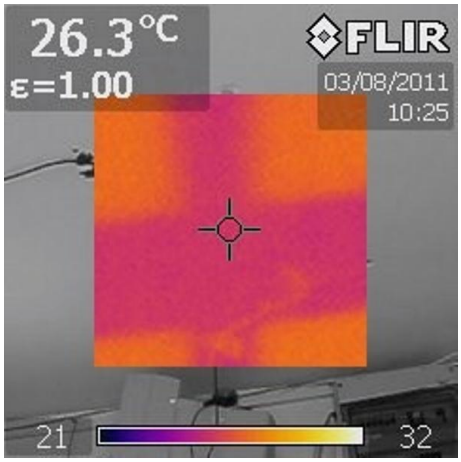

Figure 8: Photo of building ceiling taken with infrared camera.

4. EXPERIMENTAL SET-UP

The experimental records refer to the period between June and August 2011, on the Campus of Technical University of Crete in Chania – Greece. The climatic data on the site of the experiments was obtained from meteorological station of the Institute of Environmental Research, of the National Observatory of Athens. The altitude of the site is 137m, while the exact coordinates are: latitude 24 ° 04 '09 "E and longitude and 35 ° 32' 00" N.

The temperatures are recorded with 8 temperature recorders T-Logg 100 placed in the bottom of the pond. The internal conditions are recorded by 2 loggers temperature - humidity T-Logg 100E brand Greisinger electronic. The loggers have a resolution of 0.1°C and accuracy of measured values ± 0.5°C. Minisoft and GSOFT 40K software is used for data transferring.

Table 1: Thickness and U-values of the Builings envelope

Building element	Thickness (m)	U-value (W/m^{2}K)
Walls	0.26	0.806
Concrete roof	0.16	1.033 (mean U-value)
Windows		5.680

Table 2: Properties of building envelope used in simulation, that are included in the *.bui file of the TRNBuild Software. The Boundary temperature for floor is 27^{o}C.

				Solar Absorptance of wall	
	Area (m2)	Thickness (m)	U-value (W/m^{2}K)	Front	Back
Wall	32.76	0.26	0.806	0.3	0.3
Roof	7.00	0.16	1.033	0.8	0.75
Floor	7.00	0.19	2.901	0.8	0.8
Windows	2.13		2.830		

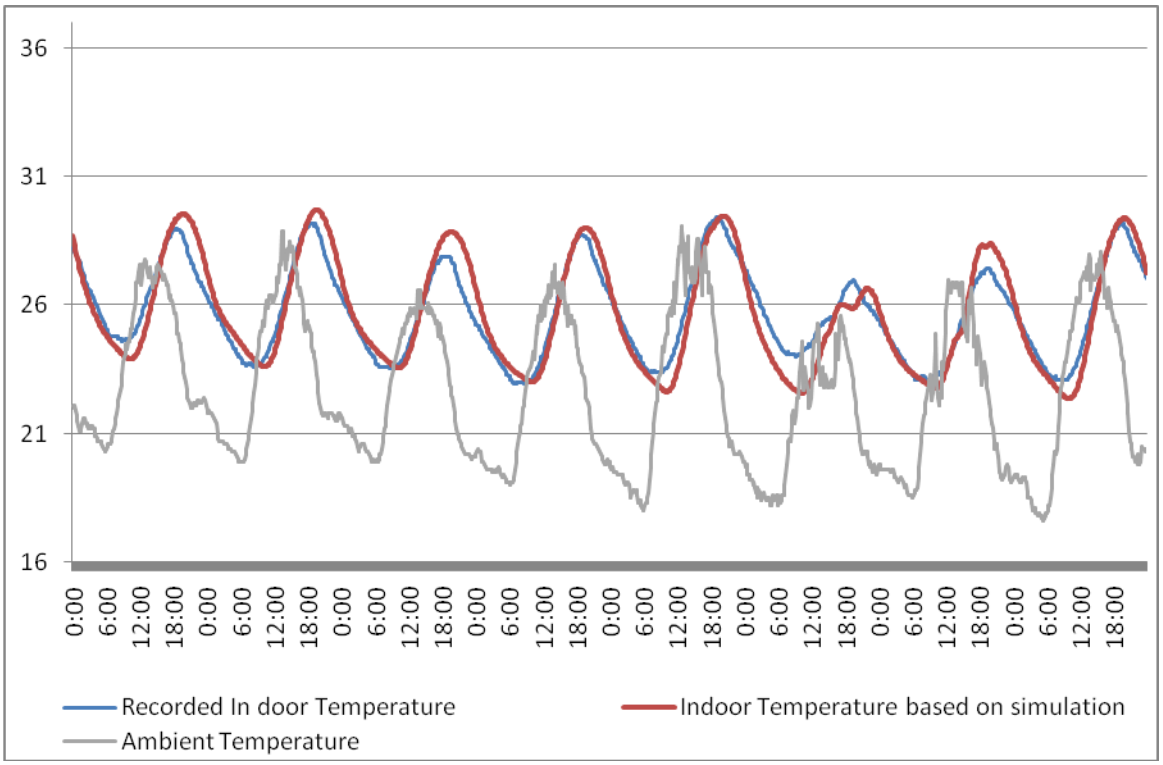

Figure 9: Indoor air temperatures according to experiments and simulation, before the application of the system in building's roof.

5. BUILDING SIMULATION

The indoor air temperature of the building before the addition of the investigated system on the roof has been recorded for a 22 days period.
The building is simulated using the parameters listed on Tables 1 and 2. The climatic data of the 22 days period are used in order to simulate the building without any roof treatment. The calculated indoor air temperatures are compared to the experimental ones, in order to validate the model. As shown in figure 9, the maximum variation of experimental and simulating values are 12%.

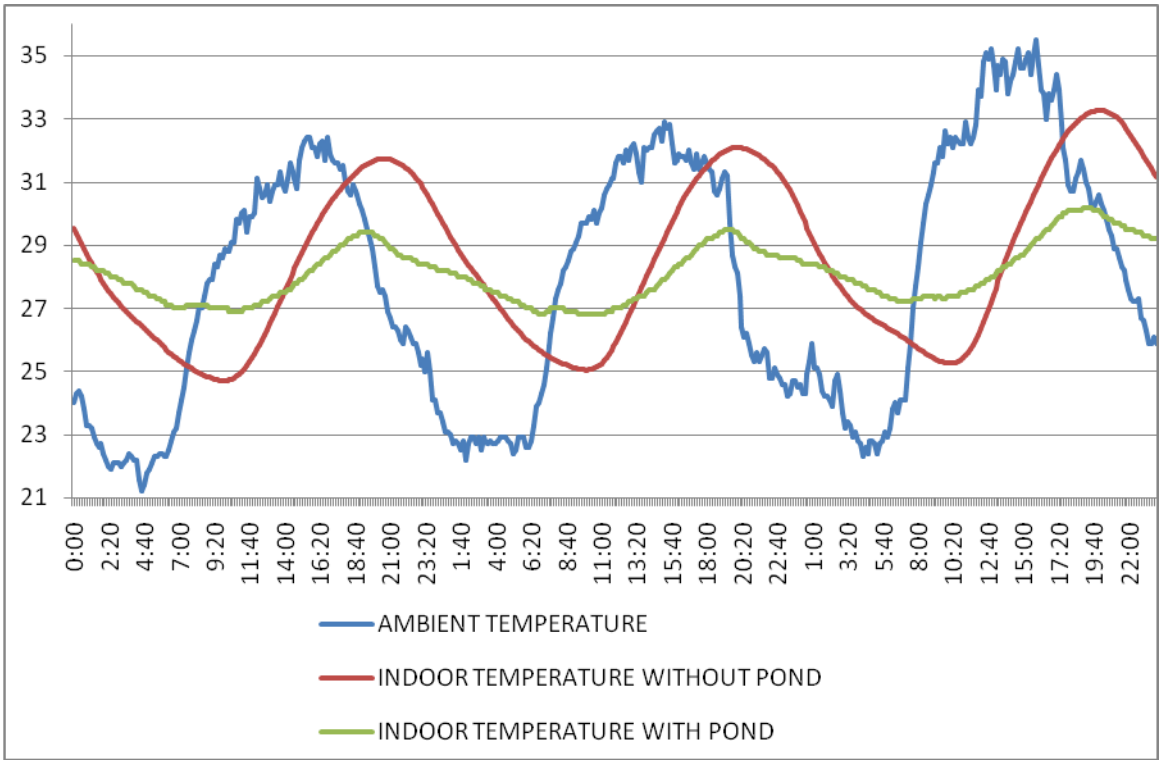

Figure 10: Indoor air temperatures according to experiments and simulation, after the application of the system in building's roof.

6. THE EFFECT OF THE VENTILATED ROOF POND WITH ALUMINIUM LAYER TO THE INDOOR AIR TEMPERATURE

Figure 10 shows the indoor air temperature of the building with the ventilated roof pond, according to the experiments, and the indoor air temperature the building would have without any roof treatment, according to the simulation.

For the whole period of experiments the fluctuation of the indoor air temperature for the building with the Ventilated pond with Aluminium layer varies from 1.6 and 3.1^{o}C. The corresponding value for the building without any roof treatment varies from 4.8 to 8.2^{o}C. As a result, the proposed technique results a reduction of indoor air temperature to the 40% compared to the building with roof pond. The indoor air temperature fluctuation of the

building with the ventilated pond with aluminium is the 25% of the ambient air temperature fluctuation.

Furthermore, the mean maximum indoor air temperature in the building without any roof treatment reaches 31.7^{o}C, almost equal to the maximum ambient air temperature (32.4 ^{o}C). The corresponding mean maximum indoor air temperature in the building with the ventilated pond with the aluminium is decreased at 29.0^{o}C. The increased heat capacity of water increases the minimum indoor air temperature by 1.3^{o}C.

7. CONCLUSION

The present investigation proposes a new passive roof cooling technique. The ventilated pond with aluminium layer can easily be constructed with common materials. According to the experiments, the system reduces the indoor air temperature fluctuation.

Further research can further investigate alternative durable and strong materials that can be used for the construction of the system. Furthermore, issues related to the thermal performance of the system in respect to climatic conditions should be also investigated.

Acknowledgements

The present investigation is a part of a Phd study supported by the Greek State Scholarships Foundation.

References

1. Dimoudi A., Androutsopoulos A., The cooling performance of a radiator based roof component, Solar Energy 80 (2006) 1039–1047
2. Erell E., Etzion Y, Analysis and Experimental verification of an improved cooling radiator, Renewable Energy 16 (1999) 700-703
3. Givoni B, Performance of the “shower” cooling tower in different climates, *Renewable Energy,* Vol. 10, No. 213, pp. 173-178, 1997
4. Givoni Baruch, Indoor temperature reduction by passive cooling systems, Solar Energy 85 (2011) 1692–1726
5. Hamza A. , Ali H., Taha I. M. S., Ismail I. M. , Cooling of water flowing through a night sky radiator, *Solar Energy* Vol. 55, No. 4, pp. 235 253, 1995
6. Spanaki Artemisia, Kolokotsa Dionysia, Tsoutsos Theocharis, Zacharopoulos Ilias (2012), Theoretical and experimental analysis of a novel low emissivity water pond in summer, Solar Energy 86, 3331–3344
7. Spanaki Artemisia, Tsoutsos Theocharis, Kolokotsa Dionysia (2011), On the selection and design of the proper roof pond variant for passive cooling purposes, Renewable and Sustainable Energy Reviews 15, 3523–3533

PASSIVE VENTILATION IN MULTI-STOREY ATRIUM BUILDINGS: A FIRST-ORDER DESIGN GUIDE

Andrew Acred[1], Gary R Hunt[2]

[1] Department of Civil & Environmental Engineering, Imperial College London, London SW7 2AZ, UK
[2] Department of Engineering, University of Cambridge, Cambridge CB2 1PZ, UK

ABSTRACT

Large, multi-storey buildings pose a particular challenge for natural ventilation design due to the interaction between heat and air flows through different building zones. We develop a demand-based preliminary design strategy for sizing ventilation openings in multi-storey buildings with heated atriums. This approach enables ventilation openings on each storey, and in the atrium, to be rapidly sized so that equal temperatures and per-person flow rates can be achieved on all storeys, regardless of the occupancy or usage. To achieve this, two key dimensionless parameters are identified which quantify the performance of the ventilation system and the effectiveness of the atrium in assisting ventilating flows. Simple analytical expressions for sizing vents are developed and an example design chart presented to provide quick and intuitive first-order design guidance.

INTRODUCTION

Passive stack ventilation has particular potential for use in multi-storey buildings. Tall vertical spaces such as atria, solar chimneys and double façades, which are common in such buildings, can enhance ventilation flows by providing a space in which buoyant air can accumulate. However, effective design remains a challenge; interacting air and heat flows can potentially result in undesirable flow patterns and an uncomfortable indoor environment **[1-3]**.

Whilst powerful computational tools – such as CFD simulations and multizone software **[4-6]** – are now commonly used for detailed design, simplified mathematical models – based on the fundamental physics governing the movement of air and heat through buildings – still form a crucial part of the preliminary design stage. Design charts and hand calculations – commonly used in best practice guidance **[7-10]** – allow designers to quickly balance core variables and provide an intuitive understanding of the behaviour of the ventilation scheme. Numerous experimental investigations, including studies of multi-compartment buildings **[11-13]**, have also shown that simplified mathematical models can capture a broad range of flow behaviours.

With this in mind, we develop a preliminary design approach for multi-storey atrium buildings based on a simplified mathematical model. We focus on sizing ventilation openings to meet design criteria for ventilation rate and thermal comfort. In particular, we use dimensionless parameters to inform design, an approach advocated and discussed by Etheridge **[14]**, for

example. Some details of the mathematical model have been omitted for brevity; for a full discussion see Acred and Hunt **[15]**. Instead, we focus herein on outlining the design method and illustrating how it may be applied to an example four-storey building.

The aim of this work is to provide a rapid and intuitive first-order design method. It is not intended to be used for detailed design, but rather to provide a starting point for software modelling with the hope of reducing the time and computational overhead associated with the design process.

OVERVIEW OF THEORY

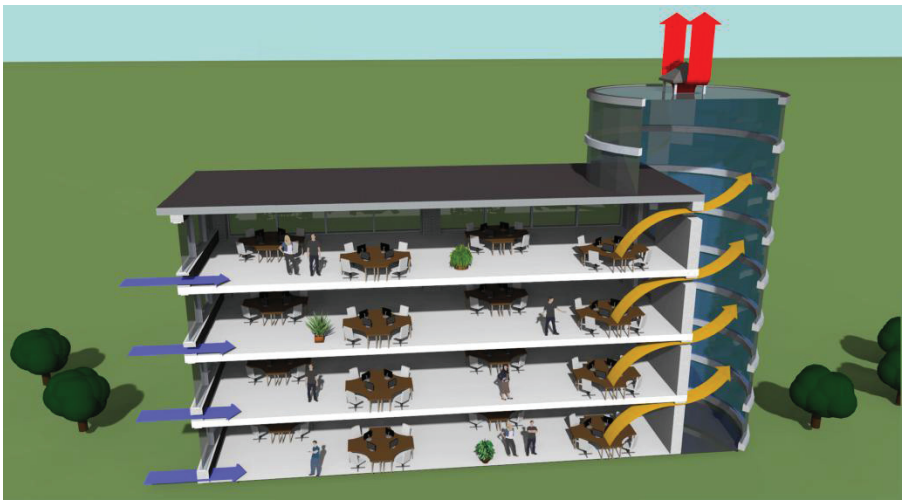

Figure 1: Visualisation of an example four-storey building with a glazed atrium. Arrows show the intended ventilation scheme: cool, fresh air enters the storey through floor-level vents, passes into the atrium via ceiling-level vents and leaves the building through the high-level atrium vent.

Figure 1 shows a visualisation of the example four-storey building considered herein, comprising open-plan occupied spaces connected to an atrium. Arrows show the intended ventilation scheme: ambient air flows into the storeys via floor-level vents, is warmed by heat gains (e.g. from office equipment, body heat and solar gains) in the storeys and passes into the atrium via ceiling-level vents. After being further heated in the atrium (e.g. due to solar gains), air then leaves the building via a high-level vent.

Building layout and core variables

Figure 2 shows a schematic in elevation of the example four-storey atrium building from Figure 1. Core ventilation variables are labelled:

The floor-to-ceiling height (m) of each storey is H; the atrium extends a height ΔH above the top storey. The flow rate (m³/s) through each storey is Q_i, where $i = 1,2,3,4$ denotes the storey number. The flow rate through the atrium vent is $Q_a = Q_1 + Q_2 + Q_3 + Q_4$. The floor- and ceiling-level vents in the storeys have cross-sectional areas $A_{in,i}$ and $A_{out,i}$, respectively. The high-level atrium vent has cross-sectional area A_a.

The air temperature (°C), net heat input (W) and number of people in each storey are T_i, W_i and n_i, respectively. The air temperature and net heat input within the atrium are T_a and W_a, respectively. The external temperature is T_0. The temperature excesses within the storeys and atrium – upon which the driving stack pressure depends – are $\Delta T_i = T_i - T_0$ and $\Delta T_a = T_a - T_0$, respectively.

We have assumed a uniform temperature in each building zone. This model is valid for buildings containing distributed heat sources which occupy more than 15% of the floor area in each zone **[16,17]**. However, we note that some stratification is likely to exist in practice, particularly in the atrium, and is closely linked to the geometry and distribution of heat sources within the building – see **[18-21]**, for example.

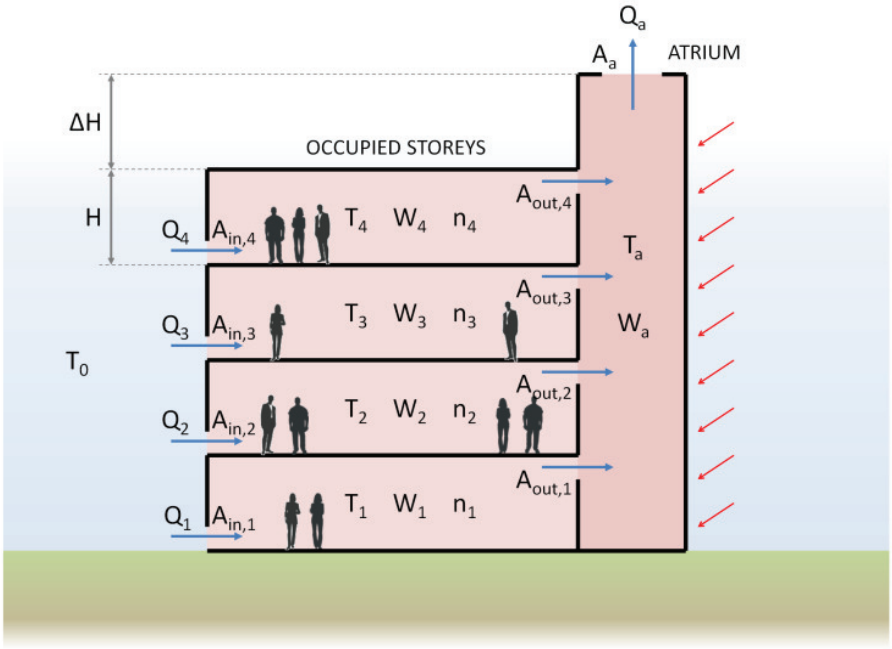

Figure 2: Schematic in elevation of a naturally ventilated four-storey atrium building. See main text for a description of the symbols shown.

Mathematical model of ventilation flows

Following **[18]** and **[22]**, the flow rates through the building can be calculated by balancing the driving stack pressure with pressure losses across vents around a closed flow loop through each storey. Pressure losses across vents are calculated using Bernoulli's theorem, which is common practice for 'purpose-built' vents **[8]**. The driving stack pressure is calculated by assuming a hydrostatic pressure distribution everywhere but at ventilation openings, and treating air as a perfect gas.

In practice, we note that other pressure terms – particularly wind – may play a role. Wind is typically harnessed to assist ventilation **[23]** (although it can also oppose stack pressure **[24]**). Flows driven by stack effect only may then be considered a 'worst case scenario', and the method presented herein gives conservative preliminary design guidance.

Applying the pressure balance to the building in Figure 2, four coupled flow equations – one for each storey – are required to describe the ventilation scheme. The flow equation for storey *i* is given by

$$\frac{Q_i^2}{a_i^2} + \frac{Q_a^2}{a_a^2} = \frac{g}{T_0}\ H\Delta T_i + \quad N - i\ H + \ \Delta H\ \ \Delta T_a\ \ , \tag{1}$$

where

$$a_i = \ \frac{1}{2c_d^2 A_{in,i}^2} + \frac{1}{2c_d^2 A_{out,i}^2}^{-\frac{1}{2}} \qquad a_a = \ \overline{2}c_d A_a \tag{2}$$

are effective vent areas for the storey and atrium vents, respectively, $N = 4$ is the number of storeys, and $g = 9.81\text{m/s}^2$.

Note that the effective storey vent area, a_i, is formed from a combination of the floor- and ceiling-level vent areas. The relative sizing of the two vents can have a significant impact on the ventilation flow **[25,26]**. Similarly, the value of the discharge coefficient, c_d – which relates effective and physical vent areas – can vary significantly based on opening geometry and flow conditions **[27,28]**. For simplicity, we do not consider these effects and focus only on how to select appropriate values of a_i and a_a.

Heat balance

The coupled equations in (1) allow the flow rates through the building to be calculated when the temperature distribution is known. The temperature distribution, in turn, depends upon the net heat gains within the building. Applying a steady heat balance to each building zone, the temperature excesses are given by

$$\Delta T_i = \frac{W_i}{\rho_0 c_p Q_i} \qquad \Delta T_a = \frac{W_{tot}}{\rho_0 c_p Q_a}, \tag{3}$$

where $W_{tot} = W_1 + W_2 + W_3 + W_4 + W_a$ is the total net heat gain within the building and ρ_0 and c_p are the density and heat capacity of ambient air, respectively. For calculations presented herein, we take $\rho_0 = 1.225$ kg/m³ and $c_p = 1.005$ kJ/kgK (corresponding to air at 15°C at sea level) **[29]**.

BALANCING DESIGN REQUIREMENTS

Typically, the coupled equations in (1) and (3) must be solved numerically to determine ventilation rates and temperatures, see **[30]** for example. However, by linking our mathematical model with ventilation design criteria based on *per-person* requirements, it is possible to solve the equations analytically and thereby allow for rapid preliminary design calculations.

Demand-based design criteria

Many ventilation guidelines are specified in terms of a minimum fresh air supply rate per person. CIBSE **[8]** and ASHRAE **[9]**, for example, stipulate a minimum requirement of 8-10l/s

per person to maintain a healthy and comfortable indoor environment. Consider the case in our example building in which each building occupant receives a given fresh air supply rate, Q_p, where the subscript p denotes 'per person'. The flow rate through a given storey can then be expressed in terms of the number of people within the storey:

$$Q_i = n_i Q_p. \tag{4}$$

Similarly, consider the case in which the net heat inputs on all storeys are divided equally between occupants such that

$$W_i = n_i W_p, \tag{5}$$

where W_p is a per-person net heat input. Note that W_p is a net heat input and includes not only body heat but also heat gains due to office equipment, lighting and so on, as well as heat losses through the building fabric. When the conditions in (4) and (5) are met, the temperatures in all storeys are equal and given by

$$\Delta T_p = \frac{W_p}{\rho_0 c_p Q_p}. \tag{6}$$

These conditions are intended to provide a convenient 'base target design' for preliminary calculations. By aiming for equal temperatures on all storeys, we target a design in which thermal comfort can be achieved in all parts of the building and avoids overheating on the upper storeys, for example.

In practice, the net heat gain per person may vary between storeys; the upper floors may receive greater solar gains, for example. This could be catered for using a weighting factor – allowing for a greater flow rate per person to maintain the desired temperature on floors with greater heat gains. However, to avoid adding additional parameters to the problem, the calculations presented herein focus on the simple 'base target design' conditions presented above.

Ventilation performance index

The balance of design criteria can be quantified using a single dimensionless 'ventilation performance index' (or VPI), λ_p, given by:

$$\lambda_p = \sqrt{\frac{Q_p^2}{\Delta T_p} \frac{T_0}{gH^5}}. \tag{7}$$

By specifying or estimating values for two out of Q_p, W_p and ΔT_p, the corresponding VPI of the design can be determined using (6) and (7). Alternatively, a design chart can be used to rapidly determine the value, or range of values, of λ_p that relates to the desired balance of design criteria. An example design chart for a building in which H = 3m is shown in Figure 3.

Various regions of Figure 3 have been highlighted to show an example of its use; the corresponding ranges of ΔT_p, Q_p, W_p and λ_p are listed in Table 1. In this example, the desired

temperature excess range is between 5 and 10°C, and the estimated per-person heat inputs lie between 100 and 200W. The region of the chart in which these ranges entirely overlap has been highlighted in dark blue. The upper and lower bounds of this range define the maximum and minimum values of λ_p for which all design criteria can be simultaneously satisfied. Flow rates within the target design range lie between 13 and 20l/s per person and therefore also satisfy the minimum flow rate requirement of 10l/s per person.

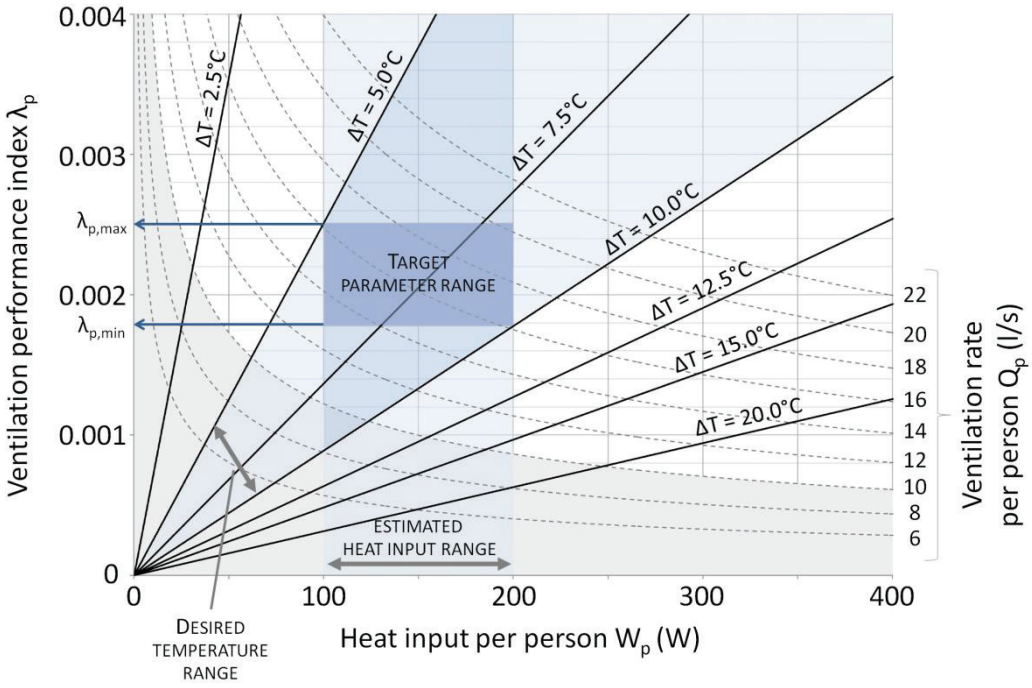

Figure 3: Design chart for selecting values of λ_P based on design requirements for a building with H = 3m. Contours of equal temperature excess (thick black lines) and equal ventilation rate per person (dashed grey lines) are shown. The chart shows an example in which the desired temperature excess is between 5 and 10°C, the estimated range of per-person heat inputs is between 100 and 200W, and the minimum required ventilation rate is 10l/s per person.

	Min	**Max**
Target temperature excess, ΔT_p (°C)	5	10
Minimum acceptable ventilation rate per person, Q_p (l/s)	10	-
Estimated heat input per person, W_p (W)	100	200
Ventilation performance index range, λ_p	0.0018	0.0025

Table 1: Ranges of ΔT_p, Q_p, W_p and λ_p for the design example shown in Figure 3.

Atrium enhancement

Atria, solar chimneys and similar vertical spaces spanning multiple storeys are typically intended to enhance stack driven ventilation flows in naturally ventilated buildings. However various studies have shown that in some cases the atrium can actually restrict flows through the building **[11,31,32]**. An effective design, therefore, should ensure that the atrium enhances

ventilation flows relative to an equivalent building without an atrium. Following a similar approach to **[11]**, we quantify this effect in a dimensionless atrium enhancement parameter:

$$E_i = \frac{Q_{i\ with\ atrium}}{Q_{i\ without\ atrium}}, \tag{8}$$

where $Q_{i\ without\ atrium}$ is the theoretical flow rate through storey i when not attached to an atrium, which can readily be calculated following **[18]**, for example. The atrium enhances ventilation flows through a given storey when $E_i > 1$. An effective design should ensure that $E_i \geq 1$ on all storeys.

Since the atrium links all storeys, the values of E_i on all storeys are linked and decrease on ascending the building **[15]**. This is an intuitive result, since flows through the lower storeys are driven by a greater depth of warm air in the atrium than flows on the upper storeys. The top storey is the 'worst performing' storey, with the lowest value of E_i, since it receives the least amount of driving from the atrium. To achieve a design with $E_i \geq 1$ on all storeys therefore requires that $E_N \geq 1$, i.e. flows through the top storey are enhanced – or at least not restricted – by the atrium.

Acred and Hunt **[15]** showed that there are limits on the maximum achievable top-storey atrium enhancement, particularly due to the possibility of undesirable exchange flows developing at the atrium outlet vent. In most scenarios, however, achieving a value of $E_N = 1$ should be possible. For the example calculations presented herein, we therefore target a design in which $E_N = 1$, thereby ensuring the atrium enhances – or at least does not restrict – flows on all storeys.

SIZING VENTILATION OPENINGS

Substituting the target design conditions into the mathematical model for ventilation flows in (1) allows us to determine simple analytical expressions for appropriately sizing ventilation openings (see **[15]** for details). The required effective vent sizes to give equal flow rates and temperatures on all storeys, for the case in which the top storey atrium enhancement is $E_N = 1$, are given by

$$a_i = \frac{n_i \lambda_p H^2}{1 + R_W (N - i)} \qquad a_a = \frac{n_{tot} \lambda_p H^2}{R_W R_H} \tag{9}$$

STOREY VENTS ATRIUM VENT

where $R_W = W_{tot}/(W_{tot} - W_a)$ is a measure of the relative heat gains in the atrium and $R_H = \Delta H/H$ is the relative height of the atrium above the top storey.

Example calculations

Table 2 shows example vent area calculations based on the design requirements and corresponding values of λ_p shown in Figure 3 and Table 1. Effective vent areas are calculated for a building with H = 3m and 30 people on each storey (i.e. n_i = 30 on all storeys). Three illustrative cases are considered in which the atrium extension above the top storey and heat input within the atrium are varied.

	Case A Short, unheated atrium: $R_H = 1$, $R_W = 1$	**Case B** Short, strongly heated atrium: $R_H = 1$, $R_W = 4$	**Case C** Tall, unheated atrium $R_H = 4$, $R_W = 1$
	Effective vent sizes (m²)		
Atrium	$1.92 < a_a < 2.71$	$0.96 < a_a < 1.36$	$0.96 < a_a < 1.36$
Storey 4	$0.48 < a_4 < 0.68$	$0.48 < a_4 < 0.68$	$0.48 < a_4 < 0.68$
Storey 3	$0.34 < a_3 < 0.48$	$0.21 < a_3 < 0.30$	$0.34 < a_3 < 0.48$
Storey 2	$0.28 < a_2 < 0.39$	$0.16 < a_2 < 0.23$	$0.28 < a_2 < 0.39$
Storey 1	$0.24 < a_1 < 0.34$	$0.13 < a_1 < 0.19$	$0.24 < a_1 < 0.34$

Table 2: Example effective vent area calculations for a building with H = 3m, 30 people on each storey and a top-storey atrium enhancement of E_N = 1. The ranges of values are based on the design requirements from Table 1.

The key result from this example calculation is that, in order to maintain equal per-person ventilation rates and temperatures on all storeys, vent sizes must increase on ascending the building. This compensates for the corresponding decrease in driving stack pressure supplied by the atrium on ascending the building, an effect which is amplified by heating the atrium.

This result agrees well with studies on this type of building. **[33]**, for example determined similar sizing rules. Numerous experimental and numerical studies have also shown that, if equal vent sizes are used on all storeys, flow rates decrease on ascending the building with the potential for overheating on upper storeys, or overcooling on lower storeys **[30,34,35]**.

Summary of preliminary design method

The steps for sizing ventilation openings to give equal flow rate per-person and temperatures on all storeys are listed below. Each step requires the designer to specify or estimate design criteria.

Note that the third step – converting effective vent areas to physical vent areas – has not explicitly been discussed herein. Should the reader wish to calculate physical vent areas, we suggest using $A_{in,i} = A_{out,i}$ for a balanced design, and taking $c_d = 0.6$, which is the commonly accepted value of the discharge coefficient for flows through 'sharp-sided' vents **[8,36]** – although this may vary with choice of ventilation opening.

1. **Determine design range of VPI, λ_p**
    a. Specify minimum acceptable ventilation flow rate per person, Q_p
    b. Specify desired temperature excess range, ΔT_p
    c. Estimate expected range of per-person heat gains, W_p
    d. Use chart in Figure 3 to determine required range of λ_p
2. **Calculate required effective vent areas**
    a. Specify desired atrium enhancement on top storey, E_N
    b. Specify occupancy levels within the building, n_i
    c. Estimate expected heat gains within the atrium
    d. Use equations in (9) to calculate required effective vent areas, a_i and a_a
3. **Calculate required physical vent areas**
    a. Estimate vent discharge coefficients, c_d
    b. Specify relative sizes of storey floor- and ceiling-level vents
    c. Use equations in (2) to calculate physical vent areas, $A_{in,i}$, $A_{out,i}$ and A_a

CONCLUSIONS

We have developed a preliminary design method for passive stack ventilation in multi-storey atrium buildings. Two dimensionless parameters – λ_p and E – have been identified and used to quantify the balance of core design variables, and the effectiveness of the atrium in enhancing ventilation flows. A design chart is presented which allows for selection of a range of values of λ_p based on the required flexibility of the ventilation scheme. Simple expressions for sizing ventilation openings based on λ_p, E and the number of people within the building are presented.

This method is intended to be as simple as possible so as to provide quick and intuitive first order guidance. It is intended to allow designers to rapidly determine preliminary requirements for a stack ventilation scheme and evaluate its potential effectiveness. We have tried to highlight some of the key limitations of the model, or suggest how it might be adapted to include more detail.

A key result is that vent sizes must increase on ascending the building, to compensate for the corresponding decrease in stack pressure available to drive flows through the upper storeys. This result agrees well with existing studies of multi-storey atrium buildings. An experimental campaign to explicitly validate the method presented herein is planned for late 2013.

ACKNOWLEDGEMENTS

The authors gratefully acknowledge the financial support of the EPSRC.

REFERENCES

[1] S. D. Fitzgerald, A. W. Woods. *Dramatic ventilation*. Building Services Journal, January:51–56, 2007.

[2] B. Krausse, M. Cook, K. J. Lomas. *Environmental performance of a naturally ventilated city centre library.* Energy and Buildings, 39:792–801, 2007.
[3] A. Acred, G. R. Hunt. *Multiple flow regimes in stack ventilation of multi-storey atrium buildings.* International Journal of Ventilation, 12:1:31-40, 2013.
[4] H. E. Feustel, A. Rayner-Hooson, editors. COMIS *Fundamentals - LBL-28560*. Lawrence Berkley Laboratory, California, 1990.
[5] G. N. Walton, W. S. Dols. *CONTAM v2.4 User Guide and Program Documentation*. National Institute of Standards and Technology, US, 2010.
[6] Y. Ji, M. J. Cook, V. Hanby. *CFD modelling of natural displacement ventilation in an enclosure connected to an atrium.* Building and Environment, 42:1158–1172, 2007.
[7] CIBSE. *Natural Ventilation in non-domestic buildings - Applications Manual AM10*. The Chartered Institution of Building Services Engineers, 2005.
[8] CIBSE. *Guide A - Environmental Design*. The Chartered Institution of Building Services Engineers, 2006.
[9] ASHRAE. *Standard 55-2010 - Thermal environmental conditions for human occupancy.* American Society of Heating, Refrigeration and Air-conditioning Engineers, Inc., 2010.
[10] D. W. Etheridge. *Natural Ventilation of Buildings: Theory, Measurement and Design*. John Wiley & Sons, Chichester, UK, 2012.
[11] J. M. Holford, G. R. Hunt. *Fundamental atrium design for natural ventilation*. Building and Environment, 38:409–426, 2003.
[12] S. R. Livermore, A. W. Woods. *Natural ventilation of multiple storey buildings: The use of stacks for secondary ventilation.* Building and Environment, 41:1339–1351, 2006.
[13] T. Chenvidyakarn and A. W. Woods. *On the natural ventilation of two independently heated spaces connected by a low-level opening*. Building and Environment, 45:586–595, 2010.
[14] D. W. Etheridge. *Nondimensional methods for natural ventilation design*. Building and Environment, 37:1057–1072, 2002.
[15] A. Acred, G. R. Hunt. *Stack ventilation in multi-storey atrium buildings: a dimensionless design approach*. Building and Environment, Submitted, 2013.
[16] G. R. Hunt, J. M. Holford, P. F. Linden. *Natural ventilation by the competing effects of localised and distributed heat sources.* 14th Australasian Fluid Mechanics Conference, pages 545–548, 2001.
[17] C. Gladstone and A. W. Woods. *On buoyancy-driven natural ventilation of a room with a heated floor.* Journal of Fluid Mechanics, 441:293–314, 2001.
[18] P. F. Linden, G. F. Lane-Serff, and D. A. Smeed. *Emptying filling boxes: the fluid mechanics of natural ventilation.* Journal of Fluid Mechanics, 212:309–335, 1990.
[19] N. B. Kaye, G. R. Hunt. *The effect of floor heat source area on the induced airflow in a room*. Building and Environment, 45:839–847, 2010.
[20] P. Cooper, G. R. Hunt. *The ventilated filling box containing a vertically distributed source of buoyancy*. Journal of Fluid Mechanics, 646:39–58, 2010.
[21] P. Cooper, P. F. Linden. *Natural ventilation of an enclosure containing two buoyancy sources.* Journal of Fluid Mechanics, 311:153–176, 1996.

[22] J. Axley. *Introduction to the design of natural ventilation systems using loop equations*. 19th AIVC Conference, Oslo, Norway, 1998.
[23] Battle-McCarthy Consulting Engineers. *Wind Towers: Detail in Building.* John Wiley & Sons, New York, 1999.
[24] G. R. Hunt, P. F. Linden. *Displacement and mixing ventilation driven by opposing wind and buoyancy*. Journal of Fluid Mechanics, 527:27-55, 2005.
[25] G. S. Larice. *Classifying steady states in emptying-filling boxes, Ph.D. thesis.* Imperial College London, 2009.
[26] C. J. Coffey and G. R. Hunt. *The unidirectional emptying box*. Journal of Fluid Mechanics, 660:456–474, 2010.
[27] A. J. Ward-Smith. *Internal fluid flow: The fluid dynamics of flow in pipes and ducts*. Clarendon Press, 1980.
[28] J. M. Holford, G. R. Hunt. *The dependence of the discharge coefficient on density contrast - experimental measurements*. 14th Australasian Fluid Mechanics Conference, pages 123–126, 2001.
[29] NASA. *U.S. Standard Atmosphere 1976*. National Aeronautics and Space Administration, 1976.
[30] J. Cooper. *The role of atria in the passive ventilation of multi-storey buildings - a steady flow analysis, Ph.D. thesis*. Imperial College London, 2010.
[31] P. M. Lynch, G. R. Hunt. *The night purging of a two-storey atrium building*. Building and Environment, 46:144–155, 2011.
[32] M. Economidou, G. R. Hunt. *The transient natural ventilation of a 2-storey atrium building - the failing atrium.* Proceedings of ROOMVENT 2009: the 11th International Conference on Air Distribution in Rooms, 2009.
[33] G. R. Hunt, J. M. Holford. *Top-down natural ventilation of multi-storey buildings*. Proceedings of the 19th AIVC Conference, pages 197–206, 1998.
[34] G. Gan. *Simulation of buoyancy-induced flow in open cavities for natural ventilation*. Energy and Buildings, 38:410–420, 2006.
[35] W. Ding, Y. Hasemi, and T. Yamada. *Natural ventilation performance of a double-skin façade with a solar chimney.* Energy and Buildings, 37:411–418, 2005.
[36] F. Flourentzou, J. Van der Maas, and C.-A. Roulet. *Natural ventilation for passive cooling: measurement of discharge coefficients.* Energy and Buildings, 27:283–292, 1998.

INVESTIGATION OF THE AIR FLOW FIELD IN FRONT OF THE REINFORCED SLOT EXHAUST HOOD

Ondřej Pech[1], Milan Pavelek[2]

1 Brno University of Technology
Technická 2896/2
Brno, Czech Republic
Pech@fme.vutbr.cz

2 Brno University of Technology
Technická 2896/2
Brno, Czech Republic

ABSTRACT

The paper deals with the investigation of air flow field in front of the reinforced slot exhaust hood with the workbench at the level of the lower edge of the exhaust opening. The reinforced exhaust hood, which is also known as the Aaberg exhaust hood, is the traditional exhaust hood equipped with an air supply jet that intensifies exhausting along the axis of the exhaust hood. By an adjustment of the air supply quantity, the reinforced exhaust hood can operate in traditional or reinforced modes. The investigation was made for the fixed air velocity in the exhaust opening and with three different momentum flux ratios of supplied and exhausted air flows. The air flow field was measured by six hot bulb thermo-anemometric sensors with the diameter of 3 mm in the vertical plane running through the axis of the exhaust opening. An obvious extension of the velocity plane in the reinforced modes was observed from the results of air velocity measurements.

KEYWORDS

Industrial ventilation, REEXS, exhausting, slot exhaust hood, velocity measurement.

1 INTRODUCTION

In industrial production different pollutants are generated from technologies. These pollutants are mostly unhealthy, and therefore the ventilation is necessary. The ventilation systems can be divided into two groups according to the air exchange rate inside a ventilated space. The first group is called the global ventilation systems and these systems control the pollution level by supplying the fresh air into the whole ventilated space. The second group is called the local ventilation systems. These systems capture pollutants at their source and reduces the load of pollutions in the area and simultaneously decrease demands on the global ventilation because the concentration of contaminants in the local exhaust air is much higher than that in global ventilation. The main part of local exhaust systems is an exhaust hood which can be traditional and reinforced. In the case of the traditional exhaust hood the air flows evenly in the direction of the exhaust opening from all the sides but its capture efficiency of pollutants rapidly decreases with an increasing distance from the source of pollutants. The traditional exhaust hood has therefore to be located as close to the source of pollutants as possible which is not always technically or technologically practicable. It is also possible to use the **Re**inforced **E**xhaust **S**ystem – REEXS invited by (Aaberg, 1977) which uses the reinforced exhaust hood. It is a traditional exhaust hood equipped with an air supply inlet that intensifies exhausting along the axis of the exhaust hood, see Fig. 1. With the suitable momentum flux ratio between supplied and exhausted air flows, the shape and the range of

the effective exhaust area are possible to be partially changed and better results of exhaustion can be reached as shown in (Pech & Pavelek, 2012) and (Pech & Pavelek, 2013).

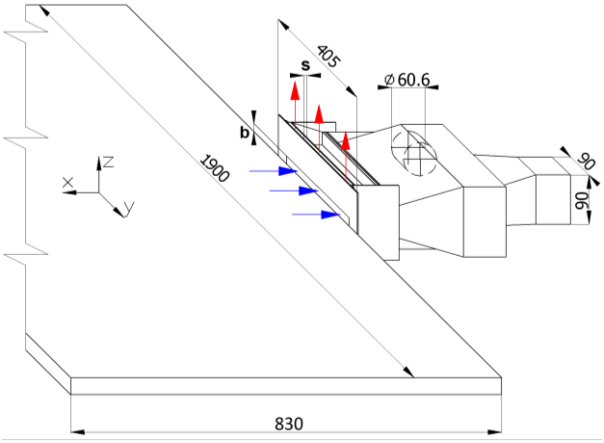

Figure 1: Reinforced slot exhaust hood with workbench

2 MEASUREMENT SETUP

In the research the reinforced slot exhaust hood (Figure 1), designed at Department of Thermodynamics and Environmental Engineering, Brno University of Technology, was used. The hood has one slot exhaust opening with the width *b* of 15 mm and a special flange with two supply slots on its long side edges. The width *s* of supply slots can by adjusted between 1 mm and 8 mm. In the investigated cases the width was set to 4 mm and the lower supply slot was blocked.

This exhaust hood enables operating in different modes which depend on the operating parameter *I* established by Hylgård (Hyldgård, 1987). For the Aaberg exhaust hood, the operating parameter is defined as the ratio between the momentum flux of supplied and the exhausted air. This operating parameter can be determined as follows,

$$I = \frac{\dot{m}_s \cdot w_s}{\dot{m}_{ex} \cdot w_{ex}}, \tag{1}$$

where $\dot{m}_s$ and $\dot{m}_{ex}$ represent the mass flow of the supply air and the mass flow of exhaust air, respectively, w_s and w_{ex} are the velocities of the supply air and the exhaust air at the slot openings, respectively. When the operating parameter is set to $I = 0$, the exhaust hood works as the traditional exhaust hood. In the case of nonzero value of the operating parameter, the exhaust hood works as the reinforced exhaust hood. Gubler (Gubler, 2002) and others shown that the higher the momentum flux ratio the higher the suction effect of the hood.

For testing and research of exhaust hoods, the measurement setup (Figure 2) was designed and assembled at our department. For measuring it is possible to use the tracer gas method (to determine the exhaust efficiency), the method of velocity measurement in front of the exhaust hood or the flow visualization method with smoke or helium bubbles.

Figure 2: Measuring setup in variant with workbench

The scheme of measurement setup is illustrated in Figure 3. It consists of three main parts: exhausting (positions 2, 3, 4 in Figure 3) and air supply (positions 5, 6, 7), both connected to the exhaust hood (position 1), and the velocity measurement part (positions 8, 9).
The workbench (position 19) with the dimension in the *x* axis of 830 mm and in the *y* axis of 1,900 mm was used. The measurement setup includes measurements of pressures and temperatures in the duct in front of the flow meters. Also the barometric pressure, ambient temperature and the temperature in the air supply slot are measured. For the measurement of velocity magnitude the velocity data logger (position 6) with six hot bulb thermo-anemometric sensors (position 8) are used.

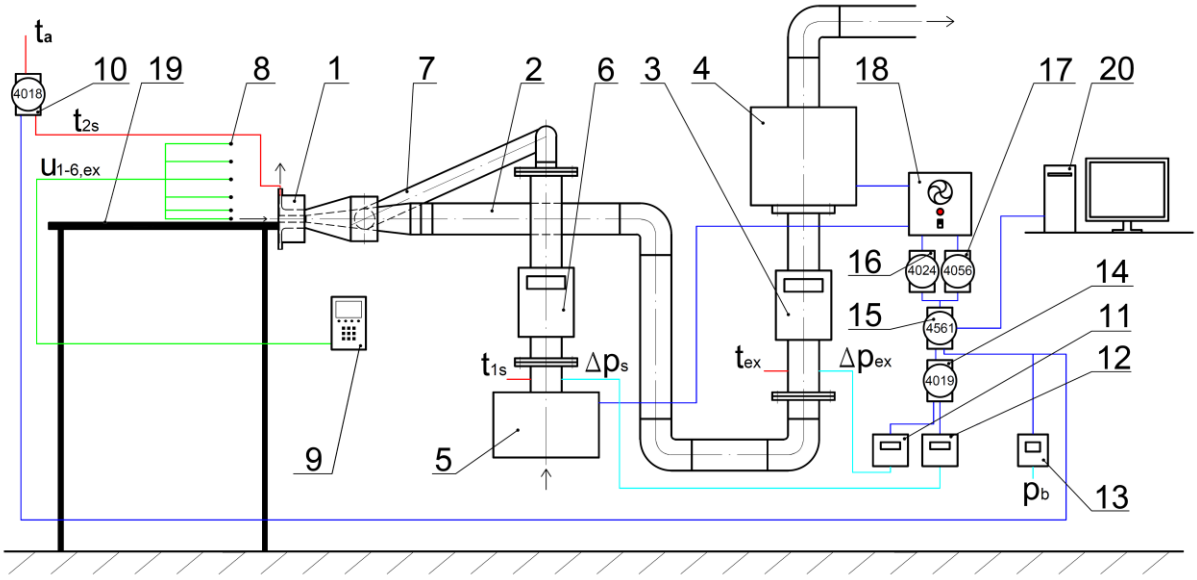

Figure 3: Scheme of the measurement setup
1 – reinforced exhaust hood, 2– exhaust air duct 3 – exhaust air flow meter, 4 – exhaust ventilators, 5 – supply air ventilator, 6 – supply air flow meter, 7 – supply air duct, 8 – thermo-anemometric sensors, 9 – velocity data logger, 10 – temperature measuring module, 11 – exhaust air pressure transmitter, 12 – supply air pressure transmitter, 13 – barometric pressure transmitter, 14 – converting module, 15 – communication module, 16 – relay output module, 17 – analogue output module, 18 – triac regulators, 19 – workbench, 20 – PC

3 VELOCITY MEASUREMENTS

The velocity field of the exhaust hood with the workbench situated at the bottom edge of the exhaust slot opening was investigated for the traditional exhaust mode ($I = 0$), and for the reinforced exhaust modes ($I = 0.3$, 0.6, and 0.9). The air was supplied only through the upper

slot opening as shown in Figure 1 and its velocity magnitude was set according to the operating parameter. The velocity magnitude in the exhaust slot opening was chosen to w_{ex} = 8.0 m/s according to the literature (Chysky & Hemzal, 1993).
For the velocity measurement of the reinforced exhaust system the constant temperature anemometry with six hot bulb sensors with the diameter of 3 mm was used. The hot bulb sensors move in the selected grid in the vertical plane ($x - z$) running through the axis of the exhaust hood located in the Cartesian coordinates system (x, y, z). Its origin was placed to the midpoint of the exhaust slot opening of the reinforced exhaust hood. The distance between measured points of the grid in the x axis was between 15 mm and 30 mm, and in z axis between 15 mm and 45 mm.

4 RESULTS AND DISCUSSION

The velocity fields from the velocity measurement by the reinforced slot exhaust hood situated over the workbench with different exhaust modes (I = 0, 0.3, 0.6 and 0.9) are shown in Figure 4. The graphs are made in dimensionless coordinates related to the width of exhaust slot opening b = 15 mm.

Owing to the nature of contaminants and to background air movements, the velocity in front of the hood must exceed a minimum velocity, known as the capture velocity, in order to draw the contaminated air into the exhaust inlet. Under normal practical conditions the capture velocity is typically of the order of 0.25 m/s, see Høgsted (Høgsted, 1987), (Saunders & Fletcher, 1993), or (Gubler, 2002). Hunt (Hunt & Ingram, 1992) defines the effective suction area, from which the air is drawn into the exhaust inlet and successfully removed from the workplace, as the area bounded by the line of constant velocity.

In the case of exhausting with the operating parameter I = 0 (position A in Figure 4), the capture velocity field is shorter in a comparison to other settings of the operating parameter I (cases of positions B, C, D). With the increasing value of operating parameter I, the capture velocity field becomes longer. In reinforced modes (cases of positions B, C, D) can be also seen the supplying air flow.

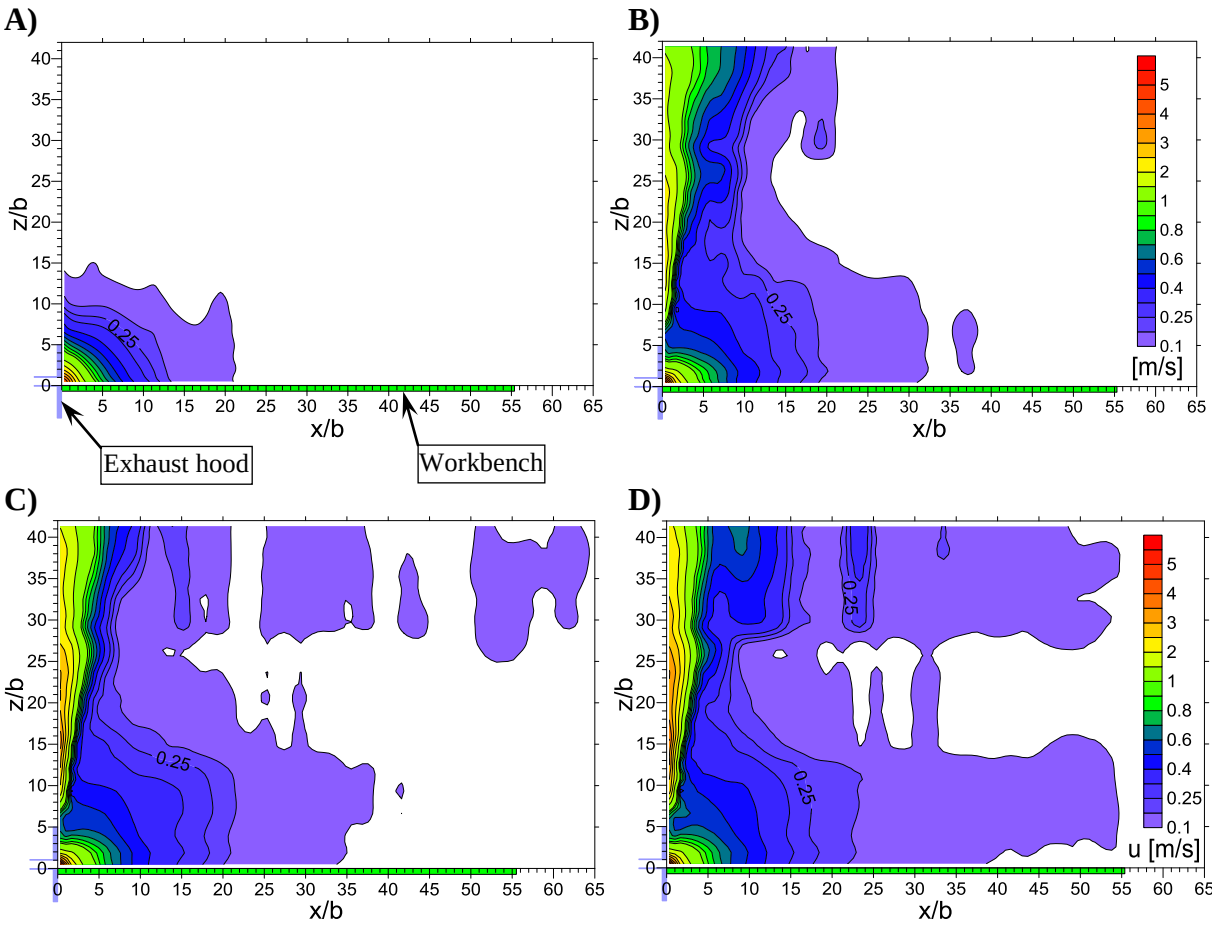

Figure 4: Velocity field in the vertical plane x – z running through the axis of the reinforced slot exhaust hood situated over the workbench with operating parameter A) I = 0; B) I = 0.3; C) I = 0.6; D) I = 0.9

In the Figure 5 there are pictured the velocity magnitudes in the axis of the reinforced slot exhaust hood with different operating parameters I. In this figure the capture velocity

u = 0.25 m/s is also drawn. As can be seen from the figure the effective suction area is shortest (x/b = 12.0) in traditional mode (I = 0). In reinforced exhaust modes the effective suction area in the axis of the reinforced slot exhaust hood is longer: in case with I = 0.3 its length equals to x/b = 16.8, with I = 0.6 to x/b = 17.6 and with I = 0.9 is its effective suction area is extended to x/b = 17.7. However, the experimentally obtained differences in the length of the effective suction area between variants with operating parameter I = 0.6 and I = 0.9 were so small that they fell into the uncertainty range of the measurements.

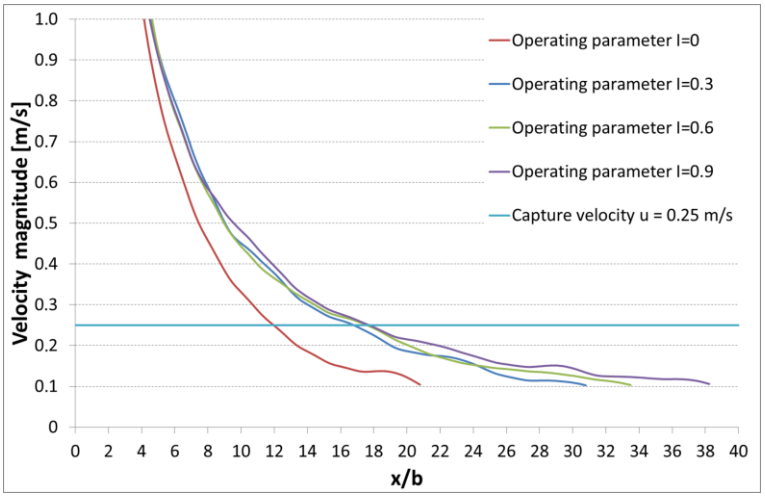

Figure 5: Velocity magnitude in the axis of the reinforced slot exhaust hood with different operating parameter I

5 CONCLUSIONS

The difference between velocity fields in front of the traditional slot exhaust hood and the reinforced slot exhaust hood situated over the workbench was observed. The velocity magnitude in the axis of the reinforced slot exhaust hood with different operating parameters I (the ratio between the momentum flux supplied and the exhausted air flow) was compared with the capture velocity in order to determine the length of the effective suction area. The results of the measurement show that in reinforced mode the effective suction area becomes longer in comparison to the traditional mode. With the increasing value of operating parameter I from 0.3 to 0.9, the effective suction area becomes longer but the difference is not as significant as in the case of comparison between traditional and reinforced modes.

6 ACKNOWLEDGEMENTS

The research leading to the presented results was supported by NETME Centre ED0002/01/01 and the Brno University of Technology project FSI-J-13-2042 for young researchers.

7 REFERENCES

Aaberg, C. P. (1977). *Patent No. 4043257.* United States.

Gubler, D. (2002). REEXS - Reinforced Exhaust System Optimization of Operating and Design Parameters. Zurich: Swiss Federal Institute of Technology.

Høgsted, P. (1987). Air movements controlled by means of exhaustion. *Proceedings of International Conference on Air Distribution in Ventilated Spaces.* Stockholm.

Hunt, G. R., & Ingram, D. B. (1992, Vol. 36). The fluid-mechanics of a 2-dimensional Aaberg exhaust hood. *Annals of Occupational Hygiene*, pp. 455-476.

Hyldgård, C. E. (1987). Aerodynamic control of exhaust. *International Conference on Air Distribution in Ventilated Spaces ROOMVENT 1987.* Stockholm.

Chysky, J., & Hemzal, K. (1993). *Ventilation and air conditioning – Design guidebook 31*. Brno: Bolit. (original in Czech).

Pech, O., & Pavelek, M. (2012). Capture efficiency of pollutants in a free space and over a workbench with reinforced slot exhaust systems. *ICCS 2012 International symposium on contamination control* (p. 31). Zurich: Swiss Federal Institute of Technology ETH Zurich.

Pech, O., & Pavelek, M. (2013, Vol. 45). Capture efficiency measurement of pollutants over a workbench with the reinforced slot exhaust system.

Saunders, C. J., & Fletcher, B. (1993, Vol.37). Jet enhanced local exhaust ventilation. *The Annals of Occupational Hygiene*, pp. 15-24.

A STUDY ON EFFECTS OF ENERGY SAVING BY APPLYING COMPLEX INSULATION INTEGRATED THE SOFT MATERIAL IN APARTMENT HOUSE

HYUNG GEUN KIM[1] , MI YEON KIM[*2] and MI YEON LEE[*3]

1 SEOUL METROPOLITAN SH CORPORATION
621, Kaepo-ro, Kangnam-Gu, Seoul,
135-988, KOREA

2 SEOUL METROPOLITAN SH CORPORATION
621, Kaepo-ro, Kangnam-Gu, Seoul,
135-988, KOREA

3 SEOUL METROPOLITAN SH CORPORATION
621, Kaepo-ro, Kangnam-Gu, Seoul,
135-988, KOREA
**Corresponding author: polonull@i-sh.co.kr*

ABSTRACT

As environmental issues are rapidly gaining more and more interest globally, various measures and standards are being set to minimize the use of energy in the architecture field, which consists about a fourth of the total use of energy. Korea, like other developed countries, is also aiming to make zero-energy buildings mandatory(by 2025) implementing various measures such as energy efficiency rating system and energy performance certification systems to gradually minimize energy consumption in buildings.
Most residential buildings of Korea are constructed using box frame using concrete walls as bearing walls and the formation of the structure is done by steel reinforced concrete. Legally obligated insulation design is mainly based on internal insulation structure with easy construction method. This design is constructed by installing an insulating material on the interior of structure. Rigid urethane with light weight and excellent waterproof property is most widely used as an insulating material in residential buildings. But rigid urethane insulating material has a concern of creating a gap when attached to the surface of concrete with uneven finishing surface due to lack of flexibility. In order to resolve such problem, this study intended to develop a complex insulating material. This material integrates an insulating material with a soft material, which acts as a buffer between the wall with uneven finishing surface and the insulating material.

KEYWORDS

Energy saving, Flexible insulating material, Airtightness, Reduction of condensation

1 INTRODUCTION

As environmental problems are coming to the fore throughout the world, diverse methods to minimize energy consumption in the construction sector, which takes up about 1/4 of total energy consumption, are being implemented. As in developed nations, Korea is also implementing various standards to minimize energy consumption in buildings. With the objective of obligating 2025 zero-energy building, energy consumption efficiency rating system and building energy performance certification system are being promoted to gradually minimize energy consumption in buildings. As a part of such methods, the law obligates buildings to have insulation design to cope with temperature changes during four seasons, regulating thermal transmittance of each part and thickness of insulating material in buildings. Most of buildings in Korea have reinforced concrete structure. Legally obligated insulation design is mainly based on internal insulation structure with easy construction method. This

design is constructed by installing an insulating material on the interior of structure. Rigid urethane with light weight and excellent waterproof property is most widely used as an insulating material in residential buildings, and it is used together with stiffeners such as gypsum board and iron plate to compensate for fragility. Rigid urethane insulating material has a concern of creating a gap when attached to the surface of concrete with uneven finishing surface due to lack of flexibility. In such gap, thermal loss can reduce insulation performance and convection phenomenon may create an unpleasant environment with condensation and inhabitation of molds. In order to resolve such problem, this study intended to develop a complex insulating material. This material integrates an insulating material with a soft material, which acts as a buffer between the wall with uneven finishing surface and the insulating material.

2 DEVELOPMENT OF INSULATING MATERIAL

Most of insulating materials used in buildings are rigid flat type materials with lack of flexibility. There is a limitation in close construction when the material is being attached to the concrete surface. The condensation phenomenon which occurs in the gap between concrete and insulating material reduces insulation performance and can create an unpleasant environment with molds.

Figure 1: Examples of Condensation phenomenon

A soft part was added in rigid insulating material to prevent occurrence of such gap. Polyethylene with elasticity and waterproof property was reviewed as the soft part. Polyethylene is chemically and physically cross-linked foam having excellent thermal insulation, buffer effect, durability and chemical resistance. Due to its light weight and easy processing, polyethylene is being widely used in civil engineering, construction, automobile interior materials, and convenience goods. Structure and outer skin of the foam can be processed according to the use, and the material shows excellent formability. The material can be used semi-permanently because of excellent durability, and the independent foam material has low thermal conductivity and desirable thermal insulation. The foam particle with high modulus of elasticity allows reduction of negative energy, excellent dimensional stability after heating, and stable dynamic modulus of elasticity and loss factor. Accordingly, there is little concern of deformation after construction with passage of time. Also, the material is flexible and not crushed by impact, allowing close construction.

Figure 2 : soft and flexible polyethylene

Rigid urethane insulating material has low thermal conductivity and excellent insulation performance. Soft polyethylene has excellent adhesion, which reduces the condensation phenomenon occurring in the gap between the wall and insulating material. The form of complex insulating material that integrated soft and flexible polyethylene with rigid urethane insulating material is as follows.

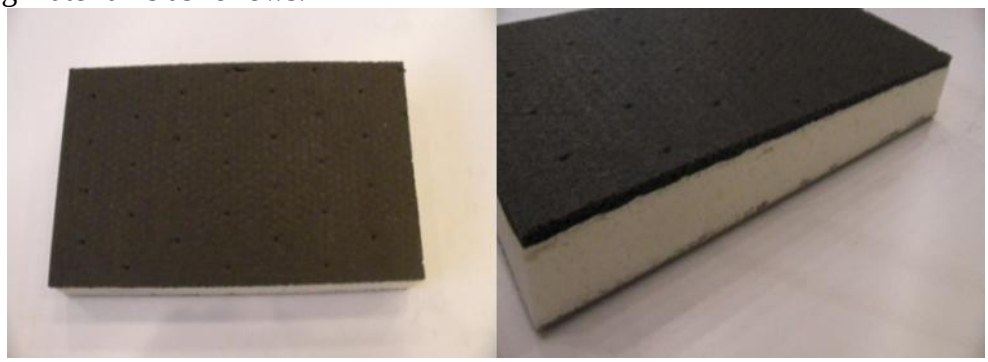

Figure 3 : The Developed insulating material

3 PERFORMANCE ASSESSMENT ON THE DEVELOPED INSULATING MATERIAL

To assess performance of the developed complex insulating material, insulation performance and occurrence of condensation were reviewed. Insulation performance assessment was conducted by comparatively analyzing thermal performance and heating load of the complex insulating material with air tightness and existing insulating materials using a computer program. For review of condensation, the developed complex insulating material was constructed in the condensed space to measure and monitor temperature and humidity.

3.1 Insulation Performance Assessment

For assessment of insulation performance, thermal performance and heating load were evaluated using a simulation program. The most general type of apartment house in Korea with the size of 84 ㎡ was selected as the simulation model, and the simulation program was based on Physibel and TRNSYS.

Table 1 : Simulation conditions

Model	Division	Design conditions
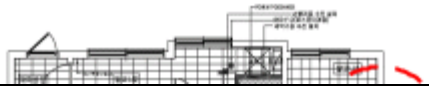	Indoor Temperature	22℃

	Outdoor Temperature		15℃
	U-Value of wall	A	0.11[W/m·K]
		B	0.12[W/m·K]
		C	0.11[W/m·K]
		D	0.11[W/m·K]

For the thermal performance simulation, heat flow performance of existing urethane insulating material was analyzed first. The developed complex insulating material was applied to the same structure to perform thermal performance assessment on the uppermost, reference and lowermost floors. Performance of the developed insulating material was reviewed by comparatively analyzing the data obtained.

Table 2 : Simulation Results

Division		Urethane Insulating material	Developed complex Insulating material
A	Uppermost Floor	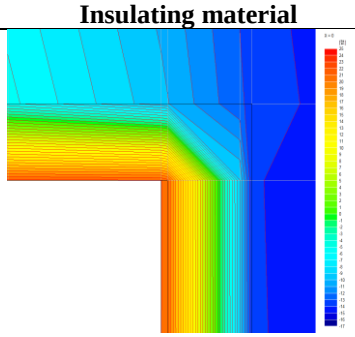	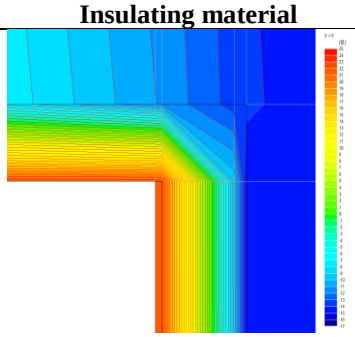
	Reference Floor	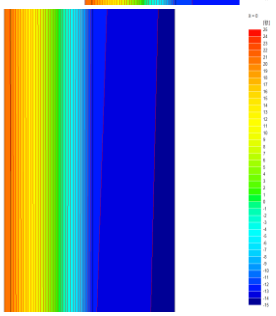	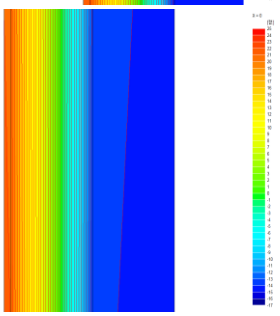
	Lowermost Floor	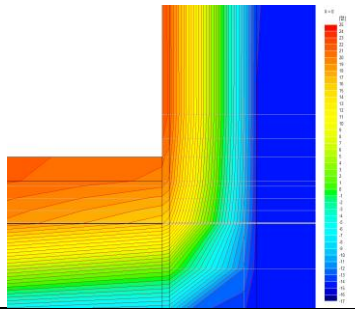	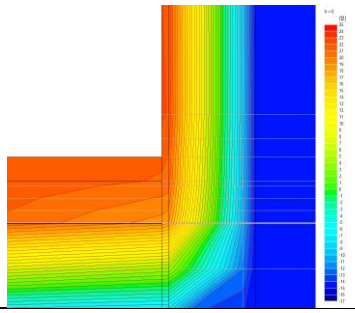

B	Uppermost Floor	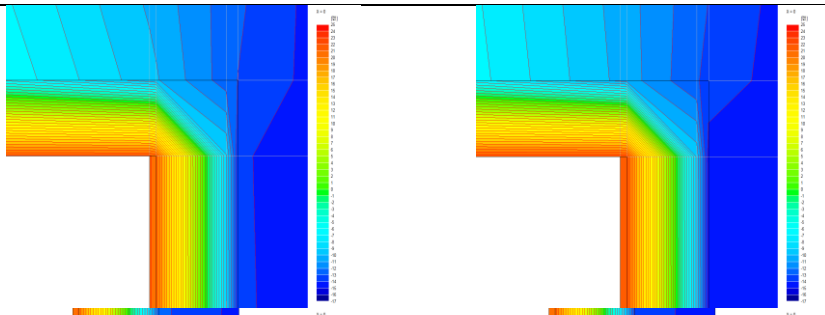
	Reference Floor	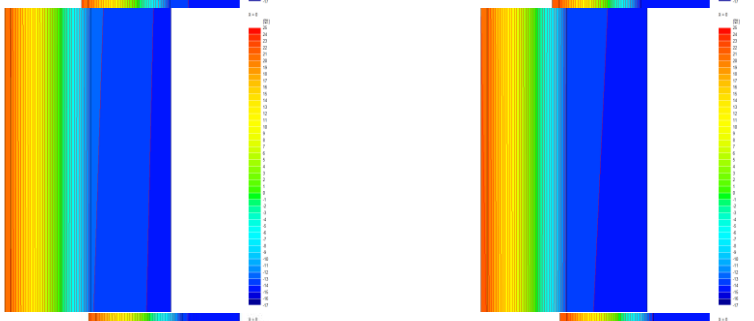
B	Lowermost Floor	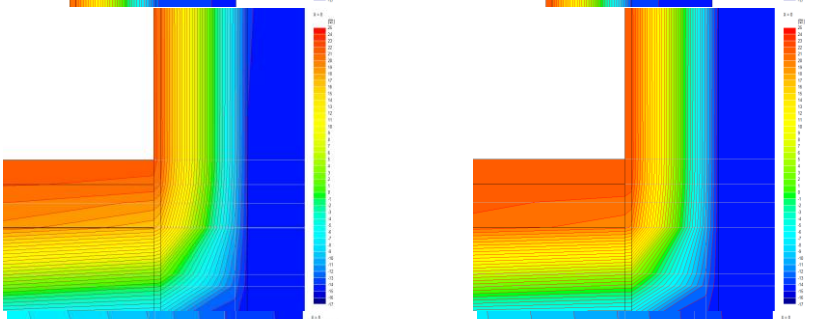
	Uppermost Floor	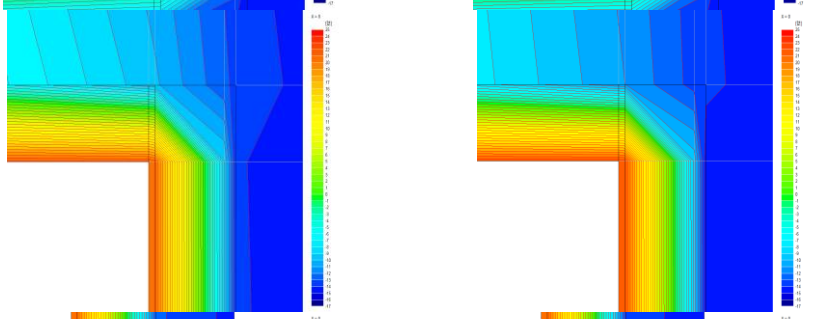
C	Reference Floor	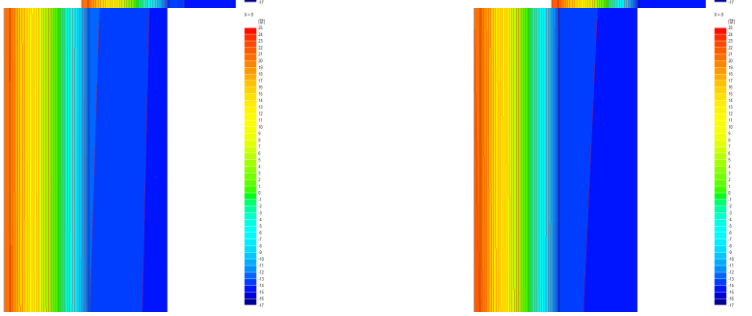
	Lowermost Floor	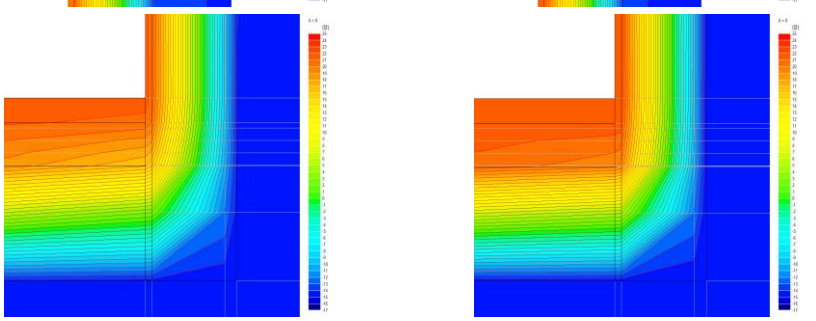

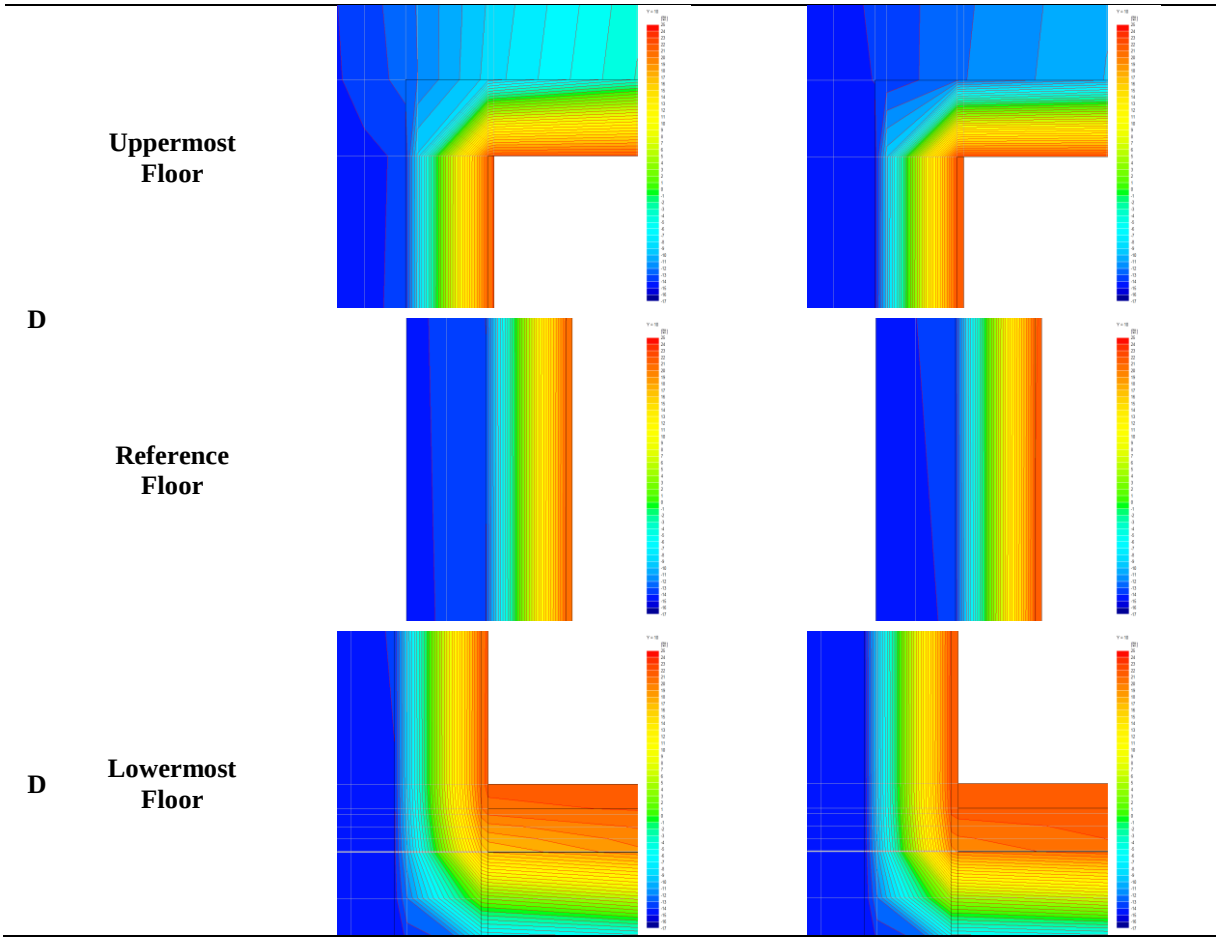

As a result of simulating the uppermost, reference and lowermost floors of Cases A, B, C and D, construction using the developed complex insulating material compared to existing insulating material was interpreted to show a difference of about 1℃ to 1.5℃~1.8℃ on top of the uppermost floor, wall of the reference floor, and bottom of the lowermost floor. Accordingly, when insulating materials with same thickness are applied, construction with complex insulating material was found to reduce heating energy due to change in temperature of about 1℃~1.8℃.

Heat load of the developed insulating material was assessed. Using the same model as in thermal performance assessment, the type of insulating material in the wall configuration according to the building part (exterior wall, uppermost floor, lowermost floor, etc.) was differentiated to evaluate heating load of each household.

Table 3 : Simulation Results

Division	Heating Load		Reduction Effect	
	Urethane Insulating material	Developed complex Insulating material	Heating Load	CO2 Emission
Lowermost Floor	8,702kWh	7,765 kWh	10.8%	12%
Reference Floor	6,422 kWh	5,883 kWh	8.4%	9%
Uppermost Floor	8,187 kWh	7,418 kWh	9.4%	10%

When constructed using the developed complex insulating material compared to existing insulating material, predicted heating load was reduced by about 10.8% for the lowermost floor, 8.4% for the reference floor, and 9.4% for the uppermost floor.

Therefore, when insulating materials with same thickness are applied, heating load was reduced by about 8~10% by constructing the building using complex insulating material.

3.2 Experimental Construction for Occurrence of Condensation

To examine occurrence of condensation, an experimental construction of existing insulating material and the developed complex insulating material was conducted on a balcony wall of an apartment house on which condensation frequently occurs during winter season due to low outdoor temperature.

After cleaning the wall surface, the insulating materials were attached to the constructed part using glue. The joint part of insulating materials was filled and straightening work was carried out.

Figure 4 : Construction Process

Occurrence of condensation was reviewed by measuring internal, external and surface temperatures.

Table 4 : Measuring Results

Division		Average Temperature
Outdoor		-3℃
Indoor		18℃
Wall	**Urethane Insulating material**	9.6℃
	Developed complex Insulating material	12.3℃

As a result of monitoring, surface temperature of the wall with the developed complex insulating material was higher than surface temperature of the wall with existing insulating material under same external temperature. In addition, while the wall with existing insulating material had its surface contaminated by condensation, the wall with the developed complex insulating material did not show occurrence of condensation.

Figure 5 : Surface of Wall – Urethane Insulation material(left), Developed complex Insulation material(right)

4 CONCLUSIONS

In this study, a complex insulating material on which a soft part was added to a rigid insulating material was developed to secure air tightness between the wall and insulating material, and performance of the material was reviewed. To examine air tightness between the insulating material and wall, an energy analysis simulation based on computer program was performed for thermal performance and insulation performance of existing insulating material

and the developed complex insulating material. Experimental construction and monitoring were carried out to observe occurrence of condensation, which can be caused by lack of air tightness. As a result of energy analysis simulation, thermal performance was improved compared to existing insulating material, and CO2 emission was reduced by decrease in heating load. Also, as a result of constructing the complex insulating material to reduce condensation that occurs on the wall surface during winter due to difference in external and internal temperatures, the material was found to be effective in preventing condensation. However, since condensation occurs as a result of complex phenomena including temperature difference, humidity, lack of ventilation and defective construction, continued monitoring and additional experimentation on the constructed parts are deemed necessary to accurately verify performance of the developed complex insulating material.

5 ACKNOWLEDGEMENTS

MIN HEE SON, SI WOO LEE(YOUNGBO Chemical Co., Ltd.)

6 REFERENCES

Kyung Hoe Lee(2007) . *Architectural Environment Design*, Munundang.

Man Taek Lim(2002). *Architectural Environment Design*, Bomundang.

ENERGY SAVING AND INDOOR AIR QUALITY IN OFFICE BUILDINGS

E. Provata[1], D. Kolokotsa [1]

[1] *Technical University of Crete, Environmental Engineering Department, 73100 Chania, Greece*

ABSTRACT

Air quality in the office room areas, as well as their energy demands for heating and cooling are directly depended on the ventilation levels in those rooms. Specifically, high internal air quality requires high levels of ventilation and therefore high energy demands. On the other hand, high energy savings can be accomplished by full building impermeability, which means low to none ventilation and at the same time low air quality. Those observations were determined from studying the effect of natural air flow in energy preservation at an extant building with office complexes, specifically the K_2 building which is part of the Environmental Engineering Department at the Technical University of Crete. The building's thermal behaviour was examined using a modelling program called TRNsys, whereas the use of a tool named COMIS allowed the modelling of air flow inside the building as well as estimating the inner pollution derived from the employees.

KEYWORDS

Energy Saving, Ventilation, Infiltration, Indoor air quality

1 INTRODUCTION

According to the European Commission, the building sector is responsible for the 40% of the final energy consumption and the 36% of carbon dioxide emissions (European Commission 2013). For this reason, the energy savings from this sector is a concern for several decades.

Since the '80s, the first draft guidelines had been set in order to reduce the energy requirements of buildings. The full insulated constructions were considered as the first improvement action for that scope because these buildings don't allow the infiltration of fresh air into the building. After that, other improvement techniques were applied that were related to the technology and the operation of the HVAC systems, as are described by Olesen et al. (Olesen, Seppanen, and Boerstra 2006)

The consequences of these actions were the energy saving from the building sector and the degradation of the indoor air quality. The lack of fresh air in the internal environment of the buildings had negative effects to the human health.

Thus were established the first actions to ensuring good indoor air quality and the prevalence of a healthy internal environment. These actions were related to the ventilation levels, the lighting level, and acoustic level etc. (Olesen 2004)

The objective of this paper is the study of the infiltration / ventilation air rates as the critical parameter which affects the most to the energy demands and the internal pollution of a building. Several studies have examined the building's energy demands and propose energy saving measures without considering the air flow or the pollutant transport (Boyer et al. 1998), (Alemu, Saman, and Belusko 2012). In this paper, the energy saving is coupled with the indoor air quality.

2 METHOLOGY

The methodology proposed in this paper is based on computer simulations using TRNsys and COMIS. TRNsys (TRaNsient SYstems Simulation program) (Solar Energy LaboratoryUniversity of Wisconsin-Madison 2010) software is used in order to provide information on the dynamics of the thermal behaviour of both the whole building, as well as for individual components (Khandelwal, Talukdar, and Jain 2011), (Al-ajmi and Hanby 2008). It can calculate a number of variables, such as the internal temperature, humidity, airflow, the power consumption, the thermal comfort etc., solving a series of differential equations that describe mass and heat transfer in buildings. COMIS (Conjunction of Multizone Infiltration Specialists) (Comis 2005) simulates multizone air flow (Li and Heiselberg 2002) and pollutant transport in buildings (Viktor Dorer, Anne Haas, Werner Keilholz, Roger Pelletret 2001). These computer simulations can be coupled by type 157 in which the COMIS gives the air flow as input to TRNsys and then the last calculates different parameters considering the infiltration or ventilation rates.

2.1 Building Description

TRNsys and COMIS were used to calculate the energy demands and the pollution levels of a building located in the area of Chania in Greece. Specifically, this building called K_2 (Figure 1) belongs to the Department of Environmental Engineering of Technical University of Crete. It's located just a few kilometres from the sea, stands at an altitude of 137 m and is orientated 45^o northwest.

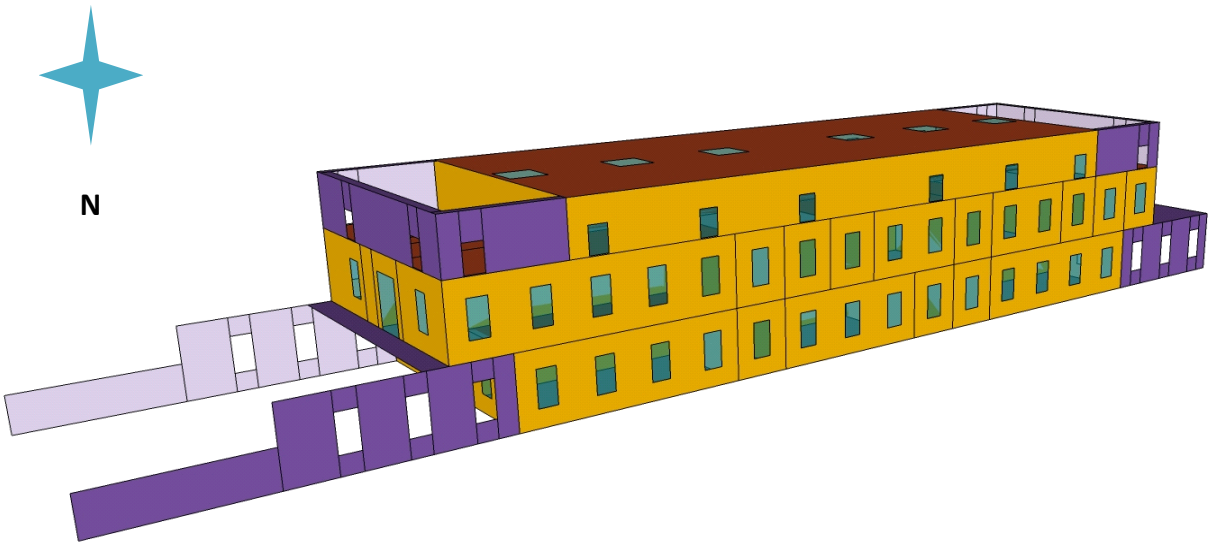

Figure 1: 3D model building

The studied building consists of a ground floor, a first floor and a second floor. At the ground floor, the computer center, a space for printings, toilets and laboratories are situated, while the first floor accommodates only offices. The last floor has no office or laboratory operation because the mechanical equipment of the building is there.

The dimensions of the building are the following: length = 42m, height = 12m and width = 14.4 m. It was separated into zones, in order to simulate and study. Specifically, thirty zones were created based on the using and the orientation of each zone. For the ground floor, 12 zones were created, 17 for the first floor, while the second floor was a single zone.

2.2 Characteristics of the building

In order to simulate the building using TRNsys, the constructive and the operating characteristics are needed.

The constructive characteristics of the building are presenting at the following table.

Table 1: Constructive characteristics

External walls	Gypsum board, Cement board, Concrete, Cement board type of Aquapanel
Internal walls	Gypsum board
Roof	Armed concrete, insulation panels
Ground Floor	Armed concrete, marble
Ceilings / Internal floors	Armed concrete, marble, Gypsum board tapes
Glazing	Aluminum frame and doubled layer

The operating characteristics that are required as inputs to each building zone include the occupants, the lights, the HVAC systems, the electronic computers, the printers and the operating schedules of all these.
The average power density of the installed lighting is 13 W/m^2 for the building under consideration. The heating system operates at 20 ° C and the cooling at 26 ° C. Computers operate at a power of 230 W and printers at 220 W. These data were entered in the modeling program considering weekly operating schedule which was a five-day work for 8 hours a day, from 8:00 until 16:00. Regarding, the occupants, it was estimated that 1 or 2 people work at each office zone doing light work and using 1 or 2 computers. At the computer center, it was set that 10 people visit this space using 10 computers from 9:00 to 15:00 daily.

3 PRESENTATION OF RESULTS

3.1 Validation of TRNsys simulation

Firstly, the validation of the simulated results was necessary. This, was achieved by comparing the measured internal air temperature with the calculated by TRNsys, at the zones which had no operation at the measuring period. The results are presented at the following figures.

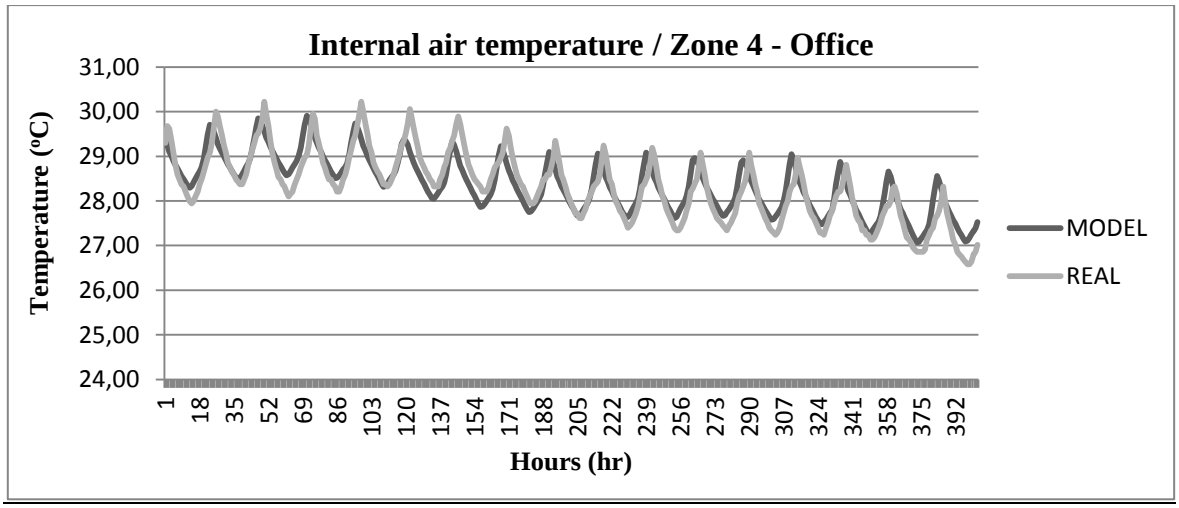

Figure 2: Comparison of internal air temperature at zone 4

Zone 4 includes one office of the building which is situated at the North West sight of the 1st floor. The internal air temperature was measured from 04/08/2012 to 21/08/2012 and its variance is shown at the figure above.

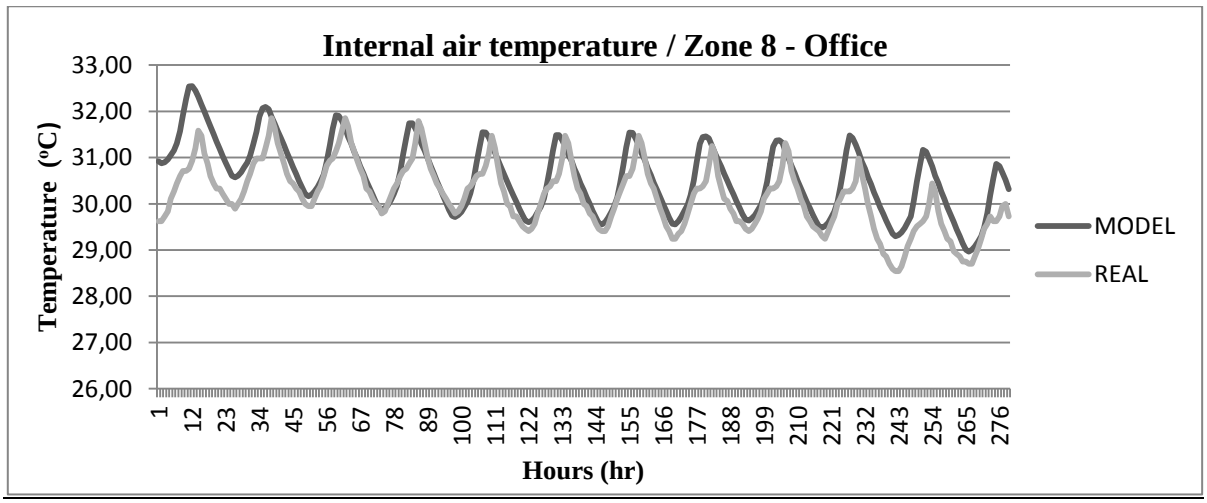

Figure 3: Comparison of internal air temperature at zone 8

At zone 8, which represents a North East office space of the 1st floor of the building, the measuring period of the internal temperature was from 08/08/2012 to 19/08/2012. The comparison between the simulated results and the measurements are shown at Figure 3.

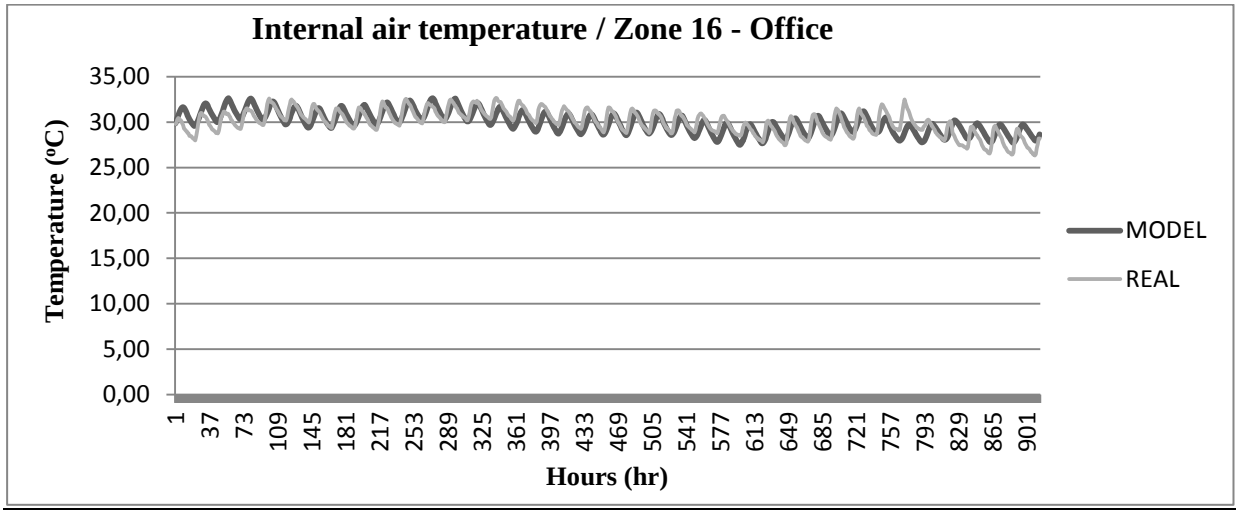

Figure 4: Comparison of internal air temperature at zone 16

The last validation was that at zone 16 which is situated at the south east corner of the 1st floor of the building. The measuring period was from 27/07/2012 to 30/08/2012 and the results are shown at Figure 4.

Regarding the three validations that were presented above, it is understandable that the building's simulation is close to the reality because of the declination between the measurements and the calculated values by the model that it was too small.

The model that was designed at TRNsys environment was validated and the next step was to calculate the energy demands of the building considering two study cases that are presented below, at the next section.

3.2 Building's energy demands

The building's energy demands were calculated considering two scenarios. At the first scenario, it was set that the building is full insulated and at the second the infiltration air rate that was calculated by COMIS for each zone is considered as an input parameter at TRNsys in order to estimate the heating and the cooling demands. The results of both scenarios are presented at the figure below.

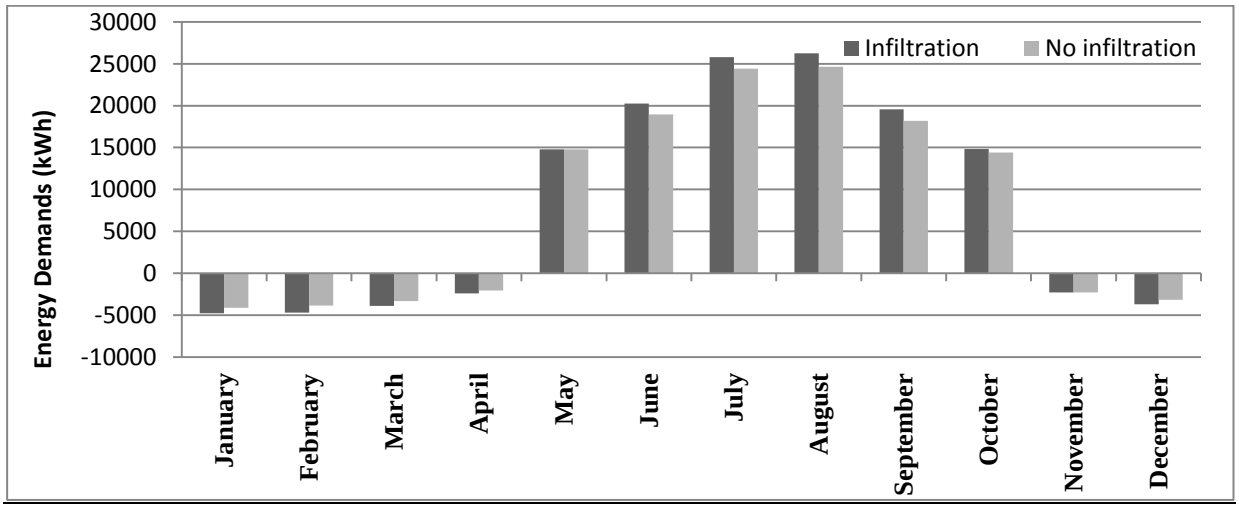

Figure 5: Building's energy demands considering infiltration and no infiltration air rates

At figure 5, the negative values represent the energy demands for heating, while the positive values show the energy demands for cooling. It is obvious that the cooling loads seems to be quite larger than the heating loads, which makes sense, as the building's geographical location is characterized by summers with intense sunshine and high temperatures, while winters are mild with median ambient temperatures. The infiltration air rate is a significant parameter for the energy saving. Regarding the results, if the building is full insulated the building needs 2947.5 kWh less for heating and 6080.1 kWh less for cooling.

In addition to energy saving, the indoor air quality should be examined in relation to the infiltration – ventilation rates, as this parameter directly affects at the health of employees in a building. As it mentioned at the beginning of this paper, the indoor air quality is depended of many pollutants and their concentrations.
In this paper only CO_2 levels were examined and calculated by using COMIS at zone 9 which represents an office space with one employee.

3.3 CO_2 levels in zone 9

Zone 9 represents an office, which is situated at the north west corner of the building at the 1st floor. In this zone, was placed equipment in order to measure the concentration of CO_2 which is produced by the human metabolism. The measuring period was from 19/08/2012 to 21/08/2012 and the measurements are presented below. The pollutant rates also were calculated by COMIS, considering that zone 9 is visited by one person who works there every day from 8:00 to 18:00. The person's characteristics that were set to COMIS are presented at Table 2.

Table 2: Person's characteristics

Sex	Male
Age	26
Height	1.80 m
Weight	80 kg
Metabolic rate	1.1 MET

The calculated concentration during the operating schedule of the office and the measurements are shown at figure 6.

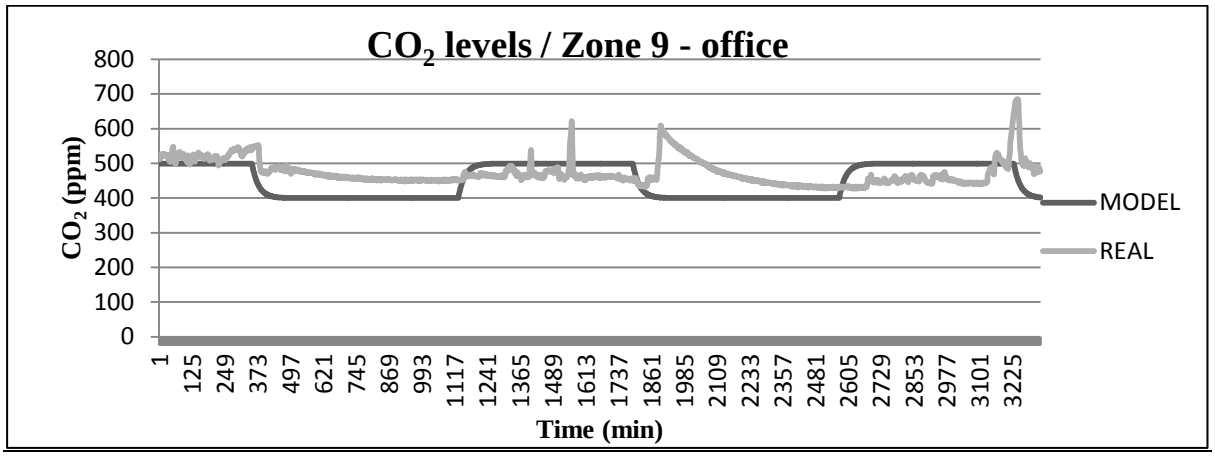

Figure 6: Comparison of calculated and measured CO_2 at zone 9

It is obvious from the figure that the calculated values are not close enough to the real measurements. However, it was estimated that the simulation represents the reality because the levels of CO_2 follows exponential increase during the time when the occupant is there, while its concentration decreases when the building is not operated.

Regarding the COMIS model is validated, the CO_2 levels was calculated at zone 9 considering 3 scenarios. The scenarios were the following:

i. The zone is full insulated
ii. The zone has not infiltration air rates
iii. The zone is ventilated every day from 11:00 to 12:00

The results are shown at the following figure. It should be noted here that the results considering the pollutant were calculated only for the period from 18/08/2012 to 26/08/2012 which includes the measuring period. That was chosen because the calculated time step was set at 60 sec in order to validate the results with the measurements and COMIS export files have capacitance limit.

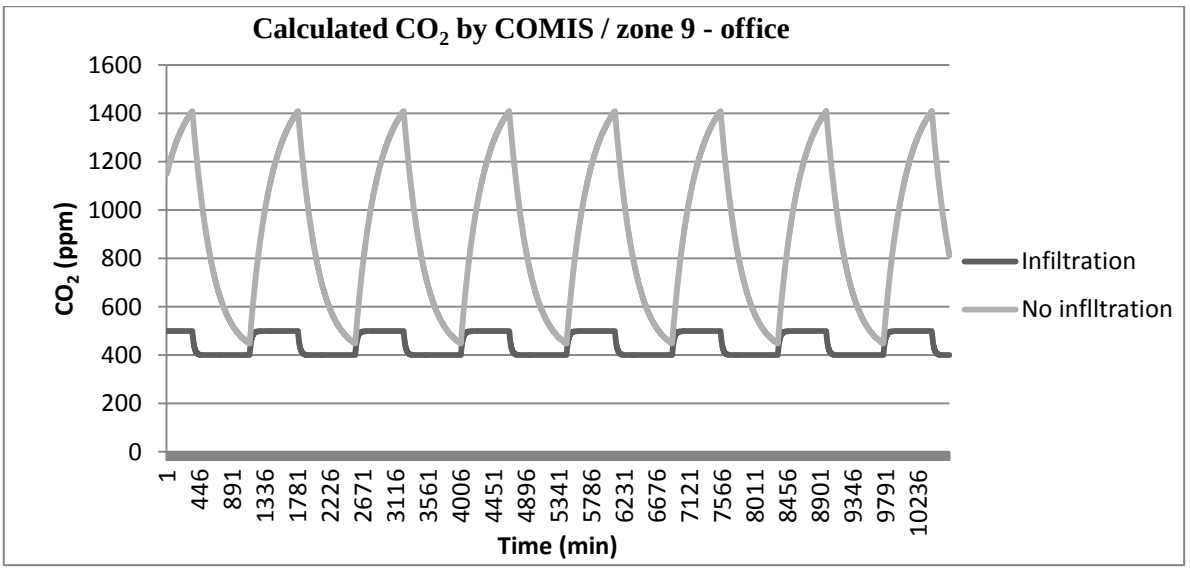

Figure 7: The variance of CO_2 concentration considering infiltration and no infiltration rates

Figure 7 shows the difference at CO_2 levels in zone 9 if the zone is infiltrated or not. At the second case, as it is obvious, the concentration increases excessively by reaching the value of 1400 ppm during the occupancy schedule.

Furthermore, as mentioned above, the natural ventilation of the zone 9 was examined. It was set at COMIS a time schedule that opens the window one hour a day daily for the simulation period. The variance of the concentration is shown below.

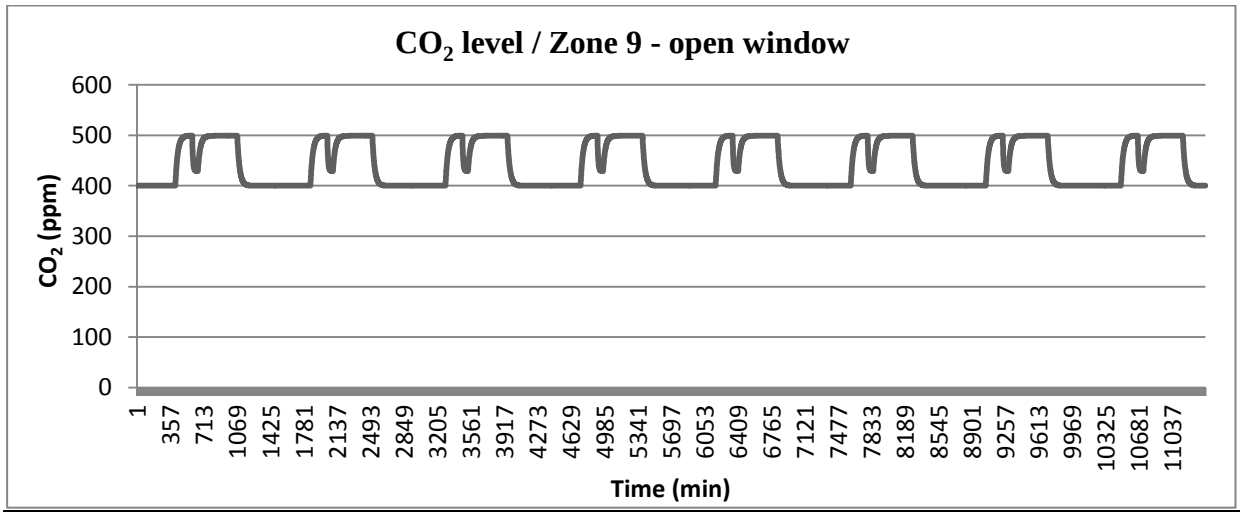

Figure 8: The concentration of CO_2 when the window is opened

As it is shown from figure 8, the CO_2 decreases when the window is opened because the air is refreshed and the concentration is diluted.

For these case studies, the energy demands of the zone also were calculated by coupling TRNsys and COMIS. The results are presented at the following figure.

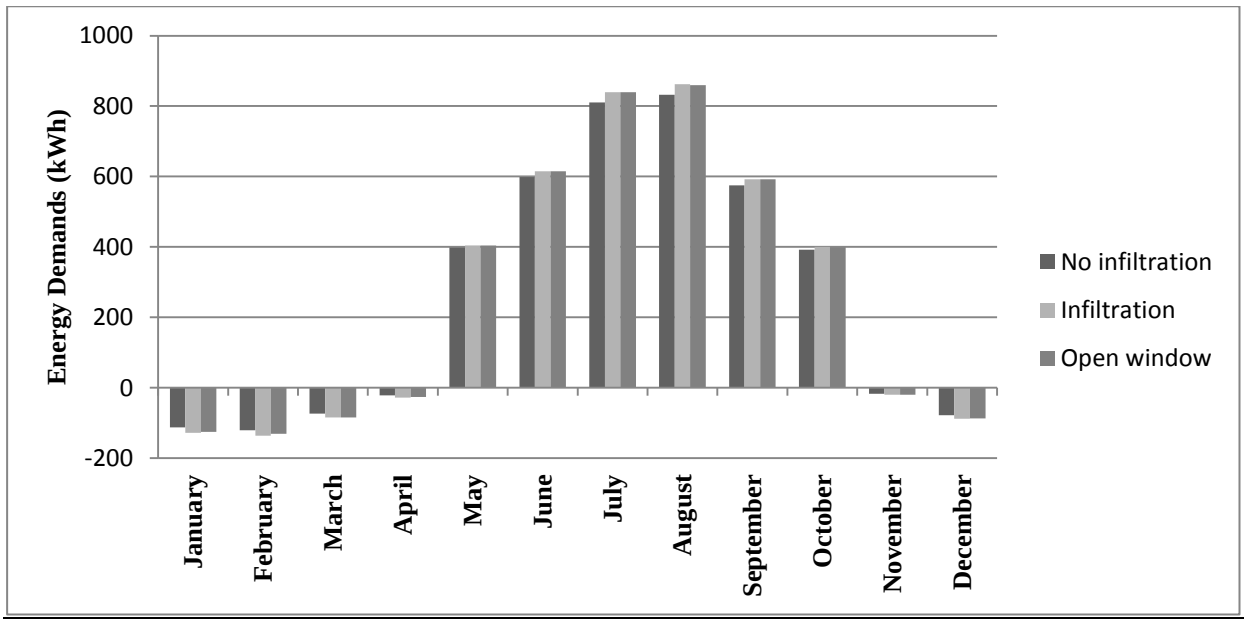

Figure 9: Energy demands of zone 9 of all the examined scenarios

Comparing the results of the three scenarios, it is concluded that the less energy consuming scenario is that it considers a full insulated building. Opening the window, the energy demands are the same as in the case of considering infiltration air rates from cracks and frames. This wasn't expected, but it was assumed that the ambient temperatures helped at the heating and the cooling of the zone.

4 CONCLUSIONS

The main objective of this report is to examine the effect of the infiltration / ventilation air rates on the energy requirements of the building and its indoor air quality. For that reason a building located at Chania of Greece was simulated by using TRNsys and COMIS software.

The calculated energy demands by TRNsys shows that the building needs more heating or cooling when it's not full insulated. However regarding the internal pollution it is obvious that low infiltration / ventilation rates create an unhealthy environment for the occupants.

At office buildings, it is important to achieve a balance between the energy demands and the quality of indoor environment, in order to minimize the consumption rates without the working conditions being unpleasant.

Finally, it would be interesting to study the case of mechanical ventilation and how this impacts on indoor pollution, the energy needs of the building and the energy cost, considering more parameters than CO_2 concentration.

5 REFERENCES

Al-ajmi, Farraj F., and V. I. Hanby. 2008. “Simulation of energy consumption for Kuwaiti domestic buildings.” *Energy and Buildings* 40(6):1101–9. Retrieved August 18, 2013 (http://linkinghub.elsevier.com/retrieve/pii/S0378778807002368).

Alemu, Alemu T., Wasim Saman, and Martin Belusko. 2012. “A model for integrating passive and low energy airflow components into low rise buildings.” *Energy and Buildings* 49:148–57.

Boyer, H., F. Garde, J. C. Gatina, and J. Brau. 1998. “A multimodel approach to building thermal simulation for design and research purposes.” 28:71–78.

Comis, Tutorial. 2005. “Comis 3.2.” 1–29.

European Commission. 2013. “Financial support for energy efficiency in buildings.”

Khandelwal, Ankur, Prabal Talukdar, and Sanjeev Jain. 2011. “Energy savings in a building using regenerative evaporative cooling.” *Energy and Buildings* 43(2-3):581–91.

Li, Yuguo, and Per Heiselberg. 2002. “Analysis Methods for Natural and Hybrid Ventilation – a Critical Literature Review and Recent Developments.” 1.

Olesen, B. W. 2004. “International standards for the indoor environment.” *Indoor air* 14 Suppl 7(Suppl 7):18–26.

Olesen, Bjarne W., Olli Seppanen, and Atze Boerstra. 2006. “Criteria for the indoor environment for energy performance of buildings: A new European standard.” *Facilities* 24(11/12):445–57.

Solar Energy LaboratoryUniversity of Wisconsin-Madison. 2010. “Trnsys 17.” 3.

Viktor Dorer, Anne Haas, Werner Keilholz, Roger Pelletret, Andreas Weber. 2001. “Rio de Janeiro, Brazil August 13-15, 2001.” 403–10.

OCCUPANCY ESTIMATION BASED ON CO_2 CONCENTRATION USING DYNAMIC NEURAL NETWORK MODEL

Hwataik Han[*1], Kyung-Jin Jang[2], Changho Han[3], and Junyong Lee[4]

1 Mechanical Engineering, Kookmin University
861-1 Jeungneung-dong, Seongbuk-gu
Seoul 136-702, Korea
**Corresponding author: hhan@kookmin.ac.kr*

2 Thermal Environmental Lab, Kookmin University
861-1 Jeungneung-dong, Seongbuk-gu
Seoul 136-702, Korea

3 Graduate School, Kookmin University
861-1 Jeungneung-dong, Seongbuk-gu
Seoul 136-702, Korea

4 Graduate School, Kookmin University
861-1 Jeungneung-dong, Seongbuk-gu
Seoul 136-702, Korea

ABSTRACT

Demand-controlled ventilation has been proposed to improve indoor air quality and to save energy for ventilation. It is important to estimate occupancy in a building precisely in order to determine adequate ventilation airflow rates, especially when people are the major source of indoor contaminants such as in office buildings. In this paper, we investigate occupancy estimation methods using a dynamic neural network model based on carbon dioxide concentration in a space. We conducted an experiment in a single room to measure carbon dioxide concentration and actual occupancy continuously in the room. We trained and tested the dynamic neural network model TDNN (time-delayed neural network) by varying the number of tapped delay lines and the number of neurons. Networks were trained using the first-day data and results were obtained for the rest of the days. The estimated results were compared with the actual number of occupants measured by a number counter installed at the entrance door. The root mean square (RMS) errors were obtained depending on system parameters. The dynamic model with tapped delay showed smaller errors in general than conventional static neural network models. The RMS errors were reduced, as the tapped delay line increased up to 15 minutes for the present experiment. The time delay has been found to be related to the dispersion time of contaminants in the space, which is again related to the dimensions of the space and the source locations relative to the sensor locations. Further research is needed to include the effect of the concentration in the adjacent rooms and the effect of other contaminants such as humidity and particle concentrations.

KEYWORDS

Occupancy estimation, Dynamic neural network, Demand-controlled ventilation, Carbon dioxide

1 INTRODUCTION

It is important to maintain indoor air quality as well as energy conservation in buildings. Energy consumption of buildings constitutes approximately 24% of the total energy consumption in Korea, more than 25% of which is consumed in ventilation for maintaining an adequate indoor environment (KEITI, 2012). Most people currently spend more than 90% of their time per day, and think it is important to provide adequate ventilation rates to maintain indoor air quality. Meanwhile, energy is wasted as buildings are often over-ventilated, especially in vacant buildings.

Recently, demand-controlled ventilation (DCV) has been investigated widely, and various DCV schemes have been developed to conserve energy for building ventilation (Emmerich and Persily, 2001). The American Society of Heating, Refrigeration and Air-Conditioning Engineers (ASHRAE, 2013) provided a standard for ventilation requirements by distinguishing the contaminants by occupants and from those by building materials. If the number of occupants in each zone is known, unnecessary ventilation can be shut off in vacant zones, and an adequate amount of ventilated air can be provided according to the occupants in the zones. Klein (2011) conducted multi-agent simulations and operated an air-conditioning system according to the number of occupants. He reported that energy consumption was saved by 12-17%, and that the indoor comfort level was improved by 5%. Xu and Wang (2007) reported that energy consumption can be reduced by as much as 8-33% by utilizing various DCV schemes.

Occupancy information can be used in various fields, such as security, lighting, fire protection, and HVAC control. Conventional methods for estimating the number of occupants include motion recognition by sensors such as passive infrared (PIR), image processing by video camera images, etc. Occupancy should be measured without hindering occupants' behavior or offending their privacy. In this context, methods using environmental sensors have been preferred, even though they can be inaccurate. Various methods have been tried by many authors in the literature. Federspiel (1997) conducted an experiment to estimate CO_2 generation rates using a Karman filter. Kar and Varsheny (2009) suggested a moment method of integration to reduce the errors occurring inherently in the process of differentiation of fluctuating CO_2 concentration data. Dong et al. (2010) revealed the correlations of occupancy with CO_2, CO, total volatile organic compounds (TVOC), particulate matter 2.5 (PM2.5), and temperature, and compared the results using the following methods: support vector machine (SVM), artificial neural network (ANN), and hidden Markov model (HMM). Lu et al. (2011) used the maximum likelihood estimation method in a mechanically ventilated room, and Mamidi et al. (2011) used a rule-based heuristic method and Gaussian process. Other than the indoor concentrations, various parameters have been tested (Hailermarium et al., 2011; Yang et al., 2012; Dodier et al., 2006) to improve accuracy in estimating occupancy, including light intensity, noise intensity, electric usage, internet usage, etc. In this paper, we investigate a simple dynamic neural network model and apply it to a single office room to figure out optimal system parameters in estimating occupancy.

2 THEORETICAL BACKGROUND

2.1 Ventilation Model

In case the indoor carbon dioxide concentration is assumed to be uniform in a zone, as shown in Fig. 1, mass conservation can be expressed as Eqn. (1). The amount of CO_2 generated in the zone is assumed to be linear with respect to the number of occupants, *N*. The metabolic emission rate per person is assumed to be constant, and there is no other generation of carbon dioxide in the room.

$$V\frac{dC}{dt} = Q\ C_{\text{out}} - C\ t\ \ + mN(t) \tag{1}$$

where *V* is the volume of the room, *Q* is the ventilation rate, m is the CO_2 generation rate per person, and C_{out} is the outdoor CO_2 concentration.

Theoretically speaking, the number of occupants can be derived from the governing equation by differentiating CO_2 concentrations with respect to time. However, because of the uncertainties involved with the concentration measurements, reliable results cannot be obtained directly from the differential equation.

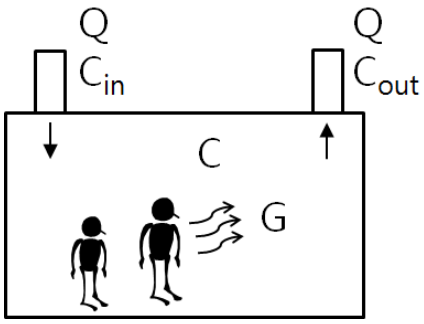

Figure 1: Concentration model in a single zone

2.2 Dynamic Neural Network

Neural networks are non-linear statistical data modeling tools that can be used to model complex relations between inputs and outputs. The design of artificial neural network was inspired by the biological neural network, which comprises neurons and synapses. ANN has been successfully applied to various fields such as system modeling, adaptive control, noise filtering, image processing, and speech recognition. ANN can be considered a black box in which the model inputs are the number of neurons in the input layer, the model parameters are the number of neurons and the values of interconnection weights, which do not have any physical meaning, in the hidden layers, and at last, the outputs are the number of neurons in the output layer.

The most common type is a static feed-forward configuration that allows the approximation of any nonlinear static mapping between input and output variables provided that certain conditions are met (Castilla, 2013). A multilayer feed-forward neural network shows outstanding performance for various functional approximations and pattern recognitions, but time series cannot be handled properly. A dynamic neural network has been developed to conduct time-series analyses (Sinha et al., 2000). A dynamic neural network uses either a tapped delay line (TDL) to delay inputs or an output feedback to provide memory functions so that time-series analyses can be conducted. Figure 2 shows the structure of a TDNN (time-delayed neural network) using a TDL. Inputs, *p*, are inputted to a hidden layer along with delayed inputs. The number of delayed inputs is *k*. The inputs are summed with weighting values, *w*, and are added with biases, *b*, and the output values, *a*, are transferred through a transfer function, *f*. For complex problems, an ANN has a large number of neurons and many hidden layers.

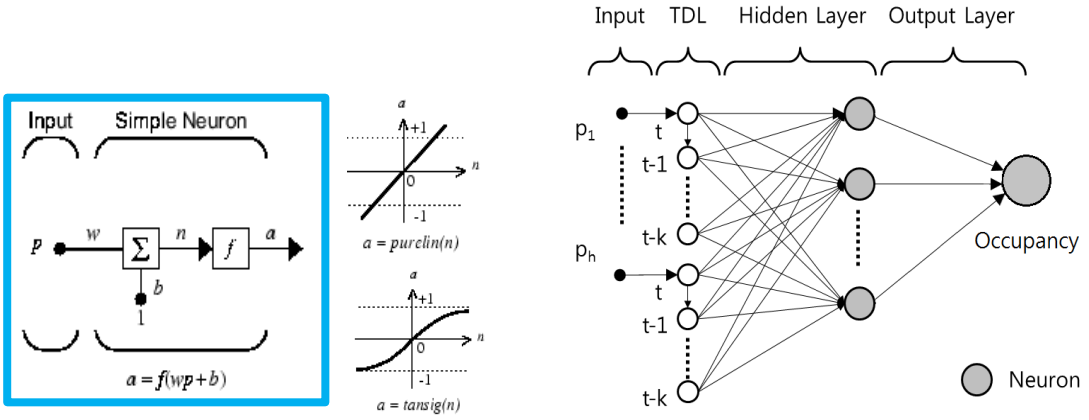

Figure 2: Structure of an artificial neural network

3 EXPERIMENTS

3.1 Test Room

The test room is located on the third floor of the five-story College of Engineering building of Kookmin University in Seoul, Korea. The configuration of the room is shown in Fig. 3. The room is an office for graduate students and is equipped with various sensors and facilities for environmental control. The room has been remodeled to conduct various DCV experiments.
Carbon dioxide concentrations were measured using a non-dispersive infrared (NDIR) type of CO_2 sensor. The measurement range is 0-20000 ppm, and the resolution is 1 ppm. Uncertainty of the CO_2 sensor is known to be within 1%. Magnetic sensors have been installed at the door and windows to detect when they are opened. A motion counter has been installed at the door to count the number of people entering and exiting the room. There are two infrared beams in the counter, which are apart horizontally to detect the direction of movement by the sequential cut-offs. Output signals were analyzed by the Lab-View counter function. The actual number of occupants is calculated by integrating the number of pulses. The time interval of data acquisition is 1 minute. The total number of data points is 1440 in 24 hours.

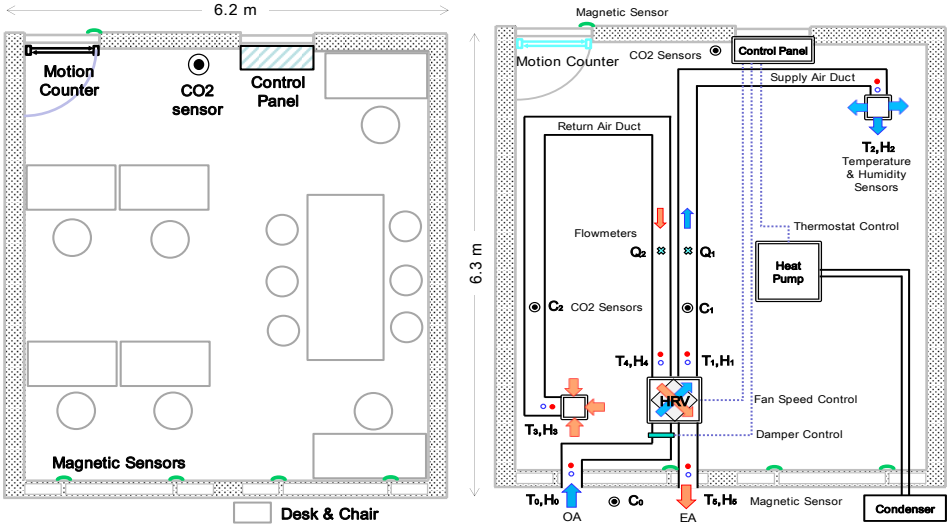

Figure 3: Test room configuration

3.2 Procedure

Experiments were conducted from May 7 to 13, 2013. Data from five days were used excluding the weekend. The number of occupants in the room varies from zero to eight irregularly. The windows were closed, and the mechanical ventilation system was not operated throughout the period. The average infiltration rate of the room is 0.29 air changes per hour (ACH) ±10%, which is obtained from the decay rate measured overnight when the room is vacant. The infiltration rate of the room is not required for neural network modeling but is shown as a reference. The infiltration rate is assumed to be constant regardless of outdoor weather conditions.
The Matlab R2012a Neural Network Toolbox was used to estimate the varying number of occupants. Network inputs are CO_2 data measured from the gas sensor, and network outputs are the number of occupants. A tangent hyperbolic function is used for the transfer function of the hidden layer, and a linear function is used for that of the output layer. In order to train

neural networks, Marquardt algorithm and Bayesian regulation were used for normalization. The maximum iteration for training is 1000, and the criterion of convergence is 10^{-10}. Training is repeated 15 times, and the output results with the minimum error were selected. Data from day 1 is used to train the neural network, and the occupancy is estimated for the rest of the days: days 2-5. The estimated occupancy is compared with the actual occupancy measured by motion sensors. The RMS of the differences is calculated according to Eqn. (2).

$$RMS = \sqrt{\frac{1}{n_{\text{total}}} \left(N_{\text{true}} - N_{\text{estimate}} \right)^2} \tag{2}$$

where n_{total} is the number of data points.

4 RESULTS AND DISCUSSION

In order to find an optimal number of TDLs, the number of input TDLs was tested from 1 to 30. The RMS error in estimating occupancy is shown in Fig. 4. As the number of TDLs increases, the RMS error decreases rapidly at first but remains nearly constant when the number of TDLs is greater than 15. The TDL value of 15 means that the inputs to the neural network are the 15 data points measured at the previous 15 time steps. The number of hidden neurons has been also tested. As the number of hidden neurons increases, the RMS error increases. The dynamic neural network model with a single hidden neuron achieves the best results and was used in the present experiment.

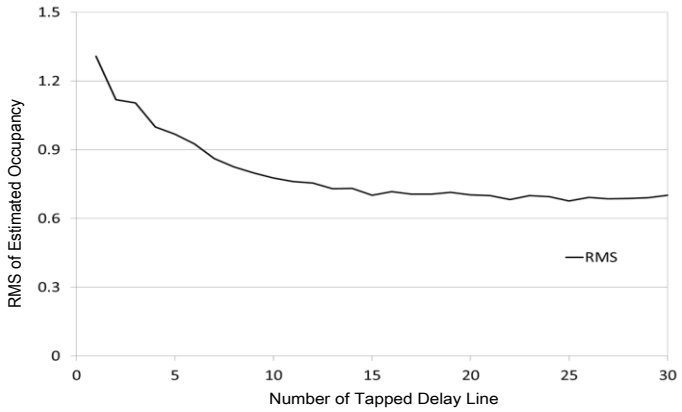

Figure 4: Effect of number of TDLs on the RMS results

The static model can be considered as a neural network with no TDLs. Without implementing the data at previous time steps, the output would be proportional to the current input. Figure 5 compares the results by the static and dynamic models. The static model gives quite a large error in estimating occupancy. The dynamic model gives much better results compared with the static model, but there remains a slight time delay in the results.

The RMS values of the dynamic model are shown in Fig. 6 with respect to the time shift of the results. The RMS error exhibits a minimum when the time shift is approximately 7 minutes. The time lag generated by the dynamic model is believed to be due partly to the sensor response time but mainly to the gas dispersion in the space. The dispersion time is considered to be proportional to the dimension of the space.

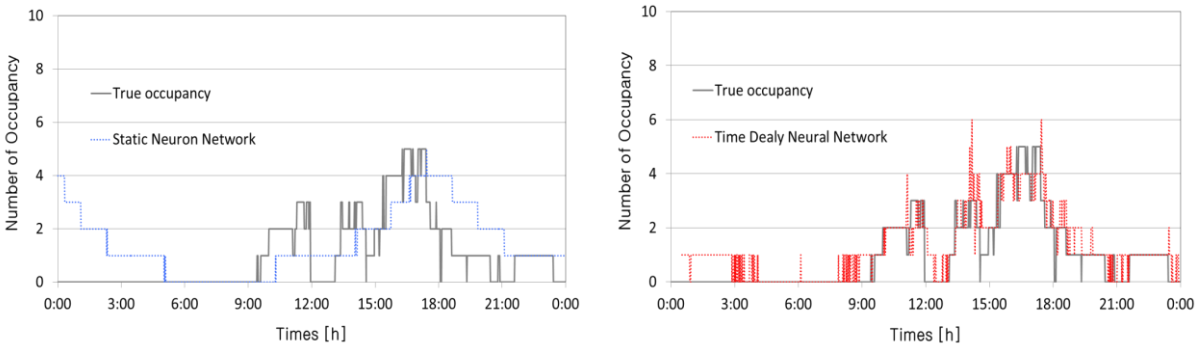

Figure 5: Comparison of static (left) and dynamic (right) models (Day 2)

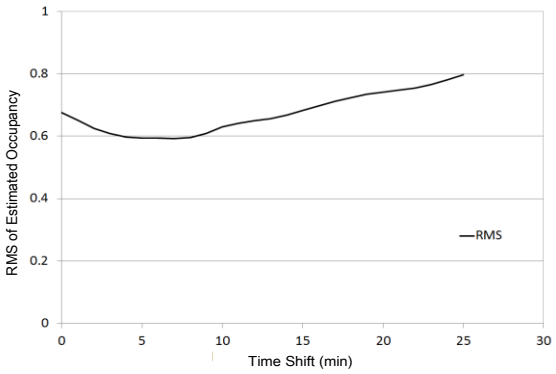

Figure 6: Effect of time shift

Figure 7 shows the final results of the estimated occupancy for the rest of the days. The figure shows the results in comparison with the actual occupancy along with the concentration variations measured in the room. The results are in good agreement with the true values. The RMS errors are found to be 0.63, 0.58, 0.63, and 0.88 respectively for days 2-5. Based on the first-day training, the average of the RMS errors is 0.68. In case we increase the number of days of training, the average RMS error decreases slowly. The average of the RMS errors by various combinations of two-day training has been found to be 0.64.

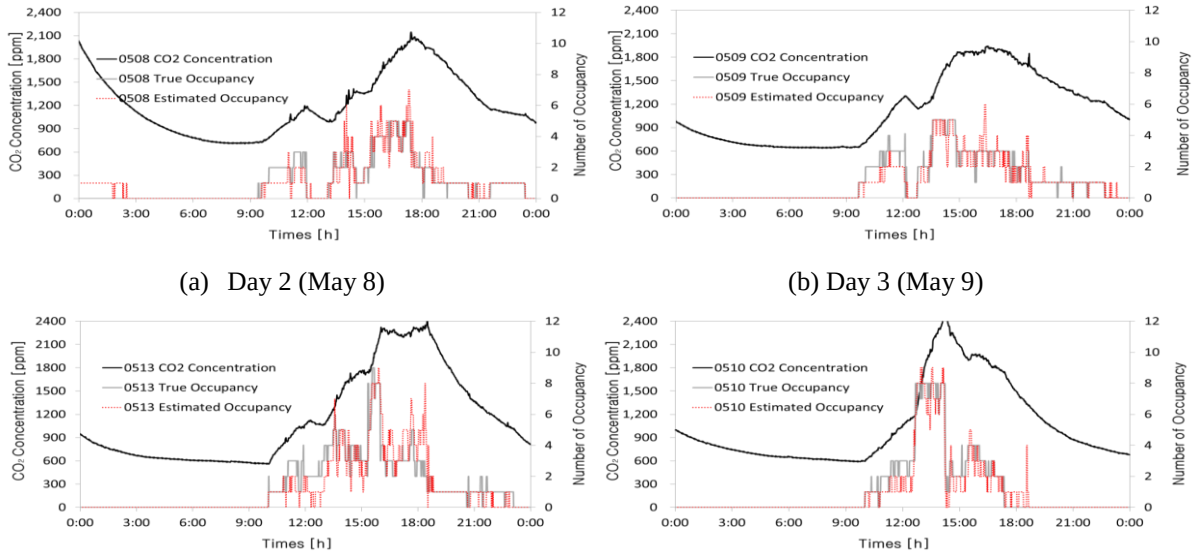

(a) Day 2 (May 8)

(b) Day 3 (May 9)

(c) Day 4 (May 10)

(d) Day 5 (May 13)

Figure 7: Comparison of estimated occupancy with true occupancy

5 CONCLUSIONS

We investigated occupancy estimation methods using the dynamic neural network model based on carbon dioxide concentration in a room with irregularly varying numbers of occupants. We trained and tested a dynamic neural network model of TDNN by varying the number of TDLs. The network model was trained using the data collected during the first day, and results were obtained for the rest of the days for various system parameters. The following conclusions have been drawn from the experimental results.

1. The dynamic model with tapped delay shows improved results compared with the conventional static neural network model. The RMS error decreases as the number of TDLs increases. The optimal number of TDLs has been found to be 15 for the present configuration.
2. Because the system-governing equation is not complicated, a simple neural network structure is sufficient to model the system with a single hidden neuron in a single layer. The RMS error rather increases as the number of hidden neurons increases.
3. The time delay of a few minutes remains in estimating occupancy using the dynamic neural network model with optimized system parameters. This issue is considered to be related to the dispersion time of contaminants in the space, which is again related to the dimensions of the space and the source locations relative to the location of sensors.

Further research needs to be conducted to include the effect of the concentration in the adjacent rooms and the effect of other parameters such as humidity and particle concentrations to improve the accuracy of the method.

6 ACKNOWLEDGMENTS

This research was supported by the Converging Research Center Program funded by the Ministry of Education (No. 2012K001383), and by the Research Policy/Infrastructure Development Program funded by the Ministry of Land, Infrastructure and Transportation (No. 11 Technique Standardization 03-01), Republic of Korea.

7 REFERENCES

KEITI. (2012). Indoor Environment Management Technology Trends of Building based on Eco-Energy. *KEITI Report*, 2012-86, 77.

Emmerich, S.J. and Persily, A.K. (2001). State-of-the-Art Review of CO_2 Demand Controlled Ventilation Technology and Application. *NISTIR 6729*.

ASHRAE. (2013). *Handbook-Fundamentals.* Atlanta: American Society of Heating Refrigerating and Air-Conditioning Engineers.

Klein, L. (2011). Coordinating Occupant Behavior for building Energy and Comfort Management using Multi-agent Systems. *Automation in Construction*, 22, 525-536.

Xu, X. and Wang, S. (2007). An Adaptive Demand-Controlled Ventilation Strategy with Zone Temperature Reset for Multi-zone Air-Conditioning Systems. *Indoor and Built Environment*, 16, 426-437.

Federspiel, C.C. (1997). Estimating the Inputs of Gas Transport Processes in Buildings. *IEEE Trans. Control System Tech.*, 5(5), 480-489.

Kar, S. and Varshney, P.K. (2009). Accurate Estimation of Indoor Occupancy using Gas Sensors, *ISSNIP*, 355-360.

Dong, B. Andrews, B. Lam, K.P. Hynck, M. Zhang, R. Chiou, Y.S. and Benitez, D. (2010). An Information Technology enabled Sustainability Test-Bed (ITEST) for Occupancy

Detection through an Environmental Sensing Network. *Energy and Buildings*, 40, 1038-1046.

Lu, X. Lu, T. and Viljanen, M. (2011). Estimation of Space Air Change Rates and CO_2 Generation Rate for Mechanically-Ventilated Buildings. *Advances in Computer Science and Engineering*, 237-260.

Mamidi, S. Maheswaran, R. Chang, Y. (2011). Smart Sensing Estimation and Prediction for Efficient Building Energy Management. In Multi-agent Smart Computing Workshop.

Hailermarium, E. Goldstein, R. Attar, R. and Khan, A. (2011). Real-time Occupancy Detection using Decision Trees with Multiple Sensor Types, *Proc. of 2011 Sym. on Simulation for Architecture and Urban Design*, 141-148.

Yang, Z. Li, N. Becerik-Gerber, B. and Orosz, M. (2012). A Non-Intrusive Occupancy Monitoring System for Demand Driven HVAC Operations, *Construction Research Congress*, 828-837.

Dodier, R.H. Henze, G.P. Tiller, D.K. and Guo, X. (2006). Building Occupancy Detection through Sensor Belief Networks, *Energy and Buildings*, 38, 1033-1043.

Castilla, M. Alvarez, J.D. Ortega, M.G. Arahal, M.R. (2013). Neural Network and Polynomial Approximated Comfort Models for HVAC Systems. *Building and Environment*, 59, 107-115.

Sinha, N.K. Gupta, M.M. and Rao, D.H. (2000). Dynamic Neural Networks: An Overview. *Industrial Technology 2000 Proc. of IEEE Int. Conference*, 1. 491-496.

ANALYSIS OF THE INDOOR AIR QUALITY IN GREEK PRIMARY SCHOOLS

Paraskevi Vivian Dorizas*, Margarita-Niki Assimakopoulos, Constantinos Helmis, and Mattheos Santamouris

Faculty of Physics, Departments of Environmental Physics and Meteorology, University of Athens, University Campus,
Athens, 157 84, Greece
**Corresponding author: p.dorizas@phys.uoa.gr*

ABSTRACT

The exposure of children to indoor air pollutants in school classrooms might cause them adverse health effects. In order to confront this issue, the in-depth study and evaluation of the indoor air quality in classrooms is necessary. The aims of this study are to characterize the environmental factors that affect indoor air quality. Several indoor air pollutants such as the concentrations of the particulate matter (PM) of several different size ranges, carbon dioxide (CO_2), carbon monoxide (CO) and VOCs, were simultaneously measured in classrooms as well as the outdoor environment in nine primary schools in Athens, Greece during April 2013. Measurements were performed for more than 7 hours per day, for a period of one to five days in a classroom, per school. The first results indicate extreme PM_{10} concentrations in many cases with varying fluctuations throughout the day, mainly attributed to the presence of students, inadequate level of ventilation and chalk dust while the ultrafine particles (UFP) remained in rather low levels. In most of the cases the indoor concentrations exceeded the outdoor ones by more than ten times. Carbon dioxide concentrations in many cases exceeded the recommended limit value indicating inadequate levels of ventilation.

KEYWORDS

Indoor Air Quality, PM, CO_2, CO, VOCs, Schools, Ventilation

1 INTRODUCTION

In recent years there is an increasing concern in the investigation of the indoor air quality (IAQ) in school buildings, since the exposure of students to indoor air pollutants may be associated with serious adverse health effects (WHO, 2005). Children are more vulnerable compared to adults, due to their growing lungs and their higher metabolic rate (Schwartz, 2004). Also they spend a considerable amount of their time within classrooms (Leickly, 2003). Apart from the impact that the exposure of indoor air pollutants have on student's health, more recent studies have shown that a degraded indoor environment may also affect their learning performance by reducing their productivity (Mendell and Health, 2005).

Particulate matter (PM) are major indoor air pollutants that depending on their size, can penetrate from the upper respiratory tract to deeper parts of the lungs and can even deposit in tracheobronchial and alveolar regions (Hinds, 1999). Numerous epidemiological studies have associated exposure to PM with morbidity or even mortality (Pope et al., 1995). Studies conducted in schools have shown that indoor PM levels are greatly affected by the presence

of pupils and the outdoor PM levels (Annesi-Maesano et al., 2007). Although major indoor PM sources such as smoking or cooking are absent in school environments, the PM concentration levels are often high (Fromme et al., 2008).

Carbon dioxide (CO_2) is another important air pollutant that in many studies has been used as an indicator of indoor air quality (Twardella et al., 2012). CO_2 concentrations levels are associated to ventilation rates and since ventilation plays a key role in maintaining IAQ, CO_2 measurements are always crucial. Studies conducted in Greek schools have found that CO_2 concentrations levels frequently exceed their recommended limit values (Synnefa et al, 2003, Santamouris et al., 2008). According to the international literature, the indoor environment of school classrooms is encumbered by air pollutants due to insufficient ventilation, inadequate maintenance and also due to lack of the necessary funding (Mendell and Health, 2005). Thus, the understanding in details of the existing situation of air pollutants in classrooms is essential in order to come up with certain proposals to improve the indoor air quality.

The main objectives of this study are: 1. to investigate the levels of air pollutants in school classrooms aiming to create an integrated concentration profile for the period of measurement, 2. to evaluate air pollutant levels based on the exceedance of their recommenced by international certification bodies limit values, 3. to compare the indoor versus the outdoor PM concentrations and to identify possible relationships between them and 4. to investigate the possible activities and to which extend they affect pollutant concentrations.

2 MATERIALS ANS METHODS

2.1 Sampling site description

Eight primary schools located in the north-western part of Attika (Thrakomakedones, Acharnae) Greece and one school located in the eastern regional area of Attika (Pallini) were monitored during spring 2013 (Figure 1). According to CORINE 2000 land cover database (Geodata, 2010), most of the schools (code names: 1, 14, 4, 18, 2, 8, see Table 1) are in areas characterized as ‘discontinuous urban fabric’ in which a great percentage of the land is covered by structures (EEA, ETC/TE, 2004). One of the schools (code 12) is at an area of ‘continuous urban fabric’ where buildings and roads cover more than 80% of the total surface, and two other schools (codes: 3 & 11) are in areas having ‘complex cultivation patterns’ where small areas of annual crops are present.

Figure 1: Map of Attika (left) and locations of schools (right)

The experimental campaign was conducted in one classroom per school. The main characteristics of the school buildings' and classrooms' where the measurements took place are summarized in Table 1.

Table 1: Characteristics of sampling sites

School name	School code name	Measurement period (Number of measurement days)	Year of construction	Classroom's floor area (m^2)	Classroom's volume (m^3)	Classroom's number of Students	Classroom's board type	Classrooms' orientation
Acharnae 14	1	1-5/4/13 (5 days)	2001	53	165	17	Chalk	North
Thrakomakedones 1	14	8-12/4/13 (5 days)	1978	64	198	25	Chalk	Northwest
Axharnae 4	4	14-18/4/13&24/4/13 (5 days)	1986	50	155	24	Chalk	Southwest
Pallini 3	3	19&22/4/13 (2 days)	-	46	137	25	Chalk	West
Acharnae 18	18	23/4/13 (1 day)	1991	47	138	18	Chalk	South
Acharnae 12	12	13-17/5/13 (5 days)	1980	49	157	25	Marker	South
Thrakomakedones 2	2	20-24/5/13 (5 days)	2003	50	162	25	Marker	East
Acharnae 8	8	27-29/5/13 (3 days)	1999	52	159	19	Marker	West
Acharnae 11	11	31/5/13 (1day)	1994	55	172	15	Chalk	South

2.2 Instrumentation and parameters measured

The indoor PM_{10}, PM_5, $PM_{2.5}$, PM_1 and $PM_{0.5}$ concentrations were measured using Handheld 3016 IAQ (Lighthouse, worldwide solutions) and the outdoor PM_{10} concentrations were sampled using Osiris, an airborne particulate monitor (Turnkey Instruments Ltd) in units of mass per unit volume ($\mu g/m^3$). Ultrafine particle (UFP) concentrations were measured using the portable counter P-Trak (TSI, Model 8525), in units of particles per unit volume (pt/cm^3), while the detection range of P-Trak is from 20nm to 1μm. CO_2, CO and Volatile organic compounds (VOCs) were measured using MultiRAE IR (RAE Systems) in units of parts per million (ppm). Particulate matter, were simultaneously monitored in the outdoor environment. The instruments measuring the outdoor air were placed at the roof terrace so as to collect a representative sample of the atmospheric air. All of the above mentioned parameters were monitored with a sampling interval of 5 min and the duration of measurement was approximately 7 hours per day.

2.3 Sampling protocol

The sampling period was during April and March 2013 (Table 1), where measurements lasted from one to five days for each of the nine schools. Measurements started 40 min prior to the arrival of students in the classrooms (at around 7:30 a.m.) and lasted until about 14:40, 40min after the students left school. Sampling took place in one classroom per school and the experimental equipment were placed at 1.1 m above the floor according to the standard ISO

7726:1998 for seated persons, as close as possible to the centre of the classroom. Any kind of indoor activities that could possibly affect the indoor air pollutant concentrations such as students' presence, window opening etc. were written on daily diaries marking the exact starting and ending time and duration of the activity.

2.4 Data processing and analysis

Statistical analysis was performed using SPSS and pollutant concentration distributions were studied through box plots calculated for every school. Descriptive statistics were estimated in order to have a clear profile of the extent to which the classrooms were polluted and the percentage of exceedance of the recommended limit value was calculated. Furthermore, ratios of indoor to outdoor concentrations were estimated. The dataset was classified in two categories of common characteristics (schools using chalk and schools using marker), whose ratios were calculated. Finally diurnal variation of pollutants was also investigated as a function of several factors that could possibly affect them.

3 RESULTS AND DISCUSSION

3.1 Distribution of indoor air pollutants

Figure 2 shows the distribution of PM_{10}, $PM_{2.5}$ and PM_1 for the entire measurement period in each of the schools in box plots. The two horizontal lines represent the recommended limit values by the WHO of 50μg/m^3 (pink line) and 25μg/m^3 (green discontinuous line) for PM_{10} and $PM_{2.5}$ respectively (WHO 2005). It is obvious that the majority of PM_{10} concentrations exceed by far the limit value. The total average value of PM_{10} in all schools is 245 μg/m^3, which is a value, exceeding by 5 times the proposed limit value. There were even cases where the indoor concentrations outreached 1,000 μg/m3 (code: 14, 1, 3 and 18). PM_{10} concentrations of school 8 schemed to be the lowest compared to all the other schools. The distribution of PM_{10} concentrations in the first seven schools (code: 14, 1, 4, 3, 18, 12, 2) is very close. The total average concentration of $PM_{2.5}$ in all schools is 18 μg/m^3, however there were several cases in which the concentrations exceeded the limit value of 25 μg/m^3 (code: 14, 1, 4, 3, 18, 12, 2). The mean PM_1 concentrations in all schools where the measurements took place was 7 μg/m^3.

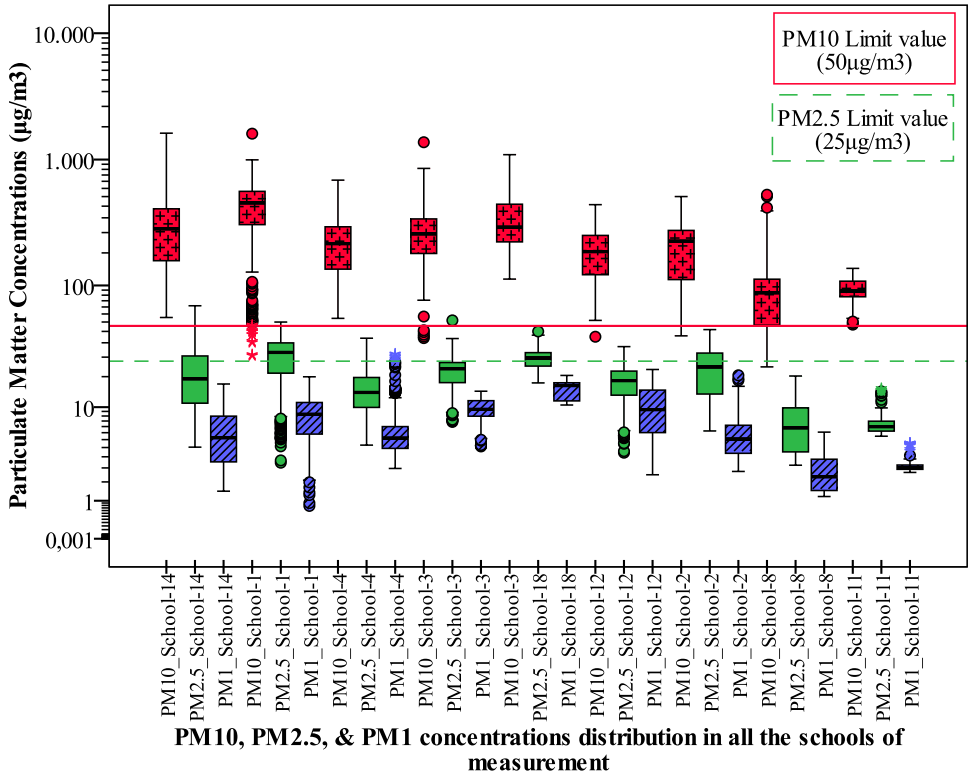

Figure 2: PM_{10}, $PM_{2.5}$ and PM_1 concentrations distribution per school

The distribution of PM in the ultrafine size range (UFP), have strong differences from school to school (Figure 3). Furthermore, one could assume that in schools 3 and 11 being at areas of 'complex cultivation patterns', away from vehicle emissions low values of UFP concentrations were expected. However the concentrations in these schools exhibit high values while the average value of UFP in all the schools is 5,584 pt/cm^3.

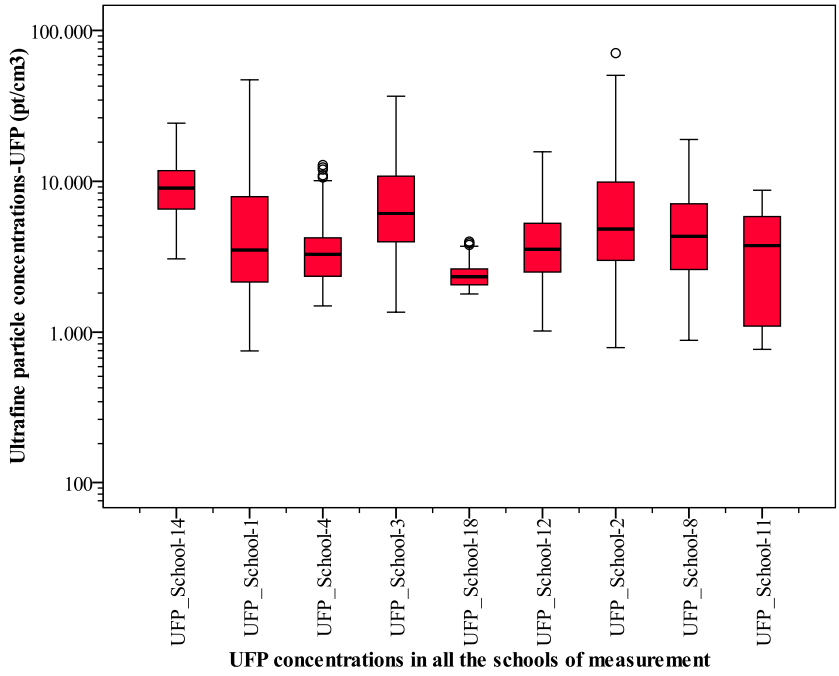

Figure 3: UFP concentrations distribution per school

Table 2 summarizes the descriptive statistics of CO, CO_2 and VOCs for the entire period of measurement in all schools. In the majority of the cases the mean value of CO_2 is above the threshold limit value of 1000 ppm (ASHRAE 62-1989), indicating inadequate levels of ventilation. CO concentrations were rather low in most schools however in schools 8 and 11 they were much higher. The mean values of VOCs concentrations were rather low in schools 14, 1, 4, 3 and 18 while in schools 12, 2, 8 and 11 the concentrations levels were higher.

Table 2: Descriptive statistics of CO, CO_2 and VOCs in all schools

School	N	CO				CO_2				VOC			
		Minimum	Maximum	Mean	Std. Dev.	Minimum	Maximum	Mean	Std. Dev.	Minimum	Maximum	Mean	Std. Dev.
14	399	0,0	0,8	0,1	0,1	556	2910	1219	604	0,0	9,4	1,0	1,1
1	428	0,0	0,9	0,1	0,2	538	5049	2082	933	0,0	5,9	1,1	1,0
4	429	0,0	1,4	0,2	0,4	546	3547	1105	601	0,0	5,7	1,1	1,0
3	191	0,0	1,1	0,2	0,3	577	2364	1209	461	0,0	5,0	1,5	1,1
18	89	0,0	0,0	0,0	0,0	566	2385	1118	536	0,0	0,8	0,2	0,2
12	406	0,2	4,0	1,3	0,8	558	4365	1437	942	0,0	51,9	6,4	9,0
2	424	0,2	8,3	2,9	2,2	587	1729	893	205	0,0	27,2	6,6	6,8
8	268	1,3	11,1	7,2	2,0	573	2207	1018	301	0,3	39,9	7,8	6,4
11	81	4,2	13,9	12,1	2,3	689	1172	971	135	3,0	39,7	15,5	8,7

Figure 4 summarizes the percentages of exceedance of the recommended limit values of CO_2, PM_{10} and $PM_{2.5}$ of the total days of measurement per school. The schools presented in the horizontal axis are shorted from low to high exceedance percentages of CO_2 concentrations. It is obvious that the majority of PM_{10} concentrations exceed by far the limit values. The limit value of $PM_{2.5}$ (25 $\mu g/m^3$) was not exceeded in schools 8 and 11.

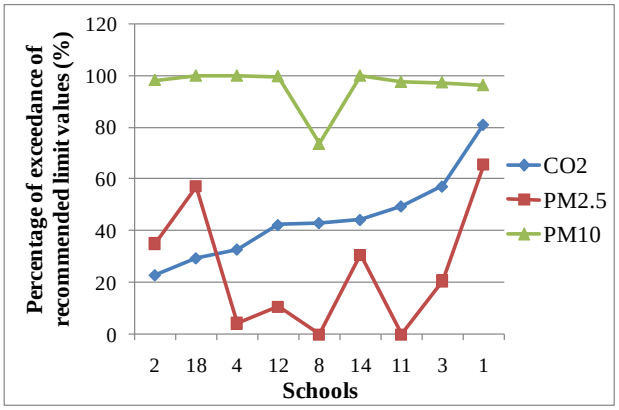

Figure 4: Percentages of exceedance of the recommended limit values

3.2 Indoor vs Outdoor particulate matter concentrations

In order to investigate if the outdoor PM_{10} concentrations affect the indoor ones, the ratio between these two concentrations has been estimated. It should be noted the indoor and outdoor concentrations were measured using two different instruments. In order to compare the results obtained from the two instruments, a correction factor has been calculated after several trial measurements took place at a lab under constant conditions without any pollutant sources.

Figure 5 presents the averaged indoor to outdoor (I/O) PM_{10} concentration ratios per school for the entire period of measurement arranged in decreasing ratios. It can be seen that for all schools the indoor concentrations are by far greater than the corresponding outdoor ones. In school 2 the I/O ratio was rather low as both the outdoor and indoor concentrations were extremely high. The extreme outdoor concentrations at this school can be possibly attributed to the fact that this school is situated at the foothill of mountain Parnitha, where on days with south-westerly winds (sea-breeze), the air pollutants exhibit high concentrations due to their transport from the city of Athens to this area, where they were trapped.

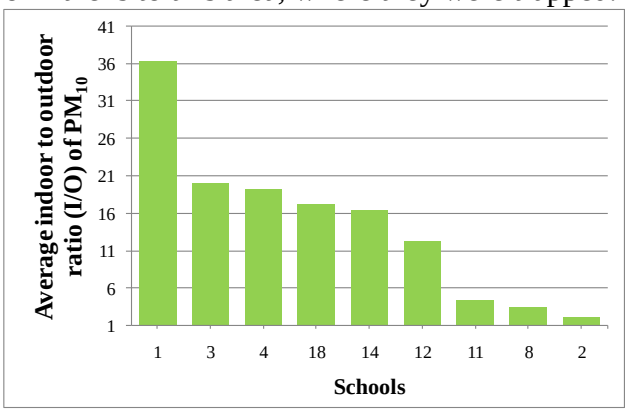

Figure 5: Average indoor to outdoor PM_{10} concentrations ratios (I/O) for the entire period of measurement in each school

3.3 Air pollutant concentrations as a function of indoor sources

3.3.1 Use of chalk (blackboard) vs the use of marker (whiteboard)

In this section the schools are divided in two categories (those using chalk -blackboard and those using marker-whiteboard) (see Table 1 column 8). Figure 6 gives the ratio of the averaged pollutant concentrations in schools using chalk (No: 14, 1, 4, 3, 18, 11) to the ones using marker (No: 12, 2, 8). It is evident that the PM concentrations in the schools using chalk are much higher that the corresponding ones using marker. The chalk dust is probably responsible for the extreme PM concentrations and especially for particles of greater size ($PM_{2.5}$ and PM_{10}). On the contrary the CO and VOCs concentrations are greater in the schools using marker as of VOCs emitted by markers. To summarise, the gain from the PM reduction using marker white boards is lost in increase of VOCs and CO concentrations.

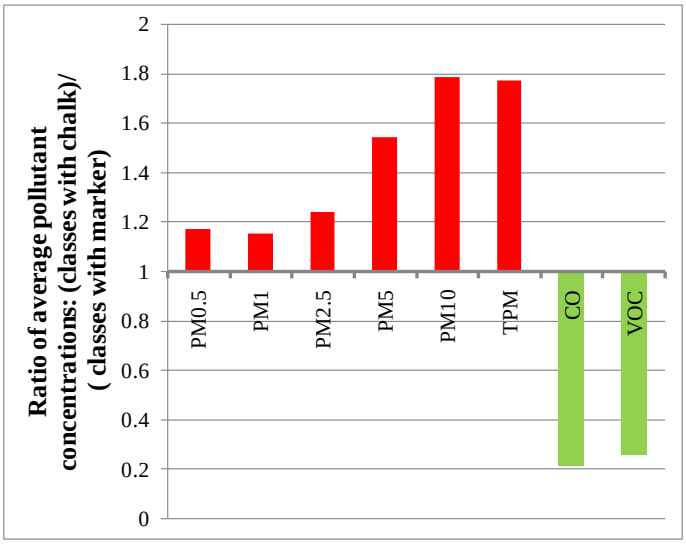

Figure 6: Ratio of the averaged pollutant concentrations of schools with blackboard using chalk to the ones with whiteboard using marker

3.3.2 PM_{10} concentrations as a function of window opening

The temporal distribution of PM_{10} concentrations was studied in detail in order to reveal the main factors responsible for the extremely high values of concentration. Figure 7 presents the diurnal PM_{10} concentrations (blue transparent area) of a representative day (15/4/2013) in school 4. In the same figure the windows opening schedule throughout the day is also marked. It can be seen that when the windows are closed (bordeaux dotted bar) the indoor concentrations significantly increase. When either half or all windows are open (purple checkered and green striped), the indoor concentrations drop significantly.

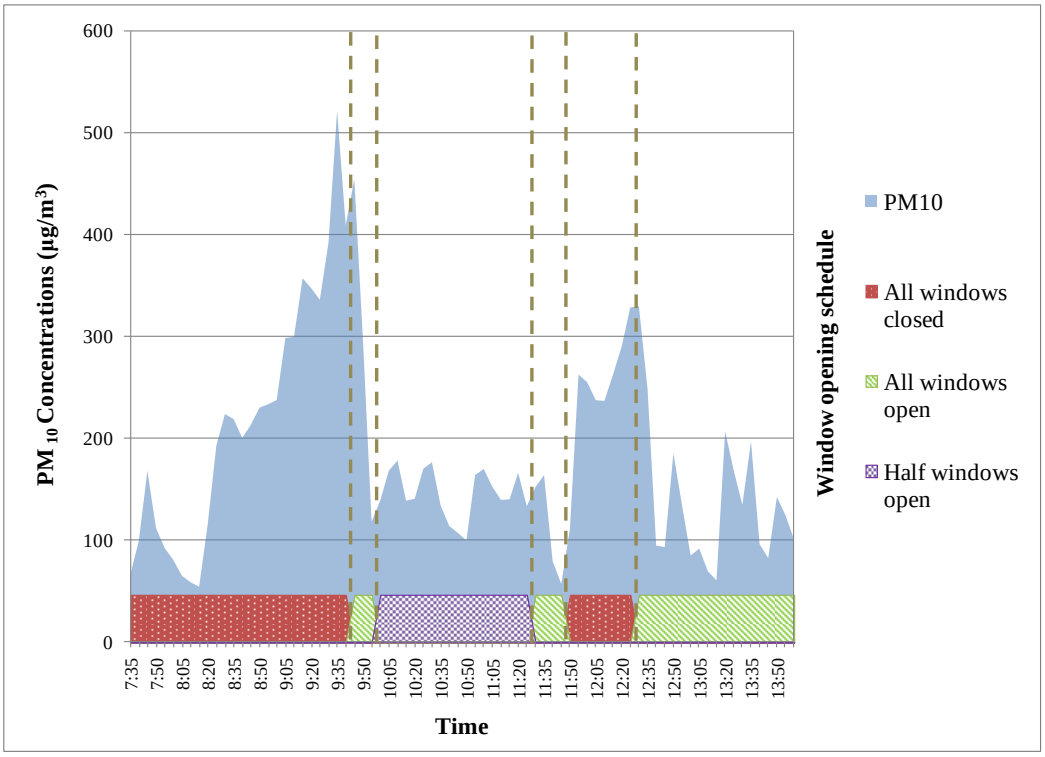

Figure 7: Diurnal variation of PM_{10} concentrations in school 4 on April 15th in relation to the window opening

Human ppresence is also important but this factor is studied separately in the next paragraph.

3.3.3 PM_{10} concentrations as a function of human presence

Figure 8 presents again the diurnal fluctuation of PM_{10} concentrations (blue striped area) throughout the same representative day as in Fig. 7 and the transparent pink area corresponds to the number of students being present in the classroom ranging, from 2 to 27.

As the students enter the classroom in the morning (08:20), the PM_{10} concentrations increase rapidly (with windows closed). At 09:40, students leave the classroom for the first break causing a fast decrease of the PM_{10} concentrations which can be also attributed to window opening (see Figure 7). When students enter again the classroom at 10:00, there is a fast increase but without reaching the peak values of the previous session, probably due to the fact that windows are now kept half open (see Figure 7). This pattern is repeated until children leave the classroom for the day.

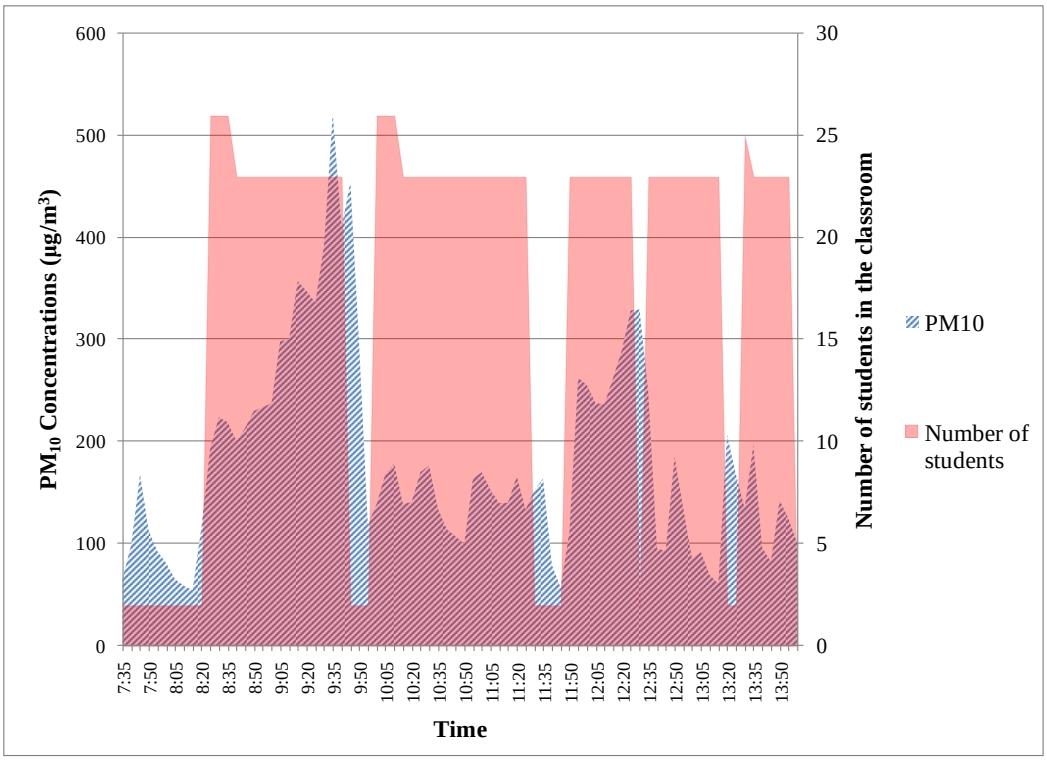

Figure 8: Diurnal variation of PM_{10} concentrations in school 4 on April 15th in relation to the number of students

4 CONCLUSIONS

The main conclusions arisen from this study are: (1) extremely high values of indoor PM_{10} concentration were measured in most of the schools, exceeding by far the recommended limit values, (2) the total average $PM_{2.5}$ concentrations from all the schools was below the limit values however, there were cases in which they were outreached, (3) ultrafine particle concentrations remained in rather low levels, (4) carbon dioxide in many cases exceeded the limit value of 1,000 ppm indicating inadequate levels of ventilation and overcrowded classrooms, (5) indoor PM_{10} concentrations are by far greater than the outdoor ones indicating that for the studied cases, the indoor environment is not affected by the outdoor environment, (6) classrooms using chalk in blackboard are characterized with significant concentrations of large sized particles ($PM_{2.5}$ & PM_{10}), while classrooms using marker in whiteboards from increased VOCs and CO concentrations, (7) window opening and the presence of students in the classrooms significantly affected the variation of the indoor PM_{10} concentrations.

5 ACKNOWLEDGEMENTS

This research has been co-financed by the European Union (European Social Fund – ESF) and Greek national funds through the Operational Program "Education and Lifelong Learning" of the National Strategic Reference Framework (NSRF) - Research Funding Program: Heracleitus II. Investing in knowledge society through the European Social Fund. We are greatly indebted to the school directors, pupils and parents, without whose consent this study would have not been possible.

6 REFERENCES

American Society of Heating, Refrigeration and Air-Conditioning Engineers (ASHRAE) (1989), Standard 62-89. *Ventilation for acceptable Indoor Air Quality*. Atlanta, USA

Annesi-Maesano, I., D. Moreau, D. Caillaud, F. Lavaud, Y. Le Moullec, A. Taytard, G. Pauli and D. Charpin (2007). Residential proximity fine particles related to allergic sensitisation and asthma in primary school children. *Respiratory medicine* 101(8): 1721-1729.

EEA, ETC/TE, (2004). Available at: http://sia.eionet.europa.eu/CLC2000/classes/Pictures?CLCcategory=1/1.1/1.1.2&CLCtitle=Discontinuous%20urban%20fabric, Accessed on July 16th, 2013

Geodata, (2010). Available at: http://www.geodata.gov.gr/maps/, Accessed on July 10th, 2013.

Fromme, H., J. Diemer, S. Dietrich, J. Cyrys, J. Heinrich, W. Lang, M. Kiranoglu and D. Twardella (2008). Chemical and morphological properties of particulate matter (PM10, PM2.5) in school classrooms and outdoor air. *Atmospheric Environment* 42(27): 6597-6605.

Hinds, W. C. (1999). *Properties, behavior, and measurement of airborne particles.* Aerosol Technology Second edition. John Wiley & Sons, inc.: pp. 206-213.

ISO 7726 (1998). Ergonomics of the thermal environment-instruments for measuring physical quantities. ISO 7726. Genève: Internationsl Organization for Standardization

Leickly, F. E. (2003). Children, their school environment, and asthma. *Annals of Allergy, Asthma and Immunology* 90(1): 3-5.

Mendell M.J. and Heath G.A, Do indoor pollutants and thermal conditions in schools influence student performance? A critical review of the literature. *Indoor Air* 2005; 15: 27-52

Pope Iii, C. A., D. V. Bates and M. E. Raizenne (1995). Health effects of particulate air pollution: Time for reassessment? *Environmental Health Perspectives* 103(5): 472-480.

Santamouris, M., A. Synnefa, M. Asssimakopoulos, I. Livada, K. Pavlou, M. Papaglastra, N. Gaitani, D. Kolokotsa and V. Assimakopoulos (2008). Experimental investigation of the air flow and indoor carbon dioxide concentration in classrooms with intermittent natural ventilation. *Energy and Buildings* 40(10): 1833-1843.

Schwartz, J. (2004). Air Pollution and Children's Health. *Pediatrics* 113(4 II): 1037-1043.

Synnefa A, Polichronaki E, Papagiannopoulou E, Santamouris M. Mihalakakou G, Doukas P, Siskos PA, Bakeas E, Dremetsika A, Geranios A and Delakou A: (2003). An Experimental Investigation of the Indoor Air Quality in Fifteen School Buildings in Athens, Greece, *International Journal of Ventilation*, **2**, (3), pp185-201.

Twardella D., Matzen W., Lahrz T., Burghardt R., Spegel H., Hendrowarsito L., Frenzel A.C., Fromme H. (2012). Effect of classroom air quality on students' concentration: results of a cluster-randomized cross-over experimental study. *Indoor Air*, (22), 378-387.

World Health Organization (WHO) 2005. *WHO air quality guidelines global update.* Report on a working group meeting, Bonn, Germany, 18-20 October

DOES INDOOR ENVIRONMENTAL QUALITY AFFECT STUDENTS PERFORMANCE?

Paraskevi Vivian Dorizas*, Margarita-Niki Assimakopoulos, Constantinos Helmis, Mattheos Santamouris, John Sifnaios, Katerina Stathi

Faculty of Physics, Departments of Environmental Physics and Meteorology, University of Athens, University Campus,
Athens, 157 84, Greece
**Corresponding author: p.dorizas@phys.uoa.gr*

ABSTRACT

There is little knowledge on if and how indoor environmental quality influences students' attendance and productivity. However, this issue has been of growing interest the recent years in the scientific community and results are showing that student learning performance is significantly affected by indoor environmental quality factors. In the present study the learning performance is examined through numerical test scores achieved by primary school students in their classrooms. The assessment of indoor environmental quality parameters such as thermal, visual, acoustic and air quality and the evaluation of Sick Building Syndrome (SBS) symptoms was conducted through questionnaires handed out to the same sample of students. Main objective of this paper is to investigate whether the degradation of the indoor environmental quality can impact the overall performance of students.

KEYWORDS

Indoor Environmental Quality, Sick Building Syndrome, student performance, schools

1 INTRODUCTION

There is an increasing concern about the negative health effects of degraded indoor environments and some of the adverse consequences are respiratory symptoms (allergies, asthma, nose and throat irritation and cough), skin symptoms (eczema) or general symptoms (fatigue, concentration difficulty, and headache) which are usually referred as Sick Building Syndrome (SBS) symptoms (WHO, 1982). The term 'Indoor Environmental Quality' (IEQ) refers to the quality of a building's environment in relation to the Indoor Air Quality (IAQ), the thermal comfort conditions as well as to the lighting and acoustics comfort (Mendell and Heath 2005).

The last ten years the scientific interest has been focused on the effects of the degraded indoor environment on the performance and productivity of students and office workers (Wargocki et al.,1999, Wargocki et al., 2000, Witterseh et al., 2004, Mendell and Heath, 2005). However the existing documentation regarding the negative effects that poor IEQ has on students' performance and attendance is still not sufficient for the creation of schools' guidelines aiming to decrease the adverse health effects and increase students' achievements (Mendell and Heath, 2005). Thus, a further knowledge on how the poor IEQ in classrooms can affect students' performance is of great importance.

The main objectives of the present study are: 1. to investigate how the students evaluated the IEQ (IAQ, Thermal comfort, lighting, acoustics) of their classrooms, 2. to evaluate their possible sick building syndrome symptoms (SBS) and 3. to assess their performance in relation to the corresponding pollutant concentration levels and to the evaluation of the IEQ.

2 METHODOLOGY

This study was carried out in nine primary schools of the Attika basin in Greece during April and May 2013 (Figure 1). The main characteristics of the schools and the classrooms where the measurements were conducted are summarized in Table 1.

Figure 1: Map of Attika (left) and locations of schools (right)

Table 1: Schools' characteristics and measurement period

School name	School code name	Measurement period (Number of measurement days)	Classroom's floor area (m^2)	Classroom's volume (m^3)	Classroom's number of Students	Classrooms' orientation
Acharnae 14	1	1-5/4/13 (5 days)	53	165	17	North
Thrakomakedones 1	14	8-12/4/13 (5 days)	64	198	25	Northwest
Axharnae 4	4	14-18/4/13&24/4/13 (5 days)	50	155	24	Southwest
Pallini 3	3	19&22/4/13 (2 days)	46	137	25	West
Acharnae 18	18	23/4/13 (1 day)	47	138	18	South
Acharnae 12	12	13-17/5/13 (5 days)	49	157	25	South
Thrakomakedones 2	2	20-24/5/13 (5 days)	50	162	25	East
Acharnae 8	8	27-29/5/13 (3 days)	52	159	19	West
Acharnae 11	11	31/5/13 (1day)	55	172	15	South

This study consists of three parts. The first part involves the measurements of concentration levels of CO, CO_2 and VOC and their analysis. The second part consists of the questionnaire survey for the subjective evaluation of the IEQ by the students and the third part includes the completion of performance tests. School headmasters' and parents' consent was necessary as the study required the participation of students. The students participated in the survey were in total 193 and the total number of answered subjective questionnaires was 655, while the total conducted performance tests were 1310. It should be mentioned that there were cases where the same students filled the same questionnaires more than one time, depending on the days of the survey's duration (Table 1, columns 2 &3).

2.1 Measurements of chemical parameters

The concentrations of CO, CO_2 and VOCs were measured in one classroom per school (the one the survey was carried on) using MultiRAE IR (RAE Systems) in units of parts per million (ppm) from 7:00 a.m. until about 14.30 p.m. However, in order to compare the pollutant concentrations to the test scores, the 15 min average of the pollutants was calculated for the corresponding time the test were filled in by the students.

2.2 Questionnaires for the subjective evaluation of IEQ

The questionnaire used for the subjective evaluation of the IEQ by the students, was divided in the following sections: 1. personal information (age, gender), 2. perception of indoor environmental conditions at that certain time (thermal comfort, IAQ, lighting and acoustics) and 3. SBS symptoms. For the evaluation of the IEQ conditions a 7-point answering scale as mentioned on the Appendix E of the CBE Occupant survey of ASHRAE 2010 was used. The SBS symptoms were answered using single Yes and No answers (HETA 1997). The questionnaires were handed out to students once every day at approximately the same time (at 10:15), just 15 min after the pupils came into the classrooms right after a 20 min break on their third class for the day.

2.3 Performance Tests

The performance tests and operative protocol were taken from the SINPHONIE project, the Schools Indoor Pollution and Health: Observation Network in Europe aiming to improve the air quality in schools. The test consisted from two parts. The first part (1a and 2a) involved 36 numerical exercises including addition, subtraction and multiplication. Students had to solve the math test in 10 min. In the second part of the test (1b and 2b), students were given a 'code' of symbols, in which each symbol was associated to a digit number. They had 120 sec. to complete the relevant symbols at a given series of numbers. This test (of both parts) was repeated by the students twice a day, during the first and last hour of lessons. The math test of the last hour was slightly changed to the one of the first hour however the code test was the same. An initial aim of this part was to investigate to the extent that is possible, if the degradation of the IAQ in classrooms throughout the day, would affect students' performance.

3 RESULTS & DISCUSSION

3.1 Subjective evaluation of IEQ

Figures 2 to 5 present the distribution of votes for the evaluation of the four major categories of the IEQ. In particular, Figure 2 presents the acceptability of the thermal environment in the 9 schools by the students. The greatest percentage of unacceptable votes appeared in schools 8, and 2, while all students of school 18 assessed the thermal environment as acceptable. In

the rest of the schools a maximum of 20% evaluated the thermal environment as unacceptable.

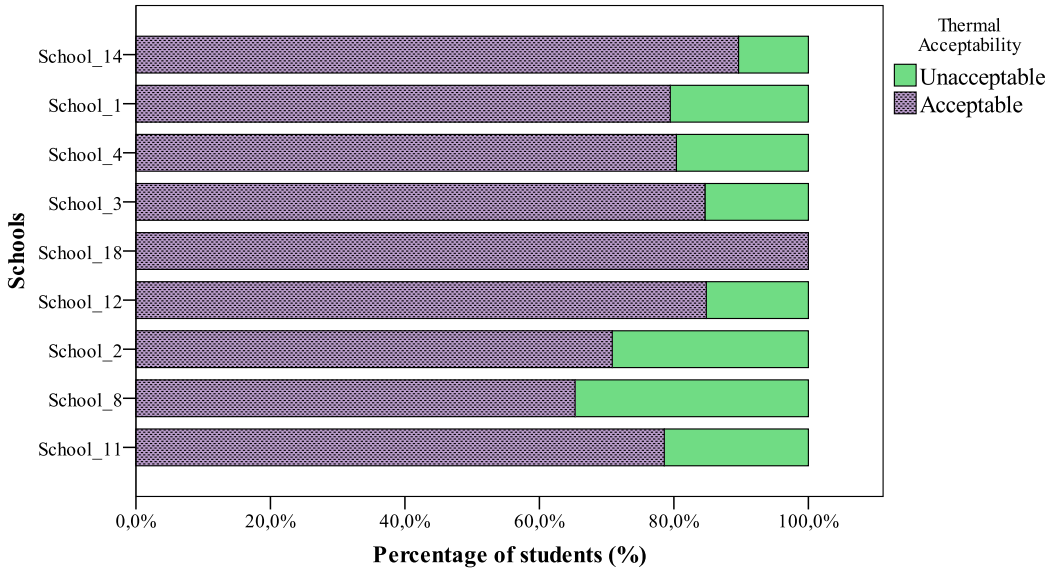

Figure 2: Distribution of votes for the assessment of the thermal environment per school

Figure 3 presents the distribution of votes per school that answer to the question: 'How satisfied are you with the air quality in the classroom'. An answering scale from zero to six was given to the students, where the vote of zero-(0) corresponds to 'very satisfied' and six-(6) to 'very dissatisfied'. In school 18 the students seemed to be the most satisfied with the air quality compared to the other schools, while school 8 had the most dissatisfied votes. Also school 2 had the less satisfied votes and a lot of dissatisfied ones (votes greater than 3). In the rest of the schools there is approximately an equal distribution (~20%) of votes from 0 to 3.

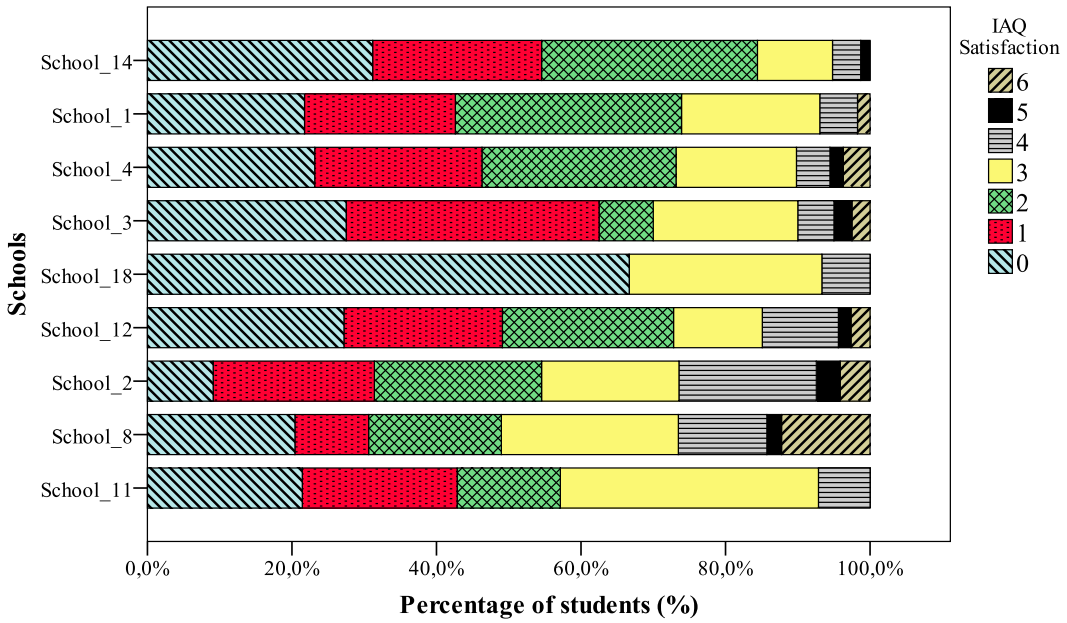

Figure 3: Distribution of IAQ satisfaction votes per school (0: totally satisfied, 6: totally dissatisfied)

The distribution of votes per school answering to the question of 'How satisfied are you with the visual comfort of the lighting?' is illustrated in Figure 4. In the 7-point scale zero-0 corresponds to 'very satisfied', while six-6 to 'very dissatisfied'. Schools 18 and 11 had the

greatest percentage of satisfied votes and none dissatisfied ones (equal or greater than 3). Schools 4, 14 and 1 had the most complains about the visual comfort of the lighting.

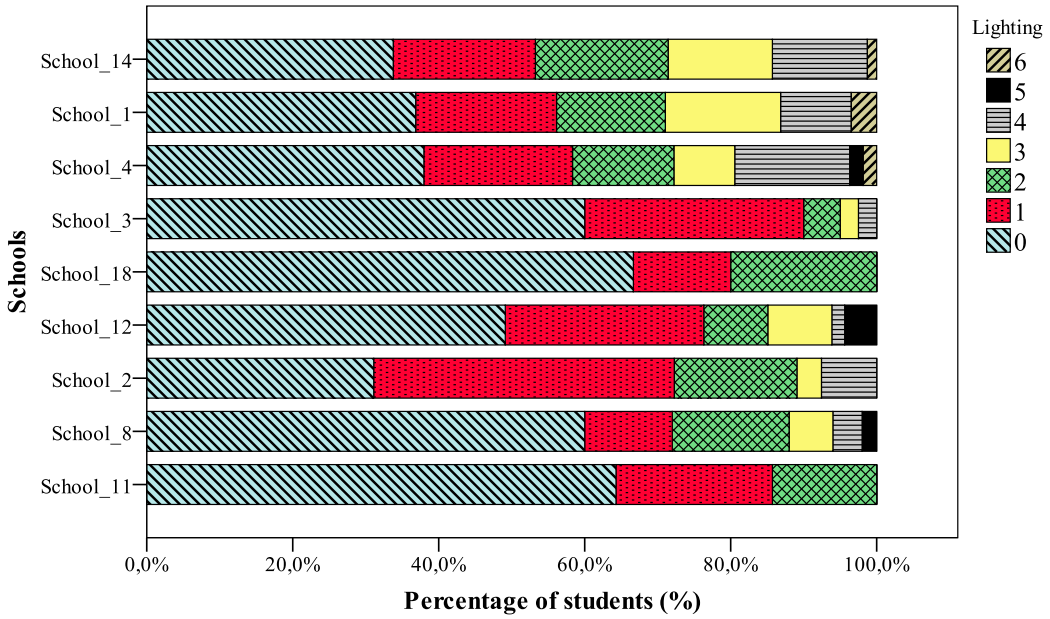

Figure 4: Distribution of votes referring to lighting satisfaction per school (0: very satisfied, 6: very dissatisfied)

Figure 5 shows the distributions of votes answering to the question of 'How satisfied are you with the noise level in your classroom?'. Once again the vote of zero-0 refers to very satisfied, while six-6 refers to very dissatisfied with the noise levels. Students in schools 1 and 11 seemed to be the most dissatisfied with the acoustics of their classrooms, while the students of schools 3 and 14 were the more satisfied as more than 50% of their students voted zero-0 meaning that they were totally satisfied with the acoustics in their classrooms without any votes of 5 and 6.

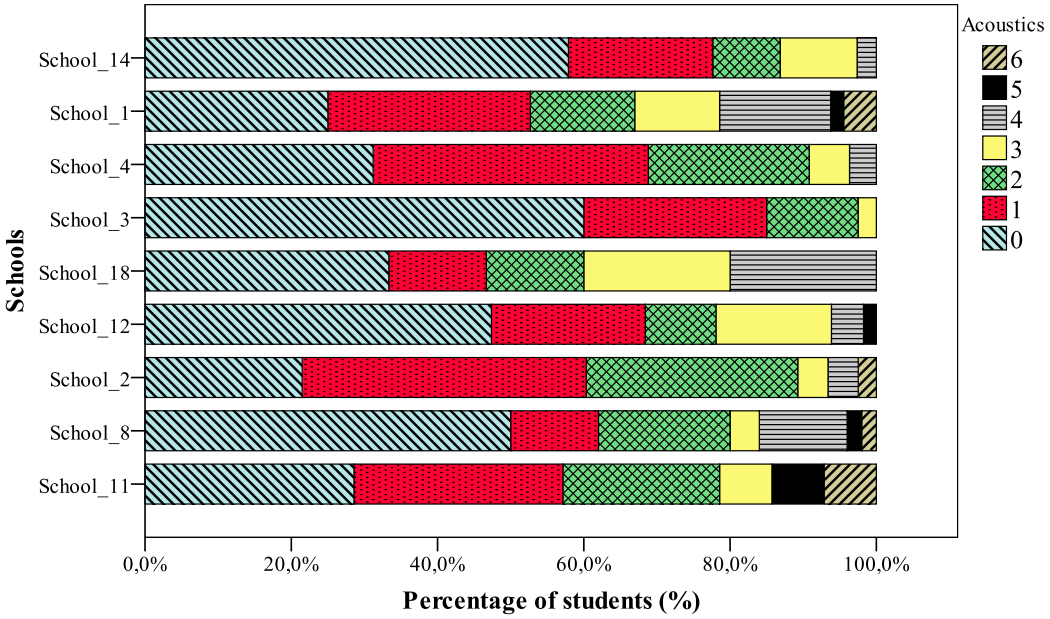

Figure 5: Distribution of satisfaction votes referring to acoustics satisfaction per school (0: totally satisfied, 6: totally dissatisfied)

The distribution of votes answering to the question: 'Overall, do the IEQ conditions of your classroom enhance or interfere with your performance?' where vote of zero-(0) corresponds to 'enhances' and vote of six-(6) to 'interferes', is presented in box plots in Figure 6 and in for

most of the schools the dispersal is identical. The greatest percentages of votes in all schools lie between zero and three. For schools 14 and 3 the distributions were exactly the same and most of the students of these schools believed that the IEQ enhanced their performance.

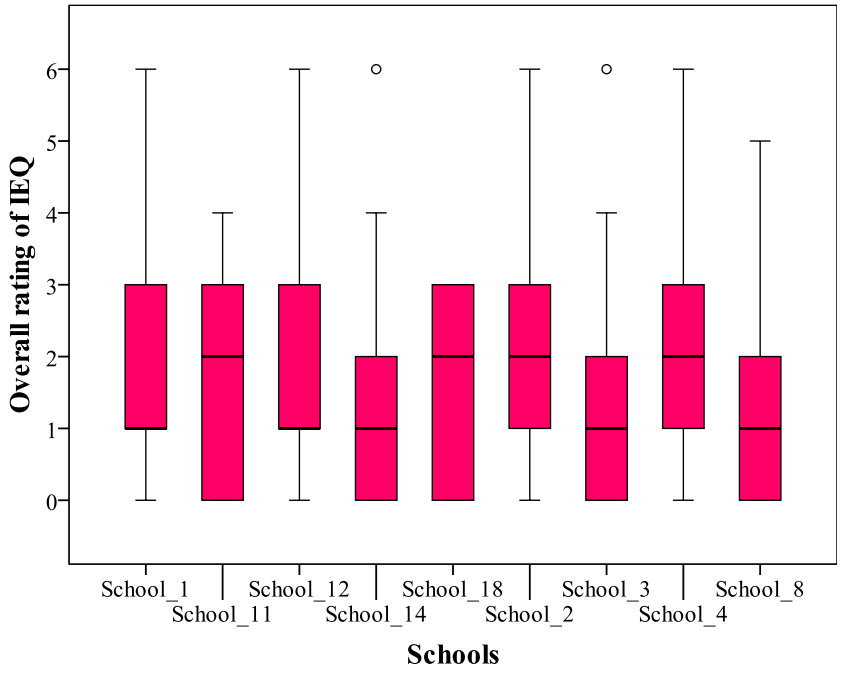

Figure 6: Distribution of votes referring on if the overall IEQ conditions encourage or not students' performance

3.2 Sick Building Syndrome-SBS symptoms

In this section the findings from the survey referring to the SBS symptoms are presented. The distribution of the percentages of students having SBS symptoms per school is indicated in Figure 7. The symptoms that occur more frequently are: allergies, fatigue, nose and throat irritation, coughing and concentration difficulty. The symptoms of headache, asthma, eye irritation and eczema are rare.

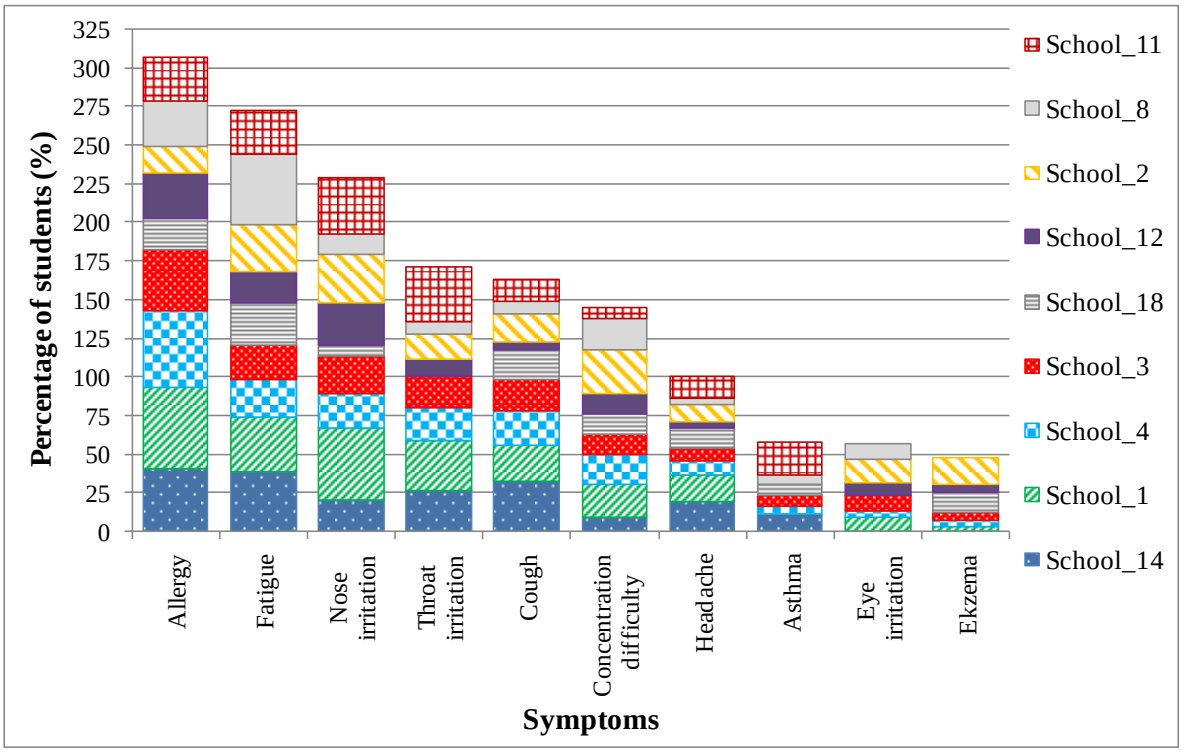

Figure 7: Distribution of students' sick building syndrome symptoms per school

In order to get a more clear virtual representation of the distribution of symptoms per school and to separate the schools whose large proportion of students is suffering from certain SBS symptoms, the dataset was divided in two parts. The one where the symptoms appear to a percentage of equal and greater than 25% of the total students per school (Figure 8) and to the one that the symptoms appear to less than 25% of the students per school (Figure 9). Great percentages of students in schools 1, 11, 14, 2 seemed to suffer more by certain symptoms (Figure 8). At least one out of four students complains about symptoms such as allergies, fatigue, nose and throat irritation, cough and difficulty in concentration (Figure 8). Figure 9 illustrates the distribution of symptoms that appear in less than 25% of the students per school. The symptoms in this case are much more, and are almost evenly distributed in each of the schools.

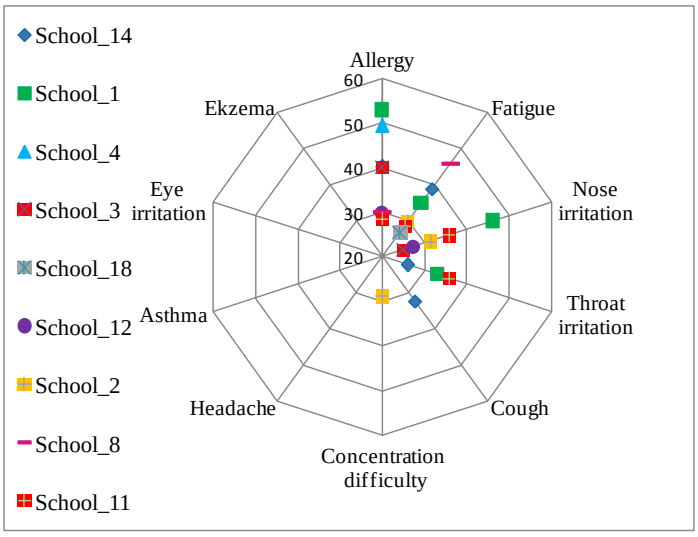

Figure 8: Distribution of students' sick building syndrome symptoms per school for cases of equal and greater than 25% of the total students per school

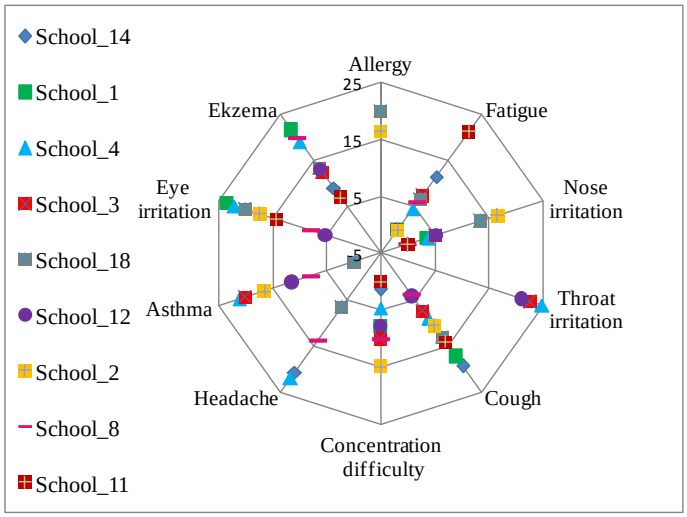

Figure 9: Distribution of students' sick building syndrome symptoms per school for cases of less than 25% of the total students per school

3.3 Performance scores vs pollutant concentrations

In order to assess the effect the pollutant concentration levels have on students' performance, the correlation coefficients were calculated between the scores achieved on the tests by the students to the corresponding concentration levels of CO, VOC and CO_2 that occurred at the time the tests were carried on. Table 2 presents the Pearson's (on the left) and Spearman's (on the right) correlations coefficients between the pollutants and the test scores. The significant correlations are marked with asterisks. As it can be seen the scores of both the 1b and 2b tests ('code test' of the first and the last hour) seemed to significantly negatively correlate to CO and CO_2, meaning that the greater the scores achieved the less concentrations occurred. The correlations were significant mainly at the level of significance 0.01.

Table 2: Pearson's (left table) and Spearman's rho (right table) correlation coefficients between test scores and pollutant levels

Pearson correlation coefficient	**CO**	**VOC**	**CO2**
Test 1a	0.014	-0.008	-0.02
Test 1b	-0.196**	-0.093*	-0.082*
Test 2a	-0.008	0.054	0.032
Test 2b	-0.013**	-0.025	-0.110**

Spearman's correlation coefficient	**CO**	**VOC**	**CO2**
Test 1a	0.039	0.025	-0.104**
Test 1b	-0.055	-0.005	-0.063
Test 2a	0.008	0.024	-0.049
Test 2b	-0.120**	-0.058	-0.208**

**Correlation is significant at the 0.01 level, *Correlation is significant at the 0.05 level

Figure 10 indicates the average scores achieved per school at each of the two 'code tests' of the first and last hour of lesson. As it can be seen, the scores of the test 2b are greater than in test 1b for all the schools. On the same figure the distribution of the average CO_2 concentrations per school are presented. In most of the cases (7 out of 9 schools) the CO_2 concentrations during the test 2b are below than the corresponding ones of the 1b test. The greater CO_2 concentrations indicate inadequate levels of ventilation which in turn also affects students' performance.

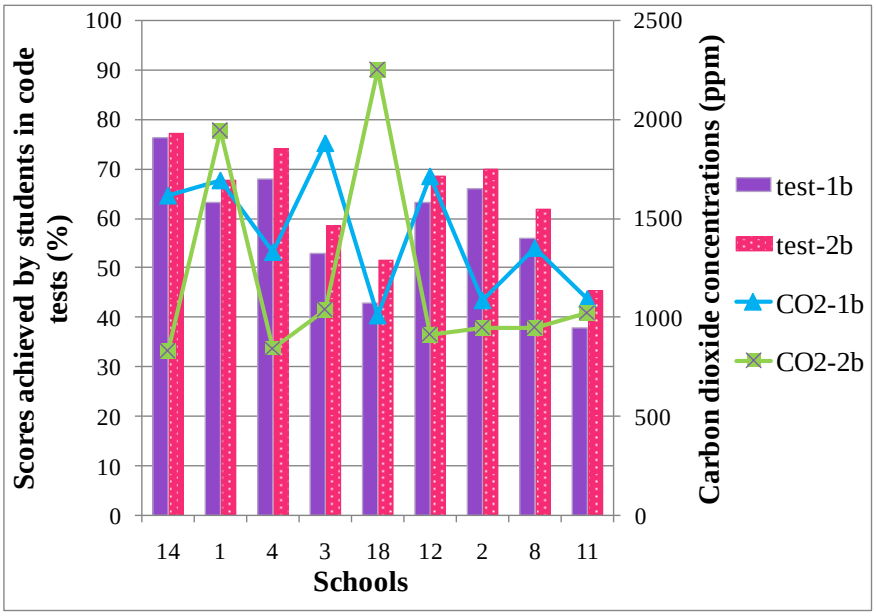

Figure 10: Averaged test scores per school and corresponding CO_2 concentrations

The correlation coefficients between the test scores and the subjective evaluation of the IEQ are shown in Table 3. Negative significant correlations mean that the greater the test scores achieved, the closer to zero (meaning satisfied, please refer to previous paragraph 3.1) are the votes of the evaluation of IEQ. Acoustics, lighting the overall rating of the IEQ on if it enhances the productivity or not and the subjective percentage of people dissatisfied (PPD) with the thermal environment seemed to be the main parameters correlating to the test scores achieved by the students.

Table 3: Pearson's and Spearman's correlation coefficients between test scores and the subjective evaluation of the IEQ

Correlation coefficients	Tests	IAQ satisfaction	Air: Fresh-Stuffy	Odor	Lighting	Acoustics	Overall rating	Subjective PPD
Pearson	Test 1a	-0.016	-0.004	-0.036	-0.081*	-0.140**	-0.083*	0.114*
	Test 1b	-0.073	-0.131**	-0.072	0.089*	-0.116**	-0.121**	0.071
Spearman's	Test 1a	-0.058	-0.051	-0.068	-0.108**	-0.152**	-0.091*	0.122**
	Test 1b	-0.067	-0.112	-0.061	0.101**	-0.07	-0.096*	0.080*

**Correlation is significant at the 0.01 level, *Correlation is significant at the 0.05 level

4 CONCLUSIONS

The main conclusions arisen from this study are: 1.Thermal comfort: in only two out of nine schools percentages of greater than 20% but less than 40% of the students evaluated the thermal environment as unacceptable. In the rest of the schools, the unacceptable votes were less than 20%. 2. IAQ: the average value of totally satisfied with the IAQ in most of the schools is approximately 20% excluding school 18 where the totally satisfied exceeded 60% of the students. Schools 2 and 8 had the highest percentages (~25%) of dis-satisfied votes (greater than 3) compared to the other schools. 3. Lighting: compared to the evaluation of IAQ, the percentage of students in all the schools that are totally satisfied with the visual

comfort is much greater. 4. Acoustics: strong differences in the distribution of votes from school to school. 5. Students in most of the schools believed that the overall IEQ enhances their performance as most of the votes lied from 3 and below. 6. Allergy, fatigue, nose and throat irritation seemed to be the main SBS symptoms of students that appeared to greater than 25 % of the students in the schools. 7. Significant negative correlations appeared between the test scores and CO and CO_2 meaning that there is evidence that the degradation of IAQ affects students' performance 8. The test scores also correlated to the evaluation of the IEQ by the students.

5 ACKNOWLEDGEMENTS

This research has been co-financed by the European Union (European Social Fund – ESF) and Greek national funds through the Operational Program "Education and Lifelong Learning" of the National Strategic Reference Framework (NSRF) - Research Funding Program: Heracleitus II. Investing in knowledge society through the European Social Fund. We are greatly indebted to the school directors, pupils and parents without whose consent this study would have not been possible.

6 REFERENCES

ASHRAE (2010). American Society of Heating, Refrigetating and Air-Conditioning Engineers, Inc. Performance Measurement Protocols for Commercial Buildings, Atlanta, 236-257.

HETA (1997). National Institute for Occupational Safety and Health's (NIOSH), Health Hazard Evaluation and Technical Assistance (HETA). Indoor Air Quality and Work Environment Symptoms Survey, Appendix 3, 297.

Mendell M.J. and Heath G.A (2005). Do Indoor Pollutants and Thermal Conditions in Schools Influence Student Performance? A critical Review of the Literature. *Indoor Air* 15: 27-32.

SINPHONIE, project. Schools Indoor Pollution and Health: Observatory Network in Europe Available at: http://www.sinphonie.eu/about, accessed on July 24th, 2013.

Wargocki, P. Wyon, D.P., Baik, Y.K., Clausen G. and Fanger, O. (1999). Perceived Air Quality, Sick Building Syndrome (SBS) and Productivity in an Office with Two Different Pollution Loads. *Indoor Air*. 9:165-179.

Wargocki, P., Wyon, D.P., Sundell, J., Clausen, G. and Fanger, O. (2000). The effects of Outdoor Air Supply Rate in an Office on Perceived Air Quality, Sick Building Syndrome (SBS) Symptoms and Productivity. *Indoor Air*. 10:222-236.

WHO (1982). World Health Organization. *Indoor Air Pollutants: Exposure and Health Effects.* Copenhagen, WHO Regional Office for Europe (Euro Reports and Studies no. 78).

Witterseh, T., Wyon, T. and Clausen, G. (2004). The effects of moderate heat stress and open-plan office noise distraction on SBS symptoms and on the performance of the office work. *Indoor Air*. 14: 30-40

INDOOR AND OUTDOOR DISTRIBUTION OF AIRBORNE POLLUTANTS IN NATURALLY VENTILATED CLASSROOMS

Paraskevi Vivian Dorizas[*1], Evangelia Kapsanaki-Gotsi[2], Margarita-Niki Assimakopoulos[1], Constantinos Helmis[1], Mattheos Santamouris[1]

[1]*Faculty of Physics, Departments of Environmental Physics and Meteorology, University of Athens, University Campus, Athens, 157 84, Greece*
**Corresponding author: p.dorizas@phys.uoa.gr*

[2]*Faculty of Biology, Department of Ecology and Systematics, University of Athens, Panepistimiopolis, GR-157 84, Athens, Greece*

ABSTRACT

The present study aims at investigating concentration levels of particulate matter PM_{10}, $PM_{2.5}$, PM_1 and UFP as well as of total airborne fungi and their vertical distribution in the indoor and outdoor environment of school classrooms. Measurements were performed in two naturally ventilated high schools in Athens, from January until May 2011. Indoor concentrations of the pollutants will be presented per floor level and indoor to outdoor (I/O) concentration ratios will be estimated as a function of the floor height. The ultimate goal is to create variations' profile of I/O pollutant ratios, so as to understand the contribution of indoor sources and the extent to which the indoor air quality is being affected by the outdoor pollutants.

KEYWORDS

Particulate Matter, Airborne Fungi, Indoor to Outdoor ratios, Vertical distributions

1 INTRODUCTION

Several studies have shown that the outdoor air pollution influences the indoor air quality (Yocom 1982). In particular, focusing on particulate matter (PM), researches have indicated that certain fractions of PM penetrate by a great percentage to the indoor environment (Koutrakis et al., 1992, Özkayanak et al., 1996). Apart from infiltration, indoor sources can also increase significantly the indoor concentrations (Khillare et al., 2004). The indoor to outdoor concentration (I/O) ratios have been studied in several researches (Cao et al., 2005),

however it is still not clear the level at which the outdoor environment affects the indoor environment.

Little is also known on how the indoor concentration levels of particulate matter (PM) and airborne fungi are distributed at various floor heights in naturally ventilated buildings. A few studies conducted in that field that are focused on PM, have shown that their rate of change is inconsistent with height due to the complex flow patterns around the buildings, to the vehicle emissions from the adjoining streets and also to particle generation affected by the vertical distribution profiles of PM concentrations (Quang et al., 2012).

The main objectives of this study are to: 1. compare the indoor to outdoor concentrations, 2. evaluate the indoor to outdoor (I/O) ratios of the pollutants and 3. examine the vertical distributions per floor of PM and airborne fungi.

2 METHODOLOGY

2.1 Sampling site description

The experimental campaign was conducted in two high schools from nearby areas just outside the city center of Athens (Dorizas et al., 2013). The first school is located in the Ymittos and the second school located in Kaisariani urban areas, hereafter denoted by Y and K respectively (Figure 1). The adjoining streets of school Y are of moderate traffic, while school K is next to a park. Both schools are naturally ventilated.

Figure 1: Map of Attica (left) and location of schools (right)

2.2 Sampling strategy

The measurements were conducted from January until May 2011 once every two weeks in each school. Air sample was collected from eight sampling sites per school, including classrooms laboratories and the outdoor environment. The windows kept closed during the measurements.

2.3 Measured parameters and instrumentation

PM_{10}, $PM_{2.5}$ and PM_1 were measured using Osiris (Turnkey Instruments Ltd), an airborne particle monitor in units of mass per unit volume (μg/m3). The ultrafine particle (UFP) concentrations were recorded using P-Trak (TSI, model 8525), a portable counter, in units of particles per unit volume (pt/cm3). Carbon dioxide (CO_2) was measured using IAQ-CALC (TSI, model 8732). Airborne fungi were recovered using a Burkard (Burkard Manufacturing Co. Ltd. Hertfordshire, UK), a portable air sampler for agar plates. Three plates with Malt Agar were exposed consecutively in each sampling site for 3 min/plate and then incubated for 2 weeks at 28 °C. The colony count was corrected and expressed as colony forming units per cubic meter (CFU/m3), a measure of viable spore concentrations. The fungal colonies were identified to genus level and *Penicillium*, *Cladosporium* and *Aspergillus* were the predominant genera.

3 RESULTS & DISCUSSION

3.1 Indoor to outdoor correlations

The indoor concentrations for all of the following cases arose from the averaged value from all of the indoor measurement sites in all of the days of measurement. The correlation coefficients between the indoor and the outdoor concentrations of pollutants are summarized in Table 1. As it can be seen for most of the cases, the correlation coefficients of particles between the indoor and the outdoor environment were high; however the correlations aren't significant. The correlation of $PM_{2.5}$ and PM_1 between the indoor and the outdoor environment are significant at the 0.01 level only in school Y. There was also found significant correlation in the UFP between the indoor and the outdoor environment. The indoor airborne fungi and their prevalent genera did not seem to correlate to the corresponding outdoor concentrations.

Table 1: Pearson and Spearman correlation coefficients of pollutants between the indoor and the outdoor environment

	Ymhttos		**Kaissariani**	
Parameter	**Pearson**	**Spearman**	**Pearson**	**Spearman**
PM_{10}	0.705	0.667	0.628	0.595
$PM_{2.5}$	0.887**	0.857**	0.606	0.690
PM_1	0.909**	0.850**	0.451	0.571
UFP	0.425	0.595	0.866**	0.833*
CO_2	0.565	0.714*	0.337	0.383
Total fungi	0.240	0.405	-0.137	0.5
Aspergillus	-0.118	-0.117	-0.199	-0.067
Cladosporium	-0.114	0.06	0.263	0.396
Penicilium	0.157	0.406	-0.034	0.446

** Correlation is significant at the level 0.01, * Correlation is significant at the level 0.05

3.2 Indoor to outdoor concentration ratios

The indoor to outdoor concentration ratios per pollutant and school are studied in this section. Figure 2 presents the I/O ratios of all the measured pollutants in school Y. As it can be seen, for most of the pollutants, the indoor concentrations are greater than the outdoor ones and most of the ratios were close to 1.5. The indoor UFP concentrations are approximately the same than the outdoor ones. *Cladosporium* was the only pollutant that its concentrations were greater outdoors than indoors. Indoor concentrations of *Aspergillus* and *Penicillium* were by more than two times greater than outdoors.

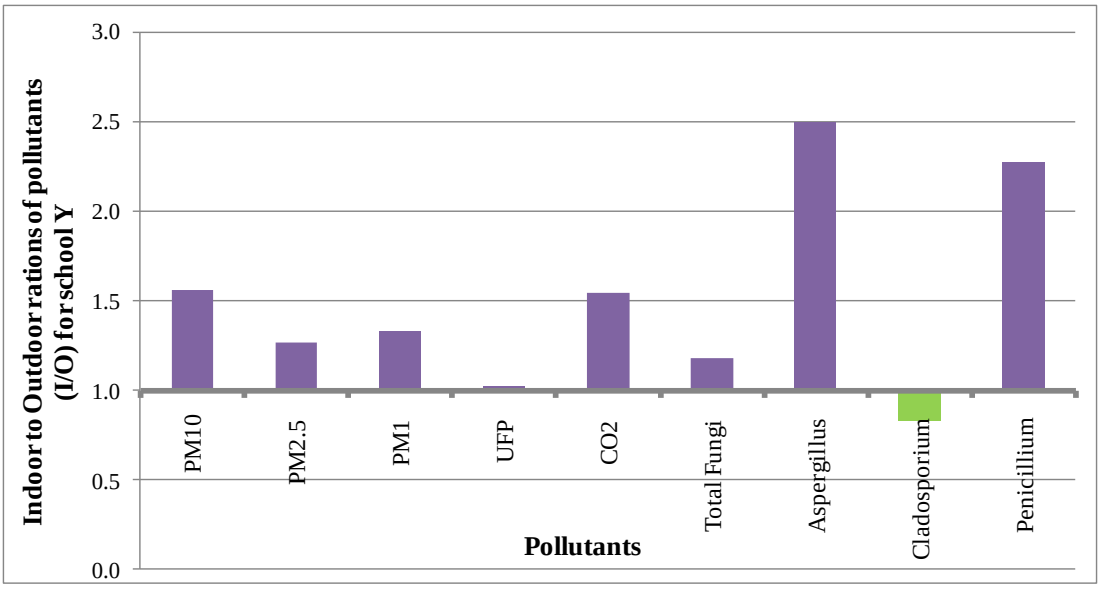

Figure 2: Indoor to outdoor (I/O) concentration ratios of pollutants in school Y

Figure 3 indicates the corresponding I/O ratios of the measured pollutants for school K. The I/O ratios of this school are slightly different than the ones of school Y for certain cases. For school K, PM_1 concentrations indoors were almost the same as outdoors. The outdoor concentrations of UFP for this school exceeded the indoor ones. Also, the indoor concentrations of *Cladosporium* were greater than the outdoor, unlike that found for school Y.

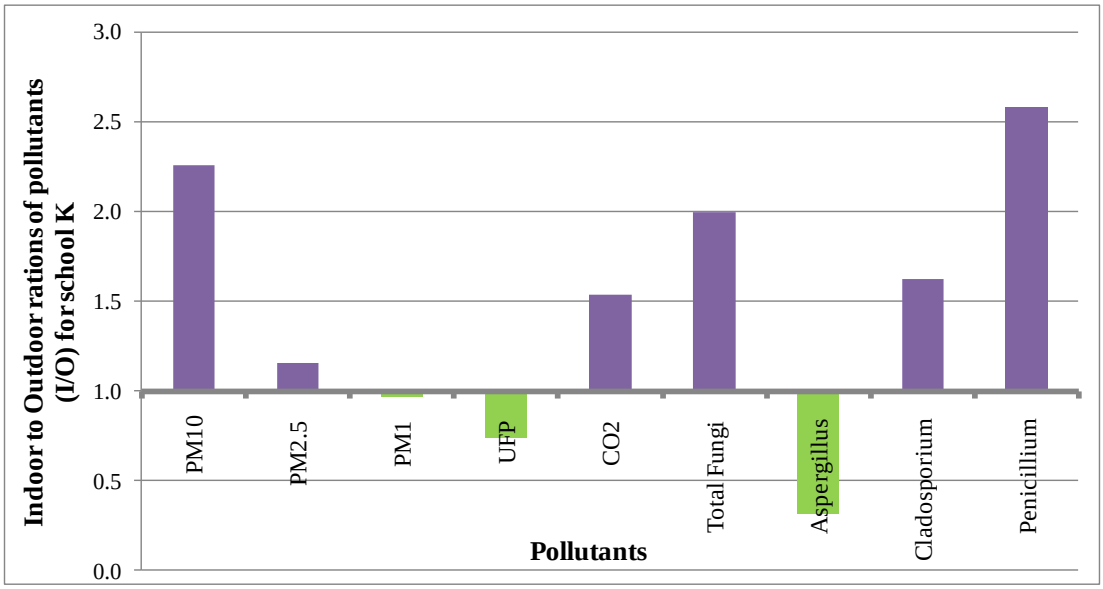

Figure 3: Indoor to outdoor (I/O) concentration ratios of pollutants in school K

The averaged I/O concentrations ratios of the two schools are shown in Figure 4. Overall, the indoor concentrations of the pollutants are greater than outdoor a fact that verifies the presence of indoor air pollutant sources, such as the increased presence of students and inadequate levels of ventilation. Only for the case of UFP concentrations the ratio was found slightly lower than 1, indicating that overall for both schools the outdoor concentrations were greater than indoors.

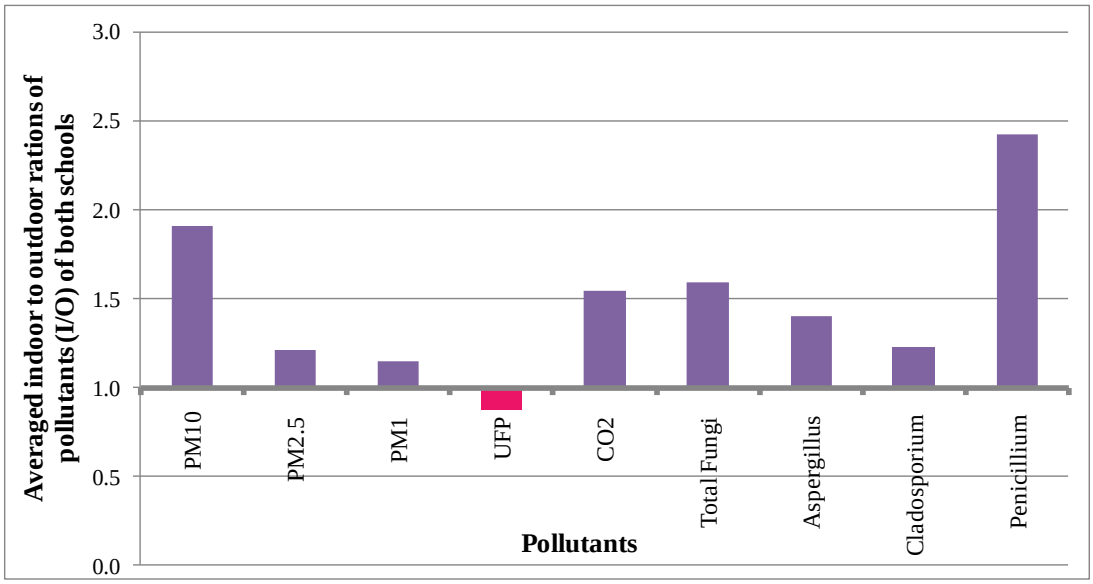

Figure 4: Averaged indoor to outdoor (I/O) concentration ratios of pollutants in both schools

3.3 Pollutant concentrations per floor level in both schools

In this section the vertical distribution of the pollutant concentrations in both schools is studied. The averaged concentrations of the pollutants per floor for all the days of measurement in both schools are presented in figures 5 – 7. The vertical distribution's profile of most of the pollutants is similar. The ground floor concentrations are approaching the outdoor concentrations and are greater than the ones of the first floor, meaning that the ground floor is probably affected by the vehicle emissions from adjoining streets (Kalaiarasan et al., 2009, Quang et al., 2012). The concentrations of the 2nd floor are greater than the ones of the 1st floor. Although the 1st floor is closer to the traffic emissions compared to the 2nd floor, the concentrations of particles and airborne fungi are lower. This fact could be due to the loss of pollutants from deflected traffic polluted air on the 1st floor from the surrounding trees that trap the particles (Cheong et al., 2007). Also, the increased concentration on the 2nd floor compared to the 1st floor could have been overwhelmed by regional sources influences (Jung et al., 2011) The indoor $PM_{2.5}$ (Figure 5, right) and PM_1 (Figure 6, left) concentrations were not greatly affected by the floor level (Jung et al., 2011, Montoya and Hildemann 2005). The airborne fungi of the ground floor were higher than in the 1st floor (Khattab and Levetin 2008).

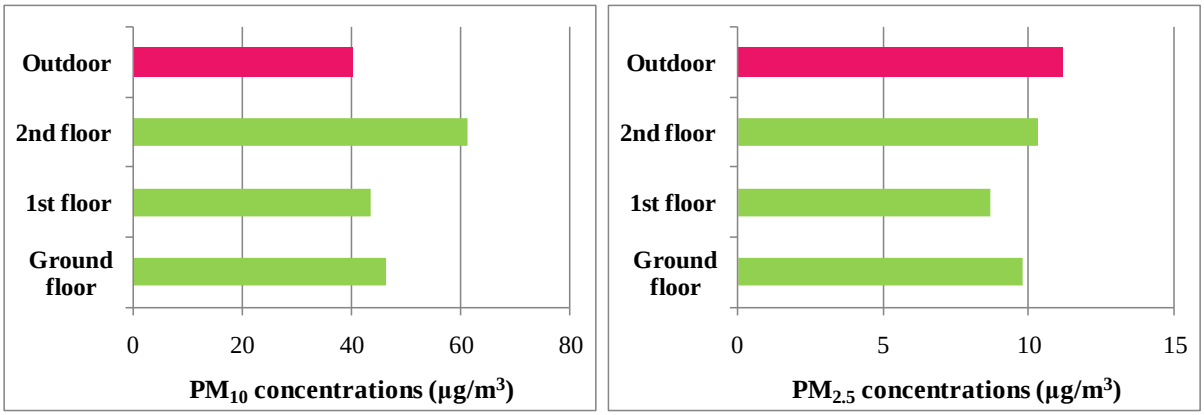

Figure 5: Averaged concentrations of PM10 (left) and PM2.5 (right) per floor in both of the schools

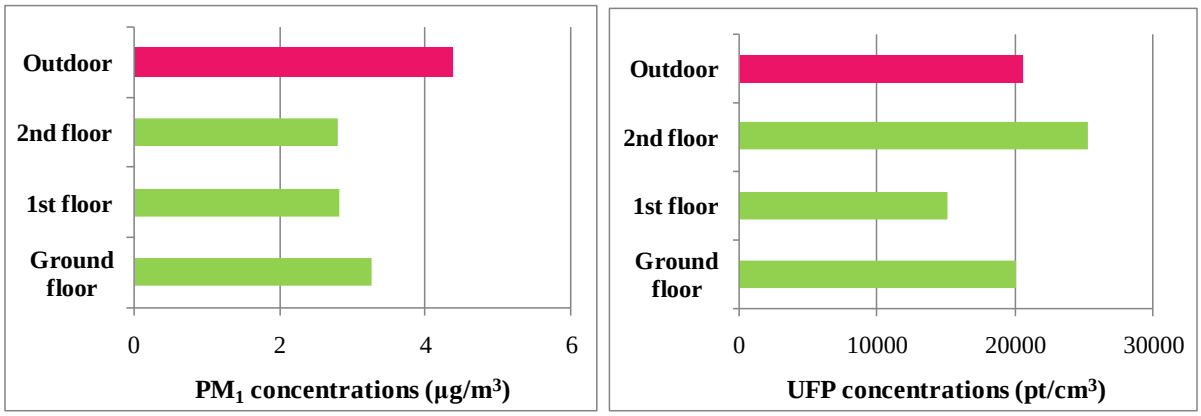

Figure 6: Averaged concentrations of PM1 (left) and UFP (right) per floor in both of the schools

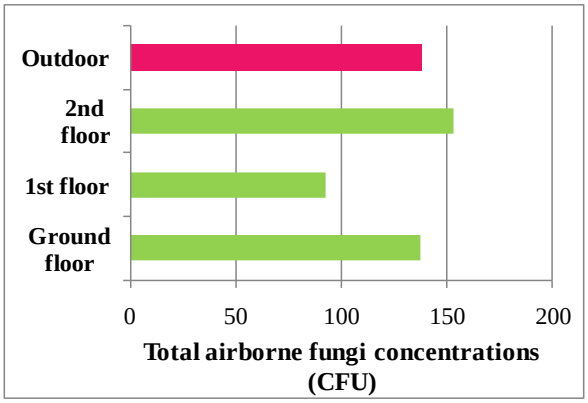

Figure 7: Averaged total airborne fungi concentrations per floor in both of the schools

4 CONCLUSIONS

The main conclusions arisen from this study are: 1. the indoor concentrations of PM correlated to the outdoor concentrations, 2. The indoor airborne fungi and their prevalent genera did not seem to correlate to the outdoor ones, 3. The indoor concentrations were greater than the outdoor concentrations for PM and airborne fungi, indicating the presence of indoor sources, 4. The vertical distribution profile of most of the measured pollutants was identical. The concentrations of the ground floor approached the outdoor levels, the concentrations of the 1st floor were lower compared to the ground floor and the ones of the 2nd floor were greater than the one of the 1st floor and in many cases exceeded the outdoor ones. Regional sources and indoor activities could have influence their vertical distribution profile.

5 ACKNOWLEDGEMENTS

This research has been co-financed by the European Union (European Social Fund – ESF) and Greek national funds through the Operational Program "Education and Lifelong Learning" of the National Strategic Reference Framework (NSRF) - Research Funding Program: Heracleitus II. Investing in knowledge society through the European Social Fund. We are greatly indebted to the school directors, pupils and parents without whose consent this study would have not been possible.

6 REFERENCES

Cao, J.J., Lee, S.C., Chow, J.C., Cheng, Y., Ho, K.F., Fung, K., Liu, S.X., Watson, J.G. (2005). Indoor/outdoor relationships for PM2.5 and associated carbonaceous pollutants at residential homes in Hong Kong-case study. *Indoor Air*. 15:197-204

Cheong, K.W.D., Balasubramanian, R. and Kalaiarasan, M. (2007). Field-based investigation on vertical distribution of airborne particulate matter in multi-storey buildings. Available at: http://www.inive.org/members_area/medias/pdf/Inive/IAQVEC2007/Cheong.pdf, Assessed on August 8th 2013.

Dorizas, P.V., Kapsanaki-Gotsi, E., Assimakopoulos, M.N., Santanouris, M. (2013). Correlation of particulate matter with airborne fungi in schools in Greece. *International Journal of Ventilation*. 12(1): 1-16.

Jung, K.H., Bernabe, K., Moors, K., Yan, B., Chillrud, Whyatt, R., Camann, D., Kinney, P.L., Perera, F.P. and Miller, R.L. (2011). Effects of floor level and building type on residential levels of outdoor and indoor polycyclic aromatic hydrocarbons, black carbon, and particulate matter in New York city. *Atmosphere.* 2:96-109.

Kalaiarasan, M., Balasubramanian, R., Cheong, K.W.D., Tham, K.W. (2009). Traffic-generated airborne particles in naturally ventilated multi-storey residential buildings of Singapore: Vertical distribution and potential health risks. *Building and Environment*, 44:1493-1500.

Khattab, A. and Levetin, E. (2008). Effect of sampling height on the concentration of airborne fungi spores. *Ann Allergy Asthma Immunol*. 101:529-534.

Khillare, P.S., Pandey, R., Balachandran, S. (2004). Characterisation of indoor PM10 in residential areas of Delhi. *Indoor and Built Environment.* 13: 139-147.

Koutrakis, P., Briggs, SLK., Leaderer B.P. (1992). Source apportionment of indoor aerosols in Suffolk and Onondaga countries, New York. *Environmental Science & Technology*. 26: 521-527

Montoya, L.D. and Hildemann L.M. (2005). Size distributions and height variations of airborne particulate matter and cat allergen indoors immediately following dust-disturbing activities. *Aerosol Science.* 36: 735-749.

Özkayanak, H., Xue, J., Spengler, J.D. Wallace, L.A., Pellizzari, L.D., Jenkins, P. (1996). Personal exposure to airborne particles ans metals: results from particles TEAM study in Riverside, C.A. Journal of Exposure Analysis and Environmental Epidemiology. 6: 57-78

Quang, T.N., He., C., Morawska., L., Knibbs, L.D. and Falk M. (2012). *Atmospheric Chemistry and Physics.* 12: 5017-5030.

Yocom, J.E. (1982). Indoor-Outdoor quality relationship. A critical review. *Journal of the Air & Waste Management Association.* 26: 521-527

INSTATIONARY OPERATION OF A VENTILATION SYSTEM

Martin Schmidt[*1], Claudia Kandzia[1] and Dirk Müller[1]

1 RWTH Aachen University
Mathieustr. 10
Aachen, Germany
**Corresponding author: mschmidt@eonerc.rwth-aachen.de*

ABSTRACT

Ensuring the thermal comfort and improving the ventilation effectiveness are important goals designing ventilation systems. This study describes effects if the ventilation system of a room is run in an instationary operation mode. That means that the inflow velocities are varied in time. The influence of different periodic times of the variation of the inflow velocities is investigated numerically with CFD simulations. The CFD simulation setup is validated by comparing CFD results with experimental data (Aachen Model Room). This comparison shows very similar results for experimental and numerical data. The CFD results show a strong reduction of the occurring time-averaged velocities inside the Aachen Model Room and they show a destruction of large-scale structure like eddies if the ventilation system is run instationary. By varying the periodic time it can be shown that longer periodic times reduce the velocities stronger than shorter periodic times.

KEYWORDS

Room airflows, CFD, instationary boundary conditions

1 INTRODUCTION

Thermal comfort and the ventilation effectiveness are important criteria for the construction of modern building ventilation supply systems. Both criteria depend mainly on air flow structures. Large scale and stable flow structures can influence the thermal comfort and ventilation effectiveness negatively. A well-designed ventilation system concerning ventilation effectiveness reduces the energy consumption of the building.

The instationary operation of a ventilation system avoids large scale flow structures. In this study the influence of the periodic time of the variation of the inlet velocity on the air flow structure is investigated numerically by Computational Fluid Dynamics (CFD). The CFD results are validated with experimental data from the Aachen Model Room.

2 VENTILATION SETUP

The investigated ventilation system is a mixing ventilation system typically occurring e.g. in meeting rooms, train and aircraft cabins. The ventilation setup for this study has been described in different studies before (Kandzia, 2011), (Kandzia, 2013). To simplify the numerical setup the CFD simulations are conducted only isothermal to investigate the effect of the periodic time T during the instationary operation. Hence, effects occurring with higher internal heat loads as describe by Linke (Linke, 1962) are not considered in this paper. In this

section the Aachen Model Room is described in detail and the experimental and numerical setup is explained.

2.1 Geometry and boundary conditions

The geometry of the Aachen model room is a simple cuboid with a length of 5 m, a width of 4 m and a height of 3 m (Figure 1). The supply air inlets are placed underneath the ceiling along the two long walls and they are built as slot diffusers with a height of 20 mm. To allow different inlet conditions along the whole length of the room, each slot diffuser is 1 m wide. Hence, 5 slot diffusers are place at each wall. With the aid of these inlet diffusers a plane wall jet enters the room. The exhaust air leaves the room above the floor. To investigate the influence of the periodic time during instationary operation three different cases are considered: The first case is the reference case. That means that the airflow rate at each diffuser is constant and the inlet velocity is 1.5 m/s. The second case is the "2D sine" case. The air flow fluctuates in form of a sine wave. The inlet velocities are calculated as:

$$v_{\text{inflow1}} = 1.5\ \text{m/s} + 0.5\ \text{m/s} \cdot \sin(\omega t) \tag{1}$$

$$v_{\text{inflow2}} = 1.5\ \text{m/s} + 0.5\ \text{m/s} \cdot \sin(\omega t + \pi) \tag{2}$$

with

$$\omega = (2\pi / T) \tag{3}$$

The corresponding inflow velocities are shown in Figure 1. For the "2D sine" case the slot diffusers at one wall supply the air with v_{inflow1} and at the opposite wall the air is supplied with v_{inflow2}. The two different inflow velocities have a phase shift of π which means that the total air flow rate of the room does not change in time. The third case is the "3D sine" which means that for each diffuser the inflow velocity fluctuates as in case "2D sine" but the opposite and the neighboring diffuser have a phase shift of π. The different inflow boundary conditions are also shown in Figure 1. To classify the investigated periodic times the periodic time is defined as a factor times the nominal time constant τ_n of the room.

$$T = a \cdot \tau_n \tag{4}$$

with

$$\tau_n = \frac{V_{\text{room}}}{V_{\text{room}}} \tag{5}$$

Four cuboids are placed inside the cabin. These cuboids serves as heat sources for non-isothermal experiments but the heat sources are switched off for this study. The walls of the room are very well isolated and an adiabatic boundary condition can be assumed.

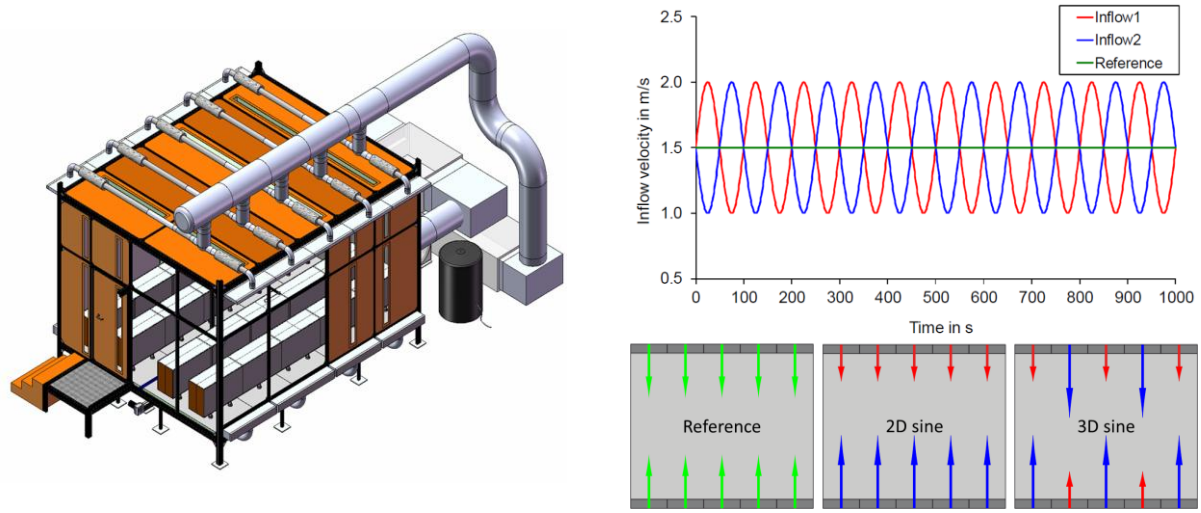

Figure 1: Experimental setup of the Aachen Model Room (left) and different conditions of the supply air (right)

2.2 Numerical Setup

Figure 2 shows the mesh for the CFD simulation. It consists of about 10 million hexahedral cells. The Simulations has been conducted with the commercial Software Ansys® CFX. The k-ω Baseline Model by Menter (Menter, 1994) is applied as turbulence model. The Walls are adiabatic and the inlets are modelled with an uniform velocity distribution. The simulations are run in transient mode with a time step of 0.25 s and a total simulation time of 1000 s according to the experiments.

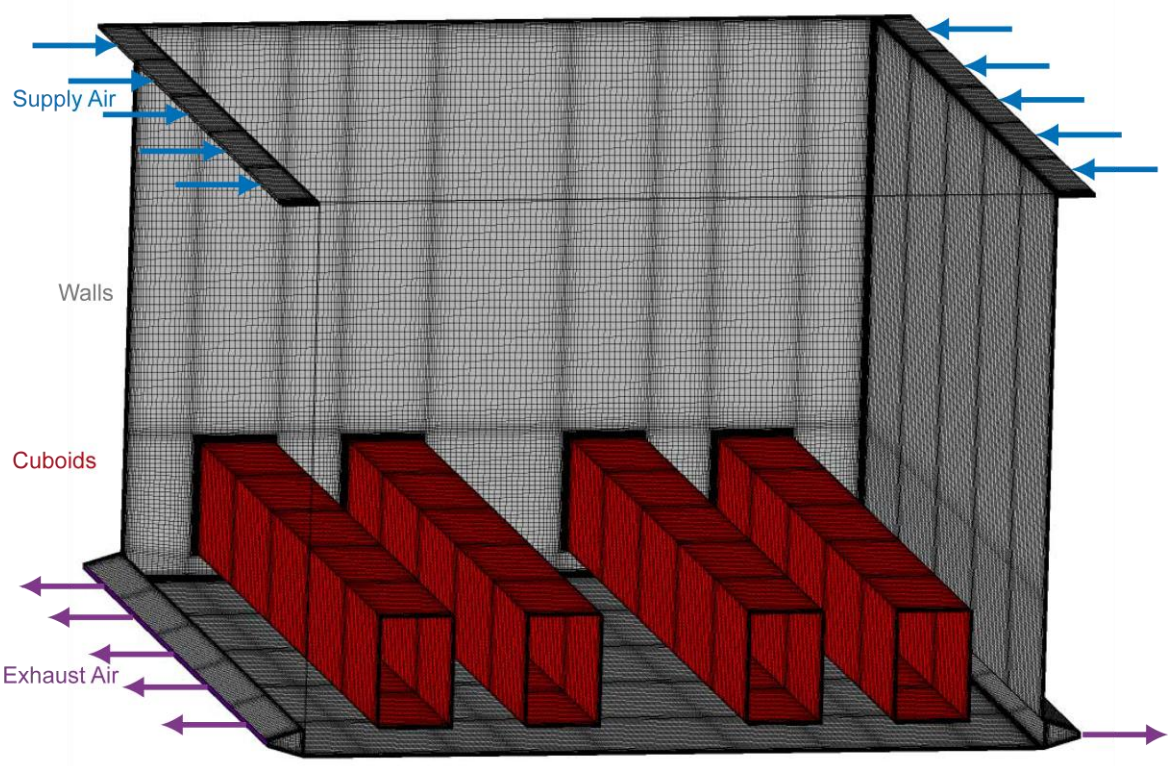

Figure 2: Mesh and boundary conditions for the CFD simulations

2.3 Validation

The numerical setup can be validated with experimental data obtained from measurements at the Aachen Model Room test bench. Inside the test bench, a traverse system with 12 omni-directional velocity probes and resistance thermometer is installed. With the aid of this traverse system the flow field inside the room can be measured in detail. In Figure 3 the comparison between experimental data and numerical data is done with the aid of time averaged velocities. The measurement points are in three different heights in a plane in the middle of the room. The plane is the same plane where the CFD results in Figure 4 and Figure 5 are presented. The Figure 3 shows well the airflow structure inside the Aachen Model Room for the reference case. The plane jets are colliding in the middle of the room and they are deflected downwards. The velocity peak in the middle is well visible. On both sides of this downward jet two large and stable eddies are established. In the lower height the velocity distribution is quite constant along the whole room width.

In the first height of 2.50 m (Figure 3a) the experimental and CFD data fit very well. This is also valid for the lowest height of 1.10 m (Figure 3c). At the height of 1.70 m (Figure 3b) some differences between CFD and experiment are visible. The minimum on both sides of the downward jet is much stronger in CFD than it is in the experiment. In CFD the center of the two large eddies is exactly at 1.70 m height while it is a little bit lower in reality. That means that the location of eddy centers cannot be predicted perfectly in CFD with two-equation turbulence models but the difference of the location is small. Based on this comparison the numerical setup is suitable for the following variation of the periodic time constant.

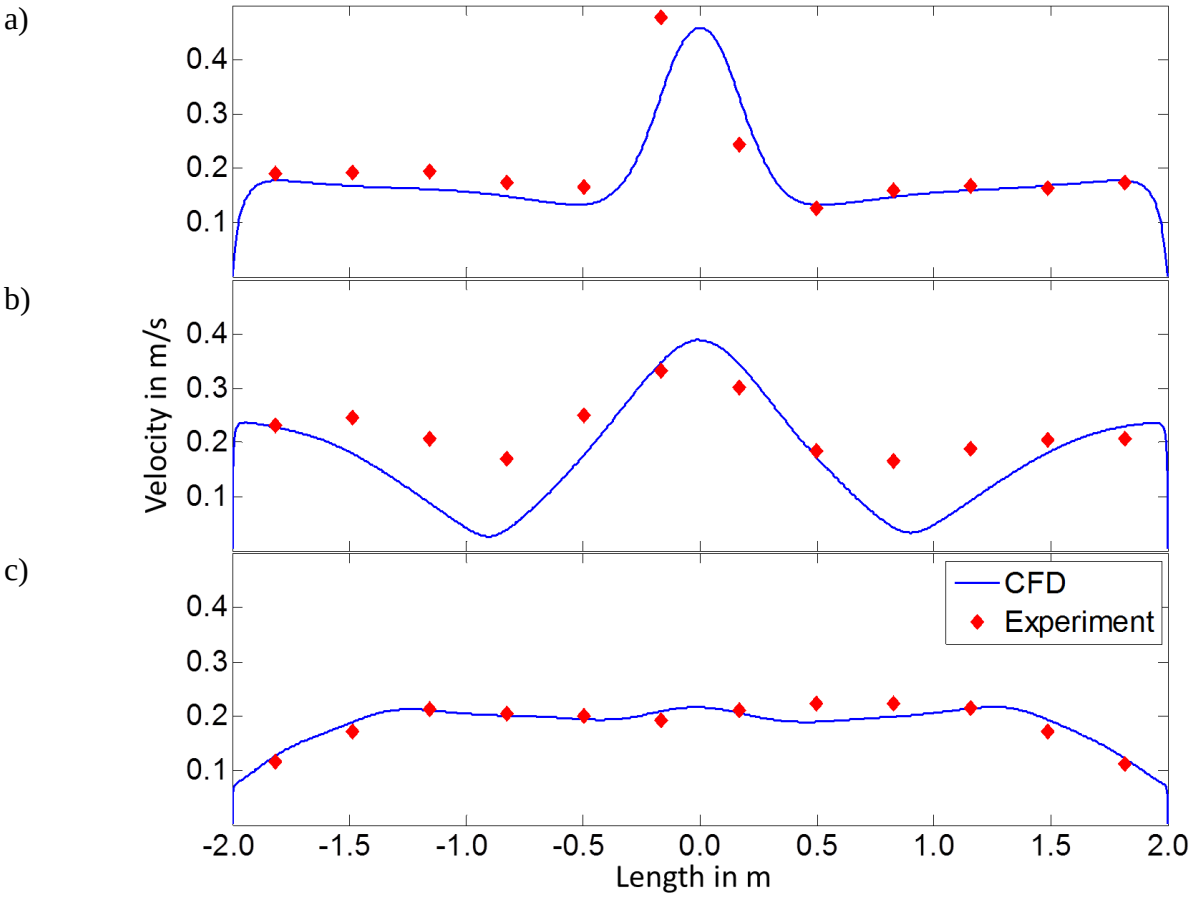

Figure 3: Comparison of the CFD simulation result and experimental data in three different heights: a) 2.50 m, b) 1.70 m, c) 1.10 m

3 RESULTS

The results of the CFD for the reference case is shown in Figure 4 as a contour plot of the time averaged velocity in the middle of the room. The air flow structure described in section 2.3 is well visible. The structure is very symmetric and the occurring velocities in the colliding jet are higher than 0.5 m/s. Two large and stable eddies exist on both sides of the colliding jet. The velocities at the edge of the eddies are still pretty high with values between 0.20 m/s and 0.25 m/s.

Figure 5 shows the results in the same plane with the same contour plot as in Figure 4. The results for the "2D sine" case are listed on the left side and the results of the "3D case" on the right side. In the first row the periodic time is a eighth of the nominal time constant, on the second row a quarter of the nominal time constant, on the third row the half of the time constant, on the fourth equal to the nominal time constant and in the last row 2.5 times the time constant.

For a short periodic time $T = 0.125 \cdot \tau_n$ and the "2D case" the velocities in the colliding jet are lower than in the reference case but the region of the colliding downward jet is wider than in the reference case. The large eddies still exist on the left and right side. For the "3D case" with the same nominal time constant the colliding jet region is only marginally visible and the large eddies disappear as well. The level of the velocities is clearly lower than in the reference case.

Doubling the periodic time $T = 0.25 \cdot \tau_n$ results in weaker but still visible colliding jet for the "2D case" while the results for the "3D case" are almost the same as for the smaller periodic time. With a periodic time $T = 0.5 \cdot \tau_n$ the colliding jet area disappears also in the "2D case" but the eddies are still visible but much weaker.With higher periodic times $T = \tau_n$ and $T = 2.5 \cdot \tau_n$ the results of the "2D case" and the "3D case are similar. The colliding jet area disappears as well as the large structures on both sides and the velocity level is clearly lower than in the reference case.

The instationary operation of a ventilation system reduces the occurring velocities and it destroys large and stable structures like eddies. The reason for this is the better mixing by increasing the velocity gradients between the jets and the surrounding air in the "2D case" and by introducing an additional velocity gradient between the neighboring jets in the "3D case". These effects can be found as well in experimental data published by Kandzia (Kandzia, 2011).The influence of the periodic time T can be also seen in Figure 5. The effect of the instationary operation increases with a longer periodic time T while the air flow structure in the "2D case" with the short periodic time $T = 0.125 \cdot \tau_n$ is still similar to the reference case with time-constant operation mode.

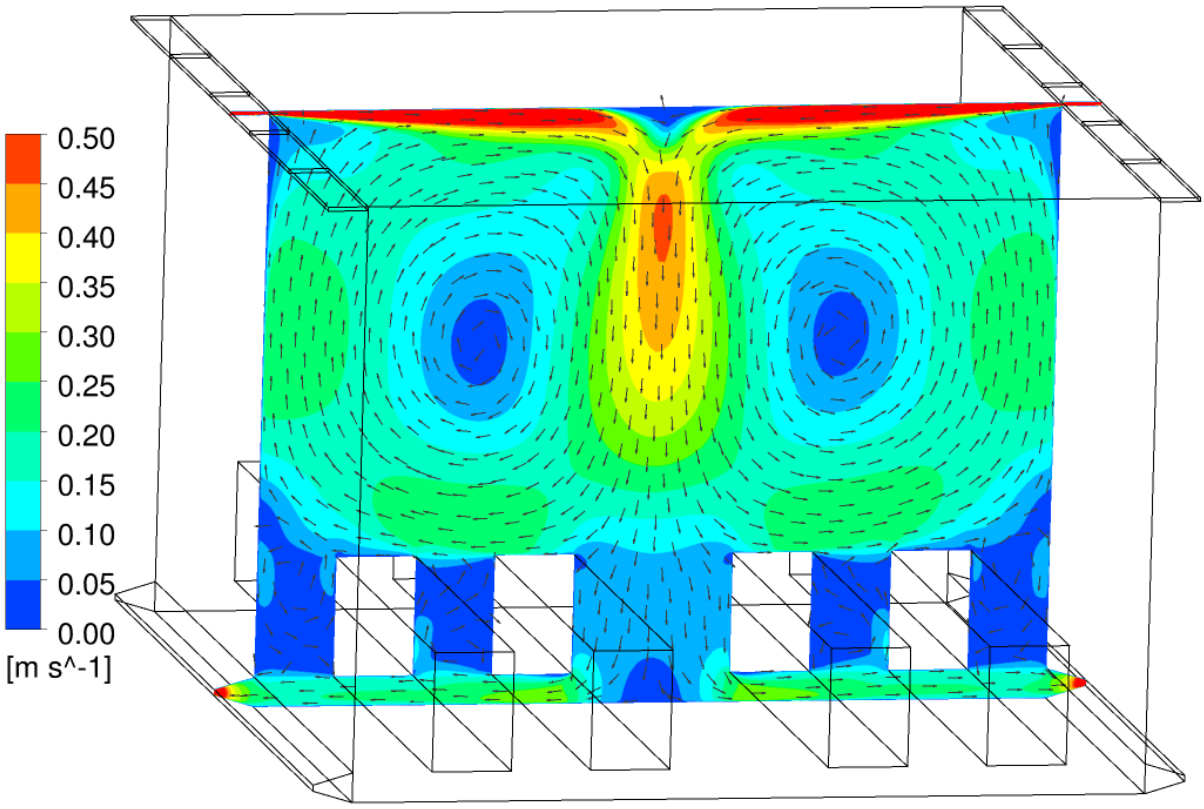

Figure 4: Velocity distribution in the middle of the room for the reference case

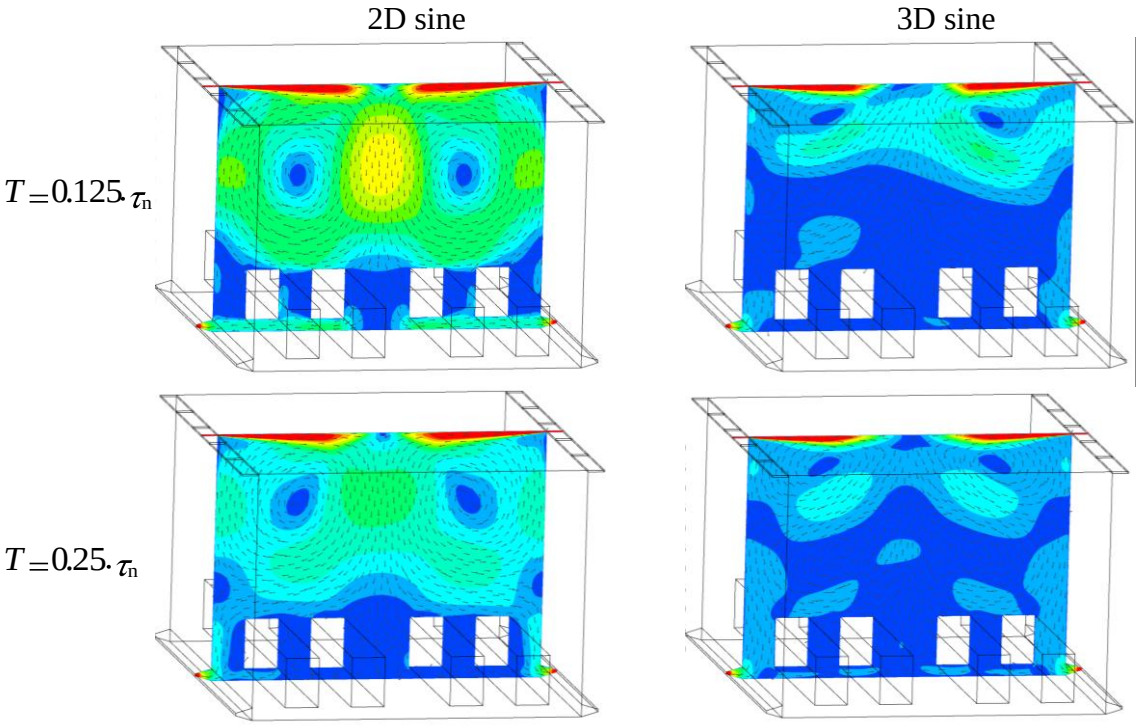

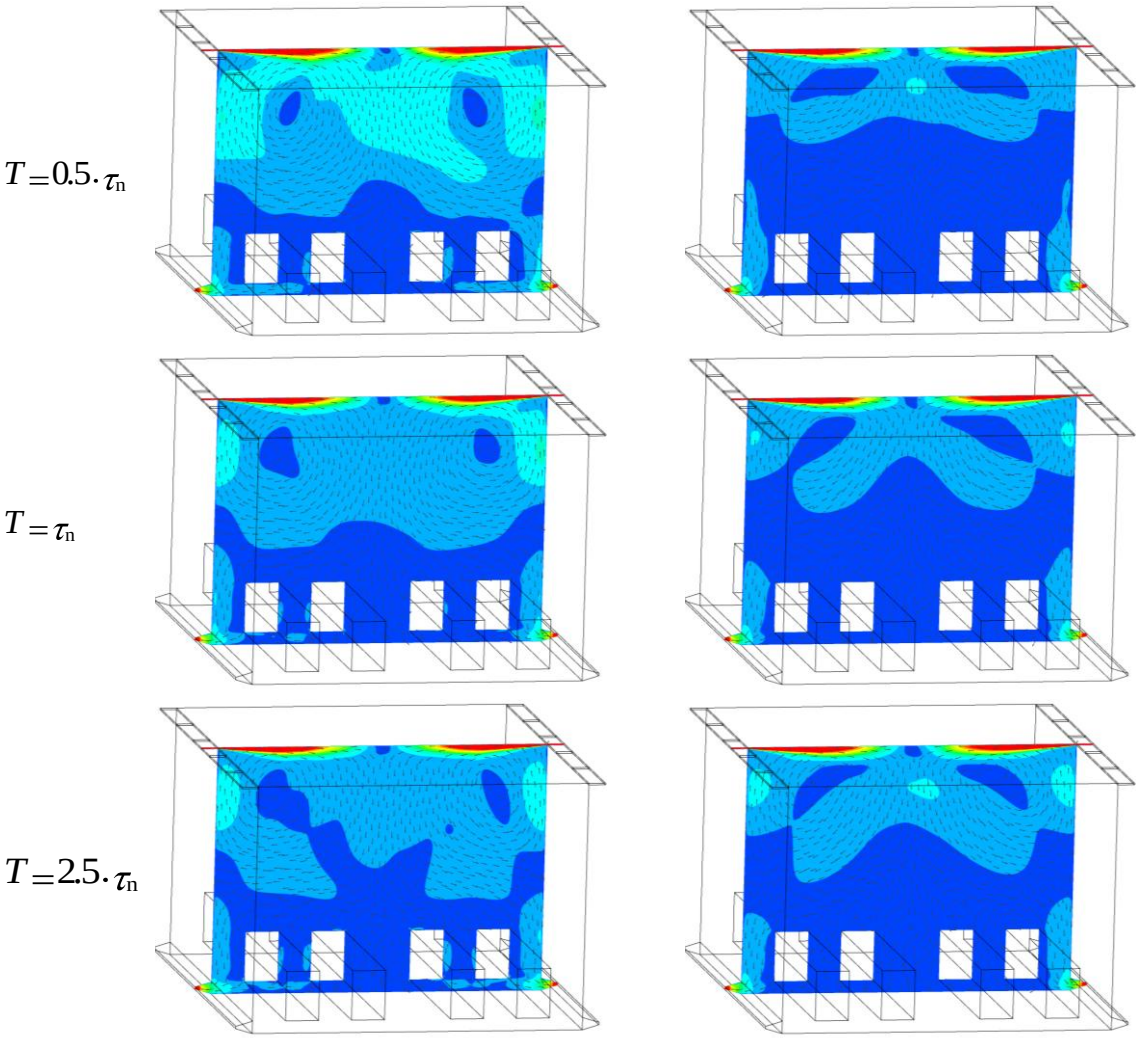

Figure 5: Velocity distribution in the middle of the room for different periodic times

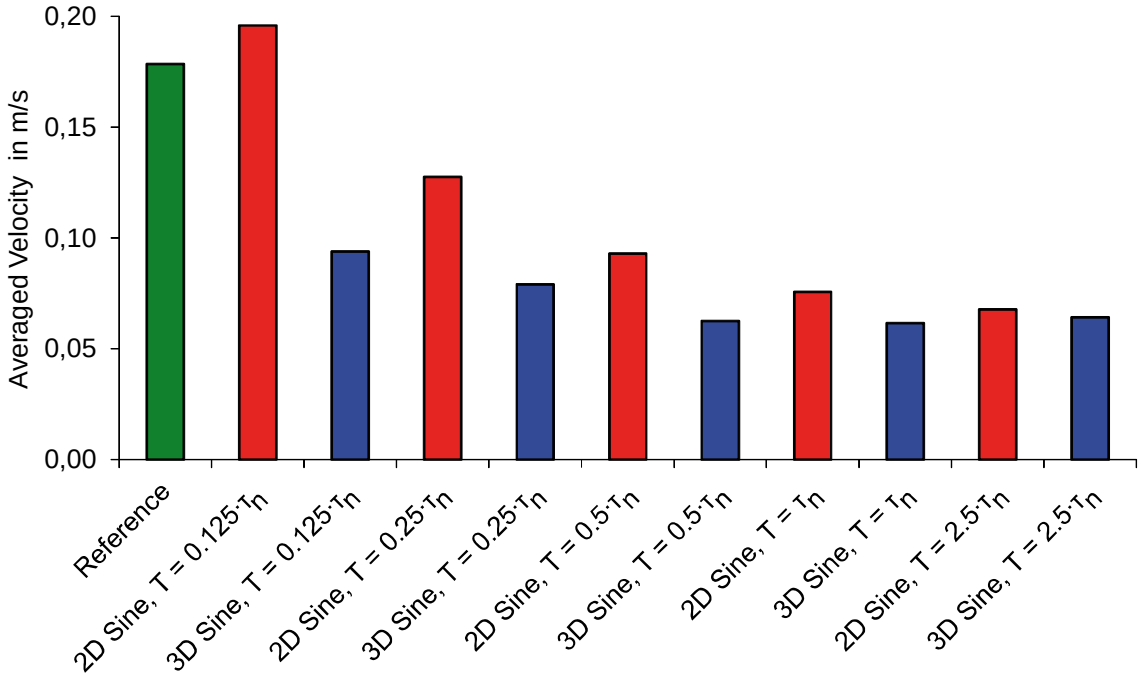

Figure 6: Averaged velocity inside the room

In Figure 6 the time-averaged velocity obtained by CFD simulations is averaged in the whole volume of the room. All eleven cases are listed in the diagram in Figure 6 and the influence of an increasing periodic time T can be seen. The volume-averaged velocity in the reference case is about 0.18 m/s and it increases up to 0.20 m/s for the "2D sine" with $T = 0.125 \cdot \tau_n$. but it decreases down to 0.09 m/s for the "3D sine" case even with the short periodic time of $T = 0.125 \cdot \tau_n$. With increasing periodic times T the volume-averaged velocity is decreasing for the "2D sine" but for the "3D sine" the volume-averaged velocity is almost constant for periodic times longer than $T = 0.5 \cdot \tau_n$.

4 CONCLUSIONS

This study shows results of CFD simulations of the Aachen Model Room with an instationary operation mode of the ventilation system. The results of the simulations confirm the results published by Kandzia (Kandzia, 2011). The occurring velocities in the Aachen Model Room can be reduced by operating the ventilation system in an instationary mode. Beside the velocity reduction large flow structure like eddies can be destroyed by the instationary effects.

The effect of the periodic time T of the operation mode has a strong influence on the results. The instationary effects are stronger with longer periodic times T. The periodic time of the instationary mode should be at least in the same dimension as the nominal time constant τ_n of the room.

The CFD simulations have been conducted only isothermal for this study. The effect of introducing heat sources into the room has to be investigated in further studies. The influence of the instationary operation mode of ventilation systems on the ventilation effectiveness has to be considered in future as well.

5 ACKNOWLEDGEMENTS

Grateful acknowledgement is made for financial support by research association for air and drying technology FLT (promotional reference 622270) and by German Research Foundation DFG (promotional reference AOBJ 579043).

6 REFERENCES

Kandzia, C. Schmidt, M and Müller, D. (2011). *Room Airflow Effects Applying Unsteady Boundary Conditions.* ROOMVENT 2011: The 12th International Conference on Air Distribution in Rooms, Trondheim, Norway, June 19-22, 2011

Kandzia, C. Schmidt, M and Müller, D. (2013). *Large Scale Flow Structures in Ventilated Rooms.* Proceedings of CLIMA 2013 : Prague 16th - 19th June, 2013

Linke, W. (1962). *Lüftung von oben nach unten oder umgekehrt?.* GI 83, vol. 5, pp. 121-152

Menter, F. (1994). *Two Equation eddy-viscosity turbulence models for engineering applications.* AAA Journal 32 (1994), pp. 1598-605

ENERGY SAVING OPPORTUNITIES BY SUITABLE HVAC MANAGEMENT: THE PROCURATIE CASE IN VENICE

Luigi Schibuola*[1], Chiara Tambani[2]

1 University IUAV of University
Dorsoduro 2206
Venice, Italy
*Corresponding author: luigi.schibuola@iuav.it**

2 University IUAV of University
Dorsoduro 2206
Venice, Italy

ABSTRACT

The thermo-hygrometric treatment related to the air change in buildings requires a relevant quota of the total energy demand for heating and air conditioning, especially when the ventilation exigency is significant. For this reason a correct energy saving strategy should always focus on the use of suitable techniques in order to reduce this consumption. For example, as the modern comfort science teaches, more flexible values can be accepted for the internal humidity set point without compromising indoor comfort conditions. But demand-controlled ventilation is the fundamental opportunity to reduce energy requirements in presence of high ventilation flow rates. An evaluation of the possible amount of the energy savings following this more flexible control strategy is here presented in a real application case. This refers to two historic buildings in Venice, the Procuratie 5 and 6 near S. Basilio harbour just transformed in modern university facilities and characterized by considerable design occupancy. As frequent in university buildings, the effective crowding has high peaks, but also an appreciable variability during the activity period. In addition to a smart humidity control, in these buildings it is therefore foreseen the presence of a variable ventilation rate on the basis of the real exigency measured by CO_2 sensors installed in the return air ducts in the classrooms and a central system based on fans equipped with inverter. In this way the strong ventilation flow rate can be controlled in each air treatment unit (from one to four units in each classroom). The central supervision system is able to perform an independent control of the air change and of the thermo-hygrometric conditions for each internal unit. An user friendly interface permits an easy intervention of the building manager on the set point values of each unit. Starting from the data of monitoring enabled by the existing supervisory system an investigation about the contribution of demand-controlled ventilation to the energy requalification of one of these two buildings is here presented. The analysis of the performance of ventilation system has pointed out the possibility of remarkable energy savings.

KEYWORDS

Demand-controlled ventilation, historic building, monitoring, ventilation valve modulation

1 INTRODUCTION

The energy demand for the ventilation air treatment can become the predominant quota of the total energy requirement for the climatization. This is particularly true for buildings characterized by high level of occupancy like for example school buildings. Already in the design phase it is therefore necessary to operate in order to reduce the energy amount adopting recovery system on the exhaust air more efficient as possible. But it is also important to investigate if the high level of the peak occupancy, foreseen in the design conditions in order to size the HVAC plant, is constant during the working hours. Otherwise the best way to reduce the energy demand for ventilation it is a modulation of the external air flow rate

following the variability of the real presence during the activity period. This precise ventilation control can be simply achieved by the use of CO_2 sensors installed inside the building or in the ducts of the return air. This is the case of the university building object of this analysis. Here the strong ventilation flow rate can be controlled for each classroom on the basis of the real presences by the use of modulating valves for the ventilation rate and a central system based on fans with inverter control. A long term monitoring has permitted to investigate the correct utilization of the ventilation control system and quantify the real amount of these savings.

2 DESCRIPTION OF THE BUILDING-PLANT SYSTEM

The analysed building is one among a group of old customs warehouses named Procuratie in the harbour area in Venice recently subjected to refurbishment . Two of them, Procuratie 5 and 6, were recently transformed in university facilities for the faculty of architecture. In the overall design and work supervision entrusted to ISP, IUAV Studies and Planning, company, the authors of this paper dealt with the plants and their subsequent monitoring (Schibuola and Tambani, 2009).

Figure 1: View of part of the warehouses

The two buildings are identical. Each presents three floors for a total of about 3210 m^2 and a climatized volume of 13450 m^3. In this paper are reported the results about Procuratie 6 which

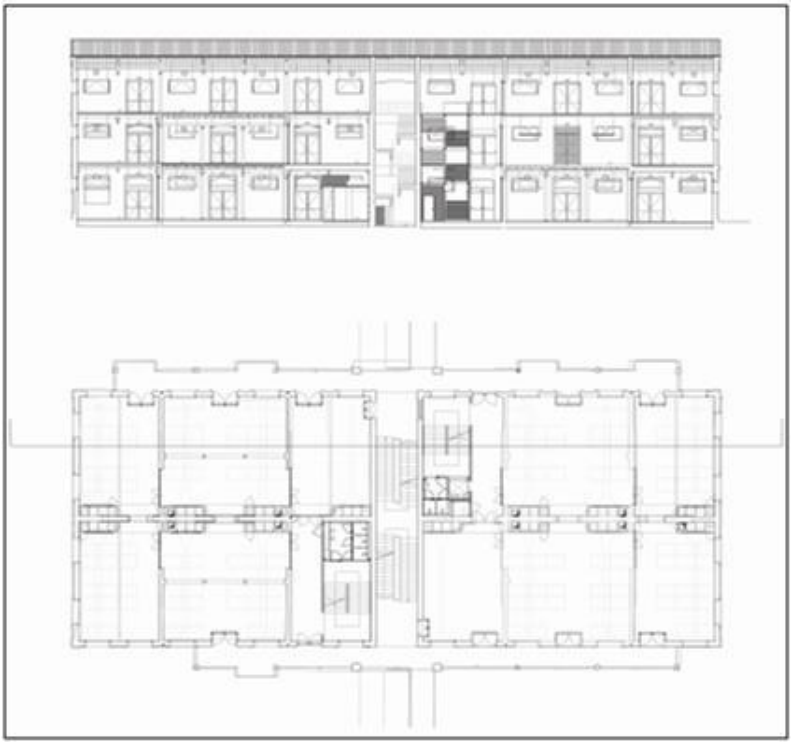

Figure 2: Longitudinal section and one floor map view of the building

is the second building from the right in the photo showed in figure 1. A longitudinal section and one floor map view of the building are reported in Figure 2. Except for one room occupied by electric equipments, the building is completely utilized for classrooms and relative toilette facilities. The entrance to the classrooms is directly from outside by balconies. All the classrooms are formed by modules of 6.4x8.9=57 m^2. Actually we have classrooms with one, two or four modules. Each module has its own internal air handling unit (internal AHU). The air conditioning plant is also equipped by two identical central air handling units installed on the top of the building (roof top AHU). Each of this two roof top AHUs serves half building (side South and North). They treat the ventilation flow rates later submitted to the inside by a network of primary air ducts which supply the internal AHUs. In Figure 3 two photos of one internal machine (a) and of the modulating valves detail (b) are reported. In winter the external air is subject to a complete treatment: preheating, humidification and post-heating. The adiabatic humidification is controlled by a humidity sensor installed in the exhaust air duct before the heat recovery system. Instead in summer we have only the cooling of the air until a fixed temperature controlled by a saturation temperature probe.

a) b)

Figure 3: Photos of one internal AHU (a) and of its air modulating valves

After this pre-treatment the cold air is submitted to the internal AHUs and here mixed with the recirculation air in the plenum installed in the lower part of each machine. In this way the strong cooling necessary to the dehumidification of the outdoor air is not lost as in the case of post-heating of the primary air. Each internal AHU is provided of two coils. The first coil is cold in summer and hot in winter. In summer this coil is driven by the two sensors of temperature and relative humidity located on the return air. The priority is the control of indoor humidity and secondly the coil avoids an increment of the indoor temperature above the set-point temperature. In winter the coil is driven only by the temperature sensor. The second coil operates only in summer in order to post-heat the air, before the introduction in the classroom, up to a minimum input temperature and also to respect a minimum indoor temperature when the exigency of dehumidification is predominant. The ventilation flow rate submitted to each internal AHU is controlled by a carbon dioxide (CO_2) concentration sensor located in the return air duct. This sensor operates on the aperture and closure of two valves installed one in the supply duct and the other in the return duct respectively, which connect each internal AHU to the primary air network. In this way it is possible to modulate the ventilation rate on the basis of the effective exigency due to the real occupancy in any moment during the working period of the building. The building is provided with a

supervisory system which permits an ongoing control and verification not only of fire and antitheft safety, but also of the production of heat and cold by a reversible air to water heat pump integrated by condensing boilers and of the working of the HVAC plant. All the measured data are shown on the computer of the management central position. They are visualized on the screen by maps which permit the operator to control the working conditions and also to modify the set-point values (Schibuola and Tambani, 2009). In Figure 4 the maps relative to a roof top AHU (a) and to one internal AHU (b) are shown. The visualized data are also recorded and in this way the supervisory system has permitted the long term monitoring used for the investigation here presented.

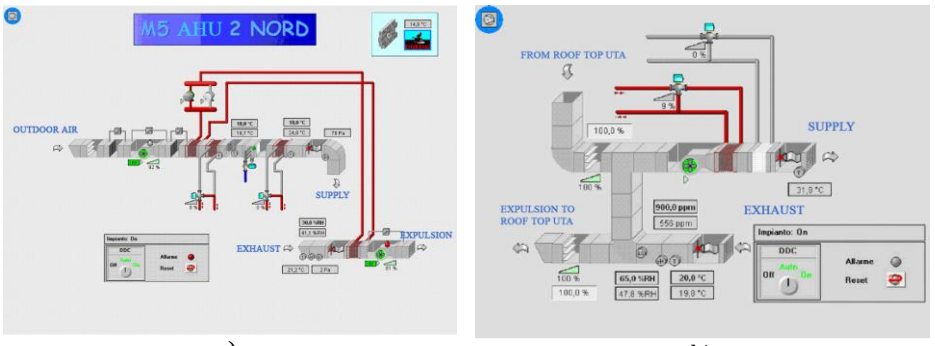

a) b)

Figure 4: Supervisory screenshots for roof top AHU (a) and internal AHU (b)

3 DESIGN OF THE VENTILATION PLANT

The realization of the classrooms is simply based on the modularity of the rooms just present in the warehouses. With a module of 57 m^2 is obtained a classroom for 45 students, with two modules for 90 and 180 seats with four module classrooms. For each classroom the specific presence is 45/57=0,79 persons per m^2. This is a value well above the average. For example the Italian standard UNI 10339 (UNI 10339, 1995) establishes a normal crowding of 0.60 pers/m^2 in the classrooms. This high value is a consequence of a precise requirement of the customer. Consequently for each internal AHU the design ventilation rate is 45x25=1125 m^3/h coming from one of the roof top AHU. In fact the ventilation quota per person is assumed to be the typical value of 25 m^3/h (7 l/s). In the end the total design ventilation rate of the building is 44000 m^3/h equally divided in the two roof top AHUs.
The high design ventilation rate and the variability of the crowding have therefore suggested the introduction of a demand-controlled ventilation (DCV) which is easily managed by the central supervision. In fact between the environmental parameters controlled for each internal AHU there is also the carbon dioxide concentration which leads the ventilation rate by the modulation of the aperture of the two motorized valves. At this moment the set-point value is 850 ppm for the CO_2 concentration measured in the return plenum box of each internal AHU. In detail the modulating valves completely open at 900 ppm and close at 800 ppm. In fact international standard (ASHRAE, 1989) recommends to maintain the internal concentration of carbon dioxide under 1000 ppm. However a minimum aperture share equal to 10% of the total is always foreseen in order to ensure a minimum air flow rate, about 0.5 ach, during the working hours. It is important to remark again that the set point of the CO_2 concentration for each AHU can be easily changed by the manager of the building plant on the basis of the requests of the users. Simple, robust and economic motorized air-tight butterfly valves have been installed and their aperture level is controlled by an electric signal coming from the central BMS.

4 EXPERIMENTAL RESULTS

The long term monitoring of the plants enabled by the building management system has provided the performance data of DCV in all the classrooms. As an example the figure 5 shows the average working conditions measured in a classroom during the school hours of a typical week. The extreme variability of the measured CO_2 concentration confirms a presence very variable and the difficult of prediction in advance. This fact is a practical demonstration of the advantage to adapt constantly the ventilation rate to the actual requirement. In addition it can be observed how it is sometimes necessary to have the total design ventilation rate as the set point value of 900 ppm fixed is exceeded. Later it will be shown as this excess is also connected to the choice of the parameters of the control system. In the bottom of figure 5 are reported the opening quotas of the valves modulating the ventilation. A high modulation can be verified. In detail it is significant that sometimes the minimum foreseen opening level (10%) is anyway able to ensure a carbon dioxide concentration within the limits. Conversely, however the total opening is sometimes not enough as already noted in the upper part of the figure 5.

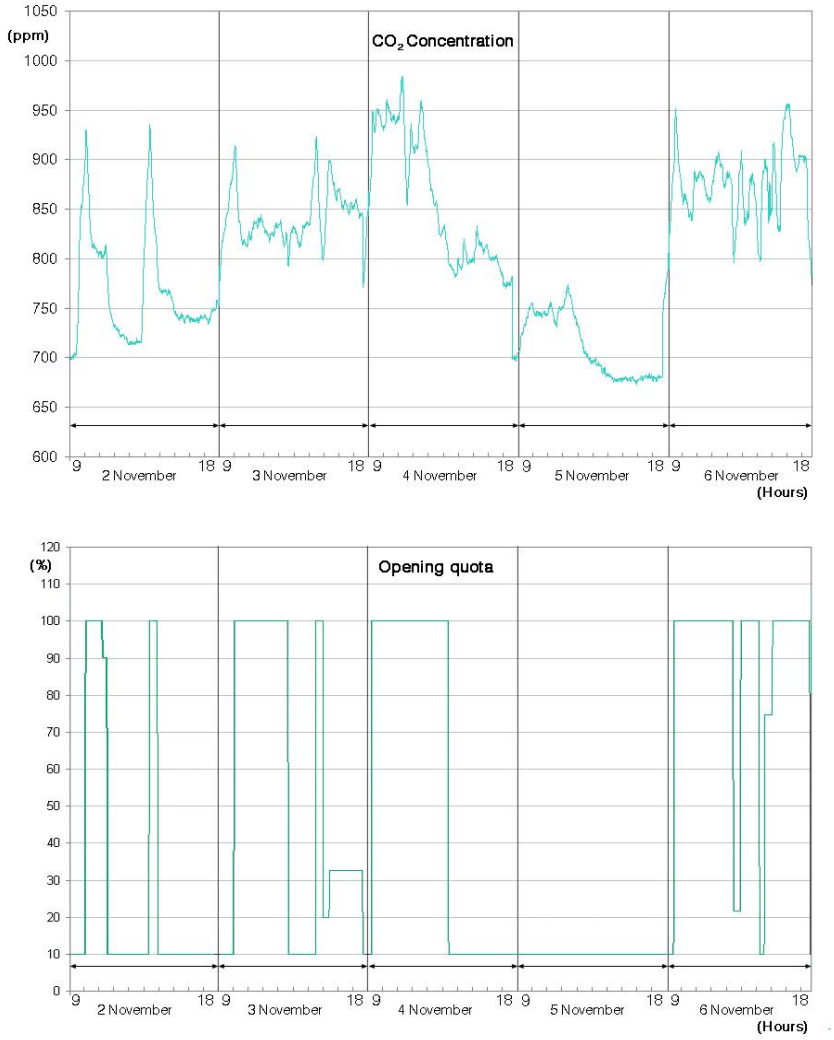

Figure 5: Trends of the CO_2 concentration (ppm) in a classroom during the working hours of a typical week (above) and the corresponding opening quota (%) of the ventilation valves (below)

In figure 6 are shown the occurrence frequencies, in percentage, of the total working hours, when the values of the CO_2 concentration are in the indicated intervals. These values are obtained by measurements recorded every ten minutes at the same time in ten classrooms for various months. It can be observed that the flexibility of the ventilation rate is able to ensure almost always a concentration within the limits fixed and in any case lower then the limit value suggested by the standard (1000 ppm).

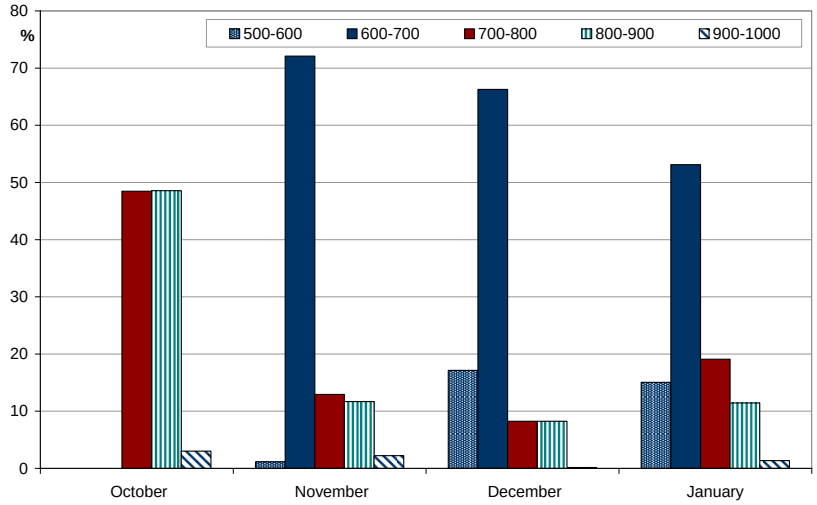

Figure 6: Time occurrence frequencies (%) of the CO_2 concentration (ppm) within different intervals in ten classrooms for three months The percentage is referred to the total of the working hours.

In addition, in December and January, it can be verified a reduction of the frequency of exceeding of the limit of 900 ppm thanks to an optimization of the control parameters obtained in this period and here explained in the next section. For example the frequency of exceeding of the limit goes from 3% in October to 1.4% in January. Figure 7 reports the means of the opening quotas (%) of the ventilation valves during the working hours recorded every minute for three classrooms in the months of November, December and January.

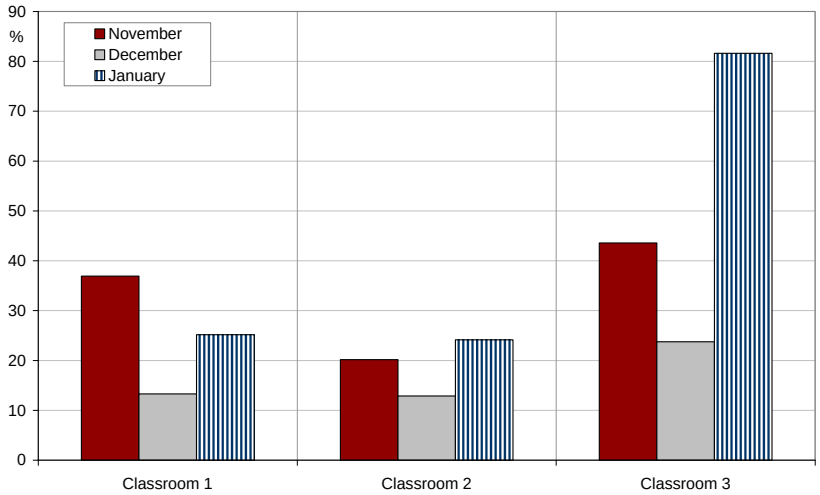

Figure 7: Means of the opening quota (%) of the ventilation valves recorded every minute for three classrooms

It can be noticed again the extreme variability of the opening quotas for each classroom which highlights the different ventilation requirement which characterizes the same classroom in different period. The high average of the opening quotas of classroom 3 (81.6%) in January demonstrates the exigency to have sometimes strong ventilation rate for long periods and at

the same time reduced rates in the other classrooms. In total of these three months the averages for the three classrooms of the percentage of opening are respectively 34.3%, 16.5% and 43%. The total average amounts to 31.3%. It is therefore evident the high energy saving which can be achieved if compared to the case of a constant ventilation flow rate.

5 OPTIMIZATION OF THE CONTROL PARAMETERS

The BMS installed in this building adopts a PID control to modulate the ventilation valves. The proportional-integrative-derivative control is a negative feedback system widely used in

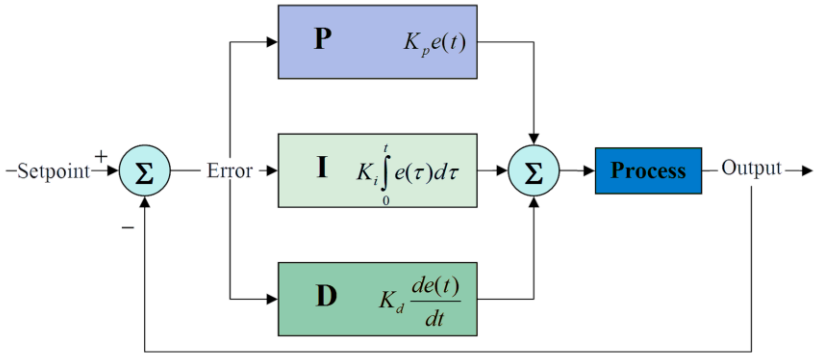

Figure 8: Scheme of a PID controller

control systems. The three actions of a PID controller are calculated separately and simply algebraically added as shown in figure 8.The choice (tuning) of the parameters K_p, K_i, and K_d can be based on experience or on the use of simplified methods (Ziegler and Nichols, Cohen and Coon or others). In the case of the BMS of the Procuratie 5 and 6 the programmers had no experience about DCV so we found butterfly valves which operate only in on-off control as the differential hysteresis was initially very little (5 ppm) causing a continuous and unacceptable oscillation between complete opening and closing. Therefore our first action was to choose a differential value appropriate for a modulating working. Even with the installation of simple butterfly valves, the presence of servomotors with proportional control has permitted to use the opportunity offered by the PID control implemented in the BMS also for the valve control system. But in this case the installed BMS allows the final user to act only on the set value of parameter K_p (gain). However this tuning was absolutely necessary as the initial value of the gain was equal to 1 (maximum possible value) and it showed to be not suitable for this application. Traditionally in cases like this it is usual to employ dedicated tools which require specialized personnel. But, exploiting the opportunities of the simplicity of the user interface typical of these modern BMS, it can be possible for the usual manager of the building to intervene directly adjusting the control values to the needs of the end users. By monitoring the response of the ventilation system, in terms of indoor comfort parameters as consequence of different set values for K_p, it was possible to individuate a more appropriate value.

In the figures 9 and 10, respectively for a classroom with average occupancy and one with a strong occupancy, are reported above the trends of CO_2 concentrations (ppm) and below the corresponding trends of the opening quota (%) of the valves. In each figure two different trends are compared obtained in two similar day (same occupancy) in the same classroom with two different values of K_p. In detail it is reported the working mode obtained with K_p equal 1, as originally set, and with K_p equal to 0.5 which is the best value among those tested.

The best performance is due to a better modulation. In fact with K_p equal to 1 there is a more drastic intervention with an increase of the oscillation.

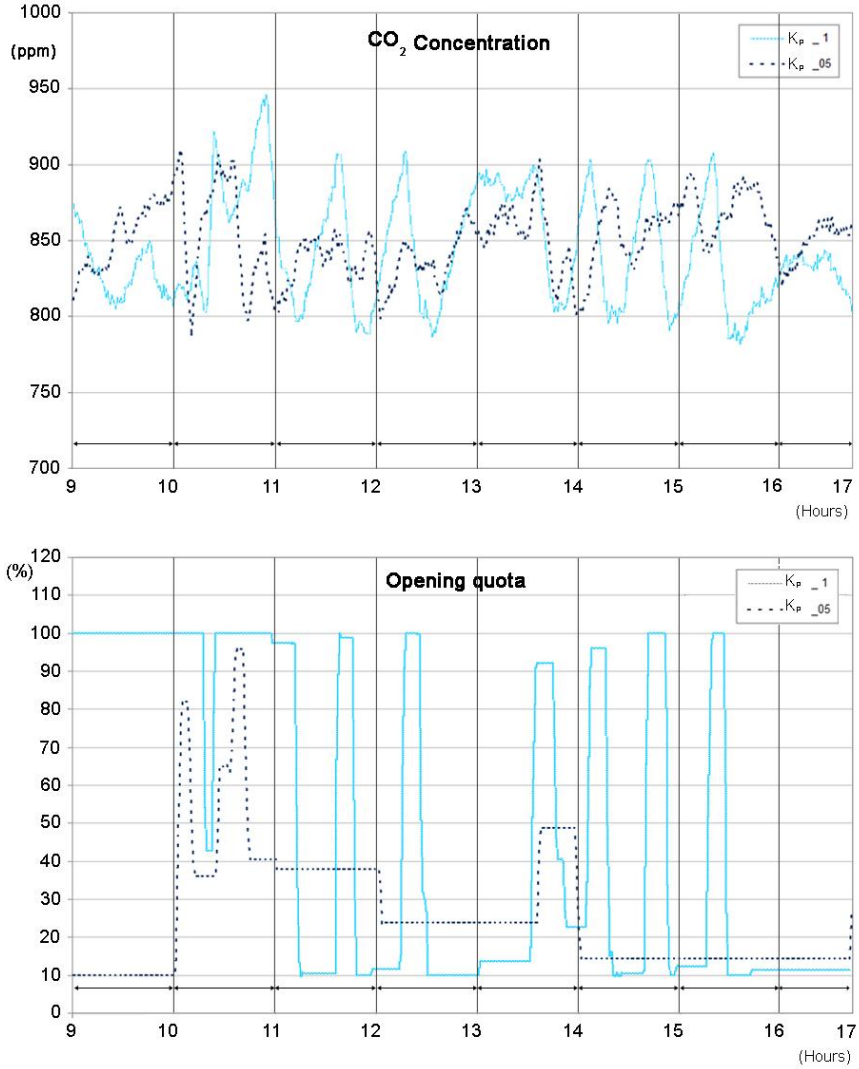

Figure 9: Comparison of the trends of CO_2 concentration (ppm) in a classroom during the working hours of two days with similar crowding but two different K_p value: 0.5 and 1,(above) and corresponding opening quota (%) of the ventilation valves (below). The values refer to a classroom with average occupancy.

Instead with K_p equal to 0.5 there is a control that more closely follows the demand. In this way it is avoided an excessive opening, if compared to the need, that moreover it is sometimes delayed. This involves a poorer control of the peaks about the limit of 900 ppm. This fact is already evident in the comparison reported in these two last figures, but in reality it is much more significant at monthly levels in the values reported in figure 6 where, as already announced, there is a clear reduction of the occurrence frequencies over 900 ppm after the adjustment with K_p equal to 0.5 in two months (December and January) if compared to the previous months.

Overall for the classroom of figure 9, in the two days with about the same occupancy there is an average opening of the valves equal respectively to 49.6% with K_p of 1 and 25.7% with K_p 0.5. In the case of strong occupancy of figure 10, there is an average opening of the valves equal respectively to 81.7% with K_p of 1 and 51.1% with K_p 0.5. Therefore thanks to the setting optimization there is a considerable reduction in the ventilation flow rate amount with a control of the CO_2 concentration even better.

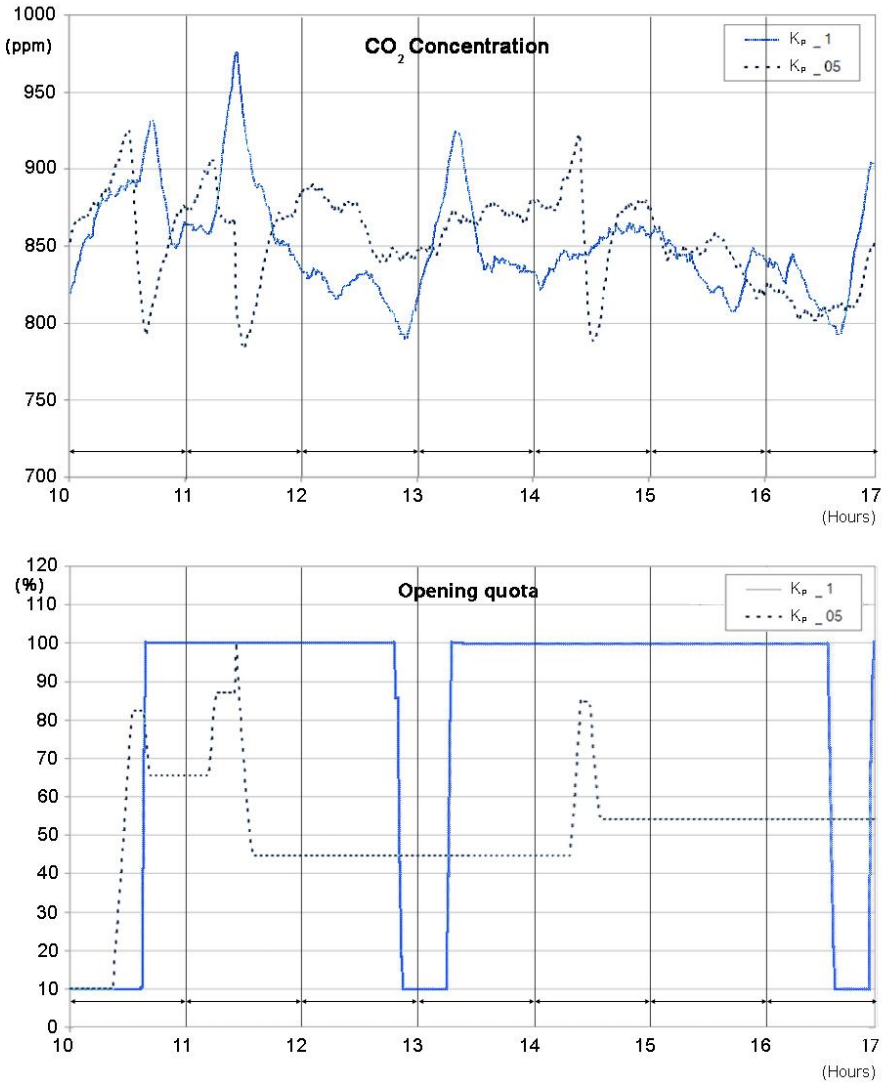

Figure 10: Comparison of the trends of CO_2 concentration (ppm) in a classroom during the working hours of two days with similar crowding but two different K_p value: 0.5 and 1,(above) and corresponding opening quota (%) of the ventilation valves (below). The values refer to a classroom with strong occupancy.

6 CONCLUSIONS

School buildings are particularly suitable to take advantage from a variable ventilation rate by an automatic control based on CO_2 sensors. Therefore especially in this case a careful management of the plants permits to achieve relevant energy and economic savings also in historic buildings subject to monumental restrictions. But a correct tuning of the parameters of the control systems is fundamental to optimize the working of the plant. In presence of a user friendly BMS, monitoring can permit an investigation of the real operating conditions of the ventilation plant in order to achieve this optimization.

7 REFERENCES

Schibuola, L., Tambani, C. (2009). "*System engineering for conservative restoration*", Refrigeration World N°4, Reed Elsevier Group.

Schibuola, L., Tambani, C. (2009). "*An assessment by monitoring and simulation of the energy savings following a correct management in school buildings*", proceedings 47th AICARR International Congress, Rome.

ASHRAE Standard 62 (1989). "*Ventilation for Acceptable Indoor Air Quality*", American Society of Heating Refrigerating and Air Conditioning Engineers, Atlanta, GA, 1992.

UNI 10339 (1995). "*Impianti aeraulici ai fini del benessere. Generalità, classificazione e requisiti. Regole per la richiesta d'offerta, l'offerta, l'ordine e la fornitura*". Italian standard UNI.

HIGH EFFICIENCY RETROFIT IN HISTORIC BUILDINGS BY DEMAND-CONTROLLED VENTILATION

Luigi Schibuola[*1], Massimiliano Scarpa[2], Chiara Tambani[3]

1 University IUAV of Venice
Dorsoduro 2206
Venice, Italy
**Corresponding author: luigi.schibuola@iuav.it*

2 University IUAV of Venice
Dorsoduro 2206
Venice, Italy

3 University IUAV of Venice
Dorsoduro 2206
Venice, Italy

ABSTRACT

Effective conservation of historic buildings subject to monumental restrictions is realized through a re-use for modern functions. In fact an attended and therefore ventilated and climatized building can be maintained in thermo-hygrometric conditions suitable controlled in order to avoid the occurrence of mold. Often only the use can justify a timely and adequate maintenance. Although the sustainability of the requalification requires acceptable management costs and therefore a limitation of the energy consumptions which must be comparable with those today prescribed for new buildings. But the monumental restrictions normally prevent interventions on building envelope. Even more than in modern buildings, it is therefore necessary to focus the efforts on plant efficiency by introducing innovative solutions.
For this goal, significant ventilation rates and high variability in the attendance suggest the realization of central plants necessary for a demand-controlled ventilation and efficient heat recovery even if their design in a monumental building can be very difficult and challenging.
In this paper are described two plants, now under construction, realized in the mainframe of the retrofit of two historic buildings in Venice. For both cases a preliminary analysis by building-plant system simulation is illustrated which was carried on to optimize the design and to assess the energy performances. The results highlight the possibility to achieve strong energy savings without compromise the monumental conservation.

KEYWORDS

Demand-controlled ventilation, historic buildings, refurbishment, energy saving

1 INTRODUCTION

The current European energy context is characterized by the adoption of the 20-20-20 Renewable Energy Directive with the goal to stop the climate change causing by greenhouse effect. The intent of the directive is a 20 percent reduction in CO_2 emissions by 2020 compared with 1990 levels, a 20 percent cut in energy consumption through improved energy efficiency by 2020 and a 20 percent increase in the use of renewable energy by 2020. The subsequent recast of the Energy Performance Building Directive, EPBD (EU Community, 2009), has focused the building energy consumption as the most important

sector where to act in order to achieve these goals. The new directive lays down mandatory national targets to be achieved by the member states. For this aim an effective action requires a widespread and incisive intervention on the existing buildings and in particular on the historic ones which constitute the greater part of the architectural heritage. But especially in the old towns full of history, we have often the presence of many buildings subject to monumental restrictions. In this case important retrofit actions regarding the building are forbidden. Therefore, even more than in the new buildings, the effort of the designer must be addressed to increase the efficiency both for energy production and its use. For monumental buildings re-used for public functions and characterized by high level of occupancy, but with significant variability, demand-controlled ventilation (DCV) can be a fundamental solution to reach important energy savings in the heating, ventilating, air conditioning (HVAC) plants.
In this paper two case studies of refurbishment of monumental buildings in Venice are described. In both cases the realization of high efficiency systems for the production of energy with the exploitation of renewable energy sources was joined with a smart management which foresees also the presence of DCV. The authors of this memory has drawn up the preliminary, defined and executive project of the plants and they are now following the work execution. The results of a preliminary study by simulation are presented here as regards the use of DCV. This analysis was carried on to optimize the plant design and to assess the real contribution in terms of energy saving and exploitation of renewable energy sources.

2 CRUCIFERS COMPLEX

The first case study is the ancient Crucifers complex which will be transformed into an university campus. For its history and architectural value the Crucifers complex is subject to heavy monumental preservation restrictions. The convent and hospital was founded in the middle of the 12th century by the order of Crucifers along the church of Santa Maria Assunta to aid and to give shelter to pilgrims and crusaders on their way to the Holy Land. It was then rebuilt after fires in 1214 and 1514, acquired by the Jesuits in 1657 following the suppression of the Crucifers order. When the Jesuits were suppressed in 1773 the monastery became a school and then, in 1808, a barrack. The Jesuits returned in 1844 and still occupy the convent parts to the North of the church. Those to the South remained used as a barrack until 1990. An aerial photo of the Southern part of the convent is showed in fig. 1a.

a) An aerial photo of the Southern part

b) The restaurant room

Figure 1: Views of the Crucifers complex

2.1 Description of building-plant system

As showed in the picture 1a the South sector of the former convent presents two cloisters on the left side and two further smaller service courtyards on the right side of the complex. In the middle of each cloister there is a well. Each well is connected to an underground cistern that collects rainwater from the above courtyard through a filtration system based on purposely placed sand. The frontal side towards Campo dei Gesuiti presents the main accesses, the back side is lapped by the channel Rio dei Gesuiti. On the left we have the church of Santa Maria and on the right side the limit is a minor channel. The complex has three long buildings (the sleeves) along the perimeter area and they present a total height of 26 m. Two other lower buildings are located in the central part and they surround the cloisters and courtyards.
This area is the object of the actual intervention of renovation and new destination for university housing for students and visiting professors and ancillary services. In detail the project foresees the creation of 177 apartments for students, each with two bed places, independent bathroom and kitchen and study area (figure 2b). Normally the ground floors are used for various services, while the upper floors are residential units. An height greater than 5 m in each floor of the sleeves has permitted the realization of mezzanines where to locate the cabinets of the rooms while the adjacent long corridors are used as recreational and meeting areas. The design was respectful of the existing architecture especially in the common areas (figure 2a). Further greater 32 residential units will be reserved for visiting professors.

a) An internal corridor

b) a room with two beds

Figure 2: Internal views of the Crucifers

In the residential unit the HVAC plant consists of fan coils embedded in the furnishings and a controlled ventilation system with delivery in the room and aspiration in the bathrooms. The centralized ventilation system allows an efficient heat recovery from exhaust air to pretreat the fresh air. Each residential unit is automatically excluded from ventilation grid in the absence of persons inside the room by two motorized valves installed on the local connections to the air supply and return ducts of the ventilation grid. The total air flow rate is controlled by inverters which act on the fan motors of the centralized recovery units. These recovery units are distributed in the various area of the Crucifers complex and each of them is installed in the garret of the corresponding supplied building.
Facilities like laundry, meeting rooms, classrooms and workshop rooms will be at disposal of the internal guests. While community services: cafe, restaurant with 150 places and

relative kitchen, gym, computer room and a library, will be opened also to the local community.
In the greater rooms at the floor level HVAC plants are based on fan coils and primary air distribution ducts. Special effort required the HVAC installation in presence of painted walls like in the restaurant room (figure 1b). In some areas there is also the contribution of radiant panels when there were no preservation restrictions on the floor. The bar and restaurant each present an independent air handling unit (AHU) for the ventilation. Both of the AHUs have a CO_2 sensors on the return duct in order to module the ventilation rate on the basis of the real occupancy of the served room by acting on the inverters which control the fans. The whole ventilation plant will be monitored by the central supervisory system where its working mode will be directly controlled on screen with the possibility of an easy introduction of the set point values The HVAC plants have been chosen to be supplied by low temperature water (40-45°C in heating mode) favorable to the working of the installed heat pump. In fact the lagoon environment has suggested the use of the surface waters coupled to a heat pump as renewable energy source. The technical centrals are located in the tower between the two courtyards on the left side and in underground room expressly dug under the widest of these two courtyards. In the tower we have the installation of the reversible water to water heat pump used to produce hot water for heating and chilled water for air conditioning in summer. The lagoon water is withdrawn from the back channel Rio dei Gesuiti sited near the back side. Auxiliary condensing boilers are also installed to integrate the heat pump.

2.2 Analysis of the performances

The analysis of the performances of the DCV plant has been carry out by simulation as the refurbishment of the building is not finished yet. The scheduling of the crowding in the various types of facilities: flats, bar and restaurant has been elaborated on the basis of an investigation expressly done in similar university buildings and commercial facilities existing in Venice. Different hourly distributions have been built up for week days and week ends. Considering the reduction of the teaching during summer, the scheduling are also diversified between summer and winter. In figure 3 the presence hourly distributions used for the simulation are shown in the case of week days during winter and summer period. These distributions in percentage are referred to the design values of occupancy (100%) which are two persons for each flat, 75 persons for the bar and 150 persons for the restaurant.

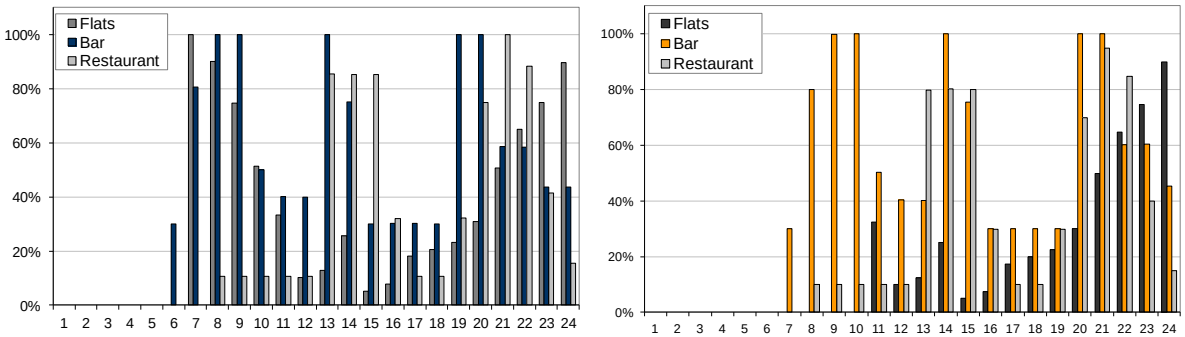

a) Winter

b) Summer

Figure 3: Distributions (in percentage) of the presences during week days in the studied rooms for winter and summer period. These trends are referred to the design values of occupancy (100%)

The ventilation rate is assumed to be equal to the design value of 25 m^3/h per persons. In this way it is possible to simulate the variation of the ventilation flow rate in presence of DCV. The energy requirement for ventilation air treatment in heating and air conditioning periods can be then calculated by a simple thermo-hygrometric calculation model on the basis of typical outdoor climatic data of Venice. The same calculation can be repeated considering a constant ventilation flow rate during the working hours of the plants and equal to the maximum design value as happens in absence of DCV.

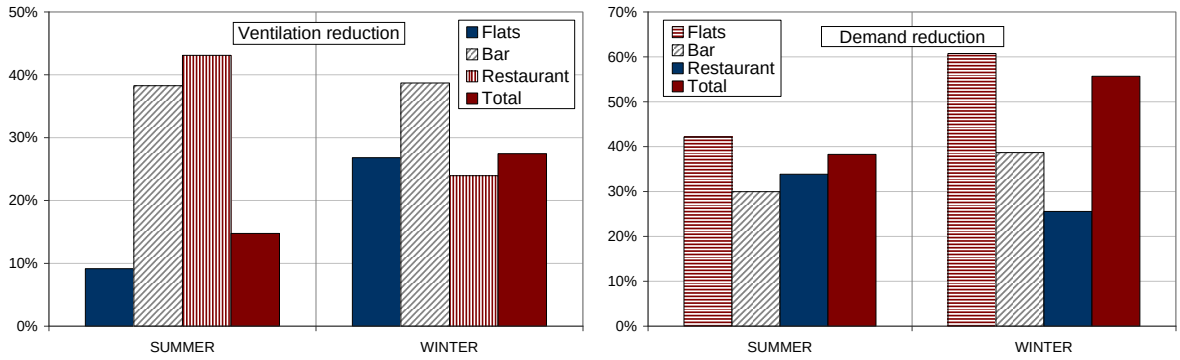

Figure 4: Ventilation rate and energy demand reductions (in percentage) during heating and air conditioning periods. These reductions are referred to the corresponding values without demand-controlled ventilation.

In figure 4 the seasonal reductions of the ventilation rate amount and of the energy demand for ventilation air treatment are reported in heating and air conditioning period for each type of facilities and the total one. These percentage reductions are referred to the corresponding ventilation amount and energy demand of the building in the case without DCV. The ventilation reduction is significant, but the benefit is remarkable especially in terms of reduction of the total energy demand for ventilation both in winter and summer.

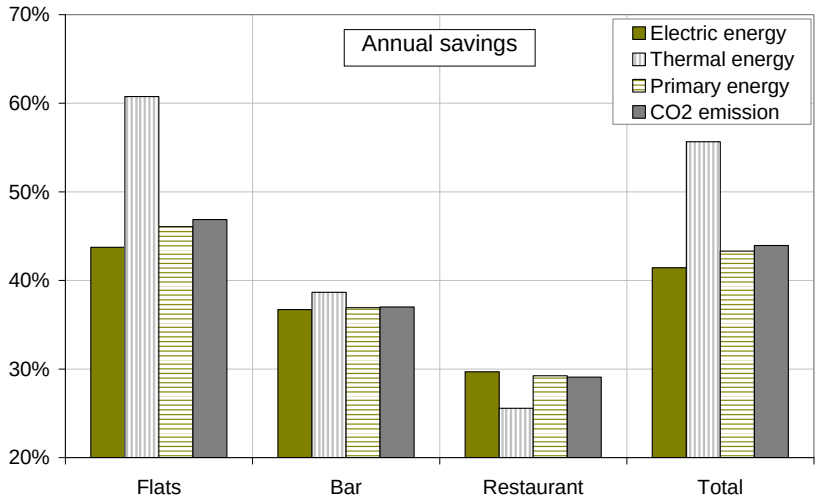

Figure 5: Annual energy savings and CO_2 emission reduction (in percent). These savings are referred to the corresponding energy requirements for ventilation and CO_2 emission without demand-controlled ventilation

The energy requirement of the HVAC plants is due to the electric energy consumption of fans and pumps supplying the coils of the AHUs, but first of all to the electric consumption of the heat pump used both for heating and air conditioning. As the heat pump is assisted by auxiliary condensing boilers, we have also a thermal energy consumption. For this reason the total energy consumption is calculated as primary energy assuming the energy

efficiencies of the condensing boilers and of the heat pump calculated by the dynamic simulation of the building-plant system (Schibuola and Tambani, 2012). To calculate the primary energy consumption for electricity production, the Italian official transformation factor of 0.45 has been used. In figure 5 the annual energy saving and CO_2 reduction in percentage obtained thanks to the introduction of DCV are reported for each facilities and the total ones. The primary energy saving about the requirement for ventilation treatment and corresponding CO_2 emission reduction are over 40% on annual basis.

3 TOLENTINI

The second case study refers to the former Convent of Tolentini commissioned by the Fathers Teatini at the end of 1500, but with the arrival of Napoleon it went to the state and became first a barrack and then a deposit. Since the 50s of last century, the property is entrusted to the IUAV University of Venice to become its main house. The movement of the teaching activities to other buildings has allowed today to schedule a transformation of part of the second and third floors already used as classrooms. In figure 6a an aerial photo of Tolentini convent is reported. The building on the left is the object of this refurbishment.

a) On the left the refurbished building

b) The main cloister

Figure 6: Views of the former Convent of Tolentini

Figure 6b shows the main cloister of the convent located on the right of figure 6a.

3.1 Description of building-plant system

In detail for a wing of the building a design was drawn up for the transformation of the old classrooms into two further new reading rooms of the library of the university, each occupying the entire second and third floor respectively which become the first and second floor of the library. In addition in the first floor of the building the complete restoration of

a) Longitudinal section

b) Cross sections

Figure 7: Sections of the building

the HVAC plant of the Aula Magna has been planned. Sections of the building in figure 7 show the characteristics of the areas subject to the interventions. In this context the design of new HVAC systems took up relevant resources. In fact the new HVAC system will substitute the existing system aimed at mere heating by radiators and it will consist, for the reading rooms, in primary air ventilation system and fan-coil terminal units whereas the Aula Magna will be totally air-conditioned by two AHUs. The first AHU is installed in a little room sited near the upper part of the bottom of the Aula Magna as shown in figure 7a and serves the area in the bottom. The second AHU is installed outside and serves the

a) Aula Magna

b) First floor of the library

Figure 8: Views of the work in progress at Tolentini

speakers area. Its final distribution ducts are under the platform of the speakers as shown in figure 8a. Demand-controlled ventilation is always adopted. In the first and second floor of the library the main ducts of the ventilation plant are installed under elevated platforms that cover part of the floor for the entire length of the room (fig.8b) without damage this ancient floor. The rebuilding foresees also the installation of a ground source heat pump with vertical double U-tube boreholes heat exchanger in the garden of the palace to produce the heat and the cold required by the new HVAC plants.

3.2 Analysis of the performances

Also for this test case the analysis is based on the simulation of the performance in presence and in absence of DCV. The scheduling of the crowding has been obtained by the monitoring of the already existing lecture rooms of this university library. For the two new

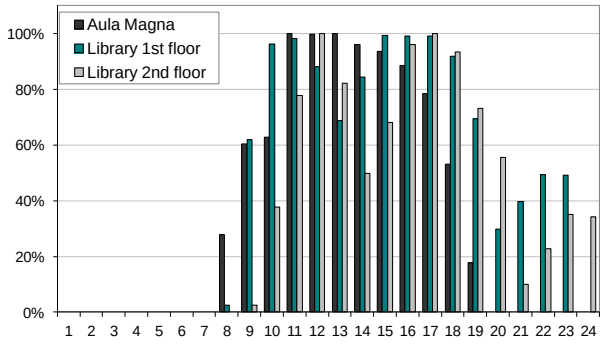

a) Winter

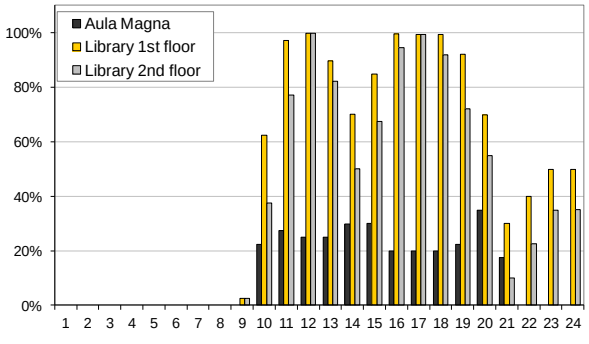

b) Summer

Figure 9: Distribution (in percentage) of the presences during week days in the studied rooms of Tolentini for winter and summer period. These trends are related to the design values of occupancy (100%).

reading rooms the ventilation AHU, with fans equipped with inverter, is only one. But as four modulating dampers are present, controlled by two different CO_2 sensors installed in the return ducts from each rooms, the DCV is independent for the first and second floor of the library. For Aula Magna DCV acts on the modulating dumpers for air intake and expulsion present in the two installed AHUs.
In figure 9 the presence hourly distributions used for the simulation are shown in the case of week days during winter and summer period. In fact different hourly distributions have been considered again for summer and winter considering the teaching reduction in summer. On Sunday the library is closed. The distributions in percentage are referred to the design values of occupancy (100%) which are 100 persons for each floor of the library and 250 persons for Aula Magna. The design value of 25 m^3/h per person is maintained also for this building. The comparison between the performances in presence or in absence of DCV permits to calculate again the reductions of the ventilation amount and of the energy demand for the studied rooms.

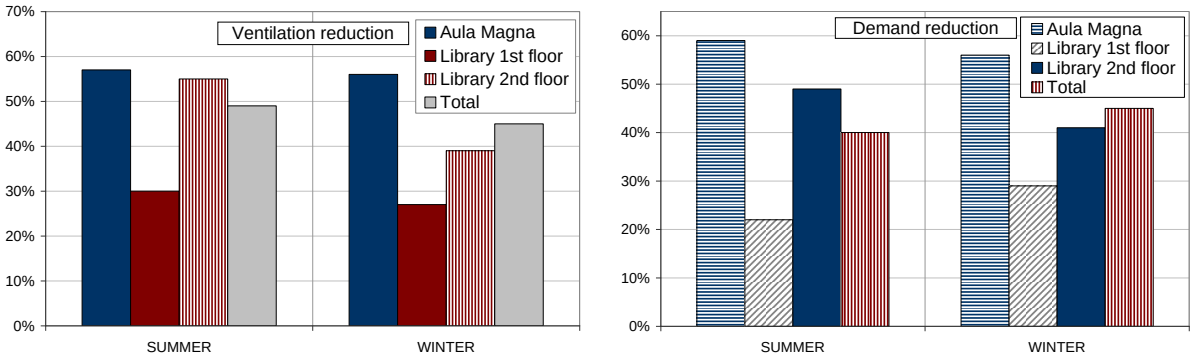

Figure 10: Ventilation rate and energy demand reductions (in percentage) during heating and air conditioning periods. These reductions are referred to the corresponding values without demand-controlled ventilation.

In figure 10 these reductions in percentage are reported for heating and air conditioning periods. They are referred to the corresponding ventilation amount and energy demand of the building in the case without DCV. The best values are in Aula Magna and in the second floor of the library where the occupancy is more flexible during the working hours. In fact

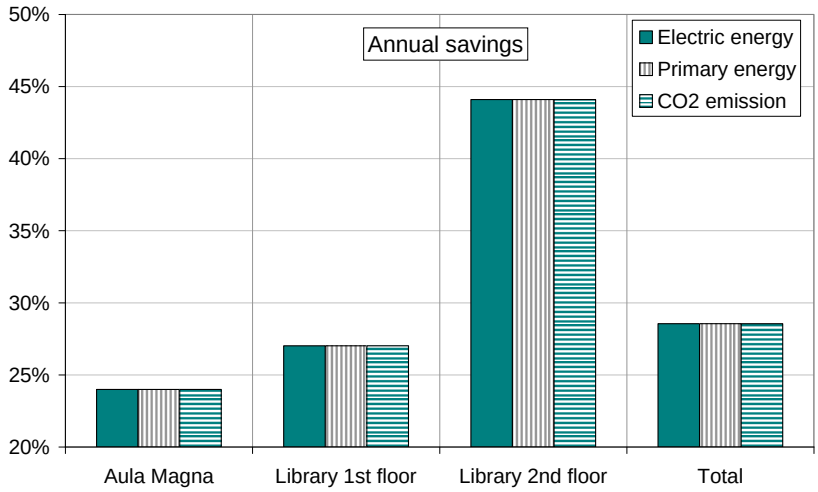

Figure 11: Annual energy savings and CO_2 emission reduction (in percent). These savings are referred to the corresponding energy requirements for ventilation and CO_2 emission without demand-controlled ventilation

Aula Magna is used not only for general meeting, but also for exhibitions and conferences characterized by variable participation. For the library the greatest occupancy is always in the first floor as it is the nearest to the distribution desk therefore we have observed that the presences in the second floor are normally less. In figure 11 the annual energy saving and CO_2 emission reduction in percentage obtained with DCV are reported for each rooms and the total ones. In this case the energy requirement for ventilation plant is only electric energy and it consists in a quota of the total electric energy absorbed by the heat pump, in heating or cooling working, to supply the AHU coils and for the relative auxiliaries, fans and pumps. To convert the energy provided by the heat pump for the ventilation treatments into the electric consumption of the machine, the coefficients of performance (COP in heating and cooling) of the heat pump have been calculated by using the results of the dynamic simulation of building-plant system (Schibuola et alia, 2011). Because of the only electric consumption, the energy savings and CO_2 emission reduction are expressed in percentage by the same value. The benefit is the greatest in the second floor as here we have the highest variability for the occupancy. The total result depends mainly on the library which is the facility more used.

4 CONCLUSIONS

These case studies have highlighted that the introduction of demand-controlled ventilation can give a fundamental contribution to the reduction of the energy requirement for ventilation also in historic buildings re-used for public functions. The consequent reduction of the emission of greenhouse gases is also remarkable. But, above all, its realization does not involve problems regarding restrictions about preservation exigencies. Therefore, among all the possible high efficiency solutions, demand-controlled ventilation should be always considered in the retrofit of HVAC plants in historic buildings. In this way also the refurbishment of monumental buildings can contribute to achieve the target of 20-20-20 within 2020 as indicated by EU parliament.

ACKNOWLEDGEMENTS

The authors wish to thank ISP, Iuav Studies & Projects, company, responsible of the general planning and architectural design of the refurbishment of Crucifers complex and Tolentini, for the availability and the sensibility in supporting the introduction of innovative design solutions with high energy efficiencies.

REFERENCES

EU Community (2009). *Energy Performance Building Directive EPBD* (recast), directive 2009/28/EC.

Schibuola, L., Tambani, C. (2012). *Renewable Energy sources for historic buildings: the Crucifers Convent in Venice.* Proceedings of the 4th International Congress of Ecoarchitecture, Wessex Institute of Technology, UK.

Schibuola, L., Scarpa, M., Tambani, C., Zarrella, A. (2011). *Prestazioni di un impianto geotermico a Venezia*. Proceedings 66° National Congress ATI Cosenza Italy.

UNCERTAINTIES IN DIFFERENT LEVEL ASSESSMENTS OF DOMESTIC VENTILATION SYSTEMS

Regina Bokel[*1], Zhiming Yang[*1], Hans Cauberg[1]

1 Faculty of Architecture and the Built Environment
Julianalaan 134
2628 BL Delft, The Netherlands
**Corresponding author: r.m.j.bokel@tudelft.nl*

ABSTRACT

In order to improve the quality of ventilation systems, assessments are widely used. In this paper, 3 main assessment levels are distinguished based on the number of ventilation systems to be assessed and the assessment objective. The main assessment levels distinguished in this paper are **global leve**l (the assessment concerns a set of ventilation systems within a country or region), **project level** (the assessment concerns a set of ventilation projects within a housing project) and **design level** (the assessment concerns one ventilation system in a housing project for different environments and different types of occupants).
Uncertainties should be considered and dealt with in assessments of domestic ventilation systems. The uncertainties that determine the in use performance of a domestic ventilation system are present in four aspects, ventilation components, building properties, outdoor environment and occupants. The structure of the uncertainties in an assessment is further studied starting from two types of uncertainties (reducible and irreducible) to two levels of uncertainty data (basic level and mixed level data).
Two different methods how to deal with different assessment levels and their uncertainties are subsequently discussed as well as how to choose a method for a specific assessment level. The methods that are developed are the accurate method and the prototype method. Finally, a brief demonstration of the described concepts and methods is given.

KEYWORDS

Assessment, uncertainties, ventilation

1 INTRODUCTION

After the energy crisis in the 70s of the last century, people realized the importance of energy saving and reducing the energy lost due to fresh air exchange became crucial. People realized that it is important to provide a sufficient, but not excessive air exchange rate, i.e. air exchange should be more controllable and efficient in the domestic setting. To achieve this goal, a properly designed ventilation system in a house is required. In order to improve the quality of ventilation systems, assessment is widely used for evaluating the performance of domestic ventilation systems and consequently improving the design of the systems. In an assessment of a domestic ventilation system, the influence of uncertainties can play an important role. In the assessment of domestic ventilation system(s), uncertainties can come into existence during 3 stages: 1) variations in the design stage; 2) variations during the construction stage; 3) variations during the measurements of the performance. The uncertainties are present in the four aspects, ventilation components, building properties,

outdoor environment and occupants, that determine the in use performance of a ventilation system for a domestic ventilation system.
These uncertainties must be considered and dealt with in an assessment process. In this paper different assessment levels are defined and it is described how the uncertainties should be treated for these different assessment levels. An example is included at the end.

2 ASSESSMENT LEVELS

Domestic ventilation systems are assessed for many different purposes. We categorised these different purposes into 3 assessment levels, i.e. the global level, the project level and the design level. The global level is used when the assessment concerns a set of ventilation systems within a country or region. The project level is used when the assessment concerns a set of ventilation projects within a housing project. The design level assessment is used when the assessment concerns one ventilation system in a housing project for different environments and different types of occupants. Each of these 3 levels can be further divided into sub-levels, see table 1. The explanations of these sub assessment levels are given below, including the scale of each assessment level and the relevant assessment objective.

Table 1: Summary of Assessment Cases by Uncertain Design Parameters

	Uncertainties in design parameters, i.e. Reducible Uncertainties		
	all four aspects: - ventilation components - building components - outdoor environment - type of occupants	**system aspects:** - ventilation components and/ or - building components	**boundary aspects:** - outdoor environment and/ or - type of occupant
A: global level	uncertain (A1)	uncertain (A2)	uncertain (A3)
B: project level	uncertain (B1)	uncertain (B2)	uncertain (B3)
C: design level	uncertain (C1); certain (C4);	uncertain (C2)	uncertain (C3)

Assessment level A, **global level**:

- Case A1: The assessment objective is to gain an overview of the performance of the domestic ventilation systems in a country or a region. Case A1 can be used to assess whether the design regulations provide sufficient guidance or governance to achieve the wanted/ required performance of the ventilation system. The set of ventilation systems under assessment contains ventilation systems with different designs, i.e. different ventilation components, building components, outdoor environments, and types of occupants.
- Case A2: The assessment objective is to determine the overall design quality, or suitability of various types of ventilation systems regulated by the design regulations, for a specific environment and specific type of occupant.
- Case A3: The assessment objective is the suitability of a specifically designed ventilation system for a different environment and/or different occupants.

Assessment level B, **project level:**

- Case B1: The assessment objective is to gain an overview of the design quality or the performance of a set of ventilation systems in a housing project. The set of ventilation systems under assessment contains ventilation systems with different designs, i.e. different ventilation components, building components, outdoor environment, and occupants.

- Case B2: The assessment objective is to gain an overview of the expected performance of the designs of the set of ventilation systems in a housing project under a specific environment and/ or type of occupant.
- Case B3: The assessment objective is to obtain the suitability of a specific ventilation system in a housing project for different environments and different types of occupants.

Assessment level C, **design level:**

- case C1: The assessment objective is to determine the possible performance range, and the important design parameters for a ventilation system. The design parameters of the ventilation components, the building components, the outdoor environment and the occupants are uncertain.
- case C2: The assessment objective is to optimize the design. the design parameters of the ventilation components and/or the design of the building components are uncertain, the design parameters of the outdoor environment and the occupants are certain.
- case C3: The assessment purpose is to determine the suitability of a design for a specific environment or a specific set of occupants. The design parameters of the outdoor environment and/or the occupants are uncertain, the design parameters of the ventilation system are certain.
- case C4: The assessment purpose is to determine the expected performance of a specific ventilation design, and/or the quality/ influence of the construction/ installation process on a design. All the design parameters of the four aspects are certain, i.e. the design is definitive, and only the irreducible uncertainties need to be considered

3 STRUCTURE OF UNCERTAINTIES IN AN ASSESSMENT

3.1 Design parameters and input parameters

In each assessment we use two types of parameters, i.e. the design parameters and the input parameters. In each of the above mentioned 4 aspects, the design parameters and input parameters must be identified. Explanations for these two types of parameters are given below.

Before we carry out the assessment of a design for a domestic ventilation system, we need to determine the design parameters which will be used to specify the design. The design parameters are, in general, not suited to be used as input of the calculation model used for the assessment, which normally consists of a calculation model or a simulation model. Thus, the input parameters, which can be used as input for the calculation model, also need to be determined.

Design parameters are specified by the designer for any system, in our case a domestic ventilation system. The form of the input parameters used depends on the calculation model that will be used to calculate the performance of the ventilation systems. One important point is that the values of the input parameters and the uncertainties in these input parameters are actually determined or highly influenced by the design parameters.

3.2 Structure of the uncertainties

Having introduced the design parameters and input parameters, we can see that eventually we need to identify and/or estimate the uncertainties in the input parameters for the assessment.

We now define two types of uncertainties that can occur in an input parameter:

- Reducible uncertainty, this is the uncertainty which can be eliminated or reduced intentionally through more detailed design. A reducible uncertainty is the uncertainty in the design parameter which is caused by the design alternative or specification uncertainty.

- Irreducible uncertainty, this is the uncertainty which cannot be eliminated or reduced by a more specified design and which is caused by the limitations of our available knowledge or techniques, or the nature of the relevant parameter. The uncertainty caused by the construction/ production deviations, modeling uncertainties or scenario uncertainties are irreducible uncertainties.

3.3 Levels of uncertainties

The considerations and treatment methods for the uncertainties for each different level of assessment are not necessarily the same. When we look at table 1.1, it can be seen that, except for the C4 case, all other cases include, to different extents, uncertainties in the design parameters, i.e. reducible uncertainties. In other words, the uncertainties in the input parameters for the C4 case only include the irreducible uncertainties, and the uncertainties in the input parameters for all other cases are combinations of reducible uncertainties and irreducible uncertainties, as explained above. This led us to come up with the concept "level of uncertainty data". This "level of uncertainty data " describes the magnitude of the existence of reducible uncertainties in the data, the data used to estimate the uncertainties in the input parameters. For practical purposes it was enough to define two levels of uncertainty data, the basic level and the mixed level:

- Basic level, i.e. the data of the uncertainties in the input parameters contain only irreducible uncertainties. For example, for the uncertainty in the leakage of windows, we may have the uncertainty data for windows with definitive design parameters, such as type and material of windows.

- Mixed level, i.e. the data of the uncertainties in the input parameters is a combination or mixture of reducible uncertainties and irreducible uncertainties. For example, the uncertainty data is only available for a set of windows, which includes windows with different design parameters, such as windows having various types and made of different materials. A worked out example is given in Yang (Yang, 2012).

4 APPROACH TO CARRY OUT THE UNCERTAINTY QUANTIFICATION ANALYSIS

Different approaches should be used to obtain the data of the uncertainties in the input parameters for the two different uncertainty levels, i.e. the accurate approach and the prototype approach as described below.

4.1 Accurate approach

When we are carrying out an assessment where a small amount of reducible uncertainties exist in the ventilation system(s) to be assessed, as in, for example, the design level assessment, then we can use the accurate approach to prepare the uncertainty data. The basic

idea for this accurate approach is that the uncertainty data used for the uncertainty quantification analysis should be the **basic level uncertainty data**.

The steps of the **accurate approach** are described below:

- step 1: Reduce the reducible uncertainty by dividing the ventilation systems under assessment into sub-sets of systems, and each set has definitive design parameters, or determining the possible definitive design combinations of the design parameters, i.e. the definitive designs.
- step 2: Estimate the basic level uncertainty data, i.e. the irreducible uncertainties in the input parameters, for each definitive design. Then, we will obtain one calculation uncertainty datasheet consisting of the irreducible uncertainties for each definitive design.
- step 3: Carry out the uncertainty quantification analysis using each calculation datasheet. For more information see (Yang, 2012) and (Yang et al. 2012).

This approach is considered to be accurate because it only estimates the irreducible uncertainties, but might only be suitable for the situation that the number of reducible uncertainties is small. If the assessment project includes a large number of reducible uncertainties, for example the global level assessment, the accurate approach may lead to a cumbersome process or is even not applicable. Thus, we developed another approach, the prototype approach, which is introduced below.

4.2 Prototype approach

When the assessment is carried out on a large set of ventilation systems, for example the global level assessment, the accurate approach introduced in sub-section 4.1 is not suitable to be used, and the prototype approach should be used.
The basic idea of the prototype approach is that the mixed level uncertainty data should be used together with the prototype ventilation systems. The detailed steps for the **prototype approach** are introduced below:

- step 1: Divide the set of ventilation systems to be assessed into sub-sets, each sub-set of the ventilation systems belongs to one prototype of the ventilation systems. A prototype of the ventilation system has a certain type of ventilation system and building floor plan. The prototypes should be developed from the whole set of ventilation systems to be assessed, and should be representative.
- step 2: Estimate the mixed level uncertainties for the whole set of ventilation systems to be assessed, or estimate the mixed level uncertainties for each sub-set of ventilation system within one prototype according to Yang (Yang, 2012). Then, these uncertainties can be used to form the calculation uncertainty datasheets, one calculation uncertainty datasheet for each prototype.
- step 3: The uncertainty quantification analysis can be carried out on every formulated calculation uncertainty datasheet in step 2.

4.3 Selection of an approach for different cases of assessments

As introduced above, different approaches, i.e. the accurate approach or the prototype approach should be used for assessments with different magnitudes of reducible uncertainties.

As shown in table 2, for different assessment cases we therefore propose to use a different approach.

Table 2: Recommended assessment approach for each assessment case

	all four aspects: - ventilation components - building components - outdoor environment - type of occupants	system aspects: - ventilation components and/ or, - building components	boundary aspects: - outdoor environment and/ or, - type of occupants
A: global level	uncertain (A1): - prototype approach	uncertain (A2): - prototype approach	uncertain (A3): - prototype approach
B: project level	uncertain (B1): - prototype approach or, - accurate approach	uncertain (B2): - prototype approach or, - accurate approach	uncertain (B3): - prototype approach or, - accurate approach
C: design level	uncertain (C1): - accurate approach certain (C4): - accurate approach	uncertain (C2): - accurate approach	uncertain (C3) - accurate approach

5 A DEMONSTRATION

In order to demonstrate the concepts and approaches introduced above, we chose to illustrate the prototype approach. Assuming an assessment was required to be carried out on the performance of ventilation systems in low-storey houses located in a certain area in Delft (NL). There are different types of houses with similar floor plan but different details. Considering the concepts and approaches introduced above, the following analysis was made:

- Two main types of ventilation systems are used in these houses, i.e. mechanical exhaust with natural supply system (MENSS) and balanced ventilation with heat recovery system (BVHRS). The assessment level is “project” and consists of two types of ventilation systems and is therefore a B2 case, see table 2. The prototype approach was chosen because of the large difference between the two ventilation systems. For the analysis, first the two prototypes were selected as shown in figure 1 a/b below. It was assumed that the systems were equally distributed over the dwellings.

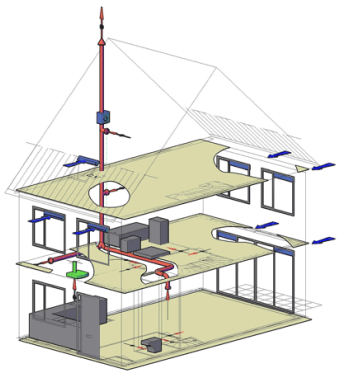

1a: MENSS system prototype

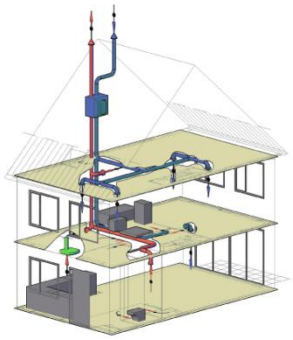

1b: BVHRS system prototype

Figure 1: Prototype ventilation system, MENSS & BVHRS (Source: ISSO 92 & 62)

- Then, in each prototype system only two uncertain design parameters were considered, i.e. building orientation and fan curve. It was assumed that the building can face any orientation in order to explore the effect of orientation on ventilation. The uncertainty in fan curve was used to see the influence of using different types of fans on the ventilation.
- After identification of the uncertainties in design parameters, the next thing is to estimate the uncertainties in the input parameters for each prototype system. The estimated uncertainties for this example of these two systems are listed in table 3 below. The designs of the ventilation components are mostly assumed to be definitive. The values of the design parameters in this example can be seen in table 3 below.

Table 3: Uncertainties used in the example

parameters	Type of PDF Variation range	unit	estimation basis
window leakage	normal (0.086, 0.41)	$dm^3/(s.m.pa^{-n})$	AIVC GUIDE 05
leakage of the joint between window/ door frame and wall	normal (0.00033, 0.012)	$dm^3/(s.m.pa^{-n})$	
internal door leakage	normal (1.1, 2)	$dm^3/(s.m.pa^{-n})$	
external door leakage	normal (0.082, 0.84)	$dm^3/(s.m.pa^{-n})$	
facade leakage	normal (0.016, 0.021)	$dm^3/(s.m^2.pa^{-n})$	
leakage through the joint wall/ ceiling	normal (0.005, 0.11)	$dm^3/(s.m.pa^{-n})$	
roof leakage	normal (0.6, 1.1)	$dm^3/(s.m^2.pa^{-n})$	
duct leakage	normal	$dm^3/(s.m^2.pa^{0.65})$	LUKA classes, & assumption
Positions of exhaust/ supply grilles	Normal (-10%, 10%)	/	Assumption
Heat recovery efficiency	Normal (70%, 90%)	/	Product information literature
Internal leakage	Normal (0, 0.0001)	$kg/(s.pa^{0.65})$	Some measurement data and inquiry
Duct pressure loss coefficient	Normal (-20%, 20%)	/	Assumption
Terrain roughness (4 directions)	Uniform (0.25, 0.4)	/	Based on the definitions in the manual of TRNFLOW
wind pressure coefficients	Uniform (-10%, 10%)	/	Cp-generator & empirical accuracy of Cp-generator
Local temperature premium	Uniform (0,1)	^oC	Literature and assumptions.
Indoor temperature set-point	Normal (12, 21) daytime (14, 21) evening (10, 19) night	^oC	Estimation from survey data from VROM

(Note: table 3 includes the uncertainties both for MENSS and BVHRS, while some uncertainties only account for BVHRS, such as heat recovery efficiency and position of supply grilles.)

- After identification of the uncertainties, the calculations were made, i.e. 140 calculations for the uncertainty propagation analysis and 116 calculations for the sensitivity analysis for each prototype system were executed. The important results are summarized below:

- Both systems had steady exhaust air flows since the variations were less than 10% because they are both provided mechanically, for example see figure 2 and 3. However, the pressure loss coefficient contributed to most variations in the mechanical air flow rates.

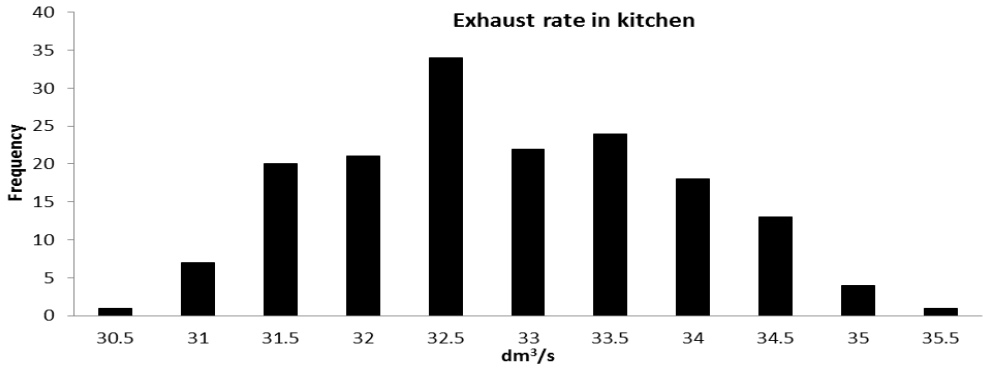

Figure 2: Annual averaged hourly exhaust air flow rate in kitchen in MENSS

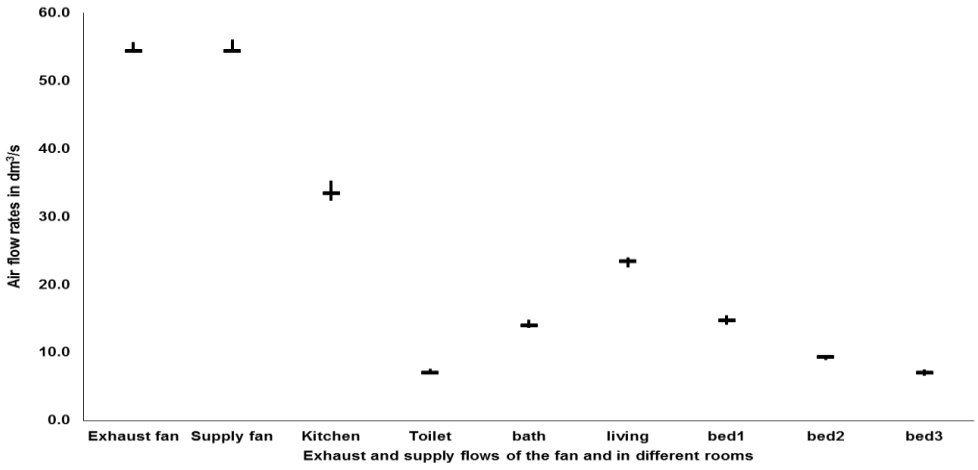

Figure 3: Annual averaged hourly exhaust/ supply air flow rates in BVHRS

- MENSS had very variable supply air flow rates as shown in figure 4 (as an example a bedroom is shown, see Yang (Yang, 2012) for more rooms), while BVHRS had quite steady supply air flow rates as shown in figure 3. The variations in the supply air flows were mostly caused by the uncertainties in the parameters "indoor temperature set point" and "building orientation".

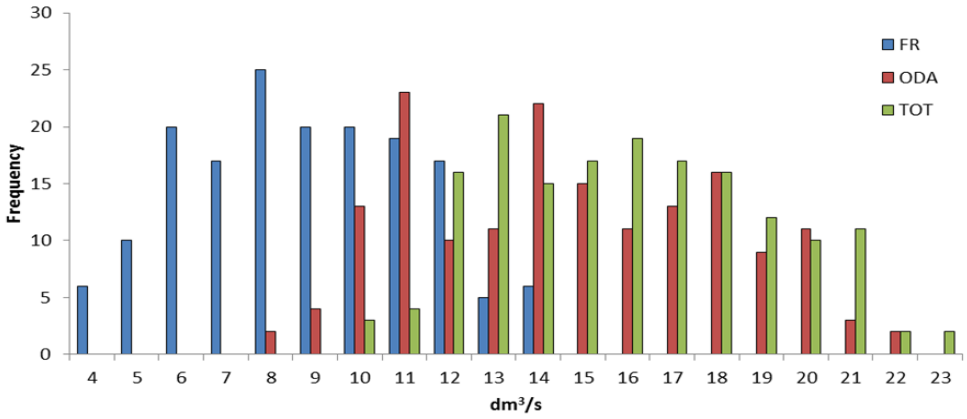

Figure 4: Annual averaged hourly supply air flow rates in bedroom in MENSS system (Note: FR accounts only fresh air from air inlets; ODA accounts FR plus inside overflow from other rooms; TOT accounts for ODA plus infiltrations)

- After the analysis of the prototype systems, the results can be combined and the overall performance of the ventilation system in this assessment can be evaluated.

6 DISCUSSION AND CONCLUSION

The main aim of this paper is to introduce concepts, i.e. level of assessment, reducible and irreducible uncertainty, and level of uncertainty data. Two approaches are given to deal with the uncertainties in an assessment of ventilation system based on the introduced concepts. A simple demonstration is given to illustrate the described concepts and to show how the approach works.

One way to deal with assessment in complex situations with significant uncertainties is to decompose the case into sub-cases where each sub-case includes fewer uncertainties and can be estimated more accurately. This is the main idea described in this paper. The given concepts and approaches are considered to be useful tools for dealing with different kinds of assessments. Although the focusing point is on ventilation systems, the concepts about uncertainties can be applied to other fields as well.

However, the attempt to quantify the uncertainties in an assessment of domestic ventilation systems led to more questions. First, the boundary between the reducible and irreducible uncertainty actually depends on the specification of the components and the available data. The irreducible level must be used when the components cannot be specified into more sub-categories or there is no more data for such sub-categories. So the boundary between a reducible uncertainty and an irreducible uncertainty depends on the user of the concepts. Furthermore, the prototype approach is demonstrated in this paper with two arbitrarily chosen prototypes. The influence of the choice of the prototypes merits a future investigation too.

7 REFERENCES

Carrie F. R, Bossaer A, Andersson J V, Wouters P, and Liddament M W, (2000). *Duct leakage in European buildings: status and perspectives.* Energy and Buildings, 2000, 32, 235-243

ISSO publication 62: Centrale gebalanceerde ventilatiesystemen met warmteterugwinning in woningen en woongebouwen. September 2010. ISBN: 978-90-5044-198-8. ISSO.

ISSO publication 92: Ventilatiesystemen met decentrale toevoer en centrale afvoer in woningen en woongebouwen. November 2009. ISBN: 978-90-5044-188-9. ISSO.

Knoll B., Phaff J. C. and Gids W. F. de, (1995). *Pressure simulation program*, Proceedings of 16th AIVC conference, Implementing the Results of Ventilation Research, Palm Springs, USA, 19-22 September.

Orme M., Liddament M. W. and Wilson A., (1998). *Numerical data for air infiltration & natural ventilation calculations*. AIVC Technical note 44, 1998.

Yang Z. (2012). *Method to assess the performance of domestic ventilation systems considering the influence of uncertainties.* PhD thesis, Delft University of Technology.

Yang Z., J.J.M. Cauberg and M. Tenpierik (2012). *Performance of counter flow heat recovery ventilation systems in dwellings considering the influence of uncertainties.* International Journal of Ventilation

MEASUREMENTS AND MODELLING OF AN EARTH-TO-AIR HEAT EXCHANGER FOR RETAIL BUILDING VENTILATION

Andrzej Górka[*1], Michał Szymański[2]

1 Institute of Environmental Engineering, Poznan University of Technology ul. Piotrowo 3a, PL 60-965 Poznan, Poland
**Corresponding author: andrzej.gorka@put.poznan.pl*

2 Institute of Environmental Engineering, Poznan University of Technology ul. Piotrowo 3a, PL 60-965 Poznan, Poland

ABSTRACT

An earth-to-air pipe type heat exchanger (EAHE) is a simple and effective ventilation system component, used for preconditioning of the fresh air supplied to a building. This paper presents two sets of results of operational parameters long-term measurements and energy analysis of EAHEs, located under two different retail buildings of floor area over 1000 square meters each.
In the second part of this paper there is described the mathematical model of the EAHE operating in a mechanical ventilation system of a retail building implementation into computer code, written in MS Excel and used for simulation of EAHE long-term operation (i.e. at least one year). The thermo-hydraulic phenomena inside the EAHE are simulated, as well as the calculation of transient three-dimensional (3-D) ground temperature field is performed with use of the method of elementary balances, in an open schema.
The elaborated model allows to analyse the impact of control strategy of ventilation system on the energy efficiency of this exchanger. As a result of this investigation, the control algorithms in described real facilities were found to be not optimal. Changes in the control strategy, leading to improvement of energy efficiency of EAHE and ventilation system in the same way, were proposed.

KEYWORDS

earth-to-air heat exchanger (EAHE), renewable energy, long-term measurements, numerical modelling, control strategy

1 INTRODUCTION

One of the most energy-intensive fields of the economy is the residential and public buildings sector. Reduction of energy demand in buildings can be obtained by improving their thermal insulation, increasing airtightness of envelopes and improving efficiency of ventilation systems. The practical result of these efforts is the idea of low-energy, passive and zero-energy buildings. In these buildings, the share of ventilation losses in total energy balance could be dominant. This situation leads in the first step to the use of heat recovery systems, which implies the application of supply-exhaust mechanical ventilation. In order to obtain further net energy demand reduction, to improve protection against freezing of heat recovery exchanger, as well as to increase the quality of climatic comfort, earth-to air heat exchangers (EAHE) are applied, as a source of renewable energy.
The EAHE is the ventilation system component – pipe buried underneath ground surface, which allows heating of fresh air in the winter period and cooling during summer time, using energy from the ground adjacent to the exchanger.

The open literature offers numerous publications on the pipe-type ground heat exchangers. The review indicates that EAHE are investigated and applied almost all over the world (from the cold climates of Scandinavia to the hot climates of Africa, Kuwait and Brazil) as well as for various types of buildings (residential, public, industrial, agricultural, etc.). All these papers can be divided into the following groups:

- describing experimental investigations of EAHEs (e.g. Eicker, 2010; Santamouris, 2007; Sawhney et al., 1999; Thanu et al., 2001),
- presenting computational models and the results of theoretical analyses (e.g. Badescu, 2007; Bojic et al., 1997; Kabashnikov et al., 2002; Tittelein et al., 2009; Wu et al., 2007),
- engineering type publications like handbooks, design guidelines, selection software descriptions / manuals, etc.

It often happens, that one item can be located in several of the above mentioned groups simultaneously – for example numerical simulations validated by measurements results (e.g. Szymanski and Wojtkowiak, 2013; Tiwari et al., 2006; Trzaski and Zawada, 2011). In each group, the authors approaches of different complexity and levels of sophistication could be found. The biggest discrepancies reveal in the description temperature changes of soil and the EAHE cooperation with other ventilation system components and the building. Another important conclusion, emerging from the analysis of the cited works, is the opinion difference on the EAHE application effectiveness.

There are more publications concerning small one-pipe installations than large multi-pipe systems. Very low number of researchers investigated EAHE and ventilation control algorithms as well as the system optimization.

In this paper two sets of results of long-term experimental investigations of earth-to-air pipe-type heat exchangers (EAHE) in mechanical ventilation systems of retail buildings are presented. There are also included results of EAHE numerical calculations. In the numerical model it is possible to apply different control strategies of the exchanger, what often influences very significantly EAHE energy efficiency. It is most important issue in moderate periods (like spring and autumn), when unwanted fresh air heating or cooling can occur. To avoid such a situation automated control dampers should by-pass the exchanger and take the fresh air directly from outside (e.g. direct wall or roof inlet to the AHU). Another possibility of these dampers use is for air mixing purpose (ambient and EAHE outlet air mixing) – to exactly meet the set point of fresh air temperature for space conditioning (especially in early summer time). The control algorithm (set points boundaries) also strongly depends on building type and climate.

2 CASE STUDIES

2.1 Investigated facilities

This study is focused on the effectiveness of two earth-to-air heat exchangers located underneath two similar one-storey retail stores in southern Poland. The floor area of the store "A" is about 1300 m^2. EAHE was installed as a system of 20 parallel pipes, Ø200 mm diameter, each 35 m long, connected in Tichelmann scheme, with manifold pipes of Ø500 mm diameter. Installation layout is presented in Figure 1. Air inlet to the exchanger is placed on the roof of the building and in opposite corner air goes out from EAHE to air handling unit (AHU). The nominal air flow rate for this EAHE is 2700 m^3/h, what corresponds to 135 m^3/h for each pipe and average air speed of 1,4 m/s inside exchanger pipes.

The second retail store "B" is quite similar to the store "A". The most important parameters of the building "B" and its EAHE are as follows:

- floor area: 1100 m^2

- air flow rate: 2400 m^3/h
- pipes: 18 parallel pipes, Ø200 mm, 38 m length, air speed: 1,4 m/s.

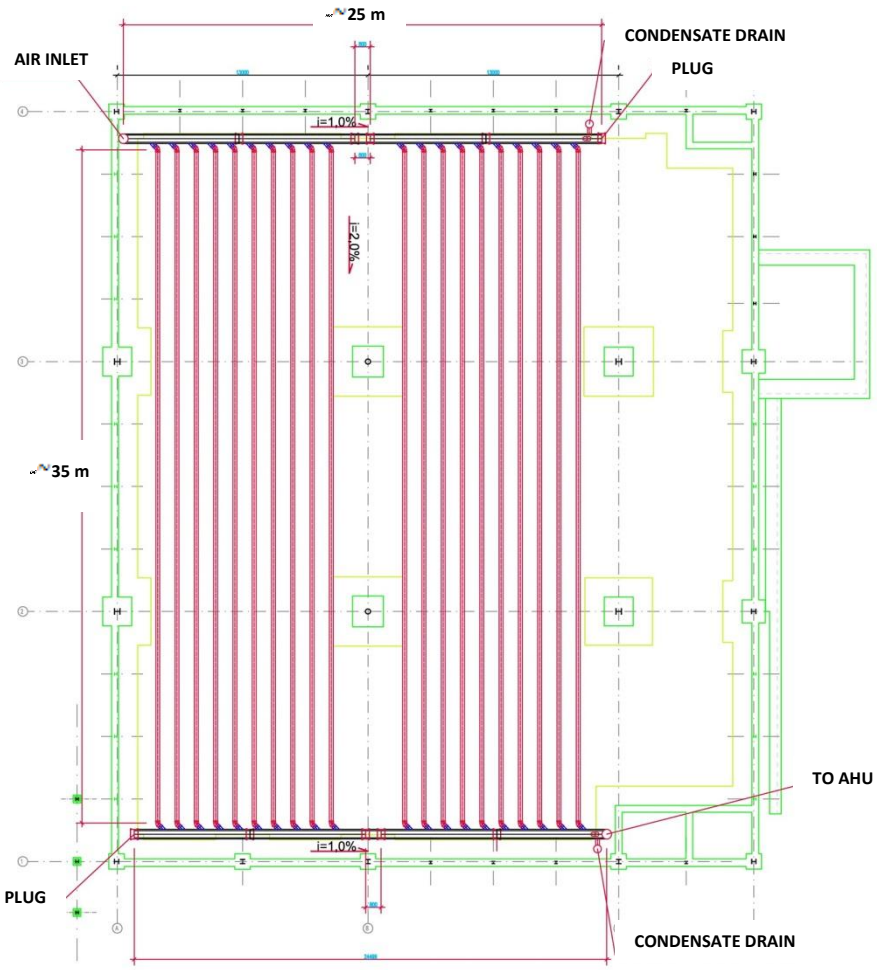

Figure 1. Layout of EAHE installation underneath the floor of commercial facility "A"

2.2 Objectives and scope of measurements

The first objective of the measurements was to precisely define the quantity of energy supplied to ventilation air in winter and recovered from ventilation air in summer, to assess the energy efficiency of EAHE in Polish climate. The second purpose of the measurements was a detailed recording of short-term and long-term variability of the operational parameters of EAHE. Collected data served later to improve of the operation of the EAHE in subsequent years.

To achieve accurate results, the following rules were adopted:

- measurements lasted for a period of one year,
- parameters were measured at short intervals of 5 minutes,
- recorded data included basic parameters allowing to define enthalpy of inlet and outlet air and to define the ventilation air flow: EAHE inlet and outlet air temperature and relative air humidity and air velocity in the duct.

2.3 Measurements results

Changes of temperature and relative humidity measured in February for case A is shown in the Figure 2 and outlet temperature as function of inlet temperature for the whole year – in Figure 3. Based on the collected data and common energy equations, the energy output of EAHE was calculated. This is shown in Figure 4.

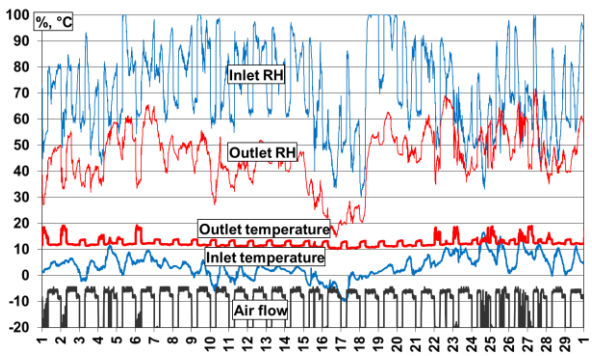

Figure 2. Measurement results for February – case A

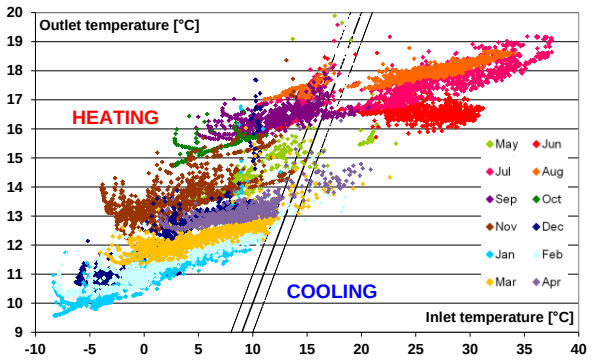

Figure 3. Distribution of outlet air temperature as a function of inlet air temperature for EAHE – case A

The control system of the air handling unit (AHU) in case A was programmed to turn on the ventilation system daily from 6:00 to 23:00 and to bypass the EAHE if the temperature difference between inlet and outlet is less than 1°C.

The winter 2007/2008 was exceptionally mild in the South of Poland – all ambient temperatures were higher than -10°C – so the maximum expected heat output of the EAHE couldn't be observed. It was however possible to investigate the influence of thermal capacity of the ground on the output air temperature: at +30°C air inlet temperature, outlet air temperatures were respectively: +16,5°C in June, +17,5°C in July and about +18,5°C in August. Basing on the data presented in Figure 3, the following remarks regarding control system can be formulated:

- the algorithm general rule, preventing use of EAHE with the temperature difference between inlet air and outlet air of less than 1°C, didn't work properly – especially in October,
- the EAHE was used sometimes in July and August to unnecessary preheat the fresh air, what prevented the use of natural cooling of the building.

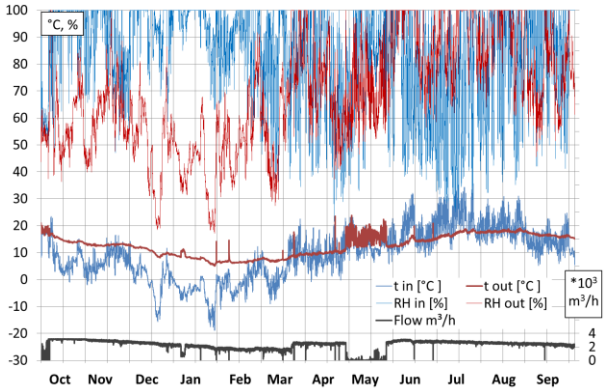

Figure 4. Annual measurement results – case B

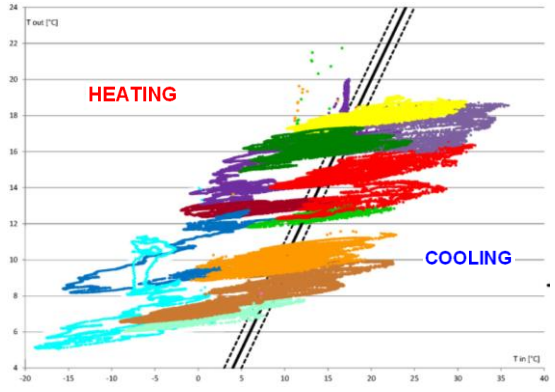

Figure 5. Distribution of outlet air temperature as a function of inlet air temperature for EAHE – case B

The EAHE investigated in case B operated nonstop all year round, because of no automated control system installed in the ventilation system. The worst consequence of the total absence of controls system was wasting energy for ventilation of an unoccupied building during nights. Other disadvantage related to EAHE was passing of the air thru the EAHE with no

effect in temperature change and the last consequence was preheating the air in summer or precooling in spring – exemplary at 26.03 the ambient air was unnecessary cooled from +22°C to +10°C. The above mentioned negative effects occurred in case B to much greater extent, than observed in case A. Essential data regarding operation of the investigated installations are presented in the Table 1 and in Figures 6 and 7.

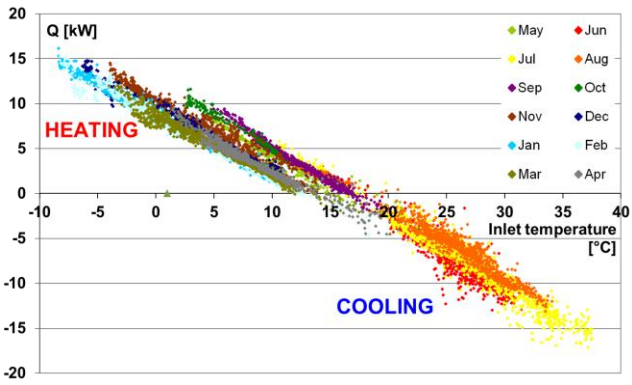

Figure 6. Heating and cooling capacity of EAHE case A as a function of outdoor air temperature

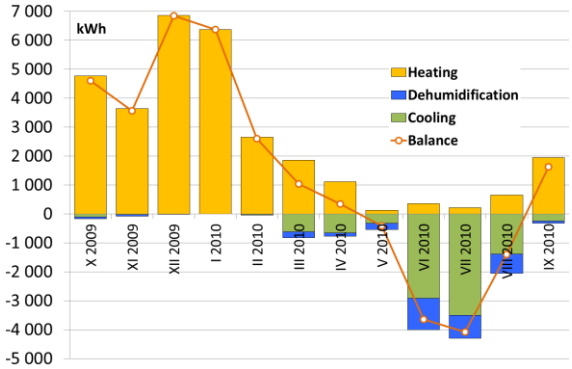

Figure 7. Monthly energy balances of EAHE – case B

As a result of EAHE application, variations of air temperature at the inlet of AHU were reduced almost 5 times in case A – from range (-8 ÷ +37°C) to range (+9,5 ÷ +19°C) and 4 times in case B. This allowed to reduce of the nominal output of heating and cooling systems required for AHU operation.

Table 1. Summary of key operating parameters of investigated installations

	Case A	Case B
Measurement period	V.2007 - IV.2008	X.2009 - IX.2010
Maximum heating output	15 kW	19 kW
Maximum cooling output	17 kW	22 kW
Energy delivered for heating	22 400 kWh	30 600 kWh
Energy delivered for cooling	9 200 kWh	13 100 kWh
Reduction of the air temperature fluctuations at the inlet to AHU	5 times	4 times

In both cases, the installations operated at air flows reduced by 10% - 50% from the design air flow. At higher, nominal air flows the heating and cooling outputs and delivered energy would be higher, however EAHE outlet temperature fluctuations would be higher too.
Despite the slightly longer pipes and air change rate in case A, output power and delivered energy are greater in case B. The reasons were mild winter occurred in case A and longer operating time in case B. Other important cause of the big difference in delivered energy is the control system. In case B there was no automated control system at all, so cooling and heating energy was delivered regardless of the real needs. It was delivered just when it was available. On the other hand, the control algorithm in case A was too complex in the first few months of measurements and EAHE was bypassed even its operation was needed.
The overall EAHE energy efficiency was very high in both cases. Amount of energy obtained from the EAHE in relation to the energy supplied to the fan was higher than 20, both in summer and in winter.

3 NUMERICAL MODELLING

3.1 Method of modelling

The numerical model is based on the method of elementary balances, in an open schema. The model is designed to simulate transient heat flow and is built of 45 sections, located perpendicular to the tubes. Each of the sections represents 1 m thick layer (Fig. 8) and was calculated in Microsoft Excel sheet (Fig. 9). There was adopted a rectangular grid in the cross-section; the pipes were approximated by squares with constant temperature equal to the average air temperature in the section (Fig. 9). The model is based on energy balances of the elements in time – equations (1) and (2). In the simplest case, temperature of the element at the end of the time step can be described by equation (3).

$$\dot{Q} \cdot \Delta\tau = m \cdot c \cdot (t'_{x,y,z} - t_{x,y,z}) \tag{1}$$

$$\dot{Q} = \sum_{i=1}^{6} \left(\frac{1}{R_i} \cdot A_i \cdot \Delta t_i\right) \tag{2}$$

$$t'_{x,y,z} = t_{x,y,z} + a \cdot \frac{\Delta\tau}{l \cdot d^2} \cdot \left[\cdot (t_{x+1,y,z} + t_{x-1,y,z} + t_{x,y+1,z} + t_{x,y-1,z} - 4\, t_{x,y,z}) + d \cdot (t_{x,y,z+1} + t_{x,y,z-1} - 2\, t_{x,y,z}) \right] \tag{3}$$

where $t_{i,j,k}$ [K] are temperatures of the "i,j,k" element at the beginning of current time step, $t'_{x,y,z}$ [K] is the temperature of the "x,y,z" element at the end of current time step, $\Delta\tau$ [s] is the length of current time step, d [m] is the distance between calculation grid nodes in x and y direction, l [m] is the distance between calculation grid nodes in z direction, a [m^2s^{-1}] is the thermal diffusivity, c [$J \cdot kg^{-1}K^{-1}$] is the specific heat capacity, m [kg] is the mass of the element, R_i [$m^2K \cdot W^{-1}$] is the heat resistance between elements and $\dot{Q}$ [W] is the heat flux.

The convective heat transfer coefficient inside the EAHE pipes was assumed as variable, air velocity dependent.

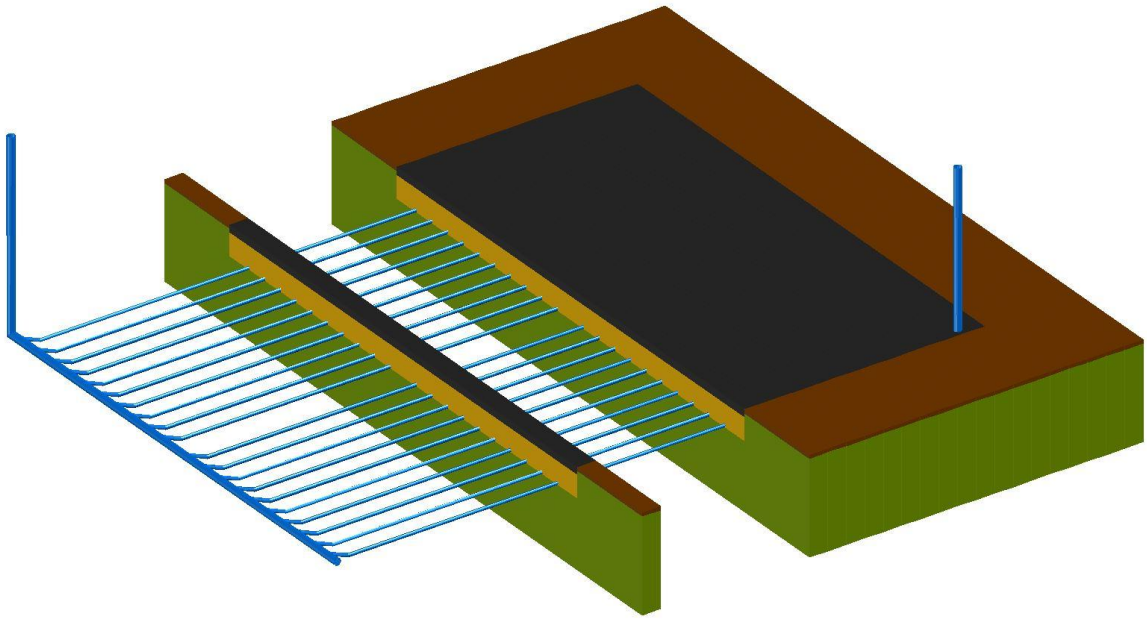

Figure 8. Division of the 3D model into layers

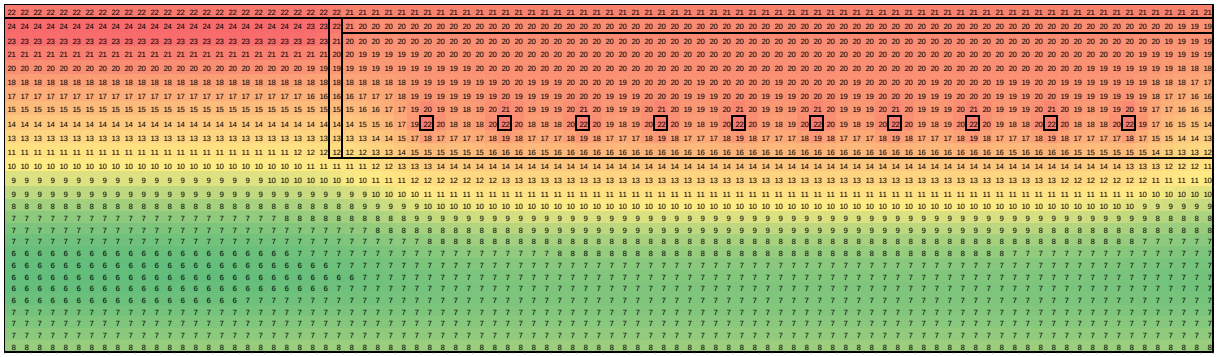

Figure 9. Exemplary, transient temperature distribution in one of the layers – air cooling mode

3.2 Control algorithms tested

Two control algorithms were tested for the same building and EAHE installation. The rules taken into account in control strategy are summarized in Table 2. It is assumed, that the EAHE is in use, when all conditions are ***TRUE***.

Table 2. Rules applied in control algorithms

	CS1	**CS2**
Condition 1	Control timer 6:00-23:00	Control timer 6:00-23:00
Condition 2	Ambient air temperature lower than +10°C or higher than +22°C	Ambient air temperature higher than +20°C in cooling mode (outlet EAHE temperature lower than inlet temperature)
Condition 3	-	Outlet EAHE temperature lower or higher than inlet temperature by at least 1°C

3.3 Modelling results

The calculations were performed for a period of one year, for ambient conditions of Poznan. The results of modelling, as plots of outlet temperature in function of inlet temperature for subsequent months are presented in Figures 10 and 11.

The control strategy in **CS1** is simple and requires only measurement of ambient air temperature. The condition 2 in **CS1** was introduced to avoid unnecessary precooling of air in spring and unnecessary preheating in summer months. This control algorithm unfortunately bypasses the EAHE also in periods, when the EAHE could preheat the air – for example from +11°C to +16°C. The heat exchanger operates also sometimes with no (or very small) temperature difference between inlet and outlet air – this is wasting of electrical energy used for powering fans.

In **CS2**, the condition 3 prevents wasting of energy for passing air thru EAHE without significant temperature change. In combination with condition 3, the temperature threshold of cooling mode (condition 2) could be safely reduced to +20°C and the temperature threshold of heating mode (+10°C) is unnecessary.

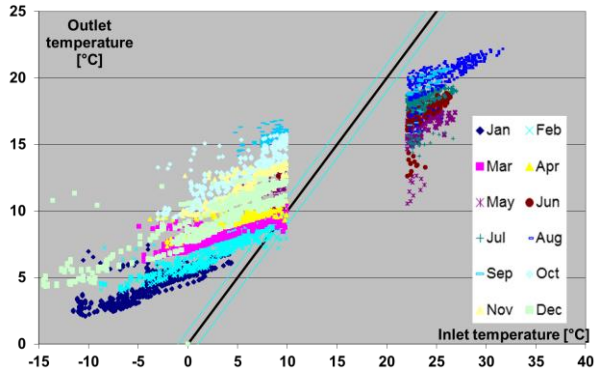

Fig. 10 Distribution of outlet air temperature as a function of inlet air temperature for EAHE – CS1

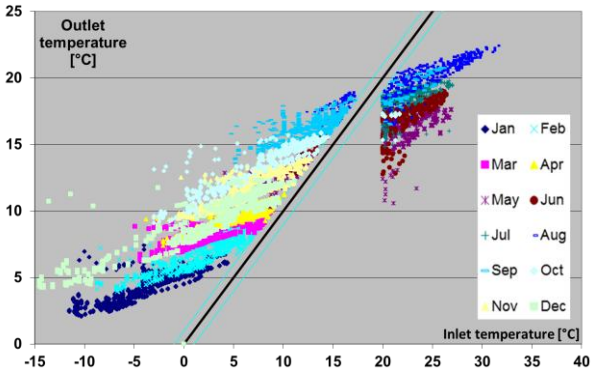

Fig. 11 Distribution of outlet air temperature as a function of inlet air temperature for EAHE – CS2

Results of the modelling are detailed annual variability of all operational parameters of the EAHE. This allows to compare and evaluate control strategies for EAHE. The developed model, after minor modifications, allows for calculation and comparison of any control strategy for the EAHE.

4 CONCLUSIONS

Earth to Air Heat Exchangers (EAHE) are energy efficient, delivering over 20 times more heating or cooling energy than they need for powering of fans. The fluctuations of temperature of inlet air in the AHU decreases 4 – 5 times as the result of EAHE application. This allows to decrease the size of heating and cooling equipment and to reduce investment costs. Applying of EAHE in investigated cases reduced the heating demand by about 17-28 kWh/(m^2·a) and cooling demand by about 7-12 kWh/(m^2·a). In similar installations even greater savings are expected, because the investigated cases didn't reach designed air flow rates. The energy saving may differ from analyzed cases, depending on operational parameters and control strategy of EAHE.

Energy efficiency of a ventilation system equipped with EAHE depends largely on the control strategy. In the second part of the paper two control algorithms of EAHE were evaluated, using numerical modeling. Algorithm **CS2**, gave 8% more heating energy and 22% more cooling energy than the algorithm **CS1**, which took into account only control timer and ambient air temperature. It is recommended to apply the algorithms similar to **CS2** in control systems of EAHE.

More energy savings are possible by application of control strategy based on control error and by use of more sophisticated control algorithms, including fuzzy logic and predictive control. The above mentioned methods of control are subjects of future research.

5 REFERENCES

Badescu V. (2007), Simple and accurate model for the ground heat exchanger of a passive house, Renewable Energy, 32/2007, p. 845-855.

Bojic M., Trifunovic N., Papadakis G., Kyritsis S. (1997), Numerical simulation, technical and economic evaluation of air-to-earth heat exchanger coupled to a building, Energy, 22/1997, p. 1151-1158.

Eicker U. (2010), Cooling strategies, summer comfort and energy performance of a rehabilitated passive standard office building, Applied Energy, 87/2010, p. 2031–2039.

Kabashnikov V.P., Danilevskii L.N., Nekrasov V.P., Vityaz I.P. (2002), Analytical and numerical investigation of the characteristic of soil heat exchanger for ventilation systems, Heat and Mass Transfer, 45/2002, p. 2407-2418.

Santamouris M. (2007), Advances in passive cooling, Earthscan.

Sawhney R.L., Buddhi D., Thanu N.M. (1999), An experimental study of summer performance of a recirculation type underground air pipe air conditioning system, Building and Environment, 34/1999, p. 189-196.

Szymanski M., Wojtkowiak J. (2013), Numerical and Experimental Investigations of Earth-to-Air Pipe Type Heat Exchanger Long-Term Operation, CLIMA 2013 - 11th REHVA World Congress and the 8th International Conference on IAQVEC, Energy Efficient, Smart and Healthy Buildings, Prague, p. 3768-3777.

Thanu N.M., Sawhney R.L., Khare R.N., Buddhi D. (2001), An experimental study of the thermal performance of an earth-air-pipe system in single pass mode, Solar Energy, 71/2001, p. 353-364.

Tittelein P., Wurtz E., Achard G. (2009), Modelling earth-to-air heat exchanger behavior with the convolutive response factors method, Applied Energy, 86/2009, p. 1683-1691.

Tiwari G.N., Akhtar M.A., Shukla A., Emran Khan M. (2006), Annual thermal performance of greenhouse with an earth-air heat exchanger: An experimental validation, Renewable Energy, 31/2006, p. 2432-2446.

Trzaski A., Zawada B. (2011), The influence of environmental and geometrical factors on air-ground tube heat exchanger energy efficiency, Building and Environment, 46/2011, p. 1436-1444.

Wu H., Wang S., Zhu D. (2007), Modelling and evaluation of cooling capacity of earth-air-pipe systems, Energy Conversion & Management, 48/2007, p. 1462-1471.

DURABILITY AND MEASUREMENT UNCERTAINTY OF AIRTIGHTNESS IN EXTREMELY AIRTIGHT DWELLINGS

Wolf Bracke[1], Jelle Laverge[*1], Nathan Van Den Bossche[1] and Arnold Janssens[1]

1 Ghent University
Jozef Plateaustraat 22
9000 Gent, Belgium

**Corresponding author: e-mail address*

ABSTRACT

In this paper we present a series of leakage tests on extremely airtight dwellings (ACH_{50} < 0.6 upon completion) in which the durability of the airtightness and the measurement uncertainty involved are assessed. In literature, repeatability and reproducibility issues have been discussed by several authors, along with influences of weather. It remains unclear, however, to what extent the available uncertainty intervals are relative or absolute. With the current tendency towards extremely low leakage levels and the introduction of airtightness requirements in building codes, the further exploration of this issue has become crucial.
In this paper, 4 aspects are studied consecutively: the repeatability and reproducibility of the fan pressurization method in extremely airtight houses, the impact of weather conditions on the measurements, the impact of the age of the construction and the reproducibility of the airtightness level in repeated construction of virtually identical houses. The latter is limited to short term effects since all dwellings (n = 15) were completed after 2010.
The results show similar relative repeatability and reproducibility intervals to those found in literature. The rather large effects of weather conditions reported in previous studies could not be reproduced. Normal wear and tear due to occupation of the dwelling proved to introduce substantial relative deterioration of the airtightness of the building shell (20-100% increase in leakage), although in absolute values, the additional leaks were modest and the buildings remained very airtight. In general, we conclude that pressurization tests render robust results in extremely tight construction, but with respect to ambitious leakage limits, test conditions and small preparation details such as the locking of window hardware can easily determine whether the dwelling will pass or fail.

KEYWORDS

Blowerdoor, reproducibility, durability, uncertainty

1 INTRODUCTION

Given Europe's ambitions to cut down CO2 emissions, all new-built houses will need to be constructed as nearly zero energy buildings by the end of 2020. While the public and building industry is well aware of the need for well-insulated buildings, there is still much room for improvement in terms of airtightness. In Belgium, for example, the median leakage level of standard construction in 2010 was just under 6 ACH at 50 Pa pressure difference (Laverge et al., 2010), about 10 times as much as the limit imposed by the Passive Haus Institut to obtain the passive house certificate (ACH_{50} < 0.6).

Since new standards are emerging and maximum air leakage limits are imposed in energy performance codes, the need for a reliable test method and reliable results is growing. Although the European standard EN 13829 (CEN, 2001) describes the preparation of the building and explains in detail how the measurements should be performed, there still is room for interpretation. In Belgium, some of this ambiguity has been addressed in a separate guideline for tests within the framework of the official Energy Performance of Buildings (EPB) calculation (2013), but a number of issues are very case dependent and decisions on how to deal with them have to be taken by the tester on site.
The growing (financial) consequences of the result of a blowerdoor measurement put increasing stress on the reliability of these tests, especially in extremely airtight construction. In these cases, a modest absolute difference in leakage can make a large difference relative to the very low leakage limit imposed. Having well-trained test operators, reliable equipment, clear standard regulations and calculation methods are evident prerequisites for reliable results. Even if all the above conditions are met, measurement uncertainties will occur due to the effects of wind and temperature or the specifics of the installation of the equipment. It's important to be able to estimate and evaluate these uncertainties in order to compare test results and to define maximum wind speeds during the test.
It's also important to study the long-term variation of air leakage. Do blowerdoor test results remain stable during the changing seasons? If not, how big is the variation that occurs? Is this variation uniform for all building methods? What's the relation to the prevailing climate? Should airtightness parameters be corrected for these seasonal effects to obtain an objective result? And for the project-owner: when is the best time to test?
Besides seasonal effects, air barriers, like all building components, may be subject to degradation due to wear and tear, resulting in a rise in the air leakage after some years. It's essential to evaluate which materials or elements are responsible for this rise in order to build future houses with a more durable airtightness barrier, as well as to estimate infiltration losses over the course of the buildings lifespan.
In addition to the reliability and reproducibility of test results, the increasing stress, with the attached financial liabilities, on tight construction also intensifies the need for data on the reproducibility of the leakage level of a construction itself. How robust is the leakage level achieved by a specific construction method?
This paper addresses these issues with respect to houses at passive house leakage levels, since these represent the lowest 10 % of the tested leakage rates included in the official EPB database in Belgium (De Baets and Jonckheere, 2013) and can therefore be considered to be representative for future airtight construction. In the next section, reproducibility issues of the pressurization test are discussed. The third section addresses the impact of weather conditions, while the fourth looks at the evolution of the leakage level over time. The reproducibility of the construction method is dealt with in the last section, followed by a conclusion section that sums up all results. For all tests a Minneapolis blower door type 4.1 was used.

2 TEST REPRODUCIBILITY

2.1 Literature

A number of studies available in literature give an idea of the expected variation when performing airtightness measurements.
A study by Delmotte and Laverge reported a standard deviation of 1,4% and maximum variation of 4,0% for 10 pressurization tests under repeatability circumstances (same operator, same test equipment) (Delmotte and Laverge, 2011). These numbers increased to 2,7% and 7,9% under reproducibility circumstances (different operators, different test equipment).

Persily performed 28 pressurization tests on a house during a three-month period and found a 5,5% standard deviation and 19,4% maximum variation (Persily, 1982). When only retaining the results from relatively calm weather days (< 2,5 m/s wind speed) these statistics decreased to 1,7% and 4,8%, showing the high impact of wind speed on the repeatability of pressurization test results. High wind speeds seem to be correlated with higher leakage results.
Kim and Shaw studied the air leakage from a house during a one-week period. They noticed similar results as the previous researches: a standard deviation of 1,7% and maximal variation of 4,2% (Kim and Shaw, 1986). The highest air leakages were measured during low wind speeds, in contrary to Persily's findings.

2.2 Measurement results

The repeatibility of the pressurization test was studied on 2 passive houses in Belgium. Passive houses are currently the only buildings subjected to maximum airtightness levels (ACH50 < 0,6 h-1) and can be regarded as 'a look in the future' of the housing market.
House 1 is a semi-detached house, built in a traditional way using masonry walls. 48 pressurization tests with identical setup were performed on 7 different days in a 5 month period between December 2012 and April 2013. On average, the measurements showed a standard deviation of 1,1 % and a maximum variation of 3,5 % within the same day (Table 1). The mean leakage measured in all tests was 230 m^3/h at 50 Pa pressure difference, corresponding to 0.54 ACH_{50}.

Figure 1. Picture of the façade of house 1 (left) and house 2 (right)

House 2 is a detached house with a wood-frame structure. It was tested 44 times in total, on 6 test days within the same period as for House 1. Here, the variation within the same day was higher with an average standard deviation of 2,7 % and an average maximum variation of 7,7 %. These uncertainties are well in line with those reported in literature. When absolute values are considered, the average standard deviation within a test day is 3.2 and 3.5 m^3/h, for house 1 and 2 resp., suggesting that the error due to repeatiblity might be more absolute in nature than relative, although Murphy suggests that, in contrast, the error is relative to the square of the leakage (Murphy et al., 1991) and Delmotte did not find a clear correlation (Delmotte and Laverge, 2011).
No relation between wind speed and air leakage could be discovered, but the results on windy days show generally more variation. Wind speeds were derived from online weather observations, which are not always reliable. A mobile weather station would be a much better option to monitor wind speed and direction.

A few additional tests were performed, to evaluate the effect of decisions in building preparation or test procedure – without neglecting EN 13829.

Table 1: Overview of air leakage measured in house 1.

	date	V_{50} (m^3/h)	ACH_{50} (-)	stdev (%)	max var (%)
day 1	17/12/2012	221.7	0.52	1.39	4.06
day 2	7/01/2013	219.8	0.51	1.18	4.32
day 3	29/01/2013	229.3	0.54	1.13	3.49
day 4	19/02/2013	223.2	0.52	1.05	2.69
day 5	11/03/2013	241.4	0.57	1.03	4.35
day 6	9/04/2013	246.2	0.58	0.92	1.83
day 7	29/04/2013	248.7	0.58	0.49	1.41

As different pressure differences over the building envelope exist due to wind and temperature effects, the place of the external pressure point might influence the measurement results. Pressurization tests were performed on both passive houses, while changing the external pressure tap around the building. Although t-tests showed no significant difference between different positions of the pressure tube in most cases, we can't conclude that this effect is negligible. Probably the effect is masked by the usual variation in airtightness measurements.

Despite well-trained test operators, reliable equipment, clear standard regulations and calculation methods, pressurization tests will always show some uncertainty due to changing natural pressure differences around the building. As wind fluctuates constantly in speed and direction, natural pressure differences across the building envelope also change. External reference taps and baseline pressure corrections are intended to cancel out these fluctuations and thereby obtain reliable test results. For this to work, however, the external reference tap should be in the 'open field'. In actual measurements, this is often impossible to achieve because of the presence of all kinds of objects around the dwelling that create wind induced turbulences.

The results of consecutively executed natural pressure difference measurements within a total time span of 5 minutes reported in Table 2, show that even 30-second averages can change substantially in a short period of time, with a difference of more than 8 Pa over 5 minutes for the south facade. Baseline pressures, measured before and after a pressurization test which typically takes 20-30 minutes, are therefore not per se representative for the natural pressure difference during the test and can lead to false corrections.

Testing at high pressure differences reduces the impact of these changing boundary conditions and, renders more robust results, as was clearly demonstrated by Delmotte (Delmotte and Laverge, 2011).

Generally, the fan should be installed in the most airtight opening of the building envelope. As this is difficult to evaluate without performing multiple tests, the test operator will use the front door in most of the cases. But when the front door is leaky, this leakage is of course not included in the measurements. In house 2, measurements were performed on both doors, showing a decrease by 22,3 m^3/h (or 15,5 %) when the fan was installed in the back door.

Standards give no clear indication whether doors should be locked during the pressurization test, or just closed, without turning the key. As leaks around doors can be almost eliminated by locking the door in case a multi-fix hardware is available, this decision can have a substantial impact on leakage results. In house 2, not locking the front or back door during a test led to an increase in leakage by 40,2 m^3/h and 41,2 m^3/h. As the overall leakage in these

dwellings is very low, this resulted in a relative increase of the total leakage of 33,4 % and 28,9 % respectively.

Table 2: consecutively measured 30-second averaged natural pressure differences at north, east and south facades for house 1.

	North	East	South
measurement 1	-0.1	0.8	-2.2
measurement 2	-0.5	0.5	-3
measurement 3	-0.5	0.9	-2.3
measurement 4	-0.4	0.4	-2.2
measurement 5	0.2	1.3	-5.6
measurement 6	-0.6	0.6	-6.9
measurement 7	-1	-0.5	-3.7
measurement 8	-0.6	-0.7	1.3
measurement 9	-0.8	-0.8	-0.8
measurement 10	-1.1	-1.2	-2.6
average	-0.54	0.13	-2.8
minimum	-1.1	-1.2	-6.9
maximum	0.2	1.3	1.3

Passive houses are equipped with mechanical supply and exhaust ventilation. These systems should be sealed off during the pressurization test, since the supply and exhaust openings represent huge leaks that are not relevant for infiltration in the building envelope.
It's up to the test operator to decide where the ventilation system will be disconnected. This can be anywhere between the external air supply/exhaust and the local air vents in the rooms. Obviously, the test result includes leakage through the ducts from the air supply/exhaust up to the point where the seals for the test are applied. Tests on House 1 show that leaks between ventilation ductwork, heat exchanger, ventilation system and silencer are responsible for an additional 43,3 m3/h, or 17,6 % of the total leakage when the ventilation system is not sealed off directly after the external air intake and discharge points.
These examples show how apparently small decisions can have an impact on the overall air leakage. This is especially true for passive houses, which have a very small air leakage and thus, although the change in absolute value of the leakage is modest, will show a huge relative difference when something in the building preparation or test procedure is changed. This makes comparing test results difficult when looking for seasonal variation or durability effects, especially when pressurization tests are not performed by the same operator.

3 SEASONAL VARIATIONS

3.1 Literature

Studies reporting seasonal variation are available in literature, but building methods and prevailing climate should be taken in mind when drawing conclusions. Persily performed multiple tests during one year on a house in Princeton (Persily, 1982). He noticed up to 30% higher air leakage in the winter compared to the lowest measurement results in summer. Air humidity on the contrary, showed peaks in the hot, humid summers and very low values in de the dry, cold winters. Persily claims the moisture in the hot summer air results in a swelling of

the wood. When the wood swells, small cracks and gaps in the construction disappear resulting in a lower air leakage.
Kim and Shaw measured a seasonal variation up to 20% when performing a similar study on two houses in Canada, with the lowest values appearing in winter (Kim and Shaw, 1986). One of these houses had an air leakage very similar to the air leakage in passive houses.
Dickinson and Feustel performed a study on 10 houses in three different climates (Dickinson and Feustel, 1986). Three houses were located in Truckee and showed a clear seasonal variation due to the extreme climate, with up to 45 % higher leakage in summer, compared to the winter measurements. This variation is very similar for all three houses, although the highest variation occurs in the house with the highest air leakage and vice versa. The fact that winter measurements show lower values is mainly attributed to the presence of large quantities of snow on and around the building envelope.

Measurement results

During the period December 2012 – April 2013, multiple pressurization tests were performed on both passive houses every three weeks. The results show an increase in average air leakage over each single test day by 13 % over the course of the 7 test days in house 1. These results are shown in Figure 2.

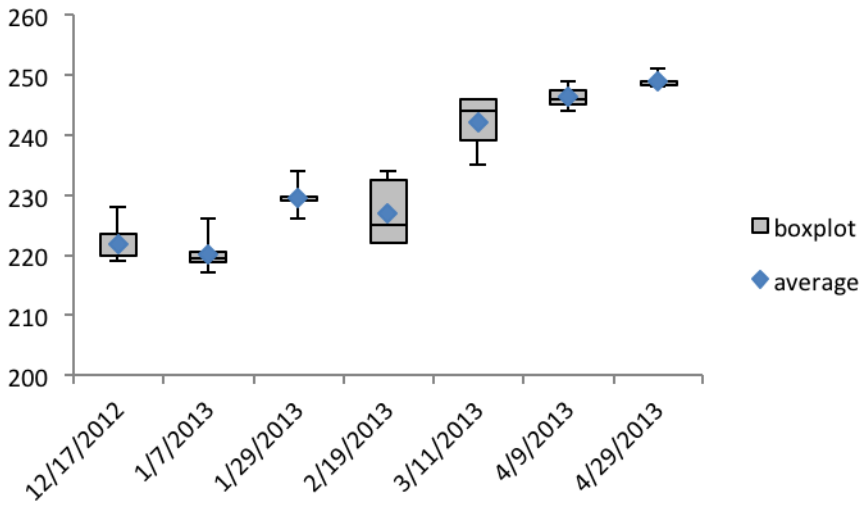

Figure 2. Boxplot and average of the leakage measured on 7 test days between December 2012 and April 2013 in house 1.

Although smaller in relative magnitude, this variation seems to follow the pattern found by Kim and Shaw (Kim and Shaw, 1986) or Dickinson and Feustel (Dickinson and Feustel, 1986). No substantial snowing occurred during the measurement period. The increase in leakage therefore has to be attributed to other factors. One potential mechanism is the differential thermal dilation of the masonry/concrete structure and the plaster that assures most of the airtightness. This would create fine cracks in the plaster, especially at edges and joints, leading to increased leakage. Another, more straightforward explanation might be a gradual deterioration of the air tightness of the ventilation ductwork due to repeated dismantling for the preparation of the pressurization test.

The air leakage results of house 2 show no clear rising or declining trend. The results fluctuate around the average value, with a slight increase of 6 % between the first and the last test day (Figure 3).
Although house 2 has a wood construction with wooden windows and doors and the Belgian climate creates a similar evolution in moisture content, it does not display the decreasing leakage in summer reported by Persily (Persily, 1982). In contrast to traditional wood frame construction, in passive houses such as this, all joints between wood panels and around envelope details such as windows etc. are sealed with tape. As these joints already are airtight, the swelling of wooden elements can't make them more airtight.

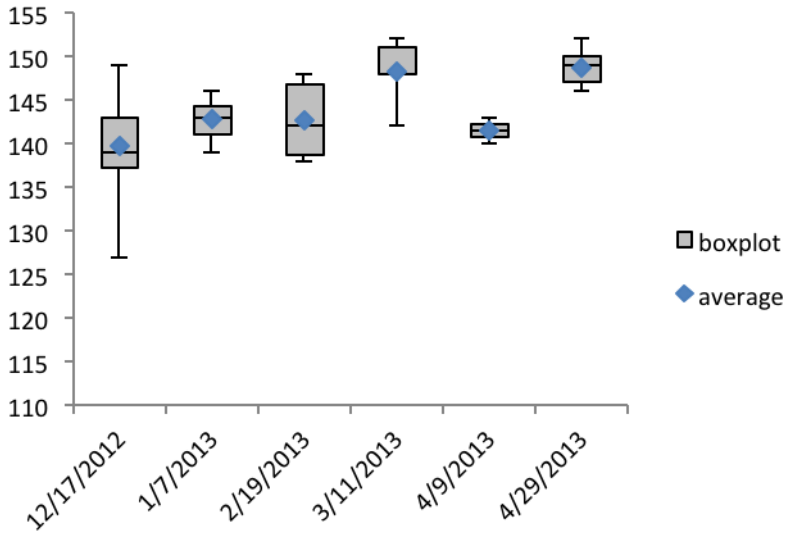

Figure 3. Boxplot and average of the leakage measured on 6 test days between December 2012 and April 2013 in house 2.

4 LEAKAGE DURABILITY

4.1 Literature

Some studies cover groups of buildings, which have been tested and retested after some years to evaluate the durability of airtightness. Due to the variation of building techniques and materials, conclusions are hard to draw. It's essential to make sure no interventions that may affect the airtightness were executed on the buildings between successive pressurization tests.
Lux tested a group of 30 relatively airtight (ACH50 < 3,0 h-1) houses six years after the original tests were carried out (Lux, 1987).
Only five houses were withheld, in which no interventions were performed. The evolution of the air leakage varies greatly, the maximum increase measured was 32% but one of the houses became 9% more airtight.
Proskiw and Eng performed tests on a group of 24 houses over a period of three years (Proskiw and Eng, 1997). The houses were on average five years old at the start of the test. Although the biggest evolution in airtightness is expected the first years after construction, Proskiw and Eng measured a maximum increase in air tightness of 37 % and a 30% decrease over this period. The leakage of a group of houses with a PE airtightness barrier increased by 3 % on average, while a group with a drywall airtightness barrier increased by 7 %.
Reiß and Erhorn compared the air leakage of 52 passive houses after construction and after a two-year period (Reiß and Erhorn, 2003). They reported an average 30% increase, which seems dramatic but corresponds to an increase of the ACH_{50} by 0,09. Increases in leakage rate as high as 216 % were seen, but a few houses also showed a decrease up to 39%.

4.2 Measurement results

Pressurization tests were performed on two estates of similar passive houses in Temse and Bredene, Belgium. The results of these tests were compared to the original test reports, generated from pressurization tests performed on completion of the dwellings one or two years earlier. No specific interventions on the dwellings occurred, making the results representative for normal wear and tear of the construction.
Eight houses were tested in Temse, as reported in Table 3, showing an average increase in air leakage by 29%. Seven tests were performed in Bredene (Table 4.), showing an average increase of 45% in air leakage. A few extreme values are responsible for this high increase. The median of 25% might be a more representative value for the increase in air leakage. Some tests were probably not performed using the same building preparation as the original tests. It's not clear whether all doors were locked during the original tests and the sealing of the ventilation system might not have been executed in exactly the same way as during the original pressurization tests. As discussed in Paragraph 2, these 'small' differences can have a serious relative impact on air leakage. This makes qualifying the individual evolutions in air tightness very difficult. Despite these uncertainties, it seems clear that there is an increase in air leakage over the years, of an order in line with findings reported in literature. Similar leaks around the doors and service penetrations in the roofs were detected in Bredene as in Temse. These leaks seem to be responsible for a good part of the measured increase.

Table 3. measured evolution in leakage rates in Temse

	ACH_{50} (-) 1	ACH_{50} (-) 2	Timespan (months)	$\Delta_{depress.}$ (%)	$\Delta_{press.}$ (%)	$\Delta_{average}$ (%)
house 1	0.43	0.56	19	30	35	32
house 2	0.55	0.81	21	38	55	47
house 3	0.56	0.54	13	2	-9	-3
house 4	0.33	0.43	13	26	34	30
house 5	0.5	0.68	13	33	36	34
house 6	0.59	0.82	19	38	42	40

house 7	0.44	0.56	13	23	27	25
house 8	0.46	0.64	18	30	30	30
mean	0.48	0.63	16	28	31	29
median	0.48	0.60	-	30	35	31
stdev (%)	18	22	-	-	-	-
max var (%)	54	62	-	-	-	-

Table 4. measured evolution in leakage rates in Bredene

	ACH_{50} (-) 1	ACH_{50} (-) 2	timespan (months)	$\Delta_{depress.}$ (%)	$\Delta_{press.}$ (%)	$\Delta_{average}$ (%)
house 1	0.41	0.51	5	43	10	25
house 2	0.58	0.68	3	14	24	19
house 3	0.59	0.69	14	23	10	17
house 4	0.41	0.75	9	115	56	86
house 5	0.5	0.64	15	21	32	27
house 6	0.34	0.75	19	127	114	120
house 7	0.6	0.73	27	21	21	21
mean	0.49	0.68	13	52	38	45
median	0.50	0.69	-	23	24	25
stdev (%)	21	12	-	-	-	-
max var (%)	53	35	-	-	-	-

The super isolating doors might suffer from high temperature differences, which cause the door to warp. These slightly warped doors create leaks at the upper and lower parts of the doors. Reinforced doors might tackle this problem. The leaks surrounding roof penetrations can be avoided by using custom airtight sockets or top hat sleeves. Not that, although considerable relative deteriorations are found, in absolute terms, the buildings remain extremely airtight.

5 WORKMANSHIP REPRODUCIBILITY

Since the dwellings in Bredene and Temse are virtually identical, the results reported above also allow to assess the reproducibility of the leakage level achieved by the used construction method and workmanship. All houses in both case studies have masonry and concrete building envelopes, with PVC window frames and a wood frame roof construction. The air barrier of the building envelope is plaster, while for the roof a poly-ethylene membrane is used.

The results from these measurements are compared to those of a similar case study in Kortrijk in Figure 4 (Laverge et al., 2010). The Kortrijk case study consists of 29 identical houses built according to standard Belgian construction methods, which is very similar to the construction of the passive houses, but without specific attention to air tightness. The variance coefficients go down from 28 % in the Kortrijk case to 12 % in Bredene. Since only passive houses are included in the measurements in Temse and Bredene and this requires a maximum leakage level of 0.6 ACH_{50}, outliers will not appear in these samples. Nevertheless, the progress in reproducibility is remarkable. Note that, although vastly improved, the reproducibility of the workmanship is still far below that of the leakage test itself, the variance coefficient of which is around 0.025 (Delmotte and Laverge, 2011).

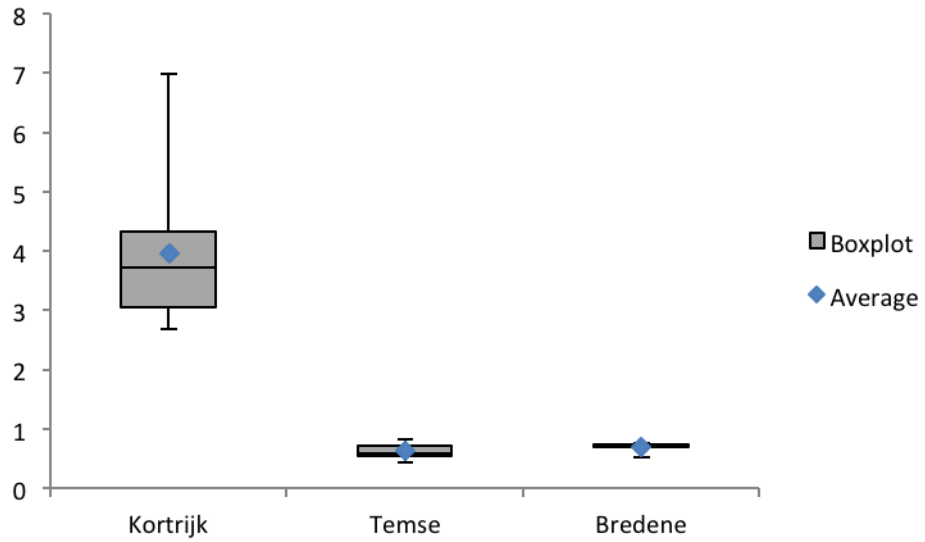

Figure 4. Boxplot of the leakage level (ACH_{50}) for the cases from 4 different case studies of quasi identical houses (N = 29, 8 and 7 respectively)

6 CONCLUSIONS

In this paper, 4 aspects of building leakage in extremely airtight houses are studied: the repeatability and reproducibility of the fan pressurization method, the impact of climate conditions on the measurements, the impact of the age of the construction and the reproducibility of the airtightness level in repeated construction of virtually identical houses. The leakage levels of the houses included in the tests are in the 10^{th} percentile of those included in the official Belgian energy performance database.

The results show similar relative repeatability and reproducibility intervals to those found in literature. The rather large effects of climate conditions reported in previous studies could not be reproduced. Normal wear and tear due to occupation of the dwelling proved to introduce substantial relative deterioration of the airtightness of the building shell (20-100% increase in leakage), although in absolute values, the additional leaks were modest and the buildings remained very airtight. The reproducibility of the workmanship in extremely airtight construction proved better than that found in standard construction.

In general, we conclude that pressurization tests render robust results in extremely tight construction, but with respect to ambitious leakage limits, test conditions and small details such as the locking of window hardware can easily determine whether the dwelling will pass or fail.

7 REFERENCES

2013. Bijkomende specificaties voor de meting van de luchtdichtheid van gebouwen in het kader van de EPB-regelgeving (in Dutch), In: Overheid, V. (ed), Brussels, 16.

Cen. 2001. Thermal performance of buildings - Determination of air permeability of buildings - Fan pressurization method (ISO 9972:1996, modified), CEN.

De Baets K. and Jonckheere T. 2013. Cijferraport energieprestatieregelgeving: Procedures, resultaten en energetische karakteristieken van het Vlaamse gebouwenbestand - periode 2006 - 2012 (in Dutch), Brussel, VEA, 51.

Delmotte C. and Laverge J. 2011. Interlaboratory tests for the determination of repeatability and reproducibility of buildings airtightness measuremetnts, *32nd AIVC conference*

and 1st TightVent Conference: Towards Optimal Airtightness Performance, Brussels, 9.

Dickinson J.B. and Feustel H.E. 1986. Seasonal variations in effective leakage area, *Thermal performance of the exterior envelopes of buildings III*, Atlanta, ASHRAE, 144-160.

Kim A.K. and Shaw C.Y. 1986. Seasonal variation in airtightness of two detached houses., *Measured Air Leakage of Buildings.*, National Research Council Canada (NRC).

Laverge J. et al. 2010. Airtightness assessment of newly build single family houses in Belgium. In: Proceedings of Buildair 2010, pp. 8.

Lux M.E. 1987. time dependent changes in air leakage of low energy houses having sealed vapour retarders, National Research Council Canada, 25.

Murphy W. et al. 1991. A round robin test of Fan Pressurization Devices, Vol. RP-594, ASHRAE.

Persily A. 1982. Repeatability and Accuracy of Pressurization Testing, *ASHRAE/DOE Conference on Thermal Performance of the Exterior Envelope of Buildings*.

Proskiw G. and Eng P. 1997. Variations in Airtightness of Houses Constructed with Polyethylene and ADA Air Barrier Systems Over a Three-Year Period, *Journal of Building Physics*, 20, 278-296.

Reiß J. and Erhorn H. 2003. Messtechnische Validierung des Energiekonzeptes einer großtechnischen umgesetzten Passivhausentwicklung in Stuttgart-Feuerbach, Fraunhofer Institute for Building Physics, 132.

AIRTIGHTNESS OF BUILDINGS - CALCULATION OF COMBINED STANDARD UNCERTAINTY

Christophe Delmotte

Belgian Building Research Institute
Avenue Pierre Holoffe 21 - 1342 Limelette, Belgium
christophe.delmotte@bbri.be

ABSTRACT

The paper presents a calculation method for the combined standard uncertainty associated with the buildings airtightness measurement done in accordance with the ISO standard 9972:2006 (or EN 13829).

The method consists in an application of the law of propagation of uncertainty (JCGM 100:2008) combined with a linear regression (y = a x + b). It goes from the measured values to the air leakage rate and the air change rate.

The ordinary method of least-squares and these of weighted least-squares (with and without negligible uncertainties of the x values) are presented. For each of these methods, the standard uncertainties of the constant a and b of the regression line and their estimated correlation coefficient are given.

The pertinence of the different methods of least-squares for the buildings airtightness measurement is discussed. It seems that the conditions of application of the unweighted method of least-squares are generally not met in the framework of the buildings airtightness measurement; it is therefore advisable to use the weighted method of least-squares.

Real measurement's data show that the combined standard uncertainty of the pressure differences is not always negligible compared with these of the airflow rates. The consideration of these two uncertainties in the calculation of the weights seems therefore necessary even if it requires a resolution by iteration.

KEYWORDS

Airtightness, blower door, uncertainty, least-squares

1 INTRODUCTION

In European countries, increasing importance has been given to airtightness of buildings since the first publication of the directive on the energy performance of buildings in 2002. In some countries there even are requirements or considerable financial incentives linked with the airtightness level. It is therefore more and more important to pay attention to the uncertainty of airtightness measurements.

The issue of uncertainty of airtightness measurements has already been dealt with in various publications (e.g. Sherman, 1994) but is still incompletely solved in practice. This is also a point of discussion in the current revision of the related ISO standard 9972:2006.

This document presents a calculation method for the combined standard uncertainty associated with the buildings airtightness measurement done in accordance with the ISO standard 9972:2006.

This method consists in an application of the law of propagation of uncertainty (JCGM 100:2008) combined with a linear regression. The ordinary method of least-squares and these of weighted least-squares are presented.
The calculation results of the combined standard uncertainty must be considered with circumspection given that various sources of uncertainty are not taken into account in the measurement method (Sherman, 1994) (Walker, 2013).

2 BUILDINGS AIRTIGHTNESS MEASUREMENT

The test is done according to the ISO standard 9972:2006 by measuring the pressure difference across the building envelope over a range of pressures applied by steps of approximately 10 Pa and the corresponding airflow rate. The range of measurement stretches from about 10 to 100 Pa.

The test is done in depressurization on the one hand and in pressurization on the other hand. The air leakage rate is equal to the mean of the air leakage rate for depressurization and these for pressurization.

3 INPUT DATA

3.1 Zero-flow pressure difference

Before and after each test, the zero-flow pressure difference ($\Delta p_{0,1}$ and $\Delta p_{0,2}$) is determined from respectively K and L measurements of the pressure difference while there is no flow through the fan (covered fan).

3.2 Temperature

Before and after each test, the temperature inside the building (T_{int}) and outside (T_e) is measured. These measurements are done punctually (single point measurement).

3.3 Pressure-airflow couples

For each of the N pressure stations, the pressure-airflow couple is determined from J measurements of the pressure difference and the corresponding airflow rate.

The measurement points are noted $\Delta p_{m,i,j}$; $q_{r,i,j}$
The pressure-airflow couples are noted ($\Delta p_{m,i}$; $q_{r,i}$).

The airflow rates are calculated from a pressure difference measurement at the fan and the calibration factors provided by the manufacturer of the fan.

These two pressure measurement are done with two different manometers or two different channels of the same manometer.

3.4 Internal volume

The internal volume of the building (V) is generally calculated on the basis of the building plans.

4 ESTIMATION OF UNCERTAINTY OF MEASUREMENT

4.1 Type A evaluation of standard uncertainty

According to JCGM 100:2008, in most cases, the best available estimate of the expectation μ_q of a quantity q that varies randomly and for which J independent observations q_j have been obtained under the same conditions of measurement, is the **arithmetic mean** of the J observations:

$$q = \frac{1}{J} \sum_{j=1}^{J} q_j \quad (1)$$

The experimental standard deviation of the mean $s\ q$ may be used as a measure of the uncertainty of q :

$$s\ q\ = \sqrt{\frac{1}{J\ J-1} \sum_{j=1}^{J} (q_j - q)^2} \quad (2)$$

This type of evaluation could be applied to the zero-flow pressure difference measurement and to the pressure-airflow couples.

4.2 Type B evaluation of standard uncertainty

According to JCGM 100 :2008, for an estimate of an input quantity q that has not been obtained from repeated observations, the standard uncertainty u(q) is evaluated by scientific judgment based on all of the available information on the possible variability of q.

The pool of information may include:

- previous measurement data;
- experience with or general knowledge of the behaviour and properties of relevant materials and instruments;
- manufacturer's specifications;
- data provided in calibration and other certificates;
- uncertainties assigned to reference data taken from handbooks.

This type of evaluation could be applied to the temperature measurement and the calculation of the internal volume.

When the pressure-airflow couples are determined from a single measurement of the pressure difference and the airflow rate for each pressure station or when each couple is considered as independent, it is advisable to estimate their Type B standard uncertainty.

4.3 Combined standard uncertainty

The standard uncertainty of the result (y) of a measurement, when that result is obtained from the values of a number (N) of other quantities (x_i) through a functional relationship (f), is termed combined standard uncertainty and denoted by u_c. It is the estimated standard deviation associated with the result and is equal to the positive square root of the combined variance obtained from all variance and covariance components, however evaluated, using the law of propagation of uncertainty (JCGM 100 :2008)

For uncorrelated input quantities:

$$u_c^2\ y\ = \sum_{i=1}^{N} \left(\frac{\partial f}{\partial x_i}\right)^2 u^2(x_i) \quad (3)$$

For correlated input quantities:

$$u_c^2\ y\ = \sum_{i=1}^{N} \left(\frac{\partial f}{\partial x_i}\right)^2 u^2(x_i) + 2 \sum_{i=1}^{N-1} \sum_{j=i+1}^{N} \frac{\partial f}{\partial x_i} \frac{\partial f}{\partial x_j}\ u\ x_i\ u\ x_j\ r(x_i, x_j) \quad (4)$$

where $r(x_i, x_j)$ is the estimated correlation coefficient of the quantities x_i and x_j.

In the framework of the buildings airtightness measurement, corrections made to the different quantities differ in case of depressurization and pressurization; it is therefore advisable to develop the combined standard uncertainties for these two modes separately.

Table 1: Development of the combined standard uncertainty for the depressurization test

Function	**Combined standard uncertainty**
$T_{int} = \frac{T_{int,1} + T_{int,2}}{2}$	$u_c\ T_{int}\ = \sqrt{\frac{u^2\ T_{int,1}}{4} + \frac{u^2\ T_{int,2}}{4}}$
$T_e = \frac{T_{e,1} + T_{e,2}}{2}$	$u_c\ T_e\ = \sqrt{\frac{u^2\ T_{e,1}}{4} + \frac{u^2\ T_{e,2}}{4}}$
$\Delta p_i = \Delta p_{m,i} - \frac{\Delta p_{0,1} + \Delta p_{0,2}}{2}$	$u_c\ \Delta p_i\ = \sqrt{u^2\ \Delta p_{m,i}\ + \frac{u^2\ \Delta p_{0,1}}{4} + \frac{u^2\ \Delta p_{0,2}}{4}}$
$q_{m,i} = q_{r,i}\ \frac{\overline{T_{int}}}{T_0}$	$u_c\ q_{m,i}\ = \sqrt{\left(\frac{\overline{T_{int}}}{T_0}\ u\ q_{r,i}\right)^2 + \left(\frac{q_{r,i}}{2\ T_{int}}\ \frac{\overline{T_{int}}}{T_0}\ u_c\ T_{int}\right)^2}$
$q_{env,i} = q_{m,i}\ \frac{T_e}{T_{int}}$	$u_c\ q_{env,i}\ = \sqrt{\left(\frac{T_e}{T_{int}}\ u_c\ q_{m,i}\right)^2 + \left(\frac{q_{m,i}}{T_{int}}\ u_c\ T_e\right)^2 + \left(\frac{q_{m,i}\ T_e}{{T_{int}}^2} u_c\ T_{int}\right)^2}$
$x_i = \ln(\Delta p_i)$	$u_c\ x_i\ = \sqrt{\left(\frac{u_c\ \Delta p_i}{\Delta p_i}\right)^2}$
$y_i = \ln(q_{env,i})$	$u_c\ y_i\ = \sqrt{\left(\frac{u_c\ q_{env,i}}{q_{env,i}}\right)^2}$
Calculation of a and b by linear regression $y = ax + b$	$u_c\ a\ , u_c\ b\ $ and $r\ a, b\ $ depending on the regression method (see hereafter)
$n = a$	$u_c\ n\ = u_c\ a$
$C_{env} = e^b$	$u_c\ C_{env}\ = e^b\ u_c\ b$
$C_L = e^b\ \left(\frac{T_0}{T_e}\right)^{1-a}$	$u_c\ C_L\ = \sqrt{\begin{aligned}&\left(e^b\ \left(\frac{T_0}{T_e}\right)^{1-a} \ln\left(\frac{T_e}{T_0}\right)\ u_c\ a\right)^2 + \left(e^b\ \left(\frac{T_0}{T_e}\right)^{1-a} u_c\ b\right)^2 \\ &+ \left(\frac{e^b\ a-1}{T_e}\ \left(\frac{T_0}{T_e}\right)^{1-a} u_c\ T_e\right)^2 \\ &+2\ e^b\ \left(\frac{T_0}{T_e}\right)^{1-a}\ \ln\left(\frac{T_e}{T_0}\right)\ u_c\ a\ u_c\ b\ r\ a, b\end{aligned}}$

$q_{50,d} = e^b \left(\frac{T_0}{T_e}\right)^{1-a} 50^a$	$u_c\ q_{50,d} = \sqrt{\left(e^b\ 50^a\ \left(\frac{T_0}{T_e}\right)^{1-a} \ln\left(50\frac{T_e}{T_0}\right)\ u_c\ a\right)^2 + \left(e^b\ \left(\frac{T_0}{T_e}\right)^{1-a} 50^a\ u_c\ b\right)^2 + \left(\frac{e^b\ (a-1)}{T_e} 50^a \left(\frac{T_0}{T_e}\right)^{1-a} u_c\ T_e\right)^2 + 2\ e^b \left(\frac{T_0}{T_e}\right)^{1-a} 50^a \ln\left(50\frac{T_e}{T_0}\right)\ u_c\ a\ u_c\ b\ r\ a,b}$

Table 2: Development of the combined standard uncertainty for the pressurization test

Function	**Combined standard uncertainty**
$T_{int} = \frac{T_{int,1} + T_{int,2}}{2}$	$u_c\ T_{int} = \sqrt{\frac{u^2\ T_{int,1}}{4} + \frac{u^2\ T_{int,2}}{4}}$
$T_e = \frac{T_{e,1} + T_{e,2}}{2}$	$u_c\ T_e = \sqrt{\frac{u^2\ T_{e,1}}{4} + \frac{u^2\ T_{e,2}}{4}}$
$\Delta p_i = \Delta p_{m,i} - \frac{\Delta p_{0,1} + \Delta p_{0,2}}{2}$	$u_c\ \Delta p_i = \sqrt{u^2\ \Delta p_{m,i} + \frac{u^2\ \Delta p_{0,1}}{4} + \frac{u^2\ \Delta p_{0,2}}{4}}$
$q_{m,i} = q_{r,i}\ \frac{\overline{T_e}}{T_0}$	$u_c\ q_{m,i} = \sqrt{\left(\frac{\overline{T_e}}{T_0}\ u\ q_{r,i}\right)^2 + \left(\frac{q_{r,i}}{2\ T_e}\ \frac{\overline{T_e}}{T_0}\ u_c\ T_e\right)^2}$
$q_{env,i} \cong q_{m,i}\ \frac{T_{int}}{T_e}$	$u_c\ q_{env,i} = \sqrt{\left(\frac{T_{int}}{T_e}\ u_c\ q_{m,i}\right)^2 + \left(\frac{q_{m,i}}{T_e}\ u_c\ T_{int}\right)^2 + \left(\frac{q_{m,i}\ T_{int}}{{T_e}^2} u_c\ T_e\right)^2}$
$x_i = \ln(\Delta p_i)$	$u_c\ x_i = \sqrt{\left(\frac{u_c\ \Delta p_i}{\Delta p_i}\right)^2}$
$y_i = \ln(q_{env,i})$	$u_c\ y_i = \sqrt{\left(\frac{u_c\ q_{env,i}}{q_{env,i}}\right)^2}$
Calculation of a and b by linear regression $y = ax + b$	$u_c\ a$, $u_c\ b$ and $r\ a,b$ depending on the regression method (see hereafter)
$n = a$	$u_c\ n = u_c\ a$
$C_{env} = e^b$	$u_c\ C_{env} = e^b\ u_c\ b$

$C_L = e^b \left(\frac{T_0}{T_{int}}\right)^{1-a}$	$u_c\ C_L\ = \sqrt{\left(e^b \left(\frac{T_0}{T_{int}}\right)^{1-a} \ln\frac{T_{int}}{T_0}\ u_c\ a\right)^2 + \left(e^b \left(\frac{T_0}{T_{int}}\right)^{1-a} u_c\ b\right)^2 + \left(\frac{e^b\ a-1}{T_{int}} \left(\frac{T_0}{T_{int}}\right)^{1-a} u_c\ T_{int}\right)^2 + 2\ e^b \left(\frac{T_0}{T_{int}}\right)^{1-a} \ln\frac{T_{int}}{T_0}\ u_c\ a\ u_c\ b\ r\ a,b}$
$q_{50,p} = e^b \left(\frac{T_0}{T_{int}}\right)^{1-a} 50^a$	$u_c\ q_{50,p} = \sqrt{\left(e^b\, 50^a \left(\frac{T_0}{T_{int}}\right)^{1-a} \ln 50\frac{T_{int}}{T_0}\ u_c\ a\right)^2 + \left(e^b \left(\frac{T_0}{T_{int}}\right)^{1-a} 50^a\, u_c\ b\right)^2 + \left(\frac{e^b\ a-1}{T_{int}}\, 50^a \left(\frac{T_0}{T_{int}}\right)^{1-a} u_c\ T_{int}\right)^2 + 2\ e^b \left(\frac{T_0}{T_{int}}\right)^{1-a} 50^a \ln 50\frac{T_{int}}{T_0}\ u_c\ a\ u_c\ b\ r\ a,b}$

Table 3: Development of the combined standard uncertainty for the calculation of the air leakage rate and the air change rate

Function	**Combined standard uncertainty**
$q_{50} = \frac{q_{50,d} + q_{50,p}}{2}$	$u_c\ q_{50} = \sqrt{\frac{u_c^2\ q_{50,d}}{4} + \frac{u_c^2\ q_{50,p}}{4}}$
$n_{50} = \frac{q_{50}}{V}$	$u_c\ n_{50} = \sqrt{\left(\frac{1}{V}\ u_c\ q_{50}\right)^2 + \left(\frac{q_{50}}{V^2}\ u\ V\right)^2}$

5 METHOD OF LEAST-SQUARES

In the framework of the buildings airtightness measurement, the relation between the airflow rate and the pressure difference has an exponential form.

$$q_{env} = C_{env}\ \Delta p^n \tag{5}$$

This exponential relation can be transformed into a linear relation as follows:

$$\ln q_{env} = \ln C_{env} + n\ \ln \Delta p \tag{6}$$

The ISO standard 9972:2006 requires the use of a least-squares technique for the calculation of the airflow coefficient C_{env} and the airflow exponent n. However it does not give more guidance.

5.1 Ordinary method of least-squares

The ordinary method of least-squares is applicable when all the y values ($y_i = \ln q_{env,i}$) are equally uncertain ($u_c\ y_1 = u_c\ y_2 = \cdots = u_c\ y$) and the uncertainties on x ($x_i = \ln \Delta p_i$) are negligible.

This method consists of finding the **regression line y = a x + b** that minimalize the sum of the squares of the difference between the measurement points and the line; which comes to minimalizing the following sum:

$$\sum_{i=1}^{N} \left(a\, x_i + b \right) - y_i \right)^2 \tag{7}$$

The constants a and b of this regression line are calculated as follows (Cantrell, 2008) (Taylor, 2000) :

Note: For the sake of simplification x_i *is used for* $\sum_{i=1}^{N} x_i$

$$a = \frac{N \sum x_i y_i - \sum x_i \sum y_i}{N \sum x_i^2 - \left(\sum x_i \right)^2} \tag{8}$$

$$b = \frac{\sum x_i^2 \sum y_i - \sum x_i \sum x_i y_i}{N \sum x_i^2 - \left(\sum x_i \right)^2} \tag{9}$$

The standard uncertainties of the constant a and b are given by :

$$u_c(a) = \sqrt{\frac{N s^2}{N \sum x_i^2 - \left(\sum x_i \right)^2}} \tag{10}$$

$$u_c(b) = \sqrt{\frac{s^2 \sum x_i^2}{N \sum x_i^2 - \left(\sum x_i \right)^2}} \tag{11}$$

where

$$s^2 = u_c^2(y) \tag{12}$$

When $u_c^2(y)$ is unknown, s² can be evaluated based on the scattering of the y_i values around the regression line [12].

$$s^2 = s^2(y) = \frac{\left(y_i - y_{i,est} \right)^2}{N-2} = \frac{\left(y_i - a\, x_i - b \right)^2}{N-2} \tag{13}$$

The estimated correlation coefficient of the constants a and b is given by :

$$r(a,b) = -\frac{\sum x_i}{\sqrt{N \sum x_i^2}} \tag{14}$$

The coefficient of determination (r²), which measures the quality of the adjustment of the measurement points by the method of least-squares, is given by (Cantrell, 2008) (Spiegel, 1996) :

$$r^2 = \frac{\left(N \sum x_i y_i - \sum x_i \sum y_i \right)^2}{\left(N \sum x_i^2 - \left(\sum x_i \right)^2 \right) \left(N \sum y_i^2 - \left(\sum y_i \right)^2 \right)} \tag{15}$$

The combined standard uncertainty associated with any estimate y, obtained through the relation $y = a\, x + b$, can be deduced trough the law of propagation of uncertainty :

$$u_c(y) = s \sqrt{\frac{1}{N} + \frac{\left(x - \bar{x} \right)^2}{\left(x_i - \bar{x} \right)^2}} \tag{16}$$

An interest of this formula is to show that the uncertainty on the estimated values through the regression line increases as one goes away from the mean value of x.

5.2 Weighted method of least-squares

Negligible uncertainties of x

When the uncertainties of the y values are not equal (and the uncertainties of the x values are negligible), it is advisable to use the weighted method of least-squares.

This method consists of finding the **regression line y = a x + b** that minimalize the sum of the squares of the weighted difference between the measurement points and the line; which comes to minimalizing the following sum:

$$\sum_{i=1}^{N} w_i \left(a\, x_i + b - y_i \right)^2 \tag{17}$$

The weight w_i applied to each measurement point i is equal to :

$$w_i = \frac{1}{s^2\ y_i} = \frac{1}{u_c^2\ y_i} \tag{18}$$

The constants a and b of this regression line are calculated as follows (Cantrell, 2008) (Taylor, 2000):

$$a = \frac{w_i \quad w_i x_i y_i - \quad w_i x_i \quad w_i y_i}{w_i \quad w_i x_i^2 - \quad w_i x_i\ ^2} \tag{19}$$

$$b = \frac{w_i\ x_i^2 \quad w_i\ y_i - \quad w_i\ x_i \quad w_i\ x_i\ y_i}{w_i \quad w_i x_i^2 - \quad w_i x_i\ ^2} \tag{20}$$

Their standard uncertainties are given by :

$$u_c\ a\ = \sqrt{\frac{w_i}{w_i \quad w_i x_i^2 - \quad w_i x_i\ ^2}} \tag{21}$$

$$u_c\ b\ = \sqrt{\frac{w_i x_i^2}{w_i \quad w_i x_i^2 - \quad w_i x_i\ ^2}} \tag{22}$$

Their estimated correlation coefficient is given by:

$$r\ a\ , b\ = -\frac{w_i x_i}{\sqrt{w_i \quad w_i x_i^2}} \tag{23}$$

The coefficient of determination (r^2) is given by :

$$r^2 = \frac{w_i \quad w_i\ x_i\ y_i - \quad w_i\ x_i \quad w_i\ y_i\ ^2}{w_i \quad w_i\ x_i^2 - \quad w_i\ x_i\ ^2 \quad w_i \quad w_i\ y_i^2 - \quad w_i\ y_i\ ^2} \tag{24}$$

The weighted method can be useful because the assumption that the uncertainties of all the y values are equal is not necessarily met in practice. It is for example the case when the measured values of the airflow rates have equal uncertainties. Indeed, the linear regression is

applied to the logarithms of the measured values and not to the measured values themselves. In that case the law of propagation of uncertainty shows that:

$$if\ u_c\ q_{env,i}\ = C \qquad (constant)$$

$$y_i = \ln(q_{env,i})$$

$$then\ u_c\ y_i\ = \sqrt{\frac{u_c\ q_{env,i}}{q_{env,i}}^2} = \frac{u_c\ q_{env,i}}{q_{env,i}} = \frac{C}{q_{env,i}}$$

$u_c\ y_i$ is therefore all the greater as $q_{env,i}$ is small. The weight w_i applied to each measurement point should therefore be equal to

$$w_i = \frac{1}{u_c^2\ y_i} = \frac{q_{env,i}^2}{C^2}$$

Which could be simplified as follows and explains the weighting proposed by the CAN standard CGSB-149.10-M86:1986:

$$w_i = q_{env,i}^2$$

Note: The formulae for $u_c(a)$ and $u_c(b)$ presented above do not accept this simplification.

Non-negligible uncertainties of x

When both x and y values have non-negligible uncertainties, the weighting can be adapted as follows (Cantrell, 2008) (Taylor, 2000) :

$$w_i = \frac{1}{u_c^2\ y_i\ + a^2\ u_c^2\ x_i} \qquad (25)$$

This method termed **effective variance** requires however a resolution by iteration given the presence of the constant a in the definition of the weighting.

Note: There are other methods in the literature that take the uncertainties of both x and y into account (Cantrell, 2008).

6 DISCUSSION

It seems that the conditions of application of the unweighted method of least-squares are generally not met in the framework of the buildings airtightness measurement; it is therefore advisable to use the weighted method of least-squares.

Real measurement's data show that the combined standard uncertainty of the pressure differences is not always negligible compared with these of the airflow rates. The consideration of these two uncertainties in the calculation of the weights seems therefore necessary even if it requires a resolution by iteration.

Taking into account the standard uncertainties of the input data of the weighted method of least-squares and not their scattering around the regression line is debatable (as would the opposite choice be). This problem could be limited by considering a large number of measurement points for each pressure station (e.g. at least 10). These points would bring information about other sources of uncertainty.

This application of the law of propagation of uncertainty is based on data's that are considered in the measurement method. However since various sources of uncertainty are not taken into account in the method (Sherman, 1994) (Walker, 2013), the combined standard uncertainty on the air leakage must be considered as a part of the total uncertainty.

7 ACKNOWLEDGEMENTS

This paper is based on a study done at the Belgian Building Research Institute in the framework of the "Etanch'Air" project with the financial support of the Walloon Region. A more extended paper is available from the author.

8 BIBLIOGRAPHY

[1] Bedfer, G. *Analyse d'erreurs et réduction de données*. http://physinfo.univ-tours.fr/Lic_Math/Default.htm (27/11/2012)

[2] CAN CGSB-149.10-M86. 1986. *Determination of the Airtightness of Building Envelopes by the Fan Depressurization* Method. Canadian General Standards Board

[3] Cantrell, C. A., (2008). *Technical Note: Review of methods for linear least-squares fitting of data and application to atmospheric chemistry problems*. Atmos. Chem. Phys., 8, 5477-5487

[4] Delmotte, C., Laverge, J. 2011. *Interlaboratory Test for the Determination of Repeatability and Reproducibility of Buildings Airtightness Measurements*. AIVC Conferences, 32nd, Proceedings. Brussels, Belgium.

[5] Guyader, A (2011). *Régression linéaire*. Université Rennes 2, France

[6] ISO 9972:2006/Amd 1:2009. *Thermal performance of buildings - Determination of air permeability of buildings - Fan pressurization method*. International Organization for Standardization, Switzerland.

[7] JCGM 100:2008. *Evaluation of measurement data — Guide to the expression of uncertainty in measurement*. Joint Committee for Guides in Metrology.

[8] Spiegel, M.R., 1996. *Probabilités et statistique. Cours et problèmes*. Mac Graw Hill, France.

[9] Okuyama, H., Onishi, Y., 2012. *Reconsideration of parameter estimation and reliability evaluation methods for building airtightness measurement using fan pressurization*. Building and Environment, Volume 47, January 2012, Pages 373–384

[10] Persily A K, Grot R A, 1985. *Accuracy in pressurization data analysis*. ASHRAE Transactions, 1985, vol. 91, pt. 2B, Honolulu, HI

[11] Sherman, M.H., Palmiter, L. 1994. *Uncertainty in Fan Pressurization Measurements*. In Airflow Performance of Envelopes, Components and Systems, Philadelphia: American Society for Testing and Materials, LBL-32115.

[12] Taylor, J.R., 2000. *Incertitudes et analyse des erreurs dans les mesures physiques - Avec exercices corrigés*. Dunod, Paris, France.

[13] Walker I.S., Sherman M.H., Joh J., Chan W. R., 2013. *Applying Large Datasets to Developing a Better Understanding of Air Leakage Measurement in Homes*. International Journal of Ventilation, Volume 11 No 4 March 2013.

IMPACT ON IAQ OF BUILDING MATERIAL EMITTED POLLUTANTS THROUGH BUILDING LEAKS : STATE OF THE ART AND SAMPLE TESTING METHODOLOGY

Sarah Juricic[1], Catherine Hung[1], Florent Boithias[1]

1 CETE de Lyon (future CEREMA)
Laboratoire d'Autun
Boulevard Giberstein
71404 AUTUN CEDEX

Sarah.juricic@developpement-durable.gouv.fr

ABSTRACT

French authorities have launched an extensive thermal renovation program aiming at retrofitting 4M dwellings over 10 years, with priority given to the most energy consuming ones. Without specific focus on airtightness, retrofitting does not achieve very low airtightness levels, which means numerous leaks in the envelope. Added to the possibility of fungus development at the junction between ancient and new wall, the possibility of airflow conveying pollutants emitted in walls into indoor air is a major concern for public health. Although this concern might apply to all types of construction, this paper will only deal with retrofitted walls, proposing a state of the art and a methodology dealing with the following issue: what is the impact of leaky retrofitted walls on indoor air pollution?

Literature shows that VOCs are commonly emitted by building construction materials. Still, the proportion of pollutants due to air leakages is scarcely documented. Hayashi et al (2008) discussed however the influence of concealed pollution sources upon IAQ in Japanese houses.

The use of a test chamber will give some valuable answers to the question raised. The chamber's purpose is to pressurize a retrofitted wall sample in order to measure the amount of pollutants released by the induced airflow through purposely made building cracks. Temperature, relative humidity and airflow being controlled, TVOC and particles concentrations will be measured in the first place.

This project will quantify by extrapolation the amount of indoor pollutants due to air leakages. Results will however only partly be generalized, as the continuous pressurization methodology only accounts for mechanical exhaust ventilation.

KEYWORDS

Airtightness, IAQ, VOC measurements, retrofit

1 INTRODUCTION

French authorities have launched an extensive thermal renovation program aiming at retrofitting 4M dwellings over 10 years, with priority given to the most energy consuming ones. Considering indoor air quality (IAQ) as a major health issue, part of the retrofit efforts should deal with it too.

Without specific focus on airtightness, retrofitting does not achieve airtightness levels as low as newly built buildings, which means numerous leaks in the envelope. Added to the possibility of fungus development at the junction between ancient and new wall, retrofitting may become a threat to IAQ if not properly managed.
This paper identifies three impacts of poor airtightness on IAQ and focuses on the leaky retrofitted wall as a possible indoor air pollution source. The paper describes a laboratory and onsite methodology to quantify and qualify this impact. The paper aims thus at dealing with following issues: what is the impact on IAQ of a leaky retrofitted wall? From the IAQ point of view, what is the importance of airtightness treatment in the success of a retrofit operation?

2 LITERATURE AND STATE OF THE ART REVIEW

2.1 Airtightness in retrofit

Retrofitting works on a dwelling aims most of the time at improving the building's envelope to lower the energy consumption. If those works are often accompanied by improvement of the airtightness level (Chan et al, 2012), the levels reached are relatively high in comparison with what can be achieved in newly built buildings.

Table 1: Airtightness in retroditted and newly built single family dwellings, in $m^3/h/m^2$

French building's airtightness Database

	Recently retrofitted single family dwellings (2010, 2011 and 2012) n=28	**Newly built single family dwellings with certification (2010, 2011 and 2012) n=13544**	**Newly built single family dwellings without certification (2010, 2011 and 2012) n=2086**
Mean	1.13	0.42	0.43
25^{th} percentile	0.78	0.31	0.31
75^{th} percentile	2.07	0.53	0.58
95^{th} percentile	3.48	0.70	1.18
Standard deviation	1.19	0.21	0.42

Table 1 shows the mean values, the 25^{th}, 75^{th} and 95^{th} percentile and the standard deviation of airtightness levels of retrofitted and low energy-consumption certified newly built single family dwellings. Whereas most of the newly built dwellings with certification achieve airtightness levels lower than 0.53 $m^3/h/m^2$ (75%), most of the retrofitted dwellings achieve airtightness levels higher then 0.78 $m^3/h/m^2$ (75%). The standard deviation of the retrofitted dwellings shows very variable airtightness levels around the mean value. The particularly low results in the newly built dwellings with certification can partly be explained by the airtightness requirement of 0,6 $m^3/h/m^2$which is inherent to the certification. However, among non certified newly built buildings, the airtightness levels are very similar to certified newly built buildings. This is why we can consider that the differences between retrofitted dwellings and newly built dwellings are still relevant.
From this table can be inferred that low airtightness is not guaranteed after a retrofit. It is very dependent on the existing structure and the retrofit itself, whether it is heavy and how it is done. Retrofitted walls are hence expected to be leakier than newly built walls.
Furthermore, the progress of airflows through building cracks is unknown. It can follow direct paths through the wall or travel between two construction layers by indirect paths. In both cases, airflows progress nearby building construction materials.

Having leaky envelopes may lead to three problems regarding IAQ :
1) transportation of outdoor pollution indoors,
2) release of sealed pollution sources in the wall itself conveyed by airflow progressing through the wall and,
3) disorders of the ventilation due to pressure variations.

1) The transfer of outdoor pollution through building cracks has been documented in the past. Liu and Nazaroff (2003) as well as Olea et al (2007) studied particle penetration through building cracks. Both papers show different penetration factors depending on the size of the building crack and the size of the particles. This paper will therefore not deal further with pollution penetration through leaky walls.

2) Building materials in the wall itself may be a source of pollution of the indoor air as well. Indeed, building construction materials are known to emit pollutants. Jones (1999) listed these pollutants in a review of existing literature on the topic: aliphatic hydrocarbons, aromatic hydrocarbons, halogenated hydrocarbons, aldehydes, ketones, ethers and esters. The author also identified VOCs to be often used in construction.

Furthermore, airflows transferring through the wall as well as vapour may condense in the wall. Not only may it damage insulation materials but it may also result in fungus development, which represents another pollution source in the wall itself. In France particularly, internal insulation is used most of the time and as soon as vapour barriers are not precautiously fitted, this risk exists.

The wall as source of indoor air pollution has of course been known for a long time. The fact that leaky walls contribute all the way more to this pollution has however scarcely been studied.
Hayashi (2008) studied from cut models, prefabricated houses and simulation tools the impact of concealed pollution sources upon indoor air quality in Japanese housing. The principle was to study the impact of known pollutant sources in the crawl, the beam and the truss spaces on the concentration of the same pollutants indoors, with calculation of the infiltration rates from these spaces to the indoor. The author concluded that seeing the concentration measured indoors, one should consider the emissions from the materials in the concealed spaces, that it is important to have low infiltration rates between those spaces and finally that the ventilation systems has to be carefully designed to fit the ventilation purposes properly. However, this paper does not study pollutants emitted by the building materials themselves.

3) The pressure variations indoors caused by poor airtightness may result in disorders of the ventilation system.
Brogat (2003) identified in a guide to retrofitting several ventilation systems unsuitable with poor airtightness. When retrofitting multi-family housing, the guide recommends not using mechanical ventilation (inlet and outlet) and any system using hygrometric controlled inlet air grids.
The impact of airtightness on ventilation is to be dissociated from its proper functioning. As a hypothesis for this paper is understood that disturbances in the ventilation system are only due to pressure variations and that the ventilation system has been properly installed and maintained.

For the purpose of this paper, only the second impact, building materials source of pollution through building cracks, will be dealt with.

3 RETROFITTING: QUANTIFYING THE IMPACT OF POOR AIRTIGHTNESS ON IAQ

Considering that building materials are a pollution source that has an impact on IAQ through envelope leakages, the question is to quantify this impact. If the impact appears to be relevant, it will be all the more important to achieve good airtightness after retrofit. This paper focuses on two methodologies which feasibility is currently being studied.

3.1 Sample testing in laboratory conditions

3.1.1 Principle

The airflow is charged with pollutants by transferring through the building cracks. In buildings, these airflows are naturally induced by wind pressure, temperature or mechanical ventilation. A wall is thus submitted to various natural pressure differences, up to ± 10 Pa.
The idea is to artificially create an airflow through previously designed building cracks on wall samples in order to measure the concentrations of VOCs released by the wall sample.
Laboratory conditions allow fixing temperature and relative humidity, which have an impact on the emission of pollutants of building materials and allow making the pressure difference on the sample vary.

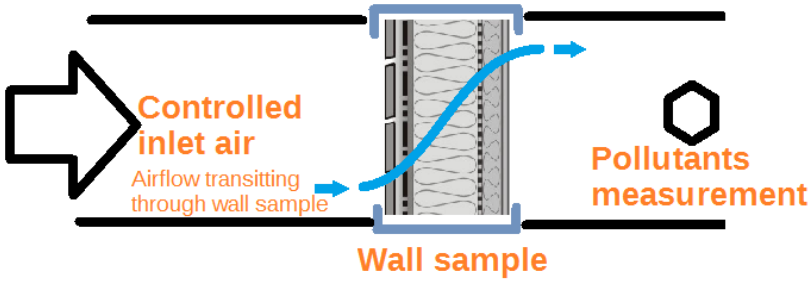

Figure 1 : Principles of the wall sample methodology. This figure does not account for the definitive design of the test chamber.

Figure 1 shows the principles of such a test. Two chambers are applied on a wall sample. The wall sample has been assembled on site specifically to have building cracks designed for the purpose of the test. Two major building cracks can be applied: direct and indirect. One chamber blows controlled air at a regulated pace, to apply various pressure differences. The sample is pressurized and air flows naturally from one side to the other. The other chamber contains pollutants measurement devices.

3.1.2 Testing methodology

The methodology has been built to be as close as possible to the ISO 16000 which describes an indoor air pollution sampling and testing methodology.

- The laboratory's air is characterised to assess the impact of indoor air pollution in the laboratory on the tests. In this case, VOCs measurements are performed before and after any test on a sample.
- The sample is tested with the following procedure. Several depressurization stages are applied to the sample. The 0 Pa measurement stage characterizes the sample emissions without any impact of poor airtightness. The following stages determine the amount and the nature of VOCs released depending on the pressure applied.

- The airtightness of the sample is determined by applying the NF EN 13829. The airtightness value is an essential parameter to understand the results of the VOCs measurements.

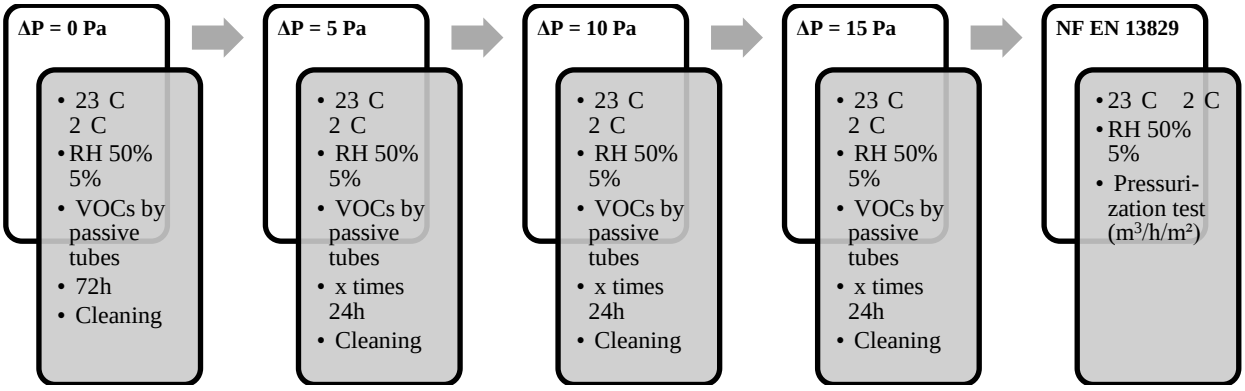

Figure 2: Test steps

3.1.3 Application to retrofit walls

The initial goal of setting up this procedure is to study the impact of retrofitting on IAQ, considering the retrofitted wall as a source of pollution when its airtightness is poor. For the need of the project, the influence of several parameters will be studied: nature of the crack, nature of the existing wall, nature of the retrofit.
The tests will focus on the most standard retrofitted walls among housing that will the most benefit from a retrofit. Indeed, this housing stock will probably be the target of the large governmental retrofit program. As for Burgundy, the housing stock which will benefit the most from retrofit is single-family dwellings, built before 1949 and which structure is stone. It represents almost 20% of the energy consumption in Burgundy and has a high potential of energy consumption savings. Furthermore, the hygro-thermal behaviour of this type of structure is particularly difficult to apprehend, because of scarce literature on the subject. Disorders due to retrofitting are even more to be expected.
The present project shall thus study the impact of retrofit, with different scenarios, of such retrofitted walls on IAQ.

3.2 On site measurements campaigns

To provide better insight on the pollution state in retrofitted dwellings, an onsite measurements campaign was considered.
In order to supplement the sample test methodology, the tests shall be performed in dwellings presenting the same construction type and the same retrofit program than the samples intended to be tested.
The goal of an onsite campaign is to quantify the VOCs pollution and compare the results with those obtained in laboratory conditions.
The campaign should deal with at least 10 dwellings. On each dwelling, three interventions are considered:

- before retrofit to provide a blank state of pollution on the dwelling,
- after retrofit to characterize the impact of the retrofit on indoor air,
- 6 months after retrofit to analyse the decrease in time of the pollutants emission.

These interventions should take place in either the living room or the bedrooms, the one that are the most impacted by the ventilation system in terms of depressurisation.

At each stage, several parameters shall be measured or controlled. Temperature and relative humidity are measured, which influence the emission rates. Ventilation system is controlled to assess the quality of its installation and the impact it could have on pollution removal. Ventilation airflows is measured, also to assess its influence on pollution removal. VOCs concentration when no depressurisation is applied, ventilation is stopped. VOCs concentrations when artificial depressurisation is applied, ventilation system still stopped. Finally, the airtightness level of the room is determined, on the basis of the NF EN 13829, which results are given in $m^3/h/m^2$, and a leakage analysis is performed.

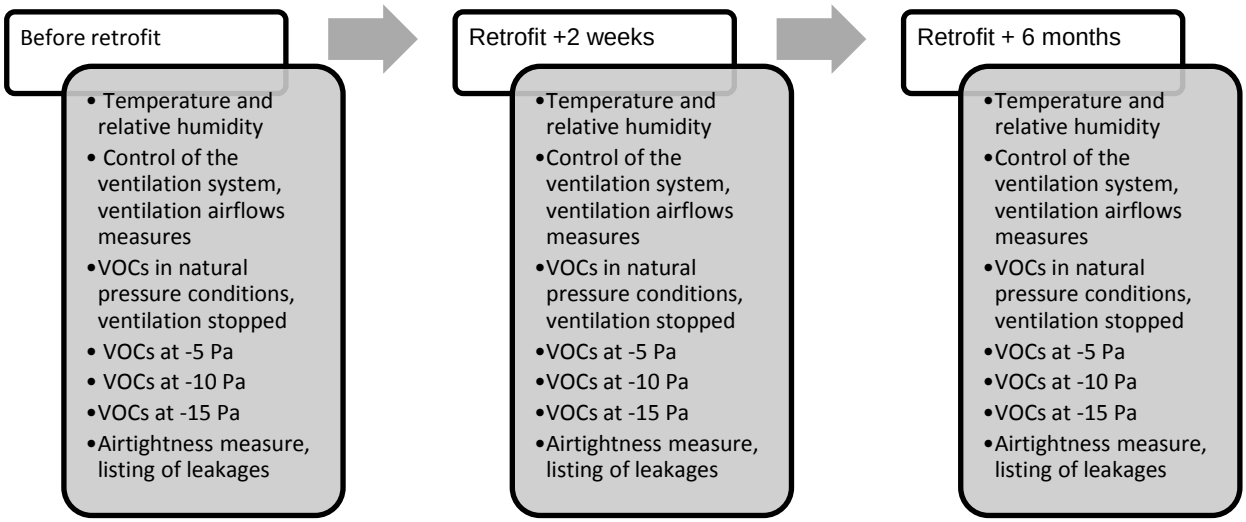

Figure 3: Steps of an onsite campaign

4 DISCUSSION AND PERSPECTIVES

4.1 Accountability of the results

This project should give valuable results on indoor air pollution by leaky retrofitted walls. Depending on the pertinence of the results, it is expected that attention should be brought to the emissions of all building materials. Moreover, an influence of the airtightness level is expected, which could show the need of treating airtightness properly during a retrofit program to avoid poor IAQ.
The results however will only account for retrofitted dwellings with ventilation systems that put the building in depression. Mechanical exhaust ventilation and natural ventilation working with stack effect are the main systems related to the results. Even so, the results are representative of the housing stock, since mechanical exhaust ventilation systems are often installed in France.

4.2 Perspectives

The tests described in this paper are part of a larger project lead by the CETE de Lyon aiming at identifying keys for retrofit strategies. Indeed, if a large set of buildings need to be retrofitted in the frame of the national retrofit program, a general reflection will have to be done on the regulatory frame of retrofitting. If energy consumption is the parameter dealt with in the current retrofit regulation, IAQ has been identified as a national public health issue by French policies and could be integrated as an important parameter if enough studies show its pertinence in a regulatory text.

Considering these challenges, the project aims at assessing the pertinence of the treatment of airtightness in retrofit programs from the IAQ point of view. Taking it further, the question to be answered is the following: from the IAQ point of view, is it relevant to set a regulatory requirement on airtightness and if so, what should it be?

5 CONCLUSIONS

In the frame of a project aiming at assessing the importance of airtightness treatment in retrofit programs, the CETE de Lyon (CEREMA) has developed a laboratory and onsite methodology to quantify and qualify COVs emissions from the building materials of leaky retrofitted walls by applying a depressurisation. The project will focus on the most energy consuming type of buildings.
The project takes place in a context of national retrofit programs and should give valuable keys to the revision of regulatory texts about retrofitting.

6 REFERENCES

Brogat, B., Lanchon, P, FONTAN, J., Millet, J.-R., Skoda-Schmoll, C., Villenave, J.-G., Brêtas, M. (2003). *Ventilation des bâtiments. Réhabilitation dans l'habitat collectif*. Edition CSTB, 88pp.

Kirchner, S., Mandin, C., Derbez, M., Ramalho, O., Ribéron, J., Dassonville, C., Lucas, J.-P., Ouatara, M. (2011). *Qualité de l'air intérieur, qualité de vie. 10 ans de recherche pour mieux respirer*. Observatoire de la qualité de l'air intérieur. OQAI. CSTB Editions.

Liu, D. L. (2002). Air pollutant penetration through airflow leaks into buildings. Dissertation for the degree of Doctor of Philosophy. University of California

Olea, L. L., Limam, K., Colda, I. (2007). Numerical simulations for particle penetration through building cracks. Proceedings of Clima 2007 Wellbeing Indoors.

Jones, A. P. (1999). Indoor air quality and health. Atmospheric Environment 33

ISO 16000-1 Indoor air – Part 1: General aspects of sampling strategy

ISO 16000-9 Indoor air – Part 9: Determination of the emission of volatile organic compounds from building products and furnishing – Emission test chamber method

APPLICATION OF BLOWER DOOR MEASUREMENTS IN THE EVALUATION OF WORKMANSHIP INFLUENCE IN AIRTIGHTNESS

Nuno M. M. Ramos[*1], Vasco P. de Freitas[1], Pedro F. Pereira[1], António Curado[2] and Alexandre Machado[1]

1 Building Physics Laboratory, Faculty of Engineering, University of Porto
Rua Dr. Roberto Frias, 4200 465 Porto
Portugal
**Corresponding author: nmmr@fe.up.pt*

2 Polytechnic Institute of Viana do Castelo - School of Technology and Management
Avenida do Atlântico, s/n, 4900-348 Viana do Castelo
Portugal

ABSTRACT

A large social housing retrofitting program was implemented in Porto, Portugal, a mild climate region. One of the features of that program was the upgrade of windows and ventilation systems. An increased airtightness was expected and mechanical extraction on kitchens and bathrooms was implemented. This work analyses the changes in building airtightness that resulted from that renovation.
A large sample of identical dwellings was analysed using the blower door test. This analysis was performed in a set of dwellings that were identical and also identically renovated. As two different contractors were involved in the renovation of specific sub sets of those dwellings, the opportunity to use the blower door test as an indicator of workmanship quality was created.
The results of this work therefore include not only the airtightness of the renovated buildings but also the variability of ACH_{50} values for each subset of dwellings, allowing for conclusions on the workmanship effect. The analysis of the adequacy of the resulting airtightness is also performed, regarding the specific climate conditions and the typical user behaviour of the dwellings. Finally, the user modifications also proved to be of high importance to the found airtightness.

KEYWORDS

Airtightness; Workmanship; Variability

1 INTRODUCTION

Workmanship quality is frequently referred as a key aspect for building airtightness (Kalamees, 2007), (Sherman, 2004), (Hens, 2011) and (Sinnott and Dyer, 2012). This paper studies that influence and tries to quantify it based on blower door measurements performed in two sets of dwellings, of identical features, renovated by two different contractors. The objective is to define if airtightness measurements allows for the comparison of different teams workmanship and which parameters are relevant for that evaluation. The authors believe that not only the average ACH_{50} is important but also the variability found in identical interventions by the same contractor.
The paper starts with a literature review intended to identify the airtightness variation ranges found in other studies that can be used as reference. The case study and measurement

procedure is presented. The results of the measurement campaign are analysed, supporting the final conclusions.

2 LITERATURE REVIEW

Many experimental studies on building airtightness, using the fan pressurization method, have been carried out in international context. Several of those studies pointed out the relevance of workmanship quality to building airtightness.

According to (Fernández-Agüera et al., 2011), despite the study had been carried out on the same types of building, which share construction processes and external variables, the results of the tests vary greatly. The authors appoint the manual processes used during construction as causes for those variances.

These variances were also detected by (Chan et al., 2005) who analysed near 70000 dwelling and denoted considerable fluctuations in the airtightness of dwelling with, apparently the same characteristics. This studied also denoted that the dwellings with bigger floor areas have smaller normalized leakage. Their explanation for this phenomenon is that larger (more expensive) homes are likely to have tighter envelopes because they are better built.

According to (Johnston and Miles-Shenton, 2009), a study carried out in seven United Kingdom dwelling, three equal dwellings in terms of construction type, built form and internal floor area, have shown airtightness results with a considerable variance. They identified the main air leakage paths as being: gaps around service penetrations through the external walls, floors and ceiling; poorly fitted and draught sealed doors, windows and loft hatch; junction between door/window frame and plasterboard drylining; and gaps between the upper floor and the external walls.

(Kalamees, 2007) studied 32 detached dwellings in Estonia. In this study the author compares the ones that were built under professional supervision and the ones built without professional supervision since it's not rare in Estonia for a house owner to build a detached house on his own, with the help of some friends or a couple of workers without professional supervision. It was found that the airtightness of the dwellings without professional supervision are significantly worse.

In a study carry out by (Pan, 2010), where the airtightness of 287 dwellings were determinate by means of a blower door, the data were collected from three house building companies in the UK. The 3 companies were independent from each other but associated in a national development group where shared some technical and managerial knowledge of the group in relation to energy efficiency design and construction. Through this, they minimise any skewed analysis which might be generated from including test results from other companies which may be associated with drastically different management context. Although the author highlights the ambiguous concept of management context (workmanship), they denoted that the analysis reveals significant difference between the airtightness of dwellings built in the three companies.

Air tightness of 28 buildings in Ireland was studied by (Sinnott and Dyer, 2012). The study grouped the dwellings in the main categories by their construction's year. Some of the oldest ones were partial or total retrofitted although, the most recent ones, newer than 2008, don't have any refurbishment. Furthermore, the newest houses are all equal to each other. The results showed that the airtightness of these houses have considerable differences. The authors made some surveys and used smoke pencil tests, in addition to common leakage paths, identified the critical leakage pathways related to poor workmanship.

The authors of (Pinto et al., 2011) studied the airtightness of 5 similar dwellings near Porto, Portugal. The 5 dwellings were part of the same building and have 2 different typologies at different stories. The results showed that the difference between them were not negligible. The authors appointed the cause as probably being due to the variation of the dimension of the

gaps surrounding the roller shutter boxes and the gaps in the lower opening joint of the external doors that strongly depends on the local installation work.
The airtightness of a dwelling were studied by (Roberts et al., 2005) at seven stages after which a pressure test were undertaken, giving an indication of the relative importance of each step in terms of airtightness. Although the different stages showed the influence of the application of some layers, they also denoted that workmanship in other vital areas that contribute to airtightness may not be as meticulous.
In the report (Sherman, 2004), the authors review over 100 of the most important international publications until 2004. That report cites a study by Shaw and Jones (1979) measured the airtightness of eleven Canadian schools. They conclude that the poor workmanship and sealing were observed to be the cause of high air leakage. The report (Sherman, 2004) conclude that in light of the fact that many of the air leakage problems are caused by poor designs and workmanship, practical guidelines for designers, contractors, and developers have been made available by various agencies. They also conclude that it is not atypical to see log-normal distributions with the standard deviation being equal to the mean. They appointed the large variation as being attributable to variations in workmanship, variations in structure use and maintenance and variations in renovation and repair activities. They finalized saying that many studies have addressed the effectiveness of air barriers and building materials to minimize leakage, but it is often the quality of workmanship and careful design that are the determining factors in achieving desirable air tightness.
According to (Hens, 2011) the results of the ACH_{50} in 14 dwellings of an estate in Belgium, showed a significant variance. According to the author, one of the main reasons for that is the lazy workmanship at the contractor's side.
From the literature review, it's possible to not only conclude on the relevance of workmanship to airtightness but also to initiate a discussion on the typical variance that can be found on measurements performed in comparable situations. The information available on ACH_{50} and q_{50} values results on the coefficient of variation (COV) presented in Table 1. It can be observed that even for identical dwellings, the COV can go up to 30% and up to 60%, on similar houses.

Table 1: Airtightness variance found in international studies

Study	Mean ACH_{50} (h^{-1})	Mean q_{50} ($m^3/h \cdot m^2$)	COV (%)	Observations
(Johnston and Miles-Shenton, 2009)	-	8.45	11.5	3 similar dwellings
(Kalamees, 2007)	3.5	-	68.5	23 houses built under professional supervision
(Kalamees, 2007)	8.4		44.0	9 houses built without professional supervision
(Sinnott and Dyer, 2012)	11.0	-	21.9	7 identical dwellings built in 2008
(Pinto et al., 2011)	6.2	-	32.0	3 identical dwellings
(Hens, 2011)	9.3	-	66.0	14 similar dwellings from the same neighbourhood

3 CASE STUDY AND METHODS

3.1 Studied buildings

A large social housing retrofitting program was implemented in Porto, Portugal. The interventions included the upgrade of windows and ventilation systems. One of the renovated neighborhoods was chosen as case study for this work. The neighbourhood has 4 detached

buildings with similar typologies. The renovation work was performed in 2009 and 2010 by two different companies, based on the same design project for all buildings.

Figure 1: Location and image of the retrofitted buildings.

The neighbourhood has a total of 179 dwellings, including the following typologies: 19 T1 dwellings, 31 T2, 72 T3, 56 T4 and 1 T5.
The dimensions of the types subject to test and the number and total area of windows is presented in Table 2.

Table 2: Dimensions of the Studied Dwellings

Typology	**Volume (m^3)**	**Net floor Area (m^2)**	**Exterior Walls Area (m^2)**	**Windows Area (m^2)**
T1	100	40	44.3	9.4
T3	160	64	36.8	12.1
T4 – A	185	74	57.5	13.4
T4 – B	185	74	46.8	13.4

The tested dwellings geometry is presented in figures 3, 4 and 5.
Natural ventilation was adopted with improvement of the air admission points, and continuous mechanical extraction was applied in the kitchens. The users, however, shut down that extraction during most of the day. A mechanical fan was installed in the bathrooms, to be turned on when the facility is used. In the main compartments self-regulating air vents were installed. The laundry had a fixed air inlet of 1x30 cm^2. Some modifications of the initial settings of the ventilation system were performed by the users, which are outlined in Table 3. If one is to interpret these dwellings as having a purpose provided natural ventilation system, than the ACH_{50} could range between 4 h^{-1} and 8 h^{-1} (Liddament, M., 1996).

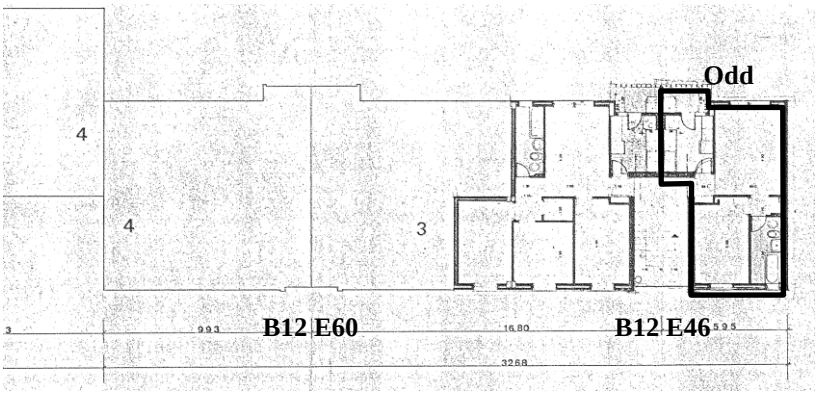

Figure 2: Plan view of building 12.

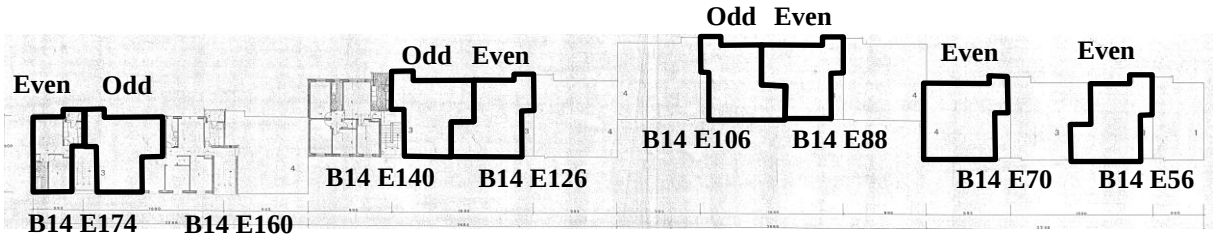

Figure 3: Plan view of building 14.

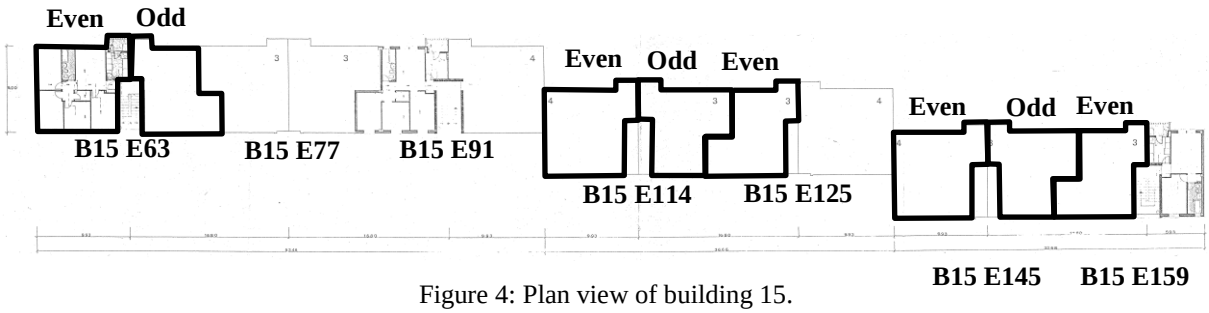

Figure 4: Plan view of building 15.

3.2 Measurement methods

The air permeability measurements were carried out using the Retrotec 1000 blower door model. The standard EN:13829-2001 was applied in the tests, following method A described in the standard. In each dwelling, both pressurization and depressurization tests were performed. The in situ measurements were done in four days of two consecutive days during spring, with average temperature ranging from 13.5 ºC to 21.0 ºC. The wind velocity during tests varied between 1.2 m/s and 2.4 m/s.

4 RESULTS AND DISCUSSION

4.1 Results

The values obtained in the tests of pressurization and depressurization were averaged and are presented in Table 3, Figure 5 and Figure 6. Table 3 also includes the description of modifications performed by the users. The dwellings without modifications are shaded in Figure 5 and Figure 6. Along with ACH_{50} values, the resulting q_{50} is presented. Two values were calculated: (A) including only vertical envelope elements and (B) including also ceiling area for dwellings located on the top floor. The hypothesis (B), although suggested by standards, should not be considered. In this type of construction, with a concrete slab in the

ceiling of the top floor, no leaks should be expected there. By considering it one would erroneously conclude that the envelope of the dwellings B12 / E46 / H11 and B12 / E46 / H41 was quite different and that's not so.

Table 3: Measured Dwellings

Dwelling (Building / Entrance / Door)	Typologies	q_{50} (A) ($m^3/h \cdot m^2$)	q_{50} (B) ($m^3/h \cdot m^2$)	ACH_{50} (h^{-1})	Modifications performed by the building users
B12 / E46 / H11	T1	28.43	28.43	12.65	No modification observed
B12 / E46 / H41	T1	29.01	15.24	12.85	No modification observed
B14 / E56 / H22	T3	19.59	19.59	4.53	Laundry opening sealed
B14 / E56 / H42	T3	19.15	6.98	4.41	Laundry opening sealed
B14 / E70 / H22	T4-B	20.79	20.79	5.34	No modification observed
B14 / E88 / H12	T3	27.84	27.84	6.44	No modification observed
B14 / E88 / H22	T3	26.70	26.70	6.18	No modification observed
B14 / E88 / H32	T3	14.50	14.50	3.35	Self-regulating devices and laundry openings sealed
B14 / E88 / H42	T3	22.85	8.32	5.26	Self-regulating devices sealed
B14 / E106 / H11	T3	31.33	31.33	7.25	No modification observed
B14 / E126 / H12	T3	28.47	28.47	6.58	No modification observed
B14 / E140 / H41	T3	29.66	10.81	6.82	No modification observed
B14 / E174 / H11	T3	35.85	35.85	8.30	No modification observed
B14 / E174 / H22	T1	16.67	16.67	7.38	No modification observed
B14 / E174 / H42	T1	20.45	10.75	9.06	No modification observed
B15 / E63 / H22	T4-A	15.82	15.82	4.92	No modification observed
B15 / E63 / H42	T4-A	16.34	7.14	5.08	No modification observed
B15 / E63 / H41	T3	21.11	7.69	4.86	Self-regulating devices sealed
B15 / E114 / H32	T4-B	31.68	31.68	7.96	No modification observed
B15 / E114 / H41	T3	13.37	4.87	3.08	Self-regulating devices and laundry openings sealed
B15 / E114 / H42	T4-B	16.91	6.55	4.28	Laundry opening sealed
B15 / E125 / H42	T3	44.16	16.11	10.16	No modification observed
B15 / E145 / H21	T3	43.31	43.31	10.02	No modification observed
B15 / E145 / H32	T4-B	28.04	28.04	7.09	No modification observed
B15 / E159 / H12	T3	41.67	41.67	9.64	No modification observed

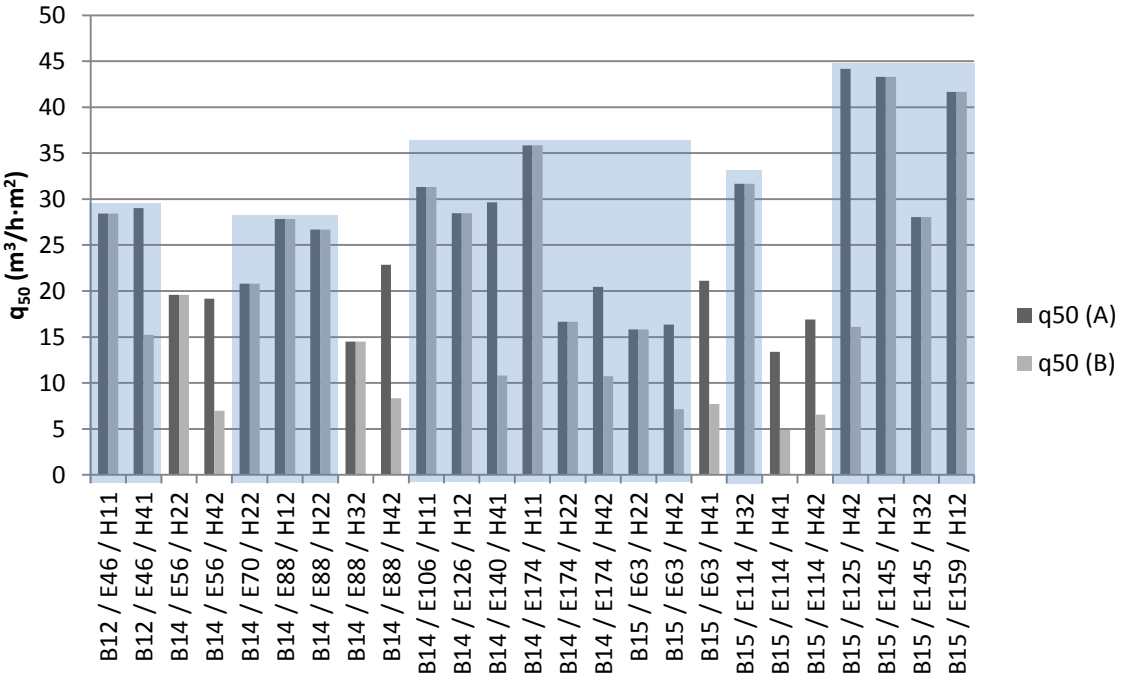

Figure 5: Values of q_{50} (A) and q_{50} (B).

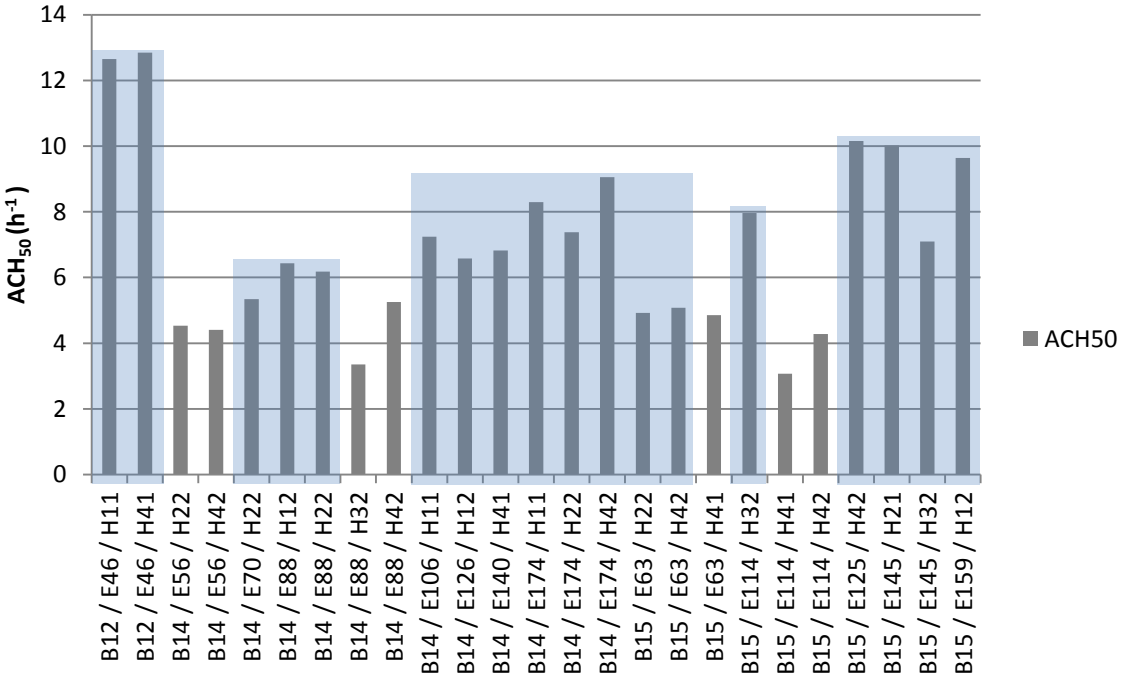

Figure 6: Values of ACH_{50}.

4.2 Discussion

The statistical analysis of the measured data is presented in Table 4, including mean and coefficient of variation (COV) of the measured ACH_{50} and q_{50} (A) values.

Table 4: Statistics of q_{50} (A) and ACH_{50}

Type of dwellings		**Specimens**	**q_{50} (A)**		ACH_{50}	
			mean ($m^3/h \cdot m^2$)	**COV (%)**	**mean** h^{-1}	**COV (%)**
All dwellings		25	25.75	35	6.94	38
All dwellings	T1	4	23.64	26	10.48	26
	T3	15	27.97	35	6.46	36
	T4 (A and B)	6	21.60	31	5.78	25
All dwellings without modifications	T1	4	23.64	26	10.48	26
	T3	9	34.33	21	7.93	21
	T4 (A and B)	5	22.53	31	6.08	22
Modified dwellings	T3	6	18.43	32	4.24	32
All dwellings without modifications by contractor	T1 - B12 (C1)	2	28.72	1	12.75	1
	T1 - B14 (C2)	2	18.56	14	8.22	14
	T3 - B14 (C2)	6	29.98	11	6.93	11
	T3 - B15 (C1)	3	43.05	3	9.94	3
	T4 (A and B) - B14 (C2)	1	20.79	-	5.34	-
	T4 (A and B) - B15 (C1)	4	22.97	35	6.26	24

The statistics presented in Table 4 support the following observations:

- The sample including all 25 measured dwellings presented a mean value of ACH_{50} = 6,9 h^{-1} and COV = 38%, Both values are in line with literature references for this type of buildings (see Table 1);

- Measurements in buildings with no modifications by the users, and separated by contractor, show that the mean ACH_{50} decreases from T1 to T4. That is not so for the q_{50} values;
- Comparing the performance of both contractors, the mean ACH_{50} by dwelling type was always lower for contractor C2, indicating better workmanship. No additional gain was introduced, in this case, with the analysis of q_{50} which could be expected given the type of construction of these buildings, where permeability is more linked to singularities than overall envelope behaviour;
- The variability of ACH_{50} dropped to a COV = 11% when considering the best contractor and the 6 T3 dwellings, the combination with the largest number of specimens;
- The modified T3 dwellings presented a mean ACH_{50} of 4.2 h^{-1}, indicating that the users tried to reduce infiltrations to its lowest value. This can be easily explained by the fact that they try to use heating the least as possible due to their low income. This value is still in the range suggested for this type of dwellings (see section 3.1) but very near its lower boundary, indicating that in some cases the ventilation rates may not be sufficient.

5 CONCLUSIONS

The main conclusions of this work are the following:

- Literature often defines workmanship as being responsible for insufficient building airtightness;
- The work by two different contractors was compared based on blower door tests, allowing to find differences of up to 50% increased ACH50 mean values in identical typologies. Based on that it's possible to say that contractor C2 was better than C1.
- A COV = 11 % was found for a sample of 6 identical dwellings retrofitted by the best contractor. A high COV could also be an indicator of poor workmanship, but in this case there was not enough data to support that.
- User action can have an important effect on building airtightness. In this case of social housing where heating is reduced to an absolute minimum, the users acted on air inlets in several apartments, reducing ACH50 mean values to almost 50% of the initial values. This action is not necessarily good as it may result in poor ventilation.

6 REFERENCES

CEN, Thermal performance of buildings - Determination of air permeability of buildings - Fan pressurization method (EN 13829-2001),

CHAN, W, R,, NAZAROFF, W, W,, PRICE, P, N,, SOHN, M, D, & GADGIL, A, J, 2005, Analyzing a database of residential air leakage in the United States, *Atmospheric Environment,* 39**,** 3445-3455,

FERNÁNDEZ-AGÜERA, J,, SENDRA, J, J, & DOMÍNGUEZ, S, Protocols for measuring the airtightness of multi-dwelling units in Southern Europe, 2011 Bologna, 98-105,

HENS, H, 2011, Dwelling air-tightness in a 55 years old estate, *9th Nordic Symposium on Building Physics - NSB 2011,* 1 of 3**,** 47 to 54,

JOHNSTON, D, & MILES-SHENTON, D, Airtightness of UK dwellings, 2009 Nottingham, 271-280,

KALAMEES, T, 2007, Air tightness and air leakages of new lightweight single-family detached houses in Estonia, *Building and Environment,* 42**,** 2369-2377,

LIDDAMENT M., 1996, A Guide to Energy Efficient Ventilation, AIVC, 254,

PAN, W, 2010, Relationships between air-tightness and its influencing factors of post-2006 new-build dwellings in the UK, *Building and Environment,* 45**,** 2387-2399,

PINTO, M,, VIEGAS, J, & DE FREITAS, V, P, 2011, Air permeability measurements of dwellings and building components in Portugal, *Building and Environment,* 46**,** 2480-2489,
ROBERTS, D,, JOHNSTON, D, & ISLE, J, A, 2005, A novel approach to achieving airtightness in drylined load-bearing masonry dwellings, *Building Services Engineering Research and Technology,* 26**,** 63-69,
SHERMAN, M, C,, C, 2004, Building Airtightness: Research and Practice, *In:* LABORATORY, L, B, N, (ed,) *REPORT N,º LBNL-53356,*
SINNOTT, D, & DYER, M, 2012, Air-tightness field data for dwellings in Ireland, *Building and Environment,* 51**,** 269-275,

CONTROL OF AIRTIGHTNESS QUALITY MANAGEMENT SCHEME IN FRANCE: RESULTS, LESSONS AND FUTURE DEVELOPMENTS

Sandrine Charrier[*1], Alexis Huet[*2], Joris Biaunier[1]

1 Centre d'Etudes Techniques de l'Equipement de Lyon
46 rue Saint Théobald. F – 38081 L'ISLE D'ABEAU Cedex, France

2 Centre d'Etudes Techniques de l'Equipement de Lyon
Boulevard Bernard Giberstein 71400 AUTUN Cedex, France

**Corresponding author:*
sandrine2.charrier@developpement-durable.gouv.fr

ABSTRACT

Since January 1st 2013, the French energy performance (EP) regulation requires building airtightness level to be justified to a lower-than-required value. These requirements represent an important change in the airtightness market. As a consequence, it is the State's responsibility to accompany this market evolution and to supervise the implementation of the quality in building airtightness. French regulation allows two ways to justify the airtightness value for the building envelope. Either the constructor performs systematic measurement on each building, or the constructor proves that a certified quality management approach is implemented.

The French State has created a specific national committee in order to evaluate the airtightness quality management schemes. The aim is to authorize constructors to justify the airtightness level of their buildings through a quality management approach. The CETE de Lyon is in charge of this committee.

In this framework, each constructor that has been certified by the committee must provide a yearly specific file. With this file, the constructor must prove the actual and yearlong application of its approach. Moreover, the committee implemented a first control campaign. It started in 2011 and ended at the end of 2012. This campaign had two goals. First, it aimed at checking the effective implementation of the quality management approach, on some buildings selected by the committee. Then, the committee wished to check the actual airtightness value of some buildings selected by the committee.

This paper will present a synthesis of the results and the lessons learnt from this control campaign. The first part will be dedicated to the analysis of the airtightness test results and to the difficulties encountered by civil servants while carrying out the control test. The second part will be dedicated to the analysis of the reality of airtightness quality management approach implementation.

The main results are 1) 75% of constructors comply with the required airtightness values, 2) but rarely, constructors fully comply with the quality management approach, 3) and constructors positively welcome the State control campaign.

The paper concludes with a synthesis of this campaign presented by a double label. The double label presents constructors results regarding levels measured and the analysis of their quality approach implementation. Finally, the paper ends with improvement proposals for the next control campaign. The State will continue to control certified constructors in two ways. Yearly file analysis will focus more on the reality of airtightness quality approach implementation. The control campaign will be maintained and will focus only on some certified constructors.

KEYWORDS

1 INTRODUCTION

Since January 1st 2013, the 2012 version of the French energy performance (EP) regulation (RT 2012) requires building airtightness level to be justified to a lower-than-required value. French regulation allows two ways to justify the airtightness value for the building envelope. Either the constructor performs systematic measurement on each building, or the constructor proves its certified quality management (QM) approach is implemented. The advantage of the QM approach is that it enables constructors to carry out measures on a restricted sample. Since 2006, the French State has implemented a committee (named the Annex VII committee) in charge of examining these approaches and proposing the certification. The certification allows constructors to justify the airtightness value of their buildings through a QM approach. The CETE de Lyon is in charge of this committee.

In the 2005 version of the French EP regulation (RT 2005), QM scheme was a constructors' voluntary approach. Since 2006, the French State has regularly certified RT2005 quality management approaches. The certification allows constructors to justify a better-than-default-value in their regular thermic calculation. Thus, constructors could use a 0.8 $m^3/h/m^2$ ($Q_{4PaSurf}$) airtightness value for their buildings envelope, instead of the 1.3 $m^3/h/m^2$ default value (for single dwellings).
In order to control the certified QM approaches, the French State planned two ways to control their real implementation. The first one is the submission by each certified constructor, of a yearly renewal file. This file is examined by the national committee presented above. The second way is a control campaign. This control campaign was carried out in its first version in 2011 and 2012. Leprince, (Leprince, 2011) describes key elements of a QM process and the control campaign process. Juricic (Juricic, 2012) presents partial results of the first year of the control campaign. The control campaign ended on December 2012.

This paper aims at presenting the control campaign process, its results and the conclusions of the whole campaign. It must be noted that RT 2005 certified approaches mainly concern single dwellings. The control campaign was therefore led on single dwellings exclusively.

This paper is organized as follows. Section 2 presents the control campaign on certified airtightness quality management approaches. Section 3 deals with quantitative results, that is to say values obtained by measures. Section 4 presents qualitative results, that is to say results of files analysis. Section 5 presents a global synthesis. Section 6 concludes with the evolutions for the next control campaign.

2 DESCRIPTION OF THE CONTROL CAMPAIGN ON AIRTIGHTNESS QUALITY MANAGEMENT PROCESS

This section presents the control campaign that was carried out.

2.1 QM approach and control principle

The underlying basis of an airtightness quality process is to implement a scheme that lasts from the genesis of the building project to the building commissioning. The QM approach is based on a precise description of "who-does-what-when-and-how". In addition, each step must be traceable and traced. The expected steps for such a process are:

- contracts between constructor and craftsmen, mentioning their involvement and fulfilment of the QM approach
- implementation of technical detailed drawings that will help craftsmen in the implementation
- craftsmen's training to the QM approach and to technical detailed drawings
- site supervision by a foreman, who must check in particular whether or not technical detailed drawings are properly applied on the construction site
- supervision documents of actions done in case of non-compliance
- detailed list of buildings applying the QM approach (address, type of construction, date of commissioning, measured value if a measure was carried out, etc.)

To justify its QM approach efficacy, a constructor must prove that airtightness measured values are lower than its QM approach airtightness limit value, on a sample of its production. With the RT 2005, these measurements were not necessarily done by an independent party (note that this part evolved with the RT2012).

The first control campaign, described in Leprince (Leprince, 2011), aimed at answering the following questions: are quality management certified approaches really implemented and fulfilled by constructors after receiving their certification? Indeed, before the implementation of the control campaign, the only official validation was based on file analysis, for initial requests or yearly certification renewal. With files inspection having a limited impact on constructors, the need for a control campaign became clear for the French State. The goal was for quality management approach certifications to be reliable and trusted.

The first control campaign was divided into two types of control:

- A quantitative control that consisted in measuring a part of the certified constructors' production. For that campaign, 5% of the yearly production of each constructor has been tested.
- A qualitative control that consisted in requiring all the documents produced in the frame of the quality approach for randomly selected buildings. For that campaign, 2% of the yearly production of each constructor has been tested.

For that first control campaign, 12 constructors have been controlled. This number corresponds to the number of certified constructors that had their certification since more than one year, at the date of the control campaign beginning (March 2011). The campaign represents 81 measures and 32 buildings qualitatively controlled. Figure 1 synthesizes numbers of qualitative and quantitative controls carried out for each constructor.

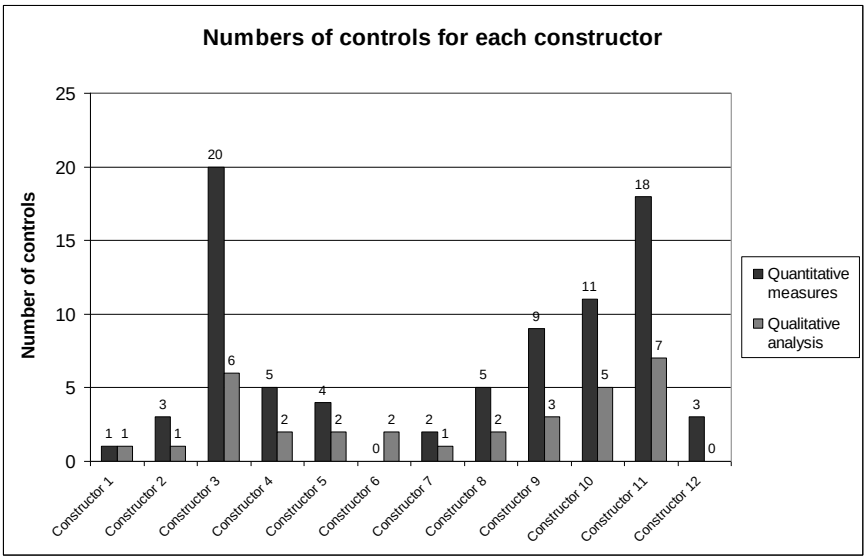

Figure 1: Numbers of qualitative and quantitative controls for each constructor

2.2 Quantitative control process

The quantitative control consisted in measuring a sample of the certified constructors' production. This control was carried out by independent state employees.

As described by Leprince (Leprince, 2011), to carry out the control campaign, the list of all constructions, which delivery is expected in the coming year, has been requested from the certified constructor. The list mentioned each construction's address, the approximate commissioning date and the name and telephone number of the future inhabitant as well as the foreman. A Microsoft Excel Solver determined how many measures had to be carried out for each constructor, in each geographical zone and by which controller (attached to a geographical zone). The same applied to the number of qualitative controls.

Requirements for that quantitative control were the same as the ones used for the yearly files control in RT 2005. For each constructor, 85% of measured values had to be below the reference value (0.8 $m^3/h/m^2$) and 100% below the default value (1,3 $m^3/h/m^2$).

2.3 Qualitative control process

The qualitative control consisted in checking the actual implementation of the certified QM approaches. In that goal, some tracing documents were requested for a set number of buildings.

The qualitative control analysed whether the documents were given or not. If files were not given, this allowed the controller to suppose that the certified QM approach was not implemented in its entirety. The five requested documents were the followings:

- List of the companies working on the site
- Contracts or subcontracts signed by all companies working on the site (that should include an airtightness statement)
- Craftsmen's certificate of training
- Site supervision documents (that must prove the fulfilment for each step of the certified QM approach)

- Tracing documents of the actions in case of non-compliance (corrective treatments, compliance of corrective treatments, results of corrections, etc.).

Each controlled building was selected by state controllers.

3 RESULTS ON QUANTITATIVE CONTROL

This section presents the results of the measures carried out on a sample of certified constructors' production. Organisational results and measured results are presented.

3.1 Not a such unexpected control

One of the goals of the quantitative controls led by neutral controllers was to verify actual airtightness value on buildings. Indeed, in RT 2005, measures were not necessarily neutral. As a consequence the random selection of tested buildings by constructors was not guaranteed. The quantitative control by independent controllers enabled one to guarantee measures and certified QM approaches reliability. In that framework, controlled buildings had to be selected by the controller.

Results of the quantitative control are the following. For 66% of constructors, the choice of the buildings was either made by the constructor, or by the controller. But in both cases, the appointment date was known soon enough (from 1 to 3 weeks before) so that constructors could organize the improvement of the tested building airtightness. This was noticed by controllers during the quantitative control, who regularly (25% of the tested buildings) encountered fresh silicon joint or polyurethane foam in inappropriate places.

Thus, this behaviour slightly modifies two aspects of the QM process. First, that behaviour reveals a more curative approach than a global approach of airtightness that must last during the whole building implementation period. Then, this puts into perspective the measured results, as they were obtained on cured buildings. Results cannot be relevant of the airtightness average value of constructors' production.
However, we should note that 4 constructors (25% of controlled ones) left the entire choice of the tested buildings to the controller. Furthermore, 2 constructors partly influenced the choice (half of tested buildings decided by controller and the other half by the constructor itself).

One of the firsts lessons of that quantitative control is that the actual unexpected in situ control is difficult to implement. A second lesson is that QM process underlined philosophy is not yet assimilated by all constructors. That philosophy lies on considering airtightness as a global issue that must be taken into account from the genesis of a project to the building commissioning. The complementary philosophy is the dissemination of good practices.

3.2 75% of constructors comply with requirements

81 measures have been carried out on 11 certified constructors' production. No measures have been carried out for one of the constructors. Figure 2 presents global results, all controlled constructors together.

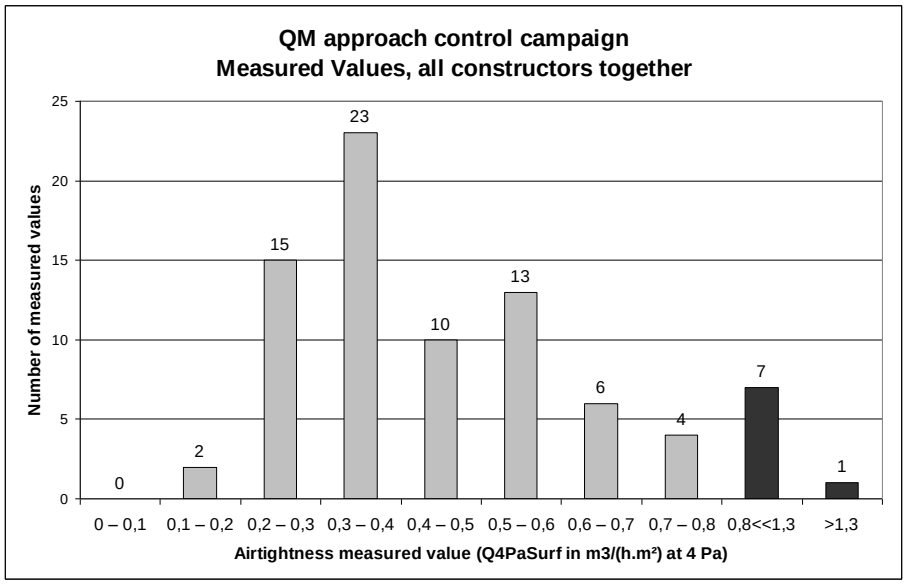

Figure 2: Measured values on 11 certified constructors

72% of measured values are between 0.2 and 0.6 $m^3/h/m^2$. These values are good results as they are far from the limit value (0.8 $m^3/h/m^2$). This tendency gives a comfortable margin in regards to the limit value. 90% of measured values are under the limit value and 10% are over.

This chart tab has been done for each constructor in order to control if their results comply with regulation.
9 constructors comply with regulation and they do not exceed the limit value, excepted for one constructor, for which 5 % (1/20) of its controlled production is between reference (0.8 $m^3/(h.m^2)$ at 4Pa) and default value (1.3 $m^3/(h.m^2)$), what remains in accordance with regulation.
2 constructors do not comply with the regulation. The first one presents only 78% (14/18) of measured values below reference value. The second one presents 78% (8/9) of measured values below reference value and 11% (1/9) above default value.

3.3 Synthesis of quantitative results: quantitative results label

In order to synthesize the control campaign results, the choice has been made to represent that synthesis into a double label. One part represents quantitative control results and the other part the qualitative control results.

For the quantitative label, a distinction has been made between different levels of conformity. Indeed, as the quantitative control was based on the constructors' production, some of them have been more controlled than others, speaking in absolute numbers (from 1 to 20 tested dwellings). Therefore, it is natural that good results on "large" constructors are statistically more reliable than results on "small" constructors, who have been concerned by fewer measures.

Thus the quantitative results label is divided into 5 levels presented below:

- Conformity, a lot of measures: All buildings comply with regulation and more than 10 buildings have been tested.

- Conformity, few measures: All buildings comply with regulation but fewer than 5 buildings have been tested.
- Conformity, word of warning: All buildings comply with regulation but measured values are close to the limit value.
- Non conformity: The measured values do not comply with the regulation that imposes 85% under referent value (0.8 $m^3/(h.m^2)$) and 100 % below default value (1.3 $m^3/(h.m^2)$).
- No data available.

The synthesis of the quantitative control results is displayed in the quantitative results label below (Figure 3).

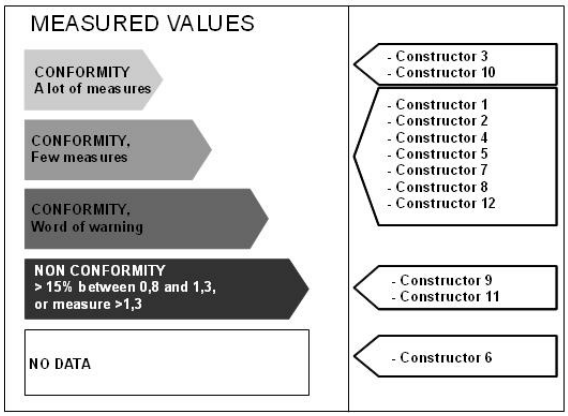

Figure 3: Label presenting quantitative control results

4 RESULTS ON QUALITATIVE CAMPAIGN

This section presents the qualitative control results. As in previous section, two points of view synthesize the results. One evaluation focuses on constructors' behaviour and control campaign welcome. The other evaluation focuses on factual results of the qualitative file analysis.

4.1 A welcomed procedure

Concerning the constructors' welcome of the control campaign, it must be noted that half of constructors did welcome the control campaign. Indeed, most of them were pioneers of airtightness QM approaches and developed that approach in order to enhance the quality in construction. Therefore, they welcomed the control campaign in order to prove their certified approaches reliability.

4.2 A different importance for each inspected file

As presented in section 2.2, 5 files were requested so that the QM approach actual implementation is verified on some randomly selected buildings. For that first control campaign, the qualitative control was only based on verifying whether each file had been given or not. The content of each file has not been evaluated.

In order to analyze and compare constructors' results, the five files have not been considered with the same degree of importance. Thus, site supervision documents and actions in case of non-compliance documents were considered of major importance, whereas craftsmen's training certificates were considered of minor importance. Nevertheless, this does not mean

that craftsmen's training is not important. It only means that, if that document was missing for a constructor and if the site supervision document was missing for another, we considered that the QM approach was less reliable for the second case than for the first one.

4.3 Results on the qualitative control

32 buildings have been qualitatively controlled, on 11 constructors' production. One constructor has not been evaluated. Figure 4 presents global results, all controlled constructors together. For each expected file, it presents whether the file has been given, has not been given or has been partially given, that is to say documents have been given but not for all craftsmen.

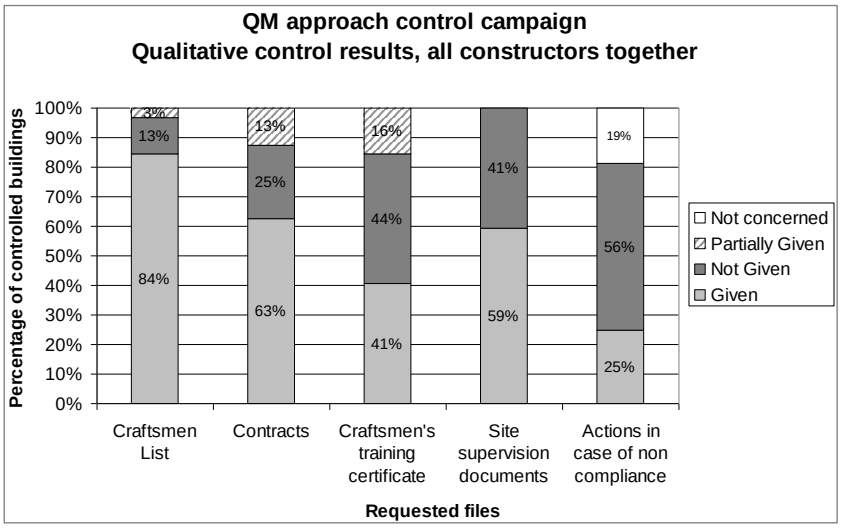

Figure 4: Results of the qualitative controls

Figure 4 shows that the list of craftsmen working on the construction site was very often given, as well as craftsmen's contracts. Then, we can note that 44% of craftsmen's training certificate has not been given. This can reveal some laxity in the constructor involvement to disseminate good practices. This is already noted as a global tendency in RT 2012 QM approaches and is revealing of the constructors' approach, who seems to consider that good practices dissemination is not helpful in obtaining airtightness values that comply with regulation.

Figure 4 also shows that 41% of site supervision documents were missing. This fact is particularly problematic. Indeed, as they are the documents that will enable the constructor to detect any non-compliance with its certified approach, these site supervision documents are one of the quality management process keystones. For instance, these documents trace the construction implementation and its compliance with technical detailed drawings. Their absence can directly lead to a non-compliant airtightness measured value.
Furthermore, 56% of the documents that should trace the implemented actions in case of a non-compliant point with the certified QM approach were not given. This represents 18 buildings (for 32 tested buildings). Among these 18 buildings, 10 buildings concerned only two constructors. Finally, 6 constructors failed in giving the file tracing the action in case of non-compliance. As the previous point, this file is essential for the QM process. Indeed, this document enables the constructor to ensure that every gap with the QM approach will be treated.

4.4 Synthesis on qualitative control: qualitative results label

As explained in section 3.3, the synthesis of the qualitative control is represented in a qualitative results label. The qualitative label is divided into 5 levels representing the fulfillment of the QM approach. These 5 levels take into consideration (1) the above results on files supplying, (2) the importance accorded to each file and described in section 4.2, (3) and the controllers' feeling on each constructor, about the collaboration and cooperation they showed.

Thus the qualitative results label is divided into 5 levels presented below:

- QM approach entirely fulfilled: all the required files have been given and comply with QM approach. The constructor expressed positive collaboration and cooperation.
- QM approach fulfilled some files missing: the majority of requested files have been given, particularly supervision files. The craftsmen's training certificates are missing. The given files comply with the QM approach. The constructor expressed positive collaboration and cooperation.
- QM approach fulfilled, but half of the documents are missing: files given comply with the QM approach. A more active collaboration was expected for that control campaign.
- Key files are missing: Site supervising and actions in case of non-compliance documents are missing. A more active collaboration was expected for that control campaign.
- No data: the committee did not receive the controller's analysis (internal issue).

The synthesis of the qualitative control is illustrated in the below qualitative results label (Figure 5).

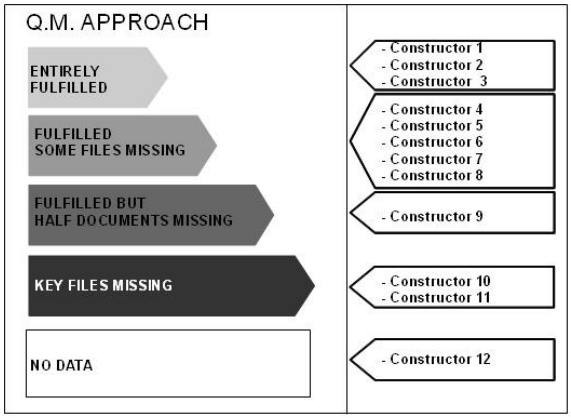

Figure 5: Label presenting the qualitative control results

We note that 25 % of controlled constructors seem to actually comply with their certified QM approach. 75% seems to apply in quasi-entirety their QM approach. 3 constructors seem to have real difficulty in applying QM approach.

5 GLOBAL SYNTHESIS: CONTROL RESULTS DOUBLE LABEL

The synthesis of the control campaign is represented by a double label, composed by both quantitative and qualitative results. The final label is presented in Figure 6.

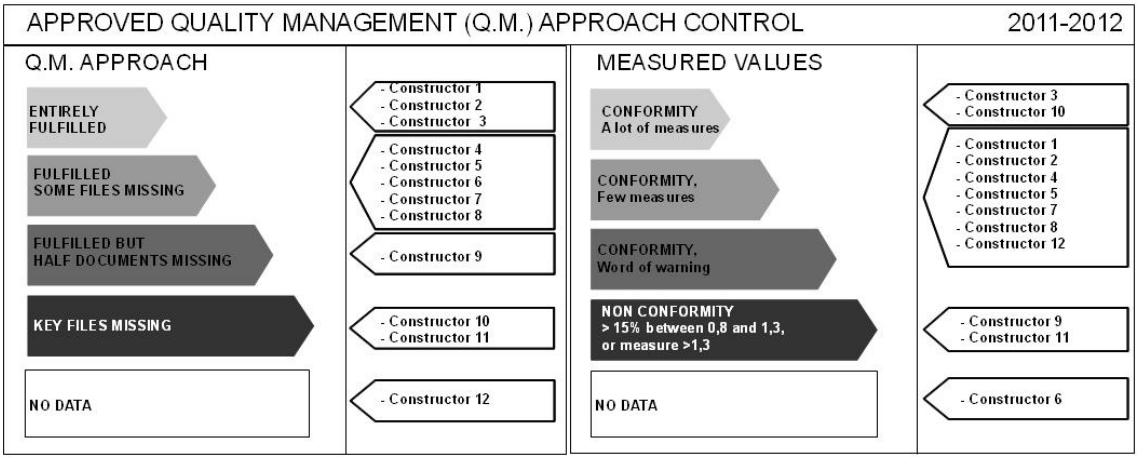

Figure 6: Control results double label

With this double label, we can note that 2 constructors came across difficulty in fulfilling the QM approach (constructors 9 and 11) and this was confirmed by measured values.
We can notice, comparing this double label with Figure 1, that the 3 constructors who have the worst results are at the same time among those who were the most controlled. However, we can also notice that constructor 3 was one of the two most controlled constructors, and its results are good. These tendencies allow us to assert that for the next control campaign, it might be fairer to define an equal controlled buildings volume for every controlled constructor.

This kind of double label has been implemented for each controlled constructor. Each constructor received a synthesis of that first control campaign, mentioning (1) its personal double label and the global label mixing all controlled constructors, (2) personal positive and negative points revealed by the control campaign and (3) the ways to improve the implementation and the measured results of their QM.

6 CONCLUSION

The control campaign has been launched in order to affirm certified QM approach reliability. As a first control campaign, the objectives were educational with a view of accompanying constructors in the application of their certified QM approach. The main conclusions of that first control campaign are that 2 constructors (on 12 controlled constructors) have difficulty in fulfilling the QM approach. The results for the other constructors are encouraging. Other main lessons learnt from that first campaign are the followings:

- We noticed a deviance in QM approach by constructors. For half of them, they seem to have a more curative approach than a global one.
- Results must be used cautiously, as some constructors have been more controlled (absolute number of controls) than others.

Thus, some improvements were put forward by controllers, for the next control campaign:

- Try to implement an actual non-expected quantitative control, if possible
- The volume of controls should be the same for each controlled constructor.
- Control only of a sample of constructors. Controlled constructors would be chosen by committee, regarding their initial file, yearly renewal file and the potential complaints.

As described in Charrier (Charrier, 2013), QM processes have become of growing interest with the RT 2012, since 2012. This growing interest and the positive results of the first QM

approach control campaign require a reliable management of the committee and of certifications. In that purpose, control campaign on certified quality management approaches is maintained and a second one will be carried out, in 2013 and 2014. The second version of the control campaign should take into consideration all the above points related by controllers (or part of). Then, the principle of qualitative and quantitative controls should be maintained. However, in situ control is a key element for certified QM approach reliability. Thus, qualitative control could be replaced by an in situ audit. This could be divided into two sequences: first, a quality management approach audit based on ISO 19001 procedures, and then, a construction site visits with craftsmen and superintendents meetings.

Then, we must bear in mind that:
- One quality management approach is certified for collective dwellings, and the QM approach committee expects more requests for such buildings in 2014.
- Ventilation ducts airtightness quality management approaches are expected, as the RT 2012 enables them.

As a consequence, it seems essential to affirm the certified quality management approach reliability. This can essentially be made thanks to the control campaign and, if possible, with more in situ controls so that constructors are aware of their responsibilities.

7 ACKNOWLEDGEMENTS

The contribution of the CETE de Lyon to the implementation of this quality framework is funded by the ministry of ecology, sustainable development and energy (MEDDE). The responsibility for the content of this publication lies with the authors. It does not necessarily reflect the opinion of the Ministry.
All the CETE civil servants that contributed to the quality management control campaign 2011-2012 are gratefully acknowledged for their mobilisation and contributions.

8 REFERENCES

Leprince, V., Biaunier, J., Carrié, F.R., Olivier, M. (2011). *Quality Management approach to improve buildings airtightness. Requirements and Verification*, 32nd AIVC Conference and 1st TightVent Conference, 12-13 October 2011, Brussels, Belgium.

Charrier, S., Ponthieux, J.(2013). *Airtigtness quality management scheme in France: assessment after 5 years operation*, 34th AIVC Conference and 3rd TightVent Conference, 25-26 September 2013, Athens, Greece

Juricic,S., Charrier, S., Boithias, F., Olivier, M. (2012). *Lessons learnt from the regulatory quality management scheme in France*, 33rd AIVC Conference and 2nd TightVent Conference, 11-12 October 2012, Copenhagen, Denmark.

Arrêté du 26 octobre 2010 relatif aux caractéristiques thermiques et aux exigences de performance énergétique des bâtiments nouveaux et des parties nouvelles de bâtiments, JO 27 octobre 2010

Arrêté du 24 mai 2006 relatif aux caractéristiques thermiques des bâtiments nouveaux et des parties nouvelles de bâtiments, JO 25 mai 2006

AIRTIGHTNESS OF VERY LARGE VOLUME BUILDINGS: MEASURING METHOD AND FIRST RESULTS

Florent Boithias[*1], Sylvain Berthault[1], Sarah Juricic[1]

1 CETE de Lyon
Département Laboratoire d'Autun
Boulevard Giberstein, 71400 Autun, France
**Corresponding author: florent.boithias@developpement-durable.gouv.fr*

ABSTRACT

CETE de Lyon gives support to French administration for thermal regulation definition and enforcement. They must therefore work on measurements in order to set appropriate requirements and give advice to professionals about building methods.
Air-tightness of very large volume buildings is a growing issue in France, as performance levels are now required by low-energy labels and energy savings can be significant in those buildings. However, to measure airtightness one must be able to induce adequate airflow-rate to get sufficient differential pressure. A high-capacity fan called MEGAFAN was bought by CETE de Lyon in 2009 to measure very large volume buildings.
This article gives a presentation of this measuring tool and deals with the first measurements made on very large volume buildings and their results.

KEYWORDS

Airtightness, large buildings, retrofit

1 INTRODUCTION

In this article, airtightness measurements on very large volume buildings are considered. For this, common measurement devices such as blowing doors are inadequate because of their too low maximum air flow rate. In such cases, more powerful devices are required.
CETE de Lyon therefore bought a high capacity fan called MEGAFAN (CETE de Lyon, 2012). MEGAFAN is needed to measure the airtightness of full commercial buildings and collective housing because it can generate a maximum air flow rate of 300 000 m^3/h. Thus, sampling is not necessary which improves the measurement's precision. For example, MEGAFAN can measure commercial buildings with a volume of 50 000 m^3 and an n_{50} of 6 h^{-1} as well as collective housing with a volume of 75 000 m^3 and an n_{50} of 4 h^{-1}.
Today, French thermal regulation (JORF, 2010) does not require any airtightness level for commercial buildings. However, low-energy label Effinergie+ requires airtightness to be lower than 1.2 $m^3/h/m^2$ (with French indicator Q_{4Pa_surf} : air flow rate at 4 Pa divided by cold surface excluding ground floor surface) for buildings with floor space lower than 3 000 m^2. Considering collective housing, thermal regulation requires 1 $m^3/h/m^2$ (French indicator Q_{4Pa_surf}). In any case, measurements must be made in accordance with NF EN 13829 (AFNOR, 2001) and French application guide GA P50-784 (AFNOR, 2011).

For legal requirements to improve, one must be able to get a good knowledge of the existing buildings' performance, in order to conclude about what appropriate airtightness level can be required.
A presentation of MEGAFAN is proposed in this article as well as results obtained on tested buildings and recurring leakage points. As a conclusion, a comparison is made between measured airtighness and French thermal regulation default value for this type of buildings.

2 PRESENTATION OF MEGAFAN

MEGAFAN is composed of a 2-meter-diameter fan placed directly on the back of a truck. A flexible tube connects the fan to a false door which must be built on site to fit to the building's opening used for measurement (Figure 1). This opening must have dimensions of at least 2.10 m by 2.10 m as the flexible tube's diameter is identical to the fan's diameter.
Fan control and collection of data needed to quantify airtightness are carried out manually. Data processing is then done automatically via the associated operating software.

Figure 1: Interior view of MEGAFAN's connection to a commercial building's opening

MEGAFAN is a unique measurement device in France. CETE de Lyon is asked to measure large volume buildings with unusual architecture, large commercial buildings or exceptional projects (Figure 2). Customers are private and public organizations as well as local authorities.
Regarding the calibration of the equipment, a procedure in accordance with ISO 5801 (ISO) is implemented in CETE de Lyon to check MEGAFAN's reliability.

Figure 2: Airtightness measurement with MEGAFAN

3 RESULTS

The airtightness results obtained for the tested buildings and a description of the buildings' specifications for existing buildings are given in Table 1 and for new buildings in Table 2. Some of these buildings were measured for a project called ACIECO (CTICM, CETE de Lyon, CSTB, LEPTIAB, 2009) whose aim was to improve knowledge about actual airtightness levels and recurring leakage spots on steel-built buildings.

Table 1: Specifications of existing tested buildings and airtightness results

Type of building	Volume (m^3)	Floor surface (m^2)	Cold surface except ground floor (m^2)	Main building materials	Year of construc-tion	Airtightness Q_{4Pa_surf} ($m^3/h/m^2$)	Airtightness n_{50} (h^{-1})
Shop	14 061	3 544	2 484	Steel, concrete, double glaze	Approx. 1970	1.8	1.25
Shopping center	27 858	6 067	7 245	Steel, concrete, simple glaze	Approx. 1970	24.3	29.2
Gymnasium	7 408	1 133	1 705	Steel, concrete, simple and double glaze	Unknown	7.85	8.98
Industrial hangar	4 083	614	1 218	Steel	2007	4.47	7.87
Industrial hangar	3 430	560	1 088	Steel	2008	4.64	7.64

Main leaks were observed at pipe passages, rooflights, window and door jambs especially at emergency exits and damage due to aging on walls and ceilings. Less leaky spots were often found at connections between walls and ceilings.

Table 2: Specifications of new tested buildings and airtightness results

Type of building	Volume (m^3)	Floor surface (m^2)	Cold surface except ground floor (m^2)	Main building materials	Year of construc-tion	Airtightness Q_{4Pa_surf} ($m^3/h/m^2$)	Airtightness n_{50} (h^{-1})
Industrial hangar	53 000	3 774	7 331	Steel	2012	2.23	0.93
Industrial hangar	53 000	3 774	7 331	Steel	2012	2.51	0.91
Industrial hangar with offices	6 982	1 548	2 417	Steel	2010	0.18	0.28

Main leaks were observed on badly joint cladding pieces and window and door jambs.

4 CONCLUSIONS

In this article, 8 commercial building were presented. 3 of them were new buildings while 5 were existing buildings. The main building material was steel.
It was observed that airtightness was poor for the measured existing buildings, as only one of them was in accordance with French thermal regulation default value for this type of buildings: Q_{4Pa_surf} = 3 $m^3/h/m^2$. The other ones were 1.5 to 8 times higher than this default value.
In parallel, it is encouraging to see that today's new buildings, even with a very large volume, can be built with a good airtightness level. Indeed, all of the measured new buildings were lower than French thermal regulation default value.
Observations made on recurring leakage points in this study are very helpful to set recommendations for professionals on new construction and retrofitting procedures, which is a growing issue to reduce global energy consumption and CO_2 production.

5 REFERENCES

CETE de Lyon (2012). *MEGAFAN, http://www.cete-lyon.equipement.gouv.fr/IMG/pdf/fiche_produit_megafan_V3-3_cle18c41c.pdf*

Journal Officiel de la République Française (2010). *Arrêté du 26 octobre 2010 relatif aux caractéristiques thermiques et aux exigences de performance énergétique des bâtiments nouveaux et des parties nouvelles de bâtiments*. Journal Officiel de la République Française.

AFNOR (2001). *Performance thermique des bâtiments – Détermination de la perméabilité à l'air des bâtiments – Méthode de pressurisation par ventilateur. Norme européenne – Norme française NF EN 13 829.*

AFNOR (2011). *Performance thermique des bâtiments – Guide d'application de la norme NF EN 13829 :2001, GA P50-784.*

ISO. *ISO 5801, International Standard.*

CTICM, CETE de Lyon, CSTB, LEPTIAB (2009). *Projet ANR-PREBAT ACIECO – Bâtiments en acier économes en énergie – Réduction de la perméabilité à l'air et traitement des ponts thermiques.* Rapport intermédiaire n°1.

COMPARISON OF DIFFERENT AIR TIGHTNESS AND AIR EXCHANGE RATE MEASUREMENTS IN A VERY SMALL TEST BUILDINGS

Stanislavs Gendelis*[1], Andris Jakovics[1], Andrejs Nitijevskis[2], Jānis Ratnieks[1]

1 University of Latvia
Zeļļu 8, Rīga, Latvia, LV-1002
**Corresponding author: stanislavs.gendelis@lu.lv*

2 Irbest, Ltd.
Kurzemes pr. 84, Rīga, Latvia, LV-1067

ABSTRACT

The airtightness of the building envelope was studied in field measurements in recently constructed experimental small test buildings. Two types of research studies were carried out: the effect of special air tight sealing and the experimental determination of air exchange rate (h^{-1}) under real operating conditions. In very small buildings with many joints between materials and construction the role of the air tight sealing is very important; the experiments show changes in measured air tightness. Another parameter – air exchange rate has been studied in different test buildings using tracer gas equipment. Results obtained from this research show the real amount of exchanged air and it is very important to evaluate ventilation heat losses for low energy buildings.

KEYWORDS

Air tightness, airtight sealing, air exchange, tracer gas, test buildings.

1 INTRODUCTION

In frame of scientific project "Development of composite building walls constructive solution from the local materials by using multiphysical modelling according to the EU energy efficiency and optimal indoor climate requirements" (UL, 2013) five similar test buildings with internal dimensions 3×3×3 m were built in Riga, Latvia (Fig. 1). The main aim of the project is to compare constructions of different materials (wood, aerated concrete, ceramics, plywood, filled ceramics) with the same or very close heat transmittance ($U \approx 0.16$ $Wm^{-2}K^{-1}$) in order to get the experimentally measurable effect of construction's heat capacity and compare different annual moisture balance (Dimdiņa et al, 2013). Buildings are equipped with *Daikin Ururu Sarara* air-air heat pumps (Daikin, 3013), which provides heating, cooling and ventilation regime by adding amount of fresh outside air into the building.

First of all, the role of air tight sealing for all indoor joints was evaluated by using *Retrotec* blower door equipment at different construction stages for most critical log house. As the internal volume of those buildings is extremely small, using of standard fan may produce results with great uncertainty; therefore also small fan was used for standard air tightness measurements and obtained results compared.

In order to determine the real value of air exchange in room, which is an important factor to model the heat balance of a building and understand the ratio of conduction and convection heat losses, air exchange measurements using special *Lumasense* tracer gas measuring system are made. The obtained air exchange rates from long-term monitoring for different buildings were analysed.

Figure 1: Experimental test buildings

2 APPROACH

2.1 Air Tightness

To measure the air tightness of the test buildings, standard pressurization and depressurization tests at 50 Pa pressure difference were carried out using *Retrotec* blower door standard testing system (Retrotec, 2013) with 2 different fans (Fig. 2(a,b)):

- model 3000 with 56 cm fan, maximum flow 14440 m^3/h,
- model 200 with 38 cm duct tester fan, maximum flow 1155 m^3/h.

Two different fans were used to compare results obtained from fans with quite different workings flows. Due to very small building volume the biggest fan (model 3000) worked very close to the accuracy limits at very low flow rate, while the flow rate for model 200 was in the middle range. To exclude all possible small air leakages around the cloth door panel, which can be very important for so small buildings, an additional special air-tight membrane has been attached for system with fan model 200 (Fig. 2(c)) for some experiments.

(a) (b) (c)

Figure 2: Different *Retrotec* fans used for air tightness measurements: (a) – model 3000, (b) – model 200, (c) – models 200 with an additional air-tight membrane

As results of pressurization/depressurization two parameters are calculated:

- n_{50} – the air exchange rate at 50 Pa pressure difference (h^{-1}),
- q_{50} – the air permeability at 50 Pa pressure difference ($m\ h^{-1}$).

To visually detect typical air leakage locations and their distribution in the buildings at different construction stages infrared image camera *Flir P620* (FLIR, 2013) was used together with blower door system. Thermography surveys were conducted twice to determine the main air leakage locations and intensity: first, before inside finishing is done, and then after air tight sealing is completed.

2.2 Air Exchange Rate

The main aim of ongoing project is to determine and analyse energy consumption for all test buildings, therefore it is very important to evaluate all the heal losses. One of them is convection heat losses through ventilation opening, which can be characterized by knowing air exchange rate in the room. Tracer gas method (Laussmann and Helm, 2011; ISO 12569, 2012) and special measuring system *Lumasense* (Lumasense, 2013) including multipoint sampler/doser *Innova 1303* and photoacoustic gas monitor *Innova 1412* are used for this purpose (Fig. 3).

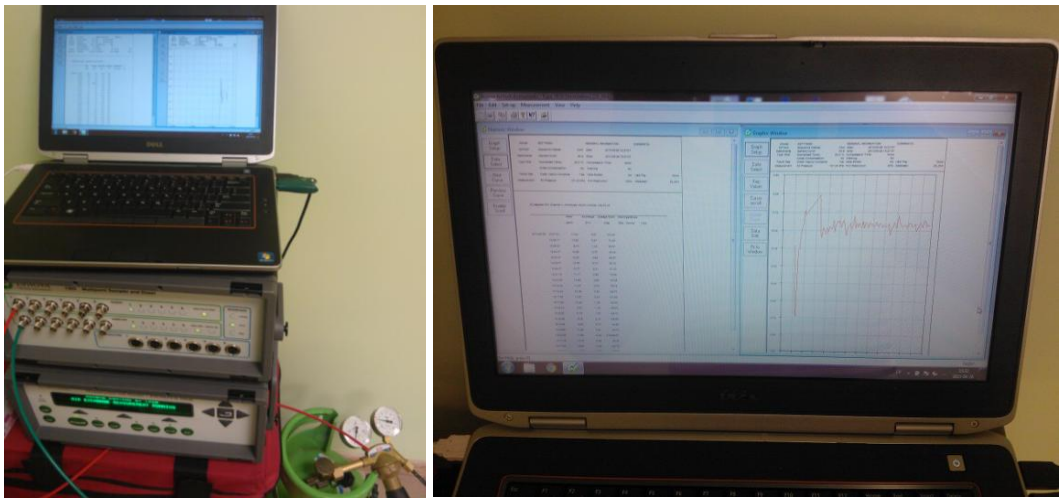

Figure 3: System and software used for tracer gas air exchange measurements

As the air volume in the room is only 27 m^3 and the expected air exchange value is small, a constant concentration method (ISO 12569, 2012) is used for long-term, continuous air change rate measurements. The principle of this method is to track the amount of tracer gas $F($ required to maintain it at a constant concentration $n($ at a constant level. To ensure better tracer gas mixing, an additional small-sized fan is used near the used doser nozzle.

3 RESULTS

3.1 Air Tightness

To control the air tightness at different construction stages, log test building is chosen with many wood construction joints, which are filled with a rubber spacer. Primarily, the air tightness measurements were carried out at the first stage of build-up process, when some places in building structures were not air-tight, e.g. window-sill is not fixed (Fig. 4(a)). After the interior finishing (Fig. 4(b)), the next air tightness measurements were carried out. Finally,

the last experiments were made after all joints between materials and constructions are tightened with permanent airtight sealing (Fig. 4(c)). All the measurements are made using small fan with diameter of 38 cm and maximum flow 1155 m^3/h. Ventilation opening was hermetically sealed too.

Results from all three mentioned construction stages are summarized in Table 1 – as one can see, air exchange rate for this building is reduced twice after interior finishing is done, but sealing of material joint reduces air exchange very slightly. This can be explained by the fact that sealed joints around walls and ceiling/floor and around biggest pipe connections (Fig. 4(c)) are only small part of leakages; the most important part of air filtration is log interconnections, what is characteristic of this type of buildings. Experimental results from other test buildings after sealing (see below) confirms this assumption.

(a) (b) (c)

Figure 4: Different construction stages in log building: (a) unfinished interior, (b) finished, not sealed, (c) sealed

Table 1: Air tightness measurement results for log building at different construction stages

	Air exchange rate n_{50} (h^{-1})	**Air permeability q_{50} (m h^{-1})**
Stage 1. Unfinished interior	4.26	2.13
Stage 2. Finished interior, not sealed joints	1.97	0.98
Stage 3. All joints are sealed.	1.91	0.94

To analyse the influence of used experimental equipment, 2 additional measurement series were made for log building at stage 2 (interior finishing is done, but joints are not sealed): with a standard fan (diameter of 56 cm, maximum flow 14440 m^3/h) and with an additional air-tight membrane, which is hermetically fitted around the blower door cloth (Fig. 2(c)).

Results get from this investigation are shown in Table 2 – there is no difference between measurements with and without the additional membrane, but the results get from system with bigger fan differ by almost 20%. The main reason of this is the accuracy of parameters' reading in the range of very low flows, which means higher uncertainty for the measurements.

Table 2: Air tightness measurement results for log building with different fan configurations

Fan model (maximum flow)	**Additional membrane**	**Air exchange rate n_{50} (h^{-1})**	**Air permeability q_{50} (m h^{-1})**
Model 200 (1155 m^3/h)	No	1.97	0.98
Model 200 (1155 m^3/h)	Yes	1.97	0.98
Model 3000 (14440 m^3/h)	No	2.36	1.18

The next series of measurements were carried out after special airtight sealing that was made in every test building. *SIGA* (SIGA, 2013) high-performance adhesives are used for the sealing of vapour control layers, wood-based panels and different junctions of pipes/cables. Examples of sealing are shown in Fig. 5.

As the main material and the type of building construction differs, the results of air tightness measurements also vary in a quite large range (Table 3) – from n_{50}=0.67 h^{-1} for building with polystyrene filled ceramics as wall material to n_{50}=1.91 h^{-1} for log building. All possible material and construction joints in every building, as well as window and door are professionally sealed; therefore the only reason for different air tightness is air filtration through building structures (aerated concrete, wood etc.).

(a) (b) (c)

Figure 5: Sealing examples in different test buildings: (a) – vapour layer, wall and cable, (b) – plywood flooring, wall and pipes, (c) – plywood ceiling panels and ventilation opening

Table 3: Air tightness measurement results for different test buildings after sealing

Test building	**Air exchange rate n_{50} (h^{-1})**	**Air permeability q_{50} ($m\ h^{-1}$)**
LOG (log house with internal insulation)	1.91	0.94
EXP (polystyrene filled ceramic blocks)	0.67	0.34
AER (aerated concrete with external insulation)	1.12	0.56
CER (ceramic blocks with external insulation)	1.47	0.70
PLY (plywood boards filled with mineral wool)	0.93	0.46

A thermographic survey is also carried out together with blower door tests in all buildings after sealing. Is shows that the thermal bridges along the doors and windows are excluded (Fig. 6) and air infiltration/exfiltration does not exist. The zones with slightly lower temperature (from the inside) are found between walls and floor/ceiling (Fig. 7), but the temperature difference there even in case of 50 Pa pressure difference is relatively small and do not exceed 3°C, thermal bridges there are small.

The difference in air tightness parameters at 50 Pa pressure difference get from experiments (Table 3) describes mainly the variable properties of boundary materials and structures, but it does not describes the real convective heat losses from buildings. To evaluate actual air exchange under given climatic conditions, a completely different approach should be used.

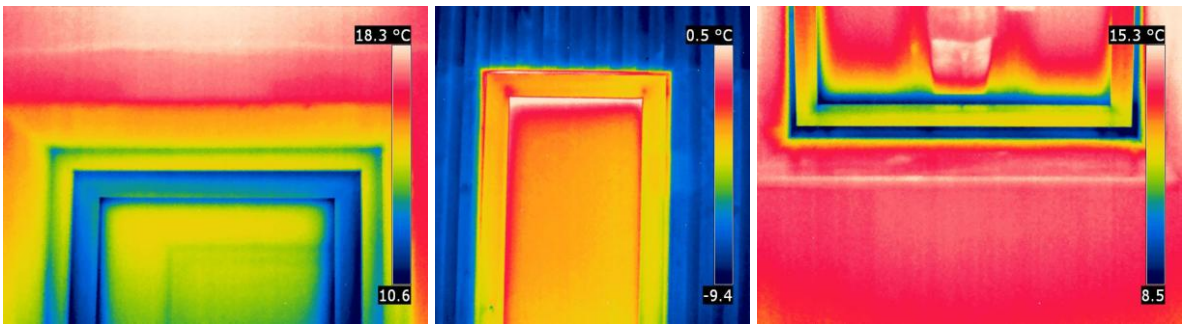

Figure 6: No thermal bridges or other defects are found for windows and doors at 50 Pa pressure difference

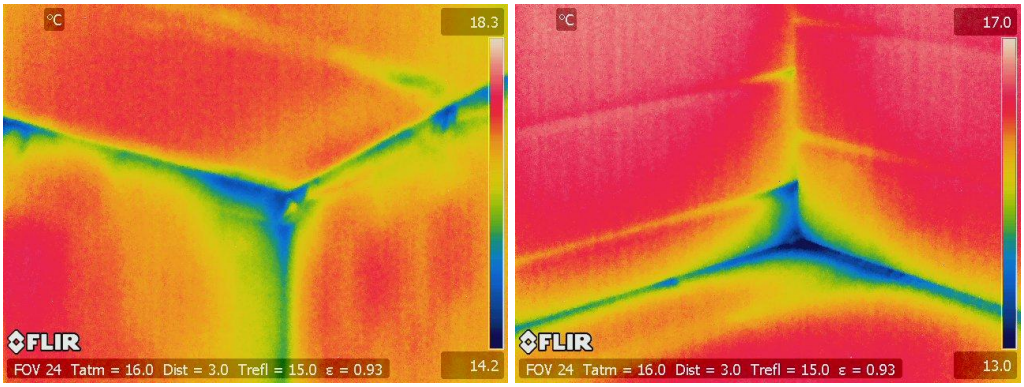

Figure 7: Ceiling/wall and floor/wall joints with decreased temperature at 50 Pa pressure difference

3.2 Air Exchange Rate

Actual air exchange rate at given climatic conditions (wind speed and direction, temperature difference etc.) and in set mechanical ventilation mode is very important factor; it describes not only the fresh air supply intensity, but also heat amount lost due to convective heat losses (air mass transfer). As the heat balance and heating/cooling energy needs in the test building are key factors, it is very important to measure the actual air exchange, which can be done by using tracer gas method.

Experimental studies of actual air change were made in all the test buildings after airtight sealing and with ventilation system running in standard mode (fresh air is added by heat pump from the outside, air exhaust is provided through the opening above the window). To ensure the air change results describing long-term building operation, measurements were carried out at least for 24 hours for every building. Obtained results (Table 4) show that the actual air change with switched on ventilation system in all test buildings is within the range of 0.43…0.50 h^{-1}. Graphical representation of calculated air exchange values for long-term monitoring period is shown on Fig. 8; it is seen, that fluctuations of the instantaneous *n* values depending on wind speed/direction for different measurement series vary.

One additional measurement was carried out in log house with switched off ventilation system and sealed ventilation opening; this study shows that air change in sealed building without operating ventilation system is very close to zero (Table 4). As blower door experiments indicated (Table 3), log building has the highest air exchange rate n_{50}; therefore it may be concluded, that all other buildings will have even lower actual air exchange rate *n*. Thus, the general finding of this experiment is that all buildings are very air-tight and the actual air exchange rates *n* with switched on ventilation system are very close, which means that more than 90% of actual air exchange is a result of mechanical ventilation system operation.

Table 4: Air exchange rate *n* for test building under actual operating conditions

Test building	**Ventilation system**	**Ventilation opening**	**Air exchange rate *n* (h^{-1})**
LOG (log house with internal insulation)	On	Open	0.45±0.03
LOG (log house with internal insulation)	Off	Sealed	0.03±0.01
EXP (polystyrene filled ceramic blocks)	On	Open	0.48±0.02
AER (aerated concrete with external insulation)	On	Open	0.5±0.03
CER (ceramic blocks with external insulation)	On	Open	0.43±0.04
PLY (plywood boards filled with mineral wool)	On	Open	0.44±0.01

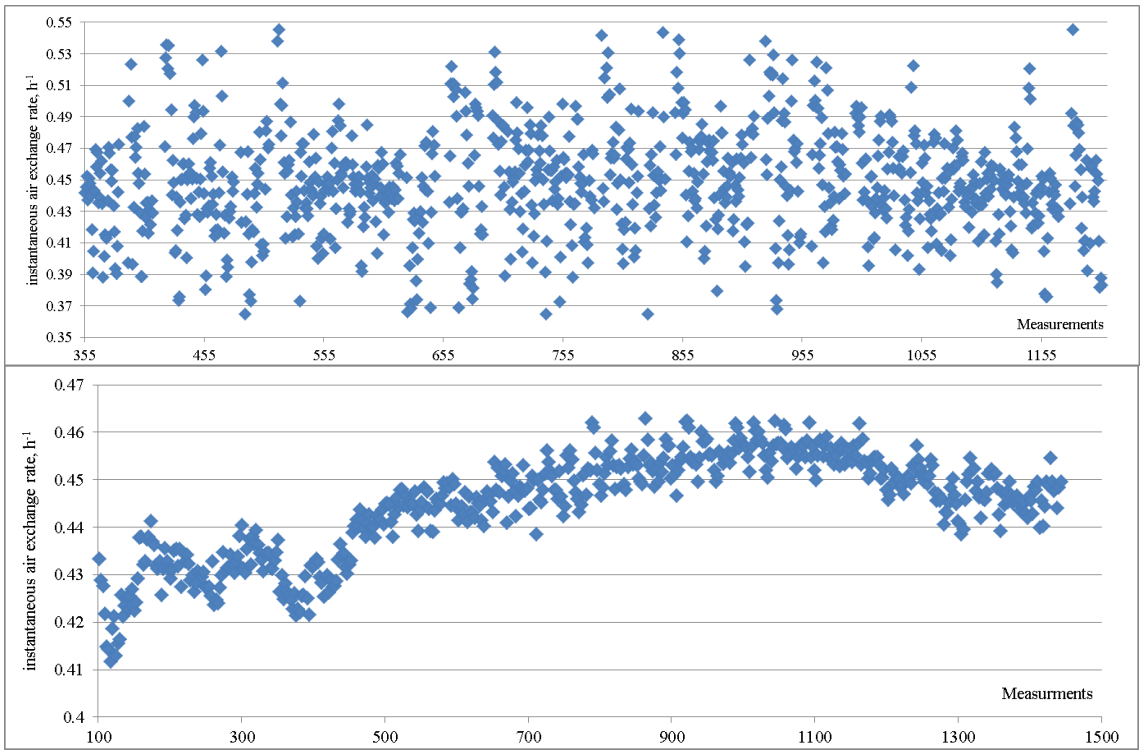

Figure 8: Examples of instantaneous air exchange rates estimated with tracer gas method

It is possible to use relationship between measured air exchange rate at 50 Pa pressure difference n_{50} and natural (actual) air exchange n, which was firstly investigated in the 80's by (Kronvall, 1978) and (Persily and Linteris, 1983):

$$n = \frac{n_{50}}{20} \tag{1}$$

Using this equation, we can calculate the actual air exchange rate for LOG building without ventilation (Table 3), n=1.91/20=0.10 h^{-1}. Comparing it with value n=0.03 h^{-1} measured by using tracer gas dilution method (Table 4), it is seen, that the difference is three times. Very simple equation (1) does not take into account neither effective average climatic conditions nor the building characteristics (shape, height etc.). Other studies (Dubrul, 1998) show that empirical correction factor between n and n_{50} changes from 10 to 30. Experiment in LOG buildings gives a result of 64; thus it can be concluded that use of blower door tests to correctly describe the real air exchange may produce very inaccurate results.

4 CONCLUSIONS

Air tightness measurements is test buildings with different structures showed that even in case when all possible joints and air gaps are perfectly sealed, there exist a small air flow, which cannot be completely excluded; one of possible explanation of this fact is air filtration through the building construction (especially for wooden materials). The use of standard blower door fan for air tightness experiments in small-sized buildings may cause serous measurement errors due to poor accuracy of equipment at very small flows; the fan with lowest airflows is recommended. Studies of actual air exchange rate using tracer gas dilution method demonstrated the dominant role of mechanical ventilation (more than 90%) in overall air exchange process in good airtightened test buildings. Comparing the results get from blower door tests and evaluated actual air exchange from tracer gas experiments, it has been established that correlation between those parameters can be fixed very approximately.

5 ACKNOWLEDGEMENTS

This research is done with financial support of ERAF, project realized by University of Latvia, No. 2011/0003/2DP/2.1.1.1.0/10/APIA/VIAA/041.

6 REFERENCES

Dimdiņa, I., Jakovičs, A., Gendelis, S., Kļaviņš J. (2013). *Testing of Energy-Efficient Building Envelope Materials in Natural Conditions.* In: Proceedings of World Sustainable Energy Days 2013, 27th February – 1st March, Wels, Austria.

Daikin (2013). Wall-mounted type Inverter Ururu Sarara [online] *www.daikin.com/global_ac/products/residential/urusara_series/outline.html* (accessed 25.08.2013).

Durbul C. (1998). *Inhabitants behaviour with respect to ventilation.* Technical note 23. Air Infiltration and Ventilation Centre (AIVC); 1988.

FLIR (2013). FLIR P620 Technical Data [online] *http://support.flir.com/DsDownload/Assets/40402-3403_en_50.pdf* (accessed 25.08.2013).

ISO 12569 (2012). *Thermal performance of buildings and materials -- Determination of specific airflow rate in buildings -- Tracer gas dilution method*. ISO Standard 12569:2012. Geneva: International Organization for Standardization.

Kronvall J. (1978). *Testing of houses for air leakage using a pressure method*. ASHRAE Trans 1978:84(1):72-9.

Laussmann D. and Helm D. (2011). *Air Change Measurements Using Tracer Gases: Methods and Results. Significance of air change for indoor air quality, Chemistry, Emission Control, Radioactive Pollution and Indoor Air Quality*, Dr. Nicolas Mazzeo (Ed.), ISBN: 978-953-307-316-3, InTech, DOI: 10.5772/18600.

Lumasense (2013). Ventilation and Air-exchange Measurements [online] *www.lumasenseinc.com /EN/products/gas-monitoring/ventilation-measurement* (accessed 25.08.2013).

Persily A., Linteris G. (1983). *A comparison of measured and predicted infiltration rates*. ASHRAE Trans 1983:89(2B):183-200.

Retrotec (2013). Air Leakage Test Systems [online] *www.retrotec.com* (accessed 25.08.2013)

SIGA (2013). Protection for House. Health. Climate [online] *www.siga.ch/en/product-overview.html* (accessed 25.08.2013).

UL (2013). University of Latvia. Project's "Development of composite building walls constructive solution from the local materials by using multiphysical modelling according to the EU energy efficiency and optimal indoor climate requirements" website [online] *www.eem.lv* (accessed 25.08.2013) (in Latvian).

USE OF COOL MATERIALS IN OUTDOOR PLACES IN ORDER TO MITIGATE THE URBAN HEAT ISLAND IN A MEDIUM SIZE CITY IN GREECE

A. Dimoudi*[1], S. Zoras[1], A. Kantzioura[1], X. Stogiannou[1], P. Kosmopoulos[1], C. Pallas[2]

1 Laboratory of Environmental and Energy Efficient Design of Buildings and Settlements, Department of Environmental Engineering, Democritus University of Thrace
Vas. Sofias 12, Greece
**Corresponding author: adimoudi@env.duth.gr*

2 Division of Technical Services, Serres Municipality
Karamanli 1,
62 122 Serres, Greece

ABSTRACT

The materials that are used in outdoor spaces are of prime importance as they modulate the air temperature of the lowest layers of the urban canopy layer, they are central to the energy balance of the surface and they form the energy exchanges that affect the comfort conditions of city people. Paved surfaces contribute to sunlight's heating of the air near the surface. Their ability to absorb, store and emit radiant energy has a substantial affect on urban microclimate.
The thermal behaviour of typical construction materials in an urban center of North Greece, at Serres, was investigated. The thermal fluctuation during the day and the surface temperature differences between different materials in a selected area inside the urban centre of the city was monitored.
The replacement of conventional materials with cool materials was evaluated to have significant benefits. CFD simulations showed that materials replacement, accompanied by other mitigation techniques in the area, result at reduction of the mean surface temperature in the streets of the area of 6.5 ºC.
The results of the measurements and the CFD simulations will be presents in the paper.

KEYWORDS

Cool materials, surface temperature, CFD simulation

1 INTRODUCTION

The thermo-physical properties of covered and construction materials in contemporary cities and the urban geometrical characteristics affect the microclimatic conditions inside the urban centers (Lau et al, 2011). The radiant balance of the urban space, the convective heat exchange between the ground and the buildings, the air flowing above the urban area and the heat generation within the city (Mihalakakou et al, 2002), (Santamouris et al, 1999) increase the air temperature in the city.
In order to improve the urban microclimate conditions, various mitigation techniques have been proposed involving the use of highly reflective materials, use of cool sinks and increased plantation (Santamouris, 2007), (Gaitani et al, 2007). Trees and green areas have a large effect at moderating the microclimate and also contribute at cooling the cities (Santamouris, 2001), (Dimoudi, 1996) as evapotranspiration from vegetation foliage reduces air temperature and increases humidity (Dimoudi, Nikolopoulou, 2003). Vegetated areas are known to be comparatively cooler during daytime than most other urban elements (Zoulia et al, 2009).

Mitigating the heat islands effect is therefore a key element to achieving sustainability in a city and it can be done by improving the urban microclimate (Gaitani et al, 2011).
The materials, which are used for the pavements of urban spaces and for the external renderings of vertical (facades) and horizontal (flat roofs) surfaces of the buildings, constitute, the ‘‘skin” of a city. These materials play a decisive role on the heat transfer processes, which take place between the city and the climatic environment. Materials influence the absorption of solar radiation, the emission of thermal radiation, the heat storage, and the evaporation processes that take place in practically every city surface.
The current study investigates the thermal behaviour of construction materials inside the urban centre. The investigation took place in a city at the North Greece, which is assumed as one of the warmest cities during summer in the North Greece.

2 MEASUREMENTS METHODOLOGY

2.1 Site description

The investigation was conducted in Serres city (Greece), located at 41°05′North and 23°33′E, in North Greece, in an altitude of about 61m above the sea level. The city has intense heat problem during summer and presents thermal episodes of high air temperature that exceed the 40 ºC. The study area is located in the central parts of the city which contains a densely urban structure. The buildings are characterized by four to five floors height and are built in the decade of 1970’s. The streets are covered by asphalt and the pavements are covered mainly by light colour, conventional pavement (concrete) tiles.
In the Table 1 the investigated materials for each measurement point are given and in the Table 2 the photo of materials are included.

Table 1: Investigated materials for each measurement point

Material	**Measurement Point (MP)**
Road asphalt	MP1 - MP11, MP14 - MP17
Light gray pavement tiles (both sides of road)	MP 1, MP3 - MP11, MP13 – MP17, MP19
Gray pavement tiles	MP8
Yellow pavement tiles	MP8
Red ground cover pavers	MP8
White pedestrian tiles	MP8

Table 2: Photo of investigated materials

 asphalt	 light gray pavement tiles	 white pedestrian tiles red ground covers pavers	 gray pavement tiles yellow pavement tiles

2.2 Monitoring procedure

A number of monitoring procedures were carried out during hot summer days, in order to investigate the thermal behaviour of construction materials which are used on buildings’

envelope, for covering pavements and open spaces. The thermal fluctuation during the day and the surface temperatures is analyzed.
The present study focuses on measurements of surface temperatures of the roads, the pavements and the vertical surfaces (Stogiannou, 2011). The field surveys involved measuring of surfaces' temperature and microclimatic monitoring of air temperature in 1.8m height. The measurement of surface temperatures took place in 20 different Measurement Points (MP).
A portable station recorded at 1.8m height the air temperature and an infrared thermometer was also employed to measure surfaces temperature at a distance of 1.2-1.3 m.
The experimental procedures were carried out at morning time 8:00am, when the absorbed solar radiation doesn't influence the materials temperature, at 13:30pm and 16:00pm and at 19:30 when the materials emitted the absorbed temperature. The experiments that are presented in this paper were performed on June and July 2011. High temperatures were prevailed during this summer period.

3 MEASUREMENTS RESULTS AND DISCUSSION

3.1 Asphalt

The surface temperatures of the asphalt road in the study area, during the experimental procedure on hot summer months (June and July) exceeded 45^{o}C during afternoon and they can reach up to 50 and 56^{o}C.
The asphalt's temperature is higher than the T_{air}. The temperature difference remains on high levels even during the afternoon, under shadowing conditions, and it is between 1,1^{o}C and 13,2^{o}C.
The mean surface temperature of asphalt of all MPs in each road, at the hottest day of measurement procedure is observed in Fig 1.

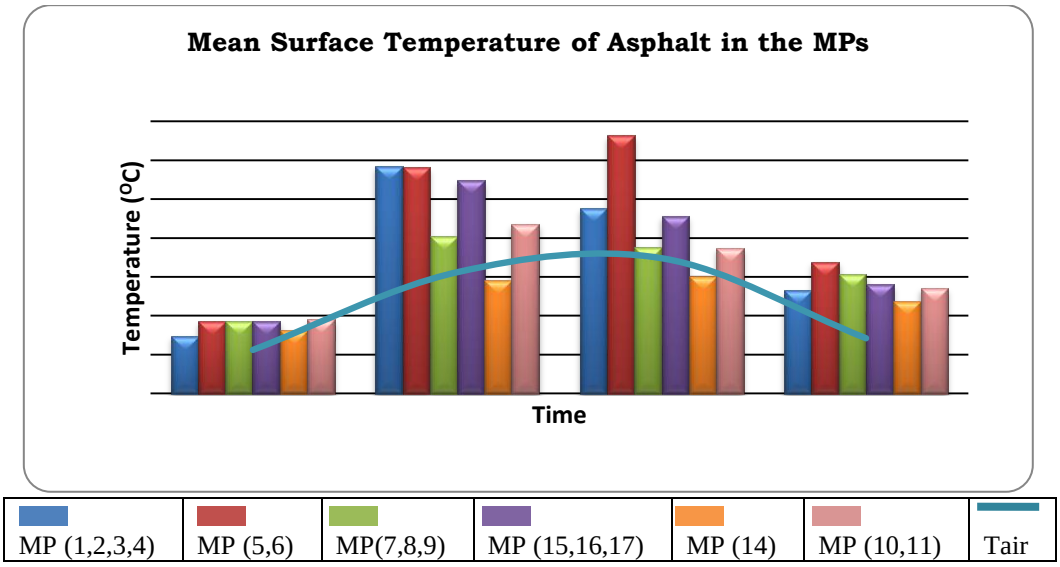

Figure 1: Mean surface temperature of asphalt in different roads of the area (mean value of different MPs in each road, each road is illustrated with a different colour)

3.2 Cement products (concrete pavement tiles)

The mainly observed cement products are pavement tiles and ground cover pavers. Their colours are light gray, gray, yellow and red.

In Fig. 2 the surface temperature on the hottest day is presented. The temperatures during the morning and afternoon time are under shadow, while in the noon, the measurement points are exposed in solar radiation. Surface temperatures are higher than air temperature. The surface temperature of gray tiles is always higher than the other colour tiles and may reach temperatures similar to asphalt, up to 56^{o}C during afternoon hours. The surface temperature in the different tiles remains higher than the air even in late afternoon, up to about 5 ^{o}C.

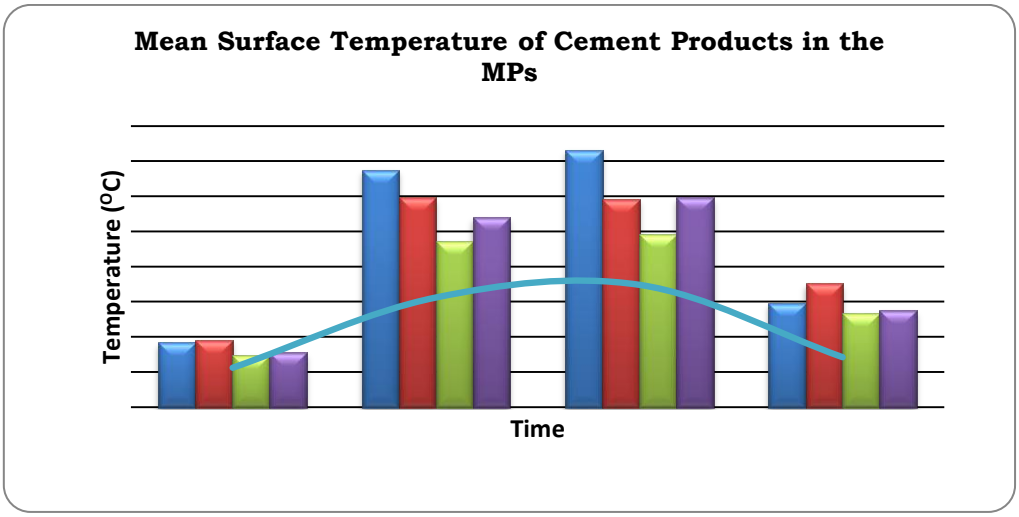

Figure 2: Mean Surface Temperature of cement products in the MPs

4 BIOCLIMATIC DESIGN SOLUTIONS

The area is currently characterised by extensive use of conventional materials in outdoor spaces, like asphalt in the streets, pavement tiles in the pavements and reduced green areas. A bioclimatic redevelopment of this part of the city is planned, for improvement of microclimate and outdoor thermal comfort conditions during summer in this area and consequently of improvement of indoor thermal comfort and improved energy performance at the surroundings buildings – lower air temperature of the external environment contributes to reduction of the hours that air-conditioning is used at buildings and at higher efficiency of the A/C units).

In the frame of the general bioclimatic redesign of the area, a total replacement of floor materials is planned with cool materials, together with increase of pavements' width, decrease of streets' width, combined with increase of green surfaces and water elements. The proposed interventions include (Drawing 1, Drawing 2) (Dimoudi et al, 2013):

- Replacement of conventional floor materials with cool materials at pedestrian streets and pavements and replacement of asphalt with cool photocatalytic asphalt at streets. The cool materials will cover the 86% of open areas and the water permeable materials (special pressed soil, low height vegetation, water surfaces) the 7% while in the existing condition the 95,5% was covered with conventional floor materials (e.g. asphalt, pavement tiles) and only the 4,5% was covered with water permeable materials (soil, low height vegetation). The thermal and optical properties of the materials are presented at Table 3.
- Shading of external places with permanent shading elements designed, mainly at sitting places that are created at selected places, but also at open spaces (e.g. park). Extensive vegetation is also used for shading that apart from other cooling benefit it contributes to psychological realm and aesthetic improvement of the area.

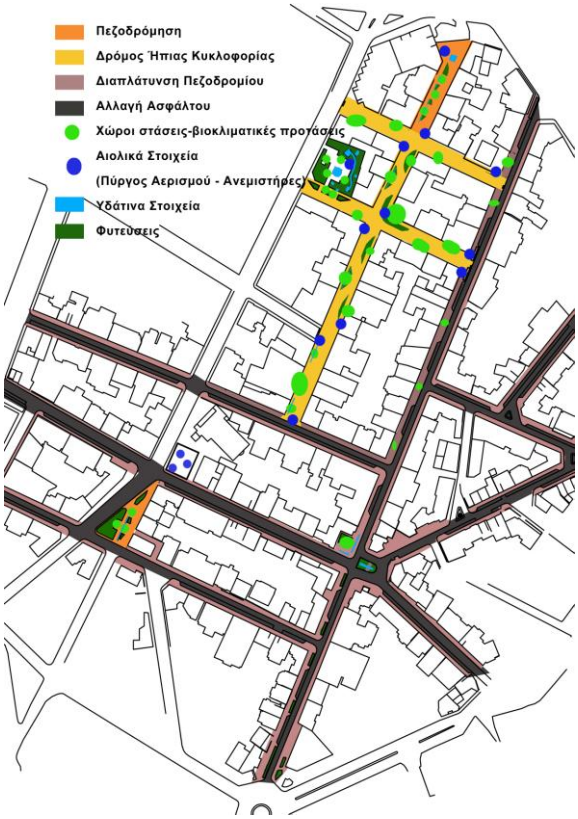

Drawing 1. Overview of the proposed interventions in the area

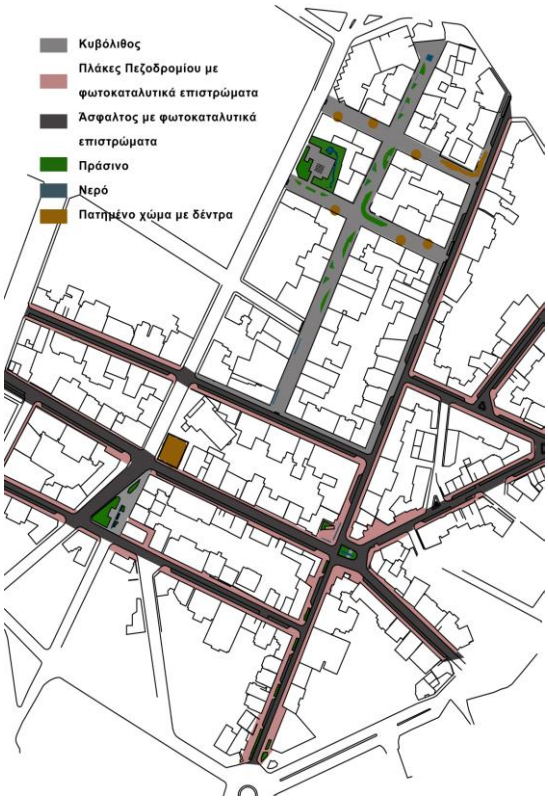

Drawing 2. Mapping of the use of new materials

Table 3 Thermal and optical properties of materials (existing condition and proposal)

	Solar reflectivity coef	Emittance coef.
Conventional materials – Floor and facades		
Street asphalt	0.10 [1]	0,85-0,93 (0,89) [2]
Light colour roof covering / flat roofs covered with pavement tiles	0.35 [1]	0.90 [3]
Light colour mortar	0.60 [1]	
Medium colour mortar (beige, grey)	0.40 [1]	
Grey colour		0.87 [3]
Dark colour mortar	0.20 [1]	
Typical structural material		0.80 [1]
Cool material - Floor coverings [4]		
Asphalt (Ecorivestimento grigio photocatalitic concrete based mortar (speciment 1)- Fotofluid	0.37	0.89
Street blocks (Street blocks CE, light grey (N° 5) or beige (N° 6))	0.67	0.89
Pavement tiles (White floor tiles (N° 12))	0.68	0.92

[1] TOTEE 20701-1 (2010)
[2] Incropera De Witt (1990
[3] Santamouris M. (2006)
[4] ABOLIN,

- Extensive use of vegetation with native species – shrubs and trees - along the streets that act as a natural conditioning system through its evapotranspiration phenomena thus, reducing the air temperature in the area.

- Enforcement of air ventilation in the outdoor spaces with outdoor fans located at selective places to increase air circulation through the streets and create comfort sitting places during hot days.
- Several water installations, like fountain - jet, water-curtains, spray-systems in selected locations in the area for introduction of direct evaporation combined with the natural evapotranspiration of vegetation.

5 SIMULATION STUDY OF THE AREA

5.1 Simulation procedure

The simulation of the thermal conditions in the study area was performed with the detailed 3-dimensional tool ANSYS CFX 13, which is an advanced general code computational fluid dynamics model that solves the Navier-Stokes differential equations and turbulence by the finite elements technique in the 3D space. It handles very detailed 3-dimensional geometry with the ability to solve efficiently heat transfer and fluid flow phenomena. Its accuracy has been widely verified against experimental and theoretical tests (http://www.ansys.com). Advanced CFD models can calculate with a high degree of accuracy microclimatic parameters at every grid point of the meshed space. However, the more complicated is the geometry of the urban open space, the more resources of input data and calculation are needed.

The 3D geometry of the area that was audited and designed by the architects' team, in a .dwg file, was imported in the CFD software. The more detailed is the structural and 3D geometry of buildings, streets, pavements, urban equipment and vegetation the more representative and accurate simulation is. This .dwg file was imported and refined in the Design Modeler module of the simulation tool where solid surfaces (buildings, streets, pavements and trees) and the fluid domain area were defined. The fluid domain area encloses the study area by a dimension of 1,000 m * 800 m * 80 m (height) – this was at least 4 times the max height of structural domains in order to avoid flow reflection at boundaries and fluid returns during simulation.

The simulation domain was meshed (solid surfaces and fluid domain volume) and mesh was created at all area's surfaces (streets, pavements, facades on streets, facades not facing streets, roofs, etc). The surfaces have been meshed by the Advanced Proximity and Curvature Function and the mesh dimensions have been selected by the criterion of the fully developed flow within the fluid domain. The typical element in the mesh had dimension of 5.0 m, with denser mesh close to solid surfaces (facades, vegetation, water elements, etc) from 0.1 to 0.5 m (tetra-, hexa-, octa- surface elements). The final mesh constituted of 2,099,018 nodes and 11,015,546 elements (Figure 3).

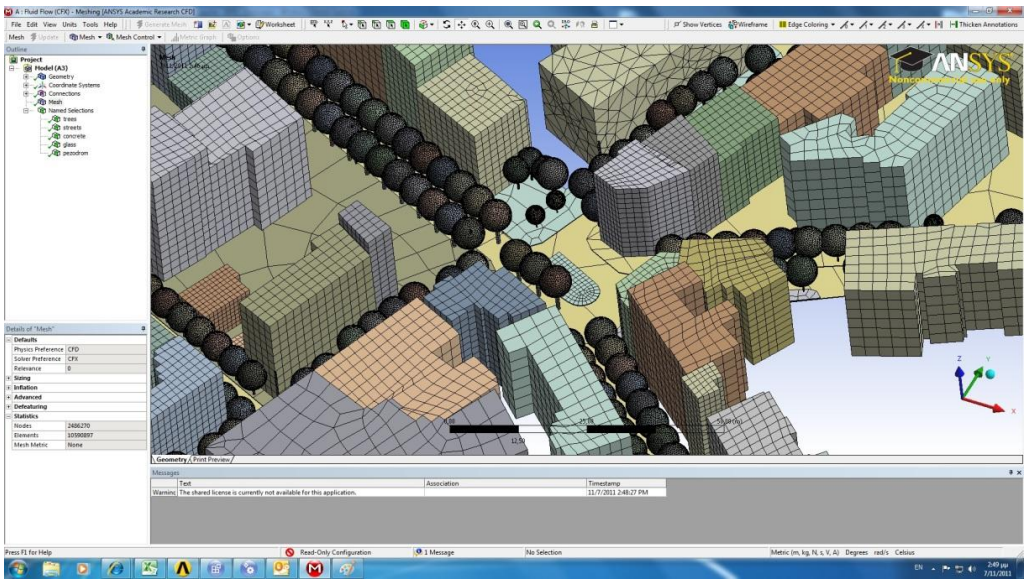

Figure 3 Mesh details in section of the study area

The meshed geometry was used to define the physical parameters in the area under consideration (CFX-Pre). Surfaces with materials (concrete, glass, pavement, water, trees) and properties (emission and reflection coefficients) have been defined. The Shear Stress Transport model with K-turbulence KE and O-Turbulence frequency was applied to simulate turbulence. Thermal energy was simulated by the discretised model in surface to surface and medium to surface modes. This takes into account opposite surfaces energy exchange that is very important in the heat balance of the open spaces in case of replacing conventional surfaces with cool materials. Solar radiation has been taken into account in slope and deviation through the top boundary. Vegetation has been considered as physical barrier to wind flow with shadowing. Water elements were defined as free surfaces (zero friction) with a constant temperature of 15 ºC.
Boundary conditions were defined by monitored data (air temperature, wind speed and direction, radiation, surface temperatures) that were taken during the summer period 2011. A time step (5 sec) and convergence criteria (10^{-4} RMS of residuals) have defined under steady state of transient calculation.
Finally, the results have been processed in the CFD Post module, provided by the software, for the final presentation.

5.2 Model validity

The ANSYS CFD model of the study area was validated against monitored data of the area that were carried out during summer 2011. The warmest day for the monitored period, with complete microclimatic data (i.e. air temperature, air velocity, surface temperature) that were monitored at different locations and heights in the area, was selected the 4th August 2011.
The data that were used for validation of the model is the monitored data in different streets and heights within the study area, i.e. the air temperature and wind velocity at heights 1.8 m and about 4.5m, the surface temperature of the facades at 1.8m height and the material surfaces of streets, sidewalks.
The climate data for that period from the Meteorological station in the city were used to simulate the climatic data in the intervention area and in the locations where measurements were carried. The simulation results were compared with the measured values of surface and air temperatures and wind speed. Since, the surface temperature measurements made during midday, the comparisons were made for the same period.

Satisfactory convergence of the values between monitored and simulation data was achieved. The difference between the monitored and simulated values range between 0.670 to -0.624 °C for the air temperature, 0.300 to -0.300 °C for the surface temperature and – 0.030, -0.090 up to -0.192 m/sec for the air velocity. Therefore, the achieved high accuracy proves that the model that was developed for the study area is reliable for assessment of the existing condition and the proposed interventions in the area.

5.3 Simulation results

The conventional materials of the streets and pavements in the area were proposed to be replaced with cool materials that are characterised by high solar reflectivity and thermal emittance (Table 1). The existing and the proposed condition of the area were simulated for the noon of the hottest day of the monitored period, thus, for the July 19th, 2011.
It was assumed that the mean maximum surface temperatures occur during the hottest day. The monitored results showed that the maximum values in the different streets in the area occur approximately the same time. Thus, the surface temperature for all surfaces in the area was simulated at the same period that is the noon of the hottest day. The mean surface temperature for each street of the area was then calculated and the mean surface temperature for the whole area was derived.
The surface temperature distribution in the area is illustrated in Figures 4 and 5 for the existing condition and the proposed interventions accordingly. The mean surface temperature in the area during noon of the July 19th reached 40.3ºC in the existing condition while the materials change together with the other interventions in the area, reduced the surface temperature to 33.8ºC, thus, obtaining a temperature reduction of 6.5 ºC.

Figure 4 Surface temperatures in the area - Existing condition

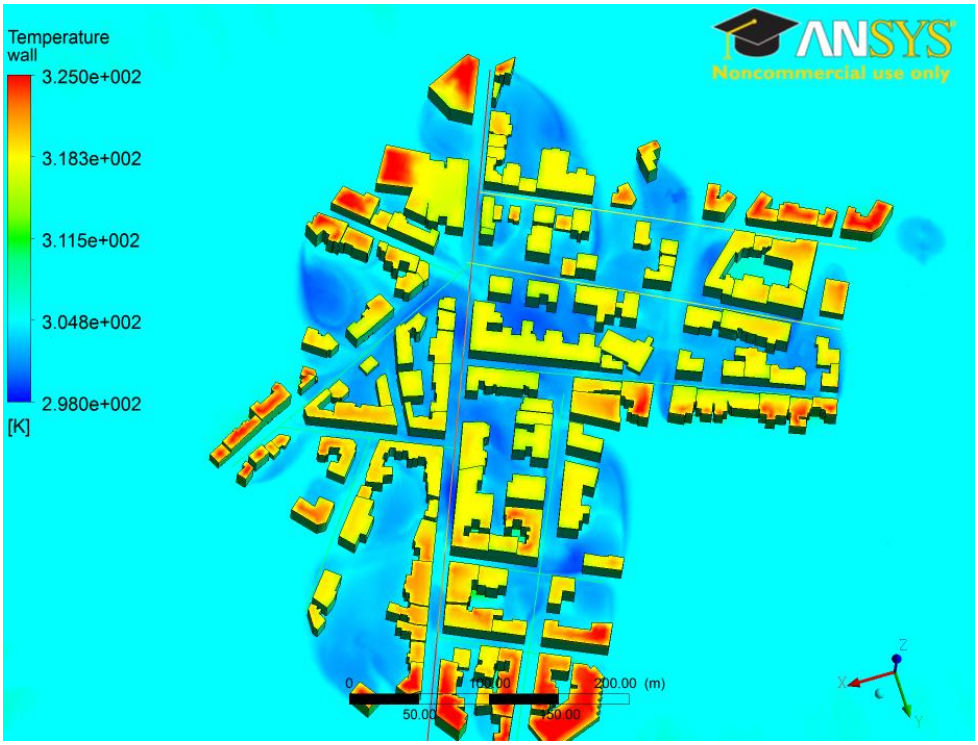

Figure 5 Surface temperatures in the area - Proposed condition

6 CONCLUSIONS

It is evident that the thermo-physical properties of covered and construction materials in contemporary cities and the urban geometrical characteristics affect the microclimatic conditions inside urban centres.

Measurements in conventional materials (asphalt, pavement tiles) in a city centre reported surface temperatures up to 50 -56 ºC during the summer period. Bioclimatic interventions combined with replacement of all conventional street and pavement materials with cool materials reduced surface temperature by 6.5 ºC.

This temperature reduction will have a big influence on the microclimate of the area, the thermal comfort of people in the outdoors spaces but also it will affect indoor conditions and houses' cooling loads.

7 ACKNOWLEDGEMENTS

The CFD simulation study was financed by the Municipality of Serres in the frame of the project "Investigation of bioclimatic rehabilitation of open spaces in an urban area of the Serres city". Special acknowledgement is made to Panos Liveris with whom we started the work together but he is not with us anymore to continue it.

8 REFERENCES

ABOLIN (2011), *Technical product leaflets & Measurements' Certificates*.

Dimoudi, A., (1996), *Urban design*, In M. Santamouris & D. Assimakopoulos (Eds.), *Passive cooling of buildings*, pp. 95–128, London: James & James Science.

Dimoudi A., Zoras S., Tamiolaki A,-M,., Dimoudi S., Liveris P., Pallas Chr., Stathis V., Varnalidou E,-E., (2013). *Microclimate improvement through redesign of open urban areas with bioclimatic criteria in a city centre.* Intern. Conf "Changing Cities: Spatial, morphological, formal & socio-economic dimensions', Skiathos, 18-21 June 2013.

Dimoudi, A., Nikolopoulou, M., (2003), *Vegetation in the urban environment: Microclimatic analysis and benefits*, Energy and Buildings, Vol. 35(1), pp. 69-76.

Gaitani, N., Spanou, A., Saliari, M., Synnefa, A., Vassilakopoulou, K., Papadopoulou, K., (2011), *Improving the microclimate in urban areas: A case study in the centre of Athens*, Building Services Engineering Research and Technology, Vol. 32(1), pp. 53-71

Gaitani, N., Michalakakou, G., Santamouris, M., (2007), *On the use of bioclimatic architecture principles in order to improve thermal comfort conditions in outdoor spaces*. Building and Environment, Vol. 42 1, pp. 317–324.

Incropera De Witt, (1990), *Fundamentals of Heat and Mass Transfer*. London: Willey

Lau, S. S. Y., Yang, F., Tai, J., Wu, X. L., & Wang, J., (2011), *The study of summer-time heat island, built form and fabric in a densely built urban environment in compact Chinese cities: Hong Kong, Guangzhou*. International Journal of Sustainable Development, Vol. 14(1-2), pp. 30-48

Mihalakakou, P., Flocas, H.A., Santamouris, M., Helmis, C.G., (2002), *Application of neural networks to the simulation of the heat island over Athens, Greece, using synoptic types as a predict*or. Journal of Applied Meteorology, Vol. 41 5, pp. 519–527.

Santamouris, M., Mihalakakou, G., Papanikolaou, N., Assimakopoulos, D.N., (1999), *A neural network approach for modeling the heat island phenomenon in urban areas during the summer period*. Geophysical Research Letters, Vol. 26 3, pp. 337–340.

Santamouris, M., (2007), *Heat island research in Europe - State of the art.* Advances Building Energy Research, Vol. 1, pp. 123–50.

Santamouris M. (Ed)., (2006), *Environmental Design of Urban Buildings*. London: Earthscan.

Santamouris, M., (Ed.), (2001), *Energy and climate in the urban built environment, The role of green spaces* (pp. 145–159), London: James & James Science.

Stogiannou X., (2011). '*Thermal Assessment of outdoor spaces structural materials'.* MSc Dissertation, MSc course 'Environmental Engineering & Science', DUTH (In Greek).

TOTEE 20701-1, (2010). *Analytical national specifications of parameters for calculation of the energy performance of buildings and issue of the energy performance certificate*. Technical Chamber of Greece.

Zoulia, I., Santamouris, M., Dimoudi, A., (2009), *Monitoring the effect of urban green areas on the heat island in Athens*. Environmental Monitoring and Assessment, Vol. 156(1-4), pp. 275-292.

COOL FLUOROCARBON COATINGS IN INDUSTRIAL BUILDINGS: OPTICAL PROPERTIES AND ENERGY PERFORMANCE

Elena Mastrapostoli[1],Theoni Karlessi[1], Alexandros Pantazaras[1], Dionysia Kolokotsa[2], Mattheos Santamouris[1]

1 1. University of Athens, Physics Department, Group Building Environmental Studies, Athens, Greece

2 1. Technical University of Crete, School of Environmental Engineering , GR 73100, Crete, Greece

Note: the contact addresses may be re-arranged

ABSTRACT

Rejection of solar gains is the aim of passive cooling strategies in any type of building and any climatic region. The extent of cool materials usefulness is dependent on the severity of external conditions and internal heat gains. The aim of the present paper is to underline the contribution of an innovative cool fluorocarbon coating in the reduction of energy demand for cooling in an industrial building with increased heat gains under temperate climatic conditions. The material is tested using accelerated weathering procedures and its optical properties, i.e. solar reflectance and infrared emmitance are measured. There is an increase of 120% of the roof's albedo by the application of cool material. Regarding the heating and cooling loads there was a decrease of 73% for cooling while there was a minor heating penalty of 5%.

Keywords: cool materials, industrial building, temperate climatic conditions, energy efficiency, reduction of cooling load

1 INTRODUCTION AND STATE OF THE ART

Rejection of solar gains is the aim of passive cooling strategies in any type of building and any climatic region. The extent of cool materials usefulness is dependent on the severity of external conditions and internal heat gains (Kolokotroni & Kolokotsa, 2013). Cool materials work by reflecting solar radiation and therefore rejecting solar heat gains at the opaque external surfaces of the building (Synnefa, Santamouris, & Apostolakis, 2007; Synnefa, Santamouris, & Livada, 2006). Heat transfer to the internal space by conduction is therefore reduced while the magnitude of the reduction will be determined mainly by the solar radiation intensity, the temperature difference between inside and outside as well as the constructional characteristics of the roof.

Climates with high solar radiation are usually associated with high external air temperatures in the summer and mild temperatures in winter. In buildings of such climates rejection of heat gains is essential to maintain comfortable conditions inside the building or the use of high quantities of air conditioning for cooling. The effect of cool materials in hot climatic conditions are studied by various researchers (H Akbari, Damon Matthews, & Seto, 2012; Boixo, Diaz-Vicente, Colmenar, & Castro, 2012; Kolokotsa, Diakaki, Papantoniou, &

Vlissidis, 2011; Romeo & Zinzi, 2011; Rose, Akbari, & Taha, 2003; Synnefa, Saliari, & Santamouris, 2012). In most cases a reduction of the cooling load varying from 20-40% is revealed by the application of cool roofs while a considerable indoor comfort improvement is noticed. Although cool materials are considered a reliable solution for hot climatic conditions, they can be a feasible solution in temperate climatic conditions, i.e. low solar radiation, moderate air temperatures in the summer and cold temperatures during the winter. In buildings of such climates, rejection of heat gains should be considered carefully because they can be useful to reduce heating requirements. On the other hand depending on the use of the building internal heat gains might be so high that air conditioning may be required throughout the year. Recent developments in materials' technology provide extra functionalities leading to the term of smart materials that provide a desired response to external stimulus, such as temperature, light, humidity, etc. Innovative materials for buildings and outdoor spaces have been developed and tested (Fufa, Hovde, Talev, & Jelle, 2010; Gustavsen, Grynninga, Arasteh, Jelle, & Goudey, 2011; Karlessi, Santamouris, Apostolakis, Synnefa, & Livada, 2009; Kolokotsa et al., 2012; Santamouris, Synnefa, Kolokotsa, Dimitriou, & Apostolakis, 2008; Syneffa, Dandou, Santamouris, Tombrou, & Soulakellis, 2008). Their durability, ageing features, UV degradation, and contribution to energy efficiency impact are still under investigation. Such materials include innovative cool coatings, phase change materials, chromotropic and photocatalytic coatings with self-cleaning functionalities, nano-composites etc. Innovative materials will have a significant impact on the built environment in the near future and their effects should be sufficiently well understood in the context of energy conservation and environmental impact.

To this end the aim of the present paper is to underline the contribution of an innovative cool fluorocarbon coating in the reduction of energy demand for cooling in an industrial building with increased heat gains under temperate climatic conditions. The material is tested using accelerated weathering procedures and its optical properties, i.e. solar reflectance and infrared emmitance are measured. The coating is then applied in an industrial building situated in the Netherlands where its contribution to the reduction of energy demand is assessed.

2 MATERIALS AND METHODS

2.1 Technical specifications of the coatings

The studied coating is a tetrafluoroethylene monomer fluorocarbon coating in a water-borne (FC coating) formula which is applied on a cement tile (7x7cm) and on an aluminum substrate (10x10cm). Each substrate was coated at a thickness of approximately 110μm.

This study includes for each sample:

- Spectral reflectance measurements over the spectrum 300-2500nm (UV-VIS-NIR)
- Calculation of the Solar Reflectance (%)
- Calculation of the Solar Reflectance Index (SRI)
- Measurement of the infrared emittance
- Calculation of maximum surface temperature
- Accelerated ageing of the samples in an Accelerated Ageing Xenon Test Chamber.

2.2 Accelerated weathering

Accelerated ageing of the concrete substrate sample (S4, cement tile) was performed in an Accelerated Ageing Xenon Test Chamber (Q-SUN, Xe-3HS) for a 60days period in a 24 hours basis according to the specifications and requirements of ISO 11341 (ISO, 2004).

With a nominal cut-on of 295 nm, the daylight filter used, provides the most accurate spectral match with direct sunlight. The filter is recommended for the best correlation between the accelerated ageing test chamber and natural outdoor exposures and conforms to the spectral requirements of ISO 4892, ISO 11341, ASTM G155, SAE J1960 and SAE J2527.

The test chamber is equipped with a precision light control system which allows the choice of the desired level of irradiance. Irradiance is monitored and controlled at 340nm.

Temperature monitoring and control is performed by a black panel temperature sensor which controls the specimen's surface temperature and simultaneously by the chamber air temperature control to give the ultimate determination of the specimen temperature. The effects of outdoor moisture are simulated by direct, pure water spray and by relative humidity control. The samples before and after weathering are depicted in Figure 1.

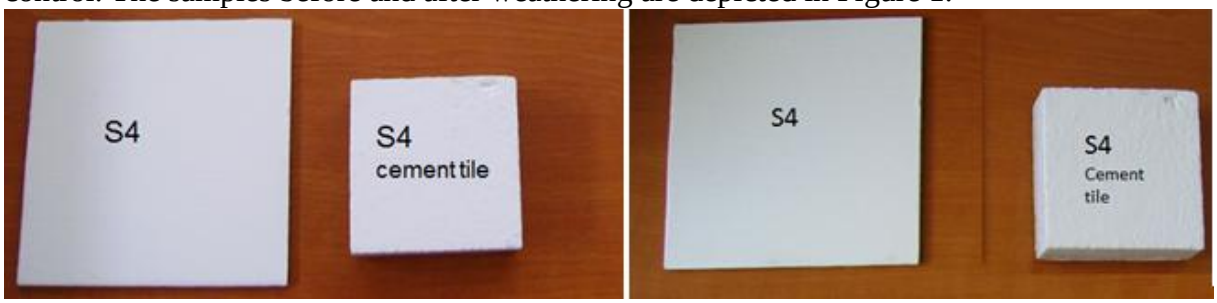

Figure 1 The samples before and after accelerated weathering

2.3 Solar reflectance

The spectral reflectance of the sample is measured in the range of 300-2500nm. The measurements for the solar spectral reflectance are conducted according to the ASTM Standard E903-96 (ASTM, 1996). The results from the spectrophotometric measurements for the specific sample before (black line) and after (red line) the artificial aging is shown in Figure 2.

The spectral reflectance data are used in order to calculate the solar reflectance of the samples. The term solar reflectance (SR) designates the total reflectance of a surface, considering the hemispherical reflectance of radiation, integrated over the solar spectrum, including specular and diffuse reflection. The calculation is done by the weighted averaging method, using a standard solar spectrum as the weighting function. The spectrum employed is that suggested by ASTM standards (ASTM, 1996, 2012a). Additionally the solar reflectance in the ultraviolet (UV: 300-400nm), the visible (VIS: 400-700nm) and the near infrared (NIR: 700-2500nm) part of the electromagnetic spectrum is calculated. The calculated values of solar reflectance are shown in Table 1.

Table 1 *Calculated values of solar, UV, VIS and NIR reflectance for all the samples.*

Sample	**Description**	**SolarReflectance (SR)**	**SR_{UV} (300-400nm)**	**SR_{VIS} (400-700nm)**	**SR_{NIR} (700-2500nm)**
S4 before	FC coating	0.89	*0.09*	0.96	0.88
S4 after	FC coating	*0.87*	0.07	*0.92*	*0.88*

The solar reflectance for the tested sample is high before the accelerated aging. The sample is characterized by high reflectance values in the visible (0.94 – 0.97) and the near infrared part of the spectrum (0.87-0.88). It exhibits strong absorption (0.08-0.09) in the UV range (300-400nm). After the accelerated aging the solar reflectance values are reduced by 0.02. Reflectance values in the near infrared part of the spectrum remained almost the same.

2.4 Measurement of the infrared emittance

The infrared emittance (e) specifies how well a surface radiates energy away from itself as compared with a black body operating at the same temperature. The measurements for the infrared emittance were conducted according to the ASTM Standard E408-71 (ASTM E408-71 (2002) - Standard Test Method for Total Normal Emittance of Surfaces Using Inspection-Meter Techniques) by using the Emissometer Model AE (Devices & Services). The results of the infrared emittance measurements are presented in Table 2 . The samples have suffered from a small reduction to the infrared emmitance values.

Table 2 Infrared emmitance for the samples

Sample	**description**	**Emmisivity**
S4 before	FC coating	0.88
S4 after	FC coating	*0.87*

2.5 Calculation of the Solar Reflectance Index (SRI) and maximum surface temperature

Based on the results of the solar reflectance and infrared emittance measurements the Solar Reflectance Index of the sample is calculated. The Solar Reflectance Index (SRI) is a measure of a surfaces ability to reject solar heat, as shown by a small temperature rise. It is defined so that a standard black (reflectance 0.05, emittance 0.90) is 0 and a standard white (reflectance 0.80, emittance 0.90) is 100 (Zerlaut, 1989).

The calculation was performed according to the ASTM standard E1980-01: Standard Practice for calculating solar reflectance index of horizontal and low sloped opaque surfaces. The SRI was calculated for medium wind conditions (convective coefficient h_c=12W/m^2 K).

The calculation of the steady state maximum surface temperature is performed as well according to the ASTM standard E1980-01 (ASTM, 2001).

The results of the calculations are shown in Table 3. The samples are characterised by very high solar reflectance index values (over 100) even after the reduction of its values after the artificial aging. SRI values exceeding 100 can be explained by the way SRI is defined: the value 100 corresponds to a standard surface with a solar reflectance of 0.8 and an infrared emittance of 0.9.

Table 3 Calculated values of Solar Reflectance Index (SRI) and maximum surface temperatures for the samples.

Sample	**description**	**SRI**	**$T_{surface}$ ^oC**
S4 before	FC coating	113	39.8
S4 after	FC coating	*110*	*41.0*

3 EXPERIMENTAL PROCEDURE

The specific sample is applied in an industrial building located in Oss, Netherlands in order to perform large scale measurements. The experimental procedure is performed in two phases, i.e. before (1st Phase) and after (2nd Phase) the FC coating application on the roof. The measurements performed are: Measurement of the roof's albedo. Thermal imaging of the roof on hourly basis. Thermal imaging of the interior spaces at 8:00, 12:00 and 16:00 Measurement of indoor temperature and humidity.

The climatic characteristics of the region are temperate, marine with cool summer and mild winter. The average air temperature is 11ºC while the relative humidity is quite high throughout the year.

3.1 Description of the Building

The building located in Oss, Netherlands has a surface area of 1685 m^2 and 7.58m height. The specific dwelling houses the production unit and storage of a chemical company and is constructed in October 1997. Its characteristics are tabulated in **Error! Reference source not found.**.

Table 4. The building's constructional and operational characteristics

	Characteristics	**Value - Description**
1.	No of stories	1
2.	Thermal zones	1
3.	Total Surface	1685 m^2
4.	Building height	7.58m
5.	Wall construction	100 mm brick-50mm insulation-19mm

		gypsum board
6.	Roof Construction	8mm metal surface-50mm insulation-8mm metal surface. Sloped roof
7.	Window type	Double U=2.720 W/m2K
8.	Overall heat transfer coefficient of walls (U_{wall})	0.482 W/m^{2}K
9.	Overall heat transfer coefficient of roof (U_{roof})	0.591 W/m^{2}K
10.	Orientation of openings	North-South.
11.	Internal gains	Electric lighting: 5.4kW Electric equipment: 43kW.
12.	Infiltration rate	3000m^3/hour
13.	Set point winter	20 ˚C
14.	Set point summer	26˚C

3.2 Measurement of the roof's albedo

The building's roof is a metal one with 50 mm insulation. The roof's characteristics are tabulated in **Error! Reference source not found.**. The roof's albedo is measured using two two Kipp & Zonen pyranometers that are positioned at 1.5m above the roof surface. Their spectral range from is from 300 to 2800nm, their response time is less than 18s, non-linearity for 0-1000W/m^2 less than 1%, temperature dependence of sensitivity from -10^{o}C to 40^{o}C less than 5%. The first pyranometer measures the incident solar radiation and the second one the reflected radiation from the roof. The albedo is measured before and after the FC coating application. The ratio between the reflected radiation from the roof and the incident solar radiation is the albedo. The average albedo is 0.3 and 0.67 for the 1st and 2nd phase of measurements respectively.

3.3 Measurement of the indoor temperature and humidity

Five TinyTag Data Loggers TGP-4500 are used for the measurement of indoor temperature and humidity (Figure 2). The reading range is from -25^{o}C to 85^{o}C and the reading resolution is 0.01^{o}C.

The maximum indoor temperatures for all sensors are recorded before the installation. The highest maximum temperature during both phases is recorded by sensor 5 is equal to 39.4°C and 30.6°C for the first and second phase respectively (Table 5). This is explained by the fact that this position is very close to the production area where heat is extracted by the machinery. The indoor temperatures measurements are used for the model validation in order to assess the energy performance of the cool material in the industrial building under temperate climatic conditions.

Table 5 Maximum and minimum temperatures for all sensors during 1st and 2nd phase of the experimental procedure

Sensor no	**T(°C)**	**1st Phase**		**2nd Phase**	
		24/7/2012	**25/7/2012**	**29/8/2012**	**30/8/2012**
1	T_{max}	35.8	**36.8**	29.6	27.0
	T_{min}	21.6	23.2	22.9	21.2
2	T_{max}	**33.8**	31.0	28.5	25.5
	T_{min}	21.5	22.4	22.0	21.0
3	T_{max}	35.5	**36.6**	28.8	26.8
	T_{min}	21.7	22.4	22.2	21.0
4	T_{max}	33.3	**34.3**	29.0	25.4

	T_{min}	21.9	22.4	22.1	21.1
5	T_{max}	38.4	***39.4***	30.6	28.9
	T_{min}	21.7	22.3	22.3	21.0

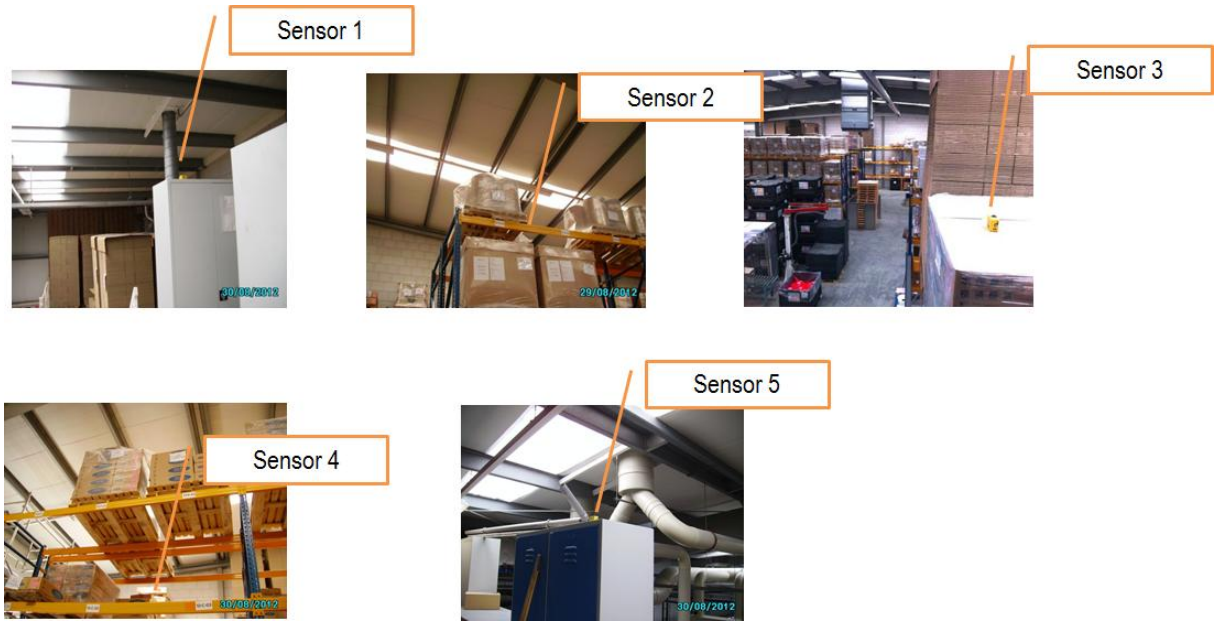

Figure 2. The temperature and humidity sensors

4 THE ENERGY PERFORMANCE OF THE COOL ROOF APPLICATION

The aim of the present analysis is to provide quantitative results on the energy efficiency that can be achieved by the application of the cool material in the specific building. The building's cooling and heating loads are calculated for the 1st and 2nd phase using EnergyPlus thermal load simulation program. The calculations are performed with an hourly time step. The values of the albedo measurements are inserted in the model together with the thermal properties of the materials. The solar absorptance of the actual roof material was set equal to 0.7 and 0.3 before and after the FC coating installation respectively. Regarding internal gains, the electric lighting is equal to 5.4kW while all the other electric equipment is measured equal to 43kW. Infiltration rate is set equal to 3000m^3/hour. The first step towards the evaluation of the energy performance is to develop validated models of that are representative of the 1st and 2nd experimental phase. The model of building that is representative for the 1st phase (before cool roof application) and its validation against the real measurements is depicted in. The specific figure illustrates the temperature variation before the application as it is derived from the measurements (red line) and from the simulation (blue line).

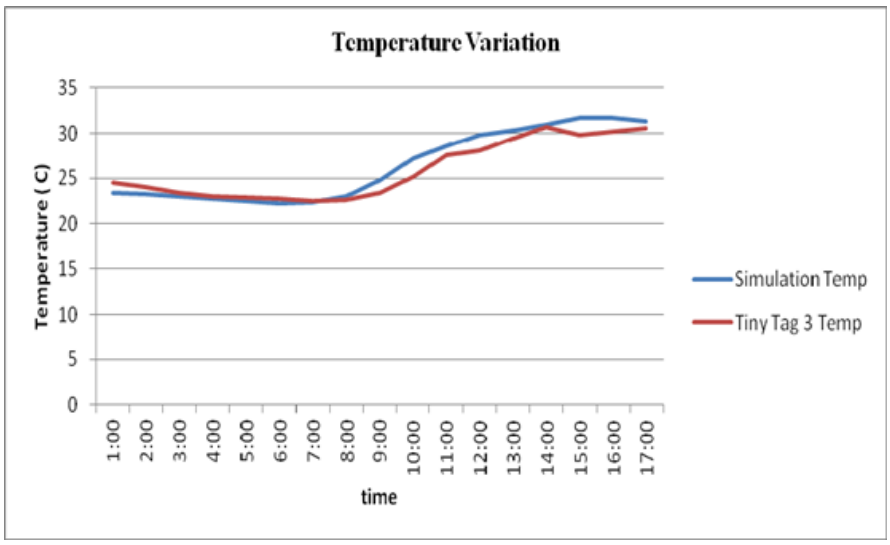

Figure 3. The measured and modeled indoor temperature fluctuation for the 24/7/2012 (1st phase)

The results indicate that before the application the indoor temperatures as calculated from the simulation vary from 22.3°C to 31.7°C while indoor temperature as recorded from sensor 3 vary from 22.4 °C to 30.7°C. After FC coating application the indoor temperature as calculated from the simulation varies from 19.4°C to 22.1°C. Maximum indoor temperature as recorded from Sensor 1 is 21.6°C and minimum indoor temperature is 20.6°C. The results show that there is a very good match between the calculated and the measured temperature values.

Furthermore, for estimating the energy demand for heating and cooling before and after the FC coating application the simulations are repeated using test reference year data on yearly basis. The thermostat set point temperatures are set equal to 26°C and 21°C for the summer and winter period repsectively. As expected, increasing roof reflectance results to reduced summer cooling loads.

The results indicated that before the application the annual cooling load was 9.7 kWh/m^2. After the application the cooling loads are equal to 2.6 kWh/m^2. The decrease in the cooling loads for an increase in roof solar reflectance of 0.4 was 73%. In order to estimate the heating penalty from increasing solar reflectance, heating loads are also calculated. Before the installation the annual heating loads are 139 kWh/m^2 and after the installation the annual heating loads are calculated to be 146 kWh/m^2.

By transforming the energy demand into final delivered energy using Energy Efficiency Ratio of 2.6 (average system efficiency) and for heating efficiency 0.75 then the energy conservation for cooling is 18.5kWh/m2 while the heating penalty is 5.3kWh/m2.

5 CONCLUSIONS

In the present study the thermal and optical characteristics of a fluorocarbon cool material are measured. The cool material is applied in an industrial building with increased internal heat gains targeting to minimise the energy demand for cooling. The value of the roof albedo has changed from 0.3 to 0.67 after the application of the cool coating. There is an increase of 120% of the roof's albedo. Regarding the heating and cooling loads there was a decrease of 73% for cooling while there was a minor heating penalty of 5%.

The overall study showed that cool materials can be a viable solution even for temperate climatic conditions and for industrial buildings where usually there is a significant burden in the cooling load due to machineries and production lines. This can make a significant difference in the use of air conditioning especially in mid seasons.

6 ACKNOWLEDGMENTS

Herewith we are acknowledging TecneXum GmbH, Essen, Germany, and Daikin Chemical Europe, Düsseldorf, Germany, for their support and to enable us to perform these studies and to publish the results.

7 REFERENCES

Akbari, H, Damon Matthews, H., & Seto, D. (2012). The long-term effect of increasing the albedo of urban areas. *Environmental Research Letters*, *7*(2).

Akbari, Hashem, & Rose, L. S. (2001). Characterizing the Fabric of the Urban Environment : A Case Study of Metropolitan Chicago , Illinois, (October).

ASTM. (1996). Standard Test Method for Solar Absorptance, Reflectance, and Transmission of Materials Using Integrating Spheres. West Conshohocken, PA.: American Society for Testing and Material.

ASTM. (2001). E1980-01: Standard Practice for calculating solar reflectance index of horizontal and low sloped opaque surfaces. American Society for Testing and Material.

ASTM. (2012a). Standard Tables for Reference Solar Spectral Irradiances: Direct Normal and Hemispherical on 37° Tilted Surface. American Society for Testing and Material.

ASTM. (2012b). E284 - 13 Standard Terminology of Appearance. American Society for Testing and Material.

Boixo, S., Diaz-Vicente, M., Colmenar, A., & Castro, M. A. (2012). Potential energy savings from cool roofs in Spain and Andalusia. *Energy*, *38*(1), 425–438.

CIE. (1987). International Lighting Vocabulary - CIE 17.4.

Fufa, S. M., Hovde, P. J., Talev, G., & Jelle, B. P. (2010). Nano-based coatings and the influence on the hygroscopic properties of wood. In *International Conference on Nanotechnology for the Forest Products Industry 2010* (pp. 147–168).

Gustavsen, A., Grynninga, S., Arasteh, D., Jelle, B. P., & Goudey, H. (2011). Key elements of and material performance targets for highly insulatingwindow frames. *Energy and Buildings*, *43*(10), 2583–2594.

ISO. (2004). Paints and varnishes -- Artificial weathering and exposure to artificial radiation -- Exposure to filtered xenon-arc radiation. International Organisation for Standardization.

Karlessi, T., Santamouris, M., Apostolakis, K., Synnefa, A., & Livada, I. (2009). Development and testing of thermochromic coatings for buildings and urban structures. *Solar Energy*, *83*(4), 538–551.

Kolokotroni, M., Gowreesunker, B. L., & Giridharan, R. (2011). Cool roof technology in London: An experimental and modelling study. *Energy and Buildings*.

Kolokotroni, M., & Kolokotsa, D. (2013). Energy and Environmental Aspects of Cool Materials. In D. Kolokotsa, M. Santamouris, & H. Akbari (Eds.), *Advances in the Development of Cool Materials for the Built Environment* (pp. 272–231). Bentham Publisher.

Kolokotsa, D., Diakaki, C., Papantoniou, S., & Vlissidis, A. (2011). Numerical and experimental analysis of cool roofs application on a laboratory building in Iraklion, Crete, Greece. *Energy and Buildings*, *55*, 85–93.

Kolokotsa, D., Maravelaki-Kalaitzaki, P., Papantoniou, S., Vangeloglou, E., Saliari, M., Karlessi, T., & Santamouris, M. (2012). Development and analysis of mineral based coatings for buildings and urban structures. *Solar Energy*, *86*(5), 1648–1659.

Kolokotsa, D., Psomas, A., & Karapidakis, E. (2009). Urban heat island in southern Europe: The case study of Hania, Crete. *Solar Energy*, *83*(10), 1871–1883.

Lowe, R. (2007). Addressing the challenges of climate change for the built environment. *Building Research & Information*, *35*(4), 343 – 350.

Nations HABITAT, U. (2011). CITIES AND CLIMATE CHANGE: POLICY DIRECTIONS.

Romeo, C., & Zinzi, M. (2011). Impact of a cool roof application on the energy and comfort performance in an existing non-residential building. A Sicilian case study. *Energy and Buildings*.

Rose, L. S., Akbari, H., & Taha, H. (2003). Characterizing the Fabric of the Urban Environment : A Case Study of Greater Houston , Texas. Berkeley, CA: Lawrence Berkeley National Laboratory.

Santamouris, M. (2012). Cooling the cities - A review of reflective and green roof mitigation technologies to fight heat island and improve comfort in urban environments. *Solar Energy*.

Santamouris, M., Pavlou, K., Synnefa, A., Niachou, K., & Kolokotsa, D. (2007). Recent progress on passive cooling techniques. Advanced technological developments to improve survivability levels in low-income households. *Energy and Buildings*.

Santamouris, M., Synnefa, A., Kolokotsa, D., Dimitriou, V., & Apostolakis, K. (2008). Passive cooling of the built environment - Use of innovative reflective materials to fight heat islands and decrease cooling needs. *International Journal of Low Carbon Technologies*, *3*(2), 71–82.

Stone, B., Vargo, J., & Habeeb, D. (2012). Managing climate change in cities: Will climate action plans work? *Landscape and Urban Planning*, *107*(3), 263–271.

Synneffa, A., Dandou, A., Santamouris, M., Tombrou, M., & Soulakellis, N. (2008). On the use of cool materials as a heat island mitigation strategy. *Journal of Applied Meteorology and Climatology*, *47*(11), 2846–2856.

Synnefa, A., Saliari, M., & Santamouris, M. (2012). Experimental and numerical assessment of the impact of increased roof reflectance on a school building in Athens. *Energy and Buildings*.

Synnefa, A., Santamouris, M., & Apostolakis, K. (2007). On the development, optical properties and thermal performance of cool colored coatings for the urban environment. *Solar Energy*, *81*(4), 488–497.

Synnefa, A., Santamouris, M., & Livada, I. (2006). A study of the thermal performance of reflective coatings for the urban environment. *Solar Energy*, *80*(8), 968–981.

Xu, T., Sathaye, J., Akbari, H., Garg, V., & Tetali, S. (2012). Quantifying the direct benefits of cool roofs in an urban setting: Reduced cooling energy use and lowered greenhouse gas emissions. *Building and Environment*, *48*(1), 1–6.

Zerlaut, G. (1989). *Solar Radiation Instrumentation, in Solar Resources*. (R. L. Hulstrom, Ed.) (pp. 173–308). MIT Press, Cambridge, MA.

USING COOL PAVING MATERIALS TO IMPROVE MICROCLIMATE OF URBAN AREAS – DESIGN REALISATION AND RESULTS OF THE FLISVOS PROJECT.

M. Santamouris*, N. Gaitani, A. Spanou, M. Saliari, K. Gianopoulou and K. Vasilakopoulou

Group Building Environmental Studies, Physics Department, Univ. Athens, Athens, Greece

And

T. Kardomateas

Prefecture of Athens, Athens, Greece

Original Paper is published in : Building and Environment, Volume 53, July 2012, Pages 128-136

ABSTRACT

The present paper deals with the application of 4500 square meters of reflective pavements in an urban park in the greater Athens area. The aim was to improve thermal comfort conditions, reduce the strength of heat island and improve the global environmental quality in the considered area. It was estimated that the use of cool pavements contributes to decrease the peak ambient temperature during a typical summer day, up to 1.9 C. In parallel, the surface temperature in the park was reduced up to 12 C while comfort conditions have been improved considerably. It is concluded that the use of reflective pavements is a very efficient mitigation technique to improve thermal conditions in open urban areas.

KEYWORDS

Heat Island, Cool materials and pavements, Heat island mitigation techniques

INTRODUCTION

Urban heat island is the more documented phenomenon of climate change. The phenomenon relies to higher urban temperatures compared to the surrounding areas because of the positive heat balance caused mainly by increased anthropogenic heat, decrease of the air flow, lack of heat sinks and increased absorption of solar radiation by the city structure.

Heat island is very well-studied and documented phenomenon for the city of Athens, Greece. Apart of the global climatic change that increases the ambient temperature and the frequency of heat waves, heat island is an additional reason that contributes to the temperature increase. The impact of heat island on the cooling energy consumption of buildings is quite important. Studies have shown that the cooling energy consumption may be doubled because of the increased ambient temperatures in the affected areas. In parallel, the environmental quality in the overheated zones is worsening as pollution is increasing, and the ecological footprint of the city is growing seriously.

To counterbalance the impact of heat island efficient mitigation techniques have been developed and applied.. This implies the use of advanced materials for the urban environment, able to amortize, dissipate and reflect heat and solar radiation strategic landscaping of cities including appropriate selection and placing of green areas, use of green roofs, solar control systems, and dissipation of the excess heat in low temperature environmental heat sinks like the ground, the water and the ambient air .

Materials presenting a high reflectance to solar radiation together with a high emmisivity factor are known as cool materials. Such materials may be used in pavements, other urban structures and building roofs Important energy benefits are also associated to the use of reflective materials as the cooling load of buildings is seriously reduced.

Although reflective materials have been extensively tested in cool roof applications, existing data on their potential to mitigate heat islands when used in pavements and other urban structures is very limited.

The present paper reports the results of a real project in Athens, Greece, where extensive use of cool colored paving materials has been made aiming to reduce ambient temperatures during summer and improve the environmental quality of a public urban park. In total, 4500 m2 of cool paving materials have been applied to the area, while extensive measurements combined to numerical modeling have been performed before and after the rehabilitation of the area to

identify the mitigation potential of the used cool materials and document the thermal performance of the whole project.

DESCRIPTION OF THE SITE AND REFURBISHMENT CHARACTERISTICS

The Flisvos urban park is a coastal area located in the south western part of Athens, Municipality of Paleon Faliron, and covers a total area close to 80000 m2. It is surrounded by a major traffic axis and the sea, Saronic Golf. The park was composed by green and paved areas that given access to the sea. The so called green part was quite sparsely planted with small trees and bushes. Paved areas were made of asphalt, concrete and quite dark paving components. The absorptivity of the used paved surfaces was measured between 0,55 to 0,65, while areas covered with concrete and asphalt presented much higher values, 0,79 and 0,89 respectively.

The local Municipality in collaboration to the Prefecture of Athens has designed and undertaken a major refurbishment plan for the area. The plan was executed in two faces. During the first one almost 2500 trees and bushes are planted while during the latest one almost 4500 m2 of existing pavements have been replaced with new cool materials presenting a high reflectivity to the solar radiation. The overall refurbishment of the park has been started at 2009 and was finalized during the summer of 2010. The first phase was finished during the end of 2009 when all green areas have been planted, while the change of the pavements has been taken place during June and part of the July 2010. The present paper concentrates on the second phase and deals with the evaluation of the thermal advantages rising from the use of the cool pavements.

CHARACTERISTICS OF THE SELECTED COOL MATERIALS

Paving materials have been selected to satisfy the following criteria :

a) To present the higher possible non specular reflectivity to solar radiation.

b) To present the lowest possible decrease of the reflectivity because of the ageing effects.

c) To present the highest possible emissivity factor something common for most of the paving materials

d) To present the highest possible durability and aesthetic value.

Based on the above, small concrete blocks of light yellow color have been designed and selected. The blocks have been colored using infrared reflective pigments mixed in the whole mass of the blocks during their preparation. For aesthetic reasons and in order to avoid a rapid degradation of the material's reflectivity a light yellow color has been selected. The solar reflectivity of the selected materials has been optimized after various tests in relation to the proportion and the characteristics of the used primary materials, (concrete, sand, gravel, etc), and the infrared reflective pigment . The global solar reflectance of the selected material was calculated close to 60 %, while the corresponding reflectivities in the visible and infrared parts are close to 47 and 71 % respectively. The emissivity of the selected concrete blocks was measured close to 0.9

EVALUATION METHODOLOGY

To evaluate the possible thermal impact of the used cool pavements on the environmental quality of the considered area, the following methodology has been designed and used. The methodology involved five distinct steps.

Step 1 :Monitoring of the Initial Situation : Detailed measurements of the main climatic parameters in the area including surface and ambient temperatures, wind speed and concentration of pollutants have been performed in the considered area prior to any intervention.

Step 2. Development of a Computational Model for the Initial Situation: A thermal model of the area has been created using CFD techniques and simulations have been performed using the boundary conditions measured during the previous step. Comparisons of the measured against the predicted values are performed and the model was improved until a very good agreement is achieved.

Step 3. Monitoring of the Final Situation : Given the installation of the cool pavements, new measurements have been carried out. All measurements have been performed according to the same experimental protocol described in step 1.

Step 4. Development of a Computational Model for the Final Situation: A new thermal model considering the installed cool pavements has been created using the same CFD tool. All other parameters and conditions stay similar as in the model described in Step2,. Simulations have been performed for the boundary conditions measured in step 3. The calculated values have

been extensively compared against the measured ones and the model improved until the best possible agreement is achieved

Step 5. Theoretical Comparisons for a Typical Summer Day : The boundary conditions corresponding to a typical summer day have been defined in details and simulations have been performed by using both calibrated thermal models. Values of the main climatic parameters in the considered area have been calculated for the initial and the final situation using exactly the same boundary conditions. Both sets of calculated data have been compared and conclusions on the thermal impact of the cool pavements have been drawn.

Such a methodology offers the possibility to identify in a quite good approximation the possible impact of a major intervention in an uncontrolled environment operating under dynamic boundary conditions.

MONITORIN STRATEGY

A complete monitoring plan has been designed and applied for both sets of measurements performed before and after the installation of the cool pavements. Ambient and surface temperatures, relative humidity, wind speed and direction as well as the concentration of suspended particles were recorded during the experiments in most of the areas of the park.

The mobile station went through the whole park following a specific route. Measurements were performed in a continuous basis, Measurements at eight reference points were recorded on an hourly basis. Comparisons between the various experimental and theoretical data sets have been performed for the reference points. In parallel to the above measurements, solar radiation data as well data on the undisturbed wind and temperature have been taken from the meteorological station

THE COMPUTATIONAL THERMAL MODEL

Computerised Flow Dynamic Techniques, CFD, have been used to evaluate the thermal environment in the considered space. For the specific work the PHOENICS CFD package has been used. As it concerns turbulence, the standard k-e model has been used. The values of the surface temperatures were calculated through the TRNSYS, simulation tool and then introduced as a boundary to PHOENICS and simulations of the ambient temperature and wind speed distributions have been performed. At the inflow boundaries, the wind field is specified.

As it concerns the interference coming from the boundaries to the flow, the distance between the object and the boundaries of the domain was set equal to 6 times the characteristic length for the position of the inlet (6H), 8 times to the position of outlet (8H) and 5 times to the lateral boundaries (5H). The top and side boundaries were considered as the symmetry conditions.

DESCRIPTION OF THE INITIAL SITUATION. MONITORING AND SIMULATION RESULTS

Detailed measurements in the park have been performed the 14th and 15th of April just before the start of the works to install the cool pavements. Both days were clear and solar radiation intensity during the noon period was close to 800 W/m2. Daily average surface temperatures in the non-shaded parts of the park varied between 24,5 C for the grass, 26,7 for the pavements, 28,4 C for the asphalt and 28,8 C for the dark bare soil. Corresponding surface temperatures in the shaded parts were 6-9 C lower. Ambient temperatures at 3.5 m height varied for both days between 16.5 C and 19.8 and for the period between 9:00 t0 17:00. The maximum spatial temperature gradient in the park was close to 2,2 C and was recorded in the early afternoon period.

Following the specific evaluation methodology described previously, specific simulations have been carried out to predict the thermal conditions in the considered space during the period of the measurements. In all simulations the undisturbed boundary conditions have been taken by the National Observatory of Athens and are used as inputs to the CFD code. In parallel, the surface temperature of the main materials in the area has been simulated and then used as inputs to the model. The maximum difference between the measured and the predicted surface temperatures never exceeded 0.4 C. Simulations have been performed for many different measured boundary conditions and the model was continuously improved to better fit the existing conditions. The agreement between the theoretical and the measured temperatures is found to be satisfactory. The maximum temperature difference between the two sets of data never exceeded 0.5 C. The spatial distribution of the temperature is also similar for both the measured and the theoretical data. Thus, it may be concluded that the developed theoretical thermal model can predict with sufficient accuracy the climatic conditions in the area prior to the installation of the cool pavements.

APPLICATION OF THE COOL PAVEMENT – MONITORING RESULTS

After the installation of the cool pavements in the park, detailed measurements have been performed using exactly the same experimental protocol as in the first monitoring campaign.

Measurements have been performed for the 27th of July and the 4th of August. Both days were clear and solar radiation intensity during the noon period was 840 and 950 W/m2 for the first and the second day respectively.

The daily surface temperature of the non-shaded cool pavements varied between 31,3 C to 33,8 C during the first day and 37,6 C and 39,9 C during the second one. The corresponding surface temperatures for the conventional pavement varied between 35,9 C and 39,2 C for the first day and 43,4 C and 47,5 C for the second one. The maximum temperature difference between the cool and conventional pavements was 5,4 C and 7,6 C for the first and the second day respectively. As expected, the temporal variation of the ambient temperature at 3.5 m height, presented the lower temperatures next to the sea front, (26 C- 28,2 C), while temperatures in the interior part of the park varied between 26.5 C to 29.5 C. The maximum spatial temperature gradient in the park was close to 1.5 C.

The same evaluation methodology described previously has been followed and CFD simulations have been performed for the 27th of July. The undisturbed climatic conditions given by the National Observatory of Athens have been used as inputs. Surface temperatures for all materials including the cool pavements have been calculated using TRNSYS and then are used as inputs to the CFD model. A very good agreement between the calculated and the measured surface temperatures has been achieved. The maximum difference between the measured and the simulated data never exceeded 0.3 C. Through repetitive runs the model has been improved the maximum possible to represent the new climatic situation in the park. The achieved agreement between the two sets of data is found quite satisfactory and the difference never exceeded 0.4 C. The predicted spatial distribution of the ambient temperature is very close to the measured one.

CALCULATION OF THE MICROCLIMATIC IMPROVEMENTS

As foreseen by the evaluation methodology, comparative simulations of the thermal conditions in the considered space have been performed for the peak period, (14:00), of a typical summer day and with and without the cool pavements. The developed and tested CFD models have been used correspondingly. The undisturbed temperature and wind speed used for the boundary conditions were 32 C and 2 m/sec blowing from northern directions. The solar radiation intensity was taken equal to 940 W/m2. Surface temperatures for all materials have been calculated using the TRNSYS thermal simulation model. The average temperature of the

non shaded cool pavement was calculated equal to 36.8 C while the temperature of the conventional pavement equal to 48.1 C.

The calculated ambient temperatures for both scenarios at the eight reference points are given in Figure 1. As expected, for the coastal part of the park, (points 6-8), temperatures are very similar and the impact of cool pavements is fully negligible. On the contrary, in the inner part of the park the impact of cool pavements is important and contributes to a decrease of the maximum ambient temperature up to 1.9 C. This is very close to the results reported in similar projects were cool pavements have been considered to improve the environmental quality of open spaces.

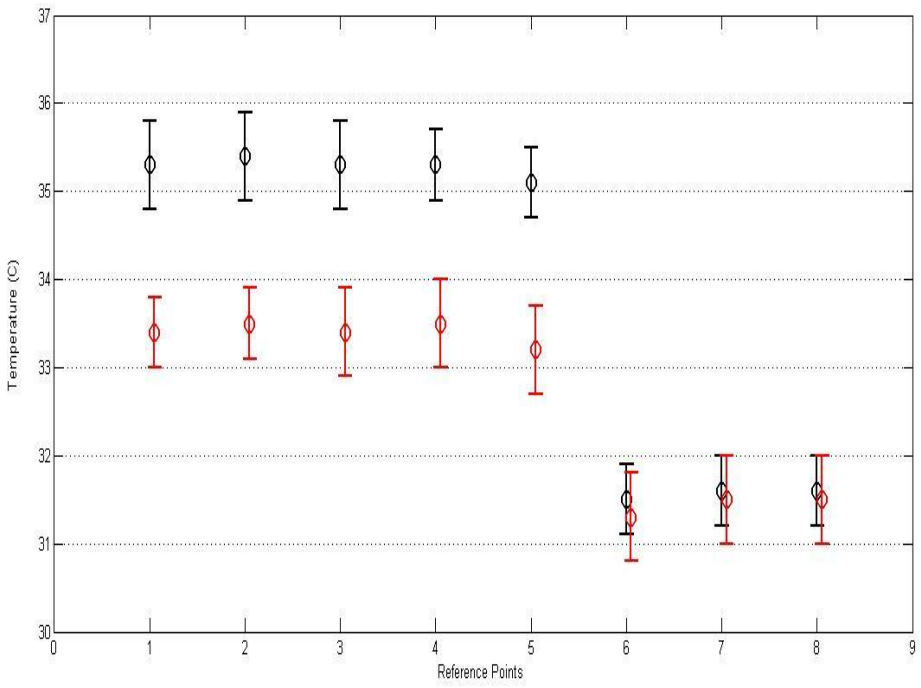

Figure 1 : Comparison of the predicted distribution of the ambient temperature in the park at 1.80 m height for 14:00 of a typical summer day before, (black), and after the installation of the cool pavements, (red)

CONCLUSIONS

Heat island increases temperature in urban areas, increase the energy consumption for cooling purposes and affect the global environmental quality of cities. Use of advanced mitigation

techniques contributes highly to decrease temperatures and improve comfort in open urban areas. Cool materials presenting a high solar reflectivity and emissivity have been proposed as an effective mitigation technique when applied to buildings and open spaces.

Almost 4500 m2 of cool pavements have been used to rehabilitate a major urban park in the greater Athens area. In order to evaluate the impact of cool pavements, measurements of the climatic conditions in the considered place have been performed before and after the installation of the cool materials. A specific evaluation methodology has been designed and applied. Computerised fluid dynamic techniques have been used to simulate the specific climatic conditions in the area before and after the installation of the new pavements. After validation against the two sets of the collected experimental data, comparative calculations have been performed with and without the cool pavements under the same climatic boundary conditions. It is found that the extensive application of reflective pavements may reduce the peak daily ambient temperature during a typical summer day up to 1.9 C while surface temperatures are reduced up to 12 C. In parallel, calculations of the thermal comfort conditions in the area have shown that cool pavements improve considerably comfort in outdoor urban spaces.

The overall analysis has shown that use of cool pavements is an efficient mitigation strategy to reduce the strength of heat island in urban areas and improve the global environmental quality of open areas.

REFERENCES

PHOENICS software tool. Available at: : http://www.cham.co.uk/.

EXPERIMENTAL DETERMINATION OF COMFORT BENEFITS FROM COOL-ROOF APPLICATION TO AN UN-CONDITIONED BUILDING IN INDIA

[1]Rathish Arumugam <rathish.iiit@gmail.com>, [1]Vishal Garg, [2]Jyothirmay mathur, [1]Niranjan Reddy, [1]Jalpa Gandhi, [3]Marc L. Fischer

1 Center for IT in Building Science, International Institute of Information Technology, Hyderabad, India

2 Center for Energy and Environment, Malviya National Institute of Technology, Jaipur, India

3 Sustainable Energy Systems Group, Environmental Energy Technologies Division, Lawrence Berkeley National Laboratory, Berkeley, California, 94720, USA

1. Abstract

Increasing roof reflectance reduces absorption of solar radiation, roof surface temperatures, and heat flux in the building interior. At the building level this leads to savings in air-conditioning energy consumption and increase in indoor comfort. At the macro level it helps in mitigating Urban Heat Island effect and reduces net solar radiation absorbed by the earth, lowering local air temperature and pollutant formation, and reducing global warming. Various studies have demonstrated energy savings in buildings using cool roofs. However, there are not many studies on the indoor comfort benefits of cool roofs for unconditioned interior spaces, especially in India. A study was performed on an un-conditioned, institutional building in a composite climate in India. Monitoring was performed for a period of six months (Jan – Jun, 2012) on two adjacent sections of continuous concrete roof surface, one of which had been previously coated with a white paint coating. The measured shortwave band-averaged (0.3-3 micron) solar reflectance was 0.28 and 0.57, for the uncoated and coated surfaces, respectively. The increased reflectivity reduced the seasonal average indoor air temperature and heat flux by 1.07^{o}C, and 14.4 W m^{-2}, respectively, with peak reductions of 1.38^{o}C and 18.3 Wm^{-2} in April, 2012. This increased the number of adaptive comfort hours by 80 hours (about 8%), providing a significant improvement in human comfort.

Keywords: Cool Roofs, Institutional Building, Un-conditional Building, Comfort Improvement, Air temperature

2. Introduction

A roof that reflects and emits the solar radiation back to the sky rather than transferring it into the building is termed as cool roof [1]. Cool roof helps in reducing air conditioning energy consumption in a conditioned building and improves thermal comfort in an un-conditioned building. The energy savings achieved in a building from cool roofs is dependent on various parameters like the location, orientation of the building, local shading by trees or other buildings, construction type, insulation type, plenum ventilation, equipment load, occupancy and operational schedules [2]. Thermal comfort benefits using cool roofs depend on other external parameters such as the location, orientation, ventilation rate, window size and type and the thermal comfort in a particular location tends to be adaptive in nature. The benefits of cool roof are summarized below.

2.1 Benefits of cool roofs:

Cools roofs have various benefits associated with them. This includes reducing heat island effect, negative radiative forcing of carbon di oxide in macro level and reducing the energy consumption of the building, increasing the comfort for the building occupants. Since our project is in building level we will look into the energy and comfort benefits of cool roofs in this section.

2.1.1 Energy savings from cool roofs:

It is notable that the maximum benefits of high albedo roofs can be seen in the hot and humid climatic zone. In one of the early experiments conducted by Florida solar energy center [3] to measure the benefits of cool roofs, an annual savings of 13,000 kWh was observed in the chiller energy consumption over 2 years period. The reduction in peak energy consumption (from 9 AM to 4 PM) was observed to by 1.5 kW (15% of the total demand) and the summer time peak reduction of 5.6 kW (35% of summer peak consumption) was observed. In an attempt to study to the impact of cool roofs on residential buildings [4], six houses were monitored in Florida. The cooling energy reduction ranged from 3% to 23%.

Researchers from Lawrence Berkeley National Laboratory conducted a series of experiments in California to quantify the benefits of high albedo roof. In a study to identify the savings from various Heat Island Effect mitigation strategies in three different climates (Baton Range, Salt Lake City and Sacramento), it was observed that the maximum savings from cool roofs occur in Hot and Dry climate [5]. A similar study [in Texas, in the city of Austin, on a retail store, showed a peak outside surface temperature reduction of 42°F (from 168°F in black roof to 126°F in a white roof). For a building which has a roof area of 10000 ft^2, an energy savings of 3.6 Wh/ft^2 (11% of total cooling energy) in cooling energy and demand reduction of 0.35 Wh/ft^2 was observed.. In terms of percentage the average summer time energy saving observed is 11% of the total cooling energy. Usage of cool roofs also reduced the insulation requirement in the building. The payback that was observed in this study was almost instantaneous [6].

In Indian context cool roofs have been demonstrated to have energy savings of 20 – 22 kWh/m^2 of roof area, corresponding to an air conditioning energy use reduction of 14 – 26% in commercial buildings by changing the previously black roofs to white roofs. This study also estimated an annual savings of 13 – 14 kWh/ m^2 of roof area by applying a white coating to concrete roof, corresponding to an energy savings of 10 – 19% in the metropolitan of Hyderabad [7].

2.1.2 Comfort improvements from cool roofs

An investigation in the city of Poitiers, France on an un-conditioned building showed a tremendous increase in the thermal comfort of the building using cool roofs [8]. Experiments were performed for both insulated and non-insulated buildings. The cool roof installed on the test building had a solar reflectivity of 0.88 and a thermal emittance of 0.9. Operative temperature was used as a parameter to estimate the comfort of the building. In case of non-insulated roof, a reduction in the operative temperature of 9.9 °C (from 32.3 °C to 23.4 °C) in the attic and a reduction of 5.8 °C (from 29.4°C to 23.6 °C) in the indoor room temperature were observed before and after installation of cool roofs. In case of insulated roof not much difference in the operative temperatures were observed. The gain observed is a maximum of 1°C (from 30.2 °C to 29.3 °C) before and after installation of cool roof.

Another study was conducted to find the impact of cool roofs and green roofs in Mediterranean climate [9]. Cities from the northern (Barcelona), southern rim (Cairo) and from the middle basins

(Palermo) of the Mediterranean area were evaluated. The indoor thermal comfort was quantified as the number of hours in which temperatures exceeded a desirable operative temperature for the room. Three different set points were chosen for this study. In Barcelona the number of unmet hours above 26^{o}C has been reduced by 46% and 26% for non-insulated and insulated roofs. Metallic roof reduces the unmet hours by 20% in both cases. No unmet hours were witnessed above 28^{o}C in case of both cool and green roofs and the un-comfort hours have been reduced by 73% in metallic roofs. Despite the energy penalties seen in Barcelona from cool roofs due the increase in the thermal comfort of the building, cool roofs may still be considered for application.

A study in London on an office space performed a parametric analysis in which the roof albedo was varied from 0.1 to 1.0 [10]. When a cool roof is applied over a building with higher ventilation rate with a higher set point is we get more energy savings. The un-comfort hours for operative temperature and air temperature were plotted for different albedo values and the internal air temperature become to dip steeper after an albedo value of 0.6.

Most of the comfort related studies have been performed over residential buildings. In our study the comfort benefits of cool-roofs for an un-conditioned institutional building in warm climate of India has been examined. This represents an important real-world evaluation of an energy-efficient retrofit that serves as part of integrated design for sustainable urban environments.

3. Methodology

3.1 Monitoring site

To find the temperature and heat flux reductions institutional building has been chosen in composite climate zone in India. The building is located in Pantnagar, Uttarkand. (28.97°N, 79.41°E). There are major agricultural industrial activities happening in Pantnagar. This leads to higher aerosol levels in the site. Due to this the soiling of the roof surfaces was expected. Temperature sensors were installed both on the inside and outside surfaces. Apart from these heat flux coming inside the building and the inside air temperature were monitored.

At Pantnagar, the College of Biological and Physical Sciences was selected as a site for the roof monitoring project as shown in **Error! Reference source not found.**.and **Error! Reference**

source not found.. The buildings that are monitored are unconditioned. The building is an educational institute with two storey structure and has grey cemented flat roof. Roof of the building was retained grey cemented and other was painted with a white coating in May, 2011. The height of the floor is 3.65m with 100cm thick concrete roof. This building has research lab, library, discussion rooms, toilets etc. The roofs were located at the east side of the building as shown in Figure 2, where "dark" denotes sensor positions for uncoated roof, and "Cool" indicates sensor positions for cool roof.

It is interesting to note that the room which had the cool coating applied on it, has two of its walls exposed to the outside atmosphere. Both walls contained windows and operation of these windows might change the infiltration rates and heat gain from the walls when compared to the dark roof.

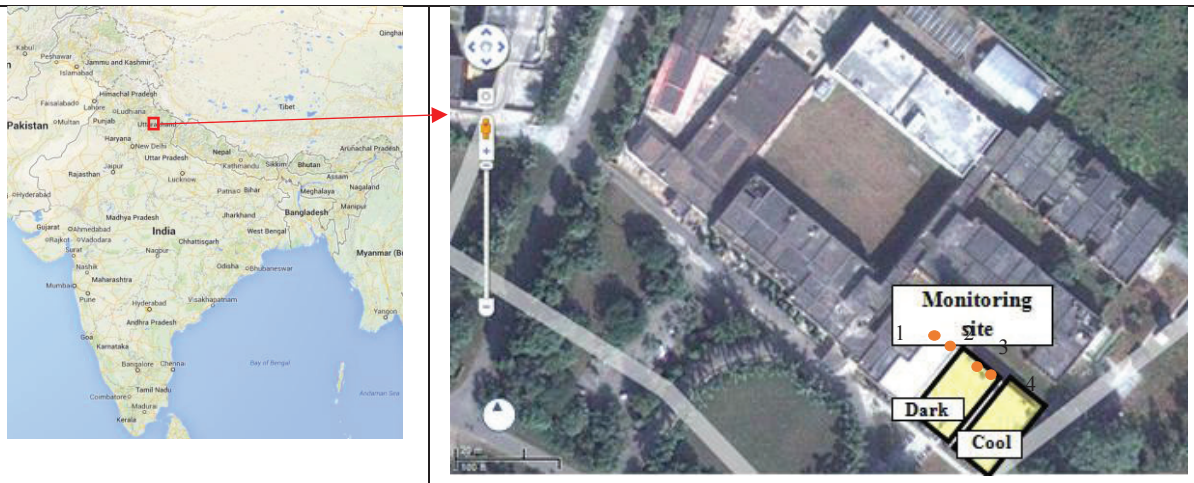

Figure 1: Satellite image of Pantnagar site: Block B Environmental Science Wing

3.2 Adaptive thermal comfort

Thermal comfort is expressed as a factor of outdoor effective temperature in various standards like ASHRAE, RP-884. This has been widely accepted method for evaluating the thermal comfort. To find the adaptive comfort, experimental data from over 22,346 building have been analyzed and it is found that indoor comfort temperatures are dependent on mean outdoor temperatures [11]. In another similar study thermal comfort can be expressed in terms of periods falling outside the desired band of adaptive temperature following the approach of Auliciems [12].

In an experiment performed to find the adaptive comfort temperatures in India, the neutral temperature, T_n [13], where found to be bound by the following relation.

$$T_n = 0.31 * T_{outside\ dry\ bulb} + 17.6^0C \qquad \text{Eq (1)}$$

$$Comfort\ Band = T_n \pm 3.5^0C$$

3.3 Roof Reflectance Measurements

Roof reflectance was measured as in support of a study of the radiative benefit of cool roofs [14]. Briefly, the shortwave reflectance was measured for the uncoated and cool roof as the ratio of up-welling to down-welling hemispheric shortwave (0.3-2 micron) radiation observed with a four-component radiometer (Kipp and Zonnen NR01) located in the middle of each roof segment. The average shortwave daytime surface reflectance of the roofs for the period from January through March, 2012 was 0.28 and 0.57 for dark roof and cool roof respectively.

3.4 Monitoring Equipment

Central data acquisition equipment was installed in the site. The measured parameters include outdoor air temperature, outdoor surface temperature, indoor surface temperature, and indoor air temperature and heat flux through the roof. The sensors used in the experiment are summarized below:

S.No	Equipment type	Equipment name
1	Data acquisition	Campbell Scientific - CR 1000
2	Heat Flux	Geothermal Heat flux sensors (ITI, GHT-2C)
3	Surface temperatures	(GG-T-30 Omega)
4	Indoor temperature	Omega: GG-T-30

Using these equipment monitoring was done for the indoor surface temperatures, outdoor surface temperatures, indoor air temperatures and heat flux for both dark roof and cool roof, through December 2011 to July 2012.

4. Results

From the collected data, over deck temperature, under deck temperature, indoor air temperature and heat flux were analyzed for the months of January through June. The data collected over 5 minutes interval was checked for its boundary values, rate of change in an interval of 5 minutes. The filtered data was averaged out to 30 minutes interval. A maximum reduction in the over deck temperature of 14.29^0C and an average reduction of 4.06^0C was observed between cool roof and dark roof. The mean reduction during operational hours (8 AM to 6 PM) for the entire period from Jan – Jun was found to be 7.74^0C. The maximum reduction in the over deck temperature was observed in the moths of April with a day time mean reduction of 9.29^0C and a 24 hours mean reduction of 4.94^0C.

In case of the under deck temperatures similar patterns have been observed compared to that of the over deck temperatures. From January through June over a period of 24 hours the mean reduction in the under deck temperature of 2.09°C is observed and a daytime reduction of 1.97°C were observed. The peak reduction happens in the month of June where a reduction of 6.7°C is observed on 24 hours basis.

A mean heat flux reduction over 24 hours for the period of Jan – Jun was found to 14.41 W/m^2 and the daytime operational hours mean reduction was found to be 21.43 W/m^2. The maximum reduction in was observed in the month of April with a 24 hours mean of 18.31 W/m^2 and a day time reduction of 26.31 W/m^2. The shift in the number of hours with higher heat fluxes from dark roof to cool roof suggest the heat entering the building is lesser in case of cool roofs. This effect might be higher since there was also heat ingress from the windows and the walls which are exposed to the outside atmosphere.

These results demonstrate that the cool roof reduces heat flux and temperatures relative to the uncoated roof. Further the scatter plots for over deck temperature for white roof vs dark roof has a slope of 0.79, which implies that the over deck temperature of cool roof increases less quickly than the over deck temperature of dark roof. Similar plots for under deck temperature shows that the building with cool roof has lower under deck temperature than the building which has dark roof.

The difference between the under deck temperature and the indoor air temperature is directly proportional to the heat flux coming inside the building. Scatter plots of ΔT and the heat flux coming inside the building for both cool roof and dark roof has similar slope, which indicate the thermal mass of the roof are of similar nature.

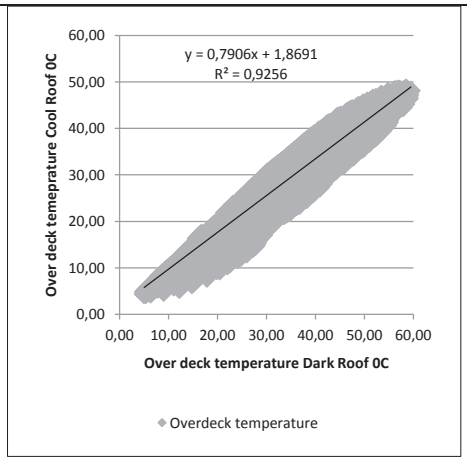

Figure 2: Over deck temperature cool roof vs. dark roofs

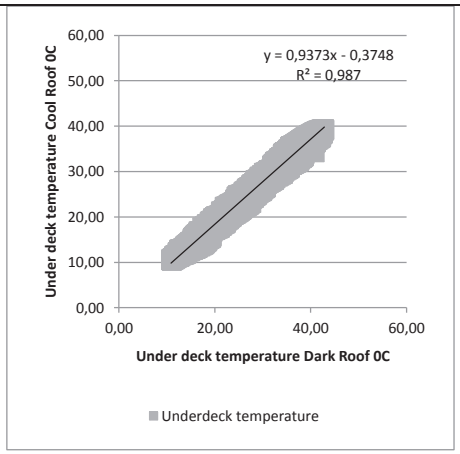

Figure 3: Under deck temperature cool roof vs. dark roof

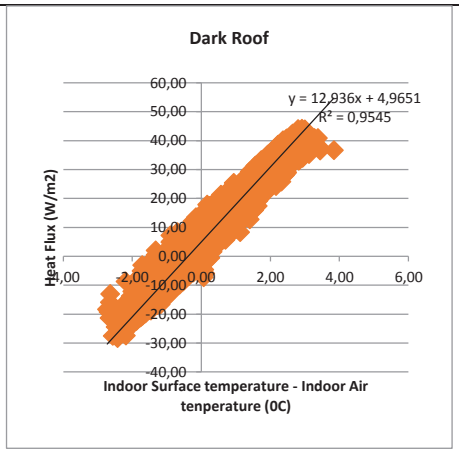

Figure 4: Heat flux vs. Delta T (Indoor surface temp - Indoor Air temp) - Dark Roof

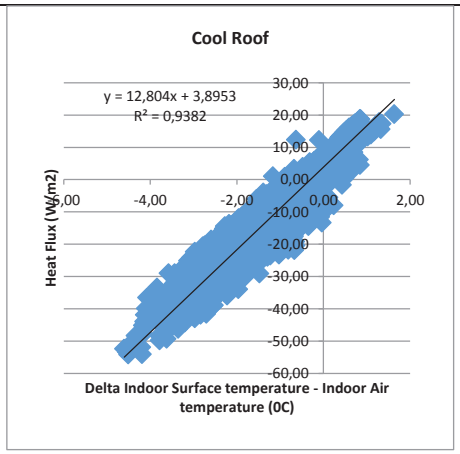

Figure 5: Heat flux vs. Delta T (Indoor surface temp - Indoor Air temp) - Cool Roof

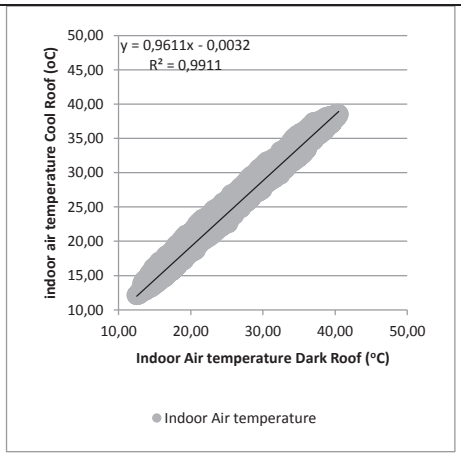

Figure 6: Indoor Air temperature Cool Roof vs Dark Roof

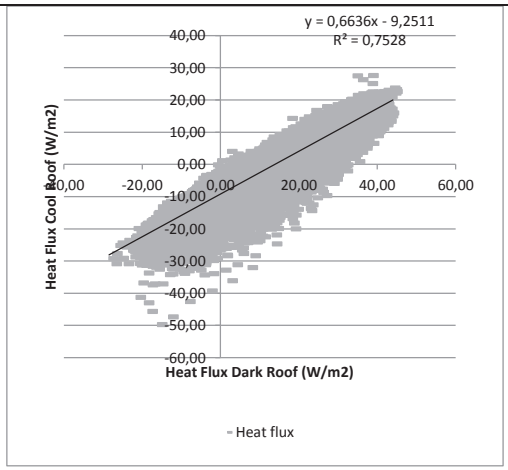

Figure 7: Heat Flux Cool Roof vs. Dark Roof

The mean reduction in the indoor air temperature in case of cool roof and dark roof was observed to 1.06^{0}C over a period of 24 hours and 0.44^{0}C over the operational hours of the building for the entire duration of analysis. This shows that the benefits from cool roof are higher in the night time than in the day. The maximum reduction in the mean indoor air temperature during day time happens in the month of June (0.89^{0}C) while the maximum reduction for 24 hours happens in the month of April (1.38^{0}C). The scatter plots between cool roof and dark roof for indoor air temperature (Figure 10) has a slope of 0.96 which implies that cool roof has lesser indoor air temperature than dark roof.

The heat flux entering the building is lower in case of cool roof than dark roof. The reduction over a period of 24 hour for the entire monitoring duration is 14.41 W/m^2 and for daytime is 21.43 W/m^2. The maximum mean reduction in flux occurs in the month of April for 24 hours (18.31 W/m^2) duration as well as daytime (26.31 W/m^2). The scatter plots between cool roof and dark roof for heat flux entering the building has a slope of 0.66 which implies that cool roof has lower heat flux than dark roof.

The following tables summarize the mean, maximum and minimum reduction for over deck surface temperature, under deck surface temperature, indoor air temperature and the heat flux.

Table 1: Over deck temperature reduction in during the Jan - Jun

Over deck temperature reduction (^{0}C)						
	Mean reduction		Max reduction		Min reduction	
	24 hrs	Daytime	24 hrs	Daytime	24 hrs	Daytime
Jan	2.82	5.21	13.06	13.06	-0.04	0.09
Feb	3.74	7.19	12.36	12.36	0.00	0.72
Mar	4.48	8.53	13.77	13.77	-0.63	2.29
Apr	4.94	9.29	14.29	14.29	-0.34	2.23
May	4.59	8.78	14.12	14.12	-0.17	2.20
Jun	4.01	7.79	13.41	13.41	-0.25	0.74
Jan - Jun	4.06	7.74	14.29	14.29	-0.63	0.09

Table 2: Under deck temperature reduction during Jan - Jun

Under deck temperature reduction (^{0}C)						
	Mean reduction		Max reduction		Min reduction	
	24 hrs	Daytime	24 hrs	Daytime	24 hrs	Daytime
Jan	1.49	1.35	3.84	3.84	0.11	0.11
Feb	1.72	1.53	3.91	3.91	-0.24	-0.24
Mar	2.13	1.90	4.62	4.47	-0.07	-0.07
Apr	2.63	2.53	5.32	5.32	0.50	0.50
May	2.45	2.39	4.88	4.88	0.48	0.48
Jun	2.25	2.24	6.70	6.70	0.39	0.39
Jan - Jun	2.09	1.97	6.70	6.70	-0.24	-0.24

Table 3: Indoor Air Temperature reduction during Jan - Jun

Indoor Air temperature reduction (^{0}C)						
	Mean reduction		Max reduction		Min reduction	
	24 hrs.	Daytime	24 hrs.	Daytime	24 hrs.	Daytime
Jan	0.70	0.35	1.80	1.51	-1.39	-1.39
Feb	0.76	0.06	2.08	1.82	-1.59	-1.59
Mar	0.94	0.05	2.66	2.19	-1.64	-1.64
Apr	1.38	0.66	2.86	2.70	-1.08	-1.08
May	1.33	0.71	2.77	2.55	-0.75	-0.75
Jun	1.30	0.89	2.45	2.43	-0.47	-0.47
Jan - Jun	1.06	0.44	2.86	2.70	-1.64	-1.64

Table 4: Heat Flux reduction during Jan - Jun

Heat Flux reduction (W/m^2)						
	Mean reduction		Max reduction		Min reduction	
	24 hrs.	Daytime	24 hrs.	Daytime	24 hrs.	Daytime
Jan	8.37	12.61	40.75	40.75	-5.39	-4.76
Feb	12.68	20.15	40.86	40.86	-5.81	-1.70
Mar	16.66	26.04	47.35	47.35	-3.73	3.66
Apr	18.31	26.31	42.85	42.85	-1.05	-1.05
May	16.70	24.14	40.30	40.30	-3.02	3.61
Jun	14.61	20.39	35.04	35.04	-0.86	-0.30
Jan - Jun	14.41	21.43	47.35	47.35	-5.81	-4.76

Since the indoor air temperature reduces with cool roof comfort analysis was performed for both the buildings. The total number of uncomfortable hours was calculated for both the buildings.

The outdoor dry bulb temperatures, and comfort band (Eq 1) are summarized in the following table:

Table 5: Comfort temperature band for Jan - Jun

	$T_{outside\ dry\ bulb}$ (^{0}C)	$T_{neutral}$ (^{0}C)	Comfort low (^{0}C)	Comfort High (^{0}C)
Jan	14	21.94	18.44	25.44
Feb	17	22.87	19.37	26.37
Mar	23	24.73	21.23	28.23
Apr	29	26.59	23.09	30.09
May	33	27.83	24.33	31.33
Jun	36	28.76	25.26	32.26

Using cool roof results in discomfort in the months of January and February and it increases the comfort in the months of March, April and it has no effect in the month of June. Though there are negative effects on comfort in winter months, the benefits from the summer months leads to a net increase in comfort. The comfort hours are summarized in the following table:

Table 6: Number of comfort hours for Jan - Jun

	Number of comfortable hours		Number of Uncomfortable hours		Change in comfort
	Dark roof	Cool Roof	Dark roof	Cool Roof	
Jan	12	0	732	744	-12
Feb	299	230.5	397	465.5	-68.5
Mar	591.5	604.5	129.5	115.5	13
Apr	122.5	224.5	453.5	351.5	102
May	36	83	708	661	47
Jun	0	0	672	672	0
Jan - Jun	1061	1142.5	3092	3009.5	81.5

Using cool roofs reduces the peak indoor air temperature and heat flux. Histogram plots of heat flux and indoor air temperatures shows shift in the peak temperatures. Even the temperature and heat flux cluster peaks have been shifted backwards in case of cool roof compared to dark roof.

Typical histogram plots of indoor air temperatures along with comfort band for all six months are shown below:

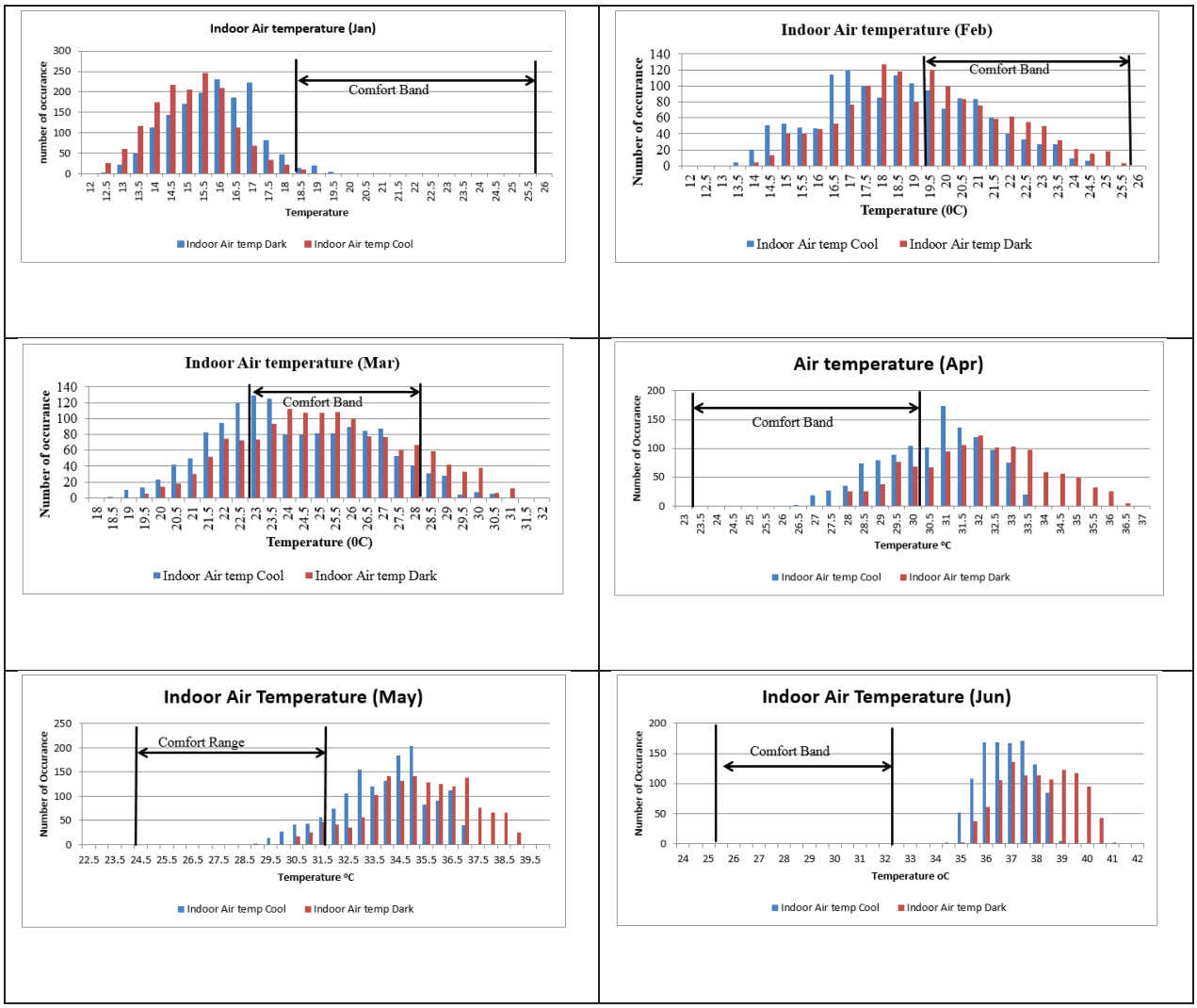

5. Conclusions

The results from the field study shows that using a cool roof (SR – 0.57) over a dark roof (SR – 0.28), results in temperature and heat flux reduction in an un-conditional institutional building. The reduced indoor air temperature levels leads to increased comfort. For the monitored period of six months (Jan - Jun), the mean reduction in indoor air temperature was 1.06^0C for 24 hours duration and 0.44^0C for the operational hours. Since there would be heat ingress in the room with cool roofs from the windows and walls that are exposed to the outside atmosphere, the savings could be higher than what is being observed in this experiment. The peak reduction in the indoor

air temperature observed was 2.86^{0}C in 24 hours duration and 2.70^{0}C in the operational hours. The heat flux coming inside the building is also reduced over the entire duration. The mean reduction over 24 hours is 14.41 W/m^2 and the daytime reduction is 21.43 W/m^2.

6 Acknowledgements

We gratefully acknowledge Prof. K.P. Singh for assistance in arranging fieldwork at the G.B. Pant University. We also thank Bipin Shah (Winbuild) for arranging the roof coatings, Ken Reichl for assistance with radiometer instrument preparation and initial data reduction. This work was supported by the US DOE Offices Energy Efficiency and Renewable Energy, and the US DOE Office of Science, Atmospheric Radiation Measurement program, under contract DE-AC02-05CH11231.

7 References

1. Cool Roof Rating Council: Resources. 03 15, 2013. http://coolroofs.org/HomeandBuildingOwnersInfo.html (accessed 03 15, 2013).
2. Konopacki S, Akbari H. "Measured energy savings and demand reduction from a reflective roof membrane on a large retail store in Austin." 2001.
3. Danny S. Parker, John R. Sherwin, Jeffrey K. Sonne, Stephen F. Barkaszi, Jr. "Demonstration of Cooling Savings of Light Colored Roof Surfacing in Florida Commercial Buildings: Our Saviour's School." 1996.
4. Danny S Parker, Jeffrey K. Sonne, Jhon R. Sherwin and Neil Moyer. "Coparative Evaluation of the Impact of Roofing Systems on Ressidential Cooling Energy Demand in Florida." ACEEE 2002 Summer Study, American Council for an Energy Efficient Economy, Washington DC. 2002.
5. Konopacki. S, Akbar. H. "Energy Savings Calculations for Heat Island Reduction Strategies in Baton Rouge, Sacramento and Salt Lake City." 2000.
6. Konopacki, Steven J, and Hashem Akbari. Measured energy savings and demand reduction from a reflective roof membrane on a large retail store in Austin. Lawerence Berkeley National Laboratory, 2001.
7. Akbari, H., Xu, T., Taha, H., Wray, C., Sathaye, J., Garg, V., Reddy, N. (2011). Using Cool Roofs to Reduce Energy Use, Greenhouse Gas Emissions, and Urban Heat island Effects: Findings from an India Experiment. Berkeley: Ernest Orlando Lawrence Berkeley National Laboratory.
8. E. Bozonnet, M. Doya, F. Allard. "Cool roofs impact on building thermal response: A French case study." Energy and Buildings, 2012.
9. M. Zinzi, S. Agnoli. "Cool and green roofs. An energy and comfort comparison between passive cooling and mitigation urban heat island techniques for residential buildings in the Mediterranean region." Energy adn Buildings, 2011.

10. M. Kolokotroni, B.L. Gowreesunker, R. Giridharan. "Cool roof technology in London: An experimental and modelling study." Energy and Buildings, 2011.
11. Richard de Dear, Gail Schiller Brager. “The adaptive model of thermal comfort and energy conservation in the built environment”. International Journal of Bio Metrology, 2001.
12. Auliciems A, R De Dear. "Airconditioning in Australia I—Human Thermal Factors." Architectural Science Review, 1986: 67-75.
13. Dhaka, Shivraj, Jyothirmay Mathur, Vishal Garg, and Vaibhav Jain. "Effect Of Envelope Properties And Thermal Adaptation On Energy Consumption And Comfort Conditions Through Simulation Of Various ECMs." 12th Conference of International Building Performance Simulation Association. Sydney, 2011
14. Salamanca, Franscisco, et al. "Top-of-atmosphere radiative cooling with white roofs: experimental verification and model-based evaluation." Environmental Research Letters, 2012.

SIMULATION OF THE COOLING EFFECT OF THE ROOF ADDED PHOTOVOLTAICS

Vasilis C Kapsalis[*1], Eftychios Vardoulakis and Dimitris Karamanis[*1]

1 Department of Environmental & Natural Resources Management, University of Patras
Seferi 2, 30100
Greece
**Corresponding authors: bkapsal@central.ntua.gr, dkaraman@cc.uoi.gr*

ABSTRACT

In this study, the TRNSYS simulation engine was used to investigate the shading and cooling effect of roof added photovoltaics. The local weather conditions were introduced in the data reader component. The sol air effective temperatures were modeled in the roof –air boundary layer, while a single zone model was used for the heat transfer calculation, both in bared and PV shaded roof. The simulation was validated by experimental data of a PV installation at the roof of the Department of Environmental & Natural Resources Management. The simulation results show that photovoltaic panels have a high impact on the roof surface temperature between shaded and exposed parts of the roof during the summer time. Heat transfer simulation with or without roof integrated photovoltaic shadings revealed the factors influencing cooling loads of a building during the year. The roof added photovoltaics can passively reduce the daily rooftop cooling energy and peak load during the hot summer days in addition to electricity production.

KEYWORDS

Roof added photovoltaics, temperature effect, heat flux, cooling load, peak power demand

1 INTRODUCTION

In countries with elevated temperatures during summer, like Greece, heat is the main problem of human thermal discomfort in buildings. The problem has intensively increased during the last 30 years since the lack of any urbanization plan led to uncontrollable growing with the subsequent environmental impact like the heat island effect in the major cities (Santamouris M. et al, 2001, Giannopoulou K. et al, 2010). The effect is lately observed regardless of the city size (Vardoulakis E. et al, 2011). Air conditioning is primary the only technique to compensate the increased temperatures and contributes a significant percentage of the total energy consumption of buildings in Greece. Subsequently, almost 25% more electricity is needed for a very short summertime period, especially July and August, and is mainly produced from fossil fuels. Many alternatives solutions have been proposed with some of them being partially effective with specific applications today (Vardoulakis E. et al., 2011, Karamanis D. et al., 2012, Synnefa A. et al, 2006, Alvarado J.L. et al, 2009). In the proposed solutions, the primary objective is the reduction of the buildings cooling load and the blocking of the temperature rise inside the urban spar during the summertime.

In addition, much research has been conducted on the direct use of rooftop building added PV (BAPV) for energy production (Strzalka A. et al, 2012, James P.A.B at al, 2009). In contrast, the possible indirect benefits of PV installations in buildings have been mainly concentrated in their integration on the building envelope and façade and their use as shading devices, blinds, walls, tiled roofs and windows. However, rooftop PV systems such as building

shading of the uncovered surface have received much less attention, while the Pv installed capacity in buildings roofs have been increased, almost linearly, approaching the 180 MW at the end of June 2012 (Greek operator of electricity market, 2012). While a number of simulation studies have been conducted, systematic experimental measurements are limited with the exception of a recent experimental study on the roof temperature variation for a limited time period (Dominguez A. et al, 2011). For example, it was demonstrated by heat transfer simulation into four different types of roofs, that BAPV can change the thermal resistance of a building by adding or replacing the building elements (Wang Y. 2006, Tian W. et al 2009). For ventilated air gap BAPV, decreases of 46% and 51% occurred for the daily heat-gain and the peak-cooling load compared with the conventional roof. Simulation results also showed that building surface temperature significantly changes while urban canyon air temperature alters only marginally. Also, Yang et al. (Yang et al, 2001) developed a simulation model for the thermal performance of PV roofs and found that the cooling load component through a PV roof is about 35% of the load of a conventional roof. In the recent experimental study, air temperature sensors and data measurements were collected for the period from 12 to 20 of August 2012. Simulations showed a reduction to the cooling load and peak power demand for the specified period. However, recent comparative simulated impact studies of roof installations, provided evidence that white and green roofs are more effective strategies for urban heat island mitigation than their PV covered ones (Scherba A. et al, 2011). In view of the above, the objective of the present study was to systematically investigate the temperature and heat gain variation of a rooftop PV installation on a university building during the summer and gain a better insight in the shading mechanism of roof added photovoltaics. PV and roof temperatures as well as meteorological parameters were recorded to estimate the differences into roof heating for shaded and non-shaded roof while the cooling and heating loads throughout the year were determined by extensive heat transfer simulation.

2 PV AND ROOF TEMPERATURES

2.1 Experimental Data

Measurements were conducted in the city of Agrinio (Western Greece) during August 2012 on a building roof of the University. Hobo dataloggers (model: Hobo ProV2) and thermocouples (Omega TMQSS-OM075G-300) connected with a fully automated meteorological station were used to collect the temperature data. The configuration and exact positions of the temperature sensors are depicted in Fig. 1.

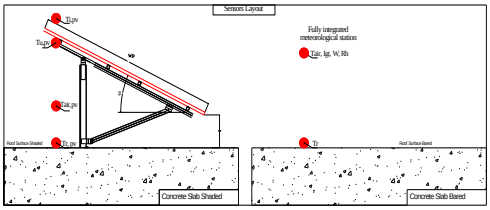

Figure 1: Sensors layout

In Figure 2.1a, temperature variations for roof surface with PV shading (Tr,pvm) and exposed roof (Tr m) are presented for the studied period from 12 to 20 August 2012. During the daytime, the temperature difference between shaded and exposed roof reached a maximum at 1:00 pm every day. At this time, maximum difference reached 16.2 ^{o}C on the first day of the measurements (12 August 2012) and a minimum difference of 10.7 ^{o}C on the ninth day of the

measurements (16 August 2012). The opposite effect was taking place after the sunset till sunrise. Exposed roof reached lower temperature levels compared to shaded roof. This difference was explained by the increased long wave radiation loss of the exposed roof surface and much more effective cooling during the night, compared to the part of the roof lying under the PV. The reason of the better and faster cooling is the increased sky view factor of the exposed roof, in addition to the shaded roof, proving that PV has also insulating properties. This result is in agreement with similar observations (Dominguez A. et al, 2011).

The variability of the roof surface temperature was also daily monitored. On a typical summer day, exposed roof summer temperature started from the value of 16.5 ^{o}C (at 6:00 am) and reached a maximum of almost 55 ^{o}C at noon. In contrast, shaded roof temperature started to rise at 20.3 ^{o}C (at 6:00) and reached a peak at 38.6 ^{o}C (at 1:00 pm). This indicates higher rates of heat absorption from exposed roof that could potentially lead to higher degradation of the roof construction materials and buildings insulation.

Figure 2.1b shows the temperatures over and under the PV module surface and air temperature between the PV tilted array and the shaded roof surface. PV surface temperature (Ti,pv) is almost 13 ^{o}C to 15 ^{o}C hotter compared to the temperature exactly under the PV module (Tu,pv) at the time period of the maximum solar radiation. This finding indicates that BAPV can act as an extra insulation over the roof during the summertime, absorbing a large amount of heat while simultaneously producing electricity.

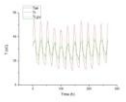

Figure 2.1a: Temperature variation for exposed and PV shaded roof

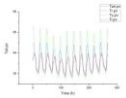

Figure 2.1b: Temperatures over and under PV

2.2 TRNSYS Simulation

Following the temperature measurements, a heat transfer simulation analysis was performed in order to examine the influence of BAPV in the building's cooling loads during the specified period. The calculation method of the program is based on the TRNSYS simulation engine (TRNSYS user manual, (2010). The local meteorological parameters were used and introduced in the program. The modelled components of the engine machine were built up through a step by step procedure. The calibration was based on several outputs of independent stages, respectively. The solar irradiation distribution produced by the TRNSYS is similar to that attained from the nearest local TMY data (Figure 2.2a). The PV array operation temperature and power at MPP are in accordance with those expected by the verified properties at STC conditions (Figure 2.2b). The single zone building utilizes the specified heat loss coefficient as of the materials properties and the capacitance is a lumped value derived from the sum of the specific heat capacities of the building's envelope. Finally the study of the roof module with and without PV panel simulated the heat transfer process with the utilization of the effective conductance and sol air temperature.

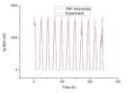

Figure 2.2a: Experiment radiation and TMY nearest local data

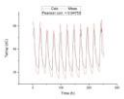

Figure 2.2b: PV array temperature at MPP power

Temperatures were modeled according to the following assumptions:

i. the body is gray
ii. the radiation properties are independent of the wavelength and
iii. the body is non transparent

According to built in components of the simulation engine, an extended analysis was performed to simulate the features of the building's response to the phenomenon. The weather conditions of a local meteorological station and the Hobo data loggers, such as total radiation Ig, wind velocity W and air temperature Tair, were collected and introduced into the data reader component. The same air velocity was used in both cases, with and without PVs, in order to express the dependence of the forced convection coefficient ho on it, as

$$ho = 5.7 + 3.8W, \quad (2)$$

in (Kj/h/m^2.^{o}C) with W, the wind velocity (m/s).
The temperature of surrounding medium was initially expressed with the solair temperature for the exposed roof surface and modeled, as the result of energy balance of total radiation and forced convection of roof – air boundary layers. The *e* correction factor was used to explain the heat flux between the internal and external roof and humidity. In our model this factor as a function of total radiation and the external convection coefficient ho, is chosen so that:

$$\lim_{Ig\to 0} e = ho \quad (3)$$

$$Tsa = Tair + \alpha Ig/ho - \varepsilon \Delta R/ho \mp e \quad (4)$$

where Tsa is the sol air temperature (^{o}C), Tair, the air temperature (^{o}C), α the absorptivity, (0<α<1), ε the emissivity coefficient (0<ε<1) Ig the total horizontal radiation ($\frac{KJ}{hm^2}$), ΔR the diffuse radiation and sky temperature effect ($\frac{KJ}{hm^2}$).
The absorption coefficient best fit value calibration was found to be α = 0.45 which is between flair flagstone's and gravel's material and denotes an albedo value for the area within the typical range of the climate conditions at the specified period (e.g dew point and participated water). The emissivity value was selected as ε=0.80. Measured and calculated data for the exposed roof sol – air temperature were validated and the results are presented in Figure 3a.
At the same time, the sol – air effective temperature of the PV shading roof, was derived from a more complicated process. The PV cell acts as an absorber with a (τα) coefficient, and its operating temperature depends on Normal Operation Cell Temperature (NOCT) conditions, the total radiation Ig and the air temperature Tair. The temperature below the array is a combined calculation between the heat transfer through the panel with a heat transfer coefficient U_L and the air convection between the cell operating temperature and the air temperature. The effective emissivity (ASHRAE, 2013) coefficient was used in this case to express the influence of the two bodies temperatures, the surface and the back edge of the array, and is deduced as.

$$\varepsilon eff = \frac{1}{\frac{1}{\varepsilon e}+\frac{1}{\varepsilon c}-1}, \quad (5)$$

where εe, the emitter's emittance with a value of 0.5 for the white plastic membrane, and εc, the collector's emittance, with a value of 0.80 for the surface material as above.
According to the observed data, during the day, the PV back temperature is higher than the one on the surface under the PV, while in the late afternoon (19:00 or 20:00) the reverse process begins and the surface temperature is slightly higher, about 1 to 3 ^{o}C, until the first sunset time.
Thus, the shaded roof absorbs the diffused only radiation and a small portion of the total, depending on the sky view factor, while the Boltzman emissivity depends on a different temperature than the sky's one, because, as denoted, it faces the PV back surface. Then the longwave emission term (LW) comes from the infrared radiation difference between the roof and the PV back edge. In this case, the total horizontal radiation has to be decomposed in $It =$ Ib + Id, which was done by the radiation processor using the Reindl model, since the roof is horizontal and the factors Fgnd = 0 and Fsky = 1. The roof fraction factor was assumed to be 0 and that only the diffused radiation affects the PV shaded roof. Roof surface was considered to be 0.81 cm^2 (0.9 cm x 0.9 cm), with one PV panel on it. The exposed roof model was extended with the available TRNSYS components and the necessary modifications to match the PV shaded roof conditions as prescribed were implemented. Also, the temperature distribution, the air gap effect and the heat flux downwards or upwards the internal roof surface have been taken into account. The effective sol air temperature and the heat rate were calculated with the TRNSYS simulation. In figure 2.2c, 2.2d the measured and calculated temperature values are presented.

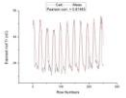

Figure 2.2c: Exposed roof surface temperature

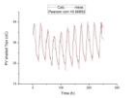

Figure 2.2d: PV shaded roof surface temperature

2.3 HEAT FLUXES IMPACT OF THE ROOF INTEGRATED PHOTOVOLTAICS ON THE BUILDING'S THERMAL BEHAVIOR

A single floor residence building of rectangular shape and 81 cm^2 flat roof was adopted for the simulation. For simulating the PV shading, a PV panel were installed on the flat roof at a tilt angle of 30 °. The lumped capacitance method was used to define the zone temperature of the building and as an input for the heat transfer simulation of the roof to the ceiling or backwards. The building's energy demand response was simulated for the specified period before and after installing the PV.
Initially, the effect of the structural materials on cooling loads was studied. Two insulation scenarios are simulated with two building thermal resistance coefficients, respectively, R high = 0.25 h.m2.K/Kj and R low = 0.5 h.m2.K/Kj) and parametric analysis of ρ = 0.2, 0.55 and 0.8 reflectivity ratio. In every case the Kirchhoff's law retained, so as,

$$\alpha + \rho = 1 \quad (6)$$

It was observed that the difference between the cooling loads of the exposed and pv shaded roof, as percentage, maximized with the decrease of their thermal resistance and increase of reflectivity value. In Figure 2.3a the pv shading effect on cooling loads of the less insulated and the more reflective roofs for the specified period is presented, while in figure 2.3b the zone temperature of the lumped capacitance model and different U factors are simulated with initial value Tz = 20oC. The more insulated buildings present larger attenuation in temperature variations, as expected. The above results are similar to those of Kolokotroni et al. (Kolokotroni M. et al, 2011)

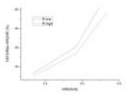

Figure 2.3a: PV shading effect vs thermal resistance R and reflectivity ρ

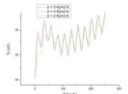

Figure 2.3b: Simulated lumped capacitance zone temperature vs U factors

The roof experimental conditions of 7.5 cm (3'') XPS extruded polystyrene insulation and concrete slab were subsequently selected to study the cooling loads and peak demand
The temperature difference between the bare and PV covered roof surface has a simultaneous impact on the heat flux downwards or upwards the building room conditions. Since the thermal resistance of the ceiling is known, according to the materials properties, the heat flux was modeled as above, taking into account the Fourier uniform heat transfer equation and the steady state heat loss coefficient. The thermal resistance was considered the same for the whole roof with a value R = 0.72 h.m2.K/Kj. In all cases the back edge pv thermal resistance is constant and equal to Rpv = 0.15 h.m2.K/Kj.

The recorded negative differences in values are corresponding to a decrease in cooling loads with the BAPV installation, primary, due to decreased heat flux (heat gain) coming from the roof surface. The peak load demand is also reduced during the on peak solar radiation hours and a cumulative effect occurs during the whole (Figure 2.3c). In a daily basis the reverse heat flux observed at night in both roofs, while at the same time the roof surface temperatures changed order with the exposed roof becoming lower (Figure 2.3d).

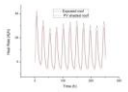

Figure 2.3c: Cooling loads and peak load demand for exposed and PV shaded roof

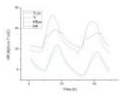

Figure 2.3d: Daily surface temperatures and heat rates comparison

At the same period a comparison made between the cumulative cooling effect and the cumulative cooling degree hours derived by the following formula,

$$CDH = \quad N_i * \quad {}_i \max\{0,\ Ti, air - Tref\ \} \quad (7)$$

where, Ni in hours, Ti,air the hourly average air temperature derived from the meteorological station and Tref a reference temperature, here 26oC (Figure 2.3e).

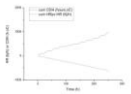

Figure 2.3e: Cumulative Cooling Degree Hours and cumulative PV shading cooling effect

The present study indicates that the roof BAPV leads to passive energy savings for an extended time period in addition to energy production for specific environmental conditions. Therefore, loads variation is highly sensitive to the selection of the environmental parameters for the particular location, PV tilt angle installation and the building structural materials. Thus, it is proposed that a detailed simulation of the building energy loads should be performed before the BAPV installation at a particular building of a specific location in order to optimize their positive shading effects in addition to their energy production.

2 CONCLUSIONS

The temperatures of the experimental study validated and simulated with quite success through TRNSYS engine. Then, the heat fluxes examined for two cases of thermal resistances and three different albedos, concluded that positive cooling effect increases at poor insulated and high reflectivity buildings. The zone temperature is simulated for three different U values and resulted to a better attenuation of the better insulated one. Eventually, the cumulative correlation of cooling effect and cooling degree hours denotes that a better insight is needed all over the year's demand response.

The cooling load study with the results presented above revealed a significant positive cooling effect of the BAPV within the specified period and conditions. The cooling energy demand response of the building reduced as well as the high cooling demand on peak or nearby radiation hours. The additional simultaneous renewable power production is an additional beneficial aspect to consider due to the environmentally cost reduction and the net metering advantages for the owner.

In a daily basis observation the surface temperature's order is reversed at night, with the exposed roof's being the smaller. It seems that at pv shaded surface the long wave radiation is trapped between the roof and the back pv array surface with reduced emissivity, while at the same time the exposed roof higher view factor at night sky leads to a faster cooling, at least at the upper and external layers of the roof.

However, the lumped capacitance method which used to analyse the effect in our model, presented limitations and is a rough estimation of the heat transfer process and the impact of the PV array which occurred. The thermal mass of the roof is unchanged, the effective temperature which depended on the effective conductance is unchanged, too, and the same zone temperature in both cases is used. On the other hand, the sensitivity of the model in different conditions and material properties should be simulated and investigated more and the findings have to exposed in a larger time period and more environmental and other factors.

3 REFERENCES

[1] Santamouris M., Papanikolaou N., Livada I., Koronakis I., Georgakis C., Argiriou A., Assimakopoulos D.N. (2001). On the impact of urban climate on the energy consumption of buildings. *Solar Energy*, 70(3), 201-216.

[2] Giannopoulou K., Livada I., Santamouris M., Saliari M., Assimakopoulos M., Caouris Y.G. (2010). On the characteristics of the summer urban heat island in Athens, Greece. *Sustainable Cities and Society*, 1(1), 16-28.

[3] Vardoulakis E., Karamanis D., Mihalakakou G., Assimakopoulos M.N. (2011). Heat island effect in Western Greece: results, statistical analysis and discussion. In: Kungolos A., Karagiannidis A., Aravossis K., Samaras P., Schramm K.W., editors. *Cemepe 2011: Proceedings of the third International Conference on Environmental Management, Engineering, Planning and Economics*, June 19-24, Skiathos.

[4] Vardoulakis E., Karamanis D., Assimakopoulos M.N, Mihalakakou G. (2011). Solar cooling with aluminium pillared clays. *Solar Energy Materials and Solar Cells*, 95(8), 2363-2370.

[5] Karamanis D., Vardoulakis E. (2012). Application of zeolitic materials prepared from fly ash to water vapor adsorption for solar cooling, 97, 334–339.

[6] Synnefa A., Santamouris M., Livada I., (2006). A study of the thermal performance of reflective coatings for the urban environment. *Solar Energy,* 80(8), 968-981.

[7] Alvarado J.L., Terrell Jr.W., Johnson M.D. (2009). Passive cooling systems for cement-based roofs. *Building and Environment*, 44(9), 1869-1875.

[8] Greek operator of electricity market. (2012). *http://www.lagie.gr/ape-sithya/miniaia-deltia-ape/*, accessed at August 5th.

[9] Strzalka A., Alam N., Duminil E., Coors V., Eicker U. (2012). Large scale integration of photovoltaic in cities. *Applied Energy*, Article in press.

[10] James P.A.B, Jentsch M.F., Bahaj A.S. (2009). Quantifying the added value of BIPV as shading solution in atria. *Solar Energy*, 83(2), 220-231.

[11] Dominguez A., Kleissl J., Luvall J.C. (2011). Effects of solar photovoltaic panels on roof heat transfer. Solar Energy, 85(9), 2244-2255.

[12] Wang Y., Tian W., Ren J., Zhu L., Wang Q. (2006). Influence of a building's intergrated-photovoltaics on heating and cooling loads. *Applied Energy*, 83, 989-1003.

[13] Tian W., Wang Y., Xie Y., Wu D. Zhu L., Ren J. (2009) Effect of building integrated photovoltaics on microclimate of urban canopy layer.

[14] Yang H., Zhu Z., Burnett J., Lu L. (2001). A simulation study on the energy performance of photovoltaic roof , *ASHRAE Transactions*, 107(2), 129-135

[15] Scherba A., Sailor D.J., Rosenstiel T.N., Wamser C.C. (2011). Modeling impacts of roof reflectivity, integrated photovoltaic panels and green roof systems on sensible heat flux into the urban environment. *Building and Environment*; 46, 2542-2551.

[16] TRNSYS, (2010). The Transient Energy System Simulation Tool, *http://www. trnsys.com/about.htm*.

[17] ASHRAE (2013). ASHRAE Handbook – Fundamentals. Atlanta, GA: *American Society of Heating, Refrigerating and Air-Conditioning Engineers*, Inc. (Chapter 26, Heat, Air and Moisture control in buildings assemblies – Material properties).

[18] Kolokotroni M., Gowreesunker B.L., Giridharan R., (2011). Cool roof technology in London An experimental and modeling study, *Energy and Buildings*, Article in press.

EXPERIMENTAL ANALYSIS OF SMALL SCALE ROOF PONDS, PROTECTED BY A VARIETY OF MATERIALS IN DIFFERENT POSITIONS IN REGARD TO WATER LEVEL

Artemisia Spanaki*[1], Dionysia Kolokotsa[2], Theocharis Tsoutsos[2], Ilias Zacharopoulos[1]

1 National Technical University of Athens, School of Architecture, Department of Architectural Technology, 42 Patission Street, 10682 Athens, Grecce

2 Technical University of Crete, Environmental Engineering Department, 73100 Chania, Crete, Greece

**Corresponding author: e-mail address Spanakiart@hotmail.com*

ABSTRACT

The experimental analysis aims to investigate ways to protect a water pond, in order to reduce bottom pond temperature. For this purpose, three identical shallow ponds are together recorded in moderate climate. The bottomless ponds are placed on a concrete roof, exposed to the ambient conditions. Water depth is kept constant in 0.10m, while each pond has an area of $1m^2$. A number of alternative materials for water protection are tested: white textile, the textile used in ironing board, aluminum layer, aluminum foil and insulation. Some of the materials are keeping afloat on water level, while other are kept below or above water level. The analysis focus on the devices that give the lowest temperatures, thus the most effective ones. The bottom pond temperatures are analyzed, in regard to the climate. Furthermore, the bottom pond temperatures are also compared to the temperatures below an insulation layer placed on a concrete slab. According to the experiments, protecting water with reflective materials can reduce bottom pond temperature, thus increasing cooling efficiency.

KEYWORDS

Roof Ponds, indirect evaporative cooling

1. INTRODUCTION

Roof ponds represent an effective passive cooling technique, especially in hot and dry climate. The heat losses mechanism is a combination of radiation, conduction and evaporation while the increased thermal capacity of the water reduces the temperature fluctuation of water.

The most investigated roof pond variation is the skytehrm (Raeissi 2008); water is enclosed to plastic bags. During the summer day the pond is protected by insulation panels which are removed during summer night. The function is revised during winter, for passive heating.

In order to overcome the maintenance issues, Tang et al (2004) proposed a roof pond with negligible maintenance, constructed by keeping gunny bags or cloth floating in the surface of water pond. In order to be afloat, the textile is supported by polystyrene strips or other floatable material attached to it underneath. The wet textile dissipates the heat through water evaporation, convection and radiation losses while capturing solar radiation. Moreover water absorbs the heat gains from the building and dissipates them. According to simulations and experiments (Tang et al., 2003 & 2005) the system prove to perform better compared to other passive cooling techniques.

According to a former parametric study of the system (Spanaki et al 2010), the efficiency of the system can be improved by placing a textile with low emissivity. Decreasing textile emissivity by 50% has a sensible effect on water temperature decreasing by 2.6 ^{o}C. The parametric study assumes that low emissivity layer acts the same way as a wet textile, allowing water evaporation through it. On the other hand low emissivity materials are commonly reflective metals. The lack of porous on the reflective layer exhibits evaporation losses.
The aim of the present study is to experimentally investigate ways to protect water pond while encouraging evaporation losses. For this purpose a number of alternative materials are used, in a variety of positions: on, below and above water layer.

2. THE TESTED MATERIALS FOR WATER PROTECTION

The tested materials have high reflectivity. Since the emissivity has proved to be a critical parameter for the bottom pond temperature of the Rood Pond with gunny bags [mine], the emissivity of the tested materials has been recorded with the D&S Emissometer, Model AE1. The emissivity values are listed in Table 1. The ironing board has lower emissivity and higher reflectivity comparing to the white textile. Aluminum foil is a reflective metallic material, differing from textile in terms of the heat dissipation mechanism, since it is not allow evaporative losses through it.

Table 1: The emissivity of the materials tested for water portection

material	White textile	Ironing Board	Aluminium layer	Aluminium foil
Emissivity	0.86	0.44	0.04	0.03

3. EXPERIMENTAL SETUP

The experiments refer to the record on three bottomless shallow ponds of 1.00 m x1.00 m x 0.16 m, constructed by stainless galvanism metal. The perimeter of each pond is externally insulated with 50 mm polystyrene panels. The ponds are filled with water 10cm deep, while a polyurethanes layer (naylon) is internally waterproofs the pond.
Water level is kept constant at 0.10m by floater in each pond, while evaporated water is supplied by a water tank. Three T-Logg 100E (Greisinger electronic GmbH – D -93126) data loggers record the temperatures on the bottom of the examined ponds.
The site where experiments were held is at Vrahokipos (Latitude 35° 19' 60N Longitude 25° 15' 0E, Elevation 25 m), a rural area of Heraklion city, on Crete island in Greece. The meteorological data were also recorded on the site of the experiments.

4. RESULTS AND DISCUSION

Three periods of experiments are analyzed. The temperature records are also referred to three ponds that are together recorded.

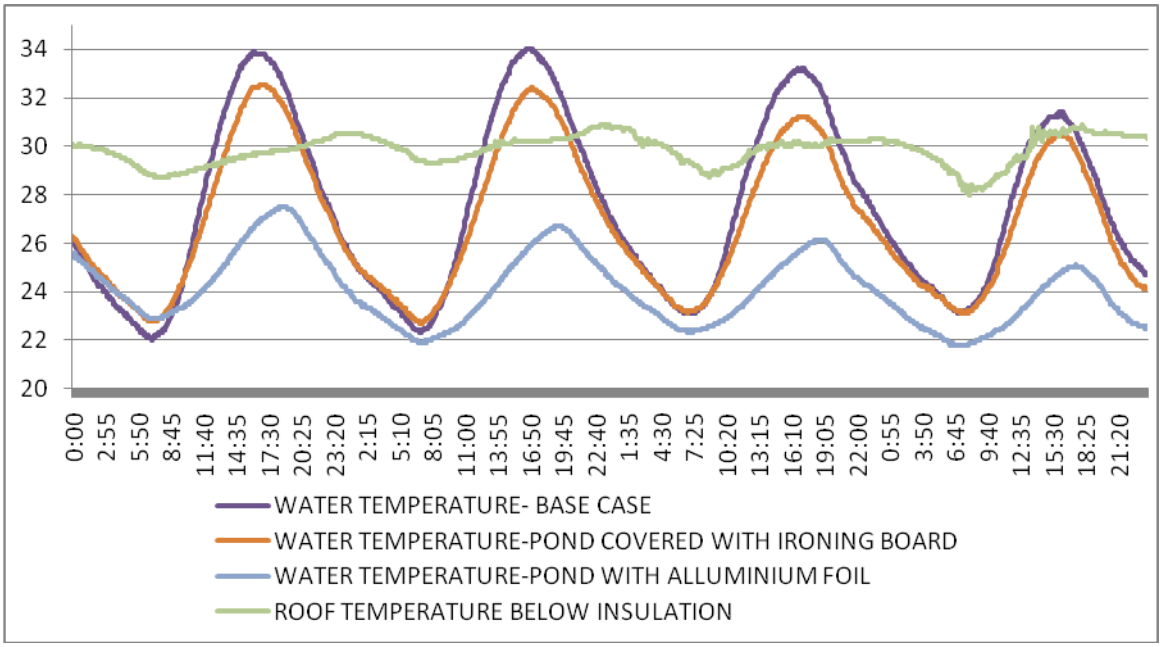

Figure 1: Bottom pond temperatures of three ponds protected with a variety of materials, placed on water level. The records are referred to the period between 2nd and 5th of July 2010.

4.1 The effect of the protection material properties to the bottom pond temperature

The first period of experiments refers, from the 2nd to the 5th of July 2010, aims to compare three ponds protected by different materials, placed on water level, as listed on Figure 1. According to the experimental records, roof temperature below insulation has lower temperatures during daytime compared to the bottom pond temperature of the base case scenario (Roof pond with white textile floating on water level). The mean daily maximum temperature of the bottom pond temperature in the Base case Scenario is 33.13°C, thus 2.63°C higher comparing to the corresponding mean maximum of the roof below insulation. The fluctuation of the temperatures of the roof below insulation is low. The mean daily minimum is 28.6°C, while the corresponding temperature of water in the Base Case scenario is 6.0°C lower.

The total thermal performance of pond with aluminum foil seems to be better compared to the other tested devices, since the daily minimum and maximum bottom pond temperatures are lower. The mean daily maximum water temperature reaches, 26.35°C, the mean daily minimum reaches 22.23°C, while the overall mean daily bottom pond temperature is 24,07°C. Concluding, the fluctuation for the roof above insulation panel and the corresponding value of bottom pond temperatures are 7.61°C and 5,27°C respectively.

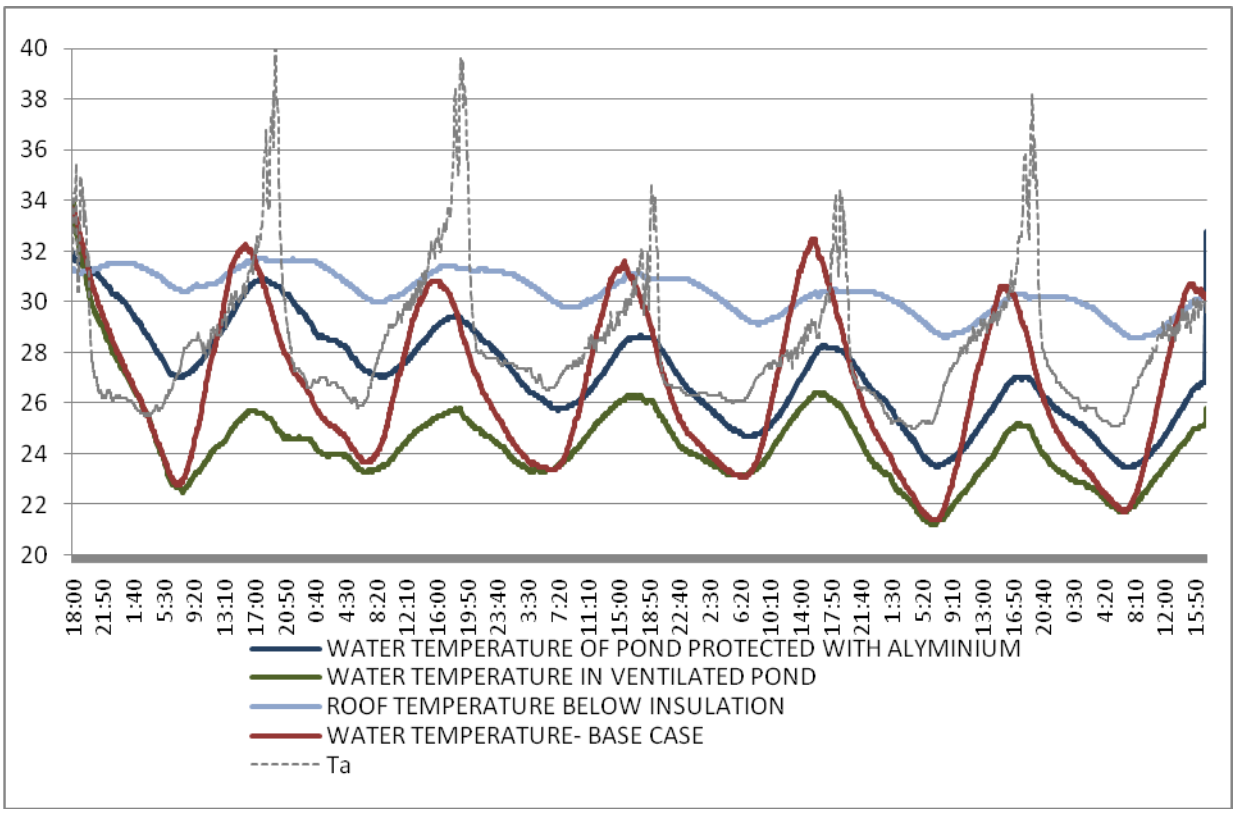

Figure 2: Bottom pond temperatures of three ponds. The aluminium foil is placed on water level, while the ventilated pond is protected by an aluminium layer above water level. The base case represents the pond with floating white textile. The records are referred to the period between 13th and 19th of July 2010.

4.2 The effect of the positions (below and above water level) of protective layer to the bottom pond temperature

The second period of experiments refers to the period between the 13th and the 19th of July 2010, as listed in Figure 3. An aluminum layer 5mm thick is placed above water level, representing a ventilated pond. The other pond has an aluminum foil, floating on water level. The third recorded pond, representing the Base Case Scenario is protected by a white textile floating on water level. Water depth is kept constant to 0.10m. Figure 2 shows the record temperatures for the second period of experiments.

Bottom pond temperature of the ventilated pond is represented by a curve that is almost parallel to the pond with a floating aluminum foil; the temperature difference between daily mean maximum is 2.68^{o}C (=28,88-31,56) while the corresponding value for the mean daily minimum values is 2,7^{o}C (=25,58-22,88). The daily minimum water temperature of the ventilated pond, is equal to the corresponding value of the Base case Scenario.

Bottom pond temperature of the ventilated pond has low fluctuation. The mean temperature for the ventilated pond is 24.32^{o}C, while the corresponding value for the roof below insulation is 6^{o}C higher. Placing an aluminum foil on water surface results daily decreased maximum water temperatures and increased minimum comparing to the corresponding values of the Base Case scenario. Concluding, the ventilated pond results a remarkable bottom pond temperature reduction, compared to the other investigated ponds.

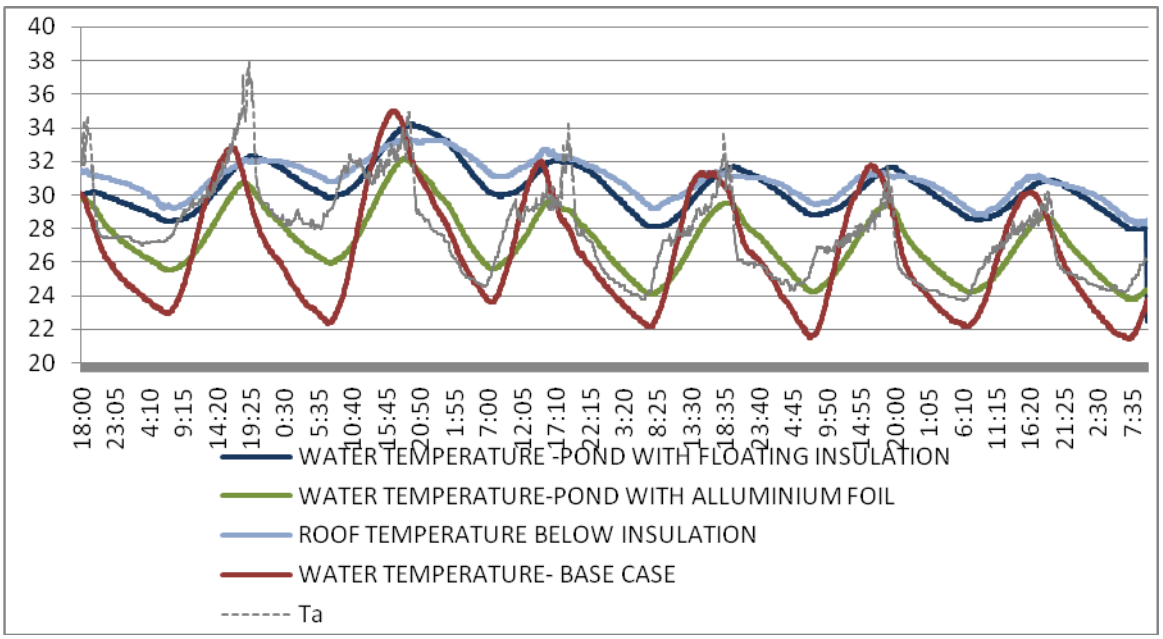

Figure 3: Bottom pond temperatures of three ponds. The aluminium foil is placed on water level, an insulating panel flows on water level. The base case represents the pond with floating white textile. The records are referred to the period between 23th and 30th of July 2010.

4.3 Comparing a roof pond with floating insulation to another one with floating aluminum foil.

An insulated panel of extruded polystyrene 3cm thick is floating on the water level of the pond. The insulating panel is covered externally to an aluminum foil, in order to reflect direct solar radiation. The other pond has an aluminum foil floating on water level, while the third one has a while textile representing the Base Case scenario. Water level is kept constant to the 10cm. The records of the period between 23rd and 30th July 2010 are listed in Figure 3.

The thermal performance of the pond with aluminum foil floating on water level has been described on the previous experimental period; the daily minimum temperatures of water are higher compared to the corresponding values of the Base Case scenario. On the other hand, the daily maximum temperatures of the pond with aluminum floating on water level are lower compared to the Base Case scenario.

The pond with the floating insulating panel, has reduced temperature fluctuations, similar to the ones of the roof avove insulation. As a result, the water below it, does not contibutes to the heat loss mechanism, since it does not encourage evaporative losses. As a result, this pond is not worth to be further investigated.

5. CONCLUSION

Roof pond with gunny bugs, is a roof pond variation proposed about a decade ago. The open pond is protected by a textile that is kept afloat on water surface. One of the advantages of the system is that it does not demand any daily operation or maintenance. The emissivity of the protective layer proved to be a critical parameter, affecting bottom pond temperature according to a parametric study.

The present study investigated a number of alternative materials for roof ponds protection in a variety of positions, thus above water level and floating on water level. The tested materials were the white textile, ironing board, and aluminum foil and aluminum layer. The pond with the white textile floating on water level represents the Base Case scenario, thus the other tested devices are being compared to that.

The experimental analysis showed that the use of reflective materials for water protection together with encouraging evaporative losses, can lead to bottom pond temperature reduction, compared to the Base case scenario. The ventilated pond, protected with an aluminum layer gave lower daily maximum temperatures, while the minimum ones are practically equal to the corresponding values of the Base case scenario (pond with floating white textile).

Further investigation should focus to a number of issues related to large scale application of the investigated system. Further analysis can propose the materials strong enough to be exposed in ambient conditions, the accomplishment to specific building regulations, and aesthetic issues. Furthermore, the performance of the system in regard to the climatic conditions could be also being investigated.

6 ACKNOWLEDGEMENTS

This investigation is a part of a Ph.D. study supported by the Greek State Scholarships Foundation.

7 REFERENCES

1. Raeissi, S., Taheri, M., 2008. *Skytherm: an approach to year-round thermal energy sufficient houses.* Renewable Energy 19, 527–543.
2. Tang, R., Etzion, Y., 2005. *Cooling performance of roof ponds with gunny bags floating on water surface as compared with a movable insulation*. Renewable Energy 30, 1373–1385.
3. Tang, R., Etzion, Y., Erell, E., 2003. *Experimental studies on a novel roof pond configuration for the cooling of buildings*. Renewable Energy 28, 1513–1522.
4. Tang, R.S., Etzion, Y., 2004a. *On thermal performance of improved roof pond for cooling buildings. Build Environment* 39, 201–209.
5. Tang, R.S., Etzion, Y., 2004b. *Comparative studies on the water evaporation rate from a wetted surface and that from a free water surface*. Building Environment 39, 77–86.
6. Artemisia Spanaki, Theocharis Tsoutsos, Dionysia Kolokotsa, *Parametric study of Roof Pond with Gunny Bags in the cooling season*, 3rd PALENC, 5th EPIC and 1st Cool Roof Conference, Rhodes, September 29-30, 2010

A CASE STUDY OF SUSTAINABLE URBAN PLANNING WITH THE USE OF A DECISION SUPPORT SYSTEM

Afroditi Synnefa*[1], Marina Stathopoulou[1], Nektaria Adaktylou[1], Denia Kolokotsa[2], Kostas Gobakis[2], Mat Santamouris[1], Nektarios Chrysoulakis[3], Costantinos Cartalis[1]

1 National and Kapodistrian University of Athens
Physics Dept., Section Applied Physics
Building of Physics - 5, University Campus
157 84 Athens, Greece
**Corresponding author: asynnefa@phys.uoa.gr*

2 Technical University of Crete
Technical University Campus, Kounoupidiana,
73100 Chania, Greece

3 Foundation for Research and Technology - Hellas
Institute of Applied and Computational Mathematics
N. Plastira 100, Vassilika Vouton,
70013, Heraklion, Crete, Greece

ABSTRACT

This paper aims to present the methodology for the development of a Decision Support System (DSS) that takes into account environmental and socioeconomic criteria, focusing on a case study that was carried out in Athens. The experimental campaign that was performed at city, neighbourhood and building scale and its main results are described. In addition, the results of the Communities of Practice that were organised are reported. A short description of the development of an ANN model for heat island prediction is given. Finally, the three different planning alternatives that were proposed and evaluated by the developed DSS are analysed.

KEYWORDS

Sustainable urban planning, Decision Support System, environmental measurements, Communities of Practice, UHI prediction

1 INTRODUCTION

In Europe, four out of every five citizens live in urban areas. Cities today face a number of environmental and socioeconomic challenges. These include environmental problems like increased levels of traffic, air pollution, and greenhouse gas emissions, neglect of the built environment, improper land-use, lack of open space, soil contamination, as well as the generation of large quantities of waste and wastewater. Increased energy consumption is another important issue taking into account Europe's increased dependence on energy imports and scarce energy resources. In addition, the generalized economic crisis and the impacts of climate change, form a new landscape within which it is required to develop coordinated and effective socioeconomic, energy and environmental strategies. Sustainable urban planning and management is a key issue in the effort to improve environmental conditions and the quality of life in cities (European Commission 2011).
In order to achieve sustainable urban planning and development, planners need to take into account environmental and socioeconomic issues and impacts simultaneously and tailor made

decision making tools provide the means to support such complex decisions and solve semi-structured or unstructured problems, presenting results in a readily understandable form.
An FP7 project called BRIDGE (sustainaBle uRban planning Decision support accountinG for urban mEtabolism), which was the joint effort of 14 Organizations from 11 EU countries, has illustrated the advantages of considering environmental issues in urban planning, focusing on specific urban metabolism components (energy, water, carbon, pollutants). The innovation of BRIDGE is the development of a Decision Support System (DSS), which assists urban planners in decision-making and provides a structured presentation of planning alternatives and the tools to evaluate them on the basis of environmental and socioeconomic impacts. The BRIDGE methodology is based on sustainability objectives and associated indicators addressing environmental, social and economic issues that are specific to each case study's planning alternatives. The indicators demonstrate the potential impact of each alternative to show the level of achievement of the sustainability objectives (based on associated defined targets and thresholds) in a quantified way. The BRIDGE project has used input from end users on their needs and requirements in the design of the DSS. A "Community of Practice" (CoP) approach was utilized to facilitate the interaction between the urban planning professionals and the BRIDGE researchers. During CoP meetings, planning priorities and core sustainability objectives were determined for each case study. Based on these, indicators were identified by participants and adjusted to the specific requirements of the planning alternatives that were analyzed. Indicators for each planning alternative were provided in quantitative and qualitative ways: environmental indicators arising from physical flows were calculated by spatial models; socioeconomic indicators reflecting objective values (number of houses constructed, number of jobs created, etc.) were given as data attached to planning alternatives and subjective value judgments (such as landscape or urban quality) were defined by end-users. In order to evaluate the biophysical/ spatial models used for the calculation of indicators in the case study cities, in situ observations were collected. Energy, water, carbon and pollutants fluxes in urban areas have been investigated by micrometeorological measurements and site studies, airborne and satellite remote sensing observations and numerical modelling approaches, leading to indicators which define the state of the urban environment. The BRIDGE DSS evaluates how the planning alternatives proposed by the end-users modify the energy, water, carbon and pollutants fluxes within the case study area. A Multi-Criteria Analysis (MCA) approach was used to address the complexity of urban metabolism issues reflected in the wide set of sustainability indicators and enabled comparison and ranking of different urban planning alternatives (Chrysoulakis et al., 2013). To develop and evaluate the DSS five case studies were chosen, each in a different city and country: Athens, Helsinki, London, Firenze and Gliwice.
This paper focuses on the Athens case study and reports the various activities performed in order to provide the required input for the development and evaluation of the DSS. More specifically, in the next sections we describe the process of consultation with end-users (CoPs) during the development of the DSS tool, the methods and results of the experimental campaign for the collection of environmental and socioeconomic data, the development of an ANN model for the prediction of heat island intensity that could potentially be included in the DSS and the use of the DSS to evaluate specific planning alternatives for the case study area. The details of the BRIDGE approach and the all the aspects of the research can be found in Chrysoulakis et al. (2013) and in the various reports and papers provided on the BRIDGE website (www.bridge-fp7.eu).

2 THE ATHENS CASE STUDY

The Athens Case Study is focused on the municipality of Egaleo, which is a densely built urban area that lies in the Western part of Athens. Five main road axes divide the area in four quarters. One of the quarters is an industrial degraded area (brownfield) called Eleonas. The total area of Egaleo is 650 ha and it is flat in general. The population is 74.046, although it is estimated that at least 120000 people, mostly medium and low income, live and work in the area. The level of education of the inhabitants is low to medium and the rate of unemployment high. The average population density is estimated to be 225 inhabitants/ha. As it appears in the land use map of Egaleo, availability of free/ green spaces is limited.
Egaleo is considered an environmentally degraded area facing problems with:

- air pollution
- traffic and transport
- thermal discomfort
- lack of green/ free spaces
- poor quality of building stock
- energy

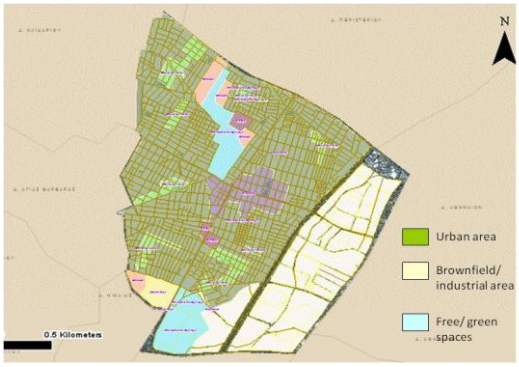

Figure 1: Land use map of Egaleo [Source: www.aigaleo.gr]

2.1 Athens CoP meetings

In the framework of the Bridge project 2 CoP meetings have been organized for the case study of Athens. These two local meetings were convened at the Municipality of Egaleo, which is the specific case study area for Athens. The participants included, apart from the BRIDGE researchers, academics, urban planners, architects, engineers and researchers all interested in sustainable urban planning. Most of them are working in the technical and planning dept. of the Municipality of Egaleo. The main outcomes of the CoP meetings were the following:

- enabling the Bridge partners and Athens planners to interact with each other and share experience on sustainable urban planning issues in Athens
- discussion of key issues of sustainable development in Athens and especially in Egaleo
- identification of planning priorities; Sustainability objectives and corresponding indicators with which to assess progress towards sustainable development (described below)
- selection, accordingly, of a planned intervention for the Athens case study and definition of underlying challenges, planning alternatives and collected indicators (described in Section 3.1)

The discussions in CoP meetings identified the following priorities for sustainable city planning in Athens:
Thermal discomfort, Energy, Quality of building stock, Transport, Green spaces and the Land use of Eleonas. Based on these sustainability priorities, and taking into account the previously defined challenges, the core sustainability objectives were established for the city by the CoP-participants: These objectives were divided to environmental and socioeconomic ones and can be summarized below:

Sustainability Objective (in order of priority)	Indicators
1. Reduce Thermal Discomfort	• Average outdoor temperature (air) and humidity; • Average surface temperature (roads, buildings, etc.); and • Wind speed.
2. Improve Air Quality and Reduce Emissions	• Concentration of pollutants (NOx, SOx, PM10, PM2.5); • CO2 concentration; • Source of emissions (% per building/sector type); • Number of days above established air quality thresholds; and • Effects of meteorological conditions (e.g. temperature) on concentrations.
3. Increase Green Space Areas	• Area (% or m2) of urban green space; • Number of trees planted; and • Types of trees planted.
4. Optimize Water Use	• Volume of water used (for irrigation).
5. Improve Energy Efficiency	• Energy consumption for lighting the avenue; and • % of energy from renewable sources (i.e. solar panels).
6. Optimize Quality of Materials Used	• Solar reflectance of materials used.

Sustainability Objective (in order of priority)	Socio-economic complement of the Environmental indicators
1. Mobility	• road traffic intensity, • quality of pedestrian sideways, • number of parking slots.
2. Public health and safety	• number and severity of road accidents and pedestrian injuries, • number of people suffering from short term effect of air pollution (upper respiratory infections such as bronchitis and pneumonia, allergic reactions) • number of people suffering from long term effects of air pollution (e.g. chronic respiratory disease, lung cancer, heart disease)
3. Social inclusion	• extent to which roads and sideways can be used by disabled or differently able people and groups (e.g. number of safe-street-crossing points, number of repose places along the street), • local community composition – compared to other areas: % of elderly people, foreigners, low-income families etc.
4. Economic criteria	• financial costs of the interventions, • estimated side-effects on local economy
5. Place identity	• aesthetic value of the area and changes due to planning intervention

Figure 2: Environmental and Socioeconomic sustainability objectives and indicators as defined by the CoPs

2.2 Experimental campaign and data collection

The main objectives of the Athens experimental campaign was to collect the necessary information needed as inputs by the models but also to estimate the urban heat island effect in the area, assess the air quality and the thermal outdoor environmental conditions, estimate the impact of outdoor environmental conditions on the cooling load of buildings in the area and the investigation of indoor environmental quality.
The observations and data collection for the Athens case study were performed at city scale, local and at building scale using different methodologies. The data collection includes tower based meteorological measurements, urban air quality data collection, heat island measurements, outdoor environmental assessment, building related observations, remote sensing and GIS data and statistical socioeconomic information. The following paragraphs briefly describe the measurement methodologies and results. All the collected data are available in the Bridge database (http://www.bridge-fp7.eu/).

a) Meteorological measurements
Meteorological measurements were taken at the Thission meteorological station of the National Observatory of Athens. The station is located on a hill in the center of Athens, very close to Egaleo. Hourly data for air temperature, RH, wind speed and direction, precipitation, diffuse and total solar radiation, sunshine duration and air pressure were collected. It was found that the case study area has high solar radiation levels and sunlight availability throughout the year and air temperatures range from 3°C (February) to 40°C (July). The yearly average value of relative humidity is about 60%. Wind directions are fairly consistent with the dominant wind direction being from the North-East reaching an average wind speed of 3m/s. Precipitation levels are quite low, especially during the summer.

b) Air quality measurements
Air quality data were retrieved from the Directorate of Air Pollution & Noise of the Greek Ministry of Energy, Environment and Climate Change, which is responsible for the operation of a network of stations, installed in the greater Athens area that measure air pollution (SO2, NOx, CO, O3, PM10, PM2.5, C6H6). The stations close to the case study area were used for analysis. It was found that exceeding of the limit occurred for certain pollutants, at the Egaleo area. PM10 pollutants exceeded limits at a number of measurement stations, NO2 presented exceedings of the indicative yearly average value and for ozone, exceedings of the warning

threshold as well as of the alert threshold occurred close to Egaleo suggesting an occurrence in Egaleo as well. These exceedings are due mostly to the high levels of sunshine and high temperatures that favour the formation of ozone.

c) Urban heat island measurements

In order to study the heat island phenomenon in the greater Athens area, a network of 17 fixed temperature stations has been set up (Table 1). These stations were located in four different zones grouped into Western, Eastern, Southern and Northern zone stations according to their geographical location and thermal balances. In all stations the data were measured with fully calibrated high precision automatic miniature sensors, which were placed in white wooden boxes with lateral slots approximating the Stevenson screen to be protected for solar radiation and rain. Temperatures were measured at 15 minute intervals.

Table 1 The location of the 17 stations and the monthly mean maximum and s.d. air temperature values for all stations for July, 2009, (*Reference station)

Station	**Lat.**	**Long.**	**July**	**Station**	**Lat.**	**Long**	**July.**
Western				**Southern**			
Egaleo	37°59'50.40"S	23°40'4.29"E	33,8 ± 2,4	Elliniko	37°54'27.35"S	23°44'32.43"E	35,0 ± 2,4
Agia Varvara	37°59'22.58"S	23°39'36.70"E	34,2 ± 2,3	Glyfada	37°51'52.72"S	23°44'39.97"E	32,8 ± 2,1
Korydallos	37°58'44.84"S	23°38'32.82"E	33,1 ± 2,1	Kallithea	37°57'25.18"S	23°42'9.91"E	35,0 ± 2,1
Haidari	38° 0'44.42"S	23°39'34.40"E	34,1 ± 2,5	Moschato	37°57'12.44"S	23°40'55.58"E	35,9 ± 1,8
Zefyri	38° 3'3.33"S	23°42'40.90"E	35,3 ± 2,8	Renti	37°57'45.94"S	23°40'27.88"E	35,9 ± 2,9
Mean			**34,1 ± 2,4**	**Mean**			**35,0 ± 2,3**
Eastern				**Northern**			
Agia Paraskevi	38° 0'50.34"S	23°49'27.79"E	31,0 ± 2,0	Kamatero	38° 3'34.80"S	23°42'50.66"E	35,3 ± 3,1
Vyronas	37°57'24.21"S	23°45'44.23"E	35,1 ± 2,7	Nea Filadelfia	38° 2'6.78"S	23°44'17.99"E	32,6 ± 2,4
Ilioupoli	37°55'57.37"S	23°45'30.88"E	33,7 ± 2,2	Nea Erythrea*	38° 5'23.69"S	23°49'9.11"E	32,4 ± 3,2
Kessariani	37°58'8.95"S	23°45'42.44"E	33,8 ± 2,9				
Mean			**33,4 ± 2,5**	**Mean**	**38° 3'34.80"S**	**23°42'50.66"E**	**33,4 ± 2,9**

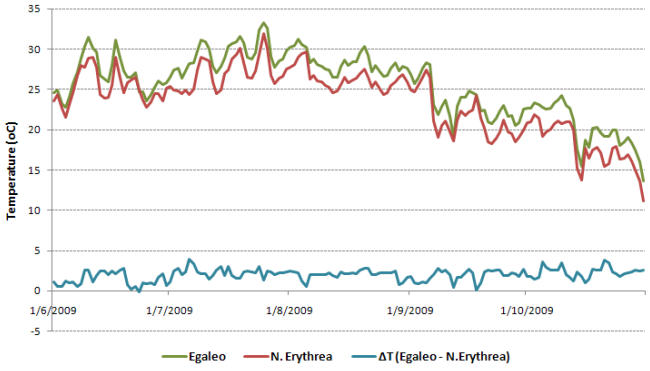

Figure 3 Daily average temperature distribution for the Egaleo and Nea Erythrea area and temperature difference, ΔT (TEgaleo – TN.Erythrea) for months June to October, 2009

The analysis showed that the case study area suffers from a strong heat island effect. Measurements between Egaleo and a suburban station indicate a mean heat island intensity for the monitoring period of 2 -3 °C, reaching however in many occasions a difference of 6 - 8 °C. Higher air temperatures were found in the industrial western part of the city and also the center while lower values (by 1-2°C) were presented at the northern and the eastern parts. More information on this work can be found in Giannopoulou et al. (2011).

d)Outdoor environmental assessment

In order to assess the quality of the outdoor environment of the case study area the following measurements have been carried out using a mobile meteorological station and portable instrumentation:

- Concentrations of PM1, PM2.5, PM10 (Lighthouse 3016 IAQ Laser Particle Counter) wind speed and direction by anemometers that have been placed in three different heights-3.5, 7.5, 15.5m – in the antenna of NKUA's mobile station.
- Air temperature, RH, air velocity and Radiant temperature at a height of 1.5m.
- Measurements of the surface temperature of the urban fabric (building facades, roads and pavements) using an infrared thermometer (Cole Palmer) and infrared camera (Thermovision 570).

The monitoring campaign was conducted during several several days the summer of 2009 between 10:00 and 17:30, in several locations in Egaleo area. The analysis of the results showed that increased surface and air temperatures and low wind speeds result in thermal discomfort for the people in the area.

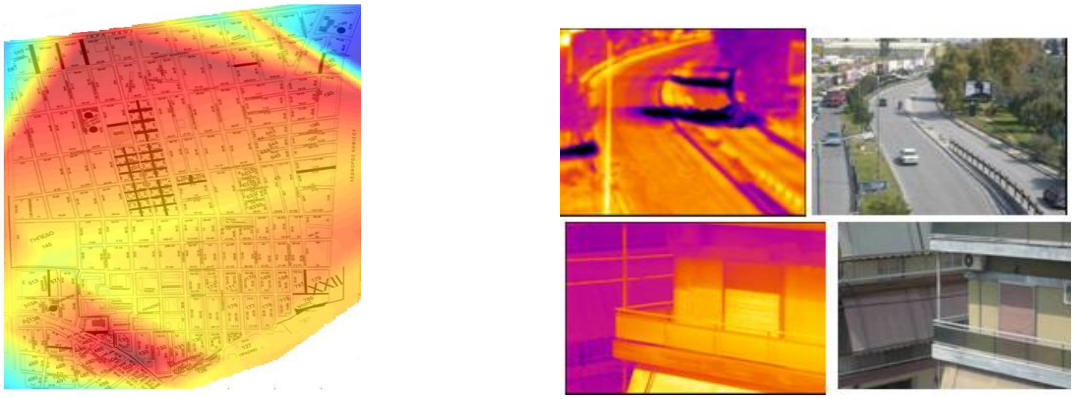

A *B*

Figure 4. Spatial air temperature distribution in the BRIDGE case study area (June 2009) (A) and infared and visible images taken in the case study area to assess the thermal environment (B)

e) Building related observations

The impact of the outdoor environmental conditions (mainly thermal comfort and air pollution) on the indoor environment of residential buildings in the case study area was also assessed. The process followed is outlined below:

a) Data collection on the residential building stock of Egaleo and selection of ten representative buildings

b) Data collection of the selected residential buildings

c) Distribution and collection of questionnaires answered by the residents

d) Indoor thermal comfort measurements: Air temperature, RH, Air velocity and mean radiant temperature

e) Measurements of PM1, PM2.5, PM10 concentrations

The results indicate that thermal discomfort inside the houses is a serious problem. It was found that over 40% of the maximum indoor temperatures are up to 35 °C, while 70% of the

mean indoor temperatures are up to 30°C for the specific monitoring period. Indoor temperatures up to 38ºC have been recorded as well as hot spells of almost 21 consecutive hours over 34ºC. Comparative analysis of the occupants' responses received from questionnaires and the measured indoor conditions indicate that the thermal comfort perception of the users is in agreement with the air temperature measurements. Also, particle number concentration measurements indoors is generally correlated with outdoor concentration characteristics in the absence of important indoor sources. In addition, although concentrations outside the residences were quite high, for well air tight buildings, concentrations were significantly lower (given the fact that no internal PM sources were found inside). On the contrary, poor construction and high infiltration rates due to e.g. old wooden frames resulted in high indoor concentrations. The presence of internal sources e.g excessive smoking and cooking (e.g. frying) as expected resulted in high concentrations during the activity. More information on this work can be found in Sakka et al. (2012).

f) Remote sensing data

High-spatial resolution satellite images were used to describe the surface characteristics of the metropolitan area of Athens: land cover and land use (LCLU), land surface albedo (LSA), land surface emissivity (LSE), land surface temperature (LST), vegetation and topography (DEM). More specifically, information on the spatial distribution of the various land cover and land use types found within the metropolitan Athens area was obtained from the Corine Land Cover 2000 (CLC00) database for Greece. Maps of LSA, LSE, LST and vegetation (NDVI index) were derived by processing of the appropriate high-spatial resolution satellite images acquired over the Athens metropolitan area from the Landsat TM sensor. It was found that the case study area is characterised by low albedo values ranging from 9% to 13% and low vegetation index with NDVI values ranging from 0.5 to 0.25.

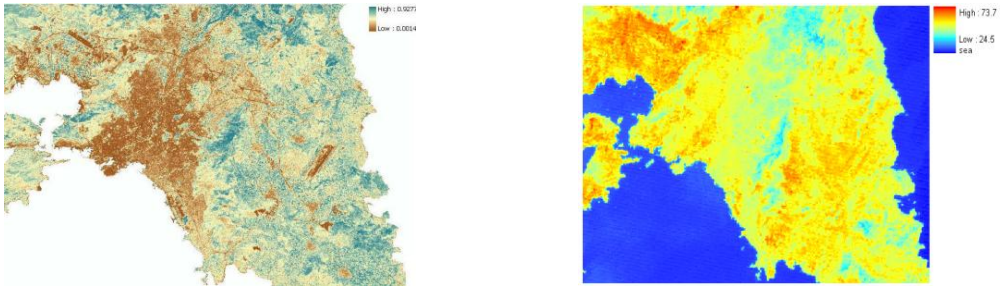

Figure 5 NDVI index and mid morning summer LST maps of Athens

g) Impact of heat island characteristics on energy loads

In an effort to estimate the impact of outdoor environmental conditions, namely of the documented urban heat island effect, on Egaleo's buildings cooling load, the following process was implemented. Based on the collected data previously analysed, a building typology that is representative of Egaleo's residential building stock was selected. Numerical analysis using TRNSYS software was then performed in order to estimate the cooling load of this same building in a)Egaleo (urban area) and b) Nea Erithrea (suburban area). In order to run the model and estimate the impact of outdoor thermal conditions on the building load, we have used the meteorological measurements performed at those sites. It was found that the assumed building in Egaleo area has an increased energy demand for cooling by 74% than the suburban area of Nea Erithrea.

3 DEVELOPMENT OF AN ANN MODEL FOR HEAT ISLAND PREDICTION

The measured data described in Section 2.2c have been used in order to develop an ANN (Artificial Neural Network) model able to predict the heat island effect in the area of Athens,

focusing on the Egaleo area. The prediction problem using neural network models is separated into three steps: designing the neural network architecture, conducting the learning or training process, and testing. From the different neural networks architectures, training and transfer functions tested, the most suitable NN architecture for the urban heat island intensity prediction in terms of accuracy was found to be the Elman type using Levenberg-Marquardt as transfer function. The specific network architecture was used for predicting the urban heat island intensity in the sites described in Table 1.

Training and verification of the ANN was performed using the data collected during the period from 06/04/2009 to 07/09/2009 for each experimental site. The remaining data was used to verify the quality of network and adaptation of the neural network to the new data.

Isothermal images have been developed to imprint the UHI intensity over Athens. For each day that the UHI over Athens is analyzed, a set of four images is constructed to visualize the ANN prediction:

- The first image maps the isotherms over Athens using the measured data of the specific day and time.
- The second image represents the isotherms of Athens urban heat island based on the 1 hour prediction results for the specific day and time.
- The third image maps the isotherms of Athens urban heat island based on the 24 hour prediction results for the specific day and time.
- The fourth image plots the isotherms of Athens urban heat island based on the 48 hour prediction results for the specific day and time.

Indicatively the isothermal maps of the UHI intensity over Athens for the day of 1/7/2009 are illustrated in Figure 6. The prediction of the maximum temperatures for the 1/7/2009 has a maximum error of 1.6 °C and 1.9 °C for the 24 hour and 48-hour prediction horizon respectively. Moreover the visualization of UHI intensity prediction shows that the isotherms of the 24 hours prediction are very close to the actual measured ones while the 48 hours prediction presents a slightly different picture.

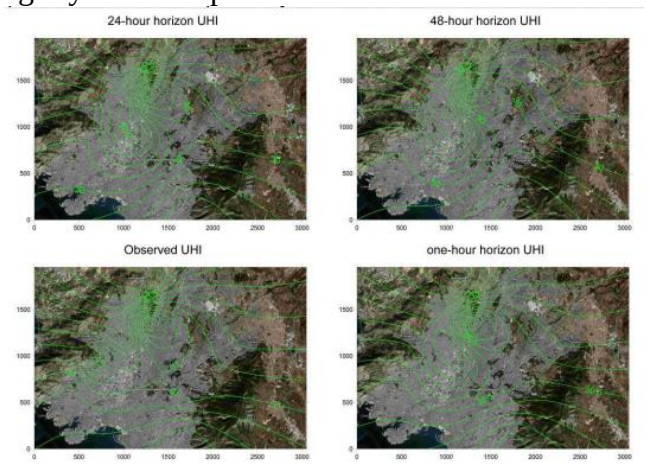

Figure 6: Measured and predicted (1h, 24h and 48h) UHI in Athens during 01/07/2009

The quality control and assurance procedures included testing of the model's accuracy in predicting temperature fluctuations, seasonal variations and sudden changes in weather conditions. It was found that the specific NN architecture and methodology is accurate for the 24 hours prediction horizon. In addition the calculation of R^2 was found to be close or higher than 0.9 for all sites which represents a good prediction of the urban heat island intensity. The methodology presented here showed that the urban heat island intensity can be predicted quite accurately for at least a 24 hours prediction horizon using a limited set of data. Therefore the NN prediction methodology can be an important tool for peak energy load predictions during heat waves and hot summer days contributing to the demand and supply energy management.

More information on the development of the ANN for the UHI prediction can be found in Gobakis et al. (2011).

4 DSS APPLICATION ON THE ATHENS CASE STUDY

In order to use the DSS for the evaluation of the planning alternatives the end user has to follow certain steps. The BRIDGE DSS allows the end user to select a specific case study with its associated urban planning alternatives. Then he has to select the sustainability objectives and indicators and define their relative importance by weighting using scale bars. The end user runs the models integrated in the DSS for specific time periods and being able to change the initial conditions for these models. He has to provide the (relative or absolute) values of socioeconomic indicators that are relevant for the case study. The outputs of the BRIDGE DSS are: a) indicators maps for each planning alternative and b) spider diagrams that show the comparative performance of each alternative for each sustainability objective (Chrysoulakis et al., 2013). The sections below describe the application of the DSS on the Athens case study.

4.1 The planning alternatives

One of the outcomes of CoP in each city was the definition of a "real life" project. A part of the city that needed to be redesigned was chosen and specific planning alternatives were proposed. For Egaleo, the discussions between the CoP participants and the results of the experimental campaign carried out in the area lead to the following three planning alternatives.

1. applying cool materials on all buildings and roads in the Egaleo municipality (Figure 7A);
2. changing the land use of Eleonas area with the municipality from its current brownfield/industrial use to urban fabric, including housing and newroads (Figure 7B);
3. changing Eleonas from brownfield/industrial to green space (Figure 7C);

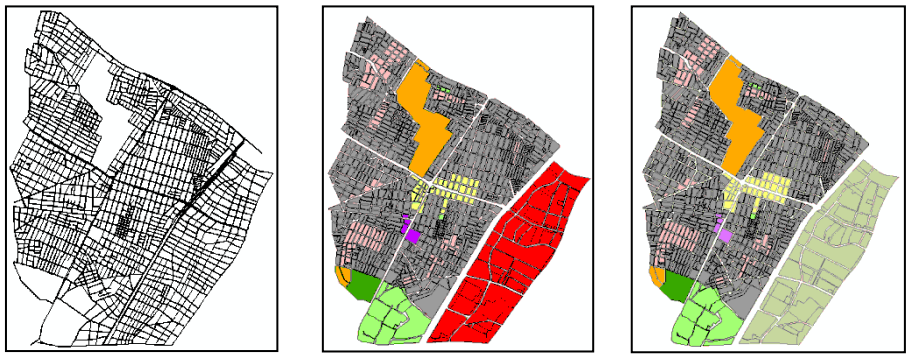

A B C

Figure 7: The three planning alternatives

These three planning alternatives are evaluated by the BRIDGE DSS.

4.2 DSS results

For the Athens case study the issue of thermal comfort was addressed. Figure 8 presents the spatial distribution of the mean evening (20:00–23:00 LST) air temperature (K) for summertime over the municipality of Egaleo. As it can be seen, Planning alternative 1 would reduce the summertime evening air temperature by approximately 0.5 K. The application of cool materials (i.e. materials with high solar reflectance and infrared emittance) on the urban

fabric of Egaleo has an impact on the urban energy budget. Solar radiation is reflected rather than absorbed by building roofs and other pavements resulting in lower surface temperatures. This means that less heat is transferred to the ambient air. Consequently, the air temperature values were lower than those of the base case. This reduction of air temperature during the evening hours was considered beneficial for the comfort of residents, as well as for the energy consumption for cooling, with obvious socioeconomic impacts. The 2nd planning alternative slightly increased the summertime evening air temperature over the brownfield of Eleonas when this was converted to residential area. However a small but measurable decrease over the residential area of Egaleo was also observed, which may have been caused by advection.

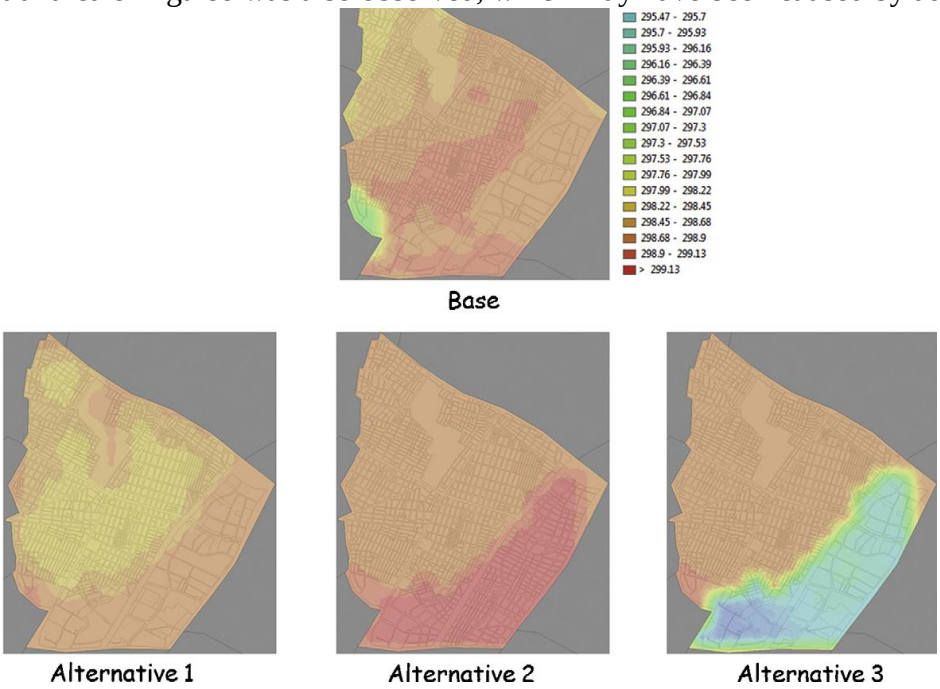

Figure 8. Mean air temperature (K) for the evening period (20:00–23:00 LST) for summertime for Athens base case (top) and planning alternatives (bottom), which are maps of differences (common scale on the right)[taken from Chrysoulakis et al. (2013)].

According to the 3rd planning alternative the brownfield of Eleonas is converted to green area. This change also affects the urban energy balance as trees and vegetation lower surface and air temperatures by providing shade and through evapotranspiration. It was found that this intervention would strongly decrease (around 1.5 K) the summertime evening air temperature. A small but detectable decrease over the residential area of Egaleo was also observed. It can be therefore concluded that all the Athens urban planning alternatives have the potential to create relatively more sustainable urban structures.

The spider diagram produced by the BRIDGE DSS for the Athens case study shows that the 2nd alternative performed better followed closely by the third alternative, although the 1st alternative obtained the highest score for the dimension "thermal comfort". For the above calculations, default weight and socioeconomic indicators values have been used.

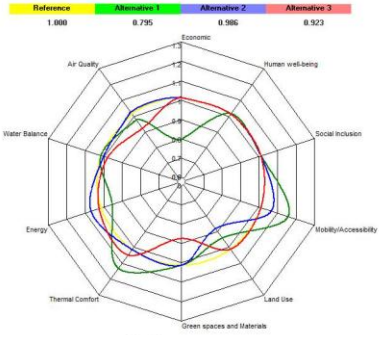

Figure 9. Spider diagram and final appraisal score the Athens case study [taken from Chrysoulakis et al. (2013)].

5 CONCLUSIONS

This paper presents the various activities performed in the framework of the BRIDGE project focusing on the case study based in Athens, in order to provide the required input for the development and evaluation of the DSS. The main outcomes of the CoP meetings were the identification of key planning issues, sustainability objectives and indicators for the city. Also, three planning alternatives were defined. The analysis of the in situ data collection that was undertaken demonstrated that the Athens case study area is characterized by: large solar availability, hot climatic conditions and low precipitation levels, low albedo and vegetation index, air quality problems for some pollutants, strong heat island effect (mean UHI intensity of 2 -3 °C reaching on occasions 6 - 8°C, increased surface and air temperatures and low wind speeds resulting in thermal discomfort for the people in the area (during summer) poor environmental conditions inside buildings (thermal discomfort and lack of IAQ) and increased cooling loads due to the heat island effect. An ANN was developed for the prediction of the urban heat island intensity and was found to accurately predict it for a 24 hours prediction horizon using a limited set of data. The evaluation of the planning alternatives by the DSS showed that all of them have the potential to create relatively more sustainable urban structures.

6 ACKNOWLEDGEMENTS

The research leading to these results has received funding from the European Community's Seventh Framework Programme (FP7/2007–2013) under grant agreement no. 211345 (the BRIDGE project: http://www.bridge-fp7.eu). The authors are grateful to all the people who have contributed to the BRIDGE research, the Municipality of Egaleo and the participants in the Athens CoP.

7 REFERENCES

N. Chrysoulakis, M. Lopes, R. S. José, S. Grimmond, M. B. Jones, V. Magliulo, J. E.M. Klostermann, A. Synnefa, Z. Mitraka, E. A. Castro, A. González, R. Vogt, T. Vesala, D. Spano, G. Pigeon, P. F. Smith, T. Staszewski, N. Hodges, G. Mills, C. Cartalis, (2013) Sustainable urban metabolism as a link between bio-physical sciences and urban planning: The BRIDGE project, Landscape and Urban Planning, Volume 112, April 2013, Pages 100-117, ISSN 0169-2046,

European Commission - Directorate General for Regional Policy (2011), Cities of tomorrow - Challenges, visions, ways forward, Luxembourg: Publications Office of the European Union, ISBN: 978-92-79-21307-6, doi:10.2776/41803

K. Giannopoulou, I. Livada, M. Santamouris, M. Saliari, M. Assimakopoulos, Y.G. Caouris, (2011), On the characteristics of the summer urban heat island in Athens, Greece, Sustainable Cities and Society, Volume 1, Issue 1, February 2011, Pages 16-28, ISSN 2210-6707, http://dx.doi.org/10.1016/j.scs.2010.08.003.

K. Gobakis, D. Kolokotsa, A. Synnefa, M. Saliari, K. Giannopoulou, M. Santamouris, (2011) Development of a model for urban heat island prediction using neural network techniques, Sustainable Cities and Society, Volume 1, Issue 2, July 2011, Pages 104-115, ISSN 2210-6707, http://dx.doi.org/10.1016/j.scs.2011.05.001.

A. Sakka, M. Santamouris, I. Livada, F. Nicol, M. Wilson (2012), On the thermal performance of low income housing during heat waves, Energy and Buildings, Volume 49, June 2012, Pages 69-77, ISSN 0378-7788,

Websites:
BRIDGE website: www.bridge-fp7.eu

URBAN GARDENS: AS A SOLUTION TO ENERGY POVERTY AND URBAN HEAT ISLAND

Vasiliki Tsilini[1], Sotiris Papantoniou[*2], Denia Kolokotsa[3], and Efpraxia Maria[4]

Technical University of Crete
School of Environmental Engineering
Greece, Crete

ABSTRACT

Urban gardens are a means of greening and are created by a local community. As regards any urban environment, urban greening helps cooling the air and provides shading, thus reducing building energy consumption and improving the outdoor conditions during the summer. In more detail, vegetation is a way to deal with the phenomenon of energy poverty in which many people cannot meet their basic energy needs as well as the phenomenon of urban heat island. This paper deals with the ways in which vegetation affects the improvement of microclimatic change, mainly through evapotranspiration. This is examined in a region of the city of Chania. More specifically, through the application of Envi-met software the current condition, a scenario with absence of vegetation and two scenarios of different vegetation are analyzed. In the last two scenarios fruit and vegetables and agro-biodiversity like herbs, which both are consumed, are used.

KEYWORDS

Energy saving, Urban Heat Island, Environmental planning, Urban green space, Community Gardening

1 INTRODUCTION

The increasing accumulation of people in cities combined with the urban heat island effect creates an urgent need to create green spaces within them. Greening is a natural method that brings many advantages depending on both techniques used and the purposes to be served.
This research concerns the creation of green urban spaces in the city of Chania, and more specifically the creation of urban gardens.

1.1 Urban Climate

The climate in every region of the globe can be described at three different levels, going from the general to the specific, from the largest scale to the smallest: the macroclimate, the mesoclimate and microclimate. The macroclimate of an area is about the general climatic characteristics and is defined by climatic conditions, such as temperature, solar radiation, sunshine, wind, humidity, clouds and rainfall. The mesoclimate of an area is the transformation of macroclimate due to local circumstances, such as the terrain, the existence of large areas of water and vegetation. The microclimate of an area is the diversification of macroclimate and mesoclimate, mainly due to human activities. (Boutagioti et al. 2009)
The continuous upward trend of agglomeration in urban centers is expected to increase the population of people living in urban areas by 60% in 2030. (Mirzaei and Haghighat 2010)This has resulted in human exposure to microclimate, specifically in "urban microclimate."
The term urban microclimate means the climatic conditions prevailing in an urban area (square, park, neighborhood, etc.), which can show significant differences compared to the

conditions prevailing in the wider area. The urban topography affects these microclimatic conditions, since it determines the shading and the flow of air between buildings to a ;arge extent.(Mirzaei and Haghighat 2010)

1.2 Urban Heat Island Effect (UHI)

Air temperatures in densely populated urban areas are higher than the temperatures of the surrounding areas. The phenomenon is known as the "heat island" effect and is the most obvious climatic manifestation of urbanization. (Santamouris et al. 2007) The causes of this phenomenon are mainly produced various sources such as anthropogenic heat, traffic, lack of green space and the construction of an urban center.

1.3 Energy poverty

According to the Greek Article 24 paragraph 1 of the 1975 Constitution there was a provision according to which, "the protection of the natural environment is an obligation of the State and a right of everyone." The right to a proper environment implies a right to energy. However, nowadays, many people are unable to meet their energy needs and even the essential ones, as it is the electricity. This phenomenon is called "energy poverty" and appears more and more as time goes by.

Energy poverty is the difficulty or inability to maintain housing at appropriate temperature (as a point of reference could be the definition used by the World Health Organization, according to which the proper temperature in the living room is 21 º C and in the other rooms 18 º C, or any another technically adequate definition) and other essential energy services: lighting, transport or electricity to use the Internet or other systems and devices. (Gazette 2011)

1.4 Biodiversity

It is obvious that in recent years there have been enormous changes in natural ecosystems. The shift of people towards urban centers, the removal of the natural environment and daily activities have led to threats to biodiversity. According to the Intergovernmental Panel on Climate Change (IPCC), human activities until 1750, were blamed for the global warming. At the same time, they argue that it is likely that 20-30% of plant and animal species will become endangered if the average amount of global temperature increase exceeds 2.3 ^{o}C. The escalating extinction crisis shows that the diversity of nature cannot support the current pressure that humanity is placing on the planet (Pia Drzewinski 2012)

The links between poverty, climate change and biodiversity are very important.

- Land use changes, leading to habitat and thus biodiversity losses, can also boost greenhouse gas emissions. (Reid and Swiderska 2008)
- Poor people are disproportionately vulnerable to the loss of biodiversity and ecosystem services. And although they are responsible for emitting the lowest levels of greenhouse gases, they suffer most from the impacts of climate change. (Reid and Swiderska 2008)
- Geographic location is a key factor in the vulnerability of poor people and poor nations. Many of these countries lie in the regions most at risk due to climate change. (Reid and Swiderska 2008)
- Biodiversity conservation and the maintance of ecosystem integrity are central to improving the ability of the poor to cope with climate change. (Reid and Swiderska 2008)

2 BIOCLIMATIC DESIGN – URBAN GARDENS

In Greece the energy demand grew rapidly after 1990 with main consumers industry or households. The main energy consumption is used for heating and cooling. According to surveys, 41% of the total energy produced is spent in European countries in order to meet buildings requirements for heating and cooling. (Axarli et al. 2008) For this reason, researchers have turned to bioclimatic design. As part of bioclimatic design green buildings, more specifically buildings whose construction and operation manual are environmentally friendly and efficient throughout its life cycle of the building, are developed. A technique of bioclimatic design for both the shell and the outside of the building, which offers better energy building performance, is urban gardens.

An urban garden is land used for growing food from people of different families, usually urban dwellers with limited access to their own land. An urban garden differs from public green spaces because the main characteristic is the familial assistance to produce their own products, vegetables, or medical herbs. (Okvat and Zautra 2011) Looking back in time, urban gardens were developed in the 80's, where cities offered to the poor a small part of land in the city to cultivate their own produce. In New York during the Great Depression nearly 5000 urban gardens were cultivated by residents in order to increase supplies of food and occupy the unemployed. (Okvat and Zautra 2011)

Nowadays that a new economic crisis affects all Europe, the idea of urban gardens is called as a solution to address energy poverty. More specifically, it examines the scenarios of cultivating horticultural or medicinal species in urban gardens (ie areas already cultivated) to lower the temperature and therefore reducing the energy needed to cool buildings.

3 STUDY AREA

3.1 Location

The study area of this research is in the city of Chania, a city located in the northwest part of Crete and the capital of the prefecture of Chania. More specifically, the block to be examined is in the region of Halepa which is one of the most historic districts of Chania, located to the east of the city. Although the area is not the direct central part of the city, it is quite densely built. Its orientation is north.

The block selected consists of five buildings, two of which are block of flats (with several floors) and the rest are smaller buildings (with two or three floors) (Figure 1).

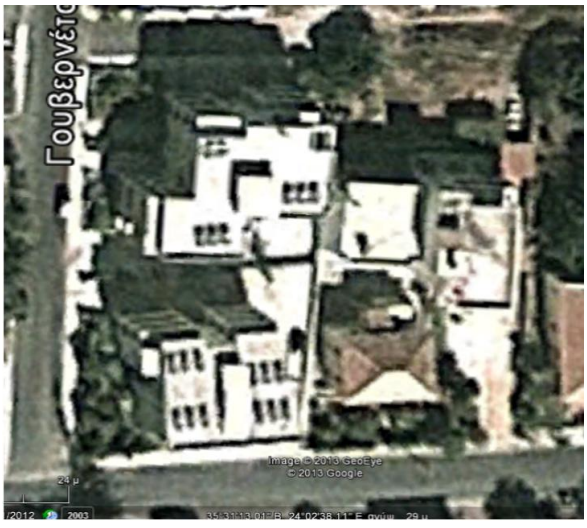

Figure 1: Study area, (*google earth*)

3.2 Climatic characteristics

The city of Chania and the region of Halepa have a typical Mediterranean climate: hot summers and mild winters. The area is also characterized by strong winds.

4 METHODOLOGY

The creation of green spaces is a technique that has been applied in the past in other studies. In those studies, as well as, in the particular one the modelling program Envi-met is used, with the difference that the concept of urban home-gardening is used and different installation scenarios and problems to address are examined.

4.1 Use of Envi-met

Envi-met is a three-dimensional microclimate model designed to simulate the interactions of the surface, plants and air in an urban environment. The spatial resolution allows the simulation of the interaction on a small scale. Envi-met is a prognostic model and is based on the Fundamental laws of fluid dynamics and thermodynamics.

The technical aspects and modules used in Envi-met are given below. (Michael Bruse & Team 2010)

Table 1: Aspects and modules of Envi-met software, (*Envi-met manual*)

Atmosphere	Soil System	Vegetation	Surfaces	Biometeorology	Behind the scenes
Wind	Temperature	Foliage temperature	Ground Surface Fluxes	PMV-Value	The Mathematics
Temperature	Water Flux	Heat exchange	Fluxes at	The climBOTs	
Vapor	Water Bodies	Vapor exchange	Walls/Roofs		
Turbulence		Water Interception	Heat transfer		
Pollutants		Water transport	through Walls		

The first step in order to use Envi-met is to create the area input file. This file combines the position and height of buildings, position of plants, distribution of surface materials and soil types, position of sources, position of receptors, database links and geographic position of the location on earth. These characteristics are set by using grids.

The next step is the creation of the configuration file which defines the settings for the simulation to run. These settings are the area input file, the name of the output file, the day the simulation runs, the meteorogical settings and the plant database. The data which were inserted are given below:

Scenarios	Summer	Spring	Autumn
Start Simulation at Day	21.07.2012	21.03.2012	21.10.2012
Start Simulation at time	00:00:00	00:00:00	00:00:00
Total Simulation Time in Hours	24.00	24.00	24.00
Save model State each min	60	60	60
Wind Speed in 10 m ab. Ground (m/s)	1.78	1.75	1.53
Wind Direction (0:N, 90:E, 180:S, 270:W)	0	270	180
Roughness Length z0 at Reference Point	0.1	0.1	0.1
Initial TemperatureAtmosphere (K)	293	293	293
Specific Humidity in 2500m (g Water/kg air)	7	7	7
Relative Humidity in 2 m(%)	50	60	65

In the end, the simulation runs and gives temperature results for every period of the time chosen by the configuration file. For the visualization of the results, Leonardo is used.

4.2 Stages

The survey examined the current state and three scenarios (no vegetation, fruit and vegetables, aromatic-medicinal species) for three seasons, summer, spring and autumn.

The plants used in each scenario are*:

Table 2: Scenarios examined

Scenarios	Vegetation
"No vegation" Scenario	No vegetation into the block, only outside
"Current state"	Ornamental plants, trees, hedges, grass
"Fruit and vegetables" scenario	Vineyard, lemon trees, tomatoes, cucumbers, onions, lettuce, red beet
"Aromatic-medicinal" scenario	Basel, miscanthus, thymus, salvia, hyssopus, oregano

The area input files created for each scenario are shown in Figure 2.

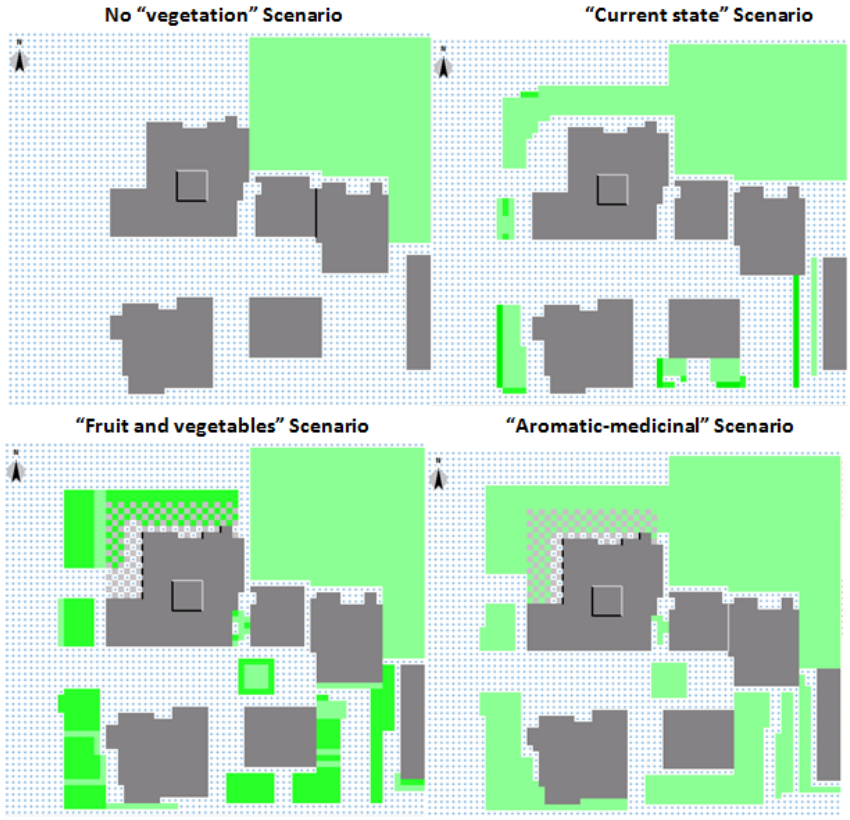

Figure 2 Study area using Envi- met in each scenario

*In order to insert the appropriate vegetation data was used the term leaf area data (LAD).

5 RESULTS

After running the simulation for each scenario summer, autumn, spring, Leonardo is used to visualize the results. The simulation was programmed to take measurements every hour but in the final tablets the results will be presented every 3 hours from 12am to 3 pm.

- **Summer**

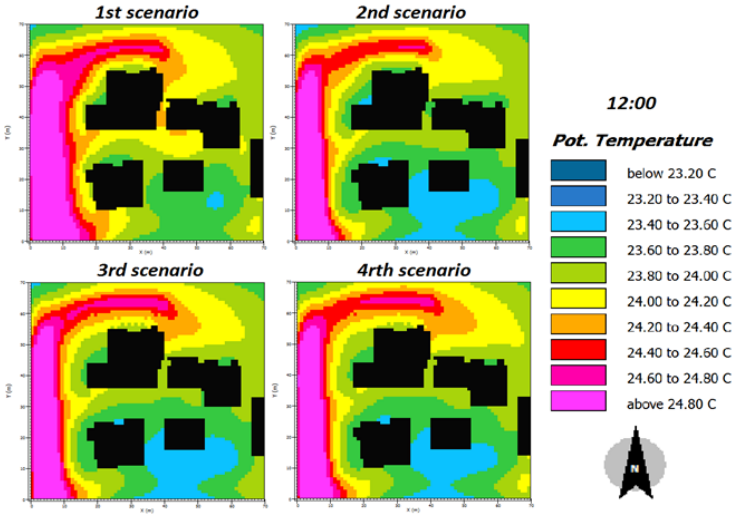

Figure 3 Summer air temperature at 12am

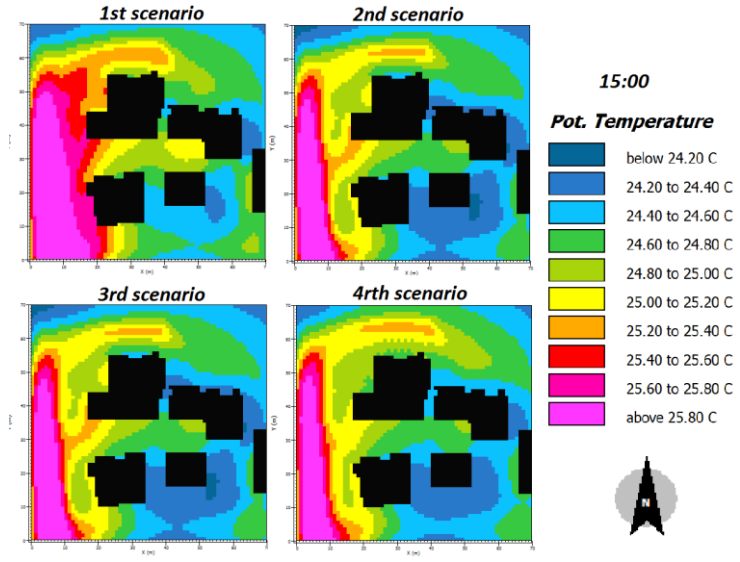

Figure 4 Summer air temperature at 15pm

The results provided above are at 12am and15pm. The maximum air temperature at a height of 1.6 m in these time periods is 26^{o}C and the minimum is below 23 ^{o}C. The temperature variation around the block is not great in any of the scenarios developed. At 12am and at 3 pm the temperature variation in the block is increased to 1.5 ^{o}C. At 12am, at 3 scenarios involving vegetation, temperature drop is felt about the same while at the table of 3pm, the fall in some places between the scenario of zero vegetation and scenario of fruits and vegetables reaches 1 ^{o}C.

➢ **Autumn**

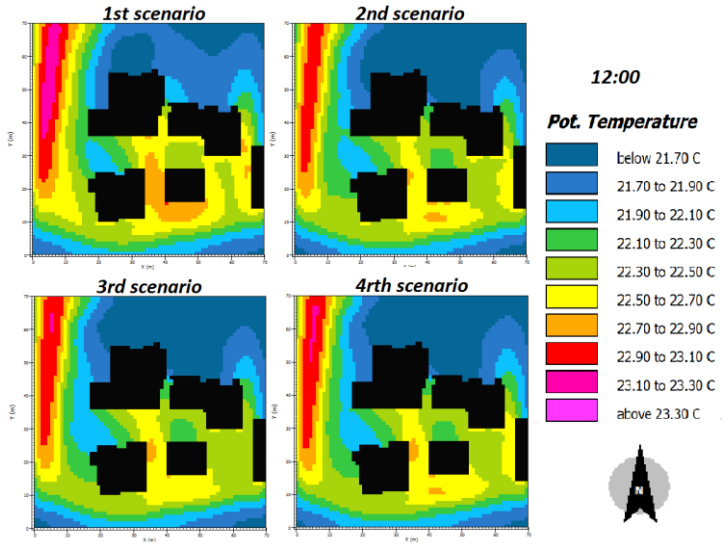

Figure 5 Autumn air temperature at 12am

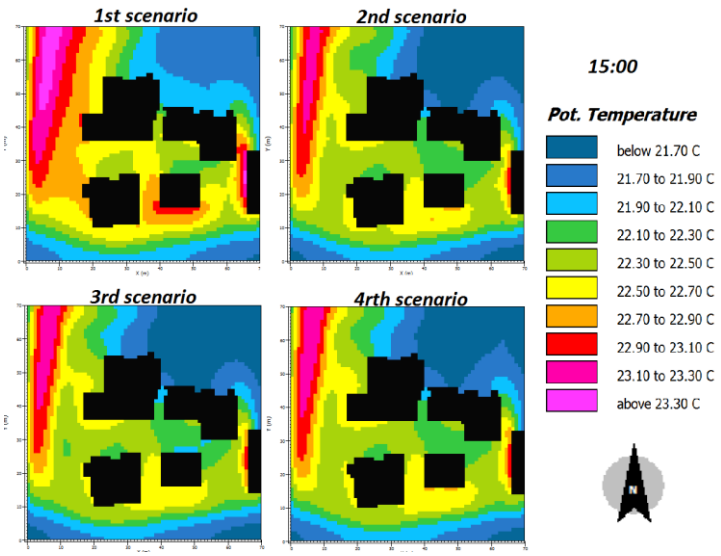

Figure 6 Autumn air temperature at 15pm

The results given above are at 12am and 15pm. The maximum air temperature at a height of 1.6 m in these periods, is above 24 ^{o}C and the minimum below 21.7 ^{o}C. At 12am and at 3pm, the temperature variation in the block is increased to 1.6 ^{o}C and with the same temperatures. In the other two cases greater temperature drop is observed in the scenario of the current state as well as scenario of fruits and vegetables, with 0.2 differences from the other two scenarios.

➢ **Spring**

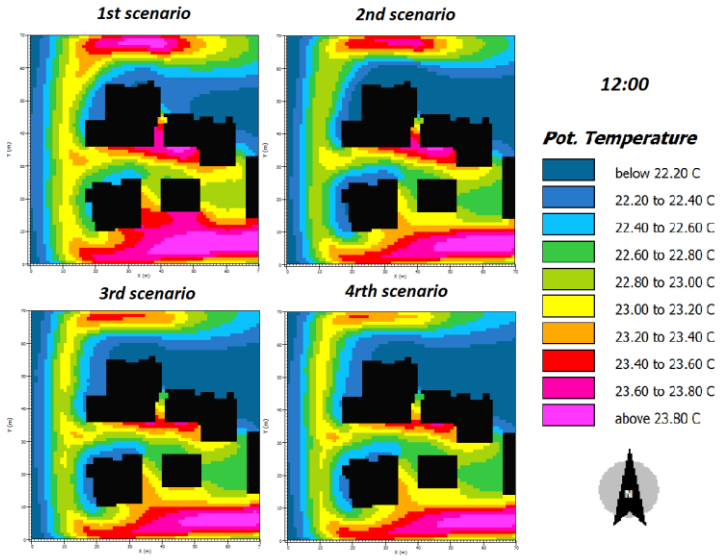

Figure 7 Spring air temperature at 12am

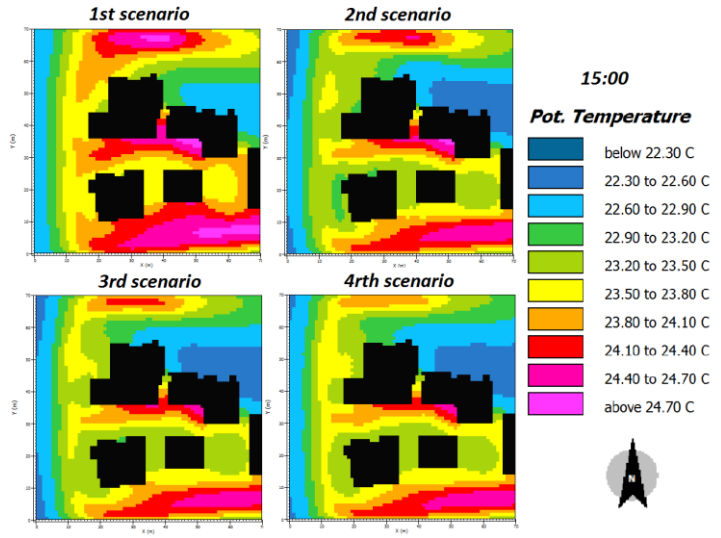

Figure 8 Spring air temperature at 15pm

Th results given above are at 12am and15pm. The maximum air temperature at a height of 1.6 m in these periods is above 24 ^{o}C and the minimum are below of 17 ^{o}C. At 12am, the temperature rises rapidly, with the lowest temperatures below 22.2 ^{o}C and the highest temperatures over 23.8 ^{o}C. At 3 pm, the temperature variation is much more than the typical temperatures frames. In this case there are areas with temperature below 22 ^{o}C and simultaneously areas with temperature above 24.7 ^{o}C. The lower temperatures in this period indicated in the second and fourth in comparison with the other scenarios.

6 CONCLUSIONS

The purpose of the scenarios examined was not to choose a unique scenario as the most appropriate but to create urban gardens with different types of vegetation. The aim of this research is to demonstrate the ways in which the greening contributes to lowering the temperature. It must be noted that in the current state, the measurements are made at a height of 1.6 m above the ground (average human height). So, it was expected that the results will be more satisfactory. However, both hypothetical scenarios are satisfactory (in terms of temperature drop). It may be possible to choose among the scenarios by performing a greater depth analysis, using other software.

The important point of this research is to assist in addressing the phenomenon of urban heat island and energy poverty.

In the first case, the results are obvious, and can be also verified at a local level by making measurements, as the three scenarios with vegetation stand out significantly from zero vegetation scenarios on the thermal behavior.

So, the use and consumption of the products cultivated into urban gardens in combination with the drop of temperature can make the difference according to the surveys carried out. It is a technique of dealing with a relatively new problem that has arisen in recent decades in rapid and natural way.

7 REFERENCES

Axarli, Klio N, AUTH Architect, 2008. “Energy planning and energy efficiency building - general principles of bioclimatic design.”

Boutagioti, Flora Maria, AUTH Architect, 2009. “The urban climate and bioclimatic interventions to improve it.”

Gazette, Government. 2011. “Government Gazette, LAW 4001.”

Michael Bruse & Team. 2010. “Envi-met Manual.”

Mirzaei, Parham A, and Fariborz Haghighat. 2010. “Approaches to Study Urban Heat Island e Abilities and Limitations.” *Building and Environment* 45 (10): 2192–2201.

Okvat, Heather a, and Alex J Zautra. 2011. “Community Gardening: a Parsimonious Path to Individual, Community, and Environmental Resilience.” *American Journal of Community Psychology* 47 (3-4) (June): 374–87.

Pia Drzewinski. 2012. “The Role of Biodiversity.” In .

Reid, Hannah, and Krystyna Swiderska. 2008. “An IIED Briefing Biodiversity , Climate Change and Poverty : Exploring the Links.”

Santamouris, M, C Pavlou, P Doukas, and G Mihalakakou. 2007. “Investigating and Analysing the Energy and Environmental Performance of an Experimental Green Roof System Installed in a Nursery School Building in Athens , Greece” 32: 1781–1788.

A HOLISTIC APPROACH OF THE DEVELOPMENT AND APPLICATION OF INNOVATIVE COMPOSITE COOL-THERMAL INSULATING MATERIALS

Sofia-Natalia Boemi[1], Stella Chadiarakou[2], Theoni Karlessi[3], Konstantina Leonidaki[1], Dimitrios Anastaselos[1], Euthimios Alexopoulos[4], Michael Kontos[2], Mat Santamouris[3], Agis Papadopoulos[1]

1 Mechanical Engineering Department,
Aristotle University of Thessaloniki
Building D, School of Engineering
Thessaloniki, Greece
**Corresponding author: nboemi@gmail.com*

2 FIBRAN SA
PO BOX 40306 56010, Stavroupoli
Thessaloniki, Greece

***3** Physics Department*
Natioan and Kapodistrian University of Athens
Athens, Greece

4 DOMOTECHNIKI S.A.
Dodecanisou 24,
Thessaloniki, Greece

ABSTRACT

The need to improve the energy performance of buildings, both new but also, and in particular, existing ones, is more imperative than ever. The "traditional" approach of thermal insulation is quite satisfactory for the reduction of thermal heating losses and loads, but it is not enough for coping with the problem of increased cooling loads, that are evolving to the single most influential problem, mainly for buildings in the densely built urban environment in Mediterranean and Southern European countries.
Aim of the ongoing DICOM project, which is co-funded by the Hellenic General Secretariat for Research and Technology, is the design, development, production, evaluation, certification and introduction to the market of innovative, composite cool - thermal insulating materials based on the new generation of extruded polystyrene (XPS) with improved vapour permeability (lower water vapour diffusion resistance factor μ) as well as with use of special plasters as a final coating with specific features of low emissivity coefficient ε. The products will be shaped in a way that makes them easily and effectively applicable for the energy upgrade of existing buildings, but will also correspond to the construction techniques of new state of the art buildings.
At the current stage, the specifications for the new products have been elaborated and their production has been launched. The whole process has been carried out in a holistic way, addressing the demands of the new energy and environmental requirements, the needs for a speedy and easy application of the materials in the construction site and the requirement to be competitive in the challenging European thermal insulation market.

KEYWORDS

Innovative insulation material, buildings, extruded polystyrene

1 INTRODUCTION

The need for the improvement of the energy efficiency of buildings, either new-built or existing ones, is already coherent and imperative. It was initially expressed by means of the Directive 2002/91/EC for the Energy Performance of Buildings, which was harmonized in the Greek legislation by the Law 3661/08 for the improvement of the energy performance of

buildings and finally the Regulation for the Energy Efficiency of Buildings, and represents the main application act of the law. Common goal of the relevant legal framework is to achieve a reduction of at least 20% in the energy consumption related to the building sector. In order to realize this aim there is a need for substantial changes regarding the existing buildings and, in addition, a new holistic approach for the thermal protection of new-built constructions (Karkanias et al., 2011). The EPBD-recast, in form of 2010/31/EU, which aims at the zero, or nearly zero, energy buildings provides a quantum leap, as it makes the ambitious goals mandatory, both for public and residential buildings. This new Directive has been harmonized in the Greek legislation by means of Law 4122/2013, which will be accompanied by a revision of the Regulation for the Energy Efficiency of Buildings.

The traditional approach of thermal insulation is quite satisfactory in reducing the thermal loads, especially considering the heating loads of buildings, as it has been proven since the introduction of the first thermal insulation regulations in Europe in the mid 1970s. On the other hand, there are limits in confronting the problem of cooling loads, especially in the warmer climatic regions, like the Mediterranean. The latter evolves to the actual problem that is traced in buildings of the dense urban environment (Papadopoulos et al., 2002; Santamouris 2001).

Cool materials present an interesting solution for the reduction of cooling loads, especially in horizontal building elements. The project discussed in this paper aims to design, develop, produce, evaluate, certify and introduce to the market highly innovative, **composite thermal insulating cool materials**, on the base of the new generation extruded polystyrene (XPS) with improved water vapor permeability properties (low water vapor diffusion coefficient μ) and with the implementation of special thermal reflective plaster, which is used as the final coating layer and comprises particular emission coefficient ε characteristics. These materials could be easily and effectively used for the energy upgrade of existing buildings, but could also cover the construction techniques of the new-built constructions (Synnefa et al 2007, Karlessi et al., 2009).

Additionally, these materials should be used for the thermal insulation of horizontal and pitch roofs, according to the current EN standards for materials and kit solutions, and for covering vertical building elements (walls and concrete elements), as it is already introduced in the External Thermal Insulation Composite Systems Guideline (ETICS, according to ETAG 004).

That project aims consequently at gaining and modulating the appropriate know-how, which will lead to the combined confrontation of the two major problems that are commonly faced in the energy performance of the building envelope today: the reduction of thermal losses through the solid building elements during the winter period and the avoidance of the overheating occurring at the same elements, which has as an impact on the reduction of cooling loads during the summer period (Papadopoulos and Giama, 2007).

Thus, on the whole, the improvement and expansion of the composite thermal insulation technological solutions, through the development of a group of products based on new generation extruded polystyrene and on new coating material with special reflection properties, for use in integrated insulation applications, in new-built and existing constructions is its scope.

At the current stage, the specifications for the new products have been elaborated and their production has been launched. The whole process has been carried out in a holistic way, addressing the demands of the new energy and environmental requirements, the needs for a speedy and easy application of the materials in the construction site and the requirement to be competitive in the challenging European thermal insulation market.

2 DICOM'S SCIENTIFIC AND TECHNICAL GOALS

In order to structure the methodology which should be implemented for combining the new insulation material in depth research analysis, theoretical, in laboratory and applied industrial, was required. That not only led to the specification of the properties but also helps to consist the need of complex insulation materials and coating matters with special thermal reflection characteristics to the widespread use in construction activities.

Major advantage of the new products, which are ranked at the peak of the technological solutions available in market is the development of an operationally, energetically and environmentally optimum manufacturing process for the generation of products which will fully cover the demands of standards, quality assurance and environmental management systems and finally, the competitiveness goals in the tough building materials market.

Also, the newly introduced products will have the ability of fast and simple in-situ application, with small inaccuracy margins, resulting in high economic competitiveness, both in new constructions and in the refurbishment and energy renovation of existing buildings.

Moreover, those new products can take advantage of the adaptability and the characteristics of cool – thermal insulating materials, consisting of ready or semi-ready thermal insulated building elements, which will feature optimal insulation properties, ease of use, minimum application cost and, additionally, will present capabilities of fire resistance, durability to impregnation and low resistance to water vapor diffusion. The thermal reflective plaster coatings will assure the maximization of the useful impacts of thermal insulation during the winter period, and simultaneously will offer overheating reduction properties during the summer period, being in the position in this way to contribute to the improvement of the exterior microclimate and ensuring quite low external surface temperatures on the applied buildings.

In parallel, the environmental friendly fabrication demands will be adopted, through modern manufacturing and managing methods of primary and secondary resources, by adopting a very lean production procedure and by using state of the art equipment, minimizing thus, the environmental impact in the production stage, and in that sense also in its entire life cycle. Finally, the material produced will be certified for the current technical directive ETAG 004 from a certified body.

As far as it concerns manufacturing, the composite product is going to allow simple and flexible high-scale production conditions. The combination of a new generation extruded polystyrene and thermal reflective plaster coatings will be achieved through a technically correct and economically viable way. The transition from one member of the family product to another member will be rapid, without the need of a major rescheduling of the production line.

Also, the methodological advantage of the Life Cycle Analysis (LCA) method was utilized in order to perceive the maximum possible of recyclable raw materials and will have the minimum possible energy and raw materials consumption (Klopffer et al., 2003; Anastaselos et al., 2008). Specifically, an extensive LCA was implemented during the distinct stages for the environmental assessment of the composite material. These stages consist of the construction, the use, the dismantling and the end of life management. The first phase includes the inventory analysis. This stage deals with the input and output flows of all the procedures concerning the under study insulation material. The inputs and outputs flows contain data of materials and energy consumption. The second phase refers to the environmental impact assessment. At this phase the environmental load calculated from the inventory analysis is transformed into environmental impacts. The environmental impacts categories' examined mainly include climate change, acidification, eutrofication and photochemical oxidation and finally the use and application of the results. At this phase and

after having analyzed the system, the crucial points are identified in order to focus on the procedures which need to be improved.
As it was mentioned before, DICOM's new composite material main goals were:

1. Simple and quick installation in new-built constructions, having low demands in planarity and parallelism of the underlying constructive layers.
2. Application without the need of major reforming works in roofs and walls of existing buildings, when the building envelope is unacceptable condition, resulting in minor charge of the present construction.
3. In any case, ability of easy transport and storage on worksite, convenience for the preparation and manufacturing of special plaster coatings (where applicable), cut and fixation.

At present, the specifications for the new products have been elaborated and their production has been launched. The whole process has been carried out in a holistic way, addressing the demands of the new energy and environmental requirements, the needs for a speedy and easy application of the materials in the construction site and the requirement to be competitive in the challenging European thermal insulation market. Thus, the product and in extension the methodology has not been tested yet because the applicability of products and techniques will arise during the implementation phase, but an effort will be made to highlight the void in ready standardized products, which will be used in the external thermal insulation of conventional existing buildings and in thermal insulation of steel construction buildings through ready building elements. In this way, the energy re-planning of existing buildings will be accomplished, having in Greece an immediate implication in near future, as a result of the aged buildings on one side, and the implementation of the Regulation for the Energy Efficiency of buildings, on the other side. Finally, these products could be used in most conventional thermal insulation practices, having the advantage of simple application.
To be more specific, their advantages are focused on:

a. The improvement of the energy performance of buildings through the substantial improvement of heat transfer and solar radiation absorption coefficient of the solid building elements of the building envelope.
b. The assurance of high thermal comfort conditions, as well as air quality in the internal environment of buildings, through the improvement of the internal surface temperatures and air permeability of the solid building elements.
c. The cost reduction compared to the currently used solutions, which apply a number of different materials and techniques, in order to achieve a comparable result.
d. The capability of microclimate improvement in local level, in case that the technology will be implemented in wide scale, e.g. in a number of continuous building blocks.
e. The overall improvement of the environmental efficiency of the building, throughout its life cycle, in terms of energy and manufacturing, use and future disposal of specific building materials.

3 LABORATORY RESULTS

The new products that will emerge should meet the requirements of European regulations. Specifically, the new composite material will be processed in accordance with the European standard EN 13164 for mechanical strength (mechanical compression and tension), behavior toward the water and thermal conductivity. Also, its suitability for applying to external insulation systems (according to Directive ETAG 004) and to inclined roof will be tested. In

the current phase, the properties of the extruded polystyrene has been evaluated (table 1) in order to meet the requirements of the new composite material.
Additionally, the new material should be included to the catalogue of cool materials (Karlessi et al., 2009; Kar1essi et al., 2011).
All in all, the new material should comply with the European Directives and marked with the CE in order to be competitive to the European market.

Table 1: Physical Properties of Extruded Polystyrene

Properties		Measure units	EN standard	
Shape of profile				I / L
Surface				Waffle
Board dimension		mm	EN 822	1250/600
				1000x600
Thickness tolerance			EN 823	T3
Declared value of compressive strength at 10% deformation		kPa	EN 826	200-300
Tensile strength perpendicular to faces		kPa	EN 1607/ ETAG 004	550
Shear Strength τ		N/mm^2	EN 12090	0,24
Shear Modulus G		N/mm^2	EN 12090	6.7
Declared thermal conductivity (after 25 years)	**20mm≤d≤60mm**	W/(m*K)	EN 12667	0,033
	>60mm			0,034
Long term water absorption by immersion	**Rough surface**	vol. %	EN 12087	1,5
Water vapour diffusion resistance factor		-	EN 12086	50
Temperature of use		°C		From -50 to +75
Reaction to fire		Class	EN 13501-1	E

4 CONCLUSIONS

The innovative composite cool-thermal insulating material that are already in the stage of pre-production combines very good mechanical and physical properties, like low thermal conductivity factor, high compressive strength, low vapor diffusion resistance factor, with the increased solar reflectance coefficient of specific plasters used for final coating.
The proposed composite material will result in lower energy consumption for heating and cooling during the use phase, compared to common insulation practice. As the use phase accounts for more than 70% of the energy consumption and hence of the total emissions, it is vital at this stage to achieve high performance in all those aspects, towards the reduction of environmental impact imposed during material's life cycle.
For the composite material's production, a combination of raw and recycled materials has been used. Sufficient quantities of the recycled materials have been supplied by a fully operational recycling line that is already installed. At the same time the manufacturing process was modified in such a way that results to the reduction of the material's ecological footprint.
The composite materials are going to be manufactured in such a way that it can be easily dismantled at the end of its useful service life. Constitute materials can be retrieved in a clean shape without mixtures and can be send either in a facility for closed-loop recycling, or to a thermal process plant for energy production. Re-use of the composite material is also possible if it's mechanical and thermal properties remain at the desirable levels.

The LCA combined with the experimental measurements that has been conducted will eventually lead to the adaptation of the eco-label sign. Finally, at the end of the research project the final products will be available to the market at a reasonable price.
The results of the project will refer to the full record of the current situation it the insulation materials' market focusing on technical and scientific attributes and to the formulation of accurate predictions for the future, that are covered in the first deliverable. Mechanical and thermal properties, manufacturing processes, potential of the usage of composite materials based on extruded polystyrene will also be thoroughly examined in order to promote energy design of new buildings and energy upgrade of existing buildings.
The design of new insulation materials, their extensive life cycle analysis and their properties specification that are covered in deliverables enhance the amplitude of scientific knowledge regarding insulation materials and provide the research organizations with the ability to evaluate and compare specific, under study, materials, in order to notify the developers and manufacturers about the environmental performance of their products.
Efficient planning of the production line, pilot study and manufacturing of the final products are the main issues examined. More specifically, from the design and the pilot study of the final products the close connection between scientific research and industry are going to be established. From the university organizations point of view industrial know-how expertise will be acquired, whereas from industrial parties' point of view several innovative insulation solutions will be produced.
Extensive laboratory measurements under real conditions will be conducted, from which certain deliverables will be produced regarding the results of these laboratory checks and measures. In this way collaborating industrial parties will improve its researching structures and quality control capabilities of their products while the university organizations will evolve and upgrade their laboratory equipment with simultaneous broadening of their research activities.

5 ACKNOWLEDGEMENTS

The authors would like to thank the Hellenic General Secretariat for Research and Technology, for providing the funds under the contract EYDE – ETAK 2787/9.11.2011

6 REFERENCES

Anastaselos D., Giama E., Papadopoulos A.M., (2008). *An assessment tool for the energy, economic and environmental evaluation of thermal insulation solutions*. Energy and Buildings 41, 1165-1171.

ETAG 004 (2000). *Guideline for European Technical Approval of External Thermal Insulation Composite Systems with Rendering*.

European Norm on Thermal insulating products for building applications — *Determination of compression behavior*, EN 826:2011, CEN TC 88.

ISO, (2006). 14040: *Environmental management - Life Cycle assessment - Principles and framework*, International Organisation for Standardisation, Geneva.

ISO, (1998). 14041: *Environmental management - Life cycle assessment -- Goal and scope definition and inventory analysis*, International Organisation for Standardisation, Geneva.

ISO, (2000). 14042: *Environmental management - Life cycle assessment – Life cycle impact assessment*, International Organisation for Standardisation, Geneva.

ISO, (2000). 14043: *Environmental management - Life cycle assessment – Life cycle interpretation*, International Organisation for Standardisation, Geneva.

Karkanias C., Boemi S.N., Papadopoulos A.M., Tsoutsos T.D., Karagiannidis A., (2010). *Energy efficiency in the Hellenic building sector: An assessment of the restrictions and perspectives of the market*, Energy Policy 38, 2776-2784.

Karlessi T., Santamouris M., Apostolakis K., Synnefa A., Livada I., (2009). *Development and testing of thermochromic coatings for buildings and urban structures*. Solar Energy 83, 538–551.

Karlessi T., Santamouris M., Synnefa A., Assimakopoulos D., Didaskalopoulos P., Apostolakis K., (2011). *Development and testing of PCM doped cool colored coatings to mitigate urban heat island and cool buildings*. Building and Environment 46, 570-576.

Klopffer W., Hutzinger O., Schmidt A., Ulf Clausen A., Astrup Jensen A., Kamstrup O.,(2003*). Comparative Life Cycle Assessment of Three Insulation Materials*, Final Report, Vol. 8.

Papadopoulos A.M., Giama E., (2007). *Environmental performance evaluation of thermal insulation materials and its impact on the building*. Building and Environment 42, 2178-2187.

Papadopoulos A.M., Theodosiou T., Karatzas K., (2002). *Feasibility of energy saving renovation measures in urban buildings: The impact of energy prices and the acceptable payback time criterion*, Energy and Buildings 34, 455-466.

Santamouris, M., (2001). *Energy and climate in the urban built environment*. London: James & James.

SETAC-Europe (1999). *Best available practise regarding impact categories and category indicators in Life Cycle Impact Assessment*. Second Working Group on LCIA., International Journal LCA 4, 66-74.

Synnefa, A., Santamouris, M., Apostolakis, K., (2007). *On the development, optical properties and thermal performance of cool colored coatings for the urban environment*. Journal of Solar Energy 81, 488–497

SOLAR OPTICAL AND THERMAL PROPERTIES OF MICRO- AND MESO-POROUS MATERIALS FOR COOLING APPLICATIONS COMPARED TO TYPICAL BUILDING MATERIALS

S. Krimpalis[*,1] and D. Karamanis[*,1]

[1]*Department of Environmental & Natural Resources Management, University of Patras, 30100 Agrinio, Greece*
Corresponding authors: skrimpalis@gmail.gr, dkaraman@cc.uoi.gr

ABSTRACT

The solar optical properties of micro- and meso-porous materials that can be building integrated or roof added for evaporating cooling purposes were studied and compared with conventional building materials. The results are interpreted in correlation with their water absorption capacity. For further studying their solar optical properties, absorbance measurements were solar-weighted in accordance with the ASTM G173 standard. Mesoporous materials presented high irradiation absorbance in the IR spectrum with significant variation depending on the water loading at different relative humidity. Strong near infrared absorptance bands of water centered at around 970 nm, 1190 nm and 1450 nm are applied to a quantitative analysis of water content. The experimental results indicate the suitability of the meso-porous primarily, and secondly the micro-porous materials under study, for building integrated solar cooling applications.

KEYWORDS

Solar cooling, water vapor cooling, micro-porous and meso-porous materials, smart materials

1 INTRODUCTION

One of the main environmental problems that big cities, and not only, have to face with the last decades is the so called urban heat island (UHI) phenomenon. Because of that, there is an increase in the demand for electric energy for cooling purposes, while also it is noted deterioration of the living environment due to higher pollutant emission and increase of the chemical weathering of building materials. Therefore the need for the development and the application of passive and efficient ways to cool down urban surfaces keeps on increasing.

Commonly used materials in the construction of buildings facades located in warm climates, often entrap a great amount of heat from the incoming solar radiation, leading to a respective thermal increase in the interior. Therefore significant effort towards energy conservation for buildings and urban structures is the research for cool materials and coatings as a passive cooling technique. However most of them target to minimize the surface temperature in roofs, masonries and pavements through the increase of solar reflectance and infrared emittance. Building integrated evaporating cooling (BIEC) is an alternative and sustainable way to cool the surfaces of a building or to cool the pavement of outdoor areas.

In the last few years the idea of using porous materials for the evaporating cooling of buildings has been started to be studied systematically. The principle of evaporative cooling is that stored water or night sorbed moisture are evaporated during the hot days and the porous surface temperature is reduced due to the release of the latent heat. The principle has been validated with the addition of liquid water [1],[2],[3] and only recently it was proved that the

principle can be applied by moisture sorption [4]. However while the IR spectroscopy of water vapor has been extensively studied [5], there are very few works in the NIR region where the solar-water interaction and absorbance behavior is important for the vapor cooling applications [6].

The aim of the present work is to examine the solar responsive performance of micro- and meso-porous materials in their perspective as passive solar cooling materials by means of moisture sorption. The solar optical and thermal properties of mesoporous materials are compared with those of typical building materials. The optical and thermal characterization of the samples are realized using a UV/VIS/NIR spectrophotometer over the solar spectrum (250– 2500 nm). Water sorption isotherms are conducted and assisted to further understand the optical behavior of the samples.

Moreover, the effect of water loading in the NIR absorbance spectrum of the porous materials is further investigated. Strong near infrared absorption bands of water applied to a quantitative analysis of water content in the porous materials after capillary condensation. By spectrum deconvolution analysis and fitting of combined Gaussian components the variation of components' heights in correlation with relative humidity is studied.

Finally the absorbance measurements are solar weighted using the standard solar spectrum ASTM G173 at air mass (AM) 1.5. In an attempt to further understandf the samples' interaction with the solar spectrum and how relative humidity can have an impact on them, the variation of the normalized solar absorbance is presented for each spectrum UV/VIS/NIR in correlation with relative humidity. Also thermal measurements were conducted by means of the transient line heat source method.

2 EXPERIMENTAL PART

Additionally with the conventional building materials, typical well ordered silicate and aluminosilicate micro- and meso-porous nanomaterials were purchased or prepared. The optical characterization of samples with pre-determined absorbed water vapor was conducted by a UV/VIS/NIR spectrophotometer (Lambda 950 of PerkinElmer fitted with a 150 mm diameter InGaAs integrating sphere that collects both specular and diffuse radiation) over the solar spectrum (200-2500 nm). The equipment was calibrated utilizing Labsphere ISO 9001:2000 certified reflectance standards. The data were solar-weighted using the reference solar spectral irradiance standard ASTM G-173 at AM 1.5.

Moisture sorption isotherms were determined by placing the samples in sealed desiccators with saturated salt solutions for controlling relative humidity while temperature was air-conditionally controlled at 25°C. Prior to measurements, samples were dried to constant mass in an air-circulated oven at 105°C. Thermal measurements were conducted by KD2 Pro from Decagon Devices. The sensor is a 30 mm dual-needle SH-1, with a size of 1.3 mm diameter x 30 mm long, 6 mm spacing, accuracy of ± 10% from 0.2 - 2 W/(m• K). The needle, in order to equilibrate to the surrounding temperature before beginning a measurement, was immersed and left into the sample's container for 10 minutes.

3 RESULTS AND DISCUSSION

First, the optical properties of the selected materials were investigated. Figure 1 shows the absorption spectrum of the samples after their saturation in desiccators with different relative humidity. For the MESO samples (a), (b) and the MICRO sample (c), the impact of relative humidity in the absorbance spectrum behavior is obvious. Especially in the NIR region of the spectrum for the MESO samples saturated at 50% as well 77% of relative humidity, four main maxima located at c. 970 nm, c. 1190 nm, c. 1450 nm and c. 1930 nm are clearly observed, indicating the water vapor condensation within the mesopores. These

maxima correspond to the second overtone of the OH stretching band (3 $\nu_{1,3}$), the combination of the first overtone of the O-H stretching and the OH-bending band ($2\nu_{1,3} + \nu_2$), first overtone of the OH-stretching band ($2\nu_{1,3}$) and combination of the OH-stretching band and the O-H bending band ($2\nu_{1,3} + \nu_2$) respectively. For the rest of the samples, which are conventional building materials, the water vapor absorption has only limited influence in their absorbance spectrum. However carbonated calcium, white cement and reflective paint, present very small absorbance for most of the spectrum. The effect is more pronounce in carbonated calcium.

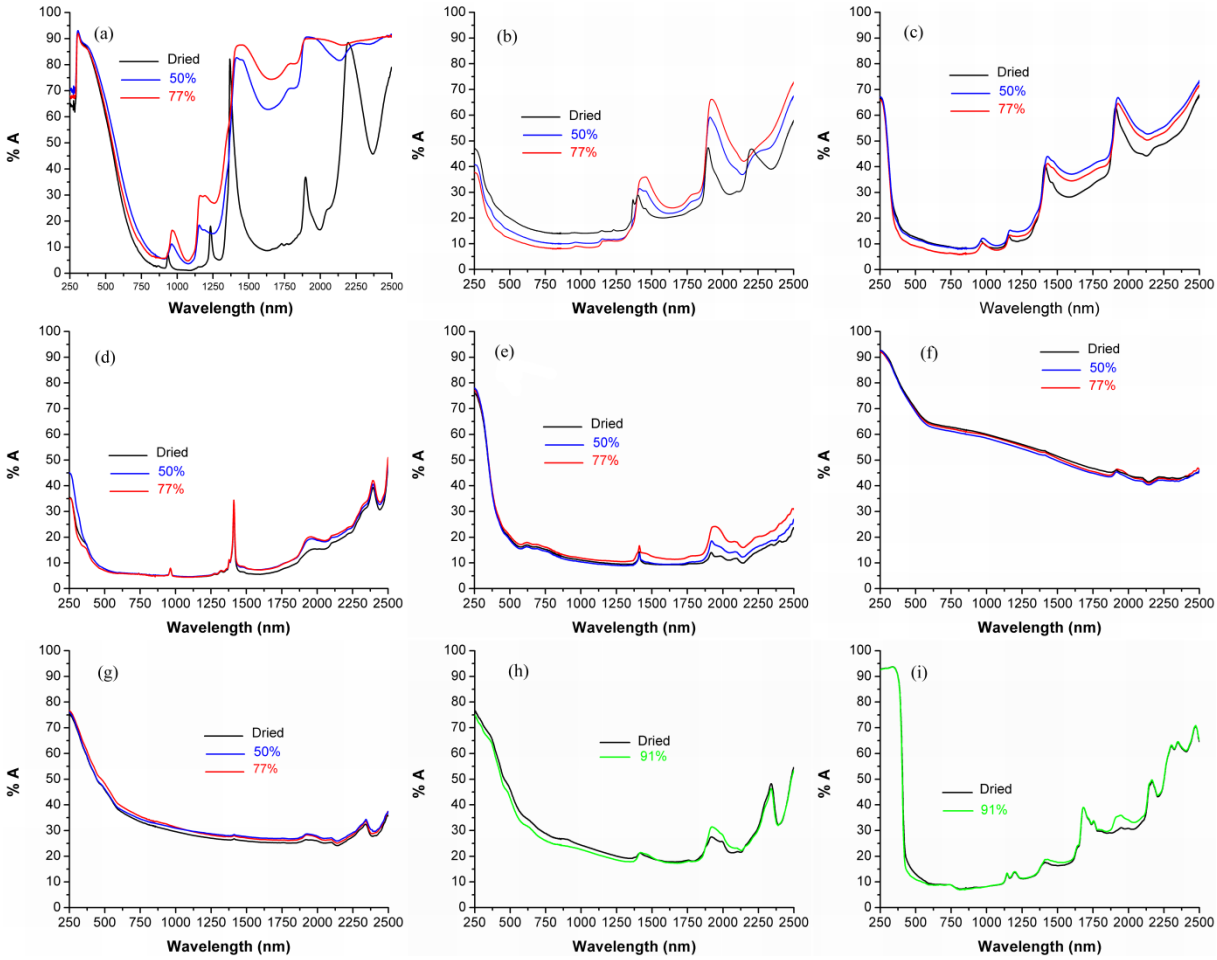

Figure 1: Absorbance spectra of a) MESO-1, b) MESO-2, c) MICRO, d) $CaCO_3$, e) Cement White, f) Cement Black, g) Plaster, h) Marble and i) Reflective Paint, for different relative humidity.

The different behavior of the porous samples' absorbance spectra presented in Figure 1, is due to the water vapor adsorption, and can be further interpreted through the moisture sorption kinetics of the samples. Figure 2 presents the water vapor sorption isotherm of the materials at 25 ^{o}C. As shown, water vapor sorption is particularly high for the porous samples, and especially for the MESO samples, while it is negligible for the conventional building materials.

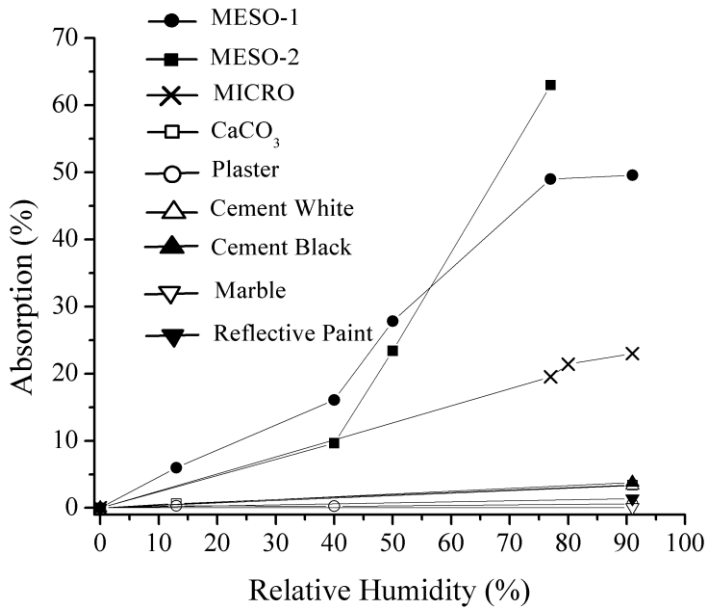

Figure 2: Water vapor sorption isotherm of the tested materials at 25 °C

The isotherms of MESO samples showed similar type behavior. The water adsorption isotherm on the MESO samples were of type V in the IUPAC classification indicating a relatively hydrophobic character in the low-pressure region of the adsorption isotherm but with a capillary condensation in regions with higher pressure leading to a total filling of the pore volume and thus to a type-V isotherm (with maximum uptake more than 60 % adsorption).

As we have already noticed from Figure 1, MESO sample's spectrum exhibits the highest variation for different relative humidity. Therefore and in order to improve our insight regarding the correlation of water absorbance and solar spectrum, the curves of three sub-bands of the spectrum with important variation in the absorbance intensity for different relative humidity were deconvoluted into their Gaussian components. These three narrow sub-bands are centered at around 970 nm, 1190 nm and 1450 nm. For the first and the second sub-bund, three Gaussian components were used in the fit, while five for the third one since it was broader than the other two. The full width at half maximum for each Gaussian component was kept constant. Figure 3 presents the behavior of the components heights in correlation with relative humidity.

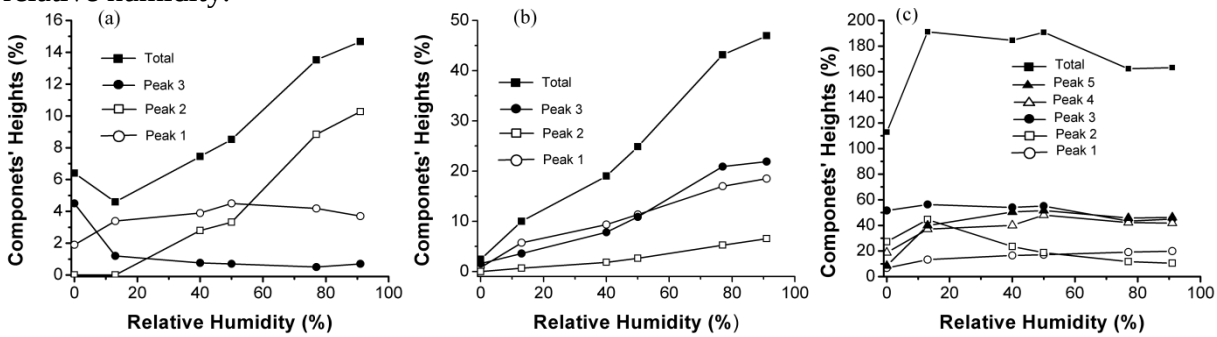

Figure 3: Variation of the Gaussian components' heights in correlation with relative humidity for three narrow sub-bands centered at around a) 970 nm, b) 1190 nm and c) 1450 nm.

Figure 3(a) corresponds to the sub-bund centered at around 970 nm. While the heights of the first and the third peak remains almost constant, the second's one keeps on increasing as relative humidity increases. Therefore, the total's peak height which results from the convolution of the three components increases almost linear as relative humidity increases. For the sub-bund centered at around 1190 nm, the increase of relative humidity results in a

linear increase of all three peaks' heights, and therefore the total's one. For the sub-bund centered at around 1400 nm, the total's peak height performs an important increase between dried mode and the 13% relative humidity, and after that exhibits only small variations. The reason for this behavior is that at about 1367 nm the SiOH stretch overtone band (2v) is diminished upon addition of water molecules while the neighboring broad H-bonded OH band at 1399 nm increases, balancing the behavior of the total [7].

In order to study the optical performance of the samples under the influence of solar irradiation, the absorbance measurements were solar weighted using the standard solar spectrum ASTM G173. Figure 4 presents the solar-weighted absorption spectrum of the samples after the absorption of water vapor at different humidity. As it was expected only the absorbance spectrum of the porous samples is notably influenced by their property to absorb vapor water. Especially for the MESO-1 sample, the absorbance intensity in the NIR spectrum, which is predominately responsible for the heating effect of the sun, is strongly influenced by the relative humidity. Consequently the water vapor loading since, as it is already presented in Figure 2, MESO samples and especially MESO-1 is highly absorbent.

Furthermore it can be seen from Figure 4 that while MESO-2 and MICRO samples have small absorption spectrum for the whole range, MESO-1 sample's absorption intensity becomes very high in the UV/VIS spectrum. In addition, carbonated calcium exhibits very small absorbance spectrum, even smaller than the reflective paint's.

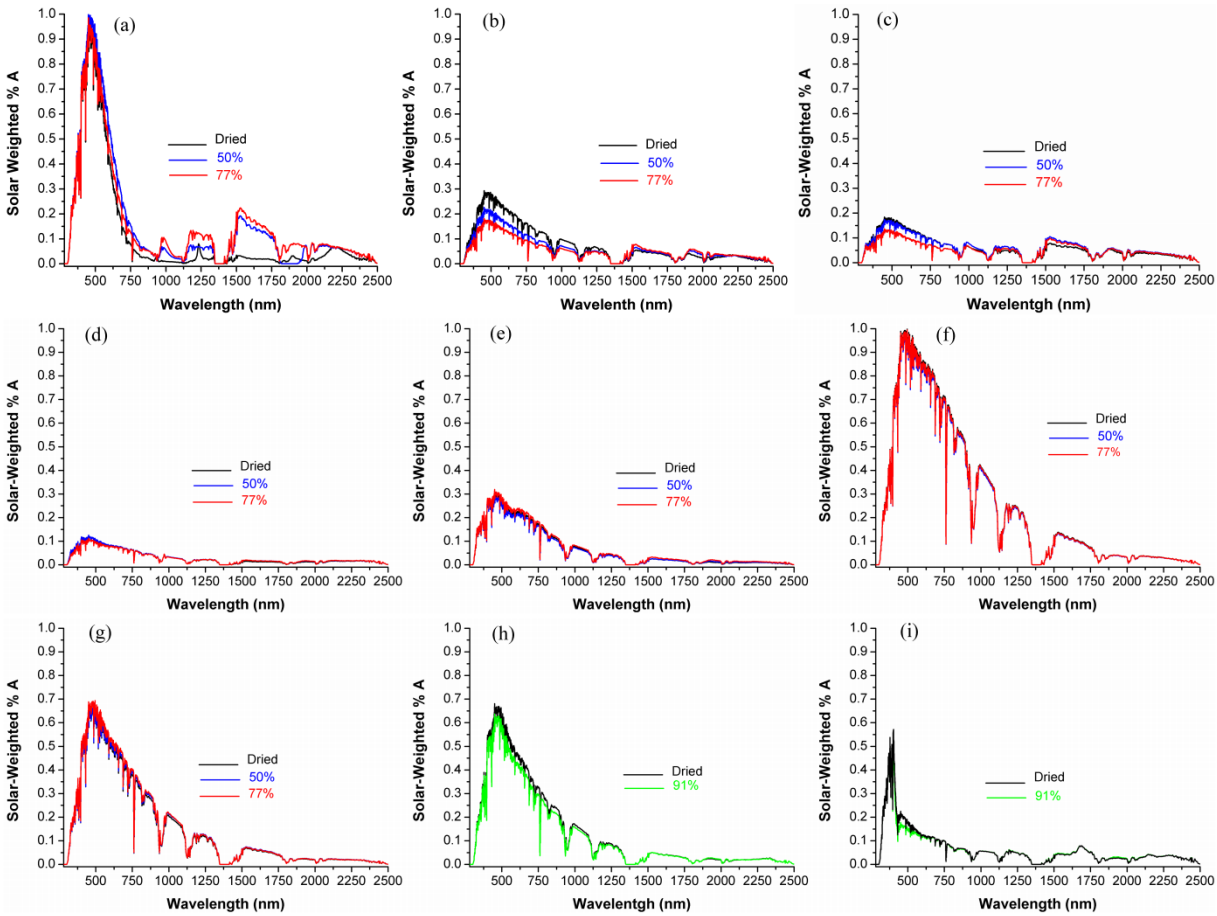

Figure 4: Solar-weighted absorbance spectra of a) MESO-1, b) MESO-2, c) MICRO, d) $CaCO_3$, e) Cement White, f) Cement Black, g) Plaster, h) Marble and i) Reflective Paint, for different relative humidity.

In order to further investigate the samples' behavior under the effect of solar irradiation, Figure 5 presents solar absorbance for each UV/VIS/NIR spectrum in correlation with the variation of relative humidity. The data are normalized to the total solar absorbance.

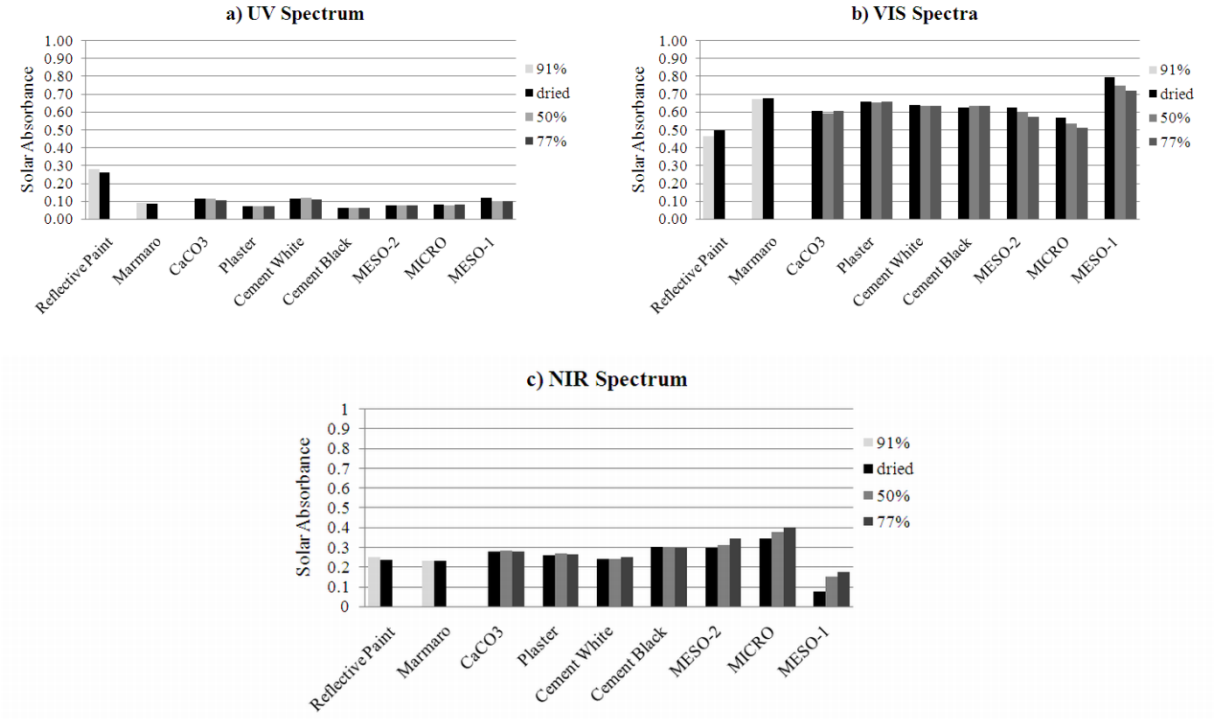

Figure 5: Variation of normalized solar absorbance in correlation with relative humidity, separately for each solar sub-bund (UV/VIS/NIR).

While for the UV spectrum normalized solar absorbance is small, with the exception of reflective paint, it becomes high for the VIS spectrum. For the NIR spectrum, normalized solar absorbance values lies between those for the UV and VIS spectra. Moreover, while for the conventional building materials the impact of relative humidity to the solar absorbance values is negligible, it is important for the MESO samples. However, in the VIS region, the increase of relative humidity results in reduced solar absorption. In the NIR region the behavior is vice versa. As it has already been presented in Figure 2 for the MESO and MICRO samples, higher relative humidity results in higher amount of absorbed water. Therefore higher amount of vapor water leads to higher solar absorbance in the NIR region.

The effect of water vapor sorption on the solar properties of the studied materials was further investigated by thermal conductivity measurements. As shown in Table 1, all samples exhibit small thermal conductivity. Moreover all of the samples show lower thermal conductivity in the dried state than the state in ambient conditions (25 °C). This is due to the water content of the MESO samples at room conditions in contrast to the empty space after drying.

Table 1. Thermal conductivity of the MESO samples

Sample (all in powder form)	**Thermal conductivity (W/m·K)**	
	Stored in Room conditions	Dried samples (200 °C for 2 h)
MESO-1	0.160	0.099
MESO-2	0.133	0.063
Cement White	0.093	0.085
Cement Black	0.124	0.108
Plaster	0.165	0.122
$CaCO_3$	0.119	0.095

4 CONCLUSIONS

The optical and thermal properties of highly absorbent synthetic porous materials for building evaporating cooling applications have been investigated. In contrast with conventional building materials, MESO and MICRO samples presented significant variation in the intensity of their absorption spectrum as a function of the relative humidity in which samples remained for specific period of time, before the absorbance measurements. Especially the MESO-1 sample presented high irradiation absorptance in the NIR spectrum for higher than 50% of relative humidity.

This behavior was explained through the investigation of the water vapor sorption isotherms. In contrast to the conventional building materials, MESO and MICRO samples exhibit high water vapor sorption which for the MESO samples is of type-V. Similar absorptance behavior was also noted, by solar-weighting the experimental optical measurements with the ASTM G173 standard spectrum. The high variation of the MESO-1 sample's absorptance for different relative humidity in the NIR spectrum, and also its high absorptance for the higher relative humidity values were revealed.

Furthermore, the absorbance intensity variation and how it is influenced by water vapor sorption was investigated by fitting Gaussian components in three sub-bunds of high variation. In many cases a linear relation between absorbance and relative humidity was determined. In addition, thermal conductivity measurements showed that all samples have similarly small thermal conductivity.

The findings of the present work show that porous samples, and particularly MESO-1 sample are good candidates for solar vapor cooling application. Therefore further investigation must be conducted in this direction.

5 ACKNOWLEDGEMENTS

This work is supported under the "ARISTEIA" Action of the "OPERATIONAL PROGRAMME EDUCATION AND LIFELONG LEARNING" and is co-funded by the European Social Fund (ESF) and National Resources.

6 REFERENCES

1. Wanphen, S., Nagano, K. (2009). Experimental study of the performance of porous materials to moderate the roof surface temperature by its evaporative cooling effect. Build Environ. 44, 338-351.
2. Vardoulakis, E., Karamanis, D., Mihalakakou, G., Assimakopoulos, M.N. (2011). Solar cooling with aluminium pillared clays. Sol. Ener. Mater. Sol Cells. 95, 2363-70.
3. Rotzetter, A.C.C., Schumacher, C. M., Bubenhofer, S. B., Grass, R. N., Gerber, L. C.,Zeltner, M., Stark, W.J. (2012). Thermoresponsive polymer induced sweating surfaces as an efficient way to pay passively cool buildings. Adv. Mater. 24, 5352-5356.
4. Karamanis, D., Vardoulakis, E., Kyritsi, E., Ökte, N. (2012). Surface solar cooling through water vapor desorption from photo-responsive sepiolite nanocomposites. Ener. Conv. Manag. 63, 118-122.
5. Ponomarev,Yu. N., Petrova, T. M., Solodov, A. M., Solodov, A. A. (2010). IR spectroscopy of water vapor confined in nanoporous silica aerogel. Opt. Express. 18(25), 26062-7.
6. Büning-Pfaue, H. (2003). Analysis of water in food by near infrared spectroscopy. Food Chemistry. 82, 107-115.
7. Zettlemoyer, A.C., Hsing, H.H. (1977). Water on Organosilane-Treated Silica Surfaces. J. Coll. Interf. Sci. 58(2), 263-274.

HEAT ISLAND PHENOMENON AND COOL ROOFS MITIGATION STRATEGIES IN A SMALL CITY OF ELEVATED TEMPERATURES

Vardoulakis Eftychios, Karamanis Dimitrios, Mihalakakou G.

ABSTRACT

High urban temperatures are observed during the last 100 years due to heat island phenomenon. The effect is intensively pronounced even in small sized cities by temperature differences between rural and urban environment reaching even 6 ^{o}C. In order to keep the phenomenon under control, mitigation strategies, especially concerning cool roofs has been established. Under hot and arid climates roof temperatures reach almost 70 ^{o}C and about 50% of heat enters into buildings through roof slab.

The aim of this paper is to present heat island phenomenon in a small city of Western Greece and propose energy saving techniques that improve overall energy performance of building stock and are easy to be applied.

KEYWORDS

Heat island, mitigation techniques, small cities

1 INTRODUCTION

Economic and social parameters modulated after the Second World War, led world population on massive displacements in large urban centers. Nowadays, almost 52% of world's population lives in cities, according to United Nations (United Nations, 2011), while in more developed nations, the percentage approaches 77% (figure 1).

Rapid and unexpected population explosion in an unprepared urban environment had serious effects on world's environmental quality and in many cases standards of living reduced. Main problems concern increased traffic, low air quality and high noise levels and also an increase of local temperatures and differentiation of microclimate. Continuous urbanization leads to cities of high population density with less area for human activities and increased energy consumption, an unsustainable way of living.

Instant corollary of the above changes in the urban environment was a change on the energy balance in cities. This resulted on serious air temperature changes in city environment and heat island effect. Heat island is the most documented phenomenon of climate change. According to that air and surface temperatures in the city are hotter than their rural surroundings. The effect has been found in cities through-out the

world, while Howard made the first documentation of it (1818) by studying London's climate (Howard, 1833).

Within the last 20 years a lot of research has been carried out on the problem and characteristics and its effect were determined (Giannaros, et al., 2012; Giannopoulou, et al., 2010; Giridharan, et al., 2004; Giridharan, et al., 2009; Kolokotroni, et al., 2006; Santamouris, et al., 2007; Stathopoulou, et al., 2007; Unger, 1996; Vardoulakis, et al., 2013; Watkins, et al., 2002). Air temperature rise, increases building cooling energy demand, which results in higher pollution emissions. Main mechanisms contributing in the phenomenon are building and road geometry, thermal and optical properties of materials used in urban spar, anthropogenic heat and lack of evaporation in the cities. The highest air temperature difference between urban and rural areas is called urban heat island intensity. According to Santamouris et al. (2001), heat island in the city of Athens, Greece is responsible for doubling building cooling load and tripling peak electricity demand. Mitigation techniques aim to reduce the impact of heat island either by increasing thermal losses in the cities or by lowering the heat gains (Santamouris, 2012).

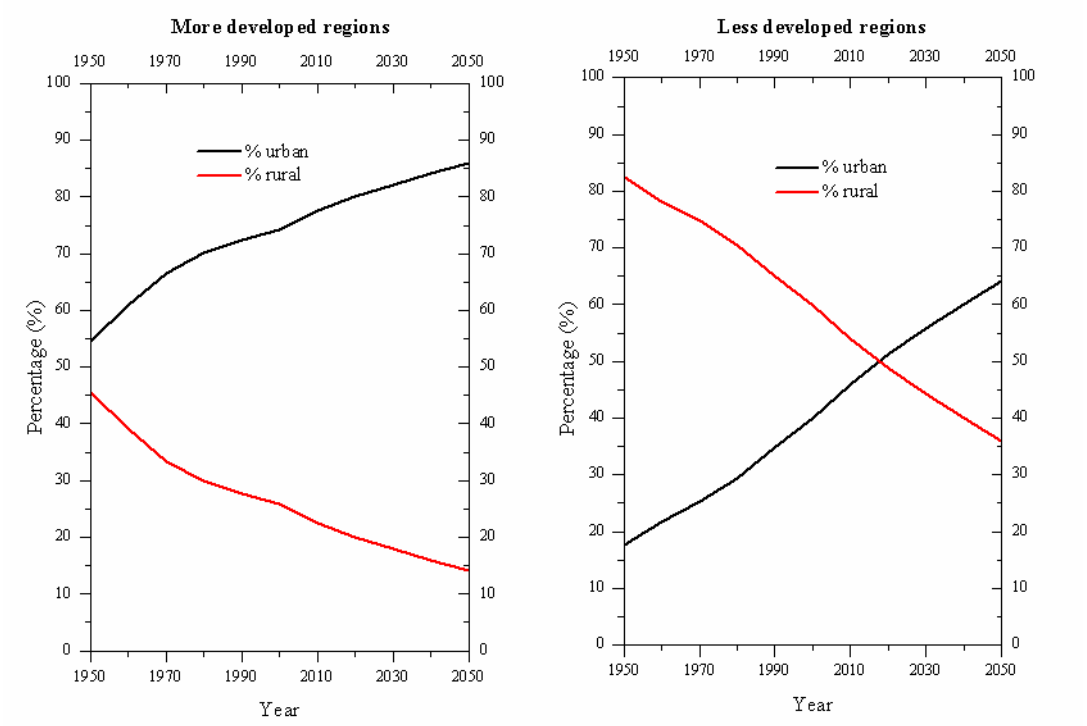

Figure 1: World percentage of urbanization after World War II and future prospects for developed and less developed countries

The objective of this paper is to describe briefly the phenomenon of heat island in a small city of Western Greece and to review mitigation techniques, developed during the last decade, easy to be applied even in small cities of elevated temperature.

2 HEAT ISLAND IN SMALL CITIES

Agrinio is a city of 93,000 inhabitants in Western Greece characterized by high temperatures and high humidity nights (55% to 78.5%), especially in the summer. According to the Hellenic National Meteorological Service the city has one of the highest mean monthly maximum temperatures in Greece during summer and usually experiences long heat wave events. A measurement network of nine datalogger devices measuring air temperature in specific locations inside and outside the city borders was installed. Also a meteorological station recorded all meteorological data at the same time. Detailed description of the city structure and characteristics of the stations are given in Vardoulakis et al. (2013).

Results show that heat island effect during summer is mainly a nocturnal effect, since city centre is warmer compared to the surrondings for more than 99% of night duration . Monthly heat island intensity reached the maximum value during August (3.8°C) at the local municipal parking station (station 7). Maximum heat island intensity approaches values of 6°C (based on mean hourly temperature record) on the same station.

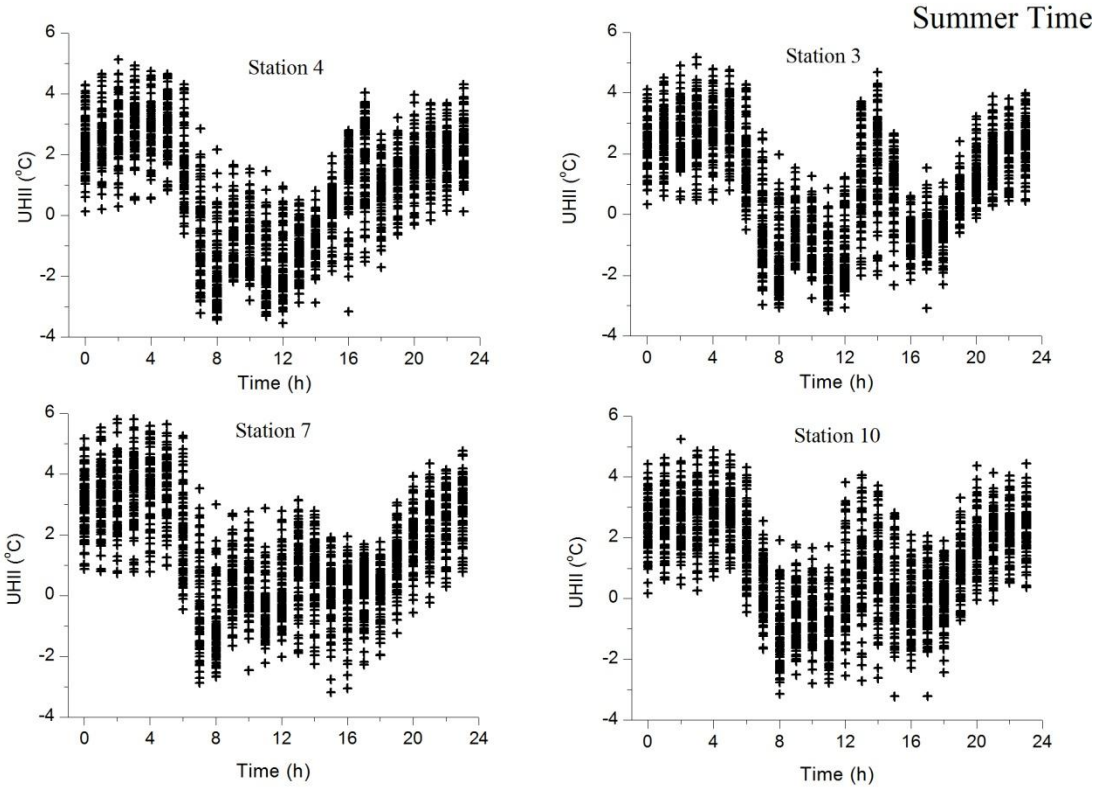

Figure 2: Heat island intensity values on 4 different urban stations during various moments of the day

On figure 2 it is very interesting to observe heat island intensities recorded during different moments of the day. Early in the morning (at 7 :00) rural environment is heated instantly and directly from the sun while at the same time large shaded areas in the city prevent a quick rise of temperature in the urban environment. As a result many times during the morning city centre seem to be cooler compared to country environment (heat sink formation). Gradually solar radiation warms up the city

environment and after 18:00 a clear heat island is present in the city until the next morning.

Heat island effect in the city of Agrinio has instant results on city energy needs in comparison to the rural area. A huge increase is observed for the cooling degree hours during the summer (+36.3%), but at the same time there is a significant gain in winter heating hours (-14.2%). According to the results of the present study heat island in small cities of elevated temperatures have a direct ascendancy on energy consumption and life quality of the city population. Therefore it is of great importance the adaptation of mitigation measures.

3 MITIGATION MEASURES FOR COOLING URBAN ENVIRONMENT

Although most of mitigation measures have been widely investigated, existing studies are offering results based on each place special characteristics, while at the same time there are few experimental studies available (Santamouris, 2012). This part of the paper presents a first attempt to categorize, propose and evaluate the ambient temperature reduction by cooling methods on roofs used in the last decade on city scale.

3.1 Use of cool roofs

Traditionally cool roof materials are stated as materials that have both high solar reflectance and high thermal emittance. Their benefits include improved building comfort, energy and money savings, reduced roof maintenance, reduction of peak electricity demand and low levels of pollution (Gartland, 2008). Increasing the roof albedo has major effect on ambient temperature.

Synnefa et al. (2008) tested several types of cool materials and a modeling study was undertaken to assess the urban heat island effect over Athens, Greece. A moderate and an extreme increase in albedo scenario were taken into account. Results estimated that a large scale increase in albedo could reduce ambient air temperature by 2°C.

Menon et al. (2010) quantified the change in land surface temperature that may be obtained by using reflective roofs of high albedo in urban areas. After performing several sets of simulations, for an average 0.003 increase in surface albedo a temperature reduction of 0.008K (for all global land areas) occurred according to the catchment land surface model.

Rosenzweig et al. (2006) deduced that substantial reductions in New York City surface and near-surface (up to 2m high) temperatures can be achieved by implementing heat island mitigation strategies. Simulations were performed with the NCAR MM5 regional climate model during the period of summer 2002. Results show that high albedo roofs can achieve a reduction of 0.4°F in New York city, while this reduction reaches 0.6°F at 3 p.m.

An important factor that usually is not measured as part of cool roof research, is the increased reflected solar radiation caused by high albedo, which might hit and be absorbed by surrounding building surfaces. This could increase the human thermal discomfort and building cooling energy use during hot periods. Therefore, attention should be given to the complete assessment of both the benefit and penalty during all year to ensure a positive net benefit will be obtained. A proposed strategy for changing albedo in a hot climate could be that: increase the albedo during summer and reduce it in winter depending on specific weather conditions. This could help to maximize thermal benefits during summer and minimize the losses during winter (Li et al., 2013).

3.2 Use of green roofs

There are a few research studies determine mitigation capabilities of green roofs on a city scale. Smith and Roebber (2011) used simulation test for a day representing average summer conditions in twenty-first century in Chicago. Chicago is a green roof leading city with 359 vegetated roofs of 5,469,463 square feet coverage in 2010. Authors calculated reduced temperatures in the urban environment as much as 3°C in addition to the temperatures estimated without the use of green roofs.

Bass et al. by using the Mesoscale Community Compressible (MC2) model for June of 2000 for the city of Toronto calculated air temperature reduction by covering 5% of the total landmass. Bass found that temperatures across the city were reduced by 1 to 2°C when sufficient moisture was provided to the plants to drive evapotranspiration (at 13:00 hours). Lower boundary layer temperatures can be reduced by using limited green roof coverage in combination with existing greenery.

Finally Chen et al. (2009) have performed coupled simulations of convection, radiation and conduction of high- and mid-rise areas in Tokyo (Otemachi and Kyobashi respectively). In both cases Chen reports that there is not a large difference and changing the roof material hardly affects the air temperature in the pedestrian area.

4 CONCLUSIONS

The existence and the intensity of the heat island effect in small cities like Agrinio were investigated. Intensity reaches a mean value of 3.82 °C on August but there are also time period of cool islands in the city centre, especially early in the morning. Present work proves that even small sized towns have serious problems, due to bad urban structure planning, which leads to an increase of energy use in urban spar. Mitigation measures like cool and green roofs are essential to improve outdoor thermal comfort conditions even in small cities and can achieve even 2°C temperature reduction.

5 REFERENCES

Bass B., Krayenhoff S., Martilli A. and Stull R. Mitigating the urban heat island with green roof infrastructure. Retrieved from http://www.cleanairpartnership.org

Chen H., Ooka R., Huang H., Tsuchiya T., 2009. Study on mitigation measures for outdoor thermal environment on present urban blocks in Tokyo using coupled simulation. Building and Environment 44(11), pp.2290-2299

Gartland Lisa, 2008. Heat Islands. Understanding and Mitigating Heat in Urban Areas, Published by Earthscan

Giannaros, T.M. and Melas, D. 2012. Study of the urabn heat island in a coastal Mediterranean City: The case study of Thessaloniki, Greece. *Atmospheric Research.* 2012, Vol. 118, pp. 103-120

Giannopoulou, K., et al. 2010b. On the characteristics of the summer urban heat island in Ahtens, Greece. *Sustainable Cities and Society.* 2010b, Vol. 1, 1, pp. 16-28.

Giridharan, R., Ganesan, S. and Lau, S. 2004. Daytime urban heat island effect in high-rise and high-density reidential developments in Hong Kong. *Energy and Buildings.* 2004, Vol. 36, pp. 525-534.

Giridharan, R. and Kolokotroni, M. 2009. Urban heat island characteristics in London during winter. *Solar Energy.* 2009, Vol. 83, 9, pp. 1668-1682.

Howard, L. 1833. *The Climate of London.* London : Harvey and Darton, 1833

Kolokotroni, M., Giannitsaris, I. και Watkins, R. 2006. The effect of the London urban heat island on building summer cooling demand and night ventilation strategies. *Solar Energy.* 2006, Τόμ. 80, σσ. 383-392.

Li H., Harvey J., Kendall A., 2013. Field measurement of albedo for different land cover materials and effects on thermal performance. Building and Environment 59, pp.536-546

Menon S., Akbari H., Mahanama S., Sednev ., Levinson R., 2010. Radiative forcing and temperature response to changes in urban albedos and associated CO_2 offsets. Environmental Research Letters 5, 014005

Rosenzweig, C., W. Solecki, L. Parshall, S. Gaffin, B. Lynn, R. Goldberg, J. Cox, and S. Hodges, 2006. Mitigating New York City's heat island with urban forestry, living roofs, and light surfaces. Presentation at 86th American Meteorological Society Annual Meeting, Jan. 31, 2006, Atlanta, Georgia. (retrieved from http://www.giss.nasa.gov)

Santamouris, M., et al. 2001. On the impact of urban climate on the energy consumption of buildings. *Solar Energy.* 2001, Vol. 70, 3, pp. 201-216.

Santamouris, M., Paraponiaris, K. and Mihalakakou, G. 2007. Estimating the ecological footprint of the heat island effect over Athens, Greece. *Climate Change.* 2007, Vol. 80, pp. 265-276.

Santamouris M.,2012. Cooling the cities – A review of reflective and green roof mitigation technologies to fight heat island and improve comfort in urban environments. Solar Energy (In Press)

Stathopoulou, M. and Cartalis, C. 2007. Daytime urban heat islands from Landsat ETM+ and Corine land cover data: An application to major cities in Greece. *Solar Energy*. 2007, Vol. 81, pp. 358-368.

Smith K.R. and Roebber P.J., 2011. Green roof mitigation potential for a proxy future climate scenario in Chicago, Illinois. Journal of Applied Meteorology and Climatology 50, pp.507-522.

Synnefa A., Dandou A., Santamouris M., Tombrou M., 2008. On the use of cool materials as a heat island mitigation strategy. Journal of applied meteorology and climatology 46, pp.2846-2856

United Nations. 2011. *World Population Prospects: The 2011 Revision and World Urbanization Prospects.* s.l. : Population Division of Department of Economic and Social Affairs of the United Nations Secretariat, 2011.

Unger, J. 1996. Heat island intensity with different meteorological conditions in a medium-sized town: Szeged, Hungary. *Theoritical and Applied Climatology.* 1996, Vol. 54, pp. 147-151.

Vardoulakis, E., et al. 2013. The urban heat island effect in a small Mediterranean city of high summr temperatures and cooling energy demands. *Solar Energy.* 2013, Vol. 94, pp. 128-144.

Watkins, R., et al. 2002. The London Heat Island: results from summertime monitoring. *Building Service Engineering Research and Technology.* 2002, Vol. 23, pp. 97-106.

ASSESSING THERMAL RISK IN URBAN AREAS – AN APPLICATION FOR THE URBAN AGGLOMERATION OF ATHENS

Polydoros T. and Cartalis C.

Department of Environmental Physics, University of Athens, University Campus, Build PHYS-V, Athens 15784
ckartali@phys.uoa.gr

Assessing thermal risk in urban areas is essential, as this can have major implications to human health and may influence quality of life in urban areas as well as the urban microclimate. Such assessment is promoted by estimating Land Surface Temperature (LST), evaluating the intensity of Surface Urban Heat Island (SUHI) and the variation of the discomfort index (DI), the latter reflecting the most common bioclimatic index used for outdoor thermal comfort applications. Calculations need to provide adequate spatial and temporal depictions of SUHI and DI, as these are correlated with such parameters as land cover/use, urban density, topography, etc. In this study an assessment of thermal risk in urban areas is made for the urban agglomeration of Athens in the event of summer heat waves.

Keywords: Thermal heat island, discomfort, urban environment and health

1. INTRODUCTION

It is usually observed that air temperatures in densely built-up urban areas are higher than the temperatures of the surrounding rural country. This phenomenon is known as 'Urban Heat Island' (UHI) and it has a significant impact on energy demand, human health and environmental conditions. The existence of the UHI is attributed to various causes: trapping of both incoming solar and outgoing longwave radiation, reduction of turbulent heat transport due to the geometry of the street canyons, decreased evapotranspiration and increased sensible heat storage due to construction materials, building and traffic heat losses as well as air pollution leading to increased long-wave radiation from the sky (Oke 1987).

The heat island phenomenon can be quantified by the maximum difference between urban temperature and the background rural temperature, which is defined as the urban heat island intensity (Oke, 1987). Heat island intensity depends on the size, population and industrial development of the city, the topography and the surface materials, the general climate of the region and the momentary meteorological conditions. In the study by Santamouris et al. (2001), it was found that during the summer period, daytime UHI intensity of Athens is close to 10°C for the central Athens area, whereas the night-time UHI intensity can rise up to 5°C.

Increased industrialization and urbanization in recent years have affected dramatically the number of urban buildings with major effects on the energy consumption of this

sector. Urban areas without a high climatic quality use more energy for air conditioning in summer and even more electricity for lighting. Moreover, discomfort and inconvenience to the urban population due to high temperatures, wind tunnel effects in streets and unusual wind turbulence due to wrongly designed high rise buildings is a very common phenomenon (Santamouris et al., 2001).

Voogt and Oke (2003) review the use of thermal remote sensing for the study of urban climates with respect to the UHI effect and describe the distinction between the atmospheric UHI and the surface UHI. Atmospheric UHI is usually detected by ground-based air temperature measurements taken from standard meteorological stations, whereas surface UHI is observed from thermal remote sensors which record the upwelling thermal radiance emitted by the surface area that lies within the instantaneous field of view (IFOV) of the sensor. In contrast to atmospheric UHIs that are best expressed under calm and clear conditions at night, surface UHIs are usually studied by using satellite thermal remote sensing data of high spatial resolution (~ 100 m) acquired at daytime when heat island intensities are greatest (Roth et al., 1989).

Many surface UHI studies have been conducted using thermal remote sensing from satellites. These studies give a spatially continuous view of the surface UHI over large urban areas than is feasible using data from meteorological station networks. In addition, remote sensing can effectively depict the thermal environment of urban areas on a repeated basis. Thus, spatial coverage and temporal repetition are the main advantages of using satellite thermal remote sensing technique in the study of the urban climates (Stathopoulou et al., 2005)

The impact of the urban microclimate on the human thermal comfort is important. In urban environments, the commonly prevalent high temperatures, especially during the summer period, that produce the urban heat island effect, also tend to aggravate the comfort conditions of the city dwellers (Stathopoulou et al.,2005). Human discomfort can be evaluated through a number of theoretical and empirical biometeorological indices requiring usually a larger or smaller number of input parameters such as air temperature, wind speed, air humidity etc. The bioclimatic index most commonly used in urban climate studies to describe the level of thermal sensation that a person experiences due to the modified climatic conditions of an urban area is the Discomfort Index (DI) of Thom (Stathopoulou et al. 2005).

This paper explores the use of thermal Advanced Very High Resolution Radiometer (AVHRR) satellite data to map bioclimatic comfort conditions by estimating the Thom's discomfort index for the urban agglomeration of Athens in the event of summer heat waves for the period from 2008 to 2012.

2. METHODOLOGY AND DATA

The datasets used were acquired from the electronic library (CLASS) of the National Oceanic and Atmospheric Administration (NOAA).AVHRR data from NOAA-18 and NOAA-19 satellites were selected for daytime because the satellites time of overpass is near noon time when the highest daily air temperatures occur. For nighttime, AVHRR data from MetOp-A satellite were selected as the overpass time is around 22.30 local time (19.30 UTC).

2.1 AVHRR data processing

AVHRR thermal images (spatial resolution at 1.1 km) were used in order to map the thermal urban environment of the city of Athens. Images were geometrically and radiometrically corrected; radiometric calibration of the images involved the conversion of the raw digital number (*DN*) values to spectral radiance and then to at-sensor reflectances for the visible channels 1 (0.58-0.68μm) and 2 (0.725 1.10μm) and to brightness temperatures for the thermal channels 4 (10.3-11.3μm) and 5 (11.5-12.5μm). The conversion to brightness temperatures from spectral radiances was performed using the inversion of Planck's blackbody equation. Next a cloud mask was applied to all images in order to ascertain their correspondence to clear sky conditions. For daytime images all pixels with channel 1 reflectance greater than 25% were considered as cloud contaminated and were rejected. For nighttime images an algorithm for cloud detection (Saunders and Kriebel, 1988) was used. The algorithm is based on channel 3, 4 and 5 temperature values as well as on the temperature differences of T4-T5 and T3-T4. Finally all images were geo-referenced to the Geographic (Lat/Lon) map projection system (Spheroid: WGS 84, Datum: WGS 84).

2.2 Urban Atlas data processing

The Urban Atlas dataset was used in order to identify the urban, suburban and rural regions of the greater Athens area. For this purpose, the initial 20 classes were merged into only three classes defined as Urban, Suburban and Rural Areas. The aggregate land cover type allows the spatial discrimination between the different urban land covers that are related to the SUHI phenomenon and also favors the spatially accurate assignment of the surface emissivity that corresponds to these urban land covers.

2.3 Land surface temperature (LST)

The algorithm selected for this study for the estimation of LST using AVHRR thermal infrared data was developed by Coll et al. (1994a). It requires the brightness temperatures in AVHRR channels 4 and 5, the mean emissivities and the spectral emissivity difference in these channels. It also uses coefficients which depend on atmospheric moisture and the surface temperature. These coefficients can be optimized according to the characteristics of a given area. The algorithm is described by the relation:

$$LST = T4 + [1 + 0.58\cdot(T4 - T5)] \cdot(T4 - T5) + 0.51 + \alpha\cdot(1 - E) - \beta\cdot(\Delta\varepsilon)$$

where:

T4 is the radiance temperature for channel 4 of AVHRR,
T5 is the radiance temperature for channel 5 of AVHRR,
E is the mean spectral emission coefficient for channels 4 and 5:

$$E = (\varepsilon 4 + \varepsilon 5)/2$$

where:

ε4 is the surface emission coefficient for channel 4,
ε5 is the surface emission coefficient for channel 5,
and Δε is the difference of the emission coefficients for channels 4 and 5:

Values for E and Δε were taken from Stathopoulou et al (2004) and are shown in Table 1. Coefficients α and β in equation (1) depend on the amount of atmospheric water vapour in the area of the satellite image and from the temperature of the surface under observation. They may be described as a function of the brightness temperature (T4) which is recorded in channel 4 of the AVHRR and the precipitable water (PW) in the area (Caselles et al. 1997).

$$\alpha = (0{,}190 \cdot PW - 0.103) \cdot T4 - 67 \cdot PW + 107$$

$$\beta = (0{,}100 \cdot PW + 1{,}118) \cdot T4 - 68 \cdot PW - 163$$

where PW is in gr/cm2 and T4 in °K. Monthly mean PW values for the region of Greece from Chrysoulakis and Cartalis (2002) were used in this study.

Table 1: Emisivity values by land cover type.

Land cover type	Mean emissivity	Emissivity difference
Urban	0.97	-0.007
Suburban	0.98	-0.003
Rural	0.989	0

2.4 Air temperature

Estimated air temperatures were derived from AVHRR surface temperatures using a simple empirical relation with coefficients determined from the comparison of air temperatures observed at meteorological stations with coincident surface temperatures of the AVHRR pixels where these stations were located. Air temperature values at each station that were coincident with the satellite overpass time were collected and results of regression analysis showed that a strong correlation (r=0.84) exist between air temperature and surface temperature (*Ts*) at night, and a moderate correlation exists at day(r=0.69) presumably reflecting stronger sub-pixel variations of surface cover and heat balance regimes. The relations derived were then applied to the AVHRR images in order to convert AVHRR surface temperatures into estimated air temperatures.

$$\text{Day: } Tair = 0.3896 \cdot Ts + 15.313$$
$$\text{Night: } Tair = 0.8246 \cdot Ts + 6.2324$$

2.5 Precipitable water (PW)

Chrysoulakis et al. (2008) studied the relation between the AVHRR temperature difference $\Delta T = T4 - T5$ (K) and the atmospheric precipitable water *PW* (cm) over Greece using daytime satellite data and radiosonde data. They found this relation to be essentially linear and approximated by the following equation:

$$PW=0.719\cdot\Delta T+0.362$$

For nighttime images a relation from Choudhury et al. (1995) was found more suitable, and for urban surfaces is expressed as:

$$PW=1.265\cdot\Delta T+ 1.493$$

It should be mentioned that **Sta**thopoulou et al. (2005) used a relation from Smith (1966) which gives precipitable water PW (cm) as a function of dew point temperature Td(°F). For the period of summer and the latitudinal zone of Greece Td in °C is obtained from the following equation:

$$T_d = \frac{5}{9}\left(\frac{lnPW + 1.2527}{0.0393} - 32\right)$$

2.4 Relative humidity (*RH*)

Relative humidity (*RH* %) is defined as the ratio of vapor pressure (*e*) to saturated vapor pressure (es) at the air temperature (Ta) expressed as a percent:

$$RH = 100\left[\frac{e}{e_s T_a}\right]$$

In this study, vapor pressure and saturated vapor pressure values (in *kPa*) were computed by using the Tetens formulae expressed as:

$$e_s T_a = 0.61078\, e^{\frac{17.269Ta}{Ta+237.29}}$$
$$e = e_s T_d$$

2.5 Discomfort index (*DI*)

Thom's discomfort index (DI) is expressed by a simple linear equation based on dry-bulb (*Tdry*) and wet-bulb (*Twet*) temperatures. Its original form is given as:

$$DI(°F)=0.4(Tdry+Twet)+15$$

If air temperature (*Ta*) as measured in degrees Celsius and relative humidity (*RH)* in % are given, DI can be computed by using the following equation:

$$DI(°C)= Ta – 0.55(1 - 0.01RH)(Ta -14.5)$$

The classes of DI are presented in Table 2 where it can be seen that the human discomfort increases as the Di values increases.

Table 2. Classes of discomfort index

Class number	Di(°C)	Discomfort conditions
1	DI<21	No discomfort
2	21≤DI<24	Less than 50% feels discomfort

3	24≤Di<27	More than 50% feels discomfort
4	27≤DI<29	Most of the population feels discomfort
5	29≤DI<32	Everyone feels severe stress
6	DI≥32	State of medical emergency

3. RESUTS AND CONCLUSIONS

Table 3 shows the mean land surface temperatures by land cover type for daytime and nighttime in the greater Athens area during heat waves. Surface urban heat island is evident at night as urban areas are 4.5°C warmer than rural areas and 2.3°C warmer than suburban areas. This is illustrated in Figure 1 where dark to bright tones indicate cooler to warmer surface temperature. At daytime urban areas are warmer than suburban areas as expected by 2°C but rural areas seem to warmer than urban areas. This can be attributed to the surface characteristics of Athens rural areas as the vegetation percentage is too low and the surface can be described as bare ground. In addition heat waves usually occur in July and August after many weeks of very low or no precipitation and the ground is deficient in moisture. Figure 2 illustrates the mean surface temperature values during heat waves at daytime.

Table 3.Mean values of Ts by land cover type

Land cover type	Daytime Ts(°C)	Nighttime Ts(°C)
Urban	51.5	29.8
Suburban	49.5	27.5
Rural	52.6	25.2

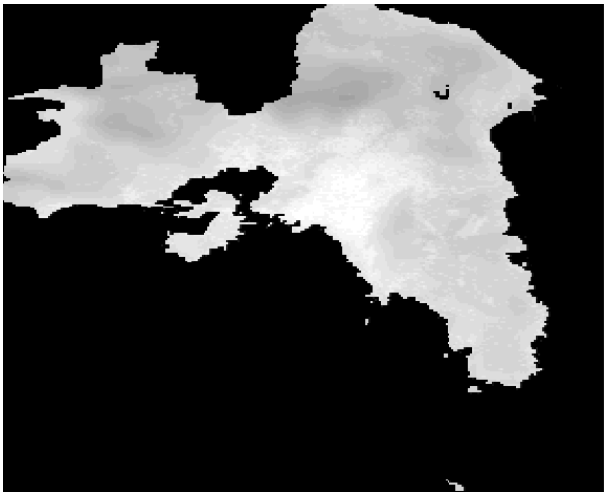

Figure1: Mean land surface temperature map at nightime.

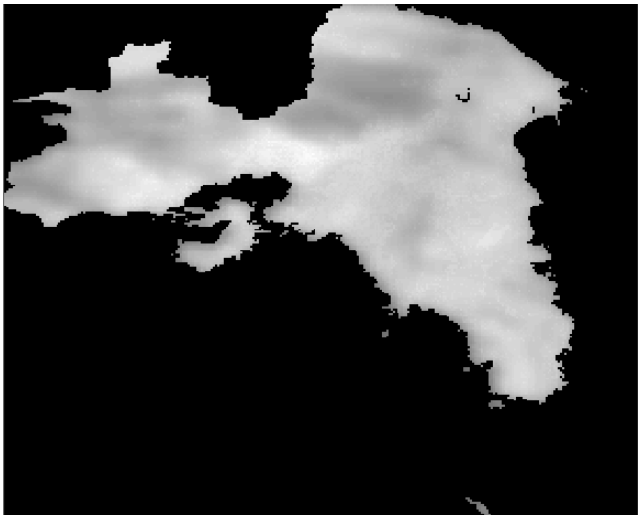

Figure 2: Mean land surface temperature at daytime.

Mean Discomfort Index values during heat waves appear in Table 4. At daytime the suburban areas of Athens have smaller DI values than urban and rural areas. Suburban areas are categorized as "Over 50% of the population feels discomfort" in the DI classification system (Table 2). Urban and rural areas are categorized as "Most of the population suffers discomfort". Figure 3 illustrates the mean DI values during heat waves at daytime where dark to bright tones indicate lower to higher DI values. At nighttime when the SUHI is relative strong, urban areas have larger DI values than suburban and rural areas. Urban and suburban are categorized as "Over 50% of the population feels discomfort" in the DI classification system. Rural areas are categorized as "Less than 50% of the population feels discomfort". This is illustrated in Figure 4.

Table 4.Mean values of DI by land cover type

Land cover type	Daytime DI(°C)	Nighttime DI(°C)
Urban	28.1	25.5
Suburban	26.7	24.3
Rural	28.1	22.7

Figure 3. Mean DI values at daytime.

Figure 4. Mean DI values at nighttime.

In this study an attempt was made to verify the presence of surface heat island, to estimate its strength as well as to evaluate Thom's discomfort index DI in the greater Athens area in the event of summer heat waves. Results demonstrate the capacity of the methodology to assess the state of thermal environment in urban agglomerations and to provide valuable information in support of the protection of the citizens during heat waves.

REFERENCES

A. Bitan The high climatic quality of city of the future Atmos. Environ., 26B (1992), pp. 313–329

Caselles, V., Coll, C., and Valor, E., 1997, Land surface emissivity and temperature determination in the whole HAPEX–Sahel area from AVHRR data. International Journal of Remote Sensing, 18, 1009–1027.

Choudhury, B.J., T.J. Dorman, and A.Y. Hsu, "Modeled and observed relations between the AVHRR split window temperature difference and atmospheric precipitable water over land surfaces", Remote Sensing of Environment, 51 p. 281-290, 1995.

Chrysoulakis, N. and C. Cartalis, "Improving the estimation of land surface temperature for the region of Greece: adjustment of a split window algorithm to account for the distribution of precipitable water". International Journal of Remote Sensing, 23(5): p. 871-880, 2002.

Chrysoulakis, N., Y. Kamarianakis, L. Xu, Z. Mitraka, and J. Ding (2008), Combined use of MODIS, AVHRR and radiosonde data for the estimation of spatiotemporal distribution of precipitable water,J. Geophys. Res., 113, D05101

Coll, C., Caselles, V., Sobrino, J. A., and Valor, E., 1994, On the atmospheric dependence of the split window equation for land surface temperature. International Journal of Remote Sensing, 15, 105–122.

G. Mihalakakou, M. Santamouris, N. Papanikolaou, C. Kartalis, A. Tsagrassoulis. Simulation of the urban heat island intensity in Mediterranean climates by neural networks—a study of the influence of climatic parameters on heat island intensity J Pure Appl Geophys, 161 (2004), pp. 429–451

M. Stathopoulou, C. Cartalis, I. Keramitsoglou, M. Santamouris. Thermal remote sensing of Thom's Discomfort Index (DI): Comparison with in situ measurements Proceedings of the Remote Sensing 2005 Symposium, (SPIE 2005), Brugge, Belgium, 19 September 2005, Environmental Monitoring, GIS Applications, and Geology V, Vol. 5983 (2005), p. 59830K

M. Stathopoulou, C. Cartalis, I. Keramitsoglou Mapping micro-urban heat islands using NOAA/AVHRR images and CORINE land cover: an application to coastal cities of Greece International Journal of Remote Sensing, 25 (12) (2004), pp. 2301–2316

Oke T.(1987) City size and urban heat island, perspectives on wilderness: Testing the theory of restorative environments, proceedings of the Fourth World Wilderness Congress, 7: 769-779

Roth, M., T.R. Oke and W.J. Emery, 1989. Satellite- Derived Urban Heat Islands from 3 Coastal Cities and the Utilization of Such Data in Urban Climatology. International Journal of Remote Sensing, 10 (11): pp. 1699-1720.

Santamouris, M., et al., 2001. On the impact of urban climate on the energy consumption of buildings. Solar Energy, 70 (3): pp. 201-216.

Saunders, R. W., and Kriebel, K. T., 1988, An improved method for detecting clear sky and cloudy radiances from AVHRR data. International Journal of Remote Sensing, 9, 123–150.

Stathopoulou M.,Cartalis C., Andritsos A., 2005. Assessing the thermal environment of major cities in Greece. In: Proc. 1st International Conference on Passive and Low Energy Cooling for the Built Environment, Santorini, Greece.

Thom, E.C., "The discomfort index", Weatherwise, 12: p.57-60, 1959.

Voogt, J.A. and T.R. Oke, 2003. Thermal remote sensing of urban climates. Remote Sensing of Environment, 86 (3): pp. 370-384.

EVALUATION OF THE APPLICATION OF COOL MATERIALS IN URBAN SPACES: A CASE STUDY IN THE CENTER OF FLORINA

Stamatis Zoras*, Antonios Tsermentselis, Panagiotis Kosmopoulos, Argiro Dimoudi

Laboratory of Environmental and Energy Efficient Design of Buildings and Settlements, Department of Environmental Engineering, Democritus University of Thrace, Vas. Sofias 12, Greece
Corresponding author*: **stamatis.zoras@gmail.com szoras@env.duth.gr,

ABSTRACT

In the last years there is a strong interest for application of bioclimatic techniques and practices in urban neighborhoods and open spaces. This paper presents a bioclimatic study of an open space in an urban area by the use of simulation tools giving emphasis on the replacement of conventional materials with cool materials. Routes linking traditional monuments in the Greek city of Florina are characterized of decreased human thermal comfort conditions during summer time. The employment of computational fluid dynamics has contributed in the understanding of what interventions should be made at urban populated routes in order to meet defined thermal related targets.

KEYWORDS

Cool materials, CFD modeling, open space

1. INTRODUCTION

It is widely approved that densely urban developments in conjunction with the use of inappropriate external materials, the increased thermal energy emission related to human related and the lack of green areas, increases environmental temperature, leading to significant environmental impacts and increased energy consumption (Fintikakis et al., 2011). Open spaces within urban developments are complicated due to thermal energy exchange between structures, shadowingand wind flow complication in comparison to general flow. Cool material and other practices (water surfaces, green roofs) are used to mitigate urban heat island effect (Gartland, 2008). The main problems that result from bad thermal conditions in settlements include decreased human thermal comfort, decreased air quality, increased heat illnesses and increased energy and water use (Stone, 2005; Baik et al., 2001).

Experimental measurements within urban developments are needed in order to identify the thermal situation. In the Greek territory there are intense thermal phenomena mainly during the summer period (Livada et al., 2002, Dimoudi et al, 2013). These are observed in open urban areas all around country. Surface temperatures in relation to microclimatic conditions (wind, temperature, radiation) must be analyzed in order to better select rehabilitating strategy of open developments.

Simulation tools must be employed (Stavrakakis et al., 2011) in order to depict the present situation around the opencast area, usually during the warmest day of the hot period.

Materials identification and constructions configuration must also be taken into account in the simulation process. New materials and bioclimatic techniques are then proposed and simulated in order to show their impact at the thermal urban environment. The aim of this procedure is to realize the microclimatic conditions improvement due to the rehabilitating bioclimatic techniques and practices. The selection of the appropriate measures depends on the targets that will be defined for achieving an improved thermal environment (e.g. thermal comfort).

Due to the complicated urban environment in terms of materials, reflection, emission, wind flows around buildings, altitude differences etc., the simulation tool must be selected very carefully. It must be able to simulate three dimensional flows with solar radiation taken into account. This inevitably leads to general codes of computational fluid dynamics tools (e.g. PHOENICS software tool) but with increased demand of computational resources. Other tools may be useful for the assessment of individual parameters, as surface materials and trees may influence thermal comfort (Matzarakis et al., 2006) but the would not assess the wind flow effect in geometrical detail.

This paper presents a bioclimatic study of an open urban complex space in a city of North Western Greece, Florina, giving emphasis on the replacement of conventional materials with cool materials. The studied area includes the routes linking traditional neighborhoods by the river side of the city. Experimental measurements, simulation tool verification and the simulation based assessment of the proposed redevelopment measures are presented. All simulations have been carried out by the ANSYS CFD software package.

The thermal targets of this study were defined in accordance with the 'Programme for Bioclimatic Redevelopment of Public Open Spaces – Study Guideline' (http://www.cres.gr/kape/Scientific_Guide_19_7.pdf). These concerned the following parameters that should be improved:

1. Mean maximum summer temperature during noon of the warmest day
2. Cooling degree hours during the typical summer day
3. Mean surface temperature during noon of the warmest day
4. Mean human thermal comfort index
5. Wind field during the typical summer day

The results of criteria 1, 3 and 5 are presented in this paper.

2. BIOCLIMATIC THERMAL PROBLEM

To examine the weather conditions in the city of Florina meteorological data of the period of 1st of January 2009 to the 31st of December 2010 were used from the meteorological stations of Florina that is located in the urban complex of the city. Hourly data were available and the meteorological parameter that was examined was the air temperature (^{o}C).

Urban climate, compared to the surrounding suburban and rural environment, varies in terms of solar radiation, characteristics of rainfall and air temperature. According to Oke (1973), almost every urban center in the world is warmer 1-4 ^{o}C than neighboring non-urban rural areas, and this enforces urban heat island effects. Also, Gilbert (1991) states that the air temperature on sunny days can be from 2.0 to 6.0 ° C higher in urban compared to suburban locations.

3. BIOCLIMATIC INTERVENTIONS

The open urban complex that was studied, belongs at the commercial and social center of Florina city, and it is heavy populated during the week. The urban summer time microclimate in this area is mainly affected by the presence of conventional surface tiles and asphalt all over the linking routes. The ground surface of the river side routes of Florina is covered by Greek (flagstone) (Figure 1).

Figure 1: River side routes in Florina

The rehabilitation strategy of the area targets to conserve human activities and improve human thermal conditions in the open urban complex. Bioclimatic interventions could be divided in two main directions.

- the river side streets
- the linking streets of the river

The main bioclimatic interventions are characterized by increasing water surfaces, vegetation, green roofs and by installing cool asphalt and flagstones.

In order to improve thermal microclimate in the area new cool materials must be used that may reduce surface temperatures of buildings, streets and sidewalks. The proposed materials have relatively high reflectivity of solar radiation and increased emission rate. The structural surfaces should be reduced and replaced by water surfaces, soil and vegetation. Green roofs in the river side buildings or where people are accommodated would also contribute in the reduction of material thermal storage.

4. MODEL VERIFICATION

Monitored data of the thermal conditions in the area of interest and surrounding locations resulted at the analytical verification of the CFD model and consequently the accurate simulation of both the current situation and proposed interventions. The ANSYS CFD model was used for the simulations.

In order to prove the ANSYS CFD model validity for the open area simulation, the model was verified against experimental data that have been carried out during September 2011. The warmest day for the period of experiment was selected in terms of the completeness of the microclimatic data (i.e. air temperature, air velocity, surface temperature). Therefore, it was chosen September the 13th, 2011, between 15:20 – 16:20 hours. The data used for validation of the model is the measurement data within the study area, i.e. the air temperature, the temperature of the material surfaces of streets, sidewalks and facades at 1.8m in height and the wind speed at the same height.

The simulation results were compared with the measured values of the surface temperature, ambient temperature and wind speed. Climate data from that period were obtained from the Florina meteorological station and used to simulate the climatic conditionin the intervention area and in places where measurement was made. Since surface temperature measurements were carried out during midday, the comparisons were made for the same period.

The concept of model validity was that meteorological input from Florina's station if are applied in ANSYS CFD then this could efficiently calculate the thermal behavior of within the urban complex. From Table 1 can be noticed a satisfactory convergence of the values between experiment and simulation. Therefore, the achieved accuracy of the model that was developed for the study area was quite high. The above comparison substantiates the high reliability of the model for the assessment of both the current situation and bioclimatic upgrade in the study area.

Table 1: Comparison between experimental and simulated data

	Experimental / Simulated		
	Tair (^{o}C)	WS(m//sec)	
Material	1.8 m	1.8 m	Tsurf (^{o}C)
Marble	27.16 / 27.85	0.70 / 0.75	27.80 / 28.3
Concrete Brick	27.40 / 27.97	0.61 / 0.66	34.50 / 34.80
Traditional flagstone of Karistos	36.23 / 36.85	0.68 / 0.63	32.0 / 32.5

5. MEAN MAXIMUM AIR TEMPERATURE AT NOON OF THE WARMEST DAY

Simulation of the average maximum summer period temperature has been carried out in the open area during noon of the warmest day. The warmest day was obtained from the period of the years 2009-2010, being the 21th of August 2010. Meteorological data from that day at noon were used in the simulation, in steady state mode, of the present and rehabilitated situation . At each case, the same meteorological data from Florina station were applied as input in ANSYS CFD with the respective materials and interventions of each configuration.

This way modeling predicted the thermal situation in the urban complex with input general meteorological data of the city.

It was assumed that in the open urban square and the linking routes in Florina, the average maximum temperatures appeared during the selected warmest day. Moreover, simulation has shown that the maximum temperatures within roads and the river side street appear at the same times. The area of interest was divided in the surface of the river side streets and river wind flow. The respective air temperatures were calculated at noon of the warmest day. Then, the resulted average maximum air temperature was compared for the case before and after rehabilitation.

Figures 2-3 depict air temperature field at each street along the river at 1.8m height during noon of the warmest day before and after rehabilitation.

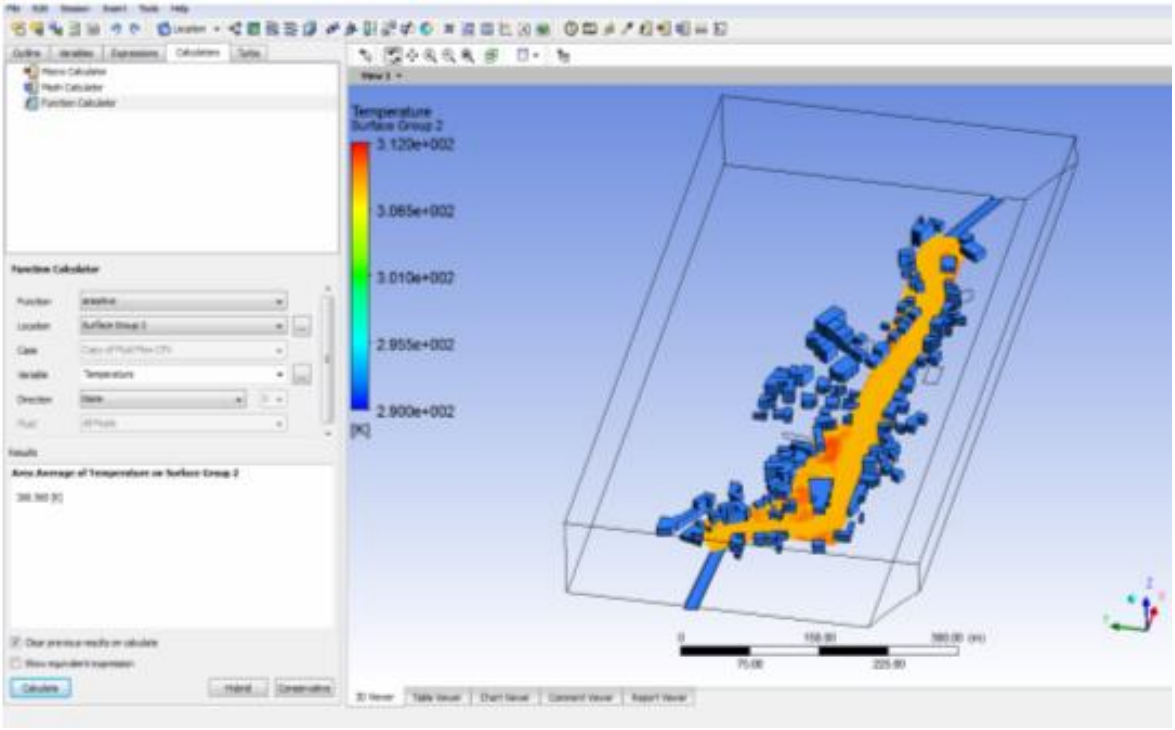

Figure 2: Present mean air temperature at 1.8 m height calculated from at least 500 grid points at each street

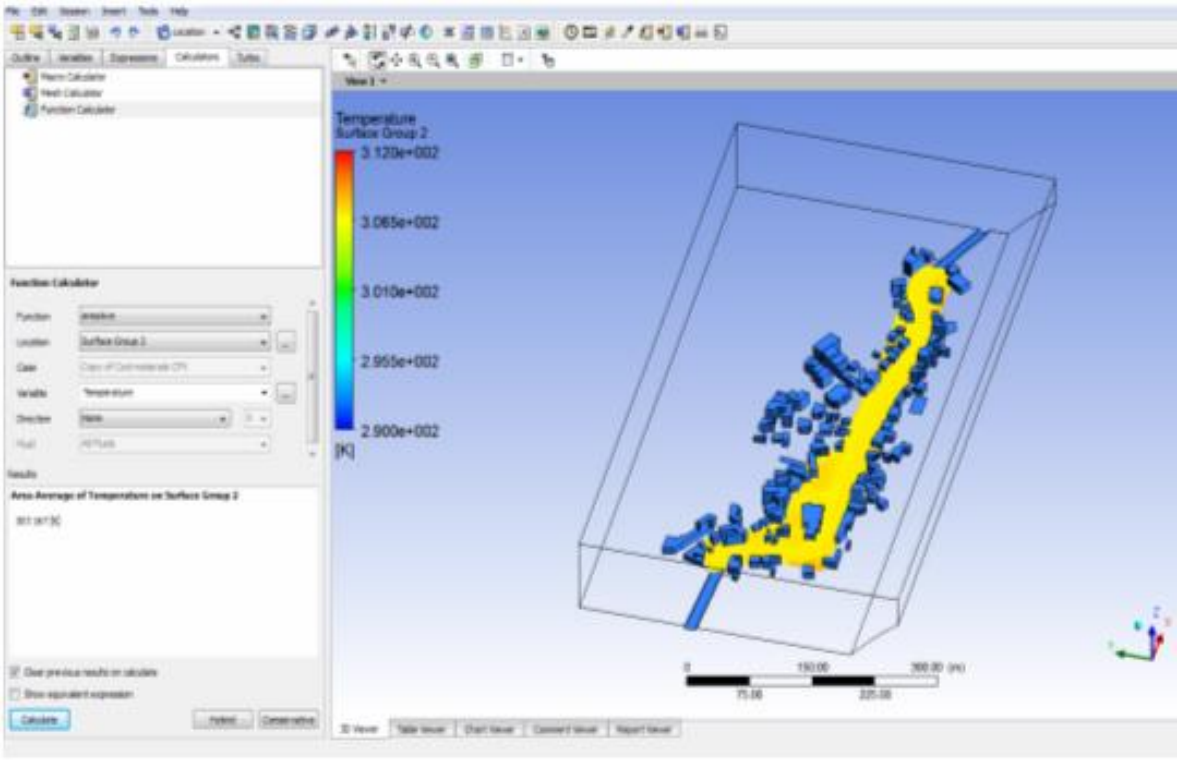

Figure 3: Mean air temperature after rehabilitation at 1.8 m height calculated from at least 500 grid points at each street

The simulated air temperature for each individual space (streets and open market) was obtained from at least 500 grid points of the mesh at 1.8m height. ANSYS CFD was applied to simulate the predicted air temperatures before and after rehabilitation with the surface areas in 21st of August 2010. The calculated total air temperature before and after case was 35,57 ºC and 34.18C, respectively. So, the air temperature improvement if bioclimatic measures are taken would be 1.39ºC.

6. MEAN SURFACE TEMPERATURE AT NOON OF THE WARMEST DAY.

CFD simulations have been carried out for the present case and for the proposed bioclimatic one. The results of the two simulations have compared concerning the warmest day of the 21st of August 2010. In the following Figures 4 and 5 display the surface temperatures for the present case and the improved one if bioclimatic techniques and practices are applied.

It was assumed that the mean surface temperature peaks during the warmest day and thus, it was calculated for all the individual roads and the market place separately. Therefore, it was assumed that the calculated surface temperatures are maximums for each individual road or open space. The mean surface temperature during noon of the 21st of August for all surfaces reached 38.21 ºC in contrast with the proposed bioclimatic configuration that reached 34.69ºC. The total predicted temperature difference was 3.52ºC. The significant material surface temperature reduction was due to shadowing from vegetation, water surfaces, green roofs, cool asphalt and cool flagstones of pavements and sidewalks.

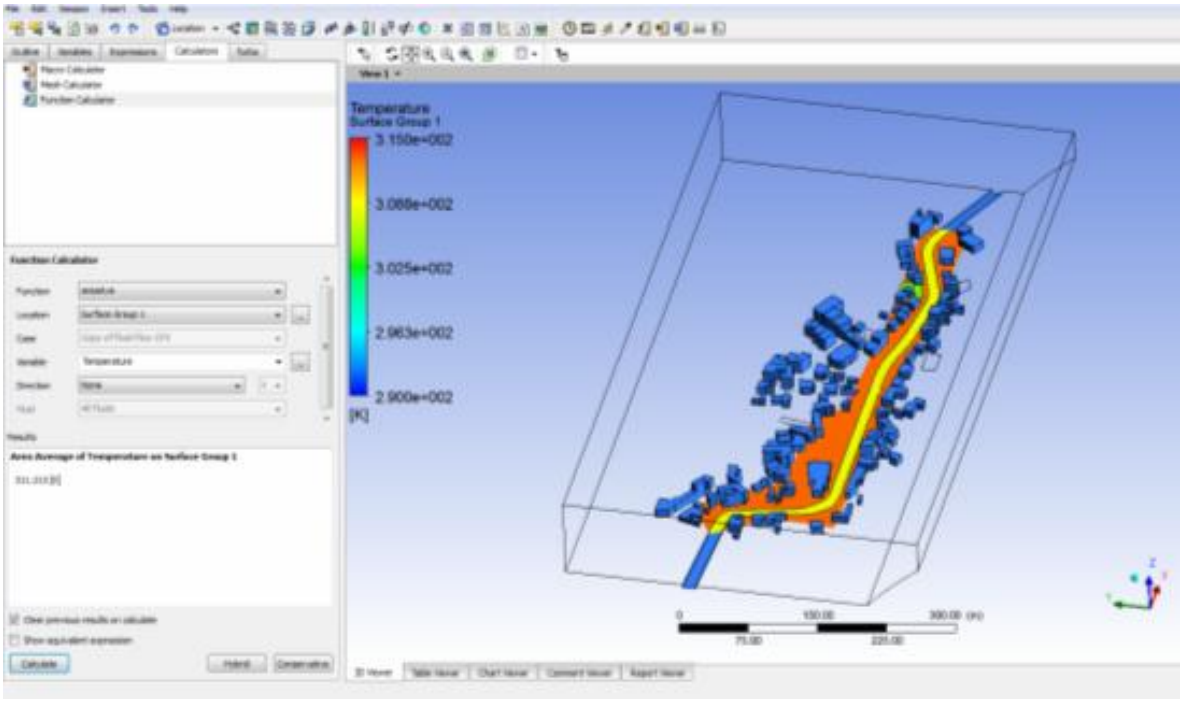

Figure 4: Mean surface temperatures of the existing condition

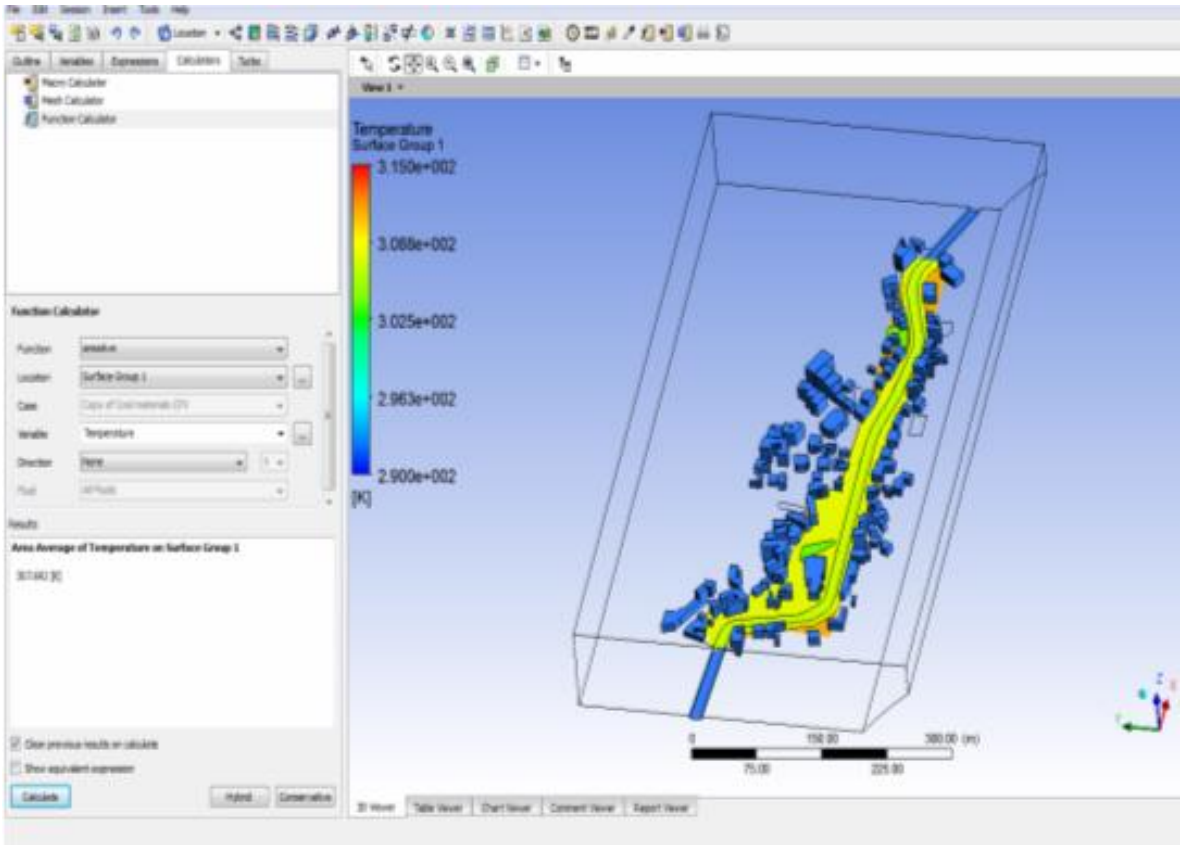

Figure 5: Mean surface temperatures of the predicted bioclimatic case

7. WIND FIELD DURING THE TYPICAL SUMMER DAY

Transient simulation of the wind field during the typical summer day with meteorological input of the area has been carried out. The typical wind field between 10:00 - 18:00 hours has been simulated in the area under consideration. From Figures 6 and 7 it was concluded that at 1.80 m height the wind velocity and turbulence would not change significantly due to the proposed bioclimatic interventions. Velocity vectors in the streets and in the open square place do not differ significantly at two cases with velocities below 1.0 m/s at all spaces (mean wind velocity before 0,578 ms-1, mean wind velocity after 0.574 ms-1). Generally, human comfort would not be affected at all open locations in relation to wind flow changes due to insignificant differences in velocities before and after rehabilitation.

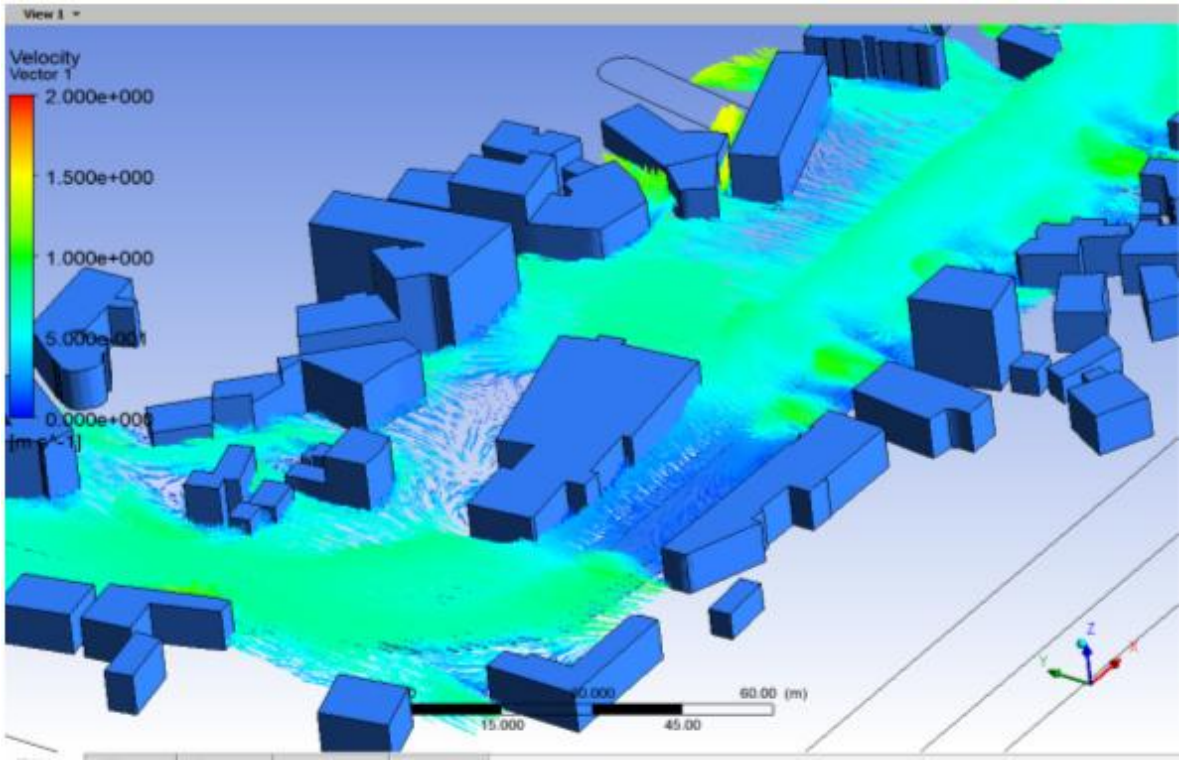

Figure 6: Mean wind field velocity in the urban complex before bioclimatic rehabilitation

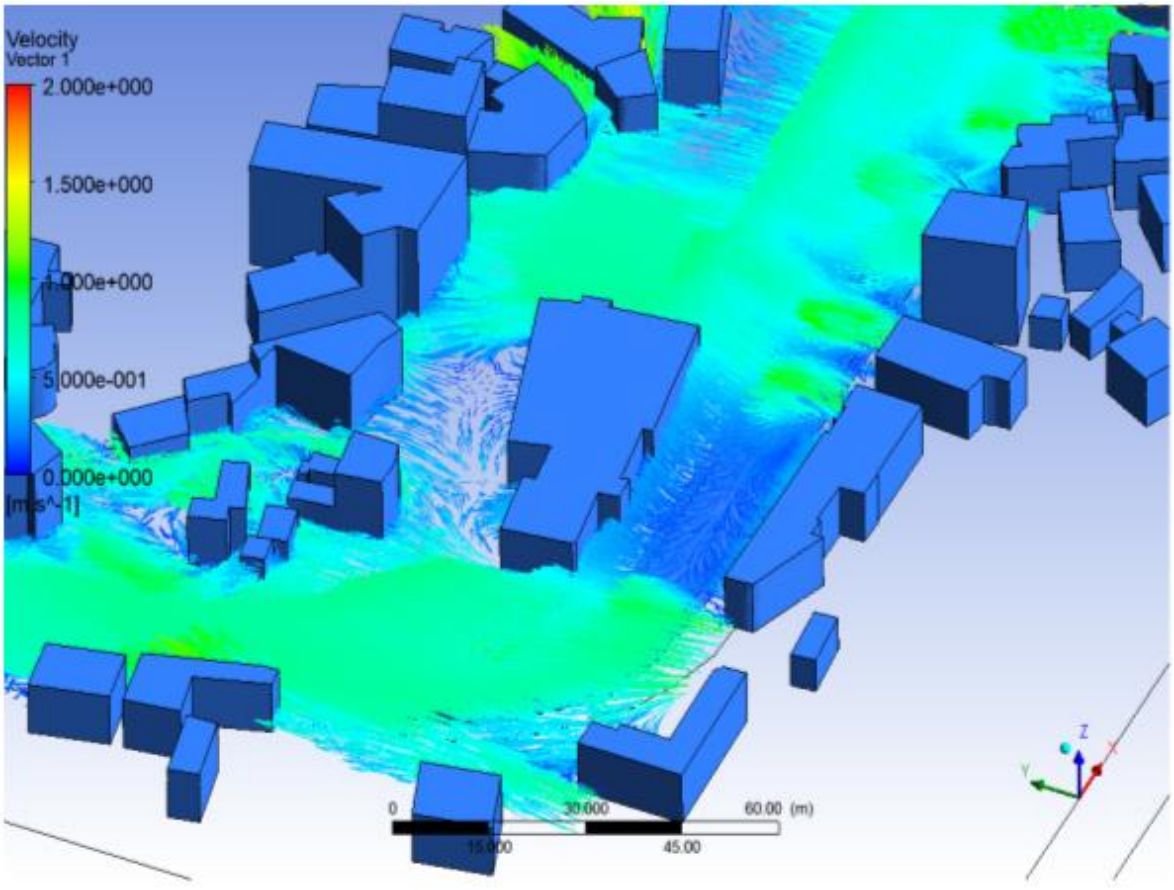

Figure 7: Mean wind field velocity in the urban complex after bioclimatic rehabilitation

8. CONCLUSIONS

Computational fluid dynamics simulation predicted the thermal conditions at the present case and the bioclimatically reformatted one. Each targeted parameter would improve if the proposed rehabilitation would take place in future. Relatively low air temperature improvement may lead to significant thermal comfort improvement. This is because thermal comfort is rather independent from air temperature but mostly correlated to radiant temperature. Note that, the wind field of velocities was approximately the same for the case before and after rehabilitation and therefore, it would not influence significantly the human thermal comfort conditions.

Reflection coefficients of cooled materials were higher than the conventional materials but emission coefficients were approximately the same. Therefore, it is rather obvious the significance of roofs, green areas and trees within the open urban complex in relation to the improvement of air temperature. Relatively high thermal comfort improvement is “easier” to be succeeded if surface thermal exchange is manipulated by any of the abovementioned ways. The exact influence of a bioclimatic intervention to microclimatic parameters must be studied in relation to urban complexity and climatic zone characteristics.

9. REFERENCES

ANSYS-CFD-SOFTWARE
http://www.ansys.com/Products/Simulation+Technology/Fluid+Dynamics.

Dimoudi, A., Kantzioura, A., Zoras, S., Pallas, C., Kosmopoulos, P. (2013). Investigation of urban microclimate parameters in an urban centre, *Energy and Buildings*, 64, 1-9.

Fintikakis, N., Gaitani, N., Santamouris, M. , Assimakopoulos, M. , Assimakopoulos, D.N., Fintikaki, M. , Albanis, G., Papadimitriou, K., Chryssochoides, E., Katopodi, K., Doumas, P. (2011). Bioclimatic design of open public spaces in the historic centre of Tirana, Albania. *Sustainable Cities and Society*, 1, 54-62.

Gartland, L. (2008). Heat *islands: Understanding and mitigating heat in urban areas*. Sterling, Virginia: Earthscan.

Gilbert, O.L. (1991). *The Ecology of Urban Habitats*. London: Chapman & Hall.

Livada, I., Santamouris, M., Niachou, K., Papanikolaou, N., & Mihalakakou, G. (2002). Determination of Places in the great Athens area where the heat island effect is observed. *Theoretical & Applied Climatology*, 71, 219–230.

Matzarakis, A., Rutz, F., and Mayer, H. (2006). Modelling the thermal bioclimate in urban areas with the RayMan model. *Proc of the PLEA 2006 Conf*, Vol. II, 449-453.

Oke, T.P. (1973). *City size and the urban heat island*. *Atmospheric Environment*, 14, 769-779.

PHOENICS software tool: http://www.cham.co.uk/.

Stavrakakis, G.M., Tzanaki, E., Genetzaki, V.I., Anagnostakis, G., Galetakis, G., Grigorakis, E. (2011). A computational methodology for effective bioclimatic-design applications in the urban environment. *Sustainable Cities and Society*, 1, 54-62.

www.cres.gr/kape/Scientific_Guide_19_7.pdf (Accessed 9th September 2013)

RECENT DEVELOPMENTS TO INTEGRATE VENTILATIVE COOLING IN THE DANISH REGULATORY CONTEXT

Per Heiselberg[1] and Karsten Duer[2]

[1]*Aalborg University*
Sohngaardsholmsvej 57
9000 Aalborg, Denmark

[2]*VELUX A/S*
Ådalsvej 99
2970 Hørsholm, Denmark

**Corresponding author: ph@civil.aau.dk*

ABSTRACT

The paper describes the actual and recent developments with regard to integration of ventilative cooling in building regulations, standards and energy compliance tool in Denmark. The paper also gives some recommendation on what is needed in the future in standards and compliance tools.

KEYWORDS

Ventilative cooling, ventilation standards, building regulation

1 INTRODUCTION

The current development in building energy efficiency in Europe towards nearly-zero energy buildings represents a number of new challenges in Denmark to design and construction of residences. One of the major new challenges is the increased need for cooling present in these highly insulated and airtight residential buildings. Also for the existing building stock energy renovations in many cases lead to elevated temperature levels and cooling needs. This is especially seen in Danish residences from the 70'ies, when large double-glazed facades towards the south are replaced with low-energy glazing and airtight facades.

In most post-occupancy studies of high performance residential buildings elevated temperature levels is the most reported problem. Aalborg University has in the last years carried out investigations of the indoor environment in both new constructions and renovated single family houses and temperature levels above 26-27 C are very often found.
The problem is not only present in the summer months but also in March-April and September-October. Even sometimes during sunny periods in January-February can high temperature levels in south facing spaces be found, (Foldbjerg 2012). Figure 1 shows measured temperatures in the south facing living room of the Active House "Home for life" in Denmark. It is seen that the periods with highest temperatures are in fact in the winter period and considering an adaptive thermal comfort criteria it is also the period with highest risk of perceived overheating. The summer period actually has acceptable conditions. The explanation is that in well-insulated and airtight residences elevated temperature levels are more correlated with the solar radiation load than with the outdoor temperature level, and

with the low level sun in Denmark in winter and spring the solar load has the same maximum radiation level this time of year as in the summer period.

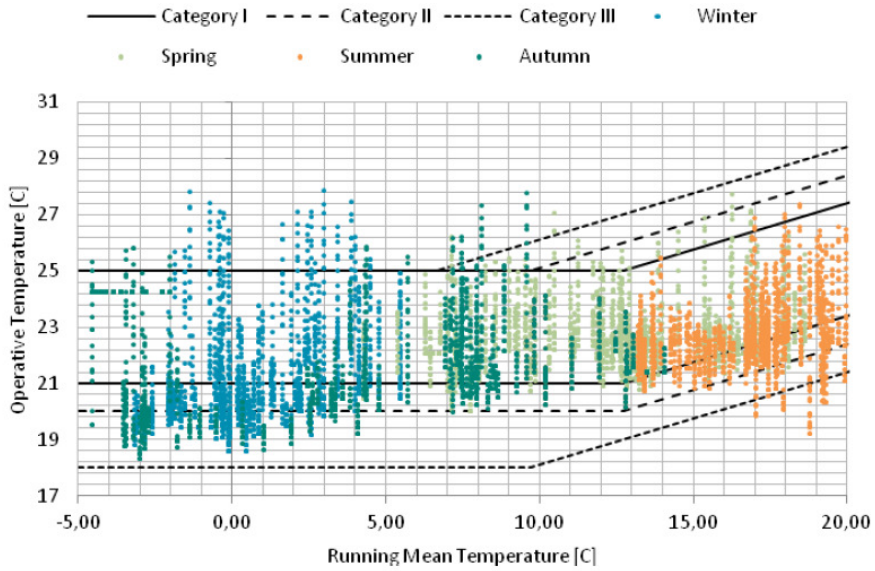

Figure 1: Measures temperature levels in the living room of Home for Life. (Foldbjerg 2012).

In the "Energiparcel project" [Larsen, 2012], where four single family houses were renovated to different energy target levels overheating was the case in three of the four cases. Only in the case with a very deep energy renovation, where energy performance and indoor environment were evaluated in the design phase was temperature levels acceptable, see table 1.

Table 1: Renovation measures and hours of overheating for four renovated single family houses.

	Mejløvænget 9 Seniorhuset	Langøvænget 1 Familiehus - Passiv	Farøvænget 4 Familiehus - Aktiv	Langøvænget 8 Prototypehuset
Tætning og isolering af facader				●
Solceller			●	●
Ovenlys			●	●
Isolering fundament				●
Isolering mod terræn, overalt		●		●
Isolering mod terræn, delvist		●	●	●
Superlavenergi-vinduer, nordfacade				●
Superlavenergi-vinduer, østfacade			●	●
Superlavenergi-vinduer, vestfacade	●	●		●
Superlavenergi-vinduer, sydfacade	●		●	●
Isolering vinduesfalse	●	●	●	●
Automatisk styring, varmeanlæg	●	●	●	●
Isolering rem	●	●	●	●
Isolering loft/tag	●	●	●	●

Temperatur Living Room	Mejløvænget 9	Langøvænget 1	Farøvænget 4	Langøvænget 8
> 26 C (hours)	181	578	180	99
> 27 C (hours)	54	370	60	28

There are a number of different reasons to why we presently are facing this situation.

For residential buildings the design process is much more simplified than for commercial buildings and are to a very large extent based on experiences and rules of thumb. To reach a

low energy need for heating in new building and in energy renovation designers apply guidelines for passive solar buildings developed in the past where insulation and airtightness levels were far from the levels of today. Similarly, designers apply guidelines on the use of building designs with a large thermal mass (energy storage) to exploit solar heat gains optimally for heating. And as they have no previous experience with overheating problems in their previous designs, they underestimate the need for cooling, they underestimate the cooling capacity needed to cool down a high thermal mass construction or might not even take it into account. Prediction of energy use in residential buildings is always based on simplified monthly methods like for example BE10 or PHPP and is estimated for the residence as a whole. Averaging the need for cooling in both time and space underestimates the need for cooling. Excess heat in spaces exposed to solar radiation is considered to be distributed fully to other spaces and excess solar radiation during daytime is partly distributed to night time. Therefore, the need for cooling to ensure acceptable temperature levels in all spaces will be higher in reality. The analysis of the risk of overheating is typically based on the calculated cooling need. Unfortunately, there is no certain correlation between the calculated cooling need with these simplified methods and the number of hours with elevated temperature levels. So, even if no cooling need is predicted and designers do not expect overheating problems, the number of hours with elevated temperature levels can be considerable.

Cooling and overheating in residences have so far not been considered as a design challenge. Therefore, the developed solutions available for application in residences to address the cooling issue are very limited and often too simplified. This leads in the few cases, where the cooling challenge is addressed to design of “one-of-a-kind” solutions, which are expensive and need careful commissioning to function. Finally, also to home owners cooling are an unknown challenge that they have not experienced before. They do not know how to reduce the overheating problem efficiently and their behaviour might in stead actually increase the problem. Or even result in the purchase and installation of air conditioning units, resulting in an increased energy use which could and should be avoided by appropriate use of ventilative cooling and other passive cooling techniques.

Ventilative cooling can be an attractive and energy efficient passive solution to avoid overheating. Ventilation is already present in most buildings through mechanical and/or natural systems using opening of windows and can both remove excess heat gains as well as increase air velocities and thereby widen the thermal comfort range. As cooling becomes a need not only in the summer period the possibilities of utilizing the free cooling potential of low temperature outdoor air increases considerably. However, it is most effective to address the challenge through a combination of passive measures and the potential of other passive measures like solar shading and thermal mass activation as well as strategies for control should be taken into account in the development of ventilative cooling solutions.

However, for the uptake of passive and ventilative cooling in order to realize the energy saving potential, it is essential that standards, regulations and compliance tools provide a fair and easy evaluation of the performance of these systems. Common principles from product solutions over standards and regulations to compliance tools are essential in order to allow ventilative cooling to be utilized in the building sector.

2 VENTILATIVE COOLING IN THE DANISH CONTEXT

The application of ventilative cooling for residential buildings in Denmark is at a low level. There is limited awareness among users and designers of low energy buildings (or deep renovations) on how to cool in an efficient and energy optimal way and except for the use of manual window opening there is no specific systems or components available in the market for automatic opening or control.
For residential buildings, small office buildings, kinder gartens and other "small building projects" the cooling need is usually calculated using the wide spread monthly demand calculation methods, although it is well-known to be quite inaccurate. Overheating risk is very rarely estimated as no easy to use methods exist and hourly based thermal building simulation tools are considered to be too expensive to use in the design process.

The architectural design solutions for residences as well as the requirements for energy performance of windows actually drives the development of building designs towards fewer and larger windows and most of them with fixed frames decreasing the possibilities and flexibilities for window airing and in some building designs airing is limited to opening of doors.

The application level of ventilative cooling for office and commercial buildings with full mechanical ventilation is high and it can be considered as a standard solution. Knowledge, systems and components are commercially available to exploit the cooling capacity of outdoor directly. However, often the increased use of electricity for fans limit the advantage compared to mechanical cooling.

Ventilative cooling with natural or hybrid ventilation is also known, but only used in a relatively few cases in offices. Many modern offices even have a limited number of windows, which can be opened.

For large office and other commercial buildings the cooling need and overheating risk is estimated during the design process using detailed thermal building simulation tools. Performance of night cooling (mechanically or naturally) might also be estimated and appropriate system designs developed.

3 VENTILATIVE COOLING IN DANISH BUILDING REGULATION

The Danish building regulations states in general terms that the thermal environment should be acceptable also in the summer period and state in the guidelines that elevated air velocities (above 0,15 m/s) are acceptable if the indoor temperature exceeds 24^{o}C. For buildings fulfilling the minimum energy requirements the regulations does not provide specific requirements to temperature levels or maximum air velocities but refers to standards (DS/EN ISO 7730 and DS447).

Recently the Danish building regulations have included a requirement for assessment of the risk of overheating in high performance buildings and for acceptable temperature levels in residences. In residences it is required that the temperature level must not exceed 26^{o}C in more than 100 hours/year and 27^{o}C in more than 25 hours/year. For other building types it is required that the building owner sets the limit for hours above 26^{o}C.

However, the methods that can be used to assess this risk convincingly are too detailed for the design of single-family houses and the existing simplified methods (it is allowed to use a simplified method for residences) are not validated for high performance residential buildings, so it is not possible to estimate their usefulness in practice. It is the intention to integrate an official simplified calculation method for overheating risk in the mean monthly energy performance calculation method, but it has not been released yet.

The Danish building regulations allows in general terms to take into account the effect of ventilative cooling, but does not give any guidelines or recommendation on how.

4 VENTILATIVE COOLING IN DANISH STANDARDS

A new Danish Standard on "Ventilation for Buildings – Mechanical, natural and hybrid ventilation systems, DS 447" was issued in the beginning of 2013. This standard is a code of practice and specifies requirements or both mechanical, natural and hybrid ventilation systems.

This standard specifies that possibilities for airing through windows or other openings to the outside are required for every room in residences. It also includes some general guidelines for ventilative cooling by natural ventilation or hybrid ventilation. However, the standard does not give any recommendation on the design of ventilative cooling systems or the calculation of ventilative cooling performance.

The standard give guidelines on the effect of elevated velocities on the thermal comfort. Figure 2 is a figure from the standard showing how much elevated air velocities will increase the acceptable operative temperature. However, the standard does not give any guidelines on how elevated velocities can be achieved and documented.

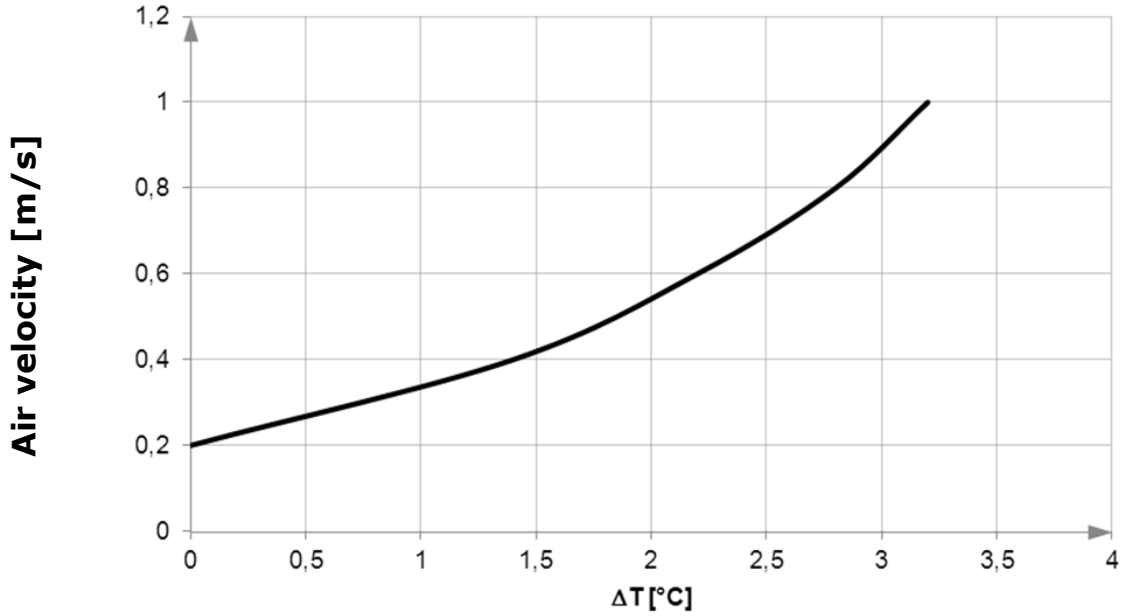

Figure 2: Air velocity vs reduction in temperature sensation. (DS447 and EN 15251).

5 VENTILATIVE COOLING IN DANISH ENERGY COMPLIANCE TOOL

In Denmark the energy compliance tool (BE10) is developed as part of the national mandatory energy rating system. It is based on the mean monthly calculation method and is capable of computing basic estimates of cooling loads, but does not yet include any calculation of the overheating risk of critical rooms.

It is possible in BE10 to specify ventilation airflow rates for ventilative cooling separated in day and night values, respectively. However, for natural ventilation it does not give any guidelines for determining the right values. Only a maximum value to use without the need for documentation is specified. For mechanical systems it is relatively easy to take ventilative cooling into account, while for natural ventilation it is difficult.

"Advanced" ventilative cooling techniques/strategies (e.g. automatic opening of windows as a function of temperature...) cannot be included in the prediction and the method is not able to model passive ventilation techniques such as natural ventilation either. All in all, the potential benefits of ventilative cooling techniques cannot be easily assessed at design stage and the performance documented.

In the design of larger office buildings and other commercial buildings more detailed thermal building calculation tools are used giving better possibilities for evaluating the cooling need and overheating risk properly and for design of ventilative cooling.

6 FUTURE NEEDS IN BUILDING REGULATIONS AND STANDARDS

For the uptake of ventilative cooling and in order to realize the energy saving potential of the technology, it is essential that standards, regulations and compliance tools provide a fair and easy evaluation of the performance of ventilative cooling systems. Common principles from product solutions over standards and regulations to compliance tools are essential in order to allow ventilative cooling to be utilized in the building sector.

At the present stage the Danish compliance tool does not support a fair evaluation of ventilative cooling as part of the calculation procedure. Building regulations and standards support the use of ventilative cooling, mainly in words but without much guidance. Likewise the existing standards are not complete - though covering several aspects.

Several issues should be dealt with consistently in future standards, eg:

- Relevant methods for calculating air change rates during nighttime and daytime in buildings with increased ventilation rates (with the purpose of cooling the building).
- Relevant methods for determining the cooling effect of increased ventilation rates.
- Relevant control for ventilative cooling based on thermal comfort criteria
- Consistent evaluation of relevant effects on indoor climate, including:
    - preference for and acceptance of increased air velocities for air temperatures above 26°C, and recognition of the associated cooling effect (decrease in operative temperature due to air motion)

- use of the adaptive approach for thermal comfort in free-running buildings as applicable to ventilative cooling scenarios in buildings for both daytime and nighttime use

The Danish compliance tool is based on a monthly method, and considers small buildings as one single zone. Averaging the need for cooling in both time and space underestimates the need for cooling. The use of available hourly methods would be an important improvement.

Secondly, there is no certain correlation between the calculated cooling need with these simplified monthly methods and the number of hours with elevated temperature levels. So, even if no cooling need is predicted and designers do not expect overheating problems, the number of hours with elevated temperature levels can be considerable. The compliance tool should facilitate a calculation of the ventilative cooling effects together with the thermal evaluation of the building (risk of overheating).

Finally, an important aspect of efficient use of ventilative cooling is the relation to thermal mass and solar shading. It is important to align the approach to these topics in relevant standards and in compliance tools.

7 REFERENCES

Foldbjerg, P., Worm, A., Asmussen, T., and Feifer, L. 2012. STRATEGIES FOR CONTROLLING THERMAL COMFORT IN A DANISH LOW ENERGY BUILDING: SYSTEM CONFIGURATION AND RESULTS FROM 2 YEARS OF MEASUREMENTS. 33rd AIVC Conference, Copenhagen, Denmark, October 10-11, 2012.

Foldbjerg, P., Hansen, E.K., Feifer, L., and Duer, K. 2011. Measurements of indoor environmental quality and energy performance of 6 European zero carbon houses – a case study from the first house. Proceedings of Indoor Air 2011, Austin, Texas.

Larsen, TS, Daniels, O, Jensen, RL & Andersen, MR 2012, *EnergiParcel-Projektet: Målinger og analyse af energiforbrug og indeklima i 4 danske parcelhusrenoveringer 2008-2011*. Aalborg Universitet. Institut for Byggeri og Anlæg, Aalborg. DCE Technical Reports, nr. 117.

DS 447 Ventilation for Buildings – Mechanical, natural and hybrid ventilations systems. 3rd , February 2013.

EN/DS ISO 7730. Ergonomics in the thermal environment – Analytical determination and interpretation of thermal comfort using calculation of the PMV and PPD indices and local thermal comfort criteria.

RECENT DEVELOPMENTS TO INTEGRATE VENTILATIVE COOLING IN THE AUSTRIAN REGULATORY CONTEXT

Peter Holzer

Dipl.-Ing. Dr. Peter Holzer
Institute of Building Research & Innovation
Luftbadgasse 3/8
1060 Wien, Austria
peter.holzer@building-research.at

ABSTRACT

Within the set of Austria´s national regulations on Thermal Protection in Building Construction the part on Avoidance of summerly Overheating (OENORM B 8110-3:2012) has been relaunched recently. The new regulation offers a method to predict the thermal summer performance of "free-running" rooms an buildings that are not equipped with means of technical cooling.

The new code suggests a dynamic calculation model with precisely defined input parameters, thus filling the gap between either very simple quasi static energy-balance approaches or very sophisticated dynamic building energy models.

The calculation method is open to taking into account measurements of ventilative cooling by night flush ventilation, both from window opening and mechanical ventilation.

The detailed calculation method is based on a dynamic heat balance of a single thermal zone model, according to ISO 13791 (ISO 13791:2004), against a periodic repetition of the very same daily runs of outside solar radiation and temperature.

The result of the detailed calculation method is a daily run of the room's operative temperature.

After one year of application the standard has proven its practical usability, with some learnings, e.g. as regards implication into commercial BEM software and as regards modelling night ventilation together with stack effect.

KEYWORDS

thermal performance of buildings, summerly overheating, night flush ventilation, periodically repeated dynamic simulation

1 INTRODUCTION

Within the set of Austria´s national regulations on *Thermal Protection in Building Construction* the part on *Avoidance of Summerly Overheating* (OENORM B 8110-3:2012) has been relaunched recently. It complies with the international standard ISO 13791 (ISO 13791:2004).

The new regulation offers a method to predict the thermal summer performance of “free-running” rooms or buildings that are not equipped with technical cooling. The calculation method newly takes into account the option of ventilative cooling by night flush ventilation, both from window opening and mechanical ventilation.

The new code suggests a dynamic calculation model with precisely defined input parameters, thus filling the gap between either very simple quasi static energy-balance approaches, offering no chance of integrating effects of ventilative cooling, or very sophisticated dynamic building energy models, being lost in details.

The paper in hands presents the new code and discusses the potentials and limitations of this approach to integrate ventilative cooling in a comparably simple calculation routine.

2 SCOPE OF APPLICATION

The regulation covers the prediction of summerly thermal comfort in buildings or rooms for constant human occupation, such as all rooms within residential flats, offices, classrooms, surgeries and else, as long as there is no mechanical cooling in operation.

Cooling effects of ventilation, both mechanical and natural, may be taken into account, being regarded as means of passive cooling apart from active mechanical cooling.

3 DEFINITION OF SUMMER COMFORT

Within the scope of the regulation, thermal summer comfort of a free running, not mechanically cooled room is defined with the room’s operative temperature, under precisely defined outdoor climate conditions, reaching not more than 27°C and additionally, for sleeping rooms only, with the night-time operative temperature between 22:00 and 06:00 staying below 25°C.

It is a specific quality of the regulation, to define summer comfort against a given outdoor situation, thus leading to robust and comparable key-figures of the thermal room’s performance and limiting the danger of chaotic and not-verifiable outputs.

The outdoor climate conditions are defined as the characteristic terrestric run of solar irradiation and outdoor temperature, at the specific site, during a mid-July clear summer day, being assumed to occur in infinite periodic repetition.

4 SIMPLIFIED CALCULATION METHOD

Remaining from the code's 1999 version there still exists a simplified calculation method, which just balances the thermal gains and the thermal masses against a very much simplified and standardized assumption of air change rate an only leads to the output of a yes/no as regards summerly overheating. Effects of Ventilative Cooling cannot be taken into account adequately with this simplified method.

5 DETAILED CALCULATION METHOD

Beside the simplified method there's the detailed one, calculating the daily operative temperature curve within the room, offering adequate options to include Ventilative Cooling both by window opening and mechanical ventilation.

5.1 The Calculation Principle

The detailed calculation method is based on a dynamic heat balance of a single thermal zone model, according to ISO 13791 (ISO 13791:2004), against a periodic repetition of the very same daily runs of outside solar radiation and temperature.

In physical means it's a periodically settled system that is investigated. Practically, the thermal performance of the room is investigated against the assumption of an ongoing summerly heat wave.

Together with a strict definition of the climatic input parameters this system delivers very accurate and highly comparable results, eliminating the confusion that's very often incorporated in results of thermal simulation runs without a strict definition of outdoor and indoor conditions.

As regards simulation tool the user is free to choose any appropriate software, as long as it complies with ISO 13791 (ISO 13791:2004).

5.2 Outdoor Climate

The outdoor temperature to be taken into account is derived from the site-sensitive daily outside mean temperature, defined as the temperature which is statistically exceeded in 130 hours within 10 years, which then is superimposed on a given daily temperature amplitude of ±7 K. The result is a site sensitive outside temperature run for a design day which represents a significantly warm summer day. Together with the principle of periodically repeated heat balance, the outdoor temperature, defined this way, characterizes a long lasting summerly heat wave.

The outdoor solar radiation is to be calculated for the solar geometry of July 15th, according to a given set of formula, including a turbidity factor according to Reitz of 0,333 and an albedo of 0,2.

For further details, the national code refers to ISO 13791 (ISO 13791:2004) as regards sky temperature and to ISO 13370 (ISO 13370:2007) as regards ground temperature.

5.3 Room Geometry and Thermal Properties

The room geometry is open to realistic modelling according to the simulation software's capabilities. It might be important to note, that, apart from the convention from simplified energy demand calculations, all heights, lengths and widths of the room's building elements should be input in their internal dimensions, not including the thickness of the building construction.

Similar, the thermal properties together with the radiation-related properties may be modelled according to ISO 13786 (ISO 13786:2007) respectively according to the algorithms of the simulation tool in use, if it's in compliance with ISO 13791 (ISO 13791:2004).

5.4 Shading

To model the effect of shading devices as well as of fixed obstacles, a number of default values are given, together with requirements as regards wind resistance and else, not at least ensuring the full operating capability of mechanical shading devices under site specific wind loads.

Solar protection devices combined with glazing according to ÖNORM EN 13363-1 (EN 13363-1:2003+A1:2007) and according to ÖNORM EN 13363-2 (EN 13363:2006)

Performance requirements of external blinds according to ÖNORM EN 13561 (EN 13561:2004+A1:2008)

Performance requirements of shutters according to ÖNORM EN 13659 (EN 13659: 2004+A1:2008)

5.5 Internal Heat Load and Hygienic Airflow Profiles

For five different kinds of characteristic room usages, hourly values are defined, covering the specific internal loads of equipment and people and covering the hygienically necessary air flow rates, apart from possible contributions of ventilative cooling, which might be superimposed. If there are higher loads or higher ventilation rates expected, they have to be taken into account alternatively.

5.6 Ventilation

Additional ventilation schedules may be introduced, beside the hygienically necessary air exchange rates. This may be done by mechanical or by natural ventilation.

If done by mechanical means, strict requirements are set to prove an acceptable level of noise imission to the room. Additionally, the thermal load from the vents has to be included into the heat balance of the room.

As regards natural window ventilation, the air flow is calculated from formula (1), estimating a window's air flow rate out of its dimensions and out of the momentary temperature difference between inside and outside air.

$$\dot{V} = 0{,}7 \cdot C_{\text{ref}} \cdot A \cdot \sqrt{H} \cdot \sqrt{\Delta T} \tag{1}$$

together with $C_{ref} = 100\ m^{0,5}/(hK^{0,5})$

together with the following interpretations of H (height) and A (area).

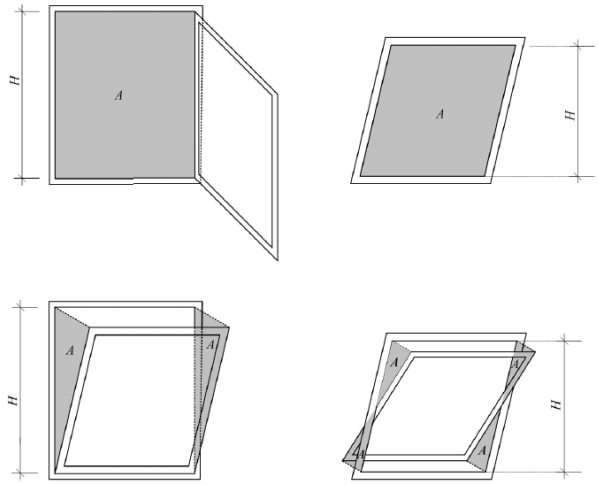

Figure 1: Interpretation of H and A within formula (1)

If windows are placed at more than one level, formula (2) is suggested.

$$\dot{V} = 0{,}7 \cdot C_{\text{ref}} \cdot A_{\text{eff}} \cdot \sqrt{H} \cdot \sqrt{\Delta T} \qquad (2)$$

together with $C_{ref} = 300\ m^{0,5}/(hK^{0,5})$

together with $A_{\text{eff}} = \sqrt{\frac{1}{\frac{1}{A^2_{\text{oben}}} + \frac{1}{A^2_{\text{unten}}}}}$

together with the following interpretations of H (height) and A (area).

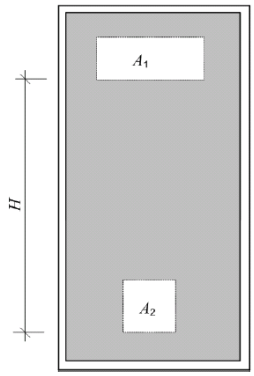

Figure 2: Interpretation of H and A within formula (2)

Both formulas take into account only the temperature driven component of the air flow, without any assumption of wind driven airflow. Thus, the outputs are conservative and “on the save side”.

Driven by the hourly values of external and internal air temperatures used in the dynamic energy balance model, the airflow through windows is calculated in hourly steps, too.

Figure (3) exemplarily shows the air flow resulting from opening tilting a window of 40 cm width and 120cm height, at increasing temperature difference between inside and outside air, according to formula (1).

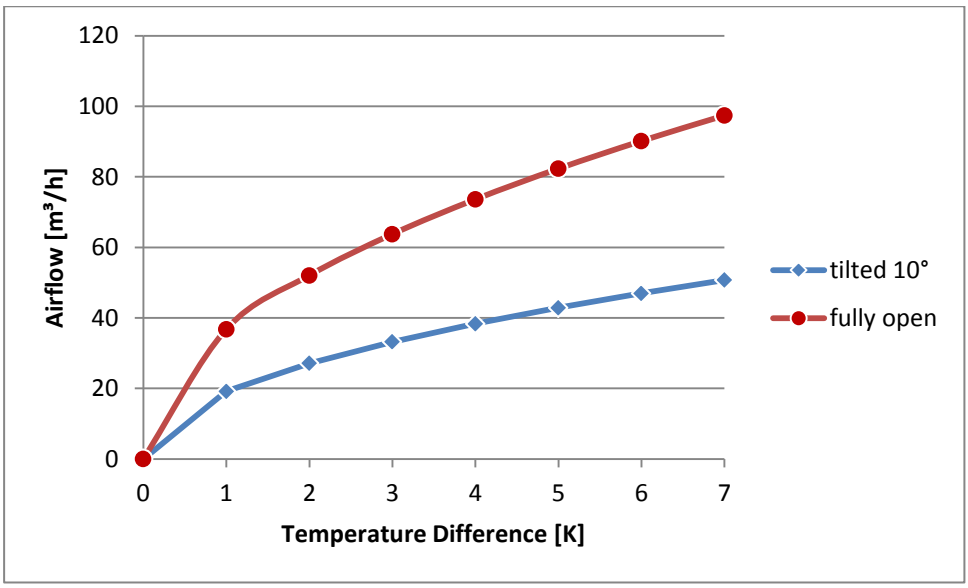

Figure 3: Air flow through a W=40cm, H=120cm window, according to formula (1)

Additional to formulas (1) and (2) the regulation sets a nuber of strict requirements as regards usability of the window opening together with weather events, safety aspects, noise emission aspects and else.

6 CRITICAL DISCUSSION AND CONCLUSION

The newly relaunched Austrian code ÖNORM B 8110-3:2012 *Thermal Protection in Building Construction - Avoidance of summerly Overheating* contains a well applicable method of predicting or restricting the danger of summerly overheating of rooms without mechanical cooling.

Effects of Ventilative Cooling can be taken into account both for mechanical and for natural, window-based solutions.

The physical principle of a periodically repeated dynamic heat balance leads to robust and highly comparable outputs, given in a daily run of the room's operative temperature.

The code offers an appreciable and practical step towards integration of ventilative cooling into the regulatory context.

Still, in practical application there occur some challenges:

Firstly commercial simulation software products usually aren't prepared to calculate the air flow through windows exactly according to formula (1). The user is forced to program workarounds, which turns out to be a bottleneck when practically integrating the calculation routine into the professional Building Energy Modelling business.

Secondly, the calculation model reaches its limits, when a number of windows at one level are combined with one or more windows at other levels. If so, it's up to the user to estimate the position of the neutral horizontal layer and to very carefully apply formula (1) and (2) in combination.

Furthermore, above the scope of the code, it still is a point of discussion, how to define the summer performance of buildings with thermal mass activation but without Air-Conditioning: By definition those buildings are mechanically cooled. By perception they are very much anticipated as free running mode buildings. It's worth a consideration to include them in the scope of the calculation methods of free running mode buildings.

7 ACKNOWLEDGEMENTS

The Austrian Standard ÖNORM B 8110-3:2012 was elaborated by the standardization committee 175, working group 01, which the author is member of, under the leadership of
Ao. Univ. Prof. Dipl-Ing. Dr. techn. Thomas Bednar,
Institute of Building Constructions and Technology
Research Center for Building Physics and Sound Protection
Vienna University of Technology, Austria

8 REFERENCES

ÖNORM EN 13363-1, Solar protection devices combined with glazing - Calculation of total solar energy transmittance and light transmittance - Simplified calculation method (EN 13363-1:2003+A1:2007)

ÖNORM EN 13363-2, Solar protection devices combined with glazing - Calculation of total solar energy transmittance and light transmittance - Detailed calculation method (EN 13363:2006)

ÖNORM EN ISO 13370, Thermal performance of buildings -- Heat transfer via the ground -- Calculation methods (ISO 13370:2007)

ÖNORM EN 13561, External blinds – Performance requirements including safety (EN 13561:2004+A1:2008)

ÖNORM EN 13659, Shutters – Performance requirements including safety (EN 13659:2004+A1:2008)

ÖNORM EN ISO 13786, Thermal performance of building components -- Dynamic thermal characteristics -- Calculation methods (ISO 13786:2007)

ÖNORM EN ISO 13791, Thermal performance of buildings -- Calculation of internal temperatures of a room in summer without mechnical cooling -- General criteria and validation procedures (ISO 13791:2004)

ÖNORM B 8110-3, Thermal Protection in Building Construction – Avoidance of summerly overheating (OENORM B 8110-3:2012)

MARKET TRANSFORMATION TOWARDS NEARLY ZERO ENERGY BUILDINGS THROUGH WIDESPREAD USE OF INTEGRATED ENERGY DESIGN

Theoni Karlessi*[1], Mat Santamouris*[1], Stefan Amann[2], Klemens Leutgöb[2]

[1]*National and Kapodestrian University of Athens, Building of Physics - 5, University Campus, 157 84 Athens, Greece*

[2] *e7 Energie Markt Analyse GmbH, Theresianumgasse 7/1/8, 1040 Vienna, Austria*
**Corresponding author: karlessith@phys.uoa.gr*

ABSTRACT

ID is a design procedure that considers the building as a whole system with the aim of optimizing it throughout the lifecycle. ID can be used to reach high ambitions by developing, discussing and evaluating a scheme using a multidisciplinary team from the initial design phases and it is a proven approach for achieving high-performance buildings with good indoor environment without sacrificing architectural quality or result in excessive costs. Integrated Design support designers in delivering buildings which satisfy occupant's needs much more than conventionally designed buildings.
Towards this direction MaTrID project supports the implementation of directive 2010/31/EU by widespread market adoption of ID on the national level. The main targets of MaTrID are:
- Establishing the general understanding on the advantages and requirements of ID
- Improving the know-how basis on ID
- Testing the practical implementation of ID on a large scale
- Development of a common tool-kit for the integrated energy design of NZEB
- Adaptation of the common tool-kit to national requirements
- Implementing EU-wide promotion and dissemination activities
- Drawing conclusions for a further market adoption

The benefit of EU collaboration is to link good practices among leading European countries (including clients, private industry, public sector, etc.). Knowledge transfer among Europe and various actors is the main benefit of MaTrID.

KEYWORDS

nearly zero energy buildings, integrated design

1 INTRODUCTION

Buildings account for around 40% of total energy consumption and 36% of CO2 emissions in Europe. The reduction of energy consumption and the use of energy from renewable sources in the buildings sector therefore constitute important measures which are needed to reduce energy dependency and greenhouse gas emissions. The mitigation potential of emissions from buildings is important and as much as 80% of the operational costs of standard new buildings

can be saved through integrated design principles, often at no or little extra cost over the lifetime of the measure. The recast Directive on the energy performance of buildings (EPBD) stipulates that by 2020 all new buildings constructed within the European Union after 2020 should reach nearly zero energy levels. This means that in less than one decade, all new buildings will demonstrate very high energy performance and their reduced or very low energy needs will be significantly covered by renewable energy sources.
In parallel, Member States shall draw up national action plans for increasing the number of nearly zero-energy buildings (NZEB). These national action plans shall include policies and measures to stimulate the transformation of existing buildings which are refurbished into nearly zero-energy buildings. In addition, by 2015 all new buildings and buildings undergoing major renovation must have minimum levels of energy from renewable sources. The implementation of these policy goals requires a major transformation in the building sector during the next few years.
The design of NZEB requires an interdisciplinary approach. Reducing the energy demand in the design phase demands specifications of the different designers and engineers such as architects, building physics or façade designers. For the demand side concept of a building the best possible heating or ventilation system should be applied. Activating of thermal mass for example requires the interaction between the structural designer and HVAC engineers. Alternative energy systems have to fit to the concept design and the building energy systems. For this reason, the introduction of a design team is compulsory for the design of NZEBs.
In this context the building design phase is of particular importance. IED is a valuable assisting approach to reduce the complexity of the design process, to ensure the implementation of defined, to identify pros and cons of alternative variants of design concepts and to allow decision makers to decide based on transparent facts. Only if IED is applied from the very beginning of the design phase we can assume that a cost-effective solution for NZEB can be identified, because only at the early design phases changes of the general design concept can be implemented at low cost. Therefore, the application of IED is part of the best way towards the intended NZEB at low cost. Experience from several demonstration and pilot projects shows that IED frequently leads to highly energy efficient solutions at least cost over the life cycle of the building, because the integration of all required expertise already in the early design phase brings forward easy and thus cost-efficient solutions.
The objectives of the proposed project have been identified based on an in- depth assessment of barriers for IED resp. on the preconditions which are required for a practical application of the IED approach. Activities are needed on the side of the building owner (developer) as well as on the side of designers. Starting from this, the following specific project objectives can be derived:

- Establishing the general understanding on the advantages and requirements of ID
- Improving the know-how basis on ID
- Testing the practical implementation of ID on a large scale
- Development of a common tool-kit for the integrated energy design of NZEB
- Adaptation of the common tool-kit to national requirements
- Implementing EU-wide promotion and dissemination activities
- Drawing conclusions for a further market adoption

The construction, architects and engineering market is very much focused on regional and local level. Additionally, the state of the art for IED in each country is different. For this reason, the emphasis of the project is on widespread market adoption on national level.

2 PRINCIPLES FOR NEARLY ZERO-ENERGY BUILDINGS

Directive 2010/31/EU (EPBD recast) Article 9 requires that "Member States shall ensure that by 31 December 2020 all new buildings are nearly zero-energy buildings; and after 31 December 2018, new buildings occupied and owned by public authorities are nearly zero-energy buildings". Member States shall furthermore *"*draw up national plans for increasing the number of nearly zero-energy buildings*"* and *"*following the leading example of the public sector, develop policies and take measures such as the setting of targets in order to stimulate the transformation of buildings that are refurbished into nearly zero-energy buildings*"*.

A nearly zero-energy building is defined in Article 2 of the EPBD recast as *"*a building that has a very high energy performance. The nearly zero or very low amount of energy required should be covered to a very significant extent by energy from renewable sources, including energy from renewable sources produced on-site or nearby*"*.

The specific EPBD Concerted Action activities around **"**Towards 2020 - Nearly zero-energy buildings**"** will support the Member States by the exchange of experiences with already existing high performance buildings(ranging from low energy buildings to passive houses, zero-energy and zero-emission buildings, and even to energy surplus houses).

The discussion topics include the most common building and service system solutions**,** calculation methods**,** promotional means, available subsidies and other incentives**,** supporting documents (e.g. guidelines), etc., as well as study tours to interact with experts at national administrations and visits to relevant sites.

The different national applications of the definition of nearly zero-energy buildings are presented and compared: front-runner countries receive a feedback and other countries gather inspiration for their own application.

Through such information exchange, Member States participants furthermore support each other in the development of the national plans for increasing the number of nearly zero-energy buildings**.**

To achieve a suitable definition, related facts and findings need to be seen in a broader societal context and need to be transferred into a practical standard, taking into account financial, legal, technical and environmental aspects. Analysing the implications identified above, it becomes obvious that most of them interact or require the consideration of one or several societal aspects. Consequently, the principles for an nZEB definition should be built on the same broad perspective, should take into account all financial, legal, technical and environmental aspects and should meet the present and future challenges and benefits. Hence, a proper and feasible nZEB definition should have the following characteristics (Thomsen, K.E., 2011):

- To be clear in its aims and terms, to avoid misunderstandings and implementation failures.
- To be technically and financially feasible.
- To be sufficiently flexible and adaptable to local climate conditions, building traditions etc., without compromising the overall aim.
- To build on the existing low-energy standards and practices.
- To allow and even foster open competition between different technologies.
- To be ambitious in terms of environmental impact and to be elaborated as an open concept, able to keep pace with the technology development.
- To be elaborated based on a wide agreement of the main stakeholders (politicians, designers, industry, investors, users etc.).
- To be inspiring and to stimulate the appetite for faster adoption.

Consequently, there are three basic principles, each one with a corollary for setting up a proper nZEB definition, addressing the three main reasons and aims for regulating the building sector: reduced energy demand, the use of renewable energy and reduced associated GHG emissions.

1. Energy demand
There should be a clearly defined boundary in the energy flow related to the operation of the building that defines the energy quality of the energy demand with clear guidance on how to assess corresponding values.
2. Renewable energy share
There should be a clearly defined boundary in the energy flow related to the operation of the building where the share of renewable energy is calculated or measured with clear guidance on how to assess this share.
3. Primary energy and CO2 emissions
There should be a clearly defined boundary in the energy flow related to the operation of the building where the overarching primary energy demand and CO2 emissions are calculated with clear guidance on how to assess these values.

3 THE INTEGRATED DESIGN PROCESS

Integrated design is an approach that considers the design process as well as the physical solutions, and the overall goal is to optimize buildings as whole systems throughout the lifecycle. Firstly, for the purpose of reaching high sustainability performance, the alternative building and technical solutions should be developed and discussed by an *integrated*, multidisciplinary team. ID emphasizes a decision process rooted in informed choices with regard to the project goals, and on systematic evaluation of design proposals. This approach for building design is paralleling the principles of environmental management referred in the international ISO 14001 standards. Here, identifying and prioritizing goals, and developing an evaluation plan with milestones for follow-up, are central issues.
A shift of approach emphasizes that the very early phases need more attention because well informed decisions here will pay off in the rest of the design process as well as in the lifecycle of the building. Well informed planning from the start can allow buildings to reach very low energy use and reduced operating costs at very little extra capital cost, if any. Considering the whole life cycle of a building, the running costs are higher than construction and refurbishment costs; thus, it becomes obvious that it is a shortsighted approach to squeeze the first design phase regarding resources. Experience from building projects applying ID shows that the investment costs may be about 5 % higher, but the annual running costs will be reduced by as much as 40-90 %. The process of ID emphasizes that the performance of buildings should be assessed in a lifecycle perspective, both regarding costs (LCC) and environmental performance (LCA). Figure 1 indicates the importance of the integrated design process at the early phases (Norby, A.S., 2013).

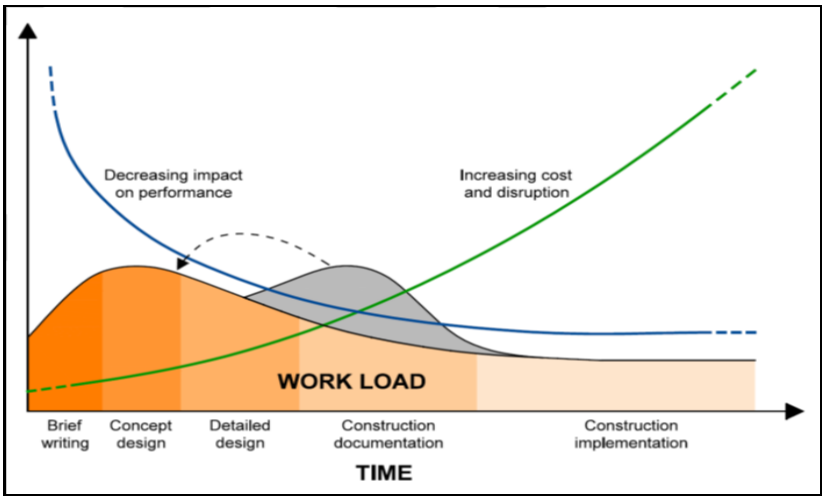

Figure 1. Early design phases offer opportunity for large impact on performance to the lowest costs and disruption. Therefore, a shift of work load and enhancement to the early phases will probably pay off in the lifecycle of the building.

3.1 The benefits

- Higher energy performance
Optimization of building form, orientation and facades is reached through open multidisciplinary discussions and design decisions in early project phases, where knowledge about important conditions is exchanged to inform the design of the building.
- Reduced embodied carbon
Optimized design is given priority before advanced technical systems and control mechanisms. The high embodied carbon of HVAC components are thus reduced.
- Optimized indoor climate
The building and technical systems work together in a logical symbiosis in order to achieve sufficient indoor air quality, temperature control and daylight access/ solar protection
- Lower running costs
Simplified technical systems are more cost efficient, both in terms of investment costs for manufacturing and installation and in terms of running costs and maintenance.
- Reduction of risks and construction defects
Improved planning leads to less building faults. Thus; less claiming, and money saved.
- More user involvement
Early involvement of users and inclusion of user needs in the design process may improve the following performance of the building in the operation phase, as well as increase user satisfaction.
- Higher value
A high performance building can yield higher rental costs which can be compensated for by a lower energy bill thus the sales value of the building will increase.
- Green image and exposure of the building
A green image can benefit the building owner or tenant organization.

3.2 The barriers

- Conventional thinking
The building sector is known for being slow accepting new ways of working. ID calls for decision processes and design methods that challenge familiar habits, and require high communication skills. Professionals on both sides of the table must practice in collaboration, and maybe adjust their working habits.
- ID seems to costs too much
Developers traditionally pay more attention to construction costs than lifecycle costs (LCC). However, when energy consumption and maintenance is included in the calculations, it usually supports investments in planning for high performance and robust solutions.
- Time constraints in initial design phase
Often developers underestimate the value of thoroughly planning, and expect high speed in conceptualizing a building. It can be challenging to convince the developer that the initial phase is crucial, and that giving time for design iterations often pay off in better concepts.
- “Skills tyranny”
As the ID process requires more collaboration between stakeholders who may have diverging goals, conflicts could be accentuated. It is therefore necessary that the team members do not insist on ultimate demands within their fields of expertise, but rather endeavour to work with a holistic approach.

3.3 The principles

Six steps can be identified for a successful integrated design implementation (Figure 2):

- Project development: this includes the discussion of the project ambitions and challenge initial client presumptions, initiating ID process and preferably make partnering contracts
- Design basis: selection of a multi-disciplinary design team, including an ID facilitator, motivated for close operation, analysis of the boundary conditions. Also refine the brief and specify the project ambitions, preferably as functional goals
- Iterative problem solving: facilitate close operation between the architect, engineers and relevant experts through workshops etc. Use of both creative and analytical techniques in the design process. Discussion and evaluation of the multiple concepts and finalise optimised design.
- On track monitoring: Use goals/ targets as means of measuring success of design proposals, make a Quality Control Plan, evaluate the design and document the achievements at critical points/milestones
- Delivery: Ensure that the goals are properly defined and communicated in the tender documents and building contracts, motivate and educate construction workers and apply appropriate quality tests, facilitate soft landing. Make a user manual for operation and maintenance of the building
- In use: Facilitate commissioning and check that the technical systems etc. are working as assumed, monitor the building performance over time regarding e.g. energy consumption, user satisfaction etc.

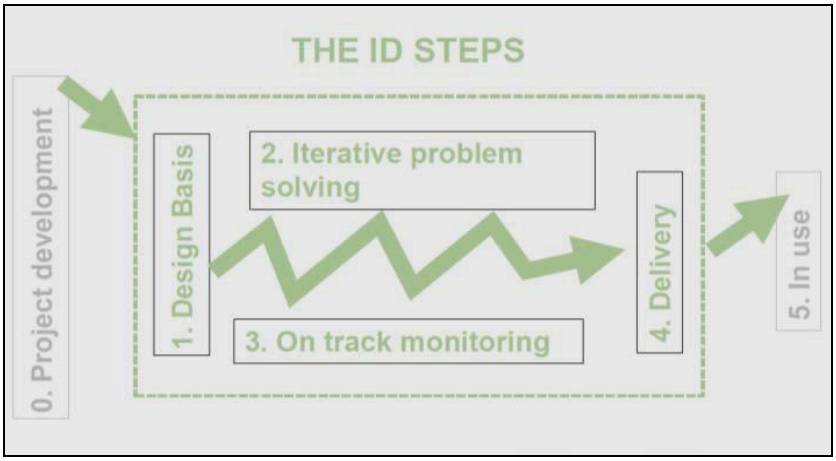

Figure 2. Overview of the ID process.

4 THE MATRID PROJECT

MaTrID aims to support the implementation of Nearly Zero Energy Buildings by 2020. In this context the building design phase is of particular importance. Integrated Energy Design (IED) is a valuable approach to reduce the complexity of the design process and facilitate the interactions between the members of the design team. IED allows them to provide the best solution for the whole building. MaTrID's targets are harmonized with the integrated design process as described in the previous section (.Leutgöb, K. 2012)

4.1 Objectives

The objectives of the proposed project have been identified based on a holistic IED approach. Activities are needed on the side of the building owner (developer) as well as on the side of designers. Starting from this, the following specific project objectives can be derived:

1. Establishing the general understanding on the advantages and requirements of IED at the side of real estate developers and building owners: In this context, the project aims at convincing opinion leaders of builder's associations, big property developers or other multipliers that IED is the way to be chosen for the design of cost-efficient NZEB.
2. Improving the know-how basis on IED: The application of IED requires practical know-how on the developer's side as well as on the designers' side. Therefore the project aims at developing practical tools, such as specific text modules for client briefs as well as for IED related contracts and remuneration models.
3. Testing the practical implementation of IED on a large scale thus setting best practice examples which can be easily copied and multiplied
4. Development of a common tool-kit for the integrated energy design of NZEB
   - Clients brief for NZEB
   - IED-related model contracts
   - IED-friendly remunerations models
   - User-friendly IED guideline
5. Adaptation of the common tool-kit to national requirements
6. Implementing EU-wide promotion and dissemination activities
7. Drawing conclusions for a further market adoption of IED in the years after the end of the project including also practical recommendations on possible policy instruments that may support the widespread use of IED on daily design practice.

4.2 Focus area

The construction, architects and engineering market is very much focused on regional and local level. Additionally, the state of the art for IED in the participating countries is very different. For this reason, the emphasis of the project is on widespread market adoption on national level. National activities are country specific and reflect the respective demand.

4.3 Benefits

The greatest benefits are provided only if applied in the earliest stages of the project, when changes to the design are still easy to implement. The benefit of EU collaboration is to cross-pollinate good practices among leading European countries (including clients, private industry, public sector, etc.). Knowledge transfer among Europe and various actors is the main benefit of MaTrID.

4.4 Outcomes

The outcomes of the project can be summarised as follows:

- A general understanding on the advantages and requirements of IED on the part of real estate developers and building owners as well as on the designers' side.
- Practical tools – such as specific text modules for client briefs as well as for IED related contracts and remuneration models – which can be directly applied in daily practice.
- Successfully tested pilot projects with practical implementation of IED on a large scale. Examples can be easily copied and multiplied.
- General acknowledgement of IED beyond the limits of the participating countries.
- Conclusions for a further market adoption of IED in the years after the end of the project including also practical recommendations on possible policy instruments that may support the widespread use of IED on daily design practice.

A specific award will give European visibility to outstanding ID processes. This award will contribute in spreading the ID approach, in highlighting its advantages and in showing possible and feasible ways to reach advanced building targets.

5 CONCLUSIONS

The European Union (EU) aims at drastic reductions in domestic greenhouse gas (GHG) emissions of 80% by 2050 compared to 1990 levels. The building stock is responsible for a major share of GHG emissions and should achieve even higher reductions of at least 88% - 91%i. Therefore, without consequently exploiting the huge savings potential attributed to the building stock, the EU will miss its reduction targets. More than one quarter of the 2050s building stock is still to be built. The energy consumption and related GHG emissions of those new buildings need to be close to zero in order to reach the EU's highly ambitious targets. The recast of the Energy Performance of Buildings Directive (EPBD) introduced, in Article 9, "nearly Zero -Energy Buildings" (nZEB) as a future requirement to be implemented from 2019 onwards for public buildings and from 2021 onwards for all new buildings

Integrated Design (ID) is necessary in managing the complex issues arising from planning buildings with high energy- and environmental ambitions. In these processes, emphasis is on collaboration in multidisciplinary teams as well as on clear goal-setting and systematic monitoring. In the early design phases, the opportunity to positively influence building performance is great, while cost and disruptions associated with design changes are very small.

The guiding strategic objective of the MarTrID project is to contribute significantly to a widespread market adoption of integrated energy design of buildings. IED should become the standard way of European building design within 2020. As a result real estate industry will find it easier to cope with the challenges coming from energy and climate change policy by producing sustainable buildings with very high energy performance in a cost-effective way, calculated over the life cycle of the building.

6 REFERENCES

Thomsen, K.E., Hermelink, A., Schimschar, S., Rose, J., Aggerholm, S., O., Boermans, T., Grozinger, J., Offermann, M. (2011) *Principles For Nearly Zero-energy Buildings, BPIE*

Leutgöb, K. (2012). *Intelligent Energy Europe- Annex 1 Description of the Action MaTrID Project* http://www.integrateddesign.eu

Norby, A. S. (2013) *MaTrID ID process guideline*

Intelligent Energy Europe (2009) *Integrated Energy Design- Some principles of low energy building design*

Official Journal of the European Union- Directive 2010/31/EU of the European Parliament and of the Council on the energy performance of buildings (recast)

THE FIRST DUTCH PASSIVE HOUSE AND PLUS ENERGY SCHOOLS: SOME DUTCH IAQ EXPERIENCES IN SCHOOLS

Wim Zeiler, Mark de Waard and Gert Boxem

TU Eindhoven
Den Dolech 2
Eindhoven, Netherlands
w.zeiler@bwk.tue.nl

ABSTRACT

Ventilation is especially important to get a good Indoor Air Quality in schools. This is important as the young children have very vulnerable still developing longs which are very sensitive to all kind of pollutions. During the last decade different types of sustainable schools were built. The first schools were like very well insulated schools up to the Passive House standard. The next step in this development are schools which generate more energy hat they need themselves: Plus Energy schools. In 2011 a first school of this type was built in the Netherlands. The evaluation of the indoor quality and comfort conditions of this school and two recently finished Passiv House schools was done by measurements as well as questionnaires. The results will be combined with those of two earlier studies on energy efficient schools (in total 8 schools) and compared with those of a recent other study in which 12 more traditionally designed and recently built Dutch schools were examined. This enabled us to compare the new sustainable school designs with the more traditional school types. It proved that the design outcome on IAQ and perceived comfort of the latest sustainable schools were on average better than the earlier designed sustainable schools however they not better than the recent traditional designed schools. So we conclude that extra care should be taken by designers to healthy indoor environment aspects especially when designing energy efficient schools.

KEYWORDS

School ventilation, sustainable schools,Indoor Air Quality

1 INTRODUCTION

The energy use of school buildings became a critical factor in the design during the last decennia as the sustainability demands are getting tighter. However although energy is very important we should not forget the indoor air quality, necessary attention level and health of the vulnerable children as they spent a large part of their time in school. Therefore it is very important that the Indoor Air Quality of a school is good. Although the indoor environment is very important for the health and concentration of children often Indoor Air Quality in schools is still problematic in many countries (Clements-Croome et al 2008, Hellwig 2010, Bakó-Biró et al 2011, Hani et al 2011, Mercier et al. 2011, Salleh et al 2011, Al-Rashidi et al 2012, Montazami et al 2012, Mydlarz et al 2012, Wargocki and Wyon 2012, Satish et al 2012).
Indoor Air Quality in schools is primarily evaluated by CO_2-concentrations. ASHRAE Standard 62-1999 recommends an indoor CO_2-concentration of less than 700 ppm above the outdoor concentration, which means around 1200 ppm, to satisfy comfort criteria with respect

to human bio effluents. Dutch schools have to meet the Dutch Building Code, which recommends a level of 1000 ppm CO_2-concentration with a maximum of 1200 ppm. The latest Dutch design guide, ISSO publication no. 89 (ISSO 2008) should lead the path to better IAQ in schools, see Table 1.

Table 1. Different classes for IAQ regarding CO2-content

Class	A (Very good)	B (Good)	C (Acceptable)	D (Insufficient)
CO_2 content (ppm)	95%of total school hours < 800	95% of total school hours 800 - 1000	95% of total school hours 1000 - 1200	95% of total school hours > 1200

However if we look at the results of earlier Dutch studies on school ventilation (Zeiler and Boxem 2007), it shows that there is no adequate Indoor Air Quality on quite a number of schools.

2 METHODOLOGY

To investigate the results of the sustainable schools during a week measurements were done concerning indoor air quality and comfort. To characterize the indoor air quality and thermal comfort in the three different schools, measurements are being executed using a measurement pole which measured 5 different parameters: Indoor temperature, Radiant temperature. Relative humidity, Indoor air velocity and CO_2 concentration. The different sensors were placed a tripod put in a classroom.

Table 2: Used measurement equipment

Type of measurement	**Equipment**	**Brand**	**TU/e ID**	**Range**
Temperature	Sensor	EE80	2335	0° - 40°C
Radiant temperature	Black sphere PT100	-	612	-100° - 300°C
Relative humidity	Sensor	EE80	2335	0 - 100%
Air velocity	Omni speedometer	Sensor HT428	708	0.05 - 5 m/s
CO_2 -concentration	Sensor	EE80	2335	0 - 5000 ppm
Log data	Data logger 2F8	Grant 2020 series	1816	n.v.t.
Process data	Laptop	Dell Latitude C840	1629	n.v.t.

In all schools also questionnaires were given to the teachers to get an impression of the satisfaction of the users, with regard to thermal comfort and perceived indoor air quality. The questionnaire used was based on the validated list which has been developed in the Health Optimization Protocol for Energy-efficient Buildings research (HOPE 2001).

2.1 School A

Number of students	285
Number of staff	24
Classrooms	11
Gross floor area	1475m²
Date completion	2012
Ventilation	Mechanical supply and exhaust
Heating/cooling	Heating by ventilation system

School A is the first passive school in the Netherlands. The construction of the school was finished in July 2011. It was build according to the passive house principle which meant extreme air tightness, triple glazing and highly insulation with a Rc = 10 m²K/W. The

conditioning is done by individual room ventilation systems with heat exchangers. The air distribution is by textile ducts, see Fig.1 .

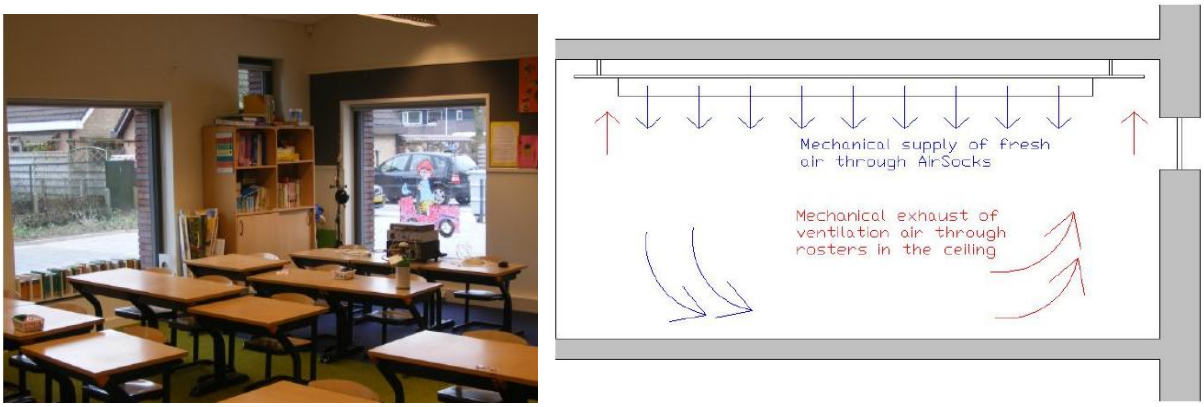

Figure 1. School A first passive house school with air distribution through textile ducts

2.2 School B

Number of students	210
Number of staff	40
Classrooms	20
Date completion	2011
Ventilation	Mechanical supply and exhaust
Heating/cooling	Heating by the ventilation system

In 2009 the Dutch government initiated the so called UKP NESK program to stimulate innovation for energy neutral buildings. UKP means unique chances projects and NESK means 'Towards energy neutral schools and offices' (Naar Energieneutrale Scholen en Kantoren). School B is the first school within the UKP NESK program that was finished, see Fig. 2. The energy concept of the school is based on applying the Passive house-concept, with an average insulation with a Rc-value of 10 m^2W/K and triple glazing. The school has a ground source heat pump, low temperature floor heating system and balanced mechanical ventilation with 85% heat recovery. IAQ is control on a maximum CO_2-level of 800 ppm.

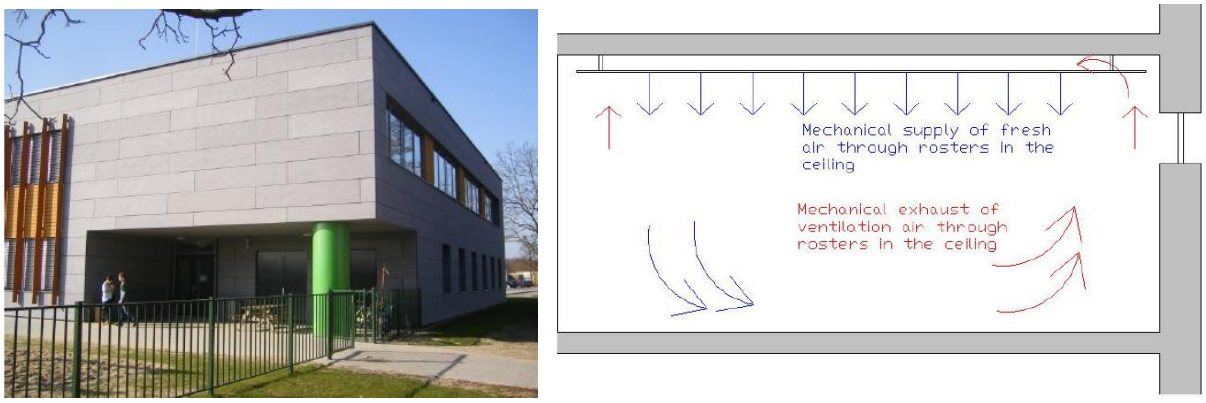

Figure 2. School B UKP NESK school with mechanical air supply through grills in ceiling

2.3 School C

Number of students	**472**
Number of staff	**73**
Classrooms	**42**

Gross floor area	**7800m²**
Date completion	**2010**
Ventilation	**Mechanical supply and exhaust**
Heating/cooling	**Floor heating/cooling**

This is the first CO2-neutral and energy plus school in the Netherlands. The indoor climate is regulated with a floor heating / cooling system with a ground source heat pump. The school has an Energy Roof, a combination of PV and thermal collectors integrated into its roof cover, which generates over a whole year more energy than the school needs for its own use. A balanced ventilation system is used to provide sufficient fresh air in the classrooms and this can be used for additional cooling during the summer, see Fig.3.

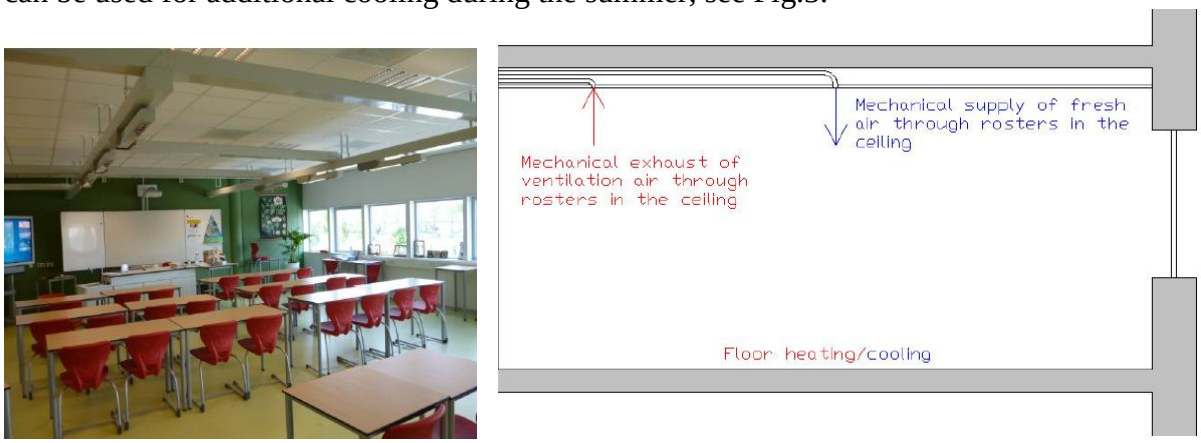

Figure 3. School C Energy plus school with mechanical air supply through grills in ceiling

3 RESULTS

3.1 Measurements

As visible in Fig.4 the three schools have a similar development in IAQ as well. During school hours the CO_2 concentration rises to a level between 800 and 1200 ppm. School C is in this case an exception. In this school the CO_2 concentration rises to a level far beyond 1200 ppm (maximum allowable concentration) and reaches concentrations around 2000 ppm. The concentrations in school C are unacceptable for buildings with an educational function.

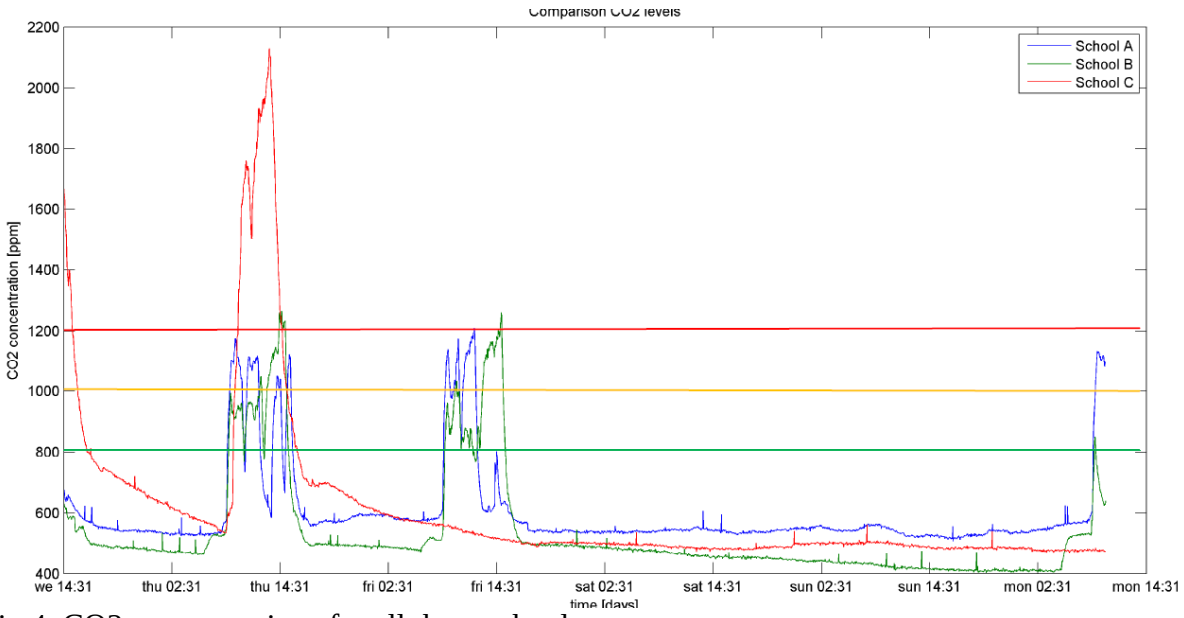

Fig 4. CO2-concentrations for all three schools

From the overview in table 3 it shows that none of the schools reach ventilation quality level A. School A en B (just!) reach level C and school C doesnot reach even that level.

Tabel 3 . Overview of the percentage of time that the conditions are in each IAQ quality level

Class	A (Very good)	B (Good)	C (Acceptable)	D (Insufficient)
CO_2 content [ppm]	percentage of school hours < 800	percentage of school hours 800 - 1000	percentage of school hours 1000 - 1200	percentage of school hours > 1200
School A	32%	22%	46%	< 1%
School B	15%	47%	32%	6%
School C	28%	12%	10%	49%

3.2 Questionnaires

The survey in school A was held among the personnel of the school (24 people). 9 members of the personnel filled in the survey which leads to a response of 37.5%. The results of this questionnaire are depicted in the figures below.

Figure 5 shows a box plot for each reviewed topic with the corresponding median, minimum and maximum value for winter and summer

.

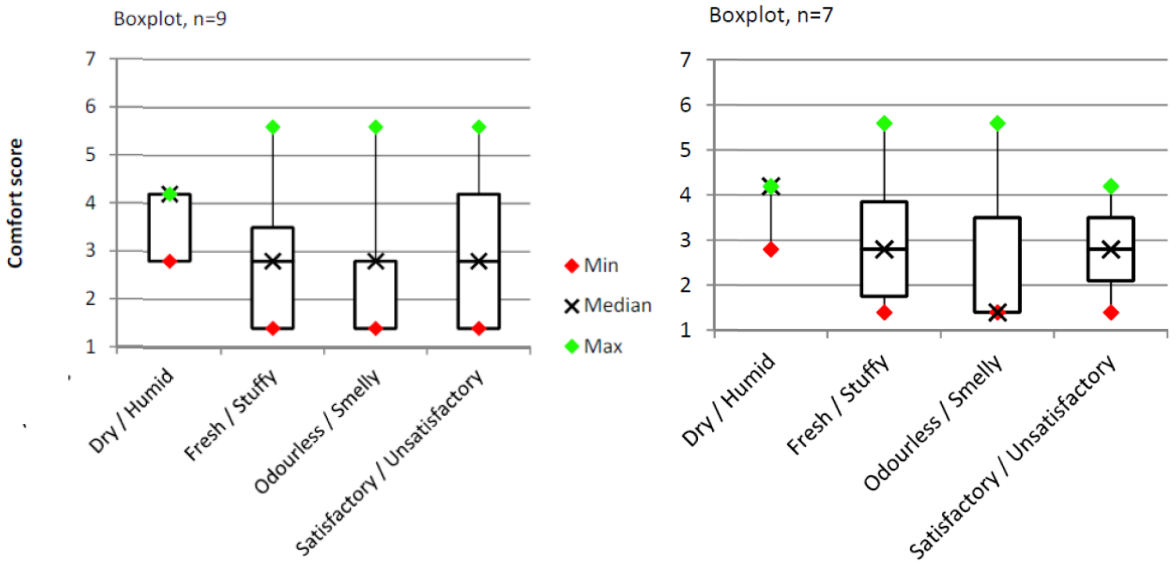

Figure 5: Results survey school A winter and summer

The survey in school B was held among the personnel of the school (40 people). Only 4 members of the personnel filled in the survey which leads to a response of 10%. The results of this questionnaire are depicted in the figure 6.

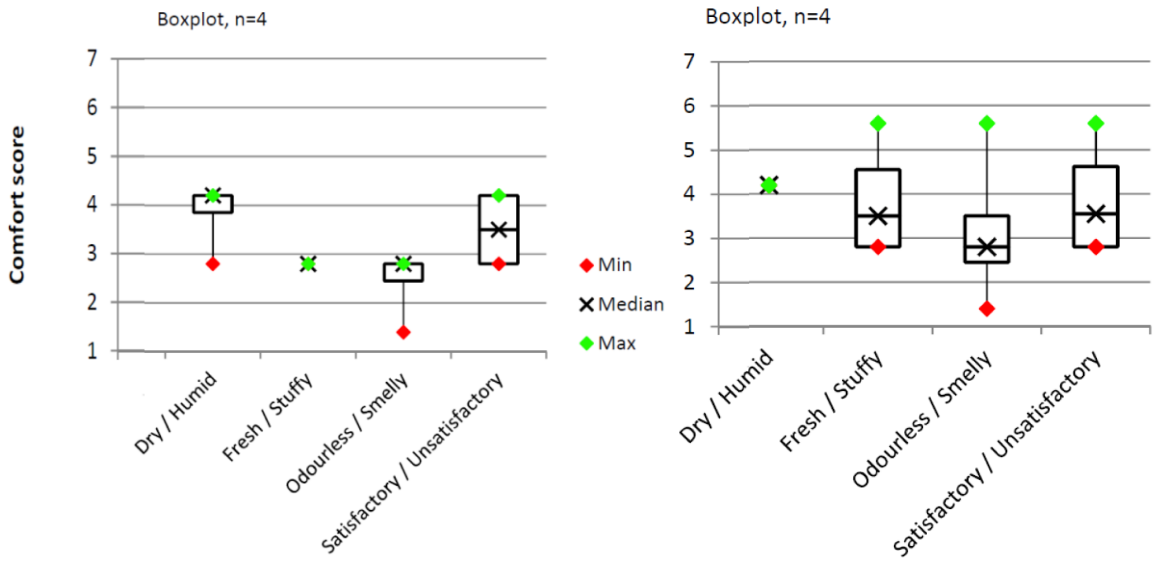

Figure 6: Results survey school B winter and summer

The survey in school C was held among the personnel of the school (73 people).18 members of the personnel filled in the survey which leads to a response of 25%. The results are given in Fig. 7.

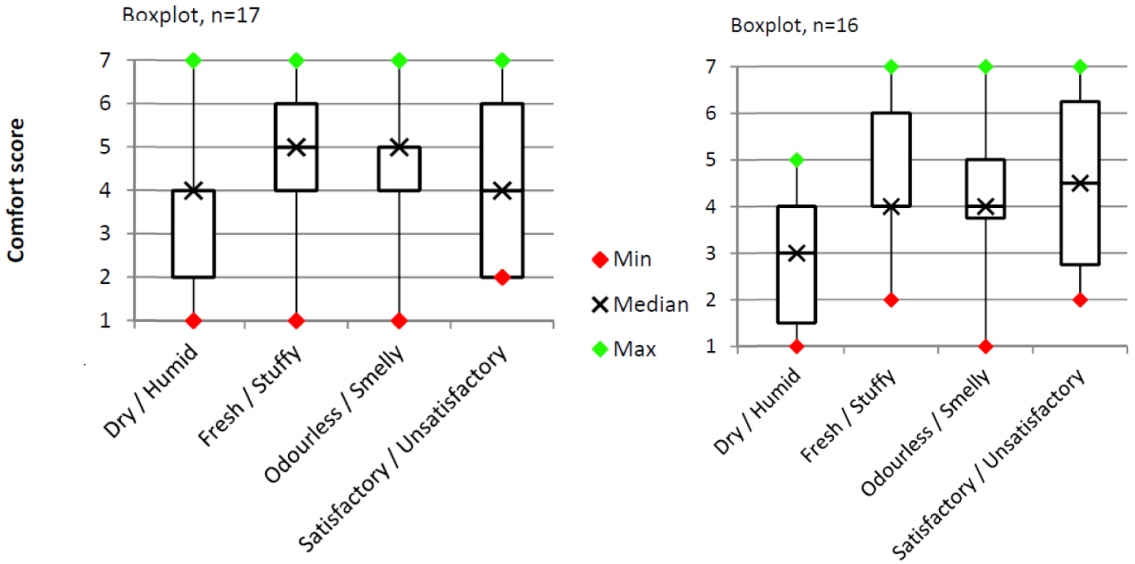

Figure 7: Results survey school A winter and summer

4 DISCUSSION

Regarding the indoor air quality in the new build sustainable schools, it can be said that the IAQ in schools A and B is good (most of the school hours between 800-1200ppm). In school C the IAQ is during a large part of the school hours insufficient (≥1200ppm). From the questionnaires of school A it followed that the IAQ in school A is reviewed by the staff as reasonably fresh and satisfactory. Compared to the actual measurement results the results of the questionnaire are in accordance. The results for IAQ in school A are categorized as class C, acceptable. School B shows quite similar results as school A. Also here the staff of the school reviews the IAQ as reasonably fresh and satisfactory, which is in accordance with the measurement results. The IAQ in school B is categorized in class B, Good. School C had the worst results regarding IAQ, most of the class hours in class D, which is unacceptable. But

the results of the questionnaire show quite neutral and stable comfort scores. So although the CO_2 concentrations inside the classroom are unacceptable, the staff does not find the IAQ uncomfortable. The scores for freshness and smelliness of the room do tend towards a bit stuffy and a bit smelly.
Clearly the ventilation of the three sustainable schools was rather disappointing as none of the schools reached class A or B. Strangely from the questionnaires is followed that the worst school based on the measurements is the school with the best perceived indoor air quality based on the questionnaires. That might be an indication that the room in which the measurements were done was not the average situation but in this case a bad example. From the questionnaires it follows that there is a slightly better perceived indoor quality in summer than in winter. As all schools had mechanical ventilation you would expect a very small difference between perceived summer and winter situation, which is the case.
To get an idea of the new schools performed better or worse than some older sustainable schools, who were not that sustainable as the new school concepts, a comparison was made with some schools of our former studies (Joosten 2004, van Bruchem 2005), see table 4.

Table 4. Some older sustainable schools for comparison

School	Date completion	Ventilation	Heating/cooling
Bruchem 3	2002	Hybrid ventilation system	Ventilated air pre-heated by thermal ceiling
Bruchem 5	2002	Exhaust-only ventilation	n.a.
Joosten C	1998	Balanced ventilation system	Central heating system with radiators
Joosten D	2000	Balanced ventilation system	Floor heating
Joosten F	2002	Balanced ventilation system	All air heating/cooling system

From the results of the comparison in Fig.8 it shows that there is not much difference in the perceived humidity, a slight improvement concerned the perceived freshness of the air, no real difference as to the perceived odour and also no real improved overall satisfaction. However when looking at the normalized CO2 concentrations, measured values recalculated to the standardized occupation of 32 pupils, there is a slight improvement, see Fig. 9

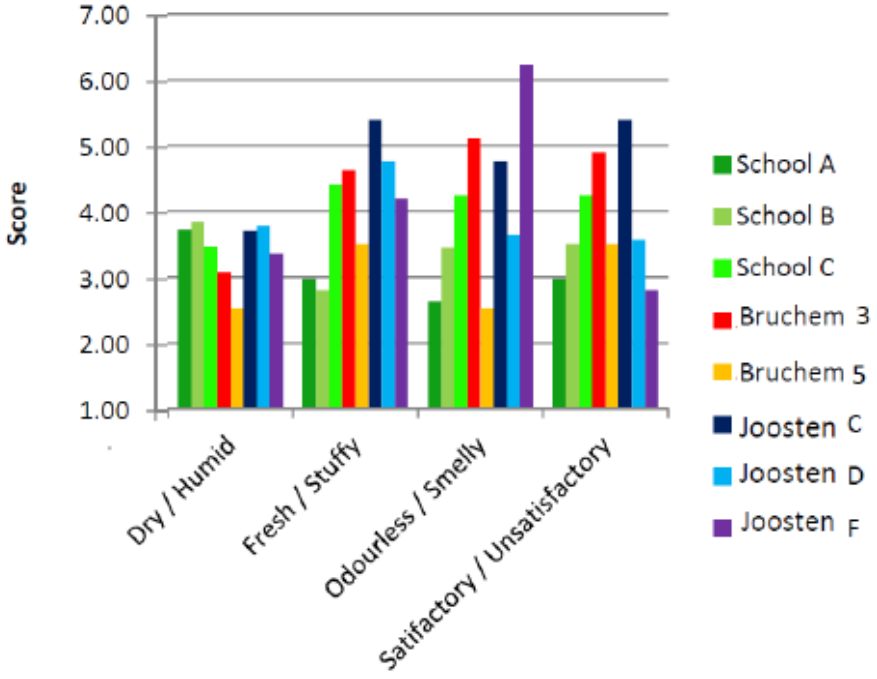

Figure 8: Perceived Indoor Air Quality aspects of sustainable schools

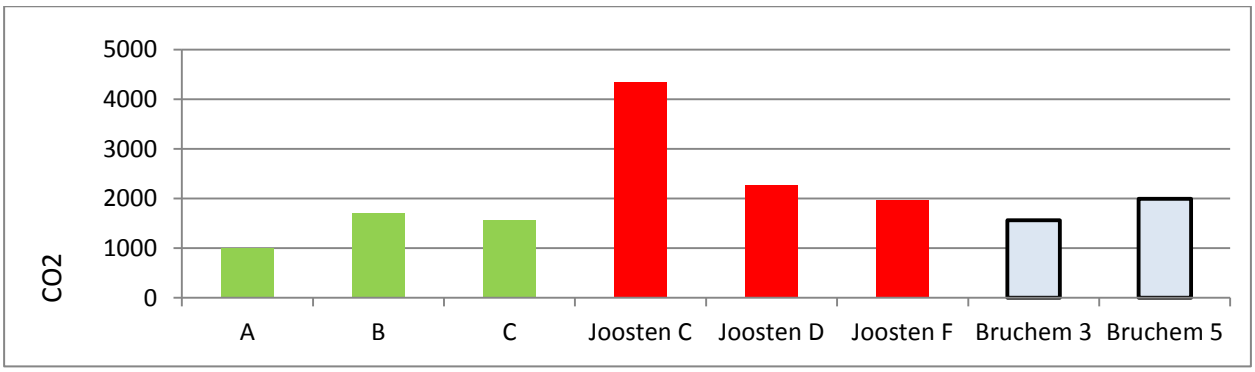

Fig 9. An overview of the normalized measured CO2 concentrations

5 CONCLUSIONS

the overall conclusion regarding IAQ is that the new build sustainable schools do not have the desired IAQ as stated in the program of demands or what was suspected during the design phase, despite of the fact that they were built with a focus on high sustainability and a high indoor air quality.

Table 5 . Claasification used in the Netherlands for school ventilation Isso 89 (2008)

Class	Description	IAQ
A	Very good	≤ 800 ppm
B	Good	≤ 950 ppm
C	Acceptable	≤ 1200 ppm

As visible in table 5, the program of demands of the investigated schools used similar values for IAQ as used in this research. Only it states that class C is below demands stated in the Dutch Building Code so class C isonly applicable for existing buildings. Since the measurements done in this research were all in newbuild schools, only the classes A and B are comparable with the results of this research. Looking at table 3 and 5 it is clear that none of the measured schools achieve an IAQ that is within the range of the classes stated in the program of demands for fresh schools. In all three schools the normalized CO_2 concentration is above 1000ppm. Looking at the development of the CO_2 concentration during atypical school day (Fig. 4), it is visible that during morning hours school B does have an IAQ which can be categorized in class B according to the program of demands for fresh schools. So it can be concluded that during parts of the day (only) school B meets the demands for fresh schools regarding CO2 concentrations, see table 6.

Table 6. Classification of the new highly sustainable schools

	Design value	Actual value
	IAQ (CO_2 [ppm])	
School A	B	C
School B	A	B
School C	n.a.	n.a.

When comparing the measurement results of this research with the results of earlier research it becomes clear that the IAQ in the new build sustainable schools does not differ (much)

from the IAQ in older less sustainable schools. Since the new build schools are built with a vision of high sustainability and a high indoor air quality, it is expected that the actual performance of the schools is slightly better and the actual CO_2 concentrations are slightly lower than older, less sustainable schools.

6 REFERENCES

Bakó-Biró Z., Clements-Croome D.J., Kochhar N., Awbi H.B., Williams M.J., 2011, Ventilation rates in schools and pupils'performance, Building and Environment 48:1-9

Bakó-Biró Z., Kochhar N., Clements-Croome D.J., Awbi H.B., Williams M.J., 2007, Ventilation Rates in Schools and Learning Performance, Proceedings Clima 2007, Antalya

Bruchem M.van, 2005, Verbeterd instalaltietechnisch ontwerp voor basisscholen om luchtkwaliteit en comfort te waarborgen, MSc thesis Technische Universiteit Eindhoven

Clements-Croome D.J., Awbi H.B., Bakó-Biró Zs., Kochhar N., Williams M., 2008, Ventilation rates in schools, Building and Environment 43: 362-367

d'Ambrosio Alfano (ed.), 2010, Indoor Environment and Energy Efficiency in schools, Part 1 Principles, REHVA Guidebook No. 13

Daisey J.M., Angell W.J., Apte M.G., 2003, Indoor air quality, ventilation and health symptoms in schools: an analysis of existing information, Indoor Air 13: 53-64

Dijken F. van, 2004, Indoor Environment in Dutch Primary Schools and Health of the Pupils, MSc thesis, Technische Universiteit Eindhoven

Grosveld G., 2011, Luisteren naar schoolgebouwen, Onderzoek naar prestaties van onderwijsgebouwen, Eindrapport BNA onderzoek, Februari 2011

Hani A., K!oiv T., Mikola A., 2011, Ventilating with room units in educational institutions, International Journal of energy and environment 5(5): 629-636

Heath G.A., Mendell M.J., 2002, Do indoor environments in schools influence student performance? A review of literature, Proceedings indoor air 2002

Hellwig R.T., 2010, How to improve the indoor climate in classrooms?, Proceedings of conference Adapting to change: New Thinking on Comfort, Cumberland Lodge, Widsor, UK

HOPE 2001. Health Optimisation Protocol for Energy-efficient Buildings: European Project No : NNE5-2001-00032;

ISSO publicatie 89, 2008. Binnenklimaat Scholen, Stichting ISSO, Rotterdam

Jago E., Tanner K., 1999. Influence of the school facility on student achievement, retrieved Kurtnitski J., 2007, Indoor Climate and Ventilation in Finnish Schools Air Distribution and Temerature Control in Classrooms, REHVA Journal june 15-22

Joosten L.A.H., 2004, Field study on the performance of exhaust-only ventilation in schools with regard to indoor air quality MSc thesis Technische Universiteit Eindhoven

Lanniello E., d'Ambrosio Alfano F.R., 2010, WS10: The REHVA guidebook on indoor environment and energy efficiency in schools – Part 1. Principles, REHVA Journal may

Mendell MJ and Heath GA, 2005, Do indoor pollutants and thermal conditions in schools influence students performance? A critical review of the literature, Indoor Air 15: 27-52

Mercier S.C., Potvin A., Tardif M., Boualem O., 2011, Hybrid ventilation in Nordic Schools, Proceedings PLEA 2011, Louvain-la-Neuve

Mi YH, Norbäck D, Tao J, Mi YL, Ferm M, 2006, Current asthma and respiratory symptoms among pupils in Shanghai, China: influence of building ventilation, nitrogen dioxide, ozone, and formaldehyde in classrooms, Proceedings Indoor Air 2006

Montazami A., Wilson M., Nicol F., 2012, Aircraft noise, overheating and poor air quality in classrooms in london primary schools, Building and Environment 52: 139-141

Mors S. ten, Hensen J.L.M, Loomans M.G.L.C., Boerstra A.C., 2011, Adaptive thermal comfort in primary school classrooms: Creating and validating PMV-based comfort charts, Building and Environment 46: 2454-2461

Mors S., 2010, Adaptive thermal comfort in primary school classrooms, Creating and validating PMV based comfort charts, MSc thesis, Eindhoven University of technology

Mydlarz C.A., Conetta R., Connolly D., Cox T.J., Dockrell J.E., Shield B.M., 2012, Comparison of environmental and acoustic factors in occupied school classrooms for 11-16 year old students, Building and Environment, doi:10.1016//j.buildenv.2012.10.020

Salleh N.M., Kamaruzzaman S.N., Sulaiman R., Mahbob N.S., 2011, Indoor Air Quality at School: Ventilation Rates and Its Impacts R\Towards Childeren – A review, Proceedings International Confernece on Environmental Science and Technology, Singapore

Al-Rashidi K., Loveday D., Al-Mutawa N., 2012, Impact of ventilation modes on carbon dioxide concentrations levels in Kuwait, Energy and Buildings 47:540-549

Shendell D.G., Prill R., Fisk W.J., Apte M.G., Blake D., Faulkner D., 2004, Associations between classroom CO2-concentrationsand student attendance in Washington and Idaho, Indoor Air 14: 333-341

Wargocki P., Wyon D.P., 2006, Research Report on effects of HVAC on student performance, ASHRAE Journal, October, 22-28

Wargocki P., Wyon D.P., 2007a. The effects of moderately raised classroom temperature and classroom ventilation rate on the performance of schoolwork by children (1257-RP). HVAC&R Research 13(2):193–220.

Wargocki P., Wyon D.P., 2007b. The effects of outdoor air supply rate and supply air filter condition in classrooms on the performance of schoolwork by children (1257-RP). HVAC&R Research 13(2):165–191.

Wargocki P., Wyon D.P., 2012, Providing Better Thermal And Air Quality Conditions in School Classrooms Would be Coat-Effective, Building and Environment, doi:10.1016//j.buildenv.2012.10.007

Satish U., Mendell M.J., Shekkar K., Hotchi T., Sullivan D., Streufert S., Fisk W.J., 2012, Is CO2 and Indoor Pollutant? Direct Effects of Low-to-Moderate CO2 Concentrations on Human Decision-Making Performance,Environmental Helath Perspectivees, http://dx.doi.org/10.1289/ehp.1104789, online 20 september 2012

Zeiler W., Boxem G., 2007, Ventilation of Dutch schools; an integral approach to improve design., Proceedings of Clima 2007 WellBeing Indoors

OPTIMIZATION METHOD FOR THE VENTILATION SYSTEM CHOICE IN ZERO ENERGY BUILDINGS

Patrick Ampe[*1], Anthony Tetaert[2], Leo Van Cauter[3], Hilde Witters[4]

1 Ghent University
ValentinVaerwyckweg 1
9000 Ghent, Belgium
**Corresponding author: Patrick.Ampe@ugent.be*

2 Ghent University
ValentinVaerwyckweg 1
9000 Ghent, Belgium

3 Ghent University
ValentinVaerwyckweg 1
9000 Ghent, Belgium

4 Ghent University
ValentinVaerwyckweg 1
9000 Ghent, Belgium

Note: the contact addresses may be re-arranged

ABSTRACT

Developing a method to optimize the investment cost of a building and the energy performance, represented by the energy consumption, one gets easily confronted with conflicting objects. As the investment cost usually rises, while the energy consumption shrinks it is somehow difficult to find an optimal solution. The utopic point would be the point where saving energy doesn't cost athing, or even better: earns the occupant extra money. Reality however shows different: restricting the energy losses almost always implies an investment. The simplest example is increasing the thermal resistance of the building envelope ((i.e. walls, roofs, floors, windows and airtightness). Since this paper handles about the ventilation system choice in zero energy buildings, it can be said that no further addition of insulation of airtightness is needed, because the heat losses through the building envelope have already been restricted to a minimum. The main issue in this paper is the control of heat losses due to the ventilation rate of the ventilation system, albeit purely hygienic or not.This paper presents a methodology for ventilation systemselection based on the total investment cost for the system and effect it has on the energy consumption of the building. Former research has shown that the choice for a cost optimal ventilation system depends on the total energy demand of the building. The proposed method makes it possible to compose a random combination of parameters (insulation thicknesses, U-values (thermal transmittance) of windows and airtightness) and calculate the heat losses through the building envelope. Through this loss of heat, the energy consumption or energy demand for the building can be calculated and an optimal choice for the ventilation system can be made, taking into account the additional cost and the system efficiency.

KEYWORDS

Optimization, ventilation system choice, zero energy building, investment cost

1 INTRODUCTION

While several studies where developed to optimize the building envelope at first and afterwards start to optimize the technical applications, this project takes a different approach. As a start, it is important to understand that every building is different. Every building has differences in geometry, orientation, material use, location (climate issues)... which means every building needs to be approached as such. Measures with respect to insulation thickness, airtightness, heating systems and ventilation units have a whole different impact depending on the architectural concept of the building. The scope of this paper is to establish a method to ease the decision making process for ventilation systems in nearly zero energy buildings.

Reviewing recent literature for European ventilation systems, it's clear that national regulations according to indoor air quality (IAQ) for buildings is a very important issue to study. Different governmental institutions in

Europe use different acceptability values for the presence of polluents in the air (Dimitroulopoulou, 2012). CO_2 is the most significant parameter in most of the cases , because it's an indication for the presence of people in a room or a building. A lot of investigations have been done on health problems and allergic reactions (asthma, rhinitis, …) of children and elderly in relation to the ventilation system installed and the amount of polluted air in rooms. Several ventilation techniques have been investigated, as for stratum ventilation (Lin ea., 2011), displacement ventilation (Lin ea., 2011, Lee and Lam, 2007), hybrid ventilation systems (Kionakis, 2005, Ji ea., 2009, Zhai ea., 2011, Kwon ea., 2013, Niachou ea., 2008), natural ventilation systems (Zhai ea., 2011, Chu ea., 2011, Niachou ea., 2008, Tan and Wong, 2012) and a whole lot of other natural and mechanical systems. The research done often focusses on the energy consumption of the systems and the impact of health considerations. These considerations imply a minimum of fresh air in a room, which means a minimum fresh air flow is required and the polluent concentration can't exceed a limit value. Moreover, the building airtightness should be taken in account for that matter. These parameters affect the energy use of a ventilation system to a significant extent (Ramponi and Blocken, 2012, Santos and Leal, 2012, Nabinger and Persily, 2011).
Authors usually allude to minimize the energy consumption by reduction of the heat losses, even apart from the building sector (Beusen ea., 2013). Increasing the airtightness of the building envelope is a strategy often used to restrict the thermal losses due to air flow. It's however important to notice that accomplishing airtightness of a construction is more effective in construction phase than as part of a retrofit operation. When making a building airtight, one should take this in account while the building is realized, not afterwards (Nabinger and Persily, 2011).
To assess the efficiency of a ventilation system, several methods are being used. A lot of research has been done using dynamic simulation software (TRNSYS) or Computational Fluid Dynamics simulation software (ANSYS). These simulation programs make iterative calculations using time steps of one hour to estimate the energy consumption of a ventilation system, based on weather data, occupancy and air humidity controlled system activation, system efficiency… The results of these investigations almost always show a reduction of the energy consumption of the ventilation system and it seems like it's always better to restrict the energy losses to a minimum. However, none of the researchers talks about the additional investment costs for a more efficient ventilation system. It's important to understand that a reduction of energy use can only be justified if the additional cost is not to high and can be paid back over a relative short period.
Some authors mention as well that occupants behavior is a very important factor to be taken into account. This parameter is very difficult to determine, because everyone behaves differently and a lot of zero-energy house owners have nor experience, nor advanced knowledge about the subject of low-energy life. It's often mentioned that ventilation systems, their settings and their functioning motives require some instructions and some education. A system that is not being used in the proper way can be very inefficient and cause additional costs or discomfort and off course due to health reasons that's not an option.
Optimization of the choice for a type of ventilation depends on a lot of parameters. Some authors use genetic algorithms [Beusen ea., 2013, Hamdy ea., 2011, Magnier and Haghighat, 2010, Wang ea., 2005, Coley and Schukat, 2002, Verbeeck, 2007) in their optimization process, others rely on a mathematical method they developed (Kapsalaki ea., 2012, Dall'O ea., 2013). In this paper we intent to explain an developed mathematical method to make a decision for a typical ventilation system, based on calculations for energy consumption and total investment cost. The methodology takes into account the budget of the client and energy performance of the ventilation system.

2 METHODOLOGY

2.1 Building design and architectural concept

To get a grip on the intentions of this paper, it's important to realize the collaboration of all parts of a building. It's impossible to state that for every building insulation measures will cause a decrease of the energy consumption. In some cases overheating will occur and a cooling device will be necessary. The same statement goes for glazing and ventilation systems. Moreover the architectural concept will influence the process of decision making. It's clear that increasing the insulation thickness in a cavity wall by 5 cm is far more expensive for a detached house than for a semi-detached or even a terraced house, since there are a lot more walls in contact with the outer environment. Dwellings with a big area of glazing on the southern façade, will profit from a change of glazing type a lot faster than building with no glazing at all in the southern walls. These examples show that every building needs to be studied as a whole, not as a combination of parts or as a simplified model.

To compare the several ventilation systems, it's necessary to know what impact the ventilation systems have on the total energy consumption. All systems have a different efficiency, blow or extract a different air flow and have (or not) a heat exchanging system with a specific efficiency. It's clear that again, not 2 systems are the same. In essence, 4 general ventilation systems can be distinguished. They are collected in

Table 1: General ventilation systems.

Table 1: General ventilation systems

Ventilation system	air supply	air extraction
System A	natural	natural
System B	mechanical	natural
System C	natural	mechanical
System D	mechanical	mechanical

Since this paper focusses on zero energy buildings some important nuances need to be made. As scientist we don't intent to decide purely on gut feeling and for that matter ventilation systems A and B cannot be excluded. It's however important to recognize that ventilation system A is not very energy efficient and that ventilation system B is almost never being applied. There is off course a reason for this trend and it has a lot to do with the controllability of the systems. Using ventilation systems A and B causes the heat losses through ventilation to be uncontrollable because there is no brake on the outgoing indoor air. Better and far more responsible would it be to apply a ventilation system C or D, where the amount of outgoing hot air is more steerable. For that reason, ventilation systems A and B are (for now) being excluded.
Ventilation systems C and D can be used for nearly zero energy buildings and can even be subdivided according to their applications, their control system and their heat exchange units. All these factors are important to be taken into account while evaluating the systems and making a comparison between them. For this study some systems C and some systems D are evaluated and compared. In *Table 2: Investigated ventilation systems and their parameters for the calculation of the energy performance and the total investment cost*, the investigated ventilation systems are listed. This list is sufficient to demonstrate the methodology of decision making, but can off course be expanded for practical applications.

Table 2: Investigated ventilation systems and their parameters for the calculation of the energy performance and the total investment cost

Ventilation system	r_{heat} [-]	r_{cool} [-]	m [-]	P_{fans} [W]	IC_T [€]
0	1,00	1,00	1,50	0,00	0
C	1,00	1,00	1,50	33,30	€ 1.500
C_{he}	1,00	1,00	1,20	27,30	€ 1.000
C^+	1,00	1,00	1,08	33,30	€ 3.300
D^+	1,00	1,00	0,94	54,50	€ 4.000
D_{he}	0,27	1,00	1,40	92,30	€ 5.000

Table 2 contains indices 'he' for 'heat exchanger' and '+' for demand controlled systems. These systems can be controlled by occupancy, CO_2 concentration or relative humidity.r_{heat} and r_{cool} are correction factors for cooling and heating modus of the ventilation system and indicate a bypass of the heat exchanger in system D, while m is a correction factor for the execution quality of the system. The energy consumption for the fans is listed below P_{fans} and contains the power for all needed fans. For systems C only 1 fan is sufficient, for systems D 2 fans are required, which explains the overall difference between the power amounts.

2.2 Energy consumption calculations

To estimate the saving of energy due to the ventilation, the norms and regulations for the Belgian building industry have been consulted. These formulas are the same formulas as the ones implemented in the EPBD, the European directive on energy efficiency of buildings.

The heat losses due to ventilation and in/exfiltration of air through the building envelope can be calculated using the following formulas. These formulas result in a value in W/K and this value needs to be multiplied by the difference in temperature between the inner and the outer environment.

For the calculation of the heat losses in heating modus:

$$H_{V,heat,seci} = 0{,}34 \,.\, V_{in|exfilt,heat,seci} + r_{preh,heat,seci} \,.\, V_{dedic,seci} + V_{over,seci} \quad W\ K \qquad (1)$$

For the calculation of the heat losses in cooling modus:

$$H_{V,cool,seci} = 0{,}34 \,.\, V_{in|exfilt,cool,seci} + r_{preh,cool,seci} \,.\, V_{dedic,seci} + V_{over,seci} \quad W \;\; K \qquad (2)$$

with:

$V_{in|exfilt,heat,seci}$

$V_{in|exfilt,cool,seci}$ airflow due to leakage through the building envelope, respectively for heating calculations and for cooling calculations. How to calculate these values doesn't belong to the scope of this investigation

$V_{dedic,seci}$ designed air flow through the ventilation system, calculated using the formula beneath.

$r_{preh,heat,seci}$

$r_{preh,cool,seci}$ the value of the reduction factor for the effect of preheating of the air flow on the net energy demand, respectively for heating calculations and for cooling calculations.

$V_{over,seci}$ the extra air flow owing to over ventilation, when systems with mechanical extraction of air are connected to a heat pump for the preparation of domestic hot water, using the extracted air as a heat source. This parameter is a very interesting one, but can't be used because a consistent calculation method hasn't been developed yet. The default value for this parameter is 0 m³/h, the parameter hasn't been taken into account.

The designed air flow through the ventilation system can be calculated using following formula.

$$V_{dedic,seci} = \quad 0{,}2 + 0{,}5 \,.\, exp\ -V_{EPW}\ \ 500 \quad .\, f_{reduc,vent,seci} \,.\, m_{seci} \,.\, V_{seci} \ \ m^3 \ \ h \qquad (3)$$

with:

V_{EPW} the total volume of the building.

$f_{reduc,vent,seci}$ a reduction factor for ventilation. The default value for this factor is 1, but more favorable can be specified, taking into account the directives from the Flemisch Minister for Energy.

m_{seci} a multiplication factor depending on the ventilation system and the execution quality of it.

V_{seci} the total volume of the studied energy sector.

Integrating these heat losses on a yearly basis, implementing hourly temperature differences, the total energy consumption due to heat losses caused by the ventilation system can be determined. Next to these heat losses, the operation energy for fans needs to be taken into account. This energy consumption can be computed on an annual basis, using a simple formula. It's important to know that this formula is only valuable for as long as the fans are only used for hygienic ventilation. If the ventilation system is designed to contribute to room heating, the ventilation rate will be much higher than just hygienic ventilation and the fans will logically be dimensioned on that basis. The energy use in that last case will be higher. For this investigation, only fans for hygienic ventilation are taken into account. The energy use is to be calculated on a monthly basis and then summed over all months to result in an annual energy consumption for the fans.

Monthly based:

$$W_{aux,fans,vent,m} = t_m \,.\, \sum_j \Phi_{fans,vent,j} \quad 3{,}6 \qquad (4)$$

Annual based:

$$W_{aux,fans,vent,a} = \sum_m W_{aux,fans,vent,m} \qquad (5)$$

with:

t_m the length of the month in Megaseconds (Ms)

$\Phi_{fans,vent,j}$ the notional value for the mean electric power of fan j. This power is determined to be half of the maximum power of the electric motor, since it is not always in use.

2.3 Total investment cost calculations

For this investigation we approached some companies to make an offer for some ventilation systems. In the research, these offer prices are being used, because of the difficulty and the uncertainty of the calculation methods used by the companies. Asking for an offer from several companies to install the exact same system, can result in a lot of different cost estimations and a solution for this kind of problem needs to be found.

Price settings and price functions are difficult enough for simple materials like insulation, bricks, concrete slabs, windows… Trying to determine a total investment cost for a system (ventilation, heating, cooling…) even goes a little further. A system not only consists of a installation unit. Ducts, controllers, distribution elements, inlet openings… need to be calculated as well, to get a reliable investment cost. It's clear that these factors are different for each investigated building and may differ depending on the system design. Two companies installing the exact same system, will handle other calculation methods and perhaps other design rules relying on their own experiences. Specifically for ventilation systems, following prices need to be added to the investment cost of a ventilation unit:

- Ducts: depending on the distance between the room and the ventilation unit. Depending on whether a system C or system D is used, the amount of ducts may double or not.
- Fans: depending on the amount of fans that need to be installed and whether or not it's necessary to add extra fans.
- Supply and extraction grilles: depending on the system and the rooms that need to be provided with grilles.
- Controllers and measuring sensors: depending on the company, the desired precision of the system control, the amount of sensors and the amount of rooms that need to be controlled independently.
- Suspension systems and placement procedures: depending on the amount of ducts, ventilation units and grilles
- Balancing procedures and balancing time: depending on the companies procedures
- …

Because of the uncertainty of all these parameters, a total cost was set for every ventilation system, as presented in *Table 2: Investigated ventilation systems and their parameters for the calculation of the energy performance and the total investment cost*. The information in this table is drawn from several offers from companies and for each system the cheapest offer, off course being conform to the demand, is taken. Doing so, the calculation procedure for the cost of a ventilation system is no longer dependent on the approach of the investigator, but only on the approach of the offering company, exactly like it is in practice.

2.4 Optimization concept

To make an optimal choice for a ventilation system, one should decide on objective, numerical operations rather than on sheer gut feeling. To make an optimized decision upon energy consumption and total investment cost, simple common sense can offer some help. We all want the best we can get out of our invested money. In means of energy that means we want as much energy savings as possible and we want the investment cost to be as low as possible. A utopic situation for that matter would be where the energy savings are infinite, while there's no investment cost at all, or even better: we get paid for it. Every kind of investment should give the most energy saving possible for the lowest marginal cost. In mathematical terms, it's fair to say:

$$Optimal\ theoretical\ solution = min\ \frac{\Delta IC_{T,i}}{-\Delta P_i} \quad (6)$$

with:

$\Delta IC_{T,i}$ the marginal investment cost for a ventilation systemi

$-\Delta P_i$ the decrease of the energy consumption due to ventilation systemi

In words, this means $\frac{\Delta IC_T}{-\Delta P}$ needs to be as small as can be. Only that solution is the optimal solution. Sometimes however, it's financially impossible to make the most optimal choice and then there's need for another solution to be chosen. In that case, the second lowest $\frac{\Delta IC_T}{-\Delta P}$ should be chosen and if that solution is financially insufficient, the third or the forth or…

Looking at *Table 2: Investigated ventilation systems and their parameters for the calculation of the energy performance and the total investment cost* and knowing you only have €1000 to spend, you always have to choose ventilation system C_{he}, no matter what. It's very probable that this solution is not the optimal one at all, but since there's no more money, it's the best there can be done. However, having €1500 at your expends, there's a decision to be made between ventilation systems C and C_{he}. System C requires a higher investment cost than system C_{he} and the investment is only justified if it makes the energy consumption drop more than system C_{he}. With some certainty it can be said that it does not, so it's smarter to choose ventilation system C_{he} and save €500. Let's however say, purely hypothetic, that ventilation system C does cause a bigger energy saving than ventilation system C_{he}. What has to be done then? This is the part, where $\frac{\Delta IC_T}{-\Delta P}$ becomes an important factor. To make a decision, $\frac{\Delta IC_T}{-\Delta P}$ has to be calculated for both ventilation systems. Only 3 situation can appear:

1) $\frac{\Delta IC_T}{-\Delta P}$ for ventilation system C is higher than $\frac{\Delta IC_T}{-\Delta P}$ for ventilation system C_{he}: Ventilation system C_{he} is the optimal solution and the decision is simple. C_{he} is chosen.
2) $\frac{\Delta IC_T}{-\Delta P}$ for ventilation system C is lower than $\frac{\Delta IC_T}{-\Delta P}$ for ventilation system C_{he}: Ventilation system C_{he} is not the optimal solution. At first ventilation system C is chosen because of it's lowest $\frac{\Delta IC_T}{-\Delta P}$. Afterwards a decision needs to be made whether it's necessary to restrict the energy consumption even more. If really required, ventilation system C_{he} has to be selected after all.
3) $\frac{\Delta IC_T}{-\Delta P}$ for ventilation system C equals $\frac{\Delta IC_T}{-\Delta P}$ for ventilation system C_{he}: Nothing can be said about the optimality of the ventilation systems. They are equally optimal, however unlikely. The decision now only depends on the need for energy reduction, since the energy performance and the investment cost for both systems are linearly related.

Mathematically spoken formula (6) can be rewritten for the real optimal solution as:

$$Optimal\ solution = \min\ \min\ \Delta IC_{T,i}\ , \min\ \frac{\Delta IC_{T,i}}{-\Delta P_i} \tag{7}$$

with:

$\Delta IC_{T,i}$ the investment cost for a ventilation system i
$-\Delta P_i$ the decrease of the energy consumption due to ventilation system i

3 CASE STUDY

To illustrate this methodology for the choice of a ventilation system, a case study has been done, using all ventilation systems in *Table 2: Investigated ventilation systems and their parameters for the calculation of the energy performance and the total investment cost*. The investigated building is a two story, detached house with a flat roof. For the ventilation calculations a family consisting of 4 people is assumed. The dwelling has a net floor area of 308 m² and a volume of about 1030 m³.
As a reference situation, the investigated case study house has been insulated up to a mean value for U of 0.4 W/m².K. Achieving a compactness of 1.49, this value results in an overall K-value of 34. The reference case has no ventilation system.

Assume in this case, a ventilation system needs to be installed, because of the bad air quality in the dwelling due to unventilated rooms. Doing some calculations with the data subtracted from *Table 2: Investigated ventilation systems and their parameters for the calculation of the energy performance and the total investment cost*, a well-founded decision can be made. The results from the calculation are collected together in

Table 3: Results of the calculations of investment costs and energy performance improvements for a list of ventilation systems applied to a case study house.

Table 3: Results of the calculations of investment costs and energy performance improvements for a list of ventilation systems applied to a case study house

Ventilation system	IC_T [€]	ΔIC_T [€]	P [W]	-ΔP [W]	$\frac{\Delta IC_T}{-\Delta P}$ [€/W]
0	€ 344.059		4158,4		
C	€ 345.559	€ 1.500	4191,7	-33,3	-45,05
C_{he}	€ 345.059	€ 1.000	4076,9	81,5	12,27
C^+	€ 347.359	€ 3.300	4042,6	115,8	28,50
D^+	€ 348.059	€ 4.000	4019,2	139,2	28,74
D_{he}	€ 349.059	€ 5.000	3589,9	568,5	8,80

The information in

Table 3: Results of the calculations of investment costs and energy performance improvements for a list of ventilation systems applied to a case study house makes it possible to decide which ventilation system to choose in the case study house. Making the simplest analysis possible at first, nobody in his right mind would choose ventilation system C. It's clear that the energy consumption for ventilation system C exceeds the energy consumption for no ventilation system at all. However, in this regard, an objection needs to be made, since a ventilation system causes an improvement of the indoor air quality. System C will perhaps not result in an energy reduction, it will make the inner environment more comfortable.

Taking into account the decision steps described in2.4Optimization concept, the path that needs to be followed is this:

1) The most optimal ventilation system would be system D_{he}. It has a $\frac{\Delta IC_T}{-\Delta P}$ of 8.8 and that's the lowest that can be found in the table. The cost however is € 5.000 and that's quite a high cost.
2) The next optimal ventilation system is ventilation system C_{he}, with a $\frac{\Delta IC_T}{-\Delta P}$ of 12.27. It only costs € 1.000 and that's the lowest investment cost in the table. Ventilation system C_{he} would be the best choice to make at first.
3) If ventilation system C_{he} doesn't imply a big enough reduction of the energy use and still some money is left to spend, the next system in line would be ventilation system C^+. $\frac{\Delta IC_T}{-\Delta P}$ of that system is 28.50 and it requires a spend of € 3.300, still less than € 5.000 for the most optimal solution.
4) If ventilation system C^+ doesn't fit the expectations in means of energy reduction, next system to choose would be ventilation system D^+, with a $\frac{\Delta IC_T}{-\Delta P}$ of 28.74 and an investment cost of € 4.000, still less than € 5.000 for system D_{he}.

In short, that means ventilation system C is not to be chosen. It is Pareto dominated by ventilation system C_{he}, because it causes a bigger energy use reduction at a cheaper price. Choosing ventilation system C, wouldn't be the smartest thing to do. In Figure 1: Graph of the optimized decision model for a ventilation system, the decision making process is illustrated through a graph, where the objective on the x-axis is the ventilation system. On the upper y-axis, $\frac{\Delta IC_T}{-\Delta P}$ for all ventilation systems can be read and on the lower y-axis the additional cost with respect to the reference case.

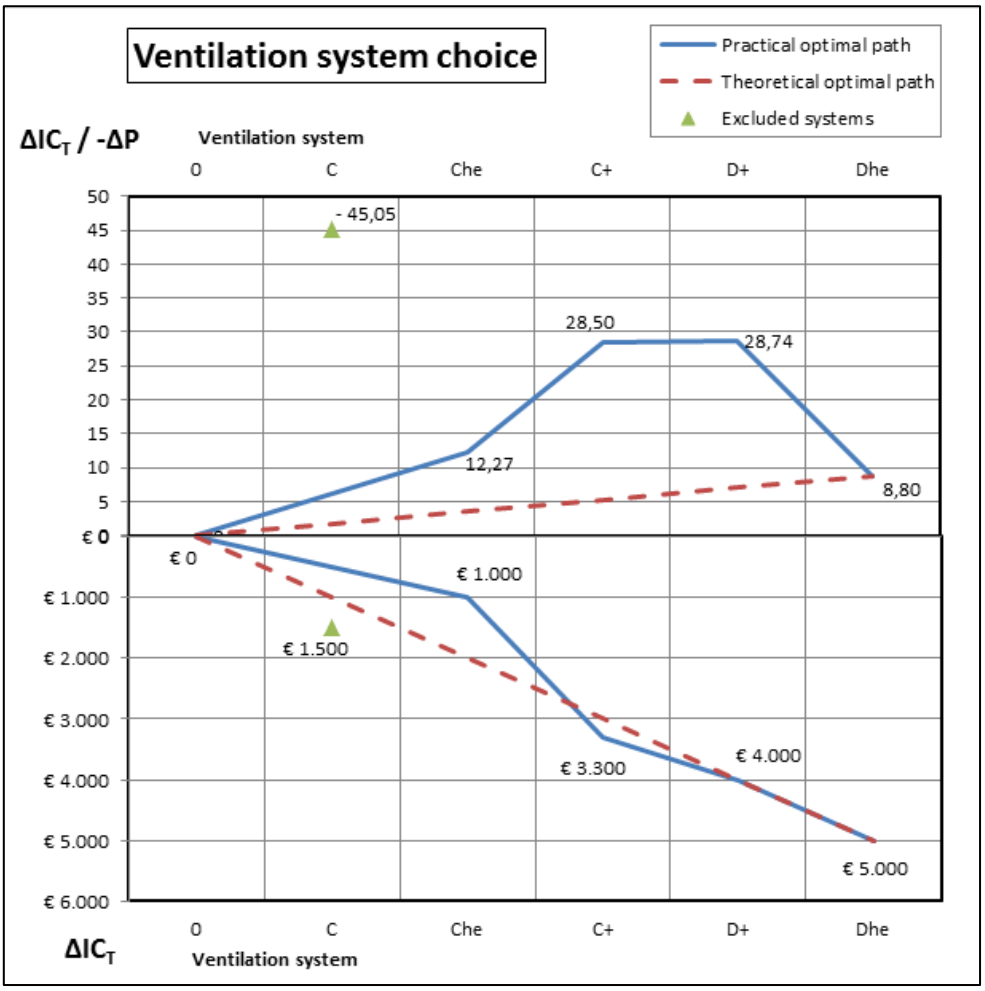

Figure 1: Graph of the optimized decision model for a ventilation system

with:

- The theoretical optimal path being the decision made when marginal investment cost doesn't matter. It is the same decision that would be made if the ventilation system was a continuous variable instead of a discrete parameter.
- The practical optimal path being the sequence of decisions made knowing the marginal investment cost may have some importance.

4 CONCLUSIONS AND DISCUSSION

The choice of a ventilation system for nearly zero energy buildings is a multi-objective problem. On one hand, the energy consumption on annual basis needs to be reduced as much as possible. On the other hand the investment cost has to be kept as low as possible. These 2 objectives are conflicting: energy reduction almost always implies an increase of the investment cost. The proposed method for the selection of a ventilation system out of a list, generates a Pareto optimal line consisting of non-dominated solutions. At that point, ventilation system drops out for the studied case. It's however important to know that a ventilation system C for another case or from another company or distributor can be optimal.

An important conclusion here can be that all ventilation systems in Table 2: Investigated ventilation systems and their parameters for the calculation of the energy performance and the total investment cost are handled with respect to each other. The list is off course non-limitative and new systems, extra systems, systems from different companies can be added as well and will be dealt with the same.

In this investigation, only ventilation systems are being optimized, but imagine what would happen when the insulation thicknesses, the airtightness, the window types, the lighting systems… are taken into account. It's not inconceivable that an additional centimeter of insulation causes a higher energy reduction at a lower price. In that case the insulation thickness dominates the ventilation system. This path is a very interesting one to follow. It means that perhaps it would be better first to insulate the building and then after a while decide to change the ventilation system.

Same thing can be said about the discrete characteristics of the ventilation systems. The investment cost for example takes jumps of about € 1.000. Between 2 systems, addition insulation measures can be taken, especially when the investment cost for the next ventilation system in line is too high.

5 ACKNOWLEDGEMENTS

This study was partly granted by IWT (Flemish Government). Thanks to all participants and counselors.

6 REFERENCES

Beusen, B., Degraeuwe, B., Debeuf, P. (2013) Energy savings in light rail through the optimization of heating and ventilation. *Transportation Research Part D 23*, pp. 50-54.
Chu, C.H., Chen, R.-H., Chen, J.-W. (2011) A laboratory experiment of shear-induced natural ventilation. *Energy and Buildings 43*, pp. 2631-2637.
Coley, D A., Schukat, S. (2002) Low-energy design: combining computer-based optimisation and human judgement. *Building and Environment 37*, pp. 1241-1247.
Dall'O', G., Bruni, E., Sarto, L. (2013) An Italian pilot project for zero energy buildings : Towards a quality-driven approach. *Renewable Energy 50*, pp. 840-846.
Dimitroulopoulou, C. (2012) Ventilation in European dwellings: A review. *Building and Environment 47*, pp. 109-125.
Hamdy, M., Hasan, A., Siren, K. (2011) Applying a multi-objective optimization approach for Design of low-emission cost-effective dwellings. *Building and Environment 46*, pp. 109-123.
Ji, Y., Lomas, K.J., Cook, M.J. (2009) Hybrid ventilation for low energy building design in south China.*Building and Environment 44*, pp. 2245-2255.
Kapsalaki, M., Leal V., Santamouris M. (2012) A methodology for economic efficient design of Net Zero Energy Buildings. *Energy and Buildings 55*, pp. 765-778.
Kionakis, C.J. (2005) Combined thermal and natural ventilation modeling for long-term energy assessment: validation with experimental measurements. *Energy and Buildings 37*, pp. 311-323.
Kwon, O.-H., Kim, M.-H., Choi, A.-S., Jeong J.-W. (2013) Energy saving potential of a hybrid ventilation system integrated with heat storage material. *Energy and Buildings 57*, pp. 346-353.
Lee, C.K., Lam, H.N. (2007) Computer modeling of displacement ventilation systems based on plume rise in stratified environment. *Energy and Buildings 39*, pp. 427-436.
Lin, Z., Lee, C.K., Fong, K.F., Chow, T.T. (2011) Comparison of annual energy performance with different ventilation methods for temperature and humidity control. *Energy and Building 43*, pp. 3599-3608.
Magnier, L., Haghighat, F. (2010) Multiobjective optimization of building design using TRNSYS simulations, genetic algorithm, and Artificial Neural Network. *Building and Environment 45*, pp. 739-746.
Nabinger, S., Persily, A. (2011) Impact of airtightness retrofits on ventilation rates and energy consumption in a manufactured home. *Energy and Buildings 43*, pp. 3059-3067.
Niachou, K., Hassid, S., Santamouris, M., Livada, I. (2008) Experimental performance investigation of natural, mechanical and hybrid ventilation in urban environment. *Energy and Buildings 43*, pp. 1373-1382.
Ramponi, R., Blocken, B. (2012) CFD simulation of cross-ventilation for a generic isolated building: impact of computational parameters. *Building and Environment 53*, pp. 34-48.
Santos, H.R.R., Leal, V.M.S. (2012) Energy vs. ventilation rate in buildings: A comprehensive scenario-based assessment in the European context. *Energy and Buildings 54*, pp. 111-121.
Tan, A.Y.K., Wong, N.H. (2012) Natural ventilation performance of classroom with solar chimney system. *Energy and Buildings 53*, pp. 19-27.
Verbeeck, G. (2007) Optimisation of extremely low energy residential buildings, PhD KU Leuven
Wang, W., Zmeureanu, R., Rivard, H. (2005) Applying multi-objective genetic algorithms in green building design optimization. *Building and Environment 40*, pp. 1512-1525.
Yasinne, B., Ghali, K., Ghaddar, N., Srour, I., Chehab, G. (2012) A numerical modeling approach to evaluate energy-efficient mechanical ventilation strategies. *Energy and Buildings 55*, pp. 618-630.
Zhai, Z.J., Johnson, M.-H., Krarti, M. Assessment of natural and hybrid ventilation models in whole-building energy simulations, in: Energy and Buildings 43,2011, pp. 2251-2261.

USING COOL PAVEMENTS AS A MITIGATION STRATEGY TO FIGHT URBAN HEAT ISLAND – A REVIEW OF THE ACTUAL DEVELOPMENTS

M. Santamouris

Group Building Environmental Studies, Physics Department, University of Athens, Athens, Greece

msantam@phys.uoa.gr

The full paper is published in **:** Renewable and Sustainable Energy Reviews, 2013

ABSTRACT

Heat island phenomenon rises the temperature of cities, increases the energy demand for cooling and deteriorates comfort conditions in the urban environment. To counterbalance the impact of the phenomenon, important mitigation techniques have been proposed and developed. The use of cool pavements presenting substantially lower surface temperature and reduced sensible heat flux to the atmosphere, appears to be one of the most important proposed mitigation solutions. The present paper investigates and describes the actual state of the art on the field of cool pavements. The existing results clearly show that the mitigation and cooling potential of cool pavements is very significant and can highly contribute to decrease temperature on the urban environment.

KEYWORDS

Heat Island, Cool Pavements, Mitigation Technologies, Reflective Pavements, Cool Materials, Permeable pavements

INTRODUCTION

Heat island refers to the development of higher urban temperatures of an urban area compared to the temperatures of surrounding suburban and rural areas Heat island has an important impact on the energy consumption of buildings and increases their energy consumption for cooling purposes. Various studies have shown that the cooling energy consumption of buildings may be doubled because of the important increase of urban temperatures

Counterbalancing the effects of urban heat island is a major priority for the scientific community. Several techniques have been proposed, developed and applied with quite high success. The impact of pavements on the development of urban heat island is very important.. Pavements cover a quite high percentage of the urban fabric and contribute highly to the development of heat island. Paved surfaces in Europe and USA, consist mainly of concrete and asphalt surfaces that present high surface temperatures during the summer period. Decreasing the surface temperature of pavements may contribute highly to improve the thermal conditions in cities suffering from high urban temperatures. This can be achieved by replacement of conventional paving surfaces with new ones presenting much lower surface temperatures during the warm period, reconstruction, preservation and rehabilitation of the existing pavements to improve their thermal performance and shading of the paved surfaces to decrease absorption of solar radiation. Advanced materials and surfaces, known as cool pavements, have been developed and are available for use in urban environments. Cool pavements are mainly based on the use of surfaces presenting a high albedo to solar radiation combined to a high thermal emissivity, (reflective pavements), or are using the latent heat of water evaporation to decrease their surface and ambient temperature, (water retention pavements). The present paper aims to present and analyse the actual status of development of the main technologies associated to cool pavements. It evaluates the recent developments concerning reflective and permeable paving surfaces while it presents new ideas and applications beyond the above technologies.

IMPROVING THE THERMAL PERFORMANCE OF PAVEMNENTS

Effective mitigation of the impact of pavements on urban heat island necessitates a serious reduction of the sensible heat flux released to the atmosphere by the paving surfaces. This is equivalent to the reduction of their surface temperature during the day and night period. Paving materials presenting a relatively reduced surface temperature are known as cool pavements.
Reduction of the surface temperature of pavements may be achieved by employing some of the following techniques :

a) To increase the albedo of the paving surfaces in order to absorb less solar radiation, (reflective pavements). Most of the existing techniques apply to asphalt, concrete and other types of pavements. Existing techniques to increase the albedo of pavements include. : The use of conventional cement concrete pavement, the use of concrete additives like slag cement and fly ash, the application of white topping and ultra thin white topping techniques, the use of roller compacted concrete pavement, the use of

light aggregates in asphalt concrete surfaces, the use of chip or sand seals with light aggregates, the application of color pigments and seals and the use of colorless and reflective synthetic binders, the painting of the surfaces with a light color using or not microsurfacing techniques, the use of sand/shot blasting and abrading binder surfaces, resin based pavements, etc. Some of the techniques are appropriate for new pavements while other for pavement rehabilitation and maintenance.

b) To increase the permeability of the surfaces, in vegetated and non vegetated pavements, in order to decrease their surface temperatures through evaporation processes. These types of pavements are known as permeable, porous, pervious or water retaining materials. As stated, the words previous and permeable are synonymous and signify that water can flow through the material through a series of pores or connected holes. In porous materials holes are available in the material mass but are not necessarily connected. In general, permeable, porous or pervious pavements present a lower albedo than the impermeable equivalents, and higher convective fluxes to the atmosphere because of their higher effective surface area created by the increased void content.. Non vegetated permeable pavements include, porous or rubberized asphalt, porous and pervious concrete, permeable interlocking concrete pavers, concrete and plastic grid pavers filled with gravels. Vegetated permeable pavements provide cooling through evapotranspiration. It includes grass pavers, reinforced turf and concrete grid pavers use lattices of different types that allow grass to grow in the interstices.

c) To increase the thermal storage capacity of the surfaces by adding ingredients of high thermal capacitance or materials of latent heat storage. Common materials used in pavements present a high thermal capacitance and is quite difficult to increase it further. However, addition of latent heat storage materials in the mass of the pavements, contribute to reduce surface temperatures during daytime and decrease sensible heat release to the atmosphere.

d) To use external mechanical systems in order to reduce the surface temperature of the paving materials. This includes among other, circulation of a fluid in the mass of the pavement to remove the excess heat, and circulation of underground water in the pavement mass.

e) Provide efficient shading of the paved areas using natural or artificial solar control devices. Shaded surfaces present a much lower surface temperature as the absorbed direct solar radiation is seriously reduced. Solar shading devices may be natural like

trees and green pergolas or artificial. Shading devices should allow infrared radiation emitted by the pavements to escape in the atmosphere to promote radiative cooling of the pavements surface.

In the following chapters the state of the art of the previously described types of pavements is presented.

REFLECTIVE PAVEMENTS

Increasing the albedo of pavements helps to decrease their surface temperature and reduce the amount of sensible heat released to the atmosphere. In parallel, it decreases the need for night lighting and increases the durability of the pavements.. Pavements consist mainly of aggregates bounded by a binder. Albedo may increase by either provide an appropriate surface coating, or aggregates of light color or a proper binder or a combination of the above.

Apart of the commercially available reflective pavements, important research developments are carried out and reported aiming to develop high reflective pavements. Five technological approaches are developed and tested.

a) The use of white high reflective paints on the surface of the pavement. New generation white paints of new generation present a very high solar reflectivity that in many cases exceeds 90 %. Use of such paints could significantly decrease the surface temperature of the pavements and decrease sensible heat released to the atmosphere. The use of high reflective paints applied on the surface or the mass of the pavements is studied. The highly reflective paints are applied on the surface of concrete pavement tiles. Albedos in both cases ranged between 0,8-0,9. Experimental testing was performed during hot summer conditions and comparative results are reported against conventional white tiles. . In particular, the thermal performance of 14 highly reflective white concrete pavement materials covered with reflective paints based on different types of technologies, were comparatively tested under hot summer conditions. The albedo of almost all tested materials was between 80-90%. The emissivity of the non-aluminum pigmented coatings was higher than 0,8, while for the aluminum based paints it varied between 0,3 and 0,4. It was found that the use of highly reflective coatings reduces the daily surface temperature of a white concrete pavement under hot summer conditions by 4 K and by 2 K during the night. The specific tiles were warmer than the ambient air by only 2 K during the day and cooler by 5,9 K during the night. A clear correlation between the emissivity of the materials and the nocturnal surface temperature was found. Pavements covered with aluminum based paints presented a

higher surface temperature than the other tiles. Aging of the used paints is found to play a very important role on the thermal performance of the pavements. It is reported that the acrylic elastomeric coatings was the coolest coating during the daytime period of the first month of the monitoring period, but became a lot warmer during the second and third month of the testing. Highly reflective white coatings, (ρ=0,88), based on the use of calcium hydroxide were also prepared and tested against conventional white pavements, (ρ=0,76), under summer conditions. The infrared emittance of the material was close to 0,85. Such a coating is inexpensive, environmentally friendly, permits the air to pass through while it presents high dirt pick up resistance. The main disadvantage of the materials is the effect of chalking. To face the problem, an acryl binder was used. It is reported that during the daytime the prototype reflective materials have lower surface temperatures ranging between 1 and 5 K, while during the night the difference was close to 1 K.

b) Use of Infrared reflective colored paints on the surface of the pavement. When nonwhite pavement materials have to be employed, infrared reflective pigments may be used to increase their global albedo.. Such a pavement surface of any color, may reflect strongly in the near infrared part and thus present a much higher solar reflectivity than a conventional material of the same color. Infrared reflective paints are used to modify the surface albedo of colored concrete and asphalt pavements by five research groups.. Infrared reflective paints were applied directly on the surface of concrete pavements . IR reflective paints were applied on the surface of asphalt together with hollow ceramic spheres to reduce the conductivity of the pavement. Thin reflective asphaltic layers of different colors developed using infrared reflective pigments were applied on conventional ashalt pavements. Ten prototype cool colored pavement materials using infrared reflective pigments were tested against conventional materials of the same color, under hot summer conditions. As reported, the reflective black material presented an albedo close to 0,27 and had a mean daily surface temperature almost 10 K lower, compared to the standard black, ρ=0,05. In parallel, the reflective blue had an albedo close to 0,33 and almost 4,5 K lower mean surface temperature compared to the conventional blue having a reflectivity of 0,18.

The use of colored reflective pavements, based on the use of inorganic infrared reflective pigments, is already commercialized in the United States. The albedo of the proposed pavements is around 0,45 to 0,55. As reported, the use of the pavements reduces surface temperatures by 11-22 K.

Thin layer asphalt pavements are developed by mixing colorless elastomeric asphalt binders with infrared reflective pigments and aggregates of special characteristics. Five samples,

(green, red, yellow, beige and off white), were developed and tested under hot summer conditions against samples of conventional asphalt. The albedo of the thin asphalt layers ranges between 27 % for the red and green samples and 55% for the off white sample. The reflectance of the conventional asphalt was measured around 4%. All samples presented a high absorptance in the UV range, while their reflectance in the infrared was high and between 39 to 56 %. Thermal monitoring of the samples has shown that during the day all samples demonstrated a surface temperature that was higher than the ambient one, while during the night time the air temperature was always higher than that of the asphalt samples, mainly because of the high emissivity of the materials. The average daytime surface temperature of the samples ranged from 36^{o} C for the off white sample to 43,6 ^{o} C for the red one. The corresponding surface temperature of the conventional asphalt was close to 60 ^{o} C. The nigh time surface temperature of all the developed samples was almost 1 to 2 K lower than that of the conventional asphalt.

c) Use of heat reflecting paint to cover aggregates of the asphalt. The use of IR reflective paints to cover the aggregates used in asphaltic pavements is proposed and tested.. The pavements are made using a heat reflecting paint that has coated each piece of aggregate, while in conventional reflective asphalt pavements the paint is applied only in the surface. The albedo of the pavements varied between 0,46 and 0,57. Monitoring showed that the developed pavements present a much lower surface temperature than a conventional drainage pavement, while temperature differences varied between 10,2 and 18,8 K. In parallel, a similar technology to prepare high albedo coatings for asphalt pavements was proposed and tested. The experiment taken place in Japan, during the summer period. It is reported that when the albedo of the pavement increased to 0,25 its surface temperature was almost 6,8 K lower than that of the conventional asphalt, while when the albedo increased to 0,6 the corresponding surface temperature decrease was close to 20 K. In a general way, it is found that when the albedo value increased by 0,1 the corresponding decrease of the surface temperature was close to 2,5 K.

d) Use of color changing paints on the surface of the pavement. Color changing coatings to be applied on pavements were proposed by several authors. In particular thermochromic coatings are able to respond thermally to the environment and change reversibly their color and reflectivity from lower to higher values, as temperature rises. Such type of pavements were developed and their thermal performance was tested in comparison to highly reflective and

common coatings. Eleven tiles of different color were developed and tested under hot summer conditions. The pavement coatings were developed using organic thermochromic pigments together with an appropriate pigment and other stabilizing components. The infrared emittance was very similar for all the tested pavements. Monitoring of their surface temperature has shown that the daily mean surface temperature of the thermochromic coatings range from 31,0 to 38,4^{o} C, from 34,4 to 45,2^{o} C for the infrared reflecting cool coatings and 36,4 C to 48,5 ^{o} C for the common coatings. In all cases, the mean daily surface temperature of the thermochromic pavements was lower than that based on the use of infrared reflecting pigments and the common coatings. The nocturnal temperature of the three types of tested coatings was almost similar. Measurements of the spectral reflectivity of the thermochromic coatings, have shown that their maximum albedo increase from colored to colorless phase was 43%.

e) Use of fly ash and slag as constituents of the concrete. In particular fly ash and slag are used as constituents for the preparation of the concrete. It is reported that when 70 % of slag is used as cement replacement the mix presented an albedo of 0,582 which is 71 % than the albedo of the conventional mix. Although the results are quite important, developments on this field are limited and may not be considered as a strong research direction.

PERMEABLE PAVEMENTS

Permeable and water retentive pavements generally include additional voids than conventional pavements in order to allow water to flow through into the sub layers and the ground while may include water holding fillers to store water. Evaporation of the water helps to reduce the surface temperature of the pavements and contribute to the mitigation of the urban heat island while the risk of flooding is reduced. Three are the performance critera for water retentive pavements : a) the ability to decrease its surface temperature under fine weather, b) sustainability to suppress the temperature rise after rainfalls and c) Maximum durability and minimum decrease of its performance over time

Important research has been carried out to improve the thermal performance of permeable and water retentive pavements. Six technological approaches are developed and tested, for asphalt, concrete and ceramic pavements.

a) Use of water holding fillers made of steel by products as an additive to porous asphalt : A new water holding pavement consisted of water holding fillers made of steel by products and integrated in porous asphalt is presented and tested both experimentally

and theoretically against porous asphalt used in permeable pavements with a porosity equal to 0,3. It is reported that the average surface temperature of the water holding pavement was 0,6 K lower than that of the infiltration porous asphalt, while the air temperature above the water holding pavement was almost 0,5 K lower than above the conventional porous asphalt. The sudden decrease of the surface temperature of the conventional porous asphalt was higher than that of the water holding pavement, however the evaporation and the cooling effect in the later continue for longer than the conventional porous pavement presenting a maximum of about 3 days.

b) Use of fine blast-furnace powder in water retentive asphalt .The development and testing of a water retentive pavement material for roads using fine blast-furnace powder is described. The fine blast furnace powder is an admixture used in cement and like and is generated by the blast furnace process. The material was tested experimentally under real conditions in roads for long periods and it is shown that the water absorbing properties of the material present only a small change after accelerated curing, while as it concerns its thermal performance it is reported that during the third year of its operation , its surface temperature was even 14 K lower that of a dense graded asphalt pavement.

c) Use of fine texture pervious mortar as an additive to pervious concrete : The development and testing of a pervious concrete pavement combined with fine texture pervious mortar is described. Mortar is produced using cementitious materials, aggregate and water and is is used in order to improve the surface texture of the pervious concrete. The water permeability of the final composition was quite low, (2-3 mm/s). No data are available about the thermal performance of the new material.

d) Use of bottom ash and peat moss as additives in pervious concrete : The development and the experimental evaluation of a novel porous pavement block using bottom ash and peat moss is described. Peat is a porous material that acts as an adsorbent to remove heavy metals from aqueous solutions. The developed pavement was tested experimentally against conventional asphalt and normal porous blocks. It is found that the proposed material presents almost 18 K lower surface temperature than asphalt after a rainfall, while the maximum surface temperature difference with the conventional porous pavement was almost 9 K.

e) Use of fly ash with very narrow particle size distribution in bricks : The development of porous bricks presenting an open porosity of 22-43 %. The bricks have an average porous size between 0,4 and 50 μm and were prepared using fly ash with very narrow particle size

distribution. Experimental work , has shown that lower surface temperatures of water retentive materials in association to the limited reflected radiation helps to improve thermal comfort of citizens.

f) Use of industrial wastes as raw material for ceramic tiles : A new water retentive ceramic tile used for pavement has been developed and experimentally tested. The tile is made using industrial wastes as raw material and is considered as one of the most water retentive ones. The pavement has been experimentally tested outdoors under saturation conditions and is found to be almost 10 K of lower temperature than a concrete roof. In parallel, the air above the tile was almost 1-2 K of lower temperature. The use of water retentive materials presenting a high capillary ability has been proposed. As reported, these materials have the ability to suck up and spread efficiently the water in the whole surface of the pavement. Measurements have shown that the surface temperature of the proposed materials was almost 10 K lower than that of the dry material and almost 25 K cooler than the surface temperature of conventional asphalt. The measured sensible and latent heat fluxes from the wet material were 70 W/m^2 and 430 W/m^2 respectively.

CONCLUSIONS

Important research is carried out aiming to better document, understand and mitigate urban heat islands. New materials, systems and technologies have been developed and proposed in order to decrease the sensible heat flux to the atmosphere from different urban structures like buildings and paved surfaces. As it concerns the research objectives on the field of cool pavements, two main research streams have been developed aiming either to develop highly reflective paved surfaces or permeable pavements making use of the cooling evaporation capacity of water.

Actual research trends to develop highly reflective pavements focus on the use of highly reflective white coatings and infrared reflective colored pigments to increase the albedo of the pavements surface, the use of reflective paints to increase the reflectance of the pavement ingredients, and also the use of color changing paints to achieve a better thermal performance all year round. .Laboratory tests have shown that the albedo achieved can be very high and the pick surface temperature of the paved materials may decrease by up to 20 K. Newly developed reflective materials and techniques were tested in many demonstration and real scale projects. Unfortunately, few projects are monitored in detail to document precisely the expected benefits from a large scale implementation of reflective pavements It is considered that there is an urgent need for more large scale demonstration projects to assess experimentally and in

details all aspects related to the modification of the local microclimate and the possible impact on thermal comfort and energy consumption.

Permeable and water retentive pavements, vegetated or not, are more appropriate for rainy and humid areas where the availability of water is not a problem. Actual research targets aim mainly to involve additional agents in the mass of the pavements like steel bioproducts, fine blast furnace powder, fine texture pervious mortar, bottom and fly ash, peat moss and industrial wastes. Research aims also to improve the capillary ability of the pavements i to increase the water content and the evaporation capacity of the materials.. Laboratory tests have shown that new generation permeable pavements seem to present a significant lower surface temperature than the corresponding conventional permeable materials. However, the thermal performance of the permeable and water retentive pavements depends highly on the availability of water.

Many demonstration and large scale applications of permeable and water retentive pavements have been realized. However, the existing scientific information regarding their thermal performance is quite limited, as very few projects have been monitored.

REFERENCES

Santamouris M : Using cool pavements as a mitigation strategy to fight urban heat island—A review of the actual developments. Renewable and Sustainable Energy Reviews. In Press, 2013

GREEN AND COOL ROOFS' URBAN HEAT ISLAND MITIGATION POTENTIAL IN EUROPEAN CLIMATES FOR OFFICE BUILDINGS UNDER FREE FLOATING CONDITIONS

Dionysia Kolokotsa[1], Mattheos Santamouris[2]

1 University of Athens, Physics Department, Group Building Environmental Studies, Athens, Greece

2 Technical University of Crete, School of Environmental Engineering , GR 73100, Crete, Greece

Note: the contact addresses may be re-arranged

ABSTRACT

Heat island which is the most documented phenomenon of climatic change is related to the increase of urban temperatures compared to the suburban. Among the various urban heat island mitigation techniques, green and cool roofs are the most promising since they simultaneously contribute to buildings' energy efficiency. The aim of the present paper is to study the mitigation potential of green and cool roofs by performing a comparative analysis under diverse boundary conditions defining their climatic, optical, thermal and hydrological conditions. The impact of cool roof's thermal mass, insulation level and solar reflectance as well as the effect of green roofs' irrigation rate and vegetation are examined. The parametric study is based on detailed simulation techniques coupled with a comparative presentation of the released integrated sensible heat for both technologies versus a conventional roof under various climatic conditions.

Keywords: green roofs; cool roofs; urban heat island; mitigation potential; sensible heat

1 INTRODUCTION AND STATE OF THE ART

The heat island effect concerns higher temperatures in central urban areas as compared to suburban areas, and is considered as the most documented phenomenon of climatic change (Santamouris 2001). Existing data shows that the intensity of the phenomenon may be very important and may reach values close to 10K. The increase of urban temperatures in association to the important climate change influences the quality of life of urban citizens. In particular, there is a considerable increase in the energy consumption for cooling buildings, while high temperatures intensify pollution problems and increase ozone concentration. In parallel, the outdoor thermal comfort conditions are deteriorated, the ecological footprint of cities is increasing, while the thermal stress is more intense for low income population (Sakka et al. 2012).

To counterbalance the aforementioned conditions various mitigation techniques have been developed. Some of the more important mitigation techniques deal with the increase of the albedo of buildings and urban structures, the use of additional green spaces in cities, (Zoulia, Santamouris, and Dimoudi 2009), the installation of green gardens on the roof of buildings, as well as the use of cool sinks for heat dissipation, such as the ground and water. In particular, the increase of urban albedo may decrease substantially carbon dioxide emissions in the atmosphere. Recent studies have shown that a long-term global cooling effect of 3×10^{-15} K corresponds to each 1 m^2 of a surface with an albedo increase of 0.01 and this is

equivalent to a CO_2 emission reduction of about 7 kg (Akbari, Damon Matthews, and Seto 2012). Increase of the albedo in the built environment can be achieved by using high reflectance surfaces in roofs, pavements and other urban surfaces. Natural materials as well as high reflectance white paints have been proposed and used with important results in buildings,(Synnefa, Santamouris, and Livada 2006). Recent studies and applications have shown that the use of cool roofs is associated to important reductions of the cooling load of the corresponding buildings, (Kolokotsa et al. 2011; Synnefa, Saliari, and Santamouris 2012; Synnefa and Santamouris 2012). Green roofs are fully or partially covered with vegetation and a growing medium over a waterproofing membrane. Two types of green roofs are available: Intensive roofs, which are heavy constructions and can support small trees and shrubs, and extensive roofs, which are covered by a thin layer of vegetation. There are several advantages associated to green roofs like decreased energy consumption, better air quality and noise reduction, increased durability of the roof materials, etc. (Mentens, Raes, and Hermy 2006; Sfakianaki et al. 2009). Important energy benefits are associated to the use of green roofs. Energy reductions depend on the design of the green roofs, the local climatic conditions and the characteristics of the building, (Castleton et al. 2010; Takakura, Kitade, and Goto 2000). A discussion on the main parameters defining the performance of the green roofs is given in (Santamouris 2012).

The total surface of roofs in the urban world is estimated close to 3.8 10^{11} m^2, while roofs constitute over 20-% of the total urban surfaces((Akbari, Menon, and Rosenfeld 2009; Akbari, Rose, and Taha 2003; Zinzi and Agnoli 2011). Thus roofs provide an excellent medium for the application of mitigation techniques as the construction cost is much lower than that of the available free ground area, while at the same time they offer additional benefits, such as the reduction of the energy consumption of the corresponding buildings.

Cool and green roofs are excellent mitigation technologies applied on the roof surface of buildings. The overall energy performance of the two examined mitigation techniques depends mainly on the climatic conditions and the constructional characteristics. A classification of the comparative performance of both roof mitigation techniques based on existing experimental and theoretical data is provided in (Santamouris 2012).

The present paper aims to investigate the comparative performance of cool roofs and green roofs under diverse boundary conditions defining their climatic, optical, thermal and hydrological condition. Parametric studies have been performed using detailed simulation techniques for both technologies and conclusions are extracted and discussed.

2 THE MITIGATION POTENTIAL OF REFLECTIVE AND GREEN ROOFS: FACTORS AFFECTING THEIR PERFORMANCE

The mitigation potential of reflective and green roofs depends on a number of parameters as summarized in (Santamouris 2012). Four categories of performance parameters have been identified as described below:

Climatic parameters like solar radiation, ambient temperature and humidity, wind speed and precipitation. Solar radiation determines the thermal balance of the roofs and defines at large their temperature. Ambient temperature regulates the amount of sensible heat released to the atmosphere as convective heat flux is a function of the temperature difference between the roof and the air. Wind speed determines the heat transfer coefficient between the roof and the atmosphere while relative humidity and precipitation define the moisture balance in green roofs.

Optical parameters like solar reflectivity and emissivity for reflective roofs and the absorptivity of the plants for the green roofs

Thermal parameters, such as the thermal capacity of the roofs and the overall heat transfer coefficient, U-value, between the roof and the building.

Hydrological parameters that define the latent heat budget in green roofs.

3 THE METHODOLOGY

The urban heat mitigation technologies associated with roofs, are: a) the cool (or reflective) roofs, and b) green roofs (or living) roofs. Both technologies can lower the surface temperatures of roofs and thus decrease the corresponding heat flux released to the atmosphere. The methodology followed in order to calculate, analyze and compare the mitigation potential of both technologies under different boundary conditions, is described below: A building model was developed using Energy Plus, which is a well-known computational package software for transient building simulation with conventional roof construction characteristics. Comparison of simulated against experimental results has shown that the model is very accurate to estimate the performance of cool and green roofs. A parametric study was performed concerning the sensible and latent heat flux released to the atmosphere for roofs under different building construction characteristics and climatic conditions. The parametric study included the following:

For the cool roofs, the impact of the albedo, the U-value of the roof and its thermal capacitance has been determined for different climatic conditions in Europe. In particular, the following sensitivity analyses have been performed: (i)Analysis of the sensible heat flux released for different solar reflectance versus the building's thermal mass. (ii)Analysis of the sensible heat flux released for different solar reflectance versus the building's insulation. (iii) Analysis of the sensible heat flux versus the climatic conditions.

For green roofs, the impact of plant characteristics and irrigation rate has been calculated for the same climatic conditions as above. In particular, the following comparisons have been performed: (i) Analysis of the sensible heat flux released versus the characteristics of the plants. (ii)Analysis of the sensible heat flux released versus irrigation rate.

Based on the sensitivity results a detailed comparison of both technologies is performed and presented below.

3.1 The building model

An office building model is developed using Energy Plus v7.1 as it offers the capability to evaluate the sensible heat flux from the roofs while latent heat flux is also calculated using the "ecoroof" module for the simulation of green roofs. The building is designed using Google Sketchup plugin for Energy Plus (Table 1).The specific characteristics of the building are tabulated in Table 1. The building was simulated as free floating without any use of heating, ventilation air conditioning system and thermostatic control during the whole day and night.

Table 1 Reference building characteristics

General Information	
Building type	Office (two storey)
Surface area	~800 m^2
Orientation	N-S
Building envelope	
Walls	brick, insulation, concrete, plasterboard total U: 0.429W/m^2K, Surface area 560 m^2
Roof	200 mm concrete, 25 mm insulation, acoustic tile ceiling of total U= 0.581 W/m^2K, Surface area 400 m^2
Windows	Double glazing windows with: U= 2.720 W/m^2K, Surface area 46 m^2 (8% of the wall area)
Floor	One layer (concrete) floor with U= 4.142 W/m^2K
Shading	Shading the south openings of the building

3.2 The mitigation potential of cool roofs

The first step in the analysis of the mitigation potential for cool roofs was to calculate the sensible heat flux released for different optical and thermal properties of cool roofs under hot

and moderate climatic conditions and in particular for various representative climatic zones. This is performed using the model described in section 3.1 for the climatic conditions of the Southern and Mid Latitude Europe. The flux of the sensible heat computed for the whole summer period, (June-August), and for roof albedos equal to 0.9, 0.8, 0.7, 0.6 and 0.3 and for the city of Chania, is depicted in Figure 1.

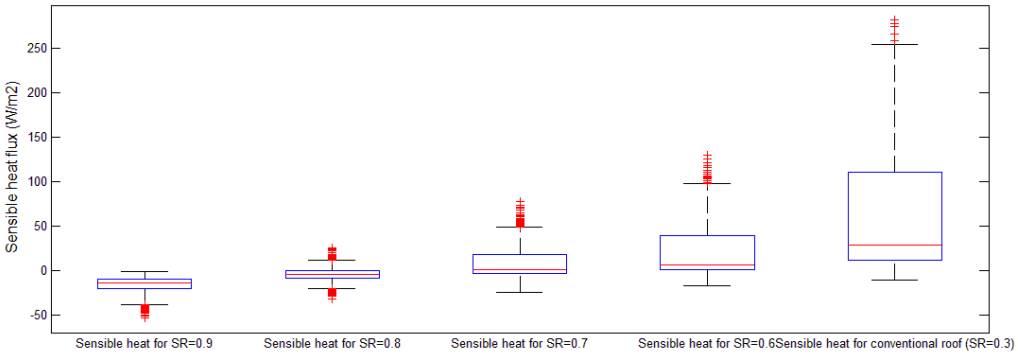

Figure 1. Comparison of heat island mitigation potential in Chania Greece, for a typical construction, between cool and conventional roof

As shown for highly reflective roofs the median sensible heat flux is negative while the maximum value is of the order of a few W/m^2. For reflectivity close to 0.8 and 0.7 the median value of the sensible heat flux is close to zero while the maximum value varies between 15 – 50 W/m^2. On the contrary, conventional roofs present a median sensible heat flux close to 30 W/m^2, and a maximum flux value around 270 W/m^2. Moreover, from the same figure it can be seen that the range of sensible heat flux values is larger for the conventional roofs compared to the cool roofs for the cooling season (summer period). This proves that the use of cool materials minimizes the roofs' heat stress.

3.2.1 Cool Roofs versus thermal mass characteristics

The combined effect of the roof's solar reflectance and thermal mass to the overall heat gain is very important but its impact sometimes is neglected or ignored. In the present section five different roof thermal mass configurations are examined through the corresponding thickness and materials, i.e. very heavyweight concrete, medium weight concrete, lightweight concrete very lightweight concrete and wooden construction roof. These configurations combined with the solar reflectance were used to calculate the sensible heat flux using Energy Plus 7.1 building model described before. Figure 2 depicts the output of the calculations in the climatic conditions of Southern Europe for SR=0.9 in different thermal mass conditions. From the specific figure it can be concluded that : a) During the night, the heat island mitigation potential for all levels of thermal mass is quite similar with a difference in the order of 2 W/m^2, b) During peak hours i.e. 11:00-17:00, the impact of the thermal mass is quite important. Heavyweight roofs present much higher mitigation potential than the lightweight roofs. The relative difference between the two cases for a roof with albedo equal to 0.9 in southern Europe is close to 13 W/m^2. The same pattern but with smaller variations for the heavyweight construction can be noticed for the other European climates. For example the daytime benefit of heavyweight roofs of very high albedo in London is close to 7 W/m^2

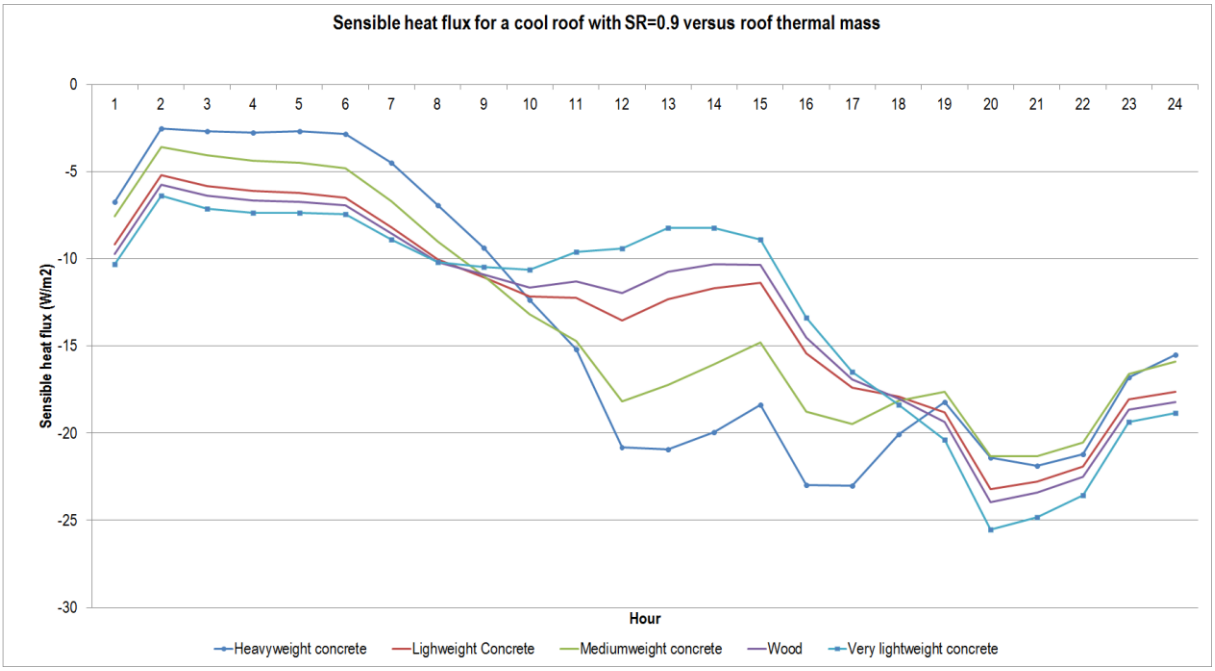

Figure 2. The sensible heat flux versus thermal mass for a cool roof with SR=0.9 and for the Southern Europe (Crete)

The day-night fluctuation of calculated sensible heat flux released by heavyweight roofs is much higher for the climatic conditions of southern Europe, while it reduces for northern climates. As shown, heavyweight roofs offer an integrated reduction of the sensible heat during the whole summer period of around 70 kWh/m^2 if compared to the lightweight constructions. Therefore the lower the albedo, the higher the benefit that heavyweight roofs offer. In particular, the sensible heat reduction for roofs with albedo equal to 0.8, 0.7, 0.6 and 0.3 are 210 kWh/m^2, 286 kWh/m^2 and 490 kWh/m^2 respectively. This is easily explained by the fact that the sensible heat flux from the roofs is inversely proportional to their albedo.

3.2.2 Cool Roofs versus thermal insulation

The present section studies the mitigation potential of the cool roofs versus the insulation level of the construction. The insulation type considered is polystyrene with thermal conductivity 0.3 W/mK while the layers used by the simulation ranged from 25mm to 150 mm with various solar reflectance characteristics. The simulation results (depicted in Figure 3) for Crete climatic conditions show that the insulation level does not influence considerably the sensible heat flux released by the roofs. The same occurs under the London climatic conditions. For albedo values of 0.9 the increase of the insulation level from 25 mm to 75 mm in Crete and London decreased the integrated summer sensible heat released by 1-2 kWh/m^2. In parallel, it decreases the peak summer indoor temperature by 0.1K in Crete and increases it by 2.2K in London. Such an increase of the temperature in London is due to the low surface temperatures at the exterior part of the roof, (almost 13-14 °C). Lower insulation levels increases the flow of heat from the interior to the exterior of the building's roof and contributes to the decrease indoor temperatures. On the contrary, in Crete, indoor and exterior roofs surface temperatures are quite similar and the flow of heat is negligible.

For lower albedo values the impact of the insulation continues to be non-important for all the thermal mass conditions. In almost all cases the increase of the insulation levels decreases the integrated summer sensible heat released. It is characteristic that in Crete and for albedo values close to 0.3 the increase of the insulation levels contribute to increase slightly the integrated summer sensible heat released. Given that for such albedo values, the maximum daily surface temperature of the roof is close to 65 °C, higher insulation levels limits the flow

of heat to the interior of the building and thus contribute to slightly higher surface temperatures, and increased integrated summer sensible heat, but also to lower indoor temperatures. In this case, summer indoor maximum temperatures for 75mm insulation are to about 0.7 °C lower than for 25mm insulation.

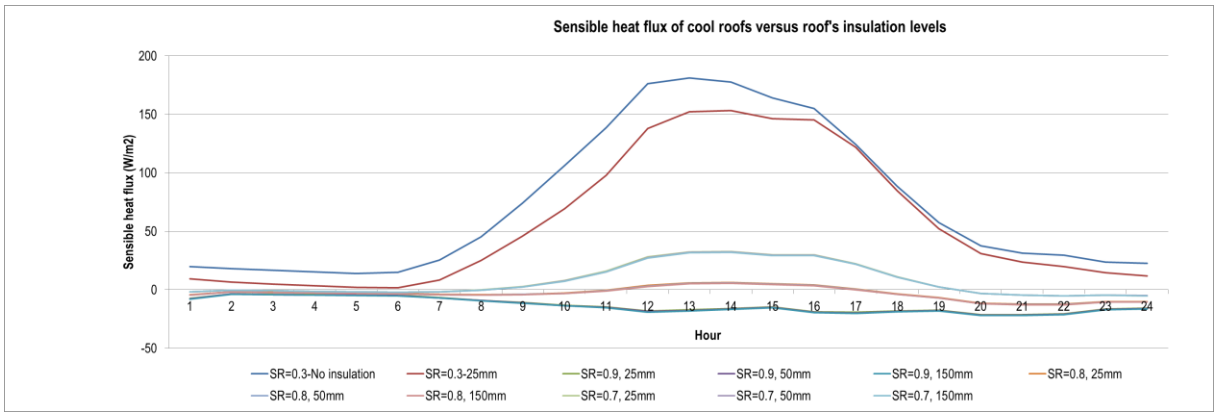

Figure 3: Sensible heat flux released from cool roofs with various insulation levels for a typical summer day

The phenomenon is more intense for less massive roofs. For northern climates, the daily surface temperature of the roof is much lower and the heat flux between the roof and the building is reduced. For example in London, the maximum daily surface temperature for albedo equal to 0.3 is close to 38°C, and the possible increase or decrease of the insulation level does not contribute to any significant variation of the integrated summer sensible flux. However, the maximum summer indoor temperature is found to increase to about 0.4K for higher insulation levels. This is explained as during the night period, the exterior surface temperature of the roof is much lower that the corresponding indoor temperature. Thus, the heat transferred from inside to the outside part of the roof during the night period is much higher for low insulation levels and the corresponding indoor temperature is also lower. Night cooling of the building contributes to lower daily indoor temperatures in low insulated buildings until the early afternoon period.

3.3 The mitigation potential of green roofs

The technology of green roofs, has gained ground during the last decades, as it reduces the energy consumption of buildings while improving the microclimate of the wider urban space where the building is situated.

The most important energy advantage of green roofs is their contribution to the insulation of the buildings, which usually results in energy savings both for heating and cooling. Apart from their impact on building energy consumption, planted roofs contribute to the mitigation of heat islands. They increase the total water-permeable city surface, helping water to be retained in the soil and allowing larger quantities to be available for evapotranspiration. At the same time, planted roofs present much higher albedo values than dark urban roof surfaces, thus reflecting off greater proportion of the incident solar radiation and not transforming it into heat (Getter et al, 2006).

3.3.1 Sensible Heat of Green Roofs as a function of LAI and Irrigation Rate

LAI represents the amount of leaf material in an ecosystem and is geometrically defined as the total one-sided area of photosynthetic tissue per unit ground surface area. Therefore the highest the LAI the denser the vegetation used in the green roof. A typical value of LAI for green roofs is LAI=1.

Sensitivity analysis has been performed for LAI values 0.05, 0.5, 1, 2 and 3 to cover all the range of possible vegetation. The maximum daily sensible heat released for a conventional roof in Crete is 157 W/m^2, while the corresponding values for LAI values 0.5,1,2,and 3 are

104 W/m^2, 70 W/m^2, 33 W/m^2 and 21 W/m^2 respectively. Values decrease by about 20-25 % for the case of an irrigated green roof. The specific values of the maximum daily sensible heat during the summer period in Crete for various LAI and irrigation rates are given in Table 3. As shown, the increase of the irrigation rate from zero to 0.1 reduces the sensible load in Crete by 20-25 %, while the increase of the irrigation rate from 0.1 to 0.3 has almost a negligible effect. As it concerns indoor ambient temperatures in Crete, green roofs with LAI=3 present almost 3°C lower maximum summer indoor temperatures than roofs with LAI=1. The sensible heat flux released by the same green roof (i.e. extensive green roof type with LAI=1 and with no irrigation rate) is calculated under different climatic conditions. The peak sensible heat released under different climatic conditions varies considerably ranging from 50-70W/m2 but it always remains lower than the conventional constructions.

Table 2. Maximum daily sensible heat released during the summer period in Crete for various LAI and irrigation rates, (W/m2).

LAI	IRRIGATION=0	IRRIGATION=0.1	IRRIGATION=0.3
0.05	157	113	113
0.5	104	79	78
1	71	54	54
2	34	25	25
3	21	15	15

In London, for LAI values close to zero, (0.05), the maximum daily sensible heat released is close to 87 W/m2, for irrigated and non-irrigated green roofs. The corresponding values for LAI equal to 0.5,1,2, and 3 are 56 W/m^2, 37 W/m^2, 17 W/m^2, and 10 W/m^2. Almost similar values are obtained for irrigated roofs.

In parallel, the sensible energy released during the whole summer period by a non-irrigated green roof in Crete is close to 176 kWh/m^2 while it is reduced to 124 kWh/m^2, 88 kWh/m^2, 73 kWh/m^2 and -8 kWh/m^2 for LAI values of 0.5,1, 2, and 3 respectively. The corresponding values for London are substantial lower and in particular: 119 kWh/m^2, 86 kWh/m^2, 62 kWh/m^2, 20 176 kWh/m^2, and 12 kWh/m^2, for LAI values of 0.05, 0.5,1,2 and 3 respectively.

4 RESULTS AND DISCUSSION

The maximum daily sensible heat flux for various cool and green roof configurations is given in a comparative way for the climate of Crete in Figure 4, in (W/m^2) and for London in Figure 5. As shown the main parameters that define the performance of cool and green roofs are the albedo and LAI value respectively. The thermal mass as well as the insulation level of cool roofs and the irrigation rate in green roofs play an important role on the sensible heat released but are less significant.

For the climatic conditions of Crete, cool roofs with an albedo of 0.9 present the best performance and the maximum daily sensible heat released is negative for the specific climatic conditions. Negative values are also obtained for green roofs with a LAI value of 3 and for irrigated and non-irrigated roofs. All other configurations present a positive maximum daily sensible heat released. When the albedo of cool roofs decreases to 0.8 the corresponding mitigation potential is very similar to that of a green roof with a LAI of 2. In this case the maximum sensible heat released is between 5 to 10 W/m^2. The better performance is achieved by very well insulated cool roofs, while well irrigated green roofs present a higher mitigation potential than non-irrigated roofs. Cool Roofs presenting an albedo of 0.7 and 0.6 release less sensible heat during the day than green roofs with a LAI of 1. When the albedo is 0.7 the released sensible heat is less than 50 W/m^2, while for albedos close to 0.6 the corresponding heat is around 60-70 W/m^2. In comparison, green roofs with LAI values equal to 1, release almost 70-80 W/m^2. When LAI decreases to 0.5 the sensible heat released is higher than 100

W/m^2 and may reach values close to 130 W/m^2. However, when the albedo decreases to 0.3 the corresponding maximum sensible heat released is higher than 150 W/m^2.

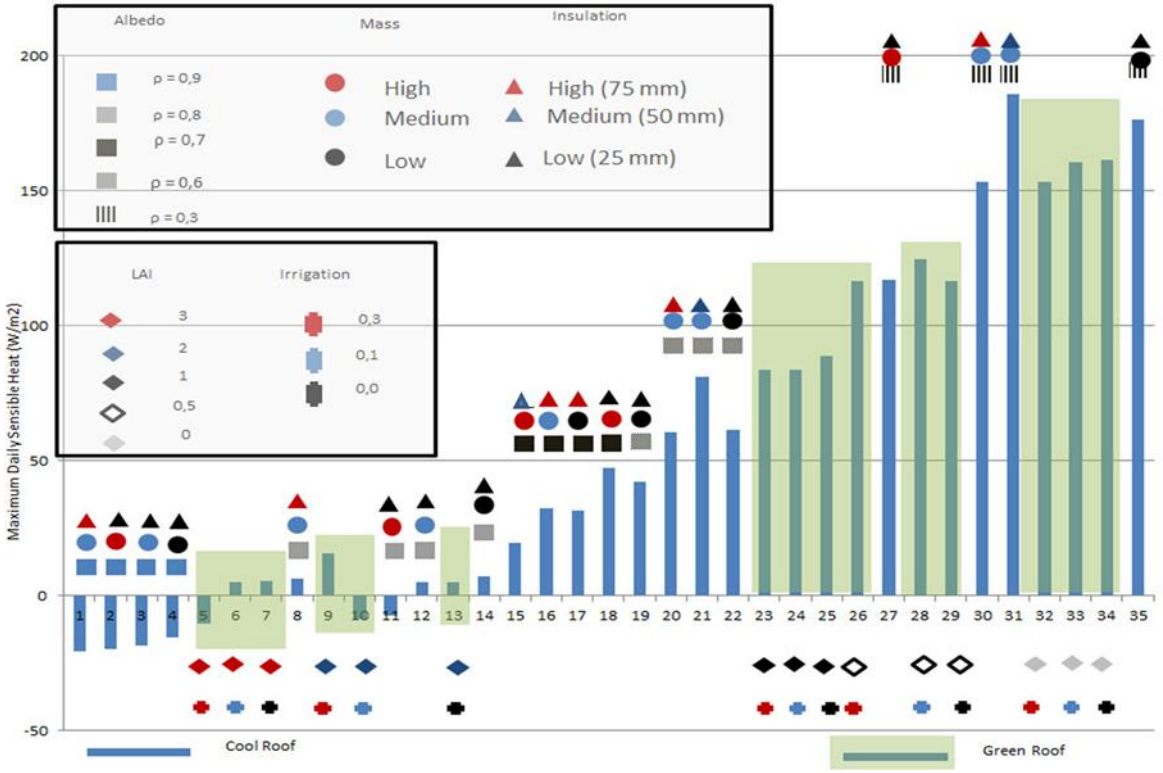

Figure 4. The maximum daily sensible heat flux extracted by cool and green roof configurations for a typical summer day in Southern Europe, (W/m^2)

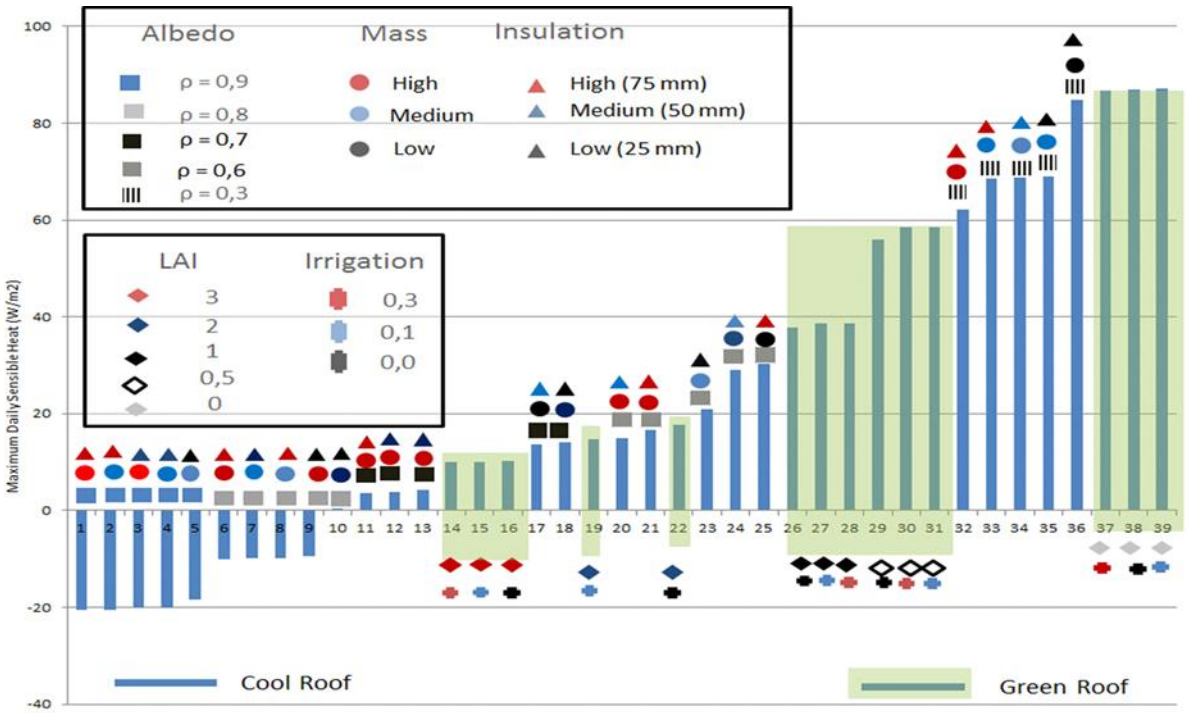

Figure 5 The maximum daily sensible heat flux extracted by cool and green roof configurations for a typical summer day in London, (W/m^2)

For Northern Europe and in particular London, cool roofs with albedos 0.9 and 0.8 present a negative daily maximum sensible heat released during the summer period and contribute highly to mitigate urban heat island. In particular, the released sensible heat is -20 W/m^2 and -10 W/m^2 for albedos of 0.9 and 0,8 respectively. Green roofs with a LAI value of 1, have also a very low daily maximum sensible heat that is close to 10 W/m^2, while for LAI values of 2 the corresponding sensible heat is below 20 W/m^2.Similar values are also obtained for cool roofs with an albedo of 0,7. When the albedo decreases to 0.6, the corresponding sensible heat increases to about 30 W/m^2. Green roofs with LAI = 1 and LAI=0.5 have a sensible load just below 40 W/m^2 and 60 W/m^2 respectively. Finally, the sensible heat released by a roof with an albedo of 0.3 releases on average about 70 W/m^2.

5 CONCLUSIONS

In this paper a comparative analysis of the green and cool roofs' urban heat island mitigation potential is performed under different climatic conditions.

By examining the overall analysis it is evident that both cool and green roofs can contribute considerably to the improvement of the urban environment while simultaneously decrease the energy demand. Since the observed high ambient temperatures intensify the energy problem of cities, deteriorate comfort conditions, put in danger the vulnerable population and amplify the pollution problems, all available solutions should be examined in order to improve the urban thermal microclimate.

As a result a careful design taking into account the specific performance of green and cool roofs but also other factors like the ageing of cool materials, the green roofs' irrigation needs as well as the climatic diversities should be taken into account to maximize the mitigation perspective.

6 REFERENCES

Akbari, H., H. Damon Matthews, and D. Seto. 2012. "The long-term effect of increasing the albedo of urban areas." *Environmental Research Letters* 7(2).

Akbari, H., S. Menon, and A. Rosenfeld. 2009. "Global cooling: Increasing world-wide urban albedos to offset CO 2." *Climatic Change* 94(3-4):275–86.

Akbari, H., L. S. Rose, and H. Taha. 2003. "Analyzing the land cover of an urban environment using high-resolution orthophotos." *Landscape and Urban Planning* 63(1):1–14.

Castleton, H. F., V. Stovin, S. B. M. Beck, and J. B. Davison. 2010. "Green roofs; Building energy savings and the potential for retrofit." *Energy and Buildings* 42(10):1582–91.

Hodo-Abalo, S., M. Banna, and B. Zeghmati. 2012. "Performance analysis of a planted roof as a passive cooling technique in hot-humid tropics." *Renewable Energy* 39(1):140–48.

Kolokotsa, D., C. Diakaki, S. Papantoniou, and A. Vlissidis. 2011. "Numerical and experimental analysis of cool roofs application on a laboratory building in Iraklion, Crete, Greece." *Energy and Buildings* 55:85–93.

Mentens, J., D. Raes, and M. Hermy. 2006. "Green roofs as a tool for solving the rainwater runoff problem in the urbanized 21st century?" *Landscape and Urban Planning* 77(3):217–26.

Sakka, A., M. Santamouris, I. Livada, F. Nicol, and M. Wilson. 2012. "On the thermal performance of low income housing during heat waves." *Energy and Buildings* 49:69–77.

Santamouris, M. 2001. *Energy and Climate in the Urban Built Environment*. edited by M Santamouris. London: James and James Science Publishers.

Santamouris, M. 2012. "Cooling the cities - A review of reflective and green roof mitigation technologies to fight heat island and improve comfort in urban environments." *Solar Energy*.

Sfakianaki, A., E. Pagalou, K. Pavou, M. Santamouris, and M. N. Assimakopoulos. 2009. "Theoretical and experimental analysis of the thermal behaviour of a green roof system

installed in two residential buildings in Athens, Greece." *International Journal of Energy Research* 33(12):1059–69.
Synnefa, A., M. Saliari, and M. Santamouris. 2012. "Experimental and numerical assessment of the impact of increased roof reflectance on a school building in Athens." *Energy and Buildings*.
Synnefa, A., and M. Santamouris. 2012. "Advances on technical, policy and market aspects of cool roof technology in Europe: The Cool Roofs project." *Energy and Buildings*.
Synnefa, A., M. Santamouris, and I. Livada. 2006. "A study of the thermal performance of reflective coatings for the urban environment." *Solar Energy* 80(8):968–81.
Takakura, T., S. Kitade, and E. Goto. 2000. "Cooling effect of greenery cover over a building." *Energy and Buildings* 31(1):1–6.
Zinzi, M., and S. Agnoli. 2011. "Cool and green roofs. An energy and comfort comparison between passive cooling and mitigation urban heat island techniques for residential buildings in the Mediterranean region." *Energy and Buildings* 55:66–76.
Zoulia, I., M. Santamouris, and A. Dimoudi. 2009. "Monitoring the effect of urban green areas on the heat island in Athens." *Environmental Monitoring and Assessment* 156(1-4):275–92.

PRELIMINARY STUDIES FOR A COOL ROOFS' ENERGY RATING SYSTEM IN ITALY

Michele Zinzi*[1], Emiliano Carnielo[2], Gaetano Fasano[1], Alessandro Federici[1]

1 ENEA Italian National Agency for New Technologies, Energy and Sustainable Economic Development
Via Anguillarese, 301
00123 Roma (I)
**Corresponding author: michele.zinzi@enea.it*

2 Università degli Studi Roma Tre, Engineering Department
Via della Vasca Navale, 79/81
00146 Roma (I)

ABSTRACT

Energy saving in the building sector is one of the key issue to achieve environmental targets at national and EU levels. Even if characterised by a large number of different climatic conditions, Italy energy policies were aimed at reducing the energy consumption related to space heating in buildings, neglecting other relevant energy uses as space cooling, which has dramatically increased in the past years. The recent EU Directive for the State Members is to assess the energy quality of buildings taking into account all the relevant energy uses.
Cool roofs are an old concept merged with new technologies that play a crucial role in the energy balance of buildings especially at Mediterranean latitudes. Reducing the solar gains thanks to the roof high solar reflectance, cool roofs keep the building cooler during cooling season, reducing the cooling demand and increasing the thermal comfort; On the other hand this technology has a negative impact on the winter energy balance. It is be noted that the performance of the roof surface also depends on the thermal emissivity, that drives the radiative exchanges of the roof towards the sky and the surrounding objects. If the performance of the cool roof products is a function of the above cited quantities, the technology impact is a function of several other parameters: climatic conditions, building geometry, thermo-physical characteristics of the building envelope.
Energy rating and labelling are a quick solution to compare energy related products, as inferred from recent EU Ecodesign Directive which requires the energy labelling not only for products that consume energy but also for energy related components, as windows.
This study presents the first studies aimed at the definition of an energy rating scheme for cool roof, starting from product properties and reaching the building performances, with a focus on dwellings. The methodology is based on a wide number of energy simulations carried out with an accurate dynamic calculation tools. The variables taken into account are:

- Roof surface radiative properties;
- Reference buildings characteristics - including solar and thermal properties, geometry, orientation;
- Climatic zones: The calculations were carried out for Palermo, Rome and Perugia in order to take into account a wide variety of summer and winter conditions of the Mediterranean areas of the country.

The calculations were performed with an insulated and not-insulated building configurations. Hourly and annual heating and cooling demands were calculated, as well as effective heating and cooling degree days.
The results were used to find out simple linear regressions, expressing the energy performance of the building as a function of the roof radiative properties and, as a consequence, measuring the performance of the cool roof product. Limits and potentialities of the method are discussed.

KEYWORDS

Cool roof, energy rating, solar reflectance, thermal emissivity

1 INTRODUCTION

Improving the energy efficiency in the building sector is one of the key issues to achieve at national and EU levels, as communicated by the EU in the 2011 Energy Efficiency Plan and

the 2020 Strategy, as well as in the 2011 Italian Energy Efficiency Plan. Even if characterised by a wide variety of climatic conditions, Italy energy policies were aimed at reducing the energy consumption related to space heating in buildings, neglecting other relevant energy uses as space cooling, which has dramatically increased in the past years (ENEA, 2012). Similar trends can be observed in other countries for residential and commercial buildings. What is highly relevant, in this sense, are the requirements set by the EPBD 2010/21/EU regarding the energy quality of buildings to be assessed by taking into account all the relevant energy uses.

Improving the energy performances on yearly basis requires the implementation of cooling efficient technologies in new and existing buildings. Cool roofs merge old concepts (white/light coloured construction materials) with new technologies. Reducing the solar gains thanks to the roof high solar reflectance allows to keep the building cooler during cooling season, decreasing the cooling demand and increasing the thermal comfort. The technology has great potentialities in the Mediterranean climate countries, but it is important to note that cool roofs also have a negative impact on the winter energy balance because of the reduced solar gains. Besides, it is important to emphasize that the performance of the roof surface also depends on the thermal emissivity that drives the radiative exchanges of the roof towards the sky and the surrounding objects. Several studies were carried out during the past years and showed potentialities and limits of the technology by means of numerical analyses (Synnefa, 2007, Akbari, 1997, Suehrcke, 2008, Zinzi, 2010) and monitoring in real buildings (Bozonnet, 2011, Kolokotroni, 2011, Romeo, 2011, Kolokotsa, 2011, Synnefa, 2012). The cool roof technology is now a well-established technology in need of proper tools to increase the market penetration.

Energy rating and labelling for windows are implemented, as voluntary schemes, in several countries: Australia, Denmark, Finland, Sweden, USA. A preliminary study was carried out in Italy (Maccari, 2000) and similar activities are on-going in several EU countries. This instrument resulted to be an important wheel in driving the market towards more efficient energy related products. No other building envelope materials and components have such instruments, while the energy labelling is spreading in EU of energy using products, as: light bulbs, refrigerators, washing machine, etc. The framework set by the Ecodesign Directive 2009/125/EC will drive a strong change in the coming years, with mandatory ecological requirements for energy-using and energy-related products.

The energy rating scheme for cool roof is, at last, a tool useful to facilitate the market penetration. It allows to properly inform the end users about energy efficient solutions and to set the boundaries for the implementation of EU Directives in the fourth coming years. Unlike products that directly use energy, the definition of a rating scheme for cool roof requires very in-depth analyses in order to take into account all the variables affecting the performance of the product and of the building, it will be installed on.

2 METHODOLOGY

The building energy performances depend on several parameters: Climatic conditions; building geometry and use; thermal and solar properties of the building envelope. A successful energy rating scheme should be, as a matter of fact, simple and general. The latter two values will ensure that the scheme will be easily understood and will reach a larger community of stakeholders. To achieve the above mentioned objective, the development of the energy rating method for cool materials is based on the effort to establish a direct relation between the energy performances of the building and its surface thermo-physical properties, without taking into account variables that are specifically building-dependent.

Cooling and heating energy calculations were performed in order to assess how different parameters affect the building and roof thermal response. The calculation results also

provided the data sets necessary to implement the mathematical functions and regressions, the energy rating should be based on.
The variables analysed in the study are described below.

2.1 The climatic conditions

The regulatory framework for the heating season is implemented since more than two decades (Decree *DPR 412/93*, 1993), with small adjustments through the years. The Italian territory is divided in six climatic zones as a function of the heating degree days, counted in base 20 °C. The zones range from A (degree days lower than 700) up to F (degree days higher than 3000). No legislative or technical standard still officially exist for the cooling season. Nevertheless, a relevant technical pre-normative work has been carried out (Iatauro, 2013) with the introduction of a climate severity index based on cumulative values of air temperature, specific humidity and solar irradiation during the cooling season. The index ranges from A (coolest zone in summer) to G. Even if the summer zoning is no yet implemented, the data are useful for the selection of the reference localities. Three exemplary cities were selected: Palermo, with hot summer and mild winter; Rome, mild summer and winter; Perugia, mild summer and colder winter. The reference climatic data are in table 1. The choice of Perugia as *cold* city depended on the focus given to the Mediterranean area of the country, where the cool roof technology has a major chance of market penetration, without considering the alpine and sub-alpine areas.

Table 1: Climatic parameters of the reference localities

City	Winter climatic zone	Winter degree days	Summer climatic zone	Summer climate severity index
Palermo	B	720	F	2014
Rome	D	1440	E	1758
Perugia	E	2289	B	1536

2.2 The reference buildings

The main choice for the reference buildings was to consider the single flat instead of the whole structure, since most of new and existing buildings use ambient regulation controls for the heating and cooling systems. The following typical apartments were selected:

- Flat with four external walls, typical configuration of detached houses;
- Flat with three external walls, typical configuration of small apartment blocks;
- Flat with two external walls, typical configuration of large and tower apartment blocks.

The base floor and the internal walls are adiabatic, the roof is flat. The geometrical characteristics were summarised in table 2.

Table 2: Geometric characteristics of chosen reference buildings

	2 External walls	3 External walls	4 External walls
Net floor area [m^2]	87	76.5	99.5
Gross Volume [m^3]	267.3	245.7	302.4
S/V Ratio [m^{-1}]	0.53	0.59	0.68
Internal Height [m]	2.7	2.7	2.7

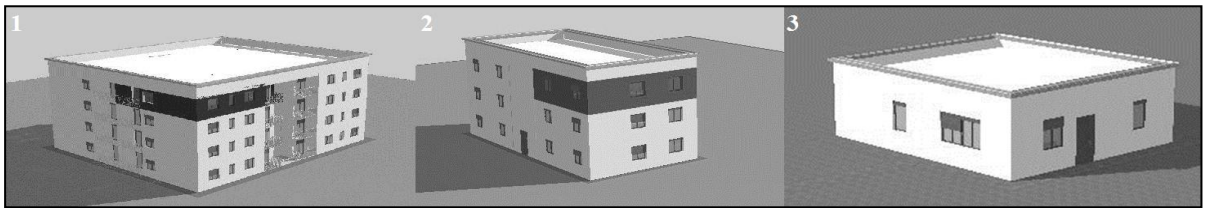

Figure 1: Apartment selected: (1) two external walls, (2) three external wall, (3) four external walls

Each building was created considering two insulation levels. The not insulated envelope was characterised by elements with the following thermal transmittances: 1.15 W/m^{2}K for the external vertical walls, 1.13 W/m^{2}K for the roof, 3.5 W/m^{2}K for the windows glass and 3.48 W/m^{2}K for the windows frame. The insulated envelope configuration, instead, presents an external walls thermal transmittance of 0.45 W/m^{2}K, a roof thermal transmittance of 0.47 W/m^{2}K, while the transmittance values for windows were set to 2.42 W/m^{2}K for the glass and 2.15 W/m^{2}K for the frame.
Other settings, common to all the three considered building models, both non-insulated and insulated, were chosen according to Italian standard reference UNI TS 11300-1 for residential structures. Internal gains were set to 4 W/m^2 with a constant occupancy density of 0.04 persons/m^2 (metabolic rate: Seated, light work). Air change value was set to 0.3 Vol/h. Net energy demands were calculated considering a temperature set-point of 20 °C during winter and a temperature set-point of 26 °C and a relative humidity set-point of 60% during summer.
The shading factor was controlled with a solar set-point. The windows shading system was modelled with a blind with low reflectivity slats activated during summer when the solar radiation is up to 150 W/m^2.

2.3 The roof surface properties

Solar reflectance (ρ_e) and thermal emissivity (ε) are surface properties of materials. The first represent the capability of material to reflect a portion of the incident solar radiation.
The second is the ability of material to emit and dissipate during the night the heat stored during the whole day.
In order to evaluate the energetic performances of cool materials, characterised by high solar reflectance and high infrared emissivity, used as roof covers, the reference buildings were studied selecting three levels of roof solar reflectance, 0.2, 0.5 and 0.8, combined with three values of thermal emissivity, 0.3, 0.6 and 0.9, obtaining nine different combinations.

3 CALCULATION RESULTS

A numerical analysis was performed using Design Builder in order to investigate the energetic performances of a cool roof application.
Design Builder is a graphical interface developed to make Energy Plus software more user-friendly. The latter is a stand-alone software for thermal simulation in a dynamic regime of building-plant systems and returns outputs in energy consumption, temperatures and heat flows. Energy Plus was developed in the laboratories of Berkeley University and Los Alamos. It has been continuously improved both in university laboratories and scientific and technical organisations such as ASHRAE that validates the calculation procedures through a special international protocol.
In essence, Design Builder combines one of the most powerful and reliable engines for calculating energy simulations with quick and easy dynamic modelling tools and also includes a simulation module for natural lighting and a powerful CFD engine calculation. Moreover it provides an easy to use OpenGL solid modeller that allows to assemble buildings models

through the positioning, the stretch and the blocks cut in three-dimensional space. Realistic three-dimensional elements determine a visual feedback of the element thickness and internal areas and volumes. Several geometric forms can be modelled as well as the optical and thermal properties of the surfaces. The templates allow to load into data projects the most common settings, activities, HVAC and lighting systems of buildings by simply selecting this features from the drop-down lists. It is also possible add or create customized templates.
More than 600 simulations were expected, taking into account: climate, building type and orientation, insulation level, roof surface properties. The first screening to reduce the number of calculations was to assess the influence of the apartment orientation. A set of simulations was performed for the eight cardinal orientations, being the apartment configured with typical values of insulation and roof properties. The orientation, whose resulted to be the closest to the average of the 8 orientation for the cooling and heating demand, was chosen as the reference, reducing to 162 the final number of simulations.
An explanatory figure is reported below to show the annual cooling, heating and global (the sum of the first two) demands as a function of the building models under study.

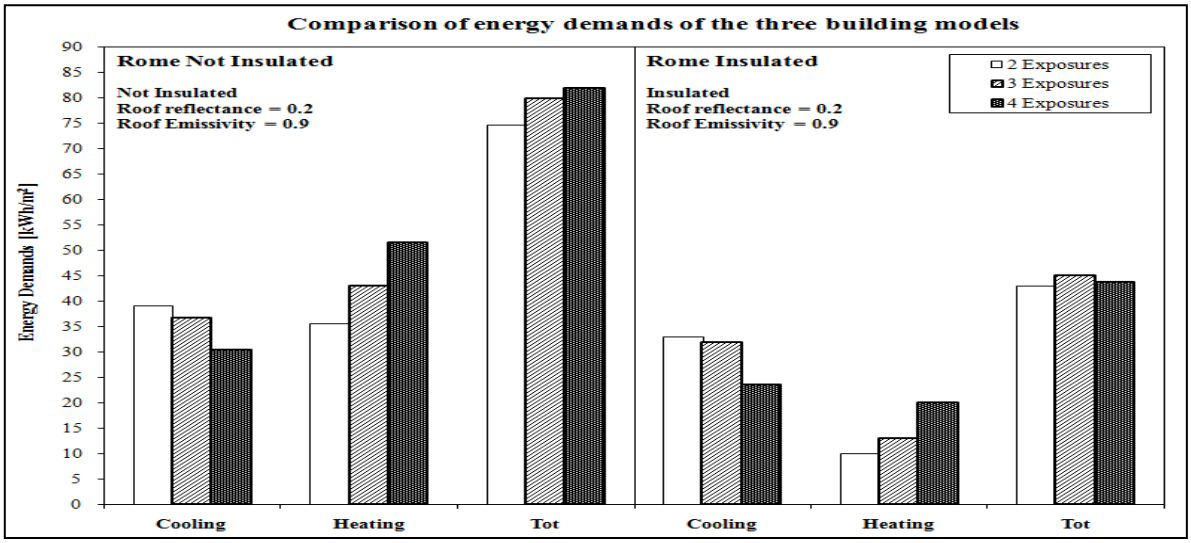

Figure 2: Annual energy demands for Rome, roof reflectance 0.2, roof emissivity 0.9

In figure 2 it is important to notice that the increase of insulation affects especially the heating demands, also by decreasing the cooling ones even if in smaller amount.
In order to assess in a more simple and general way the large number of simulation results, it was chosen to report only the average values of annual demands, summarised in table 3, obtained for the three structure types. The following figures put in evidence the impact of a cool roof application by dividing the effects due to the solar reflectance from the ones due to infrared emissivity.

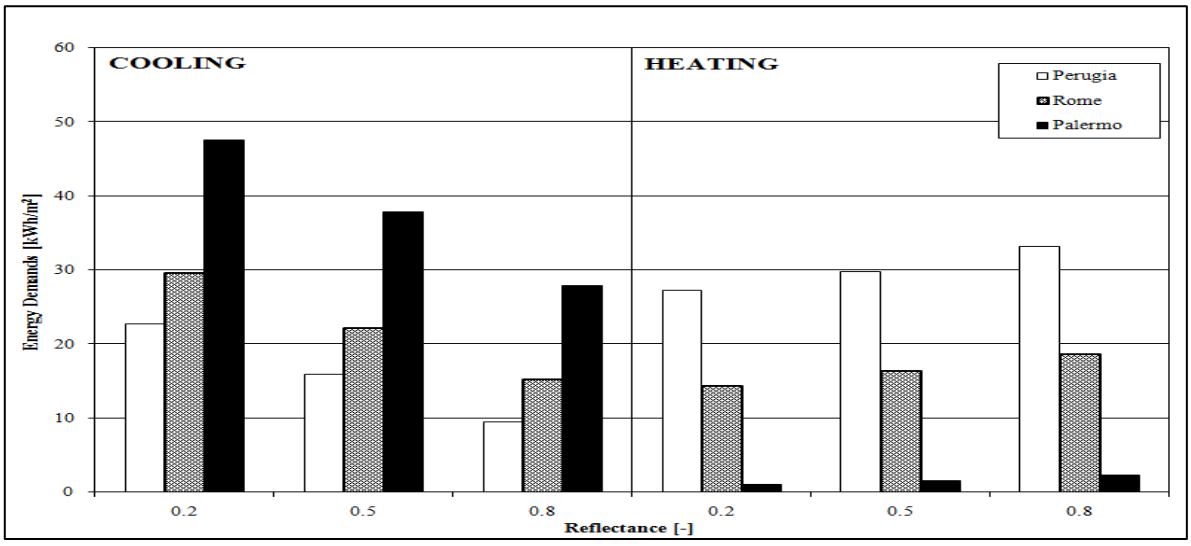

Figure 3: Insulated building: Increasing roof reflectance impact on cooling and heating demands (ε = 0.9)

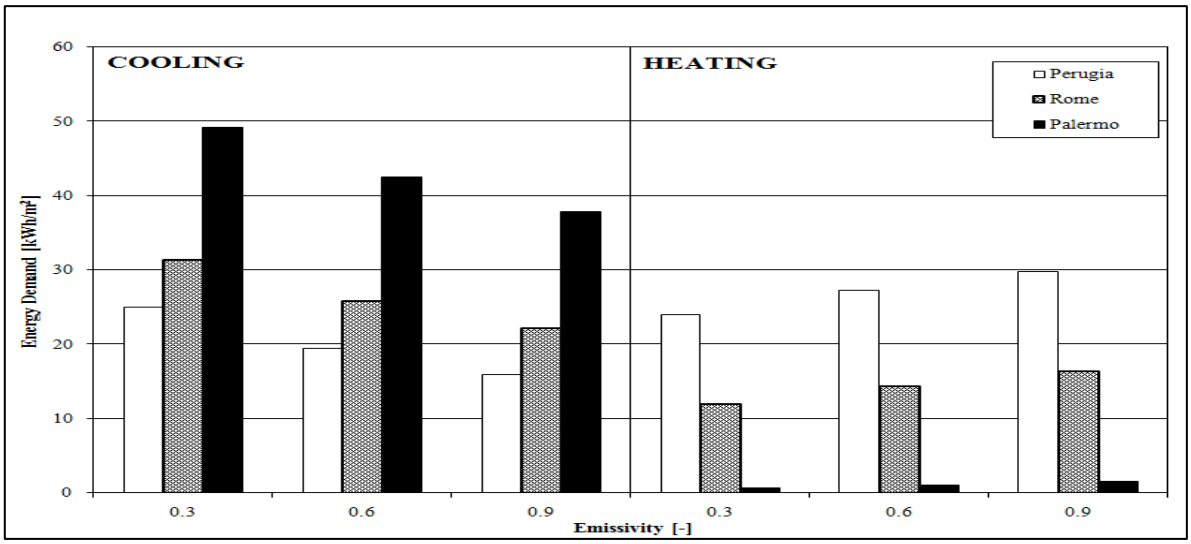

Figure 4: Insulated building: Increasing roof emissivity impact on cooling and heating loads (ρ_e = 0.5)

Figures 3 and 4, referred to the insulated building case, show how an increase both in roof reflectance and roof emissivity, can induce, during a year, a decrease in cooling demands and an increase in heating demands depending on climatic zone. The results were obtained by changing roof solar reflectance being equal emissivity set to 0.9 and by changing roof emissivity being equal solar reflectance set to 0.5.

Table 3. Design Builder results: Energy demands in kWh/m^2

			Insulated			Not Insulated		
	ρ_e	**ε**	**Cooling**	**Heating**	**Global**	**Cooling**	**Heating**	**Global**
Perugia	0.2	0.3	35.4	21.2	56.6	52.5	54.6	107.2
	0.5	0.3	25.0	24.0	49.0	31.0	63.1	94.1
	0.8	0.3	14.7	27.4	42.1	12.2	74.5	86.7
	0.2	0.6	27.7	24.7	52.4	37.0	64.4	101.4
	0.5	0.6	19.5	27.3	46.8	20.8	73.2	94.0
	0.8	0.6	11.4	30.8	42.2	7.9	84.1	92.0
	0.2	0.9	22.7	27.3	50.0	27.1	72.6	99.7
	0.5	0.9	16.0	29.8	45.8	14.6	81.2	95.8
	0.8	0.9	9.5	33.1	42.7	5.6	91.4	97.1
Rome	0.2	0.3	42.5	9.8	52.3	61.4	29.4	90.8

	0.5	0.3	31.4	11.9	43.3	38.7	35.7	74.5
	0.8	0.3	20.5	14.6	35.1	18.8	44.3	63.2
	0.2	0.6	34.7	12.3	47.0	45.7	37.0	82.7
	0.5	0.6	25.8	14.4	40.2	28.4	43.6	71.9
	0.8	0.6	17.2	16.9	34.1	13.5	52.2	65.7
	0.2	0.9	29.6	14.4	44.0	35.5	43.4	78.9
	0.5	0.9	22.2	16.3	38.6	21.8	50.1	71.9
	0.8	0.9	15.2	18.7	33.9	10.1	58.2	68.3
	0.2	0.3	62.8	0.4	63.1	90.0	5.2	95.2
	0.5	0.3	49.3	0.7	49.9	62.3	8.4	70.6
	0.8	0.3	35.0	1.2	36.2	35.0	13.2	48.2
	0.2	0.6	53.7	0.7	54.4	72.0	8.3	80.3
Palermo	0.5	0.6	42.5	1.1	43.6	49.3	12.1	61.4
	0.8	0.6	30.7	1.8	32.5	27.4	17.2	44.6
	0.2	0.9	47.6	1.1	48.7	59.5	11.4	70.9
	0.5	0.9	37.9	1.5	39.5	40.6	15.3	55.8
	0.8	0.9	27.9	2.3	30.2	22.6	20.5	43.1

4 DEVELOPMENT OF THE RATING ALGORYTHMS

The simulation results were used to develop the regressions, the energy rating should be based on. Observing the data it can be inferred that the heating and cooling demand affect the global demand in a different way as a function of the roof surface properties in the various climatic zones. Moreover the share of cooling and heating demand respect to the global energy demand dramatically depends on the insulation level for the three cities. Following the above considerations, a double track for the cool roof rating definition was implemented and it is presented in the next sub-chapters.
In the framework of the coming nearly-zero energy buildings and in order to skip the dependence on energy system efficiencies, the analyses are carried out considering on the net energy demand as provided by the simulations.

4.1 Climate dependent global energy rating

Three rating algorithms were implemented for the three selected climatic zones. A first analysis was carried out to check the impact of cool roof technologies on the global energy performances. The absolute values of the global energy demand in kWh/m^2 is strongly dependent on the insulation level, check table 3. The results can be also be presented as energy savings normalised respect to the maximum energy demand (calculated for emissivity 0.3 and solar reflectance 0.2) for each climatic zone.
Figure 5 reports the normalised energy savings for the two configurations and it can be inferred that trend and figures are similar for the two insulation levels, for the Rome case. Similar results were obtained for Palermo and Perugia, for the latter small differences of global energy demand were calculated for the not insulated configuration and for the roof properties but the trend was confirmed. For this reason the regressions were calculated starting from the global energy demand values obtained for the insulated configuration. This choice is also in accordance with the requirements of actual building codes in Italy.

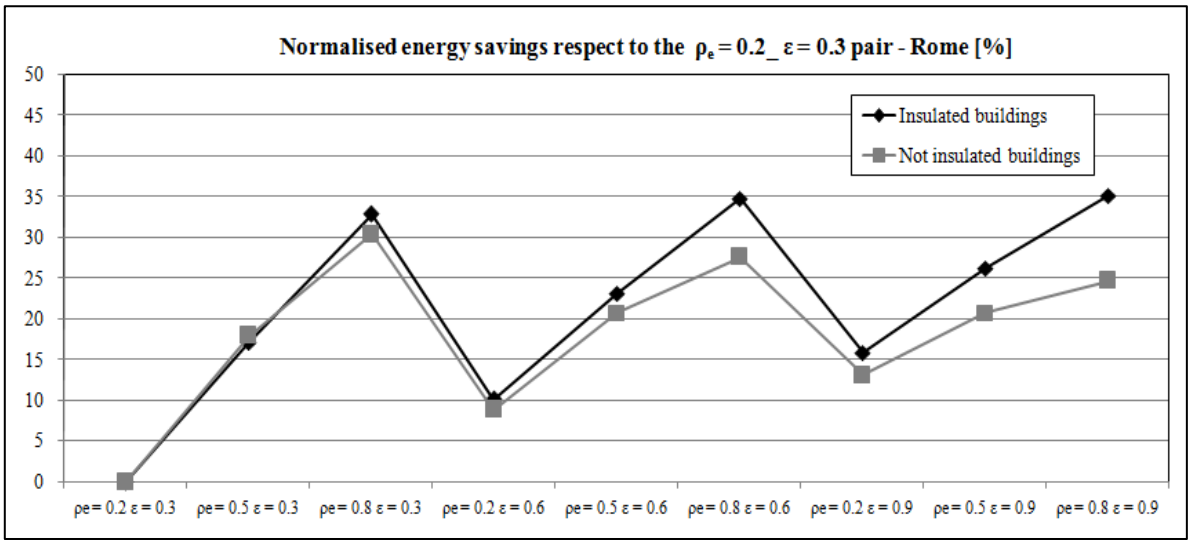

Figure 5. Comparison of the normalised global energy savings for the Rome buildings

Nine pairs of emissivity and solar reflectance values of the roof were considered in total. A linear regression for heating and one for cooling were calculated, and then combined together in a single equation for each climatic zone. Excellent r-square values were obtained, ranging from 0.964 for the heating season in Perugia to 0.995 for the cooling season in Rome. The equations for the three climatic zone are:

$$EP_{perugia} = 59.7 - 17.6\rho_e - 5.69\varepsilon \quad (1)$$

$$EP_{rome} = 56.92 - 22.4\rho_e - 8.01\varepsilon \quad (2)$$

$$EP_{palermo} = 75.8 - 39.87\rho_e - 16.68\varepsilon \quad (3)$$

4.2 Climate independent cooling energy rating

Figure 6 shows the specific cooling demand (empty red-lined boxes) for the three localities and for the insulated configuration. The results depend on the climatic zones, since significant differences can be found for the three cities and, in particular, between Palermo and the other two localities. The same results can be normalised respect to a climatic indicator as shown in figure 6, secondary Y-axis. Normalising the specific cooling demand to the Cooling Degree Days, calculated with base 10°C, a more uniform trend was obtained for the three data sets. The Degree Days are an output of the Design Builder.

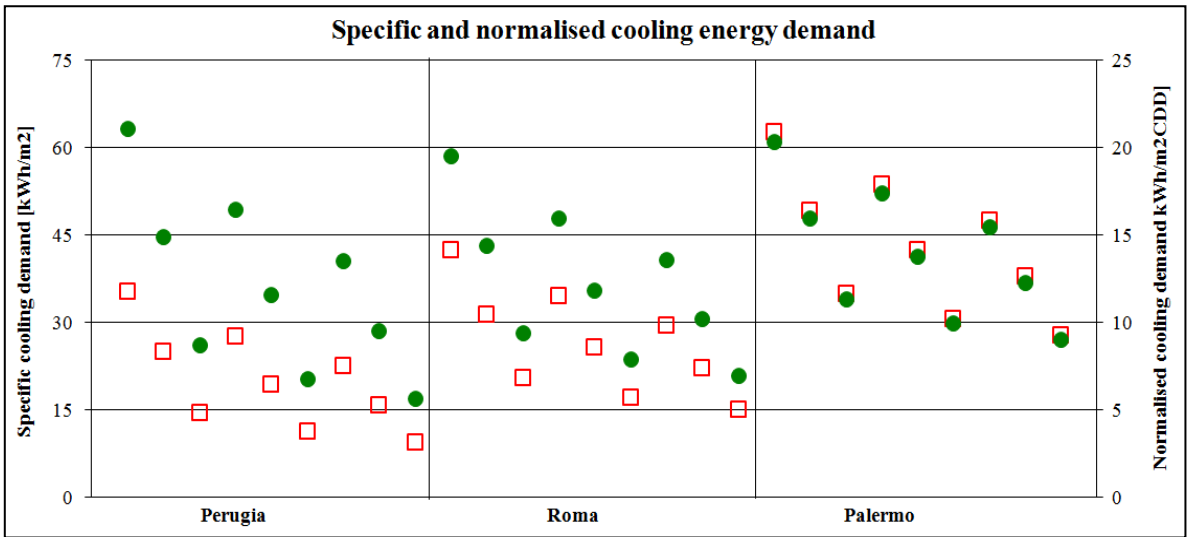

Figure 6. Effect of the cooling degree days normalisation on the climate dependence of the energy performances

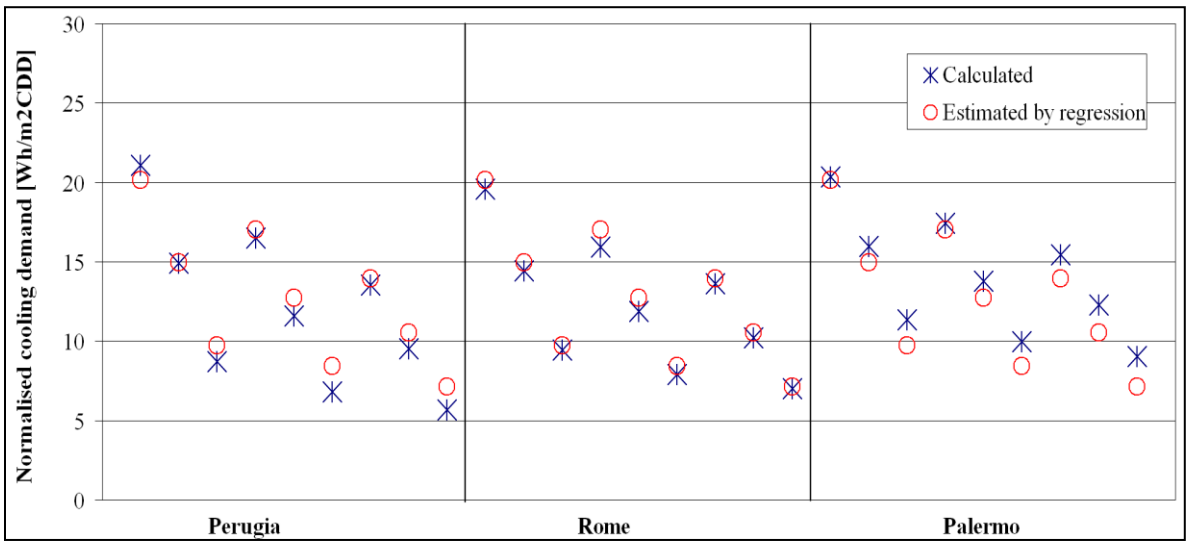

Figure 7. Comparison of the normalised cooling demand as obtained by simulations and as estimated by regression

The normalised 27 points (9 pairs of emissivity and solar reflectance values for 3 cities) were used to derive the linear regression. The indicator, expressing the performance of the cool roof product in the Italy for the cooling season (NEP_{cool}), was calculated according to the following expression:

$$NEP_{cool} = 27.32 - 20.35\rho_e - 12.35\varepsilon + 10\rho_e\varepsilon \quad (4)$$

Several regression models were tested, including different power for the reflectance and the emissivity; the best result was obtained with the above equation that include an interaction between the two physical properties. The r-square value of the regression is 0.94, which can be considered satisfactory according to the simplicity of the model. The relative error between the simulation and regression values is lower than 15% in 24 of 27 points, see figure 7. Higher discrepancies are generally found for high solar reflectance values, being lower the global energy demand.

5 CONCLUSIONS

The study demonstrated the dependence of the energy performance of residential buildings on the radiative properties of roofing products. Performances also depend on the climatic conditions and building characteristics. The insulation level was proved to be another crucial parameter affecting the amount of heating and cooling demand respect to the global energy performances.
The next step was the development of a rating system for cool roof products, starting from the results of the calculation. According to the available data two options were proposed: a climate dependent rating, assessing the performance of cool roof throughout the whole year, and an independent climate rating, actually developed for the cooling season only. The regressions are hence suitable for rating the cool roof products and define the efficiency classes in case of energy labelling.
First results of the study were promising and the research is ongoing, aimed at refining the actual algorithms as a function of more populated data sets and other more accurate normalisation procedures. The method should be next developed for other building categories were cooling demand is predominant and in dramatic increase, as office and commercial buildings

6 ACKNOWLEDGEMENTS

The authors thankfully acknowledge the Italian Ministry for Economic Development for funding the project in the framework of RSE – Ricerca Sistema Elettrico. Moreover a special thanks goes to Roberto *Berno* Pompei for his contribution to the work and in particular for the setting of calculation models used in numerical analyses.

7 REFERENCES

Rapporto Energia e Ambiente, ENEA (2012).

Synnefa, A., Santamouris, M., Akbari, H. (2007). Estimating the effect of using cool coatings on energy loads and thermal comfort in residential buildings in various climatic conditions. *Energy and Buildings*, 39(11), 1167-1174.

Akbari, H., Bretz, S., Kurn, D., Hartford, H. (1997). Peak power and cooling energy savings of high albedo roofs. *Energy and Buildings*, (25), 117-126.

Suehrcke, H., Peterson, E. L., Selby, N. (2008). Effect of roof solar reflectance on the building heat gain in a hot climate. *Energy and Buildings*, (40) 2224-2235.

Zinzi, M. (2010), Cool materials and cool roofs: Potentialities in Mediterranean buildings. *Advances in Building Energy Research*, (4) 201 - 266.

Bozonnet, E., Doya, M., Allard, F. (2011). Cool roofs impact on building thermal response: A French case study. *Energy and Buildings*, 43(11), 3006-3012.

Kolokotroni, M., Gowreesunker, B. L., Giridharan, R. (2011). Cool roof technology in London: An experimental and modelling study. *Energy and Buildings*.

Romeo, C., Zinzi, M. (2011). Impact of a cool roof application on the energy and comfort performance in an existing non-residential building. A Sicilian case study. *Energy and Buildings*.

Kolokotsa, D., Diakaki, C., Papantoniou, S., Vlissidis, A. (2011). Numerical and experimental analysis of cool roofs application on a laboratory building in Iraklion. *Energy and Buildings*.

Synnefa, A., Saliari, M., Santamouris, M., (2012). Experimental and numerical assessment of the impact of increased roof reflectance on a school building in Athens. *Energy and Buildings*, (55), 7-15.

Maccari, A., Zinzi, M. (2000). Simplified algorithms for the italian energy rating scheme for fenestration in residential buildings. *Solar Energy*, (69 Suppl.), Nos. 1 – 6, 75-92.

Decree *DPR 412/93* (1993). Regolamento recante norme per la progettazione, l'installazione, l'esercizio e la manutenzione degli impianti termici degli edifici ai fini del contenimento dei consumi di energia, in attuazione dell'art. 4, comma 4, della L. 9 Gennaio 1991, n. 10

Iatauro, D., Federici, A., Signoretti, P., Terrinoni, L., Romeo, C. (2013). Climatic Severity Index: Definition of summer climatic zones in Italy through the assesment of air conditioning energy need in buildings.

SIMULTANEOUS INTEGRATION OF URBAN HEAT ISLAND MITIGATION TECHNOLOGIES IN THE EXISTING URBAN FABRIC IN ATHENS, GREECE

Elli A. Calokerinou *, Stylianos C. Zerefos

Hellenic Open University
School of Applied Arts
Parodos Aristotelous 18,
26 335, Patra, Greece
**Corresponding author: ellisummers@gmail.com*

ABSTRACT

This research studies the possibility of introducing combinations of specific mitigation techniques for the urban heat island effect (UHI) in Athens, Greece. A variety of factors, such as surface cover, dense traffic, anthropogenic heat release and urban characteristics including geographic features and climate conditions interact with one another to create UHI, which is becoming increasingly evident also due to the changing climate, which in this region is expected to increase the duration of hot spells and the frequency of heat waves.

Mitigation techniques can contribute highly to improve the urban thermal environment, decrease the energy consumption of buildings and also decrease urban air temperatures. Proper mitigation technologies involve, among others, new building envelope technologies and the use of highly reflective materials to decrease the absorption of solar radiation by urban surfaces, the use of advanced materials adapted to the local climate, the additional use of urban green spaces and the use of appropriate heat sink technologies. Advanced mitigation techniques have been applied quite recently in many urban rehabilitation projects around the globe and have succeeded in improving the local microclimate significantly. However, each mitigation measure is often being implemented as a unique element. The focus of this research study is on their relationship and the actual feasibility for their simultaneous integration into the urban environment.

To this end this study focuses on urban architectural dynamics and the development of a methodology for the optimal simultaneous architectural integration of high performance heat-island mitigation technologies in the urban fabric. The methodology can be applied at city block or neighbourhood level and is based on the geometric characteristics and the orientation of the site, but also on the microclimatic conditions of the site. In order to achieve the aim of this study, a small typical neighbourhood in Athens, representative in terms of orientation, building height, road width etc, is analyzed as a case study. After recording each feature that describes the urban cityscape, the study presents feedback, regarding the feasibility for the integration of UHI mitigation technologies, as well as their interaction with various smart materials. Mitigation technologies studied in the present research include, but are not limited to, the reduction of anthropogenic heat release, such as the use of cooling towers, the retention of water through materials, the improvement of the reflectivity of urban surfaces, the use of green spaces, the effect of open spaces, the improvement of land usage and orientation, the use of appropriate shading, the use of natural heat sinks etc.

Finally, the study presents whether the above mentioned factors can reduce the air temperature at street level, how they affect the UHI effect and provide good air quality at the neighbourhood scale, whereas at the same time analyze possible problems or merits for their simultaneous integration.

KEYWORDS

1 INTRODUCTION

Rapidly developed urban areas, such as Athens, have a major negative impact on the outdoor environment. Urban geometry is a major factor in the urban heat island effect (UHI), as it affects airflow and mean radiant temperatures (Oke 1987, Golden 2004). Past research has focused on distinct environmental problems, such as high temperatures, wind distribution and speed in urban canyons (Oke, 1988). There are various physical and climatic factors that affect human thermal comfort in different scales, thus there is a strong need for interdisciplinary work between urban climatology, urban design and architecture (Ali-Toudert, 2005).

Mitigation techniques can contribute highly to improve the urban thermal environment and to decrease urban air temperatures. Advanced mitigation techniques have been applied quite recently in many urban rehabilitation projects around the globe (Ito et al, 2004, Slosberg et al, 2006) and have succeeded in improving the local microclimate significantly. However, each mitigation measure is often being implemented in its own as a unique element. The focus of this research is to study their relationship and the feasibility of their simultaneous integration into the urban environment.

This research studies the possibility of introducing combinations of specific mitigation techniques for the urban heat island effect (UHI) in Athens, Greece. A variety of factors, such as surface cover, traffic density, anthropogenic heat release and urban characteristics including geographic features and climate conditions, interact with each other to create UHI, which is becoming increasingly evident also due to the changing climate, which, in this region, is expected to increase the duration of hot spells and the frequency of heat waves (Climate Change Impacts Study Committee, 2011). The study focuses on urban architectural dynamics and the development of a methodology for the optimal simultaneous integration of high performance heat-island mitigation technologies in the urban fabric.

2 LITERATURE REVIEW

One of the great challenges for cities is the mitigation of the urban heat island effect (UHI). In the last years, interesting research has been presented, recognizing the root of the problem and the effects of the UHI (Golden, 2004, Kartalis, 1999) on the urban environment. The strong relationship between air pollution, anthropogenic heat, urban geometry, urban fabric and UHI density has been analyzed, introducing ways to mitigate the UHI without altering city planning (Che-Ani, 2009, Yamamoto, 2006).

The most important formative elements on the urban environment are buildings. Buildings surround urban open spaces, creating urban canyons with high temperatures. Temperature is associated with the UHI, which in turn increases the intensity of heat waves, thus humans are often exposed to extreme thermal conditions within their cities (Tan et al. 2009). There is a strong interest on the quality of open urban spaces and the relationship with various physical and climatic factors, such as surface temperatures, irradiation of canyon surfaces and wind flow at street level, decisive features that affect the microclimate of a neighbourhood. The height-to-width (H/W) ratio and street orientation were found to be the most important factors affecting thermal comfort at street level (Ali-Toudert, 2005). Surface materials were also found to affect the thermal behaviour of an urban canyon (Ali-Toudert, 2005). However, the number of interdisciplinary studies is limited (Pearlmutter et al, 1999).

Thermal sensation has been defined as the Actual Sensation Vote (ASV) (Nikolopoulou et al, 2005). Based on the ASV developed by the RUROS project (CRES, 2005),

ASV=0.034Tair_met +0.0001Sol_met – 0.086V_met – 0.001RH_met – 0.412 (r=0.27), (1)

there is an indication concerning the contribution of wind and temperature data. Analysing the data, it has been possible to examine correlations between microclimatic parameters and ASV. Through RUROS, it is becoming clear that a purely physiological approach is inadequate to characterise thermal comfort conditions outdoors. ASV has an inverse relation to wind speed. For example a case study area in Athens - which we will focus on paragraph 4 of this paper, - during the summer, records typical values of Tair_met=33°C, Sol_met=1000W/m², V_met=1m/s and RH_met=30%. This provides us with the result ASV=0.60, in between the comfortable categories -1=ASV=+1 (varying from «very cold» at -1 to «very hot» at 1). Lack of shading has a -14% impact on this value (CRES, 2005).

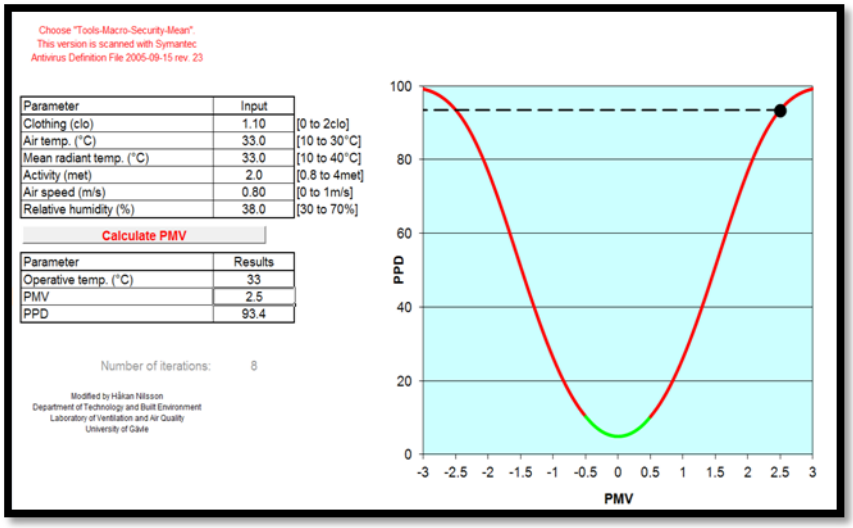

Figure 3: PMV calculation, (PMV calculation programme. Håkan Nilsson, Department of Technology and Built Environment)

The ASV is relevant only to particular meteorological factors. The subjective data collected from interviews can be compared with the thermal index Predicted Mean Vote (PMV), which is another method of predicting thermal comfort. The PMV takes into account the mean objective environmental parameters recorded for the duration of an interview, clothing levels and metabolic rate, using the ASHRAE thermal sensation scale. Comparing the PMV with the corresponding ASV, a great discrepancy was revealed between the two sets of data, since for the same area in Athens the PMV was calculated above 90% (LTPEP, 2013), when the ASV fell within comfortable limits. Therefore, we conclude to the assumption that the prediction of human thermal comfort on the outdoor environment requires a combined model.

3 METHODOLOGY

The outdoor environment is hard to quantify as it includes a multitude of factors that affect thermal comfort at pedestrian level. Critical factors for outdoor comfort include air temperature, relative humidity, air movement and mean radiant temperature. Furthermore, there are numerous unquantifiable factors affecting outdoor comfort, such as the critical importance of urban geometry, vegetation and shading. Therefore, there is a need for a quantitative assessment method for assessing the effects of climate on the urban environment and a proper implementation tool that will guide urban designers evaluate and propose coordinated UHI mitigation techniques.

This research has utilized the research of RUROS (CRES, 2004) and published research (Ali-Toudert et al. 2006, Koutsourakis 2010, Yamamura 2009, Zambrano 2006) on

thermal comfort and different factors that affect the UHI, always referring to the street level. Through a combined critical approach, our work uses a simple tool, which takes into consideration climatic and environmental factors, as well as issues and environmental problems, applicable to a wide range of Greek city typologies, adequate to guide designers and architects understand the thermal qualities and measures that create UHI. This tool has been developed through research in the urban characteristics of Greek cities and their potential to include UHI mitigation techniques used in cities around the globe.

Table 1: Site analysis -Meteorological Factors & urban parameters

factors			
meteorological factors		**air temperature** (Tair_met) oC	
		solar radiation (Sol_met) W/m²	
		wind speed (at roof level)(V_h) m/s	
		Relative humidity (RH_met) %	
		ASV (Actual Sensation Vote)	0.034(Tair_met-2)+0.0001(0.2*Sol_met)-0.086(0.4*V_met)-0.001RH_met-0.412
urban parameters	*neighbourhood*	**land use**	mixed use (residential-commercial)
			strictly residential
			strictly commercial
			industrial
			conflicting land use (residential-indastrial)
		Urban geometry	complex
			organised (with a pattern)
			no pattern
		density of built area	<40%
			40%-70%
			>70%
		free space (%)	<5%
			5%-15%
			15%-25%
			25%-50%
			>50%
	building	**characteristics**	pilotis
			atrium
			skylight
		roof type	flat roof
			roof
			terracing
	street	**street orientation**	N-S
			E-W
			NE-SW
			NW-SE
		linear street length	<90
			>90
		road classification	primary
			secondary
			pedestrian area
		height to width ratio (H/W)	<0.5
			0.5-1
			1 to 2
			2 to 3
			>3
		linear street length to height ratio (L/H)	low <3
			medium =5
			high >7
		limit to street	no extra space
			canopy
			gallery
			garden patch
		street canyon	symmetrical
			assymetrical
		sky view factor (0-1)	
		vegetation	low
			high
			linear / individual trees
			group of trees
		wind speed (at street level)(V_h) m/s	
	surface cover	**albedo (solar reflectance)**	<0.1
			0.1-0.3
			0.3-0.5
			>0.5
		thermal emission	<0.30
			0.30-0.50
			0.50-0.70
			>0.70

The referenced tool was created in response to the need for a detailed subjective analysis for case studies. This tool should be easy to use, in contrast to most urban

environment simulation programs that require more detailed technical knowledge in order to operate.

Givoni (1998) states that the differences between the urban and the rural temperatures are affected by two types of factors, the meteorological factors, such as humidity and wind speed, and various features of the urban structure, such as the density of the built-up areas, and the ratio of the height of the buildings to the distances between them. Therefore, by simply applying the meteorological factors on a site and recording the urban elements as shown in table 1, one can inspect the general characteristics for the corresponding area. All possible features can react or contradict with the restrictions of the urban geometry, thus a complete site analysis is able to provide us with the information we need to proceed with the proposal of appropriate UHI mitigation techniques.

The tool proposed in this paper is based on a database that we have developed through past research on specific UHI mitigation techniques and their implementation within the urban environment in relation to specific meteorological factors. This database is an attempt to record all possible UHI mitigation techniques and their relation to most possible urban parameters. The critical approach on their interaction, is the step towards their optimal simultaneous architectural integration in the urban fabric of Greek cities. All available mitigation techniques collected in the database have been decoded and categorized, creating an up-to-date model that suggests a 5 point scale of importance, from 1 (not important) to 5 (very important), combining urban parameters and meteorological factors and considering the analytical sensation of thermal comfort. Table 2 shows the outline of the tool, which has a tree structure that concludes to the scale of its implementation and a subjective account on the degree of effect, all considering the properties of Greek cities.

Table 2: Mitigation technique model outline

					scale of implementation	**degree of effect**
MITIGATION TECHNIQUE	**reduction in anthropogenic heat release**	control of land use			neighbourhood	**1**
		improvement control of air conditioning systems	optimal operation of air conditioning systems		buildings	**1**
			proper placing of outdor units		buildings	**2**
		use of cooling towers			buildings	**5**
		greening of building surfaces and adoption of water-retentive materials			buildings/street	**5**
		improvement in the reflectivity of walls and roofing materials			buildings	**5**
		traffic management			streets /neighbourhood	**4**
	improvement of artificial surface covers	use of cool materials	improve reflectivity of walls and roofing			
			improve reflectivity of paving materials		streets /neighbourhood	**5**
			water retentive pavement		streets /neighbourhood	**5**
		PCM Phase change materials			buildings & streets	**1**
		greening		low vegetation	streets /neighbourhood	**4**
			street greenery	row of trees		**2**
			green roof		buildings	**5**

			green walls	buildings	**3**
		pockets parks		neighbourhood	**3**
	improvement of city air ventilation	shading	artificial	street	**1**
			greenery		**3**
		use of cooling towers		buildings	**5**
		cold sinks		city	**3**
		water & green areas		neighbourhood	**3**
		windbreaks	artificial	neighbourhood	**1**
			greenery		**1**

The outcome of the process can inform architects and urban designers on the feasibility for applying each proposed mitigation technique at a certain site or neighbourhood, in terms of thermal comfort at street level. To this end the methodology proposed consists of five stages as shown in Figure 1:

Figure 1: Outline of analysis

4 CASE STUDY

The city of Athens, is dealing with the lack of green spaces and pedestrian activities, as the city centre is a vehicular environment with exposed concrete sidewalks. The present study focuses on the relation between street design, building characteristics and outdoor thermal comfort. In order to achieve the aim of the study, five city blocks representative to the city centre in terms of orientation, building height, road width etc were selected, The case study covers the district area of approximately 20.000 square meters. This district is a high density area (>70%) of mainly residential and office use. Most of the buildings are multi-storey concrete volumes (>6 floors) with flat roofs and recesses, built during the '60s, presenting high height-to-width ratio (>3), with no inner patios or an internal atrium.

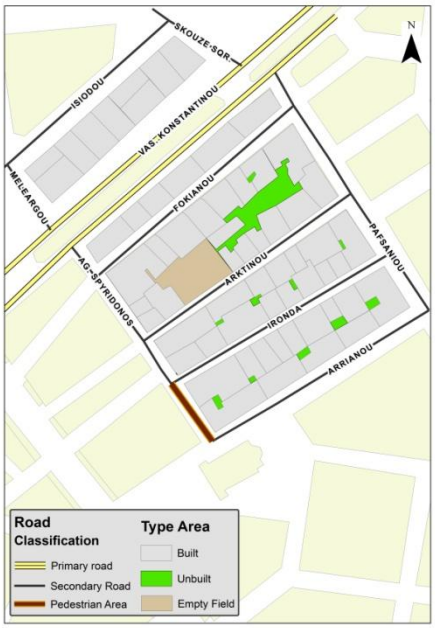

Figure 2: Area type / Road classification

The street materials are porous asphalt, concrete pavement tiles and old dirty stucco for the vertical building surfaces. Those low reflectance and high thermal emitance materials are common to the Greek urban fabric. Furthermore, the case study area consists of a sequence of urban canyons (Koutsourakis 2010), resulting to inadequate street ventilation.

The neighbourhood is facing the prevailing northeast winds on roof level. There is lack of empty space, greenery or air circulation areas in a site of flat organised topography. Being close to the city centre, dense traffic fortifies the concentration of air pollution, which

combined with encapsulated high temperatures, can be stressful and indirectly dangerous to the urban environment. Considering all of the above features and the recorded low surface reflectivity, the region, on street level, faces high temperatures.

Using Tables 3 and 4 shown below, one is able to understand specific features concerning the district of this study. While Table 3 shows the metrological factors in the area of the case study, Table 4 analyses the street characteristics, in terms of orientation, H/W ratio, material reflectance factor and surface temperature.

Table 3: Meteorological Factors – case study
(Sunday 21/07/2013, 12:00 www.airquality.gr)

meteorological factors	**PMV=4.8**	**air temperature** (Tair_met) oC	**33^{o}C**
		solar radiation (Sol_met) W/m²	**1000W/m²**
		wind speed (at roof level)(V_h) m/s	**2.1m/s**
		Relative humidity (RH_met) %	**38%**
		ASV (Actual Sensation Vote)	0.034(Tair_met-2)+0.0001(0.2*Sol_met)-0.086(0.4*V_met)-0.001RH_met-0.412

Through recording urban parameters, it is becoming clear that there are many restrictions in terms of geometry, materials and meteorological quantities. The above, set the immediate challenge to improve the qualities of artificial surfaces and the simultaneous improvement of the ventilation of the city, both without changing the urban geometry.

The most important factor is urban geometry. It is very important to analyse the urban volume (buildings) in relation to the unbuilt areas, such as streets and empty fields (which are very limited), and understand the importance of orientation. The case study area faces intermediate street orientations of NE-SW and NW-SE, which translate to short periods of thermal discomfort, as the streets are always partially in the shade (Ali-Toudert, F. et al 2006).

Table 4: Case study Street analysis

STREET ANALYSIS (air Temperature 33^{o}C)								
	Road Name	**Orientation**	**H/W**	**Materials**	**Solar reflectance/ Thermal emmitance**	**Surface T (ASTM E1980)**	**Direct Sunlight**	**Wind Speed**
1	Vas.Kon/nou	NE-SW	<1	Porous asphalt, cement pavement tiles	0.05/0.93(asphalt) 0.1/0.63(tiles)	**81.2** (asphalt) **86.3**(tiles)	Yes	0.4*2.1=**0.84m/s** (depending on the direction)
2	Fokianou	NE-SW	>3				No	
3	Arktinou	NE-SW	>3				Yes	
4	Ironda	NE-SW	>3				Yes	
5	Agiou Spiridonos	NW-SE	>3	Porous asphalt, cement pavement tiles, row of trees	0.05/0.93(asphalt) 0.1/0.63(tiles) 0.25/0.75 (trees)	**81.2** (asphalt) **86.3**(tiles) **75.6** (trees)	Yes	
6	Pausaniou	NW-SE	1-2				Yes	

The area experiences dense street canyons (H/W>3), so it is critical to understand the air movement through the canyon and the various whirls that are created near the buildings and through the vertical development of the canyons. Those whirls block the air circulation and create a heat sink, while constantly interacting with high surface temperatures. Discomfort can extend under balconies when sidewalks in the open street area already experience thermal stress (Ali-Toudert, F. Et al 2006) because of the direct irradiation, especially in wide canyons.

In the study area, there are tall building with roofs and many recesses that modify the H/W ratio. Asymmetries of street canyons tend to cause thermal stress because of direct exposure. Nevertheless, when H/W>2 (as most cases of the district), an asymmetrical canyon shows better thermal behaviour than a symmetrical (Ali-Toudert, F. Et al 2006). The use of rows of trees improves thermal comfort within a street canyon only where direct solar

radiation appears. In other cases, the use of low vegetation is ideal. Furthermore, the use of water has been found very effective at the street level, as air temperature was found to be a secondary factor in influencing thermal comfort (Ali-Toudert, F., 2005). If buildings are coated with high albedo materials or vegetation then temperatures could decrease and balance thermal comfort. The street surface temperature (table 3 surface T) can decrease up to 21.2 ^{o}C, with the implementation of >0.50 albedo street material (calculated by using the ASTM standard E1980).

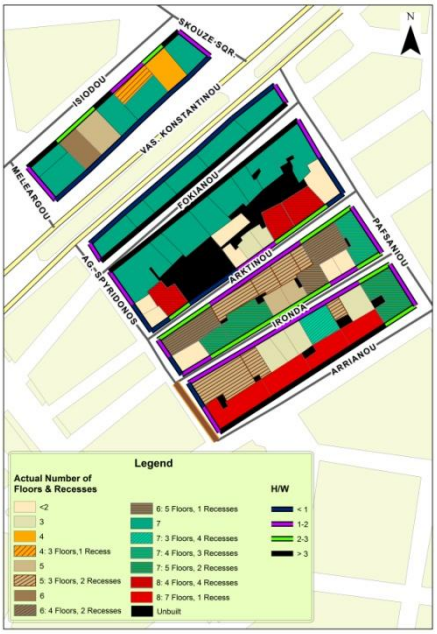

Figure 3: Actual number of floor & recesses & H/W ratio

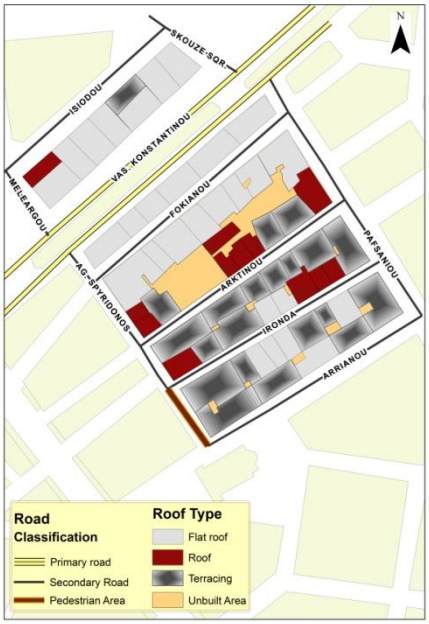

Figure 4: Road classification & roof type

5 RECOMMENDATIONS

Using the developed model (tables 2, 3 and 4), the following recommendations are suggested for improving thermal comfort in street level for the case study area by the simultaneous combination of UHI mitigation techniques:

I. Reduction in anthropogenic heat release:
   - *i. Make pedestrian paths more pleasant for walking and social interaction by eliminating traffic at NE-SW oriented streets with H/W>3*
   - *ii. Using permeable pavements*
   - *iii. Row of trees at the NW facade of the street for shading*
   - *iv. Low vegetation on the SE facade of the street to prevent whirls*

II. Improvement of artificial surface covers:
   - *i. High albedo and light colour materials for facades and building covers in order to decrease the ambient air temperature and contribute to better urban thermal comfort (as above)*
   - *ii. Creating a pocket park utilizing the only empty field of the neighbourhood connected with the private empty forgotten spaces, adjacent to the unbuilt land*
   - *iii. Permeable pavements (transpiring surfaces)*
   - *iv. Green roofs where flat roofs*
   - *v. Green walls where direct solar radiation occurs (otherwise, lack of sun implies discomfort)*
   - *vi. Canopies (shade) & vegetation where direct solar radiation occurs*

III. Improvement of city air ventilation:

i. No windbreaks needed

ii. Increasing wind speed: Warm air stagnates in the urban canyons unless ventilated with the use of water and evapotranspiration by greenery (as above)

iii. Using urban geometry vertical voids (building skylights) to create a cool tower to ventilate the existing canyon

The method applied in this study is recommended for existing locations, as it uses the real vote of the users, registered in questionnaires, making it possible to evaluate situations were inadequacies of the urban space are observed.

6 CONCLUSIONS

This paper has shown that there are ways to improve the outdoor environment in Athens, without altering the city planning by the simultaneous integration of various UHI mitigation techniques. If implemented, the recommendations gained through the model developed, have the potential to influence human thermal comfort within urban canyons.

Shading might be the key strategy in a hot and dry climate like Athens, but various urban parameters, site restriction and possibilities must be considered in the design process. Microclimatic conditions differ in the aspect ratio H/W, street orientation and a number of design details. Symmetrical and asymmetrical urban canyons with different sky view factors may occur, interacting with the same meteorological factors, requiring different implementation techniques in terms of thermal comfort. The disconnection observed so far between urban climatology on the one hand and urban geometry on the other hand, is inadequate towards the integrated sustainable urban design. This paper presented a subjective quantitative tool in the form of a computer program, that has been developed and is constantly improving (since it is under evaluation). This tool integrates climatic and environmental factors, as well as issues and environmental problems in Greece, while providing a simple design guideline understandable by practitioners, adequate for large scale implementation.

Future work can focus on the simulation of this quantitative analysis for establishing this implementation model into a simple tool for street design assessment and design guide.

7 ACKNOWLEDGEMENTS

Special thanks to Melachroini-Michaella Karageorgiou for the graphics and map processing.

8 REFERENCES

Akbari H., Pomerantz M., Taha H. (2001). *Cool surfaces and shade trees to reduce energy use and improve air quality in urban areas*, Solar energy, 70 (3)

ASTM standard E1980, (2013). http://www.astm.org/

Climate Change Impacts Study Committee. (2011). *The environmental, economic and social impacts of climate change in Greece*. Bank of Greece. http://www.bankofgreece.gr/BogEkdoseis/ClimateChange_FullReport_bm.pdf

Fazia Ali Toudert (2005). *Dependence of outdoor thermal comfort on street design in hot and dry climate*, Berichte des Meteorologischen Institutes der Universitat Freiburg Nr.15. Freibutg, November

Givoni, B. (1998) *Climate Considerations in Building and Urban Design*, Canada, John Wiley & Sons.

Golden A.S., (2004). The built environment induced urban heat island effect in rapidly urbanizing arid regions – a sustainable urban engineering complexity, Environmental Sciences, Vol.00 No.0, Taylor & Francis Ltd.

Ito M., Nitta H., Kido H., (2004). *Study on environment-friendly pavement structure for cities*, Public works research institute bulletin, Japan, April
Kartalis K. et al, (1999). *Introduction to natural and human environment: Natural environment*, Hellenic Open University
Koutsourakis N. (2010). *Flow and pollutant dispersion in urban canyons: Review*, Tech.Chron.Sci. J. TCG, I, No 1
LTPEP (laboratory of thermo physical properties and environmental processes) (2013). www.airquality.gr. Aristotle University of Thessaloniki
Nikolopoulou M. (2004). *Rediscovering the urban realm and open spaces (RUROS)*, Centre for renewable energy sources (CRES), Athens, Greece
Oke T., (1988). *Street design and urban canopy layer climate*. Energy and Building 11:103-113
Oke T.R., (1987). *Boundary Layer Climates*. Methuen, London
Pearlmutter D., Bitan A., Berliner P, (1999). *Microclimatic analysis of compact urban canyons in an arid zone*, Atmospheric environment 33
Santamouris, M. (2001) *Energy and Climate in the Urban Built Environment*, London, James & James Publication.
Slosberg R. et al (2006). *Mitigating New York s heat island with urban forestry, living roofs and light surfaces – New York city regional heat island initiative*, Columbia university center for climate systems researchi & Nasa/Goddard Institute for space studies & Department of geography, Hunter College-CUNY & SAIC
Solecki W. et al, (2004). *Urban heat island and climate change: an assessment of interacting and possible adaptations in the Camden*, New Jersey region, Environmental assessment and risk analysis element, April
Tan J. et al (2009). *The urban heat island and its impact on heat waves and human health in Shanghai*, Int J Biometeorol (2010) 54:75–84
The engineering toolbox: *Emissivity coefficients of some common materials - The radiation heat transfer emissivity coefficient of some common materials as aluminum, brass, glass and many more*, http://www.engineeringtoolbox.com/emissivity-coefficients-d_447.html
Yamamoto Y., (2006). *Measures to Mitigate urban heat islands*. Quartefly Review No.18, January
Zambrano L. et al, (2006). *Thermal comfort evaluation in outdoor space of tropical humid climate*, PLEA2006 The 23rd conference on Passive and Low energy architecture, Geneva, Switzerland, 6-8 September

URBAN REHABILITATION AT THE MUNICIPALITY OF ACHARNES, GREECE

Niki Gaitani [*1], Mat Santamouris[1], Ioannis Pappas[2], Costas Cartalis[1], Fotini Xyrafi[3], Elena Mastrapostoli[1], Panagiota Karahaliou[1], Chrysanthi Efthymiou[1]

1 National & Kapodistrian University of Athens, Faculty of Physics, Building of Physics-5, University Campus, 157 84, Athens, Greece
**Corresponding author: ngaitani@phys.uoa.gr*

2 Green- evolution, 501 Vouliagmenis Avenue, 163 41, Ilioupolis, Athens, Greece

3 ALD, Dinokratous 103, Athens, Greece

ABSTRACT

The raise of sustainability in the urban design is a key-factor for addressing the challenges in response to climate change, resource availability, environmental degradation and energy consumption. Urban planners need comprehensive microclimatic information in order to take decisions. This paper addresses the rehabilitation at the municipality of Acharnes, one of the largest municipalities of Attica, built at the southern foothills of Mt Parnitha, and 10 km north of Athens. The reintegration approach included field measurements of the thermal characteristics in the examined area. The data collected from the field measurements were analyzed according to the bioclimatic design targets of the area. The results contribute to the improvement of thermal comfort conditions and to the quality of life in municipal open spaces.

KEYWORDS

Urban design, Cool materials, Thermal Comfort

1 INTRODUCTION

The Mediterranean area has been the subject of several research studies in terms of climatic variations. The Attica basin is characterized by significant climate change as the ambient temperature has risen and the frequency of heat waves has increased (Cartalis, 2001, Santamouris, 2001). A climatic conscious design of outdoor spaces and the appropriate use of bioclimatic components are key elements to reduce the outcome of unsound development of urban areas where impermeable surfaces and denuded landscapes determine undesirable climatic effects and unhealthy environments (Gaitani, Santamouris, 2007). Various mitigation techniques have been proposed involving the use of highly reflective materials, increased plantation and the use of cool sinks large applications with cool pavements have been applied and evaluated with promising results (Akbari, 1992; Santamouris, 2007, Fintikakis,2011).
The present paper addresses the rehabilitation at the municipality of Acharnes. The main contribution of the present study is the development of an integrated approach towards the bioclimatic design of open spaces in the urban environment that ensure thermal comfort conditions at pedestrian level. A concise description of the procedure presented herein is formulated as follows: Initially, the existing microclimatic conditions are measured. Thermal comfort conditions of pedestrians are computed by implementing special thermal comfort indices.

2 FIELD SURVEY

A field survey was carried out with measurements (April-May, 2013), in three urban areas in the Municipality of Acharnes, Greece. As concerns the weather conditions, a temperate Mediterranean climate dominates, which corresponds to hot and dry summers and cool, humid winters.

2.1 Area of interest

Acharnes, is the most populous municipality in East Attica as according to the 2011 census, has a population of 107,500 inhabitants. The municipality is located about 10 km due north of Athens. (http://www .acharnes.gr/el). The regeneration approach included field measurements of the thermal characteristics in three urban areas in the centre of the municipality. The three areas under rehabilitation are shown in Fig. 1.

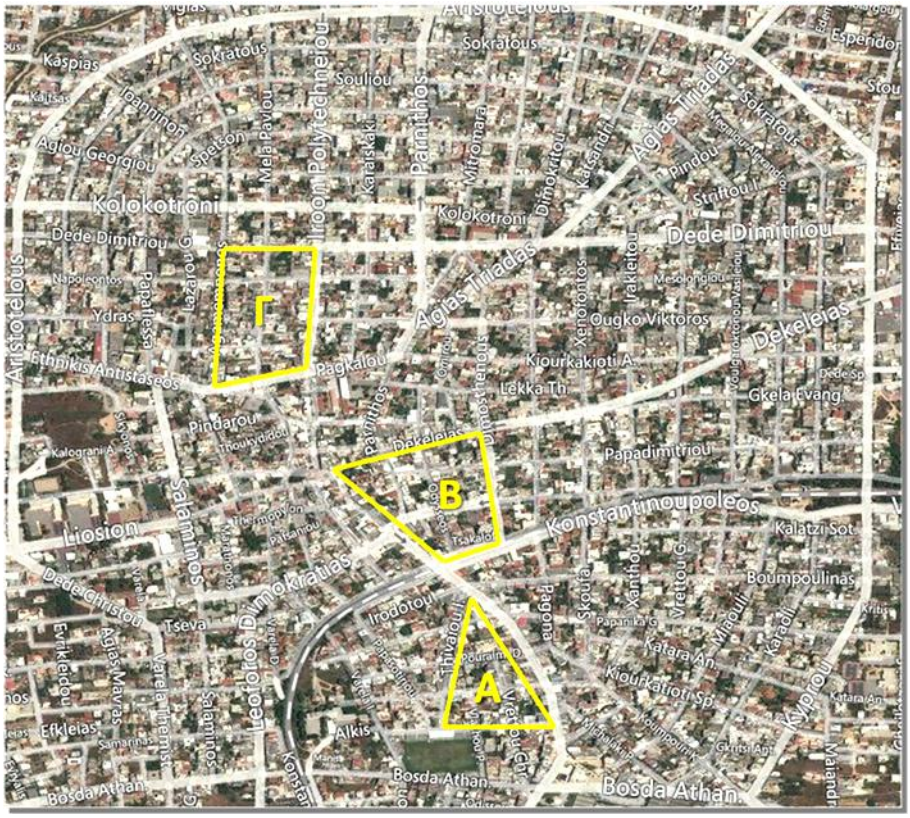

Figure 1: Survey area in GOOGLE EARTH

Local authorities have decided to regenerate the area using sustainable bioclimatic strategies. The main objective is the improvement of microclimatic conditions with the decrease of ambient temperatures during the summer period and enhancement of the thermal comfort conditions.

2.2 Field measurements of microclimatic parameters

The environmental parameters monitored were wind speed, air temperature, and relative humidity. The elements of the terrain affect the wind either by decreasing the speed and changing the direction, or by increasing the wind speed. The wind also affected by the size, the position, the orientation, the porosity and the vicinity of the buildings. For the area A the measurements indicated that the wind was varied between 0.4 m/sec to 2.7m/sec, for area B

varied from 0.3m/sec to 2.9m/sec while for the area C the wind variation was in the range 0.4m/sec to 2.4 m/sec.

The monitoring procedure included measurements of the air temperature and humidity at selected locations for each of the three areas, using data loggers (Tiny Tag TGP-4500). The data loggers were placed into weather stations located at a height of 1.80 m.

The air temperature and humidity measurements for the area A, were performed on 26th of April, 2013. The results indicated that the mean maximum air temperature was 30.0°C while the mean minimum was 24.5°C. These temperature ranges related with the geometrical characteristics of the road and the construction materials. Furthermore the anthropogenic heat that emitted during the day affected the temperature profile. Regarding the relative humidity measurements of the mean maximum value was recorded 31% while the mean minimum was 24%.

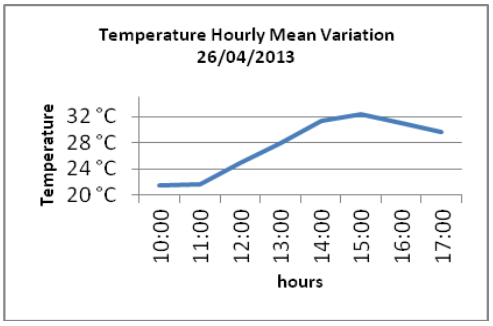

Figure 2: Maximum temperature range

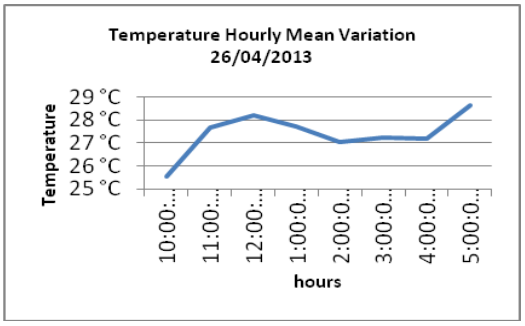

Figure 3: Minimum temperature range

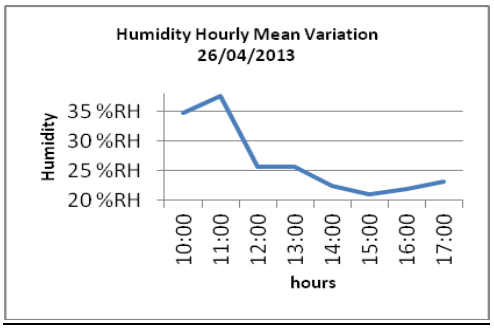

Figure 4: Maximum humidity range

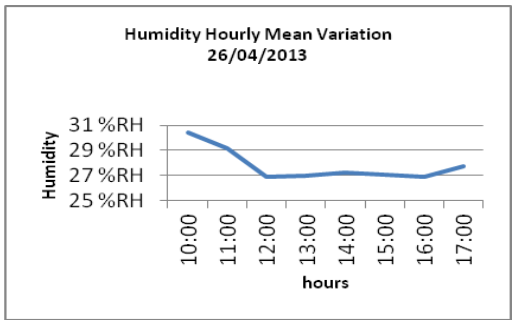

Figure 5: Minimum humidity range

The air temperature and humidity measurements for the area B were performed on 29th of May, 2013. The results indicated that the mean maximum air temperature was 31.9°C and the mean minimum was 27.0 °C. Regarding the humidity measurements the mean maximum relative humidity was 42% and the mean minimum was 35%.

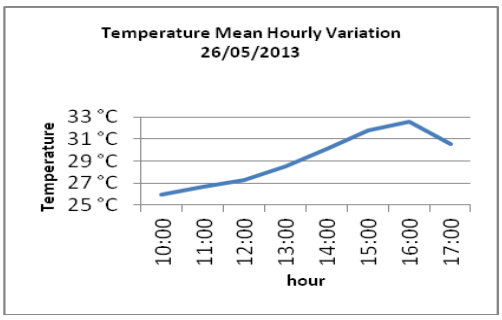

Figure 6: Maximum temperature range

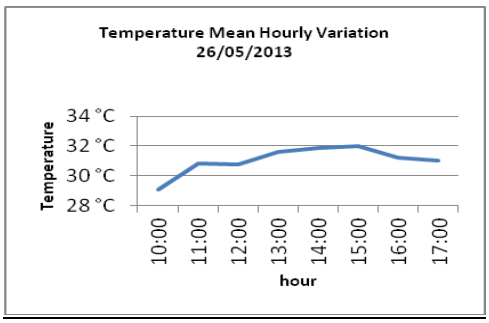

Figure 7: Minimum temperature range

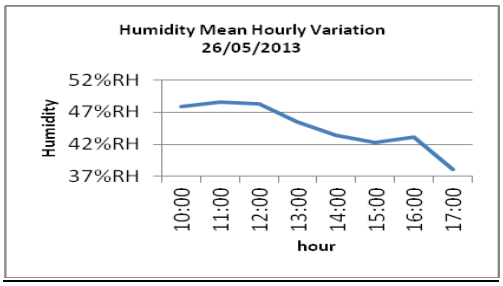

Figure 8: Maximum humidity range

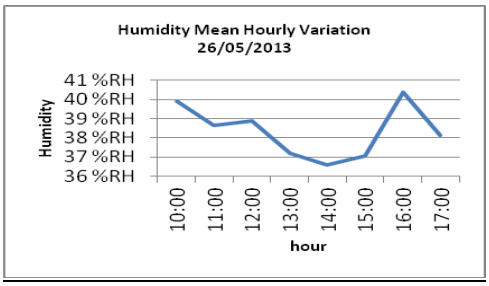

Figure 9: Minimum humidity range

The air temperature and humidity measurements for the area C were performed on 21th of May, 2013. The results indicated that the mean maximum air temperature was 33.1°C and the mean minimum was 28.5°C. Regarding the humidity measurements the mean maximum relative humidity was 39.6% and the mean minimum was 25.9%.

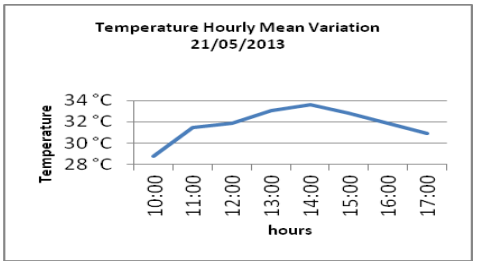

Figure 10: Maximum temperature range

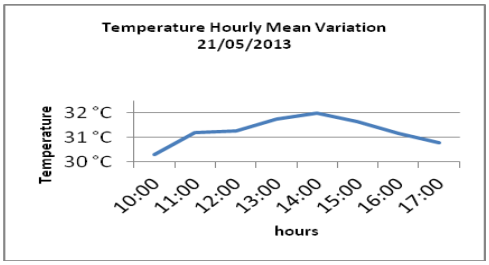

Figure 11: Minimum temperature range

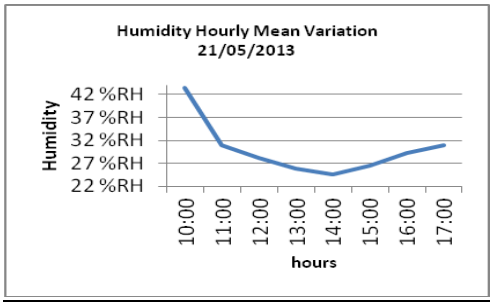

Figure 12: Maximum humidity range

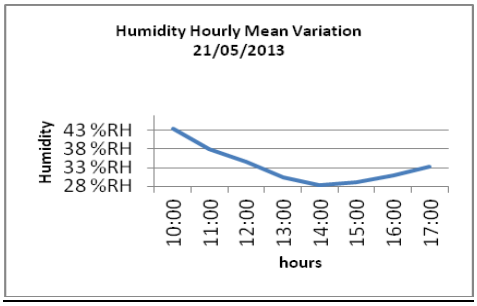

Figure 13: Minimum humidity range

2.3 Study of the materials

An important role in the microclimate of an area plays the thermal properties of the materials that compose it. For this reason the surface temperatures of paving, asphalt and other building materials of the urban planning were measured on hourly basis from morning to afternoon (10:00 to 17:00), in order to understand their thermal efficiency. Measurements were performed both under clear sky and under full or partial cloud covered conditions, provided that the measured points are completely exposed to solar radiation. For this purpose three kinds of instruments were used such as thermal camera, infrared thermometer equipped with a laser beam and a contact thermometer. The measurement results showed that for the area A, the average surface temperature of the road surface ranged from 10°C in the morning hours to 50 ° C at noon. The minimum surface temperature measured for pavement equal to 7°C, while the maximum equal to 51°C. Regarding the area B, the average surface temperature of the road surface ranged from 25°C in the morning hours to 52°C at noon. The minimum surface temperature measured for paved surfaces equal to 23°C, while the maximum equal to 49°C. While for region C the corresponding values of the asphalt ranged from 27 ° C in the morning to 52°C at noon. The minimum pavement's surface temperature reach the 26°C, while the

maximum the 48°C. The daily distribution of their surface temperature both for each selected measuring point and study area is shown in the following figures.

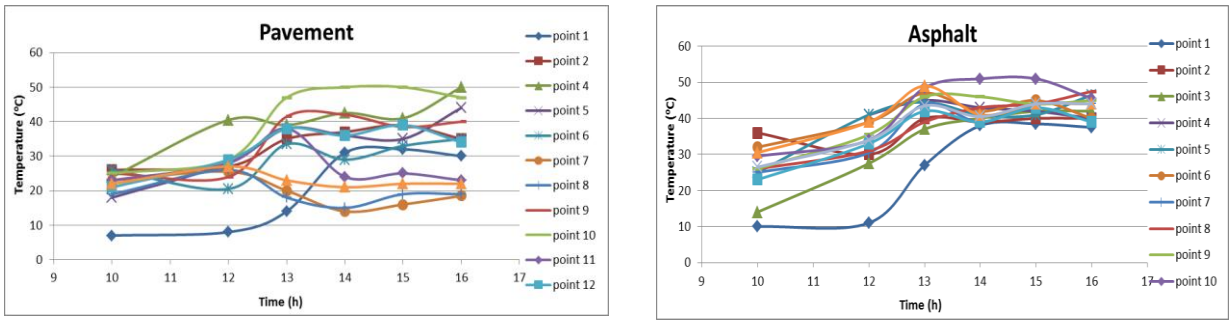

Figure 14: Comparison of daily temperature distribution a) pavement, b) asphalt of each measuring point of study area A

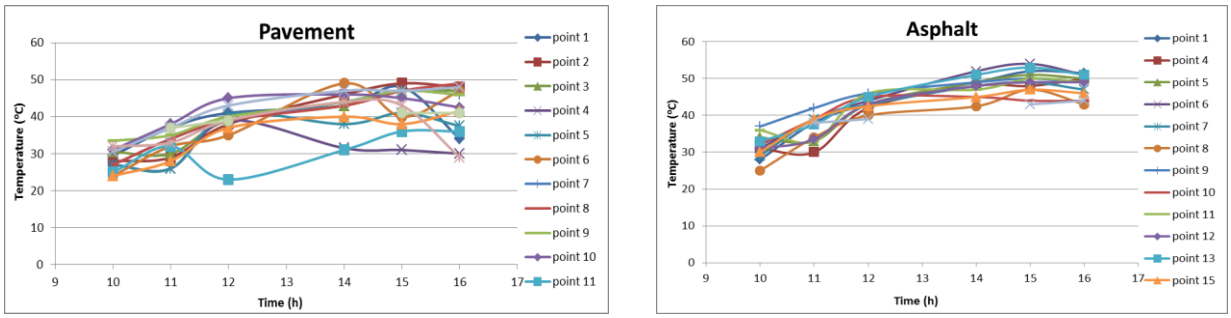

Figure 15: Comparison of daily temperature distribution a) pavement, b) asphalt of each measuring point of study area B

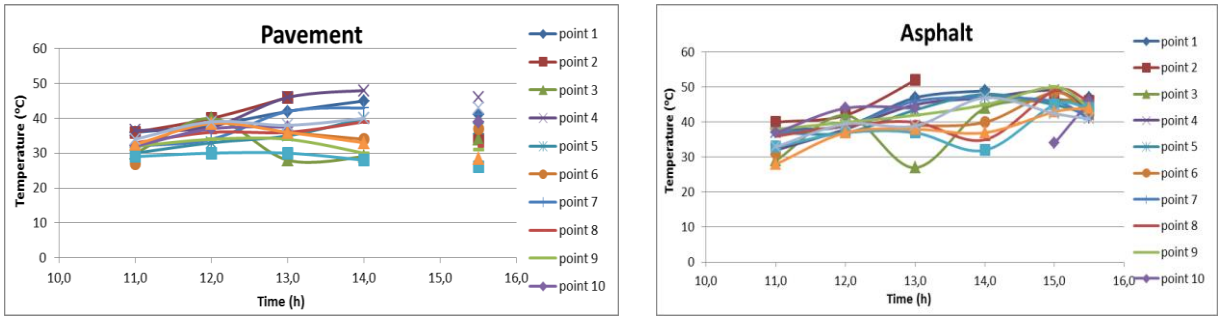

Figure 16: Comparison of daily temperature distribution a) pavement, b) asphalt of each measuring point of study area C

It is well known that sidewalks and roads as great part of urban surface, affect strongly the urban climate. The above experimental results show that the surface temperatures of the two most commonly used urban materials reach very high levels even during times of relatively low ambient air temperatures. The analysis must be taken into consideration in selecting the appropriate materials in area's rehabilitation.

2.4 Measurements of particulate matter

Particulate matter (PM) is one of the major air pollutants in urban areas. There is a clear correlation between enhanced PM_{10} and $PM_{2.5}$ levels and adverse cardiovascular and respiratory effects (C. Arden Pope, D.W. Dockery, 2006). Measurements of the levels of particulate pollution were also performed using an instrument which records the mass of airborne particles (Osiris) of an aerodynamic diameter less than 1μm (PM_1), 2.5μm ($PM_{2.5}$) and 10μm (PM_{10}). The sampling and recording time was 5 min. The airborne particles in the

outdoor air are produced by combustion processes (during the heating of buildings), by industry, by the engines of vehicles or dust and their concentration is also determined by the traffic volume, the type and quality of the fuels used. The particles of smaller diameter are more easily irrespirable and have been proven to be a source of major health problems (Kunzli, 2000, Katsoyiannietal, 2001). The limits of allowable concentration of airborne particles, established by the European Union, are 50.0μg/m^3 for PM_{10} and 25.0μg/m^3 for $PM_{2.5}$, whereas there is yet no established maximum allowed limit for PM_1. A more specific analysis of the results for each area separately is given below:

Area A

Measurements of airborne particles of an aerodynamic diameter less than 1μm (PM_1), 2.5μm ($PM_{2.5}$) and 10μm (PM_{10}) took place in the area of interest, on 26/04/2013 and during the time period 10:00 am-17:00 pm. The measured airborne particles' concentrations for area A are illustrated in box plots in the figures that follow. From the data analysis, it can be concluded that, concerning Area A, the concentrations of PM_{10} particles range in levels below the limit of 50 μg/m^3 and those of $PM_{2.5}$ and PM_1 range in levels much below the limit of 25μg/m^3.

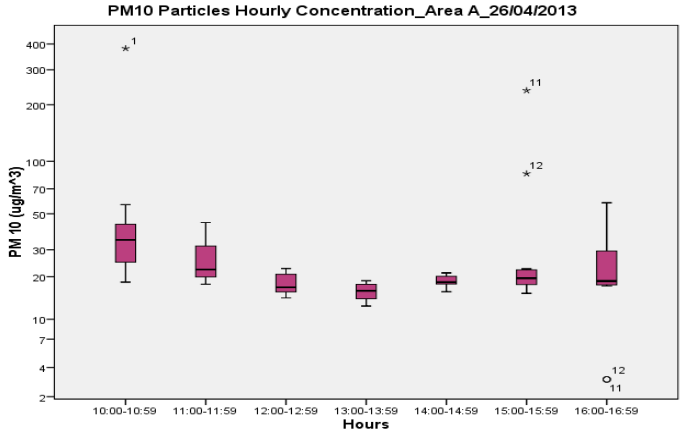

Figure 17: Mean hourly concentration of particles of diameter less than 10μm (PM_{10}) for the period 10:00 to 17:00 (26/04/2013)

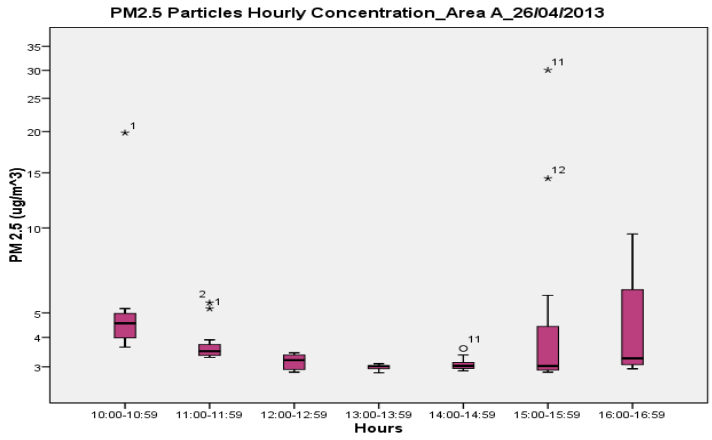

Figure 18: Mean hourly concentration of particles of diameter less than 2.5μm ($PM_{2.5}$) for the period 10:00 to 17:00 (26/04/2013)

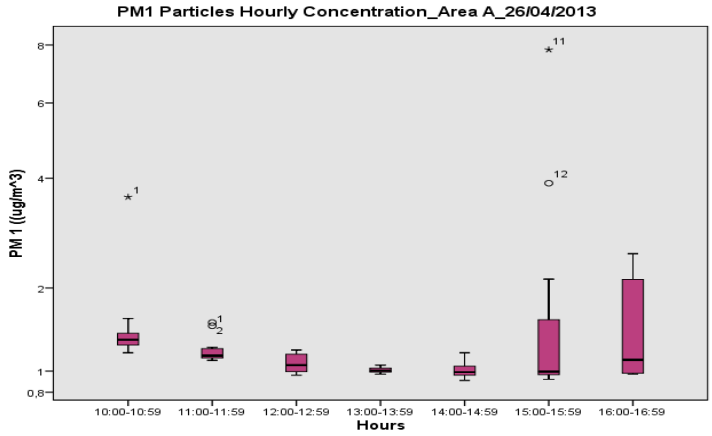

Figure 19: Mean hourly concentration of particles of diameter less than 1 μm (PM_1) for the period 10:00 to 17:00 (26/04/2013)

The maximum values occurred at 10:00 for PM_{10} and at 16:00 for $PM_{2.5}$ and PM_1 and they are much higher than the mean values as they correspond to moments when a machine was used to cut the grass of the court where the equipment was installed. The minimum values took place at 13:00 for PM_{10}, at 14:00 for $PM_{2.5}$ and at 14:20 for PM_1. The mean hourly concentration is found to be maximum from 11:00 to 11:00 for PM_{10} and from 15:00 to 16:00 for $PM_{2.5}$ and PM_1, whereas it was minimum from 13:00- 14:00 for all three types of particles.

Area B

For the second area of interest, measurements of airborne particles of an aerodynamic diameter less than 10μm (PM_{10}) took place, on 29/05/2013 and during the time period between 10:00 am and 16:00 pm. The measured airborne particles' concentrations for area B are shown in box plots in the following figures:

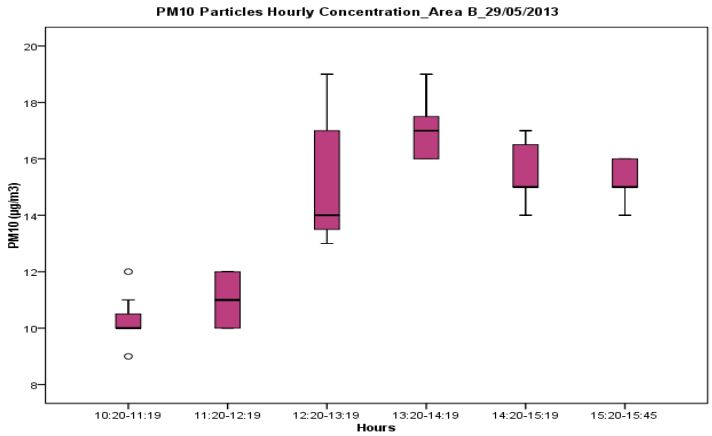

Figure 20: Mean hourly concentration of particles of diameter less than 10 μm (PM_{10}) for the period 10:00 to 16:00 (29/05/2013)

From the data analysis, it can be concluded that, concerning Area B, the concentrations of PM_{10} particles range in levels below the limit of 50μg/m^3. The mean concentration of PM_{10} particles is 13.88μg/m^3, the maximum value is 19μg/m^3 and occurred at 13:15 and the minimum value is 9μg/m^3 and appeared at 10:55.

Area C

For the third area of interest, measurements of airborne particles of an aerodynamic diameter less than 10μm (PM_{10}) took place, on 21/05/2013 and during the time period between 10:00 am and 16:00 pm. The concentrations of the PM_{10} particles for area C are given in box plot. From the data analysis, it can be concluded that, concerning Area B, the concentrations of PM_{10} particles range in levels below the limit of 50μg/m^3.

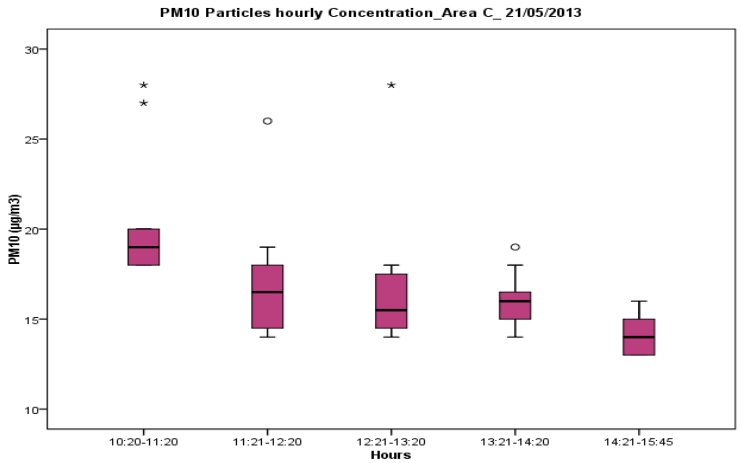

Figure 21: Mean hourly concentration of particles of diameter less than 10 μm (PM_{10}) for the period 10:00 to 16:00 (21/05/2013)

The mean concentration of PM_{10} particles is 18.26μg/m^3, the maximum value is 77μg/m^3 and occurs at 11:00 am and the minimum value is 13μg/m^3 and appears at 14:45 pm.

2.5 Thermal comfort conditions

Thermal comfort is defined as the state in which human beings feel satisfaction with the thermal environment and do not want any changes to it. The investigation and understanding of the parameters that constitute the outdoor thermal comfort is a basic requirement for the microclimatically oriented urban planning, including the planning of green areas. The extent, intensity and efficiency of activities depend on the level of comfort or discomfort experienced by humans when exposed to specific climatic conditions. Outdoor thermal comfort can be calculated using bioclimatic indices incorporating basic climatic parameters such as temperature and wind speed. In this study, in order to calculate the thermal comfort, the bioclimatic index CP is used for the selected points of the area of interest, which illustrate the different materials in the area of intervention. According to Cena, Gregorczuck, Wojcik, the CP index (in mcal cm^{-2} sec^{-1}) is calculated by the mathematical formula:

$$CP = (0.42+0.08v)(36.5-t) \quad (1)$$

Where
t: the mean air temperature in °C
v: the wind speed in m/sec

The thermal comfort levels which are defined by the index value are given in the table below:

Table 1: Estimation of human – bioclimatic environmental conditions

a/a	Values ranges of Cooling capacity (mcal $cm^{-2}sec^{-1}$)	Characterization of Environment	a/a	Values ranges of Cooling capacity (mcal $cm^{-2}sec^{-1}$)	Characterization of Environment
1	< 0.6	Extremely hot	*6*	8.1 – 10.4	Tolerably cool
2	0.6 - 2.6	Very hot	*7*	10.5 – 15.4	Cool
3	2.7 – 5.1	Annoyingly hot	*8*	15.6 – 22.4	Very cool
4	5.2 – 6.4	Tolerably hot	*9*	22.6 – 30.0	Extremely cool
5	6.5 – 8.0	Comfortable pleasant	*10*	> 30.0	Glacial

In the following figures, is given the time variation of the bioclimatic index for the three areas of interest and for the chosen positions. In that range of values, the environment is characterized as extremely hot to very hot for area A, very hot to annoyingly hot for area B and annoyingly hot to tolerably hot for area C, where its average value ranged from 3.3 to 5.6.

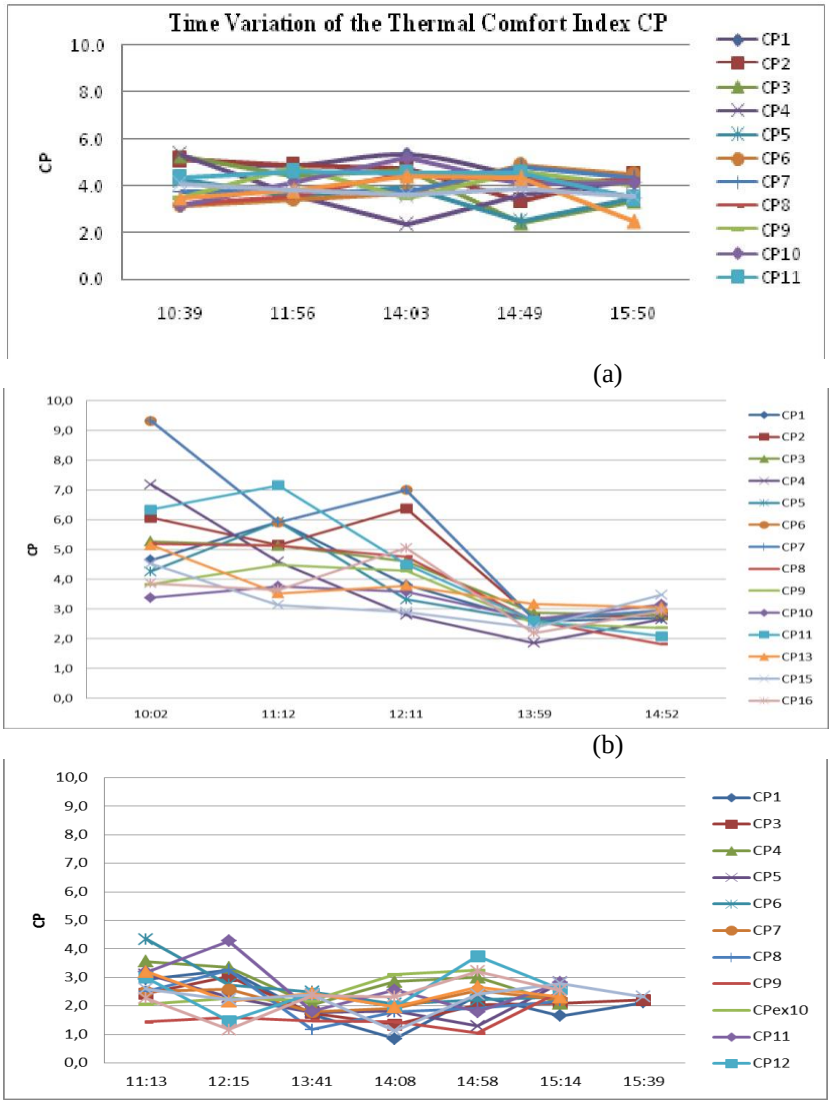

(a)

(b)

(c)

Figure 22: Time variation of the Thermal Comfort Index for (a) Area A (26/04/2013), (b) Area B (29/05/2013) and (c) Area C (21/05/2013)

3 CONCLUDING REMARKS

This paper presents the preliminary results of an ongoing study carried out for the integrated rehabilitation in three urban areas in the Municipality of Acharnes, Greece. The conclusions of the analysis presented herein are summarized as follows. The environmental parameters monitored were air temperature, wind speed and relative humidity. According to the spatial distribution of the temperature the streets showed significant heat strain during midday hours. The air temperature was ranged from 22.3°C to 32.3°C, at high levels considering the examined period (April-May, 2013).

The wind speed affected by the relative position and orientation of buildings and streets, was measured at pedestrian level in a range of 0.4-2.7m/sec.

To investigate the thermal comfort conditions, CP index was calculated at selected points according to the different materials in the area of intervention. The results indicated a high thermal stress on people and thermal discomfort at noon for the majority of the population.

Particulate matter with a diameter less than 1mm (PM_1), 2.5mm ($PM_{2.5}$) and 10mm (PM_{10}) were also measured and the concentrations for the examined period were below the permitted limits.

Detailed measurements were performed in order to investigate the temperature distribution of materials and to depict the differences in their thermal performance in the area of interest. The analysis of the results obtained have shown that the daily average surface temperatures of the materials used in the urban fabric varied between, 37.4°C for the pavements, and 41.8°C for the asphalt. The high levels of surface temperatures should be considered in selecting appropriate materials.
Furthermore, interventions (e.g. vegetation, cool materials, shading devices and water) will be proposed to eliminate these conditions. Finally, the architectural and bioclimatic design of the area will be accomplished and evaluated with the employment of advanced computer aided simulations.

4 REFERENCES

C Cartalis, A Synodinou, M Proedrou, A Tsangrassoulis, M Santamouris (2001). Modifications in energy demand in urban areas as a result of climate changes: an assessment for the southeast Mediterranean region, *Energy Conversion and Management*, 42 (14), 1647–1656.

Santamouris, M. (Ed.). (2001*). Energy and Climate in the Urban Built Environment.* James and James Science.

Santamouris, Papanikolaou, N., Livada, I., Koronakis, I., Georgakis, C., Argiriou, A., & Assimakopoulos, D. N. (2001) On the impact of urban climate to the energy consumption of buildings. *Solar Energy*, 70(3), 201–216.

Santamouris, M. (2007). Heat island research in Europe – State of the art. *Advances Building Energy Research*, 1, 123–150.

Gaitani, N., Michalakakou, G., & Santamouris, M. (2007). On the use of bioclimatic architecture principles in order to improve thermal comfort conditions in outdoor spaces. *Building and Environment*, 42(1), 317–324.

Fintikakis, N. , N. Gaitani, M. Santamouris, M. Assimakopoulos, D.N. Assimakopoulos, M. Fintikaki, G. Albanis, K. Papadimitriou, E. Chryssochoides, K. Katopodi, P. Doumas (2011) Bioclimatic design of open public spaces in the historic centre of Tirana, Albania, *Sustainable Cities and Society*, Volume 1(1), 54-62.

C. Arden Pope, D.W. Dockery (2006). Health effects of fine particulate air pollution: lines that connect. *J Air Waste Manag Assoc*, 56,709–742.

Künzli N, Kaiser R, Medina S, Studnicka M, Chanel O, Filliger P, et al. (2000). Public-health impact of outdoor and traffic-related air pollution: a European assessment. Lancet 356:795–801.

URBAN RECREATION: ENERGY EFFICIENT RETROFIT FOR CARBON ZERO AND SOCIO-ORIENTED URBAN ENVIRONMENTS

Annarita Ferrante[*1], Anastasia Fotopoulou[2], Elena Cattani[3] and Mattheos Santamouris[4]

1 DA, Department of Architecture, School of Engineering and Architecture, UNIBO, Viale Risorgimento 2, 40126 Bologna, Italy; UOA, National and Kapodistrian University of Athens, Physics Department, Group Building Environmental Research, Panepistimioupolis, 15784 Athens, Greece
**Corresponding author: annarita.ferrante@unibo.it*

2 DA, Department of Architecture, School of Engineering and Architecture, UNIBO, Viale Risorgimento 2, 40126 Bologna, Italy

3 DA, Department of Architecture, School of Engineering and Architecture, UNIBO, Viale Risorgimento 2, 40126 Bologna, Italy

4 UOA, National and Kapodistrian University of Athens, Physics Department, Group Building Environmental Research, Panepistimioupolis, 15784 Athens, Greece

ABSTRACT

Appropriate strategies to reduce energy consumption, increase Renewable Energy Sources (RES) penetration within local urban ecosystems are the higher priorities towards low carbon cities. In this context urban canyons (UCs) -conceived and investigated as a whole consisting of the buildings blocks and the related open areas- represent the core of the search for new intersections between energy issues and urban dwellers. In fact, morphological and spatial geometry of UCs, thermal properties of surface coatings and green surfaces have a strong potential on the energy performance and cooling demand reduction in urban settings.
Furthermore, the urban buildings should be also investigated to understand the potential of mutual intersections between passive components, Energy Efficient (EE) techniques and RES.
Finally, efficient schemes for zero-energy requirements, energy construction quality, technological flexibility also need to fit with different users' needs and expectation, taking into account the different economic and social possibilities, within the large building stock throughout European cities. Existing buildings in urban environments represent the biggest challenge both in carbon terms –because of the large amount of existing stock- and for the social impact they may generate on the relationship between human behaviour and urban sites.
The URBAN RECREATION project – funded within the frame EU 7th Framework Programme for Research (Marie Curie-IEF Intra-European Fellowships -IEF-) aims at achieving an effective research action exploring the socio-technical mechanisms that can promote the concrete synergies between economic constraints, users expectations, EE systems and production, in renewed forms of urban expression. In other words, URBAN RECREATION aims at demonstrating the techno-economical and social feasibility of zero energy-zero emission retrofit in existing UCs. To reach this aim the research will:
- Develop a model which spatially depicts the energy of a selected urban area as a contribution to the mapping of the city energy consumption. The principles of the model -based on the city discretization into homogeneous districts characterised by several UC types- will be therefore applicable to other districts and cities.
- Study and evaluate the energy demand/potential of the UCs by designing –in different steps of actions- retrofitted scenarios to achieve carbon neutral UCs. The study will evaluate different solutions to diffusely integrate available technologies within UCs. Therefore Energy demand in the UCs and Energy saving potential of UCs by passive and RES will be fully investigated; Zero Energy-Zero onsite emissions in the UCs, where additional energy savings production by synergies between passive and active systems will be addressed.
- Study and evaluate existing constraints (technical, economic and social constraints) and the way to overcome conflicts/barriers to the designed scenarios' penetration into real UCs. To overcome these barriers and design a framework to achieve the development of low carbon scenarios and zero energy neighbourhoods, the research

project will also develop further activities (social, technical and economic incentives/actions) to fill the knowledge gap among low carbon techniques and their adoption at social and community city level.

KEYWORDS

nZEBs – nearly Zero Energy Buildings, Energy retrofitting, RES - Renewable Energy Sources, Urban Canyons, Socio-oriented Design

1 INTRODUCTION

1.1 The energy potential of green and passive techniques in the urban microclimate

Urban growth has reached such a peak, that bypasses, reversals, or new ways of development are needed (EU Report, 2010)[1]. Increasing urbanization and deficiencies in development control in the urban environment have important consequences on the thermal degradation of urban climate and the environmental efficiency of buildings. As a consequence of heat balance, air temperatures in densely built urban areas are higher than the temperatures of the surrounding rural zones. The phenomenon, known as 'Heat Island' (HI), is due to many factors (Santamouris, 2001; Yamashita, 1996): the canyon geometry, the thermal properties of materials increasing storage of sensible heat in the fabric of the city, the anthropogenic heat, the urban greenhouse; all these factors contribute to increase urban HI effect. Research studies on this subject refer usually to the 'urban HI intensity', which is the maximum temperature difference between the city and the surrounding area (Santamouris, 2001). In this context the city of **Athens represents a highly significant pilot study**: data compiled by various sources by Ferrante (1997) and surveys performed in Athens on the HI intensity -involving more than 30 urban stations- show that during hot summer seasons urban stations present temperatures that are significantly higher than the ones recorded in the comparable suburban stations (the gap varies from 5 to 15 °C[2]). As a consequence, the **cooling load** of **reference buildings in city centre is** about **twice** the value of equivalent buildings in rural areas.

Furthermore, previous research work developed within the frame of the research project POLIS in Athens (Ferrante et al, 1998) have showed some appropriate procedures to design the use of natural components –such as green roofs and pedestrian permeable surfaces - within **Urban Canyons** (**UCs**). The design of outdoor spaces -even if reduced to the envelope of the buildings because of existing urban constraints within thickly-built urban areas as well as the use of natural components have been regarded as key means to improve urban conditions in relation to both microclimate and reduction of pollutants. By 'making-up' the building's surfaces and elevation facades with green components or shading devices, four different scenarios have been proposed in four different UCs in Athens downtown. Experimental software research models have been used to quantify the positive effects of these selected passive techniques. Obtained results clearly indicated that outer surfaces' alternative design acts as prior microclimate modifier and deeply improves outdoor air climate and quality (up to 2/3 °C reduction in ambient temperature, Santamouris, 2001).

Other significant physical factors in the thermal performance of urban environments are wind

[1] Some significant and alarming figures: the world population has grown from 2 to 6 billion, and soon will reach 7 billion, while the percentage of human beings living in cities has increased from 3% in 1800 to 14% in 1900 and is estimated to rise from the current 50% to 75% in 2050. The figure for Europe is still higher: 83% of the population are expected to live in cities by 2050 (EU Report, Brussels, 2010). The average temperature on the Earth's surface has suffered an increase of +0.6% and is estimated to reach 1.5% by 2030. The progressive increase of global warming will specifically raise urban temperatures and heat island effect. After the Messina earthquake of 1908 (which caused about 83,000 deaths) the hot summer of 2003 with ~ 70,000 deaths, mostly in the cities, was the second heaviest natural disaster of the last 100 years in Europe.

[2] Measures performed during the POLIS Research Studies by the CIENE in Athens, Prof. Santamouris. Plants have a strong effect on climate: trees and green spaces can help cool our cities (Santamouris, 2001) (Buttstädt et al, 2010) and save energy (Yamashita, 1996). Trees also help mitigate the greenhouse effect, filter pollutants, mask noise and prevent erosion (Ferrante and Mihalakakou, 2001). Results of computer simulations aimed at studying the combined effect of shading and evaporative transpiration of vegetation on the energy use of several typical one-storey buildings in US cities have showed that by adding one tree per house, the cooling energy savings varied from 12 to 24 %, while adding three trees per house can reduce the cooling load between 17 to 57 percent. According to this study, the direct effects of shading account for only 10 to 35 % of the total cooling energy savings.

flows and air circulation (Santamouris et al, 1999), (Ricciardelli et al, 2006) as well as air stratification within UCs. It is clear that In particular, the HI effect and the microclimatic conditions typical of UCs (Bitan, 1992) appear to be strongly influenced by thermal properties of the materials and components used in the buildings and on the streets (Buttstädt, 2010). The comparative research carried out by the Host Institution demonstrated that the use of cool coloured materials (Synnefa et al, 2007) and thermo-chromic building coatings can contribute to energy savings in buildings, providing a thermally comfortable indoor environment and improved urban microclimatic conditions (Karlessi et al, 2009). It is therefore evident that UCs have to be conceived and investigated as a whole consisting of the **buildings blocks** and the related **open area** along the street/square.

Thus, morphological and spatial geometry of UCs, thermal properties of surface coatings and green surfaces have a strong potential on the energy performance and cooling demand reduction in urban settings. As a first conclusion note, we can state that **microclimate in the Urban Canyons (UCs) may be assumed as the central spatial core of climatic conditions in residential urban areas**. This special context needs to be further investigated by means of a more holistic approach able to integrate the potential of mutual intersections among the different physical components (green, surfaces, coating materials, new buildings envelopes) and their effects on urban climate in a comprehensive design tool.

1.2 Policy background and zero energy case studies

Over the last decades, energy oriented innovations in building technology have emerged in many areas of the building construction sector[3] (Brown and Vergragt, 2008), till the latest experiences aiming at setting to zero the carbon emission of new developments and even of a whole City[4]: a pilot city plan to set to zero the carbon emissions of Copenhagen has been developed[5]. The increasing interest in nearly Zero Energy Buildings (nZEBs), recent European and national Directives on Energy Performance of Buildings (EPB)[6], easier accessible Best Available Techniques (BATs) and Renewable Energy Sources (RES), all seem to point to further exploitation of BAT and better penetration of RES into new building construction.

The majority of these recent case studies refer to newly conceived buildings and large development plan.

Furthermore, in spite of growing investments in RES technology (Bürer and Wüstenhagen, 2009), feed-in tariffs and, in general, the policy incentives (Bulkeley, 2010), additional investments are needed to reduce carbon emissions and fossil fuel consumption[7]. "Needless to say, this is particularly challenging in a context of global economic slowdown such as the one the world is currently experiencing" (Masini et al, 2010).

Thus, the challenge now is to **widen technical ZEB knowledge** in **existing built environments**: we need to shift our technical understanding on EE from new developments

[3] Green buildings now belongs to the "history of architecture": the first prototype buildings and their attempts to achieve zero-heating in the form of solar houses date back to 1950s (Hernandez, Kenny, 2010). Among the recent experiences is the well known urban village BedZED (Beddington Zero Emission Development), winner of the prestigious Energy Awards in Linz, Housing and Building category, Austria, 2002 (Marsh, 2002).

[4] A first zero waste-zero carbon emission City is to be constructed in Abu Dhabi, Masdar City, designed by N. Foster. Despite its location (the oil rich and hot part of the world) the development is designed as a huge, positive energy building, resulting in a self-sustaining, car-free city.

[5] The climate Plan (City of Copenhagen, 2009) demonstrates how to make Copenhagen the world's first carbon neutral capital by 2025 by means of using biomass in power stations, erecting windmill parks, increasing reliance on geothermal power and renovating the district heating network.

[6] In the frame of the legislative plane, recently the European Parliament (Directive 2010/31/EU on the EPB), amending the previous 2002 EPB Directive, has approved a recast, proposing that by 31 December 2020 all new buildings shall be nearly zero-energy consumption and will have to produce as much energy as they consume on-site. See also Task 40/Towards Zero Energy Solar Buildings, IEA SHC /ECBCS Project, Annex 52.

[7] The treaty issued by several NGOs calls for a doubling of market investments by 2012 and quadrupling by 2020 to attain the proposed carbon emission reduction targets (Meyer et al, 2009). As reported by Guy (2006), according to the United Nations Environmental Programme (UNEP) there is still an "*urgent need for the incorporation of EE issues to be included in urban planning and construction*".

and buildings to existing buildings, within UCs of active cities, since the large amount of existing stock represents the wider potential in carbon terms. In this context, recent studies and design proposals on building energy retrofitting (Ferrante et al, 2011) has proved that huge energy saving may be achieved in winter by adding different coatings to existing buildings. In particular, the combination of new building coatings like sunspaces or buffer zones (as shown in fig. 1) and RES, drastically reduce the energy performance indexes of the buildings **up to the target of nZEB**. These studies, performed during the winter season so far, need to be further investigated in order to quantify the **cooling** demand **reduction** of the proposed scenarios during hot **summer** conditions.

*Fig. 1(a, b, c, d). Energy retrofitting by new envelopes design in a reference building of Bologna. a) initial scenario; b,c) new scenario; d) different energy performance indexes (kWh/m^2*y) as a function of different retrofitting options (from left (grey) =initial state; to right (green) = final scenario)*

Thus, the context of buildings in urban areas should be further investigated, to understand the potential of mutual intersections between passive components, Energy Efficient (EE) techniques and RES. In fact, the study of the potential synergies between passive and active systems have not been fully explored; nonetheless it is particular important, since the use of EE systems and RES should provide additional energy saving deriving from passive-active interactions[8]. This represents a key added value to be gained from **closer collaborations** among **researchers**, existing business investors and **industrial partners** in the field of **RES**.
To achieve a proper **nZEB**, it is therefore crucial: i) to investigate the **cooling** demand reduction during hot **summer** conditions of retrofitted buildings; ii) to promote further investigation on synergy between passive and active energy technologies within existing urban environments, thus implementing research exchanges with economic business sectors in the common effort to activate smart and low carbon UCs.

1.3 Low Carbon Communities and Grass-root initiatives in the urban environment

Despite excellent studies and pilot zero-energy cities, an increasing societal need for human recognition in depersonalized urban environment is emerging. Furthermore, as a result of the functional or "Ford" city of the 20th century, in the open areas and along the city streets, the urban space was devalued by destroying the "transparency" of the facades on street level either by the infill of garages or by closing all doors and windows on ground level (Fig. 2).

[8] For example, the potential of PV systems in cooling, shading, increasing air stratification and vertical air extraction from UCs may produce additional energy savings, disregarded so far; wind micro-turbines may behave in interesting ways in urban environment: for example, the roof effect (Mithraratne, 2009) -which refers to wind colliding with a pitched roof- may accelerate the air movement thus improving the performance of a micro-turbine on the roof; furthermore, a micro-wind generator may help to extract air from buildings and urban environments.

Fig. 2 (a,b,c,d,e). Different urban canyons in the European cities. From the left to right: a)Vienna; b,c) Bologna; d,e) Athens.

Redesigning energy technologies in the urban areas is certainly a major scientific challenge. However, succeeding in this endeavour requires more than getting the engineering right (Webler and Tuler Seth, 2010). Thus, energy efficiency in urban settings is more than a technical problem. Recent studies have suggested that more focus should be placed on the social aspects at community level and that energy users should be engaged in their role of citizens. In fact, developing more sustainable consumption and production systems depend upon consumers' willingness to engage in "greener" and more collective behaviours (Peattie, 2010). In this frame, local urban communities have inimitable advantages in providing infrastructure for more sustainable consumption environment; in fact, different types of low-carbon communities as a context to reduce carbon intensity are emerging at different scales (Heiskanen, 2010). Existing literature (Mulugetta et al, 2010; Guy, 2006) stresses the need for a clear transfer from a technical/economically based urban theory to a human based and **socio-technical urban vision** to achieve a greener behaviour in urban environment. In this perspective, it is worth mentioning that timid attempts in the sustainable "re-design" of urban places by local-based communities are arising in the spatial sphere of the urban street environments (Fig. 3).

Fig. 3. Occupying small parking areas, the Urban Community Centotrecento Street in Bologna has encouraged small practices of self-organization among the inhabitants for a more sustainable management of space, equipment and resources.

Notably, some of Europe's leading innovation Nations have included **user-driven** or user-centred innovation as a way of providing innovative products and services that correspond better to user needs and therefore are more competitive. User-driven innovation (EU, 2009) is closely associated with design, and involves tools and methodologies developed and used by designers[9]. Practises of (re-)design of existing buildings by engaging final users are also occurring in different contexts of EU and worldwide (fig. 4).

Fig. 4 (a,b,c,d,e). User-centred design by participative process with the inhabitants in new (from left, a,b) and existing buildings (right, c,d,e).

In brief, there is a special need for efficient schemes where **zero-energy requirements, energy construction quality, technological flexibility can fit with different users' needs and expectation**, taking into account the different economic and social possibilities, within the large building stock throughout European cities. Existing buildings in urban environments represent the biggest challenge both in carbon terms –because of the large amount of existing stock- and for the social impact they may generate on the relationship between human behaviour and urban sites. Finally, we argue **UCs** (streets and connected residential buildings) are the **core of the search for new intersections** between urban dwellers and energy related issues. An effective research action should explore the socio-technical mechanisms that can

[9] EU (Commission of) Communities, 2009,"Design as a driver of user-centred innovation", Brussels, 7.4.2009, SEC(2009)501.

promote the concrete synergies between economic constraints, users expectations, EE systems and production, in renewed forms of urban self-expression.

2 CRITICAL ISSUES IN THE URBAN ENVIRONMENT

There is thus a lack of comprehensive information on the possible intersections between the BAT's options and a concrete inclusive approach to users needs. This is because close collaboration between physicians, engineers, architects, energy companies, stakeholders and urban dwellers, amongst others, is missing, which is probably why progress in this area is still limited to date. From the complexity of the state of the art in urban environment a series of missing issues arises. To sum up, there is an increasing need for:

- Further exploration of UCs' geometry for achieving better understanding of current energy demand within the different residential areas of the city. This further exploration should be observed and quantified not only with reference to the building blocks and urban textures considered as the "solid" part of the city, but also to the open streets environments, thus considering **the buildings and the related open spaces (**the UCs) as the "core" of energy investigation and the consequent global effects emerging from the cumulative effects of all the buildings and open areas in the canyons of the city;
- Energy retrofitting actions in existing building stocks within localized ground-based urban environment;
- Research studies able to bridge the knowledge gaps on the potential of both passive and active technologies by RES –solar, PV, Aeolian- and their mutual intersections in the thermal balance of UCs;
- Small scale and distributed RES penetration in local urban environments;
- Bottom-up processes aimed at including urban dwellers in low-carbon transition pathways within UCs[10].

Thus new connections between citizens, business investors and energy related issues should be investigated within localized UCs.

3 RESEARCH HYPOTHESIS

The energy of residential urban areas can be represented and estimated spatially according to a sequence of different UC types, considered as the basic urban units which characterize a whole city (as an example, see Fig. 5 -a,b,c-). Furthermore, the proposed research focuses on UCs, considering the buildings and the related open areas as a whole and the snowballing effects of all the buildings and open areas in the UCs: this holistic vision of urban energy demand can better drive urban planning decision and bottom-up, grass-root initiatives towards the adoption of alternative residential configurations/redevelopment of existing urban areas.

Fig.5 (a,b,c). a) Left: an example of discretized areas at the large urban scale within the Athens Central Area; b, c) Right part of the figure: aerial view (above) and zenith view (below) of the urban section (A) within an homogeneous district/area.

[10] "In the search of bridging the gaps between EE technology and society, we need to explore the potential links and intersections between technologies and urban dwellers in particular contexts of use, advocating the development of low-carbon and socio-oriented experiments in the urban environments" (Guy, 2006).

Thus, the assumptions of the URBAN RECREATION are the following:

i) in order to evaluate the energy demand and potential of an urban environment it is possible to develop a whole discretized city model based on different urban units (Whitehand, 2009), corresponding to the **building blocks and the related street/open area as a whole entity** (hereafter UCs);

ii) in these units retrofitting actions towards low carbon UCs have to be hypothesised and validated exploring both passive physical components (green and EE techniques for surfaces and coating materials) and energy micro-generating technologies by RES – solar, PhotoVoltaic (PV), Aeolian- etc.;

iii) the social and the economical feasibility of these actions in localized urban environments can more easily lead to bottom-up actions and drive towards a carbon neutral future (aim of the research).

4 ZERO ENERGY AND ZERO EMISSION URBAN AREAS

The goal of the URBAN RECREATION proposal is to demonstrate the feasibility of **Zero Energy and zero CO_2 emission Retrofitting** (**ZER**) throughout a whole city area. To reach this aim the research studies will:

i) - Develop a model which spatially depicts the energy of residential urban areas as a contribution to the mapping of total energy consumption in the built environment. This model will be based on the discretization of the city into different homogeneous districts, which would enable the model to be used for different case studies. Discretization of the city is a very important objective, especially considering the possible intersections with existing plan at Municipal/Regional level. The average Energy Consumption (EC) currently available in existing regulation tools will be combined with the large amount of available data (Santamouris et al, 2007) and referred to the batch of the buildings and the open areas, thus considering the UCs as the basic units for investigation of both energy and social issues in the urban environment.

ii) - Study and evaluate the energy demand/potential of the UCs; this will be achieved by designing –in different steps of actions- retrofitted scenarios in order to achieve zero energy, socially inclusive solutions by means of an inter-disciplinary research approach. The study will develop, perform and evaluate different possible solutions to achieve a sustainable and spatially localized distribution of energy, by means of technologies to be diffusely integrated in the urban buildings and canyons;

iii) - Promote further actions to contribute to fill the knowledge gap existing among low carbon passive techniques and the adoption of these technological solutions at social and community city level.

In order to investigate the validity of these hypotheses, the overall aim of URBAN RECREATION has been sub-divided into the following objectives:

4.1 Urban discretized model

Determine the instrumental values and the spatial format of the model of energy in the urban environment as a part of a broader analysis on energy consumption. In this objective we will develop a city model based on the different types of existing UCs geometry; a consistent part of the major Athens area will be mapped and 3 significant areas will be selected for further investigation.

4.2 Energy balance in the urban canyons (UCs)

Evaluate the initial energy balance of the urban environment. Estimate the thermal energy performance and the energy demand in 3 representative urban units within the major Athens area, to determine the value of the energy supply of at the initial state.

4.3 Energy saving potential of UCs

Determine the energy saving potential of the urban units. This will be achieved by designing: i) alternative urban scenarios by means of technological building

components/materials and volumes aimed at reducing the building heating and cooling loads; ii) alternative urban scenarios integrating renewable energy sources in the urban building envelope and outdoor urban sets as well. These objectives will also be connected with business economic actors, industrial associations and SMEs.

4.4 Zero Energy and Zero onsite emissions in the urban areas

Determine the final scenario to achieve zero energy and zero CO_2 emission within UCs in winter and summer conditions. The final scenario will take into account the mutual effects arising from passive and active systems within UCs. This objective is particularly important, because of possible connection/integration of the study with industrial associations, SMEs: in fact, the possible synergies between EE passive and active systems (i.e. PV panels or micro-Aeolian systems and their potential in cooling, shading, increasing air stratification and vertical air extraction) may produce significant additional energy savings and interesting added value both to RES penetration into the market; creative ideas arisen during this phase can produce the further improvement of existing products, by turning existing building and RES components into renewed or new products.

4.5 Overcoming existing constraints

Study and evaluate existing constraints and the way to overcome conflicts/barriers to the designed scenarios' penetration into real UCs. This objective is addressed to analyse and overcome the existing technical, economic and social constraints and design a framework to achieve the development of low carbon scenarios and zero energy neighbourhoods.

4.6 Outreach initiatives

Promote community of practices, dissemination and workshops about successful retrofitting actions within real urban environments.

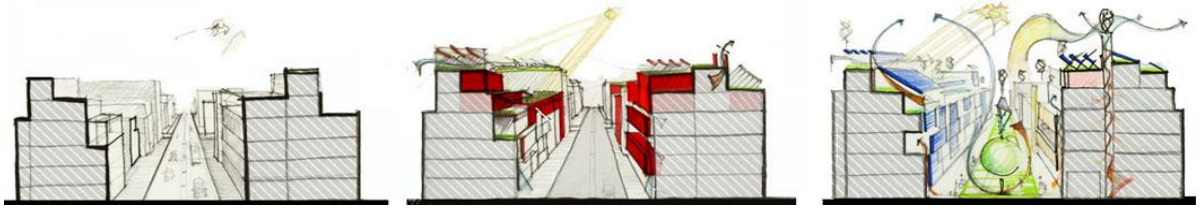

Fig. 5 (a, b, c) Different scenarios in the UCs. a) The initial scenario; b) Technological building components/materials (change of facades' surfaces, additional envelopes, additional spaces and volumes) in a first alternative UC; c) Interactions, synergies and possible additional energy saving within a complete UC scenario integrating passive and active systems (RES -PV and micro-Aeolian) in the urban building envelopes and outdoor urban sets.

5 CONCLUSIONS

Although no conclusions can be drawn (the project is just started), being a multidisciplinary and multi-scalar proposal, URBAN RECREATION may open new horizons and opportunities for research in the frame of possible intersections between social urban studies and economics, physics, technology, design disregarded until now. To sum up, the proposal will:

- √ Explore –as widely as possible- social, spatial and technical relations among urban forms, EE techniques in a neighbourhood development strategy as a part of the broader larger city scale;
- √ Demonstrate the high competitiveness of small scale energy saving and production within different urban areas;
- √ Study the mutual effects between passive systems to reduce heating and cooling loads and RES as PV and Micro-Aeolian disregarded until now; the research use of technological components such as photovoltaic panels or micro-Aeolian systems should be further investigated in order to understand additional energy saving deriving from mutual interaction among passive and active techniques;
- √ Study the actions/strategies to raise social awareness and citizens' consciousness of environment friendly tools and energy production/consumption in urban open spaces; the study will explore the actions to test social/technical feasibility in relation to alternative urban scenarios.

Therefore we foresee at least two/three research areas for possible spin off research topics, with regards to ERA competitiveness and long-term synergies: i) the social and urban sphere; ii) the industrial research implementation and design; iii) intersections between the two fields of interest.

6 REFERENCES

Bitan, A. (1992). The high climatic quality of the city of future. *Atmospheric Environment 26B*, 1992, 313-329.

Brown, H.S., Vergragt P.J. (2008). Bounded socio-technical experiments as agents of systemic change: The case of a zero-energy residential building. *Technological Forecasting & Social Change 75*, 107–130.

Bulkeley, H. (2010). Cities and the Governing of Climate Change. *Annual Review of Environment and Resources*, 229-253.

Bürer, M. J., Wüstenhagen, R. (2009). Which renewable energy policy is a venture capitalist's best friend? Empirical evidence from a survey of international cleantech investors. *Energy Policy 37*, 4997–5006.

Buttstädt, M., Sachsen, T., Ketzler, G., Merbitz, H., Schneider, C. (2010). Urban Temperature Distribution and Detection of Influencing Factors in Urban Structure. *ISUF; International Seminar on Urban Form*, Hamburg and Lubeck.

City of Copenhagen. (2009). Copenhagen Climate Plan. The Technical and Environmental Administration City Hall, 1599 Copenhagen V.

EU Report. (2010). World and European Sustainable Cities. Insights from EU research, Directorate-General for Research. Directorate L, Science, economy and society, Unit L.2. Research in the Economic, Social sciences and Humanities. *European Commission, Bureau SDME 07/34, B-1049 Brussels*. Socio-economic Sciences and Humanities; EUR 24353 EN.

EU Parliament. (2009-2010), Report on the proposal for a Directive of the European Parliament and of the Council on the Energy Performance of Buildings (recast) (COM(2008)0780-C6-0413/2008-2008/0223(COD)), 2009. *Directive 2010/31/EU of the European Parliament and of the Council of 19 May 2010 on the energy performance of buildings*.

EU Communication. (2011(a)). Energy Efficiency Plan 2011. *Comm. from the Commission to the European Parliament, the Council, the EU Economic and Social Committee and the Committee of the Regions*, Brussels.

EU Communication. (2011(b)). A resource-efficient Europe – Flagship initiative under the Europe 2020 Strategy. *Comm. from the EU Parliament, the Council, the EU Economic and Social Committee and the Committee of the Regions*. Brussels.

Energy 2020. (2010). A strategy for competitive, sustainable and secure energy. Comm. from the Commission to the European Parliament, the Council, *the EU Economic and Social Committee and the Committee of the Regions*. Brussels, 10.11.2010 COM(2010) 639 final.

EU Communication. (2009). Investing in the Development of Low Carbon Technologies (SET-Plan). *Comm. from the Commission to the European Parliament, the Council, the European Economic and Social Committee and the Committee of the Regions*, Brussels, 7.10.2009, COM(2009) 519 final.

Ferrante, A., Semprini, G. (2011). Building Energy Retrofitting in Urban areas. *Procedia Engineering 21*, 968-975. Available online at www.sciencedirect.com.

Ferrante, A., Mihalakakou G. (2001). The influence of water, green and selected passive techniques on the rehabilitation of historical industrial buildings in urban areas. *Journal Solar Energy 70*, No 3, 245-253.

Ferrante, A., Mihalakakou, G., Santamouris, M. (1999). Natural Devices in the Urban Spaces to Improve Indoor Air Climate and Air Quality of Existing Buildings. *Proceedings of International Conference of Indoor Air 99*, Edinburgh, Scotland.

Ferrante, A., Santamouris, M., Koronaki, I., Mihalakakou, G. and Papanikolau, N. (1998). The Design Parameters' contribution to Improve Urban Microclimate: An extensive analysis within the frame of POLIS Research Project in Athens. *THE JOINT MEETING OF the 2nd Eu Conference on Energy Performance and Indoor Climate In* Buildings and 3rd International Conference IAQ, Ventilation and Energy Conservation. Lyon, 19-21/11/1998.

Folke, C., Hahn, T., Olsson, P., Norberg, J. (2005). Adaptive Governance of Social-Ecological Systems. *Annual Review of Environment and Resources 30*, 441-73.

Gertz, C. (1983). Local knowledge, Basic Books, London.

Guy, S. (2006). Designing urban knowledge: competing perspectives on energy and buildings. *Environment and Planning C*: *Government and Policy 24*, 645 – 659.

Heiskanen, E., Johnson, M., Robinson, S., Vadovics, E., Saastamoinen, M. (2010). Low-carbon communities as a context for individual behavioural change. *Energy Policy 38*, 7586-7595.

Hernandez, P., Kenny, P. (2010). From net energy to zero energy buildings: Defining life cycle zero energy buildings (LC-ZEB). *Energy and Buildings 42*, 815–821.

Marsh, G. (2002). Zero Energy Buildings, Key Role for RE at UK Housing Development. *Refocus*, 58-61.

Masini, A., Menichetti, E. (2010). The impact of behavioural factors in the renewable energy investment decision making process: Conceptual framework and empirical findings. *Energy Policy*, 1-10.

Mithraratne, N. (2009). Roof-top wind turbines for microgeneration in urban houses in New Zealand. *Energy and Buildings 41*, 1013–1018.

Meyer, A. et al. (2010). A Copenhagen Climate Treaty, Version 1.0, Karlsruhe.

Mulugetta, Y., Jackson, T., Van der Horst, D. (2010). Carbon reduction at community scale. *Energy Policy 38*, 7541-7545.

Peattie, K. (2010). Green Consumption: Behaviour and Norms, *Annual Review of Environment and Resources 35*, 195-228.

Karlessi, T., Santamouris, M., Apostolakis, K., Synefa, A., Livada, I. (2009). Development and testing of thermochromic coatings for buildings and urban structures. *Solar Energy 83*, 538-551.

Synnefa, A., Santamouris, M., Apostolakis, K. (2007). On the development, optical properties and thermal performance of cool coloured coatings for the urban environment. *Solar Energy 81*, 488-497.

Santamouris, M. (2001). Energy and Climate in the Urban Built Environment. *James & James Science Publishers Ltd*, London.

Santamouris, M., Papanikolau, N., Koronakis, I., Livada, I., Asimakopoulos, D. (1999). Thermal and air flow characteristics in a deep pedestrian canyon under hot weather conditions. *Atmospheric Environment 33*, 4503-4521.

Santamouris, M., Kapsis, K., Korres, D., Livada, I., Pavlou, C., Assimakopoulos, M.N. (2007). On the relation between the energy and social characteristics of the residential sector. *Energy and Buildings 39*, 893-905.

Schultz, N. (2000). Architecture: Presence, Language, Place. *Skira (Italian Edition)*, Milan.

Ricciardelli, F., Polimeno, S. (2006). Some characteristics of the wind flow in the lower Urban Boundary Layer. *Wind Engineering and Industrial Aerodynamics 94*, 815–832.

Yamashita, S. (1996). Detailed structure of heat island phenomena from moving observations from electric tram-cars in Metropolitan Tokyo. *Atmospheric Environment 33(3)*, 429-435.

Whitehand, J.W.R. (2009). The structure of urban landscapes: strengthening research and practice. *Urban Morphology 13*, 5-27.

Webler, T., Tuler S. P. (2010). Getting the engineering right is not always enough: Researching the human dimensions of the new energy technologies. *Energy Policy 38* 2690-2691.

COMPARATIVE STUDIES OF THE OCCUPANTS' BEHAVIOUR IN A UNIVERSITY BUILDING DURING WINTER AND SUMMER TIME

D.K.Serghides[1], C.K.Chatzinikola[2], M.C.Katafygiotou[3]

[1,2,3]Cyprus University of Technology/Department of Environmental Science and Technology, Limassol, Cyprus
[1]despina.serghides@cut.ac.cy
[2]ck.chatzinikola@edu.cut.ac.cy
[3]martha.katafygiotou@cut.ac.cy

ABSTRACT

The paper focuses on the assessment of indoor comfort and the energy consumption in a University building, during winter and summer time. The examined building belongs to the Cyprus University of Technology, it is located in coastal city of Limassol and it is used for teaching and offices. The main aim of the paper is to make a comparative study of the occupants' behaviour and its effects on the building's energy consumption, as well as on the indoor thermal and optical comfort, between winter and summer season.
ASHRAE Standards (American Society of Heating, Refrigerating and Air conditioning Engineers) are used through a questionnaire campaign and the thermal comfort of occupants' is analysed with the indicator of PMV (Predicted Mean Vote), and PPD (Predicted Percent of Dissatisfied People). The occupants' answers are analyzed using SPSS (Superior Performance Software System) software.
The study and measurements are carried out during the summer and winter months of 2012 and 2013, respectively. The air temperature, the relative humidity and the levels of lighting of the building are monitored using temperature, humidity and lux meter tools. The data are collected on a daily basis for two weeks, during the period of the two seasons. The monthly energy consumption cost is calculated based on the bills of the Electricity Authority of Cyprus for 2012.
The recorded measurements; the completed questionnaires are analysed for both seasons, summer and winter. From the analysis of results, comparative studies of the occupants' behavior for the two seasons conclude to various patterns of effects on the thermal and optical comfort of the building, as well as on its energy consumption.

Keywords: Indoor comfort, occupants' behaviour, energy consumption.

1 INTRODUCTION

Inefficient energy use in buildings is both, increasingly expensive and unsustainable [1]. The increasing energy, already threatens the future of the planet, as research shows that 10% of the world population exploits 90% of energy resources [2]. Energy consumed in many ways in buildings, and the maximum consumption depends on the type of building, construction and building services details, and the climate in which the building is located [1]. Based on a research, the two characteristics with the greatest influence on energy use, is the option of building size and weather conditions [3]. Therefore, the reduction of energy consumption of a building begins from

improving the design of buildings [1] and [3]. Also, during the design phase of the building, the rate of heat loss and the number of users who are in the building, are the two parameters which must be given more attention due to high impact on building energy performance [4]. Various studies have indicated large differences in energy consumption in buildings, which are caused by the occupants' behavior of each building, which exerts a strong influence. In fact, several studies discuss that energy savings can be achieved with low-cost measures and a change in the attitude of occupants towards the energy consumption and save energy [4], [5], [6] and[10]. For example, energy is wasted needlessly if employees do not switch off their computer before they leave the job, or if they leave the lights on most of the working hours even if they are absent from the office, or even if there is sufficient natural light. By the proper use of natural lighting, the electric light can be eliminated, and so, in this way, energy saving can be achieved for lighting, cooling and electricity. Also, by switching off appliances that are not needed during the working hours, savings will be even higher. However, because of the poor occupants' energy behavior in the buildings, more energy is used during non-working hours than during working hours [5] and [7]. These are directly related to the thermal comfort of the buildings, because the use of the building by its users can lead to an improvement of the internal environment, or to degradation. However, people under the same climatic conditions do not all feel comfortable at the same time with the same conditions [11]. Of course, there are different behavioral patterns and user profiles that affect differently the energy consumption of a building. These differences in wasted energy are based on gender, age and years of service of the employees. For example, high-income couples request comfortable housing without concern for energy saving and these families are usually those which use more devices daily. Older people need higher levels of thermal comfort [5] and [8]. A study has also shown that the maximum energy consumption for heating usually is caused by bedrooms, offices and working rooms [8]. While the use of renewable sources of energy can contribute to reduce energy consumption, the focus is on the recognition of the wasting from occupants. This will facilitate the acceptance of energy-saving measures, since as a result this will improve the quality of life, protect the environment and reduce the power budget of their household, company or space [5].

2 METHODOLOGY

In the present report, the study of indoor comfort and the energy consumption in the Building Service of Academic and Student Affairs of the Cyprus University of Technology (CUT) is being studied. Specifically, the occupants' behavior affecting the energy consumption in the building, as well as the indoor thermal and optical comfort is examined during summer and winter season of 2012 and 2013, respectively. The study was carried out with questionnaires addressed to the employees and the students, instruments for daily measurements and calculations for the energy consumption.

The study compared the behavior of the occupants and the completed questionnaires. A total number of 60 occupants participated in the study, 30 occupants each season. During summer season, 60% of the participants were females and 40% males. Respectively, during winter 67% were females and 33% males. The questionnaires were given at the same time and collected after the occupants' responded. The questionnaire based on ASHRAE Standard (American Society of Heating, Refrigerating and Air conditioning Engineers) and was divided into two main

sections. The sections included: a) the thermal comfort which consists of 7 questions and b) the natural lighting with 4 questions. The occupants' answers are analyzed using SPSS (Superior Performance Software System) software and were organized in diagrams showing percentages for each question based on the total occupants' responses. Thermal comfort of occupants' is analyzed with the indicator of PMV (Predicted Mean Vote), and PPD (Predicted Percent of Dissatisfied People). For the scope of this research, employees and students in the building were chosen as the occupants under investigations.

Air temperature, relative humidity and the levels of lighting of the building are monitored using temperature, humidity and lux meter tools. The data are collected three times a day, during the period of two weeks for each season, excluding weekends. During summer season, the measurements were during 07:00 – 08:00 am, 13:30 – 14:30 pm and 17:30 – 18:30 pm, in the morning, noon and afternoon, respectively. The noon measurements were during the working hours, while the morning and afternoon hours were during non-working hours. During winter season, the measurements were during 08:00-09:00 am, 12:30-13:30 pm and 16:00-17:00 pm for the morning, noon and afternoon, respectively. The measurements were during working hours. The position and orientations of each occupant, according to that of the building, are recorded, as well as the daily observations.

The monthly energy consumption cost is calculated based on Electricity Authority of Cyprus charges for 2012 and on the data from energy bills for the building, during a summer month.

Finally, the last step was to compare the occupants' behavior for the two seasons concluding to various patterns of effects on the thermal and optical comfort of the building, as well as on its energy consumption. These were essential to evaluate how occupants may influence building energy use through their actions and behaviour.

3 THE CASE STUDY

The building of the Students Affairs of the Cyprus University of Technology is located in the center of Limassol on the corner of Athens and Nicholas Xiouta Street. Limassol has a Mediterranean and temperate climate, which is mostly hot with dry summers and mild winters. The humidity in Limassol is at high levels due to its coastal position. In the summer of 2012, the average maximum temperature in Limassol was about 34.53 °C, the average minimum temperature at 23.67 °C, while the average rainfall is 0 mm. In December of 2012, the average maximum temperature was 19.9 °C, the average minimum temperature at 12.1 °C, while the average rainfall is 48.7 mm.

Table 1: Maximum/Minimum Temperature (°C) and Precipitation (mm)

Month	Average Maximum (°C)	Average Minimum (°C)	Rain (mm)
June	32.2	22	0
July	35.2	24.9	0
August	36.2	24.1	0
December	19.9	12.1	48.7

The building was built in 1978 and functioned as a bank. In 2002 retrofitting and upgrading of 1st and 2nd floor was done, until the 1/5/2011 when the Cyprus University of Technology bought the

Figure 1: The Service of Academic and Student Affairs building.

building. In July of 2011 the renovation of the second floor of the building started; in December of 2011 that of the ground and the mezzanine. The building of Student Affairs is a three storey building with a mezzanine on the first floor. Specifically, there is a ground floor of 500 square meters (m^2), mezzanine 497 m^2, first and second floor area of 560 m^2 each one. Based on the main facade, the building has a northwest orientation.

Figure 2: Architectural Design of the building a) Ground floor, b) Mezzanine, c) First Floor, d) Second floor

The height of each floor in the building is 3.25 meters (m). The building is made of reinforced concrete frame structure and 20cm brick walls; in the interior it incorporates plasterboard panel walls of 10 cm. The facades of the building are mainly glazed, except the south façade which is opaque; the panels of windows are single glazed.

The building under study is used as offices for employees and teaching classes for students. Specifically there are offices, lecture rooms, conference rooms, computer rooms, corridors, toilets and kitchens. Also, it is equipped with all the typical appliances (computers, photocopying machines, printers, refrigerators, etc.) as well as machinery and equipment for the needs of users. On the ground floor and the mezzanine of the building, there are twenty two (22) people employed. The first and the second floor house a large number of students. The ground floor and mezzanine operates from 7:30 a.m. until 14:30 pm and from 07:30 am to 18:00 pm, in the summer and in winter periods, respectively. The first and second floor, which have classes operate from 8:00 a.m. until 20:00 pm, throughout the academic semester. However, during the 3 months of summer, the students are not attending the university, however, the staff of Student Affairs continues to work. For the summer, the survey of questionnaires was conducted in late August when the students returned to the University for their registration for the new academic year.

4 RESULTS AND DISCUSSIONS

4.1 Questionnaire Results

Prior to conducting any statistical analysis, descriptive statistics were performed. The most significant results derived from the responses given by the University's employees and students according to the questionnaire are presented below. Also, correlations between the users' responses have been made and all these are presented in Fig. 3 – 10.

4.1.1 Thermal Comfort

The first section of the questionnaire focuses on the users' thermal comfort. In Figs.3-5 indicate the relationship between indicators PMV and PPD through the question how users feel regarding thermal comfort, for summer and winter season. The predicted percentage dissatisfied (PDD) for summer is 43,35% and PMV = (-1,4). The PPD for winter is 43,35% and PMV = (+1,4). According to the standards of Ashrae the 43,35% PDD is not within accepted limits, since the PMV is -1,4 and +1,4. The majority of users indicate that in summer it feels slightly cold to cold and in winter it feels hot. The main reason that the users do not feel comfortable, in either season, is found in their answer of the question whether the air conditioning is turned on. Apparently the air conditioning was turned on at very low temperatures in summer and at very high temperatures in winter season.

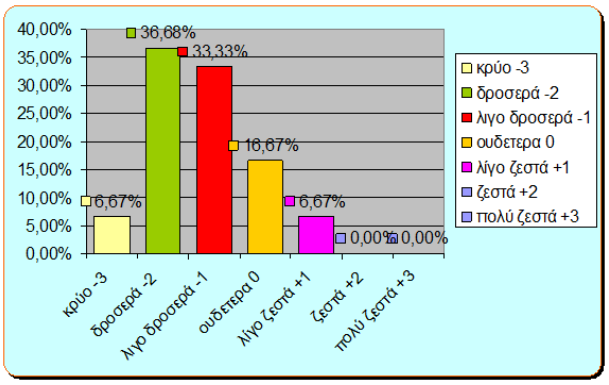

Figure 3: Percentages on the users' satisfaction for thermal comfort in summer.

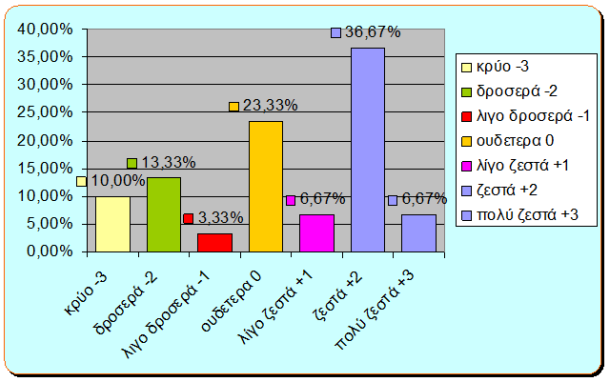

Figure 4: Percentages on the users' satisfaction for thermal comfort in winter.

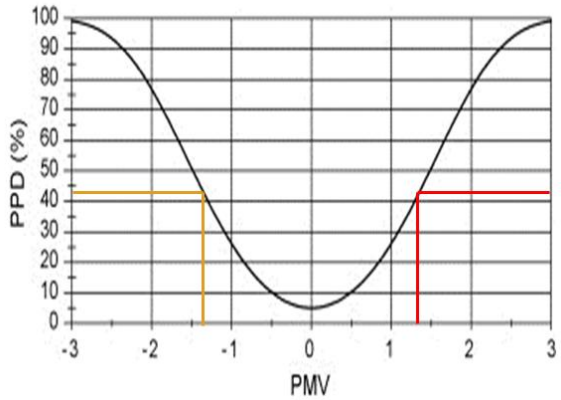

Figure 5: PPD according to the PMV. Orange colour shows the summer and red the winter

Users were asked to indicate their habits concerning the air conditioner. As shown in Fig. 6 and 7, almost 50% and 28% of employees switch off the air conditioner in their office when they leave their offices, in summer and winter, respectively. It is noteworthy that in the summer up 58,85% and in winter 62,5% of the surveyed students do not know when the air conditioner switches off, as opposed to employees. This perhaps indicates a tendency of indifference on behalf of the students concerning air conditioning in their space.

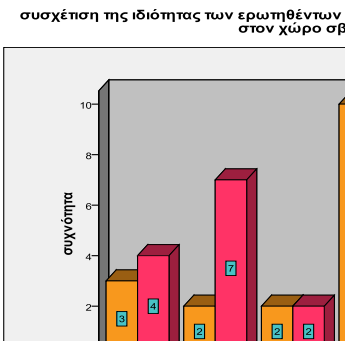

Figure 6: Correlation a (employees or students) conditione

Figure 7: Correlation and frequencies of users (employees or students) habits concerning the air conditioner in winter

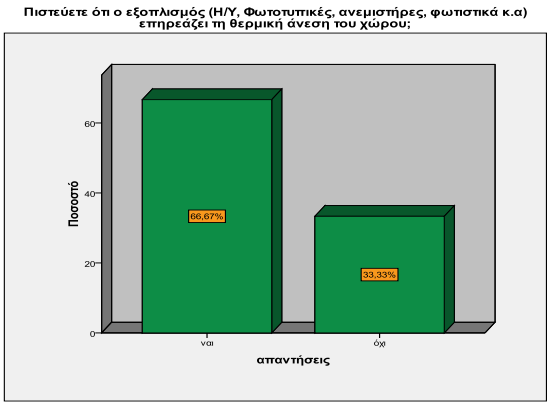

Figure 8: Percentages on the users' opinion if the equipment affects the thermal comfort in summer.

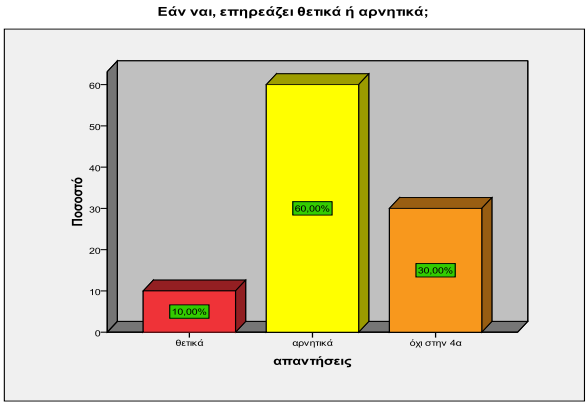

Figure 9: Percentages on the users' opinion if the equipment affects positively or negatively the thermal comfort in summer.

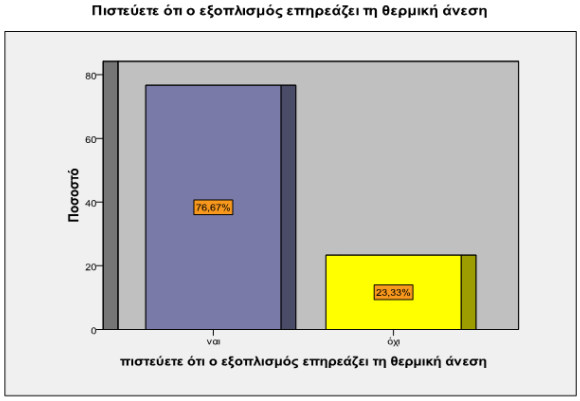

Figure 10: Percentages on the users' opinion if the equipment affects the thermal comfort in winter.

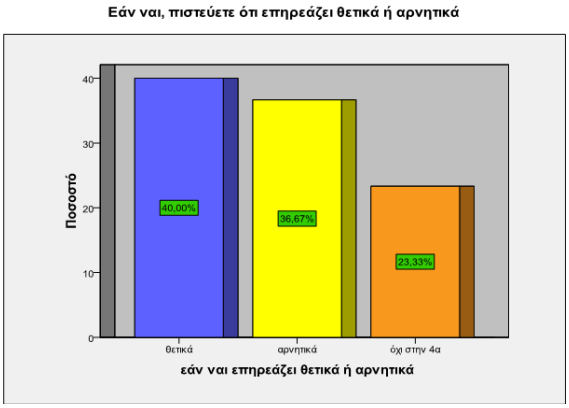

Figure 11: Percentages on the users' opinion if the equipment affects positively or negatively the thermal comfort in winter.

From the users' replies in Figs. 8 and 9, 66,67% responded positively and 33,33% responded negatively on the question of whether electronic or any other equipment affected the thermal comfort of the office/teaching areas in the summer. Also, up to 85,71% of those who responded positively in this question, believe that the electromechanical equipment adversely affects the thermal comfort of the room. During the winter, the vast majority of respondents replied positively to the specific question (76,67%), but from this percentage only 40% answered that it affects the thermal comfort positively and 36,67% that they are adversely affected (Figs. 10 and 11).Nevertheless, during the daily measurements it was observed that almost all users leave the equipment switched on for 24 hours the day.

4.1.2 Natural lighting

The second section of the questionnaire aimed in examining the natural lighting of the users' space. The users' level of satisfaction in terms of natural lighting in their office/teaching areas is presented in Fig. 12. It is shown in the figure that the employees replied that they are dissatisfied with the availability of the natural lighting in their offices in the summer. It is also shown that half of the students are dissatisfied, too. The larger numbers of the employees expressing dissatisfaction in comparison with those of the students are justified since the employees are

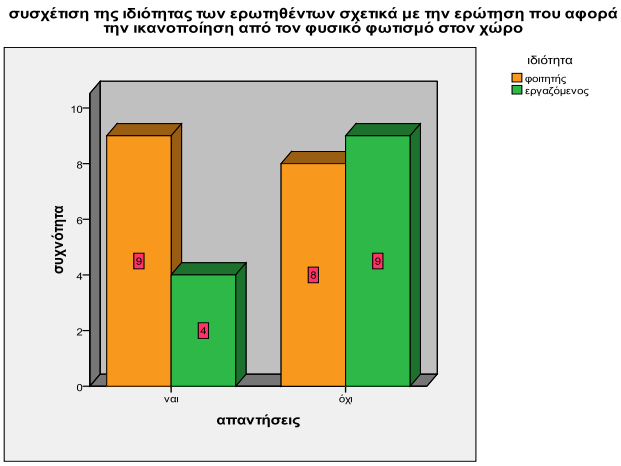

Figure 12: Correlation and frequencies of users (employees or students) habits concerning the satisfaction level for natural lighting in summer and winter.

permanently based in their offices and spend more and longer hours in the building than the students.

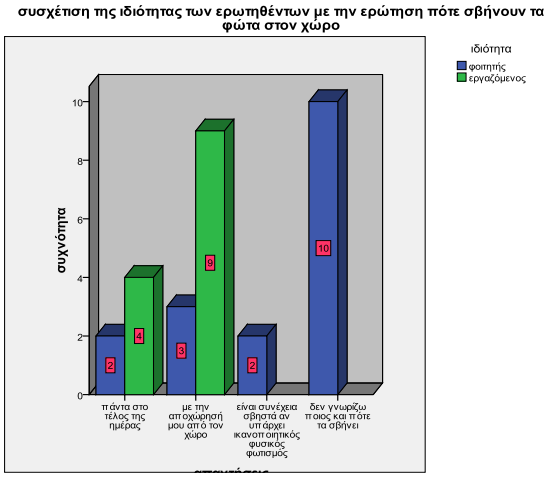

Figure 13: Correlation and frequencies of users (employees or students) habits concerning the lighting in summer and winter.

Furthermore, users were asked to indicate their habits concerning the lighting in their own space. As shown in Fig. 13, for both seasons, the majority of employees switch off the lights of their office when they leave the work. It was noted, that up to 57% of the surveyed students do not know when the lights are switched off in the teaching areas, as opposed to employees. This possibly indicates lack of the sense of responsibility on behalf of the students concerning the switching off the lights when leaving their classes.

4.2 Field measurements and indoor comfort

According to Ashrae standards, in office and educational buildings / rooms the optimal thresholds for natural lighting for open or closed-type offices and classrooms are 300 lux. In a conference room the minimum rate is 500 lux.

Figures 11 - 15 show the average temperature, humidity and lighting measurements in different spaces and orientations in the building. Figures 14a-b, show the lighting measurements in an office on the ground floor facing south. It is an open plan office for a single occupant. The light measurements in the morning and in the afternoon hours are taken with artificial lights turned on, since the specific office, as well as its adjacent one, have very porr or even no natural light at all. There are no windows or other skylights in the offices. In summer, the temperature in the afternoon with activated air conditioning is at 25,5 °C and humidity 50%. In the morning and evening measurements, the temperature in the office is around 28 °C. This is not the free running office temperature since the air conditioners remained switched on after the employee left work in the afternoon, so the temperature remains at 28 °C until the next morning. In winter the temperature measurements were at 23,5 °C and humidity 10 points lower than that of the summer.

In Figures 15a-b, measurements were made in a conference room for about 30 people, facing south with no external windows for natural light. The conference room has windows opening in an interior open space, with the shutters permanently closed. The measurements showed levels of lighting to be less than 10 lux for both seasons. The increased moisture content in the field (60 – 68 %) is due to the fact that is aired and illuminated only when in use, which is not daily. In the summer, half of the days of measurements, the temperature is around 26 °C, with air-conditioning on in the room, without any occupants. In winter, the temperature was at about 23 °C.

Figures 16a-b, illustrate measurements performed in a lecture room of the first floor with northwest orientation, with 21 computers. The room has glass panes with north, northwest and west orientation. In the summer, the measurements were taken with the air conditioning off and it was observed that the temperature in the morning hours, compared with that of other rooms in which the air conditioning was also closed, was higher at about 2-2,5 °C. This is probably due to the fact that the

mechanical equipment in the room (computers and printer) affects the natural temperature of the room. During the days that the measurements were taken, in both seasons, it was observed that more than half of the computers were in operation, even if there were no lessons in session. The lighting in the room at the location of the measurements was very low and this is because the shutters of the windows were all closed. Based on measurements of adjacent rooms / offices with the same orientation, it is speculated that during the midday hours if the shutters of the windows were open, natural light is largely satisfactory. Nevertheless, based on field visits on a daily basis, it was observed that the users, choose not to open the shutters of the windows, instead they turn on the lights.

Figures 17a-b, show the measurements of a classroom of 20 people (60 m^2) with southwest orientation on the second floor. Based on the measurements in the room, with the lights and shutters closed, the levels of natural light was measured to be about 100-110 lux, whereas with the blinds open it exceeded the 290 Lux at midday. On the west side of this room there are windows that cover an area of approximately 20 m^2. However, natural light is not allowed in the room; during the field visits, it was noticed that the occupants preferred the artificial light instead of opening the shutters. The natural temperature of the room without air conditioning is 31 to 33 degrees in the morning until the afternoon and humidity 55– 60 %, in the summer season. In winter, the temperature measured at about 21-22 °C and humidity 49-50%.

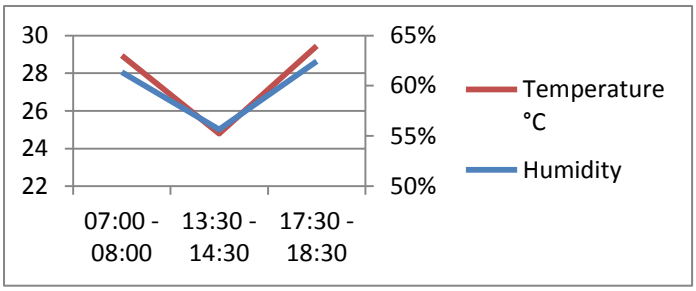

Figure 14a: Results of temperature and humidity measurements in an office at south in summer.

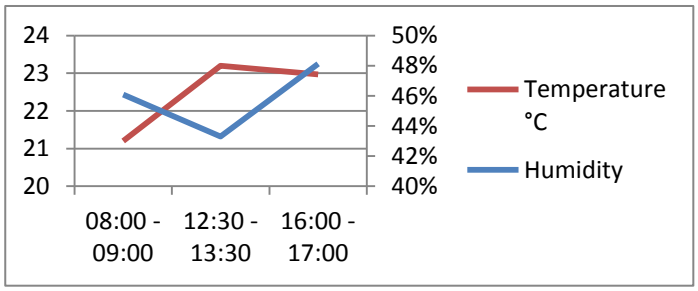

Figure 14b: Results of temperature and humidity measurements in an office at south in winter.

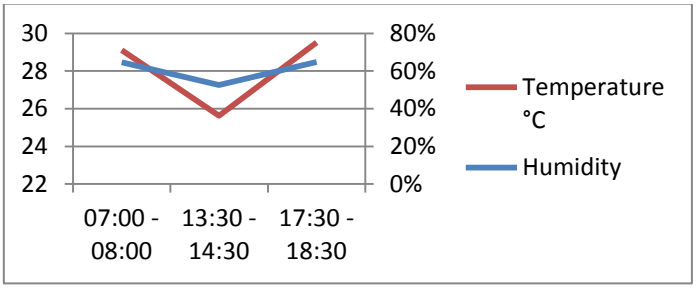

Figure 15a: Results of temperature and humidity measurements in a conference room at south in summer.

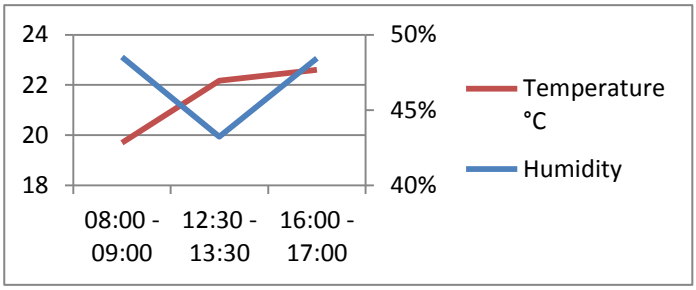

Figure 15b: Results of temperature and humidity measurements in a conference room at south in winter.

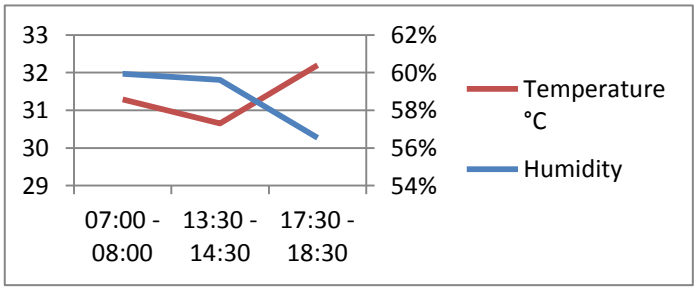

Figure 16a: Results of temperature and humidity measurements in a lecture room at northwest in summer.

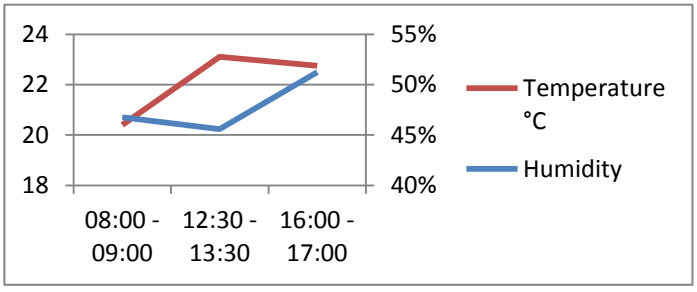

Figure 16b: Results of temperature and humidity measurements in a lecture room at northwest in winter.

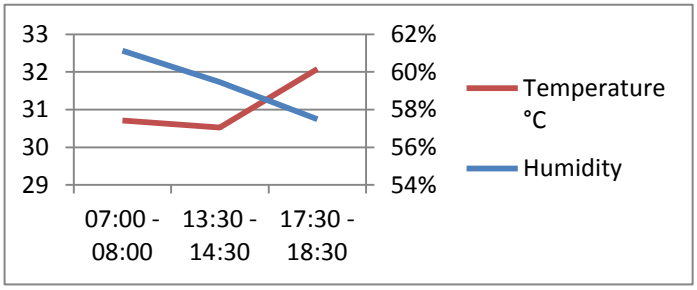

Figure 17a: Results of temperature and humidity measurements in a lecture room at southwest in summer.

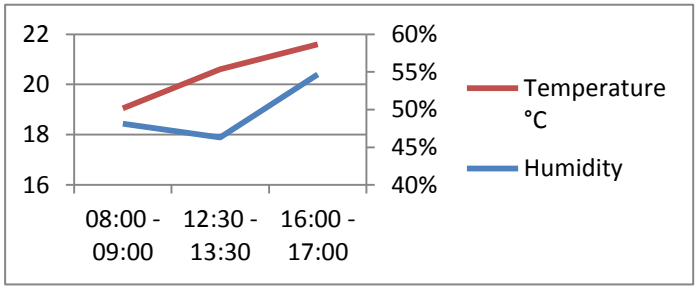

Figure 17b: Results of temperature and humidity measurements in a lecture room at southwest in winter.

4.3 Energy consumption and occupants' behavior

The official working time for the building is the crucial time for energy demand charge. However, by visiting the building in the early morning hours that no one was in it, it was confirmed that some occupants leave their computers on over-night and over the weekends. Also, all the equipment was left running throughout the semester even though no one was in the building. Fig.ure 18 shows two scenarios of consumption by equipment of the building, including air conditioners and lamps, representing the apportionment of energy between 24 and 12 hours per day. According to measurements and calculations, if all equipment remains open 24 hours a day, then consumption amounts to 1505,76 kWh for 1 day. This amounts to 33126,72 kWh for 1 month. Therefore the monthly cost of consumption amounts to 10931 €. It is estimated that if all the equipment is reduced to 12 hours of operation, then there is a great energy saving and consumption descends to 970,38 kWh for one day and therefore to 21438,36 kWh for one month. Thus, the monthly cost of consumption drops to 7044 €. However in order to achieve this, it is necessary to raise the energy awareness and change the behaviour of the occupants in order to consume less.

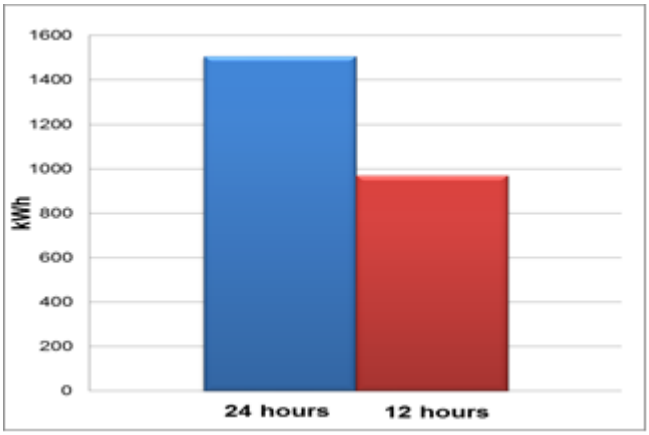

Figure 18: Scenarios of energy consumption

5 CONCLUSIONS

Indoor comfort and energy consumption has been examined in the Building of Student Affairs of the Cyprus University of Technology (CUT) during summer and winter time. Specifically, a comparative study between winter and summer season was carried out of the occupants' behaviour and its effects on the building's energy consumption, as well as on the indoor thermal and optical comfort. The survey was

conducted using both questionnaires regarding thermal comfort and natural light, and field measurements with appropriate instruments for daily measurements. Also, the energy consumption of the building is calculated for two scenarios.
Thermal comfort of occupants in the building, during the summer and winter months, is not satisfactory in the office / lecture room, given that the predicted percentage dissatisfied PPD is 43.35% and 43.34%, respectively, and PMV -1.4 and 1.4, respectively. According to the results, the thermal comfort is affected negatively by the equipment in use in summer and positively in winter. Also, the majority of users and especially the students, leave the air conditioning, lights and equipment on when they are leaving the room / office and throughout the day. This indicated the lack of proper energy use from the occupants of the building.
The south and southwest side of the building can be an important advantage for space heating naturally by solar radiation (with horizontal blinds to avoid overheating in summer), as for ventilation in the use of the building, such as offices, classrooms and conference rooms. This is not possible since the entire south side of the building is built and enclosed, without any benefit for heating and ventilation. Additionally, every effort is made to improve the many weaknesses of internal and external layout of the building and in turn the occupants' behavior (employees and students) adapt accordingly, but indicate an intense indifference in regards to the energy consciousness and behavior.
For energy benchmarking, if air conditioners, lamps and general building equipment are used only during the operating hours and not 24 hours per day, then a high amount of energy could be saved and the cost of the consumption for the building will be much lower. Simply by switching off appliances at the end of the day could save energy. The savings will be higher if the equipment is switched off when is not required even during the operating hours. Meanwhile, ongoing studies in the same sector for this building will be carried out for the other two seasons.

6 REFERENCES

[1] Harris, D. J. (2012). A guide to energy management in buildings.
[2] Paksoy, H. Ö. (2007). *Thermal Energy Storage for Sustainable Energy Consumption Fundamentals, Case Studies and Design.*
[3] Menassa, E. A. (December 2012). A comprehensive analysis of the impact of occupancy parameters in energy simulation of office buildings .
[4] Zhun Yua, B. C. (June 2011). A systematic procedure to study the influence of occupant behavior on building energy consumption.
[5] O.A. Nisiforou, S. P. (December 2012). Behaviour, attitudes and opinion of large enterprise employees with regard to their energy usage habits and adoption of energy saving measures.
[6] É. Mata, F. L. (December 2009). Optimization of the management of building stocks: An example of the application of managing heating systems in university buildings in Spain.
[7] O.T. Masoso, L. G. (February 2010). The dark side of occupants' behaviour on building energy use.
[8] Santin, O. G. (October 2011). Behavioural Patterns and User Profiles related to energy consumption for heating.
[9] *ΠΡΟΣΦΑΤΑ ΜΕΤΕΩΡΟΛΟΓΙΚΑ ΔΕΔΟΜΕΝΑ*. (2012-2013). Ανάκτηση από ΜΕΤΕΩΡΟΛΟΓΙΚΗ ΥΠΗΡΕΣΙΑ: http://www.moa.gov.cy/moa/ms/ms.nsf/DMLmeteo_reports_gr/DMLmeteo_reports_gr?OpenDocument&Start=1&Count=300&Expand=1.4
[10] Serghides D.K. 2008: "Integrated Design for the Zero Energy House and the Human Factor– PLEA towards Zero Energy Building PLEA Conference Proceedings Paper ID. 745
[11] Serghides D. K. (1993). Zero Energy of the Mediterranean Houses, ISES '93 Solar World Congress, *Solar Architecture*. **7**(2): 48-256.

FUEL POVERTY AND THE FINANCIAL CRISIS: A HOUSEHOLD SURVEY IN GREECE

Mathew Santamouris[*1], John A. Paravantis[2], Dimitra Founda[3], Dionysia Kolokotsa[4], Giouli Michalakakou[5], Agis M. Papadopoulos[6]

1 University of Athens
School of Sciences, Faculty of Physics
Panepistimioupolis, 15771 Ilissia, Greece
**Corresponding author: msantam@phys.uoa.gr*

2 University of Piraeus
80 Karaoli & Dimitriou Street
18534 Piraeus, Greece

3 National Observatory of Athens
Lofos Nymfon,
11810 Thiseio, Greece

4 Technical University of Crete
Saint Titos Square
73132 Chania, Greece

5 University of Patras
Panepistimioupolis
26504 Rio, Greece

6 Aristotle University of Thessaloniki
Panepistimioupolis
54124 Thessaloniki, Greece

ABSTRACT

This research aims to investigate, analyse and characterize the relation between the economic crisis and energy consumption in Greece. A survey held in the spring and summer of 2012 collected data of the heating energy consumption for 2010-2011 and 2011-2012, from 598 households via a questionnaire. Comparing the 2010-11 winter to the harsher winter of 2011-12 showed that inhabitants consumed less energy during the winter of 2011-12 because of the rapid economic degradation. Important conclusions were drawn regarding the energy consumption of the households which during the harsh winter 2011-12 was 37% less than expected. Cluster analysis rendered two distinct clusters: three fourths of the households belonged to the lower income group that lived in a smaller space, had half the income and consumed more specific energy compared to the high income group, although much less than expected based on the degree hours of the second winter. One out of three higher-income and one out of four lower-income households adopted some conservation measures after the first winter while 2% of the higher income households and 14% of the lower-income households were below the fuel poverty threshold. Directions for further research include monitoring of low income households with sensors.

KEYWORDS

Energy consumption; fuel poverty; economic crisis; cluster analysis.

1 INTRODUCTION

It has been asserted that one of the most eminent social problems of the 21st century is fuel poverty, which has been recognized as a distinct form of inequality and an unacceptable feature of the present time (Boardman, 1991; 2010). It affects the poor and its roots are detected in the quality of the housing stock and the cost of fuel, particularly high in these times of global financial crisis and peak oil. A sufficient standard of warmth is usually identified as 21 degrees Centigrade for the main living area, and 18 degrees for other occupied rooms (WHO, 1987). The Fuel Poverty Ratio (FPR) is identified as

$$\text{Fuel poverty ratio} = \frac{\text{energy consumption} \times \text{price}}{\text{income}} \quad (1)$$

and if it is greater than 0.1, the household is considered to be fuel poor (DECC, 2012). FPR compares the cost of energy consumption to the income of a household (Hill, 2012) and is an interaction of three factors: the energy efficiency of the household, the cost of energy and the household income (DECC, 2010). Although FPR does not reflect underlying problems and causes, it is the only indicator that shows both the extent and the depth of fuel poverty.

The term fuel poverty has been used since the early 1980s (Bradshaw & Hutton, 1983) and was defined by in 1991 as the difficulty or even inability of a family to afford the funds for proper heating at home (Boardman, 2010). Fuel poverty was officially recognized as a problem when the United Kingdom (UK) Minister at the Department of the Environment, Transport and the Regions (DETR) stated that an integrated approach across government to tackle fuel poverty and energy efficiency would be taken and that coherent policies should be produced aiming to go to the heart of the problem (Boardman, 2010). When the Third Energy Package led to the integration of energy poverty, within Directives 2009/72/EC and 2009/73/EC of the European Parliament and of the Council, it was the first time energy poverty entered the vocabulary of European Union (EU) institutions.

Poverty and fuel poverty are linked, but not synonymous concepts (Boardman, 2010). A vulnerable household is defined as one that contains children, elderly people and persons that are disabled or have a long term illness (Boardman, 2010; Hill, 2012). In the UK, the fuel poor have been categorized into poor households, vulnerable households and households with high energy bills with payment difficulties. Unfortunately, it is difficult to identify fuel poor households because the information needed is never held by one single entity and often cannot be communicated for reasons of privacy (Dubois, 2012). The calculation of fuel poverty is based on annual fuel costs set against annual income. Fuel costs in winter are likely to be more difficult to be paid by poorer households that pay for their gas and electricity using pre-payment meters and quarterly standard credits (compared to those that pay a set monthly amount by direct utility bill). A recent EC Working Paper suggests that those in fuel poverty could be defined as *"households that spend more than a pre-defined threshold share of their overall consumption expenses on energy products"* with the threshold set at *"double of the national average ratio number"* (EC, 2010; Moore, 2012).

In addition to space heating, fuel-related costs may include spending on energy for water heating, lights, appliances and cooking. Fuel poverty is therefore not based on what a household actually spends on energy. As fuel poverty is a measure of what a household needs to spend on energy rather than what it actually spends, total energy needs are modeled by various factors, including the size and energy efficiency of the property, household size and type and the type of heating (Bolton & Richards, 2012). Energy efficiency is very important as it affects the fuel requirement of a household and it is affected by energy efficiency measures (DECC, 2010).

Fuel poverty is primarily a determinant of three household factors: income, energy prices and energy efficiency of dwellings. In most cases the profile of fuel poor people are those who receive social security payments, work part time or are in debt. Unemployment rates, growing job insecurity (part time employment, short-term jobs) lead a lot of people to live below the poverty threshold (DECC, 2012). Beyond building degradation, fuel poverty translates into physical and mental health issues, e.g. cold temperatures can affect the immune and the cardiovascular system while damp cold houses influence negatively people who suffer from

respiratory problems and allergies. A survey conducted among five countries (Belgium, France, Italy, Spain and United Kingdom) analyzed causes and consequences of fuel poverty, helped realize the difficulties faced by the people living in such a situation, and gave the opportunity for reflection on an appropriate strategy to wipe out this phenomenon (EPEE, 2009). At the same time, this study revealed the lack of data and of relevant studies beyond the UK.

Only three out of the 27 EU member states have officially defined fuel poverty. All existing definitions stress the relationship between low income and energy efficiency (Thomson & Snell, 2013). According to its most widely accepted definition (UK), a fuel poor household is one that needs to spend more than 10% of its income to achieve adequate energy services in the home (DTI, 2001). This threshold figure was adopted in an investigation of the problem of affordable warmth by the Energy Report of the 1991 English House Condition Survey (EHCS) (DOE, 1991), an annual survey, commissioned by the Department of Communities and Local Government (CLG), which involves physical inspection of properties by professional surveyors. In April 2008, EHCS merged with the Survey of English Housing (SHE) to create the English Housing Survey (DECC, 2010). In the UK in particular, because of the pre-payment systems, the problem of debt is not as great as in other countries although it is still estimated that around one billion British pounds of debt is owed to energy suppliers by consumers. Unfortunately, the recent rise of energy prices (and further rise expected) will make it more and more difficult for this category of people to pay energy bills (EPEE, 2009). In the UK, fuel poverty is seen as a rights-to-warmth issue and it has become a matter of justice and entitlement to healthy living (Walker & Day, 2012). In fact, the UK appears to be the only country that has presented policies and scientific programs on fuel poverty, supporting vulnerable households that face inadequate heated homes and health problems (Boardman, 2010).

Turning to European countries, the UK is a pioneer on fuel poverty surveys. Fuel poverty in England is researched with the English Housing Survey (EHS); in Scotland, by the Scottish House Condition Survey (SHCS); the Living-in-Wales Survey is used to estimate fuel poverty in Wales; finally, the Northern Ireland House Condition Survey is used to calculate the Northern Ireland fuel poverty levels (DECC, 2010). There is also the National Ecosystem Assessment (NEA), which is the UK's leading fuel poverty charity campaigning for affordable warmth. Finally, a European project called European Fuel Poverty and Energy Efficiency (EPEE), aims to improve the knowledge of fuel poverty and identify operational mechanisms to fight against this phenomenon (DECC, 2010).

In a survey of energy efficient British households, it was shown that fuel poverty is a complex socio-technical problem that may be explained using a combination of physical, demographic and behavioral characteristics of a residence and its occupants (Kelly, 2011). A Structural Equation Model (SEM) was introduced to calculate the magnitude and significance of explanatory variables on dwelling energy consumption. Using the English House Condition Survey (EHCS) consisting of 2531 unique cases, the main drivers behind residential energy consumption were found to be: number of household occupants, floor area, household income, dwelling efficiency (determined by the Standard Assessment Procedure or SAP), household heating patterns and living room temperature. The number of occupants living in a dwelling was shown to have the largest magnitude of effect, floor area and household income while there is strong mediation between causal variables. Statistical analysis implied that homes with a propensity to consume more energy will be more expensive to decarbonize due to the law of diminishing returns, a finding of concern in the context of global climate change.

In another UK study, strategies of low-income households for coping with limited financial resources and cold homes in the winter months were investigated (Anderson, White & Finney, 2012). The sample of 699 households with an income below 60% of the national median income included in-depth interviews of a subsample of 50 households. Findings showed that the primary strategy adopted by low-income households to cope with financial pressure was to reduce spending, including spending on essentials such as food and fuel. Just below two out of every three (63%) of low-income households had cut their energy consumption in the previous winter and almost half (47%) had experienced cold homes. Very low income households could not afford any heating. For households surviving on very small domestic budgets, it is a sad truth that the extra cash-in-hand could be more attractive than a warmer home.

The Irish government defines fuel poverty as "the inability to afford adequate warmth in a home, or the inability to achieve adequate warmth because of the energy inefficiency of the home". A survey conducted in Ireland noted that existing households needed more fuel than others either because their circumstances imposed that they be heated for longer periods of time or because they were occupied by the elderly or those with very young children so they demanded higher temperatures (Healy & Clinch, 2004). Households were investigated based on demographic, educational and socioeconomic variables. A very strong relationship was found between the incidence of fuel poverty and social class. As expected, there was a very strong correlation between fuel poverty and income. Results regarding the severity of fuel poverty by income level were mixed, as they revealed both high-and low-income households suffering from high levels of chronic fuel poverty (Whyley & Callender, 1997). Many large families find it difficult to heat their home adequately over time, a troublesome result as health effects of cold and damp exposure are particularly intense among children. It was also found that housing tenure gave households varying levels of control over their home, heating systems and their energy consumption and was identified as an important dynamic of fuel poverty.

In France a person is considered fuel poor "if he/she encounters particular difficulties in his/her accommodation in terms of energy supply related to the satisfaction of elementary needs, this being due to the inadequacy of financial resources or housing conditions" (Thomson & Snell, 2013). The first measures targeting low-income fuel-poor households in France, were developed in the middle of 1980s (Dubois, 2012). However, it was only in 2010 that the current fuel poverty policy was instituted. Its basis is a program called *habiter mieux,* which supports the thermal renovation of low income households, which are located in rural areas. The aim was for 300 thousand households to be thermally renovated with financial support from a budget of 750 million euros managed by the National Agency for Habitat Improvement (ANAH). It is noted that a household may benefit from the program *habiter mieux*, if it has a project of thermal renovation that would result in an improvement of at least 25% of its energy efficiency.

A survey of 964 houses in Belgium compared insulated to non-insulated homes (Hens, Parijs & Deurinck, 2002). Calculation tools were found to predict heating energy consumption assuming typical dwelling use although this was subjected to physical restrictions and the average temperature in partially heated homes increased with higher insulation quality as expected. An average indoor temperature of 18 degrees Celsius was considered usual.

In a German survey, Michelsen & Madlener (2012) investigated the preferences of home owners for applying improved Residential Heating Systems (RHS) and found incentives for adopting RHS to vary among families. Homes that use gas and oil for heating were found to

prefer energy savings whereas the ones using heat pumps or wood pellet fired boilers prefer to be independent of fossil fuels. Analysis of the data also showed that the grant from the Federal Office of Economics and Export Control (*Bundesamt für Wirtschaft und Ausfuhrkontrolle*, BAFA), which would be important for the adoption of RHS, does not play a role in the decision-making process. It was suggested that RHS manufacturers in Germany improve their marketing strategies in order for home owners to take the adoption decision, having in mind not only their behavior but also age, size etc. of their homes. In another German study, Schuler, Weber and Fahl (2000) found both technical characteristics of buildings and utilization patterns of households to be essential factors of the demand of space heating of private West-German households. The paper considered that the energy consumption for space heating may vary broadly and depends not only on socio-economic developments but on political actions as well. Such considerations may motivate governments lower the barrier for energy investments and apply policies that provide incentives for insulation of dwellings. Energy consumption related behavior was also targeted by Braun (2010) who investigated both East and West German households. Braun asserted that socio-economic characteristics together with building type and region are important determinants of the space heating technology applied. The paper focused on building features such as construction age that was found to play a more important role than home ownership.

In nearby Austria, the NELA project (German acronym for "Sustainable Energy Consumption and Lifestyles in Poor and at-Risk-of-Poverty Households") investigated energy consumption in households in Vienna, Austria (Brunner, Spitzer & Christanell, 2011). NELA surveyed 50 Viennese households afflicted by poverty and compared them to ten better-off households. The interviews were conducted during the summer of 2009 and the spring of 2010.The results identified four distinct types of households: ''the overcharged'', ''the modest fuel poor'' (fuel poor), ''the modest non-fuel poor'', and the ones ''on a low income'' (non-fuel poor). Similar classifications were found by a survey conducted in France by Devaliere (2010) as quoted by Brunner, Spitzer & Christanell (2011). It was confirmed that low income households try to cope by adopting various energy conservation measures.

Buzar (2007) claims that fuel poverty is apparent in post socialist countries of Eastern and Central Europe and the Former Soviet Union. The author mentions to the *"hidden"* geography of poverty, referring to the lack of heating in the households of these countries. A survey held in FYROM and the Czech Republic showed that low income households are energy poor and areas of energy poverty (called "hidden") appear dull and messy due to specific circumstances of the post-socialist frame of these regions.

Turning to Southern Europe, in Italy, the E-SDOB (Statistical Distribution of Buildings) tried to address heating energy issues by defining the performance scale for energy certification of buildings, and evaluating the building volume falling in different classes (Fracastoroa & Serraino, 2010). E-SDOB has also been used to evaluate the energy saving potential of large scale retrofit actions on the building envelope. E-SDOB seems to be a useful tool for a better knowledge of the regional building stock as well as the adoption of coherent energy regulations. As the authors point out though, the global overview of the building stock energy performance provided by E-SDOB may provide further insight but it cannot replace specific analyses at a building level when retrofit actions have to be implemented.

In Spain, the Environmental Science Association (*Asociación de Ciencias Ambientales*, ACA) started a project named REPEX aiming to research the relationship between fuel poverty and unemployment. This project claims that fuel poverty in Spain is caused by unemployment and that the renovation of houses, in order to be efficiently heated, could offer employment to

workers that lost their jobs because of the financial crisis. However, fuel poverty in Spain is not a first priority issue neither to the Spanish Political Parties nor to the media (EU Fuel Poverty Network, 2012).

All in all, since fuel poverty lacks an official Europe-wide definition, comparing fuel poverty among European countries is not trivial (Hill, 2012).

A United States (US) survey conducted among families of equal economic status over a 15-year period (1987–2002) during the winter heating season in Seattle, Washington, USA (which has a climate similar to that of the eastern Mediterranean) showed that, regardless of life style, the space heating energy behavior of the tenants remained constant (Emery & Kippenhan, 2006). The results of the survey suggested that estimates of energy savings could be based upon envelope thermal resistance for moderate occupant behavior. For such behavior, space heating was well characterized by the difference between house temperature and outside air temperature. It is encouraging to note that over 15 years in which houses sustained considerable wear and tear as expected of rental properties, the space heating behavior did not change, i.e. the envelope tightness did not seem to degrade and the sensitivities remained constant.

A survey carried out in New Zealand, with houses poorly insulated and rental properties not required to have insulation or heating, showed the inability of many households to afford adequate heating (Howden-Chapman et al., 2009). Three of the main factors included: the poor quality of housing in terms of thermal efficiency; relatively high levels of income inequality compared to other Organization of Economic Cooperation and Development (OECD) countries (Wilkinson & Pickett, 2009); and an increase in the real price of residential electricity, which occurred mainly after the deregulation of the industry in 1996 and 1998. Vulnerable population groups particularly those on low income, the old and the young (who are more likely to suffer health consequences) pressured the New Zealand governments to translate research into policy. The problem's antecedents were targeted, including inadequate standards for existing houses, rising income inequality and the need to protect low-income households from the rising price of heating fuels. A suggested policy to face fuel poverty in New Zealand was prepayment metering as a method to pay for electricity, helping households that faced disconnection and wished to lower their expenditure (O'Sullivan, Howden-Chapman & Fougere, 2011). As in many areas of Southeaster Europe and Greece, economic difficulties faced by the lower income clusters in New Zealand mean that as both unemployment and fuel poverty will intensify.

An energy conservation survey of 10 Japanese residential buildings, showed that energy-saving consciousness was raised and energy consumption reduced by energy saving activities of the household members (Ueno et al., 2006). An improved online tool for the registration of energy consumption information revealed that the power consumption of many appliances and the total energy consumption of the household were reduced by 18% and the total city-gas consumption decreased by 9%. Also, savings of 20% in space heating were achieved by residents that switched to more energy saving sources or reduced the duration of space heating.

During the winter of 2003-04, a questionnaire survey was undertaken of more than 200 residential households in the rural fringe of Xian City in China (Tonooka et al., 2006). Fuel consumption, including the use of biomass for cooking and space heating, was investigated; stove types, stove use and characteristics of residents as well as residential houses were also reported and analyzed. The survey aimed to quantify energy consumption, emissions of

greenhouse gases and air pollutants in rural areas of China. The survey showed that energy consumption in rural areas in China includes biomass fuel, in particular a mixture of agricultural waste and twigs commonly used for *kang* (a traditional cooking stove), coal and Liquefied Petroleum Gas (LPG). It was proposed that there is a relationship between income level and priority of LPG use and that the energy consumption level of rural households in China remains a subject for further work.

In wrapping up this section, it is added that surveys on fuel poverty during the last decade in Europe have not come up with dramatic changes from year to year (Palmer, MacInnes & Kenway, 2008).

Nowadays, with the global financial crisis, it is suspected that fuel poverty is a substantial problem especially in areas of lower income such as southeastern Europe. Given the dearth of published research on fuel poverty in these areas, this research measures fuel poverty in Greece and investigates the impact of the global financial crisis on the energy consumption of households via a number of questions that look into how various socioeconomic, environmental and consumption variables relate to fuel poverty.

Literature review will be completed with a look into empirical research in Greece, carried out in the next section.

2 ENERGY CONSUMPTION AND ECONOMIC SITUATION IN GREECE: EXISTING RESEARCH

Turning to investigations in Greece about the specific energy consumption of households and its relation to the economic situation, a 2004 survey held in Athens, collected social, financial, energy and technical data from about 1110 households (Santamouris et al, 2007a). These households were divided into seven income groups and a detailed analysis showed that there was an almost direct relationship between income and household area. It was also found that higher income was associated with newer buildings and that almost 64% of the families in the lower income group lived in apartments (the corresponding number for the more affluent group was 48%). Low income families lived mostly in the lower part of multistory buildings while high income households live mainly in the higher part of the buildings. Only 28% of people in the poorest group dwelled in insulated buildings, with the corresponding figure for the richest group being close to 70%. High income families paid almost 160% higher annual costs than the low income ones. Low income households paid nearly 67% higher electricity cost per person and square meter than high income households. Furthermore 1.63% of the households suffered from fuel poverty and 0.35% from severe fuel poverty (2004 values). Fuel poverty in low income groups, was in the region of 16%. Severe fuel poverty, in the low income group, was calculated close to 4%. Concerning energy poverty, the average percentage of the households spending more than 10% of their income for energy was close to 11.3%, while 2% spent more than 20%. Almost 40% of the low income group, called the energy poor, spent more than 10% of their income for energy while almost one fifth of the poor households, called the severely energy poor, spent more than 20% of their income for energy. Fuel and energy poverty reached quite high levels in the low income groups, with a dramatic increase attributed to the fuel prices. It was concluded that energy policies addressed to the dwelling sector should set as a priority the improvement of the envelope quality of residents where low income people are living.

In another study referring mainly to the summer conditions (Santamouris et al., 2007b), it was found that low income population in Athens, lives in areas where the heat island is well

developed. Recent studies have shown that temperature increase in high density areas suffering from heat island may reach 5-7 K, depending on the local climatic conditions, (Santamouris, 2007; Livada et al., 2002). Higher urban temperatures increase considerably the necessary energy consumption for cooling purposes (Hassid et al., 2000; Santamouris et al., 2001), affect thermal comfort conditions (Pantavou et al., 2011) and increase pollution levels (Stathopoulou et al., 2008). Monitoring of a high number of low income households in Athens during the heat waves of 2007 (Sakka et al., 2012) shown that Indoor temperatures as high as 40 C occurred while the average indoor minimum temperature was always above 28 C.

A study of a typical multi-family Greek building in 2007 compared commonly used heating sources (including oil), natural gas and autonomous systems (Papadopoulos, Oxizidis & Papandritsas, 2007). The cost distribution of central heating was determined to favor penthouses over apartments in intermediate floors, possibly failing to motivate some occupants to promote energy conservation while at the same time not providing motivation for superior insulation of the roof of a building. The authors asserted that the use of electrically driven heat pumps can be a very good solution for heating Greek buildings, since (at the time of writing) they were in some cases equally expensive to other fuels. It was also suggested that the increased potential of renewable energy sources in electricity generation (mainly wind power) might also be improved. The authors expected the rationalization of electricity tariffs to enable the installation and use of heat pumps as central heating systems, increasing in turn their market infiltration.

Sardianou (2008) highlighted the use of statistical models in determining domestic consumption of Greek households. The results of the survey held in 2003 in Greece, unveiled that various characteristics such as the number of persons in a household, the type of the building and the ownership status, influence the domestic demand for heating. Findings confirmed that there is a relationship between household annual income and annual fuel consumption while there were already (back then) households that had decreased their heating consumption in view of increasing oil prices.

Finally, according to the most recent opinion survey of fuel poverty in Greece (Panas, 2012), the median specific energy consumption of buildings in Athens was found to equal 29 kWh per cubic meter**,** greater (the author asserted) than that of other countries with more adverse weather conditions such as Denmark, Germany and the Netherlands. Fuel poverty was calculated with three different methods based on (a) the proportion of energy expenditures of a household, (b) the opinion of residents on their energy coverage and (c) the condition and conveniences of the household. From 1988 to 1997 Greece was found to have a seasonal rate of mortality of 18%, which ranked it at a position higher than that of other countries with heavier winters. Panas refers to the relation between the inadequate heating of households and the increased mortality rate during the winter season. However, through a recent questionnaire survey in northern Greece conducted in November of 2012, 814 people were asked whether they paid more than 10% of their annual income for heating (it is noted that this is a subjective method of documenting fuel poverty). According to the survey, respondents declared their inability to pay the heating bills and their fear for consequences of the current economic crisis in the future, supporting the notion that Greek households are not presently energy efficient.

Important research has been carried out to develop and propose proper mitigation and adaptation techniques to improve the environmental performance of low income households, (Santamouris, 2012); Santamouris & Kolokotsa, 2013). Applications in real scale projects showed that it is possible to improve considerably the environmental quality of buildings and

open spaces, decrease the energy consumption and improve the quality of life of low income citizens (Santamouris et al., 2012).

3 METHODOLOGY

3.1 Research questions

A number of key research questions are gleaned from the literature and are listed below:

1. How do building characteristics and socioeconomic data relate to fuel poverty?
2. In particular, how does family income impact fuel poverty?
3. How do different heating sources relate to fuel poverty? Fuel poor cannot afford relatively expensive high fuel such as electricity, natural gas and liquid petroleum.
4. How are heating hours and other measures of energy use related to fuel poverty? Fuel poor households try to curb energy consumption by reducing their heating hours oftentimes irrespective of climatic conditions.
5. What conservation measures are usually taken by households in order to combat energy consumption and fuel poverty in a time of falling incomes? Such measures may depend on factors such as household size, heating sources and energy efficiency.
6. What are typical values of specific energy consumption measured in kWh per m²? It is noted that electricity prices for household consumers should not exceed 0.10 euros per kWh in order to be considered affordable (Bouzarovski, Petrova & Sarlamanov, 2012).
7. Are households typically clustered into groups that indicate social class? How big a role is played by annual family income and the type of family i.e. number of children, senior citizens, members or with disabilities? What percentage of each cluster is fuel poor?
8. What policies and measures have been adopted especially in Southern East Europe and the Mediterranean? This question will be partially addressed as results are synthesized into conclusions.

To answer many of these questions, a survey was carried out in this work as explained below.

3.2 Survey

This survey focused on Greece, covering a wide variety of bioclimatic types. The survey was done in the spring and summer of 2012. A total of 598 households were polled with a questionnaire and data were gathered for the winter of 2010-11 (milder) and the winter of 2011-12 (harsher). The climatic conditions that prevailed over Greece during the two successive winters of 2010-2011 and 2001-2012 were remarkably different. Winter 2010-2011 ranks among the warmest winters on record in Greece according to the historical archives of the National Observatory of Athens, dating back to 19th century. In particular, winter 2010-2011 was the 3rd warmest on record with a maximum temperature averaging 16.6^{0} C from November to February, 2°C above normal (with respect to the 1961-1990 period) for the 4-month period. It is notable that November 2010 was the second warmest recorded ever. On the contrary, winter 2011-2012 ranks among the 15% of coldest winters on record, with maximum and minimum temperatures averaging 13.5°C and 6.6°C respectively from November to February, approximately 3°C lower than the corresponding temperatures of winter 2010-2011. It is also remarkable that November 2011 ranks among the 5 coldest on record.

The data were collected either by live interview of members of the household (adhering completely to the questionnaire) or by e-mailing the questionnaire. A follow-up by telephone of the households was carried out in order to confirm that collected data were correct; these households were selected from the sample systematically so as to cover both data collection modes and all personnel that collected data in the field.

Data were inspected for outliers; some rather large income values were located but none so large as to warrant exclusion from the data set. For buildings that were renovated, the renovation year was used to estimate the age of the buildings. As regards insulation, it is noted that buildings constructed: prior to 1980 lack insulation; from 1980 to 1990 have some ("flexible") insulation; and after 1990 are properly insulated.

A question relates to the energy consumption of apartments (as opposed to that of detached houses): does the reported energy consumption of households that live in apartments represent the energy consumption of the apartment or the entire apartment building? In many cases energy consumption was reported in monetary terms and, thus, represented correctly the energy consumption of the household.

4 RESULTS

Variable names and selected descriptive statistics are shown in Table 1.

Table 1. Basic statistics for quantitative variables

Variable name		min	max	mean	mode
DEGRDAYRATIO	degree days ratio of area of household	1.26473	1.40310	1.35606	1.34897 (n=469)
Q3MEMBERS	number of persons in household	1	8	2.99497	4 (n=180)
Q4M2	household surface area (m²)	25	400	96.4573	120 (n=56)
Q5RENAGE	building age since construction of last renovation (years)	2	112	28.6173	32 (n=53)
Q7FLOOR	household floor (if apartment)	-0.5	12	–	1 (n=136)
Q9SALAR09	2009 income (euros)	0	200000	26221	30000 (n=38)
Q10SALAR10	2010 income (euros)	0	200000	24900.2	
Q11SALAR11	2011 income (euros)	0	200000	22497.8	10000 (n=34)
Q12OIL	heating oil dummy variable	0 (n=131)	1 (n=465)		1
Q13GAS	natural gas dummy variable	0 (n=519)	1 (n=63)		0
Q14AC	air conditioning dummy variable	0 (n=193)	1 (n=405)		1
Q16BTU	installed air conditioning (BTUs)	6000	84000	25390.1	9000.0 (n=52)
Q18HOUR	hours of operation of air conditioning	0.140	24	3.89724	2 (n=61)
Q31CONSERV	conservation measures dummy	0 (n=386)	1 (n=196)		0 (n=386)
FUELPOVRAT1	fuel poverty ratio (winter 2010-11)	0.0015	0.6	0.051171	0.05
FUELPOOR1	fuel poor dummy (winter 2010-11)	0 (n=415, 88.9%)	1 (n=52, 11.1%)		0
FUELPOVRAT2	fuel poverty ratio (winter 2011-12)	0.001	0.666667	0.0550866	0.0333333
FUELPOOR2	fuel poor dummy(winter 2011-12)	0 (n=399, 88.3%)	1 (n=53, 11.7%)		0
Q48HEATHRS1	hours of heating (winter 2010-11)	0.570	24	6.90073	4 (n=83)
Q49HEATHRS2	hours of heating (winter 2011-12)	0.570	24	5.92486	4 (n=86)
KWHM2TOTAL1	actual specific energy consumption (kWh/m², winter 2010-11)	0.0351695	882.793	134.034	82.1642 (n=8)
KWHM2TOTAL2	actual specific energy consumption (kWh/m², winter 2011-12)	0.0351695	676.798	114.172	90.1362 (n=7)
KWHM2DEGRD	specific energy consumption based on degree days (kWh/m², winter 2010-11)	0.0474425	1190.86	182.404	110.837 (n=6)

The sample comprised 598 households that were located in a wide variety of geographical regions and bioclimatic types of Greece, including: Attica, Crete, parts of Peloponnese and the Cyclades islands (intense thermo-Mediterranean); Mainland Greece (weak to intense Thermo-Mediterranean); Thessaly (weak to intense meso-Mediterranean); Macedonia (i.e. northern Greece, sub-Mediterranean); and other local bioclimatic types in Peloponnese (weak to intense meso-Mediterranean, intense thermo-Mediterranean).

Most households were located in Athens and Attica (78.4%) with a 10.2% in Crete and a 9.7% in Peloponnese. Greek Macedonia and the rest of Northern Greece were underrepresented, something that may be addressed in a future work.

4.1 Descriptive analysis

Of the 598 households that were surveyed, three-fourths (452, i.e. 75.6% if the total) lived in apartments with the rest one-fourth (146, i.e. 24.4% of the total) living in detached houses. Buildings were constructed (or renovated) from 1900 to 2010, i.e. building age varied from 2 to 112 years with an average value of 28.6 years; age distribution is shown in Figure 1 and shows two peaks corresponding to periods of pronounced building activity fueled by economic growth (circa 1980 and 2000).

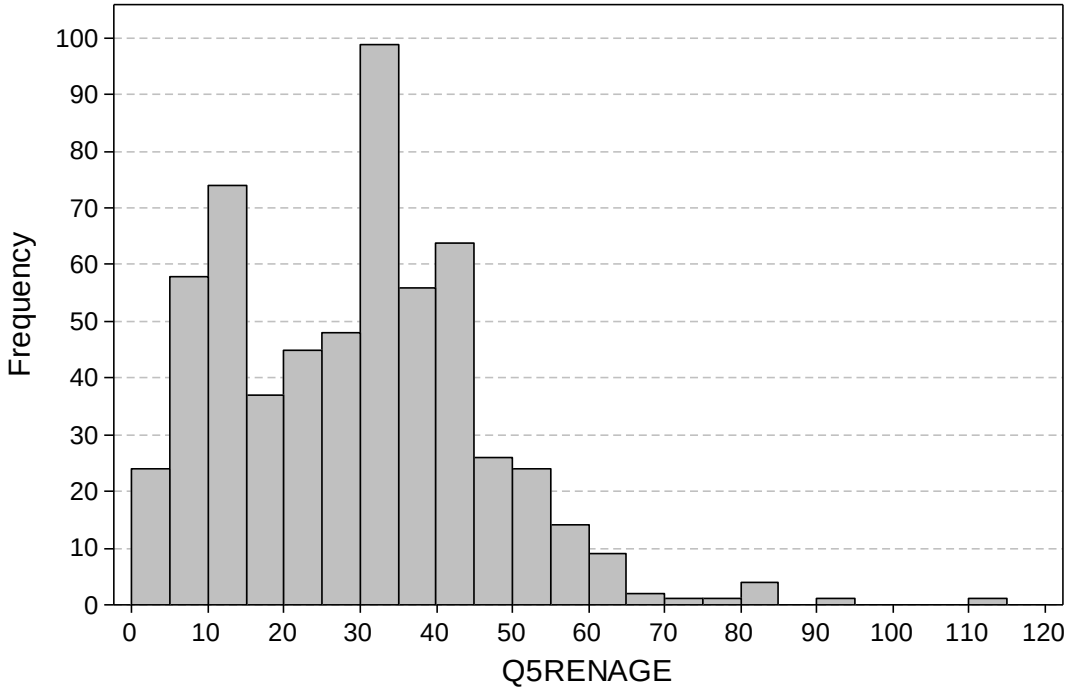

Figure 1. Building age (since construction or last renovation)

On the average, detached houses (31.3 years of age) were a little older than apartments (27.8 years). Surface area varied from 25 to 252 m² for apartments and from 50 to 400 for detached houses. The average surface area of apartments equaled 88.7 m²; for detached houses it equaled 120.5 m². The mode (i.e. most frequent value) of surface area was equal to 120 m² for both subsets i.e. apartments and detached houses (and was valid for a total of 56 households). The median floor for apartments was 2 with a mode of one (valid for 136 apartments). Households had one to 8 members, with an average household size of 3.5 (and mode of 4) in the case of detached houses and an average of 2.8 (with a mode of 2) in the case of apartments. These figures corresponded to an average of 37 m² per household member (and a mode of 30 m² which was valid for 50 households) with no difference between apartments and detached houses.

The effect of the global financial crisis and resulting austerity measures in Greece is depicted in the average household income that was reduced from 26221 euros (2009), to 24900 (2010) and 22498 (2011), a total reduction of 14%. Changes in the distribution of annual household income are shown in Figure 2.

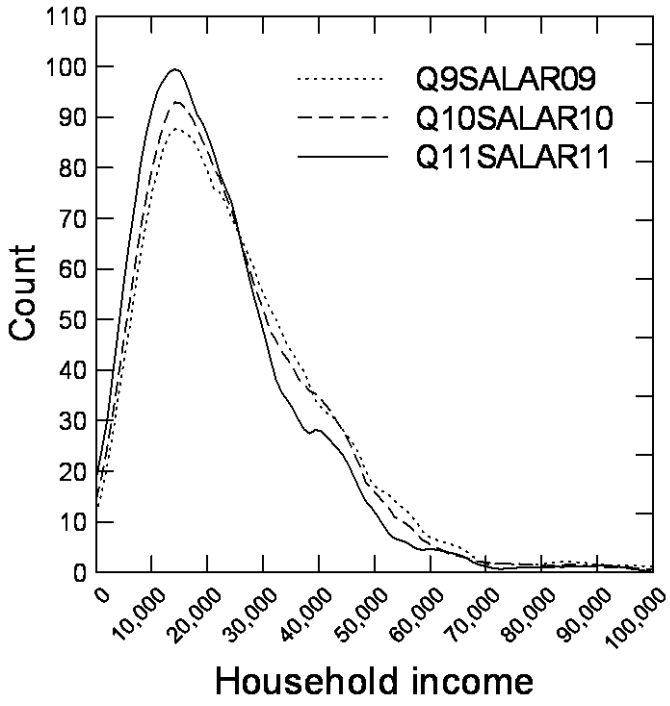

Figure 2. Annual household income distribution (2009 to 2011)

Household income changes were different across income classes as shown in Table 2.

Table 2. Household income changes across income classes

2009 income (thousands of euros)	Income change until 2012 (euros)	% change relative to average 2009 income in class
0~10	+1682	+26.1
10~20	-1778	-12.7
20~30	-3539	-15.1
30~40	-5056	-15.4
40~50	-5545	-13.2
50~60	-9496	-18.5
60~70	-8615	-14.2
70~80	-21667	-31.0
80~90	-19400	-23.4

Interestingly, the lowest income class gained about a fourth of its 2009 income probably because more household members joined the work force due to the worsening economic conditions. All other classes lost 12.7 to 31% of their 2009 income.

Looking at heating sources for the (colder) winter of 2011-12, it was found that: 18 households (3.1% of the total) did not use oil, natural gas or air conditioning; 141 households (24.3%, i.e. about one in four) were heated with oil alone; 29 households (5%, i.e. one in twenty) used only natural gas; and 51 households (8.8%) employed only air conditioning. Turning to mixtures of energy sources, it was found that: 309 households (53.2% of the total) were heated with oil and air conditioning; natural gas with air conditioning was by used by 32 households (5.5%); finally, only one household apparently had the opportunity to use all three heating sources (oil, gas and air conditioning). In the previous winter, 2010-11 (that was warmer), only 40 households (6.7% of the total) declared a different heating source; of these, 17 (2.8%) changed from oil to natural gas. In the 405 households (67.7% of the total or three out of four) that had air conditioning, the number of units varied from one to 7 with 9000

BTUs (2.64 kW) being the most prevalent unit type; three-fourths (74.4%) of the households had up to two units with 2 units being the mode (valid for 131 households). On the average, households with air conditioning turned on their unit(s) for 3.8 hours daily and when the temperature fell below 17.3 degrees Centigrade. Finally, 280 households (71.6% of the 391 that had air conditioning) did not use their units at night.

Based on the consumption of the first (milder) winter and degree hours of the second (colder) winter, specific energy consumption in the second winter should have an average of 182.40 and a median of 138.40 kWh/m². Yet, the average specific consumption of the second winter equaled 114.17 kWh/m² (with a median of 88.052) so it more than a third (37.4%) smaller than expected. Breaking specific energy consumption by income class, shown in Table 3, shows that specific energy consumption in the second winter (2011-12) was up to 20.9% smaller than the first (2009-10) and up to 72.1% smaller than what was expected been based on degree hours.

Table 3. Specific energy consumption per income class

2009 income (thousand euros)	Median consumption 2010-11 (kWh/m²)	Median consumption 2011-12 (kWh/m²)	was reduced by (%)	Expected consumption 2011-12 (kWh/m²)	Should be bigger by (%)
0-10	115.06	102.41	-11.0	156.84	53.1
10-20	127.57	110.06	-13.7	173.53	57.7
20-30	140.52	118.25	-15.8	191.24	61.7
30-40	165.41	130.88	-20.9	225.29	72.1
40-50	127.33	109.47	-14.0	173.61	58.6
50-60	123.85	115.01	-7.1	168.26	46.3
60-70	160.78	134.70	-16.2	217.19	61.2
70-80	202.25	166.41	-17.7	272.83	64.0
80-90	184.13	177.49	-3.6	248.99	40.3

Energy consumption in the first (milder) winter (2010-11) varied from 0 to 883 kWh/m² with an average of 134 and a median of 102 kWh/m²; 12 large values varying from 514 to 883 were retained in the analysis because they appeared to be correct. Energy consumption in the second (colder) winter (2011-12) varied from 0 to 676 kWh/m² with an average of 109.6 and a median of 88 kWh/m²; again, 5 large values (567 to 677) were nevertheless correct and were retained in the analysis. Households used an average of 20.1 kWh/m² less energy in the second winter (a 15% reduction) despite the fact that it was colder.

As mentioned in the literature review section, if the Fuel Poverty Ratio (FPR) is greater than 0.1, the household is considered to be fuel poor (DECC, 2012). Two FPRs were calculated, based on fuel expenses for the winters of 2009-10 and 2010-11 and the household income of the years 2010 and 2011. Average FPR was 0.05 for the 2009-10 winter and 0.055 for the 2010-11 winter, with the second value being bigger than the first at a significance level higher than 99.99% (t-test for paired samples: t=2.620; p=0.0045). It is concluded that the fuel poverty of households deteriorated very significantly during the duration of the study. The ratio of fuel poor households was 11.1% (52 cases) for the first winter and 11.7% for the second (53 cases). These figures underline the importance of fuel poverty in Greece during this time of global financial uncertainty.

In the 452 apartments (75.6% of the total) that had an average age of 27.8 years and an average surface area of 88.69 m², dwelled an average of 2.82 persons, with an average three-year (2010, 2011 and 2012) household income of 23034 euros and an average energy

consumption of 124.8 kWh/m² in the first winter (2010-11) and 103.4 kWh/m² in the second winter (2011-12), i.e. a reduction of 17%. In comparison, in the 146 detached houses (24.4% of total households) that had an average age of 31.3 years and an average surface of 120.5 m², dwelled an average of 3.5 persons, with an average three-year household income of 27126 euros and an average energy consumption of 163.1 kWh/m² for the first winter and 148 kWh/m² for the second winter (a reduction of 9.3%). It is worth noting that the bigger reduction that is observed in apartments may be (in part) due to the more accurate measurement of energy consumption in detached houses.

More interesting comparisons are presented in the next section that documents the clustering of households into a low and a high income group.

4.2 Cluster analysis

To achieve a distinct clustering of cases, a relatively small number of variables (representing salient features of households) should be included in the analysis. Of the many variables available, those (a) holding data considered to be of high quality and (b) having only a handful of missing values were considered for cluster analysis (so that a listwise deletion of cases with missing data would not result in a dramatic reduction of cases available for clustering). Data quality and missing data consideration along with a priori expectations as to which variables should characterize the profile of a household, lead to the following variables being selected for possible inclusion in cluster analysis:

- socioeconomic (Q9SALAR09/Q10SALAR10/Q11SALAR11, Q3MEMBERS);
- building related (property type i.e. apartment/house, Q5RENAGE, Q4M2);
- energy consumption related (Q12OIL, Q13GAS, Q14AC, Q31CONSERV, Q48HEATHRS1/Q49HEATHRS2, KWHM2TOTAL1/KWHM2TOTAL2);
- environmental (DEGRDAYRATIO) variables.

Fuel poverty ratio information, in particular, could not be included in the analysis due to more than 150 missing values.

Prior to the analysis it was noted that some quantitative variables measured the same quantity at different times and were thus highly collinear. Retaining all such variables in the analysis would result in their overrepresentation (Mooi & Sarstedt, 2011). On the other hand, extracting factors from such variables (via factor analysis) may result in several problems and is advised against by Dolnicar and Grun (2009) with arguments that are valid in the case of principal component analysis as well. Based on these recommendations, it was decided that:

- only the 2011 income (Q11SALAR11) with the 2011-2009 income reduction (DIFFSALARY) be retained in the analysis, as the smallest number of income variables that still convey a measure of (a) income size and (b) income reduction due to the financial crisis;
- only the difference in heating hours (DIFFHEATHOURS) between the two winters be selected for inclusion in the analysis;
- energy consumption be represented by (a) the specific energy consumption of the second (harsher) winter (KWHM2TOTAL2) and (b) its difference from the specific consumption (of the same winter) expected from degree hours (DIFFKWHM2DEGRD).

Trying different two-step clustering schemes (carried out with IBM SPSS version 21) with the categorical variables (such as property type, Q12OIL and Q31CONSERV) included, showed that no stable number of clusters could be reached at. Dummy variables were found to exert

an undue amount of influence in shaping the number and size of the clusters; when one relatively unimportant dummy variable (such as Q13GAS) was taken out, an entirely different number of clusters of different size resulted. Much stabler clustering schemes were obtained when only quantitative variables were included in the analysis and hierarchical clustering was used.

On the issue of sample size, Formann (1984) as quoted by Mooi and Sarstedt (2011) recommends a sample of at least 2^m cases, where m equals the number of clustering variables. Although these are just recommendations, it follows that it would be good to not exceed 8 (sample size of 256) to 9 (sample size of 512) variables in order to cluster analyze the available 598 cases (not all of which will be complete).

The final list of 8 variables included in hierarchical cluster analysis along with complete cases is shown in Table 4.

Table 4. Variables used in cluster analysis

	Variable	Complete cases	Range
1	Q11SALAR11	585	0 to 200000
2	DIFFSALARY (=Q11SALAR11- Q11SALAR9)	579	-80000 to 40000
3	Q3MEMBERS	596	1 to 8
4	Q5RENAGE	588	2 to 112
5	Q4M2	597	25 to 400
6	DIFFHEATHOURS (=Q49HEATHRS2- Q49HEATHRS1)	563	-22.5 to 20.0
7	KWHM2TOTAL2	560	0.0352 to 676.798
8	DIFFKWHM2DEGRD (=KWHM2TOTAL2- KWHM2DEGRD)	558	-757.463 to 364.833
	complete cases after listwise deletion of missing data:	508	

It was decided that hierarchical cluster analysis be carried out with Ward's linkage method and the squared Euclidean as the appropriate distance measure (Romesburg, 2004). On the number of clusters, some exploratory graphs (Figure 1 and Figure 2) had previously indicated the presence of two clusters (Everitt et al., 2011), a scheme that was confirmed by the analysis. The presence of two clusters was validated by rerunning the analysis on randomly sorted data (Mooi & Sarstedt, 2011) and is shown in Table 5.

Table 5. Cluster centroids (eq. var.: equal variances t-test; uneq. var.: unequal variances t-test;

	Variable	Cluster 1 ("low income")	Cluster 2 ("high income")	t-test H0: μ1=μ2 Ha: μ1≠μ2
1	Q11SALAR11	18006	39744	t= -9.18; p=0.0000 (uneq. var.)
2	DIFFSALARY	-4355	-2174	t=-2.52; p=0.0120 (eq. var.)
3	Q3MEMBERS	2.8	3.7	t=-7.16; p=0.0000 (eq. var.)
4	Q5RENAGE	30.5	21.8	t=6.32; p=0.0000 (uneq. var.)
5	Q4M2	83.2	136.3	t=-13.82; p=0.0000 (uneq. var.)
6	DIFFHEATHOURS	-1.3	-0.3	t=-3.29; p=0.0010 (eq. var.)
7	KWHM2TOTAL2	120.7	102.4	t=2.28; p=0.0234 (uneq. var.)
8	DIFFKWHM2DEGRD	-76.6	-54.6	t=-3.22; p=0.0014 (uneq. var.)
	cases in cluster	389	119	
		(76.57%)	(23.43%)	

The 508 complete cases were classified into two clusters:

1. The first cluster included about three-fourths (76.6%) of the cases and evidently represented lower-income households. These had a 2011 income of 18006 euros, 4355 euros lower than their 2009 income; had 2.8 members per household; lived in an apartment of a house with an area of 83.2 m², in a building that was 30.5 years old (or last renovated); and had a specific energy consumption of 131.5 kWh/m² for the second (harsher) winter, a full 76.6 kWh/m² lower than expected from climatic conditions (degree hours);
2. The second cluster included the rest one-fourth (23.4%) of the cases, that represented higher-income households. These had a 2011 income of 39744 euros (more than twice the income of the first cluster), that was only 2174 euros lower than their 2009 income; had 3.7 members per household, one more than the previous cluster; lived in an apartment of a house with an larger area of 136.3 m², in a building that was only 21.8 years old (or last renovated); and had a lower specific energy consumption of 102.4 kWh/m² for the second winter, 54.6 kWh/m² lower than expected from climatic conditions.

As noted by the t-tests for independent samples (with equal or unequal sample variances assumed as indicated by Levene's test) in the rightmost column of Table 5, all variable values at the cluster centroids were significantly different between the two clusters at a confidence level of 97% or higher. This provides an initial confirmation of the validity of the classification of households in two distinct clusters. Further validation is provided by comparing the values of other criterion variables at the cluster centroids – these are provided in Table 6, the last column of which tests indicates the results of independent sample t-tests or proportion z-tests (as appropriate).

Table 6. Values of selected criterion variables at cluster centroids (eq. var.: equal variances t-test; uneq. var.: unequal variances t-test;

Variable	Cluster 1 ("low income")	Cluster 2 ("high income")	t or z test: H0: μ1=μ2 Ha: μ1≠μ2
Q9SALAR09	22361	41918	t= -7.96; p=0.0000 (uneq. var.)
Q10SALAR10	20707	41865	t=-8.38; p=0.0000 (uneq. var.)
income per household member (SAL11PCAP)	7638.69	12590.8	t=-5.42; p=0.0000 (uneq. var.)
% of households dwelling in house	19.54%	39.50%	z =-4.45; p=0.0000
% of households dwelling in apartment	80.46%	60.50%	z =4.45; p=0.0000
Q7FLOOR	1.8	1.5	t=1.70; p=0.0906 (eq. var.)
Q13GAS	9.95%	15.97%	z =-1.81; p=0.0710
Q16BTU	23953	30410	t=-3.14; p=0.0022 (uneq. var.)
Q17TEMP	17	18.4	t=-1.56; p=0.1200 (eq. var.)
Q18HOUR	4.01	3.46	t=1.49; p=0.1398 (uneq. var.)
% of households that took conservation measures (Q31CONSERV)	35.60%	24.79%	z=2.17; p=0.0297
DIFFTEMPIN	-0.54	-0.4	t= -1.05; p=0.2943 (uneq. var.)
DIFFTEMPOUT	-0.69	-0.59	t=-0.55; p=0.5836 (uneq. var.)
FUELPOVRAT1	0.055	0.033	t=5.02; p=0.0000 (uneq. var.)
% of households above fuel poverty line (2010-11) (FUELPOOR1)	13.87%	2.06%	z=3.24; p=0.0012
FUELPOVRAT2	0.061	0.040	t=4.18; p=0.0000 (uneq. var.)
% of households above fuel poverty line (2011-12) (FUELPOOR2)	14.71%	3.06%	z=3.10; p=0.0019
Q48HEATHRS1	6.9	7.1	t=-0.33; p=0.7408 (eq. var.)
Q49HEATHRS2	5.6	6.8	t=-2.27; p=0.0244 (uneq. var.)
KWHM2TOTAL1	145.1	115.4	t= 3.22; p=0.0014 (uneq. var.)

It is seen that:

- the income of Cluster 2 (higher income) is twice that of Cluster 1 (lower income) and that even the per capita income is different between the two clusters at a confidence level higher than 99.99%;
- twice (i.e. 39.5%) the number of households of Cluster 2 live in houses compared to those of Cluster 1 (i.e. 19.54%) and this also reflects on the value of Q7FLOOR;
- more Cluster 2 households (15.97%) are heated with natural gas and have more installed air conditioning power (30410 BTU) compared to those of Cluster 1 (9.95% and 23953 BTU respectively);
- one out of three Cluster 1 households (i.e. 35.6%) adopted some conservation measures after the first winter, compared to one out of four for Cluster 2 (24.79%);
- only 2.06% of the households of Cluster 2 households were above the fuel poverty line, compared to 13.87% for Cluster 1;
- finally, Cluster 2 households consumed less specific energy in the first winter as well (115,4 kWh/m² compared to 145.1 for Cluster 1).

Many of these findings are in agreement with Santamouris et al. (2007a).

Cluster analysis is thus brought to conclusion, having obtained a clear picture of the classification of households: one out of four household is of higher income that suffered a

smaller loss since 2009; has more members; lives in a newer and larger house or apartment; and consumes less specific energy. It is the other three in four households that fuel poverty policies should target so that the 13.9% fuel poor proportion of this group is controlled even if the economic crisis in Greece deepens.

5 CONCLUSIONS

The survey presented in this paper focused on Greece and analyzed the energy consumption of households located in a wide variety of geographical regions and bioclimatic types. Many of the findings are in agreement with Santamouris et al. (2007a). Clearly, the lower-income three out of four households are the ones that fuel poverty policies should target, so that the 13.87% fuel poor proportion of this group is controlled as best as possible, given the financial crisis in Greece. Energy policies should take into account social consequences so as to avoid causing further human misery (Bradshaw & Hutton, 1983). Energy counselling together with energy saving packages for emergency relief (e.g. energy saving bulbs, radiator reflectors), pointed out by the French survey reviewer earlier, would help in this direction.

As regards the means, in Ireland, fuel allowance does reduce the severity of experience of fuel poverty among the low-income households. As pointed out by Kelly (2011), homes with a propensity to consume more energy should be targeted using behavioural strategies combined with economic penalties and incentives; homes with low Standard Assessment Procedure (SAP) rates should be targeted for whole home efficiency upgrades in order to break through the energy efficiency barrier. The (SAP) is the methodology used by the Department of Energy & Climate Change (DECC) in UK which assesses and compares the energy and environmental performance of dwellings. In Greece, Santamouris et al. (2007a) concluded that energy policies addressed to the dwelling sector should set as a priority the improvement of the envelope quality of residents where low income people are living.

One should be beware of the economic means though, especially at this time of great financial crisis and hardship in Greece. The consequences of a liberal energy market without any regulations regarding the prevention of energy debts may be seen in Austria (Brunner, Spitzer & Christanell, 2011). All the measures suggested should be integrated into a national strategy for the reduction of fuel poverty. The Austrian study suggests all proposed measures not be applied singularly but instead be integrated into a national strategy for the reduction of fuel poverty.

The UK Department of Energy (DOE), has claimed that the achievement of energy conservation together with affordable warmth are the two central aims of efficiency policies and even the slightest improvement in energy efficiency would help in providing affordable warmth to the poorest households (DOE, 1991). The importance of this study is further underscored by the fact that the building sector in Greece represents 36% of total energy consumption and consumes around 450 million euros per year (Panas, 2012).

Turning to directions for further study, an important task that complements the present study is the monitoring of low income households with sensors in order to investigate temperature levels for the case of families that can barely purchase heating energy. This research is underway by some of the authors of this paper and its results are expected to shed more light on the relationship between energy and poverty and how these affect survivability at this time of a global financial crisis. Other tasks that would be beneficial to carry out in a future investigation include: collection and analyses of more household data from Northern Greece; an in-depth comparison of apartments versus detached houses; the impact of specific energy

conservation measures adopted by households; and an examination of alternative policies designed to address fuel poverty in Greece and Southeastern Europe.

6 ACKNOWLEDGMENTS

Thanks are due to numerous undergraduate students of the University of Athens, the University of Piraeus and the Technical University of Crete who helped with data collection.

7 REFERENCES

Anderson, W., White, V. & Finney, A. (2012).Coping with Low Incomes and Cold Homes. *Energy Policy*, 49, 40-52.

Boardman, B. (1991). *Fuel Poverty: From Cold Homes to Affordable Warmth*. Belhaven Press, London.

Boardman, B. (2010). *Fixing Fuel Poverty: Challenges and Solutions*. Earthscan, London.

Bolton, P. & Richards, P. (2012). *Fuel Poverty*. House of Commons Library, United Kingdom.

Bouzarovski, S., Petrova, S. & Sarlamanov, R. (2012). Energy Poverty Policies in the EU: A Critical Perspective. *Energy Policy*, 49, 76-82.

Bradshaw, J. & Hutton, S. (1983). Social policy options and fuel poverty. *Journal of Economic Psychology*, 3, 249-266.

Braun, F. (2010). Determinants of Households' Space Heating Type: A Discrete Choice Analysis for German Households. *Energy Policy*, 38, 5493-5503.

Brunner, K. M., Spitzer, M. & Christanell, A. (2011). Experiencing Fuel Poverty. Coping Strategies of Low-Income Households in Vienna/Austria. Energy Policy, 49, 53-59.

Buzar, S. (2007). The "Hidden" Geographies of Energy Poverty in Post-Socialism: Between Institutions and Households. *Geoforum*, 38, 224-240.

Department of Energy and Climate Change (DECC) (2010). *Fuel Poverty Methodology Handbook*. Crown Copyright, URN 10D/825.

Department of Energy and Climate Change (DECC) (2012). *Annual Report on Fuel Poverty Statistics 2012*. A national statistics publication, United Kingdom.

Department of the Environment (DOE) (1991). *English House Condition Survey 1991: Energy report*. DOE, London.

Department of Trade and Industry (DTI) (2001). *The UK Fuel Poverty Strategy*. London, Department of Trade and Industry, available at http://webarchive.nationalarchives.gov.uk/+/http://www.dti.gov.uk/energy/fuel-poverty/strategy/index.html, accessed on 11/2007.

Devaliere, I. (2010). *Identification des Processus de Précarisation Energétique des Ménages et Analyse des Modes d'intervention*. CSTB, Paris.

Dolnicar, S. & Grun, B. (2009). Challenging "Factor-Cluster Segmentation". *J. Travel. Res.*, 47, 63-71.

Dubois, U. (2012). From Targeting to Implementation: The Role of Identification of Fuel Poor Households. *Energy Policy*, 49, 107-115.

Emery, A. F. & Kippenhan, C. J. (2006). A Long Term Study of Residential Home Heating Consumption and the Effect of Occupant Behavior on Homes in the Pacific Northwest Constructed According to Improved Thermal Standards. *Energy*, 31, 677-693.

EU Fuel Poverty Network (2012). *Fuel Poverty in Spain*. Available at http://fuelpoverty.eu/2012/02/10/fuel-poverty-in-spain/, accessed on 04/2013.

European Commission (EC) (2010). An Energy Policy for Customers. Commission Staff Working Paper, EC, Brussels, SEC, 1407 final.

European Fuel Poverty and Energy Efficiency (EPEE) (2009). Diagnoses of causes and consequences of fuel poverty in Belgium, France, Italy, Spain and the United Kingdom. EPEE.

European Parliament (EP). *Directive 2009/72/EC of the European Parliament and of the Council of 13 July 2009 concerning common rules for the internal market in electricity and repealing Directive 2003/54/EC (Text with EEA relevance)*. Available at http://eur-lex.europa.eu/LexUriServ/LexUriServ.do?uri=OJ:L:2009:211:0055:0093:EN:PDF, accessed on 02/2013.

Everitt, B. S., Landau, S., Leese, M. & Stahl, D. (2011). *Cluster Analysis*. 5th ed., Wiley & Sons, United Kingdom.

Formann, A.K. (1984). *Die Latent-Class-Analyse: Einführung In Die Theorie Und Anwendung*. Beltz, Weinheim, Germany.

Fracastoroa, V. & Serraino, M. (2010). A Methodology for Assessing the Energy Performance of Large Scale Building Stocks and Possible Applications. *Energy and Buildings*, 43, 844-852.

Hassid, S., Santamouris, M., Papanikolaou, N., Linardi, A., Klitsikas, N., Georgakis, C. & Assimakopoulos, D.N. (2000). The Effect of the Athens Heat Island on Air Conditioning Load. *Energy and Buildings*, 32, 131-141.

Healy, J. D. & Clinch, J. P. (2004). Quantifying the Severity of Fuel Poverty, its Relationship with Poor Housing and Reasons for Non-Investment in Energy-Saving Measures in Ireland. *Energy Policy*, 32, 207-220.

Hens, H. , Parijs, W. & Deurinck, M. (2002). Energy Consumption for Heating and Rebound Effects. *Energy and Buildings*, 42, 105-110.

Hill, J. (2012). *Getting the Measure of Fuel Poverty: Final Report of the Fuel Poverty Review*. CASE report 72.

Howden-Chapman, P., Viggers, H., Chapman, R., O' Dea, D. & Sarah, F. (2009). Warm Homes: Drivers of the Demand for Heating in the Residential Sector in New Zealand. *Energy Policy,* 37, 3387-3399.

Kelly, S. (2011). Do Homes That Are More Energy Efficient Consume Less Energy?: A Structural Equation Model of the English Residential Sector. *Energy,* 36, 5610-5620.

Livada, I., Santamouris, M., Niachou, K., Papanikolaou, N. & Mihalakakou, G. (2002). Determination of Places in the Great Athens Area Where the Heat Island Effect Is Observed. *Theoretical Appl. Climatol.*, 71, 219-230.

Michelen, C. & Madlener, R. (2012). Homeowners' Preferences for Adopting Innovative Residential Heating Systems: A Discrete Choice Analysis for Germany. *Energy Economics,* 34, 1271-1283.

Mooi, E. & Sarstedt, M. (2011). *A Concise Guide to Market Research: The Process, Data, and Methods Using IBM SPSS Statistics*. Springer.

Moore, R. (2012). Definitions of Fuel Poverty: Implications for Policy. *Energy Policy*, 49 19-26.

O'Sullivan, Howden-Chapman, K. & Fougere, G. (2011). Making the Connection: The Relationship between Fuel Poverty, Electricity Disconnection, and Prepayment Metering. *Energy Policy*, 39, 733-741.

Palmer, G., MacInnes, T. & Kenway, P. (2008). COLD AND POOR: *An Analysis of the Link between Fuel Poverty and Low Income.* New Policy Institute, London, United Kingdom.

Panas, E. (2012). *Research of Fuel Poverty in Greece November 2012* [in Greek]. Department of Statistics, Athens University of Economics and Business, Greece.

Pantavou, K., Theoharatos, G., Mavrakis, A. & Santamouris, M. (2011). Evaluating Thermal Comfort Conditions and Health Responses during an Extremely Hot Summer in Athens. *Building and Environment*, 46, 339-344.

Papadopoulos, A. M., Oxizidis, S. & Papandritsas, G. (2007). Energy, Economic and Environmental Performance of Heating Systems in Greek Buildings. *Energy and Buildings,* 40, 224-230.

Romesburg, C. H. (2004). *Cluster Analysis for Researchers*. Lulu Press, North Carolina, United States of America.

Sakka, A., Santamouris, M., Livada, I., Nicol, F. & Wilson, M. (2012). On the Thermal Performance of Low Income Housing during Heat Waves. *Energy and Buildings,* 49, 69-77.

Santamouris, M. & Kolokotsa, D. (2013). Passive Cooling Dissipation Techniques for Buildings and Other Structures: The State of The Art (Review Article). *Energy and Buildings,* 57, 74-94.

Santamouris, M. (2007). Heat Island Research in Europe, the State of the Art. *Journal of Advances in Building Energy Research* (Review Paper), 1, 23-150.

Santamouris, M. (2012). Cooling the Cities - A Review of Reflective and Green Roof Mitigation Technologies to Fight Heat Island and Improve Comfort in Urban Environments. *Solar Energy*, available online 30 July 2012, ISSN 0038-092X, http://dx.doi.org/10.1016/j.solener.2012.07.003. (http://www.sciencedirect.com/science/article/pii/S0038092X12002447).

Santamouris, M., Gaitani, N., Spanou, A., Saliari, M., Gianopoulou, K. & Vasilakopoulou, K. (2012). Using Cool Paving Materials to Improve Microclimate of Urban Areas - Design Realisation and Results of the Flisvos Project. *Building and Environment*, 53, 128-136.

Santamouris, M., Kapsis, K., Korres, D., Livada, I., Pavlou, C. & Assimakopoulos, M. N. (2007a). On The Relation between the Energy and Social Characteristics of The Residential Sector. *Energy and Buildings*, 39, 893-905.

Santamouris, M., Papanikolaou, N., Livada, I., Koronakis, I., Georgakis, C., Argiriou, A. & Assimakopoulos, D. N. (2001). On the Impact of Urban Climate to the Energy Consumption of Buildings. *Solar Energy*, 70 201-216.

Santamouris, M., Pavlou, K., Synnefa, A., Niachou, K. & Kolokotsa, D. (2007b). Recent Progress on Passive Cooling Techniques. Advanced Technological Developments to Improve Survivability levels in Low - Income Households. *Energy and Buildings*, 39 859-866.

Sardianou, E., (2008). Estimating Space Heating Determinants: An Analysis of Greek Households. *Energy and Buildings*, 40, 1084-1093.

Schuler, A., Weber, C. & Fahl, U. (2000). Energy Consumption for Space Heating Of West-German Households: Empirical Evidence, Scenario Projections and Policy Implications. *Energy Policy*, 28, 877-894.

Stathopoulou, E., Michalakakou, G., Santamouris, M. & H. S. Bargiorgas (2008). Impact of Temperature on Tropospheric Ozone Concentration Levels in Urban Environments. *Journal of Earth System Science*, 117, 227-236.

Thomson, H. & Snell, C. (2013). Quantifying the Prevalence of Fuel Poverty across the European Union. *Energy Policy*, 52, 563-572.

Tonooka, Y., Liu, J., Kondou, Y. & Fukasawa, O. (2006). A Survey on Energy Consumption in Rural Households in the Fringes of Xian City. *Energy Buildings*, 38, 1338-1342.

Ueno, T., Inada, R., Saeki, O. & Tsuji, K. (2006). Effectiveness of an Energy-Consumption Information System for Residential Buildings. *Applied Energy*, 83, 868-883.

Walker, G. & Day, R. (2012). Fuel Poverty as Injustice: Integrating Distribution, Recognition and Procedure in the Struggle for Affordable Warmth. *Energy Policy*, 49, 69-75.

Whyley, C. & Callender, C. (1997). Fuel Poverty in Europe: Evidence from the European Household Panel Survey. Policy Studies Institute, London, United Kingdom.

Wilkinson, R. & Pickett, K. (2009). *The Spirit Level: Why More Equal Societies Almost Always Do Better*. Allen Lane, London, 2009.

World Health Organization (WHO) (1987). *Health Impact of Low Indoor Temperatures: Report on a WHO Meeting*. Copenhagen: World Health Organization.

MICRO-CLIMATE MODIFICATION AND POTENTIAL FOR REDUCTION IN SUMMERTIME OVER-HEATING IN SOCIAL HOUSING, SOUTH WALES (UK)

David Holmes[*1], Tim Taylor[1], John Counsell[1]

1 Cardiff Metropolitan University
Llandaff Campus, Western Avenue
CF5 2YB, United Kingdom
**Corresponding author: daholmes@cardiffmet.ac.uk*

ABSTRACT

There is a growing consensus that the climate is changing faster than at any time in the past millennium. This is likely to have major effects upon many aspects of the built environment. UK Climate Impact Projections 09 indicate significant increases in Summer Mean Temperatures. This may suggest a requirement for cooler buildings during the summer months. In consequence, that would likely lead to an increase in demand for mechanical ventilation and comfort cooling. In the UK, the energy balance used in modifying environmental conditions could change from one predominantly concerned with winter heating, to a situation in which more energy is used to provide summertime cooling.
This paper reports a research project, funded by the European Union Social Fund, in collaboration with United Welsh (Housing Association).The project aims to develop guidance for low carbon and ecological social housing in South Wales and is concerned with design and construction. Evidence already suggests recently constructed dwellings are overheating even now, under current summertime conditions. With a possible life span in excess of sixty years, they must be suitably adapted for changed climatic conditions, if they are to remain fit for purpose throughout. With the prospect of a Mediterranean type climate, external spaces around dwellings will become more important as levels of outdoor activity increase. The psychological benefits of green space, and its amenity value to residents is well recognised. Some innovative approaches to surface water management and enhancement of biodiversity focus upon the benefits of external landscaping. This research investigates whether a better understanding of how such factors influence the local micro-climate could deliver benefits in terms of improved internal conditions, and reduced energy use.
The methodology adopted takes a recently completed new-build social housing scheme from the portfolio of the industrial partner, and using recognised thermal modelling packages, seeks to establish if, and to what extent summertime overheating is currently an issue, and how this may be impacted by climate change. Utilising 'ENVI-met', a micro-climate simulation model, notional changes in the form of specific landscape measures are then assessed in terms of their influence upon the local environment. This data is finally used in a further iteration of modelling, to evaluate the impact of micro-climatic modification and ventilation strategies on the internal environment of adjacent dwellings.
This paper will be useful to Registered Social Landlords, Local & Regional Government Agencies, and Private Sector organisations engaged in the planning, design and procurement of residential buildings.

KEYWORDS

Adaptation, Climate Change, Overheating, Micro-climate.

1 INTRODUCTION

There is a growing consensus that the climate is changing faster than at any time in the past millennium, and that further change is inevitable. This is likely to be long-lasting and have a significant impact on the built environment (IPCC, 2007). UK Climate Impact Projections 09, indicate possible increases in Summer Mean Temperatures for South Wales (UK), of 2-3°C by the middle of the century (Met Office, 2010). This suggests a requirement for cooler buildings during the summer months, and would likely lead to an increase in demand for

mechanical ventilation and comfort cooling. In the UK, the energy balance used in modifying environmental conditions could change from one predominantly concerned with winter heating, to a situation in which more energy is used to provide summertime cooling (Gething, 2010).

With the prospect of a Mediterranean type climate, external spaces around dwellings will become more important as levels of outdoor activity increase. The psychological benefits of green space and its amenity value to residents is well recognised (Winson, 2011). In the UK, the 'Oil Crisis' of the 1970's provided the stimulus for research activity aimed at energy conservation and demand reduction. The principle of utilising external landscape measures was identified as a passive approach to the design of energy efficient buildings (BRE, 1990). Political and economic changes however, resulted in a reduction in the perceived threat to national fuel security, and interest in this alternative approach declined.

This paper reports a research project, funded by the European Union Social Fund, in collaboration with United Welsh (Housing Association). The project aims to develop guidance for low carbon and ecological social housing in South Wales and is focussed upon adaptation measures in relation to micro-climatic modification. Current U.K. standards largely focus on reducing heating demand. Evidence suggests that recently constructed dwellings are overheating even now, under current summertime conditions (NHBC, 2012). With a possible life span in excess of sixty years, these dwellings must be suitably adapted for changed climatic conditions, if they are to remain fit for purpose throughout their lifecycle. Predicted demographic changes also suggest higher levels of vulnerability to excess heat, as an aging population begins to exhibit increases in long term health conditions and increased susceptibility to heat stress.

Using contemporary modelling techniques this research investigates whether a better understanding of how such measures influence the local micro-climate could deliver improved internal conditions, and reduced energy use.

The methodology adopted looks at a recently completed new-build social housing scheme from the portfolio of the industrial partner. In the first part of a two-stage modelling process, 'ENVI-met', a micro-climate simulation modelling platform (Bruse, 2010), is utilised to assess the impact of specific landscape components. Solar shading, and localised air temperature data are then used to produce amended Energy Plus weather files. In the second part, natural ventilation simulations, using DesignBuilder, a computer based thermal modelling package (Designbuilder, n.d.) are completed using weather files edited to reflect output data from stage one. Results are analysed to assess the impact of micro-climatic modification upon the ventilation and internal temperatures of domestic living space within the dwelling.

2 METHODOLOGY

2.1 Case Study: Unit 5, Heol Elan, Rassau, Ebbw Vale.

A 5 person, 4 bedroom, detached, south-facing dwelling was selected as the basis for this case study. Constructed in 2010, and built using lightweight timber frame construction, to Code for Sustainable Homes Level 4. The detached nature of the property provides the greatest ratio of external wall to floor area, and likely to most clearly demonstrate the impact of external conditions.

2.2 ENVI-met

2.1.1 Area Input File

A notional layout was utilised in the Area Input File (AIF), and built around a $1m^2$ grid. The geographic location was designated as latitude 51.80137, longitude -3.224734 (junction of Honeyfield Road and Glyndwr Road). The dwelling footprint is represented by a rectangular

plan form 8m x 8m, and a total plot area of 240 m^2, (12m wide and 20m deep). The front bay window was simplified, and the roof assumed to be flat, to accommodate limitations within the model. The overall building height was designated as 7m. Distances to boundaries were representative of average plot sizes within the development, with a distance of 2m to side boundaries and 6m from the front and rear facades. In the first of two area input layouts, ground treatment is limited to two surface types. A paved concrete hard-standing, sized to accommodate one parked vehicle within the front garden area, and concrete paving along the side elevation to the rear access door, were also included. The remaining ground surface was assigned to 'grass'. To account for the impact of adjacent units the basic plan was repeated to each side, giving an overall grid size of X=36 Y=20. A telescoping vertical grid was employed, consisting of 9 modules to the top of the 3D model (Z=9). A number of 'receptors', capable of sensing and recording model data at a specific point were referenced and located at strategic points around the building perimeter.

2.1.2 Configuration Input

Input data specified a 24 hour period for the total simulation time with a start time of 04:00 to allow for initialisation prior to sunrise. The simulation date 21.06.2002 was assigned to provide maximum sun altitude, and to align the data output with Designbuilder, for use in the second stage of the process. Input data for wind speed, wind direction, initial temperature, specific and relative humidity were specified as daily average values taken from the Prometheus current weather file for Cardiff (Exeter University, n.d.). Initial temperature and specific humidity were calculated using a constant value for atmospheric pressure of 1027 hPa. A Roughness Length of 1.0 was considered to be an appropriate value for a suburban area with regular large obstacle coverage.(DWIA, n.d.). Configuration data as Table 1.

Table 1: Configuration Input File data

Input	Value	Unit	Input	Value	Unit
Start Simulation at Day	21.06.2002	DD.MM.YYYY	**[SOILDATA] Settings for Soil**		
Start Simulation at Time	04:00:00	HH:MM:SS	Initial Temperature Upper Layer (0-20 cm	293	K
Total Simulation Time	24.00	Hours	Initial Temperature Middle Layer (20-50 cm)	293	K
Save Model State	60	min	Initial Temperature Deep Layer (below 50 cm)	293	K
Wind Speed in 10 m ab. Ground	7	m/s	Relative Humidity Upper Layer (0-20 cm)	50	%
Wind Direction (0:N,90:E,180:S,270:W)	246		Relative Humidity Middle Layer (20-50 cm)	60	%
Roughness Length z0 at Reference Point	1.0		Relative Humidity Deep Layer (below 50 cm)	60	%
Initial Temperature Atmosphere	284	K	**[TIMESTEPS] Dynamical Timesteps**		
Specific Humidity in 2500 m	5.69	g Water/kg air	Sun height for switching dt(0) -> dt(1)	40	
Relative Humidity in 2m	73	%	Sun height for switching dt(1) -> dt(2)	50	
Database Plants	[input]\Plants.dat		Time step (s) for interval 1 dt(0)	2.0	
[BUILDING] Building properties			Time step (s) for interval 2 dt(1)	2.0	
Inside Temperature	293	K	Time step (s) for interval 3 dt(2)	2.0	
Heat Transmission Walls	0.29	W/m²K	[PMV] Settings for PMV-Calculation		
Heat Transmission Roofs	0.16	W/m²K	Walking Speed	0.0	m/s
Albedo Walls	0.3		Energy-Exchange	58	Col. 2 M/A
Albedo Roofs	0.25		Mech. Factor	0.0	
[PLANTMODEL] Settings for plant model			Heat transfer resistance cloths	0.5	
Stomata res. approach (1=Deardorff, 2=A-gs)	2				
Background CO2 concentration	350	ppm			

The internal temperature was specified as 293K (22°C) and maintained throughout the simulation period. Thermal transmission values for walls and roof were taken from specification by Stride Treglown (architects), and albedo ratings for external facing materials taken as mid-range values published by NASA (National Aeronautics and Space Administration, 1999). Values for 'Timestep Intervals' were reduced to 2.0 to increase model stability. Following completion, data output from the ATM (atmosphere) files was imported in to Leonardo (information visualisation software) for analysis, and sense checking. The DesignBuilder 'Sun Path Tool' was used to evaluate MRT (mean radiant temperature) output to ensure model behaviour was in line with expectations. Data output from receptors was checked against output from the main ATM files and used to check model performance in the vertical plane (Z axis).

2.1.3 Suburban scale garden trees

A second area input file was created, based upon the original layout and incorporating 13 standardised trees. A deciduous, 6.5 m high 'Field Maple' (acer campestre) was selected for suitability in terms of size, crown/root spread, tolerance of variable soils, exposure and local conditions (Cardiff City Council, 2013). A local specimen was identified and surveyed using a calibrated surveying staff, ranging rods, tripod mounted Leica D5, laser distance meter, and Canon Eos 400D digital SLR camera. A modification of the photographic technique introduced by Peper and McPherson (1998), and later developed by Shinzato and Duarte (2012) was used to calculate the Leaf Area Index (LAI). This was converted into ten values for Leaf Area Density by re-scaling profiles established by Spangenberg, Shinzato et al. (2008). This data was used to define the modelled tree within the database. Two trees were allocated to each front garden, positioned 5m apart, at a distance of 5m from the front and rear facades. A row of trees, 5m apart was positioned along the northern boundary. All other variables remained consistent with those originally specified, and formed the basis of the second simulation of stage one.

2.1.4 ENVI-met output

Data output from both simulations was interrogated using Leonardo. Horizontal sections for Z=1, at hourly intervals throughout the simulation period, were evaluated and compared. Output for this level (1.5m above external ground level) was selected as representative of conditions likely to be experienced by a pedestrian within the model space. MRT was selected as an appropriate parameter for analysis. The process of temperature scale selection indicated that values for MRT were higher than expected. Guidance literature suggested over estimation of solar radiation, to some degree, was a recognised characteristic of the ENVI-met model. Future iterations could include the application of a solar correction factor. In this study, comparative analysis of relative values is adopted. The range and bandwidth of temperatures were adjusted to provide clarity of detail to areas and time-frames of particular interest. Standardised field maple trees, were also added to the DesignBuilder model. Using the 'Sun Path Tool', shadow analysis was completed to produce rendered images as a further basis for comparison. Vertical sections taken through the model at X=15 were also analysed to investigate temperature distribution in the vertical plane.

2.3 Impact on internal environment

To determine if, and to what extent, modification of the external micro-climate, by the planting of suburban scale trees impacts upon environmental conditions within the dwelling, it was necessary to link the ENVI-met outputs to a process of internal modelling. In a two-stage simulation study on a residential building in Cairo, reported by Famy, Sharples and Eltropolsi (2009) average data output from a series of receptors within an ENVI-met model is used to amend EnergyPlus weather files, in turn used for internal thermal simulation of a

single zone domestic dwelling. For the purposes of this study, a similar approach has been adopted and modified to investigate an individual ground floor living space within a multi-zone dwelling, and in the context of a northern European climate.

2.4 Amended Energyplus Weather Files

Drawings and specification for the dwelling were utilised to generate a three dimensional 'zoned' model in DesignBuilder. The lounge, a single, ground floor living space, is selected as the focus of study, and amended EnergyPlus weather files are created for each scenario and for use in simulating the environment within this zone. Output for level Z=1 from ENVI-met receptor R5, located immediately adjacent to external window W1, is used to modify climatic data held within the standard current weather file for Cardiff. Modified parameters include, air temperature, relative humidity, dew-point, short-wave direct solar radiation, short-wave diffuse solar radiation, and global horizontal radiation. Separate files are created for simulating internal conditions within the zone, and tagged to identify each scenario (ground cover with and without trees), zone, receptor, z value, and simulation date.

2.5 Natural Ventilation Simulations

For each scenario, the relevant amended weather file was loaded, and natural ventilation simulations completed. Graphical outputs and numerical data were exported as .wmf and .csv files for analysis and comparison, and the CFD capability within Designbuilder utilised to interrogate the output data. Slice and variable settings were adjusted to enable analysis of different parameters, with adjustment of value ranges and band widths as necessary to access detailed information and assist interpretation.

3 RESULTS

3.1 Stage One: Comparative analysis of ENVI-met Simulations (Figure 1.)

Results for the simulation based upon ground cover only are compared with those in which field maple trees were added. Micro-climatic conditions are evaluated and the impact of upon the external area is analysed by reference to differential MRT values as observed at time-frames throughout the simulation period and to corresponding solar shadow analysis.

3.2 Stage Two: Comparative Analysis of Natural Ventilation Simulations

The graphical output from DesignBuilder natural ventilation simulations for scenario AL3 (based upon weather conditions modified to include data output from the ENVI-met simulation for 'ground cover only') and AL6 (based upon external conditions modified by the addition of field maple trees.) is analysed to assess the effective air movement, in terms of in-flow and out-flow through individual openable windows..

3.2.1 Temperature Distribution (Figure 2.)

In accounting for radiant influences, analysis of internal temperature distribution concerns values for both operative and air temperatures. Interrogation of output for 15:00 hours on 21.06.2002 is taken as the basis for analysis. Plan view CFD slices taken at floor and cill level, and cross-sectional slices at W1 and W4, analysed using filled temperature contours, suggest the room in simulation AL6 is significantly cooler than in simulation AL3.

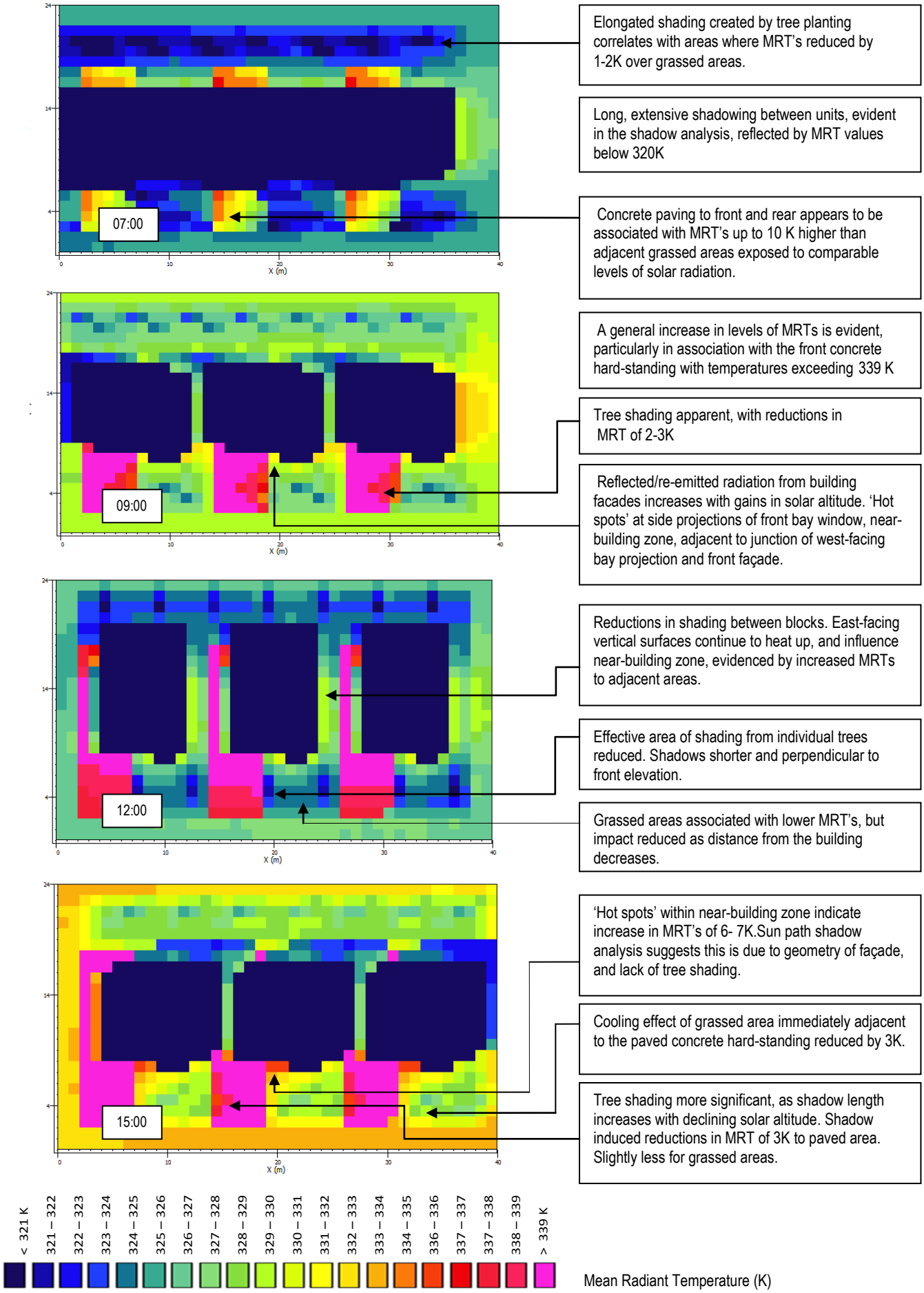

Figure 1. Analysis of ENVI-met Output for Simulation with Field Maple TreeS

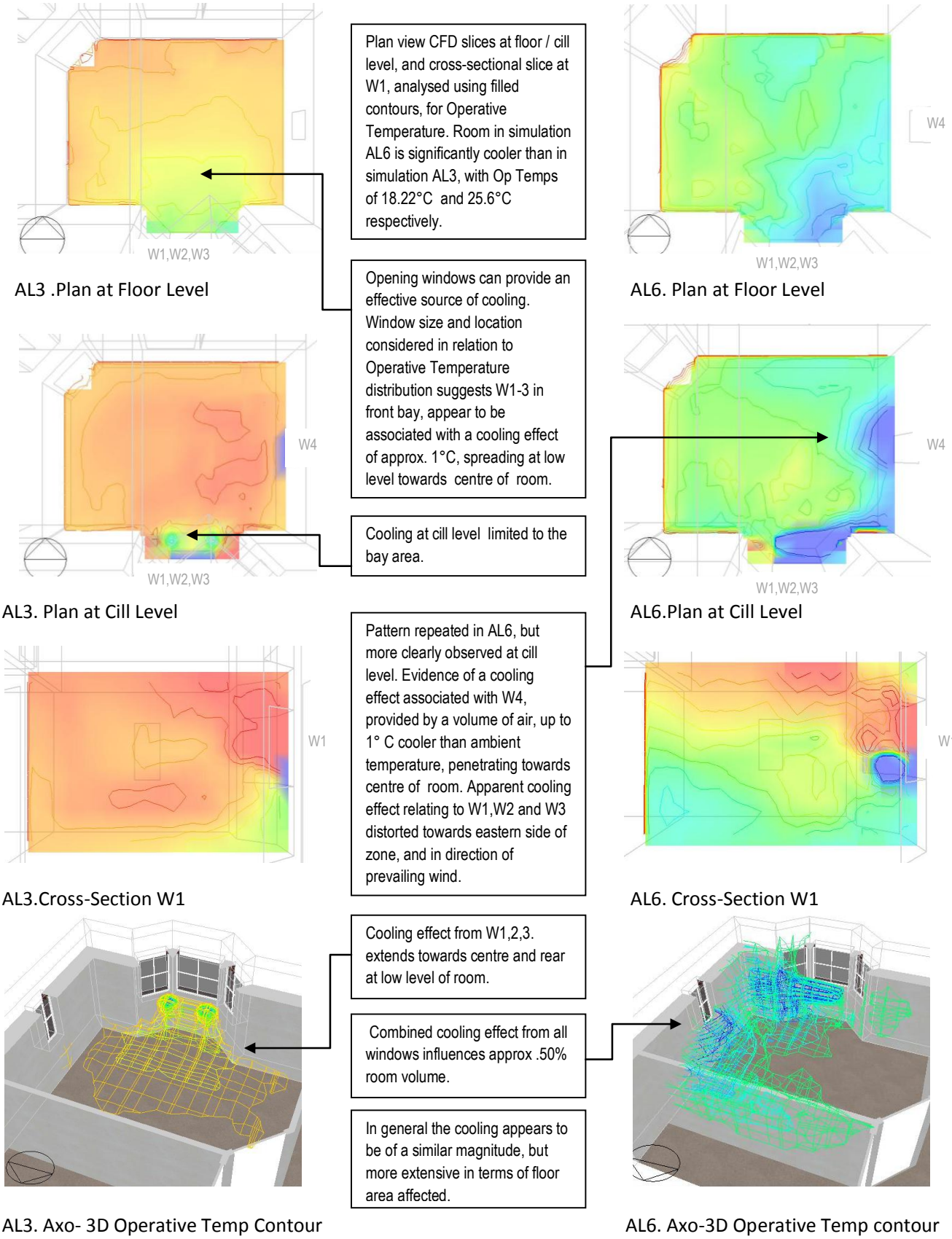

Figure 2. Comparative Analysis of Operative Temperature Distribution

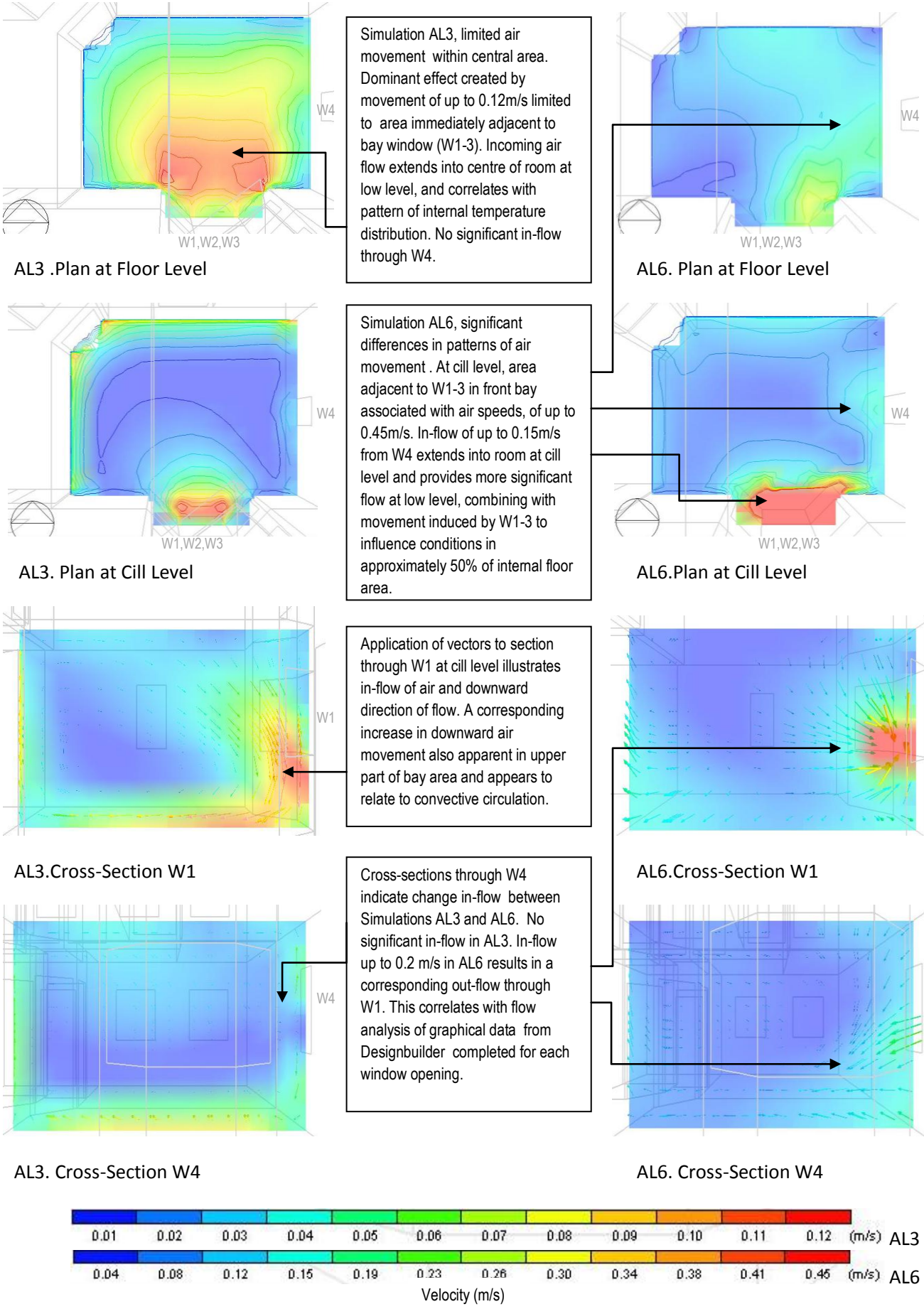

Figure 3. Comparative Analysis of Air Movement

Table 2: Comparison of Zone Temperature Distribution and Solar Gain for 15:00, 21st June

Variable	AL3 - Ground Cover Only	AL6 – Ground Cover With Trees	Reduction	Percentage Reduction (%)
Air Temperature °C	23.2	16.89	6.31	27.19
Operative Temperature °C	24.76	18.00	6.76	27.3
Outside Dry bulb Temperature °C	22.4	15.1	7.13	32.58
Solar Gain To External Windows kW	0.4516385	0.2046927	0.2469431	54.68

South-facing glazed openings in the building form suggest solar gain is likely to be a significant influence upon internal environmental conditions. Output data for solar gain to external windows is provided in Table 2 and illustrates that a reduction of 54.68% is achieved by the introduction of solar shading in the form of field maple trees. Analysis of axonometric images of the south-facing, front bay window showing 3-D contour mapping of mean radiant temperatures for each scenario also demonstrates the impact. At 15:00 hours the data for AL3 indicates significantly higher MRT values, at or above 26.5°C, compared to 19.5°C for scenario AL6. The beneficial effect of solar shading during the earlier part of the day is also illustrated by the relative distribution of values across the three windows. In simulation AL6, W1 (facing due south) and W3 (facing south-east) appear to be associated with lower MRT values.

3.2.2 Air Movement (Figure 3.)

The same series of plan views and sections were analysed for each scenario, using air velocity filled contours and vectors to interpret the speed and direction of air movement. It seems probable that increased levels of air movement and through ventilation evident in scenario AL6 are due to localised external air turbulence created by the interaction of prevailing winds and field maple trees.

4 CONCLUSIONS

Shading from the Field Maple trees appears to result in lower temperatures to both grassed and paved areas. This is more apparent in areas of concrete paving, where the thermal mass responds more quickly to insolation, and retains higher temperatures for longer. Tree shading appears to be most effective in reducing MRTs during the mid-morning and mid-afternoon, and could assist in alleviating the cumulative effect of heat gain throughout the day. The relative alignment and proximity of adjacent units could be significant in providing shadow and preventing higher temperatures between dwellings. Interaction of the building façade with cooling effects delivered by landscape elements suggests the supply of inflow air for natural ventilation and cooling, could be adversely influenced by hot spots. Specification of surface materials aiming to reduce this phenomenon could be advantageous within the near building zone, and wall construction adjacent to external ground level could also be significant in this respect. Vehicular access restricting hard surfaced areas to the shaded north side of the dwelling, could also be of benefit, and a consideration in terms of site layout.

The addition of the Field Maple trees reduces external air temperature by more than 30 percent and appears to have a positive impact upon internal comfort conditions. Shading reduces solar gain by more than 50 percent, and mid afternoon, mean operative temperatures are significantly reduced. Natural ventilation, limited by the size, and position of openable windows, is enhanced by the trees. Increased in-flow, contrary to wind direction, promotes through ventilation, and cooling influences a greater proportion of the living space. It seems probable this is due to localised external air turbulence created by the interaction of prevailing wind and field maple trees.

5 ACKNOWLEDGEMENTS

Thanks for assistance in supporting this study are extended to Mr Gareth Davies, *United Welsh*, and Mr Ian Standen, *Stride Treglown*. The PhD project is funded by Cardiff Metropolitan University, United Welsh, and the European Social Fund through the European Union's Convergence programme administered by the Welsh Government.

6 REFERENCES

BRE. 1990. Building Research Establishment Digest 350 Climate and Site Development Part 2:Influence Of Micro-climate.
BRUSE, M. 2010. *ENVI-met Help System* [Online]. Available: www.envi-met.com.
CARDIFF CITY COUNCIL. 2013. *Trees in Cardiff:A Householders Guide* [Online]. Available: http://www.cardiff.gov.uk/content.asp?nav=2,2870,3139,3942.
DESIGNBUILDER. *Building Simulation Software* [Online]. Available: http://www.designbuilder.co.uk/ Accessed 14 October 2012
DWIA. *Danish Wind Industry Association:Wind Energy Concepts* [Online]. Available: http://www.windpowerwiki.dk/index.php/Wind_energy_concepts Accessed 14 August 2013
EXETER UNIVERSITY. *Prometheus:The Use of Probabilistic Climate Change Data to Future-proof Design Decisions in the Building Sector* [Online]. Available: http://emps.exeter.ac.uk/research/energy-environment/cee/projects/prometheus/ Accessed 14 August 2013.
FAMY, M., SHARPLES, S. & ELTRAPOLSI, A. 2009. Dual stage simulations to study the microclimatic effects of trees on thermal comfort in a residential building Cairo Egypt. . *Eleventh International IBPSA Conference.* Glasgow, Scotland
GETHING, B. 2010. Design for Future Climate:Opportunities for adaptation in the built environment. London: Technology Strategy Board.
IPCC 2007. Intergovernmental Panel on Climate Change
Summary for Policymakers. In: Climate Change 2007: Mitigation. Contribution of Working Group III to the Fourth Assessment
Report of the Intergovernmental Panel on Climate Change. *In:* METZ, B., DAVIDSON, O. R., BOSCH, P. R., DAVE, R. & MEYER, L. A. (eds.). Cambridge
MET OFFICE. 2010. *UK Climate Projections 09: Briefing Report Summary* [Online]. Available: http://ukclimateprojections.defra.gov.uk/ Accessed 03 November 2011.
NATIONAL AERONAUTICS AND SPACE ADMINISTRATION. 1999. *Urban Climatology and Air Quality* [Online]. Available: http://www.ghcc.msfc.nasa.gov/urban/urban_heat_island.html Accessed 24 march 2013.
NHBC 2012. National House Building Council Overheating in new homes:A review of the evidence. IHS BRE Press on behalf of the NHBC Foundation
PEPER, P. J. & MCPHERSON.E.J 1998. Comparison of five methods for estimating leaf area index of open-grown trees. *Journal of Arboriculture* 24.
SHINZATO, P. & DUARTE, D. 2012. Microclimatic Effect of Vegetation for Different Leaf Area Index. *PLEA 2012 - 28th Conference, Opportunities, Limits & Needs Towards an environmentally responsible architecture.* Lima, Perú.
SPANGENBERG, J., SHINZATO, P., JOHANSSON, E. & DUARTE, D. 2008. Simulation of the influence of vegetation on microclimate and thermal comfort in the city of Sao Paulo. *Piracicaba,* 3**,** 1-19.
WINSON, A. Trees people and the built environment
Urban Trees Research Conference 13–14 April 2011 Edgbaston,Birmingham. Forestry Commission, Silvan House, 231 Corstorphine Road, Edinburgh EH12 7AT, 94-103.

IMPACT OF CLIMATE CHANGE ON INDOOR THERMAL COMFORT OF NATURALLY VENTILATED PUBLIC RESIDENTIAL BUILDINGS IN SINGAPORE

Nyuk Hien Wong[1], Erna Tan[*2], and Steve K. Jusuf[3]

1 National University of Singapore
Department of Building
4 Architecture Drive
Singapore

2 National University of Singapore
Department of Building
4 Architecture Drive, Singapore
**Corresponding author: erna.tan@nus.edu.sg*

3 National University of Singapore
Environmental Research Institute
5A Engineering Drive 1, Singapore

1 ABSTRACT

Public residential buildings in Singapore are designed as naturally ventilated. As climate changes, the indoor thermal comfort becomes critical as it depends greatly on the outdoor weather condition. The Predicted Mean Vote (PMV) model developed for Singapore (Givoni, et al., 2006) which depends on indoor air temperature and air speed is used to predict the indoor thermal comfort. The objectives are to determine the current level of PMV and the future level of PMV due to climate change, and to simulate whether proposed mitigation method on the building envelope can bring back the future PMV level back to current level.

The paper discusses the changes in the indoor air temperature, the indoor air movement and the subsequent thermal comfort due to the climate change by simulating two main typologies of typical public housing, i.e. point block (model Point) and slab block (model Slab), at three different heights of the building (level 2, mid-level and top-level), and under current (reference) and projected weather conditions (future). The 24-hour indoor air temperature is simulated in IES-VE, while the indoor air movement is simulated in CFD Fluent under four external wind scenarios, i.e. Northeast (NE) and Southwest monsoon (SW), ambient prevailing wind (Generic set) and a simulated wind in an estate (Local set).

The changes in indoor air temperature, indoor air speed and the compilation of PMV results are presented in the paper.

The simulation study shows that there is increase of the indoor air temperature, but no significant difference of the indoor air speed due to the climate change. The resulting PMV index shows that climate change causes longer duration of warm thermal

discomfort throughout the day. Implementing a mitigation method proposed from other study on cooling load e.g. a combination of lower solar absorption for wall and roof surface, lower u-value of wall and lower shading coefficient of glass, the thermal comfort level on the Top level in each model in the future can be brought back to current level.

2 KEYWORDS

Climate change, public residential buildings, natural ventilation, thermal comfort, Singapore

3 INTRODUCTION

Public residential buildings in Singapore are designed as naturally ventilated. As climate changes, the indoor thermal comfort becomes critical as it depends greatly on the outdoor weather condition. This paper discusses the impact of climate change on the indoor thermal comfort in the public residential buildings in Singapore. Predicted Mean Vote (PMV) index can be used to predict the mean value of the subjective ratings of a group of people in a given environment. Using the PMV model developed for Singapore which depends on indoor air temperature and air speed, the current level of PMV can be determined, and the future level of PMV due to climate change can be predicted. Mitigation methods on the building envelope to reduce the heat gain are proposed to bring back the future PMV level back to current level.

4 METHODOLOGY

4.1 The approach of study

The study is based on the PMV model developed for Singapore (Givoni, et al., 2006) as shown below.

$$PMV = 1.2*((0.4257*Temperature-12.04) + (0.26-1.231*Wind)) \quad (1)$$

The perception of the PMV value is shown in Table 1.

Table 1: PMV value

PMV value	Perception
3 to 2	Hot
2 to 1	Warm
1 to 0	Neutral
0 to -1	Neutral
-1 to -2	Cool
-2 to -3	Cold

The study found that higher wind speed allows a person to tolerate higher air temperatures and yet still achieve thermal comfort (Givoni, et al., 2006).

The indoor air temperature data were gathered from simulations using Integrated Environmental Solution <Virtual Environment> software. The models were simulated using the historical weather data of year 1990 as Reference Case and then simulated using the projected weather data (Future Case) to predict the increase of indoor air temperature from year 1990. Average indoor air temperature for each room in each

unit is used for the analysis. The indoor air speed data were from simulations using CFD Fluent. The models were simulated using historical wind data of year 1990 as Reference Case and projected wind data in the future due to climate change (Future Case), based on Northeast (NE) and Southwest monsoon (SW) for two scenarios, i.e. ambient/ prevailing wind condition (Generic set) and localized wind condition in an estate in Singapore (Local set). Average air speed at 1.20m above the floor for each room in each unit is used for the analysis.

The paper then discusses the changes in the indoor air temperature, the indoor air movement and the subsequent thermal comfort due to the climate change.

4.2 The models

There are two models of public residential buildings used in the study, i.e. model for point block (model Point) and model for slab block (model Slab). Model Point is a 40-storey high building with overall window-to-wall ratio (WWR) of 0.108 and east-west orientation WWR of 0.023, while model Slab is a 16-storey high building with overall WWR of 0.114 and east-west orientation WWR of 0.04. The east-west openings are mainly from the bathrooms. Model Point and model Slab are shown in Figure 1 and Figure 2 respectively.

The properties of the models are as follows: the thermal transmittance (u-value) of opaque wall is 2.6087 W/m^2K, the u-value of roof is 0.5363 W/m^2K, the u-value of ceiling is 2.4275 W/m^2K, the solar absorptance of wall and roof surface is 0.70, the u-value of fenestration is 6.9326 W/m^2K, and the shading coefficient of glass is 0.7016. Each window has 300mm wide horizontal shading.

Naming of the rooms in each unit of model Point and model Slab can be referred to Figure 1 and Figure 2 respectively. MBR is Master Bedroom, BR1 is Bedroom 1, BR2 is Bedroom 2, K is Kitchen, and LR is Living Room.

The models were simulated as naturally ventilated all the time. The analysis was conducted for low level (Level 2), middle level (Mid level) and top level (Top level) of the block.

4.3 The boundary conditions

For the indoor air temperature simulation, the Reference Case is based on historical weather data of 20-year observation. The projected weather data used shows an average increase of 1.3°C.

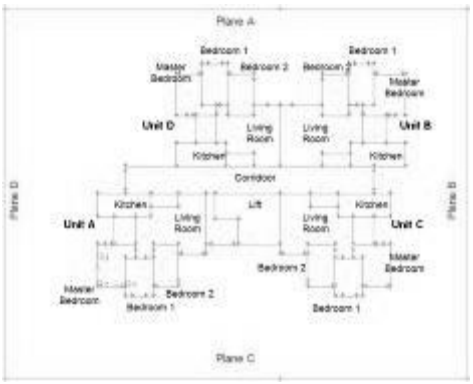

Figure 1: Model Point

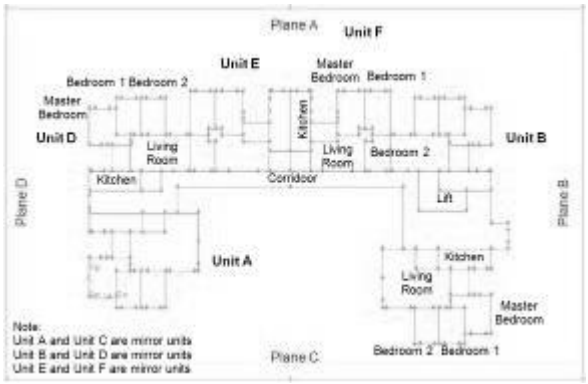

Figure 2: Model Slab

For the air movement simulation, the simulations were performed under turbulence k-ε realizable model with standard wall function. Uniform meshes were used with length of 0.10m. For the Level 2, the plane containing the ceiling of the second level was defined as symmetrical plane. Similarly, for the Top level, the plane containing the floor of the top level was defined as symmetrical plane. For the Mid level, both the planes containing the floor and ceiling of the mid-level were defined as symmetrical planes.

For the Generic set, the external environment is typically a residential unit length away from the block; while for the Kallang set, the external environment is 10m and 8m away from the model Point and model Slab respectively.

4.4 The mitigation method

From other study on cooling load using the same models and boundary conditions, a mitigation method was implemented in this study. The mitigation method (Mitigation Case) uses 1.03 W/m^2K for u-value of wall, 0.45 for shading coefficient of glass and 0.25 for solar absorptance of both wall and roof. This case uses the projected weather data.

5 RESULT ANALYSIS AND DISCUSSION

In average, the impact of climate change is predicted to increase the indoor air temperature of around 1.2°C for all levels in model Point. The mitigation method can reduce the indoor air temperature at Mid and Top levels back to the current level. It only can reduce 0.9°C for Level 2.

Table 2: Range of air temperature across the units for model Point in Reference Case

	Level 2		Mid level		Top level	
Unit	**Min (°C)**	**Max (°C)**	**Min (°C)**	**Max (°C)**	**Min (°C)**	**Max (°C)**
A	28.5	30.3	28.9	30.7	28.7	31.6
B	28.6	30.4	29.1	30.8	28.7	31.7
C	28.6	30.3	28.7	30.7	28.7	31.7
D	28.6	30.2	29.1	30.6	29.1	31.5

Table 3: Range of air temperature across the units for model Point in Future Case

	Level 2		Mid level		Top level	
Unit	**Min (°C)**	**Max (°C)**	**Min (°C)**	**Max (°C)**	**Min (°C)**	**Max (°C)**
A	29.8	31.5	30.1	31.9	29.8	32.8
B	29.8	31.6	30.3	32.0	30.3	32.9
C	29.8	31.5	30.2	31.9	29.8	32.8
D	29.8	31.4	30.2	31.8	30.3	32.7

Table 4: Range of air temperature across the units for model Point in Mitigation Case

	Level 2		Mid level		Top level	
Unit	**Min (°C)**	**Max (°C)**	**Min (°C)**	**Max (°C)**	**Min (°C)**	**Max (°C)**
A	29.5	30.6	29.6	30.6	29.4	30.8
B	29.6	30.6	29.7	30.7	29.5	30.9
C	29.6	30.6	29.6	30.6	29.4	30.8
D	29.6	30.6	29.6	30.6	29.5	30.9

In model Slab, the increase of indoor air temperature is predicted to be around 1.2°C, 0.9°C and 1.1°C for Level 2, Mid level and Top level respectively. The mitigation method can reduce the indoor air temperature at Mid and Top level back to the current level. It only can reduce 0.8°C for Level 2.

Table 5: Range of air temperature across the units for model Slab in Reference Case

	Level 2		Mid level		Top level	
Unit	**Min (°C)**	**Max (°C)**	**Min (°C)**	**Max (°C)**	**Min (°C)**	**Max (°C)**
A	28.5	30.4	28.4	30.8	28.5	32.2
B	28.5	30.4	28.4	30.8	28.5	32.2
C	28.5	30.4	28.5	30.9	28.5	32.2
D	28.5	30.1	28.9	30.5	28.7	31.5
E	28.7	30.2	29.1	30.7	29.2	31.6
F	28.7	30.3	29.1	30.7	29.2	31.7

Table 6: Range of air temperature across the units for model Slab in Future Case

	Level 2		Mid level		Top level	
Unit	**Min (°C)**	**Max (°C)**	**Min (°C)**	**Max (°C)**	**Min (°C)**	**Max (°C)**
A	29.7	31.6	30.0	31.9	29.7	33.3
B	29.8	31.4	30.2	31.8	29.8	32.8
C	29.7	31.7	29.4	30.3	29.6	33.3
D	29.8	31.4	30.1	31.7	30.2	32.7
E	29.9	31.5	30.3	31.9	30.4	32.8
F	29.9	31.5	30.3	31.9	30.4	32.8

Table 7: Range of air temperature across the units for model Slab in Mitigation Case

	Level 2		Mid level		Top level	
Unit	**Min (°C)**	**Max (°C)**	**Min (°C)**	**Max (°C)**	**Min (°C)**	**Max (°C)**
A	29.6	30.7	29.7	30.8	29.5	31.3
B	29.5	30.5	29.6	30.5	29.4	30.8
C	29.6	30.8	29.7	30.9	29.5	31.3
D	29.5	30.5	29.5	30.5	29.4	30.8
E	29.6	30.6	29.7	30.7	29.5	30.9
F	29.6	30.6	29.7	30.7	29.5	30.9

For Generic set, as the ambient wind speeds are fairly high, ranging from a magnitude of 2.52 m/s to 2.87 m/s, the indoor air speeds are correspondingly higher. The maximum air speeds for model Point and model Slab are 1.97 m/s (NE monsoon for Future Case in the kitchen of Unit B on the Mid level) and 2.90 m/s (SW monsoon for Future Case in the living room of Unit F on the Top level) respectively. Comparing between Reference Case and Future Case, no significant difference in indoor air speeds are observed among the units and all three levels for both models.

For Local set, the ambient wind speeds are lower, ranging from a magnitude of 0.07 m/s to 2.35 m/s, and the indoor air speeds are correspondingly lower. The maximum air speeds for model Point and model Slab are 4.21 m/s (SW monsoon for Future Case in the master

bedroom of Unit C on the Top level) and 1.44 m/s (NE monsoon for Future Case in the bedroom 2 of Unit C on the Top level) respectively. Comparing between Reference Case and Future Case, the difference in indoor air speeds for model Point are greater, although not very significantly. For model Slab, significant difference is observed during the SE monsoons, where an order of magnitude decrease in indoor air speed across all units is found in the Future Case. Furthermore, the Top level experiences a twofold increase in indoor air speeds for both NE and SW monsoons.

Figure 3 and Figure 4 show the compilation of all hourly PMV results for model Point based on Generic set and Local set wind conditions respectively for different cases. Figure 5 and Figure 6 show the compilation of all hourly PMV results for model Slab based on Generic set and Local set wind conditions respectively for different cases. The compilation is a 24-hour hourly PMV results for all units in the three different levels in a residential model.

In all figures, the left column shows the Reference Case, the middle column shows the Future Case, and the right column shows the Mitigation Case. The rows show different levels of the building and different wind directions. From top to bottom, in Figure 3 and Figure 4, the rows represent Level 2 with NE wind, Level 2 with SW wind, Mid level with NE wind, Mid level with SW wind, Top level with NE wind and Top level with SW wind. In Figure 5 and Figure 6, the rows represent Mid level with NE wind, Mid level with SW wind, Top level with NE wind and Top level with SW wind. In each row, the vertical axis shows the 24-hour of a day, while the horizontal axis shows the different rooms in all units in a building level. Green color represents neutral PMV of between -1 to 1, red color represents warm to hot PMV of between 1 to 3, and blue color represents cool to cold PMV of between -1 to -3.

Figure 3 shows that based on NE wind on Level 2, climate change increases the percentage of warm discomfort from 20% in Reference Case to 55% in Future Case, but by implementing Mitigation Case, the percentage of warm discomfort in the future can be reduced back to 33%.

Based on SW wind on Level 2, climate change increases the percentage of warm discomfort from 21% in Reference Case to 56% in Future Case, but by implementing Mitigation Case, the percentage of warm discomfort in the future can be reduced back to 37%.

Based on NE wind on Mid level, climate change increases the percentage of warm discomfort from 12% in Reference Case to 47% in Future Case, but by implementing Mitigation Case, the percentage of warm discomfort in the future can be reduced back to 30%.

Based on SW wind on Mid level, climate change increases the percentage of warm discomfort from 19% in Reference Case to 49% in Future Case, but by implementing Mitigation Case, the percentage of warm discomfort in the future can be reduced back to 28%.

Based on NE wind on Top level, climate change increases the percentage of warm discomfort from 23% in Reference Case to 51% in Future Case, but by implementing Mitigation Case, the percentage of warm discomfort in the future can be reduced back to 24%.

Based on SW wind on Top level, climate change increases the percentage of warm discomfort from 21% in Reference Case to 56% in Future Case, but by implementing Mitigation Case, the percentage of warm discomfort in the future can be reduced back to 24%.

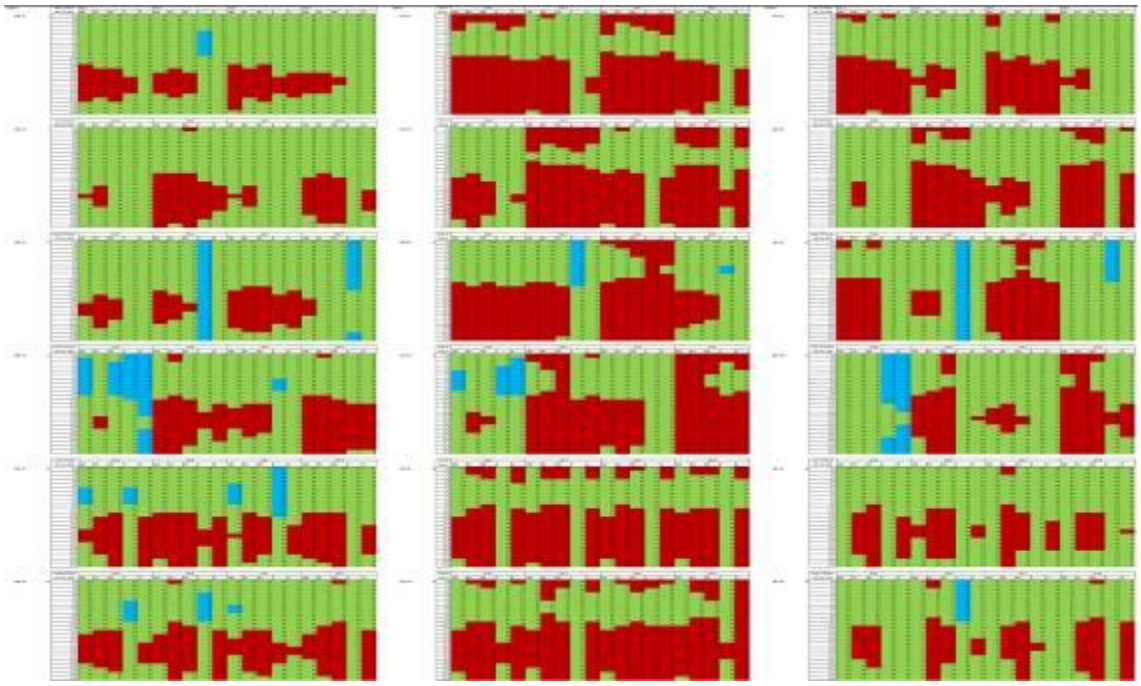

Figure 3: Compilation of PMV results for model Point Generic set: Reference Case (left), Future Case (middle), and Mitigation Case (right)

Figure 4 shows that based on NE wind on Mid level, climate change increases the percentage of warm discomfort from 44% in Reference Case to 75% in Future Case, but by implementing Mitigation Case, the percentage of warm discomfort in the future is reduced to 68%.

Based on SW wind on Mid level, climate change increases the percentage of warm discomfort from 33% in Reference Case to 84% in Future Case, but by implementing Mitigation Case, the percentage of warm discomfort in the future is reduced to 72%.

Based on NE wind on Top level, climate change increases the percentage of warm discomfort from 14% in Reference Case to 25% in Future Case, but by implementing Mitigation Case, the percentage of warm discomfort in the future can be reduced back to 6%.

Based on SW wind on Top level, climate change increases the percentage of warm discomfort from 12% in Reference Case to 31% in Future Case, but by implementing Mitigation Case, the percentage of warm discomfort in the future can be reduced back to 10%.

Figure 5 shows that based on NE wind on Level 2, climate change increases the percentage of warm discomfort from 7% in Reference Case to 26% in Future Case, but by implementing Mitigation Case, the percentage of warm discomfort in the future can be reduced back to 13%.

Based on SW wind on Level 2, climate change increases the percentage of warm discomfort from 8% in Reference Case to 31% in Future Case, but by implementing Mitigation Case, the percentage of warm discomfort in the future can be reduced back to 14%.

Based on NE wind on Mid level, climate change increases the percentage of warm discomfort from 12% in Reference Case to 8% in Future Case, but by implementing Mitigation Case, the percentage of warm discomfort in the future can be reduced back to 11%.

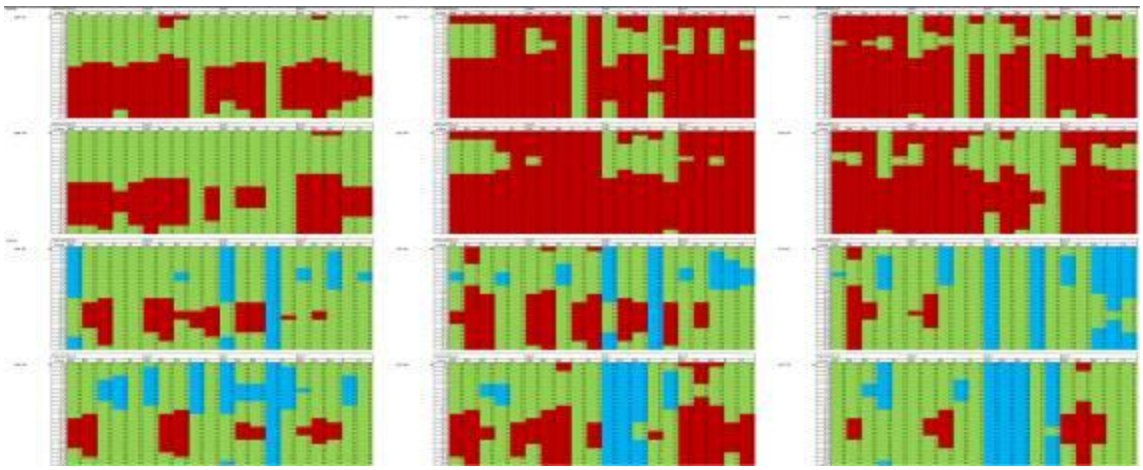

Figure 4: Compilation of PMV results for model Point Local set: Reference Case (left), Future Case (middle), and Mitigation Case (right)

Based on SW wind on Mid level, climate change increases the percentage of warm discomfort from 10% in Reference Case to 28% in Future Case, but by implementing Mitigation Case, the percentage of warm discomfort in the future can be reduced back to 14%.

Based on NE wind on Top level, climate change increases the percentage of warm discomfort from 3% in Reference Case to 9% in Future Case, but by implementing Mitigation Case, the percentage of warm discomfort in the future can be reduced back to 0%.

Based on SW wind on Top level, climate change increases the percentage of warm discomfort from 1% in Reference Case to 13% in Future Case, but by implementing Mitigation Case, the percentage of warm discomfort in the future can be reduced back to 0.3%.

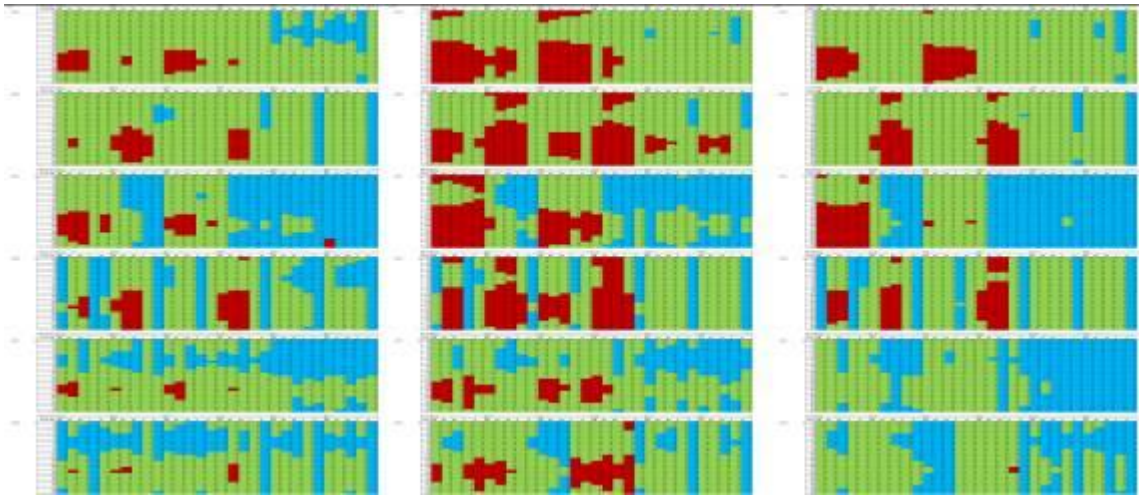

Figure 5: Compilation of PMV results for model Slab Generic set: Reference Case (left), Future Case (middle), and Mitigation Case (right)

Figure 6 shows that based on NE wind on Mid level, climate change increases the percentage of warm discomfort from 56% in Reference Case to 95% in Future Case, but by implementing Mitigation Case, the percentage of warm discomfort in the future is still at 92%.

Based on SW wind on Mid level, climate change increases the percentage of warm discomfort from 36% in Reference Case to 99% in Future Case, but by implementing Mitigation Case, the percentage of warm discomfort in the future is still at almost 100%.

Based on NE wind on Top level, climate change increases the percentage of warm discomfort from 50% in Reference Case to 70% in Future Case, but by implementing Mitigation Case, the percentage of warm discomfort in the future can be reduced back to 34%.

Based on SW wind on Top level, climate change increases the percentage of warm discomfort from 57% in Reference Case to 71% in Future Case, but by implementing Mitigation Case, the percentage of warm discomfort in the future can be reduced back to 36%.

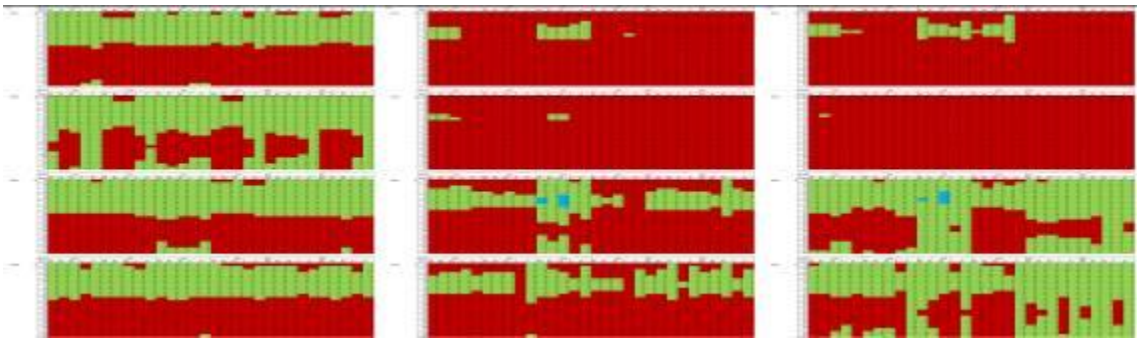

Figure 6: Compilation of PMV results for model Slab Local set: Reference Case (left), Future Case (middle), and Mitigation Case (right)

In overall, the thermal comfort becomes warmer more frequently for all the units in a particular floor in Future Case due to climate change, but with implementing mitigation methods in Mitigation Case, the thermal comfort condition in the future, except for Local set at Mid level, can be brought back to current level.

The thermal comfort condition on the Top level is better than the Mid level as the mitigation method which provides insulation works on both roof and wall for the Top level, compared with only on wall for the Mid level.

6 CONCLUSION

Using PMV model for Singapore, the impact of climate change on the indoor thermal comfort of naturally ventilated public residential buildings in Singapore has been analysed. The main variables are the indoor air temperature and indoor air movement. Using historical weather data as Reference Case and projected weather data and wind condition as Future Case, the changes in the indoor thermal comfort have been analysed. Mitigation Case analysis which combines a lower solar absorption for wall and roof surface, lower u-value of wall and lower shading coefficient of glass has also been done to see whether the mitigation method can improve the indoor thermal comfort on the Top level in the future back to the current level.

Air temperature simulations were conducted. The results show that there is increase in indoor air temperature due to climate change. Due to the insulation provided by the mitigation method, the Mitigation Case reduces the maximum air temperature in the Future Case.

Air movement or wind speed simulations were conducted based on two wind conditions, i.e. prevailing wind condition (Generic set) and localized wind condition (Local set) as a representative of residential area. The unit arrangements of each model are found to significantly affect the average indoor air speed, and cross ventilation is found to have increased the indoor air speed.

The calculation of PMV shows the there is increase of percentage dissatisfaction towards warm or hot sensations due to climate change. Implementing the Mitigation Case can only

help to bring down the discomfort level on the Top level back to the current level. The mitigation method is less effective on the Mid level due to the lower wind speed and the less insulation effect. Further study can be carried out to assess if mitigation methods such as introducing a “void deck” or sky garden at the Mid level will improve ventilation for Mid level units.

From the study, besides improving the insulation of the opaque walls to reduce solar heat gain, it is recommended to optimize cross ventilation as it helps to increase wind speed through the units and improve thermal comfort. It is to be reminded that all the simulations were conducted based on ideal situation on which all windows are fully opened during natural ventilation period, and did not consider occupants’ behavior to close the windows.

7 ACKNOWLEDGEMENTS

The study is part of the research project “Study on Long Term Impact due to Climate Change: Impact on Urban Temperature Profile and Energy Consumption of Buildings” funded by National Environment Agency (NEA) and coordinated by Institute of High Performance Computing (IHPC). The indoor air movement simulations were conducted by Alex Tan.

8 REFERENCES

Givoni, B., Khedari, J., Wong, N. H. & Noguchi, M., 2006. Thermal sensation responses in hot, humid climates: effects of humidity. *Building Research and Information,* 34(Special on Indoor Environmental Quality), p. 5.

POTENTIAL OF NIGHT VENTILATIVE COOLING STRATEGIES IN OFFICE BUILDINGS IN SPAIN. COMFORT ANALYSIS

Olatz Irulegi[*1], Álvaro Ruiz-Pardo[2], Antonio Serra[1], and José M. Salmerón[3]

1
University of the Basque Country
Plaza Oñate, 2
20018, San Sebastian (Spain)

2
University of Cadiz
C/ Chile, 1
11002, Cádiz Spain

3
University of Seville
Camino de los descubrimientos S/N
41092,Seville, Spain

**Corresponding author: o.irulegi@ehu.es*

ABSTRACT

Night ventilation has been applied successfully to many passively-cooled or low-energy office buildings. This paper analyses the thermal comfort achievable according to European standard EN 15251:2007 by applying this strategy in office buildings in Spain. Specifically, the comfort level is evaluated using the Degree Hours (DH) criteria and the maximum indoor temperature. For the DH criteria, four base temperatures are considered: 25ºC and the three Categories for acceptable ranges of operative temperature around the adaptive comfort temperature established in the standard for free running buildings. Considering the interest of architects and engineers in the prediction of optimal comfort condition as a function of building typology (8 typologies), glazing ratio (30% and 60%) and climate (12 different Climate Zones), a total of 192 different study cases are obtained where an optimal air change per hour (ACH) that ranges from 1 to 50 ACH is defined. As an example of the obtained results, in Almeria, a city in the south of Spain characterized by hot summers with average daily temperature of 26ºC, in the case of a Linear Typology with 30% glazed façade, the best comfort result is achieved by a night ventilation flow of 20 ACH for Limit of Category II. Further increases in night ventilation flow produces marginal improves. In this case, the Mean Peak Temperature is reduced in 0.5ºC. Furthermore, in Soria, a city in the north of Spain characterized by mild summers with average daily temperature of 20ºC, in the case of a Linear Typology with 30% glazed façade, the best comfort result is achieved by a night ventilation flow of 6 ACH for Limit of Category II In this case Peak Temperature is reduced 0.6ºC. The research shows that passive night ventilation should be considered as an effective strategy to reduce cooling demand in buildings with high daily internal gains (i.e. offices buildings), improving comfort conditions and flattening peak temperatures.

KEYWORDS

Night Ventilation, Offices, Comfort, Building Typology, Climate Zones

1 INTRODUCTION

The use of air conditioning in the building sector is increasing rapidly. In almost the 46% of the houses in the Organisation for Economic Co-operation and Development (OECD) it has been rising by 7% each year. It is reasonable to think that in the case of office buildings this figure is even higher. Since 1990 the energy consumption in office buildings has increased by 300%, becoming, in 2008, the responsible for the 47.84% of energy consumption in the service sector (6% of the total energy consumption in Spain) (Segurado de Arriba, 2008).

Furthermore, the energy impact of this sector is expected to increase considering the proliferation of squanderer glass buildings in the last decade, since concepts related to modernity, technology and transparency are playing a predominant role in their design (Coyne

Intensive use of air conditioning is the result of many processes (Santamouris, 2007), in particular:

- adoption of an universal style of buildings that does not consider climatic issues and results in increasing energy demands during the summer period;
- increase of ambient temperature, particularly in the urban environment, owing the heat island phenomenon, which exacerbates cooling demand in buildings;
- changes in comfort culture, consumer behaviour and expectations;
- improving of living standards and increased affluence of consumers;
- increase in buildings' internal loads.

The environmental impact associated to the intensive use of air conditioning in terms of CO_2 emissions will have achieved the value of 18.1 Mt in Europe by 2020, far cry from the figure 0.516 Mt registered in 1990 (Adnot, 1999). This disproportioned increase in CO_2 levels does not reflect the international compromise adopted with the Kyoto protocol, where a reduction of 5% in CO_2 and CFC emissions, habitual in air condition systems, was established for the period 2008-2012,

In Spain, the panorama is particularly alarming. In 2007 the United Nations presented a report before the Bali Climate Change Conference (2007) exposing that Spain was at the head unfulfilling the Kyoto Protocol considering that the CO_2 emissions increased to 53% between 1990-2005, when a limit of 15% was defined. The level of CO_2 associated to air conditioning in Spain was 1.12Mt in 1996 and it is expected to increase to 7.13Mt by 2020 (Adnot, 1999).

Because of all these reasons, counteracting the environmental and energy impact of air conditioning is one of the main objectives in the near future. Passive cooling is presented as an effective strategy in order to achieve the Kyoto Agreement, reducing the energy demand of buildings and providing an adequate thermal comfort (Santamouris, 2004).

2 OBJECTIVE

This work continues the research line started by the project "Energy Efficiency of Ventilated Active Façades applied to office buildings in Spain". The project was financed by the Spanish National Plan for Research and finished on 2009. Its main objective was to determine the energy saving achievable (reduction of cooling demand) by the use of a Ventilated Active Façade - VAF. For the analysis 192 study cases were considered. The study cases represented the 8 most common typologies of offices in Spain, the typical glazed surface in façades (30% and 60%) and 12 Spanish climate zones (Table 1). The software used in the study was LIDER.

The simulation results demonstrated that the achievable energy saving is very dependent on the building typology, the glazed surface and the climate zone. Furthermore, the work stated that using the VAF technology the cooling demand of office buildings could be reduced averagely into a 20%, and even up to a 40% in many cases.

Table 1: Denomination of the 8 most common typologies of office buildings in Spain. The number in the nomenclature of each building represents the percentage of glazed facade (30% and 60%)

U Typology (U30 / U60)	**Tower with communication core in façade** (TF30 / TF60)	**Tower with central communication core** (TC30 / TC60)	**Ring typology** (O30 / O60)
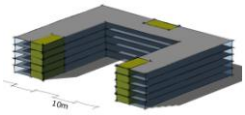	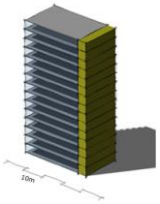	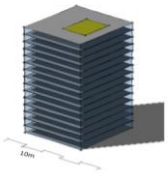	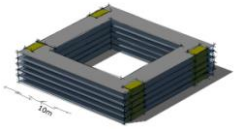
L-Typology (L30 / L60)	**Linear Typology** (LI30 / LI60)	**Disperse Typology** (D30 / D60)	**Compact typology** (CP30 / CP60)
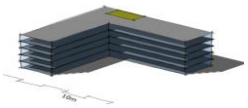	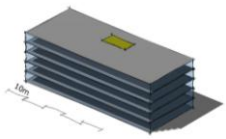	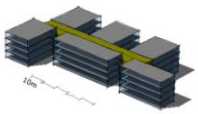	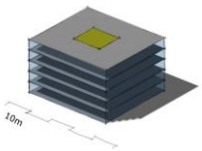

The present work evaluates a different strategy to reduce the cooling demand of office buildings in Spain. Night ventilation is particularly suited to office buildings because these are usually not occupied during the night.

Many studies evaluate the benefits of night ventilation (Kolokotroni 2006, Kolokotroni 2010, Santamouris 2007). Some researches state that the peak temperature inside office buildings can be reduced between 0ºC and 2.6ºC for cross ventilated buildings and between 0.2ºC and 3.5ºC in single-sided ventilation buildings (Geros, 1999). Other studies show that for day and night ventilation of 4 ACH, internal temperature is reduced about 1ºC and 1.5ºC in UK (Kolokotroni, 1998).

Based on it, this article studies the impact of applying passive night ventilation in the Spanish climate and the thermal comfort achievable, according to European standard EN 15251:2007.

Specifically, the comfort level is evaluated using the Degree Hours (DH) criteria and the maximum indoor temperature. For the DH criteria, four base temperatures are considered: 25ºC and the three categories for acceptable ranges of operative temperature around the adaptive comfort temperature established in the standard for free running buildings.

The Category III corresponds to a moderate expectation of the occupants, the Category II corresponds to a mid-expectation, the Category I is related to a high level of expectation.

Considering the significant influence of the air flow (air changes per hour - ACH) in the efficacy of night ventilation, a wide range of them is considered. The air changes per hour range from 1 to 50, while the operating period goes from 02:00 to 08:00 hours (coolest outdoor temperature).

The results of the research show, for every typology, glazed surface in façade and climate zone, an optimal night ventilation pattern to achieve the highest level of comfort.

As an example of the results, in Almeria, a city in the south of Spain characterized by hot summers with average daily temperature of 26ºC, in the case of a Linear Typology with 30% glazed façade, the best comfort result is achieved by a night ventilation period of 6 hours, from 02 to 08 solar time, and 20 ACH. Further increases in air ventilation flow produces marginal improves in the comfort variables.

In comparison with the Base Case (1 ACH) the DH are reduced from near to 90% for the case of Category III to 68% for Category I, that means a very significant improve of the comfort level. The peak temperatures are reduced near to 2ºC.

The research show that passive night ventilation should be considered as an effective strategy to reduce cooling demand in buildings with high daily internal gains (i.e. offices buildings), improving comfort conditions and flattening peak temperatures.

3 SIMULATIONS

In order to analyse the influence of night ventilation on the comfort of office building occupants in Spanish climates, a sample of 16 buildings representing the most common building typologies in Spain (8 different typologies and 30% and 60% of glazed surface in façade) is considered. The buildings are simulated in a free-floating mode in the 12 climate zones defined in the Spanish Technical Code -CTE. The results of the simulations cover a wide range of possible combinations providing very useful information to architects and designers.

The simulation program used is LIDER (Ministerio de Vivienda de España 2009), the calculation engine of the Spanish national tool used for regulation purposes in Spain performing dynamic and multi-zone simulations of buildings.

The Table 2 shows the 12 different Spanish Climate Zones and their representative cities considered for this study. The denomination of the Climate Zone is given by a letter and a number. The letter represents the winter climate severity, where "A" is the less severe zone, thus, the case with less heating demand. The letter "E" is the climate with most severe winter. The number represents the summer climate severity, where the number "1" is the climate with less cooling demand and the number "4" is the climate with highest cooling demand.

Table 2: Climate Zones in CTE and representative cities

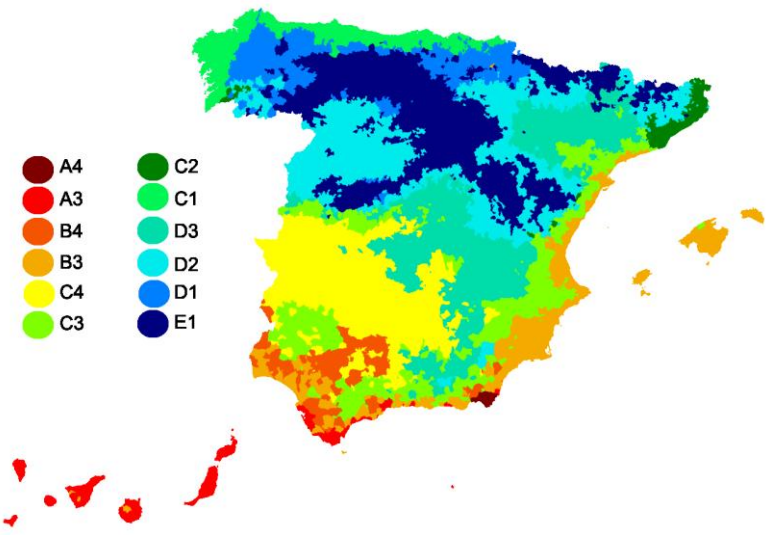

Climate zone	Representative City
A4	Almeria
C4	Badajoz
C2	Gerona
C3	Granada
B4	Huelva
D3	Madrid
A3	Malaga
C1	Pontevedra
E1	Soria
D2	Valladolid
B3	Valencia
D1	Vitoria

3.1 Definition of buildings

The main constructive characteristics of the 16 study cases are described in the Table 3. The denomination and model of each case is depicted in Table 1.

Table 3. Main construction and geometrical characteristics of the 16 buildings

Building nomenclature	Floors	Construction surface	Total Façade Surface	Façade surface facing South	Total glazed surface	Glazed surface facing South	Shape Factor: S/V
CP30	B+4	6480m^2	3240 m^2	810 m^2	972 m^2	243 m^2	0.2 m^{-1}
CP60	B+4	6480m^2	3240 m^2	810 m^2	1944 m^2	486 m^2	0.2 m^{-1}
DS30	B+3	12240m^2	8262 m^2	1620 m^2	2478,6 m^2	486 m^2	0.242 m^{-1}
DS60	B+3	12240m^2	8262 m^2	1620 m^2	4957,2 m^2	972 m^2	0.242 m^{-1}
L30	B+4	4680 m^2	4050 m^2	945 m^2	1215 m^2	283,5 m^2	0.281 m^{-1}
L60	B+4	4680 m^2	4050 m^2	945 m^2	2430 m^2	567 m^2	0.281 m^{-1}
LI30	B+4	7200 m^2	3780 m^2	1350 m^2	1134 m^2	405 m^2	0.205 m^{-1}
LI60	B+4	7200 m^2	3780 m^2	1350 m^2	2268 m^2	810 m^2	0.205 m^{-1}
O30	B+4	12960 m^2	9720 m^2	1620 m^2	2916 m^2	486 m^2	0.200 m^{-1}
O60	B+4	12960 m^2	9720 m^2	1620 m^2	5832 m^2	972 m^2	0.200 m^{-1}
TC30	B+14	18900 m^2	9720 m^2	2835 m^2	2916 m^2	850,5 m^2	0.145 m^{-1}
TC60	B+14	18900 m^2	9720 m^2	2835 m^2	5832 m^2	1701 m^2	0.145 m^{-1}
TF30	B+14	9720 m^2	7290 m^2	2430 m^2	2187m^2	729 m^2	0.196 m^{-1}
TF60	B+14	9720 m^2	7290 m^2	2430 m^2	4374 m^2	1458 m^2	0.196 m^{-1}
U30	B+4	7920 m^2	6480 m^2	1350 m^2	1944 m^2	405 m^2	0.270 m^{-1}
U60	B+4	7920 m^2	6480 m^2	1350 m^2	3888 m^2	810 m^2	0.270 m^{-1}

Following this geometrical parameters, all the buildings are modelled using the software LIDER. The configuration of the façade in every case is adapted to the severity of the climate zone, to comply with the minimum requirements of energy demand established in CTE. The impact produced by the variation of the thermal inertia, is not studied in this work.

3.2 Description of simulations

The method followed for simulating all the buildings in every climate zone is described below:

a) Firstly, a Base Building is defined in order to have a comparison pattern that permits to evaluate the benefits of applying night ventilation. The Base Building consists of a building with 1 ACH, a daily constant value. 1 ACH is the typical ventilation flow for office buildings according to the Spanish Regulation about Salubrity – HS3. There are 16 Base Buildings in each of the 12 climate zones, this is, 192 Base Buildings.

b) For every building, simulations with different night ventilation flows are then conducted, considering the following ACH: 2, 4, 6, 8, 10, 13, 16, 20, 25, 30, 40, 50. Night Ventilation is applied during 6 hours (02:00 a 08:00), coinciding with the lowest exterior temperatures.

c) The occupancy schedule is set from 07:00 to 15:00 and from 17:00 to 20:00 during the week and from 07:00 to 15:00 on Saturdays. Internal loads in this period are:

-People: 10 W/m^2
-Lighting: 7.5 W/m^2
-Appliances: 7.5 W/m^2

The results obtained are an hourly register of air temperature for every space of the building and for the whole year. For evaluating the benefits obtained by applying night ventilation in every case, the following variables are considered:

a) Weighing factor, (wf). It is used the definition given in the Standard EN 15251:2007, Annex F, Method B "Degree hours criteria". With it, long term thermal comfort conditions are evaluated. Wf consists of an *hourly cumulative calculation of the difference between the operative temperature registered for one space and the acceptable maximum temperature*. In the A.2 Section of the former Standard there are defined three different Categories where a specific acceptable limit of operative temperature is as well determined. Category III (moderate expectation of the occupants), Category II (normal expectation of the occupants), Category I (high expectation of the occupants). These limits are calculated using an adaptive comfort method, so that do not correspond to a fix limit, but change with the time and the exterior temperature of every location. In this study, apart from the given three temperature limits, the limit of 25ºC is as well considered, that is the usual upper value for non-adaptive thermal comfort analysis.

b) Maximum interior temperature. This variable permits to evaluate, in a quite direct way, the effect of night ventilation since it is expected that interior temperature will reduce when ventilation flow increases. However, the inconvenience is that, for every space in a building, a different maximum temperature is registered. For this reason, the average maximum temperature for every room is calculated and then a weighted average value for the whole building is obtained, where the weight of every room is proportional to its surface area.

4 RESULTS

The results obtained for each variable are shown separately in the following two sections. In the first one it is studied the influence of night ventilation in the Degree Hours, while in the other one it is shown the effect on the interior maximum air temperature.

4.1 Weighing factor

As mentioned before, due to the wide range of building typologies and climate zones considered in this study, for the evaluation of the variation of the weighing factor, the "degree hour variation" (∇wf) will be used.

This variable is defined as the ratio between the weighing factor of the building with different ventilation flows (case_study) and the Base Building (1ACH).

$$\nabla wf = \frac{wf_{case\_study}}{wf_{base\_building}} \quad (1)$$

As an example of it, in the following graphs (Figure 1) the results for *Almeria (Climate Zone A4)* are represented. Almeria is a city in the South of Spain characterized by hot summers with average daily temperature of 26ºC. In the graphs, the former defined Categories III, II and I and the limit of 25ºC are studied. Each line represents the deviation of ∇wf for every building respect to its Base Building as the ventilation flow increases.
When the variation of ∇wf is *zero*, it means that the interior temperature is within the comfort boundaries.

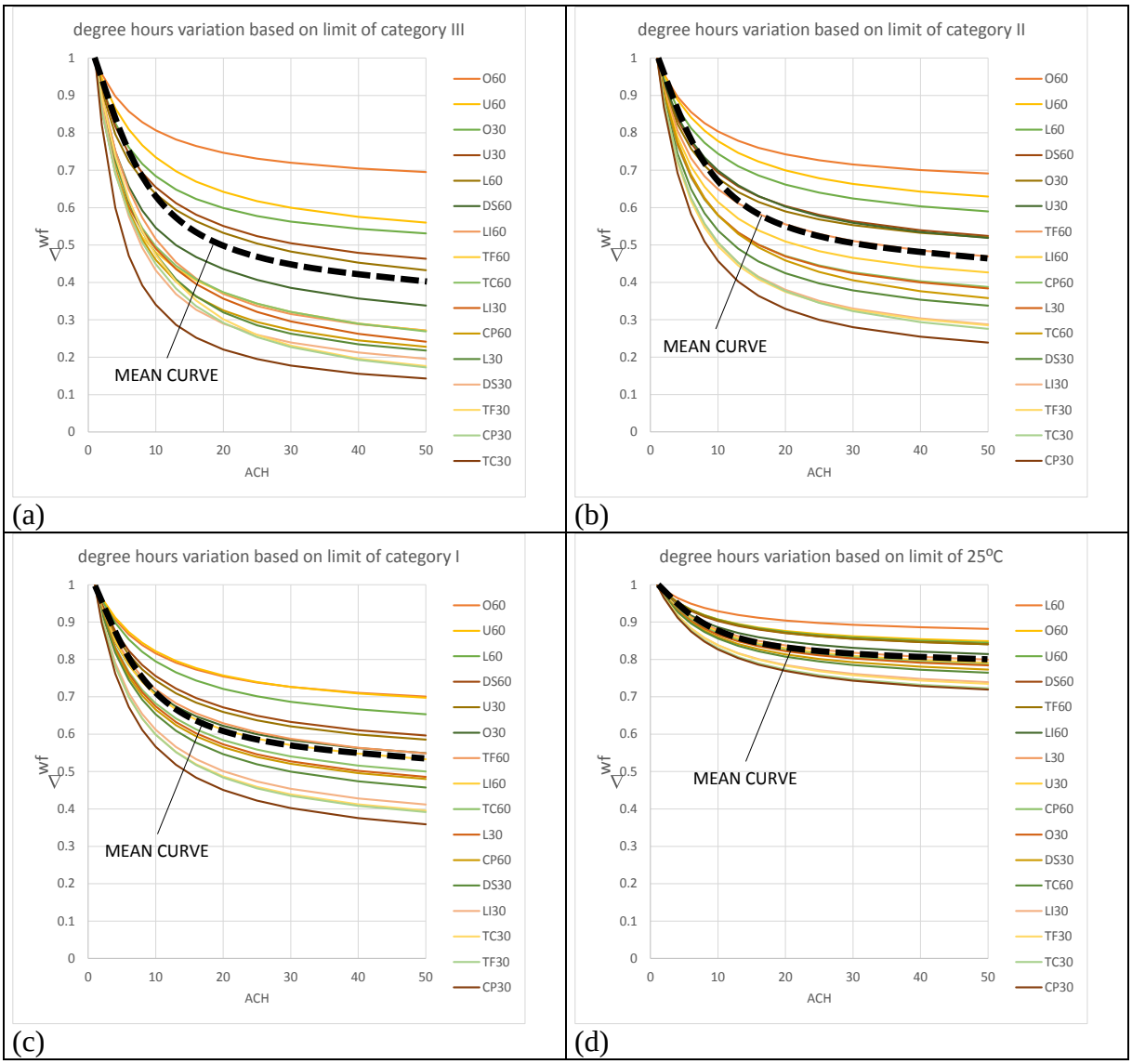

Figure 1. Degree Hours based on the limit of Category I (c), Category II (b), Category III (a) and limit of 25ºC (d) in Climate Zone A4

It has to be highlighted that the influence of the building typology on ∇wf is very significant, but a detailed study of it exceeds the scope of the present article.

In the Figure 2 the values for 10, 20 and 50 ACH of the "mean curve" for every climate zones are shown.

a)Mean values of ∇wf for Limit of Category III

b) Mean values of ∇wf for Limit of Category II

c) Mean values of ∇wf for Limit of Category I

d) Mean values of ∇wf for Limit of 25ºC

Figure 2. Degree Hours variation respect to Base Building (∇wf), for all the climatic zones

It is observed that in warm climate zones, the ∇wf value is higher than in cool climates, that indicates that the reduction of the DH is lower in warmer climates than in the cooler ones. The reason for it is that the night-time temperature in cool climates is usually lower and the daytime temperature is not very distanced from the comfort limit.

In addition, for the ∇wf variation based on the limits of Category II and I, (Figure 2, b, c) the reduction of DH is similar in the climate zones with a climatic severity for summer of 4, 3 and 2, resulting remarkable that the same occurs for all the climates zones with limit of 25ºC (Figure 2, d).

The results show that:

- Considering the comfort limits established for Category II and I, the proportional improvement of the comfort is almost the same in the warm and moderate climates. In the coolest climates, it is possible to achieve the comfort in a greater number of hours.

- If the limit is 25ºC, for all the climate zones, the interior temperatures are located in a distance from the comfort that is proportionally very similar in all the cases.

The variables considered in this study measure the relative variation of the DH. Although the variation is proportionally similar in warm and cool climates, the absolute value is different, resulting lower in the coolest ones. Relating this fact with the values of the variation shown for the limits of Category II and I, thanks to night ventilation in the coolest climates it is possible to stay within comfort limits in almost the whole day.

4.2 Effect on maximum temperature

The Table 4 shows the influence of night ventilation in the maximum indoor temperature for every building, climate zone and ventilation flow respect to its Base Building (1 ACH). The temperature difference is represented by ∇Tmax. In the Table, for every climate zone the "coldest case" corresponds to the building with the lowest maximum temperature. "the hottest case" to the building with the higher maximum temperature and the "Mean" corresponds to the average value for all the buildings.

Table 4: Variation of the peak temperature (∇Tmax) for the coldest, hottest and mean building, for every climate zone and ventilation flow. The temperature difference is respect to its Base Building (1 ACH)

Climate Zone		1 ACH			10 ACH			20 ACH			50 ACH		
		Coldest case	Mean	Hottest case	Coldest case	Mean	Hottest case	Coldest case	Mean	Hottest case	Coldest case	Mean	Hottest case
A3	Tmax	28.6	30.2	31.3	28.5	29.1	30.9	28.4	29.0	30.7	28.3	28.9	30.6
	∇Tmax				-0.1	-0.3	-0.4	-0.2	-0.4	-0.6	-0.3	-0.5	-0.8
A4	Tmax	29.3	31.1	31.9	29.2	29.8	31.5	29.1	29.7	31.4	29.0	29.5	31.2
	∇Tmax				-0.1	-0.3	-0.4	-0.2	-0.4	-0.6	-0.3	-0.5	-0.8
B3	Tmax	27.9	28.6	30.5	27.7	28.3	30.0	27.6	28.2	29.9	27.5	28.1	29.7
	∇Tmax				-0.2	-0.3	-0.5	-0.2	-0.4	-0.6	-0.3	-0.5	-0.8
B4	Tmax	29.3	30.0	32.1	29.1	29.7	31.6	29.0	29.6	31.4	28.9	29.5	31.2
	∇Tmax				-0.2	-0.3	-0.5	-0.2	-0.4	-0.7	-0.3	-0.6	-0.9
C1	Tmax	24.3	25.1	27.2	24.3	25.0	26.7	24.3	24.9	26.6	24.3	24.9	26.4
	∇Tmax				0.0	-0.1	-0.5	0.0	-0.2	-0.8	0.0	-0.2	-1.0
C2	Tmax	26.4	27.2	29.0	26.4	26.8	28.4	26.2	26.7	28.2	26.0	26.6	28.1
	∇Tmax				0.0	-0.4	-0.6	0.0	-0.5	-0.8	0.0	-0.6	-1.0
C3	Tmax	28.7	29.6	31.8	28.4	29.1	31.0	28.2	28.9	30.8	27.9	28.7	30.5
	∇Tmax				-0.3	-0.5	-0.8	-0.4	-0.7	-1.1	-0.6	-1.0	-1.4
C4	Tmax	29.5	30.5	32.6	29.2	30.0	31.9	29.1	29.8	31.6	28.8	29.6	31.4
	∇Tmax				-0.3	-0.5	-0.7	-0.4	-0.7	-1.0	-0.6	-0.9	-1.3
D1	Tmax	22.9	23.7	25.6	22.9	23.6	25.1	22.9	23.5	24.9	22.9	23.5	24.8
	∇Tmax				0.0	-0.1	-0.5	0.0	-0.1	-0.8	0.0	-0.2	-1.0
D2	Tmax	26.0	26.9	29.3	25.7	26.4	28.5	25.5	26.2	28.3	25.2	26.0	28.1
	∇Tmax				-0.3	-0.5	-0.8	-0.5	-0.8	-1.1	-0.6	-1.0	-1.4
D3	Tmax	28.0	29.0	31.3	27.7	28.5	30.6	27.5	28.3	30.4	27.4	28.1	30.2
	∇Tmax				-0.3	-0.5	-0.7	-0.4	-0.6	-0.9	-0.5	-0.8	-1.2
E1	Tmax	24.6	25.5	28.0	24.6	25.3	27.2	24.6	25.2	27.0	24.6	25.1	26.8
	∇Tmax				0.0	-0.2	-0.8	0.0	-0.3	-1.1	0.0	-0.3	-1.3

In general, the temperature variation (∇Tmax) is relatively little. The value decreases when the ventilation flow increases, with an asymptotically trend. It is clear that for some buildings the peak temperature reduction continues increasing for high ventilation flows, when in other cases, the reduction is almost marginal. It is observed that the difference between the minimum and maximum values for every case moves around 0.5ºC. Moreover, the results achievable by increasing the ventilation flow or changing the climate zone are similar. That confirms, once again, that the building typology is more significant than the absolute increase of ventilation flow when night ventilation is applied.

In order to describe a detailed performance of buildings according to the variation of peak temperature, a detailed example for Almeria (Climate Zone A4) is described in the Figure 3. It is perceived that for all the cases, the maximum temperature shows a decreasing trend with an asymptotic trend by increasing the ACH. The values of maximum temperature vary appreciably among buildings.

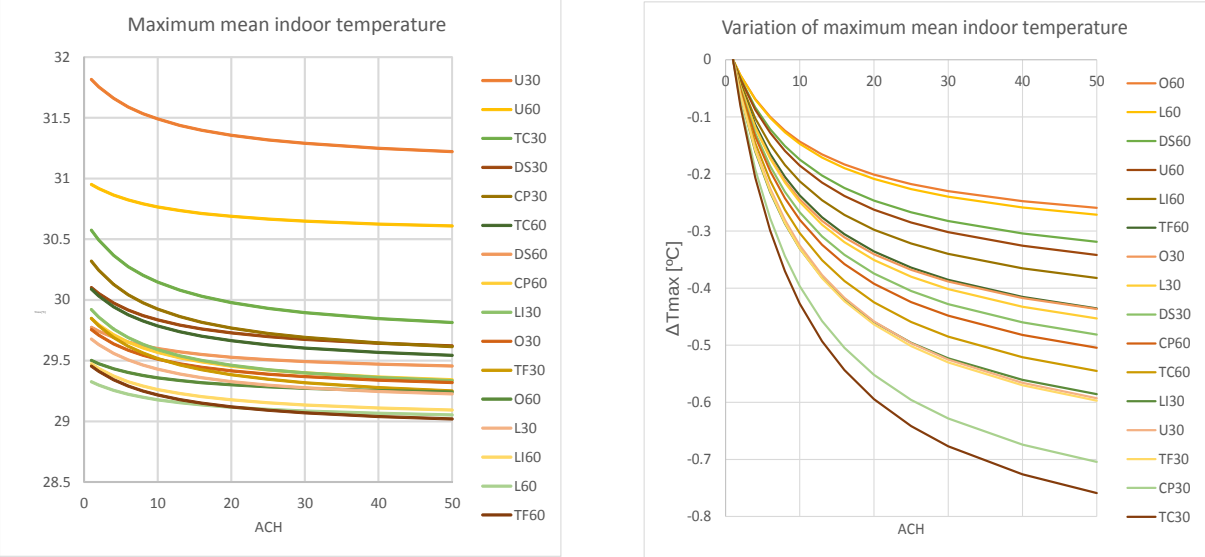

Figure 3 Maximum mean indoor temperature for all the buildings situated in Almeria, Climate Zone A4. Variation of the maximum mean indoor temperature for all the buildings situated in Climate Zone A4

5 CONCLUSIONS

Night ventilation is an operative strategy to improve comfort conditions in the users of office buildings in Spain. Depending on the level of request and the climate zone it is possible to maintain comfort conditions in 100% of the working schedule, making not necessary the use of air conditioning. Some studies suggest (Geros 1999, Kolokotroni 1998, Kolokotroni 2007) that peak temperature can be reduced up to 3.5ºC. The results of this paper show that in the case of Spain, the achievable reduction is approximately 1ºC. It has to be pointed that this variations are the mean of the maximum temperatures and not the maximum absolute. In addition, different construction materials were not considered in this work, where the influence of thermal inertia could help to reduce peak temperatures.

Although it was not an initial objective of this work, the results show that the building typology is an important factor for evaluating night ventilation as *effective or significant* to improve comfort conditions. Two main variables in buildings are identified as relevant for optimal and effective night ventilation: low glazed surfaces in façade and a low shape factor (compact buildings).

6 REFERENCES

Adnot, J. (ed) (1999). *Energy Efficiency of Room Air-conditioners (EERAC),* Study for the Directorate General for Energy (DG XVII) of the Commission of the European Communities, Luxembourg.

Akbari, H. (2007). *Opportunities for Saving Energy Improving Air Quality in Urban Heat Islands*, Earthscan, UK and USA.

Coyne, R., Snodgrass, R. (1994). Metaphors in the design studio. *Journal of Architectural Education,* **48** 2 pp. 113–125.

Geros, V., Santamouris, M., Tsangrassoulis, A., Guarracino, G. (1999). Experimental evaluation of night ventilation phenomena, *Energy and buildings*, vol 29, pp141-154.

Givoni, B. (1998) Effectiveness of mass and night ventilation in lowering the indoor daytime temperatures. Part I: 1993 experimental periods. *Energy and Buildings* 2, 25-32.

IEA (International Energy Agency) (2003). *Cool Appliances*, International Energy Agency, Paris.

Kolokotroni, M. (1995) *Night ventilation in commercial buildings. In: Review of Low Energy Cooling Technologies.* Internationl Energy Agency, Energy Conservation in Buildings and Community Systems Programme. Annex 28 Low Energy Cooling, Subtask 1, United Kingdom, pp. 7-11.

Kolokotroni, M. and Santamouris, M. (2007). *Ventilation for Cooling*, Earthscan, UK and USA.

Kolokotroni, M.,Giannitsaris, I. and Watkins, R. (2006). The effect of the London urban heat island on building summer cooling demand and night ventilation strategies. *Solar Energy,* 80 (4) : 383-392.

Kolokotroni, M.; Davies, M., Croxford, B., Bhuiyan, S. and Mavrogianni, A. (2010). A validated methodology for the prediction of heating and cooling energy demand for buildings within the Urban Heat Island Case-study of London, *Solar Energy,* 84 (12): 2246-2255.

Kolokotroni, M., Webb, B.C., Hayes, S.D. (1998). Summer cooling with night ventilation for office buildings in moderate climates. *Energy and buildings,* vol 27, pp 231-237.

Ministerio de Vivienda de España, Instituto para la Diversificación y Ahorro de la Energía (IDAE). LIDER. 2009.

Santamouris, M. (2001). *Energy and Climate in the Urban Built Environment*, James and James, London.

Santamouris, M. (2004). Night ventilation strategies. *AIVC Ventilation information paper*, no. 4, INIVE eeig, Brussels, Belgium.

Santamouris, M. (2007). *Advances in passive cooling*, Earthscan , UK and USA.

Segurado de Arriba, P., García Montes, J.P. (2008), *Evolución del consumo y de la intensidad energética en España, Análisis Global y Sectorial de la evolución del consumo y de la intensidad energética en España. Comparación a nivel europeo*, IDAE, Dpto. Planificación y Estudios.

STUDY OF FUTURE WEATHER DATA CONSIDERING GLOBAL AND LOCAL CLIMATE CHANGE FOR BUILDING ENERGY SIMULATION

Hideki Kikumoto[1], Ryozo Ooka[2], Yusuke Arima[3],
And Toru Yamanaka[4]

1 Research Associate,
Institute of Industrial Science,
the University of Tokyo,
Ooka Lab. CW403 IIS,
4-6-1 Komaba, Meguro-ku, Tokyo, Japan,
kkmt@iis,u-tokyo.ac.jp

2 Professor,
Institute of Industrial Science,
the University of Tokyo,
Ooka Lab. CW403 IIS,
4-6-1 Komaba, Meguro-ku, Tokyo, Japan,
ooka@iis,u-tokyo.ac.jp

3 Faculty of Engineering,
The University of Tokyo,
Ooka Lab. CW403 IIS,
4-6-1 Komaba, Meguro-ku, Tokyo, Japan,
arima-y@iis,u-tokyo.ac.jp

4 Kajima Technical Research Institute,
Kajima Corporation,
t-yamanaka@kajima.com

ABSTRACT

Climate change phenomena such as global warming and urban heat island effects cause serious problems for the development of building technology. Therefore, it is imperative that architects and designers consider the effects of climate change on long-term building performance. At present, energy simulations are often used to evaluate the indoor thermal environment and energy consumption of buildings. In these simulations, it is common to use regional weather data that are usually based on current or past weather conditions. However, most buildings have a lifespan of several decades, during which climate can gradually change. Therefore, the design of energy conservation systems such as ventilative cooling strategies and energy simulations should incorporate climate change predictions in order to ensure that buildings are adaptable to future climatic conditions. As a result, future weather scenarios are very important for simulating building performance.

The purpose of this study is to construct future standard weather data using numerical meteorological models, for use in architectural designs. At present, the climatic data used for this purpose are obtained from a Global Climate Model (GCM). Although a GCM can predict long-term global warming, its coarse grid resolution (~100 km) cannot describe the details of local phenomena. Therefore, we employ a downscaling method. We input GCM data into a Regional Climate Model (RCM) as initial and boundary conditions, and physically downscale the data using the RCM. RCM uses nested regional climate modeling and can analyze the local climate at fine grid resolutions (~1 km). The climatic scenarios obtained via this method are expected to accurately predict local phenomena such as the urban heat island effect.

The results confirm that the weather data generated via the dynamical downscaling method can predict local climate. We subsequently constructed a prototype of the future standard weather data based on the Model for Interdisciplinary Research On Climate (MIROC) and the Weather Research and Forecasting (WRF) Model, and simulated building energy consumption using regional climate data. By comparing present and future energy simulations, we estimated the impact of climate change on the energy performance of a building.

KEYWORDS

Climate change / Future Standard Weather Data / Building Energy Simulation / Dynamical Downscaling

1 INTRODUCTION

In building energy simulations, it is common to use regional weather data that are usually based on current or past weather conditions. However, most buildings have a lifespan of several decades, during which climate can gradually change. Therefore, energy simulations

should incorporate climate change predictions in order to ensure that buildings are adaptable to future climatic conditions. The purpose of this study is to make future standard weather data for building energy simulation. This study employs a dynamical downscaling method to derive future standard weather data at a local scale, which are used to simulate the energy performance of buildings under future climate change scenarios. We first review the literature on standard weather data and dynamical downscaling.

1.1 Standard Weather Data

Standard weather data are useful in a wide range of applications. Generally, standard weather data are obtained by combining monthly weather data representing average monthly weather over several years. In Japan, expanded AMeDAS (Automated Meteorological Data Acquisition System) weather data are published and used as standard data. AMeDAS uses regional climate information that is collected across the country at intervals of about 16 km [Akasaka et al., 2004]. The standard weather data set requires 8 weather components: temperature, humidity, solar radiation, sky radiation, wind velocity and wind speed, precipitation, sunshine hours. However, most AMeDAS stations observe only temperature, wind direction and wind velocity, precipitation, sunshine hours, and include some missing data due to automated observation. It is therefore necessary to interpolate the required regional climate information omitted by AMeDAS. As a result, standard weather data will include uncertainness associated with estimation and interpolation. Alternatively, the use of a dynamical downscaling method can provide all of the components needed for a standard weather data set. In addition, regional climate information can be calculated for any location without being restricted to observation stations.

1.2 Dynamical Downscaling

There is a climate data predicted by a Global Climate Model (GCM). GCM is a mathematical model of the general circulation of the planetary atmosphere and ocean. Although a GCM can predict long-term climatic trends, but its coarse grid resolution (~100 km) cannot describe the details of local phenomena. The use of GCM data is problematic in applications that need more detailed regional climate information. The objective of downscaling is to bridge the spatial gaps in data sets between the climate information predicted by GCM and the regional climate information needed for other applications. Downscaling uses two methods: statistical downscaling (SD) or dynamical downscaling (DD). In SD, statistical relationships derived from regional data are used to downscale large-scale climate data, so this method requires regional observations. When using this method in predicting future regional climate, an important question is whether the relationship derived from current data can apply to future conditions influenced by global warming. In order to resolve this problem, we use a dynamical downscaling method. In DD, GCM data are input as initial- and boundary conditions to a Regional Climate Model (RCM); the RCM analysis is then used to physically downscale the GCM data. RCM uses nested regional climate modeling, and can analyze the local climate at high resolutions (~1 km). Previous studies have successfully reproduced regional climate from GCM data [Yuqing et al., 2004]. Using dynamical downscaling, we can obtain all of the detailed spatial–temporal information required for a standard weather data model.

2 DETAILS OF DYNAMICAL DOWNSCALING METHOD

The process of dynamical downscaling to produce future standard weather data utilizes a GCM and RCM. In this study, we use the MIROC4h (Model for Interdisciplinary Research On Climate version4) as GCM and WRF (Weather Research and Forecasting) as RCM.

2.1 MIROC

This study uses MIROC4h developed by the Center for Climate System Research (CCSR), the National Institute for Environmental Studies (NIES), the Frontier Research Center for Global Change (FRCGC), as GCM. MIROC4h reproduces global warming at a horizontal scale of approximately 60 km [Nozawa, 2007]. Fig. 1 shows that monthly mean temperature and annual specific humidity change at surface 2 m in August in Otemachi in Tokyo, Japan. In this study, we use present weather data for the period 2006 to 2010, and use future weather data for from 2031 to 2035. In Otemachi, the monthly average surface temperature in August increases by 0.87℃ between the present (2006–2010) and the future (2031–2035) study periods, and specific humidity increases by 0.00144 [kg/kg].

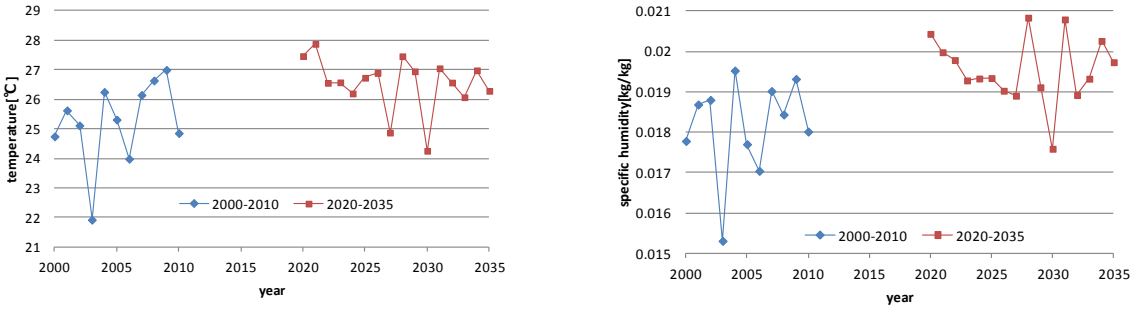

a) Temperature b) Specific humidity

Fig. 1 Trend in monthly average surface temperature and humidity in August in Tokyo predicted by MIROC.

2.2 Description of WRF Model

We use the weather research and forecasting model (WRF, version 3.4) as the RCM [William, C. S., et al., 2008]. The WRF model was mainly developed by the National Center for Atmospheric Research (NCAR), and is commonly used for local climate studies.

2.3 Analysis

We use USGS (U.S. Geological Survey) 24-category land use data. Fig. 2 and Table 1 show the nesting regions of the WRF. The target areas in this study are the Kanto region in Japan, and Tokyo and its surrounding area. We use four levels of nested regional climate modeling, where the first and fourth levels have horizontal spatial resolutions of 54 km and 2 km respectively. We use the Noah land surface model (Noah LSM) as a land physics scheme. Noah LSM requires soil temperature and humidity which are not predicted by MIROC, so we also use National Centers for Environmental Prediction (NCEP) Final Operational Global Analysis (FNL) data for soil temperature and humidity. Table 2 shows the weather component list of MIROC and FNL data, and Table 3 shows the applied physics scheme. We simulated from 1 July to 31 August, and the target analysis term is the period 1–30 August in each year.

Table 1 Nesting region in WRF simulation

Items	Content
Map projection system	Lambert conformal conic projection
Horizontal grid dimensions and grid spacing	Domain 1: 38×38 (horizontal scale 54 [km]) Domain 1: 49×49 (horizontal scale 18 [km]) Domain 1: 49×49 (horizontal scale 6 [km]) Domain 1: 61×52 (horizontal scale 2 [km])
Vertical levels	28 (from surface to the 50 hPa level)

Time step	Domain 1: 180 sec; Domain 2: 60 sec; Domain 3: 20 sec; Domain 4: 20/3 sec.
Nesting	Two-way nesting

Fig. 2 The nesting region

Table 2 Weather component used as initial and boundary conditions in WRF simulation

a) MIROC4h

Longitude, Latitude	0.5625°
Time	6 hour
Geopotential height	17 layers※
Temperature	17 layers※
Specific humidity	17 layers※
Wind velocity	17 layers※
Sea surface pressure	Surface
Surface temperature	Surface
Sea surface temperature	Surface

※17 layers (1000, 950, 900, 850, 700, 500, 400, 300, 250, 200, 150, 100, 70, 50, 30, 20, 10 [hPa])

b) FNL°

Longitude, Latitude	1
Time	6 hour
Soil temperature	4 layers※
Soil water	4 layers※

※4 layers (0–10, 10–40, 40–100, 100–200 [cm])

Table 3 WRF physics scheme

Cumulus parameterization	Domains 1&2: Grell 3D scheme; Domains 3&4: none
Microphysics	WRF Single-moment 6-class scheme
Planetary boundary layer	Yonsei University scheme
Longwave radiation	RRTM scheme
Shortwave radiation	Dudhia scheme
Land surface	Noah Land Surface Model (Noah LSM)

3 DYNAMICAL DOWNSCALING USING MIROC AND WRF

3.1 Locality Reproduced by Dynamical Downscaling

Fig. 3 shows surface temperature at 2 m and wind field at 10 m above the surface, as predicted by MIROC and WRF at 21:00 hr on 16 August 2006. The 60-km horizontal grid scale of MIROC is too coarse to represent local climate information. On the other hand, the high resolution of WRF can reproduce the locality considering the regional topographic effects.

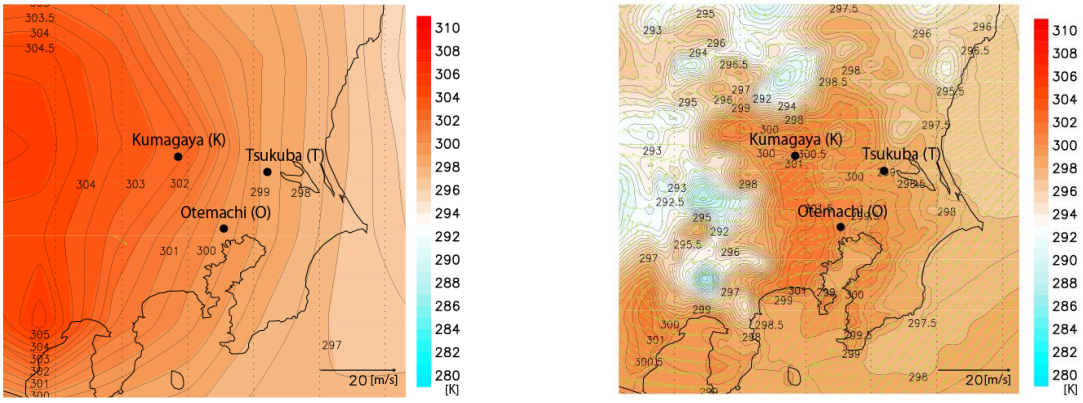

a) MIROC b) WRF

Fig. 3 Temperature at 2 m and wind field at 10 m predicted by MIROC and WRF at 21:00 hr on 16 August 2006

Fig. 4 represents the mean daily changes in weather components and the mean wind direction (according to frequency of direction) from August 2006–August 2010 for each of the three study locations: Otemachi (lat 35.9, long 39.76), Tsukuba (lat 36.65, long 40.12), and Kumagaya (lat 36.15, long 39.38). As shown in Fig. 4 a), the night-time temperature in Otemachi is higher than that in Tsukuba and Kumagaya due to urban heat retention. It is noticeable that the maximum daytime temperature in Kumagaya is attributed to heat

generated in urban areas south of Kumagaya, which is transported by the south sea breeze from Tokyo Bay. Fig 4 b) show that humidity increases during the morning in Tsukuba and Kumagaya, but not in Otemachi. Wind velocity is low at Kumagaya due to its inland location (Fig.4 c)) and wind direction is different among 3 cities (FIg.4 d)). Thus, we can derive local climate information from a GCM via dynamical downscaling, by employing land use data in the WRF.

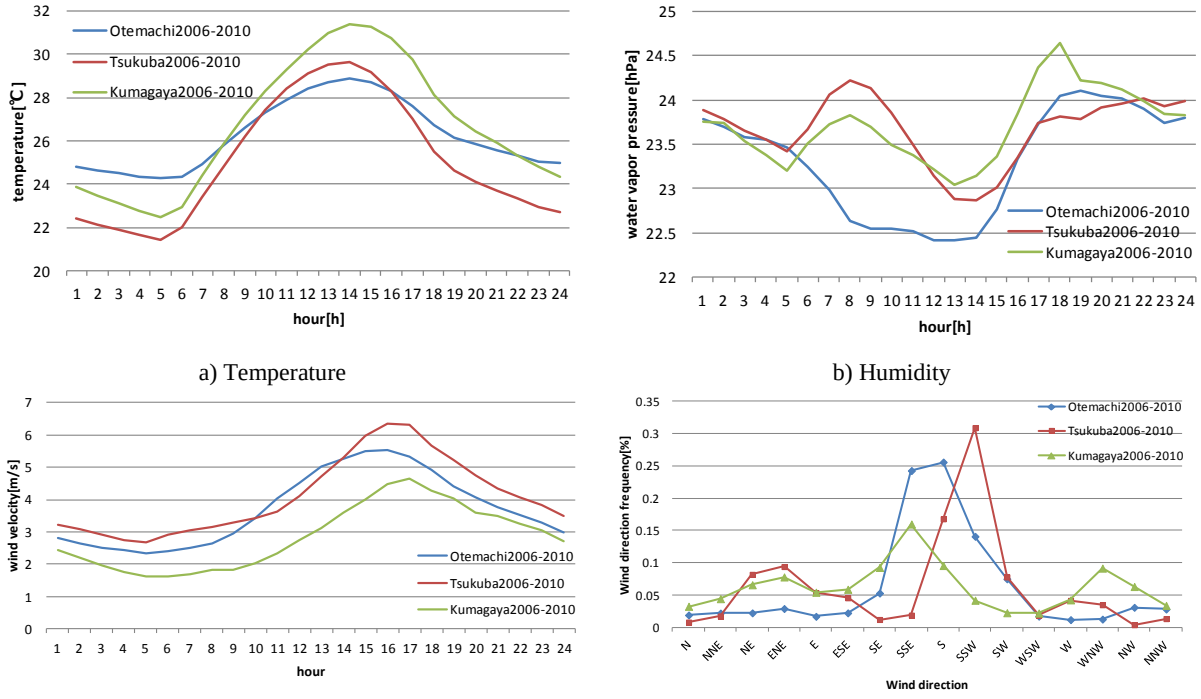

a) Temperature

b) Humidity

c) Wind velocity

d) Wind direction

Fig. 4 Daily changes five-year (August 2006–August 2010) mean weather component and wind direction distribution for each of the three cities, predicted by WRF

3.2 Changes in Weather Components between Present and Future

Fig. 5 shows the mean daily weather components for August 2006–August 2010 in Otemachi compared with the changes predicted for 2031–2035. The data predict future increases in both temperature and humidity. We can see the increases in other cities, and Table 4 shows the present and future five-year mean temperature and humidity, and the temperature and humidity increase reproduced by WRF and MIROC. From the WRF result, it is evident that the maximum temperature change is at Tsukuba, (1.27°C), and the minimum temperature change is at Kumagaya; and that the maximum change in specific humidity is at Tsukuba, (0.00173 [kg/kg]), and the minimum change at Kumagaya (0.00111 [kg/kg]). However, in the MIROC result, the predicted temperature and humidity changes at Otemachi and Tsukuba are smaller than those predicted by WRF; in contrast, WRF predicts smaller changes at Kumagaya. Based on the results, it is evident that local climate change can be reproduced using a dynamical downscaling method.

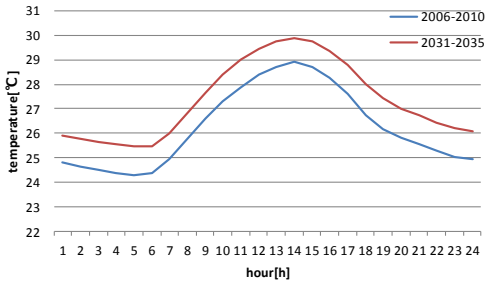

a) Temperature

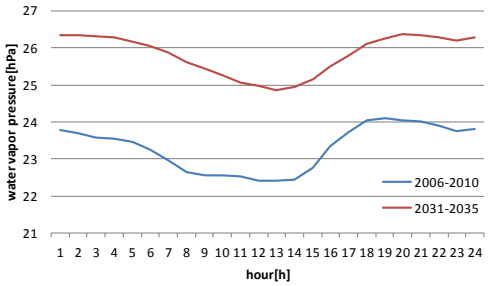

b) Humidity

Fig. 5 Five-year mean temperature and humidity daily change in August in Otemachi predicted by WRF comparing the present and future

Table 4 Present and future 5-year mean temperature and humidity in August reproduced by MIROC and WRF

	Temperature [°C]		Specific humidity [kg/kg]		Temperature Increase [°C]		Specific humidity Increase [kg/kg]	
	MIROC	WRF	MIROC	WRF	MIROC	WRF	MIROC	WRF
Otemachi 2006–2010	25.72	26.24	0.0187	0.0147	0.86	1.12	0.00144	0.0016
Otemachi 2031–2035	26.59	27.36	0.0198	0.0163				
Tsukuba 2006–2010	26.27	25.06	0.0187	0.0149	0.92	1.27	0.0015	0.00173
Tsukuba 2031–2035	27.19	26.33	0.0202	0.0166				
Kumagaya 2006–2010	24.89	26.67	0.0181	0.0150	0.81	0.50	0.00144	0.00111
Kumagaya 2031–2035	25.70	27.17	0.0196	0.0161				

4 APPLICATON OF WEATHER DATA TO ENERGY SIMULATION

4.1 Selecting Standard Weather Data

Generally, when standard weather data are estimated, data from the same month are selected over a period of several years, and then these standard months are combined to produce standard weather data for one year. Fig. 6 a) shows frequency distribution for temperature in August 2006–2010, and Fig. 7 a) shows the same for August 2031–2035 in Tokyo. Here, we selected the standard month that represents average temperature for the present (2006–2010) using temperature frequency deviation from 5-year (August 2006–2010) average temperature frequency V_y defined by formula (1). Here, $F_{y,i}$ is the frequency of temperature i in year y, and F_i is the average frequency of temperature i over 5 years (2006–2010). Table 5 shows deviation V_y from the mean in each of the present five years (2006–2010). As shown in Table 5, the smallest deviation during the present period (2006–2010) is during 2007. We therefore select weather data from 2007 as standard weather data for the present five-year period; similarly, the period 2031–2035 is represented by data for 2034. Fig. 6 b) and Fig. 7 b) show good agreement in the temperature frequency of the standard year and the five-year mean.

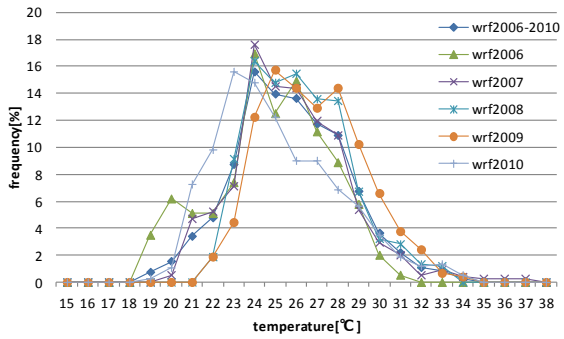

a) 5 yr in August in the present and 5-year mean

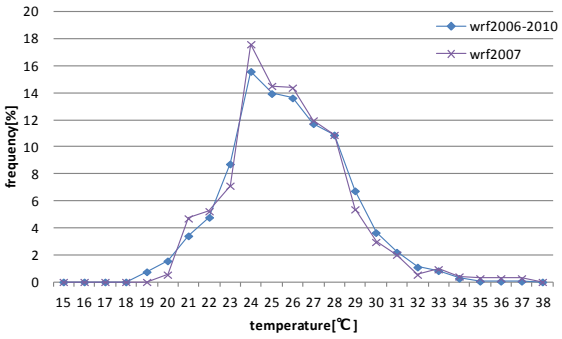

b) August 2007 and 5-year mean

Fig. 6 Temperature frequency distributions predicted by dynamic downscaling in present

$$V_y = \left(F_{y,i} - F_i \right)^{2}{}^{1/2} \quad (1)$$

Table 5 Standard deviation of temperature frequency from 5 years mean distribution

Year	2006	2007	2008	2009	2010
V_y	7.2	3.7	19.4	9.7	11.7

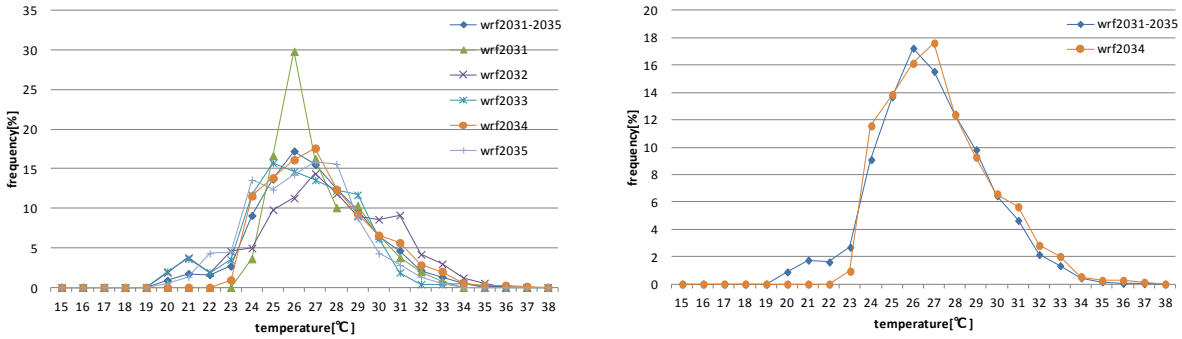

a) for 5 yr in August in the 2030s and 5-year mean b) August in 2034 and 5-year mean

Fig. 7 Future temperature frequency distributions predicted by dynamic downscaling

Table 6 Standard deviation of annual temperature frequency from 5-year mean (2031–2035)

Year	2031	2032	2033	2034	2035
V_y	14.8	10.5	6.5	4.8	7.9

4.2 Sample Standard Weather Data

The WRF results show an average temperature of 26.23°C in August 2007, which increases by 1.52°C to 27.75°C in August 2034. Fig. 8 compares daily temperature and solar radiation between August 2007 and August 2034. These hourly weather data for a month generated by dynamical downscaling are used to simulate the energy consumption of buildings.

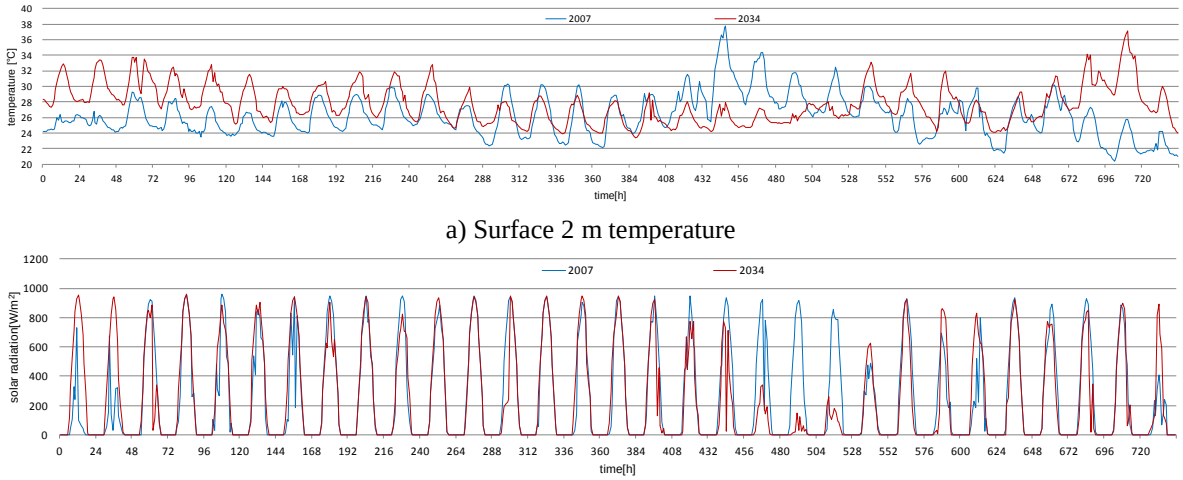

a) Surface 2 m temperature

b) Solar radiation

Fig. 8 Temporal variation in surface temperature and solar radiation in Tokyo during August (2007 and 2034) generated by WRF

4.3 Building Energy Simulation Conditions

We used energy simulation to analyze the impact of climate change on the energy consumption [Urano, 2009] of a standard detached house located in Tokyo. Fig. 9 illustrates plans for a typical house used for environmental studies of architecture in Japan. TRNSYS

software (University of Wisconsin, USA) was used for the energy simulations. The weather data generated by WRF were used to analyze the energy consumption of the house during August under present (2007) and future (2034) climate scenarios. We assumed a cooling system with units located in the combined living and dining room with a kitchen (termed LDK), a bedroom, and a child's room (A); these rooms had areas of 29.8 m^2, 13.3 m^2, and 10.8 m^2, respectively. The cooling equipment was assumed to be activated when the air temperature in these rooms exceeded 26°C in accordance with the time schedule shown in Table 8. The thermal properties of the house are illustrated in Table 9. The simulation term is for one month, from 1–31 August of each year.

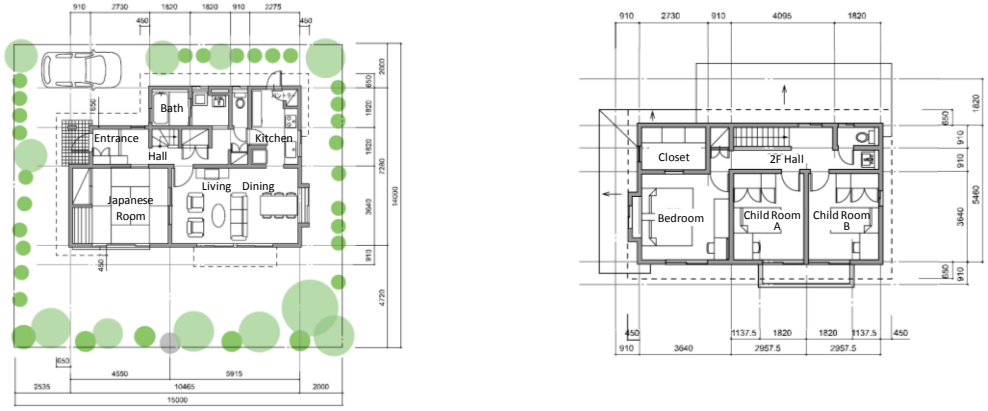

a) First floor b) Second floor

Fig. 9 Plans for a model house (the standard house model in Japan) used in the building energy simulation

Table 8 Air conditioning setting

ROOM	Preset Temperature [°C]	Schedule of air conditioning
LDK	26	6:00–10:00, 12:00–14:00, 16:00–24:00
BEDROOM	26	21:00–23:00
CHILD ROOM (A)	26	20:00–21:00, 22:00–24:00

Table 7 Thermal property of a model house

ROOM	Heat transmission coefficient [W/m^2K]	Solar absorptance [-]	Convective heat transfer coefficient [W/m^2K]
External wall	1.671	0.8	3.05 (indoor), 17.7 (outdoor)
Roof	2.591	0.8	3.05 (indoor), 17.7 (outdoor)

4.4 Building Energy Simulation Result

Fig. 10 presents times series of the variation in sensible heat load in the LDK area. Small and large of heat load of each cases differ from day to day. For example, on 20 August, the sensible heat load in 2007 is greater than that for 2034, because the outdoor temperature in 2007 is higher than that predicted in 2034 (Fig. 10). Fig. 11 show mean daily sensible heat load in the LDK and bedroom. The mean daily sensible heat load in future is higher than that at present. Table 9 show the total sensible heat load for the month of August in Otemachi. In August 2007, total sensible heat load is 2.35×10^6 [MJ/month], compared with 2.70×10^6 in August 2034. The sensible heat load is predicted to increase by 15% between the two study periods, which is considerable for simulation of a building's thermal performance.

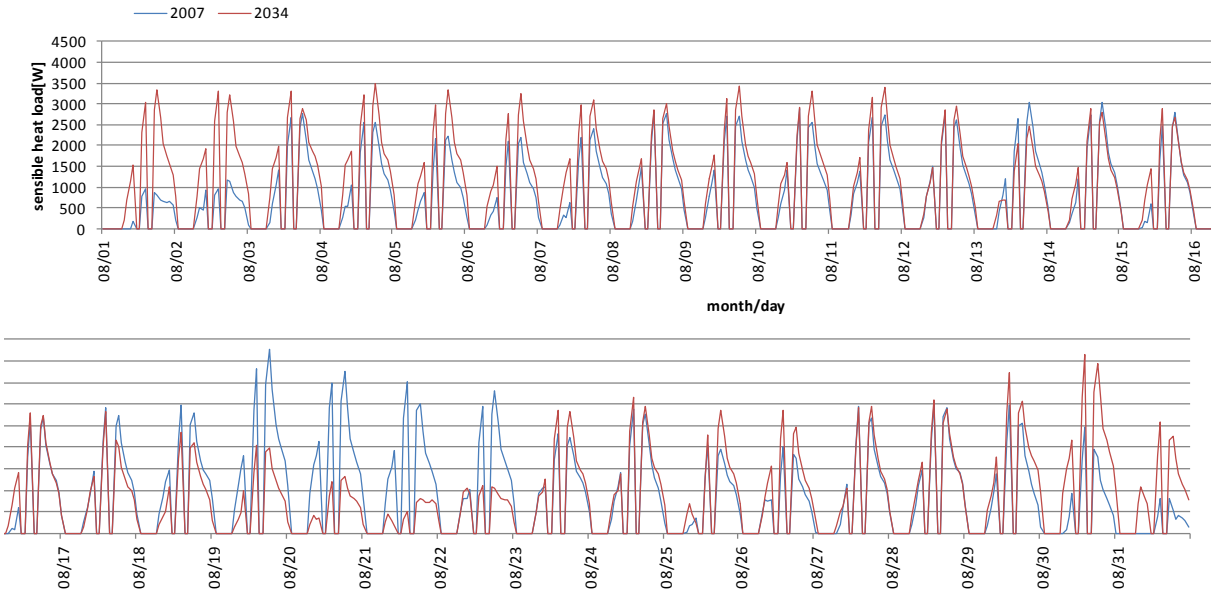

Fig. 10 Change in sensible heat load in LDK area during August. Simulated by TRNSYS using standard weather data generated by WRF

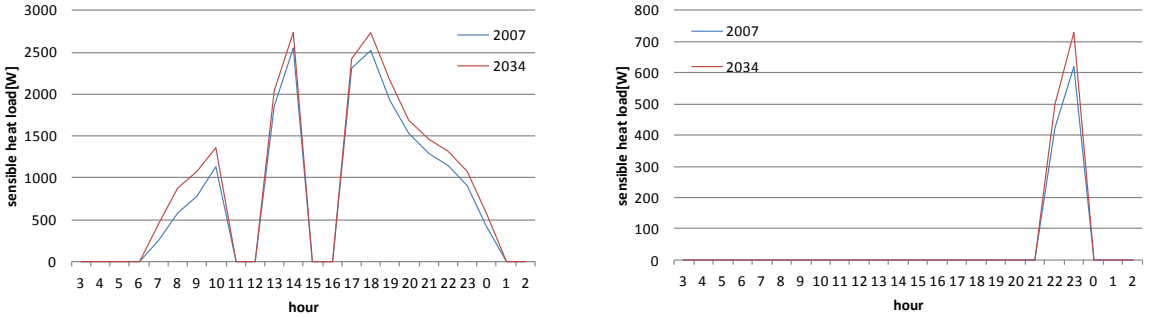

a) LDK b) Bedroom

Fig. 11 Change in mean daily sensible heat load in LDK area and bedroom between August 2007 and 2034

Table 9 Total sensible heat load of model house during August: 2007 and 2034

Case	Sensible heat load for one month [MJ/month]
2007	2.35×10^{6}
2034	2.70×10^{6}

5 CONCLUSIONS

Using a dynamical downscaling method with the WRF model, we can obtain regional climate information and local climate changes. In other existing methods, climate change is predicted by GCM and added to current weather data in order to predict future local weather data, but the effect of local climate change is not considered. To create future standard weather data, which requires high-resolution climate information at scales of a few km, this dynamical downscaling method is a useful way to consider regional characteristics and regional climate change. Future weather data derived from dynamical downscaling are expected to represent both global climate change and local climate phenomena, and by using this method, designers can take future local climatic conditions into consideration.

We assessed the impact of climate change from the present to the 2030s in terms of the energy consumption of a detached house in Tokyo, Japan. We simulated climate using the downscaling technique with global and regional climate models to derive regional weather data for August for the present (2006–2010) and during the 2030s (2031–2035). Standard

weather data predict that outdoor temperature will increase by 1.52°C (from 26.23°C to 27.75°C) from the present (2007) to the future (2034). As a result, the sensible heat load for the house was predicted to increase by 15% under the study conditions.

6 ACKNOWLEDGEMENTS

This study represents part of research conducted by the working group on near-future standard weather data using global climate modeling (project general manager; Ryozo OOKA). The authors are deeply grateful to WG members (Satoru IZUKA, Toru MOCHIDA, Akira KONDO, Hideyo NIMIYA, Ryuichiro YOSHIE, Shinji YOSHIDA); and express their gratitude to Kimoto lab. in the Atmosphere and Ocean Research Institute, University of Tokyo, who provided MIROC4h data for the present study.

7 REFERENCES

Akasaka, H., 2003: Current state of the availability and required future work on the Expanded AMeDAS Weather Data, Summaries of Technical Papers of Annual Meeting, AIJ, pp. 57-60.

Soga, K., Akasaka, H., 2004: Study on the Method for Constructing a Reference Weather Year. A comparison of the EA method and the SHASE method, J. Environ. Eng., AIJ, No 581, pp. 21-28.

Soga, K., Murakami, S., Akasaka, H., Nimiya, H, 2009: Development of an Integrated Energy Simulation Tool for Buildings and MEP Systems, the BEST(Part44) Development of EA Weather Data and Future Weather Data, J. SHASE, pp. 659-662.

Yuqing, W., et al., 2004: Regional climate modeling: progress, challenges, and prospects, J. Meteorol. Soc. Jpn. 82, pp. 1599-1628.

Lo, J. C.-F., et al., 2008: Assessment of three dynamical climate downscaling methods using the Weather Research and Forecasting (WRF) model, J. Geophys. Res. 113, D09112.

Nozawa, T., et al., 2007: Climate change simulations with a coupled ocean-atmosphere GCM called the model for interdisciplinary research on climate: MIROC, CGER's Supercomputer Monograph Report 12 (NIES).

Mochizuki, T., et al., 2012: Decadal Prediction Using a Recent Series of MIROC Global Climate Models. J. Meteorol. Soc. Jpn. 90A, pp. 378-383.

Skamarock, W. C., et al., 2008: A Description of the Advanced Research WRF Version 3. NCAR Tec. Note.

Urano, A., 2009: Influence of global warming on office building cooling loads, 7th ICUC.

PROPOSED RESEARCH AGENDA FOR ACHIEVING INDOOR AIR QUALITY SUPPORTING HEALTH AND COMFORT IN HIGHLY ENERGY EFFICIENT BUILDINGS

Pawel Wargocki[1*], Max Sherman[2], Willem de Gids[3], Peter Wouters[4], Francis Allard[5], François Rémi Carrié[4], Paolo Carrer[6], and Stylianos Kephalopoulos[7]

[1]*International Centre for Indoor Environment and Energy, DTU Civil Engineering, Technical University of Denmark*

[2]*Residential Building Systems Group, Lawrence Berkeley National Laboratory, USA*

[3]*VentGuide, the Netherlands*

[4]*International Network for Information on Ventilation and Energy Performance, INIVE EEIG, Belgium*

[5]*University of La Rochelle, France*

[6]*The University of Milan, Italy*

[7]*European Commission, Joint Research Centre, Ispra, Italy*

ABSTRACT

Research topics that need to be addressed so that the future highly energy efficient buildings do not compromise health and comfort of the building occupants were identified. They can be used to form the short-term and long–term research agenda. Research priorities were identified during two workshops. During first workshop, the stakeholders involved in the building design, construction and operation, and invited experts from different disciplines formed the first list of the priorities. The list was subjected to public review and supplemented in the subsequent workshop held during large international congress. The impact of user behavior with respect to control of the indoor environmental quality was the topic that received distinctively higher priority than the other topics. It was also highly advised to benchmark differences in health risks, exposures and sources of these exposures in the traditional buildings, energy retrofitted buildings and new highly energy-efficient buildings. Many other research topics identified received quite similar priority; the effort needed to accomplish the research work was estimated. Developing databases with benchmarking results and information on past and current projects was seen as an important task for the future. The research agenda includes also developing policies and training courses, which have been considered as an important step to promote highly efficient energy buildings with high indoor environmental quality. Crosscutting and harmonization of different policies needs to be promoted in that process.

KEY WORDS

Energy efficient buildings; Research priorities; Effort; Indoor air quality; Ventilation

1 INTRODUCTION

Buildings create shelter and conditions for working, learning, leisure and comfortable living. A built environment should be safe with no health hazards for its users either due to poor design and construction, or due to poor operation, maintenance and performance. Negligence and/or compromise of any of the actions required to achieve high criteria set for the conditions indoors can bring about serious problems resulting in the substantial costs and numerous undesirable consequences (Wargocki, 2011). The holistic approach for creating

indoor environmental quality in buildings is hence required involving different disciplines and harmonization with policies and regulations. Numerous determinants of healthy, productive and comfortable indoor environments must be considered comprising among others outdoor air pollution and climate, as well as the expectations and behavior of buildings' users to name just few (Oliveira Fernandes et al., 2009). The approach should also take into account the potential limitations defined, e.g. by the access to the necessary technologies and energy resources.

A considerable amount of energy is used in buildings to support the processes, which ensure that the indoor environment is of a high quality promoting healthy living. This situation is changing at present as a response to the stringent requirements and limitations for energy use in buildings. These requirements are imposed by the policies and regulations having aim to reduce the carbon footprint and slow down the process of climate change. An example of such policy includes the Energy Performance of Building Directive released by European Commission in 2002 with a recast in 2010 (EPBD, 2002; 2010). Voluntary building certification schemes contribute to this change, as well. They are considered signatures of modernism, prestige and excellence. The building stock portfolio is changing, too. The number of highly energy efficient buildings (termed also nearly zero energy buildings) is increasing at a high rate. Many existing buildings also fall into this category after undergoing the renovation and retrofit processes in order to reduce substantially the energy use.

This fairly radical and rapid change is not adequately supported by the scientific evidence on the effects (both benign, positive and negative) on health and comfort of users of highly energy efficient buildings. Among others, it is important to understand what the common perception is of highly energy efficient buildings, what the health implications are including occupant behavior and the parameters of indoor air quality as well as what the trade-offs are between different factors including energy and indoor environmental quality.

The urgency for developing research agenda addressing these issues thus exists. The agenda should identify the most critical aspects of highly energy efficient buildings that need to be examined, as well as the proper steps that need to be taken to avoid the potential negative consequences of the ubiquitous strive for meeting the rigorous targets for maximum energy use in buildings.

The present paper describes an attempt to develop such an agenda. It is achieved by defining research topics that need to be addressed so that the future energy efficient buildings do not compromise health and comfort of the building occupants. Indoor air quality in highly energy efficient buildings is the main focus of the agenda but it is recognized that thermal, acoustical and visual environment are also components of the indoor environmental quality (Frontczak et al., 2012); they are not directly addressed here.

2 METHODS

Two workshops were held to create the research agenda.

During the first workshop, experts from the following disciplines were invited: ventilation, medicine, epidemiology, building systems and building policies. The legislators and stakeholders involved in the building design, construction and operation were invited too. During two-day interactions and discussions, they identified research issues that need to be addressed to ensure that a built environment in highly energy efficient buildings, both new ones and those that have undergone the energy retrofit, is safe and comfortable for its users. The issues addressed broad areas related to basic human requirements, technical solutions,

policies and training programs supporting implementation. The results of the workshop were used to draft the first version of the research agenda, which was then reviewed and agreed upon by the participants of the workshop.

In the next step, the agenda was subjected to external review during during a specific workshop held at the 2012 AIVC conference in Copenhagen (Denmark); its content was presented and discussed with the workshop participants. One aim of this additional workshop was to supplement the agenda with the new topics potentially overlooked during the first workshop. Another aim was to prioritize the identified topics and estimate how much effort is expected for their accomplishment.

The agenda was developed following the conceptual framework presented in Figure 1. This framework defines the steps, which are needed to achieve healthy comfortable and productive indoor environments in the highly energy efficient buildings. The steps are as follows:

- Step 1. Definition of performance parameters needed for achieving high indoor air quality. These parameters should consider among others expectation and needs of the users, as well as the known evidence on the conditions having potentially harmful effects, and those promoting well-being.
- Step 2. Definition of processes for controlling the release and distribution of contaminants having harmful effects on humans, as well as the precursors for such contaminants. These processes should include among others careful selection of building materials, furnishing and consumer products, and the use of technologies for dilution, removal, filtration and air cleaning, as well as defining the proper use and maintenance routines.
- Step 3. Implementation of the design methods supporting the creation of high indoor air quality in the built environment. This pertains predominantly to ventilation systems.
- Step 4. Proper implementation and execution of the systems ensuring that air quality levels are high. This again mainly pertains to ventilation systems.
- Step 5. Diligent, practical and judicious operation and maintenance of buildings and all systems installed in buildings.

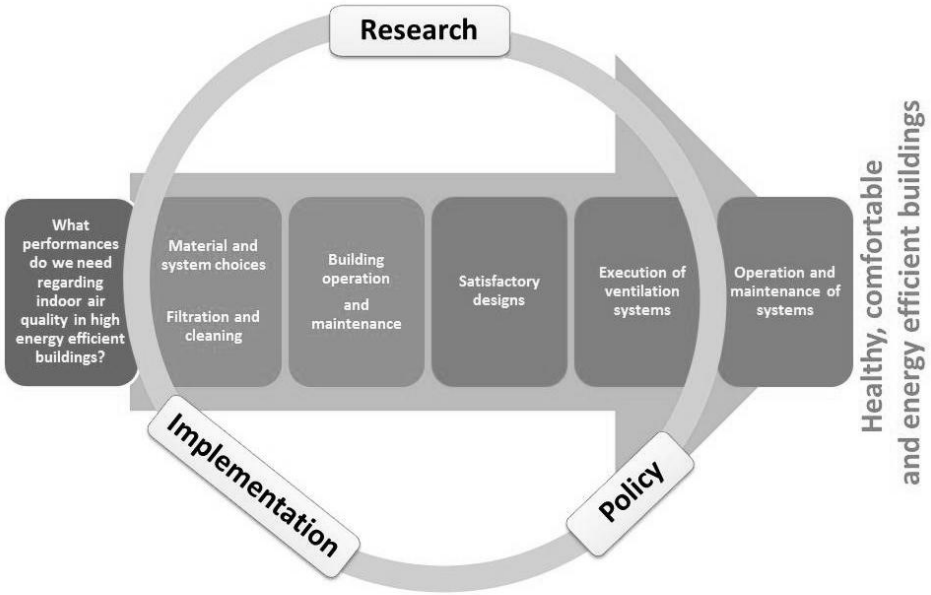

Figure 1: Framework for achieving indoor air quality supporting healthy, comfortable and productive highly energy efficient buildings

3 RESULTS

Research priorities identified by the participants of the two workshops are presented in Tables 1 to 3. They list the topics that need an action in highly energy efficient buildings. The topics are grouped to address basic research requirements, the issues related to the solutions for achieving healthy and comfortable highly energy efficient buildings, as well as the policies and training programs needed to support the implementation of solutions.

Basic research requirements include issues such as identification of health and comfort problems experienced by the users of highly energy efficient buildings, definition of the needs and expectation of users of highly energy efficient buildings as regards indoor air quality, prioritization of health and comfort endpoints, and identification of hazardous sources and pollutants.

The topics related to solutions include both the existing solutions that are effective and efficient for mitigating and preventing potential problems, as well as identification of the missing solutions.

The topics related to the implementation of solutions try to determine, whether there are any barriers experienced during design, construction, operation and maintenance of highly energy efficient buildings that can compromise indoor environmental quality, in particular air quality, whether they are perceived similarly by different stakeholders and how they should be mitigated and prevented.

Tables 1-3 indicate also, how the topics were prioritized by 30 participants of the second workshop on the scale from 5= high priority to 1=low priority, and whether they were considered to require 5=large or 1=small effort in order to be accomplished. The topics having high priority can be considered as topics, which require immediate action and attention (short-term priority topics). Those with the lower priority should not be considered as irrelevant. They still need to be resolved to ensure that health and comfort requirements are met in highly energy efficient buildings but their implementation and execution can be delayed (long-term priority topics).

Table 1: The proposed research agenda for achieving indoor air quality supporting healthy, comfortable and energy efficient energy buildings – Basic research needs

Topic/issue	**Priority***	**Effort****
1-1 Impact of user behavior with respect to control of the indoor environmental quality	4.2	3.7
1-2 Development and implementation of new advanced methods for monitoring indoor air quality, and monitoring of health and comfort in relation to indoor air quality	3.8	3.1
1-3 Definition of ventilation requirements and the parameters defining these requirements	3.5	2.9
1-4 Definition of the pollutants of concern in highly energy efficient buildings	3.5	3.1
1-5 Definition of expectations of users of highly energy efficient buildings in relation to indoor air quality, and their change compared with the expectations in traditional and retrofitted buildings	3.1	3.0
1-6 Exploration of differences in health risks in traditional buildings, energy retrofitted buildings and new highly energy efficient buildings	3.1	4.0
1-7 Examination of the impact of non-building related variables (gender, age, social and work status) on the requirements related to health and comfort	2.9	3.1
1-8 Development of improved and simplified toxicological characterization of pollutants	2.4	3.5

*Indicated on an interval scale from High=5 to Low=1 with step of 1; ** Effort to accomplish the task indicated on an interval scale from Large=5 to Small=1 with step of 1; the average scores of 30 participants are presented

Table 2: The proposed research agenda for achieving indoor air quality supporting healthy, comfortable and energy efficient energy buildings – Solutions

Topic/issue	**Priority***	**Effort****
2-1 Evaluation of new advanced ventilation strategies on health and comfort	3.6	3.3
2-2 Identification of the barriers that block innovation in building process relative to the indoor environment	3.3	2.9
2-3 Development of means for active involvement of building users in creation of healthy and comfortable indoor air quality (intervening on people's habits)	3.3	3.5
2-4 Flexibility of design to account for variations	3.2	3.1
2-5 Comparison of natural ventilation, mechanical ventilation, ventilation on demand or other ventilation solutions in the context of highly energy efficient buildings taking into account the purpose and circumstances of their use	3.0	3.2
2-6 Development of harmonized methodology for measurements of emissions from building materials and consumer products, and simple, i.e. comprehendible emission classes	2.8	2.6
2-7 Impact of labeling of building materials and consumer products on health and comfort	N/A***	N/A***

*Indicated on an interval scale from High=5 to Low=1 with step of 1; ** Effort to accomplish the task indicated on an interval scale from Large=5 to Small=1 with step of 1; the average scores of 30 participants are presented; *** the topic was proposed during workshop but no vote was taken

Table 3: The proposed research agenda for achieving indoor air quality supporting healthy, comfortable and energy efficient energy buildings – Policy needs, methods of harmonization between policies, proper execution, better management and implementation

Topic/issue	Priority*	Effort**
3-1 Development of methods assuring more responsibility of contractors, designers and installers	3.7	3.3
3-2 Tools and methods for ensuring performance-based design operation and maintenance of building systems securing indoor air quality	3.7	3.5
3-3 Examination of the importance of health and comfort outcomes in terms of public health, economy and costs	3.7	3.8
3-4 Methods securing robust design assuring high indoor air quality	3.6	3.3
3-5 Guidelines for operating buildings in multi-objective environment as well as simple manuals and user-interfaces for building users	3.5	2.9
3-6 Development of educational and training programs for different stakeholders involved in building processes including the provision of certification for different stakeholders from architects, designers and engineers to installers and facility managers	3.3	2.9
3-7 Development of long-term economic incentives for creation of healthy and comfortable indoor environments in form of add-on-values rather than penalties	3.1	3.4
3-8 Development of methods assuring more responsibility of contractors, designers and installers	N/A***	N/A***
3-9 Development of training programs including provision of certification for different stakeholders	N/A***	N/A***

*Indicated on an interval scale from High=5 to Low=1 with step of 1; ** Effort to accomplish the task indicated on an interval scale from Large=5 to Small=1 with step of 1; the average scores of 30 participants are presented; *** the topic was proposed during workshop but no vote was taken

4 DISCUSSION

Present agenda, though not reviewed and discussed publicly by wide groups of scientists and stakeholders involved in the building process, can still be considered to provide a reasonable and useful appraisal of what is needed as regards the research, the implementation of solutions and policies in highly energy efficient buildings. It is interesting to see that many of the research topics have been indicated to have generally similar priority. This may suggest that the agenda has a very wide scope, and that many stakeholders and disciplines involved in the building process and creation of indoor environmental quality were represented when the agenda was created.

The impact of user behavior with respect to control of the indoor environmental quality was the only topic to receive distinctively higher priority than the other topics. This reflects well the current intensive discussions on the importance of human behavior among the stakeholders and scientists involved in the research, construction, design and operation of the buildings. New research data indicate that humans, their actions, attitudes and behaviors are an important and in some cases even a dominant element in the entire approach for creation of healthy and comfortable built environment. The data imply that even best policies, technology and regulation are not going to be effective unless behavioral aspects are taken into account. Still the panels providing the input to the present agenda consider that information on this issue is insufficient and it should have high priority in research. In particular, the reasons should be investigated behind certain actions taken by the users of the buildings. In addition, their motivation to perform these actions needs to be examined. In addition, future research should investigate the extent to which the control should be delegated to humans as well as which aspects of control of indoor environmental quality should be delegated to humans. The studies need to determine the balance between the fully automated building and a building with as few controls as possible. Another important topic is to study how to engage and motivate the occupants to be more responsible for the environments, in which they live.

Benchmarking differences in health risks in the traditional buildings, energy retrofitted buildings and new highly energy-efficient buildings were considered to take the largest effort to complete. It was strongly voiced that these studies should be accompanied by examining the exposures and the sources, which are responsible for the effects observed. Although quite elaborate and intensive, it was felt that these measurements can create a true reference point (benchmark) for the future developments of built environment. In particular, such reference is needed to assess the performance, effectiveness and success of the mitigation practices, as well as the performance of future technologies. There is an apparent lack of such reference and benchmark at present. The benchmarking should not only include buildings with problems but also buildings in which there are no problems (the successful projects) to cover the whole representative range of the buildings. This will also facilitate understanding of the differences between well-performing buildings and the buildings where the problems are observed. Benchmarking allows collection of the comparable data across different countries and characterization of exposures using similar methods and approaches, which is yet additional value. However, it also needs standardized measuring protocols to achieve this goal; their development can be considered as an additional deliverable of developing and using the benchmarking protocols. The multi-disciplinary approach is needed in this endeavor. It should integrate not only the “traditional” disciplines involved in the indoor air research, but also social sciences and anthropological approaches. Health impact assessment and risk monitoring should receive similar importance as the traditional methods for examining the effects of indoor environmental quality on health and comfort.

Methodological aspects of the experimental studies are of paramount importance for collection of decent scientific evidence. Traditionally funding is however not given for the research on the methodological aspects of experiments. This is one of the reasons, why topics related to the experimental design are not listed in Tables 1 to 3. The proper characterization of research methods would require an elaborate and comprehensive multidisciplinary approach beginning with the decent review of the literature and the assessment of the data presented therein. Examples of such effort include reviews by Nordworks and Euroworks (Sundell et al., 1999). The methodological aspects worth investigating are among others proper control of confounding and bias through selection of reference and control groups. They also include the sufficient and representative size of the studied building populations and human cohorts. Long-term data are also of the importance considering that so far research has been using monitoring of the data for short periods usually being non-representative fractions of actual indoor exposures. Examining advantages and disadvantages of using different experimental designs in the context of indoor air research has been encouraged. These designs include large cross-sectional studies taking a snap-shot of the conditions in the buildings through longitudinal prospective cohort studies monitoring the same population for the extended period of time, to intervention studies which again should use different length of examination periods. The advantages of chamber and field studies need to be considered as well. Toxicological methods should further be developed including both methods involving humans and animals. Especially the latter is the largest source of error and uncertainties, and therefore the improved toxicological information on this aspect is necessitated. The new advanced objective methods for measuring the effects on health comfort and mental performance should learn largely from the past evidence. The methods that have been shown to be ineffective should be rejected.

No specific pollutants have been specified that should be especially examined as regards their impact on health and comfort in highly energy efficient buildings. As a minimum approach, the compliance with WHO Air Quality Guidelines (WHO, 2006; 2010) and the recommendations of INDEX project (Kotzias et al., 2005) has been recommended; the data in these documents are based on the available scientific evidence that has been scrutinized carefully and thoroughly. At the same time it must be acknowledged that neither WHO Guidelines nor INDEX project have specified all pollutants of concern. Therefore, in the proposed studies characterizing exposures in highly energy efficient buildings strong effort should be placed on exploring which pollutants should be specifically addressed in the future highly energy efficient building. Among the pollutants that potentially need a special focus are ambient and indoor generated particles (both submicron, nano- and ultrafine particles as well as traditionally recognized PM2.5 and PM10) and the composition of pollutants adsorbed on their surfaces, dust depots and reactive indoor air chemistry pollutants, gaseous pollutants with a special emphasis on formaldehyde and acrolein and other pollutants which in risk modeling are shown to be mainly responsible for reduced healthy life years expressed as DALYs (Oliveira Fernandes et al., 2009; Jantunen et al., 2011; Logue et al., 2012), new emerging pollutants such as SVOCs, PCBs, phthalates, flame retardants, persistent occurring pollutants and endocrine disrupting pollutants, moisture and biological pollutants, as well as contagions and viruses responsible for communicable infectious diseases so far studied to a lesser extent in connection with the impact of indoor air quality on their transmission in the built environment (except hospitals and medical care buildings). Definition of pollutants of concern should also take into account the effects of mixtures, even when individual components are clearly below their low effect level, as well as the potential additive, adjuvant and synergistic effects, which have so far been studied to much lesser extent than the effects of individual pollutants, except for the studies with ozone and its capacity to modify the

exposures through reactive products (Weschler, 2011). The limitations for advanced characterization of exposures have been one reason while so called “cocktail effects” of many contaminants present have been studied to a lesser extent. These methods have advanced in the recent years, and it is expected that they will advance even more. It is likely that there could be pollutants of concern that are yet not identified but may have significant health effects considering the constant change in chemical composition of indoor air. Thus, only systematic monitoring through proper experimental approach with representative groups and control for confounding would be able to assess their importance. Relationships between indoor conditions and wellbeing of occupants are complex because many pollutants contribute to annoyance, irritation and perception. This is also because different parameters (e.g., age, gender, and health status) and conditions not related to indoor environment (e.g., psychosocial stressors, type of work, social status) have been hypothesized to make individuals more susceptible to environmental exposures. Their role and subsequent confounding of the experimental data collected especially in field measurements is not fully understood and requires further elucidation.

Definition of pollutants of concern should also be accompanied by examination of methods for effective control of exposure to these pollutants. They can at best include source and emission control, but may also need to include local exhausts, dilution and removal through ventilation, passive and active air cleaning using the specialized equipment, and perhaps materials having properties to seal emission of pollutants or clean the air from unwanted pollution already released into the air (Darling et al., 2012). In any case, the impact on health and comfort should always be examined after the different exposure and emission control methods have been applied in existing buildings; this applies particularly to air cleaning which often is tested under experimental conditions in the laboratory for specific contamination and no tests are performed under real conditions and for mixtures of pollutants (Zhang et al., 2011).

Traditionally acute effects on humans are monitored and there is quite limited research data on the chronic comfort and health effects in the built environment including serious chronic effects such as cancer. Without finding the reasons on why these data re missing, it should be underlined that the future research needs to document the relationship between the chronic and acute effects, and whether the decision criteria for setting the requirements regarding indoor air quality in buildings should be based on the chronic or on acute effects, or both. In addition, it should be decided whether the requirements should be based on health or comfort end-points, or both, most of the current ventilation standards are using comfort as decision criteria. The expectations of the users of highly energy efficient buildings regarding their performance should not be neglected. They should include opinions of all different stakeholders involved in the building process and not only users of the buildings.

It is clear from Figure 1 that achieving healthy and comfortable highly energy efficient buildings require not only sufficient scientific evidence but also proper solutions, implementation and support in form of the regulations and policies. Although not traditionally included in the research agenda the topics dealing with the implementation and policies have been considered in the present work. It was felt that they were as important as purely scientific topics. The listed policies should appeal to the authorities for taking responsible role for creating conditions in built environment supporting healthy and comfortable living.

The present research agenda only indirectly discusses the potential impact of climate change on the built environment and the indoor environmental quality. This issue has been considered

to have high priority especially in relation to the effects of overheating (often reported in modern energy efficient buildings), on morbidity, as well as on the aspects of aging population (longer at work, long exposure times indoors, etc.). The definition of climate severity index was proposed during workshops as a tool for design of the built environment to address somehow this issue. Since the climate change and the related research agenda has been covered previously (IOM, 2011), it was therefore decided to exclude it from the present work.

There is no doubt that implementation of the actions illustrated in Tables 1-3 need a substantial funding. The listed topics can be used when the funding programs, research directions and priorities are formed by different public, private, national and international agencies supporting research.

The research agenda and their outcomes need to be properly communicated not only in the form of the scientific discourse, but also in form that can be easily comprehended by the average citizen. She/he should understand the implications of certain actions and behaviors and the needs for application of specific solutions and undertakings, which at first may be even considered as costly and unjustified. Proper PR is an important key especially when it is intended to increase the delegation of responsibility to building users that are important link in the successful operation of building systems, as indicated above. Consequently, it is very important that the users of highly energy efficient buildings are properly informed and instructed among others on how to use the building and the different technologies so that their health and comfort are not compromised.

5 CONCLUSIONS AND OUTLOOK INTO THE FUTURE

The future work should take into consideration the past and current research programs, partially to learn what issues have not been addressed already that are on the list of research priorities identified in the present paper, which issues need further elucidation, and also in order not to repeat the work that has already been completed. The topics/issues presented in Tables 1-3 could form the basis to classify new initiatives and contributions in the area of health and comfort in highly energy efficient buildings.

Developing an open-source Internet-based database assembling the information, or search engine finding information on research studies investigating the impact of indoor environmental quality on health and comfort in modern and traditional buildings would be useful tool for advancing the sciences in this context. The information on the running and completed projects is already available on web sites of different funding agencies, but it is difficult to access and is not available in the standardized format.

Developing databases with benchmark measurements would be useful as well.

Future policies should build upon the existing ones and the particular focus should be directed towards achieving crosscutting, integration, harmonization and compliance between different policies.

6 ACKNOWLEDGMENTS

Present work was supported by the Joint European Medical Research Board (JEMRB) through funding provided by the European Insulation Manufacturers' Association

(EURIMA). The work was overviewed by and consulted with JEMRB Trustees through regular contact with Prof. Thomas Schneider to whom many thanks are directed for very valuable comments and suggestions. The Authors thank the participants of the workshop held in Brussels on May 2-3, 2012 and the workshop held during AIVC 2012 conference in Copenhagen on October 10-11, 2012 for the valuable contributions to the proposed research agenda.

7 REFERENCES

Darling, E.K., Cros, C.J., Wargocki, P., Kolarik, J., Morrison, G.C., and Corsi, R.L. (2012). Impacts of a clay plaster on indoor air quality assessed using chemical and sensory measurements, *Building and Environment*, 57, 370-376.

EPBD (2002). *Directive 2002/91/EC of the European Parliament and of the Council of 16 December 2002 on the energy performance of buildings*.

EPBD (2010). *Directive 2010/31/EU of the European Parliament and of the Council of 19 May 2010 on the energy performance of buildings (recast)*.

Frontczak, M., Schiavon, S., Goins, J., Arens, E., Zhang, H. and Wargocki, P. (2012). Quantitative relationships between occupant satisfaction and satisfaction aspects of indoor environmental quality and building design, *Indoor Air*, 22: 119–131. doi: 10.1111/j.1600-0668.2011.00745.x

IOM (Institute of Medicine) (2011). *Climate Change, the Indoor Environment, and Health.* Washington DC, The National Academy Press.

Kotzias, D., Koistinen, K., Kephalopoulos, S., Schlitt, C., Carrer, P., Maroni, M., Jantunen, M., Cochet, C., Kirchner, S., Lindvall, T., McLaughlin, J., Mølhave, L., Fernandes, E., and Seifert, B. (2005). *The INDEX project. Critical Appraisal of the Setting and Implementation of Indoor Exposure Limits in the EU. Final Report*. EUR 21590 EN. European Commission, Directorate General, Joint Research Centre.

Logue, J.M, Price, P.N., Sherman, M.H., and Singer, B.C. (2011) A Method to Estimate the Chronic Health Impact of Air Pollutants in U.S. Residences. *Environmental Health Perspectives*, 120, 216-222.

Jantunen, M., Oliveira Fernandes, E., Carrer, P., Kephalopoulos, S. (2011). *Promoting actions for healthy indoor air (IAIAQ)*. European Commission Directorate General for Health and Consumers. Luxembourg. ISBN 978-92-79-20419-7.

Oliveira Fernandes, E., Jantunen, M., Carrer, P., Seppänen, O., Harrison, P., Kephalopoulos, S., (2009). *Co-ordination Action on Indoor Air Quality and Health Effects (ENVIE). Final report*.

Sundell, J. and Bornehag, C-G. (1999). Nordic interdisciplinary reviews of the scientific literature concerning the relationship between indoor environmental factors and health, Nordworks. in Raw, G., Aizlewood, C. and Warren, P. (eds) *Proceedings of Indoor Air '99*, Edinburgh, The 8th International Conference on Indoor Air Quality and Climate, vol 1, pp 177-182

Wargocki, P. (2011). Productivity and Health Benefits. *Encyclopaedia of Environmental Health*, Nriagu, J.O. ed., Burlington: Elsevier, pp. 688-693.

Weschler, C. J. (2011). Chemistry in indoor environments: 20 years of research. *Indoor Air*, 21: 205–218. doi: 10.1111/j.1600-0668.2011.00713.x

WHO (2006): Air quality guidelines. Global update 2005. Particulate matter, ozone, nitrogen dioxide and sulfur dioxide. Copenhagen, WHO Regional Office for Europe, 2006.

WHO (2010): WHO Guidelines for Indoor Air Quality: Selected pollutants. Copenhagen, WHO Regional Office for Europe, 2010.

Zhang, Y., Mo., J., Li, Y., Sundell, J., Wargocki, P., Zhang, J., Little, J.C., Corsi, R., Deng, Q, Leung, M., Fang, L., Chen, W., Li, J., Sun, Y. (2011) Do commonly-used air cleaning technologies improve indoor air quality? A literature review, *Atmospheric Environment*, 45(26), pp. 4329-4343.

WHY WE VENTILATE

Max Sherman, Jennifer M. Logue, Phillip N. Price, and Brett C. Singer

Lawrence Berkeley National Laboratory
1 Cyclotron Road
Berkeley, California, USA

ABSTRACT

It is widely accepted that ventilation is critical for providing good indoor air quality (IAQ) in homes. However, the definition of "good" IAQ, and the most effective, energy efficient methods for delivering it are still matters of research and debate. This paper presents the results of work done at the Lawrence Berkeley National Lab to identify the air pollutants that drive the need for ventilation as part of a larger effort to develop a health based ventilation standard. First, we present results of a hazard analysis that identified the pollutants that most commonly reach concentrations in homes that exceed health-based standards or guidelines for chronic or acute exposures. Second, we present results of an impact assessment that identified the air pollutants that cause the most harm to the U.S. population from chronic inhalation in residences. Lastly, we describe the implications of our findings for developing effective ventilation standards.

KEYWORDS

Indoor air quality; hazard analysis; residential; DALYs; ventilation

INTRODUCTION

The primary purposes of ventilation in buildings are to provide a sufficient oxygen supply for the occupants and to remove any hazardous substances or noxious odors in the indoor air. For thousands of years societies have realized the need to set or adjust ventilation for specific indoor tasks. The initial inception of residential ventilation is unknown, but likely was from neolithic times and used to remove combustion gases from indoor heating and cooking such as introducing vents for fires. According to Kuhnl-Kinel [1], ancient Egyptians noticed that stone cutters working outdoors had fewer respiratory problems, people in the middle ages realized that air in building could transmit disease, and in 1600 the king of England required buildings to be a certain height with tall, slim windows to facilitate the removal of smoke from heating and cooking.

Traditionally in residences the dominant form of ventilation has been natural ventilation including infiltration. In older, leakier homes infiltration from weather driven flows through cracks in the building's exterior may provide sufficient ventilation for residents. In the 1960s and 1970s home construction shifted from natural materials to new synthetic materials and new construction products; and there was increasing interest in tightening homes to conserve energy due to the energy crisis of the 1970s. The increased tightness in homes reduced ventilation that, along with synthetic materials, led to dramatic increases in residential mold related problems and potential issues with combustion spillage. There was also increasing concern about the impact of material emissions on the health of residences as new materials were introduced.

People spend the majority of their time in residences [2], making indoor air quality an increasing concern. It has been widely recognized that the health burden of indoor air is significant [3-4]. Current ventilation standards are ostensibly set to protect the health of residents. The American Society of Heating, Refrigerating and Air Conditioning Engineer's (ASHRAE's) Standard 62.2 is the most widely accepted residential ventilation standard in the United States. ASHRAE developed Standard 62.2 "Ventilation and Acceptable Indoor Air Quality in Low-Rise Residential Buildings" to address indoor air quality (IAQ) issues (ASHRAE 2010). ASHRAE 62.2 is now required in some building codes, such as California's Title 24, and treated as a standard of practice in many energy efficiency programs and by organizations that train and certify home performance contractors. The standard specifies an overall, residence-level outdoor air ventilation rate as a function of floor area (a surrogate for material emissions) and the number of bedrooms (a surrogate for occupant-related emissions) and requires bathroom and cooking exhaust fans. The focus of the standard generally is considered to be the overall ventilation rate. This emphasis has been based on the idea that risks indoors are driven by continuously emitted, distributed sources such as formaldehyde from furnishings and bio-effluents (including odors) from humans. The required level of whole residence mechanical ventilation was based on the best judgment of experts in the field, but was not based on any analysis of chemical pollutant concentrations or other health-specific concerns.

While whole residence ventilation has been recognized as an effective method for reducing many indoor risks, there are significant costs associated with high ventilation rates due to moving and conditioning the air. While certain human needs likely set the minimum for ventilation, based on the requirements for providing sufficient oxygen and removing CO_2, source control and efficient task ventilation can remove other contaminates of concern effectively while lowering energy demands and reducing associated green house gas emissions. To effectively design residential ventilation systems to maximize health, while minimizing ventilation costs, we first need to specify our objectives for ventilation.

This paper will present a summary of the ongoing work at the Lawrence Berkeley National Laboratory to develop a health based ventilation standard. This work focuses on non-biological indoor air pollutants. Ventilation affects moisture in the indoor environment, and moisture affects mold development. However, ventilation is not an effective method of controlling whole residence moisture loads (although it is effective in bathrooms) because many locations have higher outdoor than indoor humidity. First we will discuss a hazard assessment of indoor pollutants that identified the air pollutants in residences that exceed health based standards and guidelines. Second, we present the results of a study that determined the relative importance of different pollutants to health. Lastly, we will discuss the impact of these results on ventilation standards.

HAZARD ASSEMENT OF INDOOR POLLUTANTS

The initial step in this broad effort was to conduct a hazard assessment of non-biological air pollutants – i.e., including chemical gases and particles – in residences[5]. The analysis compiled data from published studies reporting measurements of air pollutants in residences. That literature review identified 86 articles that were relevant to acute and chronic exposure in residences and considered a broad collection of contaminants measured indoors regardless of source. The contaminants included some emitted purely from indoor sources, some that enter predominantly from outdoors, and some having both indoor and outdoor sources.

Summary results were compiled and used to calculate representative mid-range and upper-bound concentrations relevant to chronic exposures for over 300 pollutants and peak

concentrations relevant to acute exposures for a few pollutants. For over 100 pollutants, measured concentrations were compared to available chronic and acute health-hazard standards and guidelines from the U.S. Environmental Protection Agency (USEPA), California Office of Environmental Health Hazard Assessment (OEHHA), the U.S. Occupational Safety and Health Administration (OSHA), the Agency for Toxic Substances and Disease Registry (ATSDR), and the World Health Organization. Fifteen diverse pollutants were identified as potential chronic or acute health hazards for many homes. A subset of pollutants were identified as priority chemical pollutants based on the prevalence of the pollutant in homes and the quality of available measurements in homes. Table 1 lists the identified priority hazards.

Priority Pollutants for Chronic Exposure	Potential Acute Exposure Concerns
Acetaldehyde	Acrolein
Acrolein	Chloroform
Benzene	Carbon Monoxide
Butadiene, 1,3-	Formaldehyde
Dichlorobenzene,1,4-	NO_2
Formaldehyde	
Naphthalene	
NO_2	
$PM_{2.5}$	

Table 1. Pollutants that potentially pose an adverse indoor health risks.

The hazard assessment narrowed the list of hundreds of chemicals to a much smaller group of pollutants of concern. But this approach considered only disease incidence for cancer standards and disease potential for non-cancer standards; it did not consider disease severity. Prioritizing mitigation efforts among residential indoor air pollutants, and comparing their cumulative health damage to other environmental hazards requires a consistent and comparative metric that accounts for both disease incidence and the severity or costs of the health endpoints. This need motivated development of an impact assessment methodology for indoor air pollutant inhalation.

HEALTH DAMAGE OF CHRONIC INDOOR AIR EXPOSURE

We synthesized disease incidence and health damage models to develop a methodology for quantifying indoor air quality and applied the methodology to calculate the population average health damage due to chronic inhalation of non-biological air pollutants in U.S. residences[6]. We first analyzed published data to calculate mean exposure concentrations and then estimated age-dependent inhalation air intake over the course of a year. We used disease incidence and disease damage models to predict the pollutant-specific and total health damage in Disability Adjusted Life Years and to identify the pollutants that dominate impacts on human health.

Determining Annual Population Health Damage

To determine the annual population health damage we compared estimates of current air pollutant intake in U.S. homes (using measurement based estimates of population-averaged, residential chronic exposure concentrations) to the theoretical case of a home with no indoor pollutant sources and no pollutants infiltrating from outdoors, i.e. with homes having no pollutants in the indoor air. Population intake via other micro-environments was held constant as a baseline for which inhalation in residences adds an increment of harm.

The Disability Adjusted Life Year (DALY) metric is a powerful tool for quantifying and inter-comparing the damages from health endpoints that can result from specific pollutant

intake. DALYs quantify overall disease damage including both mortality and morbidity. DALYs are the equivalent years of life lost to illness or disease and include years lost to premature death (YLL) and equivalent life years lost to reduced health or disability (YLD).

$$DALY = YLL + YLD \quad (1)$$

The years of reduced health are weighted from 0 to 1, based on the severity of disease, to calculate equivalent years lost. For example, a 5 year illness that reduces quality of life to 4/5 that of a healthy year is valued at 1 DALY lost.

Several authors have determined the DALYs lost per incidence of specific diseases using the preeminent work of Murray and Lopez [7-11]. Multiplying a disease incidence rate by a "damage factor" yields a rate of lost DALYs per disease incidence.

$$DALYs = \frac{\partial Damage}{\partial Disease\ incidence} * Disease\ Incidence \quad (2)$$

Damage rates multilplied by available disease incidence statistics , integrated over all diseases of interest, are often used to determine the total burden of disease in a community. This method was used by the World Health Organization to determine the disease damage for 192 countries [11].

Our analysis used the compilation of measured concentration data to calculate total DALYs lost due to inhalation of air pollutants in residences. We approached this using three different methods. The first method was for criteria pollutants, which are more extensively studied and have a larger body of available epidemiological studies. We aggregated the available Concentration-Response (C-R) functions in the literature to determine disease incidence as a function of a change in airborne concentrations. For each health outcome for each criteria pollutant we multiplied the change in disease occurrence rate by the damage factor for that disease. This level of epidemiological data was not available for the majority of remaining pollutants. The second method that we used was primarily for air toxics or hazardous air pollutants which have limited epidemiological data, but extensive data from toxicological studies. This method used the work of Huijbregts et al. [7] to calculate the health damage associated with the intake of non-criteria pollutants. Huijbregts et al. [7] determined cancer and non-cancer mass intake-based damage factors by synthesizing disease damage factors and animal toxicology based disease incidence rates. This method is much more uncertain than using C-R functions which is reflected by significantly larger uncertainties. The third method was used for pollutants that had already had been significantly studied and had available literature studies apportioning specific disease rates to exposure. This applied to radon and secondhand tobacco smoke (SHS). The population average DALYs lost due to radon, acute carbon monoxide (CO) and SHS were determined based on estimates of disease incidence by multiplying them by the damage factors for those diseases.

Figure 1 shows the damage in DALYs per year per 100,000 people from exposure to the 15 pollutants with the highest central estimate of damage. The whiskers indicate the aggregate uncertainty (95th percentile confidence interval) in the disease incidence and disease damage factors. Figure 1 shows the clear result of our analysis: on a population average, the most harmful pollutants in residential indoor air are $PM_{2.5}$, SHS, formaldehyde, acrolein, radon and ozone. The hazards of SHS and radon are more widely recognized and focused in a smaller fraction of homes. By contrast, $PM_{2.5}$, acrolein, and formaldehyde are present at substantial levels in most homes yet there may be less widespread recognition of these hazards. Formaldehyde is primarily emitted from materials throughout the home. Acrolein is primarily

emitted from materials and cooking [12]. $PM_{2.5}$ concentrations indoors, unlike acrolein and formaldehyde, are due to both indoor and outdoor sources and outdoor concentrations may exceed indoors in many locations [4].

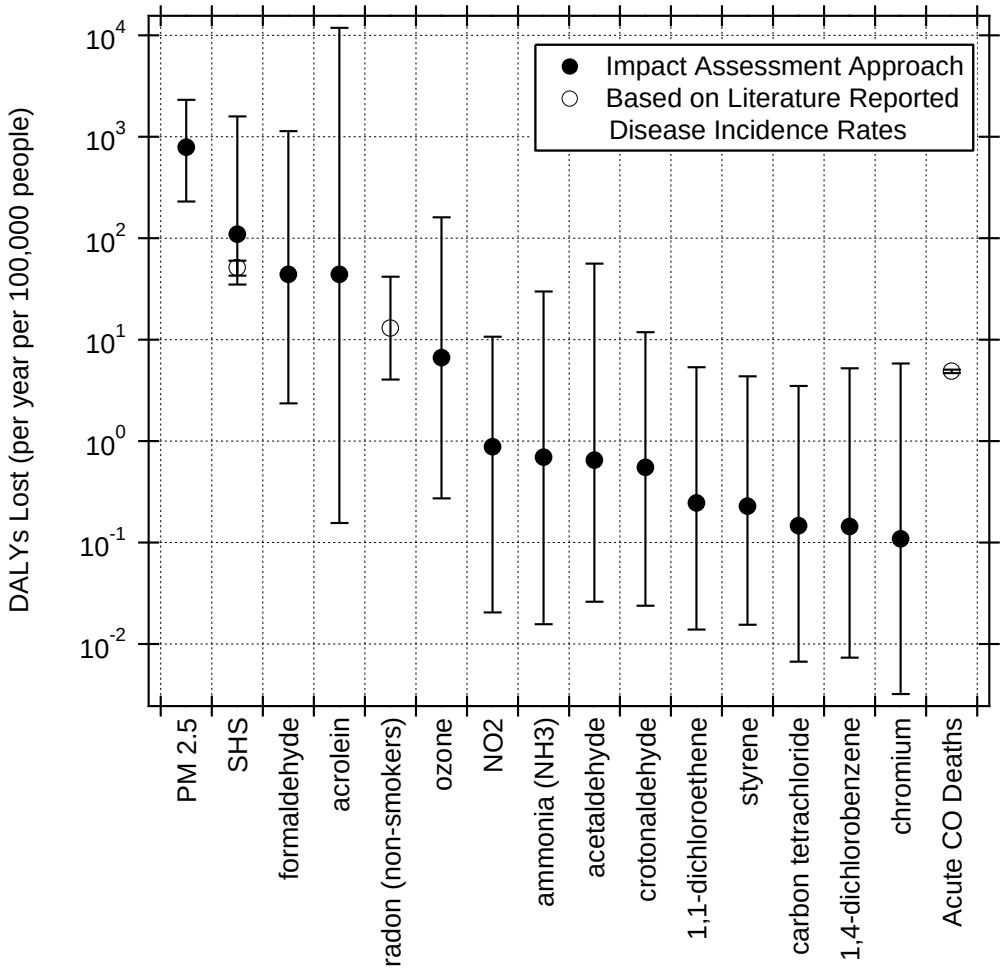

Figure 1. Estimated population averaged annual cost, in DALYs, of chronic air pollutant inhalation in U.S. residences; results for the 15 pollutants with highest mean damage estimates.

To explore possible variations in the health impact rankings of pollutants across homes, we used a Monte Carlo approach to calculate the total chronic health damage from exposure to all pollutants included in our analysis, except radon and SHS. For each home, we sampled with replacement from the distribution of estimated damage for each pollutant and calculated an estimate of total health damage for the home. We assumed independent variability of all pollutants. This was repeated for a sufficient number of homes to yield a stable mean and standard deviation for the total health damage. We assumed that individual pollutant damages vary independently. This approach did not explicity account for any synergistic or antagonistic interactions of pollutant health effects. The resulting distribution of total health damage and the characteristics of each set of individual pollutant contributions to the total health damages were analyzed. For 80% of the sample sets (calculated damages for individual homes), $PM_{2.5}$ was the largest contributor. For 16% of the sample sets acrolein was the dominant contributor and for 4% of the sample sets it was formaldehyde. The dominant contributor was a compound other than these three in less than 0.25% of the sample sets. For 90% of the sample sets, acrolein, formaldehyde, and $PM_{2.5}$ contributed more than 80% of the

total health damage. This reinforces the finding that these three pollutants account for the majority of chronic health from intake of air pollutants in non-smoking homes. We estimate that the current indoor air quality related heath damage to the U.S. population from all sources, excluding SHS and radon, is in the range of 4-11 mili-DALY/p/yr (mili-DALYs per person per year). This indicates that the damage attributable to indoor air is, comparatively, somewhere between the health effects of road traffic accidents (4 mili-DALY/p/yr) and all-cause heart disease (11 mili-DALY/p/yr) in the U.S. The compounds that dominate that total are $PM_{2.5}$, acrolein, and formaldehyde.

IMPLICATIONS FOR VENTILATION STANDARDS

Ventilation standards have the potential to significantly improve indoor air quality (IAQ) in the vast majority of homes. Identifying the pollutants that drive the risks will allow us to make suggestions for modifying the current ventilation standards and identify areas where further research is needed. This section describes how two particular elements of ventilation standards can improve IAQ: overall air exchange rate and localized exhaust ventilation.

Current ventilation standards focus primarily on providing the right amount of overall ventilation for a home based on the idea that the main drivers for pollutant concentrations are furnishings and occupants themselves. A reasonable lower bound for the overall ventilation rate would likely be the airflow needed to control for body odor [13]. Additional air flow is needed to control concentrations of pollutants that have diffuse emission sources in residences. Our analysis indicated that material emissions of acrolein and formaldehyde are the main pollutants that need to be controlled with an overall ventilation rate and the rate should be set at levels that would provide safe indoor concentrations of these pollutants.

There is insufficient material emission data currently to set a ventilation rate based on acrolein, however an appropriate ventilation rate for formaldehyde has been suggested based on California health standards of 0.3 air changes per hour for existing homes and 0.5 for new homes [14]. There are two main concerns with providing ventilation at these levels: 1) the cost of conditioning the extra airflow and 2) bringing in outdoor pollutants.

One way of reducing needed overall ventilation for a home, and the associated energy and cost penalty, would be source control. Currently in the U.S. there is not sufficient information to estimate the benefits of source reduction by simulating the replacement of specific materials or applying specific existing standards or guidelines for material emissions [15]. Developing these databases could aid in the reduction of material loading of formaldehyde and acrolein. Implementing standards that reduced material loading in homes would reduce the required ventilation rate and save energy.

Increasing air flow through the home increases the rate at which outdoor pollutants are brought indoors. Our study identified $PM_{2.5}$ as the most important pollutant for health in residential environments. While indoor sources such as combustion and chemistry significantly impact indoor $PM_{2.5}$ concentrations, a significant fraction of homes may have higher concentrations outdoors than indoors indicating that more ventilation may actually increase health risks [4]. Providing ventilation air via filtered supply or filtered balanced ventilation using heat/enthalpy recovery ventilators is one potential solution. Another option is to filter the indoor air independent of the ventilation system to reduce indoor $PM_{2.5}$ concentrations. Including measures to reduce indoor particle concentrations in ventilation standards could greatly improve IAQ from a health perspective.

Our analysis indicates that effective localized exhaust ventilation is key to maintaining good IAQ. The two main types of localized exhaust in ventilation standards are kitchen and bath ventilation. Effective kitchen ventilation is needed to mitigate acute pollutant events resulting from combustion based cooking appliances and food preparation activities. Task ventilation can also significantly mitigate chronic exposures by removing pollutants at their source. ASHRAE 62.2 requires a kitchen exhaust fan that is above the cooktop and provides at least 100 cubic feet per minute (roughly 50 $m^3 h^{-1}$) of airflow while producing 3 sones or less of noise. The standard doesn't specify a minimum pollutant capture efficiency or sound limits at higher flow rates. Requiring a high pollutant capture efficiency and potentially requiring automatic fan use when the range is operated could significantly improve indoor air quality. Four out of five of the identified acute contaminates of concern (except chloroform) are emitted by combustion or cooking. It is critically important to make sure that there is effective ventilation for all indoor combustion. Research is needed to determine if the health benefit of adding a commissioning requirement to ventilation standards is worth the cost.

Effective bath fans are also critical for providing good indoor IAQ. Bath fans remove bio-effluence, moisture and pollutants generated in bathroom activities such as personal care product use and showering. Showering has been shown to elevate concentration of chloroform above acute thresholds[16]. Bathroom exhaust flow rate requirements should be designed to keep chloroform levels below acute thresholds. Further research is needed to determine which episodic activities in bathrooms may lead to acute exposures.

CONCLUSION

The main air pollutants of concern when setting residential ventilation standards are formaldehyde, acrolein, and $PM_{2.5}$. Whole residence ventilation rates should be based on controlling formaldehyde and acrolein. Filtration of incoming or house air to remove $PM_{2.5}$ would substantially improve indoor air quality.

Effective task ventilation is critical for controlling acute exposures in residences. All combustion in homes should be effectively vented and cooking exhaust systems should be required to meet minimum pollutant capture efficiency standards.

The identification of formaldehyde, acrolein and $PM_{2.5}$ as the highest priority pollutants for chronic exposure opens opportunities to improve energy efficiency through consideration of control measures complementary to ventilation.

ACKNOWLEDGEMENTS

Funding was provided by the U.S. Dept. of Energy Building Technologies Program, Office of Energy Efficiency and Renewable Energy under DOE Contract No. DE-AC02-05CH11231; by the U.S. Dept. of Housing and Urban Development Office of Healthy Homes and Lead Hazard Control through Interagency Agreement I-PHI-01070, by the U.S. Environmental Protection Agency Office of Air and Radiation through Interagency Agreement DW-89-92322201-0 and by the California Energy Commission through Contract 500-08-061.

REFERENCES

[1] Kuhnl-Kinel, J. *The History of Ventilation and Air Conditioning: Is CERN up to date with the latest technological developments?* in *Proceedings of the Third ST Workshop-CERN*. 200. Chamonix, France: European Organization for Nuclear Research (CERN).

[2] Klepeis, N.E., et al., *The National Human Activity Pattern Survey (NHAPS): a resource for assessing exposure to environmental pollutants.* Journal of Exposure Analysis and Environmental Epidemiology, 2001. **11**(3): p. 231-252.

[3] Edwards, R.D., et al., *VOC concentrations measured in personal samples and residential indoor, outdoor and workplace microenvironments in EXPOLIS-Helsinki Finland.* Atmospheric Environment, 2001. **35**: p. 4531-4543.

[4] Weisel, C.P., et al., *Relationships of Indoor, Outdoor, and Personal Air (RIOPA) Part I. Collection Methods*. 2005, Health Effects Institute, Mickely Leland National Urban Air Toxics Research Center and Descriptive Analysis.

[5] Logue, J.M., et al., *Hazard assessment of chemical air contaminants measured in residences.* Indoor Air, 2011. **21**(2): p. 92-109.

[6] Logue, J.M., et al., *Chronic Health Damage of Residential Indoor Air.* Submitted to Environmental Health Perspectives, 2011.

[7] Huijbregts, M.A.J., et al., *Human-toxicological effect and damage factors of carcinogenic and noncarcinogenic chemicals for life cycle impact assessment.* Integrated Environmental Assessment and Management, 2005. **1**(3): p. 181-244.

[8] Lvovsky, K., et al., *Environmental costs of fossil fuels: a rapid assessment method with application to six cities*. 2000, The World Bank Environment Department: Washington, D.C.

[9] Murray, C.L. and A.D. Lopez, *The global buden of disease: a comprehensive assessment of rmortality and disability from diseasees, injuries, and risk factors in 1990 and projected to 2020.* Global Burden of Disease and Injury Series. Vol. 1. 1996, Cambridge, MA: Harvard University. 990.

[10] Murray, C.L. and A.D. Lopez, *Global health statistics: A compendium of incidence, prevalence, and mortality estimates for over 200 conditions*, in *Global burden of disease and injury series*. 1996, Harvard University: Cambridge, MA. p. 906.

[11] WHO, *Global Health Risks: Mortality and burden of disease attributable to selected major risks*. 2009, World Health Organization: Geneva, Switzerland.

[12] Seaman, V.Y., D.H. Bennett, and T.M. Cahill, *Origin, occurrence, and source emission rate of acrolein in residential indoor air.* Environmental Science & Technology, 2007. **41**: p. 6940-6946.

[13] Cain, W.S., et al., *Ventilation requirements in buildings: I. Control of occupancy odor and tobacco smoke odor.* Atmospheric Environment, 1983. **17**(6): p. 1183-1197.

[14] Sherman, M.H. and A.T. Hodgson, *Formaldehyde as a basis for residential ventilation rates.* Indoor Air, 2004. **14**(1): p. 2-8.

[15] Willem, H. and B.C. Singer, *Chemical Emissions of Residential Materials and Products: Review of Available Information*. 2010, Lawrence Berkeley National Laboratory: Berkeley, CA. p. 48.

[16] Kerger, B.D., C.E. Schmidt, and D.J. Paustenbach, *Assessment of airborne exposure to trihalomethanes from tap water in residential showers and baths.* Risk Analysis, 2000. **20**(5): p. 637-651.

GREEN ROOFS AND VERTICAL GREENERY SYSTEMS EVALUATION – HEAT AND MASS TRANSFER MODELLING AND EXPERIMENTAL QUANTIFICATION

Marija S. Todorovic

Academy of Engineering Sciences of Serbia, Postal address,
Zeleni Venac 2/III, Belgrade, 11000, Serbia
deresmt@eunet.rs

ABSTRACT

Green roofs and vertical greenery systems present an interesting approach to enhance building's natural ventilation and cooling, improving fresh air quality and building's energy efficiency, reducing building's energy consumption, and reducing an urban heat island, but it is not easy to make reliable prediction on the resulting energy savings, as well as the estimate of the realized ventilation effectiveness. However, over the past decades, green roofs and vertical greenery systems technology have evolved into a viable design component that can provide multiple benefits and aesthetic value to a wide variety of buildings projects. World wide has been collected significant knowledge, observation, implementation, and experimentation to describe successful strategies that include system selection, design, plant selection, maintenance and client/owner education. There are studies stressing benefits of green roofs and green facades as passive systems in the energy efficiency of buildings. These benefits depend very much on the ability of plants to intercept solar radiation, and proceed steadily to grow. On the other hand, design of these systems is difficult because it is not easy to predict relevant extreme climatic conditions, and to obtain reliable data of their biodynamic behavior under different local conditions. In addition, some authors consider the use of these green systems as a thermal storage technology for buildings. Hence, there are reasons to intensify similar investigations to evaluate experimentally the energy impact of using green roof and vertical greenery systems in Mediterranean-continental conditions.

KEYWORDS

Green roof and vertical greenery systems, energy simulation, heat and mass transfer, model validation, experimental quantification.

1 INTRODUCTION

The concept of green walls is an ancient one, with examples in architectural history reaching back to the Babylonians – with the famous Hanging Gardens of Babylon, one of the seven ancient wonders of the world. Highlights of the history of green walls listed in "Green Roofs for Healthy Cities" (September 2008) are: 3rd C. BCE to 17th: Throughout the Mediterranean, Romans train grape vines (Vitis species) on garden trellises and on villa walls. Manors and castles with climbing roses are symbols of secret gardens. 1920s**:** The British and North American garden city movement promote the integration of house and garden through features such as pergolas, trellis structures and self-clinging climbing plants. 1988: Introduction of a stainless steel cable system for green facades. Early 1990s: Cable and wire-rope net systems and modular trellis panel systems enter the North American marketplace. 1993: First major application of a trellis panel system at Universal CityWalk in California. 2002**:** The MFO Park, a multi-tiered 300' long and 50' high park structure opened in Zurich, Switzerland. 2005: The Japanese federal government sponsored a massive Bio

Lung exhibit, the centerpiece of Expo 2005 in Aichi, Japan.

Today, in the world, at the far east and far west, the rapid pace of urbanization and the growing concern for climate change have led to the increasing trend of bringing nature back into cities, and building's greening became a key element of urban transformation and the exterior surfaces of buildings have been deemed to offer vast opportunities for greening - the insertion of greenery into urban-scapes; planting on roofs and walls becoming one of the most innovative and rapidly developing features of city planning, architecture and ecological landscaping. In addition to green roofs, vertical greenery represents a new dimension in greenery-related infrastructure, where plants are incorporated within the vertical surfaces of buildings. The concept itself is not new and there are a few R&D studies conducted in the world in this field, implementation of vertical greenery is yet expected to be on an extensive scale. Concerning the large surface areas on existing buildings which are to be energy refurbished, these technologies are excellent candidates for the two-fold greening: positive environmental change in dense urban areas, and real simple via plants greening.

Building roofs and facades are under permanent environmental influences, such as sun and acid rain, which age and can ultimately destroy them. Living wall systems can protect them. A view back in history shows that green facades are not new technology but can offer multiple benefits as a component of current urban design. In the 19th century, in many European and some North American cities, woody climbers were frequently used as a cover for simple facades writes White Paper version: September 2012.

In Central Europe in the 1980s, a growing interest in environmental protection, resulted in the vision to bring back nature into cities (in many German cities incentive programmes were developed, supporting tenant to plant and maintain climbers in their backyards, roofs and facades). Since the 1980s, research has been conducted on series of relevant topics as follows: the insulating effects of plants on facades, the ability of plants to mitigate dust, plants evaporative cooling effects, and even habitat creation for urban wildlife, including birds and spiders etc.

The aim of this paper is to review research activities on the green roofs and vertical greenery facade technologies, focusing mainly the most intensive research areas on far East and far West. Although, there was a widespread development and presence of attractive technologies in Germany, a lack of implementation guidelines and incentives was dominant in other European countries. Green roof (GR) and vertical greenery systems (VGS) technologies have been recognized in United States as a sustainable technology for saving energy and increasing indoor and outdoor air quality (**P**aulo Cesar Tabares-Velasco, Jelena Srebric 2009). However, until recently, none of the models had been neither enough analyzed nor validated by the experimenting. Although, obvious important, both heat and mass fluxes and surface temperatures were not objective of serious study. A recently developed green roof thermal performance model by Paulo Cesar Tabares-Velasco and Jelena Srebric 2012, was experimentally quantified by Paulo Cesar Tabares-Velasco et. al 2012. Further studies and discussions are necessary to clarify considerations for successful green facade installations and projects, although green facade systems have a history of durability and functionality, compared with other green wall systems, that can make their inclusion cost effective into projects of all scales.

2 GREEN ROOF MODELLING AND VALIDATION

2.1. Green Roof Modeling

The green roof model with plants has been defined by Paulo Cesar (Paulo Cezar Tabares-Velasco and Jelena Srebric 2012) as an extension of the model for green roof without plants.

Assuming negligible thermal storage and metabolic rate, the energy balance for the plant canopy and for the substrate underneath the plants they formulated by the following two equations, respectively:

$$R_{sh,abs,plants} = Q_{film,plants} + Q_{IR,S,P} \quad (1)$$

$$R_{sh,abs,substrate} = Q_{IR,S,P} + Q_{s,s} + Q_{conduction} + Q_{IR,subs,cov,sky} + Q_E \quad (2)$$

where $R_{sh,abs,plants}$ is the absorbed short-wave radiation by the plants, and $Q_{film,plants}$ represents the heat transfer between plants and the surrounding environment by means of latent (transpiration), convective, and radiative heat transfer. In Equation (1), $R_{sh,abs,substrate}$ is the absorbed solar radiation by substrate underneath the plants, $Q_{IR,S,P}$ is the radiative or long-wave radiative heat transfer between the plant layer and the top substrate layer, $Q_{S,S}$ is the convective heat transfer between the top substrate layer and the surrounding air, $Q_{conduction}$ is the conductive heat flux through green roof substrate, and $Q_{IR,subs,cov,sky}$ is the thermal radiation exchanged between substrate and sky.

The amount of solar radiation absorbed by the plants ($R_{sh,abs,plants}$) and substrate underneath the plants ($R_{sh,abs,substrate}$) depends on the spectral properties of both surfaces, as well as the vegetation density in terms of LAI, which is mostly defined as the projected or shadow leaf area divided by the ground area. Absorbed solar radiation by the plants is calculated using Equation (3) as follows:

$$R_{sh,abs,plants} = (1 - \rho_{plants} - \tau_{plants,solar})(1 + \tau_{plants}\rho_{substrate})R_{sh} \quad (3)$$

where $\tau_{plants,solar}$ is short-wave transmittance of a canopy ($\tau_{splants,solar} = e^{-ksLAI}$), and k_s is the extinction coefficient, the amount of intercepted solar radiation depends on the transmittance of the plant layer, what depends on the solar altitude and leaf orientation.

Furthermore, the absorbed solar radiation for the substrate underneath the plants ($R_{sh,abs,substrate}$) represents the amount of radiation that is not intercepted by the leaves, transmitted ($\tau_{plants,solar}$) or reflected ($r_{substrate}$) to the substrate as follows:

$$R_{sh,abs,substrate} = \tau_{plants,solar}(1 - \rho_{substrate})R_{sh} \quad (4)$$

In addition to the solar radiation, the thermal radiation exchange between sky, plants, and green roof substrate is to be taken in account:

$$Q_{IR,plants,sky} = (1 - \tau_{plants,IR})\varepsilon_{plants}\sigma(T_{plants}^4 - T_{sky}^4) \quad (5)$$

$$Q_{IR,substrate,cov,sky} = (\tau_{plants,IR})\varepsilon_{substrate}\sigma(T_{plants}^4 - T_{sky}^4) \quad (6)$$

Long-wave radiation exchange between plants and substrate is very complex and difficult to be determined. But using appropriate assumptions calculations is simplified. So, assuming that plants and substrate are infinite parallel plates/surfaces following equation is obtained by Paulo Cesar (Paulo Cezar Tabares-Velasco and Jelena Srebric 2012):

$$Q_{IR,S,P} = (1 - \tau_{IR})\frac{\sigma(T_{plants}^4 - T_{top,substrate}^4)}{\frac{1}{\varepsilon_{substrate}} + \frac{1}{\varepsilon_{plants}} - 1} \quad (7)$$

As a next step, the convective heat transfer coefficient is calculated using equation (4), developed for horizontal flat plates, but adding a correction coefficient to account for the roughness of the plants. In addition, convective heat transfer at the substrate is calculated using an equation developed for convection of porous media Paulo Cesar (Paulo Cezar

Tabares-Velasco and Jelena Srebric 2012):

$$Q_{convection,plants} = 1.5.\,\mathrm{LAI}.\,h_{conv}(T_{plants} - T_{air}) \quad (8)$$

$$Q_{convection,substrate,cov} = h_{sub}(T_{substrate,top} - T_{air}) \quad (9)$$

A particularly important heat fluxes shown in the energy balance Equations (1 and 2) are substrate evaporation and plant transpiration, particularly if reductions of building's cooling loads are focused. Plant transpiration can be is calculated using Equation (10), and the stomatal resistance, rs, using the Equation (11):

$$Q_T = \mathrm{LAI}\frac{\rho C_p}{\gamma(r_s + r_a)}(e_{s,plants} - e_{air}) \quad (10)$$

$$r_s = \frac{r_{stomatal,min}}{\mathrm{LAI}} \cdot f_{solar} \cdot f_{VPD} \cdot f_{vwc} \cdot f_{temperature} \quad (11)$$

The empirical functions "f" in Equation (21) represent a role that different environmental and plant variables (solar radiation - f_{solar}, vapor pressure deficit – f_{VPD}, water content – f_{VWC}, and temperature – $f_{temperature}$), play in stomatal resistance/aperture and, consequently, in plant transpiration.

2.2. Green Roof Modeling Validation via Green Roof Field Data

Presented modeling approach has been experimentally explored by same authors Paulo Cesar (Paulo Cesar Tabares-Velasco, Jelena Srebric (2011). They conducted measurements aimed to determine whether their model is correctly predicting the real green roof physics, by the measuring technical characterization of the heat and mass transfer fluxes under quasi-steady state conditions in the environmental chamber within a specially designed laboratory apparatus, named "Cold Plate".

However, as that heat and mass transfer model was only validated in quasi-steady-state conditions, in order to assure the accuracy of the model, authors further research resulted in physically more sound description and dynamic validation of the model based on the field data from a green roof installed on a commercial building in Chicago during summer weather conditions (published by Paulo Cesar Tabares-Velasco, Mingjie Zhao, Nicole Peterson, Jelena Srebric, Robert Berghage, 2012 in paper entitled "Validation Of Predictive Heat And Mass Transfer Green Roof Model With Extensive Green Roof Field Data").

The instrumented green roof total area was about 14,000 m^2 and about half of that area was covered with a green roof. From top to bottom, the installed green roof consisted of: (1) a plant layer of mixed Sedum species, (2) 7.5 cm substrate layer, (3) two layers of polypropylene fabric layers, (4) 2.5 cm of thick foam drainage/protection board made from chunks of recycled closed cell polystyrene, and (5) 0.2 cm PVC waterproof membrane layer. The substrate used was based on expanded clay and has a dry bulk density of 650 kg/m^3 , bulk density at the maximum water-holding capacity of 1130 kg/m^3, and a maximum volumetric water-holding capacity of 49.6%. The green roof was instrumented with temperature, heat flux, water content sensors and a weather station recording outdoor weather data every 1 min and averaging every 15 min. The roof was instrumented with a net solar radiometer, but without a pyrgeometer for measuring incoming long wave radiation, and consequently the sky temperature was not measured directly, disabling accurate determination of the sky temperature. There are several models to calculate the sky temperature and sky radiation, but for their implementation is necessary to assume clear sky conditions and consequently, the simulated results can over or under-predict the actual sky temperature (approx. by up to 10^oC). Main reason for this discrepancy is the fact that the model does not consider the cloud

cover, and, therefore, the sky temperature can have different trends when compared to the real weather conditions. As a result, it is important to use real weather data, when performing simulations with the green roof model, or in the case that predictions and optimization of the green roof is to be done, it is necessary to implement dynamic, numerical simulations and/or co-simulations and use Typical Meteorological Year data.

Limited by the permitted paper length, details of experimental apparatus and measurements protocols, here are not to be reviewed, but a few figures with graphically presented the measurements results (published by Paulo Cesar Tabares-Velasco, Mingjie Zhao, Nicole Peterson, Jelena Srebric, Robert Berghage, 2012) to illustrate green roof effects demonstrating reached verification of individual heat transfer processes as well as the validation of the modeling quality and accuracy are shown on Figures 1 – 3., as follows.

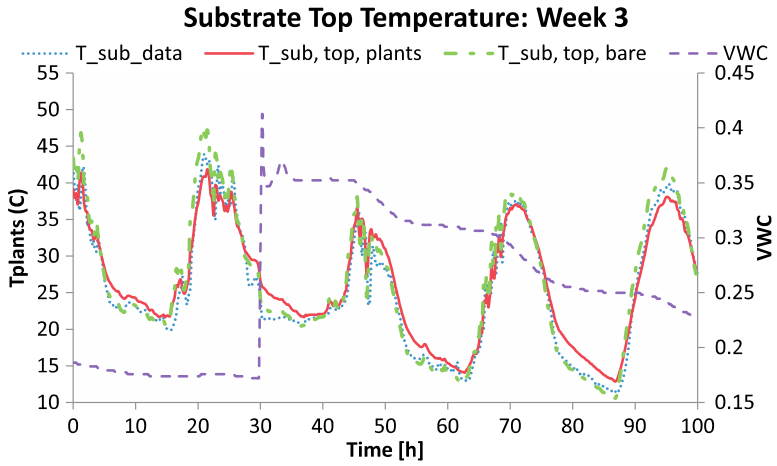

Fig. 1. Substrate top temperature measured data ($T_{sub,\ data}$), calculated substrate top temperatures for bare substrate roof ($T_{sub,\ top,\ bare}$), and calculated substrate top temperatures for substrate covered by plants ($T_{sub,\ top,\ plants}$) during the third week of July, VWC is the amount of moisture that the soil will hold; it is defined as the volume of water divided by the total volume of the sample

Overall, the results in Figs. 1 show that the model accurately predicted the substrate top temperature of the green roof. Comparing, simulated and measured temperatures, can be seen good qualitative results agreement, and that the plants of the green roofs reduced the substrate top temperature significantly. Measured and calculated substrate heat flux dynamics is shown on the Figure 2., and as it values are directly proportional to the temperature gradients and substrate's thermal conductivity, presented curves pattern are demonstrating similarity to the related temperature lines pattern.

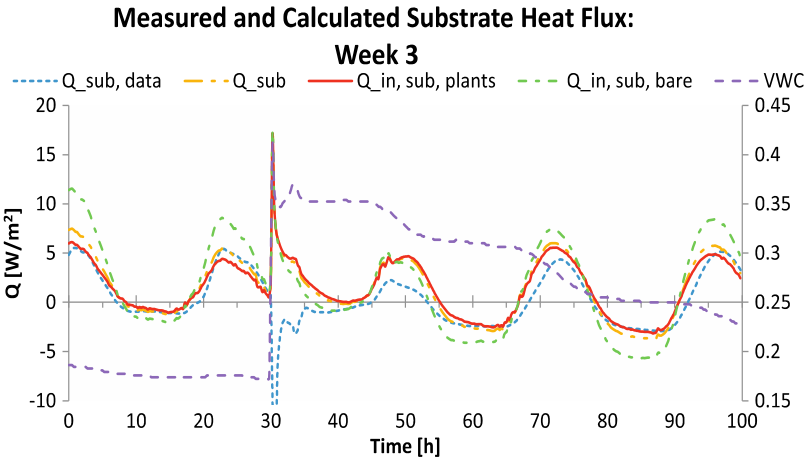

Fig. 2. Substrate heat flux data ($Q_{sub,\ data}$), calculated combined heat fluxes (Q_{sub}), calculated heat fluxes for bare substrate roof ($Q_{in,\ sub\ bare}$) and calculated heat fluxes for green roof covered by plants ($Q_{in,\ sub,\ plants}$) during the second week of July.

2.3. Validation Results and Model Performance Evaluation

The dynamic validation was performed by the comparing substrate surface temperature, heat flux through the roof, and net radiation, and results did show that the green roof thermal

model predicts the heat and mass transfer appropriately as long as the long-wave radiation data from a weather station are used to reduce a possible bias resulting from the sky condition, but discrepancy is significantly increased if sky temperature was calculated by the assumption about the sky conditions.

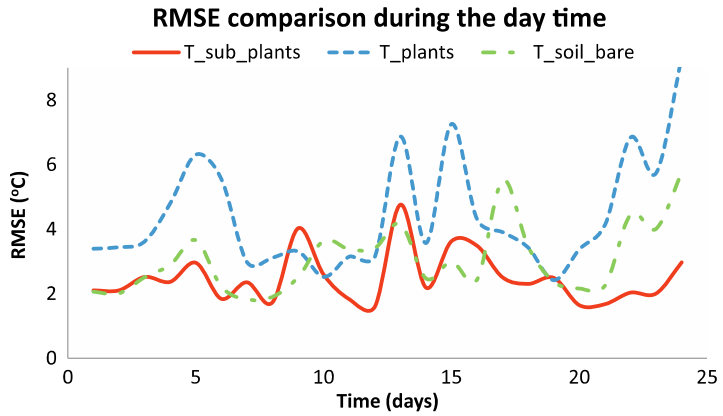

Fig. 3. RMSE (the root mean square error) for top substrate temperatures calculated by the model without plants ($T_{sub\ bare}$), top substrate temperatures covered by plants ($T_{sub\ plants}$) and plant surface temperatures (T_{plants}) during

It is clear, that a green roof has a different thermal performance from a bare substrate roof because of the plants shading, transpiration, and wind shielding, but it is also important to carefully model green roof without plants because green roofs are not 100% covered by plants all time. Therefore, two models - bear and fully covered green roof model, are to be combined in a third model – partially covered green roof, which is most probably the dominant situation on some buildings green roofs.

In addition to the validation diagrams as shown on Fig.1 and 2. validation procedure (Paulo Cesar Tabares-Velasco at. al, 2012) encompassed the proposed Root Mean Square Error (RMSE) analysis illustrated in Fig. 3. In order to further analyze the performance of the model, also normalized root mean square error (NRMSE) values were calculated for surface temperatures, heat fluxes through the roof, and radiation. Comparison of the RMSE values of surface temperatures during the day time and night time, show better agreement during the day than during the night, what is mainly result of inadequate accuracy of the sky temperatures and related long-wave radiation predictions. The long-wave radiation exchange between the sky and the substrate is underestimated, especially during the night when the long wave radiation has a significant role in the heat transfer.

3 VERTICAL GREENERY MODELLING AND VALIDATION

The importance of the outdoor environment greening is growing in synergy with the raising intensity of the worldwide enormous urbanization and urban population growth. Consequences of increased population density in cities and municipalities are increased corresponding infrastructure quality and demands as water quality, storm water management and Urban Heat Island (UHI). White Paper version: Sep. (2012) outlines examples of Seattle and Chicago (Fig. 4) which have implemented design recommendations for the integration of organic, living systems within the built environment, such as green roofs, green walls and vegetated swales, that can act as a bridge to alleviate the increased demands placed on existing infrastructure. This concept known as Living Architecture, promotes biomass to cool urban areas, support the growth of tree canopies to improve air quality and rain gardens to mitigate storm water runoff. It is multi- and cross-disciplinary approach which outlines deep cooperation between architects, architecture and civil engineers, building physics and HVAC engineers, landscape architects, agriculture engineering and horticulture experts.

As a very special example can be, by Kelly Chiang, Alex Tan (2009), described Singapore's vision to be a "City in a Garden" where nature is closely intertwined with the urban fabric,

existing not only as parks and gardens but also becoming an integral part of buildings and of people's lives, and where vertical greenery, together with the other forms of sky-rise greenery, is important segment of the development of the green urban infrastructure.

Fig. 4. Freestanding green facade integrated into a green street demonstration project, Chicago (left), east facing, three story, green facade attached to an urban parking structure, Seattle (right), White Paper version: Sep. (2012).

The fact that Singapore became hotter $0.6^{O}C$ over the last 50 years (The Straits Times, 2009), contributed very much to the raising trend of vertical greenery. There have been more and more systems - installations of vertical greenery in building developments: airport, hotels, residential and public buildings, shopping malls and other. The Singapore National Climate Change Strategy recognized that the UHI effect in Singapore can lead to the greater use of air-conditioning and increase the energy demand, and as a measure to lower the surface and ambient temperatures proposed the amount of greenery to be increased in the city, including rooftop gardens and vertical greening systems on buildings. As these new greenery systems should be designed as buildings adaptable and activated subsystems, related R&D needs are outlined.

3.1. Vertical Greenery Research and Demonstration Project

With an aim to introduce and evaluate various vertical greenery systems (VGS) has been conducted R&D project, results of which are presented by Wong Nyuk Hien (2013). Project objectives were to asses the efficiacy of installing VGS, the maintenance required and the benefits that such installations bring to buildings and to the environment of the tropical climate.

The project encompassed testing of eight VGS, each constructed to fit an industry standard reinforced concrete wall measuring 6 m high by 4 m wide – the equivalent of two storeys of a building. The systems were tested to measure their environmental impact - the benifits of VGS: thermal-, plant shading-, acoustic- and air quality-impact.

Thermal impact - surface temperature. The VG walls and the control wall (a bare surfaced wall) were set up with thermocouple wires for temperature measurements, with an aim to determine the extent of the surface temperature reduction in the presence of VGS (temperature measurements were taken at the wall surface directly behind the VGS and the substrate surface on the system that is covered with plants. In addition, the vertical greenery walls showed a reduced day – night fluctuation of wall surface temperature .

Measurement results showed a distinct reduction in the wall surface temperature with the VGS installation for all eight systems, but the size of reduction varied with each system. The reduction in the wall surface temperature was result of the insulation and shading effect of the

VGS and its associated plants. The recorded substrate temperatures for all eight vertical greenery walls were measurable lower than the wall surface temperature of the control walls and the substrate temperatures were lower than the temperature of the bare control wall as a result of the shading and evapotranspiration cooling effect of the plants Figure 5. Wong Nyuk Hien (2013). Concerning the thermal impact, general concluding remark is that results confirm the potential thermal benefits of the VGS in reducing the surface temperatures of building façades in climatic conditions which deserve air-conditioning. The significant reductions in wall temperatures lead to a corresponding reduction in the cooling loads, air-conditioning needs and brings related savings in energy consumption.

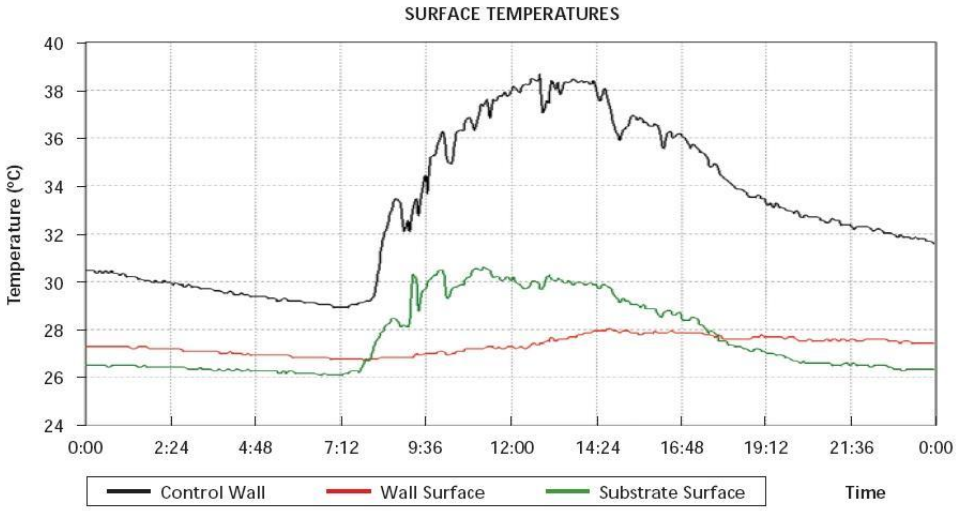

Fig. 5. Temperature readings on bare control wall surface (black) as well as the wall (red) and substrate (green) surfaces of vertical greenery wall 4 in HortPark, Wong Nyuk Hien (2013).

Thermal impact efficiency was influenced by: system typology, substrate profile thickness, type of substrate media, irrigation frequency and substrate media's moisture retention rate, as well as of the plant shading coefficient. Further, VGS can be also used as means to stabilise the daily fluctuation of surface wall temperatures. As constant expansion and contraction of the façade's material is avoided, this feature contributes to the prolonged lifespan of building façades leading to a cost savings in maintenance and replacement of façade cladding.

It is to be stressed according to Wong Nyuk Hien (2013), that similar results are shown by the experiments in Germany where a vertical greenery surface was recorded to be 10°C cooler than a bare wall when observed at 1:30 pm in September (Wilmers, 1990). Also, similar experiments in Hong Kong did show that a maximum temperature decrease of 8.4°C can be achieved. It is interesting that VGS have a stronger effect than rooftop gardens in decreasing the urban canyon air temperature (Alexandri and Jones, 2008).

Thermal impact - ambient temperature. The ambient temperature was defined as the air temperature at distances of 0.15 m, 0.30 m and 0.60 m away from the substrate surface. The difference in ambient temperature between the control wall and the VGS is most significant at 0.15 m away from the vertical greenery systems or control wall surface. Graph 2 on Figure 6. shows that a reduction of ambient temperature was highest when the outdoor air temperature was highest and was as high as 3.3°C. Naturally, this difference decreases with a further distance away from the VGS. By 0.60 m, there was no significant difference. Also temperature decrease depends on the: system typology, density of greenery coverage.

Concerning the quantity of wall façades area in the built environment, the use of VGS to cool the ambient temperature in building canyons can result in lower temperature of air entering air conditioning systems what will have as a savings in the energy cooling loads and demands.

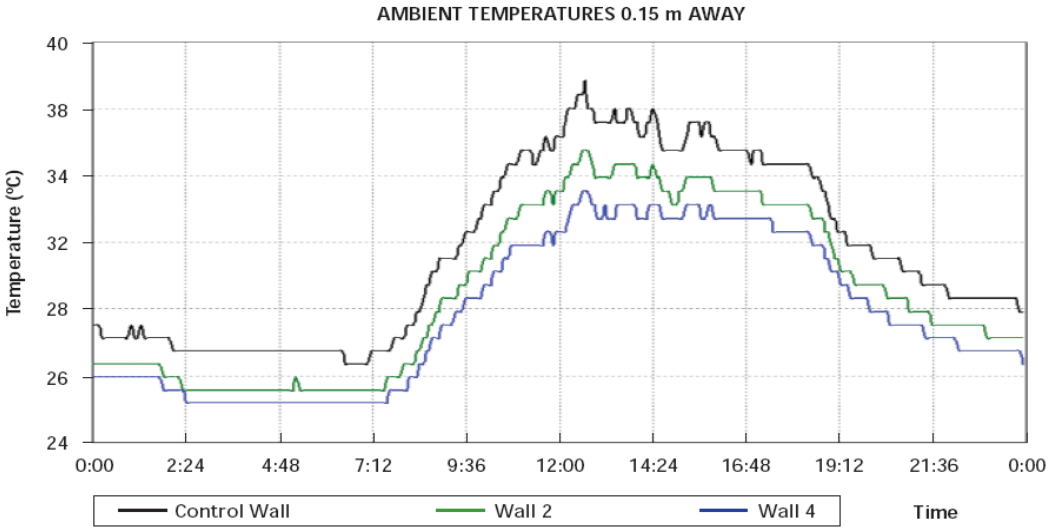

Fig. 6. Graph 2 : Ambient temperatures 0.15 m away from wall – source Wong Nyuk Hien (2013).

Improving Air Quality – Outdoor and Indoor via Ventilation and Air-conditioning. Greenery improves air quality by its intrinsic ability to absorb carbon dioxide and pollution, as well as dust. In Frankfurt, Germany, it was found that streets without trees had an air pollution count of 10,000 to 20,000 dirt particles per litre of air, whereas a street in the same neighbourhood with trees had only 3,000 dirt particles per litre of air (Minke and Witter, 1982).

VGS, when cladded on the façades of buildings situated next to roads with heavy traffic, can absorb and break down a variety of pollutants, notably volatile organic compounds and un-burnt vehicle exhaust's hydrocarbons. Studies on climber plants show that they are highly effective trapping and filtering dust in their tissues (Johnston and Newton, 1993; Peck *et al.,* 1999).

With the widespread adoption of GR and particularly VGS, the amount of biomass in an urban area can be increased, thus contributing to the reduction of carbon dioxide levels produced by vehicles, industrial processes and mechanical systems. This reduction leads to improved outdoor air quality and reduced respiratory problems among the people living in the city, and helps to increase quality of fresh air used for ventilation either natural or mechanical, as well as within air-conditioning system.

3.2. Vertical Greenery Systems Investigation via Energy Simulations

A review of studies on the VGS thermal effects is valuable to get insight in ranges of related quantification results. For example, the shading effect of vertical greenery systems reduces the energy used for cooling by approximately 23% and the energy used by fans by 20%, resulting in 8% reduction in annual energy consumption (Bass and Baskaran, 2003). Projected energy savings range from 90% to 35% for various cities when all possible façades are implemented with vertical greenery systems (Alexandri and Jones, 2008). The presence of vertical greenery systems is effective in lowering the mean radiant temperature of a building if the entire glass façade is covered. Similarly, the energy cooling load will be significantly reduced if the plant shading coefficient is low and the greenery coverage is high (Wong *et al.,* 2009a).

To get better insight in VGS dynamics and try to advance the knowledge, a series of simulations were run - Wong Nyuk Hien (2013), with a direct goal to find out the effect of VGS on the thermal comfort and cooling energy loads while relevant quantities were the mean radiant temperature (MRT) - the average mean temperature of all the objects surrounding a person, and the energy cooling load - the energy required to cool the interior space to the temperature set by the controller.

A comparative study of three different scenarios was studied to obtain the MRT of a hypothetical 10-storey building, measuring 30.0 m in length by 30.0 m in width and 4.0 m high for every floor.

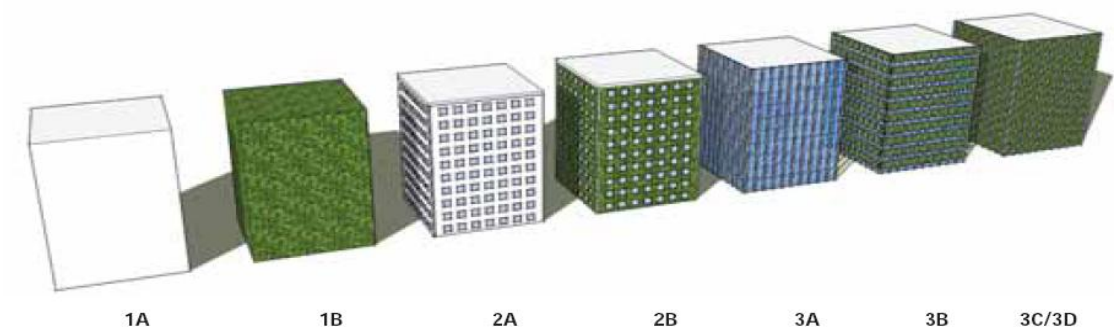

Fig. 7. Scenarios of energy simulations – source Wong Nyuk Hien (2013).

In the Table 1. are presented Scenarious analysed by the simulation, their relevant characteristics and quantities, and corresponding simulations results.

Table 1. Summary of energy simulations

Scenarios	Greenery Coverage	MRT (^{o}C)		Reduction in Energy Consumption (%)
		Maximum	Minimum	
Full Opaque Wall				
1A	0%	34.39	30.28	–
1B	100%	24.01	23.20	74.29%
Opaque Wall With About 25% Window Perforations				
2A	0%	36.57	27.71	–
2B	100%	35.30	27.82	10.35%
Full 6 mm Thick Clear Glass Façade				
3A	0%	49.94	27.63	–
3B	50%	45.81	27.73	12.45%
3C	100% (SC = 0.5)	45.03	27.48	17.93%
3D	100% (SC = 0.1)	45.72	27.75	31.75%

Plant Shading Coefficient and Envelope Thermal Transfer Value ETTV. The plant shading coefficient study was carried out in HortPark in Singapore to determine the plant shading coefficient of different types of plants as well as the correlation between the plant shading coefficient and leaf area index (LAI). The plant shading coefficient of each species allows a quantitative calculation of the vertical greenery systems. The plant shading coefficient is the ratio of the average solar radiation of the plant species over the average solar radiation of the control wall at the same period of time, while the LAI is defined as the single-side leaf area per unit ground area of a plant (Ong, 2003).

Correlation Between Plant Shading Coefficient and Leaf Area Index (LAI). Field studies results show that VGS block incident solar radiation, reducing the amount of heat through the concrete façade. This performance depends on the system structure, substrate and plant characteristics. Thicker the overlaps and coverage of leaves is, their shading is better.

The correlation equation between the plant shading coefficient and LAI shows an inversed linear relationship, as a consequence of the plant shading coefficient (PSC) definition. PSC is defined as the ratio of the average solar radiation beneath a plant to the control wall. A low

solar radiation value beneath the plant signifies that the plant can shade the wall effectively. Hence, with the same incoming solar radiation, a plant that shades better will have a corresponding lower shading coefficient. Relevant mathematical formulation is as follows:

$$PSC = - 0.3043\ LAI + 0.8112 \quad (12)$$

Its meaning is: a lower plant shading coefficient means denser greenery coverage, leading to greater thermal insulation and a lower LAI. VGS is to have denser greenery coverage in order to provide more shade and insulation for the building. In the comparison study of all the plants that were planted on eight vertical greenery systems, it was observed that plants which achieve optimum results (high LAI and low plant shading coefficient) were species with denser leaves and wider greenery coverage.

Envelope Thermal Transfer Value (ETTV) Calculations. By Wong Nyuk Hien the ETTV is a measure of the average heat gain into a building through its envelope by taking into account the three basic components of heat transfer, namely heat conduction through opaque walls, heat conduction through glass windows and solar radiation through glass windows. The conducted research project Wong Nyuk Hien (2013), particularly its research component of the plants shading coefficient has lead to the possibility to include greenery into the calculation of ETTV by the following equation:

$$EETV = \frac{12(A_{w1}.U_{w1} + A_{w2}.U_{w2} + \ldots + A_{wn}.U_{wn})}{A} + \frac{3.4(A_{f1}.U_{f1} + A_{f2}.U_{f2} + \ldots + A_{fn}.U_{fn})}{A_o} + \frac{211(A_{f1}.SC_{f1} + A_{f2}.SC_{f2} + \ldots + A_{fn}.SC_{fn})(CF)}{A_o} \quad (13)$$

where:

- A_{w1}, A_{w2}, A_{wn} : areas of different opaque wall (m^2)
- A_{f1}, A_{f2}, A_{fn} : areas of different fenestration (m^2)
- A_o : gross area of the exterior wall (m^2)
- U_{w1}, U_{w2}, U_{wn} : thermal transmittances of opaque walls (W/m^2 K)
- U_{f1}, U_{f2}, U_{fn} : thermal transmittances of fenestrations (W/m^2 K)
- SC_{f1}, SC_{f2}, SC_{fn} : shading coefficients of fenestrations
- CF : correction factor for solar heat gain through fenestration

The calculations for the Scenarios given in the Table 1. show that the presence of a VGS on a full glass façade is effective in reducing the building's façade's ETTV, and that its effectiveness is raising with the decrease of the plant shading coefficient. For example with a plant shading coefficient of 0.500, VGS has helped to reduce the ETTV by more than 40%.

Table 2. ETTV calculation for scenarios 1A and 1B, source Wong Nyuk Hien (2013).

Plant Shading Coefficient	ETTV (W/m^2)		ETTV Reduction
	Scenario 1A	Scenario 1B	
0.986	59.537	59.184	0.59%
0.500	59.537	46.909	21.21%
0.041	59.537	35.316	40.68%

Also and example: with the presence of VGS, an envelope thermal transfer value (ETTV) of a building with full glass façade is effectively reduced with a greenery effectiveness of 40.68% (Wong et al., 2009a).

4 CONCLUSIONS

In this paper presented is a review of the state of the art of the energy impact of the GR (green roofs) and VGS (vertical greenery systems), and a review of recent research results, focusing GR and VGS evaluation, particularly their thermal performance of extensive roof and vertical greenery systems – heat and mass transfer modelling and experimental quantification. In particular, study focuses the role of plants for the heat flux reduction through the building's roof and façade's structures and the plants role in reducing air pollution and increasing air quality.

Overall, plants are reducing the heat flux through the building's envelope and roof via water management and additional water storage in the plant leaves/roots, and via sensible heat flux through additional shading provided by the plant leaves.

Further, paper reviews a quasi-steady state heat and mass transfer green model that can be incorporated in different energy simulation software or calculation procedures. The model considers heat and mass transfer processes between the sky, plants, and substrate, and is validated by the conducted experimental data that consists of surface temperatures, conduction heat flux, convection heat flux, net radiation and evapotranspiration. The validation shows that the model predicts the heat and mass transfer pretty accurately, but it tends to underestimate peak evapotranspiration rates and there is a need for its further development and improvement. However, it is not to be neglected, that there is a need for introduction some missing factors in existing research studies, as for example wind impact.

Dynamic validation under outdoor conditions after detailed steady state validation have shown the model produces accurate and reliable results for variables such as evapotranspiration. Based on the agreement shown in these studies, this could be one step farther in demonstrating how accurately the modeling can perform predictions in summer conditions, and users of the model have an opportunity to implement fully validated green roof model.

In addition, reviewed studies also produced and recommended inputs needed for simulating green roofs and vertical greeneries such as LAI, stomatal resistance, and substrate resistance to evaporation. The next step is to be R&D of the physically sound - dynamic energy and mass transfer simulation modeling, which will encompass all relevant transfer processes, and energy and mass balance equations relevant for the whole complex of occurring, and in synergy acting phenomena, including outdoor ambient, and Earth – Sun and surrounding objects relation's pattern. Final result is to be/or are to be developed specific simulations and co-simulations algorithms, ready for the introduction into a building energy simulation programs such as TRNSYS, EnergyPlus, etc.

5. REFERENCES

Alexandri E. and Jones P. (2008). Temperature Decreases in an Urban Canyon due to Green Walls and Green Roofs in Diverse Climates. *Building and Environment*, 43: 480-493.

Bass B. and Baskaran B. (2003). *Evaluating Rooftop and Vertical Gardens as an Adaptation Strategy for Urban Areas.* Institute for Research and Construction. NRCC-46737, Project number A020, CCAF Report B1046. National Research Council, Ottawa, Canada.

BCA. (2008). *Code on Envelope Thermal Performance for Buildings.* Building and Construction Authority, Singapore.

Gabriel Pérez, L. Rincón, A.Vila, J.M. González, L. F. Cabeza (2010), *Energy Efficiency Of Green Roofs And Green Facades In Mediterranean Continental Climate,*

http://intraweb.stockton.edu/eyos/energy_studies/content/docs/effstock09/Session_11_1_Case%20studies_Overviews/102.pdf.

Green Roofs for Healthy Cities (September 2008), *Introduction to Green Walls Technology, Benefits & Design*, www.greenroofs.org.

Johnston J. and Newton J. (1993). *Building Green: A Guide to using Plants on Roofs, Walls and Pavements.* London Ecology Unit, London, UK. Kang J. (2007). *Urban Sound Environment.* Taylor and Francis, New York, USA.

Kelly Chiang, Alex Tan (2009), *Vertical Greenery*, National University of Singapore, ISBN no • 978-981-08-3973-4.

Minke G. and Witter G. (1982). Haeuser mit Gruenem Pelz. *Ein Handbuch zur Hausbegruenung.* Verlag Dieter Fricke GmbH, Frankfurt, Germany.

Ong B. L. (2003). Green Plot Ratio: an ecological measure for architecture and urban planning. *Landscape and Urban Planning*, 63: 197-211.

Paulo Cesar Tabares-Velasco, Jelena Srebric (2009). *The Role of Plants in the Reduction of Heat Flux through Green Roofs: Laboratory Experiments,* ASHRAE Transactions, Volume 115, Part 2.

Paulo Cesar Tabares-Velasco, M. Zhao, N. Peterson, J. Srebric, R. Berghage, (2012). *Validation Of Predictive Heat And Mass Transfer Green Roof Model With Extensive Green Roof Field Data*, Ecological Engineering 47, 165–173.

Paulo Cesar Tabares-Velasco and Jelena Srebric (2012). *A Heat Transfer Model For Assessment Of Plant Based Roofing Systems In Summer Conditions*, Building and Environment 49, 310-323.

Paulo Cesar Tabares-Velasco, J. Srebric (2011). *Experimental Quantification Of Heat And Mass Transfer Process Through Vegetated Roof Samples In A New Laboratory Setup,* International Journal of Heat and Mass Transfer 54, 5149–5162.

White Paper version: Sep. (2012), *Considerations for Advanced Green Facade Design*, http://www.greenscreen.com/direct/GS_AdvancedGreenFacadeDesign.pdf.

Wilmers F. (1990). Effects of Vegetation on Urban Climate and Buildings. *Energy and Buildings*, 15: 507-514.

Wong Nyuk Hien (2013). *Evaluation of Vertical Greenery Systems for Building Walls,* National University of Singapore Department of Building, bdgwnh@nus.edu.sg.

THE EFFECT OF SOLAR RADIATION ON THERMOCHROMIC BUILDING COATINGS: TESTING THE PERFORMANCE AND PROPOSING METHODS FOR THEIR IMPROVEMENT

Theoni Karlessi*[1], Mat Santamouris*[1]

[1]*National and Kapodestrian University of Athens, Building of Physics - 5, University Campus, 157 84 Athens, Greece*

ABSTRACT

The improvement of the urban microclimate combined with the reduction of the energy loads is a highly important target that requires the research and development of innovative solutions with advanced thermal and optical properties. Color changing thermochromic coatings being reflective in summertime and absorptive in wintertime can address to the demand of lower surface temperatures and lower cooling loads. The interaction though with the solar radiation results in the breaking of the chemical bonds and the degradation of their performance.
The present work aims to investigate various methods and techniques for the improvement of the coatings performance. Towards this direction an important step is to identify the factors that affect thermochromism. Combinations of UV and optical filters were used on thermochromic coatings applied on concrete tiles under accelerated ageing conditions of one month period in order to isolate the parts of solar spectrum that cause the photodegradation. Covering the sample with red filter which cuts off wavelengths below 600nm protects most efficiently the reversible color change of the thermochromic coating as the solar reflectance at the dark phase remains unaffected during the whole experimental period.
The promising results of this research in addition to the advantages from the color changing properties concerning energy efficiency in buildings, indoor air environment and urban microclimate, encourages further investigation of the materials and the techniques.

KEYWORDS

thermochromic coatings, photodegradation, , accelerated ageing

1 INTRODUCTION

The materials used in the urban fabric play a very important role for the microclimatic thermal balance. They absorb solar and infrared radiation and dissipate part of the accumulated heat through convective and radiative processes to the atmosphere increasing ambient temperature. Thus, the optical and thermal characteristics of the materials used determine to a high degree the energy consumption and comfort conditions of individual buildings as well as of open spaces [1-6].
The main properties of a material that control its surface temperature are the solar reflectance and the infrared emittance [7]. New generation materials and techniques that present advanced

thermal characteristics, dynamic optical properties, increased thermal capacitance and a much higher heat island mitigation potential have been developed[6]. Innovative materials have the ability to be more reflective and present lower surface temperatures during the cooling period, while being more absorptive and taking advantage of the solar gains during the heating period [8]. This property can be described and analysed by thermochromism. The thermochromic effect is a change in the spectral properties of an organic or inorganic substance caused by heating or cooling. In intrinsically reversible organic thermochromic systems, heating above a defined temperature causes a change in color from darker to lighter tones. This transition is achieved by a thermally reversible transformation of the molecular structure of the pigments that produces a spectral change of visible color. When temperature decreases below the color-changing point, the system returns to its thermally stable state [11-16].

Towards this direction, thermochromic color-changing coatings have been developed and tested. Thermochromic pigments have been developed as three component organic mixtures and they were incorporated into common white coating [13, 14]. After an hour of exposure to solar radiation and for ambient temperatures below 20^{o}C the thermochromic coating could absorb almost the same amount of solar energy as an ordinary colored coating, but when the temperature was above 20^{o}C it could reflect more solar energy, presenting 4^{o}C lower temperature than the ordinary colored coating [14]. Karlessi et al. developed eleven thermochromic coatings at 30^{o}C color changing temperature by using thermochromic pigments into an appropriate binder system and tested their thermal and optical characteristics against color matching conventional and cool (highly reflective) coatings [10]. The results for the brown thermochromic coating indicate higher values for the solar reflectance (SR=0.55 for the colored and SR=0.76 for the coloreless phase) compared to the common (SR=0.18) and cool coating (SR=0.41) of the same color. Mean daily surface temperature during a hot summer was also measured and the temperature difference between common and thermochromic coatings was ΔT= 11.3 ^{o}C, and between cool and thermochromic coatings was ΔT= 9.2 ^{o}C. These results reveal the potential of thermochromic materials to avoid overheating in summertime, and absorb heat in wintertime when it is necessary.

However, photodegradation is a major problem for thermochromic materials when exposed to outdoor conditions. Interaction with solar radiation cause the breaking and/or crosslinking of the polymer chains, leading to altered chemical and mechanical properties, and loss of the reversible thermochromic effect [15, 16].

Various techniques have been tested to decrease the degradation of the thermochromic coatings and improve their outdoor performance. Experiments proved that when UV absorbers are incorporated in the thermochromic coatings the optical efficiency is not improving and the ageing problems remain. Efficiency is improved when the UV protectors are applied on the surface of the coatings but still the problem of degradation is important. UV filters with a transmittance at the UV part of the solar radiation close to zero have also been used for the photostabilization of the thermochromic coatings [6, 17-19]. Results however showed that although the optical performance improves considerably but the problem remains. This indicates that not only the ultraviolet but also other parts of the solar radiation interact with the molecular bonds, having a negative effect on thermochromism. The advantages that can be derived from their color changing properties concerning energy efficiency in buildings, indoor air environment and urban microclimate encourages further investigation [10] and results in this work.

The following study aims at the investigation of the optical performance of a thermochromic coating under accelerated ageing conditions, using combinations of UV and optical filters in order to isolate the influence of different parts of the solar radiation.

2 PRODUCTION AND APPLICATION OF THERMOCHROMIC COATINGS

For the production of the thermochromic coating, organic water based red thermochromic pigments of powder form and color changing temperature of 25^{o}C were used. An appropriate binder system that should not itself absorb infrared radiation was produced for the development of the thermochromic coatings. The system composed of water (32%), thermochromic pigment red (12%), titanium dioxide (9%) in order to avoid transparency at the colorless state and other additives. With a temperature increase above 25^{o}C the thermochromic coating becomes transparent, revealing the color of the substrate.
The thermochromic coating was applied on concrete tiles, size of 6cm x 6cm. In Fig.1 the thermochromic sample in three different thermal phases before the exposure to accelerated ageing conditions is presented. Figure 1(a) depicts the sample in full coloration at a temperature of 10^{o}C, while in Figure 1(c) the sample is completely decolorized at a temperature of 35^{o}C. An intermediate phase is presented in Fig.1(b).

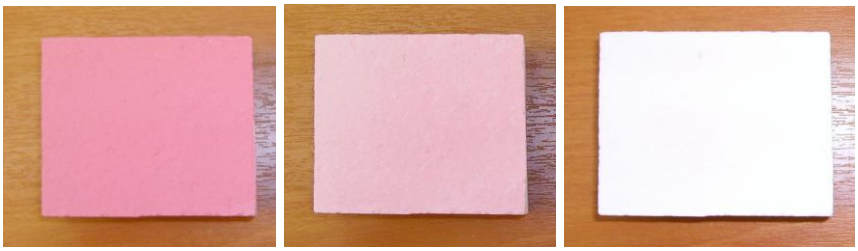

a. b. c.
Figure1(a) Full coloration, (b) Intermediate phase, (c) Full decoloration

3 EXPERIMENTAL PROCEDURE OF ACCELERATED AGING

Accelerated ageing of the samples was performed in an Accelerated Ageing Xenon Test Chamber (Q-SUN, Xe-3HS) [20] for one month period in a 24 hours basis according to the specifications and requirements of ISO 11341: Paints and varnishes -Artificial weathering and exposure to artificial radiation- Exposure to filtered xenon arc radiation [21]
In order to protect the samples from the exposure to accelerated ageing conditions optical and UV filters were used: red filter, yellow blue and green filters and UV glass filter. The filters were placed on top of the samples covering the thermochromic surface. All measurements were performed every five days of exposure for a total time period of 30 days.
The transmittance of the filters at a range of 300-2500nm is presented at Fig.2.The appropriate selection of the filters was based on their transmittance range and the aim was to cover partially the whole wavelength range, providing thus the ability to isolate the influence of the ageing conditions in each part of the spectrum and for each filter.

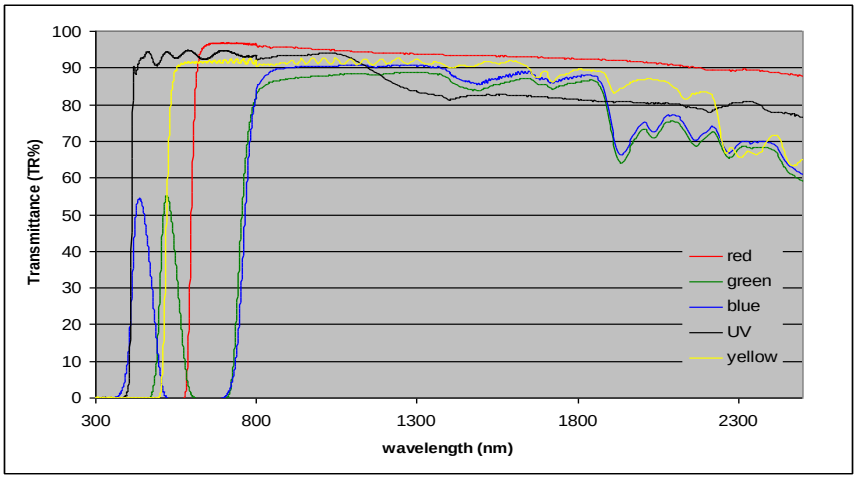

Figure 2: Transmittance of the filters at a range of 300-2500nm

3.1 Measurements of solar reflectance

The spectral reflectance of the samples was measured at a range of 300-2500nm of the solar spectrum that includes a part of the ultraviolet radiation (UV: 300-400nm), the visible (VIS:400-700nm) and the near infrared part (NIR: 700-2500nm). A UV/vis/NIR spectrophotometer (Varian Carry 5000), was used for measuring the spectral reflectance of the samples. Figure 3 presents the spectral reflectance for every five days of exposure of the uncovered and the sample with the UV and the optical red filter in the dark phase.

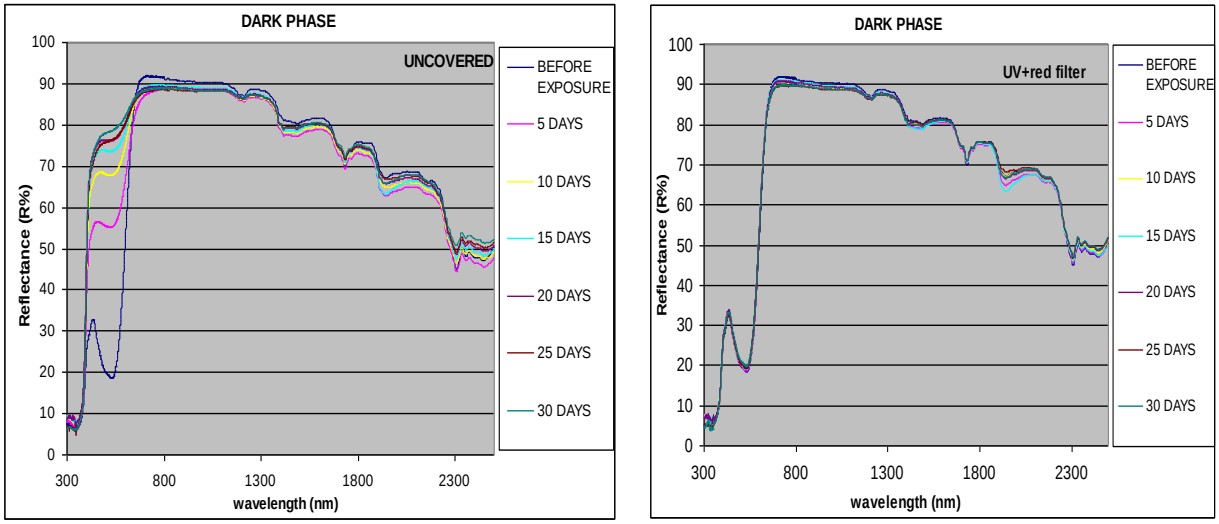

Figure 3: Spectral reflectance of the uncovered and UV+red filter sample at the dark phase

Tables 1, 2 present the calculated values of solar reflectance for the sample covered with UV+red filter for the dark and white phase respectively. Tables 3, 4 present the calculated values of solar reflectance for the uncovered sample.

Table 1 Solar reflectance (%) of the sample covered with UV+red filter at the dark phase

UV+red filter	BEFORE EXPOSURE	5 DAYS	10 DAYS	15 DAYS	20 DAYS	25 DAYS	30 DAYS
SR	68	67	68	68	68	67	67

SRir	**86**	**85**	**85**	**85**	**85**	**85**	**85**
SRvis	**45**	**45**	**45**	**45**	**45**	**45**	**45**
SRuv	**7**	**7**	**7**	**7**	**7**	**6**	**6**

Table 2 Solar reflectance (%) of the sample covered with UV+red filter at the white phase

UV+red filter	BEFORE EXPOSURE	5 DAYS	10 DAYS	15 DAYS	20 DAYS	25 DAYS	30 DAYS
SR	**84**	**84**	**84**	**84**	**84**	**83**	**83**
SRir	**85**	**85**	**85**	**85**	**85**	**85**	**84**
SRvis	**88**	**89**	**89**	**88**	**88**	**86**	**85**
SRuv	**7**	**8**	**8**	**8**	**8**	**6**	**6**

Table 3 Solar reflectance (%) of the uncovered sample at the dark phase

UNCOVERED	BEFORE EXPOSURE	5 DAYS	10 DAYS	15 DAYS	20 DAYS	25 DAYS	30 DAYS
SR	**68**	**74**	**78**	**79**	**80**	**80**	**80**
SRir	**86**	**83**	**84**	**84**	**84**	**84**	**84**
SRvis	**45**	**64**	**73**	**77**	**79**	**78**	**80**
SRuv	**7**	**8**	**8**	**9**	**9**	**7**	**7**

Table 4 Solar reflectance (%) of the uncovered sample at the white phase

UNCOVERED	BEFORE EXPOSURE	5 DAYS	10 DAYS	15 DAYS	20 DAYS	25 DAYS	30 DAYS
SR	**84**	**77**	**80**	**80**	**78**	**76**	**75**
SRir	**85**	**83**	**84**	**84**	**85**	**84**	**83**
SRvis	**88**	**73**	**78**	**80**	**73**	**69**	**68**
SRuv	**7**	**8**	**8**	**9**	**7**	**5**	**5**

3.2 Measurements of color coordinates

The Carry Color Calculations application is an module which allows to perform calculations on data collected by Varian Carry 5000. Calculations are performed for tristimulus values X, Y, Z, chromaticity coordinates x, y, z and color coordinates for CIE L*a*b*. Color difference ΔE^*_{ab} is also calculated. The set-up is for a selectable wavelength range of 380-780nm at an interval of 1nm, with a D65 illuminant and a CIE (1964) 10° degrees observer. Figure 4 shows the color difference the last day of exposure for each sample for the dark and the white phase.

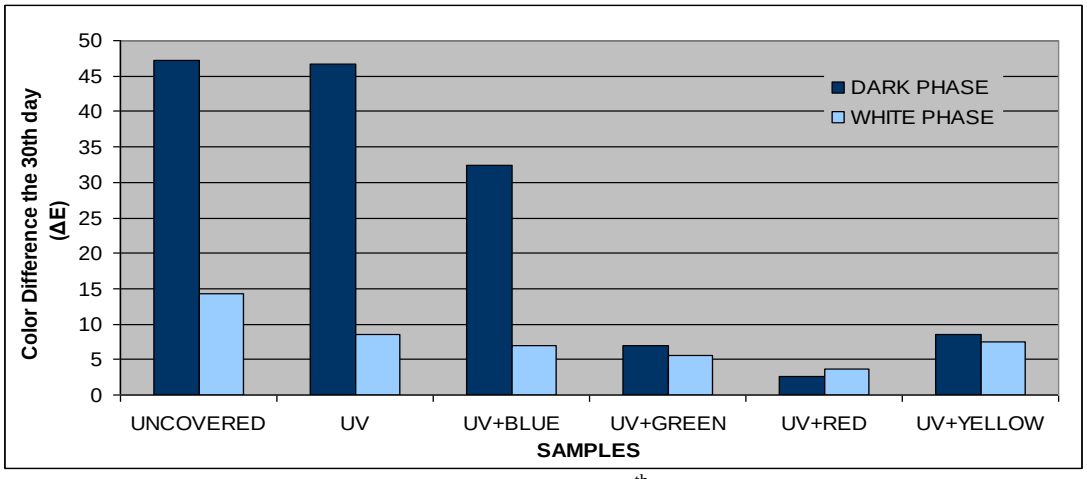

Figure 4: Color Difference (ΔE) the 30th day for each sample

Figures 4, 5 present the variation of brightness L* for the whole experimental period for the uncovered sample and the sample covered with UV and red filter respectively.

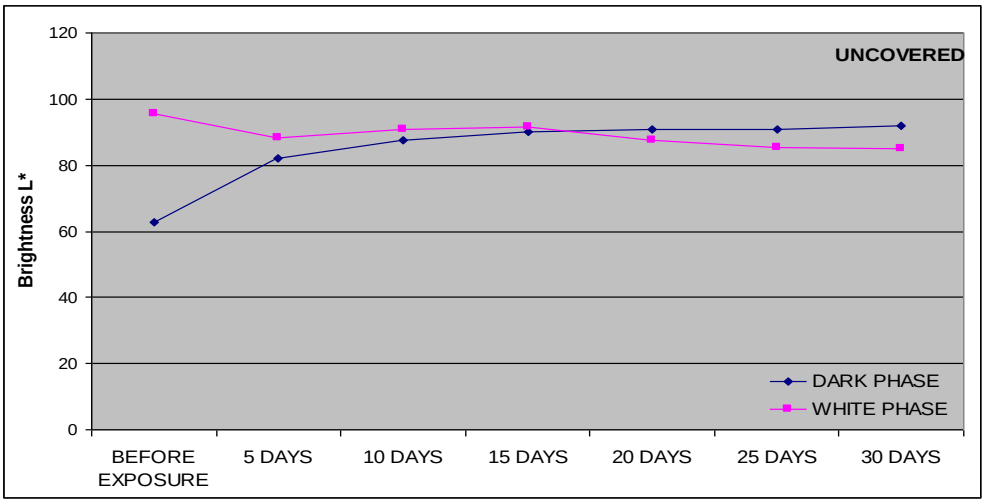

Figure 4: Variation of brightness L* for the uncovered sample

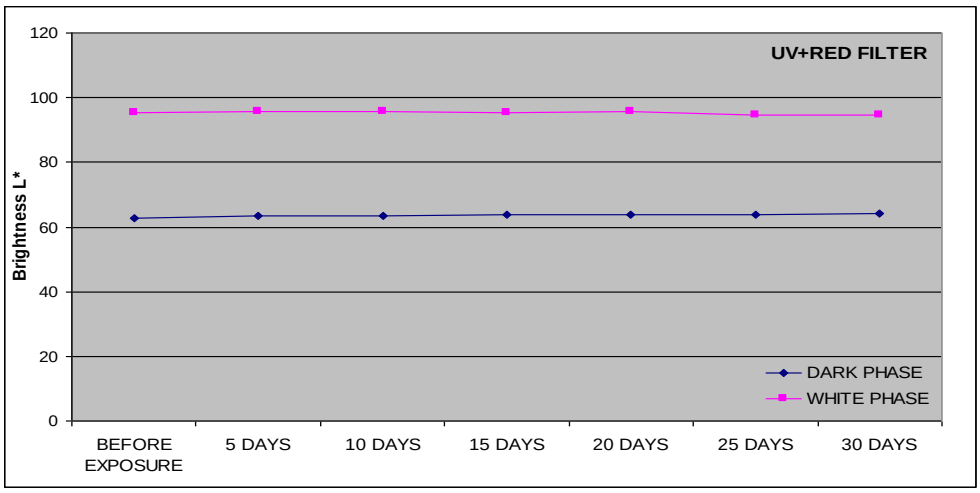

Figure 4: Variation of brightness L* for the sample covered with UV+red filter

4 ANALYSIS OF THE RESULTS

Solar reflectance for all the samples tested increases in the dark phase, while in the white phase decreases. The variation of solar reflectance is mainly in the visible part of the

spectrum. The uncovered sample, 30 days after the exposure to accelerated ageing conditions has increased SR value by 8% and SRvis by 16% at the dark phase compared to its condition before exposure. At the white phase, the reduction of SR is 7.6% and of SRvis is 17.6%. The use of UV filter did not improve significantly the dark phase of thermochromic effect. Thus, the cut-off of the ultraviolet radiation does not ensure the improvement of the thermochromic behaviour of the samples. The results of the use of optical filters prove that besides the UV part of the radiation, there are parts of the visible that also affect and degrade the thermochromic properties. The greatest degradation is presented to the sample with the blue filter. Covering the sample with red filter which cuts off wavelengths below 600nm protects most efficiently the reversible color change of the thermochromic coating as the solar reflectance at the dark phase remains unaffected during the whole experimental period. The white phase presents the lowest change compared to the other samples, 0.8% for SR and 2.6% for SRvis.

The results are confirmed by the color measurements. Brightness L* at the dark phase increases, while at the white increases. For the uncovered sample and the sample with the UV filter the biggest change in brightness is remarked during the first 10 days of exposure. Afterwards, the brightness in both phases matches as the thermochromic properties are lost and the color change is irreversible. At the sample with the red filter that provides the best protection of thermochromic characteristics the change of brightness is 2.5% for the dark and 1% for the white phase. The results of color change ΔE are in accordance with the previous results. As observed in Fig.4, the higher values until the last day of exposure are remarked for the uncovered sample and the sample with the UV filter, equal to 47 in both samples at the dark phase and 7 and 8.5 in the white phase respectively. The results for the combination of UV and red filter present the lowest ΔE equal to 2.6 at dark phase and 3.6 at white. The variation of ΔE at the sample with the red filter is minor.

5 CONCLUSIONS

Thermochromic systems can contribute to the improvement of the urban microclimate and the decrease of energy loads. For high temperatures, during summertime thermochromic coatings have the ability to reflect solar energy, reducing the surface's temperature, while in wintertime absorb solar energy, increasing the surface's temperature as reversible color change takes place.

However, photodegradation is a major problem for thermochromic materials when exposed to outdoor environment. Various methods have been tested by applying different UV absorbers with different techniques in the thermochromic coatings, in order to photostabilise the color changing effect of the material. The results though show that the performance of the thermochromic material was not improved and the degradation problems remain. This indicates that not only the ultraviolet but also other parts of the solar radiation interact with the molecular bonds, having a negative effect on thermochromism.

The scope of this work is to detect the parts of solar radiation that damage thermochromism. For this reason six samples of red thermochromic coating applied on concrete tiles were prepared and covered with different combinations of UV and optical filters. The samples were submitted to accelerated aging conditions for one month period and their optical characteristics (reflectance, color coordinates and color difference) were periodically measured.

Variation of SR is mainly detected at the visible part of the spectrum. The uncovered sample, 30 days after the exposure to accelerated ageing conditions has increased SRvis value by 16% at the dark phase compared to its condition before exposure. At the white phase, the reduction of SRvis is 17.6%. The degradation of thermochromic properties was observed mostly at the samples were the filters are transparent at the parts of the visible spectrum closer to the

ultraviolet, mainly in blue, green and yellow, while the sample with red filters remained unaffected at the dark phase and changed slightly at the white.
The results of color change ΔE are in accordance with the reflectance results. The higher values until the last day of exposure are remarked for the uncovered sample and the sample with the UV filter, equal to 47 in both samples at the dark phase. The results for the combination of UV and red filter present the lowest ΔE equal to 2.6 at dark phase and 3.6 at white. The variation of ΔE at the sample with the red filter is minor.
The stabilization of one thermochromic sample under intense and prolonged weathering conditions that is accomplished in this work is a breakthrough in the field of thermochromism. Considering also the advantages that can be derived from the color changing properties concerning energy efficiency in buildings, indoor air environment and urban microclimate encourages further investigation.

6 REFERENCES

[1] Doulos, L., Santamouris, M., Livada, I., Passive cooling of outdoor urban spaces. The role of materials. Solar Energy 77 (2001), 231–249.

[2] Synnefa, A., Santamouris, M., Apostolakis, K., 2007a. On the development, optical properties and thermal performance of cool colored coatings for the urban environment. Journal of Solar Energy 81, 488–497.

[3] Synnefa, A., Santamouris, M., Akbari, H., 2007b. Estimating the effect of using cool coatings on energy loads and thermal comfort in residential buildings in various climatic conditions. Journal of Energy and Buildings 39, 1167–1174.

[4] Akbari, H., Davis, S., Dorsano, S., Huang, J., Winert, S., 1992. Cooling our Communities – A Guidebook on Tree Planting and White Colored Surfacing. US Environmental Protection Agency, Office of Policy Analysis, Climate Change Division.

[5] Santamouris, M., Adnot, J., Alvarez, S., Klitsikas, N., Orphelin, M., Lopes, C., Sanchez, F., 2004. Cooling the Cities. Eyrolees, Paris, France, ISBN: 2-911762-54-1.

[6] Santamouris, M., Synnefa, A., Karlessi, T., Using advanced cool materials in the urban built environment to mitigate heat islands and improve thermal comfort conditions, Solar Energy, Volume 85, Issue 12 (2011), 3085-3102

[7] Akbari, H., Bretz, S., Taha, H., Kurn, D., Hanford, J., Peak power and cooling energy savings of high albedo roofs. Journal of Energy and Buildings – Special Issue on Urban Heat Islands and Cool Communities, 25(2) (1997), 117–126.
[8] Karlessi, T., Santamouris, M., Apostolakis, K., Synnefa, A., Livada, I., Development and testing of thermochromic coatings for buildings and urban structures, Solar Energy, 83 (2009), 538–551.

[9]White, M.A., LeBlanc, M., 1999. Thermochromism in commercial products. Journal of Chemical Education 76, 1201–1205.

[10] Ma,Y., Zhu, B., Research on the preparation of reversibly thermochromic cement based materials at normal temperature, Cement and Concrete Research 39 (2009) 90-94

[11] Ma, Y., Zhu, B., Wu, K., Preparation and solar reflectance spectra of chameleon-type building coatings, Journal of Solar Energy 70 (2001), 417–422.

[12] Ma, Y., Zhang, X., Zhu, B., Wu, K., Research on reversible effects and mechanism between the energy-absorbing and energy-reflecting states of chameleon-type building coatings. Journal of Solar Energy 72 (2002), 511–520.

[13] Lopes, F., Neves, J., Campos, A., Hrdina, R., Weathering of Microencapsulated Thermochromic Pigments, Research Journal of Textile and Apparel 13 (2009), 78-89

[14] Bamfield, P., 2001. Chromic phenomena, technological applications of color chemistry. Royal Society of Chemistry, 33–41.

[15] Pospisil, J., Nespurek, S., Photostabilization of coatings. Mechanisms and performance. Progress in Polymer Science 25 (2000), 1261–1335

[16] Berdahl, P., Akbari, H., Levinson, R., Miller, W.A., Weathering of roofing materials – an overview, Construction and Building Materials 22 (2008), 423–433.

[17] Pospısil,J., Pilar,J., Billingham, N.C, Marek, A., Horak Z., Nespurek,S., Factors affecting accelerated testing of polymer photostability Polymer Degradation and Stability 91 (2006) 417-422

[18] ODA, H., PHOTOSTABILIZATION OF ORGANIC THERMOCHROMIC PIGMENTS: ACTION OF BENZOTRIAZOLE TYPE UV ABSORBERS BEARING AN AMPHOTERIC COUNTER-ION MOIETY ON THE LIGHT FASTNESS OF COLOR FORMERS DYES AND PIGMENTS VOLUME 76, ISSUE 1 (2008) 270–276

[19] ODA, H., PHOTOSTABILIZATION OF ORGANIC THERMOCHROMIC PIGMENTS. PART 2: EFFECT OF HYDROXYARYLBENZOTRIAZOLES CONTAINING AN AMPHOTERIC COUNTER-ION MOIETY ON THE LIGHT FASTNESS OF COLOR FORMERS DYES AND PIGMENTS VOLUME 76, ISSUE 2,(2008) 400–405

[20] Q-Lab http://www.q-lab.com/products/q-sun-xenon-arc-test-chambers/q-sun-xe-3

[21] ISO 11341: Paints and varnishes -Artificial weathering and exposure to artificial radiation- Exposure to filtered xenon arc radiation.

INFLUENCE OF THE IRRADIANCE SPECTRUM ON SOLAR REFLECTANCE MEASUREMENTS

Chiara Ferrari[1], Antonio Libbra[1], Alberto Muscio[*1], and Cristina Siligardi[1]

[1] *EELab – Dept. of Engineering "Enzo Ferrari"*
University of Modena and Reggio Emilia
Via Vignolese 905
41125 Modena (ITALY)
**Corresponding author: alberto.muscio@unimore.it*

ABSTRACT

Solar reflectance is the key performance parameter of cool roof and cool pavement materials. For its assessment, the measured spectral reflectivity of the sample is weighted by a reference spectrum of solar irradiance. Several standard and non-standard spectra are however available, taking into account different climate conditions, angle of incidence of the solar beam, contribution of the diffuse radiation content.
This study is aimed at investigating the impact of using different solar irradiance spectra as specified by existing standards or suggested by qualified research institutions, and verifying if those spectra can yield equivalent solar reflectance values from the viewpoint of assessment of standard performance and comparison of commercial products. Several actual material are considered, either white or coloured ones and with assorted spectral behaviour.

KEYWORDS

Cool roof, cool pavements, cool colours, solar reflectance, solar irradiance spectrum

1 INTRODUCTION

Cool roof and cool pavement materials, characterized by high values of solar reflectance and thermal emittance, are probably the best solution to limit summer overheating of buildings and the urban heat island effect (Akbari, 2012; Santamouris, 2011, 2012). In particular, solar reflectance is the key parameter as it measures the ability of a material to immediately reflect the incident sunlight. In order to calculate this parameter, the measured spectral reflectivity of the samples is integrated with spectral values of the solar irradiance that try to reproduce the actual amount of solar radiation reaching a building or pavement surface. As it is generally easier to measure the reflected fraction of incident sunlight than the absorbed one (Levinson, 2010), solar reflectance is commonly specified for cool materials, whereas solar absorptance is more often found in standards for calculation of building performance such as ISO 13790. For an opaque surface, however, its solar absorptance is usually determined by subtracting the solar reflectance from unity.
Several standard spectra of solar irradiance are available, taking into account different climate conditions, angle of incidence of the solar beam, contribution of the diffuse radiation content, etc. A largely used hazy sky air mass 1.5 beam normal spectrum (E891BN) is provided by the ASTM E891 standard. In fact, while ASTM E891 was withdrawn in 1999, its E891BN spectrum is still employed via ASTM E903 and it is someway incorporated (see Levinson

2010, 2010a) also into ASTM C1549 – currently the most utilized standards for calculation of solar reflectance.
The E891BN spectrum takes into consideration bean normal solar radiation because it was intended for prediction of solar concentrator performance. For the same reason, air mass 1.5 is considered as it is close to the mean condition at which beam-normal solar energy is delivered in most relevant locations of the U.S.A. A hazy sky condition is also considered, with spectral optical depth of the atmospheric aerosol as large as 0.270 at 500 nm, since this was assumed to be an average condition for the U.S.A. Usage of the E891BN spectrum, however, is questioned by Levinson et Al. (Levinson, 2010) as it allows best predicting mean solar heat gain along the whole year, whereas it is a matter of fact that building overheating and the urban heat island phenomenon show up mostly in summer, that is for peak solar heat gain. Building air conditioning systems are typically sized to meet annual peak cooling load rather than annual mean cooling load. Moreover, most pavements and large roofs are approximately horizontal and, consequently, they tend to be most strongly irradiated when the sun is high and the sky is clear. On the other hand, a zenith sun (air mass 1) is shown to reasonably approximates the solar position of annual peak global horizontal solar irradiance in the mainland U.S.A. (Levinson, 2010), and the same can be shown to occur in Southern Europe, where air mass is always below 1.2 throughout the whole summer (Fig. 1: Athens, Rome).

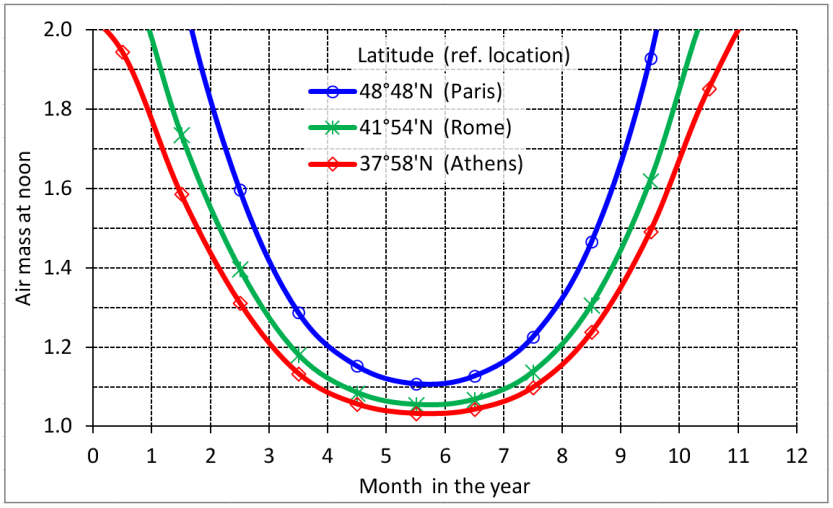

Figure 1: Minimum air mass for reference locations in Southern and Central Europe

In view of the results of their above mentioned theoretical analysis, Levinson et Al. recommend using a clear sky air mass 1 global horizontal solar spectrum (AM1GH) for calculation of the solar reflectance value, and they show that solar heat gain computed from that value approximates the instantaneous annual peak solar heat gain of a horizontal surface in the U.S.A. to within 2 W m^{-2}. Nonetheless, AM1GH is not a standard spectrum such as EN891BN or another widely used one (EN410) provided by the European standard EN 410, which is similar to AM1GH but is available with a relatively coarse wavelength step size (20 nm in the range 300-800 nm, 50 nm in the range 800-2100 nm, and 100 nm in the range 2100-2500 nm). Two other interesting standard spectra provided by ASTM G173 for clear sky but air mass 1.5 are the spectral global irradiance (*i.e.* from the solar disk plus sky diffuse and diffuse reflected from ground) on a south facing surface tilted 37° from the horizontal (G173GT), and the spectral direct + circumsolar irradiance (*i.e.* in a field of view centred on the solar disk and with 5° diameter) on a surface pointing to the sun (G173DC).
AM1GH and the other above mentioned standard spectra E891BN, EN410, G173GT, and G173DC are summarized in Tab. 1. A dimensionless spectral irradiance is also represented in

Fig. 2 in terms of percentage of the total solar irradiance that falls in the unit wavelength, evaluated by the formula

$$100 \cdot S_\lambda \delta\lambda / S_{tot} \quad (\%) \tag{1}$$

where S_λ (W $m^{-2}nm^{-1}$) is the spectral irradiance, $\delta\lambda$ (nm) is the wavelength step size, and S_{tot} (W m^{-2}) is the total irradiance in the range 300-2500 nm, which includes about 99% of total solar irradiance at the earth surface and can be estimated from spectral data as follows:

$$S_{tot} = \int_{300}^{2500} S_\lambda d\lambda \cong \sum S_\lambda \delta\lambda_{\lambda=300..2500} \tag{2}$$

Linear interpolation of available data was generally applied to obtain a common wavelength step size or to match that of the measured reflectivity spectrum. In Fig. 3 the discrepancy of the dimensionless spectral irradiance with respect to E891BN is also presented for all spectra.

Table 1: Summary of the considered solar irradiance spectra

Initialism	Description	Aerosol optical depth at 500nm	UV/Vis/NIR (%)	Source
AM1GH	Clear sky AM1 global horizontal irradiance	0.084	6.5/45.0/48.5	NREL SMARTS 2.9.5
EN410	Clear sky AM1 global horizontal irradiance	0.1	6.2/44.3/49.5	EN ISO 410:2011
G173GT	Clear sky AM1.5 global irradiance on a south facing surface tilted 37°	0.084	4.5/43.5/52.0	ASTM G173-03
G173DC	Clear sky AM1.5 direct irradiance on a surface normal tracking the sun	0.084	3.3/42.2/54.5	ASTM G173-03
EN891BN	Hazy sky AM1.5 beam-normal irradiance	0.270	2.8/39.2/58.0	ASTM E891-87(1992)

As pointed out by Levinson et Al. (Levinson, 2010), direct solar irradiance has a higher NIR content than diffuse solar irradiance. As a result, E891BN and also G173DC have a significantly higher NIR content than all other spectra (see Tab. 1 and Figs. 2-3). In principle, since vertical and/or north facing surfaces mostly collect diffuse irradiance, whereas horizontal or south facing surfaces mostly collect direct irradiance, different spectra should be used to integrate the spectral reflectivity for surfaces having different orientation and inclination, thus obtaining different solar reflectance values even if the material is the same. On the other hand, unique values are surely preferred by either material manufacturers or building designers, in order to more easily define the product specification or calculate the building performance. A spectrum selected for integration of spectral reflectivity data should therefore realize a compromise between ease of operation and correctness of performance prediction. The NIR content of solar irradiance spectra is also affected the by the air mass, which depends on the location and the time in the year, as well as by the sky clearness, which can be quite variegated throughout the U.S.A., and at an even greater extent throughout Europe due to higher population and industry concentration and the existence of heavily polluted areas with permanent low wind condition.

While the impact of the spectrum selection on the calculated values of solar reflectance can be expected to be small for cool white materials with flat spectral reflectivity, it can become significant with cool coloured materials having selective reflective properties (Levinson, 2010). A non-negligible impact may even arise for cool white surfaces, since white ceramic materials can show an almost flat spectral reflectivity, whereas organic materials often show a strong absorption in the range above 1500-1700 nm (Libbra, 2011). Generally speaking, the spectrum selection may affect competition between manufacturers of cool solutions because it may arbitrarily induce differences in the solar reflectance estimate up to a few percentage

points, almost negligible in terms of solar heat gain but evident enough to influence the choice of an inexperienced designer or end user.

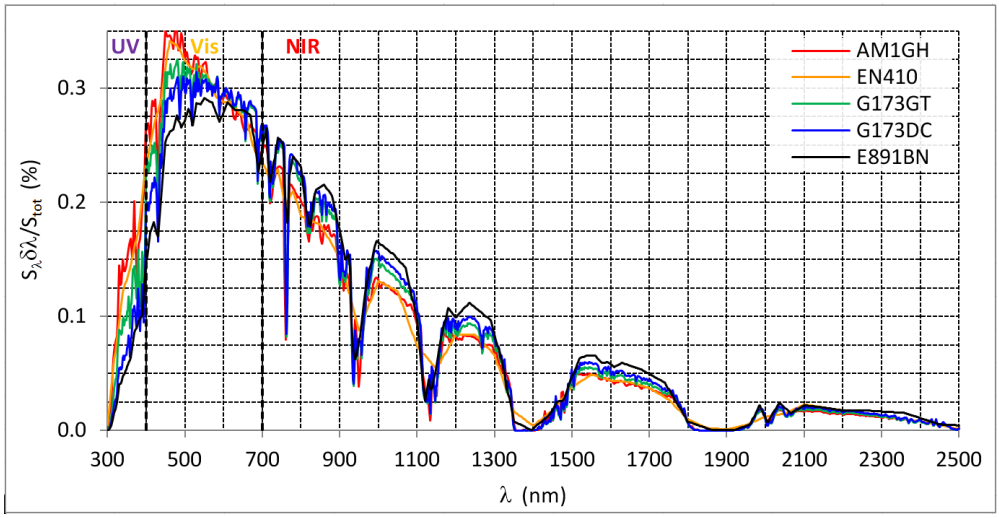

Figure 2: Dimensionless spectral irradiance expressed in terms of percentage of the total solar irradiance falling in the unit wavelength

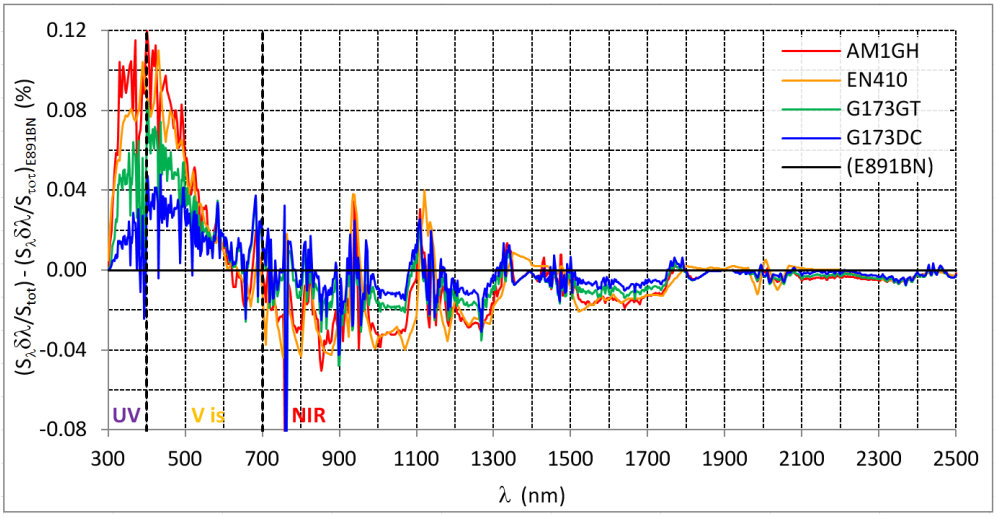

Figure 3: Discrepancy of dimensionless spectral irradiance of the considered spectra with respect to E891BN

This study is part of an investigation campaign on cool roofing solutions (Libbra, 2011, 2011a, 2013; Ferrari, 2013) and it is aimed at investigating the use of the solar irradiance spectra as specified by common existing standards or proposed by Levinson at Al. (Levinson, 2010), summarized in Tab. 1, and verifying if those spectra can yield equivalent solar reflectance values from the viewpoint of standard performance assessment, in order to enable the comparison of commercial products within the framework of a certification program like that of the Coor Roof Council of the U.S.A. (CRRC, 2013) or that under development by the European Cool Roof Council (ECRC, 2013). Actual materials are considered, either white or coloured ones and with assorted spectral behaviour, most of them commercially available.

2 EXPERIMENTAL ANALYSIS AND TESTED MATERIALS

Samples of several different materials were analysed in this study, representative of commercial products of the same type tested at the Energy Efficiency Laboratory (EELab) at Modena in terms of qualitative spectral behaviour. Those samples can be divided into three sets, identified in the following as ‘cool white samples’, ‘white samples’, and ‘coloured

samples'. The first sample set consists of five different 'cool' white samples (SR>65%): a glazed tile, an unglazed tile, a single ply membrane, painted bitumen shingle, and a thin organic coating applied onto a metallic substrate. The second sample set consists of three (non-bright) white samples with relatively low solar reflectance: white concrete, coated basalt grit, and slate shingle. The third sample set consists of mass coloured concrete samples with six different colours: yellow, orange, brick, ocra, brown, and red. These colours are representative of common surfaces of the Mediterranean architectures and the selected samples show a NIR reflectivity spectrum significantly higher than that in the visible range, thus approaching the concept of cool colour surface with selective behaviour. If fact, the coloured sample set is not representative of all possible cool coloured materials and coatings, nonetheless cool colours are a product category still under development and with marginal commercial impact.

Table 2: Summary of the measured values of solar reflectance

Sample	**AM1GH SR (%)** (UV/Vis/NIR)[a]	**EN410 SR (%)** (UV/Vis/NIR)[a]	**G173GT SR (%)** (UV/Vis/NIR)[a]	**G173DC SR (%)** (UV/Vis/NIR)[a]	**EN891BN SR (%)** (UV/Vis/NIR)[a]
Cool white samples					
Glazed tile	82.8 (51.4/85.4/84.6)	83.0 (52.5/85.4/84.6)	83.6 (52.8/85.5/84.6)	84.0 (54.4/85.6/84.6)	84.2 (56.1/85.6/84.5)
Unglazed tile	79.9 (53.5/81.1/82.2)	80.0 (54.3/81.2/82.2)	80.6 (54.5/81.2/82.3)	81.0 (55.7/81.3/82.2)	81.2 (57.0/81.4/82.2)
Single ply	76.4 (9.7/84.9/77.5)	76.5 (10.1/85.0/77.2)	77.8 (9.7/85.1/77.6)	78.5 (10.2/85.4/77.4)	78.4 (11.0/85.6/76.8)
Painted bit. shingle	74.7 (8.8/81.0/77.7)	74.9 (9.1/81.2/77.5)	76.2 (8.8/81.3/77.9)	77.0 (9.2/81.6/77.7)	77.1 (9.9/81.8/77.2)
Metallic substrate	66.7 (11.2/74.2/67.2)	66.9 (11.5/74.3/67.2)	67.8 (11.2/74.5/67.2)	68.5 (11.7/74.7/67.1)	68.6 (12.5/74.9/67.0)
White samples					
White concrete	56.1 (42.8/56.7/57.4)	56.1 (43.1/56.7/57.2)	56.6 (43.1/56.9/57.6)	56.8 (43.5/57.0/57.4)	56.7 (44.0/57.1/57.1)
Basalt grit	42.4 (14.4/44.6/44.1)	42.5 (14.6/44.7/44.0)	43.1 (14.4/44.8/44.1)	43.5 (14.6/45.0/44.1)	43.6 (15.0/45.1/43.9)
Slate shingle	42.4 (14.4/44.6/44.1)	42.5 (14.6/44.7/44.0)	43.1 (14.4/44.8/44.1)	43.5 (14.6/45.0/44.1)	43.6 (15.0/45.1/43.9)
Coloured samples					
Yellow	33.5 (11.5/29.0/40.7)	33.7 (11.5/29.1/40.6)	34.6 (11.5/29.7/40.7)	35.2 (11.5/30.1/40.7)	35.8 (11.5/30.5/40.6)
Orange	25.4 (9.0/19.5/33.1)	25.7 (9.0/19.6/33.2)	26.4 (9.0/20.1/33.2)	27.0 (9.0/20.4/33.2)	27.6 (9.0/20.7/33.2)
Brick	22.3 (12.2/18.8/26.9)	22.5 (12.2/18.9/27.0)	22.9 (12.2/19.2/26.9)	23.3 (12.2/19.4/27.0)	23.7 (12.2/19.6/27.0)
Ocra	20.6 (9.7/19.1/23.4)	20.7 (9.7/19.1/23.4)	21.0 (9.7/19.4/23.4)	21.3 (9.7/19.6/23.4)	21.6 (9.7/19.8/23.4)
Brown	18.8 (8.5/15.7/23.0)	18.9 (8.5/15.7/23.0)	19.3 (8.5/16.0/23.0)	19.7 (8.5/16.2/23.0)	20.0 (8.5/16.4/23.0)
Red	16.5 (6.4/11.4/22.6)	16.7 (6.4/11.5/22.7)	17.2 (6.4/11.8/22.6)	17.6 (6.3/12.0/22.7)	18.1 (6.3/12.1/22.8)

[a] The UV, Vis, and NIR solar reflectance values reported between brackets are calculated by means of Eq. (3) but applied to the UV (<400 nm), Vis (400-700nm), and NIR (>700 nm) ranges

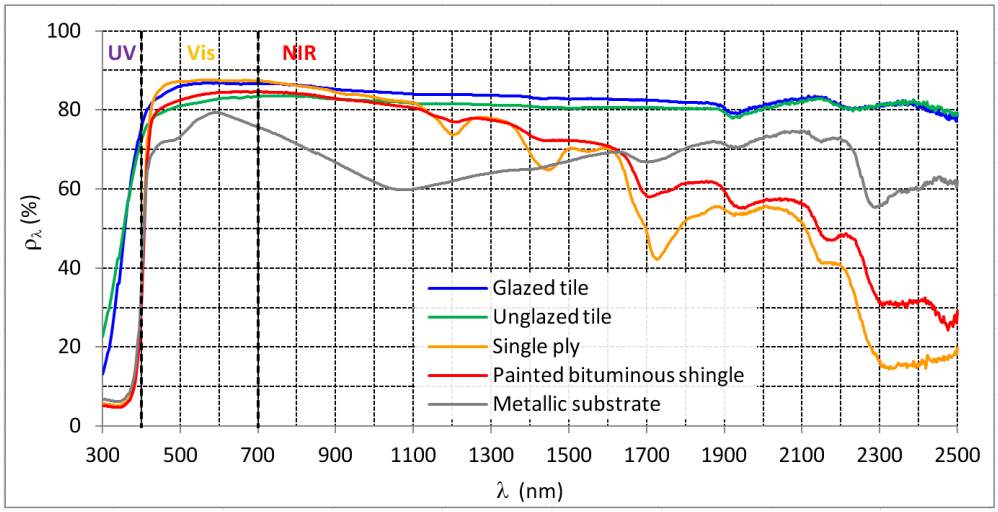

Figure 4: Reflectivity spectra of the 'cool' white samples

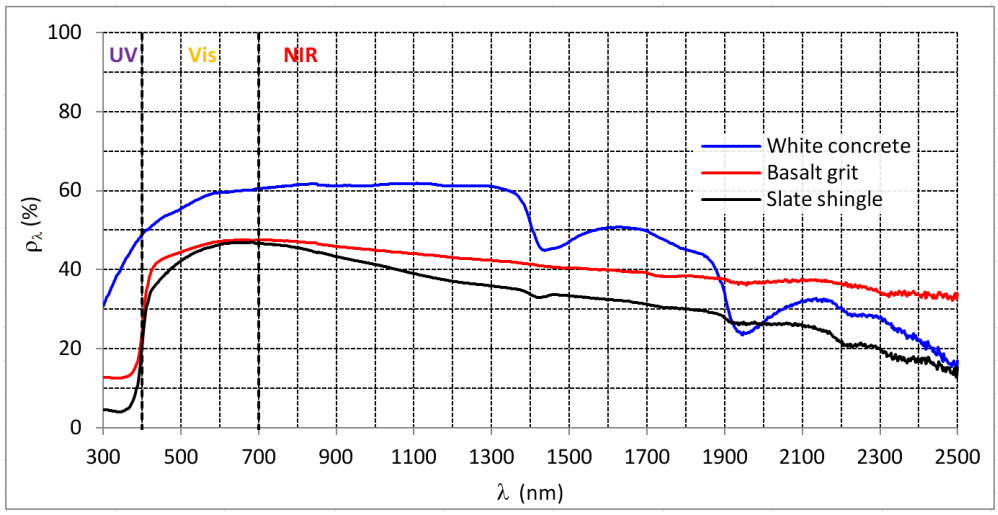

Figure 5: Reflectivity spectra of the white samples

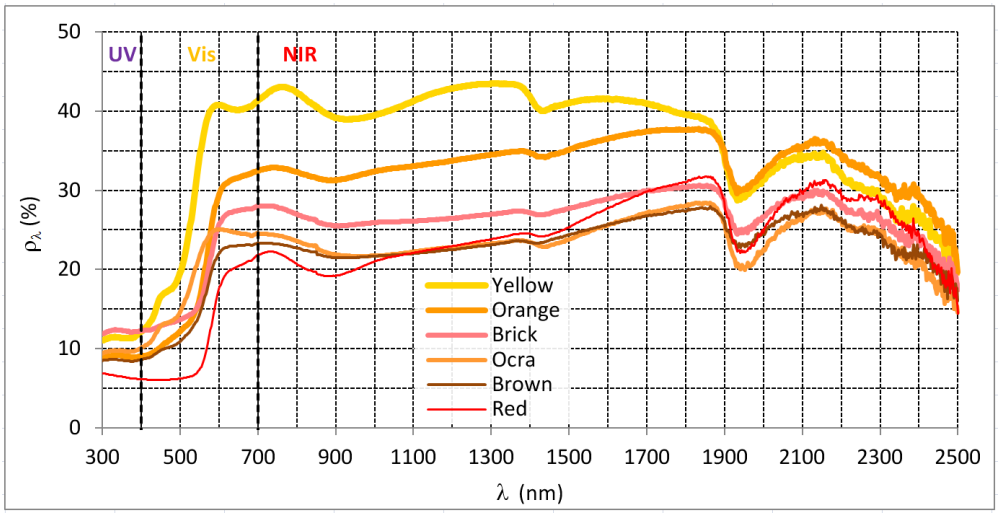

Figure 6: Reflectivity spectra of the coloured samples

The solar reflectance of each sample was calculated according to ASTM E903, using a Jasco V-670 UV/Vis/NIR spectrometer with 150 mm integrating sphere to measure the reflectivity spectrum. In order to compute the solar reflectance value SR, the reflectivity spectrum is then integrated with the five considered spectra of solar irradiance (AM1GH, EN410, G173GT, G173DC, and E981BN):

$$SR = \frac{\int_{300}^{2500} \rho_\lambda S_\lambda d\lambda}{\int_{300}^{2500} \rho_\lambda S_\lambda d\lambda} \cong \left(\frac{\sum \rho_\lambda S_\lambda \delta\lambda}{\sum S_\lambda \delta\lambda} \right)_{\lambda=300..2500} \quad (3)$$

where ρ_λ is the spectral reflectivity. The measured solar reflectance (SR) values are summarized in Tab. 2, while the measured reflectivity spectra are shown in Figs. 4-5-6.

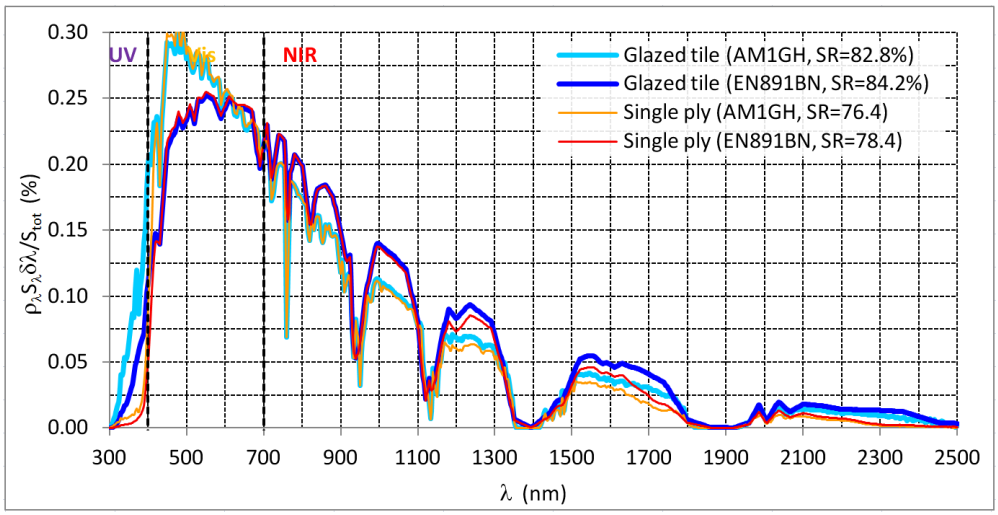

Figure 7: Comparison of dimensionless spectral reflection (dimensionless reflectivity x irradiance) for a ceramic and an organic 'cool' white solutions

3 DISCUSSION AND CONCLUSIVE REMARKS

The spectral reflectivity data in Figs. 4-5 illustrate the almost flat spectrum that white ceramic materials can have, as well as the strong absorption in the range above 1500-1700 nm (Libbra, 2011) often shown by organic materials. Intermediate results are generally obtained when an organic coating is applied onto a metallic or inorganic substrate with very different behaviour and the coating is not thick enough to mask the substrate. Close values of solar reflectance can thus be provided by materials with quite dissimilar spectral behaviours and reflective properties in the UV, Vis and NIR ranges (Tab. 2). As a result, the choice of the reference spectrum with which the spectral reflectivity data are integrated, with its peculiar distribution of radiant energy in the different spectral ranges, may affect the returned SR value. The problem was already extensively investigated by Levinson et Al. (Levinson, 2010) from the viewpoint of theoretical prediction of mean and peak solar heat gain in function of all most relevant parameters. Therefore, this study is focused on the solar reflectance values returned by the use of selected solar spectra when actual materials are tested, in order to verify if the emerging discrepancies are large enough to influence product comparison and competition.
A main result of this analysis is that the UV, Vis, and NIR solar reflectance values, calculated by means of Eq. (3) applied to the UV (<400 nm), Vis (400-700nm), or NIR (>700 nm) ranges, are almost the same with all solar spectra (Tab. 2). Discrepancies for a same material and a same spectral range are generally well below one percentage point. Larger discrepancies, however, arise in the values of total solar reflectance. These discrepancies can be as high as a couple of percentage points and are basically due to the different fractions of total radiant energy that fall in the UV, Vis, and NIR ranges: for instance, the NIR range includes as much as 58% of total radiant energy in the EN891BN spectrum, but only 48.5% and 49.5% in the AM1GH and EN410 spectra, respectively (Tab. 1). As easily predictable, ceramic surfaces with a relatively flat reflectivity spectrum show the smallest discrepancies,

nonetheless these can be as high as a percentage point due to the relatively low solar reflectance in the UV range, which includes as much as 6.5% and 6.2 of total radiant energy in AM1GH and EN410, respectively, but only 2.8% in EN891BN. Over evidence of the consideration above can be provided by the reflection spectra in Fig. 7, where the dimensionless spectral reflectivity of a ceramic surface and that of an organic coating, which show very different spectral behaviour, are multiplied by the dimensionless spectral irradiance from the E891BN and AM1GH spectra, the two ones showing the largest differences.
While passing from one solar spectrum to the other, the arising discrepancies always show the same sign and, for a same sample set, the same magnitude. Therefore a fair product comparison is likely to be allowed if a same reference spectrum is always used. In fact, the maximum discrepancies evidenced here are scarcely significant in terms of solar heat gain and, moreover, below the accuracy of commonly used measurement methods such as those based on spectrometers or reflectometers, nevertheless situations can be envisaged in which the choice of an inexperienced designer or end user can be influenced.
In conclusion, EN891BN is the most widely used standard spectrum for solar reflectance measurement and, therefore, it is the current reference, but AM1GH or EN410 may provide more accurate predictions in terms of peak solar heat gain of horizontal or low-sloped surfaces in regions like mainland U.S.A. or Southern Europe. Other standard spectra like G173DC and G173GT generally return intermediate results. Any one among them can probably be chosen for assessment of standard performance and product comparison, at least for white products, but a unique choice can be recommended.

4 REFERENCES

Akbari, H., and Matthews, H.D. (2012). Global cooling updates: Reflective roofs and pavements, *Energy & Buildings*, 55, 2-6.

ASTM C1549 (2009). *ASTM* C1549-*09 – Standard Test Method for Determination of Solar Reflectance Near Ambient Temperature Using a Portable Solar Reflectometer.* ASTM International, West Conshohocken, PA (U.S.A.).

ASTM E891 (1992). *ASTM E891-87(1992) – Tables for Terrestrial Direct Normal Solar Spectral Irradiance for Air Mass 1.5.* ASTM International.

ASTM E903 (1996). *ASTM E903-96 – Standard test method for solar absorptance, reflectance, and transmittance of materials using integrating spheres.* ASTM International.

ASTM G173 (2003). *ASTM G173-03 – Standard Tables for Reference Solar Spectral Irradiances: Direct Normal and Hemispherical on 37° Tilted Surface.* ASTM International.

Cool Roof Rating Council (CRRC, 2013). *Product rating program manual (CRRC-1).* Retrievable in 2013 at the address: www.coolroofs.org/alldocs.html#crrc1.

EN 410 (2011). *EN 401:2011 – Glass in building — Determination of luminous and solar characteristics of glazing*. European Committee for Standardization, Brussels (Belgium).

EN ISO 13790 (2008). *EN ISO 13790:2011 – Energy performance of buildings – Calculation of energy use for space heating and cooling.* European Committee for Standardization.

European Cool Roof Rating Council (ECRC, 2013). *EU-Cool Roofs Strategic Plan*. Retrievable in 2013 at the address: http://coolroofcouncil.eu/index.php?option=com_docman&task=cat_view&gid=68&Itemid=51&lang=en.

Ferrari, C., Libbra, A., Muscio, A., and Siligardi, C. (2013). Design of ceramic tiles with high solar reflectance through the development of a functional engobe. *Ceramics International*, in press.

Levinson, R., Akbari, H., and Paul Berdahl, P. (2010). Measuring solar reflectance—Part I: Defining a metric that accurately predicts solar heat gain. *Solar Energy*, 84(9), 1717-1744.

Levinson, R., Akbari, H., and Paul Berdahl, P. (2010a). Measuring solar reflectance—Part II: Review of practical methods. *Solar Energy*, 84(9), 1745-1759.

Libbra, A., Muscio, A., Siligardi, C., and Tartarini, P. (2011). Assessment and improvement of the performance of antisolar surfaces and coatings. *Progress in Organic Coatings*, 72, 73-80.

Libbra, A., Tarozzi, L., Muscio, A., and Corticelli, P. (2011a). Spectral response data for development of cool coloured tile coverings. *Optics & Laser Technology*, 43, 394-400.

Libbra, A., Muscio, A., and Siligardi, C. (2013). Energy performance of opaque building elements in summer: analysis of a simplified calculation method in force in Italy. *Energy & Buildings*, 64, 384-394.

Santamouris, M., Synnefa, A., and Karlessi, T. (2011). Using advanced cool materials in the urban built environment to mitigate heat islands and improve thermal comfort conditions. *Solar Energy*, 85(12), 3085-3102.

Santamouris, M. (2012). Cooling the cities – A review of reflective and green roof mitigation technologies to fight heat island and improve comfort in urban environments. *Solar Energy*, in press, doi:10.1016/j.solener.2012.07.003.

PERFORMANCE OF SELF-CLEANING COOL CEMENTITIOUS SURFACE

Ana Paula Werle[*1], Vanderley M. John[2], Kai Loh[3], Rômulo Ando[4] and Michele Lemos de Souza[5]

1 University of São Paulo
School of Engineering
São Paulo, Brazil
**ana.werle@lme.pcc.usp.br*

2 University of São Paulo
School of Engineering
São Paulo, Brazil

3 University of São Paulo
School of Engineering
São Paulo, Brazil

4 University of São Paulo
Chemistry Institute
São Paulo, Brazil

5 University of São Paulo
Chemistry Institute
São Paulo, Brazil

ABSTRACT

A strategy to reduce global warming is to increase the reflectance and thermal emittance of the built environment (Akbari, Menon, e Rosenfeld 2008). The urban heat islands usually increase the temperature by more than 10ºC (Santamouris et al. 2001). A cool roof can reduce the temperature up to 3.3ºC (Synnefa, Santamouris, e Akbari 2007) and improve indoor thermal comfort and reduce energy consumption. A comfortable indoor temperature in the buildings represents a better quality of life for those who cannot afford air conditioning besides reducing the cooling energy, costs and environmental impacts.

Most horizontal surfaces in cities are constituted by roofs and pavements and even cool when exposed to natural environment, degradation of these surfaces can occur due to factors such as UV radiation, wind and rain, biodeterioration and soiling.

Cool roofs and cool pavements constitute most of the horizontal surfaces in cities and interfere with the urban climate. The environmental exposure can cause degradation of these surfaces due to factors such as UV radiation, wind and rain, biodeterioration and soiling. Biodeterioration and soiling can be partially controlled by periodical cleaning but this procedure is time consuming, expensive and wastes water and detergents; moreover, roof cleaning is only possible when the surface is accessible and this is not always possible. Therefore, the best solution is a durable self-cleaning cool surface.

The aim of this research is to develop a durable self-cleaning cool cement-based surface. Three samples of TiO2 (anatase) products (P25, US NANO - IV and Millenium – TiONA) - added to cement pastes for self-cleaning solution - were studied. All the samples were characterized by X-ray Fluorescence Spectroscopy (XRF), while other tests focused on the measurement of the photocatalytic activity of TiO_2, using Congo Red dye on white cement paste specimens. 5% and 30% of TiO_2 were added, and the paste without addition was used as a reference. The changes after 5h of UV exposure were measured by surface analysis using absorbance measurements with UV-VIS Spectrophotometer, Raman Spectroscopy and Scanning Electron Microscopy, with EDS. The results showed that cement paste with addition of TiO_2 degrades the Congo Red dye more than the reference one and degradation is a function of the availability of TiO_2 on the surface.

Keywords
Self-cleaning, cementitious surface, TiO_2, Congo Red dye, photocatalytic degradation.

1 INTRODUCTION

TiO_2 (anatase) nanoparticles have been of interest due to their capacity to generate functional surfaces. When activated by UV radiation, TiO_2 is capable of oxidizing pollutants (Chen e

Poon 2009a; Destaillats et al. 2012; Janus et al. 2008), has biocide effect (Gumy et al. 2006), and concurrently generates self-cleaning inorganic surfaces (Aïssa et al. 2011).
It is clear that self-cleaning surfaces can reduce the cleaning process, lower maintenance costs and are associated to environmental impact. Commercial applications include self-cleaning glasses (Chabas et al. 2008; TX ACTIVE® 2006; Yu et al. 2006) and cement-based surfaces (Aïssa et al. 2011; Chen e Poon 2009b; Chen, Kou, e Poon 2011; Hüsken, Hunger, e Brouwers 2009). Research interest includes long-term performance of cement-based materials (Maury e De Belie 2010), special application on large cementitious surfaces, such as pavements (Chen, Kou, e Poon 2011) and also capability to degrade atmospheric pollution (Ai et al. 2011).
There are several anatase nanoparticle products in the international market. These products have different characteristics, including mineralogical composition, particle size distribution and surface area (Hussain et al. 2010). A systematic comparison among thirteen different samples showed significant differences in the inactivation of E coli bacteria (Gumy et al. 2006). However, a comparison of different anatase products performance when mixed with cement is not yet available.
Our objective wass to study three different TiO_2 anatase types from the market added to white cement paste and compare their performance to produce cement-based cool photocatalytic surfaces.

2 METHODS

The tests were divided into characterization of TiO2 powder by X-ray Fluorescence Spectroscopy (XRF) and quantitative measurements of the photocatalytic effect of TiO_2, added into white cement paste, using Congo Red (CR) dye. The degradation was measured by Absorbance with Spectrophotometer Shimadzu UV-VIS, Scanning Electron Microscopy (SEM) and Raman Spectroscopy.
The cementitious pastes were produced adding TiO_2 (0%, 5% and 30%) and water to white cement powder. The content of 5% of TiO_2 was defined based on the literature (Diamanti, Ormellese, e Pedeferri 2008; Aïssa et al. 2011; Lucas, Ferreira, and de Aguiar 2013) and the 30% content was defined so as to have an excess of TiO_2 in the specimens. Ø 25mm x h 2mm specimens were cast with the mixtures and cured for 24 hours in high humidity environment and dried at 40 ° C in oven, for 7 days;

2.1 X-RAY Fluorescence Spectroscopy (XRF)

Bulk semi-quantitative chemical composition was carried out in 3 samples of TiO_2 powder, by standardless XRF (Axios Advanced, PANalytical) from fluorine to uranium in glass samples. Loss of ignition was carried out at 1.050°C by 1 h.

2.2 Photocatalytic activity of TiO_2 using Congo Red (CR) dye degradation

The activity was determined by CR dye degradation, after 5 hours of UV radiation exposure.
The cementitious specimens, with TiO_2 additions, adsorbed CR dye (solution of 7 mg / L) on the surface. The specimens were in contact with the dye for 1 h, in constant stirring, in an environment protected from light. After this period, the specimens were washed with deionised water, without abrasion, to remove the possible excess of dye on the surface, and dried in an oven (40°C) for 2h.
The degradation test was carried out in a ventilated chamber with a source of UV radiation (Phillips lamp HPL-N 125 W high pressure mercury bulb with no glass). The specimens were placed on a glass base, at a 10cm distance of the UV radiation source for 5h. The experiment was monitored over time, with intervals of 1 hour. The specimens were removed from the chamber after each hour and the absorbance was measured in a spectrophotometer. Absorption changes were measured using integrating sphere, in which the reflectance data were transformed into absorbance using the Kubelka-Munk equation. Beam size at openings (at 20 nm slit width): Nearly 7 mm wide, 9 mm high - reflection side. Detectors:

photomultiplier and PbS cell. Through this procedure, it was possible to determine, in visible range (400-700nm), changes in colour after UV exposure time.

2.2.1 Absorbance Measurements

The measurements were performed with Spectrophotometer Shimadzu UV-3101 PC, in UV and Visible range (200 – 800nm).

2.2.2 Scanning Electron Microscopy with EDS (SEM)

SEM was performed on cement paste specimens, with 0% and 5% of TiO_2. The specimens were dried at 40 ° C for 48h. After dried, they were metallized with carbon in a Bal-tec Leica, Model SCD-050 and tested in the equipment FEI - Quanta600 EGF.

2.2.3 Raman Spectroscopy

RS was carried out on cement paste specimens; the measurements were performed at room temperature using a wavelength of 647.1nm in a Spectra Physics Kr + ion laser. The scattered light beams were analysed with Raman Dilor XY spectrometer, equipped with optical multichannel charge-coupled devices, with liquid nitrogen cooled detector.

3 RESULTS AND DISCUSSION

3.1 X-RAY Fluorescence Spectroscopy

The results of X-Ray spectroscopy are focused on Cl and SO_3, the main constituents detected in the test are presented in Table 1.

Table 1 Main elements identified in the chemical analysis of TiO_2 P 25 Degussa, US NANO, Millenium and LPC samples.

Components	P25 – Degussa (%)	US NANO (%)	Millenium (%)
SO_3	Nd	0.37	0.31
Cl	0.09	0.01	0.02
TiO_2	97.6	95.9	96.2
PF	2.23	3.14	3.01

nd = non detected compound

X-ray fluorescence results showed the presence of different components/elements in the samples. However, the amount of those components does not exceed 1% of the chemical composition of the material. U.S. NANO and Millenium samples have a considerable amount of SO_3, while the P25 sample presents a larger amount of Cl than the others. Such differences might be related to the products production route, which could have some influence on the products performance.

Most of the information about composition and structure of TiO_2 lies in the percentages of crystallite phases, as observed by Xu e Zhang (2009); León-Ramos et al. (2010); Hussain et al. (2010). According to the literature, the crystallographic characteristics are more important than the chemical analysis for photocatalytic activity. However, this test was performed to verify whether the impurities detected could influence photocatalytic performance.

3.2 Absorbance Measurements

The test was performed in three specimens of each formulation and showed similar results; thus, only one result was presented. Specimens containing TiO_2 addition present much more higher absorption in UV wavelengths fraction as compared to the reference specimen (figs. 1 and 2). The difference between the specimens in the UV spectrum is a function of the amount of TiO_2 added to the cement paste. Specimens with 30% TiO_2 in the mixture absorb a higher percentage of UV radiation as compared with the 5% addition. Data demonstrate the availability of TiO_2 for photocatalytic activity. In visible range, the behavior is the same for all samples with absorbance ratio of 0.01, or 99% reflectance.

The absorption of UV radiation test shows that each TiO_2 sample provides a specific absorption band, i.e., a unique absorption profile. The differences in profile could be attributed to the chemical composition of each product and result from the difference in elements on the surface of the particle.

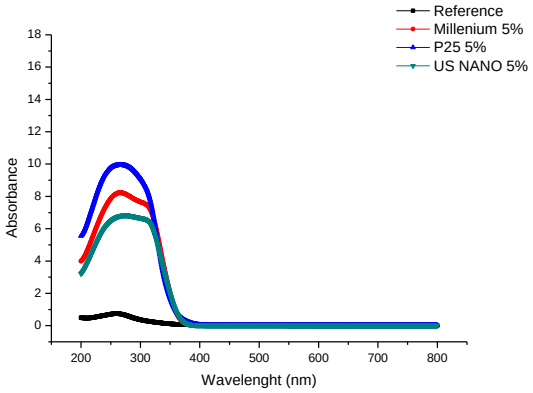

Figure 1 – Absorbance results for reference and paste with 5% TiO2

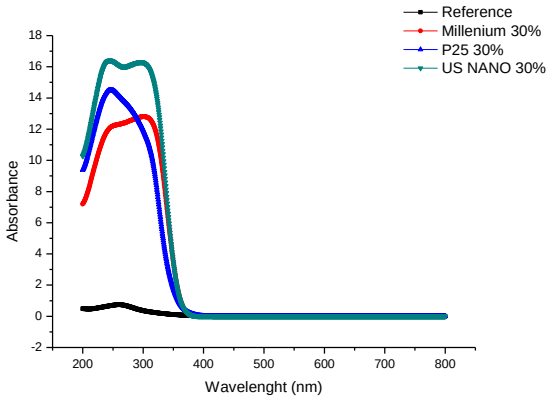

Figure 2 – Absorbance results for reference and paste with 30% of TiO2

3.3 Scanning Electron Microscopy (SEM) with EDS

SEM with EDS mapping is not usual to verify TiO_2 particles in self-cleaning solutions. This technique is a useful tool for checking TiO_2 availability on the surface. Fig. 1 shows the image of cement paste with 0% addition of TiO_2. Figs. 2, 5 and 6 show images of cement paste with 5% addition of TiO_2, from three different products. The analysis was performed in three different spots of the specimens in each sample. Fig. 3, 4, 7 and 8 are the EDS spectra which show the components present on the specimens surface. The test shows the availability of TiO_2 on the surface and also shows the distribution of these particles. Only specimens with 5% TiO_2 addition were tested because this content is a more problematic scenario. The surface of the specimen is mostly covered by $CaCO_3$, from cement carbonation (blue spots/dark color) and by TiO_2 (yellow spots/bright colors). Hence, if only 5% of the TiO_2 added to the cement paste was sufficient to identify TiO_2 on the surface, it is possible to assume that specimens prepared with 30% of TiO_2 will have much more of these particle available on the surface.

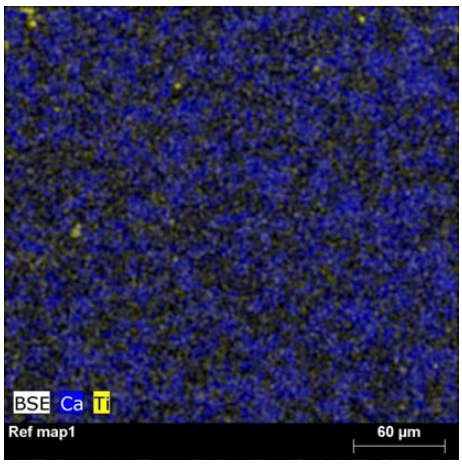

Figure 1 - Reference Sample - White cement

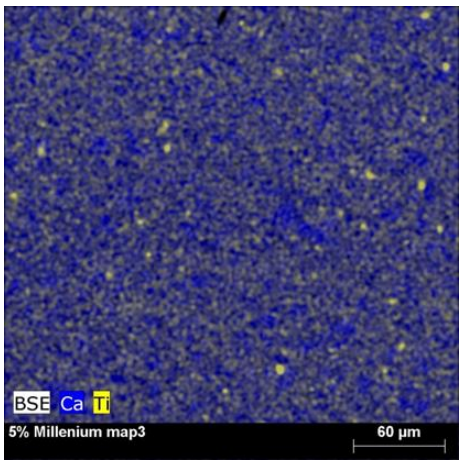

Figure 2 - Sample - White cement + 5% TiO_2 Millenium

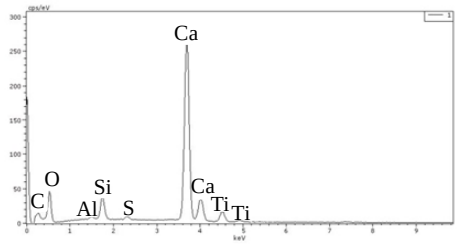

Figure 3 - Components present in the reference sample with white cement

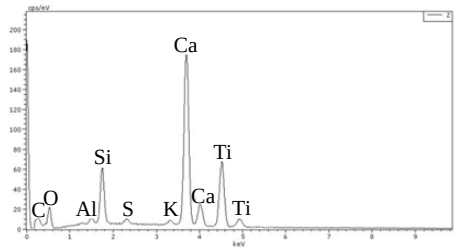

Figure 4 - Components present in the sample with white cement + 5% of TiO_2 Millenium

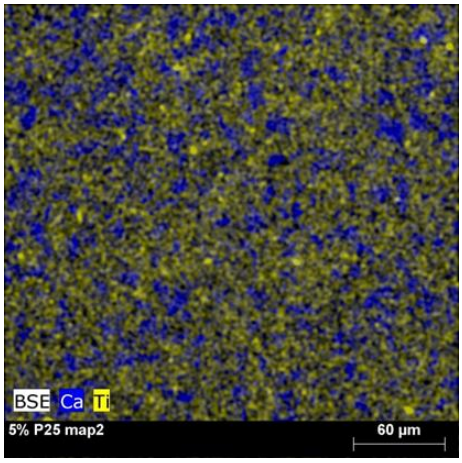

Figure 5 - Sample with white cement + 5% TiO_2 P25

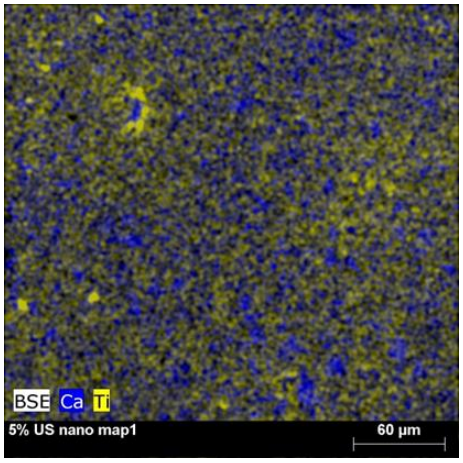

Figure 6 - Sample with white cement + 5% TiO_2 US NANO

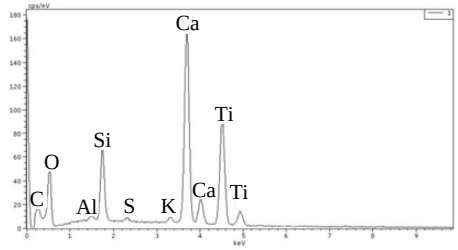

Figure 7 - Components present in the sample with white cement + 5% TiO_2 P25

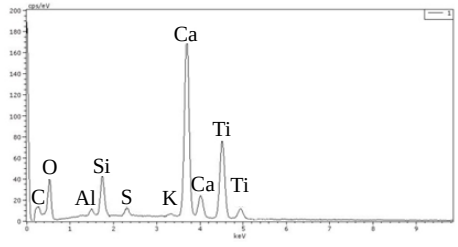

Figure 8 - Components present in the sample with white sample + 5% TiO_2 US NANO

3.4 Raman Spectroscopy

The crystallographic phases found on the specimens surfaces were calcium carbonate, liberated from cement hydration and carbonation phenomena, identified at 714 and 1087 cm^{-1} band, hydrated compounds, such as C-S-H (988 cm^{-1}) and ettringite (850 cm^{-1}). The same peaks were found by Deng et al. (2002); the authors also identified the hydrated cement compounds by Raman spectroscopy, which agrees with the peaks identified in this work, such as C-S-H, ettringite and $CaCO_3$.

TiO_2 samples exhibited a similar feature by Raman, peaks 395, 514, and 640 cm-1 bands, corresponding to the Raman fundamental modes of anatase phase (Li et al. 2011); however, the samples in this study showed peaks with distinct intensity. This evidences that each product has its own surface particle characteristics.

Raman spectroscopy makes clear how different the spectra of the specimens that have TiO2 in the mixture are when compared with the reference specimen. The reference specimen presents a characteristic and intense peak of calcium carbonate in the 1087 cm^{-1} band while specimens with TiO_2 present the same peak, but much less intense. Raman spectroscopy profiles are shown in fig. 9.

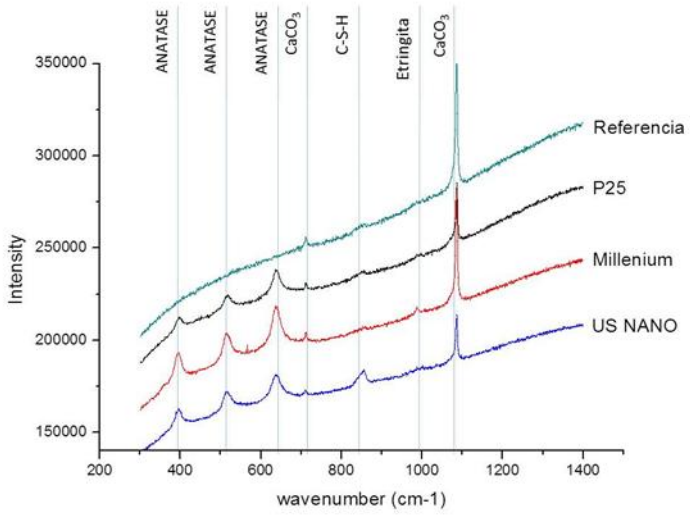

Figure 9 - Identification of elements over the sample surfaces by Raman Spectroscopy

3.5 Congo Red (CR) Dye Degradation

The dye degradation represents the photocatalytic activity of specimens containing TiO_2 comparatively to the reference. After 5h of exposure to UV radiation, the pastes prepared with 5% TiO_2 were observed to present more data variation and results of paste with TiO_2 and reference are very close to each other.

Specimens mixed with 30% TiO_2 present greater degradation than specimens with 5% TiO_2 showing that additions of over 5% are necessary.

Considering the final absorbance (300min of exposure) with 5% and 30% TiO_2 additions, it can be observed that absorbance reduced in the order of 8% for sample Millenium, 28% for US NANO and 94% for P25 and the reference presented 2%, 23% and 57%, respectively of absorbance decrease.

Results show the efficiency of the amount of product added to the mixture, as well as the efficiency of the P25 product for photocatalytic activity.

Da Costa, Zamora, e Zarbin (2011) studied the effect photocatalytic of different samples of TiO2, including P25, to degrade Reactive Blue-19 dye in solutions. The dye solution was observed to degrade 99% in the visible spectrum, with P25, after 60 minutes of UV radiation

exposure. The equipment used was an UV-VIS Spectrophotometer, similar to the equipment used in this study.

Devi, Murthy, e Kumar (2010) studied the TiO_2 photocatalytic effect using aqueous solution of Congo Red dye, exposed to natural UV radiation. The degradation of the dye was measured with UV-VIS equipment in the visible spectrum (400 - 700nm). The authors showed that after sun exposure, the sample anatase doped with V, Zn, present higher photodegradation (38% to 100%) than undoped anatase and sample P25 presented photodegradation of 06% to 18%, respectively.

Janus et al. (2008) tested samples of artificially modified TiO_2 (doped with carbon nanotubes) and samples of P25. For the P25 sample, after 5.5 hours of UV radiation exposure, 100% of degradation of the mono azo dye was verified. The test shows that the two samples have equivalent performance in relation to photodegradation. The TiO_2 modified dye degradation occurred after 5h, while for P25 the dye degradation occurred after 5.5h.

The results of Congo Red dye degradation is presented in Figs. 10 and 11.

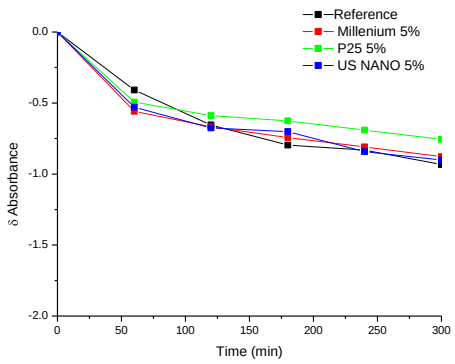

Figure 10 – CR dye degradation with 5% TiO2 in the matrix

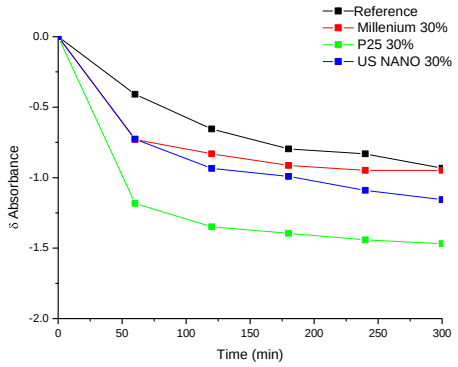

Figure 11 – CR dye degradation with 30% TiO2 in the matrix

4 CONCLUSION

The XRF test confirmed that each of the 3 samples of the study has a specific chemical composition.

SEM with EDS showed that there is TiO_2 available for photo catalytic activity on the surface of the white cement specimens and that these particles are quite well distributed on the surface.

Raman spectroscopy identified the crystalline phases of TiO2 and products of cement hydration and carbonation on the surface of the specimens as well as C-S-H and etringite.

Photocatalytic activity, verified by Congo Red dye degradation, demonstrated that the paste with TiO_2 addition exhibited higher degradation than the reference samples. Specimens with 30% TiO_2 in the paste degrade more than the specimens with 5% due to the greater availability of TiO_2 on the surface. The different types of TiO_2 have different degradation performance. Such differences can be attributed to the specificities of the products, such as different chemical elements or contents. In the experimental conditions of the P25 study, TiO_2 showed the best performance when compared with the reference, Millenium and U.S. NANO, when added to the paste at 30%.

The literature revue showed that UV–VIS spectroscopy is a very common and precise method to quantify dye degradation. However, there is still no consensus about the most appropriate type of dye for test procedures. Along the same lines, research is showing testing

methodologies in aqueous solution. Nevertheless, this situation does not represent the scenario of TiO_2 application for building materials, with air purification and self-cleaning solutions. The procedure used in this study permitted to select the more photoactive TiO_2 sample showing that the test performance using cement paste is appropriate for TiO_2 photocatalitic studies for application in building surfaces.

ACKNOWLEDGEMENTS

The authors thank the Chemistry Institute of the University of São Paulo and student Larissa Nardi for all their support and dedication. The main author thanks FAPESP for the scholarship.

REFERENCES

Ai, Zhihui, Linli Zhu, Shuncheng Lee, e Lizhi Zhang. 2011. "NO Treated TiO2 as an Efficient Visible Light Photocatalyst for NO Removal". *Journal of Hazardous Materials* (maio). doi:10.1016/j.jhazmat.2011.05.033. http://linkinghub.elsevier.com/retrieve/pii/S0304389411006728.

Aïssa, Aurélie Hadj, Eric Puzenat, Arnaud Plassais, Jean-Marie Herrmann, Claude Haehnel, e Chantal Guillard. 2011. "Characterization and photocatalytic performance in air of cementitious materials containing TiO2. Case study of formaldehyde removal". *Applied Catalysis B: Environmental* 107 (1-2) (agosto): 1–8. doi:10.1016/j.apcatb.2011.06.012.

Akbari, Hashem, Surabi Menon, e Arthur Rosenfeld. 2008. "Global cooling: increasing world-wide urban albedos to offset CO2". *Climatic Change* 94 (novembro 20): 275–286. doi:10.1007/s10584-008-9515-9.

Chabas, A., T. Lombardo, H. Cachier, M. H. Pertuisot, K. Oikonomou, R. Falcone, M. Verità, e F. Geotti-Bianchini. 2008. "Behaviour of self-cleaning glass in urban atmosphere". *Building and Environment* 43: 2124–2131. doi:10.1016/j.buildenv.2007.12.008.

Chen, Jun, Shi-cong Kou, e Chi-sun Poon. 2011. "Photocatalytic cement-based materials: Comparison of nitrogen oxides and toluene removal potentials and evaluation of self-cleaning performance". *Building and Environment* 46 (9) (setembro): 1827–1833. doi:10.1016/j.buildenv.2011.03.004.

Chen, Jun, e c Chi-sun Poon. 2009a. "Photocatalytic construction and building materials: From fundamentals to applications". *Building and Environment* 44: 1899–1906. doi:10.1016/j.buildenv.2009.01.002.

Chen, Jun, e Chi-sun Poon. 2009b. "Photocatalytic Cementitious Materials: Influence of the Microstructure of Cement Paste on Photocatalytic Pollution Degradation". *Environmental Science & Technology* 43 (23) (dezembro): 8948–8952. doi:10.1021/es902359s.

Da Costa, Elias, Patricio P. Zamora, e Aldo J.G. Zarbin. 2011. "Novel TiO2/C nanocomposites: Synthesis, characterization, and application as a photocatalyst for the degradation of organic pollutants". *Journal of Colloid and Interface Science* (outubro). doi:10.1016/j.jcis.2011.10.028. http://linkinghub.elsevier.com/retrieve/pii/S0021979711013014.

Deng, C.-S., C. Breen, J. Yarwood, S. Habesch, J. Phipps, B. Craster, e G. Maitland. 2002. "Ageing of oilfield cement at high humidity: a combined FEG-ESEM and Raman microscopic investigation". *Journal of Materials Chemistry* 12 (10) (setembro 26): 3105–3112. doi:10.1039/b203127m.

Destaillats, Hugo, Mohamad Sleiman, Douglas P. Sullivan, Catherine Jacquiod, Jean Sablayrolles, e Laurent Molins. 2012. "Key parameters influencing the performance of

photocatalytic oxidation (PCO) air purification under realistic indoor conditions". *Applied Catalysis B: Environmental* 128 (novembro): 159–170. doi:10.1016/j.apcatb.2012.03.014.

Devi, L. Gomathi, B. Narasimha Murthy, e S. Girish Kumar. 2010. "Photocatalytic activity of TiO2 doped with Zn2+ and V5+ transition metal ions: Influence of crystallite size and dopant electronic configuration on photocatalytic activity". *Materials Science and Engineering: B* 166 (1) (janeiro): 1–6. doi:10.1016/j.mseb.2009.09.008.

Gumy, D., C. Morais, P. Bowen, C. Pulgarin, S. Giraldo, R. Hajdu, e J. Kiwi. 2006. "Catalytic activity of commercial of TiO2 powders for the abatement of the bacteria (E. coli) under solar simulated light: Influence of the isoelectric point". *Applied Catalysis B: Environmental* 63 (março): 76–84. doi:10.1016/j.apcatb.2005.09.013.

Hüsken, G., M. Hunger, e H.J.H. Brouwers. 2009. "Experimental study of photocatalytic concrete products for air purification". *Building and Environment* 44 (12) (dezembro): 2463–2474. doi:10.1016/j.buildenv.2009.04.010.

Hussain, M., R. Ceccarelli, D.L. Marchisio, D. Fino, N. Russo, e F. Geobaldo. 2010. "Synthesis, characterization, and photocatalytic application of novel TiO2 nanoparticles". *Chemical Engineering Journal* 157 (1) (fevereiro): 45–51. doi:10.1016/j.cej.2009.10.043.

Janus, Magdalena, Beata Tryba, Ewelina Kusiak, Tomoki Tsumura, Masahiro Toyoda, Michio Inagaki, e Antoni W. Morawski. 2008. "TiO2 Nanoparticles with High Photocatalytic Activity Under Visible Light". *Catalysis Letters* 128 (1-2) (outubro): 36–39. doi:10.1007/s10562-008-9721-0.

León-Ramos, J. A., D. Kibanova, P. Santiago-Jacinto, Y. Mar-Santiago, e M. Trejo-Valdez. 2010. "Synthesis, characterization and photocatalytic properties of tungsten-doped hydrothermal TiO2". *Journal of Sol-Gel Science and Technology* 57 (1) (setembro): 43–50. doi:10.1007/s10971-010-2322-6.

Li, Z, L Mi, PN Wang, e JY Chen. 2011. "Study on the visible-light-induced photokilling effect of nitrogen-doped TiO2 nanoparticles on cancer cells". http://openi.nlm.nih.gov/detailedresult.php?img=3211446_1556-276X-6-356-1&req=4.

Maury, A., e N. De Belie. 2010. "Estado del arte de los materiales a base de cemento que contienen TiO_2: propiedades auto-limpiantes". *Materiales de Construcción* 60 (298) (maio): 33–50. doi:10.3989/mc.2010.48408.

Santamouris, M, N. Papanikolaou, I. Livada, I. Koronakis, C. Georgakis, A. Argiriou, e D. N. Assimakopoulos. 2001. "ON THE IMPACT OF URBAN CLIMATE ON THE ENERGY CONSUMPTION OF BUILDINGS". *Solar Energy* 70: 201–216.

TX ACTIVE®. 2006. "TX ACTIVE®: PRESENTATION OF THE FIRST ACTIVE SOLUTION TO THE PROBLEM OF POLLUTION". http://www.italcementigroup.com/NR/rdonlyres/2062CB8F-6FAB-4C3B-86EB-28AE17D68913/0/Comunicato_TXActive_UK.pdf.

Xu, Hua, e Lizhi Zhang. 2009. "Controllable One-Pot Synthesis and Enhanced Photocatalytic Activity of Mixed-Phase TiO Nanocrystals with Tunable Brookite/Rutile Ratios". *The Journal of Physical Chemistry C* 113 (5) (fevereiro): 1785–1790. doi:10.1021/jp8089903.

Yu, Jiaguo, Huogen Yu, Bei Cheng, Minghua Zhou, e Xiujian Zhao. 2006. "Enhanced photocatalytic activity of TiO2 powder (P25) by hydrothermal treatment". *Journal of Molecular Catalysis A: Chemical* 253 (1-2) (julho): 112–118. doi:10.1016/j.molcata.2006.03.021.

DEVELOPMENT AND TESTING OF PHOTOVOLTAIC PAVEMENT FOR HEAT ISLAND MITIGATION

Chrysanthi Efthymiou[1], Mat Santamouris[*2], Denia Kolokotsa[3], Andreas Koras[4]

1 Group Building Environmental Physics, Physics Department, Division of Applied Physics, University of Athens, Panepistimioupolis, 15784 Athens, Greece
2 Group Building Environmental Physics, Physics Department, Division of Applied Physics, University of Athens, Panepistimioupolis, 15784 Athens, Greece
**Corresponding author: msantam@phys.uoa.gr*
3 Energy Management in the Built Environment Research Unit, Environmental Engineering Department, Technical University of Crete, Technical University Campus, Kounoupidiana, GR 73100 Chania
4 Sector of Aerodynamics and Flight Mechanics, Hellenic Air Force Academy, HAFA, Dekelia Attica, TGA 1010

ABSTRACT

The present article deals with the development and testing of photovoltaic pavement for heat island mitigation. The scope of this study is to evaluate its contribution to the balance of the Urban Heat Island phenomenon. For this reason, we made a photovoltaic pavement for purely experimental reasons (dimensions 3.5x1.3m) that consists of two different voltage polycrystalline photovoltaic panels. On top of them, a triplex security glass with a nonslip silk screen, PVB standard 1.14 mm was placed. We measured their surface temperature, from morning till noon, each and every hour, for several months (summer-autumn-spring). It was proven that, in comparison with other respective asphalt street and ground measurements, it has essentially lower values. In addition, in order to find out the degree witch the photovoltaic pavement contributes to the improvement of the urban microclimate, a simulation took place.

KEYWORDS

Heat island, photovoltaics, simulation, mitigation

1. INTRODUCTION

The growing population in urbanized areas, in 1950 30% of the world population lived in urban areas and this price is expected to rise to 60% in 2030, causes an increase of anthropogenic heat and thus, the center of the cities, in temperate zones, become hotter than their periphery, forming an urban heat island (UHI). (Essa et al., 2013)

In recent decades, the scientific community has shown great interest in both the recording of urban heat island effect and the mitigation techniques of it. The reason behind such intensive monitoring of this effect is its significant energy and environmental impact on the urban environment, which can be considered as the most significant recorded event of what we call climate change. The main

energy impact of heat island, is associated to the high energy consumption for cooling in buildings (Giannopoulou et al., 2011), which increases the production of smog, contributes to high production of pollutants from power plants (SO_2, CO, NO_X) and acts as a trap for pollutants, reducing therefore the quality of life and resulting in a social - economic impact on urbanized areas. Moreover reduces the levels of thermal comfort and creates additional health problems and mortality due to high temperatures (Gobakis et al., 2011, Giannaros et al., 2013).

The existence of the phenomenon is perceived by calculating the difference in air temperature between urban and non-urban areas, called intensity of the urban heat island effect and depends on the size, topography and geometry of urban areas, the size of population and industrial growth of the city, the heat balance of the urban area, topography, local climate and weather conditions. This phenomenon is observed both day and night and the spatiotemporal evolution depends on the unique characteristics of each urban area (Gobakis et al., 2011).

The thermal properties of construction materials (cement, asphalt, concrete, glass) play a very important role, namely the high heat capacity and low reflectivity in the sunlight. More particularly, the structured surfaces characterized by sensitivity to heat storage during the day which is retransmitted during the night, produce a positive thermal anomaly over the urban area (Papangelis et al., 2012). Furthermore, help to reduce wind speed by approximately 25% in the cities due to increased roughness and urban geometry. An additional feature of cities that creates - intensify the phenomenon is the reduced latent heat of evaporation or the replacement of natural green areas with dry surfaces and rapid runoff of water from rainfall thereby reducing the storage of rainwater on the surface of the earth. Finally, active role played by air pollution over the city, and the anthropogenic heat released from urban activities (cars, air conditioning, etc.). (Stathopoulou et al., 2007)

It has been found that the average spatial extent of urban heat island in Athens is 55.2 km^2 and the average intensity of 5.6^oC. The effect is less pronounced in the early morning and afternoon hours. The intensity of UCL island follows a typical daily cycle by taking the minimum and maximum values, the early hours (sharp decrease after sunrise) and during the night (increase after sunset), respectively (Giannaros et al., 2013). The maximum values occur during the summer and especially in mid-July for day while on the night there is a shift of the maximum about two weeks. Identified and some extremely hot areas (hot spots) where the temperatures differ on average 4-6^oC (with a maximum of up to 9-10^oC) compared to the surrounding suburban. (Keramitsoglou et al., 2011)

Despite the general picture of the phenomenon, there are variations of intensity in the different areas of the basin due to the existence or not of green areas and uncovered areas with bare ground (mines, dumps, stadiums and extensive pedestrianization), the density of buildings, traffic, industrial activity and thermal properties of materials. Topography plays an important role too, which is evident by the lowest temperatures found near the shoreline, probably due to the phenomenon of the sea breeze, but also from the different heating of the slopes of the mountains (eastern warmer than the west) and the cutoff of summer northern winds (annual) by them. (Livada et al., 2002; Stathopoulou and Cartalis, 2006; Stathopoulou et al., 2009; Giannopoulou et al., 2011; Keramitsoglou et al., 2011; Gobakis et al., 2011; Giannaros et al., 2013)

There are many techniques to improve the urban microclimate and mitigation of the heat island phenomenon. Materials play a very important role and determine the thermal balance in the urban environment. The use of materials with high reflectivity to solar radiation and high emissivity in the thermal radiation, called cool materials, both in buildings envelopes and in other urban surfaces, contributes to reduce thermal loads through transport phenomena (convection, radiation). (Santamouris et al., 2011)

Cool materials are characterized by high solar reflectance and infrared emittance values. These two properties result in lower external surface temperatures and reduce heat penetrating into the building and decrease the ambient air temperature.

Sidewalks are a big piece of urban surface and affect strongly the urban climate. Their thermal balance is determined by the amount of the absorbed solar radiation, the emitted infrared radiation, the heat transferred by convection to the atmospheric air, the heat stored in to the mass of the material and the heat conducted to the ground. When latent heat

phenomena are present, evaporation or even condensation affect the thermal regime of the pavement surfaces as well, while the effect of rain and icing has to be considered as well. The use of cool pavement surface with lower temperatures and reduced flow sensible heat in the atmosphere is one of the most important solutions proposed (Santamouris, 2013). Cool pavements refer to a range of established and emerging materials that tend to store less heat and may have lower surface temperatures compared to conventional products. Conventional pavements are usually impervious made of concrete and asphalt, with solar reflectance values ranging between approximately 4% and 45%, which can reach peak summertime surface temperatures of 48–67^{o}C. Increasing the solar reflectance of a paved surface keeps it cooler under the sun. Measured data clearly indicate that increasing the pavement's solar reflectance by 0.25 can decrease the pavement temperature by up to 10^{o}C.

Another proposal is to use photovoltaic panels for the mitigation of the phenomenon as mentioned at work of Golden et al., 2006, in which pavement's surface temperatures were measured in three cases: unshaded, shaded by PV canopy and shaded by urban forestry canopy. It was proved that HMA surface shaded by a PV canopy achieves a 55.8^{o}F (13.2^{o}C) surface temperature reduction in comparison to the adjacent fully exposed HMA, while the HMA surface mitigated (covered) by the urban forestry achieves a maximum reduction of 43.2^{o}F (6.2^{o}C) in comparison to the adjacent fully exposed HMA. Photovoltaic panels provide a greater thermal reduction benefit during the diurnal cycle in comparison to urban forestry while also providing the additional benefits of supporting peak energy demand, conserving water resources and utilizing a renewable energy source.

This paper focuses to the use of photovoltaics directly as pavements. Experiments and simulations have been performed to assess the mitigation potential of cool photovoltaic pavements. New technologies for photovoltaic pavements based on the use of PV tiles made with glass integrated over ceramic, enables walking on and placing of furniture. Photovoltaic pavements may provide electricity, save space and in case their surface temperature is appropriate, they could contribute to mitigate heat islands in cities. (Santamouris, 2013)

2. EXPERIMENTAL AND SIMULATION ANALYSIS

To conduct this research an experimental device was developed and built. The device is depicted in the following photos (figure 1, 2). It is a metallic construction, the dimensions and the shape of which are almost similar to those of a conventional pavement, namely 3.5m in length and 1.3m in width. Enough room under the surface of the pavement is provided, appropriate for the storage and safety of the various equipment, (batteries, inverter, etc) required for the operation of the PVs. Two different voltage polycrystalline photovoltaic panels, where their characteristics are given in Table 1, reside at the horizontal surface of the device, able to generate enough electricity for the lighting of the pavement. A triplex security glass with a nonslip silk screen, PVB standard 1.14mm is mounted above the PV panels at a distance of 5cm from the latter and its properties are mentioned in Table 2.

Table 1: Characteristics of PV panels

Panel 1	**Panel 2**
P = 145 W_P	P = 220 W_P
U_{MPP} = 34.1 V	U_{MPP} = 29.3 V
U_{OC} = 42.2 V	U_{OC} = 36.4 V
I_{MPP} = 4.24 A	I_{MPP} = 7.51 A
I_{SC} = 4.69 A	I_{SC} = 8.18 A
V = 840V	V = 1000 V

Table 2: Glass properties

	Luminous factors	**Energy factors**
Nominal thickness = 21.1 mm	Transmittance = 83%	Transmittance = 60%
Weight = 51.2 kg/m^2	Outdoor reflectance = 8%	Solar factor g = 0.68%
Normal outdoor	Indoor reflectance = 8%	U_g = 5.3

emissivity = 0.89		W/(m^{2}K)

Figure 1: The experimental PV pavement

Figure 2: Closer look to the glass above the panels

During the summer of 2013 (June-July) the surface temperatures of asphalt, pv pavement and soil surfaces were measured using a contact thermometer. Thus, as shown in the figure 3, the soil has higher temperature than the other two surfaces in the early hours and a sharp drop immediately after the local noon. The photovoltaic pavement on the other side increases gradually its surface temperature in the morning and performs a delay compared to the soil, about 2 hours, when it starts reducing its temperature in smoother way than the soil. Finally, concerning the asphalt, lower temperature observed in the morning, but increases during the day and remains higher than the other two surfaces during evening hours.

To prove, however, that such an application, beyond the benefits of photovoltaics in energy production without the emission of pollutants, helps in urban heat island mitigation, an appropriate three-dimensional microclimate model (Envimet 3.1) is used to calculate the mitigation potential of pv pavements. The thermal regime in the area was calculated considering a) conventional asphaltic pavements and b) pv pavements. For the simulation of the above mentioned phenomena a main street (Fragoklissias) in Maroussi was selected, the coarse urban formation and the dense planting of which ensures big amounts of insolation during the day time (figure 4).

Figure 4: Image of analysis area as shown in Google earth

This model takes into account all types of solar radiation (direct, diffuse and reflected) and thermal radiation flows from the atmosphere, soil and walls. The calculation of the radiation flow includes shading, absorption and reradiation of plants.

To obtain results an input file feeds the software with the required data, the latter given in a matrix format. Such data include the geometry of the site and neighboring buildings, the selected step of the simulation grid (grid), the atmospheric and climatic conditions, types of plantings, paving materials, and elevations of the perimeter buildings and levels.

A grid was used over the study area, consisting of 220x60x20 nodes (x, y, z) with a resolution of 3.4m x 3.4m. The total simulation time was 24 hours from midnight of one day to midnight the next day, the meteorological start data of the simulation, defined by meteorological data for the region during summer 2013 by the National Observatory of Athens and paving materials of status quo and their characteristics are shown in table 3.

Table 3: Characteristics of conventional paving materials

material	reflectance	Emissivity
asphalt	0.1	0.9
Pavement tiles	0.2	0.9
soil	0.0	0.98

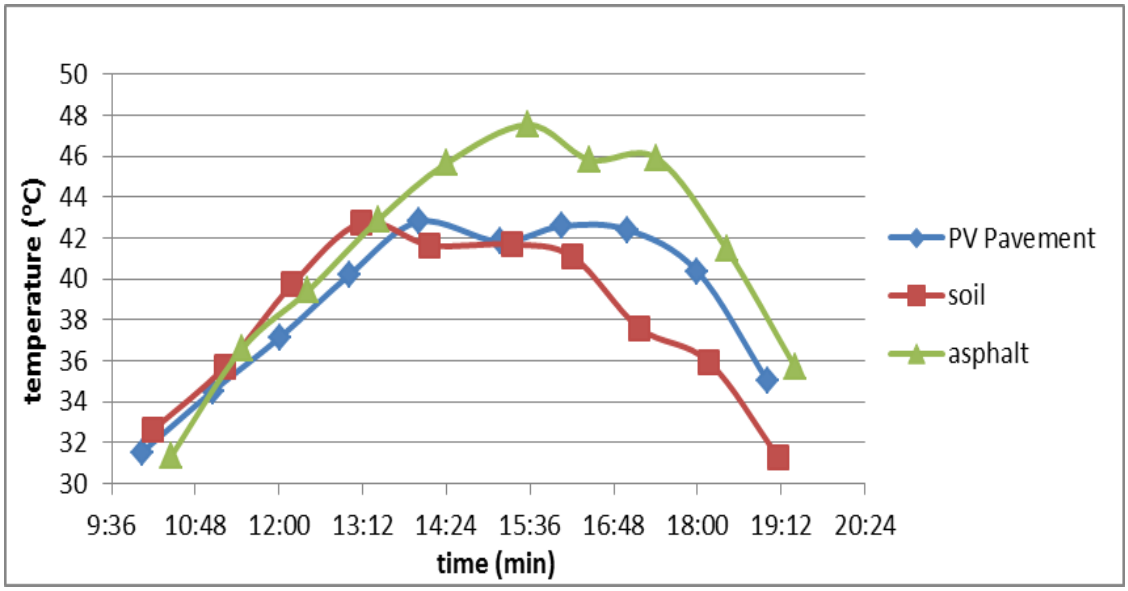

Figure 3: Comparison of daily temperature distribution of three different materials

At a first step, the distribution of the surface temperature in the street, on the current situation, has been calculated for a typical summer day with specific boundary conditions (temperature, wind direction and velocity, solar radiation). Secondly, the same calculations have been carried out for the same boundary conditions as the ones used in the initial phase a) for the new situation. The different optical properties of the materials have been taken into account. For solar radiation values corresponding to 12:00h and 15:00h (Local Time) and for undisturbed ambient temperature and wind speed, the calculated surface temperatures for both situations are shown in the following figures.

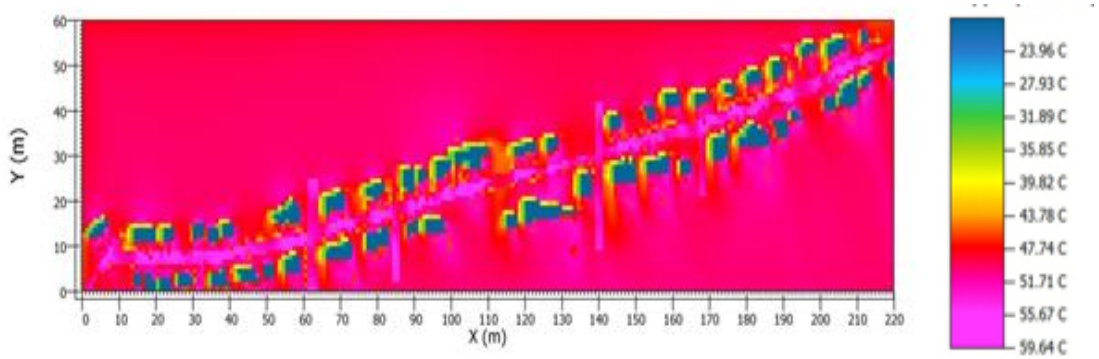

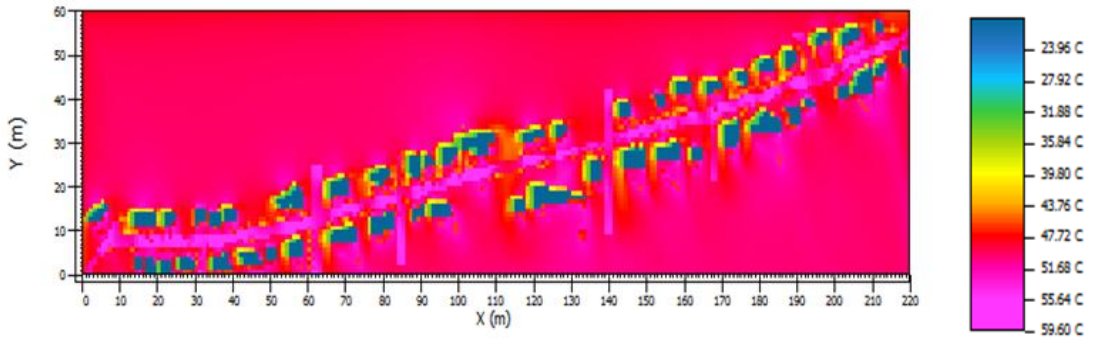

b)

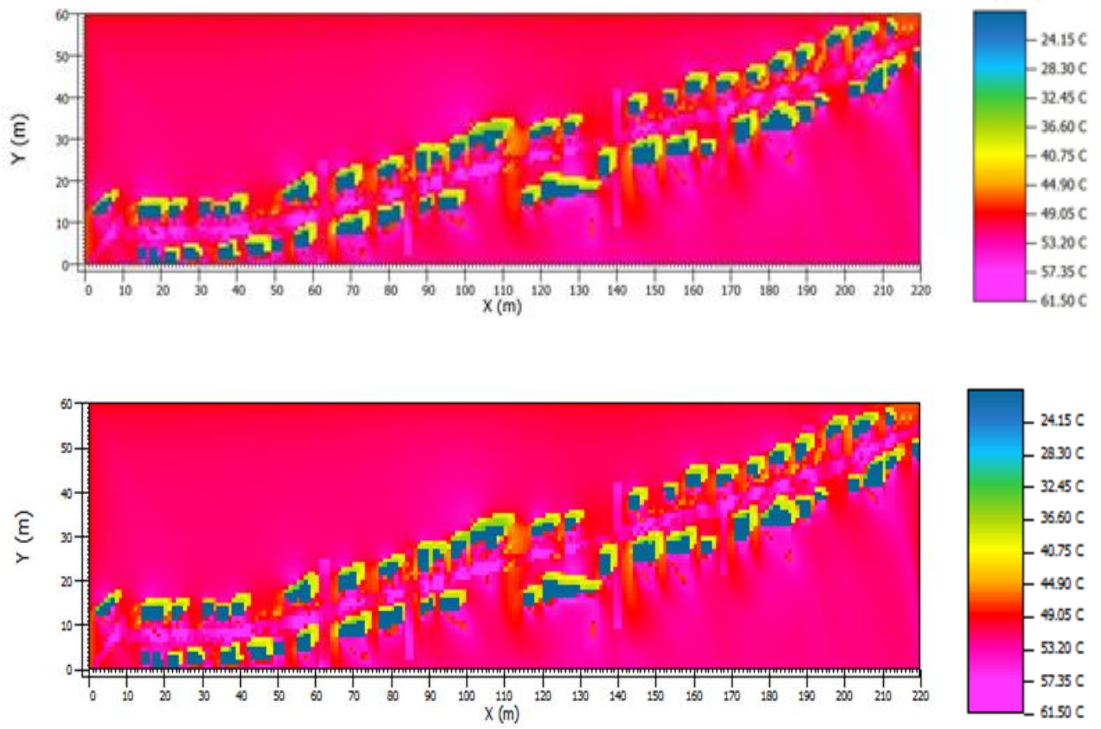

Figure 5: surface temperature before and after the application of pv pavements respectively at a) 12:00h, b) 15:00h

Simulations of the ambient temperature, in height of 1.80m, have been carried out for the same climatic boundary conditions as used previously in order to be able to quantify the possible microclimatic improvements. In particular, simulations have been carried out for an undisturbed ambient temperature and wind speed taking into account the considered improvements. The calculated distribution of the surface temperature has been introduced to the computerized tool as a new boundary. The results of this simulation both with and without the interventions, at 12:00h and 15:00h o clock as before, are given in figures below.

a)

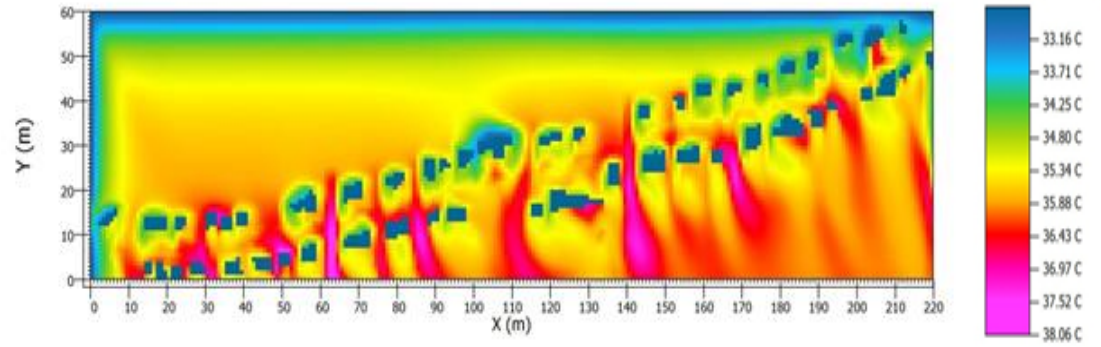

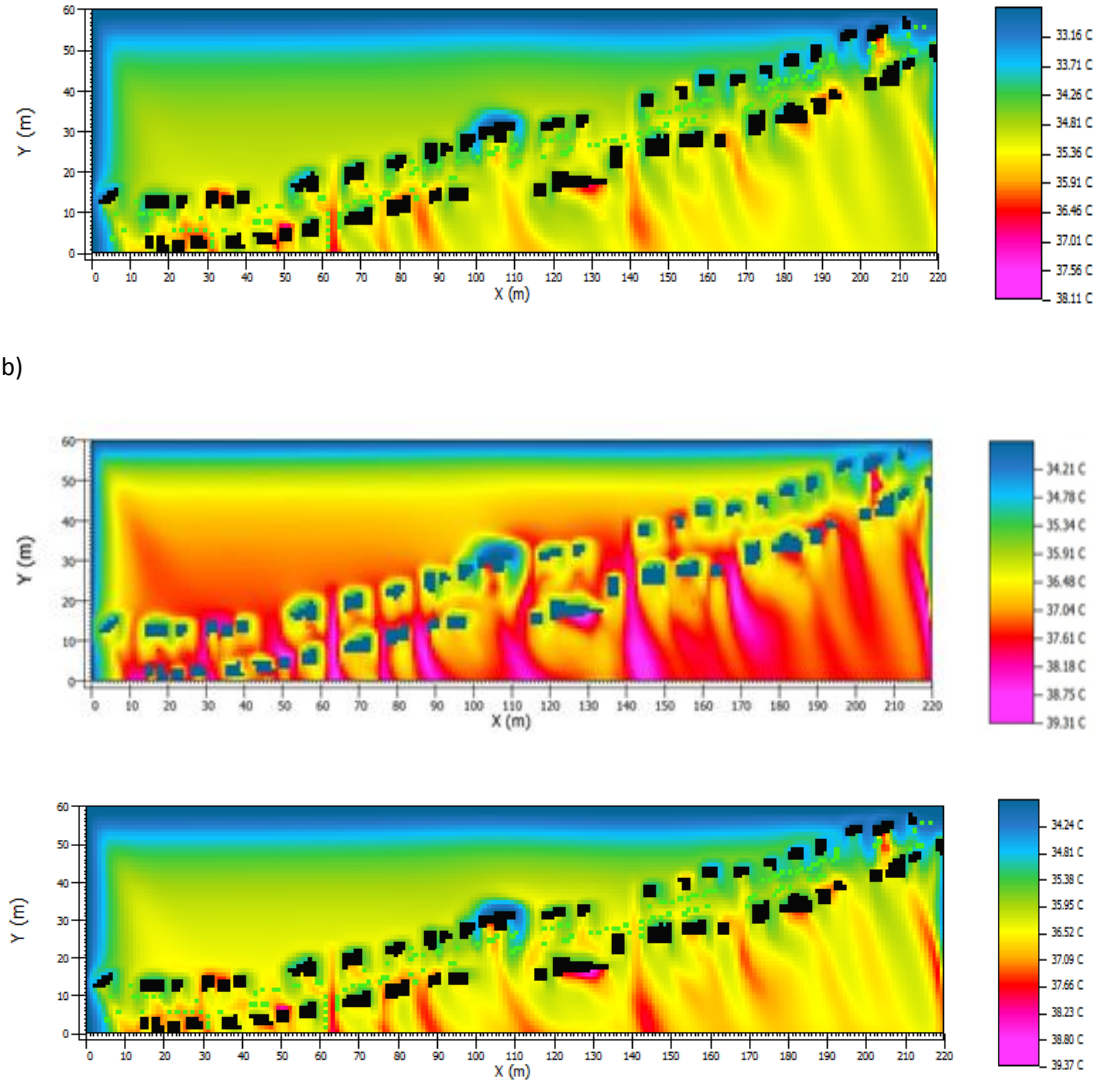

Figure 6: air temperature (1.80m) before and after the application of pv pavements respectively at a) 12:00h, b) 15:00h

Obviously, replacing conventional pavements with PV ones results in a drop of both surface and air temperature, whereas these temperature differences are with time, which is well validated against the above obtained experimental data. More specifically there is a maximum decrease of the surface temperature close to 4°K and to the ambient air close to 2°K. Speaking for the surface temperatures, they have been substantially decreased because of the different thermal properties of pv pavements against the conventional ones. Concerning the ambient air temperatures, there is a remarkable drop due to lower surface temperatures of pv pavements, which cause a reduction in heat exchange.

3. CONCLUSIONS

Heat island increases temperature in urban areas, increases the energy consumption for cooling purposes and affects the global environmental quality of cities. The use of advanced mitigation techniques highly contributes to decrease temperatures and improve comfort in open urban areas. (Santamouris et al., 2012)

New materials, systems and technologies have been developed and proposed in order to decrease the sensible heat flux to the atmosphere from different urban structures like buildings and paved surfaces. Business around pavements present an extreme commercial importance and employ hundreds thousands of workers, engineers and administrators. It is

during the very recent years that researcher working on pavement technologies started to look on their optical and thermal properties and the possible impact on urban climate.

Photovoltaics were only known about their use in energy production. The present paper presents a mitigation technique for urban heat island phenomenon with the use of photovoltaics and in particular the application of photovoltaics directly in pavements. This technique has direct and indirect effects on the microclimate. The analysis of the results obtained through the monitoring and the detailed simulations have shown that the considered microclimatic improvement technique have helped to decrease substantially both the surface and ambient temperatures up to 5^{o}K and to 2^{o}K respectively against the conventional pavements. Also the power generated from the PV will depend on the rating of the system and the available electricity generating potential hours. PV pavements can be used to provide supplemental base load and peak power electricity for urban open areas.

4. REFERENCES

Essa, W., van der Kwast, J., Verbeiren, B., Batelaan, O., (2013). *Downscaling of thermal images over urban areas using the land surface temperature–impervious percentage relationship. International Journal of Applied Earth Observation and Geo-information*, 23, 95–108

Gaitani, N., Spanou, A., Saliari, M., Synnefa, A., Vassilakopoulou, K., Papadopoulou, K., Pavlou, K., Santamouris, M., Papaioan-nou, M., Lagoudaki, A., (2011). *Improving the microclimate in urban areas: a case study in the center of Athens. Building Serv. Eng. Res. Technol.*, 32.1, pp. 53–71

Giannaros, T. M., Melas, D., Daglis, I. A., Keramitsoglou, I., Kourtidis, K., (2013). *Numerical study of the urban heat island over Athens (Greece) with the WRF model. Atmospheric Environment*, doi: 10.1016/j.atmosenv.2013.02.055.

Giannopoulou, K., Livada, I., Santamouris, M., Saliari, M., Assimakopoulos, M., Caouris, Y.G., (2011). *On the characteristics of the summer urban heat island in Athens, Greece. Sustainable Cities and Society*, 1, 16–28

Gobakis, K., Kolokotsa, D., Synnefa, A., Saliari, M.,Giannopoulou, K., Santamouris, M., (2011). *Development of a model for urban heat island prediction using neural network techniques. Sustainable Cities and Society*, 1, 104–115

Golden, J.S., Carlson, J., Kaloush, K.E., Phelan, P., (2007). *A comparative study of the thermal and radiative impacts of photovoltaic canopies on pavement surface temperatures. Solar Energy*, 81, 872–883

Keramitsoglou, I., Kiranoudis, C. T., Ceriola, G., Weng, Q., Rajasekar, U., (2011). *Identification and analysis of urban surface temperature patterns in Greater Athens, Greece, using MODIS imagery. Remote Sensing of Environment*, 115, 3080–3090

Livada, I., Santamouris, M., Niachou, K., Papanikolaou, N., Mihalakakou, G., (2002). *Determination of places in the great Athens area where the heat island effect is observed. Theoretical and Applied Climatology*,71,219-230

Papangelis, G., Tombrou, M.,Dandou, A., Kontos, T., (2012). *An urban "green planning" approach utilizing the Weather Research and Forecasting (WRF) modeling system. A case study of Athens, Greece. Landscape and Urban Planning*, 105, 174–183

Santamouris, M., Synnefa, A., Karlessi, T., (2011). *Using advanced cool materials in the urban built environment to mitigate heat islands and improve thermal comfort conditions. Solar Energy*, 85, 3085–3102

Santamouris, M., Gaitani, N., Spanou, A., Saliari, M., Giannopoulou, K., Vasilakopoulou, K., Kardomateas, T., (2012). *Using cool paving materials to improve microclimate of urban areas - Design realization and results of the flisvos project. Building and Environment*, 53,128-136

Santamouris, M. (2013*). Using cool pavements as a mitigation strategy to fight urban heat island – a review of the actual developments. Renewable and Sustainable Energy Reviews*, 26, 224–240

Stathopoulou, M, Cartalis, C.,(2006). *Daytime urban heat islands from Landsat ETM+ and*

Corine land cover data: An application to major cities in Greece. Solar Energy, 81, 358–368

Stathopoulou, M., Cartalis, C., Petrakis, M., (2007). *Integrating Corine Land Cover data and Landsat TM for surface emissivity definition: application to the urban area of Athens, Greece. International Journal of Remote Sensing*, Vol. 28, No. 15, 3291–3304

Stathopoulou,M., Synnefa, A.,Cartalis, C., Santamouris, M, Karlessi,T. and Akbari, H.,(2009). *A surface heat island study of Athens using high-resolution satellite imagery and measurements of the optical and thermal properties of commonly used building and paving materials. International Journal of Sustainable Energy*, Vol. 28, Nos. 1–3, 59–76

Synnefa, A., Dandou, A., Santamouris, M., Tombrou, M., (2008). *On the Use of Cool Materials as a Heat Island Mitigation Strategy. Journal of Applied Meteorology and Climatology*, Vol. 47

A NUMERICAL AND EXPERIMENTAL ANALYSIS OF THE AGING OF THE COOL ROOFS FOR BUILDINGS IN GREECE

E. Mastrapostoli[1], M. Santamouris[*2], Dionysia Kolokotsa[3], Perdikatsis Vassilis[4], Danae Venieri[3], Kostas Gompakis[3]

1 Group Building Environmental Studies
Physics Department, University of Athens
Athens, Greece

2 Group Building Environmental Studies
Physics Department, University of Athens
Athens, Greece
**Corresponding author:* msantam@phys.uoa.gr

3 School of Environmental Engineering
Technical University of Crete
Kounoudipiana, Crete, Greece

4 School of Mineral Resources Engineering,
Technical University of Crete
Kounoudipiana, Crete, Greece

ABSTRACT

Cool roof coatings remain cooler than absorptive roofs and thus predominantly are used in buildings that require the reduction of the indoor temperature and the cooling loads. Cool roofs can also reduce the ambient temperature. A currently contentious aspect of solar reflective cool coatings is the extent to which an initially high solar reflectance decreases with time.

In the present study, the aging effect on the optical and thermal characteristics of two cool roofs is reported. The buildings under investigation are two schools in Greece, in the city of Athens. The research in this field is roughly divided in four phases and includes the assessment of the optical and thermal performance of the cool roof. For each one of the phases the documentation of the building's profile includes albedo measurements and infrared imaging of the roof. The first phase includes the above measurements on the existing roof. In the second phase the roof was cleaned at the points where the measurements were taken. The third phase includes albedo measurements and infrared imaging at the cleaned points. In order to estimate the change of the albedo and the surface temperature of the cool roof with time, the same cool coating was applied in a part of the roof. In the fourth phase the measurements were repeated for the new part of the cool roof.

With the aim of investigating what may cause this aging of the cool coating, chemical and biological analysis for two samples from the old and the new cool coating was also carried out.

This study also presents simulations of the buildings in order to estimate the effect of the aging of the cool roofs on the thermal comfort and the alteration of the cooling and heating loads using the EnergyPlus simulation Program.

KEYWORDS

High albedo roof coatings, albedo degradation, cooling energy savings

1 INTRODUCTION

Cool roof coatings remain cooler than absorptive roofs due to their properties of the high solar reflectivity and the high infrared emittance. Roofs with high albedo are used in buildings that require the reduction of the indoor temperature and the cooling loads. Cool roofs can also reduce the ambient temperature through the reduction of the sensible heat emmited. To maximize cooling energy savings, high albedo roof coatings should maintain the above properties for the service life of the coating (Bretz, 1997).

Roofing materials are exposed to environmental conditions (wind, sunlight, rain, hail, snow, atmospheric pollution) and consequently degrade over time (Berdahl, 2006). Weatherisation is a serious problem for

reflective roofs. Experimental data suggests that the reflectance of roofs decreases because of the dust load, ultraviolet radiation, microbial growth, acid rain, moisture penetration and condensation, wind and biomass accumulation. Other research shows that black carbon particles, known as soot particles, is the primary cause of reflectance loss. Reflective surfaces may have a longer useful life if surface temperature keeping low during the sunlight hours, because that result in less diurnal thermal expansion and contraction (Akbari, 2005).
This paper assesses the aging effect on the optical and thermal characteristics of two school buildings in Athens, Greece. A simulation analysis is carried out in order to estimate the alteration in the cooling and heating loads. The building description, the experimental and modeling procedure and the results are being discussed in the following sections.

2 DESCRIPTION OF THE BUILDINGS

The buildings under investigation are two schools located in Kaisariani, a densely built urban area near the centre of Athens, Greece. School A (Figure 1) was built in 1929 and School B (Figure 2) was built in 1980. The two schools share the same school-courtyard.

Figure 1 The location (a) and the school building A (b) at Kaisariani Athens

Figure 2 The location (a) and the school building B (b) at Kaisariani Athens

2.1 SCHOOL A

The school building A is a rectagular two-floor building. In the ground floor seven classrooms are located, the office of the staff as well as auxilary storage space's. In the first floor there are six classrooms, the principal's office and two more storage spaces. The ground floor and the first floor are connected with an internal staircase. The total area of the roof is 614.9 m^2. The masonry construction of the school building is stone without any insulation and the windows are simple glasses. Figure 3 describes the lay out and the orientation of the building. Each one of the two floors constitutes a thermal zone of the building that was used in the simulation model.
Regarding internal gains the artificial lighting was set equal to 16W/m^2 . Infiltration is being used by opening the windows during recess and it is considered to be 108m^3/hour. Each classroom is occupied by twenty three children and fifteen adults in total as the school's staff. The operation schedule of the building is from 8:00 to

14:00 from Monday to Friday excluding national holidays Christmas (23 December–8 January), Easter (two weeks) and summer holidays (22 June–31 August).

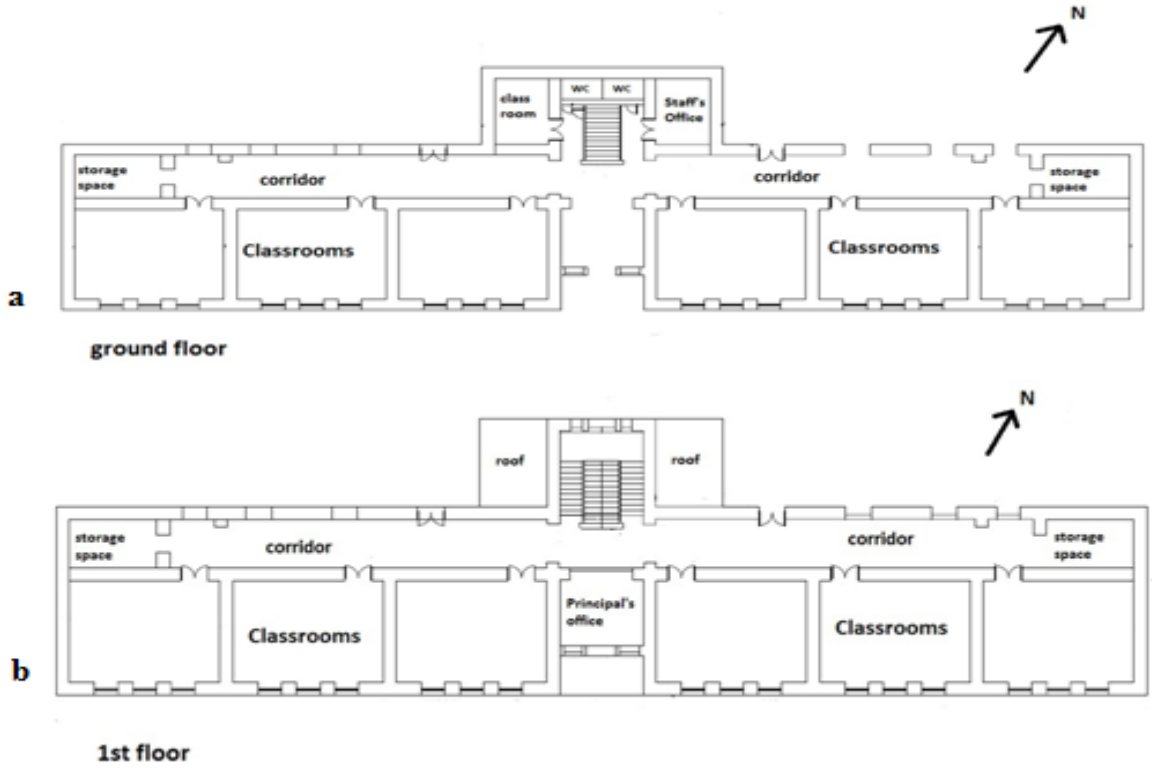

Figure 3 Plans of the school building A with lay out

2.2 SCHOOL B

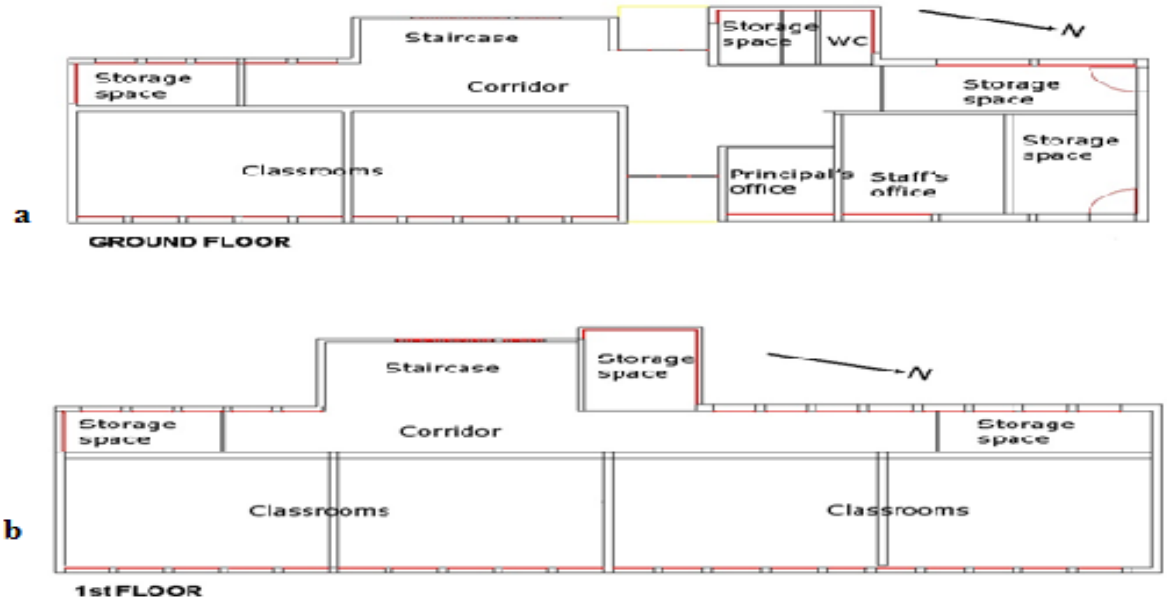

Figure 4 Plans of the school building B with lay out.

The school building B is also a rectagular two-floor building. In the ground floor two classrooms are located, the principal's office and the office of the staff as well as auxilary storage space's. In the first floor there are four classrooms and three more storage spaces. The ground floor and the first floor are connected with an internal staircase. The total area of the roof is 410 m^2. The masonry construction of the school building is

reinforced concrete without any insulation and the windows are double-glazing windows. Figure 4 describes the lay out and the orientation of the building. For the simulation model each one of the two floors of the building constitutes a thermal zone.

Regarding internal gains the artificial lighting was set equal to 16W/m^2 . Infiltration is being used by opening the windows during recess and it is considered to be 108m^3/hour. Each classroom is occupied by twenty children and fifteen adults in total as the school's staff. The operation schedule of the building is from 8:00 to 14:00 from Monday to Friday excluding national holidays, Christmas (23 December–8 January), Easter (two weeks) and summer holidays (22 June–31 August).

For the simulations carried out, which are described in the next sections, the set point temperature for heating is considered to be 21°C and for cooling is considered to be 26°C.

3 METHODOLOGY

The research for the assessment of the optical and thermal performance of the cool roof for the school building A is roughly divided in four phases and for school building B in two phases. For each one of the phases the documentation of the building's profile includes albedo measurements and infrared imaging of the roof.

3.1 Instrumentation

Albedo measurements were carried out in order to analyze the effective reflectance of the roof using two pyranometers (Kipp & Zonen), one for the incident solar radiation and one for the reflected radiation from the roof. The spectral range of the pyranometers is from 300 to 2800nm. Albedo was measured on clear days between 09:00am to 02:00 pm.
An infrared camera (AGEMA Thermovision) was used to detect heat patterns and temperature changes on the roof.

3.2 Monitoring Procedure

The monitoring procedure for school building A includes different phases. The first phase includes the albedo measurements and infrared imaging of the existing roof after 4 years of operation. In the second phase the roof was cleaned at the temperature as well the albedo are measured again. Figure 5 depicts the measured roof temperature of a cleaned point of the roof by using an infrared camera.

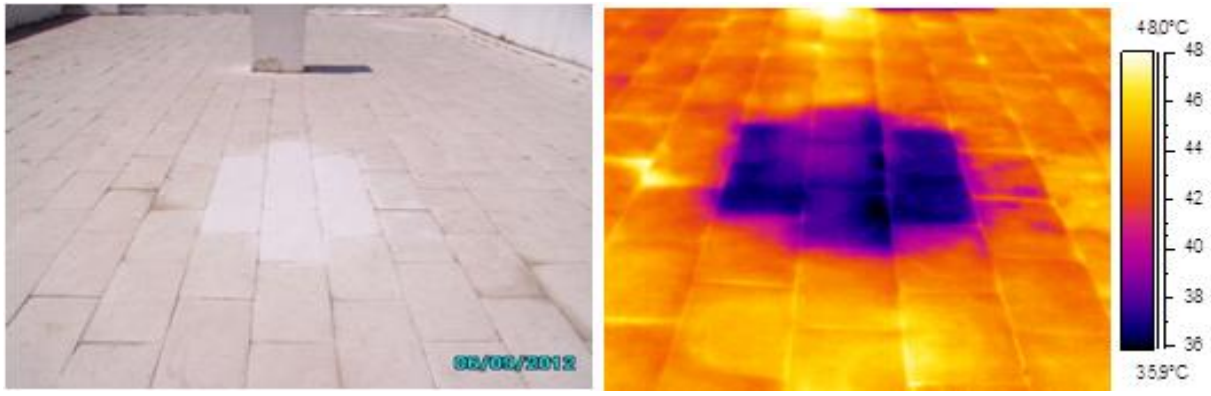

Figure 5 Visible and infrared imaging of the roof depicting the difference in the surface temperature between the existing roof and the cleaned point.

In order to estimate the change of the albedo and the surface temperature of the cool roof with time, the same cool coating was applied in a part of the roof. In the fourth phase the measurements were repeated for the new part of the cool roof. Figure 6 depicts the temperature difference between the existing cool coating and the new part of the cool coating.

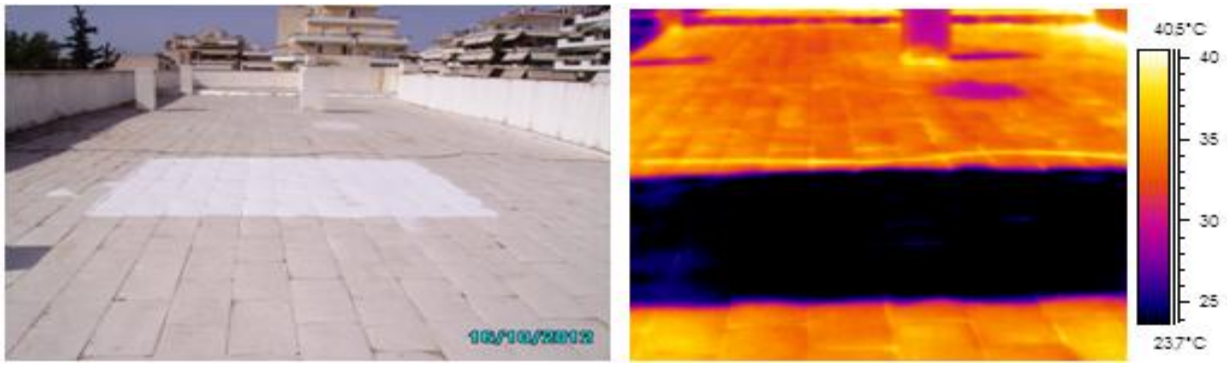

Figure 6 Visible and infrared imaging of the roof depicting the difference in the surface temperature between the existing cool roof and the new part of the cool roof

The monitoring procedure for school building B includes albedo measurements and infrared imaging of the existing roof and the same measurements for a new part of the cool coating in order to estimate the differences in albedo and surface temperature of the roof. Figure 7 depicts the difference on the surface temperature of the cool roof.

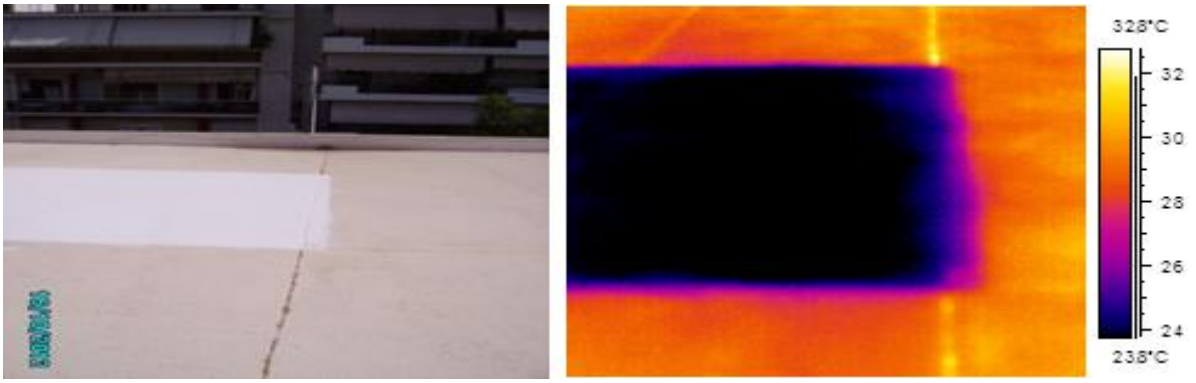

Figure 7 Visible and infrared imaging of the roof depicting the difference in the surface temperature between the existing cool roof and the new part of the cool roof

4 RESULTS

4.1 Measured decrease in albedo

In Figure 8 the albedo of the school buildings under study is given for all phases.

Figure 8a depicts the alteration of the albedo of the school building A as recorded during the measuring procedure. The results indicated that the albedo of the existing cool roof was decreased by 25% compared with the albedo of the new cool coating. Furthermore the increase in albedo resulting from washing the roof was significant (10%).

The results for the albedo of the school building B as presented in Figure 8b indicated a decrease of 23.5% for the albedo value of the existing roof.

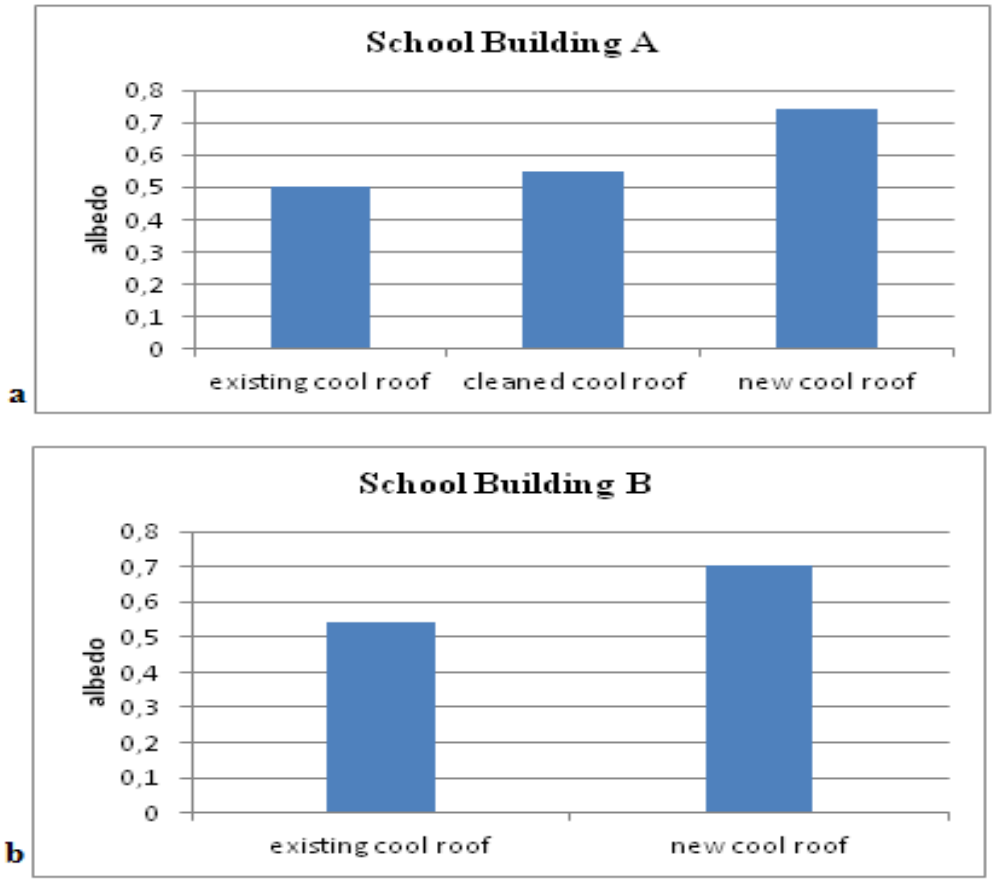

Figure 8 Albedo measurements for the different measuring phases for building A (a) and building B (b)

4.2 Chemical and biological analysis of the samples

The samples studied are extracted by the cool roof of building school A. Moreover a clean sample is also tested as reference. For the analysis the following techniques are used:

1. Optical stereoscopic microscopy and polarizing microscopy. The samples were impregnated in epoxy resin and the surface to be studied was polished in order to study a possible layer of pollutants in the cross section of the samples.
2. X-ray Diffractiometry using X-ray Powder Diffraction Spectrometer D8000 Advance by Bruker, with copper lamp. The qualitative analysis was performed with the Diffrac Plus software and database. The quantitative analysis was performed using the Rietveld method. Measurements were made directly on the surface of the samples while the X-ray beam's penetration on the sample's surface is 100 to 150 μm.
3. Scanning Electron Microscopy (SEM) in order to study the distribution of contaminants on the surface of samples

Table 1 The XRD quantitative analysis of samples

	Calcite	Rutile	Huntite	Quarz	Kaolinite	Illite	Talc	Dolomite	Epsomite	Albite
Koul 0/Ref.	50.2	46.3	-	-	2.6	-	-	-	-	0.9
Koul 1/1st sample	40.2	35.9	3.2	1	3.9	4.3	11.4	-	-	-
Koul 2/2nd sample	47.4	24.1	2.3	1.9	3.2	10.0	-	2.0	8.9	-

The KOUL0 sample's analysis shows that it is a plastic color. Calcite ($CaCO_3$), and Rutile (TiO_2) are the major mineral aggregates that are the plastic's fillers. Kaolinite ($Al_2Si_2O_5(OH)_4$) and Albite ($NaAlSi_3O_8$) and Albite (NaAlSi3O8) also belong to the inorganic inert of plastic color.

In KOUL1 sample, which is a part of the cleaned cool roof, we can see apart from the minerals of the reference sample, the existence of Quartz (SiO_2), Illite ($KAl_4Si_2O_9(OH)_3$), Huntite($CaMg_3(CO_3)_4$) and Talc ($Mg_3Si_4O_{10}(OH)_2$). The minerals Huntite και Talc can be found as Calcite and Rutile in high quality plastics.
The minerals Quartz and Illite are atmospheric pollutants that are disposed on the samples surface. Moreover is it very possible that part of the Calcite in KOUL1 sample is pollutant since the ratio Calcite/Rutile is higher than the one of the reference sample.
In the KOUL2 sample, which is a part of the existing cool roof, we can find Dolomite ($CaMg(CO_3)_2$) Epsomite ($MgSO_4 \cdot 7H_2O$) apart from the other minerals that exist in KOUL1 sample. Epsomite is attributed to water that has increased concentration in sulphates.

4.3 Implications for cooling energy use

In order to estimate the implications of cool roof aging on the cooling needs of the buildings, the schools have been simulated for a complete year, using Energy Plus simulation program. Simulations have been performed for all the measured cases of the roof albedo. Energy Plus is an energy analysis and thermal load simulation program. The following graphs (Figure 9-Figure 10) depict the annual cooling and heating loads for the school building A and school building B.

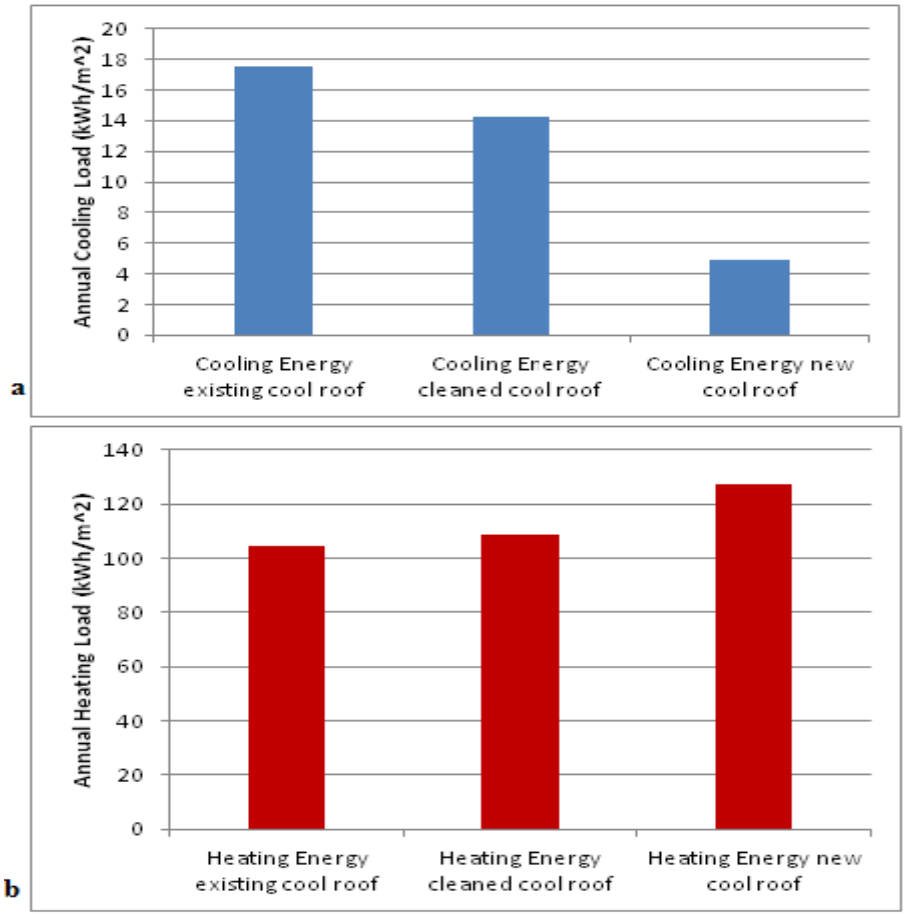

Figure 9 annual cooling (a) and heating (b) loads for building school A

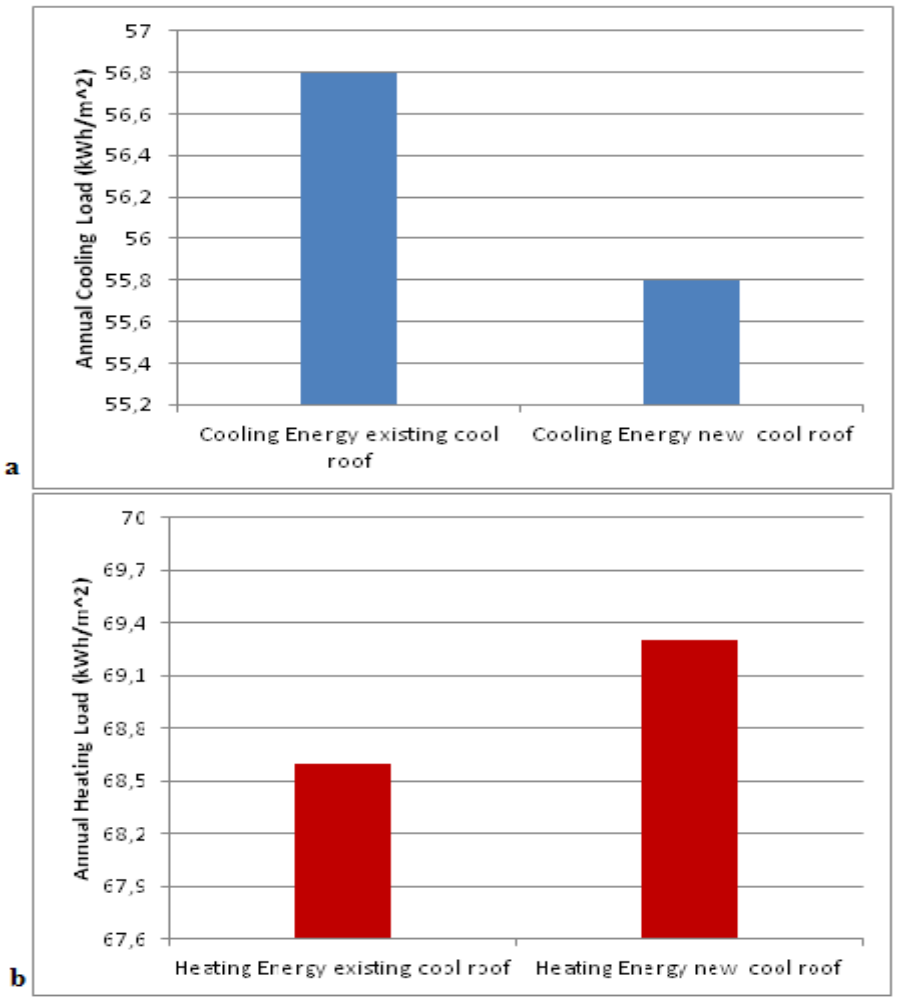

Figure 10 annual cooling (a) and heating (b) loads for building school B

After the cleaning of the cool roof the results of the annual cooling loads for the school A presents a decrease of 18.8% while after the application of the new cool coating there was a significant decrease of 72%. The simulation results indicated that after the cleaning of the roof the annual heating penalty was 4.2kWh/m^2, and after the application of the new cool roof was 23kWh/m^2.
For building school B the application of the new cool roof results to a decrease in the annual cooling load of 1.76 % while the heating penalty was 1% for a complete simulation year.

5 CONCLUSIONS

This paper describes a case study that examines the impact of the aging of the cool roof on energy loads and surface temperature through experimental and modeling testing. The buildings selected involve two school buildings located near the centre of the Athens, Greece. The solar reflectance of the school A roof has changed from 0.5 (existing cool roof) to 0.55 (washed cool roof) and finally to 0.74 after the new application of the same cool coating while the albedo of the school B has shown an alteration from 0.54 to 0.71 for the existing and the new cool coating application respectively. The results of the chemical and biological analysis of the samples of school building A suggest the presence of atmospheric pollutants. In both school roofs the surface temperature has a significant decrease between the part of the existing cool coating and the application of the new part. The simulation results indicated that the annual cooling load for school A has a decrease from 18.8% to 72% for the part of the cleaned roof and the part of the new cool roof respectively. The heating penalties were no as significant as the cooling potential savings.
The results of this study indicate the impact of the aging of the cool roof on the cooling and heating loads, the indoor and the surface temperature.

6 REFERENCES

Akbari, H. e. (2005). *Aging and Weathering of Cool Roofing Membranes.* California: Lawrence Berkeley National Laboratory.

Berdahl, P. A. (16 de December de 2006). Weathering of roofing material - An overview. *Construction and Building Materials* , pp. 423-433.

Bretz, S. ,. (1997). Long-term performance of high albedo roof coatings. *Energy and Buildings* , pp. 159-167.

NEARLY ZERO ENERGY HOTELS THE EUROPEAN PROJECT NEZEH

Theocharis Tsoutsos[1*], Stavroula Tournaki[1], Zoritsa Urosevic[2], Anita Derjanecz[3], Cristina Nunez[4], Stephane Pouffary[5], Nigel Claridge[6], Stefania Mauro[7], Camelia Rata[8], Rodrigo Morell[9] and Marco Biscan[10]

1 Technical University of Crete, School of Environmental Engineering, Renewable and Sustainable Energy Systems Lab, TUC Campus Greece
Theocharis.Tsoutsos@enveng.tuc.gr

2 United Nations World Tourism Organization Madrid, Spain

***3** Federation of European Heating and Air-conditioning Associations Brussels, Belgium*

4 Network of European Region for a Sustainable and Competitive Tourism Brussels, Belgium

5 ENERGIES 2050 Biot, France

6 Sustainable Innovation Stockholm, Sweden

7 Istituto Superiore sui Sistemi Territoriali per l'Innovazione Torino, Italy

8 Agency of Brasov for Energy Management and Environment Protection Brasov, Romania

9 Creara Consultores S.L. Madrid, Spain

10 Energy Institute Hrvoje Pozar Zagreb, Croatia

Note: the contact addresses may be re-arranged

ABSTRACT

The European Union (EU) aims to a 20% reduction of the Europe's annual primary energy consumption by 2020. Furthermore, EU commits to reduce GHG emissions to 80-95% below 1990 levels by 2050. One of the main issues of the EU energy strategy is the radical improvement of the energy performance of new as well as existing buildings.

Within this frame, the rate of renovations needs to be increased, as the existing building stock represents the largest potential sector for energy savings. For new buildings, the EPBD recast fixes 31 December 2020 as the deadline for all new buildings to be "nearly zero energy" (NZEB).
Focusing our attention on the hospitality industry, which is responsible for 2% of the world's CO_2 emissions, NZEB applications could add important advantages:

- Energy consumption is usually higher in hotels than in residential buildings, so there is a larger margin for energy saving measures;
- Hotel guests can experience the comfort of living in NZEB, learning how relevant architectural and technical solutions can also be replicated at home;
- The competitive advantages gained by the initiators will push other hotels to imitate.

Currently the NZEB market is limited. Significant efforts are required to promote the concept to the stakeholders, to link the demand and supply side and to challenge further replication.
This paper presents the methodology, activities and outcomes of the EU initiative NEZEH (Nearly Energy Zero Hotels) including examples of NZEH and the legal and institutional framework status in various EU countries in order to tackle the main market barriers that prevent SME hotels from investing in major refurbishment projects towards nearly zero-energy consumption levels.
In long-term, the NEZEH initiative will support the hospitality sector to reduce operational costs and to improve its image and services, so as to enhance their competiveness and sustainability contributing in parallel to the EU fight against the climate change and energy uncertainty.

KEYWORDS

Zero energy buildings; NZEB; hotels; energy saving; high energy performance buildings

1 INTRODUCTION

There is an urgent need to increase the energy efficiency of European building stock. Buildings account for approximately 40 percent of total energy consumption and 36% of greenhouse gas (GHG) emissions in Europe (Farrou et al 2012) in the European Union. To face this problem the European Union (EU) has set ambitious targets for 2020 and even more ambitious for 2050 (European Commission 2010; 2011; 2012). Among them, EU aims to the drastic reduction of the domestic GHG emissions by 80-95%, compared to 1990 levels, by 2050. The building sector is one of the key sectors to contribute to this aim and has to do its part through brave refurbishments.
Nearly zero energy buildings (NZEBs), a new generation of low energy buildings, with integrated renewable energy sources, increased levels of comfort and limited environmental impact, will play a critical role in improving European building stock.
Focusing on the hospitality industry, which is responsible for 2% of the world's CO_2 emissions, Near Zero Energy Hotel (NEZEH) applications could add important advantages since:

- Energy consumption is usually higher in hotels than in residential buildings, presenting so a larger potential for energy saving measures;

- Hotel guests can experience the comfort of living in NZEB, learning relevant architectural and technical solutions, which could also be replicated at home;
- The competitive advantages gained by the pioneers will push other hotels to imitate.

Within this frame, the rate of building renovations needs to be increased, as the existing building stock represents the field with the higher potential for energy savings.

Currently, there is low awareness of the Nearly Zero Energy Buildings (NZEB) concept and there are limited successful demonstrations at EU level to inspire and drive replications in the private non-residential sector (Karagiorgas et al, 2007). National markets lack familiarity and expertise with integrated design process and interventions and there are an inadequate number of qualified craftsmen and designers for NZEB. The national applications of NZEB definition are still under development in most EU MS; in March 2013, only six Member States had their national application of the Nearly Zero-Energy Buildings definition legally fixed (EC, 2013).

In the participating countries, there are, if any, different national approaches for the NZEB definition. The NZEB concept is not yet understood by the majority of developers/providers/suppliers. Even the NZEB early adopters cannot easily find the appropriate technical actors.

To counter this, as a follow up of other EU initiatives (Karagiorgas et, 2006; various, 2013), the European project "Nearly Zero-Energy Hotels" (NEZEH) will link the supply and demand side, bridging the gap between industry and the interested SME hotel owners and will mobilise major key actors of the building construction industry increasing awareness about the challenges ahead with regard to NZEB targets. The NEZEH's main objective is to accelerate the rate of refurbishment of existing buildings into Nearly Zero Energy Buildings (NZEB), focusing to the hotels sector:

a) providing technical advice to hoteliers determined to go for NZEB renovations;
b) demonstrating the competitive advantages and sustainability of such projects in order to increase the rate of renovation in the hotels industry;
c) challenging further large scale renovations through capacity building activities and showcases of the front runners.

The methodological approach, the outcomes and the first findings of the new European project NEZEH is presented in the current paper.

2. THE NZEB DEFINITION

An overview of the European Energy-in-Buildings policy is depicted in fig.

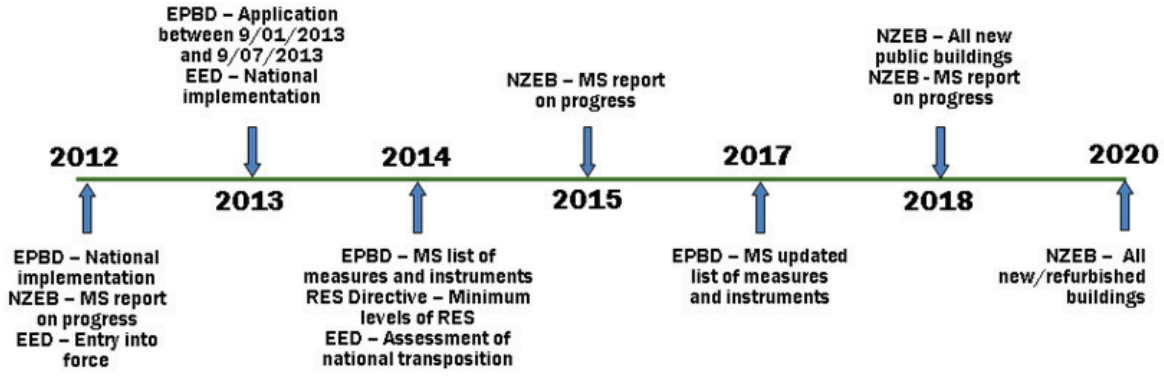

Figure 1: Energy in Buildings-Policy overview

Table 1 provides a summary of the interaction between the three relevant EU Directives.

Table 1: Interaction between the three EU Directives - EBPD, EED and RED (EC 2013)

	EPBD recast	**EED - ESD**	**RED**
Target	No	Indicative	Binding
Scope	Heat, Power	Heat, Power, Transport	Heat, Power, Transport
Actions	Yes	Yes	Yes
Action Plan required	No	Article 14	Article 4
Reporting	Yes	Article 14	Article 22
Pubic/visited buildings	Article 7	Article 5	No
Information & Training	Article 20	Article 7	Article 14
Energy Certificates/Audits	Articles 11,12	Article 12	
Competent persons	Article 17	Article 8	Article 14
Financial instruments	Article 10	Article 9,11	Some
Energy suppliers	No	Articles 6,10,11,13	Yes
Metering and billing info	Article 20	Article 8	Some
Smart metering/building monitoring	Articles 8,14,15	Articles 12,13	Some

The EPBD recast obliges the Member States (MS) to ensure that minimum Energy Performance requirements are set with a view to achieving cost-optimal levels (art. 4). The MS should also take the necessary measures to ensure that new buildings, buildings undergoing a major renovation, and replaced or retrofitted building components that form part of the building envelope, meet the requirements set with a view to achieving cost-optimal levels (art. 6 & 7) (EC, 2013).
The cost-optimal level is *"the energy performance level which leads to the lowest cost during the estimated economic lifecycle"* (art. 2.14).

Article 9 of the EPBD recast puts deadlines, such as that "*Member States shall ensure that (a) by 31 December 2020 all new buildings are nearly zero-energy buildings; and (b) after 31 December 2018, new buildings occupied and owned by public authorities are nearly zero-energy buildings*".
MS shall furthermore "*draw up national plans for increasing the number of nearly zero-energy buildings*" and "*following the leading example of the public sector, develop policies and take measures such as the setting of targets in order to stimulate the transformation of buildings that are refurbished into nearly zero-energy buildings*".
It is estimated that there are at least 23 different terms for high performance buildings used in the EU MS: e.g. passive house, law-energy house, green building, eco-building etc. Especially for NZEB, this term is defined in article 2 of the recast EPBD as "*a building that has a very high energy performance... . The nearly zero or very low amount of energy required should be covered to a very significant extent by energy from renewable sources, including energy from renewable sources produced on-site or nearby*".
Annex I of the recast EPBD gives a common general framework for the calculation of the EP of buildings, including NZEB, as follows: "*The energy performance of a building shall be determined on the basis of the calculated or actual energy that is consumed in order to meet the different needs associated with its typical use, and shall reflect the heating energy needs and cooling energy needs (energy needed to avoid overheating) to maintain the envisaged temperature conditions of the building, and domestic hot water needs.*"
Furthermore, the Annex lists the aspects that should be taken into consideration for the methodology applied. These aspects include natural and mechanical ventilation, and built-in lighting installation (mainly in the non-residential sector).

3. METHODOLOGY

The geographical coverage at local and national level of the project is:

- six (6) Southern European countries: Spain, Greece, Italy, Romania, Croatia and France
- one (1) Nordic country (Sweden).

The consortium also involves:

- two (2) European networks the Federation of European Heating and Air-conditioning Associations and the Network of European Regions for a Sustainable and Competitive Tourism, and
- one (1) international organisation the United Nations World Tourism Organization, which will contribute to spread the effects of the project across EU.

All targeted regions have a robust tourism industry, but in different typology (geographic/climate zone, diverse touristic products, different technical solution).

At the same time, they face different level of maturity in terms of market's experience at EE and RE technologies and with regard to the NZEB concept familiarity and know-how.
The NEZEH consortium is consist of the:

- Technical University of Crete, Renewable and Sustainable Energy Systems Lab-TUC (project coordinator, GR)
- United Nations World Tourism Organization-UNWTO (ES)
- Network of European Region for a Sustainable and Competitive Tourism-NECSTour (BE)
- Federation of European Heating and Air-conditioning Associations-REHVA (NL)
- Agency of Braşov for Energy Management and Environment Protection-ABMEE (RO)
- Creara consultants (ES)
- ENERGIES 2050 (FR)
- Energy Institute Hrvoje Požar-EIHP (HR)
- Istituto Superiore sui Sistemi Territoriali per l'Innovazione-SITI (IT)
- Sustainable Innovation (SE)

4. MAIN OUTPUTS

The major outputs of the NEZEH initiative will be:

- An integrated set of decision support tools to assist hoteliers in identifying appropriate solutions and designing feasible and sustainable NZEB projects.
- A dynamic communication channel between the building sector and the hotels industry, which will enable the exchanging between demand and supply side and the endorsement of the NZEB concept.
- Demonstration pilot projects in 7 countries to act as "living" examples, aiming to increase the rate of NZE renovation projects in the targeted countries.
- Practical training and informational materials and capacity building activities to support nationally the implementation and dissemination of NEZEH projects.
- Integrated communication tools to increase awareness for the NZEB benefits, to promote front runners and to foster replication; challenging much more SMEs to invest in refurbishment projects in order to achieve NZE levels.

In the long term the project will help the European hospitality sector to reduce operational costs, to improve their image and products and so to enhance their competiveness contributing in parallel to the EU efforts for the reduction of GHGs.

5. ENERGY INDICATORS IN HOTELS

The selection criteria during the initial research phase include:

1) Declared energy performances and renewable energy production
2) Emissions from energy certificates

3) Potential labelling and certifications
4) Sustainable management strategies
5) Geographical location and climate conditions

A list was then integrated including hotels identified by desk research and also the hotels suggested by the NZEH project's partners who provided national examples of high energy performance hotels. The second step for the selection of potential hotel examples analyses the profile of the 27 sustainable hotels identified so far, in order to assess which hotels can be defined as nearly zero energy buildings.

Table 1 presents indicative data of selected hotels during the NEZEH activities.

Table 1: Examples of hotels committed to achieve these targets within NEZEH project

Location of the hotel	No of rooms	Floor area (m^2)	Electricity use (kWh/year)	Gas / heat use (kWh/year)	Total energy use per floor area ($kWh/m^2.year$)	Floor area to be renovated (m^2)	Energy savings (%)	RES integration* (%)
Chania Crete GR	225	20,300	1.007.050	563.225	77,3	2.000	20	70
Rethymno Crete GR	100	2.570	196.640	74.607	105,5	600	20	60
Lassithi Crete GR	270	13.458	1.500.000	832.560	173	2.500	25	50
Peloponnese GR	27	1.220	35.747	41.137	63	1.220	16	70
Karlovac, HR	40	1.610	160.000	260.000	261	1.000	40	70
Zagreb, HR	44	3.000	185.000	274.000	153	300	10	50
Briancon, FR	20	500	38.500	108.254	294	500	25	40
Bari Sardo IT	30	2.200	129.000	38.000	75,9	400	50	40
Turin, IT	106	4.000	583.644	1.342.188	481,5	1.000	25	40
Brasov, RO	14	2.000	59.753	211.309	135,5	2.000	20	60
Minorca, ES	243	13.500	1.141.628	770.072	141,6	1.475	12	50
Palma de Mallorca, ES	356	20.000	2.000.000	2.000.000	200	20.000	20	50
Palma de Mallorca, ES	183	16.500	1.700.000	140.000	112	16.500	25	40

6. CONCLUSION

For the assessment phase of existing successful NZEH examples it was proved that the number of realised high performance buildings of general use seems to be rather low (< 200 in total) in most countries, with the exception of Austria, Germany, Czech Republic, and Slovenia.
The NEZEH initiative will have a positive impact in reducing the building sector. During the project: 15.000 hotel owners are going to be informed and gain access to the project results in EU level. Pilot projects, in seven (7) countries, will demonstrate the profitability and benefits of such an investment and will become a powerful example to inspire emulation by other hotel owners.
The increasing number of NEZEH may:

- inspire the supply side to provide more suitable solutions, reducing the costs for the demand side;
- raise the visibility of the NZEB concept to a large number of hotel owners;
- increase the number of "green" hotels thus having a positive effect over the demand;
- In the long-term, NEZEH will support the hospitality sector to reduce operational costs and to enhance competiveness and sustainability.

A prerequisite of the success of the NEZEH initiative is the commitment of the tourism industry to increase the visibility and promote the NEZEH hotels challenging much more SME hotels to invest in refurbishment projects that achieve NZE levels.

7. ACKNOWLEDGEMENTS

This publication is supported by the European Commission under the Intelligent Energy Europe Programme, within the framework of the project NEZEH (Nearly Energy Zero Hotels). The sole responsibility for the content of this paper lies with the authors. It does not necessarily reflect the opinion of the European Union. The European Commission is not responsible for any use that may be made of the information contained therein.

NOMENCLATURE

EPBD	Energy Performance of Building Directive
EU	European Union
GHG	GreenHouse Gas
HES	Hotel Energy Solutions (project)
IEA	International Energy Agency
IPCC	Intergovernmental Panel on Climate Change
MS	Member State(s)
NZE	Near Zero Energy
NZEB	Near Zero Energy Building
NEZEH	Near Zero Energy Hotels
RELACS	Renewable Energy for Tourist Accommodation Building s(project)
SME	Small and Medium Enterprise
UNWTO	United Nations World Tourism Organisation

8 REFERENCES

European Commission (2010). Directive 2010/31/EU of 19 May 2010 on the energy performance of buildings (recast), *Official Journal* 2010; L 153/13.

European Commission (2011). A Roadmap for moving to a competitive low carbon economy in 2050, COM(2011) 112 final; 2011.

European Commission (2012). Commission Delegated Regulation (EU) No 244/2012 of 16 January 2012 supplementing Directive 2010/31/EU on the energy performance of buildings, *Official Journal* 2012; L 081.

European Commission (2013). Implementing the Energy Performance Building Directive (EPBD), Porto, June 2013.

European Commission, Ecofys (2013) Towards nearly zero-energy buildings, Definition of common principles under the EPBD, February 2013.

Farrou, I., Kolokotroni, M., Santamouris M. (2012). A method for energy classification of hotels: A case-study of Greece. *Energy and Buildings*, 55**,** 553-62.

Karagiorgas M, Tsoutsos T, Drosou V, Pouffary S, Pagano S, Lopez Lara G, Melim Mendes , JM. (2006). HOTRES: Renewable energies in the hotels. An extensive technical support for the hotel industry. *Renewable and Sustainable Energy Reviews* 10(3), 198-224.

Karagiorgas M, Tsoutsos T¸ Moiá-Pol A. (2007). Analysis, simulation and monitoring of energy consumption in Mediterranean hotels. Application in Greece. *Energy and Buildings* 39(4), 416-26.

Tsoutsos, T., Tournaki, S., Avellaner de Santos, C., Vercellotti, R. (2013). Nearly Zero Energy Buildings. Application in Mediterranean hotels, Mediterranean Green Energy Forum, Fez, Morocco, 17-19 June 2013.

various (2013), hotel energy solutions, hotelenergysolutions.net/ accessed 01/2013.

THE IMPACT OF TEMPERATURE INCREASE IN GREECE ON THE ENERGY DEMAND OF BUILDINGS

Triantafyllia Nikolaou[*1], John Kapsomenakis[2], Dionysia Kolokotsa[3], Mattheos Santamouris[4], and Stylianos Zerefos[5]

1 Technical University of Crete,
Electronic & Computer Engineering Department
University Campus Kounoupidiana
73100 Chania, Greece
**Corresponding author: tnikolaou@isc.tuc.gr*

2 Centre for Atmospheric Physics
& Climatology, Academy of Athens,
84 Solonos Str.
10680 Athens, Greece

3 Technical University of Crete,
Environmental Engineering Department
University Campus Kounoupidiana
73100 Chania, Greece

4 University of Athens, Physics Department,
Group Building Environmental Studies,
University Campus
15784 Athens, Greece

5 Hellenic Open University,
18 Aristotelous Str.
26335 Patras, Greece

ABSTRACT

The increase of the ambient air temperatures in urban areas during the past few decades, due to the heat island phenomenon and the warming of the lower atmosphere, has strong impact on the energy profile of buildings, the comfort conditions, the air pollution and the indoor environment, especially in the Mediterranean regions with hot climate conditions. The present paper focuses on the investigation of the impact of the temperature increase in nine Greek cities over the last forty years on the energy demand of buildings. This research is very crucial in order to understand climatic future trends, to establish the development of new technologies and techniques (such as ventilation strategies and smart materials) aiming to reduce the energy consumption of buildings, to improve the urban microclimate, as well as to steer specific policy actions. The methodology developed for this research includes: a) Analysis of climatic data: hourly data series of air temperature and relative humidity covering the forty year period 1970-2010 from nine Greek meteorological stations of the Hellenic National Meteorological Service (HNMS) are presented and analysed. b) Simulation studies: In order to evaluate the potential impact of temperature variation on the energy demand of buildings, specific energy simulation studies have been performed using the Virtual Building Dataset (VBD) tool. The simulation process includes the determination of typical building for the simulations, the development of the required climate data files and the performance of 369 simulations using the VBD tool, which has been developed by coupling TRNSYS with Matlab. c) Analysis of the simulation results: the annual heating and cooling loads of the typical building for the nine Greek cities and for the period 1970-2010. The analysis showed that for the period in question the heating load in the Greek building sector has decreased by about 1 kWh/m^2 per decade, while the cooling load has increased by about 5 kWh/m^2 per decade. This phenomenon has major environmental, economic and social consequences, which will be amplified in the upcoming decades in view of the expected man-made climatic changes in this geographic area.

KEYWORDS

Temperature increase, heating demand, cooling demand, climatic change

1 INTRODUCTION

The phenomenon of climatic change in association with local ambient air temperatures increase due to urban heat island is very intense the major cities of South East Mediterranean, where recent studies have shown unusual temperature anomalies (Mihalakakou et al., 1998; Livada et al., 2007; Founda, 2011 and Zanis et al., 2009). In the case of the Greek capital city of Athens, the specific topography combined with the augmenting urbanisation and industrialisation contributed to a significant increase of the ambient temperature during the last 30 years (Giannopoulou et al., 2011; Mihalakakou et al., 2002). Multiyear studies have shown that the intensity of the average summer period heat island intensity may reach values close to 7-8 ºC (Santamouris et al., 1999). Consequently, the urban heat island acts in local level by increasing the outdoor temperature, while extreme phenomena are attributed to climate change.

Based on the outcomes of numerous studies the increase of urban temperatures has a serious impact on the energy consumption of buildings. In (Hassid et al., 2000; Santamouris et al., 2001) the spatial distribution of the cooling needs of different typical buildings was calculated for different urban zones in the city of Athens. It is calculated that the cooling needs as well as the peak electricity demand for cooling in the affected areas, increased up to 100 % compared to the corresponding load in the suburban areas around the city. A review on the impact of climate change on air condition systems in terms of performance and reliability is performed in (Yau and Pean, 2011) showing that the research should focus on the future energy needs for heating and cooling due to climate change.

Monitoring studies of low income housing in the areas affected by the heat island in Athens were performed during the period of heat waves. The experiments have shown that indoor temperatures exceeded 30ºC for almost 85% of the hot period, while periods of about 216 continuous hours above 30 ºC were recorded (Santamouris et al., 2007b; Pantavou et al., 2011; Sakka et al., 2012).

Climatic model forecasts of future ambient temperatures in the specific geographical area, as well as projections of the expected energy consumption of the building sector reveal an important temperature increase followed by a considerable increase of the energy consumption for cooling purposes. In (Cartalis et.al, 2001) the energy impact of the climatic change in the area was evaluated using various climatic models for the next twenty years. It was found that a significant increase of the cooling and decrease of the heating degree days have to be expected. The area of Athens as well as Central Macedonia, Crete and the Aegean islands may be the areas most affected during the summer period. Another similar study (Asimakopoulos et al., 2012) has evaluated the energy impact of the climatic change in Greece up to 2100, using various climatic models. It was reported that the energy demand of buildings for cooling purposes may increase up to 248%, while the heating demand may decrease up to 50 % until 2100.

The aim of the present research is to investigate the energy and environmental impact of climate change and the trends recorded over the last forty years on the building sector in Greece. The results of this work are very crucial for determining the climatic future trends, establishing the development of new technologies and techniques, such as ventilation strategies and smart materials for reducing the energy consumption of buildings, for improving the urban microclimate, as well as for steering specific policy actions (Kapsomenakis et al., 2013).

2 ANALYSIS OF THE CLIMATIC DATA

Hourly values of air temperature and relative humidity covering the period 1970-2010 from nine Greek meteorological stations of the Hellenic National Meteorological Service (HNMS) were used in the present study. The locations of the meteorological stations are shown in

Figure 1. It is noted that the accuracy of temperature measurement devices (thermometers) is 0.2 °C and of the relative humidity measurement devices is 1%.

Figure 1: The nine meteorological stations

2.1 Temperature and relative humidity trends

The intra-annual variability of the mean temperature along with the intra-annual variability of diurnal temperature range are analyzed in details in (Kapsomenakis et al., 2013). From the data the trends of hourly air temperature have been calculated for each station using the least square linear regression method. It is interesting to note that all the hourly temperatures of every station show generally upward trends during the period under study. These upward trends are more prominent during the summer and in general are statistically significant at a 95% confidence level (Welch test) during all seasons except winter. In winter, upward trends are also statistically significant, but at a lower confidence level. These climatic trends are in agreement with the findings of other researchers, especially for summer trends (Feidas et al., 2004; Philandras et al., 2008; Nastos et al., 2011). Relative humidity trends are doubtful. More specifically, over Eastern Continental Greece relative humidity shows a statistically significant (at 95 % confidence level) downward trend during spring and summer. On the contrary, upward trends are observed over South and South-eastern Aegean which, in some cases, are statistically significant at a 95 % confidence level. Finally in Western Greece weak and not statistically significant -upward or downward- trends prevail. To summarize, statistically significant upward trends are observed in air temperatures at all stations.
The results discussed above for individual stations in Greece are also evident when we calculate the average values of air temperature for all 9 stations as can be seen in Figure 2 for 02:00 and 14:00 Local Time (LT). The temperature increase trends per decade for 2:00 as well as for 14:00 LT can be extracted by the trend lines. For 2:00 the temperature increase per decade is 0.58°C, 0.37°C, 0.27°C and 0.14°C for June – July – August (JJA), September – October – November (SON), March – April – May (MAM) and December – January – February (DJF) respectively. Therefore it is clear that upwards trends in Figure 2 are larger at night and significantly greater during summertime.

2.2 Heating & cooling degree hours trends

Furthermore, the number of Heating/Cooling Degree-Hours is calculated in a seasonal base as well as their linear trends (using Mann-Kendall statistical test) for the period 1970-2010. As depicted in Figure 3 the average increase of Cooling Degree Hours (CDH) based on the trend lines is 472 CDH, 21.5 CDH and 16.8 CDH per decade for JJA, SON and MAM respectively. (Kapsomenakis et al., 2013).

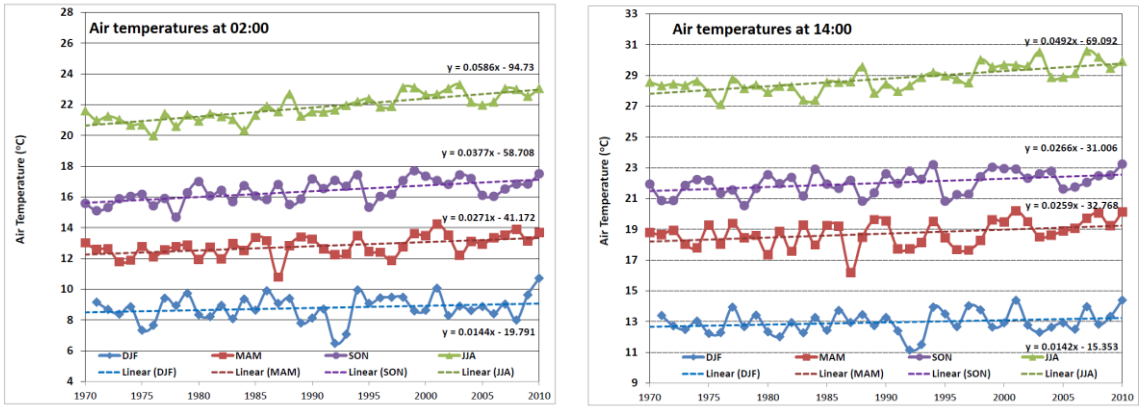

Figure 2: Mean seasonal air temperature average over all stations time-series at 02h and 14h local time. Linear trend lines are dashed

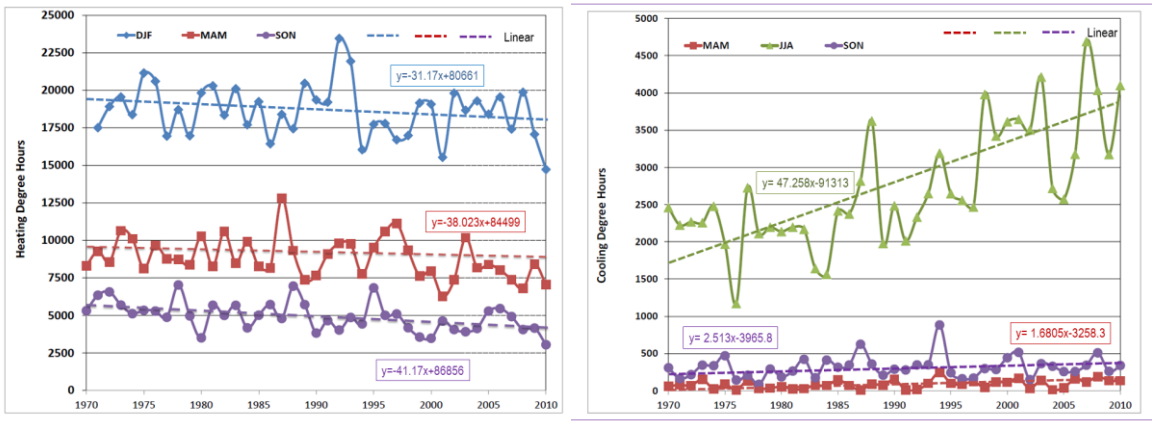

Figure 3: Mean seasonal heating and cooling degree hours average over all stations time-series. Linear trend lines are dashed.

3 THE IMPACT ON THE ENERGY CONSUMPTION OF BUILDINGS

In order to evaluate the potential impact of temperature variation on the energy consumption of buildings, specific energy simulation studies have been performed using the Virtual Building Dataset (VBD) tool, described in detail in (Nikolaou et al., 2009). The VBD consists of 30,000 buildings with detailed constructional, operational, energy and indoor thermal comfort annual data. The overall procedure for the creation of this tool was developed by coupling TRNSYS with Matlab. The simulation process has been conducted following 3 steps:

Step 1: Typical office building selection: The building that has been used for the simulations was chosen as "typical office building" in Greece taking as a criterion its annual heating and cooling load (kWh/m2y) that has to correspond to the 50% of the cumulative frequency distributions of thermal and cooling loads respectively of the 30,000 buildings included in

VBD. In (Kapsomenakis et al., 2013) the constructional, operating and energy characteristics of the selected typical office building for the purpose of this research are analyzed in detail.
Step 2: Development of climate data files: Based on the records of the data for the years 1970-2010, 41 files according to TMY2 format for each city (one file for each year) were created, by developing a suitable program in Matlab, in order to be used as inputs to the VBD tool. Since only Dry Bulb Temperature and Relative Humidity values were included in the files of the records, the remaining required data (except the Dew Point Temperature values) are derived from hourly meteonorm files for each city. Regarding the values of the Dew Point Temperature, they have been calculated in an hourly base of each year from the respective hourly data of Dry Bulb Temperature and Relative Humidity, using part of the Bögel modification, also known as the Arden Buck equation (Buck, 1981).
Step 3: Simulations and results: Forty one simulations for the nine Greek cities (totally 369 simulations) have been performed using the VBD tool along with the climate data files developed in step 2. The results include annual heating and cooling load values for the years 1970-2010 for each city and they are analysed below.
Figure 4 provide the calculated values of the annual heating and cooling load for four cities covering the four climatic zones in Greece. As can be seen from these figures an important temporal decrease of the heating load and a significant increase of the cooling loads, are calculated. As expected, the calculated increase of the cooling load is much higher than the corresponding decrease of the heating load. More specifically, in Heraklion, which is situated at the southern part of the country, the annual heating load has been reduced by 23%, i.e. from 34.3 kWh/m^2/y to 26.5 kWh/m^2/y. The reduction of the heating load is of similar order in Athens and Corfu and approaches 20%. The heating load has been reduced from 39.4 kWh/m^2/y to 31.7 kWh/m^2/y and from 45.5 kWh/m^2/y to 36.2 kWh/m^2/y in Athens and Corfu respectively. In Larisa, the reduction is much lower and close to 6% i.e. from 48.2 kWh/m^2/y to 45.5 kWh/m^2/y. Concerning the annual cooling load, the calculated increase varies between 15% to 29% for the overall forty year period. In particular, in Heraklion the cooling load has been increased from 93.7 kWh/m^2/y to 120.9 kWh/m^2/y, in Athens from 99.5 kWh/m^2/y to 124.8 kWh/m^2/y, in Corfu from 81.9 kWh/m^2/y to 101.2 kWh/m^2/y, while in Larisa the load has been increased from 87.2 to 100.7 kWh/m^2/y. The annual variation of the heating and cooling load has a symmetrical temporal variation per year. Figure 5 presents the relationship between the annual heating and cooling load in the four selected cities. As shown, the higher the annual cooling load the lower the heating one.
Figures 6 and 7 present a linear fit of the annual variation of the heating and cooling load in the four selected cities respectively. It is calculated that the average reduction of the heating load is close to 1.0 kWh/m^2 per decade. In particular, it is 0.84 kWh/m^2 in Larisa, 1.01 kWh/m^2 in Heraklion, 1.04 kWh/m^2 in Athens and 1.4 kWh/m^2 in Corfu. As for the increase of the cooling load, it is much higher than the corresponding decrease of the heating load and ranges between 4.5 to 6.2 kWh/m^2 per decade. In particular, the maximum increase is presented in Athens, 6.2 kWh/m^2, mainly because of the complementary effect of the urban heat island phenomenon. For the rest of the cities, the calculated increase per decade is close to 5.6 kWh/m^2 in Corfu, 4.5 kWh/m^2 in Heraklion and 4.4 kWh/m^2 in Larisa.
Increase of the cooling and decrease of the heating load of buildings may have a very serious impact on the energy balance of the country. Cooling in Greece is mainly provided by air conditioners and heat pump systems while oil and natural gas are mainly used for heating purposes. In addition electricity production in Greece relies upon fossil fuels, i.e. lignite, and oil (Agoris et al., 2004). The Increase of the cooling loads will raise the peak electricity demand in the country and will oblige utilities to build additional power plants to satisfy the demand. Such a scenario will increase the cost of electricity as kWh produced during peak conditions is more expensive.

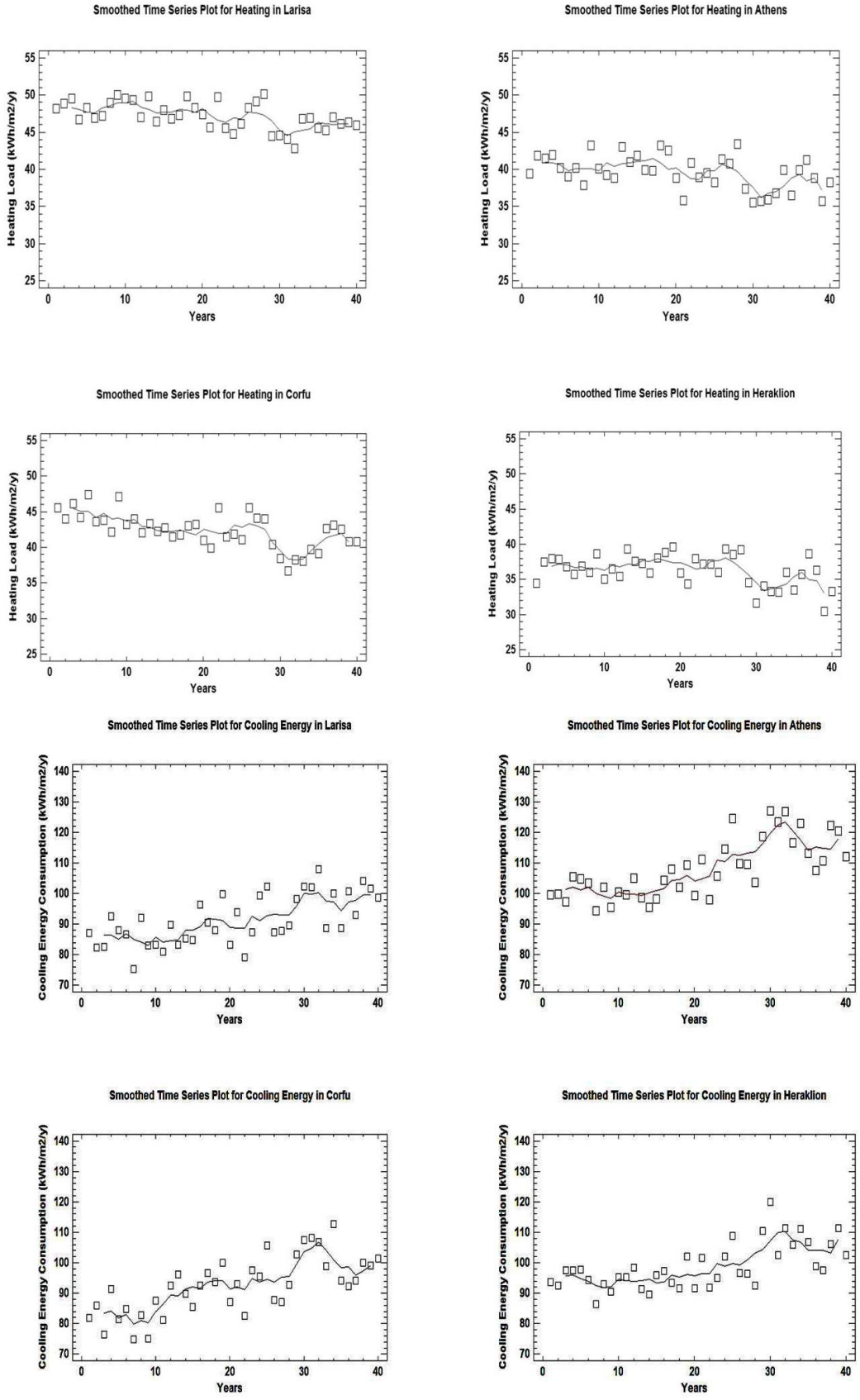

Figure 4: Annual variation of the heating and cooling load in four Greek cities.

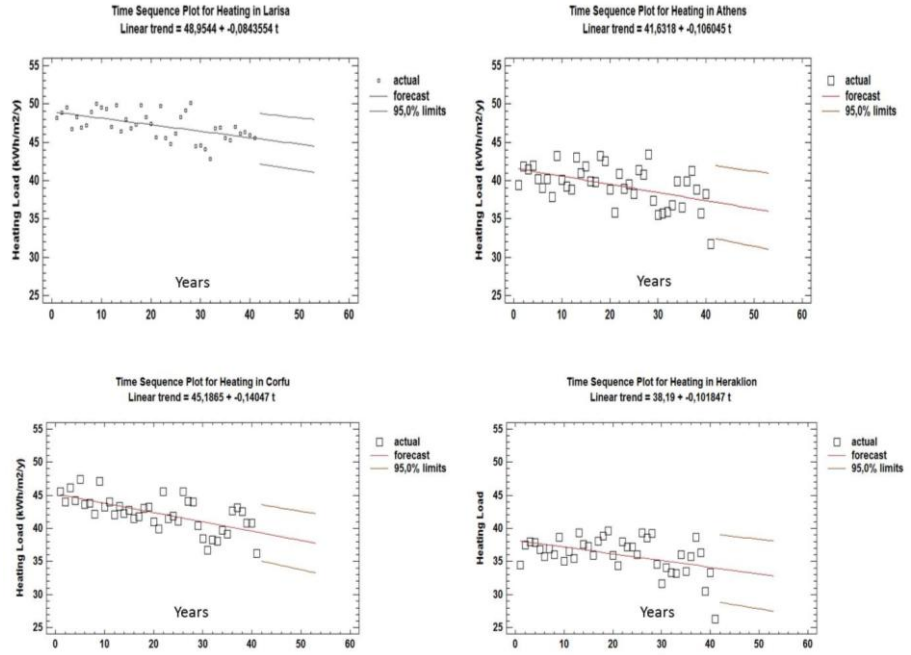

Figure 5: Correlation between the annual heating and cooling load for the four selected Greek cities.

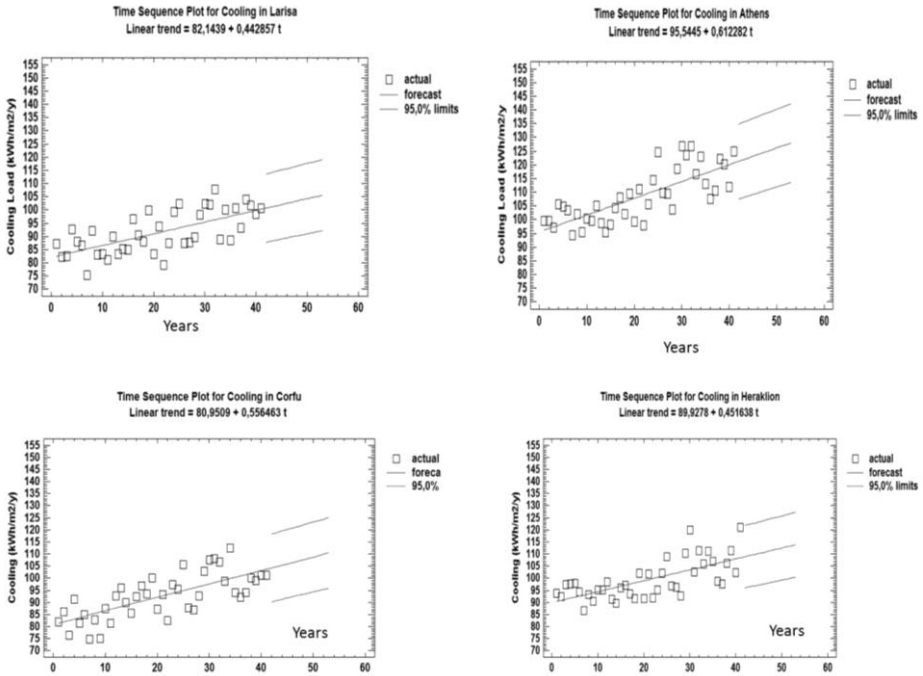

Figure 6: Linear Correlation of the annual variation of the heating load for four Greek cities.

Higher ambient temperatures will also oblige more citizens and in particular low and mid income households to install air conditioners to provide indoor comfort. Actually, the penetration of air conditioners in low and mid income residential buildings is quite limited. Additional users will increase the absolute energy consumption for cooling and will further increase the peak electricity demand. This will increase the energy cost especially of low income citizens in the country. According to (Santamouris et al., 2007a), the annual cost of cooling in low income households in Greece is almost the double per unit of surface and person than in high income households. This is because the high majority of low income citizens lives in non-insulated and non-thermally protected buildings. Decrease of the heating

needs may contribute towards lower imports of oil and natural gas, however, the relative benefit is much lower than the damage caused by the increase of the cooling demands.

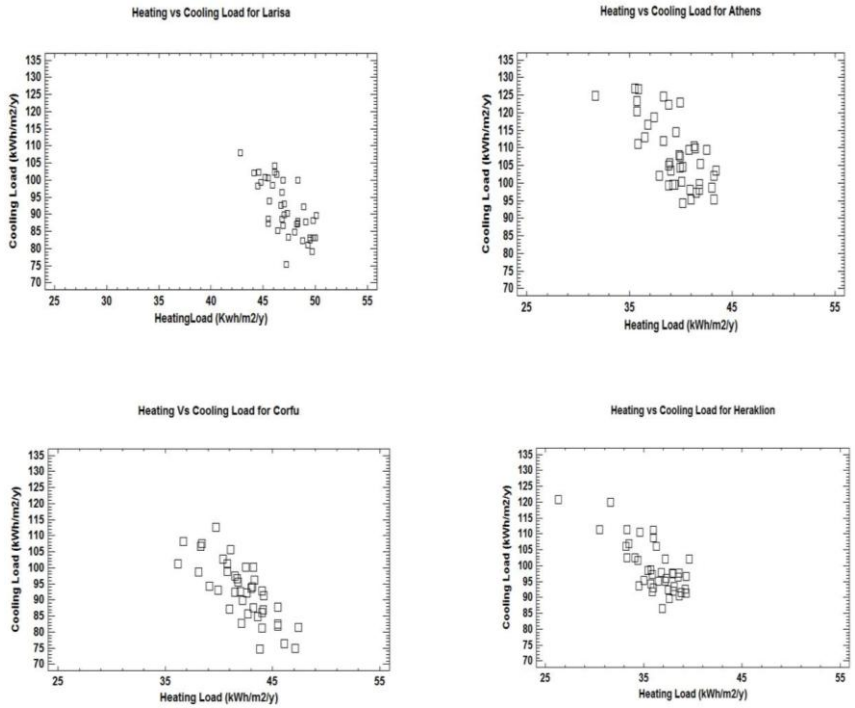

Figure 7: Linear Correlation of the annual variation of the cooling load for four Greek cities.

4 CONCLUSIONS

The last forty years have been characterized by very important anomaly trends of the ambient air temperatures in Greece and the South Eastern Mediterranean. These trends are the resultant of man-made global climatic change in the area and the augmentation of the heat island phenomenon in the major urban zones in Greece. The increase of the ambient air temperature is found to be more significant during the summer than during the winter period. Important increasing and decreasing trends have been calculated for the annual cooling and heating degree days in major urban locations of the country (Kapsomenakis et al., 2013).The phenomenon is statistically significant at a 95% confidence level.

Higher ambient air temperatures have a significant impact on the energy consumption of buildings. Detailed simulations performed for four major urban areas of Greece using hourly climatic data for a forty year period, have shown that the heating load of buildings decreases by about 1.0 kWh/m^2 per decade while the cooling load increases by almost 5.0 kWh/m^2 per decade. Thus, this important climatic phenomenon increases considerably the total energy consumption of the buildings sector and has significant economic and social consequences. Given that climatic forecasts for this geographic area predict an important amplification of the climate change phenomena for years to come (Asimakopoulos et al., 2012) the expected energy penalty is expected to increase considerably in the future.

The results of the study make evident that proper mitigation and adaptation techniques have to be undertaken in order to confront global climatic change and local heat island phenomena and also counterbalance their impact on the energy and environmental quality of buildings. In our opinion it is the main research priority for the future. Several studies presenting suggested mitigation and adaptation techniques for different countries have been already carried out (Gupta and Gregg, 2011). Simulation studies have shown that when proper mitigation and

adaptation techniques are undertaken, both the energy consumption and the environmental quality in the built environment can be improved considerably (Asimakopoulos et al., 2012).
Mitigation techniques should include any anthropogenic intervention to reduce heating sources and enhance the sinks of temperature anomalies. Mitigation technologies are not sufficiently promoted, although there are significant research actions. In particular research on materials for the outdoor urban environment, is of high importance (Karlessi et al., 2011). On the other hand, the adaptation of the building sector deals with possible technological adjustments to climatic anomalies in order to moderate the energy and environmental impact and cope with the consequences.
Adaptation technologies are very well developed, and are the subject of sophisticated and advanced research that has permitted to develop materials, systems and techniques for the building sector that contribute highly in the reduction of energy consumption and the improvement of indoor environmental quality, In particular, the development and use of passive and advanced cooling techniques for buildings offer very significant possibilities to improve the energy performance of buildings during the summer period (Santamouris and Kolokotsa, 2013).

5 REFERENCES

Agoris, D., Tigas, K., Giannakidis, G., Siakkis, F., Vassos, S., Vassilakos, N., Kilias, V., and Damassiotis, M. (2004). An analysis of the Greek energy system in view of the Kyoto commitments, Energy Policy, 32(18), 2019–2033.

Asimakopoulos, D.A., Santamouris, M., Farrou, I., Laskari, M., Saliari, M., Zanis, G., Giannakidis, G., Tigas, K., Kapsomenakis, J., Douvis, C., Zerefos, S.C., Antonakaki, T., and Giannakopoulos, C. (2012). Modelling the energy demand projection of the building sector in Greece in the 21st century, *Energy and Buildings*, 49, 488-498.

Buck, A. L. (1981). New equations for computing vapor pressure and enhancement factor, *Applied Meteorology*, 20, 1527–1532.

Cartalis, C., Synodinou, A., Proedrou, M., Tsangrassoulis, A., and Santamouris, M. (2001). Modifications in energy demand in urban areas as a result of climate changes: an assessment for the southeast Mediterranean region, *Energy Conversion and Management*, 42(14), 1647–1656.

Feidas, H., Makrogiannis, T., and Bora-Senta, E. (2004). Trend analysis of air temperature time series in Greece and their relationship with circulation using surface and satellite data: 1955-2001, *Theoretical and Applied Climatology*, 79 (3–4), 185–208.

Founda, D. (2011). Evolution of the air temperature in Athens and evidence of climatic change: A review, *Advances in Building Energy Research*, 5(1), 7–41.

Giannopoulou, K., Livada, I., Santamouris, M., Saliari, M., Assimakopoulos, M., and. Caouris, Y. G. (2011). On the characteristics of the summer urban heat island in Athens, Greece, *Sustainable Cities and Society*, 1(1), 16–28.

Gupta R., and Gregg, M. (2011). Adapting UK suburban neighbourhoods and dwellings for a changing climate, *Advances in Building Energy Research*, 5(1), 81–108.

Hassid, S., Santamouris, M., Papanikolaou, N., Linardi, A., Klitsikas, N., Georgakis, C., and Assimakopoulos, D. N. (2000). Effect of the Athens heat island on air conditioning load, *Energy and Buildings*, 32(2), 131–141.

Kapsomenakis, J., Kolokotsa, D., Nikolaou, T., Santamouris, M., Zerefos S. (2013). Forty Years Increase of the Air Ambient Temperature in Greece: The Impact on Buildings. *Energy Conversion and Management*, 74, 353 – 365.

Karlessi, T., Santamouris, M., Synnefa, A., Assimakopoulos, D., Didaskalopoulos, P., and Apostolakis, K. (2011). Development and testing of PCM doped cool colored coatings

to mitigate urban heat island and cool buildings, *Building and Environment*, 46(3), 570–576.

Livada, I., Santamouris, M., and Assimakopoulos, M. (2007). On the variability of summer air temperature during the last 28 years in Athens, *Journal of Geophysical Research D: Atmospheres*, 112(12).

Mihalakakou, G., Santamouris, M., Papanikolaou, N., Cartalis, C., and Tsangrassoulis, A. (2004). Simulation of the urban heat island phenomenon in Mediterranean climates, *Pure and Applied Geophysics*, 161(2), 429–451.

Mihalakakou, G., Santamouris, M., and Asimakopoulos, D. (1998). Modeling ambient air temperature time series using neural networks, *Journal of Geophysical Research D: Atmospheres*, 103(D16), 19509–19517.

Nastos, P. T., Philandras, C. M., Kapsomenakis, J., and Eleftheratos, K. (2011). Variability and trends of mean maximum and mean minimum air temperature in Greece from ground-based observations and NCEP-NCAR reanalysis gridded data, *International Journal of Remote Sensing*, 32(21), 6177–6192.

Nikolaou, T., Skias, I., Kolokotsa, D., and Stavrakakis, G. (2009).Virtual Building Dataset for energy and indoor thermal comfort benchmarking of office buildings in Greece, *Energy and Buildings*, 41(12), 1409–1416.

Pantavou, K., Theoharatos, G., Mavrakis, A., and Santamouris, M. (2011). Evaluating thermal comfort conditions and health responses during an extremely hot summer in Athens, *Building and Environment*, 46(2), 339–344.

Philandras, C. M., Nastos, P. T., and Repapis, C. (2008). Air temperature variability and trends over Greece, *Global Nest Journal*, 10(2), 273–285.

Sakka, A., Santamouris, M., Livada, I., Nicol, F., and Wilson, M. (2012). On the thermal performance of low income housing during heat waves, *Energy and Buildings*, 49, 69–77.

Santamouris M., and Kolokotsa, D. (2013). Passive cooling dissipation techniques for buildings and other structures: The state of the art, *Energy and Buildings*, 57, 74–94.

Santamouris, M., Pavlou, K., Synnefa, A., Niachou, K., and Kolokotsa, D. (2007a). Recent progress on passive cooling techniques, Advanced technological developments to improve survivability levels in low-income households, *Energy and Buildings*, 39(7), 859–866.

Santamouris, M., Kapsis, K., Korres, D., Livada, I., Pavlou, C., and Assimakopoulos, M. (2007b). On the relation between the energy and social characteristics of the residential sector, *Energy and Buildings*, 39(8), 893–905.

Santamouris, M., Papanikolaou, N., Livada, I., Koronakis, I., Georgakis, C., Argiriou, A., and Assimakopoulos, D.N. (2001). On the impact of urban climate on the energy consumption of buildings, *Solar Energy*, 70(3), 201–216.

Santamouris, M., Mihalakakou, G., Papanikolaou, N., and Asimakopoulos, D.N. (1999). A neural network approach for modeling the heat island phenomenon in urban areas during the summer period, *Geophysical Research Letters*, 26(3), 337–340.

Zanis, P., Kapsomenakis, I., Philandras, C., Douvis, K., Nikolakis, D., Kanellopoulou, E., Zerefos, C., and Repapis, C. (2009). Analysis of an ensemble of present day and future regional climate simulations for Greece, *International Journal of Climatology*, 29(11), 1614–1633.

DEVELOPMENT OF AN ALGORITHM FOR PREDICTING THE PERFORMANCE AND OPTIMIZING THE DESIGN OF AN ENERGY EFFICIENT LIGHTING SYSTEM

Konstantina Vasilakopoulou[1,2], Afroditi Synnefa[1], Dionisia Kolokotsa[2], Theoni Karlessi[1], Mattheos Santamouris[1]

1 Group Building Environmental Studies, Physics Department, National Kapodistrian University of Athens, Panepistimioupoli Zografou Athens Greece

2 Environmental Engineering Department, Technical University of Crete, Kounoupidiana, Chania Crete, Greece
**Corresponding author: kvasilakopoulou@isc.tuc.gr*

ABSTRACT

This paper describes part of the research that is being done on the prediction of the performance of light pipes and the ways to optimize their design, in order to house artificial lighting, able to supplement daylight in a space. The research has up to date resulted in an algorithm for the easy and quick calculation of the interior illuminance provided by light pipes and in a procedure for the calculation of the power of the necessary artificial lighting (LEDs) and the energy savings for lighting, due to the daylight provided by the light pipes and the daylight linked controls of the LEDs.

KEYWORDS

Light pipes, performance algorithm, LEDs, energy savings

1. INTRODUCTION

Lighting is one of the most important energy consumers among the building mechanical systems, especially in public buildings and office premises located in city centres. During the last decades, daylight systems, more sophisticated than the usual side windows, are commonly used both in new and in renovated buildings, in order to satisfy the users' requests for access to daylight and to provide for reduced energy consumptions. One of the most common daylight systems, mainly used in the countries of north-western Europe is a category of Tubular daylight guidance systems, the passive zenithal guidance system, more commonly referred to as light pipe. Light pipes permit the entrance of skylight and sunlight through a transparent dome, placed on the building roof, into a highly reflective tube. After internally reflected, light is guided at ceiling level, where an opal or prismatic diffuser, diffuses the light emitted in the space. The tubes can either be straight or have bends, and the system diameter and length may vary significantly, depending on application.

A respectful number of scientists has studied the performance of passive light pipes and developed algorithms for the calculation of the light emitted by this type of daylight system. The Luxplot method, for example, can be applied to pipes of any size, with any number of bends of any angle, with a diffuser (Jenkins and Muneer, 2003). It calculates the luminous flux and then estimates the illuminance distribution at any point on the reference plane. The method does not involve solar altitude and sky clearness parameters. From this methodology, the authors have developed a tool with an output of a colour luxplot (Jenkins et al 2005). The tool developed by Zhang and Muneer (Zhang and Muneer, 2002) is for use with light pipes with opal or cloudy diffuser, straight or elbowed. The input parameters are more than those of the Luxplot method, as it requires solar altitude and sky clearness. The quantity used to describe the light pipe performance is the "Daylight Penetration Factor" (DPF). A third methodology, which is included in the Technical Report CIE 173:2006, is described in the following paragraphs, as it was used for the development of the proposed algorithm.

The following paragraphs include part of a study conducted within the framework of the European project HERB (Holistic energy efficient retrofitting of residential buildings), aimed to develop an algorithm for the calculation of the performance of light pipes and for the integration of energy efficient artificial lighting controlled by daylight linked controllers.

2. DEVELOPMENT OF AN ALGORITHM FOR THE CALCULATION OF THE ILLUMINANCE PROVIDED BY LIGHT PIPES

2.1 General

The methodology for defining the specifications of an optimum light pipe with integrated artificial lighting (LEDs in particular) for a certain space with specific lighting requirements, would lead to the appropriate light pipe sizing and/or number of pipes and the number/wattage of the LEDs required for the system to provide the minimum illuminance needed on the reference plane. The two main parameters that have to be determined are:

a. The illuminance E_{pipe} that the light pipe can provide under specific external conditions. The daylight availability from other natural light sources (for example windows, skylights, etc) is not investigated in this paper.

b. The illuminance E_{LED} that the artificial lighting sources will provide, in order to supplement the natural lighting.

These terms are associated with the following relation:

$$E_{LED} = E_{int} - E_{pipe} \text{ (lux)} \quad (1),$$

where E_{int} is the desired illuminance level on the reference plane.

2.2 Description of the TTE method and of the simulation procedure

CIE Technical report 173:2006 "Tubular Daylight Guidance Systems" describes one analytical method for the performance calculation of passive zenithal systems, based

on the concept of Transmission Tube Efficiencies (TTE). TTE is a term that expresses the efficiency of the tube, taking into account the losses on the output of a light pipe due to the light absorbed by the guide material, the multiple reflections of light that occur within the tube, the tube length, the presence of pipe elbows, etc, under overcast sky conditions. The relationship for the TTE calculation incorporates the length, diameter and reflectance of the guide. However, the Technical Report provides TTE values for different pipe diameters, lengths and reflectances, as well as for various angles and number of elbows, in a tabulated form for a more straightforward application.

The methodology firstly calculates the flux Φ_i emerging from the diffuser of a light pipe, for specific external global illuminance, TTE and dome and diffuser transmittances. In order for an indication of the interior lighting levels, provided by a number of light pipes N in a space, to be provided, the Technical report provides a relation for the Daylight Penetration Factor (DPF).

After the flux Φ_i emerging from the output device of the light pipe is calculated, it can be used with any lighting software, in order to simulate the illuminance levels on the reference plane. The procedure includes finding (or constructing) a luminaire with circular polar diagram, setting the diameter of the luminaire the same as the light pipe diameter, replacing the lumen output of the original luminaire with the flux derived from the TTE method and replacing the luminaire Utilization Factor with the light pipe Utilization factor (UF). This is a Utilization factor for passive light guides, based on the assumption that the light pipe output devices can resemble flush mounted luminaires, with an approximate cosine luminous intensity distribution. The values of Lower Flux Utilance can be used as Utilization factors (Carter, 2002), which are given by the Technical report, according to the room index and reflectances of the interior surfaces.

2.3 Calculations performed with the TTE method

The TTE method was applied to light pipes of two reflectance values (0.95 and 0.98) five diameters (0.25, 0.35, 0.53, 0.65, 0.9 m) and seventeen lengths (0.25, 0.5, 0.75, 1, 2, 3, 4, 5, 6, 8, 10, 12, 14, 15, 16, 18, 20, 25 m) in order for the flux Φ_i to be determined, for an external illuminance of 5,000lux. The transmission of both the clear dome and the diffuser was considered to be 0.82.

For the light pipe characteristics previously described, the TTE values were read from the table of the CIE technical report. For any length that is not included in the CIE technical report, the TTE value of the light pipes with one of the diameters mentioned above and of tube reflectances 0.92, 0.95, 0.98 or 0.995, can be derived from Table 1. These relations emerged from regression analysis, estimating the relationships between the length (L), the diameter (D) and the reflectance (R) of the tube.

Table 1: Relationships for the calculation of the TTE values

D \ R	0.92	0.95	0.98	0.995
0.25	$-0,235\ln(L) + 0,678$	$0,9268e^{-0,144L}$	$0,9817e^{-0,063L}$	$0,9985e^{-0,017L}$
0.35	$0,9007e^{-0,164L}$	$0,9504e^{-0,12L}$	$0,9901e^{-0,046L}$	$0,999e^{-0,012L}$
0.53	$0,9502e^{-0,114L}$	$0,9768e^{-0,074L}$	$0,9949e^{-0,031L}$	$1,0004e^{-0,008L}$
0.65	$0,9679e^{-0,096L}$	$0,9795e^{-0,073L}$	$0,9958e^{-0,025L}$	$e^{-0,007L}$
0.9	$0,9767e^{-0,071L}$	$0,9875e^{-0,045L}$	$0,9985e^{-0,019L}$	$1,0009e^{-0,005L}$

After the flux values for the aforementioned cases were calculated with the TTE method, they were assigned to a luminaire with cosine luminous intensity distribution and simulations were performed with the IES VE pro software. The light pipes were simulated in eight different types of rooms of varying sizes which are commonly met in residential buildings (Room Length/Width/Height (m): 4/4/3, 4/4/5, 6/4/3, 4/7/3, 5/5/4, 6/6/2.5, 4/3/3, 4/5/3). The reflectance values of the interior surfaces were considered to be: walls: 50%, ceiling: 70%, floor: 30%. The working plane on which the illuminance levels were calculated was 0.85m above the room floor and was 0.50m offset to the walls. In total, 1,728 scenarios were calculated.

2.4 Deriving relationships for a simplified algorithm for illuminance calculation

The above described calculations and simulations were aimed to provide data for the development of an algorithm that would enable the calculation of the light output of light pipes in a certain room, in order to estimate the interior lighting conditions that are established and for the artificial lighting equipment to be defined and sized, in terms of wattage and/or number of LED lamps.

The correlation of the calculated illuminance values with the room dimensions and the TTE, led to the following relationships, depending on the light pipe diameter (D):

$$\text{For } D=0.25,\ E_i = 5,73 - 0,64 \times L - 0,31 \times W - 0,95 \times H + 4,34 \times TTE \quad (3)$$

$$\text{For } D=0.35,\ E_i = 14,22 - 0,90 \times L - 1,30 \times W - 2,30 \times H + 7,59 \times TTE \quad (4)$$

$$\text{For } D=0.53,\ E_i = 34,63 - 2,96 \times L - 2,29 \times W - 6,02 \times H + 19,03 \times TTE \quad (5)$$

$$\text{For } D=0.65,\ E_i = 59,79 - 4,52 \times L - 4,08 \times W - 10,06 \times H + 25,53 \times TTE \quad (6)$$

$$\text{For } D=0.90,\ E_i = 101,68 - 6,26 \times L - 9,59 \times W - 18,08 \times H + 58,22 \times TTE \quad (7)$$

where L= the room length, considered to be larger than the room width (m),W= the room width (m), H= the room height (m) and TTE= the transmission tube efficiency.

The particular relations are valid for specific conditions (E_{ex}=5,000lux, τ_c=0,82, etc), however they can be easily transformed to take into account different exterior and interior conditions and light pipe characteristics, by multiplying the result with the following product:

$$k = (Eex/5{,}000) \times (\tau_{dome} \times \tau_{diffuser}/0{,}82) \times (MF/0.9) \quad (8)$$

where MF is a maintenance factor, participating in the flux calculation, related to the positioning of the light pipe dome and the pollution of the specific location.

3. DEVELOPMENT OF A METHOD FOR THE OPTIMISATION OF THE DESIGN OF LED ASSISTED LIGHT PIPES

3.1 Calculation of the illuminance from the LEDs

Since daylight levels are not stable throughout a certain time period, the light emitted from a light pipe, should be supplemented by artificial lighting, in order to achieve a certain interior design illuminance E_{int}. The design interior illuminance on a reference plane, is determined by the space's function and the users' needs. Usually, indicative illuminance values for interior spaces, depending on their use, are given by Standards. For domestic environments, such limits are not provided by Standards, so the design illuminance value should be set depending on the users' needs and activities. The design illuminance E_{int} is given by relation (1).

The illuminance from the light pipes of a room can be calculated from the algorithms described previously, for a given external illuminance. However, the maximum illuminance from the LEDs, needed to reach the design illuminance in a room, is the value that defines the installed power of the lamps used in the light pipe system. The maximum E_{LED} should be adequate in order to provide the necessary supplementary illuminance levels to the illuminance levels provided by the natural light sources of a room, at the time when the external illuminance is relatively low for the location where the room is situated. One such external illuminance could be the average external global illuminance $E_{ex,min}$, of the month with the lowest average external global illuminance, compared to the rest of the eleven months of the year, for a specific location. This data can be obtained from organizations that perform climatic measurements in every country, or by climatic files included in software databases.

By calculating the emitted flux Φ_i for external illuminance $E_{ex,min}$, the illuminance values provided by a light pipe $E_{pipe,min}$ under relatively low levels of external illuminance can be simulated or calculated by relations 3-7. If $E_{pipe,min}$ is then used in relation (1), the $E_{LED,max}$ that is calculated, is going to cover the needs for supplementing the natural light in order for the design illuminance to be achieved in a room, in the majority of the sky conditions.

For maximum energy savings for lighting, the lamps' output should be controlled by a dimmer, receiving input from a daylight sensor. The control pattern would turn the artificial lighting on, when E_{pipe} is less than the E_{int} that has been set for the specific room and increase the output of the LEDs as E_{pipe} falls. When $E_{pipe} \leq E_{pipe,min}$, the LEDs are going to work in maximum output. As users of rooms usually forget to turn off the lights of systems that are daylight linked when the daylight is adequate, it is important for the control system to automatically turn off the lamps when they are not needed. When emitting 1% of their maximum output, artificial lighting systems consume 8% of their full power, leading to unnecessary waste (Reinhart, 2004).

An alternative way to define the $E_{LED,max}$, is to set it equal to the design illuminance E_{int}, so that the light pipe system can provide the necessary light levels in the room, even during the nighttime. However, this approach is not followed here, as it would not result in an optimized design of the daylight system comprised from the light pipe and the LEDs.

3.2 Calculation of necessary installed power of the LEDs

The calculation of the necessary installed power of the light pipe LEDs that are going to supplement the natural lighting provided by the light pipes of a space, requires the steps analyzed in the following paragraphs.

1. Calculation of the flux (lm) emitted by the lamps.

After the maximum light output from the LEDs in terms of illuminance is known, the $E_{LED,max}$ value can be used with the following relation of the lumen method, in order for the necessary LED lumens to be calculated.

$$E_{LED}=(\Phi_{LED} \text{ x } N \text{ x } UF \text{ x } MF)/A \quad (9)$$

Where Φ_{LED}= the flux emitted by all the LED lamps included in one light pipe, N=the number of light pipes in the room, UF =the utilization factor of the luminaire, MF= the maintenance factor of the luminaire, A= the area of the working/reference plane.

From relation (9) the flux Φ_{LED} of the LEDs that will be included in one light pipe can be calculated.

2. Estimation of the LEDs luminous efficacy (lm/W). This step is needed only when the lamps of the system have not yet been precisely specified, in which case, the luminous efficacy is provided by the manufacturer. If, however, an estimate has to be made, the parameters that have to be considered are the desired correlated colour temperature (CCT) of the lamps, the losses due to temperature and the losses caused by the optical system -lenses or diffusers- and from the light that reaches some part of the luminaire and never reaches the reference plane.
3. Calculation of the LEDs wattage.

By dividing the total flux Φ_{LED} coming from the LEDs of one light pipe with the luminous efficacy value of a LED lamp η, the wattage P_{LED} of the lamps of one light pipe is calculated (10).

$$P_{LED}= \Phi_{LED}/\eta \text{ (W)} \quad (10)$$

3.3 Energy savings for lighting

The energy savings for lighting can be calculated with a number of ways. A simplified but indicative way has been selected, in order to calculate the percentage of the energy saved by the use of the LED lamps and a daylight linked-dimming profile.

Relation (10) gives the wattage of the LEDs that have to be installed in each light pipe of a space, in order to provide the supplementary lighting, when natural lighting is not enough for the needs of the users. Since the mean monthly external global illuminance

of a specific location is known, the wattage of the LEDs that is needed to provide for the supplementary illuminance can be calculated for every month. By multiplying this wattage P_{LED} to the average daylight hours of each month of the year, the energy consumption for lighting (if the LEDs were on during all the daylight hours) is calculated. From this value and from the energy consumption for the same external conditions but with no daylight availability, the percentage of energy savings can be calculated.

This method gives a rough estimate for the energy savings that result from the use of light pipes and artificial lighting controlled to supplement the daylight systems, employing only the necessary wattage.

3.4 Application of the procedure for the LED power specification and of the calculation of energy savings for lighting

The procedure analyzed in the previous chapters, has been implemented in four rooms, of dimensions frequently met in residences, with different light pipe characteristics (diameter, length) and different window areas. The calculations were performed for seven European cities: Nottingham-UK, Geneva-Switzerland, Lisbon-Portugal, Madrid-Spain, Amsterdam-Netherlands, Bologna-Italy and Athens-Greece. The mean daylength of every month in hours and the monthly mean of daily sums of global illuminance in kluxh, were obtained by www.satel-light.com. December was for every city the month with the less hours of day and with the lowest mean global illuminance value. By dividing the global illuminance of December with the hours of day of the same month, the $E_{ex,min}$ for which the sizing of the artificial lighting system will be calculated, was obtained.

$E_{ex,min}$, i.e. the global illuminance of December for every city, was used with equations (3)-(7) and the average illuminance from one light pipe was calculated for the "worst sky conditions", on a reference plane covering the room area, with an offset to the walls of 0.50m. These values were subtracted from the E_{int} of each room and E_{LED} was obtained. Based on this illuminance that has to be provided by the LEDs, the flux of all the LEDs (Φ_{LED}) in one light pipe was calculated, from relation (9). The luminous efficacy η that was assumed for the LEDs was 70lm/W. By dividing Φ_{LED} with η, the watts P_{LED} of the LEDs that have to be installed in each light pipe were calculated.

In order to calculate the energy savings for lighting, P_{LED} was multiplied with the mean daylength of December. This consumption was compared to the consumption of a system that would provide E_{int} only with the use of the LEDs for the same time period. The same procedure was followed for the rest of the months, for every city.

Some indicative results of the application of the algorithm for the calculation of E_{pipe} and of the determination of P_{LED} and of the energy savings in various rooms, locations and months, are given in Table 2.

4. RESULTS & DISCUSSION

4.1 General

The methodologies and algorithms previously described are part of a more general study, aiming to provide easily and quickly applied tools for the optimization of daylight systems, that include light pipes with integrated LED lighting, within the framework of the European project HERB (Holistic energy efficient retrofitting of residential buildings). Specifically, the light pipes are intended to be installed in domestic environments, which explains the small size of the room types used for the above analysis. Analysis for light pipes with elbows has also been performed, but is not presented in this paper.

The TTE method, as the analytical methodology proposed by the Technical Report CIE:173:2006, was chosen as the most accurate theoretical algorithm for the calculation of light pipes' performance. The flux Φ_i that resulted, was used as the lumen output of a luminaire with a perfect diffuser, with a lighting software (IES VE pro). The assumption that the light pipe is a luminaire enabled the simulation of the average illuminance in the studied rooms. A forward Raytracing tool, which would be able to dynamically simulate the interior lighting conditions and the energy savings from the use of the daylight system, is going to be used in a later stage of the study. Also, an experiment under laboratory conditions is already prepared, in order to validate the results obtained by the previously mentioned methods.

4.2 Assessment of the developed algorithm

The algorithm that was developed was intended to calculate the average illuminance on the reference plane of residential rooms, which usually have small dimensions. The proportions of the rooms would probably make the light pipe diffuser an area and not a point source, to which the inverse square law applies. For that reason, the assumption that the lumen method can be applied, for the calculation of the E_{LED}, is considered to be acceptable. However, the results of the calculation of the LEDs' wattage were tested with simulations. An LED luminaire with a diffuser, of approximately the same luminous efficacy and wattage as the ones used for the calculations, gave approximately the same average interior illuminance.

The comparison of the illuminance levels, from the light pipes in a room, calculated with the TTE method and the above described simulations and with the algorithms that resulted from the correlation of the various parameters (relations 3-7), shows great consistency.

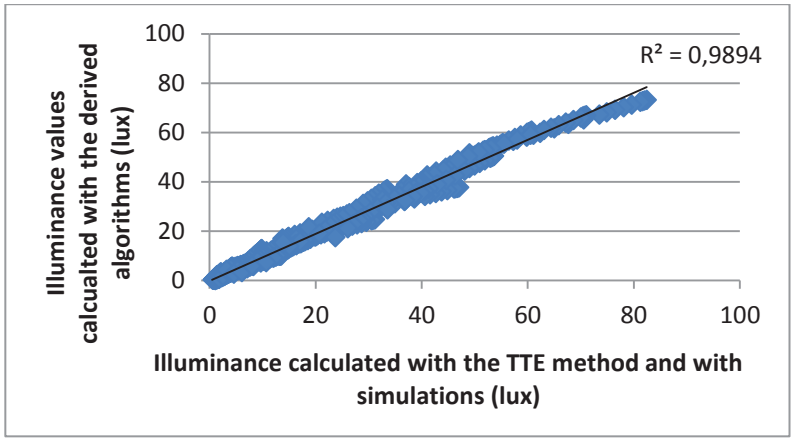

Figure 1.Correlation of the illuminance calculated with relations (3-7) and with the TTE methodology-simulation of the light pipe as a luminaire with "perfect diffuser".

4.3 Assessment of the energy savings due to the daylight system

The application of the calculation procedure for the estimation of the wattage of the LEDs needed and for the energy savings that arise, show that light pipes can provide substantial savings in locations with high external illuminances and more moderate savings in locations with lower external illuminances, for the same time interval. However, countries with "darker" external conditions are probably going to use a daylight system with integrated artificial lighting for longer periods, which will lead to increased savings. The energy savings exceed 14%, even in the "darkest" month of the northest city of the study, for internal illuminance of 150 lux, which is a rather appreciable percentage for energy savings for lighting.

5. CONCLUSIONS

This paper describes part of the research that is being done on the performance of light pipes and the ways to optimize their design, in order to house artificial lighting, able to supplement daylight in a space. The research is performed within the framework of HERB, a European project that investigates the application of various innovative energy efficiency technologies in residential buildings.

The research has up to date resulted in an algorithm for the easy and quick calculation of the interior illuminance provided by light pipes (based on the methodology described in Technical Report CIE:173:2006 and lighting simulations) and in a procedure for the calculation of the power of the necessary artificial lighting (LEDs) and the energy savings for lighting, due to the daylight provided by the light pipes and the daylight linked controls of the LEDs. Much work needs to be done on the field, with simulations with forward Raytracing and optical design software and an experiment under laboratory conditions being currently prepared.

ACKNOWLEDGEMENTS

The authors would like to express their thanks to Aris Tsangrassoulis, Ass. Professor at the Architectural Department of the University of Thessalia, for his precious help.

This work was realized within the framework of the European project HERB: Holistic energy efficient retrofitting of residential buildings, (project number 314283).

Table 2.Results from the application of the algorithm for the illuminance from the light pipe and the LED power estimation process for different room types, months and European cities (tube reflectance=0.98, MF=0.8, room surface reflectances: ceiling/walls/floor=0.7/0.5/0.3, reference plane height=0.85, η_{LED}=70lm/W, τdome x τdif=0.72, reference plane at 0.85m above floor and 0.5m offset to walls)

Month	City	Room length/ width/ height (m)	Pipe diameter/ length (m)	External illuminance (lux)	E_{pipe} (lux)	E_{int} (lux)	E_{LED} (lux)	P_{LED} (W)	Daylight hours (h)	Energy consumption for lighting (kWh)	Energy savings (%)
Dec.	Amsterdam			8467,53	23,97		126,03	67,77	7,7	0,52	15,98
	Nottingham			8064,93	21,86		128,14	68,90	7,7	0,53	14,57
	Madrid			19273,68	52,25		97,75	52,57	9,5	0,50	34,83
	Lisbon	4/7/3	0.65/3	24115,79	65,37	150	84,63	45,51	9,5	0,43	43,58
	Bologna			14460,67	39,20		110,80	59,58	8,9	0,53	26,13
	Athens			20375	55,23		94,77	50,96	9,6	0,49	36,82
	Geneva			12034,09	32,62		117,38	63,12	8,8	0,56	21,75
Jun.	Amsterdam			34801,20	85,49		214,51	97,84	16,6	1,62	28,50
	Nottingham			30440,48	74,78		225,22	102,73	16,8	1,73	24,93
	Madrid			56880,79	139,72		160,28	73,10	15,1	1,10	46,57
	Lisbon	6/4/3	0.53/6	55026,85	135,17	300	164,83	75,18	14,9	1,12	45,06
	Bologna			47083,87	115,66		184,34	84,08	15,5	1,30	38,55
	Athens			55844,59	137,18		162,82	74,27	14,8	1,10	45,73
	Geneva			42987,34	105,60		194,40	88,67	15,8	1,40	35,20
Sept.	Amsterdam			26158,73	62,30		137,70	73,45	12,6	0,93	31,15
	Nottingham			24417,32	58,15		141,85	75,66	12,7	0,96	29,08
	Madrid			44888,89	106,90		93,10	49,65	12,6	0,63	53,45
	Lisbon	5/5/4	0.375/5	48298,39	115,02	200	84,98	45,32	12,4	0,56	57,51
	Bologna			39280,00	93,55		106,45	56,78	12,5	0,71	46,77
	Athens			45620,97	108,65		91,35	48,72	12,4	0,60	54,32
	Geneva			34642,86	82,50		117,50	62,67	12,6	0,79	41,25

REFERENCES

Jenkins, D., Muneer, T. (2003). Modelling light-pipe performances—a natural daylighting solution. Building and Environment 38, 965 – 972

Jenkins, D., Muneer, T. Kubie, J. (2005). A design tool for predicting the performances of light pipes. Energy and Buildings 37, 485–492

Carter, D.J. (2002). The measured and predicted performance of passive solar light pipe systems. Lighting Research and Technology, vol. 34 no. 1 39-51

Zhang, X., Muneer, T. (2002). A design guide for performance assessment of solar light guide. Lighting Research and Technology, 34(2), 149-169

Technical Report, CIE 173:2006. Tubular daylight guidance systems.

Reinhart, C.F. (2004). Lightswitch-2012: a model for manual and automated control of electric lighting and blinds. Solar Energy 77, 15-28

Satel light website: www.satel-light.com

HERB project website: http://www.euroretrofit.com/

A DEVELOPMENT OF A LIGHTING CONTROLLER USING SMART SENSORS

Sotiris Papantoniou[1], Denia Kolokotsa[1], Kostas Kalaitzakis[1], Davide Nardi Cesarini[2], Eduard Cubi[3] and Cristina Cristalli[2]

1 Technical University of Crete
Technical University of Crete Campus
Greece
**Corresponding author: spapantoniou@isc.tuc.gr*

2 Loccioni Group
Via Fiume 16
Ancona, Italy

3 Institut de Recerca en Energia de Catalunya
Jardins de les Dones de Negre 1, 2ª pl.
Barcelona, Spain

ABSTRACT

The aim of this paper is to present an advanced controller for artificial lights developed and tested using validated light models for several rooms in two European Hospitals located in Chania, Greece and Ancona, Italy respectively. Fuzzy techniques have been used for the architecture of the controller. The efficiency of the controllers has been tested using validated models of the RADIANCE back-wards ray tracing model. The input of the controller is the error between the current value of the photo sensor and the desired one, and the output is the change of the light level that should be applied (S.I.S.O). The controller has been tested on 2 different artificial light systems (On/ off switching, Dimming). Measurements and simulation indicate significant energy saving in both systems. Results are compared to the current use of the artificial lights by the users. All work has been contacted using Matlab's and RADIANCE's environment.

KEYWORDS

Fuzzy control, artificial lights, energy consumption, artificial lights dimming,

1 INTRODUCTION

Although classic passive energy saving techniques are trying to reduce energy losses from the fabric of the buildings, primary energy can also be saved from the reduction of the internal gains which affect the electricity spent and the cooling loads required to remove them. Among the most common internal gains available in most of the buildings, are those which come from artificial lights. Artificial lights in the office buildings consume significant amount of energy all around the world compared to the whole building's consumption as presented by Santamouris (Santamouris et al. 1994) and Lam (Lam et al. 2003) and increase the internal gains affecting the cooling loads of buildings as reported by Franzetti (Franzetti et al. 2004) According to Dr. Santamouris research artificial lights consume 10% of total energy consumption based on measurements in buildings of Greece. Most recent lighting systems are based on fluorescent lamps and only very recent ones allow dimming using electronic ballasts which replace the older magnetic ones. Before fluorescent lights, most buildings had incandescent lights which were very inefficient. Electronic ballasts can dim up and down the artificial lights linearly, adjusting the indoor light level to comfort levels while saving energy. Dimming of artificial lights can be combined with a recent daylight harvesting systems, which

reduce furthermore the requirements for artificial lights according to Raphael (Raphael 2011). A smart controller is reading inputs from a light sensor and a presence indicator can adjust the light level automatically, maximizing the comfort level and the energy saving.

2 AVAILABLE CONTROL TECHNIQUES FOR ENERGY SAVINGS OF LIGHTING SYSTEMS

The issue of energy savings from the artificial lights, maximizing the benefits from natural daylight has been raised by many researchers for many years. Wen (Wen and Agogino 2010) estimated through a combination of measurements and simulations that a controller with a photo sensor connected to each light fixture can save up to 60% of energy or up to 23% if there is only one photo centre installed in the centre of the room. Kumaar (Nippun Kumaar et al. 2010) propose an intelligent lighting system which can save up to 40% of energy during daytime. Furthermore according to Frattari et. al. (Frattari et al. 2009) dimming of artificial lights perform much better comparing to manual on/ off or automatic on/off but the performance depends on the season of the year. According to his research dimming is performing better during the summer comparing to autumn.
Among these techniques fuzzy control techniques are also well-known for their efficiency in many controllable systems. Although fuzzy technology has been developed since 1965 their application is continuously increased due their main advantage which is the users' knowledge inserted in the form of rules. Another advantage of fuzzy control is their adaptability to actual measurements using the ANFIS (Adaptive Neuro Fuzzy Inference System) (Jang 1993) architecture, in which the fuzzification and de-fuzzification parameters are updated based on measurements. A light controller based on ANFIS is presented by Kurian et. al (Kurian et al. 2008; Kurian et al. 2006), where the controller is fuzzy based, but the parameters are adapted based on results from a model developed using RADIANCE software.

3 DEVELOPED FUZZY CONTROLLER ANALYSIS

The current fuzzy controller developed for the lighting systems is based on the 'Sugeno' Type fuzzy model. The specific architecture is selected because it can update the fuzzification parameters using measured data. (Papantoniou et al. 2012) The controller can be trained with the specific data using the ANFIS architecture, in order to adapt it to current conditions. The architecture of the system can be seen in Figure 1. The sensors which are used are an indoor light sensor and a presence indicator. When presence is detected the controller will estimate the change of the artificial lights level in order to meet the users' requirements. When users are not detected inside the room lights will be either switched off or dim further down in order to maximize energy saving.

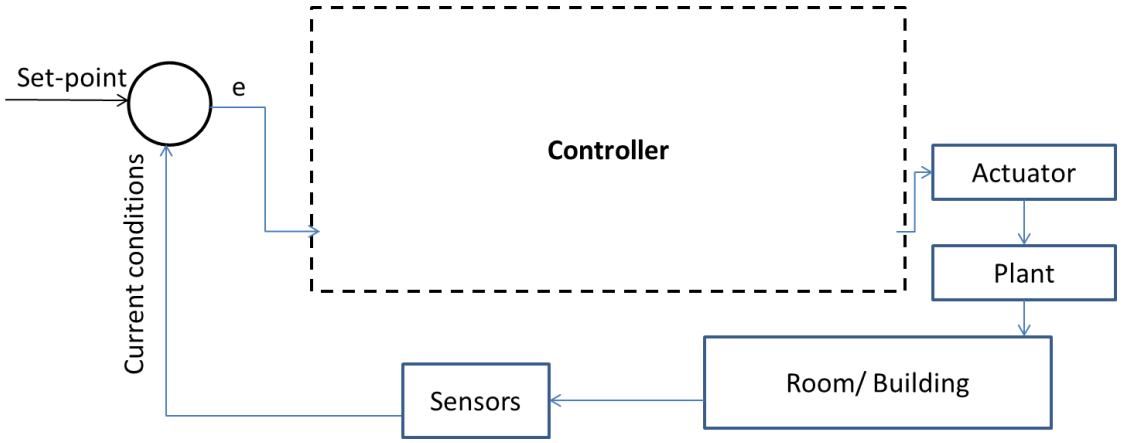

Figure 1: Architecture of the system

The controller is having as input the difference between current and desired light level (error) and as an output the new state of the artificial lights that should be applied. The architecture of the controller can be seen in Table 1.

Table 1: Architecture of the fuzzy controller

Type of fuzzy controller	‘Sugeno’			
N. of inputs	1: error between current and desired light level			
N. of outputs	1: change in the artificial lights state			
Fuzzification membership functions	5			
Fuzzification parameters (‘trapmf’)	'NE':	[-1000 -200 -150 -50]		
	'ZERO':	[-50 -25 25 50]		
	'PO':	[150 200 2000 2800]		
	'SNE':	[-150 -75 -25 0]		
	'SPO':	[20 50 100 200]		
De-fuzzification parameters (constant)	'NE':	[-1]		
	'SNE':	[-0.3]		
	'ZERO':	[0]		
	'SPO':	[0.3]		
	'PO':	[1]		
User’s knowledge	1, 5 (1): 1		4, 4 (1): 1	
	2, 3 (1): 1		5, 2 (1): 1	
	3, 1 (1): 1			
Further fuzzy parameters	AndMethod: 'prod'		OrMethod: 'probor'	
	ImpMethod: 'prod'		AggMethod: 'sum'	
	DefuzzMethod:'wtaver'			

3.1 Application of the controller in different lighting systems

The controller can be applied in artificial lighting systems with dimming systems or in on/off systems as long as more than 1 light fixture with different circuits are installed. In case of systems with dimming possibilities, the output of the controller should be confined to the limits of the dimming device (ex. 10% step of dimming, linear or not dimming etc.). In case of dimming systems the output of the controller has to be filtered in order to meet the requirements of the dimming system.

In case of using on/ off with different light fixtures systems, a different approach is required in which lights are switched on or off properly. For the on/ off systems the system is initially switching on the light fixtures closer to the entrance of the room, and if the light level is not sufficient the light fixture close to the window is activated as well. Thus, daylight level is

used as much as possible, since the daylight factor's value is higher close to the window comparing its value close to the entrance of the room. (Li et al. 2006)

4 APPLICATION OF THE FUZZY CONTROLLER IN HOSPITALS' WARDS

In the framework of the European Project: "Green@Hospital", measurements concerning lighting and thermal conditions is performed using smart sensors. Preliminary analysis of lighting measurements indicates that energy savings are possible if a smart lighting controller is developed and applied. A numerical estimation of the energy savings per year is presented in Table 2 and Table 3.

Table 2: Energy saving potential in artificial lights, Hospital of Ancona

Ward	Room Id	Room	Savings due to		Combined savings
			Presence detection	Dimming	
Hematology	1	Warehouse	55%	16%	62%
	2	Nurse office	34%	16%	44%
	3	Doctors office	35%	53%	70%
Oncology	4	Visitors waiting room	39%		39%
	5	Nurse office	7%	50%	54%
	6	Archives (2 rooms)	NA		
	7	Ambulatory	18%	21%	35%
	8	Patients waiting room	36%	35%	58%
	9	Day hospital room	NA		

Table 3: Energy saving potential in artificial lights, Hospital of Chania

Ward	Room Id	Room	Savings due to		Combined savings
			Presence detection	Set point	
Paediatric	1	Patients' room	65.7 %	25 %	72.60 %
	2	Doctors' room	82.17%	21.95%	88.39 %
	3	Doctors' rest room	99.65%	0.0%	99.65%

As it can be seen in Table 2 and Table 3, energy savings can be obtained by dimming down the artificial lights when the selected rooms are not occupied and dim the artificial when natural daylight is sufficient. Moreover, significant high levels of sunlight indicate possible over-heating condition during summer which could be reduced by using controllable internal or external movable shades. However, this use is not possible during the current project. For each room an annual emulation is conducted using RADIANCE Software (Ward and Shakespeare 1998) with the controller developed in the Matlab environment. The RADIANCE model is measuring the light level in a specific point selected in the room and it can also create photorealistic images to show visually the light distribution in the room. The process for developing the RADIANCE models can be seen in Figure 2. The control algorithm developed in Matlab apart from estimating the new light level is recording the selected light state in order to estimate the annual consumption and savings.

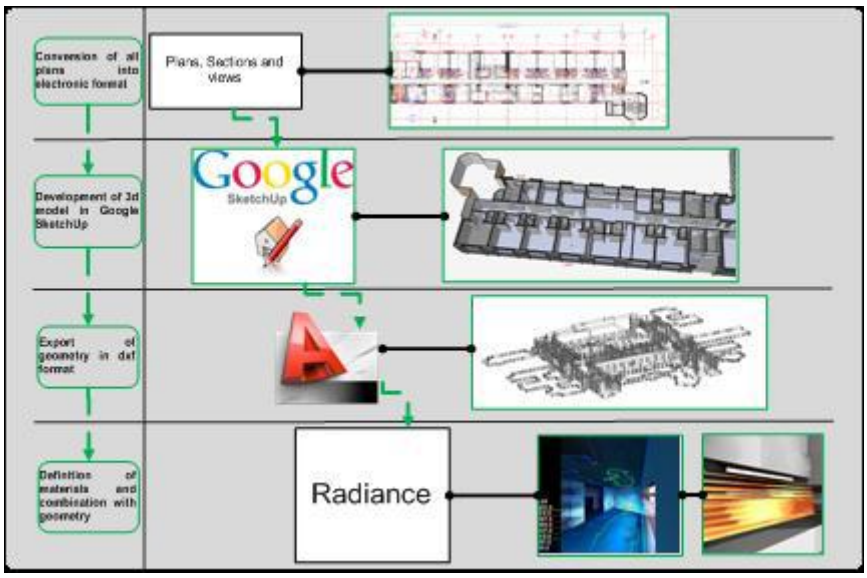

Figure 2: Schematic description of the development of the necessary geometry in RADIANCE

4.1 Application of the fuzzy controller in the Paediatric department of the Hospital of Chania

A 3D model of the hospital of Chania has been developed, enhancing the geometric details in the paediatric department as it can be seen in Figure 3 with the validation results for the Patients' room for 29th till the 31st of July 2013. The model has been validated with indoor measurements collected from the rooms and outdoor horizontal radiation measured from Technical University of Crete 7.5 km from the Hospital of Chania. The required plans and sections have been obtained by the personnel of the hospital of Chania and the technical characteristics of the light fixtures have been developed using Software Relux. (Relux Informatik AG 2012) The lighting system in the hospital is based on switching the lights on/ off.

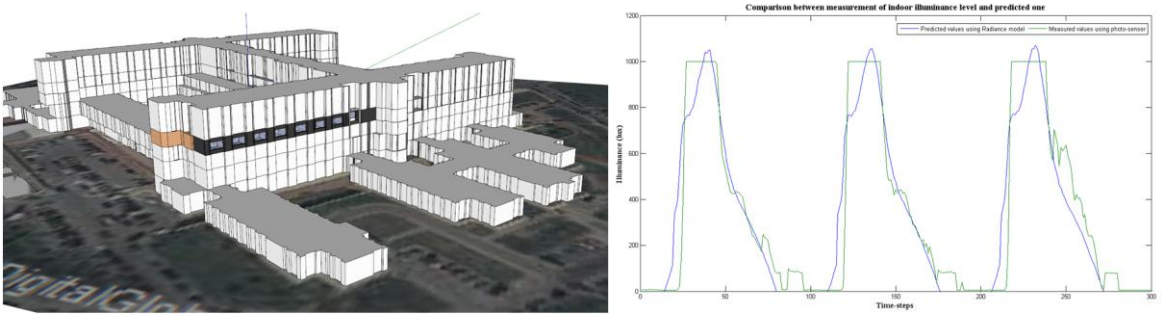

Figure 3: 3D model and validation results of the Hospital of Chania

In the 3 selected rooms where the controller will be implied 2 different light fixtures are installed. For each room, the controller selects which fixture will operate based on photo sensor and presence measurements in-situ. In Figure 4 the indoor light level can be seen under 3 different operations for 2 days.

At first the RADIANCE model is estimating light level based only on daylight (green line), with lights fully operating (red line) and with the developed fuzzy control (blue line). In the right side of Figure 4, the light level can be seen in all 3 different conditions. As it can be seen in the right part of Figure 4 the fuzzy system is switching off the second light fixture (closer to the window) saving energy while indoor light level is sufficient.

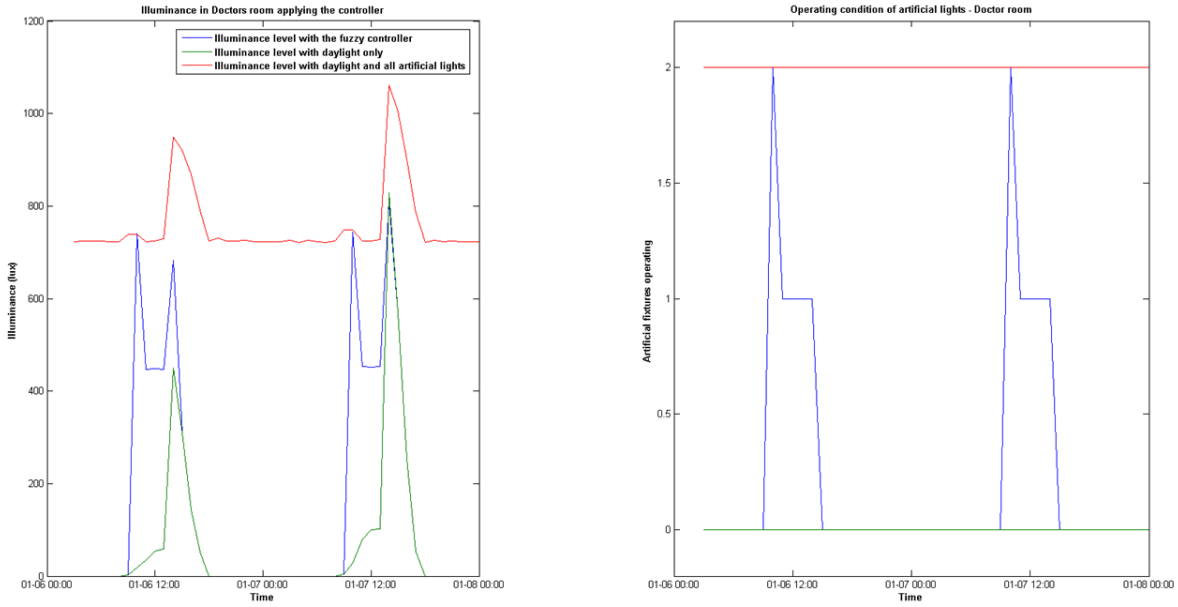

Figure 4: Indoor light level in the Doctors' room Hospital of Chania under different artificial lights conditions

Although an annual emulation has not been performed yet due to significant increased computational time (greater than a week for annual simulation), it can be seen from the results that energy can be saved during the course of the day where daylight is not sufficient but combined with partial usage of artificial lights, indoor light level can be sufficient.

4.2 Application of the fuzzy controller in the Oncology and Haematology department of the Hospital of Ancona

Similarly to the Hospital of Chania, 10 rooms have been selected in the Hospital of Ancona in order to save energy from artificial light control by dimming the artificial lights based on available daylight and presence indication. Measurements have been collect during the time period between November 2012 and January 2013, collecting 1 week data per selected room.
The developed 3D model in SketchUp can be seen in Figure 5. The required plans and sections have been obtained by the personnel of the hospital of Ancona and the technical characteristics of the light fixtures have been developed using Software Relux. (Relux Informatik AG 2012)

Figure 5: 3D model of the Ancona Hospital

In the Hospital of Ancona the artificial lights will dim based on the decisions of the fuzzy controller and presence indication. Outdoor horizontal radiation data are collected from

Loccioni Group head-quarters which are located only few kilometres from the hospital of Ancona. The application of the fuzzy controller for 2 selected day in the warehouse of the haematology department can be seen in seen in Figure 6 where the light level inside the room can be seen with the lights operating under the current system (green line), with the fuzzy controller (blue line) and only natural daylight (red line). On the right side of Figure 6 the lights operating conditions can be seen. From the dimming level of the artificial lights the energy consumption of the artificial lights can be estimated as a relation between the dimming level and the maximum consumption when lights are operating under maximum power.

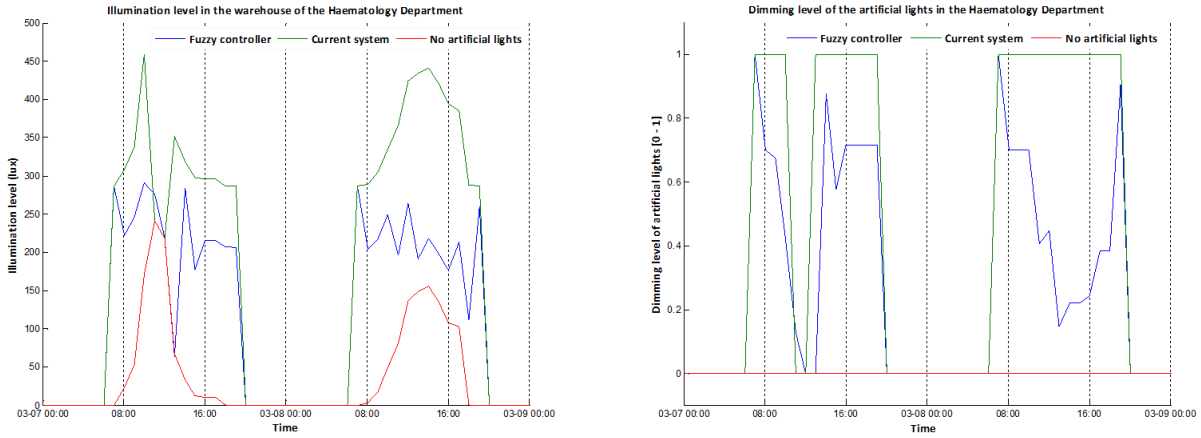

Figure 6: Indoor light level in the warehouse of the Ancona Hospital under different artificial lights conditions

As it can be seen in Figure 6, the controller is keeping the light level stable around the desired set point (200 lux) dimming the artificial lights from 0 to 1 with a step of 0.1, saving energy assuring the indoor level. Savings can be increased if the controller is applied more frequently (ex. 10 min).

An annual emulation has been performed combining the controller developed in Matlab and the RADIANCE developed model of the hospital of Chania. A representative presence schedule has been established for the selected rooms to provide the necessary inputs to the controller. The presence schedule and the necessary set points for the selected rooms are presented in Table 4.

Table 4: Provided parameters for the annual emulation

Selected rooms of AOR	**Time**	**Presence indication**	**Light set point**
Visitors waiting room (Room 7)	00:00 – 01:59 02:00 – 05:59 06:00 – 20:59 21:00 – 21:59 22:00 – 23:59	1 0 1 0 1	200 lux 50 lux 200 lux 50 lux 200 lux
Nurse office (Room 9)	00:00-06:59 07:00 – 18:59 19:00 – 23:59	0 1 0	0 lux 500 lux 0 lux
Doctors office (Room 10)	00:00-06:59 07:00 – 18:59 19:00 – 23:59	0 1 0	0 lux 500 lux 0 lux

Running the emulation the following energy savings are estimated based on the state of the artificial lights. The results from the emulation can be seen in Table 5.

Table 5: Estimated energy savings from the annual emulation

Selected rooms of AOR	Estimated energy savings
Visitors waiting room	36%
Nurse office	54%
Doctors office	45%

Comparing Table 2 and Table 5 it can be seen that the estimation of possible energy savings due to dimming are similar for the visitors' waiting room. For the other 2 rooms located in the Haematology department the emulation show that the savings are much higher comparing to initial estimation. This difference is reasonable if we assume that the initial estimations have been calculated using measurements collected during the winter. The rooms are self-shaded by hospital and thus daylight is much lower comparing to the summer.

5 CONCLUSIONS

In this paper the possibilities of primary energy savings from artificial lights operating in two hospitals of Europe have identified based on measurements. A fuzzy controller has been developed in Matlab environment and tested on validated RADIANCE models developed for the selected hospitals. The application of the controller in the RADIANCE model indicates that energy saving in the hospital of Chania and the 3 selected rooms of the hospital of Ancona can be achieved. Furthermore, running a full annual emulation combining the use of the controller and developed model in RADIANCE, energy saving based on dimming is estimated to be more than 35% in all selected rooms.

6 ACKNOWLEDGEMENTS

This work is partly funded by the EU Commission, within the research contract GREEN@Hospital (Contract Nr. 297290) a three year European Project co-funded by the ICT Policy Support Programme as part of the Competitiveness and Innovation framework Programme (CIP).

7 REFERENCES

Franzetti, C., Fraisse, G. and Achard, G. 2004. Influence of the coupling between daylight and artificial lighting on thermal loads in office buildings. *Energy and Buildings* 36(2), pp. 117–126.

Frattari, A., Chiognm, M. and Boer, J. 2009. AUTOMATION SYSTEM FOR LIGHTING CONTROL: COMPARISON BETWEEN DATA RECORDED AND SIMULATION MODEL. *International Journal for Housing Science* 33(1), pp. 45–56.

Jang, J.-S. (Computer S.D.T.H.U. 1993. ANFIS: Adaptive-Network-Based Fuzzy Inference System. *IEEE Transactions on Systems, Man, and Cybernetics* 23(3), p. 21.

Kurian, C., Aithal, R., Bhat, J. and George, V. 2008. Robust control and optimisation of energy consumption in daylight--artificial light integrated schemes. *Lighting Research and Technology* 40(1), pp. 7–24.

Kurian, C.P., George, V.I., Bhat, J. and Aithal, R.S. 2006. ANFIS MODEL FOR THE TIME SERIES PREDICTION OF INTERIOR DAYLIGHT ILLUMINANCE. *International Journal on Artificial Intelligence and Machine Learning (AIML)* 6(3), pp. 35–40.

Lam, J.C., Li, D.H.W. and Cheung, S.O. 2003. An analysis of electricity end-use in air-conditioned o ce buildings in Hong Kong. 38, pp. 493–498.

Li, D.H.W., Cheung, G.H.W. and Lau, C.C.S. 2006. A simplified procedure for determining indoor daylight illuminance using daylight coefficient concept. *Building and Environment* 41(5), pp. 578–589.

Nippun Kumaar, a. ., Kiran, G. and Sudarshan, T. 2010. Intelligent Lighting System Using Wireless Sensor Networks. *International Journal of Ad hoc, Sensor & Ubiquitous Computing* 1(4), pp. 17–27.

Papantoniou, S., Kolokotsa, D. and Pouliezos, A. 2012. Neuro-fuzzy model based predictive algorihm for environmental management of buildings. , pp. 1–8.

Raphael, B. 2011. Active Control of Daylighting Features in Buildings. *Computer-Aided Civil and Infrastructure Engineering* 26(5), pp. 393–405.

Relux Informatik AG 2012. Relux Suite.

Santamouris, M., Argiriou, a., Dascalaki, E., Balaras, C. and Gaglia, a. 1994. Energy characteristics and savings potential in office buildings. *Solar Energy* 52(1), pp. 59–66.

Ward, G. and Shakespeare, R. 1998. *Rendering with Radiance The Art and Science of Lighting Visualization*. Morgan Kaufmann.

Wen, Y.-J. and Agogino, a. 2010. Control of wireless-networked lighting in open-plan offices. *Lighting Research and Technology* 43(2), pp. 235–248.

DEVELOPMENT OF AN INNOVATIVE ENERGY MANAGEMENT SYSTEM FOR UNIVERSITY CAMPUSES

Ariadni Vasilomichelaki[1], Kolokotsa Dionysia[*2], Kalaitzakis Kostas[3]

1 Department of Electronics and Computer Engineering, Technical University of Crete, University Campus, Kounoupidiana, GR-73100, Chania, Greece

2 Department of Environmental Engineering, Technical University of Crete, University Campus, Kounoupidiana, GR-73100, Chania, Greece
**Corresponding author: dkolokotsa@enveng.tuc.gr*

3 Department of Electronics and Computer Engineering, Technical University of Crete, University Campus, Kounoupidiana, GR-73100, Chania, Greece

ABSTRACT

Universities' campuses can be viewed as small communities considering their size, users and mixed complex activities. The energy and environmental impact caused by universities due to activities and operations in teaching and research could be considerably reduced by an effective choice of organizational and managerial measures. In addition, there is considerable room for improvement and research potential in energy management, when leaving from the single building aspect and moving towards a "district" approach, where a set of different buildings and outdoor spaces are considered. The aim of this paper is to present an integrated and holistic indoor - outdoor Web-based Energy Management System for Campuses, which is developed, tested and validated through the accurate modeling of two Campus buildings and their outdoor spaces, as well as the corresponding expert systems and control algorithms. Thus, the load demand in real-time can be predicted, giving the capability of providing optimal or nearly-optimal demand balance, while maintaining the users' safety, health and comfort. The overall concept is estimated to contribute at least a 25% reduction of the primary energy consumption, due to reduction of energy waste. The proposed system will create the basis for a future Smart Grid community.
The system will be developed under the Project CAMP_IT, financed by General Secretariat for Research and Technology.

KEYWORDS

Please provide a maximum of five keywords which reflect the content of the paper Energy efficiency, energy consumption, Building Management System, zero- energy buildings, control algorithms, smart grid

1 INTRODUCTION

Considering the size of Universities' campuses it can be said can be viewed as small cities due to their size, users and mixed complex activities. The energy and environmental impact caused by universities via activities and operations in teaching and research, as well as provision of support services could be considerably reduced by an effective choice of organizational and managerial measures (Alshuwaikhat et al, 2008). Since the University campuses natural land is replaced with artificial surfaces and buildings with undesirable thermal effects, the overheating by human energy release and absorption of solar radiation on dark surfaces and buildings is possible. Hence, campuses create an urban-kind climate which cannot be neglected. To design and operate a sustainable campus, it is necessary to factor the

indoor-outdoor environment and information holistically and strategically into the planning and operational process.
Nowadays, the improvement of the outdoor environment has gained a substantial attention. Open urban spaces can contribute to the quality of life within cities, or contrarily, enhance isolation and social exclusion. The major factor that determines the quality of the open urban spaces is the climate conditions that occur in the micro scale environment. The strategies to improve urban environment include the use of smart materials, the increase of vegetation, ventilation, shading and evaporation. On the other hand, ICT for energy management has evolved considerably the last decades. Advances in the design, operation optimization, and control of energy-influencing building elements (e.g., HVAC, solar, fuel cells, CHP, shading, natural ventilation, etc.) unleashed the potential for realization of significant energy savings and efficiencies in the operation of both, new and existing building sites worldwide. Last but not least nowadays it is vital that Europe's electricity networks are able to integrate all low carbon generation technologies as well as to encourage the demand side to play an active part in the supply chain. In this part, ICT technology plays a vital role. Currently the issue of Energy Management for large sites, such University Campuses is addressed by the Energy Information Systems (EIS) which have evolved out of the electric utility industry in order to manage time-series electric consumption data. However, other energy management technologies have also expanded their functionalities, and have partly come to merge with EIS technology. Since EIS products are relatively new technologies, they are changing quickly as the market unfolds (Motegi et al, 2003).

2 OBJECTIVES – EXPECTED RESULTS

Based on the above analysis, there is a considerable room for improvement and research potential in energy management, when leaving from the single building aspect and moving towards a "district" approach where different buildings and outdoor spaces are considered. Towards this "district approach" the use of University Campuses, as a field of application, is considerably advantageous compared to a community or city district as the overall area belongs to a single owner. Therefore the aim of the CAMP-IT is to develop, test and validate an integrated and holistic indoor - outdoor Web based Energy management System for Campuses. This major objective is pursued within CAMP-IT via a number of multifaceted actions and S&T Objectives: (a) Advance the state of the art in modeling of buildings and outdoor spaces by creating a modeling procedure and a holistic methodology. In addition a simplification process will be developed to provide "district models" "as accurate as possible". (b) Advance the state of the art in expert systems and control algorithms for energy load prediction and shaping in small communities by developing an efficient, robust and rapidly-adapting real-time expert system capable of providing optimal – or nearly-optimal – demand balance, while maintaining users' safety and health and, most importantly, complying with end-users comfort-related commands and requests. (c) Advance the state-of-the-art in user-interaction, sensoring and interfacing by either employing wireless technologies or using the existing IP infrastructure and connectivity of Campuses to ensure interoperability, expandability, flexibility and easiness of installation. (d) Integrate the above-mentioned systems and designs in order to come up with a fully-functional system capable of providing efficient, robust, safe and user-acceptable conditions on Campus level. (e) Application and validation of the developed system in TUC Campus during their ordinary operation. The Campus buildings selected (Annex 1) cover a wide range of different building designs and operations, self-generating components, automatically and manually-controlled energy-influencing elements and environmental conditions. (f) Evaluation of the impact of the CAMP-IT system with emphasis on its effect in significantly contributing towards the easy

and cost/energy-efficient deployment and operation of an Advanced Campus Web Based Energy Management, as well as the user-friendliness and user-acceptance of the CAMP-IT concept. In CAMP-IT we have chosen to move rapidly towards commercially viable prototyping and proof-of-concept systems by deploying and testing the system in real time conditions.

Therefore the specific system by exploiting the existing Internet connectivity and infrastructure of the University Campuses, as well as existing knowledge and experience of the involved teams will cover the aforementioned specific objectives for two TUC Campus buildings and the space of public use around them (see Annex 1). The overall concept is depicted in

Figure 1 and is estimated to contribute to at least 25% reduction of the primary energy consumption due to reduction of energy waste. Moreover the CAMP-IT system will create the basis for a future smart grid community.

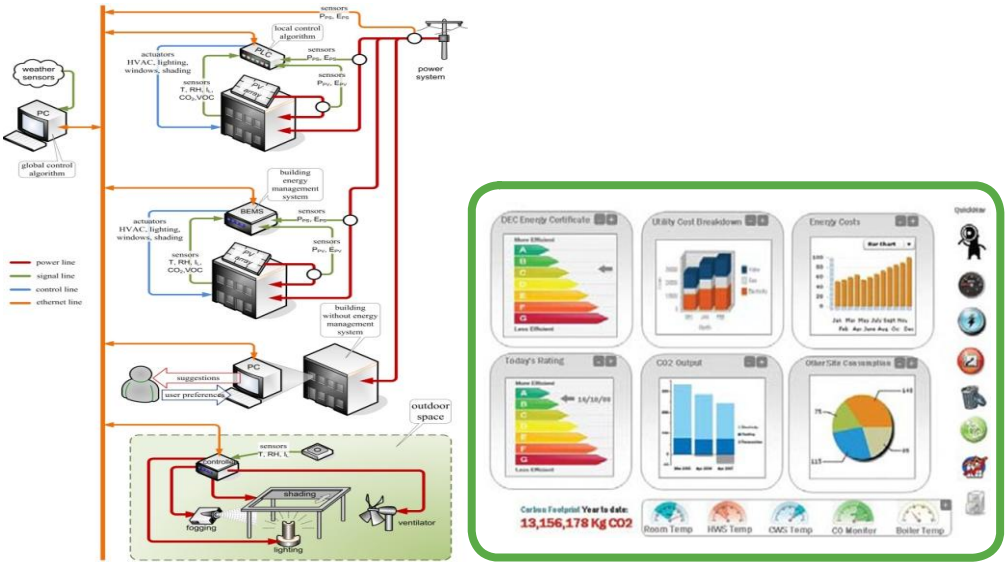

Figure 1. The Concept and a view of the CAMP-IT custom application using industrial automation products and services

Progress beyond the state-of-the-art: The building services management systems and control are now approximately thirty years old. Their increasing use during the last decades has led to the collection of significant experience and the market is approaching maturity. Simulation and application of artificial intelligence control techniques (such as fuzzy logic and artificial neural networks), has indicated that they have the potential to make significant energy savings in buildings, especially when the renewable energy sources are controlled in an integrated fashion with the rest of the building system. The development and demonstration of CAMP-IT system involves groundbreaking innovations and progress beyond the state-of-the-art in various fields. This includes the indoor-outdoor modeling and integration, real-time expert system and system connectivity. In the following paragraphs the key S&T questions of the proposal are shortly addressed and the state-of-the-art is discussed.

Apart from progress in the different fields presented below, the system integration plays a key role for reaching and validating the set goals.

Indoor – outdoor modeling and interaction: In the last two decades, a considerable amount of research studies show that the air movement in and around buildings may be predicted using Computational Fluid Dynamics (CFD) models (for example, in the year 2007 the 70% of publications dealing with airflow in buildings include CFD models) (Chen et al, 2009;

Chen et al, 2010). The implementation of comfort and environmental indices into a CFD model leads to local information about the living conditions in buildings. Currently, numerous

studies dealing with the evaluation of indoor thermal comfort and environmental conditions using CFD models exist (Zhou & Haghighat, 2009a&b; Stavrakakis et al., 2011). It should be mentioned, however, that researches which utilize appropriately modified thermal and environmental indices (e.g. for non air-conditioned spaces) are few and they focus mainly on outdoor or semi-outdoor spaces (Bouyer et al., 2007). On the other hand, various researches focus in the improvement of outdoor comfort conditions by applying several techniques based on bioclimatic architecture criteria and on passive cooling and energy conservation principles (Gaitani et al, 2007). It is noticeable that until now, there exists no integrated and holistic approach for buildings' operation optimization by taking advantage of the indoor-outdoor full-scale simulations. The proposed system targets to fulfill requirements beyond the state-of-the-art and to expand the existing knowledge in the built environment' modeling by: (a) creating a modeling methodology for the functioning of the building throughout its all life cycle (design, operation, etc.); (b) using a single methodology and tools to model the overall process. Finally a Meta program developed by Lawrence Berkley National Laboratory, where EnergyPlus (CFD is integrated), Radiance, Modelica and Matlab are interconnected, will be used for the CAMP-IT; (c) providing a simplification methodology for modeling Campus areas.

Development of a decision support tool and optimization method for web based energy management system: The main challenge in the design of control systems for energy performance of buildings is to find the balance between implementation costs, operation costs, energy consumption, indoor climate quality, users' satisfaction and contribution to sustainable building. Intelligently designed buildings are those that involve environmentally responsive design, taking into account the surroundings and building usage and involving the selection of appropriate building services and control systems to further enhance building operation with a view to the reduction of energy consumption and environmental impact over its lifetime. This procedure requires advanced control techniques to establish a balance among user comfort requirements, energy consumption, passive solar design concepts, solar heating and cooling technologies, as well as photovoltaics. A significant attention is drawn by the model based predictive systems as the intelligent combination of all available energy-generation, together with automatically- and manually-controlled building elements, cannot be achieved if simple heuristic or data-driven strategies are employed. Therefore decision support systems that compute their control and optimization decisions based on efficient and accurate built environment models are required in order to obtain efficient and nearly-optimal operation on a community level. Based on the analysis presented in the previous subsection, a prerequisite for the deployment of an efficient web based energy management system for Campuses is the development of an expert system which: (a) Manages in an energy efficient way the Campus buildings and spaces of public use. (b) Monitors the energy load and perform load balancing and load shaping per building and per Campus and as a whole. (c) Interacts with each building's BEMS and each user through e-mails and web forms. (d) Optimizes of the overall strategy based on historical data. (e) Focuses on the Campus as a district and creates a holistic methodology for buildings and outdoor spaces of public use.

Integration into campus existing infrastructure- Interconnection of buildings and outdoor spaces: Sensors, actuators and interfaces are essential components for the successful implementation and real-time operation of a web based energy management system. The evolution of the specific components was quite rapid during the last decades leading to the intelligent buildings' concept derived from artificial intelligence and information technology. While ICT infrastructure networks are seen as an important part in emerging building and community energy management systems through i.e. Metropolitan Area Networks, the

integration of sensor networks with future energy management systems is still an open problem. The aim of the present project is to advance the existing knowledge in ICT for energy management infrastructure by establishing an IP-based sensor network system, where nodes communicate their information using Web services, allowing direct integration in modern IT systems. To guarantee the system scalability and respect consolidated and diffused standards, the logical/architectural level of the whole Campus Energy Management System will be linked to an infrastructure based on Internet Protocol (IP). The IP choice will lead to wired networks realization in combination with Wi-Fi networks. Another advantage of the Ethernet protocol must be searched in the possibility to realize networks even in already existing buildings. The system will be exposed towards the external part of the network by means of Web Services, enabling the XML information exchange through communications on Internet channels (according to the SOAP standard). The same architectural approach will be guaranteed both, in the transport with the IP standard and in the application with the data flows exchange in XML. The Campus Energy Management System and Hub will be designed to integrate different communication protocols for recovering the field data. The model logics will follow a plug-in approach for the insertion of modules dedicated to the analysis of specific sub-systems.

3 TECHNICAL DESCRIPTION, S&T METHODOLOGY, OVERALL STRATEGYAND ASSOCIATED WORK PLAN

Campus sustainability has become an issue of global concern as a result of the realization of the impacts which the activities and operations of universities have on the environment. On July 2000, the U.S. Environmental Protection Agency (EPA) issued an Enforcement Alert which explained that the agency was now holding colleges and universities to the "same standards as industry" in order to "create a safe haven for human health and the environment" (Savely et al, 2007). The energy management on Campus level is not a straightforward issue. It includes the management of multi buildings with different operational characteristics and schedules such as labs, auditoriums, classrooms, small shops, coffee areas, together with the outdoor environment (outdoor lighting, shading, etc.). The general framework of analysis, CAMP-IT will develop a web based energy management for measuring and mitigating the possible dimensions of energy and environmental impact that the University Campuses can generate. The overall methodology is based on 5 phases:

Phase 1: Development of the necessary models for indoor-outdoor environment interaction and load prediction - The objective is to create and deliver indoor-outdoor interactions models to assist the development of the expert system as well as the overall Campus Energy Management system validation

Phase 2: Development of the expert system and control algorithms for campus energy management-The objective is to develop the suitable control strategy to be incorporated in the Web based Campus Management System. The control strategy will monitor and control the building systems and outdoor environment. In addition, the system will analyze the performance during operation and will therefore be able to detect buildings or parts of buildings with performance problems

Phase 3: Development and Specifications for the necessary infrastructure and communication technologies for Campus networking- The objective is to prepare the installation procedure and the integration of the Web based Campus Energy Management into the TUC Campus

Phase 4: Installation of the necessary components at the Campus case study and demonstration-Objective is to test the developed Web based campus energy management system by implementing it to the TUC Campus

Phase 5: Validation of the methodology- The objective is the evaluation of the CAMP-IT system and its impact on the energy performance terms of technical, operational, and economic aspects. The evaluation will be based on: (a) quantitative performance indices, like primary energy savings and demand reductions from external sources, and (b) qualitative features, like user's response to the systems, as well as indoor and outdoor comfort and satisfaction

4 CONCLUSION

The ICT for energy efficiency has been identified as a key major player in the fight against climate change being the fastest, cheapest and cleanest way to address energy resources issues. Today there are two major challenges in ICT for the built environment as far as enabling the vision of intelligent community. First is how the different elements can cooperate together in an integrated manner, and second, how the buildings can be connected in real-time to a web based ICT enterprise or Community systems. In the CAMP-IT project a web based ICT energy management in district–campus level will be developed to support the interconnection of multi buildings and spaces of public use. CAMP-IT is not just about the installation of another advanced energy management system in buildings, it is about utilizing harmoniously, and most effectively all buildings in a district level, taking into account buildings' interaction and outdoor spaces in a holistic approach and adapting the decisions in real-time based on a predictive and integrative manner. Furthermore CAMP-IT is not just about improved energy-efficiency in a fragmented way. The holistic but realistic view taken by the proposed system along with the potential of harmoniously regulating multiple buildings with outdoor spaces makes it an ICT-based "enabler of energy efficiency and comfort" and along with a reasonable installation of renewable sources will help realize significant energy savings and carbon emissions reduction reaching or even surpassing a target of 25% reduction. Another critical issue is the support of smart grids' effective deployment which is vital for Europe's electricity networks liberalization. Those networks should be able to integrate all low carbon generation technologies as well as to encourage the demand side to play an active part in the supply chain in a district and community level. Therefore a number of further R&D activities need to be initiated now, in order to deliver applications and solutions for the long term perspective of 2050 and beyond. To move towards an increasing low-carbon economy, European electricity networks will need to evolve to provide support for possible future energy vectors, for effective introduction of carbon credits, taxes and trading, for generating buildings integrated with energy distribution and finally for massive combination of renewable generation in the built environment. The CAMP-IT project contributes towards this perspective by providing the necessary knowledge and state of the art uptake to move towards smart grids integration in a large scale by starting the demand-supply integration in communities with only one owner as University Campuses where the various decisions are easier to be undertaken. Overall through integrated approaches, understanding and tools, the CAMP-IT project will reinforce the European

industrial and technological position in ICT-enabled technologies for multi buildings and outdoor spaces and, more importantly, lead to reduced energy intensity of the economy.

5 ACKNOWLEDGEMENTS

The research project is implemented within the framework of the Action «Supporting Postdoctoral Researchers» of the Operational Program "Education and Lifelong Learning" (Action's Beneficiary: General Secretariat for Research and Technology), and is co-financed by the European Social Fund (ESF) and the Greek State.

6 REFERENCES

Alshuwaikhat, H. M., & Abubakar, I. (2008). An integrated approach to achieving campus sustainability: Assessment of the current campus environmental management practices. *Journal of Cleaner Production, 16*(16), 1777-1785.

Bouyer, J., Vinet, J., Delpech, P., & Carré, S. (2007). Thermal comfort assessment in semi-outdoor environments: Application to comfort study in stadia. *Journal of Wind Engineering and Industrial Aerodynamics, 95*(9-11), 963-976. Retrieved from www.scopus.com

Bushby, S. T. (1997). BACnet™: A standard communication infrastructure for intelligent buildings. Automation in Construction, 6(5-6), 529-540.

Camacho, E.F., Rubio, F.R., Berenguel, M. & Valenzuela, L. 2007, "A survey on control schemes for distributed solar collector fields. Part I: Modeling and basic control approaches", Solar Energy, vol. 81, no. 10, pp. 1240-1251.

CEN 15217:2007a, Energy performance of buildings - Methods for expressing energy performance and for energy certification of buildings, Centre Europeen de Normalisation.

CEN 15251:2007a, Indoor environmental input parameters for design and assessment of energy performance of buildings- addressing indoor air quality, thermal environment, lighting and acoustics, Centre Europeen de Normalisation.

Chen, Q. (2009). Ventilation performance prediction for buildings: A method overview and recent applications. *Building and Environment, 44*(4), 848-858.

Chen, Q., Lee, K., Mazumdar, S., Poussou, S., Wang, L., Wang, M., et al. (2010). Ventilation performance prediction for buildings: Model assessment. *Building and Environment, 45*(2), 295-303.

Gaitani, N., Mihalakakou, G., & Santamouris, M. (2007). On the use of bioclimatic architecture principles in order to improve thermal comfort conditions in outdoor spaces. *Building and Environment, 42*(1), 317-324.

Gobakis, K., Kolokotsa, D., Synnefa A., Santamouris, M. (2010) Development of a model for urban heat island prediction using neural network techniques, The SET 2010 (9th International Conference on Sustainable Energy Technologies) Shanghai 24 to 27 August 2010.

Kalaitzakis, K., Stavrakakis, G. S., & Anagnostakis, E. M. (2002). Short-term load forecasting based on artificial neural networks parallel implementation. *Electric Power Systems Research, 63*(3), 185-196.

Motegi, N. Piette, M.A. Kinney, S., Herter, K. 2003, Web-based energy information systems for energy management and demand response in commercial buildings, Lawrence Berkeley National Laboratory. http://escholarship.org/uc/item/5z796433

Savely SM, Carson AI, Delclos GL. 2007.An environmental management system implementation model for U.S. colleges and universities. Journal of Cleaner Production;15:660.

Stavrakakis, G. M., Zervas, P. L., Sarimveis, H., & Markatos, N. C. (2010). Development of a computational tool to quantify architectural-design effects on thermal comfort in naturally ventilated rural houses. *Building and Environment, 45*(1), 65-80.

Zhou, L., & Haghighat, F. (2009a). Optimization of ventilation systems in office environment, part II: Results and discussions. *Building and Environment, 44*(4), 657-665.

Zhou, L., & Haghighat, F. (2009b). Optimization of ventilation system design and operation in office environment, part I: Methodology. *Building and Environment, 44*(4), 651-656.

Annex 1: Description of the buildings

Technical University of Crete

Building K1 AND K2 – Environmental engineering department buildings

Buildings data

- Location (ZIP code, climate zone)
    - Technical University of Crete Campus, Chania, Crete, 73100
    - Climate of South Europe – mild Winter, hot Summer
- Year of construction
    - 2002
- Three main types of building utilization, f.i. office, laboratory, lecture hall, storage
    - Office, Laboratory, computer room
- Reference area, f.i. net floor area and conditioned net floor area, fraction of different building utilizations
    - Floor area: 2450 m^2
- Number of storeys, rough sketch of building shape and floor plan
    - Two storeys, Figures show the view and the layout of the building
- Building envelope (i.e. type of façade, fraction of total window area, …)
    - The construction is a combination of concrete and metal. Specifically, the ground floor is made of concrete while the second floor has metal framework and cement plates as external walls. The building is insulated and double glazed.
- Technical installations (i.e. type of ventilation, air conditioning, fraction of conditioned net floor area, …)
    - The building serviced by FCU systems with thermostats available in each room.
- Building energy management systems (BEMS)
    - 2 different BEMS are used in the building The first is used for controlling cooling and heating while the second for lights, fire systems and elevators
- Current state of repair and year of latest major renovation of building envelope and main technical installations respectively
    - Building is fairly maintained but has not been upgraded considerably in terms of energy performance during the recent years

Energy Data

- Estimated consumption of electricity for 2009
    - Electricity 136 kWh/m^2
- Utilizations of electricity included in the measured values (i.e. lighting, ventilation, air conditioning, cooking, IT, elevators …)
    - Not available
- Measured consumption of fuels for 2009
    - The building is heated using electricity for the FCU systems.
- Utilizations of thermal energy included in the measured values (i.e. heating, hot water, absorption chillers …)
    - Heating
- Energy generation in the building (cogeneration, solar thermal, PV, …), measured production of the last 3 years

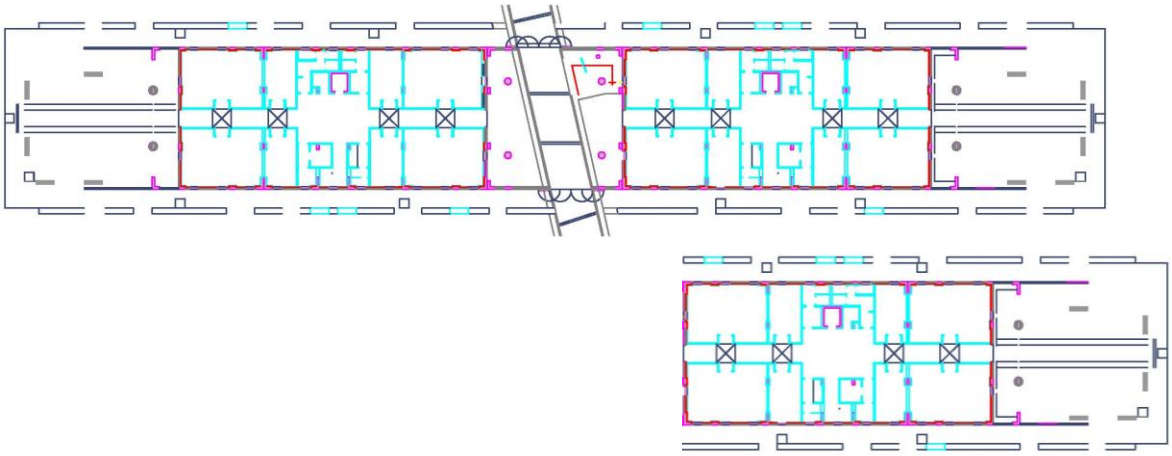

Figure 1: Floor plans of environmental engineering department buildings

Figure 2: Back view of environmental engineering department main building

Figure 3: Internal views of the buildings

Figure 4: Outdoor space of environmental engineering building

GUIDELINES FOR HEALTH-BASED VENTILATION IN EUROPE

Pawel Wargocki[*1], Paolo Carrer[2], Eduardo de Oliveira Fernandes[3], Otto Hänninen[4], Stylianos Kephalopoulos[5], and HEALTHVENT[6] Group

1 Department of Civil Engineering
Technical University of Denmark
**Corresponding author: paw@byg.dtu.dk*

2 Milan University
Italy

3 Faculty of Engineering
Porto University
Portugal

4 National Institute for Health and Welfare
Finland

5 European Commission, Joint Research Centre
Institute for Health and Consumer Protection
Italy

6 See Acknowledgments

ABSTRACT

Guidelines for health-based ventilation in Europe are proposed. They take the premise in control of exposures to air pollutants indoors having both indoor and outdoor origin. Exposures are controlled through a double sequential approach, in which source control is the primary strategy while ventilation is the secondary strategy only after all options for source control have been fully implemented. The World Health Organization (WHO) air quality (AQ) guidelines are used to set the exposure limits. A decision diagram is created to guide through the process of source control and to aid the choice of the ventilation rate for a specific building. Ventilation rate is called health-based, when the WHO AQ guidelines have been met both regarding the pollutants in the air used for ventilation and in the indoor air. If the WHO AQ guidelines are met through source control, then the health-based ventilation rate is equal to the base ventilation rate. This is the rate required to handle primarily human bioeffluents. Based on the literature review of epidemiological studies and other considerations, the base ventilation rate has been set at 4 L/s per person. The health-based ventilation rate cannot in any case be lower than the base ventilation rate. If WHO AQ guidelines cannot be met through source control, then the health-based ventilation rate is a multiple of the base rate, high enough to satisfy the WHO AQ guidelines for a specific building. Health-based ventilation guidelines do not define or promote a specific system to provide ventilation. They only advise on design, operation and maintenance of such systems so that the air supplied can always comply with the WHO AQ guidelines. They advise additionally on the separation of health-based ventilation rate for air quality control from the air used to achieve thermal requirements (heating/cooling), and on the use of volume flow per person as the main metric for ventilation. Implementation of the health-based ventilation guidelines is estimated to halve the loss of healthy life years in Europe from indoor exposure to poor air quality from 2 to 1.1 million without significant impact on energy. Harmonized regulation of product labelling and ventilation is needed to implement and get benefit from the guidelines for health-based ventilation. Additionally indoor air quality requirements must be integrated across different legislative acts including the Ambient Air Directive and the Energy Performance Building Directive. These actions will result in advancement in knowledge and technological innovation, and will secure the basic human rights to breathe clean air.

KEYWORDS

Ventilation; Health; Public buildings; Residential buildings; Ventilation system; Guidelines

1 INTRODUCTION

Indoor air has been recognized as a significant determinant of population health. The burden of disease associated with major air exposures indoors in 26 European countries was recently accounted for loss of two million healthy life years annually expressed as disability adjusted life years (DALYs) (de Oliveira-Fernandes et al. 2009; Jantunen et al., 2011). More than half of this is attributable to indoor exposure to pollutants originating from the outdoor air, the rest to pollutants having indoor sources. The development of health-based ventilation guidelines has been recommended as one of the strategic priorities to reduce the burden of disease associated with exposure to air pollution (de Oliveira-Fernandes et al., 2009).

Current ventilation standards in Europe do not adequately address the health-relevant aspects of indoor air quality. They provide different categories of comfort as the main decision criteria for designing ventilation requirements (EN15251, 2007; EN 13779, 2007).

The HealthVent project was funded by the European Commission's Directorate General (DG) for Health and Consumers (2010-2012) and developed a guidelines framework for health-based ventilation in public and residential buildings in Europe. The consequences for health and energy of implementing these guidelines are discussed bearing in mind future trends in the indoor built environments as well as environmental sustainability issues.

2 GUIDELINES FOR HEALTH-BASED VENTILATION

The guidelines developed by the HealthVent project acknowledge that proper indoor exposure control requires regulations to be developed and implemented in a co-ordinated framework where priority is given to source control measures and in second place to ventilation. They must be consequently based on two fundamental prerequisites: (1) The air indoors must fulfil the requirements of the air quality (AQ) guidelines defined by the World Health Organization (WHO, 1987; 2000; 2005; 2009; 2010); and (2) The priority in terms of strategy for controlling indoor air quality and reducing the health risks associated with indoor exposures is given to source control. Ventilation is only used as a supplementary strategy to control exposure in support to the source control strategy when the source control latter is not sufficient to guarantee the fulfilment of the WHO AQ guidelines inside buildings.

Health-based ventilation rate is defined for a specific building so that exposures to pollutants meet the WHO air quality guideline values through a double sequential approach integrating at first place source control measures and then the appropriate ventilation rate.

A decision diagram was developed for determining the actual health-based ventilation rate for a specific building. This diagram provides possibilities to explore and implement source control strategies at both outdoor air and building level before the final required health-based ventilation rate is determined.

The health-based ventilation rate cannot be lower than the base ventilation rate (Seifert et al., 1993). The base ventilation rate has been set at 4 L/s per person taking into account the results of review of epidemiological literature on ventilation and health and modelling of exposure to human bioeffluents using carbon dioxide (CO_2).

The base ventilation rate is intended to dilute and exhaust occupant bioeffluents. It is a basic requirement that should always be satisfied. The base ventilation rate has been defined to create a true benchmark and reference point for defining ventilation rates based on health

criteria admitting that rates lower than the base ventilation rate are not allowed. The base ventilation rate will be sufficient unless there are indoor sources other than the occupants' bioeffluents. If the WHO AQ guidelines are not met after all options of source control indoors have been exploited, then the actual health-based ventilation rate is higher than the health-related base ventilation rate and calculated by selecting a multiplying factor (>1) of the base ventilation rate.

Health-based ventilation rate only deals ultimately with indoor air quality, is based on health requirements and should not be confused and must be treated separately from the air required for achieving thermal comfort (for cooling and/or heating).

The proposed guidelines neither specify nor promote which system for air delivery should be used. Cultural and climatic aspects should be considered in this decision process. The guidelines do require however that the air delivery does not increase the risk for health indoors by creating exposures to pollutants that exceed the WHO AQ guidelines values due to inadequate design, operation and maintenance procedures during the entire life-time of a building. The set of recommendations addressing these aspects of air delivery and minimizing the health risks are defined as a part of the guidelines.

3 IMPLICATIONS FOR HEALTH AND ENERGY

Potential health implications of implementing the health-based ventilation guidelines were estimated by assessing the expected health gains (i.e. reduction of the burden of disease) based on current levels of exposure to air pollution indoors in Europe. Three alternative methods for controlling exposures were simulated including (a) adjustment of ventilation rates, (b) efficient filtration of outdoor air and (c) source control of pollutants originating outdoors and indoors combined with the defined base ventilation rate to match the proposed criteria of the health-based ventilation guidelines. In the latter case, maximum reduction in the burden of disease was achieved up to 55%, which corresponds to almost a million DALYs per year.

Potential energy implications of implementing the health-based ventilation guidelines were examined by simulating energy needs for heating and cooling in relation to the ventilation needs. A comprehensive set of scenarios was examined with different input parameters representing different performance of the ventilation systems and climatic conditions. Energy simulations showed that health benefits could be achieved if the health-based ventilation guidelines would be integrated with energy efficient designs.

4 IMPLEMENTATION AND GAPS IN KNOWLEDGE

Proper implementation of the health-based ventilation rate requires a holistic approach for the built environment ensuring that both indoor and ambient air quality is adequately addressed in all relevant documents and EU regulations such as the Ambient Air Directive and the Energy Performance Building Directive. This was proposed by the former DG RTD funded EnVIE project (de Oliveira-Fernandes et al., 2009), which additionally indicated the need for the Green Paper on indoor air quality.

Implementation of the guidelines supports the potential development of the following policies and regulations: (a) common regulation on ventilation in Europe; (b) harmonized product labelling criteria; (c) building regulations requiring products with certified emissions already at the design stage; (d) regulations for indoor air quality maintenance, auditing and operation

procedures; (e) criteria for energy requirements decoupling ventilation from indoor air quality control and ventilation from thermal comfort; and (f) European regulation providing guidance on proper scope, design, construction, maintenance and inspections of ventilation systems.

Gaps in knowledge were defined and further research needs concerning the relationship between ventilation and health were identified especially focusing on a proper characterization of exposures and ventilation, chronic health effects and subpopulations with special needs (i.e. vulnerable groups).

5 CONCLUSIONS

Implementation of the health-based ventilation guidelines will promote advancement of knowledge, technological innovation and will secure competitiveness of the European market. At the same time, the basic rights stated by WHO (2000b) to grow up, live, work and learn in healthy indoor environments will be also secured.

6 ACKNOWLEDGEMENTS

The present work was supported by a grant from the Second Programme of Community Action in the Field of Health 2008-2013, European Commission - Directorate General (DG) for Health and Consumers, Executive Agency for Health and Consumers, through the contract no 2009 12 18 for conducting the project on "Health-Based Ventilation Guidelines for Europe (HealthVent)" in the period from June 1, 2011 to March 31, 2013.

The project was performed by the consortium composed of eleven partners, as follows: Technical University of Denmark; Jena University Hospital, Germany; University of Milan, Italy; National and Kapodistrian University of Athens, Greece; University of Porto, Faculty of Engineering, Portugal; National Institute for Health and Welfare, Finland; University of La Rochelle, France; SINTEF Energy Research, Norway (until May 2012); REHVA, Federation of European Heating & Air-conditioning Associations REHVA, Belgium; Association Asthma, Bulgaria; and EFA, European Federation of Asthma and Allergy Associations, Belgium. Recognitions are due to the project's collaborative partners WHO, European Centre for Environment and Health in Bonn, Germany; and European Commission, DG Joint Research Centre, Institute for Health and Consumer Protection in Ispra, Italy.

7 REFERENCES

EN Standard 15251 (2007) *Indoor environmental input parameters for design and assessment of energy performance of buildings addressing indoor air quality, thermal environment, lighting and acoustics*. CEN.

EN Standard 13779 (2007) *Ventilation for non-residential buildings - Performance requirements for ventilation and room-conditioning systems*. CEN.

Jantunen M., de Oliveira Fernandes E., Carrer P., Kephalopoulos S. (2011) *Promoting actions for healthy indoor air (IAIAQ)*. European Commission Directorate General for Health and Consumers. Luxembourg. ISBN 978-92-79-20419-7.

De Oliveira Fernandes E., Jantunen M., Carrer P., Seppänen O., Harrison P., Kephalopoulos S., (2009). *Co-ordination Action on Indoor Air Quality and Health Effects (ENVIE).* Final

report, 165 pp.

Seifert B., Levin H., Lindvall T., Moschandreas D., (1993). A critical review of criteria and procedures for developing indoor air quality guidelines and standards. Proceedings of Indoor Air, Vol. 3, pp. 465-470.

WHO (1987). *Air quality guidelines for Europe.* Copenhagen, WHO Regional Office for Europe, 1987 (WHO Regional Publications, European Series, No. 23).

WHO (2000). *Air quality guidelines for Europe, 2nd ed.* Copenhagen, WHO Regional Office for Europe, 2000 (WHO Regional Publications, European Series, No. 91).

WHO (2000b). *The right to healthy indoor air.* Report on a WHO meeting, Bilthoven, Netherlands, 15–17 May 2000. Copenhagen, WHO Regional Office for Europe, 2000.

WHO (2005). *Air quality guidelines. Global update 2005. Particulate matter, ozone, nitrogen dioxide and sulfur dioxide.* Copenhagen, WHO Regional Office for Europe.

WHO (2009). *WHO guidelines for indoor air quality: dampness and mould.* Copenhagen, WHO Regional Office for Europe.

WHO (2010). *WHO Guidelines for Indoor Air Quality: Selected pollutants.* Copenhagen, WHO Regional Office for Europe.

FILTER PRESSURE DROP CONTROL IN BALANCED VENTILATION SYSTEMS FOR DWELLINGS

Alain Ginestet[*1], Dominique Pugnet[1], and Laure Mouradian[1]

1 CETIAT
Centre Technique des Industries Aérauliques et Thermiques
Domaine scientifique de la Doua, 25 avenue des Arts
69100 Villeurbanne, FRANCE
**Corresponding author: alain.ginestet@cetiat.fr*

ABSTRACT

As a consequence of the energy and environmental issues, it is necessary to reduce the energy consumption of buildings. So, the air tightness of building envelopes is being improved and the air change rate due to infiltration is decreasing. It is then even more important than in the past that the buildings are equipped with well designed and working ventilation systems in order that the air renewal within buildings is ensured. In this context, the market of balanced ventilation systems with heat recovery for dwellings is growing.
In order to maintain the air flows of the balanced ventilation systems and to control their electricity consumption (one fan on each air circuit), it is necessary to define a maximum pressure drop value for the filters above which they should be replaced.
The objective of our study was to determine the pressure drop increase of commercially available filters in balanced ventilation systems for dwellings as they are continuously used for long-term (1 year) with real outdoor air. The efficiency by particle size as well as the mass of dust collected were also reported.
A very popular filter for balanced ventilation systems for dwellings is the panel mini-pleated filter type and this is why it has been considered in our study. It has been decided to study G4, F5 and F7 panel mini-pleated filters. Some of the studied F7 filters have been tested with and without a prefilter (class G4) installed upstream.
Choosing a filter for balanced ventilation systems if not only a question of class. It has been shown that from the energy consumption point of view, it is better to use a F7 filter protected by a prefilter installed upstream instead of the same F7 filter alone because the increase of pressure drop is lower. A G4 prefilter appears suitable for the protection of the panel mini-pleated F7 filters but a more efficient prefilter can be necessary if the efficiency of the fine filter is high. Regarding the popular panel mini-pleated technique, the pleat width is an important parameter that has to be high enough to prevent fast surface loading of the filter. So a pleat width smaller than about 5 mm should be avoided.
Energy savings issues should not reduce indoor air quality. The efficiency of the filters has to be high enough to insure that the balanced ventilation systems will provide clean air to the building and its occupants (well being and health issues).
Finally, the results of our study are of a great interest for the design of filters for balanced ventilation systems in the context of low energy buildings.

KEYWORDS

Ventilation, Balanced ventilation, Air filtration, Filter pressure drop, Indoor air quality

1 INTRODUCTION

The European Commission (European Commission, 2013) claims that buildings consumed 41 % of the final energy in Europe in 2010. Moreover, the average energy consumption of the building sector (220 kWh/m^2 in 2009) has increased by around 1 % per year since 1990, with residential buildings (around 200 kWh/m^2 on average) representing a 0.6 % per year increase compared to 1.5 % per year for non-residential buildings (around 200 kWh/m^2 on average).

As a consequence of the energy and environmental issues, it is necessary to reduce the energy consumption of buildings. So, the air tightness of building envelopes is being improved and the air change rate due to infiltration is decreasing. It is then even more important than in the past that the buildings are equipped with well designed and working ventilation systems in order that the air renewal within buildings is ensured.
In this context, the stock of balanced ventilation systems with heat recovery in existing dwellings is still small (only 1.5 % of European residential one or two family houses and only 7 % of non-residential and collective residential buildings are equipped (European Commission, 2012)) but the market is growing. EVIA (the European Ventilation Industry Association) estimates that the 2012 market of balanced ventilation systems for residential buildings in Europe exceeded the 400 000 units, with an annual increase of 25 % from 2010 (EVIA, 2012).
Balanced ventilation systems with heat recovery include air filters used to protect the heat exchanger (both on the fresh air and exhaust air sides) and to enhance the quality of supplied air. The assessment of thermal, acoustic and airflow performances of balanced ventilation systems for dwellings relies on the European standard EN 13141-7 (2011). National labels provide additional requirements. For example, the French "NF" mark requires that the system provides the air flow required by the French regulation (French regulation, 1982) when used with a typical ductwork. This mark also requires that the filter classes according to EN 779 (2002) are at least F5 (since the revision of EN 779 in 2012, F5 class has been replaced by M5 class, all the performances being equal) on the outdoor air side and G4 on the exhaust air side. All the tests for certification are operated on new systems. One of the issues is the guarantee of those performances during their real use. In spite of the recent development of the balanced ventilation systems market, almost no information is available on the filters characteristics and performance changes along time when used in real life.
In order to maintain the air flows of the balanced ventilation systems and to control their electricity consumption (one fan on each air circuit), it is necessary to define a maximum pressure drop value for the filters above which they should be replaced. So, the initial pressure drop of the filters as well as the increase of their pressure drop as function of time have to be as low as possible.
The objective of our study was to determine the pressure drop increase of commercially available filters in balanced ventilation systems for dwellings as they are continuously used for long-term (1 year) with real outdoor air. The efficiency by particle size as well as the mass of dust collected were also reported.

2 AIR FILTERS FOR BALANCED VENTILATION SYSTEMS

A balanced ventilation system for dwellings is typically composed of one ductwork for supply of air from outside and one other ductwork for indoor air exhaust. In balanced ventilation systems with heat recovery, heat transfer between exhaust and outdoor air is made possible thanks to an air-to-air heat exchanger inserted in a ventilation box together with 2 fans. The ventilation box is placed at the crossing of the 2 ductworks. Heat transfer allows to heat supplied air during the cold season and to cool it during the warm season. The heat exchanger is protected upstream by 2 sets of filters, one on the outdoor air side and the other on the exhaust air side. There is a wide variety of filters on the market including different sizes, shapes, filter medium, medium configuration and class efficiency. A very popular filter for balanced ventilation systems for dwellings is the panel mini-pleated filter type and this is why it has been considered in our study.

3 EXPERIMENTAL METHOD

Two different balanced ventilation boxes with heat recovery were installed at CETIAT (Villeurbanne, France) for continuous long term running at more or less constant air flow rate (120 m³/h) in order to allow long time (1 year between May 2010-May 2011 or May 2011-May 2012 or May 2012-May 2013) filter testing with natural dust loading. The 2 circuits of each ventilation box that are normally used for respectively outdoor and exhaust air flows were connected to a same outdoor air inlet. Because of the symmetry of the systems with respect to outdoor vs. exhaust air circuits, this allows to test 4 different filtration configurations in parallel with the same outdoor air (typical of that of a large European city) without changing the way in which the filters are normally installed.

It has been decided to study G4 (equivalent to MERV7 or MERV8 class according to ANSI/ASHRAE Standard 52.2 (2012)), F5 (equivalent to MERV9 to MERV11 class) and F7 (equivalent to MERV13 class) panel mini-pleated filters. Some of the studied F7 filters have been tested with and without a prefilter (class G4) installed upstream. F7 filter class is widely used in balanced ventilation systems for dwellings and the prefilter is intended to prevent fast filter pressure drop increase due to the loading of the F7 filters by particles. In that case, for each ventilation box, the F7 filter is used alone in one circuit and protected by a G4 filter in the other circuit.

The main characteristics of the studied filters are reported in Table 1. Filtering medium of filters B and C is made of glass fibres while that of filter D, E and F is made of electrostatically charged synthetic fibres (electret). Filters E and F have approximately the same filtration area, are manufactured with the same filtering medium but have different pleat width and also different thickness.

F7 filters C and D have been studied with and without a G4 filter installed upstream (bag filter installed upstream of filter C and plan filter installed upstream of filter D).

The 2 balanced ventilation systems were regularly stopped (every 6 to 8 weeks) in order to remove the filters for performance measurements (pressure drop, mass of retained dust and efficiency by particle size). The amount of dust retained by the filters was determined by direct weighing of the filters. A test rig used for EN 779 filter testing was used for pressure drop and fractional efficiency (by particle size with DEHS aerosol in the particle size range 0.2 to 5 µm) measurements.

Table 1 : Main filter characteristics

Filter	**A**	**B**	**C**	**D**	**E**	**F**
Filtering medium	Unknown	Glass fibre	Glass fibre	Electret synthetic fibre	Electret synthetic fibre	Electret synthetic fibre
Class (EN 779)	G4	F5*	F7**	F7**	F7**	F7**
Filtration area (m²)	0.42	0.88	1.00	0.66	0.49	0.50
Thickness (mm)	10	42	44	18	20	48
Number of pleats	139	54	59	97	65	26
Pleat width (mm)	2.8	4.8	4.4	4.0	6.1	10.4
Initial pressure drop at 120 m³/h (Pa)	15	9	20	70	24	20

** Since the revision of EN 779 in 2012, F5 class has been replaced by M5 class, all the performances being equal*

*** Since the revision of EN 779 in 2012, F7 class takes into account not only the average efficiency but also the minimum efficiency at 0.4 µm*

4 RESULTS

The results of the measurements of the filter performances are shown in Figures 1 to 6.
The filtration efficiency (left ordinate axis) is plotted for 2 different particle sizes (0.4 µm for the 0.3-0.5 µm optical particle counter channel and 2.5 µm for the 2-3 µm optical particle counter channel) representative of the whole particle size range studied (0.2 to 5 µm) for a fine (0.4 µm) and a coarse (2.5 µm) fraction consideration.
The filter pressure drop increase (current pressure drop minus initial pressure drop) is shown on the right ordinate axis. Filtration efficiency and pressure drop increase are expressed as function of time (abscissa axis) over a 1 year period of time. It has to be noted that filter B (Figure 2) was not fed with air for about 2 weeks at the end of 2012 because of electrical failure of the motor of the fan.
Tests have been stopped after 9 months for filter D (Figure 4) because the pressure drop increase was too big (approximately 1000 Pa) for this kind of application.

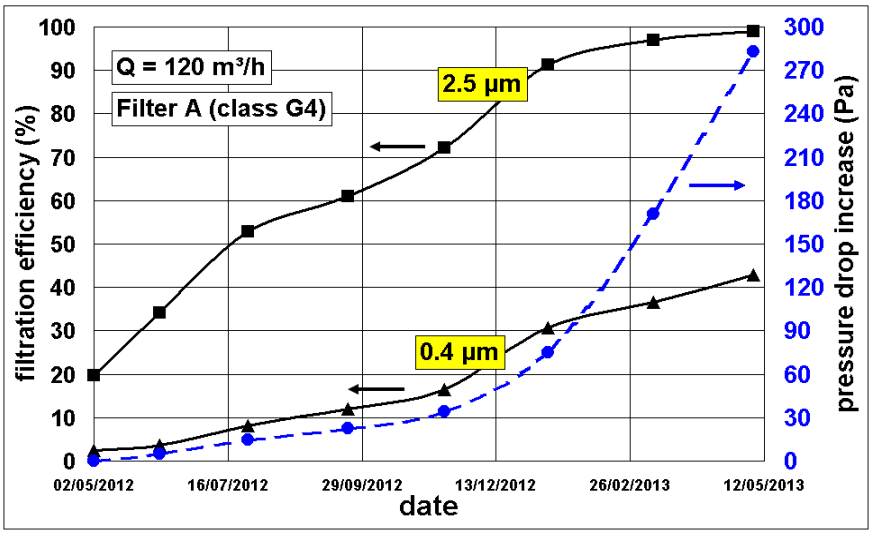

Figure 1 : Performances of filter A

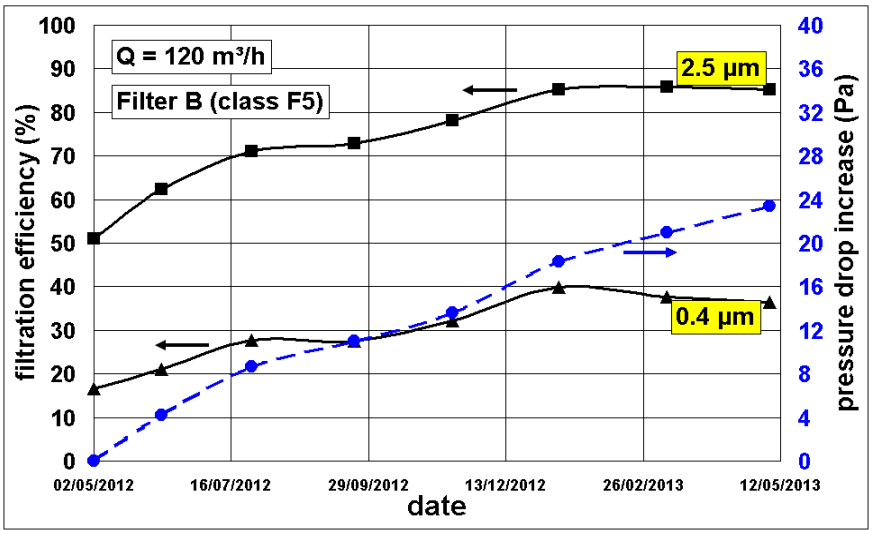

Figure 2 : Performances of filter B

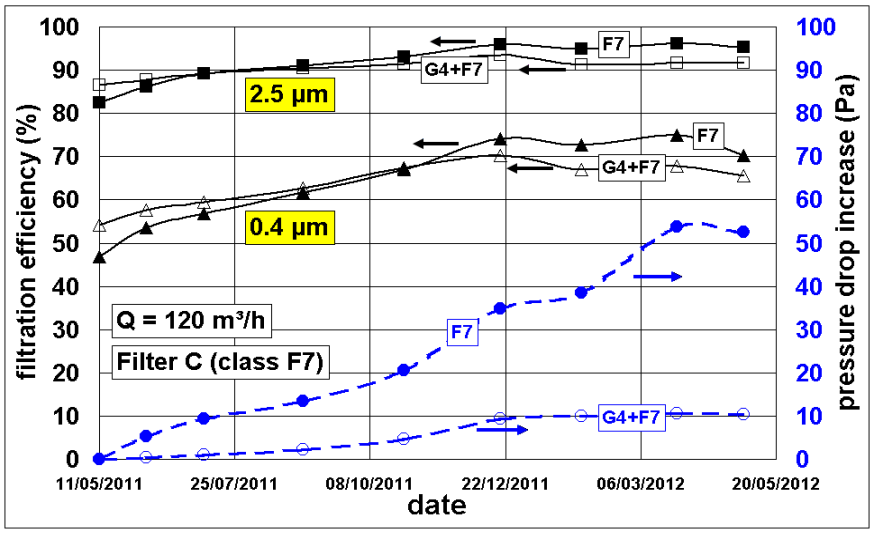

Figure 3 : Performances of filter C

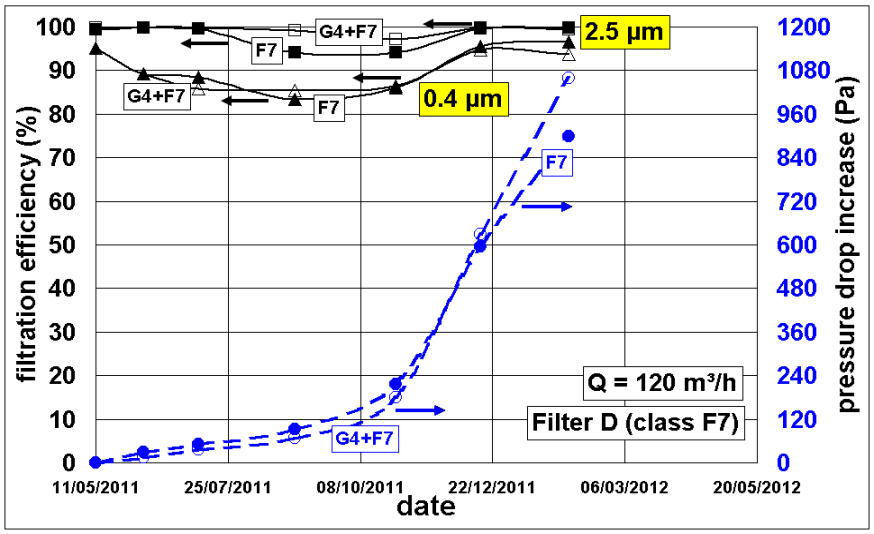

Figure 4 : Performances of filter D

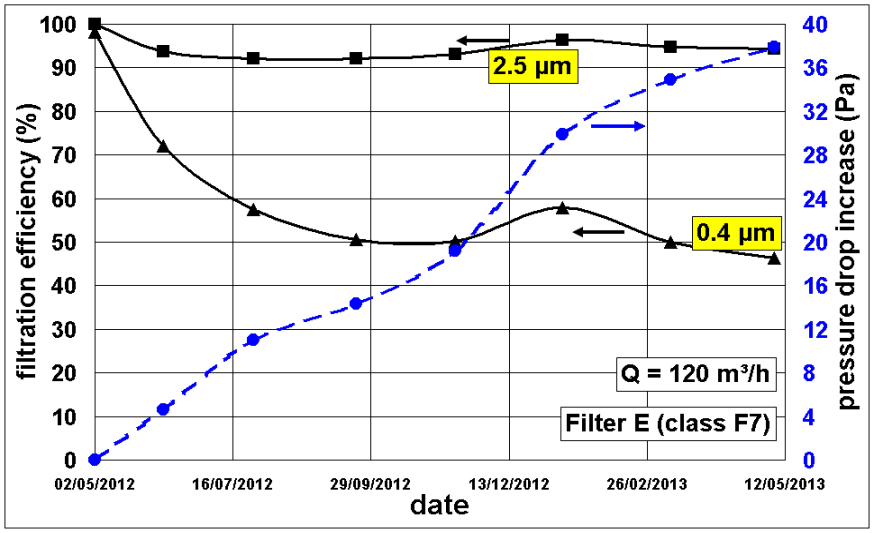

Figure 5 : Performances of filter E

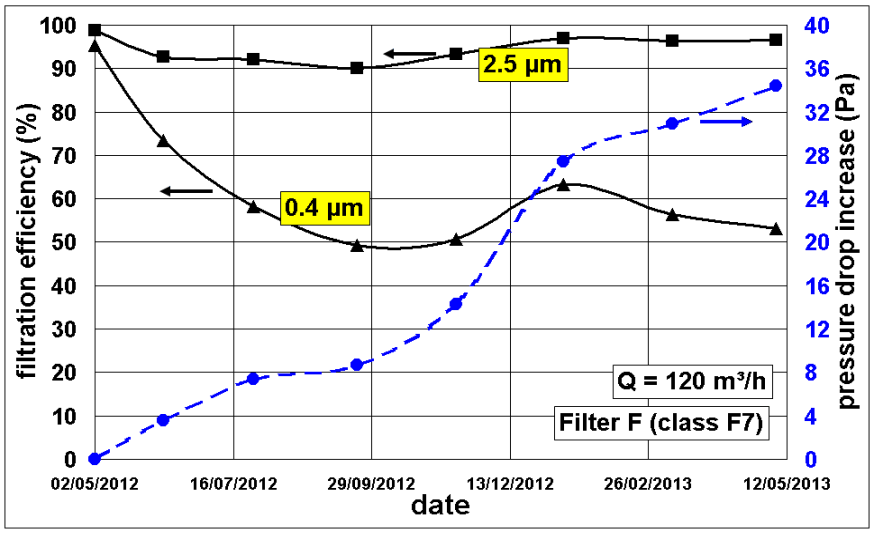

Figure 6 : Performances of filter F

5 DISCUSSION

5.1 Filter performances

The initial efficiency of the G4 filter (filter A, Figure 1) is the lowest of all the tested filters. Its initial efficiency at 0.4 µm was only a few percents (3.2 %) in line with was is expected for a G filter. Its efficiency has increased a lot after 1 year, reaching more than 40 % at 0.4 µm and 99 % at 2.5 µm. This especially high level is associated to a very high pressure drop increase, more than 280 Pa after 1 year, due to a very high loading by particles on the filter surface (Figure 7). The pressure drop has increased linearly for 6 months then has increased much more rapidly after a transition point between depth loading and surface loading.
The pressure drop increase of the F5 filter (filter B, Figure 2) has been controlled with a maximum value of 23 Pa reached after 1 year despite a high loading by particles (Figure 8). Its efficiency has increased linearly for about 8 months then it has remained more or less constant. The same phenomenon has been observed with filter C (class F7, Figure 3) made of the same material and using the same pleat technique ; its maximum pressure drop increase after 1 year was 54 Pa.


Figure 7 : Filter A after 1 year of use

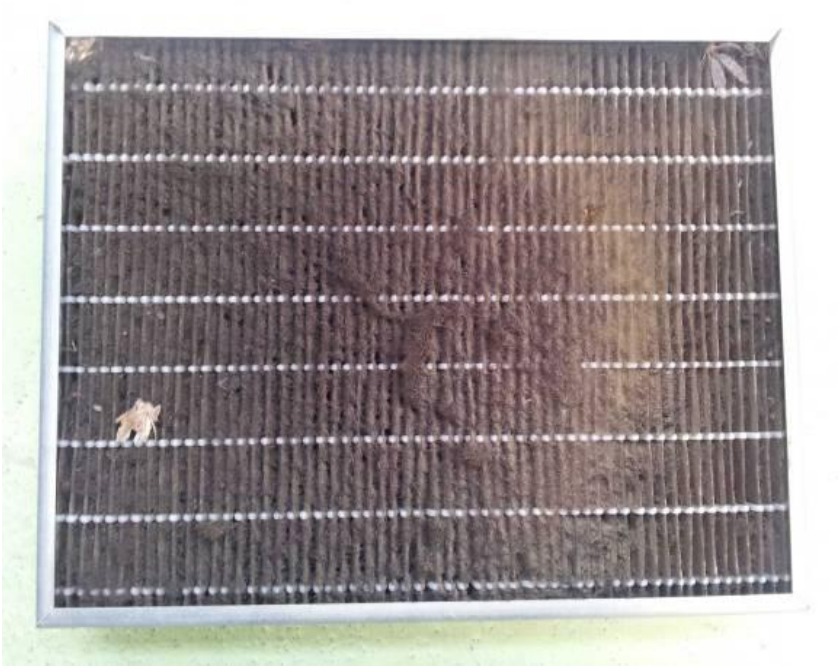

Figure 8 : Filter B after 1 year of use

The pressure drop of filter D (class F7, Figure 4) has increased linearly for 4 months then has increased much more quickly after a transition point between depth loading and surface loading. A lot of dust has deposited on the surface of the filter. Moreover, the pleat structure has been deformed (see next paragraph). Its efficiency has decreased a bit due to the loss of the electrostatic effects. This phenomenon has been met during testing of other type of electret filters whose results have been published in others papers (Ginestet et al, 2011 and 2013).
The 2 F7 electret filters (filters E and F, Figures 5 and 6) made of the same filtering medium and having the same filtration area behaved in the same way. Their pressure drop has increased more or less linearly while their efficiency has decreased due to the loss of the electrostatic effects. The pressure drop increase has been limited to respectively 38 Pa (filter E) and 34 Pa (filter F) after 1 year.

5.2 Influence of the use of a prefilter

The use of a G4 prefilter upstream of the F7 filter C has allowed to limit the pressure drop increase to 10 Pa instead of 54 Pa when no prefilter is used (Figure 3). 60 % to 80 % in mass of the particles challenging the filters have been retained by the G4 filter and thus loading of the F7 filter C is limited. When the F7 filter is not protected by the G4 prefilter, a thin layer of fibres and particles covers the front area of the filter (Figure 9) which is not observed when the prefilter is used (Figure 10). This phenomenon and this kind of results (less pressure drop increase with the use of a prefilter) have been observed during testing of other types of F7 filters whose results have been published in others papers (Ginestet et al, 2011 and 2013).
For F7 filter D, the pressure drop increase was not different with or without the use of a prefilter (Figure 4). The efficiency of this F7 filter is very high, as well as its initial pressure drop, and the amount of dust retained by the prefilter was not enough to slow down its loading and pressure drop increase. Nevertheless, the amount of dust covering the front surface of the F7 filter not protected by the prefilter (Figure 11) appears higher than that of the protected F7 filter (Figure 12) (the mass increase of the non protected filter D is higher than that of the protected filter D). For this F7 filter a more efficient prefilter would have been necessary.

Figure 9 : Filter C not protected by a prefilter, after 1 year of use

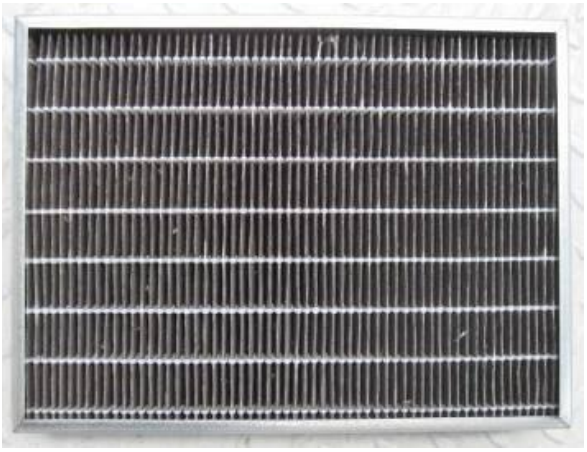

Figure 10 : Filter C protected by a prefilter, after 1 year of use

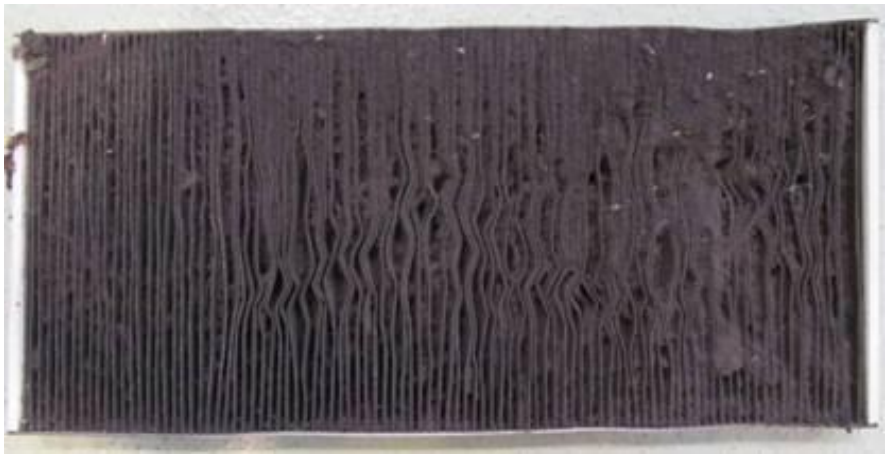

Figure 11 : Filter D not protected by a prefilter, after 9 months of use

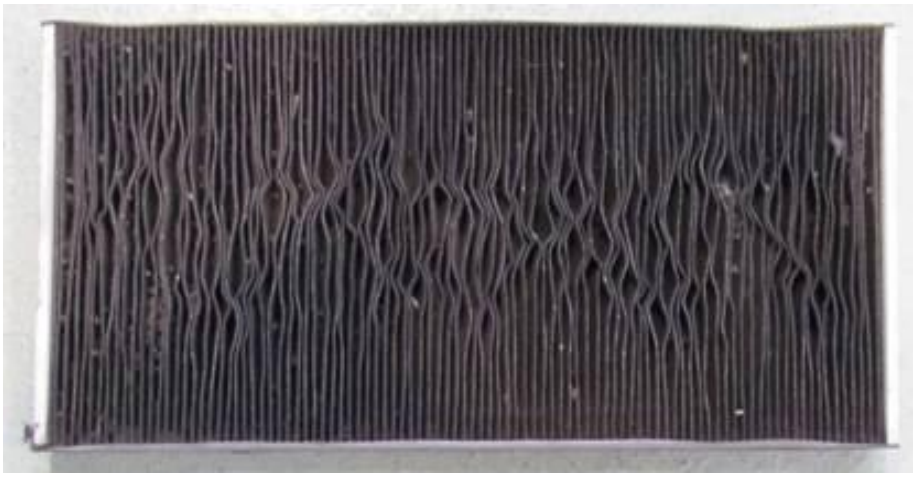

Figure 12 : Filter D protected by a prefilter, after 9 months of use

5.3 Influence of the pleat width

The results for filters E (Figure 5) and F (Figure 6) (these filters have the same filtration area and are made of the same filtering medium but have a different pleat width) show that a more opened pleat structure (10.4 mm pleat width for filter F and 6.1 mm pleat width for filter E),

reduces by more than 10 % the pressure drop increase (34 Pa for filter F instead of 38 Pa for filter E) because of less risk to promote loading and blocking of pleat opening by particles (Figures 13 and 14). The initial pressure drop of the more opened filter is also lower (20 Pa for filter F instead of 24 Pa for filter E, see Table 1).

Figure 13 : Filter E after 1 year of use (pleat width 6.1 mm)

Figure 14 : Filter F after 1 year of use (pleat width 10.4 mm)

Despite its low efficiency, the pressure drop increase of G4 filter A (Figure 1) was particularly high because its pleat width is very small (2.8 mm) then many pleats were blocked and overloaded by particles (Figure 7). The low pleat depth (10 mm) can also explain fast loading of the pleats.

6 CONCLUSIONS

As the balanced ventilation with heat recovery is more and more used in dwellings and because it is necessary to reduce the energy consumption of the fans of these systems, the pressure drop increase of the filters along their life must be limited.
On the occasion of long term tests of filters typically used in balanced ventilation boxes (panel mini-pleated filters), it has been shown that from the energy consumption point of

view, it is better to use a F7 filter protected by a prefilter installed upstream instead of the same F7 filter alone because the increase of pressure drop is lower. A G4 prefilter appears suitable for the protection of the panel mini-pleated F7 filters but a more efficient prefilter can be necessary if the efficiency of the fine filter is high. More generally, the filtration of the balanced ventilation systems has to be well designed in such a way that a prefilter and a fine filter are used in series (in separate units or in one unit), the efficiency of the prefilter being adapted to the efficiency of the fine filter in order to ensure lower pressure drop increase, reduced filter maintenance and lower energy consumption.
Choosing a filter for balanced ventilation systems with heat recovery is not only a question of class. Regarding the popular panel mini-pleated technique, the pleat width is an important parameter which has to be high enough to prevent fast surface loading of the filters. So a pleat width smaller than about 5 mm should be avoided.
Energy savings issues should not reduce indoor air quality. The efficiency of the filters has to be high enough to ensure that the balanced ventilation systems will provide clean air to the building and its occupants (well being and health issues). Engineers have to design filters with acceptable pressure drop increase together with high filtration efficiency : this compromise is still difficult to achieve.

7 ACKNOWLEDGEMENTS

This study has been financially supported by both the Ventilation and Filtration CETIAT technical committees. The authors are grateful to the manufacturers who have provided the balanced ventilation systems used for the tests as well as the filters under study.

8 REFERENCES

ANSI/ASHRAE Standard 52.2 (2012). *Method of testing general ventilation air-cleaning devices for removal efficiency by particle size*.

EN 13141-7 (2010). *Ventilation for buildings – Performance testing of components/products for residential ventilation – Part 7: Performance testing of a mechanical supply and exhaust ventilation units (including heat recovery) mechanical ventilation systems intended for single family dwellings*.

EN 779 (2002). *Particulate air filters for general ventilation – Determination of the filtration performance*.

EVIA (2012). *European Ventilation Industry Association EVIA - The Industry Platform for Ventilation and Fans*. K. Händel. Slide presentation at Chillventa, Nuremberg, Germany. October 2012 (www.chillventa.de).

European Commission (2012). *Possible Ecodesign and Energy Labelling Measures for Ventilation Units*. Consultation document, October 2012.

European Commission (2013). *Report from the Commission to the European Parliament and the Council - Financial support for energy efficiency in buildings – Commission staff working document accompanying the document*. Document SWD (2013) 143 final, April 2013.

French regulation (1982). Arrêté du 24 mars 1982 relatif à l'aération des logements (in French).

Ginestet, A., Pugnet, D. and Mouradian, L. (2011). *Filters for balanced ventilation systems : design, long-term performances and energy considerations*. 32nd AIVC Conference and 1st TightVent Conference, Brussels, Belgium, 12-13 October 2011.

Ginestet, A., Pugnet, D. and Mouradian, L. (2013). *Air filters for balanced ventilation systems*. Filtration+Separation, 50(1): 30-33.

AIR FLOW MODEL FOR SUB-SLAB DEPRESSURIZATION SYSTEMS DESIGN

Thierno M.Oury Diallo[1,2], Bernard Collignan[1], Francis Allard[2]

1 CSTB Health Division,
84 avenue Jean-Jaurès
77447 Marne-la-Vallée, France

2 University of La Rochelle-
(LaSIE, FRE-CNRS 3474)
Avenue Michel Crépeau
17042 La Rochelle, France
**Corresponding author:thierno.diallo@cstb.fr*

ABSTRACT

Soil gas pollutants (Radon, VOCs, etc...) entering buildings are known to pose serious health risks to building's occupants, and various systems have been developed to lower this risk. Soil Depressurization Systems (SDS) are among the most efficient mitigation systems protecting buildings against soil pollutants. Two kinds of SDS are currently used: active and passive systems. Active systems are mainly use fans, which enables the mechanical sub-slab's air extraction. Passive systems use natural thermal forces and wind effect to extract air from the sub-slab. Until now, no airflow model effective enough has been developed to help design those systems. In this paper, a novel method, based on analytical models of soil gas transfer, is presented to design Soil Depressurization Systems. The developed air flow models take into account various kinds of substructures: slab-on-grade and basement (supported slab and floating slab). These airflow models are integrated in a multizone airflow and heat transfer building code. This integration takes into account various parameters such as meteorological conditions (stack effect, wind), building characteristics (e.g. building envelope, airtightness…) and ventilation systems. Preliminary field verification results for extracted flow using passive sub-slab depressurization in an experimental house are presented and discussed. The results obtained show that, depending on local meteorological conditions and building characteristics, the airflow model is accurate enough, and represents a useful SDS design tool.

KEYWORDS

Soil gas, passive sub-slab depressurisation, active sub-slab depressurisation, airflow model, design.

1 INTRODUCTION

Radon migration from subsurface soil to indoor air can represents a major health risk, as it increases the risk of lung-cancer. The most effective system preventing soil gas pollutants entering buildings is the Soil Depressurisation System (SDS). It prevents the convective transfer of the soil gas pollutant towards the building (USEPA, 1993; Collignan and O'Kelly, 2003; Collignan et al., 2004). This system is generally equipped with an exhaust fan which maintains a constant depressurisation beneath the building. It is sometimes mentioned that this depressurisation could be obtained naturally using natural buoyancy and wind effect. The advantages of this system include lower operation and maintenance costs. The ability and the efficiency of this technique have not yet been assessed properly, and need to be tested. In the literature, some analytical (Reddy et al., 1991; Cripps, 1998) and numerical (Gadjil et al., 1991; Bonnefous, 1992; Halford and Freeman, 1992) models have been developed to characterize such systems. Reddy et al. (1991) used an analytical airflow SDS model based on the exponential non-Darcy flow. As explained by Gadjil et al. (Gadjil et al., 1991), this model has a certain limit, since it is assumed that there are no cracks in building's slab, and that the interface between the sub slab gravel and the soil is impermeable. In fact, the presence of crack in building slab can have a significant impact on the pressure field and velocity in the gravel layer. According to experiments of Turk (Turk, 1991), 40-90% of the air drawn in by the SDS comes from inside of the building. The Reddy et al. model is only valid when soil

permeability is higher than gravel permeability by a considerable margin. This model cannot be used when the soil is proven permeable. Cripps (Cripps, 1998) has developed also an analytical model based on the Darcy-Forchheimer equation. Counter to Reddy et al. model, this model includes a peripheral crack of the slab. However, it considers the soil impermeable just like the Reddy et al. model. Gadjil et al. (Gadjil et al., 1991) and Bonnefous (Bonnefous, 1992) used a 3 D finite element model to study the performance of SDS systems. This model takes into account the diffusive and convective transport in the soil and sub slab gravel. However, the transport (convection and diffusion) within the slab is ignored. It considers the airflow through the peripheral crack of the slab. Despite its assumptions, this model allows the identification of mechanisms and factors contributing to the performance of SDS systems. To study the effectiveness of passive SDS in reducing radon entry rate in building, Harold and Freeman (Harold and Freeman, 1996) used the finite element model Rn3D, which simulates the convective and diffusive transport in a porous medium. Transport in the porous medium is governed by Fick's law of diffusion and Darcy's law of convection. This model considers both the building slab permeability and the peripheral crack of the slab. Compared to numerical models, analytical models are more attractive in terms of use by professionals, even if they represent fewer of the phenomenon involved. A one year monitoring of a passive Soil Depressurisation System has been undertaken in an experimental dwelling on the CSTB site (Abdelouhab et al., 2010; Collignan et al, 2008). The ongoing mechanical efficiency of the whole system was recorded. Those experimental results show the potential advantage of passive SDS for protecting buildings against the soil gas pollutants. Its efficiency, however, depends on meteorological conditions and buildings characteristics.

In this context, it appeared necessary to have a tool for the design of such a system, which may take into account these different parameters. Such a tool could enable testing of the availability of passive SDS in a specific context and helps with its design. In this paper, an analytical model developed to characterise mechanical running of passive and active SDS is presented. Compared with the existing SDS analytical airflow models, this model considers the permeability of the soil, witch affects the effectiveness of the SDS. It assumes the permeability of the slab, and the existence of the slab’s peripheral crack. The airflow in the subslab gravel layer is governed by the Darcy-Forchehimer equation. Two slab substructures are considered: the floating slab and the supported slab. This model is coupled with a ventilation model and enables the verification of passive SDS functionning, during a year, for given specific meteorological conditions and building characteristics. Results obtained have been compared with experimental results and some sensitivity studies were presented.

2 PRESENTATION OF PREVIOUS EXPERIMENTAL STUDY

A one year monitoring of a passive Soil Depressurisation System had been undertaken in an experimental dwelling on CSTB site. The objective of this study was to assess the mechanical efficiency of such a system during a year. This experiment and the main results obtained are summarized below (Abdelouhab et al., 2010; Collignan et al., 2008). During its construction, an SDS has been installed into the experimental dwelling. For the purpose of this experiment, it had been conceived to be monitored in a passive way. To analyse the performance of such a system during time, the air velocity in the duct and the air temperature at the entrance of the duct were measured each minute with a probe. The indoor temperature in following analyses is the average temperature measured in different rooms. Likewise, basement depressurization has been measured between the gravel layer and indoor environment at floor level with a differential manometer. Wind (velocity and direction) and external temperature have been recorded from a weather station located close to the experimental dwelling (figure 1 a)

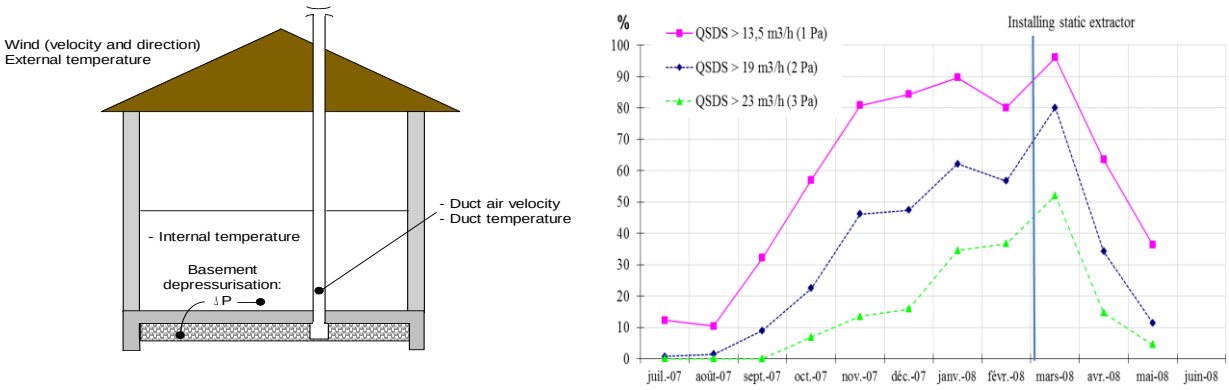

a b

Figure 1: a) Parameters measured during the one year follow up b) Percentage of running time of the system along year above three thresholds.

Results obtained consist of an important database of the physical variables measured each minute during the year. One of the main results obtained during this experiment is presented in figure 1 b. It shows the percentage of running time of the system during the year above three thresholds of extracted air flow rates from the basement. These experimental results showed the advantage of passive SDS, on the one hand to protect the building against the soil gas pollutants. On the other hand, this technique works at a marginal cost, unlike mechanical SDS. It appears also that natural running of SDS is highly variable during the year. However, in these experiments, percentage of running time could be significant and mainly during the winter season. This is an interesting result because a preventive solution is mainly needed during this period to block soil gas pollutants entrance due to convective fluxes between ground and inhabited volume. A secondary result showed the advantage of installing an efficient static extractor at the exit of the duct to ameliorate the running of the system. As a conclusion, it could be said, that efficient running of passive SDS depends on weather conditions and some building and environmental parameters. So that, it appears interesting to develop a model that can assess performance of such a system in specific conditions. This model could help to design the passive SDS.

3 DEVELOPMENT OF ANALYTICAL AIR FLOW MODEL

An analytical model has been developed to determine the mechanical running characteristics of a passive SDS (air flow and depressurization) as a function of building characteristics and meteorological conditions (wind and temperature difference). The conceptual model to quantify airflow through porous media is based on an analogy between the heat transfer conduction and the air flow as presented in previous works (Diallo et al. 2012). Airflow through porous media follows generally Darcy law except in gravel layer where Darcy-Forchheimer law is used. Air flow through passive SDS duct is due to pressure difference between gravel layer and the environment. It can come from indoors and from the soil:

$$Q_{SDS} = Q_{ind} + Q_{soil} \quad (1)$$

Q_{SDS}, Q_{ind} and Q_{soil} (in m^3/s) are respectively air flow into the duct, from indoors and from the soil respectively. Figure 2 shows a scheme of passive SDS integrated in its environment

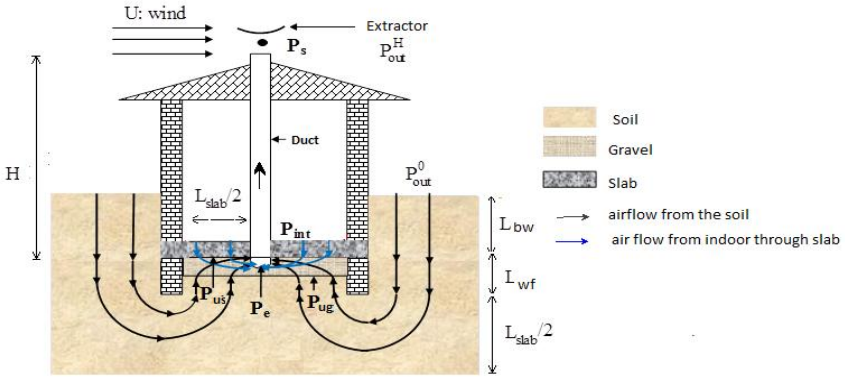

a

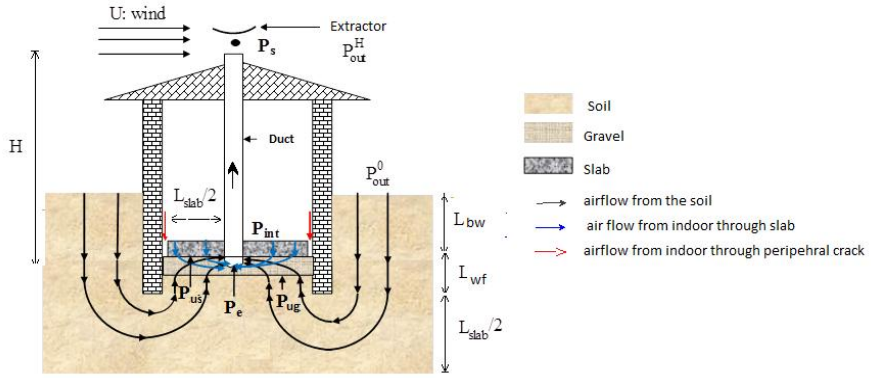

b

Figure 2: SDS integrated in a dwelling, with different pressures to be considered: a) supported slab substructure b) floating slab substructure.

3.1 Determination of air flow from indoors (Q_{IND}) for supported slab (figure 2 a)

Pressure loss between indoors and duct entrance can be written as follows:

$$P_{ind} - P_e = (P_{ind} - P_{US}) + (P_{US} - P_e) \quad (2)$$

with P_{ind} being the pressure above the floor, P_e the pressure at duct entrance and P_{US} the pressure under the slab, in Pa. Pressure loss between indoors and under slab can be expressed as:

$$(P_{ind} - P_{US}) = R_{slab} \times Q_{ind} \quad (3)$$

with (Diallo et al., 2012):

$$R_{slab} = \frac{e_{slab} \times \mu}{k_{slab} \times S_{slab}} \quad (4)$$

with e_{slab} (m) being the thickness of the slab, μ (Pa.s) the dynamic viscosity of air, k_{slab} (m²) the air permeability of slab and S_{slab}(m²) the surface of the slab.

Based on expressions presented in Annex for the determination of pressure loss in gravel between two surfaces, pressure loss between under slab and duct entrance is as followed:

$$P_{US} - P_e = R_{g1} c A_h^{-1} Q_{ind}^2 + R_{g1} Q_{ind} \quad (5)$$

with c the Forchheimer coefficient, R_{g1} (Pa/m^3/s) the gravel resistance between under slab and duct entrance and A_h (m²) the surface of the hemisphere at the entrance of the duct. Replacing eq. (3) and eq. (5) in eq. (2), we obtain:

$$\left(\frac{R_{g1} c}{A_h}\right) Q_{ind}^2 + (R_{g1} + R_{slab}) Q_{ind} - (P_{ind} - P_e) = 0 \quad (6)$$

Solving eq. (6) with positive discriminant, air flow from indoors can be expressed:

$$Q_{ind}=\left[-\left(R_{g1}+R_{slab}\right)+\left[\left(R_{g1}+R_{slab}\right)^2+4\left(\frac{R_{g1}c}{A_h}\right)(P_{ind}-P_e)\right]^{0.5}\right]\left[2\left(\frac{R_{g1}c}{A_h}\right)\right]^{-1} \quad (7)$$

3.2 Determination of air flow from indoors (Q_{IND}) for floating slab (figure 2 b)

To determine the air flow indoors for floating slab, the resistance of the slab R_{slab} in eq. (7) is just replaced by the total resistance R_{tot} of the slab and the peripheral crack which are in parallel.

$$Q_{ind}=\left[-\left(R_{g1}+R_{tot}\right)+\left[\left(R_{g1}+R_{tot}\right)^2+4\left(\frac{R_{g1}c}{A_h}\right)(P_{ind}-P_e)\right]^{0.5}\right]\left[2\left(\frac{R_{g1}c}{A_h}\right)\right]^{-1} \quad (8)$$

The total resistance R_{tot} is:

$$R_T=\left[\left(R_{crack}\right)^{-1}+\left(R_{slab}\right)^{-1}\right]^{-1} \quad (9)$$

The resistance of the slab R_{slab} is given by eq.4 and the resistance of the crack is:

$$R_{crack}=\frac{12\times e_{slab}\times\mu}{d^3 P} \quad (10)$$

With d (m) being the width crack, P (m) the perimeter of the slab.

3.3 Determination of air flow from the soil (Q_{SOIL})

Pressure loss between outdoors and duct entrance can be written as followed:

$$P_{out}^0-P_e=\left(P_{out}^0-P_{ug}\right)+\left(P_{ug}-P_e\right) \quad (11)$$

with P_{out}^0 and P_{ug} being the outdoor pressure at ground level and the pressure under gravel layer respectively, in Pa. Pressure loss between outdoors and under slab can be expressed:

$$\left(P_{out}^0-P_{ug}\right)=R_{soil}\times Q_{soil} \quad (12)$$

with (Diallo et al. 2012):

$$R_{soil}=\left[\frac{k_{soil}P}{\pi\mu}\ln\left(\frac{1+\left(\frac{\pi}{2L_{wf}+L_{bw}}\right)\left(\frac{L_{slab}+e_m}{2}\right)}{1+\left(\frac{\pi}{L_{wf}+L_{bw}}\right)\left(\frac{e_m}{2}\right)}\right)\right]^{-1} \quad (13)$$

with k_{soil} (m²) the air permeability of the soil, P (m) the perimeter of the slab, L_{wf} (m) the length of foundation, L_{slab} (m) the length of the slab and e_m (m) the thickness of the foundation wall. L_{bw} (m) is the basement wall height. If L_{bw}=0 in eq., we get slab-on-grade substructure. Based on expressions presented in Annex for the determination of pressure loss in gravel between two surfaces, pressure loss between under gravel and duct entrance is as followed:

$$P_{ug}-P_e=R_{g2}cA_{duct}^{-1}Q_{soil}^2+R_{g2}Q_{soil} \quad (14)$$

with R_{g2} (Pa/m^3/s) the gravel resistance between under gravel and duct entrance and A_{duct} (m²) the surface of the cylinder at the entrance of the duct. Replacing eq. (12) and eq. (14) in eq. (11), we obtain:

$$\left(\frac{R_{g2}c}{A_{duct}}\right)Q_{soil}^2+\left(R_{g2}+R_{soil}\right)Q_{soil}-(P_{out}^0-P_e)=0 \quad (15)$$

Solving eq. (15) with positive discriminant, air flow from the soil can be expressed:

$$Q_{soil}=\left[-\left(R_{g2}+R_{soil}\right)+\left[\left(R_{g2}+R_{soil}\right)^2+4\left(\frac{R_{g2}c}{A_{duct}}\right)(P_{out}^0-P_e)\right]^{0.5}\right]\left[2\left(\frac{R_{g2}c}{A_{duct}}\right)\right]^{-1} \quad (16)$$

Replacing eq. (16) and eq. (7) in eq. (1), air flow into the duct for supported slab can be deduced:

$$Q_{SDS} = \left[-\left(R_{g1} + R_{slab}\right) + \left[\left(R_{g1} + R_{slab}\right)^2 + 4\left(\frac{R_{g1}\,c}{A_h}\right)(P_{ind} - P_e) \right]^{0.5} \right] \left[2\left(\frac{R_{g1}\,c}{A_h}\right) \right]^{-1} + \left[-\left(R_{g2} + R_{soil}\right) + \left[\left(R_{g2} + R_{soil}\right)^2 + 4\left(\frac{R_{g2}\,c}{A_{duct}}\right)(P^0_{out} - P_e) \right]^{0.5} \right] \left[2\left(\frac{R_{g2}\,c}{A_{duct}}\right) \right]^{-1} \quad (17)$$

By replacing R_{slab} by R_{tot} in eq. 17, air flow into the duct for floating slab is deducted.

3.3.1. Determination of pressure difference into the duct

This pressure difference is the result of the equilibrium between pressure losses and stack effect. It can be expressed as:

$$(P_e - P_s) = \Delta P_{friction} + \Delta P_{singularity} + \Delta P_{stack} \quad (18)$$

with pressure losses due to friction into the duct and due to singularity, respectively:

$$\Delta P_{friction} = \lambda \frac{H}{D_H} \times \frac{1}{2}\rho\left(\frac{Q_{SDS}}{A_{duct}}\right)^2 \; ; \; \Delta P_{singularity} = \sum \zeta_i \times \frac{1}{2}\rho\left(\frac{Q_{SDS}}{A_{duct}}\right)^2$$

with λ and ξ_i are the linear and singular pressure loss coefficients respectively (I.E. IDEL'CIK, 1969). D_H (m) is the hydraulic diameter of the duct, ρ (kg/m^3) the volumic mass of the air and h (m) the height of the duct. The stack effect into the duct ΔP_{Stack} is:

$$\Delta P_{stack} = (\rho_e - \rho_s) g H \quad (19)$$

with ρ_e and ρ_s(kg/m^3) the densities of the air at the entrance and at the exit of the duct respectively. It is assumed that T_e and ρ_e are known. The unknown is:

$$\rho_s = \rho_e T_e / T_s \quad (20)$$

To determine T_s and based on enthalpy balance into the duct, temperature along the duct for a given height (h) can be written (Mounajed, 1989):

$$T(h) = T_{int} + (T_e - T_{int})\exp(-\omega \alpha_m h), \text{ with: } \omega = \frac{\pi D}{\rho Q_{SDS} C_p} \quad (21)$$

In eq. (21), T_{int} is supposed to be known. α_m is a global exchange coefficient between indoors and air flow into the duct. It could be determined considering three resistances in parallel as followed:

$$\frac{1}{\alpha_m S_{int}} = \frac{1}{S_{int} h_{int}} + \frac{\ln(r_1 / r_2)}{2\pi\lambda H} + \frac{1}{h_{ext} S_{ext}} \quad (22)$$

With S_{int} (m²) and S_{ext} (m²) the internal and external surface of the duct respectively, r_1 (m) and r_2 (m) the internal and external radius of the duct respectively. h_{int} and h_{ext} are classical heat exchange coefficients for natural convection that can be found in Elenbass (1942). Eq. (21) enables to determine T(H) (= T_s). Once T_s determined, as a function of Q_{SDS}, we can write ρ_s as a function of Q_{SDS} with eq. (20) and as a function of P_{ind}, P_e and P^0_{out} using eq. (17).

3.3.2. Determination of pressure loss at the exit of the duct (static extractor)

In presence of wind, shape of the extractor diminishes outdoor pressure at the exit of the duct and we have:

$$P_s - P^H_{out} = \frac{1}{2}\rho C_{p,out} U^2 \quad (23)$$

with P^H_{out} the outdoor pressure at the exit duct level in Pa, $C_{p,out}$ a suction coefficient depending on the shape of the extractor and U (m/s) wind velocity.

3.3.3. Determination of pressure loss at the exit of the duct (mechanical extractor)

The depression created by a mechanical extractor can be expressed by a quadratic law (Mounajed, 1989):

$$\Delta P_{ext} = \frac{\rho}{\rho_0}\left(P_x + C_x Q_{sds}^2\right) \quad (24)$$

Where Px and Cx are coefficients from the overall characteristic of the extractor used. ρ and ρ_0 are respectively the reference density of air at 20 ° C and the actual density. This depression can also be obtained by polynomial from the fan characteristic used (Koffi, 2009) regression. This type of extractor is not used in this study; this extractor model is presented just to show that the SDS model developed can be adapted for this type of extractor. In this study we focused on the passive extractor because the experiments are conducted with this type of extractor.

3.3.4. Determination of Q_{SDS}

Using eq. (18) to eq. (23), pressure difference between the entrance of the duct and outdoors can be written:

$$(P_e - P_{out}^H) = (P_e - P_S) + (P_S - P_{out}^H) = \left(\lambda\frac{L}{D_H} + \sum_1 \zeta_i\right) \times \frac{1}{2}\rho\left(\frac{Q_{SDS}}{A_{duct}}\right)^2 - (\rho_s - \rho_e)gH + \frac{1}{2}\rho C_{p,out} U^2 \quad (25)$$

From eq. (20), air flow into the duct can be deduced:

$$Q_{SDS} = A_{duct}\left(2\left[(P_e - P_{out}^H) + (\rho_e - \rho_s)gH - \frac{1}{2}\rho C_{p,out} U^2\right]\left[\rho\left(\lambda\frac{L}{D_H} + \sum\zeta_i\right)\right]^{-1}\right)^{0.5} \quad (26)$$

Using the two expressions of Q_{SDS} (eqs. (17) and (26)), we can write:

$$\begin{aligned}
&\left[-(R_{g1} + R_{slab}) + \left[(R_{g1} + R_{slab})^2 + 4\left(\frac{R_{g1}c}{A_h}\right)(P_{ind} - P_e)\right]^{0.5}\right]\left[2\left(\frac{R_{g1}c}{A_h}\right)\right]^{-1} \\
&+\left[-(R_{g2} + R_{soil}) + \left[(R_{g2} + R_{soil})^2 + 4\left(\frac{R_{g2}c}{A_{duct}}\right)(P_{out}^0 - P_e)\right]^{0.5}\right]\left[2\left(\frac{R_{g2}c}{A_{duct}}\right)\right]^{-1} \\
&-A_{duct}\left(2\left[(P_e - P_{out}^H) + (\rho_e - \rho_s)gH - \frac{1}{2}\rho C_{p,out} U^2\right]\left[\rho\left(\lambda\frac{L}{D_H} + \sum\zeta_i\right)\right]^{-1}\right)^{0.5} = 0
\end{aligned} \quad (27)$$

In this equation, if P_{ind}, P_{out}^0 and P_{out}^H are known. As explained previously in §3.3.1, ρ_s can be expressed as a function of P_{ind}, P_e and P_{out}^0. The only unknown is P_e. Once P_e is calculated, Q_{SDS} can also be calculated for given conditions.

3.4 Integration in a ventilation model

For this study a numerical ventilation model developed under Mathlab-Simulink environment has been used (Koffi, 2009). Equation (27) can be integrated. This equation can be solved using Newton method. For a given time step, P_{ind}, P_{out}^0 and P_{out}^H are given by ventilation model. P_e, Q_{SDS}, Q_{soil} and Q_{ind} are calculated. Determination of Q_{ind} could modify indoor mass balance, so it is needed to have a loop on mass balance of ventilation model; to obtain a converged result.

This integration allows us to obtain mechanical running characteristics of a passive SDS all along the year for given environmental conditions (meteorology) and building characteristics (dimensions, ventilation system, air permeability). It makes it possible to conduct relevant studies on given parameters to test the ability of passive SDS to run in given conditions and to dimension it.

4 RESULTS

4.1 Confrontation with experimental results

Passive SDS model presented in § 2 has been compared to results of the experiment presented in § 1. For this confrontation, it was needed to have additional data as soil and slab permeabilities. For slab permeability, value obtained during complementary experiments using tracer gas (Abdelouhab, 2011) is used. For soil permeability and thanks to a collaboration with IRSN (IRSN, 2012), soil permeability had been assessed. It had appeared that soil permeability around the experimental dwelling was relatively heterogeneous and some averages were necessary to be used in our model. Figure 3 presents a confrontation of experimental and numerical results obtained for air flow through passive SDS and for gravel depressurization between July 2007 and February 2008 in the experiment.

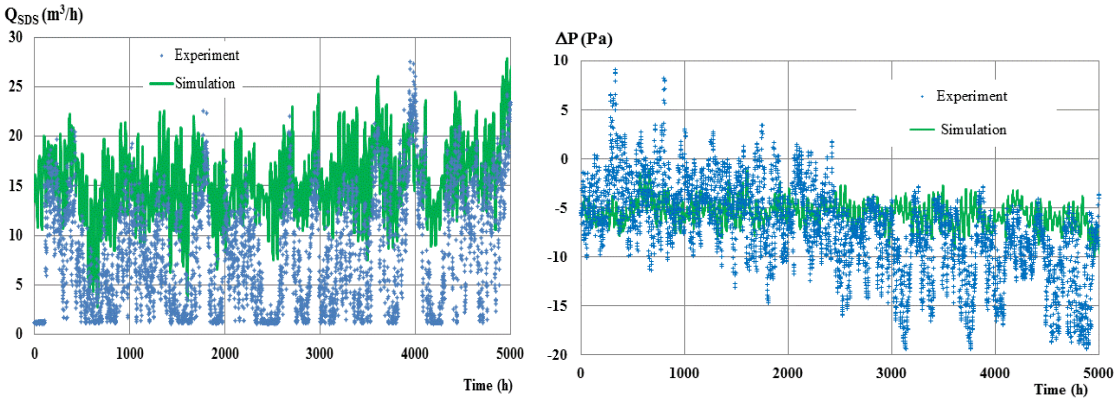

(a) (b)

Figure 3: comparison between experimental and numerical for air flow through passive SDS (a) and gravel depressurization (b) between July 2007 and February 2008.

Based on these results, it can be said that numerical results obtained with our model are relevant. However, it is observed that experimental results are more variable than numerical ones. Also, there is generally an overestimation of the air flow through the SDS duct with calculations, which implies an underestimation of depressurization in the gravel layer. Those findings could be explained by different reasons. Firstly, from a numerical point of view, wind effect on extractor is always beneficial. It is not necessary the case in a real environment due to the possible angle between wind direction and exit of the duct which can have its flow blocked. Secondly, the wind's turbulence and fluctuations can have a negative impact on air flow that is not taken into account in the calculations. Finally, results obtained with the model can be sensitive to the variation of some parameters used. Figure 4 show the impact of the variation of relevant parameters on averaged air flow from duct during the period.

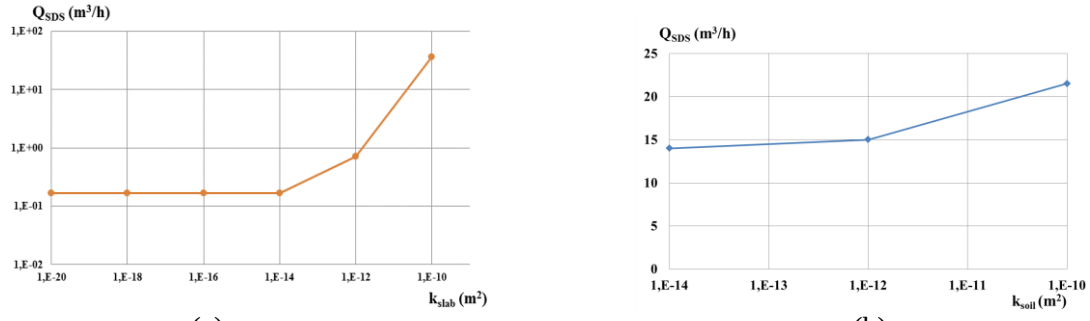

(a) (b)

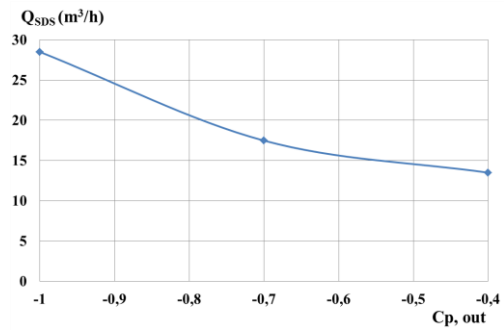

(c)

Figure 4: impact of variations of (a) slab permeability, (b) soil permeability and (c) extractor suction coefficient on averaged air flow from the SDS duct.

Despite assumptions of the model and some uncertainties due to a lack of knowledge on some relevant parameters, it can be concluded that numerical results obtained are more satisfactory compared than the experimental ones. As complementary results and with an analogy with experimental results presented in figure 1 b, figure 5 shows the percentage of running time of the system along the considered period above three thresholds. The same remarks can be made with the other numerical and experimental results.

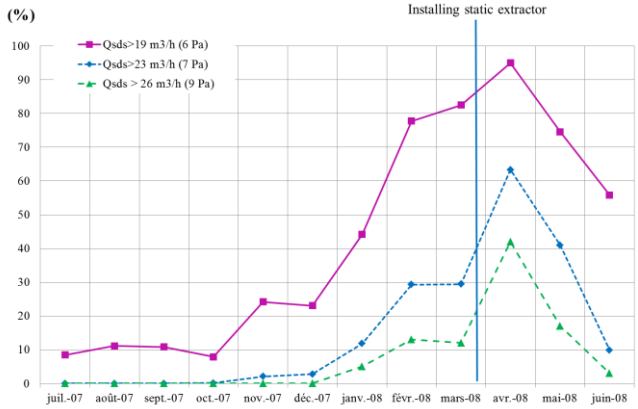

Figure 5: Percentage of running time of the system along the considered period above three thresholds.

4.2 Sensitivity study on the impact of meteorological conditions

To show the interest of this model, a sensitivity study has been conducted to analyze the impact of different meteorological conditions on mechanical running characteristics of passive SDS, for a given dwelling. Figure 6 show meteorological conditions used for this study.

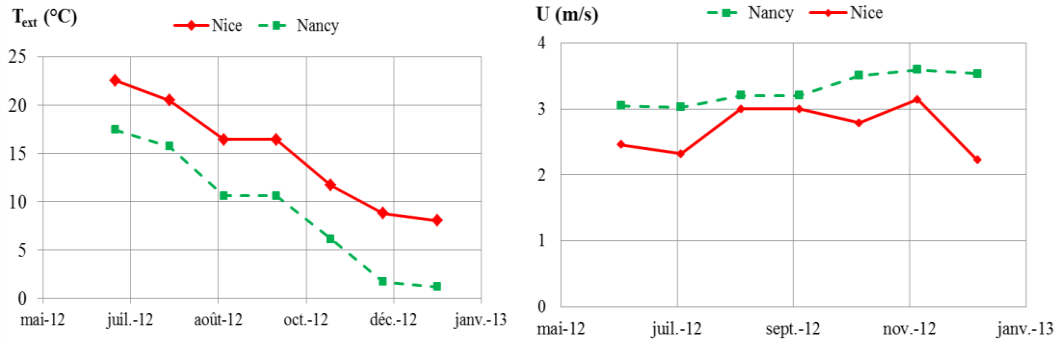

(a) (b)

Figure 6: external temperature (a) and wind velocity (b) for two different cities, Nancy and Nice, in France (monthly averaged).

It can be seen that external temperature is always lower in Nancy compared to Nice. The monthly averaged force of the wind is higher. Figure 7 presents numerical results obtained for air flow through passive SDS and for gravel depressurization along time for the two towns and during the considered period

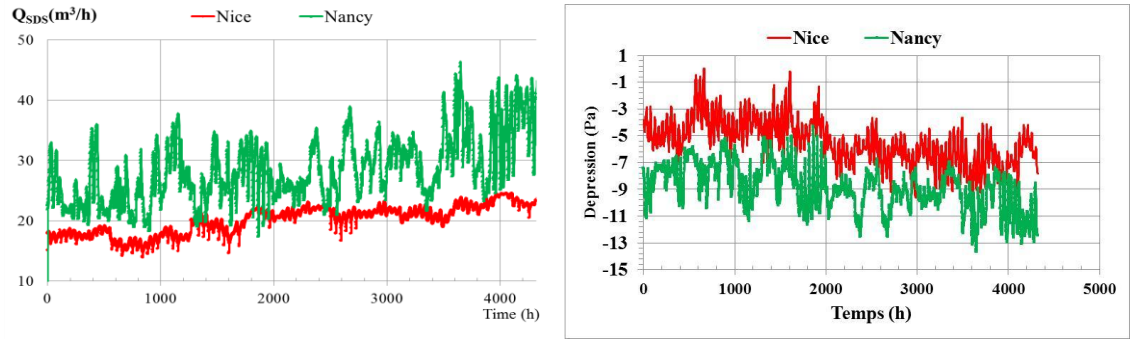

(a) (b)

Figure 7: numerical air flow through passive SDS (a) and gravel depressurization (b) for Nice and Nancy.

It can be seen that mechanical running of passive SDS is more effective in Nancy than in Nice. For the same result, figure 8 shows the percentage of running time of the system along the considered period above three thresholds for the two towns.

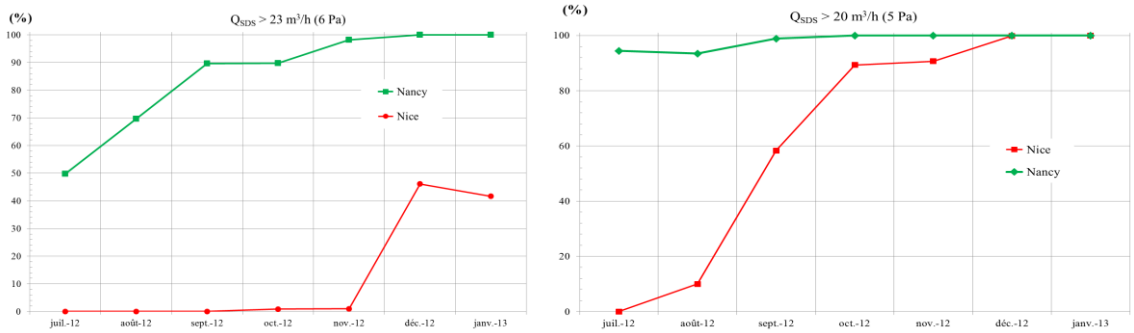

Figure 8: Percentage of running time of the system along the considered period above two thresholds for Nice and Nancy.

This figure allows us to say that for dwelling considered in these calculations, passive SDS can be more efficient if the dwelling is in Nancy region and less efficient if it is in Nice region. As shown in figure 6, the reason is that Nancy has a colder climate with wind generally slightly higher. This first sensitivity study show the potential interest of the model developed to test the ability of the passive SDS to be efficient for a considered building in given meteorological conditions. It could then be an help to dimension the system.

5 CONCLUSION

In this paper, a method based on the development of analytical air flow models to study soil gas transfer is presented to design passive Soil Depressurization System (SDS). This airflow model developed to study mechanical running of passive SDS is integrated in a multizone airflow building code. This integration allows to take into account the impact of meteorological conditions (stack effect, wind), building characteristics (height, diameter of duct for SDS, airtightness of building) and ventilation systems.

Preliminary field verification results for extracted flow using passive soil depressurization in an experimental dwelling are presented and discussed. The results obtained are quite satisfactory. Also preliminary sensitivity studies were conducted to analyze the impact of different meteorological conditions on mechanical running characteristics of passive SDS, for

a given dwelling. This study shows that the airflow model developed is accurate enough to design passive SDS systems, depending on local meteorological conditions and building characteristics.

6 ACKNOWLEDGMENT

This study was conducted in the framework of a Ph.D at CSTB (Scientific and Technical Center for Building) in collaboration with LaSIE (Laboratory of Engineering Sciences for Environment) at University of La Rochelle and partly supported by the ADEME (French Environment and Energy Management Agency).Complementary experiments needed for this study to determine soil permeability were conducted by IRSN (Institute for Radiological Protection and Nuclear Safety Institut).

Annex: Pressure loss in gravel layer

Air flow in a gravel layer can be approached by the nonlinear equation of Darcy-Forchheimer (Bonnefous, 1992):

$$\nabla P = -\frac{\mu}{k} c u^2 - \frac{\mu}{k} u \tag{A1}$$

with μ (Pa.s) the dynamic viscosity of air, k (m²) the air permeability of the gravel, c the Forchheimer coefficient and u (m/s) the velocity of air.

On this basis, we assume that the pressure difference between two interfaces in gravel layer can be written as followed:

$$P_g - P_e = a_1 Q^2 + b_1 Q \tag{A2}$$

The analogy with Darcy-Forchheimer equation (A1) implies that a_1 et b_1 coefficients are respectively proportional to à k_c/μ et k/μ.

$$a_1 = \frac{\mu}{k} c \alpha_1 \; ; \; b_1 = \frac{\mu}{k} \beta_1 \tag{A3}$$

Equation (A2) becomes:

$$P_g - P_e = \frac{\mu}{k} c \alpha_1 Q^2 + \frac{\mu}{k} \beta_1 Q \tag{A4}$$

In this equation, $\frac{\mu}{k} c \alpha_1$ and $\frac{\mu}{k} \beta_1$ need to have the dimension of a resistance (Pa.s/m^3). Using dimensional analysis, it can be concluded that:

$$\alpha_1 = \left[\frac{1}{M^3}\right] \text{and} \beta_1 = \left[\frac{1}{M}\right] \tag{A5}$$

It is assumed that a1 and b1 include a shape factor S(m),depending on geometry considered between the two interfaces. So that:

$$\alpha_1 = A_c^{-1} S^{-1} \text{and} \beta_1 = S^{-1} \tag{A6}$$

with A_c (m²) a surface depending on shape of fluid interface. Replacing eq. (A6) in eq. (A4) and considering a resistance of gravel layer as Rg = μ/(kS), eq. (A4) becomes:

$$P_g - P_e = R_g c A_c^{-1} Q^2 + R_g Q \tag{A7}$$

For model presented in this paper, it is needed to define Rg and Ac for the two configurations as presented below:

Configuration 1:

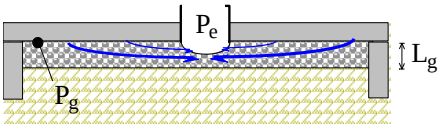

Configuration 2:

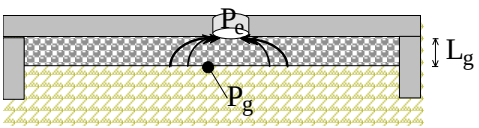

$$R_{g1} = \frac{\mu}{k}\frac{1}{\pi D} \quad ; \quad A_c = A_h = 2\pi D^2/4$$

$$R_{g2} = \frac{\frac{\mu}{k}\left[1-\left(\frac{D}{5.66L_g}\right)\right]}{1.85D} \quad ; \quad A_c = A_{duct} = \pi D^2/4$$

For configuration 1, it is based on the definition a thermal flux between a semi-infinite surface and a hemisphere (Holman, 2010), with D (m) the diameter of the hemisphere and A_h (m²) the surface of the hemisphere.

For configuration 2, it is based on the definition of thermal flux between an infinite surface and a cylinder (Sunderland and Johnson, 1964), with L_g (m), the depth of gravel layer and A_{duct} (m) the surface of cylinder entrance. Please refer to the main conclusions of the work.

7 REFERENCES

Abdelouhab M. (2011). *Contribution à l'étude du transfert des polluants gazeux entre le sol et les environnements intérieurs des bâtiments*. Thèse Université de La Rochelle.

Abdelouhab M., Collignan B. and Allard F. (2010). *Experimental study on passive Soil Depressurization System to prevent soil gaseous pollutants into building*. Building and Environment, 45, 2400-2406.

Bonnefous Y. (1992). *Étude numérique des systèmes de ventilation du sol pour diminuer la concentration en radon dans l'habitat*. Thèse de doctorat en Génie Civil : sols, matériaux, Structures et Physique du bâtiment, Institut National des Sciences Appliquées de Lyon, 256 p.

Collignan B., Abdelouhab M. Allard F., 2008. *Experimental study on passive sub-slab depressurisation system. Proceedings of the American Association of Radon Scientists and Technologists 2008*. International Symposium, September 14-17, 2008, Las Vegas USA. AARST © 2008.

Collignan B. O'Kelly P., 2003. *Dimensioning of soil depressurisation system for radon remediation in existing building.* Proceedings of Healthy Building conference, 7th- 11th Dec. 2003, Singapore, 517-523.

Collignan B., O'Kelly P. Pilch E., 2004. *Basement depressurisation using dwelling mechanical ventilation system.* 4th European Conference on Protection against radon at home and at work, 28th June- 2nd July 2004 Praha, Czech republic.

Cripps A.J. (1998). *Air Modeling and measurement of soil gas flow*. AIVC 11619, Construction Research communication Ltd.

Diallo T.M.O., Collignan B., Allard F. (2012), *Analytical quantification of airflows from soil through building substructures*, 10.1007/s12273-012-0095-2,2012. Building Simulation Journal.

Elenbaas W. (1942). *Heat Dissipation of Parallel Plates by Free Convection*,Physica, Vol. IX, No.1, p.1–28.

Gadgil A.J., Bonnefous Y.C., Fisk W.J. *Relative effectiveness of Sub-Slab Pressurization and Depressurization Systems for Indoor Radon Mitigation: Studies with an Experimentally Verified Numerical Model*. In: Proceedings of the 1992 international symposium on Radon

Gray A., Read S., McGale P. Darby, S., 2009. *Lung cancer deaths from indoor radon and the cost effectiveness and potential of policies to reduce them.* Brit Med J. 338, 3110-3121.

Holford, D.J. & Freeman, H.D. (1996) *Effectiveness of a Passive Subslab Ventilation Systemn in Reducing Radon Concentrations in a Home.* Environ. Sci. Technol. 30, 2914-2920.

Holman J. P. (2010). *Heat Transfer*, 10th Edition, Jack P. Holman, Southern Methodist University McGraw-Hill, New York, 2010. ISBN-13 9780073529363

I.E IDEL'CIK, (1969). *Memento des pertes de charge – Coefficients de pertes de charge singulières et de pertes de charge par frottement*. Traduction du Russe par Madame M. Meury. Collection n°13 du Centre de Recherches et d'essais du Chatou. Eyrolles, Paris.

IRSN, (2012). *Mesure de la perméabilité effective du sol aux gaz autour de la maison expérimentale MARIA du CSTB*. RT/PRP-DGE/2012-00019.

Koffi J. (2009) *Analyse multicritère des stratégies de ventilation en maisons individuelles*. Thèse Université de la Rochelle.

Mounajed, M.R., (1989). *La modélisation des transferts d'air dans les bâtiments application â l'étude de la ventilatio*n. PhD thèse. L'École Nationale des Ponts et Chaussées.

Sunderland J. E., Kenneth R.J. (1964). *Shape factors for heat conduction through bodies with isothermal or convective boundary conditions*. ASHRAE 71st Annual Meeting in Cleveland, Ohio.

Turk B.H., Harrison J.and Sextro R. G. (1991). *Performance of radon control systems. Energy and Buildings*.Vol.17, pp. 157-175.

USEPA, 1993. *Radon reduction techniques for existing detached houses. Technical guidance (third edition) for Active Soil Depressurization systems*. EPA/625/R-93/011.

HEATING ENERGY PENALTIES OF COOL ROOFS: THE EFFECT OF SNOW ACCUMULATION ON ROOF

Hashem Akbari, Mirata Hosseini

Heat Island Group
Building, Civil and Environmental Engineering Department
Concordia University
1455 De Maisonneuve Blvd. W.
Montreal, Quebec, Canada

Email: Hashem.Akbari@Concordia.ca

ABSTRACT

Utilizing a cool roof is an efficient way to reduce the cooling energy use of a building. Cool roofs, however, may increase heating energy use in winter. In cold climates, during the winter the sun angle is lower, days are shorter, sky is cloudy, and most heating occur during early morning or evening hours when the solar intensity is low. In addition, the roof may be covered with snow for most of the heating season. All these lead to a lower (than what is commonly thought) winter time heating penalties for cool roofs.

We used DOE-2.E to simulate energy consumption in an office building in four cold climate cities in North America: Anchorage (AK), Milwaukee (WI), Montreal (QC), and Toronto (ON). The effect of sun angle, clouds, daytime duration, and heating schedules can be modelled with existing capabilities of DOE-2. Snow on the roof provides an additional layer of insulation and increases the solar reflectance of the roof. To simulate the effect of snow, we defined a function consisting of U-value and absorptivity of the roof on a daily basis to simulate four different types of snow on the roof. We used an average of six years meteorological data from National Oceanic and Atmospheric Administration (NOAA) and Environment Canada to estimate the snow thickness on the roof. Results show that the heating penalties of cool roof are significantly lower (than what is commonly thought) considering snow on the roof. Annual heating energy consumption of the building with dark and cool roof without considering the snow are 85 and 88 MJ/100 m^2, respectively (3 MJ/100 m^2 penalty for cool roof) in Anchorage whereas, the annual heating energy for the dark and cool roof considering the effect of Late-Winter Packed snow are 83 and 84 MJ/100 m^2, respectively (1 MJ/100 m^2 penalty for the cool roof). For a typical office building with electricity as cooling fuel and natural gas as heating fuel, cool roofs save \$0.08/ m^2 in Montreal and in Toronto the saving for cool roof is \$0.04/ m^2 (not accounting for the effect of peak demand savings and potential downsizing of the HVAC systems).

KEYWORDS

Cool Roof, Heating Energy, Cold Climate, Office Building, DOE-2.E

1 INTRODUCTION

Cool roofs reduce the heat flux penetration into a building through the roof. Solar reflectance, infrared emittance, and thermal insulation are three parameters affecting roof heat flux. When a roof absorbs solar radiation, it is transformed into heat and some of this heat is emitted back as infrared radiation according to the infrared emittance property of the roof (in the 4-80 μm spectrum). Thus, a roof with a high solar reflectance and a high infrared emittance will absorb

less energy and will be cooler than a regular roof (Akbari and Levinson 2010). When a roof is cooler, the heat flux through the roof decreases, therefore, less cooling energy is needed to provide thermal comfort inside the building. Thermal insulation of the roof is the third parameter that influences the heat flux through the roof. During the winter, because of lower solar radiation absorption, a cool roof may increase the heating energy of the building.

Akbari et al. (2004) state that for cold climates with hot summers, a roof with solar reflectance and high emmitance is preferred as the heating penalty during the year will be less important. In addition, for cold climates with no summer cooling, using cool roof is not suggested. Some factors that make the heating energy penalties small include: lower wintertime sun angle, shorter days (sun light hours), cloudy skies, and heating period (early in the morning and evening hours). In cold climates the roof may be covered by snow during some months of the heating season and there would not be a significant difference in heating energy use of a building with cool and dark roof. The focus of this study is to quantify the heating energy penalties of a cool roof accounting for the effect of roof snow.

2 METHODOLOGY

The effect of sun angle, clouds, daytime duration, and heating schedules can be modelled with existing capabilities of DOE-2. Snow on the roof provides an additional layer of insulation and increases the solar reflectance of the roof. To simulate the effect of snow, we defined a function consisting of U-value and absorptivity of the roof on a daily basis to simulate four different types of snow on the roof. We used an average of six years meteorological data to estimate the snow thickness on the roof.

2.1 Study sites and data

We studied four cold climate cities in North America: Anchorage (AK), Milwaukee (WI), Toronto (ON), and Montreal (QC). In order to estimate the thicknesses of snow cover, we applied previous meteorological data provided by National Oceanic and Atmospheric Administration (NOAA) for the first two cities and Environment Canada for the next two cities. Figure 1 shows the snow cover on a flat surface and outside air temperature in Anchorage. Note that snow is covering a flat surface from mid-October to mid-April.

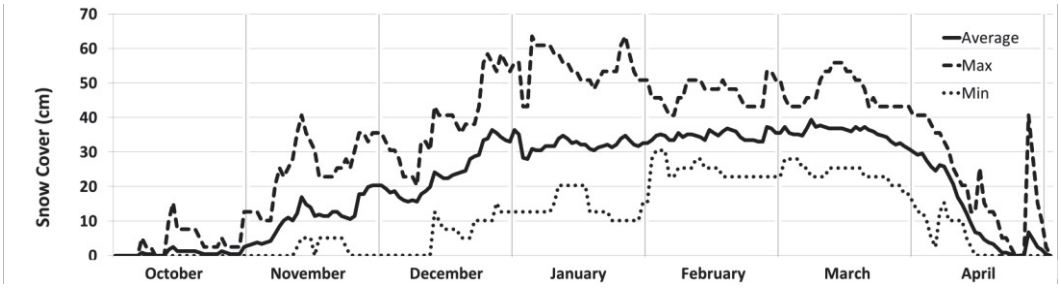

a) Snow cover

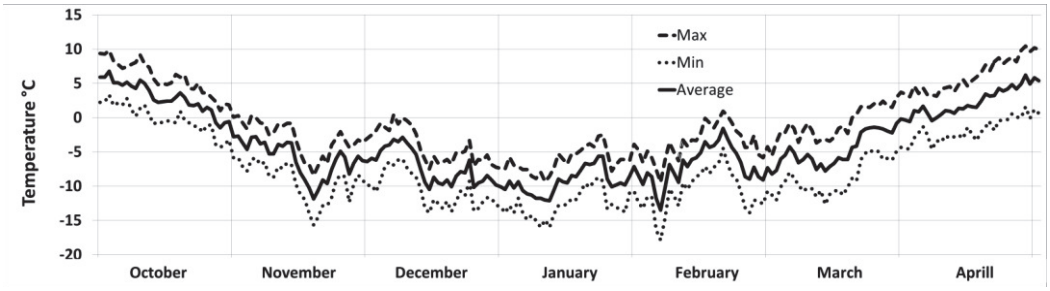

b) Outdoor air temperature

Figure 1. Snow cover and outdoor air temperature in Anchorage, AK

2.2 Snow Properties

Gray (1970) and Raab and Vedin (1995) have documented the density for different types of snow as in Table 1.

Table 1: Density of different type of snow (kg/m^3)

Type of Snow	Raab and Vedin	Gray
Very loos new snow	<30	10-30
Newly-fallen dry snow	30-100	70-190
Wet, new snow	100-200	
Wind-packed snow	200	200-350
Late-winter Packed snow	200-300	400-550
Thawing snow in spring	>400	600-700

Hedstrom and Pomeroy (1998) provide an equation to calculate the density of fresh and dry snow based on the air temperature as follow:

$$\rho_s = 67.9+51.25\ e^{Ta/2.59} \quad (1)$$

Where: ρ_s is density of snow in kg/m^3 and T_a is the air temperature in °C.

Sturm et al. (1997) provide an equation for to calculate the snow effective conductivity based on the density of snow as below:

$$k_{eff} = 0.138\text{-}1.01\ \rho+3.233\ \rho^2 \qquad \{0.156 < \rho < 0.6\} \quad (2)$$

$$k_{eff} = 0.023+ 0.234\ \rho \qquad \{\rho < 0.156\}$$

Where ρ is in g cm^{-3} and k_{eff} is in Wm^{-1} K^{-1}.

The heat transport through the snow has three components: (1) conduction through the ice lattice, (2) conduction through the air in the pore spaces, and (3) latent heat transport across pore spaces because of vapour sublimation and condensation. Radiation and convection heat transfer is considered small and ignored in our analysis. An effective thermal conductivity (k_{eff}) is used to combine all three main mechanisms (Sturm et al, 1997). We calculated k_{eff} of for snow using Eq. 2 and density of snow listed in Table 1 (see Table 2).

Table 2: Effective thermal conduction for different snow type

Type of Snow	$k_{eff}(Wm^{-1}\ K^{-1})$
Very loos new snow	0.0276
Newly-fallen dry snow	0.059
Wind-packed snow	0.1259
Packed late-winter snow	0.4412

In this study we considered four types of snow based on thermal conductivity. Since in our methodology we change the U-value of the roof on a daily basis, we modelled the roof as a quick wall in DOE-2 (this approach ignores thermal storage effect of the roof materials). Much of the shortwave radiation incident on a snow surface is reflected, with albedos as high as 0.9 for compact, dry, clean snow, dropping to 0.5-0.6 for wet snow (Pomeroy and Brun, 2001). Hence, the absorptance of the snow was assumed to be as 0.2 as an average.

2.3 Simulated building characteristics

We studied a small (465 m²) office as prototype Building with flat roof consisting of six zones (four perimeters, one central, and a plenum zone). A VAV system with natural gas boiler together with an electric chiller as one case and a packaged variable volume variable temperature with heat pump system (using electricity for both heating and cooling) as second

system serve the building. For the period that snow exists on the roof, we assumed that the absorptance of the roof is 0.2 and when snow disappears, the absorptance would be 0.85 and 0.4 for dark roof and cool roof, respectively. Table 3 presents the characteristics of the prototype building and HVAC system.

2.4 DOE-2 simulations

To simulate the effect of snow, we defined a function consisting of U-value and absorptivity of the roof on a daily basis to simulate four different types of snow on the roof.

2.4.1 Overall U-value of the roof with snow

In our modelling effort, we calculate the U-value of the snow based on its thermal conductivity and thickness. We considered density of four snow types (Late-winter packed, Wind packed, Newly-fallen dry, and Very loose new snow) and simulated the building energy consumption using DOE-2.E.

In order to find the overall U-value of the roof considering the snow, we used the following equation:

$$\frac{1}{U_{overall}} = \frac{1}{U_{roof}} + \frac{1}{U_{snow}} \quad (4)$$

Where, $U_{overall}$ is the overall U-value of the roof with snow, U_{roof} is U-value of the roof including inside film resistance (but not outside film resistance), and U_{snow} is U-value of snow. $U_{snow} = \frac{k_{eff}}{d}$, k_{eff} is thermal conductivity of snow from Table 2 which is result of equation 2, and d is daily thickness of snow. Thus, depend on the type and the thickness of snow we assumed a particular $U_{overall}$ for each day.

2.4.2 Duration of snow

Among the four cold-climate cities, in Anchorage the roof of the building is covered by snow for six months: mid-October to mid-April. Whereas, in other three cities the roof is covered by snow for almost four months and half: November 21 to April 8.

2.4.3 Slope of the roof

Here, we simulate the effect of the snow on flat roofs. Sloped roofs are designed to shed snow. Hence the period of snow cover on the roof is shorter and depends on the roof slope and frequency of snow storm.

2.4.4 Snow thickness

For all four simulated climate regions, we calculated the six-year daily average thickness snow cover on the surface and used the data to simulate the prototype building heating energy use with the snow on the roof.

3 RESULTS

We first simulated the office building with dark and cool roof without snow to compare heating and cooling energy consumption. Then, we simulated the effect of snow, taking into account as a layer of the roof.

Table 3: Prototype office building and HVAC system characteristics

Characteristic	Old Vintage	Old Vintage New HVAC	New Vintage
Construction			
Floor Area (m^2)	464.5		
Number of Floors	1		
Floor Materials	4IN Concrete Slab-On-Grade		
Roof Materials	Roof Gravel, Built-up-roof, R-7 Mineral Board insulation, Wood Sheathing (U-Value=0.63W/m^2K)		R-20 insulation(U-Value=0.251W/m^2K)
Wall Materials	Wood Shingles, Plywood, R-7 Fiber insulation, Gypsum Board (U-Value=0.555W/m^2K)		R-19 insulation (U-Value=0.241W/m^2K)
Window Characteristics			
Number of Panes	2	2	2
Shading Coefficient	0.76	0.76	0.76
Interior Loads			
Occupancy (Person)	50		
Interior Lights (W/m^2)	16.14		
Miscellaneous (W/m^2)	10.76		
HVAC System			
Type 1	Variable Air Volume (VAV)		
Schedule	8 am – 9 pm Weekdays Jan1 – Dec 31		
Ventilation	Supply		
Capacity	Zonal/Local	Zonal/Local	Zonal/Local
Efficiency	0.55		
Economizer	Temperature		
Economizer Limit Temperature(°C)	18.3		
Outside Air (m^3/h/person)	34		
Natural Ventilation	No		
Cooling			
Type	Air-Cooled Hermetic Reciprocating Chiller		
Capacity	Zonal/Local	Zonal/Local	Zonal/Local
COP	3.65	4.54	4.54
Setpoint (°C)	25		
Setup (°C)	37		
Heating			
Type	Natural Gas Hot Water boiler		
Capacity	Zonal/Local	Zonal/Local	Zonal/Local
Efficiency (%)	80	84	84
Setpoint (°C)	21		
Setup (°C)	13		
Type 2	Packaged Variable Volume and Temperature (VVT)		
Cooling			
Type	Direct-Expansion		
Capacity	Zonal/Local	Zonal/Local	Zonal/Local
COP	2.77	3.57	3.57
Setpoint (°C)	25		
Setup (°C)	37		
Heating			
Type	Heat Pump		
Capacity	Zonal/Local	Zonal/Local	Zonal/Local
COP	2.7	3.5	3.5
Setpoint (°C)	21		
Setup (°C)	13		

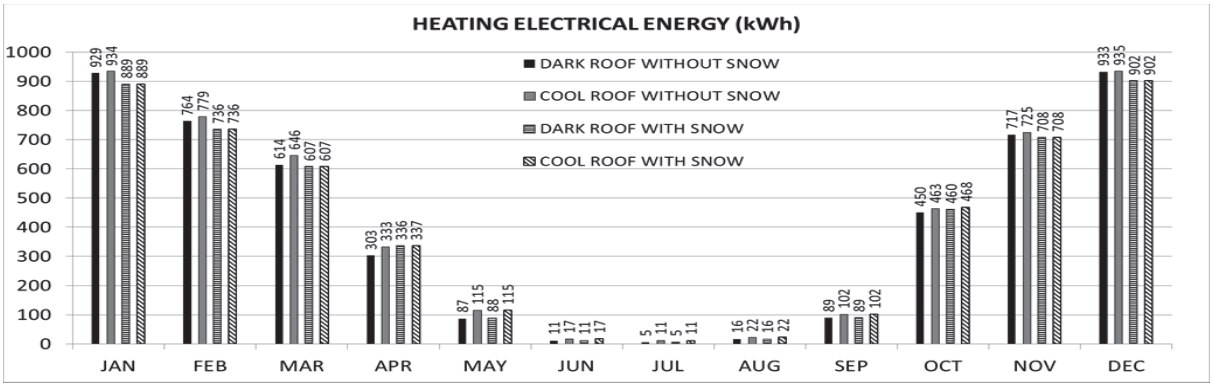

a) Monthly electrical heating energy consumption

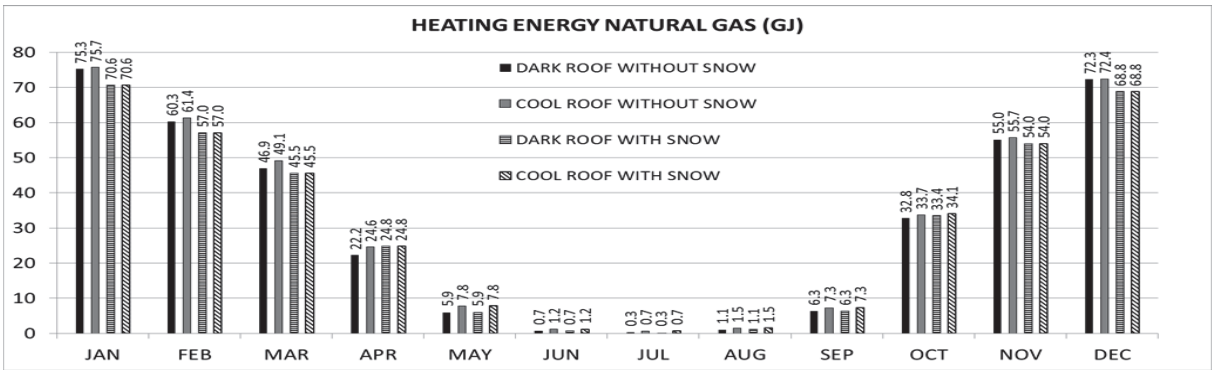

b) Monthly natural gas heating energy consumption

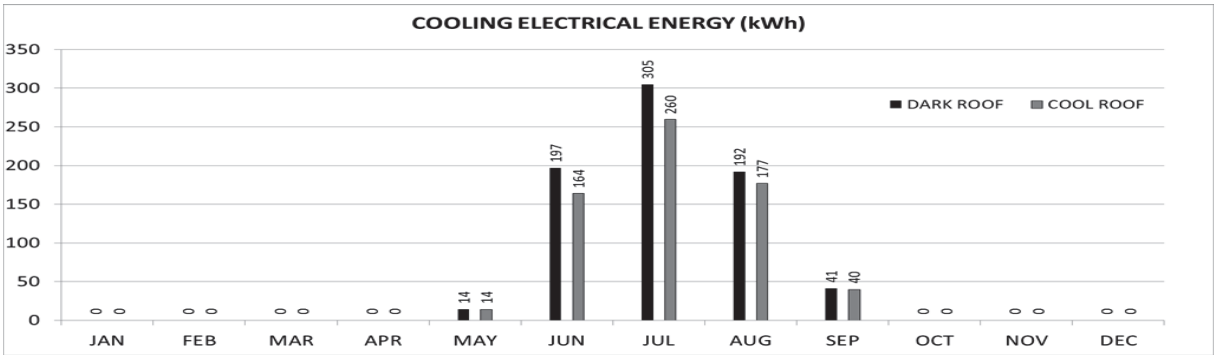

c) Monthly electrical cooling energy consumption

Figure 3: Small office building monthly electrical and gas heating energy (a,b) and electrical cooling (c) consumption in Anchorage

For Anchorage, Figure 3 shows that using a cool roof for the building is associated with heating energy consumption penalties primarily during October through April. Accounting for the effect of snow, these penalties no longer exists for six months (Nov-Apr) of the year and the heating energy for the building with cool and dark roofs are the same. Cooling energy use (and hence savings) are fairly small.

We calculated annual expenditure for electricity and natural gas using local cost as in Table 4 for all the four cities.

Table 4: energy rates in the four locations

	Anchorage[1]	Milwaukee[1]	Montreal	Toronto
Electricity ($/kWh)	0.116	0.077	0.089 (HydroQuebec)	0.078 (OntarioHydro)
Natural Gas ($/therm)	0.49	1.01	0.31(Gaz Metro)	0.57 (Energy Shop)

1. Akbari and Levinson (2010)

Table 5 shows the annual heating penalties and cooling savings for cool roof with and without snow, for the building with VAV and PVVT system in all four cities. Considering the effect of snow on the roof, conditioning cost penalties for cool roof decreased in Anchorage (from 0.14 to 0.04 $/m^2 for gas-heating system and from 0.29 to 0 $/m^2 for electric-heating system). In Milwaukee for gas-heating system, conditioning penalties for cool roof reduced from 0.16 to 0.01 $/m^2 and for electric-heating system from 0.13 to 0.07 $/m^2.

Accounting for the effect of snow in Montreal, conditioning savings for cool roof increased from 0.01 to 0.08 $/m^2 for gas-heating system and 0.18 $/m^2 penalties for cool roof reached to 0.13 $/m^2 savings for that of electric-heating system. In Toronto, for gas-heating system 0.05 $/m^2 penalties for cool roof altered to a 0.04 $/m^2 savings.

As the roof insulation in buildings increases (new construction), the energy consumption differences between dark roof and cool roof decreased significantly. For instance, in Anchorage penalties for cool roof decreased from 0.04 to 0.01$/m^2 and in Milwaukee this amount reduced from 0.01 to 0 $/m^2. For Montreal and Toronto also savings for cool roof decreased from 0.08 to 0.03 $/m^2 and from 0.04 to 0.01 $/m^2, respectively. These same results are obtained by Syneffa et al. (2007).

4 CONCLUSIONS

Utilizing cool roof is an efficient way to reduce building cooling energy use and urban heat island. Cool roofs, however, may increase the heating energy use. In this study, we simulated the annual heating and cooling energy use in conventional and cool roof buildings in four cities in cold climates. Results show that annual energy expenditure for an small office prototype building in cold climates with cool roofs is lower than those of dark roofs.

Accounting for the effect of roof snow, conditioning cost penalty for cool roof reduced dramatically in Anchorage (0.14 to 0.04 $/m^2 for gas-heating system and 0.29 to 0 $/m^2 for electric heating system). In Milwaukee for gas-heating system, conditioning penalties for cool roof reduced from 0.16 to 0.01 $/m^2 whereas for electric-heating system 0.13 $/m^2 penalty for cool roof altered to a 0.07 $/m^2 savings.

In Montreal also conditioning savings for cool roof increased from 0.01 to 0.08 $/m^2 for gas-heating system and 0.18 $/m^2 penalty for cool roof changed to 0.13 $/m^2 savings for electric-heating system. In Toronto for using gas-heating system, 0.05 $/m^2 penalties for cool roof altered to a 0.04 $/m^2 savings.

These simulations show that penalties for cool roofs in cold climates are very small, if any. Cool roofs also save peak demand electricity use during the summer (saving $) and potentially lead to down-sizing of the HVAC equipment (saving more $). Accounting for the peak demand savings and downsizing will only make cool roofs more economical. Also, it should be noted that a cool roof replacing a dark roof leads to cooling of the globe. The heat island reduction and air quality benefits of cool roof are also significant.

5 ACKNOWLEDGEMENTS

Funding for this research was provided by the National Science and Engineering Research Council of Canada under discovery program.

Table 6: Annual heating penalty and cooling saving for cool roof with and without snow in the building with VAV and PVVT system

City	Gas heating (heating in GJ/100 m2, cooling in kWh/100 m2)										Heat pump (heating and cooling in kWh/100 m2)									
	No snow on roof		LWP* snow on roof		WP* snow on roof		NFD* snow on roof		VLN* snow on roof		No snow on roof		LWP snow on roof		WP snow on roof		NFD snow on roof		VLN snow on roof	
	D*	C*	D	C	D	C	D	C	D	C	D	C	D	C	D	C	D	C	D	C
a) Anchorage											**Old construction with old systems**									
Heating energy use	85	88	83	84	77	78	73	74	70	71	12468	12800	11792	11885	10511	10604	9678	9771	8994	9086
Cooling energy use	161	141	161	141	161	141	161	141	161	141	216	135	227	135	227	135	227	135	227	135
Conditioning expenditure ($)	520	534	508	512	474	479	451	455	431	435	1471	1500	1394	1394	1246	1246	1149	1149	1070	1070
											Old construction with new systems									
Heating energy use	81	84	79	80	74	75	70	71	66	67	11545	11874	10916	10990	9685	9758	8888	8961	8238	8311
Cooling energy use	129	113	129	113	129	113	129	113	129	113	176	105	176	105	176	105	176	105	176	105
Conditioning expenditure ($)	498	512	487	491	454	459	432	436	413	417	1360	1390	1287	1287	1144	1144	1051	1052	976	976
											New construction with new systems									
Heating energy use	60	61	60	61	58	58	56	56	54	54	8084	8225	8001	8023	7571	7593	7192	7214	6801	6823
Cooling energy use	126	116	126	116	126	116	126	116	126	116	187	148	187	148	187	148	187	148	187	148
Conditioning expenditure ($)	373	378	372	373	360	361	349	350	337	338	959	971	950	948	900	898	856	854	811	809
b) Milwaukee											**Old construction with old systems**									
Heating energy use	54	57	55	56	53	55	52	53	49	50	7043	7399	7215	7318	6844	6948	6470	6574	6030	6134
Cooling energy use	1385	1252	1385	1252	1385	1252	1385	1252	1385	1252	1359	1167	1359	1167	1359	1167	1359	1167	1359	1167
Conditioning expenditure ($)	654	670	666	667	647	648	628	629	604	605	647	660	660	653	632	625	603	596	569	562
											Old construction with new systems									
Heating energy use	52	54	53	54	51	52	49	50	47	48	6410	6730	6560	6646	6197	6282	5837	5922	5419	5504
Cooling energy use	1112	1005	1112	1005	1112	1005	1112	1005	1112	1005	1067	912	1067	912	1067	912	1067	912	1067	912
Conditioning expenditure ($)	609	626	621	623	603	605	584	587	562	564	576	588	587	582	559	554	532	526	499	494
											New construction with new systems									
Heating energy use	37	38	38	38	37	38	37	37	36	36	4329	4460	4436	4465	4348	4377	4243	4271	4084	4113
Cooling energy use	1046	994	1046	994	1046	994	1046	994	1046	994	1047	971	1047	971	1047	971	1047	971	1047	971
Conditioning expenditure ($)	458	465	465	465	460	460	453	453	443	443	414	418	422	419	415	412	407	404	395	391
c) Montreal											**Old construction with old systems**									
Heating energy use	70	73	71	72	68	69	65	66	62	63	10054	10492	10194	10289	9537	9631	8930	9025	8279	8374
Cooling energy use	1176	1029	1176	1029	1176	1029	1176	1029	1176	1029	1176	938	1176	938	1176	938	1176	938	1176	938
Conditioning expenditure ($)	377	376	381	373	370	362	359	351	347	339	999	1017	1012	999	953	941	899	887	841	829
											Old construction with new systems									
Heating energy use	67	70	68	69	65	66	62	63	59	60	9318	9712	9357	9516	8808	8884	8227	8303	7602	7678
Cooling energy use	944	826	944	826	944	826	944	826	944	826	918	730	918	730	918	730	918	730	918	730
Conditioning expenditure ($)	347	349	351	345	341	335	330	324	319	313	911	929	914	912	866	856	814	804	758	748
											New construction with new systems									
Heating energy use	50	51	51	51	50	50	49	49	47	48	6623	6798	6760	6788	6605	6633	6418	6446	6140	6168
Cooling energy use	874	818	874	818	874	818	874	818	874	818	854	766	854	766	854	766	854	766	854	766
Conditioning expenditure ($)	274	274	277	274	275	271	271	267	265	262	665	673	678	672	664	658	647	642	622	617
d) Toronto											**Old construction with old systems**									
Heating energy use	54	57	56	57	54	56	53	54	51	52	6502	6884	6724	6850	6426	6552	6106	6232	5715	5841
Cooling energy use	1365	1204	1365	1204	1365	1204	1365	1204	1365	1204	1435	1182	1435	1182	1435	1182	1435	1182	1435	1182
Conditioning expenditure ($)	440	445	449	445	440	436	431	427	418	414	619	629	636	627	613	603	588	578	558	548
											Old construction with new systems									
Heating energy use	51	54	52	54	51	52	50	51	48	49	5686	6056	5883	6020	5601	5734	5304	5435	4943	5061
Cooling energy use	1109	978	1109	978	1109	978	1109	978	1109	978	1117	891	1117	891	1117	891	1117	891	1117	891
Conditioning expenditure ($)	400	406	409	407	401	399	392	390	380	378	531	542	546	539	524	517	501	493	473	464
											New construction with new systems									
Heating energy use	37	38	37	38	37	38	37	37	36	36	4156	4304	4286	4325	4222	4261	4136	4175	3999	4038
Cooling energy use	1024	963	1024	963	1024	963	1024	963	1024	963	942	866	942	866	942	866	942	866	942	866
Conditioning expenditure ($)	305	308	310	309	308	307	305	304	300	299	398	403	408	405	403	400	396	393	385	383

***LWP=Late Winter Packed WP=Wind Packed NFD=Newly Fallen Dry VLN=Very Loose New D=Dark C=Cool**

6 REFERENCES

Levinson R, Akbari H. Potential benefits of cool roofs on commercial buildings: conserving energy, saving money, and reducing emission of greenhouse gases and air pollutants. Energy Efficiency 2010; 3:53-109.

Miller WA, Parker DS, Akbari H. Painted metal roofs are energy-efficient, durable and sustainable. Cool Metal Roofing Coalition; 2004:1-13.

Gray, D.M., (ED). 1970. Handbook on the Principles of Hydrology. Canadian National Committee for the International Hydrological Decade, Ottawa.

Raab B, Vedin H (eds). 1995. Sweden's National Atlas: Climate, Lakes and Waters. Bokf□orlaget Bra B□ocker (ISBN 91-7024-898-2).

Hedstrom, N.R., and Pomeroy, J.W. 1998. Accumulation of intercepted snow in the boreal forest: measurements and modelling. Hydrol. Processes**,** 12, 161 1-1623.

Sturm, M., Holmgren, J., Konig, M., and Morris, K. 1997. The thermal conductivity of seasonal snow.3 Glaciology**,** 43(143), 26-41.

Pomeroy, J.W. and E. Brun. 2001. "Physical properties of snow" In, (eds. H.G. Jones, J.W. Pomeroy, D.A. Walker and R.W. Hoham) *Snow Ecology: an Interdisciplinary Examination of Snow-covered Ecosystems*. Cambridge University Press, Cambridge, UK. 45-118.

A. Synnefa, M. Santamouris, H. Akbari Estimating the effect of using cool coatings on energy loads and thermalComfort in residential buildings in various climatic conditions, Energy and Buildings 39 (2007) 1167–1174

Hydro-Quebec http://www.hydroquebec.com

Gaz Metro http://www.gazmetro.com/

Ontario Hydro http://www.ontario-hydro.com

Energy shop http://www.energyshop.com/natural-gas-prices-Enbridge-residential.cfm

INFLUENCE OF COOL MATERIALS ON BUILDING ENERGY DEMAND AT DISTRICT SCALE

Adrien Gros[1], Petroula Alexaki[2], Emmanuel Bozonnet[*1], and Christian Inard[1]

1 LaSIE, La Rochelle University
Pole science et technologie
Avenue Michel Crépeau
17000 La Rochelle
France

2 Grenoble INP
11, rue des Mathématiques
38402 Saint Martin d'Hères
France

ABSTRACT

Since 2007, more than half of world population lives in urban areas and its activity leads to an increase of building energy demand notably in summer. The temperature rise of densely built areas is mainly due to landscaping and anthropogenic heat fluxes such as air conditioning systems. Acting on urban landscaping, building density, surface albedo or green area can mitigate the urban heat island with direct and indirect improvement of building energy performances.

In the present study, a new numerical approach was developed to assess the building energy demand including microclimate interactions on buildings. The different physical phenomena are computed at the district scale with different meshes, for the surfaces and the volumes, of the tridimensional numerical mockup. The urban microclimate is assessed thanks to specific models developed for the outdoor airflows, the longwave and shortwave radiative exchanges. The thermal behaviour of buildings is computed by a model developed on the basis of the weighting factor method which saves computation time. Then, a coupling method was implemented in order to match the results from the various meshes. The thermal balances are computed simultaneously for the whole district cells, including indoor and outdoor balances, for each time step.

A case study was selected and studied: a district located in Nantes, France, named Pin Sec district. A parametric study is carried out considering cool materials. The results are displayed as the cooling demand of buildings for each case studied. The impact of cool material areas on both building energy demand and urban microclimate are clearly shown through the results obtained.

KEYWORDS

Zonal model, district scale, urban microclimate, building energy demand, weighting factor method

1 INTRODUCTION

Between 1950 and 2007, the urban population has grown from 30% to 50% of the world population. The associated growth of the urban area has amplified urban microclimate. The modification of the local wind fields and the increase of the heat transfers between walls, ground and air, changed the microclimatic parameters at local scale. The most known urban microclimate aspect engendered is the Urban Heat Island (UHI). It is characterised by higher temperatures in urban area than in rural area, leading to an increase of the cooling energy demand in the towncenter (Santamouris et al. 2001) . The use of air-conditioning systems to maintain indoor inhabitant comfort, reject anthropogenic heat fluxes in the atmosphere. The result is a negative feedback that increases the UHI and the building energy demand. The building energy demand management have to be more efficient with limiting the air-conditioning systems use. Modification of urban landscaping, such as building morphology, surface albedo or green areas, can mitigate UHI, which consequently reduces energy demand.

The simulation of the different physical processes in urban areas can be used to compute the building energy demand. Traditionally the thermal dynamic building tools are used to optimise the energy consumption of building by computing annual or seasonal building energy demand. The meteorological data files used are generally issued from standard data (as the airport) and are not representative of the urban microclimate conditions. The outdoor physical phenomena are generally very briefly described and the interaction with the urban environment is not taken into account. Microclimatic models enable to compute precisely all the physical processes in the urban areas (Martilli 2007). But the building indoor description is generally very simplified and CPU times needed to achieve simulation are too high to simulate the building energy demand during a year or a season.

We propose in this paper an intermediate model dealing with the local urban climate with building energy demand at the district scale. The goal of this model is to couple the climatic field of the urban canopy with thermal fluxes inside buildings. The detailed description of all the physical processes inside and outside the building are not adapted to annual prediction of energy consumption at the district scale. Thus a simplified model of the urban canopy based on zonal model is used. Initially developed to compute temperature fields in canyon street (Bozonnet et al. 2005; de la Flor and Domínguez 2004), this method was improved to be applied on any urban geometric configuration. A reduced thermal building model based on the weighting factor method (Depecker et al. 2001; Rousseau 1978) is used to compute the building thermal load.

In the first part, the meshes used in order to simulate the canopy, as well as buildings are described. In the last part, a case study i.e a district located in Nantes, France, named Pin Sec district, is used to compute the building energy demand during the summer season. A parametric study is carried out considering cool materials. Cool materials are characterised by high albedo and emissivity (Santamouris et al. 2011). By decreasing the solar irradiance absorbed by the facades, cools materials allow reducing the surface temperatures and thus minimizing the UHI intensity and the cooling load associated. The results are displayed as the cooling demand of buildings for each case studied.

2 URBAN DISTRICT MESH FOR URBAN FLUXES

An adapted meshing was developed to model at the district scale. The Pin Sec district located in the North-East of Nantes city centre, in France (Figure 1), is used to illustrate the meshes developed. Pin Sec is a residential district of 136.000 m² composed of 40 residential buildings, 4 scholar buildings, 1 scholar gymnasium, 2 sport buildings and 11 utility buildings.

Figure 1 : Topview (a) and localisation (b) of Pin Sec district in Nantes, France


(a)

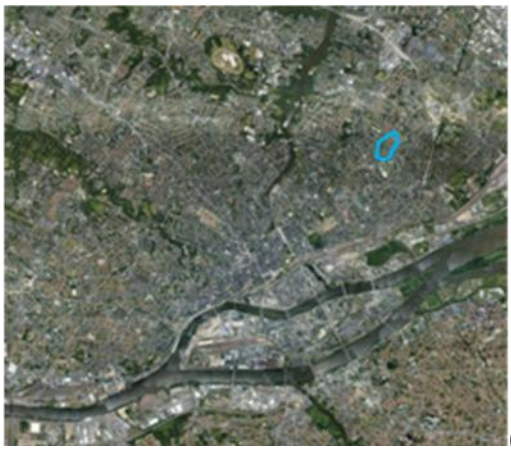
(b)

The district is split into in two domains, the urban canopy, divided in canopy cells and the building divided in building cells (Figure 2). The canopy cells are used to compute the outdoor air temperature and the building cells are used to compute the power needed to maintain a given temperature set point. The urban surfaces are the interfaces between the canopy cells and building cells. They are used to calculate the surface outside temperatures of the ground and the buildings walls.

Figure 2 : Representation of the different physical domains

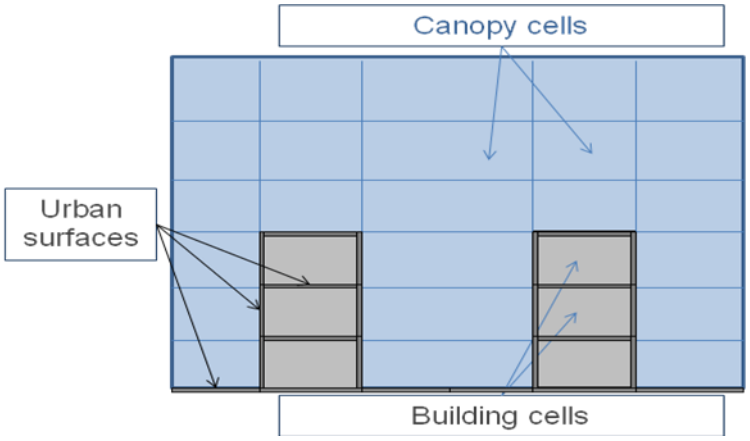

The coupled model allows computing surfacic physical values (surface temperatures) and volumic physical values (outdoor air temperatures and heating/cooling powers). Thus, two categories of mesh have to be distinguished: the surfacic mesh and volumic mesh. For the surfacic mesh, the discretization is chosen like in the building thermal dynamic simulation. Each wall with different orientation and physical properties are defined by its own node. Thus the Pin Sec district is composed of 1551 surfaces (Figure 3 (a).) with surfaces ranging from 50 m² to 1000 m². In the volumic mesh, each floor of a building represents a building cell with a height equal to 3 m. The canopy cells are built by extrusion of the ground urban surface. To simplify the simulation, height of the building cells and canopy cells are equal and fixed to 3 m i.e the height of a floor. Thus the Pin Sec district is composed of 3122 canopy cells and 149 building cells (Figure 3 (b)).

Figure 3 : District surfacic (a) and volumic (b) model

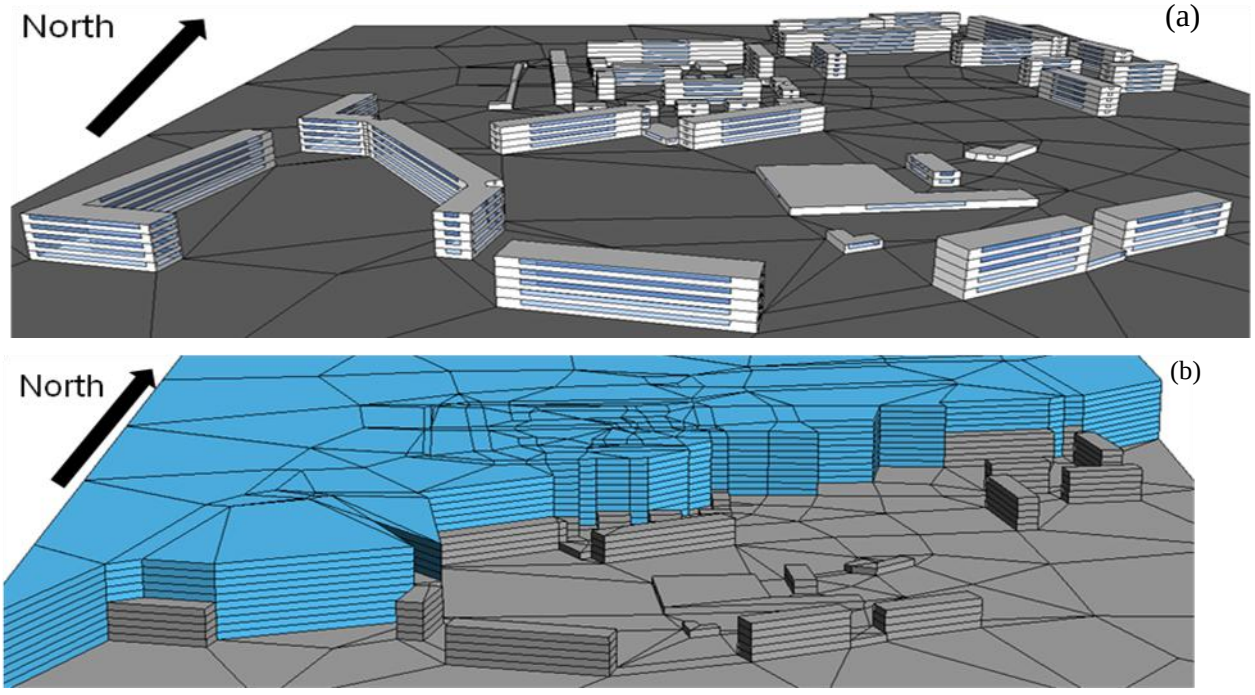

Some physical phenomena need a more precise mesh. To compute solar irradiance received by each wall, it is necessary to determine the mask effect created by the urban environment. Each urban surface is split into triangles to obtain 15 887 submeshes (Figure 4 (a)).
To compute the airflow around the building a more precise mesh is used too. The volumic district model is meshed with a regular hexahedral meshing. Thus, the Pin Sec district is composed of 13 584 688 hexahedra (Figure 4 (b))

Figure 4 : Surfacic (a) and volumic (b) submesh

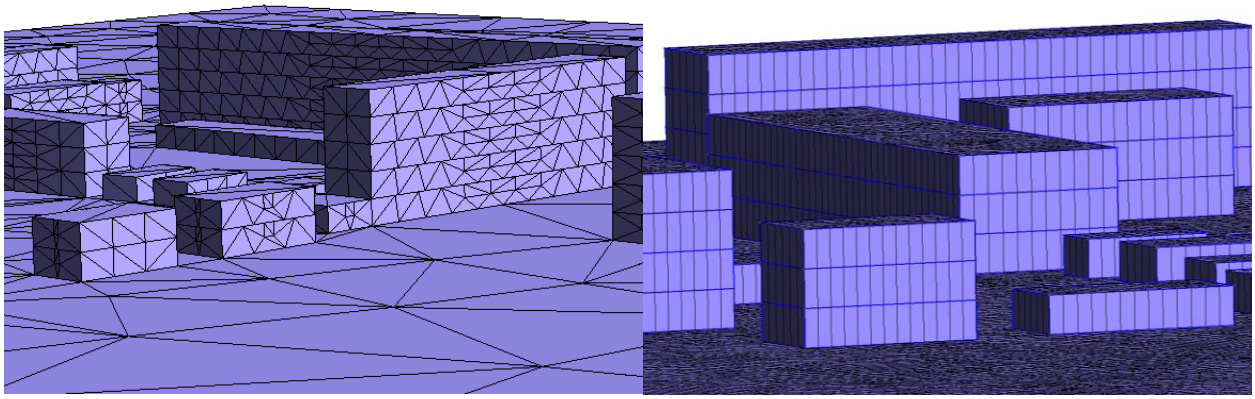

(a) (b)

3 URBAN CANOPY MODEL

3.1 Temperature field simulation

The canopy cells are composed of five or six faces indexed *n*. These faces are either an interface with another canopy cell or an urban surface.
Each face is crossed by mass and heat fluxes. The temperature of the canopy cell $T^t_{e,k}$ at time *t* can be computed thanks to the thermal balance (Equation (1)) with V_k, the cell volume [m^3], C_p, the air specific heat [J/(kg.K)], ρ the air density [kg/m^3], $\phi_{k,n}$ the heat flux through the face *n* [W] and ϕ_s the heat production in the cell [W].

$$\rho C_p V_k \frac{dT^t_{e,k}}{dt} = \sum_n \phi_{k,u} + \phi_s \quad (1)$$

For a face in contact with urban surface *i* at the temperature $T^t_{se,i}$ the flux through the face is defined by:

$$\phi_{k,n} = h_{ce,i} A_i (T^t_{se,i} - T^t_{e,k}) \quad (2)$$

Where A_i is the area of the urban facet *i* [m^2] .
Else if the face *n* is an interface with another cell at the temperature $T^t_{e,j}$, the heat flux through is defined by:

$$\phi_{k,n} = C_p Q_n (T^t_{e,j} - T^t_{e,k}) \quad (3)$$

Where, Q_n is the mass flow through the face *n* [kg/s].
To respect the mass conservation the air mass flow sum of each canopy cell must be equal to zero.

3.2 Flow field simulation

The Computational Fluid Dynamic models are often used to simulate the flow field in urban areas and to study pedestrian comfort or outdoor air quality. These models are very precise but the computing time and the power necessary is not adapted to achieve annual or seasonal simulation. To simplify the flow field computation, the urban aeraulic model QUIC (Pardyjak and Brown 2003) is used. This model is based on empirical laws developed by Rockle (1990) to provide flow fields which comply with continuity equation (Kaplan and Dinar 1996; Kastner-Klein et al. 2004). The velocities calculated are then used to compute the air mass flows through each canopy cell interface. The QUIC aeraulic simulation is used to compute the velocity components *u*, *v* or *w* for the facet of each hexahedral submesh aligned in the *x*, *y* or *z* directions. The air mass flow $Q_{f,p}$ [kg/s] through the facet *p* is given by:

$$Q_{f,p} = \rho V_{f,p} A_{f,p} \tag{4}$$

Where $A_{f,p}$ is the area [m²] and $V_{f,p}$ the normal velocity [m/s]of facet *p*.
Each interface from canopy cells can be represented as facet set oriented in the x, y or z direction corresponding to the hexahedral meshing. The air mass flow through the interface is the sum of each air mass flow through each corresponding facet.

$$Q_n = \sum_{p=0}^{Np} Q_{f,p} \tag{5}$$

4 THERMAL BUILDING MODEL

4.1 Building demand model

To simplify the calculation building energy load, the weighting factor method is used. This method consists in computing all the thermal processes inside building cells for a unit excitation. The weighting factor W^n_E is the discrete value of the thermal load induced by the unit excitation E_u, *n* hours after the excitation. The thermal load Q^t_E [W] induced by a excitation E^t is expressed with the convolution product (equation (6)).

$$Q^t_E = \sum_{n=0}^{\infty} W^n_E E^{t-n} \tag{6}$$

To compute the total thermal load of a building cell, three categories of unit excitation are considered:

- T_c, the temperature set point of the building cell,
- E_{clo} , the solar irradiance through the windows incoming in the building cell,
- $T_{se,j}$, the outdoor surface temperature of the walls

Thus the power P^t [W] needed to maintain the temperature set point is computed as the sum of the thermal load induced by each excitation, the internal gain Q^t_{int} and the thermal load due to the air exchange with a canopy cell *k*

$$P^t = \rho C_p V \frac{dT^t_c}{dt} + \rho C_p D_v \left(T^t_c - T^t_{e,k}\right) - Q^t_{int} - Q^t_{E,clo} - Q^t_{T_c} - \sum_{j=1}^{Np} Q^t_{T_{se,j}} \tag{7}$$

Where, D_v is the ventilation air flow [m^3/s] in the building cell due to the infiltration and the mechanical ventilation.

4.2 Thermal surface model

The urban surfaces are interface between urban canopy and building. The surface temperature calculation allows coupling the outdoor air temperature with indoor thermal load simulation.
A thermal balance is used to compute the outdoor surface temperature $T^t_{se,i}$ of the urban surface *i*.

$$\varphi^t_{ce,i} + \varphi^t_{pe,i} + I^t_{GLO,i} = I^t_{CLO,i} \tag{8}$$

The conductive heat flux is calculated by using the response factor method (Depecker et al. 2001; Mitalas and Stephenson 1967).

$$\varphi^t_{pe,i} = \sum_{n=0}^{\infty} Y^n_i \cdot T^{t-n}_{si,i} - \sum_{n=0}^{\infty} Z^n_i \cdot T^{t-n}_{se,i} \tag{9}$$

If the urban surface is a building wall, weighting factors are defined to calculate the conductive heat flux with excitation defined in the previous section (Gros 2013). Thus the conductive heat flux is calculated by:

$$\varphi^t_{pe,i} = \varphi^t_{int} + \varphi^t_{E,clo} + \varphi^t_{T_c} + \sum_{j=1}^{Np} \varphi^t_{T_{se,j}} - \sum_{n=0}^{\infty} Z^n_i \cdot T^{t-n}_{se,i} \tag{10}$$

With

$$\varphi^t_E = \sum_{n=0}^{\infty} YW^n_E E^{t-n} \tag{11}$$

The convective heat flux is calculated by using the outdoor air temperature of the canopy cell in contact with the surface:

$$\varphi^t_{ce,i} = h_{ce,i}(T^t_{e,k} - T^t_{se,i}) \tag{12}$$

The direct solar irradiance $I^t_{b,i}$ and the diffuse solar irradiance received by the urban surface *i* are calculated by using the solar irradiation simulation software SOLENE (Miguet and Groleau 2002). The overall surfaces of the urban scene form a closed envelope, including the sky as a hemisphere with an infinite radius (Bozonnet et al. 2005). By using the view factors between the urban surfaces, the radiosity method can be used to compute the total irradiance considering the multiple reflexion $I^t_{CLO,T,i}$ (Equations 13 and 14).

$$J^t_{CLO,i} = \rho_{CLO,i}(I^t_{b,i} + I^t_{d,i} + \sum_{j=1}^{Ns} F_{ij} J^t_{CLO,j}) \tag{13}$$

$$I^t_{CLO,t,i} = \frac{J^t_{clo,j}}{\rho_{CLO,i}} \tag{14}$$

Considering the urban surface as black body, the longwave irradiance reflections are neglected. The view factors are then used to compute the longwave irradiance received by each urban surface through a linear model.

$$I^t_{GLO,i} = h_{re} F_{ij}(T^t_{se,j} - T^t_{se,i}) \tag{15}$$

5 CASE STUDIES

5.1 Description

The coupled model is applied to the Pin Sec district in Nantes, to study the influence of the cool painting. The goal is to study the impact of different cool painting application on the cooling energy demand corresponding to the period from 1st May to the 30th September. The building walls are composed of 20 cm of concrete and 10 cm of insulation and double-glazed windows. Cool paints are applied to increase the reflectivity from 0.3 to 0.9 and to maintain a high emissivity of 0.9. The coupled model is used to simulate the energy demand of the Pin Sec district for 4 different cases. The first case is without cool painting (case A), the second case concerns cool paint only on building vertical walls (case B), the third is with cool paint only on the roofs (case C) and the last case gathers case B and C (cool paint on roofs and vertical walls, case D).

Table 1: Description of studied cases

Case A	Case B	Case C	Case D
Without cool paint	With cool paint on building vertical walls	With cool paint on building roofs	With cool paint on building roofs and walls

5.2 Microclimatic aspect

The coupled model allows computing the air temperature of each canopy cell for each hour of the year. These results can be aggregated to calculate for each canopy cell, the number of degree-hours [D-h] higher than the indoor temperature set point (26°C). This process allows determining which cells are the most influenced by the urban environment. The canopy cells located in the centre of the district have the highest values, reaching values of 6000 D-h higher than 26°C (zone 1
Figure 5).

Figure 5 : Degree-hours number of urban cells (3m< Z< 6m)

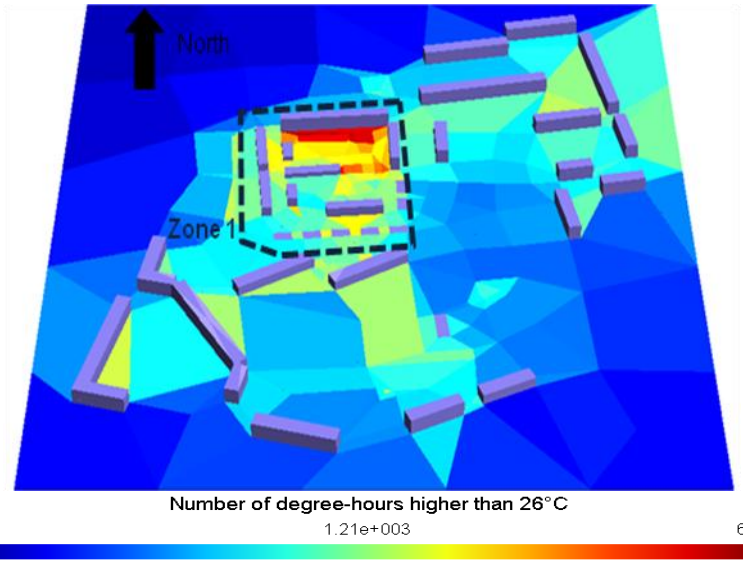

The canopy cells located in the district side have the smallest values close to 243 D-h higher than 26°C. The values located on the boundaries of the studied domain are equal to the meteorological data used for the simulation. Thus the more the canopy cells are located in high density area, the more the number of degree-hours is high. Thus the numbers of degree-hours increases for canopy cells located in high density areas.

The differences between the number of degree-hours for case A and B or C respectively for canopy cells located between 0 m and 3 m due to the cool paint application are shown in Figure 6. The more sensitive zones correspond to the denser zones. Indeed, in zone 1 (Figure 6) the contact surface between canopy and urban area is more important than in the other zones. The air is more influenced by the surface temperatures and thus by cool paint. As presented on the Figure 6, the use of cool paint on facades (case B) is the most efficient way to decrease UHI effects. It allows a more important decrease (97% for case B, and 91% for the case C) and a better distribution in the whole district.

Figure 6 : Difference of number of degree-hours for urban cells (0m< Z< 3m) between case A and B (a) and case A and C (b)

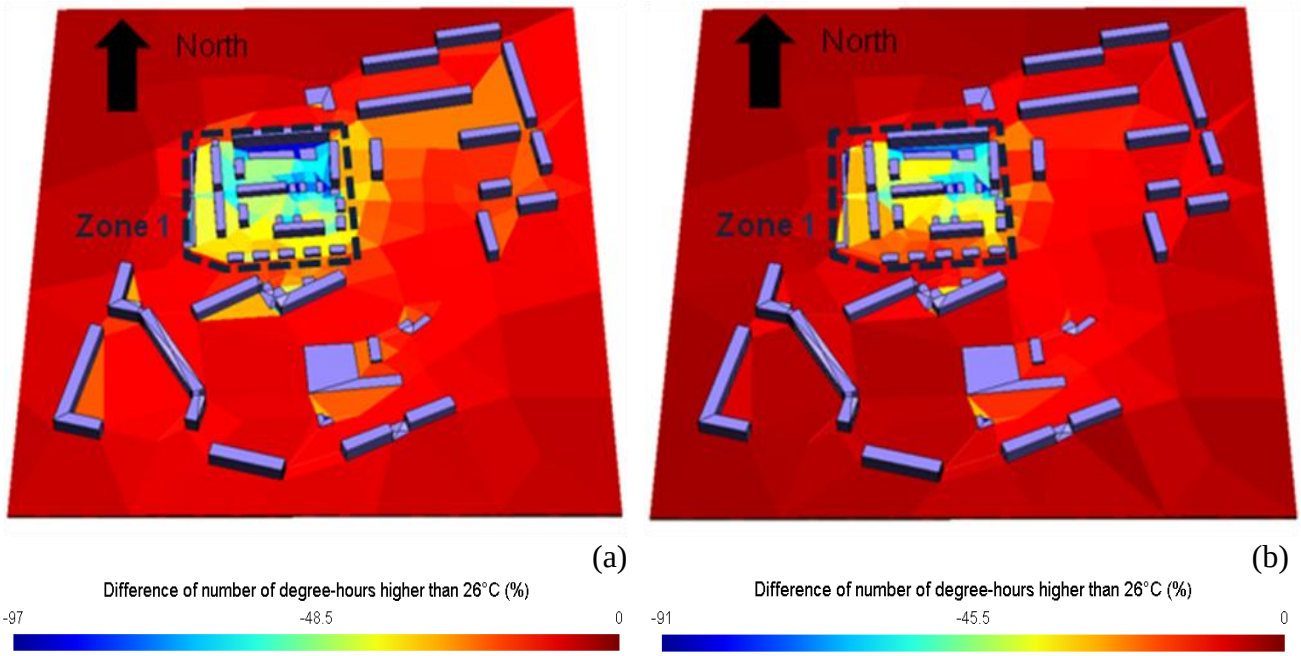

5.3 Building demand impact

Figure 7 (a) shows cumulative frequency of cooling demand for the four cases. For case A, 8% of building cells, corresponding to the 11 utility buildings are not air conditioned. 60 % of building cells have cooling need ranging from 15 kWh/m²/year to 40 kWh/m²/year and 32% ranging from 40 kWh/m²/year to 87 kWh/m²/year. Figure 7 (b) shows cooling energy demand distribution in the district. The areas with the most important cooling energy demand are located in zone 1, in accordance to the result presented in
Figure 5.

Figure 7 : Cooling demand cumulative frequency for the cases A, B, C and D (a) and tri-dimensional energy demand representation of the district for case A (b)

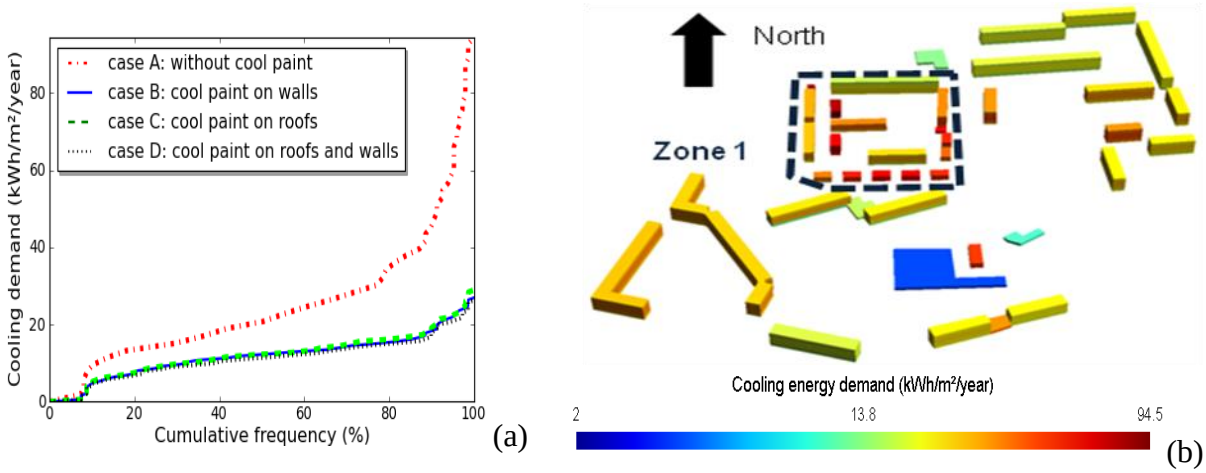

Using cool paint reduces the disparity of cooling energy demand between the different buildings. All the cooling energy demands are ranged from 0 to 20 kWh/m²/year. For both cases of cool paint either on the roofs or on the walls, the decrease is the same but the spatial distribution changes. The use of cool paint on roofs favours the decrease of energy demand of the last floor of the buildings (Figure 8 (b)), and the use of cool paint on facades favours the decrease of energy demand of the intermediate floors of the buildings (Figure 8 (a)). Energy demand decrease is not uniform in the district. It is more important in zone 1, corresponding to the most important decrease of the number of degree-hours higher than 26°C (Figure 6). Furthermore, the buildings with the higher energy demand of case A, are those with the higher cooling energy decrease due to the cool paint (cases B, C and D).

Figure 8 : Energy demand decrease between case A and B (a) and between case A and C (b)

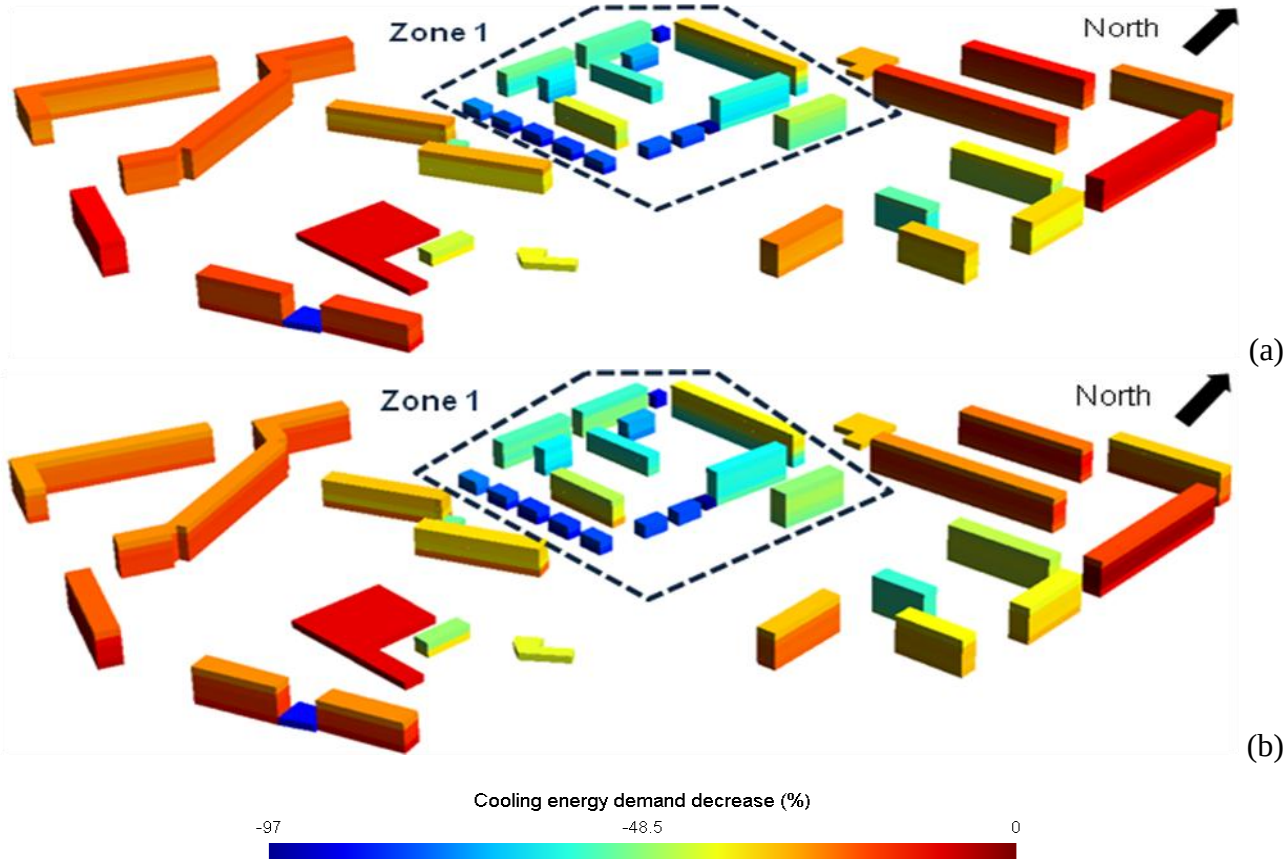

6 CONCLUSIONS

In this paper, a model based on the coupling between building energy model and urban canopy at a district scale is presented. This coupled model highlights the microclimatic effect on the building energy demand. It was used to study the impact of different cool paints on the Pin Sec district in Nantes, France. Then, the impact of cool paints on building energy demand and urban microclimate could be assessed. The calculation of the Degree-hours inside the urban canopy shows zones where energy demand is less important. The densest built areas are the most sensitive ones to the urban microclimate impact: the cooling energy demands are the most important and the cool paint use is the most efficient. Whatever the cool paint method used, the decrease of cooling energy demand is roughly equal to 78%. Using cool paint on facades seems the most efficient to reduce the UHI effects. By applying cool paint on the facades of a given building enables reducing the energy demand of surrounding buildings. Applying cool paint on the roofs has less impact on the urban microclimate than when applied on walls. It seems that it is not necessary to combine roof and wall cool painting. Indeed the benefits of cool paints seem to reach a threshold. So, to further decrease cooling demand it's necessary to work on removing indoor heat by using an appropriate ventilation strategy. Finally in order to improve the cool paint effect at the district scale, it could be interesting to carry out a parametric study in order to determine how each building influences the urban microclimate.

7 ACKNOWLEDGEMENTS

The authors are grateful to the Poitou-Charentes Region and the ADEME (French Environment and Energy Management Agency) for the financial support of this study.

8 REFERENCES

Bozonnet, E., Belarbi, R., and Allard, F. (2005). "Modelling solar effects on the heat and mass transfer in a street canyon, a simplified approach." *Solar Energy*, 79(1), 10–24.

Depecker, P., Menezo, C., Virgone, J., and Lepers, S. (2001). "Design of buildings shape and energetic consumption." *Building and Environment*, 36(5), 627–635.

De la Flor, F. S., and Domínguez, S. A. (2004). "Modelling microclimate in urban environments and assessing its influence on the performance of surrounding buildings." *Energy and Buildings*, 36(5), 403–413.

Gros, A. (2013). "Modélisation de la demande énergétique des bâtiments à l'échelle d'un quartier."Thèse de Doctorat, université de La Rochelle.

Kaplan, H., and Dinar, N. (1996). "A lagrangian dispersion model for calculating concentration distribution within a built-up domain." *Atmospheric Environment*, 30(24), 4197–4207.

Kastner-Klein, P., Norman, O. K., and Clark, J. V. (2004). "Modeling of flow and dispersion characteristics in typical urban building configurations with the fast-response model QUIC." *13th Confernce on the Applications of Air Pollution Meteorolgy with the Air and Waste Management Assoc*.

Martilli, A. (2007). "Current research and future challenges in urban mesoscale modelling." *International Journal of Climatology*, 27(14), 1909–1918.

Miguet, F., and Groleau, D. (2002). "A daylight simulation tool for urban and architectural spaces–application to transmitted direct and diffuse light through glazing." *Building and Environment*, 37(8-9), 833–843.

Mitalas, G. P., and Stephenson, D. G. (1967). "Room thermal response factors." *ASHRAE Trans.;(United States)*, 73.

Pardyjak, E. R., and Brown, M. (2003). *QUIC-URB v. 1.1: Theory and User's Guide*. LA-UR-07-3181.

Rockle, R. (1990). "Bestimmung der Stomungsverhaltnisse im Bereich komplexer Bebauungsstrukturen." der Technischen Hochschule Darmstadt,, Germany.

Rousseau, S. (1978). "Simulation numérique du comportement thermique des locaux d'habitation. Evaluation de l'influence de la radiation solaire, des conditions climatiques et des paramètres caractéristiques du bâtiment."Thèse de Doctorat, INSA de Lyon.

Santamouris, M., Papanikolaou, N., Livada, I., Koronakis, I., Georgakis, C., Argiriou, A., and Assimakopoulos, D. . (2001). "On the impact of urban climate on the energy consumption of buildings." *Solar Energy*, 70(3), 201–216.

Santamouris, M., Synnefa, A., and Karlessi, T. (2011). "Using advanced cool materials in the urban built environment to mitigate heat islands and improve thermal comfort conditions." *Solar Energy*, 85(12), 3085–3102.

DESIGN IMPACTS OF COOL ROOF COATING, VENTILATION AND THERMAL INERTIA ON COMMERCIAL LOW-RISE BUILDING ENERGY DEMAND AND SUMMER COMFORT

Remon Lapisa[1], Emmanuel Bozonnet[1], Marc O. Abadie[1], Patrick Salagnac[1], Rémi Perrin[2]

[1]LaSIE (FRE-CNRS 3474), Université de La Rochelle, La Rochelle, France
[2]SOPREMA, 14 Rue de Saint-Nazaire-67025, Strasbourg Cedex 01, France
Email: emmanuel.bozonnet@univ-lr.fr

ABSTRACT

Few studies focus on commercial low-rise buildings which are often characterized by low-cost constructions materials and weak energy performances. For these large volumes, the heat transfers with the roof and the ground are prevalent. In this article, we show how the analysis of heat transfers through both the roof and the ground can achieve their thermal performance. The roof design and its opening systems is a key factor of the thermal and lighting performance. Roof openings (skylight) and radiative properties of roof coating (cool roof) have a direct impact on solar gains, thermal losses and natural ventilation potential. The overall building thermal behavior depends both on the combination of these design parameters (solar reflectance, opening size, etc.) and weather conditions. Yet, the inertia of these lightweight structures is mainly given by the slab on the ground; and the performance of the roof design cannot be separated from the type of soil and slab which determine the dynamic behavior of these buildings.
A simple and typical case study is presented and modeled and, an extensive parametric study (840 annual simulations) is performed to point out these key parameters impacts on building energy demand and comfort. The mixed use of efficient roof techniques (skylights and cool roof) combined with a high inertia of the building can be an adequate passive cooling solution in summer, with a 99.8% drop of degree hours above the discomfort temperature in summer. Nevertheless, we show that these passive strategies could not be totally efficient without taking care of the ground thermal inertia which account up to 58.6%.

KEYWORDS

Commercial building, thermal inertia, ventilation, cool roof, passive cooling, simulations

1 INTRODUCTION

With a growth of 1% per year, the world population estimated at 8.2 billion in 2030 will rise energy demand up to 87% (2006-2030) especially for non-OECD countries (IAE, 2008). The main part of energy use is dedicated to supply the building energy needs in urban areas. In France, 43.87% of the global annual primary energy consumption in 2010 (*Chiffres clés de l'énergie édition 2012*) is allocated for building sector (71 MTep). 20.9% of this energy is required by the tertiary and commercial sector (Rabai, 2012). The part dedicated to the tertiary sector has continuously increased up, and is 15% higher than in 2001. Commercial buildings' energy consumption associated to heating and air-conditioning accounts for 57% of total expenses (Balaras et al., 2000; Chwieduk, 2003).

The present study aims at defining design key-factors to improve the energy performance of commercial low-rise buildings by seeking to reduce the heating energy demand while providing thermal comfort in summer without cooling system. The combination of cool roof to limit the solar heat gains through the roof and ventilation to reject the heat stored by the building is investigated here as passive cooling techniques to meet thermal comfort requirements in summer.

The main principle of cool roof is to reduce radiative heat gain by modifying its solar reflectance and thermal emittance. With this technique, outer surface of roof coated by high solar reflectance material will reflects more solar radiation, while the absorbed heat is emitted to the sky due to the high thermal emittance. Cool roof technologies on a commercial building can reduce the peak temperatures of roof surfaces about 33°C to 42°C in summer (Akbari et al., 2005; Xu et al., 2012). In these studies, cooling energy demand was reduced up to 20 $Wh/m^2/day$ (52% of total energy requirement) and CO_2 emission decreased from 11 to 12 kg CO_2/m^2 of flat roof area. (Bozonnet et al., 2011) conducted a study for moderate climate in France that shows a result of 10°C roof surface mean temperature decrease, in summertime, due to cool roof technology.

Natural and night ventilation can help to mitigate overheating by removing out the warm indoor air. A study conducted by (Wang et al., 2009) indicated that the night ventilation is quite effective especially in northern hemisphere to be a passive-cooling way. The night ventilation can reduce the average indoor temperature from 1.5°C up to 4°C (Blondeau et al., 1997; Geros et al., 1999; Kubota et al., 2009; Shaviv et al., 2001) according to the location, envelopes and building usage scenarios.

As for the roof, the large surface of slab on ground and the ground characteristics are key-parameters in the energy balance and performance of roof techniques for commercial low-rise building. Most studies focus on typical houses, but even in those studies the role of ground floor is not negligible; thus a study conducted by (Labs K et al., 1988) on heat loss through a non-insulated floor showed that 10% of the energy losses are attributed to the floor for poorly-insulated and up to 30% to 50% for well-insulated walls/roof building. Moreover, the ground is a key factor considering its thermal inertia potential for low-rise buildings which are often built with low inertia materials (mainly metal construction). The study of a test cell (small building) by (Aste et al., 2009) showed a 10% difference in the heating loads between high and low thermal inertia envelopes. Ground properties and thermal inertia (including shelving) of low-rise buildings can contribute to the dynamic of passive cooling techniques, and we focus on these combinations as it has to be handled properly to reduce building energy consumption.

In this paper, we will demonstrate the effect of cooling strategies (cool roof and natural ventilation) on a very simple case study of low-rise commercial building. The building energy demand and thermal comfort model is detailed in the following parts and takes into account all the main parameters with coupled heat and airflow transfers. Parametric analyses are performed to highlight the single and combined impacts of the cool roof, natural ventilation and ground/shelving thermal inertia.

2 CASE STUDY DESCRIPTION AND PASSIVE COOLING STRATEGIES

2.1 Description of the typical commercial building

The study is carried out on a cubic-shape one-floor commercial building (*Figure 1*) located in temperate climate (Marseille, France). The base of the building is a square of 36 m sides. The building height is 6 m, and its steel structure with a large flat roof surface is covered by 16 skylights, i.e. 2.4% (31.36 m^2) of the roof area.

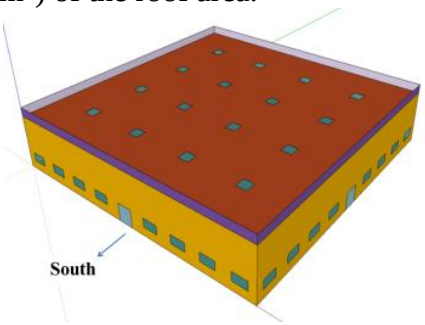

Figure 1. Geometry of the studied commercial building

The vertical walls (except the northern one) include 30 m^2 of windows. The vertical exterior walls are well insulated and have a total thickness of 30.5 cm (1.3 cm of gypsum, 14 cm of glass wool, 15 cm of rock wool and an outer steel cladding of 2 mm). The ground thermal inertia of the building is mainly due to the concrete slab (160 mm thick with no thermal insulation) which directly lies on sand. Besides, thermal inertia of the commercial shelves is considered with 10% of the building volume (787.9 m^3). It consists of 40% cardboard, 30% liquids/oils, 10% metals and 20% plastics. The building is equipped with a heating system and no cooling system is installed. To ensure the fresh air renewal, a heat recovery ventilation (HRV) system provides 0.75 air changes per hour (ACH) during daytime. The occupancy period of this building is 07.00 AM-10.00 PM every day except on Sunday.

2.2 Cooling strategies: cool roof and natural ventilation

A roof surface albedo of 0.3 is given for this reference building. For the parametric study, the cool roof strategy is studied through the modification of the roof coating albedo, within the interval 0.1-0.9. The high thermal emissivity (0.9) is considered constant.

Natural ventilation is provided by opening some skylights and windows. This ventilation is carried out on summer during night from 08.00 PM to 06.00 AM only when the indoor air temperature is 2°C higher than the ambient temperature. Mechanical ventilation remains in operation during the summer and can be adjusted based on requirements.

3 BUILDING MODELS

The simulation of the commercial low-rise building has been performed using the coupling between the TRNSYS building model (Type 56) and the CONTAM airflow model under the TRNSYS 17 simulation environment. As illustrated in *Figure 2*, the building is modeled as a unique zone (nodal approach) that interacts with the following main elements: the *Airflow Model* used to calculate the airflow rates through the openings and the envelope, the *Roof Thermal Model* to account for the cool roof radiative properties and the *Ground Thermal Model* to evaluate the heat transfer through the ground.

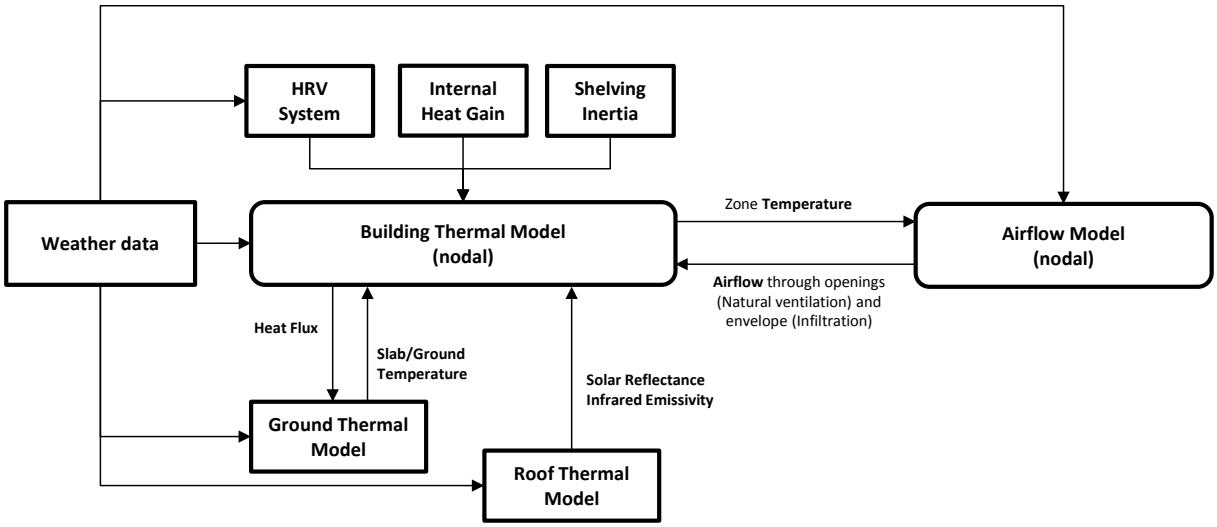

Figure 2. Schematic representation of the building energy simulation coupling process

Two modeling levels have been used to calculate heat transfer through the ground: the so-called one-dimensional (1D) and adiabatic models. Note that those models account for heat transfer only, no moisture transfer is considered here.

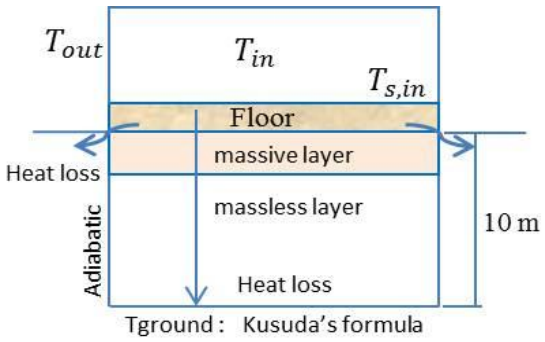

Figure 3. One-dimensional model of ground heat transfer

The 1D model, illustrated in *Figure 3*, splits the ground below the concrete slab into two layers of the same soil materials. The first layer, modeled as a massive layer, accounts for thermal inertia and is defined as a wall in TRNSYS building model. The second layer is modeled as a resistance layer, with no thermal inertia, and is referred as massless layer. A shown by (Adjali et al., 2000), the temperature of the ground at 10 m can be considered independent of the building behavior so that the total thickness above the building has been set to 10 m. The required temperature in the model at this depth is calculated by the model of Kusuda (Eckert and Drake Jr, 1987; Kusuda and Bean, 1984):

$$T\ z,t\ = T_m - T_a\, e^{-z\times\ \sqrt{\frac{\pi}{365\alpha}}} \times \cos\ \frac{2\pi}{365}\ \ t - t_p - \frac{z}{2}\ \ \sqrt{\frac{365}{\pi\alpha}} \quad (1)$$

Parametric simulations have been performed to evaluate the necessary thickness of the massive layer in a previous study (Lapisa et al., 2013). Results show that this building model using a 30 cm massive layer gives comparable results regarding the heat transfers through the ground than a more complicated, and heavy computation time, three-dimensional ground model (McDowell et al., 2009; Zhou et al., 2002).

A simplified model (adiabatic) is also used in order to characterize the effect of the ground inertia on the building energy demand and thermal comfort. For this model, there is no heat transfer below the concrete slab and no ground thermal inertia is taken into account.

For both models, the cold bridges between the slab and outside are calculated according to the standards (French building regulation).

4 PASSIVE COOLING POTENTIAL OF COOL ROOF AND NATURAL VENTILATION

All the studies are based on the previously defined reference building: low roof solar reflectance (0.3), mechanical ventilation operating only during the occupancy period and skylights closed (no natural ventilation). In the following parts, the criteria for indoor overheating (based on operative temperature) during summertime and occupancy hours are:

- The **degree-hours** (DH) above the adaptive summer comfort temperature defined by the standard EN-ISO-1525. DH [°C.h] drops are proportional to cooling energy gains required for a mechanically cooled building.
- The **discomfort ratio** based on the occupancy hour's ratio above summer comfort temperature (EN-ISO-1525).

4.1 Impact of cool roof

Temperature evolutions are compared, see *Figure 4*, for three days in summer (1-3 August) using both ground heat transfer models and 2 roof solar reflectance values (0.3 for standard roof and 0.9 for cool roof): ambient temperature ($T_{outside}$), roof surface temperature ($T_{s\text{-}roof}$) and indoor operative temperature (T_{op}).

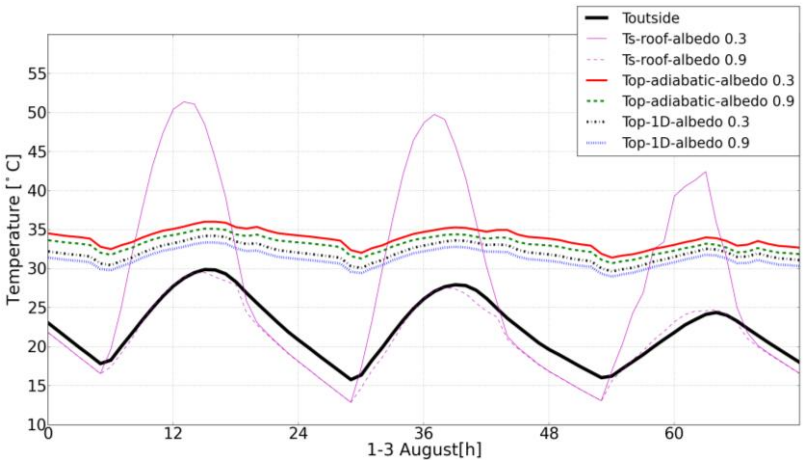

Figure 4. Ambient, operative and roof surface temperature in summer

The temperature peaks occur on the interval 12.00 AM-03.00 PM. With cool coating the solar absorption decreases and the roof external surface temperature drastically drops of 22°C, but the operative temperature drop is here only 1°C. This mainly comes from the highly insulated roof that lessens the effect of very high temperatures at the external side. However, the ground thermal inertia impact, assessed from results difference between both 1D and adiabatic

models, is more significant on the operative temperature with a difference of 2.5°C (*Figure 4*) for all albedo values. This inertia effect and heat transfers to/from the ground are facilitated by the lack of insulation below the slab on ground which mitigates the indoor air overheating.

Figure 5 presents the cool roof effects on previously defined summer comfort criteria (DH and discomfort ratio) evaluated with or without ground thermal inertia (two ground models), and with or without shelving.

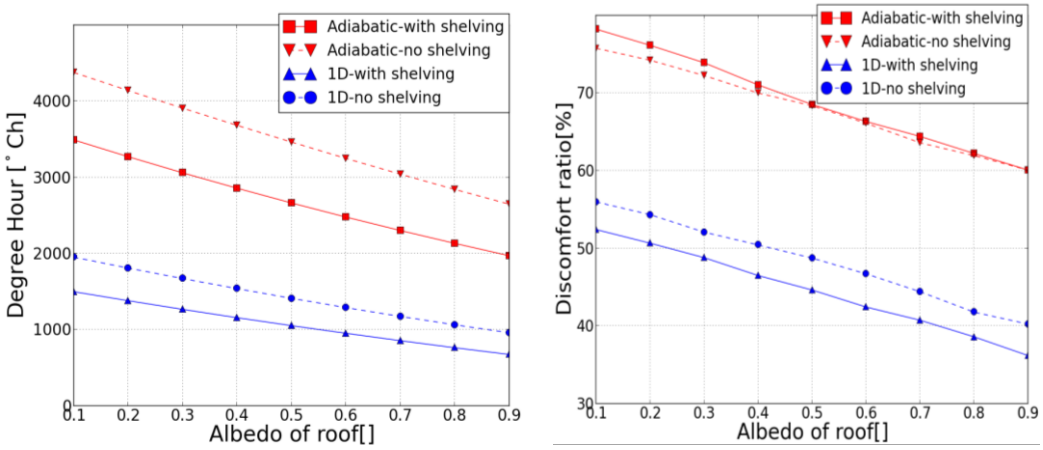

Figure 5. Effect of the roof albedo on a) DH [°Ch] and b) Discomfort ratio

DH decreases vary from 46.8% for the ground coupled building and 35.6% for the adiabatic one for an albedo variation from 0.1 to 0.9. The ground inertia participates in reducing the degree hours from 3060°Ch to 1265°Ch (58.6%) for the reference building (0.3 of albedo) and from 1970°Ch to 673°Ch (65.8%) for the building with cool roof. On the other side, the shelving also absorbs a notable portion of the heat from the indoor air and reduces the DH value of about 24.2% compared to the empty building. For this type of well-insulated roof building, the cool roof effect is lower than ground inertia impact.
Figure 5.b presents the discomfort ratio versus albedo. The albedo effect follows the same global trend as for the DH; except for the shelving only effect which does not have a significant impact on the discomfort ratio. This is due to the too small shelving inertia and it highlights the importance of the design and the minimum inertia needed for summer thermal comfort.

4.2 Impact of ventilation

4.2.1 Impact of natural ventilation

Figure 6 shows the impact of opening the skylights on the natural ventilation flow rate and the degree hours (DH) above adaptive temperature. The flow rate increases almost linearly with the skylight opening area. Among the different calculations, the flow rate only slightly differs at the highest opening area showing that wind is the predominant parameter, and not the ambient to indoor temperature difference. The adiabatic case (red curves) with higher indoor temperatures (see previous section) presents the highest flow rate which demonstrates that the temperature gradient acts with the wind-driven ventilation in the present configuration.

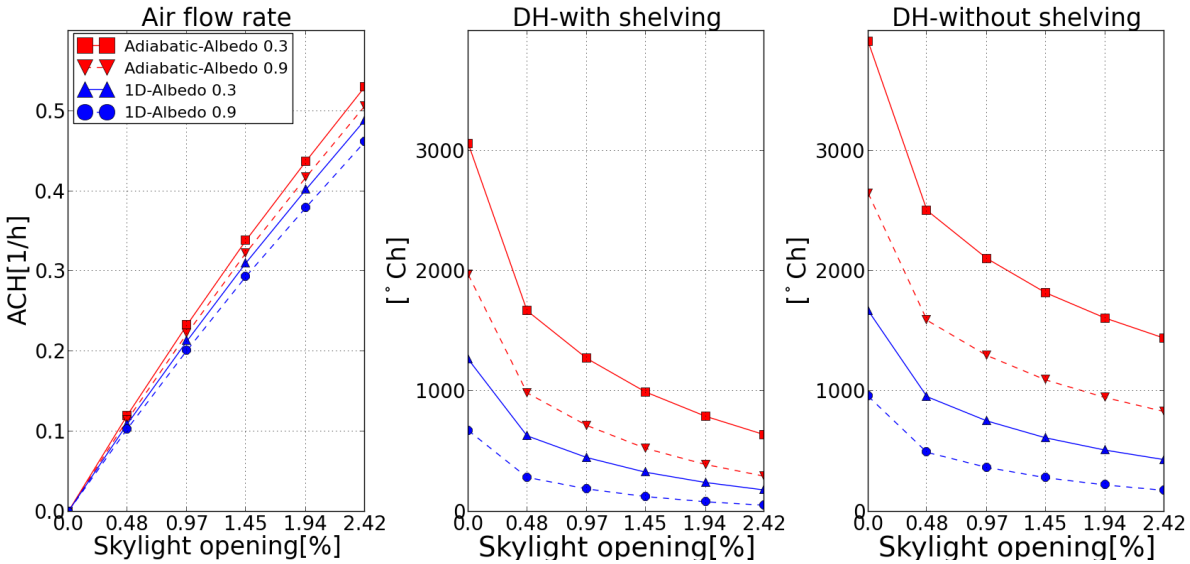

Figure 6. Skylight ratio effect on (a) natural ventilation rate (ACH), and (b) DH with shelving and (c) without

As illustrated by the other two graphs, *Figure 6.b* and *c*, using natural ventilation during night to decrease DH is very efficient even at very low airflow. DH values (for occupancy period) sharply decrease with the increase of the skylight opening, dropping up to 79.2% for the maximal opening value. In this case, the shelving is also important as the night cooling participates to the indoor temperature reduction during daytime. Combined effects of ground and shelving thermal inertia are obviously as important as the natural ventilation, giving very good results with high inertia and skylight opening.

4.2.2 Impact of mechanical ventilation scenario

Two mechanical ventilation scenarios have been defined: ventilation during the occupation period (*occ*) and permanent (*occ + Nighttime*). Without natural ventilation, the permanent mechanical ventilation (*Figure 7*) brings a reduction of DH from 1265°Ch to 221°Ch (6 times smaller). Mechanical ventilation during night is actually effective enough in reducing temperatures for the next day. Note that the mechanical ventilation rate (0.75 ACH) is on the same order of the mean nighttime natural ventilation with all the skylights opened (about 0.5 ACH). The combination of mechanical and natural ventilation during the night can avoid thermal discomfort during occupancy by reducing the DH by 97.6% as illustrated by *Figure 7*.

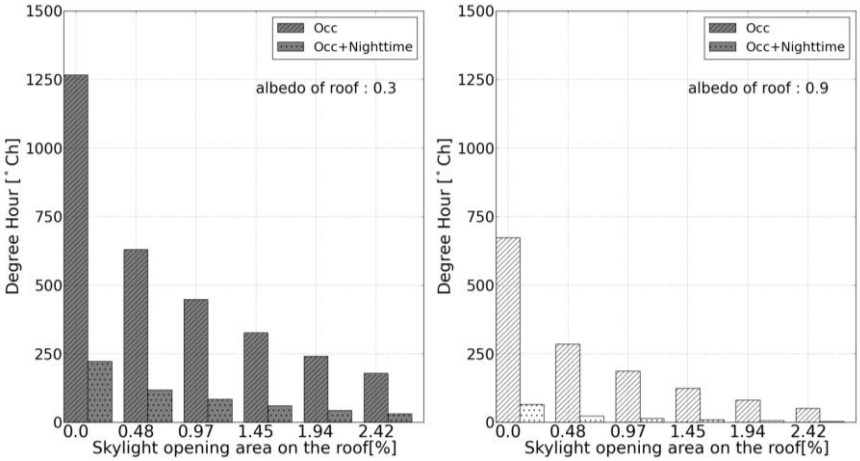

Figure 7. Degree Hours above adaptive temperature (DH) for mechanical and natural ventilation scenarios

4.3 Passive cooling strategies

Following this study of passive cooling strategies alone (i.e. cool roof and natural ventilation), the present section aims at evaluating their combined effect along with the thermal inertia

brought by the ground and the shelving. Here, the indoor overheating during summertime and occupancy hours is highlighted by the average of maximum daily temperatures and the degree-hours (DH above adaptive comfort temperature following EN-ISO-15251).

4.3.1 Cool roof and natural ventilation coupled effects

The potential of the coupling of both cool roof and natural ventilation is analyzed *Figure 8* varying both parameters skylight opening and roof albedo. The two graphs have the same tendencies and both passive-cooling strategies have a similar and significant effect.

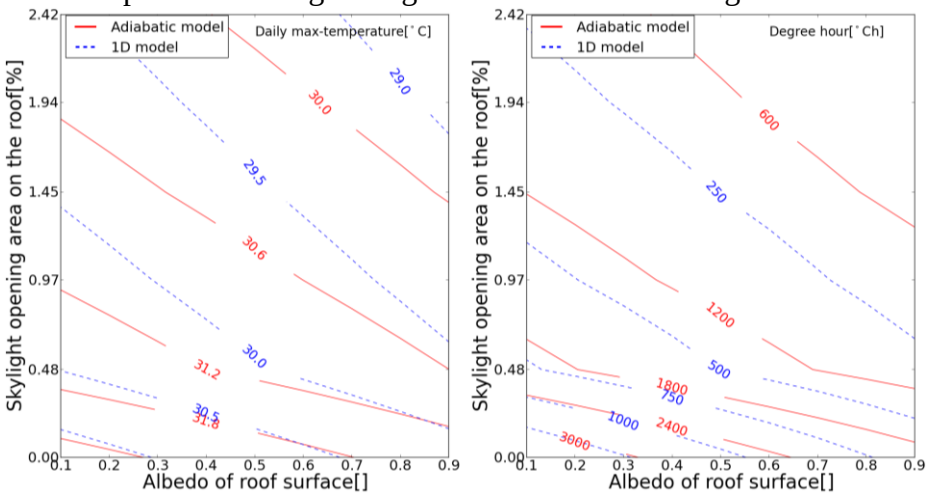

Figure 8. Skylight ratio of roof and roof albedo effects on both:
a) Average of daily max operative temperature [°C], b) DH above comfort temperature [°Ch]

From no skylights to 0.5% of skylight ratio of roof surface, the natural ventilation effect is the most efficient with almost 1°C gain on maximum temperature, *Figure 8.a*, and around 1000°Ch gains on DH, *Figure 8.b*, whatever is the albedo. The gains of cool roof decrease with the increase of skylight opening ratio, mainly considering the degree hours. Yet the relative gains are always important and these two figures can be helpful in building design phase to help defining balanced requirements for roof albedo and skylights' ratio.

4.3.2 Effectiveness comparison of all natural cooling strategies

In order to compare all previous cooling strategies, we analyzed, see *Figure 9*, the absolute temperatures and the DH mitigation for cool roof (albedo 0.9), night natural ventilation and night mechanical ventilation (with ref. building characteristics). In this case study, considering the Mediterranean weather of Marseille, ventilation alone (natural or/and mechanical) provides more gains in cooling effect when compared to cool roof alone. For the considered three days, see *Figure 9.a*, the operative temperature drops from around 1°C with cool roof, and up to 3°C with night natural ventilation. With additional nighttime mechanical ventilation, the operative temperature drops only slightly below the natural ventilation case. Here, ventilation effectiveness is highly dependent on the air flow rate and outside air temperature. The last cooling strategy by combining natural-mechanical ventilation and cool roof allows a temperature drop above 5°C (*Figure 9.a*). DH [°Ch] of discomfort drops by 46.8% due to cool roofs, by 82.5% due to night mechanical ventilation, by 86% due to night natural ventilation and by 99.8% due to the combination of the passive solutions (*Figure 9.b*). For well-insulated roof building, the most effective passive cooling potential could be improved by increasing the air flow rate through ventilation. Natural ventilation is preferred here because it does not require any energy. Enlarging the surface area of skylights offer more effective passive cooling gains and replaces mechanical ventilation needs.

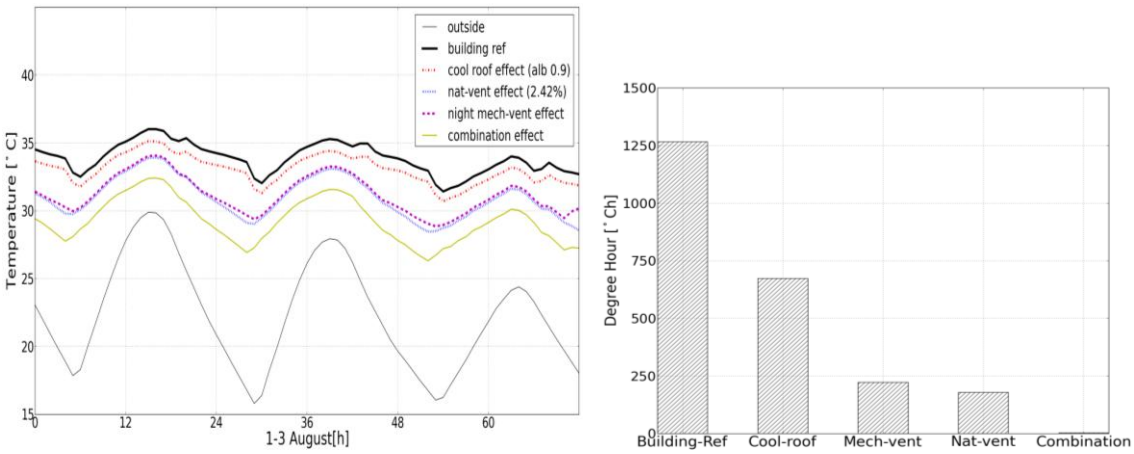

a. b.

Figure 9. a. Effects of cooling strategies on operative temperature,
b. Effects of cooling strategies on DH above adaptive discomfort temperature

5 CONCLUSIONS

The typical commercial building analyzed here, located in a Mediterranean climate and well insulated, has demonstrated the interest of passive cooling strategies such as natural ventilation ensured by skylights (2.4% of roof surface) which alone contributes to a strong reduction of summer discomfort with a 86% drop of degree hours (DH) above discomfort temperatures. The cool roof technique alone is also valuable with a 46.8% drop of DH of discomfort. The use of mechanical ventilation at night performed not better than natural ventilation with a 82% drop of DH. But these well-known techniques can operate in a very efficient way when combined together; night natural and mechanical ventilation together with cool roof give a huge drop of DH up to 99.8%. These tendencies of DH can be used also to design mechanically cooled buildings, as the energy consumption varies in the same way, even if a good design could give in this case a satisfactory solution.

Moreover, we have demonstrated that these solutions could be not totally effective without the contribution of the ground thermal inertia. Indeed, it contributes up to a 58.6% drop of DH compared to an adiabatic floor model. This mean that for large-volume low-rise buildings, the ground floor is a key factor to be considered; and its insulation from the ground could be counterproductive. The shelving inertia participates also in the passive cooling process, and it was assessed to a 24.2% DH drop compared to a building without shelving.

These parametric results and the methodology used have given first results which could be used in commercial building design phase, but it has to be extended. The ongoing work and the outlooks on this topic is now to assess the optimal ratio of skylights in order to provide the best passive cooling effects and checked against additional heat losses in winter. Moreover, the model has to be refined in order to take into account thermal stratification within the building and to study comfort zones.

6 ACKNOWLEDGEMENTS

The authors wish to thank the Indonesian government for its financial support.

7 REFERENCES

Adjali, M. H., Davies, M., Rees, S. W., and Littler, J. (2000). “Temperatures in and under a slab-on-ground floor: two- and three-dimensional numerical simulations and comparison with experimental data” Building and Environment 35, 655–662.

Akbari, H., Levinson, R., and Rainer, L. (2005). “Monitoring the energy-use effects of cool roofs on California commercial buildings” Energy and Buildings 37, 1007–1016.

Aste, N., Angelotti, A., and Buzzetti, M. (2009). "The influence of the external walls thermal inertia on the energy performance of well insulated buildings" Energy and Buildings 41, 1181–1187.

Balaras, C. A., Droutsa, K., Argiriou, A. A., and Asimakopoulos, D. N. (2000). "Potential for energy conservation in apartment buildings" Energy and Buildings 31, 143–154.

Blondeau, P., Spérandio, M., and Allard, F. (1997). "Night ventilation for building cooling in summer" Solar Energy 61, 327–335.

Bozonnet, E., Doya, M., and Allard, F. (2011). "Cool roofs impact on building thermal response: A French case study" Energy and Buildings 43, 3006–3012.

Chiffres clés de l'énergie édition 2012 (n.d.). (MEDDE, Commissariat général au développement durable), p. 40.

Chwieduk, D. (2003). "Towards sustainable-energy buildings" Applied Energy 76, 211–217.

Eckert, E. R. G., and Drake Jr, R. M. (1987). *Analysis of heat and mass transfer* (New York), Hemisphere Publishing.

Geros, V., Santamouris, M., Tsangrasoulis, A., and Guarracino, G. (1999). "Experimental evaluation of night ventilation phenomena" Energy and Buildings 29, 141–154.

IAE (2008). "World Energy Outlook 2008-2009, International Agency Energy."

Kubota, T., Chyee, D. T. H., and Ahmad, S. (2009). "The effects of night ventilation technique on indoor thermal environment for residential buildings in hot-humid climate of Malaysia" Energy and Buildings 41, 829–839.

Kusuda, T., and Bean, J. W. (1984). "Simplified methods for determining seasonal heat loss from uninsulated slab-on-grade floors" ASHRAE Trans.;(United States) 90.

Labs K, Shen L, Huang Y, Parker D, and Carmody J (1988). "Building Foundation Design Book" Oak Ridge National Lab., TN (USA); Minnesota Univ., Minneapolis (USA). Underground Space Center RNL/Sub-86-72143/1.

Lapisa, R., Bozonnet, E., Abadie, M., Salagnac, P., and Perrin, R. (2013). "Effect of ground thermal inertia on the energy balance of commercial low-rise buildings" Building Simulation 2013 (Chambéry, France) . Presented at the BS2013.

McDowell, T. P., Thornton, J. W., and Duffy, M. J. (2009). "Comparison of a Ground-Coupling Reference Standard Model to Simplified Approaches" Eleventh International IBPSA Conference, Glasgow, Scotland.

Rabai, Y. (2012, November). "Dix ans de consommation d'énergie dans le secteur tertiaire [Publications, Chiffres & statistiques, 2012] : Observation et statistiques."

Shaviv, E., Yezioro, A., and Capeluto, I. G. (2001). "Thermal mass and night ventilation as passive cooling design strategy" Renewable Energy 24, 445–452.

Wang, Z., Yi, L., and Gao, F. (2009). "Night ventilation control strategies in office buildings" Solar Energy 83, 1902–1913.

Xu, T., Sathaye, J., Akbari, H., Garg, V., and Tetali, S. (2012). "Quantifying the direct benefits of cool roofs in an urban setting: Reduced cooling energy use and lowered greenhouse gas emissions" Building and Environment 48, 1–6.

Zhou, Z., Rees, S. W., and Thomas, H. R. (2002). "A numerical and experimental investigation of ground heat transfer including edge insulation effects" Building and Environment 37, 67–78.

COOL ROOF FOR PASSIVE COOLING: SIMULATIONS OF AN EXISTING BUILDING IN SOUTHERN ITALY

Vincenzo Costanzo[*1], Gianpiero Evola[1], Antonio Gagliano[1], Luigi Marletta[1]

1 Department of Industrial Engineering, University of Catania
Viale Andrea Doria 6
95125, Catania, Italy
**Corresponding author: costanzo.vincenzo@gmail.com*

ABSTRACT

Roofs are the envelope component more severely hit by solar radiation in summer (1470 kWh/m^2 on average in Italy), hence one may expect that using *cool materials* on the finishing layer of a roof should provide a significant reduction in the heat flow entering the building, with sensible relief in terms of building cooling load.
In this paper a case study is presented, based on the dynamic simulation of an existing office building in Catania (Southern Italy). In this building, a part of the roof has been recently treated with a commercial cool painting, with the aim of improving the thermal comfort in summer. Hence, the simulations represent a preliminary study, that will allow to assess the expected effectiveness of the intervention. More in detail, the results of the simulations will be discussed both in terms of thermal comfort and energy savings due to the use of the cool painting, through the evaluation of parameters such as the roof surface temperature, the operative temperature and the cooling load for both conditions, i.e with and without the cool painting on the roof.
The paper also discusses the potential increase of the energy needs for winter heating, and looks at the overall balance in terms of primary energy. These aspects are usually not well highlighted in the current scientific literature.

KEYWORDS

Cool Roof case study, occupants' comfort, building energy performances, design suggestions

1 INTRODUCTION

The roof surface represents about 20-25% of urban surfaces and 60-70% of the building envelope on average in Italy, depending on the building typology (Corrado, 2011); thus, it plays a very important role in the energy balance of buildings, and it is important to find appropriate solutions to improve its energy performance, also in relation to the specific climate.
In this context, *cool materials* represent an efficient way to cope with the increase of energy consumption in summer and the urban heat island effect, without a sensible change in the aesthetic feature (Synnefa, 2007). As an example, Levinson (Levinson, 2007) have developed some materials (mainly paintings) whose chromatic result is as close as possible to the existing original color of the untreated roof, showing how this is obtainable by maximizing the near infrared reflectance without affecting the behavior of the painting in the visible field, which is strictly related to the perceived color.
Cool materials are characterized by high values of solar reflectance ($r > 0.6$), which strongly reduces the amount of solar radiation absorbed by the roof outer layer, and by high infrared emissivity values ($\varepsilon > 0.8$), which contributes to dissipate the heat accumulated during the day through an intensive radiant heat exchange at night.

In order to discuss the suitability of the cool roof technology as a passive cooling strategy for hot climates, this paper presents the results of a case study in Catania (southern Italy), based on simulations with the software tool EnergyPlus.
The simulations will allow to evaluate the results to be expected from the application of a commercial cool painting on a low-rise office building; this intervention has already been performed, and it will be the object of an experimental monitoring campaign.
The results of the simulations will show the benefits of using cool roofs on existing buildings, both in terms of reduction of cooling demand and decrease of the hours of thermal discomfort. However, attention will be also paid to the winter condition, when the presence of the cool painting lowers the heat absorbed by the roof, with consequences in terms of heating demand. Actually, this is a drawback of cool materials not always addressed in the scientific literature.

2 METHODOLOGY

The study has been developed in two different phases: the first stage involved the characterization of the building envelope in terms of thermal and optical properties, whereas in the second stage the calculation of the energy performance and the study of the thermal comfort were carried out through a series of dynamic simulations.

2.1 Characterization of the building envelope

The evaluation of the thermal transmittance (*U-value*) of the opaque envelope components was supported by a measurement campaign of the envelope transmittance values, carried out through a Heat Flux Meter; the instrument chosen to this purpose is the TESTO 435-2 multifunction instrument.
On the other hand, before applying the product to the roof, laboratory tests were conducted to characterize its spectral reflectance. To this aim the Perkin Elmer Lambda 750 UV/Vis/NIR spectrophotometer was used, according to ASTM E 903-96 standard (ASTM, 1996).
In this way the global reflectance value *r* was calculated, while the same value for the untreated roof has been deduced from Levinson (Levinson, 2010) and Romeo's (Romeo, 2011) studies.
Both the *U-value* of the envelope components and the *r* value of the existing clay tiles and of the cool painting are summarized in Table 1.

2.2 Assessment of the thermal and energy performance of the building

The assessment of the energy performance and the thermal comfort conditions in the sample building are carried out using the software for dynamic thermal analysis EnergyPlus v.7.0.
In order to carry out a thermal comfort analysis of the building, the operative temperature has been chosen as an index closely related to the comfort condition perceived by the occupants, so a reduction of its value during the period of observation implies better conditions for the building occupants.
An effective way to quantify the intensity of uncomfortable thermal sensation due to overheating in a living space is the measure of the difference between the room operative temperature and a threshold value; however, the duration of such overheating should also be taken into account.
To this aim we will adopt an indicator called *Intensity of Thermal Discomfort* for overheating (ITD_{over}), introduced by Sicurella (Sicurella, 2012), which is defined as the time integral, over the occupancy period *P* (from 9:00 to 18:00 for weekdays in this case), of the positive differences between the current operative temperature and the upper threshold for comfort:

$$ITD_{over} = \int_P \Delta T^+(\tau)\, d\tau \quad (1)$$

where :
$$\Delta T^+ = \begin{cases} T_{op}\ \tau - T_{lim}\ \tau & \text{if } T_{op}\ \tau > T_{lim}\ \tau \\ 0 & \text{if } T_{op}\ \tau < T_{lim}\ \tau \end{cases} \quad (2)$$

The value of the threshold temperature T_{lim} depends on the choice of a specific thermal comfort theory. In this paper, the adaptive approach is chosen, as described in the ISO EN 15251 Standard (EN Standard 15251, 2007): hence, the threshold value is not constant in time, but it should be determined daily as a function of the running mean outdoor air temperature T_{rm}. The formulation of the threshold temperature is given in Eq. (3), and corresponds to the fulfillment of Category I introduced by the EN Standard (high level of expectation):

$$T_{lim} = 20.8 + 0.33 \cdot T_{rm} \quad (3)$$

3 THE CASE STUDY

3.1 Description of the building

The building considered in this case study is an existing office building in Catania (Southern Italy), a town on the Eastern coast of Sicily, whose main features are summarized in Table 1. The ground floor hosts a series of offices used by the teachers of the local University, while the basement is occupied by laboratories; the roof is walkable and hosts the air-conditioning devices.

Table 1: Features of the building

General information	
Location	Catania, Italy (LAT. 37°31□N, LONG.
Building type	15°04□E)
Surface area	Office building
Operation hours	207 m^2
Main orientation	09:00-18:00 form Monday to Friday
	NE-SO
Building envelope	
S/V ratio	0.47 [m^{-1}]
Walls – U value	U = 0.80 [W m^{-2} K^{-1}]
Roof – U value	U = 0.70 [W m^{-2} K^{-1}]
Floor – U value	U = 1.90 [W m^{-2} K^{-1}]
Windows – U value	U = 2.80 [W m^{-2} K^{-1}]
Shading	White blinds
Clay tiles – r value	0.25 [-]
Cool painting – r value	0.45 [-]

Figure 1: Ground plan with building orientation and picture of the main façade

The composition of the outer walls and the roof is reported in Table 2, from the outermost to the innermost layer.
The windows consist of double-glazing filled with Argon (4-12-4 mm), whose aluminum frame is provided with thermal cutting; the shading system consists of white curtains. The whole window system shows a thermal transmittance value U = 2.80 $W \cdot m^{-2} \cdot K^{-1}$, calculated according to (UNI EN ISO 10077-1, 2007).
In Table 2 the most important thermal properties of the building materials are also collected, as reported by the national standards (UNI 10351, 1994) and (UNI 10355, 1994), as well as by the international standard (UNI EN ISO 6946, 2008).

Table 2: Characteristics of the opaque envelope

Materials	**Thickness [cm]**	**Density [$kg \cdot m^{-3}$]**	**Specific heat [$J \cdot kg^{-1} \cdot K^{-1}$]**	**Conductivity [$W \cdot m^{-1} \cdot K^{-1}$]**
Roof				
Clay shingles	1.2	1800	840	0.72
Mortar	2	2000	840	1.40
Sand	2	1700	840	0.60
Polyester membrane	0.8	1120	1460	0.16
Light cement screed	10	1600	880	0.65
Mineral wool	3	35	840	0.044
Reinforced base	6	2000	840	1.40
Prefabricated slab	6	2000	840	1.16
Air gap	30	1.20	1000	*
False ceiling	2	900	840	0.21
Outer walls				
Plates of basalt stone	3	2800	840	3.50
Mortar	3	2000	840	1.40
Concrete block	12	1400	880	0.43
Polystyrene	3	20	1400	0.036
Air gap	17	1.20	1000	**
Hollow clay block	8	750	840	0.40
Inner plaster	2	1400	840	0.70

*R = 0.23 [$m^2 \cdot K \cdot W^{-1}$] **R = 0.18 [$m^2 \cdot K \cdot W^{-1}$]

3.2 Description of the simulations

In order to simulate the dynamic energy performance of the building with EnergyPlus, the following assumptions were made:

- annual simulation period with hourly time step;
- the local weather file for the site of Catania is derived from the library available on the EnergyPlus weather data;
- occupancy pattern: from Monday to Friday, 09:00-18:00;
- electrical heat gains: 150 W per workstation;
- lighting systems: 6 $W \cdot m^{-2}$;
- people sensible load: 60 W per person;
- outdoor air infiltration rate: 0.5 h^{-1} during the occupancy period, 0.2 h^{-1} during the remaining time.

In the next section the results of the simulations will be presented under four different scenarios:

1. no painting (solar reflectance r = 0.25 for the non-treated existing roof);
2. cool painting actually applied on the roof (r = 0.45);
3. more performing painting (r = 0.65);
4. best performing painting (r = 0.85).

The simulations are focused both on the thermal comfort and energy performance of the building, as well as on the thermal behavior of the cool painting:

- the study of the thermal behavior of the cool painting estimates the temperature reduction of the roof outer surface;
- the comfort analysis shows the hourly evolution of the operative temperature for a reference room of the building. In addition, an indicator for measuring the duration and the intensity of thermal discomfort is calculated for three rooms with different exposures;
- the energy analysis evaluates the hourly heating and cooling loads, the design loads for summer and winter and the global annual energy need. In addition, a comparison between different heating systems will show the most performing equipment for the case study.

4 RESULTS AND DISCUSSION

4.1 Roof temperature

One of the most noticeable aspects related to the use of a cool painting on the finishing layer of a roof is the sharp reduction of its outer surface temperature: according to Levinson (Levinson, 2010), Romeo (Romeo, 2011) and Bozonnet (Bozonnet, 2011), a mean reduction of 12°C is expected when using a product with average quality (r = 0.45), whereas the use of a high-reflective painting (r = 0.85) can introduce a temperature reduction up to 25°C.
As concerns this case study, Figure 2 shows that the outer surface temperature for the existing roof is always higher than that reached by the painted roof. The minimum difference pertains to the less performing painting (r = 0.45) and ranges around 5-10°C, but in the case of the best performing painting such temperature difference actually increases up to 20-30°C.

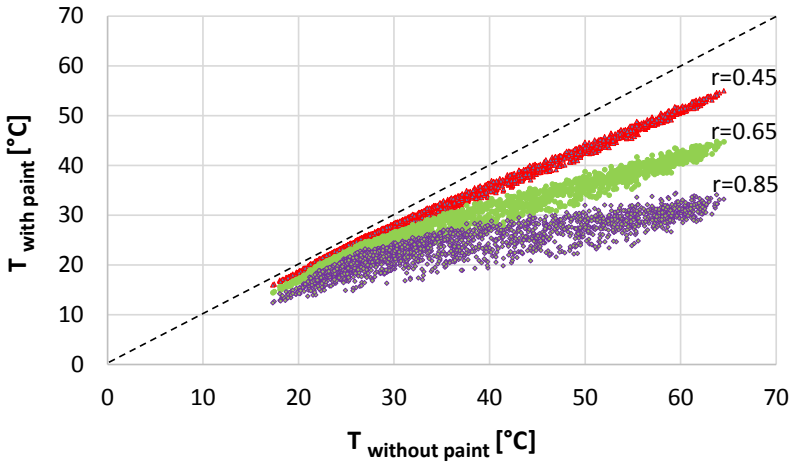

Figure 2: Comparison between the outer surface temperature of the roof without painting and with growing reflectance values

Furthermore, as shown in Figure 3 for the hottest days of the year, the use of a cool painting on the roof leads to a sensible reduction of the peak outer surface temperature, while at night the effect is more evident. In fact, when the solar irradiance is at its maximum (12:00 – 14:00) and a peak of about 60°C is reached for the untreated roof, a paint with r = 0.45 shows a reduction of 10°C and the one with r = 0.85 has a reduction of 25°C.
At night, these differences amounts to 1°C and of 3°C respectively, which lowers the risk of vapor condensation on the roof.

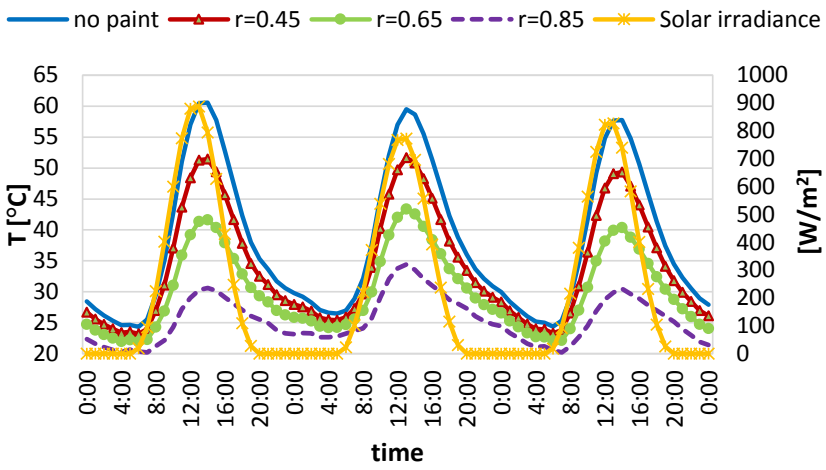

Figure 3: Outer surface temperature of the roof during the hottest days of the year (August 8th – 10th)

4.2 Comfort analysis

The sensible reduction in the surface temperature of the roof leads to a significant reduction in the operative temperature of the underneath rooms. The reference room for this analysis is the office n.3, placed in the middle of the northern side of the building (see Fig. 1). This office is representative of the whole set of offices due north-east.
As shown in Fig. 4, during the three hottest days of the year (from the 8th to the 10th of August) a peak value of 36°C for the operative temperature is expected without painting during the occupancy period (9:00-18:00); it can also be observed that a reduction of around 1 °C every $\Delta r = 0.20$ is achieved when using cool paintings with increasing reflectance.

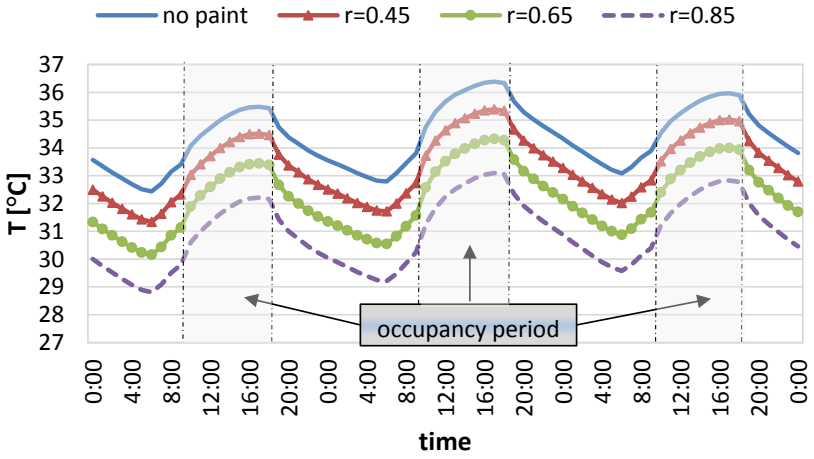

Figure 4: Operative temperature in the office n.3 during the hottest days of the year (August 8th – 10th)

In this case study, three rooms are investigated from the comfort perspective: the office n.3 which is representative of the north-east rooms, the office n.6 which is due south-west and the assembly room that is characterized by many glazed surfaces and by a double exposure.
The values of the ITD discomfort index, calculated as described in Section 2.2, are shown in Fig. 5. Here, the expected effectiveness of the real cool painting (r = 0.45) in reducing the thermal discomfort of the occupants is clear, as it implies a reduction of the ITD of about 21% with respect to the case without cool painting.
However, even better results can be obtained if using the most performing painting (r = 0.85), since the expected reduction of ITD is 63%, and this is true for all the rooms considered.

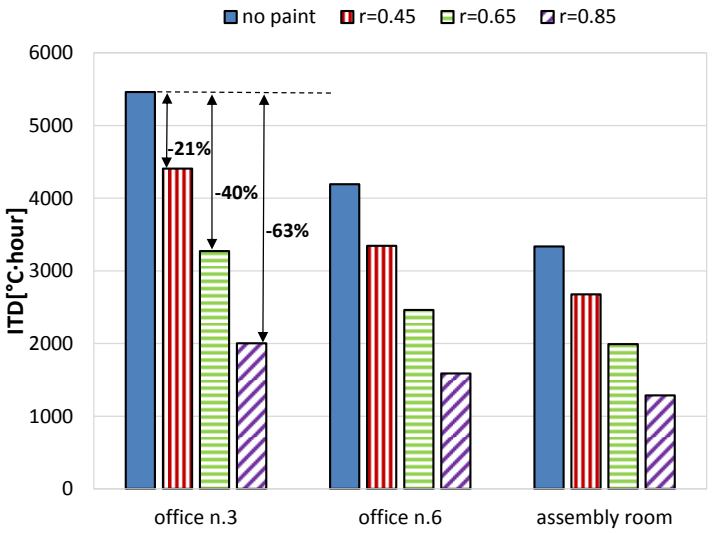

Figure 5: ITD index for three different rooms over the whole summer season

4.3 Energy analysis

Another positive aspect closely related to the use of the cool roof technology is the sensible reduction of the cooling load of the building, thanks to the lower rate of heat flux penetrating through the plain roof. This effect is shown in Fig. 6 with reference to the hottest days of the year; the curves represent the building sensible cooling load, determined through the simulations with a cooling set point temperature of 26°C during the occupancy period in summer (09:00 - 18:00 for weekdays, from May to September).
As one can observe, the peak of the cooling load can be cut by 14% in comparison with the case without cool painting if using the real paint with r = 0.45 (from 8440 W to 7230 W): The result is far more encouraging if using a very performing pain (r = 0.85), as the peak load is reduced by 44%, i.e. from 8440 W to 5206 W.

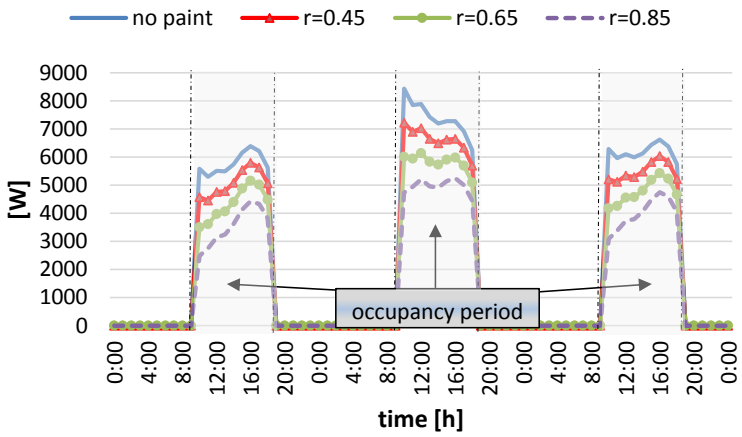

Figure 6: Sensible cooling load of the building during the hottest days of the year (August 8th – 10th)

However, the reduction of the cooling load in summer is not the only effect of the cool painting on the energy performance of the building. In fact, the low absorptivity of the roof also implies lower heat gains in winter, which determines a potential increase of the winter heating load. To this aim, the simulations were repeated for the winter season (from October to April), by imposing a heating set point temperature of 20°C during the occupancy period.
The resulting trend of the design thermal loads as a function of the solar reflectance *r* is reported in Table 3 for summer and winter: as a matter of fact, the increase of the peak

heating load due to the presence of the cool painting in winter is not negligible. Actually, the peak heating load raises from 14.9 kW to 15.6 kW (+ 4.7%) if using a paint with r = 0.45, and from 14.9 kW to 17.1 kW (+ 14.7%) if using a paint with r = 0.85.

Table 3: Design thermal loads for heating and cooling

	r = 0.25	**r = 0.45**	**r = 0.65**	**r = 0.85**
Sensible cooling load [W]	8442	7299	6473	5613
Sensible heating load [W]	14885	15661	16299	17083

In any case, the most important parameter from the perspective of the overall energy savings is the annual energy need of the building for space heating and cooling, obtained by integrating over time the curves of the sensible load for heating and cooling.
As shown in Table 4, the annual energy need for space cooling Q_s is strongly reduced by increasing the value of the roof solar reflectance r : the expected reduction is around 15% if using a paint with r = 0.45, and around 45% for a paint with r = 0.85. On the other hand, an increase of the energy need for space heating Q_w should be expected (11% for a paint with r = 0.45 and 31% with r = 0.85).
As a result, the total expected annual energy need is reduced by 5% (from 8787 to 8347 kWh) and by 12% (from 8787 to 7742 kWh) in comparison with the case without cool painting, respectively when r = 0.45 and r = 0.85.
Thus, the results of the simulations seem to be very encouraging, and to justify the use of very performing cool painting for roofs in hot climates.

Table 4: Annual building energy need as a function of the solar reflectance of the roof

	r = 0.25	**r = 0.45**	**r = 0.65**	**r = 0.85**
Summer energy need Q_s [kWh]	5565	4726	3891	3042
Winter energy need Q_w [kWh]	3222	3621	4110	4700
Total energy need [kWh]	8787	8347	8001	7742

4.4 Comparison in terms of Primary Energy

From the previous analysis, one can conclude that the adoption of cool paintings always allows a reduction in the annual building energy needs in hot climates. However, in the authors' opinion this conclusion should also be supported by the calculation of the overall Primary Energy consumption.
In this case, one needs to define the plant solutions adopted to provide both heating and cooling to the sample building. In fact, the Primary Energy consumption (PE) strongly depends on the efficiency of the conversion process, which is expressed by the Primary Energy Ratio *PER*.
Now, in this study air-conditioning in summer is supposed to be provided through fan-coil units fed by a reversible electric air-to-water vapour-compression chiller. As concerns space heating, two different solutions will be investigated: air-to-water electric reversible heat pump and conventional gas-fired heat generator. The annual primary energy need for both cooling and heating need is expressed by the following equation:

$$PE = \frac{Q_s}{PER_s} + \frac{Q_w}{PER_w} \tag{4}$$

Table 5: Primary Energy Ratio of different plant systems

	PER
Vapour-compression Chiller	PER_s = EER·0.46
Air-to-water Heat Pump	PER_w = COP·0.46
Gas-fired heat generator	$PER_w = \eta$

Here the first addend is the primary energy consumption for cooling in summer (S), while the second one is the primary energy consumption for heating in winter (W); the primary energy ratios PER_s and PER_w depend on the plant configuration and are summarized in Table 5.
For the calculation of the system efficiency, the following mean values were assumed:

- Energy Efficiency Ratio of the vapour-compression chiller: *EER* = 3.65;
- Coefficient of Performance of the heat pump: *COP* = 3.76;
- global efficiency of the gas-fired heat generator: η = 0.75;
- Italian electricity grid efficiency coefficient: 0.46.

As shown in Fig. 8, the primary energy demand for cooling (blue columns) always benefits from an increase in the solar reflectance of the cool painting. As concerns the primary energy demand for heating (red columns), its increase with *r* is less significant when using the heat pump than with a conventional gas-fired heat generator, thanks to the high PER of the heat pump. This allows an overall primary energy saving, as the annual PE drops from 5960 kWh without cool painting to 5289 kWh with a very performing painting (*r* = 0.85), so showing a reduction of 11%.
On the other hand, the use of a gas-fired heat generator leads to an increase of the overall primary energy need, so nullifying the benefits originating from the use of the cool painting in summer: the energy demand raises from 8068 kWh to 8461 kWh (increase of 5%).
These results suggest that the use of the cool roof technology has to be carefully evaluated also considering the winter period, and not only the summer period. The calculation should also account for the type of system adopted for space heating, since this choice may strongly influence the overall balance in terms of primary energy.

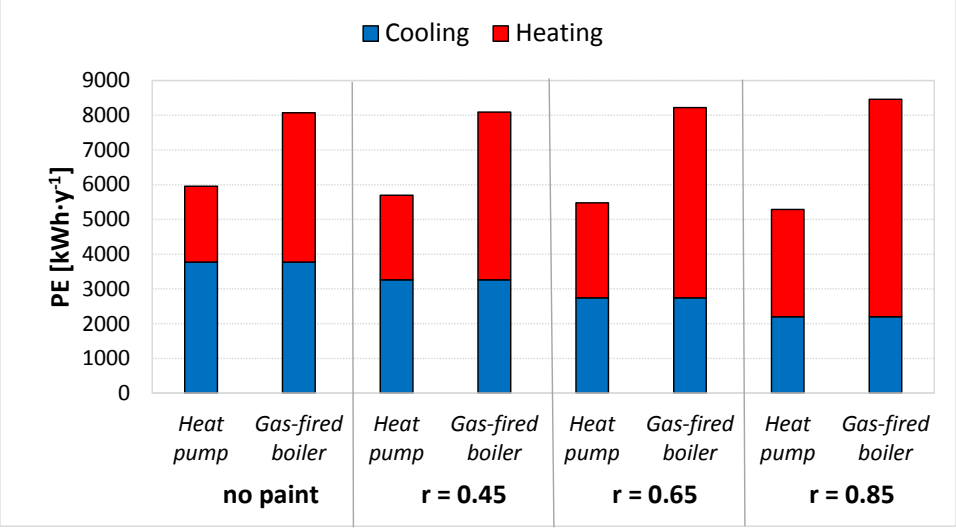

Figure 8: Comparison between different plant technologies in terms of annual primary energy need

5 CONCLUSIONS

The aim of this paper was to investigate the effectiveness of the cool roof technology for the refurbishment of an existing low-rise office building in Catania, a city in southern Italy with a

hot-humid climate, in which the energy demand for space cooling in summer is predominant if compared to that for space heating in winter.
The simulations carried out with the software EnergyPlus have pointed out that the comfort sensation of the occupants in free running conditions in summer can be significantly improved by applying a cool painting with an average value of solar reflectance (r = 0.45), which corresponds to the performance of a commercial painting actually applied to the roof in the framework of an experimental campaign. However, further enhancements might be expected if using a very-performing cool painting (up to r = 0.85).
Moreover, the application of the cool painting leads to a noticeable reduction of the building energy needs for space cooling; however, an increase of the energy needs for space heating in winter should also be expected. Such a drawback provides a sensible increase of the primary energy consumption for heating, that may also overcome the advantages achieved in summer.
In conclusion, the adoption of cool paintings for roofs is a solution that must be carefully evaluated in regions with intense or long winter period and in buildings where the heating system has not a very high performance.

6 REFERENCES

Bozonnet, E. (2011). Cool roofs impact on building thermal response: a French case study. *Energy and Buildings, 43*(11), 3006-3012.

Corrado, V. (2011). Building Typology Brochure – Italy. Politecnico di Torino, Dipartimento di Energetica, Gruppo di ricerca Tebe.

Levinson, R. (2007). Methods of creating solar – reflective nonwhite surfaces and their application to residential roofing materials. *Solar Energy Materials and Solar Cells, 91*(4), 304-314.

Levinson, R. (2010). A novel technique for the production of cool colored concrete tiles and asphalt shingle roofing products. *Solar Energy Materials and Solar Cells, 94*(6), 946-954.

Romeo, C. (2011). Impact of a cool roof application on the energy and comfort performance in an existing non – residential building. A Sicilian case study. *Energy and Buildings doi:10.1016/j.enbuild.2011.07.023 (In Press, Corrected Proof).*

Sicurella, F. (2012). A statistical approach for the evaluation of thermal and visual comfort in free – running buildings. *Energy and Buildings, 47,* 402-410.

Synnefa, A. (2007). On the development, optical properties and thermal performance of cool colored coatings for the urban environment. *Solar Energy, 81*(4), 488-497.

ASTM E 903-96 (1996). Standard Test Method Solar Absorptance, Reflectance and Transmittance of Materials Using Integrating Spheres.

EN Standard 15251 (2007). Indoor environmental input parameters for design and assessment of energy performance of buildings addressing indoor air quality, thermal environment, lighting and acoustics.

UNI EN ISO 6946 (2008). Building components and building elements. Thermal resistance and thermal transmittance. Calculation method.

UNI EN ISO 10077-1 (2007). Prestazione termica di finestre, porte e chiusure oscuranti – Calcolo della trasmittanza termica – Parte 1: Generalità.

UNI 10351:1994 (1994). Materiali da costruzione. Conduttività termica e permeabilità al vapore.

UNI 10355:1994 (1994). Murature e solai, valori della resistenza termica e metodo di calcolo.

DEVELOPMENT AND APPLICATION OF 'THERMAL RADIATIVE POWER' FOR URBAN ENVIRONMENTAL EVALUATION

Yupeng Wang[*1], Hashem Akbari[2]

1 Concordia University, Canada
1455 de Maisonneuve Blvd. West EV006.415
Montreal, Quebec, Canada H3G 1M8
**Corresponding author:*
wangyupeng0628@gmail.com

2 Concordia University, Canada
1455 de Maisonneuve Blvd. West EV006.409
Montreal, Quebec, Canada H3G 1M8

ABSTRACT

We have developed a new evaluation method of "thermal radiative power" (TRP) for investigating the impact of building surface material albedo on urban environment. The simulation system ENVI-met is used. This system is a 3D computer model which analyzes micro-scale thermal interactions within urban environments. It simulates urban-scale environmental conditions such as roofs, exterior wall, and ground surface temperatures. Focuses of this research are on the climate change in urban and community scale in cold climates. The urban environmental analysis is carried out in a typical residential area in the central city of Montreal. The model for simulation is based on the existing urban conditions (building layout, building volume and ground surface properties). The TRP with varied building roof materials is calculated and compared. The effect of building surface materials on local climate is analyzed. The selected simulation area in this research is 300m by 300m. Each urban surface (ground, walls, and roofs) is analyzed individually, in order to determine the urban environmental contribution. The interaction between reflective surfaces is discussed. Representing the environmental conditions by TRP could help to define the impact of urban surfaces on the macro-climate (urban level) and micro-climate (community level).

KEYWORDS

Urban Climate; Thermal Radiative Power; Air Temperature; Mean Radiation Temperature; Relative Humidity

1 INTRODUCTION

The Urban heat island (UHI) effect is the phenomenon that a metropolis is usually significantly warmer than its rural surroundings. It occurs because city centre buildings and street surface materials, which have high heat capacities, store heat during the day, and release heat slowly at night. The adverse energy and environmental effects of UHIs, and methods to alleviate them, has become a major research topic in sustainability programs. Decreasing the energy consumption of buildings is an important topic in environmental engineering. Daytime solar energy absorption is the primary cause of the urban heat island effect in summer. Pavements and roofs comprise over 60% of urban surfaces. Dark materials, dark pavements and roofs, absorb 80-90% of sunlight. Lighter materials, white roofs and lighter colored pavements, absorb only 30-65% of sunlight. There is an interaction of thermal radiation between roof, wall and ground surfaces. The use of reflective building surface materials is a critical solution for UHI mitigation [1, 4, 5, 6, 10, 21, 22, 23].
A large number of studies are currently attempting to demonstrate the extent of the UHI effect in cities. Some studies are using averaged Land Surface Temperature (LST) [15, 18, 20],

derived from satellite data. However, observed LST depends on spatial resolution, because of the different land cover types. In most present studies, a spatial resolution of 1 km^2 is used. This ignores land cover characteristics on a community scale.
Furthermore, LST derived from the satellite database ignores the contribution from the surface of exterior building walls. This is a serious deficiency for the consideration of urban solar heat absorption and reflection. This is especially relevant for mega cities that have a high density of high-rise buildings. This research will provide a new evaluation method for assessing the impact of building surface solar reflectance on the UHI effect. The TRP, released from the urban surfaces, is not used in existing studies, even though it is a suitable indicator to represent the impact of solar heat absorption.
Many researchers have focused on the building surface materials, LST and urban heat island problem. Most studies have analyzed measured climatological data and demonstrated the correlations with urban development [3, 9, 15, 18, 20]. Very few have studied the UHI contribution from each environmental effector in micro scale, that directly affect the outdoor thermal comfort. In this research, the thermal radiation from urban surfaces (such as building roofs, exterior walls and ground surfaces) will be simulated, using a micro-scale urban simulation model. Both an urban and a community scale will be analyzed. The simulation will be helpful to determine the contributions of each component, and to determine the optimal combination of urban surface properties.
In addition, most present studies are focused on the UHI effect in hot and dry cities. The UHI effect in cold climates, such as Canada cities, should be further investigated. In this research, a new UHI evaluation system is proposed and applied in the city of Montreal. The objectives of our study are to: (1) define the new UHI evaluation method TRP, and (2) demonstrate the qualification of the TRP to express the extent of UHI. This research will be an investigation of the methodology for UHI study, which contributes to environmental urban planning standards providing, that can be used in urban developments and redevelopments.

2 METHODOLOGY

2.1 Selected Simulation Area

The selected area is a high-density residential area, next to the city's main commercial area and a university. There are many high-rise residential buildings of more than 15 floors. Most of the ground surface is asphalt road. The area was 300 meters by 300 meters.

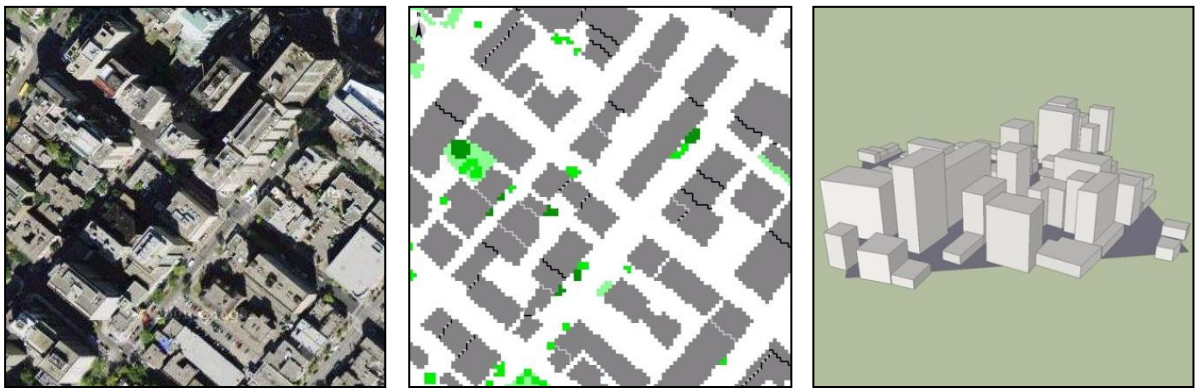

Aerial satellite view | Area input file to the ENVI-met | 3D image

Figure 1. Images of the selected area: 1) aerial satellite view pictures, 2) input file images for ENVI-met simulations, based on the aerial satellite view pictures, and 3) 3D images of the buildings volumes.

2.2 Urban Environmental Simulation

We used ENVI-met simulation model (a three-dimensional computer model that analyzes micro-scale thermal interactions within urban environments) to simulate the environmental

conditions in the selected area. ENVI-met is designed to simulate the surface-plant-air interactions in urban environments. It has a typical spatial resolution of 0.5m to 10m, and a temporal resolution of 10 seconds. A simulation is typically carried out for at least 6 hours, usually for 24-48 hours. The optimal time to start a simulation is at night or sunrise, so that the simulation can follow the atmospheric processes. ENVI-met requires an area input file which defines the 3-dimensional geometry of the target area. This includes buildings, vegetation, soils and receptors. A configuration file, which defines the initialization input, is also required [12, 14, 16].

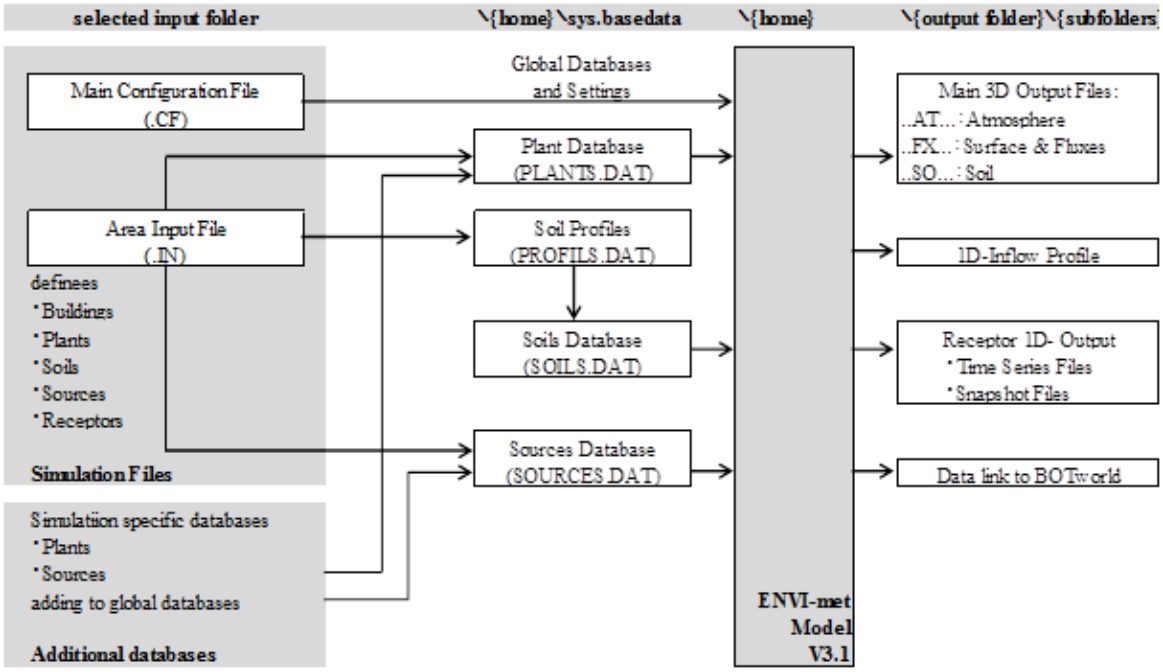

Figure 2. Data flow in ENVI-met V3.1 (http://www.envi-met.com/)

The data flow shown in figure 2 summaries the general interaction between input and output data. ENVI-met carries out detailed calculation in regards to [13]:

- shortwave and long-wave radiation fluxes with respect to shading, reflection and re-radiation from building systems and the vegetation
- evapotranspiration and sensible heat flux from the vegetation into the air, including full simulation of all physical plant parameters (e.g. photosynthesis rate)
- surface and wall temperatures for each grid point
- water and heat exchange inside the soil system
- the calculation of biometeorological parameters, such as Mean Radiant Temperature (MRT) or Fanger's Predicted Mean Vote (PMV) value
- the dispersion of inert gases and particles, including sedimentation of particles at leaves and surfaces.

For these simulations, the geometry of urban street canyons in selected area is identified using satellite pictures and street maps from Google Map. Area input files were built by ENVI-met; we input satellite pictures into the editing files, and defined the ground, vegetation, building facade and building layout by cubic grids of $27m^3$ (3m×3m×3m). The simulations were run for 24 hours, starting from one hour before sunrise (4am). We simulated this area in summer. The weather data was obtained from the “Weather Spark” database. However, with the spatial limitation of the simulation model, a deviation will emerge around the edge of simulation model. This deviation will also affect the UHI simulation results with ENVI-met.

2.3 Definition of 'Thermal Radiative Power'

The thermal radiative power (TRP) of a black surface, given by the Stefan–Boltzmann law is obtained by:

$$P = \dot{O} \bullet A \bullet T^4 \quad (1)$$

For surfaces which are not black bodies, one has to consider the (generally frequency dependent) emissivity Ɛ . This emissivity has to be multiplied with the radiation spectrum formula before integration over the wavelength spectrum. If it is taken as a constant, the resulting formula for the power output can be written in a way that contains Ɛ as a factor. The following equation is used for calculating the TRP in this research:

$$P = Ɛ \bullet \dot{O} \bullet A \bullet T^4 \quad (2)$$

Where:

P: Thermal Radiative Power (W)

Ɛ : Emissivity (Soil: 0.92-0.96; Concrete: 0.94; Asphalt: 0.9-0.98)

$\dot{O}$: Stefan-Boltzmann Constant = 5.67×10-8 ($W \bullet m^{-2} \bullet K^{-4}$)

A: Radiating Surface Area (m^2)

T: Absolute Temperature (K)

3 RESULTS

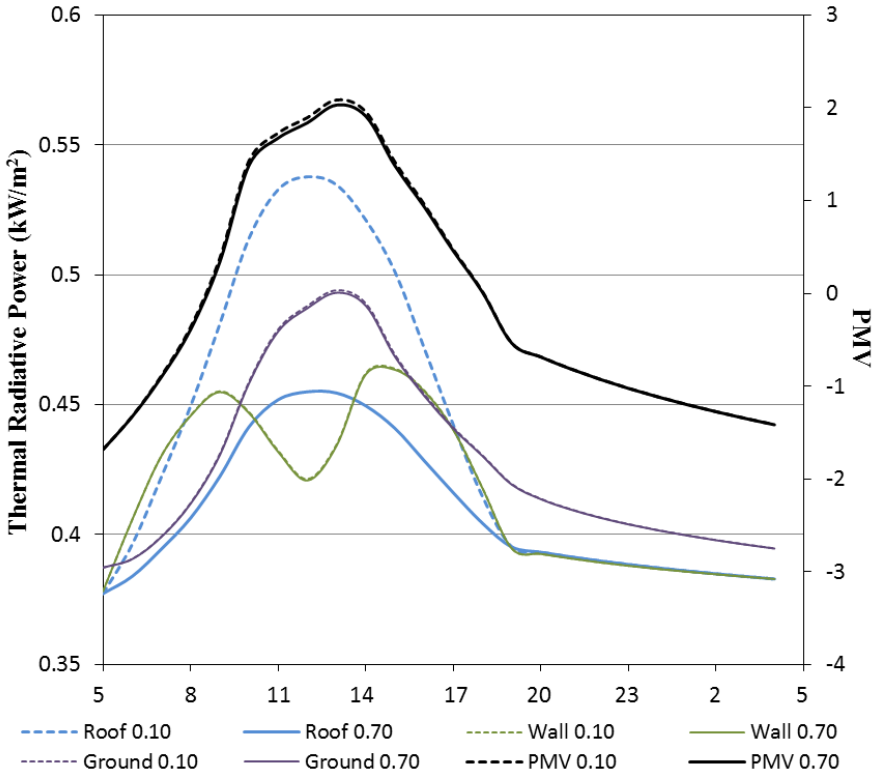

Figure 3. Averaged TRP of each urban surface elements (Roof, Wall, and Ground) per m^2, and averaged diurnal PMV at 1.8m above the ground on a typical Summer day (from 5am, 22 July, to 4am the next day) in the selected area, with two roof types (Type 1: albedo 0.10; Type 2: 0.70). Diurnal PMV with lower roof albedo is slightly higher than that with higher roof albedo.

The Averaged TRP per m^2, from each element of urban surfaces at daytime and night time is calculated and showed in figure 3. Type 1 represents the model with roof albedo of 0.10; type 2 represents the model with roof albedo of 0.70. With increasing the roof albedo, the TRP from roof is decreased 15.4% (0.08kW/m^2) at 1pm. Meanwhile, the TRP from walls and ground is also slightly decreased (0.2% from ground, and 0.1% from walls). This could be considered as the reason of the PMV difference. PMV that observed in type 2 is 0.05 lower than that in type 1 in the midday from 10am to 2pm. At midnight (1am), the TRP from

ground, building walls, and roofs in two types of model are almost the same. This could explain the same PMV that observed during the night time; the difference is lower than 0.01 after 6pm. This comparison demonstrated the interactions among each urban surface, because the TRP of ground and walls are reduced by increasing the albedo of the roofs.

Figure 4 compares T_a, T_{mrt}, and relative humidity with two model types. Diurnal T_a and T_{mrt} with lower roof albedo are slightly higher than that with higher roof albedo, and relative humidity is lower for the model with lower roof albedo. The effect of roof albedo on T_a, T_{mrt}, and relative humidity is pronounced during daytime (from 11am to 7pm). During this period, T_a difference is around 0.2^OC, T_{mrt} difference is around 0.06^OC, and relative humidity difference is over 0.8%. At nighttime (after 7pm), the temperature difference between two models is close to 0^OC. This is to say, the effect of roof albedo on community-scale thermal environment is mainly during daytime. Additionally, higher roof albedo could also reduce the surface temperature of buildings, leading to a higher indoor comfort, lower energy consumption, and lower heat emission. However, the impact of heat emission from indoor of buildings is not included in this simulation. Therefore, the environmental benefits of high albedo roof are even higher than the results shown by these simulations.

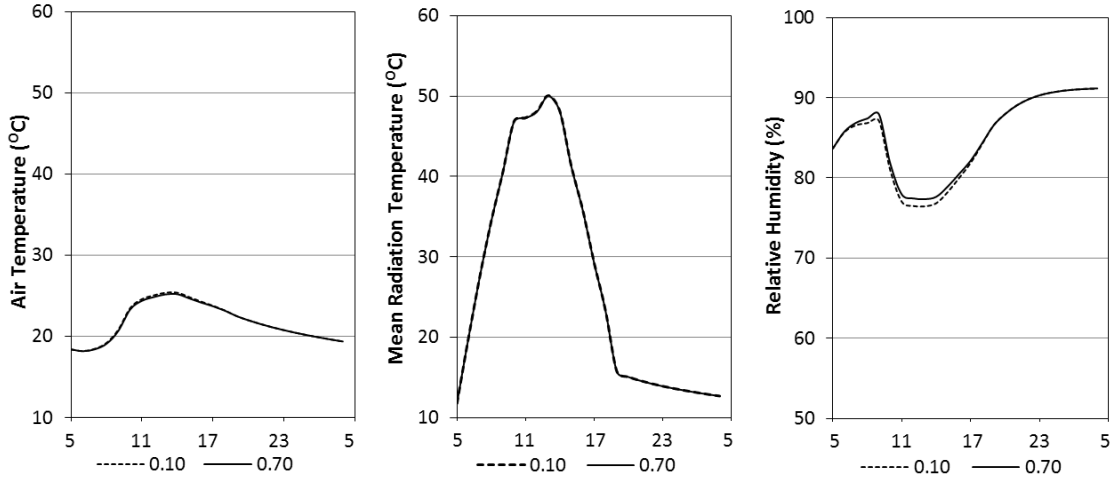

Figure 4. Averaged diurnal air temperature (T_a), mean radiation temperature (T_{mrt}), and relative humidity at 1.8m above the ground on a typical Summer day (from 5am, 22 July, to 4am the next day) in the selected area, with two roof types (Type 1: albedo 0.10; Type 2: 0.70).

Furthermore, the correlation between TRP change (TRP change = TRP of type 1 – TRP of type 2) and urban environmental condition changes (T_a change = T_a of type 1 – T_a of type 2; T_{mrt} change = T_{mrt} of type 1 – T_{mrt} of type 2; Relative humidity change = Relative humidity of type 1 – relative humidity of type 2; PMV change = PMV of type 1 – PMV of type 2) are indicated in figure 5. All coefficients of determination (R^2) are greater than 0.80. Inspecting the correlation between TRP change and T_{mrt} change, the impact from the TRP change of the ground (R^2=0.99) is much bigger than that from the walls (R^2=0.95) and roofs (R^2=0.83). On the other hand, comparing TRP change from roofs , walls and ground, the TRP change of the roofs is showing a higher impact on T_a (R^2=1), relative humidity (R^2=0.99) and PMV (R^2=0.99). The effect of TRP and T_{mrt} at ground level is highly correlated. The effect of each urban surface element (roofs, walls, and ground) on the urban thermal comfort is investigated separately. The result verified the TRP as an urban environmental evaluation index.

The interactions among the ground, building walls, and roofs are observed in this comparison. TRP from Ground contributes almost 100% to the radiative environment in community scale, because the released radiative power directly effects to the human height level. The effect of TRP from building walls on comfort is somewhat lower. This is because some part of the TRP from walls will be directly reflected to the sky, and some part of it will be locked in the

urban canyon. Inter-reflection also occurs between surrounding walls and ground. TRP from roofs slightly affects the urban radiative environment, because very small part of TRP will be reflected to the surrounding walls (this fraction becomes obvious with big differ of building height, such as central area of cities), and most part of it will be released to the sky.

The estimation of TRP can make a significant contribution to the process of urban environmental analysis for urban development or redevelopment, helping to develp policies and guidelines. TRP could also be carried out by field measurement for existing urban environmental evaluation, in order to develop specific promotion scenarios. In such case, measuring the surface temperature, calculating the emitted radiation intensity, and multiplying it by the area of each surface (walls, roofs, and ground), one can develop a TRP index for each community area.

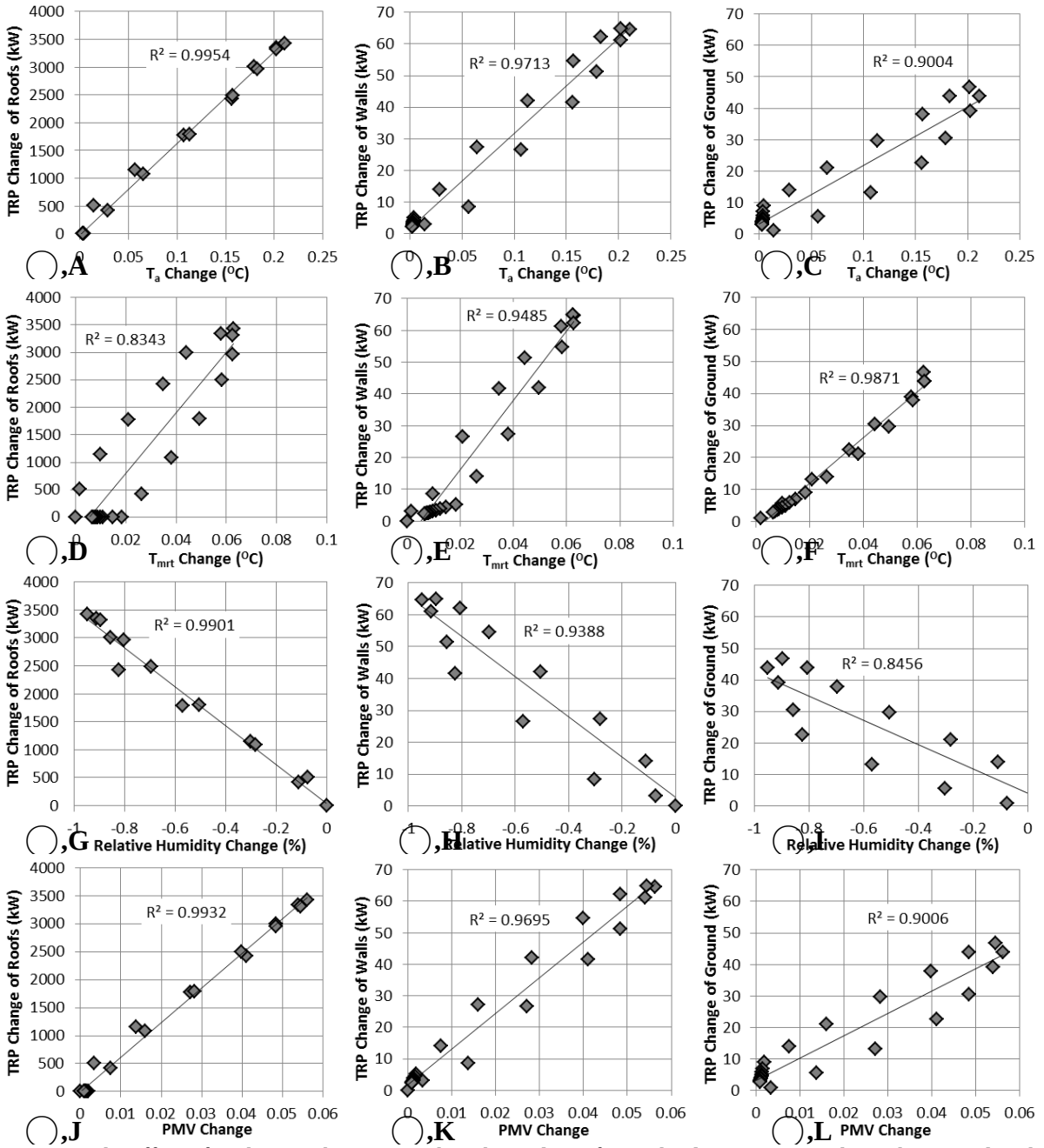

Figure 5. The effect of each TRP changes to urban thermal comfort. The data is at 1.8m above the ground in the selected areas 24 hours of a typical day in summer (from 5am, 22 July, to 4am the next day). R^2= coefficient of determination. TRP changes are proportional to T_a, T_{mrt} and PMV changes, inversely correlated to relative humidity change.

4 CONCLUSION

In this study, TRP is introduced as a new standard for evaluating urban environment. Compared to LST, TRP could indicate the thermal effect from each urban surface element in community scale, and evidence the impact from each surface element. Two types of urban model are simulated and compared. Changing the albedo of building roofs from 0.1 to 0.7, the TRP from roofs during the typical summer day is decreased obviously (around 6% to 15% during 7am to 5pm). The TRP from walls and ground are also somewhat decreased (around 0.02% to 0.20% during 7am to 5pm). The impact of TRP from each urban surface element on the urban thermal comfort are compared and discussed. Changing of TRP shows a strong correlation with changing of urban thermal comfort indicators, such as T_a, T_{mrt}, relative humidity, and PMV. It is investigated that, TRP is a qualified index for urban environmental evaluation in the three-dimensional urban respect.

Development and application of this index could help to specific the phenomenon of urban climate change, and helps to figure out the solution scenarios for urban climate change mitigation. In addition, application studies in various urban areas with various building types, vegetation plans, and urban surface materials should be carried out in the next stages.

5 ACKNOWLEDGEMENTS

This research was partially funded by an NSERC Discovery grant. The authors wish to express appreciation to Professor Michael Bruse (University of Mainz, Germany) for providing the advanced free environmental simulation program (ENVI-met).

6 REFERENCES

[1] Akbari, H., Bretz, S., Taha, H., Kurn, D. and Hanford, J. Peak power and cooling energy savings of high albedo roofs. Energy and Buildings – Special Issue on Urban Heat Islands and Cool Communities 1997; 25 (2): pp. 117-126.

[2] Akbari H., Pomerantz M. and Taha H. Cool surfaces and shade trees to reduce energy use and improve air quality in urban areas. Solar Energy 2001; 70(3): pp. 295-310.

[3] Arathyram.R.S and K.Venugopala Raoa. Characterisation of urban heat islands in one of the most urbanized corridors of India from space based multi-sensor, spatio-temporal data. Applied Geo-informatics for Society and Environment Proceeding 2012; pp. 25-31.

[4] Berdahl P. and Bretz S. Spectral solar reflectance of various roof materials. Cool Building and Paving Materials Workshop, Gaithersburg, MD 1994.

[5] Bretz, S., Akbari, H. and Rosenfeld, A. Practical issues for using solar reflective materials to mitigate urban heat islands. Atmospheric Environment 1997; 32: pp. 95-101.

[6] Bretz, S. and Akbari, H. Long-term performance of high albedo roof coatings. Energy and Buildings 1997; 25: pp. 159-167.

[7] D. J. Unwin. The synoptic climatology of Birmingham's urban heat island, 1965-74. Weather 1980; 35 (2): pp. 43-50.

[8] Hideki, T. and Masakazu, M. Surface heat budget on green roof and high reflection roof for mitigation of urban heat island. Building and Environment 2007; 42: pp. 2971-2979.

[9] Kayleigh A. Somers, Emily S. Bernhardt, James B. Grace, Brooke A. Hassett, Elizabeth B. Sudduth, Siyi Wang and Dean L. Urban. Streams in the urban heat island: spatial and temporal variability in temperature. Freshwater Science 2013; 32 (1): pp. 309-326.

[10] Konopacki, S. and Akbari, H. Measured energy savings and demand reduction from a reflective roof membrane on a large retail store in Austin. Lawrence Berkley Laboratory Report No. LBNL-47149, CA. 2001.

[11] Levinson, R., Akbari, H., Konopacki, S. and Bretz, S. Inclusion of cool roofs in nonresidential Title 24 prescriptive requirements. Energy Policy 2005; 33: pp. 151-170.
[12] M. Bruse. ENVI-met website: www.envimet.com; 2013.
[13] M. Bruse. ENVI-met 3.0: Updated model overview; 2004.
[14] M. Bruse. The influences of local environmental design on microclimate – development of a prognostic numerical model ENVI-met for the simulation of Wind, temperature and humidity distribution in urban structures. Ph.D. Thesis, Germany: University of Bochum; 1999
[15] Menglin S. Jin. Developing an index to measure urban heat island effect using satellite land skin temperature and land cover observations. American Meteorological Society 2012; 25: pp. 6193-6201.
[16] Ozkeresteci I, Crewe K, Brazel A.J. and Bruse M. Use and evaluation of the ENVI-met model for environmental design and planning: an experiment on linear parks. Cartographic Renaissance, Document Transformation Technologies 2003; 402-409.
[17] Rosenfeld A., Akbari H., Bretz S., Fishman B.L., Kurn D.M., Sailor D. and Taha H. Mitigation of urban heat islands: materials, utility programs, updates. Energy and Buildings 1995; 22: pp. 255-265.
[18] Rupesh Gupta. Temporal and spatial variations of urban heat island effect in Jaipur city using satellite data. Environment and Urbanization ASIA 2012; 3 (2): pp. 359-374.
[19] Santamouris M., Papanikolaou N., Livada I., Koronakis I., Georgakis C., Argiriou A., et al. On the impact of urban climate to the energy consumption of buildings. Solar Energy 2001; 70(3): 201e16.
[20] Shushi Peng, Shilong Piao, Philippe Ciais, Pierre Friedlingstein, Catherine Ottle, Francois-Marie Breon, Huijuan Nan, Liming Zhou and Ranga B. Myneni. Surface urban heat island across 419 global big cities. Environmental Science & Technology 2012; 46: pp. 696-703.
[21] Synnefa A., Santamouris M. and Apostolakis K. On the development, optical properties and thermal performance of cool colored coatings for the urban environment. Solar Energy 2007; 81: pp. 488-497.
[22] Synnefa, A., Santamouris, M. and Livada, I. A study of the thermal performance and of reflective coatings for the urban environment. Solar Energy 2006; 80: pp. 968-981.
[23] Taha H., Akbari H. and Rosenfeld A., Residential JH. Residential cooling loads and the urban heat island—The effects of albedo. Building and Environment 1988; 23(4): pp. 271-83.
[24] Winston T.L. Chow, Anthony J. Brazel. Assessing xeriscaping as a sustainable heat island mitigation approach for a desert city. Building and Environment 2012; 47: 170-181.
[25] Yarbrough D.W. and Anderson R.W. Use of radiation control coatings to reduce building air-conditioning loads. Energy Sources 1993; 15: pp. 59-66.

DEVELOPMENT OF SELF-CLEANING TOP-COAT FOR COOL ROOF

Takeshi Sonoda[1], Yasushi Nakanishi[*1], Takahiro Hamamura[2], Hiroki Ueda[1], Taizo Aoyama[1], and Hideki Takebayashi[3]

1. Kaneka Corporation
Miyamae-cho 1-8, Takasago-cho
Takasago, Hyogo, JAPAN
** yasushi_nakanishi@kn.kaneka.co.jp*

2. Kaneka Corporation
5-1-1 Torikai-nishi,
Settsu, Osaka, Japan

3. Kobe University
Rokkodai-cho 1-1, Nada-ku
Kobe, Hyogo, JAPAN

ABSTRACT

Our recent study has shown that the acrylic silicon polymer is useful to formulate self-cleaning topcoat which may maintain the thermal insulation effect of cool roof effectively.
A 2K self-cleaning topcoat was formulated with a water-borne type acrylic silicon polymer. Its effect to maintain high solar reflectance was confirmed by outdoor exposure test in comparison with coatings having no self-cleaning function. The solar reflectance performance was well maintained regardless of installation angle, lightness of colour or pigment type.
After outdoor exposure, drop of solar reflectance was found. It had clear correlation to change in lightness of colour for light coloured coatings. In the meantime, for dark coloured coatings, the above-mentioned correlation was relatively low. This suggests that the decline of solar reflectance was caused by dirt pick up rather than drop in the lightness of colour.
The decline of solar reflectance, that is supposed to be caused by dirt pickup, started just after installation and it was saturated in 3 to 6 months. After a 6-months exposure, the solar reflectance of the self-cleaning topcoat dropped by about 2% while the subject decline of non-self-cleaning topcoat was about 11%. A simulation study was also done to compare the electricity consumption for air conditioning, which showed that saving of electricity consumption could be 10% more with the self-cleaning topcoat.

KEYWORDS

self-cleaning, cool roof, acrylic silicon polymer, heat island, energy saving

1 INTRODUCTION

Cool Roof coating is drawing social attention worldwide, as one of solutions against “Heat Island” effect in urban area. However, it is pointed out that drop of solar reflectance of cool roof coating happens in rather short period after installation[1)]. Supposedly, the drop of the solar reflectance is due to dirt pickup.
Self-Cleaning paint is widely used for building wall coating, and effect to avoid dirt pick-up is proven. Acrylic silicon polymer is one of base resins which is useful to formulate self-cleaning paint.
In this paper, we will discuss effect of the self-cleaning technology to maintain the solar reflectance in cool roof coating application. The first part of the paper is discussing results of outdoor exposure using test specimens.
The second part of the paper is discussing result of a real building installation test. In this test, temperature inside and outside of the building, electricity consumption for air conditioning, and roof surface heat balance were measured to prove effect of cool roof coating. And also, the measured data was used for simulation study of air conditioning energy saving effect based on cooling load calculation[2)].

2 EXPERIMENTS AND RESULTS

2.1 Outdoor exposure with test specimens

2.1.1 Experimental

2.1.1.1 Material

Water-borne 2K acrylic silicon polymer system was used as binder in self-cleaning paint. The binder consists of 2 parts. Part A contains base polymer emulsion with alkoxysilyl group. Part B contains hydrolysis/condensation catalyst and alkyl silicate (Table 1). Alkyl silicate is to form hydrophilic layer on the surface of the coating, and results in self-cleaning effect (Figure 1). Non-self-cleaning paint was formulated only with Part A.
To colour the paint, white and black pigments were used to formulate paints of white, black and grey of various lightness. 2 different types of titanium dioxide were chosen as white pigments.Wpg1 is large particle size type, which has average diameter around 1μm. Wpg2 is general type , of which has average diameter around 0.36μm.For black pigments, various types, BkPg1 – BkPg5, were chosen from commercially available products.

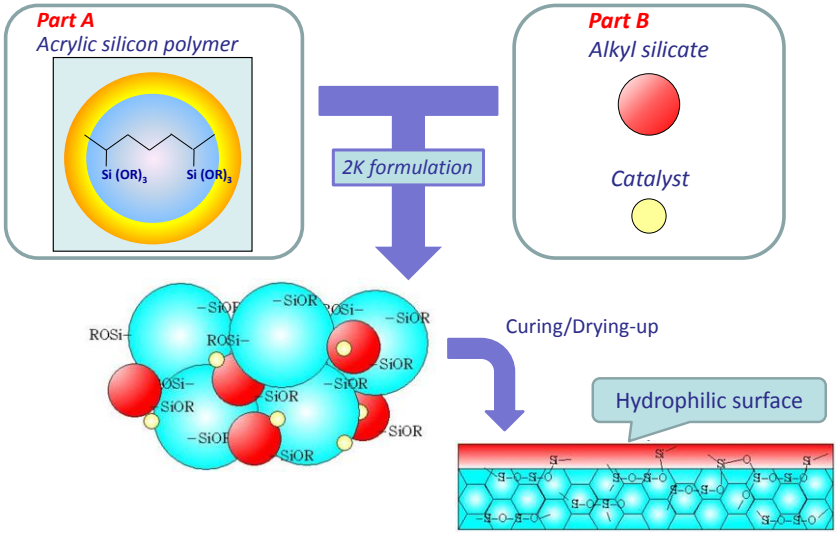

Figure 1: Image of the film-forming

. Table 1: Binder of test paint

	Part A	Part B
Main component	Acrylic silicon polymer	Alkyl silicate + Catalyst
Non-volatile content	ca. 50%	ca. 43%
Viscosity	ca. 200mPa·s	ca. 13mPa·s
pH	ca. 8	-
Minimum film formation temperature	ca. 40℃	-
Particle size	ca. 190nm	-
Surfactant	Anionic/Nonionic	-
Blend ratio	Part A : Part B = 6 : 1	

Table 2: pigments of test paint

Colour	Mark	Pigments	Concentration
White	WPg1	Titanium White (PW6) (large particle, 1μm)	100%
	WPg2	Titanium White (PW6) (general, 0.36μm)	100%
Black	BkPg1	Carbon Black (PBk6)	22%
	BkPg2	Paliogen Black (PBk31)	30%
	BkPg3	Bismuth Vanadate Yellow (PY184) / Quinacridone Violet (PV19) / Phthalocyanine Blue BGS (PB15:3) / Barium Sulfate(Synthetic) (PW21) mixture	29%
	BkPg4	Composite oxide pigment of copper and bismuth	60%

	BkPg5	Azo Methyne Black	30%

Colour Index Name is indicated in bracket.

2.1.1.2 Test paints formulation

Binder and pigments, which are mentioned above, are used to formulate test paints together with other additives. Black colour and white colour were formulated first. Then, various lightness of grey was formulated by mixing the black and white.

2.1.1.3 Test specimen

Epoxy based sealer and commercially available cool roof paint (white colour) were painted on anodic oxidized aluminium plate (70x150x0.8mm) to make base plate.
Test paints were applied on it, and cured for no shorter than 14days at room air temperature to come up with test specimen.

Photo 1: Exposure test

2.1.1.4 Outdoor exposure

All the specimens were situated at 3 different angles to horizon (0, 30, and 45degrees) facing to south in Settsu, Osaka, Japan.
In the course of the exposure test, lightness (L^*), and solar reflectance were measured periodically. The lightness was measured with Color Meter ZE2000 (Nippon Denshoku Industries). The solar reflectance was calculated with the method described on JIS K5602 (Determination of reflectance of solar radiation by paint film) based on spectral reflectance measure by Spectrophotometer SolidSpec-3700 (Shimadzu) in the wave length range of 300nm – 2500nm.

2.1.2 Results

2.1.2.1 Effect of exposure angle

Lightness and solar reflectance change after outdoor exposure were compared at different exposure angles (0, 30, and 45degrees). The comparison was made with white coloured coating. The results are shown on figure 2 and 3.

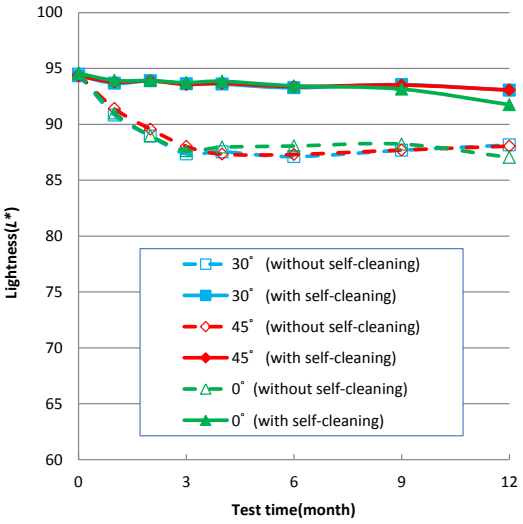

Figure 2: Effect of exposure angle on lightness (L^*)

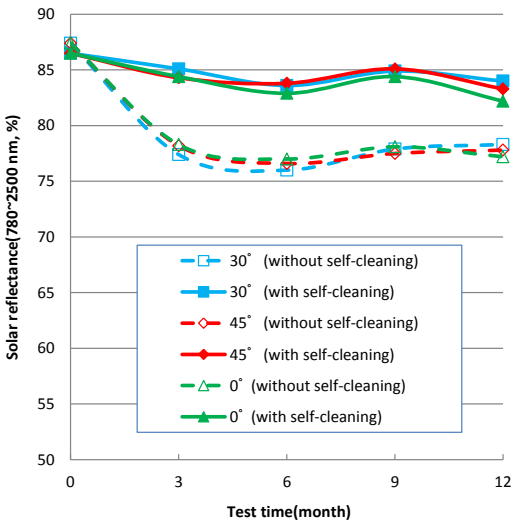

Figure 3: Effect of exposure angle on solar reflectance

No clear differences on both lightness and solar reflectance were found at different exposure angles. Self-cleaning paint maintained higher lightness and solar reflectance compared to non-self-cleaning paint.

For the case of non-self-cleaning paint both lightness and solar reflectance dropped in first 3-6 months to stay low after that.

2.1.2.2 Effect of lightness of the paint colour

In order to simulate effect of colour variation in cool roof paint, lightness and solar reflectance were compared with differently coloured specimens.

Test paints were formulated in black, white and 2 greys. The grey was adjusted to 70% and 50% lightness. White pigment was Wpg1 and black pigment was BkPg3.

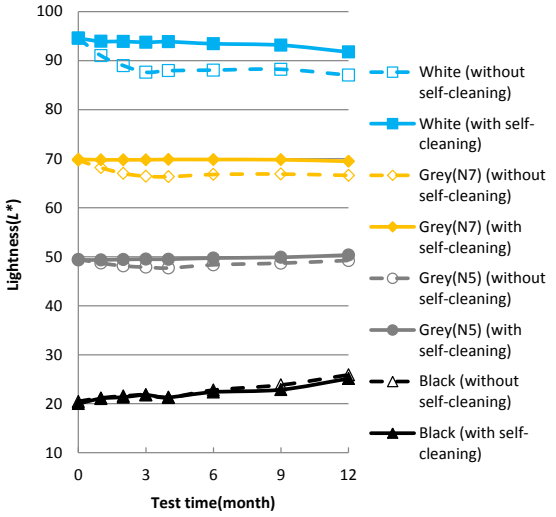

Figure 4: Effect of lightness of the paint colour on lightness (L^*)

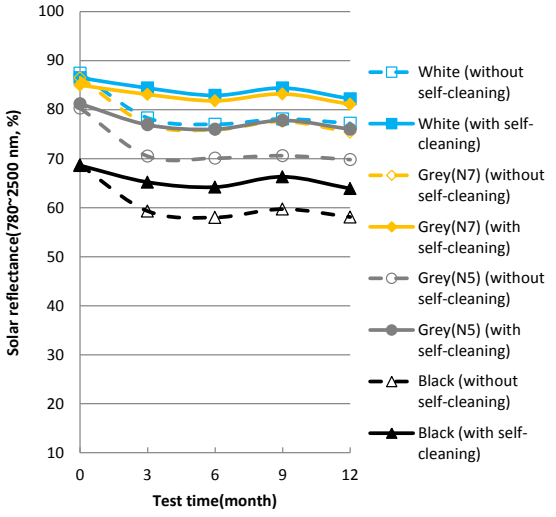

Figure 5: Effect of lightness of the paint colour on solar reflectance

On solar reflectance, effect of self-cleaning function was clearly seen even with black colour as much as white colour.

Contrary, on lightness, effect of self-cleaning function was only seen on brighter colour. The darker the colours, the less difference in lightness was found between with and without self-cleaning function. There was virtually no difference of the lightness for black coloured paint with and without self-cleaning function.

This results suggests that it is difficult to tell drop of solar reflectance by appearance for darker colours.

2.1.2.3 Effect of pigment

One of the most important aspects of cool roof paint is to maximize solar reflectance. In this aspect, choice of pigment is essential. In this section, we compared several pigments, which can be used for cool roof coating, in combination with self-cleaning technology.

Table 3: Effect of the solar reflectance(780~2500nm) by change of pigment

Mark	Colour	Self-cleaning function	Change of the solar reflectancereflectance (780~2500nm)					Change of the solar reflectance retention (780~2500nm)			
			Initial	3 months	6 months	9 months	1 year	3 months	6 months	9 months	1 year
WPg1	White	Without	87.4	78.3	77.0	78.1	77.2	90	88	89	88
		With	86.5	84.4	82.9	84.4	82.2	98	96	98	95
WPg2	White	With	85.2	82.1	81.6	82.5	80.6	96	96	97	95
	Grey(N7)	With	82.2	79.2	77.7	80.5	77.5	96	95	98	94
BkPg3	Black	Without	68.7	59.3	58.0	59.7	58.1	86	84	87	85
		With	68.6	65.1	64.2	66.3	63.9	95	94	97	93
	Grey(N7)	Without	86.5	77.0	75.9	77.6	75.4	89	88	90	87
		With	85.0	83.1	81.8	83.2	81.1	98	96	98	95
BkPg2	Black	With	72.3	69.1	67.8	68.3	66.8	96	94	94	92
	Grey(N7)	With	87.1	85.6	84.5	85.1	83.8	98	97	98	96
BkPg4	Black	With	54.7	51.3	50.0	51.5	49.5	94	91	94	90
	Grey(N7)	With	81.6	79.4	78.3	77.8	78.4	97	96	95	96
BkPg5	Black	With	72.1	68.8	67.8	70.0	67.9	95	94	97	94
	Grey(N7)	With	86.8	84.3	83.4	83.6	83.0	97	96	96	96
BkPg1	Black	With	4.1	4.5	4.4	4.4	4.7	110	107	107	115
	Grey(N7)	With	33.0	32.6	32.1	32.6	32.3	99	97	99	98

Table 4: Effect of the solar reflectance(300~2500nm) by change of pigment

Mark	Colour	Self-cleaning function	Change of the solar reflectancereflectance (300~2500nm)					Change of the solar reflectance retention (300~2500nm)			
			Initial	3 months	6 months	9 months	1 year	3 months	6 months	9 months	1 year
WPg1	White	Without	85.1	74.5	73.0	74.0	72.8	88	86	87	86
		With	84.9	82.8	81.5	82.4	79.9	98	96	97	94
WPg2	White	With	87.1	83.9	83.6	83.5	82.1	96	96	96	94
	Grey(N7)	With	63.1	61.1	60.2	61.5	60.1	97	95	97	95
BkPg3	Black	Without	34.4	30.3	29.8	30.5	29.9	88	87	89	87
		With	34.3	32.9	32.5	33.4	32.6	96	95	97	95
	Grey(N7)	Without	62.8	56.0	55.4	56.3	55.0	89	88	90	88
		With	62.5	61.2	60.5	61.4	60.0	98	97	98	96
BkPg2	Black	With	41.1	39.2	38.4	38.5	37.9	95	93	94	92
	Grey(N7)	With	67.4	66.4	65.7	66.2	65.5	99	97	98	97
BkPg4	Black	With	28.0	26.7	26.2	26.9	26.2	95	94	96	94
	Grey(N7)	With	60.9	62.4	63.0	63.1	64.2	102	103	104	105
BkPg5	Black	With	36.7	35.6	35.2	36.0	35.2	97	96	98	96
	Grey(N7)	With	64.8	65.5	66.0	66.4	67.0	101	102	102	103
BkPg1	Black	With	4.2	4.6	4.6	4.5	4.9	110	110	107	117
	Grey(N7)	With	30.2	29.9	29.6	29.9	29.7	99	98	99	98

Table 5: Effect of lightness(L^*) by change of pigment

Mark	Colour	Self-cleaning function	Change of Lightness(L^*)					Change of Lightness Difference(ΔL^*)			
			Initial	3 months	6 months	9 months	1 year	3 months	6 months	9 months	1 year
WPg1	White	Without	94.6	87.6	88.1	88.2	87.0	-6.9	-6.5	-6.3	-7.5
		With	94.6	93.7	93.4	93.2	91.8	-0.8	-1.1	-1.4	-2.8
WPg2	White	With	96.6	95.0	95.6	94.2	94.5	-1.6	-1.0	-2.4	-2.2
	Grey(N7)	With	72.6	71.9	72.1	71.5	71.9	-0.8	-0.5	-1.1	-0.7
BkPg3	Black	Without	20.5	21.8	22.8	23.7	25.9	1.4	2.3	3.3	5.4
		With	20.0	21.8	22.4	22.9	25.1	1.8	2.4	2.9	5.1
	Grey(N7)	Without	69.7	66.4	66.8	66.9	66.6	-3.3	-2.9	-2.8	-3.1
		With	69.9	69.8	69.8	69.8	69.5	-0.1	-0.1	-0.1	-0.4
BkPg2	Black	With	14.0	17.0	17.4	17.8	21.0	3.0	3.4	3.8	7.0
	Grey(N7)	With	71.1	71.1	71.3	71.1	71.4	0.0	0.3	0.1	0.3
BkPg4	Black	With	17.6	21.1	21.9	22.5	24.7	3.5	4.3	4.9	7.1
	Grey(N7)	With	70.6	74.3	75.9	75.9	77.0	3.8	5.3	5.3	6.4
BkPg5	Black	With	8.8	13.2	13.9	14.7	18.0	4.4	5.1	5.9	9.2
	Grey(N7)	With	68.2	71.4	73.1	73.1	74.9	3.2	4.9	4.9	6.7
BkPg1	Black	With	5.7	11.1	12.5	13.1	16.9	5.4	6.8	7.4	11.3
	Grey(N7)	With	57.5	57.5	57.7	57.7	57.8	0.0	0.2	0.2	0.4

As a result, it was found that self-cleaning paint kept 90% or higher solar reflectance retention after 1 year exposure, regardless of the pigment types.
One remark to be made is increase in lightness (L^*) for some pigments. All the black colour and some greys. Although there has not been precise investigation of cause of the colour change, decomposition of the pigments is suspected.

2.2 Experiments in the actual building

2.2.1 Objective material

Self-cleaning paint was formulated with 2K water borne acrylic silicon binder. 1K water borne acrylic silicon based paint, which does not have self-cleaning function, was chosen as a reference. Colour was white for both paints.

2.2.2 Outline of measurement

The measurement is being executed through 18th July 2012 and 30th September 2013 in Osaka, Japan. A cross-sectional schematic view of the roof is shown on figure 5. Data without cool roof paint was taken from 18th July to 7th Aug. 2012, then cool roof paint was applied on 8th Aug. 2012. Centre of the roof was remained un-painted, and self-cleaning and non-self-cleaning paint were applied on east side and west side of the roof.

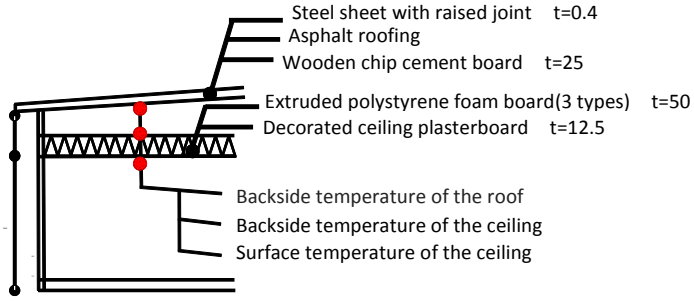

Figure 5: Cross-sectional structure of the roof and temperature measurement point

Solar reflectance measurement was done with 2 points correction method, in which black standard colour plate and white standard colour plate are used in order to remove the effect of ambient[3)]. Measurements were made at 7 positions on the roof, where self-cleaning paint (3 positions), non self-cleaning paint (3 positions), and no paint (1 position) were applied respectively. Colour measurement was also made at same positions using a handy type spectrophotometric color difference meter NF333 (Nippon Denshoku Industries).
On top of above, 3 net pyranometers and 3 infrared thermocouples were equipped to measure continuous measurement of solar reflectance and surface temperature. (Figure 6)
A sketch in the building is shown on the Figure 7. In the meeting room, air conditioner was running continuously setting point at 26°C. In the thermostatic room, air conditioner was running continuously set point at 23°C. In the office room, air conditioner was periodically running at 27°C. And there was no air conditioning in the storage room.

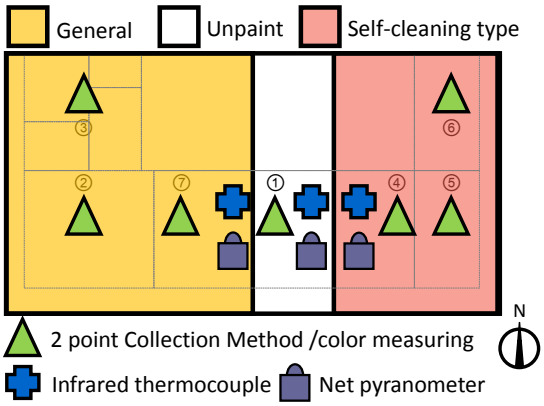

Figure 6: Measurement points on the roof

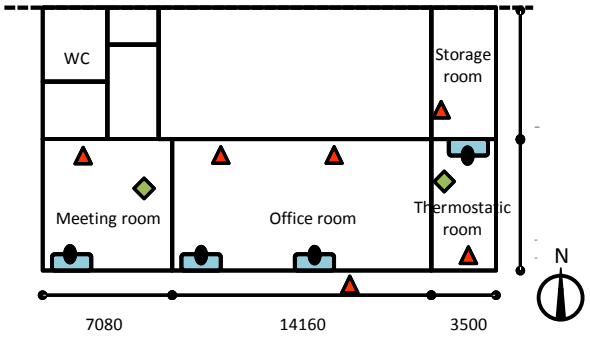

Temperature of the roof section
Air temperature of indoor and outdoor
Temperature of the air conditioning outlet
Consumption electricity of the air conditioner
Figure 7: Measurement points in the room

2.2.3 Temporal change of solar reflectance and lightness

Change of solar reflectance with time is shown on figure 8. There are some differences according to the measurement position, however, in general, the value showed its maximum just after the paint application and gradually comes down.
Average values of solar reflectance and lightness are shown on figure 9. Average was made by measurement values from 3 positions each for self-cleaning paint and non-self-cleaning paint.
For self-cleaning paint, drop of solar reflectance in 6 months was 1.8% (82.9 → 81.1%), meanwhile it was 10.7% (84.7 → 74.0%) for non-self-cleaning paint. Besides it, lightness dropped 3.3 for self-cleaning, and 5.9 for non-self-cleaning. We suppose that the drop of the lightness is due to dirt pickup. Self-cleaning paint showed clear advantage over non-self-cleaning paint in maintenance of solar reflectance and lightness after exposure.

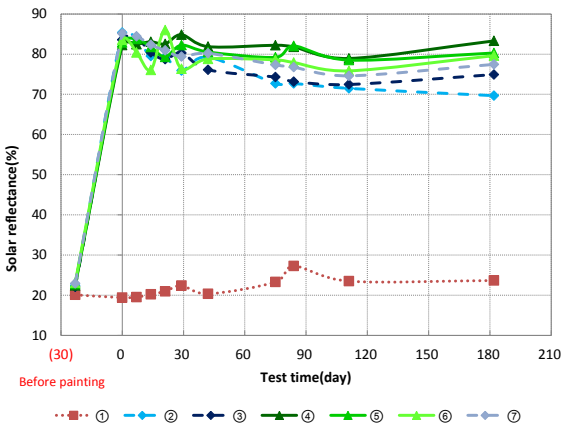

Figure 8: Temporal change of solar reflectance calculated by 2 points collection method

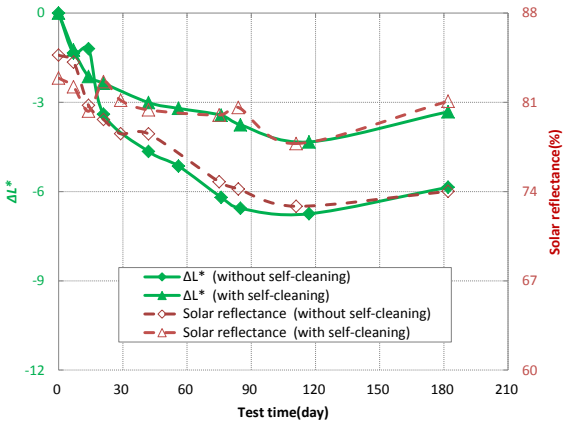

Figure 9: Temporal change of solar reflectance and lightness difference(ΔL^*) averaged in 3 measurement points

2.2.4 Room air temperature without air conditioner before and after painting

Air temperature trends in a day are compared before and after the cool roof coating installation. The comparison was made choosing typical sunny day with much solar radiation and cloudy day with less solar radiation. Outside air temperature and air temperature in the storage room (without air conditioning), before and after the cool roof paint, are shown on figure 10 and figure 11. 1-2°C drop of air temperature was observed after cool roof paint. Supposedly, it is due to decline of heat transmission by cool roof paint. It was also noticed that peak of room air temperature comes about 1hr after the peak of the outside air temperature.
The clear drop of the air temperature in the storage room and on the roof surface was only observed on fine days and not observed on cloudy days.

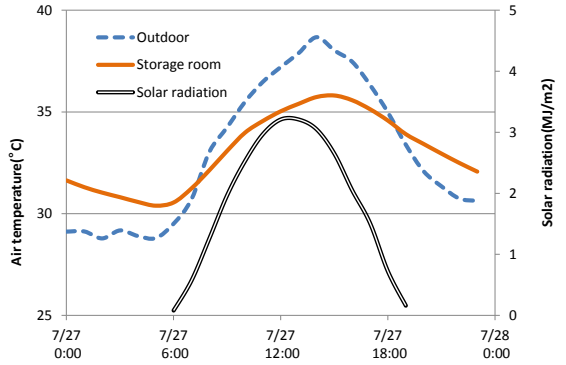

Figure 10: Room air temperature without air conditioner on sunny day **before painting**

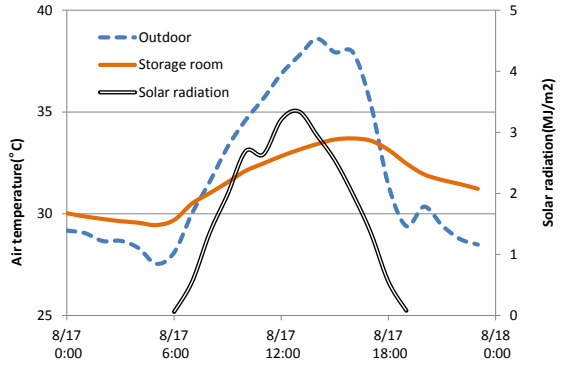

Figure 11: Room air temperature without air conditioner on sunny day **after painting**

2.2.5 Energy saving of air conditioner

In order to compare energy consumption before and after the cool roof coating installation, effect of several factors needs to be taken into account, i.e. heat of transmission, internal heat generation, temperature difference between inside and outside of the building. Because of this complexity, energy saving effect of cool roof paint was not so clear on raw data. In this section we'll discuss effect of cool roof coating on energy saving by separating effect of some factors.
Following equation is proposed to describe effect of factors on air conditioning energy consumption.

$$E = A \times I + B \times \Delta T + C$$

Here, E is a day accumulated air conditioning energy consumption (Wh/day), I is a day accumulated solar radiation (Wh/day), and ΔT is difference between outside air temperature and room air temperature a day average. A, B and C are constant coefficients which have correlation to solar radiation absorption (A), heat transmission (B), and internal heat generation (C). In this study E, I and ΔT are measured. We can assume that B and C stay unchanged before and after the cool roof paint installation.

Correlations between E and ΔT of the meeting room and the thermostatic room are shown on figure 12 and 13.

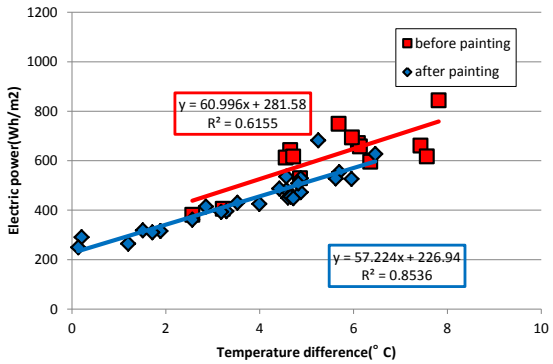

Figure 12: Relationship between daily integrated power consumption and daily averaged air temperature difference of meeting room and outdoor

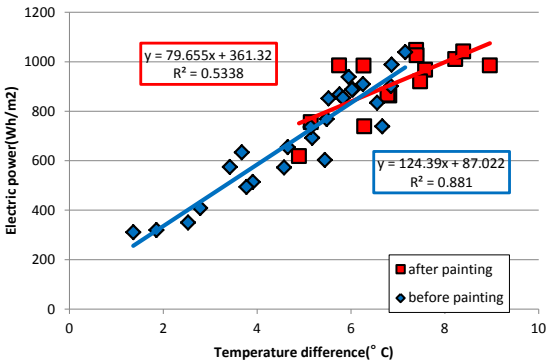

Figure 13: Relationship between daily integrated power consumption and daily averaged air temperature difference of thermostatic room and outdoor

We could see difference in energy consumption before and after the cool roof coating application in the meeting room, and we estimated the energy saving was 54.6 Wh/day/m^2. The slopes of the correlation lines (B) were close as assumed.

On the other hand, energy saving was not observed in the thermostatic room. It should be due to too low capacity of air conditioner in the room. It cannot maintain setting air temperature when too much load is applied. For example, data on 27th Jul. is shown on figure 14. The room air temperature went up to 25°C while setting point was 23°C. At the same time power consumption was saturating around 1100 Wh. For the reference, air conditioner's capacity was 1.13kW in the thermostatic room, and 3.31kW in the meeting room.

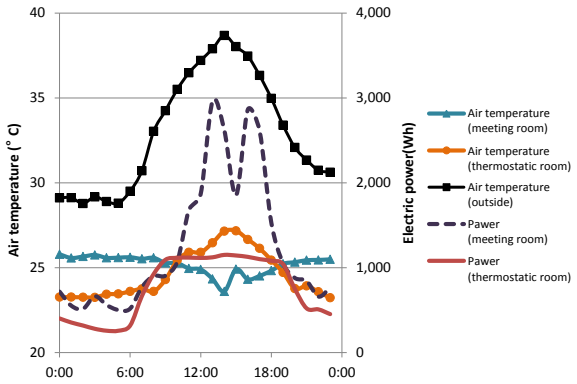

Figure 14: Air temperature and power consumption on sunny day before painting

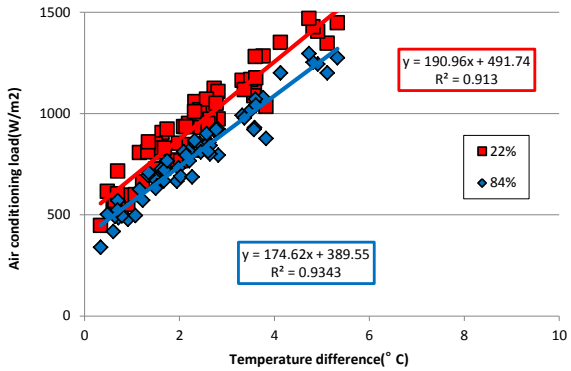

Figure 15: Relationship between daily integrated cooling load and daily averaged air temperature difference of meeting room and outdoor

2.3 Cooling load calculation

2.3.1 Outline of cooling load calculation

A cooling load calculation was carried out using computer software "SMASH". On the SMASH, a model of the building is built up with "room data", "position data" and "room relation data". Air conditioning load is calculated based on thermal circuit networks taking "area data" as boundary condition. We used average weather condition in Osaka as the "area data".

Solar reflection for the calculation was chosen based on actual measurement results. They are 22% for before painting, 84% for just after painting, 80% for self-cleaning coating after weathering, and 74% for non-self-cleaning coating after weathering.

2.3.2 Result of cooling load calculation

The calculation results for the meeting room is shown on figure 15, which compares before and after the cool roof coating installation. Energy saving effect of cool roof paint was estimated around 102.2 W/day/m^2. Energy

saving effect after exposure drop was estimated 6.58 W/day/m^2 for self-cleaning coating and 16.41 W/day/m^2 for non-self-cleaning coating.

3 CONCLUSIONS

- Self-cleaning coating keeps higher solar reflectance after outdoor exposure when used for cool roof coating.
- The decline of solar reflectance, that is supposed to be caused by dirt pickup, started just after installation and it was saturated in 3 to 6 months.
- Maintenance of solar reflectance by self-cleaning function is good regardless of colour (lightness).
- It is not possible to judge visually the drop of solar reflectance of dark coloured coating.
- Drop of solar reflectance was also noticed on the coating applied on roof of actual building. It was confirmed that self-cleaning paint gives smaller drop of solar reflectance and lightness after weathering, and it resulted in slightly lower roof surface temperature.
- Temperature, electricity consumption and heat balance on the roof were measured and energy saving by the effect of cool-roof coating was estimated.
- Result of cooling load calculation was similar to the electricity consumption measurement, and also energy saving effect of self-cleaning paint over non self-cleaning paint was estimated.

4 REFERENCES

1)Daisuke Itoh, Hitoshi Takeda, Tetsuo Fujimoto, Yasushi Kondo, Yasunobu Ashie: Study on change of performance by outdoor exposure of reflective paints, *AIJ Journal of Technology and Design*. Vol.17, No. 35, pp.217-220, 2011

2) Chihiro Yamada, Hideki Takebayashi, Etsuko Ishii, Katsuo Miki: Study on the Introduction Effect of High Reflectance Paint -Part1 reduction of air conditioning load, *AIJ Journal of Summaries of Technical Papers of Annual Meeting*, D-1, 875-876, 2012

3) Yasutaka Murata, Koji Sakai, Hiroshi Kanamori, Hideki Takebayashi, Yoh Matsuo, Masakazu Moriyama, Atsumasa Nishioka, Naomichi Yano, Ryosaku Shimizu, Katsuo Miki, Toshikazu Murase, Hashem Akubari: a study on insolation reflectivity measurement of the cool painting surface : a proposal of measuring method by the 2 point correction and accuracy testing on the horizontal surface, *Journal of environmental engineering (Transaction of AIJ)*. Vol.73, No.632, pp.1209-1215, 2008-10-30

EFFECT OF COOL ROOFS AND GREEN ROOFS ON TEMPERATURE IN THE TROPICAL URBAN ENVIRONMENT

Chun Liang Tan[1], Nyuk Hien Wong[2], Steve Kardinal Jusuf[2], Pei Yu Chia[2]

1 National University of Singapore
School of Design and Environment
Centre for Sustainable Asian Cities
4 Architecture Drive, Singapore
tcl@nus.edu.sg

2 National University of Singapore
School of Design and Environment
Department of Building
4 Architecture Drive, Singapore

ABSTRACT

The treatment of roof space with cool paint or vegetation is a widely employed urban heat mitigation strategy. As the allocation of roof space for social activity becomes more prevalent in the urban environment, there is a need to understand how cool roofs and green roofs can affect the outdoor thermal comfort of its users.

The study seeks to quantify the cooling effect of cool roofs and green roofs. Six plots, each measuring 3.0 m by 3.0 m, are set up at a rooftop. The setup consists of four plots of vegetation, one plot painted with cool paint and one with exposed concrete. The type of vegetation used for the green roofs are categorized according to regulatory guidelines. Analysis of air, surface and mean radiant temperature is conducted for the six plots.

Results show the effectiveness of cool roofs and green roofs in reducing surface temperature under direct sunlight. Significant reduction in mean radiant temperature is observed for plots with vegetation. The Leaf Area Index and physical dimension of plants do not show good correlation with the reduction mean radiant temperature. This study confirms the need for cool roofs and green roofs to be strategically sited to achieve optimal cooling effect.

KEYWORDS

Cool roof; green roof; mean radiant temperature; outdoor thermal comfort

1 INTRODUCTION

Cities around the world are expanding at a rapid pace. With rapid urbanization, rural hinterland is converted to concrete urban sprawls, resulting in numerous environmental issues such as pollution and the Urban Heat Island (UHI) effect. The rise in temperature, especially in the city, has a severe impact to our physiological well-being. Numerous thermal comfort and heat stress indices have been developed to indicate our willingness to accommodate to various thermal conditions (Epstein and Moran, 2006). Many strategies have been developed to improve thermal comfort. The introduction of cool roofs and green roofs are common methods employed to mitigate this change in climate. Cool roofs are characterised by their high solar reflectance and high thermal emittance. Heat transfer to the environment is reduced by reflecting incident solar irradiance in the day and by emitting heat stored in the roof surface at night. Green roofs reduce the thermal load by blocking incident solar irradiance using plant foliage and soil substrate, as well as by cooling the ambient temperature by means of evapotranspiration. The result is either a direct improvement in occupancy thermal comfort

or a lessening of overall building cooling load through heat gain reduction (Akbari et. al, 2001; Santamouris, 2012).

Many studies on the effects of cool roofs and green roofs have focused on the surface temperature of roofs as well as the quantification of cooling energy savings for the building (Arthur et. al, 1998; Synnefa et. al, 2007). Research on green roofs often focus on the quantification of roof surface temperature. There are also studies into various aspects of rooftop greenery such as the types of plants used, growth substrates, acoustic performance, air quality and maintainability (Akbari, 2002; Parizotto and Lamberts, 2011; Baik et. al, 2012; Saadatian et. al, 2013). Various feasibility studies have also been conducted to determine the structural and logistical considerations for green roof implementation (Castleton et. al, 2010).

The reviewed literature suggests that most studies conducted for cool roofs and green roofs tend to focus on their impact to the indoor environment. There is little information on how cool roofs and green roofs will affect the outdoor environment. This is much more pertinent to green roofs, as green roofs are often designed as roof gardens and can be used as outdoor social spaces. The evaluation of thermal environments by most comfort or stress indices often requires the measurement of the air temperature, mean radiant temperature, air velocity and relative humidity. The mean radiant temperature (t_{mrt}) can be considered as one of the main factors contributing to both indoor and outdoor thermal comfort, as indicated in various studies which have showed that thermal comfort is highly dependent on the shortwave and long wave radiation fluxes from the surroundings (Mayer and Höppe, 1987; Mayer, 1993). In this study, in addition to surface and air temperature, t_{mrt} is quantified to determine the impact due to exposure to different types of green roofs and a cool roof.

2 METHODOLOGY

2.1 Measurement

The experiment is conducted at the National University of Singapore, School of Design and Environment (SDE 1) rooftop. Six plots are measured. Each plot has a dimension of 3.0 m by 3.0 m. The first four plots are plots with vegetation. The fifth plot is covered with an acrylic sheet painted with cool paint. The sixth plot is bare concrete roof, used as a control for the measurement. The characteristics of each plot are shown in Table 1.

Table 1. Plot characteristics

Plot	**Characteristic**	**Specification**
1	Shrub	Phyllanthus cochinchinensis
2	Shrub	Heliconia American Dwarf
3	Shrub	Sphagneticola trilobata
4	Turf	Cow grass
5	Cool Paint	*JOTUN* Jotashield extreme
6	Concrete	Control

Each plot is placed at regular intervals of 3.0 m to minimize interference from neighbouring plots. Sensors are deployed to measure the air temperature (t_a) and globe temperature (t_{globe}) of the different plots (Figure 1). Measurements are made at one minute intervals. A total of 36 sensors are deployed. Each globe temperature sensor is attached to a survey pole and measure t_{globe} at 1.3 m above the plots. Six sensors are placed underneath each plot to measure the roof surface temperature.

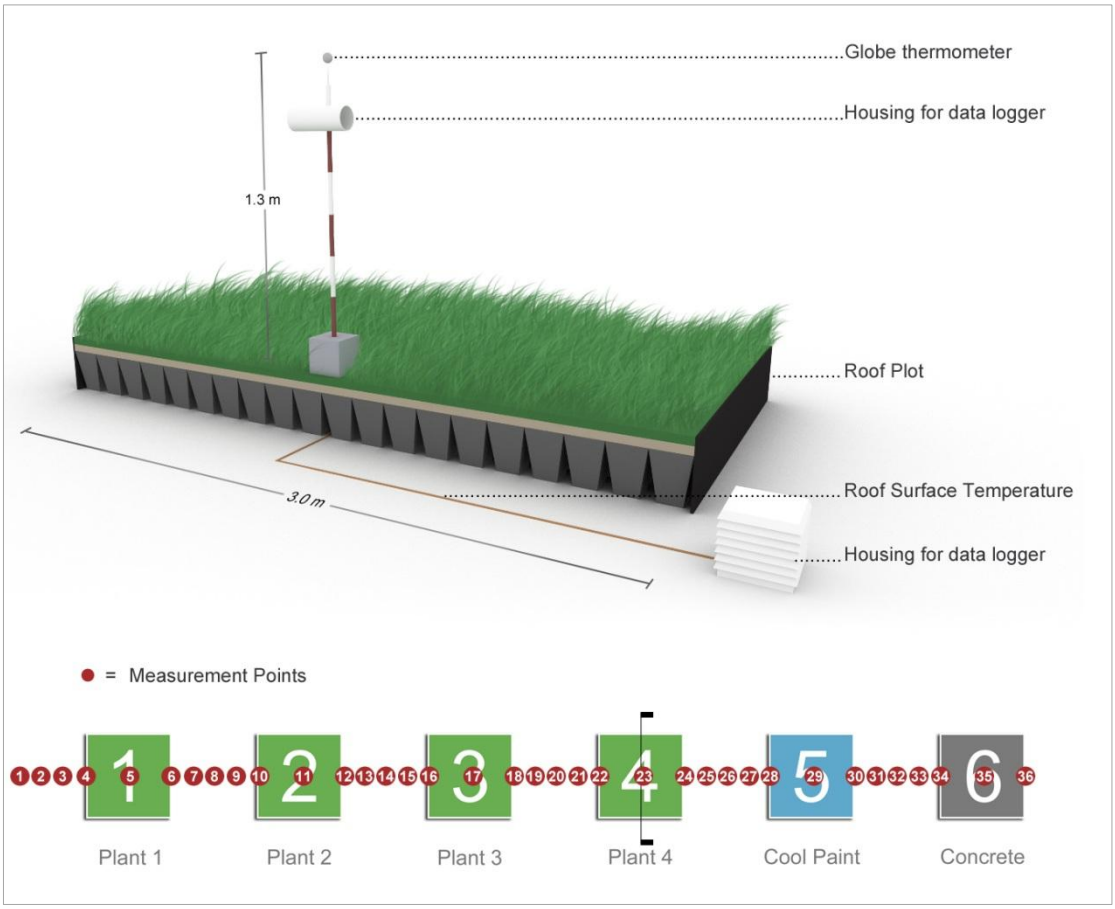

Figure 1. Measurement points and sectional perspective of setup

Thermocouples are used for surface temperature measurement. The LAI of plants used in Plots 1 to 4 is measured using both direct and indirect methods. The LAI-2000 is utilized for indirect measurement. The leaves are subsequently scanned using a flatbed scanner and the total leave area calculated using image editing software. A reflectivity test is performed for materials from the six plots. A total of six samples, each measuring 0.05 m by 0.05 m, are used for the reflectivity test. For the Plots 1 to 4, the selected leaves are glued onto a sample board and cover the surface entirely. Measurements from 23 days with clear sky conditions are averaged and used for analysis.

2.2 Customized globe thermometers

Estimation of t_{mrt} is done using the globe thermometer. Initially developed for indoor usage, the globe thermometer has since been adapted for outdoor use. For outdoor measurement, the 38 mm globe thermometer is a common option as the globe used is a table tennis ball, which can be readily purchased and conveniently replaced. The accuracy of the 38 mm globe thermometer can be adjusted to cater to outdoor conditions by recalibrating the mean convection coefficient. In this study, t_{mrt} is estimated using a formula specifically recalibrated for tropical outdoor use (Tan et al., 2013).

$$Tmrt = \left(Tg + 273.15\right)^4 + \frac{3.42 \times 10^9 Va^{0.119}}{\varepsilon D^{0.4}} \times \left(Tg - Ta\right)^{0.25} - 273.15 \quad (1)$$

where,

t_g = Globe temperature (°C)
V_a = Air velocity (ms^{-1})
t_a = Air temperature (°C)
D = Globe diameter (mm)
ε = Globe emissivity

3 RESULTS AND DISCUSSION

The average diurnal air temperature profile is shown in Figure 2. The maximum and minimum air temperature recorded is 33.0 °C and 26.9 °C respectively. In general, plots with vegetation exhibit lower t_a during the day (With the exception of Plot 2). Plot 5 reached a peak temperature of 33.0 °C while Plot 1 registered the lowest peak temperature of 31.9 °C. Plot 2, which consists of Heliconia American Dwarf, is observed to be slightly higher than Plot 5. Both Plots 2 and 5 show higher air temperature readings than Plot 6, the control plot. At night, the air temperature for Plot 1 remains the lowest, while Plots 2 and 6 exhibit the highest air temperature. A lag of 1 hour is observed between the peak of the averaged solar irradiance and the peak of all the 6 plots.

The maximum and minimum values of t_{mrt} recorded are 63.0 °C and 24.9 °C respectively (Figure 3). The maximum difference during the hottest time (14:00 hrs) is approximately 6.0 °C. It is observed that Plots 4, 5 and 6 exhibit similar t_{mrt} profiles, peaking at approximately 63.0 °C. Of the six plots, Plot 1 (Phyllanthus cochinchinensis), has the coolest diurnal t_{mrt} profile, followed by Plot 2 (Heliconia American Dwarf) and Plot 3 (Sphagneticola trilobata). In the absence of sunlight (01:00 hrs – 07:00 hrs and 19:00 hrs to 00:00 hrs), the t_{mrt} profile for all six plots remain stable without much fluctuation.

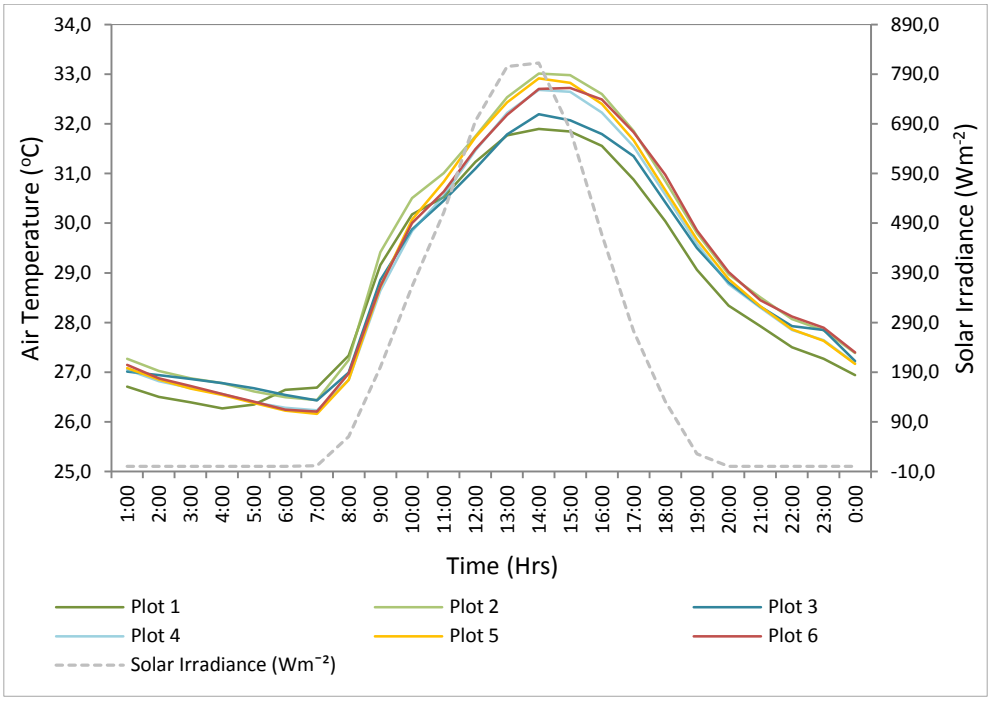

Figure 2. Diurnal t_a profile for clear sky conditions

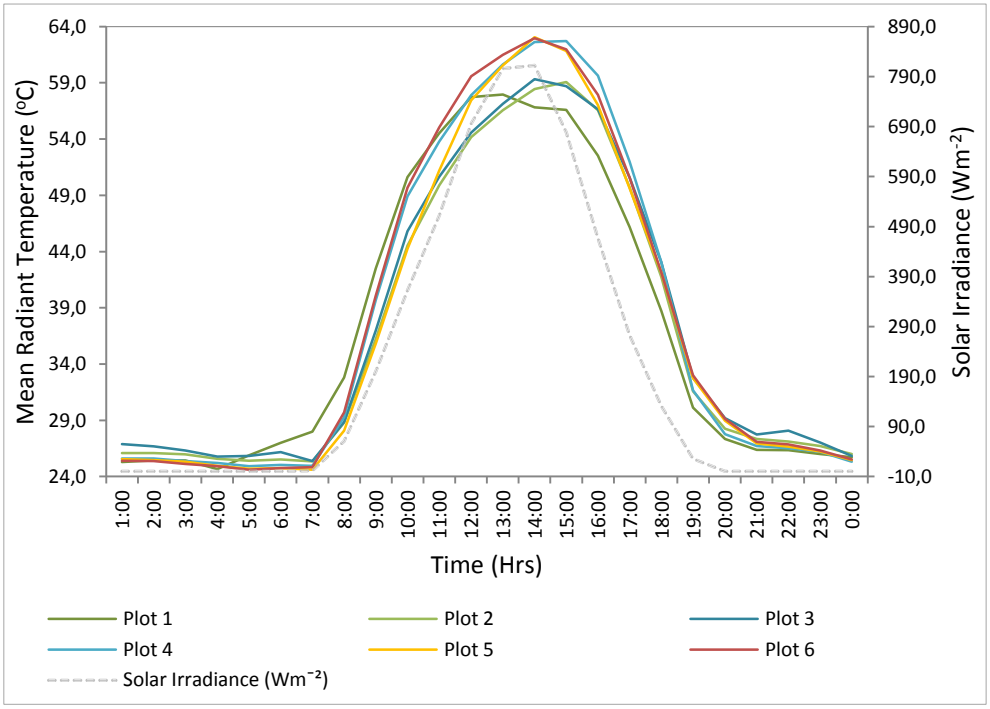

Figure 3. Diurnal t_{mrt} profile for clear sky conditions

3.1 Comparison of t_{mrt} and t_a between plots

The average t_a and t_{mrt} profiles of all 36 measurement points are shown in Figure 4. Only hourly profiles from 11:00 hrs to 15:00 hrs are displayed. This period is considered to be the hottest part of the day, with average solar irradiance ranging from 680.0 Wm^{-2} to 810.0 Wm^{-2}. In general, t_a is lower for Plots 1 to 3. Measurement Points 4 and 16 exhibits the lowest t_a profile at the hottest period (14:00 hrs), with temperatures of 32.1 °C and 31.9 °C respectively. In general, higher fluctuations in t_{mrt} can be observed in Plots 3, 4 5. The t_{mrt} profiles for Plots 1 and 2 have significantly less fluctuation.

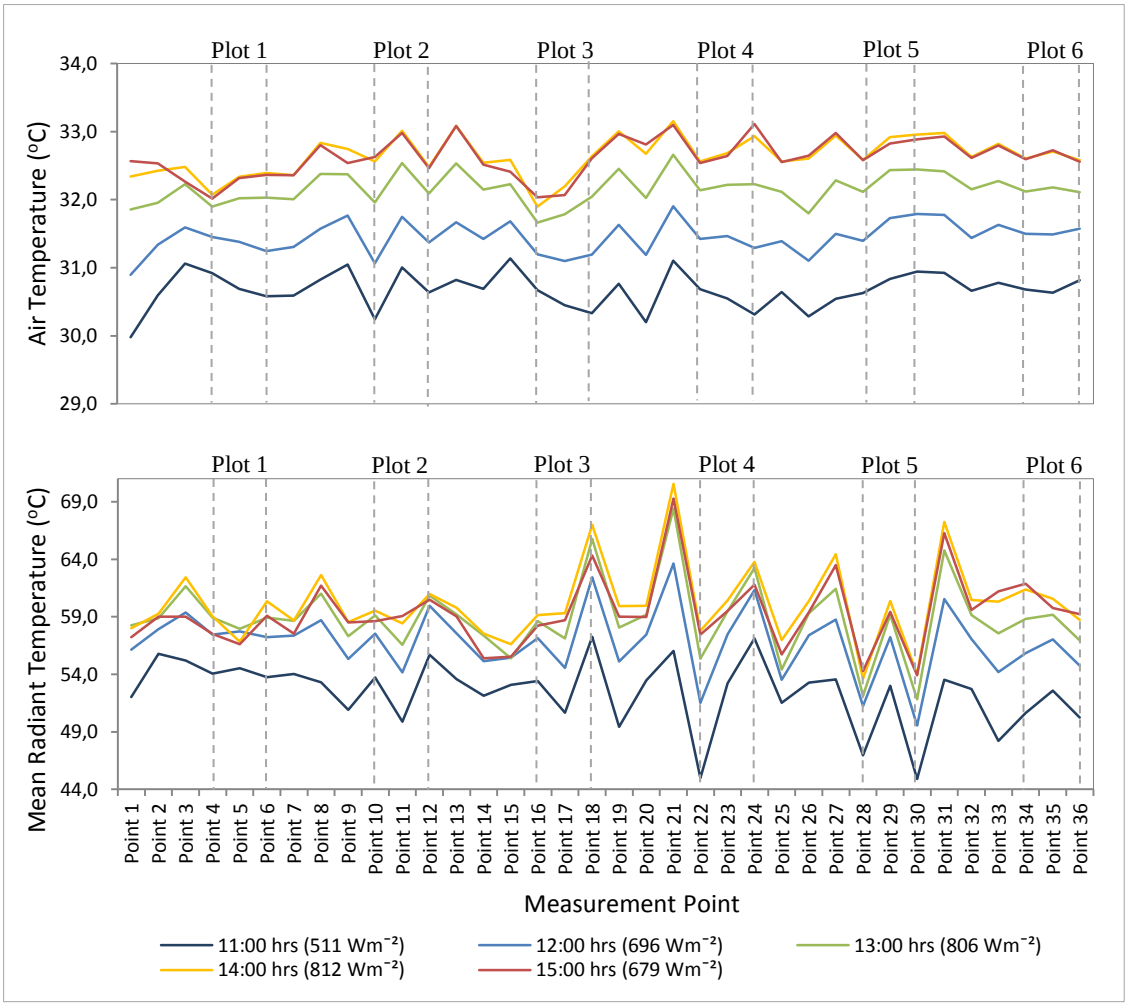

Figure 4. Profiles of t_a and t_{mrt} across 36 measurement points

3.2 Measurement of Leaf Area Index (LAI)

The LAI of all plants used in this study is shown in Table 2. The corresponding LAI for each plant provided by the Singapore National Parks Board (NParks) are also listed as reference (Tan and Sia, 2009). Using the indirect measurement method, Plots 1 and 3 show higher LAI values of 4.34 and 4.60 respectively. When the direct measurement method is utilized, the results are reversed. Plots 2 and 4 show much higher LAI values of 7.21 and 4.45, whereas Plots 1 and 3 show lower LAI values. The difference in both methods may be due to the excess direct shading captured by the LAI-2000 plant canopy analyzer to obtain measurement using the indirect measurement method.

Table 2. LAI values for Plots 1 to 4

Plot	Plant Species	LAI Indirect measurement (Averaged)	LAI Direct measurement	LAI Recommended by Nparks
1	Phyllanthus cochinchinensis	4.34	2.78	Shrub (Dicot) 4.50
2	Heliconia American Dwarf	3.47	7.21	Shrub (Monocot) 3.50
3	Sphagneticola trilobata	4.60	3.59	Ground cover 4.50
4	Cow grass	2.28	4.45	Turf 2.00

3.3 Reflectivity test

Material reflectivity is tested using a spectrophotometer and the results are shown in Figure 5. Under the visible light spectrum, which spans from approximately 380 nm to 700 nm, cool paint exhibits the highest reflectivity of above 80.0 %. This is followed by concrete with a peak of 40.4 %. Vegetation under visible light displays relatively lower reflectivity, peaking at 25.2 % (Plot 4), 21.6 % (Plot 3), 14.5 % (Plot 1) and 13.8 % (Plot 2) at around 550 nm.

For wavelengths in the near-infrared range (700 nm to 2500 nm), the reflectivity of cool paint reduces gradually, while the reflectivity of concrete increases at a similar pace. The reflectivity of the plants increases significantly from 700 nm to 1400 nm and undergoes a series of fluctuations, rising again from 1600 nm to 1800 nm and 2200 nm. It can be seen that the reflectivity of plants from the range of 701 nm to 1300 nm can equal that of cool paint.

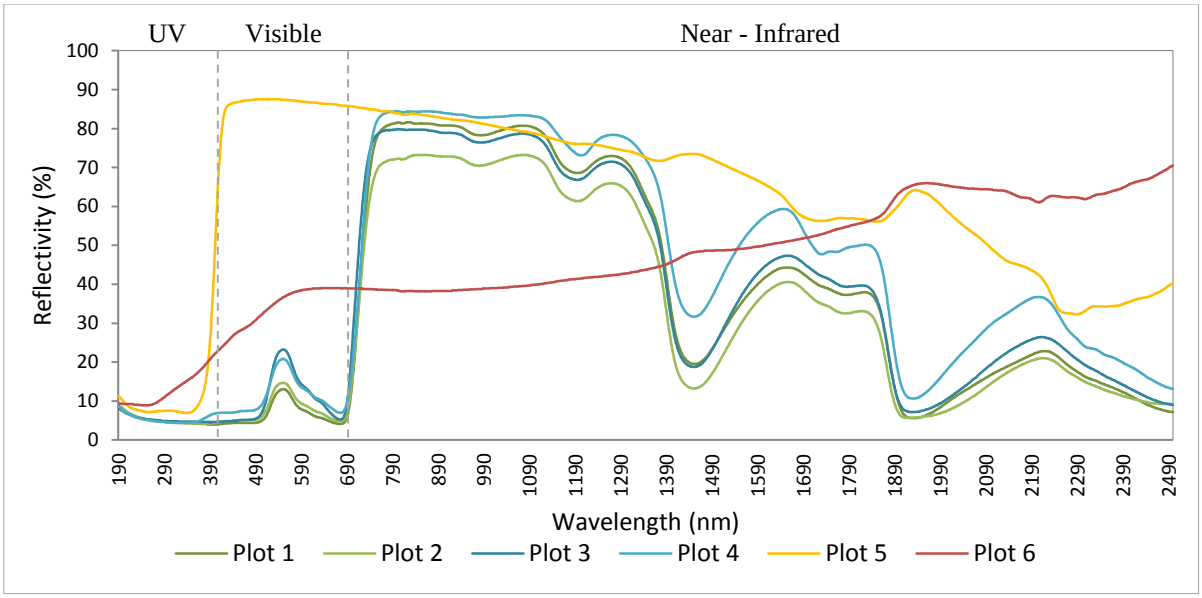

Figure 5. Spectrometer test results

3.4 Roof surface temperature

The average diurnal roof surface temperature profile is shown in Figure 6. The solar irradiance peaked at 1004.4 Wm^{-2} at 14:00 hrs. The surface temperature under Plots 1 to 4 is significantly lower than Plots 5 and 6 during daytime. The maximum difference between Plot 6 and Plot 3 is approximately 14.4 °C. The surface temperature of Plots 1 to 4 is maintained at between 26.0 °C to 29.0 °C throughout the day. In contrast, the surface temperature of Plots 5 and 6 increases greatly during the day. A peak of 45.9 °C is observed at 13:25 hrs for Plot 6, while the corresponding temperature of Plots 1 to 4 is only in the range of 27.0 °C to 27.5 °C. It can be observed that the diurnal surface temperature profile for Plots 5 and 6 are similar for large parts of the day, except for periods of high solar irradiance (11:00 hrs to 14:00 hrs), where temperature readings for Plot 5 are slightly lower than that of Plot 6. From 03:00 hrs to 07:00 hrs, it can be observed that Plots 5 and 6 (Cool paint and concrete roof) have a slightly lower temperature compared to the other plots.

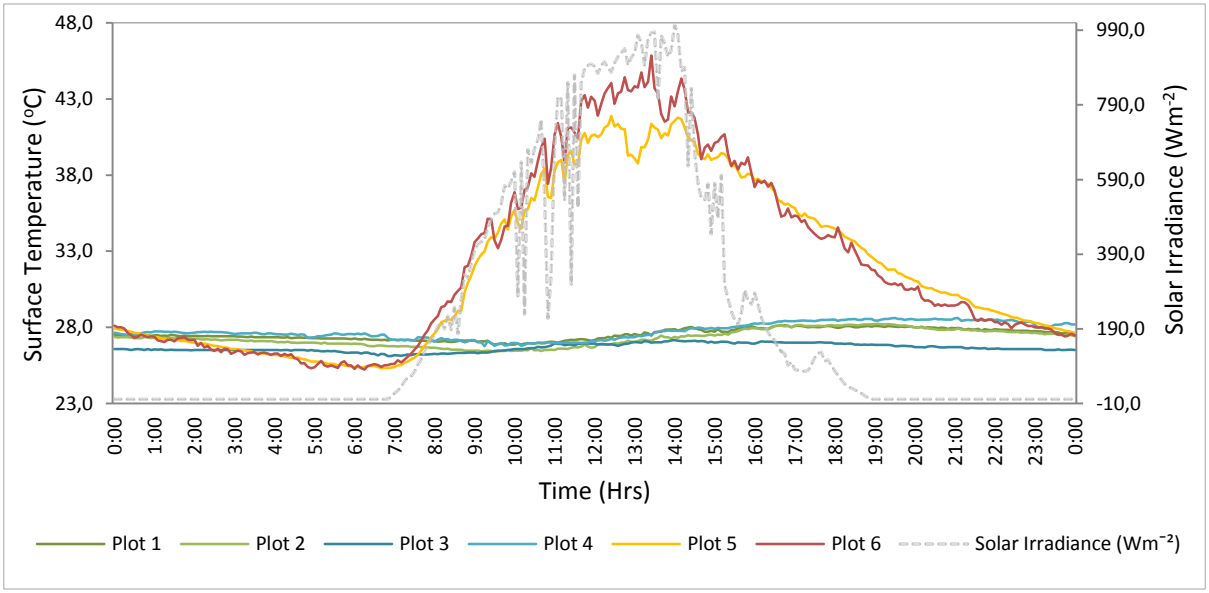

Figure 6. Roof surface temperature - 9th October 2012

3.5 Cooling effect of cool roofs and green roofs

Results from the various measurements show that when cool roofs and green roofs are exposed to direct solar irradiance, the surface temperature is significantly lower compared to the exposed concrete roof (Figure 6). However, only green roofs provide a substantial reduction in air and mean radiant temperature. At peak temperature, air temperature 1.3 m above the cool roof can reach up to 32.9 °C, which is 1.0 °C higher than Plot 1.

A possible reason for the lower air and mean radiant temperature experienced by Plots 1 to 4 may be due to the evapotranspiration of plants. The presence of moisture in the soil and emancipation of water from the plant stomata increases the latent heat of vaporization and cools the surrounding air. As shown in Figure 4, the cooling effect of Plot 1 is not just limited to Measurement Point 5, but for up to 3.0 m away.

Besides lowering the t_a and t_{mrt}, the introduction of green roofs can also help to minimize temperature fluctuations. Figure 4 shows that the t_{mrt} around Plots 1 to 4 fluctuate less than around Plots 5 and 6, and Figure 6 shows that the surface temperature for Plots 1 to 4 exhibit

a diurnal temperature differential of about 3.0 °C, while Plots 5 and 6 show a diurnal temperature differential of about 20.0 °C. Fluctuations in radiant temperature will drastically change the solar radiation absorbed by an individual and the energy budget of the person, affecting the overall thermal comfort (Brown and Gillespie, 1995).

Results from the reflectivity test shows that for the visible light range (380 nm to 700 nm), the cool roof can have a reflectivity of more than 80 %. In comparison, the reflectivity of plants is in the range of 20 %, which is rather low. However, at the near-infrared range, especially from the range of 700 nm to 1400 nm, the reflectivity of plants can almost equal that of cool paint (Figure 5). Since up to 50 % of the solar irradiance distribution is in the near-infrared zone, this attribute may be crucial for reflecting heat back to the atmosphere. The high reflectivity of plants, in addition to the inherent cooling effect through evapotranspiration, may be the main factors leading to significantly lower t_s, t_a and t_{mrt} values.

4 CONCLUSIONS

Results from this study show that for clear sky conditions, the plots with vegetation can reduce the surrounding t_a and t_{mrt} by about 1.0 °C and 6.0 °C respectively. Reduced fluctuation in diurnal t_{mrt} is also observed for the plots with vegetation. The effect in temperature reduction is evident up for to 3.0 m away from the midpoint of the green plots.

Results from the reflectivity test show that cool paint has high reflectivity in the visible light range, and plants have comparable reflectivity in the near-infrared range (Figure 5). It is important to note that only a flat piece of leaf is used for testing with the spectrometer. Therefore, test results may not indicate the reflectivity of the entire shrub. Also, due to varying leave orientation, incident solar radiation may not be reflected directly back to the atmosphere. While cool roofs exhibit a high solar reflectance, the performance may decline over time due to aging, dirt and weathering (Bretz and Akbari, 1997; Synnefa et al., 2007). Studies have shown that due to dirt accumulation, the reflectivity of white-coated roofs may drop approximately 15 % in the first year, followed by a decline of 2 % annually (Bretz et al., 1998).

The installation of green roofs is much more complex and costlier than cool roofs. Most green roofs require a support tray or waterproofing membrane, soil substrate and plants. For cool roofs, the roofs only need to be painted with cool paint. Green roofs are also prone to maintainability issues. There will be inevitable drawbacks, such as the penetration of plant roots into the roof waterproofing membrane, damaging the roof insulation (Chew, 2010). Recognizing the challenges of installation and maintenance, countries such as Singapore have introduced incentive schemes to promote the incorporation of green roofs into building design (National Parks Board, 2013).

Cool roofs and green roofs are common staples in the design palette of architects and designers. In quantifying the cooling effect of different plants and cool material, objective criteria can be used to assess the performance of the outdoor roof space in terms of thermal comfort.

5 REFERENCES

Akbari, H. (2002). Shade trees reduce building energy use and CO_2 emissions from power plants. *Environmental Pollution*, 116, 119-126.

Akbari, H., Pomerantz, M., Taha, H. (2001). Cool surfaces and shade trees to reduce energy use and improve air quality in urban areas. *Solar Energy*, 70(3), 295-310.

Arthur, H.R., Akbari, H., Romm, J.J., Pomerantz, M. (1998). Cool communities: strategies for heat island mitigation and smog reduction. *Energy and Buildings*, 28, 51-62.

Baik, J.J., Kwak, K.H., Park, S.B., Ryu, Y.H. (2012). Effects of building roof greening on air quality in street canyons. *Atmospheric Environment*, 61, 48-55.

Bretz, S. E., Akbari, H. (1997). Long-term performance of high-albedo roof coatings. *Energy and Buildings*, 25(2), 159-167.

Bretz, S.E., Akbari, H., Rosenfeld, A. (1998). Practical issues for using solar-reflective materials to mitigate urban heat islands. *Atmospheric environment*, 32(1), 95-101.

Brown, R. D., Gillespie, T. J. (1995). *Microclimatic landscape design: creating thermal comfort and energy efficiency*, John Wiley & Sons.

Castleton, H.F., Stovin, V., Beck, S.B.M., Davison, J.B. (2010). Green roofs; building energy savings and the potential for retrofit. *Energy and Buildings*, 42, 1582-1591.

Chew, M. (2010). *Maintainability of facilities: for building professionals*, World Scientific.

Epstein, Y., Moran, D.S. (2006). Thermal comfort and heat stress indices. *Indust Health*, 44, 388-398.

Mayer, H. (1993). *Urban bioclimatology*. Experientia, 49, 957-63.

Mayer, H., Höppe, P. (1987). Thermal comfort of man in different urban environments. *Theoretical and Applied Climatology*, 38, 43-9.

National Parks Board. (2013). Skyrise Greenery Incentive Scheme 2013. <http://www.skyrisegreenery.com/index.php/home/incentive_scheme/about/>

Parizotto, S., Lamberts, R. (2011). Investigation of green roof thermal performance in temperate climate: A case study of an experimental building in Florianópolis city, Southern Brazil. *Energy and Buildings*, 43, 1712-1722.

Saadatian, O., Sopian, K., Salleh, E., Lim, C.H., Riffat, S., Saadatian, E., Toudeshki, A., Sulaiman, M.Y. (2013). A review of energy aspects of green roofs. *Renewable and Sustainable Energy Reviews*, 23, 155-168.

Santamouris, M. (2012) Cooling the cities – A review of reflective and green roof mitigation technologies to fight heat island and improve comfort in urban environments. *Solar Energy*, http://dx.doi.org/10.1016/j.solener.2012.07.003

Synnefa, A., Santamouris, M., Akbari, H. (2007). Estimating the effect of using cool coatings on energy loads and thermal comfort in residential buildings in various climatic conditions. *Energy and Buildings*, 39, 1167-1174.

Tan, P. Y., Sia, A. (2009). *Leaf Area Index of tropical plants: A guidebook on its use in the calculation of green plot ratio*. National Parks Board.

Tan, C. L., Wong, N. H., Jusuf, S. K. (2013). Outdoor mean radiant temperature estimation in the tropical urban environment. *Building and Environment*, 64, 118-129.

VENTILATION AND ENERGY ASPECTS OF FOOD RETAIL BUILDINGS

Maria Kolokotroni*, Savvas Tassou and Baboo Lesh Gowreesunker

RCUK Centre for Sustainable Energy Use in Food Chains
Brunel University,
Kingston Lane, Uxbridge,
UB8 3PH, UK
**Corresponding author: maria.kolokotroni@brunel.ac.uk*

ABSTRACT

Worldwide the food system is responsible for 33% of GHG emissions. It is estimated that by 2050, total food production should be 70% more than current food production levels. In the UK, food chain is responsible for around 18% of final energy use and 20% of GHG emissions. Estimates indicate that energy savings of the order of 50% are achievable in food chains by appropriate technology changes in food production, processing, packaging, transportation, and consumption.

Ventilation and infiltration accounts for a significant percentage of the energy use in food retail (supermarkets) and catering facilities service buildings such as restaurants and drink outlets. In addition, environmental conditions to maintain indoor air quality and comfort for the users with minimum energy use for such buildings are of a primary importance for the business owners and designers. In particular, supermarkets and restaurants present design and operational challenges because the HVAC system has some unique and diverse conditions that it must handle.

This paper presents current information of energy use in food retail and catering facilities and continues by focussing on the role of ventilation strategies in food retail supermarkets. It presents the results of current studies in the UK where operational low carbon supermarkets are predicted to save 66% of CO_2 emissions compared to a base case store. It shows that low energy ventilation strategies ranging from improved envelope air-tightness, natural ventilation components, reduction of specific fan power, novel refrigeration systems using CO_2 combined with ventilation heat recovery can lead to significant savings with attractive investment return. Finally, the potential of ventilation coupled with sensible and latent energy storage for load shifting is proposed as an area worth investigating.

KEYWORDS

energy use, food chain, ventilation, supermarkets, heat recovery, refrigeration

1 INTRODUCTION

The food chain comprises agricultural production, manufacturing, distribution, retail, consumption and waste disposal. In Europe, there were just over 48 million people employed within the EU-27s food chain in 2008; this equated to more than one in five of the EU's total workforce. The food chain was made-up of close to 17 million different holdings/enterprises

and generated EUR 751 billion of added value, equivalent to just under 6 % of the EU-27's GDP, (Eurostat, 2011). In 2010, the food and tobacco industry sector accounted for almost 10 % share of the total energy consumed by the EU-27 industry (29 Mtoe vrs 292 Mtoe total), (Eurostat, 2012).

In the UK alone, it is estimated that the food chain is responsible for 195 $MtCO_2e$ emissions from domestic food chain activity in 2010, of which 118 $MtCO_2e$ are from UK food chain activity and the remainder from food imports; retail and catering account for 7.7 Mtoe/year or 18 $MtCO_2e$ emissions. Figure 1 shows these statistics diagrammatically. The food chain is also responsible for 15 Mt of food waste, with households generating 7.2 Mt/year and 3.2 Mt/year from manufacturing. In terms of economic activity the agri-food sector contributed £96.1 billion or 7.3% to national Gross Value Added in 2011, an increase of 7.8% on 2010 and employed 3.3 million people in the third quarter of 2012 (13% of GB employment), (Defra, 2012).

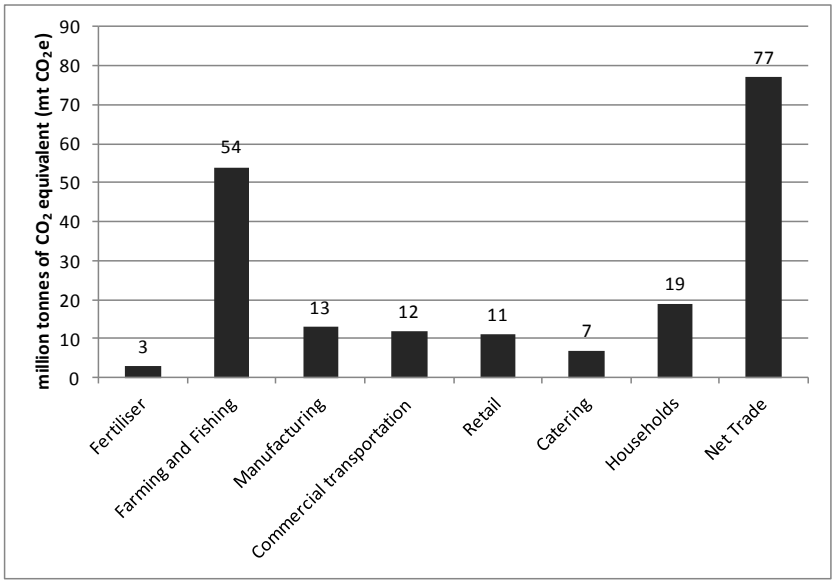

Figure 1: Greenhouse gas emission from the UK food chain (reproduced from Defra 2012, p43)

A study in the US (Canning et al, 2010) estimating changes in energy flows, shows the food-related share of the national energy budget at 15.7% for 2007 based on 2002 data. The authors note that this estimate does not account for any technology changes, including energy technologies that may have occurred after 2002. The study shows that food related aggregated energy flow rose by 12.7% vrs 3.8% of the total.

The statistics quoted above indicate that energy use in the food chain is a significant proportion of the total energy use and estimates indicate that energy savings of the order of 50% are achievable in food chains by appropriate technology changes in food production, processing, packaging, transportation, and consumption. In recent years, progress has been made in the reduction of energy consumption and emissions from the food chain primarily through the application of well proven technologies that could lead to quick return on investment. To make further progress, however, significant innovations will have to be made in approaches and technologies at all stages of the food chain, taking a holistic view of the chain and the interactions both within the chain and the external environment.

This paper focuses on part of the food chain, that of retail and public consumption. Through a literature review and a UK focus, it aims to show how low energy ventilation technologies can be used in food retail buildings in order to reduce their energy use.

2 ENERGY USE IN FOOD RETAIL AND CATERING

Recent statistics of energy use in the UK, indicate that 40 MWh (21% of total energy use in 2011) are used by general retail buildings and 24 MWh (almost 13% of total energy use by non-domestic buildings) are used by hotel and catering buildings (Figure 2). Of this, 27% is for catering and 5 % is for ventilation and cooling (Figure 3). Ventilation also has an impact on the energy use of heating (32% of total) and lighting in many cases (15% of the total). (DECC, 2013).

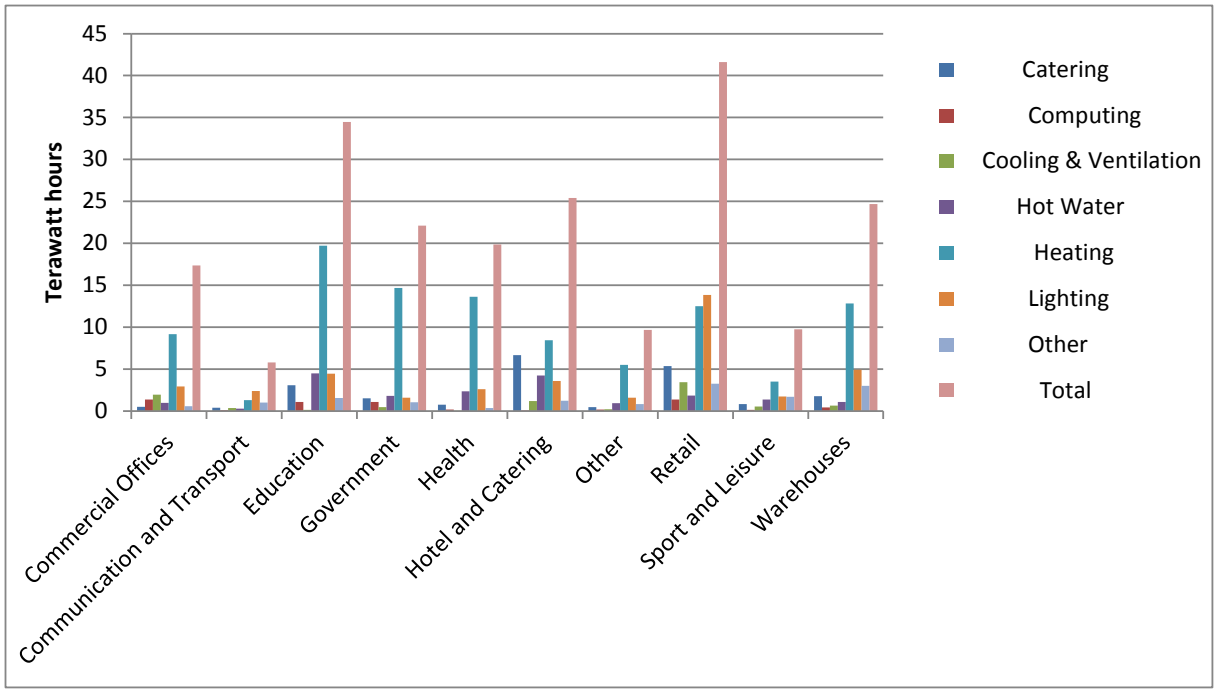

Figure 2: Final energy consumption in the service sector in the UK by sub-sector and end use 2012 (DECC 2013, Table 5.09).

Figure 3: Final energy consumption in 'retail' and 'hotel & catering' in the UK by end use in 2012. Legend categories are the same as in Fig 2. (DECC 2013, Table 5.09).

In addition, energy for cooking and refrigeration in the domestic sector is a sizeable percentage of the energy use. Cooking accounts for 5% of energy use in the home for a group of 19 IEA countries (IEA19), a number similar to energy use for lighting. The IEA

publication (IEA, 2008) also notes that appliance energy use (mostly electricity) is growing very rapidly and has overtaken water heating as the second most important household energy demand; in 2005 home appliances use 21% of households energy. In EU15, the diffusion of energy efficient large appliances such as refrigerators and freezers is improving but is still a large percentage of the appliance energy use in households (IEA, 2008).

In the light of the above statistics, this project will investigate energy use reduction technologies, starting with food retail buildings which is the focus of the remainder of this paper.

3 ENERGY REQUIREMENTS OF SUPERMARKETS

There is evidence that UK supermarkets have significantly improved their operational efficiency over the period 2000–2010. Figure 4 presents (Sullivan and Couldson, 2013) total greenhouse gas emissions relative to 2007 baseline of six supermarket chains; it can be seen that the majority have improved emissions; the increased case is mainly due to the expansion of operations outside the UK but its UK emissions reduced by 5%.

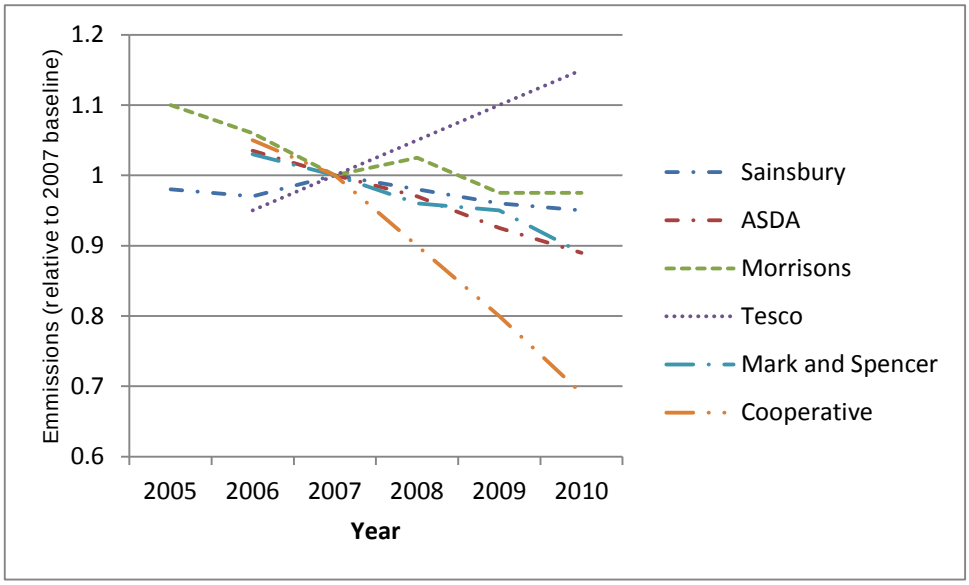

Figure 4: Total Greenhouse Gas Emissions form UK Retailers (2005-2010) (source Sullivan and Couldson 2013)

Despite this improvement, ***retail food stores*** are large consumers of energy. Food retailing in the UK is responsible for around 12.0 TWh and around 3% of total electrical energy consumption (Tassou et al, 2011). Estimates for GHG emissions from food retail operations vary between 6 and 9.5 MtCO2e (Stanford, 2010). Retail food stores are a part of the commercial sector of buildings which accounted for 7% of the total delivered energy consumption worldwide, with an expected yearly increase of 1.5% up to 2035 (IEA, 2011). It remains unclear what percentage of the energy consumption is covered by supermarkets alone, since very few studies make a distinction between building types in the non-domestic or commercial sector. In the USA, the average energy use intensity of supermarkets is 631 kWh/m^2 per year (Energy Information Administration, 2003 cited in Pérez-Lombard et al. (2008)). The corresponding figure for the U.K. varies between 700 kWh/m^2 per year for hypermarkets, to 2000 kWh/m^2 per year for convenience stores (Tassou et al., 2011). Current benchmarks (CIBSE, 2012) indicate 261 kWh/sales floor area of fossil fuel and 1026 kWh/sales floor area of electricity for typical supermarkets.

The energy use in supermarkets will depend on business practices, store format, product mix, shopping activity, the equipment used for in-store food preparation, preservation and display. Figure 5 shows diagrammatically the energy use by various parts in a hypermarket. In general, the refrigeration systems account for between 30% and 60% of the electricity used (taking into consideration smaller stores), whereas lighting accounts for between 15% and 25% with the HVAC equipment and other utilities such as bakery, for the remainder. Gas is normally used for space heating, domestic hot water and in some cases for cooking and baking and can be as high as 250 kWh/m^2 per year in hypermarkets.

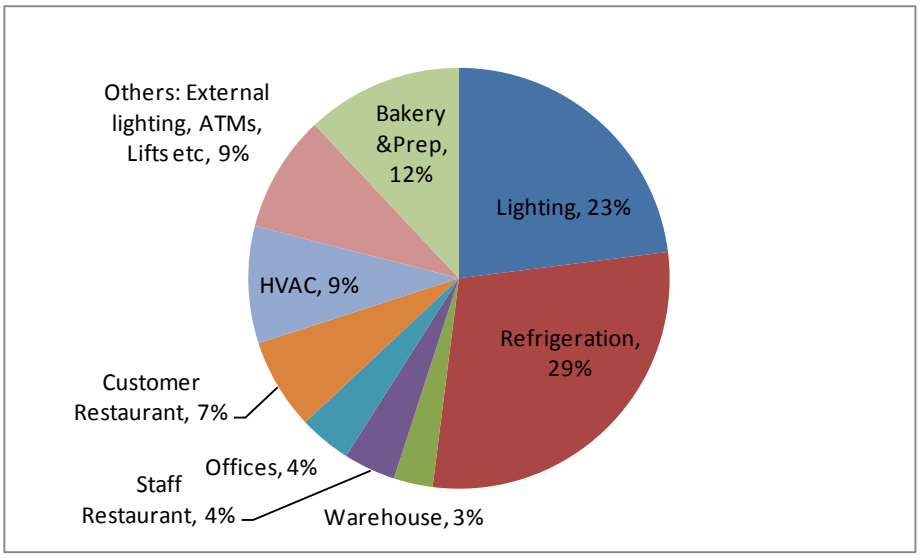

Figure 5: Percentage contribution of electrical energy use processes in a hypermarket.(source Tassou 2011).

Therefore, significant energy savings can be achieved by improving the efficiency of refrigeration systems, refrigeration and HVAC system integration, heat recovery and amplification using heat pumps, demand side management, system diagnostics and local combined heat and power generation and tri-generation. Energy saving opportunities also exist from the use of low energy lighting systems, improvements in the building fabric, integration of renewable energy sources, and thermal energy storage (Tassou et al 2011, Carbon Trust 2010). Another area that provides significant opportunities for energy savings is the design of more efficient refrigerated display fixtures. Figure 6 shows the contribution to the load of a vertical multi-deck open form chilled food display cabinet. As indicated, infiltration accounts for more than ¾ of the energy load which has led to proposed and implemented solutions on how to minimise it (Tassou et al 2011).

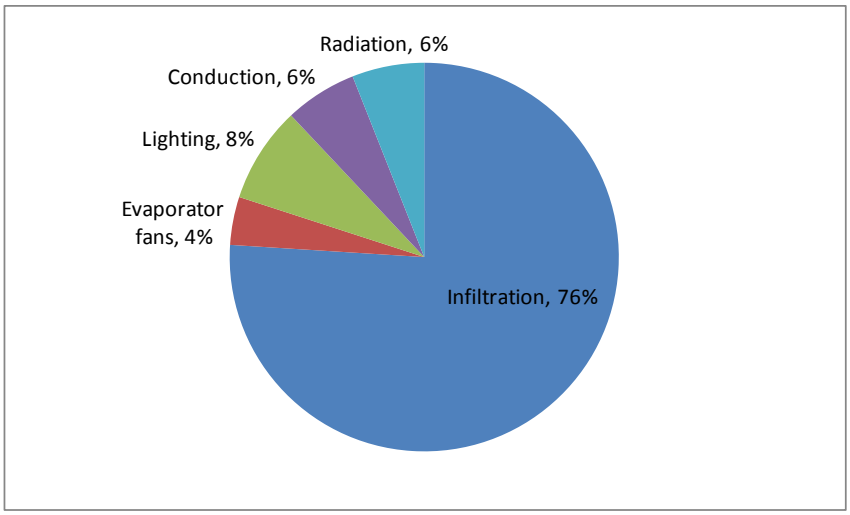

Figure 6: Contributions to the load of a vertical multi-deck open front chilled food display cabinet. (Tassou 2011)

4 EXAMPLES OF LOW CARBON SUPERMARKETS IN THE UK AND VENTILATION FEATURES

A study carried out in 2010 investigated the potential for a zero energy store (Hill et al, 2010) based on available data from supermarkers and thermal modelling. It suggests that:

- Refrigeration accounts for 40-50% of electricity consumption, with lighting and store heating/cooling systems accounting for most of the remainder.

- The need to heat or cool air introduced for ventilation purposes may account for around twice as much energy consumption as the heat lost or gained through conduction across the walls, roof and floor of the store.

Therefore ventilation is an area where further energy efficiency improvements are possible and natural ventilation systems have started being introduced in UK stores in many cases linked with natural lighting systems.

Envelope infiltration: In the UK, air-tightness tests are mandatory for buildings with a floor area of more than 1000m^2 and should be less than a maximum (or limiting) air permeability of 10 m^3.h^{-1}.m^{-2} at a test pressure differential of 50 Pa (ATTMA 2010, Part L, 2010). In general, the envelope area of the building is the total area of all floors, walls and ceilings bordering the internal volume subject to the test. Overall internal dimensions are used to calculate this area. The limiting air permeability is the worst allowable air permeability. The design air permeability is the value used in establishing the Building Emission Rate (BER expressed as kgCO_2/(m^2.year)), and is based on a specific measurement of the building concerned. So, air-tightness of supermarket envelope is regulated under the energy efficiency building regulations and in many cases 5 m^3.h^{-1}.m^{-2} at 50Pa is the desirable design value for low carbon supermarkets.

Ventilation strategies can be divided to those (a) integrated with other low carbon design strategies for the building and (b) integrated with the equipment of the supermarket.

4.1 Low carbon design and ventilation

There are examples of low carbon supermarkets and guidelines on how to achieve such buildings. Two reports sponsored by leading UK supermarket chains have been published in the last few years (Hill et al, 2010, Target Zero, 2011). In both reports, a base case supermarket was created based on the operational details of an existing store and energy efficiency measures were investigated including renewables. In this paper, only the energy efficiency improvements are reviewed.

The results of the (Target Zero, 2011) study are shown in Table 1; the energy efficiency improvements introduced were divided into three packages each with increased energy savings. Table 1 shows that all three energy efficiency packages are predicted to save money. Package B which includes ventilation features such as reduction of specific fan power and ventilation heat recovery has a lower NPV than Package A and therefore more attractive. For package C which includes additionally highly improved air-tightness at 5 $m^3.h^{-1}.m^{-2}$ @ 50 Pa, despite the greater reduction in carbon emissions, its economic performance is less attractive.

Table 1: Energy Efficiency Measures for zero carbon stores (source Target Zero, 2011 p. 21)

Option	Energy Efficiency Measures	Total operational CO_2 emissions ($kgCO_2/yr$) [change from base case total emissions]	Change in capital cost from base case building [%]	Change in 25 year NPV from base case building (£)
Base case building	-	699,289	-	-
Package A	Composite internal floor High efficiency lamps and luminaires Specific fan power reduced by 20% Motion sensing control throughout Improved chiller efficiency SEER = 6 Improved boiler efficiency to 95% Building oriented so that glazed façade faces south	508,196 [-27%]	[-0.36%]	-973,545
Package B	Package A plus (or superseded by): Very high efficiency lamps and luminaires Specific fan power reduced by 30% Roof lights 10% with daylight dimming Improved chiller efficiency SEER = 7 Ventilation heat recovery (60% efficient) Improved air tightness 7m3/hr per m2 @ 50 Pa	419,895 [-51%]	[0.90%]	-1,053,332
Package C	Package B plus (or superseded by): Specific Fan power reduced by 40% Roof lights 15% with daylight dimming Improved chiller efficiency SEER = 8 Highly improved air tightness 5m3/hr per m2 @ 50 Pa Active chilled beam / radiant ceiling Advanced thermal bridging (0.013W/m2K) Improved wall U-value to 0.25W/m2K	379,548 [-46%]	[5.1%]	-495,153

(Hill et al, 2010) report has summarised low energy design initiatives as:

- Enhanced utilisation of daylight
- A combination of natural and mechanical ventilation, with heat exchange
- Improved refrigeration cabinets, with doors on frozen food cabinets
- Improved control over lighting and ventilation, and acceptance of a wider range of internal temperatures
- LED display lighting
- Renewable energy sources, such as biomass or wind power

The overall effect of these measures is typically to reduce energy consumption to around 400kWh/m², with the proportional reduction in energy use for lighting and refrigeration being slightly higher than for heating and cooling. This sets a baseline for considering future reductions in energy use and emissions.

The same report (Hill et al, 2010) has identified a number of low carbon supermarkets and in particular an exemplar low carbon supermarket was constructed by one of the leading supermarket chains in the UK which has been monitored and studied by a number of research teams in the UK (Hill et al, 2010). The low carbon features of this supermarket are presented in Table 2.

Table 2: Emission Reduction Measures for zero carbon stores (Hill et al, 2010 p 22)

Envelope/Glazing	Nanogel sandwich skylihgts 1200mm clerestory glazing
Lighting	900 Lux instead of 1200 lux DALI control system – individually addressable fittings LED lighting in display cabinets
Ventilation/Cooling	Windcatchers roof vents Control by CO2 concentration
Refrigeration	Doors on freezer cabinets Anti-sweat coatings CO_2 refrigerant
Energy supply	CHP system powered by biofuel derived from wastes Micro-wind turbine
Forecast energy savings	50% energy use reduction compared with the base case (2006 regulations store) 66% emissions reduction

It can be seen that roof vents were used as well as CO_2 ventilation control. A recent example of such installation is in a superstore which opened in January 2013 (see Figure 7). This followed the installation of bespoke windcatchers at the Cheetam Hill Store which has achieved 37% energy use reduction based on energy efficiency measures and a total of 66% CO_2 reduction if the combined cooling heating and power plant room utilising absorption chiller technology is included (Campbell and Riley, 2009).

Figure 7: Windcatchers of a supermarket opened in January 2013 (courtesy of Monodraught Ltd).

4.2 Refrigeration plant and ventilation

CO_2 refrigeration systems have been used in recent years because of the environmental benefits they offer in terms of energy use reduction and avoidance of harmful refrigerant leakage to the atmosphere. At Brunel University, novel CO_2 refrigeration systems have been developed for supermarkets, notably with the integration of CO_2 refrigeration and trigeneration systems where the refrigeration generated by the trigeneration system is used to condense the CO_2 refrigerant in a cascade arrangement (Suamir et al, 2012). The trigeneration system consists of a natural gas engine based CHP system and a sorption refrigeration system. The heat rejected by the CHP system is used to drive the sorption chiller, with the cooling energy produced employed to condense the CO2 refrigerant of the subcritical CO_2 refrigeration system. Table 3 shows energy performance of a conventional and the proposed system for a case study supermarket and it indicates that 30% fuel energy savings; the case-study supermarket is the Cheetam Hill Store, also referred to in the previous section. Figure 8 shows a conventional and the proposed supermarket energy systems.

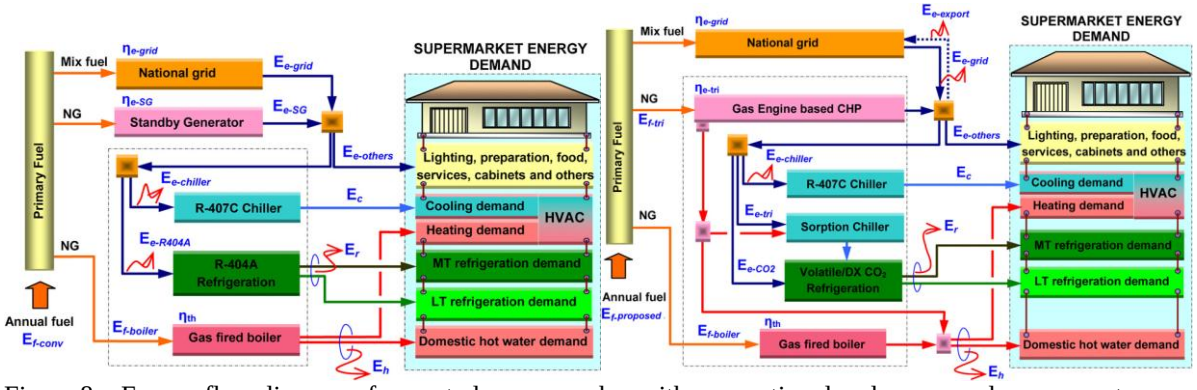

Figure 8: Energy flow diagram of case study supermarker with conventional and poroposed energy system, (Source Suamir and Tassou, 2013).

Table 3: Energy savings systems for supermarkets [Source Suamir et al, 2012]

Fuel Utilisation Components	Supermarket energy systems		**Unit**
	Conventional	Proposed	
Trigeneration Fuel	-	7,450,016	kWh
Boiler Fuel	874,068	24,670	kWh
Improted Electricity	2,817,321	62,343	kWh

Fuel of imported electricity	8,537,338	188,919	kWh
Exported electricity	-	332,962	kWh
Fuel saving to grid supply	-	1,008,975	kWh
Total fuel required	9,411,406	6,654,630	kWh
Fuel Energy savings	-	2,756,776	kWh/year
Fuel energy savings ration (FESR)	-	29.29	%

The cooling/heating demands for the building are usually provided by an air handling unit (AHU) with pre- and re-heat and cooling coils supplied by the gas fired boiler and compression chiller. The integration of the CO_2 cascade refrigeration system with the HVAC system and the AHU for heat recovery was investigated using the supermarket simulation model 'supersim' developed under the TRNSYS simulation environment (Ge and Tassou 2011). The results show that by controlling the head pressure of the refrigeration system a proposrtion or all the heat demand of the supermarket can be satisfied with heat recovery (Ge and Tassou, 2013).

Finally, in recent years Phase Change Materials (PCM) have been used in passive and active ventilation systems to maximise heat recovery applications and free cooling using external air. There is a vast amount of research in this area but has not been applied directly to supermarkets. The authors have developed a modelling method using CFD and thermal modelling to investigate the impact of active PCM systems in displacement ventilation in large enclosures. It was found that the addition of the PCM-HX in the DV diffuser reduces the energy requirement for heating in the intermediate and summer periods when 'no-night-ventilation' and 'limiting-control ventilation' night charging strategies for the PCM are used. These PCM charging strategies lead to annual energy demand reductions of 22% (Gowreesunker et al, 2013). These strategies might have good effectiveness in specific areas of a supermarket such as refrigerated warehouses for occupant comfort as well as the general customer areas.

5 CONCLUSIONS AND PLANNED WORK

This paper presented current energy use statistics of food retail and catering facilities buildings to demonstrate the high potential for the application of energy efficient technologies in the design of these buildings and their HVAC equipment. It focussed on UK examples of latest 'low carbon' supermarkets and showed that there is potential for significant energy savings with attractive financial return. It outlined current development in refrigeration systems and their integration with the energy management of the building for potential savings in the provision of environmental conditions.

Future work will target the goal of zero or near zero emission store whilst improving service and shopper experience. Investigations will involve future concept store design and building envelope for both small urban and out of town hypermarkets, to improve thermal performance and allow optimum integration of renewable energy and natural technologies (such as natural ventilation, day-lighting and thermal storage using PCMs) with HVAC equipment and their optimum integration within the constraints and objectives to provide flexibility and lower environmental impacts. Shopper surveys will be carried out to find how to improve their shopping experience.

6 ACKNOWLEDGEMENTS

This work is carried out as part of the RCUK Centre for Sustainable Energy Use in Food Chains (EP/K011820/1) project.

7 REFERENCES

ATTMA (2010), Technical Standard L2. Measuring Air permeability of Building Envelopes (Non-Dwellings), October 2010. (http://www.attma.org/downloads/ATTMA%20TSL2%20Issue%201.pdf)

Campbell A and Riley O (2009), Building Services For Low Carbon Supermarkets, Proc. Inst. R. 2009-10. 3-1

Canning P, Charles A, Huang S, Polenske KR, and Waters A (2010), *Energy Use in the U.S. Food System*, United States Department of Agriculture, Economic Research Service, Economic Research Report Number 94 March 2010.

Carbon Trust (2010).Refrigeration road map, CTG021, 56 pgs. www.carbontrust.co.uk.

CIBSE (2012), Guide F: Energy Efficiency in Buildings, CIBSE

Defra, 2012. *Food Statistics Pocketbook*. (http://www.defra.gov.uk/statistics/foodfarm/food/).

DECC, (2013), Energy consumption in the UK, Chapter 5: Services Sector Energy consumption, https://www.gov.uk/government/organisations/department-of-energy-climate-change/series/energy-consumption-in-the-uk

Eurostat, 2011. *Food: from farm to fork statistics*. http://epp.eurostat.ec.europa.eu/cache/ITY_OFFPUB/KS-32-11-743/EN/KS-32-11-743-EN.PDF

Eurostat, 2012. *Energy, transport and environment indicators*. (http://epp.eurostat.ec.europa.eu/portal/page/portal/product_details/publication?p_product_code=KS-DK-12-001

Ge YT and Tassou SA, (2011). Performance evaluation and optimal design of supermarket 4refrigeration systems with supermarket module 'supersim', Part I: Model Description and Validation, International Journal of Refrigeration, 34: 540-549

Ge YT and Tassou SA, (2013). Control strategies to maximise heat recovery form CO2 refrigeration systems in supermarket applications in the UK, 2nd IIR International Conference on Sustainable and the Cold Chain, April 1-3, 2013, Paris, France.

Gowreesunker BL, Tassou SA, Kolokotroni M (2013). Coupled TRNSYS-CFD simulations evaluating the performance of PCM plate heat exchangers in an airport terminal building displacement conditioning system, Building and Environment 65: 132-145

Hill, F., Courtney, R. & Levermore, G. 2010. Towards a zero energy store - a scoping study (ZEST). Manchester: University of Manchester. *www.sci.manchester.ac.uk/uploads/**zest**finalreport.pdf*

IEA. 2011. International Energy Outlook 2011. Available: http://www.eia.gov/forecasts/ieo/pdf/0484(2011).pdf [Accessed 15 June 2013].

IEA (2008)Worldwide Trends in Energy Use and Efficiency *Key Insights from IEA Indicator Analysis. IEA*

Part L (2010), Building Regulations Part L2A Conservation of Fuel and Power in new buildings other than dwellings, http://www.planningportal.gov.uk/buildingregulations/approveddocuments/partl/approved

Pérez-Lombard, L., Ortiz, J. & Pout, C. 2008. A review on buildings energy consumption information. *Energy and Buildings,* 40**,** 394-398.

Stanford J (2010). Reducing energy Consumption and GHG Emissions in the Food Supply Chain, Food Processing Farada, Interim Report, 40 pgs, Project No. 1125.
Sullivan R and Gouldson A. 2013. Ten years of corporate action on climate change: What do we have to show for it? Energy Policy, in press, June 2013
Target Zero (2011), Guidance on the design and construction of sustainable, low carbon supermarket buildings, http://www.steelconstruction.info/index.php?title=Special:ImagePage&t=Supermarket+guidance+doc+v2.pdf
Tassou, S. A., Ge, Y. T., Hadawey, A., Marriott, D.(2011).Energy consumption and conservation in food retailing, Applied Thermal Engineering, 31 (2011) 147-156.
Suamir IN, Tassou SA and Marriot D (2012). Integration of CO2 refrigeration and trigeneration systems for energy and GHG emission savings in supermarkets, International Journal of Refrigeration 23, 407-417
Suamir IN and Tassou SA (2013). Performance evaluation of integrated trigeneration and CO2 refrigeration systems, Applied Thermal Engineering 50, 1487-1495

.

OPTIMIZING THE OPERATION OF EARTH-TO-AIR HEAT EXCHANGERS IN HIGH-PERFORMANCE VENTILATION SYSTEMS FOR LOW-ENERGY BUILDINGS – A CASE STUDY

Alexandru Tudor*[1], Jens Pfafferott[2], Nico Maier[3]

1 Politechnic University of Bucharest
Spl. Independentei 313,
060042 Bucharest, Romania
**Corresponding author: allex_tudor@yahoo.com*

2 Hochschule Offenburg - University of Applied Sciences
Badstrasse. 24
77652 Offenburg, Germany

3 Hochschule Offenburg - University of Applied Sciences
Badstrasse. 24
77652 Offenburg, Germany

ABSTRACT

Earth-to-air heat exchangers are energy-efficient systems that use the ground for cooling in summer and heating in winter. Design, simulation and planning tools are available in the market, and earth-to-air heat exchangers are well-accepted in the built environment. Furthermore, there is a wide knowledge on their performance in operation. Based on long experiences in the design and operation of earth-to-air heat exchangers, pre-defined operation strategies are applied in ventilation concepts. In ventilation concepts with highly efficient heat recovery systems, optimized operation strategy should optimized rather in a combined optimization of air-handling unit and earth-to-air heat exchanger than a single optimization of the earth-to-air heat exchanger.

The study is based on monitoring data from a sports hall which was built in Passivhaus style. The heating and cooling concept is based on thermo-active building systems which are supplied by a ground-coupled absorption heat pump. The supply air is heated in winter and cooled in summer by an earth-to-air heat exchanger. The air-handling unit is directly coupled to the earth-to-air heat exchanger without bypass option and doesn't contain any additional heating or cooling.

A coupled plant-and-building simulation model is set up for the design and development of an optimized operation strategy. The model is developed in the R program.

A monitoring campaign in summer is used for the model validation. The simulation models is based on the simple-hourly-method building model according to ISO 13790, a simplified heating and cooling system, a characteristic-line model for the heat recovery system, and a detailed earth-to-air heat exchanger model. The building is controlled by a building-energy-management-system (BEMS) which is modeled according to the current operation (for model validation) and is used for the optimization of the operation strategy.

The improved control strategy takes the indoor temperature and the outdoor temperature into account. The outlet temperature is not suitable as input for the control strategy since the monitoring value is only indirectly available in operation.

KEYWORDS

earth-to-air heat exchanger, passive house, model

1 INTRODUCTION

The atmospheric air thermal inertia is lower than that of the soil. The thermal energy accumulated in the soil can be used through an earth-to-air heat exchanger (EAHE) consisting

in one or more tubes buried in the ground. The air entering the tube is heated in winter and cooled in summer, due to the temperature difference between the incoming outdoor air and soil. Using this type of renewable energy, the energy consumption required by a buiding can be reduced (Zhao, 2004). Several simple EAHE design solutions exist, such as single pipe EAHEs (Badescu, 2007) and two-pipe EAHEs (Bojic et al, 1997). More involved solutions consist of register type systems (Badescu and Isvoranu, 2011).

Earth-to-air heat exchangers may be used to save the energy in those buildings which are equipped with an active ventilation system (Badescu, 2007). This is particularly easy in case of passive houses (PH) where the active ventilation system makes part of the standard.

Earth-to-air heat exchangers are energy-efficient systems that use the ground for cooling in summer and heating in winter. Design, simulation and planning tools are available in the market, and earth-to-air heat exchangers are well-accepted in the built environment. Furthermore, there is a wide knowledge on their performance in operation. Based on long experiences in the design and operation of earth-to-air heat exchangers, pre-defined operation strategies are applied in ventilation concepts. In ventilation concepts with highly efficient heat recovery systems, optimized operation strategy should optimized rather in a combined optimization of air-handling unit and earth-to-air heat exchanger than a single optimization of the earth-to-air heat exchanger.

Passive houses are buildings in which a high level of comfort is achieved in winter and in summer without a separate heating system or air-conditioning system - the house 'heats' and 'cools' itself purely 'passively' (Adamson, 1987), (Feist, 1988). The *Passivhaus concept* originated from a collaboration between Bo Adamson at Lund University in Sweden and Wolfgang Feist at the Institute for Housing and the Environment, Germany. The concept has been implemented by W. Feist in Germany in 1992, when the first passive house has been built. The two basic criteria for a passive house are: 15kWh/(m^2/year) for annual heating demand and 120 kWh/(m^2/year) for total primary energy consumption (Badescu et al, 2010), (Feist, 1993).

The present paper aims describes a passive building and its earth-to-air heat exchanger system and air-handling unit. A coupled plant-and-building simulation model is set up for the design and development of an optimized operation strategy. The model is developed in the R program and validated with monitoring data. The building is controlled by a building-energy-management-system (BEMS) which is modeled according to the current operation (for model validation) and is used for the optimization of the operation strategy. The improved control strategy takes the indoor temperature, the CO2 level (as an indicator for the actual use) and the outdoor temperature into account. In this example, the overall efficiency of the existing heating, cooling and ventilation system can be improved by an optimized operation strategy.

The Gerhard Grafe Sports Complex (Figure 1) is located in Germany, in the northern part of Dresden. The building was opened in June 2012 and has a total surface of 1360 square meters with a volume of 8935 cubic meters. Glazing area is 300 square meters and in figure 2 it can be seen a picture of the layout of the interior space and glazing. According to the heating and cooling required by the customer, this building passive requires only 32.65 kWh / m² as the main requirement and 24 kWh / m² as heating requirement, including photovoltaic system performance computing (Pfafferott, 2013).

Figure 1: Gerhard Grafe Building

To protect the building from outside influences, the building is embedded halfway down in the ground. This causes the building to be more resistant to changes in outside air temperature. For this reason even built-in heating system, heating the wall and the floor heating, are heat really slowly the building. A number of systems are installed in the gym, which must be coordinated: solar panels on the roof that can be used to supply hot water, power to the primary circuit of the heat pump, air is sucked and circulated through the earth-to-air heat exchanger.

Figure 2: Opening day

The energy used for air conditioning inside the building can be significantly reduced by using an earth-to-air heat exchanger system. Using the ground as a seasonal energy buffer allows here in winter pre-heating the incoming air and improves the reliability of the heat exchanger of the ventilation system. In summer the low temperature level of the earth can be used to cool the outside air entering the building. Active cooling of the areas of use is not necessary.
In the ventilation system of Gerhard Grafe sports hall in Weixdorf the earth-to-air heat exchanger is therefore upstream of an air handling unit.

The ground heat exchanger consisting of two pipe registers with eight parallel polyethylene pipe is laid along the east and west side of the hall at a depth of 2 m to 3 m. The tube length is 40 m with a nominal diameter of 250 mm. The outside air is filtered before entering the earth-to-air heat exchanger. There are two intake towers and after emerging from

the EAHE reach in a suction building in the basement together, from which the ventilation device gets the air.

For indoor climate monitoring, mobile measurement technology is used to temperature and microclimate. The system consists of a station located inside the sports hall and two remote stations, weather station and the facade. The two outer stations can transmit recorded data archiving by Wirelles (W-LAN) station inside. A datalogger records ambient temperature and humidity in the gym and the operating temperature of the ventilation system [Pfafferott, 2013].

In the first data measurement campaign were collected data between June 9, 2012 (Sunday) 00:00 until July 11, 2012 (Tuesday) at 24:00. The measurements were made at a time interval of 3 to 6 minutes. After the test of plausibility, the measured values were converted into average for every 60 minutes.

2 MODEL VALIDATION

In this chapter, the simulation model of the building was implemented in the "R" programming language. It follows two main purposes:
- the possibility of a standardized comparison between measurement and simulation;
- in the future, this model can be used / developed on a large scale, as the model based on data analysis;

Measurement data can be stored and updated in R. The model can run at the same time a simulation and produce results and graphics with simulation and measurement data. Thus, a direct comparison between real and simulated operation may be possible without the need for additional interfaces.

For modelling the earth–to-air heat exchanger system and especially for a realistic view of the behaviour of the earth, it has been taken into account a number of complex relationships. First, knowledge of soil structure is necessary to determine the thermal conductivity and temperature. Individual parameters are taken from [VDI, 2006] or experience.

Regarding the time of using the building, a comparison between measurements made and the occupancy data given by the user did not provide a useful correlation. The use of the building was considered to be 12 hours per day from Monday to Friday. In the following we will present some computational relations and some parameters used in the model:

The building requires as input a number of parameters such as inlet temperature, air temperature at the output from earth-to-air heat exchanger, the temperature inside the building, the air velocity measured at the outlet of air handling unit, global solar radiation, diffuse solar radiation. Direct radiation is calculated as the difference between global solar radiation and diffuse solar radiation. The model includes some of the differential equations from ISO 13790 and the method is described in the standard. The time plan is set between 10:00 and 22:00, and the information is taken from the owner of the building.

In Figure 3 it can be seen simulate the operation of the building in the measurement campaign (33 days) and the comparison between the calculated temperature (model) and the measured temperature.

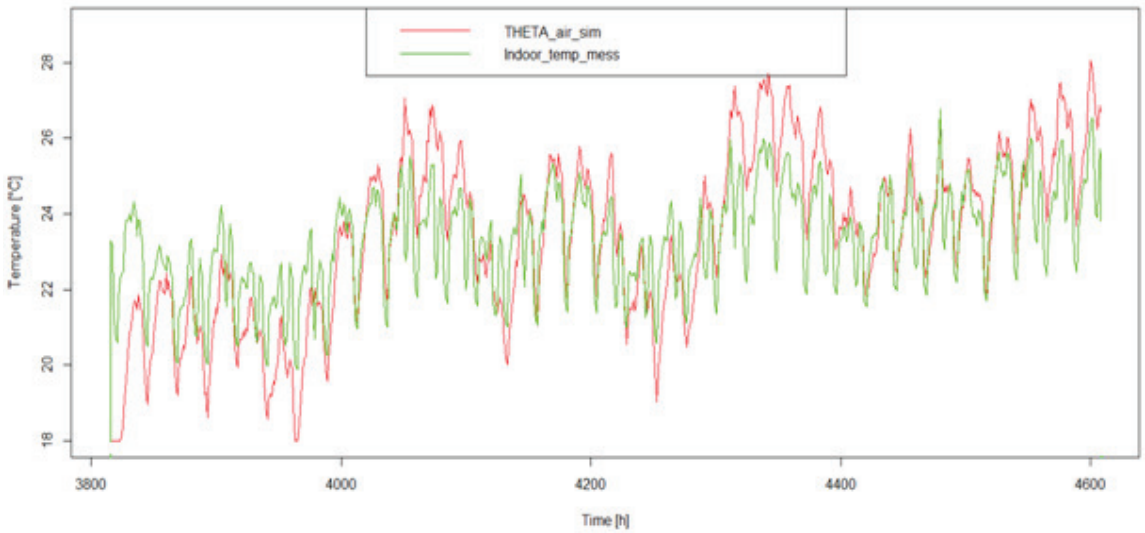

Figure 3: Comparison between the measured outlet temperature (Indoor_temp_mess) and the calculated outlet temperature (THETA_air_sim)

The average difference between the calculated temperature (model) and the measured temperature is 0.09 °C. The maximum temperature difference between the same values was 5.15 °C recorded on June 9, 2012 at 1:00, and the minimum temperature difference was 0.009 °C recorded on 4 July 2012 at 14:00.

Usual statistical indicators of accuracy are the mean bias error (MBE) and the root mean square error (RMSE) [Badescu, 1988], [Badescu and Isvoranu, 2011] defined by:

$$MBE = \frac{1}{n}\sum_1^n (T_{out,c,i} - T_{out,m,i}) \qquad (1)$$

and

$$RMSE = \sqrt{\frac{1}{n}\sum_1^n (T_{out,c,i} - T_{out,m,i})^2} \qquad (2),$$

where

$T_{out,c,i}$ is the computed outlet temperature, $T_{out,m,i}$ is the measured outlet temperature, while n is the number of values. MBE value for the indicated period was 0.09 °C and the RMSE value was 1.37 °C.

3 AIR COOLING AND HEATING

After achieving validation of the model, we simulated the functioning of the building for a period of one year. Since there were recorded data only for 33 days, we used annual reference test TRY [Deutscher Wetterdienst 2013 - http://www.dwd.de] to have hourly temperature values for a year (8760 hours). TRY appeared in 1985 and is updated annually. It contains hourly weather data that is based on records from previous years. It has been used for the same purpose in works such as [Janssens et al, 2005], [Breesch et al, 2005], [Pfafferott, 2004]. Annual reference test provides data for 15 different areas of Germany, of which obviously was chosen Dresden region. The system is simulated for a constant flow rate of 3000 m3 / h.

The building is controlled by a building-energy-management-system (BEMS) which is modeled according to the current operation (for model validation) and is used for the optimization of the operation strategy.

The improved control strategy takes the indoor temperature and the outdoor temperature into account. The outlet temperature is not suitable as input for the control strategy since the monitoring value is only indirectly available in operation.

Using the simulation model, it can be calculated the amount of energy provided by the efficient systems installed in the building. As it can be seen in figure 4, the yearly total amount of energy for the building is 68.59 MWh. The figure shows that in the winter period the amount is bigger than the rest of the year.

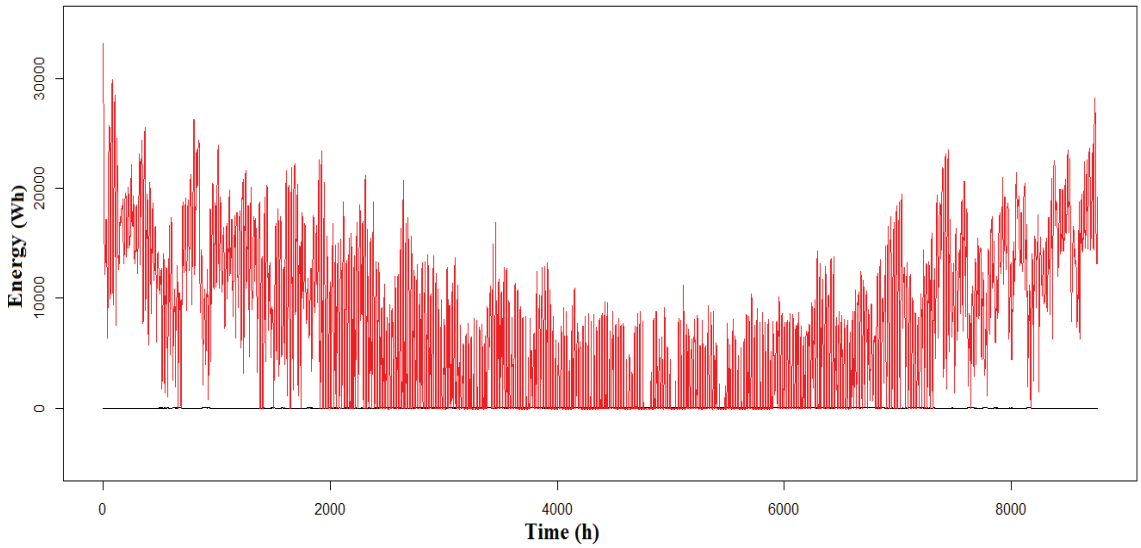

Figure 4: The yearly (8760h) amount of energy of the building

The distribution per season of the amount of energy is: 15.49 MWh in the spring, 4.99 MWh in the summer, 16.51 MWh in the autumn, and 31.59 MWh in the winter.

In the figure 5 it can be seen the temperature distribution for a year. Generally, in the winter (or when there are low temperatures) the outlet air temperature is higher than the inlet air temperature. Similarly, in the summer the outlet temperature (or when there are high temperatures) is lower than the inlet temperature, like it is expected. Overall, the EAHE system fulfills the functions for which it was built.

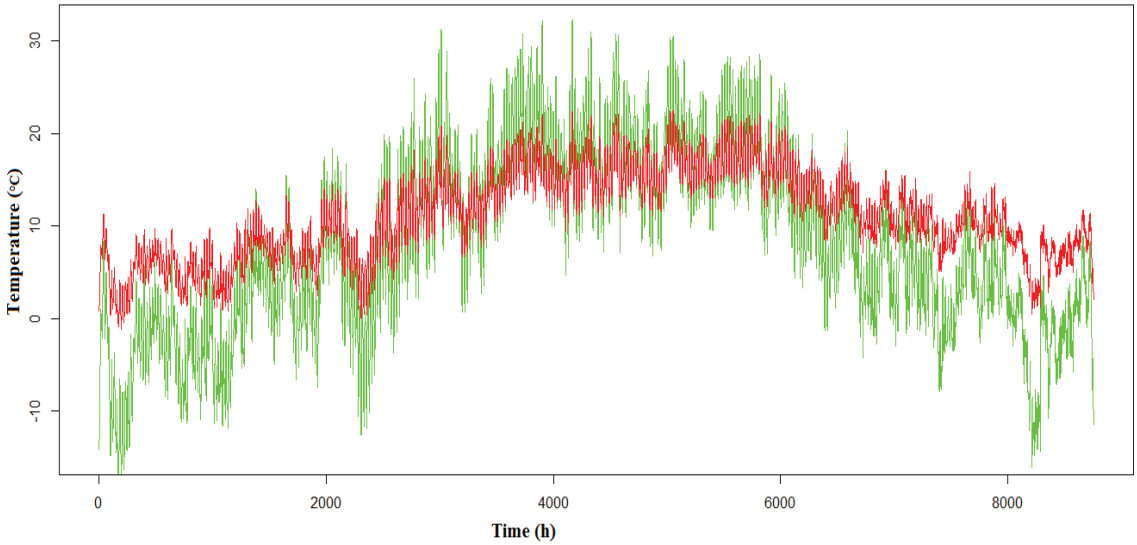

Figure 5: The yearly (8760h) temperature distribution; green – inlet air temperature (outside); red – outlet air temperature

However, analyzing the simulation data for a full year, not always the system provides useful energy. For example, in a day like March 25, at 9:00 the inlet air temperature is 10.7 °C and the outlet air temperature is 10.92 °C. All the night until that hour the EAHE was heating the air, providing useful energy. At 10:00 the inlet air temperature is 12.4 °C and the outlet air temperature is 12.18 °C. Similarly, at 11:00 the inlet air temperature is 14.7 °C and the outlet air temperature is 12.79 °C. It is clear that from 10:00 the system is not providing any more useful energy but is consuming electric energy and should be switched off. In this way, the BEMS can be set up for the heating the air if the inlet air is lower or equal with 10.7 °C.

Similarly, in the summer there is no need for cooling all the time. This aspect depends on the user and his preferences about the temperature in the building. It can be considered an ambient temperature of 22 °C. It is clear that, in the summer when the inlet air temperature is below this, value there is no need for cooling. The summer had 2208 hours and in 1539 hours the temperature was below 22 °C. In the same spirit the night ventilation concept can be used (Geros et al, 2005; Breesch, 2006; Pfafferott, 2004).

4 CONCLUSIONS

The Gerhard Grafe Sports Complex is briefly presented. The paper focuses on the earth-to-air heat exchanger system attached to this building. A new simulation model is proposed to predict the EAHE operation. The model was validated using experimental data recorded during 33 days in the summer period.

An improved control strategy is developed and takes the indoor temperature and the outdoor temperature into account. As a conclusion we can say that the bypass option can be used in several cases during a year. The recommendation is to use when the inlet air temperature is between 10.7 °C and 22 °C. The importance of this optimization is shown here and can improve the operation of those systems and electricity savings.

5 REFERENCES

Adamson Bo 1987. “Passive Climatization of Residential Houses in People’s Republic of China”; Lund University, Report BKL 1987:2

Badescu V. - Economic aspects of using ground thermal energy for passive house heating, Renewable Energy 32 (2007) 895–903

Badescu V., Isvoranu D. - Pneumatic and thermal design procedure and analysis of earth-to-air heat exchangers of registry type, Applied Energy 88 (2011) 1266–1280

Badescu V., Laaser N., Crutescu R.- Warm season cooling requirements for passive buildings in Southeastern Europe (Romania), Energy 35 (2010) 3284-3300

Bojic M, Trifunovic N, Papadakis G, Kyritsis S. - Numerical simulation, technical and economic evaluation of air-to-earth heat exchanger coupled to a building. Energy 1997;22:1151–8.

Breesch H., Bossaer A., Janssens A. - Passive cooling in a low-energy office building. Solar Energy 79 (2005) 682-696

Breesch, H. 2006. *Natural night ventilation in office buildings: performance evaluation based on simulation, uncertainty and sensitivity analysis*, Ghent University, Belgium

Deutscher Wetterdienst 2013 - http://www.dwd.de

Feist W. 1988. "Forschungsprojekt Passive Hauser." Institut Wohnen und Umwelt, Darmstadt: 1988

Feist W. - Passive Houses in Central Europe; Thesis, University of Kassel, 1993

Geros, V., Santamouris, M., Karatasou, S., Tsangrassoulis, A., Papanikolaou, N. 2005. On the cooling potential of night ventilation techniques in the urban environment. *Energy And Buildings* 37(3): 243-257.

Janssens A., M. Steeman, J. Desmedt, H. Hoes, M. De Paepe, Energy Performance Of Earth-Air Heat Exchanger In A Belgian Office Building, AIVC 26th conference, Brussels, Belgium, 21-23 September 2005, pp 15-20.

Pfafferott J. - Enhancing the Design and the Operation of Passive Cooling Concepts. Fraunhofer IRB-Verlag, Stuttgart (2004)

Pfafferott J., Abschlussbericht Projekt „Passivhaus Sporthalle Weixdorf", 2013

Zhao Z. M. – 2004. Simulation of earth-to-air heat exchanger systems, National Library of Canada, ISBN: 0-612-91158-6

ARE HEAT RECOVERY SYSTEMS NECESSARY FOR NEARLY ZERO ENERGY BUILDINGS IN MILD CLIMATES?

Flourentzos Flourentzou[1], Samuel Pantet

1 Estia SA
Parc Scientifique EPFL
1015 Lausanne, Switzerland
**flou@estia.ch*

ABSTRACT

Heat recovery ventilation became an unavoidable element of a passive or nearly zero energy building in Northern and Central Europe countries. Airtightness standards became very tight so that the building is compatible with this ventilation system. As frosting of heat recovery unit consumes a lot of electrical energy, a buried pipe system to smooth air temperature variations became also a necessary system in order to avoid defrosting. All these systems cost a lot of money and grey energy to get the benefit of 60 to 70% global net heat recovery of ventilation losses and some freshness in the summer. Southern countries, copying energy saving practices from the north, sometimes without a serious critical approach, adopted this practice and some of them even impose it for low energy consumption buildings.

This article presents the results of a life cycle assessment, taking into account all the consumed primary energy of the system, integrating also the grey energy of the machines and ducts. Heat recovery becomes a questionable principle, in climates where temperature differences and heat recovery potential are low. In cases where high-energy performance heat and cooling production, is used like heat pumps of COP higher that 4, the study shows that unfortunately the system consumes more electricity, than the electricity needed to produce the recovered heat or coolness. The study shows also the limited potential of the buried pipe technique compared to natural ventilation.

The analysis shows that heat recovery in mild climates can be considered as an energy saving measure only where mechanical ventilation is imposed for other reasons (very high external noise pollution, special uses needing high standard controlled ventilation, etc).

KEYWORDS

Ventilation, heat recovery, nearly zero energy buildings.

1 INTRODUCTION

Nearly zero energy buildings bring a new fundamental change in building energy behaviour in southern climates: Energy for heating is reduced to extremely low levers and the main energy needs are for cooling. Table 1 shows that in an almost zero energy building in Nicosia, energy demand for heating is 8 kWh/m^{2}y while energy demand for cooling is 34 kWh/m^{2}y. These values are without any ventilation heat recovery. In old, non-insulated, buildings these values where 149 kWh/m^{2}y for heating and 43 kWh/m^{2}y for cooling. The ratio heating energy

demand/cooling energy demand passes from 8/10 in non-insulated buildings to 2/10 in almost zero energy buildings (Flourentzou 2012 - 1).

Insulation	Heating demand	Cooling demand	Total demand
A. 0 cm, single glazing	149 (78%)	43 (22%)	192
B. 4 cm, double glazing - 3.5 W/m^{2}k	21 (25%)	64 (75%)	85
C. 10 cm, double glazing - 1.3 W/m^{2}k	8 (19%)	34 (81%)	42

Table 1. Heat and cooling demand of 3 building scenarios for an office building in Lefkosia – Cyprus, simulated dynamically with DIA+.

This means that the effort in well-insulated and well-shaded buildings in the south should be concentrated on low primary energy cooling technics. The most efficient low energy cooling technic is night ventilation. This means that half of the year, the building should be open or ventilated with high airflow rates, and this is a very significant difference between building thermal behaviour in southern and northern climates (Flourentzou 2012 -2). Designers attitude towards infiltration level and heat recover should be re-examined with the new reality.

To aboard this question, we take a real simple office building which is under construction, and we simulate heating and cooling demand, and we evaluate ventilation heat recovery and buried pipe energy savings. Simulations are performed with DIAL+, 2013 version (Paule, 2013).

2 TECHNICAL CHARACTERISTICS OF THE BUILDING

2.1 Typology and dimensions

We choose as typical office space a typical floor of a high-rise building under construction in Lefkosia. The floor total height is 3.84m, while the clear internal height is The building is well insulated and well shaded. East and west façades are equipped with a combination of fixed and movable solar protection and south façade is equipped with a 1.5m overhangs and internal solar protection. East, South and West facades are 50% glazed (glazing height = 1.8 m). North façade has 4 windows of 2X2.5m.

The total rough surface area is 486 m^2. The useful area without the external walls and the staircase is 479xx

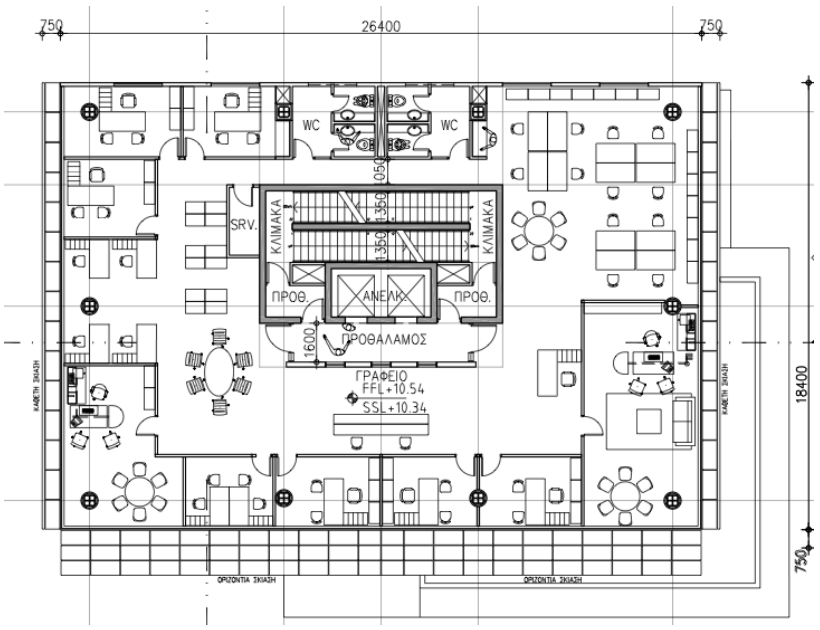

Figure 1: plan of a standard storey

2.2 Simulation parameters

The envelope characteristics are different for the cold and hot climates according to table 2. They are unchanged for all simulations.

	Cold climates	**Hot climates**
Thermal insulation position	external	external
Wall thermal insulation thickness	30 cm	10 cm
Roof thermal insulation thickness	30 cm	10 cm
Glazing g value	0.6	0.4
Window U value	0.8 W/m^{2}K	1.3 W/m^{2}K
Glazing light transmittance	O,55	0.65
Ventilation opening dimensions	1X1.8	1X1.8
Number of occupants	35	35
Ventilation airflow (30 m^3/pers)	1250/146 m^3/m^{2}h	1250/146 m^3/m^{2}h
Internal gains (7 W/m^2)	3400W	3400W
Lighting power (15.9 W/m^2)	7223W	7223W
Solar protection g value	0.15	0.15
Glazing control	Automatic if >90 W/m^2	Automatic if >90 W/m^2

Table 2. Building thermal characteristics for cold (Geneva and Copenhagen) and hot (Athens and Lefkosia) climates.

We vary climatic conditions for cold and hot climates: Stockholm - SE, Geneva - CH, Athens – GR and Lefkosia – CY. We consider DK and CH as cold climates while GR and CY hot climates. Climatic data come from a meteonorm standard file except for CY coming from real data of a standard year according the local energy department. This variation will change the building energy balance. Heating and cooling needs will be different.

We also vary the building thermal mass. We consider low thermal mass a space with suspended ceiling and raised floor and light façades with insulation within plaster boards. High thermal mass keeps the same façade but with apparent concrete floor and ceiling. This will change the dynamic behaviour of the building, especially during summer. It will change the free cooling potential and the overheating risks.

We will compare the effect of heat recovery for the 8 combinations of light and heavy buildings for the 4 climatic conditions.

3 SIMULATION RESULTS

3.1 Heating and cooling energy demand without heat recovery

Dynamic simulations are performed according to ISO EN 15791 with DIAL+ software.

Simulation	Light Building			Massive Building		
	Cooling	Heating	Total	Cooling	Heating	Total
CY Nicosia	42	5	47	41	2	43
GR Athens	31	8	39	30	5	35
CH Bern	9	25	34	7	22	28
SE Stockholm	9	33	42	9	31	40

Table 3. Cooling energy demand in hot climates represents 80 to 95% of the total energy demand while heating energy demand represents 70 to 80% of the total in cold climates. Light buildings consume 5 to 15% more than massive buildings depending of the meteorological conditions.

As we can see from table 3, in hot climates cooling energy demand for passive buildings is of the same order of magnitude as heating energy demand for cold climates but the total energy demand is of similar magnitude for hot and cold climates.

3.2 Effect of heat recovery in hot and cold climates

Simulation	Light Building			Massive Building		
	Cooling	Heating	Total	Cooling	Heating	Total
CY Nicosia	42	2	44	41	0.4	41
GR Athens	34	3	37	32	0.8	33
CH Bern	9	7	16	7	5	12
SE Stockholm	9	12	21	9	10	19

Table 4. Cooling energy demand in hot climates represents 80 to 95% of the total energy demand while heating energy demand represents 70 to 80% of the total in cold climates. Light We choose as typical

Tables are numbered. The table caption is above the table.

Table 5: Table Caption

Column Title	Column Title	Column Title	Column Title	Column Title
Table content				

Figures are numbered. The figure caption is below the figure.

Figure 2: Figure caption

Equations are numbered:

$$A = B + C \quad (1)$$

$$D + E = F \quad (2)$$

4 CONCLUSIONS

Please refer to the main conclusions of the work.

5 ACKNOWLEDGEMENTS

Please list the individuals that provided help to this work, if any.

6 REFERENCES

Flourentzou, F., Irwin, D., Kritioti, M., Stasis, T., Zachopoulos, N., (2012). Hybrid ventilation and cooling technics for the new Nicosia Townhall, AIVC conference, Copenhagen, 2012.

Flourentzou, F., Paule, B., Pantet, S., (2012). Natural ventilation and passive cooling simulation is not any more a privilage for experts, AIVC conference, Copenhagen, 2012.

Paule, B., et al, (2012). DIAL+Suite : a new suite of tools to optimize the global energy performance of room design, Status Seminar, Zurich..

‘INDOOR ENVIRONMENTAL QUALITY IN VERY LOW INCOME HOUSEHOLDS DURING THE WINTER PERIOD IN ATHENS

Alevizos S, Aslanoglou L, Mantzios D, Milonas P, Sarelli I, Santamouris M.

Group Building Environnemental Studies, Physics Department, University of Athens, Athens, Greece

and

Paravantis J.A.

University of Pireas, 18534 Pireas, Greece

Abstract

This paper presents and discusses monitored data of the indoor temperature in almost 50 low income houses in Athens Greece during the winter of 2012-2013. The aim of the research was to identify the degree that the actual economic crisis in the country influences the indoor environmental conditions, comfort and health in low income households. Analysis of the data has shown that indoor temperatures in the monitored low income houses were much lower than the appropriate threshold set for comfort and health. It is concluded that the actual economic crisis decreases seriously the potential of residents to buy energy and heat their houses and puts the local population under a serious environmental and health risk.

Introduction

It is well known that low indoor temperatures in houses have very serious environmental and health consequences [1]. Adequate heating is necessary to achieve temperatures that provide thermal comfort and does not threat the health of the residents. According to the World Health Organisation, [2], the benchmark indoor temperature for vulnerable population is 20ºC, while Boardman suggested a temperature around 18ºC, (3). As mentioned in [4], medical literature asks for a minimum temperature of 21ºC for the more vulnerable population, 18ºC for sedentary activities and 18ºC for able healthy people.

The association of low indoor temperatures and human health is extremely well documented. Exposure to low indoor temperatures in cold houses may cause serious respiratory deceases, increased blood pressure, risk of stroke, frequent accidents, arthritis, deceases of mental nature [5]. A 2007 study of WHO [2] carried out in eight European countries has shown that residents in cold houses and also non properly insulated houses as well as houses with single glazing or houses without a tight roof, may suffer from respiratory diseases at a much higher percentage than those living in properly heated homes. Low temperatures were highly associated with bronchitis and pneumonia, cold/throat illnesses, allergies and asthma. Similar results are also reported by Shortt and Rugkasa [6], for Northern Ireland. It is important that aged people (older than 65 years of age), shown an increased rate of respiratory problems, they are exposed to an important physiological health risk, as ageing may cause a diminished cold induced thermoregulation that results to a reduced body temperature, hypothermia and death. Low indoor temperatures are highly associated with poor mental health. Cold homes may have a damaging psychosocial impact including depression, stress, social isolation and constraints of mobility.

Previous research has shown that the thermal quality of low income houses in Greece is poor [7]. Only a very small part of the low income housing stock is insulated and has double glazing while the energy spent for heating purposes is quite high because of the poor envelope quality. As a consequence of the insufficient housing quality, low income residents experience extreme environmental conditions especially during the warm summer period and heat waves [8]. The economic crisis that started in the country after 2009, has created very important financial problems to the low income households. Their income has been seriously diminished while a high percentage of the population is unemployed. As a matter of fact, a study carried out during the winter period of 2011-2012 found that the energy spent for heating purposes has been seriously reduced and homes were not kept at adequate conditions [9].

The present study is a follow up of the previous research carried out in Greece to investigate indoor environmental conditions in low income houses. This study aimed to identify the levels of indoor temperature in the houses and associate them with social and economic parameters. This is a preliminary presentation of the results.

Description of the Study

In order to assess the environmental quality of low income households in Athens, Greece, almost fifty residences have been selected for monitoring. In each house a miniature temperature sensor has been placed measuring indoor temperature at 15 minutes interval. Sensors were placed in a well-ventilated and heat protected part of each house. All sensors were properly calibrated. Measurements are performed for the period between December 2012 and April 2013.

All information about the main characteristics defining the thermal performance of the houses, such as the existence and the type of insulation or the heating system, have been collected. Information on the social and economic status of the households was collected as well. The possible energy consumption of the present and past years was also collected when available. All houses were regularly visited by trained surveyors to download the recorded data and get a report on the actual problems and the applied conditions in the households. All data were subjected to quality control and measurements not satisfying the requirements were rejected and not taken into any futher account.

Main Results

This paper presents a preliminary analysis of the collected data from the monitored houses. Following a quality control procedure, data from 44 houses (out of a total of 50) are selected and analysed. Statistical analysis is performed for the whole set of the considered data and every month separately. In the remainder of this paper, data and analysis concerning just January 2013 are presented. It is noted that January was the coldest month of the specific winter period and presents the highest interest concerning the severity of the results. The whole analysis will be presented in an extended paper to be submitted in the near future.

The winter of 2012-2013 was a very mild one. According to the National Observatory of Athens, the average ambient temperature during January 2013 was close to 10.6ºC, while the absolute maximum and minimum were 19.0ºC and 0.9ºC. In parallel, the number of heating degree days was 228. Temperature levels during January were quite high compared to past years. Only three days of low ambient temperature were recorded, in particular, the 8th, 9th and 10th of January with average temperatures around 2.5, 3.9 and 6.8ºC, respectively. The cumulative frequency distributions of the average and minimum ambient temperatures for the whole month are given in Figure 2.

Figure 1 shows the variability of the indoor temperature in all 44 houses. The average temperature varied between 11.7 and 21,1ºC with the vast majority being below the threshold of 18ºC. Minimum temperatures ranged between 5.2 and 18.8ºC and in most of the buildings, minimum temperatures were below 15ºC. It is characteristic that in almost two thirds of the houses, the maximum temperature was always below 20ºC. It has to be pointed out that in about 5% of the sample, indoor temperature was at freezing levels. The specific buildings were characterized by a very low quality of envelope while the tenants could not afford (for economic reasons) the use of any kind of energy.

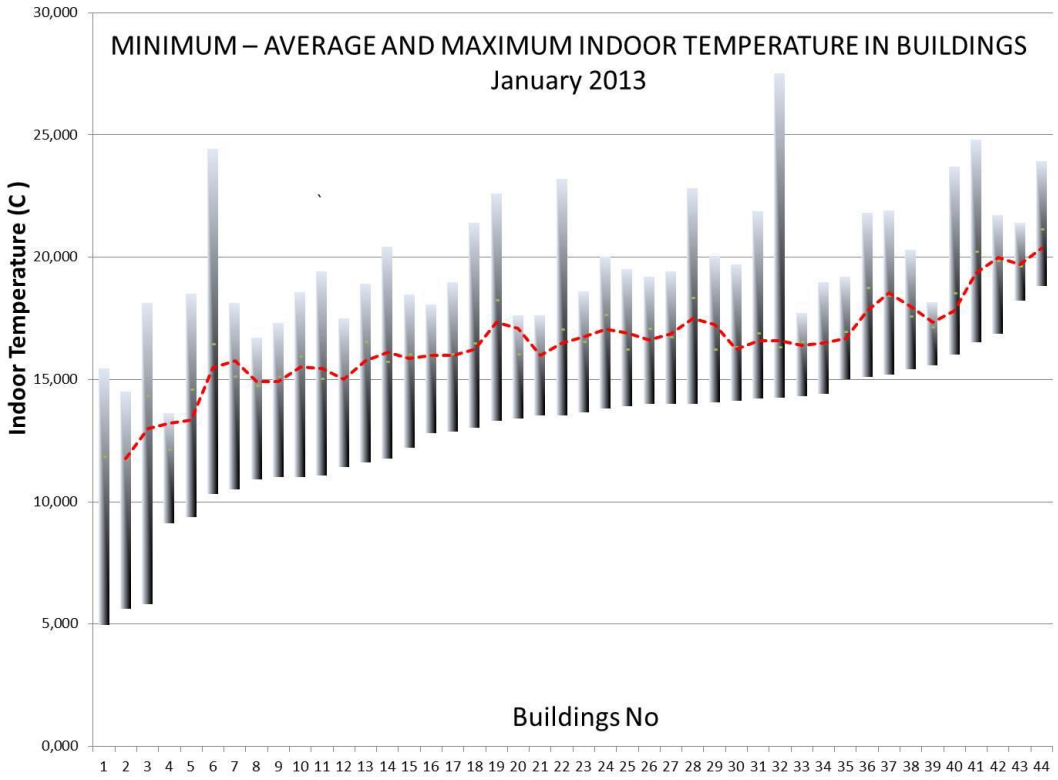

Figure 1. Variability of the measured indoor temperature in the 44 houses. Median temperature (line) and minimum and maximum temperatures are shown (bars).

A better representation of the indoor average and minimum temperatures are given in comparison to the corresponding ambient temperatures in Figure 2. As shown in almost 90% of the houses the levels of the indoor average temperature were below 18ºC, while for about 25% of the house, the average indoor temperature was below 15ºC. In parallel, indoor minimum temperature in all buildings was below 18ºC, while for 70% of the buildings the minimum

temperature was below 14ºC. Finally, the 17% of the buildings was below 10ºC and the 10% of the houses it was below 7ºC.

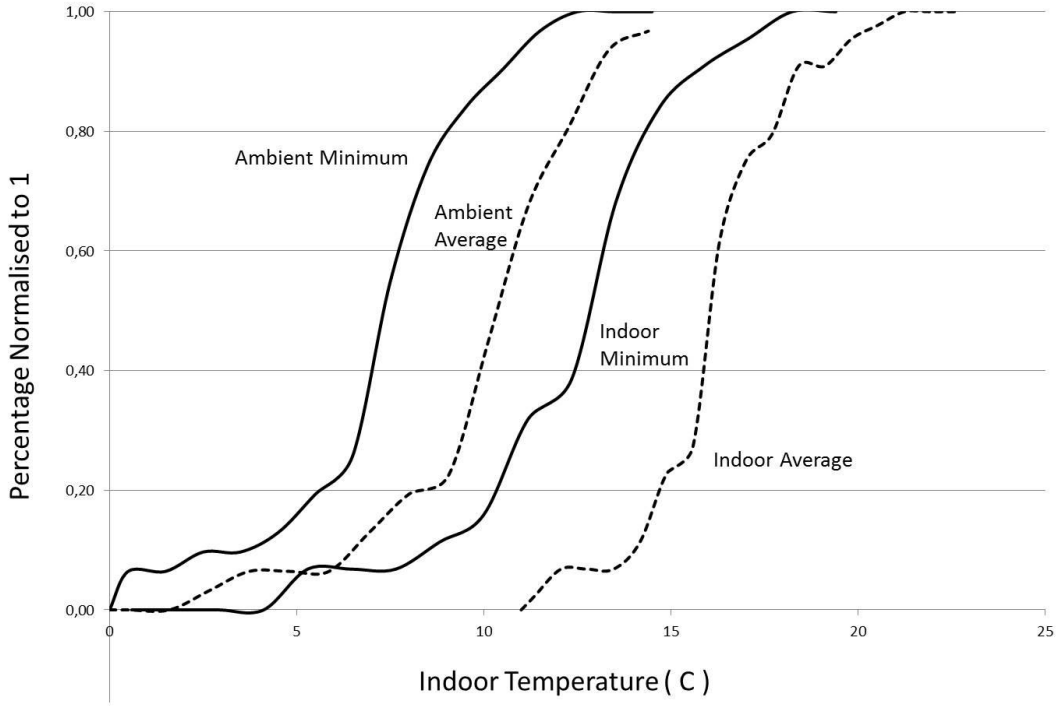

Figure 2. Cumulative frequency distribution of indoor and ambient minimum and average temperatures for January 2013. All 44 houses are included.

As it concerns the indoor environmental conditions during the entire January period, it is found that almost 79% of the global monitoring period for all houses (44 houses × 31 days × 24 hours), indoor temperature was below 18ºC, while for the 22% of the monitoring period, indoor temperature was below 15ºC. The specific percentage of the monitoring period for each house, (31 days × 24 hours), for which indoor temperatures were below 18 and 15ºC, is given in Figure 3. As shown, for almost 18 out of the 44 houses, indoor temperature was below 18ºC, for the whole monitoring period, while for almost 35 houses, temperature was below 18ºC for 80 %of the time. Only four houses have succeeded to keep indoor temperatures above 18 C for more than 80 % of the time. For three houses, indoor temperatures were below 15ºC for almost the whole period and for 10 houses, temperature was below 15ºC for more than 60% of

the monitoring period. For almost half of the houses, indoor temperature was lower than 15ºC for almost 20% of the time.

As already mentioned, the month of January was quite mild and it was quite difficult to extract specific information on the behaviour of the buildings and the families under extreme weather conditions. To evaluate the performance of buildings as well as the indoor conditions during low temperature periods, a specific analysis is performed for the two cold days of 8th and 9th of January.

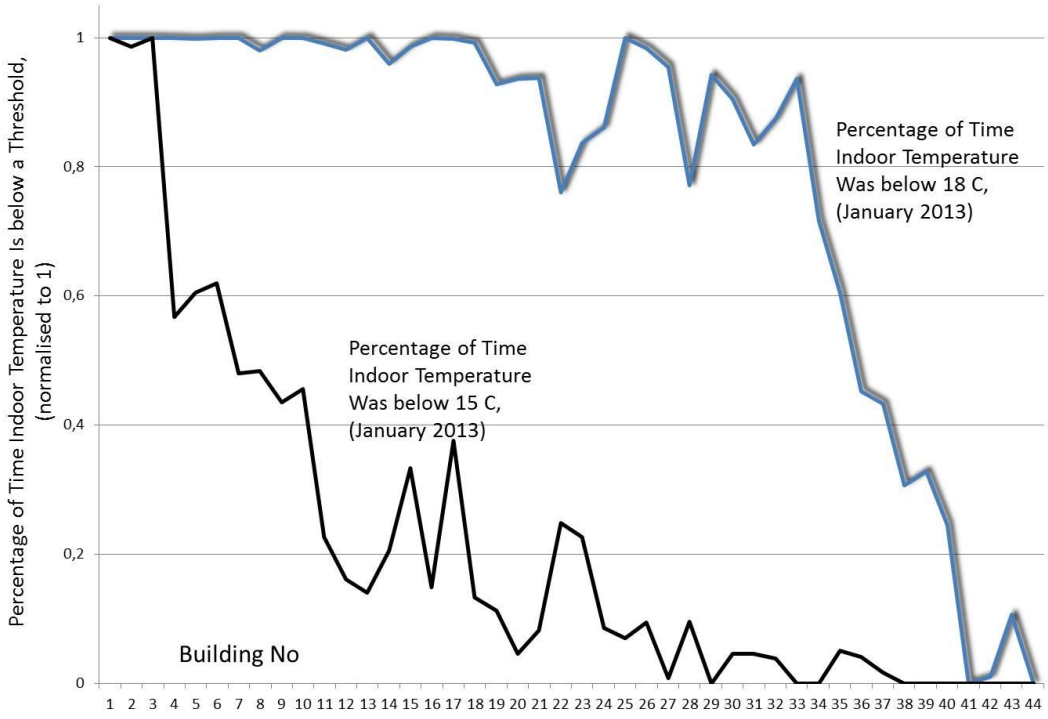

Figure 3. Percentage of the total monitoring period for each house with indoor temperatures below 18 and 15ºC.

The variability of the indoor temperature of all the monitored houses for these two specific days is given in Figure 4.

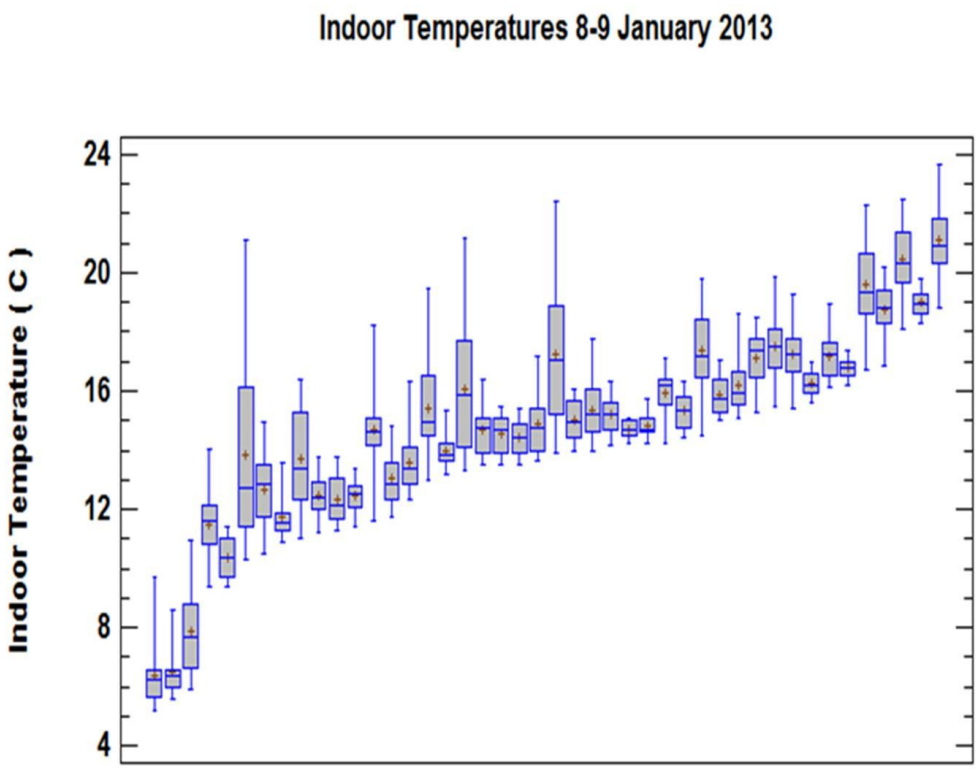

Figure 4. Variability of indoor temperatures in all monitored buildings during the cold days of 8th and 9th of January 2013.

Study of Figure 4 shows clearly that during the two specific days, indoor temperatures in most of the buildings was very low and much below the proper thresholds. The average median temperature for all houses was close to 14.7ºC, while the average and absolute minimum were 13.2 and 5.5ºC respectively. For two of the houses, indoor temperature was below 8ºC for almost the entire two days period, while for almost 25% of the houses the average indoor temperature was below 12ºC. The variation of the indoor temperature in the three coldest houses as well as the variation of the ambient temperature for the period of the two specific days, is given in Figure 5.

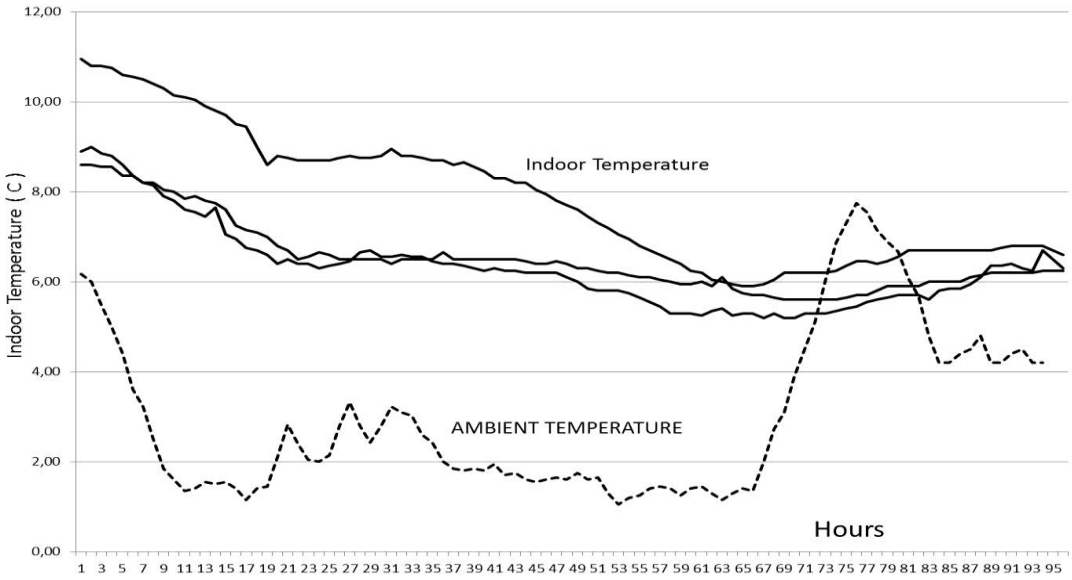

Figure 5. Indoor temperature variation for the three coldest buildings during the two specific days of low ambient temperature.

It is more than evident that indoor environmental conditions in the specific low income houses is completely unacceptable and put the life of the residents at high risk. At the same time, the levels of indoor temperature in almost 95% of the monitored houses are found much below the appropriate thresholds. A more detailed and specific analysis associating the specific levels of indoor environmental quality against economic, social and health characteristics is going to be published in the near future.

Conclusions

Low income population in Greece lives in badly protected houses that need a quite high energy load to heat and cool. Previous studies have shown that low income population has to spend much higher energy amounts per capita and area compared to high income population as their houses are improperly insulated and thermally protected. It is also known that the serious decrease of the financial income caused by the economic crisis had a serious impact on the energy spent for heating purposes by low income population and has tremendously decreased the heating bills. This new financial situation has an important impact on the indoor environmental quality in the houses as the lack of resources does not allow the achievement of proper indoor temperatures. Monitoring of about 50 low income houses during the winter of 2012 – 2013 in Athens has shown that indoor temperatures are much lower than the threshold

values set for comfort and health purposes. In most of the houses, long spells of low indoor temperatures are recorded while during periods of low ambient temperatures the specific indoor conditions in selected houses were completely unacceptable and for most of the houses much below the internationally accepted conditions.

It is a serious need to improve indoor temperatures in low income houses in Greece. It is obvious that there is a very serious environmental and health risk for the residents. Programs to supply cheap energy for heating together with programs to improve the thermal performance of the low income houses have to be defined and undertaken urgently.

References

1. Wilkinson, P., Armstrong, B., Fletcher, T., Landon, M., Mckee, M., Pattenden, S., Stevenson, S., 2001. Cold Comfort: the Social and Environmental Determinants of Excess Winter Deaths in England. 1986–96. The Policy Press, Bristol.
2. World Health Organisation , 2007: Large analysis and review of European housing and health status (LARES), WHO Regional Office for Europe, DK-2100 Copenhagen , Denmark
3. B. Boardman, 1991, Fuel Poverty: From Cold Homes to Affordable Warmth, Belhaven, Press, London
4. John D. Healy and J. Peter Clinch, 2002 : Fuel Poverty in Europe : A cross country analysis using a new composite measurement, University College Dublin
5. National Heart Forum, 2003. Fuel poverty and health toolkit: A guide for primary care organisations, and public health and primary care professionals. National Heart Forum, London
6. Shortt N. and Jorun Rugkasa, 2007 : ‘‘The walls were so damp and cold’’ fuel poverty and ill health in Northern Ireland: Results from a housing intervention, Health & Place 13, 99–110.
7. M. Santamouris, K. Kapsis, D. Korres, I. Livada, C. Pavlou and M.N. Assimakopoulos, 2007 : On the Relation Between the Energy and Social Characteristics of the Residential Sector. Energy and Buildings. 39, 893–905
8. Sakka, M. Santamouris, I. Livada, F. Nicol, M. Wilson, 2012 : On the thermal performance of low income housing during heat waves, Energy and Buildings, Volume 49, Pages 69-77

9. M. Santamouris, J. A. Paravantis, D. Founda, D. Kolokotsa, P. Michalakakou, A. M. Papadopoulos, N. Kontoulis, A. Tzavali, E. K. Stigka, Z. Ioannidis, P. Mexil, A. Matthiessen & E. Servou, 2013 : Financial Crisis and Energy Consumption: A Household Survey in Greece, Energy and Buildings, Volume 65, October 2013, Pages 477-487.

DWELLING ENVIRONMENTAL QUALITY INDEX: AN INDICATOR OF INDOOR ENVIRONMENTAL QUALITY IN RESIDENTIAL BUILDINGS

Marina Laskari[*1], Stavroula Karatasou[1], and Mat Santamouris[1]

1 Group Building Environmental Studies
Department of Applied Physics, National and Kapodistrian University of Athens
Athens, Greece
**Corresponding author: mlaskari@phys.uoa.gr*

ABSTRACT

Efforts to save energy may easily lead to the compromisation of indoor environmental conditions and vice-versa. This study suggests an indicator for indoor environmental quality classification, developed with the purpose of assisting households that are trying to save energy, to maintain optimum levels of indoor environmental quality during this effort. The "Dwelling Environmental Quality Index" (DEQI) is a comprehensive indoor environmental quality indicator, reported to occupants as an easily understood number (percentage). The DEQI is calculated for a thermal zone in which indoor air temperature, relative humidity and CO2 levels are monitored. It expresses in a single value the prevalent indoor environment quality category for the monitored period, based on the four indoor environment categories defined in standard EN 15251. Calculations for the DEQI rely on actual hourly measurements which may correspond to an entire-day, a week, a season or to a whole year, and as a result is capable of acting as a performance indicator for short-, medium- and long-term energy conservation measures implemented during the measured period.

KEYWORDS

Indoor environment, quality classification, residential buildings

1 INTRODUCTION

Based on health considerations, and depending on the indoor air quality indicator, acceptable exposure ranges exist for short-term and for long-term exposure (Health Canada, 1995; ASHRAE, 2007). Furthermore, seasonal variations in outdoor environmental conditions cause for relevant changes in the expectations of occupants from their thermal environment and therefore different criteria exist for evaluating the indoor environment during different seasons (CEN 2007b; ISO 2005).

The European Standard EN 15251 (2007b) and ASHRAE Standard 55 (2004) provide guidelines for the measurement of the indoor environment in buildings. In general, it is suggested that measurements are conducted in the spaces where occupants spend most of their time, at a floor height representative of the activity performed in that space. In residential buildings the space in which all occupants commonly spend most of their time is the living room, while activities performed there are mainly sedentary. Therefore, for residential buildings the optimum position for locating sensors is the living room at sedentary head height.

Marino et al. (2012) defined an indoor environmental quality index that can evaluate and classify the indoor environment in both single environments and whole buildings based on numerical values from either actual measurements or from numerical simulations.

This paper presents the application of this environmental quality index in one social housing dwelling in Belgium for a 2 week period in December 2012. This dwelling is one of the (approximately) 300 dwellings from 10 different European countries participating in the EC funded ICE-WISH project. The ICE-WISH project was launched in 2011 with the primary objective of improving energy efficiency in social housing using ICTs, while ensuring that implemented conservation measures will have no adverse influence on the indoor environment. For this purpose the project foresees for the installation of utility meters and sensors for monitoring the indoor environment, namely indoor air temperature, indoor relative humidity and indoor CO_2 concentrations. These three parameters form the indoor environmental parameters used for the evaluation of the dwellings' indoor environment.

2 METHODOLOGY

The proposed methodology allows for the calculation of an indoor environmental quality index that can evaluate and classify the indoor environment in dwellings based on measurements of indoor environmental parameters. It is based on the methodology developed by Marino et al. (2012) for the environmental quality classification of both single environments and whole buildings.

For residential buildings, like in the case of this study, it is considered sufficient to assess conditions in a single zone, namely the living room, where occupants spend most of their time. The methodology is consisting of four main steps. Firstly, the comfort factors and corresponding parameters to be considered in the assessment of indoor environmental quality are identified. Secondly, target values are assigned to each of the comfort parameters. Thirdly, the indoor environmental quality of the dwelling is evaluated through the calculation of the DEQI; and lastly, the dwelling's indoor environment is assigned a comfort class based on the DEQI score.

The first step involves the definition of the comfort factors and parameters to be assessed or, in the case that an assessment has already been performed, the selection of comfort factors and parameters that should be included in the environmental quality assessment. The evaluated period depends on the scope of the study and may be short, like for example a day or week, or longer, like for example a season or a year.

Comfort factors may be from any of the comfort aspects: thermal comfort, visual comfort, acoustic comfort and indoor air quality. Chiang and Lai (2002) and Chan et al. (2008) provide a list of comfort factors and associated parameters that can be included in the DEQI. Indoor air quality for example, may be evaluated through one or more of e.g. suspended particles ($PM_{2.5}$ or PM_{10}), carbon monoxide (CO), carbon dioxide (CO_2), formaldehyde (HCHO) etc.

European Standard EN 15251 (2007b), the Standard that connects energy performance of buildings with indoor environmental input parameters, defines four categories of environmental quality, that can be considered for any comfort factor (Table 1).

Table 1: Environmental quality categories

Category	Explanation
I	High level of expectation and is recommended for spaces occupied by very sensitive and fragile persons with special requirements like handicapped, sick, very young children and elderly persons.
II	Normal level of expectation and should be used for new buildings and renovations.
III	An acceptable, moderate level of expectation and may be used for existing buildings.
IV	Values outside the criteria for the above categories. This category should only be accepted for a limited part of the year.

The next step, after having identified comfort factors and parameters to include in the evaluation, is to define target values for each of the selected parameters and environmental

quality categories. The target values may differ from one study to another depending on the specifics of the zone under study (e.g. sensitivity of the occupants or of the space to specific parameters).
Next, with the help of the *Time Fraction Matrix [F]*, the time fraction for which hourly values for each of the studied parameters and for the study period expected, fall within each of the four quality categories, is determined.

$$F = \begin{matrix} f_{1,I} & f_{1,II} & f_{1,III} & f_{1,IV} \\ f_{2,I} & f_{2,II} & f_{2,III} & f_{2,IV} \\ f_{3,I} & f_{3,II} & f_{3,III} & f_{3,IV} \\ \dots & \dots & \dots & \dots \\ f_{n,I} & f_{n,II} & f_{n,III} & f_{n,IV} \end{matrix} \quad (1)$$

with $\sum_{j=I}^{IV} f_{i,j} = 1$

This matrix is made up of as many rows as the number of selected parameters and of four columns (the number of quality categories), with the generic matrix element $f_{i,j}$ representing the fraction of time for which the values of parameter *i* are in the ranges of quality category *j*.
Depending on the priorities and scope of each study, one might want to assign specific weights to each studied comfort parameter. Weighting is incorporated in the calculations for the DEQI through the *Relative Weight Vector {w}:*

$$w = \begin{matrix} w_1 \\ w_2 \\ w_3 \\ \dots \\ w_n \end{matrix} \quad (2)$$

Ways of obtaining the weighting value for each parameter include the Analytical Hierarchy Process (AHP) (Chiang and Lai, 2002) or through the calculation of a relative weight (Marino et al. 2012).
The multiplication of the *Time Fraction Matrix transpose* $[F]^T$ with the *Relative Weight Vector {w}* produces the *Time Fraction Weighted Mean Vector {f}:*

$$f = F^T w = \begin{matrix} f_I \\ f_{II} \\ f_{III} \\ f_{IV} \end{matrix} \quad (3)$$

with the generic vector element f_j indicating the persistence of the indoor environmental conditions in the j_{th} quality category.
Finally, the DEQI is calculated through the following relationship:

$$DEQI = 100f_I + 70f_{II} + 35f_{III} + 0f_{IV} \quad (4)$$

The scores of the DEQI may range from 0, when all values for the measured parameters fall in quality category IV, to 100, when all values for the measured parameters fall in quality category I. In a similar manner, when all values fall in Category II or III, the DEQI results to a

score of 70 or 35, respectively. Overall, the higher the DEQI score the better the overall indoor environmental conditions were in the dwelling for the period of time studied.
Marino et al. (2012) also adapted the energy performance classification of buildings described in European Standard EN 15217 (2007a) according to the definition of the environmental quality categories in EN 15251 (2007b) to establish a seven point scale (scale A to G) classification of the indoor environment as shown in the Table 2.

Table 2: DEQI results for each of the studied periods

DEQI	Indoor Environment Quality Class
90-100	A
75-90	B
60-75	C
45-60	D
30-45	E
15-30	F
0-15	G

The idea behind this is that the higher the DEQI score, the closer the indoor environmental quality is to the optimum class A.

3 APPLICATION OF THE DEQI IN AN ACTUAL DWELLING

The methodology presented earlier was adapted to the needs of the ICE-WISH project. This section presents the application of a preliminary version of the DEQI in a dwelling in Belgium.

3.1 The application environment

The dwelling studied here is an apartment in a social housing block located in Genk, Belgium and it is one of the 30 dwellings participating in ICE-WISH from the specific pilot. The total floor area of the dwelling is 43.26m^2 and it is comprised of 5 spaces: living/dining room, bedroom, kitchen, bathroom and a corridor. The floor plan of the apartment is presented in Figure 1. The building was constructed between 1965-1975 and was fully renovated in 2006. After the renovation individual condensing gas-boilers were installed in all apartments used for space heating and domestic hot water, and the thermal performance of the envelope was also significantly improved (with additional insulation and installation of high performance window systems with ventilation grids). Fresh air is supplied through the ventilation grids to the living room and bedroom while a ventilation shaft in the bathroom, kitchen and toilet provides exhaust ventilation. The apartment is occupied by one person. The structure presents no issues with condensation or mould.

Figure 1: Test dwelling

For the purposes of the project utility meters were installed for the measurement of total energy and water consumption and sensors for monitoring the indoor environment, namely indoor air temperature, indoor relative humidity and indoor CO_2 concentrations were installed in the living room. These three parameters will form the environmental parameters studied in the application of the DEQI in this section.
The measurement data used in this study are in hourly intervals and correspond to two consecutive weeks in December of 2012. The comfort factors considered in the study along with the corresponding parameters are listed in Table 2.

Table 2: Comfort factors and corresponding representative parameters

Comfort factors	**Representative parameters**
Winter thermal conditions	Indoor Temperature (^oC)
	Relative Humidity (%)
Air Quality	CO_2 concentrations (ppm)

Because this is a preliminary study to validate the basic concept of the DEQI, all measured comfort parameters were assigned with the same weighting.
The target values for the monitored environmental parameters are presented in Table 3.

Table 3: Parameters values for the four environmental categories for winter

Parameter	**Environmental quality category**			
	I	**II**	**II**	**IV**
Indoor Temperature (^oC)	21-25	20-21 25-25.5	18-20 25.5-26	<18 >26
Relative Humidity (%)	35-50	30-35 50-60	25-30 60-70	>70 <25
CO_2 concentrations (ppm)	<600	600-1000	1000-1500	>1500

3.2 Results

The time fraction matrix for weeks 1 and 2 and as a total for the two weeks, respectively, is presented in a graphical manner in Figure 2 and Figure 3. It is calculated through Equation 1.

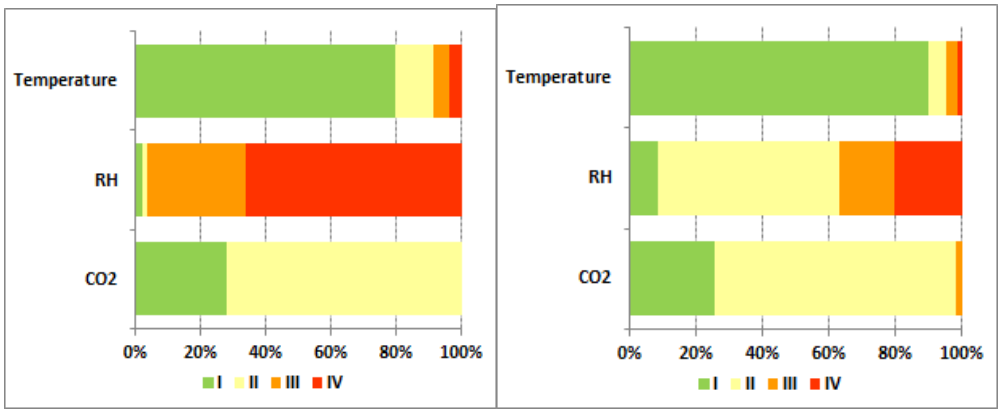

(a) (b)

Figure 2: Time Fraction matrix for a) week 1 and b) for week 2

As pointed out from the results, temperature is at optimum levels (Category I) for the majority of time for both weeks. CO_2 levels are at normal levels for a renovated building (Category II)

for the majority of time and at optimum levels for part of the time also. Relative humidity in week 1 had an average value of 24%. This is clearly illustrated in Figure 2a where Relative Humidity is below the moderate level (Category IV) for the majority of time. In week 2, Relative Humidity levels are slightly improved (weekly average is 30%) and this is also clearly illustrated in Figure 2b.
Figure 3 gives the time fraction matrix for weeks 1 and 2 combined. Temperature and CO_2 levels do not differ significantly from the individual values for weeks 1 and 2 shown in Figure 2. Contrarily, the distribution of Relative Humidity hourly values in the four environmental quality categories differs significantly between weeks 1 and 2 combined and individual weeks. This is because Relative Humidity is so different between weeks 1 and 2, that even the average of these two cases (weeks 1 and 2 combined) differs importantly from conditions in individual weeks (weeks 1 and 2, individually).

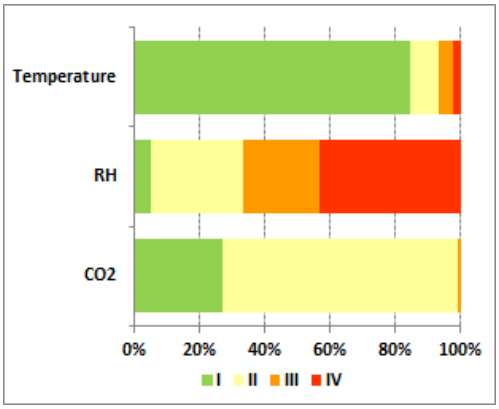

Figure 3: Time Fraction matrix for weeks 1 and 2 combined

What is important to notice here is that if one would study only week 1 (Figure 2a only), then the immediate conclusion would be that the dwelling has a significant Relative Humidity issue, while if week 2 was studied independently (Figure 2b only), then conclusions for temperature and CO2 levels would be similar to those of week 1, but conclusion for Relative Humidity would be that for a significant amount of time Relative Humidity is at normal levels of expectation. The study of the biweekly results on the other hand would give a more representative picture of the dwelling's conditions as it covers both periods of time (week 1 and week 2). Since the calculated biweekly values are the average of the two individual weeks they would show an intermediate condition between normal (week 2) and rather unacceptable (week 1) for Relative Humidity.

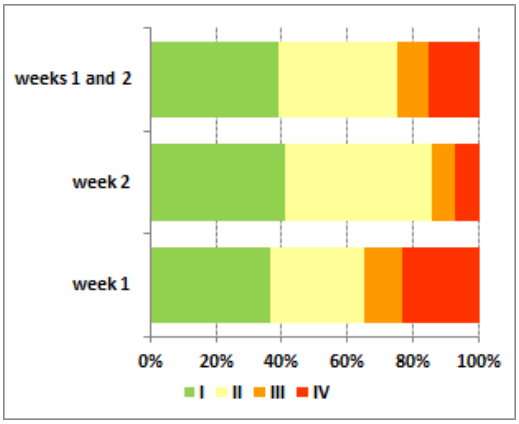

Figure 4: Time Fraction Weighted mean vectors for all studied periods

Figure 4, enhances the value of this observation by showing the overall impact that the variation in one single parameter (in our case that of Relative Humidity) can have on the Time Fraction Weighted mean vectors. It is calculated with the help of Equation 3. In addition, the same Figure also suggests the importance of a DEQI evaluating the indoor environment at a short-term (weeks 1 and week 2 individually) and at longer-term (weeks 1 and 2 combined), since the combined results show that the dwelling is not performing neither as bad as noticed for week 1 nor as good as noticed for week 2. However, both cases, the short-term and longer-term have their importance. The short-term helps the user to focus on the problems better, while the longer-term gives the bigger and more representative picture of indoor environmental conditions.
Next, the DEQI is determined, with the help of Equation 4. Results are presented in Table 4. As shown, during week one the DEQI score is 61 and very close to quality class D, while during week 2 the DEQI is at the boundary between class B and C. Looking at the 2 weeks combined the DEQI is at the middle of class C and the value of the DEQI is the average of the DEQI score for week 1 and 2, respectively.

Table 4: DEQI results for each of the studied periods

Study period	DEQI	Indoor Environment Quality Class
Week 1	61	C
Week 2	75	C
Weeks 1 and 2	68	C

4 CONCLUSIONS

The Dwelling Environmental Quality Index is able to communicate to occupants a large and significant amount of information regarding their indoor environmental conditions in a single value.
When the DEQI is calculated for a short period of time (i.e. a day or a week) it can assist in the identification of activities that affect the indoor environment in a positive or negative manner. It can also help occupants stay updated and even set short-term targets for the improvement of the quality of their indoor environment.
When considering measured values for a longer period of time the DEQI provides a more objective overview of the indoor environment as it helps mitigate the effects on the indoor environment of casual activities or events taking place inside or outside the dwelling in the short-term.
When only a small number of environmental parameters is considered in the DEQI then the impact that each of the parameters may have on the DEQI score is significant. On the other hand when a large number of parameters are considered in the DEQI then the impact of individual parameters on the DEQI is less profound. This also shows how important and delicate the matter of assigning weighting factors to each environmental parameter included in the DEQI calculations can be. Especially when occupants or the building structure have problems that are impacted by specific parameters (i.e. humidity, temperature etc) extra care should be put in the weighting assignment.
The individual study of parameters considered in the DEQI is important for understanding the impact that each parameter has had on the final DEQI score and consequently the areas where occupants should focus their efforts for improving their indoor environment, but also the areas were no additional or significant effort is necessary.
Finally, the DEQI can prove to be a very useful tool for occupants that receive energy consumption feedback at the same frequency as they receive the DEQI score. Just by comparing the DEQI score to the percentage of energy savings for e.g. one day or one week to

the day or week before, respectively, one can determine whether energy savings were compromised in favour of better environmental conditions, or vice versa. In time, the comparison of the two values (% savings and DEQI score) could help occupants become more aware of the interactions between energy consumption and the indoor environment in their home and as a result help them find the balance that they prefer for their own home between the two.

5 ACKNOWLEDGEMENTS

The authors gratefully acknowledge partners from the ICE-WISH Project: Kristien Van Hemelryck and Bernard Wallyn from VMSW (Belgium); Guy Bartlett, Hayley Cloud, Jonathan Perry and Bethan Jones from UPL (UK). The project was made possible through funding from the European Commission.

6 REFERENCES

ASHRAE 55 (2010). Thermal environmental conditions for human occupancy. ANSI/ASRAE Standard 55. Atlanta: American Society of Heating, Refrigerating, and Air-Conditioning Engineers, Inc.

ASHRAE 62-1 (2007). Ventilation for acceptable Indoor Air Quality. ANSI/ASRAE Standard 62-1. Atlanta: American Society of Heating, Refrigerating, and Air-Conditioning Engineers, Inc.

CEN (2007a). EN 15217: Energy performance of buildings - methods for expressing energy performance and for energy certification of buildings. Bruxelles: European Standardisation Organisation.

CEN (2007b). EN 15251: Indoor environmental input parameters for design and assessment of energy performance of buildings addressing indoor air quality, thermal environment, lighting and acoustics. Bruxelles: European Standardisation Organisation.

Chan, E.H.W., Lam, K.S., Wong, W.S. (2008). Evaluation of indoor environment quality of dense urban residential buildings. *Journal of Facilities Management 4(6),* 245-265.

Chiang, C. M., Lai, C. M. (2002). A study of the comprehensive indicator of indoor environment assessment for occupants' health in Taiwan. *Building and Environment 37,* 387-392.

Health Canada. (1995). *Exposure Guidelines for Residential Indoor Air Quality.*

ICE-WISH - Demonstrating through Intelligent Control (smart metering, wireless technology, cloud computing, and user-oriented display information), Energy and Water wastage reductions In European Social Housing. http://www.ice-wish.eu/uk/icewish.asp

ISO (2005). EN ISO 7730: Moderate thermal environments - analytical determination and interpretation of thermal comfort using calculation of the PMV and PPD indices and local thermal comfort. Geneva: International Standard Organization.

Marino, C., Nucara, A., Pietrafesa, M. (2012). Proposal of comfort classification indexes suitable for both single environments and whole buildings. *Building and Environment 57,* 58-67.

UNCERTAINTIES IN AIR EXCHANGE USING CONTINUOUS-INJECTION, LONG-TERM SAMPLING TRACER-GAS METHODS

Max Sherman[1], Iain Walker[2], and Melissa Lunden[3]

1 Lawrence Berkeley National Laboratory
1 Cyclotron Road
Berkeley, CA 94720, United States
**mhsherman@lbl.gov*

2 Lawrence Berkeley National Laboratory
1 Cyclotron Road
Berkeley, CA 94720, United States

3 Lawrence Berkeley National Laboratory
1 Cyclotron Road
Berkeley, CA 94720, United States

ABSTRACT

The PerFluorocarbon Tracer (PFT) method is a low-cost method commonly used for measuring air exchange in buildings. This is a specific instance of the more general *Continuous-Injection, Long-Term Sampling (CILTS)* approach for using tracer gasses. The technique is widely used but there has been little work on understanding the uncertainties (both precision and bias) associated with its use, particularly given that it is typically deployed by untrained or lightly trained people to minimize experimental costs. In this article we will conduct a first-principles error analysis to estimate the uncertainties and then compare that analysis to CILTS measurements that were over-sampled, through the use of multiple tracers and emitter and sampler distribution patterns, in three houses. We find that the CILTS method can have an overall uncertainty of 10-15% in ideal circumstances, but that even in highly controlled field experiments done by trained experimenters, one should expect more like 20%. There many realistic field conditions (such as open windows) where CILTS is not likely to provide any quantitative data. Even avoiding the worst situations CILTS should be considered as having a *factor of two* uncertainty for the broad field trials that it is typically used in. We provide guidance on how to deploy CILTS and design the experiment to minimize uncertainties.

1 INTRODUCTION

Building ventilation is the primary process used to insure acceptable indoor air quality by removing pollutants from indoor sources as well as conditioning the air for occupant comfort. In many buildings, ventilation occurs by the uncontrolled leakage of air through the building envelope termed infiltration. Efforts to improve building energy efficiency have focused on reducing infiltration by making homes more airtight. In the absence of designed ventilation, reduced infiltration can lead to elevated concentration of pollutants indoors. However, the use of mechanical ventilation can offset the energy gained thought improved airtightness. Thus, accurate measurement of the ventilation rate, or air exchange rate, is key to assess the energy and air quality impacts of infiltration. Having a reliable estimate of building

ventilation can also be necessary to characterize other indoor phenomena, such as the emission rate of contaminants indoors.

The constant injection method involves placing a number of emission sources, whose emission rate is well known or controlled – often using sophisticated mass flow controllers - of one or more tracer gases in a house together with samplers to measure the concentration of the gas over a period of time that can range from hours to days. The time-averaged air exchange rate is determined from the volume of gas tracer emitted into the house and the concentration of that tracer measured by the sampler. Simpler methods utilize a passive technique to obtain relatively constant emission of tracer, such as the evaporation of a liquid through a controlling membrane. This method is often called the "PFT" method because it used PerFluorocarbon Tracer gases. The defining characteristic of this technique is not the tracer gasses themselves but the fact that they use Constant Injection and Long-Term Sampling in the field. We shall refer to this technique with a more generic title of CILTS.

The CILTS method is widely used due to the small size and low cost of the sources and samplers, the flexibility in measurement duration, and because to can be deployed using personnel with limited training. This is particularly important for applications such as field projects that require the measurement of the air exchange rate in large numbers of homes. There is general guidance regarding the number of gas sources that should be placed based on the total area of the space [ASTM E741 2000]; sources and samplers are largely placed in a locations within a home based on the convenience for occupants and engineering judgment.

Due to its widespread use, it is important to have a reasonably good idea of the uncertainties associated with the CILTS method, but limited analyses exist. The factors that affect measurement uncertainty include uncertainties in the tracer emission rate, the measured tracer concentration, the time rate of change in the tracer concentration, and the spatial variability of tracer concentration within the house. Some earlier research investigated some of these uncertainties [Dietz and Cole, 1982; Leaderer et al, 1985], but do not explicitly discuss the implications for the resulting air exchange rate. D'Ottavio et al, 1988, shows how to analyze the data but contains no error analysis. The objective of this work is to estimate the sources and magnitude of errors for a typical single-zone application of CILTS. These uncertainties will be examined thought analysis of field data using a theoretical uncertainty analysis method developed by Sherman (1989). Based on the analysis, recommendations for reducing the errors of using the CILTS method will be listed.

A more extensive version of this article has been submitted for publication.

2 UNCERTAINTIES ESTIMATES FOR THE CILTS METHOD

All tracer gas methods use the continuity equation to calculate the air exchange rate from the measured tracer concentrations and other experimental parameters. The continuity equation for a single zone is as follows:

$$V \times \dot{C} + Q \times C = S \quad \textbf{(1)}$$

where V is the zone volume (m^3), Q is the ventilation rate of the zone (m^3/h), C is the tracer concentration (g/m^3), $\dot{C}$ is the time rate of change of tracer concentration ($g/m^3/h$) and S is the tracer emission rate (g/h). The ventilation rate generally varies as a function of time, which is directly reflected in the term for the time rate of change of tracer concentration. However,

the CILTS method results in a single measurement of tracer gas concentration averaged over the time period of the experiment. Therefore, the use of the continuity equation to calculate the air exchange rate measured using the CILTS method requires that sampling time period be sufficiently long that the transient changes in concentration can be neglected. When this is the case, an average air exchange rate, A (1/h) can be determined from the measured tracer emission rate and the measured concentration as follows

$$Q = S / C = A \times V \quad \textbf{(2)}$$

When the emitters are first placed in the building there is an additional transient period during which the tracer reaches equilibrium in the home. It is also important that the tracer sampling period either avoids this initial transient period or that the sampling period is long enough so that this transient period is inconsequential to use Eq. 2 to calculate the air exchange rate.

There are a number of errors to consider when calculating the air exchange rate using Eq. 2 with the CILTS method. The first types are instrumentation errors associated with the measurement of the tracer gas emission rate and concentration. The second type of errors are those arising from the simplified model of the continuity equation used to interpret the data. The subsequent discussion will discuss these different sources of error in detail.

2.1 Instrumentation Error

Instrumentation error encompasses all of the errors in the directly measured quantities of average emission and concentration. The contribution to the uncertainty to the calculated air exchange rate follows from Eq. 2 and can be expressed as:

$$\left(\frac{\delta Q}{Q}\right)^2 = \left(\frac{\delta A}{A}\right)^2 = \left(\frac{\delta S}{S}\right)^2 + \left(\frac{\delta C}{C}\right)^2 \quad \textbf{(3)}$$

There can also be an error term for the uncertainty in the volume of the space, but for this effort, we shall assume that is small.

Estimating the uncertainty of the average tracer emission rate, S, is a straightforward exercise. The total mass emitted is often measured gravimetrically by weighing the emitter before and after the tracer gas sampling period, and the result can be highly accurate. If the emitter is calibrated in the laboratory and an emission curve is used, it may be less accurate. The emission rate may not be constant, but if the changes in the emission rate are not correlated with variations in the air change rate, small variations in time will not affect the results. We will, therefore, consider the tracer emission rate to be constant in time.

The error in the measured tracer gas concentration is due to errors in both sample collection and analysis. The analytical technique used to measure the amount of tracer gas in the sample can have precision errors due to variability in instrument response and bias errors due to imperfect calibration. The errors in sample collection are primarily due to uncertainly in the value of sampling rate and a sampling rate that may not be constant. Both of these errors are of particular important with concentrating samplers (e.g. sorbent tubes) due to potential effects of temperature and potential sample saturation. Non-concentrating sampling techniques such as bag sampling are much less likely to experience non-constant sampling rates. There is a modelling error (discussed later) associated with assuming the concentration is spatially homogeneous at the spatial average, but there is also a measurement error associated with determining the average concentration. This uncertainty can be reduced by using multiple samplers, but the modelling error cannot.

Most experiments using the CILTS technique do not analyse the concentration data in the field, which can result in an additional source of measurement error. Transporting the sample to the laboratory for analysis allows for an opportunity for sample degradation. For instance, some of the sample may be lost in transit or storage through leaks. This is particularly important for concentrating samplers where the concentration measurement is a function of the total collected mass. For non-concentrating samplers, such as units that directly sample room air into a bag, the loss of part of the sample is less important because analysis results directly in a concentration. For concentrated samples any loss will create a negative bias. For all kinds of samples, contamination of the sample in transportation can result in error in either direction.

2.2 Model Errors

Model errors result from the fact that the model one is using to interpret the data is a simplification of reality. This is, of course, intrinsic in any scientific experiment, but it is important to recognize the simplifications that may lead to significant error and to reduce them or at least estimate their impact.

To analyse the data in the CILTS approach it is assumed that the system is in steady-state (i.e. that the concentration has had sufficient time to reach equilibrium that transient effects are unimportant), that the parameters are stationary (i.e. that the air exchange is truly a constant over the measurement period), and that space is a single-zone (i.e. that the concentration is homogenous throughout the space). Each of these assumptions has an intrinsic error that is dependent on the system being measured rather than the instruments measuring that system. We will examine each of these errors individually (i.e. assuming no instrumentation or other model errors contribute) and then combine them assuming they are independent.

2.3 Steady-State

The time dependent continuity equation, Eq. 1, includes the time rate of change of the tracer concentration, thus a complete solution will have include a term that accounts for the initial concentration. The CILTS method assumes that transient changes in concentration can be neglected, and so represents a source of error that depends on the difference between the initial and final concentrations.

$$\left(\frac{\delta Q}{Q}\right)_{steady-state} = \left(\frac{\delta A}{A}\right)_{steady-state} = -\frac{V}{S}\frac{\Delta C}{\Delta t} = -\frac{1}{A\Delta t}\frac{\Delta C}{C} \quad \textbf{(4)}$$

The bias from this error at could be corrected if we knew the initial and final concentration. Since CILTS only measures the average concentration over the sampling period, we cannot correct the result without some prior knowledge of the system. For instance, if we know that the initial concentration was zero, Eq. 4 can be used recursively to correct the CILTS result. However, as previously discussed, successful implementation of the CILTS method requires sufficiently long sampling times that these transient changes in concentration, which should make this error quite small. We shall assume this is the approach taken and that any calculable biases have been taking into account.

2.4 Constant Air Exchange

A sufficiently long sampling period is necessary to allow for the transient changes in concentration to be neglected. The air exchange rate, however, will most likely vary over the sampling period, so the tracer gas concentration will be varying over time. The CILTS

method measures the average concentration, but the air exchange rate is inversely related to the concentration. Thus, the CILTS analysis will underestimate air exchange rather than providing in a true average air exchange rate. This effect has been previously investigated (Sherman LBL-23088). If the variation is small, the bias can be corrected for, however, the bias can be intractably large if the variation in air exchange is large - as might be the case for an experiment where windows are opened and closed during the testing or the weather changes significantly. This magnitude is important when the measured average air exchange rate is used for energy calculations. However, some analyses do not use the average air exchange, but rather the effective air exchange as described by Sherman and Wilson (1986). For instance, the effective air exchange is more useful for understanding the dilution of indoor contaminants. The CILTS method does not result in a bias in the effective air exchange rate from variations in tracer gas concentration that occur during the measurement period.

2.5 Homogeneity

The CILTS analysis assumes that the space can be treated as a single zone and that the concentration is the same everywhere in this zone. Incomplete mixing, however, can result in substantial variability in tracer concentration within the zone resulting in a measured concentration that may not be representative of the space as a whole. In addition, the average concentration measured in the zone may not be the representative concentration needed in the CILTS analysis. The continuity equation requires that the representative concentration must be the flow-weighted average concentration of the air flowing from the space to outside.

To investigate the errors due to inhomogeneity, we have broken down the putative single zone into a set of N interacting multizone spaces starting from the derivation of Sherman (1989). The results show that, even if the average concentration could be measured with minimum uncertainty, there would be an error in the calculated average air exchange rate induced from the spatial inhomogeneity as follows:

$$\left(\frac{dQ}{Q}\right)_o^2 = \left(\frac{dA}{A}\right)_o^2 = N\frac{d^2C_o}{C^2} + N\frac{d^2S}{S^2} \qquad \textbf{(5)}$$

This is a new term not usually considered in error analysis, but can be combined with other errors in a straightforward manner

3 ERROR ANALYSIS OF CILTS DATA

An intensive investigation of the CILTS method was recently performed in three test homes (Lunden et al, 2012)), which can only be summarized herein. The tests used multiple simultaneous PFTs sampling at high spatial density in multiple configurations to evaluate the precision of the technique and to provide guidance on the best way to deploy it. This data set, hereafter referred to as the "Lunden data", is uniquely able to help us examine the errors that result from the CILTS method using the error analysis presented above. Each test house used four different PFTs with different sample densities and two different sampling methods essentially resulting in four separate experimental measurements of the same air exchange rate. The differences between the experiments serve to identify which factors are most important with regards to experimental uncertainty. In addition, the high spatial density of sampling locations in the experiments – larger than a typical experiment – will help to quantify the spatial variability in tracer concentration.

The experiments were designed to investigate a series of ventilation conditions. These experimental ventilation conditions included no forced air system operation, normal operation of an air conditioner, constant operation of the forced air system fan, and other variations. Estimates of precision and bias errors that are the same for each experiment are as follows:

- Emission source: The PFTs emission sources were the same for all experiments, and consisted of liquid in a glass vial with a septa through which the gas diffused. The vials were placed in dry block heaters to keep the emitters at a constant temperature. The emission rate for each vial was measured gravimetrically on site using a high precision scale, which generally give results on the order of 1% or better. The accuracy of these scales can be hard to assess, but can be assumed to be on the order of 1%. Sources can sometimes undergo more transport and handling that will affect the precision of the measured emission rate, i.e. when sources are shipped to and from experimental locations by mail. For these situations, the precision error may be on the order of 5%.

- Collection and Transport: In the Lunden data, there were large numbers of emitters and, most importantly, samplers. We shall assume that any precision errors due to sample collection will be reflected in any inhomogeneity of the measured concentrations, and will thus only consider bias errors. While there is no evidence of a significant bias in sample collection, for the purposes of this analysis, we shall assume a bias error of 3% and no transportation error.

- Analysis: The tracer gas analyser had a precision error of 5%. This uncertainty reduces as multiple sampler are used to estimate the mean concentration. During the analysis of the tracer gas samples, a significant bias was discovered and corrected, with no residual bias reported. For the purposes of this analysis, we shall assume a bias error of 2%, which is not reduced by multiple samples.

One of the samplers used in the experiment collected time resolved gas samples, resulting in 15 measurements of the tracer gas concentration every 24 hours. While these concentrations were averaged in order to calculate the average ACH over the experimental period, the time resolved results provide a measure of the size of the time varying concentration term. We estimate the magnitude of this variation as the average concentration plus and minus two times the standard deviation of the time resolved measurements. The variation in concentration generally occurs over a 24-hour period. Using these estimates, the magnitude of the time varying term ranges from 3% to 16%. For our experimental homes, the largest values tended to occur when there was no central air handling fan operating. The average value of the time varying term for all conditions with central forced air fan operation was 4%.

Putting this all together (assuming we have many samples), the Lunden study error becomes

$$\left(\frac{dQ}{Q}\right)^2_{effective} = \left(\frac{dA}{A}\right)^2_{effective} = \left(\frac{1}{ADt}\frac{DC}{C}\right)^2 + 0.0034 + N\left(0.0001 + \frac{d^2C_o}{C^2}\right) \quad \textbf{(6)}$$

If we disregard the time varying term and assume that the space is truly a homogeneous single zone, the air exchange rate resulting from the CILTS method as deployed by Lunden et al (2012) would have an uncertainty of 6%. Assuming a value of 4% for the time varying term increases the uncertainty to 7%. These uncertainty estimates represent the minimum uncertainty in the measured air exchange rate. It is highly unlikely that the tracer gas concentration in a home would ever be truly homogeneous. The extent to which spatial

homogeneity contributes to the uncertainty can be assessed for the Lunden data due to the relatively high spatial density of samplers deployed in their experiments.

3.1 House 1

House 1 in the experiments conducted by Lunden et al (2012) is a 93 m^2 single story house with a simple, compact floor plan. Four different PFTs were deployed, each with a different spatial distribution of emitters, and in some cases, samplers. The tracer gases were over-sampled (i.e., using more locations) compared to a typical CILTS measurement to allow a better estimate of the spatial variation. In their report, Lunden et al. (2012) divided the space into 9 zones. Some of the zones are small enough to ignore or sufficiently well coupled to be considered a single zone. As a result, we shall assume 4 zones in our error calculations, recognizing that this may be an under estimate. The air handler in house 1 turns over the air seven times per hour.

In the test in which the central air handler was not run the average air exchange rate from the four tracers was 0.5 ACH with a standard deviation from the different tracer approaches of 13%. The four tracer gasses all showed a spatial variation on the order of 20% (16%-22%). Using Equation 10 to estimate the error we expect an uncertainty of 40%. This value is much larger than the 6 to 7% uncertainty due to all other sources of error and bias, showing that the heterogeneity in the measured tracer concentration dominates the overall uncertainty of the measured air exchange rate. The air change rate measured with this data has an unknown bias, but the standard deviation of 13% between the four tracer gases is well within the 40% estimate of the overall uncertainty.

The average air exchange rate for the experiment with constant central forced air fan operation was 0.87ACH with a standard deviation of 29%. This is higher than with the air handler off likely due to the contribution of duct leakage and with a larger standard deviation between the four tracers. The average spatial variation, 12%, was smaller for this condition, but had a larger range of values. The larger range of spatial variation is largely due to the results from tracer 3, which had only two emitters in the house. Discounting this value, the total uncertainty we would expect in this test is 18% but because of the outlier we see 25%.

Lunden attributes the outlier to the fact that the concentrations analyzed were low and close to the detection threshold for the analyzer. This type of error can happen because of the difficulties of knowing the air exchange rate and therefore the required emission rate as well as the appropriate number and location of emitters and samplers before starting the experiments. This problem is particular to these passive measurements that lack the instant feedback from real time measurements.

3.2 House 2

House 2 was a 325 m^2 ranch style home with a long narrow floor plan. This house had two central forced air systems and with them both operating the air was circulated 4.3 times per hour. The house was divided into 9 zones. Unlike the more compact configuration of house 1, these zones do not combine so easily and 9 may be an under-estimate. In the error calculations, we shall use 9 as the physical number of zones.

During economizer operation, one of the central systems supplied air from outside at the airflow rate used by the central system in normal recirculation mode – in this case about 3 ACH. This is a much higher flow than natural infiltration or most mechanical ventilation. For the three experimental conditions, it appears that the results from the tracer which has only one emitter, has a higher spatial variability than that observed for the other three tracers.

This is similar to the results for house 1, where there was a significantly higher spatial variability for one of the experimental conditions for the tracer with only two emitters.

In normal operation, we see a tracer variation of 15%-28% averaging to 18%. An 18% variation corresponds to an estimate ACH total uncertainty of 55%. The average measured ACH from the 4 tracer gasses is 0.27 ACH with a standard deviation of 10%. Similarly, the concentration variation for the Continuous Fan data is between 12% and 22%, with an average of 15%, leading to an overall estimated uncertainty of 45%, while the measured air change is 0.42 ACH with a standard deviation of %. When the system utilizes an Economizer fan, which operates occasionally, the variation in concentration is between 10% and 25% with an average of 20%, leading to an estimated uncertainty of 60%. The measured air change rate is 0.29 ACH with a standard deviation of 7%.

We note that the standard deviations of our measured values are significantly smaller than our estimated uncertainty. If all one cared about were repeatability this would indicate that our error estimate was too large, but our error estimate includes errors caused by model violations—in particular the fact that the average concentration may not be the same as the exfiltration weighted concentration. An example of this from the House 2 experiments was that a couple of rooms on the windward side had slightly open windows. This resulted in a net flow of air across the house leaving the windward rooms at lower concentrations. These rooms likely had less exfiltration and the samples from these rooms should have been weighted less. Thus we might expect a positive bias in the results, i.e., the experiment overestimated the air change rate.

The increased mixing due to central forced air heating and cooling system air handler operation reduces the variability in concentrations from zone to zone. It also shows increased air exchange - probably due to leaky ducts. The improvement in homogeneity is most noticeable for the experiments that had the fewest number of emitters.

3.3 House 3

House 3 experiments were designed to evaluate the effects of different distributions of emitters. House 3 was a 237 m^2, 3 story, open-plan house. Unlike houses 1 and 2, the tracer gas emitters were placed differently in house 3. Each floor had a unique tracer associated with in order to quite clearly see distribution patterns. In addition, one tracer was evenly distributed. Operation of the air handler fan introduced 3.4 ACH of internal mixing. House 3 was divided into 12 zones within the space spread over 3 floors. Because of the large stack effect in this home, there are generally much larger differences in tracer gas concentration from floor to floor than between most rooms within a single floor. Since the spatial variability is driving by vertical stratification in the house, we shall the three floors as the number of zones.

If we look at the case where the tracer was emitted everywhere the air exchange was 0.26±40% when the air handler was not running and 0.3±29% when the air handler was running. (Based on a concentration inhomogeneity of 23% and 17% respectively.) Since the natural ventilation air change rate was stack dominated for this house we would expect that the single tracer emitted only on the lower floor would give results similar to the tracer emitted everywhere. The air exchange for this single tracer was 0.26±47% with the air handler off and 0.32±9% with the air handler on confirms that this is indeed the case. By contrast if we use the data from the tracer injected only on the upper floor the result is quite different: 1.3±211% with the air handler off and 0.98±124% with the air handler on. The very large positive bias is the result of there being very little third floor tracer on the lower

two floors due to the internal stack driven airflow from the lower to upper floors. These results indicate that if sampler locations are poorly chosen the errors are so large that the results are not useable. Again, we have the problem for passive methods that we do not know a priori (or even during the experiment) that these errors are occurring. The best we can do to minimize this problem it to emit and sample tracers on all floors of buildings and in more than one location per floor.

Averaging tests for all four tracers gives an average of 0.56 ACH±156% (based on a 90% concentration inhomogeneity) with the air handler off and 0.48 ± 121% (based on a 70% inhomogeneity) with the air handler on. The vast majority of the differences between the tracer gases is due to the very high air flow rate estimate from the tracer emitted only on the upper floor. This also biases the mean of the four tracers to be much higher than for the tracer emitted everywhere or the tracer emitted on the ground floor.

Additional experiments were performed in house 3 with interior doors closed and a kitchen exhaust on the second floor operating. With no air handler fan, this mode of operation showed the biggest special variation for each tracer with a range of 68% to 196% and a mean of 114% for an estimated error of 197%. The mean of the four tracer gas results was 0.52 ACH. With the air handler fan operating the spatial variation was reduced to a mean of 64% with a range of 19% to 146% (for an error estimate of 111%) and the mean of the four tracer gas results was 0.48 ACH. This result shows that even with the air handler operating it could not overcome the compartmentalization due to closed doors combined with tracers not emitted uniformly throughout the house.

4 RECOMMENDATIONS FOR CILTS APPLICATIONS

CILTS can be an accurate and precise method for determining air exchange when the system being measured matches the model assumptions—in particular that the air exchange and source emission be constant and that the system is in fact a single, isolated, well-mixed zone. Such a situation may occur in the laboratory or field studies with low air exchange rates and high internal mixing (e.g., due to operating a central forced air heating or cooling system air handler).However, CILTS is most used in situations where we know the assumptions are violated to at least some non-trivial degree. The uncertainties associated with these violations can be minimized by careful experimental design and deployment. The recommendations below will reduce the uncertainty of the CILTS result:

- *Emission Rate*: The emitters typically used by CILTS are passive emitters whose rate changes slowly over time, but more importantly is a function of temperature. The emitters should be placed in a temperature controlled environment to keep their emission rate constant during the experiment. The emitters should be calibrated for each experiment or they should be gravimetrically weighed before and after each experiment such that the total amount of emission is determined and no extrapolation of the concentration calibration curve is necessary to analyse the samples.
- *Emitter Deployment*: Emitters should be deployed in proportion to the local ***in***filtration to improve homogeneity. Of course the infiltration is not actually known; so this becomes a judgment by the experimenter. In many instances the best strategy is to deploy them evenly around the perimeter on all floors of the building. In instances where we know the air flow patterns, such as in the winter in a stack-dominated building, we know that the infiltration will predominantly happen in the lower parts of the building; so our emitter deployment should be predominantly in the lower parts of the building
- *Sampler Deployment*: As with the emitters, if we have no a priori knowledge, the samplers should be deployed evenly throughout the building. However if we can predict some of

the air flow patterns in advance the emitters should be placed near areas of ***ex***filtration. For example, if there is a prevailing wind direction, the samplers should preferentially be placed away from the windward side.

- *Sampler Number*: At least four samplers should be used per floor, and more in a large or complex floorplan. We recommend using a sampler for every 25-30 sq. m). An advantage of using multiple samples in addition to improving special averaging is that we can use the results to improve uncertainty estimates based on the standard deviation of the sampler results.
- *Mechanical Mixing*: When additional mixing (e.g. by use of air handler) can be applied it will improve homogeneity and reduce uncertainty. Care must be taken, however, to assure that the mixing does not change the system being measured
- *Experiment Duration*: To avoid issues from initial equilibrium transient effects a good practice is to deploy emitters for 24 hours before sampling begins. If this cannot be done, the integration time for CILTS must be at least 24 hours and preferably longer—especially for low air change rates. The integration time, however, should not be so long that the fundamental flow paths have changed—for example going from a stack dominated to wind dominated pattern. In such a case there will be a bias to the results and the estimate of the uncertainty from the spatial concentration variance will be under estimated.

5 CONCLUSIONS

We have taken oversampled field measurements with multiple gases and sampler/emitter locations and combined them with an error analysis to show that the CILTS method can have an uncertainty of 10-15% under ideal conditions. Ideal conditions include quality calibration of experimental equipment, correct placement of samplers and emitters relative to air flow patterns in the building, and a constant ventilation rate.

Deviations from ideal conditions include several issues related to effective sampling. Overall the most important factor about the system is the degree of mixing. It is not enough to measure the average concentration correctly as spatial inhomogeneities themselves introduce additional uncertainties. The experimental data suggests that even with optimum emitter and sampler placement, CILTS uncertainties of 20-25% should be expected when no special provisions are made for mixing.

When the infiltrating and exfiltrating flows are not evenly distributed around the parts of the building errors increase. The induced errors can, in principle, be mitigated by careful placement of the samplers (near exfiltrating areas) and the emitters (near infiltrating areas). This requires that those patterns persist through the experiment and that the experimenter knows what the pattern is.

Another factor related to persistence is the errors caused by having the air exchange itself vary during the course of the experiment. Variations in the air exchange have a biased effect on the inferred average air change rate independent of the issues of mixing and the need to change the optimal deployment. CILTS measures the effective air exchange not the average air exchange. The effective air exchange is the value relevant for dilution and most IAQ purposes, but not for energy purposes.

In general CILTS is not a very good method for estimating air exchange when there are large intermittent air exchanges going on (e.g., through open windows). In most circumstances it will be practically impossible to deploy samplers and emitters to accommodate this situation

and it is unlikely that sufficient mechanical mixing can be supplied to minimize its impact. CILTS is best deployed over a period of time where the weather conditions are stable such that the air exchange is reasonably constant..

The typical use of CILTS is in high-volume or low cost situations where it is deployed by technicians (or even occupants) who are not highly trained in its application. Very often no prior estimate of the air exchange (rate or pattern) has been made. Under these more typical conditions, one might consider CILTS to provide results in the range of a "factor of 2" of the right answer.

6 ACKNOWLEDGEMENTS

Funding was provided by the U.S. Dept. of Energy Building Technologies Program, Office of Energy Efficiency and Renewable Energy under DOE Contract No. DE-AC02-05CH11231; by the U.S. Dept. of Housing and Urban Development Office of Healthy Homes and Lead Hazard Control through Interagency Agreement I-PHI-01070; by the U.S. Environmental Protection Agency Office of Air and Radiation through Interagency Agreement DW-89-92322201-0 and by the California Energy Commission through Contract 500-08-061.

7 REFERENCES

ASTM, E741-00 (2000) Standard test method for determining air change in a single zone by means of a tracer gas dilution, *American Society for Testing Materials*, West Conshocken, PA.

D'Ottavio, T.W., Senum, G.I., and Dietz, R.N. (1988). Error analysis techniques for perfluorocarbon tracer derived multizone ventilation rates. *Building and Environment*, 23(3), 187-194.

Leaderer, B.P., Schaap, L., and Dietz, R.N. (1985) Evaluation of the perfluorocarbon tracer technique for determining infiltration rates in residences. *Environ. Sci. Tech*., 19, 1225-1232.

Lunden, M., Faulkner, D., Heredia, E., Cohn, S., Dickerhoff, D.J., Noris, F., Logue, J., Toshifumi, H. Singer, B. and Sherman, M. 2012. *Experiments to Evaluate and Implement Passive Tracer Gas Methods to Measure ventilation Rates in Homes.*

Sherman M.H. , "Uncertainty in Air Flow Calculations Using Tracer Gas Measurements", *Building and Environment*, 24(4), pp. 347-354, 1989. [LBL-25415]

Sherman, M.H., "On Estimation of Multizone Ventilation Rates from Tracer Gas Measurements," *Building and Environment* 24 355-362, 1989. LBL-25772.

Sherman, M.H., "Analysis of Errors Associated with Passive Ventilation Measurement Techniques," *Building and Environment* 24 (No. 2): 131-139, 1989. LBL-23088.

Sherman, M H., and David J. Wilson. "Relating Actual and Effective Ventilation in Determining In-door Air Quality." *Building and Environment* 21, no. 3/4 (1986): 135-144.

ON INVESTIGATING INSTANTANEOUS WIND-DRIVEN INFILTRATION RATES USING CO_2 DECAY METHOD

Dimitrios Kraniotis*, Tormod Aurlien, Thomas K. Thiis

Department of Mathematical Sciences and Technology, Norwegian University of Life Sciences
Drøbakveien 31, P.O. box: 5003, IMT, N-1423, Ås, Norway
**Corresponding author: dimitrios.kraniotis@umb.no*

ABSTRACT

Carbon dioxide has been already recognized as a potential tracer gas towards estimation of the mean air exchange rates (ACH) of a room or building. The wind direction and mean wind velocity have been also clarified as critical factors that affect the air infiltration. In this study, the indoor CO_2 concentration is detected and logged at three specific points in an office room for seven selected measurement-periods. The decay method is used to estimate the leakage rates. In parallel, an ultrasonic anemometer is used outdoors for monitoring wind characteristics, as the direction angle and the instantaneous velocity components, while the turbulence intensity is calculated. The results of ACH vary from $0,32h^{-1}$ to $0,75h^{-1}$ from measurement to measurement and thus an investigation is carried out from the perspective of unsteady windy conditions. A spectral analysis of the wind measurements is applied and the corresponding power spectra $S_{vv}(f)$ are correlated to the mean ACH of the room, giving a better understanding of wind-driven infiltration and depicting the role of the wind fluctuations frequency. In addition, a hypothesis of using the spatial distribution of CO_2 concentration indoors as airflow pattern tracer is presented respect to the location of the leakages and the local [CO_2] fluctuations are discussed as an indicator of leakage detection.

KEYWORDS

Wind-driven infiltration, Wind power spectral analysis, FFT, Turbulence intensity, Tracer gas, CO_2 decay method, Indoor building dynamics

1 INTRODUCTION

Air infiltration in buildings refers to the uncontrolled flow of outside air to the internal space through leakages in the envelope. Its impact on the energy consumption has been studied and clarified in a very early stage even (e.g. Caffrey, 1979; Persily, 1982; Anderlind, 1985). Air infiltration is caused either by wind-induced pressure differences across the building envelope or by the gradients between internal and external temperatures (Etheridge and Sandberg, 1996). Especially when the buoyancy forces are small, the wind-driven infiltration could potentially be the dominant mechanism (Shaw, 1981). The influence of climate characteristics, as the wind direction and the wind speed has been stated as factors that affect the air exchanges (Sherman, 1987).
Furthermore, the dynamic characteristics of air infiltration have been pointed (e.g. Hill and Kusuda, 1975) and therefore challenges arise upon that field. In particular, in low-rise

buildings the unsteady wind seems to govern the leakage rates (Brownell, 2002). Fluctuating wind causes unsteady flow phenomena that affect the instantaneous airflow rates across cracks and openings resulting to a deviation from the mean ones (e.g. Etheridge, 1999, Chaplin, 2000).
To estimate the infiltration rates of a building or a room, tracer gas techniques has been recognised as valuable and the their principles have been discussed (e.g. Sherman, 1990). In particular, carbon dioxide (CO_2) has been stated as a simple, cheap and proper gas to use for this purpose (Roulet, 2002). Recently, Labat *et al*. (Labat *et al.*, 2013) discussed the variation of the buildings air change rate (ACH) under natural conditions.
In this paper, CO_2 decay method is employed to estimate the mean leakage rates of a room and to correlate them to the wind direction and the wind velocity. In order to have a better understanding of wind-driven infiltration, a spectral analysis is performed providing additional information about the dynamic nature of wind and its impact on ACH. The results in the frequency-domain are presented and the role of the wind fluctuations frequency is discussed. Furthermore, the potential of using the indoors [CO_2] spatial distribution and the local [CO_2] fluctuations for leakages detection and as an airflow pattern tracer is asserted and linked to the outdoors wind conditions.

2 SETUP OF EXPERIMENT

2.1 Experimental field

The experimental work was carried out in the field of the meteorological station of the Norwegian University of Life Sciences (UMB) in Ås (59,66°N / 10,78°E). Figure 1a shows the field of the station and Figure 1b highlights the building in which the CO_2 measurement took place. The building is located at the south-west corner of the site. The orientation of the building deviates from the N-S axis by 6,5°. It consists of two compartments: an office room and a garage. The dimensions of each room as well as those of the whole building are shown in the Figure 2a.
The building is a typical Norwegian wooden construction of 70's (Fig. 2b). In particular, the garage is a non-heated space and consequently not insulated. Its external wall consists of only one layer (wooden cladding of 2*cm* thickness). In contrast, the office room is heated and insulated. The assembly of the external walls (~ 12,5*cm*) consists of five layers: wooden panel (1*cm*), vapor barrier, insulation (10*cm*), wind barrier and an external wooden cladding (1,5*cm*). The internal wall that separates the office from the garage is also insulated and wooden panels had been placed on both the interior and the 'exterior' surface (12*cm*). Finally, the ceiling is also insulated and its inner side consists of a wooden panel.
The measurements were carried out in the office room of the building. The dimensions of the net space of the room is 3,8*m* x 2,8*m* x 2,15*m* (V = 22,876m^3). The volume used hereinafter in the calculations refers to these dimensions. Figure 2c and 2d show the existence of a hole, in the north external wall of the building, in 2,1*m* height from the floor of the office room. The hole is circular (d_h = 2,5*cm*) and it services electrical issues as a cable (d_{cab} = 1*cm*) is fixed passing through. Based on the construction of the office room, it would be reasonable to claim that this hole constitutes a severe leakage path and probably the most important one. More precisely, the net area of the leakage-opening is ~ 4,12cm^2. In addition, the joints alongside the two windows of the room are taken into account as potential leakages. Finally, the door of the room was kept closed and sealed during the measurements.

Figure 1. (a) A satellite view of the experimental field and its surroundings. (b) The location of the building, at the SW corner of the experimental field.

2.2 Instruments

As mentioned above, the objective of this paper is to investigate the dynamic nature of air infiltration in buildings under unsteady wind conditions using CO_2 as tracer gas. In order to study the unsteady wind characteristics, an ultrasonic anemometer was used. Its principle is based on the transit time of ultrasonic acoustic signals. In particular, the following magnitudes were measured by the anemometer and logged in a PC: the three dimensional (3D) wind speed v, the three orthogonal velocities u, v and w, the wind direction angle θ_w, the wind elevation angle φ and the sonic-temperature of the ambient air.
The anemometer was placed on a mast at the same height as the hole-leakage (2,2m from the ground level) and in a distance of 11,5m from the north-oriented wall of the building (Fig. 1b). The sampling frequency was chosen as $f_w = 32Hz$, the fastest possible output rate given by the instrument, so that the dynamic wind characteristics would be detected. In order to be in harmony with other studies, the hourly 3D wind velocity on 10m from the main anemometer of the meteorological station was recorded as well.
For the purpose of measuring the infiltration rates of the office room, CO_2 detectors - loggers were used. In order to study the dynamics of the indoor, a frequency sampling of $f_g = 1Hz$ was chosen for logging the gas concentration. In total, three loggers were used, distributed at three different locations in the office room aiming to research the spatial variations of CO_2. The loggers were placed close to the hole-leakage (point A), close to the west-oriented window (point B) and the third one close to the sealed door (point C). All of them were on the same height that was defined as 0,8m. The logging points are noted in the Figure 2 by the red spots.
Finally, a pressurization test was applied in the office room, in order to get the air changes at 50Pa. The result showed that the $ACH_{50} = 8{,}17h^{-1}$, giving a general magnitude of the airtightness level. Consequently, following the relative 'rule-of-thumb', the annual infiltration rate of the room in operation is $n = 0{,}41h^{-1}$ (Sherman, 1998).

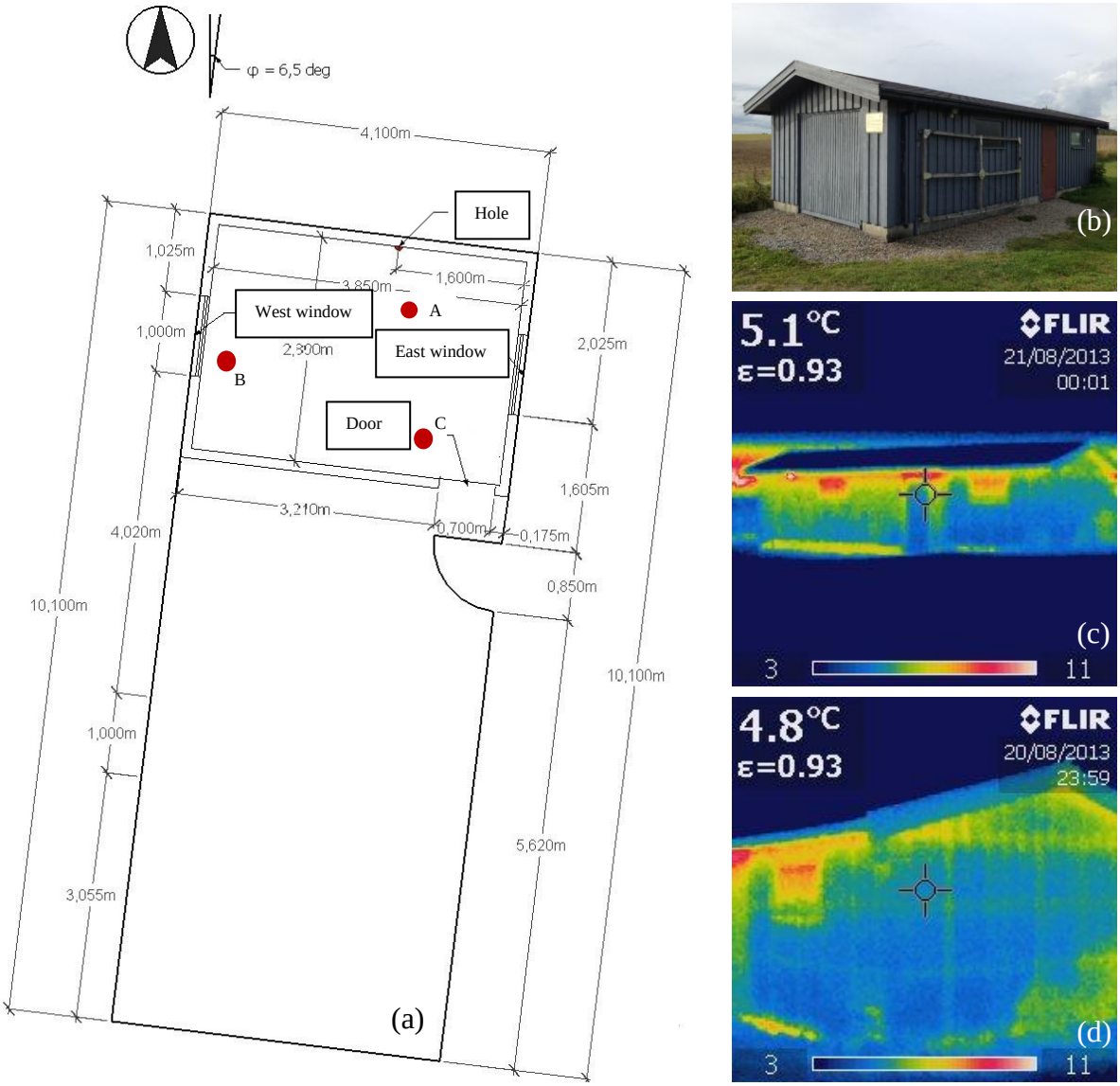

Figure 2. (a) Plan of the building, with the logging points A, B and C. The location of the hole across the north wall, the two windows and the door are shown as well. (b) The building is a typical Norwegian wooden construction of 70's. (c) Infrared picture of the building. (d) Infrared picture of the NE corner of the building.

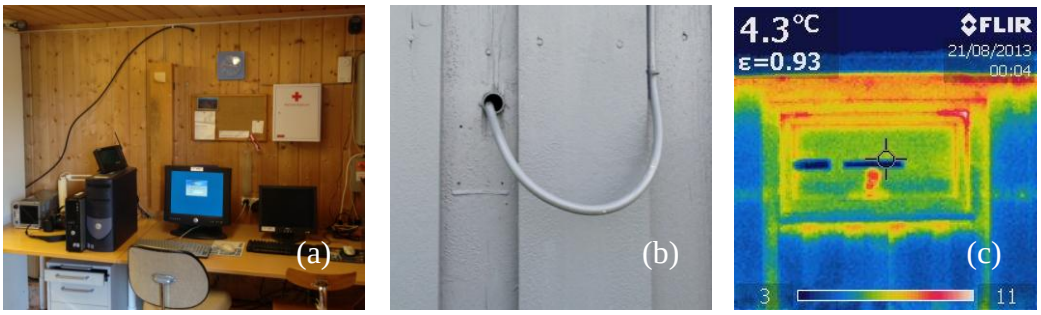

Figure 3. (a), (b) View of the leakage – hole, from inside and outside respectively. (c) Infrared picture of the leakages in the window that is west-oriented.

3 METHODOLOGY

The measurements were carried out during approximately periods of 3*h* on seven selected days and the annotation 'Day n' (n=1-7) is employed hereinafter. In order to have an overview of the wind conditions in each day, the Reynolds averaged wind velocity U was calculated as follows:

$$U = \overline{u^2 + v^2 + w^2} \quad (1)$$

where u, v and w are the three mean wind velocity components.
As mentioned above, the orientation of the building deviates from the N-S axis by only 6,5°. Thus, it is reasonable to claim that the longitudinal velocity component *v* in the axis N-S incidents by 90° angle on the north-oriented wall. In a similar way, we assume that the window close to the point B is west-oriented, while the other window east-oriented respectively.
The combined and synchronized use of an ultrasonic anemometer and CO_2 detectors with high sampling frequency provides the chance of investigating the dynamics of the wind-driven infiltration under unsteady conditions. Towards this scope, the calculation of the wind turbulence intensity I and the wind power spectrum, on each measurement day, seems to be helpful.
Wind turbulence can be generally described as fluctuations in the flow of air. The turbulence intensity is a scale characterizing turbulence as percent. In fact, it gives a picture of how large are the fluctuations of the wind flow compared to the mean value of the velocity. In other words, turbulence intensity *I* 'describes' the unsteadiness of wind and is calculated from the orthogonal velocity components *u*, *v* and *w* as follows:

$$I = \frac{\overline{\frac{1}{3}(u'^2 + v'^2 + w'^2)}}{\overline{u^2 + v^2 + w^2}} \quad (2)$$

where *u'*, *v'* and *w'* are the turbulent velocity fluctuations in E-W (lateral) axis, in N-S (longitudinal) axis and in the 'updraft' (normal) axis respectively. In the denominator, $U = \overline{u^2 + v^2 + w^2}$ is the Reynolds averaged velocity.
Furthermore, a spectral analysis is carried out in order to provide information about the wind energy distribution with respect to frequency. Thus, in this paper a Fast Fourier Transform (FFT) algorithm is applied into the fluctuations of the three orthogonal wind velocity components (here for the longitudinal velocity *v* in the N-S axis), in order to compute the Discrete Fourier Transform (DFT) and the frequency domain (Newland, 1975):

$$V'\,k = \sum_{n=0}^{N-1} v'\,n\; e^{-j2\pi nk/N} \quad (3)$$

where *V'*: the frequency domain representation of the wind fluctuations *v'* of the longitudinal velocity *v* in the axis N-S,
k: the k[th] frequency component,
n: the n[th] sample (in the time domain)
N: the total number of samples of *v*,
j: the imaginary unit.
Finally, the wind spectrum is calculated based on the following equation:

$$S_{vv}\ f\ =\ v'(f)\ ^2 = \int_{-\infty}^{\infty} v'(t)e^{-ift}dt \qquad (4)$$

In addition, the CO_2 'concentration test decay method' (ASTM – E741, 2006) is employed during the analysis of the data from the loggers placed indoors. In this way, the infiltration rates can be calculated in each case (day). The highest gas concentration that the loggers could detect and record was approximately 4000*ppm*. For each day, the initial and final times were determined and a normalized concentration C_N is calculated in each measurement time:

$$C_N = \ln \frac{C\ t\ - C_o}{C\ 0\ - C_o} \qquad (5)$$

where *C(t)*: the CO_2 concentration in the office room, as an average of the CO_2 concentrations detected in the three loggers,

C(0): the initial CO_2 concentration in the office room at t = 0*s*,

Co: the outdoors CO_2 concentration (it was about 410ppm).

Since the CO_2 concentration fluctuating as decaying, the 'average method' cannot be applied. Thus, in order to compute the ACH, the 'optional regression method' is used and a regression of ln*C(t)* needs to be performed according to (ASTM – E741, 2006):

$$\ln C_N = -At + \ln C_N(0) \qquad (6)$$

In the graphs of the C_N versus time a fitting line is added, the slope of which represents the mean infiltration rate ACH.

4 RESULTS AND DISCUSSION

4.1 ACH and wind characteristics

The normalized CO_2 concentration C_N for each measurement-day is computed and shown in the Figure 4. It is clear that the decay of the tracer gas is characterized by fluctuations. The necessary regression analysis is thus performed and the linear fitting line is presented in the Figure 4 along with the decay. As mentioned above, the slope of the fitting line is the mean ACH of the office room.

The values of the infiltration rates vary from 0,32h^{-1} to 0,75h^{-1}. The temperature gradients between outside and inside varies during the measurement-periods from 3$^{\circ}C$ to 7$^{\circ}C$, thus it would be reasonable to claim that the wind is the dominant mechanism of infiltration (Shaw, 1981). The lowest ACH took place on the day 1 and day 2 (ACH = 0,32 h^{-1}). During the measurement periods of those days the wind blows mainly from South (SSW-S on day 1 and SSE-S on day 2). The south-oriented side of the office room is wind-shielded, since it is the internal wall that separates the office from the garage. Given that the main leakages of the office are located on the east, west and north façade of the room, the relatively low ACH seem reasonable, despite of the large wind velocity (day 1: υ = 5,3*m/s* at 10*m* height and *U* = 3,7*m/s* at 2,2*m*, while for the day 2: υ = 5,0*m/s* at 10m and *U* = 3,4*m/s* at 2,2*m*).

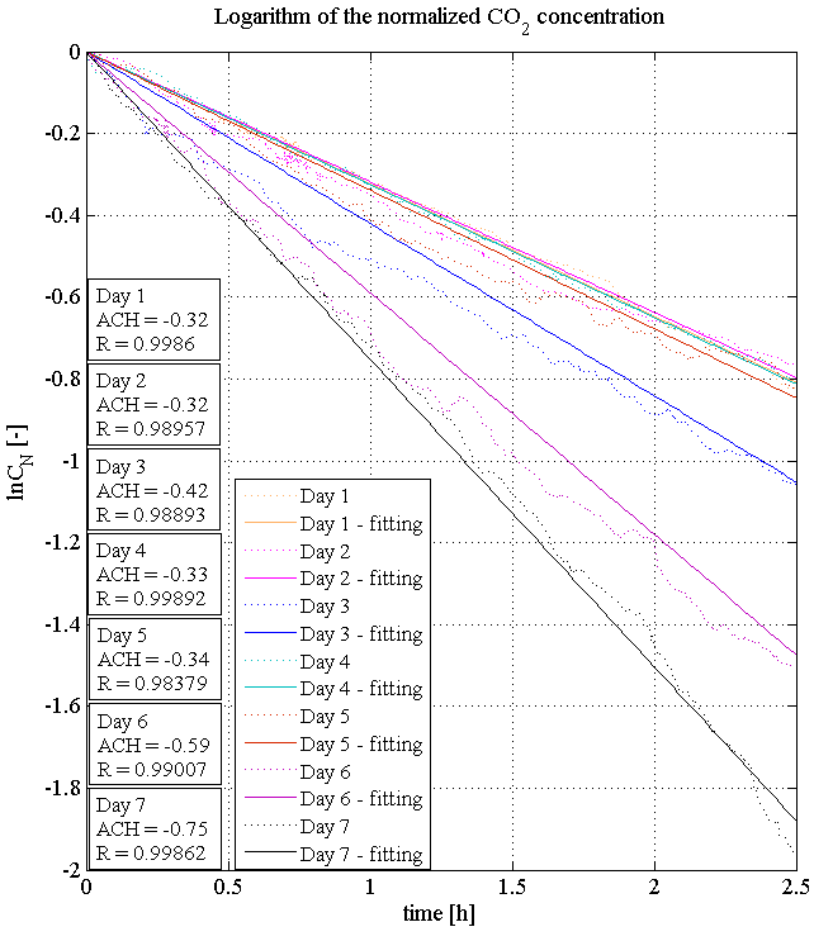

Figure 4. Logarithm of the average value of the CO_2 concentration in the three measurement locations versus the elapsed time since the start of decay.

During the days 3-7 the wind was blowing mainly from the North (or NNE and NE). A detailed overview of the wind direction angles during the measurements is provided in the Figure 5.

The higher infiltration rates during the days 3-7 can be explained by the fact that the north wall of the office room, where the hole is located, is in these cases exposed. Even though the wind direction is during those days fairly the same, the ACH vary from $0{,}33h^{-1}$ to $0{,}75\ h^{-1}$. The variations of the Reynolds averaged velocity U (or of 3D speed υ at 10m) can provide some arguments about these differences. Table 1 shows among other the 3D velocity υ at 10m, the Reynolds averaged velocity U at the height of the ultrasonic anemometer ($2{,}2m$) and the main wind direction angle θ_w. Since the main θ_w is in N-S axis, the respective wind velocity v was decided to be shown as well. In addition, the ACH rates for each measurement are summarized again and presented in Table 1 as well as the confidence intervals representing the dispersion of the [CO_2] around the fitting lines (using 99,9% confidence).

From the Table 1, it is clear that among the days 3-7 (that all correspond to the N or NE wind direction), the days 4 and 5 appear to have low ACH. Indeed, during these measurements the wind is milder compared to the other measurements. Thus, the impact of the wind velocity is getting justified as critical towards the estimation of building infiltration rates. In harmony with this, it is also the fact that during the day 7, when the highest velocity occurs ($\upsilon = 5{,}5m/s$ at $10m$ height and $U = 4m/s$ at $2{,}2m$), the ACH are the highest as well (ACH = $0{,}75\ h^{-1}$).

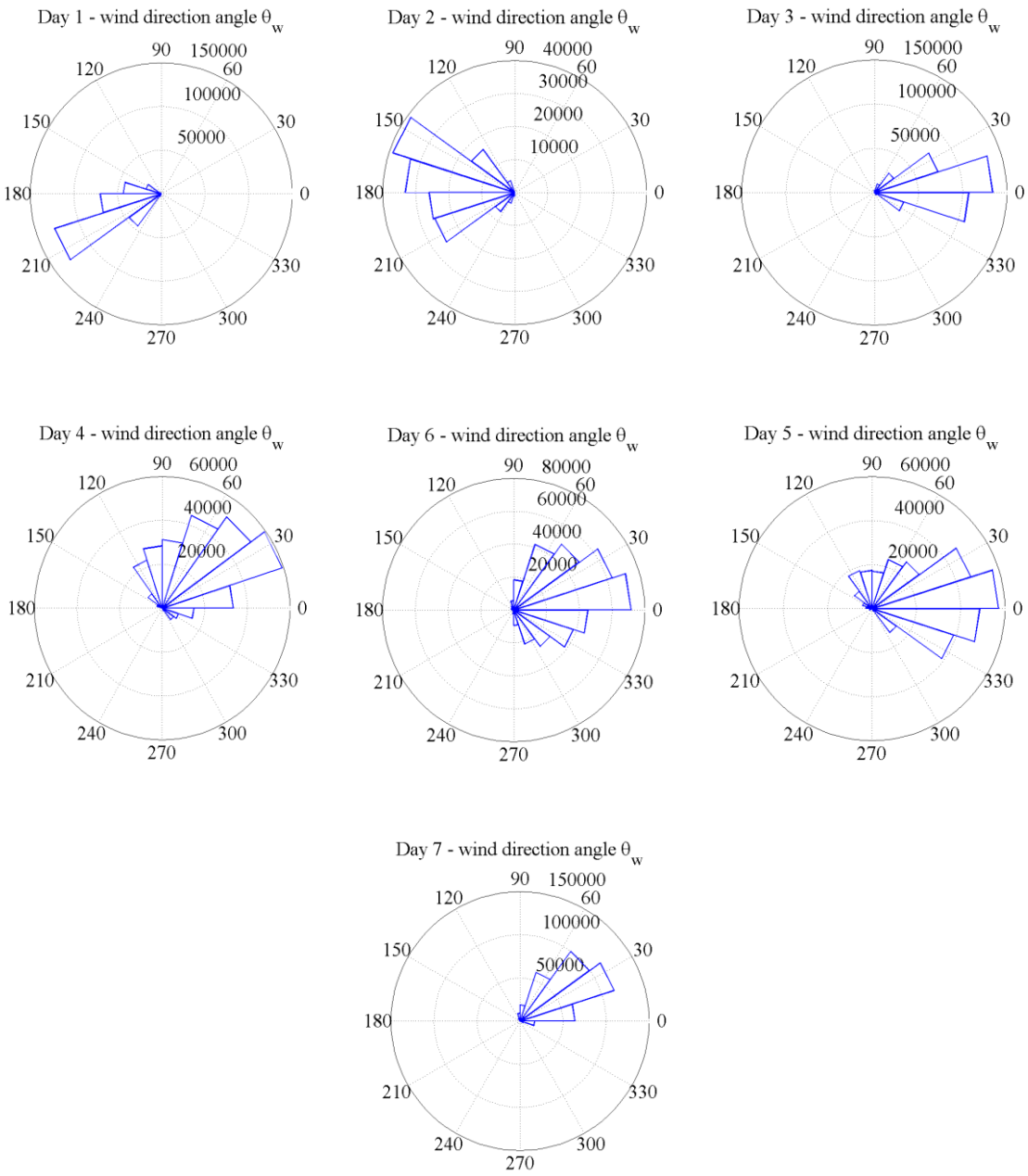

Figure 5. 'Windroses' depicting the variation of the wind direction angle θ_w during each measurement – day ($\theta_w = 0^\circ$ corresponds to North, $\theta_w = 90^\circ$ to East, $\theta_w = 180^\circ$ to South and $\theta_w = 270^\circ$ to West).

Table 1: Overview of the wind characteristics during the measurements and the respective ACH as calculated after a regression analysis applied.

	Wind speed *υ* (10m) [*m/s*]	**Reynolds averaged velocity *U* [*m/s*]**	**Wind velocity *v* in N-S axis [*m/s*]**	**Main wind angle θ_w [°]**	**Wind turbulence intensity I [%]**	**ACH [h^{-1}]**
Day 1	5,3	3,7	-3,2	SSW - S	28	0,32 ± 0,0004
Day 2	5,0	3,4	-3,0	SSE - S	36	0,32 ± 0,0012
Day 3	3,7	3,1	2,8	N	28	0,42 ± 0,0017
Day 4	3,4	2,5	1,2	NE	44	0,33 ± 0,0004
Day 5	2,9	2,1	1,5	N	47	0,34 ± 0,0016
Day 6	3,5	2,7	2,0	N - NNE	44	0,59 ± 0,0023
Day 7	5,5	4,0	2,9	NE	32	0,75 ± 0,0012

However, the results from the day 3 and 6 seem not to follow this 'rule'. In fact, even though the Reynolds averaged velocity *U*, as well as the longitudinal wind velocity component *v* in N-S axis, is higher in the day 3 than in the day 6, the ACH detected in the day 3 is lower than the respective in the day 6 ($ACH_3 = 0{,}42\ h^{-1}$, while $ACH_6 = 0{,}59\ h^{-1}$).
Thus, it would be reasonable to claim that neither the wind direction nor the wind velocity can fully play the role of safe criterion in order to determine the in-situ wind-driven infiltration. To research this 'disharmony' the turbulence intensity *I* (Table 1) and the wind power spectrum $S_{vv}(f)$ (Figure 6 and Figure 7) are computed, as has been described analytically in the methodology section. The turbulence intensity gives a magnitude of the amplitude of the fluctuations compared to the mean velocity. It can be extracted from the Table 1 that the intensity is not consistent with the results of ACH, thus no safe conclusion could be drawn.
In contrast to the intensity *I* (and the amplitude of the wind fluctuations) the wind power spectrum $S_{vv}(f)$ gives the energy distribution of the wind respect to the frequency of the fluctuations. The wind fluctuations frequency has already implied as critical parameter in a previous numerical study (Kraniotis *et al*., 2013). Since the wind angle is mainly North, the spectra of the longitudinal velocity *v* is decided to be presented.
As seen in Figure 6, even though the day 3 has slightly more energy than the day 6 in the very low frequencies (f~ <0,05*Hz*), the picture is opposite in higher frequencies. The spectrum of day 6 has more energy (two large peaks) than the respective of the day 3 in frequencies around $f = 0{,}15Hz$ ($0{,}1Hz < f < 0{,}2Hz$). Furthermore, the spectrum of day 6 seems also to include more energy than the day 3 in the high frequencies $0{,}5\ Hz < f < 1Hz$. In the very high frequencies, $f > 2Hz$, the two spectra appear to have similar picture.
Consistent with the previous research are the spectra of the other measurements as well. The day 7 seem to contain the higher energy among the measurement-days 3-7 in the frequencies f > 0,5Hz. Moreover, it appears to have by far higher energy than the other spectra in the very high frequencies f > 1Hz. The spectrum of the day 4 (that has the lowest ACH among the days 3-7) shows the highest energy in the very low frequencies (f ~ 0,03*Hz*), but it contains very little in the high frequencies (for $f < 0{,}7Hz$). The spectrum of the day 5, that it has also low ACH, seems to have fairly similar picture to the latter in the high frequencies. After all, it would be reasonable to claim that the high wind frequencies can play a determined role towards the evaluation of building ACH rates.

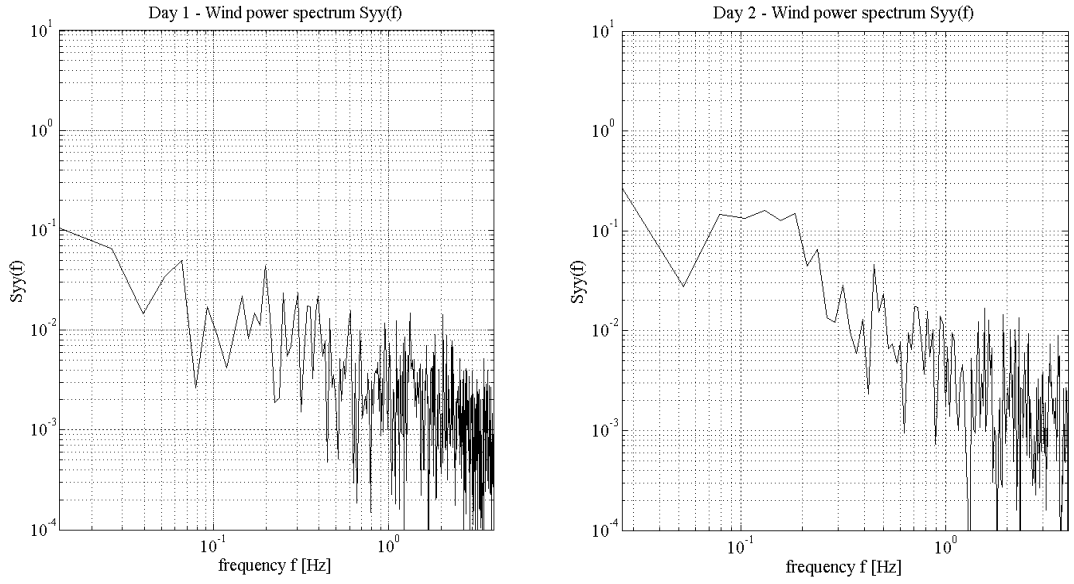

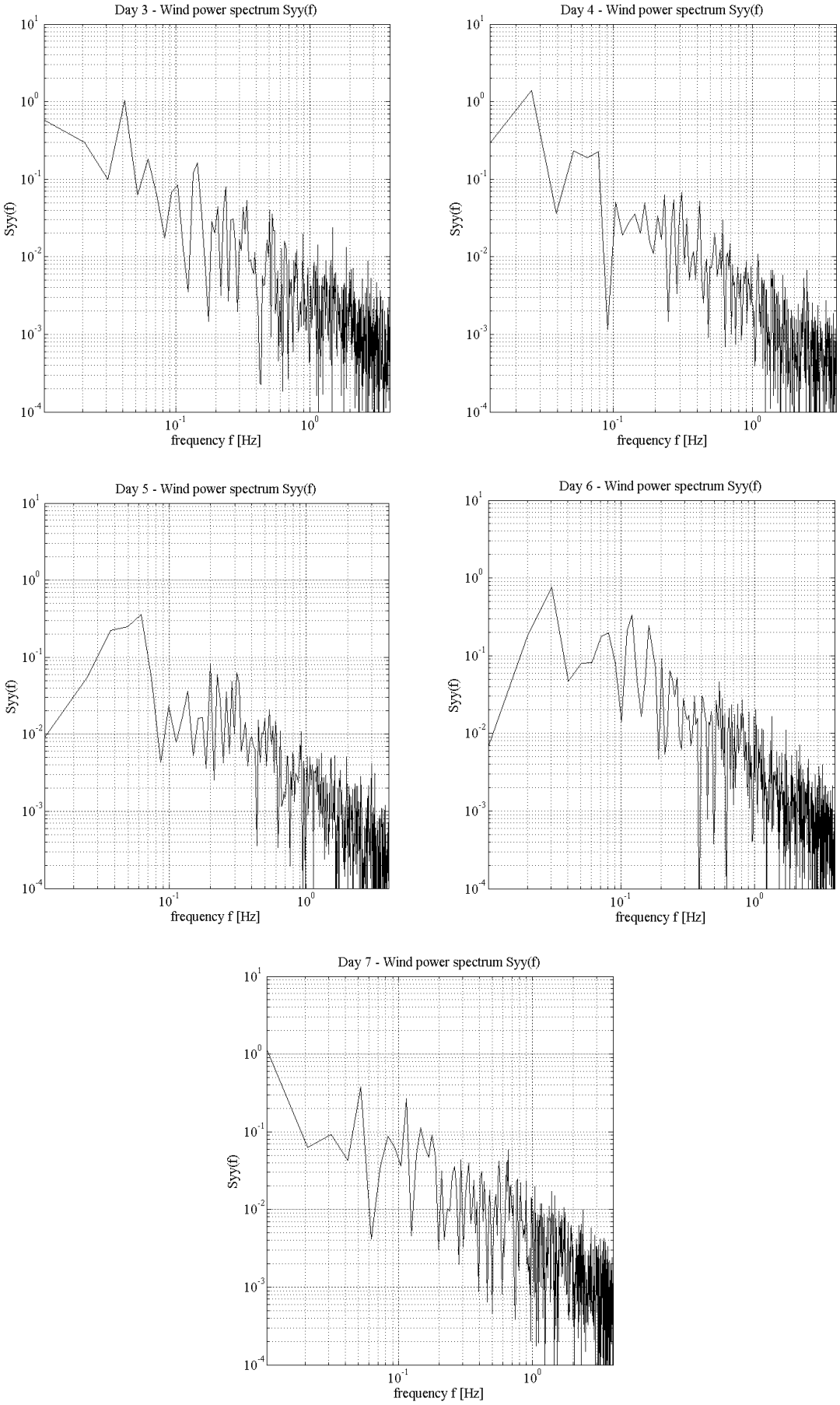

Figure 6. Wind power spectra of the longitudinal wind velocity *v* in the axis N-S.

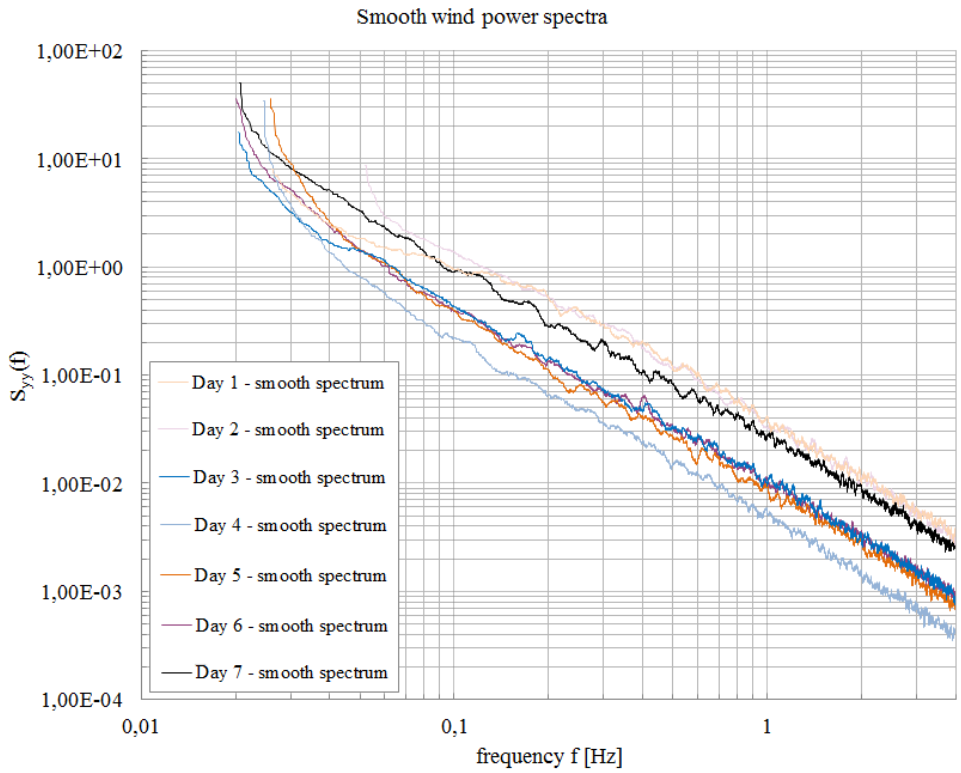

Figure 7. Smooth wind power spectra of the longitudinal wind velocity *v* in the axis N-S.

4.2 Spatial distribution of [CO_2]

Among the objectives of this paper is also the investigation of the spatial distribution of the CO2 concentration as well as its time variation. Detecting and logging the [CO_2] at multiple positions in the room may provide information regarding the indoor airflow patterns. The hypothesis is based on the fact that when the air enters the room is getting accelerated close the respective leakage (from it mainly enters), resulting in relatively higher ACH. In contrast, relatively lower ACH could imply a 'recession' of air flow, tending to a more 'stationary' regime. It should be noted that the logging-points A and C are located on an imaginary axis N-S, while the logging points B and C on an axis E-W. Figure 7 shows the ACH as calculated in each logging-point (A, B and C) after the regression analysis applied.

For the measurement-day 1, when the wind direction is SSW-S, it happens that $ACH_C = ACH_B > ACH_A$. Following the hypothesis stated above, the air flows from the axis C - B $\rightarrow$ A. Indeed, respect to the wind direction, it would be reasonable to claim that the air may enters from the west-oriented window, which is very close located to the logging-point C and then it follows the 'axis' C – B. It finally results into the point A, which is north-oriented and consequently well-shielded from a SSW-S wind.

For the measurement-day 2, $ACH_B > ACH_C > ACH_A$. In this case the wind direction is SSE-S, it could be assumed that the air mainly flows into the room from the east-oriented window (close to logging point B) and following the 'axis' B – C, results into the leakage A.

All the measurement-days 3-7 (apart from the day 3) seem to respect the hypothesis as well respect to the corresponding wind direction. In all those cases it happens that $ACH_A > ACH_C > ACH_B$, implying that the air enters from the leakage A and respecting the mainly North wind, flows on the 'axis' A – C, which is parallel to N-S, and then is getting dissipated and 'stationary' at the point B.

Finally, table 2 shows the standard deviation σ of the ACH at each logging-point for all the measurement-periods. The values imply the 'fluctuations' of the [CO_2] at the certain point. It seems that for the point C the σ is higher compared to the points A and B, for all the cases. Given that the point C is close to the sealed door, it would be reasonable to claim that the [CO_2] fluctuates because of the wall boundary conditions on the that side of the office room. Again, the relatively small leakage area of the point C most likely 'blocks' the flow when it is normal (90° angle) to it, resulting in oscillations of the [CO_2]. In contrast a logger close to a relatively bigger leakage area may detects less [CO_2] fluctuations, as the air could exfiltrate or infiltrate more easily and the flow is more 'smooth', implying boundary conditions more similar to an 'opening'.

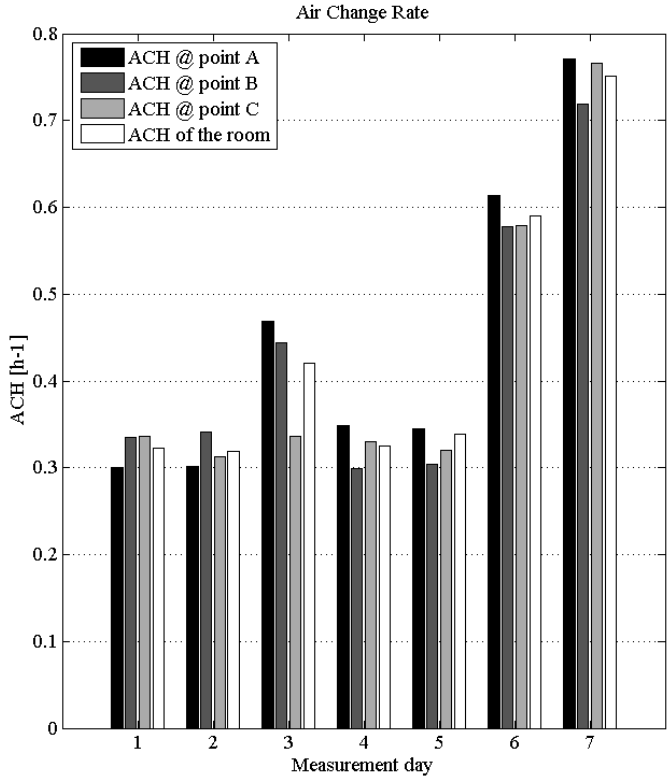

Figure 7. Air change rates (after the regression analysis) at each logging-point for each measurement-day.

Table 2: Standard deviation σ of the ACH at the three logging-points.

	Day 1	**Day 2**	**Day 3**	**Day 4**	**Day 5**	**Day 6**	**Day 7**
σ of point A	0,0139	0,0405	0,0705	0,0182	0,0534	0,0795	0,0410
σ of point B	0,0102	0,0387	0,0726	0,0160	0,0371	0,0998	0,0407
σ of point C	0,0304	0,0481	0,0834	0,0392	0,0675	0,1008	0,0607

5 CONCLUSIONS

The indoor CO_2 concentration ([CO_2]) is detected and logged at three specific points in the office room of the meteorological station of the Norwegian University of Life Sciences

(UMB). In parallel, an ultrasonic anemometer is used outdoors for monitoring wind characteristics, as the direction angle and the instantaneous velocity components. In total seven measurement-periods are presented in this paper.
The CO_2 decay method is employed to calculate the infiltration rates of the room in each measurement (day 1-7), using a regression analysis. The results show that ACH vary from $0{,}32h^{-1}$ to $0{,}75h^{-1}$. The south wall of the room is wind-shielded and the lowest values take place when the wind is South, justifying the influence of wind direction angle. However, the ACH show large differences even among the measurement-days that the main wind direction is the same (North wind). A study on the wind speed, the Reynolds average wind velocity and the longitudinal velocity component provides some arguments for the variation of the leakage rates. Nevertheless, the mean values of the wind velocity are not enough to explain the whole picture of ACH variation. Therefore, the turbulence intensity is calculated and a spectral analysis is performed in order to investigate the dynamic characteristics of the unsteady wind. The amplitude of wind fluctuations (turbulence intensity) cannot be straightforward correlated to the ACH, while their frequency characteristics (wind power spectra) provide a better understanding of wind-driven infiltration, implying the role that high wind fluctuations frequency and the potential to cause higher ACH.
Finally, a hypothesis of using the spatial distribution of $[CO_2]$ indoors as airflow pattern tracer is presented respect to the location of the leakages. It seems low $[CO_2]$ levels (and consequently high ACH) characterise positions close to where air flows into the room, while higher values of $[CO_2]$ (and consequently low ACH) take place at positions that the flow is getting recessed, described by a more 'stationary' regime. In addition, the fluctuations of the indoors $[CO_2]$ seem that potentially could be an indicator of the boundary conditions of the respective position. When the airflow is normal (90° angle) to relatively small leakage areas is reasonable to claim that is getting 'blocked' ('wall' boundary conditions), resulting in a locally oscillating phenomenon. In contrast, an area close to a relatively big leakage path is more likely characterized by a 'smooth' flow, when the angle is 90°, and thus the local $[CO_2]$ fluctuations may be relatively small, implying 'opening-type boundary conditions.
The paper sets up issues regarding the impact of the unsteady wind on the air exchanges. Maybe a more detailed study of the dynamic wind characteristics through a spectral analysis ought to provide a more detailed view of the wind-driven infiltration, especially in cases that the latter is more important mechanism than the buoyancy forces. Further research need to be done in order to enhance the results regarding the role of the wind fluctuations frequency and to investigate the local building dynamic phenomena with respect to the leakage magnitude and distribution.

6 REFERENCES

Anderlind, G. (1985). *Energy consumption due to air infiltration*. Proceedings of the 3rd ASHRAE/DOE/BTECC Conference on Thermal Performance of Exterior Envelopes of Buildings, Clear Water Beach, FL, 201–208.

ASTM International (2006). *Standard test method for determining air change in a single zone by means of a tracer gas dilution*.

Brownell, C., 2002. *Infiltration heat recovery*. Duke University, Durham, NC.

Caffey, G.E. (1979). *Residential air infiltration*. ASHRAE Transactions (85), 919–926.

Chaplin, G.C., Randall, J.R., Baker C.J. (2000). *The turbulent ventilation of a single opening enclosure*. Journal of Wind Engineering and Industrial Aerodynamics (85), 145–161.

Etheridge, D.W., Sandberg, M. (1996). *Building ventilation: Theory and measurement*. Wiley.

Etheridge, D.W. (1999). *Unsteady wind effects in natural ventilation design*. CIBSE National Conference, Harrogate

Hill, J.E., Kusuda, T., 1975. *Dynamic characteristics of air infiltration*. ASHRAE Transactions. (81)1, 168–185.

Kraniotis, D., Thiis, T.K., Aurlien, T. (2013). Wind direction and leakage distribution. A CFD transient analysis of their impact on air exchange rates under unsteady wind conditions. 6th European – African Conference on Wind Engineering, Cambridge, UK.

Labat, M., Woloszyn, M., Garnier, G., Roux, J.J. (2013). *Assessment of the air change rate of airtight buildings under natural conditions using the tracer gas technique. Comparison with numerical modelling.* Building and Environment (60) 37–44.

Newland, D.E. (1975). An introduction to random vibrations, spectral and wavelet analysis. Longman Scientific & Technical.

Persily, A. (1982). *Understanding air infiltration in homes*. Report PU/CEES No. 129. Princeton University Center for Energy and Environmental Studies, Princeton, NJ.

Roulet, C.A., Foradini, F. (2002). Simple and cheap air change rate measurement using CO_2 concentration decays. International Journal of Ventilation (1), 39–44.

Shaw, C.-Y. (1981). *A correlation between air infiltration and air tightness for houses in a developed residential area*, National Research Council Canada, Ottawa.

Sherman M.H. (1987). *Estimation of infiltration from leakages and climate indicators*. Energy and buildings (10), 81–86.

Sherman M.H. (1990). *Tracer-gas techniques for measuring ventilation in a single zone*. Building and Environment (25) 4, 365–374.

Sherman, M.H. (1998). *The use of blower-door data*, Lawrence Berkeley National Laboratory.

EXPERIMENTAL PERFORMANCE CHARACTERIZATION OF A NEW SINGLE ROOM VENTILATION DEVICE WITH HEAT RECOVERY

Samuel Gendebien[*1], Emeline Georges[1], Luc Prieels[2], and Vincent Lemort[1]

1 University of Liege
Thermodynamics Laboratory
Chemin des Chevreuils, 7
4000 Liège
Belgium
**Corresponding author: sgendebien@ulg.ac.be*

2 Greencom Development SCRL
Rue Gilles Magnée, 92/3
4430 Ans
Belgium

ABSTRACT

Nowadays, important efforts are made to reduce the residential building energy consumption. In this context, a growing interest for heat recovery ventilation has been observed during the last decades. The present paper focuses on a new single room ventilation with heat recovery. Double flow ventilation is achieved through the integration of the unit into windows ledges. The developed device is particularly suitable compared to traditional centralized heat recovery ventilation units for retrofitted houses due to the absence of air extracting and air pulsing ducts through the house.

The first part of the paper consists in describing the characteristics and properties of the developed device (volume, components, flow configuration, advantages and drawbacks).

In the second part of the paper, an experimental approach is presented to characterize the unit. The criteria of performance are based on:

- Thermal effectiveness of the unit (testing of a recovery heat exchanger),
- Hydraulic aspects (flows delivered by the unit vs energy supplied to the unit),
- Acoustic aspects.

The overall performance of the unit can be established based on the experimental results described here above. Cartography of performance (ratio between the recovered heat and the supply electrical power) can be drawn, depending on the flow rates delivered by the unit and the indoor/outdoor temperature difference.

The last part of the paper compares the new system with natural, simple exhaust ventilation and traditional centralized systems in terms of primary energy, consumer price and carbon dioxide emissions. Results show that the presented device seems more competitive than natural and simple exhaust ventilation for the Belgian climate. The single room ventilation investigated in this paper also shows better performance than most of the centralized ventilation systems tested on site.

KEYWORDS

Ventilation, heat recovery, laboratory measurement, air-to-air heat exchanger

1 INTRODUCTION

According to Pérez-Lombard (2008), in 2004, energy consumption of buildings represented 37% of the total final energy consumption of the EU, corresponding to a larger share than industry (28%) and transports (32%) sectors respectively.

The residential sector accounts for the major part (70%) of this building energy consumption. As referred in the Trias Energetica concept (2012), the first step to make a building climate-friendly is to reduce the energy demand by implementing energy-saving measures. To this end, the first retrofit options to be considered for existing residential buildings are the improvement of the thermal insulation and air tightness. Improving the building envelope tends to increase the relative part of the energy consumption due to ventilation. According to Roulet et al. (2001), more than 50% of the total energy losses can be due to ventilation losses, in building with a high thermal insulation. In this context, a large amount of heat recovery technologies have been developed in the last decades (Mardiana-Idayu and Riffat (2012)).

As referred by Fehrm et al. (2002), heat recovery ventilation dedicated to residential building started in the late seventies in Sweden. Heat recovery ventilation has now acquired a status of efficient ventilation strategy, especially for buildings with low or zero energy consumption (Handel (2011)). The supplementary study on Ecodesign Lot 10 (2012) estimates a potential market of 937500 mechanical heat recovery units to be met in 2025 in the EU 27, with an explosion of sales in the medium climate market. As reported by Wouters et al. (2008), this trend was already observed in Belgium (in the frame of the Walloon project *"Construire avec l'énergie"*) with an increasing of the share of the balanced mechanical ventilation systems.
Recently, a large amount of papers about heat recovery ventilation has been released in the scientific literature but these papers focus more precisely on the heat recovery exchanger. Adamski (2008a) carried out experimental studies and developed correlations on a longitudinal flow spiral recuperator. Fernandez-Seara et al. (2010) experimentally studied an off-the-shelf air-to-air heat recovery device for balanced ventilation. Kragh et al. (2008) also experimentally investigated a new counter-flow heat exchanger but focused more precisely on the frosting issue. A thermoeconomic investigation was carried out by Söylemez (2000) in order to optimize heat recovery exchanger size. Adamski (2008b) (2010) also estimated the financial effect due to the use of heat recovery ventilation instead of a simple ventilation system.
The present paper focuses on the performance characterization of a balanced single room ventilation unit with heat recovery. To the best knowledge of the authors, only the papers of Manz et al. (2000) and Schwenzfeier et al. (2009) presents experimental investigation of such units. The present investigated device is rather different in terms of components/flows configuration, dimensions and flow inlet/outlets geometry. Volume of the whole investigated unit is 0.041 [m^3] (1.05 X 0.148 X 0.265 [m^3]).
Finally, it should also be noticed that recent studies (Laverge (2011), Maripuu (2011)) investigated the potential of demand controlled ventilation (DCV), which could be particularly suitable with balanced single room ventilation.

2 PRESENTATION OF THE DEVICE

2.1 Centralized ventilation vs single room ventilation with heat recovery

As already specified, the principle of heat recovery ventilation is well-known, but most of already commercialized units are centralized (the supplementary study on Ecodesign Lot 10 (2012)), which involves air extracting and air pulsing ducts through the house. Usually, vitiated air is extracted from wet rooms such as bathroom, kitchen and fresh air is pulsed into dry rooms such as living room, bedroom (Dimitroulopoulou (2012)). This system is known in Europe as system D with heat recovery (NBN D50-001).

Some advantages of single room ventilation are listed by Manz et al. (2000):

- *Local ventilation units do not need any ducting within the dwelling and are therefore very suitable for retrofitting use.*
- *Independent ventilation per room is possible with optimal adjustment to local needs.*
- *Local room ventilation allows quick removal of pollutants from a source-room, before they mix up with the air in other rooms as might happen with central dwelling ventilation.*
- *A direct sound transmission from room to room through the ventilation system cannot occur.*

Others advantages can be added to this list:

- Avoiding ducts means shortening the hydraulic circuits, and hence the pressure drops related to the passage of air flow rates through them. From this fact, the specific fan power (SFP) can be reduced.

- Given their placement in habitable rooms and the accessibility of each component, the maintenance of the system (particularly, the filters replacement) is easier and cheaper than in centralized heat recovery ventilation systems.
- As referred by Wouters and Van den Bossche (2005), possible problems of installed centralized ventilation systems are leaking air ducts. According to Andersson (2013), *"many studies have identified defective ventilation and insufficient air flow as a mean reason for occurrence of sick building… Duct systems accounts for a large fraction of the energy use in a building. This is further increased with a leaky duct system."* These potential issues are avoided in single room units.
- Dust accumulation in ducting can lead to a performance degradation of the installation due to a rising of the pressure drop (Anon (2000)). Moreover, the indoor air quality can decrease due to a contamination of air flow rate by particles, micro-organisms or volatile organic compound (Barbat and Feldmann (2010)). Once again, these problems are avoided in single room ventilation units.

But these advantages imply a considerable challenge: developing a competitive heat recovery ventilation system despite of a small available volume by taking care of the aesthetic aspects. As for every heat recovery ventilation system, the developed device faces with a trade-off between a high thermal effectiveness and a related rise of pressure drops inducing a degradation of the global performance of the unit due to a higher energy use for the fan. Greater attention is paid to hydraulic performance than in centralized systems since they are directly related to the noise generated by the fans. Indeed, in the design step of this kind of device, it is important to keep in mind that the heat recovery device will be installed in life rooms and has to be as silent as possible. In Belgium, according to the NBN S01-400-1, requirements for each type of local are summarized in Table 1:

Table 1: Requirement in terms of acoustic comfort according to the Belgian norm NBN S01-400-1 for mechanical ventilation

Local	Normal acoustic comfort level	Superior acoustic comfort level
Bathroom, toilets	≤ 35 dB	≤ 30 dB
Kitchen	≤ 35 dB	≤ 30 dB
Life room	≤ 30 dB	≤ 27 dB
Bedroom	≤ 27 dB	≤ 25 dB

The World Health Organization recommends two values in the report *"Guideline values for community noise in specific environments"(1999)*: respectively, 35 dB for life rooms and30 dB inside bedrooms.

2.2 Investigated device characteristics

The investigated device has been recently developed in the frame of the Green + project. Several aspects of the device have been the object of several papers during the development steps:

- Aparecida et al. (2011) presents the main design steps of the unit,
- Masy et al. (2011) focuses on the interaction with the building air tightness and indoor hygro-thermal climate,
- Ajaji and André (2012)) focuses on the ventilation efficiency.

The present paper aims to compare the overall performance (hydraulic, thermal and acoustic) of the final unit with the natural, simple exhaust ventilation and traditional centralized systems. The investigated device consists of a parallelepiped box containing two fans and two

filters (for both fresh and indoor air flow rates), an electronic fan control, a set of sensors (depending of the model) and a heat recovery exchanger. Flow configurations inside the unit are represented in Figure 1.
The specificity of the units is the easiness of integration in the windows ledge, which makes them especially convenient in the frame of a house retrofitting (windows removal). Most single room ventilation with heat recovery units are installed on a wall with air inlet and air outlet through the building façade.

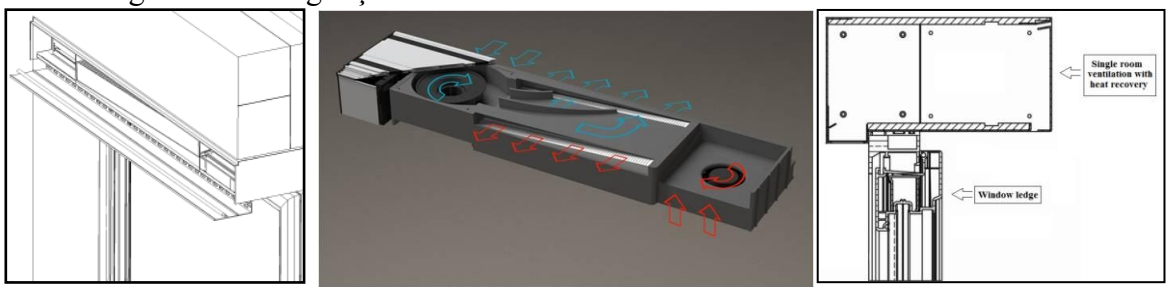

Figure 1: Investigated single room ventilation unit and flow configurations inside the device

The heat exchanger is the key component of the unit. The heat exchanger under investigation is a U-flow configuration heat exchanger. Nasif et al. (2010) has already investigated an enthalpy heat exchanger that presents a quite similar flow configuration (Z-flow configuration). Such exchangers (also called quasi-counter flow heat exchanger) present a counter flow configurations over the major part of their heat transfer area. The investigated heat recovery exchanger is made in polystyrene. The main disadvantage of polystyrene heat exchangers concerns their low thermal conductivity. However, this disadvantage can be counter-balanced by the high enlargement factor (ratio of the developed length to the protracted length) that can be reached with polystyrene heat exchangers compared to traditional plate heat exchangers made of metal (rarely superior to 1.5 according to Ayub et al. (2003)). The enlargement factor is close to 4 in the central part of the heat exchanger.
Filters dedicated to the indoor and outdoor air flow rates are placed upstream the fans and hence upstream the heat exchanger in order to protect the unit and its component against dust accumulation. Moreover, the system is designed in such a way that both filters are accessible from the inside of the house. The range of classification of available filters for the unit is comprised between G3 to F7 types, according to EN 779. The investigated single room ventilation was tested with G4 filters.

3 PERFORMANCE OF THE DEVICE

3.1 Components performance of the unit (design step)

In the design step of the device, several components and several combination of their integration have been investigated a large amount of time. From this fact, it was important to develop test benches that could be easily used for several geometries and configurations.
A test bench dedicated to the thermal/hydraulic performance of the heat exchanger has been constructed. Another test bench was developed to investigate the hydraulic performance of the device through the determination of the fan performance and the relation between the flow delivered and the electrical power supplied to the device. These test benches, their characteristics and some of intermediate experimental performance results are given by Gendebien (2012).

3.2 Final overall performance of the unit

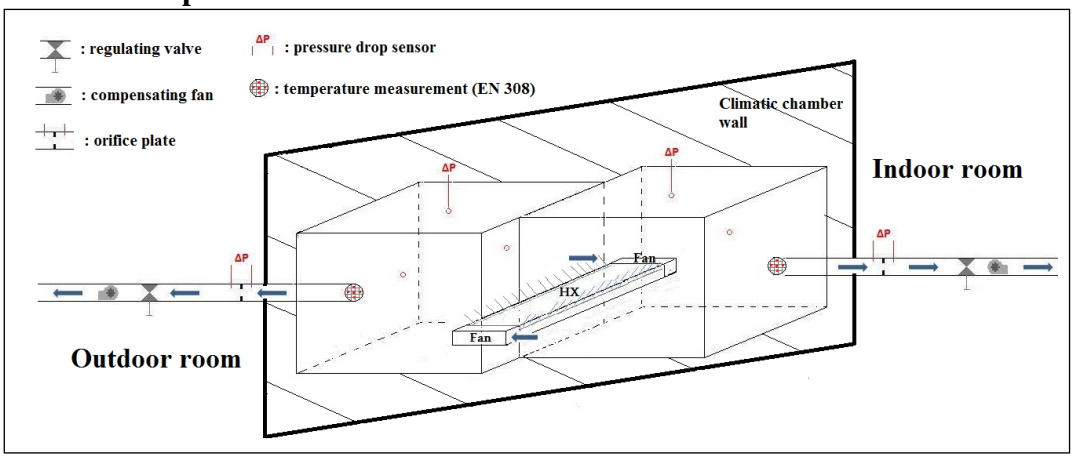

Figure 2: Schematic representation of the experimental apparatus dedicated to the thermal performance of the entire unit

In order to take into account the conduction effects in the unit and an eventual degradation of thermal performance due to a mis-distribution of the flow rate through the heat exchanger, the best way to determine the overall performance of the final device is to test it into a climatic chamber, as schematically shown in Figure 2.

The idea is to place the unit in a wall separating an outdoor and an indoor room of a climatic chamber. Flow rate delivered by each side of the unit are measured by the pressure compensated box method (Lebrun and Hannay, 1972). The mean outlet temperature of each side of the device is determined by means of five thermocouples T (placed as mentioned by NBN 308) situated at the exhaust of the pressure-compensated box. COP of the system is directly deduced by measuring the supply electrical power delivered to the unit.
Since the exhaust and the inlet of the unit consists of slits, it is important to mention that ensuring the air tightness between the unit and the experimental apparatus takes a large amount of time. That is the reason why this experimental apparatus is not suitable for the design step of the device but only for the overall performance of the final version of the device.

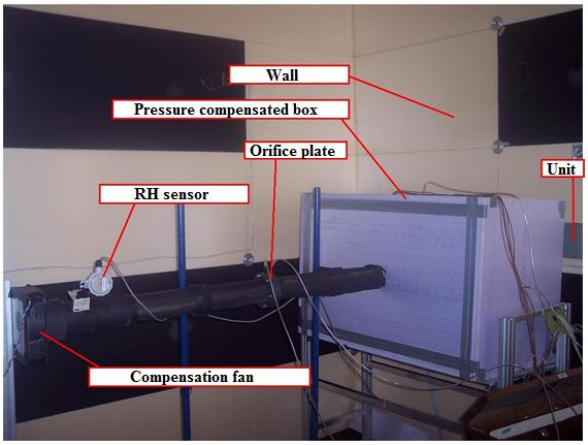

Figure 3: Climatic chamber test (outdoor side)

The overall performance of a centralized heat recovery ventilation is highly dependent on the hydraulic circuit (length and bending of the pulsing and extracting ducts) and so on the house and ducts configuration. In contrary, the overall performance of a single room heat recovery ventilation is not influenced by the rest of the installation.

Previous studies (Gendebien et al., 2013) have highlighted the fact that the annual amount of latent heat rate compared to sensible recovered heat can be neglected in moderate climates such as Belgian climate. From this fact, it is has been decided that the following results do not take into account the potential latent heat transfer rate in the establishment of the recovered heat transfer rate. The overall performance of the unit can be defined by the ratio of the recovered heat transfer rate to the electrical power of the fans and is given by Equation 1:

$$COP = \frac{Q_{recovered}}{W_{fans}} \quad (1)$$

By neglecting the potential increase of heat recovered due to latent term, the recovered heat transfer rate is given by Equation 2 and depends on the heat exchanger effectiveness (varying with the mass flow rate), the delivered mass flow rate and on the indoor/outdoor difference temperature:

$$Q_{recovered} = M_{fresh} \cdot cp \cdot \varepsilon \cdot (T_{ind} - T_{out}) \quad (2)$$

with M_{fresh} the fresh air mass flow rate in [kg/s], *cp* the air capacity in [J/kg-K], ε the heat exchanger effectiveness [-], T_{ind} the indoor temperature and T_{out} the outdoor temperature. Cartography of performance can be drawn, depending on the delivered flow rate by the unit and the indoor/outdoor temperature difference, as shown in *Figure 4*:

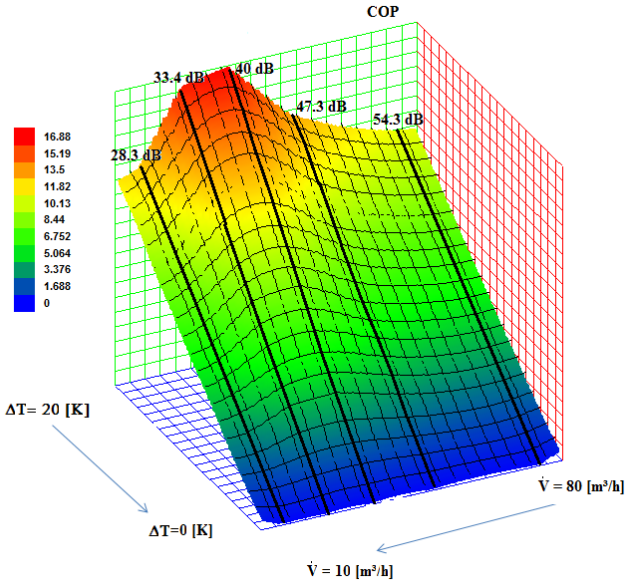

Figure 4 : COP [-] vs flow rate in [m^3/h] and difference indoor/outdoor temperature in [K] (performance cartography of the unit)

Sound pressure levels have been determined on the inner side of the unit. In order to have a complete cartography of performance of the device (thermal and hydraulic), the level of generated noise related to a specific flow rate is also indicated in Figure 4.

4 CO2 EMISSIONS, PRIMARY ENERGY AND ENERGY COSTS OF THE DEVICE

4.1 Competitiveness of the device

As shown in the previous section, the energy saved by the investigated device is highly dependent on the indoor/outdoor temperature difference. Many authors use a heating degree days (HDD) method to determine how much a heat recovery system is competitive in a given

climate. For example, Adamski (2010) used it to estimate the financial effects of a ventilation system with a spiral recuperator in Poland. Kristler and Cussler (2002) combined the heating degree days and the absolute humidity days to define a cost effectiveness ratio (division of the actual energy cost savings of the investigated device by these energy costs) to optimize the performance of their membrane heat exchanger. More recently, Laverge and Janssens (2012) used the heating degree day method to evaluate the advantage of natural, simple exhaust mechanical ventilation and heat recovery ventilation over each others for European countries. In the frame of this study, the method is applied for mean average values for Europe and Belgium which can be considered as a typical moderate European climate.

The total annual heat recovered in [J/year] by the investigated device can be determined by integrating Equation 3 over one typical year:

$$Q_{recovered} = \quad V(t).\rho\ t\ .cp(t).\ \varepsilon\ \ V\ \ .\ \Delta T\ (t)\ \ dt \tag{3}$$

The total electrical energy delivered to the unit over one year in [J/year] can be determined by Equation 4:

$$E_{el} = \quad [\ W_{fan,fresh}(V) + \ W_{fan,out}\ \ V\ \ ]\ dt \tag{4}$$

Equations 3 and 4 are quite difficult to evaluate since the flow rate delivered by the unit and hence the effectiveness and the electrical fan consumption vary with time and is dependent on many factors (type of ventilation control, type of room where is placed the unit, user's behavior,…). In the frame of this study, it has been decided to make some assumptions to solve them. Some assumptions are the same than the one used by Laverge and Janssens (2012):

- the ventilation system is considered to permanently run all along the year,
- the specific heat capacity cp [J/kg-K] and the air density ρ [kg/m³] are considered constant all year long and their products are equal to 1224 [J/m³-K],
- integration of the indoor/outdoor temperature difference over a year can be realized through the use of the number of heating degree days HDD [K day]. According to Eurostat (2013), the heating degree for a given day is equal to the difference between 18°C and the mean outdoor temperature but only if this average daily outdoor temperature is inferior to 15°C. On the contrary, it is assumed equal to zero. The mean outdoor temperature is defined as the mathematical average of the minimum to the maximum temperature of that given day.
  Values used in the frame of this study for Europe and Belgium come from Eurostat (2013) and corresponds to the mean heating degree days over the period 1980-2004. They are respectively for Europe and Belgium equals to 3253 and 2872 [K day],
- effectiveness of the system is considered constant all year long.

By using the enounced assumptions and by normalizing Equation 3 and 4, one can determine the total annual heat recovered per m³/h $q_{recovered}$ in [Jh/m³-year] and the annual electrical energy delivered to the unit per m³/h for both fans e_{el} in [Jh/m³-year]. For the completeness of the paper, the main equations proposed by Laverge et Janssens (2012) are recalled here:

$$q_{recovered} = \ 24\ .1224\ .HDD.\varepsilon \tag{5}$$

$$e_{el} = \ 24\ .365\ .\ SFP \tag{6}$$

with SFP, the specific fans power in [J/m³]. In order to take into account some potential variation of the ventilation flow rate, the value used for the SFP of the unit and the

effectiveness of the unit in Equations 5 and 6 is the mean average value related to five rotational speeds covering the flow rate range of the unit. The average effectiveness is equal to 0.748 and the total SFP for both fans is equal to 1376 [J/m^3].

The device can be evaluated by means of three performance parameters: CO_2 emissions, primary energy and energy costs of the device. Hence, the competitiveness of the heat recovery device is demonstrated if the dimensionless number Ω, defined in Equation 7, is superior to one for each of the investigated performance parameters:

$$\Omega = \frac{q_{recovered} \cdot f_{fuel}}{e_{el} \cdot f_{el}} = \frac{q_{recovered}}{e_{el} \cdot f} > 1 \quad (7)$$

with f_{fuel} and f_{el}, the traditional conversion factors for the space heating fuel and electricity. It is assumed that the equivalent of the recovered heat is generated with a100% efficient natural gas combustion. f is the conversion factor for 1J of electricity to 1J of gas fired heating for $C0_2$ emissions, primary energy and energy costs. Values used for f in the frame of the study for Europe and Belgium are listed in Table 2:

Table 2 : Used value for conversion factor for Europe and Belgium

Conversion factors	**Values**		**References**	
	UE	**BE**	**UE**	**BE**
CO2	1.72	1.16	Laverge and Janssens (2012)	Stabbat (2009)
Primary energy	2.74	2.5		Walloon EPB decree (2008)
Energy costs	2.8	2.9		Eurostat (2013)

Numerical values for Ω_{SRVHR}, determined from Equation 7, for CO2, primary energy and household consumer prices are resumed in Table 3 :

Table 3 : Ω_{SRVHR} values

	Ω_{SRVHR}	
	UE	**BE**
CO2	3.89	4.51
Primary energy	2.437	2.09
Energy costs	2.12	1.80

As shown in Table 4, Ω_{SRVHR} is higher than one as well for the UE as for Belgium. From this fact, the investigated device seems to be competitive from an environmental and economic point of view.

It is also possible to use the method to determine the minimal HDD from which the device is competitive given several values of conversion factor. For Belgium, the most restrictive conversion factor concerns the energy costs. By taking this latter, the minimal HDD from which the device is competitive is 1600 [K day]. That corresponds to HDD of a low energy building in Belgium (base temperature chosen for the determination of the HDD is 12.5 °C).

4.2 Comparison with other ventilation systems

In the present section, the device is compared with three other ventilation systems: natural, simple exhaust and "traditional" centralized heat recovery ventilation. Given results in Table 3, it is clear that the system is more competitive than natural ventilation since Ω_{SRVHR} is higher than one for each investigated case as well for Belgium as for Europe. The investigated system is even more competitive compared to the simple exhaust ventilation since the latter involves a supplementary electrical consumption related to exhaust fans compared to natural

ventilation. The comparison with traditional centralized heat recovery ventilation appears to be more complicated since the SFP of traditional centralized system is highly dependent on the used fan and on the hydraulic characteristics of ducts. According to the European standard EN 13779 [XX], Laverge and Janssens [XX] propose to take the boundary between SFP 3 and SFP 4 (1250 [J/m^3] per fan), as reference for heat recovery system.
A centralized ventilation system with heat recovery is assumed to be as competitive as the investigated device if Ω_{CHRV} is at least equal to the determined Ω_{SRVHR}. In other terms, the minimum effectiveness for centralized systems required to be as competitive as the investigated device is given by Equation 8:

$$\varepsilon_{min,CHRV} = \varepsilon_{SRVHR} \cdot \frac{SFP_{CHRV}}{SFP_{SRVHR}} \quad (8)$$

So, by assuming a total SFP of 2500 [J/m^3] (1250 [J/m³] per fan) for a centralized heat recovery device, the required minimum effectiveness has to be equal to 1.35 [-], which is physically unrealistic. Recently, Caillou [XX] presented in situ measurements of SFP for centralized heat recovery ventilation systems. Results are given in Figure 5.

The required minimum effectiveness to be as competitive as the investigated single room ventilation is superior to unity (which is physically unrealistic) for more than half of the investigated systems (17 out of 28). By considering an average effectiveness equal to 0.9 for a centralized heat recovery exchanger, the investigated single room ventilation shows better performance for 75% of the investigated cases. To conclude, from an energetic point of view and compared to other systems on the market, performance of the investigated device sounds promising.

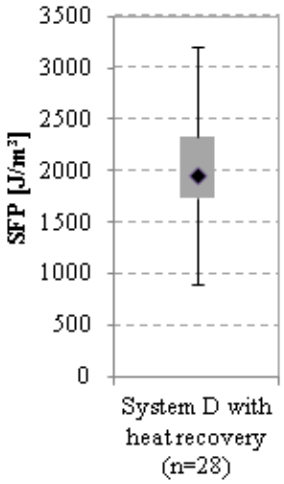

Figure 5: measurement of SFP in situ (Caillou [XX])

5 DISCUSSION

The presented COP of the device is determined in conservative conditions and takes into account the electrical conversion losses: transformation from AC (230~) to DC (24V). These losses are not negligible compared to the electrical power delivered to the fans, (especially for the low rotational speeds) and are entirely dependent on the current transformers used. In the determination of the SFP, these losses could be neglected if one assumes the presence of a DC domestic network, resulting from the use of photovoltaic panels for example.

By only taking a unique reference temperature, the method of the HDD is debatable since it doesn't take into account the thermal properties of the building, its air tightness

characteristics, the solar and internal gains as well as the device operation/use. However, despite its simplicity, the method allows pointing out some trends (at a national/regional level) and permits to compare different types of heat recovery balanced ventilation in a fair way (see Equation 8). Moreover, the method also allows to determine a minimal HDD from which the device is competitive.

6 CONCLUSIONS

The present paper investigates a new single room ventilation unit with heat recovery particularly suitable in the frame of a house retrofitting. The main specificity of the investigated device is its possible integration into windows ledge. A single room ventilation unit with heat recovery presents a large range of advantages compared to centralized heat recovery ventilation but this implies a difficult trade-off between hydraulic (and hence fan noise generated by the unit) and thermal performances. An experimental procedure is presented in order to characterize the performance of the entire unit. This is realized by determining the thermal performance of the heat exchanger and the hydraulic interaction between the fans and the unit. It is proposed to graphically represent the measured overall performance of the device by means of a cartography taking into account the difference outdoor/indoor difference and the delivered flow rates. In order to have a comprehensive representation of the performance in one graphic, the generated noise level corresponding to specific delivered flow rates is also indicated. The competitiveness of the device is evaluated by means of a heating degree day method through three performance parameters: CO_2, primary energy, and energy costs. The method also permits to highlight the competitiveness of the investigated system from an energy point of view compared to other ventilation systems. As expected, the main negative aspect of the investigated device concerns the generated average noise levels which are higher for the highest delivered flow rates than the requirements provided in the standard NBN S01-400-1. However, the studied device responds to an actual growing need (high rate of retrofitting in EU). Some improvements concerning the acoustic performance of the device are currently under development.

ACKNOWLEDGEMENTS

This study has been carried out in the frame of the Green+ project. This project is performed with the support of the Walloon Region of Belgium and is carried out by a large consortium of research centers and industrial partners such as Greencom sprl and ACTE s.a.

REFERENCES

Pérez-Lombard, L., Ortiz, J., Pout, C. 2008. *A review on buildings energy consumption information*. Energy and building 40, (2008), 394-398

Trias energetic concept website. Visited on the 6th of March 2012. www.triasenergetic.com

Roulet, C.-A., Heidt F.D., Foradini F., Pibiri M.-C. 2001. Real heat recovery with air handling units. Energy and Buildings 33, (2001), 495–502

Mardiana-Idayu, A., Riffat, S.B., 2012. *Review on heat recovery technologies for building applications.* Renewable and Sustainable Energy Reviews 16 (2012) 1241– 1255

Fehrm M, Reiners W., Matthias Ungemach, M. 2002. *Exhaust air heat recovery in buildings.* International Journal of Refrigeration 25 (2002) 439–449

Handel, C., 2011. *Ventilation with heat recovery is a necessity in « nearly zero » energy buildings.* REHVA Journal – May 2011.

Supplements to Preparatory Study on Residential Ventilation LOT 10. 2012. Fachinstitut Gebäude-Klima e.V.

Wouters, P., Heijmans, N., Delmotte, C., Van den Bossche, P., Wuyts, D. 2008. *Trends in the Belgian building ventilation market and drivers for change.* AIVC. Ventilation Information Paper n° 18. May 2008.

Adamski, M., 2008a. *Heat transfer correlations and NTU number for the longitudinal flow spiral recuperators.* Applied Thermal Engineering 29, (2009), 591-596

Fernandez-Seara , J., Diz, R., Uhia, F., Dopazo, A., Ferro, M., 2010. *Experimental analysis of an air-to-air recovery unit for balanced ventilation systems in residential building.* Energy conversion and management (2010)

Kragh, J., Rose, J., Nielsen, T.R., Svendsen, S. 2008. *New counter flow heat exchanger designed for ventilation systems in cold climate.* Energy and buildings 39, (2008), 1151-8

Söylemez, M.S. 2000. *On the optimum heat exchanger sizing for heat recovery.* Energy Conversion and Management 41, (2000), 1419-1427

Adamski, M., 2008b. *Longitudinal flow spiral recuperators in building ventilation systems.* Energy and Buildings 40, (2008), 1883–1888

Adamski, M., 2010. Ventilation system with spiral recuperator. Energy and buildings 42, (2010), 674-677

Manz. H., Huber, H., Schalin A., Weber, A., Ferrazzini M., Studer, M., 2000. *Performance characterization of single room ventilation unit with recuperative or regenerative heat recovery.* Energy and building 31 (2000) 37-47

Schwenzfeier, L., Akoua, J-J., Bianchina, M., Buseyne, S., Limoges, D., and Morel, R. 2009. *Use of compact balanced single room ventilation units with heat recovery in existing dwellings.* Proceedings of the 2009 AIVC Conference, Berlin.

Laverge J., Van den Bossche, N., Heijmans, N., Janssens, A. 2011. *Energy saving potential and repercussions on indoor air quality of demand controlled residential ventilation strategies.* Building and environment 46 (2011) 1497-1503

Maripuu, M-L, 2011. *Demand controlled ventilation (DCV) for better IAQ and energy efficiency.* REHVA journal. March 2011

Dimitripoulo, C., 2012. *Ventilation in European dwellings: A review.* Building and environment 47 (2012) 109-125

NBN D 50-001. 1991. *Dispositifs de ventilation dans les bâtiments d'habitation.* Belgian standard.

Wouters, P., Van den Bossche, P. 2005. Ventilation system quality for dwellings: a pragmatic approach. AIVC 26th conference - Brussels, Belgium, 21-23 September 2005 - pp 187

Andersson, J., 2013. *Swedish experience with airtight ductwork.* REHVA Journal - January 2013

Anon. 2000. *Nettoyer et décontaminer les gaines de climatisation*, L'entrepreneur, juin/juillet 2000, N° 164, pp. 42-43

Barbat, M., Feldmann, 2010. *Besoins et méthodes de nettoyage des conduits d'air en France.* AIVC. Ventilation Information Paper n° 34. Juillet 2010.

NBN S01-400-1. *Norme nationale belge. Critères de l'isolation acoustique pour les immeubles d'habitation.* Janvier 2008.

Berglund B, Lindvall T, Schwela DH, editors. Guidelines for Community Noise. Geneva: World Health Organization; 1999.

Aparecida Silva, C., Gendebien, S., Hannay, J., Hansen, N., Lebrun, J., Lengele, M., Masy, G., Prieels, L. 2011. *Decentralized mechanical ventilation with heat recovery. Proceedings of the 32nd AIVC Conference.* Bruxelles.

Masy, G., Lebrun, J., Gendebien, S., Hansen, N., Lengele, M., Prieels, L. 2011. *Performances of DAHT connected to building airthightness and indoor hygrothermal climate. Proceedings of the 32nd AIVC Conference.* Bruxelles.

Ajaji, Y., André, P., 2012. *Ventilation performance measurement of a decentralized mechanical system with heat recovery using Tracer gas decay method.* Proceedings of the Healthy Buildings 2012 conference.

Nasif, M., Al-Wacked, R., Morrison, G., Behnia, M., 2010. *Membrane heat exchanger in HVAC energy recovery systems, systems energy analysis.* Energy and buildings 42, (2010), 1833-1840

Ayub, Z. H. 2003. Plate heat exchanger survey and new heat transfer and pressure drop correlations for refreigerant evaporators. Heat Transfer Engineering. 24(5):3-16, 2003

EN 779. 2012. New European Standard for General Ventilation Filters.

Gendebien, S., Prieels, L., Lemort, V. 2012. *Experimental investigation on a decentralized air handling terminal: procedure of aeraulic and thermal performance determination of the entire unit under several operating conditions.* Proceedings of the 6th European Thermal Sciences Conference

Hannay, J., Lebrun, J., (1972). *Méthode d'essais applicable aux ventilos convecteurs*, Thermique et aéraulique, Juin 1972.

European Standard EN 308. *Heat exchangers – test procedures for establishing performance of air to air and flue gases heat recovery devices*. European committee for standardization; 1997.

Gendebien, S., Bertagnolio, S., Lemort, V., 2013. *Investigation on a ventilation heat recovery exchanger: modeling and experimental validation in dry and partially wet conditions.* Energy and buildings (In press).

Kistler K.R. and Cussler E.L., 2002. *Membrane modules for building ventilation.* Chem. Eng. Res. Des. 80, pp. 53–64.

Laverge and Janssens. 2012. *Heat recovery ventilation operation traded off against natural and simple exhaust ventilation in Europe by primary energy factor, carbon dioxide emission, household consumer price and exergy*. Energy and buildings. 50 (2012) 315-323

http://epp.eurostat.ec.europa.eu/cache/ITY_OFFPUB/KS-SF-09-055/EN/KS-SF-09-055-EN.PDF

Eurostat, Heating degree day by NUTS 2 regions- annual data. Mean heating degree-days over period 1980-2004.

Stabbat, P. 2009. *Analysis of building heating and cooling demands in the purpose of assessing the reversibility and heat recovery potentials. Annexes.* IEA-ECBS Annex 48. Heat Pumping and Reversible Air conditioning. http://www.ecbcs.org/docs/ECBCS_Annex_48_Final_Report_R1_Annexes.pdf

Walloon EPB decree. 2008. *Arrêté du gouvernement wallon déterminant la méthode de calcul et les exigences, les agréments et les sanctions applicables en matière de performance énergétique et de climat intérieur des bâtiments.*
http://www.cstc.be/homepage/download.cfm?dtype=na_energy&doc=EPB_RW_MB20080730.fr.pdf&lang=fr

EN 13779. 2007. CEN Ventilation for Non-residential Buildings-Performance Requirements for Ventilation and Room conditioning Systems, Brussels, 2007.

Caillou, S., 2012. *Impact des systèmes de ventilation.* Séminaire bâtiment durable du 23 Novembre 2012. Améliorer et garantir la qualité de l'air intérieur. IBGE. Institut bruxellois pour la gestion de l'environnement. http://www.icedd.be/downloads/data/Semi_3_231112_livret_FR.pdf

MODELLING OF URBAN CANYON: ANALYTICAL AND EXPERIMENTAL REMARKS

F.Rossi[1], F. Cotana[1], V. Coccia[*1], A.L. Pisello[1], E. Bonamente[1], M. Palombo[1], G. Pignatta[1], and E. Morini[1]

1 CIRIAF – Interuniversity Research Center on Pollution and Environment "M. Felli"
University of Perugia, Italy
Via G. Duranti, 06125, Perugia, Italy
**Corresponding author: e-mail coccia@crbnet.it*

ABSTRACT

The urban climate of high-density areas is often affected by an increase of the air temperature known as Urban Heat Island (UHI) phenomenon.
UHI is strongly influenced by the solar reflectance of conventional materials used for building envelope and urban coatings, i.e. streets and square pavings.
The present work proposes an original method to predict the temperature of both facades and local air mass on urban scenarios. The effect of changes on coatings may also be estimated.
The proposed method is based on an Experimental Facility (EF) and a Theoretical Model (TM) which are jointly taken into account for UHI predictions.
EF is located at the University of Perugia which is composed of two separate metal rails incorporating several insulating frames, resembling a urban canyon, positioned at different mutual height/distance ratios (i.e. H/D = 0.5, 1.0, 2.0). Each frame can be equipped with particular reflective films (e.g. cool roofs coatings) in order to assess variation of radiative exchanges as a function of geometry, meteorological conditions, and radiative properties of walls. The monitoring system is equipped with temperature sensors, a pyranometer and an anemometer. A weather station is located nearby.
EF may be used directly to estimate UHI by a mechanical analogy which however introduces strong limitation on real scenario dimensions and operative conditions.
By validating the TM via EF the range of real scenario may be studied and predicted is widely extended and the proposed method may be applied virtually for any case.
The preliminary calibration of the methodology using measured data is also presented.

KEYWORDS

Urban Heat Island effect, Urban canyon, Climate modelling, Building envelope, Cool roofs

1 INTRODUCTION

UHI is a well-known urban phenomenon which witnesses an increase of air temperature especially on summer time; the main consequences of UHI are an increase on building energy demand and a reduction of comfort condition [1]. Howard et al. [2] were the first who documented the temperature differences between an urban area and a rural one; this phenomenon was later named ‘‘Urban Heat Island’’ by Manley [3]. Although UHI related to winter time is not as much studued as for summer time, a few interesting contributions focused on the overall year-round have been issued, such as the work by Giridharan et al. [4], where a 9.0 °C difference between urban-rural conditions on winter time was registered.

The most relevant parameters impacting UHI are urban surfaces albedo, evapotranspiration and anthropogenic heating [5]. Many research contributions showed that an effective strategy to mitigate UHI consists of the implementation of high-reflective

envelopes (e.g. cool roofs [6]) on behalf of conventional "darker" coatings [7]. Most of the research investigation on technologies to mitigate UHI were aimed to reduce energy

demand for cooling and GHG emissions.

At a local scale, UHI mitigation also improved the indoor thermal comfort of buildings [8]. The thermal behavior of a case-study scholar building in Athens was analysed through dynamic simulation modelling, showing a decrease in the annual cooling load of 40% after the installation of cool roofs. The same fundamental results were also experimentally documented by the same study and other scientists' contributions [9]. In fact, Kolokotsa et al. [10] showed that also the indoor thermal performance of non–conditioned buildings is influenced by UHI. This work concerning a university lab building located in Iraklion, Crete, demonstrated an year-round energy saving of 19.8%, and 27% for the summer period, achieved by applying cool roofs as a strategy to mitigate the urban temperature increase. Additionally, together with such inter-building effect [11], the potentialities of high-reflective irradiated surfaces have important impacts also on the global warming reduction. Akbari et al. [12] demonstrated that the increase in global average air temperature is directly linked to the reflectance capability of coatings exposed to solar radiation and located in urban areas.

A tool to estimate UHI and to test different material for coating would help researcher, administrators and low makers to better design urban ambient.

In this paper an original method to predict the temperature of both facades and local air mass on urban areas is proposed. By that the effect of changes on coatings is estimated which may be helpful for the energy design of a building. The proposed method is based on an Experimental Facility (EF) and a Theoretical Model (TM) which are jointly taken into account for UHI predictions. EF may be used directly to estimate UHI by a mechanical analogy which however introduces strong limitation on real scenario dimensions and operative conditions. By validating the TM via EF the range of real scenario may be studied and predicted is widely extended and the proposed method may be applied virtually for any case. Preliminary experimental data are presented.

1.1 Urban Canyon models

Numerical and analytical models can predict the spatial and temporal variation of UHI as a function of the relevant geometries of the urban context and reflectance features of building envelopes and urban coverings.

Gobakis et al. [13] applied neural-network techniques to the urban heat island modelling: the work showed the correlation between measured and predicted UHI parameters for several sites: the UHI intensity can be predicted quite accurately for at least a 24-h time horizon using a limited set of data.

The urban canyon effect was also modelled by Allegrini et al. in [14], by applying building dynamic simulation tools. Simulations were carried out for stand-alone buildings and buildings located in street canyons; the study showed the importance of accounting for the local urban microclimate when predicting the energy demands for buildings in urban areas. Geometry (i.e. aspect ratio) of urban canyons is also a key factor regulating the radiative flux exchange among different surfaces. With dynamic thermal simulations, Strømann-Andersen et al. [15] found that geometry variation is able to modify the overall energy consumption up to +30% for offices and +19% for housing. Also reflectivity features of the canyon surfaces play an important role in the thermal behavior of buildings. For instance, Doya et al. [16]

Figure 1: Panoramic view of the test field installation.

showed the positive effect of cool roofs against urban heat island, by monitoring a micro-scale experimental case study representing a typical urban canyon geometry. Additionally, the canyon geometry plays an important role also in terms of streets air quality. In fact, Chan et al. [17] showed that the pollutant transport and diffusion is influenced by the canyon aspect ratio.

The UHI can be influenced by the micro-climate conditions as well. In particular, with respect to the climate characterization, Krüger et al. [18] studied the impact of canopy geometry and building orientation on building cooling loads. Also the average wind speed is taken into account in the calculations and it was found that the highest increase in cooling loads is related to the highest urban concentration geometry. For particular cases, the simulation showed an increase in energy demand for cooling up to 250% and a decrease for winter heating up to 40%.

A urban heat storage model (UHSM) has been proposed by Bonacquisti et al. [19]. The authors used this urban canopy layer model to study the thermal anomalies between central Rome and its sub-urban surroundings. The validated results showed that the greatest difference between urban and rural temperatures is about 2°C during winter and 5°C during summer. As expected, such differences are directly related to the urban geometry and the optic-energy properties of materials.

The influence of the urban texture on building energy consumption was also studied by Ratti et al. [20] applying Digital Elevation Model (DEM). The surface-to-volume parameter was considered as representative to describe the urbanization rate of several cities such as London, Toulouse and Berlin. The work showed that the DEMs analysis could be used to explore the effects of the urban texture on the energy performance of buildings by taking into account the canyon geometry, the mutual shadowing, and window-to-wall ratios.

In this articulate research perspective, the model of the Urban Canyon as a function of its aspect ratio and radiative properties of its surfaces represents the focus of the work. The proposed analytic model is based on an energy-balance approach, and it takes into account the incoming solar radiation, the reflective properties of the canyon surfaces (both vertical walls and the ground surface), the convective heat transfer, and the characteristic height to distance ratio (H/D). As a result, the temperatures of the canyon surfaces can be estimated.

The present work proposes an original method to predict the temperature of both facades and local air mass on urban scenarios. The effect of changes on coatings may also be estimated.

The proposed method is based on an Experimental Facility (EF) and a Theoretical Model (TM) which are jointly taken into account for UHI predictions.

EF may be used directly to estimate UHI by a mechanical analogy which however introduces strong limitation on real scenario dimensions and operative conditions.

By validating the TM via EF the range of real scenario may be studied and predicted is widely extended and the proposed method may be applied virtually for any case.

The preliminary calibration of the methodology using measured data is also presented.

2 THE EXPERIMENTAL FACILITY (EF)

The EF is located on the roof of one the buildings at the University of Perugia, Italy (lat. 43° 6' 44"N), as shown in Figure 1. It consists of two twin arrays, designed to monitor and compare the thermal behavior of two canyons featuring the same geometry and different reflective properties. Each test field is composed of four metal frames (0.6 m high, 4.2 m long) supporting insulating panels (0.2 m thick). The orientation of the frames, currently South-North, can be adjusted. The panel pitch can also be changed to reproduce different aspect ratios (H/W). In the presented configuration the investigated values of the aspect ratios are 0.5, 1.0 and 2.0 (Figure 2). A bituminous membrane was laid on the ground to resemble the radiative properties of the road surface. A total of 48 surface temperature sensors (i.e. type K thermocouples) were installed on the 16 sides: each side is instrumented with 2 sensors positioned along the vertical axis (to minimize boundary effects) at 0.2 and 0.4 m from the ground. The ground temperatures of each inner canyon, and open north- and south-facing canyons are also measured. Two sensors are used for each inner canyon (at 1/3 and 2/3 of the canyon width) and one sensor is used for each open canyon (0.4 m far from the vertical surface). One air temperature sensor is also positioned at the centre of each inner canyon (0.3 m high) and another one on each open canyon (0.3 m above the ground temperature sensor). An upward-facing pyranometer is also used. Continuous monitored data by a fully equipped meteorological station, positioned in the same experimental site are also available.

3 THE THEORETICAL MODEL (TM)

The TM proposed here is based on an energy-balance approach. The incoming solar energy enters the canyon and it is reflected or absorbed by the sun-exposed surface. It is supposed that no energy is transmitted through the ground nor through the vertical walls. When the

Figure 2: Close view of the West (in front) and East (behind) test fields before cabling. Each field is composed of 3 canyons with H/D ratios equal to 1.0, 0.5, and 2.0 (from left to right respectively).

radiant flux strikes a sun-exposed surface, part of it is diffusively reflected and part is absorbed as in the following equations:

$$R_{refl} = r \cdot R_{sun}$$
$$R_{abs} = a \cdot R_{sun}$$

$$r + a = 1 \quad (1)$$

where R_{sun} is the incoming solar radiation normal to the surface, R_{refl} and R_{abs} the reflected and absorbed radiations, respectively. The reflection (r) and absorption (a) coefficients in eq. (1) are associated to the visible portion of the electromagnetic spectrum, and, more precisely, they have to be interpreted as solar reflection and absorption indices [21-22]. As in the common real case, the reflection is considered to be diffused. According to the proper view factor, the reflected light can escape from above and/or strike another surface of the canyon (e.g. a shadowed wall or the ground) where part of it is absorbed and part is reflected again. This process is iterated until all the visible light is either absorbed or exits the canyon. At each step the absorbed energy produces an increase of the surface temperature (T), and it is re-emitted according to:

$$G = \epsilon \cdot \sigma_0 \cdot T^4 \quad (2)$$

being ϵ the surface emissivity and σ_0 the Stefan-Boltzmann constant. For temperatures close to the standard ambient conditions the radiation is emitted at infrared wavelengths. Infrared radiation undergoes a multiple reflection/absorption/reemission process, similar to that of visible light but characterized by infrared absorption (α) and reflection (ρ) coefficients. As for the visible spectrum it is assumed that there is no transmitted infrared radiation:

$$\rho = 1 - \alpha, \ \alpha = \epsilon \quad (3)$$

The canyon is modelled as a parallelepiped. It is delimited by 6 surfaces: the ground, the sun-exposed and shadowed surfaces, the sides and the top of the canyon (

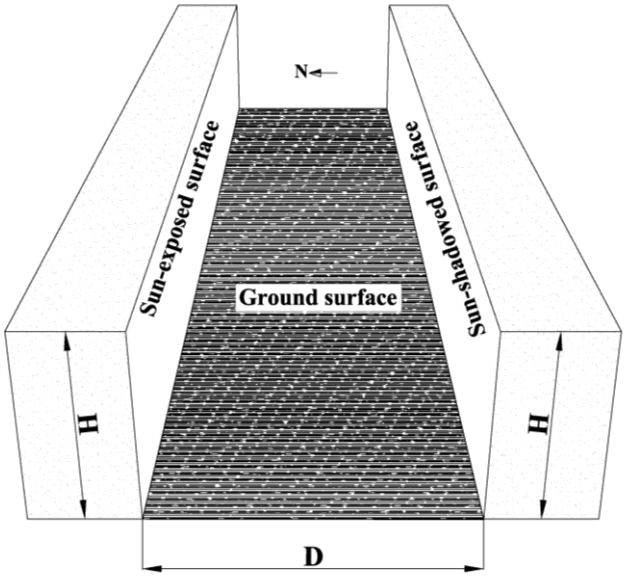

Figure **3**). These last three surfaces are opened and solar radiation (both visible and infrared) can exit the canyon through them.

The canyon is parameterized by three linear dimensions: length (hereafter referred to as L), height (H) and distance (D). Changing their values, it is possible to produce differently shaped canyons, spanning over all possible aspect rations (H/D) and enhancing or dimming side-effects (depending on L).
For a given geometry, an energy balance is run considering the total energy reaching and leaving each surface. Three sets of equations are used: one for the visible radiation, one for the infrared radiation, and one for the overall energy balance, including convection.
The visible radiosity (R) is defined as the radiant visible flux (W/m^2) leaving a surface. It is given by:

$$R_i.S_i = r_i \cdot \quad _{j \neq i} R_j \cdot S_j \cdot F_{j \to i} + R_{sun,i} \cdot S_i \tag{4}$$

where $S_{i(j)}$ is the extension of surface *i(j)*, r_i is the visible reflection coefficient, and $F_{j \to i}$ is the view factor from surface *j* to surface *i*. $R_{sun,i}$ is the normal component of the solar flux on the surface *i*

$$R_{sun,i} = R_{sun} \cdot cos\ \theta \tag{5}$$

where θ, the angle between the normal to the surface and the sun beam, is a function of the solar altitude (β) and azimuth (φ) angles, and the orientation and inclination of the surface itself. $R_{sun,i}$ is zero for a shadowed surface.
The infrared radiosity (*G*), defined similarly to *R*, includes the thermal flux radiated from the surface:

$$G_i.S_i = \alpha_i \cdot \sigma_0 \cdot T_i^4 \cdot S_i + \rho_i \cdot \quad _{j \neq i} G_j \cdot S_j \cdot F_{j \to i} \tag{6}$$

The global energy balance on each surface is defined by the following equation:

$$R_{sun,i} \cdot S_i + \quad _{j \neq i}\ R_j + G_j\ \cdot S_j \cdot F_{j \to i} = \ R_i + G_i\ \cdot S_i + h_i^c \cdot\ T_i - T_{in}\ \cdot S_i \tag{7}$$

where h^c_i is the heat transfer coefficient of surface *i* and T_{in} is the air temperature inside the canyon. The convection coefficient h^c_i can be directly computed from the surface and air properties, and the system geometry.
A final equation defines the energy balance on the top open surface (S_{sky}):

$$_i R_{sun,i} \cdot S_i = \quad _{j \neq sky}\ R_j + G_j\ \cdot S_j \cdot F_{j \to sky} \tag{8}$$

where *i* marks the sun-exposed surfaces, *j* marks all the canyon surfaces, and $F_{j \to sky}$ is the

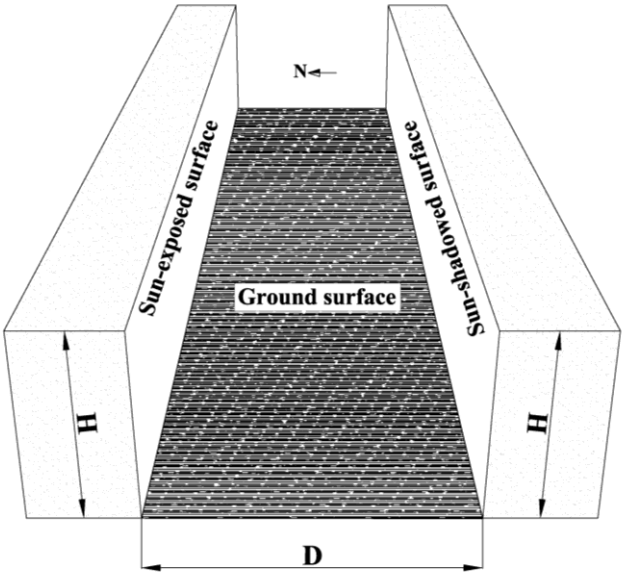

Figure **3:** Sketch of the urban canyon geometry parameters. The aspect ratio is defined by the ration of the height (H) over the distance (D).

view factor form surface *j* to the top surface (i.e. the sky).
The TM is defined by a total of 10 equations, 3 for visible radiosities (eq. (4)), 3 for infrared radiosities (eq. (6)), 3 for the total energy on the canyon surfaces (eq. (7)), and 1 for energy through the top surface (eq. (8)). The system is fully determined, having a total of 10 unknown variables R_1, R_2, R_3, G_1, G_2, G_3, T_1, T_2, T_3, and T_{in}, where subscripts from 1 to 3 mark the canyon inside surfaces and T_{in} is the inside air temperature.

Two different scenarios can be reproduced for the convective heat exchange, one for dominant natural convection and one for dominant forced convection.

Natural convection

In the case of natural convection, h_c is given by:

$$hc = Nu \cdot \frac{\lambda}{l} \tag{9}$$

$$Nu = c_{h,v} \cdot Ra^{1/3} \tag{10}$$

$$Ra = \frac{a \cdot g \cdot \theta \cdot l^3 \cdot \rho^2 \cdot \gamma}{\mu \cdot \lambda} \tag{11}$$

where *Nu* is the Nusselt number, $c_{h,v}$ a constant taking different values for horizontal and vertical surfaces, and *Ra* the Rayleigh number [23].
Since in eq. (11) the term $A = \frac{(a \cdot g \cdot \rho^2 \cdot \gamma)}{\mu \cdot \lambda}$ is only dependent on the specific properties of the fluid participating in the convective heat transfer, it is univocally calculated. Therefore, the Rayleigh number can be written as

$$Ra = A \cdot \theta \cdot \mathrm{L}^3 \tag{12}$$

A mechanical analogy (i.e. similitude approach) is needed to relate the experimental data found on the EF to a real-size scenario. The same convective exchange is guaranteed if the two systems have the same the Rayleigh number:

$$\mathrm{Ra} = \mathrm{Ra_M} \tag{13}$$

$$\theta \cdot \mathrm{L}^3 = \theta_M \cdot L_M^3 \tag{14}$$

In the case of a EF with a characteristic length L_M, the above condition can be achieved forcing an appropriate θ_M. Changing the EF parameters, different real scenarios, characterized by L and θ, can be reproduced. For example, forcing θ_M=55°C and using typical real-condition values θ=5°C, a scale factor of $L_M/L \approx 0.3$ is achieved:

$$L_M = \sqrt[3]{\frac{\theta}{\theta_M}} \cdot L \tag{15}$$

An alternative, hard to carry out, solution is represented by the replacement of the fluid (i.e. the A parameter of eq. 12).
The condition given by eq. (15) may be achieved making adjustments on the EF, that are:

- to use a protection barrier from the external wind without modifying the insolation conditions;
- to install adjustable warming plates on EF pavement.

In addition, the next configuration of the EF will include a rotating platform to follow the Sun-path. Figure 4 shows the configuration of the EF for the natural convection experinces.

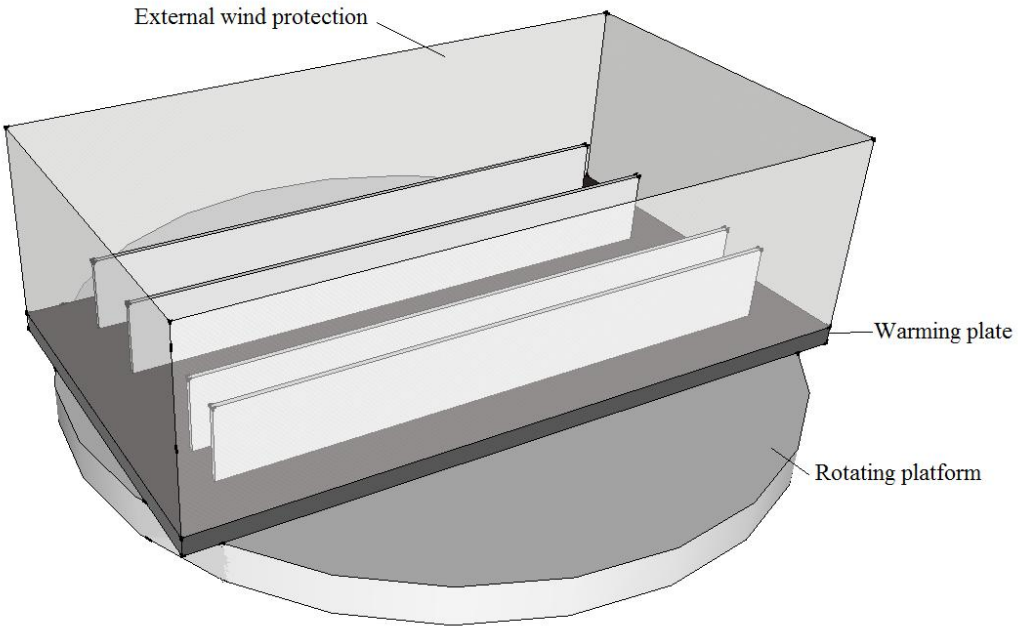

Figure **4:** Adaptation of the EF to the natural convection conditions

Forced convection

In the case of forced convection, h_c is given by:

$$hc = Nu \cdot \frac{\lambda}{l} \tag{16}$$

$$Nu = C \cdot Re^m \cdot Pr^n \tag{17}$$

$$Pr = \mu \cdot \frac{Cp}{k} \tag{18}$$

$$Re = \frac{\rho \cdot u \cdot L}{\mu} \tag{19}$$

where *Nu* is the Nusselt number, *Pr* is the Prandtl number, and *Re* Reynolds number with their usual definitions [24].

Since in eq. (19) the term $B = \frac{\rho}{\mu}$ is only dependent on the specific properties of the fluid participating to the convective heat transfer, it is univocally calculated. Therefore, the Reynolds number can be expressed by:

$$Re = B \cdot (u \cdot L) \tag{20}$$

The EF and the real scenario are connected by the following analogy relation:

$$u \cdot L = u_M \cdot L_M \tag{21}$$

The EF dimension (L_M) may be set forcing the longitudinal air velocity (u_M) (e.g. using a fan): For example, considering u=5 m/s and u_M=50 m/s, the scale ratio is L_M/L=0.1:

$$L_M = \frac{u}{u_M} \cdot L \tag{22}$$

The condition given in eq. (22) may be achieved making adjustments on the EF, that are:

- to use a protection barrier from the external wind without modifying the insolation;
- to install a fan producing an air flow in the longitudinal direction of each canyon; the air flow will be laminated prior entering each canyon.

In addition, the next configuration of the EF will include a particular rotating platform enabling to follow the Sun-path.

Figure 5 shows the EF configured for forced convection conditions.

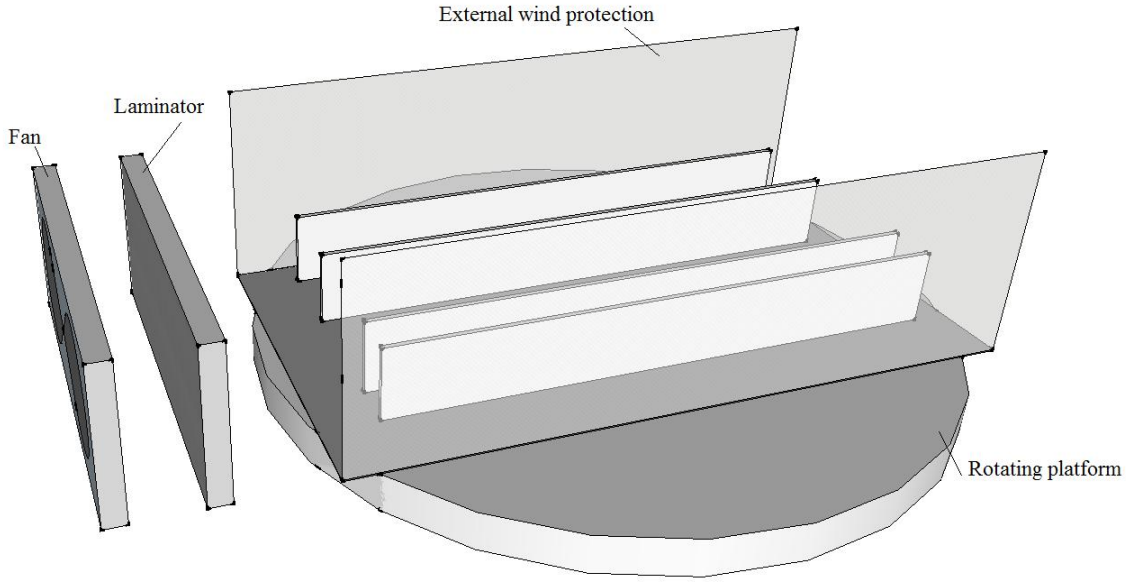

Figure **5:** Adaptation of the EF to the forced convection conditions.

4 TM VALIDATION AND BASELINE ANALYSIS

EF may be used directly to estimate UHI by a mechanical analogy which however introduces strong limitation on real scenario dimensions and operative conditions.
By validating the TM via EF the range of real scenario may be studied and predicted is widely extended and the proposed method may be applied virtually for any case.
The TM validation via EF may be done without using analogy relations; it will be carried out comparing the experimental results and the predicted values using appropriate geometric, radiative, and convective parameters.
Figure 6 provides a logical pattern between the real scenario, the EF, and the TM.

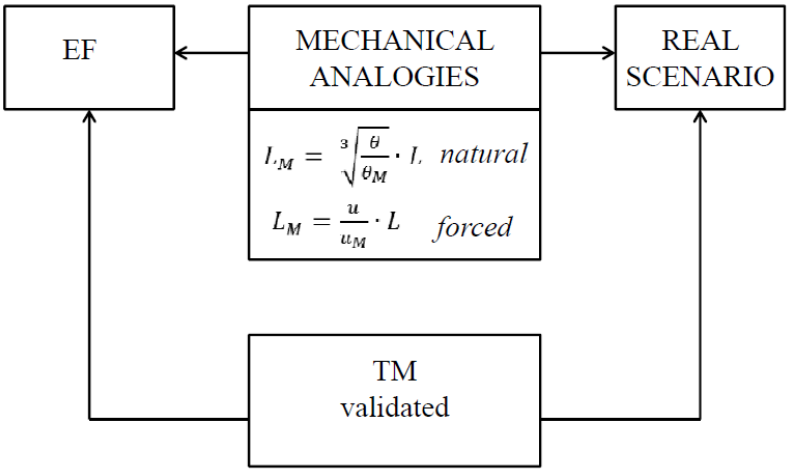

Figure 6: Logical pattern between the real scenario, the EF, and the validated TM.

The analysis of the surface properties bases on the difference observed the two test fields when the vertical surfaces have different reflective properties (e.g. to test the cooling performances of highly-reflective "cool" coverings). In an ideal case, i.e. identical canyons on both sides instrumented with equal-response sensors, each difference in the characteristic

temperature can be attributed to the surface property change alone. In the real case, it is necessary to perform a baseline analysis to estimate the sensitivity of the EF to the specific parameter.

A preliminary calibration campaign was run from July 24th to July 29th 2013. Both of the test fields were South oriented and equipped with the same surface finishing (i.e. white extruded polystyrene) and instrumented with a limited number of sensors positioned at specular positions (i.e. at each West sensor corresponds the mirror East sensor). Ground and vertical surface temperatures and solar radiation were measured every 10 mins.

The result of the baseline shows that the average difference between mirror sensors is 0.45°C for the entire dataset and 0.05°C considering night-time data only. The slightly larger daylight difference suggests that the difference is attributable either to reflectivity or geometric differences between the two test fields. The average standard deviation is 0.77°C. This value represents the estimation of the sensitivity of the EF to a change of the reflective properties of the surfaces. This value of standard deviation is expected to be at about one order of magnitude lower than the temperature difference produced by the reflective films applied on the two mirror setup facilities. First results from the monitored data, carried out during the first week of August 2013, confirm this expectation. The maximum ground temperature (r = 7.5 %) is between 60 and 75°C, depending on the sensor position, produced with a maximum solar radiation of 1014 W/m^2.

5 CONCLUSIONS AND FUTURE DEVELOPMENT

A comprehensive approach to the Urban Heat Island effect, including analytical modelling and experimental measurements, is presented.

As a first result, an energy-balance analytic model (TM), predicting the behavior of a urban heat canyon as a function of meteorological conditions, geometry, and surface reflective properties was elaborated. The TM bases on a set of 10 equations taking into account separately visible and infrared radiosities and the total energy balance on each of the canyon surface. The system is fully determined (it involves a total of 10 variables), and returns the characteristic canyon temperatures for different boundary conditions.

As a second result, an EF was designed, implemented, and instrumented to resemble typical urban canyon conditions. The EF is composed of two twin test fields with adjustable height/distance ratios and interchangeable surface coverings. A total of 58 temperature sensors, a pyranometer and an anemometer were deployed.

In the first data taking period (July 24th to July 29th) the system stability was tested and an estimation of the sensitivity to the change of surface reflective properties was performed. The two test fields were equipped with the same covering and same geometry. Temperature measurements from specular sensor couple show an overall stability over the time, with an averaged standard deviation of 0.77°C. This result defines the sensitivity of the EF when comparing the performances of different-reflectivity coverings applied on equal-geometry urban canyons. First results confirm that this sensitivity value is less than one order of magnitude with respect to the expected difference produced by the application of films with different reflectance capability in the two parallel test facilities (EF), as carried during the first week of August 2013.

An intensive data-taking campaign is currently on-going. On each test field, the vertical surfaces of the canyons have the same reflective properties (high reflectivity on one side and low reflectivity on the other side). The results will be used to relate the reflectivity to the canyon characteristic temperature change. Measured wind speed will be included to correctly account for the convection heat transfer. A wind protective barrier will be also arranged. As a final step, the data will be used to validate the TM.

6 REFERENCES

[1] Shahidan, M. F., Jones, P. J., Gwilliam, J., Salleh, E. (2012). An evaluation of outdoor and building environment cooling achieved through combination modification of trees with ground materials. *Building and Environment*, 58, 245-257.

[2] Manley, G. (1958). On the frequency of snowfall in metropolitan England. Quarterly *Journal of the Royal Meteorological Society*, 84, 70-72.

[3] Taha, H. (1997). Urban climates and heat islands: albedo, evapotranspiration, and anthropogenic heat, *Energy and Buildings*, 25, 99-103.

[4] Giridharan, R., Kolokotroni, M. (2009). Urban heat island characteristics in London during winter, *Solar Energy*, 83, 1668-1682

[5] Howard, L. (2012). *Climate of London Deduced from Meteorological Observations*, Harvey and Darton 3rd ed.

[6] Pisello, A.L., Cotana, F., Nicolini, A., Brinchi, L. (2013). Development of Clay Tile Coatings for Steep-Sloped Cool Roofs. *Energies*, 6, 3637-3653.

[7] Santamouris, M. (2007). Heat island research in Europe—the state of the art, *Advances Building Energy Research*, 1(1), 123-150.

[8] Synnefa, A., Saliari, M., Santamouris, M. (2012). Experimental and numerical assessment of the impact of increased roof reflectance on a school building in Athens, *Energy and Buildings*, 55, 7-15.

[9] Pisello, A. L., Rossi, F., Cotana, F. (2012). On the impact of cool roofs in Italian residential buildings: experimental assessment of summer and winter performance, ICHMT Digital library on line, DOI: 10.1615/ICHMT.2012.SEBUA-12.220.

[10] Kolokotsa, D., Diakaki, C., Papantoniou, S., Vlissidis, A. (2012). Numerical and experimental analysis of cool roofs application on a laboratory building in Iraklion, Crete, Greece, *Energy and Buildings*, 55, 85-93

[11] Xu, X., Taylor, J.E., Pisello, A.L., Culligan, P. (2012). The impact of place-based affiliation networks on energy conservation: An holistic model that integrates the influence of buildings, residents and the neighborhood context, Energy and Buildings, 55, 637-646.

[12] Akbari, H., Matthews, D. H. (2012). Global cooling updates: Reflective roofs and pavements, Energy and Buildings, 55, , pp. 2-6.

[13] Gobakis, K., Kolokotsa, D., Synnefa, A., Saliari, M., Giannopoulou, K., Santamouris, M. (2011). Development of a model for urban heat island prediction using neural network techniques, *Sustainable Cities and Society*, 1, 104-115.

[14] Allegrini, J., Dorera, V., Carmelieta, J. (2012). Influence of the urban microclimate in street canyons on the energy demand for space cooling and heating of buildings, *Energy and Buildings*, 55, 823-832.

[15] Strømann-Andersen, J., Sattrup, P.A. (2011). The urban canyon and building energy use: Urban density versus daylight and passive solar gains, *Energy and Buildings*, 43, 2011-2020.

[16] Doya, M., Bozonnet, E., Allard, F. (2012). Experimental measurement of cool facades' performance in a dense urban environment, *Energy and Buildings*, 55, 42-50.

[17] Chan, A. T., So, E. S. P., Samad, S. C. (2001). Strategic guidelines for street canyon geometry to achieve sustainable street air quality, *Atmospheric Environment*, 35, 4089-4098.

[18] Krüger , E., Pearlmutter, D., Rasia, F. (2010). Evaluating the impact of canyon geometry and orientation on cooling loads in a high-mass building in a hot dry environment, *Applied Energy*, 87, 2068-2078.

[19] Bonacquisti, V., Casale, G.R., Palmieri, S., Siani, A.M. (2006). A canopy layer model and its application to Rome, *Science of the Total Environment*, 364,1-13.

[20] Ratti, C., Baker, N., Steemers, K. (2005). Energy consumption and urban texture, *Energy and Buildings*, 37, 762-776.

[21] ASTM International. Standard test method for solar absorptance, reflectance, and transmittance of materials using integrating spheres. 2012, ASTM 903-12, DOI: 10.1520/E0903-12.

[22] European Committee for Standardization. Glass in building – determination of luminous and solar characteristics of glazing. 2011, UNI EN 410:2011.

[23] M. Felli and C. Buratti. Lezioni di Fisica Tecnica 2. 2004. ISBN 88-89422-14-9.

[24] Y.A. Cengel, Termodinamica e trasmissione del calore, ed. McGraw-Hill, 1998.

ON THE ANALYSIS OF COOL ROOFS FOR COOLING SYSTEM EFFICIENCY

Anna Laura Pisello[1*], Mattheos Santamouris[2], Franco Cotana[1]

1 CIRIAF – University of Perugia
Via G. Duranti 67,
06125 Perugia, Italy
**Corresponding author: Pisello@crbnet.it*

2 Group Building Environmental Studies,
Physics Department
University of Athens, Athens

ABSTRACT

Cool roof is a well-documented passive cooling strategy for buildings in several climate conditions. The mechanism consists of the reduction of the heat load entering the roof, which is characterized by high solar reflectance and high thermal emittance. The purpose of this paper is to study the coupled effect produced by such a technology. First, the passive cooling contribution is quantified, then, the "active" contribution is investigated. This latter effect consists of the cool roof capability to decrease the suction air temperature of heat pump external units, when these units are located over the same roof. This "cooling" benefit produce an extra-increase of the energy performance of the heat pump in cooling mode, given that it produces the decrease of the temperature lift between the source and the output. In order to study this twofold effect, an industrial building with an office area located in Rome, Italy, was continuously monitored in summer 2012. The thermal behavior of the roof, of the indoor environment, and the energy requirement for cooling were evaluated. The main results showed that the cool roof allows to decrease the roof overheating up to 20°C. The office indoor air temperature was lowered, even if the same set-point temperature was kept constant during the whole campaign. The energy requirement for cooling decreased by about 34% during the working time of the office. In order to investigate the "active" contribution, suction air temperature was monitored and a new simple analytical model is proposed in order to estimate the cool roof effect in reducing the air overheating over the roof and, therefore, the temperature lift to be smothered with the cooling system.

KEYWORDS

Cool roof; Energy saving in buildings; roof albedo; passive cooling; office building; energy efficiency.

1 INTRODUCTION

Cool roofs are those roofs that are able to reflect solar radiation and emit heat, keeping the roof cooler than a traditional roof even when subject to high solar radiation [1]. In cool roof applications, the incident solar radiation is reflected by roof, and the absorbed radiation entering the roof is consequently decreased. This passive phenomenon implies lower heat load penetrating the roof and into the thermal zones of the building, with the following reduction of energy requirement for cooling. Cool roof performance represents the object of many important studies concerning cool coating application over the roof of residential and non-residential buildings, which behavior is analyzed through experimental and numerical analysis [2].

Haberl and Cho, in their literature review about the effect of cool roofs on building energy saving for cooling [3], showed that the achievable energy saving amount is about 20% in residential and commercial buildings. They reported a cooling energy saving average range of 2-44% , and the reduction of the cooling peak of 3-35%. Cool roof performance is influenced by several parameters such as the ceiling insulation level, the attic configuration, climate conditions, occupancy schedules and inter-building phenomena in general. The effect of cool roofs in determining cooling load and thermal comfort conditions was investigated by Synnefa et al. in [4] for residential buildings. The study consisted of an integrated

experimental and numerical assessment aimed at estimating the effect of cool colored materials for envelopes in 27 cities around the world. They investigated cool roof potentialities in different climatological conditions, such as: (i) Mediterranean area, (ii) humid continental area, (iii) subtropical arid area, and (iv) desert. They considered the same building layout for modeling the case study prototype and its technical-architectural features. Therefore, they estimated the cooling energy savings, together with the potential wintertime penalties. The main findings show that the increase in roof solar reflectance by 0.65 is able to reduce: (i) cooling loads of 8-48 kWh/m^2, (ii) discomfort hours by 9-100%, and (iii) peak temperature by 1.2°C to 3.7°C. The main variables to consider, when performing cool roof assessment, are climate and roof insulation level. Winter potential penalties (0.2-17 kWh/m^2) are in general lower than summer benefits (9-48 kWh/m2) and they could be worsen by high-transmittance level of the roof. In fact, the roof reflectance increase could potentially increase the heating energy demand. Several numerical and experimental studies have shown that this winter penalty is basically far less incisive than the cooling benefit, producing an overall year-round energy saving in both mild and moderate climate regions [5].

Important studies also took into account cool roof effect in determining indoor thermal comfort conditions, especially for free floating buildings, where the cool roof, as passive solution, is able to produce an operative temperature average decrease of 2.3°C in Sicily [6].

A successful European project specifically concerned the investigation around this technique. Thanks to the findings of this project [7], huge research effort was dedicated to this theme. Many cool roof applications were analyzed through experiments and numerical analyses also in those European countries which are not characterized by southern Mediterranean climate, such as London area and Andalusia, Spain. For instance, Kolokotroni et al. in [8] investigated the effect of a cool roof coating applied on the roof of a naturally ventilated office building in London. The cool roof application represented an effective building passive retrofit solution even in temperate climates, where the optimum reflectance value is around 0.6-0.7. Sprawling the boundary of this technique at larger scale, Boixo et al. in [9] focused on the potential energy saving achievable by cool roof implementation at regional scale. The case study consisting of Andalusia region allowed to quantify an overall energy saving of around 295,000 kWh per year. In fact, important cool roof effects were also carried out through larger scale studies, in particular considering the effect of high reflective surfaces in improving urban climate condition [10]. In order to be able to apply such a technique to existing buildings located in urban area, new less impacting materials and roof elements were developed, where infra-red reflectance is optimized, but visible aspect is maintained as traditional roof covering or tiles for example [11]. Therefore, cool roof strategy could become an effective and feasible solution even in urban historic centers and for existing buildings in general [12].

2 ACTIVE AND PASSIVE BENEFITS OF COOL ROOFS

As already described, cool roof as passive strategy aimed at reducing building energy requirement for cooling have already been widely investigated, in several climate conditions, building operations and architectures [13]. The potential further benefit produced by cool roofs arises from the observation that in several Italian commercial and industrial buildings, the external units of the heat pumps, commonly used for cooling, are located over the roof, especially if they have flat configuration. This positioning determines the energy efficiency of such a technology because the roof is exposed to the solar radiation all day long and during the overall year. Therefore, the thermal characteristics of the roof, and the consequent thermal environment of the air adjacent to the roof, are of primary importance in determining heat pump energy efficiency. In fact, the performance of heat pumps for cooling is affected by several factors [14], such as: (i) climate (cooling demand and maximum peak loads); (ii) temperature of the cooling source and distribution system; (iii) auxiliary energy consumption;

(iv) technical standard of the heat pump; (v) sizing of the heat pump in relation to the cooling demand and the operating characteristics; (vi) control system. Additionally, it is known that the coefficient of performance of heat pumps in cooling mode increases as outdoor temperature decreases, because it is strictly related to the temperature lift between the source and the output [14].

In this work, the cool roof effect in decreasing the suction air temperature of heat pumps with external units located over the roof is investigated, by assuming that all the other characteristics affecting heat pump efficiency do not vary due to cool roof application, except for (ii). To this aim, the suction air temperature of the cooling system is monitored before and after the cool roof installation over the case study building. Then, the passive cooling benefits are evaluated when combined with the "active" benefits in increasing cooling energy efficiency.

3 METHODOLOGY

3.1 Main steps of the research work

This research concerns the analysis of the results of an experimental campaign carried out during summer 2012 in Rome, Italy. The step-by-step methodology is described below.

- Choice of the building. Typical Italian industrial building is chosen, where an open office area, located in the mezzanine adjacent to the roof, is monitored for the purpose of the study. The roof is represented by a non-insulated roof with precast reinforced concrete structure. The external units of the heat pumps are located over the roof of the office, which is characterized by the application of the innovative cool roof coating.
- Continuous monitoring. The indoor-outdoor thermal-energy monitoring began on July 2012 and it ended on October 2013. The scenario B as "before" and the scenario A as "after" the cool roof application are monitored.
- In-field albedo and thermography measurement. Two kinds of measurements are carried out during the experiment, in order to measure the in-field albedo of the studied roof and evaluate the superficial temperature of the monitored roof [15].
- Evaluation of the passive cooling cool roof effect. The analysis of the roof thermal behavior and of the indoor thermal behavior is carried out, in order to quantify the passive cooling benefit produced by the cool coating.
- Evaluation of the active cool roof effect. The energy consumption of the heat pump system of the open office area is investigated. Additionally, a new simple procedure investigating the relationship between the outdoor temperature and the suction air temperature of the external units of the heat pump located over the monitored roof is proposed, with the purpose to estimate cool roof benefits produced by the decrease of suction air temperature in summer.

3.2 Analysis of the active cool roof effect

The evaluation of the cooling efficiency is performed by taking into account the capability of the cool coating to reduce the temperature of the suction air of the external unit of the heat pump, located over the roof of the monitored office. A 12-day period for each scenario is chosen in order to have similar climate conditions to compare scenario B and A. August 9th-20th is chosen for scenario B, and August 23rd-September 3rd for scenario A. The average day is elaborated for each scenario, by calculating the average value of all the data collected during these 12 days, every 5 minutes. Therefore, the temperature T(t) of each scenario is calculated, for each instant t, as follows (1):

$$T_B(t) = \frac{\sum_{i=1}^{n} T_{B,i}(t)}{n} \qquad T_A(t) = \frac{\sum_{i=1}^{n} T_{A,i}(t)}{n} \tag{1}$$

Where n=12 is the number of days for each scenario; $T_{B,i}$ and $T_{A,i}$ are the temperature values at each instant t, in each day i, for scenario B and A, respectively.

The daily overheating of the suction air temperature, with respect to the reference outdoor dry bulb temperature, is analysed through sinusoidal wave equations, in order to evaluate the cool roof contribution in reducing the wave amplitude A^* and the non-zero central amplitude T^* of the daily wave. Therefore, the 24-hour behavior of scenario B is described as follows for suction air temperature $T_{s,B}(t)$ and outdoor temperature $T_{o,B}(t)$ (2):

$$\begin{cases} T_{s,B}(t) = T^*_{s,B} + A^*_{s,B} \cdot \sin\left(\frac{2\pi}{T} t + \varphi^*\right) \\ T_{o,B}(t) = T^*_{o,B} + A^*_{o,B} \cdot \sin\left(\frac{2\pi}{T} t + \varphi^*\right) \end{cases} \qquad 0 \le t < 24 \tag{2}$$

Eq. (3) describes the thermal behavior of suction air $T_{s,A}(t)$ and outdoor $T_{o,A}(t)$ temperature for scenario A:

$$\begin{cases} T_{s,A}(t) = T^*_{s,A} + A^*_{s,A} \cdot \sin\left(\frac{2\pi}{T} t + \varphi^*\right) \\ T_{o,A}(t) = T^*_{o,A} + A^*_{o,A} \cdot \sin\left(\frac{2\pi}{T} t + \varphi^*\right) \end{cases} \qquad 0 \le t < 24 \tag{3}$$

Where:

- $T^*_{s,B}$ and $T^*_{s,A}$, $T^*_{o,B}$ and $T^*_{o,A}$ are the non-zero center amplitudes of the suction air/outdoor temperature sine wave, optimized to minimize in least square sense the error between real data and the sine curve for scenario B and A, respectively;
- $A^*_{s,B}$ and $A^*_{s,A}$, $A^*_{o,B}$ and $A^*_{o,A}$, are the amplitude values of the sinusoidal curves, which are manually tuned and optimized in such a way to minimize in least square sense the error between real data and the sine curve, in scenario B and A, respectively;
- φ^* is the phase values of the sinusoidal curves, manually tuned and optimized to minimize in least square sense the error between real data and the sine curve;
- T is the period of the oscillation, which corresponds to 24 hours.

The analysis of the amplitude T* and the non-zero center amplitude A* of the sine wave equation, allows to evaluate the contribution produced by cool roof in terms of overheating of the suction air with respect to the outdoor air temperature. This same overheating is calculated through the difference between the $T_s(t)$ and $T_{o,B}(t)$, in (4-5) for scenario B and A, respectively:

$$\Delta T_B(t) = T_{s,B}(t) - T_{o,B}(t) = \left(T^*_{s,B} - T^*_{o,B}\right) + \left(A^*_{s,B} - A^*_{o,B}\right) \sin\left(\frac{2\pi}{T} t + \varphi^*\right) \qquad 0 \le t < 24 \tag{4}$$

$$\Delta T_A(t) = T_{s,A}(t) - T_{o,A}(t) = \left(T^*_{s,A} - T^*_{o,A}\right) + \left(A^*_{s,A} - A^*_{o,A}\right) \sin\left(\frac{2\pi}{T} t + \varphi^*\right) \qquad 0 \le t < 24 \tag{5}$$

Given that the "active" cool roof effect could be described as the capability to decrease the difference of the amplitudes and of the non-zero center amplitudes, these parameters are synthetically defined as $\bar{T}$ and $\bar{A}$. Therefore, eq. (4-5) could be rewritten as follows (6-7), for scenario B and A, respectively:

$$\Delta T_B(t) = \bar{T}_B + \bar{A}_B \sin\left(\frac{2\pi}{T} t + \varphi^*\right) \qquad 0 \le t < 24 \tag{6}$$

$$\Delta T_A(t) = \bar{T}_A + \bar{A}_A \sin\left(\frac{2\pi}{T} t + \varphi^*\right) \qquad 0 \le t < 24 \tag{7}$$

4 EXPERIMENTAL CAMPAIGN

4.1 Case study

The chosen case study consists of an industrial building located in Rome, Italy. The industrial production area occupies the ground floor of the building, around 1000 m^2 of ground surface, and an open office area occupies the mezzanine. This thermal zone is monitored and the cool roof twofold effect is investigated.

The case study industrial building was constructed in 1969 (Figure 1). The monitored office is represented by a rectangular 60 m^2 mezzanine, which longer side (10 m long) is coincident with the South-East façade of the building. The structural system of the case study consists of a precast reinforced concrete columns and beams; the opaque façade elements are concrete non-insulated panels. The roof structure consists of canal beams integrated with sloped glass panels. The structure is not provided with any insulation panel, such as all the industrial buildings constructed before the building energy efficiency regulation, forced in Italy in 1976 [16].The office basically consists of three rooms, where the main zone is monitored and where the heat pump system is located. The nominal cooling capacities of the system is 3604-5569-7034 W, while the nominal heating capacity is 3809-5862-7327 W.

Fig. 1 View of the façade and the open office of the case study building.

The thermal zone occupancy is from 8:00 a.m. to 5:00 p.m. from Monday to Friday, national holidays excluded. The monitored office is typically occupied by 6 sales-people, each one working on his desk position. According to the occupants, the cooling plants are kept at the same constant temperature set-point, in the weekends and nights as well, for the entire duration of the campaign described in this paper.

4.2 In-field thermal-energy monitoring

The thermal-energy monitoring of the open office is carried out both before and after the cool roof implementation, i.e. during what is named scenario B (before) and scenario A (after). The B scenario began on July 25th, 2012 and it ended on August 20th. The scenario A began on August 23rd, after the cool roof application (August 20th -22nd) and it ended on September 28th. Roof thermography and albedo in-field measurement are operated on August 8th and September 6th, for scenario B and A, respectively.

The monitoring setup is composed by a series of temperature probes and energy meters collecting data every 5 minutes, and connected to a data-logger station, and then to a web-based platform. The temperature probes are positioned as follows: (i) in the middle of the thermal zone (indoor air temperature), (ii) on the roof external surface, (iii) on the roof internal surface, (iv) in correspondence to the position of the suction air flux of the external unit of the heat pump, as indicated by the technology producer (Figure 2). As already mentioned, on two selected days, spot thermography and albedo measurements are performed.

Thermography is operated at three different times during each day (at about 10:00 a.m., 12:30 p.m., 3:00 p.m.) both before and after the cool roof implementation.

Figure 2(a-e): Monitoring system: (a) external surface temperature probe, (b) internal surface temperature probe, (c) indoor air temperature probe, (d-e) albedo in-field measurement before and after cool roof application.

A FLIR i3 infrared camera is used to analyze both the internal and external envelope surfaces of the building, with a <0.15°C precision and -20ºC÷250ºC temperature range. The albedo is measured by a double pyranometer DPA 568 produced by LSI-Lastem, where the first pyranometer is upward oriented and the second one is downward oriented. Both these instruments are able to measure the radiation every 20 seconds, and to report the values of average, minimum, maximum, and standard deviation every 10 minutes (Figure 2) [15].

5 RESULTS AND DISCUSSION

5.1 In-field preliminary measurements

The optical-thermal performance of the chosen cool roof coating is characterized by in-field albedo measurement through albedometer facility. The global radiation data collected every 10 minutes shows that, by selecting the 12:00 – 2:00 p.m. time interval, in order to avoid mutual shading disturbing phenomena produced by the shape of the roof, the albedo of the scenario B is 0.07 (bitumen covering) while the albedo of the scenario A is 0.75 [15]. Thermography images show that the cool roof benefit consists of the reduction of the internal and external surface temperature of the roof, and also the reduction of the thermal dissimilarities between temperature of the beam and of the concrete shingle [14].

5.2 Cool roof effect on roof thermal behavior

Figure 3 reports the temperature values of roof external surface T_{surf} and outdoor temperature T_{out}, monitored in August 9^{th}-12^{th} and August 23^{rd}-26^{th} for scenario B and A, respectively. The periods are chosen for the similar weather and temperature conditions to compare the two considered scenarios. The effect of the cool coating is evident in decreasing the daily thermal peak of 10-15°C. Nevertheless, during the night, the surface temperature does not highlight any evident difference between the two configurations.

Figure 4 describes roof external surface temperature versus the outdoor temperature, taking into account the overall 12 days of monitoring for both scenarios. By reporting the tendency line for each series of data, which is able to describe the trend (R^2>0.8), the cool roof contribution is evident at high temperature in particular. In fact, when outdoor temperature is higher than 30°C, the solar radiation is supposed to be an important contribution such as during sunny daily hours, and cool roof is able to decrease T_{surf} up to 20°C in the monitored period. Consistently with the previous consideration, the night behavior, when T_o is around 20-25°C, the roof surface temperature is not much affected by cool roof implementation.

5.3 Cool roof effect on indoor thermal behavior

Figure 5 reports the comparison between the indoor air temperature of the open office area and the outdoor temperature measured during the same days of the previous analysis. It is evident that the cool roof, despite the slightly hotter conditions registered in scenario A, is able to cool the indoor office area, even if the set-point temperature of the cooling system is kept at 23°C by the occupants during the whole period. In particular, given the cool roof capability to reduce the heat gain entering the roof in scenario A, the indoor air temperature in

the afternoon is even lower than during morning, and the difference between the two considered scenarios is around 2-4°C from 2:00 pm to 10:00pm. The same phenomenon is confirmed by occupants' perception. In fact, they asked to increase the set-point temperature because of their freezing perception, after the cool roof application.

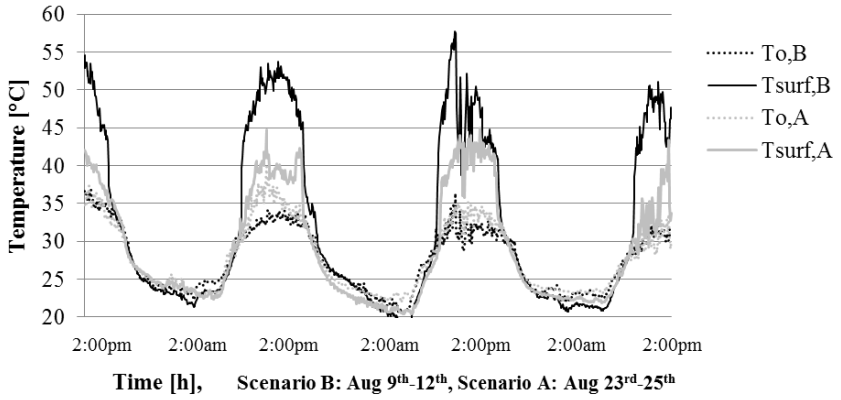

Figure 3: Superficial temperature of the roof T_{surf} with respect to outdoor temperature T_{out} for scenario B and A.

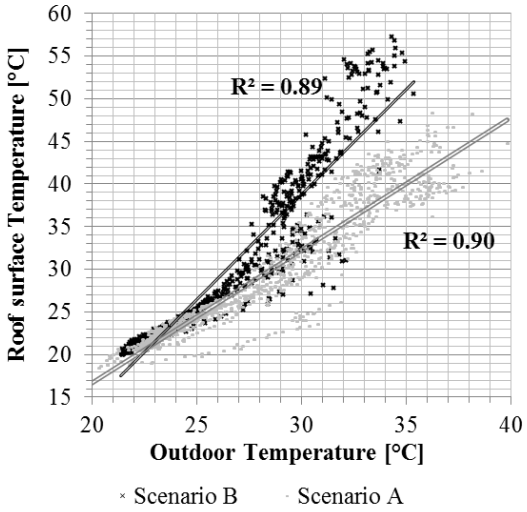

Figure 4: External surface temperature of the roof vs. outdoor temperature for scenario B and A.

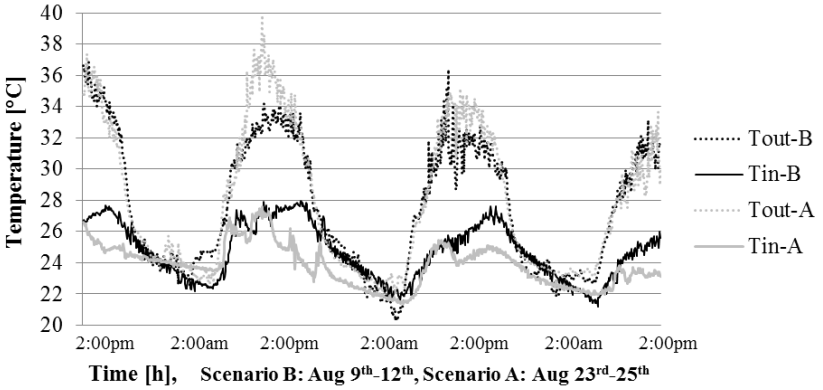

Figure 5: Indoor air temperature T_{in} with respect to outdoor temperature T_{out} for scenario B and A.

5.4 Cool roof effect on suction air temperature

As previously mentioned, the suction air temperature mainly affects the efficiency of the heat pump systems, given that it determines the temperature lift between the source and the output.

In order to evaluate the cool roof effect of this parameter, a temperature probe is installed in the proper position close to the external unit of the heat pump located over the roof, and the air temperature of this position is monitored. Section 3.1 describes the methodology proposed to investigate such an effect. The main purpose of defining a simple curve to describe the potential overheating reduction produced by cool roof, is to provide a sort of preliminary estimation that could be useful to evaluate the increase of the Energy Efficiency Ratio (EER) of the heat pumps when their external units are located in "colder" environment produced by cool roof application. This benefit, that here is defined as "active" cool roof effect, has to be added to the passive cooling contribution produced by the same cool roof application.

Figure 6 reports the daily profiles of measured suction temperatures $T_{s,B(meas)}$ and $T_{s,A(meas)}$, measured outdoor temperatures $T_{o,B(meas)}$ and $T_{o,A(meas)}$ for scenario B and A, respectively. Additionally, the sine wave equations of the same parameters are represented, as described in (2-3). Table 1 reports the descriptive parameters of the sine wave equations, calculated to minimize the error in least square sense. Therefore, the cool roof "active" effect consists of the reduction of the amplitude difference between T_s and T_o by 1.2°C, i.e. from 0.7°C to -0.5°C. Additionally, cool roof application is able to decrease the non-zero center amplitude T_s^* with respect to T_0^* by 0.4°C, when scenario B is characterized by higher T_s^* with respect to T_0^* by 0.5°C.

Figure 7 reports the difference between suction air temperature and air temperature for both the scenarios, described in eq. (6-7) and Table 2 reports the descriptive parameters of the sine waves equations (6-7). Figure 8 highlights how the cool roof effect is able to decrease the overheating of the suction air temperature, in particular during the hottest hours of the day, when the overheating decreases from 1.2°C (scenario B) to -0.9°C (scenario A). Additionally, the difference between the two non-zero center amplitudes of the overheating wave $\overline{T_B} - \overline{T_A}$ is 0.9°. The cool roof is also able to decrease the overall amplitude of the sine wave ($\overline{A_B} - \overline{A_B}$), by 1.2°C, which represent the two key parameters of the analysis of the "active" affect.

Table 1: Descripting parameter of the sine wave function of eq. (5-6).

Parameters	Scenario B	Scenario A
T_s^*	29.0°C	25.2°C
T_o^*	28.5°C	25.6°C
A_s^*	5.9°C	4.7°C
A_o^*	5.2°C	5.2°C
φ^*	0.5π rad	0.5π rad

Table 2: Descripting parameter of the sine wave function of eq. (7-8).

Parameters	Scenario B	Scenario A
$\overline{T} = T_s^* - T_o^*$	0.5°C	-0.4°C
$\overline{A} = A_s^* - A_o^*$	0.7°C	-0.5°C

5.5 Energy consumption

The energy consumption of the monitored heat pump of the open office area is collected twice a day, at the beginning and at the end of the working time, for the entire duration of the campaign. The results of two climatically similar weeks are compared in Figure 8. The graph reports the values collected at 8:00am and at 5:00pm, in order to investigate the cool roof contribution in decreasing energy requirement for cooling during the night and during the day, respectively.

The overall cool roof benefit corresponds to 34% of energy saving during the day and to 47% of the energy saving during the night, calculated by comparing scenario B with scenario A and then, calculating the average value of the week. This important reduction in energy requirement for cooling is therefore produced by the passive cool roof cooling effect, coupled with the described active effect.

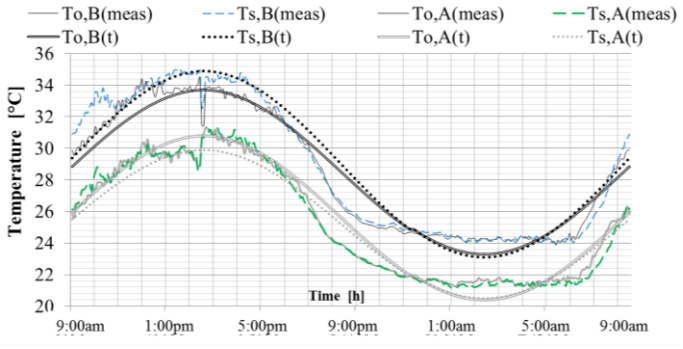

Figure 6: Daily (measured and simulated) profiles of T_s with respect to T_o in B and A scenarios.

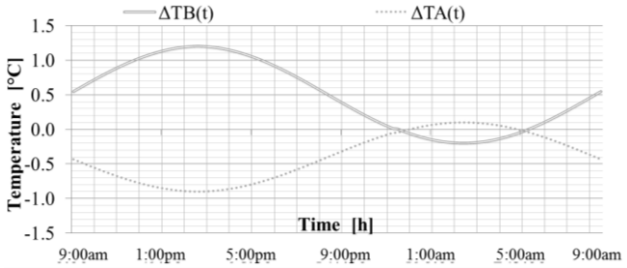

Figure 7: Daily overheating (simulated) profiles in B and A scenarios.

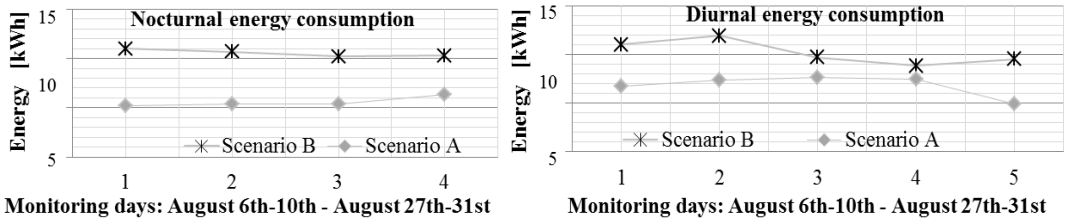

Figure 8: Daily overheating (simulated) profiles in B and A scenarios.

6 CONCLUSIONS

This study describes the twofold effect of the cool roof application on a case study industrial-office building in Italy. First, cool roof passive cooling contribution is investigated, then, specific attention is paid in order to evaluate its "active" contribution. This latter aspect consists of the cool roof capability to decrease the air temperature of the ambient over the roof, when the external units of the heat pumps in cooling mode are located. This contribution is able to decrease the suction air temperature, and then also the temperature lift between the source and the output air. For this reason, the energy efficiency of the heat pump during the cooling season increases.

The selected building is a non-insulated 1000 m^2 industrial building where the office, 60 m^2 area, occupies the mezzanine. The in-field albedo increased from 7% to 75%. The thermography showed cool roof capability to homogenize the temperature of the roof, and to lower the internal surface temperature of about 10°C. The indoor-outdoor continuous monitoring carried out during summer 2012, showed that the cool roof was able to decrease the heat gain entering the roof and the indoor air temperature of the office area by 2-4°C, even if the set-point temperature of the cooling system was kept constant for the period of the

study. A comparison between two similar weather periods is operated, in order to quantify the benefit in terms of electricity saving for cooling. It corresponded to 34% during the daily work shifts of the monitored period. Finally, a new procedure was proposed to evaluate the decrease of the suction air temperature after cool roof application. The main results showed that the cool roof is able to annul the suction air overheating with respect to the outdoor air temperature.

7 ACKNOWLEDGEMENTS

This work was carried with the technical support of TecneXum GmbH.

8 REFERENCES

[1] Akbari, H., Levinson R., Rainer L. (2005) Monitoring the energy-use effects of cool roofs on California commercial buildings. *Energy and Buildings*, 37, 1007-1016.

[2] Borge-Diez, D., Colmenar-Santos A., Pérez-Molina C., Castro-Gil M.. Passive climatization using a cool roof and natural ventilation for internally displaced persons in hot climates: Case study for Haiti. *Building and environment*, 59, 116-126.

[3] Haberl, J.S., Cho S. (2004). Literature review of uncertainty of analysis methods (Cool Roofs) Report to the Texas Commission on Environmental Quality. Texas A&M.

[4] Synnefa, A., Saliari M., Santamouris M. (2012). Experimental and numerical assessment of the impact of increased roof reflectance on a school building in Athens. *Energy and buildings*, 55, 7-15.

[5] Pisello, A.L., Rossi, F., Cotana, F. (2012). On the impact of cool roofs in Italian residential buildings: experimental assessment of summer and winter performance. DOI: 10.1615/ICHMT.2012.SEBUA-12.220.

[6] Romeo, C., Zinzi, M. (2011) Impact of a cool roof application on the energy and comfort performance in an existing non-residential building. A Sicilian case study. *Energy and buildings*. DOI:10.1016/j.enbuild.2011.07.023.

[7] Synnefa, A., Santamouris, M. (2012). Advances on technical, policy and market aspects of cool roof technology in Europe: The Cool Roofs project. Energy and buildings. *Energy and Buildings*, 55, 35-41.

[8] Kolokotroni, M., Gowreesunker, B.L., Giridharan, R. (2011). Cool roof technology in London: An experimental and modelling study. Energy and buildings. DOI: 10.1016/j.enbuild.2011.07.011.

[9] Boixo, S., Diaz-Vicente, M., Colmenar, A., Castro M.A. (2012). Potential energy savings from cool roofs in Spain and Andalusia. *Energy*, 38, 425-438.

[10] Santamouris, M., Synnefa, A., Karlessi, T. (2011). Using advanced cool materials in the urban built environment to mitigate heat islands and improve thermal comfort conditions. *Solar Energy*, 85, 3085-3102.

[11] Santamouris, M., Synnefa, A., Karlessi, T. (2011). Using advanced cool materials in the urban built environment to mitigate heat islands and improve thermal comfort conditions. *Solar Energy*, 85 (12), 3085-3102.

[12] Pisello, A.L., Cotana, F., Nicolini, A., Brinchi, L. (2013). Development of Clay Tile Coatings for Steep-Sloped Cool Roofs. *Energies*, 6, 3637-3653.

[13] Synnefa, A., Santamouris, M., Akbari, H. (2007). Estimating the effect of using cool coatings on energy loads and thermal comfort in residential buildings in various climatic conditions. *Energy and Buildings*, 39 (11), 1167-1174.

[14] Liu, X., Ni, L., Lau, S.-K., Li, H. (2013). Performance analysis of a multi-functional heat pump system in cooling mode, *Applied Thermal Engineering*, 59 (1-2), 253-266.

[15] Pisello, A.L., Thiemann, A., Santamouris, M., Cotana, F. (2013). Analysis of a Cool Roof System for Reducing Cooling Loads and Improving Cooling System Efficiency. Proceedings of CLIMA2013 International Conf. Prague. 16-18 June.

[16] Pisello, A.L., Cotana, F. (2013). Pisello, A.L.; Cotana, F. The thermal effect of an innovative cool roof on residential buildings in Italy: Results from two years of continuous monitoring. Submitted for publication in Energy and Building on May 2nd, 2013.

TOWARD DESIGNING STRATEGIES FOR URBAN HEAT ISLAND MITIGATION BASED ON MULTISCALE FLOW CONSIDERATIONS

Marina K.-A. Neophytou[1*], Eleonora Tryphonos[1], Paris Fokaides[1], Mats Sandberg[2], Ekaterina Batchvarova[3], Harindra J.S. Fernando[4], Jos Lelieveld[5,6], Georgios Zittis[5]

[1] *Environmental Fluid Mechanics Laboratory, Department of Civil and Environmental Engineering, University of Cyprus, CYPRUS*
**Corresponding author: neophytou@ucy.ac.cy*

[2] *KTH Research School, Univeristy of Gavle, SWEDEN*

[3] *National Hydrometeorological Institute, BULGARIA*

[4] *Department of Civil & Environmental Engineering and Earth Sciences, University of Notre Dame, USA*

[5] *Energy, Environment and Water Research Center, The Cyprus Institute, CYPRUS*

[6] *Max Planck Institute for Chemistry, Mainz, GERMANY*

ABSTRACT

Much of the on-going discussion on urban heat island mitigation and proposed measures for cooling is based on case-studies taken at a specific scale and settings; the evaluation of the effectiveness of proposed cooling measures is therefore made using performance criteria derived for that specific scenario. The transferability of this knowledge to other sites and climatologies is not ensured. This is because the phenomena dictating the urban climate are inherently multi-scale and the contribution of heating sources or cooling mechanisms as well as their interaction with other ongoing-possibly physical phenomena can be different. Therefore, strategies for urban cooling in a city should consider the mutli-scale nature of urban climate, based on which mitigation actions and costs must be considered. In this work we report results from a multi-scale field experiment conducted in Nicosia-Cyprus in July 2010 to investigate the Urban Heat Island (UHI) in Nicosia capital city and its interaction with multi-scale meteorological phenomena that take place in a broader region over Cyprus. Specifically, the results are analysed and interpreted in terms of a non-dimensional/scaling parameter dictating the urban heat island circulation reported from laboratory experiments (Fernando, 2010). We find that the field measurements obey the same scaling law during the day, in the absence of any other flow phenomena apart from the urban heating. During the night we find that the deduced non-dimensional value reduces to half (compared to that during the day); this is due to the presence of katabatic winds from Troodos mountains into the urban center of Nicosia and their cooling effect superimposed on diurnal urban heating. Based on this deduction, we evaluate the impact of various proposed heat island mitigation measures in urban planning.

KEYWORDS

Field experiments, urban meteorology, mediterranean urban climate

1 INTRODUCTION

Urbanization has been increasing at an alarming rate: while in the 1800's, only 3% of the world's population lived in urban areas, by the 1950's the urban population increased to 30% and in 2000 it reached 47%. With this ever increasing growth, numerous issues have been raised, such as air quality issues, sustainable use of energy, maintenance of waste materials and socio-economic status of urban inhabitants as well as on the presence of the urban heat

island phenomenon [6]. Much of the on-going discussion on urban heat island mitigation and proposed measures for cooling is based on case-studies taken at a specific scale and settings; the evaluation of the effectiveness of proposed cooling measures is therefore made using performance criteria derived for that specific scenario. The transferability of this knowledge to other sites and climatologies is not ensured. This is because the phenomena dictating the urban climate are inherently multi-scale and the contribution of heating sources or cooling mechanisms as well as their interaction with other ongoing-possibly physical phenomena can be different. Therefore, strategies for urban cooling in a city should consider the mutli-scale nature of urban climate, based on which mitigation actions and costs must be considered. In this work we report results from a multi-scale field experiment conducted in Nicosia-Cyprus in July 2010 to investigate the Urban Heat Island (UHI) in Nicosia capital city and its interaction with multi-scale meteorological phenomena that take place in a broader region over Cyprus. Specifically, the results are analysed and interpreted in terms of a non-dimensional/scaling parameter dictating the urban heat island circulation reported from laboratory experiments (Fernando, 2010). Therefore strategic urban design decisions for UHI mitigation should take into account any scaling laws that bound the behaviour of the built environment in order to develop measures that would mitigate UHI.

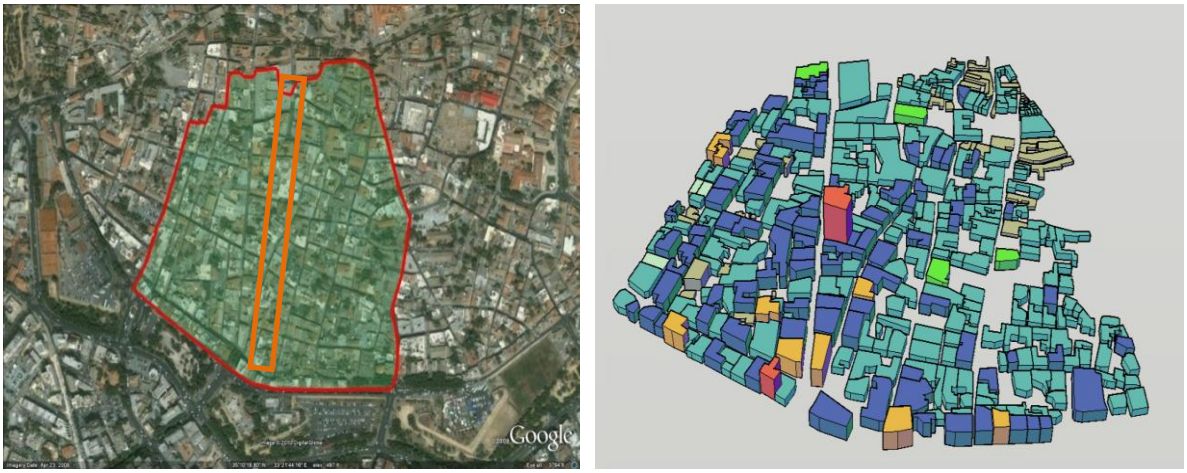

Figure 1: The investigated Nicosia's old city centre encircled with the red continuous line (on the Right-Hand-Side); the orange line encircles the steet (Ledras Street) under investigation. On the Right-Hand_Side, the AUTOCAD model mapping of the region is shown taking account coloured according to the building height of each building volume.

2 METHODOLOGY

2.1 Field Site

In terms of the site selection, the parameters of building height, building density and paved and unpaved area coverage were examined. This analysis provided fundamental data for all the subsequent tasks and actions. The objective was to create a complete database of the investigated area in order to assess the status of urban environment in Cyprus. Hence, major groups of building blocks (approximately 350 building blocks) were analyzed and scaled down for the applied channel, in order to support the parameterization studies for the investigated scenarios. Within this task, the geometries under investigation were also be modelled for the purposes of the CFD study. The building energy behaviour and performance are heavily influenced by the density of the building space that is why the facades chosen have different SVF. For example facades that are placed in front of an open parking area (H/W<1) can be compared with some others that are placed in a canyon. Some other

important factors were the orientation of the chosen facades and the properties of the surrounding surfaces in the same canyon.
Among the investigated neighbourhoods, the old city centre of Nicosia appeared as being the most representative for the Mediterranean-like architecture, therefore it was decided that the field campaign should be carried out in this area (see Fig. 1). The old town centre, which is the historical centre of the city, is delimited by Venetian type walls. It is generally characterized by narrow canyons with Mediterranean-style planning but also includes some buildings of contemporary architecture and also some large squares. From the West to East, four major sub-neighbourhoods (SN) could be identified according to homogeneity and packing building density SN1 to SN4. SN1 includes some larger open spaces/parking lots so that it has an overall lower packing density and it is less homogeneous. SN2 is homogeneous over relatively large distances in neighbourhoods units. SN3 has some broader avenues and squares so that it has a lower packing density. SN4 has a very large packing density being also relatively uniform.

2.2 Intensive observation periods

During the field measurement campaign, different types of measurements were taken. As the collected data are too many and complex, Table 1 summarizes briefly the collected data of the field campaign measurements. The period of the campaign is divided in three periods. The intensive observation period, 01-20/07/2010 where meteorological data are collected from different scales, the intensive observation period 10-12/07/2010, where with meteorological data buildings' temperature and humidity are collected and the peak day 12/07/2010 where radiosoundings and aerial thermography took place. Additionally, a supplementary investigation about the influence of the trees of the street temperature took place during 14-16/07/2010.

2.2.1 Meteorology across the scales – measurement procedure

2.2.1.1 Synoptic Scale

Meteorology at the synoptic scale was recorded during the observation period from 7th to 15th July 2010 using a radiosounding system. It is noted that the radiosounds were released from Nicosia old city centre area at (33.3613˚ E, 35.1741˚ N), in order to capture the urban profile characteristics of the lower layers. The sounding system provided measurements of the air pressure, temperature and humidity as well as of the wind speed and direction in corresponding altitudes. Sets of the measured data were sent down to a receiving station (ground station) as the radiosond was carried aloft by a balloon. For the days of the 7th , 10th , 11th and 15th of July 2010, the radiosoundings were released at a sporadic rate, while for the observation day of the 12th July 2010, radiosounds were released every three hours, in order capture the profile variation throughout the day.

2.2.1.2 Regional Scale

In order to examine the phenomenon of UHI in the city of Nicosia, meteorological data from Cyprus Meteorological Service for Nicosia and its surroundings are collected. Because of the Turkish occupation on the northern part of the island, meteorological data from this direction were not available. The five stations from where data were collected and analyzed from Nicosia broader surroundings are Nicosia_PASYDY, Athalassa, Athienou, Astromeritis and

Table 1: List of TOPEUM collected data according to the scale of observation, both for Meteorology and Building

Surface Temperature Respond; starting from the data of the observation period 01-20 of July 2010, moving to the data of intensive observation period 10-12 of July 2010 and ending with the data of the peak day 12th of July 2010.

Category	Scale	Collected Data	Stations	Data Time Interval	Data Origin
Meteorology	**Regional Scale**	Meteorological Data: WS and WD (10m Height), T (2m Height)	*Nicosia_Pasydy* *Athalassa* *Tamasos* *Athienou* *Astromeritis*	Hourly	Cyprus Meteorological Service
Meteorology	**Local Scale**	WS, WD, T patterns	*Sonic 1* (Ariadnis str. _ 5m height) *Sonic 2* (Rooftop in Ledras str. _ 5m height from rooftops, 26.8m from the ground) *Sonic 3* (Ledras str. _ 5m height) *Sonic 4* (Arsinois str. _ 5m height)	Hourly	TOPEUM Field Experiment
Meteorology	**Synoptic Scale**	Meteorological Maps (500hPa and surface)		00UTC and 12UTC	Cyprus Meteorological Service
Building Surface Temperature Response	**Neighborhood Scale**	On ground thermography	*Building 1* Exhibition Hall-Municipality of Nicosia, Ledras str. *Building 2* CYTA, Arsinois and Onasagorou str. *Building 3* Church, Solonos str. *Building 4* Onasagorou str. *Building 5* Fokionos str.	Every 2 hours	TOPEUM Field Experiment
Building Surface Temperature Response	**Building Scale**	Termocouples in 4 levels a) ground level b) 0,40m height c) 1,20m height d) 2,00m height	*Building 1* Exhibition Hall-Municipality of Nicosia, Ledras str. *Building 2* CYTA, Arsinois and Onasagorou str. *Building 6* Ledras str.	Every 10 minutes	TOPEUM Field Experiment
		in situ temperature and relative humidity measurements	*Building 1* Exhibition Hall-Municipality of Nicosia, Ledras str. *Building 2* CYTA, Arsinois and Onasagorou str. *Building 6* Ledras str.	Every 6 hours	TOPEUM Field Experiment
Meteorology	**Synoptic Scale**	Radiosoundings	*Theatre of Bank of Cyprus Cultural Foundation* Faneromenhs str.	Every 3 hours	TOPEUM Field Experiment
Building Surface Temperature Response	**Urban Scale**	Aerial thermography	*Old City Centre*	Morning: 8am Afternoon: 3pm Night: 10 pm	TOPEUM Field Experiment
Meteorology	**Synoptic Scale**	Radiosoundings	*Theatre of Bank of Cyprus Cultural Foundation* Faneromenhs str.	**7 of July 2010**_07:30 and 11:30pm **11 of July 2010**_1:30pm **15 of July 2010**_02:30 and 11:30 pm	TOPEUM Field Experiment
Building Surface Temperature Response	**Building Scale with trees influence**	Thermocouples in 3 levels on two different walls (east and west) of each building a) 2m height b) 3m height c) 4m height	*Building 7* Flo Café (with trees) *Building 8* Toy store (without trees)	**14-16 of July 2010** Every 10 minutes	TOPEUM Field Experiment

Tamasos for the period from the 1st to the 20th July 2010. Information on the surrounding wind directions as well as wind speeds was recorded at a height of 10m above the ground in the corresponding areas. It is noted however, that the anemometer of the Nicosia-PASYDY station is placed at a height of 2m, in the vicinity of buildings, hence comparisons of wind data from this station was avoided.

2.2.1.3 Urban and Local Scale

The smallest scale analyzed is the local scale. For the investigation of the wind direction, wind speed and wind temperature, four places in Ledras Street neighborhood are examined during the period from the 7th to 20th July 2010. A sonic anemometer (denoted as Sonic 2 in figures), was placed at the rooftop of the University of Cyprus Architecture School in Ledras Street, which is the second highest building of the region, in order to capture the meteorology of the urban scale. Another sonic was placed on School of Architecture building in the street canyon, in Ariadnis street (denoted as Sonic 1). In addition, a sonic was placed in Ledras Street (denoted as Sonic 3), and another one in the perpendicular street to Ledras Street, Arsinois street (denoted as Sonic 4).

2.2.2 Building surface Temperature response – measurement procedure

2.2.2.1 Urban Scale

In order to capture the impact at the urban scale of the solar radiation exposure of the built environment, aerial thermography took place during the morning, afternoon and night of 12th July 2010, above the historical centre of Nicosia, which is also the geometrical centre of the city. The three different times of the day, in which aerial thermography took place were chosen in order to capture buildings' thermal response. Hence, as during the observation period, sun rise was at about 5:40-6:00 the morning aerial thermography took place at 8:00, two hours after sunrise in order to allow enough time for the building thermal response. In a similar way afternoon aerial thermography took place at 15:00, two hours after the corresponding solar zenith at the intensive observation period. Finally, aerial thermography took also place at night 22:00, about three four hours after the sunset, during which city's activities minimized. It is noted that during the aerial thermography, there were important restrictions; due to the Turkish-occupied part of central Nicosia and the restricted activities allowed by the Turkish occupying army, aerial thermography could not take place from a distance closer than 1km south of United Nations buffer zone. Hence infrared images were taken under an angle of about 45˚. Additionally, the minimum height in which helicopter could fly was about 400m from the ground. In order to verify the quality of the infra-red images captured by the thermocamera, a verification thermocouple measurement was simultaneously conducted from a public school rooftop (Archibishop Makarios Lyceum, Nicosia), recording the corresponding temperature, and at the same time an infrared image of the rooftop from the thermocamera at angle of 45˚ and height of 400m was captured. Temperatures recorded with the thermocouple and the infra-red thermocamera differed by 7% providing an acceptable accuracy.

2.2.2.2 Neighborhood Scale

Moreover, five buildings, made of similar materials, are chosen in the broader neighborhood of Ledras Street in order to the record the thermal response of several materials during different times of the day for the intensive observation period 10th to 12th July 2012. Infra-red images were taken approximately every two hours during the three-day intensive

observation period, following a circuit path between the five different buildings. Buildings' selection criteria included their orientation, the street canyon height-to-width ratio and the material of the façade.

2.2.2.3 Building Scale

At the local-building scale, the surface temperature and humidity over a building wall were recorded during the three-day intensive observation period at different times of the day. Specifically measurements were taken locally at four different elevation points over each building wall (of the different buildings), ranging from ground level up to 2.00 m heigh.

3 RESULTS

3.1 Summarised results: multi-scale meteorology and urban building thermal response

Multiscale meteorological measurements and simulations were recorded. Figure 2 shows simulation results from different resolutions for the background wind fields at different resolutions. Figure 3 shows the results from the radiosoundings tracking and processing; this enables the estimation of the boundary layer height. Radiosoundings indicate the structure of the atmosphere depending on the vertical height. Several radiosondes were released in the period 7th -15th July 2010. Radiosoundings on 7th, 11th and 15th of July were diagnostic, while during the peak observation period, on the 12th of July, one radiosonde was released every three hours creating the vertical profile of the atmosphere during the day. The position of each radiosound during the recording period is illustrated in Figure 3. Radiosounding results showed that the troposphere height in Cyprus is slightly higher than its nominal height of 11 km. According to radiosounding profiles for potential temperature, the height of inversion layer was deduced to be approximately 17km, corresponding to the troposphere height in Cyprus.

Supplementary information on weather conditions during the days of IOP was obtained using the Weather and Research Forecasting (WRF) model - version 3.4, which was run at the Cyprus Institute High Performance Computing. WRF is a state-of-the-art mesoscale model designed to serve both operational forecasting and atmospheric research needs (Skamarock et al., 2007). To drive the model, the NCEP FNL (Final) Operational Global Analysis data of 1.0 x 1.0 degree resolution updated every six hours (http://rda.ucar.edu/) is used; this product is from the Global Data Assimilation System (GDAS), which continuously collects observational data. In relation to the topography, during 22:00-03:00 katabatic winds from Troodos mountain take place, and start to get disorganized at 04:00 to 05:00 in the morning, as sun rises. At 06:00 in the morning, as the heating of the ground surface begins, anabatic winds appear and are observed until 15:00. At the same time such an activity is not observed for Pentadaktulos mountain. Moreover, at 06:00 in the morning eastern winds are observed in Nicosia and Athienou and these speeds are increased at 08:00 and become SE. At the same time SW winds are observed in Astromeritis due to sea breezes and then get strengthened at 11:00. In the noon, 13:00-14:00, the two flows, are merged indicating tunnel phenomenon in Nicosia, which disappear at 15:00-16:00. Finally, from 17:00 until the first hours in the morning, west winds are observed northern of Troodos Mountain, with speeds which are continuously decreasing until 19:00 to 3m/s and then increased to approximately 6m/s until 03:00.

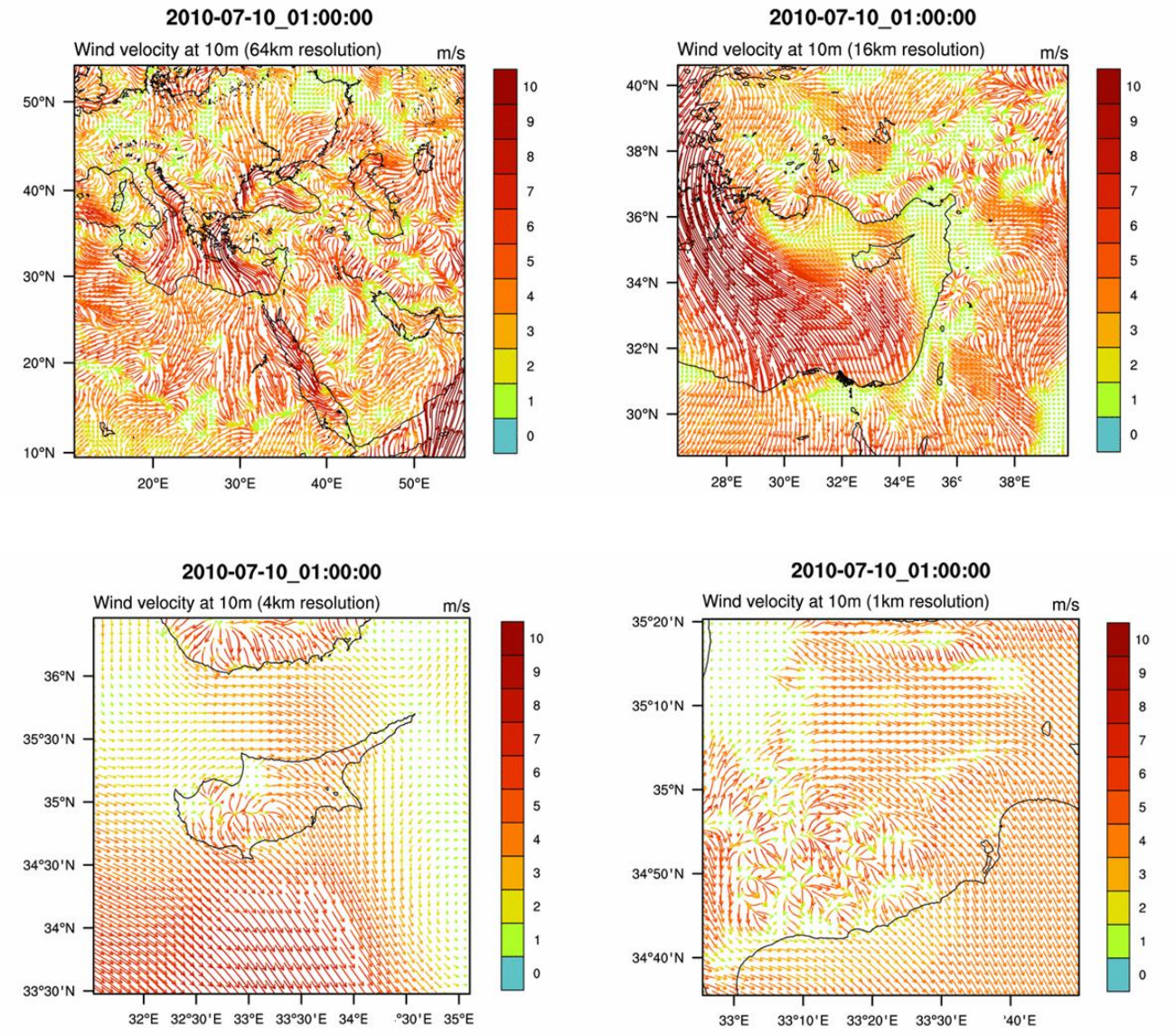

Figure 2: Wind flow in the region of Cyprus, from WRF model results (Produced by Georgios Zittis – Cyprus Institute, 2012). Video provided in the appended cd.

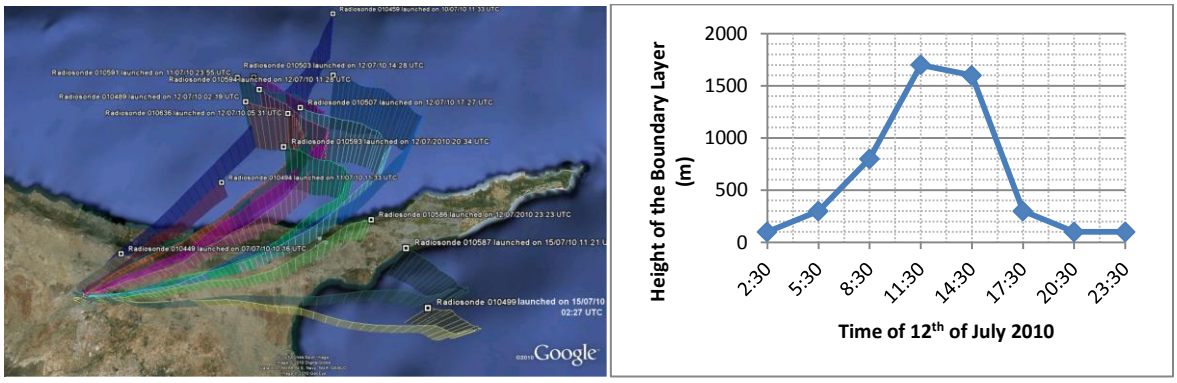

Figure 3: Radiosoundings traces during the intensive observation period (left); the evolution of the height of the atmospheric boundary layer during 12th of July 2010 (right)

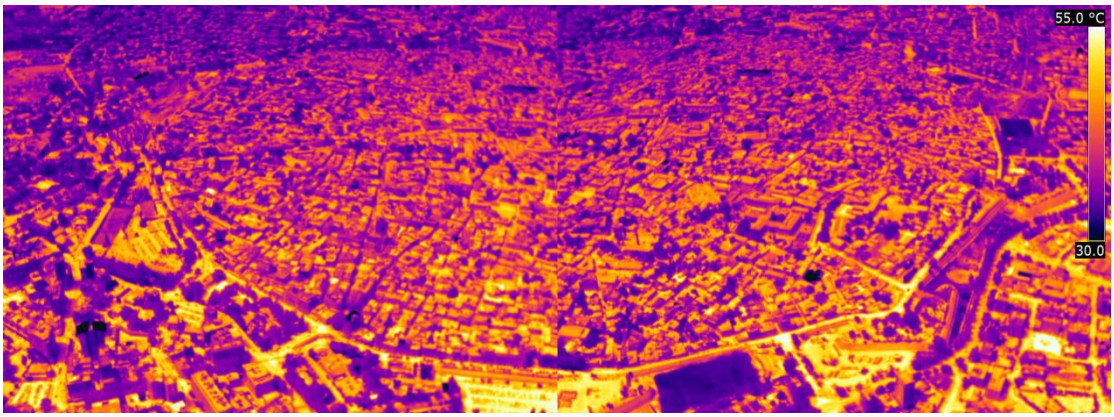

Figure 3: Aerial infrared image during the afternoon, of 12th July 2010 at 3pm.

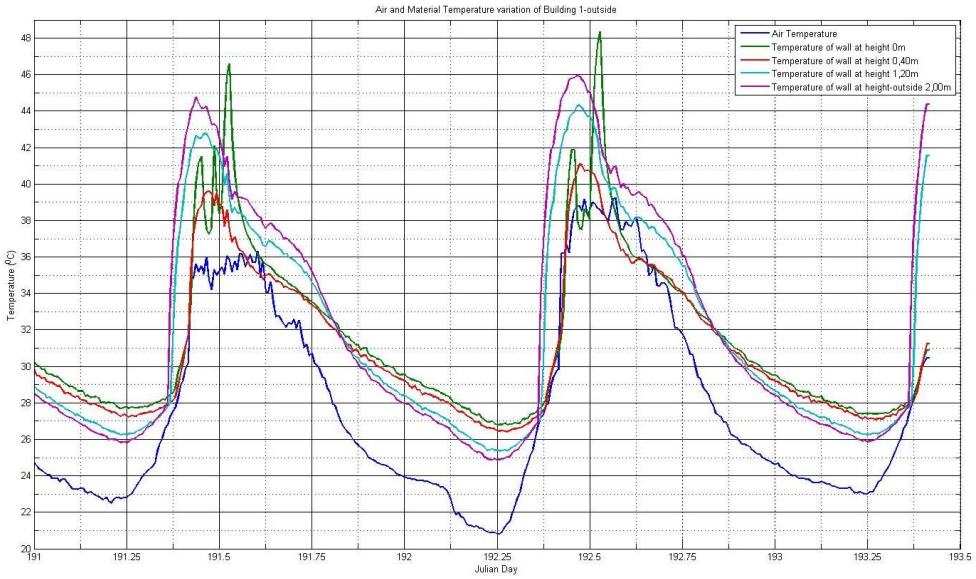

Figure 4: Air temperature variation in comparison with material temperature variation recorded from the thermocouples outdoor of Building 1, Ledras street.

3.2 Analysis and interpretation of the observed Urban Heat Island

Meteorological conditions across various scales were monitored in order to account appropriately for the influence of such phenomena possibly contributing to the Urban Heat Island (UHI) phenomenon. Urban area data were taken from those recorded at Nicosia-PASYDY station while rural area data were taken from Astromeritis and Athienou: Astromeritis is closer to the sea-coast than Athienou, and as observed from WRF simulations it is mainly affected by sea breezes, hence cooling effects are taking place.

The magnitude of a UHI is defined as the temperature difference between urban and rural areas, ΔT_{U-R}. No standard protocol exists on measurement stations used for ΔT_{U-R}. During the day, air temperatures of Nicosia- PASYDY are greater than the temperature in Athienou by $\Delta T_{U-R} = 0.5 - 3.5\,^{\circ}C$. However during the night the temperature difference is not as large as during the day. The nocturnal temperature difference varies from $\Delta T_{U-R} = 0.5 - 1.5\,^{\circ}$C. The results show that the existence of UHI

is provident, although its magnitude is not as large as compared to other south-european studies eg in Athens (Kolokotsa et al, 2000).

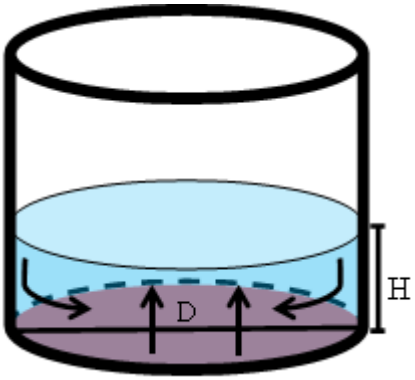

Laboratory experiments conducted by Fernando et al. (Fernando et al, 2010), considered the city as a circular source of heat taking into account the convergence flow that arises as a result of the thermal flows due to the UHI phenomenon. A dimensionless parameter, independent from Reynolds number, was proposed. In the experiments, the bottom of the tank was a heated disk, of diameter D, in a stably stratified fluid; the results show that for a uniform heat flux Q_0 (or a buoyancy flux $q_0 = gaQ_0\ \ \rho_0 c_p$) the resulting ground level convergence velocity U_r (of buoyancy frequency N) is given by $U_r \approx 0.7(q_0 D)^{1/3}$, and when the temperature difference between the disk and ambient fluid ΔT_{U-R} is specified, then $U_r \quad ga\Delta T_{U-R} D\ ^{1/2} = 0.08 \pm 0.01$.

For the calculation of this dimensionless parameter, data from Architecture Rooftop - Sonic 2 as representative of the heated urban area urban area are taken into account, as the data of this height approaches better the heated disk. Data from street, Sonics 1, 3 and 4 have not been considered as most suitable for the β-parameter calculation as the conditions in the canyons, are affected also by shading, trees etc. During the day, due to the fact that sea breezes from Astromeritis reach Nicosia, Athienou is considered as rural area in our analysis. Consequently, the dimensionless parameter as deducted from our field experiments (for diurnal variations) is $\beta = 0.0789$, approximately equal with the idealized laboratory value 0.08 ± 0.01. This indicates the existence of UHI during the day in Nicosia, which is in agreement with the high temperature difference between Nicosia-PASYDY and Athienou.

During the night, katabatic winds from Tamasos affect Nicosia. In the nocturnal case, the non-dimensional β parameter is found to be 0.0346, approximately half compared of the value during the day and the laboratory value. Again this lower value indicates the lower magnitude of UHI during the night, as temperature difference form Nicosia-PASYDY and Athienou shows. Despite the small value of β, it could be said that UHI also exists during the night, at a lower intensity, of 50% of the value reported in laboratory experiments. This difference is due to the contribution of katabatic winds.

4 CONCLUSIONS

A multiscale consideration of the urban heat island phenomenon has proven necessary as manifested through a field measurement campaign taken place in Nicosia-Cyprus during July 2010. It was shown with regard to the meteorology that during the summer, Cyprus is characterized by the etesian winds from Westerly to Northwesterly directions, high stability and small variations of atmospheric pressure. At the same time topography has a special role in the air circulation. Coastal regions are mainly affected by sea and land breezes, whereas anabatic and katabatic winds from mountain enhance the development of local wind systems, specifically anabatic and katabatic winds are observed to originate from Troodos Mountain.

Athalassa, which is a suburban area, has greater temperature values and night that urban Nicosia, both during the day, as NW winds are dominant, particularly during the day, and warm air from Nicosia is advected to Athalassa. Athienou is considered as the rural station to Nicosia, as this region is not affected from sea breezes as much as Astromeritis does, not only because is farther away from the sea than Astromeritis is, but also because the effect of the sea breezes are nearly cancelling out with the etesian winds and hence any cooling effect is not enhanced. Furthermore Athienou is closer to Nicosia than Astromeritis, which provides

better comparison conditions. Moving closer to the urban area, air temperature variations are observed to be the same both for the height of rooftop and the street canyons conditions. Wind speeds in street canyons are much lower than wind speeds at rooftop level. Furthermore, wind directions in the street canyon are completely different compared to the rooftop level, however wind directions appear to be the same both during day and night in different street canyons even though the canyons may be perpendicular to each other.

Finally, UHI phenomenon is present in the city of Nicosia, with higher magnitude during the day than during the night due to the effect of katabatic winds, specifically the temperature difference between urban and rural area, $\Delta T_{U-R_{day}}$ ranges $0.5 - 3.5\ ^{\circ}C$ while during night ranges in $0.5 - 1.5\ ^{\circ}\mathrm{C}$. Moreover, calculation of the scaling dimensionless parameter β during the day is found to be 0.0789 while during the night is 0.0346; this compares quite well with values obtained in laboratory measurements where $\beta = 0.08 \pm 0{,}01$ not indicating other effects such as katabatic cooling.

5 ACKNOWLEDGEMENTS

The authors wish to acknowledge a number of organisations and persons for their contribution and assistance during the field measurement campaign, without which this work would not have been possible: Cyprus Police for providing the helicopter for 4 flights and assistance during the flights, Nicosia District Mayor, Cyprus Meteorological Service, United Nations as well as a large number of volunteers who helped at various stages for this work to be realised. The project is funded through the ERA-NET (Urban-Net Call) and the Cyprus Research Promotion Foundation under the contract ΔΙΕΘΝΗ/URBAN-NET/0308/02.

6 REFERENCES

Akbari, et al. (1996): Policies to reduce heat island: magnitudes of benefits and incentives to achieve them, in proceedings ACEEE Summer Study on Energy Efficiency in Buildings, vol. 9,. Pp. 177.

Batchvarova and Gryning (2006). Progress in Urban Dispersion Studies. Journal of Theoretical and Applied Climatology, Vol. 84, Nos. 1-3, pp 57-67.

De Ridder Koen, et al., 2006: The impact of urban sprawl on air quality and population exposure: a case study in the German Ruhr area; EURASAP Newsletter 60, April 2006, ISSN-1026-2172, 13-29.

Fernando, H.J.S. (2010). Fluid dynamics of urban atmospheres in complex terrain. Annual

Jian Hang et al.: Studies of wind environment in simple compact square, round or long cities by CFD simulation and wind tunnel measurements, Project No. HKU 7145 /07E

Review of Fluid Mechanics Vol. 42, pp. 365-389.

Neophytou, M., Fokaides, P., Panagiotou, I., Ioannou, I., Petrou, M., Sandberg, M., Wigo, H., Linden, E., Batchvarova, E., Videnov, P., Dimitroff, B., Ivanov, A. (2011). Towards optimization of urban planning and architectural parameters for energy use minimization in Mediterranean cities (TOPEUM). Conference Proceedings of the World Renewable Energy Congress, May 2011, Linkoping – Sweden.

T.R. Oke et al. (1991): „Simulation of surface urban heat islands under ‚ideal' conditions at night. – Part 2: Diagnosis and causation, Boundary Layer Meteorology, Vol. 56. pp.339-358

Santamouris (2001): „Energy and Climate in the Urban Building Environment. James and James Science Publishers, London".

Synnefa et al. (2005): A study of the thermal performance of reflective coatings for the urban environment, Solar Energy, Vol. 80, pp. 968-981.

STUDING THE EFFECT OF "COOL" COATINGS IN STREET URBAN CANYONS AND ITS POTENTIAL AS A HEAT ISLAND MITIGATION TECHNIQUE

Chrissa Georgakis[a,*] Stamatis Zoras[b], Mat Santamouris[a]

[a] Group of Building Environmental Physics, University of Athens, Building Physics 5, University Campus, 157 84 Athens, Greece

[b] Laboratory of Environmental and Energy Design, Department of Environmental Engineering, Polytechnic School of Xanthi, Democritus University of Thrace, Greece

Abstract

Surface temperature measurements were performed in a deep street canyon, during summer period, in the center of Athens. Surface temperature was measured on an hourly basis, at several spots, in the external facades of buildings, pavements and at ground level inside an urban canyon. At the same time experimental data of air temperature were collected through extensive monitoring at four different heights in the center of the urban canyon. Based on these measurements air temperature vertical stratification was analyzed and interpreted as a function of the coating used.

Computational fluid dynamics (CFD) simulation were performed for evaluating surface temperature in the external facades of the buildings and at ground level in the urban canyon, for the coating used in the urban street canyon. CFD simulations based on the orientation of the street, the geometrical characteristic of the street (Height/Width), together with the type of coating used to define the surface temperature at different spot inside the canyon. At the same time air temperature was calculated in the center of the canyon for the specific four heights. Computational results were compared to field data in order to validate the accuracy of the CFD model used for the prediction both of surface and air temperature inside an urban street canyon. Secondly, by the means of the computational fluid dynamics model for the various types of "cool" coatings used for the buildings facades and smart materials for the ground level, i) air temperature was calculated at four different heights inside the urban canyon and ii) surface temperature in the canyons facades and at ground level. The calculated data have been thoroughly analyzed.

Aim of the work was the comparison between measurements of the vertical stratification of air temperature inside a deep street urban canyon with the calculated ones for different “cool” coatings and smart materials and give evidences for the possible mitigation of the heat island effect. The use of “cool” coatings in buildings has been estimated as crucial for the energy consumption and thermal comfort conditions in cities. Their albedo to solar radiation and emissivity to long-wave radiation, are very important parameters for the reduction of absorbed solar radiation and air temperature inside street canyons.

Corresponding author Tel: +30-210-7276849; fax: +30-210-7295282; email address: cgeorgakis@phys.uoa.gr

KEYWORDS

Surface temperature measurements and calculated values, cfd tool, vertical stratification of air temperature, cool coatings

1. INTRODUCTION

“Cool communities” strategies reroof and repave in lighter colors and new materials in order to reduce air temperature in cities and decrease the increased heat island effect. Planting trees is also an effective way to cool communities, mainly effective if they shade buildings, though savings are significant if they merely cool air by evapotranspiration. It was estimated that 50% of the temperature decrease could be arise from planting trees and 29% could be the benefits from the lighter-colored roofs and 21% from the light-colored pavements (Rosenfeld et al., 1998). In this study it was indicated that “cool communities” strategies, can lead to air temperatures’ reduction in LA as much as 3^0C.

In a recent study a smaller scale project carried out to optimize the rehabilitation of specific urban zone in a dense urban area in Maroussi, Athens (Santamouris et al., 2012). The project dealt with the rehabilitation of a zone of 16,000 m2, using new high reflectivity pavements, green spaces and earth to air heat exchangers. The repaving consisted of colored asphaltic material presenting a reflectivity close to 0.35 in the place of paving surfaces consisted of black asphalt for roads and dark concrete tiles for pavements with albedo lower than 0.4. The initial colored concrete pavements with reflectivity of 0.78 replaced with natural reflective materials, marbles, and concrete pavements colored with higher reflectivity paints. Computational analysis indicated that the use of cool pavements may lead to a decrease of the peak ambient

temperature in the build area by 1.2–2.0 degrees. The application of all measures may raise up to 3.4 degrees the decrease of the air temperature, in the area.

In this study we focus on two different tasks. The first task is the comparison between the measured and calculated values for the a) surface temperature for the initial coating of the pavements and b) the air temperature in the center of a deep street urban canyon. The second task of this work is the calculation of the surface and the air temperature, inside the deep urban canyon, by using a "cool" coating and the possible mitigation of the heat island effect in the specific urban area.

2. DESCRIPTION OF THE MEASUREMENTS

Measurements of several meteorological parameters were performed, during summer period, in the center of Athens. The mobile meteorological station of the University of Athens (Figure 1) was parted from: a) a vehicle and b) a telescopic mast PT8 Combined Collar Mast Assembly with extended height of 15.3 meters, retracted height 3.43 meters and maximum head load 15 kgr. The experimental site was a deep street urban canyon, which is oriented in the center of Athens with the long axis in a NW'N-SE'S direction (33^0 from real North counter-clockwise). The in-canyon measuring point was located in the middle of a cross-canyon distance, 20 m from the North intersection. The mean buildings height was 23 meters and the distance between buildings was equal to 8 meters. The geometrical characteristics of the street canyon were H/W=3 and L/W=6.9.

The first type of measurements was:

a) Air temperature measurements in the centre of the canyon. Miniature thermometers were placed on the telescopic mast at 3.5-7.5-11.5-15.5 meters, measured air temperature every 30 seconds. The miniature screen formed housing for a range of temperature sensing elements, proving weather protection while allowing the free passage of air b) Wind speed and direction measurements in the centre of the canyon. Anemometers were placed on the telescopic mast at 3.5-7.5-11.5-15.5 meters height, measured and recorded wind speed and direction every 30 seconds. Pulse output anemometer 10 Hz per knot, for recording the air wind speed inside the canyon and W200 Porton Windwane, $\pm 300^0$ ranges for recording the wind direction respectively. The meteorological data were monitored from 9:00LT-18:00LT each day of the experimental campaign, which lasted three consecutive days.

The *second type of measurements was:*

Hourly surface temperature measurements at a cross section in the middle of the street canyon. An infrared thermometer equipped with a laser beam used to measure the surface temperatures of the exterior building façades facing the canyon. Measurements were performed from the bottom to the top of both façades of the canyon in steps of 1-1.5 m. All measurements were performed from street level. In addition, the pavement and road temperatures were measured at different points along the width of the canyon. All measurements were performed on an hourly basis during the twelve experimental hours.

For the recording of the meteorological data acquisition modules have been placed inside the vehicle. LabView was the software used for the recording and storing of the meteorological data.

3. DEDCRIPTION OF THE CFD SOFTWARE

The efficient simulation of the thermal energy condition in the area of interest the detailed three dimensional tool ANSYS CFX 13 has been used. ANSYS CFX is an advanced general code computational fluid dynamics model that solves the Navier Stokes differential equations and turbulence by the finite elements technique in the 3D space. It is a commercial software package that handles very detailed 3D geometry with the ability to solve efficiently heat transfer and fluid flow phenomena. Its accuracy has been widely verified against experimental and theoretical tests (www.ansys.com). Advanced CFD models can calculate with a high degree of accuracy microclimatic parameters at every grid point of the meshed space. However, the more complicated is the geometry of the urban open space the more resources of input data and calculation are needed.

ANSYS CFD is managed by its own desktop (Workbench) that the user handles the whole simulation process. It can simulate in steady state or transient mode the microclimatic parameters', heat transfer and fluid flows' distributions in time and space. This is the ideal approach of the three dimensional urban environment.

Simulation setup constituted of four stages, 1) Geometry integration and domain definitions, 2) Meshing, 3) Physics definition and 4) Solution and result representation. The more detailed is the structural and 3D geometry of buildings, streets, pavements, urban equipment and vegetation the more representative and accurate simulation will be.

The meshed geometry is used to define the physical parameters in the area under consideration (CFX-Pre). Surfaces with materials (concrete, glass, pavement, water, trees) and properties (emission and reflection coefficients) have been defined. Turbulence was simulated by the Shear Stress Transport model with K-Turbulence KE and O-Turbulence frequency. Thermal energy was simulated by the discritised model in surface to surface and medium to surface modes. This takes into account opposite surfaces energy exchange that is very important in the heat balance of the open spaces in case of replacing conventional surfaces with cool materials. Solar radiation has been taken into account in slope and deviation through the top boundary. Boundary conditions were gathered by the experimental data (air temperature, wind speed and direction, radiation, surface temperatures) that have been described on the previous paragraph. The simulation time step (5 sec) and convergence criteria (10^{-4} RMS of residuals) have been defined under steady state and transient calculation. Finally, the results have been processed in the CFD Post provided by the software according to the required challenges.

4. COMPARISON BETWEEN MEASURED AND CALCULATED VALUES

For the purpose of this study measurements inside the canyon estimated for 2-5.5-9.5-15.5 meters height since the levels where surface temperature was measured at the canyons' walls were 2.5-6-9.5-13-15.5-20 meters. It is important all measurements to be in the same level so differences between air and surface temperature to derive. The following equation (equation 1) can be used for the calculation of air temperature, where T_1 and T_2 are the temperatures at two heights Z_1, and Z_2 and a is the angle of elevation of the sun

$$T_1 - T_2 = N(1.2 - 6.8\sin a)\log_{10}(Z_1 / Z_2) \quad (1)$$

where N is the effective absence of cloudiness (N= 1 corresponding to a clear sky). The angle of elevation of the sun was calculated for all the experimental days (Tait, 1949; Georgakis et al., 2010).

Measurements depicted in box plots. The line in the middle of the box is the median, or the 50^{th} percentile of the sample. The lower and upper lines of the box are the 25^{th} and 75^{th} percentiles, representing the lower and upper quartile, respectively. Data are considered outliers if they are located 1.5 times the interquartile range away from the

top or bottom of the box. Figures 2-4 present measurements and calculated values for surface temperatures at the SW wall of the canyon, the NE wall of the canyon and at ground level, for 10:00LT in the morning -13:00LT at noon and 16:00LT in the afternoon, as representative hours for the experimental period.

In the same box plots two different calculated values depicted. The albedo of a smooth concrete asphalt grey slab is close to 0.36 and in walls painted with grey plaster does not exceed the value of 0.4 (Taha et al., 1992), so for the CDF simulations the albedo of the canyons' initial surfaces coating considered equal to 0.3 and for the case of the "cool" coating equal to 0.6 (Figures 2-4). For all calculations the emissivity of the canyons' materials was considered equal to 0.9.

According the plots in the morning the surface temperature on the sunny NE wall is almost 5^0C higher than the opposite SW wall and the grounds' surface temperature is close to 29^0C (Figure 2). At noon (13:00LT) grounds' average surface temperature approaches 41^0C, close to 10^0C higher than the corresponding walls surface temperature (Figure 3). In the afternoon (16:00LT) average surface temperature on the SW wall reaches 35^0C, while grounds' corresponding surface temperature is 4^0C lower (Figure 4). The average calculated values (for albedo equal to 0.3) were very close to average values of measurements. Differences between average measurements and calculated values did not exceed 0.3^0C strengthen the value of the CFD tool used. The measured mean values of surface temperature were always least high than the temperatures calculated for albedo equal to 0.3, which was chosen based the literature, as an appropriate value for the CFD simulations. The reason is that after the years the albedo of coatings decreases and the real value can be measured close to 0.2. In the second task of our study the use of a "cool" coating with higher albedo (equal to 0.6) decreased average calculated values of surface temperature. Almost for all cases after the use of a "cool" material can lead surface temperature 2^0C lower at canyons' walls and 3^0C lower at ground level (Figures 2-4). This conclusion is strongly linked with the angle of elevation of the sun; the thermal properties of the canyons' materials and the geometry of the experimental site.

Air temperature calculated values followed the vertical stratification of the measured ones, during experimental period (Table 1). The range of air temperature differences, between measured and calculated values (for materials with albedo value equal to 0.6), was up to 0.9^0C. These differences depended from the distance from ground

level and the time period. This conclusion provided evidences that the increase of materials' albedo can lead to reduction of ambient temperature inside the canyon.
The wind flow as expected cannot be influenced by the change of the surfaces' material (Table 2) since calculated values derived from the CFD simulations did not differ from measurements.

5. CONCLUSIONS

The alternative way to fight heat island in dense urban cities is to increase urban albedo. Difficult is to reconstruct cities, with huge green areas and lower building factor, so in the effort to decrease air temperature in the center of cities scientists focus nowadays in optimization for the reflectivity of the pavements, roofs and walls.

It was proved that an increase on the albedo of a coating in surfaces of a deep street canyon can lead to 3^0C decrease of surface temperature on ground level. The decrease on walls' surface temperature may reach 2^0C. All these conclusions are strongly related to the geometry of the canyon and the solar incidence angle. Ambient air temperature inside the canyon, strongly depending from canyons' covering, may decrease close to 1^0C. Advanced reflective materials for roof and pavements, the "cool materials", are strongly considered as the solution in the fight of the heat island effect (Akbari et al., 2009; Santamouris et al., 2012). Materials "cool" colored painted can contribute to the decrease of surface temperatures and energy consumption in urban areas (Synnefa et al, 2007).

The conclusions of this study are valid for the specific boundary conditions, strongly related to the micro-climatic conditions of the studied area. In the forthcoming study, the t-test of the difference of the means will be applied, in order to prove the goodness of fit between the measurements derived from the extended experimental campaign and the ones raised from the application of the theoretical model. This test will be performed for all measured data and not only for selected hours.

REFERENCES

Rosenfeld AH, Akbari Hashem, Romm Joseph J, Pomerantz Melvin (1998). Cool communities: strategies for heat island mitigation and smog reduction. *Energy and Buildings, 28, 51–62.*

Santamouris M, Xirafi F, Gaitani N, Spanou A, Saliari M, Vassilakopoulou K. (2012). Improving the microclimate in a dense urban area using experimental and theoretical techniques. The case of Marousi, Athens. *International Journal of Ventilation, 11(1), 1–16.*

Georgakis C., Santamouris M., Kaisarlis G. (2010). The vertical stratification of air temperature in the center of Athens, *Journal of Pure and Applied Meteorology and Climatology, 49 (6), 1219-1232.*

Tait G. W. C. (1949). The vertical temperature gradient in the lower atmosphere under daylight conditions. *The Quarterly Journal of the Royal Meteorological Society, 75, 325, 287-292.*

Akbari, H., Menon, S., & Rosenfeld, A. (2009). Global cooling: Increasing world-wide urban albedos to offset CO2. *Climatic Change, 94, 275–286. doi:10.1007/s10584- 008-9515-9.*

Synnefa A, Santamouris M, Akbari H. (2007). Estimating the effect of using cool coatings on energy loads and thermal comfort in residential buildings in various climatic conditions, *Energy and Buildings, 2007, 39,11, 1167-1174.*

Taha H, Sailor D, Akbari H. (1992). High albedo materials for reducing cooling energy use. Lawrence Berkeley Laboratory Report 31721, University of California, Berkeley, CA 94720.

FIGURES

Figure 1: Mobile Meteorological Station of the University of Athens

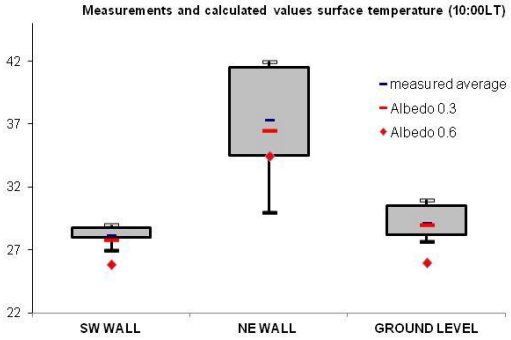

Figure 2: Measured and calculated values at 10:00LT

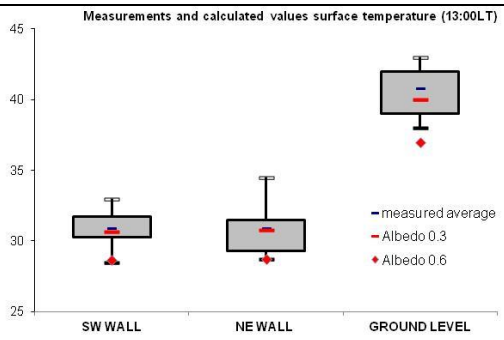

Figure 3: Measured and calculated values at 13:00LT

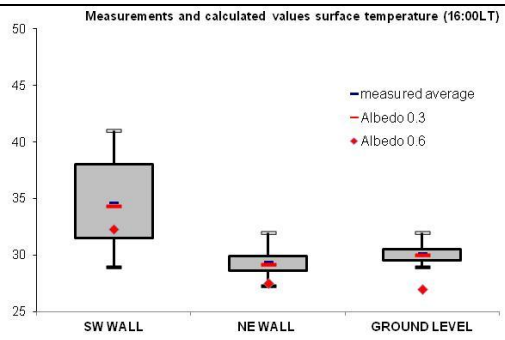

Figure 4: Measured and calculated values at 16:00LT

Table 1 Measurements and calculated values for air temperature inside the canyon

HEIGHT LEVEL	2 m	5.5m	9.5m	15.5m
Measurements 10:00LT	26.9	25.9	26.1	26.2
Calculated vales (albedo 0.3)	27.5	26.3	26.5	26.2
Calculated vales (albedo 0.6)	27.3	25.9	25.9	25.7
Measurements 13:00LT	29.5	28.7	28.8	28.8
Calculated vales	29.6	29.0	29.0	28.5

(albedo 0.3)				
Calculated vales (albedo 0.6)	29.0	28.5	28.3	28.0
Measurements 16:00LT	29.0	29.0	29.3	29.2
Calculated vales (albedo 0.3)	29.5	29.0	29.3	29.2
Calculated vales (albedo 0.6)	28.9	28.5	28.4	28.5

Table 2 Measurements and calculated values for wind speed inside the canyon

HEIGHT LEVEL	**2 m**	**5.5m**	**9.5m**	**15.5m**
Measurements 13:00LT	0.33	0.28	0.65	1.16
Calculated vales (albedo 0.3)	0.31	0.27	0.58	1.20
Calculated vales (albedo 0.6)	0.30	0.26	0.59	1.22
Measurements 16:00LT	0.30	0.38	0.35	0.18
Calculated vales (albedo 0.3)	0.32	0.39	0.34	0.23
Calculated vales (albedo 0.6)	0.30	0.35	0.40	0.50

THE THERMAL CHARACTERISTICS AND THE MITIGATION POTENTIAL OF A MEDIUM SIZE URBAN PARK IN ATHENS, GREECE

Fotini Skoulika[1], Mattheos Santamouris [*2], Dionysia Kolokotsa[3]

1 Group Building Environmental Research, Physics Department, University of Athens
University Campus, Buid. PHYS-V
Athens GR 15784, Greece

2 Group Building Environmental Research, Physics Department, University of Athens
University Campus, Buid. PHYS-V
Athens GR 15784, Greece
**Corresponding author: msantam@phys.uoa.gr*

3 Technical University of Crete
Chania, Crete, Greece
Polytedhnioupolis, Kounoupidiana
73100 Chania, Crete, Greece Group Building

ABSTRACT

An urban park located in a densely built area of Western Athens, Greece is monitored. Temperature data from 15 urban and suburban stations are also used to perform comparative analysis at the city level. The park presents an important temperature inhomogeneity during day and night due to the variable radiative cooling capacity and shading potential between its various zones. Average nocturnal Cool Island Intensities (CII) against the reference urban stations varied between – 0.7 K to – 2.8 K while during the daytime the maximum CII was between -0.2 to -2.6 K. A statistical significant correlation between the magnitude of the CII and the population density index is found for both day and night. The data analysis showed that the park was warmer than the urban stations for ambient temperatures lower than 34 °C, while for higher urban temperatures the park remained cooler. Moreover the absolute CII increased as a function of the ambient temperature. A strong correlation with the wind speed is observed for speeds higher than 6 m/sec. The mitigation potential of the park was assessed by using three traverses in and around the park. The analysis of the Park Cooling Index (PCI) showed a variation from 3.3 to 3.8 K. The traverses' temperature gradient was estimated to be between 0.16 to 1.4/100m.The climatic influence of the park was extended up to 300 m away from the borders of the park.

KEYWORDS

Urban Heat Island, Urban Park, Cool Park Intensity, Cool Island Intensity

1 INTRODUCTION

The urban heat island is one of the more studied phenomena of climate change. It deals with higher ambient temperatures in the central areas of the cities compared to their suburban or rural surroundings (Santamouris, 2001). Heat island is a very well documented phenomenon for the city of Athens, Greece (Livada et al, 2007, Santamouris et al, 1999, Kassomenos and Katsoulis 2006, Gobakis et al 2011) and is observed mainly in the Central and Western zones of the city. The increase of green spaces in the city under the form of green roofs, urban parks and other green zones is a known and efficient mitigation technique. Trees and green spaces

contribute highly to the improvement of the urban climate as they provide solar protection, affect air movements and heat exchange, absorb solar radiation and cool the air through evapotranspiration processes. Consequently, decrease of the temperature is achieved. The present paper reports the analysis of the field measurements performed in and around a medium size park in Western Athens, Greece during the summer period. Data from 15 urban stations are used in a comparative way to understand and analyse the relative climatic conditions in the park and the reference urban areas as well as to evaluate its climatic distribution. The specific objectives of the present study are to analyse the thermal conditions and the temperature inhomogeneity in the park during the day and the night period, to investigate the climatic influence of the park in its immediate surroundings during the warm summer period and to compare the temperature status in the park against other city zones presenting different urban characteristics, thermal conditions and heat balances.

2 EXPERIMENTAL SITE DESCRIPTION

2.1 DESCRIPTION OF THE PARK AND THE AREA

The studied urban park is located in the Municipality of Peristeri, a suburb located in the western part of Athens, Greece, 37.58 ° N and 23.43 ° E. The total surface area of the park is 60.000 m^2 while it is surrounded by a densely built urban area involving medium size residential and commercial buildings with a heavy traffic. The park is covered by grass, various types of bushes, low trees dense medium and high size trees and it is watered during summer just after sunrise and sunset. The suburb of Peristeri is characterized by a strong heat island phenomenon ranging between 6 to 12 K (Mihalakakou et al, 2002, Gianopoulou et al, 2011) because of the very high density, the accelerated industrialization and the very significant anthropogenic heat.

2.2 Experimental Procedure

A series of measurements of the ambient temperature inside and in the surrounding of the park were performed during the period 29/7/2012-2/9/2012. The measurements were recorded by nine fixed meteorological sensors distributed inside the park, combined with measurements of the ambient temperature conducted inside the park and its immediate surroundings using a calibrated hand held thermometer. Three different traverses were designed and followed towards different directions around the park. Measurements were performed under hot stable climatic circumstances, clear skies and peak solar radiation conditions, and finally moderate to strong wind speeds from NE directions during the day period. Data from eighteen meteorological stations located around the Athens area have been also collected for the whole experimental period.

3 RESULTS

3.1 Temperature Distribution in the Park

The distribution of the minimum and maximum daily temperatures in the park as

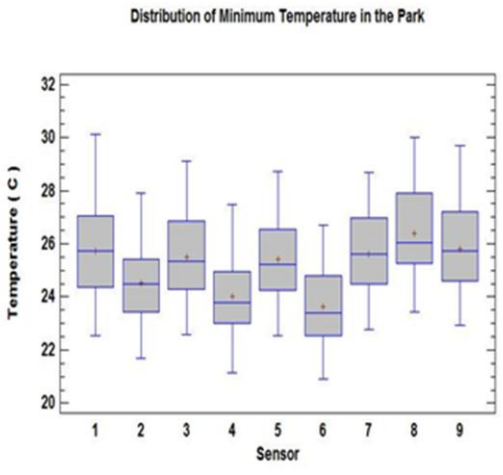

Figure 1: Distribution of the Daily Minimum Temperature in the Park during the experimental period.

recorded by the nine sensors is given in Figures 1 and 2 respectively. Minimum temperatures in the park recorded around sunrise. No important time lag is found between the different sensors. Minimum temperatures varied between 21 ° C to 30.5 ° C, with an average minimum temperature close to 25.2 ° C. The maximum temperature difference between the nine sensors was recorded around sunrise time and ranged from 1.0 to 3.0 K. Significant recorded temperature differences may be justified as a) the wind speed around sunrise was low during the whole experiment, (< 2 m/sec), advection phenomena were very weak and thus the transfer of air masses between the various zones of the park was insignificant; b) the sky view factor in the area around the sensors varied considerably and therefore the corresponding radiative cooling potential was very different. The maximum daily temperature in the park varied between 30 ° C and 41.4 ° C with an average value close to 34.8 ° C. Maximum daily temperatures are recorded around 14:30 - 15:30 local time, for all sensors. The average maximum temperature difference between nine sensors in the park was close to 2.5 K, however in specific days the daily maximum temperature difference in the park reached values close to 5 K. Daytime temperature differences inside the park are strongly related to the shading conditions in every zone.

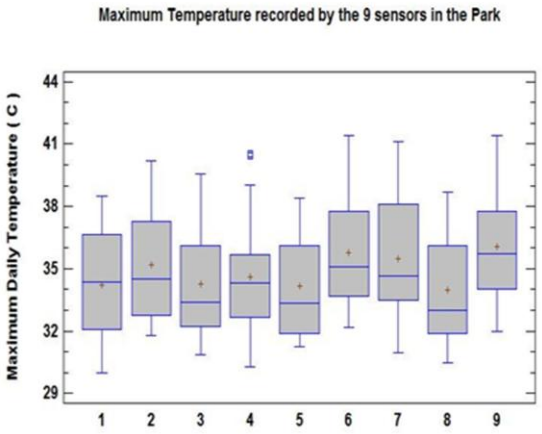

Figure 2: Distribution of the Daily Maximum Temperature in the Park during the experimental period.

3.2 Analysis of the Nocturnal Cool Island Intensity

In order to calculate the Cool Island Intensity of the Peristeri Park during the night and day period, the hourly, minimum and maximum daily temperatures measured inside the park have been compared against the corresponding data from 15 meteorological stations located in the major Athens area. In fact, seven of the stations are situated close to the park in the area of Western Athens, six of the stations are in and around the Athens Municipality and two of the stations are in the Northern part of the city. The distribution of the night time minimum temperatures recorded in the park as well in the 15 reference stations is given in Figure 3 for the whole period of measurements. Analysis of the night time temperature difference between the park and the urban stations revealed that the maximum ΔT occurs just after the sunset period and before midnight. During this period the average CII between the park and the urban stations varied between -0.7 K to -2.8 K. The

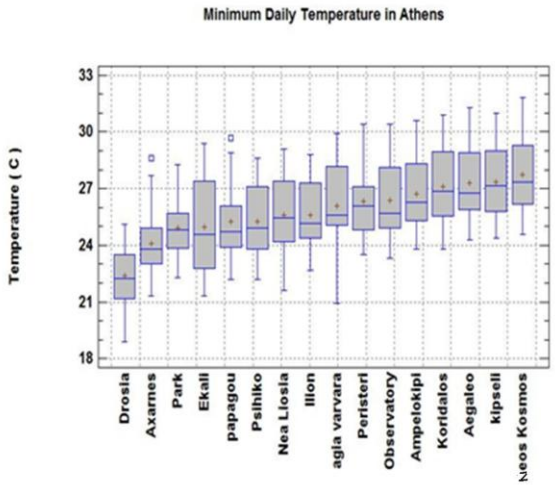

Figure 3: Distribution of the Minimum Daily Temperature in the Park and the other 15 stations in Athens.

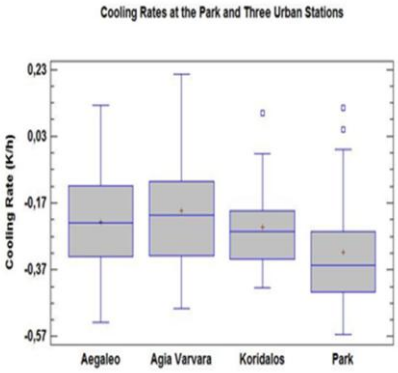

Figure 4: Cooling Rates, (K/h) for the park and three urban stations.

cooling rate of the park as well as of three surrounding urban stations was calculated for the period between sunset to sunrise, and for all days of the experiment (Figure 4). The average cooling rate in the park was calculated close to 0.32 K/h, a much lower value than the ones reported for Gothenburg, Sacramento and Vancouver. This may attributed to the much higher urban density in the considered area compared to the previously mentioned cities. In parallel, the cooling rate of the urban stations varied between 0.19 K/h to 0.24 K/h, values to about 60-70 % lower than in the park. As shown (Figure 3), the average minimum temperature in the park was lower than the corresponding value of all the urban reference stations (-0.7 to -2.4 K), while it was slightly higher than that of the three stations located in green areas in the borders of the city (+2.5 K and +0.8 K). Lower minimum nocturnal temperatures in the park and higher cooling rates should be attributed: a) to the higher radiative cooling capacity in the park because of the much higher sky view factor, and b) to the high convective thermal gains released in the reference urban areas by buildings and urban structures heated during the day time. Both of the parameters are related to the density and the characteristics of the buildings and in a way to the population density in a region .There is a statistically significant strong correlation between the observed nocturnal CII and the corresponding population density for every considered urban area that confirms the importance of the urban density on the development of lower nocturnal temperatures in the park (Figure 6). The night time temperature difference, CII, calculated for each reference station presents a high daily variability. Figure 5 gives the daily variation of the calculated CII around the sunrise period, for four reference urban stations presenting high temperature differences against the park. As shown, the daily fluctuation of the temperature difference in all stations is very significant and may reach values between -4.7 to 0.6 K. However, it is important to note that the pattern of the four curves is very similar although the magnitude of the corresponding CII differs between the stations. This signifies that the daily evolution of the temperature difference is mainly affected by global changes at the city level, like synoptic scale phenomena, than changes of local scale. To better understand the daily fluctuation of the nocturnal temperature differences, the relation between the daily minimum temperature and the corresponding CII in five urban stations were calculated (Figure 7). As shown the higher the minimum ambient temperature in the urban station, the higher the nocturnal temperature difference value. A similar pattern is also found between the maximum temperature of the previous day and the corresponding nocturnal Cooling Island Intensity. Higher daytime ambient temperatures result to an important increase of the minimum night-time temperatures

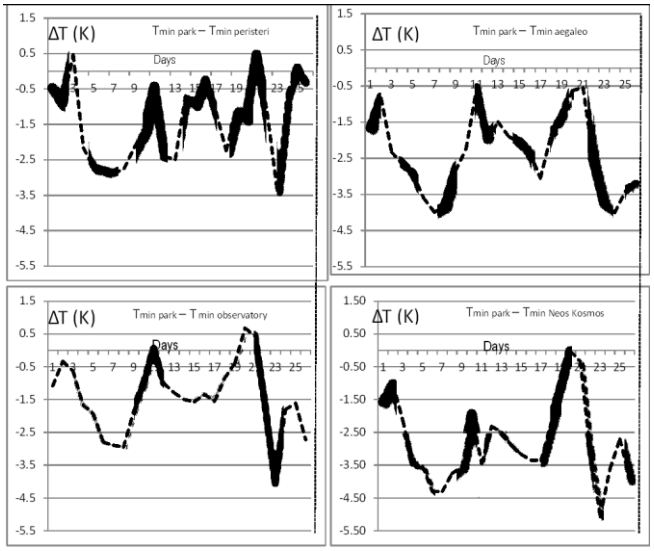

Figure 5: Daily Nocturnal Difference of Minimum Temperatures between the park and four Urban Stations.

and a significant decrease of the daily temperature amplitude in the urban stations. On the contrary, higher urban temperatures affect much less the magnitude of the daily temperature amplitude in the park than in urban areas as their thermal capacity is much lower and the anthropogenic heat is almost negligible. The daily amplitude for the urban stations and the park is quite similar for ambient temperatures close to 30 ° C however, for temperatures around 40 ° C the amplitude in the urban stations may be 4-5 K lower than that in the park.

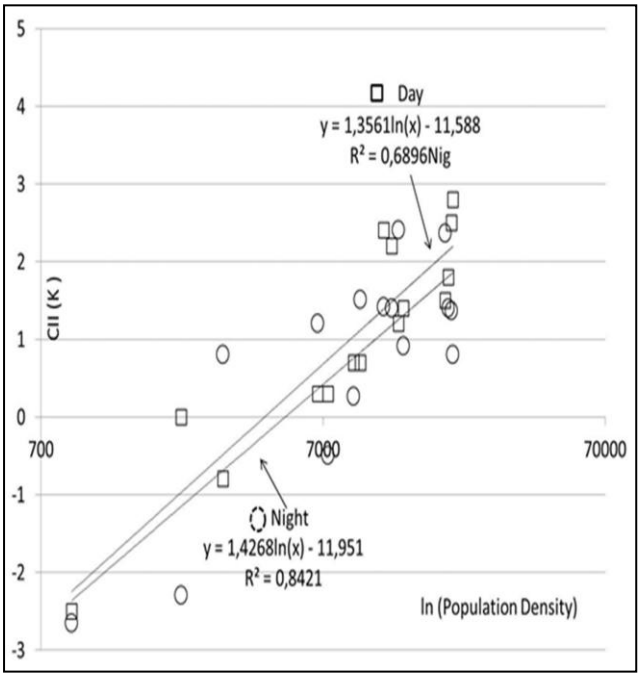

Figure 6: Relation of the daytime and nocturnal Cool Island Intensity with the Population Density.

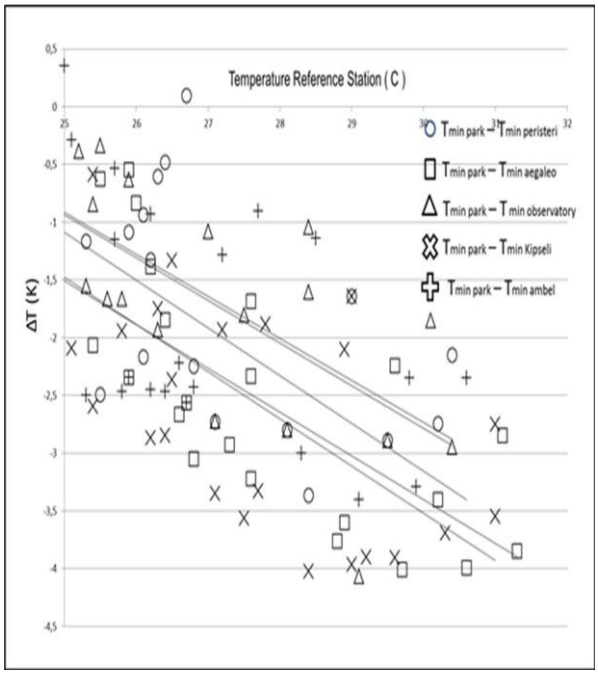

Figure 7: Relation between the daily minimum temperature and the corresponding ΔT for five urban stations.

3.3 Analysis of the Day Time Cool Island Intensity

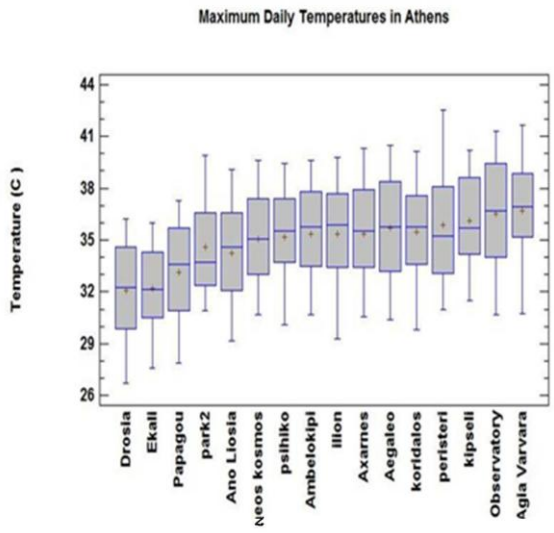

Figure 8: Distribution of the Daytime Maximum Temperature in the Park as well as in 15 urban stations.

The distribution of the daytime maximum temperatures recorded in the park during the whole period of the measurements as well as in the 15 previously presented reference stations indicate that the average maximum temperature of the park was lower than all the urban stations (Figure 8). However, it was warmer than the two stations located in suburban areas around the city, Ekali and Drosia, and an urban station located in a quite green zone of Athens. The Cool Island Index against the 12 urban stations was varied between -0.2 K and -2.6 K with an average value close to -1.4 K. The park presented almost 2.5 K higher maximum temperature than the suburban stations of Ekali and Drosia. Lower daytime maximum temperatures in the park compared to the urban stations are mainly attributed to the increased shading in the park provided by the plants that decreases the soil surface temperatures and the corresponding convective gains to the ambient air, the lack of antropogenic heat, the evaporation losses, and the absence of convective gains from high temperature urban structures and buildings. It is characteristic that the reported Cool Island Intensity values increase by -1.2 K when the temperature of the more shaded part of the park is used as reference while it decreases by the same absolute value when the more exposed to solar radiation part of the park is used as a reference instead of the average park temperature. In parallel, an important correlation between the daytime Cool Island Intensity and the population density is found (Figure 6). The relation is statistically significant although is less strong than the one found for the nighttime period. Like during the night period, the daily variability of the daytime Cool Island Intensity in the park is high. Particularly, varies between + 2.5 K to -7.0 K, while the pattern of the daily evolution is similar for all stations. A very important correlation between the maximum ambient temperature and the corresponding Cool Island Index in the park, is obtained, (Circle points). It is found that that the higher the maximum daytime temperature in the urban station, the higher the CII in the park (Figure 9). However, it is very interesting to note that when the temperature in the city is higher than 38 to 39 ° C the Cool Island Intensity of the park is decreasing seriously and does not

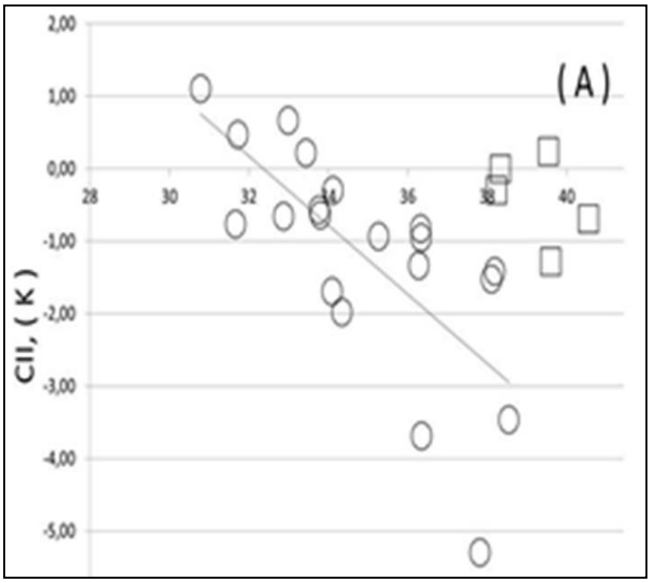

Figure 9: Relation between the daily average maximum ambient temperature of eight urban stations with the corresponding average Cool Island Intensity in the park.

follow the previous found trend between the CII and the ambient temperature (Figure 9, square points).

3.4 Mitigation Potential and Analysis of the Traverses around the Park

As already mentioned, three types of traverses were designed and carried out to estimate the climatic influence of the park in the surrounding area during and around the noon period. The first and the second traverses were performed on a daily basis since the 23rd of August to the 2nd of September 2012. For the first traverse, monitoring of the temperature was extended up to 420 m from the park towards NE directions and on a principal street with quite heavy traffic. The traverse included eight dense residential blocks with buildings of 2 or 3 stores. The street has a width close to 7 m, is covered by asphalt and has very few trees around it, while its H/W ratio varies from 1.0 to 1.Eight measurements are taken along the road as shown in Figure 10. The second traverse was carried out along the same road but towards NW direction. The street continues to have the same characteristics as described previously, however the first 120 meters immediately after the park exit, are surrounded from both sides by a non-built open space (Figure 10). Measurements are taken at seven specific points.

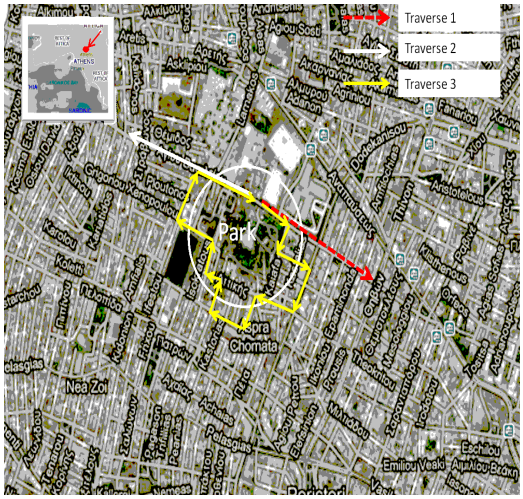

Figure 10: Traverses around the park area.

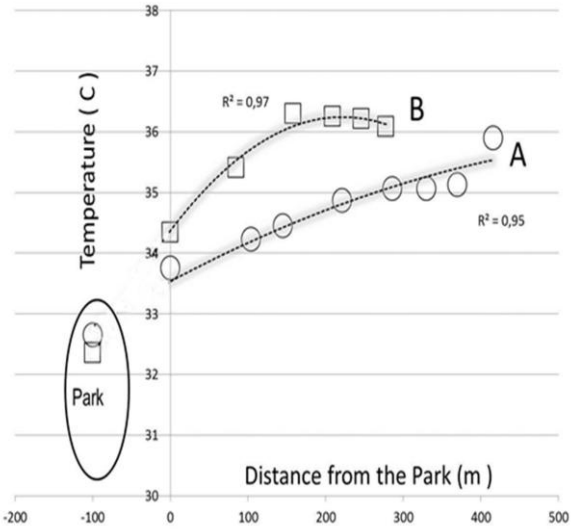

Figure 11: Distribution of the average ambient temperatures along the first, (A) and the second, (B), traverse. Also, the average temperatures of the park are given.

The distribution of the average temperature along the first and the second traverses are given in Figure 11. As shown, the distribution of the temperature along the traverse follows a second order polynomial relation with R^2= 0.95-0.97 for both cases. The calculated average Park Cooling Index PCI, was close to 3.3 K. During the first traverse, while the average temperature in the park was 32.6 ° C, the temperature increased by 1.1 K just out of the main entrance of the park and reached values close to 35.9 at the end of the traverse. This last point of the traverse corresponds to an intersection with a major traffic artery of the city where the generated anthropogenic heat is high. Temperatures tend to stabilize at about 300 m beyond the park, while the high value measured at the end of the traverse was influenced by the traffic. Interpretation of the complete set of measurement permits to consider that the climatic influence of the park should not exceeded 300-350 meters. During the second traverse, the PCI was 3.8 K, while a very rapid increase of the temperature was observed for the initial 150 meters because of the vicinity with the non shaded open space.

Temperatures increased along the initial 220 meters end then were stabilized or even slightly decreased. The temperature gradient along the first traverse varied between 0.16 K/100 meters and 0.84 K/100 meters with the average value of 0.52 K/100 meters. Calculations are based using as initial reference temperatures that out of the park and as final the one at the end of the traverse. For the second traverse, the temperature gradient was higher because of the proximity with open field and varied between 0.75 K/100 meters and 1.4 K/100 meters. When as reference the average temperature in the park is used than the temperature at the exit of the park, the temperature gradient varied between 0.45 K/100 meters to 1.1 K/100 meters with an average value of 0.78 K/100 meters for the first traverse, and values between 1.0-1.8 K/100 meters for the second traverse with an average close to 1.2 K/100 meters. These values are much higher than the temperature gradients reported by Lindqvist S. (1992), for a low density area in Gothenburg and considerably lower than those reported by Lee et al, (2009) for a very dense commercial area in Seoul. It is found that the temperature gradient along both the traverses is strongly influenced by the wind speed, especially for values higher than 5 m/sec (Figure 12). Increase of the wind speed tends to rise in a statistical significant way the temperature gradient beyond the park limit. Higher wind speed towards the windward side of the park, create a high pressure that seriously limits the flow of cool air from the park to the surrounding area. The third traverse around the park perimeter had as objective to investigate the temperature differences between the windward and the leeward sides of the park. Traverses have been carried out 24 times during the experimental period between 13:00-14:00. The main conclusion of the analysis is that the park is in average 0.8-1.2 K cooler than its immediate surroundings. In parallel, it is found that temperature around the park is very similar and there no significant temperature differences between the leeward and windward sides. This happens because of the density, the layout and the generated anthropogenic heat around the park vary considerably involving non shaded open spaces, partly or fully shaded urban canyons and some green spaces. Thus, the possible thermal benefits from the park are counterbalanced by various thermal gains.

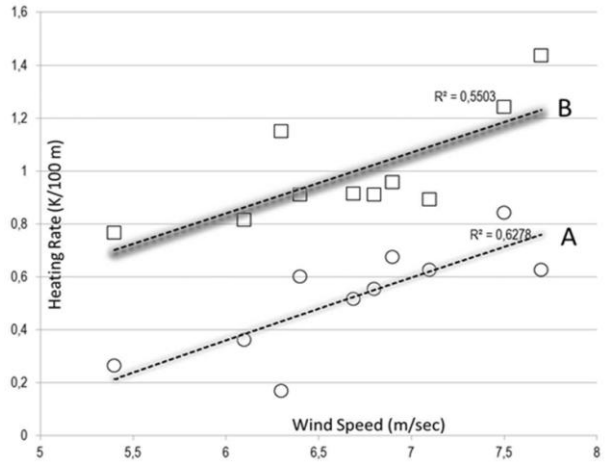

Figure 12: Relation between the wind speed and the heating rate for wind speeds higher than 5 m/sec for the first, (A) and the second traverse, (B).

4 CONCLUSIONS

It is demonstrated that even medium size urban parks can create local cool islands during the day and the night period. During the night time the average cooling rate in the studied park was 0.32 K/h, much higher than in the reference urban stations where values ranged between 0.19 to 0.24 K/h. This has resulted to important night time Cool Island Intensities in the park (-0.7 K/h to -2.8 K/h) against 13 urban stations. Temperature differences varied as a function of the urban characteristics and found to correlate in a statistical significant level with the population density index of the considered urban areas. Higher maximum daytime temperatures correspond to lower day-night temperature amplitudes in the urban stations while a strong correlation has been found between the daily maximum temperatures and the nocturnal Cool Island Intensities in the park. During the day period, the average maximum temperature in the park was lower than in 12 reference urban stations and the magnitude of

the corresponding daily Cool Island Intensity varied between -0.2 K and -2.6 K with an average value close to -1.4 K. The CII found to have a strong correlation with the population density in the corresponding urban areas. The park is found to be warmer than the urban areas for ambient temperatures lower than 34 C, however the CII increased as a function of the ambient temperature for values higher than 34 C. The calculated PCI was between 3.3 K and 3.8 K, while the temperature gradient along the traverses from the park to the urban areas varied between 0.16 to 1.4 K/100 meters connected strongly with wind speeds higher than 5 m/sec. Parks may contribute highly to mitigate urban heat islands, however their climatic influence is subject to the characteristics of the park and the thermal properties of neighbouring urban areas.

5 ACKNOWLEDGEMENTS

This work would not have been possible without the considerable help of the Professor Mathheos Santamouris.

6 REFERENCES

Giannopoulou K., I. Livada, M. Santamouris, M. Saliari and M. Assimakopoulos, Y.G. Caouris, (2011) : On the Characteristics of the Summer Urban Heat Island in Athens, Greece. Journal Sustainable Cities and Society, Volume 1, Issue 1, Pages 104-115

Gobakis, D. Kolokotsa, A. Synnefa, M. Saliari, K. Giannopoulou, M. Santamouris, (2011) : Development of a model for urban heat island prediction using neural network techniques, Sustainable Cities and Society, Volume 1, Issue 2, Pages 104-115

Kassomenos, P.A. and Katsoulis, B.D, (2006) : Mesoscale and macroscale aspects of the morning Urban Heat Island around Athens, Greece, Meteorology and Atmospheric Physics, Volume 94, Issue 1-4, Pages 209-218

Lee Sang-Hwa, Kyoo-Seock Lee and Wen-Cheng Jin, (2009) : Effect of an urban park on air temperature differences in a central business district area, Landscape Ecol. Eng, 5:183–191

Lindqvist S. (1992) : Local climatological modelling for road stretches and urban areas. Geograjska Annaler 14A,265-274.

Livada – M.Santamouris, M.N.Assimakopoulos, (2007) : On the variability of summer air temperature during the last 28 years in Athens, JGR, 2007, Journal of Geophysical Research, Vol. 112, D12103.

Mihalakakou P., H.A. Flocas, M. Santamouris and C.G. Helmis, (2002) : 'Application of Neural Networks to the Simulation of the Heat Island over Athens, Greece, Using Synoptic Types as a Predictor, J. Applied Meteorology, 41,5,519-527.

Santamouris, G. Mihalakakou, N. Papanikolaou and D. N. Assimakopoulos, (1999) : ' A Neural Network Approach for Modeling the Heat Island Phenomenon in Urban Areas During the Summer Period' Geophysical Research Letters, 26, 3, p.p. 337-340.

Santamouris, M. (Ed.), (2001). Energy and Climate in the Urban Built Environment. James and James Science Publishers, London.

EVOLUTION OVER TIME OF UV-VIS-NIR REFLECTANCE OF COOL ROOFING MATERIALS IN URBAN ENVIRONMENTS

Riccardo Paolini*[1,2], Michele Zinzi[3], Tiziana Poli[1], Emiliano Carnielo[4], Matteo Fiori[1], Andrea Giovanni Mainini[1]

1 Politecnico di Milano, Dept. of Architecture, Built environment and Construction engineering
Via Ponzio, 31
20133 Milano, Italia
**Corresponding author: riccardo.paolini@polimi.it*
3 ENEA – UTEE-ERT Italian National Agency for New Technologies, Energy and Sustainable Economic Development
s.p. 104 - st. 113, via Anguillarese, 301
00123 Roma, Italia

2 Heat Island Group, Environmental Energy Technology Division, Lawrence Berkeley National Laboratory
1 Cyclotron Road
94720 Berkeley (CA), USA
4 Università degli Studi Roma Tre
Via della Vasca Navale 79/81
00146 Roma, Italia

ABSTRACT

Highly reflective building envelope materials are widely identified as an effective design option to limit the peak surface temperatures of roofs in summer conditions, thus mitigating the urban microclimates and the energy demand for cooling. However, especially surfaces having high solar reflectance are subject to soiling (i.e. deposition of soot and other airborne particles), in addition to ageing, and biological growth. All these processes reduce the reflectance of bright surfaces (and increase the reflectance of surfaces having reflectance lower than roughly 0.20). As a result, a decrease in the solar reflectance of a cool roof yields to higher surface temperatures and a reduction in the energy savings expected thanks to high albedo roofing. Furthermore, the durability is also impacted.

To quantify this effects, we exposed in the urban environment in Milano and in Roma (Italy) 14 roofing membranes, including synthetic, factory applied coating on synthetic membranes, field applied coatings on modified bitumen, asphalt shingles. For each product class (e.g. synthetic membranes) we selected a high reflectance product and a mid-low reflectance one. We measured the UV-Vis-NIR spectral reflectance of three samples per product before the exposure – begun in April 2012 – and after 3, 6, and 12 months. Herein we present the results of the first year of natural exposure, reporting a remarkable loss in the solar reflectance, sometimes exceeding 15% of the initial value already after the first three months of natural exposure and in some cases by more than 30% after one year, depending on their initial value.

With the measured curves of solar reflectance over time as input data, we performed finite differences numerical modelling (by means of the software tool WUFI 5.2) of heat and moisture transport through typical roof assemblies. We analyzed the variation in the surface temperature and heat flux due to the change in solar reflectance, and we obtained relevant differences. For instance, in case of a highly reflective flat roof (with initial solar reflectance equal to 0.852, reduced to 0.624 after one year) over 14 cm of expanded polystyrene on a reinforced concrete slab (U-value of the roof assembly equal to 0.267 W m^{-2} K^{-1}) we computed a significant increase in peak surface temperatures (during the first summer up to 7°C, and up to 14°C more at the end of the first year , assessed in the context of Milano, Italy). Knowledge about the soiling trends for different building envelope materials allows to better estimate the cooling energy demand of buildings, plan cleaning and maintenance operations (whether viable and sustainable), and to assess the service life and the life cycle, and eventually study the benefits of possible anti-soiling treatments.

KEYWORDS

Cool materials; solar reflectance; soiling; ageing; natural exposure.

1 INTRODUCTION

In the Literature there are several studies assessing the evolution over time of the solar reflectance of building envelope materials (e.g. Berdahl *et al.*, 2002; Bretz & Akbari, 1997). In addition, data can be retrieved from the databases made available by the U.S. Environmental Protection Agency (U.S. EPA) and by the U.S. Cool Roofing Rating Council (CRRC), which report clean and aged - after three years of natural exposures - solar reflectance (SR) and thermal emittance (TE) for 2469 products (as of August 2013). More in detail, the CRRC manages the natural exposure of roofing products at three sites in the U.S. (and the aged SR and TE are the average after three years at the three sites): one in a temperate and polluted sub-urban environment (in Ohio), one in a hot-dry extra-urban climate (in Arizona), and one in a hot and humid extra-urban context (in Florida). It is interesting to note that none of the exposure fields is located within an urban area (for obvious reasons of space required for the exposure facilities and the cost of land use). At the CRRC's exposure sites, as analysed by Sleiman *et al.* (2011), excluded the roofing products with initial solar reflectance (SR_{T0}) lower than 0.20, all the exposed products present losses in SR increasing with SR_{T0}. For instance, for products with SR_{T0} of more than 0.80, after three years SR is in average about 20% lower than the initial value, with a variation of about 15% depending on the exposure site. Moreover, as noted by Sleiman *et al.* (Sleiman *et al.*, 2011) these databases do not include spectral data, useful for understanding the agents producing the variation in reflectance, and study possible countermeasures. This aspect has been investigated on a set of roofing membranes by Berdahl *et al.* (Berdahl *et al.*, 2002), who identify the atmospheric soot particles deposing onto the buildings' surfaces as the main agent producing the variation in reflectance; they also observe that soot absorbs more at low wavelengths than in the NIR, leading to yellowing of surfaces. However, even if data are available - alas seldom spectral - about the magnitude of the variation of optical and radiative properties over time of roofing materials and even about the effect of alternative cleaning procedures (Levinson *et al.*, 2005), these concern almost only the North American contexts.

Herein we present the results of the first year of natural exposure in urban environments in Milano and in Roma (Italy) of 16 roofing materials, including roofing membranes (single-ply synthetic, field applied coating on modified bitumen, asphalt shingles). For each product class (e.g. synthetic membranes) we selected a high reflectance product and a mid-low reflectance one. We measured the UV-Vis-NIR spectral reflectance of three samples per product before and after 3, 6, and 12 months of natural exposure. Using the measured data, we computed - for Milano's climate context - the exterior surface temperatures and heat fluxes for flat roofing assemblies typical of industrial and commercial buildings, both well insulated and with no insulation. The purpose of this study, thus, is to portray the early trends (after the first year of natural exposure) of the solar reflectance of roofing membranes when exposed to the environmental conditions typical of European cities. Moreover, with this work we aim to assess the impact of soiling on the exterior surface temperatures and the heat flux of flat roofs.

2 SELECTED MATERIALS

To assess the effect of soiling on roofing materials we selected from the market 14 roofing membranes, trying to include all the possible features that could lead to a different dirt pickup. For each product class we chose a "standard" option, a "cool" alternative (namely having higher reflectance in the NIR than in the visible portion of the solar spectrum), and, if

available, a photocatalytic alternative. We included products with SR_{T0} ranging from 0.237 to 0.868, having a smooth or rough surface (to different degrees); moreover, some membranes are somewhat glossy (with a perceivable specular component) while others are matte (Tab. 1).

Table 1: Selected roofing membranes, and initial solar reflectance.

Code	Description	Initial solar reflectance
m1	Grey flexible polyolefin (matte and with anti-slip surface)	0.256
m2	Grey flexible polyolefin with white factory applied elastomeric coating (glossy)	0.852
m3	White flexible polyolefin (matte and with anti-slip surface)	0.762
m4	White thermoplastic polyolefin (glossy)	0.824
m5	Grey PVC membrane (glossy)	0.464
m6	White PVC membrane (matte)	0.838
m7	Cool beige thermoplastic polyolefin (matte)	0.593
m8	Polymer-bitumen with extra white field applied elastomeric coating	0.805
m9	Polymer-bitumen with white field applied elastomeric coating	0.731
m10	Polymer-bitumen with white TiO_2 photoactive field applied coating	0.765
m11	Polymer-bitumen with white field applied elastomeric coating type B (glossy)	0.718
m12	Polymer-bitumen with cool coloured elastomeric field applied coating	0.386
m13	Photoactive asphalt shingle	0.282
m14	Standard asphalt shingle	0.234

3 NATURAL EXPOSURE AND MEASUREMENT PROCEDURES

Since cool roofing products are widely recommended as an option to mitigate urban climates, we decided to expose the selected samples at two locations within two urban areas with different climates: Roma and Milano, in both cases about halfway between city centre and periphery. The exposure is performed on two non-shaded roofs and distant from main specific sources of pollution (e.g. a particular industrial plant), thus subject to the background pollution and soil deposition (in addition, in Milano a weather station is positioned on the same roof and an air quality station is less than 300 m far). The roofing membranes were exposed low sloped (1.5% as recommended by both Italian and Swiss application standards); in Milano replicates were also exposed south oriented with a slope of 45 degrees. For each product three samples of 10 cm x 10 cm in size each were exposed for each site and exposure condition, and they had been fastened to metal frames, 80 cm above the roof.

The same samples were measured when clean, and after 3, 6, and 12 months of natural exposure, begun on April 18th 2012, they were retrieved, measured in the laboratory, and re-exposed. All the measurements were performed with a UV-Vis-NIR spectrometer (Perkin Elmer Lambda 950 with 150 mm integrating sphere with PMT/PbS detectors) from 300 to 2500 nm, sampling each 5 nm. Each sample was just measured in the central point, considering as representative the portion of the sample lit by the measurement beam, namely a rectangle of about 3 mm x 20 mm, thus using the rest of the 100 mm x 100 mm samples just to exclude the edge effects. As averaging procedure (to compute the solar, UV, visible and NIR integrated values) we used that detailed in the ISO 9050 standard (ISO, 2003), which uses an air mass 1.5 global horizontal solar spectral distribution. For each product and exposure condition (i.e. site, orientation, and slope), for the three replicates we computed the average spectral curve, and then the integrated values.

4 UV-VIS-NIR REFLECTANCE WITH TIME: FIRST YEAR RESULTS

Herein we present the solar reflectance trends (absolute and as a percentage of the initial value) for the three exposure conditions (Roma and Milano horizontal, and Milano facing south with a slope of 45 degrees) for all the aged membranes, while for the sake of synthesis we present the spectral data only for the eight membranes which are mostly differentiated in terms of spectrum among those tested.
At both the exposure sites we observe remarkable variations of solar reflectance after one year of natural exposure, and in any case the changes at the CRRC's sites after three years are of the magnitude of the variations that we measured after six months of exposure in Milano and Roma. For instance, for membranes with initial solar reflectance greater than 0.80 (Sleiman *et al.*, 2011), at the Florida exposure site the average absolute loss in SR for the tested products is of 0.238 ± 0.146, while it is of 0.077 ± 0.060 and 0.173 ± 0.092 respectively in Arizona and in Ohio, namely, in average roughly 0.162, or 18% of the initial value after three years. For products within the same range (0.8-1.0) of SR_{T0} (namely membranes, m2, m4, m6, and m8 of our collection, see Tab. 1) we computed after just six months absolute losses of 0.171 (Fig. 1a) in Milano (of 0.158 for 45° slope, Fig. 1c), as in Ohio (the most urban site among those managed by the CRRC), and of 0.116 in Roma (Fig. 1e), while after one year we measured in Milano losses equal to 0.223 (0.217 for 45° slope) and of 0.154 in Roma. Considering any possible term of comparison, we see that after one year of natural exposure at the two polluted urban sites in Roma and Milano we observe the same or a greater magnitude of solar reflectance loss than at the CRRC's sites. In general, the membranes that we exposed having SR_{T0} between 0.2 and 0.3 (e.g. m1, m13, and m14) do not show relevant absolute variations over time (roughly 0.02-0.05). It is however interesting to note that the SR of the single-ply grey membrane (m1) shows a monotonic decreasing trend, while for the asphalt shingles (m13 and m14) SR fluctuates over time, sometimes exceeding the initial value when the gaps between beads are filled with soot (and other particulate matter), which has higher reflectance than the bitumen substrate (as discussed in detail by Berdahl *et al.*, 2012). Considering the general trend of losses in solar reflectance for all the membranes having SR_{T0} greater than 0.40 (i.e. all but m1, m13, and m14), we note that, after one year the average absolute loss in Milano ranges from 0.15 to 0.25 for low sloped membranes (from 0.10 to 0.25 for 45° tilted samples), in Roma it ranges roughly from 0.08 to 0.16. The loss of solar reflectance of samples low sloped and tilted by 45° (south oriented) in Milano is not remarkably different. Once again looking at the most reflecting membranes of the collection (i.e. with SR_{T0} greater than 0.80), we compute that the relative (as a percentage of the initial value) solar reflectance loss is of about 26.7% for low sloped samples, and of about 26.1% for 45° tilted samples. Differences are larger at 3 and 6 months, thus when the soiling is less conspicuous.

The spectral curves (Fig. 2 and Fig. 3) allow a deeper understanding of the action of depositions on the reflectance of roofing membranes. The abatement of reflectance is evident mainly in the visible and in the first part of the near infrared, and it is interesting to note that for all the bright membranes, the shape of the spectra is altered especially in the first part of the visible portion of the spectrum (more precisely between 420 and 600 nm), while after about 600-800 nm the spectrum is substantially shifted down, retaining the original shape. Although, as obvious, the absolute values of reflectance of samples exposed at the two sites are different, is noticeable that the shape of the spectra of the aged membranes is almost the same both in Roma and Milano, suggesting that in metropolitan areas just the intensity of deposition is different, while the basic ingredients of soiling (e.g. products of combustion from vehicles' engines and heating plants) are the same. There is actually a difference in terms of shape of the spectra between the horizontally exposed samples and those tilted of 45°. For the latter ones the effect of depositions between 420 and 600 nm is slightly less pronounced than for the low sloped specimens. In addition, comparing the results for clean and soiled membranes with different initial spectral reflectances, we note that when the reflectance is

lower than 0.40 after 1500 nm the impact of soiling in the last portion of the NIR seems to be negligible (Fig. 2 d, e, and f). Similarly, the case of membrane m12 (Fig. 3 g, h, and i), a cool coloured field applied coating on modified bitumen, is remarkable in showing which is the optical behaviour of soot in the visible, since the spectral reflectance of that membrane is unchanged just in the visible.

a)

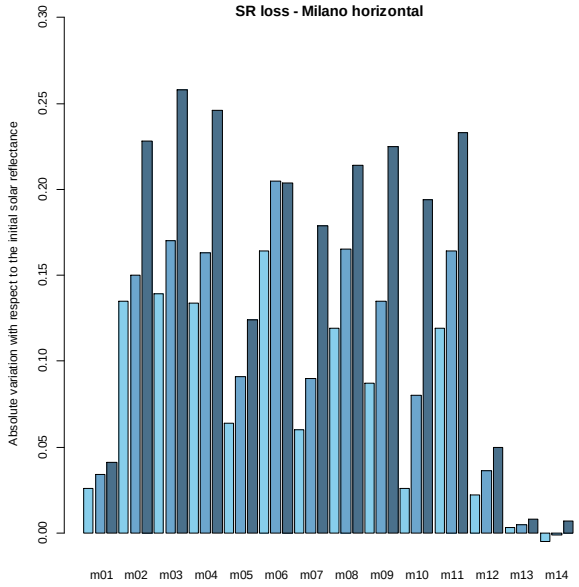

b)

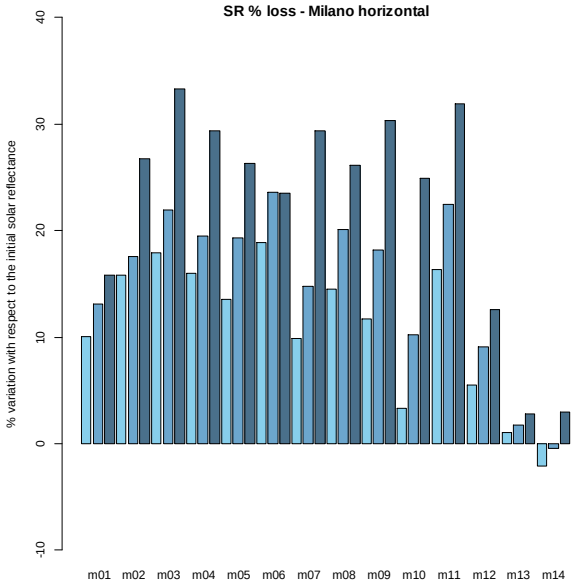

c)

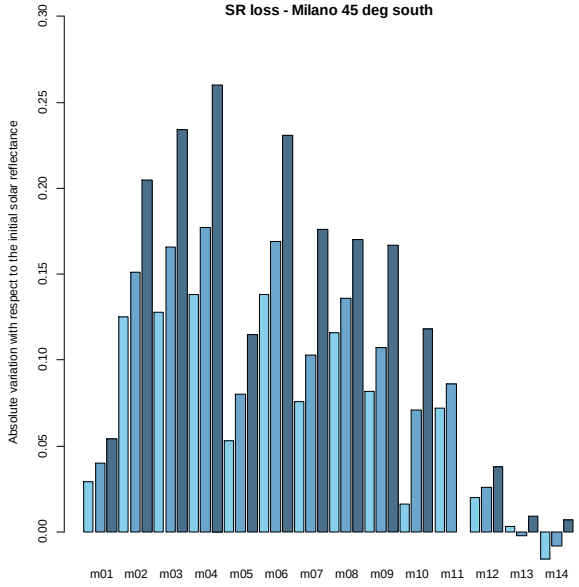

d)

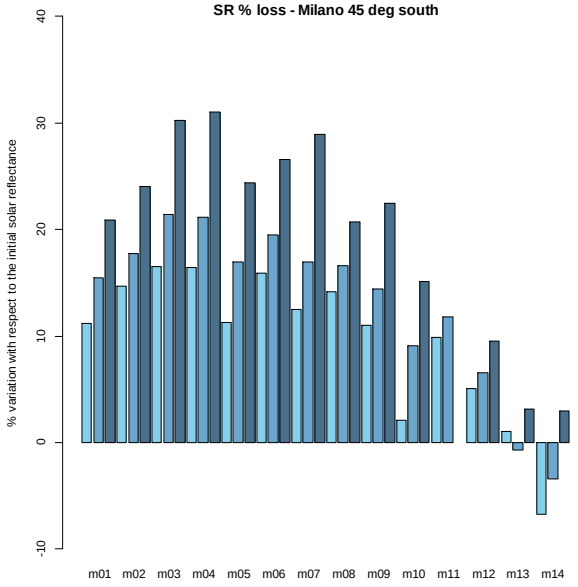

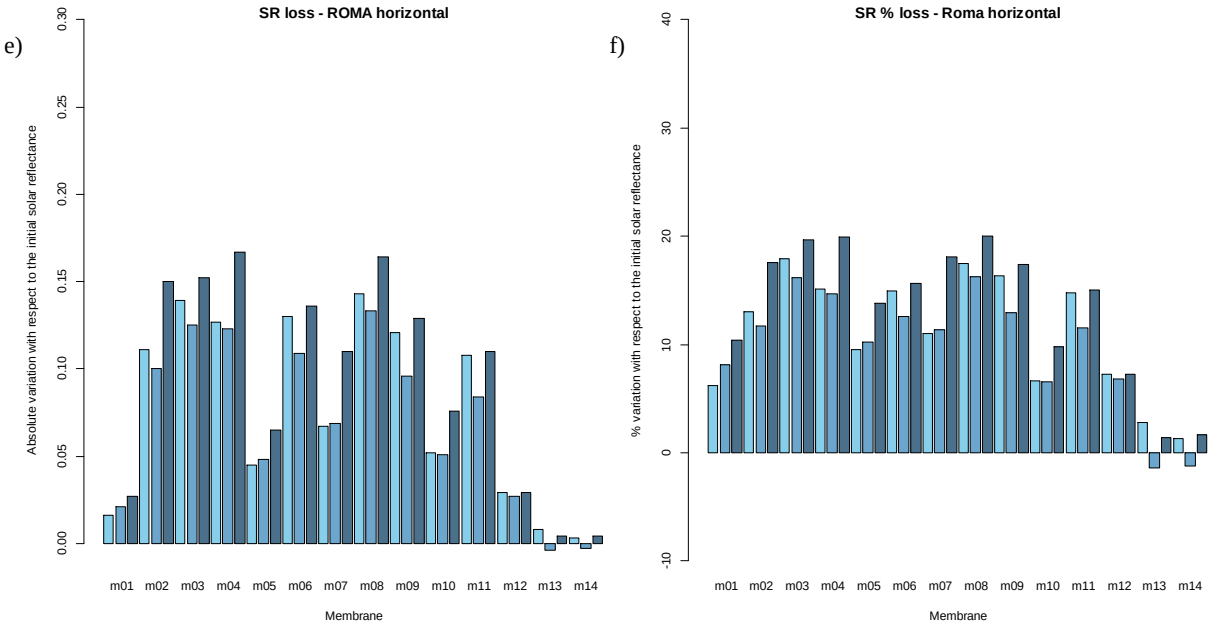

Figure 1: Absolute solar reflectance variation after 3 (light blue), six (blue), and 12 months (dark blue) in Milano for low sloped samples (a) and samples tilted by 45° (c) and low sloped in Roma (e). Relative (percentage of the initial value) loss of solar reflectance in Milano low sloped (b), Milano 45° tilted (d), and Roma (f).

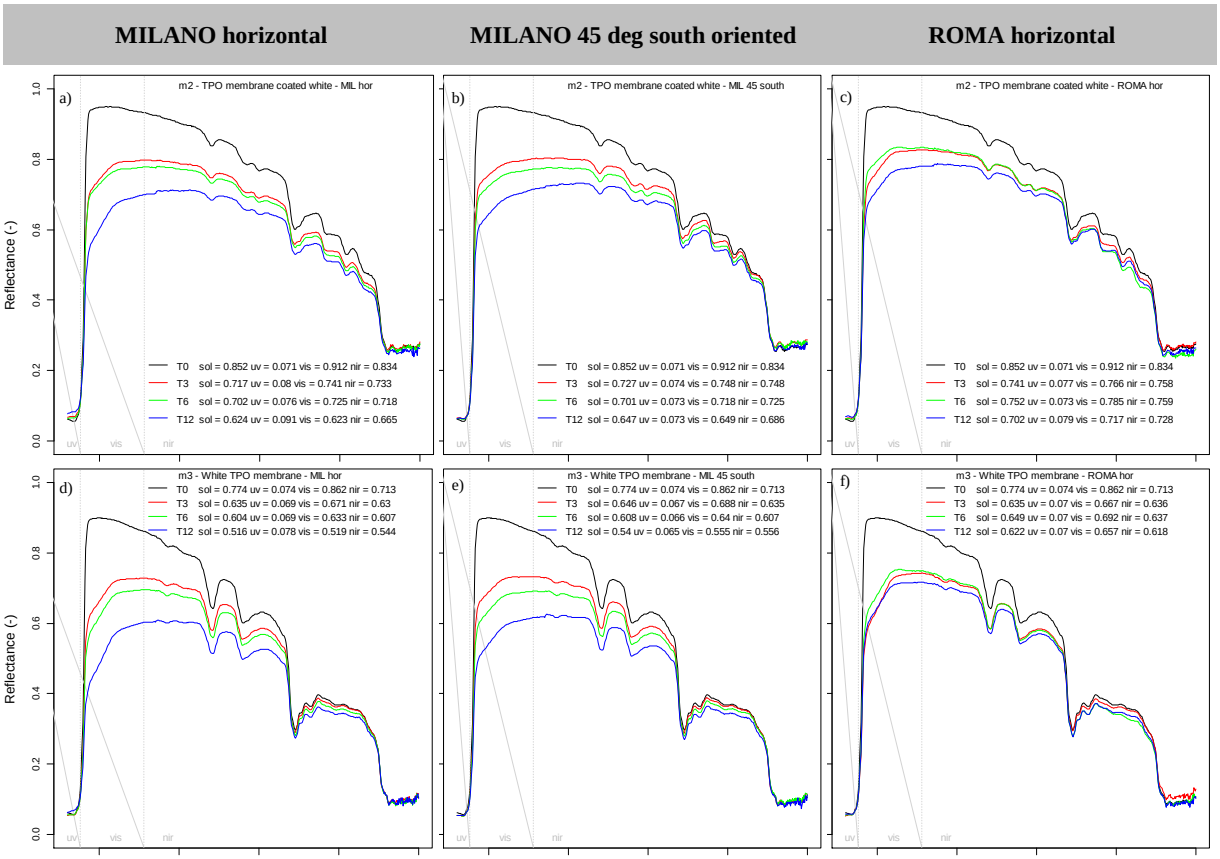

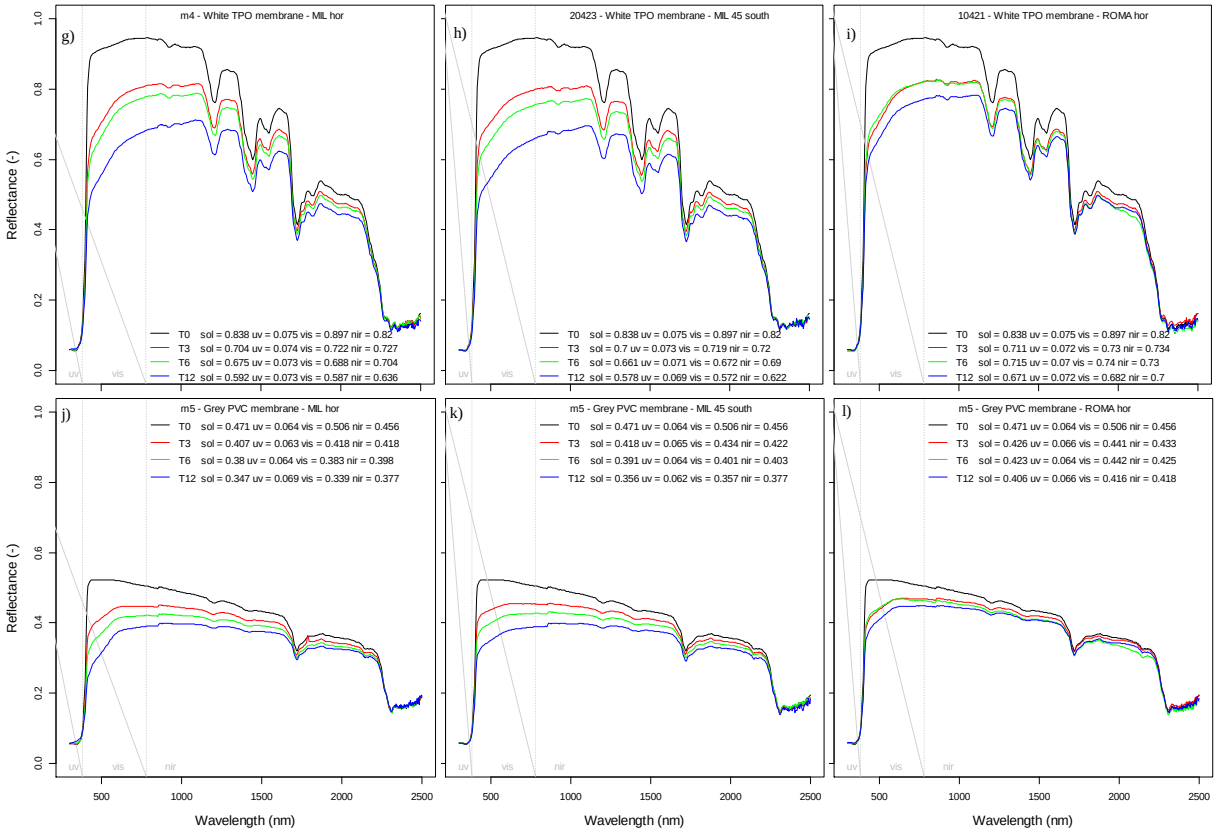

Figure 2: Spectral reflectance and computed solar, UV, visible, and NIR reflectance for the membranes m2, m3, m4, and m5 after 3, 6 and 12 months in Milano (low sloped and 45° sloped south oriented) and in Roma.

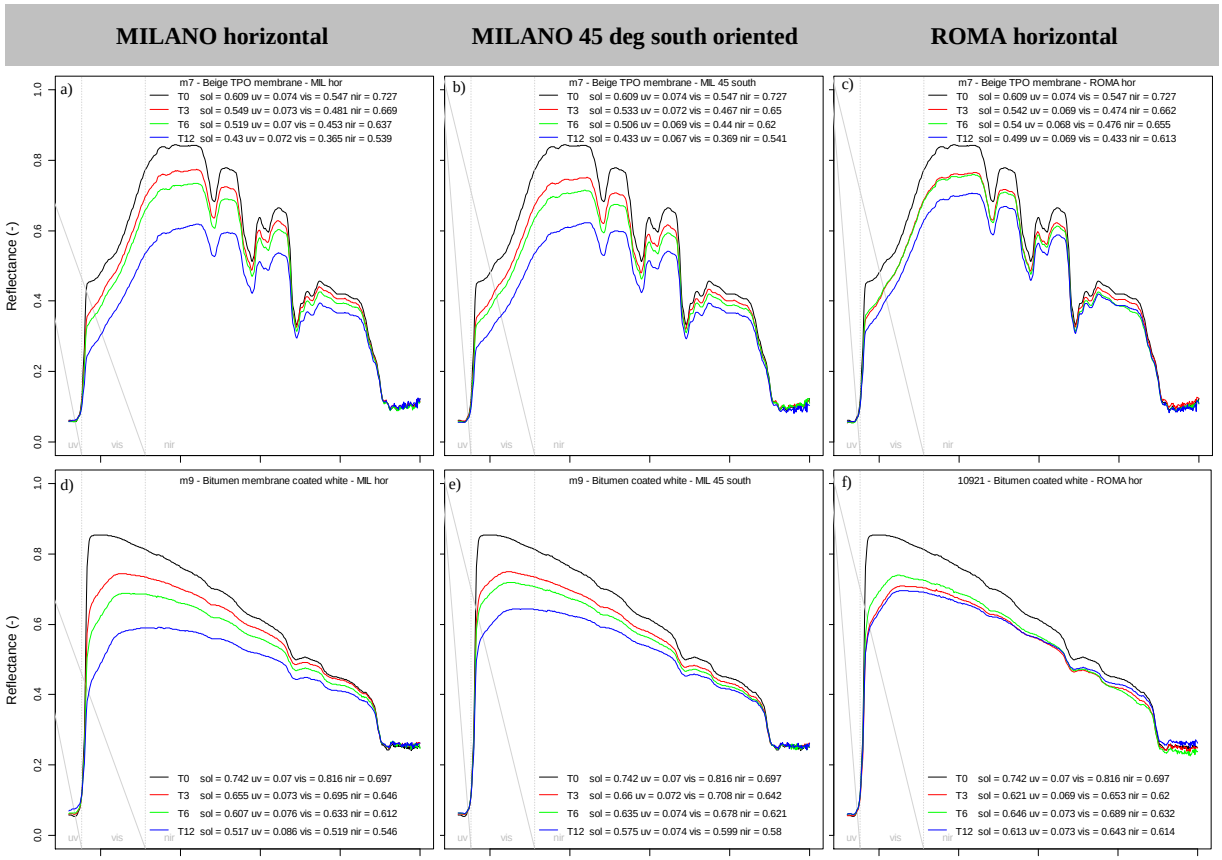

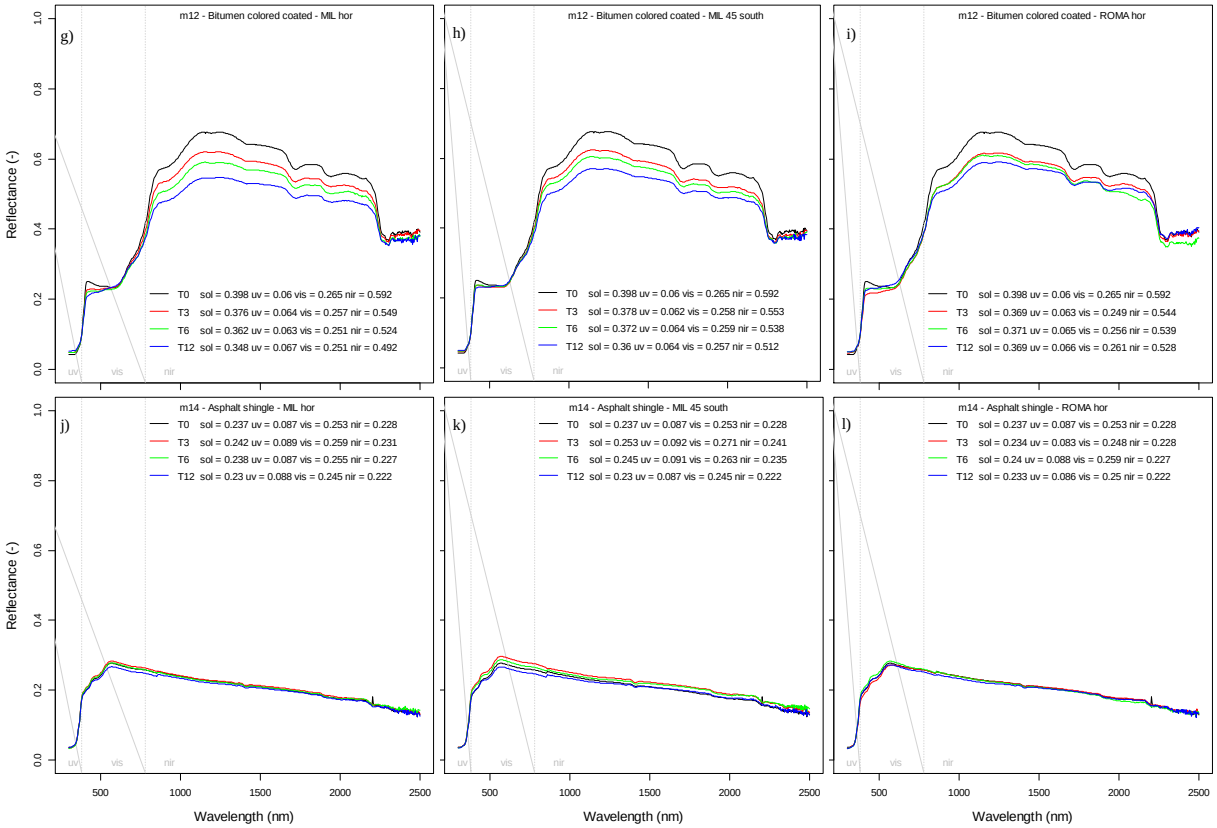

Figure 3: Spectral reflectance and computed solar, UV, visible, and NIR reflectance for the membranes m7, m9, m12, and m14 after 3, 6 and 12 months in Milano (low sloped and 45° sloped south oriented) and in Roma.

5 COMPUTED SURFACE TEMPERATURES AND HEAT FLUXES

Once that the evolution over time of the solar reflectance of a given roofing product is known for a specific context - or a reliable estimate is made using a regression representative for a class of products in a possible context of application, such as urban climates in Southern Europe - it is important to assess when and whether these changes are relevant for the building energy demand and the microclimate. To investigate this aspect we performed numerical modelling of heat and moisture transport through typical (for the Italian context) precast flat roofing assemblies for industrial and commercial buildings, considering the case of well insulated roofs and woofs without insulation. In detail, we considered a double-T precast concrete slab, with a wing 5 cm thick, with additional 5 cm of concrete screed and, in case of insulation, a vapour retarder (1 mm of polyethylene), 14 cm of expanded polystyrene (EPS) and the roofing membrane (U-value = 0.267 W m^{-2} K^{-1}), while in case of no insulation the membrane is applied onto the screed (U-value = 4.087 W m^{-2} K^{-1}). The case without insulation is representative for either a non-retrofitted building or a building where an industrial activity takes place (e.g. with a furnace or computer servers) dissipating heat and keeping the indoor temperature constant at 20°C in winter without the need of a heating plant, while demanding cooling in summer.

The numerical simulations were performed by means of the software tool WUFI 5.2 (www.wufi.de), based on a finite volumes physically based model, which couples and resolves numerically (up to convergence) two equations dealing, respectively, with one-dimensional transient heat and moisture transport, and is capable of taking into account the latent transformations, as well as the dependency of the thermal properties on temperature and

moisture content. For the exterior climate, we used hourly data from 15 April 2012 to 15 April 2013 - namely the period of exposure of the membranes - collected by a weather station in Politecnico di Milano (latitude: 45.4798; longitude: 9.2297) on the same roof were the samples were exposed. For the indoors, we assumed 20°C when the exterior temperature is lower than 10°C, 25°C when the exterior temperature higher than 20°C, and linearly interpolated values in between. Then, we considered the case of membrane m2, a flexible polyolefin topped by a white glossy elastomeric coating, with SR_{T0} equal to 0.852, and 0.717 after 3 months, 0.702 after 6 months, and 0.624 after one year of natural low sloped exposure in Milano (Fig. 2a). Then we modelled two cases: with constant SR (as clean), and with SR as a function of time using the measured data (intermediate values were linearly interpolated).

Considering peak summer conditions, for instance close to solar noon in a typical clear sky summer day (in this case July 21st), we see that the exterior surface temperature of a well insulated flat roof is 7°C hotter just after 3 months of natural exposure than if kept clean (Fig 4a), while there is little difference at the interior surface temperature, given that the building is conditioned. In case of a non-insulated roof, instead, the difference between soiled and clean condition is smaller (about 4.5°C) at the exterior surface, while it is of about 2.5°C at the interior surface (Fig. 4b). Looking at hourly values all through the year we see that, already in its first summer of service life, the soiled roof is 7-8°C hotter than the clean roof if insulated, and 5°C if not insulated. In the end of the first year of service life, the roof is dirtier, and already in the first part of April the soiled roof is hotter than the clean roof by about 14°C or 8°C, respectively if insulated or not. Finally, considering the heat fluxes at the interior surface we note that, not surprisingly, in case of high insulation, the difference between soiled and clean roof is negligible. On the other hand, for a non-insulated roof, the peak incoming heat fluxes when the roof is soiled (in average 38 W m^{-2}) are more than double than when the roof is clean (in average 16 W m^{-2}). In winter condition, instead, a non-insulated clean roof transfers more heat than the soiled one even by about 15 W m^{-2}.

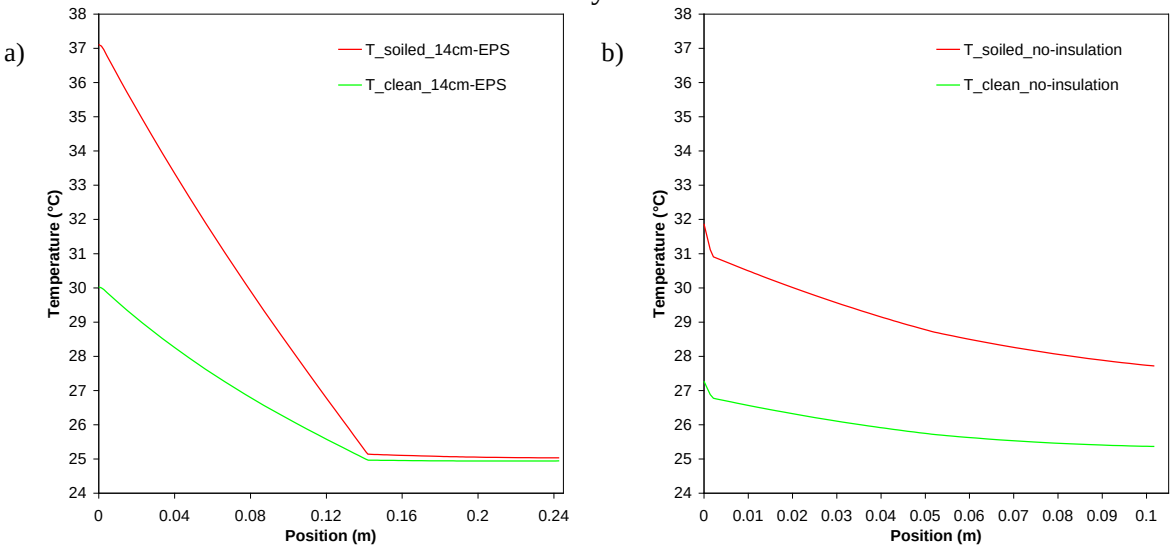

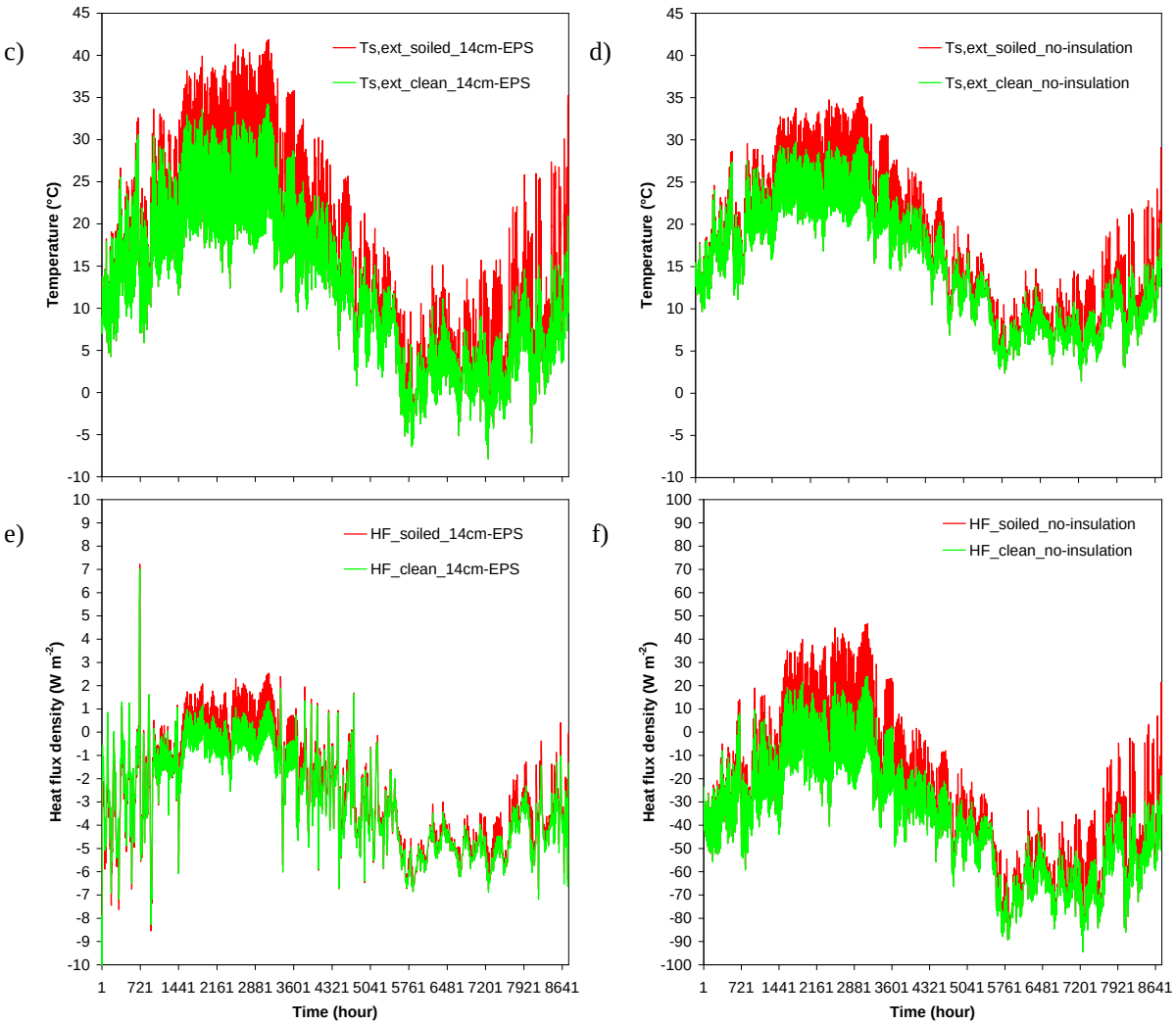

Figure 4: Temperature profiles (from the exterior surface to the interior) with 14 cm of EPS (a) and with no insulation (b) on a typical summer day (21st July) at 13:00 local time; hourly exterior surface temperatures with high (c) or no insulation (d); and hourly heat flux density at the interior surface with high (e) or no insulation (f).

6 CONCLUSIONS

Since cool roofs are identified as an effective option to mitigate heat islands and reduce the cooling energy demand of buildings, several studies were performed in the U.S. to determine how long a roof may retain its high albedo, but there are only few experiences in Europe. Thus, to assess the effect of dirt deposition on albedo in Italian cities, in April 2012 we exposed both in Milano and in Roma 14 roofing membranes retrieved from the market, measuring their reflectance when clean and after 3, 6, and 12 months. After the first year of natural exposure in Milano we compute a reduction of SR by sometimes more than 30% of the initial value, for instance for the membranes with initial SR greater than 0.80, while for the samples exposed in Roma the peak reductions are of about 20%. Especially, we note that the losses observed after three years of exposure at the CRRC's sites were achieved in Roma and Milano just after six months. We also computed the surface temperatures and the heat fluxes for typical roof assemblies for industrial and commercial buildings, when the roof is soiled and when is modelled as always clean. In summer, just after 3 months of service life, the soiled roof is 7-8°C hotter than the clean roof if insulated, and 4-5°C if not insulated. In the end of the first year of service life, the roof is dirtier, and already in the first part of April the soiled roof is hotter than the clean roof by about 14°C or 8°C, respectively if insulated or

not. If for well insulated roofs the influence of soiling on interior surface temperatures and heat fluxes is negligible, for a non-insulated roof, the peak incoming heat fluxes when the roof is soiled are more than double than for a clean roof (in average 38 vs. 16 W m^{-2}).

7 ACKNOWLEDGEMENTS

The authors thankfully acknowledge the Italian Ministry for Economic Development for funding the projects "Valutazione delle prestazioni di cool materials esposti all'ambiente urbano" and "Sviluppo di materiali e tecnologie per la riduzione degli effetti della radiazione solare". Exposure facilities and spectrometer at Politecnico di Milano, and numerical modelling activity were funded by Politecnico di Milano - Agenzia delle Entrate in support to the project "Rivestimenti fluorurati avanzati per superfici edilizie ad alte prestazioni".

8 REFERENCES

Berdahl, P., H. Akbari, L.S. Rose. (2002). Aging of reflective roofs: soot deposition. *Applied Optics*, 41(12), 2355-2360

Berdahl, P., H. Akbari, R. Levinson, J. Jacobs, F. Klink, R. Everman. (2012). Three-year weathering tests on asphalt shingles: Solar reflectance. *Solar Energy Materials and Solar Cells*, 99(special issue), 277–281.

Bretz, S.E., H. Akbari. (1997). Long-term performance of high-albedo roof coatings. *Energy and Buildings*, 25(2), 159-167

ISO, ISO 9050. (2003). Glass in building — Determination of light transmittance, solar direct transmittance, total solar energy transmittance, ultraviolet transmittance and related glazing factors. Geneva (CH)

Levinson, R., P. Berdahl, A.A. Berheb, H. Akbari. (2005). Effects of soiling and cleaning on the reflectance and solar heat gain of a light-colored roofing membrane. *Atmospheric Environment*, 39(40), 7807–7824

Sleiman, M., G. Ban-Weiss, H.E. Gilbert, D. Francois, P. Berdahl, T.W. Kirchstetter, H. Destaillats, R. Levinson. (2011). Soiling of building envelope surfaces and its effecton solar reflectance - Part I: Analysis of roofing product databases. *Solar Energy Materials and Solar Cells*, 95(12), 3385–3399

EXPERIMENTAL INVESTIGATION OF THE THERMAL AND OPTICAL BEHAVIOR OF AN INTENSIVE GREEN ROOF SYSTEM INSTALLED IN AN OFFICE BUILDING IN ATHENS

Panagiota Karachaliou[1], Mattheos Santamouris[1]

1 Group of Building Environmental Studies, Building of Physics-5,Section of Applied Physics, Physics Department, University Campus, National and Kapodistrian University of Athens, 15784, Athens, Greece

ABSTRACT

The aim of this paper is to experimentally investigate and analyze the thermal and optical behavior of a Green Roof System (GRS) installed in the 10000 m^2 roof of a fully insulated, bioclimatic office building in Peania. More specifically, during the experimental procedure, measurements of the outdoor temperature and relative humidity have been performed, as well as of the air temperature inside the building and the surface temperature of the ceiling. Furthermore, the surface temperatures of the roof were measured using thermographic imaging, as well as the optical properties such as the albedo of the roof's covering materials. The GRS is an intensive green roof and it consists of almost 16000 indigenous plants of at least 14 different kinds which cover the largest part of the roof surface. The rest of the area is covered by a running truck of made by a bioclimatic stabilized ceramic floor. The ceramic material was found to be 5.1 ^{0}C – 7.2 ^{0}C cooler than the soil or other common materials and the planted area 10.1 ^{0}C - 16.1 ^{0}C cooler than the ceramic floor. The different species of plants were also studied and the conclusion that the density of the foliage plays a primary role was extracted, as there was a difference of 11.8 ^{0}C between a plant with and a plant without dense foliage. It was observed that the different surfaces present their maximum temperature at different hours. The ceramic floor, at 14:00 for the 46.7% of the time and at 15:00 for the 40 %, while the planted area at 14:00 for the 53.3 % of the days, at 13:00 for the 26.6% and, oppositely to the ceramic floor, never at 15:00.

KEYWORDS

Green roof, urban heat island

1. INTRODUCTION

Most of the Mediterranean cities suffer from a quite strong heat island phenomenon (Santamouris, 2007). In particular, in Athens, where its intensity causes important energy and environmental problems (Sfakianaki et al., 2009), mitigation techniques aim to balance the thermal budget by increasing thermal losses and decreasing the corresponding gains. Among the most important of the proposed techniques are those targeting to increase the albedo of the urban environment (Santamouris et al., 2011) and to expand the green spaces (Zoulia et al., 2009). Because of the lack of open spaces where green could be integrated and as the total surface of roofs constitutes over 20% of the total urban surfaces (Akbari et al., 2009), Green Roof strategy is one of these practices that not only provides heat island amelioration and thermal comfort but also reduces energy consumption of buildings (Saadatian et al., 2013).

There are two main available types of green roofs:

- Extensive roofs: light and covered by a thin layer of vegetation with soil thickness less than 10-15 cm where only small herbaceous species can survive, low maintenance requirement, no load consideration
- Intensive roofs: heavy constructions with soil thickness more than 15-20 cm that can support small trees and shrubs, large-scale plants and facilities (Sfakianaki et al., 2009,Kolokotsa et al., 2013, Jaffal et al., 2012, Lin et al. 2013)

There are several advantages associated to green roofs like:

They reduce the flux of heat through the planted area, the heating and cooling needs of buildings and the temperature fluctuation during the day resulting to decreased energy consumption (Santamouris et al., 2007), especially for the building's top floor. Evapotranspiration from the plants and convective losses to the ambient air may contribute to reduce the temperature in urban areas and mitigate heat island. They provide better air quality, absorb atmospheric pollutants and particulate matter, mitigate the greenhouse effect, filter pollutants (Sfakianaki et al., 2009) and they reduce a city's carbon footprint by converting carbon dioxide to oxygen through photosynthesis (Jaffal et al., 2012). They also reduce noise, help with the storm water runoff management, prevent erosion and increase the durability of the roof materials. (Santamouris, 2012). Major disadvantages associated with planted roofs are the additional load that the building has to support and the relatively high investment cost. (Sfakianaki et al., 2009)

The mitigation potential of green roofs depends on several parameters as summarized in (Santamouris, 2012):

(a) Climatic parameters: solar radiation, ambient temperature and humidity, wind speed and precipitation

(b) Optical Variables: albedo to solar radiation, emissivity of the roofing systems and absorptivity of the plants

(c) Thermal parameters: thermal capacity of the roofs and overall heat transfer coefficient, U value

(d) Hydrological variables: all parameters defining latent heat phenomena.

Several studies that have been performed for buildings in Athens analyze the thermal properties and the energy performance of green roofs. It has been shown that they reduce the cooling load at 6 – 49% for the whole building and 12 – 87% for the last floor (Santamouris et al., 2007). For non-insulated building, the temperature of the roof without planting is 42 - 48^0C while it is 28 - 40^0C with planting, ie occurs a decrease of 10 ^{0}C (Niachou et al., 2001). According to Sfakianaki et al., 2009, for a spring sunny day with ambient temperature 23.1 ^{0}C, the average temperature of the green roof was approximately 6.5 – 9.1 ^{0}C lower than that of a conventional roof. Furthermore, it was found that a green roof was able to effectively reduce the cooling load by approximately 11% for thermostatically controlled buildings and to improve heat comfort in summer with a maximum expected temperature drop of approximately 0.6 ^{0}C between the roof surface and the interior. A study on the energy-saving effectiveness of a green roof showed it reduced the electricity consumption for air conditioning in summer approximately 40%, however, the results showed no significant savings in heating (Spala et al., 2008).

2. DESCRIPTION OF THE BUILDING AND THE GREEN ROOF

Measurements have been performed in an office building located in the sparsely built industrial zone of Peania, an east suburb of the area of Athens. It is a three-storey building with three basements, equipped with a Green Roof System (GRS). It has a surface of almost 10000 m^2 per floor and 60000 m^2 in total while the elevation of each floor is equal to 3.60 m. The main axis of the building is northwest – southeast oriented and all external surfaces are exposed to solar radiation as it stands by itself and there is no shading from neighboring buildings.

Figure 1: The office building in Peania

The aspect ratio, which is the ratio of the building's height over its width, is equal to 0.07, as it is a very long building with only three floors, while the ratio of the surface covered by windows over the surface covered by wall is equal to 0.53.

It is fully insulated: the exterior walls consist of heavyweight reinforced concrete and insulation of extruded polystyrene, the floors are made of heavyweight reinforced concrete, a particle board and a linoleum coating, while the ceilings of a metal false ceiling and mineral wool. The whole façade is also covered by metal shades which have the ability to move.

The GRS is an intensive green roof installed on the 10000 m^2 roof of the building and it consists of almost 16000 indigenous plants of at least 14 different kinds which are listed in table 1.

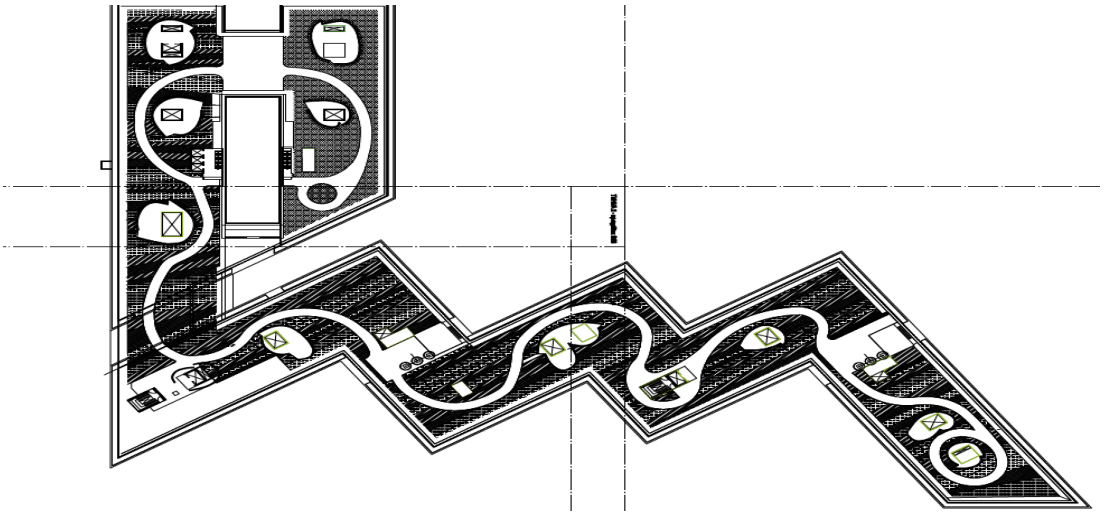

Figure 2: A plan view of the roof

Figure 3: A panoramic view of a part of the green roof

The rest of the area is covered by a running truck of 2000 m^2 made by stabilized ceramic floor. It is an ecological, bioclimatic and water permeable material which consists from ground tiles, mosaic, quartz, sand and pumice.

The materials and the structural elements of the GRS (the layers from outside to inside) are the following:

1. The plant level: local, dry – tolerant plants.
2. A mechanical substrate, a vegetation layer
3. A geotextile filter sheet from thermally strengthened polypropylene
4. A drainage system from thermoformed recycled polyethylene.

5. A moisture retention substrate from recycled fiber of polyester/polypropylene.
6. A waterproofing membrane – root barrier.
7. An elastomeric bitumen membrane.
8. A waterproofing bitumen membrane.
9. Lightweight concrete.
10. Polyethylene insulation
11. Extruded polystyrene insulation.
12. A vapor barrier (elastomeric, waterproofing, asphalt emulsion).
13. Heavyweight reinforced concrete.

Table 1: Kinds of different plants

Plant species	Measured height (2/07/2013, cm)	Flowering season
Artemisia ludoviciana	20	Summer - Autumn
Helichrysum italicum	32	Summer
Artemisia Alba	32	Autumn
Artemisia Absinthium	15	Summer
Satureja thymbra	40	Spring – Summer
Origanum dictamus	25	Summer
Origanum majorana	45	Summer – Autumn
Lavandula stoeches	30	Spring – Summer
Lavandula dentata green	60	Summer
Lavandula dentata		
Salvia fructicosa	25	Summer
Salvia farinacea	35	Spring – Summer
Salvia sclarea	60	Spring – Summer
Salvia of purpurea	65	Summer
	30	Summer

3. DESCRIPTION OF EQUIPEMENT AND EXPERIMENTAL MEASUREMENTS

The experimental investigation of the present study has been performed during the period 30/05/07/2013 – 30/07/2013 and consists of the following measurements:

- The outdoor and indoor temperature and relative humidity were measured with an interval of 5 minutes, with calibrated data loggers Tinytag Plus 2 placed in meteorological cages. The accuracy is $\pm 0.1^0$C, the temperature range is -40 to 85 ^{0}C and the humidity range 0-100. One sensor was installed on the roof and one in one of the top floor's offices.
- The solar and the reflected from the different roof surfaces radiation was measured every hour (10 am – 16 pm) with a double pyranometer in order to calculate the albedo of four different surfaces of the roof, as the ratio between the reflected from the roof radiation and the solar radiation.
- The top floor's ceiling's surface temperature was measured with a portable infrared thermometer with a laser pointer (range -22^0C–550^0C) and an infrared thermographic camera (Thermovision 570) in three spots (in an office, in the corridor and in the entrance) every hour.
- The surface temperature of the stabilized ceramic floor was measured hourly with an infrared thermometer and an infrared thermographic camera at two spots (in the sun and in the shade), as well as at the three spots situated exactly over those where the ceiling's temperature was measured.
- The illustration of the surface temperature of the different kinds of plants was performed with the infrared thermographic camera. There are hourly measurements for every different species of plants (Table 1) as well as for the whole vegetated area in order to study the differences between the different plants.

4. RESULTS AND ANALYSIS OF THE MEASUREMENTS

The experimental procedure took place for the time period of 30/05/2013 – 30/07/2013 during which the mean air temperature was 26.4 ^{0}C, while the maximum and the minimum values were 40.4 ^{0}C and 15.5 ^{0}C respectively. Figure 4 shows the fluctuation of the outdoor air temperature during this period, measured at a height of 1.80 m over the roof's surface.

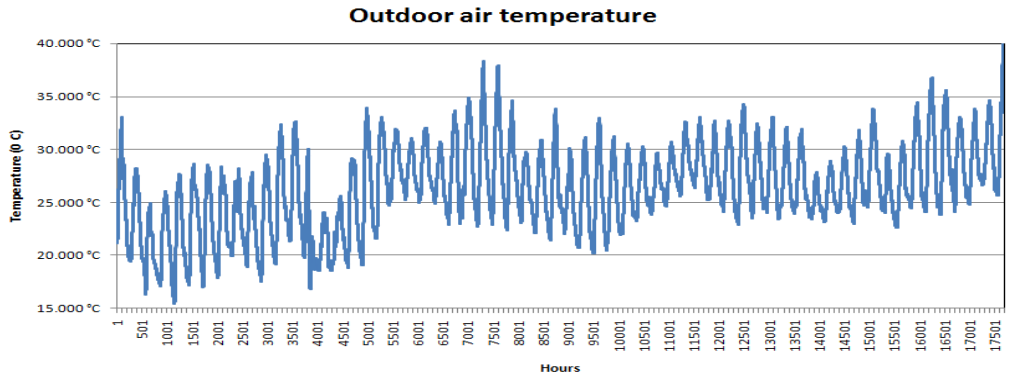

Figure 4: Variation of the outdoor air temperature for the whole measurements period

Several observations were made and the following conclusions were extracted for a typical summer (warm and sunny) day (25/07/2013):

The mean ambient temperature was 34.7 ^{0}C and the mean relative humidity 29.9%, while the respective maximum values were 36.8 ^{0}C and 34.7 %. The hourly mean variation of the air temperature on the roof is shown in figure 5.

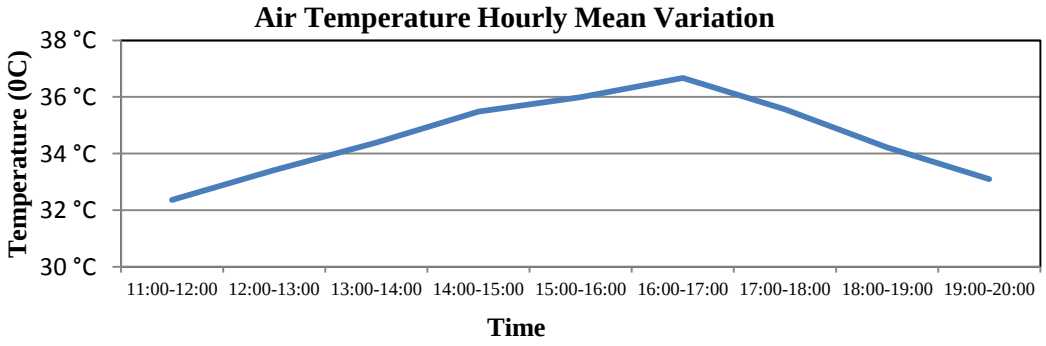

Figure 5: Hourly mean variation of the air temperature during the day 25/07/2013

In the following figure a comparison between the basic measured temperatures is presented. The mean surface temperature (Figure 6a) of the planted area is significantly lower than the ceramic floor's, with the temperature difference varying from 10.1 ^{0}C (at 11:00) to 16.1 ^{0}C (at 15:00). At the same time, the ceramic floor's mean surface temperature is from 5.1 ^{0}C (at 13:00) to 7.2 ^{0}C (at 13:00) lower than the soil's. The ceiling's surface temperature varies between 25.1 ^{0}C and 26.4 ^{0}C. The maximum value occurs at 15:00 for the ceramic roof floor and the soil while for the planted area at 14:00 and for the ambient air at 16:00. As far as maximum values are concerned (Figure 6b), the ceramic floor is also 6.6 ^{0}C (at 12:00) to 9.8 ^{0}C (at 15:00) cooler than the soil but, oppositely to the mean values, the maximum ones are higher for the planted area than for the ceramic floor

since they correspond to spots of soil. The measurement is taken for the whole vegetated area which includes foliage and soil at the same time, and this is the reason the maximum values for the planted area and the soil are close. It is particularly interesting to examine separately and compare the temperatures of the foliage, the soil and the ceramic floor.

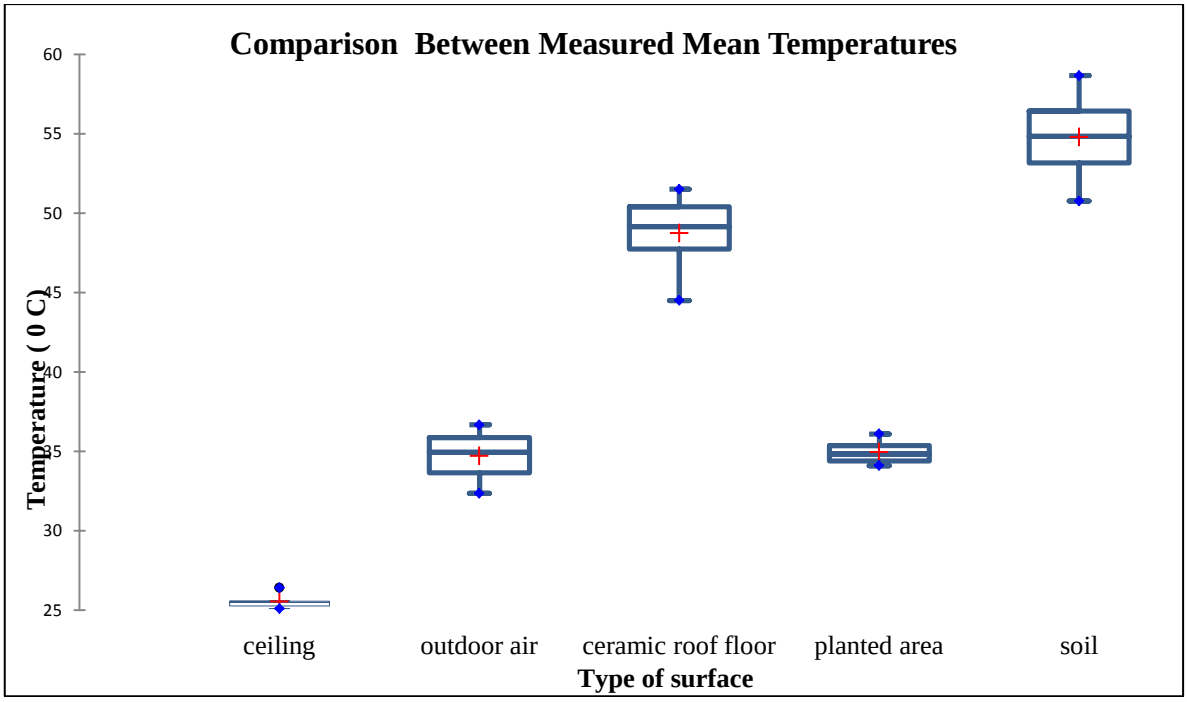

(a)

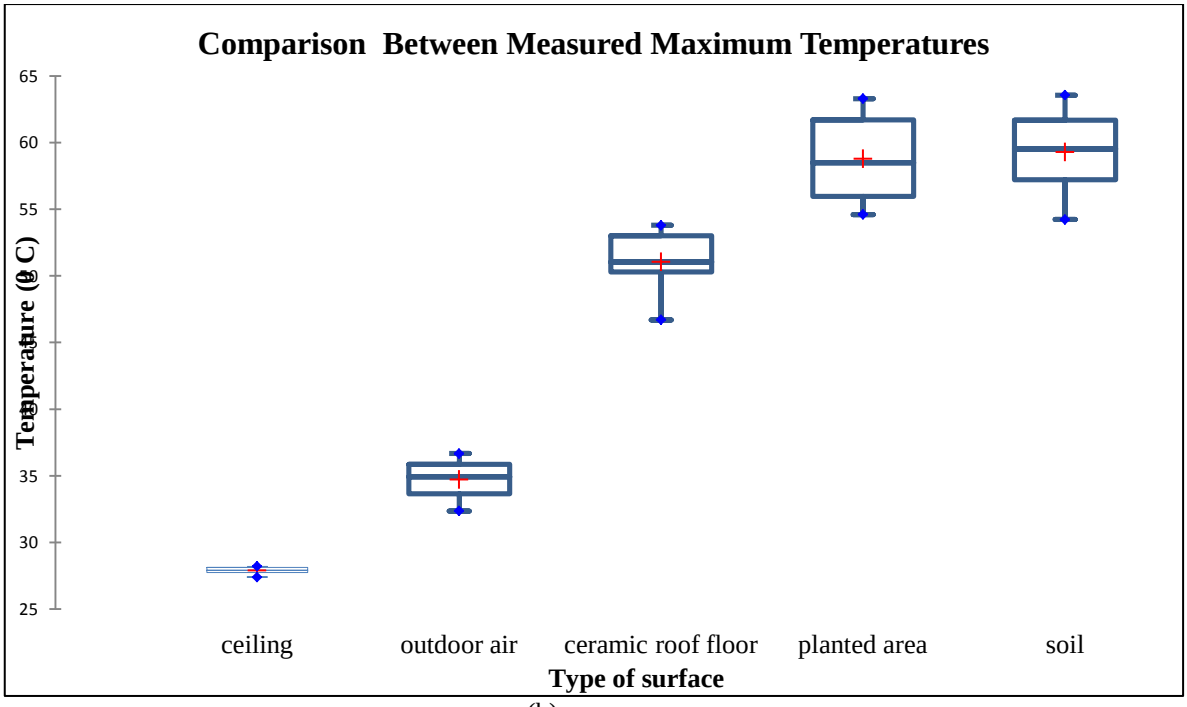

(b)

Figure 6: Comparison between the (a) mean and (b) maximum measured temperatures of the outdoor air, and the surface temperatures of the top floor's ceiling, the soil, the ceramic floor and the planted area

As it can be seen in a comparative graph that shows the variation of the mean temperature of all the different species of plants, the one which presented the lower mean surface temperature is plant 11 (Salvia fructicosa) because of its dense foliage and those with the highest are plants 12 (Salvia farinacea) and 13 (Salvia sclarea) because their foliage's low density lets a considerable area without leaves, covered only by soil. Plant 4, which also presents high temperatures, is ignored because its foliage had been dried.

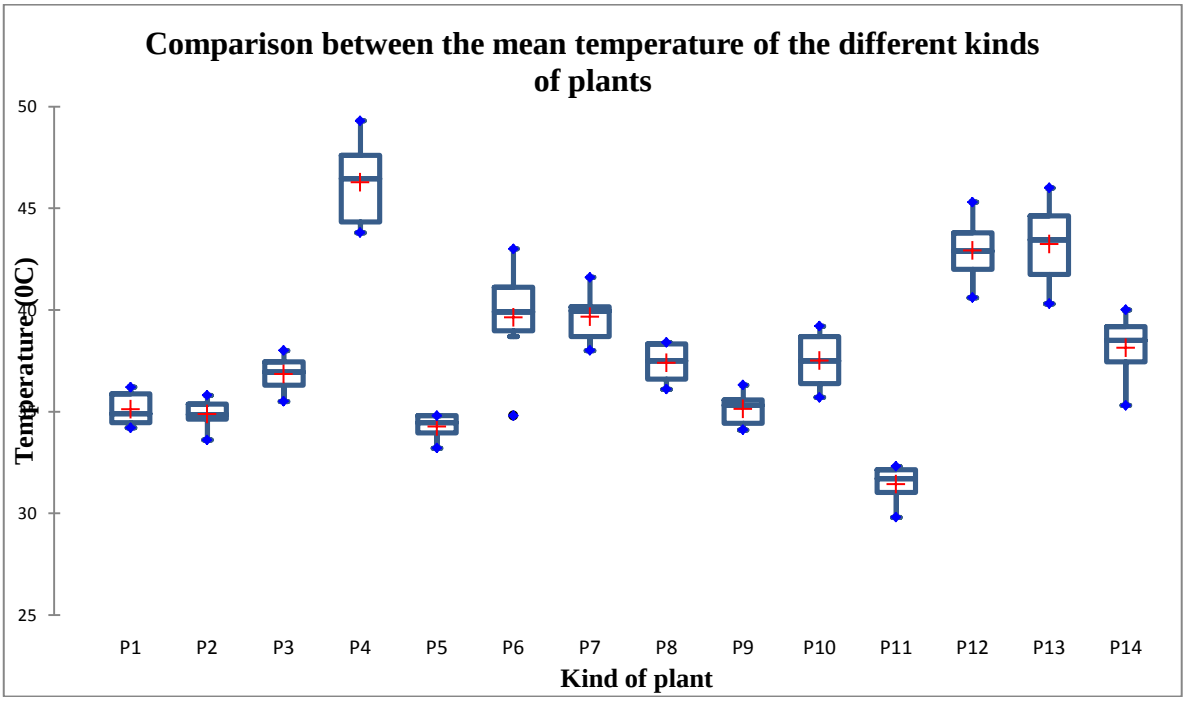

(a)

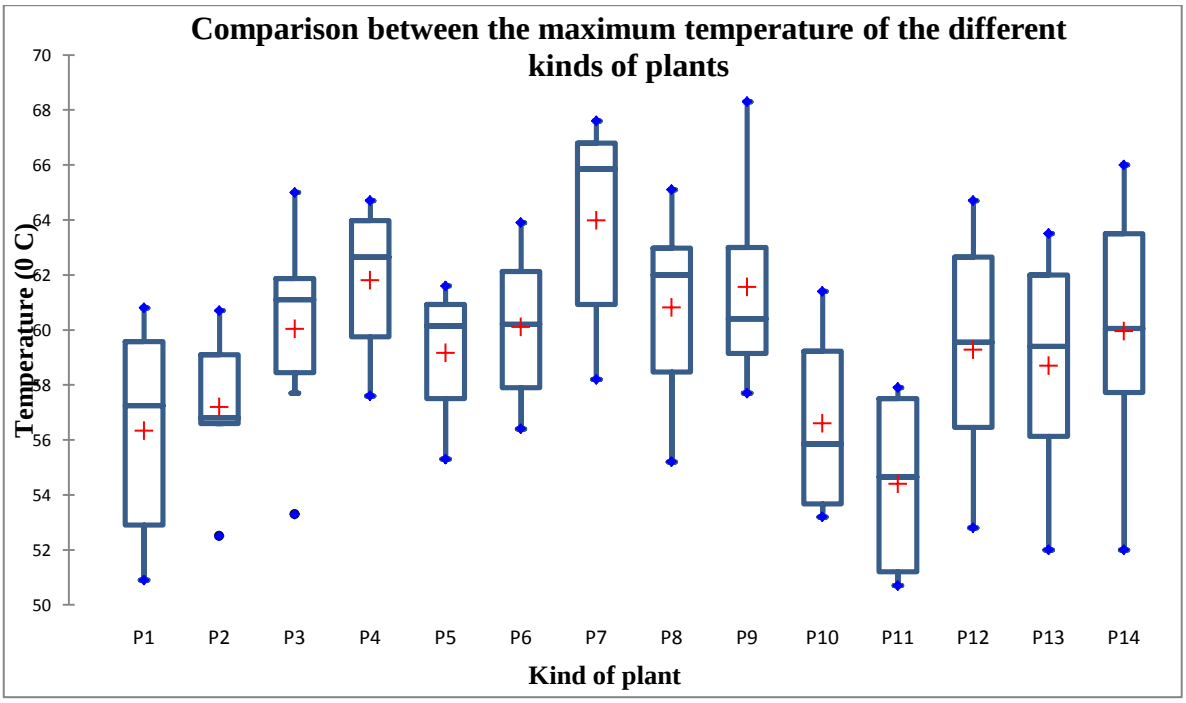

(b)

Figure 7: Comparison between the (a) mean and (b) maximum temperatures of the different kinds of plants

A comparison between the temperatures of the ceramic floor not only with the general planted area but with the foliage and the soil separately follows. Plants 11(dense foliage) and 13 (not dense foliage) were chosen because they presented the lowest and highest surface temperatures. The soil for plant 13 is presented 4.3 ^{0}C in average warmer than for plant 11 and the foliage itself is only 3.2 ^{0}C warmer for plant 13. At the same time, the whole planted area of plant 13 is 11.8 ^{0}C warmer than the one of plant 11. The curves for the foliage and the general planted area are similar and close for plant 11, while there is a greater temperature difference between the foliage and the general area for plant 13. More specifically, for plant 11 the average temperature difference between the foliage and the general planted area is 4.3 ^{0}C while for plant 13 it is 9.3 ^{0}C. All this illustrates strongly the importance of the foliage's density and the percentage of area covered by leaves. Finally, it can be remarked that the foliage of plant 11 is 18 ^{0}C cooler than the ceramic floor at the same time that the one of plant 13 is 14.8 ^{0}C cooler.

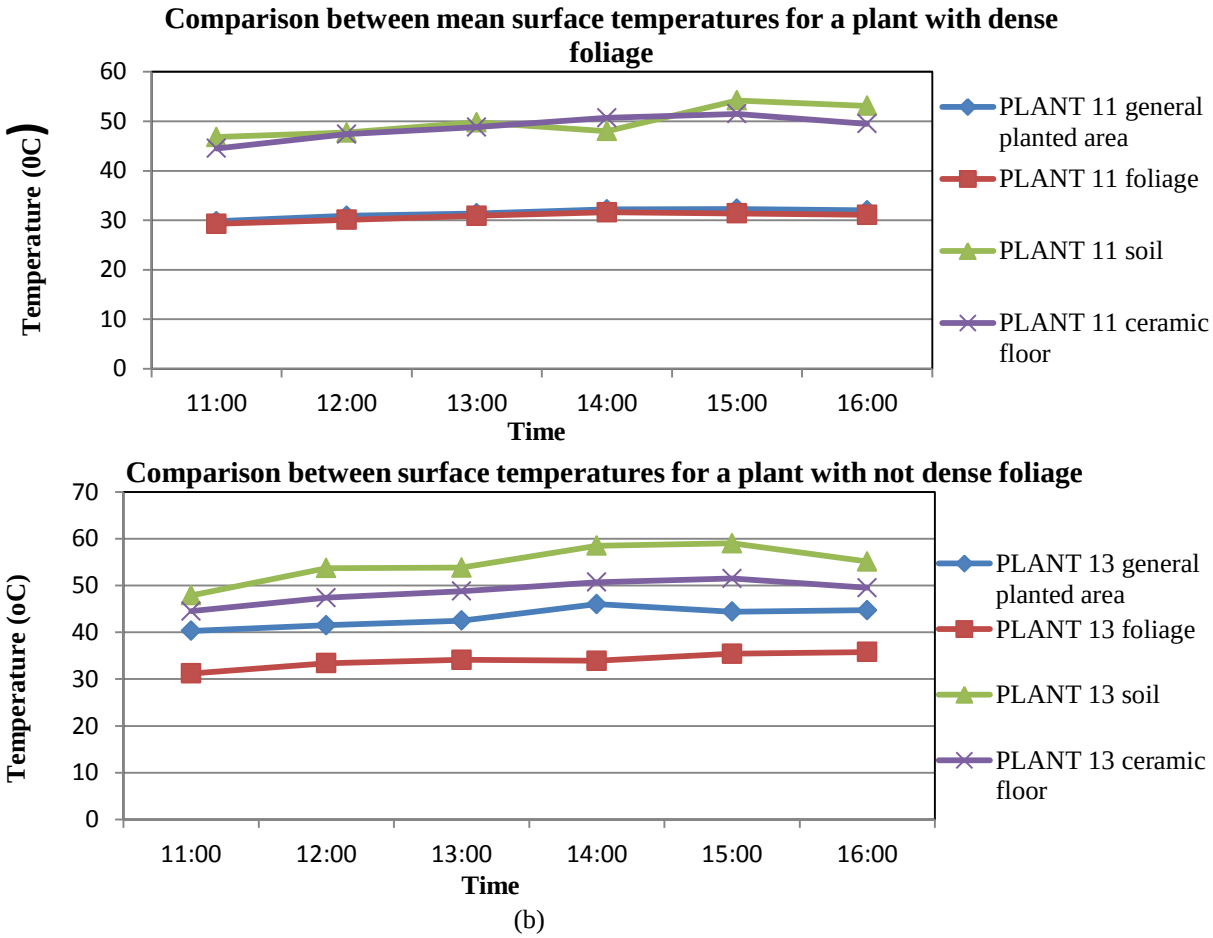

(b)

Figure 8: Comparison between the mean surface temperatures of the general planted area, the foliage, the soil and the ceramic floor for (a) a plant with high foliage density (plant 11: Salvia fructicosa) and (b) a plant with low foliage density (plant 13: Salvia sclarea)

A statistical analysis that corresponds to the entire set of measurements was also performed. In the figures that follow is given in boxplots the statistical distribution of the measured surface temperatures for every hour and for the ceramic floor, the soil and the whole planted area, where the median, the mean, the maximum and the minimum value, as well as the 25th and the 75th percentile are illustrated. Figure 10 shows the distribution of surface temperatures of the foliage only,

of each different kind of plant for the measurements of 14:00, when the highest temperatures occurred.

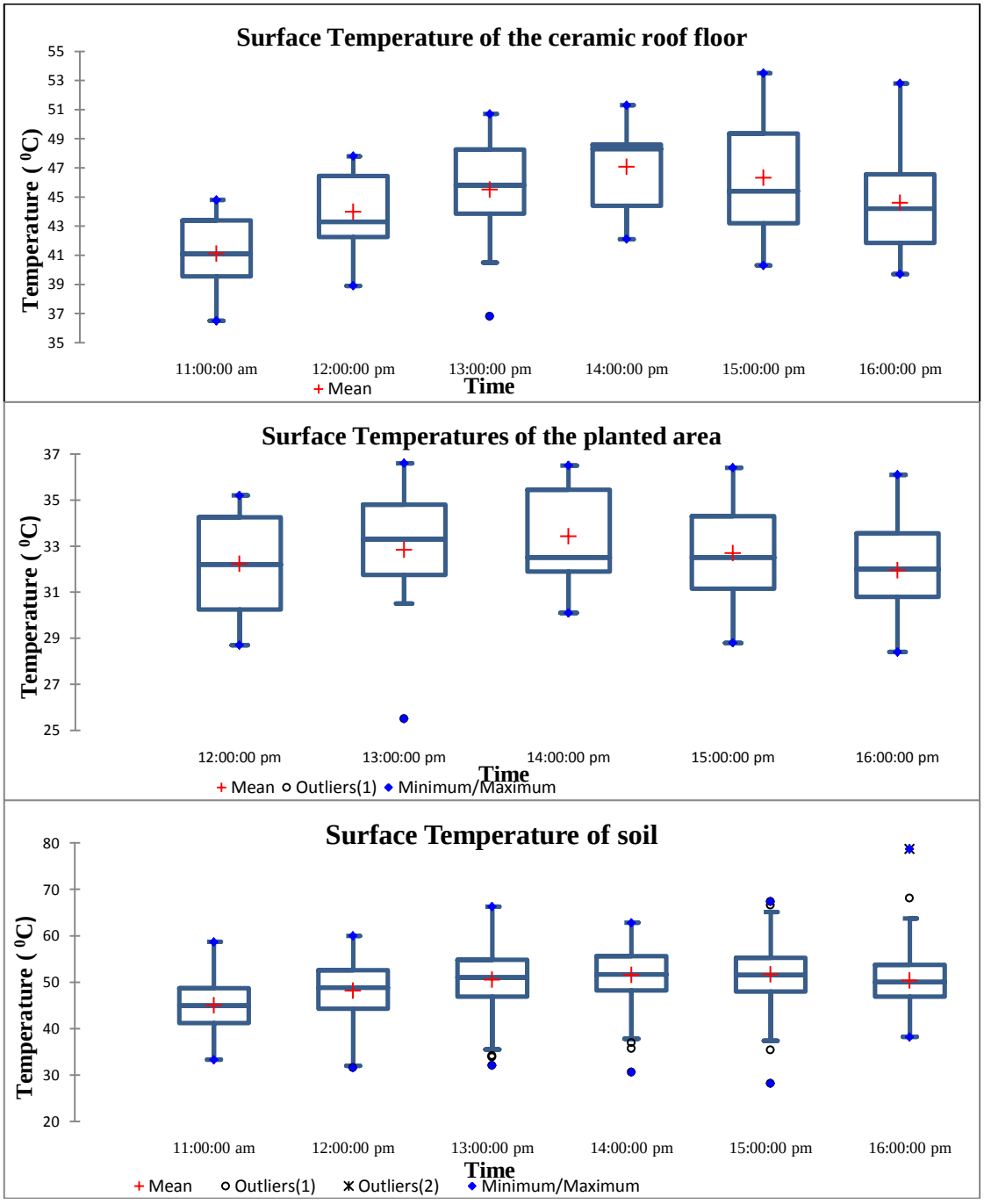

Figure 9: Comparison of the statistical distribution of the measured surface temperatures for every hour and for the ceramic floor, the planted area and the soil.

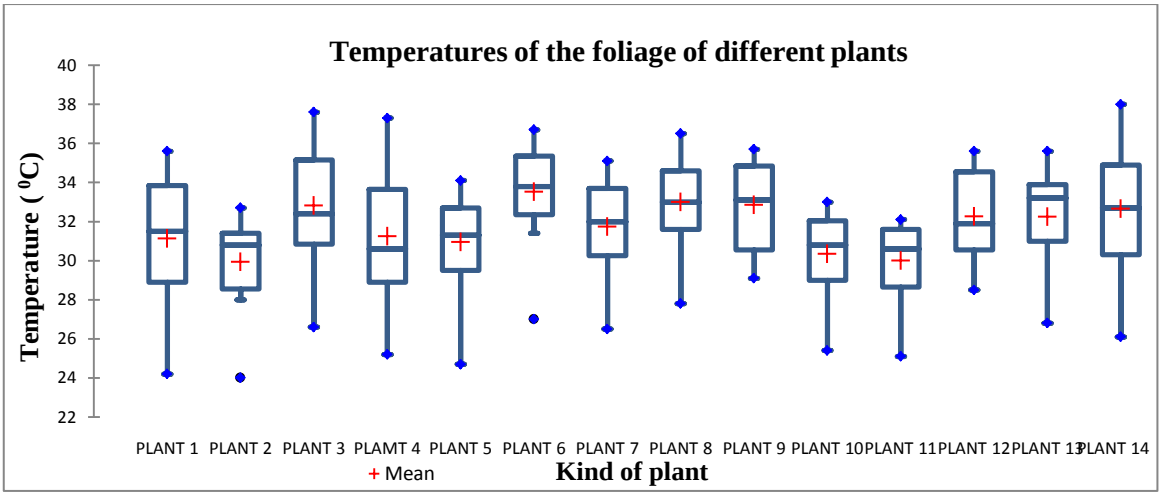

Figure 10: Distribution of surface temperatures of the foliage only of each different kind of plant for the measurements of 14:00, when the highest temperatures occurred

In Table 2 are presented the mean and the maximum values that appeared during the whole experimental period for every hour of measurements and for the ceramic floor, the planted area and the soil. The ceramic floor and the soil present the highest temperature at 15:00 (53.5 ^{0}C and 67.4 respectively)), while the planted area presents it at 13:00 and it is significantly lower (35.3 ^{0}C). Taking into account the mean values, it is concluded that the temperature difference between the planted area and the ceramic floor takes its greatest value at 14:00 when it is 13.66 ^{0}C and varies between 11.8 ^{0}C (at 12:00) and 13.6 (at 15:00). In Table 3 the frequencies of the hour that the maximum temperature appears are given. The result is that for the ceramic floor, the maximum occurred at 14:00 for the 46.7% of the time, at 15:00 for the 40 % and at 13:00 and 16:00 for 6.6% each. Concerning the planted area, the highest temperature appeared at 14:00 for the 53.3 % of the days, at 13:00 for the 26.6%, at 12:00 and 16:00 for 6.6% each and, oppositely to the ceramic floor, it never occurred at 15:00.

Table 2: Mean and maximum temperature for every hour and for different surfaces

	11:00		**12:00**		**13:00**		**14:00**		**15:00**		**16:00**	
	mean	max	mean	max	mean	max	mean	max	mean	max	mean	max
Ceramic floor	41.1	44.8	44	47.8	45.5	50.7	47.06	51.3	46.3	53.5	44.6	52.8
Soil	45	58.7	48.2	60	50.5	66.3	51.6	62.8	51.7	67.4	50.4	78.7
Planted area	31.6	35.3	32.2	35.2	32.8	36.6	33.4	36.5	32.7	36.4	32	36.1

Table 3: % Frequencies of the hour that the maximun temperature appears

Hour of appearance of max Temperatures (frequencies %)	**11:00**	**12:00**	**13:00**	**14:00**	**15:00**	**16:00**
Ceramic floor	0	0	6.6	46.7	40	6.6
Planted area	0	6.6	26.6	53.3	0	6.6

5. CONCLUSIONS

By conducting the experimental procedure and the present study, it was mainly concluded that the Green Roof System which is installed in the office building in Peania, is a particularly interesting case study and its thermal and optical behavior is greatly promising concerning its energy and environmental efficiency. The ceramic material that covers a part of the roof was found to be 5.1^{0}C – 7.2 ^{0}C cooler than the soil or other common materials and the planted area, which is the main surface cover for the roof, was 10.1 ^{0}C - 16.1 ^{0}C cooler than the ceramic floor. The different species of plants were also studied and the conclusion that the density of the foliage plays a primary role was extracted, as there was a difference of 11.8 ^{0}C between a plant with and a plant without dense foliage. A final difference that was observed is the fact that the different surfaces present their maximum temperature in different hours. The ceramic floor, at 14:00 for the 46.7% of the days and at 15:00 for the 40 %, while the planted area at 14:00 for the 53.3 % of the days, at 13:00 for the 26.6% and, oppositely to the ceramic floor, never at 15:00. The analysis of the experimental results is still in progress and a theoretical approach is also ongoing using the simulation programs Energy+ and EnviMet in order to extract some conclusions on the efficiency of the green roof and its contribution not only to the energy consumption of the building and the indoor thermal comfort, but also to the urban microclimate and the mitigation of the urban heat island phenomenon.

REFERENCES

Akbari, H., Menon, S., Rosenfeld, A.(2009). Global cooling: increasing world-wide urban albedos to offset CO2. Climatic Change 94, 275–286.

Cook – Patton, S., Bauerle, T.L. (2012). Potential benefits of plant diversity on vegetated roofs: A literature review. Journal of Environmental Management 106 (2012) 85e92

Dunnett, N., Nagase, A., Booth, R., Grime, J.P. (2008). Influence of vegetation composition on runoff in two simulated green roof experiments. Urban Ecosyst. 11, 385e398.

Jaffal, I., Ouldboukhitine, S., Belarbi R. (2012). A comprehensive study of the impact of green roofs on building energy performance. Renewable Energy 43 (2012) 157e164.

Kolokotsa, D., Santamouris, M., Zerefos, S.C. (2013). Green and cool roofs' urban heat island mitigation potential in European climates for office buildings under free floating conditions. Solar Energy 95 (2013) 118–13.

Kolb, W., Schwarz, T.(1986). Zum Klimatisierungseffekt von Pflanzbeständen auf Dächern, Teil I. Zeitschrift für Vegetationstechnick 9. Republished in Veitshoechheimer Berichte, Heft 39, Dachbegrünung. (cf. Dunnett and Kingsbury 2004a).

Lin,B., Yu, C., Su,A.T., Lin, Y.J. (2013). Impact of climatic conditions on the thermal effectiveness of an extensive green roof. Building and Environment 67 (2013) 26e33.

Mihalakakou, G., Flocas, H.A., Santamouris, M., Helmis, C.G. (2002). Application of neural networks to the simulation of the heat island over Athens, Greece, using synoptic types as apredictor. Journal of Applied Meteorology, 41 (5), pp. 519-527.

Mulder, C.P.H., Uliassi, D.D., Doak, D.F.(2001). Physical stress and diversityproductivity relationships: the role of positive interactions. Proc. Natl. Acad. Sci. USA 98, 6704e6708.

Niachou, A., Papakonstantinou, K., Santamouris, M., Tsangrassoulis, A., Mihalakakou, G. (2001). Analysis of the green roof thermal properties and investigation of its energy performance. Energy and Buildings 33, 719–729.

Saadatian,O., Sopian, K., Salleh, E., Lim, C.H., Riffat, S., Saadatian, E., Toudeshki, A., Sulaiman, M.Y. (2013). A review of energy aspects of green roofs. Renewable and Sustainable Energy Reviews 23 (2013) 155–168.

Santamouris M. Heat island research in Europe—the state of the art. Advances in Building Energy Research (2007). 1:123–150.

Santamouris, M. (2012). Cooling the cities – A review of reflective and green roof mitigation technologies to fight heat island and improve comfort in urban environments. Solar Energy.

Santamouris, M., Pavlou, C., Doukas, P., Mahalakakou, G., Synnefa, A., Hatzimpiros, A., Patargias, P. (2007). Investigating and analysing the energy and environmental performance of an experimental green roof system installed in a nursery school building in Athens, Greece. Energy 32 (2007) 1781–1788.

Santamouris, M., Synnefa, A., Karlessi, T. (2011). Using advanced cool materials in the urban built environment to mitigate heat islands and improve thermal comfort conditions. Sol. Energy 85, 3085–3102.

Sfakianaki, A., Pagalou, E., Pavlou, K., Santamouris, M., Assimakopoulos, M. N. (2009). Theoretical and experimental analysis of the thermal behavior of a green roof system installed in two residential buildings in Athens, Greece. International Journal of Energy Research,33:1059–1069.

Spala A, Bagiorgas HS, Assimakopoulos M, Kalavrouziotis J, Matthopoulos D, Mihalakakou G.(2008). On the green roof system. Selection, state of the art and energy potential investigation of a system installed in an office building in Athens, Greece. Renewable Energy 2008;33:173e7.

Theodosiou TG.(2003). Summer period analysis of the performance of a planted roof as a passive cooling technique. Energy and Buildings 2003;35:909e17.

Zoulia, E., Santamouris, M., Dimoudi, A. 2009. Monitoring the effect of urban green areas on the heat island in Athens. Environmental Monitoring and Assessment 156 (1–4), 275–292.

CONSIDERING THE ATTICA EXAMPLE: HOTEL LOCATION AS A DETERMINANT FACTOR OF TOURIST CARBON FOOTPRINT

Stella Panayiota Pieri[1*], Panayiotis Kouyias[1], Vasiliki Milioni[1], Athanasios Stamos[1], Ioannis Tzouvadakis[1]

1 National Technical University of Athens
Iroon Polytexneiou 9
15780, Zografou
Athens
**Corresponding author: cpieris@tee.gr*

ABSTRACT

The tourism industry is responding to the widespread concern over the future of the global climate. However, little quantitative work has been done on carbon dioxide emissions associated with tourism destinations. This paper proposes a framework illustrating how this can be done. The tourist carbon footprint (TCF) is a result of tourists' personal consumption, transportation, activity, and accommodation costs. In this study we evaluate the tourist carbon footprint associated with tourist transportation to and in the vicinity of the prefecture of Attica, Greece. The research, conducted in three stages, aims to demonstrate how important is hotel location as a determinant factor of tourist carbon footprint and to propose measures to reduce CO2 emissions through the implementation of policies that are environmentally friendly and are aiming to facilitate the transport of the tourists and promote the use of public transport.

KEYWORDS

Tourist carbon footprint (TCF), Tourist transportation, CO2 emissions, hotel location

1 INTRODUCTION

Tourism is travel for recreational, leisure, or business purposes. The World Tourism Organization defines tourists as people "traveling to and staying in places outside their usual environment for not more than one consecutive year for leisure, business and other purposes" (World Tourism Organization, 1995). The tourist carbon footprint (TCF) is a result of tourists' personal consumption, transportation, activity, and accommodation costs. The study evaluates the TCF associated with tourist transportation. The first part of the paper portraits the research tool used to acquire the input data and the methodology used for analyzing and processing this data. The second part of the paper presents the mathematical formula and the calculations made for each of the 21 hotel units that took part in the survey. Calculations are made of the TFC produced by the transportation of tourists of each hotel. Consequently, the results are presented and evaluated in a series of tables and diagrams. Finally, the study puts forward proposals for a series of low-cost measures which could be adopted by the hotels management and tourist stock. The aim of the research is to determine the importance of hotels location in a reduced TFC. The hotels included in the study vary in size and category but are all city-hotels.

2 THE RESEARCH TOOL AND METHODOLOGY

Most research on Tourist carbon footprint draws almost exclusively on tourists retrospective self-reporting. According to Nielsen and Blichfeldt (Nielsen, Blichfeldt, 2009) although any vacation contains many in situ decision-making processes, most research on vacation decision-making emphasizes up-front decision-making (and especially the generic decision 'to go' and choice of destination) whereas research on in situ decision-making is very sparse (Nielsen, Blichfeldt, 2009). Apart from the obvious methodological problems with retrospective self-reporting, such reporting is especially problematic in relation to in situ decision-making due to the simple fact that tourists make so many decisions in situ (some of which are indeed minor) that it is highly doubtful if (1) tourists even remember them when they are later interviewed or fill out a questionnaire and/or (2) the interview/questionnaire situation actually allows tourists to go into details to the extent necessary in order to uncover in situ choices and movements. Accordingly, any 'new' methods that (could) provide knowledge on tourist mobility at the destination would undoubtedly be a valuable tool in the quest to fill the knowledge gap pertaining to touristic behaviour at the destination (Nielsen, Blichfeldt, 2009).

In this study, we decided to deliberately ignore the individual tourists in-situ decision making and focus on net road distances and numerical statistical data. The questionnaire was thus addressed to the management of the hotels instead of the tourists, in an effort to actually approximate the value of the tourist carbon footprint which could be attributed to each hotel. In order to draw valid conclusions a significant number of hotels from the existing hotel stock in Attica had to be studied. Additional data were collected from personal interviews with accommodation managers at each location and incorporated into the TCF calculation.

Consequently, the tourist attractions of the hosting prefecture Attica were highlighted and all tourist destinations were hierarchized and matched in weighting factors according to their rate of popularity which was decided after thorough bibliographical research.

Information about the road distance between each hotel and each of the previously mentioned tourist destination was calculated with a GPS system. The following map illustrates the location of the hotels that participated in the research whereas the adjacent table presents the places of tourist interest considered in the study.

Map 1. Geographical sites of tourist interest in Attica

3 DATA COLLECTION

Out of the 50 hotels originally approached only 21 responded positively and provided all necessary information. In the research sample the hotels vary both in size and category and range from a 2* thirty bed hotel to a 5* star 374 bed hotel. They all consist of city hotels and they are all located in the prefecture of Attica in Greece.

The data collected consisted of:

i. The annual number of clients staying in a hotel
ii. The percent of each customer type.
iii. The duration of the stay of the various types of tourists.
iv. The percent of tourists visiting each of the different sites of tourist interest previously specified.
v. The percent of tourists visiting each of the different sites with each of the different means of transportation.
vi. The Carbon emissions factor of the various modes of transportation.

As far as transport modes are concerned, it should be noted that air travel is clearly the most significant overall source of greenhouse gas emissions in land-based tourism out weighting any other emissions resulting from in-land mobility.

4 CALCULATION OF TOURIST CARBON FOOTPRINT ASSOCIATED WITH TRANSPORTATION

All data collected were processed individually for each hotel unit with the software Microsoft Excel and the following mathematical formula:

$$TCF_{transport} = 2 \times S_i \times \lambda \times X \times P_i \times k \quad (1)$$

Where:

$2 \times S_i$: two-way distance of hotel development from sites of tourist attraction

X: annual number of tourists staying in a hotel

λ: estimated percentage of tourists visiting each site of tourist attraction

P_i: estimated rate of use of each mode of transport

k: Carbon Emissions factor for each means of transport

Table 1. Carbon Emissions Factor per unit of measurement of each mode of transport.

Transportation	Unit of measurement	Kg CO2 / unit of measurement
Metro(fixed rail)	Passenger kilometre (pkm)	0,07801
Bus	Passenger kilometre (pkm)	0,10351
Taxi	Distance vehicle (vkm)	0,22169
Car	Distance vehicle (vkm)	0,15

5 THE RESULTS

Table **2** illustrates the results that came out from the analysis of each one of the hotels under study, as far as, their tourist carbon footprint is concerned. It is obvious that tourists staying in hotels located in the wider area of Athens city centre have a lower carbon footprint as a result of: 1) their proximity to the most popular sites of tourist attraction, some of which are even within walking distance and 2) the better network of Public Transport. The crucial role, that hotel proximity to the city center plays in the formulation of the tourist carbon footprint of each hotel is easily perceived by a close observation of Map no.1 illustrating the dispersion of sites of tourist attraction on the map of Attica.

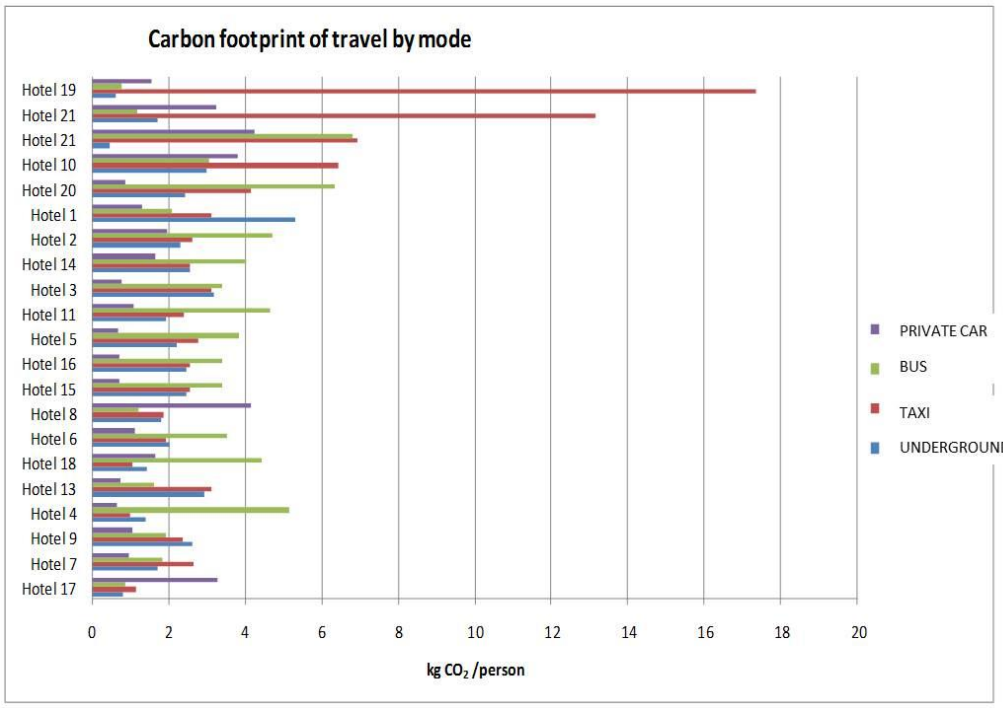

Figure 1. Calculation of TFC by mode of travel for each hotel

Table 2. Annual Carbon Emissions per hotel and per customer

A/A	Location	Annual emmissions kgCO2/Hotel	Annual emmissions kgCO2/Person
1	Southwest Attica (Pireus)	51543.46	11.86
2	Southwest Attica (N. Smirni)	622804.68	11.63
3	Downtown Athens (close to Larisis st.)	504639.24	10.05
4	Downtown Athens	152811.18	8.23
5	Downtown Athens	419219.83	9.55
6	Downtown Athens	380511.64	8.67
7	Downtown Athens	203917.29	7.17
8	Southwest Attica (Moshato)	36143.97	9.01
9	Downtown Athens	147670.18	8.02
10	Southwest Attica (Glyfada)	271067.5	16.31
11	Southwest Attica (Ampelokipi)	786353.02	10.08
12	North section of Athens (Kifisia)	128190.77	19.31
13	Downtown Athens	227618.83	8.43
14	Downtown Athens (Siggrou Av.)	324083.83	10.82
15	Downtown Athens (Ilissia)	140242.45	9.17
16	Downtown Athens (Ilissia)	41652.01	9.17
17	Downtown Athens	54709.93	6.13
18	Downtown Athens	28756.86	8.6
19	Eastern Attica	144623.36	20.29
20	Southwest Attica (Paiania)	239611.92	13.83
21	Southwest Attica (Vouliagmeni)	403515.27	18.48

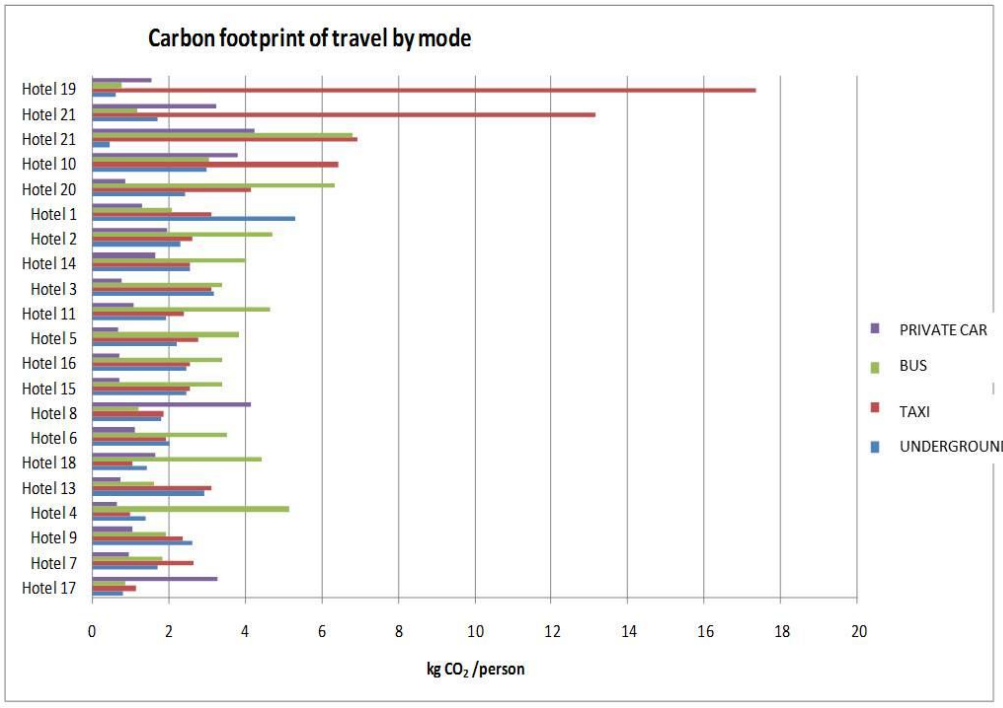

Figure **1** presents the TCF by mode of transport for each one of the hotels under study. The hotels on the vertical axis are classified in ascending value depending on their annual carbon TFC. The fact that the distance between a hotel and the center of Athens influences the transportation TCF, can be better understood by comparing the results of all hotels under study in relation to their distance from the center. For this purpose, we selected a fixed point and measured the distance of each hotel from it. The point chosen as benchmark was Omonia Square. Generally, it is observed that the carbon footprint tends to increase as the distance from Omonia Square increases. Nevertheless, the relationship between distance and the TFC is not strictly proportional. This is due to the fact that TFC is also influenced by a series of other the factors incorporated in the formula.

Table 3. Distance of hotels from Omonia Square (km)

A/A	Distance from Omonia Sq. (km)
D1	9
D2	6,4
D3	1,2
D4	0,8
D5	1,2
D6	1,4
D7	2,4
D8	6,7
D9	1,1
D10	14,9
D11	3,6
D12	15
D13	1,2
D14	3,7
D15	2,9
D16	2,8
D17	0,3
D18	1
D19	18,5
D20	12,3
D21	18,4

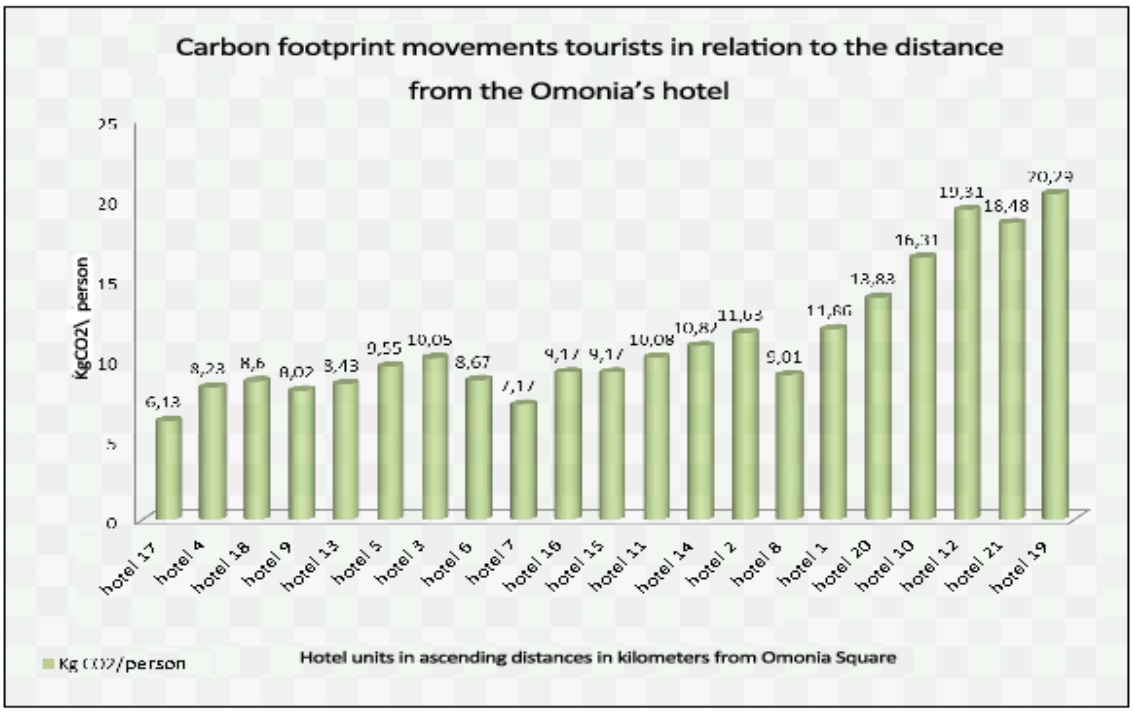

Figure 2. TCF analysis in relation to the distance from the city center.

6 MAPPING THE RESULTS

To visualize the influence of hotel location in determining the tourist carbon footprint that results from tourist trips, we invented the iso-pollutant curves map. The iso-pollutant curves map is a detailed and accurate graphic representation of the typical value of carbon footprint at a particular geographical area or point. In particular, the map below illustrates the areas of

Attica, that tend to have more or less the same carbon footprint per hotel guest. Specifically, it appears that the areas near the center of the capital have less carbon footprint than the regional areas, mainly because of there is a concentration of the most important sites of tourist attraction such as museums , the Acropolis , Plaka , Monastiraki, shopping centers etc.

These areas are clearly separated in zones by their respective iso-pollutant curves shown on the map with red lines:

1. Zone A : City Center, with Tourist Carbon footprint (TCF) : TCF < 8.5 kgCO2/ tourist
2. Zone B: peripheral kgCO2/ tourist with 8.5 < = TFC < 15.0 kgCO2/ tourist (ie Piraeus)
3. Zone C: Suburbs with TCF > = 15 kgCO2/ tourist

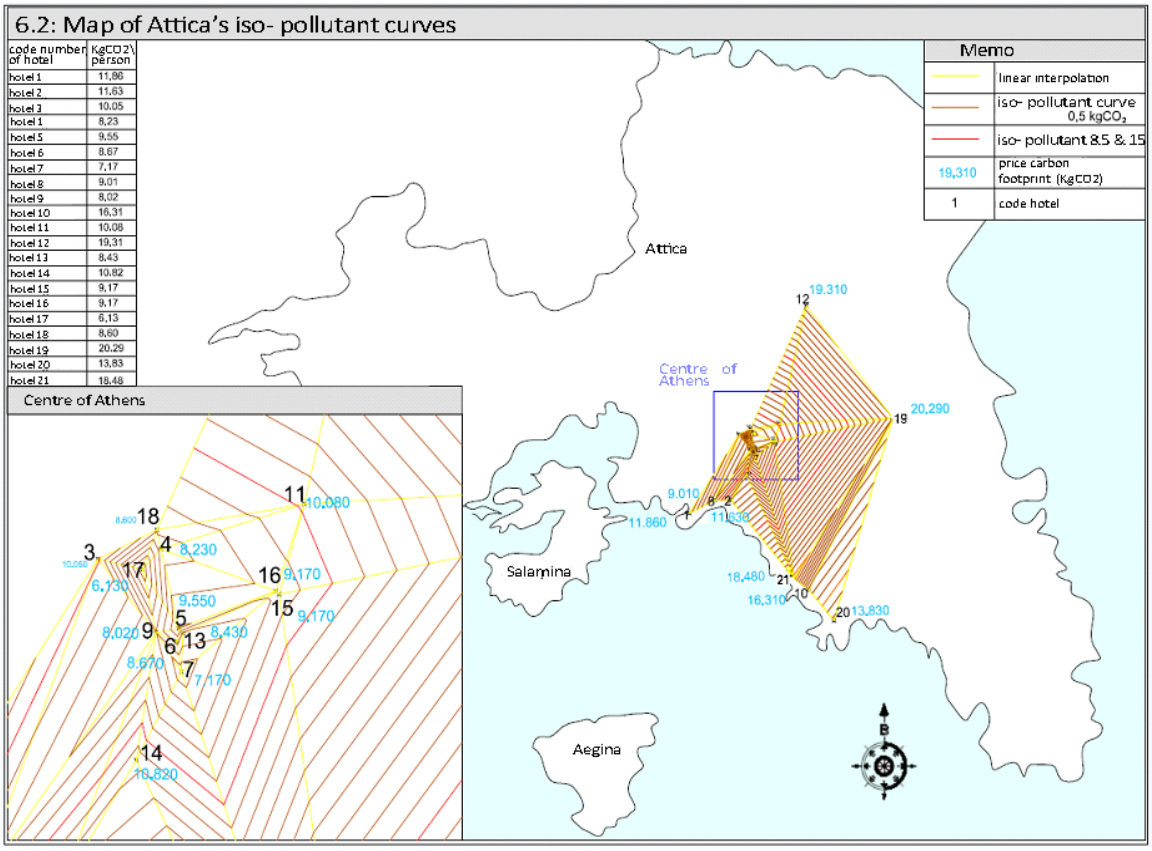

Map 2. Atttica - TCF iso-pollutant curves map

7 CONCLUSION AND PROPOSALS

By collecting hotel reservations statistics concerning the hotel occupancy, the hotel category, the per cent of each customer type hosted yearly, the length of stay, the country of origin, the mode of transport to the area of their destination and identifying the most popular tourist sites, we managed to have a value of the TCF which could be attributed to the hotel and which is a function of the hotel location as illustrated by the mathematical formula and the iso-pollutant curves map.

To sum up, in Attica the tourist carbon footprint varies between 28.756 Kg CO2 to 786.353 Kg CO2 per hotel and between 6,13 KgCO2 to 20,29 Kg CO2 per tourist yearly. Hotel no. 17, which is located at Omonia Square has the lowest carbon footprint., whereas Hotel no. 19

located at Attiki Odos, Paiania has the highest value.Furthermore, the further away a hotel is from the city center the higher the tourist carbon footprint.

It is therefore evident, that the TCF could be minimized through the choice of the appropriate location for a new hotel development at the earlier stages of strategic planning. Low TCF is associated with proximity to sites of tourist interest, which is also a requirement for the convenience of most tourists. The hotel management could reduce the TFC of the hotel through a series of measures that encourage customers to use public transport, bicycles or move on foot for their transportation during their stay. Low TCF could also be achieved in various ways through the information and awareness of the customers of their impact on the environment and of their carbon footprint, but also through the organization and planning of group excursions to sites of tourist attraction. Finally, the hotels through the purchase and use of hybrid cars and mini-vans for the transportation of their customers to the city center or other places of tourist interest, could reduce further their TFC.

In the same time, the government and in particular the ministry of transport by strengthening the existing grid of Public Transport (grid frequency) and replacing conventional fuels with biofuels could enhance the hotel sectors effort towards a lower TFC.

REFERENCES

"UNWTO technical manual: Collection of Tourism Expenditure Statistics". World Tourism Organization. 1995. p.10. Retrieved 26 March 2009.

European Commission Directorate - General for Energy and Transport, EU Energy in Figures. (2009). Greenhouse Gas Emissions by Sector. European Communities.

National Emission Inventory of Greenhouse Gases, submitted to the EU by the Ministry of Environment (EAA, 2007)

Organisation for Economic Co-operation and Development (OECD)

Hyde, R., Watson, S., Cheshire, W., Thomson, M. (2006) The Environmental Brief-Pathways for Green Design, Taylor & Francis.

Nielsen, N. C., Blichfeldt, B. S. (2009). Where do they go? Monitoring Mobility at the destination, 18th Symposium in Tourism and Hospitality Research

RESOURCE- AND COST-EFFECTIVE INTEGRATION OF RENEWABLES IN EXISTING HIGH-RISE BUILDINGS

Theoni Karlessi*[1], Mat Santamouris*[1], Tilmann Kuhn[2]

[1]*National and Kapodestrian University of Athens, Building of Physics - 5, University Campus, 157 84 Athens, Greece*

[2]*Fraunhofer Institute for Solar Energy Systems ISE, Heidenhofstraße 2. 79110 Freiburg, Germany*

**Corresponding author: karlessith@phys.uoa.gr*

ABSTRACT

In 2009 the regulatory framework and the business environment for the construction sector has changed significantly in order to reduce the CO2-emissions of existing and new buildings. New buildings have to be net-zero after 2020, some public buildings already after 2018. Several national Governments try to achieve a net-zero primary energy balance for the complete building stock until 2050 which is truly a grand challenge. In order to reach these goals two things have to be done:

- increase the efficiency, especially in case of existing buildings
- cover the remaining energy demand with renewable sources.

The two most challenging aspects resulting from these goals are:

- the number of buildings which have to renovated is really huge, which means that a lot of investments have to be done and which also means that much more labour for construction works is needed than currently available.
- in many cases, current processes and building components are not ready for a widespread and cost-effective implementation of energy-harvesting functionalities in the building skin.

Therefore a fundamental transformation of the construction sector is necessary in order to streamline the fragmented responsibilities and to develop business models which are attractive for third-party financing.

The main objective of the EU Cost Effective project is to convert facades of existing high-rise buildings into multifunctional, energy gaining components. This target includes new façade components, business models, technical concepts and the demonstration in two pilot buildings.

KEYWORDS

high-rise buildings, multifunctional façade components, integrated concepts

1 INTRODUCTION

The use of renewable energy in the building sector is nowadays dominated by the application of solar domestic hot water and PV systems in single-family houses. In order to significantly increase the use of renewable energy in the building sector, concepts have to be developed for large buildings. In these buildings high fractions of the energy demand can only be met with renewable energy sources, when the façade is used for energy conversion in addition to the roof. This is especially true for buildings with a small roof area compared to the floor area ("high-rise buildings") and for existing buildings which generally have a higher energy demand than new buildings. Therefore the main focus is to convert facades of existing "high-rise buildings" into multifunctional, energy gaining components. This goal can be achieved through the development of new multi-functional façade components which combine standard features and the use of renewable energy resources and the development of new business and cost models which consider the whole life cycle of a building and which incorporate the

benefits from reduced running costs and greenhouse-gas emissions. The new components will in particular profit from the application of nano-structured coatings and films which will enhance their performance and durability due to antireflective, anti-soiling and seasonal shading functionality. In order to achieve a successful development and implementation of these new technologies and concepts European key actors from construction industry and energy research have been involved.
The main purpose of the actions is to reach the goals of the EC set forth for 2020 and 2050 to address climate change issues and to contribute to improve EU energy independence. In 2009 the regulatory framework and the business environment for the construction sector has changed significantly in order to reduce the CO_2-emissions of existing and new buildings. It is now officially agreed within Europe that Net-Zero-Energy buildings are the goal for the future. New buildings have to be net-zero after 2020, some public buildings already after 2018. Several national governments try to achieve a net-zero primary energy balance for the complete building stock until 2050 which is truly a grand challenge. In order to reach these goals two things have to be done: increase the efficiency, especially in case of existing buildings and cover the remaining energy demand with renewable sources. The challenges resulting from these goals are:

- the number of buildings which have to renovated is really huge, which means that a lot of investments are to be done and which also means that much more labour for construction works is needed than currently available.
- in many cases, current processes and building components are not ready for a widespread and cost-effective implementation of energy-harvesting functionalities in the building skin.

Therefore a fundamental transformation of the construction sector is necessary in order to streamline the fragmented responsibilities and to develop business models which are attractive for third-party financing (Tilmann et al.,2011) .

The main objectives include new façade components, business models, technical concepts and the demonstration in two pilot buildings. In more detail, the following items have been reached:

- a set of 5 of new façade components and systems:
  - a glazing integrated transparent solar thermal collector
  - air-heating vacuum tube collectors for façade application
  - an angle-selective transmittance BIPV-component
  - a facade integrated natural ventilation system with heat recovery
  - a solar assisted decentralized heat pump system using unglazed solar thermal collectors with plaster covering.
- developed integrated (techno-economic) concepts consisting of technical concepts and corresponding business-models for the most important categories of existing high-rise buildings in Europe (EU25). This includes also the identification of the most important categories of existing high-rise buildings.
- demonstrated the practical feasibility in two pilot buildings in Spain and Slovenia.

2 STATE OF THE ART ANALYSIS AND PROBLEM IDENTIFICATION

2.1 Statistical evaluation of high-rise buildings

Statistical information on existing and new high-rise buildings has been collected in order to determine the geographical distribution and the corresponding characteristics of high-rise buildings.

The data acquisition for the different countries is done using a variety of different sources. Where applicable, direct data from the building owners or building maintenance is included. In addition to such direct information, databases with information, e.g. from different EU research projects is used to mainly provide specific values for specific groups of buildings. National statistical and meteorological (for climatic data) organizations and EUROSTAT are evaluated. Additionally, a literature research is conducted, trying to identify relevant literature-values and a significant share of information on single buildings is taken from the "EMPORIS" database, which is commercially available from Emporis Corp. For single buildings, a total of 18.402 datasets are provided. For economic data, a total of 133 different datasets are given, for energy data, the total number of datasets amounts to 409 and for climatic data, a total of 500 datasets is listed in the database. The statistical evaluation includes the following topics:

- overall building situation and general historic trends
- technical and constructional building data including building use
- façade related building data
- energy related building data
- economic building data
- climate related building data

The majority of the investigated buildings are office use buildings. In terms of used facade material, glass facades (usually post-mullion-structures) dominate the distribution, followed by natural stone facades and concrete based facades. Metal facades and other materials are of reduced significance for high-rise buildings.
Figure , which presents the average construction costs in € / m² GFA[1], shows a clear trend of increasing construction costs for the USA and no clear patterns for Europe and China, presumably due to the limited number of data.

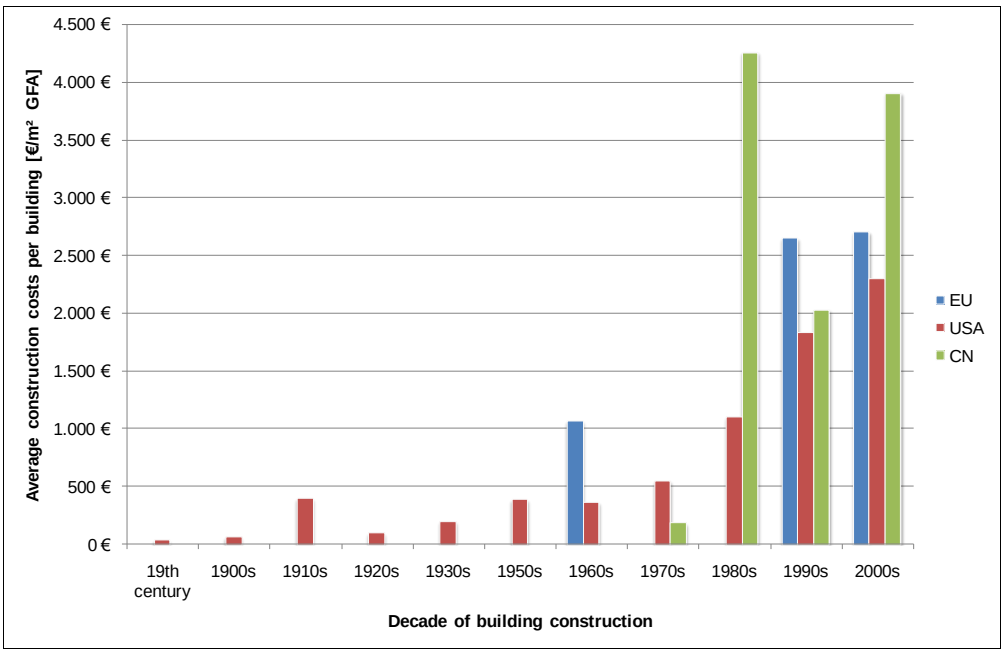

Figure 1: Average construction costs in € per m² gross floor area per decades of construction – separately given for the EU, the USA and China[2].

1 GFA = Gross Floor Area

2.2 Problems and opportunities related to the installation of low energy and renewable energy systems in high-rise buildings

The main focus of the project is to convert façades of existing "high-rise buildings" into multifunctional, energy-gaining components. The implementation of this goal requires the determination and classification of the building characteristics in order to investigate the application of innovative systems in existing high-rise buildings. The first step for the development of new multifunctional components which combine conventional and innovative low energy features is the identification of the problems and opportunities related to their installation (Synnefa et al., 2009).

Twenty two high-rise buildings with different architectural, constructive, systems and energy characteristics from Greece, Germany, Austria, Slovenia, Switzerland, France and Spain were selected for data acquisition. Figure 2 presents the transparent share of the total facade area of the investigated buildings.

Building analysis related to the installation of innovative energy systems require the consideration of building characteristics and the occupant's perception of the building conditions and controls. For this reason data acquisition from high-rise buildings was performed by the completion of two questionnaires, an extended one to be fill in by the building manager concerning building information (General Information, Building Description -Envelope-Interior Surroundings, Heating- Cooling- Ventilation System, Lighting System, Other Equipment, Building Energy Management, Indoor Conditions, Environmental Performance) and a short questionnaire for the occupants with information for indoor conditions and system controls.

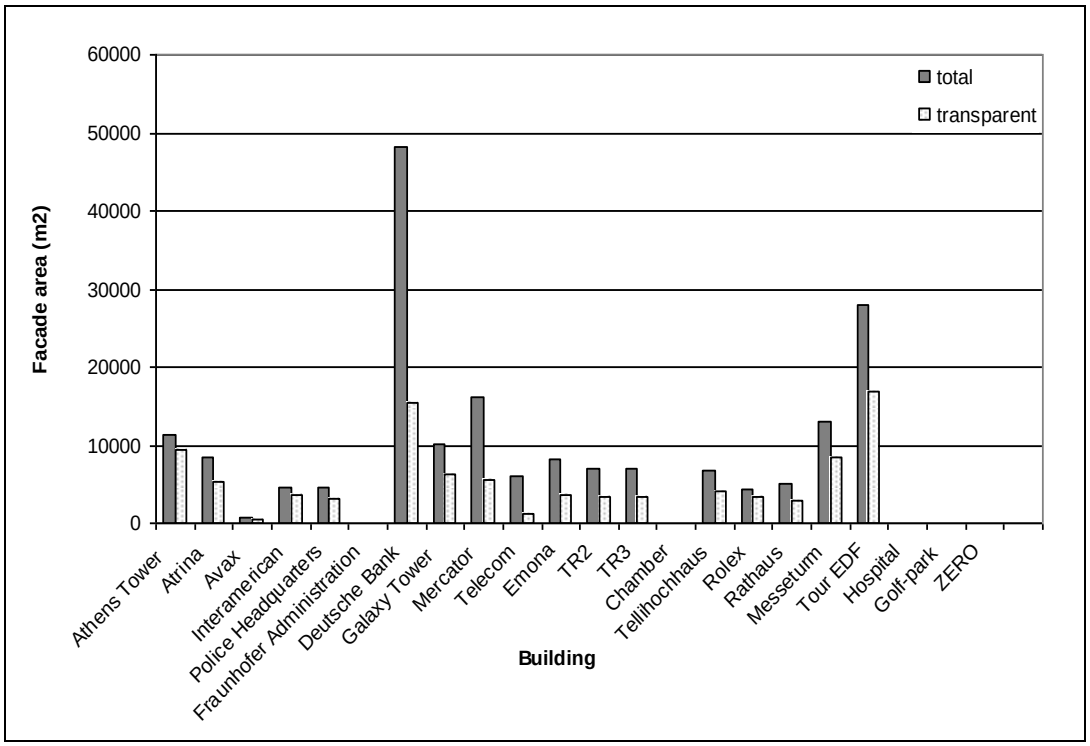

Figure 2: Façade area of the buildings and the non-opaque share

3 BUILDING PERFORMANCE CRITERIA, SPECIFICATIONS FOR INTEGRATED CONCEPTS AND CLASSIFICATION

The specifications of the various building components with regard to energy consumption reduction goals and user comfort have been defined. In addition to that various new technical concepts for whole buildings have been developed and the potential performance of the new concepts has been assessed. Finally high-rise building categories together with typical buildings for each category have been established. The categorization is essential for the development of the facade components which is the core of this assessment (Koene, F. et al., 2009).

The five main building categories identified as predominant for the existing high-rise buildings are:

- Category 1, 1945-1960 Post-war, massive facade in reinforced concrete structure
- Category 2, 1960-1980 Reinforced concrete with perforated façade
- Category 3, 1975-1990 Skeleton construction with precast concrete
- Category 4, 1975-1995 Skeleton construction with curtain-wall façade
- Category 5, 1980-2005 Tall buildings, Skeleton construction with all-glazed facade, air-conditioned.

The main constructive and facade characteristics are presented in Figure 3.

Building categories	Post-war, reinforced concrete structure with massive facade	Reinforced concrete with (precast) concrete façade	Skeleton construction with precast concrete panels (strip windows)	Skeleton construction with curtain-wall façade	Tall buildings, Skeleton construction with curtain-wall facade, air-conditioned
Image					
category	1	2	3	4	5
time line	1945-1965	1960-1980	1975-1990	1975-1995	1980-2005
main construction	reinforced concrete	reinforced concrete	reinforced concrete	reinforced concrete	reinforced concrete / steel
precast	no	possible	possible	no	no
facade	load bearing	load bearing	non bearing	non bearing	non bearing
stability	facade	facade/core	core	core	core
material facade	massive brick, brick cavity wall	brick, natural stone, stucco, ceramic tiles, glass cladding	concrete, metal cladding	metal profiles, metal cladding	metal profiles, metal cladding
glazing	single	single/double	double	double	double coated
windows	openable	openable	openable	openable/closed	closed
floor plan	lineair cell structure	lineair cell structure	core cell structure	cell/open structure	cell/open structure
air-conditioning	no	no	no	no	yes

Figure 3: Building categories and their characteristics

The five building categories are further presented with the identification of representative buildings in each category. Cost-effective partners were asked for collaboration by sending detailed information on selected high-rise buildings representing building categories. The description of the building included general information of the building size, insulation, heating/cooling and ventilation supply systems and controls, energy consumption, indoor environment quality and user satisfaction. The information gives broader insight into building categories and their relating building problems through real building examples.

4 DEVELOPMENT OF NEW MULTIFUNCTIONAL COMPONENTS

Based on the experience of the previous work which included detailed specifications and overall information on high-rise buildings, prototype multifunctional facade components have been developed (Tilmann, K.,2013).

4.1 Transparent solar thermal façade collector

Two generations of prototypes of new transparent solar thermal façade collectors (TSTC) have been developed (Fig.4). The first generation is integrated in a sealed glazing unit, the second generation is integrated in a closed cavity façade. They have been characterised with detailed measurements and concepts for their integration in whole high-rise building heating, ventilation and cooling (HVAC) concepts have been developed.

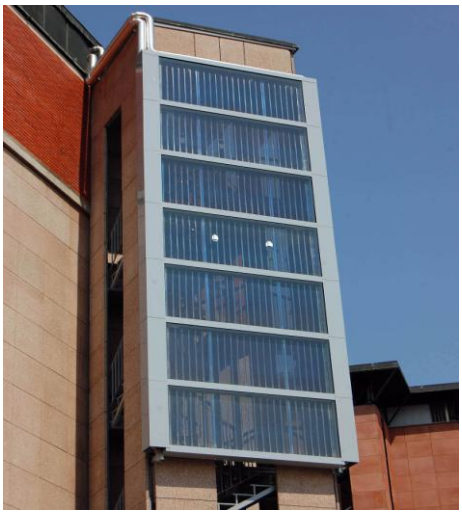

Figure 4: Prototype transparent solar thermal façade collectors, installed at the pilot building in Slovenia

4.2 Solar thermal vacuum tube collector

Prototypes of façade-integrated solar-thermal vacuum tube collectors are used to heat air directly and have been developed successfully (Fig.5). The heated air can be used directly for room heating in winter or in combination with solar heating and cooling systems. Because air is used as the heat transfer medium (simple handling of stagnation situations), easy façade integration is possible.

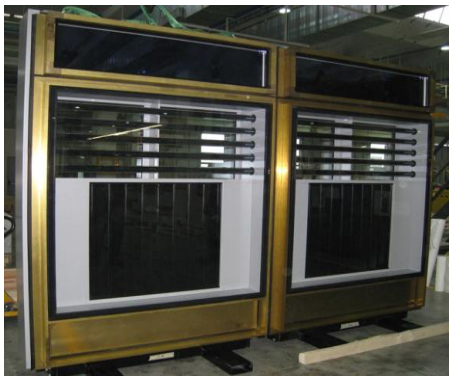

Figure 5: Air-heating vacuum tube collectors (tubes in the middle) at the international trade fair Bau 2011 in Munich.

4.3 Building integrated PV component

Prototypes of a glazing unit with integrated PV, which generates electricity and simultaneously provides solar control and glare protection have been developed successfully (Fig.6). The solar control functionality significantly reduces the energy consumption of buildings because of lower cooling loads. The generated electricity helps to cover the primary energy demand of the building itself.

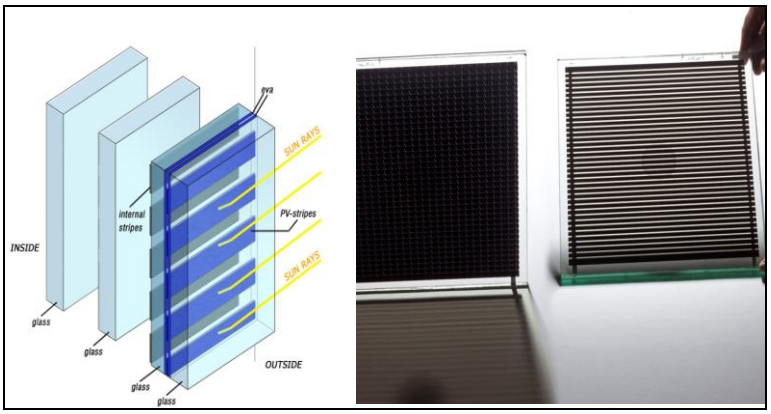

Figure 6: PVShade®

4.4 Facade integrated natural ventilation system with heat recovery

A façade-integrated natural ventilation concept with heat recovery has been developed and demonstrated successfully (Fig.7). The cost effectiveness has been improved by eliminating the supply air ducting by using decentralized supply. The concept consists of local HVAC units placed in the façade which, without air ducting or fans (no noise!), supply preheated or cooled outside air to users. The unit can be driven by low-temperature energy sources, e.g. originating from exhaust air (twin coil) or from renewable energy sources.

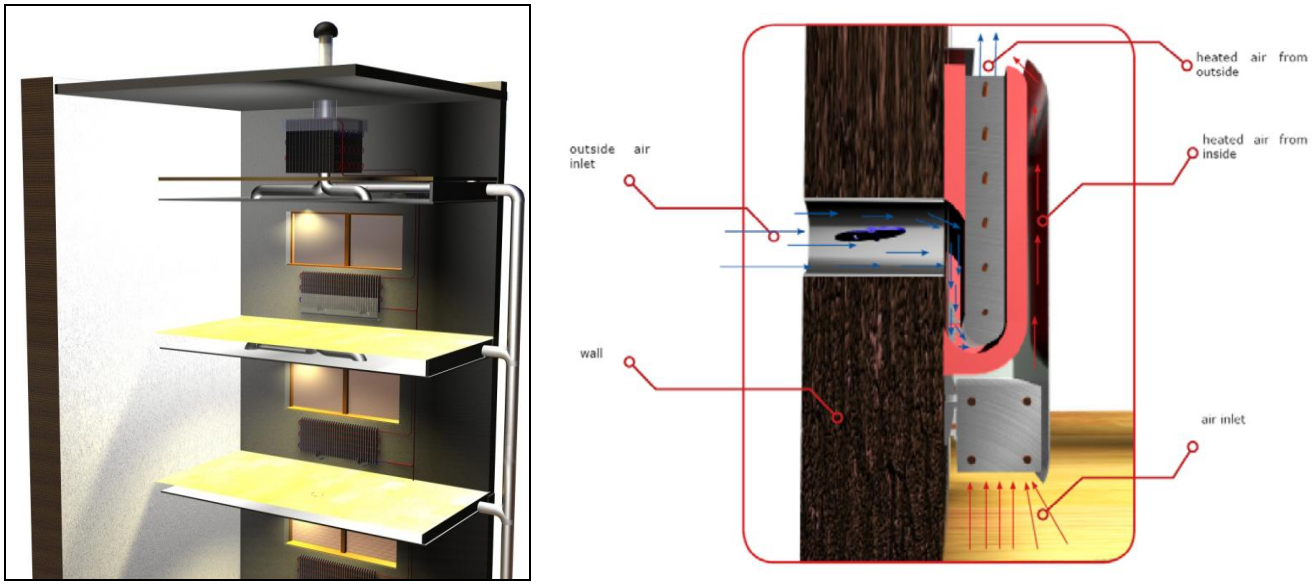

Figure 7: Natural ventilation with heat recovery. The right side shows a sill area integrated device. On the left hand side the device is integrated in the suspended floor.

4.5 Solar assisted decentralised heat pump system

A heating/cooling system for high-rise buildings using active solar façade elements to take advantage of the available unglazed vertical surface was successfully developed. The system is composed of an active solar façade coupled to a reversible heat pump. The active façade works as a low temperature solar collector as well as an atmospheric heat exchanger and a nighttime heat-dissipater in order to boost the heating/cooling efficiency of the system. The first exchanges have pointed out the technical issues and limitation such as condensation or frost formation on the façade and the need for heat storage means. Following, a number of concepts have been proposed, analysed and discussed, sometimes with the help of simulations. The concept of the active solar façade system is presented in Figure 8.

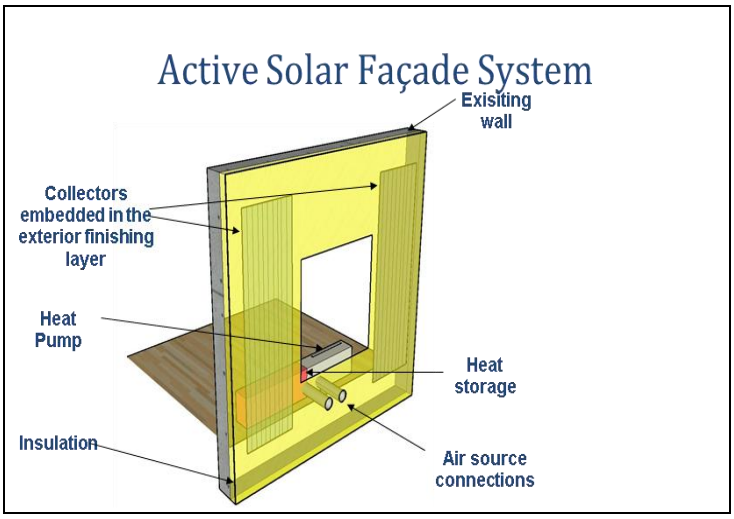

Figure 8: Unglazed collector & heat-pump

5 INTEGRATED CONCEPTS OF RENEWABLES

A number of technical renovation concepts were developed to address the high energy consumption of high rise buildings as well as address challenges in comfort and user satisfaction that are commonly encountered in these buildings. In the concepts, conventional components, such as high quality glazing, as well as novel components analyzed in the previous section are used. The economic feasibility of these concepts is also a crucial topic of the present study. The problem to be adressed is how to make it financially attractive to renovate a building in an energy efficient way, which generally is more expensive than a 'business as usual' renovation. The technical renovation concepts are taken as the starting point for a techno-economic analysis. Energy data, calculated with the building simulation software TRNSYS, and cost data of components are fed into a business model which was developed in this project (Koene, F. et al. 2012).

For each of the technical concepts, dynamic TRNSYS simulations were carried out to calculate the thermal behaviour of the building, the energy demand for heating, cooling, electricity consumption (for lighting and installation) and, when applicable, the electricity generated by photo voltaic panels.In addition, TRNSYS modules were developed to represent the novel components, such as the Active Solar Façade (ASF), the vacuum tube collector, the Transparent Solar Thermal Collector (TSTC) and the semi-transparent PV-shade modules.In addition, cost data were supplied for both conventional and novel components in the concepts. The business model developed calculates the NPV (Net Present Value) of a number of costs and revenues over a period of 15 years. The business model identifies three stakeholders: 1)

building owner, 2) building user or tenant and (optionally) 3) a third party called ESCO (Energy Service Company).

5.1 Construction aspects

A catalogue of solutions and ideas has been produced that helps the planners to integrate the new components (Pfenninger, E.,2012). In general the visual aspects are proposed by the Building Owner/Building Developer and the Architect to achieve the overall investment and maintenance cost as well as the user requirements. The technical requirements of the building envelope are driven by the optimal implementation of the architectural requirements, considering the following aspects:

- Agreed budget (investment and maintenance costs)
- User requirements (natural ventilation, glare-, darkening-, privacy-, energy aspects)
- Physical requirements (thermal-, shading-, glare-, privacy-, acoustic-, structural-, seismic-, wind load-, day light-, weather/air/vapour tightness aspects)
- Local codes/statutory requirements
- Sustainability certificates and labels such as "Leed,"Breeam" etc.
- Technical guidance and recommendations
- Industrial Standards/Quality requirements
- Safety, security and fire rating requirements
- Cleaning access
- Gain energy from the building envelope

In order to meet and comply with all the above requirements a highly successful functional and efficient building envelope shall be designed, which becomes a more and more complex task, thus requires additional input and assistance from a specialised Facade Engineer/Consultant.

5.2 Environmental aspects

This task focuses on the assessment of the environmental impacts of different integrated concepts taking into account retrofit activities for high-rise buildings of all categories and the adequate integration of new developed components. For the assessment, the whole life cycle of the concepts will be considered by taking into account:

- the manufacturing of the components,
- the building construction and retrofit measures,
- maintenance activities for components and buildings,
- the operation of the component and the building where the concepts are applied
- the End-of-Life for building and components.

Parameterized, generic LCA models are built up to assess the whole life cycle of the multifunctional components including the production, the use phase (maintenance and operation) as well as the End-of-Life phase (Lenz, K. et al. 2012). The software provides a graphical user interface where life cycle phases, production steps, maintenance activities or End-of-Life scenarios are represented by so called "plans" and "processes" which are connected by flows (e.g. material flows and energy flows) for modelling purpose.

The LCA model built up is hierarchically structured (meaning plans may consist of processes and other sub-plans), having an overall life cycle plan on the top level and detailed sub-plans for different life cycle phases on sub levels.

5.3 Architectural and aesthetical integration

The aesthetic aspects are based on slightly different façade typologies than the construction aspects. Architects might choose for the feeling or the color of a material like brick, natural stone, metal cladding, glass or wood. In general the material for high-rise are limited. The

wind pressure and the difficulty in the maintenance on the higher levels ask for materials that can withstand the climate influence with less maintenance (Reijenga, T.,2012). Main typologies are:

1. Massive or cavity wall with or without openings
2. Precast element wall
3. Curtain wall

Beside this there are many hybrid façade solutions. Mainly based on additional elements like a second layer for the façade and with both aesthetic and quality improving reasons. These are:

1. Integrated systems
2. Climate façade or box windows
3. Second skin (double façade)
4. Second layers (louvers, shading)

5.4 Socio-economic aspects

Under this field, case studies have been chosen as a research tool in order to measure in detail the socio-economic aspects of the integrated concepts for cost-effective integration of renewables (Kowalska, A. et al. 2011). In order to achieve this, context and perception of Most Important Customers (MIC) (investor/owner and tenant/occupant) were investigated in terms of investing in building integrated solutions. What is more, willingness and policy of ESCO financing/co-financing of such projects was explored. The new approach to investment (elaborated within Cost-Effective) was presented to the respondents and their opinion on this issue was gathered and analysed in a further step. To explain further the rationale how the barriers of implementing building integrated renewables have been overcome, non-residential high-rise buildings in which renewables (solar/PV) are already implemented (or there is an ongoing project of implementing) were also investigated. In relation to the previous, societal acceptance of applied technology and stakeholder involvement were investigated as well as the involvement of ESCO, as an important key stakeholder for the Cost-Effective project Under the case studies the following type of respondents were interviewed:

1. Investors/owners
2. Tenant/occupant
3. ESCO (Energy Service Companies) in relevant country

5.5 Integration in building management systems

A holistic strategy has been implemented for each component, facilitating the integration procedure. This strategy includes initially an analysis of the BMS concepts, introducing the main features and functionalities of BMS system including control level, management level, service level and backbone network (Maseda, J., 2011). Independence and autonomy of management and optimization of the energy and maintenance processes are two important features of BMS design. Main commercial implementations in PLC platforms, bluetooth platforms, ZigBee platforms, PLC media and wireless media are stated. The methodology designed and implemented to interface with the technology developers is described and in parallel fundamental questions related to decision making, control and data reporting are answered through a questionnaire, highlighting the importance of the BMS integration of the components developed in the Cost-Effective project. Main topics are technology characteristics, building and BMS integrations considerations and hardware characteristics. The core contribution of the report is an in-depth analysis of the integration of the different components in a BMS. The analysis has been done as an independent process for every component as the characteristics and functionality provided is different for each one.

5.6 Development of a Decision Support Tool

This DST is a tool, containing simple guidelines to give information on energy-efficient and sustainable renovation of high rise buildings focusing on decision makers like architects and building owners (Fig.9). The tool is designed for use in the initial phase, and should inspire decision makers to implement energy efficient renovation measures (Karlessi, T., 2012). Main decisions in relation to ambitions in energy-efficiency, sustainability, economic feasibility and occupants' participation take place in the first, or the initiative phase of building renovation projects.

The DST tool provides practical and in-depth information of relevance by:

• case studies with examples and pictures of virtual and real buildings
• support for planners on how to integrate the new concepts in BMS
• best practice catalogues
• examples of business models
• test results for components
• support for design and commissioning of BMS

The tool works by defining the renovation case selecting:

- Location: Western or Southern Europe
- Building type, according to year of construction, type of building
- Preference for mainly thermal (heat) or photovoltaic (PV, electricity) energy

This will result in:

1) Example of a Cost Effective concept for each situation
2) More detailed information, to support your decisions, on:

• Economic support
• Case Studies
• Components & costs
• Other support

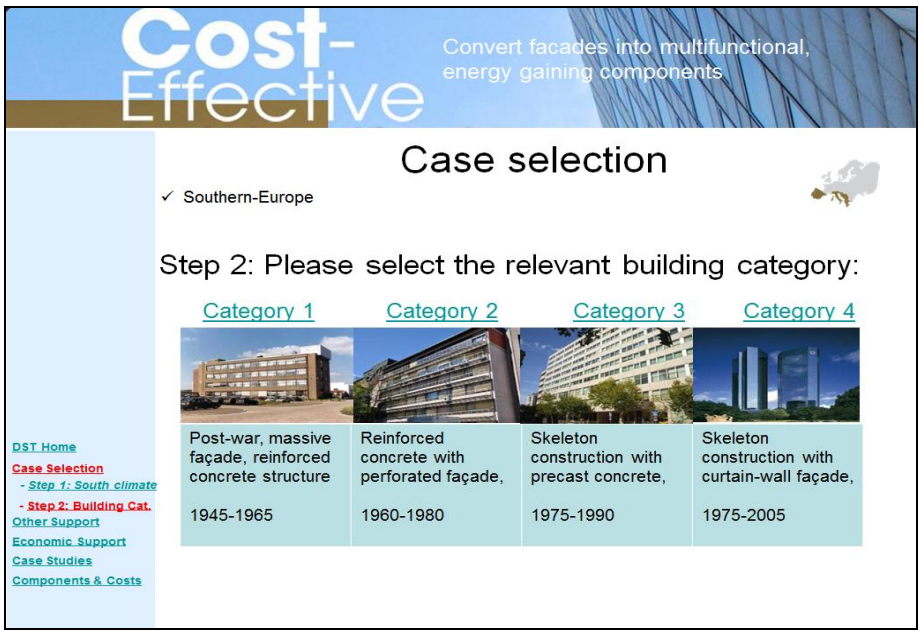

Figure 9: The Decision Support Tool

6 CONCLUSIONS

The main task achieved in the framework of the Cost-Effective project is the development and implementation of new and highly advanced integrated cost-effective façade concepts, based on new multifunctional components and/or new combinations of (improved) existing high-rise building envelope technologies in order to improve the primary energy balance of the building.
This goal is achieved through the development of new multi-functional façade components which combine standard features and the use of renewable energy resources and the - development of new business and cost models which consider the whole life cycle of a building and which incorporate the benefits from reduced running costs and greenhouse-gas emissions. All relevant aspects (construction, environmental, architectural and aesthetical, socio-economic) have been considered. The practical feasibility was tested in two pilot buildings in Spain and Slovenia
Thus the project contributes (1) to convert renewable energy into useful forms for specific applications and (2) to significantly improve the building energy performance through cladding and ventilation technologies and utilisation of embedded renewable energy sources. All outcomes are available at the project site http://www.cost-effective-renewables.eu

7 REFERENCES

Tilmann, K., Werner, W., (2011) SEVENTH FRAMEWORK PROGRAMME COOPERATION - THEME 4 NMP-2007-4.0-5 Grant Agreement for: Collaborative Project Resource- and Cost-effective integration of renewables in existing high-rise buildings

Tilmann, K., (2013) Deliverable D0.1.4 Final publishable summary report

Karlessi, T., (2012) D4.1.8. A DST tool including case studies with examples and pictures of virtual and real buildings. Support for planners and how to integrate the new concepts in BMS. Best practice catalogues, examples of business models, test results for components. Support for design and commissioning of BMS

Koene, F., Oleksik, A.,(2012) D4.1.1 Report on the developed techno-economic integrated concepts.

Pfenninger, E., (2012) D4.1.2 Integrated Concepts - Construction Aspects

Lenz, K., Schneider, S. (2012) D4.1.3 Report on the assessment of the environmental impacts of different integrated concepts - LCA of new developed components

Reijenga, T., (2012) D4.1.4 Integrated concepts – technical composition

Synnefa, A., Karlessi, T., Santamouris, M., Bastian, W., Cacavelli, D., (2009) D1.4.1 Report on performance evaluation and documentation of state-of-the-art technologies in EU25, USA and China

Koene, F., Kondratenko, I., Reijenga, T., (2009) D2.1.2 Report on identification of representative buildings per building category (set of representative buildings)

Maseda, J., (2011) D4.1.4 Integrated Concepts- Integration in Building Management System

Kowalska, A., Oleksik, A. (2012) D.4.1.5 Socio-economic aspects of integrated concepts

RETROFITTING AN OFFICE BUILDING TOWARDS A NET ZERO ENERGY BUILDING (NZEB)

Eleni Pyloudi[1], Sotiris Papantoniou[1], Dionysia Kolokotsa[1]

1 Technical University of Crete
School of Environmental Engineering
Technical University of Crete, Crete, Greece

ABSTRACT

Energy consumption in buildings for heating, cooling and lighting needs to be reduced in all European countries in order to achieve the goals set by the latest European Directives for reducing energy consumption by 20% and increase the introduction of Renewable energy sources by 20%. The present paper focuses initially on the reduction of energy consumption for a university building in Crete and then covering the minimized energy demands with renewable energy sources. The approach is simulation based. At first, current heating and cooling demands of the building are estimated. Subsequently, through the application of basic energy conservation techniques, such as applying cool materials in the façade of the building, a detailed analysis is performed for the energy requirements to cover new demands. Finally, Renewable Energy Sources are implemented in order to provide energy to the building or directly into the grid, thus having a zero energy building.

KEYWORDS

Zero Energy Building (ZEB); Net Zero Energy Building; Office building; Simulation-based approach; Renewable Energy Sources

1 INTRODUCTION

One of the most controversial issues nowadays is Global Warming which concerns not only the scientific realm, but it also has obvious impacts on various sciences such as economics and sociology. Both the impact of global warming and the increase of primary energy demand and electrical energy, is forcing international communities to propose future targets in order to deal with this threat, mainly through public awareness, new standards/regulations and other measures (Silva et al. 2013).

Buildings today account for 40% of the world's primary energy use and 24% of the greenhouse gas emissions (IEA 2011). It is estimated that 26% of the total final energy consumption of Europe was consumed in residential buildings and 13% in non-residential buildings (Berggren et al. 2013). The tertiary sector (non-residential building and agriculture) is one of the fastest growing energy demand sectors and it is expected to be 26% higher in 2030 than it was in 2005, compared to only 12% higher for residential buildings (Boyano et al. 2013). This estimation makes it necessary to investigate the use of energy in the non-residential buildings sector, but the difficulty is to find the way to achieve smart consumption strategies without causing negative consequences to people's standard of living and productivity.

The ZEBs have great potential in helping to alleviate the problems related to the deterioration of the environment and the depletion of energy sources. In the building sector, net energy is considered as the balance between the energy consumption in a building and the energy produced by its renewable energy systems. To this respect, the Net ZEB refers to

buildings which are connected to the energy grids and the ZEB is more general and may include autonomous buildings (Li et al. 2013). Several countries have proposed future building energy targets to establish ZEBs such as the Building Technology Program of the US Department of Energy and the EU Directive on Energy Performance of Buildings (Sartori et al. 2012). Achieving a Net ZEB includes two main strategies; firstly by minimizing the required energy through energy efficient measures and then by meeting the minimal energy needs by adopting renewable energy.
Energy-efficient measures, applied to existing buildings during minor/major retrofits, which can reduce the energy consumption in buildings, can be grouped into three categories (Li et al. 2013):

- Building envelopes - thermal insulation, thermal mass, windows/ glazing (including daylighting) and reflective/green roofs.
- Internal conditions - indoor design conditions and internal heat loads (due to electric lighting and equipment/appliances).
- Building services systems - HVAC (heating, ventilation and air conditioning), electrical services (including lighting) and vertical transportation (lifts and escalators).

Even if the most effective energy-efficient measures are applied, energy will still be required in order to power the daily running of a building. The main difference between energy efficient buildings and ZEBs is that in ZEBs the minimized energy is covered by the use of renewable energy. The most common technologies which are adopted for onsite applications are the following (Li et al. 2013):

- PV (Photovoltaic) and BIPV (building-integrated photovoltaic)
- Wind turbines
- Solar thermal (solar water heaters)
- Heat pumps

This paper will examine the potential of retrofitting an office building in order to become Net Zero Energy Building using TRNSYS and HOMER software. Thus, this paper has two objectives; applying energy efficient measures divided in the basic three categories listed above and the adoption of renewable energy technologies which includes the combination of Photovoltaic panels and Wind turbines. Especially, the methodology will be presented in chapter 2, the simulation details, in which all scenarios will be explained, are presented in chapter 3 and finally, the results and the conclusions are in chapter 4 and 5 respectively.

2 METHODOLOGY

Firstly, the present building was modeled on TRNSYS software and its energy behavior was examined. The second step was the minimization of energy consumption applying energy-efficient measures. Finally, the minimized energy was covered applying Renewable Energy Sources on building in order to try to achieve the conversion of the present building into Net Zero Energy Building. The steps are presented in the Figure 1.

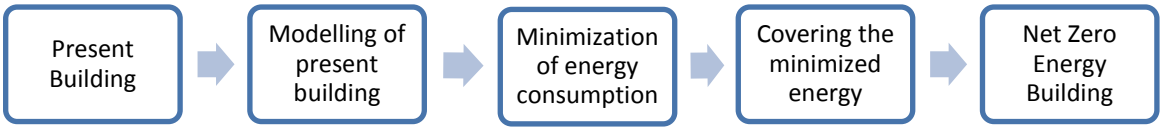

Figure 1: The steps of the project

The minimization of energy consumption requires energy-efficient measures to be applied. Energy efficient measures can be classified into three categories; Measures which could be applied in Building Envelopes, in Internal Conditions and in Building Services Systems (Li et al. 2013).

Four different scenarios were examined in order to minimize the consumption of the building and three more scenarios in order to cover this minimized energy with renewable energy sources. Thus, the following scenarios are going to be presented in Table 1.

Table 1: Description of scenarios

Description of Scenarios					
Initial condition	Present condition of the building				
Scenario 1	Combination of the following improvements on **building envelopes**	Insulation on walls	Replacement of windows	Cool coating on external walls	Insulation of ceiling
Scenario 2	Combination of the following improvements on **internal conditions**	Replacement of the present lights		Reduction of consumption of computers	
Scenario 3	Combination of the following improvements on **building services systems**	Changes on heating and cooling settings		Changes on ventilation settings	
Scenario 4	Combination of Scenarios 1,2 and 3				
Scenario 5	Installation of photovoltaic panels				
Scenario 6	Installation of wind turbines				
Scenario 7	Combination of Scenarios 5 and 6				
Best case scenario	Combination of scenarios 4 and 7				

3 SIMULATION DETAILS

The TRNSYS software (Klein S.A. et al 2012) was used in order to simulate the building and find its yearly consumption. The central part of the simulation was the Type-56 (multi-zone building) which gives the opportunity to divide the office building into 31 thermal zones (Provata 2012). After minimizing the consuming energy, HOMER software ((Kassam & Implementation n.d.), (Giatrakos et al. 2009)) was used in order to combine two Renewable Energy Sources - PVs and Wind turbines - in the most appropriate way, aiming at covering the remaining energy.

3.1 Initial condition of the building

General building description

The office building of Environmental Engineers at Technical University of Crete is situated in the campus of the Technical University of Crete in the suburbs of Chania, Greece and its coordinates are 24°A (longitude) and 35°B (latitude). The building was constructed in 1997 and it is a two-storey building with a total height of 11m and total length of 48m. The ground floor (605 m^2) and the first floor (610 m^2) consist of office rooms, laboratories, stairways, elevators, toilets, hallways and PC labs and concerning the second floor (421 m^2), it

accommodates the mechanical equipment as no employees work there. The electricity demands of the building are covered by the grid.
It is considered that the building is occupied by 56 persons performing seated, light work such as typing. Its operating schedule is from 8:00 am until 6:00 pm every weekday.
The ventilation rate depends on the size of each zone, the number of persons and the use of each zone. The infiltration rate is considered constant value of 0.5 ach.

The characteristics of the building (Katerina Paulidou 2008) are presented in Figure 2.

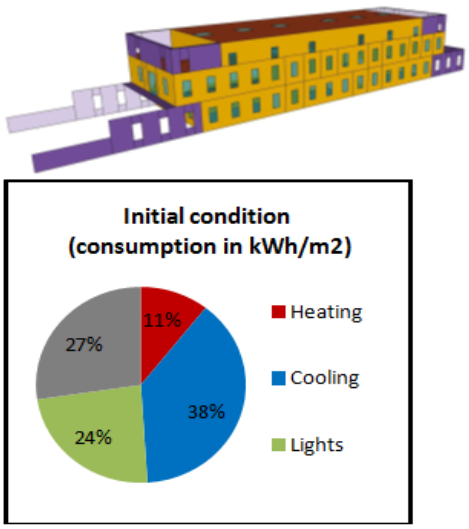

Characteristics of the building	
General information	
Location	Chania, Crete, Greece
Building type	Office building
Floors	3 (The ground and the first floor are in operation and the second floor is used for the installation of HVAC systems
Surface area	1296 m2 (including the surface area of ground and first floor)
Operation hours	08:00 - 18:00 Monday - Friday
Orientation	SE
Building envelope	
Walls	Three-layer (plasterboard, polysterine, concreteboard) outer walls of total U-value = 0.915W/m2K
Roof	Two-layer (concrete iron, polysterene) ceiling of total U-value = 1.449W/m2K
Windows	Double glazing windows with U-value = 2,83 W/m2K)
Floor	Two-layer (polysterene and marble) with U-value = 0,945 W/m2K)
Building services	
Cooling system	VRV system (6.44 kW) with separate mechanical ventilation support
Heating system	Same with cooling system

Figure 2: Initial Characteristics of the Building

The energy consumption is approximately 37600 kWh (29 kWh/m^2) for cooling and 10400 kWh (8 kWh/m^2) for heating. The electricity consumption for lighting and computers is 23300 kWh (18 kWh/m^2) and 26800 kWh (20.7 kWh/m^2) respectively.

Initial Building Envelopes

Thermal insulation of external walls (See

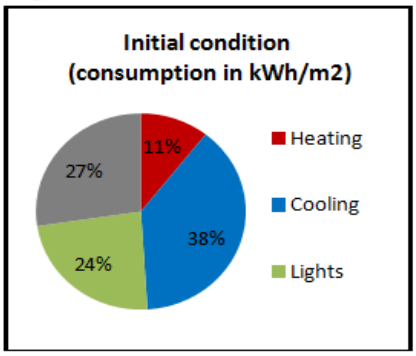

Characteristics of the building	
General information	
Location	Chania, Crete, Greece
Building type	Office building
Floors	3 (The ground and the first floor are in operation and the second floor is used for the installation of HVAC systems
Surface area	1296 m2 (including the surface area of ground and first floor)
Operation hours	08:00 - 18:00 Monday - Friday
Orientation	SE
Building envelope	
Walls	Three-layer (plasterboard, polysterine, concreteboard) outer walls of total U-value = 0.915W/m2K
Roof	Two-layer (concrete iron, polysterene) ceiling of total U-value = 1.449W/m2K
Windows	Double glazing windows with U-value = 2,83 W/m2K)
Floor	Two-layer (polysterene and marble) with U-value = 0,945 W/m2K)
Building services	
Cooling system	VRV system (6.44 kW) with separate mechanical ventilation support
Heating system	Same with cooling system

Figure 2: Initial Characteristics of the Building

-)

Windows (See

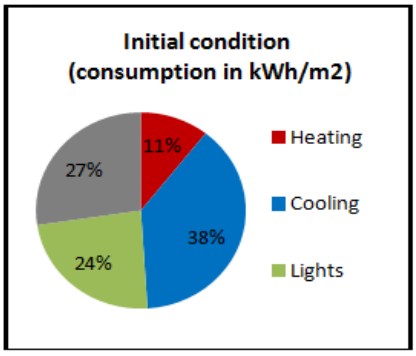

Characteristics of the building	
General information	
Location	Chania, Crete, Greece
Building type	Office building
Floors	3 (The ground and the first floor are in operation and the second floor is used for the installation of HVAC systems
Surface area	1296 m2 (including the surface area of ground and first floor)
Operation hours	08:00 - 18:00 Monday - Friday
Orientation	SE
Building envelope	
Walls	Three-layer (plasterboard, polysterine, concreteboard) outer walls of total U-value = 0.915W/m2K
Roof	Two-layer (concrete iron, polysterene) ceiling of total U-value = 1.449W/m2K
Windows	Double glazing windows with U-value = 2,83 W/m2K)
Floor	Two-layer (polysterene and marble) with U-value = 0,945 W/m2K)
Building services	
Cooling system	VRV system (6.44 kW) with separate mechanical ventilation support
Heating system	Same with cooling system

Figure 2: Initial Characteristics of the Building

-)
- Solar absorption of external walls; the solar absorption of the external area of the walls is equal to 90%, which means that part of the reflected radiation is only 10%.

Thermal insulation of the ceiling (See

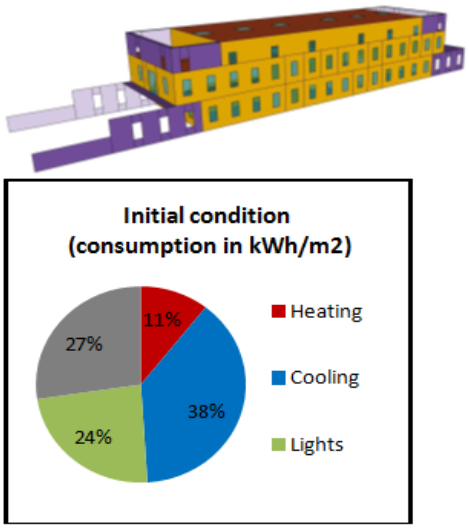

Characteristics of the building	
General information	
Location	Chania, Crete, Greece
Building type	Office building
Floors	3 (The ground and the first floor are in operation and the second floor is used for the installation of HVAC systems
Surface area	1296 m2 (including the surface area of ground and first floor)
Operation hours	08:00 - 18:00 Monday - Friday
Orientation	SE
Building envelope	
Walls	Three-layer (plasterboard, polysterine, concreteboard) outer walls of total U-value = 0.915W/m2K
Roof	Two-layer (concrete iron, polysterene) ceiling of total U-value = 1.449W/m2K
Windows	Double glazing windows with U-value = 2,83 W/m2K)
Floor	Two-layer (polysterene and marble) with U-value = 0,945 W/m2K)
Building services	
Cooling system	VRV system (6.44 kW) with separate mechanical ventilation support
Heating system	Same with cooling system

Figure 2: Initial Characteristics of the Building

-)

Initial Internal Conditions

- **Electric lighting;** It is considered that lighting is provided 8:00-10:00a.m. and 16:00-18:00a.m. every workday, while the rest of the daytime, lighting is provided mainly from the windows. The present lights consume 19 W/m^2.
- **Appliances;** The main appliances which are used are the computers which consume 140 W when they are in operation.

Initial Building Services Systems

- Infiltration; The infiltration of the present building is 0.5 ach
- Ventilation; According to the HVACs' characteristics, the average ventilation rate of each thermal zone of the office building is estimated at 20 L/s/person.
- Heating; Temperature set point is defined to be 20 ^{o}C in winter months only when the building is operating.
- Cooling; cooling system is responsible to keep the temperature at 26 ^{o}C only when the building is operating.

3.2 Scenarios of minimizing the consuming energy of the building

➢ **Scenario 1** - Energy-efficient measures in **Building Envelopes**

Table 2: Measures of Scenario 1 (Building Envelopes)

		Walls	**Ceiling**	**Windows**			**Walls**	**Ceiling**	**Windows**
Initial condition	Polysterene insulation (cm)	2	1	-	**Scenario 1**	Polysterene insulation (cm)	5	3	-
	Total U-value (W/m^2)	0.915	1.449	2,83		Total U-value (W/m^2)	0.436	0.671	1,04
	g-value	-	-	0,755		g-value	-	-	0,227
	Solar reflectance (%)	10	-	-		Solar reflectance with **cool paint**	89	-	-

(%)

In this scenario changes in the building envelope are examined. These changes include firstly the increase of wall insulation which achieves the reduction of the U-value. The next measure is to replace the present windows with windows with lower U-value and g-value. One more change in the building envelope which can be applied is to paint the external walls with cool paint in order to increase the reflective radiance from 10 % to 89 % (Kolokotsa et al. 2012). The last measure to be applied is the increase of the ceiling insulation. Those measures are presented in the Table 2.

- **Scenario 2** - Energy-efficient measures in **Internal Conditions**

Table 3: Measures of Scenario 2 (Internal Conditions)

	Lights (W/m^2)	**Computers (W)**
Initial condition	19	140
Scenario 2	10	98

In this study the internal conditions include the lights and the computer (Table 3). The present lights consume $19W/m^2$ and the total consumption of lights is 23300 kWh. In terms of the computers, taking under consideration that each computer consumes 140 W and that there are 92 computers which operate when the offices are open, the total consuming energy of computers is 26800 kWh.
The change which is examined in this scenario is to reduce the consuming energy of lights and computers. In terms of lights, the scenario studies the case of the replacement of the present lights with others which consume $10W/m^2$ instead of 19 W/m^2. Regarding the computers, one possible scenario is to replace the power supply of personal computers with new ones which consume 30 % less energy.

- **Scenario 3** - Energy-efficient measures in **Building Services System**

Table 4: Measures of Scenario 3 (Building Services System)

	Heating in common areas (^OC)	**Cooling in common areas (^OC)**	**Ventilation (L/s/person)**
Initial condition	20	26	20
Scenario 3	17	28	8.3

Heating, cooling and ventilation conditions in one office are very important factors in order to make people feel comfortable and productive. For this reason it was impossible to increase the temperature in winter and to reduce the temperature in summer time in offices for energy saving reasons. But, one scenario which can be examined is to apply this energy saving in common areas such as corridors, stairways and toilets. So, one part of scenario 3 is to reduce the heating set point in common areas from 20 ^OC to 17 ^OC and to increase the cooling set point in those areas from 26 ^OC to 28 ^OC. This change will prove effective because the comfort conditions of workers will not be degraded as they stay in these locations for only a limited time.
The second part of scenario 3 is to change the ventilation settings. According to the constructor, the air which is delivered for each person is approximately 20 L/s, but regarding to (Greece 2010), 8.3 L/s/person are satisfactory for offices. The changes made in Scenario 3 are shown in Table 4.

- **Scenario 4** – **Combination** of Scenarios **1,2 and 3**

In this scenario it is examined how energy consumption can be achieved applying measures on building envelopes, internal conditions and building services system. Table 5 describes the combination of measures taken in each scenario.

Table 5: Measures of Scenario 4 (Combination of scenarios 1, 2 and 3)

		Walls	Ceiling	Windows	Lights (W/m^2)	Computers (W)	Heating (common areas) (^OC)	Cooling (common areas) (^OC)	Ventilation (L/s/person)
Initial	insulation (cm)	3	2	-	19	140	20	26	20
	Total U-value (W/m^2)	0.915	1.449	2,83					
	g-value (0 - 1)	-	-	0,755					
	Solar reflectance (%)	10	-	-					
Scenario 4	insulation (cm)	5	3	-	10	98	17	28	8.3
	Total U-value (W/m^2)	0.436	0.671	1,04					
	g-value (0 - 1)	-	-	0,227					
	Solar reflectance with **cool paint** (%)	89	-	-					

3.3 Measures for covering the minimized energy

HOMER software was used for finding the best combination of photovoltaic panels and wind turbines, aiming at producing the same quantity of energy which is consumed.

- **Scenario 5** – Installation of **photovoltaic panels** on the roof

Table 6: Characteristics of photovoltaic panels

Electrical dara (STC)	
Rated power (W)	265
Rated voltage (V)	31.4
Rated current (A)	8.44
Open-circuit voltage (V)	38.3
Short-circuit current (A)	8.91
Efficiency (%)	16.1
Length x width x height (mm^3)	1660*990*50
Weight (kg)	20

The case of installing 76 photovoltaic panels on the roof of the building with south direction was examined in order to produce energy and give this to the building or directive into the grid. Each photovoltaic panel has the characteristics which are presented in Table 6.

- **Scenario 6** – Installation of **wind turbines**

Four Wind Turbines Roof Mount Towers are selected to be installed in order to cover a significant part of the remaining energy. The main characteristics of these turbines are presented in the Figure 3.
and the power curve is presented in Figure 3.

Wind Turbin characteristics	
Rated power (kW)	3
Output Voltage (V)	120/220
Rotor Blade Diameter (m)	4.8
Start-up Wind Speed (m/s)	2.5
Generator Efficiency	>0.96
Turbine Weight (kg)	138
Noise (db(A))	40@5m/s
Temperature Range (Oc)	-20 to +50

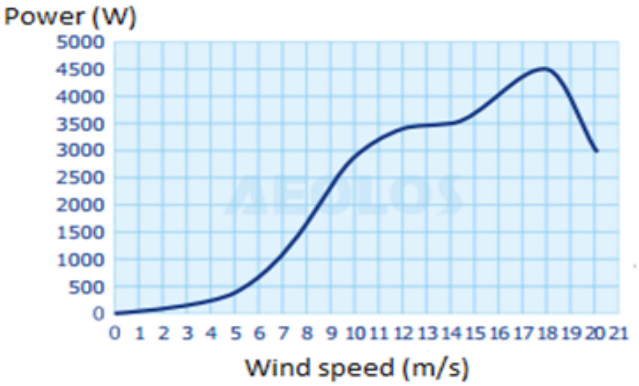

Figure 3: Characteristics of wind turbines

- **Scenario 7** – **Combination** of scenarios **5 and 6**

It is obvious that in this scenario the case of having photovoltaic panels and wind turbines to function at the same time will be examined. The target of this scenario is to produce as much energy as possible.

4 RESULTS

- Concerning the measures for minimizing the consuming energy

In the initial condition, the higher proportion (38 %) of the energy is consumed for cooling needs and it is logical taking into consideration that the building is situated at Chania, Greece, which is categorized in A category (Greece 2010). The lower proportion (11 %) is consumed for the heating needs and approximately the same proportion of the energy used for lighting and computers (24 % and 27 % respectively).

It can be inferred from Figure 4 that the changes in the building envelope (Scenario 1) cause on important reduction on the consumption for cooling that reaches 69%. In this Scenario, the energy which is consumed is reduced from 76 kWh/m^2 (initial condition) to 56 kWh/m^2. So, by applying measures on building envelopes a 26% reduction on the total consuming energy is achieved.

Applying Scenario 2, the total energy consumed by lights will be reduced from 76 kWh/m^2 kWh to 66 kWh/m^2, achieving 13% energy saving and the total energy consumed by computers will be reduced from 76 kWh/m^2 kWh to 68.5 kWh/m^2, achieving 9 % energy saving. It can be inferred that these measures cause a slight decrease in consumed energy for cooling and a slight increase in energy for heating.

Examining the case of applying measures on Building Services System (Scenario 3), it can be inferred that both heating and cooling requirements are reduced approximately 3 kWh/m^2. The energy saving application of this scenario reaches the rate of 9 % having reduced the energy requirement from 76 kWh/m^2 to 69 kWh/m^2.

The combination of all previous scenarios which is presented from Scenario 4 shows that all consuming energy sources reduce their needs. The major reduction can be detected in cooling needs in which a reduction of 83 % occurs. The reduction of lighting, heating and computer needs follow with the rates of 47 %, 38 % and 30 % respectively. In general, the total consuming energy is reduced from 76 kWh/m^2 to 34 kWh/m^2 and the energy saving reaches the value of 55 %.

	Energy consumption (kWh/m²)				
	Initial	Scen. 1	Scen. 2	Scen. 3	Scen. 4
Heating	8.0	8.0	9.5	4.0	5.0
Cooling	29.0	9.0	26.0	26.0	5.0
Lights	17.8	17.8	9.4	17.8	9.4
Computers	20.7	20.7	14.5	20.7	14.5
Total	75.5	55.5	59.4	68.5	33.9
Energy Saving		26%	21%	9%	55%

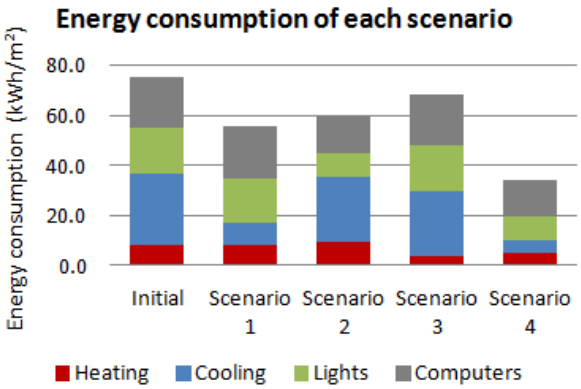

Figure 4: The reduction of energy consumption applying different scenarios

- Regarding the measures for covering the minimized energy

The minimized energy, which needs to be covered by renewable energy sources, is 44000 kWh/yr. The photovoltaic panels installed on the roof of the building produce approximately 24000 kWh/yr and the wind turbines Roof Mount Towers produce 20000 kWh annually. So, the renewable energy sources produce almost the same quantity of energy which is consumed. But the photovoltaic panels and wind turbines cannot function every day due to different daily weather conditions. For this reason, it is necessary to have 23000 kWh/yr grid purchases.

Figure 5 shows how much energy is covered by each source.

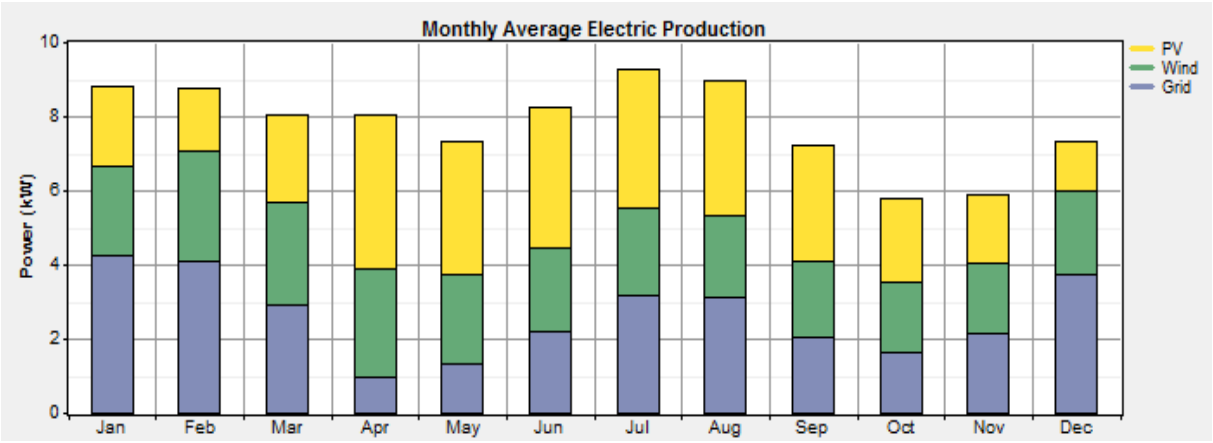

Figure 5: Monthly average electric production

5 CONCLUSIONS

Considering only the energy reduction by applying energy efficient measures without considering the cost required to apply the measures, it can be concluded that the most energy-efficient scenario is Scenario 4. It is expected to be the best scenario while it is the combination of three other energy-efficient scenarios each of which cause a reduction in the required energy.

Scenario 1, according to which changes on Building Envelope were applied, proved the more energy-efficient among the first three scenarios. This was caused because it managed to reduce the cooling needs, which are the main source of consuming energy in the building, by

69 %. The less effective scenario proved to be Scenario 3 while it brought about only a slight reduction in required energy.

To sum up, the energy-efficient measures with ascending order are the following;

- Increasing the insulation on the walls and ceiling, replacement of windows and applying cool paint to the external walls.
- Replacement of lights and power supply of personal computers.
- Changing the temperature setpoint in common areas and adjusting the ventilation rate in required values.

Concerning the renewable energy sources, it can be inferred that the more energy is produced by photovoltaic panels (24000 kWh/yr) in contrast to the production by the wind turbines (20000 kWh/yr). It can also be inferred from Figure 5 that the photovoltaic panels produce the most significant quantity of energy during the months of February until April while wind turbines produce an almost stable quantity of energy during all months with only a slight difference from February and April, when the quantity of energy produced is higher. In general, the building needs more energy than what is offered by renewable energy sources during the months of November until March and July and August, but the opposite is true in the other months. Thus, the energy production come from Renewable Energy Sources has the same quantity with the energy consumption of the building. Subsequently, applying the best case scenario (energy efficient measures in combination with Renewable Energy Sources) the retrofitting of the present building in order to become a Net Zero Energy building is achieved.

6 REFERENCES

Berggren, B. et al., 2013. Net ZEB office in Sweden – A case study, testing the Swedish Net ZEB definition. *International Journal of Sustainable Built Environment*.

Boyano, a., Hernandez, P. & Wolf, O., 2013. Energy demands and potential savings in European office buildings: Case studies based on EnergyPlus simulations. *Energy and Buildings*, 65, pp.19–28.

Giatrakos, G.P. et al., 2009. Sustainable energy planning based on a stand-alone hybrid renewableenergy/hydrogen power system: Application in Karpathos island, Greece. *Renewable Energy*, 34(12), pp.2562–2570.

Greece, T.C. of, 2010. Analytic national standards of parameters for the calculation of energy performance of buildings and issuing of energy performance certificate. In *TOTEE 20701-1*.

IEA, 2011. Towards Net Zero Energy Solar Buildings – Fact sheet.

Kassam, A. & Implementation, F., HOMER Software Training Guide for Renewable Energy Base Station Design.

Katerina Paulidou, 2008. Environmental and Economic Assessment of Energy Behavior of an Office Building in Crete.

Klein S.A. et al, 2012. *TRNSYS 17: A Transient System Simulation Program*, University of Wisconsin, Madison, USA.

Kolokotsa, D. et al., 2012. Numerical and experimental analysis of cool roofs application on a laboratory building in Iraklion, Crete, Greece. *Energy and Buildings*, 55, pp.85–93.

Li, D.H.W., Yang, L. & Lam, J.C., 2013. Zero energy buildings and sustainable development implications e A review. *Energy*, 54, pp.1–10.

Provata, E., 2012. "Energy Saving and Indoor Environmental Quality in Office Buildings."

Sartori, I., Napolitano, A. & Voss, K., 2012. Net zero energy buildings: A consistent definition framework. *Energy and Buildings*, 48, pp.220–232.

Silva, P.C.P. et al., 2013. Development of prefabricated retrofit module towards nearly zero energy buildings. *Energy and Buildings*, 56, pp.115–125.

DEVELOPMENT OF A SMART SENSOR FOR CONTROLLING ARTIFICIAL LIGHTS AND VENETIAN BLINDS

Pantelis Foutrakis [1], Sotiris Papantoniou [2], Kostas Kalaitzakis [1], and Denia Kolokotsa [2]

1 Technical University of Crete
Department of Electronics and Computer Engineering
Chania, Greece

2 Technical University of Crete
Department of Environmental Engineering
Chania, Greece

ABSTRACT

Cooling loads in office buildings with large glazing facades are increase due to solar radiation penetrating the windows and over-heating the rooms. Moreover solar radiation provides natural lighting in the rooms, which might be higher than expected in the summer months and causes glare problems. In order to balance optimally between the reduction of cooling loads and natural lighting a controller can be applied to select the best combination between the position of blinds and whether the artificial lights will operate or not.
The developed controller, arduino based, is applied in an office building and is controlling the level of venetian blinds and their angle. The application is using as input an indoor and outdoor illuminance sensor, and an occupancy sensor. The controller is based on fuzzy rules and the fuzzification parameters are optimized offline using matlab's optimization algorithms.

KEYWORDS

Energy Saving, smart sensors, Control, Arduino, Matlab

1 INTRODUCTION

Energy efficiency in buildings is becoming a crucial issue nowadays as it contributes simultaneously to conventional fuels consumption reduction, energy costs cut for building owners and decrease in global warming gas release to the atmosphere. Buildings consume 40% of the energy used worldwide, and it is widely accepted that measures and changes in the buildings operation can achieve substantial savings. Moreover buildings are expected to meet very high standards in the near future. They should be created in a sustainable way, achieve zero-net energy equilibrium, be healthy, comfortable, responsive to the power grid, and economical to build and maintain (Kolokotsa et al. 2010).
In a typical office building, the energy-saving of lighting is an important problem because the lighting accounts for 40% of the total electric power consumption in the entire building. However, the lighting affects the amenity of an office space, and inappropriate energy-saving

of the lighting decreases the productivity of office workers. Therefore, a lighting control system for the office building must achieve the appropriate energy-saving based on careful and accurate control of light. In any case, energy efficiency must never compromise indoor comfort for building users. Lack or poor indoor comfort has a direct affect on users' productivity and an indirect effect to actual buildings' energy efficiency. Unreasonable users' reaction is proved to be disastrous for energy efficiency, i.e. heating greenhouse extensions to buildings, using internal blinds during the day to cut daylight and keeping electric lights on. Building energy management systems (BEMS) contribute to energy efficiency, maintaining indoor and visual comfort. Most BEMS applied in buildings store measured data for energy analysis, control and optimization of energy management, preserve indoor and visual comfort. Although the implementation of BEMS used to be cost effective only in new buildings due to extended wiring required for the communication demands, recent developments in the building automation and control sector by the introduction of various transmission media, helped considerably the feasibility of energy management in existing buildings. Moreover the requirement for a global interoperability in heterogeneous building automation environment consisting of different fieldbuses and data networks is recently a field of continuous research that is still far from being satisfied. Generally, interoperability is achieved when heterogeneous operating entities can communicate transparently and work together for a common scope. One major scope of BEMS is to satisfy the thermal and visual comfort, the air quality demands as well as reduce the energy consumption. Factors that influence the users' comfort are the indoor thermal comfort, the indoor visual comfort and the indoor air quality.

Artificial Intelligence (AI) has been applied to advanced building environmental controls such as thermal-, lighting-, and air-quality controls. With the substantial advantage of applicability in non-linear systems or systems with unclear dynamics, AI-based control methods incorporating Fuzzy Logic (FL), Adaptive Neuro-Fuzzy Inference System (ANFIS), and Artificial Neural Network (ANN) successfully have created more comfortable environments in buildings. In visual comfort, advanced logics using AI models are being investigated for optimal control of lighting conditions with improved energy efficiency.

In research, the field of modeling the behavior of occupants in a building and the field of developing smart controllers (especially for lighting and blinds) are evolving alongside each other. So on one hand, there is a large variety of control algorithms for blinds and lighting, on the other hand, multiple stochastic models have been developed to mimic the behavior of an occupant regarding the use of blinds, light, and ventilation. By combining stochastic models with control algorithms for lighting and blinds, higher simulation accuracy can be reached, and additionally, the saving potential of a controller can be better estimated. Controlling blinds and lighting not only changes the consumption of electric energy for lighting but also that of heating and cooling. Interior venetian blinds are widely used in office spaces to control solar heat gain and prevent visual discomfort. Their properties have significant impact on office daylight availability, and hence on energy demand for office lighting, heating and cooling. Recent studies on automated operation of shading devices have shown great potential for energy savings.

The scientific and the political communities have been aware for several years of the global warming problem. By consequence, a European target is the reduction of greenhouse gases by 20% until 2020 while allowing economic and demographic growths. This can be reached only if the energy consumption is optimized. According to, in 2007 the services and households sectors use 40% of the total final European (EU-27) energy. Within the buildings, the heating systems consume more than 50% which means about 23% of total energy consumption. Even if the trends are to construct new energy-efficient buildings, an overall energy consumption reduction cannot be achieved without an optimization in the existing buildings. As renovations and isolations have high costs and are time demanding, in this context, an advanced control system is the optimal solution. The challenges of indoor lighting system

control are to find a compromise between the user visual comfort and the energy consumption.

2 EXISTING LIGHTING AND BLIND CONTROL MODELS

Blind controllers have either been time dependent or have been based on a threshold value, for example, solar radiation. Over the years, more input variables have been added and the outcome was no longer linearly dependent on input variables. In recent years, automatic adaptation to the occupant and acceptance by the occupant has attracted the attention of researchers and developers in this field. In the early approaches, blinds were adjusted based on one input variable, for example, (Inoue et al. 1988) or (Leslie et al. 2005). In (Newsham et al. 1994) model, the blinds were lowered if the intensity of the sunlight, which fell on the occupants, exceeded 233W/m2. With this rather simple rule, it was already possible to lower the mean PPD (predicted percentage of occupants dissatisfied with the thermal environment) from 22% to 13%. More sophisticated controllers include more than one variable and are closed-loop algorithms. (Trobec Lah et al. 2006) built a fuzzy logic system for managing a roller blind with respect to lighting levels inside the building. The inputs for the system are internal illuminance, global and reflected solar radiation, as well as the current position of the roller blind. The system was applied to a test chamber where it showed a solid performance in controlling the inside illuminance in correlation with the available solar radiation. Thermal comfort is not controlled by the system.

Another improvement is the adaptation of the system according to the needs of the occupants. In (Guillemin and Morel 2002), an integrated self-adaptive controller for heating, shading, and lighting is proposed. The inputs for the controller are current time, indoor and outdoor temperature, solar radiation, presence or absence of occupants in the room, and, additionally, set points (concerning lighting and temperature) expressed by the user. The controller consists of two artificial neural networks (ANN) for the prediction of room temperature and weather, a fuzzy logic for controlling heat and a fuzzy logic for controlling artificial lighting and blinds, which also controls the blinds. To continuously optimize the system, each night, a self-adaption process, using Genetic Algorithms, looks for the most efficient set of parameters for the controllers.

The process and controller are described in separate papers ((Guillemin and Morel 2001), (Guillemin and Molteni 2002)). (Kolokotsa et al. 2006) presents a fuzzy logic controller for indoor thermal and visual comfort and air quality based on the EIB (European Installation Bus) and Matlab. The system was tested and implemented in an experimental chamber (size: 1 m x 1 m x 2 m) equipped with sensors for outdoor and indoor temperature, humidity, illuminance, airflow, and CO2 concentration. The fuzzy controller is fed the following parameters: Predicted Mean Vote (PMV), outdoor temperature, heating or cooling requirements, window opening, indoor illuminance, level of electric lighting, and shading. This produces the following outputs: artificial lighting level and shading position. The system was tested for a period of 3 days, which is short, and showed a good performance in terms of keeping the target values (temperature, PMV index, and illuminance) in the defined range. There is no information given about energy savings resulting from the system. In most publications, it has been shown that the proposed controllers in terms of energy consumption are superior to an on-off controlled counterpart ((Kolokotsa et al. 2001), (Kolokotsa 2003), (Galasiu, Atif, and MacDonald 2004)). Thus, it would generally seem that blind controller development has maintained the focus on providing a comfortable environment and saving energy. However, the adaptation to, and the acceptance of, the occupant is increasingly the centre of interest. Another trend is that more input variables are used for the controller. This

may not be a problem in a laboratory setting but in the real world the additional sensors often make the controller expensive, complicated to install and hence unattractive for users.
(Kurian et al. 2008) developed a combined system for controlling blinds and lighting. This system consists of three fuzzy logic controllers: glare, visual comfort, and energy effectiveness (user absent). For controlling blinds and artificial light, an adaptive neuro-fuzzy inference system (ANFIS) (Kurian et al. 2005) was implemented. The controller was compared with a base case, a simple on/off scheme that yielded energy reductions between 5% and 60%. Lighting controls should not only optimize the energy consumption but also aim to provide comfortable lighting to produce a good working environment. Additionally, it needs to be shown that daylight may have a positive influence on the body and can raise worker productivity, which is very important for office buildings (Berson, Dunn, and Takao 2002). An overview of current research regarding the affect of daylight on people is given in (Galasiu and Veitch 2006).
Although it is rather clear that lighting control systems have a positive impact on energy consumption when maintaining a high level of lighting, comparing the level of savings is rather difficult. This is due to the different profiles of setups as well the requirements of occupants.

3 DEVELOPMENT OF CONTROL MODEL

3.1 Development of fuzzy code

If we analyze a fuzzy controller, we notice that there are a couple of basic elements that describe its function, or its input-output relation. Creation of zero-order Takagi-Sugeno fuzzy system implies the defining of input and output, their respective domains, input membership function, values of output constants and a rule base.

In order to control both blinds and lights in an office using Takagi-Sugeno fuzzy system two models were created with 2 inputs and 1 output, one for blinds and the other for lights.

For inputs the illuminance sensors are used. The indoor sensor value minus a constant of 500 lux is called error and the outdoor sensor value in lux is the second input called outside. We used trapezoidal continuous membership functions for the inputs of the system and they have 4 parameters. The range for error is [-500 2000] and for outside is [0 1000]. The parameters of membership functions are stored as a matrix in a memory card in two separate files one for each input.

Output membership functions of the zero order Takagi-Sugeno system are constants and are stored in a file in memory card as a column-vector.

Rule base is one of the basic elements of the fuzzy system. One rule can be represented by four elements. This way for a system with n rules, a matrix with nx4 dimension is formed.
Rules applied in this fuzzy system have the following form:

If error is A1 and outside is B1 then Y1
If error is A2 and outside is B1 then Y2
If error is A3 and outside is B1 then Y3

For a system with two inputs and one output, this is a general format of rules. So, membership functions linked with both inputs, operator which links the inputs in premises (AND or OR), value of output in the consequence, which is also called a membership function although in zero-order Takagi-Sugeno system it is a constant, are important. In order to create a numerical representation of the rules, each function is marked with a number, for instance the value of its index. That way, three elements of a row-vector for this rule are specified. It remains to find a number to represent the AND or OR operation. That can be solved by marking AND with 1 and OR with 2. Membership function of the first input is the first element in the row, the second is the membership function of the second input, the third is a membership function of the output, and the fourth is the value defining AND or OR operation. So the first rule can be presented with the following vector [1 1 1 1], the second is [2 1 2 1] and the third is [3 1 3 1].

This way there are two files in memory card for the rule base, one for blinds and another for lights.

The rule base for lights and shades are shown in the following figures:

1. If (error is ZERO) then (lights is stable) (1)
2. If (error is NE) and (outside is low) then (lights is up) (1)
3. If (error is NE) and (outside is normal) then (lights is up) (1)
4. If (error is NE) and (outside is high) then (lights is lup) (1)
5. If (error is SNE) and (outside is low) then (lights is lup) (1)
6. If (error is SNE) and (outside is normal) then (lights is stable) (1)
7. If (error is SNE) and (outside is high) then (lights is ldown) (1)
8. If (error is SPE) and (outside is low) then (lights is ldown) (1)
9. If (error is SPE) and (outside is normal) then (lights is ldown) (1)
10. If (error is SPE) and (outside is high) then (lights is ldown) (1)
11. If (error is PE) and (outside is low) then (lights is down) (1)
12. If (error is PE) and (outside is normal) then (lights is down) (1)
13. If (error is PE) and (outside is high) then (lights is down) (1)

Figure 1: Rules for the fuzzy controller of the artificial lights

1. If (error is ZERO) then (shades is stable) (1)
2. If (error is NE) and (outside is low) then (shades is stable) (1)
3. If (error is NE) and (outside is normal) then (shades is up) (1)
4. If (error is NE) and (outside is high) then (shades is up) (1)
5. If (error is SNE) and (outside is low) then (shades is stable) (1)
6. If (error is SNE) and (outside is normal) then (shades is lup) (1)
7. If (error is SNE) and (outside is high) then (shades is lup) (1)
8. If (error is SPE) and (outside is low) then (shades is stable) (1)
9. If (error is SPE) and (outside is normal) then (shades is stable) (1)
10. If (error is SPE) and (outside is high) then (shades is ldown) (1)
11. If (error is PE) and (outside is low) then (shades is stable) (1)
12. If (error is PE) and (outside is normal) then (shades is down) (1)
13. If (error is PE) and (outside is high) then (shades is down) (1)

Figure 2: Rules for the fuzzy controller of the shades

The membership functions for inputs and outputs can be seen in Table 1 and Table 2:

Table 1: Architecture of the fuzzy controller for lights

Type of fuzzy controller	'Sugeno'
N. of inputs	2: error between current and desired light level, outside light level
N. of outputs	1: change in the artificial lights state

Fuzzification parameters error('trapmf')	'NE':	[-1000 -550 -400 -300]
	'ZERO':	[-200 -100 100 250]
	'PE':	[400 550 2200 2500]
	'SNE':	[-400 -300 -200 -100]
	'SPE':	[100 250 400 550]
Fuzzification parameters outside('trapmf')	'low':	[-450 0 250 450]
	'normal':	[250 450 550 950]
	'high':	[550 950 1050 1450]
De-fuzzification parameters (constant)	'down':	[-100]
	'ldown':	[-50]
	'stable':	[0]
	'lup':	[50]
	'up':	[100]

Table 2: Architecture of the fuzzy controller for shades

Type of fuzzy controller	'Sugeno'	
N. of inputs	2: error between current and desired light level, outside light level	
N. of outputs	1: change in the venetian blinds level	
Fuzzification parameters error('trapmf')	'NE':	[-1000 -550 -400 -300]
	'ZERO':	[-200 -100 100 250]
	'PE':	[400 550 2200 2500]
	'SNE':	[-400 -300 -200 -100]
	'SPE':	[100 250 400 550]
Fuzzification parameters outside('trapmf')	'low':	[-450 0 250 450]
	'normal':	[250 450 550 950]
	'high':	[550 950 1050 1450]
De-fuzzification parameters (constant)	'down':	[-100]
	'ldown':	[-50]
	'stable':	[0]
	'lup':	[50]
	'up':	[100]

The structure of the fuzzy controller for shades and lights can be seen in Figure 3:

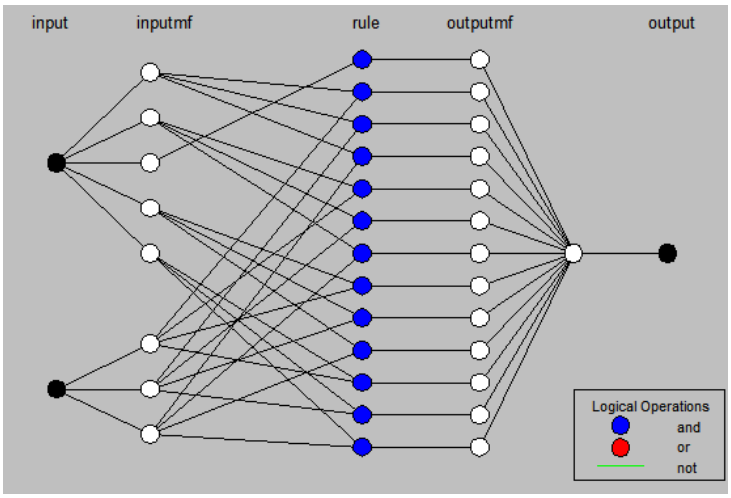

Figure 3: Structure for shades and art. lights

3.2 Sensor arrangement in building

The arduino is placed on the ceiling in the office. The PIR sensor (presence sensor), the inside illuminance sensor, the memory card module (for storing files and writing sensor values, fuzzy outputs and arduino outputs in a txt file) and the xbee module (for wireless communications) are placed on a detachable shield properly designed to attach on arduino and for use with this system. The outdoors illuminance sensor is placed outside the office window and is connected with cable to our arduino system. The system can be both battery and mains powered.

3.3 Zigbee protocol for wireless communications

The system uses xbee modules to communicate with computer through zigbee protocol. It sends the outputs, sensor values, current position of blinds and lights state to computer that monitors the system or to an arduino equipped with an LCD screen in the office room. Also the system can be programmed through zigbee from distance, send and receive files from and to memory card. The personnel of the office can bypass with zigbee the system for using their own parameters of the lighting and blinds state to match their needs.

4 RESULTS

In this chapter the results of the developed controller can be seen. At first in Figure 4, the inputs and outputs of the two developed fuzzy controllers can be seen. The hardware connection of the sensors with the arduino micro-controller can be seen in Figure 5.

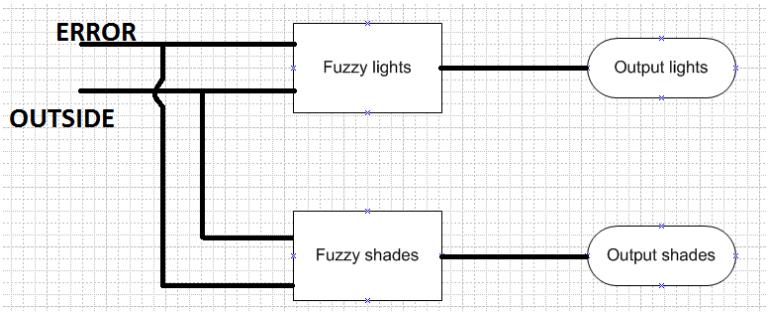

Figure 4: Fuzzy model for our system

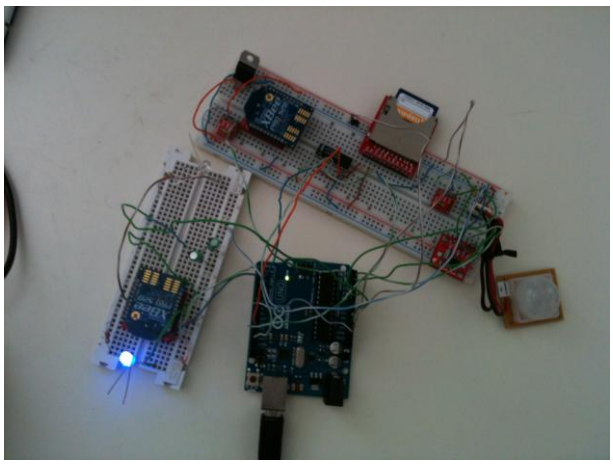

Figure 5: The developed system applied in a breadboard

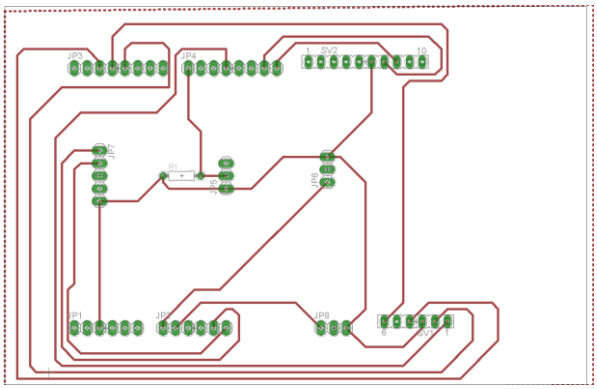

Figure 6: Designed Shield for the necessary sensors

The change in the light level due to outdoor illuminance and difference between the current and desired illuminance can be seen in Figure 8, while the change in the shades position using the same inputs can be seen in Figure 7.

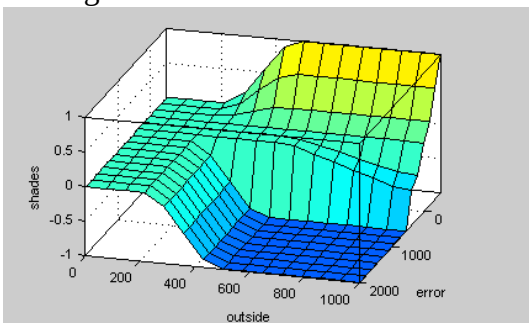

Figure 7: Structure from MATLAB for shades

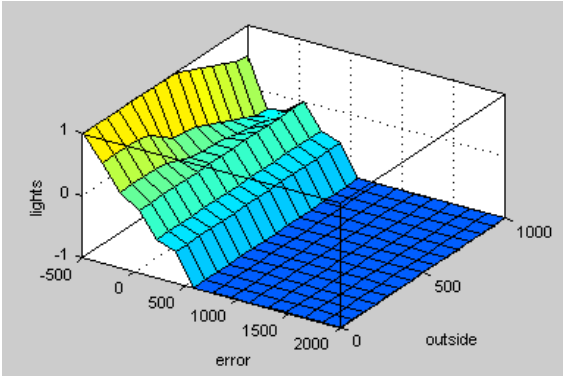

Figure 8: Structure from MATLAB for lights

5 CONCLUSIONS

This smart controller effectively uses fuzzy logic to properly control lights and venetian blinds in an office space with little power needed. It communicates with computer systems to become more accurate and flexible. It stores fuzzy rules and membership functions in memory card and this way is easily accessible to users.

6 SUGGESTIONS

Using arduino and sensors in an office control system is easy-adaptable and very flexible. More sensors can be added and with proper arduino coding, more functions can be performed with little effort. We can add to this system a CO2 sensor, a humidity sensor, a temperature sensor to entirely control an office room with one exclusive system and provide a complete controlled working environment with little to none human interference and save space because this system is very small and can pass unnoticed.

7 ACKNOWLEDGEMENTS

This work is partly funded by the EU Commission, within the research contract GREEN@Hospital (Contract Nr. 297290) a three year European Project co-funded by the ICT Policy Support Programme as part of the Competitiveness and Innovation framework Programme (CIP).

8 REFERENCES

Berson, David M., Felice A. Dunn, and Motoharu Takao. 2002. “Phototransduction by retinal ganglion cells that set the circadian clock.” *Science* 295:1070–73.

Galasiu, Anca D., Morad R. Atif, and Robert A. MacDonald. 2004. “Impact of window blinds on daylight-linked dimming and automatic on/off lighting controls.” *Solar Energy* 76:523–44.

Galasiu, Anca D., and Jennifer A. Veitch. 2006. “Occupant preferences and satisfaction with the luminous environment and control systems in daylit offices: a literature review.” *Energy and Buildings* 38:728–42.

Guillemin, A., and S. Molteni. 2002. “An energy-efficient controller for shading devices self-adapting to the user wishes.” *Building and Environment* 37:1091–97.

Guillemin, A., and N. Morel. 2001. “An innovative lighting controller integrated in a self-adaptive building control system.” *Energy and Buildings* 33:477–87.

Guillemin, A., and N. Morel. 2002. “Experimental results of a self-adaptive integrated control system in buildings: a pilot study.” *Solar Energy* 72:397–403.

Inoue, T., T. Kawase, T. Ibamoto, S. Takakusa, and Y. Matsuo. 1988. “The development of an optimal control system for window shading devices based on investigations in office buildings.” *ASHRAE Transactions* 94:1034–49.

Kolokotsa, D. 2003. “Comparison of the performance of fuzzy controllers for the management of the indoor environment.” *Building and Environment* 38:1439–50.

Kolokotsa, D., D. Rovas, E. Kosmatopoulos, and K. Kalaitzakis. 2010. “A roadmap towards intelligent net zero- and positive-energy buildings.” *Solar Energy* 85:3067–84.

Kolokotsa, D., G. Saridakis, A. Pouliezos, and G. S. Stavrakakis. 2006. “Design and installation of an advanced EIB^{TM} fuzzy indoor comfort controller using Matlab.” *Energy and Buildings* 38:1084–92.

Kolokotsa, D., D. Tsiavos, G. S. Stavrakakis, K. Kalaitzakis, and E. Antonidakis. 2001. “Advanced fuzzy logic controllers design and evaluation for buildings’ occupants thermal-visual comfort and indoor air quality satisfaction.” *Energy and Buildings* 33:531–43.

Kurian, C., R. Aithal, J. Bhat, and V. George. 2008. “Robust control and optimisation of energy consumption in daylight--artificial light integrated schemes.” *Lighting Research and Technology* 40:7–24.

Kurian, Cp, S. Kuriachan, J. Bhat, and Rs Aithal. 2005. “An adaptive neuro-fuzzy model for the prediction and control of light in integrated lighting schemes.” *Lighting Research and Technology* 37:343–52.

Leslie, R. P., R. Raghavan, O. Howlett, and C. Eaton. 2005. “The potential of simplified concepts for daylight harvesting.” *Lighting Research and Technology* 37:21–40.

Trobec Lah, Mateja, Borut Zupančič, Jože Peternelj, and Aleš Krainer. 2006. “Daylight illuminance control with fuzzy logic.” *Solar Energy* 80:307–21.

EXERGY ANALYSIS OF BIOGAS-FED SOFC

G. Fragoyiannis, D. Mytakis and F.A. Coutelieris

Department of Environmental & Natural Resources Management, University of Patras, Seferi 2, 30100, Agrinio, Greece, Tel: +302641074196; Fax: +30 2641074176, fcoutelieris@upatras.gr

ABSTRACT

Fuel cells are highly efficient energy conversion systems that have recently gained significant interest in terms of both science and applications. Exergy analysis is adopted here for a power plant involving SOFC with external steam reforming that is fuelled by modeled biogas/steam mixtures. The electrical efficiency has been estimated and the effect of various operational parameters on the process efficiency has been investigated. The optimal operation parameters of the integrated SOFC plant are specified by pinpointing and minimizing the existing losses, while a parametric analysis has been also performed to provide guidelines for practical design.

KEYWORDS

SOFC, biogas, Power plant, Energy, Exergy analysis.

1 INTRODUCTION

From the very beginning of the systematic development of actual electricity generating systems based on fuel cells, research was guided by endeavors to approximate their optimal theoretical patterns of operation as dictated by the first law of thermodynamics. Given that the first law (energy) analysis has been generally regarded as capable and sufficient to determine real design optima, the analysis according to the second law was usually underestimated. In fact, it was not until the term "exergy" became a synonym of monetary value when the second law acquired practical significance in the optimization of energy systems. Since this had happened, the "exergy analysis" has been accepted as a sound method for the interpretation of the axiomatic role of the second law in the design and optimization of energy systems in terms of both efficiency and cost, and as a supplementary tool to aid in decision making about the parameters and criteria that may lead to optimality in terms of the impact of engineering systems to environment (Rosen &Dincer, 2001).

Biogas is a renewable fuel containing 50 – 80 %v CH4 diluted by 50 – 20 %v CO2 reforming agent. Only 10 % of the readily exploitable biogas resources are estimated to be used today due to the local nature of biogas production, which implies the use of internal combustion engines of small nominal power and low electrical conversion. Moreover, landfill biogas (almost 80 % of current biogas production) often contains less than 50 % CH4, hindering its use in conventional power systems. On the contrary, solid oxide fuel cells (SOFCs) can be directly fed with CH4/H2O mixtures and by-pass the need to pre-reform biogas or to eliminate CO through successive catalytic reactors (Singhal & Kendall, 2003). Internal steam reforming is the dominant route for biogas-fed SOFCs commercialization, while only few preliminary studies, mostly triggered by the prospects of direct biogas SOFC applications, had examined internal dry reforming (Yentekakis, 2006, Shiratori et al., 2008).

In general, the advantageous position of fuel cells as highly efficient energy conversion systems has been indemnified by numerous projects for installation in central or distributed power plants (see for example Bedringas et al., 1997). Accumulation of experience from these early fuel cell programs revealed that it would be useful to recognize the exergetic

optimization criteria for effective performance, as these could allow engineering modifications to attain optima unconceivable from energy conservation law. The present work is devoted to the examination of this specific problem, assuming a stationary power plant fed by biogas and comprised of a SOFC with the ability of internal steam reforming, while peripheral devices were also considered.

2 ENERGY AND EXERGY BALANCES

Exergy is the thermodynamic property that describes the "useful energy" content, or the "work producing potential" of a system at a certain state (Kotas, 1985). Hence, exergy can be calculated assuming the reversible thermal, mechanical and chemical transition of the system to a state that is in equilibrium with its environment. A clarification of the exergy concept can be presented by considering a one inlet – one outlet device as a system with a flow of a mixture of i chemical species of known composition at elevated temperature and high pressure. The energy balance for this system, ignoring the changes in kinetic and potential energies, may be expressed as

$$\sum_j \dot{Q}_j - \dot{W} = \left(\sum_i \dot{m}_i h_i \right)_{in} - \left(\sum_i \dot{m}_i h_i \right)_{out} \tag{1}$$

where $\dot{Q}_j$ is the heat flux from the environment to the system, $\dot{W}$ is the power produced by the system, $\dot{m}_i$ is the mass flowrate and h_i is the specific enthalpy of the species i, respectively. On the other hand, the exergy balance for this system is,

$$\sum_{i=1}^{p} \left(1 - \frac{T_0}{T_i} \right) \dot{Q}_i + \sum_{i=1}^{n} [(\bar{h}_i - T_0 \bar{s}_i)_{in} - \mu_{0,i}] \dot{N}_{i,in} = \dot{W} + \sum_{i=1}^{n} [(\bar{h}_i - T_0 \bar{s}_i)_{out} - \mu_{0,i}] \dot{N}_{i,out} + T_0 \dot{s}_{gen} \tag{2}$$

where $T_0 \dot{s}_{gen}$ is the rate of exergy destruction in the system due to the irreversibility (heat dissipation, mixing, chemical reactions etc.), $\dot{N}_{i,in}$ and $\dot{N}_{i,out}$ are molar flow rates and the bar over some quantities of Eq. (2) denotes averaged quantities referred to mixture of chemical species. The first term of the left hand side of Eq. (2) describes the exergy in heat flows and the second the exergy in inlet mass flows. The second term of the right hand side describes the exergy in outlet mass flows.

Based on the energy and exergy balances of Eqs. (1) and (2), the analysis of the power plant is possible given the exact definition of the physical and chemical properties of each stream of matter and the environment. For the purposes of this work, the "standard reference environment" proposed by Szargut et al. (1988) has been adopted and an environmental composition of 75.67% N2, 20.35% O2, 0.03% CO2, 3.03% H2O(g) and 0.92% Ar in volume basis was assumed at T_0 = 298.13 K and p_0 = 1.013 bar.

3 THE POWER PLANT

The architecture of the system that has been taken under consideration in the present study is presented in Figure 1. A range of biogas/steam mixtures of constant molar flowrate ($2.9\ 10^{-6}$ mol/sec) were fed to the anode compartment in parallel (co-flow) to a cathodic air flowrate ($4.0\ 10^{-5}$ mol/sec), adequate to ensure a slight variation of the oxygen content, throughout the unit volume. The, preheated at 1073 K in a heat exchanger biogas/steam mixtures are mixed with steam in the mixer before supply the cell and internally reformed through the linearly independent reactions of steam reforming and water gas shift (WGS):

$$CH_4 + H_2O \leftrightarrow CO + 3H_2 \quad (3)$$

$$CO + H_2O \leftrightarrow CO_2 + H2 \quad (4)$$

The anodic electro-oxidation of both H2 and CO at the triple phase boundary is given as:

$$H_2 + CO + 2O^{2-} \rightarrow H_2O + CO_2 + 4e^- \quad (5)$$

Although only one device is actually required for both reforming and electro-oxidation, it is necessary to distinguish reformer from fuel cell, in terms of processing, as presented in Figure 1. In order to express the incompleteness of the above mentioned reforming process, the extensions of reforming, ε_{CH4} were used as conversion factors of reaction (3). It is also assumed that reaction (5) takes place with an extent below 100% by employing the factor of hydrogen utilization, U. In practice, a portion of hydrogen would not react in the SOFC since the cell voltage adjusts to the lowest chemical potentials for the gas mixture at the exit of the anode. Unreformed methane and residual hydrogen are considered to undergo complete combustion in the burner providing heat for vaporization and reforming. The reformer and the vaporizer are heated by the burner while a heat exchanger is used to increase the temperature of the incoming air. A part of the heat produced in the burner is released to the environment. Finally, the overall energy efficiency (η_I, %) is defined as the ratio of the produced electrical work to the lower heating value of biogas and the overall exergy efficiency (η_{II}, %) as the ratio of the produced electrical work to the standard chemical exergy of biogas. Obviously, the aforementioned values depend on biogas composition.

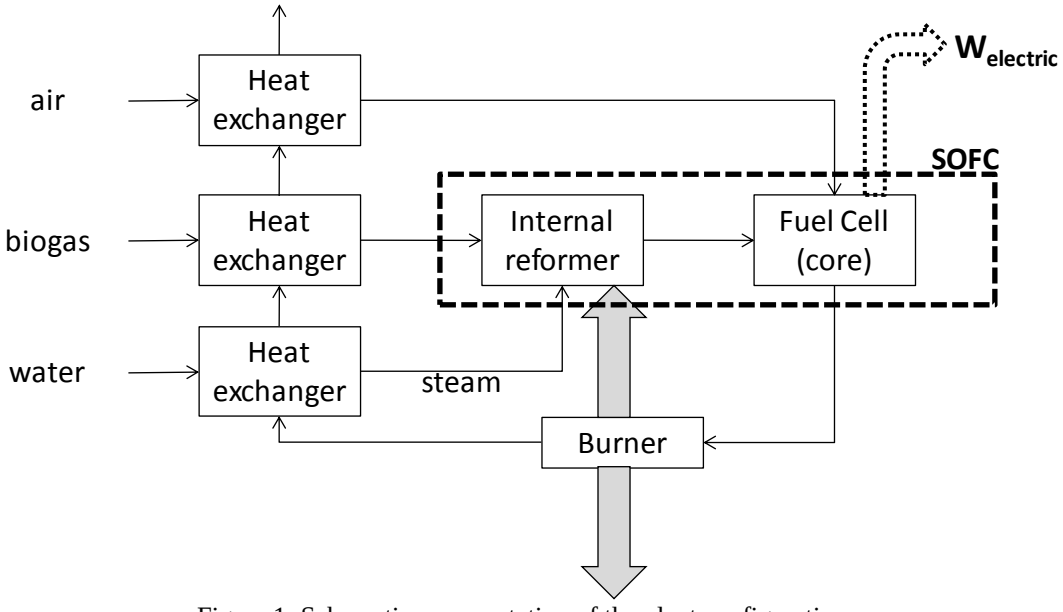

Figure 1: Schematic representation of the plant configuration.

4 RESULTS & DISCUSSION

Fully-customizable modular software, based on the above mentioned mathematical principles, has been developed to simulate the processes that take place in the described system. This program represents the power plant with a circuit-like structure consisted of nodes and connection branches. Each separate device of the system is assumed to be a node of the equivalent circuit. The most significant independent variables that affect on the efficiency have been considered to be the extension of reforming (ε_{CH4}) and the fuel utilization (U). The flow, the temperature, the energy and the exergy in every branch as well as the irriversibilities in every node were calculated as functions of these operational parameters with high accuracy (error < 0.1%). For the calculation of the exact temperatures in the sites of the power cycle, an iterative method has been employed by considering the variation of the thermal capacities with temperature.

Table 1 presents the operational flow-sheet of the system, where all the operational parameters (namely, the temperatures of any device as well as the mass flow-rate in any branch of the apparatus) have been justified so that maximum efficiency can be obtained. This maximization procedure aims at the satisfaction of the following criteria:

I. Air temperature just before the fuel cell should be as closer to the operational temperature of the cell as it can
II. Thermal energy and exergy releases from burner to environment should be minimal.
III. Temperature of flue gases must be minimized, as well.

It is obvious that all the above criteria are satisfied by the operational procedures described in the present work.

Table 1: Operational Flowchart

Branch	Flowrate (moles/s)	Temperature (K)	Energy (% of Biogas HHV)	Exergy (% of Biogas Standard Chemical Exergy)
1	3.7×10^{-6}	298	100	100
2	4.0×10^{-5}	298	0	0
3	3.2×10^{-6}	298	0	0
4	3.7×10^{-6}	1073	112.3	107.6
5	1.1×10^{-5}	1073	131.2	121.4
6	3.2×10^{-6}	1073	27.0	15.5
7	4.0×10^{-5}	1045	82.8	59.5
8	4.0×10^{-5}	1200	51.2	30.8
9	4.0×10^{-5}	1199	39.1	22.3
10	4.0×10^{-5}	1186	16.4	10.9
11	4.0×10^{-5}	1132	6.1	4.8
12	4.0×10^{-5}	1065	22.7	16.0

Device	Energy Balance (% of Biogas HHV)	Exergy destructed (% of Biogas Standard Chemical Exergy)
Heat Exchanger 1	0	0.5
Heat Exchanger 2	0	2.4
Heat Exchanger 3	0	3.0
Reformer	0	0.1
Fuel Cell	0	0.4
Burner	0	7.9
Electricity Produced	**81.3**	**78.5**

The influence of the extension of reforming as well as of the fuel utilization is presented in the following Figures. Power output of the fuel cell system is obviously positively affected by the increases of both the extension of the reforming and fuel utilization (see Figures 2a & 3a).

Furthermore, fuel utilization affects on cell outlet in an almost identical linear manner for values lower than 70% while a quite higher increment rate is presented as U values reach their upper limit (74%). It is obvious that the influence of these two parameters should be only on the devices that are related to reforming and electrochemical reactions. Thus, (see Figure 2b) its increase affects on the reformer, the fuel cell and the burner. This influence is positive in the direction of the efficiency maximization because the higher the ε_{CH4}, the richer in hydrogen the gas mixture that fed the cell and, thus, the lower the energy dissipations of the whole system. It must be noted that ε_{CH4} is limited at 93% because higher values correspond to conditions where the burner becomes insufficient for the coverage of the total energy needs of the system. System response to the variations of the fuel utilization is quite analogous (see Figure 3b). The only significant difference can be focused on the limit of the increament, which is 78%.

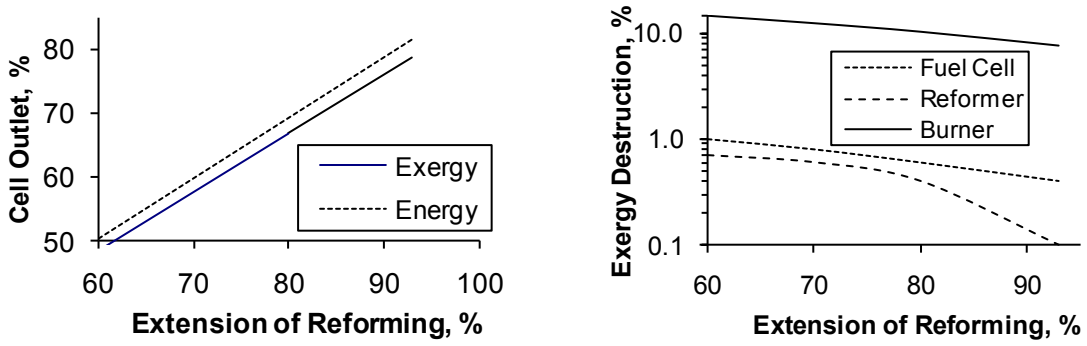

(a) **(b)**

Figure 3: Extension of reforming influence on cell outlet (a) and exergy destruction (b) (U = 78%, Tair = 1040K, CH4/CO2/H20=30/30/40).

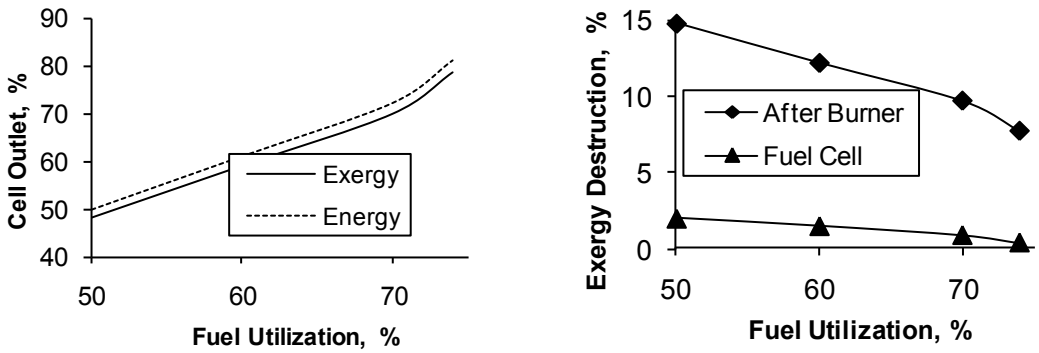

(a) **(b)**

Figure 4: fuel utilization influence on cell outlet (a) and exergy destruction (b) (ε_{CH4} = 93%, Tair = 1040K, CH4/CO2/H20=30/30/40).

5 CONCLUSIONS

The overall performance of a fuel cell system fed by biogas according to the first and the second law of thermodynamics, is presented here. The analysis was directed to the optimization of the operational condition, while both energy and exergy balances as functions

of the principal operational parameters have been postulated and used. A computer program with advanced optimization abilities was developed and used for simulation purposes. After the optimization took place, efficiencies of the order of 81.3% of the low heating value and 78.5% of the standard chemical exergy of biogas are obtained.

6 REFERENCES

Bedringas, K.W., Ertesvag, I.S., Byggstoyl, S., Magnussen, B.F. (1997) Exergy analysis of solid-oxide fuel-cell systems. *Energy*, 22, 403-412.

Kotas, T.J. (1985). *The exergy method of thermal plant analysis*. London: Butterworths.

Rosen, M.A., Dincer, I. (2001). Exergy as the confluence of energy, environment and sustainable development. *Exergy An International Journal*, 1, 3-13.

Shiratori, Y., Oshima, T., Sasaki, K. (2008). Feasibility of direct-biogas SOFC. *International Journal of Hydrogen Energy*, 33, 6316-6321.

Singhal, S.C., Kendall, K. (2003). *High Temperature Solid Oxide Fuel Cells*. New York: Elsevier.

Szargut, J., Morris, D.R., Steward, F.R. (1988)). *Exergy analysis of thermal, chemical and metallurgical processes*. New York: Hemisphere.

Yentekakis I.V. (2006). Open- and closed-circuit study of an intermediate temperature SOFC directly fueled with simulated biogas mixtures. *Journal of Power Sources*, 160, 422–425.

PILOT APPLICATION OF FLYWHEELS IN RES-BASED POWER PLANTS

G. N. Prodromidis and F.A. Coutelieris

Department of Environmental & Natural Resources Management, University of Patras, Seferi 2, 30100, Agrinio, Greece, Tel: +302641074196; Fax: +30 2641074176, fcoutelieris@upatras.gr

ABSTRACT

The present study deals with the feasibility of Flywheel Energy Storage Systems (FESS) in several RES-based stand-alone electricity production systems. Energy buffering is necessary in any RES-based off-grid system, however conventional energy storage systems (batteries, hydrogen etc.) suffer from limited equipment lifetime, high initial costs, and negative environmental impact during their operation as well as after their life-cycle. This study combines the mature technology of storing kinetic energy through a flywheel, with more conventional technologies such as electrochemical batteries. Through an extensive study of existing technologies, it is proved that an off-grid project with advanced and totally "green" technologies is feasible, and of comparable cost to more conventional RES-based systems. Furthermore, this study presents general information on FESS operation in several projects.

KEYWORDS

Flywheel, Hybrid System, Energy Storage System, Renewables, Zero emissions.

1 INTRODUCTION

Over the last 20 years, the world's population has increased by approx. 1.6 billion people and is expected to rise by 1.4 billion over the next 20 years (REN21, 2011). The above trend corresponds to an analogous increment in electricity demands due to industrialization, urbanization and motorization that are strongly associated with increased energy consumption, which consequently affects the fossil fuel process. In addition, the wasteful use of fossil fuels aggravates climate change due to continuous environmental pollution. The efficiency of energy production processes as well as the optimal adjustment between the load coverage and the consumption of specific parts of a stand-alone power system is crucial to eliminate energy waste. Therefore, the use of Renewable Energy Sources (RES), which are usually characterized by efficient energy conversion cycles, is further strengthened.

An attractive option towards optimization of global electrification in terms of environmentally friendly solutions is the development of off-grid supplied electricity systems. These hybrid systems are characterized by zero pollutant emissions and the lack of excessive operation and maintenance costs. Such systems are currently established in isolated remote areas for rural electrification where connection to the national grid is difficult and expensive (Bekele and Tadesse, 2012). During the last decades, renewable technologies such as photovoltaic panels/arrays (PVs) and wind turbines became popular in projects providing electricity to several one-way, grid connected and autonomous power plants up to 10kW.

The main drawback characterizing all RES-based autonomous systems is that the environmental energy potential is quite unpredictable since it fluctuates with time and is strongly dependent on local meteorological conditions (Prodromidis and Coutelieris, 2011). Temporary energy buffering in storage systems is crucial for an uninterruptable energy

supply, especially for standalone RES-based systems. Besides the well-known electrochemical batteries, numerous buffering technologies are used in mobile or medium-scale applications such as hydrogen technologies, super capacitors and compressed air pumps (Wang et al., 2013). To conclude, the development a low-cost, state-of-the-art eco-friendly device, which can be charged and discharged several times with high efficiency and has stable performance during a project's lifetime, is crucial for the total commercialization of buffering technologies based on RES. To this end, flywheels appear to provide a feasible solution, since they have numerous advantages compared to other technologies such as electrochemical batteries and hydrogen-based equipment. Their long lifespan is one of their main advantages as they can be charged and discharged at high rates for many cycles without efficiency losses. Their efficiencies are quite high (Liu and Jiang, 2007) while they can be connected either to an AC-bus, offering a huge variety of frequencies, or a DC-bus depending on the demands of the established hybrid system to cover the desirable load (Bolund et al. 2007). Drawbacks of such a solution include limited storage times as a significant percentage of commercialized flywheel stored capacity is wasted through the marvel of self-discharge. In optimum operation conditions (magnetic bearings, vacuum enclosed device, etc.), these rates are found to be in the range of 0.18 to 2.0 times stored capacity per hour (Farret and Simoes, 2006). These values are valid for very low friction losses and are significantly higher in real-life scenarios. This phenomenon can be reduced by using state-of-the-art construction materials such as carbon fibres, or by the combined use of more conventional technologies. However, this does increase the cost of such an installation dramatically, therefore the combination of different technologies prevents a more suitable solution for real-life RES-based systems.

This paper focuses on the involvement of renewable sources in off-grid systems, which constitute the starting point for the inclusion of off-grid supplied electricity into real-life projects. The current trends on designing an FESS and its implementation into an RES-based autonomous system are also discussed.

2 MATERIALS & METHODS

A laboratory-scale FES system was designed and constructed by using an electric motor of 1hp that would be fed by the excess energy from RES technologies when the environmental potential fluctuates at high levels. This electric energy is transformed into kinetic energy and stored in a rotational mass. By following the reverse path it can be given back to the system via the electric motor, acting as an alternator. The power of the specific motor is determined by the power of the battery (approx. 660W) and by the rotational speed (peak at approx. 1800rpm≈188.5rad/sec). Measured without load, the angular velocity was found higher than that given by the manufacturer because the standard value of 1800 rpm corresponds to standard supply voltage under the manufacturer's standard conditions, not attained in laboratory experiments. Here after, the higher rotational velocity is the experimental velocity (approx. 2150 rpm), measured under 12 V DC continuous supply without loads on the motor.

Several problems had to be overcome during the construction of the experimental FES system, mostly concerning the solidity of the rotational parts and the stability of the whole project. Numerous small-sized parts were designed from scratch. All the apparatus is presented in Fig. 1 and described in Table 1

(a)

b.

c.

d.

e.

f.

g.

h.

i.

Figure 1: The experimental apparatus (a) and its specific parts: (b) electric motor, (c) axle, (d) electromagnetic clutch, (e) roller bearings with housing, (f) adapter for axle, (g) adapter for rotational mass, (h) steel base, (i) frame.

Table 1: Description of the parts of the established FES system.

Parts	Description	Quantity
Axle	Aluminum, 15 cm long, supports the rotational mass.	1
Bearing housing	Steel case, oil lubricated for the roller bearing at the end of the axle which is supported on the frame.	1
Adapters	Aluminum, one to adapt the clutch to the motor's axle and one to permanently connect the rotational mass with the axle.	2
Electromagnetic clutch	Mayr ROBATIC, 24V, 20W and 20 Nm. Engages the rotational mass when appropriate.	1
Roller bearing	Diameter of 0.02 m. Responsible for reducing friction losses during rotation.	2
Rotational mass	Stores the kinetic energy from the electric motor; inner radius: 0.19m, outer radius: 0.25m, mass: 1.8kg, thickness: 0.005m and 8 connecting radii included.	1
Steel base	Mounted onto the electric motor to keep the outer housing of the clutch stable for the rotation of its internals.	1
Voltage source	Fed by the grid and offers 24V to the clutch during its engagement to the system: Phoenix Contact, 100V-240V AC input, 22.5-29.5V DC output.	1

Given the 1 hp electric motor, it is easy to calculate the torque provided at maximum power, which is approx. 3.956Nm. Two layouts (solid and hollow cylinder) and two different materials (steel and aluminium) have been taken into account for the simulations (see Table 2). It was found that the best option is the hollow aluminium rotational mass, presented in detail in Fig. 2, while the differences observed between the ideal mass and the constructed one can be attributed to safety reasons (avoid damage due to vibrations). One of the fundamental differences is the number and size of the connecting radii (eight instead of the four initially designed). This design eliminates the distortion of the rotational mass during rotation due to its higher thickness. The mass of the final construction was 0.700 kg heavier than the ideal because the adapter is also included with the axle.

Table 2: Ideal vs. constructed rotational mass.

Motor info				
P_{motor} (W)	745.69			
ω (rad/sec)	188.5			
Rotational mass	**Solid steel**	**Solid aluminum**	**Hollow steel**	**Hollow aluminium**
R_{max} (m)	0.215	0.310	0.270	0.380
R_{min} (m)	-	-	0.235	0.325
m (kg)	1.940	1.390	1.600	1.070
ω_{rot} (rad/sec)	181.88	176.95	181.99	187.50
L (m)	0.0017			
Operational results				
$E_{kinetic}$ (Wh)	0.207	0.290	0.317	0.473
I (kg m^2)	0.045	0.067	0.069	0.097
n (%)	0.0278	0.0389	0.0425	0.0634

a. b.

Figure 2: The rotational mass: (a) design, (b) construction.

3 THEORETICAL AND EXPERIMENTAL RESULTS & DISCUSSION

In the present study, the efficiency is calculated by dividing the mean energy stored in a specific time interval by the energy consumed by the electric motor in the same period. This magnitude depends on the time-scale of the whole process since, in a flywheel system, the duration of the rotational motion of the cylindrical mass is a crucial parameter for the estimation of the system's efficiency. For the optimal case of Table 2, the value of 0.0634% corresponds to a one-hour time-scale while the flywheel can be rotated for less than one minute. This very low percentage can be increased by changing the rotational time taken into account to calculate the efficiency of an FES system. By decreasing the time step of charging, the energy consumed by the electric motor can be directly comparable to that given back to system through the reverse path by the rotation of the mass.

Table 3: Experimental measurements.

t (sec)	ω(rad/sec)	E_{FES} (kWh)	Mean E_{FES} (kWh)	$E_{consumed}$ (kWh) $\left[=\frac{745.69}{3600}t\right]$	n (%) $\left[\frac{\text{Mean } E_{FES}}{E_{consumed}}\right]$
1	199.77	0.000357		0.000207	
2	194.05	0.000337	0.000347	0.000414	83.78
3	186.97	0.000313	0.000336	0.000622	54.02
4	179.49	0.000288	0.000324	0.000829	39.09
5	172.11	0.000265	0.000312	0.001036	30.13
6	164.94	0.000244	0.000301	0.001243	24.19
7	158.26	0.000224	0.000290	0.001450	19.98
8	151.86	0.000207	0.000279	0.001658	16.86
9	145.75	0.000190	0.000270	0.001865	14.45
10	140.58	0.000177	0.000260	0.002072	12.56
11	136.01	0.000166	0.000252	0.002279	11.04
12	131.20	0.000154	0.000244	0.002487	9.79
13	126.52	0.000143	0.000236	0.002694	8.75

The experimental process demonstrates that an FES system is capable of being rotated for a couple of seconds and then it stops due to friction losses because the apparatus is not vacuum-enclosed. In addition, the whole rotation of the axle is based on typical roller bearings with high friction losses compared to electromagnetic bearings. The efficiencies ranged between 83.78% and 8.75% and the operational time fluctuated from 2 to 13 sec (Table 3), although the flywheel can be rotated for 40 sec due to the moment of inertia. The analysis is

meaningless for such long time periods because the angular velocity of the flywheel decreases under 126.5 rad/sec for t>13 sec, thus the motor can return voltages lower than 12V. The time-dependent efficiency (last column in Table 3), could be improved by the use of an electric motor of higher angular velocity consuming the same amount of energy.

4 CONCLUSIONS

In this study, an FES system was simulated under different scenarios, and one of which (laboratory-scale) was implemented to validate the theoretical analysis. This process revealed the outstanding characteristics of flywheels during their operation. More precisely, two different materials and shapes were simulated for the rotational mass. It is proved that a hollow aluminium cylindrical mass is the preferable option since it can give better energy storage results. This mass shape was included into the experimental apparatus, designed and built to validate the theoretical results. As efficiency decreases rapidly with time due to friction losses, such an FES system can rival competitive storage technologies widely available on the market, but only for applications that use a storage energy bank to support a system for a very short-time during its operation or to cover a peak load for a limited time during a single day such as UPSs.

5 REFERENCES

Bekele, G., Tadesse, G. (2012). Feasibility study of small Hydro/PV/Wind hybrid system for off-grid rural electrification in Ethiopia. *Applied Energy*, 97, 5-15.

Bolund, B., Bernhoff, H., Leijon, M. (2007). Flywheel energy and power storage systems. *Renewable and Sustainable Energy Reviews*, 11, 235-258.

Farret, F.A., Simoes, M.G. (2006). *Integration of Alternative Sources of Energy*. New York: John Wiley & Sons.

Liu, H., Jiang, J. (2007). Flywheel energy storage-An upswing technology for energy sustainability. *Energy and Buildings*, 39, 599-604.

Prodromidis, G.N., Coutelieris, F.A. (2011). A comparative feasibility study of stand-alone and grid connected RES-based systems in several Greek Islands. *Renewable Energy*, 36, 1957-63.

REN21 Steering Committee (2011). *Renewables 2011 Global Status Report.* www.REN21.net

Wang, Y., Ronilaya, F., Chen, X., Roskilly, A.P. (2013). Modelling and simulation of a distributed power generation system with energy storage to meet dynamic household electricity demand. *Applied Thermal Engineering*, 50, 523-535.

ISBN 978-2-930471-42-6